Scientific and Technical Aerospace Reports

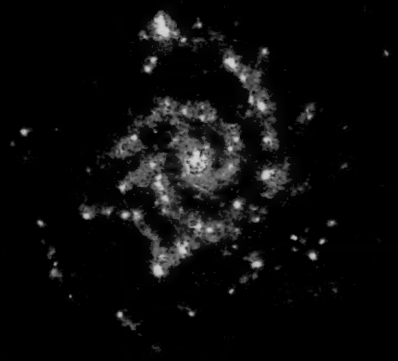

An Abstract Journal

Volume 32, Number 8
August 1994
N94-28399 to N94-30980

The NASA STI Program ... in Profile

Since its founding, NASA has been dedicated to the advancement of aeronautics and space science. The NASA Scientific and Technical Information (STI) Program plays a key part in helping NASA maintain this important role.

The NASA STI Program provides access to the NASA STI Database, the largest collection of aeronautical and space science STI in the world. The Program is also NASA's institutional mechanism for disseminating the results of its research and development activities.

Specialized services that help round out the Program's diverse offerings include creating custom thesauri, translating material to or from 34 foreign languages, building customized databases, organizing and publishing research results ... even providing videos.

For more information about the NASA STI Program, you can:

- **Phone** the NASA Access Help Desk at (301) 621-0390
- **Fax** your question to the NASA Access Help Desk at (301) 621-0134
- **E-mail** your question via the **Internet** to help@sti.nasa.gov
- **Write** to:

NASA Access Help Desk
NASA Center for AeroSpace Information
800 Elkridge Landing Road
Linthicum Heights, MD 21090-2934

Scientific and Technical Aerospace Reports

Scientific and Technical Aerospace Reports (STAR), is published each month as a major product of the NASA Scientific and Technical Information (STI) Program.

Inside this issue you will find:

- **Front Matter** containing a typical citation and abstract sample explaining the standard format, including codes for ordering reports
- **An Abstract Section** containing citations and abstracts of reports and publications that provide comprehensive coverage of worldwide aerospace-related topics including aeronautics and space science technology. *STAR* lists published and publicly available reports entered into the NASA STI Database during the four weeks preceding publication of this issue. These citations and abstracts are listed by subject categories.
- **An Index Section**
  - Subject
  - Personal author
  - Corporate source
  - Contract number
  - Report number
- **An Appendix** containing a guide for ordering cited reports, registering with the NASA STI Program, and using the available products and services. Additionally, price schedules, phone numbers, and addresses are included in this information packed section.

NASA also sponsors the companion journal, *NASA Open Volumes on Aerospace (NOVA)*, which lists abstracts of the open literature on aerospace subjects available worldwide. *NOVA* is for internal NASA use only, available from the NASA Center for AeroSpace Information (CASI).

Entries found in *STAR* are available through the NASA online retrieval service, RECON, and through DIALOG as the Aerospace Database.

The NASA STI Program gathers information through national and international agreements and exchanges and makes this information available to the NASA community and to the public in many forms through various outlets.

For additional information on the NASA STI Program, call the NASA Access Help Desk at (301) 621-0390, or write to:

NASA Center for AeroSpace Information
800 Elkridge Landing Road
Linthicum Heights, Maryland 21090-2934

US ISSN 0036-8741

This publication was prepared by the NASA Center for AeroSpace Information,
800 Elkridge Landing Road, Linthicum Heights, MD 21090-2934, (301) 621-0390.

Volume 32 Number 8 / August 1994

TABLE OF CONTENTS

AERONAUTICS For related information see also *Astronautics.*

01 AERONAUTICS (GENERAL) **3121**

02 AERODYNAMICS **3122**
Includes aerodynamics of bodies, combinations, wings, rotors, and control surfaces; and internal flow in ducts and turbomachinery. For related information see also 34 *Fluid Mechanics and Heat Transfer.*

03 AIR TRANSPORTATION AND SAFETY **3135**
Includes passenger and cargo air transport operations; and aircraft accidents. For related information see also *16 Space Transportation* and *85 Urban Technology and Transportation.*

04 AIRCRAFT COMMUNICATIONS AND NAVIGATION **3136**
Includes digital and voice communication with aircraft; air navigation systems (satellite and ground based); and air traffic control. For related information see also *17 Space Communications, Spacecraft Communications, Command and Tracking* and *32 Communications and Radar.*

05 AIRCRAFT DESIGN, TESTING AND PERFORMANCE **3145**
Includes aircraft simulation technology. For related information see also *18 Spacecraft Design, Testing and Performance* and *39 Structural Mechanics.* For land transportation vehicles see *85 Urban Technology and Transportation.*

06 AIRCRAFT INSTRUMENTATION **3149**
Includes cockpit and cabin display devices; and flight instruments. For related information see also *19 Spacecraft Instrumentation* and *35 Instrumentation and Photography.*

07 AIRCRAFT PROPULSION AND POWER **3150**
Includes prime propulsion systems and systems components, e.g., gas turbine engines and compressors; and onboard auxiliary power plants for aircraft. For related information see also *20 Spacecraft Propulsion and Power, 28 Propellants and Fuels,* and *44 Energy Production and Conversion.*

08 AIRCRAFT STABILITY AND CONTROL **3154**
Includes aircraft handling qualities; piloting; flight controls; and autopilots. For related information see also *05 Aircraft Design, Testing and Performance.*

09 RESEARCH AND SUPPORT FACILITIES (AIR) **3155**
Includes airports, hangars and runways; aircraft repair and overhaul facilities; wind tunnels; shock tubes; and aircraft engine test stands. For related information see also *14 Ground Support Systems and Facilities (Space).*

ASTRONAUTICS For related information see also *Aeronautics.*

12 ASTRONAUTICS (GENERAL) **3158**
For extraterrestrial exploration see *91 Lunar and Planetary Exploration.*

13 ASTRODYNAMICS **3159**
Includes powered and free-flight trajectories; and orbital and launching dynamics.

14 GROUND SUPPORT SYSTEMS AND FACILITIES (SPACE) **3160**
Includes launch complexes, research and production facilities; ground support equipment, e.g., mobile transporters; and simulators. For related information see also *09 Research and Support Facilities (Air).*

15 LAUNCH VEHICLES AND SPACE VEHICLES **3160**
Includes boosters; operating problems of launch/space vehicle systems; and reusable vehicles. For related information see also *20 Spacecraft Propulsion and Power.*

16 SPACE TRANSPORTATION **3164**
Includes passenger and cargo space transportation, e.g., shuttle operations; and space rescue techniques. For related information see also *03 Air Transportation and Safety* and *18 Spacecraft Design, Testing and Performance.* For space suits see *54 Man/System Technology and Life Support.*

17 SPACE COMMUNICATIONS, SPACECRAFT COMMUNICATIONS, COMMAND AND TRACKING **3164**
Includes telemetry; space communications networks; astronavigation and guidance; and radio blackout. For related information see also *04 Aircraft Communications and Navigation* and *32 Communications and Radar.*

N.A.—No abstracts were assigned to this category for this issue.

18 SPACECRAFT DESIGN, TESTING AND PERFORMANCE **3164**
Includes satellites; space platforms; space stations; spacecraft systems and components such as thermal and environmental controls; and attitude controls. For life support systems see *54 Man/System Technology and Life Support.* For related information see also *05 Aircraft Design, Testing and Performance*, *39 Structural Mechanics*, and *16 Space Transportation.*

19 SPACECRAFT INSTRUMENTATION **3171**
For related information see also *06 Aircraft Instrumentation* and *35 Instrumentation and Photography.*

20 SPACECRAFT PROPULSION AND POWER **3171**
Includes main propulsion systems and components, e.g., rocket engines; and spacecraft auxiliary power sources. For related information see also *07 Aircraft Propulsion and Power*, *28 Propellants and Fuels*, *44 Energy Production and Conversion*, and *15 Launch Vehicles and Space Vehicles.*

CHEMISTRY AND MATERIALS

23 CHEMISTRY AND MATERIALS (GENERAL) **3174**

24 COMPOSITE MATERIALS **3175**
Includes physical, chemical, and mechanical properties of laminates and other composite materials. For ceramic materials see *27 Nonmetallic Materials.*

25 INORGANIC AND PHYSICAL CHEMISTRY **3186**
Includes chemical analysis, e.g., chromatography; combustion theory; electrochemistry; and photochemistry. For related information see also *77 Thermodynamics and Statistical Physics.*

26 METALLIC MATERIALS **3201**
Includes physical, chemical, and mechanical properties of metals, e.g., corrosion; and metallurgy.

27 NONMETALLIC MATERIALS **3211**
Includes physical, chemical, and mechanical properties of plastics, elastomers, lubricants, polymers, textiles, adhesives, and ceramic materials. For composite materials see *24 Composite Materials.*

28 PROPELLANTS AND FUELS **3224**
Includes rocket propellants, igniters and oxidizers; their storage and handling procedures; and aircraft fuels. For related information see also *07 Aircraft Propulsion and Power*, *20 Spacecraft Propulsion and Power*, and *44 Energy Production and Conversion.*

29 MATERIALS PROCESSING **3227**
Includes space-based development of products and processes for commercial application. For biological materials see *55 Space Biology:*

ENGINEERING For related information see also *Physics.*

31 ENGINEERING (GENERAL) **3229**
Includes vacuum technology; control engineering; display engineering; cryogenics; and fire prevention.

32 COMMUNICATIONS AND RADAR **3240**
Includes radar; land and global communications; communications theory; and optical communications. For related information see also *04 Aircraft Communications and Navigation* and *17 Space Communications, Spacecraft Communications, Command and Tracking.* For search and rescue see *03 Air Transportation and Safety*, and *16 Space Transportation.*

33 ELECTRONICS AND ELECTRICAL ENGINEERING **3261**
Includes test equipment and maintainability; components, e.g., tunnel diodes and transistors; microminiaturization; and integrated circuitry. For related information see also *60 Computer Operations and Hardware* and *76 Solid-State Physics.*

34 FLUID MECHANICS AND HEAT TRANSFER **3269**
Includes boundary layers; hydrodynamics; fluidics; mass transfer and ablation cooling. For related information see also *02 Aerodynamics* and *77 Thermodynamics and Statistical Physics.*

35 INSTRUMENTATION AND PHOTOGRAPHY **3286**
Includes remote sensors; measuring instruments and gauges; detectors; cameras and photographic supplies; and holography. For aerial photography see *43 Earth Resources and Remote Sensing.* For related information see also *06 Aircraft Instrumentation* and *19 Spacecraft Instrumentation.*

36 LASERS AND MASERS **3292**
Includes parametric amplifiers. For related information see also *76 Solid-State Physics.*

37 MECHANICAL ENGINEERING 3297
Includes auxiliary systems (nonpower); machine elements and processes; and mechanical equipment.

38 QUALITY ASSURANCE AND RELIABILITY 3315
Includes product sampling procedures and techniques; and quality control.

39 STRUCTURAL MECHANICS 3316
Includes structural element design and weight analysis; fatigue; and thermal stress. For applications see *05 Aircraft Design, Testing and Performance* and *18 Spacecraft Design, Testing and Performance.*

GEOSCIENCES For related information see also *Space Sciences.*

42 GEOSCIENCES (GENERAL) 3324

43 EARTH RESOURCES AND REMOTE SENSING 3325
Includes remote sensing of earth resources by aircraft and spacecraft; photogrammetry; and aerial photography. For instrumentation see *35 Instrumentation and Photography.*

44 ENERGY PRODUCTION AND CONVERSION 3336
Includes specific energy conversion systems, e.g., fuel cells; global sources of energy; geophysical conversion; and windpower. For related information see also *07 Aircraft Propulsion and Power, 20 Spacecraft Propulsion and Power,* and *28 Propellants and Fuels.*

45 ENVIRONMENT POLLUTION 3341
Includes atmospheric, noise, thermal, and water pollution.

46 GEOPHYSICS 3354
Includes aeronomy; upper and lower atmosphere studies; ionospheric and magnetospheric physics; and geomagnetism. For space radiation see *93 Space Radiation.*

47 METEOROLOGY AND CLIMATOLOGY 3368
Includes weather forecasting and modification.

48 OCEANOGRAPHY 3376
Includes biological, dynamic, and physical oceanography; and marine resources. For related information see also *43 Earth Resources and Remote Sensing.*

LIFE SCIENCES

51 LIFE SCIENCES (GENERAL) 3379

52 AEROSPACE MEDICINE 3387
Includes physiological factors; biological effects of radiation; and effects of weightlessness on man and animals.

53 BEHAVIORAL SCIENCES 3397
Includes psychological factors; individual and group behavior; crew training and evaluation; and psychiatric research.

54 MAN/SYSTEM TECHNOLOGY AND LIFE SUPPORT 3399
Includes human engineering; biotechnology; and space suits and protective clothing. For related information see also *16 Space Transportation.*

55 SPACE BIOLOGY ..... N.A.
Includes exobiology; planetary biology; and extraterrestrial life.

MATHEMATICAL AND COMPUTER SCIENCES

59 MATHEMATICAL AND COMPUTER SCIENCES (GENERAL) ..... N.A.

60 COMPUTER OPERATIONS AND HARDWARE 3404
Includes hardware for computer graphics, firmware, and data processing. For components see *33 Electronics and Electrical Engineering.*

61 COMPUTER PROGRAMMING AND SOFTWARE 3406
Includes computer programs, routines, algorithms, and specific applications, e.g., CAD/CAM.

62 COMPUTER SYSTEMS 3430
Includes computer networks and special application computer systems.

63 CYBERNETICS **3434**
Includes feedback and control theory, artificial intelligence, robotics and expert systems. For related information see also *54 Man/System Technology and Life Support.*

64 NUMERICAL ANALYSIS **3451**
Includes iteration, difference equations, and numerical approximation.

65 STATISTICS AND PROBABILITY **3463**
Includes data sampling and smoothing; Monte Carlo method; and stochastic processes.

66 SYSTEMS ANALYSIS **3466**
Includes mathematical modeling; network analysis; and operations research.

67 THEORETICAL MATHEMATICS **3466**
Includes topology and number theory.

PHYSICS For related information see also *Engineering.*

70 PHYSICS (GENERAL) **3468**
For precision time and time interval (PTTI) see *35 Instrumentation and Photography*; for geophysics, astrophysics or solar physics see *46 Geophysics, 90 Astrophysics*, or *92 Solar Physics.*

71 ACOUSTICS **3477**
Includes sound generation, transmission, and attenuation. For noise pollution see *45 Environment Pollution.*

72 ATOMIC AND MOLECULAR PHYSICS **3481**
Includes atomic structure, electron properties, and molecular spectra.

73 NUCLEAR AND HIGH-ENERGY PHYSICS **3494**
Includes elementary and nuclear particles; and reactor theory. For space radiation see *93 Space Radiation.*

74 OPTICS **3498**
Includes light phenomena and optical devices. For lasers see *36 Lasers and Masers.*

75 PLASMA PHYSICS **3503**
Includes magnetohydrodynamics and plasma fusion. For ionospheric plasmas see *46 Geophysics.* For space plasmas see *90 Astrophysics.*

76 SOLID-STATE PHYSICS **3510**
Includes superconductivity. For related information see also *33 Electronics and Electrical Engineering* and *36 Lasers and Masers.*

77 THERMODYNAMICS AND STATISTICAL PHYSICS **3522**
Includes quantum mechanics; theoretical physics; and Bose and Fermi statistics. For related information see also *25 Inorganic and Physical Chemistry* and *34 Fluid Mechanics and Heat Transfer.*

SOCIAL SCIENCES

80 SOCIAL SCIENCES (GENERAL) **3526**
Includes educational matters.

81 ADMINISTRATION AND MANAGEMENT **3526**
Includes management planning and research.

82 DOCUMENTATION AND INFORMATION SCIENCE **3528**
Includes information management; information storage and retrieval technology; technical writing; graphic arts; and micrography. For computer documentation see *61 Computer Programming and Software.*

83 ECONOMICS AND COST ANALYSIS **3536**
Includes cost effectiveness studies.

84 LAW, POLITICAL SCIENCE AND SPACE POLICY **3537**
Includes NASA appropriation hearings; aviation law; space law and policy; international law; international cooperation; and patent policy.

85 URBAN TECHNOLOGY AND TRANSPORTATION **3537**
Includes applications of space technology to urban problems; technology transfer; technology assessment; and surface and mass transportation. For related information see *03 Air Transportation and Safety, 16 Space Transportation,* and *44 Energy Production and Conversion.*

SPACE SCIENCES For related information see also *Geosciences.*

88 SPACE SCIENCES (GENERAL) ..... **N.A.**

89 ASTRONOMY **3538**
Includes radio, gamma-ray, and infrared astronomy; and astrometry.

90 ASTROPHYSICS **3542**
Includes cosmology; celestial mechanics; space plasmas; and interstellar and interplanetary gases and dust. For related information see also *75 Plasma Physics.*

91 LUNAR AND PLANETARY EXPLORATION **3549**
Includes planetology; and manned and unmanned flights. For spacecraft design or space stations see *18 Spacecraft Design, Testing and Performance.*

92 SOLAR PHYSICS **3550**
Includes solar activity, solar flares, solar radiation and sunspots. For related information see also *93 Space Radiation.*

93 SPACE RADIATION **3552**
Includes cosmic radiation; and inner and outer earth's radiation belts. For biological effects of radiation see *52 Aerospace Medicine.* For theory see *73 Nuclear and High-Energy Physics.*

GENERAL

Includes aeronautical, astronautical, and space science related histories, biographies, and pertinent reports too broad for categorization; histories or broad overviews of NASA programs.

99 GENERAL **3553**

SUBJECT INDEX **I-1**

PERSONAL AUTHOR INDEX **I-169**

CORPORATE SOURCE INDEX **I-189**

CONTRACT NUMBER INDEX **I-219**

REPORT NUMBER INDEX **I-223**

APPENDIX **A-1**

TYPICAL CITATION AND ABSTRACT

NASA SPONSORED — ON MICROFICHE

ACCESSION NUMBER → **N94-12270*#** United Technologies Corp., West Palm Beach, FL. ← CORPORATE SOURCE
Pratt and Whitney.

TITLE → **ADVANCED CONTROL FOR AIRBREATHING ENGINES, VOLUME 1: PRATT AND WHITNEY**

AUTHOR → J. A. Ralph Jul. 1993 83 p ← PUBLICATION DATE

CONTRACT OR GRANT → (Contract NAS3-25952; RTOP 505-62-61)

REPORT NUMBERS → (NASA-CR-189203; E-8006; NAS 1.26:189203) Avail: CASI HC A05/MF A01 ← AVAILABILITY SOURCE AND PRICE CODE

The application of advanced control concepts to air breathing engines may yield significant improvements in aircraft/engine performance and operability. Screening studies of advanced control concepts for air breathing engines were conducted by three major domestic aircraft engine manufacturers to determine the potential impact of concepts on turbine engine performance and operability. The purpose of the studies was to identify concepts which offered high potential yet may incur high research and development risk. A target suite of proposed advanced control concepts was formulated and evaluated in a two phase study to quantify each concept's impact on desired engine characteristics. To aid in the evaluation specific aircraft/engine combinations were considered: a Military High Performance Fighter mission, a High Speed Civil Transport mission, and a Civil Tiltrotor mission. Each of the advanced control concepts considered in the study are defined and described. The concept potential impact on engine performance was determined. Relevant figures of merit on which to evaluate the concepts are determined. Finally, the concepts are ranked with respect to the target aircraft/engine missions. A final report describing the screening studies was prepared by each engine manufacturer. Volume 1 of these reports describes the studies performed by Pratt & Whitney. Author (revised)

VOLUME 32 NUMBER 8 / August 1994

Scientific and Technical Aerospace Reports

A Monthly Publication of the National Aeronautics and Space Administration

01 AERONAUTICS (GENERAL)

N94-28537* National Aeronautics and Space Administration, Washington, DC.
AERONAUTICAL ENGINEERING: A CUMULATIVE INDEX TO A CONTINUING BIBLIOGRAPHY (SUPPLEMENT 300)
Feb. 1994 673 p
(NASA-SP-7037(300); NAS 1.21:7037(300)) Avail: CASI HC A99

This publication is a cumulative index to the abstracts contained in supplements 288 through 299 of Aeronautical Engineering: A Continuing Bibliography. The bibliographic series is compiled through the efforts of the Center for Aerospace Information of the National Aeronautics and Space Administration (NASA). Seven indexes are included: subject, personal author, corporate source, foreign technology, contract number, report number, and accession number. Author

N94-28666# Naval Aviation Logistics Center, Patuxent River, MD. Maintenance Office.
AIRCRAFT AGE IMPACTS ON MAINTENANCE REQUIREMENTS
John Johnson Sep. 1993 21 p
(AD-A275701) Avail: CASI HC A03/MF A01

Under the current defense environment, decreasing economic resources limit new aircraft acquisition programs. As a consequence the Services will be forced to operate aging aircraft without replacement for many critical missions. The impact of this average age increase upon future Operating and Support (O&S) costs must be assessed properly if the Department of Defense decision makers are to make properly informed downsizing decisions. The Naval Aviation Maintenance Office, Logistics Engineering Department, Resource Analysis Division, has developed methodology, techniques and procedures for evaluating potential relationships between the age of in service aircraft and their O&S costs using existing data bases. The incidence of verified material failures (VF) and the Direct Maintenance Manhours (DMH) expended to correct them are correlated to the aircraft's age during its in-service operational life and are potential indicators of increased O&S Costs. The Naval Aviation Logistics Data Analysis (NALDA) data bases for Navy and Marine Corp aircraft contain historical operations and maintenance data which can serve as age indicators. DTIC

N94-28732# Naval Aviation Logistics Center, Patuxent River, MD. Maintenance Office.
AIRCRAFT AGE IMPACT ON INDIVIDUAL OPERATING AND SUPPORT COST ELEMENTS
Laurence Stoll and Stan Davis Sep. 1993 40 p
(AD-A275739) Avail: CASI HC A03/MF A01

This study develops methodology, techniques and procedures for evaluation of age related cost trends associated with major categories of Operating and Support cost. Data sources including Naval Aviation Logistics Data Analysis (NALDA) history, Chief of Naval Operations Flying Hour Projection System Budget Analysis Reports, Visibility and Management of Operating and Support Cost Maintenance Subsystem and Total Support System reports, and Naval Depot Production Performance Reports (PPR's) were used to evaluate cost trends over the most recent ten years of cost data. Detailed data was collected on ten major Type Model Series aircraft including the P-3C, S-3A, F/A- 18A/B, F-14A, CH-53E, SH-60B, E-2C, SH-3H, CH-46E and A-6E. Evaluations of age related trends and recommendations for changes in current estimating processes when appropriate have been developed for the following cost categories; (1) O&I Level Consumables/Repair Parts (2) AVDLR's; (3) Aircraft Overhaul/Support; (4) Engine Overhaul/Support; (5) Petroleum, Oil, Lubricants (POL); (6) O and I level labor requirements. Results of this study clearly demonstrate age related trends of increasing costs linked to aircraft service life 'fleet age' for most of the categories under examination. DTIC

N94-28743# Air Force Inst. of Tech., Wright-Patterson AFB, OH. School of Logistics and Acquisition Management.
DEMONSTRATION OF IMPROVED SOFTWARE SUPPORT LABOR ESTIMATION FOR AIR FORCE OPERATIONAL FLIGHT PROGRAMS THROUGH FUNCTIONAL ORIENTATION M.S. Thesis
Ronald R. Warner, Jr. and Darrel L. Wright Dec. 1993 251 p
(AD-A275789; AFIT/GSS/LAS/93D-7) Avail: CASI HC A12/MF A03

This study demonstrated two approaches to improve current software support effort estimation models for aircraft software. Both approaches involved a functional orientation not used by existing models. The first approach demonstrated how to orient a model to reflect the block change cycle modification process and how to represent support effort changes over time in order to improve effort estimation accuracy. Current software models do not reflect the support environment or the temporal characteristics of aircraft software support. The second approach demonstrated how to calibrate a model by properly selecting source data in order to increase accuracy. Support calibration is not addressed by current models. A literature search affirmed the validity of both approaches and the methodology. In addition, a standard description of the block change cycle was developed and validated. A prototype estimation model was derived from the COCOMO model and included a unique support calibration. Data was obtained from Air Force Software Support Centers but was unusable, so data was generated from the prototype for the demonstration. A method that was developed to compare the prototype with current models demonstrated that the prototype is an acceptable model. DTIC

N94-29090 Aeronautical Research Labs., Melbourne (Australia).
FISHERMANS BEND: A CENTRE OF AUSTRALIAN AVIATION
J. L. Kepert Sep. 1993 75 p Limited Reproducibility: More than 20% of this document may be affected by microfiche quality
(AD-A274981; ARL-GD-39; DODA-AR-008-377) Avail: CASI HC A04

Since 1919, Fishermens Bend, Victoria, has been a major center of Australian aviation. Many of Australia's great aviation achievements were born there. From its formation in 1939, the Aeronautical Research Laboratory, situated astride this activity at the Bend, has provided scientific and technical support to numerous aeronautical endeavors occurring in its surrounds. This report summarizes the many activities at the Bend from the first flight of an S11 Shorthorn from the Carey Airfield in 1919 to the production to the last indigenously built aircraft, the Nomad, in 1984. The aerodromes have long gone, the roar of aero-engines are contained within test cells, but the strong tradition of Australian aviation still lives on at the Bend today. DTIC

N94-29160 Sumitomo Heavy Industries Ltd., Tokyo (Japan).
[STUDY OF BRIDGE DESIGN AND TECHNOLOGY]
1993 89 p In JAPANESE
(PB94-137916) Copyright Avail: Issuing Activity (National Technical Information Service (NTIS))

Contents: Study of Super Long-span Bridge; ATMD System for Vibration Suppression on Bridge Tower; Effects of Turbulence Flow on Aerodynamic Characteristics of Box Girder Bridges; Aerodynamic Stability of Bridge Tower;

Fabrication of 780N/mm2 Class High Tensile Steels Made Truss Member Chord; Structural Analysis System of Long Span Bridge; Design of Akashikaikyo-ohashi Bridge; Design and Vibration Control of Tsurumi Fairway Bridge; Fabrication, Erection and Cable Vibration Control of Kemi 1-gousen Bridge; Repair Work of Girder on Hanshin Expressway Accidentally Damaged by Falling Heavy Load; Countermeasure for Infra-sound and Erection of Dodairazawabashi Bridge; Design, Fabrication, and Laying Down of 4A Steel Caisson for Kurushima-ohashi Bridge. NTIS

N94-29463# Aerospatiale, Paris (France).
A TIME REASONING SYSTEM BASED ON THE EVENT CALCULUS FOR SCHEDULING IN AERONAUTIC MAINTENANCE Ph.D. Thesis - Toulouse Univ. [UN SYSTEME DE RAISONNEMENT TEMPOREL BASE SUR LE CALCUL D'EVENEMENTS POUR L'ORDONNANCEMENT EN MAINTENANCE AERONAUTIQUE]
Denys Bernard 1993 214 p In FRENCH
(Rept-932-710-101; ETN-94-95487) Avail: CASI HC A10/MF A03

Problems specific to the planning and scheduling of aircraft maintenance work sites are addressed. Methods presently employed and their associated problems are considered. The event calculus of Kowaslki and Sergot is introduced. Its adaptation to the domain of aircraft maintenance is considered, together with the associated inference rules. This permits an appropriate representation of the whole of the actions which are treated in a particular problem. A description of all the axioms characterizing the different types of situation for which a plan is to be prescribed is given. This presupposes that the scheduling takes out or prevents intervention of 'bugs' which could constrain the time organization of the actions. The sequencing processed by the computer architecture is considered. The organization of the system is explained. The last program tested is presented. ESA

N94-29842# Lawrence Livermore National Lab., CA.
DUAL-BAND INFRARED (DBIR) IMAGING INSPECTIONS OF BOEING 737 AND KC-135 AIRCRAFT PANELS
N. K. DelGrande, K. W. Dolan, P. F. Durbin, M. R. Gorvad, and A. B. Shapiro 27 Aug. 1993 55 p
(Contract W-7405-eng-48)
(DE94-005700; UCRL-CR-115237) Avail: CASI HC A04/MF A01

We apply dual-band infrared (DBIR) imaging as a dynamic thermal tomography tool for wide area inspection of a Boeing 737 aircraft and several Boeing KC-135 aircraft panels. Our analyses are discussed in this report. After flash-heating the aircraft skin, we record synchronized DBIR images every 40 ms, from onset to 8 seconds after the heat flash. We analyze selective DBIR image ratios which enhance surface temperature contrast and remove surface-emissivity clutter (from dirt, dents, tape, markings, ink, sealants, uneven paint, paint stripper, exposed metal, and roughness variations). The Boeing 737 and KC-135 aircraft fuselage panels have varying percent thickness losses from corrosion. We established the correlation of percent thickness loss with surface temperature rise (above ambient) for a partially corroded F-18 wing box structure and several aluminum reference panels. Based on this correlation, lap splice temperatures rise 1 C per 24 +/- 5 % material loss at 0.4 s after the heat flash. We show tables, charts and temperature maps of typical lap splice material losses for the riveted (and bonded) Boeing 737 and the riveted (but unbonded) Boeing KC-135. We map the fuselage composite thermal inertia, based on the (inverse) slope of the surface temperature versus inverse square root of time. Composite thermal inertia maps characterize shallow skin defects within the lap splice at early times (less than 0.3 s) and deeper skin defects within the lap splice at late times (greater than 0.4 s). Late time composite thermal inertia maps depict where corrosion-related thickness losses occur. Lap splice sites on a typical Boeing KC-135 panel with low composite thermal inertia values had high skin-thickness losses from corrosion. DOE

02 AERODYNAMICS

Includes aerodynamics of bodies, combinations, wings, rotors, and control surfaces; and internal flow in ducts and turbomachinery.

For related information see also *34 Fluid Mechanics and Heat Transfer.*

N94-28658*# National Aeronautics and Space Administration. Langley Research Center, Hampton, VA.
STEADY PRESSURE MEASUREMENTS ON AN AEROELASTIC RESEARCH WING (ARW-2)
Maynard C. Sandford, David A. Seidel, and Clinton V. Eckstrom Feb. 1994 537 p
(RTOP 505-63-50-15)
(NASA-TM-109046; NAS 1.15:109046) Avail: CASI HC A23/MF A04

Transonic steady and unsteady pressure tests have been conducted in the Langley transonic dynamics tunnel on a large elastic wing known as the DAST ARW-2. The wing has a supercritical airfoil, an aspect ratio of 10.3, a leading-edge sweep back angle of 28.8 degrees, and two inboard and one outboard trailing-edge control surfaces. Only the outboard control surface was deflected to generate steady and unsteady flow over the wing during this study. Only the steady surface pressure, control-surface hinge moment, wing-tip deflection, and wing-root bending moment measurements are presented. The results from this elastic wing test are in tabulated form to assist in calibrating advanced computational fluid dynamics (CFD) algorithms. Author (revised)

N94-28674# Naval Postgraduate School, Monterey, CA.
AERODYNAMIC DESIGN USING PARALLEL PROCESSORS Ph.D. Thesis
Stephen C. Brawley Sep. 1993 152 p
(AD-A275470) Avail: CASI HC A08/MF A02

An airfoil design technique has been developed which decreases the computational processing time by more than an order of magnitude when optimizing aerodynamic performance. The practicality of airfoil design using parallel processors and Navier-Stokes flow solvers has been demonstrated. Typically, an airfoil is designed to meet certain criteria based upon its aerodynamic performance at set flight conditions. If an optimization technique is used for airfoil design, the shape of the airfoil is varied, and the aerodynamic performance of numerous airfoil geometries are evaluated using computational fluid dynamics. Multiple aerodynamic performance evaluations require the vast majority of computational processing time used in airfoil design optimization. DTIC

N94-28899# Polytechnic Univ., Brooklyn, NY. Dept. of Aerospace Engineering.
EXPERIMENTAL INVESTIGATION OF THREE-DIMENSIONAL VORTEX-AIRFOIL INTERACTION IN A SUPERSONIC STREAM Final Report, 15 Oct. 1992 - 14 Oct. 1993
Iraj M. Kalkhoran Dec. 1993 30 p
(Contract F49620-93-1-0009)
(AD-A275107; POLY-AE-93-8; AFOSR-94-0027TR) Avail: CASI HC A03/MF A01

An experimental study involving interaction between streamwise wing-tip vortices and a two-dimensional lifting surface in a supersonic stream was conducted. The experiments were designed to simulate interaction of supersonic vortices with aerodynamic surfaces of high-speed aircraft and missiles. The experimental scheme involves positioning an instrumented two-dimensional wedge downstream of a semi-span wing so that the trailing tip-vortex from the wing interacts with the aerodynamic surface. Experimental results indicate that the interaction strongly depends on the vortex strength and vortex proximity to the wedge leading edge. In their most organized form, distortion of streamwise vortices upon interacting with the wedge was found to result in formation of symmetric detached shock fronts far upstream of the wedge leading edge followed by an apparent slip surface separating a subsonic region from a supersonic zone. Interaction of vortices with oblique shock wave over the wedge section indicates that interaction of a relatively weak vortex with a moderate strength oblique shock does not lead to significant changes in the vortex structure. On the other hand, interaction of a moderate strength vortex with a strong oblique shock results in the formation of a detached shock wave upstream of the oblique shock front. DTIC

N94-28946# National Aerospace Lab., Tokyo (Japan).
PROCEEDINGS OF THE 10TH NAL SYMPOSIUM ON AIRCRAFT COMPUTATIONAL AERODYNAMICS [DAI 10 KAI KOKUKI KEISAN KUKI RIKIGAKU SHINPOJIUM U RONBUNSHU]
Dec. 1992 268 p In ENGLISH and JAPANESE Symposium held in Tokyo, Japan, 10-12 Jun. 1992
(ISSN 0289-260X)
(NAL-SP-19; JTN-94-80612) Avail: CASI HC A12/MF A03

The following topics were discussed: Monte Carlo simulation using variable soft sphere model, numerical simulation of shock wave, airfoil design using Navier-Stokes code, numerical analysis of supersonic flow, numerical simulation of three dimensional shear flow, and programming and interface for numerical wind tunnel. For individual titles, see N94-28947 through N94-28993.

N94-28947# National Aerospace Lab., Amsterdam (Netherlands).
ENGINEERING OF SYSTEMS FOR APPLICATION OF SCIENTIFIC COMPUTING IN INDUSTRY **c61**
W. Loeve *In* NAL, Proceedings of the 10th NAL Symposium on Aircraft Computational Aerodynamics Dec. 1992 p 1-5 (For primary document see N94-28946 08-02)
Avail: CASI HC A01/MF A03

Mathematics software is of growing importance for computer simulation in industrial computer aided engineering. To be applicable in industry, the mathematics software and supporting software must be structured in such a way that functions and performance can be maintained easily. In the present paper, a method is described for development of mathematics software in such a way that this requirement can be met.
Author (NASDA)

N94-28948# National Aerospace Lab., Tokyo (Japan).
MONTE CARLO SIMULATION OR NORMAL SHOCK WAVE. PART 2: VHS MODEL AND VSS MODEL [SHOGEKIHA NO MONTE KARURO SHIMYURESHON. 2: VHS MODERU TO VSS MODERU] **c34**
Hiroaki Matsumoto and Katsuhisa Koura *In its* Proceedings of the 10th NAL Symposium on Aircraft Computational Aerodynamics Dec. 1992 p 7-10 In JAPANESE (For primary document see N94-28946 08-02)
Avail: CASI HC A01/MF A03

The validity of the Variable Soft Sphere (VSS) molecular model, which is consistent with both the viscosity and diffusion coefficients of any intermolecular potential, is investigated by the Monte Carlo simulation of the shock wave structure in binary gas mixtures of Maxwell molecules. Calculations are made by the null-collision direct-simulation Monte Carlo method. The VSS model yields the same shock wave structures as Maxwell molecules even when the Variable Hard Sphere (VHS) molecular model reveals a different structure. The computation time and simplicity of the VSS model are confirmed to be almost the same as those of the VHS model. The VSS model is, therefore, preferable to the VHS model in practical use. Using the reliable values of the VSS parameters, the shock wave structure in He and Xe gas mixtures is investigated to compare with the measured density profiles. The density gradient and separation distance are in reasonable agreement with the experimental results.
Author (NASDA)

N94-28949# National Aerospace Lab., Tokyo (Japan). Aerodynamics Div.
VARIABLE SOFT SPHERE MOLECULAR MODEL IN THE MONTE CARLO SIMULATION OF AIR SPECIES [KUKI BUNSHI NO MONTE KARURO SHIMYURESHON NIOKERU VSS BUNSHI MODERU] **c34**
Katsuhisa Koura, Hiroaki Matsumoto, and Mikinari Takahira *In its* Proceedings of the 10th NAL Symposium on Aircraft Computational Aerodynamics Dec. 1992 p 11-15 In JAPANESE (For primary document see N94-28946 08-02)
Avail: CASI HC A01/MF A03

The Variable Soft Sphere (VSS) molecular model is developed so that both the viscosity and diffusion coefficients are consistent with those for any intermolecular potential. The values of the VSS cross-section parameters are listed for air species together with the viscosity coefficients, which may be required in the evaluation of the Knudsen number. The VSS model is applied to the 'Rarefied Gas Numerical Wind Tunnel (RGNWT)' and some results obtained using the RGNWT are presented for the flowfield around the H-2 Orbiting Plane (HOPE). Author (NASDA)

N94-28950# National Aerospace Lab., Tokyo (Japan). Aerodynamics Div.
RAREFIED GAS NUMERICAL WIND TUNNEL. PART 8: HOPE [KIHAKU KITAI SUCHI FUDO. 8: HOPE] **c09**
Katsuhisa Koura, Mikinari Takahira, and Hiroaki Matsumoto *In its* Proceedings of the 10th NAL Symposium on Aircraft Computational Aerodynamics Dec. 1992 p 17-20 In JAPANESE (For primary document see N94-28946 08-02)
Avail: CASI HC A01/MF A03

The Rarefied Gas Numerical Wind Tunnel (RGNWT) developed for the simulation of rarefied gas flows around three dimensional whole flight bodies is applied to the H-2 Orbiting Plane (HOPE). Some flowfield properties and aerodynamic characteristics are presented. Author (NASDA)

N94-28951# National Aerospace Lab., Tokyo (Japan).
NUMERICAL SIMULATION OF ARC HEATED WIND TUNNEL FLOW [AKU KANETSU GATA FUDO NO SUCHI KAISEKI] **c09**
Ryoji Takaki, Yasuhiro Wada, and Yasuo Watanabe *In its* Proceedings of the 10th NAL Symposium on Aircraft Computational Aerodynamics Dec. 1992 p 21-26 In JAPANESE (For primary document see N94-28946 08-02)
Avail: CASI HC A02/MF A03

A numerical analysis of thermochemical nonequilibrium inviscid flow is made for the arc heated wind tunnel at NAL (National Aerospace Laboratory). The calculation is carried out with the Harten-Yee type TVD (Total Variation Diminishing) scheme, using finite-rate seven species chemical reactions and the Park's 2-temperature model in order to take account of nonequilibrium thermochemistry. Results of numerical simulations for three models (perfect gas model, 1-temperature model, and 2-temperature model) are presented and are compared with each other. Author (NASDA)

N94-28952# Kyushu Univ., Fukuoka (Japan). Dept. Aeronautics and Astronautics.
NUMERICAL SIMULATION OF UNSTEADY AERODYNAMIC HEATING INDUCED BY SHOCK REFLECTIONS [SHOGEKIHA NI YUKISARETA HITEIJO KURIKI KANETSU GENSHO NO SUCHI SHIMYURESHON]
Shigeru Aso, Kenichi Ohyama, and Masanori Hayashi *In* NAL, Proceedings of the 10th NAL Symposium on Aircraft Computational Aerodynamics Dec. 1992 p 27-32 In JAPANESE (For primary document see N94-28946 08-02)
Avail: CASI HC A02/MF A03

Numerical simulations on unsteady shock reflections by a ramp have been conducted in order to investigate unsteady aerodynamic heating due to shock reflection processes at higher incident shock Mach number. The two-dimensional Navier-Stokes equations with thin layer approximation are solved numerically by a TVD (Total Variation Diminishing) scheme. The effect of mesh refinement to the calculated results is investigated carefully. The results show the smaller mesh size is necessary for calculating precise aerodynamic heating loads and capturing the fine structure of the shock reflection patterns. Author (NASDA)

N94-28953# National Aerospace Lab., Kakuda (Japan).
NUMERICAL SIMULATION OF STEADY MACH REFLECTION BY SHOCK CAPTURING SCHEMES [SHOGEKIHA HOKAKUHO NIYORU TEIJO MAHHA HANSHA NO SUCHI SHIMYURESHON]
Takeshi Kanda, Katsuhiro Ito, Kouichiro Tani, and Masahiro Takahashi *In its* Proceedings of the 10th NAL Symposium on Aircraft Computational Aerodynamics Dec. 1992 p 33-37 In JAPANESE (For primary document see N94-28946 08-02)
Avail: CASI HC A01/MF A03

Modern shock capturing schemes, i.e., solution adaptive interpolatory schemes, supply beautiful solutions, so they are used generally even in the industrial world. There is a problem in shock capturing schemes, however, when there are plural shocks within the grid points constructing a numerical flux. In order to stabilize a numerical solution in such a scheme, the accuracy must be degenerated. Such a situation can be often seen in two dimensional flow field, and steady Mach reflection is a typical example of the plural shock flow. An analytical solution of the steady Mach reflection was shown, and an investigation of shock capturing scheme performance by comparing it with present analysis was proposed. In this report, a newly developed scheme was also used to investigate the characteristics of the shock capturing schemes, and the performances of TVD (Total

Variation Diminishing) scheme and of the new scheme were compared. Carbuncle phenomena and entropy layer on the wall were also discussed.
Author (NASDA)

N94-28954# Tohoku Univ., Sendai (Japan). Div. of Engineering.
HIGHER-ORDER ACCURATE NUMERICAL SIMULATION OF 3D SUPERSONIC MIXING LAYERS [SANJIGEN CHOONSOKU KONGOSO NO KOJI SEIDO SUCHI SHIMYURESHON]
Koichi Ishizaka, Satoru Yamamoto, and Hisaaki Daiguji *In* NAL, Proceedings of the 10th NAL Symposium on Aircraft Computational Aerodynamics Dec. 1992 p 39-44 In JAPANESE (For primary document see N94-28946 08-02)
Avail: CASI HC A02/MF A03

The purpose of the present paper is to perform direct numerical simulations of the time-developing subsonic and supersonic mixing layers. In order to simulate unsteady shock-vortex interactions accurately, a fourth-order accurate shock capturing scheme is used. This scheme is based on the third-order accurate upwind finite-difference scheme and the accuracy can be extended to fourth(fifth)-order by adopting additional compact terms into the schemes. The resolution is higher than the existing scheme and the algorithm is simpler than the ENO (Essentially Non-Oscillatory) scheme. Finally, some numerical results of subsonic and supersonic mixing layers are shown and the reliability is discussed in comparison with the ordinary numerical scheme. Author (NASDA)

N94-28955# National Aerospace Lab., Tokyo (Japan).
NUMERICAL SIMULATION OF AEROTHERMODYNAMIC HEATING OF HYPERSONIC SPACE TRANSPORTATION VEHICLES [CHOKOSOKU HIKOTAI NO KURIKI KANETSU: CFD TO FUDOSHIKEN]
Yukimitu Yamamoto *In its* Proceedings of the 10th NAL Symposium on Aircraft Computational Aerodynamics Dec. 1992 p 45-50 In JAPANESE (For primary document see N94-28946 08-02)
Avail: CASI HC A02/MF A03

Numerical hypersonic aerodynamic studies of space planes, H-2 Orbiting Plane (HOPE). and OREX (Orbital Re-entry EXperiment) have been conducted for several years. In this paper, the analysis of the aerodynamic heating and real gas effects is described. Numerical results are compared with the heat transfer data obtained by various experimental techniques.
Author (NASDA)

N94-28956# National Aerospace Lab., Amsterdam (Netherlands).
ENGRID: A GRAPHICAL INTERACTIVE CODE FOR THE COMPUTATION OF STRUCTURED GRIDS FOR BLOCKED FLOW DOMAINS **c34**
S. P. Spekreijse *In its* Proceedings of the 10th NAL Symposium on Aircraft Computational Aerodynamics Dec. 1992 p 51-56 Prepared in cooperation with Alenia, Rome, Italy Sponsored by Netherlands Agency for Aerospace Programs, Delft, Netherlands (For primary document see N94-28946 08-02)
Avail: CASI HC A02/MF A03

The underlying idea of the widely used and accepted multiblock approach for flow analysis is to subdivide a geometrical complex flow domain region into several smaller, more manageable regions, referred to as blocks. Typically there are several individual blocks in a given flow domain, each block having three computational coordinates. In the present approach the grid generation process is divided into two sub-processes: (1) block decomposition, i.e., the creation of blocked flow domains; and (2) grid generation, i.e., the computation of structured grids in the blocks. The ENGRID code is a general purpose multi-block grid generation code for the computation of Euler or Navier-Stokes types of grids in flow domains which are already subdivided into blocks. The two required input files for ENGRID are a topology and a geometry file. The topology file defines the topology of a multi-block flow domain. The topology of a blocked flow domain describes how the blocks are connected to each other. The geometry file contains the geometrical information of a multi-block flow domain. The file contains the geometrical definition of all vertices, all non-default elementary edges, and all non-default elementary faces. Author (NASDA)

N94-28957# Fuji Heavy Industries Ltd., Tokyo (Japan).
A DESIGN OF THIRD-GENERATION AIRFOILS FOR HELICOPTER ROTOR BLADES USING NAVIER-STOKES [NABIE SUTOKOSU KAISEKI O MOCHIITA HERIKOPUTA ROTA BUREDO YO DAI 3 SEDAI KOUSEINO YOKUGATA NO SEKKEI] **c05**
Masaaki Nakadate and Masahiro Obukata *In* NAL, Proceedings of the 10th NAL Symposium on Aircraft Computational Aerodynamics Dec. 1992 p 57-62 In JAPANESE (For primary document see N94-28946 08-02)
Avail: CASI HC A02/MF A03

Recent progress in the performance of helicopters has been so remarkable that maximum speeds of over 200 knot are not uncommon among experimental helicopters. Such high performance owes much to the progress in rotor aerodynamics, especially the development of advanced airfoils. Additionally, the recent progress in Computational Fluid Dynamics (CFD) and supercomputers has been quite remarkable. These improvements make it possible to accurately predict airfoil performance up to and beyond maximum lift, where viscous and vortical effects prevail. A practical design target was identified. The target was to obtain airfoil shapes with comparable performance to that of Boeing Helicopter's third-generation airfoils, VR-12 through VR-15. Prior to the design, a parametric study on leading edge thickness and camber was carried out. The study depended upon the fact that the maximum lift of airfoils is related to leading edge shape. An optimal combination of leading edge thickness and camber was decided during the parametric study. Then, the shape, especially around the leading edge, was successively refined by relaxing the leading edge pressure peak to realize much higher maximum lift without spoiling other performance. Finally, off-design and overall characteristics were verified up to transonic Mach numbers. The airfoil U896H thus designed, has a thickness over chord ratio of 0.10 and has symmetric section shape except for the optimized cambar around the leading edge. Wind tunnel results of the airfoil showed high maximum lift and high drag divergence Mach number as expected and enough to be among third-generation airfoils. Author (NASDA)

N94-28958# Mitsubishi Heavy Industries Ltd., Tokyo (Japan).
NUMERICAL ANALYSIS OF AIRFOIL FOR HELICOPTER BLADE AT HIGH ANGLE OF ATTACK USING NAVIER-STOKES CODE [NABIE SUTOKUSU KAISEKI NIYORU HERI BUREDO YOKUGATA NO KOGYOKAKU TOKUSEI SUISAN NO KOKOROMI]
Naohito Adachi, Mitsuo Ishiguro, Masahiro Nakao, Naoki Hirose, and Mamoru Satou *In* NAL, Proceedings of the 10th NAL Symposium on Aircraft Computational Aerodynamics Dec. 1992 p 63-68 In JAPANESE (For primary document see N94-28946 08-02)
Avail: CASI HC A02/MF A03

Numerical analysis using an Navier-Stokes code is conducted in order to develop a method to simulate flow fields around helicopter airfoils at high angle of attack. The results are compared with experimental data to investigate the subject for the simulation of the flow fields at high angle of attack. Based on the investigation, the effect of the grid system is examined. It is shown that the concentration of the grid at the trailing edge is important. Author (NASDA)

N94-28959# Fuji Heavy Industries Ltd., Tokyo (Japan).
NUMERICAL ANALYSIS OF SUPERSONIC TRANSPORT WINGS [CHOONSOKU YUSOKI SHUYOKU KEIJO NO SUCHI KAISEKI]
Tetsuo Yamazaki and Takashi Uchida *In* NAL, Proceedings of the 10th NAL Symposium on Aircraft Computational Aerodynamics Dec. 1992 p 69-74 In JAPANESE (For primary document see N94-28946 08-02)
Avail: CASI HC A02/MF A03

Numerical analysis of supersonic transport wings was carried out. The drag reduction obtained by using the warped wing design technique is from 0.0006 to 0.0010 in supersonic cruise condition. It is also clarified that the drag reduction by use of Euler analysis is less than that by the linear method, because the flow mechanism in supersonic region is essentially non-linear. Finally it is shown that the cranked arrow wing-body configuration has the best lift to drag ratio in supersonic cruise condition in comparison with delta or ogee wing-body configuration.
Author (NASDA)

N94-28960# Tokyo Univ. (Japan). Graduate School.
NUMERICAL STUDY ON THE INTERACTION BETWEEN SCRAMJET ENGINE MODULES CAUSED BY THERMAL CHOKE [SAMARU CHOKU NITORU SUKUMARA JETTO ENJIN NO MOJURU KANNO KANSHO] **c07**

Takuo Onodera and Shojiro Kaji *In* NAL, Proceedings of the 10th NAL Symposium on Aircraft Computational Aerodynamics Dec. 1992 p 75-80 In JAPANESE (For primary document see N94-28946 08-02)
Avail: CASI HC A02/MF A03

Airframe-integrated scramjet engines are now proposed as one of the most promising propulsion systems for hypersonic transports and transatmospheric vehicles for single-stage-to-orbit. Such engines are composed of several modules, each of which consists of an air-intake, a combustion chamber, and a nozzle, and these modules are attached side by side to the bottom surface of the fuselage of a vehicle. In such a configuration, it is considered that when disturbances cause one of the modules to be unstarted, such influences propagate to the adjoining modules through the intake and/or the nozzle, and that the normal operation of the propulsion system should be destroyed. In this study, such interactions between modules of the airframe-integrated scramjet engines are investigated numerically. Shock waves generated by thermal choke in the heating region of the module are used to trigger unstart. The flow field, including the yaw cross section of the modules, is approximated. An inviscid compressible flow is assumed, so Euler equations with heating terms are used as the governing equations. The explicit symmetric TVD (Total Variation Diminishing) scheme is used. From the two-dimensional calculations, the following conclusions are obtained: (1) when thermal choke occurs in one module of a scramjet engine, its influence reaches the adjoining modules through shock wave propagation and they become unstarted; and (2) the transient process from the started condition to unstarted is completed in about 30 msec, and the unstarted modules generate not thrust but drag.
Author (NASDA)

N94-28961# Ishikawajima-Harima Heavy Industries Co. Ltd., Tokyo (Japan).
NUMERICAL SIMULATION OF SUPERSONIC FLOW AROUND SPACE PLANE WITH ENGINE INSTALLED [ENJIN TSUKI SUPESPUREN ZENKI KEIJO MAWARI NO NAGARE NO SUCHI SHIMYURESHON]

Shinichi Kuroda and Kozo Fujii *In* NAL, Proceedings of the 10th NAL Symposium on Aircraft Computational Aerodynamics Dec. 1992 p 81-86 In JAPANESE (For primary document see N94-28946 08-02)
Avail: CASI HC A02/MF A03

Airframe-engine integration is one of the most important problems in the area of supersonic inlet technologies. In the present paper the flow around an airframe-engine integration model is numerically simulated. Because of the geometrical complexity, the overlaid composite grid approach, based on the Fortified Solution Algorithm (FSA) concept, is used for the discretization strategy. In the present computation, the composite grid consists of four component grids. The primary grid is constructed with respect to the airframe, and the subsidiary grids are generated about the nacelle, duct, and diverter. The minor grids are used to resolve the features of the engine geometry and are overlaid on the main grid. The inviscid flow field is solved for this configuration at a Mach number of 2.75 and zero deg angle of attack. Although the overall flow features are successfully simulated by this preliminary computation, further improvement of the solution quality by grid enrichment and the discussion about the flow field are left as future work.
Author (NASDA)

N94-28962# Osaka Prefecture Univ., Sakai (Japan). Graduate School.
NUMERICAL ANALYSIS OF SONIC BOOM IN THE NEAR FIELD [KINOBA NIOKERU SONNIKKU BUMU NO SUCHI KAISEKI]

Akihiko Yoshida, Kazuhiro Nakahashi, and Shoichi Fujii *In* NAL, Proceedings of the 10th NAL Symposium on Aircraft Computational Aerodynamics Dec. 1992 p 87-92 In JAPANESE (For primary document see N94-28946 08-02)
Avail: CASI HC A02/MF A03

Numerical solutions of 3-D Euler equations are obtained for supersonic flows in order to investigate the sonic boom pressure signatures in the near field. The models used in the calculations are a body of revolution and two wing-body configurations. The results for the body of revolution indicate good agreement with the experimental data. A solution-adaptive-grid method which uses tension and torsion spring analogies is applied. The results show that this method improves the accuracy of solutions, and that sharper pressure signatures can be calculated than those in the initial grid.
Author (NASDA)

N94-28963# Mitsubishi Electric Corp., Kamakura (Japan).
NUMERICAL ANALYSIS OF TWO DIMENSIONAL/AXISYMMETRIC NON-EQUILIBRIUM HYPERSONIC FLOW [NIJIGEN/JIKU TAISHO GOKU CHOONSOKU HIHEIKORYU NO SUCHI KAISEKI]

Takuji Kurotaki *In* NAL, Proceedings of the 10th NAL Symposium on Aircraft Computational Aerodynamics Dec. 1992 p 93-98 In JAPANESE (For primary document see N94-28946 08-02)
Avail: CASI HC A02/MF A03

Numerical analysis of chemically and thermally non-equilibrium hypersonic flow around a sphere are carried out. Two-dimensional and axisymmetric full Navier-Stokes equations which have chemical and thermal non-equilibrium effects are considered by using Park's two-temperature model and the Landau-Teller vibrational relaxation model. An efficient numerical algorithm is constructed which consists of the combination of LU-SGS (Lower Upper-Symmetric Gauss-Seidel) schemes and the implicit diagonal method for a source Jacobian matrix for the time integration of an implicit finite difference method and MUSCL-type (Monotonic Upstream Centered Schemes for Conservation Laws) TVD (Total Variation Diminishing) scheme based on Roe-type flux splitting for convective terms. Shock location of both numerical results and experimental data are compared and good agreement is obtained in the wide range of Mach numbers up to M(sub infinity) = 16. Shock capturing capability is good enough to describe very strong discontinuity with no more than three grid points. Author (NASDA)

N94-28964# Kawasaki Heavy Industries Ltd., Gifu (Japan).
ROLE OF COMPUTATIONAL FLUID DYNAMICS IN AERONAUTICAL ENGINEERING. PART 10: NUMERICAL ANALYSIS OF FLOW AROUND 2-D MULTI-ELEMENT HLD [SEKKEI NICKERU SUCHI KAISEKI NO KATSUYO NITSUITE. SONO 10: 2 JIGEN TAYOKUSO MAWARI NAGARE NO SUCHI KAISEKI] **c34**

Koichi Egami, Eiji Shima, Kanichi Amano, and Shingo Nakamura *In* NAL, Proceedings of the 10th NAL Symposium on Aircraft Computational Aerodynamics Dec. 1992 p 99-104 In JAPANESE (For primary document see N94-28946 08-02)
Avail: CASI HC A02/MF A03

A 2-D Navier-Stokes analysis of flow around multi-element high lift devices was carried out. In order to calculate the aerodynamic characteristics in a wide range of angle of attack, the q-omega 2-equations turbulence model was used. Numerical results show flowfields with large viscous wake region without flow separation on the top surface of the flap at large angle of attack. In high Reynolds number cases, numerical results of decrease in lift coefficient were computed.
Author (NASDA)

N94-28965# National Aerospace Lab., Tokyo (Japan).
NUMERICAL SOLUTION OF INVERSE PROBLEM IN AERODYNAMICS [KOKU RIKIGAKU NIOKERU GYAKUMONDAI TO SONO KAIHO]

Susumu Takanashi *In its* Proceedings of the 10th NAL Symposium on Aircraft Computational Aerodynamics Dec. 1992 p 105-108 In JAPANESE (For primary document see N94-28946 08-02)
Avail: CASI HC A01/MF A03

One of the most important inverse problems in aerodynamics is defined as the problem of finding the wing section contour given the desired surface pressure distribution for a fixed wing planform. This problem can be solved by the 'residual-correction' method based on the transonic integral equations. In this paper, some of the recent applications of the integral equation method using various analysis codes including Navier-Stokes codes are presented.
Author (NASDA)

N94-28966# Mitsubishi Heavy Industries Ltd., Tokyo (Japan).
CODE DEVELOPMENT FOR HYPERSONIC REAL-GAS FLOW SIMULATIONS TOWARD THE DESIGN OF SPACE VEHICLES, PART 2 [KURIKI SEKKEI TSURU TOSHITE NO GOKU CHOONSOKURYU KEISANN KODO NO KAIHATSU. SONO 2]

Masahiro Nakao and Kozo Fujii *In* NAL, Proceedings of the 10th NAL Symposium on Aircraft Computational Aerodynamics Dec. 1992 p 109-114 In JAPANESE (For primary document see N94-28946 08-02)
Avail: CASI HC A02/MF A03

A hypersonic flow simulation system is under development. A flow analysis code, an adaptive grid generation code, and a computation code of equilibrium chemical composition as a post process routine have been developed. The flow analysis code that is based on 3-D upwind flux splitting scheme using the VEG (Variable Equivalent Gamma) method has been improved in order to simulate heat transfer distributions. Numerical simulations are conducted for flow fields around HOPE (H-2 Orbiting Plane). Flow conditions are Mach number of 15 and angle of attack of 30 degrees. Computed heat transfer ratio distributions are obtained. Results are compared with experimental data and good agreement is shown along a body symmetrical line of the lower surface. Author (NASDA)

N94-28967# Shimizu Corp. (Japan).
THREE DIMENSIONAL SIMULATION OF COMPRESSIBLE FLOW INDUCED BY A HIGH-SPEED TRAIN MOVING INTO A TUNNEL [TONNERU NI TOTSUNYUSURU KOSOKU SHARYO NIYOTTE YUKISARERU NAGAREBA NO SUCHI SHIMYURESHON]
Takanobu Ogawa, Kozo Fujii, and Yoshiaki Tamura *In* NAL, Proceedings of the 10th NAL Symposium on Aircraft Computational Aerodynamics Dec. 1992 p 115-120 In JAPANESE (For primary document see N94-28946 08-02)
Avail: CASI HC A02/MF A03

A three dimensional compressible flow induced by a practical high-speed train moving into a tunnel is numerically simulated. The flow field is decomposed with the zonal method and the Fortified Solution Algorithm (FSA) is used as an interface scheme. The result indicates that the algorithm is efficient to handle the moving boundary configurations which include a complicated geometry. The flow features, such as a compression wave and an expansion wave created by the train and an increment of drag force acting on the train are clarified. Author (NASDA)

N94-28968# Toyota Motor Co., Aichi (Japan).
NUMERICAL ANALYSIS OF INCOMPRESSIBLE VISCOUS FLOW AROUND A BUBBLE [HENKEI WO TOMANAU KIHO MAWARI NO NAGARE NO SUCHI KAISEKI] **c34**
Minoru Sugano, Ryuji Ishii, and Shigeki Morioka *In* NAL, Proceedings of the 10th NAL Symposium on Aircraft Computational Aerodynamics Dec. 1992 p 121-126 In JAPANESE Prepared in cooperation with Kyoto University, Kyoto, Japan (For primary document see N94-28946 08-02)
Avail: CASI HC A02/MF A03

A numerical simulation of flows around a deformable gas bubble rising through an incompressible viscous fluid is carried out on a supercomputer Fujitsu VP-2600 at the Data Processing Center of Kyoto University. The solution algorithm is a modified MAC (Marker And Cell) method. For the grid generation, an orthogonal mapping proposed by Ryskin and Leal is applied. The numerical results are compared with Ryskin and Leal's results and previous experiments. It will be shown that a good agreement is obtained between them. Author (NASDA)

N94-28969# Ishikawajima-Harima Heavy Industries Co. Ltd., Tokyo (Japan).
UNSTEADY AERODYNAMIC COMPUTATIONS AROUND NACA0012 AT HIGH ANGLES OF ATTACK [NACA0012 YOKUGATA MAWARI NO KOGYOKAKU NIOKERU HITEIJO KUKIRYOKU NO KEISAN]
Kazuhito Miyata, Jiro Nakamichi, and Rinichi Murao *In* NAL, Proceedings of the 10th NAL Symposium on Aircraft Computational Aerodynamics Dec. 1992 p 127-132 In JAPANESE (For primary document see N94-28946 08-02)
Avail: CASI HC A02/MF A03

In the present study, periodic flows are simulated around NACA 0012 airfoil at high angle of attack to validate the unsteady Navier-Stokes code. Thin-layer approximated unsteady Navier-Stokes equations are integrated in a time-dependent manner with Baldwin-Lomax turbulence model. With Mach number, 0.3 and Reynolds number, 6 x 10(exp 6), characteristics of lift, drag and moment coefficients are investigated at a variety of angles of attack. The simulated flows are compared qualitatively with experimental results obtained by flow visualization conducted in a low-speed tunnel at higher angles of attack than that at which 'stall' occurs. The similar periodicity of the flows is found in the experimental result. Author (NASDA)

N94-28970# Shimizu Corp. (Japan).
STUDY OF MODELING OF TURBULENCE OF RENORMALIZATION GROUP ANALYSIS [KURIKOMIGUN NIYORU RANRYU MODERU NO ICHI KOSATSU] **c34**
Wako Takanashi *In* NAL, Proceedings of the 10th NAL Symposium on Aircraft Computational Aerodynamics Dec. 1992 p 133-134 In JAPANESE (For primary document see N94-28946 08-02)
Avail: CASI HC A01/MF A03

This paper presents the renormalization group analysis for the turbulence problem. This procedure does not require any experimentally adjustable parameters. The following numerical values for important constants of turbulent flows can be derived; for instance, the Kolmogorov constant for the inertial-range spectrum C(sub k) = 1.605. A differential LES (Large Eddy Simulation) model is also derived, as is the Smagorinsky constant C(sub s) = 0.00615. Author (NASDA)

N94-28971# Nagoya Univ. (Japan). Dept. of Aeronautical Engineering.
THE UPSILON-q METHOD AND THE PSI-q METHOD FOR INCOMPRESSIBLE FLOWS [HIASSHUKUSEI RYU NITAISURU UPUSHIRON-Q HO TO PUSAI-Q HO] **c34**
Wei Jia and Yoshiaki Nakamura *In* NAL, Proceedings of the 10th NAL Symposium on Aircraft Computational Aerodynamics Dec. 1992 p 135-140 In JAPANESE (For primary document see N94-28946 08-02)
Avail: CASI HC A02/MF A03

This paper proposes a new formulation for the incompressible N-S (Navier-Stokes) equations by introducing a new variable q, the rotation of which represents the convective and pressure gradient terms of the momentum equations. The derived governing equations consist of the linear dynamic equations and the Poisson equation for the new variable q with the nonlinear source. These equations automatically satisfy the divergence free condition. The boundary condition for the new variable q is the Dirichlet type, the Poisson equation can be quickly solved by the conventional point relaxation method. Furthermore, a new method to economically obtain the corresponding pressure field is also proposed. Applications to a driven cavity flow and the flow around a circular cylinder show excellent performances of the new method. Author (NASDA)

N94-28972# National Aerospace Lab., Tokyo (Japan).
ON THE NUMERICAL ANALYSIS OF SHEAR FLOWS [SENDANRYU NO SUCHI KAISEKI NITSUITE] **c34**
Satoru Ogawa and Yoko Takakura *In its* Proceedings of the 10th NAL Symposium on Aircraft Computational Aerodynamics Dec. 1992 p 141-144 In JAPANESE (For primary document see N94-28946 08-02)
Avail: CASI HC A01/MF A03

Numerical simulations of 3-D shear flows are carried by solving the pseudo-compressibility equations for incompressible fluid proposed by Chakravarthy. Governing equations are integrated explicitly in time by a third order upwind finite volume scheme. A steady 3-D duct flow over a backward-facing step, and 3-D spatially developing incompressible mixing layer are solved, and it is shown the results of numerical simulation using the present methods is reasonable. Author (NASDA)

N94-28973# National Aerospace Lab., Tokyo (Japan). Computational Sciences Div.
ON APPROXIMATE RIEMANN SOLVERS: IMPROVEMENT OF HLLEM SCHEME AND ITS GENERALIZATION FOR CHEMICALLY REACTING FLOWS [KINJI RIMAN KAIHO NITSUITE: HLLEM SUKIMO NO KAIRYO TO HANNOURYU ENO KAKUCHO] **c34**
Yasuhiro Wada *In its* Proceedings of the 10th NAL Symposium on Aircraft Computational Aerodynamics Dec. 1992 p 145-152 In JAPANESE (For primary document see N94-28946 08-02)
Avail: CASI HC A02/MF A03

Investigated are characteristics of the approximate Riemann solvers, which are used as a building block for construction of modern shock-capturing schemes. Then a new approximate Riemann solver is proposed, which is a result of an improvement of HLLEM (Harten Lax van Leer Einfeldt Modified) scheme, satisfying the positivity condition and entropy one. Also its generalization for nonequilibrium flows such as high-temperature gas is described. Some numerical results are presented as well.
Author (NASDA)

N94-28974# Science Univ. of Tokyo (Japan). Faculty of Science.
ANALYSIS OF 3-D ACOUSTIC PROBLEMS USING BOUNDARY ELEMENT METHOD [KYOKAI YOSOHO NIYORU SANJIGEN ONKYO KAISEKI] **c71**
Mitsunori Yanagizawa *In* NAL, Proceedings of the 10th NAL Symposium on Aircraft Computational Aerodynamics Dec. 1992 p 153-156 In JAPANESE (For primary document see N94-28946 08-02)
Avail: CASI HC A01/MF A03

This paper is concerned with the development of a numerical method for the prediction of the characteristics of a sound field using boundary element analysis. An acoustics field in inner or exterior problems of harmonic vibration is governed by the Helmholtz equation. It can be solved by a boundary condition and an initial condition being given. Unknown values of acoustic pressure on the boundary are analyzed by the boundary element method using boundary conditions. After this procedure, the values of acoustic pressure at the inside point can be calculated from those of the boundary. This procedure allowed substantial saving of memory. Analysis with a personal computer became possible. According to these results, it was shown that the calculations can be carried out sufficiently with a small computer in spite of the small memory capacity. Small computers, which are very popular, will become an effective tool in numerical simulation with boundary element method. Author (NASDA)

N94-28975# Tokyo Univ. (Japan). Graduate School.
STUDY ON MIXING AND INJECTION OF HYDROGEN INTO A SUPERSONIC FLOW [CHOONSOKURYU CHU ENO SUISO NO FUKIDASHI TO KONGO NIKANSURU KENKYU]
Kazuhiko Yokota and Shojiro Kaji *In* NAL, Proceedings of the 10th NAL Symposium on Aircraft Computational Aerodynamics Dec. 1992 p 157-162 In JAPANESE (For primary document see N94-28946 08-02)
Avail: CASI HC A02/MF A03

The effects of the injection methods on mixing of hydrogen in the free stream are investigated. The numerical simulations are performed by solving the full two-dimensional Navier-Stokes equations using the explicit symmetric total variation diminishing (TVD) scheme. As for the injection methods, single injection, tandem injection, and parallel injection are examined. The injected hydrogen mass flow is constant in all cases. Injection methods are evaluated by the correlation between the mixing efficiency and the mass flow averaged total pressure loss at the outlet boundary of the computational region. First, the injection angle is varied in case of single injection. The results show that the more forward the injection angle is leaned, the more deeply hydrogen penetrates into the free stream. Second case is tandem injection, and the distance between or mass flow ratio of two injections is varied. The results show that the upstream injection blocks the main stream, so the barrel shock of the downstream injection becomes larger and dominant in mixing in tandem injection. Last is parallel injection, and the distance from the wall to the injection is varied. The results show that parallel injected hydrogen can be mixed in the free stream in spite of the fact that it has no momentum perpendicular to the free stream. The correlations between the mixing efficiency and the total pressure loss in all cases show that the mixing efficiency in the parallel injection is two times as much as in other methods of injection. Author (NASDA)

N94-28976# Kawasaki Heavy Industries Ltd., Tokyo (Japan).
VERIFICATION OF A THREE-DIMENSIONAL VISCOUS FLOW ANALYSIS FOR A SINGLE STAGE COMPRESSOR [NS KAISEKI NIYORU TANDAN ASSHUKUKI YOKURETSU NAGARE NO KENSHO] **c34**
Akinori Matsuoka, Keisuke Hashimoto, Osamu Nozaki, Kazuo Kikuchi, Masahiro Fukuda, and Atsuhiro Tamura *In* NAL, Proceedings of the 10th NAL Symposium on Aircraft Computational Aerodynamics Dec. 1992 p 163-168 In JAPANESE (For primary document see N94-28946 08-02)
Avail: CASI HC A02/MF A03

A transonic flowfield around rotor blades of a highly loaded single stage axial compressor was numerically analyzed by a three dimensional compressible Navier-Stokes equation code using Chakravarthy and Osher type total variation diminishing (TVD) scheme. A stage analysis which calculates both flowfields around inlet guide vane (IGV) and rotor blades simultaneously was carried out. Comparing with design values and experimental data, computed results show slight difference quantitatively. But the numerical calculation simulates well the pressure rise characteristics of the compressor and its flow pattern including strong shock surface. Author (NASDA)

N94-28977# National Aerospace Lab., Tokyo (Japan).
NUMERICAL STUDY ON INTERNAL FLOWS OF CENTRIFUGAL COMPRESSORS [ENSHIN ASSHUKUKI NO NAIBU NAGARE NIKANSURU SUCHI KAISEKI] **c07**
Takashi Yamane and Toshio Nagashima *In its* Proceedings of the 10th NAL Symposium on Aircraft Computational Aerodynamics Dec. 1992 p 169-174 In JAPANESE (For primary document see N94-28946 08-02)
Avail: CASI HC A02/MF A03

Numerical calculations have been performed for the analysis of internal flow structures of centrifugal compressors. Computational results reveal the jet and wake structure at the impeller exit. The effects of the wake against diffuser vanes were also investigated by an unsteady rotor-stator interaction calculation and a steady stage calculation. Author (NASDA)

N94-28978# Ishikawajima-Harima Heavy Industries Co. Ltd., Tokyo (Japan).
APPLICATION OF FLOW FIELD SIMULATION TO TURBINE VANE DESIGN [SUCHI SHIMYURESHON TO TABIN YOKURETSU SEKKEI] **c07**
Koji Matsunaga, Hisao Takeuchi, Atsushige Tanaka, Ruriko Yamawaki, Hiroshi Hamazaki, Kazuo Kikuchi, and Osamu Nozaki *In* NAL, Proceedings of the 10th NAL Symposium on Aircraft Computational Aerodynamics Dec. 1992 p 175-180 In JAPANESE (For primary document see N94-28946 08-02)
Avail: CASI HC A02/MF A03

This paper presents an application of the three dimensional Navier-Stokes computations in designing a turbine vane cascade. The accurate prediction of the cascade flow characteristics such as total pressure loss and outlet flow angle is important for aerodynamic engineers to evaluate the performance of airfoil contour shapes. Curvilinear leaned and swept stator vanes, adopted to suppress the secondary flow and reduce the losses, are studied in detail. The advanced design based on the three dimensional Navier-Stokes computations succeeded in reducing the losses, showing the capability of the code as a design tool. Author (NASDA)

N94-28979# Osaka Prefecture Univ., Sakai (Japan). Dept. of Aeronautical Engineering.
THREE-DIMENSIONAL EXTERNAL FLOW COMPUTATIONS USING PRISMATIC GRID [PURIZUMU KOSHI NIYORU SANJIG EN GAIBURYU NO SUICHI KEISAN] **c34**
Kazuhiro Nakahashi *In* NAL, Proceedings of the 10th NAL Symposium on Aircraft Computational Aerodynamics Dec. 1992 p 181-186 In JAPANESE (For primary document see N94-28946 08-02)
Avail: CASI HC A02/MF A03

A new approach to compute external viscous flows around three dimensional configurations is proposed. A prismatic grid is used where the three dimensional surface is covered by triangles similar to the unstructured grid. The direction away from the body surface is structured so as to achieve efficient and accurate computations for high Reynolds number viscous flows. The prismatic grid is generated by a newly developed marching-type procedure in which grid spacings are controlled by a variational method. The capability of the method is demonstrated by applying it to a viscous flow computation around a complete aircraft configuration. Author (NASDA)

N94-28980# Kyoto Univ., Sakyoku (Japan).
APPLICATION OF DIGITAL CONTROL THEORY TO ADAPTIVE GRID GENERATION [SAITEKI SEIGYO O MOCHIITA TEKIO KOSHI SEISEIHO] **c63**
Makoto Kobayakawa and Eitaro Yamada *In* NAL, Proceedings of the 10th NAL Symposium on Aircraft Computational Aerodynamics Dec. 1992 p 187-192 In JAPANESE (For primary document see N94-28946 08-02)
Avail: CASI HC A02/MF A03

New methods for adaptive grid generation through optimal regulator of digital control are presented. The performance index of linear optimal regulator problem has a strong relation to the characteristics of adaptive

grid generation. Paying attention to this point, one and two dimensional Poisson equations are transformed into the state-space form. The numerical examples of NACA-0012 airfoil flow field and supersonic flow around corners show strong clustering of grid lines at shock waves through these two kinds of adaptation. Author (NASDA)

N94-28981# National Aerospace Lab., Tokyo (Japan). Aeroengine Div.
AN ELLIPTIC-HYPERBOLIC GRID GENERATION METHOD AND APPLICATION TO COMPRESSOR FLOWS [DAEN-SOKYOKUSEN GATA KOSHI SEISEIHO TO ASSHUKUKI NAGARE ENO OYO] **c07**
Kazuomi Yamamoto *In its* Proceedings of the 10th NAL Symposium on Aircraft Computational Aerodynamics Dec. 1992 p 193-198 In JAPANESE (For primary document see N94-28946 08-02)
Avail: CASI HC A02/MF A03

A three dimensional grid generation method was developed in which an elliptic grid generation equation can be locally changed into a simple hyperbolic type to specify exact grid spacings and directions explicitly. Some simple weighting functions are utilized in order to change the equation type smoothly. Resultant grids for several kinds of blade rows show the method's robustness in the convergence characteristics and its flexibility in application to a variety of complicated geometries. Author (NASDA)

N94-28982# SofTek Systems, Inc., Tokyo (Japan).
UPWIND METHOD USING LOCAL INTERPOLATION [KYOKUSHOTEKINA HOKAN O MOCHIITA KAZAKAMIHO NITSUITE] **c34**
Susumu Shirayama *In* NAL, Proceedings of the 10th NAL Symposium on Aircraft Computational Aerodynamics Dec. 1992 p 199-204 In JAPANESE (For primary document see N94-28946 08-02)
Avail: CASI HC A02/MF A03

Several approaches based on the polynomial which approximates the local solutions to the governing equations have been proposed. The polynomial is piecewisely determined by interpolating the physical quantities on a point aimed at solving the equations and an adequate number of surrounding points. The derivatives at the point are evaluated by using this interpolated polynomial. Most of the conventional methods can be classified by the kinds of polynomial and the use of the interpolation. It may be considered that this basic concept is useful for constructing a method in which the results are independent of grid systems. Also, it seems that to find an appropriate interpolation may contribute to constructing a multidimensional upwind scheme. Author (NASDA)

N94-28983# Kyushu Univ., Fukuoka (Japan). Dept. of Mechanical Engineering for Power.
AN IMPLICIT UPWIND SCHEME FOR THE THREE-DIMENSIONAL EULER EQUATIONS USING A POINTWISE RELAXATION METHOD [TEN KANWAHO O MOCHIITA SANJIGEN OIRA HOTEISHIKI NO INTEKI KAZAKAMI KAIHO] **c34**
Masato Furukawa, Seiichi Ibaraki, Eito Matsuo, and Masahiro Inoue *In* NAL, Proceedings of the 10th NAL Symposium on Aircraft Computational Aerodynamics Dec. 1992 p 205-210 In JAPANESE (For primary document see N94-28946 08-02)
Avail: CASI HC A02/MF A03

An implicit upwind relaxation scheme has been developed for computing compressible inviscid flows using a composite zonal grid system or an unstructured grid. The three dimensional Euler equations are discretized spatially by a cell-centered finite volume formulation, in which the inviscid fluxes are evaluated using a highly accurate upwind scheme based on the Roe's approximate Riemann solver. A new time-linearization of the inviscid fluxes evaluated by the Roe's approximate Riemann solver is presented. No approximate factorization is introduced, and unfactored implicit equations are solved by a pointwise relaxation method. Numerical examples are presented for the inviscid flows through a transonic duct and a diagonal flow impeller. The present scheme was found to be stable at CFL (Courant Friedrichs Lewy) numbers of over 10(exp 5). Author (NASDA)

N94-28984# National Aerospace Lab., Kakuda (Japan).
FLOW AND HEAT TRANSFER IN A ROTATING SQUARE SECTIONED U-BEND [KAITENSURU U-BENDO NAI NO NAGARE TO NETSUDENTATSU] **c34**
Hiroshi Tamura and Hiroshi Ishigaki *In its* Proceedings of the 10th NAL Symposium on Aircraft Computational Aerodynamics Dec. 1992 p 211-214 In JAPANESE (For primary document see N94-28946 08-02)
Avail: CASI HC A01/MF A03

Numerical analysis was conducted for the laminar flow and heat transfer in a square sectioned U-bend which rotates at constant angular velocity about an axis parallel to a center of the bend curvature. In a rotating U-bend, secondary flow develops under the effects of Coriolis force and centripetal force which affects its friction and heat transfer. The flow was characterized by five parameters: K(sub LC), Ro, lambda, lambda/Ro, and Pr. The calculations were conducted with various combinations of these parameters. Author (NASDA)

N94-28985# Tokyo Inst. of Tech. (Japan). Dept. of Energy Sciences.
TRANSONIC EXPANDING FLOW THROUGH AXIALLY SYMMETRIC ORIFICES [JIKU TAISHO ORIFISU O TORU SENONSOKU BOCHORYU] **c34**
Yuminobu Igarashi and Hisashi Mikami *In* NAL, Proceedings of the 10th NAL Symposium on Aircraft Computational Aerodynamics Dec. 1992 p 215-220 In JAPANESE (For primary document see N94-28946 08-02)
Avail: CASI HC A02/MF A03

This paper describes a method of finding the flow pattern of an axially symmetric transonic gas jet through a circular orifice. Numerical solutions were obtained by hodograph transformation and the method of characteristics. The contraction coefficient, velocity profiles and centerline Mach number distributions were calculated. The numerical results are found to agree with the experimental data by Sherman. Author (NASDA)

N94-28986# National Aerospace Lab., Kakuda (Japan).
SIMILARITY BETWEEN TURBULENT FLOWS THROUGH CURVED PIPE AND ORTHOGONAL ROTATING PIPE [NIJI NAGARE O TOMONAU KANNAI RANRYU NO SOJISEI] **c34**
Hiroshi Ishigaki *In its* Proceedings of the 10th NAL Symposium on Aircraft Computational Aerodynamics Dec. 1992 p 221-224 In JAPANESE (For primary document see N94-28946 08-02)
Avail: CASI HC A01/MF A03

The secondary flow due to Coriolis force takes place when viscous fluid flows through a straight pipe rotating about an axis perpendicular to the pipe axis. This is analogous to the secondary flow due to centrifugal force in the flow through a stationary curved pipe. The quantitative similarities between the two flows are demonstrated for turbulent flow by the similarity arguments and computational study using kappa-epsilon turbulence model. It is demonstrated that the mutual similarity between two flows is established for friction factors and flow patterns. Author (NASDA)

N94-28987# National Aerospace Lab., Kakuda (Japan).
NUMERICAL ANALYSIS OF LAMINAR FLOW IN S-CURVED SQUARE DUCT WITH INLET AND OUTLET STRAIGHT REGION [S-GATA BENDO NO NAGARE NO SUCHI KAISEKEI] **c34**
Hitoshi Yamada, Hiroshi Ishigaki, and Munekazu Mochizuki *In its* Proceedings of the 10th NAL Symposium on Aircraft Computational Aerodynamics Dec. 1992 p 225-228 In JAPANESE (For primary document see N94-28946 08-02)
Avail: CASI HC A01/MF A03

Developing laminar flow in a S-curved square duct with an inlet and outlet straight region, is studied numerically by using a finite volume method. In this study, Dean number is 299 and curvature ratio is 7 and S-curved duct angle is 22.5 degrees respectively. Calculated results are compared with the experimental data by Taylor et al.. The calculated results showed good agreements with the experimental data. Author (NASDA)

N94-28988# National Aerospace Lab., Kakuda (Japan).
DEVELOPMENT OF BUOYANCY AFFECTED LAMINAR FLOW IN A HEATED PIPE [FURYOKU GA SAYOSURU KANETSU KANNAI NAGARE NO HATTATSU] **c34**
Munekazu Mochizuki and Hiroshi Ishigaki *In its* Proceedings of the 10th NAL Symposium on Aircraft Computational Aerodynamics Dec. 1992 p 229-233 In JAPANESE (For primary document see N94-28946 08-02)
Avail: CASI HC A01/MF A03

The effects of buoyancy on developing laminar flow and heat transfer in a horizontal pipe are analyzed numerically. Thermal boundary conditions

are axially constant wall heat flux and peripherally constant wall temperature. The results on friction factor, flow pattern, and Nusselt number are discussed. Author (NASDA)

N94-28989# National Aerospace Lab., Kakuda (Japan).
MUTUAL SIMILARITY OF DEVELOPING LAMINAR FLOWS WITH SECONDARY STREAMS IN DUCTS: CURVED PIPE FLOW AND ORTHOGONAL ROTATING PIPE FLOW [NIJI NAGARE O TOMANAU KANNAI SORYU JOSO NAGARE NO SOJISEI: KYOKKAN TO CHOKKO KAITENKAN] **c34**
Hiroshi Ishigaki *In its* Proceedings of the 10th NAL Symposium on Aircraft Computational Aerodynamics Dec. 1992 p 235-239 In JAPANESE (For primary document see N94-28946 08-02)
Avail: CASI HC A01/MF A03

Similarity between the developing laminar flows in a curved pipe and an orthogonally rotating pipe is discussed. Two nondimensional parameters and nondimensional axial distance Z are obtained properly for each flow. When the second parameters become large, computational results show that friction factors, flow patterns and flow characteristics become very similar for same value of K(sub L) and Z. Author (NASDA)

N94-28990# National Aerospace Lab., Tokyo (Japan).
PARALLELIZATION TECHNIQUES FOR HIGHLY PARALLEL VECTOR COMPUTER [KOHEIRETSU BEKUTORU KEISANKI NIOKERU HEIRETSUKA GIHO] **c62**
Kinuyo Nakamura, Noriyuki Ando, and Naoki Nishi *In its* Proceedings of the 10th NAL Symposium on Aircraft Computational Aerodynamics Dec. 1992 p 241-246 In JAPANESE (For primary document see N94-28946 08-02)
Avail: CASI HC A02/MF A03

The assumed highly parallel vector computer with hierarchical memory that consists of many vector computers with local memory and one common memory is the main theme. To speed up parallel processing of CFD (Computational Fluid Dynamics) programs on that parallel computer, it needs parallelization techniques such as enlarging parallel portion, equal work load, enlarging task granularity and minimizing volume of data access between local memory and common memory. In this paper high efficiency of parallel processing of that parallel computer obtained by applying parallelization techniques to a CFD program is described.
Author (NASDA)

N94-28991# National Aerospace Lab., Tokyo (Japan).
PARALLEL FORTRAN PROGRAMMING FOR NWT [NWT MUKE HEIRETSU FORTRAN PUROGURAMINGU NITSUITE] **c62**
Masahiro Yoshida, Takashi Nakamura, Masahiro Fukuda, Shin Okada, and Shuichi Nakamura *In its* Proceedings of the 10th NAL Symposium on Aircraft Computational Aerodynamics Dec. 1992 p 247-252 In JAPANESE Prepared in cooperation with Fujitsu Ltd., Tokyo, Japan (For primary document see N94-28946 08-02)
Avail: CASI HC A02/MF A03

The Numerical Wind Tunnel (NWT) is under research and development by NAL-Fujitsu joint activity. It is a parallel computer system of distributed memory architecture composed of vector processors. In this paper, the programming method of parallel Fortran by gradually catching the descriptions for high-speed execution, in the case of parallelizing and tuning usual Fortran programs for NWT is shown. The examination results using a concrete procedure are presented. Author (NASDA)

N94-28992# National Aerospace Lab., Tokyo (Japan).
PERFORMANCE EVALUATION OF THE NWT WITH PARALLEL FORTRAN [NWT HEIRETSU FORTRAN NI MOTODUKU HEIRETSU HYOKA] **c62**
Takashi Nakamura, Masahiro Yoshida, Masahiro Fukuda, Shuichi Nakamura, Takeo Murase, and Tatsuya Matsuzaki *In its* Proceedings of the 10th NAL Symposium on Aircraft Computational Aerodynamics Dec. 1992 p 253-258 In JAPANESE Prepared in cooperation with Fujitsu Ltd., Tokyo, Japan (For primary document see N94-28946 08-02)
Avail: CASI HC A02/MF A03

The Numerical Wind Tunnel (NWT) is under research and development by NAL-Fujitsu joint activity. It is a parallel computer system of distributed memory architecture composed of vector processors. In this paper, the performance on the desk of two application programs that were parallelized by current parallel language processor is shown. The performance using network simulator and evaluation software 'VTAP' which is based on VP400 performance analysis is evaluated. The estimation that the present machine performs CFD (Computational Fluid Dynamics) simulation about 100 times faster than Fujitsu VP400 is presented. Author (NASDA)

N94-28993# National Aerospace Lab., Tokyo (Japan).
A METHOD OF USER INTERFACE FOR NWT [NWT NO YUZA INTAFEISU JITSUGEN HOSHIKI] **c62**
Masako Tsuchiya, Kazuyo Suematsu, Shunji Suematsu, Haruo Hatama, Hiroshi Morishige, Yasushi Yamaguchi, and Yukihiro Karube *In its* Proceedings of the 10th NAL Symposium on Aircraft Computational Aerodynamics Dec. 1992 p 259-264 In JAPANESE (For primary document see N94-28946 08-02)
Avail: CASI HC A02/MF A03

Numerical Wind Tunnel (NWT) is a CFD (Computational Fluid Dynamics)-oriented parallel computer system with distributed memory, and the operating system of NWT is UNIX. In order to provide users much convenience and to maintain efficient functions of management on 'MSP' operating system, it is preferable to use NWT with user interface of MSP which is the operating system up to this time. In this paper the procedure how to construct user interface of MSP for NWT is presented.
Author (NASDA)

N94-29197 JAI Associates, Inc., Mountain View, CA.
A FREE-WAKE EULER AND NAVIER-STOKES CFD METHOD AND ITS APPLICATION TO HELICOPTER ROTORS INCLUDING DYNAMIC STALL Final Report, 1 May 1990 - 30 Sep. 1993
Ganapathi R. Srinivasan Nov. 1993 127 p Limited Reproducibility: More than 20% of this document may be affected by microfiche quality
(Contract DAAL03-90-C-0013)
(AD-A275416; TR-93-01; ARO-27752.8-EG-S) Avail: CASI HC A07

This report summarizes the results of the research in two parts. Part I describes the development and application of a free-wake Euler and Navier-Stokes computational fluid dynamics method, called 'TURNS', for helicopter applications. This finite-difference, implicit, upwind numerical method uses structured grids, and has been used for calculating the viscous, three-dimensional flow-fields of rotors in hover, forward flight, blade-vortex interactions, and high speed impulsive noise. The good agreement of numerical results with experiments for surface pressures, wake trajectory, thrust, power, Figure of Merit, and acoustic wave forms indicate the accuracy and suitability of the numerical method. It is demonstrated that both aerodynamics and acoustics information can be obtained in a single solution of the governing equations. In Part II, the unsteady flowfield results of a two-dimensional oscillating wing are presented for five widely used turbulence models and compared with experiments. The accuracy and suitability of turbulence models for unsteady separated flow are discussed. DTIC

N94-29306# Washington State Univ., Pullman.
AN EXPERIMENTAL STUDY OF WING TIP VORTEX IN THE NEAR WAKE OF A RECTANGULAR WING Interim Report, 1 Feb. 1991 - 31 May 1993
Youxin Zheng and B. R. Ramaprian Jun. 1993 209 p
(Contract DAAL03-91-G-0026)
(AD-A275389; MME-TF-93-1; ARO-28159.6-EG) Avail: CASI HC A10/MF A03

An experimental study of the tip vortex behind a NACA 0015 rectangular wing of aspect ratio 4 was carried out to understand the structure and evolution of the vortex in the near-wake region. The results of these experimental studies are presented in this report. These measurements were made nonintrusively using three-component laser-Doppler velocimetry (LDV). The experiments were carried out at a Reynolds number of about 180,000 in a low-speed wind tunnel. Two cases were studied, namely: (1) stationary wing, and (2) wing oscillating in pitch sinusoidally about its quarter-chord axis. The flow properties measured were the three components of the instantaneous velocity. These data were processed to obtain time-mean and phase-locked flow properties such as velocity, vorticity and turbulence. The data were obtained at several locations at 0.15 - 3.0 chord lengths downstream from the trailing edge. The typical distributions of mean velocity, vorticity, circulation and turbulent intensity in the near wake are presented and discussed for the stationary wing. In the case of the oscillating wing, the phase-locked velocity, vorticity and turbulence data

show details of the evolution of the unsteady tip vortex downstream from the trailing edge. The results also show that the flow is strongly non-quasi-steady at the oscillation frequency studied. The results are fully archived on tape and are available to any interested reader. These can be used as database in the development of wake models for the finite wing, and in studies of three-dimensional wing aerodynamics DTIC

N94-29443*# National Aeronautics and Space Administration. Langley Research Center, Hampton, VA.

LOW-SPEED LONGITUDINAL AERODYNAMIC CHARACTERISTICS OF A FLAT-PLATE PLANFORM MODEL OF AN ADVANCED FIGHTER CONFIGURATION

Brian E. McGrath (Lockheed Engineering and Sciences Co., Hampton, VA.), Dan H. Neuhart (Lockheed Engineering and Sciences Co., Hampton, VA.), Gregory M. Gatlin, and Pat ONeil Mar. 1994 36 p Original contains color illustrations

(RTOP 505-68-70-05)

(NASA-TM-109045; NAS 1.15:109045) Avail: CASI HC A03/MF A01; 8 functional color pages

A flat-plate wind tunnel model of an advanced fighter configuration was tested in the NASA LaRC Subsonic Basic Research Tunnel and the 16- by 24-inch Water Tunnel. The test objectives were to obtain and evaluate the low-speed longitudinal aerodynamic characteristics of a candidate configuration for the integration of several new innovative wing designs. The flat plate test allowed for the initial evaluation of the candidate planform and was designated as the baseline planform for the innovative wing design study. Low-speed longitudinal aerodynamic data were obtained over a range of freestream dynamic pressures from 7.5 psf to 30 psf (M = 0.07 to M = 0.14) and angles-of-attack from 0 to 40 deg. The aerodynamic data are presented in coefficient form for the lift, induced drag, and pitching moment. Flow-visualization results obtained were photographs of the flow pattern over the flat plate model in the water tunnel for angles-of-attack from 10 to 40 deg. The force and moment coefficients and the flow-visualization photographs showed the linear and nonlinear aerodynamic characteristics due to attached flow and vortical flow over the flat plate model. Comparison between experiment and linear theory showed good agreement for the lift and induced drag; however, the agreement was poor for the pitching moment. Author (revised)

N94-29473*# National Aeronautics and Space Administration. Langley Research Center, Hampton, VA.

AN EXPERIMENTAL AND THEORETICAL STUDY OF THE AERODYNAMIC CHARACTERISTICS OF SOME GENERIC MISSILE CONCEPTS AT MACH NUMBERS FROM 2 TO 6.8

M. Leroy Spearman and Dorothy O. Braswell Apr. 1994 31 p

(RTOP 505-69-20-01)

(NASA-TM-109110; NAS 1.15:109110) Avail: CASI HC A03/MF A01

A study has been made of the experimental and theoretical aerodynamic characteristics for some generic high-speed missile concepts at Mach numbers from 2 to 6.8. The basic body for this study had a length-to-diameter ratio of 10 with the forward half being a modified blunted ogive and the rear half being a cylinder. Modifications made to the basic body included the addition of an after body flare, the addition of highly swept cruciform wings and the addition of highly swept aft tails. The effects of some controls were also investigated with all-moving wing controls on the flared body and trailing-edge flap controls on the winged body. The results indicated that the addition of a flare, wings, or tails to the basic body all provided static longitudinal stability with varying amounts of increased axial force. The control arrangements were effective in producing increments of normal-force and pitching-moment at the lower Mach numbers. At the highest Mach number, the flap control on the winged body was ineffective in producing normal-force or pitching-moment but the all-moving wing control on the flared body, while losing pitch effectiveness, still provided normal-force increments. Calculated results obtained through the use of hypersonic impact theory were in generally good agreement with experiment at the higher Mach numbers but were not accurate at the lower Mach numbers.

Author (revised)

N94-29545*# National Aeronautics and Space Administration. Langley Research Center, Hampton, VA.

EXPERIMENTAL STUDIES OF TRANSONIC FLOW FIELD NEAR A LONGITUDINALLY SLOTTED WIND TUNNEL WALL Ph.D. Thesis - George Washington Univ., 1988

Joel L. Everhart and Percy J. Bobbitt Apr. 1994 73 p

(RTOP 506-40-41-01)

(NASA-TP-3392; L-16423; NAS 1.60:3392) Avail: CASI HC A04/MF A01

The results of detailed parametric experiments are presented for the near-wall flow field of a longitudinally slotted transonic wind tunnel. Existing data are reevaluated and new data obtained in the Langley 6- by 19-inch Transonic Wind Tunnel are presented and analyzed. In the experiments, researchers systematically investigate many pertinent wall-geometry variables such as the wall openness and the number of slots along with the free stream Mach number and model angle of attack. Flow field surveys on the plane passing through the centerline of the slot were conducted and are presented. The effects of viscosity on the slot flow are considered in the analysis. The present experiments, combined with those of previous investigations, give a more complete physical characterization of the flow near and through the slotted wall of a transonic wind tunnel.

Author (revised)

N94-29674 Illinois Univ., Urbana-Champaign.

AN EXPERIMENTAL STUDY OF THE FLOWFIELD ON A SEMISPAN RECTANGULAR WING WITH A SIMULATED GLAZE ICE ACCRETION Ph.D. Thesis

Abdollah Khodadoust 1993 252 p

Avail: Univ. Microfilms Order No. DA9314893

The effect of a simulated glaze ice accretion on the flowfield of a semispan, reflection-plane, rectangular wing at Re = 1.5 million and M = 0.12 was investigated. A laser Doppler velocimeter was used to map the flowfield on the upper surface of the model in both the clean and iced configurations at alpha = 0, 4, and 8 degrees angle of attack. At low angles of attack, the massive separation bubble aft of the leading edge ice horn behaved in a manner similar to laminar separation bubbles. At alpha = 0 and 4 deg, the locations of transition and reattachment, as deduced from momentum thickness distributions, were in good agreement with transition and reattachment locations in laminar separation bubbles. These values at y/b = 0.470, the centerline measurement location, matched well with data obtained on a similar but two dimensional model. The measured velocity profiles on the iced wing compared reasonably with the predicted profiles from Navier-Stokes computations. The iced-induced separation bubble also had features similar to the recirculating region aft of rearward-facing steps. At alpha = 0 and 4 deg, reverse flow magnitudes and turbulence intensity levels were typical of those found in the recirculating region aft of rearward-facing steps. The calculated separation streamline aft of the ice horn at alpha = 4 deg, y/b = 0.470, coincided with the locus of the maximum Reynolds normal stress. The maximum Reynolds normal stress peaked at two locations along the separation streamline. The location of the first peak-value coincided with the transition location, as deduced from the momentum thickness distributions. The location of the second peak was just upstream of reattachment, in good agreement with measurements of flows over similar obstacles. The intermittency factor in the vicinity of reattachment at alpha = 4 deg, y/b = 0.470, revealed the time-dependent nature of the reattachment process. The size and extent of the separation bubble were a function of angle of attack and spanwise location. Three dimensional effects were strongest at alpha = 8 deg. The calculated separation and stagnation streamlines varied little with spanwise location at alpha = 0 deg. The calculated separation streamlines at alpha = 4 deg revealed that the bubble was largest near the centerline measurement plane, whereas the tip-induced vortex flow and the model root-tunnel wall boundary layer interaction reduced the size of the bubble. These effects were most dramatic at alpha = 8 deg. Dissert. Abstr.

N94-29760*# Stanford Univ., CA. Dept. of Aeronautics and Astronautics.

NUMERICAL STUDY OF THE TRAILING VORTEX OF A WING WITH WING-TIP BLOWING

Hock-Bin Lim Mar. 1994 136 p Sponsored by NASA. Ames Research Center

(NASA-CR-195803; NAS 1.26:195803; JIAA-TR-112) Avail: CASI HC A07/MF A02

Trailing vortices generated by lifting surfaces such as helicopter rotor blades, ship propellers, fixed wings, and canard control surfaces are known to be the source of noise, vibration, cavitation, degradation of performance, and other hazardous problems. Controlling these vortices is, therefore, of practical interest. The formation and behavior of the trailing vortices are studied in the present research. In addition, wing-tip blowing concepts employing axial blowing and spanwise blowing are studied to determine their effectiveness in controlling these vortices and their effects on the performance of the wing. The 3D, unsteady, thin-layer compressible Navier-Stokes equations are solved using a time-accurate, implicit, finite difference scheme that employs LU-ADI factorization. The wing-tip blowing is simulated using the actuator plane concept, thereby, not requiring resolution of the jet slot geometry. Furthermore, the solution blanking feature of the chimera scheme is used to simplify the parametric study procedure for the wing-tip blowing. Computed results are shown to compare favorably with experimental measurements. It is found that axial wing-tip blowing, although delaying the rolling-up of the trailing vortices and the near-field behavior of the flowfield, does not dissipate the circulation strength of the trailing vortex farther downstream. Spanwise wing-tip blowing has the effect of displacing the trailing vortices outboard and upward. The increased 'wing-span' due to the spanwise wing-tip blowing has the effect of lift augmentation on the wing and the strengthening of the trailing vortices. Secondary trailing vortices are created at high spanwise wing-tip blowing intensities. Author (revised)

N94-29826 Maryland Univ., College Park.
AN ANALYTICAL STUDY OF UNSTEADY ROTOR/FUSELAGE INTERACTION IN HOVER AND FORWARD FLIGHT Ph.D. Thesis
Gilbert Lewis Crouse, Jr. 1992 265 p
Avail: Univ. Microfilms Order No. DA9315626

An analytical study of the coupled rotor/fuselage aerodynamic environment is presented. Results from the analysis are used to help understand the nature of interactional phenomena on helicopters. Two analytical methods have been developed, and results from these models are compared with experimental measurements on a representative rotor/body model. The first method is a simplified analysis that treats the fuselage as a planar surface. This model is very computationally efficient, and is particularly useful for studying the pressure on the upper surface of the fuselage induced by the rotor and its wake. The second, and more comprehensive, model is the MURFI (Maryland Unsteady Rotor/Fuselage Interaction) model and consists of an unsteady source panel representation of the fuselage coupled with a lifting line rotor model and several different wake models. This analysis is more computationally expensive than the simplified model, but is capable of studying the entire coupled rotor/fuselage flowfield. In addition, the latter model is also used for the prediction of the effects of the fuselage on the rotor flowfield. A new helicopter free-wake methodology is also presented. The new model overcomes the well known instability of traditional free-wake methods in hover and in low-speed flight. In addition, the new method achieves this capability without an appreciable increase in computational effort. This model is particularly useful for interactional aerodynamics since the most severe wake/fuselage interactions occur in the hover and low-speed flight regime. Using these analytical models, results are shown that clearly demonstrate the capability of potential flow analyses to predict interactional effects, provided that all of the pertinent unsteady terms are included in the analysis. In particular, it is shown that the unsteady terms due to the time-rate-of-change of the surface source elements are very important to prediction of the surface pressure response. The analysis has also provided an improved understanding of the effects of the fuselage on the rotor loads and performance. Dissert. Abstr.

N94-29877 Purdue Univ., West Lafayette, IN.
TIME-MARCHING AEROELASTIC AND SPATIAL ADAPTATION PROCEDURES ON TRIANGULAR AND TETRAHEDRAL MESHES USING AN UNSTRUCTURED-GRID EULER METHOD Ph.D. Thesis
Russ David Rausch 1992 301 p
Avail: Univ. Microfilms Order No. DA9314067

Two- and three-dimensional, unstructured-grid, upwind-type Euler codes were modified to include time-marching aeroelastic and spatial adaptation procedures on triangular and tetrahedral meshes. The modifications for the time-marching aeroelastic procedures involve the addition of the structural equations of motion for their simultaneous time integration with the governing flow equations. A detailed description of the time-marching aeroelastic procedures is presented along with comparisons of computed results with experimental data to assess the accuracy of the capability. Flutter results are shown for both two and three-dimensional configurations including a NACA 0012 airfoil, an isolated 45 deg swept-back wing, and a supersonic transport configuration with a fuselage, clipped delta wing, and two identical rearward-mounted engine nacelles. The spatial adaptation procedures involve mesh enrichment and mesh coarsening to either add points in high gradient regions of the flow or remove points where they are not needed, respectively, in order to produce time-accurate solutions of high spatial accuracy at minimal computational cost. A detailed description of the enrichment and coarsening procedures is presented along with comparisons of computed results with experimental data to assess the accuracy of the capability. Steady results using the spatial adaptation procedures are shown for a NACA 0012 airfoil, an F-5 fighter wing, and an ONERA M6 wing. Unsteady results are shown for a NACA 0012 airfoil and a three dimensional simulation of a one-dimensional shock tube problem. The computed results are shown to be of high spatial accuracy, primarily in that shock waves are sharply captured. Dissert. Abstr.

N94-29879 Kansas Univ., Lawrence.
UNSTEADY TRANSONIC AERODYNAMICS IN FREQUENCY DOMAIN FOR FLUTTER ANALYSIS Ph.D. Thesis
Tai-Hsing Tom Sun 1992 100 p
Avail: Univ. Microfilms Order No. DA9313180

A finite difference method for calculating the three dimensional nonlinear transonic flow in the frequency domain is presented for the solution of unsteady pressure distribution. The averaging technique is employed to separate the governing equation into the in-phase and the out-of-phase equations. These two equations are then solved simultaneously with the finite difference scheme adopted in an existing steady code. The modified code is verified by comparing the calculated results with experimental data and existing computational method for a uniform rectangular wing with NACA 64A010A airfoil, ONERA M6 wing, a uniform rectangular wing with symmetrical circular arc airfoil in pitching or structural bending oscillations. The results are shown in good agreement in most cases. The effects on the unsteady characteristics of grid number and convergence criterion are discussed. A new methodology for solving the nonlinear flutter condition is also discussed. The formulations using the Beecham-Titchner method shows that the flutter conditions can be easily determined. Dissert. Abstr.

N94-29893*# Eloret Corp., Palo Alto, CA.
PARTICLE KINETIC SIMULATION OF HIGH ALTITUDE HYPERVELOCITY FLIGHT Final Technical Report, 1 Jan. 1989 - 31 Jan. 1994
Iain Boyd and Brian L. Haas 19 Apr. 1994 17 p
(Contract NCC2-582)
(NASA-CR-194535; NAS 1.26:194535) Avail: CASI HC A03/MF A01

Rarefied flows about hypersonic vehicles entering the upper atmosphere or through nozzles expanding into a near vacuum may only be simulated accurately with a direct simulation Monte Carlo (DSMC) method. Under this grant, researchers enhanced the models employed in the DSMC method and performed simulations in support of existing NASA projects or missions. DSMC models were developed and validated for simulating rotational, vibrational, and chemical relaxation in high-temperature flows, including effects of quantized anharmonic oscillators and temperature-dependent relaxation rates. State-of-the-art advancements were made in simulating coupled vibration-dissociation recombination for post-shock flows. Models were also developed to compute vehicle surface temperatures directly in the code rather than requiring isothermal estimates. These codes were instrumental in simulating aerobraking of NASA's Magellan spacecraft during orbital maneuvers to assess heat transfer and aerodynamic properties of the delicate satellite. NASA also depended upon simulations of entry of the Galileo probe into the atmosphere of Jupiter to provide drag and flow field information essential for accurate interpretation of an onboard experiment. Finally, the codes have been used extensively to simulate expanding nozzle flows in low-power thrusters in support of propulsion activities at NASA-Lewis. Detailed comparisons between continuum calculations and DSMC results helped to quantify the limitations of continuum CFD codes in rarefied applications. Author

N94-29920*# Princeton Univ., NJ. Dept. of Mechanical and Aerospace Engineering.

WALL PRESSURE FLUCTUATIONS IN THE REATTACHMENT REGION OF A SUPERSONIC FREE SHEAR LAYER Final Technical Report, 1 Jan. 1991 - 30 Jun. 1991

Alexander J. Smits 14 Apr. 1994 10 p

(Grant NAG1-1072)

(NASA-CR-195790; NAS 1.26:195790) Avail: CASI HC A02/MF A01

The primary aim of this research program was to investigate the mechanisms which cause the unsteady wall-pressure fluctuations in shock wave turbulent shear layer interactions. The secondary aim was to find means to reduce the magnitude of the fluctuating pressure loads by controlling the unsteady shock motion. The particular flow under study is the unsteady shock wave interaction formed in the reattachment zone of a separated supersonic flow. Similar flows are encountered in many practical situations, and they are associated with high levels of fluctuating wall pressure. The free shear layer is formed by the flow over a backward facing step, using an existing model, with the base pressure on the step adjusted so that there is no pressure discontinuity at the lip. The shear layer therefore develops in a zero pressure gradient. The primary advantage of this flow configuration is that the reattachment process can be studied in the absence of a separation shock. The mean flow data, and some preliminary hot-wire measurements of the mass-flux fluctuations were made by Baca and Settles, Baca, Williams and Bogdonoff, who showed that the shear layer became self-similar at about 17 delta(sub 0) downstream of the lip, and that it grew at a rate typical of the observed Mach number difference (about 1/3rd the incompressible growth rate). The turbulence measurements were later extended by Hayakawa, Smits and Bogdonoff under NASA Headquarters support. Derived from text

N94-29937*# National Aeronautics and Space Administration. Langley Research Center, Hampton, VA.

AERODYNAMIC CHARACTERISTICS OF A PROPELLER-POWERED HIGH-LIFT SEMISPAN WING

Garl L. Gentry, Jr., M. A. Takallu, and Zachary T. Applin Apr. 1994 70 p

(RTOP 535-03-10-02)

(NASA-TM-4541; L-17259; NAS 1.15:4541) Avail: CASI HC A04/MF A01

A small-scale semispan high-lift wing-flap system equipped under the wing with a turboprop engine assembly was tested in the LaRC 14- by 22-Foot Subsonic Tunnel. Experimental data were obtained for various propeller rotational speeds, nacelle locations, and nacelle inclinations. To isolate the effects of the high lift system, data were obtained with and without the flaps and leading-edge device. The effects of the propeller slipstream on the overall longitudinal aerodynamic characteristics of the wing-propeller assembly were examined. Test results indicated that the lift coefficient of the wing could be increased by the propeller slipstream when the rotational speed was increased and high-lift devices were deployed. Decreasing the nacelle inclination (increased pitch down) enhanced the lift performance of the system much more than varying the vertical or horizontal location of the nacelle. Furthermore, decreasing the nacelle inclination led to higher lift curve slope values, which indicated that the powered wing could sustain higher angles of attack near maximum lift performance. Any lift augmentation was accompanied by a drag penalty due to the increased wing lift. Author (revised)

N94-29973 Kansas Univ., Lawrence.

AIRCRAFT AERODYNAMICS WITH DEFLECTED JETS IN GROUND EFFECT Ph.D. Thesis

Chyuan-Hsyan Paul Liaw 1992 116 p

Avail: Univ. Microfilms Order No. DA9313133

A computational method by combining a potential flow approach with a Navier-Stokes solver is developed to analyze the flow field and predict the aerodynamics for three-dimensional configurations with deflected jet in ground effect. The potential flow method, PMARC/VSAERO, is a low-order panel code solving the potential flow over three-dimensional geometries. The Navier-Stokes code (NS3D) is based on the vorticity transport equation and the Poisson equation for the vector velocity potential in viscous, incompressible flow. Calculations for a rectangular flat plate and a wing-body combination with a single normal-deflected jet in ground effect with and without free stream are conducted. The computed results indicate that due to the induced velocity of a constant-thrust jet, the suck-down force (-L) is increased when the ground height (h) decreases. Calculated results for a 90 degree lifting jet issuing from a flat plate and for a wing-body configuration show good agreement in trend with available data. The computed moment coefficient versus ground height is also compared with data for the wing-body configuration. It also shows a good agreement in trend. However, the magnitude of the suck-down effect is under predicted. The discrepancy between the computational results and the experimental data is most likely due to a lack of an accurate simulation of turbulence effect, a fine enough grid system, an accurate specified vorticity distribution at the jet exit, or unknown experimental errors. The calculated flow field of roll-up jets is also presented. The flow patterns of a 90 degree jet impinging on the ground without the free stream effect has a stagnation point on the ground and symmetric with respect to the jet core. Due to the effect of the free stream, the stagnation point occurs ahead of the jet core, and the flow pattern is no longer symmetric. For deflected jets with any deflection angle other than 90 degrees, the vortex roll-up is stronger in the direction of the jet deflection, and the vortex shape is deformed. With a free stream combined with deflected jet, the flow pattern becomes more complicated. The jet core is deformed and the vortex roll-up is obvious. For lower ground height, the vortex becomes flatter. In summary, the flow patterns are affected by jet velocity, free stream velocity, deflected angles and ground height. Dissert. Abstr.

N94-30124*# Illinois Univ., Urbana-Champaign. Dept. of Aeronautical and Astronautical Engineering.

THE 3-D LDV MEASUREMENTS ON A 30-DEGREE SWEPT WING WITH A SIMULATED ICE ACCRETION Final Report

Michael B. Bragg and Michael K. Kerho Apr. 1994 63 p

(Grant NAG3-1134; RTOP 505-68-10)

(NASA-CR-195327; E-8778; NAS 1.26:195327) Avail: CASI HC A04/MF A01

Three dimensional flowfield measurements have been obtained for a semispan 30-degree swept wing with a simulated glaze ice accretion. The model tested has a NACA 0012 section perpendicular to the leading edge. Measurements were made using a two-component laser Doppler velocimeter (LDV) system. Mean velocity measurements were obtained for all three velocity components. Streamwise turbulence intensities were also obtained. All measurements were taken in the University of Illinois 3 by 4 foot subsonic wind tunnel at a Reynolds number of 1 million and 8 degrees angle of attack. The data is presented in tabular form. Author (revised)

N94-30151*# National Aeronautics and Space Administration. Ames Research Center, Moffett Field, CA.

COMPUTATION OF WIND TUNNEL WALL EFFECTS FOR COMPLEX MODELS USING A LOW-ORDER PANEL METHOD

Dale L. Ashby and Scott H. Harris Feb. 1994 19 p

(RTOP 505-59-53)

(NASA-TM-104019; A-93077; NAS 1.15:104019) Avail: CASI HC A03/MF A01

A technique for determining wind tunnel wall effects for complex models using the low-order, three dimensional panel method PMARC (Panel Method Ames Research Center) has been developed. Initial validation of the technique was performed using lift-coefficient data in the linear lift range from tests of a large-scale STOVL fighter model in the National Full-Scale Aerodynamics Complex (NFAC) facility. The data from these tests served as an ideal database for validating the technique because the same model was tested in two wind tunnel test sections with widely different dimensions. The lift-coefficient data obtained for the same model configuration in the two test sections were different, indicating a significant influence of the presence of the tunnel walls and mounting hardware on the lift coefficient in at least one of the two test sections. The wind tunnel wall effects were computed using PMARC and then subtracted from the measured data to yield corrected lift-coefficient versus angle-of-attack curves. The corrected lift-coefficient curves from the two wind tunnel test sections matched very well. Detailed pressure distributions computed by PMARC on the wing lower surface helped identify the source of large strut interference effects in one of the wind tunnel test sections. Extension of the technique to analysis of wind tunnel wall effects on the lift coefficient in the nonlinear lift range and on drag coefficient will require the addition of boundary-layer and separated-flow models to PMARC. Author

N94-30152*# Illinois Univ., Urbana-Champaign. Dept. of Aeronautical and Astronautical Engineering.

AN EXPERIMENTAL STUDY OF THE AERODYNAMICS OF A SWEPT AND UNSWEPT SEMISPAN WING WITH A SIMULATED GLAZE ICE ACCRETION Final Report

Michael B. Bragg May 1994 232 p

(Grants NAG3-1134; NAG3-28; RTOP 505-68-10)

(NASA-CR-195330; E-8813; NAS 1.26:195330) Avail: CASI HC A11/MF A03

Two semispan wings, one with a rectangular planform and one with 30 degrees of leading edge sweep were tested. Both had a NACA 0012 airfoil section, and both were tested clean and with simulated glaze ice shapes on their leading edges. Several surface roughness were tested. Each model geometry is documented and each surface roughness is explained. Aerodynamic performance of the wing in the form of sectional lift and integrated three-dimensional lift is documented through pressure measurements obtained from rows of surface pressure taps placed at five span locations on the wing. For the rectangular wing, sectional drag near the midspan is obtained from wake total pressure profiles. The data is presented in tabular and graphical form and is also available on computer disk. Author

N94-30176*# National Aeronautics and Space Administration. Langley Research Center, Hampton, VA.

USER'S MANUAL FOR THE MODEL INTERFACE AND PLUGBOARD CABINETS IN THE 14- BY 22-FOOT SUBSONIC TUNNEL

Robert B. Askew and P. Frank Quinto Apr. 1994 55 p

(RTOP 505-59-10-13)

(NASA-TM-109062; NAS 1.15:109062) Avail: CASI HC A04/MF A01

The primary method of connection between the wind tunnel model instrumentation and the data acquisition system in the 14- by 22-Foot Subsonic Tunnel is through the Model Interface (MIF) and Plugboard cabinets. The MIF and Plugboard cabinets allow versatility in the connection of the instrumentation to the different data systems in the facility. The User's Manual describes the components inside the MIF cabinet, the input and output of the MIF, and the MIF patchboard, and the Plugboard cabinets. There are examples of standard connections for most of the instrumentation used in the facility. Author (revised)

N94-30387 National Aerospace Lab., Amsterdam (Netherlands). Informatics Div.

THE DESIGN OF A SYSTEM OF CODES FOR INDUSTRIAL CALCULATIONS OF FLOWS AROUND AIRCRAFT AND OTHER COMPLEX AERODYNAMIC CONFIGURATIONS

J. W. Boerstoel (Technische Univ., Delft, Netherlands.), S. P. Spekreijse, and P. L. Vitagliano 9 Apr. 1992 16 p Presented at the 10th AIAA Applied Aerodynamics Conference, Palo Alto, CA, 22-24 Jun. 1992 See also N92-45492 Limited Reproducibility: More than 20% of this document may be affected by microfiche quality

(Contract NIVR-01604N)

(PB94-125598; NLR-TP-92190-UP; AIAA Paper 92-2619-CP; Alenia-TR-57X92054; CIRA-DLC-EST-271; ETN-94-95581) Avail: CASI HC A03

For industrial calculations of three dimensional flows around transport aircraft, a system of Computational Fluid Dynamics (CFD) codes for flow calculations is developed. This system includes codes for aerodynamic geometry modeling in block decomposition work, multiblock grid generation, Euler and Navier-Stokes flow calculations, and flow visualization. The codes are tuned to each other. Two examples of this tuning are discussed. Analytic representations for geometric shapes of aerodynamic curves and surfaces are presented that may be used for several tasks in CFD work (geometric modeling of surface, refacing of aerodynamic configuration surfaces). Multiblock grid generation is simplified by allowing grid lines to be only C(sup 0)- continuous over block faces. Block coupling algorithms for the flow solvers are discussed, that prevent accuracy loss due to the nonsmoothness of the grid over block faces. ESA

N94-30388 National Aerospace Lab., Amsterdam (Netherlands). Fluid Dynamics/Informatics Div.

NUMERICAL INVESTIGATION INTO HIGH-ANGLE-OF-ATTACK LEADING-EDGE VORTEX FLOW

J. I. vandenBerg, H. W. M. Hoeijmakers, and H. A. Sytsma 26 May 1992 29 p Presented at the AIAA 10th Applied Aerodynamics Conference, Palo Alto, CA, 22-24 Jun. 1992 See also N92-45477 Sponsored by Netherlands Agency for Aerospace Programs Limited Reproducibility: More than 20% of this document may be affected by microfiche quality

(PB94-125564; NLR-TP-92248-U; AIAA Paper 92-2600-CP; ETN-94-95584) Avail: CASI HC A03

A Euler method is applied to the steady subsonic (M(infinity) = 0.50) leading edge vortex flow about a 65 deg sharp edged cropped delta wing at incidences close to the incidence at which vortex breakdown is observed in wind tunnel experiments. Above a critical value of the incidence the pseudo time dependent numerical procedure fails to attain a steady state solution. This occurrence of 'solution breakdown' indicates the limits of the domain of applicability of the steady flow Euler method for the case of subsonic leading edge vortex flow. Analysis of the converged solution at incidences just below the critical value reveals that above the aft part of the wing the velocity and vorticity distribution within the vortex core undergo a remarkable change. ESA

N94-30389 National Aerospace Lab., Emmeloord (Netherlands). Aerodynamics Div.

EXPERIMENTS AND THEORETICAL CONSIDERATIONS REGARDING THE ALLOWABLE ROUGHNESS HEIGHT IN LAMINAR FLOW

A. C. deBruin 15 Jun. 1992 12 p Presented at the 1st European Forum on Laminar Flow Technology, Hamburg, Germany, 16-18 Mar. 1992 Limited Reproducibility: More than 20% of this document may be affected by microfiche quality

(Contract NIVR-01506N)

(PB94-125556; NLR-TP-92252-U; ETN-94-95585) Avail: Issuing Activity (European Space Agency (ESA))

The results of detailed experiments with single cylindrical roughness elements in a favorable pressure gradient laminar boundary layer are described. Based on these results, the allowable roughness height is analyzed for a family of similarity type laminar boundary layers. Subsequently, the problem of optimum airfoil shape with maximum resistance against surface roughness is addressed. The scaling laws for allowable roughness height are also discussed from a more global viewpoint. ESA

N94-30401 National Aerospace Lab., Amsterdam (Netherlands). Aerodynamics Div.

CALCULUS OF VARIATIONS APPLIED TO 2D MULTI-POINT AIRFOIL DESIGN

T. E. Labrujere and J. vanderVooren 1 Sep. 1992 32 p Presented at the 1st European Computational Fluid Dynamics Conference, Brussels, Belgium, 7-11 Sep. 1992 Limited Reproducibility: More than 20% of this document may be affected by microfiche quality

(PB94-125457; NLR-TP-92361-U; ETN-94-95594) Avail: CASI HC A03

Aspects of a residual correction method to solve the multipoint airfoil design problem for subsonic and transonic conditions are discussed. The method is based on full potential theory and minimizes a cost function weighting the deviations from specified target pressure distributions for each design condition in a least squares sense. Deviations from specified target pressure distributions (residuals) are translated into airfoil geometry corrections, using an approximate inverse method derived from solving an equivalent incompressible multipoint airfoil design problem using calculus of variations and numerical optimization. The feasibility of introducing the equivalent incompressible multipoint design problem is demonstrated for a two point reconstruction test case. First results of a two point example design are presented. ESA

N94-30492 National Aerospace Lab., Amsterdam (Netherlands). Fluid Dynamics Div.

ASPECTS OF THE MODELING AND NUMERICAL SIMULATION OF LEADING-EDGE VORTEX FLOW

H. W. M. Hoeijmakers 4 Dec. 1992 23 p Presented at the IUTAM Symposium on Fluid Dynamics of High Angle of Attack, Tokyo University, Japan, 13-17 Sep. 1992 Sponsored by Netherlands Agency for Aerospace Programs Limited Reproducibility: More than 20% of this document may be affected by microfiche quality

(AD-B179108; NLR-TP-92521-U; ETN-94-95965) Avail: CASI HC A03

A cell centered central difference finite volume Euler method is applied to the steady subsonic flow about a 65 degree sharp cropped delta wing at incidences close to the incidence at which leading edge vortex breakdown

is observed in wind tunnel experiments. Above a critical value of the incidence the pseudo-time dependent numerical procedure fails to attain a steady state solution. For the case of subsonic leading edge vortex flow the occurrence of 'solution breakdown' indicates the limits of the domain of applicability of the steady flow Euler method. In the search for the critical incidence it is found that for a given grid and for a given setting of the parameters controlling the artificial dissipation two distinct, steady state solutions exist. Analysis of the two solutions obtained at one incidence reveals that within the vortex core above the aft part of the wing these solutions feature remarkably different velocity and vorticity ditributions. ESA

N94-30493 National Aerospace Lab., Amsterdam (Netherlands). Aerodynamics Div.

A RESIDUAL CORRECTION METHOD APPLIED TO 2D MULTI-POINT AIRFOIL DESIGN AND 3D SINGLE-POINT WING DESIGN

T. E. Labrujere and J. vanderVooren 31 Jan. 1993 25 p Submitted for publication Limited Reproducibility: More than 20% of this document may be affected by microfiche quality

(Contract AERO-1082)

(NLR-TP-92524-U; ETN-94-95966) Avail: CASI HC A03

Results of a residual correction method to solve the multipoint airfoil design problem for subsonic and transonic conditions are presented. The method is based on full potential theory and minimizes a cost function weighting the deviations from specified target pressure distributions for each design condition in a least squares sense. Deviations from specified target pressure distributions (residuals) are translated into airfoil geometry corrections, by means of an approximate inverse calculation using a linearized panel method. The feasibility of introducing an equivalent incompressible multipoint design problem is demonstrated for a two point reconstruction test case. First results of a two point example airfoil design case are presented. The applicability of the residual correction methodology to three dimensional single point wing design is demonstrated as well. ESA

N94-30525 Virginia Polytechnic Inst. and State Univ., Blacksburg.

SENSITIVITY ANALYSIS OF THE STATIC AEROELASTIC RESPONSE OF A WING Ph.D. Thesis

Lloyd Byron Eldred 1993 147 p

Avail: Univ. Microfilms Order No. DA9319768

A technique to obtain the sensitivity of the static aeroelastic response of a three dimensional wing model is designed and implemented. The formulation is quite general and accepts any aerodynamic and structural analysis capability. A program to combine the discipline level, or local, sensitivities into global sensitivity derivatives is developed. A variety of representations of the wing pressure field are developed and tested to determine the most accurate and efficient scheme for representing the field outside of the aerodynamic code. Chebyshev polynomials are used to globally fit the pressure field. This approach had some difficulties in representing local variations in the field, so a variety of local interpolation polynomial pressure representations are also implemented. These panel based representations use a constant pressure value, a bilinearly interpolated value, or a biquadratically interpolated value. The interpolation polynomial approaches do an excellent job of reducing the numerical problems of the global approach for comparable computational effort. Regardless of the pressure representation used, sensitivity and response results with excellent accuracy have been produced for large integrated quantities such as wing tip deflection and trim angel of attack. The sensitivities of such things as individual generalized displacements have been found with fair accuracy. In general, accuracy is found to be proportional to the relative size of the derivatives to the quantity itself. Dissert. Abstr.

N94-30740 National Aerospace Lab., Amsterdam (Netherlands). Unsteady Aerodynamics and Aeroelasticity Dept.

PROSPECTS OF TIME-LINEARIZED UNSTEADY CALCULATION METHODS FOR EXPONENTIALLY DIVERGING MOTIONS IN AEROELASTICITY

M. H. J. Hounjet and B. J. G. Eussen 22 Apr. 1992 21 p Presented at the AIAA Dynamics Specialist Conference, Dallas, TX, 16-17 Apr. 1992 Limited Reproducibility: More than 20% of this document may be affected by microfiche quality

(PB94-126224; NLR-TP-92163; ETN-94-95578) Avail: CASI HC A03

A demonstration is given of a simple procedure which was used to generate unsteady loads for oscillating wings in a two dimensional and three dimensional subsonic, transonic and supersonic flow for an almost complete range of existing time linearized methods including a method allowing for wind tunnel wall interference. The method transforms real unsteady data obtained for diverging exponential motions of the wind to unsteady complex data for harmonic oscillations by means of fitting the real data by Pade polynomials and using these approximations for harmonic oscillations assuming the analytical continuation is valid. ESA

N94-30858 National Aerospace Lab., Amsterdam (Netherlands). Aerodynamics Div.

GRID ADAPTION IN COMPUTATIONAL AERODYNAMICS

R. Hagmeijer and K. M. J. deCock 1 Apr. 1992 23 p Submitted for publication Sponsored in part by National Aerospace Lab. Limited Reproducibility: More than 20% of this document may be affected by microfiche quality

(Contract AERO-0018-C(H))

(PB94-126240; NLR-TP-92139-U; ETN-94-95575) Avail: CASI HC A03

An algorithm to adapt computational grids is applied to aerodynamic problems. The algorithm is described and the main features are discussed. Applications to both inviscid and viscous flows around two dimensional airfoils show that the algorithm is robust and almost fully automatic, and that shocks, expansion zones, boundary layers and shear layers are well resolved by the adapted grid. ESA

N94-30865 Air Force Inst. of Tech., Wright-Patterson AFB, OH.

HOPF BIFURCATION IN VISCOUS, LOW-SPEED FLOWS ABOUT AN AIRFOIL WITH STRUCTURAL COUPLING Ph.D. Thesis

Mark John Lutton 1993 152 p

Avail: Univ. Microfilms Order No. DA9324933

The locations of Hopf bifurcation points associated with the viscous incompressible flow about a NACA 0012 airfoil with structural coupling are computed for very low Reynolds numbers (less than 2000). A semi-implicit, first-order-accurate time-integration algorithm is employed to solve the streamfunction-vorticity form of the Navier-Stokes equations. The formulation models the inclusion of simple structural elements affixed to the airfoil and captures the resulting airfoil motion. The equations describing the airfoil motion are integrated in time using a fourth-order Runge-Kutta algorithm. The dissertation is divided into two parts. In Part 1, numerical experiments are performed in the laminar regime to determine if the structural model of the airfoil has an effect upon the location of the Hopf bifurcation point when compared with the fixed airfoil. Results are reported for a variety of structural characteristics, including variation of torsional and linear spring constants, inertial properties, structural coupling, and structural damping. The structure of the solution space is explored by means of phase plots. In Part II, the Baldwin-Lomax turbulence model is implemented to model turbulent flow. A numerical effort is made to predict the onset of unsteady flow and the results are compared to theory and experiment. A comparison is undertaken with the compressible and incompressible form of the Navier-Stokes equations to assess the correspondence of the unsteady lift evolved by pitching the airfoil at a prescribed frequency and amplitude. Comparisons are made with the lift predicted by the potential flow method of Theodorsen. Dissert. Abstr.

N94-30871 National Aerospace Lab., Amsterdam (Netherlands). Theoretical Aerodynamics Dept.

NUMERICAL SIMULATION OF LEADING-EDGE VORTEX FLOW

H. W. M. Hoeijmakers (Technische Univ., Eindhoven, Netherlands.) 30 Nov. 1991 31 p Sponsored by Netherlands Agency for Aerospace Programs, and Ministry of Defence Limited Reproducibility: More than 20% of this document may be affected by microfiche quality

(AD-B175154; PB94-125481; NLR-TP-91471-U; ETN-94-95568) Avail: CASI HC A03

An analysis of results of a computational method to simulate the steady compressible vortical type of flow around a 65 deg sharp edged cropped delta wing is presented. Some more fundamental aspects of the numerical simulation such as the separation of the flow, the structure of the leading edge vortex core and the flow inside the free shear layer are emphasized. For the vortex core in isolation as well as for the free shear layer, closed form solutions are presented which might assist in the analysis of the numerical results. ESA

N94-30916# National Aerospace Lab., Amsterdam (Netherlands). Fluid Dynamics Div.
AERODYNAMIC ANALYSIS OF SLIPSTREAM/WING/NACELLE INTERFERENCE FOR PRELIMINARY DESIGN OF AIRCRAFT CONFIGURATIONS
C. M. vanBeek, W. J. Piers, and B. Oskam 22 Nov. 1991 25 p Presented at the AGARD Fluid Dynamics Panel Symposium on Aerodynamic Engine/Airframe Integration for High Performance Aircraft and Missiles, Fort Worth, TX, 7-10 Oct. 1991 Sponsored by Netherlands Agency for Aerospace Programs
(AD-B173651; NLR-TP-91453; ETN-94-95567) Avail: CASI HC A03/MF A01

A panel method based model for the computation of the time averaged influence of a propeller slipstream on the aerodynamic characteristics of an aircraft configuration is described. The slipstream model is based on the simplifications that the single rotating propeller is replaced by an actuator disk and that all the vorticity of the slipstream is represented on a cylindrical sheet of fixed geometry which envelops the slipstream in combination with a discrete vortex at the axis of the slipstream. Appropriate jump conditions across the actuator disk and boundary conditions on the cylindrical sheet, solved simultaneously with the boundary conditions on the aircraft configuration, yield the mutual influence of the propeller and the slipstream on the aerodynamic characteristics of the aircraft. This slipstream model is incorporated in a three dimensional panel method. Computed lift increments due to the slipstream are presented for a realistic wing/nacelle/fuselage configuration and compared with wind tunnel data for several thrust coefficients and angles of attack of the aircraft. ESA

N94-30949*# National Aeronautics and Space Administration. Lewis Research Center, Cleveland, OH.
EVALUATION OF FLIP-FLOP JET NOZZLES FOR USE AS PRACTICAL EXCITATION DEVICES
Ganesh Raman (NYMA, Inc., Brook Park, OH.), Edward J. Rice, and David M. Cornelius Apr. 1994 13 p Proposed for presentation at the ASME Fluids Engineering Division Summer Meeting, Lake Tahoe, NV, 19-23 Jun. 1994; sponsored by ASME
(Contract NAS3-27186; RTOP 505-62-52)
(NASA-TM-106377; E-8190; NAS 1.15:106377) Avail: CASI HC A03/MF A01

This paper describes the flowfield characteristics of the flip-flop jet nozzle and the potential for using this nozzle as a practical excitation device. It appears from the existing body of published information that there is a lack of data on the parameters affecting the operation of such nozzles and on the mechanism of operation of these nozzles. An attempt is made in the present work to study the important parameters affecting the operation and performance of a flip-flop jet nozzle. Measurements were carried out to systematically assess the effect of varying the nozzle pressure ratio (NPR) as well as the length and volume of the feedback tube on the frequency of oscillation of this device. Flow visualization was used to obtain a better understanding of the jet flowfield and of the processes occurring within the feedback tube. The frequency of oscillation of the flip-flop jet depended significantly on the feedback tube length and volume as well as on the nozzle pressure ratio. In contrast, the coherent velocity perturbation levels did not depend on the above mentioned parameters. The data presented in this paper would be useful for modeling such flip-flop excitation devices that are potentially useful for controlling practical shear flows. Author

03 AIR TRANSPORTATION AND SAFETY

Includes passenger and cargo air transport operations; and aircraft accidents.

For related information see also *16 Space Transportation* and *85 Urban Technology and Transportation.*

N94-28799# Arizona State Univ., Tempe. Dept. of Mechanical and Aerospace Engineering.
CRASHWORTHINESS ANALYSIS OF COMMUTER AIRCRAFT SEATS Technical Note
David H. Laananen Nov. 1993 20 p
(Contract DTFA03-90-P-00447)
(AD-A275889; CR-R-91012; DOT/FAA/CT-TN-91/28) Avail: CASI HC A03/MF A01

During the past several years, the Federal Aviation Regulations (FAR) were significantly modified with respect to seat/restraint system strength, attachment of seats to the aircraft structure, and the means by which they are to be evaluated. Aircraft accident data, human tolerance levels, and aircraft structural characteristics have been considered in the development of these new standards. Dynamic testing is now required for seats to be installed in general aviation aircraft, transport category aircraft, and rotorcraft. Performance criteria are similar to those specified by the Federal Motor Vehicle Safety Standards for automobiles but also include a limit on pelvic force, in order to prevent spinal injuries which may be caused by the vertical component of impact force. A category of aircraft that has not as yet been affected by the rule modifications is the commuter type aircraft, which seats 10 to 19 passengers. Since this airplane is closer in size to general aviation aircraft than to large transports, it is also covered by FAR Part 23. The Federal Aviation Administration is currently involved in the conduct of a test program addressing commuter aircraft occupant crash safety. In support of this effort, a research program the includes full-scale aircraft drop tests, sled tests of seats, and computer simulations is being conducted. This report describes the use of the SOM-LA (Seat/Occupant Model-Light Aircraft) program in modeling three commuter aircraft seats. The predicted response of the seats to a potential set of test conditions is described. DTIC

N94-29185 National Transportation Safety Board, Washington, DC.
NATIONAL TRANSPORTATION SAFETY BOARD ANNUAL REVIEW OF AIRCRAFT ACCIDENT DATA. US GENERAL AVIATION, 1990
17 Dec. 1993 84 p Limited Reproducibility: More than 20% of this document may be affected by microfiche quality
(PB94-126869; NTSB/ARG-93/02) Avail: CASI HC A05

The report presents a statistical compilation and review of general aviation accidents which occurred in 1990 in the United States, its territories and possessions, and in international waters. The report is divided into five sections: All Accidents; Fatal Accidents; Serious Injury Accidents; Property Damage Accidents and Midair Collision Accidents. Several tables present accident parameters for 1990 accidents only, and each section includes tabulations which present comparative statistics for 1990 and for the five-year period 1985-1989. NTIS

N94-29402# National Transportation Safety Board, Washington, DC.
AIRCRAFT ACCIDENT/INCIDENT SUMMARY REPORT: IN-FLIGHT LOSS OF CONTROL, LEADING TO FORCED LANDING AND RUNWAY OVERRUN, CONTINENTAL EXPRESS, INC., N24706 EMBRAER EMB-120 RT, PINE BLUFF, ARKANSAS, 29 APRIL 1993
29 Apr. 1993 51 p
(PB94-910404; NTSB/AAR-94/02/SUM) Avail: CASI HC A04/MF A01

This report explains the in-flight loss of control of N24706, leading to a forced landing and runway overrun at Pine Bluff, Arkansas, on 29 April 1993. The safety issues discussed in the report are flight crew professionalism, inattentiveness, and fatigue. A recommendation concerning fatigue was made to the Federal Aviation Administration. Author (revised)

N94-29862# Systems Control Technology, Inc., Arlington, VA.
POTENTIAL HAZARDS OF MAGNETIC RESONANCE IMAGERS TO EMERGENCY MEDICAL SERVICE HELICOPTER OPERATIONS Final Report
Robert B. Newman Jan. 1993 56 p
(Contract DTFA01-87-C-00014)
(DOT/FAA/RD-92/15; SCT-92RR-14) Avail: CASI HC A04/MF A01

In recent years, there have been several incidents with helicopters where magnetic resonance imagers (MRI's) have interferred with the operation of magnetic sensors such as compasses and directional gyroscopes. The magnetic fields generated by the MRI magnet causes magnetic sensors to give aberrant readings. This report documents the characteristics of MIR's and how they operate. It discusses relevant federal regulations of MRI and all magnetic effects and hazards involved with operating helicopters in a strong static magnetic field for both personnel and equipment. Finally, the report makes recommendations for safe helicopter operations in and around MRI's. Author

N94-30144 Manitoba Univ., Winnipeg. Dept. of Actuarial and Management Science.

A CAPACITY PLANNING MODEL FOR CANADIAN MILITARY AIRLIFT REQUESTS M.S. Thesis

Barry Anthony Stannard Aug. 1993 150 p

(ISBN-0-315-86079-0; CTN-94-61178) Copyright Avail: Micromedia Ltd., Technical Information Centre, 240 Catherine Street, Suite 305, Ottawa, Ontario, K2P 2G8, Canada HC/MF

The problem of the constrained assignment of n variable length tasks (missions), integrating many airlift requests from 13 users with eight priorities, to m parallel machines (CC130 Hercules airframes) is presented. A general mathematical model was developed which is suitable for assisting airlift planners in deciding which airlift mission requests to accept. The model can be implemented on a microcomputer and is essentially a computational subroutine for a larger decision support system. A high quality airlift capacity plan resulted from the application of a group of management science techniques. Analytic hierarchy process was used to quantify each mission request. A sequential linear programming model proved to be a computationally efficient approach for producing an automated planning aid to assist the airlift capacity planners. The model is flexible, computationally fast, and accurate. It handles linked missions, either as a pair or as a minimum out of an optimal number. User hour and fleet flying hour constraints are modelled and missions can be added, deleted, or modified. While the model was developed for the Canadian Forces, it can be adapted for other similar military and civilian situations. Author (CISTI)

N94-30890 National Oceanic and Atmospheric Administration, Boulder, CO. Environmental Technology Lab.

REMOTE SENSOR OBSERVATIONS DURING WISP91: THE USE OF MICROWAVE RADIOMETERS, RASS, AND LIDAR CEILOMETERS FOR DETECTION OF AIRCRAFT ICING CONDITIONS

B. B. Stankov, J. B. Snider, E. R. Westwater, R. H. Beeler, and L. S. Fedor Oct. 1993 85 p See also PB91-131839 Limited Reproducibility: More than 20% of this document may be affected by microfiche quality

(PB94-142106; NOAA-TM-ERL-ETL-236) Avail: CASI HC A05

From Jan. 15 through Mar. 31, 1991, the National Oceanic and Atmospheric Administration's (NOAA) Wave Propagation Laboratory (WPL) participated in the Winter Icing and Storms Project (WISP91). Several remote sensors were used in the study: an array of four dual-channel microwave radiometers, Wind Profilers and Radio Acoustic Sounding Systems (RASS) at 915, 405, and 50 MHz; operational National Weather Service (NWS) lidar ceilometers; and infrared radiometers operating at 10.6 micrometers. One of the principal objectives of the project was to determine the utility of combined sensors to detect supercooled liquid water. After describing the changes in the system relative to the 1990 experiments, results of two representative cases are presented to illustrate the capabilities and limitations of the combined system. NTIS

04 AIRCRAFT COMMUNICATIONS AND NAVIGATION

Includes digital and voice communication with aircraft; air navigation systems (satellite and ground based); and air traffic control.

For related information see also *17 Space Communications, Spacecraft Communications, Command and Tracking* and *Communications and Radar.*

N94-28744# Air Force Inst. of Tech., Wright-Patterson AFB, OH. School of Logistics and Acquisition Management.

EVALUATION OF ACCESS/NAVIGATIONAL FEATURES OF A GRAPHICAL-USER INTERFACE INSTALLED ON A PORTABLE MAINTENANCE AID M.S. Thesis

Lisa A. Carney and Roger A. Quinto Sep. 1993 146 p

(AD-A275791; AFIT/GLM/LAL/93S-9) Avail: CASI HC A07/MF A02

Portable maintenance aids (PMA's) are being developed to access and store electronic technical information on the flightline. The prototype PMA designed by Armstrong Laboratory personnel has redundant access/navigational features. Redundancy increases software memory usage and adds unnecessary weight to the PMA. The purpose of this research was to determine the best access/navigational feature installed on the PMA. The best feature is the feature that provides the highest degree of user satisfaction. An experiment was conducted to evaluate the following features for screen and menu access and navigation, respectively: dedicated/hardware keys, programmable soft keys, and push button keys, and number keys, cursor control keys, and programmable soft keys. Modified computer screens from the prototype PMA were used on a laptop personal computer, which simulated the PMA, to evaluate each feature, one at a time. Twenty-eight maintenance technicians rated and ranked each access/navigational feature. The results indicated that the best feature for screen access and navigation was the dedicated/hardware keys and the best feature for menu access and navigation was the number keys. DTIC

N94-28914# Federal Aviation Administration, Atlantic City, NJ. Technical Center.

LOS ANGELES INTERNATIONAL AIRPORT INSTRUMENT LANDING SYSTEM APPROACH DATA COLLECTION AND REDUCTION, PHASE 1 Final Repoort, Nov. 1991 - Apr. 1992

J. Thomas, D. Timoteo, and P. Hoang Nov. 1993 72 p

(AD-A275115; DOT/FAA/CT-TN93/12) Avail: CASI HC A04/MF A01

Position data on aircraft flying Instrument Landing System (ILS) approaches from 40 nautical miles (nmi) down to runway threshold were collected at Los Angeles International Airport (LAX) between November 26, 1991 and April 25, 1992. The purpose of the data collection was to provide an accurate database of navigational performance of aircraft flying ILS approaches at distances between 10 nmi and 32 nmi. Aircraft position data were collected using the in-place LAX surveillance primary and secondary radars. The data were reduced and analyzed at the Federal Aviation Administration (FAA) Technical Center by ACD-340 personnel. The discussion in this Final Report concerns the accuracy of the collected position data and possible sources of error in the data collection. DTIC

N94-29445# Federal Aviation Administration, Washington, DC.

THE 1993 FEDERAL AVIATION ADMINISTRATION AVIATION SYSTEM CAPITAL INVESTMENT PLAN

Dec. 1993 304 p

Avail: CASI HC A14/MF A03

Based on a total system approach, the Aviation System Capital Investment Plan (CIP) relates user community needs to technical opportunities, human factors, and operational considerations. The systematic implementation of the projects defined in this CIP will result in improved safety and efficiency, while accommodating spiraling demands at constrained cost. It supports a more complex system and creates a foundation for continued evolution that uses modern technologies and capabilities. The CIP also recognizes that continuing upgrades and enhancements are necessary to meet evolving national airspace system (NAS) user needs. It includes the following: Original NAS Plan (Chapter 2)--Preservation of the original NAS Plan projects; Growth (Chapter 3)--Projects that expand, relocate, or consolidate existing facilities/capabilities in response to changing demand on the system. Each potential metroplex control facility (MCF) is identified in this chapter; Infrastructure Replenishment (Chapter 4)--Projects identified since the original NAS Plan that refurbish structures, replace obsolete equipment, or relocate facilities to maintain service, improve effectiveness, and/or reduce cost; Supportability (Chapter 5)--Capital improvement projects that support logistics, provide spares, train personnel, and manage the human resource aspect of modernizing the NAS; and New Capabilities (Chapter 6)--Projects identified since the original NAS Plan which, if implemented, are expected to add significant new capabilities to the system. The new TRACON Automation System project is contained in this chapter. Author (revised)

N94-29558# Advisory Group for Aerospace Research and Development, Neuilly-Sur-Seine (France). Guidance and Control Panel.

MACHINE INTELLIGENCE IN AIR TRAFFIC MANAGEMENT [L'INTELLIGENCE ARTIFICIELLE DANS LA GESTION DU TRAFIC AERIEN]

Andre Benoit, ed. (European Organization for the Safety of Air Navigation, Brussels, Belgium.) Oct. 1993 400 p In ENGLISH and FRENCH The 56th Symposium was held in Berlin, Germany, 11-14 May 1993

(AGARD-CP-538; ISBN-92-835-0724-X) Copyright Avail: CASI HC A17/MF A04

This volume contains the Technical Evaluation Report and the 30 papers, presented at the Guidance and Control Panel Symposium held in Berlin,

Germany from 11th to 14th May 1993. The papers were presented covering the following headings: Air Traffic Processes; Novel Approaches; Transition to Operation; Human/Machine Relationship; Air/Ground Integration; PHARE; and Ground Movements Control. For individual titles, see N94-29559 through N94-29587.

N94-29559# Mitre Corp., McLean, VA. Center for Advanced Aviation Systems Development.

ADVANCES IN DEVELOPMENT CAPABILITIES FOR INTELLIGENT AIR TRAFFIC MANAGEMENT SYSTEMS

Kerry M. Levin and John J. Fearnsides *In* AGARD, Machine Intelligence in Air Traffic Management Oct. 1993 18 p (For primary document see N94-29558 08-04)

Copyright Avail: CASI HC A03/MF A04

Visual presentation is a major source of information for air traffic control. Significant advances in computers, display technology, and the tools used by developers of intelligent air traffic management (ATM) systems pose challenges for the development of computer-human interfaces (CHI's) associated with the new automation. The CHI must be designed to be both usable and suitable. This paper reviews three capabilities available to developers of intelligent ATM systems: case-based reasoning system design, rule-based system design, and individually tailored CHI. It recommends that any intelligent ATM system be examined early in its development cycle in a laboratory environment, where it can be tested in concert with other elements of the ATM system. Author

N94-29560# CompEngServ Ltd., Ottawa (Ontario).

INTELLIGENT SYSTEMS FOR AIR SPACE CONTROL AND MANAGEMENT

David Bowen and Andrzej Hlibowicki *In* AGARD, Machine Intelligence in Air Traffic Management Oct. 1993 11 p Sponsored by Transportation Development Centre (For primary document see N94-29558 08-04)

Copyright Avail: CASI HC A03/MF A04

Complete automation of an air traffic control system requires the identification of functions and their allocation to a distributed system, part of which is on the ground and part of which flies. The evolution of current systems appears to be taking place with ill-defined visions of what the final system will or should look like. In some cases this fuzzy view of the future is purposely carried because of the implications of proposing a view which antagonizes various groups or associations representing those already engaged in the process. Yet, each step along the way implies explicitly or implicitly some final target system. As each year goes by, we move toward a system which may be a long way from what is really desirable in the next century. It seems reasonable that some versions of the ideal future system should be understood within the community. At least one of these options should be what is technically feasible. From this, an acceptable system can be negotiated. The first step in this process is to determine the desired functionality without regard to any other factors. From this, technical feasibility can be determined and/or predicted; and finally, the allocation of the functions to humans or machines can be debated. The management of a dense cluttered air space requires a set of skills and capabilities on the part of an air traffic control team which, in some of their functions, cannot be represented algorithmically. Successful automated air traffic management systems will necessarily emulate the intuitive portions of the human management capability using various technologies drawn from the broad field of artificial intelligence. Indeed portions of the overall management system have been the subject of research and development efforts in many laboratories around the world. The integration of these fragments into an overall scheme is often left as an implicitly understood architecture. This paper begins by presenting CompEngServ (CES) Ltd.'s view of an automated airspace management system. The paper then presents an overview of the prototype of an advanced controller workstation developed by CES (under contract to Transport Canada) which prototypes various portions of this architecture for Airspace Management. This system represents the state of the art in Air Traffic Control (ATC) research. This prototype is also an example of multiple hardware and software technologies being harnessed to develop a solution to a problem initially thought to be too complex for automation. The paper then presents the future direction of research at CES and then closes with the issues which have been raised by our work that need addressing before an automated system will be practical. Author

N94-29561# Centre d'Etudes de la Navigation Aerienne, Toulouse (France).

USE OF ADVANCED TECHNOLOGIES IN ATM (AIR TRAFFIC MANAGEMENT) DOMAIN

P. Planchon and M. Bonnard *In* AGARD, Machine Intelligence in Air Traffic Management Oct. 1993 11 p (For primary document see N94-29558 08-04)

Copyright Avail: CASI HC A03/MF A04

The CENA is in charge of studies related to Air Traffic Management and therefore to some of the communication, navigation, and surveillance means. The work is carried out to support French and European ATC (air traffic control) in an international cooperation. It encompasses studies and experimental development aiming at operational implementation within the CAUTRA 5 program. The different CENA projects are integrated in an experimental simulator frame named ADER. This test-bed will support one of the demonstrations within PHARE, a joint European experimental program. The CENA organization is based upon a technical directorate in charge of the horizontal projects as previously described and 10 divisions located either at Athis-Mons (near Paris) or in Toulouse. One of these divisions, called COA (Control Organization and Automation), deals mainly with studies aiming at providing ATM (air traffic management) operators with helpful decision tools, using advanced methods and technologies. In this paper, it can be found a short description of COA division activities and a more precise analysis of one of the projects, called GOETHE, aiming to provide ATFM (Air Traffic Flow Management) regulators with a more user-friendly tool. Derived from text

N94-29562# Princeton Univ., NJ. Dept. of Mechanical and Aerospace Engineering.

AIR TRAFFIC MANAGEMENT AS PRINCIPLED NEGOTIATION BETWEEN INTELLIGENT AGENTS

Robert Stengel and John Wangermann *In* AGARD, Machine Intelligence in Air Traffic Management Oct. 1993 10 p (For primary document see N94-29558 08-04)

(Contract DT-FA01-92-G-0011)

Copyright Avail: CASI HC A02/MF A04

The major challenge facing the world's aircraft/airspace system (AAS) today is the need to provide increased capacity, whilst reducing delays, increasing the efficiency of flight operations, and improving safety. Technologies are emerging that should improve the performance of the system, but which could also introduce uncertainty, disputes, and inefficiency if not properly implemented. The aim of our research is to apply techniques from intelligent control theory and decision-making theory to define an Intelligent Aircraft/Airspace System (IAAS) for the year 2025. The IAAS would make effective use of the technical capabilities of all parts of the system to meet the demand for increased capacity with improved performance. Author

N94-29563# Shape Technical Center, The Hague (Netherlands).

USE OF GPS IN AUTOMATED AIR TRAFFIC CONTROL

Hermann F. Hegels and Willem E. Hoekstra *In* AGARD, Machine Intelligence in Air Traffic Management Oct. 1993 26 p (For primary document see N94-29558 08-04)

Copyright Avail: CASI HC A03/MF A04

The Global Positioning System NAVSTAR is rapidly becoming the world standard for navigation and timing. Although primarily designed to be a military system, the civil user community is expanding at a breathtaking pace. After an introduction to the general GPS policies and the technical fundamentals this paper presents an idea on how to use GPS NAVSTAR to improve Air Traffic Control. Existing selective identification features will form the key to a GPS-based position, velocity, and acceleration message. Higher update rates and the vastly improved information on each aircraft will provide the input for a flight plan correlation function enabling an automatic air traffic monitoring and control far beyond current standards. Author

N94-29564# Raumfahrt Systemtechnik G.m.b.H., Salem (Germany).

GROUND INDEPENDENT LANDING SYSTEM

Hans Martin Braun and Philipp Hartl *In* AGARD, Machine Intelligence in Air Traffic Management Oct. 1993 6 p (For primary document see N94-29558 08-04)

Copyright Avail: CASI HC A02/MF A04

Air traffic in Central Europe is dramatically increasing today. There are some indications that present upgrades of the air traffic control system might not be efficient and that planned upgrades will not be realized in time due to budgetary restrictions. One key element in air traffic control is a precise navigation of the aircraft during landing, the most critical part of the flight. It is presently performed by use of the instrument landing system ILS and in some areas already by the microwave landing system MLS. The latter provides a very high navigation performance and allows a high landing sequence under all weather conditions. However, it requires extensive ground equipment at the airports and hence, only a few airports in Central Europe are equipped with it today. This paper presents the results of a study on a new microwave landing system with a spaceborne radar transmitter and airborne radar receivers. Based on this bistatic radar system, navigation in landing phase could also be performed independently from weather conditions. However, it does not require any active equipment at the landing site. Even taxi way guidance could be performed with this system. It is called 'Ground Independent Landing System' (GILS). Author

N94-29565# Deutsche Aerospace A.G., Ulm (Germany).
GPS/GNSS FOR ATM
Thomas Jacob, Jochen Meyer-Hilberg, Gerhard Bantle, Winifred Roesch, Heinz-Georg Wippich, and Horst Schmidt *In* AGARD, Machine Intelligence in Air Traffic Management Oct. 1993 10 p (For primary document see N94-29558 08-04)
Copyright Avail: CASI HC A02/MF A04

The actual implemented Air Traffic Control (ATC) systems have radar coverage gaps on the Northern Atlantic and Trans-Siberian Routes as well as in the Pacific area. This situation results in insufficient air traffic surveillance information in the corresponding control sectors and larger separation between aircraft on these routes to ensure safe operation. Unfortunately, this procedure reduces the capacity and limits air traffic flow. These problems can be overcome by the worldwide use of the high accurate position data from Global Navigation Satellite Systems (GNSS) such as the U.S. Global Positioning System (GPS) and the Russian Global Navigation System (GLONASS) aboard the aircraft as proposed by the ICAO-FANS plan. In combination with the Automatic Dependent Surveillance (ADS) function as specified by ARINC 745, the onboard computed position and flight path data is transmitted to the Aeronautical Telecommunication Network (ATN) for further use by ATM and ATC. Based on these principles, Deutsche Aerospace AG, Airborne Systems Division has developed a demonstrator. This system integrates the precise (Differential) GNSS information with the data from an Inertial Measurement Unit (e.g. AHRS) aboard the demonstrator aircraft to fulfill the accuracy and consistency/integrity requirements during all phases of flight. This system integration has been done to ensure integrity of GNSS position information during satellite outages or satellite masking, e.g. during turns. For demonstrating ADS-functionality, the onboard computed position and flight path velocity is transmitted in combination with flight management information to the ground system using a data link. In addition to this en-route ADS function with medium accuracy requirements, a high accuracy mode using Differential GNSS data for conflict detection calculations between low separated aircraft has been implemented. The conflict detection and alert functions are based on a special designed Expert System capable of real time operation. A taxi monitoring function can also be performed by the system. All system functions have been tested and demonstrated during flight trials using a VHF data link for communication. Results of these flight tests will be presented. Author (revised)

N94-29566# Shape Technical Center, The Hague (Netherlands).
ACCS SURVEILLANCE EXPLORATORY PROTOTYPE (ASEP) **c32**
K. Gaebler *In* AGARD, Machine Intelligence in Air Traffic Management Oct. 1993 18 p (For primary document see N94-29558 08-04)
Copyright Avail: CASI HC A03/MF A04

The increasing sophistication of surveillance systems, both civilian and military, has generated a great deal of interest in techniques of multi-target tracking and sensor integration. To help SHAPE and the NATO Air Command and Control System (ACCS) Management Agency (NACMA) to specify and implement the ACCS surveillance subsystem, in particular in the areas of data fusion and identification, the SHAPE Technical Center (STC) is currently developing an ACCS Surveillance Exploratory Prototype (ASEP) as an element of its new integrated testbed. The purpose of the ASEP is to demonstrate the feasibility and operational benefits of future air picture generation systems. The significant difference between this advanced system and currently available systems is that ASEP will provide better tracking continuity, more accurate estimates of track positions, velocity, acceleration, and additional information on targets. The provision of this information on air targets is also of great importance for civil ATC systems, especially in view of growing requirements for ATC planning, conflict alert and conflict resolution. The use of multiple sensors and sources requires the fusion of different types of data, including sensor reports containing measured attributes such as the target type and other target features. Since advanced fusion algorithms are using kinematic data as well as attribute data for the identification process, the majority of all air targets can be identified automatically. This paper gives an overview of the following components that are implemented in the ACCS Surveillance Exploratory Prototype at STC: scenario generation and sensor simulation; real-time multi-sensor tracking; real-time radar data integration; external track and flight plan data integration; and air picture presentation on a Surveillance Workstation using new human-computer interface (HCI) techniques. Derived from text

N94-29567# Deutsche Forschungsanstalt fuer Luft- und Raumfahrt, Brunswick (Germany). Inst. of Flight Guidance.
CONTRIBUTIONS OF DLR TO AIR TRAFFIC CAPACITY ENHANCEMENT WITHIN A TERMINAL AREA
U. Voelckers, U. Brokof, D. Dippe, and M. Schubert *In* AGARD, Machine Intelligence in Air Traffic Management Oct. 1993 11 p (For primary document see N94-29558 08-04)
Copyright Avail: CASI HC A03/MF A04

Enhancement of air traffic capacity within the TMA cannot be achieved easily. Single solutions and improvements of technical equipment, procedures and standards, with automation support for human operators in isolated areas, e.g. for the management of the airport, airspace and Air Traffic Control very often will only yield marginal capacity increases. Whether it is: new concrete (runways, taxiways, aprons), reduced separation minima, or advanced ATM functions, all these measures will only result in significant capacity increases, if they are designed, developed and implemented in a comprehensive, combined effort, making use of set of complementary measures and functions in a well structured, optimized architecture and implementation strategy. This comprehensive approach is especially true for high density TMA's/airports, operating close to capacity limits, where any capacity enhancement measure will directly affect and/or require capacity related issues in other areas. Based upon the specific needs of the Frankfurt airport and TMA, DLR is working on a variety of tools and functions, which--combined and implemented in a well designed strategy plan--can yield significant capacity increases without the construction of new runways. Three candidate systems--under development or even already in operation--which mutually depend on and complement one another will be presented as examples of an even larger capacity enhancement plan for the TMA. Derived from text

N94-29568*# National Aeronautics and Space Administration. Ames Research Center, Moffett Field, CA.
DESIGN OF CENTER-TRACON AUTOMATION SYSTEM
Heinz Erzberger, Thomas J. Davis, and Steven Green *In* AGARD, Machine Intelligence in Air Traffic Management Oct. 1993 12 p (For primary document see N94-29558 08-04)
Copyright Avail: CASI HC A03/MF A04

A system for the automated management and control of terminal area traffic, referred to as the Center-TRACON Automation System (CTAS), is being developed at NASA Ames Research Center. In a cooperative program, NASA and FAA have efforts underway to install and evaluate the system at the Denver area and Dallas/Ft. Worth area air traffic control facilities. This paper will review CTAS architecture, and automation functions as well as the integration of CTAS into the existing operational system. CTAS consists of three types of integrated tools that provide computer-generated advisories for both en-route and terminal area controllers to guide them in managing and controlling arrival traffic efficiently. One tool, the Traffic Management Advisor (TMA), generates runway assignments, landing sequences and landing times for all arriving aircraft, including those originating from nearby feeder airports. TMA also assists in runway configuration control and flow management. Another tool, the Descent Advisor (DA), generates clearances for the en-route controllers handling arrival flows to metering gates. The DA's clearances ensure fuel-efficient and conflict free descents to the metering gates at specified crossing

times. In the terminal area, the Final Approach Spacing Tool (FAST) provides heading and speed advisories that help controllers produce an accurately spaced flow of aircraft on the final approach course. Data bases consisting of several hundred aircraft performance models, airline preferred operational procedures, and a three dimensional wind model support the operation of CTAS. The first component of CTAS, the Traffic Management Advisor, is being evaluated at the Denver TRACON and the Denver Air Route Traffic Control Center. The second component, the Final Approach Spacing Tool, will be evaluated in several stages at the Dallas/Fort Worth Airport beginning in October 1993. An initial stage of the Descent Advisor tool is being prepared for testing at the Denver Center in late 1994. Operational evaluations of all three integrated CTAS tools are expected to begin at the two field sites in 1995. Derived from text

N94-29569# National Aerospace Lab., Amsterdam (Netherlands).
SIMULATION OF FULLY AUTOMATED AIR TRAFFIC CONTROL CONCEPTS
Wim denBraven and Hans vandenBos *In* AGARD, Machine Intelligence in Air Traffic Management Oct. 1993 16 p Sponsored by Schiphol Airport Authorities (For primary document see N94-29558 08-04)
Copyright Avail: CASI HC A03/MF A04

In order to be able to investigate various aspects of the complex Air Traffic Control (ATC) system of the future, a real-time ATC simulation facility has been constructed at NLR. The ATC automation environment of this simulator is provided by CTAS, the Center/TRACON Automation System, developed by the NASA Ames Research Center. For the simulation of air traffic, radar observations, and data link, the NLR ATC Research Simulator (NARSIM) is used. The facility can be used at various levels of automation, ranging from conventional, 'manual' ATC to fully automatic control. For the latter, CTAS has been extended with various decision and control algorithms, dealing with tasks normally executed by the air traffic controller. In a set of real-time simulation experiments different concepts of fully automated ATC are investigated, characterized by various combinations of control functions and different levels of air-ground interaction. Furthermore, the effect of different levels of aircraft navigation performance is studied. The traffic samples are based on single-runway IFR operations for Schiphol Airport, with the traffic mix and distribution based on predictions for the year 2000. The Dutch airspace is simulated with one overall area control sector, controlling traffic from all directions to the three arrival gates, and one Schiphol approach sector, merging the aircraft from these gates into a properly spaced sequence on final approach. For the analysis of the simulations, methods are under development to present overall ATC system performance in terms of safety, flight efficiency, capacity, and control performance. The results of the simulations are used to determine critical areas in ATC system automation, as well as potential benefits thereof. They can also contribute to an optimal distribution of tasks between man and machine in the ATC system of the future. Author (revised)

N94-29570# European Organization for the Safety of Air Navigation, Brussels (Belgium).
DECISION MAKING AIDS (DMA) IN ON-LINE ATC SYSTEMS
Andre Benoit, Jean-Marc Pomeret, and Sip Swierstra *In* AGARD, Machine Intelligence in Air Traffic Management Oct. 1993 11 p (For primary document see N94-29558 08-04)
Copyright Avail: CASI HC A03/MF A04

This paper covers the potential of Decision Making Aids to be implemented before the year 2000 and, within the time frame considered, covers all of the aspects of automated assistance, based on flight path prediction and monitoring, which help air traffic controllers to establish and assess the predicted traffic situation more efficiently. Problem detection, problem minimization, and 'best next clearance' advisories will permit the reduction of the controller's mental workload without decreasing the level of safety or the controller's situational awareness. Author (revised)

N94-29571# Centre d'Etudes de la Navigation Aerienne, Toulouse (France).
COGNITIVE APPROACH TO SPECIFICATIONS ON AIR TRAFFIC CONTROLLERS' DECISION ASSISTANCE SYSTEMS [UNE APPROCHE COGNITIVE POUR LA SPECIFICATION D'AIDES A LA DECISION POUR LES CONTROLEURS AERIENS]
Marcel Leroux *In* AGARD, Machine Intelligence in Air Traffic Management Oct. 1993 10 p In FRENCH (For primary document see N94-29558 08-04)
Copyright Avail: CASI HC A02/MF A04

The central problem of this investigation is the creation of an Air Traffic Control System (ATC) involving both man and machine. The present document reports on two examples which typify the man-machine relationships in systems which are partly automated. In one case, the part played by the machine is detrimental to man's involvement; in the other case, man and machine work together for better results. The manner in which this second approach was used during the development of the CENA's ERATO project is described. Transl. by FLS

N94-29572# Deutsche Forschungsanstalt fuer Luft- und Raumfahrt, Brunswick (Germany). Inst. for Flight Guidance.
CONSIDERATIONS ON GRAPHICAL USER INTERFACES FOR INTELLIGENT ATM SUPPORT SYSTEMS
R. Beyer *In* AGARD, Machine Intelligence in Air Traffic Management Oct. 1993 13 p (For primary document see N94-29558 08-04)
Copyright Avail: CASI HC A03/MF A04

Considerations on the design of graphical user interfaces (GUI's) for air traffic controllers are presented in the context of a European Air Traffic Management System (EATMS). The fundamental issues discussed include the following: air traffic controller tasks; human information processing and mental models; and automation strategies with respect to the GUI design. The more specific issues of GUI design which are also discussed include the following: GUI programming environments and standards; development tools; design principles and human factors/human engineering standards; and usability testing. Conclusions are drawn regarding the current background of GUI design with respect to an EATMS and necessary future developments. Author (revised)

N94-29573# Deutsche Forschungsanstalt fuer Luft- und Raumfahrt, Brunswick (Germany). Inst. for Flight Guidance.
INTERACTIVE ANALYSIS AND PLANNING TOOLS FOR AIR TRAFFIC AND AIRSPACE MANAGEMENT
S. E. Mahlich *In* AGARD, Machine Intelligence in Air Traffic Management Oct. 1993 13 p (For primary document see N94-29558 08-04)
Copyright Avail: CASI HC A03/MF A04

Since 1989, the Institute for Flight Guidance of the German Aerospace Research Establishment (DLR) has been developing prototypes of interactive tools in close cooperation with the German Air Navigation Services (DFS) in order to achieve gradual improvements in the efficiency and productivity of the air traffic control system. The paper briefly describes the potential of a selection of analysis and planning tools that have been developed in this framework. After an introduction into the 'planning world' of tactical and strategical air traffic planning, the objectives and potentials of four tools will be demonstrated as applied to real traffic scenarios and actual problems of the current ATM system. Author (revised)

N94-29574# Alcatel ISR, Evry (France).
DAISY: A DECISION AID FOR AN AIR SITUATION INTERPRETATION SYSTEM
N. Bichat, R. Allouche, and A. Bories *In* AGARD, Machine Intelligence in Air Traffic Management Oct. 1993 8 p (For primary document see N94-29558 08-04)
Copyright Avail: CASI HC A02/MF A04

Due to increases in air traffic volume and the evolution of operational missions, Alcatel ISR has been awarded a contract to analyze the requirements of military air traffic controllers, especially in the area of the air situation interpretation and the implementation of a mock-up. DAISY is aimed at providing controllers with a decision aid for an air situation interpretation system. In this context, interpretation stands for all the rules and combined information which give an operational meaning to the air situation. Abnormal situations are highlighted, a diagnosis is given, and a proposal is made for decision. After a requirements analysis is conducted, both by experts and controllers during six months, a twelve-month technical feasibility study was led by Alcatel ISR, and a mock-up was developed dealing with typical interpretation scenario such as trajectory prediction. Author (revised)

N94-29575# Deutsche Forschungsanstalt fuer Luft- und Raumfahrt, Brunswick (Germany). Inst. for Flight Guidance.

DLR'S ATM DEMONSTRATION PROGRAMME

V. Adam, E. Klostermann, and M. Schubert *In* AGARD, Machine Intelligence in Air Traffic Management Oct. 1993 12 p (For primary document see N94-29558 08-04)

Copyright Avail: CASI HC A03/MF A04

The Institute for Flight Guidance of DLR is involved in medium and long term research and development of concepts, procedures, functions, and components for a future integrated Air Traffic Management System. The medium term work concentrates on improvements concerning the capacity of Frankfurt airport. This paper describes a planned demonstration program which is designed to prove concepts and tools developed by the Institute in cooperation with the German ATC Authority (DFS) and the operator of Frankfurt airport (FAG) as well as with PHARE. The aim of these experiments is to demonstrate the feasibility and merits of integration of onboard avionics with advanced ATC systems on the ground. For this purpose an Air Traffic Management Demonstrator System will be employed, which comprises an air segment and a ground segment connected via an automatic data link and voice communication. The demonstration program will be performed in several phases comprising simulation runs in an air traffic simulator as well as flight tests with a real aircraft. Author (revised)

N94-29576# Honeywell, Inc., Minneapolis, MN. Systems and Research Center.

ADVANCED AIR TRAFFIC CONTROL AND FLIGHT MANAGEMENT SYSTEM CONCEPTS

Robert L. Schultz *In* AGARD, Machine Intelligence in Air Traffic Management Oct. 1993 11 p (For primary document see N94-29558 08-04)

Copyright Avail: CASI HC A03/MF A04

A time-based air traffic control (ATC) system where vehicles are sequenced on desired time of arrival (TOA) has been proposed as one way that might help increase airport capacity. This paper evaluates three time-based ATC system concepts: (1) ground based (computing trajectories on the ground), (2) aircraft based (computing trajectories on the aircraft), and (3) ground and air based (generating parametrized velocity and acceleration profiles on the aircraft and transmitting them to the ground where trajectories are recomputed). The parameters compared are amount of database, complexity of communications, computational requirements, autonomy of aircraft, and similarity to current procedures. The ground-and-air-based approach using parametrized profiles has the best potential for providing a high-landing-rate ATC system with minimal processing and communications requirements. In this approach, ATC assigns time slots at the metering fix based on desired time of arrival (TOA) and range-TOA windows generated on the aircraft. The aircraft sends a simple set of parametrized deceleration and velocity profiles to the ground. The ground processor uses these profiles to generate trajectories and identify conflicts. The ground processor resolves conflicts by examining nearby trajectories using both the sets of parametrized deceleration and velocity profiles and the range-TOA windows. The new horizontal plan and the new profile parameters are sent to the aircraft, where the aircraft flight management system (FMS) regenerates the trajectory and precisely flies it. The advantages of such a system are that it is a natural extension of the current system; it does not require massive ground databases of aircraft thrust, drag and FMS models; it uses a ground processor generating simple models to examine and resolve conflicts; it requires only one air-to-ground interaction; and the aircraft is autonomous. A simulation was used to evaluate the concept. The models used in the simulation are ATC trajectory generator, aircraft FMS, aircraft path controller, and vehicle motion. Multiple-aircraft scenarios, starting in cruise and descent, were examined. Factors examined were separation distances between aircraft on different approach trajectories, accuracy of TOA, and effects of wind-forecast errors on TOA errors.

Author

N94-29577# Federal Aviation Administration, Washington, DC.

OPPORTUNITIES FOR INTEGRATING THE AIRCRAFT FMS, AERONAUTICAL OPERATIONAL CONTROL CENTERS, AND FUTURE AIR TRAFFIC MANAGEMENT SYSTEMS IN OCEANIC AIRSPACE

Clyde Miller, Bill Blake, John Sorensen, and Joseph Miller *In* AGARD, Machine Intelligence in Air Traffic Management Oct. 1993 10 p (For primary document see N94-29558 08-04)

Copyright Avail: CASI HC A02/MF A04

Rapid technological changes are taking place in the aviation system user facilities - both on the aircraft flight deck and at the aeronautical operational control (AOC), or flight dispatch centers. On the flight deck, the flight management system (FMS) is bringing capability for precise three-dimensional guidance, flight path optimization, and speed control to meet required time-of-arrival (RTA) constraints at key route waypoints. This is enhanced by the precision global navigation satellite system (GNSS), use of digital datalink for communications, and automatic dependent surveillance (ADS). At AOC facilities, advancements in flight planning, flight following, weather information and datalink allow the dispatcher greater flight operations management capability over the airline fleet. This is especially significant for oceanic airspace operations. In parallel, the oceanic air traffic management (ATM) system is undergoing an evolution in automation that will enhance the overall aviation system productivity. Much of the information that each of the three system components - flight deck/FMS, AOC, and ATM - have would be very useful to the other two components for flight efficiency and overall productivity enhancements. Worldwide datalink technology will provide a universal and reliable data communication capability between these components to allow this information sharing. This paper discusses the opportunity to integrate the functions of the FMS, AOC, and ATM computers by exploiting the capabilities of worldwide ground and air data link. First, the outstanding needs of both the oceanic airspace user and traffic management provider are stated. Then, the emerging technological capabilities of ATM automation, FMS and AOC are summarized. This is followed by explicit operational applications where the integration of these capabilities can bring incremental benefits to flight efficiency and human productivity. Needs of both the airspace user and air traffic management service provider are addressed. Operations using today's organized oceanic track system as well as the future free route system are discussed. The opportunities for FMS-AOC-ATM integration are illustrated by three scenarios for oceanic operation. These include a mid-oceanic route replanning task to respond to weather change, a passing maneuver to allow more flexibility in flight speed and altitude when flying along a track system, and use of the FMS RTA capability to meet scheduled track entry gate times with precise accuracy. Author (revised)

N94-29578*# National Aeronautics and Space Administration. Langley Research Center, Hampton, VA.

PROFILE NEGOTIATION: AN AIR/GROUND AUTOMATION INTEGRATION CONCEPT FOR MANAGING ARRIVAL TRAFFIC

David H. Williams, P. Douglas Arbuckle, Steven M. Green, and Wim denBraven *In* AGARD, Machine Intelligence in Air Traffic Management Oct. 1993 11 p (For primary document see N94-29558 08-04)

Copyright Avail: CASI HC A03/MF A04

NASA Ames Research Center and NASA Langley Research Center conducted a joint simulation study to evaluate a profile negotiation process (PNP) between a time-based air traffic control ATC system and an airplane equipped with a four dimensional flight management system (4D FMS). Prototype procedures were developed to support the functional implementation of this process. The PNP was designed to provide an arrival trajectory solution that satisfies the separation requirements of ATC while remaining as close as possible to the airplane's preferred trajectory. The Transport Systems Research Vehicle cockpit simulator was linked in real-time to the Center/TRACON Automation System (CTAS) for the experiment. Approximately 30 hours of simulation testing were conducted over a three week period. Active airline pilot crews and active Center controller teams participated as test subjects. Results from the experiment indicate the potential for successful incorporation of airplane preferred arrival trajectories in the CTAS automation environment. Controllers were able to consistently and effectively negotiate nominally conflict-free trajectories with pilots flying a 4D-FMS-equipped airplane. The negotiated trajectories were substantially closer to the airplane's preference than would have otherwise been possible without the PNP. Airplane fuel savings relative to baseline CTAS were achieved in the test scenarios. The datalink procedures and clearances developed for this experiment, while providing the necessary functionality, were found to be operationally unacceptable to the pilots. Additional pilot control and understanding of the proposed airplane-preferred trajectory and a simplified clearance procedure were cited as necessary for operational implementation of the concept. From the controllers'

perspective, the main concerns were the ability of the 4D airplane to accurately track the negotiated trajectory and the workload required to support the PNP as implemented in this study. Author

N94-29579# European Organization for the Safety of Air Navigation, Brussels (Belgium).
AIR-GROUND INTEGRATION OF THE ATM SYSTEM IN PHARE
B. Kirstetter and R. D. Hunter *In* AGARD, Machine Intelligence in Air Traffic Management Oct. 1993 11 p (For primary document see N94-29558 08-04)
Copyright Avail: CASI HC A03/MF A04

This paper provides a general introduction into the Programme of Harmonised Air Traffic Management Research in EUROCONTROL (PHARE). It describes the objectives of the research program and addresses the benefits of the integration of the automated systems onboard the aircraft with those of the ATC systems on the ground using a digital air-ground data link. The assumptions on the expected infrastructure and environment are explained and the possible automation and air-ground negotiation strategies discussed. Finally descriptions of the experimental facilities available or under development and of the planned experiments are provided. Author

N94-29580# Deutsche Forschungsanstalt fuer Luft- und Raumfahrt, Brunswick (Germany). Inst. for Flight Guidance.
EXPERIMENTAL FLIGHT MANAGEMENT SYSTEM
V. Adam, G. Ingle, and R. Rawlings *In* AGARD, Machine Intelligence in Air Traffic Management Oct. 1993 21 p (For primary document see N94-29558 08-04)
Copyright Avail: CASI HC A03/MF A04

The paper reviews the requirements for an Experimental Flight Management System (EFMS) and the methods adopted for its development. The functionality is described and the future application of the system is summarized. Author

N94-29581# National Aerospace Lab., Amsterdam (Netherlands).
THE PHARE ADVANCED TOOLS
Henk A. P. Blom, Garfield Dean, Marc LeGuillou, Eric Petre, and Uwe Voelckers *In* AGARD, Machine Intelligence in Air Traffic Management Oct. 1993 8 p (For primary document see N94-29558 08-04)
Copyright Avail: CASI HC A02/MF A04

The Programme for Harmonisation of ATM Research in Eurocontrol (PHARE) has undertaken to perform the required research work necessary for the introduction of advanced ATM. Within this PHARE framework, it is the task of the PHARE Advanced Tools (PAT's) group to develop the appropriate automation and communication tools to support the air traffic controller. Although the principles for computation, prediction and control of air traffic trajectories are well developed, the various future ATM scenarios reflect different views on the way automation and communication technology can best be applied. The consequence of this is that PHARE research has to be directed towards multiple ATM scenarios, and that the PAT's to be developed should be applicable to automation and communication under different ATM scenarios. The paper gives an overview of the approach taken by the PAT's group in facing this challenge. Author

N94-29582# Centre d'Etudes de la Navigation Aerienne, Toulouse (France).
THE COMMON MODULAR SIMULATOR (CMS): AN ARCHITECTURE TEST BED FOR FUTURE ADVANCED ATM SYSTEMS
J. R. Velten *In* AGARD, Machine Intelligence in Air Traffic Management Oct. 1993 8 p (For primary document see N94-29558 08-04)
Copyright Avail: CASI HC A02/MF A04

The Common Modular Simulator (CMS) project is part of the Program for Harmonized ATM Research in Eurocontrol (PHARE). The main objective of this project is to provide a common integration environment which shall allow the creation of a homogeneous infrastructure in order to facilitate and harmonize the development as well as the evolution of ATM simulators in the different research establishments. To meet such an ambitious objective, CMS partners have adopted a system architecture based on a client-server model with active servers providing event subscription and event notification mechanisms. The main advantages of such client-server models are to offer a very modular system architecture and to provide, through the associated application programming interface (API), a very powerful mechanism of abstraction. This leads to a very flexible, evolutive, open, scalable and adaptable system. CMS will offer an architecture test bed for future advanced ATM systems. As a consequence, this project should be of great benefit to many other ATM projects. Author (revised)

N94-29583# Eurocontrol Experimental Centre, Bretigny (France).
ARC2000: AUTOMATIC RADAR CONTROL
Xavier Fron, Bernard Maudry, Jean-Pierre Nicolaon, and Jean-Claude Tumelin *In* AGARD, Machine Intelligence in Air Traffic Management Oct. 1993 14 p (For primary document see N94-29558 08-04)
Copyright Avail: CASI HC A03/MF A04

The 'Studies, Tests, and Applied Research' (STAR) program of the EUROCONTROL Agency is addressing several implementation timescales for air traffic management (ATM) systems and procedures. ARC2000 (automatic radar control 2000) is presently the major long-term component of the STAR program, for implementation beyond 2015. ARC2000 is addressing the enroute ATC capacity issue, which is severe in Europe, by investigating the limit case where both major constraints, workload and sectorization, are eliminated. It is often easier to solve a complex problem by first looking at the limit case. ARC2000 could not be implemented as such, but should provide precious information with respect to feasible levels of automation in the long term. There are also significant by-products which will speed up shorter term research. Indeed, ARC2000 provides a 20-30 minute conflict-free planning which is a key feature of the European Air Traffic Management System (EATMS) concept. Author (revised)

N94-29584# Technische Univ., Brunswick (Germany). Inst. of Flight Guidance and Control.
AUTOMATIC CONTROL STEPS FOR AIRCRAFT TAXI GUIDANCE
Klaus Moehlenkamp and Gunther Schaenzer *In* AGARD, Machine Intelligence in Air Traffic Management Oct. 1993 5 p Sponsored by German Research Society (For primary document see N94-29558 08-04)
Copyright Avail: CASI HC A01/MF A04

Modern high precision navigation systems based on satellite and inertial navigation provide a positioning accuracy that has never been achieved before, for aircraft enroute as well as during approach and on the airfield. By using such combined accurate positioning systems it is possible to guide aircraft on the ground and to perform automatic taxiing, which further increases the safety of ground operations. Whenever high precision terrestrial navigation is needed, common aeronautical navigation displays are not able to provide the information, which easily can be combined with the pilot's view from the cockpit, to deliver the necessary guidance aid. A flexible map display is desired to be shown in the cockpit. The new taxi guidance system GINaS, presented in this paper, is based on an integrated navigation system (DGPS/INS) and a digital map using only the standard display and navigation hardware of modern commercial aircraft. The system was successfully tested in one of our testbeds, a van. This van can be driven automatically by the system as well as by the pilot using the information of the digital map and a drive-director. The accuracy reaches submeter level. Author (revised)

N94-29585# Marconi Radar Systems Ltd., Chelmsford (England).
AIRSIDE GROUND MOVEMENTS SURVEILLANCE
D. R. Corrall, A. N. Clark, and A. G. Hill *In* AGARD, Machine Intelligence in Air Traffic Management Oct. 1993 13 p Sponsored in part by Commission of the European Communities (For primary document see N94-29558 08-04)
Copyright Avail: CASI HC A03/MF A04

In the modern world there is an increasing need for surveillance, and a consequent need for automatic or semi-automatic methods for processing dynamic input data and presenting it in a form which is useful to the end user. This paper outlines advanced knowledge-based techniques for monitoring such data. The techniques have been applied to airport ground traffic applications and demonstrated in particular on data from actual turn-round scenarios for stand area servicing of an aircraft as observed by a single camera. Results are output in real-time as a status report by an integrated system which is designed to handle the vagaries of real data in respect to incompleteness and uncertainty. The new techniques developed can also be applied to other ground movements surveillance applications which have multiple sensor inputs of the same or different modalities.
Author (revised)

N94-29586# Deutsche Forschungsanstalt fuer Luft- und Raumfahrt, Wessling (Germany). Inst. of Radiofrequency Technology.

A NOVEL NEAR-RANGE RADAR NETWORK FOR AIRPORT SURFACE CONTROL

K.-H. Bethke, B. Roede, M. Schneider, and A. Schroth *In* AGARD, Machine Intelligence in Air Traffic Management Oct. 1993 14 p (For primary document see N94-29558 08-04)

Copyright Avail: CASI HC A03/MF A04

This contribution describes a radar network for airport surface movement guidance and control. The network comprises several low power radar stations which are organized in modules of four stations each. All antennas are staring and illuminating the area continuously. Moving objects are localized by range profile measurements and a subsequent multilateration. Each module runs autonomously. The module computer at the master station calculates the multilaterations and controls the communication with three slave stations. The measured data from these stations are transferred via the radar transmitters to the master station, while the multilateration and imaging results are sent via data cables to the central computer. There, the information from all modules will be merged and tracks will be constructed; furthermore, a classification process on the basis of the images will be executed. Author (revised)

N94-29587# Federal Aviation Administration, Washington, DC. Research and Development Service.

DEVELOPMENT OF PRECISION RUNWAY MONITOR SYSTEM FOR INCREASING CAPACITY OF PARALLEL RUNWAY OPERATIONS

Gene A. Wong *In* AGARD, Machine Intelligence in Air Traffic Management Oct. 1993 12 p (For primary document see N94-29558 08-04)

Copyright Avail: CASI HC A03/MF A04

This paper describes the results of a research program to investigate the use of advanced radar, display systems, and controller alert automation aid to increase capacity at airports with closely spaced parallel runways. Analysis has indicated that the runway spacing could be reduced without adversely affecting capacity if a surveillance radar of higher update and accuracy and a high resolution color display system with controller alert automation aid are used. This paper first describes a research program to demonstrate the feasibility of using a precision runway monitor (PRM) system for conducting independent simultaneous approaches to parallel runways spaced at less than 3400 ft (1035 m) apart. A PRM system consists of an improved radar system that provides high azimuth and range accuracy and higher data rates than the current terminal airport surveillance radar (ASR), a processing system that monitors all approaches and generates controller alerts when an aircraft appears to be blundering, and a high resolution color display. Two airports were selected to serve as the demonstration and test facilities of the PRM system. This paper describes the key elements of the demonstration program including test criteria and scenarios, controller and pilot/aircraft response times, and risk analysis. Results of the demonstration program on the feasibility of the 3400 ft runway spacing standards using PRM are presented. Recommendations on radar update rate, accuracy, and display requirements for the PRM system are summarized. This paper also describes the follow-on research activities to investigate further reduction of parallel runway spacing standards to below 3400 ft using the PRM system and advanced navigation and landing systems. Applications and extension of research results to triple and quadruple closely spaced parallel runways are discussed.

Author (revised)

N94-29837 Texas Univ., Austin.

A GUIDANCE AND NAVIGATION SYSTEM FOR TWO SPACECRAFT RENDEZVOUS IN TRANSLUNAR HALO ORBIT Ph.D. Thesis

Brian Leigh Jones 1993 203 p

Avail: Univ. Microfilms Order No. DA9323444

This research considers the design of a representative end-to-end guidance and navigation system for the terminal phase rendezvous of two spacecraft in the circular restricted three-body problem. It assumes the target vehicle is in a small radius translunar halo orbit; the target vehicle remains passive with respect to the rendezvous profile. The chaser vehicle is in an independent small radius translunar halo orbit and executes all rendezvous maneuvers. First, the halo orbit guidance problem is formulated in the frequency-domain from which an output feedback guidance law is developed using H(sub 2) control theory. Linear simulation results validate the guidance law and provide data which quantify the effect of control inputs, noise characteristics and halo orbit characteristics on the steady state halo orbit station-keeping costs. Secondly, a two space-craft terminal phase rendezvous targeting law is derived; nonlinear simulation results validate the targeting law. Using these results, the three-body terminal phase rendezvous problem is further characterized and contrasted with the two-body problem. Thirdly, a rendezvous navigation filter is constructed to supply the targeting law with chaser vehicle state information. Nonlinear simulation results validate the filter design and provide data to assess the filter performance. Lastly, two rendezvous scenarios are examined to demonstrate the complete system design. Dissert. Abstr.

N94-30189# Advanced Aviation Concepts, Jupiter, FL.

EXTREMELY LOW VISIBILITY IFR ROTORCRAFT APPROACH (ELVIRA) OPERATIONAL CONCEPT DEVELOPMENT. VOLUME 1: EXECUTIVE SUMMARY Final Report

Catherine A. Adams, Richard J. Adams, Scott A. Fontaine, and Howard A. Wheeler Mar. 1994 51 p

(Contract DTFA01-89-C-00016)

(DOT/FAA/RD-94/1,I) Avail: CASI HC A04/MF A01

The Extremely Low Visibility IFR Rotorcraft Approach (ELVIRA) workshop was the second since 1987 to address the enhancement of safety and reliability of helicopter operations by improving the attractiveness of IFR operations in lieu of special VFR operations. The 1993 workshop was the next logical step in the FAA's Vertical Flight research and development program since significant, relevant analyses, simulation and flight test work has been accomplished in the past six years. The workshop was held in Santa Fe, New Mexico on August 24-26, 1993. The participants were a select group of 59 industry and government experts in each of their individual disciplines. The group was charged with the task of defining an ELVIRA operational concept in the areas of: operational needs, infrastructure requirements, procedural changes, technology requirements, night tests, and public benefits. These experts were asked explicitly to address affordable and practical near term solutions to issues previously identified through their experience. The deliberations at the workshop resulted in the identification near term needs of the operator types who would use ELVIRA, activity regions, safety factors and operational improvements. These needs were analyzed and the operational changes responsive to the needs were documented. The proceedings of the workshop culminated with a recommendation of ten IFR enhancements that would eliminate current penalties for using the IFR system. If action is taken to achieve these changes, safety and mission reliability will be increased through increased flight hours under positive control. Volume 1 summarizes the activities and contributions of the participants. Volume 2 provides an overview of the presentations at the workshop. Volume 3 documents the perspectives of the participants as recorded by Technical Monitors and observers. Author

N94-30243*# Texas Univ., Austin. Center for Space Research.

TOWARDS 10(EXP 9) GPS GEODESY: VECTOR BASELINES, EARTH ROTATION AND REFERENCE FRAMES Annual Progress Report, 1 Jan. 1993 - 31 Dec. 1993

Bob E. Schutz 10 Mar. 1994 25 p

(Grant NAG5-1936)

(NASA-CR-195768; NAS 1.26:195768) Avail: CASI HC A03/MF A01

Effort during the period form January 1, 1993 to December 31, 1993 were in the following areas: GPS orbit accuracy assessments and efforts to improve the accuracy; analysis and effects of GPS receiver antenna phase center variation; analysis of global GPS data being collected for the IGS campaign; and analysis of regional (south west Pacific) campaign data. A brief summary of each of the above activities is presented.

Derived from text

N94-30439 National Aerospace Lab., Amsterdam (Netherlands). Informatics Div.

A SIMULATOR FOR MULTI-RADAR ANALYSIS FOR REALISTIC TRAFFIC

R. A. Hogendoorn, F. Heerema, and P. Sauer 12 Jan. 1992 19 p Presented at the Workshop on RASS, Eurocontrol Institute, Luxembourg, 14-16 Dec. 1992 Limited Reproducibility: More than 20% of this document may be affected by microfiche quality

(AD-B179099; NLR-TP-92481-U; ETN-94-95964) Avail: CASI HC A03

An overview of the SMART (Simulator for Multiradar Analysis for Realistic Traffic) radar simulator is given. A generic simulator model is presented

and the two major subsystems of SMART, the Traffic Subsystem (TSS) and the Radar Subsystem (RSS) are described. Software engineering aspects are discussed and samples of test results are presented in order to show the simulator operation. ESA

N94-30853 National Aerospace Lab., Amsterdam (Netherlands). Flight Div.

A STOCHASTIC CONTROL APPROACH TO FLIGHT PATH MONITORING

B. A. vanDoorn and H. A. P. Blom 31 Jan. 1992 99 p Limited Reproducibility: More than 20% of this document may be affected by microfiche quality

(AD-B174630; NLR-TP-92020-U; ETN-94-95570) Avail: Issuing Activity (European Space Agency (ESA))

A stochastic control approach used to obtain an idea of the qualitative aspects of flight path monitoring is described and first results achieved with it are reported. Two kinds of stochastic control are dealt with: stochastic impulse control and stochastic continuous control. For the latter one, a LQG problem formulation (a Linear model under Gaussian noise with a Quadratic cost function) is considered. For this type of problem formulation, the optimal control is known. A number of experiments are executed to illustrate the optimal control for a simple flight path monitoring problem. The results of these experiments, in combination with the analytical results from impulse control theory, provide a sound basis for the design of a flight path monitoring tool. ESA

N94-30854 National Aerospace Lab., Amsterdam (Netherlands). Flight Div.

A REVIEW OF THE STATUS AND CAPABILITIES OF NAVSTAR GPS

N. vanDriel 10 Feb. 1992 12 p Presented at the Netherlands Institute of Navigation Navstar Global Positioning System Workshop, Amsterdam, Netherlands, 27 Sep. 1991 Limited Reproducibility: More than 20% of this document may be affected by microfiche quality

(AD-B174629; PB94-126281; NLR-TP-92042-U; ETN-94-95571) Avail: CASI HC A03

A general description of the Navstar Global Positioning System (GPS) is given. A technical description of the space segment, control segment, and user segment is also given. The program history and present status are recalled. The system performance is evaluated considering the levels of service, precise positioning service, and standard positioning service. Implications related to the possible use of GPS as an operational navigation system are discussed. In order for the system to be used as an operational navigation system for mariners or aviators, it is required that certain criteria for availability, accuracy and integrity are met. Some evolving new techniques are discussed: differential GPS, dynamic carrier tracking, and attitude determination. ESA

N94-30915 National Aerospace Lab., Amsterdam (Netherlands). Flight Div.

FLIGHT SIMULATOR EVALUATION OF ADVANCED MLS PROCEDURES

L. J. J. Erkelens and J. H. vanDronkelaar 29 Nov. 1991 201 p Sponsored by FAA, and Rijksluchtvaartdienst Limited Reproducibility: More than 20% of this document may be affected by microfiche quality

(AD-B174270; NLR-TP-91446-U; ETN-94-95566) Avail: CASI HC A10

Simulator testing, conducted to collect and analyze crew performance and crew response in order to address several issues on equipment failures, is reported. The testing provided both quantitative measures such as aircraft positional errors, aircraft state and control parameters, and qualitative data such as responses to pilot questionnaires and pilot comments. The specific objectives of the present tests are: to expose crews, while flying a moving base flight simulator programmed with the flying qualities of a wide body transport aircraft, to Microwave Landing Systems (MLS) based curved path approach and departure procedures which have been found to be beneficial from an air traffic control point of view; to collect pilot perception and performance data while flying these curved path procedures; to measure crew ability to detect insidious failures and to respond to these failures; to measure crew performance and to collect perception data when the crew must revert to basic MLS position awareness data in the presence of a navigation or guidance failure; to evaluate performance on a complex approach path with one (critical) engine inoperative. ESA

N94-30933# Civil Aeromedical Inst., Oklahoma City, OK.

MAINTAINING VIGILANCE ON A SIMULATED ATC MONITORING TASK ACROSS REPEATED SESSIONS Final Report

D. J. Schroeder, R. M. Touchstone, J. A.. Stern, N. Stoliarov, and R. Thackray Mar. 1994 13 p Prepared in cooperation with Massachusetts Inst. of Tech., Cambridge

(Contract DTFA02-90-R-00149)

(DOT/FAA/AM-94/6) Avail: CASI HC A03/MF A01

Maintaining alertness to information provided visually is an important aspect of air traffic controllers' work. Improper or incomplete scanning and monitoring behavior is often referred to as one of the causal factors associated with operational errors and deviations. This study was undertaken to assess changes in vigilance/attention across 3 separate days as subjects performed on an Air Traffic Control (ATC) simulation task. Information was gathered as part of a larger study of attention and 'gaze control inefficiencies.' Twenty paid subjects on 3 separate days monitored a simulated ATC task for 44 critical events over a 2 hour session. The complex monitoring task included the detection of: (1) altitude malfunctions; (2) aircraft conflict/no conflicts where 2 aircraft were at the same altitude on an airway simultaneously; and (3) triangular targets representing VFR aircraft that appeared either centrally or peripherally on the screen during the course of each session. Changes in performance on the complex monitoring task associated with either time-on-task or repeated sessions were dependent on nature of the task. Performance on the component involving detection and decision-making (conflict/no conflict detection) evidenced a decrement associated with time-on-task on each of the 3 days. Improvement was evident from the first to the third day. Performance on the identification of the altitude malfunctions remained relatively immune to the effects of time-on-task or repeated sessions. Detection of the VFR aircraft intruders presented a mixed picture, with improvement noted in some aspects of performance but not in others, and some evidence of time-on-task effects. Outcomes were generally consistent with previous findings with this task and consistent with other literature with respect to the presence of performance decrements associated with time-on-task. The results were consistent with a view that the decrements are associated with lapses in attention or 'blocks,' rather than a generalized fatigue effect or a general modification in overall scanning behavior. Furthermore, the results suggest that there were aspects of monitoring performance that remain relatively immune to time-on-task effects, even during the course of the three 2-hour sessions. Author

N94-30943 National Aerospace Lab., Amsterdam (Netherlands). Flight Div.

THE EXPERIMENTAL FLIGHT MANAGEMENT SYSTEM: AN AIR TRAFFIC MANAGEMENT RESEARCH TOOL

Job Brueggen 29 Jun. 1992 14 p Presented at the 1992 SFTE Annual Symposium on Flight Testing in the Global Environment, Long Island, NY, 3-7 Aug. 1992 Limited Reproducibility: More than 20% of this document may be affected by microfiche quality

(NLR-TP-92253-U; ETN-94-95972) Avail: CASI HC A03

The Experimental Flight Management System (EFMS) program, part of a European collaborative research program called PHARE (Program for Harmonized ATM (Air Traffic Management) Research in Eurocontrol), which aims to investigate a future ATM scenario, is described. The EFMS will incorporate some revolutionary features, of which the most important are to plan and fly a four dimensional trajectory and to negotiate that trajectory via a digital data link with air traffic control. Development is a multinational activity of the aerospace centers of Germany, France, England and the Netherlands, coordinated by Eurocontrol. A first demonstration is planned for Jan. 1993. A number of applications of the EFMS program are described, most notably the avionic research test bed. ESA

N94-29323# Wright Lab., Wright-Patterson AFB, OH.

OBJECT ORIENTED DESIGN OF THE AUTONOMOUS FIXTAKING MANAGEMENT SYSTEM

Joseph Diemunsch and John Hancock *In* AGARD, Aerospace Software Engineering for Advanced Systems Architectures Nov. 1993 14 p

(For primary document see N94-29315 08-61)

Copyright Avail: CASI HC A03/MF A03

N94-29614*# Jet Propulsion Lab., California Inst. of Tech., Pasadena.
COMBINING GPS AND VLBI EARTH-ROTATION DATA FOR IMPROVED UNIVERSAL TIME
A. P. Freedman *In its* The Telecommunications and Data Acquisition Report 15 May 1991 p 1-12 (For primary document see N94-29613 08-32)
(RTOP 310-10-61-87-02)
Avail: CASI HC A03/MF A02

N94-29772*# Jet Propulsion Lab., California Inst. of Tech., Pasadena.
MICRO GUIDANCE AND CONTROL TECHNOLOGY OVERVIEW
Glen J. Kissel and Fred Y. Hadaegh *In its* Proceedings of the Workshop on Microtechnologies and Applications to Space Systems 15 Jun. 1993 p 75-81 (For primary document see N94-29767 08-31)
Avail: CASI HC A02/MF A03

N94-29788*# Draper (Charles Stark) Lab., Inc., Cambridge, MA.
EMERGING TECHNOLOGIES IN MICROGUIDANCE AND CONTROL
Marc S. Weinberg *In* JPL, Proceedings of the Workshop on Microtechnologies and Applications to Space Systems 15 Jun. 1993 p 247-25 (For primary document see N94-29767 08-31)
Avail: CASI HC A02/MF A03

N94-29792*# Jet Propulsion Lab., California Inst. of Tech., Pasadena.
MICRO GUIDANCE AND CONTROL SYNTHESIS: NEW COMPONENTS, ARCHITECTURES, AND CAPABILITIES
Edward Mettler and Fred Y. Hadaegh *In its* Proceedings of the Workshop on Microtechnologies and Applications to Space Systems 15 Jun. 1993 p 289-304 (For primary document see N94-29767 08-31)
Avail: CASI HC A03/MF A03

N94-29794*# OCA Applied Optics, Inc., Garden Grove, CA.
MINIATURE WIDE FIELD-OF-VIEW STAR TRACKERS FOR SPACECRAFT ATTITUDE SENSING AND NAVIGATION
William McCarty, Eric Curtis, Anthony Hull, and William Morgan *In* JPL, Proceedings of the Workshop on Microtechnologies and Applications to Space Systems 15 Jun. 1993 p 317-32 (For primary document see N94-29767 08-31)
Avail: CASI HC A03/MF A03

N94-30281 University of Western Ontario, London.
EXTENDED OCCUPANCY GRID METHOD FOR MODELLING UNKNOWN DYNAMIC ENVIRONMENTS
Robert E. Webber and Yue-Feng Zhang *In* Defence Research Establishment Suffield, Proceedings of the 3rd Conference on Military Robotic Applications 1991 p 54-60 (For primary document see N94-30275 08-37)
Avail: Issuing Activity (Defence Research Establishment Suffield, P.O. Box 4000, Medicine Hat, AB T1A 8K6 Canada)

N94-30282* National Aeronautics and Space Administration, Washington, DC.
NAVIGATION OF MILITARY AND SPACE UNMANNED GROUND VEHICLES IN UNSTRUCTURED TERRAINS
Paul Lescoe (Army Tank-Automotive Command, Warren, MI.), David Lavery, and Roger Bedard *In* Defence Research Establishment Suffield, Proceedings of the 3rd Conference on Military Robotic Applications 1991 p 61-67 (For primary document see N94-30275 08-37)
Avail: Issuing Activity (Defence Research Establishment Suffield, P.O. Box 4000, Medicine Hat, AB T1A 8K6 Canada)

N94-30285 Defence Research Establishment Suffield, Medicine Hat (Alberta).
THE USE OF LOW COST DIFFERENTIAL MODE GPS RECEIVERS IN UNMANNED VEHICLES
Thomas E. Ollevier *In its* Proceedings of the 3rd Conference on Military Robotic Applications 1991 p 81-85 (For primary document see N94-30275 08-37)
Avail: Issuing Activity (Defence Research Establishment Suffield, P.O. Box 4000, Medicine Hat, AB T1A 8K6 Canada)

N94-30286 Ottawa Univ. (Ontario). Dept. of Electrical Engineering.
ENCODING TECHNIQUE FOR AUTOMATED GUIDED VEHICLE POSE RECOVERY IN A STRUCTURED ENVIRONMENT
E. Petriu, T. Bieseman, N. Trif, W. S. McMath, and S. K. Yeung *In* Defence Research Establishment Suffield, Proceedings of the 3rd Conference on Military Robotic Applications 1991 p 86-92 (For primary document see N94-30275 08-37)
Avail: Issuing Activity (Defence Research Establishment Suffield, P.O. Box 4000, Medicine Hat, AB T1A 8K6 Canada)

N94-30643*# Air Force Systems Command, Falcon AFB, CO.
AN OPERATIONAL CONTROL SEGMENT (OCS) UPDATE ON GPS CONSTELLATION STATUS AND FUTURE PROGRAM DIRECTIONS
Harrison C. Freer *In* NASA. Goddard Space Flight Center, The 25th Annual Precise Time and Time Interval (PTTI) Applications and Planning Meeting May 1994 p 65-78 (For primary document see N94-30639 08-70)
Avail: CASI HC A03/MF A06

N94-30644*# Coast Guard, Washington, DC.
LORAN-C TIME MANAGEMENT
Charles Justice, Norm Mason, and Doug Taggart *In* NASA. Goddard Space Flight Center, The 25th Annual Precise Time and Time Interval (PTTI) Applications and Planning Meeting May 1994 p 79-92 (For primary document see N94-30639 08-70)
Avail: CASI HC A03/MF A06

N94-30648*# Bureau International des Poids et Mesures, Sevres (France).
GPS COMMON-VIEW TIME TRANSFER
W. Lewandowski *In* NASA. Goddard Space Flight Center, The 25th Annual Precise Time and Time Interval (PTTI) Applications and Planning Meeting May 1994 p 133-148 (For primary document see N94-30639 08-70)
Avail: CASI HC A03/MF A06

N94-30650*# Jet Propulsion Lab., California Inst. of Tech., Pasadena.
TIME AND POSITION ACCURACY USING CODELESS GPS
C. E. Dunn, D. C. Jefferson, S. M. Lichten, J. B. Thomas, Y. Vigue, and L. E. Young *In* NASA. Goddard Space Flight Center, The 25th Annual Precise Time and Time Interval (PTTI) Applications and Planning Meeting May 1994 p 169-182 (For primary document see N94-30639 08-70)
Avail: CASI HC A03/MF A06

N94-30651*# Bureau International des Poids et Mesures, Sevres (France).
THE USE OF THE AOA TTR-4P GPS RECEIVER IN OPERATION AT THE BIPM FOR REAL-TIME RESTITUTION OF GPS TIME
Claudine Thomas *In* NASA. Goddard Space Flight Center, The 25th Annual Precise Time and Time Interval (PTTI) Applications and Planning Meeting May 1994 p 183-196 (For primary document see N94-30639 08-70)
Avail: CASI HC A03/MF A06

N94-30652*# Hydro-Electric Power Commission, Burnaby (British Columbia).
DEVELOPMENT OF AN ACCURATE TRANSMISSION LINE FAULT LOCATOR USING THE GLOBAL POSITIONING SYSTEM SATELLITES
Harry Lee *In* NASA. Goddard Space Flight Center, The 25th Annual Precise Time and Time Interval (PTTI) Applications and Planning Meeting May 1994 p 197-204 (For primary document see N94-30639 08-70)
Avail: CASI HC A02/MF A06

N94-30655*# Graz Univ. (Austria).
TROPOSPHERIC CORRECTIONS TO GPS MEASUREMENTS USING LOCALLY MEASURED METEOROLOGICAL PARAMETERS COMPARED WITH GENERAL TROPOSPHERIC CORRECTIONS
D. Kirchner, C. Lentz, and H. Ressler *In* NASA. Goddard Space Flight Center, The 25th Annual Precise Time and Time Interval (PTTI) Applications and Planning Meeting May 1994 p 231-248 (For primary document see N94-30639 08-70)
Avail: CASI HC A03/MF A06

N94-30660*# National Inst. of Standards and Technology, Boulder, CO. Time and Frequency Div.
A COMPARISON OF GPS BROADCAST AND DMA PRECISE EPHEMERIDES
Marc A. Weiss, Gerard Petit, and Steve Shattil *In* NASA. Goddard Space Flight Center, The 25th Annual Precise Time and Time Interval (PTTI) Applications and Planning Meeting May 1994 p 293-306 (For primary document see N94-30639 08-70)
Avail: CASI HC A03/MF A06

N94-30661*# Beijing Inst. of Radio Metrology and Measurements (China).
SOME APPLICATIONS OF GPS TIMING INFORMATION
Yinbai Zhang *In* NASA. Goddard Space Flight Center, The 25th Annual Precise Time and Time Interval (PTTI) Applications and Planning Meeting May 1994 p 307-315 (For primary document see N94-30639 08-70)
Avail: CASI HC A02/MF A06

N94-30662*# Naval Observatory, Washington, DC.
A COMPARISON OF SEVERAL GPS DATA REDUCTION METHODS
H. Chadsey *In* NASA. Goddard Space Flight Center, The 25th Annual Precise Time and Time Interval (PTTI) Applications and Planning Meeting May 1994 p 317-328 (For primary document see N94-30639 08-70)
Avail: CASI HC A03/MF A06

N94-30663*# Rockwell International Corp., Colorado Springs, CO.
CESIUM AND RUBIDIUM FREQUENCY STANDARDS STATUS AND PERFORMANCE ON THE GPS PROGRAM
M. J. VanMelle *In* NASA. Goddard Space Flight Center, The 25th Annual Precise Time and Time Interval (PTTI) Applications and Planning Meeting May 1994 p 329-344 (For primary document see N94-30639 08-70)
Avail: CASI HC A03/MF A06

N94-30665*# Bureau International des Poids et Mesures, Sevres (France).
COMPARISON OF LASSO AND GPS TIME TRANSFERS
W. Lewandowski, G. Petit, F. Baumont, P. Fridelance, J. Gaignebet, P. Grudler, C. Veillet, J. Wiant, and W. J. Klepczynski *In* NASA. Goddard Space Flight Center, The 25th Annual Precise Time and Time Interval (PTTI) Applications and Planning Meeting May 1994 p 357-366 (For primary document see N94-30639 08-70)
Avail: CASI HC A02/MF A06

N94-30677*# Osborne (Allen) Associates, Westlake Village, CA.
IONOSPHERIC CORRECTIONS TO PRECISE TIME TRANSFER USING GPS
Robert W. Snow, Allen W. Osborne, III, John A. Klobuchar, and Patricia H. Doherty *In* NASA. Goddard Space Flight Center, The 25th Annual Precise Time and Time Interval (PTTI) Applications and Planning Meeting May 1994 p 495-504 (For primary document see N94-30639 08-70)
Avail: CASI HC A02/MF A06

05 AIRCRAFT DESIGN, TESTING AND PERFORMANCE

Includes aircraft simulation technology.

For related information see also *18 Spacecraft Design, Testing and Performance* and *39 Structural Mechanics*.For land transportation vehicles see *85 Urban Technology and Transportation*.

N94-28647# Battelle Columbus Labs., OH.
EFFECTS OF REPAIR ON STRUCTURAL INTEGRITY Final Report, Jan. 1990 - Sep. 1992
R. Rice, R. Francini, S. Rahman, M. Rosenfeld, S. Rust, S. Smith, and D. Broek Dec. 1993 156 p
(Contract DTRS57-89-C-00006)
(AD-A275756; DOT-VNTSC-FAA-93-11; DOT/FAA/CT-93/79) Avail: CASI HC A08/MF A02

FAA regulations require commercial aircraft operators to repair damaged aircraft structures. These repairs must be performed in a timely manner to reduce aircraft downtime and loss of revenue. A guiding principal for such repairs is to restore the structure to the original (or better) static strength and stiffness. However, the repair can also be designed for adequate fatigue resistance, damage tolerance, and inspectability. Fatigue and damage tolerance (DT) analyses should be based on realistic stress histories which, in turn, should be derived from realistic load spectra. Thus, an algorithm for the development of a stress history should be included in a comprehensive analysis of repairs. Since many damage repair stations and airlines do have at least basic computer facilities that can be used for fatigue and damage tolerance analysis, one goal has been the development of a relatively simple, yet accurate analytical tool to design aircraft repairs more effectively. The structural analysis and stress spectrum development procedures described in this report are approximate and, therefore, have certain limitations. These procedures might be used to qualitatively compare the quality of different repair options with the original structure. DTIC

N94-28657# Foster-Miller Associates, Inc., Waltham, MA.
FULL-SCALE TESTING AND ANALYSIS OF CURVED AIRCRAFT FUSELAGE PANELS Final Report, May 1991 - Mar. 1992
G. Samavedam, D. Hoadley, and D. Thomson Dec. 1993 58 p
(Contract DTRS57-89-D-00009)
(AD-A275666; DOT-VNTSC-FAA-93-10; DOT/FAA/CT-93/78) Avail: CASI HC A04/MF A01

This report presents data on (1) residual strength of aircraft panels containing Multiple-Site Damage (MSD) in tap splices, and (2) fatigue strength of panels subjected to cyclic pressure loading. The testing was conducted using the dedicated Aging Aircraft Test Facility previously built in the Foster-Miller laboratory. A previous report describes the work in the first phase involving the design and operation of the facility and the test data generated on residual strength of panels with longitudinal midday skin cracks. In the Phase II work presented here, several residual strength tests were conducted to develop a relationship between failure pressure and the lead crack length in the critical upper rivet line of the lap joint. In some of the panels multiple-site damage was also built in the rivet line during fabrication. The reduction in the residual strength due to MSD has been experimentally quantified. Conditions of crack arrest at tear straps and panel flapping were also investigated. Fatigue testing of the panel, with no initial damage in the tap splice except an unbonded lap joint area, was conducted to investigate the crack initiation at multiple sites, crack growth rates and eventual linkup of the ligaments and fracture failure. The ultimate life of the panel, and the damage in critical upper and lower skin rivet rows was determined. Conclusions of practical interest were drawn from the test data. DTIC

N94-28660# Naval Postgraduate School, Monterey, CA.
A MOMENT PLOTTING METHOD FOR CHARACTERIZING AIRCRAFT FATIGUE DATA POPULATION DISTRIBUTIONS M.S. Thesis
Rolf M. Lokensgard Sep. 1993 106 p
(AD-A275500) Avail: CASI HC A06/MF A02

A method was developed where, by statistically analyzing samples of aircraft fatigue data from a population, the population's probability distribution function is determined. The method uses plots of a sample's coefficient of variation, and measures of skewness and kurtosis, superimposed on templates of curves created from the moment functions of normal, lognormal, Weibull, and exponential distributions. The moment functions are derived for each distribution. The plotting technique is combined with a comparison of goodness of fit statistics to form the complete distribution selection method. The method is first tested on random numbers generated from known distributions to see if the correct distributions are selected; then the method is applied to helicopter loads data, fatigue life characterization test data, and counting accelerometer data. DTIC

N94-28817*# California Polytechnic State Univ., San Luis Obispo. Dept. of Aeronautical Engineering.
MODIFICATION OF ACSYNT AIRCRAFT COMPUTER PROGRAM FOR PRELIMINARY DESIGN Semiannual Progress Report, Oct. 1993 - Mar. 1994
Daniel J. Biezad and Ruben Rojos-Oviedo 31 Mar. 1994 13 p
(Contract NCC2-834)
(NASA-CR-195737; NAS 1.26:195737) Avail: CASI HC A03/MF A01

This paper presents the development of a computer simulation of agility flight test techniques. Its purpose is to evaluate the agility of aircraft

configurations early in the preliminary design phase. The simulation module is integrated into the NASA Ames aircraft synthesis design code. Trade studies using the agility module embedded within the design code to simulate the combat cycle time agility metric are illustrated using a Northrop F-20 aircraft model. Results show that the agility module is effective in analyzing the influence of common parameters such as thrust-to-weight ratio and wing loading on agility criteria. The module can also compare the agility potential between different configurations and has the capability to optimize agility performance early in the design process. Author

N94-28837# Naval Postgraduate School, Monterey, CA.
ACQUISITION, DESIGN MODIFICATION, ASSEMBLY, AND GROUND TEST OF NPS HUMMINGBIRD REMOTELY PILOTED HELICOPTER M.S. Thesis
Gregory J. Fick Sep. 1993 93 p
(AD-A275546) Avail: CASI HC A05/MF A01

The Hummingbird is a 150-lb. gross weight, remotely piloted helicopter (RPH) with a 50-lb. payload and a rotor radius of 10.25 ft. It is powered by a 25 h.p. air cooled two-cylinder Westlake engine. As such it represents one of the largest RPH's in the world. It was purchased from Gorham Model Products in 1992 to provide a suitable rotorcraft research flight test platform for the Department of Aeronautics and Astronautics at the Naval Postgraduate School. The helicopter was delivered disassembled and was accompanied by an ample supply of replacement and spare parts. Also included was a second helicopter in a partially assembled condition that had been previously flown. Assemblies provided comprised the chassis, main rotor transmission, rotor head assembly, and tailboom with tail rotor gear box and rotor. The task undertaken by this thesis was to fabricate one operable RPH and to design, fabricate, and install whatever new assemblies that were required for its NPS mission and to make up for deficiencies in the previous design. The work completed required: (1) design, fabrication, and installation of a new skid-type landing gear system; (2) redesign and incorporation of a new engine mount system; (3) modification of the engine and main rotor transmission coupling; (4) upgrade of the electrical system and elongation of the nose section; and (5) initial engine testing. Recommendations for future modifications to the helicopter and laboratory facilities and development of a static hover test fixture are also included. DTIC

N94-28870# Naval Postgraduate School, Monterey, CA.
PROCEDURAL GUIDE FOR MODELLING AND ANALYZING THE FLIGHT CHARACTERISTICS OF A HELICOPTER DESIGN USING FLIGHTLAB M.S. Thesis
Gary P. McVaney 23 Sep. 1993 150 p
(AD-A275077) Avail: CASI HC A07/MF A02

This thesis presents one method for modeling and analyzing a helicopter design using Flightlab. Flightlab is a computer program that provides for engineering design, analysis, and simulation of aircraft using nonlinear dynamic modeling techniques. The procedure to model a single main rotor helicopter is outlined using a sample helicopter design. The analysis procedure contains computer program scripts for determining the time response of the helicopter to standard control inputs such as a longitudinal impulse, a lateral step, and a pedal doublet. A linear model of the helicopter can be extracted from the nonlinear model, and a comparison of the time response to the control inputs based on these two models is presented. The procedure for conducting frequency sweep testing for the linear model is also discussed. This guide to using Flightlab for aircraft modelling and analysis is designed to make it easier to use Flightlab for creating additional aircraft models for use in control system analysis and additional engineering design. DTIC

N94-28998# Air Force Inst. of Tech., Wright-Patterson AFB, OH. School of Engineering.
EXPLORING QDES AS A TOOL FOR DETERMINING LIMITS OF ACHIEVABLE PERFORMANCE IN AIRCRAFT DESIGN M.S. Thesis
Mark F. Reidinger Dec. 1993 151 p
(AD-A275359; AFIT/GAE/ENY/93D-23) Avail: CASI HC A08/MF A02

This thesis explores the usefulness of a computer aided control design software package called QDES in determining the limits of achievable aircraft performance as it relates to controller capability. Modern aircraft, particularly fighters, are being designed to be statically unstable to enhance their maneuverability and performance. It is possible that the aircraft, although physically capable of a certain level of performance due to its engine/airframe combination, may be uncontrollable up to this level. This study sought to develop a methodology to use QDES to make a preliminary analysis of an aircraft design to determine if there exists a controller that will enable this design to meet its performance goals and, if not, to determine what the limits of achievable performance are. DTIC

N94-29042# Logicon, Inc., Dayton, OH.
BACKSCATTER HAZE DEVICE FOR MEASUREMENT OF HAZE IN AIRCRAFT TRANSPARENCIES Final Report, Jan. 1991 - Dec. 1992
H. L. Task (Air Force Systems Command, Wright-Patterson AFB, OH.), Richard J. Bartell, and Sheldon E. Unger May 1993 36 p
(AF Proj. 7184)
(AD-A275127; AL/CF-TR-1993-0102) Avail: CASI HC A03/MF A01

The method currently used throughout the aircraft transparency industry to measure haze is ASTM Test Method D1003. This procedure was originally developed for applications involving small, thin, and flat transparent parts. Major limitations of Test Method D1003 include its restriction to small, flat samples and its requirement for having the source and detector on opposite sides of the sample under test. In order to facilitate field testing of installed aircraft windscreens, a test method was developed which overcomes the limitations of Test Method D1003. The new method determines haze values by measuring the amount of light backscattered off the surface of the transparency under test. A prototype instrument was developed and tested against D1003. The results of those tests are presented. The new instrument consists of an integrating sphere, a mechanically chopped incandescent light source, a silicon detector, and supporting electronics. This report describes the device, which is based on U.S. Patent Number 4,687,338, in detail. Use of this type of device in the field could provide quantitative data for determining when an installed aircraft windscreen should be replaced or refinished in place. DTIC

N94-29200# Naval Postgraduate School, Monterey, CA.
A NON-LINEAR SIMULATION FOR AN AUTONOMOUS UNMANNED AIR VEHICLE M.S. Thesis
David R. Kuechenmeister Sep. 1993 123 p
(AD-A275062) Avail: CASI HC A06/MF A02

Unmanned Air Vehicles have become increasingly important on the modern battlefield. The restrictive requirement for runways and special equipment to take off and land was partially solved by the vertical take off and landing Airborne Remotely Operated Device, AROD. Work done at the Naval Postgraduate School has modified the AROD to not only land and launch vertically, but to fly horizontally for the majority of the mission. To realize these capabilities, as well as that of autonomous flight, an accurate computer model was required of both the AROD and the avionics test bed aircraft, Bluebird, in order to design the control and navigation systems. High fidelity, non-linear equations of motion were derived in matrix form that represented any six degree of freedom aircraft model, and they were then tailored for use on specific aircraft. Computer modeling of the resulting equations of motion, as well as the sensors used on the aircraft, was done using SIMULINK and MATLAB software. The resulting computer model provides a non-linear system of equations, which are easily linearized at any desired flight condition, as required by the proposed control and navigation system design. DTIC

N94-29391# Aeronautical Systems Div., Wright-Patterson AFB, OH.
KC-135 COCKPIT MODERNIZATION STUDY AND CREW REDUCTION FEASIBILITY DEMONSTRATION Final Report, 15 Aug. 1992 - 31 Aug. 1993
John E. Ehrhart, Jr., Jordan R. Kriss, Janet M. Emerson, and Thomas C. Hughes Oct. 1993 123 p
(AD-A275230; ASC-TR-93-5023) Avail: CASI HC A06/MF A02

Future KC-135 missions will require significant increases in aircraft flexibility to respond to the Air Force vision of Global Reach, Global Power. Such flexibility typically translates into advanced avionics systems and system capabilities; however, a large percentage of the avionics systems currently installed on the KC-135 are late 1950's and 1960's technology which has degraded the efficiency, reliability, maintainability and safety of the KC-135 mission. Strategic Air Command (SAC), now Air Mobility Command (AMC) issued a statement of need (SON, 1987) addressing the need to modernize the KC-135 cockpit avionics to attend to these problems. This report documents the evaluation phase of this program and for the first time

directly compares the two-man and three-man cockpit configurations. The validation of the reduced crew consisted of a comparison of crew performance across three distinct missions - Minot, Castle and Desert. Results supported the two-person (No Nav) cockpit, given certain modifications. Based on these results, the CSEF recommended follow-on flight test of the KC-135. Recommendations are based upon using the final design, identical in system capabilities, as developed at the Crew Station Evaluation Facility. The key to the success of this program lies in the utilization of the modifications discussed in this report and the proper implementation of those modifications in future KC-135 cockpits. DTIC

N94-29594 Georgia Inst. of Tech., Atlanta.
HELICOPTER MISSION AND ROTOR PERFORMANCE OPTIMIZATION WITH QUASI-LINEAR INFLOW THEORY Ph.D. Thesis
Azhar Mansur Khan 1992 149 p
Avail: Univ. Microfilms Order No. DA9315887

The enhanced performance envelope of a future generation rotorcraft is greatly desired by all the designers. This design goal can be achieved through rotor performance optimization design methodology, which in simple words is a numerical technique for obtaining the design goals by satisfying the design requirements. The design goal for rotorcraft performance optimization is the reduction of rotor power for a specific weight and mission while the design variables are the rotor chord and twist which define the rotor blade geometry. Constraints are applied to satisfy certain minimum design requirements. Since optimization is a complex numerical iterative procedure, which utilizes a considerable amount of computation time, it is desired by all designers to come up with such an aerodynamic model for helicopter performance calculations which utilizes minimum amount of computer processing time. In view of the above, a steady non-uniform inflow model is used to calculate the rotor performance for both hover and forward flight. The main emphasis of this research work has been to simplify the inflow model without loss of accuracy since, ultimately, this research work is going to be a part of the multidisciplinary helicopter design optimization. Therefore, all time dependent terms have been neglected and all pressure functions and power expressions have been time averaged. After neglecting unsteady terms it was required to take care of the blade tip loss; for which the Prandtl's tip loss function has been used. All complex integrals have also been calculated ahead of time and stored in data files to be used as input to the main program as and when required. The rotor performance code is then modified to a nonlinear constrained optimization problem to be used as input to the optimization routine. The updated version of a FORTRAN routine (CONMIN) for constrained function minimization is used for optimization purpose. Finally, the most optimum planform for the rotor is obtained from the point of view of taper and twist, that requires the least amount of power for a given thrust for hover, for forward flight, and for certain specified missions. The missions to be optimized are a combination of both hover and forward flight. Thus, this research work is an analytical formulation of an optimum rotor for various pre-defined missions. Dissert. Abstr.

N94-29685*# Lockheed Aircraft Service, Inc., Ontario, CA.
AIRCRAFT SYSTEM AFT TELESCOPE CAVITY CONFIGURATION STUDY FOR STRATOSPHERIC OBSERVATORY FOR INFRARED ASTRONOMY (SOFIA), PHASE 2 Final Report
22 Apr. 1994 171 p Original contains color illustrations
(Contract NAS2-13872)
(NASA-CR-194266; NAS 1.26:194266; R54045007) Avail: CASI HC A08; 62 functional color pages color pages

The SOFIA Aircraft System (AS) Phase 1 Study was a broad-based study which addressed itself to satisfying technical and programmatic requirements by drawing from existing technology and applying cost-efficient commercial approaches to the aircraft modification. In this SOFIA AS Phase 2 Study, five critical areas of the aircraft were selected for more detailed investigation: forward pressure bulkhead, aft bulkhead, 'free' shell to bulkhead interface, shell cut-out to bulkhead interface, and flooring. The in-depth investigation of these areas upon a finite element model (FEM), with a fine grid model in areas of particular interest, is discussed. The FEM code used is called 'STRAP' and was developed by the engineering firm, Rasmussen and Associates. STRAP is NASTRAN compatible to within 1%. The loads applied to the model were approximated from known 747 envelope conditions. The areas of investigation, and a section through the fuselage is shown. The thrust of this investigation was to develop the design concepts conceived under phase 1 to the point where detailed design could be undertaken with a high level of confidence.
Derived from text

N94-29721*# Eloret Corp., Palo Alto, CA.
ADVANCED VEHICLE CONCEPTS SYSTEMS AND DESIGN ANALYSIS STUDIES Final Technical Report, 1 Apr. 1992 - 31 Jan. 1994
Mark H. Waters and Loc C. Huynh 20 Apr. 1994 10 p
(Contract NCC2-746)
(NASA-CR-195115; NAS 1.26:195115) Avail: CASI HC A02/MF A01

The work conducted by the ELORET Institute under this Cooperative Agreement includes the modeling of hypersonic propulsion systems and the evaluation of hypersonic vehicles in general and most recently hypersonic waverider vehicles. This work in hypersonics was applied to the design of a two-stage to orbit launch vehicle which was included in the NASA Access to Space Project. Additional research regarded the Oblique All-Wing (OAW) Project at NASA ARC and included detailed configuration studies of OAW transport aircraft. Finally, work on the modeling of subsonic and supersonic turbofan engines was conducted under this research program.
Author (revised)

N94-29854 Purdue Univ., West Lafayette, IN.
INTEGRATED PROPULSION-AIRFRAME DYNAMICS AND CONTROL Ph.D. Thesis
Ronald A. Perez 1990 329 p
Avail: Univ. Microfilms Order No. DA9313941

The development of an integrated control scheme to enhance the performance of a generic interconnected multivariable dynamical system, consisting of a turbofan engine and an airframe, in the presence of predominantly destructive dynamical interactions over the flight envelope is considered in this research. The control scheme consists of two components: a simple static forward loop or feedback loop precompensator to improve the interactions followed by a forward or feedback loop controller to improve the performance. System performance specifications dictate zero steady state errors in the engine and airframe controlled output variables as well as minimal overshoot with rapid and smooth acceleration and deceleration profiles. Furthermore the system must be tolerant to soft and hard output sensor failures by means of analytic redundancy only. A control methodology to satisfy the above specifications is presented here. Necessary and sufficient conditions are presented in order to achieve stable closed loop performance of the overall system by tuning every loop separately (i.e., decentralized stability). This leads to very simple control structures, but even for these rather simple control schemes, a significant improvement over previous integration schemes is obtained. Dissert. Abstr.

N94-29878 Georgia Inst. of Tech., Atlanta.
ROTORCRAFT AIRFRAME STRUCTURAL OPTIMIZATION FOR VIBRATION AND DYNAMIC STRESS REDUCTION INCLUDING DAMPING TREATMENT Ph.D. Thesis
Ashish Kumar Sareen 1992 129 p
Avail: Univ. Microfilms Order No. DA9315910

This work focuses on the development of finite element based methodologies for mass, stiffness, and damping modifications of practical airframe structures. This preliminary design type of engineering methodology of analysis and optimization allows rapid and accurate engineering prediction and placement of responses while guiding the structural designer-dynamicist in determining the location, type and quantity of structural modifications when the airframe is sustaining severe forced vibrations. For new airframe structures, minimum weight structures can be designed with proper placement of airframe natural frequencies and subject to constraints on forced response displacements and dynamic stresses by systematic nonlinear programming-based modifications of mass, stiffness and damping of the structure. In the case of an existing design, when significant mass and stiffness modifications cannot be affected, the designer can resort to viscoelastic type energy-dissipation damping treatments and determine their efficacy. Furthermore, should the change of excitation frequency bring about modal resonance, damping treatments can control response due to resonating modes, without resorting to stiffness or mass changes. This work focuses on the development of necessary computational tools for airframe structural optimization and implements the sensitivity analysis procedures for the various design constraints encountered in vibration and fatigue design of structures. The application of the optimization procedure

is demonstrated using both an elastic-line as well as a built-up finite element model of the Bell AH-1G helicopter airframe structure.

Dissert. Abstr.

N94-29887 Civil Aviation Authority, London (England).

AIRCRAFT EVACUATIONS: THE EFFECT OF A CABIN WATER SPRAY SYSTEM UPON EVACUATION RATES AND BEHAVIOUR

D. M. Bottomley (Cranfield Inst. of Tech., Bedford, England.), H. C. Muir (Cranfield Inst. of Tech., Bedford, England.), and M. C. Lower (Southampton Univ., England.) Mar. 1993 71 p Original contains color illustrations

(CAA-Paper-93008; ISBN-0-86039-547-2; ETN-94-95514) Copyright Avail: Issuing Activity (Civil Aviation Authority, Greville House, 37 Gratton Road, Cheltenham, England, HC)

An experiment which investigated the human factors aspects of water spray systems, proposed as a means of reducing the effects of fire occurring in an aircraft cabin, is reported. The potential effects of such systems upon evacuation rates and other issues such as visibility and audibility within the cabin were investigated. In total, eight full scale aircraft evacuations were conducted using a 707 airframe. Each evacuation involved a group of around forty five adults who performed one evacuation only. Four groups evacuated in dry conditions, the remaining four evacuated in the water spray. Video cameras were positioned both inside the aircraft cabin and on the platform outside to provide objective measures of evacuation performance. Subjective accounts were also obtained using post evacuation questionnaires. The results revealed that the evacuation times for the two conditions were virtually identical, the lack of a statistically significant difference suggesting that the presence of the water spray did not affect evacuation rates. Other results are given. ESA

N94-30129# Royal Military Coll. of Canada, Kingston (Ontario). Dept. of Physics.

ACOUSTIC EMISSION MONITORING OF AGING AIRCRAFT STRUCTURES

S. L. McBride, M. R. Viner, and M. D. Pollard Mar. 1993 13 p

(DREP-93-17; CTN-94-61135) Avail: CASI HC A03/MF A01

Acoustic emission measurements were used to detect fatigue cracks in a full-scale aircraft structure during ground durability and damage tolerance testing. Measurements were made using a 16-channel data acquisition system receiving signals from piezoelectric sensor elements. Fatigue cycling loads were applied at various loading points on the aircraft structure to simulate the known flight load spectra measured in flight. Acoustic emission data were recorded for 700 equivalent flying hours and analyzed at intervals. After 700 hours of testing it was clear from the acoustic emission data that significant crack growth was occurring in the starboard wing skin. Fasteners were removed to inspect fastener holes in the damage area identified by acoustic emission. Fatigue cracks were detected in several holes using eddy current only after the structure was loaded to open the cracks. Acoustic emission data were further analyzed to reconstruct the history of defect growth and to separate the crack growth emission data from crack face rubbing data. The tests show that cracks originating inside fastener holes can be detected easily by acoustic emission without the removal of fasteners. Acoustic emission monitoring is shown to be superior to conventional nondestructive testing in locating fatigue cracks and can be used to determine load conditions leading to crack growth.

Author (CISTI)

N94-30131# Royal Military Coll. of Canada, Kingston (Ontario). Dept. of Physics.

ENHANCED FATIGUE CRACK DETECTION IN AGING AIRCRAFT USING CONTINUOUS ACOUSTIC EMISSION MONITORING

Stuart L. McBride, Yanhua Hong, and Michael Pollard Feb. 1993 12 p

(DREP-93-16; CTN-94-61137) Avail: CASI HC A03/MF A01

Acoustic emission measurements were used to detect fatigue cracks in a full-scale aircraft structure during ground durability and damage tolerance testing. Data are presented for about 3,000 equivalent flying hours of continuous monitoring. Acoustic emission data were acquired via piezoelectric sensors using a 32-channel instrumentation system. The regions of the aircraft structure monitored were located on the lower wing skin, particularly the 15 percent, 39 percent, and 44 percent spar regions. Fatigue cycling loads were applied at various loading points to simulate the known flight load spectra measured on flying aircraft. Defects detected by acoustic emission and confirmed by conventional nondestructive methods were of two types: fatigue cracks in fastener holes repaired at or before 9,754 equivalent flying hours or new defects occurring principally at the wing skin edge aft of the 44 percent spar. For a number of defects, acoustic emission detection preceded conventional detection by about 3,000 equivalent flying hours. Compared to periodic monitoring, continuous acoustic emission monitoring increases the number of crack advance events available for analysis and enables more secure confirmation of their source. Continuous monitoring also improves the location of crack advance sources and provides a better estimate of distributed structural noise.

Author (CISTI)

N94-30342 National Aerospace Lab., Amsterdam (Netherlands). Fluid Dynamics Div.

DEVELOPMENT OF A METHOD TO PREDICT TRANSONIC LIMIT CYCLE OSCILLATION CHARACTERISTICS OF FIGHTER AIRCRAFT (CONTINUED)

Jos J. Meijer and Atlee M. Cunningham, Jr. 10 Apr. 1992 21 p Presented at the 33rd AIAA/ASME/AHS/ASC Structures, Structural Dynamics and Materials Conference/Dynamics Specialist Conference, Dallas, TX, 16-17 Apr. 1992 Sponsored by USAF; General Dynamics Corp.; Ministry of Defence; and National Aerospace Lab. Limited Reproducibility: More than 20% of this document may be affected by microfiche quality

(Contract NIVR-07801N)

(NLR-TP-92156-U; ETN-94-95576) Copyright Avail: Issuing Activity (European Space Agency (ESA))

The continued development of a method to predict the transonic limit cycle oscillation characteristics for a fighter aircraft is reported. An earlier analysis of steady wind tunnel data, obtained for a fighter type aircraft, indicated that shock induced and trailing edge separation play a dominant role in the development of Limit Cycle Oscillations (LCO) at transonic speeds. On the basis of these data, a semi-empirical LCO prediction method is being developed. Its preliminary version was applied to several configurations and correctly identified those which have encountered LCO. It showed the potential for application early in the design process of new aircraft to determine and understand the nonlinear aeroelastic characteristics. The method has been upgraded since. It is described in its present form and results of the latest predictions are used to further assess various parametric effects. The ultimate refinements are expected from recent unsteady wind tunnel force and pressure measurements of which a few preliminary results are analyzed. ESA

N94-30516 Maryland Univ., College Park.

EXPANDING THE WAVERIDER DESIGN SPACE USING ARBITRARY GENERATING FLOWFIELDS Ph.D. Thesis

Frederick Ferguson 1993 227 p

Avail: Univ. Microfilms Order No. DA9327413

The present analysis deals with a quantum leap in the design space of hypersonic vehicles by carefully constructing aircraft from arbitrary flowfields. The design philosophy followed is basically that of finding a shape with a theoretically known and acceptable flowfield in the cruise condition. The ultimate goal is to obtain a complete aircraft configuration with integrated lift surface, stowage volume and propulsion unit, which will have satisfactory low speed, low supersonic speed and cruise Mach number performance. In order to construct shapes, whose behavior in an inviscid fluid stream may be calculated exactly, stream surfaces chosen according to certain rules from assumed shock shapes are replaced by solid boundaries. A combination of such a stream surface, coupled with reliable engineering approximations for the calculations of local shear stress and pressure distribution, are built up piecemeal into complete aircraft configurations. To accomplish the task of designing waveriders a new numerical technique is developed. This numerical method uses the speed and simplicity of spatial marching techniques and the efficiency of the method of characteristics. It is shown that the design process is greatly simplified. Furthermore, this method is sufficiently flexible to allow for considerable freedom of choice in the disposition of lift, volume, and base and platform shapes. Included in this analysis are methods which indicate how the lifting efficiencies of the resulting vehicles may be investigated, and to some extent, optimized. Emphasis is placed on the influence of the shock wave shape and its relationship with the aerodynamic characteristics of the resulting waverider. A systematic approach, based on the Rosenbrock optimization routine, is developed in an effort to carved waveriders with optimal aerodynamic characteristics for given dimension and free stream

conditions. A new class of viscous optimized waveriders, possessing very high L/D ratios, are presented. Finally, since the present method provides a very rapid computational procedure, it is used in parametric studies to provide preliminary data on the off design and high altitude performance of waverider configurations. Dissert. Abstr.

N94-30687 Lawrence Livermore National Lab., CA.
DUAL-BAND INFRARED IMAGING FOR QUANTITATIVE CORROSION DETECTION IN AGING AIRCRAFT
N. K. DelGrande Nov. 1993 5 p Presented at the Autumn Conference of the American Society for Nondestructive Testing (ASNT), Long Beach, CA, 8-12 Nov. 1993 Limited Reproducibility: More than 20% of this document may be affected by microfiche quality
(Contract W-7405-eng-48)
(DE94-004187; UCRL-JC-115167; CONF-931193-1) Avail: CASI HC A01/MF A01

Aircraft skin thickness-loss from corrosion has been measured using dual-band infrared (DBIR) imaging on a flash-heated Boeing 737 fuselage structure. We mapped surface temperature differences of 0.2 to 0.6 C for 5 to 14% thickness losses within corroded lap splices at 0.4 seconds after the heat flash. Our procedure mapped surface temperature differences at sites without surface-emissivity clutter (from dirt, dents, tape, markings, ink, sealants, uneven paint, paint stripper, exposed metal and roughness variations). We established the correlation of percent thickness loss with surface temperature rise using a partially corroded F-18 wing box and several aluminum panels which had thickness losses from milled flat-bottom holes. We mapped the lap splice composite thermal inertia, (kpc)(sup (1/2)), which characterized shallow skin defects within the lap splice at early times (less than 0.3 s) and deeper skin defects within the lap splice at late times (greater than 0.4 s). Corrosion invaded the inside of the Boeing 737 lap splice, beneath the galley and the latrine, where we observed 'pillowing' from volume build-up of corrosion by-products. DOE

N94-30787 Rensselaer Polytechnic Inst., Troy, NY.
NONLINEAR MULTIBODY FORMULATION FOR ROTORCRAFT ANALYSIS Ph.D. Thesis
Nam Kook Kang 1993 281 p
Avail: Univ. Microfilms Order No. DA9325247

Rotorcraft systems include a wide range of different types of vehicles such as single, or tandem rotor helicopters and tilt rotors. Therefore a typical rotorcraft system can have several blades and rotors, fuselage and possibly wings. Similarly a variety of rotors such as articulated hingeless and bearingless rotor types have different physical characteristics, and rotor blades become complex with sweep, and twist, as well as composite materials. In view of these aspects, nonlinear multibody formulation for rotorcraft analysis has been developed. The formulation is based on the finite element method, allowing to model arbitrary complex multibody configurations. Two alternative multibody approaches are pursued and compared in terms of accuracy, computational efficiency and numerical stability and the final nonlinear multibody formulation is expressed in a single inertial system, using Cartesian coordinates to represent the configuration of each body. Elastic bodies are modeled as nonlinear beam elements which are naturally curved and twisted, and undergoing arbitrarily large deflections and rotations. Kinematic constraint elements allow an accurate modeling of multibody rotorcraft system and the constraint equations are enforced via an augmented Lagrangian formulation. After comparing various finite element and finite difference methodologies, a displacement based finite element method with Hilber-Huges-Taylor time integration scheme is used. This integration scheme introduces numerical dissipation into the time integration process to control high frequency numerical oscillations. This nonlinear multibody formulation is coupled with simplified aerodynamic model to treat realistic rotorcraft problems. Numerical results of nonlinear static problem of tension-bending-torsion coupled beam and rigid body dynamic problems show an excellent correlation with experimental data, or analytical results. Practical applications of this formulation are made for the airloads calculation in forward flight of the Sikorsky's H-34 and ground resonance prediction of the Boeing's 'Advanced Chinook' tandem helicopter. Dissert. Abstr.

N94-30905 FractuResearch, Inc., Galena, OH.
ANALYSIS CONCERNING THE INSPECTION THRESHOLD FOR MULTI-SITE DAMAGE Final Report, Apr. - Jun. 1991
D. Broek Dec. 1993 51 p Limited Reproducibility: More than 20% of this document may be affected by microfiche quality
(Contract DTRS57-91-P-80859)
(PB94-142429; AD-A276593; DOT-VNTSC-FAA-93-7; DOT/FAA/CT-93/77) Avail: CASI HC A04

Periodic inspections, at a prescribed interval, for Multi-Site Damage (MSD) in longitudinal fuselage lap-joints start when the aircraft has accumulated a certain number of flights, the inspection threshold. The work reported here was an attempt to obtain justification for the threshold. It is based upon an analysis of fatigue data for lap-joints (riveted as well as riveted plus bonded) of a configuration closely resembling those in several types of aircraft. Depending upon the definition of threshold, the results show that it will be around 30,000 flights. Graphs are supplied upon the basis of which airworthiness authorities can determine a threshold in accordance with their preferred definition, and for different service conditions. NTIS

N94-30947# Aeronautical Research Inst. of Sweden, Stockholm.
FATIGUE MANAGEMENT AND VERIFICATION OF AIRFRAMES
A. F. Blom and H. Ansell Dec. 1993 30 p Presented at the 77th AGARD Structures and Materials Panel Meeting, Bordeaux, France, 27 Sep. - 1 Oct. 1993 Sponsored by Aeronautical Research Inst. of Sweden; Saab Military Aircraft; and Swedish Defence Material Administration
(FFA-TN-1993-55; ETN-94-95858) Avail: CASI HC A03/MF A01

The methodology currently used in Sweden for fatigue management and verification of airframes is described. Applications from the new fighter aircraft JAS39 Gripen are included in order to illustrate the various concepts being considered. Additional experience from recent work on the older fighter 37 Viggen is also included to highlight certain differences in the detail analyses, stemming from rather different nominal stress levels in the two aircraft. The following are discussed: the handling of load sequences and load spectra development, stress analyses and fracture mechanics analyses, fatigue crack growth modeling, component and full scale testing, service load monitoring regarding both the dedicated test aircraft, which is used to verify basic load assumptions, and also the individual load tracking program developed for the new fighter. ESA

N94-28957# Fuji Heavy Industries Ltd., Tokyo (Japan).
A DESIGN OF THIRD-GENERATION AIRFOILS FOR HELICOPTER ROTOR BLADES USING NAVIER-STOKES [NABIE SUTOKOSU KAISEKI O MOCHIITA HERIKOPUTA ROTA BUREDO YO DAI 3 SEDAI KOUSEINO YOKUGATA NO SEKKEI]
Masaaki Nakadate and Masahiro Obukata *In* NAL, Proceedings of the 10th NAL Symposium on Aircraft Computational Aerodynamics Dec. 1992 p 57-62 In JAPANESE (For primary document see N94-28946 08-02)
Avail: CASI HC A02/MF A03

N94-30293 Defence Research Establishment Suffield, Ralston (Alberta).
HATT-X: A HIGH PERFORMANCE FLYING LABORATORY FOR AUTONOMOUS UNMANNED AIRCRAFT RESEARCH AND DEVELOPMENT
Alex B. Markov and Robert W. Herring *In its* Proceedings of the 3rd Conference on Military Robotic Applications 1991 p 136-142 (For primary document see N94-30275 08-37)
Avail: Issuing Activity (Defence Research Establishment Suffield, P.O. Box 4000, Medicine Hat, AB T1A 8K6 Canada)

06 AIRCRAFT INSTRUMENTATION

Includes cockpit and cabin display devices; and flight instruments.

For related information see also *19 Spacecraft Instrumentation* and *35 Instrumentation and Photography.*

N94-29005# Texas Univ., Arlington. Dept. of Industrial Engineering.
INFORMATION PRESENTATION FOR EXPERT SYSTEMS IN FUTURE FIGHTER AIRCRAFT Final Report, Dec. 1992 - Aug. 1993
Mica R. Endsley and Esin O. Kiris Sep. 1993 31 p
(Contract F33616-89-C-0532)
(AD-A275126; AL/CF-TR-1993-0164) Avail: CASI HC A03/MF A01

This study explored the method for presentation of information in the context of a crew-aiding intelligent associate. Forty-five male Air Force pilots and forty-five male and female students served as subjects in the evaluation of prototype display designs. Categorical information coding produced the shortest processing and response times for both groups of subjects. Confidence in decision making was shown to be affected by both coding schema and subject experience level. DTIC

N94-29048# Logicon, Inc., Dayton, OH.
A COMPARISON OF THREE AIRCRAFT ATTITUDE DISPLAY SYMBOLOGY STRUCTURES Interim Report, Dec. 1990 - Dec. 1991
Eric E. Geiselman, Robert K. Osgood, and David W. Biers Jun. 1993 106 p Prepared in cooperation with Dayton Univ., OH
(Contract F33615-89-C-0532)
(AD-A275172; AL/CF-TR-1993-0134) Avail: CASI HC A06/MF A02

This study evaluated the attitude information conveyance of a new aircraft attitude display concept. The new symbology format, called the THETA symbology, was developed by integrating the shape of the conventional ADI and the transparency of the HUD into a single format. This research addressed whether or not there was a significant performance advantage or decrement incurred by the symbology integration. The THETA symbology, ADI, and HUD were evaluated during an attitude maintenance task and an attitude recovery task. The results of the study suggest few differences between the THETA and ADI formats while performance and training time were better with both the THETA symbology and the ADI than with the HUD format. The findings of the study lend support to the hypothesis that an attitude display formed of the integration of ADI and HUD type symbology will demonstrate a performance benefit over a pure HUD format. DTIC

N94-29377*# Honeywell Information Systems, Inc., Minneapolis, MN. Systems and Research Center.
FUTURE MANNED SYSTEMS ADVANCED AVIONICS STUDY Final Report
Bob Sawamura and Kathie Radke Jan. 1992 251 p Prepared for NASA. Johnson Space Center
(NASA-CR-188277; NAS 1.26:188277) Avail: CASI HC A12/MF A03

COTS+ was defined in this study as commercial off-the-shelf (COTS) products, ruggedized and militarized components, and COTS technology. This study cites the benefits of integrating COTS+ in space, postulates a COTS+ integration methodology, and develops requirements and an architecture to achieve integration. Developmental needs and concerns were identified throughout the study; these needs, concerns, and recommendations relative to their abatement are subsequently presented for further action and study. The COTS+ concept appears workable in part or in totality. No COTS+ technology gaps were identified; however, radiation tolerance was cited as a concern, and the deferred maintenance issue resurfaced. Further study is recommended to explore COTS+ cost-effectiveness, maintenance philosophy, needs, concerns, and utility metrics. The generation of a development plan to further investigate and integrate COTS+ technology is recommended. A COTS+ transitional integration program is recommended. Sponsoring and establishing technology maturation programs and COTS+ engineering and standards committees are deemed necessary and are recommended for furthering COTS+ integration in space. Derived from text

N94-29389# Air Univ., Maxwell AFB, AL. Airpower Research Inst.
COCKPIT VIDEO: A LOW COST BDA SOURCE
Kevin W. Smith Dec. 1993 96 p
(AD-A275228; AU-ARI-93-1) Avail: CASI HC A05/MF A01

This research can not address all the bomb damage assessment (BDA) problems experienced during the Gulf War, as time and classification would preclude such an analysis. Instead, it will focus on unit level war-fighting interfaces, particularly those to which onboard video was a key contributor. DTIC

N94-29316# Aerospatiale, Toulouse (France).
HOW TO CONTROL THE INCREASE IN THE COMPLEXITY OF CIVIL AIRCRAFT ON-BOARD SYSTEMS
P. Chanet and V. Cassigneul *In* AGARD, Aerospace Software Engineering for Advanced Systems Architectures Nov. 1993 10 p (For primary document see N94-29315 08-61)
Copyright Avail: CASI HC A02/MF A03

N94-29331# Wright Lab., Wright-Patterson AFB, OH.
A COMMON Ada RUN-TIME SYSTEM FOR AVIONICS SOFTWARE
Clive L. Benjamin, Marc J. Pitarys, Eliezer N. Solomon, and Steve Sedrel *In* AGARD, Aerospace Software Engineering for Advanced Systems Architectures Nov. 1993 11 p (For primary document see N94-29315 08-61)
Copyright Avail: CASI HC A03/MF A03

N94-29332# Alsys, Inc., Saint Cloud (France).
Ada RUN TIME SYSTEM CERTIFICATION FOR AVIONICS APPLICATIONS
Jacques Brygier and Marc Richard-Foy *In* AGARD, Aerospace Software Engineering for Advanced Systems Architectures Nov. 1993 9 p (For primary document see N94-29315 08-61)
Copyright Avail: CASI HC A02/MF A03

N94-29334# Alenia, Torino (Italy).
ON GROUND SYSTEM INTEGRATION AND TESTING: A MODERN APPROACH
B. DiGiandomenico *In* AGARD, Aerospace Software Engineering for Advanced Systems Architectures Nov. 1993 7 p (For primary document see N94-29315 08-61)
Copyright Avail: CASI HC A02/MF A03

N94-29336# Wright Lab., Wright-Patterson AFB, OH. Avionics Logistics Branch.
VALIDATION AND TEST OF COMPLEX WEAPON SYSTEMS
Mark M. Stephenson *In* AGARD, Aerospace Software Engineering for Advanced Systems Architectures Nov. 1993 12 p (For primary document see N94-29315 08-61)
Copyright Avail: CASI HC A03/MF A03

N94-29348# International Business Machines Corp., Owego, NY.
DSSA-ADAGE: AN ENVIRONMENT FOR ARCHITECTURE-BASED AVIONICS DEVELOPMENT
Louis H. Coglianese and Raymond Szymanski *In* AGARD, Aerospace Software Engineering for Advanced Systems Architectures Nov. 1993 8 p Sponsored in part by DARPA (For primary document see N94-29315 08-61)
Copyright Avail: CASI HC A02/MF A03

07 AIRCRAFT PROPULSION AND POWER

Includes prime propulsion systems and systems components, e.g., gas turbine engines and compressors; and onboard auxilliary power plants for aircraft.

For related information see also *20 Spacecraft Propulsion and Power, 28 Propellants and Fuels,* and *44 Energy Production and Conversion.*

N94-28923*# National Aeronautics and Space Administration. Lewis Research Center, Cleveland, OH.
A RANDOM DISTRIBUTION REACTING MIXING LAYER MODEL
Richard A. Jones (Rensselaer Polytechnic Inst., Troy, NY.), C. John Marek, Leik N. Myrabo, and Henry T. Nagamatsu Mar. 1994 13 p Proposed for the 30th Joint Propulsion Conference, Indianapolis, IN, 27-29 Jun. 1994; sponsored by AIAA, ASME, SAE, and ASEE
(RTOP 505-62-52)
(NASA-TM-106517; E-8636; NAS 1.15:106517; AIAA Paper 94-3050)
Avail: CASI HC A03/MF A01

A methodology for simulation of molecular mixing, and the resulting velocity and temperature fields has been developed. The ideas are applied to the flow conditions present in the NASA Lewis Research Center Planar Reacting Shear Layer (PRSL) facility, and results compared to experimental data. A gaussian transverse turbulent velocity distribution is used in conjunction with a linearly increasing time scale to describe the mixing of different regions of the flow. Equilibrium reaction calculations are then performed on the mix to arrive at a new species composition and

temperature. Velocities are determined through summation of momentum contributions. The analysis indicates a combustion efficiency of the order of 80 percent for the reacting mixing layer, and a turbulent Schmidt number of 2/3. The success of the model is attributed to the simulation of large-scale transport of fluid. The favorable comparison shows that a relatively quick and simple PC calculation is capable of simulating the basic flow structure in the reacting and nonreacting shear layer present in the facility given basic assumptions about turbulence properties. Author

N94-29103*# Sverdrup Technology, Inc., Brook Park, OH.
STRUCTURAL/AERODYNAMIC BLADE ANALYZER (SAB) USER'S GUIDE, VERSION 1.0 Final Report
M. R. Morel Mar. 1994 112 p
(Contract NAS3-25266; RTOP 505-63-5B; RTOP 535-03-10; RTOP 505-62-10)
(NASA-CR-194460; E-8490; NAS 1.26:194460) Avail: CASI HC A06/MF A02

The structural/aerodynamic blade (SAB) analyzer provides an automated tool for the static-deflection analysis of turbomachinery blades with aerodynamic and rotational loads. A structural code calculates a deflected blade shape using aerodynamic loads input. An aerodynamic solver computes aerodynamic loads using deflected blade shape input. The two programs are iterated automatically until deflections converge. Currently, SAB version 1.0 is interfaced with MSC/NASTRAN to perform the structural analysis and PROP3D to perform the aerodynamic analysis. This document serves as a guide for the operation of the SAB system with specific emphasis on its use at NASA Lewis Research Center (LeRC). This guide consists of six chapters: an introduction which gives a summary of SAB; SAB's methodology, component files, links, and interfaces; input/output file structure; setup and execution of the SAB files on the Cray computers; hints and tips to advise the user; and an example problem demonstrating the SAB process. In addition, four appendices are presented to define the different computer programs used within the SAB analyzer and describe the required input decks. Author (revised)

N94-29291# Advisory Group for Aerospace Research and Development, Neuilly-Sur-Seine (France). Propulsion and Energetics Lab.
RESEARCH AND DEVELOPMENT OF RAM/SCRAMJETS AND TURBORAMJETS IN RUSSIA [LA RECHERCHE ET LE DEVELOPPEMENT DES STATOREACTEURS, DES STATOREACTEURS A COMBUSTION SUPERSONIQUE ET DES TURBOSTATOREACTEURS EN RUSSIE]
Dec. 1993 230 p Lecture series held in Laurel, MD, 1-2 Dec. 1993, in Cologen, Germany, 13-14 Jan. 1994, and in Paris, France, 17-18 Jan. 1994
(AGARD-LS-194; ISBN-92-835-0732-0) Copyright Avail: CASI HC A11/MF A03

Russia has a long tradition of achievement in ramjet research and development. The need for new and effective products has led to the establishment of ramjet research as a priority in Russian research and development. This Lecture Series will present and discuss the scientific problems associated with the development of ramjets/scramjets and turboramjets. Some specific aspects of liquid/solid ramjet development, the concepts of LH2 high efficiency RAM combustors, the results of full scale turboramjet testing, scramjet or CFD analyses, and ground flight tests will be studied. This Lecture Series, endorsed by the Propulsion and Energetics Panel of AGARD, has been implemented by the Consultant and Exchange program. For individual titles, see N94-29292 through N94-29301.

N94-29292# Central Inst. of Aviation Motors, Moscow (Russia).
[INTRODUCTION AND OVERVIEW OF RESEARCH AND DEVELOPMENT OF SOLID PROPELLANT RAMROCKETS, LIQUID FUEL RAMJETS AND EXPERIMENTAL HYDROGEN RAM COMBUSTORS]
V. Sosounov *In* AGARD, Research and Development of Ram/Scramjets and Turboramjets in Russia Dec. 1993 19 p (For primary document see N94-29291 08-07)
Copyright Avail: CASI HC A03/MF A03

Ramjets, turboramjets, and scramjets have been studied intensively as possible propulsion systems for missiles, high velocity planes, and aerospace planes, which would use this type of propulsion during the atmospheric acceleration phase. All of these propulsion system configurations have a degree of commonality: ram ducts. This fact is discussed in this section of the Lecture Series. CASI

N94-29293# Central Inst. of Aviation Motors, Moscow (Russia).
TURBORAMJET ENGINES: TYPES AND PERFORMANCES
M. M. Tskhovrebov *In* AGARD, Research and Development of Ram/Scramjets and Turboramjets in Russia Dec. 1993 22 p (For primary document see N94-29291 08-07)
Copyright Avail: CASI HC A03/MF A03

In this report on turboramjet engines, some of the properties of variable cycle propulsion plants based on a combination of ramjet and various turbine-type engines are considered. Various measures of engine thrust performance vs. Mach number are represented. Turboramjet engines (TRE) are classified according to their manner of energy transfer to the ramjet parts. The defining principles of essential TRE propulsion plant working parameters are considered. TRE's with various levels of thrust performance are presented. An effectiveness comparison of various combined propulsion plants for future hypersonic transport planes and a TSTO first stage with LH2 fuel is given. A preference is shown for the turboramjet engine as a universal multimode propulsion plant. The optimization of operating modes in response to changing conditions is adopted as an approach to governing the operation of a combined engine working process. Author (revised)

N94-29294# Central Inst. of Aviation Motors, Moscow (Russia).
RESEARCH AND DEVELOPMENT OF RAMJETS/RAMROCKETS. PART 1: INTEGRAL SOLID PROPELLANT RAMROCKETS
V. Sosounov *In* AGARD, Research and Development of Ram/Scramjets and Turboramjets in Russia Dec. 1993 31 p (For primary document see N94-29291 08-07)
Copyright Avail: CASI HC A03/MF A03

Solid propellant ramrockets (SPRR) combine the exclusive operational advantages of solid rockets with the higher fuel efficiency of air breathing engines. The specific feature of an SPRR which differs from a liquid fuel ramjet is the arrangement of the ram combustor in which the products of the primary burning of the solid propellant inside the gas generator are injected through nozzles and reburned. The second feature of the SPRR combustion process is that the gas by-products of primary gas generator are reburned in the ram combustor as turbulent or quasi-turbulent gas flames. Usually there is no need for special flameholders. These special features can lead to some peculiarities in the inserted booster case and to rather complicated gasified fuel supply devices. The third special (negative) feature of SPRR is the constant or programmed fuel supply rate during the flight. Hence, the problem of SPRR fuel flow rate control arises. This lecture discusses the following topics: integration of SPRR with a booster rocket engine; the energy capabilities of different ramjet solid propellants and their application; the effectiveness of secondary fuel combustion in the ram combustor; model and full scaled ramrocket ground testing; and fuel flow rate control in ramrockets. Author (revised)

N94-29295# Central Inst. of Aviation Motors, Moscow (Russia).
SOME PROBLEMS OF SCRAMJET PROPULSION FOR AEROSPACE PLANES. PART 1: SCRAMJET: AIMS AND FEATURES
A. Roudakov *In* AGARD, Research and Development of Ram/Scramjets and Turboramjets in Russia Dec. 1993 20 p (For primary document see N94-29291 08-07)
Copyright Avail: CASI HC A03/MF A03

This lecture addresses problems of scramjet propulsion for single-stage aerospace planes. The aerospace plane main objective is acceleration of some payload up to orbital speed. It defines a requirement for the propulsion system to be frugal in the wide flight speed range under conditions of propulsion mass limitation and thrust compared with flight vehicle weight. In accordance with modern estimations, real hydrogen fuel scramjet specific impulse may be several times more than that of a rocket engine in the wide flight speed range, from Mf = 5...6 up to Mf = 15...20. But hydrogen scramjet propulsion requires significant air ram connected with high heating of vehicle structure, large hydrogen tanks (and vehicle), and special forms of the flight vehicle. As a result the scramjet advantage, as well as any other air breathing engine advantage, over the modern liquid rocket engines is not doubtless. Nevertheless scramjets can provide good efficiency in aerospace planes if each scramjet element and units are developed very carefully and have high performances. In another case, scramjet may lose

competition with liquid rocket engines and a full scale scramjet will be never created. Theoretical and experimental investigations, ground and flight model tests have demonstrated the possibility of supersonic combustion ramjet for hypersonic flights. But we must carry out serious investigations to obtain high efficiency of scramjet elements and scramjet propulsion as a whole to be sure of scramjet success in aerospace plane competition with liquid rocket engine. Author (revised)

N94-29296# Central Inst. of Aviation Motors, Moscow (Russia).
SCRAMJET CFD METHODS AND ANALYSIS. PART 1: SCRAMJET CFD METHODS. NUMERICAL SIMULATION OF THE FLOW IN SCRAMJET DUCT
V. Kopchenov, K. Lomkov, L. Miller, V. Krjukov, I. Rulev, V. Vinogradov, V. Stepanov, N. Zacharov, R. Taguirov, and M. Aukin *In* AGARD, Research and Development of Ram/Scramjets and Turboramjets in Russia Dec. 1993 20 p (For primary document see N94-29291 08-07)
Copyright Avail: CASI HC A03/MF A03

The computer analysis of scramjet flow became of great importance because of the limited possibilities of ground tests and difficulties of measurements in high speed/enthalpy flows. This fact is a powerful stimulus in CFD development. A short description and examples of applications of the mathematical model for scramjet duct flow developed in CIAM are presented in this paper. Derived from text

N94-29297# Central Inst. of Aviation Motors, Moscow (Russia).
RESEARCH AND DEVELOPMENT OF RAMJETS/RAMROCKETS. PART 2: INTEGRAL LIQUID FUEL RAMJETS
V. Sosounov *In* AGARD, Research and Development of Ram/Scramjets and Turboramjets in Russia Dec. 1993 23 p (For primary document see N94-29291 08-07)
Copyright Avail: CASI HC A03/MF A03

Integral liquid fuel ramjets (LFRJ) have some specific features influencing their arrangement and construction. Among such features are: a larger size and working duration than solid propellant ramjets (SPRR), the necessity of fuel manifolds and flameholders, the wall cooling system arrangement in the combustion chamber, and the possibility of fuel flow and nozzle position control during flight on different speed/altitude trajectories. This lecture will discuss some items concerning the mentioned LFRJ features: the integration of ram combustor and booster; duct flow instability during the ejection of booster case; fuel supply device and effective combustion in ramjet; and adaptive control of ramjet on different flight trajectories. Author (revised)

N94-29298# Central Inst. of Aviation Motors, Moscow (Russia).
RESEARCH AND DEVELOPMENT OF RAMJETS/RAMROCKETS. PART 3: THE STUDY OF GASEOUS HYDROGEN RAM COMBUSTORS
V. A. Sosounov *In* AGARD, Research and Development of Ram/Scramjets and Turboramjets in Russia Dec. 1993 6 p (For primary document see N94-29291 08-07)
Copyright Avail: CASI HC A02/MF A03

The peculiarities of H2 ramjet turboramjet high efficiency ram combustors are discussed which include some special topics such as: flame stabilization behind the nozzle edge; increase of the number of nozzles and ram combustor length reduction; separate combustion without mixing of flames; uniform spread of fuel and air in chamber section; the experiment on model burner series; and methods of effective H2 combustion in a short combustor. Author (revised)

N94-29299# Central Inst. of Aviation Motors, Moscow (Russia).
CIAM EXPERIMENTAL TURBORAMJETS
M. M. Tskhovrebov, V. I. Solonin, and P. A. K. Adjardouzov *In* AGARD, Research and Development of Ram/Scramjets and Turboramjets in Russia Dec. 1993 23 p (For primary document see N94-29291 08-07)
Copyright Avail: CASI HC A03/MF A03

In this report, some results of the TRE operating process including those performed on specially developed demonstrator engines are considered. Essential technical requirements and design features of the experimental TRE designed and developed at CIAM for investigatory study on a test bench are shown. Test facilities for experimental investigations of TRE in 'connected tube' manner and experimental work technology features are presented. Some results of the CIAM TRE experimental study included engine parameters on changing to ramjet operation mode variation. Working parameters in the windmilling (ramjet) mode of operation, and flow characteristics in the afterburner-ramjet combustion chamber are shown. A TRE based on TF parts characteristics matching on changing to ramjet operation mode and engine working parameter variations when going to windmilling in the ramjet mode are discussed. Author (revised)

N94-29300# Central Inst. of Aviation Motors, Moscow (Russia).
SCRAMJET CFD METHODS AND ANALYSIS. PART 2: SCRAMJET CFD ANALYSIS. NUMERICAL SIMULATION OF SUPERSONIC MIXING AND COMBUSTION APPLIED TO SCRAMJET COMBUSTOR
V. Kopchenov, K. Lomkov, S. Zaitsev, and I. Borisov *In* AGARD, Research and Development of Ram/Scramjets and Turboramjets in Russia Dec. 1993 30 p (For primary document see N94-29291 08-07)
Copyright Avail: CASI HC A03/MF A03

A short description of a mathematical model developed in CIAM for numerical simulation of supersonic mixing and combustion, which permits the analysis of the three-dimensional effects, is presented. Some aspects of mixing and combustion enhancement will also be considered on the base of CIAM experience. Derived from text

N94-29301# Central Inst. of Aviation Motors, Moscow (Russia).
SOME PROBLEMS OF SCRAMJET PROPULSION FOR AEROSPACE PLANES. PART 2: SCRAMJET: DEVELOPMENT AND TEST PROBLEMS
A. Roudakov *In* AGARD, Research and Development of Ram/Scramjets and Turboramjets in Russia Dec. 1993 26 p (For primary document see N94-29291 08-07)
Copyright Avail: CASI HC A03/MF A03

The topics covered include the following: SCRAMJET development strategy; subscale model SCRAMJET flight tests; hypersonic flying laboratory and experimental double mode SCRAMJET; SCRAMJET operation in flight conditions; and experimental dual model SCRAMJET parameters. Derived from text

N94-29438*# General Motors Corp., Indianapolis, IN. Gas Turbine Div.
INVESTIGATION OF ADVANCED COUNTERROTATION BLADE CONFIGURATION CONCEPTS FOR HIGH SPEED TURBOPROP SYSTEMS. TASK 2: UNSTEADY DUCTED PROPFAN ANALYSIS COMPUTER PROGRAM USERS MANUAL Final Report, Mar. 1990 - Mar. 1991
Edward J. Hall, Robert A. Delaney, and James L. Bettner May 1991 116 p
(Contract NAS3-25270; RTOP 535-03-10)
(NASA-CR-187105; NAS 1.26:187105) Avail: CASI HC A06/MF A02

The primary objective of this study was the development of a time-dependent three-dimensional Euler/Navier-Stokes aerodynamic analysis to predict unsteady compressible transonic flows about ducted and unducted propfan propulsion systems at angle of attack. The computer codes resulting from this study are referred to as Advanced Ducted Propfan Analysis Codes (ADPAC). This report is intended to serve as a computer program user's manual for the ADPAC developed under Task 2 of NASA Contract NAS3-25270, Unsteady Ducted Propfan Analysis. Aerodynamic calculations were based on a four-stage Runge-Kutta time-marching finite volume solution technique with added numerical dissipation. A time-accurate implicit residual smoothing operator was utilized for unsteady flow predictions. For unducted propfans, a single H-type grid was used to discretize each blade passage of the complete propeller. For ducted propfans, a coupled system of five grid blocks utilizing an embedded C-grid about the cowl leading edge was used to discretize each blade passage. Grid systems were generated by a combined algebraic/elliptic algorithm developed specifically for ducted propfans. Numerical calculations were compared with experimental data for both ducted and unducted propfan flows. The solution scheme demonstrated efficiency and accuracy comparable with other schemes of this class. Author

N94-29860*# Eloret Corp., Palo Alto, CA.
A STUDY OF LOW EMISSIONS GAS TURBINE COMBUSTIONS Final Technical Report, 1 Oct. 1990 - 31 Jan. 1994
Henry G. Adelman 25 Apr. 1994 11 p
(Contract NCC2-699)
(NASA-CR-195763; NAS 1.26:195763) Avail: CASI HC A03/MF A01

Analytical studies have been conducted to determine the best methods of reducing NO(x) emissions from proposed civilian supersonic transports.

Modifications to the gas turbine engine combustors and the use of additives were both explored. It was found that combustors which operated very fuel rich or lean appear to be able to meet future emissions standards. Ammonia additives were also effective in removing NO(x), but residual ammonia remained a problem. Studies of a novel combustor which reduces emissions and improves performance were initiated. In a related topic, a study was begun on the feasibility of using supersonic aircraft to obtain atmospheric samples. The effects of shock heating and compression on sample integrity were modeled. Certain chemical species, including NO2, HNO3, and ClONO2 were found to undergo changes to their composition after they passed through shock waves at Mach 2. The use of detonation waves to enhance mixing and combustion in supersonic airflows was also investigated. This research is important to the use of airbreathing propulsion to obtain orbital speeds and access to space. Both steady and pulsed detonation waves were shown to improve engine performance.

Author (revised)

N94-30013*# Duke Univ., Durham, NC. Dept. of Mechanical Engineering and Materials Science.

AEROACOUSTIC SENSITIVITY ANALYSIS AND OPTIMAL AEROACOUSTIC DESIGN OF TURBOMACHINERY BLADES Status Report, 11 Jul. 1993 - 10 Jan. 1994

Kenneth C. Hall 10 Jan. 1994 24 p

(Grant NAG3-1433)

(NASA-CR-195786; NAS 1.26:195786) Avail: CASI HC A03/MF A01

During the first year of the project, we have developed a theoretical analysis - and wrote a computer code based on this analysis - to compute the sensitivity of unsteady aerodynamic loads acting on airfoils in cascades due to small changes in airfoil geometry. The steady and unsteady flow though a cascade of airfoils is computed using the full potential equation. Once the nominal solutions have been computed, one computes the sensitivity. The analysis takes advantage of the fact that LU decomposition is used to compute the nominal steady and unsteady flow fields. If the LU factors are saved, then the computer time required to compute the sensitivity of both the steady and unsteady flows to changes in airfoil geometry is quite small. The results to date are quite encouraging, and may be summarized as follows: (1) The sensitivity procedure has been validated by comparing the results obtained by 'finite difference' techniques, that is, computing the flow using the nominal flow solver for two slightly different airfoils and differencing the results. The 'analytic' solution computed using the method developed under this grant and the finite difference results are found to be in almost perfect agreement. (2) The present sensitivity analysis is computationally much more efficient than finite difference techniques. We found that using a 129 by 33 node computational grid, the present sensitivity analysis can compute the steady flow sensitivity about ten times more efficiently that the finite difference approach. For the unsteady flow problem, the present sensitivity analysis is about two and one-half times as fast as the finite difference approach. We expect that the relative efficiencies will be even larger for the finer grids which will be used to compute high frequency aeroacoustic solutions. Computational results show that the sensitivity analysis is valid for small to moderate sized design perturbations. (3) We found that the sensitivity analysis provided important insight into how airfoils should be modified to improve their aeroelastic stability. Using this insight, we redesigned an aeroelastically unstable cascade to produce a stable cascade. Derived from text

N94-30130# Atlantis Scientific Systems Group, Inc., Ottawa (Ontario).

RADAR JET ENGINE HEALTH MONITORING PROJECT Final Report

Catherine Harrison, Nicholas Wise, Leonard Lighstone, and L. Philip Carr Jun. 1993 47 p

(ASSGI-301; CTN-94-61136) Avail: CASI HC A03/MF A01

Radar returns of aircraft exhibit jet engine modulation (JEM) lines. The JEM lines are caused by the rotating parts in the turbine engines. The radar returns from the engines suggest that it may be possible to monitor the health of the engine, more specifically blade damage and possibly blade tip rub, by using radar as a sensor. A feasibility study was conducted using continuous wave K-band and X-band radar on CF-700 and J-85 engines. Results showed that to make realistic JEM measurements, a radar with two channels (in-phase and quadrature) is required and that there are optimal viewing angles for different fan blade configurations. Radars were accordingly modified and tested including an X-band cross polarization radar for seeing further into the engine and a X-band dual channel radar. It is not yet known if the radar can see into the engine beyond the second compressor stage. Work remains to be done in order to decide whether radar as an engine health monitoring device would present any advantages over conventional maintenance methods.

Author (CISTI)

N94-30914 National Aerospace Lab., Amsterdam (Netherlands). Structures and Materials Div.

FRACTOGRAPHIC AND MICROSTRUCTURAL ANALYSIS OF FATIGUE CRACK GROWTH IN Ti-6Al-4V FAN DISC FORGINGS

R. J. H. Wanhill and C. E. W. Looije 30 Sep. 1991 46 p Limited Reproducibility: More than 20% of this document may be affected by microfiche quality

(AD-B174765; NLR-TP-91142-U; ETN-94-95565) Avail: CASI HC A03

The constant amplitude and flight simulation (TURBISTAN) fatigue crack growth behavior of Ti-6Al-4V fan disc forgings, tested in an engine disc cooperative test program, was investigated by fractographic and microstructural analysis. The crack growth curve shapes and fractographic characteristics were similar. Transitions in the fatigue crack growth curves correlated with a change from structure sensitive to continuum mode crack growth, primarily in the transformed and aged beta grains, and decreased fracture surface roughness. The transitions were most probably caused by the maximum plane strain cyclic plastic zone sizes becoming equal to and exceeding the average platelet alpha packet sizes. The significance of such transitions for prediction of fatigue crack growth and service failure analysis is discussed. ESA

N94-30935 Ohio State Univ., Columbus.

POTENTIAL OF THE RAMJET ENGINE FOR HYPERSONIC FLIGHT SPEEDS Ph.D. Thesis

Sami Jamil Antoun 1993 203 p

Avail: Univ. Microfilms Order No. DA9325456

Although the concept of the supersonic combustion ramjet (scramjet) is not new, the maximum flight speed that can be achieved by this power plant has not been established to date. The purpose of this dissertation is to determine the maximum flight speed at which the scramjet is capable to produce enough thrust to overcome its own external drag. In order to determine the maximum flight speed, the net thrust developed by the scramjet is compared to the external drag acting on it for flight Mach numbers 7 to 25. Using an ideal engine cycle, it will be shown that the maximum flight Mach number of the scramjet is approximately 23. When more realistic assumptions are used to include the effects of stagnation pressure loss due to viscous effects and combined friction at the wall of the combustion chamber, the maximum flight Mach number which the scramjet engine may produce is about 12. In this analysis, the flow at the end of each of the engine components is assumed to be one dimensional and in chemical and thermodynamic equilibrium. Performance losses due to incomplete mixing and combustion of fuel and air have not been considered. Dissert. Abstr.

N94-28960# Tokyo Univ. (Japan). Graduate School.

NUMERICAL STUDY ON THE INTERACTION BETWEEN SCRAMJET ENGINE MODULES CAUSED BY THERMAL CHOKE [SAMARU CHOKU NITORU SUKUMARA JETTO ENJIN NO MOJURU KANNO KANSHO]

Takuo Onodera and Shojiro Kaji *In* NAL, Proceedings of the 10th NAL Symposium on Aircraft Computational Aerodynamics Dec. 1992 p 75-80 In JAPANESE (For primary document see N94-28946 08-02)

Avail: CASI HC A02/MF A03

N94-28977# National Aerospace Lab., Tokyo (Japan).

NUMERICAL STUDY ON INTERNAL FLOWS OF CENTRIFUGAL COMPRESSORS [ENSHIN ASSHUKUKI NO NAIBU NAGARE NIKANSURU SUCHI KAISEKI]

Takashi Yamane and Toshio Nagashima *In its* Proceedings of the 10th NAL Symposium on Aircraft Computational Aerodynamics Dec. 1992 p 169-174 In JAPANESE (For primary document see N94-28946 08-02)

Avail: CASI HC A02/MF A03

N94-28978# Ishikawajima-Harima Heavy Industries Co. Ltd., Tokyo (Japan).
APPLICATION OF FLOW FIELD SIMULATION TO TURBINE VANE DESIGN [SUCHI SHIMYURESHON TO TABIN YOKURETSU SEKKEI]
Koji Matsunaga, Hisao Takeuchi, Atsushige Tanaka, Ruriko Yamawaki, Hiroshi Hamazaki, Kazuo Kikuchi, and Osamu Nozaki *In* NAL, Proceedings of the 10th NAL Symposium on Aircraft Computational Aerodynamics Dec. 1992 p 175-180 In JAPANESE (For primary document see N94-28946 08-02)
Avail: CASI HC A02/MF A03

N94-28981# National Aerospace Lab., Tokyo (Japan). Aeroengine Div.
AN ELLIPTIC-HYPERBOLIC GRID GENERATION METHOD AND APPLICATION TO COMPRESSOR FLOWS [DAEN-SOKYOKUSEN GATA KOSHI SEISEIHO TO ASSHUKUKI NAGARE ENO OYO]
Kazuomi Yamamoto *In its* Proceedings of the 10th NAL Symposium on Aircraft Computational Aerodynamics Dec. 1992 p 193-198 In JAPANESE (For primary document see N94-28946 08-02)
Avail: CASI HC A02/MF A03

N94-29254# Technische Hochschule, Darmstadt (Germany). Inst. fuer Energie- und Kraftwerkstechnik.
NUMERICAL MODELLING OF TURBINE COMBUSTION CHAMBERS
S. Maidhof and J. Janicka *In* AGARD, Fuels and Combustion Technology for Advanced Aircraft Engines Sep. 1993 10 p (For primary document see N94-29246 08-25)
Copyright Avail: CASI HC A02/MF A04

N94-29255# Alfa Romeo S.p.A., Naples (Italy). Research and Development Dept.
NUMERICAL SIMULATION OF AEROTHERMAL CHARACTERISTICS IN GAS TURBINE COMBUSTORS WITH COMPLEX GEOMETRIES
P. DiMartino, G. Cinque, and C. Paduano *In* AGARD, Fuels and Combustion Technology for Advanced Aircraft Engines Sep. 1993 14 p (For primary document see N94-29246 08-25)
Copyright Avail: CASI HC A03/MF A04

N94-29256# General Motors Corp., Indianapolis, IN. Gas Turbine Div.
APPLICATION OF CFD IN COMBUSTOR DESIGN TECHNOLOGY
Hukam C. Mongia *In* AGARD, Fuels and Combustion Technology for Advanced Aircraft Engines Sep. 1993 18 p (For primary document see N94-29246 08-25)
Copyright Avail: CASI HC A03/MF A04

N94-29257# Pratt and Whitney Aircraft of Canada Ltd., Mississauga (Ontario).
RECENT CFD APPLICATIONS IN SMALL GAS TURBINE COMBUSTION SYSTEMS DEVELOPMENT
T. C. J. Hu and L. A. Prociw *In* AGARD, Fuels and Combustion Technology for Advanced Aircraft Engines Sep. 1993 12 p (For primary document see N94-29246 08-25)
Copyright Avail: CASI HC A03/MF A04

N94-29258# Societe Nationale d'Etude et de Construction de Moteurs d'Aviation, Moissy-Cramayel (France).
AEROTHERMOCHEMICAL CALCULATIONS IN AFTERBURNERS [CALCULS AEROTHERMOCHIMIQUES DANS LES FOYERS DE RECHAUFFE]
C. Dejeu, J. L. Schultz, and S. Meunier *In* AGARD, Fuels and Combustion Technology for Advanced Aircraft Engines Sep. 1993 8 p In FRENCH Original contains color illustrations (For primary document see N94-29246 08-25)
Copyright Avail: CASI HC A02/MF A04

N94-29263# General Electric Co., Cincinnati, OH. Advanced Engine Combustor Aero Design.
FUEL INJECTOR DESIGN FOR HIGH TEMPERATURE AIRCRAFT ENGINE
R. W. Stickles, W. J. Dodds, T. R. Koblish, J. Sager, and S. Clouser *In* AGARD, Fuels and Combustion Technology for Advanced Aircraft Engines Sep. 1993 12 p (For primary document see N94-29246 08-25)
(Contract N00140-87-C-6321)
Copyright Avail: CASI HC A03/MF A04

N94-29264# Pratt and Whitney Aircraft of Canada Ltd., Mississauga (Ontario).
DESIGN ASPECTS IN SMALL AIRCRAFT GAS TURBINE FUEL INJECTORS
K. McCaldon, L. A. Prociw, and P. Sampath *In* AGARD, Fuels and Combustion Technology for Advanced Aircraft Engines Sep. 1993 10 p (For primary document see N94-29246 08-25)
Copyright Avail: CASI HC A02/MF A04

N94-29267# Leeds Univ. (England). Dept. of Fuel and Energy.
ULTRA LOW NO(x) ULTRA LEAN GAS TURBINE PRIMARY ZONES WITH LIQUID FUELS
G. E. Andrews, H. S. Alkabie, U. S. AbdulHussain, and M. AbdulAziz *In* AGARD, Fuels and Combustion Technology for Advanced Aircraft Engines Sep. 1993 14 p Sponsored in part by Science Research Council (For primary document see N94-29246 08-25)
Copyright Avail: CASI HC A03/MF A04

N94-29269# United Technologies Research Center, East Hartford, CT. Aerothermal Technology/Chemical Sciences.
EVALUATION OF THE TRANSIENT OPERATION OF ADVANCED GAS TURBINE COMBUSTORS
T. J. Rosfjord and J. M. Cohen *In* AGARD, Fuels and Combustion Technology for Advanced Aircraft Engines Sep. 1993 10 p Sponsored by Pratt and Whitney Aircraft (For primary document see N94-29246 08-25)
(Contract N00140-87-C-9902)
Copyright Avail: CASI HC A02/MF A04

N94-29270# Fiat Aviazione S.p.A., Turin (Italy). Direzione Progettazione.
TECHNOLOGY RIGS: A TOOL FOR AFTERBURNER DEVELOPMENT
G. Riccardi, A. Tasselli, and A. Trovati *In* AGARD, Fuels and Combustion Technology for Advanced Aircraft Engines Sep. 1993 17 p (For primary document see N94-29246 08-25)
Copyright Avail: CASI HC A03/MF A04

08 AIRCRAFT STABILITY AND CONTROL

Includes aircraft handling qualities; piloting; flight controls; and autopilots.

For related information see also *05 Aircraft Design, Testing and Performance.*

N94-28632# Michigan Univ., Ann Arbor. Dept. of Electrical Engineering and Computer Science.
CLOSED LOOP VIBRATIONAL CONTROL: THEORY AND APPLICATIONS Final Report, 1 Jan. 1990 - 30 Sep. 1993
Semyon M. Meerkov, Pierre T. Kabamba, and Eng-Kee Poh 15 Dec. 1993 95 p
(Contract DAAL03-90-G-0004)
(AD-A275451; ARO-27510.3-EG) Avail: CASI HC A05/MF A01

In this project, a novel control technique, referred to as Closed Loop Vibrational Control, is developed and applied to the problem of fuselage vibrations suppression in helicopter dynamics. This technique is applicable to systems where the control input enters the open loop dynamics as an amplitude of a periodic, zero average function, and this amplitude can be chosen to depend on the systems outputs. An example of such a system is the helicopter with Higher Harmonic Control (HHC) where periodic feathering of rotor blades around a fixed pitch angle is introduced in order to suppress the fuselage vibrations. For systems with this structure, a number of control-theoretic problems, including stabilizability, pole placement and robustness, have been solved, and the results are reported in this document. DTIC

N94-29532 Texas A&M Univ., College Station.
CONCURRENT SIMULATION AND CONSTRAINT STABILIZATION FOR FLEXIBLE MULTIBODY SYSTEMS Ph.D. Thesis

Ramesh Gopal Menon 1992 147 p
Avail: Univ. Microfilms Order No. DA9315104

This dissertation presents a family of computationally efficient methods for the simulation of large, flexible multibody systems. Nonrecursive order N formulations for the transient dynamic analysis of multibody systems can be achieved using range space methods. Unlike the recursive methods, this formulation does not rely on system topology to induce parallelism. These methods induce concurrency via the method of subdomain decomposition, and it is shown that they are amenable to implementation on the forthcoming class of highly parallel architectures. This class of formulations can be distinguished from other variants of subdomain decomposition in that redundant degrees of freedom are retained, and the coupling of substructures is achieved by explicitly calculating the coupling forces in an order N computational cost. A preconditioned conjugate gradient method is used for the range space solution, with a preconditioner motivated by the directed graph of multibody systems with no closed chains. The method is shown to be rapidly convergent for linear and nonlinear structural systems with a large number of degrees of freedom. One potential drawback of the range space formulation is the well known constraint violation drift associated with redundant formulations of transient multibody dynamics. This dissertation introduces a family of concurrent constraint violation stabilization algorithms that retain the order N computational cost of the range space formulation, while ensuring simulation fidelity. The hybrid methods introduced are based upon penalty multibody formulations and augmented Lagrangian formulations. Explicit bounds on measures of the constraint violation are presented. It is shown that, in the augmented Lagrangian method, the number of fixed iterations per time step dictate the diameters of the attractors of constraint violations in phase space. Several numerical examples of simulation and control are presented including simulations of the Space Station Freedom, the NASA Langley control structure interaction evolutionary model, and nonlinear, multirigid bodies articulating in space. Dissert. Abstr.

N94-29728 Kansas Univ., Lawrence.
AN EXPERIMENTAL INVESTIGATION OF THE EFFECT OF LEADING EDGE EXTENSIONS ON DIRECTIONAL STABILITY AND THE EFFECTIVENESS OF FOREBODY NOSE STRAKES Ph.D. Thesis
An-Kuo Fu 1992 197 p
Avail: Univ. Microfilms Order No. DA9323014

Low speed wind tunnel testing was conducted at Aeronautical Research Laboratory in Taiwan, ROC, using a generic configuration, to investigate the effect of leading-edge extensions (LEX) on directional stability and the effectiveness of forebody nose strakes. To help interpret the wind tunnel measurements, flow visualization including dye and laser sheet was also conducted. It was found that for the present configuration, the LEX vortices dominated the flow field such that the forebody vortices were depressed to stay close to the body surface. Because of this, the nose strakes on this configuration were found to be ineffective in reducing directional instability and producing control moment with a single strake. Directional instability for the configuration with the LEX's was mainly caused by the vertical tail. However, for the configuration with a single small nose strake at very high angles of attack, the instability was caused by a second forebody vortex formed under the nose strake which stayed close to the body surface. Using a single large nose strake, effectiveness for yaw control was significantly improved. However, for sideslip control, the proper forebody side for its deployment depends on the angle of attack. In addition, with a pair of large nose strakes, the untrimmed yawing moment was almost eliminated at zero sideslip. A bi-stable condition was identified for the configuration without the LEX's at alpha = 46 deg. in the water tunnel and 48 deg. in the wind tunnel. For the baseline configuration with the LEX's, a bi-stable condition was also found at alpha = 55 deg.
Dissert. Abstr.

N94-29850 Wichita State Univ., KS.
DECOUPLED FLIGHT CONTROL SYSTEM DESIGN USING THE SINGULAR PERTURBATION METHOD
Sukjune Park 1992 209 p
Avail: Univ. Microfilms Order No. DA9311976

A new approach is developed to design the high gain output feedback with proportional plus integral (P-I) controller. The singular perturbation theory is utilized for the theoretical development. This approach is simpler and more comprehensive than the other methods. The controller produces desirable closed-loop response with minimal interaction between outputs. The new design method is applied to the design of decoupling flight control systems for the full aircraft model (i.e., lateral and longitudinal dynamics). The complete process used to obtain a decoupling flight control law is presented. A robustness study is included to test the controller performance with parameter variations. The results show that the controller is robust with respect to varying maneuver commands. Also, this study includes the six degree of freedom nonlinear simulation to validate the design method. The nonlinear simulation results show that output-feedback solutions from the linear case satisfy the required conditions for application to nonlinear systems. A computer aided design program is developed to assist in the interactive design process. Dissert. Abstr.

N94-30204*# National Aeronautics and Space Administration. Lewis Research Center, Cleveland, OH.
A NOVEL APPROACH TO NOISE-FILTERING BASED ON A GAIN-SCHEDULING NEURAL NETWORK ARCHITECTURE
T. Troudet (Sverdrup Technology, Inc., Brook Park, OH.) and W. Merrill Apr. 1994 10 p
(Contract NAS3-25266; RTOP 584-03-11)
(NASA-TM-106563; E-8739; NAS 1.15:106563) Avail: CASI HC A02/MF A01

A gain-scheduling neural network architecture is proposed to enhance the noise-filtering efficiency of feedforward neural networks, in terms of both nominal performance and robustness. The synergistic benefits of the proposed architecture are demonstrated and discussed in the context of the noise-filtering of signals that are typically encountered in aerospace control systems. The synthesis of such a gain-scheduled neurofiltering provides the robustness of linear filtering, while preserving the nominal performance advantage of conventional nonlinear neurofiltering. Quantitative performance and robustness evaluations are provided for the signal processing of pitch rate responses to typical pilot command inputs for a modern fighter aircraft model. Author (revised)

N94-29317# Societe de Fabrication d'Instruments de Mesure, Massy (France). Industries Groupe Avionique.
PERFORMING SPECIFICATIONS FOR COMPLEX SYSTEMS' SOFTWARE [SPECIFICATIONS EXECUTABLES DES LOGICIELS DES SYSTEMES COMPLEXES]
F. Delhaye and D. Paquot *In* AGARD, Aerospace Software Engineering for Advanced Systems Architectures Nov. 1993 14 p In FRENCH
(For primary document see N94-29315 08-61)
Copyright Avail: CASI HC A03/MF A03

N94-30284 Combustion Dynamics Ltd., Medicine Hat (Alberta).
PAYLOAD CENTRAL CONTROL FOR UNMANNED AIRCRAFT
D. R. Weiler, M. G. Henders, R. H. Chesney, and D. Ehman *In* Defence Research Establishment Suffield, Proceedings of the 3rd Conference on Military Robotic Applications 1991 p 74-80 (For primary document see N94-30275 08-37)
Avail: Issuing Activity (Defence Research Establishment Suffield, P.O. Box 4000, Medicine Hat, AB T1A 8K6 Canada)

09 RESEARCH AND SUPPORT FACILITIES (AIR)

Includes airports, hangars and runways; aircraft repair and overhaul facilities; wind tunnels; shock tubes; and aircraft engine test stands.

For related information see also *14 Ground Support Systems and Facilities (Space).*

N94-28510*# General Electric Co., Cincinnati, OH. Advanced Technology Operations.
DESIGN AND FABRICATION OF FORWARD-SWEPT COUNTERROTATION BLADE CONFIGURATION FOR WIND TUNNEL TESTING Final Report
G. H. Nichols 1 Mar. 1994 164 p
(Contract NAS3-25269)
(NASA-CR-194868; NAS 1.26:194868) Avail: CASI HC A08/MF A02

Work performed by GE Aircraft on advanced counterrotation blade configuration concepts for high speed turboprop system is described. Primary emphasis was placed on theoretically and experimentally evaluating the

aerodynamic, aeromechanical, and acoustic performance of GE-defined counterrotating blade concepts. Several blade design concepts were considered. Feasibility studies were conducted to evaluate a forward-swept versus an aft-swept blade application and how the given blade design would affect interaction between rotors. Two blade designs were initially selected. Both designs involved in-depth aerodynamic, aeromechanical, mechanical, and acoustic analyses followed by the fabrication of forward-swept, forward rotor blade sets to be wind tunnel tested with an aft-swept, aft rotor blade set. A third blade set was later produced from a NASA design that was based on wind tunnel test results from the first two blade sets. This blade set had a stiffer outer ply material added to the original blade design, in order to reach the design point operating line. Detailed analyses, feasibility studies, and fabrication procedures for all blade sets are presented. Author (revised)

N94-28749*# National Aeronautics and Space Administration. Lewis Research Center, Cleveland, OH.

THE NOZZLE ACOUSTIC TEST RIG: AN ACOUSTIC AND AERODYNAMIC FREE-JET FACILITY

Raymond S. Castner Apr. 1994 12 p Presented at the 18th AIAA Aerospace Ground Testing Conference, Colorado Springs, CO, 20-23 Jun. 1994; sponsored by AIAA

(RTOP 505-62-84)

(NASA-TM-106495; E-8485; NAS 1.15:106495; AIAA Paper 94-2565)

Avail: CASI HC A03/MF A01

The nozzle acoustic test rig (NATR) was built at NASA Lewis Research Center to support the High Speed Research Program. The facility is capable of measuring the acoustic and aerodynamic performance of aircraft engine nozzle concepts. Trade-off studies are conducted to compare performance and noise during simulated low-speed flight and takeoff. Located inside an acoustically treated dome with a 62-ft radius, the NATR is a free-jet that has a 53-in. diameter and is driven by an air ejector. This ejector is operated with 125 lb/s of compressed air, at 125 psig, to achieve 375 lb/s at Mach 0.3. Acoustic and aerodynamic data are collected from test nozzles mounted in the free-jet flow. The dome serves to protect the surrounding community from high noise levels generated by the nozzles, and to provide an anechoic environment for acoustic measurements. Information presented in this report summarizes free-jet performance, fluid support systems, and data acquisition capabilities of the NATR.

Author (revised)

N94-28752# IBM Federal Systems Div., Gaithersburg, MD.

CLEANROOM ENGINEERING HANDBOOK. VOLUME 3: PROJECT EXECUTION IN THE CLEANROOM ENVIRONMENT

Ara Kouchakdjian, Richard H. Cobb, Alan R. Hevner, and James A. Whittaker 31 Jul. 1993 69 p

(Contract F19628-88-C-0032)

(AD-A275860) Avail: CASI HC A04/MF A01

This is one of a series of six engineering handbooks prepared for and used by the engineering staff at Picatinny Arsenal for the STARS technology transfer demonstration. The handbooks define the engineering process and algorithms that will be used in Cleanroom projects. They are designed to provide support to trained engineers using Cleanroom Engineering, not to substitute for training. This handbook, Volume 3, provides managers and team leaders with guidance in the planning, directing, and controlling of Cleanroom projects. Project execution is the planning for, and the controlling of the solution to the four major decisions within a software project. These decisions are: (1) to assign tasks to specific team members in the execution of the project; (2) to determine the expected completion date for some phase of the project; (3) to determine if the progress made toward developing the desired software and the resources consumed to date are in balance with each other and with the project's Business Plan; and (4) to determine if some aspect of the design is acceptable and the design effort should continue in the current direction or if the direction should be altered. If the direction is to be altered then a replanning effort must be initiated. This volume covers topics such as completion conditions, metrics collection, forms driven process management system, file and tool reference table, and an automated process management system named CEPA (Cleanroom Engineering Process Assistant). DTIC

N94-28753# IBM Federal Systems Div., Gaithersburg, MD.

CLEANROOM ENGINEERING HANDBOOK. VOLUME 4. SPECIFICATION TEAM PRACTICES

Ara Kouchakdjian, Richard H. Cobb, Alan R. Hevner, and James A. Whittaker 31 Jul. 1993 69 p

(Contract F19628-88-D-0032)

(AD-A275861) Avail: CASI HC A04/MF A01

This is one of a series of six engineering handbooks prepared for and used by the engineering staff at Picatinny Arsenal for the STARS technology transfer demonstration. The handbooks define the engineering process and algorithms that will be used in Cleanroom projects. They are designed to provide support to trained engineers using Cleanroom Engineering, not to substitute for training. This handbook, Volume 4, explains the set of specific tasks performed by the Cleanroom Specification Team for each cycle of a project. Specification tasks are described and the relationship among tasks are defined. The Cleanroom specification team's mission is to create the system specification in six specification volumes. Templates are proposed as recommended formats for the presentation of information and tasks results. Techniques for revising the specifications throughout the system life cycle are described. The Cleanroom process model for software system development projects is presented in Volume 1 - Cleanroom Process Overview - of this series of Cleanroom Handbooks. This handbook, Volume 4, describes the activities of the Specification Team for each cycle of project development. The specification activity may include the preparation of both system and software specifications, depending on the needs and status of the project. Specifications define the requirements placed on the system so it can satisfy its mission and the behavior the system must exhibit to fulfill the assigned requirements. A system specification defines requirements and behavior for a solution which integrates some combination of hardware, software, communications, human behavior, etc. DTIC

N94-28772 IBM Federal Systems Div., Gaithersburg, MD.

CLEANROOM ENGINEERING HANDBOOK. VOLUME 2: ORGANIZATION AND PROJECT FORMATION IN THE CLEANROOM ENVIRONMENT

31 Jul. 1993 55 p Limited Reproducibility: More than 20% of this document may be affected by microfiche quality

(Contract F19628-88-D-0032)

(AD-A275809) Avail: CASI HC A04

The purpose of this handbook is to provide managers with guidance in developing plans on the organization and project levels for the development of software using the Cleanroom process. Additionally, guidance on directing and controlling the implementation of the plan will be presented to help managers ensure that projects are properly executed. Planning, directing, and controlling are just a few of the aspects of a manager's role in the Cleanroom process. The planning, directing, and controlling requirements for managers at different levels differ as do the requirements at different stages of the project. DTIC

N94-29047# Nottingham Univ. (England).

GRANULAR BASES FOR HEAVILY LOADED PAVEMENTS Final Report, Feb. 1988 - Dec. 1990

W. K. Chan and S. F. Brown Mar. 1993 170 p

(AD-A275171; AFCESA/CEL-TR-91-06) Avail: CASI HC A08/MF A02

This research improves the understanding of the permanent deformation characteristics of granular materials under repeated, reversed shear loadings in flexible pavements. In the laboratory, triaxial tests provided vertical repeated loadings, and a hollow cylinder apparatus was used to apply reversing shear stresses and associated rotating principal planes. The laboratory tests were analogous to larger scale tests that were run, using vertical plate and tire loadings. It was found that higher material densities lead to large improvements in permanent deformation resistance, and permanent deformation is significantly more when stresses are reversed in both the laboratory and in the field. The findings were validated using two fully-instrumented pilot scale trafficking tests. DTIC

N94-29052*# Texas A&M Univ., College Station. Engineering Experiment Station.

WIND TUNNEL TESTING AND RESEARCH Final Report, 25 Jan. 1990 - 12 Mar. 1993

Oran W. Nicks 15 Nov. 1993 21 p

(Contract NAS9-18261)

(NASA-CR-188273; NAS 1.26:188273) Avail: CASI HC A03/MF A01

The topics covered include the following: a test of a Space Shuttle model with various base enhancements intended to help reduce the drag of the Shuttle in the landing configuration; further tests conducted using a Shuttle model to explore base drag improvement techniques; testing of parafoils having different airfoil shapes and line lengths; a study of ground effects on a Shuttle model; and three dimensional velocity profiles in the wake aft of the Space Shuttle were determined to study the effects of wake velocities on the Orbiter drag chute. Derived from text

N94-29151# Air Force Civil Engineering Center, Tyndall AFB, FL. Engineering and Services Lab.

ASPHALTIC CONCRETE PERFORMANCE UNDER HEAVY FIGHTER AIRCRAFT LOADING Final Report, Apr. 1988 - Nov. 1990

D. A. Timian, S. M. Dass, W. C. Dass, R. H. Sues, and M. B. Hardy Feb. 1993 359 p

(AD-A275046; AFCESA/ESL-TR-91-26; XC-AFCESA/ESL) Avail: CASI HC A16/MF A03

Rutting of asphaltic concrete pavements is rapidly becoming a cause for concern among AF civil engineers. Modern fighter aircraft often have operating tire pressures well above the capacity of the existing pavements. To reduce rutting, a mix design technique that explicitly considers the expected loading was investigated. Pavement test sections were constructed and trafficked by high pressure tires. Variations in test sections included mix design (Marshall and gyratory), airfield design (4- and 6-inch flexible and rigid composite), and wheel loading (F-15C/D). Pavement loading was monitored throughout trafficking, including dynamic load magnitude, position, and velocity. Pavement response was measured by taking profilographs before, during, and after trafficking. Damage parameters were defined and calculated to evaluate test section response and performance. Damage varied significantly between test sections, with the most obvious factors being the mix design and the base layer support. The gyratory test sections outperformed their Marshall counterparts with the gyratory composite section performing the best. This study has shown that pavements can be designed using gyratory methods. However, improvements in base layer performance are needed to improve the overall performance of flexible airfield pavements. DTIC

N94-29754# Systems Control Technology, Inc., Arlington, VA.

ROOFTOP EMERGENCY HELIPORTS Final Report

William T. Sampson, III, Sandra Henninger, and Richard S. Fixler Jun. 1993 61 p

(Contract DTFA01-87-C-00014)

(DOT/FAA/RD-93/2) Avail: CASI HC A04/MF A01

The research for this project included an in-depth analysis of high-rise fire incidents in which helicopters have been used. Following this effort, a survey was conducted of building codes that were applicable to the construction of heliports and helistops on the roofs of high-rise buildings. These codes were examined to determine common and uncommon elements and to identify strengths and weaknesses. After analyzing this data, the FAA's Heliport Design Advisory Circular (AC) 150/5390-2 was reviewed. This data was then used to develop recommendations for additions or changes to the AC. Author

N94-29904*# National Aeronautics and Space Administration. Lewis Research Center, Cleveland, OH.

LARGE SCALE CRYOGENIC FLUID SYSTEMS TESTING

May 1992 13 p Original contain color illustrations

(NASA-TM-109735; B-0426; NAS 1.15:109735) Avail: CASI HC A03/MF A01; 6 functional color pages

NASA Lewis Research Center's Cryogenic Fluid Systems Branch (CFSB) within the Space Propulsion Technology Division (SPTD) has the ultimate goal of enabling the long term storage and in-space fueling/resupply operations for spacecraft and reusable vehicles in support of space exploration. Using analytical modeling, ground based testing, and on-orbit experimentation, the CFSB is studying three primary categories of fluid technology: storage, supply, and transfer. The CFSB is also investigating fluid handling, advanced instrumentation, and tank structures and materials. Ground based testing of large-scale systems is done using liquid hydrogen as a test fluid at the Cryogenic Propellant Tank Facility (K-site) at Lewis' Plum Brook Station in Sandusky, Ohio. A general overview of tests involving liquid transfer, thermal control, pressure control, and pressurization is given. Derived from text

N94-29956*# Alabama Univ., Huntsville.

VACUUM CHAMBER AND ADAPTORS FOR SHEAROGRAPHY AND HOLOGRAPHY Final Technical Report, 8 Apr. 1992 - 8 Jan. 1993

James R. Clark, Charles M. Horton, and Robert J. Campbell Jan. 1993 37 p Original contains color illustrations

(Contract NAS8-38609)

(NASA-CR-192467; NAS 1.26:192467; UAH-5-32902) Avail: CASI HC A03/MF A01; 1 functional color page

Study methods to excite aerospace components using a vacuum to induce deformations are presented. The deformations will be measured by shearography, holography, and image correlation. Author

N94-30200*# National Aeronautics and Space Administration. Langley Research Center, Hampton, VA.

APPLICATION OF FUZZY LOGIC TO THE CONTROL OF WIND TUNNEL SETTLING CHAMBER TEMPERATURE

David A. Gwaltney and Gregory L. Humphreys Mar. 1994 16 p

(RTOP 505-70-59-03)

(NASA-TM-109105; NAS 1.15:109105) Avail: CASI HC A03/MF A01

The application of Fuzzy Logic Controllers (FLC's) to the control of nonlinear processes, typically controlled by a human operator, is a topic of much study. Recent application of a microprocessor-based FLC to the control of temperature processes in several wind tunnels has proven to be very successful. The control of temperature processes in the wind tunnels requires the ability to monitor temperature feedback from several points and to accommodate varying operating conditions in the wind tunnels. The FLC has an intuitive and easily configurable structure which incorporates the flexibility required to have such an ability. The design and implementation of the FLC is presented along with process data from the wind tunnels under automatic control. Author

N94-30268# Japan Machinery Federation, Tokyo.

THE 1992 REPORT ON THE NEXT GENERATION ULTRA CLEAN TECHNOLOGY FOR ADVANCED MICROFABRICATION

Mar. 1993 666 p In JAPANESE

(DE94-744171; ETDE/JP-MF-94744171) Avail: CASI HC A99/MF A06

The paper studies the next generation ultraclean technology for the manufacture of ultrahigh integrated and ultrahigh functional electronic devices. To effectively fabricate ultrahigh performance LSI at a low cost, the first thing needed is checking of the capital investment. The equipment cost makes up 74 percent of the capital investment. It becomes extremely important to reduce the process number by simplification of device structure, to increase operational rates of the equipment, and to reduce the number of the equipment. On the other hand, it is necessary to give the equipment continued cleaning in order to prevent a decrease in yield caused by attachment of foreign substances and to assure quality. It is also necessary to introduce facilities with such high performance as plasma in-situ cleaning. The paper gives detailed explanations of the future semiconductor manufacturing system and fabrication facilities technology and the technology for the reactive/corrosive particular gas which is expected to be increasingly used for CVD and RIE (reactive ion etching). Detailed explanations are also given of the water evaluation technology, microvibration prevention necessary for ultra-microprocessing, the contamination control system, and the water surface processing and measuring technology. DOE

N94-30399 National Aerospace Lab., Amsterdam (Netherlands). Fluid Dynamics Div.

CORRECTION OF X HOT-WIRE MEASUREMENTS FOR GRADIENTS NORMAL TO THE PLANE OF THE WIRES

J. H. M. Gooden 9 Jul. 1992 53 p Limited Reproducibility: More than 20% of this document may be affected by microfiche quality

(PB94-125473; NLR-TP-95592; ETN-94-95592) Avail: CASI HC A04

A gradient correction method, which allows correction of the results obtained from X hot wire measurements for flow gradients normal to the plane of the hot wires, is described. The influence of these gradients on the hot wire response is determined from the hot wire response equations. A data processing method which allows a correction of the measured data after the measurements have been completed is described. The method was applied to hot wire measurements of the mean and fluctuating flow velocities in the turbulent wake shed from a two dimensional wing above a single trailing edge flap. ESA

N94-30423 National Aerospace Lab., Amsterdam (Netherlands). Fluid Dynamics Div.
A MODERNISED HST OF NLR
F. Jaarsma, J. Smith, and R. K. vanderDraai 31 Oct. 1992 22 p Presented at the European Windtunnels and Forum on Windtunnel Test Techniques, Southampton Univ., England, 14-17 Sep. 1992 Limited Reproducibility: More than 20% of this document may be affected by microfiche quality
(AD-B179220; NLR-TP-92420-U; ETN-94-95961) Avail: CASI HC A03

The modernization underway and plans for the future of the High Speed Tunnel (HST) are reported. The improvement comprised three main objectives, namely: improvement of testing capabilities; improvement of Reynolds number range; and improvement of productivity. Because of budget limitations the total plan will be executed in phases. The first phase, now under full execution, concerns the following more specific items: extension of test section length to reduce buoyancy effects; adaptability to two different test section heights (1.6 and 1.8 m) allowing extended incidence range; new model support system allowing a selection between slender sting support boom with limited incidence range (30 deg), double roll sting boom with moderate incidence range (30 deg in a single sweep) and limited yaw (+ and -10 deg), or articulated sting boom with large incidence range (50 deg) and large yaw (+ and - 30 deg); automated tunnel operation for improved productivity and improved accuracy; and modernization of the controls of the power plant. Wall and support interference effects were studied in detail in order to arrive at improved mechanical systems and correction methods. Further improvements planned in the future include application of adaptive walls and an increase of power to extend the range in terms of Reynolds number testing. ESA

N94-30788 George Washington Univ., Washington, DC.
ANALYSIS OF FLUCTUATING STATIC PRESSURE MEASUREMENTS IN A LARGE HIGH REYNOLDS NUMBER TRANSONIC CRYOGENIC WIND TUNNEL Ph.D. Thesis
William B. Igoe 1993 258 p
Avail: Univ. Microfilms Order No. DA9329869

Dynamic measurements of fluctuating static pressure levels were made using flush mounted high frequency response pressure transducers at eleven locations in the circuit of the National Transonic Facility (NTF) over the complete operating range of this wind tunnel. Measurements were made at test section Mach numbers from 0.2 to 1.2, at pressure from 1 to 8.6 atmospheres and at temperatures from ambient to -250 F, resulting in dynamic flow disturbance measurements at the highest Reynolds numbers available in a transonic ground test facility. Tests were also made independently at variable Mach number, variable Reynolds number and variable drivepower, each time keeping the other two variables constant thus allowing for the first time, a distinct separation of these three important variables. This report contains a description of the NTF emphasizing its flow quality features, details on the calibration of the instrumentation, results of measurements with the test section slots covered, downstream choke, effects of liquid nitrogen injection and gaseous nitrogen venting, comparisons between air and nitrogen, isolation of the effects of Mach number, Reynolds number and fan drive power, and identification of the sources of significant flow disturbances. The results indicate that primary sources of flow disturbance in the NTF may be edge-tones generated by test section sidewall reentry flaps and the venting of nitrogen gas from the return leg of the tunnel circuit between turns 3 and 4 in the cryogenic mode of operation. The tests to isolate the effects of Mach number, Reynolds number and drive power indicate that Mach number effects predominate. A comparison with other transonic wind tunnels shows that the NTF has low levels of test section fluctuating static pressure especially in the high subsonic Mach number range from 0.7 to 0.9. Dissert. Abstr.

N94-30856 National Aerospace Lab., Amsterdam (Netherlands). Fluid Dynamics Div.
'REAL TIME' AND THE NLR AERODYNAMIC FACILITIES
R. K. vanderDraai 23 Mar. 1992 16 p Presented at the NLUUG Conference, Ede, Netherlands, 6 May 1992 Limited Reproducibility: More than 20% of this document may be affected by microfiche quality
(AD-B173626; NLR-94-92113-U; ETN-94-95573) Avail: CASI HC A03

Reasons for the real time characteristics of the computer systems directly connected to a wind tunnel, and which are used for data acquisition, process control and data processing, are given. The choice of a computer to perform any of these tasks is described, and strategies to do so are given. An example of choosing a real time control system for use in aerodynamic facilities is outlined. The choice of the computer was made in the HP computer domain. Therefore, the choice between UNIX or a real time environment was needed. It turned out that the UNIX (HP-UX) computers (HP9000) do not respond as fast as RTE-A computers, while the RTE-A computers (HP1000) are not as fast as the HP9000 computers. After precise definition of the problem and careful analysis of the computer properties for this particular problem, HP1000 RTE-A machines were chosen. ESA

N94-28950# National Aerospace Lab., Tokyo (Japan). Aerodynamics Div.
RAREFIED GAS NUMERICAL WIND TUNNEL. PART 8: HOPE [KIHAKU KITAI SUCHI FUDO. 8: HOPE]
Katsuhisa Koura, Mikinari Takahira, and Hiroaki Matsumoto *In its* Proceedings of the 10th NAL Symposium on Aircraft Computational Aerodynamics Dec. 1992 p 17-20 In JAPANESE (For primary document see N94-28946 08-02)
Avail: CASI HC A01/MF A03

N94-28951# National Aerospace Lab., Tokyo (Japan).
NUMERICAL SIMULATION OF ARC HEATED WIND TUNNEL FLOW [AKU KANETSU GATA FUDO NO SUCHI KAISEKI]
Ryoji Takaki, Yasuhiro Wada, and Yasuo Watanabe *In its* Proceedings of the 10th NAL Symposium on Aircraft Computational Aerodynamics Dec. 1992 p 21-26 In JAPANESE (For primary document see N94-28946 08-02)
Avail: CASI HC A02/MF A03

N94-29649*# National Aeronautics and Space Administration. Ames Research Center, Moffett Field, CA.
LAMINAR FLOW SUPERSONIC WIND TUNNEL PRIMARY AIR INJECTOR
Brooke Edward Smith *In its* The 27th Aerospace Mechanisms Symposium May 1993 p 333-348 (For primary document see N94-29627 08-15)
Avail: CASI HC A03/MF A03

12 ASTRONAUTICS (GENERAL)

For extraterrestrial exploration see *91 Lunar and Planetary Exploration.*

N94-28583# Japan Space Utilization Promotion Center, Tokyo.
SURVEY REPORT OF JSUP SPACE ENVIRONMENT UTILIZATION RESEARCH COMMITTEE IN FISCAL YEAR 1992: PROTEIN CRYSTAL GROWTH SESSION [HEISEI 4 NENDO JSUP UCHU KANKYO RIYO KENKYUKAI HOKOKUSHO: TANPAKUSHITSU KESSHO SEICHO KENKYUKAI]
Yuhei Morita (Fuji Oil Co. Ltd., Tsukuba, Japan.), Nobuo Tanaka, Yukio Mitsui, Tomoya Ogawa, Tamaichi Ashida, Shinya Yoshikawa, Mitsuo Ataka, Nobuya Nagashima, Junichi Shigeta, and Koji Watanabe Mar. 1993 67 p In JAPANESE Sponsored by Japan Motorcycle Racing Organization, Tokyo, Japan
(JTN-94-80584) Avail: CASI HC A04/MF A01

This report reviews the protein crystal growth experiments under microgravity. The objective is to verify the potentials of protein crystal growth in the spacecraft. Principles of crystal growth, examples of the actual experiments such as cytochrome oxidized enzymes crystallization are introduced. The following concluding remarks were confirmed: (1) crystal growth is slower in microgravity. Crystal nucleus generation and crystal growth take place in a diffused rate-determining step due to lack of weight differences between solute and protein molecules; (2) protein molecules behave differently at crystal nucleus generation. Even in the same crystallization conditions, nucleus generation strongly depends on the electric charge on protein molecule surfaces, generating crystal nuclei with different physical properties from those of the earth counterparts; and (3) single crystals in high quality are obtained in microgravity, however, this does not necessarily depend on the shape or size of the single crystals. The possible cause is that because crystal nucleus generation is mainly determined by

the physical properties on the molecule surfaces, molecules meet more accurately, making better molecule arrangement within crystal nuclei.
Author (NASDA)

N94-30162# Japan Space Utilization Promotion Center, Tokyo.
SURVEY REPORT OF JSUP SPACE ENVIRONMENT UTILIZATION RESEARCH COMMITTEE IN FISCAL YEAR 1992: FUNCTIONAL NEW MATERIALS SESSION [HEISEI 4 NENDO JSUP UCHU KANKYO RIYO KENKYUKAI HOKOKUSHO: KINOSEI SHINSOZAI KENKYUKAI]
Yoshihiro Hamakawa, Akira Kinbara, Hiroshi Takimoto, Hideyuki Takakura, Takanobu Hori, Joji Shinohara, Yoji Ishikawa, Kenichi Sano, Shigenobu Okada, and Yoshinobu Yamamoto Mar. 1993 69 p In JAPANESE Sponsored by Japan Motorcycle Racing Organization
(JTN-94-80582) Avail: CASI HC A04/MF A01

Materials with super high purity can be obtained that benefit from the evolution in material refining and high-vacuum technologies for these past ten years. Taking advantages of microgravity environment, amorphous semiconductors made a remarkable improvement both in quality and quantity. Although there has not been an experiment utilizing the merit of high-vacuum environment, the environment is essential for film fabrication, from spattering to MBE (Molecular Beam Epitaxy) and plasma CVD (Chemical Vapor Deposition). It also has a potential function as a heat sink. Space is considered to be a favorable environment for many things including the followings that were investigated: semiconductor joining by atomic adhesion, fabrication of thin films of diamond and amorphous silicon alloys, CVD processes, production of super-minute grains, light element analysis by SIMS (Secondary Ion Mass Spectrometry), and anti-proton generation by laser accelerators. A solar breeder allows for the amount of solar batteries transported from the earth to be minimized, cutting down transportation costs tremendously. This report reviews the potentials of material processing in space. Processing technologies of spacecraft construction materials, thin solid films, and fine alloys are reviewed. Light element analyzing method and antiproton storing technology for liquid metal MHD (Magnetohydrodynamic) power generator are also reviewed.
Author (NASDA)

N94-30794# Japan Space Utilization Promotion Center, Tokyo.
SURVEY REPORT OF JSUP SPACE ENVIRONMENT UTILIZATION RESEARCH COMMITTEE IN FISCAL YEAR 1992: METALLIC MATERIALS SESSION [HEISEI 4 NENDO JSUP UCHU KANKYO RIYO KENKYUKAI HOKOKUSHO: KINZOKUKEI ZAIRYO KENKYUKAI]
Michio Yamazaki (Nishi-Tokyo Univ., Yamana, Japan.), Akihiko Kamio, Tetsuichi Motegi, Kazuhiko Kuribayashi, Takanobu Hori, Akira Tanji, Toshihiro Inatani, Yoshihiro Iwata, Masami Miyauchi, and Shigeru Oyama Mar. 1993 94 p In JAPANESE Sponsored by Japan Motorcycle Racing Organization
(JTN-94-80583) Avail: CASI HC A05/MF A01

This report describes space processing research conducted by NASA. The in-situ observation of separate liquid phase behavior of Al-Pb and Al-Bi alloys conducted in Japan is also reported. The following topics are included: space environment, space processing, microgravity, microgravity experiments, Hg-Cd-Te alloy, Ni-Sn alloy, Fe-Ni alloy, Al-Ga-As alloy, MBE (Molecular Beam Epitaxy), Ga-As crystal growth, semiconductor junctions, directional solidification, immiscible alloys, binary mixtures, succinonitrile solution, pushing phenomenon, containerless processing, containerless capsule dropping process, undercooling, Ostwald growing process, IML-1 (International Microgravity Laboratory-1), IML-2, Marangoni effect, liquid flow, ammonium chloride, molding, convection, segregation, metal combustion, flames, droplets, bubbles, STEP (Space Technology Experiment Platform), solid solution, sintering, metallic glasses, and viscosity. Author (NASDA)

13 ASTRODYNAMICS

Includes powered and free-flight trajectories; and orbital and launching dynamics.

N94-30237 Laval Univ. (Quebec). Dept. des Sciences Geodesiques et Teledetection.
APPLICATION OF EXTENDED LAGRANGE SERIES TO THE PRECISE DETERMINATION OF GLOBAL POSITIONING SATELLITE ORBITS M.S. Thesis [APPLICATION DES SERIES DE LAGRANGE ETENDUES A LA DETERMINATION PRECISE DES ORBITES DES SATELLITES GPS]
Caroline Huot Sep. 1993 128 p In FRENCH
(ISBN-0-315-85724-2; CTN-94-61152) Copyright Avail: Micromedia Ltd., Technical Information Centre, 240 Catherine Street, Suite 305, Ottawa, Ontario, K2P 2G8, Canada HC/MF

A new semi-analytical method is presented for solving the calculation of the perturbed orbits of Global Positioning System (GPS) satellites. Preliminary notions concerning coordinates, Keplerian orbits, and the perturbed orbit are established. The basic principles of the analytical and numerical method are introduced along with the models of the principal perturbations affecting the GPS satellites. Different methods of orbit calculation are reviewed to demonstrate the main advantages and drawbacks of each. A comparison proves that the method of extended Lagrange series has many advantages. Contrary to Cowell's method, the extended Lagrange series method does not require any starting algorithm. The proposed method is distinguished from other techniques of integration by its simple formulation and for its facility in analyzing one or many perturbations. Results obtained using the MicroCosm program are presented which indicate that calculation of the orbit by the extended Lagrange series method is accurate to within 4 cm and 70 cm for short arcs of 6 and 10 hours respectively.
CISTI

N94-30961 Iowa State Univ. of Science and Technology, Ames.
OPTIMAL LOW-THRUST, EARTH-MOON TRAJECTORIES Ph.D. Thesis
Craig Allen Kluever 1993 146 p
Avail: Univ. Microfilms Order No. DA9321183

A variety of optimal trajectories from a circular low-Earth parking orbit to a circular low-lunar parking orbit are computed for a range of low-thrust spacecraft. The problem is studied in the context of the classical restricted three-body problem. Minimum-fuel, planar trajectories with a fixed thrust-coast-thrust engine sequence are computed for both a 'high-end' low-thrust spacecraft and 'moderate' low-thrust nuclear electric propulsion (NEP) spacecraft. Since a low-thrust trajectory is a long duration transfer with slowly developing spirals about the Earth and Moon, the minimum-fuel Earth-Moon trajectory is obtained by formulating and successively solving a hierarchy of subproblems. The subproblems include optimal Earth-escape and Moon-capture trajectories and sub-optimal translunar trajectories. The complete minimum-fuel trajectory problem is eventually solved using a 'hybrid' direct/indirect method which utilizes the benefits of a direct optimization method and an indirect method from optimal control theory. Minimum-fuel transfers are also computed using a switching function structure which results in multiple thrust and coast arcs. In addition, a new combined vehicle and trajectory optimization problem of maximum payload fraction is formulated and solved. Finally, 3-D minimum-fuel trajectories are obtained for both the 'high-end' and 'moderate' low-thrust spacecraft. Numerical results are presented for various optimal Earth-Moon trajectories.
Dissert. Abstr.

N94-29655*# Jet Propulsion Lab., California Inst. of Tech., Pasadena.
ENHANCED ORBIT DETERMINATION FILTER SENSITIVITY ANALYSIS: ERROR BUDGET DEVELOPMENT
J. A. Estefan and P. D. Burkhart *In its* The Telecommunications and Data Acquisition Report 15 Feb. 1994 p 24-36 (For primary document see N94-29652 08-32)
(RTOP 310-10-63-50-00)
Avail: CASI HC A03/MF A03

N94-29656*# Jet Propulsion Lab., California Inst. of Tech., Pasadena.
ENHANCED ORBIT DETERMINATION FILTER: INCLUSION OF GROUND SYSTEM ERRORS AS FILTER PARAMETERS
W. C. Masters, D. J. Scheeres, and S. W. Thurman *In its* The Telecommunications and Data Acquisition Report 15 Feb. 1994

p 37-41 (For primary document see N94-29652 08-32)
(RTOP 310-10-63-50-00)
Avail: CASI HC A01/MF A03

N94-29666*# Jet Propulsion Lab., California Inst. of Tech., Pasadena.
TOPEX/POSEIDON OPERATIONAL ORBIT DETERMINATION RESULTS USING GLOBAL POSITIONING SATELLITES
J. Guinn, J. Jee, P. Wolff, F. Lagattuta, T. Drain, and V. Sierra *In its* The Telecommunications and Data Acquisition Report 15 Feb. 1994 p 163-174 (For primary document see N94-29652 08-32)
(RTOP 314-40-22-42-05)
Avail: CASI HC A03/MF A03

14 GROUND SUPPORT SYSTEMS AND FACILITIES (SPACE)

Includes launch complexes, research and production facilities; ground support equipment, e.g., mobile transporters; and simulators.

For related information see also *09 Research and Support Facilities (Air).*

N94-28413# Technical Research Centre of Finland, Espoo.
TESTING LABORATORIES AS NOTIFIED BODIES
Jarl Forsten 1993 13 p
(PB94-132396; VTT/RN-1458; ISBN-951-38-4352-1) Copyright Avail: CASI HC A03/MF A01

Testing laboratories can - if they fulfil the requirements - be appointed as notified bodies responsible for certain EC Directives. The notification process has been analyzed from the viewpoint of testing laboratories. The tasks the testing laboratory must take on board when acting as a notified body have been identified. As testing laboratories can also act as notified bodies, many laboratories will expand their activities in that direction. They have to, of course, demonstrate their capability, but the decision will mainly be related to expected market developments. The questions of financing certain infrastructural costs as well as of challengability are open for further discussion. NTIS

N94-29470*# National Aeronautics and Space Administration. Marshall Space Flight Center, Huntsville, AL.
NASA MARSHALL SPACE FLIGHT CENTER SOLAR OBSERVATORY REPORT, JULY - OCTOBER 1993
J. E. Smith Apr. 1994 20 p
(NASA-TM-108448; NAS 1.15:108448) Avail: CASI HC A03/MF A01

This report provides a description of the NASA Marshall Space Flight Center's Solar Vector Magnetograph Facility and gives a summary of its observations and data reduction during June-October 1993. The systems that make up the facility are a magnetograph telescope, an H-alpha telescope, a Questar telescope, and a computer code. Author

15 LAUNCH VEHICLES AND SPACE VEHICLES

Includes boosters; operating problems of launch/space vehicle systems; and reusable vehicles.

For related information see also *20 Spacecraft Propulsion and Power.*

N94-28836*# Virginia Polytechnic Inst. and State Univ., Blacksburg. Dept. of Electrical Engineering.
BEAM SCANNING OFFSET CASSEGRAIN REFLECTOR ANTENNAS BY SUBREFLECTOR MOVEMENT Final Report
James W. LaPean, Jr. and Warren L. Stutzman Mar. 1994 208 p
(Grant NAG1-859; RTOP 233-01-03-22)
(NASA-CR-191604; NAS 1.26:191604; SATCOM-93-19) Avail: CASI HC A10/MF A03

In 1987 a NASA panel recommended the creation of the Mission to Planet Earth. This mission was intended to apply to remote sensing experience of the space community to earth remote sensing to enhance the understanding of the climatological processes of our planet and to determine if, and to what extent, the hydrological cycle of Earth is being affected by human activity. One of the systems required for the mission was a wide scanning, high gain reflector antenna system for use in radiometric remote sensing from geostationary orbit. This work describes research conducted at Virginia Tech into techniques for beam scanning offset Cassegrain reflector antennas by subreflector translation and rotation. Background material relevant to beam scanning antenna systems and offset Cassegrain reflector antenna system is presented. A test case is developed based on the background material. The test case is beam scanned using two geometrical optics methods of determining the optimum subreflector position for the desired scanned beam direction. Physical optics far-field results are given for the beam scanned systems. The test case system is found to be capable of beam scanning over a range of 35 half-power beamwidths while maintaining a 90 percent beam efficiency or 50 half-power beamwidths while maintaining less than I dB of gain loss during scanning. Author

N94-29369*# National Aeronautics and Space Administration. Lyndon B. Johnson Space Center, Houston, TX.
HEAVY-LIFT VEHICLE-LAUNCHED SPACE STATION METHOD AND APPARATUS Patent Application
Donald C. Wade, inventor (to NASA), Horatio DeLaFuente, inventor (to NASA), Reginald B. Berka, inventor (to NASA), Steven L. Rickman, inventor (to NASA), Edgar O. Castro, inventor (to NASA), Kornel Nagy, inventor (to NASA), Clarence J. Wesselski, inventor (to NASA), Timothy E. Pelischek, inventor (to NASA), and John A. Schleisling, inventor (to NASA) 3 Dec. 1993 40 p
(NASA-Case-MSC-21760-1; NAS 1.71:MSC-21760-1; US-Patent-Appl-SN-161038) Avail: CASI HC A03/MF A01

Methods and apparatus are provided for a single heavylift launch to place a complete, operational space station on-orbit. A payload including the space station takes the place of a Shuttle Orbiter using the launch vehicle of the Shuttle Orbiter. The payload includes a forward shroud, a core module, a propulsion module, and a transition module between the core module and the propulsion module. The essential subsystems are pre-integrated and verified on Earth. The core module provides means for attaching international modules with minimum impact to the overall design. The space station includes six control moment gyros for selectably operating in either LVLH (local-vertical local-horizontal) or SI (solar inertial) flight modes. NASA

N94-29627*# National Aeronautics and Space Administration. Ames Research Center, Moffett Field, CA.
THE 27TH AEROSPACE MECHANISMS SYMPOSIUM
Ron Mancini, comp. May 1993 384 p Symposium held in Moffett Field, CA, 12-14 May 1993; sponsored by NASA, Washington, California Inst. of Tech., and LMSC
(NASA-CP-3205; A-93053; NAS 1.55:3205) Avail: CASI HC A17/MF A03

The proceedings of the 27th Aerospace Mechanisms Symposium, which was held at ARC, Moffett Field, California, on 12-14 May 1993, are reported. Technological areas covered include the following: actuators, aerospace mechanism applications for ground support equipment, lubricants, latches, connectors, robotic mechanisms, and other mechanisms for large space structures. For individual titles, see N94-29628 through N94-29651.

N94-29628*# European Space Agency. European Space Research and Technology Center, ESTEC, Noordwijk (Netherlands).
COLLECTING COMETARY SOIL SAMPLES? DEVELOPMENT OF THE ROSETTA SAMPLE ACQUISITION SYSTEM **c90**
P. A. Coste, M. Fenzi, and Michael Eiden *In* NASA. Ames Research Center, The 27th Aerospace Mechanisms Symposium May 1993 p 1-19 (For primary document see N94-29627 08-15)
Avail: CASI HC A03/MF A03

In the reference scenario of the ROSETTA CNRS mission, the Sample Acquisition System is mounted on the Comet Lander. Its tasks are to acquire three kinds of cometary samples and to transfer them to the Earth Return Capsule. Operations are to be performed in vacuum and microgravity, on a probably rough and dusty surface, in a largely unknown material, at temperatures in the order of 100 K. The concept and operation of the Sample Acquisition System are presented. The design of the prototype corer and surface sampling tool, and of the equipment for testing them at

cryogenic temperatures in ambient conditions and in vacuum in various materials representing cometary soil, are described. Results of recent preliminary tests performed in low temperature thermal vacuum in a cometary analog ice-dust mixture are provided. Author

N94-29629*# National Aeronautics and Space Administration. Lewis Research Center, Cleveland, OH.

A COMPACT ROLLER-GEAR PITCH-YAW JOINT MODULE: DESIGN AND CONTROL ISSUES **c37**

Mark E. Dohring (Case Western Reserve Univ., Cleveland, OH.), William J. Anderson (NASTEC, Inc., Cleveland, OH.), Wyatt S. Newman (Case Western Reserve Univ., Cleveland, OH.), and Douglas A. Rohn *In* NASA. Ames Research Center, The 27th Aerospace Mechanisms Symposium May 1993 p 21-36 (For primary document see N94-29627 08-15)

Avail: CASI HC A03/MF A03

Robotic systems have been proposed as a means of accomplishing assembly and maintenance tasks in space. The desirable characteristics of these systems include compact size, low mass, high load capacity, and programmable compliance to improve assembly performance. In addition, the mechanical system must transmit power in such a way as to allow high performance control of the system. Efficiency, linearity, low backlash, low torque ripple, and low friction are all desirable characteristics. This work presents a pitch-yaw joint module designed and built to address these issues. Its effectiveness as a two degree-of-freedom manipulator using natural admittance control, a method of force control, is demonstrated. Author (revised)

N94-29630*# Jet Propulsion Lab., California Inst. of Tech., Pasadena.

MARS ROVER MECHANISMS DESIGNED FOR ROCKY 4 **c37**

Tommaso P. Rivellini *In* NASA. Ames Research Center, The 27th Aerospace Mechanisms Symposium May 1993 p 37-49 (For primary document see N94-29627 08-15)

Avail: CASI HC A03/MF A03

A Mars rover prototype vehicle named Rocky 4 was designed and built at JPL during the fall of 1991 and spring 1992. This vehicle is the fourth in a series of rovers designed to test vehicle mobility and navigation software. Rocky 4 was the first attempt to design a vehicle with 'flight like' mass and functionality. It was consequently necessary to develop highly efficient mechanisms and structures to meet the vehicles very tight mass limit of 3 Kg for the entire mobility system (7 Kg for the full system). This paper will discuss the key mechanisms developed for the rover's innovative drive and suspension system. These are the wheel drive and strut assembly, the rocker-bogie suspension mechanism and the differential pivot. The end-to-end design, analysis, fabrication and testing of these components will also be discussed as will their performance during field testing. The lessons learned from Rocky 4 are already proving invaluable for the design of Rocky 6. Rocky 6 is currently being designed to fly on NASA's MESUR mission to Mars scheduled to launch in 1996. Author (revised)

N94-29631*# Nippon Telegraph and Telephone Public Corp., Yokosuka (Japan). Radio Communication Systems Labs.

A MODULE CONCEPT FOR A CABLE-MESH DEPLOYABLE ANTENNA **c32**

Akira Meguro *In* NASA. Ames Research Center, The 27th Aerospace Mechanisms Symposium May 1993 p 51-66 (For primary document see N94-29627 08-15)

Avail: CASI HC A03/MF A03

This paper describes the design, manufacture, and deployment tests of a modular mesh deployable antenna. Reaction forces and moments created by a mesh and cable network are estimated using CASA. Deployment analysis is carried out using DADS. Three types of deployable antenna modules are developed and fabricated. Their design approach and deployment characteristics are also presented. Ground deployment tests are performed to verify design criteria. Author

N94-29632*# Astro Aerospace Corp., Carpinteria, CA.

WAVES IN SPACE PLASMA DIPOLE ANTENNA SUBSYSTEM **c32**

Mark Thomson *In* NASA. Ames Research Center, The 27th Aerospace Mechanisms Symposium May 1993 p 67-82 (For primary document see N94-29627 08-15)

Avail: CASI HC A03/MF A03

The Waves In Space Plasma (WISP) flight experiment requires a 50-meter-long deployable dipole antenna subsystem (DASS) to radiate radio frequencies from the STS Orbiter cargo bay. The transmissions are to excite outer ionospheric plasma between the dipole and a free-flying receiver (Spartan) for scientific purposes. This report describes the singular DASS design requirements and how the resulting design satisfies them. A jettison latch is described in some detail. The latch releases the antenna in case of any problems which might prevent the bay doors from closing for re-entry and landing of the Orbiter. Author

N94-29633*# National Aeronautics and Space Administration. Langley Research Center, Hampton, VA.

DESIGN AND TESTING OF THE LITE VARIABLE FIELD STOP MECHANISM **c37**

Robert A. Dillman *In* NASA. Ames Research Center, The 27th Aerospace Mechanisms Symposium May 1993 p 83-92 (For primary document see N94-29627 08-15)

Avail: CASI HC A02/MF A03

The Variable Field Stop (VFS) is a rotary mechanism that reliably positions any of four aperture plates in the optical path of a spaceflight experiment, limiting the amount of light reaching the detectors. This paper discusses the design, operation, and testing of the VFS. Author

N94-29634*# National Aeronautics and Space Administration. Langley Research Center, Hampton, VA.

INTEGRATION OF PYROTECHNICS INTO AEROSPACE SYSTEMS **c28**

Laurence J. Bement and Morry L. Schimmel *In* NASA. Ames Research Center, The 27th Aerospace Mechanisms Symposium May 1993 p 93-106 (For primary document see N94-29627 08-15)

Avail: CASI HC A03/MF A03

The application of pyrotechnics to aerospace systems has been resisted because normal engineering methods cannot be used in design and evaluation. Commonly used approaches for energy sources, such as electrical, hydraulic and pneumatic, do not apply to explosive and pyrotechnic devices. This paper introduces the unique characteristics of pyrotechnic devices, describes how functional evaluations can be conducted, and demonstrates an engineering approach for pyrotechnic integration. Logic is presented that allows evaluation of two basic types of pyrotechnic systems to demonstrate functional margin. Author

N94-29635*# Space Industries, Inc., League City, TX.

RETENTION LATCH MECHANISM FOR THE WAKE SHIELD FACILITY **c37**

Timothy G. Vendrely *In* NASA. Ames Research Center, The 27th Aerospace Mechanisms Symposium May 1993 p 107-120 (For primary document see N94-29627 08-15)

Avail: CASI HC A03/MF A03

The Wake Shield Facility (WSF) is a space transportation system (STS) payload that is scheduled for launch on STS-60 in November, 1993. It is being designed, tested and integrated into the STS by Space Industries Inc. for the University of Houston's Space Vacuum Epitaxy Center, a NASA Center for the Commercial Development of Space. The WSF is composed of two main components: a cross-bay carrier and a free-flying experimental platform. The WSF's primary objective is the epitaxial growth of thin films by controlled beam techniques in the ultra-high vacuum that exists in the wake of the free-flyer. The Retention Latch Mechanism (RLM) has been developed to act as the structural interface between the free-flyer and the carrier. Author

N94-29636*# National Aeronautics and Space Administration. Marshall Space Flight Center, Huntsville, AL.

DEVELOPMENT AND TESTING OF THE AUTOMATED FLUID INTERFACE SYSTEM **c18**

Martha E. Milton and Tony R. Tyler *In* NASA. Ames Research Center, The 27th Aerospace Mechanisms Symposium May 1993 p 121-135 (For primary document see N94-29627 08-15)

Avail: CASI HC A03/MF A03

The Automated Fluid Interface System (AFIS) is an advanced development program aimed at becoming the standard interface for satellite servicing for years to come. The AFIS will be capable of transferring propellants, fluids, gasses, power, and cryogens from a tanker to an orbiting satellite. The AFIS program currently under consideration is a joint venture

between the NASA/Marshall Space Flight Center and Moog, Inc. An engineering model has been built and is undergoing development testing to investigate the mechanism's abilities. Author

N94-29637*# Starsys Research Corp., Boulder, CO.
METAL BAND DRIVES IN SPACECRAFT MECHANISMS **c37**
Daryl Maus *In* NASA. Ames Research Center, The 27th Aerospace Mechanisms Symposium May 1993 p 137-146 (For primary document see N94-29627 08-15)
Avail: CASI HC A02/MF A03

Transmitting and changing the characteristics of force and stroke is a requirement in nearly all mechanisms. Examples include changing linear to rotary motion, providing a 90 deg change in direction, and amplifying stroke or force. Requirements for size, weight, efficiency and reliability create unique problems in spacecraft mechanisms. Flexible metal band and cam drive systems provide powerful solutions to these problems. Band drives, rack and pinion gears, and bell cranks are compared for effectiveness. Band drive issues are discussed including materials, bend radius, fabrication, attachment and reliability. Numerous mechanisms are shown which illustrate practical applications of band drives. Author

N94-29638*# Jet Propulsion Lab., California Inst. of Tech., Pasadena.
POINTING MECHANISMS FOR THE SHUTTLE RADAR LABORATORY **c37**
Gerald W. Lilienthal, Argelio M. Olivera, and Lori R. Shiraishi *In* NASA. Ames Research Center, The 27th Aerospace Mechanisms Symposium May 1993 p 147-164 (For primary document see N94-29627 08-15)
Avail: CASI HC A03/MF A03

The Shuttle Radar Laboratory (SRL) is scheduled for launch in December of 1993 on the first of its two missions. The SRL has three major radar instruments: two distributed phased-array antennas, which make up the Spaceborne Imaging Radar-C System (SIR-C) and are capable of being electronically steered, and one X-Band Synthetic Aperture Radar (X-SAR), which is pointed mechanically by a suite of mechanisms. This paper will describe these mechanisms and summarize the development difficulties that were encountered in bringing them from the design stage through prototype development and protoflight testing. Author

N94-29639*# Honeywell, Inc., Glendale, AZ. Satellite Systems Operation.
OPTICAL CHOPPER ASSEMBLY FOR THE MARS OBSERVER **c74**
Terry Allen *In* NASA. Ames Research Center, The 27th Aerospace Mechanisms Symposium May 1993 p 165-180 (For primary document see N94-29627 08-15)
Avail: CASI HC A03/MF A03

This paper describes the Honeywell-developed Optical Chopper Assembly (OCA), a component of Mars Observer spacecraft's Pressure Modulator Infrared Radiometer (PMIRR) science experiment, which will map the Martian atmosphere during 1993 to 1995. The OCA is unique because of its constant accurate rotational speed, low electrical power consumption, and long-life requirements. These strict and demanding requirements were achieved by use of a number of novel approaches. Author

N94-29640*# Teldix Luftfahrt-Ausruestungs G.m.b.H., Heidelberg (Germany). Space Dept.
A GIMBALED LOW NOISE MOMENTUM WHEEL **c19**
U. Bichler and T. Eckardt *In* NASA. Ames Research Center, The 27th Aerospace Mechanisms Symposium May 1993 p 181-196 Sponsored in part by ESA (For primary document see N94-29627 08-15)
Avail: CASI HC A03/MF A03

The bus actuators are the heart and at the same time the Achilles' heel of accurate spacecraft stabilization systems, because both their performance and their perturbations can have a deciding influence on the achievable pointing accuracy of the mission. The main task of the attitude actuators, which are mostly wheels, is the generation of useful torques with sufficiently high bandwidth, resolution and accuracy. This is because the bandwidth of the whole attitude control loop and its disturbance rejection capability is dependent upon these factors. These useful torques shall be provided, without - as far as possible - parasitic noise like unbalance forces and torques and harmonics. This is because such variable frequency perturbations excite structural resonances which in turn disturb the operation of sensors and scientific instruments. High accuracy spacecraft will further require bus actuators for the three linear degrees of freedom (DOF) to damp structural oscillations excited by various sources. These actuators have to cover the dynamic range of these disturbances. Another interesting feature, which is not necessarily related to low noise performance, is a gimballing capability which enables, in a certain angular range, a three axis attitude control with only one wheel. The herein presented Teldix MWX, a five degree of freedom Magnetic Bearing Momentum Wheel, incorporates all the above required features. It is ideally suited to support, as a gyroscopic actuator in the attitude control system, all High Pointing Accuracy and Vibration Sensitive space missions. Author

N94-29641*# Aerospace Corp., El Segundo, CA. Mechanics and Materials Technology.
THE USE OF SCREENING TESTS IN SPACECRAFT LUBRICANT EVALUATION **c27**
Chris Kalogeras, Mike Hilton, David Carre, Stephen Didziulis, and Paul Fleischauer *In* NASA. Ames Research Center, The 27th Aerospace Mechanisms Symposium May 1993 p 197-217 (For primary document see N94-29627 08-15)
(Contract F04701-88-C-0089)
Avail: CASI HC A03/MF A03

A lubricant screening test fixture has been devised in order to satisfy the need to obtain lubricant performance data in a timely manner. This fixture has been used to perform short-term tests on potential lubricants for several spacecraft applications. The results of these tests have saved time by producing qualitative performance rankings of lubricant selections prior to life testing. To date, this test fixture has been used to test lubricants for 3 particular applications. The qualitative results from these tests have been verified by life test results and have provided insight into the function of various anti-wear additives. Author

N94-29642*# Lockheed Missiles and Space Co., Palo Alto, CA.
THREE HIGH DUTY CYCLE, SPACE-QUALIFIED MECHANISMS **c37**
David Akin, Ralph Horber, and Jake Wolfson *In* NASA. Ames Research Center, The 27th Aerospace Mechanisms Symposium May 1993 p 219-236 (For primary document see N94-29627 08-15)
(Contracts NAS5-30386; NAS5-26813; NAS8-37334)
Avail: CASI HC A03/MF A03

The Michelson Doppler Imager (MDI) is a scientific instrument aboard the Solar and Heliospheric Observatory (SOHO) spacecraft. In 1995, the spacecraft will be put into a halo orbit about the L1 Lagrangian point (equal Sun and Earth gravity). The MDI looks at the sun continuously and takes a picture with a large format CCD camera every 3 seconds. The design goal of the mission is 6 years, so over 60 million pictures will be taken. The sun, being a high intensity source, provides a signal with a single pixel noise level of 0.2 percent. Many images are combined to measure the oscillatory motion of the sun so very high performance is required of the mechanisms in order that they not add noise to the data. The MDI instrument is made up of two parts, the electronics package and the optics package. This paper describes the design and testing of three mechanisms on the MDI which are required to operate large numbers of times. Derived from text

N94-29643*# Deutsche Aerospace A.G., Munich (Germany).
PARACHUTE SWIVEL MECHANISM FOR PLANETARY ENTRY **c18**
R. Birner, J. Kaese, F. Koller, E. Muehlner, and H.-J. Luhmann *In* NASA. Ames Research Center, The 27th Aerospace Mechanisms Symposium May 1993 p 237-254 Sponsored by ESA and DASA (For primary document see N94-29627 08-15)
Avail: CASI HC A03/MF A03

A parachute swivel mechanism (PSM) for planetary entry missions such as a Mars probe (MARSNET) or return of cometary material samples (ROSETTA mission) has been developed. The purpose of the PSM is to decouple the spin of the probe from the parachute, with low friction torque, during both the deployment and descent phases. Critical requirements are high shock loads, low friction, low temperatures, and several years of storage in the deep space environment (during the cruise phase of the probe, prior to operation). The design uses a main thrust ball bearing to cope with the load requirement and a smaller thrust ball bearing for guiding of the shaft. Except for use on the Viking and Galileo swivels, it appears that this type of bearing has very rarely been employed in space mechanisms, so that little is known of its friction behavior with dry lubrication. A slip

ring assembly allows the transfer of electrical power for post-reefing of the parachute. A test program has been conducted covering the environmental conditions of Mars entry and Earth reentry. This paper describes requirement constraints, model missions of planetary entries, a bearing trade-off, analyses performed, design details, the lubrication system, and test results (friction torque versus load/spin rate). In addition, the design of the test rig is addressed. Author (revised)

N94-29644*# Hughes Space and Communications Group, El Segundo, CA.
LOW MELTING TEMPERATURE ALLOY DEPLOYMENT MECHANISM AND RECENT EXPERIMENTS **c26**
M. J. Madden *In* NASA. Ames Research Center, The 27th Aerospace Mechanisms Symposium May 1993 p 255-266 (For primary document see N94-29627 08-15)
Avail: CASI HC A03/MF A03

This paper describes the concept of a low melting temperature alloy deployment mechanism, U.S. Patent 4,842,106. It begins with a brief history of conventional dimethyl-silicone fluid damped mechanisms. Design fundamentals of the new melting alloy mechanism are then introduced. Benefits of the new over the old are compared and contrasted. Recent experiments and lessons learned complete this paper. Author (revised)

N94-29645*# National Aeronautics and Space Administration. Goddard Space Flight Center, Greenbelt, MD.
THE SOLAR ANOMALOUS AND MAGNETOSPHERIC PARTICLE EXPLORER (SAMPEX) YO-YO DESPIN AND SOLAR ARRAY DEPLOYMENT MECHANISM **c18**
James W. Kellogg *In* NASA. Ames Research Center, The 27th Aerospace Mechanisms Symposium May 1993 p 267-282 (For primary document see N94-29627 08-15)
Avail: CASI HC A03/MF A03

The SAMPEX spacecraft, successfully launched in July 1992, carried a yo-yo despin system and deployable solar arrays. The despin and solar array mechanisms formed an integral system as the yo-yo cables held the solar array release mechanism in place. The SAMPEX design philosophy was to minimize size and weight through the use of a predominantly single string system. The design challenge was to build a system in a limited space, which was reliable with minimal redundancy. This paper covers the design and development of the SAMPEX yo-yo despin and solar array deployment mechanisms. The problems encountered during development and testing will also be discussed. Author (revised)

N94-29646*# Lockheed Missiles and Space Co., Sunnyvale, CA.
LOCK-UP FAILURE OF A FOUR-BAR LINKAGE DEPLOYMENT MECHANISM **c37**
Michael Zinn *In* NASA. Ames Research Center, The 27th Aerospace Mechanisms Symposium May 1993 p 283-298 (For primary document see N94-29627 08-15)
Avail: CASI HC A03/MF A03

A successful failure investigation of a four-bar linkage deployment mechanism has been performed. Possible failure causes such as the mismatch of material coefficient of thermal expansion (CTE), excessive hinge friction, limit switch interference, and thermal gradient induced resistive preload were investigated and are discussed. The final conclusions and corrective actions taken are described. Finally, valuable lessons learned during the investigation are discussed. Author (revised)

N94-29647*# National Aeronautics and Space Administration. Langley Research Center, Hampton, VA.
MINIATURE LINEAR-TO-ROTARY MOTION ACTUATOR **c37**
Michael R. Sorokach, Jr. *In* NASA. Ames Research Center, The 27th Aerospace Mechanisms Symposium May 1993 p 299-314 (For primary document see N94-29627 08-15)
Avail: CASI HC A03/MF A03

A miniature hydraulic actuation system capable of converting linear actuator motion to control surface rotary motion has been designed for application to active controls on dynamic wind tunnel models. Due to space constraints and the torque requirements of an oscillating control surface at frequencies up to 50 Hertz, a new actuation system was developed to meet research objectives. This new actuation system was designed and developed to overcome the output torque limitations and fluid loss/sealing difficulties associated with an existing vane type actuator. Static control surface deflections and dynamic control surface oscillations through a given angle are provided by the actuation system. The actuator design has been incorporated into a transonic flutter model with an active trailing edge flap and two active spoilers. The model is scheduled for testing in the LaRC 16 Foot Transonic Dynamics Tunnel during Summer 1993. This paper will discuss the actuation system, its design, development difficulties, test results, and application to aerospace vehicles. Author

N94-29648*# National Aeronautics and Space Administration. Ames Research Center, Moffett Field, CA.
PORTABLE LINEAR SLED (PLS) FOR BIOMEDICAL RESEARCH **c51**
Will Vallotton (Sverdrup Technology, Inc., Moffett Field, CA.), Dennis Matsuhiro, Tom Wynn, and John Temple *In its* The 27th Aerospace Mechanisms Symposium May 1993 p 315-331 (For primary document see N94-29627 08-15)
(RTOP 199-16-12-17; RTOP 199-16-12-19; RTOP 199-90-63-20)
Avail: CASI HC A03/MF A03

The PLS is a portable linear motion generating device conceived by researchers at Ames Research Center's Vestibular Research Facility and designed by engineers at Ames for the study of motion sickness in space. It is an extremely smooth apparatus, powered by linear motors and suspended on air bearings which ride on precision ground ceramic ways. Author

N94-29649*# National Aeronautics and Space Administration. Ames Research Center, Moffett Field, CA.
LAMINAR FLOW SUPERSONIC WIND TUNNEL PRIMARY AIR INJECTOR **c09**
Brooke Edward Smith *In its* The 27th Aerospace Mechanisms Symposium May 1993 p 333-348 (For primary document see N94-29627 08-15)
Avail: CASI HC A03/MF A03

This paper describes the requirements, design, and prototype testing of the flex-section and hinge seals for the Laminar Flow Supersonic Wind Tunnel Primary Injector. The supersonic atmospheric primary injector operates between Mach 1.8 and Mach 2.2 with mass-flow rates of 62 to 128 lbm/s providing the necessary pressure reduction to operate the tunnel in the desired Reynolds number (Re) range. Author

N94-29650*# National Aeronautics and Space Administration. Marshall Space Flight Center, Huntsville, AL.
DESIGN AND TEST OF ELECTROMECHANICAL ACTUATORS FOR THRUST VECTOR CONTROL **c37**
J. R. Cowan and Rae Ann Weir *In* NASA. Ames Research Center, The 27th Aerospace Mechanisms Symposium May 1993 p 349-366 (For primary document see N94-29627 08-15)
Avail: CASI HC A03/MF A03

New control mechanisms technologies are currently being explored to provide alternatives to hydraulic thrust vector control (TVC) actuation systems. For many years engineers have been encouraging the investigation of electromechanical actuators (EMA) to take the place of hydraulics for spacecraft control/gimballing systems. The rationale is to deliver a lighter, cleaner, safer, more easily maintained, as well as energy efficient space vehicle. In light of this continued concern to improve the TVC system, the Propulsion Laboratory at the NASA George C. Marshall Space Flight Center (MSFC) is involved in a program to develop electromechanical actuators for the purpose of testing and TVC system implementation. Through this effort, an electromechanical thrust vector control actuator has been designed and assembled. The design consists of the following major components: Two three-phase brushless dc motors, a two pass gear reduction system, and a roller screw, which converts rotational input into linear output. System control is provided by a solid-state electronic controller and power supply. A pair of resolvers and associated electronics deliver position feedback to the controller such that precise positioning is achieved. Testing and evaluation is currently in progress. Goals focus on performance comparisons between EMA's and similar hydraulic systems. Author

N94-29651*# General Electric Co., San Jose, CA.
SP-100 CONTROL DRIVE ASSEMBLY DEVELOPMENT **c73**
Thomas Gleason, A. Richard Gilchrist, and Gary Schuster *In* NASA.

Ames Research Center, The 27th Aerospace Mechanisms Symposium May 1993 p 367-375 (For primary document see N94-29627 08-15)
Avail: CASI HC A02/MF A03

The SP-100 is an electrical generating nuclear power system for space operation. This paper describes the nuclear reactor control systems and the methods used to assure reliable performance for the 10-year design life. Reliable performance is achieved by redundancy and by selecting highly reliable components and design features. Reliability is quantified by analysis using established reliability data. Areas lacking reliability data are identified for development testing. A specific development test description is provided as an example to demonstrate how this process is meeting the system reliability goals. Author

16 SPACE TRANSPORTATION

Includes passenger and cargo space transportation, e.g., shuttle operations; and space rescue techniques.

For related information see also *03 Air Transportation and Safety* and *18 Spacecraft Design, Testing and Performance.* For space suits see *54 Man/System Technology and Life Support.*

N94-28827# RADEX, Inc., Bedford, MA.
SOCRATES SIMULATION OF THE EMISSION AT WAVELENGTH 6300 A GENERATED BY THE INTERACTION BETWEEN THE ATMOSPHERE AND THE SPACE SHUTTLE EXHAUST Scientific Report No. 2, 18 Feb. 1988 - 31 Dec. 1992
A. Setayesh and M. F. Tautz 31 Aug. 1993 44 p
(Contract F19628-93-C-0023)
(AD-A275567; RXR-93082; PL-TR-93-2186; AD-E201744) Avail: CASI HC A03/MF A01

The SOCRATES contamination-interaction code has been used to simulate the reactions between the space shuttle exhaust and the atmosphere at an altitude of 320 km. The investigation carries out the simulations for regions extending to 15 km from spacecraft. These simulations calculate the radiation from O(D1) - O(P3) photons as function of time for orientations of engine firing into the ram, perpendicular, and into the wake of the shuttle motion. The IRMA plotting program has been used to depict in color the time development of the shuttle plume. DTIC

N94-29355*# Raytheon Co., Waltham, MA. Electronic Components Div.
A TRANSPORTRONIC SOLUTION TO THE PROBLEM OF INTERORBITAL TRANSPORTATION
William C. Brown Jul. 1992 178 p
(Contract NAS3-25066)
(NASA-CR-191152; NAS 1.26:191152; PT-7452) Avail: CASI HC A09/MF A02

An all-electronic transportation system described by the term 'transportronics' is examined as a means of solving the current problem of the high cost of transporting material from low-Earth orbit (LEO) to geostationary orbit (GEO). In this transportation system, low cost electric energy at the surface of the Earth is efficiently converted into microwave power which is then efficiently formed into a narrow beam which is kept incident upon the orbital transfer vehicles (OTV's) by electronic tracking. The incident beam is efficiently captured and converted into DC power by a device which has a very high ratio of DC power output to its mass. Because the mass of the electric thruster is also low, the resulting acceleration is unprecedented for electric-propelled vehicles. However, the performance of the system in terms of transit times from LEO to GEO is penalized by the short time of contact between the beam and the vehicle in low-Earth orbits. This makes it necessary to place the Earth based transmitters and the vehicles in the equatorial plane thus introducing many geopolitical factors. Technically, however, such a system as described in the report may out-perform any other approach to transportation in the LEO to GEO regime. The report describes and analyzes all portions of the beamed microwave power transmission system in considerable detail. An economic analysis of the operating and capital costs is made with the aid of a reference system capable of placing about 130,000 kilograms of payload into GEO each year. More mature states of the system are then examined, to a level in which 60,000 metric tons per year could be placed into GEO. Author

N94-29714# Ministry of Education, Science and Culture, Sagamihara (Japan).
START OF SPACE TOURISM [SUPESU TSURIZUMU KENKYU KOTOHAJIME]
Makoto Nagatomo *In* Society of Medical Research for Space Station, The MERSS 5th Symposium on Space Medicine: Medical and Physiological Experiment Utilizing Parabolic Flight Mar. 1993 p 26-33 In JAPANESE (For primary document see N94-29709 08-52)
Avail: CASI HC A02/MF A01

17 SPACE COMM., SPACECRAFT COMM., COMMAND & TRACKING

Includes telemetry; space communications networks; astronavigation and guidance; and radio blackout.

For related information see also *04 Aircraft Communications and Navigation* and *32 Communications and Radar.*

N94-29880*# New Mexico State Univ., Las Cruces. Center for Space Telemetering and Telecommunications Systems.
AN ANALYSIS OF CARRIER PHASE JITTER IN AN MPSK RECEIVER UTILIZING MAP ESTIMATION Ph.D. Thesis Semiannual Status Report, Jul. 1993 - Jan. 1994
William P. Osborne 2 May 1994 321 p
(Grant NAG5-1491)
(NASA-CR-195806; NAS 1.26:195806) Avail: CASI HC A14/MF A03

The use of 8 and 16 PSK TCM to support satellite communications in an effort to achieve more bandwidth efficiency in a power-limited channel has been proposed. This project addresses the problem of carrier phase jitter in an M-PSK receiver utilizing the high SNR approximation to the maximum aposteriori estimation of carrier phase. In particular, numerical solutions to the 8 and 16 PSK self-noise and phase detector gain in the carrier tracking loop are presented. The effect of changing SNR on the loop noise bandwidth is also discussed. These data are then used to compute variance of phase error as a function of SNR. Simulation and hardware data are used to verify these calculations. The results show that there is a threshold in the variance of phase error versus SNR curves that is a strong function of SNR and a weak function of loop bandwidth. The M-PSK variance thresholds occur at SNR's in the range of practical interest for the use of 8 and 16-PSK TCM. This suggests that phase error variance is an important consideration in the design of these systems. Author

N94-29621*# Jet Propulsion Lab., California Inst. of Tech., Pasadena.
PHASING THE VERY LARGE ARRAY ON GALILEO IN THE PRESENCE OF JUPITER'S STRONG RADIO EMISSION
J. S. Ulvestad *In its* The Telecommunications and Data Acquisition Report 15 May 1991 p 69-82 (For primary document see N94-29613 08-32)
(RTOP 314-40-31-30-03)
Avail: CASI HC A03/MF A02

18 SPACECRAFT DESIGN, TESTING AND PERFORMANCE

Includes satellites; space platforms; space stations; spacecraft systems and components such as thermal and environmental controls; and attitude controls.

For life support systems see *54 Man/System Technology and Life Support.* For related information see also *05 Aircraft Design, Testing and Performance, 39 Structural Mechanics,* and *16 Space Transportation.*

N94-28417*# Martin Marietta Corp., Denver, CO. Astronautics Group.
INTEGRATED ACTIVE AND PASSIVE CONTROL DESIGN METHODOLOGY FOR THE LaRC CSI EVOLUTIONARY MODEL Final Report
Christopher T. Voth, Kenneth E. Richards, Jr., Eric Schmitz, Russel N. Gehling, and Daniel R. Morgenthaler Apr. 1994 366 p

(Contract NAS1-19371; RTOP 590-14-91-52)
(NASA-CR-4580; NAS 1.26:4580) Avail: CASI HC A16/MF A03

A general design methodology to integrate active control with passive damping was demonstrated on the NASA LaRC CSI Evolutionary Model (CEM), a ground testbed for future large, flexible spacecraft. Vibration suppression controllers designed for Line-of Sight (LOS) minimization were successfully implemented on the CEM. A frequency-shaped H2 methodology was developed, allowing the designer to specify the roll-off of the MIMO compensator. A closed loop bandwidth of 4 Hz, including the six rigid body modes and the first three dominant elastic modes of the CEM was achieved. Good agreement was demonstrated between experimental data and analytical predictions for the closed loop frequency response and random tests. Using the Modal Strain Energy (MSE) method, a passive damping treatment consisting of 60 viscoelastically damped struts was designed, fabricated and implemented on the CEM. Damping levels for the targeted modes were more than an order of magnitude larger than for the undamped structure. Using measured loss and stiffness data for the individual damped struts, analytical predictions of the damping levels were very close to the experimental values in the (1-10) Hz frequency range where the open loop model matched the experimental data. An integrated active/passive controller was successfully implemented on the CEM and was evaluated against an active-only controller. A two-fold increase in the effective control bandwidth and further reductions of 30 percent to 50 percent in the LOS RMS outputs were achieved compared to an active-only controller. Superior performance was also obtained compared to a High-Authority/Low-Authority (HAC/LAC) controller. Author (revised)

N94-28477# Sandia National Labs., Albuquerque, NM.
BAG: A CODE FOR PREDICTING THE PERFORMANCE OF A GAS BAG IMPACT ATTENUATION SYSTEM FOR THE PATHFINDER LANDER
J. K. Cole and D. E. Waye Nov. 1993 57 p
(Contract DE-AC04-94AL-85000)
(DE94-003688; SAND-93-2133) Avail: CASI HC A04/MF A01

The National Aeronautics and Space Administration (NASA) is planning to launch a network of scientific probes to Mars beginning in late 1996. The precursor to this network will be PATHFINDER. Decelerating PATHFINDER from the high speed of its approach to Mars will require the use of several deceleration techniques working in series. The Jet Propulsion Laboratory (JPL) has proposed that gas bags be used to cushion the payload's ground impact on Mars. This report presents the computer code, BAG, which has been developed to calculate the pneumatic performance of gas bag impact attenuators and the one-dimensional rigid-body dynamic performance of a payload during ground impact. DOE

N94-28697*# National Aeronautics and Space Administration. Lewis Research Center, Cleveland, OH.
SECOND NASA WORKSHOP ON WIRING FOR SPACE APPLICATIONS
Jan. 1994 196 p Workshop held in Cleveland, OH, 6-7 Oct. 1993; sponsored by NASA, Washington and NASA. Lewis Research Center Original contains color illustrations
(RTOP 323-57-4A)
(NASA-CP-3244; E-8294; NAS 1.55:3244) Avail: CASI HC A09/MF A03; 8 functional color pages

This document contains the proceedings of the Second NASA Workshop on Wiring for Space Applications held at NASA LeRC in Cleveland, OH, 6-7 Oct. 1993. The workshop was sponsored by NASA Headquarters Code QW Office of Safety and Mission Quality, Technical Standards Division and hosted by NASA LeRC, Power Technology Division, Electrical Components and Systems Branch. The workshop addressed key technology issues in the field of electrical power wiring for space applications. Speakers from government, industry, and academia presented and discussed topics on arc tracking phenomena, wiring system design, insulation constructions, and system protection. Presentation materials provided by the various speakers are included in this document. For individual titles, see N94-28698 through N94-28717.

N94-28698*# European Space Agency. European Space Research and Technology Center, ESTEC, Noordwijk (Netherlands).
ESTEC WIRING TEST PROGRAMME MATERIALS RELATED PROPERTIES **c33**
M. D. Judd *In* NASA. Lewis Research Center, Second NASA Workshop on Wiring for Space Applications Jan. 1994 p 15-18 (For primary document see N94-28697 08-18)
Avail: CASI HC A01/MF A03; 8 functional color pages

Electrical wires are considered as EEE parts and are covered within the ESA SCC specification series (ESA SCC 3901/XXX). This specification defines the principal properties of the wires including insulation/lay-up and electrical properties. Some additional space related materials requirements are also included, requirements such as outgassing and silver plating thickness. If a project has additional materials requirements over and above those covered by the relevant SCC specification, then additional testing is required. This is especially true for crewed spacecraft. The following topics are discussed in this context: additional requirements for manned spacecraft; flammability; arc tracking; thermal decomposition; microbial surface growth; and ageing. Author (revised)

N94-28699*# Wright Lab., Wright-Patterson AFB, OH.
ROBUST 300 C WIRE INSULATION SYSTEM **c33**
John G. Nairus *In* NASA. Lewis Research Center, Second NASA Workshop on Wiring for Space Applications Jan. 1994 p 19-23 (For primary document see N94-28697 08-18)
Avail: CASI HC A01/MF A03; 8 functional color pages

The objective of this program is to identify, develop, and demonstrate an optimum wire insulation system that is capable of continuous operation at 300 C. The system is to possess a combination of superior electrical (AC or DC), mechanical, and physical properties over the KAPTON (trademark) derived insulations described in MIL-W-81381 and those hybrid constructions identified in Air Force contract F33615-89-C-5606, commonly known as TKT constructions. Author (revised)

N94-28700*# Sverdrup Technology, Inc., Brook Park, OH.
NASA WIRING PROGRAM: SURVEY OF NASA EXPERIENCES IN WIRING SYSTEM SAFETY **c33**
Mark W. Stavnes *In* NASA. Lewis Research Center, Second NASA Workshop on Wiring for Space Applications Jan. 1994 p 27-39 Original contains color illustrations (For primary document see N94-28697 08-18)
Avail: CASI HC A03/MF A03; 8 functional color pages

The objective of this program is to address safety and reliability issues of complete wiring systems. The plans for carrying out the objective include the following: determine the wiring system design factors; investigate circuit protection technologies; and address manufacturing and maintenance procedures. Author (revised)

N94-28701*# National Aeronautics and Space Administration. Lewis Research Center, Cleveland, OH.
SELECTION OF THE SPACE STATION FREEDOM (SSF) FLAT COLLECTOR CIRCUIT (FCC) INSULATION MATERIAL **c33**
Dawn Emerson *In its* Second NASA Workshop on Wiring for Space Applications Jan. 1994 p 41-49 (For primary document see N94-28697 08-18)
Avail: CASI HC A02/MF A03; 8 functional color pages

The topics are presented in viewgraph form and include the following: function of the Space Station Freedom (SSF) Flat Collector Circuit (FCC); requirements of the FCC which affect the selection of the insulation material; data to support the selection of the FCC insulation material; development history; modified design; coverlay testing; effects on modified design on FCC; arc tracking tests performed on FCC; and arc tracking test results. CASI

N94-28702*# National Aeronautics and Space Administration. Goddard Space Flight Center, Greenbelt, MD.
NASA PARTS PROGRAM OFFICE RESPONSIBILITIES **c33**
Patrick L. Kilroy *In* NASA. Lewis Research Center, Second NASA Workshop on Wiring for Space Applications Jan. 1994 p 51-53 (For primary document see N94-28697 08-18)
Avail: CASI HC A01/MF A03; 8 functional color pages

The topics are presented in viewgraph form and include the following: NASA Parts Program Office responsibilities; NASA Parts Project Office responsibilities; development priorities; and candidate functions for EPIMS baseline. CASI

N94-28703*# Paramax Systems Corp., Lanham, MD.
NASA PARTS PROJECT OFFICE: BASIC GOALS **c33**
Jeannette Plante *In* NASA. Lewis Research Center, Second NASA Workshop on Wiring for Space Applications Jan. 1994 p 55-57 (For primary document see N94-28697 08-18)
Avail: CASI HC A01/MF A03; 8 functional color pages

The topics are presented in viewgraph form and include the following: a standard part per MIL-STD-975; standard wire in MIL-STD-975; what is space grade, grade 1, and grade 2; conduit and catalyst for information transfer; NASA Interconnection Standardization Working Group; and present and past wire issues. CASI

N94-28704*# Naval Air Warfare Center, Indianapolis, IN.
NAVAIR AIRCRAFT WIRING STANDARDIZATION AND QUALIFICATION PROGRAM **c33**
Thomas Meiner *In* NASA. Lewis Research Center, Second NASA Workshop on Wiring for Space Applications Jan. 1994 p 59-61 (For primary document see N94-28697 08-18)
Avail: CASI HC A01/MF A03; 8 functional color pages

The topics are presented in viewgraph form and include the following: wiring responsibilities; purpose of the program; measurement of program effectiveness; results; and summary. CASI

N94-28705*# Naval Air Warfare Center, Indianapolis, IN.
ORGANIZED WIRING SYSTEMS **c33**
Thomas Meiner *In* NASA. Lewis Research Center, Second NASA Workshop on Wiring for Space Applications Jan. 1994 p 63-77 Original contains color illustrations (For primary document see N94-28697 08-18)
Avail: CASI HC A03/MF A03; 8 functional color pages

The topics are presented in viewgraph form and include the following: wiring systems, quality control, qualification and standardization, and maintenance costs. CASI

N94-28706*# National Electrical Mfrs. Association, Washington, DC. Wire and Cable Div.
NEMA WIRE AND CABLE STANDARDS DEVELOPMENT PROGRAMS **c33**
Robert W. Baird *In* NASA. Lewis Research Center, Second NASA Workshop on Wiring for Space Applications Jan. 1994 p 79-93 (For primary document see N94-28697 08-18)
Avail: CASI HC A03/MF A03; 8 functional color pages

The National Electrical Manufacturers Association (NEMA) is the nation's largest trade association for manufacturers of electrical equipment. Its member companies produce components, end-use equipment and systems for the generation, transmission, distribution, control and use of electricity. The wire and cable division is presented in 6 sections: building wire and cable, fabricated conductors, flexible cords, high performance wire and cable, magnet wire, and power and control cable. Participating companies are listed. Derived from text

N94-28707*# National Aeronautics and Space Administration. Marshall Space Flight Center, Huntsville, AL.
MSFC INSPECTIONS OF INSTALLED POLYIMIDE WIRE **c33**
Joe C. Landers *In* NASA. Lewis Research Center, Second NASA Workshop on Wiring for Space Applications Jan. 1994 p 95-102 (For primary document see N94-28697 08-18)
Avail: CASI HC A02/MF A03; 8 functional color pages

An alert was issued because of the arc-tracking possibilities of installed polyimide wire harnesses. MSFC undertook a program to try to enhance the safety and reliability of these harnesses. Photographs are presented showing the need for inspections of installed wiring harnesses. Derived from text

N94-28708*# Sverdrup Technology, Inc., Cleveland, OH.
WIRING FOR SPACE APPLICATIONS PROGRAM **c33**
Ahmad Hammoud *In* NASA. Lewis Research Center, Second NASA Workshop on Wiring for Space Applications Jan. 1994 p 105-108 (For primary document see N94-28697 08-18)
Avail: CASI HC A01/MF A03; 8 functional color pages

The insulation testing and analysis consists of: identifying and prioritizing NASA wiring requirements; selecting candidate wiring constructions; developing test matrix and formulating test program; managing, coordinating, and conducting tests; and analyzing and documenting data, establishing guidelines and recommendations. Derived from text

N94-28709*# National Aeronautics and Space Administration. White Sands Test Facility, NM.
FLAMMABILITY, ODOR, OFFGASSING, THERMAL VACUUM STABILITY, AND COMPATIBILITY WITH AEROSPACE FLUIDS OF WIRE INSULATIONS **c27**
David Hirsch (Lockheed Engineering and Management Services Co., Inc., Las Cruces, NM.) and Harry Johnson *In* NASA. Lewis Research Center, Second NASA Workshop on Wiring for Space Applications Jan. 1994 p 109-120 (For primary document see N94-28697 08-18)
Avail: CASI HC A03/MF A03; 8 functional color pages

The NASA Lewis Research Center requested NASA Johnson Space Center White Sands Test Facility to conduct flammability, odor, offgassing, thermal vacuum stability, and compatibility tests with aerospace fluids of several wire insulations. Derived from text

N94-28710*# McDonnell-Douglas Aerospace, Saint Louis, MO.
ELECTRICAL AND MECHANICAL TESTING OF WIRE INSULATION FOR SPACE APPLICATIONS **c27**
Linda A. Burkhardt *In* NASA. Lewis Research Center, Second NASA Workshop on Wiring for Space Applications Jan. 1994 p 121-129 (For primary document see N94-28697 08-18)
Avail: CASI HC A02/MF A03; 8 functional color pages

Results of tests comparing M81381/7 versus Gore HSCR wire insulation on corona inception and extinction, time and current to smoke, wire fusing time, abrasion, flex life, and dynamic cut-through are presented in view-graph format. Results show that Gore is not comparable to M81381 in performance at elevated temperatures, that mechanical properties of M81381 are superior, and that corona and wire fusing times are equivalent. CASI

N94-28711*# Sverdrup Technology, Inc., Brook Park, OH.
EVALUATION OF PYROLYSIS AND ARC TRACKING ON CANDIDATE WIRE INSULATION DESIGNS FOR SPACE APPLICATIONS **c27**
Thomas J. Stueber and Kenneth Hrovat *In* NASA. Lewis Research Center, Second NASA Workshop on Wiring for Space Applications Jan. 1994 p 131-145 Original contains color illustrations (For primary document see N94-28697 08-18)
Avail: CASI HC A03/MF A03; 8 functional color pages

The ability of wire insulation materials and constructions to resist arc tracking was determined and the damage caused by initial arcing and restrike events was assessed. Results of arc tracking tests on various insulation constructions are presented in view-graph format. Arc tracking tests conducted on Champlain, Filotex, and Teledyne Thermatics indicate the Filotex is least likely to arc track. Arc tracking occurs more readily in air than it does in vacuum. CASI

N94-28712*# National Aeronautics and Space Administration. Lewis Research Center, Cleveland, OH.
WIRE INSULATION DEGRADATION AND FLAMMABILITY IN LOW GRAVITY **c27**
Robert Friedman *In its* Second NASA Workshop on Wiring for Space Applications Jan. 1994 p 147-164 Original contains color illustrations (For primary document see N94-28697 08-18)
Avail: CASI HC A03/MF A03; 8 functional color pages

This view-graph presentation covers the following topics: an introduction to spacecraft fire safety, concerns in fire prevention in low gravity, shuttle wire insulation flammability experiment, drop tower risk-based fire safety experiment, and experimental results, conclusions, and proposed studies. CASI

N94-28713*# State Univ. of New York, Buffalo.
BREAKDOWN TESTING OF WIRING INSULATION **c27**
Javaid R. Laghari *In* NASA. Lewis Research Center, Second NASA Workshop on Wiring for Space Applications Jan. 1994 p 165-172 (For primary document see N94-28697 08-18)
Avail: CASI HC A02/MF A03; 8 functional color pages

The dielectric strength of potential wiring insulation, recommended by NASA Lewis Research Center to replace existing M81381 (polyimide), was evaluated at high temperature. Results, given in view-graph format, show

that their is no dependence of breakdown strength on temperature for the constructions tested and that their was little effect of frequency on the breakdown characteristics. CASI

N94-28714*# Technische Univ., Darmstadt (Germany).
A NEW TEST METHOD FOR THE ASSESSMENT OF THE ARC TRACKING PROPERTIES OF WIRE INSULATION IN AIR, OXYGEN ENRICHED ATMOSPHERES AND VACUUM **c33**
Dieter Koenig *In* NASA. Lewis Research Center, Second NASA Workshop on Wiring for Space Applications Jan. 1994 p 173-188 (For primary document see N94-28697 08-18)
Avail: CASI HC A03/MF A03; 8 functional color pages

Development of a new test method suitable for the assessment of the resistance of aerospace cables to arc tracking for different specific environmental and network conditions of spacecraft is given in view-graph format. The equipment can be easily adapted for tests at different realistic electrical network conditions incorporating circuit protection and the test system works equally well whatever the test atmosphere. Test results confirm that pure Kapton insulated wire has bad arcing characteristics and ETFE insulated wire is considerably better in air. For certain wires, arc tracking effects are increased at higher oxygen concentrations and significantly increased under vacuum. All tests on different cable insulation materials and in different environments, including enriched oxygen atmospheres, resulted in a more or less rapid extinguishing of all high temperature effects at the beginning of the post-test phase. In no case was a self-maintained fire initiated by the arc. CASI

N94-28715*# TRW, Inc., Redondo Beach, CA.
HIGH TEMPERATURE POLYMER DIELECTRIC FILM INSULATION **c27**
Robert J. Jones *In* NASA. Lewis Research Center, Second NASA Workshop on Wiring for Space Applications Jan. 1994 p 189-191 (For primary document see N94-28697 08-18)
Avail: CASI HC A01/MF A03; 8 functional color pages

PFPI polymers were invented in the late 1970's. Assessment of emerging requirements has dictated that 300 C performance is the goal for next generation wire insulation. TRW PFPI as superior 300 C polymer candidates is presented. Included is a comparison of promising PFPI film properties with Kapton. Also included are the promising bulk polymer or coating properties. CASI

N94-28716*# Foster-Miller Associates, Inc., Waltham, MA.
HIGH TEMPERATURE ARC-TRACK RESISTANT AEROSPACE INSULATION **c27**
William Dorogy *In* NASA. Lewis Research Center, Second NASA Workshop on Wiring for Space Applications Jan. 1994 p 193-201 (For primary document see N94-28697 08-18)
Avail: CASI HC A02/MF A03; 8 functional color pages

The topics are presented in viewgraph form and include the following: high temperature aerospace insulation; Foster-Miller approach to develop a 300 C rated, arc-track resistant aerospace insulation; advantages and disadvantages of key structural features; summary goals and achievements of the phase 1 program; performance goals for selected materials; materials under evaluation; molecular structures of candidate polymers; candidate polymer properties; film properties; and a detailed program plan. CASI

N94-28717*# Minnesota Mining and Mfg. Co., Saint Paul. Electrical Products Div.
A 3M HIGH TEMPERATURE DIELECTRIC FILM **c27**
Edward Hampl, Jr. *In* NASA. Lewis Research Center, Second NASA Workshop on Wiring for Space Applications Jan. 1994 p 203-210 (For primary document see N94-28697 08-18)
Avail: CASI HC A02/MF A03; 8 functional color pages

The performance characteristics of a dielectric film are summarized. Additionally, the film's environmental and chemical properties are listed: low shrinkage to 300 C; moisture insensitive; low outgassing under vacuum; excellent surface qualities--easy metallization of film; flame retardant; and low smoke generation. A series of graphs that display the performance characteristics of the film are also presented. Author (revised)

N94-28814*# National Aeronautics and Space Administration. Lewis Research Center, Cleveland, OH.
HYPERVELOCITY IMPACT INDUCED ARCING AND KAPTON PYROLIZATION IN A PLASMA ENVIRONMENT
Robert J. Christie (Rockwell International Corp., Cleveland, OH.), Steve R. Best (Auburn Univ., AL.), and Craig A. Myhre Mar. 1994 7 p
(RTOP 474-46-10)
(NASA-TM-106528; E-8656; NAS 1.15:106528) Avail: CASI HC A02/MF A01

Tests were performed on the Space Station Freedom (SSF) solar array flat conductor circuit (FCC) to determine if hypervelocity impacts could induce pyrolization of Kapton and/or cross-conductor arcing. A sample piece of FCC was placed in a plasma environment and biased to +200 V relative to the plasma potential. The FCC was then impacted with particles in the 100 micron size range with hypervelocities of about 7 km/s. These tests were unable to induce Kapton pyrolization, cross-conductor arcing, or any other plasma interaction. Author (revised)

N94-29002# California Univ., Santa Barbara. Dept. of Mechanical Engineering.
GENERAL THEORY AND ALGORITHMS FOR THE NON-CASUAL INVERSION, SLEWING AND CONTROL OF SPACE-BASED ARTICULATED STRUCTURES Final Report
E. Bayo and B. Paden Oct. 1993 197 p
(Contract F49620-91-C-0095)
(AD-A275118; AFOSR-94-0015TR) Avail: CASI HC A09/MF A03

The following final report describes the accomplishments obtained by the research team at UCSB sponsored by the Directorate of Aerospace Sciences of the AFOSR. The major accomplishments are the following: General Procedures for the Non-Causal Inverse Dynamics of Nonlinear Articulated Structures; Inverse Dynamics of Nonlinear Articulated Structures; Simultaneous Trajectory Tracking and Vibration Reduction; Buckling Control of a Flexible Beam Using Piezoelectric Actuators; Nonlinear Inversion-Based Regulation. DTIC

N94-29022# Aerospace Corp., El Segundo, CA. Technology Operations.
PROTON SWITCHES Technical Report
J. B. Blake and S. S. Imamoto 1 Nov. 1993 6 p
(Contract F04701-88-C-0089)
(AD-A275150; TR-0091(6940-05)-7; SMC-TR-93-61) Avail: CASI HC A02/MF A01

An overview is given of the design and performance of two simple omnidirectional proton sensors included in the payload of the CRRES mission. These sensors measured the proton fluxes in the energy range of approximately 20 MeV to 100 Mev. DTIC

N94-29383*# National Aeronautics and Space Administration. Lewis Research Center, Cleveland, OH.
HYPERVELOCITY IMPACT TESTING OF SPACE STATION FREEDOM SOLAR CELLS
Robert J. Christie (Rockwell International Corp., Cleveland, OH.), Steve R. Best (Auburn Univ., AL.), and Craig A. Myhre Mar. 1994 10 p
(RTOP 474-46-10)
(NASA-TM-106509; E-8618; NAS 1.15:106509) Avail: CASI HC A02/MF A01

Solar array coupons designed for the Space Station Freedom electrical power system were subjected to hypervelocity impacts using the HYPER facility in the Space Power Institute at Auburn University and the Meteoroid/Orbital Debris Simulation Facility in the Materials and Processes Laboratory at the NASA Marshall Space Flight Center. At Auburn, the solar cells and array blanket materials received several hundred impacts from particles in the micron to 100 micron range with velocities typically ranging from 4.5 to 10.5 km/s. This fluence of particles greatly exceeds what the actual components will experience in low earth orbit. These impacts damaged less than one percent of total area of the solar cells and most of the damage was limited to the cover glass. There was no measurable loss of electrical performance. Impacts on the array blanket materials produced even less damage and the blanket materials proved to be an effective shield for the back surface of the solar cells. Using the light gas gun at MSFC, one cell of a four cell coupon was impacted by a 1/4 inch spherical aluminum projectile with a velocity of about 7 km/s.

The impact created a neat hole about 3/8 inch in diameter. The cell and coupon were still functional after impact. Author (revised)

N94-29405*# Analex Corp., Brook Park, OH.
CRYOGENIC ON-ORBIT LIQUID DEPOT STORAGE ACQUISITION AND TRANSFER (COLD-SAT) EXPERIMENT SUBSYSTEM INSTRUMENTATION AND WIRE HARNESS DESIGN REPORT Final Report
Lawrence G. Edwards Mar. 1994 72 p
(Contract NAS3-25776; RTOP 506-48-00)
(NASA-CR-189172; E-8098; NAS 1.26:189172) Avail: CASI HC A04/MF A01

Subcritical cryogens such as liquid hydrogen (LH2) and liquid oxygen (LO2) are required for space based transportation propellant, reactant, and life support systems. Future long-duration space missions will require on-orbit systems capable of long-term cryogen storage and efficient fluid transfer capabilities. COLD-SAT, which stands for cryogenic orbiting liquid depot-storage acquisition and transfer, is a free-flying liquid hydrogen management flight experiment. Experiments to determine optimum methods of fluid storage and transfer will be performed on the COLD-SAT mission. The success of the mission is directly related to the type and accuracy of measurements made. The instrumentation and measurement techniques used are therefore critical to the success of the mission. This paper presents the results of the COLD-SAT experiment subsystem instrumentation and wire harness design effort. Candidate transducers capable of fulfilling the COLD-SAT experiment measurement requirements are identified. Signal conditioning techniques, data acquisition requirements, and measurement uncertainty analysis are presented. Electrical harnessing materials and wiring techniques for the instrumentation designed to minimize heat conduction to the cryogenic tanks and provide optimum measurement accuracy are listed. Author (revised)

N94-29415# Aerospatiale, Cannes (France).
MICROVIBRATIONS ON A GEO TELECOMMUNICATION SATELLITE
J. M. Betermier (Centre National d'Etudes Spatiales, Toulouse, France.), M. C. Charmeau (Centre National d'Etudes Spatiales, Toulouse, France.), P. Rideau, and C. Garnier 1993 15 p
(Rept-932-440-101; ETN-94-95472) Avail: CASI HC A03/MF A01

Analyses carried out to assess the microvibration characteristics on a geostationary (GEO) satellite are reported. The aims of these studies were both to increase the knowledge of the levels of dynamic perturbations transmitted to the optical terminal on board the geostationary satellite, and to develop methods and tools able to deal with emerging applications such as SILEX (Semiconductor laser Intersatellite Link Experiment). The simulations and tests which were performed on the TDF1 satellite in order to characterize the microvibration levels at a simulated point of interface between TDF1 and a mounted instrument are summarized. The analysis of the complete transmission of the disturbances generated by onboard pieces of equipment such as momentum wheels and thrusters up to the instrument's line of sight is presented. A general simulation model was developed using JAMES software means to further investigate the coupled system: spacecraft and aerial part. Parameters which may affect microvibration transmission, such as unbalances, friction, gimbal configuration, were tuned and many simulations were run in order to quantify their impacts. A comparison between levels at the interface and on the instrument's line of sight was established for the main sources of disturbance. The adequacy of methods and tools developed for future applications is presented. ESA

N94-29419# Aerospatiale, Cannes (France).
SATELLITES: RELIABILITY AND OPERATION SECURITY [LES SATELLITES: FIABILITE ET SURETE DE FONCTIONNEMENT]
Philippe Giudicelli and Dominique Demarquilly 1993 4 p In FRENCH
(Rept-932-440-108; ETN-94-95478) Avail: CASI HC A01/MF A01

The importance of safety and reliability analysis is underlined. It is a crucial point for designing systems, such as satellites, in which neither failure repairing can be easily performed nor unoperating broken equipment can be replaced. A system's reliability and security can be assessed by computerized simulations, which also allow solution finding. The major difficulties concerning satellites is searching for errors in nonelectronic equipment. ESA

N94-29543# Aerospatiale, Cannes (France). Div. Espace et Defense.
APPLICATION OF FLUIDNET-G SOFTWARE TO THE PRELIMINARY THERMAL AND HYDRAULIC DESIGN OF HERMES SPACEPLANE
J. N. Chelotti, S. Andre, T. Maciaszek, A. Thuaire, and A. Ferro 1993 14 p See also N93-41459
(Rept-932-440-107; ETN-94-95477) Avail: CASI HC A03/MF A01

FLUIDNET-G is a 'workstation' based graphic's orientated software package. The package performs single phase fluid loop thermal and hydraulic preliminary design. The main characteristics of this tool are as follows: the user friendliness of the graphics and the workstation concept; and the 'upstream compatibility' towards others analysis tools. An application illustrates FLUIDNET-G's ability to perform tradeoff and sensitivity studies. ESA

N94-29757*# National Aeronautics and Space Administration. Lewis Research Center, Cleveland, OH.
SUMMARY REPORT OF MISSION ACCELERATION MEASUREMENTS FOR SPACEHAB-01, STS-57 LAUNCHED 21 JUNE 1993
Brian Finley (Sverdrup Technology, Inc., Brook Park, OH.), Carlos Grodsinsky, and Richard DeLombard Mar. 1994 286 p Original contains color illustrations
(Contract NAS3-25266; RTOP 694-03-011)
(NASA-TM-106514; NAS 1.15:106514; MMAP-STS-57; E-8631) Avail: CASI HC A13/MF A03; 162 functional color pages

The maiden voyage of the commercial Spacehab laboratory module onboard the STS-57 mission was integrated with several accelerometer packages, one of which was the Space Acceleration Measurement System (SAMS). The June 21st 1993, launch was the seventh successful mission for the Office of Life and Microgravity Sciences and Application's (OLMSA) SAMS unit. This flight was also complemented by a second accelerometer system. The Three Dimensional Microgravity Accelerometer (3-DMA), a Code C funded acceleration measurement system, offering an on-orbit residual calibration as a reference for the unit's four triaxial accelerometers. The SAMS accelerometer unit utilized three remote triaxial sensor heads mounted on the forward Spacehab module bulkhead and on one centrally located experiment locker door. These triaxial heads had filter cut-offs set to 5, 50, and 1000 Hz. The mission also included other experiment specific accelerometer packages in various locations. Author (revised)

N94-29828 Wisconsin Univ., Madison.
THE INFLUENCE OF APPENDAGE VIBRATION ON THE ATTITUDE DYNAMICS OF A DUAL-SPIN SATELLITE Ph.D. Thesis
Mark Channing Stabb 1992 124 p
Avail: Univ. Microfilms Order No. DA9306484

In order to complete mission requirements, many spacecraft must undergo a specific motion. Accurate prediction of a satellite's attitude over time can be very important to mission planners and satellite designers. This thesis develops a perturbation method which is used to obtain an approximate analytical solution to the equations of motion for a dual-spin satellite with a flexible appendage. The perturbation of the motion from the ideal rigid body case is obtained as a function of system parameters. With this result, the relationships between spacecraft attitude dynamics and values of the system parameters can be found and examined without having to know specific values for the parameters themselves. The flexible appendage is modeled as a nonlinear beam with a finite sized tip mass at the end. Previous studies have not examined a tip mass with finite dimensions in conjunction with the full nonlinear equations of motion for a three dimensional case. The work presented here allows for all of these effects to be considered. Examples for specific configurations of the spacecraft are presented showing the magnitudes of the perturbations as functions of system parameters. This allows for investigation of minima of the perturbations in the parameter space of the satellite, a useful tool for spacecraft designers. In addition, comparisons of the perturbation solution with a numerically integrated solution of the full equations of motion for specific values of the system parameters are also presented. The results show that the perturbation method is in very close agreement with the numerical solution for the specific configurations chosen. Dissert. Abstr.

N94-29896 City Univ. of New York, NY.
HIGH-RESOLUTION ROBOT TRACKING AND DIRECTION FINDING FOR SPACE STATION ENVIRONMENT Ph.D. Thesis

Kamal Shahrabi 1993 178 p
Avail: Univ. Microfilms Order No. DA9315502

In the past few years the problem of location finding and tracking of extravehicular robots in space station environment, and the related problem of estimating the parameters of signals in noise, have attracted considerable interest. Conventional direction finding, tracking, and locating techniques such as maximum likelihood (ML) and multiple signal characterization (MUSIC) are proving inadequate to support the full and effective utilization of robotics in a space station environment. The scope of this work is to provide a new and more efficient signal processing technique for a space station robotic tracking system which overcomes existing technical limitations such as radio transmission multipath, station reflections, the number of robots, space station environment, stringent resolution requirements, and space station architecture. In general, this work contains block level design and study of a communication system for a space station involving spread spectrum and digital processing of signal techniques that achieves as space station robotic tracking implementation. This report contains an extensive analysis of the system performance from the following points of view: utilization of a chirp signal, which, in conjunction with a polling procedure, allows for individual robot identification, location and tracking; estimate the number of antennae; determine the location of the antennae on the space station; generate a detailed block diagram design; and perform an overall system analysis that considers the effects of signal multipath.
Dissert. Abstr.

N94-29917*# Alabama Univ., Huntsville. Dept. of Electrical and Computer Engineering.
WAVE GENERATION BY CONTAMINANT IONS NEAR A LARGE SPACECRAFT Final Technical Report, 1 Oct. 1992 - 30 Nov. 1993
N. Singh 1993 59 p
(Grant NAG3-1373)
(NASA-CR-195797; NAS 1.26:195797) Avail: CASI HC A04/MF A01

Measurements from the space shuttle flights have revealed that a large spacecraft in a low earth orbit is accompanied by an extensive gas cloud which is primarily made up of water. The charge exchange between the water molecule and the ionospheric O(+) ions produces a water ion beam traversing downstream of the spacecraft. In this report we present results from a study on the generation of plasma waves by the interaction of the water ion beams with the ionospheric plasma. Since velocity distribution function is key to the understanding of the wave generation process, we have performed a test particle simulation to determine the nature of H2O(+) ions velocity distribution function. The simulations show that at the time scales shorter than the ion cyclotron period tau(sub c), the distribution function can be described by a beam. On the other hand, when the time scales are larger than tau(sub c), a ring distribution forms. A brief description of the linear instabilities driven by an ion beam streaming across a magnetic field in a plasma is presented. We have identified two types of instabilities occurring in low and high frequency bands; the low-frequency instability occurs over the frequency band from zero to about the lower hybrid frequency for a sufficiently low beam density. As the beam density increases, the linear instability occurs at decreasing frequencies below the lower-hybrid frequency. The high frequency instability occurs near the electron cyclotron frequency and its harmonics. Author (revised)

N94-30123*# National Aeronautics and Space Administration. Lewis Research Center, Cleveland, OH.
ELECTRIC POWER SYSTEM TEST AND VERIFICATION PROGRAM
Daniel S. Rylicki and Frank Robinson, Jr. Mar. 1994 36 p
(RTOP 474-12-10)
(NASA-TM-106405; E-8241; NAS 1.15:106405) Avail: CASI HC A03/MF A01

Space Station Freedom's (SSF's) electric power system (EPS) hardware and software verification is performed at all levels of integration, from components to assembly and system level tests. Careful planning is essential to ensure the EPS is tested properly on the ground prior to launch. The results of the test performed on breadboard model hardware and analyses completed to date have been evaluated and used to plan for design qualification and flight acceptance test phases. These results and plans indicate the verification program for SSF's 75-kW EPS would have been successful and completed in time to support the scheduled first element launch. Author (revised)

N94-30161*# National Aeronautics and Space Administration. Marshall Space Flight Center, Huntsville, AL.
VULNERABILITY OF MANNED SPACECRAFT TO CREW LOSS FROM ORBITAL DEBRIS PENETRATION
J. E. Williamsen Apr. 1994 206 p
(NASA-TM-108452; NAS 1.15:108452) Avail: CASI HC A10/MF A03

Orbital debris growth threatens the survival of spacecraft systems from impact-induced failures. Whereas the probability of debris impact and spacecraft penetration may currently be calculated, another parameter of great interest to safety engineers is the probability that debris penetration will cause actual spacecraft or crew loss. Quantifying the likelihood of crew loss following a penetration allows spacecraft designers to identify those design features and crew operational protocols that offer the highest improvement in crew safety for available resources. Within this study, a manned spacecraft crew survivability (MSCSurv) computer model is developed that quantifies the conditional probability of losing one or more crew members, P(sub loss/pen), following the remote likelihood of an orbital debris penetration into an eight module space station. Contributions to P(sub loss/pen) are quantified from three significant penetration-induced hazards: pressure wall rupture (explosive decompression), fragment-induced injury, and 'slow' depressurization. Sensitivity analyses are performed using alternate assumptions for hazard-generating functions, crew vulnerability thresholds, and selected spacecraft design and crew operations parameters. These results are then used to recommend modifications to the spacecraft design and expected crew operations that quantitatively increase crew safety from orbital debris impacts. Author (revised)

N94-30264# Sandia National Labs., Albuquerque, NM.
SPACE DEBRIS REMOVAL USING A HIGH-POWER GROUND-BASED LASER
D. K. Monroe 1993 20 p Presented at the OE/LASE 1994: Conference on Optics, Electro-Optics, and Laser Applications in Science and Engineering, Los Angeles, 22-29 Jan. 1994
(Contract DE-AC04-94AL-85000)
(DE94-006363; SAND-93-1523C; CONF-940142-6) Avail: CASI HC A03/MF A01

The feasibility and practicality of using a ground-based laser (GBL) to remove artificial space debris is examined. Physical constraints indicate that a reactor-pumped laser (RPL) may be best suited for this mission, because of its capabilities for multimegawatt output long run-times, and near-diffraction-limited initial beams. Simulations of a laser-powered debris removal system indicate that a 5-MW RPL with a 10-meter-diameter beam director and adaptive optics capabilities can deorbit 1-kg debris from space station altitudes. Larger debris can be deorbited or transferred to safer orbits after multiple laser engagements. A ground-based laser system may be the only realistic way to access and remove some 10,000 separate objects, having velocities in the neighborhood of 7 km/sec, and being spatially distributed over some 10(exp 10) km(exp 3) of space. DOE

N94-30350# Advisory Group for Aerospace Research and Development, Neuilly-Sur-Seine (France). Avionics Panel.
TACSATS FOR NATO [LES SATELLITES TACTIQUES POUR L'OTAN]
Feb. 1994 70 p
(AGARD-AR-322; ISBN-92-835-0733-9) Copyright Avail: CASI HC A04/MF A01

Tactical satellites (TacSats) are studied to determine their utility in meeting the needs of theater commanders. Six mission areas are studied: battlefield surveillance, communications, tactical missile warning and assessment, regional maritime surveillance, navigation, and weather. The synergistic role between strategic and tactical satellites is also considered. TacSat system concepts are provided in most mission areas as are means of implementing TacSat systems, including the launch and ground system segments. Issues raised in these areas are discussed. Finally, TacSat costs are discussed and the Working Group's conclusions and recommendations are provided.
Author (revised)

N94-30811# National Space Development Agency, Tokyo (Japan).
DEVELOPMENT STATUS OF THE COMMUNICATIONS AND BROADCASTING ENGINEERING TEST SATELLITE (COMETS) [KOMETTSU SHISUTEMU NO KAIHATSU]
Keisuke Ozawa, Kazuhiko Oshida, Junichi Aoyama, Naoki Sato, Masayoshi Kawaguchi, Katsumi Oishi, and Mizuho Ikeda Aug. 1993 8 p Repr.

from Technical Report of IEICE (Tokyo, Japan) SANE-93-25, Aug. 1993 p 5-12 In JAPANESE
(JTN-94-80545) Avail: CASI HC A02/MF A01

COMETS (Communications and Broadcasting Engineering Test Satellite) is the research and development purpose satellite in the area of satellite communications and broadcasting technologies, to be launched in 1997 by H-2 launch vehicle. The main mission is to experimentally demonstrate and evaluate the technologies on inter-orbit communications, advanced satellite broadcasting on Ka-band and advanced mobile satellite communications on Ka-band and millimeter-wave band. The development of COMETS has been started on March 1991 as the preliminary design phase, and the preliminary design reviews of the subsystems and systems of COMETS had been held between June 1992 to April 1993, in which the feasibility of COMETS system was confirmed. This paper presents the outline of S/C (spacecraft) mission, system configuration, S/C operation plan and development plan of COMETS based on the results of the preliminary design. Author (NASDA)

N94-30857 National Aerospace Lab., Emmeloord (Netherlands). Space Div.
THE MACS-TSA APPLIED IN THE ISO AND SAX SPACECRAFT PROJECTS
Frans J. Sonnenschein and Henk Keppel 30 Mar. 1992 10 p Presented at the 1992 European Simulation Multiconference, York, England, 1-3 Jun. 1992 Sponsored by ESA; Netherlands Agency for Aerospace Programs; Fokker Space and Systems; and Alenia Spazio SPA Limited Reproducibility: More than 20% of this document may be affected by microfiche quality
(PB94-126257; NLR-TP-92134-U; ETN-94-95574) Avail: CASI HC A02

The place of a Modular Attitude and Orbit Control Subsystem Test and Simulation Assembly (MACS-TSA) in the development process of the ISO (Infrared Space Observatory) and SAX (Italian X-ray Astronomy Satellite) spacecrafts is given, with emphasis on the simulation aspects. The MACS-TSA is used as checkout equipment during the integration of Attitude and Orbit Control System (AOCS) hardware and software at subsystem level. The other spacecraft subsystems are simulated, as well as their dynamic behavior in the orbital environment. A description of the components of the TSA is given. ESA

N94-30864 Texas A&M Univ., College Station.
DYNAMICS AND CONTROL OF TETHERED SATELLITE SYSTEMS Ph.D. Thesis
Euisok Kim 1993 130 p
Avail: Univ. Microfilms Order No. DA9328752

The purpose of this research is to investigate the dynamics of a tethered satellite system in which the flexibility of the tether is considered and to design control laws for the deployment and retrieval of the tethered subsatellite using a method based on the Lyapunov stability theory. The dynamics of the system considered is modelled with as little simplifications and assumptions as possible to keep the problem tractable and at the same time physically realistic. Effects of geometric nonlinearity is taken into account. The hybrid governing equations are discretized by using the Galerkin's method. The flexible tether is also modelled as a series of beads which are connected in series by massless springs. Several tension and reel rate feedback control laws for deployment and retrieval are designed using Lyapunov's method when flexibility of the tether is neglected. It was found that the tension control laws designed or the simplified system can have a stabilizing effect on the vibrations of the tether. The performance of the full dynamic system with the designed control laws is investigated via simulations using both the Galerkin and bead model. At the same time, observations regarding the dynamics of the system and the validity of using the Galerkin's discretization procedure for a variable length tether are investigated. It is shown that the effects of geometric nonlinearity is significant during retrieval and that when geometric nonlinearity is included, an artificial instability is introduced into the Galerkin model causing sudden divergence of the system response during retrieval. This behavior is reproduced even for a simplified two dimensional example problem. It was found that the bead model produces a response that is physically realistic. Simulation studies using the bead model show that when reel rate control laws are used, vibrations grow to the point where the system becomes unstable. However, the tension control laws successfully retrieve the tethered subsatellite and were found to be effective in damping the elastic longitudinal vibrations in the early stages of retrieval. A nonrecursive order-N method for efficiently simulating the bead model is also introduced. The feasibility of implementing the order-N method for parallel computation is investigated using two parallel computer architectures. It was found that, due mostly to communication time, the use of the parallel computers do not offer any improvement in overall computation time. Dissert. Abstr.

N94-30932# National Space Development Agency, Tokyo (Japan).
DEVELOPMENT STATUS OF COMETS MISSIONS [KOMETTSU MISSHON SHISUTEMU NO KAIHATSU]
Kazuhiko Oshida, Chiharu Ouchi, Toyohachi Yokota, Shozo Nakazato, Minoru Takahasi, Sinji Suzuki, and Daisuke Miyajima Aug. 1993 6 p Repr. from Technical Report of IEICE (Tokyo, Japan), SANE-93-27, Aug. 1993 p 21-26 In JAPANESE
(JTN-94-80544) Avail: CASI HC A02/MF A01

Missions of Communications and Broadcasting Engineering Test Satellite (COMETS) are to develop and evaluate the new technologies in the field of Inter-orbit Satellite System (ISS), advanced Broadcasting Satellite System (BSS) and advanced Mobile Satellite System (MSS). Mission system of COMETS, presented in this report, includes an allocation of the overall function and performance to earth station, spacecraft and user terminal, an arrangement of the frequency assignment without interference between these three mission subsystems with telemetry command subsystem, and hardware integration. This report presents the outline of COMETS mission, overall system performance, function and performance requirements for each subsystem, and hardware configuration based on the results of the preliminary design. Author (NASDA)

N94-30960 Colorado Univ., Boulder.
LOCAL INTERACTION CONTROL FOR SPACE CONSTRUCTION Ph.D. Thesis
Philip Graham Good 1993 167 p
Avail: Univ. Microfilms Order No. DA9320422

A control scheme for assembling flexible substructures is developed using sensors and actuators local to the interaction point and without the need to modify existing controllers on the interacting substructures. It assumes a nominal interaction controller is first developed to produce the desired performance for the interaction, then the stability of the system is addressed by the use of an auxiliary interaction controller, which is the focus of this dissertation. Two types of auxiliary interaction control were investigated: (1) the open loop mode (OLM) auxiliary interaction controller uses open loop modal information to stabilize the system and is based on the residual mode filter (RMF) scheme; and (2) the closed loop mode (CLM) auxiliary interaction controller uses closed loop modal information to stabilize the system and is based on the disturbance accommodation control (DAC) scheme. Theory is developed for the stability of each method under ideal actuator conditions and under conditions where actuator dynamics are present. Exponential stability theory is developed for the OLM and CLM methods to bound the slowest rate of decay of the closed loop systems. Implementation of the local interaction controllers is investigated on a computer model designed to simulate a simple space station to space shuttle docking maneuver. Dissert. Abstr.

N94-29324# National Aerospace Lab., Amsterdam (Netherlands).
THE DEVELOPMENT PROCEDURES AND TOOLS APPLIED FOR THE ATTITUDE CONTROL SOFTWARE OF THE ITALIAN SATELLITE SAX
G. J. Hameetman and G. J. Dekker *In* AGARD, Aerospace Software Engineering for Advanced Systems Architectures Nov. 1993 8 p (For primary document see N94-29315 08-61)
Copyright Avail: CASI HC A02/MF A03

N94-29636*# National Aeronautics and Space Administration. Marshall Space Flight Center, Huntsville, AL.
DEVELOPMENT AND TESTING OF THE AUTOMATED FLUID INTERFACE SYSTEM
Martha E. Milton and Tony R. Tyler *In* NASA. Ames Research Center, The 27th Aerospace Mechanisms Symposium May 1993 p 121-135 (For primary document see N94-29627 08-15)
Avail: CASI HC A03/MF A03

N94-29643*# Deutsche Aerospace A.G., Munich (Germany).
PARACHUTE SWIVEL MECHANISM FOR PLANETARY ENTRY
R. Birner, J. Kaese, F. Koller, E. Muehlner, and H.-J. Luhmann *In*

NASA. Ames Research Center, The 27th Aerospace Mechanisms Symposium May 1993 p 237-254 Sponsored by ESA and DASA (For primary document see N94-29627 08-15)
Avail: CASI HC A03/MF A03

N94-29645*# National Aeronautics and Space Administration. Goddard Space Flight Center, Greenbelt, MD.
THE SOLAR ANOMALOUS AND MAGNETOSPHERIC PARTICLE EXPLORER (SAMPEX) YO-YO DESPIN AND SOLAR ARRAY DEPLOYMENT MECHANISM
James W. Kellogg *In* NASA. Ames Research Center, The 27th Aerospace Mechanisms Symposium May 1993 p 267-282 (For primary document see N94-29627 08-15)
Avail: CASI HC A03/MF A03

N94-29782*# General Electric Co., Schenectady, NY. Corporate Research and Development.
ADVANCED MICROFABRICATION TECHNOLOGIES FOR MICROSPACECRAFT
M. Ghezzo, B. Bagepalli, S. Kodiyalam, C. Korham, K. Browall, and Norman Alexander *In* JPL, Proceedings of the Workshop on Microtechnologies and Applications to Space Systems 15 Jun. 1993 p 157 (For primary document see N94-29767 08-31)
Avail: CASI HC A01/MF A03

N94-30672*# Johns Hopkins Univ., Columbia, MD. Applied Physics Lab.
TIME MAINTENANCE SYSTEM FOR THE BMDO MSX SPACECRAFT
Martin J. Hermes *In* NASA. Goddard Space Flight Center, The 25th Annual Precise Time and Time Interval (PTTI) Applications and Planning Meeting May 1994 p 433-444 (For primary document see N94-30639 08-70)
Avail: CASI HC A03/MF A06

19 SPACECRAFT INSTRUMENTATION

For related information see also *06 Aircraft Instrumentation* and *35 Instrumentation and Photography.*

N94-29035*# Boeing Defense and Space Group, Seattle, WA.
FAULT TOLERANT TESTBED EVALUATION, PHASE 1 Final Report
V. Caluori, Jr. and T. Newberry 30 Sep. 1993 26 p
(Contract NAS9-18878)
(NASA-CR-188275; NAS 1.26:188275) Avail: CASI HC A03/MF A01

In recent years, avionics systems development costs have become the driving factor in the development of space systems, military aircraft, and commercial aircraft. A method of reducing avionics development costs is to utilize state-of-the-art software application generator (autocode) tools and methods. The recent maturity of application generator technology has the potential to dramatically reduce development costs by eliminating software development steps that have historically introduced errors and the need for re-work. Application generator tools have been demonstrated to be an effective method for autocoding non-redundant, relatively low-rate input/output (I/O) applications on the Space Station Freedom (SSF) program; however, they have not been demonstrated for fault tolerant, high-rate I/O, flight critical environments. This contract will evaluate the use of application generators in these harsh environments. Using Boeing's quad-redundant avionics system controller as the target system, Space Shuttle Guidance, Navigation, and Control (GN&C) software will be autocoded, tested, and evaluated in the Johnson (Space Center) Avionics Engineering Laboratory (JAEL). The response of the autocoded system will be shown to match the response of the existing Shuttle General Purpose Computers (GPC's), thereby demonstrating the viability of using autocode techniques in the development of future avionics systems. Author

N94-29640*# Teldix Luftfahrt-Ausruestungs G.m.b.H., Heidelberg (Germany). Space Dept.
A GIMBALED LOW NOISE MOMENTUM WHEEL
U. Bichler and T. Eckardt *In* NASA. Ames Research Center, The 27th Aerospace Mechanisms Symposium May 1993 p 181-196 Sponsored in part by ESA (For primary document see N94-29627 08-15)
Avail: CASI HC A03/MF A03

N94-29791*# National Aeronautics and Space Administration. Lyndon B. Johnson Space Center, Houston, TX.
THE APPLICATION OF MICROMACHINED SENSORS TO MANNED SPACE SYSTEMS
Aldo Bordano, Gary Havey, Jerry Wald, and Hatem Nasr *In* JPL, Proceedings of the Workshop on Microtechnologies and Applications to Space Systems 15 Jun. 1993 p 279-28 (For primary document see N94-29767 08-31)
Avail: CASI HC A02/MF A03

20 SPACECRAFT PROPULSION AND POWER

Includes main propulsion systems and components, e.g., rocket engines; and spacecraft auxilliary power sources.

For related information see also *07 Aircraft Propulsion and Power, 28 Propellants and Fuels, 44 Energy Production and Conversion,* and *15 Launch Vehicles and Space Vehicles.*

N94-28736*# TRW, Inc., Redondo Beach, CA.
ARCJET SYSTEM INTEGRATION DEVELOPMENT Final Report
Sidney Zafran Mar. 1994 59 p
(Contract NAS3-25603; RTOP 506-42-31)
(NASA-CR-187147; E-8655; NAS 1.26:187147) Avail: CASI HC A04/MF A01

Compatibility between an arcjet propulsion system and a communications satellite was verified by testing a Government-furnished, 1.4 kW hydrazine arcjet system with the FLTSATCOM qualification model satellite in a 9.1-meter (30-foot) diameter thermal-vacuum test chamber. Background pressure was maintained at 10(exp -5) torr during arcjet operation by cryopumping the thruster exhaust with an array of 5 K liquid helium cooled panels. Power for the arcjet system was obtained from the FLTSATCOM battery simulator. Spacecraft telemetry was monitored during each thruster firing period. No changes in telemetry data attributable to arcjet operation were detected in any of the tests. Electromagnetic compatibility data obtained included radiated emission measurements, conducted emission measurements, and cable coupling measurements. Significant noise was observed at lower frequencies. Above 500 MHz, radiated emissions were generally within limits, indicating that communication links at S-band and higher frequencies will not be affected. Other test data taken with a diagnostic array of calorimeters, radiometers, witness plates, and a residual gas analyzer evidenced compatible operation, and added to the data base for arcjet system integration. Two test series were conducted. The first series only included the arcjet and diagnostic array operating at approximately 0.1 torr background pressure. The second series added the qualification model spacecraft, a solar panel, and the helium cryopanels. Tests were conducted at 0.1 torr and 10(exp-5) torr. The arcjet thruster was canted 20 degrees relative to the solar panel axis, typical of the configuration used for stationkeeping thrusters on geosynchronous communications satellites.
Author

N94-28800*# Auburn Univ., AL. Engineering Experiment Station.
DEVELOPMENT OF A NEW GENERATION SOLID ROCKET MOTOR IGNITION COMPUTER CODE Final Report
Winfred A. Foster, Jr., Rhonald M. Jenkins, Alessandro Ciucci, and Shelby D. Johnson 10 Feb. 1994 173 p
(Grant NAG8-683)
(NASA-CR-195734; NAS 1.26:195734) Avail: CASI HC A08/MF A02

This report presents the results of experimental and numerical investigations of the flow field in the head-end star grain slots of the Space Shuttle Solid Rocket Motor. This work provided the basis for the development of an improved solid rocket motor ignition transient code which is also described in this report. The correlation between the experimental and numerical results is excellent and provides a firm basis for the development of a fully three-dimensional solid rocket motor ignition transient computer code. Author

N94-28833*# National Aeronautics and Space Administration. Lewis Research Center, Cleveland, OH.
NUCLEAR ELECTRIC PROPULSION: A BETTER, SAFER, CHEAPER TRANSPORTATION SYSTEM FOR HUMAN EXPLORATION OF MARS
John S. Clark, Jeffrey A. George, Leon P. Gefert, Michael P. Doherty, and

Robert J. Sefcik Mar. 1994 17 p Presented at the 11th Symposium on Space Nuclear Power and Propulsion Systems, Albuquerque, NM, 9-13 Jan. 1994; sponsored by Univ. of New Mexico
(RTOP 593-71-00)
(NASA-TM-106406; E-8242; NAS 1.15:106406) Avail: CASI HC A03/MF A01

NASA has completed a preliminary mission and systems study of nuclear electric propulsion (NEP) systems for 'split-sprint' human exploration and related robotic cargo missions to Mars. This paper describes the study, the mission architecture selected, the NEP system and technology development needs, proposed development schedules, and estimated development costs. Since current administration policy makers have delayed funding for key technology development activities that could make Mars exploration missions a reality in the near future, NASA will have time to evaluate various alternate mission options, and it appears prudent to ensure that Mars mission plans focus on astronaut and mission safety, while reducing costs to acceptable levels. The split-sprint nuclear electric propulsion system offers trip times comparable to nuclear thermal propulsion (NTP) systems, while providing mission abort opportunities that are not possible with 'reference' mission architectures. Thus, NEP systems offer short transit times for the astronauts, reducing the exposure of the crew to intergalactic cosmic radiation. The high specific impulse of the NEP system, which leads to very low propellant requirements, results in significantly lower 'initial mass in low earth orbit' (IMLEO). Launch vehicle packaging studies show that the NEP system can be launched, assembled, and deployed, with about one less 240-metric-ton heavy lift launch vehicle (HLLV) per mission opportunity - a very Technology development cost of the nuclear reactor for an NEP system would be shared with the proposed nuclear surface power systems, since nuclear systems will be required to provide substantial electrical power on the surface of Mars. The NEP development project plan proposed includes evolutionary technology development for nuclear electric propulsion systems that expands upon SP-100 (Space Power - 100 kw(e)) technology that has been developed for lunar and Mars surface nuclear power, and small NEP systems for interplanetary probes. System upgrades are expected to evolve that will result in even shorter trip times, improved payload capabilities, and enhanced safety and reliability. Author

N94-28834*# National Aeronautics and Space Administration. Lewis Research Center, Cleveland, OH.
PERFORMANCE AND DURABILITY OF HIGH EMITTANCE HEAT RECEIVER SURFACES FOR SOLAR DYNAMIC POWER SYSTEMS
Kim K. deGroh, David M. Roig, Christopher A. Burke, and Dilipkumar R. Shah Mar. 1994 16 p Presented at the 1994 ASME International Solar Energy Conference, San Francisco, CA, 27-30 Mar. 1994; sponsored by ASME
(RTOP 585-03-21)
(NASA-TM-106549; E-8700; NAS 1.15:106549) Avail: CASI HC A03/MF A01

Haynes 188, a cobalt-based superalloy, will be used to make thermal energy storage (TES) containment canisters for a 2 kW solar dynamic ground test demonstrator (SD GTD). Haynes 188 containment canisters with a high thermal emittance (epsilon) are desired for radiating heat away from local hot spots, improving the heating distribution, which will in turn improve canister service life. In addition to needing a high emittance, the surface needs to be durable in an elevated temperature, high vacuum environment for an extended time period. Thirty-five Haynes 188 samples were exposed to 14 different types of surface modification techniques for emittance and vacuum heat treatment (VHT) durability enhancement evaluation. Optical properties were obtained for the modified surfaces. Emittance enhanced samples were exposed to VHT for up to 2692 hours at 827 C and less than or equal to 10(exp -6) torr with integral thermal cycling. Optical properties were taken intermittently during exposure, and after final VHT exposure. The various surface modification treatments increased the emittance of pristine Haynes 188 from 0.11 up to 0.86. Seven different surface modification techniques were found to provide surfaces which met the SD GTD receiver VHT durability requirement. Of the 7 surface treatments, 2 were found to display excellent VHT durability: an alumina based (AB) coating and a zirconia based coating. The alumina based coating was chosen for the epsilon enhancement surface modification technique for the SD GTD receiver. Details of the performance and vacuum heat treatment durability of this coating and other Haynes 188 emittance surface modification techniques are discussed. Technology from this program will lead to successful demonstration of solar dynamic power for space applications, and has potential for application in other systems requiring high emittance surfaces. Author (revised)

N94-28999*# National Aeronautics and Space Administration. Lewis Research Center, Cleveland, OH.
LOW EARTH ORBIT DURABILITY EVALUATION OF PROTECTED SILICONE FOR ADVANCED REFRACTIVE PHOTOVOLTAIC CONCENTRATOR ARRAYS
Kim K. deGroh and Timothy A. McCollum Apr. 1994 13 p Presented at the AIAA 32nd Aerospace Sciences Meeting and Exhibit, Reno, NV, 10-13 Jan. 1994; sponsored by AIAA
(RTOP 506-41-11)
(NASA-TM-106543; E-8687; NAS 1.15:106543; AIAA Paper 94-0374)
Avail: CASI HC A03/MF A01

The need for efficient, cost effective sources of electrical power in space has led to the development of photovoltaic power systems which make use of novel refractive solar concentrators. These concentrators have been conceived in both point-focus and linear-focus designs. Current concentrator lenses are fabricated from flexible silicones with Fresnel facets along their inside surface. To insure the efficient operation of these power systems, the concentrator lenses must be durable and the silicone material must remain specularly transmitting over a reasonable lifetime in low Earth orbit (LEO) and other space environments. Because of the vulnerability of silicones to atomic oxygen and ultraviolet radiation in LEO these lenses have been coated with a multi-layer metal oxide protective coating. The objective of this research was to evaluate the LEO durability of the multilayer coated silicone for advanced refractive photovoltaic concentrator arrays with respect to optical properties and microstructure. Flat metal oxide coated silicone samples were exposed to ground-laboratory and in-space atomic oxygen for durability evaluation. Author

N94-29097*# National Aeronautics and Space Administration. Lewis Research Center, Cleveland, OH.
EVALUATION OF OXIDE-COATED IRIDIUM-RHENIUM CHAMBERS
Brian D. Reed Mar. 1994 15 p Presented at the 1993 JANNAF Propulsion Meeting, Monterey, CA, 15-19 Nov. 1993; sponsored by the JANNAF Interagency Propulsion Committee
(RTOP 506-42-31)
(NASA-TM-106442; E-8286; NAS 1.15:106442) Avail: CASI HC A03/MF A01

Iridium-coated rhenium (Ir-Re) provides long life operation of radiation-cooled rockets at temperatures up to 2200 C. Ceramic oxide coatings could be used to increase Ir-Re rocket lifetimes and allow operation in highly oxidizing environments. Ceramic oxide coatings promise to serve as both thermal and diffusion barriers for the iridium layer. Seven ceramic oxide-coated Ir-Re, 22-N rocket chambers were tested with gaseous hydrogen/gaseous oxygen (GHz/G02) propellants. Five chambers had thick (over 10 mils), monolithic coatings of either hafnia (HfO2) or zirconia (ZrO2). Two chambers had coatings with thicknesses less than 5 mils. One of these chambers had a thin-walled coating of ZrO2 infiltrated with sol gel HfO2. The other chamber had a coating composed of an Ir-oxide composite. The purpose of this test program was to assess the ability of the oxide coatings to withstand the thermal shock of combustion initiation, adhere under repeated thermal cycling, and operate in aggressively oxidizing environments. All of the coatings survived the thermal shock of combustion and demonstrated operation at mixture ratios up to 11. Testing the Ir-oxide composite-coated chamber included over 29 min at mixture ratio 16. The thicker walled coatings provided the larger temperature drops across the oxide layer (up to 570 C), but were susceptible to macrocracking and eventual chipping at a stress concentrator. The cracks apparently resealed during firing, under compression of the oxide layer. The thinner walled coatings did not experience the macrocracking and chipping of the chambers that was seen with the thick, monolithic coatings. However, burn-throughs in the throat region did occur in both of the thin-walled chambers at mixture ratios well above stoichiometric. The burn-throughs were probably the result of oxygen diffusion through the oxide coating that allowed the underlying Ir and Re layers to be oxidized. The results of this test program indicated that the thin-walled oxide coatings are better suited for repeated

thermal cycling than the thick-walled coating, while thicker coatings may be required for operation in aggressively oxidizing environments. Author

N94-29216 Air Force Inst. of Tech., Wright-Patterson AFB, OH. School of Engineering.

ORBITAL APPLICATIONS OF ELECTRODYNAMIC PROPULSION M.S. Thesis

Troy Irwin Dec. 1993 125 p Limited Reproducibility: More than 20% of this document may be affected by microfiche quality

(AD-A275413; AFIT/GA/ENY/93D-4) Avail: CASI HC A06

Electrodynamic propulsion (EDP) uses forces resulting from electric currents in conductors as a spacecraft travels through a magnetic field. A vehicle-independent expression for the specific power required for any maneuver is derived and used to assess EDP feasibility. Analytical expressions for the accelerations and combined current-conductor vector required to change the orbital plane or the argument of perigee are developed based on Lagrange's planetary equations. Solutions to the forced Clohessy-Wiltshire equations are developed to study iii-plane rendezvous. Results show EDP can change inclination or right ascension of the ascending mode at approximately 0.4 degrees/day with current spacecraft specific power technology. The effects of the Earth's oblateness on a 24 hour, 90 degree inclination Molniya orbit can be negated. Rendezvous is possible with EDP, and approaches along the target velocity vector with no attitude change are possible with current spacecraft specific power. Approaches involving altitude changes will be possible when modest spacecraft power improvements are made. EDP allows a soft dock - velocities and accelerations decay to zero as the chase vehicle the target - and there is no thruster plume to impart momentum or contaminate the target. DTIC

N94-29403*# National Aeronautics and Space Administration. Lewis Research Center, Cleveland, OH.

ROCKET ENGINE SYSTEM RELIABILITY ANALYSES USING PROBABILISTIC AND FUZZY LOGIC TECHNIQUES

Terry L. Hardy and Douglas C. Rapp Apr. 1994 18 p Proposed for presentation at the 30th Joint Propulsion Conference, Indianapolis, IN, 27-29 Jun. 1994; sponsored by the AIAA, ASME, SAE, and ASEE

(RTOP 506-42-72)

(NASA-TM-106519; E-8640; NAS 1.15:106519; AIAA Paper 94-2750) Avail: CASI HC A03/MF A01

The reliability of rocket engine systems was analyzed by using probabilistic and fuzzy logic techniques. Fault trees were developed for integrated modular engine (IME) and discrete engine systems, and then were used with the two techniques to quantify reliability. The IRRAS (Integrated Reliability and Risk Analysis System) computer code, developed for the U.S. Nuclear Regulatory Commission, was used for the probabilistic analyses, and FUZZYFTA (Fuzzy Fault Tree Analysis), a code developed at NASA Lewis Research Center, was used for the fuzzy logic analyses. Although both techniques provided estimates of the reliability of the IME and discrete systems, probabilistic techniques emphasized uncertainty resulting from randomness in the system whereas fuzzy logic techniques emphasized uncertainty resulting from vagueness in the system. Because uncertainty can have both random and vague components, both techniques were found to be useful tools in the analysis of rocket engine system reliability. Author (revised)

N94-29444*# Space Power, Inc., San Jose, CA.

NON-ISOLATED 30 kW CLASS ARCJET PCU Final Report

See-Pok Wong and Edward J. Britt Mar. 1994 40 p

(Contract NAS3-25609; RTOP 506-42-31)

(NASA-CR-189148; E-7426; NAS 1.26:189148; SPI-39-10) Avail: CASI HC A03/MF A01

A 30 kW class arcjet Power Conditioning Unit, PCU, was built and tested during this Phase 2 SBIR contract. The PCU is an improved version of two previously developed PCU's. All of these units are 3-phase, 20 kHz buck regulators with current mode feed back to modulate the duty cycle to control the arcjet current at any selected operating point. The steady state control can assure arcjet stability despite the negative dynamic resistance of the arc discharge. The system also has a circuit to produce a high voltage start pulse to breakdown the gas and initiate the arc. The start pulse is formed by temporarily switching a short current path across the output terminals with a special solid state switching array. The switches then open rapidly, and the energy stored in the output inductors of the buck regulator produces a pulse of approximately 2500 V for approximately 500 nsec. The system was tested and modified until the transition to steady operation occurred after start up with a very small surge current overshoot. The system also can withstand a direct short circuit across the output without damage. The automatic feed back control simply reduces the duty cycle to hold the current at the set point. When the short is removed the full power output is immediately restored. This latest version arcjet PCU is conduction cooled to remove waste heat by conduction to the base plate. This unit is closer to flight a type of design than the previous functional bread boards. Waste heat is small because the PCU has a very high efficiency, 296 percent. The PCU was extensively tested with resistor loads to simulate operation with an arcjet. The unit was tested with ammonia arcjets at the Jet Propulsion Laboratory. Approximately 400 hours of testing were completed, with several starts. Many hours were also demonstrated with resistive loads. Some testing with hydrogen arcjets was also carried out at NASA LeRC. This system concept is now the design base for the ATTD program. Author (revised)

N94-29544 Alabama Univ., Huntsville.

A VARIABLE SELECTION HEURISTIC FOR SOLID ROCKET MOTOR DESIGN Ph.D. Thesis

J. Wayne McCain 1993 202 p

Avail: Univ. Microfilms Order No. DA9324488

This dissertation research enhances an existing solid rocket motor design code by implementing an independent variable selection heuristic to precede the code's pattern search optimizer. The heuristic analyzes the effect of altering each independent SRM design variable and selects, by comparing calculated partial derivatives with an experimental threshold value, the parameters to be varied during design. By employing the heuristic, subjectivity is reduced, the design process is more efficient, and the risk of selecting a 'local optimum' is mitigated. Use of the new code's heuristic is illustrated with six test cases. The Fortran source code is listed in an appendix. Dissert. Abstr.

N94-29546*# Colorado State Univ., Fort Collins. Dept. of Mechanical Engineering.

DEVELOPMENT AND VERIFICATION OF A MODEL TO PREDICT IMPINGEMENT CURRENTS FOR ION THRUSTERS

Jeffery Monheiser Apr. 1994 101 p

(Grant NAG3-1206)

(NASA-CR-195322; E-8756; NAS 1.26:195322) Avail: CASI HC A06/MF A02

A One Dimensional model describing the production of ions that impinge on accelerator grids and cause them to erode is developed. Experimental data are obtained that show measured impingement currents agree with currents computed using this model to within +/- 30 percent. Data are also presented which show that impingement current ions are produced by charge exchange rather than single or multistep electron-impact reactions. Electrical potentials measured in the regions adjacent to and downstream of an accelerator grid are presented to show that charge exchange ions that impinge on the grid can be conveniently separated into two groups, one created upstream and the second created downstream of an ion beam neutralization boundary. All of the ions created in the first region impinge on accelerator grids while only a fraction of those created downstream of the neutralization boundary do. Data are also presented to show that experimentally measured values of the distance from the accelerator grid to this neutralization boundary agree with values computed using an equation developed by Kerslake. The One Dimensional model can be used to separate the relative contributions to impingement current ions produced from background atoms and atoms that come from the thruster. The model is applied to show that ions produced from xenon background atoms dominate impingement currents measured in many ground tests. Impingement currents in space should be substantially less because this contribution to the current will be negligible. Author (revised)

N94-29848*# Alabama Univ., Huntsville. Dept. of Mechanical and Aerospace Engineering.

ASPECTS OF MODEL-BASED ROCKET ENGINE CONDITION MONITORING AND CONTROL Final Report

Gerald R. Karr and Arthur J. Helmicki Apr. 1994 33 p

(Grant NAG8-212)

(NASA-CR-195116; NAS 1.26:195116; UAH-5-30175) Avail: CASI HC A03/MF A01

A rigorous propulsion system modelling method suitable for control and condition monitoring purposes is developed. Previously developed control oriented methods yielding nominal models for gaseous medium propulsion systems are extended to include both nominal and anomalous models for liquid mediums in the following two ways. First, thermodynamic and fluid dynamic properties for liquids such as liquid hydrogen are incorporated into the governing equations. Second, anomalous conditions are captured in ways compatible with existing system theoretic design tools so that anomalous models can be constructed. Control and condition monitoring based methods are seen as an improvement over some existing modelling methods because such methods typically do not rigorously lead to low order models nor do they provide a means for capturing anomalous conditions. Applications to the nominal SSME HPFP and degraded HPFP serve to illustrate the approach. Derived from text

N94-29868*# Wyle Labs., Inc., Huntsville, AL.
SPECIALIZED DATA ANALYSIS OF SSME AND ADVANCED PROPULSION SYSTEM VIBRATION MEASUREMENTS Final Report, Jun. 1989 - Oct. 1993
Thomas Coffin, Wayne L. Swanson, and Yen-Yi Jong Oct. 1993 430 p
(Contract NAS8-38156)
(NASA-CR-193940; NAS 1.26:193940; ER-60900-93-F) Avail: CASI HC A19/MF A04

The basic objectives of this contract were to perform detailed analysis and evaluation of dynamic data obtained during Space Shuttle Main Engine (SSME) test and flight operations, including analytical/statistical assessment of component dynamic performance, and to continue the development and implementation of analytical/statistical models to effectively define nominal component dynamic characteristics, detect anomalous behavior, and assess machinery operational conditions. This study was to provide timely assessment of engine component operational status, identify probable causes of malfunction, and define feasible engineering solutions. The work was performed under three broad tasks: (1) Analysis, Evaluation, and Documentation of SSME Dynamic Test Results; (2) Data Base and Analytical Model Development and Application; and (3) Development and Application of Vibration Signature Analysis Techniques. Derived from text

23 CHEMISTRY AND MATERIALS (GENERAL)

N94-28557# Sandia National Labs., Albuquerque, NM.
ALKYLENE-BRIDGED POLYGERM- AND POLYGERMSILSESQUI-OXANES: NEW HYBRID ORGANIC-INORGANIC MATERIALS
G. M. Jamison, D. A. Loy, G. Zender, and K. J. Shea 1993 9 p Presented at the 207th Spring National Meeting of the American Chemical Society, San Diego, CA, 13-18 Mar. 1994
(Contract DE-AC04-94AL-85000)
(DE94-005096; SAND-93-2514C; CONF-940301-5) Avail: CASI HC A02/MF A01

Alkylene-bridge polygerm- and polygermsilsequioxanes have been formed by hydrolysis-condensation of their corresponding (EtO)(sub 3)M(CH(sub 2))(sub n)Ge(OEt)(sub 3) monomers under HCl- and NEt(sub 3)-catalyzed conditions in ethanol. Solid state (sup 13)C and (sup 29)Si NMR indicate the retention of the alkylene bridging moiety during polymerization. The resulting aerogels are mesoporous materials with high surface areas. Incorporation of the short ethylene bridging unit results in higher surface areas than when heylene bridges are present. The porous nature of hexylene-bridged hybrid network Si(CH(sub 2))(sub 6)GeO(sub 3))(sub n) appears insensitive to the acidic or basic nature of the catalyst employed in it formation, in contrast to its polysilsesquioxane counterpart. Work is underway to determine the origin of porosity in these materials, and to characterize xerogel materials generated from these monomers. DOE

N94-28747*# National Aeronautics and Space Administration. Lewis Research Center, Cleveland, OH.
FORMATION AND CHEMICAL REACTIVITY OF CARBON FIBERS PREPARED BY DEFLUORINATION OF GRAPHITE FLUORIDE
Ching-Cheh Hung Apr. 1994 29 p Presented at the 21st Biennial Conference on Carbon, Buffalo, NY, 13-18 Jun. 1993; sponsored by the American Carbon Society
(RTOP 506-41-41)
(NASA-TM-106398; E-8228; NAS 1.15:106398) Avail: CASI HC A03/MF A01

Defluorination of graphite fluoride (CFX) by heating to temperatures of 250 to 450 C in chemically reactive environments was studied. This is a new and possibly inexpensive process to produce new carbon-based materials. For example, CF 0.68 fibers, made from P-100 carbon fibers, can be defluorinated in BrH2C-CH = CH-CH2Br (1,4-dibromo-2butene) heated to 370 C, and graphitized to produce fibers with an unusually high modulus and a graphite layer structure that is healed and cross-linked. Conversely, a sulfur-doped, visibly soft carbon fiber was produced by defluorinating CF 0.9 fibers, made from P-25, in sulfur (S) vapor at 370 C and then heating to 660 C in nitrogen (N2). Furthermore, defluorination of the CF 0.68 fibers in bromine (Br2) produced fragile, structurally damaged carbon fibers. Heating these fragile fibers to 1100 C in N2 caused further structural damage, whereas heating to 150 C in bromoform (CHBr3) and then to 1100 C in N2 healed the structural defects. The defluorination product of CFX, tentatively called activated graphite, has the composition and molecular structure of graphite, but is chemically more reactive. Activated graphite is a scavenger of manganese (Mn), and can be intercalated with magnesium (Mg). Also, it can easily collect large amounts of an alloy made from copper (Cu) and type 304 stainless steel to form a composite. Finally, there are indications that activated graphite can wet metals or ceramics, thereby forming stronger composites with them than the pristine carbon fibers can form. Author

N94-28924*# National Aeronautics and Space Administration. Lewis Research Center, Cleveland, OH.
GRAPHITE INTERCALATION COMPOUNDS PREPARED FROM GRAPHITE FLUORIDE
Ching-cheh Hung Mar. 1994 15 p Presented at the 21st Biennial Conference on Carbon, Buffalo, NY, 13-18 Jun. 1993; sponsored by the American Carbon Society
(RTOP 506-41-41)
(NASA-TM-106447; E-8299; NAS 1.15:106447) Avail: CASI HC A03/MF A01

The intercalation reaction between graphite fluoride and ferric chloride was observed in the temperature range of 300 to 400 C. The graphite fluorides used for this reaction have an sp(sup 3) electronic structure and are electrical insulators. They can be made by fluoridating either carbon fibers or powder having various degrees of graphitization. Intercalation is fast and spontaneous and can occur in the presence of air. The ferric chloride does not have to be predried. The products have an sp(sup 2) electronic structure and are electrical conductors. They contain new types of graphite intercalated compounds (GIC), which are mostly first stage and have an identity period near 11.1 A. This value is different from the 9.3 A value for first-stage GIC made by direct FeCl3-graphite intercalation. The new GIC contains iron and chlorine. It also contains fluorine, in concentrations that depend on the intercalation condition. This GIC deintercalated slowly in air at room temperature, but deintercalated quickly and completely at 370 C. Deintercalation is accompanied by the formation of rust (hematite) distributed unevenly on the fiber surface. When heated to 400 C in pure N2 (99.99 vol percent), this new GIC deintercalates without losing its staging structure. However, when the GIC is heated to 800 C deintercalation is complete and accompanied by the formation of iron oxides (other than hematite), distributed evenly in or on the fiber. This iron-oxide-covered fiber may be useful in making carbon-fiber/ceramic-matrix composites with strong bonding at the fiber-ceramic interface. Author (revised)

N94-29307# Pittsburgh Univ., PA. Dept. of Chemistry.
ORGANIC MATERIALS THAT RESPOND TO MOLECULES Final Report, 1 Mar. 1990 - 31 Aug. 1993
A. D. Hamilton and S. G. Weber 11 Jan. 1993 12 p
(Contract DAAL03-90-G-0051)
(AD-A275392; ARO-27724-6-MS-SM) Avail: CASI HC A03/MF A01

Materials have been developed in which symmetry and structure are tunable by control of the molecular size of one of the partners in the A-B pair. Materials have been studied in which a reversible crosslinking agent's

concentration is used to control material properties. The two systems are understood in quantitative detail. DTIC

N94-29458*# Boeing Defense and Space Group, Seattle, WA.
ANALYSIS OF SELECTED MATERIALS FLOWN ON INTERIOR LOCATIONS OF THE LONG DURATION EXPOSURE FACILITY Report, Oct. 1989 - Dec. 1993
H. A. Smith, K. M. Nelson, D. Eash, and H. G. Pippin Apr. 1994 111 p
(Contracts NAS1-18224; NAS1-19247; RTOP 506-43-61-02; RTOP 233-03-02-04)
(NASA-CR-4586; NAS 1.26:4586) Avail: CASI HC A06/MF A02

This report documents the post-flight condition of selected hardware taken from interior locations on the Long Duration Exposure Facility (LDEF). This hardware was generally in excellent condition. Outgassing data is presented for heat shrink tubing and fiberglass composite shims. Variation in total mass loss (TML) values for heat shrink tubing were correlated with location. Nylon grommets were evaluated for mechanical integrity; slight embrittlement was observed for flight specimens. Multi-layer insulation blankets, wire bundles, and paints in non-exposed interior locations were all in visibly good condition. Silicon-containing contaminant films were observed on silver-coated hex nuts at the space- and Earth-end interior locations. Author

N94-29554* National Aeronautics and Space Administration. Langley Research Center, Hampton, VA.
POLYIMIDES CONTAINING THE PENTA FLUORO SULFANYL BENZENE MOIETY Patent
Anna K. St.Clair, inventor (to NASA) and Terry L. St.Clair, inventor (to NASA) 12 Apr. 1994 9 p Filed 27 May 1993 Continuation-in-part of US-Patent-Appl-SN-755207, filed 5 Sep. 1991
(NASA-Case-LAR-15082-1; US-Patent-5,302,692;
US-Patent-Appl-SN-077132; US-Patent-Appl-SN-755207;
US-Patent-Class-528-353; US-Patent-Class-528-125;
US-Patent-Class-528-128; US-Patent-Class-528-170;
US-Patent-Class-528-172; US-Patent-Class-528-173) Avail: US Patent and Trademark Office

The diamine, 1,3-diamino 5-penta fluoro sulfanyl benzene (DASP), was reacted with various dianhydrides to form polyimides containing an SF5 moiety. These polyimides exhibit high glass transition temperatures, high density, low solubility, and low dielectric properties. These polymers were used to prepare semipermeable membranes, wire coatings, and films and are useful for electronic, space, and piezoelectric applications.
Official Gazette of the U.S. Patent and Trademark Office

N94-30242*# Alabama Univ., Huntsville. Center for Microgravity and Materials Research.
PROCESS MODELLING FOR MATERIALS PREPARATION EXPERIMENTS Semiannual Progress Report No. 9, 1 Aug. 1993 - 31 Jan. 1994
Franz Rosenberger and J. Iwan D. Alexander 31 Jan. 1994 7 p
(Grant NAG8-790)
(NASA-CR-195782; NAS 1.26:195782) Avail: CASI HC A02/MF A01

The main goals of the research under this grant consist of the development of mathematical tools and measurement techniques for transport properties necessary for high fidelity modelling of crystal growth from the melt and solution. Of the tasks described in detail in the original proposal, two remain to be worked on: development of a spectral code for moving boundary problems, and development of an expedient diffusivity measurement technique for concentrated and supersaturated solutions. We have focused on developing a code to solve for interface shape, heat and species transport during directional solidification. The work involved the computation of heat, mass and momentum transfer during Bridgman-Stockbarger solidification of compound semiconductors. Domain decomposition techniques and preconditioning methods were used in conjunction with Chebyshev spectral methods to accelerate convergence while retaining the high-order spectral accuracy. During the report period we have further improved our experimental setup. These improvements include: temperature control of the measurement cell to 0.1 C between 10 and 60 C; enclosure of the optical measurement path outside the ZYGO interferometer in a metal housing that is temperature controlled to the same temperature setting as the measurement cell; simultaneous dispensing and partial removal of the lower concentration (lighter) solution above the higher concentration (heavier) solution through independently motor-driven syringes; three-fold increase in data resolution by orientation of the interferometer with respect to diffusion direction; and increase of the optical path length in the solution cell to 12 mm. Derived from text

24 COMPOSITE MATERIALS

Includes physical, chemical, and mechanical properties of laminates and other composite materials.

For ceramic materials see *27 Nonmetallic Materials*.

N94-28528# Lawrence Livermore National Lab., CA.
FILAMENT TO MANDREL GAP ANALYSIS: RESULTING GAP FROM FILAMENT WINDING OVER A CONE-CYLINDER TRANSITION MANDREL (REFERENCE NMTP NO. 93838)
P. Geraghty 27 Oct. 1993 18 p
(Contract W-7405-eng-48)
(DE94-004225; UCRL-ID-115701) Avail: CASI HC A03/MF A01

The composites industry employs a method of high speed continuous reinforcement lay-down called filament winding. This is a process where resin impregnated tows, bundles of filament, are wound over a rotating mandrel. The tows, hereafter referred to as filament, are laid down over the rotating mandrel at a prescribed wind angle. Consider a cylindrical filament winding mandrel with conical features such that the filament is tangent to both the cylinder and the cone simultaneously. A gap is formed between the points of tangency. The gap distance measured along a line normal to the filament and intersecting the mandrel's axis of rotation. The maximum distance occurs between the filament and a point on the intersection of the cylinder and the cone. The problems this paper addresses are: given a cylindrical filament winding mandrel with conical features, what is the gap size for a given wind angle?; conversely, what is the wind angle for a given gap size?; and what does the geometry need to be in the mandrel transition area between the cylinder cone such that the filament remains in contact with the mandrel at all times?. DOE

N94-28579# Los Alamos National Lab., NM.
CHARACTERIZATION OF STRUCTURE AND MECHANICAL PROPERTIES OF MoSi2-SiC NANOLAYER COMPOSITES
H. Kung, T. R. Jervis, M. Nastasi, T. E. Mitchell, and J. P. Hirvonen 1993 9 p Presented at the Fall Meeting of the Materials Research Society, Boston, MA, 29 Nov. - 3 Dec. 1993
(Contract W-7405-eng-36)
(DE94-004982; LA-UR-93-4274; CONF-931108-33) Avail: CASI HC A02/MF A01

A systematic study of structure-mechanical properties relation is reported for MoSi2-SiC nanolayer composites. Alternating layers of MoSi2 and SiC were synthesized by DC magnetron and RF-diode sputtering, respectively. Cross-sectional transmission electron microscopy was used to examine three distinct reactions in the specimens when exposed to different annealing conditions: crystallization and phase transformation of MoSi2, crystallization of SiC, and spheroidization of the layer structures. Nanoindentation was employed to characterize the mechanical response as a function of structural changes. As-sputtered material exhibits amorphous structures in both types of layers and has a hardness of 11 GPa and a modulus of 217 GPa. Subsequent heat treatment induces crystallization of MoSi2 to form the C40 structure at 500 C and SiC to form the alpha structure at 700 C. The crystallization process is directly responsible for hardness and modulus increase in multilayers. A hardness of 24 GPa and a modulus of 340 GPa can be achieved through crystallizing both MoSi2 and SiC layers. Annealing at 900 C for two hours causes the transformation of MoSi2 into the C11(sub b) structure, as well as spheroidization of the layering to form a nanocrystalline equiaxed microstructure. A slight degradation in hardness but not in modulus is observed accompanying the layer breakdown. DOE

N94-28581# Los Alamos National Lab., NM. Materials Div.
FABRICATION AND TESTING OF PLASMA-SPRAY FORMED MoSi2 AND MoSi2 COMPOSITE TUBES
R. G. Castro, J. R. Hellman, A. E. Segall, and D. L. Shelleman 1993 7 p Presented at the Fall Meeting of the Materials Research Society, Boston, MA, 29 Nov. - 3 Dec. 1993

(Contract W-7405-eng-36)
(DE94-004995; LA-UR-93-4230; CONF-931108-35) Avail: CASI HC A02/MF A01

Plasma-spray forming has been used to fabricate thick-wall tubes of MoSi2 and MoSi2 containing concentric layers of Al2O3. This process is being investigated as a potential fabrication method for producing tubular components of MoSi2 and MoSi2 composites for use in high temperature fuel-burner applications. Results are reported on spray forming method used to produce various tube sizes. Room temperature strength of pure MoSi2 tubes in the as-deposited condition, and after heat treating at 1500 C for two hours in vacuum, is also reported. Strength of plasma sprayed MoSi2 tubes were measured via diametral compression of O-ring and C-ring sections in air at room temperature. Prediction of the strength distribution was based on Weibull statistical theory. DOE

N94-28653# Martin Marietta Labs., Baltimore, MD.
COMPOSITE PANEL FAILURE ANALYSIS AND IMPROVEMENT PLAN Final Report, Jun. - Oct. 1993
David K. McNamara 21 Dec. 1993 116 p
(Contract DAAK70-90-C-0019)
(AD-A275655; MML-TR-93-17) Avail: CASI HC A06/MF A02

Engineering test specimens and prototype XM19 Landing Mat sections were examined to determine the reasons for below-standard performance. Electron microscopy, x-ray photoelectron spectroscopy and thermal analyses were used in addition to visual microscopy, to determine the locus of failure, residual adhesive cure, and identify contributing causes of the failures. A number of poor production practices were identified, and a prototype process improvement plan proposed. DTIC

N94-28654# Naval Postgraduate School, Monterey, CA.
SERVICE LIFE PREDICTION OF COMPOSITE STRUCTURES THROUGH FIBER TESTING M.S. Thesis
Gregory S. Morin Sep. 1993 94 p
(AD-A275661) Avail: CASI HC A05/MF A01

Increasing the severity of the stress history of a structure reduces its service life. Feasibility studies to increase the zero fuel weight of the P-3 Orion depend heavily on the resulting decrease in service life of the wing box and airframe. One option of extending the service life of existing aircraft is through the replacement or augmentation of critical structural members with composite materials. Since structural composites do not yet have adequate service life statistics, life predication must be through probability modeling. Such modeling can begin with experimental data on accelerated testing of fiber life under several sustained load levels. This data can be the basis for an appropriate strength-life model of the fiber which can in term be related to the strength-life model of the composite by the local-load sharing model. The local-load sharing model captures the physical failure sequence of fiber failure within a composite. Such a strength-life model, when combined with structural analysis, can be used to predict an airframe's service life under the changed conditions associated with the zero fuel weight increase. DTIC

N94-28655# Naval Postgraduate School, Monterey, CA.
SAFETY ENHANCEMENT OF COMPOSITES VIA PERIODIC PROOF TESTING M.S. Thesis
Joseph H. Woodward Sep. 1993 74 p
(AD-A275662) Avail: CASI HC A04/MF A01

The development of new composite materials, which lack the historical field data base, has led to the need for an accelerated life testing method applicable to composites. Accelerated life testing by increasing the sustained stress levels requires the modeling and validation of a strength-life relation. Proof testing of composite fibers by over-loading is one step in the understanding of the relationship. It is also important in the reliability and safety assurance in deployment of composite structures. A parametric study examined the strength-life relation of composite fibers and a methodology to analyze the fiber failures after proof testing. The fiber statistical strength was modeled by a probability of failure model while a deterministic approach was taken considering individual fibers and the associated life reduction each fiber experienced during the proof testing procedure. Also studied was the distribution of the first failure to occur after proof testing in order to understand the effects of the sustained load and the proof load on fiber life. DTIC

N94-28673 Air Force Inst. of Tech., Wright-Patterson AFB, OH. School of Engineering.
FATIGUE BEHAVIOR OF A CROSS-PLY CERAMIC MATRIX COMPOSITE AT ELEVATED TEMPERATURES UNDER TENSION-TENSION LOADING M.S. Thesis
Richard J. Tuznik Dec. 1993 99 p Limited Reproducibility: More than 20% of this document may be affected by microfiche quality
(AD-A275466; AFIT/GAE/ENY/93D-28) Avail: CASI HC A05

A study was conducted which investigated the behavior of a Nicalon/calcium aluminosilicate (Nicalon/CAS) cross-ply (0/90)(sub 2S) ceramic matrix composite at elevated temperatures under tension-tension fatigue loading. Tension-tension fatigue tests were performed with a load ratio of R = 0.10 and a frequency of 10 Hertz at 700 C and 850 C. These results were compared to results from a previous study conducted at room temperature. Material behavior and damage was recorded by fatigue life curves, elastic modulus' maximum and minimum strain, acetate replication techniques, and post-mortem fractography. Analysis of these results showed identical matrix dominated damage behavior at RT and 700 C. Ultimate failure was caused by an accumulation of matrix damage, most of which occurred on the first cycle. However, at 850 C, significantly less damage occurred to the matrix and failure was fiber dominated. Fiber debonding was identified as the major damage mechanism responsible for final failure at this elevated temperature. DTIC

N94-28688 BDM Corp., McLean, VA.
TECHNOLOGY BASE ENHANCEMENT PROGRAM. METAL MATRIX COMPOSITES
30 Aug. 1993 215 p Limited Reproducibility: More than 20% of this document may be affected by microfiche quality
(Contract DAAA08-91-D-0008)
(AD-A275531) Avail: CASI HC A10

In an era of declining defense budgets, the North American defense industrial base faces the challenges of advancing and maintaining technological superiority with reduced government research and development funding. In response to this challenge, the North American Defense Industrial Base Organization (NADIBO) sponsored the Metal Matrix Composites (MMCs) assessment as a case study to assess the potential for emerging technologies to continue to advance and to remain viable in the current and projected economic environment. This assessment provides a methodology and framework for conducting similiar studies in the future and identifies opportunities to enhance the level of joint effort between the U.S. and Canada in creating and sustaining a viable MMC marketplace. DTIC

N94-28729 Florida Univ., Gainesville. Dept. of Materials Science and Engineering.
INNOVATIVE PROCESSING OF COMPOSITES FOR ULTRA-HIGH TEMPERATURE APPLICATIONS, BOOK 1 Annual Report
Reza Abbaschian Nov. 1993 101 p Limited Reproducibility: More than 20% of this document may be affected by microfiche quality
(Contract N00014-91-J-4075)
(AD-A275597) Avail: Issuing Activity (Defense Technical Information Center (DTIC))

The overall objective of this program was to provide a fundamental understanding of the processing science and technology necessary to fabricate ceramic-matrix, intermetallic-matrix, and metal-matrix composites with superior mechanical properties in high temperature and oxidizing environments. The composites are intended for use as structural materials for advanced aerospace applications at temperatures exceeding 1200 deg C (2200 deg F). In order to accomplish the program objective, interactive research groups were established in three key areas of (1) Fiber Fabrication, (2) Coatings and Infiltration, and (3) Composite Fabrication. The objective of the fiber fabrication group was to develop new fibers which have superior strength and toughness at high temperatures and in oxidizing environments. The research effort focused on the development of two types of fibers: (1) glass-free mullite-based fibers, and (2) oxygen-free silicon carbide fibers. The coatings program had two primary objectives: (1) to control the characteristics of matrix/reinforcing phase interfaces (e.g., to control chemical reactions and bonding at a matrix/fiber interface) and (2) to develop coatings that will improve the oxidation resistance of metal-matrix and intermetallic-matrix composites. Coatings methods utilized included

chemical vapor deposition, sol-gel processing, and solution coating with polymeric precursors to ceramics. DTIC

N94-28730 Florida Univ., Gainesville. Dept. of Materials Science and Engineering.
INNOVATIVE PROCESSING OF COMPOSITES FOR ULTRA-HIGH TEMPERATURE APPLICATIONS, BOOK 2 Annual Report
Reza Abbaschian Nov. 1993 154 p Limited Reproducibility: More than 20% of this document may be affected by microfiche quality
(Contract N00014-91-J-4075)
(AD-A275598) Avail: Issuing Activity (Defense Technical Information Center (DTIC))

The overall objective of this program is to develop intermetallic-matrix composites for structural application above 1200 deg C. The development of intermetallic-matrix composites is motivated by their inherent useful properties such as excellent oxidation resistance, high melting points and relatively low densities. The main disadvantages of intermetallics are poor fracture toughness at ambient temperature and low creep resistance and strength at high temperatures. It is expected that their inherent advantages can be effectively utilized via artificial compositing. The approaches used are to improve fracture toughness via ductile phase toughening, and to increase the creep resistance and strength via high strength ceramic reinforcements such as SiC whiskers. Two classes of alloys have been selected for investigation: (1) molybdenum disilicide (MoSI2), and (2) Nb-based aluminides with the major focus on NbAl3. DTIC

N94-28731 Florida Univ., Gainesville. Dept. of Materials Science and Engineering.
INNOVATIVE PROCESSING OF COMPOSITES FOR ULTRA-HIGH TEMPERATURE APPLICATIONS, BOOK 3 Annual Report
Reza Abbaschian Nov. 1993 169 p Limited Reproducibility: More than 20% of this document may be affected by microfiche quality
(Contract N00014-91-J-4075)
(AD-A275599) Avail: Issuing Activity (Defense Technical Information Center (DTIC))

The overall objectives of this program are: to develop improved processing methods for enhancing densification, controlling shrinkage and tailoring microstructure development in ceramic-matrix composites; and to develop ceramic-matrix composites with high temperature properties (mechanical, chemical, and dielectric) suitable for high temperature structural applications. These objectives are currently being pursued throughout two projects: Viscous, Transient Viscous and Pressure-Assisted Transient Viscous Sintering of Ceramics and Composites Using Submicron Composite Particles; and Processing of Ceramics and Composites by Liquid Infiltration Processing. DTIC

N94-28735 Army Natick Labs., MA. Research, Development and Engineering Center.
BALLISTIC PERFORMANCE OF POLYCARBONATE/POLYESTER AND POLYCARBONATE/STYRENE- ACRYLONITRILE MICROLAYER SHEETS Final Report, Oct. 1991 - Jun. 1993
William G. Kohlman Jan. 1994 28 p Limited Reproducibility: More than 20% of this document may be affected by microfiche quality
(DA Proj. 1L1-62786-AH-98)
(AD-A275462; Natick/TR-94/005) Avail: CASI HC A03

Extruded microlayer sheets of polycarbonate / polyester (PC/PCTG) and polycarbonate / styrene-acrylonitrile (PC/SAN) were tested for ballistic performance and chemical resistance. Composition of the microlayer sheets ranged from 60 to 100 percent polycarbonate. The number of layers in the approximately one-eighth inch thick sheets ranged from one for the blend control samples to 3713 layers in the PC/PCTG sheets. The normalized ballistic test results showed that some samples performed as well as and slightly better than injection molded polycarbonate samples. The failure mechanism was affected by the composition and the number of layers. Increasing composition of polycarbonate and number of layers decreased the percent of brittle failures. Immersion studies showed that the PC/PCTG microlayer sheets were attacked by diethylene triamine and xylene but slower than polycarbonate by itself. The diethylene triamine drop testing demonstrated that the microlayer sheets were attacked but the PC/SAN sheets showed the least effect. DTIC

N94-28823*# National Aeronautics and Space Administration. Langley Research Center, Hampton, VA.
PREDICTION OF STRESS-STRAIN RESPONSE OF SCS-6/TIMETAL-21S SUBJECTED TO A HYPERSONIC FLIGHT PROFILE
Massoud Mirdamadi (Analytical Services and Materials, Inc., Hampton, VA.) and W. Steven Johnson Feb. 1994 32 p
(RTOP 505-63-50-04)
(NASA-TM-109026; NAS 1.15:109026) Avail: CASI HC A03/MF A01

Thermomechanical response of a cross-ply SCS-6/Timetal-21S composite subjected to a generic hypersonic flight profile with the temperature ranging from -130 C to 816 C was evaluated experimentally and analytically. A two dimensional micromechanical anlaysis, VISCOPLY, was used to predict the stress-strain response of the laminate and of the constituents in each ply during thermomechanical loading conditions. In the analysis, the fiber was modeled as elastic with transverse orthotropic and temperature dependent properties and the matrix was modeled using a thermoviscoplastic constitutive relation. The fiber transverse modulus was reduced in the analysis to simulate fiber-matrix interface failure. Reasonable agreement was found between measured and predicted laminate stress-strain response when fiber-matrix debonding was modeled. Author

N94-28865# Drexel Univ., Philadelphia, PA. Dept. of Materials Engineering.
ON THE DYNAMIC MECHANICAL BEHAVIOR OF 3-D INTEGRATED FABRIC REINFORCED COMPOSITES Final Report
Frank K. Ko and Harry C. Rogers 5 Nov. 1993 120 p
(Contract DAAL03-86-G-0069)
(AD-A275424; ARO-23798.2-MS-F) Avail: CASI HC A06/MF A02

In order to elucidate the role of fiber architecture and test geometry on the impact behavior of 3-D braided composites, 3-D braided preforms having thicknesses varying form 0.3 in. to 1.0 in. were prepared for resin transfer molding with a vinylester resin system. Angle ply composites were fabricated for comparison with the 3-D composites to investigate the role of yarn interlacing in their dynamic impact response. The yarn interlacing was found to play an important role in raising the composites' ability to absorb impact energy, increasing its damage threshold and improving its damage containment. The 3-D network of fibrous reinforcement adds through-thickness strength and creates a complex path for crack growth. The superiority of the 3-D yarn interlacing was most obvious in the thicker structures where the degree of interlacing is more pronounced. During the course of this study, two non-destructive evaluation techniques (x-ray transmission and light transmission) were developed and utilized. X-ray transmission techniques were useful in detecting voids, improper wetting and fiber alignment in the as-molded composite plates. Light transmission was effective in characterizing the extent of damage by showing areas of delamination, debonding and cracking. DTIC

N94-29008# Air Force Inst. of Tech., Wright-Patterson AFB, OH. School of Engineering.
STATIC FRACTURE BEHAVIOR OF A CERAMIC MATRIX COMPOSITE AT ELEVATED TEMPERATURES M.S. Thesis
David M. Agins Dec. 1993 75 p
(AD-A275363; AFIT/GAE/ENY/93D-1) Avail: CASI HC A04/MF A01

This study investigated systematically the damage initiation, damage progression, and failure modes of a ceramic matrix composite, Nicalon/CAS, when loaded in tension at elevated temperatures in the presence of air. A cross-ply lay-up, (0/90)2s, was studied. The primary means of analysis were stress-strain data taken during monotonic and incremental load tests and crack density assessments. Testing was conducted at room temperature, 700 deg C, and 850 deg C. The stress-strain response was consistent for monotonic and incremental loading, except for a decrease in failure load at the elevated temperatures. Initial damage progression was also consistent, but the damage leading to failure and the final failure mode at 850 deg C were different due to the oxidation of the fibers. The oxidation created a brittle interface between the fiber and matrix, which resulted in an increase in fiber pull-out at the failure surface. DTIC

N94-29012# Air Force Inst. of Tech., Wright-Patterson AFB, OH. School of Engineering.
FATIGUE BEHAVIOR OF A CROSS-PLY CERAMIC MATRIX COMPOSITE UNDER STRAIN CONTROLLED TENSION-TENSION AND

TENSION-COMPRESSION LOADING M.S. Thesis
James J. Gudaitis Dec. 1993 207 p
(AD-A275374; AFIT/GAE/ENY/93D-17) Avail: CASI HC A10/MF A03

The purpose of this study was to investigate the fatigue response of a cross-ply (0/90)2s Nicalon/Calcium-Aluminosilicate (Nicalon/CAS) ceramic matrix composite at room temperature under strain controlled tension-tension and tension-compression fatigue loading. The primary objectives were to determine strain fatigue limits (fatigue life of at least 1,000,000 cycles) for both loading cases and to complete a fatigue life diagram (i.e. strain range versus fatigue life) for all tests. Failure mechanisms were also studied. The average initial modulus value for this lay-up was 120 GPa. DTIC

N94-29024# Quadrax Advanced Materials Systems, Inc., Portsmouth, RI.
3-D BRAIDED, CONTINUOUS FIBER CERAMIC COMPOSITES PRODUCED BY CHEMICAL VAPOR INFILTRATION Final Report, 18 Jan. 1991 - 2 Jan. 1992
Mark D. Mello and Robert A. Florentine Dec. 1993 28 p
(Contract DAAL04-91-C-0004)
(AD-A275192; ARL-CR-111) Avail: CASI HC A03/MF A01

Continuous fiber reinforced ceramic composites were successfully fabricated by chemical vapor infiltration of silicon carbide and silicon nitride matrix materials. Fiber preforms were three dimensionally braided with Nicalon(TM) and Nextel(TM) fiber materials forming a network of through thickness fiber architectures. Three unique material compositions were produced with the objective of demonstrating the capability of braiding brittle ceramic fibers and producing quality composites structurally capable of performing in a ballistic environment. It is anticipated that the continuous fiber architecture will be a significant technical advantage towards improvements in ceramic armor applications where non-catastrophic failure and increased toughness are a concern. DTIC

N94-29100*# National Aeronautics and Space Administration. Langley Research Center, Hampton, VA.
TEST AND ANALYSIS OF A STITCHED RFI GRAPHITE-EPOXY PANEL WITH A FUEL ACCESS DOOR
Dawn C. Jegley and W. Allen Waters, Jr. Mar. 1994 53 p
(RTOP 510-02-12-01)
(NASA-TM-108992; NAS 1.15:108992) Avail: CASI HC A04/MF A01

A stitched RFI graphite-epoxy panel with a fuel access door was analyzed using a finite element analysis and loaded to failure in compression. The panel was initially 56-inches long and 36.75-inches wide and the oval access door was 18-inches long and 15-inches wide. The panel was impact damaged with impact energy of 100 ft-lb prior to compressive loading; however, no impact damage was detectable visually or by A-scan. The panel carried a failure load of 695,000 lb and global failure strain of .00494 in/in. Analysis indicated the panel would fail due to collapse at a load of 688,100 lb. The test data indicate that the maximum strain in a region near the access door was .0096 in/in and analysis indicates a local surface strain of .010 in/in at the panel's failure load. The panel did not fail through the impact damage, but instead failed through bolt holes for attachment of the access door in a region of high strain. Author

N94-29126# California Univ., Santa Barbara. Dept. of Materials.
EFFECT OF MICROSTRUCTURE ON THE STRENGTH AND FRACTURE ENERGY OF BIMATERIAL INTERFACES Final Report, 1 Jan. 1990 - 31 Dec. 1993
Anthony G. Evans 31 Dec. 1993 349 p
(Contract N00014-90-J-1300)
(AD-A274987) Avail: CASI HC A15/MF A03

The annual report of the Office of Naval Research grant at UCSB on strength and fracture energy of bimaterials interfaces includes three sections: mechanics of interfaces, coating design for composite systems, and mechanics of brittle matrix composites. DTIC

N94-29135# SRI International Corp., Menlo Park, CA.
MICROSTRUCTURE/PROPERTY RELATIONSHIPS FOR SCS6/TIMETAL 21-S COMPOSITE Annual Report, 1 Sep. 1992 - 31 Aug. 1993
Charles G. Schmidt, Takao Kobayashi, Christine H. Kanazawa, and Donald A. Shockey Oct. 1993 21 p
(Contract F49620-92-C-0063)
(AD-A275056; AFOSR-94-0034TR) Avail: CASI HC A03/MF A01

Fracture surfaces of tensile test specimens from SCS6/Timetal 21-S composites with (0)4 or (0/90)s ply sequences were examined to characterize the failure processes. Fracture surface topography analysis (FRASTA) was used to quantitatively characterize the fracture surfaces. Results indicate that the topographies of the matrix fracture surfaces are a strong function of processes that occur during the rapid reduction in load after the maximum load. Failure of the matrix in all composites occurs after the maximum load is reached and after some or all of the 0 deg fibers have failed. Only part of the matrix phase of the 90 deg plies in a (0/90)s composite contributes to the tensile strength. The interface strength between the fibers and the matrix is negligible and does not contribute significantly to the strength of the composite. DTIC

N94-29166# Naval Postgraduate School, Monterey, CA.
AN ANALYSIS OF THE MICROSTRUCTURE AND REINFORCEMENT DISTRIBUTION OF AN EXTRUDED PARTICLE-REINFORCED Al 6061-10 VOLUME PERCENT Al2O3 METAL MATRIX COMPOSITE M.S. Thesis
Fredric W. Longenecker Sep. 1993 81 p
(AD-A275050) Avail: CASI HC A05/MF A01

This research was performed in conjunction with funding by DURALCAN-USA through a Cooperative Research and Development Agreement (CRDA). The program seeks to improve the ductility of cast and extruded Al 6061-Al2O3 metal matrix composite (MMC) materials. Annealing stages were designed to be introduced into combined extrusion and drawing operations during the processing of the MMC's. This work has included a comprehensive analysis of a composite's microstructure as related to processing strains ranging from zero to 5.32 during extrusion/drawing operations. As the strains were increased, particle clusters present in the as-cast material were dispersed and the particle distribution became more uniform. Strains of greater than 4.0 were required in order to disperse the clusters and substantially eliminate banding of the particle distribution. The recrystallized grain size in the Al matrix decreased as increased processing strain was applied to the material. The grain size appeared to be stable and resistant to coarsening during subsequent solution heat treatment. Quantitative image analysis revealed no change in apparent particle size or aspect ratio indicating no fracturing of the particles during processing. The image analysis revealed no readily measurable feature to be used to assess uniformity of the particle distribution. DTIC

N94-29208*# Case Western Reserve Univ., Cleveland, OH.
PROPERTIES OF GRAPHITE FIBER REINFORCED COPPER MATRIX COMPOSITES FOR SPACE POWER APPLICATIONS Final Report
David L. Ellis Aug. 1992 14 p
(Contract NCC3-94; RTOP 590-13-11)
(NASA-CR-191026; E-7491; NAS 1.26:191026) Avail: CASI HC A03/MF A01

The thermal and mechanical properties of pitch-based graphite fiber reinforced copper matrix (Gr/Cu) composites usable for space applications such as radiator fins were investigated. Thermal conductivity was measured as a function of fiber volume fraction and architecture. Results showed for unidirectional P-100 Gr/Cu composites, the longitudinal thermal conductivity was nearly independent of fiber volume fraction. Transverse thermal conductivities (perpendicular to the fibers) were strongly affected by the fiber volume fraction with higher volume fractions resulting in lower thermal conductivities. The effect of architecture on thermal conductivity followed the cosine squared law for simple architectures. Insufficient data are available currently to model more complex architectures, but adding fibers in the direction of the heat flow increases the thermal conductivity as low conductivity plies are supplemented by high conductivity plies. Thermal expansion tests were conducted on the Gr fibers and Gr/Cu composites. The results show a considerable thermal expansion mismatch between the fibers and the Cu matrix. The longitudinal thermal expansion showed a strong dependence on the architecture of the Gr/Cu composites. The composites also show a thermal expansion hysteresis. The hysteresis was eliminated by an engineered interface. Mechanical testing concentrated on the dynamic modulus and strength of the composites. The dynamic modulus of the Gr/Cu composites was 305 GPa up to 400 C, a value equivalent to Be. The strengths of the composites were less than expected, but this is attributed to the poor bond across the interface between the Gr fibers and Cu matrix. Testing of composites with an engineered interface is expected to yield strengths nearer the values predicted by the rule of mixtures.
Author (revised)

N94-29412# Aerospatiale Aquitaine, Saint-Medard en Jalles (France).
CHARACTERISATION AND PROCESSING OF SiC/MAS-L GLASS CERAMIC MATRIX COMPOSITE [ELABORATION ET CARACTERISATION DU COMPOSITE A MATRICE VITROCERAMIQUE SIC/MAS-L]
G. Larnac, P. Peres, and J. M. Donzac 1993 22 p In FRENCH Submitted for publication
(Rept-932-430-111; ETN-94-95469) Avail: CASI HC A03/MF A01

Results concerning microstructural studies as well as mechanical property evaluations carried out on SiC-MAS-L composites under air and inert atmosphere as a function of temperature are presented. MAS is MgO-Al2O3-SiO2. These ceramic fiber reinforced glass-ceramic matrix composites were made by hot unidirectional pressing. Two types of thermal cycling were determined leading to different matrix microstructures. In one case, the matrix was composed of a mixture of crystalline and amorphous phases, and in the other the matrix was totally ceramicized. The mechanical characterization in an inert atmosphere as a function of temperature showed that these two matrices behaved differently. When the composite is tested in air, it produces, above 800 C, an increase in the constraint of interfacial strength and a modification of the mode of rupture. It is concluded that ceramic fiber reinforced glass-ceramic composites represent potential materials for thermomechanical applications up to 1000 C. ESA

N94-29413# Aerospatiale Aquitaine, Saint-Medard en Jalles (France). Espace et Defense.
GLASS-CERAMIC MATRIX COMPOSITES
Jean F. Jamet 1993 11 p Presented at the A.A.A.F. Conference, Bordeaux, France, 12-13 Oct. 1992
(Rept-932-430-112; ETN-94-95470) Avail: CASI HC A03/MF A01

The history of glass-ceramic matrices is given and reasons for the present interest in these materials are also given: their state of the art is considered taking into account the glass composition, glass synthesis (the melting route and the chemical route), the densification technology (hot pressing, injection molding of short fiber matrix compound, matrix transfer molding, hot isostatic pressing), and sandwich structrure feasibility. The glass-ceramic matrices were characterized taking into account their high temperature behavior, mechanical fatigue behavior, and creep behavior. Main application aims of aerospace companies with this composite are listed. ESA

N94-29425# Aeronautical Research Inst. of Sweden, Stockholm. Structures Dept.
ASSESSMENT OF THE FIBRE VOLUME DISTRIBUTION AROUND OPTICAL FIBRES
Klas Levin and Pavel Sindelar Jun. 1993 30 p
(Contract FMV52700-90-066-16-001)
(FFA-TN-1993-12; ETN-94-95526) Avail: CASI HC A03/MF A01

The disturbance of embedded optical fibers on fiber distribution in carbon fiber reinforced plastics is addressed. Results for a number of configurations in terms of the variation of fiber volume content around optical fibers in laminates are presented. The width of the wedge shaped matrix pocket, which occurs when the angle between the optical fiber and adjacent plies differ, was determined for different configurations. The results showed that a region with low fiber volume content appeared extending out from the optical fiber despite the same orientation of optical fiber and the surrounding carbon fibers in the adjacent plies. The size of the region was affected by the direction: namely, the region was greater in the horizontal than in vertical direction. Besides different coating materials, neither diameter of optical fiber, its location in the laminate, nor type of laminate had any significant effect on the distribution of the fiber volume content. The smallest region was detected for the polyimide coated optical fiber with the stiffest coating tested. Only the angle between the optical fiber and the adjacent carbon fiber orientation did contribute to the width of the matrix pocket. The largest matrix pockets were observed when the optical fiber was oriented perpendicular to the surrounding carbon fibers. Even for fairly large variation of the optical fiber diameters, the width of the matrix pocket was almost similar. ESA

N94-29442# Aerospatiale Aquitaine, Saint-Medard en Jalles (France). Espace et Defense.
DAMAGE MESO-MODELING OF 3D EVOLUTIVE COMPOSITES [MESO-MODELISATION DE L'ENDOMMAGEMEMT DE COMPOSITES EVOLUTIFS TRIDIRECTIONNELS]
O. Allix (Ecole Normale Superieure, Cachan, France.), C. Cluzel (Ecole Normale Superieure, Cachan, France.), P. Ladeveze (Ecole Normale Superieure, Cachan, France.), and P. Peres 1993 12 p In FRENCH Presented at the 8th Journees Nationales sur les Materiaux Composites, 16-18 Nov. 1992
(Rept-932-430-106; ETN-94-95464) Avail: CASI HC A03/MF A01

An evolutive Three Dimensional (3D) carbon-carbon composite developed for thermostructural applications is dealt with. The composite looks like a plate reinforced in the normal direction by fiber yarns in order to prevent delamination. The choice of the stacking sequence and the proportion of normal reinforcement lead to a range of materials. Two mesomodelings are proposed. In the first the composite is modeled as a stacking of damageable and slightly inelastic single layers. This enables the prediction of the inner rupture of a structure under complex loadings. This approach provides a simple tool for the optimization of the choice of a stacking sequence as regards to the inner deteriorations. Another aspect concerns the understanding of the 3D mechanisms of degradation, especially delamination in order to optimize the distribution of the normal reinforcements. This second approach is in progress and is, at present, developed in elasticity only. Asymptotic developments are used to obtain, by means of finite elements, the 3D distribution of stresses. ESA

N94-29454# Aerospatiale Aquitaine, Saint-Medard en Jalles (France). Dept. Qualite.
MICROFOCUS RADIOSCOPY, A HIGH RESOLUTION MEANS OF INSPECTING COMPOSITE MATERIALS [LA RADIOSCOPIE A MICROFOYER, UN MOYEN D'INSPECTION HAUTE RESOLUTION DES MATERIAUX COMPOSITES]
Daniel Loubet 1993 5 p In FRENCH
(Rept-932-430-109; ETN-94-95467) Avail: CASI HC A01/MF A01

Several examples of the use of microfocus radioscopy in the field of aeronautics and space are given. The use of microfocus X-ray set compensates for the weak geometric resolution of classic radioscopy by magnification of the radiologic image. Enlargements in ratios of 1 to 100 or 200 do not pose any problems and defects as small as a few tens of microns will be easily detected. A digital treatment set of radioscopic images is a very important complement for this type of installation. Several examples of use in the field of aeronautics and space are given, using this installation. The examples given concern the control of the redressing of anti oxidation protection of thermostructural parts in which eventual cracks must be detected, and the control of the homogeneity of ceramic composites in which the porosity must be detected. ESA

N94-29462# Aerospatiale, Suresnes (France). Dept. Materiaux.
CORRELATION BETWEEN WET AGEING, HUMIDITY ABSORPTION AND PROPERTIES ON COMPOSITE MATERIALS BASED ON DIFFERENT RESINS FAMILY
J. Cinqin and P. Abjean 1993 14 p
(Rept-932-600-107; ETN-94-95486) Avail: CASI HC A03/MF A01

The material humidity content influence on the Interlaminar Shear Stress (ILSS) and on the glass transition temperature (T(sub g)) properties is pointed out. Three composite families were investigated: Bismaleimide (BMI), cyanate, and epoxy. Experimental data on humidity absorption show that for BMI and cyanate, the data can be fitted with Fick's law to follow the humidity absorption kinetics. For expoxy, the data can be fitted with Langmuir's law. Regarding the T(sub g) values, for the epoxy, the drop of T(sub g) between the dry state and the wet state occurs during the first step of humidity absorption. For the cyanate, the drop of T(sub g) appears during the last step of humidity absorption. For the BMI, no influence of humidity content on the T(sub g) values was noticed. Concerning the ILSS, for the epoxy a linear relationship between the humidity content and the ILSS was observed. For the cyanate, no influence of the humidity content on the ILSS was noted. For the BMI, a humidity content over 0.6 results in a important decrease of the ILSS. ESA

N94-29472*# National Aeronautics and Space Administration. Langley Research Center, Hampton, VA.
PRELIMINARY EVALUATION OF HYBRID TITANIUM COMPOSITE LAMINATES
J. L. Miller, D. J. Progar, W. S. Johnson, and T. L. St.Clair Apr. 1994 31 p
(RTOP 505-63-50-04)
(NASA-TM-109095; NAS 1.15:109095) Avail: CASI HC A03/MF A01

In this study, the mechanical response of hybrid titanium composite laminates (HTCL) was evaluated at room and elevated temperatures. Also, the use of an elastic-plastic laminate analysis program for predicting the tensile response from constituent properties was verified. The improvement in mechanical properties achieved by the laminates was assessed by comparing the results of static strength and constant amplitude fatigue tests to those for monolithic titanium sheet. Two HTCL were fabricated with different fiber volume fractions, resin layer thicknesses, and resins. One panel was thicker and was more poorly bonded in comparison to other. Consequently, the former had a lower tensile strength, while fewer cracks grew in this panel and at a slower rate. Both panels showed an improvement in fatigue life of almost two orders of magnitude. The model predictions were also in good agreement with the experimental results for both HTCL panels. Author (revised)

N94-29475 National Defence Research Establishment, Stockholm (Sweden). Dept. of Weapon Systems, Effects and Protection.
INTELLIGENT MATERIAL SYSTEMS AND STRUCTURES. PART 7: DEBONDING AND PULL-OUT OF TWO OPTICAL FIBERS FROM TWO EPOXIES [INTELLIGENTA MATERIAL SYSTEM OCH STRUKTURER. DEL 7: DEBONDING OCH PULL-OUT AV TVA SLAGS OPTISKA FEBRER]
T. Karlsson Oct. 1993 21 p In SWAHILI Limited Reproducibility: More than 20% of this document may be affected by microfiche quality
(ISSN 0347-3694)
(PB94-137767; FOA-C-20945-8.4-Pt-7) Avail: CASI HC A03

With the pull-out method one can monitor the load during debonding and pull-out of optical fibers from plastics and probably from fiber composites. Both of the fibers used debonded between the cladding and the skin. The bond strength between them showed great local variations which might constitute a problem for their use as sensors. The fragmentation method was shown to be useless to determine the shear strength between the optical fibers and plastics as the former are too ductile. The ultimate strength of the quartz fiber deteriorated rapidly after it had been stripped of its skin. NTIS

N94-29478# Aerospatiale Aquitaine, Saint-Medard en Jalles (France). Div. Espace et Defense.
RELIABILITY OF COMPOSITE MATERIAL STRUCTURES. APPLICATION: HIGH PRESSURE SPHERICAL CODED TANKS [FIABILITE DES STRUCTURES EN MATERIAUX COMPOSITES. APPLICATIONS: RESERVOIRS SPHERIQUES BOBINES HAUTEPRESSION]
J. Mendez 1993 8 p In FRENCH Sponsored by ESA
(Rept-932-430-103; ETN-94-95461) Avail: CASI HC A02/MF A01

Theoretical and practical analysis of the reliability of critical non electronic components of a spacecraft, of which failure would lead to the termination of a mission, are reported. Application is made to high pressure spherical coiled tanks which stock high pressure gas and release it at precise moments during a mission. The theoretical probability of structural or functional failure is made using the 'resistance-constraint' method. The practical probability of failure of a component is estimated by identifying all the potential causes of failure which may arise during manufacture, assembling, integration, use, etc. The global probability of failure is the sum of the theoretical and practical probabilities. ESA

N94-29485*# National Aeronautics and Space Administration. Langley Research Center, Hampton, VA.
NON-RECTANGULAR TOWPREG ARCHITECTURES Patent Application
Donald A. Sandusky, inventor (to NASA) (College of William and Mary, Williamsburg, VA.), Joseph M. Marchello, inventor (to NASA) (Old Dominion Univ., Hampton, VA.), and Robert M. Baucom, inventor (to NASA) 20 Oct. 1993 8 p
(NASA-Case-LAR-14863-1-CU; NAS 1.71:LAR-14863-1-CU; US-Patent-Appl-SN-141293) Avail: CASI HC A02/MF A01

A shaped towpreg ribbon having a cross-sectional geometry which promotes intimate lateral contact between adjacent composite tows was prepared. The cross-sectional geometry is non-rectangular and promotes intimate lateral contact between adjacent towpreg ribbons during normal processing. NASA

N94-29496*# National Aeronautics and Space Administration. Langley Research Center, Hampton, VA.
APPARATUS FOR PROVIDING A UNIFORM, CONSOLIDATED, UNIDIRECTIONAL, CONTINUOUS, FIBER-REINFORCED POLYMERIC MATERIAL AND METHOD RELATING THERETO Patent Application
Donald A. Sandusky, inventor (to NASA) (College of William and Mary, Williamsburg, VA.) 20 Oct. 1993 19 p
(NASA-Case-LAR-15173-1-CU; NAS 1.71:LAR-15173-1-CU; US-Patent-Appl-SN-141292) Avail: CASI HC A03/MF A01

An apparatus and method were developed for providing a uniform, consolidated, unidirectional, continuous, fiber-reinforced polymeric material. The apparatus comprises a supply means, a forming means, a shaping means, and a take-up means. The forming means further comprises a pre-melting chamber and a stationary bar assembly. The shaping means is a loaded cooled nip-roller apparatus. Forming takes place by heating a polymeric prepreg material to a temperature where the polymer becomes viscous and applying pressure gradients at separate locations along the prepreg material. Upon exiting the forming means, the polymeric prepreg material is malleable, consolidated, and flattened. Shaping takes place by passing the malleable, consolidated, flattened prepreg material through a shaped, matched groove in a loaded, cooled nip-roller apparatus to provide the final solid product. NASA

N94-29508* National Aeronautics and Space Administration. Lewis Research Center, Cleveland, OH.
METHOD OF PRODUCING A CERAMIC FIBER-REINFORCED GLASS-CERAMIC MATRIX COMPOSITE Patent
Narottam P. Bansal, inventor (to NASA) 25 Jan. 1994 6 p Filed 30 Jun. 1993 Supersedes N93-31299 (31 - 12, p 3700) Continuation-in-part of US-Patent-Appl-SN-872262, filed 16 Apr. 1992
(NASA-Case-LEW-15264-2; US-Patent-5,281,559; US-Patent-Appl-SN-084058; US-Patent-Appl-SN-872262; US-Patent-Class-501-8; US-Patent-Class-501-32; US-Patent-Class-501-95; US-Patent-Class-264-58; Int-Patent-Class-C03C-10/06; Int-Patent-Class-C03C-14/00) Avail: US Patent and Trademark Office

A fiber-reinforced composite composed of a BaO-Al2O3-2SiO2 (BAS) glass ceramic matrix is reinforced with CVD silicon carbide continuous fibers. A slurry of BAS glass powders is prepared and celsian seeds are added during ball melting. The slurry is cast into tapes which are cut to the proper size. Continuous CVD-SiC fibers are formed into mats of the desired size. The matrix tapes and the fiber mats are alternately stacked in the proper orientation. This tape-mat stack is warm pressed to produce a 'green' composite. The 'green' composite is then heated to an elevated temperature to burn out organic constituents. The remaining interim material is then hot pressed to form a silicon carbide fiber-reinforced celsian (BAS) glass-ceramic matrix composite which may be machined to size.
Official Gazette of the U.S. Patent and Trademark Office

N94-29509* National Aeronautics and Space Administration. Ames Research Center, Moffett Field, CA.
COMPOSITE FLEXIBLE BLANKET INSULATION Patent
Demetrius A. Kourtides, inventor (to NASA) and David M. Lowe, inventor (to NASA) 11 Jan. 1994 23 p Filed 1 Aug. 1991 Supersedes N94-15926 (32 - 3, p 934) Continuation-in-part of US-Patent-Appl-SN-700368, filed 6 May 1991 which is a division of US-Patent-Appl-SN-410576, filed 21 Sep. 1989
(NASA-Case-ARC-11955-1-CU; US-Patent-5,277,959; US-Patent-Appl-SN-739026; US-Patent-Appl-SN-700368; US-Patent-Appl-SN-410576; US-Patent-Class-428-116; US-Patent-Class-112-415; US-Patent-Class-112-420; US-Patent-Class-112-440; US-Patent-Class-139-420A) Avail: US Patent and Trademark Office

An improved composite flexible blanket insulation is presented comprising top silicon carbide having an interlock design, wherein the reflective shield

is composed of single or double aluminized polyimide and wherein the polyimide film has a honeycomb pattern.
Official Gazette of the U.S. Patent and Trademark Office

N94-29524 National Physical Lab., Teddington (England).
STRESS TRANSFER MECHANICS FOR MULTIPLE PERFECTLY BONDED CONCENTRIC CYLINDER MODELS OF UNIDIRECTIONAL COMPOSITES
L. N. McCartney 1993 43 p
(PB94-138633; NPL-DMM(A)-129) Copyright Avail: Issuing Activity (National Technical Information Service (NTIS))

The problem of predicting the stress and displacement distributions in an assembly of perfectly bonded multiple cylinders subject to load transfer has been reduced to manipulating sets of recurrence relations that generate a set of fourth order simultaneous ordinary differential equations. Each cylinder is assumed to be a transverse isotropic solid and account is taken of the residual stresses arising from thermal expansion mismatch effects. Numerical solutions of the problem are readily obtained using a desk-top computer and experience of application of the technique to unidirectional carbon fiber epoxy composites has shown that the new technique is robust. For a unidirectional composite with fiber fractures, by representing the fibers by one set of cylinders, the matrix by another set, and surrounding effective composite material by a third set, accurate solutions for stress and displacement distributions can be found in the vicinity of a fiber fracture that agree closely with finite element solutions. The value of the stress concentration is found to be slightly higher than that predicted by local load sharing if account is taken of the axial stress gradient in the nearest neighbor fibers, and smaller if the stress concentration is based on the average axial stress in these fibers. NTIS

N94-29541*# National Aeronautics and Space Administration. Langley Research Center, Hampton, VA.
EFFECTS OF PHYSICAL AGING ON LONG-TERM CREEP OF POLYMERS AND POLYMER MATRIX COMPOSITES
L. Catherine Brinson (Northwestern Univ., Evanston, IL.) and Thomas S. Gates Feb. 1994 34 p
(RTOP 505-63-50-04)
(NASA-TM-109081; NAS 1.15:109081) Avail: CASI HC A03/MF A01

For many polymeric materials in use below the glass transition temperature, the long term viscoelastic behavior is greatly affected by physical aging. To use polymer matrix composites as critical structural components in existing and novel technological applications, this long term behavior of the material system must be understood. Towards that end, this study applied the concepts governing the mechanics of physical aging in a consistent manner to the study of laminated composite systems. Even in fiber-dominated lay-ups the effects of physical aging are found to be important in the long-term behavior of the composite. The basic concepts describing physical aging of polymers are discussed. Several aspects of physical aging which have not been previously documented are also explored in this study, namely the effects of aging into equilibrium and a relationship to the time-temperature shift factor. The physical aging theory is then extended to develop the long-term compliance/modulus of a single lamina with varying fiber orientation. The latter is then built into classical lamination theory to predict long-time response of general oriented lamina and laminates. It is illustrated that the long term response can be counterintuitive, stressing the need for consistent modeling efforts to make long term predictions of laminates to be used in structural situations.
Author (revised)

N94-29593 Georgia Inst. of Tech., Atlanta.
ACTIVE CONTROL OF DELAMINATIONS IN SMART COMPOSITE STRUCTURES Ph.D. Thesis
Lakshmana Nagesh Bab Gummadi 1992 217 p
Avail: Univ. Microfilms Order No. DA9315877

Delaminations are one of the most commonly observed defects in laminated composite structures. Presence of delaminations significantly degrade the performance of a structure. Under certain loading conditions, these delaminations may grow and the growth of such delaminations may eventually lead to catastrophic failures. In this thesis, control of growth of delaminations is studied using the concepts of smart structures. As a first step, a detailed dynamic model of a delaminated beam, is studied. Effects of the delamination on dynamic characteristics such as natural frequencies, mode shapes and dynamic response under various loading conditions are studied. It is observed that the presence of delaminations not only affect the natural frequencies but also significantly alter the mode shapes when compared with the natural frequencies and mode shapes of a perfect beam. Later, this dynamic model has been improved to study the effects of shear deformation and rotary inertia on dynamic characteristics. Elements based on first order and third order shear deformation theories that include rotary inertia effects are developed to study the dynamics of the delaminated beam. It is observed from these studies, that shear deformation effects are quite significant for small delamination sizes. Observed changes in the dynamic behavior of the delaminated beam and the perfect beam are used to detect the size and the location of the delamination. Ibrahim time domain identification technique that uses the free response data is used for identifying natural frequencies and mode shapes. From the identified natural frequencies and mode shapes, it is concluded that changes in dynamic responses of delaminated beams can be used for the detection of the size and the location of a delamination. As a next step, growth of this identified delamination is controlled by using active control techniques. Since growth of delamination is due to high interlaminar stresses, an active control scheme that reduces the high interlaminar stresses is proposed to control the growth of delamination. Fracture mechanics based total energy release rate criterion is used to characterize the growth of delamination. Robustness aspects in the design of active control schemes are discussed for a smart structure. A robust controller that reduces vibrations even when the sensors are partially debonded is designed. Mu synthesis is used for the design of robust controllers. Dissert. Abstr.

N94-29684*# Sverdrup Technology, Inc., Brook Park, OH.
THERMODYNAMIC ANALYSIS OF CHEMICAL COMPATIBILITY OF SEVERAL COMPOUNDS WITH Fe-Cr-Al ALLOYS Final Report
Ajay K. Misra Jul. 1993 32 p
(Contract NAS3-25266; RTOP 510-01-50)
(NASA-CR-191166; E-8009; NAS 1.26:191166) Avail: CASI HC A03/MF A01

Chemical compatibility between Fe-19.8Cr-4.8Al (weight percent), which is the base composition for the commercial superalloy MA956, and several carbides, borides, nitrides, oxides, and silicides was analyzed from thermodynamic considerations. The effect of addition of minor alloying elements, such as Ti, Y, and Y2O3, to the Fe-Cr-Al alloy on chemical compatibility between the alloy and various compounds was also analyzed. Several chemically compatible compounds that can be potential reinforcement materials and/or interface coating materials for Fe-Cr-Al based composites were identified. Author (revised)

N94-29735 Purdue Univ., West Lafayette, IN.
FREE EDGE AND SIZE EFFECTS ON FAILURE INITIATION AND ULTIMATE STRENGTH OF LAMINATES CONTAINING A CENTER HOLE Ph.D. Thesis
Gou-Don Chu 1992 158 p
Avail: Univ. Microfilmes Order No. DA9313967

A failure analysis method that includes free edge and size effect was proposed for failure prediction in composite laminates containing a center hole. Categorically, this failure analysis consists of three major parts. The first is the size effect on the strength of an unnotched coupon specimen under off-axis loading. The relationship between ultimate strength and volume of the specimen was established by curve fitting the experimental results. From those test results, the strength of the composite laminate with respect to the dimension of the specimen was determined. After finding the relation between size and strength, the location of the onset of failure in the hole can be determined by comparing the strength of off-axis unnotched specimens with the hoop stress around the hole. The corresponding strength in this location was defined as the initial failure strength. From the specified failure location and stress, subsequent failure progression was performed by ply-by-ply classical laminate failure analysis in addition to free edge failure analysis of the laminate at the free surface of the hole. Experiments on (0/90/(+/- 45))(sub s) and (0/90)(sub s) laminates and their off-axis specimens were Performed to verify the present method. Dissert. Abstr.

N94-29810 Nebraska Univ., Lincoln.
PERFORMANCE OF A HIGHER-ORDER TRIANGULAR FINITE ELEMENT FOR COMPOSITE LAMINATED STRUCTURES Ph.D. Thesis

Hao Yu 1993 144 p
Avail: Univ. Microfilms Order No. DA9322819

In general, the shear stiffness of composite materials is much lower than that of conventional engineering materials and the transverse shear deformation is not negligible in analyzing composite structures. Unfortunately, many finite elements which include transverse deformation become too stiff when dealing with thin composite laminated plates. Therefore, a new higher-order triangular finite element model with six nodes, which includes transverse shear effects and can deal with both very thin and thick composite laminated structures, is developed in this dissertation. The basic element tests for isotropic and orthotropic materials are conducted and the results are compared with the theoretical solutions. Also, several typical bending problems for composite laminated structures, such as cross-ply, angle-ply, sandwich and swept plates and cantilever laminated beams with different stack sequences, are solved using the present finite element model, and the results are compared with their corresponding exact solutions wherever possible or those of some other existing finite element models. Interlaminar shear stress calculation and comparisons for isotropic and anisotropic plates are also presented. Dissert. Abstr.

N94-29852 New Mexico Inst. of Mining and Technology, Socorro.
INTERFACE ENGINEERING IN ALUMINA FIBER/GLASS COMPOSITES Ph.D. Thesis
Ramanan Venkatesh 1992 274 p
Avail: Univ. Microfilms Order No. DA9313001

The goal of the present study is the development of tough alumina fiber/glass composites. Alumina and glass form a chemical bond and hence the resulting composite is brittle. SnO2 has been shown to have no solubility in alumina and very little diffusion in glass. A weakly bonded SnO2 interphase would aid in crack deflection, fiber debonding, and/or fiber pullout in alumina/SnO2/glass composites. The proposed study modifies the interface of alumina fiber/glass composites by incorporating a layer of SnO2, and characterizes the physical and mechanical properties of the resultant composites. Thermal stresses evaluated from a three-element cylindrical model showed radial tensile stress in both PRD-166/SnO2/glass and single crystal alumina Saphikon/SnO2/glass matrix composites. Even though there was weak mechanical bonding and tensile radial thermal stress at the PRD-166/SnO2 interface, the fibers could not be pushed out during a nanoindentation test. This was attributed to fiber roughness causing a compressive clamping stress at the PRD-166/SnO2 interface. PRD-166/glass matrix composites failed in a brittle manner whereas PRD-166/SnO2/glass matrix composites exhibited nonplanar failure with crack deflection and fiber bridging as the major toughening mechanisms. Saphikon/SnO2/glass matrix composites failed in a tough manner with extensive fiber pullout. This difference in the mode of failure was due to a relatively smooth Saphikon fiber. Fracture toughness of PRD-166/glass and PRD-166/SnO2/glass matrix composites measured with a chevron notch showed that the toughness of PRD-166/SnO2/glass matrix composite was higher than that of PRD-166/glass matrix composites because of crack deflection, fiber bridging, partial fiber debonding, and some fiber pullout. A judicious interplay of roughness induced radial stress and thermal stress distribution can be used to make a tough CMC. Dissert. Abstr.

N94-29875 Illinois Univ., Urbana-Champaign.
FAILURE STRENGTH AND MECHANISM OF COMPOSITE LAMINATES UNDER MULTIAXIAL LOADING CONDITIONS Ph.D. Thesis
Jerry Zhiqi Wang 1993 140 p
Avail: Univ. Microfilms Order No. DA9314957

An experimental study of strength and failure behavior of orthotropic G-10 glass fiber reinforced composite laminates in an in-plane stress state was conducted. Different types of biaxial specimens and associated test fixtures were developed and employed in the study. Standard IITRI specimens were wed to determine tensile and compressive failure strengths of G-10 composite laminates in both fill and warp directions. Biaxial tension-compression (BTC) and biaxial compression-compression (BCC) flat coupon specimens with flexible end reinforcements were designed and tested to study failure behaviors and mechanisms of composite laminates under a biaxial tension-compression and biaxial compression-compression stress states. Tubular specimens loaded in axial tension, axial compression, torsion, internal pressure, and external pressure were employed to produce desired combinations of in-plane stresses and strains. Based on the biaxial failure envelopes obtained from the tests, notched BCC specimens (BCC(n)) were tested in a biaxial compression loading condition to study failure behavior of notched laminates under a biaxial stress state. Failure mechanisms of notched and unnotched composite laminates were studied based on the test data and failure surface examination. Dissert. Abstr.

N94-29876 Washington Univ., Seattle.
FRACTURE PROCESS ZONE OF BRITTLE COMPOSITES Ph.D. Thesis
Chang-Te Yu 1992 211 p
Avail: Univ. Microfilms Order No. DA9312767

An experimental-numerical analysis was used to study the fracture process zone (FPZ) trailing the crack tip in brittle composites. Two major parts are included in this dissertation. Part 1 is a static mode 1 fracture analysis of ceramic matrix composites. Part 2 is a mixed mode 1 and mode 2 dynamic fracture analysis of concrete. In Part 1, the FPZ which trailed a stably growing crack in SiC(w)/Al2O3 ceramic matrix composite was investigated through a hybrid experimental-numerical analysis. Surface displacements on the sides of three-point bend and wedge loaded-double cantilever beam (WL-DCB) specimens with chevron notch starter cracks were measured with moire interferometry during crack growth. The three-point bend specimens were precracked by the single edge precrack bend (SEPB) method. The experimental data was then input to two and three dimensional finite element models of the three-point bend and WL-DCB specimens, respectively, to determine by an inverse analysis the crack closure stress (CCS) versus crack opening displacement (COD) relations for SiC(w)/Al2O3. Energy dissipation rates in the trailing process zone plus the matrix fracture and fiber breakage accounted for about 80 percent of the release energy rate with the remainder being dissipated through the frontal process zone. In Part 2, a hybrid experimental-numerical procedure was used to analyze rapid crack growth in an impact loaded three-point bend concrete specimen with an offset straight precrack. Two-beam dynamic moire interferometry was used to record eight sequential moire patterns of the horizontal or vertical displacements by a ultra-high speed camera with an exposure of 2 microseconds and a framing rate of 100,000 frames/sec. The fracture responses of ceramic composites and concrete were both characterized by FPZ models which are the dominant fracture energy dissipation mechanism in this type of brittle composite. Dissert. Abstr.

N94-29933# Los Alamos National Lab., NM.
BRITTLE COMPOSITES MODELING: COMPARISONS WITH MoSi2/ZrO2
S. P. Chen 1993 6 p Presented at the Fall Meeting of the Materials Research Society (MRS), Boston, MA, 29 Nov. - 3 Dec. 1993
(Contract W-7405-eng-36)
(DE94-004978; LA-UR-93-4307; CONF-931108-43) Avail: CASI HC A02/MF A01

We have calculated the mechanical properties of brittle composites with a spring-network (SN) model. The composites that we studied involve transformation toughening effects and the accompanying micro-cracking. Our simulation results are consistent with experiments of MoSi2 toughened with ZrO2. We found that the continuum mechanics predictions on linear dependence in e(sup T) and f about the transformation toughening are correct except for some differences in the critical transformation stress dependence. By monitoring the stress changes due to the transformation and micro-cracking we are able to separate, for the first time, the contributions from these two competing effe-ts. We found that the fracture toughness due to micro-cracks accompanying the transformation is a decreasing function of f and may be negative for large f. We also found that the fracture toughness of the composites increases as the modulus, interfacial cohesion, and uniformity of particle distributions increases.
DOE

N94-29964 Georgia Inst. of Tech., Atlanta.
INTERLAMINAR FRACTURE ANALYSIS FOR LAMINATED COMPOSITES UNDER COMBINED LOADING Ph.D. Thesis
Jian Li 1992 146 p
Avail: Univ. Microfilms Order No. DA9315889

Two analytical models based upon a shear deformation theory and a sublaminate approach have been developed to analyze composite laminates under extension, bending, torsion and combined loading. The first model is used to predict the free edge interlaminar stresses for composite laminates under extension, bending and torsion. The interlaminar stresses are obtained in closed form. The effectiveness of this model is validated by comparisons with a benchmark elasticity solution for unidirectional and cross-ply laminates

under torsion loading. Excellent agreement is observed. Further comparisons with finite element simulation and a Lekhnitskii's stress functions approach for off-axis and angle-ply laminates under various loading conditions are performed. Good agreement with both methods are demonstrated. The second model is for the analysis of delaminated unsymmetrical laminates subjected to extension, bending, torsion and combined loading. Closed form expressions for interlaminar stresses, total strain energy release rate and strain energy release rate components are obtained. The model is applied to the prediction of the critical interfaces, in a class of unsymmetrical laminates with (-theta,(90-theta)2, -theta,(theta-90)2, theta)T lay-ups. A comparison between the critical interfaces predicted based on the peel stress distribution through the thickness and the total strain energy release rate is presented. It is shown that the critical interface predictions based on the peel stress is consistent with the total strain energy release rate approach for most of the cases considered. It is also shown that combined loading has significant effect on potential delamination sites. Free-edge delamination may reduce or increase the extension-twist coupling depending on the location and length of the delamination, and the lay-up of the laminate. Tests of both damaged and undamaged specimens showed the same trend as the analytical predictions. This indicates that free edge delamination has a significant effect on the coupling at low level of applied loads and therefore could be easily detected at an early stage. Furthermore, the influence should be considered in the design of elastically tailored composites in order to ensure their damage tolerance. Dissert. Abstr.

N94-30016*# Washington Univ., Saint Louis, MO. Lab. for Ultrasonics.
PHYSICAL INTERPRETATION AND DEVELOPMENT OF ULTRASONIC NONDESTRUCTIVE EVALUATION TECHNIQUES APPLIED TO THE QUANTITATIVE CHARACTERIZATION OF TEXTILE COMPOSITE MATERIALS Semiannual Progress Report, 15 Sep. 1993 - 14 Mar. 1994
James G. Miller 11 Apr. 1994 19 p Original contains color illustrations
(Grant NsG-1601)
(NASA-CR-195766; NAS 1.26:195766) Avail: CASI HC A03/MF A01; 2 functional color pages

In this Progress Report, we describe our continuing research activities concerning the development and implementation of advanced ultrasonic nondestructive evaluation methods applied to the inspection and characterization of complex composite structures. We explore the feasibility of implementing medical linear array imaging technology as a viable ultrasonic-based nondestructive evaluation method to inspect and characterize complex materials. As an initial step toward the application of linear array imaging technology to the interrogation of a wide range of complex composite structures, we present images obtained using an unmodified medical ultrasonic imaging system of two epoxy-bonded aluminum plate specimens, each with intentionally disbonded regions. These images are compared with corresponding conventional ultrasonic contact transducer measurements in order to assess whether these images can detect disbonded regions and provide information regarding the nature of the disbonded region. We present a description of a standoff/delay fixture which has been designed, constructed, and implemented on a Hewlett-Packard SONOS 1500 medical imaging system. This standoff/delay fixture, when attached to a 7.5 MHz linear array probe, greatly enhances our ability to interrogate flat plate specimens. The final section of this Progress Report describes a woven composite plate specimen that has been specially machined to include intentional flaws. This woven composite specimen will allow us to assess the feasibility of applying linear array imaging technology to the inspection and characterization of complex textile composite materials. We anticipate the results of this on-going investigation may provide a step toward the development of a rapid, real-time, and portable method of ultrasonic inspection and characterization based on linear array technology. Derived from text

N94-30125*# Virginia Univ., Charlottesville. Dept. of Civil Engineering and Applied Mechanics.
MULTIPLE CONCENTRIC CYLINDER MODEL (MCCM) USER'S GUIDE Final Report
Todd O. Williams and Marek-Jerzy Pindera Apr. 1994 80 p
(Contract NAS3-26571; RTOP 505-63-12)
(NASA-CR-195299; E-8689; NAS 1.26:195299) Avail: CASI HC A05/MF A01

A user's guide for the computer program mccm.f is presented. The program is based on a recently developed solution methodology for the inelastic response of an arbitrarily layered, concentric cylinder assemblage under thermomechanical loading which is used to model the axisymmetric behavior of unidirectional metal matrix composites in the presence of various microstructural details. These details include the layered morphology of certain types of ceramic fibers, as well as multiple fiber/matrix interfacial layers recently proposed as a means of reducing fabrication-induced, and in-service, residual stress. The computer code allows efficient characterization and evaluation of new fibers and/or new coating systems on existing fibers with a minimum of effort, taking into account inelastic and temperature-dependent properties and different morphologies of the fiber and the interfacial region. It also facilitates efficient design of engineered interfaces for unidirectional metal matrix composites. Author (revised)

N94-30178*# Virginia Univ., Charlottesville. Dept. of Civil Engineering and Applied Mechanics.
MICROMECHANICAL ANALYSIS OF THERMO-INELASTIC MULTIPHASE SHORT-FIBER COMPOSITES Final Report
Jacob Aboudi Mar. 1994 19 p
(Grant NAG3-1377; RTOP 505-63-12)
(NASA-CR-195290; E-8650; NAS 1.26:195290) Avail: CASI HC A03/MF A01

A micromechanical formulation is presented for the prediction of the overall thermo-inelastic behavior of multiphase composites which consist of short fibers. The analysis is an extension of the generalized method of cells that was previously derived for inelastic composites with continuous fibers, and the reliability of which was critically examined in several situations. The resulting three dimensional formulation is extremely general, wherein the analysis of thermo-inelastic composites with continuous fibers as well as particulate and porous inelastic materials are merely special cases. Author (revised)

N94-30190*# Akron Univ., OH.
COMPUTATIONAL SIMULATION OF COMPOSITE STRUCTURES WITH AND WITHOUT DAMAGE M.S. Thesis Final Report
Thomas F. Wilt Mar. 1994 105 p
(Grant NAG3-50; RTOP 505-63-5B)
(NASA-CR-194433; E-8240; NAS 1.26:194433) Avail: CASI HC A06/MF A02

A methodology is described which uses finite element analysis of various laminates to computationally simulate the effects of delamination damage initiation and growth on the structural behavior of laminated composite structures. The delamination area is expanded according to a set pattern. As the delamination area increases, how the structural response of the laminate changes with respect to buckling and strain energy release rate are investigated. Rules are presented for laminates of different configurations, materials and thickness. These results demonstrate that computational simulation methods can provide alternate methods to investigate the complex delamination damage mechanisms found in composite structures. Author

N94-30256 Stanford Univ., CA.
DELAMINATION GROWTH IN COMPOSITES UNDER CYCLIC LOADS Ph.D. Thesis
Christian Ulf Dahlen 1993 103 p
Avail: Univ. Microfilms Order No. DA9326454

A semi-empirical model was developed for estimating the growth of delaminations inside fiber reinforced organic matrix composites subjected to cyclic loads. At any point of the circumference of the delamination mode 1, mode 2, or mixed mode conditions may exist. The form of the proposed delamination growth model follows Elber's expression for the growth of a mode 1 crack in an aluminum sheet. By employing dimensional analysis, the parameters were established which are to be included in the model. The expression obtained depends on the material properties (transverse tensile ply strength, transverse tensile ply modulus, longitudinal ply shear strength, critical energy release rate) and on the energy release rate at the location under consideration. Tests were conducted with Fiberite T300/976 and IM7/977-2 graphite epoxy composites under mode 1, mode 2, and mixed mode conditions using double cantilever beam, end notched cantilever beam, and mixed mode bending test coupons subjected to both static and cyclic loads. From these tests, first, the constants needed in the model, were determined. Second, data were generated and compared

to predictions of the model, and good agreement was found between measured and predicted delamination growths. Results of the present model were also compared to data reported previously, and the model predictions agreed well with these previous data. Dissert. Abstr.

N94-30257 Maryland Univ., College Park.
THREE-DIMENSIONAL FREE VIBRATION ANALYSIS OF THICK ARBITRARILY LAMINATED, RECTANGULAR, CYLINDRICAL AND SPHERICAL COMPOSITE PANELS Ph.D. Thesis
Kuan Hong Huang 1993 203 p
Avail: Univ. Microfilms Order No. DA9327430

A layer-wise theory was established to solve the free vibration problem of thick, arbitrarily laminated composite panels of rectangular, cylindrical, and spherical geometry. The boundary conditions at four edges of these panels can be any combination of simply supported, free clamped, and guided, and can be varied through the thickness to model the effects of three-dimensional boundary conditions. In this three dimensional semi-analytical method, the displacement field is modeled by finite element interpolation shape functions along the thickness direction and by beam function expansions in the two in-plane directions. The natural frequencies obtained show this method to be more accurate, especially for predicting higher modes, than previous models based on the first-order transverse shear deformation theory (FSDT) or the higher-order transverse shear deformation theory (HSDT). Some in-plane vibration modes which were found to be missing in previous models are obtained in the present study. The improved accuracy of the present method can be attributed partly to the three-dimensional displacement field which allows prediction of truly three-dimensional mode shapes in thick laminates, and partly, to the layer-wise displacement field which provides the ability to model more complicated layer-wise boundary conditions, as well as layer-wise continuous stiffness properties for heterogeneous laminates. Dissert. Abstr.

N94-30343 Technische Univ., Delft (Netherlands). Structures and Materials Lab.
THE MACHINING OF FIBER METAL LAMINATES. PART 1: AN INVENTORY OF FORMING PROCESSES [HET BEWERKEN VAN VEZELMETAALLAMINATEN. DEEL 1: EEN IVENTARISATIE VAN DE VERVORMINGSPROCESSEN]
R. vanPraag Feb. 1993 183 p In DUTCH Sponsored by IOP-Metalen Limited Reproducibility: More than 20% of this document may be affected by microfiche quality
(LR-710-Pt-1; ETN-94-95527) Avail: CASI HC A09

The forming process characteristics of fiber metal laminates were inventorized with a view to aircraft construction. The following forming processes are described: several bending processes, deep drawing, peen forming, metal spinning, and autoclave edge forming. A number of adaptations to processes to enhance the deformation possibilities are discussed. ESA

N94-30355 Stanford Univ., CA.
DAMAGE IDENTIFICATION IN COMPOSITES USING BUILT-IN PIEZOELECTRICS Ph.D. Thesis
Charles Henry Keilers, Jr. 1993 172 p
Avail: Univ. Microfilms Order No. DA9326494

An identification method was developed that uses measured responses from piezoelectrics built into laminated composite beams to detect a delamination and estimate its size and location. This development involved both experimental and analytical work. Experiments were performed using surface-mounted piezoceramics on composite beams with and without an artificial delamination. Some of these piezoceramics were used as actuators to dynamically excite specimens while others were used as sensors to measure strains. These experiments showed that a delamination changes the dynamic forced response. Therefore, when a measured response differs from an undamaged structure's baseline response, damage could exist and the identification procedure is run. The identification procedure consists of a response comparator, a damage selector and a model. The model is run repeatedly to predict the changes in response due to different possible delaminations. After each run, the damage selector chooses the next assumed delamination size and location randomly, using an approach related to simulated annealing that improves agreement between the measured and calculated responses. The response comparator then compares these two responses using a weighted quadratic objective function. When the objective function is minimized, the responses agree, and the assumed delamination dimensions are also best estimates for the actual dimensions. The technique has been estimates for the actual dimensions. The technique has been tested using measured responses and has successfully identified artificially implanted beam delaminations. Dissert. Abstr.

N94-30419 National Physical Lab., Teddington (England). Materials Metrology Div.
PARTICULATE METAL MATRIX COMPOSITES: DRAFT PROCEDURE FOR TENSILE TESTS AT AMBIENT TEMPERATURE
B. Roebuck and J. D. Lord Dec. 1993 20 p
(NPL-DMM(A)-100; ETN-94-95829) Copyright Avail: Issuing Activity (National Physical Lab., Teddington, Middlesex TW11 0LW, England)

A draft procedure for the tensile testing of particulate reinforced metal matrix composites at ambient temperatures is reported. It recommends appropriate rectangular cross section test piece dimensions, testing rates and methods of gripping and strain measurement. The method of measurement of Young's modulus, proportional limit, proof stress, tensile strength and elongation to failure are defined. A recommended proforma for the test report is enclosed. ESA

N94-30438 National Physical Lab., Teddington (England). Materials Metrology Div.
STANDARDISATION REQUIREMENTS FOR ULTRASONIC C-SCANNING OF POLYMER MATRIX COMPOSITES: AN INITIAL ASSESSMENT
J. L. Lesniarek-Hamid and G. D. Sims Jun. 1993 18 p Sponsored by Dept. of Trade and Industry
(ISSN 0959-2423)
(PB94-139318; NPL-DMM(A)-105; ETN-94-95830) Copyright Avail: Issuing Activity (National Physical Lab., Teddington, Middlesex TW11 0LW, England)

As part of a wider program aimed at new or improved test methods for quality control, qualification and design data purposes, an assessment was undertaken on the 'standardization' requirements for the use of the ultrasonic C scan technique for evaluating polymer matrix composites. A compilation of that assessment, which covered current practices used by industry and requirements in terms of defect detection and measurement, is reported. Calibration of the equipment, determination of porosity and detection and measurement of all types of defects are covered. The requirements for standards was investigated. The principle needs identified are for standards for calibration of the equipment and defect detection. The large majority of participants do not measure porosity using the ultrasonic C scan technique and there was not a strong requirement for standards in this area. Very few participants were aware of the requirements in the draft European standard, pr EN2565, to measure porosity using ultrasonic methods. The results of the assessment will be used to guide a research program to satisfy the identified needs. ESA

N94-30524 National Physical Lab., Teddington (England). Materials Metrology Div.
A REVIEW OF MECHANICAL TEST METHODS FOR CERAMIC MATRIX COMPOSITES
R. Morrell Oct. 1993 23 p Sponsored by Dept. of Trade and Industry, London, England
(PB94-147576; NPL-DMM(A)-122; ETN-94-95841) Copyright Avail: Issuing Activity (National Physical Lab., Teddington, Middlesex TW11 0LW, England)

The current state of mechanical test methodology for continuous fiber reinforced ceramic matrix composites is described and analyzed based on testing experience accumulated during the last four years. Practical problems of testing are discussed in relation to the development of ASTM and CEN standardized test methods. Topics covered include, flexural, tensile, compressive and shear testing, determination of elastic moduli and fracture toughness, extensometry and high temperature testing. ESA

N94-30589# Sandia National Labs., Albuquerque, NM.
SIMULATION OF COMPOSITE MATERIAL RESPONSE UNDER DYNAMIC COMPRESSIVE LOADING
S. A. Silling and P. A. Taylor 1993 12 p Presented at the International Union of Theoretical and Applied Mechanics (IUTAM) Symposium on Computational Mechanics of Materials, Providence, RI, 15-18 Jun. 1993

(Contracts DE-AC04-94AL-85000; DE-AC04-76DP-00789)
(DE94-005272; SAND-93-1490C; CONF-9306291-1) Avail: CASI HC A03/MF A01

Realistic computer prediction of high-velocity impact and penetration events involving composite materials requires a knowledge of the material behavior under large compressive stresses at high rates of deformation. As an aid to the development of constitutive models for composites under these conditions, methods for numerical simulation of the material response at the microstructural level are being developed. At present, the study is confined to glass fiber/epoxy composites. The technique uses a numerical model of a representative sample of the microstructure with randomly distributed fibers. By subjecting the boundary of this numerical sample to prescribed loading histories, a statistical interpretation allows prediction of the global material response. Because the events at the microstructural scale involve locally large deformation, and because of the constantly changing picture with regard to contact between the fibers, the Eulerian code CTH is used for these calculations. Certain aspects of material failure can also be investigated using this approach. The method allows the mechanical behavior of composite materials to be studied with fewer assumptions about constituent behavior and morphology than typically required in analytical efforts. DOE

N94-30593 Argonne National Lab., IL.
EFFECT OF FIBER COATING ON MECHANICAL PROPERTIES OF NICALON FIBERS AND NICALON-FIBER/SiC MATRIX COMPOSITES
J. P. Singh, D. Singh, and R. A. Lowden Dec. 1993 10 p Presented at the 18th Annual Conference on Composites and Advanced Ceramics, Cocoa Beach, FL, 9-14 Jan. 1994 Limited Reproducibility: More than 20% of this document may be affected by microfiche quality
(Contract W-31-109-eng-38)
(DE94-005477; ANL/ET/CP-80555; CONF-940135-2) Avail: CASI HC A02

The effect of fiber-coating thickness on retained in-situ fiber strength and the resulting mechanical properties of composites was investigated. Flexure tests in a four-point-bend mode were used to evaluate ultimate strength and work-of-fracture of the composites with various fiber-coating thicknesses. Retained in-situ fiber strength in the fractured composites was evaluated by fractographic techniques. Retained in-situ fiber strength, ultimate strength, and work-of-fracture of the composites increased with increasing fiber-coating thickness, reaching a peak value at a coating thickness of approximately 0.3 microns. Further increases in coating thickness did not improve the mechanical properties of either the fibers or the composites. A direct correlation between retained in-situ fiber strength and mechanical properties of the composites suggests that retained in-situ fiber strength has a significant influence on the mechanical properties of composites. DOE

N94-30693# Los Alamos National Lab., NM.
CREEP BEHAVIOR OF MoSi2-SiC COMPOSITES
D. P. Butt, S. A. Maloy, H. Kung, D. A. Korzekwa, and J. J. Petrovic 1993 7 p Presented at the Fall Meeting of the Materials Research Society (MRS), Boston, MA, 29 Nov. - 3 Dec. 1993
(Contract W-7405-eng-36)
(DE94-004980; LA-UR-93-4288; CONF-931108-30) Avail: CASI HC A02/MF A01

Using a cylindrical indenter, indentation creep behavior of hot pressed and HIPed MoSi2-SiC composites containing 0-40% SiC by volume, was characterized at 1000-1200C, 258-362 MPa. Addition of SiC affects the creep behavior of MoSi2 in a complex manner by pinning grain boundaries during pressing, thus leading to smaller MoSi2 grains; by obstructing or altering both dislocation motion and grain boundary sliding; and by increasing the overall yield stress of the material. Comparisons are made between indentation and compressive creep studies. It is shown that under certain conditions, compressive creep and indentation creep measurements yield comparable results after correcting for effective stresses and strain rates beneath the indenter. DOE

N94-30704 Ames Lab., IA.
STUDIES ON THE OPTIMIZATION OF DEFORMATION PROCESSED METAL-METAL MATRIX COMPOSITES Ph.D. Thesis
T. W. Ellis Jan. 1994 141 p Limited Reproducibility: More than 20% of this document may be affected by microfiche quality
(Contract W-7405-eng-82)
(DE94-006033; IS-T-1676) Avail: CASI HC A07

A methodology for the production of deformation processed metal-metal matrix composites from hyper-eutectic copper-chromium alloys was developed. This methodology was derived from a basic study of the precipitation phenomena in these alloys encompassing evaluation of microstructural, electrical, and mechanical properties. The methodology developed produces material with a superior combination of electrical and mechanical properties compared to those presently available in commercial alloys. New and novel alloying procedures were investigated to extend the range of production methods available for these materials. These studies focused on the use of high pressure gas atomization and the development of new containment technologies for the liquid alloy. This allowed the production of alloys with a much more refined starting microstructure and lower contamination than available by other methods. The knowledge gained in the previous studies was used to develop two completely new families of deformation processed metal-metal matrix composites. These composites are based on immissible alloys with yttrium and magnesium matrices and refractory metal reinforcement. This work extends the physical property range available in deformation processed metal-metal matrix composites. Additionally, it also represents new ways to apply these metals in engineering applications. DOE

N94-30771# Los Alamos National Lab., NM.
MICROWAVE ASSISTED CHEMICAL VAPOR INFILTRATION
D. J. Devlin 1993 11 p
(Contract W-7405-eng-36)
(DE94-005005; LA-UR-93-4343) Avail: CASI HC A03/MF A01

The purpose of this program is to develop a new process for the fabrication of ceramic matrix composites by chemical vapor infiltration. This period has been devoted in part to the exploration of material systems suitable for MACVI processing. A number of potential processing schemes are possible using combinations of absorbing and transparent material as composite components. This includes the use of an absorbing preform (nicalon fiber) combined with a transparent matrix (silicon nitride). Composites 5 cm in diameter by 1 cm. thick have been fabricated to densities of 65% theoretical. Processing times for these materials are under 20 hours. Higher densities will require additional microwave power now possible with the new reactor. The most effective MACVI scheme will involve the use of a transparent fiber with an absorbing matrix. The hot spot will be initiated by appropriate treatment of the central region of the preform. To this end, alumna fibers with pretreatments to control thermal gradients has been explored. Nextel 610 fibers have been effectively pretreated carbon coating resulting in preferential heating in the interior of the preform. Possible matrix materials include siliconized silicon carbide, doped silicon carbide, alumna, and zirconia. A patent for MACVI has been issued 10/19/93. DOE

N94-30827# Sandia National Labs., Albuquerque, NM.
DELAMINATION OF WOVEN E-GLASS FABRIC COMPOSITES
M. L. Dunn (Colorado Univ., Boulder.), E. D. Reedy, Jr., and T. R. Guess 1993 20 p Presented at the 39th International Symposium of the Society for the Advancement of Material and Process Engineering and Exhibition, Anaheim, CA, 11-14 Apr. 1994
(Contract DE-AC04-94AL-85000)
(DE94-003227; SAND-93-1442C; CONF-940412-1) Avail: CASI HC A03/MF A01

An experimental/analytical study investigating delamination growth in E-glass fabric/polyester composites was carried out. Double cantilever beam and end-notched flexure delamination specimens were tested, and the measured data was compared to calculated results. A stacked shell finite element methodology was developed to perform the analysis. This approach breaks the composite into sublaminate shells connected by springs spanning the delamination plane. The stacked shell analyses can use either a critical stress or a critical energy release rate criterion to propagate the delamination, and both criteria are shown to yield similar predictions. Role of connecting springs, and proper choice for spring constants has also been investigated in detail. The spring constants must be chosen in a physically meaningful way to develop consistent values of energy release rate, compliance, and the stress distribution ahead of the delamination. Calculated results for the

double cantilever beam and end-notched flexure specimens are in good agreement with measured test data and continuum finite element solutions. DOE

N94-30956 Massachusetts Univ., Lowell.
NUMERICAL MODELING AND PREDICTION OF THE THERMOMECHANICAL BEHAVIOR OF FIBER-REINFORCED COMPOSITES Ph.D. Thesis
Panagiotis Blanas 1993 231 p
Avail: Univ. Microfilms Order No. DA9322413

This research effort investigates the behavior of continuous fiber reinforced, unidirectional composite materials under mechanical and thermal loads. A numerical procedure is developed that allows for the prediction of composite effective properties. A micromechanical approach and the finite element method of analysis are used to model and determine the composite material response under loading. The representative volume element concept along with assumptions of regular and periodic fiber distribution arrays are employed in the micromechanics problem formulation. Both square and hexagonal fiber arrays are utilized to model the microstructure of the composite material. The composite is treated as a macroscopically homogeneous, linearly elastic and transversely isotropic medium. Linear elastic behavior is also assumed for the homogeneous fiber and matrix constituent phases. The finite element method is employed in the solution of the micromechanics boundary value problem. Two and three dimensional finite element models of the representative volume element are generated. Various layouts of these models in single and multiple cell configurations are developed and utilized in the modeling and analysis of the unidirectional composite. A number of boundary conditions and load cases are also used in the analysis to determine the behavior of the composite. Displacement and stress fields produced in the composite under the various loading conditions are obtained and used in the computation of effective property values. Effective material properties are obtained for two composite material systems. Results are compared with results from micromechanics equations and experimental data. The effect of boundary conditions on predicted effective property values is also addressed and discrepancies that occur at the free boundaries of the composite are examined.
Dissert. Abstr.

N94-30959 Rutgers - The State Univ., New Brunswick, NJ.
A CLASS OF INCLUSION PROBLEMS FOR THE STRENGTHENING OF BRITTLE AND DUCTILE COMPOSITES Ph.D. Thesis
Huang-Hsing Pan 1992 232 p
Avail: Univ. Microfilms Order No. DA9321318

Using Eshelby's solution of an ellipsoidal inclusion as the point of departure, a class of inhomogeneity and transformation problems for the strengthening of brittle and ductile composites are investigated in this thesis. First, the effective elastic moduli of a two-phase composite containing aligned, two dimensional, and three dimensional randomly oriented ellipsoidal inclusions are derived. The nine, five, and two independent elastic constants for these three different classes of composites are found as a function of inclusion shape and volume concentration. The moduli are found to always lie in or on the bounds of Willis and of Hashin and Shtrikman. These results are then developed into a form suitable for the elliptic cracks, and then the influence of crack density parameters on the reduction of the effective moduli of cracked bodies is brought about. The established results for the effective moduli with softer inclusions, and with elliptic cracks, are then applied to study the microcracks and inhomogeneity, as well as the transformation, toughening of brittle solids. It is found that the toughness of brittle materials (e.g. ceramics) can always be enhanced by addition of soft particles, and by the dilatational nature of the phase transformation from tetragonal to monoclinic crystal structure. In the case of microcrack toughening, the theory derived is shown to be very close to Hutchinson's modified lowest order formula. The investigation finally is directed towards the thermal stress problems in dual-phase solids during a cooling process. For a dual-phase steel, it is found that dilational tensile stress develops in the ferrite matrix during martensitic transformation. The volume of the dual-phase steel is found to decrease first during cooling, but increase upon the occurrence of phase transformation. The thermal stress analysis is finally studied for the two-phase metal-matrix composites. An exact, local theory is derived to determine the extent of thermal stress in the inclusions and the ductile matrix for both particle and fiber-reinforced composites. For a two-phase composite containing aligned spheroidal inclusions, an energy approach is developed at the end. It is demonstrated that the thermal stress in the ductile matrix can be significantly relieved by its plastic flow.
Dissert. Abstr.

N94-30447*# Idaho National Engineering Lab., Idaho Falls.
NEAR-NET-SHAPE MANUFACTURING: SPRAY-FORMED METAL MATRIX COMPOSITES AND TOOLING
Kevin M. McHugh *In* NASA, Washington, Technology 2003: The Fourth National Technology Transfer Conference and Exposition, Volume 1 Feb. 1994 p 64-73 (For primary document see N94-30440 08-99)
(Contract DE-AC07-76ID-01570)
Avail: CASI HC A02/MF A04

N94-30452*# Phillips Lab., Edwards AFB, CA.
THE UNIVERSAL APPLICATIONS OF MICROTUBES AND MICROTUBE COMPOSITES
Wesley P. Hoffman and Kamleshwar Upadhya *In* NASA, Washington, Technology 2003: The Fourth National Technology Transfer Conference and Exposition, Volume 1 Feb. 1994 p 108-113 (For primary document see N94-30440 08-99)
Avail: CASI HC A02/MF A04

N94-30481*# National Aeronautics and Space Administration. Langley Research Center, Hampton, VA.
FOUR ADVANCES IN CARBON-CARBON MATERIALS TECHNOLOGY
Howard G. Maahs, Wallace L. Vaughn, and Witold Kowbel *In* NASA, Washington, Technology 2003: The Fourth National Technology Transfer Conference and Exposition, Volume 1 Feb. 1994 p 361-370 (For primary document see N94-30440 08-99)
Avail: CASI HC A02/MF A04

N94-30482*# National Aeronautics and Space Administration. Marshall Space Flight Center, Huntsville, AL.
CASTING OF WELDABLE GRAPHITE/MAGNESIUM METAL MATRIX COMPOSITES WITH BUILT-IN METALLIC INSERTS
Jonathan A. Lee, Uday Kashalikar, and Patricia Majkowski *In* NASA, Washington, Technology 2003: The Fourth National Technology Transfer Conference and Exposition, Volume 1 Feb. 1994 p 371-376 (For primary document see N94-30440 08-99)
Avail: CASI HC A02/MF A04

25 INORGANIC AND PHYSICAL CHEMISTRY

Includes chemical analysis, e.g., chromatography; combustion theory; electrochemistry; and photochemistry.

For related information see also *77 Thermodynamics and Statistical Physics.*.

N94-28407# Technical Research Centre of Finland, Espoo. Lab. of Heating and Ventilation.
MEASUREMENT OF VOLATILE METAL SPECIES AT ELEVATED TEMPERATURES Ph.D. Thesis
Kari Larjava 1993 125 p
(ISSN 1235-0621)
(PB94-132321; VTT/PUB-137; ISBN-951-38-4255-X) Copyright Avail: CASI HC A06/MF A02

The thesis consists of the following publications: Development of the volatile metal aerosol sampler based on vaporization/condensation; (2) Fate of some trace elements in fluidized-bed combustion and gasification processes; (3) Development and laboratory investigations of a denuder sampling system for the determination of heavy metal species in flue gases at elevated temperatures; (4) Application of diffusion separators for measurement of metal emissions; (5) Measurement and control of mercury species after liquid waste incineration; (6) Application of the diffusion screen technique to the determination of gaseous mercury and mercury(II)chloride in flue gases.
NTIS

N94-28483# Ames Lab., IA.
MEASUREMENT OF ELEMENTAL SPECIATION BY LIQUID CHROMATOGRAPHY: INDUCTIVELY COUPLED PLASMA MASS SPECTROMETRY (LC-ICP-MS) WITH THE DIRECT INJECTION NEBULIZER (DIN) Ph.D. Thesis
S. Shum May 1993 168 p
(Contract W-7405-eng-82)
(DE94-005261; IS-T-1644) Avail: CASI HC A08/MF A02

This thesis is divided into 4 parts: elemental speciation, speciation of mercury and lead compounds by microbore column LC-ICP-MS with direct injection nebulization, spatially resolved measurements of size and velocity distributions of aerosol droplets from a direct injection nebulizer, and elemental speciation by anion exchange and size exclusion chromatography with detection by ICP-MS with direct injection nebulization. DOE

N94-28519# Ames Lab., IA.
INSTRUMENTAL DEVELOPMENT OF NOVEL DETECTION AND SEPARATION METHODS FOR CAPILLARY ELECTROPHORESIS Ph.D. Thesis
T. Garner Jul. 1993 117 p
(Contract W-7405-eng-82)
(DE94-005554; IS-T-1614) Avail: CASI HC A06/MF A02

After a general introduction, this thesis is divided into 3 parts: indirect fluorescence detection of sugars separated by capillary zone electrophoresis with visible laser excitation, absorption detection in capillary electrophoresis by fluorescence energy transfer, and increased selectivity for electrochromatography by dynamic ion exchange. DOE

N94-28561# Ames Lab., IA.
GAS PHASE THERMOCHEMISTRY OF ORGANOGERMANIUM COMPOUNDS Ph.D. Thesis
J. P. Engel Dec. 1993 140 p
(Contract W-7405-eng-82)
(DE94-004885; IS-T-1687) Avail: CASI HC A07/MF A02

A variety of silyl- and alkyl-germylene precursors have been synthesized and subsequently pyrolyzed in the gas phase. Arrhenius parameters were obtained employing a pulsed-stirred flow reactor for these unimolecular decompositions. These precursors are divided into two major categories by mechanism of germylene extrusion: (alpha)-elimination precursors and germylacetylenes. The extrusion of germylenes from germylacetylene precursors is of primary interest. A mechanism is proposed employing a germacyclopropene intermediate. Evidence supporting this mechanism is presented. In the process of exploring germylacetylenes as germylene precursors, an apparent dyatropic rearrangement between germanium and silicon was observed. This rearrangement was subsequently explored. DOE

N94-28567# Sandia National Labs., Albuquerque, NM.
SOLUBILITY OF Nd IN BRINE
F. Khalili, V. Symeopoulos, J. F. Chen, and G. R. Choppin 1993 14 p Presented at the 4th International Conference on Chemistry and Migration Behavior of Actinides and Fission Products in the Geosphere, Charleston, SC, 12-17 Dec. 1993
(Contract DE-AC04-94AL-85000)
(DE94-005099; SAND-93-7113C; CONF-931201-10) Avail: CASI HC A03/MF A01

The solubility of Nd(III) has been measured in a synthetic brine at pcH 6.4, 8.4, 10.4 and 12.4. The brine consisted predominantly of (Na+K)Cl and MgCl2, with an ionic strength of 7.8M (9.4m). The experimental solubility is much less than that estimated from modeling of the species in solution in equilibrium with the Nd solid using S.I.T. The predominant solid compound of Nd (III) at each pcH was determined from X-ray diffraction patterns. DOE

N94-28675# National Inst. for Resources and Environment, Ibaraki (Japan).
JOURNAL OF NIRE, VOL. 2, NO. 2 [SHIGEN TO KANKYO, VOL. 2, NO. 2]
Takeshi Usami, ed., Yoshihiro Ogisu, ed., Masayoshi Saito, ed., Nobuo Kido, ed., Koichi Mizuno, ed., Akira Miyazaki, ed., Hiroaki Kondo, ed., Yoshio Yamada, ed., Mikio Kobayashi, ed., and Katsuya Tsurusaki, ed. et al 25 Mar. 1993 74 p In JAPANESE
(ISSN 0916-9997)
(JTN-94-80552) Avail: CASI HC A04/MF A01

The following topics were discussed: coal, coal molecular structure, coal liquefaction, solvent extraction, bioconversion, biomass, microorganisms, hydrocarbons, hydrocarbon fuels, coal carbonization, coal oxidation, phenols, methanol, chlorofluorocarbons, adsorvents, desorption, aceton, iodine, complex compound, molecular vibrational frequency shift, MO (Molecular Orbital) method, plasma diagnosis, RF (Radio Frequency) plasma, temperature distribution, electron density, spectral analysis, refraction, silica tubes, marine resources, underwater resources, marine mining, international cooperation, nuclear magnetic resonance, and gas chromatography. For individual titles, see N94-28676 through N94-28683.

N94-28676# National Inst. for Resources and Environment, Ibaraki (Japan). Gasification Div.
MOLECULAR STRUCTURE OF COAL STUDIED BY SOLVENT EXTRACTION [SEKITAN NO KOZO TO YOZAI KAYOKA]
Osamu Yamada *In its* Journal of NIRE, Vol. 2, No. 2 25 Mar. 1993 p 1-7 In JAPANESE (For primary document see N94-28675 08-25)
Avail: CASI HC A02/MF A01

Coal has been known to consist of solvent soluble 'mobile phase' and solvent insoluble 'immobile phase'. This concept, which is called two phase model, is based on the idea that coal is a three dimensionally cross-linked macromolecular network. Molecular structure of coal and various coal conversion reactions have been discussed using this model. Recently, a high performance solvent system is found to solubilize coal much higher than conventional solvents. A new coal structure model other than two phase model is proposed. This report reviews recent studies on high performance solvents and new concepts of structural model of coal derived from the solvent extraction experiments. Author (NASDA)

N94-28677# National Inst. for Resources and Environment, Ibaraki (Japan).
RESEARCHES ON BIOCONVERSION OF COAL INTO LIQUID PRODUCT [BISEIBUTSU NI YORU SEKITAN NO KAYOKA NARABINI BUNKAI]
Keiji Miki *In its* Journal of NIRE, Vol. 2, No. 2 25 Mar. 1993 p 9-17 In JAPANESE (For primary document see N94-28675 08-25)
Avail: CASI HC A02/MF A01

The first evidence of biosolubilization or biodegradation of brown coal using wood-decaying fungi prompted the identification of other organisms capable of growing on and solubilizing coal. The isolation of extracellular lignin peroxidase from white-rot fungi also accelerated the enzymatic degradation study of coal. The bacterial processing revealed the effects of alkaline substances and chelator in addition to enzymatic action on coal solubilization. However, the characterization of solubilized products, attributed to high molecular weight aromatic carboxylate, raised the question about the practical application of such aerobic biological treatments which are unable to improve quality as alternative fuels and chemicals. On the other hand, recent reports suggest that coal is degraded by anaerobic microorganisms and hydrogenase/cytochrome c without an increase in oxygen and a decrease in carbon content. These results may offer a promising approach to feasible bioprocessing of coal. Author (NASDA)

N94-28678# National Inst. for Resources and Environment, Ibaraki (Japan). Fundamental Research Div.
STRUCTURAL CHANGES DURING CARBONIZATION AND OXIDATION OF COAL [SEKITAN NO TANKA OYOBI SANKA NI TOMONAU KOZO HENKA]
Hiroyuki Kawashima, Yasumasa Yamashita, John Anthony MacPhee, Yoshio Yamada, and Ikuo Saito *In its* Journal of NIRE, Vol. 2, No. 2 25 Mar. 1993 p 19-26 In JAPANESE (For primary document see N94-28675 08-25)
Avail: CASI HC A02/MF A01

Solid state C-13 NMR (Nuclear Magnetic Resonance) spectra of carbonized and oxidized coal were measured to investigate the structural changes during carbonization and oxidation. By oxidation, coal produces gas mainly by oxidation of aliphatic chain and fraction of the aromatic carbon (fa) increased. By carbonization, all coal showed little structural changes lower than 350 C and significant changes from 350 to approximately 450 C. Aromatic carbons of all coal apparently remained in coke or char and were condensed while aliphatic carbons were decomposed to produce

tar and gas. All samples showed the same structural changes during carbonization but the degrees of the changes differed greatly according to the coal species and lower rank coal showed a much bigger change. The rate of chemical structural change during this temperature range seems to decide each coal's reactivity. Author (NASDA)

N94-28679# National Inst. for Resources and Environment, Ibaraki (Japan). Heteroatoms Div.

METHANOL-MEDIATED CONTINUOUS EXTRACTION OF PHENOLIC COMPOUNDS FROM COAL LIQUID [METANORU O BAITAI TO SURU SEKITAN EKIKAYUCHU NO FENORURUI NO RENZOKU CHUSHUTSU]

Yoichi Kodera, Akimitsu Matsumura, and Koji Ukegawa *In its* Journal of NIRE, Vol. 2, No. 2 25 Mar. 1993 p 27-32 In JAPANESE (For primary document see N94-28675 08-25)

Avail: CASI HC A02/MF A01

A methanol-mediated extraction method was utilized in the separation of phenolic compounds from coal liquids. A naphtha distillate of Wandoan coal liquid was treated in a continuous extraction apparatus. Flow rates of the feed oil, methanol, and water were 0.25 - 1.0, 0.125 - 0.5, and 0.125 - 0.5 L/h, respectively. Run times were three to 10 hours. The effect of varied methanol-to-oil weight ratio on extraction yields of phenolic compounds was examined. As in corresponding batch experiments, extraction yields of phenol, o-, m-, and p-cresol increased as the amount of methanol increased. However, increased addition of water reduced the yields of phenolic compounds. Removal of methanol under reduced pressure caused an oily mixture of phenolic compounds to separate from the extract. The amount of separated oil was dependent on MeOH/water, weight ratio.

Author (NASDA)

N94-28680# National Inst. for Resources and Environment, Ibaraki (Japan). Air Quality Measurement Div.

PROPERTIES OF ADSORBENTS FOR COLLECTION AND ANALYSIS OF TRACE AMOUNT OF CHLOROFLUOROCARBONS IN AIR [TAIKICHU NO BIRYO CFC RUI SOKUTEI NO TAME NO HOSHUYO KYUCHAKUZAI NO KENTO]

Toshiyuki Tanaka and Heita Murakoshi *In its* Journal of NIRE, Vol. 2, No. 2 25 Mar. 1993 p 33-40 In JAPANESE (For primary document see N94-28675 08-25)

Avail: CASI HC A02/MF A01

Adsorption and desorption properties of adsorbents are investigated for measuring trace amounts of CFC (chlorofluorocarbons) in the air. Micropore structures and the breakthrough volume are measured for Tenax GC, Tenax TA, Tenax GR, Carbotrap, Carbotrap C, Carboxen 563, Carboxen 564, and Controlled-pore glass. Tenax GC was inadequate for collecting ambient chlorofluorocarbons quantitatively, and other Tenax type adsorbents are almost the same as regards their properties. Carboxen 563 and 564 showed an adequate capacity for the sampling of chlorofluorocarbons in air. However, these absorbents need a desorption temperature higher than 300 C, and produce ghost peaks and/or broad peaks during gas chromatographic analysis. Author (NASDA)

N94-28681# National Inst. for Resources and Environment, Ibaraki (Japan). Excited State Chemistry Div.

AB INITIO STUDY OF VIBRATIONAL FREQUENCY SHIFT UPON THE 1:1 ACETONE-IODINE COMPLEX FORMATION [ASETON-YOSO SAKUTAI NO SHINDOSU SHIFUTO NI KANSURU RIRONTEKI KENTO]

Osamu Setokuchi and Masaru Sato *In its* Journal of NIRE, Vol. 2, No. 2 25 Mar. 1993 p 41-50 In JAPANESE (For primary document see N94-28675 08-25)

Avail: CASI HC A02/MF A01

Vibrational frequency shift upon the 1 : 1 acetone-iodine complex formation was determined from geometries optimized at the SCF (Self Consistent Field) and MP2 (Moeller-Plesset Second Order Perturbation) levels using the ab initio MO (Molecular Orbital) theory, and comparison was made with experimental results. The SCF calculation with DZ (Double Zeta) basis sets augmented by a single set of d polarization functions gave values consistent with experimental results. The MP2 calculation failed to indicate even the sign of the shift, when using DZ basis sets without d polarization functions. Also, the shift of the nu(sub 19) acetone vibrational band was over estimated. These results are discussed from structural and energetical points of view. The origin of vibrational frequency shift is explained as being due to the behavior of orbital electrons, based on the natural bond orbital theory. Author (NASDA)

N94-28682# National Inst. for Resources and Environment, Ibaraki (Japan). Siliceous Materials Div.

A NOVEL SPECTROSCOPIC MEASUREMENT METHOD OF RF PLASMA FOR TEMPERATURE AND ELECTRON DENSITY DIAGNOSES [KOSHUHA NETSU PURAZUMA NO ONDO-DENSHI MITSUDO BUNPU NO SOKUTEI NO TAME NO BUNKO KEISOKU SHUHO NO KENTO]

Nobuyuki Kikukawa, Masami Sugasawa, and Masakazu Nakamura *In its* Journal of NIRE, Vol. 2, No. 2 25 Mar. 1993 p 51-59 In JAPANESE (For primary document see N94-28675 08-25)

Avail: CASI HC A02/MF A01

A new scanning method for spectroscopic data acquisition of RF (Radio Frequency) plasma suitable for Abel inversion was proposed. A small telescope was mounted on a theta-stage outside the 'shield box', with only the front end being inserted through a minimum opening in the shield box. Therefore, more than several tens of spectroscopic data points required for Abel inversion can be quickly measured with minimum RF noise disturbance. The influence of quartz walls and cooling water surrounding RF plasma on the light path of this 'theta-scan' was discussed and it was found that the true lateral position chi can be deduced without knowledge of refractive indices of media. Using this method, the temperature and electron density profile in argon-hydrogen RF plasma were derived preliminarily through the Arl Boltzmann-plot and H(sub beta) Stark broadening methods. The effect of the carrier gas flow rate on the temperature profiles was also discussed. Author (NASDA)

N94-28683# National Inst. for Resources and Environment, Ibaraki (Japan). Mining and Geotechnology Dept.

ON UNITED STATES-JAPAN CONFERENCE ON DEVELOPMENT AND UTILIZATION OF NATURAL RESOURCES: REPORT OF THE 14TH JOINT MEETING OF U. S. AND JAPAN MARINE MINING PANEL [TENNEN SHIGEN NO KAIHATSU RIYO NI KANSURU NICHIBEI KAIGI (UJNR) NI TSUITE: KAITEI KOBUTSU SHIGEN SENMON BUKAI NO DAI 14 KAI GODO KAIGI HOKOKU]

Takeshi Usami *In its* Journal of NIRE, Vol. 2, No. 2 25 Mar. 1993 p 61-67 In JAPANESE (For primary document see N94-28675 08-25)

Avail: CASI HC A02/MF A01

The US-Japan Conference on Development and Utilization of Natural Resources (UJNR) had their first conference in Tokyo in 1964. Marine Mining Panel (MMP), one of the panels of UJNR, has had 14 meetings so far since 1970, involving in joint research activities including information and researchers exchange. The cooperation themes of MMP are: (1) Mn lumps on abyssal floors; (2) Co crust mineral deposits and underwater hydrothermal mineral deposits; and (3) sands and gravels on continental shelves. The 14th MMP meeting was held at the University of Hawaii in June 1992. After reporting and discussion on the cooperation themes, participants went on field trips to relevant organizations and facilities such as MMTC's (Marine Minerals Technology Center) and PMEL (Pacific Marine Environmental Laboratory). MMP will continue their regular meeting with the same themes once in one and half or two years. 'Natural gas and oil' may be added to the cooperation themes. Author (NASDA)

N94-28777 George Washington Univ., Washington, DC. Dept. of Chemistry.

SIMILARITY SOLUTIONS AND NUMERICAL MODELING IN BUOYANCY CONTROLLED TURBULENT DIFFUSION FLAMES

David E. Ramaker 3 Feb. 1994 8 p Limited Reproducibility: More than 20% of this document may be affected by microfiche quality

(Contract N00014-93-1-G014)

(AD-A275820) Avail: CASI HC A02

The objective of this research was to develop a fundamental understanding of the behavior of buoyancy controlled axisymmetric diffusion gas flames and liquid pool fires. Specifically, we attempted to simulate two-dimensional axisymmetric profiles of the velocity, temperature, and species and soot concentrations. Knowledge of these profiles allowed us to determine the main characteristics of the flame; i.e., the heat feed back, which in turn determines the mass burning rate of a liquid pool, the height of the flame and the power output of a fire source to the surrounding environment. DTIC

N94-28789# Helsinki Univ. of Technology, Espoo (Finland). Lab. of Chemical Engineering.
QUALITATIVE VECTOR OPTIMIZATION OF A CONDENSATE STABILIZER PROCESS Plant Design Report Series
M. Hurme, J. Dohnalova, and M. Dohnal 1994 17 p
(PB94-133246; Rept-11) Avail: CASI HC A03/MF A01

A method of qualitative vector optimization is presented with an application to reasoning on a condensate stabilizer process. The method can be applied to the early stages of process design where the comparison of different alternatives is based both on quantitative and qualitative knowledge. The optimization goals are not single-criteria type but exhibit a qualitative multicriteria problem. The presented approach disintegrates one general goal into a set of subgoals which can be more objectively evaluated. NTIS

N94-28832*# National Aeronautics and Space Administration. Lewis Research Center, Cleveland, OH.
MATRIX ISOLATION STUDIES OF THE INTERACTIONS OF BF3 WITH WATER AND SUBSTITUTED DIETHYL ETHERS. CHEMICAL IONIZATION MASS SPECTROMETRIC DETERMINATION OF THE PROTON AFFINITY OF (CF3CH2)2O
David W. Ball (Cleveland State Univ., OH.) and Michael J. Zehe Dec. 1993 18 p
(RTOP 505-63-5A)
(NASA-TM-106422; E-8259; NAS 1.15:106422) Avail: CASI HC A03/MF A01

BF3 was co-condensed with H2O, D2O, (C2H5)2O, (CF3CH2)2O, and (C2F5)2O in excess argon at 15 K. Infrared spectra of BF3/water isolated in solid argon provided a more complete analysis of the BF3--H2O complex than previously published. Infrared spectra of the matrices showed a definite Lewis acid-base interaction between BF3 and diethyl ether; a weak but definite interaction with bis (2,2,2-trifluorodiethyl) ether, and no observable interaction with perfluorodiethyl ether. Thus, the ether data indicate a clear trend between strength of interaction with BF3 and the degree of F substitution. To support and explain the emerging relationship between interaction strength and the basicity of the oxygen-containing molecule, the proton affinity of (CF3CH2)2O was measured using chemical ionization mass spectrometry. The implications of the results for lubricant/metal oxide surface interactions are discussed. Author (revised)

N94-29004# Princeton Univ., NJ. Dept. of Mechanical and Aerospace Engineering.
FUELS COMBUSTION RESEARCH Annual Technical Report, 1 Oct. 1992 - 30 Sep. 1993
Irvin Glassman and Kenneth Brezinsky 10 Dec. 1993 24 p
(Grant AF-AFOSR-0431-91)
(AD-A275122; AFOSR-94-0032TR) Avail: CASI HC A03/MF A01

Future Air Force aircraft fuels will contain chemical constituents that not only contribute to the propulsion of the aircraft but also to the temperature control of both the combustor walls and the aircraft body. Temperature control may require the use of new, endothermic fuels such as methylcyclohexane (MCH). This cycloalkane in the presence of a catalyst dehydrogenates to toluene. The toluene and hydrogen product, containing a small amount of unreacted MCH, fuel the combustor. The burning characteristics of the mixture as well as its temperature stability as it is transferred to the combustor, most likely as a supercritical fluid, are largely unknown. Clarifying the combustion and thermal stability characteristics of both gaseous and supercritical fluid mixtures of toluene and methylcyclohexane has been the focus of the past year's research. Gas phase flow reactor studies of the pyrolysis and oxidation of pure MCH and of the oxidation of mixtures of MCH and toluene have revealed the chemical means by which MCH affects the oxidation chemistry of toluene. Supercritical fluid flow reactor examinations of the thermolysis of MCH and toluene mixtures have suggested chemical routes to deposit formation in the fluid fuels. These results are described in greater detail in this report. DTIC

N94-29010# Cornell Univ., Ithaca, NY. Dept. of Chemistry.
SWEEP RATE AND CONCENTRATION EFFECTS ON METASTABLE STRUCTURES FORMED IN THE UNDERPOTENTIAL DEPOSITION OF SILVER ON Pt(111)
D. L. Taylor and H. D. Abruna 1993 17 p
(AD-A275369) Avail: CASI HC A03/MF A01

We report on the effects of concentration and scan rate on the underpotential deposition of silver onto a Pt(111) surface. We note that the voltammetry at a silver concentration of 0.10 mM is highly dependent on the scan rate whereas it is virtually unchanged at a silver concentration of 1.0 mM. Derived from text

N94-29058# Oregon Univ., Eugene. Dept. of Chemistry.
CRYSTALLIZATION OF SILVER CHROMATE FROM ETHANOL VIA SALT METATHESIS REACTIONS OF SOLUBILIZED PRECURSORS Technical Report No. 7, 1 Jun. 1993 - 31 Aug. 1993
Kenneth M. Doxsee 14 Oct. 1993 3 p
(AD-A275178) Avail: CASI HC A01/MF A01

Admixture of aqueous solutions of silver nitrate and potassium chromate results in immediate precipitation of silver chromate as a red-brown microcrystalline powder, while addition of aqueous silver nitrate solution to a solution of potassium chromate/18-crown-6 in ethanol gives a bright-red precipitate. X-ray powder diffraction shows both materials to be orthorhombic silver chromate. The ethanol-derived sample displays broader diffraction peaks, suggesting smaller crystallite size. Scanning electron microscopy confirms this. The ethanol-derived sample appears amorphous, while the aqueous sample displays well-faceted crystallites approximately 0.5 - 1 micron in size. DTIC

N94-29140# Duke Univ., Durham, NC. Dept. of Chemistry.
TRIS(TRIMETHYLSILY)ARSINE AND LITHIUM BIS(TRIMETHYLSILY)ARSENIDE
Richard L. Wells, Mark F. Self, James D. Johansen, Janeen A. Laske, and Steven R. Aubuchon 18 Jan. 1994 12 p
(Contract N00014-89-J-1545)
(AD-A275075; DU/DC/TR-39) Avail: CASI HC A03/MF A01

The reported syntheses of the title compounds are a modification of the published procedures of Becker et al., designed to minimize Schlenk techniques and allow researchers to prepare two very useful compounds with a minimum of danger. DTIC

N94-29246# Advisory Group for Aerospace Research and Development, Neuilly-Sur-Seine (France). Propulsion and Energetics Panel.
FUELS AND COMBUSTION TECHNOLOGY FOR ADVANCED AIRCRAFT ENGINES [LES PROPERGOLS ET LES SYSTEMES DE COMBUSTION POUR LES MOTEURS D'AERONEFS]
Sep. 1993 495 p In ENGLISH and FRENCH Symposium held in Fiuggi, Italy, 10-14 May 1993 Original contains color illustrations
(AGARD-CP-536; ISBN-92-835-0719-3) Copyright Avail: CASI HC A21/MF A04

The conference proceedings contains 38 papers that cover new technologies for low NO(x) combustors and advanced high pressure/high temperature cycle engines. The technical evaluation report and the keynote address are included at the beginning, and discussions follow most papers. The symposium was arranged in the following sessions: technology overview papers (two papers); modeling: pollutant formation (four); modeling: combustor design (five); high temperature fuels and fuel systems (six); combustion research: performance (six); combustion research: emissions (five); fuel atomization: diagnostics and modeling (five); and combustion research: flowfield and mixing (four). The last paper is a contribution from Russia not allocated to a session. For individual titles, see N94-29247 through N94-29285.

N94-29247# Deutsche Forschungsanstalt fuer Luft- und Raumfahrt, Oberpfaffenhofen (Germany). Inst. fuer Physik der Atmosphaere.
ON THE EFFECT OF EMISSIONS FROM AIRCRAFT ENGINES ON THE STATE OF THE ATMOSPHERE **c45**
U. Schumann *In* AGARD, Fuels and Combustion Technology for Advanced Aircraft Engines Sep. 1993 19 p Sponsored by DFG; BMFT; and Commision of the European Communities (For primary document see N94-29246 08-25)
Copyright Avail: CASI HC A03/MF A04

Emissions from aircraft engines include carbon dioxide, water vapor, nitrogen oxides, sulphur components, and various other gases and particles. Such emissions from high-flying global civil subsonic aircraft contribute to anthropogenic climate changes by increase of ozone and cloudiness in the upper troposphere, and by enhanced greenhouse effect. The absolute emissions by air traffic are small (a few percent of total) in comparison to

surface emissions. However, the greenhouse effect of emitted water and of nitrogen oxides at cruise altitude is large in comparison to that of the same emissions near the earth's surface because of relatively large residence times at flight altitudes, low background concentrations, low temperature, and large radiative efficiency. At present, it appears that the emissions of nitrogen oxides have changed the background concentration in the upper troposphere in between 40 deg N and 60 deg N by 100 percent, causing an increase of ozone by about 20 percent. Regionally the observed annual mean change in cloudiness is of order 0.4 percent. The resultant greenhouse effect of changes in ozone and thin cirrus cloud cover causes a climatic surface temperature change of the order 0.01 to 0.1 K. These temperature changes are small in comparison to the natural variability. Recent research indicates that the emissions at cruise altitude may increase the amount of stratospheric aerosols and polar stratospheric clouds and thereby may have an impact on the atmosphere environment, to a yet unknown degree. Air traffic is increasing by about five to six percent per year; fuel consumption grows by about three percent per year. Moreover, the climatic changes due to air traffic enhance other environmental problems originating, e.g., from anthropogenic carbon dioxide or methane emissions. Hence, air traffic induced emissions are of growing importance. This calls for the development of efficient and low-emission propulsion systems and other means to reduce the emissions. This paper surveys the state of knowledge and describes several items of results from recent and ongoing research.

Author (revised)

N94-29248# Naval Air Warfare Center, Trenton, NJ. Aircraft Div.

COMBUSTION TECHNOLOGY NEEDS FOR ADVANCED HIGH PRESSURE CYCLE ENGINES

Stephen D. Clouser and Richard A. Kamin *In* AGARD, Fuels and Combustion Technology for Advanced Aircraft Engines Sep. 1993 8 p (For primary document see N94-29246 08-25)

Copyright Avail: CASI HC A02/MF A04

The challenges in designing high performance aircraft combustion systems have not changed significantly over the years, but the approach has shifted towards a more sophisticated analytical process. Initially an overview of the U.S. Navy's component technology development procedure is presented to show how technology development is still tied into mission requirements. A more technical discussion on combustion technology status and needs will show that the classic impediments that have hampered progress towards near-stoichiometric combustion still exist. Temperature rise, mixing, liner cooling, stability, fuel effects, temperature profile control, and emissions continue to confront the aerodynamic and mechanical designers with a plethora of engineering dilemmas and trade-offs. In addition, new materials such as ceramic matrix composites (CMC) and intermetallics like titanium aluminides (TiAl) are now being incorporated into every advanced design. The process of combustion design has taken on a new meaning over the past several years as three dimensional codes and other advanced design and validation tools have finally changed the approach from a 'cut and burn' technique to a much more analytical process. All of these new aspects are now integral elements of the new equation for advanced combustion design that must be fully understood and utilized. Only then will the operable, high temperature capable combustion systems needed for future military aircraft be developed. Author

N94-29249# Rolls-Royce Ltd., Bristol (England).

COMBUSTION FOR FUTURE SUPERSONIC TRANSPORT PROPULSION

B. W. Lowrie *In* AGARD, Fuels and Combustion Technology for Advanced Aircraft Engines Sep. 1993 6 p (For primary document see N94-29246 08-25)

Copyright Avail: CASI HC A02/MF A04

Even with it's marginal performance, Concorde has demonstrated that supersonic civil aircraft are a practical proposition. A second generation machine will need sufficiently good performance for a robust operating system that can provide reliable, frequent service with competitive economics. Additionally, the propulsion system must be acceptable environmentally. That is it must create acceptable noise levels around airports and have acceptable emissions throughout its mission including cruise. Whatever devices may be used to improve the acceptability at subsonic flight conditions, the high operating temperatures at cruise can create difficult targets for the operation of the combustion system both mechanically and in the combustion process itself. While the driving force is ever better fuel consumption and weight to achieve economic viability, a future supersonic transport engine will have cycle temperatures limited only by the mechanical integrity of the major components. The environment of the major components in modern gas turbine engines is dominated by the air delivered by the compressor system. Consequently the maximum compression temperature is governed by materials available for the turbine and compressor discs. The continued improvement of the disc material leads to combustion inlet temperatures beyond today's experience and sets difficult targets for combustion system emissions. This is worsened by the requirement being at cruise and therefore maintained for the major part of the mission. Problems such as creep and oxidation of metallic parts are also considered. Author (revised)

N94-29250# Leeds Univ. (England). Dept. of Fuel and Energy.

PREDICTION OF PROMPT NO(x) IN HYDROCARBON AIR FLAMES

Valerie Dupont, M. Pourkashanian, and A. Williams *In* AGARD, Fuels and Combustion Technology for Advanced Aircraft Engines Sep. 1993 13 p (For primary document see N94-29246 08-25)

Copyright Avail: CASI HC A03/MF A04

The gas turbine industry is directing particular attention to very low NOx combustors, whether for aircraft or land based CCGT systems. These low NOx combustors frequently use liquid fuels or natural gas burning under very lean premixed conditions with air or under rich-lean conditions, although only the first case is studied here. In land based systems, diluted steam or nitrogen are sometimes injected into the combustion chambers to reduce flame temperature. The NOx emissions from such systems are the product of three chemical mechanisms which are interrelated: the hydrocarbon prompt NO, the thermal NO (extended Zeldovich mechanism), and the nitrous oxide route to NO. Formation of NO2 from NO also occurs, as well as emission of carbon monoxide and unburnt hydrocarbons. When the fuel-oxidant proportion decreases towards leaner conditions, flame temperatures are lowered, resulting in the total NO being reduced and the thermal-NO contribution greatly diminished to the benefit of the remaining two mechanisms of NO formation. While knowledge of the elementary reactions and their chemical kinetics concerning methane and simple hydrocarbons combustion has existed for a number of years, its use for computer modeling is limited to simple flow dynamics configurations. Nevertheless, understanding of such combusting flows under a wide range of experimental conditions allows for analogies or speculations with more complex actual systems. Such understanding can be achieved by means of one dimensional laminar premixed flame modeling, with a full chemical mechanism which incorporates the three routes of NO formation. Complementary to this understanding is the modeling of the actual combustion system using a full description of the fluid dynamics coupled with a reduced chemical scheme, which is then compared against the first model. The objective of this investigation is to evaluate the relative importance of the three mechanisms of NO formation in lean premixed methane-air combustion with increasing pressure using the one dimensional plug flow package PREMIX, and to test the validity of a three dimensional model with a global chemical mechanism against the one dimensional model in the atmospheric pressure case. Methane is chosen because it is the only mechanism which is reasonably well known and is a good guide to the behavior of other hydrocarbons. The mixture ratio chosen is richer than that in lean gas turbines, but the combustion of this mixture with the low preheat gives realistic gas turbine final flame temperatures. Conditions of NO2 formation are also analyzed in the one dimensional model and results extrapolated to the case of gas turbines. Derived from text

N94-29251# Centre National de la Recherche Scientifique, Paris (France).

SIMULATION OF POLLUTANT FORMATION IN TURBULENT COMBUSTORS USING AN EXTENDED COHERENT FLAME MODEL

E. Djavdan, D. Veynante, J. M. Duclos, and S. Candel *In* AGARD, Fuels and Combustion Technology for Advanced Aircraft Engines Sep. 1993 8 p Sponsored by SNECMA (For primary document see N94-29246 08-25)

Copyright Avail: CASI HC A02/MF A04

An extension of a flame surface density model, combining flamelet concepts and homogeneous reactor combustion, is proposed to predict NO and CO formation. Results for CO in propane-air premixed flames for different equivalence ratios are compared to available experimental measurements. The agreement is good but the model is sensitive to the

determination of the flamelet model parameters such as those governing the effective strain rate. Author (revised)

N94-29252# Cranfield Inst. of Tech., Bedford (England). School of Mechanical Engineering.

FLOWFIELD PREDICTION OF NO(x) AND SMOKE PRODUCTION IN AIRCRAFT ENGINES

S. Alizadeh and J. B. Moss *In* AGARD, Fuels and Combustion Technology for Advanced Aircraft Engines Sep. 1993 20 p Sponsored by Science Research Council (For primary document see N94-29246 08-25)

Copyright Avail: CASI HC A03/MF A04

CFD predictions of nitric oxide and smoke production in a tubular combustor are described for a range of inlet temperature and pressure conditions up to 800 K and 8 bar, chosen to distinguish the effects of both state properties and turbulence on formation rates. Combustion models based on both laminar flamelet and chemical equilibrium representations are contrasted and compared with measurements in the literature. While uncertainties persist with respect to the detailed mechanisms, notably for soot formation, a strategy is identified which extends the role of mixture fraction in the calculation of the influence of turbulent scalar fluctuations on emissions prediction. Author (revised)

N94-29253# Technical Univ. of Lisbon (Portugal). Dept. of Mechanical Engineering.

NUMERICAL PREDICTION OF TURBULENT SOOTING DIFFUSION FLAMES

P. J. Coelho, T. L. Farias, J. C. F. Pereira, and M. G. Carvalho *In* AGARD, Fuels and Combustion Technology for Advanced Aircraft Engines Sep. 1993 16 p (For primary document see N94-29246 08-25) (Contract BD/860/90-IB)

Copyright Avail: CASI HC A03/MF A04

Soot formation is an important but poorly understood subject. Although significant advances have been made in the last few years, soot formation models for numerical calculation still present recognized shortcomings. Different soot formation models are compared in the calculation of a propane turbulent diffusion flame and the influence of soot agglomeration and refractive index on soot volume fraction values inferred from extinction measurements are investigated. The time-averaged equations governing conservation of mass and momentum are closed by the k-epsilon eddy viscosity/diffusivity model and combustion is modeled using the laminar flamelet approach. Soot prediction involves the solution of transport equations for soot particle number density and soot mass fraction. The uncertainties of soot volume fractions obtained from extinction measurements due to agglomeration and the value of the complex refractive index were studied. Results using Rayleigh approximation were compared with predictions using the model presented by Iskander et al. for scattering and extinction of light by an ensemble of spherical particles. Author (revised)

N94-29254# Technische Hochschule, Darmstadt (Germany). Inst. fuer Energie- und Kraftwerkstechnik.

NUMERICAL MODELLING OF TURBINE COMBUSTION CHAMBERS **c07**

S. Maidhof and J. Janicka *In* AGARD, Fuels and Combustion Technology for Advanced Aircraft Engines Sep. 1993 10 p (For primary document see N94-29246 08-25)

Copyright Avail: CASI HC A02/MF A04

This paper focuses on the calculation of the flow and scalar fields of axisymmetric gas turbine combustion chambers with non-premixed combustion. Modelling of the turbulent swirling flow is carried out both by viscosity and Reynolds stress closure. It is our intention to specify the shortcomings as well as the potential of the different schemes with regard to prediction capabilities, numerical performance, and economic worth. The various aspects of modelling are discussed. A short description of the governing transport equations as well as the turbulence closure is given. An equilibrium chemistry model is compared to a laminar flamelet model, both schemes applied in conjunction with a probability density formulation for scalar properties. Numerical results of velocities and temperature in model gas turbine combustion chambers are compared with experimental results. Probable reasons for deviations are deduced and some prospects for possible future development of numerical simulation of gas turbine combustion are given. Author (revised)

N94-29255# Alfa Romeo S.p.A., Naples (Italy). Research and Development Dept.

NUMERICAL SIMULATION OF AEROTHERMAL CHARACTERISTICS IN GAS TURBINE COMBUSTORS WITH COMPLEX GEOMETRIES **c07**

P. DiMartino, G. Cinque, and C. Paduano *In* AGARD, Fuels and Combustion Technology for Advanced Aircraft Engines Sep. 1993 14 p (For primary document see N94-29246 08-25)

Copyright Avail: CASI HC A03/MF A04

A method is presented for calculating steady three-dimensional two-phase turbulent reactive flows with curved irregular boundaries. The gas phase equations are solved in an Eulerian frame of reference by a numerical technique based on the finite volume approach, while the equations describing droplet motion, evaporation, and burning are treated in a Lagrangian frame of reference. Turbulent transport is described by the standard k-epsilon model. The combustion model utilizes a conserved scalar formulation and an assumed shape probability density function to account for chemistry-turbulence interaction. The numerical scheme employs structured non-orthogonal grids, a node-centered variable arrangement, and Cartesian velocity components. A special interpolation procedure is used to avoid checkerboard oscillations due to pressure-velocity coupling, and a low diffusive and bounded scheme is introduced to approximate the convective terms in the transport equations. The capabilities of the numerical procedure are demonstrated by simulating an annular combustion chamber for which experimental results were available. The agreement between calculation and experiments ranges from fair to good. Author (revised)

N94-29256# General Motors Corp., Indianapolis, IN. Gas Turbine Div.

APPLICATION OF CFD IN COMBUSTOR DESIGN TECHNOLOGY **c07**

Hukam C. Mongia *In* AGARD, Fuels and Combustion Technology for Advanced Aircraft Engines Sep. 1993 18 p (For primary document see N94-29246 08-25)

Copyright Avail: CASI HC A03/MF A04

Multidimensional computational combustion dynamics has been used over the last twenty years to provide improved insight during gas turbine combustor design and development processes. The empirical/analytical combustor design methodology that was first demonstrated under the Army sponsored Combustor Design Criteria Validation program conducted during 1974-1978 has been used in the design and demonstration of 15 advanced rig combustors, four technology demonstrator engine combustors, three engine combustors, and one small turbine augmentor. Recognizing the limitations of turbulent combustion models, numerics, and the assumptions required to fully specify the boundary conditions for practical gas turbine combustion systems, a new technique that combines state-of-the-art turbulent combustion models with 'consistent' macro-volume expressions ('hybrid combustor modelling') was proposed. This hybrid modeling approach has been calibrated with combustors that include diffusion flame, lean premix/prevaporized, or rich-lean types of combustion processes. The hybrid modeling technique gives good 'quantitative' agreement with measured data on gaseous emissions, smoke, combustion efficiency, lean blowout fuel-air ratio, pattern factor, liner wall temperature levels, and gradients of a number of combustors. Author (revised)

N94-29257# Pratt and Whitney Aircraft of Canada Ltd., Mississauga (Ontario).

RECENT CFD APPLICATIONS IN SMALL GAS TURBINE COMBUSTION SYSTEMS DEVELOPMENT **c07**

T. C. J. Hu and L. A. Prociw *In* AGARD, Fuels and Combustion Technology for Advanced Aircraft Engines Sep. 1993 12 p (For primary document see N94-29246 08-25)

Copyright Avail: CASI HC A03/MF A04

A typical small gas turbine combustor is modelled using CFD, and the numerical results are compared with laser doppler velocimetry (LDV) measured data. The predicted flow characteristics are in excellent agreement with the measurements. Some aspects of CFD application in combustor design are discussed. CFD can be used in the following ways: as a tool in studying the flowfield development; in the optimization of location, size, and quantity of flow devices; in monitoring flow performance; and in correlating important design parameters. Use of CFD can significantly reduce the lapse time and the development cost of gas turbine combustors.

Author

N94-29258# Societe Nationale d'Etude et de Construction de Moteurs d'Aviation, Moissy-Cramayel (France).

AEROTHERMOCHEMICAL CALCULATIONS IN AFTERBURNERS [CALCULS AEROTHERMOCHIMIQUES DANS LES FOYERS DE RECHAUFFE] **c07**

C. Dejeu, J. L. Schultz, and S. Meunier *In* AGARD, Fuels and Combustion Technology for Advanced Aircraft Engines Sep. 1993 8 p In FRENCH Original contains color illustrations (For primary document see N94-29246 08-25)

Copyright Avail: CASI HC A02/MF A04

The detailed study of the aerodynamics and the thermodynamics of systems is an important part in the process of dimensioning and optimizing the afterburning chambers of modern turbojets. In this context, the article presents two examples of geometries and recent results drawn from concrete cases. The aerothermochemical code which was used was developed by ONERA within the framework of the Cooperative Action for Combustion Chambers (A3C). It is based on a volumes type technique finished with a structured three-dimensional mesh adapted to the walls. The model of combustion used of the generalized type 'Eddy Break Up' is the subject of a more detailed presentation. Author (revised)

N94-29259# Pratt and Whitney Aircraft, West Palm Beach, FL. Fuels and Lubricants Group.

HIGH TEMPERATURE FUEL REQUIREMENTS AND PAYOFFS **c28**

Tedd B. Biddle and Bennett M. Croswell *In* AGARD, Fuels and Combustion Technology for Advanced Aircraft Engines Sep. 1993 12 p Sponsored by AFWAL and Naval Air Propulsion Test Center (For primary document see N94-29246 08-25)

Copyright Avail: CASI HC A03/MF A04

This paper describes a study performed under contract to Air Force Wright Laboratory, Wright-Patterson Air Force Base, Dayton, OH in association with the Naval Air Propulsion Laboratory, Trenton, NJ. The study projected fuel temperature capability requirements for future tactical fighter applications and the payoffs that would be realized by achieving these capabilities. The study was approached on the basis of the maximum benefit that might be realized through the use of high temperature fuels, i.e. elimination of the recirculation system. Heat loads were projected for different missions spanning IHPTET technology phases 1, 2, and 3 at different flight conditions. Fuel temperatures across fuel system components were calculated at these heat loads. Shortfalls of the current 163 C fuel capability were shown, and minimun fuel temperature requirements were defined. The study concluded that elimination of the recirculation system is not feasible but shows how high temperature fuel capability can minimize the weight penalty associated with fuel recirculation. In this way, potential payoffs for high temperature fuel development were shown in the form of reduced weight penalties that would normally be encountered as larger and larger recirculation systems are required to accommodate the increasing heat loads projected for advanced aircraft. Author (revised)

N94-29260# Instituto Nacional de Tecnica Aeroespacial, Madrid (Spain). Fuels and Lubricants Lab.

HIGH TEMPERATURE RESISTANT JET FUELS **c28**

Luis M. Peloche and Santiago Asensio *In* AGARD, Fuels and Combustion Technology for Advanced Aircraft Engines Sep. 1993 9 p Sponsored by British Petroleum Oil, Inc. (For primary document see N94-29246 08-25)

Copyright Avail: CASI HC A02/MF A04

The thermal stability of aviation fuels is evaluated according to the ASTM D 2341 method. This characteristic is linked to the presence of generators of instability, mainly diolephins and N and S derivates. The objectives of the present work are as follows: to obtain, in the laboratory, kerosene which is thermally stable; the isolation and identification of generators of instability; and the regeneration of thermally unstable kerosenes. Author (revised)

N94-29261# Wright Lab., Wright-Patterson AFB, OH.

RESEARCH AND DEVELOPMENT OF HIGH THERMAL STABILITY FUELS **c28**

T. Edwards, W. M. Roquemore, W. E. Harrison, and S. D. Anderson *In* AGARD, Fuels and Combustion Technology for Advanced Aircraft Engines Sep. 1993 19 p (For primary document see N94-29246 08-25)

Copyright Avail: CASI HC A03/MF A04

Increases in aircraft performance are leading to increases in the thermal stress on the primary aircraft coolant--the fuel. Fuel thermal stability limitations may offset future aircraft performance gains. The Air Force's Wright Laboratory is sponsoring several research programs to address this problem. The development of an additive package for JP-8 to improve its thermal stability is the primary focus of this paper. This program involves extensive testing of fuels and additives in a variety of test devices, culminating in tests in a fuel system simulator and engine tests. These tests involve Air Force personnel, on-site contractors (University of Dayton Research Institute, Systems Research Laboratories), Pratt and Whitney Aircraft Co., additive manufacturers, and Sandia National Laboratory. The test devices include several flowing and static tests, where the behavior of a fuel is investigated in a wide variety of environments. The study of several baseline fuels in these devices has led to some new insights into the mechanisms of fuel thermal (in)stability. It is becoming clear that a fuel's tendency to oxidize (to form peroxides, for example) is often inversely proportional to its tendency to form insoluble deposits. Author (revised)

N94-29262# Systems Research Labs., Inc., Dayton, OH.

DEVELOPMENT OF GLOBAL/CHEMISTRY MODEL FOR JET-FUEL THERMAL STABILITY BASED ON OBSERVATIONS FROM STATIC AND FLOWING EXPERIMENTS **c28**

V. R. Katta, E. G. Jones, and W. M. Roquemore *In* AGARD, Fuels and Combustion Technology for Advanced Aircraft Engines Sep. 1993 11 p (For primary document see N94-29246 08-25)

(Contract F33615-90-C-2033)

Copyright Avail: CASI HC A03/MF A04

Two global-chemistry models for oxidative deposition of jet fuels are evaluated by integrating them into a Computational Fluid Dynamics with Chemistry (CFDC) code. A previously developed two-step global-chemistry model was found to be insufficient to describe the thermal-oxidation and -deposition rates associated with a Jet-A fuel. A new global-chemistry model has been developed systematically based on observations from flowing and static experiments. The global-autoxidation reaction is modified such that the reaction rate becomes zeroth-order with respect to the dissolved oxygen concentration. The generation of deposit-forming precursor is coupled with the autoxidation reaction by introducing a radical species ROO. A formulation for the sticking probability has also been developed. Deposition profiles are well represented by this new model under a variety of temperature and flow conditions. The model correctly predicts the changes in magnitude and spatial location of the deposition peak due to changes in flow. The CFDC model, which is designed for flowing systems, has been extended to static experiments. The model incorporates a non-depleting species F(sub s) representing all non-oxygen compounds responsible for deposition. Static experiments were found to provide a useful and inexpensive method for estimating the concentration of F(sub s) in the fuel. Author

N94-29263# General Electric Co., Cincinnati, OH. Advanced Engine Combustor Aero Design.

FUEL INJECTOR DESIGN FOR HIGH TEMPERATURE AIRCRAFT ENGINE **c07**

R. W. Stickles, W. J. Dodds, T. R. Koblish, J. Sager, and S. Clouser *In* AGARD, Fuels and Combustion Technology for Advanced Aircraft Engines Sep. 1993 12 p (For primary document see N94-29246 08-25)

(Contract N00140-87-C-6321)

Copyright Avail: CASI HC A03/MF A04

The objective of the Innovative High Temperature Aircraft Engine Fuel Nozzle Program was to design and evaluate a nozzle capable of operating at a combustor inlet air temperature of 1600 F (1144 K) and a fuel temperature of 350 F (450 K). The nozzle was designed to meet the same performance requirements and fit within the size envelope of a current production dual orifice fuel nozzle. The design approach was to use improved thermal protection and fuel passage geometry in combination with fuel passage surface treatment to minimize coking at these extreme fuel and air temperatures. Heat transfer models of several fuel injector concepts were used to optimize the thermal protection, while sample tube coking tests were run to evaluate the effect of surface finish, coatings and tube material on the coking rate. Based on heat transfer analysis, additional air gaps, reduced fuel passage flow area and use of ceramic tip components reduced local fuel wetted wall temperatures by more than 200 F (100 K) when compared to a current production fuel nozzle. Sample tube coking test results showed the importance of surface finish on the fuel coking

rate. Therefore, a one micro-inch (0.025 micron) roughness was specified for all fuel passage surfaces. A novel flow divider valve in the tip was also employed to reduce weight, allow room for additional thermal protection, and provide back pressure to reduce the risk of fuel vaporization. The fuel nozzle was fabricated and evaluated in a series of high temperature coking tests. Initial results of these tests indicate that thermal protection and surface treatments were partially successful in preventing nozzle fouling, but additional refinement of the internal flowpath is needed to prevent buildup of coke particles that partially blocked the spin slots which meter the nozzle fuel flow. Author

N94-29264# Pratt and Whitney Aircraft of Canada Ltd., Mississauga (Ontario).

DESIGN ASPECTS IN SMALL AIRCRAFT GAS TURBINE FUEL INJECTORS **c07**

K. McCaldon, L. A. Prociw, and P. Sampath *In* AGARD, Fuels and Combustion Technology for Advanced Aircraft Engines Sep. 1993 10 p (For primary document see N94-29246 08-25)

Copyright Avail: CASI HC A02/MF A04

The causes of fuel injector spray deterioration and the effects of this deterioration on engine durability and performance are discussed. Small aircraft gas turbine fuel injectors present special design challenges due to low fuel flow rates involved and the physical size limitations. The principal fuel injector performance requirements are discussed in relation to their effect on the hydraulic, aerodynamic, and thermal design of aerating fuel injectors. Author

N94-29265*# Pennsylvania State Univ., University Park. Dept. of Mechanical Engineering.

THE EFFECT OF INCOMPLETE FUEL-AIR MIXING ON THE LEAN LIMIT AND EMISSIONS CHARACTERISTICS OF A LEAN PREVAPORIZED PREMIXED (LPP) COMBUSTOR

D. A. Santavicca, R. L. Steinberger, K. A. Gibbons, J. V. Citeno, and S. Mills *In* AGARD, Fuels and Combustion Technology for Advanced Aircraft Engines Sep. 1993 12 p Sponsored by NASA. Lewis Research Center and GE (For primary document see N94-29246 08-25)

Copyright Avail: CASI HC A03/MF A04

Results are presented from an experimental study of the effect of incomplete fuel-air mixing on the lean limit and emissions characteristics of a lean, prevaporized, premixed (LPP), coaxial mixing tube combustor. Two-dimensional exciplex fluorescence was used to characterize the degree of fuel vaporization and mixing at the combustor inlet under non-combusting conditions. These tests were conducted at a pressure of 4 atm., a temperature of 400 C, a mixer tube velocity of 100 m/sec and an equivalence ratio of .8, using a mixture of tetradecane, 1 methyl naphthalene and TMPD as a fuel simulant. Fuel-air mixtures with two distinct spatial distributions were studied. The exciplex measurements showed that there was a significant amount of unvaporized fuel at the combustor entrance in both cases. One case, however, exhibited a very non-uniform distribution of fuel liquid and vapor at the combustor entrance, i.e., with most of the fuel in the upper half of the combustor tube, while in the other case, both the fuel liquid and vapor were much more uniformly distributed across the width of the combustor entrance. The lean limit and emissions measurements were all made at a pressure of 4 atm. and a mixer tube velocity of 100 m/sec, using Jet A fuel and both fuel-air mixture distributions. Contrary to what was expected, the better mixed case was found to have a substantially leaner operating limit. The two mixture distributions also unexpectedly resulted in comparable NO(x) emissions, for a given equivalence ratio and inlet temperature, however, lower NO(x) emissions were possible in the better mixed case due to its leaner operating limit. Author

N94-29266# Dayton Univ., OH.

STUDIES OF LEAN BLOWOUT IN A RESEARCH COMBUSTOR

D. R. Ballal, M. D. Vangsness, S. P. Heneghan, and G. J. Sturgess *In* AGARD, Fuels and Combustion Technology for Advanced Aircraft Engines Sep. 1993 9 p (For primary document see N94-29246 08-25)

(Contract F33615-92-C-2207)

Copyright Avail: CASI HC A02/MF A04

A prime requirement in the design of a modern gas turbine combustor is good lean blowout (LBO) stability to ensure an adequate stability margin. Therefore, a geometrically simple, optically accessible, and acoustically decoupled research combustor was designed to reproduce the gross features of the flow field in a modern annular gas turbine combustor. Its LBO was measured using methane and propane fuels. We successfully observed and documented a systematic and detailed sequence of events comprising an attached flame, a lifted shear flame, an intermittent shear flame, the large-scale instability of the flame front, and LBO. Also, for the sake of comparison, a generic gas turbine combustor was tested and its LBO limits were measured. We found that LBO in the research combustor behaved like a perfectly stirred reactor (PSR) for values of combustor-loading spanning three orders of magnitude. Also, LBO was successfully correlated using a simple PSR theory. Finally, Swithenbank's dissipation gradient approach and an eddy dissipation model with a built-in characteristic extinction time criterion, when coupled with CFD, offer the possibility of an a priori calculation of LBO. The lean stability of a generic gas turbine combustor at peak heat release rates was less than that in a research combustor. Also, in the generic combustor, the flame changes from a lifted to an attached position depending upon how combustor loading is achieved. Due to such complications, modeling of the LBO process that works reasonably well with the research combustor will be seriously challenged by the blowout behavior evidenced in the generic gas turbine combustor. Author

N94-29267# Leeds Univ. (England). Dept. of Fuel and Energy.

ULTRA LOW NO(x) ULTRA LEAN GAS TURBINE PRIMARY ZONES WITH LIQUID FUELS **c07**

G. E. Andrews, H. S. Alkabie, U. S. AbdulHussain, and M. AbdulAziz *In* AGARD, Fuels and Combustion Technology for Advanced Aircraft Engines Sep. 1993 14 p Sponsored in part by Science Research Council (For primary document see N94-29246 08-25)

Copyright Avail: CASI HC A03/MF A04

Three low NOx gas turbine combustor design concepts, Jet Mix, Grid Mix and radial swirlers, which have been demonstrated to give very low NOx emissions using gaseous fuels have been successfully tested on liquid fuels and low NOx emissions demonstrated. The Jet Mix was shown to have low NOx emissions at atmospheric pressure and has been tested at pressure, with similar low NOx results. Kerosene performance and emissions was very similar to that for propane as the fuel. The scale up of the Jet Mix was found to be possible without increasing the NOx emissions greatly and is a preferable design option to the use of large numbers of smaller Jet Mix modules. Sector tests at pressure showed the Jet Mix design produced emission reductions close to the best of the NASA clean combustor results. The Grid Mix low NOx design was shown to be capable of low NOx performance using kerosene. There was a much wider flame stability than for the Jet Mix design and lower NOx emissions were demonstrated. The radial swirler with vane passage of 76mm wall fuel injection was shown to have ultra low NOx emissions with liquid fuels, only slightly higher than for gaseous fuels. For a high air flow radial swirler it was found that central kerosene injection gave lower NOx emissions than for gaseous fuels and had the potential to yield a NOx EI of below 10 at simulated take off conditions. Author

N94-29268# Centro Applicazioni Militari dell'Energia Nucleare, Pisa (Italy).

COMPUTATIONAL AND EXPERIMENTAL RESULTS IN HIGH PRESSURE COMBUSTIONS OF H2/AIR AND H2/O2/H2O

Dino Dini *In* AGARD, Fuels and Combustion Technology for Advanced Aircraft Engines Sep. 1993 10 p (For primary document see N94-29246 08-25)

Copyright Avail: CASI HC A02/MF A04

The first results of a research and development program on combustion characteristics of gaseous hydrogen fuel in a 'can' type gas turbine combustor, both in combination with air or with oxygen and water, are here presented. Application of a H2/O2/H2O combustion chamber is suggested for the launch-boost phase of an advanced turboramjet. Experiments have been conducted to determine the configuration and the operation of the hydrogen-air combustion chamber test facility, to be transferred to two different kinds of small power turboshafts. Computations, project details and tests, are presented regarding high pressure and temperature stoichiometric H2/O2 combustion in which water is gradually injected. Referring to an already realized and operated (on behalf of the author) H2/O2/H2O combustor for a water steam closed cycle in a turbine/alternator electrically propelled automobile, a detailed design is

developed for a quite higher steam temperature, as required in high performance boost phase of a low noxious emission advanced turboramjet, in which H2 and O2 are stored in liquid form. Author

N94-29269# United Technologies Research Center, East Hartford, CT. Aerothermal Technology/Chemical Sciences.

EVALUATION OF THE TRANSIENT OPERATION OF ADVANCED GAS TURBINE COMBUSTORS **c07**

T. J. Rosfjord and J. M. Cohen *In* AGARD, Fuels and Combustion Technology for Advanced Aircraft Engines Sep. 1993 10 p Sponsored by Pratt and Whitney Aircraft (For primary document see N94-29246 08-25)

(Contract N00140-87-C-9902)

Copyright Avail: CASI HC A02/MF A04

A unique test capability has been defined and used at the United Technologies Research Center to evaluate the transient response of advanced gas turbine combustors. This UTC Transient Combustion Facility offers the opportunity to achieve pre-defined time variations of the air and fuel flow rates and air temperature delivered to a combustor model. This capability can be used for model scales ranging from multi-nozzle combustor sectors to smaller setups focusing on one component or process. A dedicated control computer aids in establishing time profiles for the input parameters and automatically executing the transient test. Among its applications, the facility has been used to study the occurrence of in-nozzle fuel vaporization during Bodie cycles and to assess the tolerance of a fuel-staged combustor to rapid fuel redistribution. Author

N94-29270# Fiat Aviazione S.p.A., Turin (Italy). Direzione Progettazione.

TECHNOLOGY RIGS: A TOOL FOR AFTERBURNER DEVELOPMENT **c07**

G. Riccardi, A. Tasselli, and A. Trovati *In* AGARD, Fuels and Combustion Technology for Advanced Aircraft Engines Sep. 1993 17 p (For primary document see N94-29246 08-25)

Copyright Avail: CASI HC A03/MF A04

To develop a component of an advanced aircraft engine, heavy experimental activities are necessary. To avoid very long and expensive test campaigns on development engines, tests on the so-called technology rigs are fundamental. Particularly in the case of combustion components, whose analytical simulations by means of computer code are still not completely satisfactory and where very high gas temperatures may cause important problems of mechanical integrity, it is essential to check the behavior of the component on the rig before testing on the engine. This paper gives an overview of the test rigs which are used by FiatAvio in the development of the afterburner system for an advanced fighter aircraft engine. The tests which are carried out on these rigs are described and some of the most important results are reported, discussing the benefit they have given to the engine development. Even if this paper obviously does not cover all the results obtained from rig tests over years of engine development, the few examples reported clearly show the importance of these rigs and confirm that the financial outlay to build and update the rigs, test plants and models is worthwhile. Author

N94-29271*# California Univ., Irvine. Combustion Lab.

POLLUTANT EMISSIONS FROM AND WITHIN A MODEL GAS TURBINE COMBUSTOR AT ELEVATED PRESSURES AND TEMPERATURES

S. A. Drennan, C. O. Peterson, F. M. Khatib, W. A. Sowa, and G. S. Samuelsen *In* AGARD, Fuels and Combustion Technology for Advanced Aircraft Engines Sep. 1993 10 p Sponsored by Northrop Corp. (For primary document see N94-29246 08-25)

(Contract NAG3-1124; F08635-90-C-0100)

Copyright Avail: CASI HC A02/MF A04

Conventional and advanced gas turbine engines are coming under increased scrutiny regarding pollutant emissions. This, in turn, has created a need to obtain in-situ experimental data at practical conditions, as well as exhaust data, and to obtain the data in combustors that reflect modern designs. The in-situ data are needed to (1) assess the effects of design modifications on pollutant formation, and (2) develop a detailed data base on combustor performance for the development and verification of computer modeling. This paper reports on a novel high pressure, high temperature facility designed to acquire such data under controlled conditions and with access (optical and extractive) for in-situ measurements. To evaluate the utility of the facility, a model gas turbine combustor was selected which features practical hardware design, two rows of jets (primary and dilution) with four jets in each row, and advanced wall cooling techniques with laser drilled effusive holes. The dome is equipped with a flat-vaned swirler with vane angles of 60 degrees. Data are obtained at combustor pressures ranging from 2 to 10 atmospheres of pressure, levels of air preheat to 427 C, combustor reference velocities from 10.0 to 20.0 m/s, and an overall equivalence ratio of 0.3. Exit plane and in-situ measurements are presented for HC, O2, CO2, CO, and NO(x). The exit plane emissions of NO(x) correspond to levels reported from practical combustors and the in-situ data demonstrate the utility and potential for detailed flow field measurements. Author

N94-29272# Pratt and Whitney Aircraft, East Hartford, CT.

REDUCTION OF NO(x) BY FUEL-STAGING IN GAS TURBINE ENGINES: A COMMITMENT TO THE FUTURE

I. Segalman, R. G. McKinney, G. J. Sturgess, and L.-M. Huang *In* AGARD, Fuels and Combustion Technology for Advanced Aircraft Engines Sep. 1993 17 p (For primary document see N94-29246 08-25)

Copyright Avail: CASI HC A03/MF A04

As part of an ongoing program of continuous improvement by control of gaseous emissions from the combustors of gas turbines, a unique fuel-staged annular combustor is being developed for application to current and future Pratt & Whitney aircraft engines. The configuration advantages of this combustor are outlined, and discussions are presented on staging considerations and fuel system impacts. Development of the fuel-staged combustor is described by reference to supporting mixing experiments and computational fluid dynamic studies, and rig tests at high pressures. Measured results are given appropriate for the International Aero Engines (IAE) V2500 engine that show progressive reductions in achieved emissions compared to the goals established for this program. Author

N94-29273# Societe Nationale d'Etude et de Construction de Moteurs d'Aviation, Moissy-Cramayel (France). Dept. YKC.

CHAMBERS OF TURBOREACTORS WITH VARIABLE GEOMETRY: A RESPONSE TO THE MATRIX OF POLLUTION IN CYCLES AT HIGH TEMPERATURE, HIGH PRESSURE [LES FOYERS DE TURBOREACTEURS A GEOMETRIE VARIABLE: UNE REPONSE A LA MAITRISE DE LA POLLUTION DANS DES CYCLES A HAUTE TEMPERATURE, HAUTE PRESSION]

S. Meunier, D. Ansart, and P. Ciccia *In* AGARD, Fuels and Combustion Technology for Advanced Aircraft Engines Sep. 1993 4 p In FRENCH (For primary document see N94-29246 08-25)

Copyright Avail: CASI HC A01/MF A04

The pollutants emissions decrease doesn't seem easily achievable, particularly with advanced engines cycles conditions with high pressure, temperature, and fuel to air ratio. For a given fuel and air split, the combustor size can't be reduced without leading to relight altitude, combustion stability, and emissions concerns. In addition, the liners areas to be cooled remain considerable, the cooling airflow increase leads to higher fuel to air ratio in the primary zone and finally to unacceptable Nox emissions levels due to higher flame temperatures. In order to satisfy the trade off in between the combustor performance at low and high engine ratings, several combustor concepts are in development. Among them, the use of variable geometries to modulate the primary zone airflow seems promotive. Indeed, this concept allows to satisfy the compromise between the different ratings taking into account the decrease of the combustor panels areas to be cooled. That is the reason why this variable geometry concept is particularly suitable to high pressure and temperature engines cycles. In this paper, test results recorded on a five-cups sector fitted with a variable geometry injection system, and some measured performance on a full annular combustor are commented. It appeared that acceptable performance in term of combustion stability can be met with a low volume combustor. The cooling airflow reduction and the primary zone fuel to air ratio control allow to meet quite good and homogeneous combustor exit temperature profiles whatever the engine rating. Author

N94-29274# Defence Research Agency, Farnborough (England).

THE INFLUENCE OF AIR DISTRIBUTION ON HOMOGENEITY AND POLLUTANT FORMATION IN THE PRIMARY ZONE OF A TUBULAR COMBUSTOR

J. R. Tilston, M. I. Wedlock, and A. D. Marchment *In* AGARD, Fuels and Combustion Technology for Advanced Aircraft Engines Sep. 1993

12 p (For primary document see N94-29246 08-25)
(BRITE/EURAM-1019)
Copyright Avail: CASI HC A03/MF A04

This paper summarizes the work undertaken by the Defense Research Agency (DRA Pyestock) for the BRITE/EURAM Low Emissions Combustor Technology Project No 1019. The work was jointly funded by the CEC (DGXIIH), the UK DTI (CARAD - ATF4) and the UK MOD (DCSA). The gas turbine emissions problem is summarized and the design philosophy of the experimental program is described. The principal objective was to demonstrate a simultaneous reduction of NO(x) and smoke emissions together with acceptable idling emissions and stability in an unstaged combustor. A secondary objective was to demonstrate the extent to which NO(x) and smoke could be reduced if the combustor was to be used as the main stage of a staged combustor where a poorer idling performance could be accepted. The work consisted of a parametric investigation of the principal factors controlling the emissions produced in the combustor primary zone. Particular emphasis was placed on the influence of the distribution, number, and size of air entry holes and of residence time on pollutant formation. The results from the complete experimental program are summarized. These suggest that NO(x) reductions of about 30-40 percent should be possible together with excellent smoke and idling performance. The results suggest that NO(x) was formed very close to stoichiometric flame temperatures even at very weak combustor mixture strengths and under well mixed conditions. The reductions that were achieved were largely as a result of reductions of residence time. Author

N94-29275# Universidad Politecnica de Madrid (Spain). Dept. de Motopropulsion y Termofluidodinamica.
EFFECTS OF HYDROGEN ADDITION ON POLLUTANT EMISSIONS IN A GAS TURBINE COMBUSTOR
J. Salva and G. Lopez *In* AGARD, Fuels and Combustion Technology for Advanced Aircraft Engines Sep. 1993 9 p (For primary document see N94-29246 08-25)
Copyright Avail: CASI HC A02/MF A04

This paper presents an experimental work on the control of pollutants produced in a tubular hydrocarbon fueled combustor, by the injection of hydrogen in small quantities (less than 4 percent of total fuel). Hydrogen is introduced in the primary zone premixed with the air. Using this technique, with lean primary zone, it is possible to reduce the NO(x) emission level while maintaining CO and HC emission index at normal levels (CO and HC levels are greater without hydrogen injection). Injecting butane, instead of hydrogen, shows that there is no beneficial effect, so the influence of hydrogen in CO and HC reduction is due mainly to factors such as hydrocarbon substitution and chemical kinetics. An analysis to estimate the contribution of these factors is also included. Author

N94-29276# Imperial Coll. of Science and Technology, London (England). Dept. of Mechanical Engineering.
DUCTED KEROSENE SPRAY FLAMES
R. M. Perez-Ortiz, S. Sivasegaram, and J. H. Whitelaw *In* AGARD, Fuels and Combustion Technology for Advanced Aircraft Engines Sep. 1993 16 p Sponsored by Rolls-Royce Ltd. (For primary document see N94-29246 08-25)
(Contract N00014-89-J-1721)
Copyright Avail: CASI HC A03/MF A04

Reaction progress in premixed methane-air flames in round ducts without and with kerosene sprays has been quantified on the basis of species concentration measurements for different fueling arrangements of kerosene with equivalence ratio, proportion of liquid to gaseous fuel, duct length and air preheat temperature as variables in smooth and in rough combustion. The intensity of heat release close to the flame holder in rough combustion was greater than that in smooth combustion, and the duct length necessary to ensure complete combustion decreased with air preheat temperature and upstream turbulence intensity and was weakly dependent on the proportion of methane to kerosene in flow arrangements where the kerosene was sprayed upstream of the flame-holder. The injection of kerosene through the flame holder at a velocity larger than that of the mean flow past the disk led to uneven mixing and incomplete combustion. Pulsed injection of kerosene through a pintle-type injector also resulted in incomplete combustion due to the larger droplet size than in arrangements with a steady flow of kerosene. Oscillations of large amplitude were induced at equivalence ratios usually associated with smooth combustion and oscillations in rough combustion ameliorated by pulsed injection of kerosene comprising around 10 percent of the total fuel. Author

N94-29277*# National Aeronautics and Space Administration. Lewis Research Center, Cleveland, OH.
SPRAY COMBUSTION EXPERIMENTS AND NUMERICAL PREDICTIONS
Edward J. Mularz (Army Research Lab., Cleveland, OH.), Daniel L. Bulzan, and Kuo-Huey Chen *In* AGARD, Fuels and Combustion Technology for Advanced Aircraft Engines Sep. 1993 21 p Original contains color illustrations (For primary document see N94-29246 08-25)
Copyright Avail: CASI HC A03/MF A04

The next generation of commercial aircraft will include turbofan engines with performance levels significantly better than those in the current fleet. Control of particulate and gaseous emissions will also be an integral part of the engine design criteria. These performance and emission requirements present a technical challenge for the combustor: control of the fuel and air mixing and control of the local stoichiometry will have to be maintained much more rigorously than with combustors in current production. A better understanding of the flow physics of liquid fuel spray combustion is necessary. This paper describes recent experiments on spray combustion where detailed measurements of the spray characteristics were made, including local drop-size distributions and velocities. Also, an advanced combustor CFD code has been under development and predictions from this code are compared with experimental results. Studies such as these will provide information to the advanced combustor designer on fuel spray quality and mixing effectiveness. Validation of new fast, robust, and efficient CFD codes will also enable the combustor designer to use than as valuable additional design tools for optimization of combustor concepts for the next generation of aircraft engines. Author

N94-29278# Centre d'Etudes et de Recherches, Toulouse (France).
MODELING OF THE PHASE LIQUIDATES IN COMBUSTION CHAMBERS [MODELISATION DE LA PHASE LIQUIDE DANS LES CHAMBRES DE COMBUSTION]
P. Hebrard, G. Lavergne, P. Beard, P. Donnadille, and P. Trichet *In* AGARD, Fuels and Combustion Technology for Advanced Aircraft Engines Sep. 1993 12 p In FRENCH (For primary document see N94-29246 08-25)
Copyright Avail: CASI HC A03/MF A04

This paper presents experimental results, numerical models, and simulations relating to the behavior of the liquid phase in combustion chambers. These studies concern the initial conditions, boundary conditions, and validations of the models of the various physical processes which must be integrated into the computer codes of reactive flows. Several experiments are presented: characterization of a jet of drops at the aerodynamic exit of a burner, dispersion of the drops in a screen turbulence and a strongly nonstationary flow, trajectories and evaporation of the drops in a turbulent flow, and interaction of the drops with a hot wall. The characterizations of the diphasic flows are carried out by LDA and hot wire for the gas phase and by phase Doppler anemogranulometry and rapid video techniques associated with image processing for the liquid phase. Video techniques and image processing make it possible to restore the trajectories of the drops, their speed as well as the main statistics of dispersion (average trajectory, envelope, and presence rate). The experimental results, in particular those coming from the dispersion of the drops, are compared with the numerical results of simulations. The Lagrangian method is used for transport of the drops, and their dispersion can be calculated starting from the following two approaches: the gas phase is calculated by direct simulation and a deterministic model is retained for the transport of the drops; and the gas phase is calculated starting from a model of turbulence of the type K- and stochastic models are used for the transport of drops. In conclusion, the models most appropriate to the diphasic flows studied are deduced. Author (revised)

N94-29279# Karlsruhe Univ. (Germany). Lehrstuhl und Inst. fuer Thermische Stroemungsmaschinen.
A NEW EULERIAN MODEL FOR TURBULENT EVAPORATING SPRAYS IN RECIRCULATING FLOWS
S. Wittig, M. Hallmann, M. Scheurlen, and R. Schmehl *In* AGARD, Fuels and Combustion Technology for Advanced Aircraft Engines Sep.

1993 11 p Sponsored by Arbeitsgemeinschaft Hochtemperatur Gasturbine and DFG (For primary document see N94-29246 08-25)
Copyright Avail: CASI HC A03/MF A04

A new Eulerian model for the computation of turbulent evaporating sprays in recirculating flows is derived. It comprises droplet heating and evaporation processes by solving separate transport equations for the droplet's temperature and diameter. Full coupling of the droplet and the gaseous phase is achieved by the exchange of source terms due to momentum, heat, and mass transfer. The partial differential equations describing the droplet's transport and evaporation in the new method can be solved using the same numerical procedure as for the gas phase equations. The validity of the model is established by comparison with a well known Lagrangian approach and with experimental data. For this purpose calculations of a recirculating droplet charged air flow within a model combustor are presented. Author (revised)

N94-29280*# National Aeronautics and Space Administration. Lewis Research Center, Cleveland, OH.
EXPERIMENTAL STUDIES ON EFFERVESCENT ATOMIZERS WITH WIDE SPRAY ANGLES **c34**
J. D. Whitlow (Purdue Univ., West Lafayette, IN.), A. H. Lefebvre (Purdue Univ., West Lafayette, IN.), and R. J. Rollbuhler *In* AGARD, Fuels and Combustion Technology for Advanced Aircraft Engines Sep. 1993 11 p (For primary document see N94-29246 08-25)
Copyright Avail: CASI HC A03/MF A04

An experimental investigation was conducted to examine the operating and spray characteristics of two internal-mixing twin-fluid atomizers that were designed to produce effervescent atomization at low air/liquid mass ratios (ALR's). These two experimental atomizers ejected the two phase flow so as to produce a wide spray angle. One atomizer was a plain orifice design that used a four-hole exit orifice which divided and turned the two phase flow just prior to ejection. The other atomizer, called the conical sheet atomizer, ejected the two phase flow through an annular passage in such a way as to form a hollow cone spray. The atomizer operating parameters varied during this investigation were the air/liquid mass ratio, atomizer operating pressure, and, in the case of the conical sheet atomizer, the exit gap width. Studies of spray characteristics included measurements of the spray Sauter mean diameter (SMD), drop size distribution, and, for the conical sheet atomizer, circumferential distribution of the liquid mass within the spray. For both atomizers it was found that SMD decreases with an increase in either ALR or operating pressure. The effect of ALR on SMD diminishes as the value of ALR increases. For the conical sheet atomizer, when operating at low values of pressure and ALR, SMD increases with increase in gap width, but the influence of gap width on SMD diminishes with an increase in either pressure or ALR. At the highest operating pressure of the conical sheet atomizer (552 kPa), SMD is independent of gap width at all ALR's. For both atomizers, changes in operating pressure and ALR have little effect on the distribution of drop sizes in the spray. Author (revised)

N94-29281# Technische Hochschule, Darmstadt (Germany). Flight Propulsion.
THE MIXING PROCESS IN THE QUENCHING ZONE OF THE RICH-LEAN-COMBUSTION CONCEPT
Th. Doerr and D. K. Hennecke *In* AGARD, Fuels and Combustion Technology for Advanced Aircraft Engines Sep. 1993 9 p Sponsored by DFG Original contains color illustrations (For primary document see N94-29246 08-25)
Copyright Avail: CASI HC A02/MF A04

The rich burn/quick quench/lean burn (RQL) combustion system is a potential concept to reduce both NO(x) and CO, UHC emissions. In view of the concept's crucial mixing process, an experimental investigation of a nonreacting multiple jet mixing with a confined crossflow has been conducted. Temperature distributions, mixing rate, and standard deviation were determined for measurements with round jet orifices by parametric variation of flow and geometric conditions. The results show that best mixing strongly depends on an optimum momentum flux ratio. Too high ratios yield a deterioration of mixing process, due to the mutual impact of opposed entraining jets. Furthermore, over a wide range of geometries investigated, inline and staggered configurations provide similar mixing rates. An appreciable enhancement of mixing with staggered orifice configurations only occurs for high momentum flux ratios and large spacings. Author

N94-29282# Deutsche Forschungs- und Versuchsanstalt fuer Luft- und Raumfahrt, Cologne (Germany). Inst. for Propulsion Technology.
INVESTIGATION OF THE TWO-PHASE FLOW IN A RESEARCH COMBUSTOR UNDER REACTING AND NON-REACTING CONDITIONS **c34**
C. Hassa, A. Deick, and H. Eickhoff *In* AGARD, Fuels and Combustion Technology for Advanced Aircraft Engines Sep. 1993 12 p Sponsored by TECFLAM (For primary document see N94-29246 08-25)
Copyright Avail: CASI HC A03/MF A04

The flow resulting from an airblast atomizer with prefilmer and corotating swirl was investigated in a cylindrical combustion chamber. Gas and droplet velocities were measured by a phase Doppler anemometer and species and gas temperature by gas sampling probes respectively, thermoelements at atmospheric conditions and without fuel and air preheat. Because of interference with the liquid phase, the species measurements were restricted to a minimum distance of 40 mm from the atomizer lip. The temperature measurements showed the dominating influence of the external recirculation zone on flame stabilization for the investigated nozzle configuration with a small expansion angle of the swirling flow. The species concentration fields exhibit homogeneous radial profiles at an axial distance of 100 mm behind the atomizer, although droplets are observed up to 140 mm. Integrating the measured liquid volume flux density profiles, it was found that the fuel flux at 45 mm behind the atomizer had diminished to 14 percent of the maximum measured value. The axial profile of the liquid flux weighted Sauter mean diameter is almost linearly increasing from 22 to 31 micrometers. Systematic experimental errors and losses of the system sensitivity, which enter the results partly with opposite signs, have an influence on the measured flux densities and moments of the particle size distribution. The measurement of individual flux density profiles was reproducible to within 45 percent. A comparison between the gas flow in the nearfield of the atomizer under reacting and nonreacting conditions showed a partial suppression of the expansion of the velocity profiles by the hot corner vortex. Together with the combustion induced axial acceleration, the thus effected reduction of the effective swirl number leads to the breakdown of the recirculation at 29 mm. Author (revised)

N94-29283# Karlsruhe Univ. (Germany). Lehrstuhl und Inst. fuer Thermische Stroemungsmaschinen.
TIME-RESOLVED MEASUREMENTS IN A THREE DIMENSIONAL MODEL COMBUSTOR **c34**
R. Jeckel and S. Wittig *In* AGARD, Fuels and Combustion Technology for Advanced Aircraft Engines Sep. 1993 15 p Sponsored by Arbeitsgemeinschaft Hochtemperatur Gasturbine and BMFT (For primary document see N94-29246 08-25)
Copyright Avail: CASI HC A03/MF A04

Locally and time-resolved measurements of the velocity, temperature, and species concentration in a three dimensional jet-stabilized combustor are presented. The combustor was developed at the Institute for Thermal Turbomachinery, University of Karlsruhe, for extended benchmark experiments. For the present investigation, the combustor was fired by propane. The profiles of the velocity, temperature, and species distribution were determined at seven planes along the combustor axis. A comparison between the cold flow and the reacting hot gas conditions is given. The time-resolved velocity and temperature measurements were performed by a two component LDA-system as well as specially designed and optimized thermocouple probes. The time-dependent analysis demonstrates that the velocity and turbulence and/or the temperature fluctuations are dramatically increased under hot combusting conditions. Finally, the locally determined species distributions are compared with the global concentrations at the exit of the combustor providing a data base for numerical tests.
Author (revised)

N94-29284# Calgary Univ. (Alberta). Dept. of Mechanical Engineering.
TEMPERATURE AND COMBUSTION ANALYSIS OF COMBUSTOR WITH ACOUSTICALLY CONTROLLED PRIMARY ZONE AIR-JET MIXING
P. J. Vermeulen, V. Ramesh, B. Sanders, and J. Odgers *In* AGARD, Fuels and Combustion Technology for Advanced Aircraft Engines Sep. 1993 13 p (For primary document see N94-29246 08-25)
(Grant NSERC-A-7801)
Copyright Avail: CASI HC A03/MF A04

A small tubular combustor of normal design and behavior, employing acoustically controlled primary zone air-jet mixing processes, has been

successfully tested at scaled 1/4 load operating conditions, and some data was obtained at 1/2, 3/8, and 3/4 loads. The acoustic control produced a distinct richening effect, measured just downstream of the primary zone, which produced a decrease in combustion efficiency and a somewhat increased and flatter combustion gas temperature distribution. The prime cause of richening was due to combustor flow blockage caused by acoustically enhanced jet penetration. This, and the secondary effect of acoustically shed jet toroidal vortices, resulted in up to 35 percent increase in mixing, relative to 'no-drive' measured just downstream of the primary zone. The acoustic drive produced a more uniform exit plane temperature pattern, resulting in up to 35 percent improvement in mixing relative to 'no-drive' and in up to 20 percent relative improvement in the temperature pattern quality. The effects depend on air/fuel ratio and, in general, improved relative to 'no-drive' with richening. At 3/4 load, 150 W single driver power, the acoustic driving effectiveness was reduced by about 80 percent with correspondingly reduced improvements in mixing and quality. The effects of acoustic drive were favorably controllable by means of the driving power, and the exit plane data showed increased flow blockage caused by increased jet penetration by the acoustic drive was the major control mechanism.

Author (revised)

N94-29285# Central Inst. of Aviation Motors, Moscow (Russia).

ENDOTHERMIC FUELS FOR HYPERSONIC AVIATION c28

Leonid S. Ianovski and Clifford Moses *In* AGARD, Fuels and Combustion Technology for Advanced Aircraft Engines Sep. 1993 8 p (For primary document see N94-29246 08-25)

Copyright Avail: CASI HC A02/MF A04

The creation of hypersonic vehicles and the use of jet engines with higher temperature cycles has resulted in a significant increase in the thermal stresses of the engine elements. In order to use the fuel as the coolant for these elements, it is necessary to increase the heat capacity of hydrocarbon fuels. This problem can be solved by taking advantage of such high temperature chemical processes as catalytic dehydrogenation and thermal cracking or pyrolysis of hydrocarbon fuels, including the addition of the initiators and catalysts. The chemical heat capacity of hydrocarbon fuels can be used for the direct cooling of such elements as combustion chambers, nozzles, and front wing edges; indirect cooling of these elements can be accomplished by using a heat-transport medium in the fuel/air or fuel/gas heat exchangers. The gaseous products of the decomposed fuels can be used as a working medium for the drive of the equipment of a fuel/feeding system.

Author (revised)

N94-29312# Colorado State Univ., Fort Collins. Dept. of Chemistry.

TEMPLATE SYNTHESIZED NANOSCOPIC GOLD PARTICLES: OPTICAL SPECTRA AND THE EFFECTS OF PARTICLE SIZE AND SHAPE

Colby A. Foss, Jr., Gabor L. Hornyak, Jon A. Stockert, and Charles R. Martin 25 Jan. 1994 43 p

(Contract N00014-82-K-0612)

(AD-A275378; TR-91) Avail: CASI HC A03/MF A01

We have prepared nanoscopic gold cylinders of controlled radius and aspect ratio via electrodeposition of the metal within the pores of anodically-grown porous aluminum oxide membranes. The nanocylinder radii are determined by the pore dimensions of the host alumina which, in turn, depend on anodization conditions. The particle aspect ratios were controlled by varying the amount of Au deposited within the pores. The optical spectra of the gold nanocylinder/alumina composites exhibit strong absorption bands in the visible spectrum. The extinction maxima (Lambda max) values for gold particles approaching sphere-like geometry agree well with Mie Theory calculations. The blue shift of Lambda max as the particle aspect ratio is increased in qualitative agreement with Maxwell-Garnett Theory. We propose a simple modification of Maxwell-Garnett Theory that addresses both size and shape effects.

DTIC

N94-29356*# National Aeronautics and Space Administration. Lewis Research Center, Cleveland, OH.

FUEL-RICH CATALYTIC COMBUSTION OF A HIGH DENSITY FUEL

Theodore A. Brabbs (Sverdrup Technology, Inc., Brook Park, OH.) and Sylvia A. Merritt Washington Jul. 1993 13 p

(RTOP 505-62-52)

(NASA-TP-3281; E-7298; NAS 1.60:3281) Avail: CASI HC A03/MF A01

Fuel-rich catalytic combustion (ER is greater than 4) of the high density fuel exo-tetrahydrocyclopentadiene (JP-10) was studied over the equivalence ratio range 5.0 to 7.6, which yielded combustion temperatures of 1220 to 1120 K. The process produced soot-free gaseous products similar to those obtained with iso-octane and jet-A in previous studies. The measured combustion temperature agreed well with that calculated assuming soot was not a combustion product. The process raised the effective hydrogen/carbon (H/C) ratio from 1.6 to over 2.0, thus significantly improving the combustion properties of the fuel. At an equivalence ratio near 5.0, about 80 percent of the initial fuel carbon was in light gaseous products and about 20 percent in larger condensable molecules. Fuel-rich catalytic combustion has now been studied for three fuels with H/C ratios of 2.25 (iso-octane), 1.92 (jet-A), and 1.6 (JP-10). A comparison of the product distribution of these fuels shows that, in general, the measured concentrations of the combustion products were monotonic functions of the H/C ratio with the exception of hydrogen and ethylene. In these cases, data for JP-10 fell between iso-octane and jet-A rather than beyond jet-A. It is suggested that the ring cross-linking structure of JP-10 may be responsible for this behavior. All the fuels studied showed that the largest amounts of small hydrocarbon molecules and the smallest amounts of large condensable molecules occurred at the lower equivalence ratios. This corresponds to the highest combustion temperatures used in these studies. Although higher temperatures may improve this mix, the temperature is limited. First, the life of the present catalyst would be greatly shortened when operated at temperatures of 1300 K or greater. Second, fuel-rich catalytic combustion does not produce soot because the combustion temperatures used in the experiments were well below the threshold temperature (1350 K) for the formation of soot. Increasing the temperature above this value would remove the soot-free nature of the process. Since all the fuels studied show a similar breakdown of the primary fuel into smaller molecular combustion products, this technique can be applied to all hydrocarbon fuels.

Author (revised)

N94-29457# Aerospatiale, Suresnes (France). Dept. Materiaux.

FIRE BEHAVIOR OF AERONAUTICAL MATERIALS [COMPORTEMENT AU FEU DES MATERIAUX AERONAUTIQUES]

B. Costes, C. Kuras, and B. Carriere 1993 25 p In FRENCH

(Rept-932-600-105; DCR/M-61546/C-92; ETN-94-95484) Avail: CASI HC A03/MF A01

A set of graphics that introduce the aeronautical problems of toxicity and safety linked to fire in an aircraft and the combustion of aircraft construction materials are presented. Materials currently used, their certification, and present solutions to their associated problems, are considered. Previous aircraft accidents and their causes are addressed as case studies. Combustion tests and environmental constraints are reported.

ESA

N94-29592 California Univ., Irvine.

LIQUID-OXYGEN DROPLET VAPORIZATION AND COMBUSTION: ANALYSIS OF TRANSCRITICAL BEHAVIOR AND APPLICATION TO LIQUID-ROCKET COMBUSTION INSTABILITY Ph.D. Thesis

Jean-Pierre Delplanque 1993 223 p

Avail: Univ. Microfilms Order No. DA9315775

The behavior of a liquid-oxygen (LOX) droplet vaporizing and burning in gaseous hydrogen at conditions supercritical for both propellants is investigated using modelling/numerical techniques. First, high-pressure phase-equilibrium computations are implemented for the oxygen/hydrogen system using the Redlich-Kwong equation of state. The chosen approach is then to consider the idealized case of an isolated LOX droplet in a quiescent environment and successively include consequential features such as convection, combustion, and the effect of neighboring droplets in an array. Results show that in a quiescent environment the surface temperature reaches the critical mixture value and the droplet lifetime is subsequently controlled by the regression of the critical interface. The details of the diffusion layer of dissolved hydrogen do not affect the results significantly. However, when convection is included, it is shown that, at the conditions prevalent in a rocket engine, the reduced surface tension causes a LOX droplet to undergo boundary layer stripping for most of its lifetime. Evaluation of the stripping rate shows that it is much larger than the vaporization rate and reduces the predicted droplet lifetime by at least one order of magnitude. The film model is modified to include the effect of stripping on the heat transfer into the droplet. In most cases, stripping precludes criticality at the interface. Application of this new model to the prediction of flame spread in an idealized LOX droplet array configuration shows that high

temperatures in the reaction zone cause the droplet surface temperature to reach the critical mixing conditions even when stripping is included. However, the droplet lifetime is still controlled by the stripping rate. The model is then applied to oscillatory LOX droplet vaporization (isolated) and combustion (array). The predicted response factor spectra are compared to the results yielded by the (n - tau) model and show that the gasification process can drive the instability if it is rate-controlling. Stripping is shown to affect significantly the range of frequencies in which the gasification process is driving combustion instabilities. In view of liquid-rocket combustion instability applications, the response of a droplet in an array is compared to the response of an isolated droplet. Dissert. Abstr.

N94-29676 California Inst. of Tech., Pasadena.
LIFTED TURBULENT JET FLAMES Ph.D. Thesis
Jay Alan Hammer 1993 155 p
Avail: Univ. Microfilms Order No. DA9325355

Experiments were conducted on lifted, turbulent jet diffusion flames. An automated technique was implemented to measure the temporal history of the liftoff height h. For the fuels investigated, the mean liftoff height h-bar has a linear dependence on exit velocity U(sub s), with a slight dependence on Reynolds number. A strain-rate model for liftoff, based on far-field scaling of turbulent jets, provides an explanation for the linear dependence of h-bar on U(sub s). When air is premixed with the fuel, the slope of the h-bar versus U(sub s) line increases faster than predicted by far-field scaling of turbulent jets. The amplitudes of the fluctuations of h are of the order of the local large scale of the jet. As h-bar increases, there is a slight increase in normalized fluctuation level h'/h-bar. The time scales of the fluctuations of h are considerably longer than the local large-scale time of the turbulence tau(sub delta). By using fuels of different chemical times to vary tau(sub delta), the measured correlation time tau(sub 1/2) normalized by tau(sub delta) was found to collapse with Richardson number xi(sub h). Experiments in which the nozzles were oriented horizontally showed no change in tau(sub 1/2), however. To investigate alternative explanations for the collapse of tau(sub 1/2)/tau(sub delta) with xi(sub h), the flame length L was measured simultaneously with h. L(t) is nearly uncorrelated with h(t), dismissing the possibility that a feedback mechanism from L to h controls the fluctuations of h. Simultaneous measurements of h and the visible radiation I were also made. For the most sooting fuel, acetylene, I(t) is highly correlated with h(t). This correlation is not the cause of the large values of tau(sub 1/2)/tau(sub delta) for that fuel, however. Non-sooting hydrogen/ethane flames were found to have values of tau(sub 1/2)/tau(sub delta) comparable to those of acetylene. Another experiment was conducted in which two dimensional images of fuel concentration (CH4) and reaction zones (indicated by CH) were obtained. The images showed a wide variety of structure types. The flame stabilization position showed large fluctuations in both the axial and radial directions. The shot to shot variation in methane number density at the flame base was also large. Dissert. Abstr.

N94-29857*# Omitron, Inc., Greenbelt, MD.
CAMERA ARTIFACTS IN IUE SPECTRA Final Report
O. W. Bruegman and D. M. Crenshaw 31 Mar. 1994 58 p
(Contract NAS5-31234)
(NASA-CR-189337; NAS 1.26:189337) Avail: CASI HC A04/MF A01

This study of emission line mimicking features in the IUE cameras has produced an atlas of artifacts in high-dispersion images with an accompanying table of prominent artifacts and a table of prominent artifacts in the raw images along with a medium image of the sky background for each IUE camera. Author

N94-29881 Illinois Univ., Urbana-Champaign.
NON-INVASIVE TEMPERATURE MEASUREMENTS USING ELECTRON PARAMAGNETIC RESONANCE SPECTROSCOPY Ph.D. Thesis
Joseph John Eckburg 1993 120 p
Avail: Univ. Microfilms Order No. DA9314862

A system has been developed that may be used for noninvasive in vivo temperature measurements in living systems. We use the nitroxide, 3-doxyl-5 alpha-cholestane, mixed in 1 mol percent cholesterol and 99 mol percent methyl docosanoate and encapsulated in proteinaceous microspheres (average diameter less than 2 micron). We have shown a dramatic and measurable change in the EPR spectral line shape between 38 and 48 C. This technique has many potential clinical applications, especially in optimizing the treatment of cancer with hyperthermia. Using the mid-field to high-field peak height ratio of the EPR spectra as the temperature dependent parameter, the temperature resolution for this system is 0.2 C. Encapsulation of the mixture in the microspheres provides two critical functions. First, the microspheres are easily injectable since they are smaller than the diameter of capillaries and are suspended in water. Second, the microspheres separate the mixture from the surrounding environment, thereby protecting the nitroxide from bioreduction and ensuring that the shape of the EPR spectrum is greatly affected by temperature in the range of the medium's liquid-solid transition. There was a hysteresis effect seen in the spectral line shape for this system as the temperature was raised and then lowered between 37 and 48 C. However, if the temperature of the system is kept above or below a certain critical temperature and within a small temperature range (less than 3 C), the hysteresis can be avoided and accurate temperature measurements can be made. In order to increase the temperature resolution, computer simulation of the EPR spectra for the temperature measurement system was attempted. The no motion limit and fast motion limit spectra for the system were successfully simulated. Initial attempts to simulate the spectra for the system between 38 and 48 C were unsuccessful. Dissert. Abstr.

N94-29938*# Texas A&M Univ., College Station. Dept. of Chemistry.
ELECTROCHEMICAL INCINERATION OF WASTES Final Report
J. O. M. Bockris, R. C. Bhardwaj, and C. L. K. Tennakoon Jan. 1993 49 p
(Grant NAGw-1779)
(NASA-CR-195262; NAS 1.26:195262) Avail: CASI HC A03/MF A01

There is an increasing concern regarding the disposal of human wastes in space vehicles. It is of utmost importance to convert such wastes into harmless products which can be recycled into an Environmental Life Support System (CELSS), which incorporates the growth of plants (e.g. wheat) and algae to supplement the diet of the astronauts. Chemical treatments have proven relatively unsatisfactory and tend to be increasingly so with increase of the mission duration. Similarly, the use of heat to destroy wastes and convert them to CO2 by the use of air or oxygen has the disadvantage and difficulty of dissipating heat in a space environment and to the inevitable presence of oxides of nitrogen and carbon monoxide in the effluent gases. In particular, electrochemical techniques offer several advantages including low temperatures which may be used and the absence of any NO and CO in the evolved gases. Successful research has been carried out in the electrochemical oxidation of wastes over the last several years. The major task for 1992 was to conduct parametric studies in preparation for the building of a breadboard system, i.e., an actual practical device to consume the daily waste output of one astronaut in 24 hours, electrochemical incineration of human wastes in space vehicles. One of the main objectives was to decide on the type of three dimensional or other electrode system that would suit this purpose. The various types of electrode systems which were considered for this purpose included: rotating disc electrode, micro-electrode (an array), vibrating electrode, jet electrode, and packed bed electrode. Derived from text

N94-30017# National Research Council of Canada, Ottawa (Ontario). Combustion and Fluids Engineering.
MEASUREMENTS AND PREDICTIONS OF THE COMBUSTION CHARACTERISTICS OF ENCLOSED SWIRL-STABILIZED PROPANE FLAMES
J. H. Lau, I. G. Campbell, K. Depooter, and M. V. DSouza Sep. 1993 61 p
(IECE-CFE-TR-001; NRC-36246; CTN-94-61131) Avail: CASI HC A04/MF A01

A computer code containing submodels for propane combustion, soot formation, and radiation is described. Propane combustion is represented by the minimum of either the reaction rate of a four-step chemical scheme or a turbulence mixing rate. Soot concentration is calculated using the formation submodel of Magnussen et al (1978) and a suitable oxidation submodel. Radiative transfer due to soot particles is determined assuming spherical absorbers and emitters, while that of the gas phase is computed using a discrete transfer method which solves the intensity equation along discrete rays. The code was applied to swirl stabilized propane flames and experimentally evaluated in an atmospheric chamber representing an axisymmetric step combustor, with the reactants introduced at the plane of the step. Radial profiles of gas temperature, velocity, and species

concentration were measured at several axial planes, along with axial profiles of soot volume concentration and radiative heat transfer. The results revealed a complex flow structure downstream of the nozzle. Agreement with numerical predictions is good once the flow is fully developed. The radiation submodel performs satisfactorily, but the soot submodel requires further development. Author (CISTI)

N94-30111# Weizmann Inst. of Science, Rehovoth (Israel). Dept. of Physics.
BOUNDARY-INDUCED PHASE TRANSITIONS IN EQUILIBRIUM AND NON-EQUILIBRIUM SYSTEMS
M. Henkel (Geneva Univ., Switzerland.) and G. Schuetz Aug. 1993 11 p
(DE94-608137; WIS-PH-93-73) Avail: CASI HC A03/MF A01 (US Sales Only)

Boundary conditions may change the phase diagram of nonequilibrium statistical systems like one dimensional asymmetric simple exclusion process with and without particle number conservation. Using quantum Hamiltonian approach, the model is mapped onto an XXZ quantum chain and solved using the Bethe ansatz. This system is related to a two dimensional vertex model in thermal equilibrium. The phase transition caused by a point-like boundary defect in the dynamics of the one dimensional exclusion model is in the same universality class as a continuous (bulk) phase transition of the two dimensional vertex model caused by line defect at its boundary. DOE

N94-30137 British Columbia Univ., Vancouver. Dept. of Physics.
THE FAR-INFRARED ABSORPTION SPECTRUM OF LOW TEMPERATURE HYDROGEN GAS Ph.D. Thesis
Edward Hyman Wishnow Feb. 1993 192 p
(ISBN-0-315-85432-4; CTN-94-61158) Copyright Avail: Micromedia Ltd., Technical Information Centre, 240 Catherine Street, Suite 305, Ottawa, Ontario, K2P 2G8, Canada HC/MF

The far infrared spectrum of normal hydrogen gas was measured over the temperature range 21-38 K and the pressure range 0.6-3 atmospheres. The spectra cover the very weak and broad collision induced translational absorption band of H2, well isolated from the H2 rotational lines at these temperatures. To observe the weak translational absorption band, a long pathlength multireflection He-cooled absorption cell was designed and constructed. The cell is coupled to a Fourier transform interferometer and H2 spectra were obtained at a resolution of 0.24/cm. The integrated absorption of the measured H2 translational spectrum is consistent with the binary absorption coefficient calculated using the Poll and Van Kranendonk theory of collision induced absorption. No sharp spectral features were observed that can be attributed to dimer transitions. The H2 spectra show the sharp R(0) line of hydrogen deuteride (HD) superposed on the translational band at 89.2/cm, where the HD is present in the gas at natural abundance. Since the experimental conditions were close to those found in the atmospheres of Uranus and Neptune, the observed spectra have relevance to astronomical observation of H2, in particular to the determination of planetary deuterium hydrogen ratios. Spectra of other gases and gas mixtures (including He, N2, O2, CH4, CO, Ar) at 78 K and 88 K were also obtained. Author (CISTI)

N94-30260# Sandia National Labs., Albuquerque, NM.
DIRECT MEASUREMENT OF THE REACTIVITY OF NH AND OH ON A SILICON NITRIDE SURFACE
R. J. Buss, P. Ho, W. G. Breiland, and E. R. Fisher 1993 5 p Presented at the Fall Meeting of the Materials Research Society (MRS), Boston, MA, 29 Nov. - 3 Dec. 1993
(Contract DE-AC04-94AL-85000)
(DE94-005286; SAND-93-1456C; CONF-931108-43) Avail: CASI HC A01/MF A01

In order to understand and successfully model the plasma processing used in device fabrication, it is important to determine the role played by plasma-generated radicals. The authors have used the IRIS technique (Imaging of Radicals Interacting Surfaces) to obtain the reactivity of NH(X(exp 3)S(-)) and OH(X(exp 2)P) at a silicon nitride film surface while the film is exposed to a plasma-type environment. The reactivity of NH was found to be zero both during exposure of the surface to an NH3 plasma and during active deposition of silicon nitride from a SiH4/NH3 plasma. No NH surface reaction was detectable for any rotational states of NH and over a surface temperature range of 300-700 K. OH radicals generated in an H2O plasma were found to have a reactivity of 0.57 on a room temperature oxidized silicon nitride surface. The OH reactivity falls to zero as the temperature of the substrate is raised. DOE

N94-30266# California Univ., Berkeley. Lawrence Berkeley Lab.
APPLICATION OF SEMICLASSICAL METHODS TO REACTION RATE THEORY Ph.D. Thesis
R. Hernandez Nov. 1993 147 p
(Contract DE-AC03-76SF-00098)
(DE94-007041; LBL-34925) Avail: CASI HC A07/MF A02

This work is concerned with the development of approximate methods to describe relatively large chemical systems. This effort has been divided into two primary directions: First, we have extended and applied a semiclassical transition state theory (SCTST) originally proposed by Miller to obtain microcanonical and canonical (thermal) rates for chemical reactions described by a nonseparable Hamiltonian, i.e. most reactions. Second, we have developed a method to describe the fluctuations of decay rates of individual energy states from the average RRKM rate in systems where the direct calculation of individual rates would be impossible. Combined with the semiclassical theory, this latter effort has provided a direct comparison to the experimental results of Moore and coworkers. In SCTST, the Hamiltonian is expanded about the barrier and the 'good' action-angle variables are obtained perturbatively; a WKB analysis of the effectively one dimensional reactive direction then provides the transmission probabilities. The advantages of this local approximate treatment are that it includes tunneling effects and anharmonicity, and it systematically provides a multidimensional dividing surface in phase space. The SCTST thermal rate expression has been reformulated providing increased numerical efficiency, an appealing link to conventional transition state theory, and the ability to go beyond the perturbative approximation. DOE

N94-30267# Central Research Inst. of Electric Power Industry, Tokyo (Japan). Energy and Environment Lab.
ANALYSIS OF INFRARED RADIATION HEATING PROCESS CONSIDERING CHEMICAL REACTION OF MATERIAL TO BE HEATED
T. Miyanaga, T. Onuma, and Y. Nakano Apr. 1993 26 p In JAPANESE
(DE94-744116; CRIE-T-92039) Avail: CASI HC A03/MF A01

A one dimensional infrared radiation heating simulation method was developed that considers chemical changes in materials to be heated. The simulation method analyzes processes to heat polyethylene glycol with far infrared radiation and near infrared radiation, and compares the results with experimental results. The analytical results indicated relatively well the trends of temperature rise in parts of a material to be heated, proving the suitability of this method as a simplified method to investigate heating internal to a material. Identical result was obtained in heating the white of an egg. As a result of using this method to calculate infrared radiation energy absorption in parts of the material being heated, it was found that heating with far infrared radiation has its energy absorbed in the vicinity of the surface of the heated material, and the trend would not change even if chemical change has been caused in the heated material. In addition, the present method can estimate complex infrared radiation heating processes in materials to be heated and the required amount of infrared ray irradiation relatively easily. The method can also be utilized for selection of infrared radiating bodies suitable for particular materials to be heated, as well as for rational designs of heating furnaces. DOE

N94-30723# Oak Ridge National Lab., TN.
STRUCTURAL ANALYSIS OF AMORPHOUS PHOSPHATES USING HIGH PERFORMANCE LIQUID CHROMATOGRAPHY
B. C. Sales, L. A. Boatner, B. C. Chakoumakos, J. C. McCallum, J. O. Ramey, and R. A. Zuhr 1993 13 p Presented at the Fall Meeting of the Materials Research Society (MRS), Boston, MA, 29 Nov. - 3 Dec. 1993
(Contract DE-AC05-84OR-21400)
(DE94-004791; CONF-931108-29) Avail: CASI HC A03/MF A01

Determining the atomic-scale structure of amorphous solids has proven to be a formidable scientific and technological problem for the past 100 years. The technique of high-performance liquid chromatography (HPLC) provides unique detailed information regarding the structure of partially disordered or amorphous phosphate solids. Applications of the experimental

technique of HPLC to phosphate solids are reviewed, and examples of the type of information that can be obtained with HPLC are presented. Inorganic phosphates encompass a large class of important materials whose applications include: catalysts, ion-exchange media, solid electrolytes for batteries, linear and nonlinear optical components, chelating agents, synthetic replacements for bone and teeth, phosphors, detergents, and fertilizers. Phosphate ions also represent a unique link between living systems and the inorganic world. DOE

N94-30748# Los Alamos National Lab., NM.
LATTICE GAS SIMULATIONS OF REPLICATING DOMAINS
S. P. Dawson, B. Hasslacher, and J. E. Pearson 1993 13 p Presented at the NATO Workshop on Pattern Formation and Lattice Gas Automata, Waterloo, Canada, 7-14 Jun. 1993
(Contract W-7405-eng-36)
(DE94-005008; LA-UR-93-4331; CONF-9306294-1) Avail: CASI HC A03/MF A01

We use the lattice gas cellular automation (LGCA) developed to simulate a process of pattern formation recently observed in reaction-diffusion systems. We study the reaction mechanism, which is an extension of the Selkov model for glycolytic oscillations. We are able to reproduce the self-replicating domains observed in this work. We use the LGCA simulation to estimate the smallest length-scale on which this process can occur under conditions encountered in the cell. These estimates are similar to those obtained for Turing patterns in the same setting. DOE

N94-30769# Ohio State Univ., Columbus. Dept. of Chemistry.
PHOTOCHEMISTRY IN CONSTRAINED SPACES: ZEOLITES AND LAYERED DOUBLE METAL HYDROXIDES
P. K. Dutta 1993 6 p
(Contract DE-FG02-90ER-14105)
(DE94-004958; DOE/ER-14105/4) Avail: CASI HC A02/MF A01

The authors have continued their research in the field of preparation and reactions of photochemical systems in zeolites and layered lithium aluminates. The study on zeolite focused on faujasitic zeolites. The experimental strategy is to build Ru(bpy)(sub 3)(2+) inside the supercage and examine the photoelectron transfer from this entrapped complex to acceptor molecules (viologens) through the ring openings. The effort on layered lithium aluminum double hydroxides (LDH) of composition LiAl2(OH)6(+)X(-) has been on incorporation of photoactive molecules in these interlayers, with particular emphasis on pyrene and Zn porphyrins. DOE

N94-30770# State Univ. of New York, Buffalo. Dept. of Chemistry.
GROUP TRANSFER AND ELECTRON TRANSFER REACTIONS OF ORGANOMETALLIC COMPLEXES: SUMMARY OF RESEARCH ACCOMPLISHED IN 1993
1993 4 p
(Contract DE-FG02-87ER-13775)
(DE94-004963; DOE/ER-13775/5) Avail: CASI HC A01/MF A01

In the past year, the research on mechanisms of electron transfer processes between organometallic complexes has continued to progress with emphasis on two electron processes and on reactions of organometallic radicals. This summary will highlight the research on: (1) halide transfer reactions, (2) alkyl and acyl transfer reactions, and (3) reactions of seventeen-electron organometallic complexes. At this point, some conclusions on the transfer of hydrogen, halogen, and methyl as the cation, radical, and anion can be made. For each group, transfer as the cation is more facile. For hydrogen, transfer as the hydride is considerably slower, but H* transfers nearly as rapidly as H(+). Methyl could be transferred as CH3(+) or CH3(-), but not as the radical. Halogens transfer readily as X(sup +), more slowly as X* and not at all as X(-). DOE

N94-30877# Notre Dame Univ., IN. Dept. of Chemical Engineering.
TRANSIENT STUDIES OF LOW TEMPERATURE CATALYSTS FOR METHANE CONVERSION
E. E. Wolf 1993 7 p
(Contract DE-FG22-92PC-92529)
(DE94-005767; DOE/PC-92529/T4) Avail: CASI HC A02/MF A01

This report summarizes studies on the oxidative coupling of methane on metallo oxide catalysts. Results are reported for LaCoO3 and LaNiO3, both unpromoted and Li promoted. DOE

N94-30880# Oak Ridge K-25 Site, TN.
REINTERPRETATION OF RATE DATA FOR THE REACTION OF ClF AND F2
L. D. Trowbridge Jan. 1994 12 p
(Contract DE-AC05-84OR-21400)
(DE94-005819; K/TCD-1091) Avail: CASI HC A03/MF A01

Experimental data on the rate of recombination of ClF + F2 have been reinterpreted to yield a single rate equation. This reinterpretation assumes that the recombination reaction is surface area dependent and is first order in partial pressure of each of F2 and ClF. The recombination rate equation used fits quite well three data sets which varied significantly in available NiF2 surface area. The resulting equation is dn(ClF3)/dt = A S P(F2) P(ClF) (1 - Theta) e(exp -E/RT), where dn(ClF3)/dt is the rate of formation of ClF3 in mol/s, S is the surface area of NiF2 catalyst in square centimeters, P(X) is the partial pressure of species X in Torr, R is the gas constant (1.987 cal/mol-K), and T is the temperature in Kelvin. The pre-exponential A and activation energy E are given by: A = 2.853 x 10(exp -8) mole/s-cm(exp 2)-Torr(exp 2) and E = 11,665 cal/mole. The term (1 - Theta), a product surface-coverage related inhibition factor, is given by: (1 - Theta) = (1 + 0.184 P(ClF3))(exp -1), although (1 - Theta) is never allowed to be less than 16 percent. DOE

N94-30911 California Inst. of Tech., Pasadena.
AN INVESTIGATION OF THE REACTING VORTEX STRUCTURES ASSOCIATED WITH PULSE COMBUSTION Ph.D. Thesis
Thomas William Zsak 1993 166 p
Avail: Univ. Microfilms Order No. DA9325399

An investigation of the reacting vortex structures associated with pulsating combustion is performed using a laboratory dump combustor in order to gain an understanding of the controlling physical and chemical processes present during the burning of the vortex structures. Stabilized on the lip of a rearward-facing step flame holder, the vortices are shed at acoustic longitudinal modes of the apparatus. In all cases examined, a fuel-rich mixture of methane and air is used, 30 percent greater than stoichiometric, and the velocity at the dump plane is 21 m/sec. Results are presented for the expansion ratios of 4.0 and 12.0. A linearized one-dimensional acoustic model is developed to predict the resonant acoustic modes and mode shapes of the system for the two configurations. Heat addition is modeled as a sinusoidally varying volumetric mass source which can be placed at any location within the combustion chamber. Good agreement is found between the natural frequencies predicted by the model and those obtained experimentally under both hot- and cold-flow conditions. The effects of different combustion chamber temperatures on the pressure and velocity responses are revealed as are the effects of placing the heat addition at different axial locations downstream of the dump plane. It is shown that the pressure amplitude spectra for each expansion ratio can be successfully predicted given the relationship between heat release in the chamber and frequency. The ignition mechanisms of the vortex structures are found to be different for the two chamber configurations, and the bulk of the heat release is shown to occur much closer to the dump plane for the chamber with the smaller expansion ratio. The influence of the lower wall of the combustor on the burning of the structures is shown to be weaker for the chamber with the larger expansion ratio. The additions of ionization probes and an intensified, charge-injection-device (CID) camera to the experimental program have allowed the burning histories of the shed vortex structures to be recorded. Capturing an image of the chemiluminescence from the burning of the vortices at nearly the same instant as a shadowgraph image of the density gradients within the chamber completely describes the reacting flow field. Temperature measurements made with fine-wire thermocouples complete the experimental investigation and complement the results obtained above. Dissert. Abstr.

N94-30938 Politecnico di Milano (Italy). Dipt. di Elettronica e Informazione.
APPLICATION OF THE EXTENDED KALMAN FILTER TO THE ESTIMATION OF THE CHAR MASS IN A FLUIDIZED BED COMBUSTOR
Luigi Piroddi 1993 25 p Sponsored in part by Ministry of University and Scientific and Technological Research; CNR; and Ente Nazional per l'Energia Elett
(Rept-93-065; ETN-94-95825) Avail: Issuing Activity (Politecnico di Milano, Piazza Leonardo da Vinci 32, 20133 Milan, Italy)

Research aiming at the design of real time estimation techniques of

the mass of char starting from available Fluidized Bed Combustor (FBC) plant measurements is presented. To this purpose, the Extended Kalman Filter (EKF) was adopted as the basic estimation tool. The following subprocesses of the combustion process are described in order to develop an appropriate mathematical model of the plant: fluid dynamics, coal drying and devolatilization, char combustion, fines combustion, oxygen concentration, and energy storage and heat transfer. A model of the plant (char mass conservation equation and bed energy conservation equation) is given. An estimation oriented model is given and the char mass estimation is described. ESA

N94-29514# National Inst. for Resources and Environment, Ibaraki (Japan). Rare Metals Div.
PREPARATION OF MONODISPERSED FINE PARTICLES CONTAINING RARE METALS AND RARE EARTHS [EKISOHO NI YORU REAMETARU REAASU KEI TANBUNSAN BIRYUSHI NO GOSEI]
Mikio Kobayashi and Yoshihiro Nishisu *In its* Journal of NIRE, Vol. 2, No. 3 25 May 1993 p 11-20 In JAPANESE (For primary document see N94-29512 08-99)
Avail: CASI HC A02/MF A02

N94-30220 Clemson Univ., SC. Dept. of Physics and Astronomy.
CHARGE COLLECTION SPECTROSCOPY APPLIED TO MOS RAM'S
P. J. McNulty, D. R. Roth, W. J. Beauvais, and W. G. Abdel-Kader *In* Defence Research Establishment, Proceedings of the 1991 Single Event Upset Symposium 1991 13 p (For primary document see N94-30211 08-73)
Avail: Issuing Activity (Defence Research Establishment, Ottawa, ON K1A 0Z4 Canada)

26 METALLIC MATERIALS

Includes physical, chemical, and mechanical properties of metals, e.g., corrosion; and metallurgy.

N94-28456# Pacific Northwest Lab., Richland, WA.
RELATIONSHIP BETWEEN SWELLING AND IRRADIATION CREEP IN COLD-WORKED PCA STAINLESS STEEL IRRADIATED TO APPROXIMATELY 178 DPA AT APPROXIMATELY 400 C
M. B. Toloczko (California Univ., Santa Barbara.) and F. A. Garner Sep. 1993 16 p Presented at the 6th International Conference on Fusion Reactor Materials, Stresa, Italy, 27 Sep. - 1 Oct. 1993
(Contracts DE-AC06-76RL-01830; DE-FG06-89ER-75522)
(DE94-004368; PNL-SA-22456; CONF-930928-19) Avail: CASI HC A03/MF A01

The eighth and final irradiation segment for pressurized tubes constructed from the fusion prime candidate alloy (PCA) has been completed in the Fast Flux Test Facility (FFTF). At 178 dpa and approximately 400 C, the irradiation creep of 20% cold-worked PCA has become dominated by the 'creep disappearance' phenomenon. The total diametral deformation rate has reached the limiting value of 0.33%/dpa at the three highest stress levels employed in this test. The stress-enhancement of swelling tends to camouflage the onset of creep disappearance, however, requiring the use of several nontraditional techniques to extract the creep coefficients. No failures occurred in these tubes, even though the swelling ranged from approximately 20 to approximately 40%. DOE

N94-28460# Pacific Northwest Lab., Richland, WA.
RADIATION EFFECTS IN BERYLLIUM USED FOR PLASMA PROTECTION
D. S. Gelles, M. DalleDonne, G. A. Sernyaev, and H. Kawamura Sep. 1993 22 p Presented at the 6th International Conference on Fusion Reactor Materials, Stresa, Italy, 27 Sep. - 1 Oct. 1993
(Contract DE-AC06-76RL-01830)
(DE94-004599; PNL-SA-22668; CONF-930928-18) Avail: CASI HC A03/MF A01

Beryllium is presently a leading candidate material for fusion reactor first wall coating and divertor applications. This paper reviews the literature on beryllium, emphasizing the effects of irradiation on essential properties. Swelling and embrittlement experiments as a function of irradiation temperature and dose, and as a function of neutron spectrum, are described, and the results are quantified where possible. Effects of impurity content are also reported, from which optimum composition specifications can be defined. Microstructural information has also been obtained to elucidate the processes controlling the property changes. The available information indicates that beryllium divertors can be expected to embrittle quickly and may need frequent replacement. DOE

N94-28479# Brookhaven National Lab., Upton, NY.
COMPUTER SIMULATION OF MARTENSITIC TRANSFORMATIONS Ph.D. Thesis
Ping Xu Nov. 1993 198 p
(Contract DE-AC03-76SF-00098)
(DE94-005213; LBL-34908) Avail: CASI HC A09/MF A03

The characteristics of martensitic transformations in solids are largely determined by the elastic strain that develops as martensite particles grow and interact. To study the development of microstructure, a finite element computer simulation model was constructed to mimic the transformation process. The transformation is athermal and simulated at each incremental step by transforming the cell which maximizes the decrease in the free energy. To determine the free energy change, the elastic energy developed during martensite growth is calculated from the theory of linear elasticity for elastically homogeneous media, and updated as the transformation proceeds. DOE

N94-28525# Ames Lab., IA.
INTERSTITIALLY STABILIZED PHASES IN THE ZIRCONIUM-NICKEL SYSTEM Ph.D. Thesis
R. A. MacKay Jul. 1993 133 p
(Contract W-7405-eng-82)
(DE94-005561; IS-T-1647) Avail: CASI HC A07/MF A02

Addition of nonmetal interstitial atoms to Zr-Ni compounds has resulted in several new phases. A single-crystal x-ray study was carried out for Zr3NiO.Zr4Ni2O is a high-temperature phase, forming in samples annealed at 1250 C. Huekel band calculations led to prediction and confirmation of additional phases in more electron rich systems. Other phases studied by XRD are Z6Ni4Ti2O(0.6), Nb6Ni6O, and Nb6Ni4Ta2O2. Phases identified by powder diffraction are Nb4Ni2O, Zr4Cu2O, and Zr6Co4Ti2O. New Zr kappa phases in space group P6s3/mmc were found: Zr9Mo4SO(x) and Zr9W4(S,Ni)O3. A new structure type was discovered with Zr6Ni6TiSiO(1.8). In all these interstitially stabilized phases, O is coordinated in Zr octahedral; there are no Ni-O interactions. DOE

N94-28527# Ames Lab., IA.
DIRECTIONAL SOLIDIFICATION STUDIES IN Ni-Al ALLOYS Ph.D. Thesis
Je-hyun Lee May 1993 214 p
(Contract W-7405-eng-82)
(DE94-005562; IS-T-1653) Avail: CASI HC A10/MF A03

Three solid phases are involved in the phase equilibria of the intermetallic compound Ni3Al near its melting point, beta, gamma'(Ni3Al), and gamma. The generally-accepted phase diagram involves a eutectic reaction between beta' and gamma, but some recent studies agree with an older diagram due to Schramm, which has a eutectic reaction between the beta and gamma' phases. The phase equilibria near Ni3Al compositions was evaluated using quenched directional solidification experiments, that preserve the microstructures tonned at the solidification front, and using diffusion couple experiments. These experiments show that eutectic forms between beta and gamma' phases, as in the Schramm diagram. Growth and phase transformations of these three phases are also studied in the directional solidification experiments. Microstructure analysis shows that etching of Ni3Al(gamma') is very sensitive to small composition variations and crystallographic orientation changes. The eutectic solidification study confirms that the equilibrium eutectic is gamma' + beta, and that the metastable gamma + beta eutectic might be also produced in this system according to the impurities, solidification rates, and composition variations. DOE

N94-28544# Los Alamos National Lab., NM.
FAILURES TO MODEL THE DEVELOPMENT OF A CUBE TEXTURE DURING THE HIGH TEMPERATURE COMPRESSION OF Al-Mg ALLOYS
U. F. Kocks, Shuh Rong Chen, and P. R. Dawson 1993 6 p Presented at the International Conference on Textures of Materials, Clausthal, Germany, 20-24 Sep. 1993

(Contract W-7405-eng-36)
(DE94-005013; LA-UR-93-4521; CONF-9309231-6) Avail: CASI HC A02/MF A01

A strong (100) fiber texture has been observed under some circumstances after the compression and tension of Al-Mg alloys. It is not due to static recrystallization after the text, but probably connected with some form of dynamic recrystallization. Possibilities that this unusual texture might rise from some unconventional deformation mechanisms were searched for but not found. DOE

N94-28551 Gosudarstvennyi Komitet po Ispolzovaniyu Atomnoi Energii, Obninsk (USSR).
ANALYSIS OF DATA BY LONG-TIME MECHANICAL PROPERTIES OF 08KH18N10T STEEL IRRADIATED BY NEUTRONS
O. V. Sopov and V. A. Solovev 1992 7 p In RUSSIAN Limited Reproducibility: More than 20% of this document may be affected by microfiche quality
(DE94-605337; FEI-2247) Avail: Issuing Activity (Department of Energy (DOE)) (US Sales Only)

The results of the experimental data analysis on a radiative variation of durable mechanical properties of the austenite chromonickel steel C8X8H10T which is a material of the internal structures of PWR's, are given. The equations for the calculation of the time up to the damage are recommended. The equations of a maximum relative elongation at a durable rupture are given. DOE

N94-28562# Ames Lab., IA.
FUNDAMENTAL STUDIES OF HYDROGEN INTERACTION WITH SUPPORTED META AND BIMETALLIC CATALYSTS Ph.D. Thesis
S. Bhatia Dec. 1993 178 p
(Contract W-7405-eng-82)
(DE94-004887; IS-T-1682) Avail: CASI HC A09/MF A02

The thesis is divided into 3 parts: interaction of H with silica supported Ru catalysts (high pressure in situ NMR), in situ NMR study of H interaction with supported Ru-group IB bimetallic catalysts, and in-situ NMR study of H effects on silica-supported Pt, Rh and Ru catalysts. DOE

N94-28643# Naval Postgraduate School, Monterey, CA.
INTERMETALLIC GROWTH AT THE INTERFACE BETWEEN COPPER AND BISMUTH-TIN SOLDER M.S. Thesis
Fred O. Vollweiler Sep. 1993 80 p
(AD-A275716) Avail: CASI HC A05/MF A01

Tin-bismuth alloys have been proposed as alternatives to lead containing solders for interconnection and packaging applications. Consequently, the interface between copper metallizations and bismuth-tin solders needs to be evaluated with respect to brittle intermetallic formation. In the binary Bi-Sn alloys, both the Cu6Sn5 and Cu3Sn intermetallic phases were found at the Cu/solder interface after exposure at 250 C, 300 C, and 350 C. Bi-Sn-Sb alloys were also studied and in addition to the aforementioned intermetallic compounds Cu-Sb intermetallics were found. Kinetic growth laws have been established for the intermetallics at various temperatures and solder compositions. In addition, bulk samples of the solder were tested in compression in the furnace-cooled and quenched condition. Quenching appeared to result in higher strain rate dependence. Furthermore the tin-rich compositions were more strain rate sensitive than the bismuth-rich composition. DTIC

N94-28793# North Carolina State Univ., Raleigh. Dept. of Chemistry.
ANODIZATION OF COPPER IN CHLORIDE MEDIA Technical Report, 1 Feb. 1993 - 31 Jan. 1994
Janet G. Osteryoung 31 Jan. 1994 21 p
(Contract N00014-93-1-0375)
(AD-A275565; TR-1) Avail: CASI HC A03/MF A01

The main objective of this phase was to lay the theoretical and experimental groundwork for the determination of standard potentials and complex ion formation constants for metal-metal ion-ligand systems. The metal of interest is copper and the ligands initially of interest chloride and ethylene glycol. The approach employs exact analysis of pulse voltammograms at copper microelectrodes. DTIC

N94-28822*# National Aeronautics and Space Administration. Lewis Research Center, Cleveland, OH.
EFFECTS OF THERMOMECHANICAL PROCESSING ON TENSILE AND LONG-TIME CREEP BEHAVIOR OF Nb-1 PERCENT Zr-0.1 PERCENT C SHEET
Robert H. Titran and Mehmet Uz Mar. 1994 17 p Presented at the Metallurigal Society Annual Meeting, San Francisco, CA, 27 Feb. - 3 Mar. 1994 Prepared in cooperation with DOE, Washington, DC
(RTOP 583-02-21)
(NASA-TM-106319; E-8065; NAS 1.15:106319; DOE/NASA/26310-19)
Avail: CASI HC A03/MF A01

Effects of thermomechanical processing on the mechanical properties of Nb-1 wt. percent Zr-0.1 wt. percent C, a candidate alloy for use in advanced space power systems, were investigated. Sheet bars were cold rolled into 1-mm thick sheets following single, double, or triple extrusion operations at 1900 K. All the creep and tensile specimens were given a two-step heat treatment 1 hr at 1755 K + 2 hr 1475 K prior to testing. Tensile properties were determined at 300 as well as at 1350 K. Microhardness measurements were made on cold rolled, heat treated, and crept samples. Creep tests were carried out at 1350 K and 34.5 MPa for times of about 10,000 to 19,000 hr. The results show that the number of extrusions had some effects on both the microhardness and tensile properties. However, the long-time creep behavior of the samples were comparable, and all were found to have adequate properties to meet the design requirements of advanced power systems regardless of thermomechanical history. The results are discussed in correlation with processing and microstructure, and further compared to the results obtained from the testing of Nb-1 wt. percent Zr and Nb-1 wt. percent Zr-0.06 wt. percent C alloys. Author

N94-28830 Aluminum Co. of America, Alcoa Center, PA.
ROLE OF MICROSTRUCTURE ON THE FATIGUE DURABILITY OF ALUMINUM AIRCRAFT ALLOYS Progress Summary Report, Mar. - Dec. 1993
J. R. Brockenbrough, R. J. Bucci, A. J. Hinkle, P. E. Magnusen, and S. M. Miyasato 29 Dec. 1993 40 p Limited Reproducibility: More than 20% of this document may be affected by microfiche quality
(Contract N00014-91-C-0128)
(AD-A275814) Avail: CASI HC A03

The goal of this program is to provide a framework through which metallic alloy development programs and aircraft life assessment methodologies may exploit the potentially significant advantages in performance, weight reduction, and cost savings offered by quality improved materials and processes. The key performance attribute studied in this investigation is fatigue durability as identified by cracking which originates from microstructural features and grows to an inspectable dimension of economic consequences (i.e., a crack requiring diagnostic or corrective action during the operational lifetime of a part). Meeting the program objective consists of the following steps: (1) coupling historical material performance data with new data to formulate the opportunity and validate the concept, (2) quantifying the relationship between microstructure and performance, (3) synthesizing and verifying analytical models for predicting statistical fatigue response from microstructure data, and (4) developing test/evaluation protocols to facilitate technology implementation and concept scale-up to quantify payoff potential. DTIC

N94-28867# Northwestern Univ., Evanston, IL. Materials Research Center.
TOUGHENING MECHANISMS IN ULTRAHIGH-STRENGTH STEELS Final Report, 1 Sep. 1989 - 31 Aug. 1993
G. B. Olson and T. Mura 1 Dec. 1993 173 p
(Contract DAAL03-89-K-0152)
(AD-A275439; ARO-27163.5-MS) Avail: CASI HC A08/MF A02

A systems approach to materials design is extended to adaptive microstructures undergoing a programmed dynamic evolution in both processing and service to achieve novel combinations of properties. Fundamental principles are developed to support rational design of high-toughness ultrahigh-strength martensitic steels of interest for advanced armor and high performance gear applications. Theoretical modelling and high resolution microanalytical experiments in the martensitic alloys address control of autocatalytic coherent precipitation to achieve efficient strengthening without embrittlement, and the controlled precipitation of

optimal stability metastable austenite for adaptive dilatant transformation plasticity tuned to crack-tip stress states for efficient interaction with strain localization processes in ductile fracture. DTIC

N94-28900 Tennessee Univ., Knoxville. Dept. of Materials Science and Engineering.
FUNDAMENTAL STUDIES ON THE CORROSION BEHAVIOR OF WELDMENTS IN MARINE MICROBIAL ENVIRONMENTS Annual Report, 30 Sep. 1992 - 29 Sep. 1993
R. A. Buchanan, C. D. Lundin, P. Angell, A. Kovacs, and K. K. Khan Nov. 1993 22 p Limited Reproducibility: More than 20% of this document may be affected by microfiche quality
(Contract N00014-92-J-4116)
(AD-A275247) Avail: CASI HC A03

During the first year of this project, comprehensive literature reviews were completed in the areas of (1) weldments employed in marine applications, (2) microbially influenced corrosion (MIC) in marine environments, and (3) MIC of weldments in marine environments. Specific weldment types covering a wide range of materials were selected for MIC evaluation. Laboratory MIC evaluations were initiated on a prototype weldment (as-welded 304L stainless steel base metal, 308L filler metal) in the crevice condition. Combinations of variables were employed to enhance MIC attack of the weldment during bacterial exposures, as compared to the corrosion observed during sterile control exposures. The variables included three different consortia of marine bacteria, different degrees of solution aeration, and different solution replacement rates (dilution rates) during continuous low-flow conditions. Unfortunately, little differentiation between the bacterial and sterile-control results have been obtained to date. When corrosion occurred, either in the bacterial or control experiments, it always occurred as general or pitting-type corrosion at crevice sites within the weld-modified (weld-metal/HAZ) surface area, never within the unaffected base-metal area. Corrosion potential and solution-redox-potential measurements suggested that oxygen concentration cells contributed to the sterile-control results, but due to the uniform and highly-deaerated condition at the bacterial specimen surfaces, did not contribute to the bacterial results. DTIC

N94-28921*# National Aeronautics and Space Administration. Lewis Research Center, Cleveland, OH.
CYCLIC AXIAL-TORSIONAL DEFORMATION BEHAVIOR OF A COBALT-BASE SUPERALLOY
Peter J. Bonacuse (Army Research Lab., Cleveland, OH.) and Sreeramesh Kalluri (Sverdrup Technology, Inc., Brook Park, OH.) Nov. 1992 25 p Presented at the Second Symposium on Cyclic Deformation, Fracture, and Non-Destructive Evaluation of Advanced Materials, Miami, FL, 16-17 Nov. 1992; sponsored by the American Society for Testing and Materials
(Contract NAS3-25266; RTOP 584-03-11)
(NASA-TM-106372; E-8182; NAS 1.15:106372; ARL-MR-113) Avail: CASI HC A03/MF A01

Multiaxial loading, especially at elevated temperature, can cause the inelastic response of a material to differ significantly from that predicted by simple flow rules, i.e., von Mises or Tresca. To quantify some of these differences, the cyclic high-temperature, deformation behavior of a wrought cobalt-based superalloy, Haynes 188, is investigated under combined axial and torsional loads. Haynes 188 is currently used in many aerospace gas turbine and rocket engine applications, e.g., the combustor liner for the T800 turboshaft engine for the RAH-66 Comanche helicopter and the liquid oxygen posts in the main injector of the space shuttle main engine. The deformation behavior of this material is assessed through the examination of hysteresis loops generated from a biaxial fatigue test program. A high-temperature axial, torsional, and combined axial-torsional fatigue data base has been generated on Haynes 188 at 760 C. Cyclic loading tests have been conducted on uniform gauge section tubular specimens in a servohydraulic axial-torsional test rig. Test control and data acquisition were accomplished with a minicomputer. In this paper, the cyclic hardening characteristics and typical hysteresis loops in the axial stress versus axial strain, shear stress versus engineering shear strain, axial strain versus engineering shear strain, and axial stress versus shear stress spaces are presented for cyclic, in-phase and out-of-phase, axial torsional tests. For in-phase tests three different values of the proportionality constant, lambda (ratio of engineering shear strain amplitude to axial strain amplitude), are examined, viz., 0.86, 1.73, and 3.46. In the out-of-phase tests, three different values of the phase angle, phi (between the axial and engineering shear strain waveforms), are studied, viz., 30, 60, and 90 deg with lambda = 1.73. The cyclic hardening behaviors of all the tests conducted on Haynes 188 at 760 C are evaluated using the von Mises equivalent stress-strain and the maximum shear stress-maximum engineering shear strain (Tresca) curves. Comparisons are also made between the hardening behaviors of cyclic axial, torsional, and combined in-phase and out-of-phase axial-torsional fatigue tests. These comparisons are accomplished through simple Ramberg-Osgood type stress-strain functions for cyclic, axial stress-strain and shear stress-engineering shear strain curves. Author (revised)

N94-29015 Centre National de la Recherche Scientifique, Thiais (France). Molecular Materials Lab.
REPORT ON SMART MATERIALS [RAPPORT: MATERIAUX INTELLIGENTS]
F. Garnier 29 May 1992 38 p In FRENCH Sponsored by Direction des Recherches, Etudes et Techniques and Centre de Documentation de l'Armenebt
(PB94-137528) Avail: Issuing Activity (National Technical Information Service (NTIS))

Smart materials are defined as complex materials able to function as sensors (for detecting physical or chemical changes inside or outside the material), data-transfer and -processing devices (for responding to outside changes), and actuators (enabling the material to modify itself or the physical or chemical environment around it). Despite widespread use of the term, a review of the literature shows that, strictly speaking, no such materials exist. The author believes the value of the smart materials concept lies in the joint development of a set of themes by physicists, chemists, biologists, computer specialists and mathematicians, which can be used to advance materials toward real possession of multiple functions. NTIS

N94-29043# Cornell Univ., Ithaca, NY. Dept. of Chemistry.
SYNTHESIS AND NEUTRON DIFFRACTION STUDY OF Na3WN3 AND Na3MoN3 Technical Report No. 19, 1990 - 1993
P. E. Rauch, F. J. DiSalvo, N. E. Brese, D. Partin, and M. OKeeffe 17 Jan. 1994 21 p
(Contract N00014-91-J-1269)
(AD-A275158) Avail: CASI HC A03/MF A01

We have extended our ambient pressure method for the synthesis of ternary alkali metal nitrides to synthesize a new class of nitrides, Na3MN3 (M = Mo or W). These compounds were synthesized from the metal nitride and NaNH2 at 500 C under flowing ammonia at atmospheric pressure. The structures were examined using X-ray powder diffraction and neutron powder diffraction and found to be identical with that obtained from single crystal prepared by Ostermann, Zachwieja and Jacobs at high pressure. DTIC

N94-29056# Minnesota Univ., Minneapolis. Office of Research and Technology Transfer Administration.
RESEARCH ON THE IMPROVEMENT OF SHAPE-MEMORY AND MAGNETOSTRICTIVE MATERIALS Report, 1 Aug. 1989 - 31 Jul. 1993
Richard D. James 13 Oct. 1993 5 p
(Contract DAAL03-89-G-0081)
(AD-A275397; ARO-27063.12-MA-SM) Avail: CASI HC A01/MF A01

The goals of this research are to give predictive, quantitative models that can be used to improve shape-memory and magnetostrictive materials, and that can guide the development of new materials. A new theory of martensite and a new theory of magnetostriction were found, both of which predict accurately observed domain structures in these alloys. The principal findings based on these theories are (1) the importance of the precise values of the lattice parameters in determining the microstructure, and therefore the behavior of these materials; (2) the presence of the growth twins in Tb(x)Dy(1-x)Fe2, the material with the largest known magnetostriction, do not decrease the magnetostrictive strain in this alloy, as was formerly thought; (3) thermoelastic theory gives a mechanism for increased strain-rate dependence in uniaxial tension experiments on TiNi. A unique experimental facility was built for fundamental experimental studies on stress and magnetic field-induced phase transformation. DTIC

N94-29089# Utah Univ., Salt Lake City. Dept. of Chemistry.
PITTING CORROSION OF TITANIUM Interim Report, Jun. - Dec. 1993
Norberto Casillas, Steven J. Charlebois, William H. Smyrl, and Henry S.

White 20 Jan. 1994 37 p
(Contract N00014-91-J-1927)
(AD-A274980; TR-28) Avail: CASI HC A03/MF A01

The breakdown of native and anodically-grown oxide films on Ti electrodes is investigated by scanning electrochemical microscopy (SECM), video microscopy, transmission electron microscopy, and voltammetry. SECM is used to demonstrate that the oxidation of Br(-) on Ti occurs at microscopic surface sites (10 to 50 micrometer diameter, 30 sites/sq cm) that are randomly positioned across the oxide surface. After determining the position of the active sites for Br(-) oxidation, breakdown of the oxide is initiated by increasing the electrode potential to more positive values. Direct correspondence is observed between the location of the electroactive sites and corrosion pits, indicating that oxide breakdown is associated with a localized site of high electrical conductivity. The potential at which pitting is observed in voltammetric experiments is found to be proportional to the average oxide thickness, for values ranging between 20 and 100 A, indicating that breakdown is determined either by the magnitude of the electric field within the oxide or by the interfacial potential at the oxide/Br(-) solution interface. Pitting occurs at significantly lower potentials in Br(-) solutions than in Cl(-) solutions, suggesting a strong chemical interaction between the TiO2 surface and Br(-). A mechanism of oxide breakdown is proposed that is based on the potential-dependent chemical dissolution of the oxide at microscopic surface sites. DTIC

N94-29119 National Physical Lab., Teddington (England). Div. of Materials Metrology.
SURFACE TENSION OF TIN AND ITS ALLOYS WITH PARTICULAR REFERENCE TO SOLDERS
B. J. Keene 1993 134 p
(PB94-138302; NPL-DMM(A)-113) Copyright Avail: Issuing Activity (National Technical Information Service (NTIS))

The report collates, in graphical form, the literature data which relate to the influence of composition and of temperature on the surface tension of Sn alloys. Curves have been traced directly from diagrams given in the relevant references. Brief comments on the extant data are given for each system. For some systems the comments also include suggested relations for the particular metal which is alloyed with Sn. NTIS

N94-29142# Helsinki Univ. of Technology, Espoo (Finland). Lab. of Engineering Materials.
LOW TEMPERATURE BEHAVIOR OF VIRGIN MARTENSITE Ph.D. Thesis
L. Yong 28 Jun. 1993 154 p See also PB93-226280
(ISSN 0785-1294)
(PB94-132925; ISBN-951-22-1629-9; Rept-5/1993/MTR) Avail: CASI HC A08/MF A02

Three aspects of the virgin martensite at low temperatures have been studied; namely, internal friction behavior of virgin lenticular martensite, effect of martensite morphology on the aging behavior of virgin martensite, and the zig-zag martensite formed at low temperatures. NTIS

N94-29196 Martin Marietta Labs., Baltimore, MD.
ELECTROCHEMICAL BEHAVIOR AND SURFACE CHEMISTRY OF NONEQUILIBRIUM ALUMINUM ALLOYS: PASSIVITY MECHANISM AND FABRICATION METHODS Final Report, 1 Dec. 1992 - 30 Nov. 1993
G. D. Davis, B. A. Shaw, B. J. Rees, A. Lyengar, and E. L. Principe 17 Jan. 1994 30 p Limited Reproducibility: More than 20% of this document may be affected by microfiche quality
(Contract N00014-C-93-0007)
(AD-A275401; MML-TR-94-02) Avail: CASI HC A03

The electrochemical behavior of sputter-deposited nonequilibrium stainless aluminum alloys and different methods to produce bulk or thick-film material have been investigated. Nonequilibrium Al-Ta and Al-W alloys exhibit enhanced passivity over a wide pH range even though the passive film chemistry varies considerably. This enhanced passivity can be explained by the solute-rich interphase mechanism (SRIM) which states that formation and passivation of occluded cells stabilize the passive film from continued Cl(-) attack and dissolution. The best material is produced by sputter deposition; however, physical vapor deposited and plasma sprayed material also exhibit some enhanced passivity. DTIC

N94-29205 Virginia Univ., Charlottesville. Dept. of Materials Science and Engineering.
MECHANICAL ALLOYING PROCESSING WITH APPLICATION TO STRUCTURAL MATERIALS: ASSERT SUPPLEMENT Final Report, 1 Jun. 1992 - 31 May 1993
T. H. Courtney 23 Nov. 1993 2 p Limited Reproducibility: More than 20% of this document may be affected by microfiche quality
(Contract DAAL03-92-G-0096)
(AD-A275400; ARO-29728.1-MS-AAS) Avail: CASI HC A01

When two-phase mixtures of ductile metals are mechanically alloyed, they often assume a convoluted lamellar structure. Since these powders are consolidated at elevated temperatures, their structures (and therefore properties) are likely be altered by consolidation processing. We have investigated microstructural changes that take place upon heat-treating mechanically alloyed Cu-20 vol.% NB alloys. The transition from a plate-like to a spherical microstructure is described, and the kinetics of this process appear controlled by a type of boundary diffusion even though the coarsening temperature was high in terms of the homologous temperature of Cu. Reasons for this behavior are suggested. Finally, during heat treatment (carried out in hydrogen), a Nb layer forms around the particles. The thickness of this layer (and the corresponding zone denuded of Nb within the particle) increases with continued elevated temperature exposure at a rate that is consistent with the process being driven by curvature forces. DTIC

N94-29380*# National Aeronautics and Space Administration. Marshall Space Flight Center, Huntsville, AL.
CHAMBER FREE FUSION WELDING ROOT SIDE PURGING METHOD AND APPARATUS Patent Application
William F. McGee, inventor (to NASA) (Martin Marietta Space Systems, Inc., Huntsville, AL.) and Daniel J. Rybicki, inventor (to NASA) (Martin Marietta Space Systems, Inc., Huntsville, AL.) 29 Nov. 1993 14 p
(NASA-Case-MFS-28832-1; NAS 1.71:MFS-28832-1;
US-Patent-Appl-SN-158331) Avail: CASI HC A03/MF A01

A method and apparati are presented for non-chamber root side purging in fusion welding of oxygen reactive metals which require that the molten weld zone and local solid areas of the weld seam remaining at high temperatures be shielded from normal atmosphere to prevent degradation of the welded area. The apparati provide an inert atmosphere to the root side of a weld joint through a porous medium whereby the jet-like thrust of the plasma arc actually draws the continuously supplied inert atmosphere into the path of the molten or high temperature solid weld zone. The porous medium is configured so it can be placed at the borders of the weld seam and substantially parallel to the seam without restricting the view of the root side of the seam. The inert gas is dispersed evenly through the porous media and across the weld seam, at the point of arc penetration and in front of and behind the arc. The apparati can be constructed so as to limit the amount of inert gas flow and can be mobile and travel synchronously with the welding arc. NASA

N94-29387 Helsinki Univ. of Technology, Espoo (Finland). Labs. of Metallurgy and Engineering Materials.
EFFECT OF NON-METALLIC INCLUSIONS ON THE MACHINABILITY OF STEEL
Aino Helle, Reima Vaeinoelae, and Juha Pietikaeinen 1993 62 p Sponsored by Suomen Akatemja, Helsinki, Finland Limited Reproducibility: More than 20% of this document may be affected by microfiche quality
(ISSN 0785-5168)
(PB93-230233; TKK-V-B85; ISBN-951-22-1536-5) Avail: Issuing Activity (National Technical Information Service (NTIS))

The research project was commenced in order to obtain a deeper understanding of the basic phenomena behind the effect of inclusions on the machinability of steel and, particularly, of the prerequisites and mechanisms of the formation of a protective layer by the inclusions on the cutting tool during machining of steel. The main object of the research work was to find new types of inclusions with which the machinability of steel could be improved without any deterioration of its mechanical properties. NTIS

N94-29395# Cornell Univ., Ithaca, NY. Dept. of Chemistry.
THE SYNTHESIS AND STRUCTURAL CHARACTERIZATION OF Na3WO3N Technical Report, 1990 - 1993

S. H. Elder, F. J. DiSalvo, J. B. Parise, J. A. Hriljac, and J. W. Richardson, Jr. 17 Jan. 1994 24 p
(Contract N00014-91-J-1269)
(AD-A275243; TR-18) Avail: CASI HC A03/MF A01

We report the discovery of a new ternary oxynitride, Na3WO3N. Na3WO3N is synthesized by exposing a eutectic melt consisting of 1/2Na2O: 1Na2WO4 to a flow of ammonia gas at 695 C. The compound crystallizes in the acentric space-group Pmn2(1) with a = 7.2481 (3), b = 6.2728 (3) and c = 5.6493 (2) A. The structure was determined from synchrotron X-ray powder diffraction data and refined using the Rietveld analysis on neutron powder diffraction data. It is isostructural to the low temperature form of Li3PO4, which can be derived from an ordered wurtzite structure-type with all the atoms having tetrahedral coordination. Alternatively, the structure can be described as being 'salt-like' consisting of isolated (WO3N)(-3) tetrahedral poly-anions separated by Na(+). DTIC

N94-29447*# National Aeronautics and Space Administration. Marshall Space Flight Center, Huntsville, AL.
ROTARY ACTUATOR Patent Application
Myron Brudnicki, inventor (to NASA) (Allied-Signal Corp., Morristown, NJ.) 12 Oct. 1993 12 p
(NASA-Case-MFS-28581-1; NAS 1.71:MFS-28581-1;
US-Patent-Appl-SN-134441) Avail: CASI HC A03/MF A01

Rotary actuators and other mechanical devices incorporating shape memory alloys are provided herein. Shape memory alloys are a group of metals which when deformed at temperatures below their martensite temperatures, resume the shapes which they had prior to the deformation if they are heated to temperatures above their austensite temperatures. Actuators in which shape memory alloys are employed include bias spring types, in which springs deform the shape memory alloy (SMA), and differential actuators, which use two SMA members mechanically connected in series. Another type uses concentric cylindrical members. One member is in the form of a sleeve surrounding a cylinder, both being constructed of shape memory alloys. Herein two capstans are mounted on a shaft which is supported in a framework. Each capstan is capable of rotating the shaft. Shape memory wire, as two separate lengths of wire, is wrapped around each capstan to form a winding around that capstan. The winding on one capstan is so wrapped that the wire is in a prestretched state. The winding on the other capstan is so wrapped that the wire is in a taut, but not a prestretched, state. Heating one performs work in one direction, thus deforming the other one. When the other SMA is heated the action is reversed. NASA

N94-29507* National Aeronautics and Space Administration. Lewis Research Center, Cleveland, OH.
PLASMA SPRAYED CERAMIC THERMAL BARRIER COATING FOR NiAl-BASED INTERMETALLIC ALLOYS Patent
Robert A. Miller, inventor (to NASA) and Joseph Doychak, inventor (to NASA) 12 Apr. 1994 6 p Filed 26 Oct. 1992 Supersedes N93-31294 (31 - 12, p 3705)
(NASA-Case-LEW-15535-1; US-Patent-5,302,465;
US-Patent-Appl-SN-970669; US-Patent-Class-428-552;
US-Patent-Class-428-553; US-Patent-Class-428-565;
Int-Patent-Class-B22F-7/00) Avail: US Patent and Trademark Office

A thermal barrier coating system consists of two layers of a zirconia-yttria ceramic. The first layer is applied by low pressure plasma spraying. The second layer is applied by conventional atmospheric pressure plasma spraying. This facilitates the attachment of a durable thermally insulating ceramic coating directly to the surface of a highly oxidation resistant NiAl-based intermetallic alloy after the alloy has been preoxidized to promote the formation of a desirable Al2O3 scale.
Official Gazette of the U.S. Patent and Trademark Office

N94-29525# Aerospatiale, Chatillon (France).
ELECTRON MICROSCOPY: METAL ALLOY X RAY MICROANALYSIS [MICROSCOPIE ELECTRONIQUE: MICROANALYSE X DES ALLIAGES METALLIQUES]
F. Cournut, C. Becker, and C. Patoz 1993 11 p In FRENCH
Presented at the Symposium on Analytical Sciences, 6 May 1993
(Rept-932-600-101; ETN-94-95480) Avail: CASI HC A03/MF A01

A method for estimating the feasibility of metal alloy microanalysis and the possible analytical performances are investigated. The aim is the optimization of the equipment's use and costs. Moreover, the procedure is a decision making tool concerning analysis orientation and feasibility. The principles of scanning electron microscopy are given, together with the device description. Possible applications of scanning electron microscopy on qualitative and quantitative analysis are summarized. X-ray emission spectra and equipment parameters are characterized. ESA

N94-29736*# University of Eastern Kentucky, Richmond. Dept. of Physics and Astronomy.
STUDY OF ACTIVATION DATA OF METAL SAMPLES FROM LDEF-1 AND SPACELAB-2 Final Technical Report, 27 Mar. 1993 - 1 Mar. 1994
C. E. Laird 15 Apr. 1994 27 p
(NASA Order H-13029-D)
(NASA-CR-195802; NAS 1.26:195802) Avail: CASI HC A03/MF A01

Gamma-ray spectra obtained from samples flown aboard the Long Duration Exposure Facility have been analyzed to obtain the nuclear species produced in this material by the interaction of this material with protons and neutrons in this material by the interaction of this material with protons and neutrons encountered in its 69 month orbital flight as well as to quantify the specific activity (pCi/kg) of these nuclear species. This quantification requires accurate corrections of efficiency, self-attenuation, and background. Plans have been developed for archival of the spectra in a form readily accessible to the scientific, engineering and technical community engaged in space research and application. Work has been initiated in the process of estimating the flux of activating particles encountered by material at various locations of the spacecraft.
Derived from text

N94-29758*# National Aeronautics and Space Administration. Lewis Research Center, Cleveland, OH.
THE EFFECT OF VARIOUS METALLURGICAL PARAMETERS ON THE FLOW AND FRACTURE BEHAVIOR OF POLYCRYSTALLINE NiAl NEAR THE BRITTLE-TO-DUCTILE TRANSITION
Ronald D. Noebe Apr. 1994 254 p
(RTOP 505-63-52)
(NASA-TM-106534; E-8669; NAS 1.15:106534) Avail: CASI HC A12/MF A03

An investigation of the effect of various metallurgical parameters such as interfaces, allowing additions, test temperature, and strain rate on the flow and fracture behavior of polycrystalline NiAl is summarized. From this study, a more complete understanding of the deformation and fracture behavior of polycrystalline NiAl near the brittle-to-ductile transition temperature has been developed. A mechanism for the BDTT is proposed that is based on the operation of localized dislocation climb processes that operate within the vicinity of the grain boundaries and provide the additional deformation mechanisms necessary for grain-to-grain compatibility during plastic deformation. Finally, methods for improving the low temperature mechanical behavior of NiAl were considered and reviewed within the context of the present knowledge of NiAl-based materials and the operative deformation and fracture mechanisms determined in this study. Special emphasis was placed on the use of second phases for improving low temperature properties. Author (revised)

N94-29900 Wichita State Univ., KS.
THE EFFECT OF MECHANICAL PAINT STRIPPING ON THE FATIGUE AND FRACTURE OF THIN ALUMINUM AIRPLANE SKIN Ph.D. Thesis
Joe P. Amro 1992 150 p
Avail: Univ. Microfilms Order No. DA9311975

An experimental investigation has been carried out to evaluate the affects of dry stripping (paint removal by plastic particle blasting) on aluminum aircraft skins (2024-T3). Analytical procedures were carried out for determining changes in fatigue life and relevant fracture resistance parameters such as number of cycles required to generate a surface crack of certain length, crack propagation rate, and number of cycles to failure while indicating the dependence of these parameters on the surface condition (morphology). The surface morphology dependence on deformation, fracture resistance properties, and defects presented on the surface were characterized using scanning electron microscopy, optical microscopy, and other modern metallographic techniques. The results indicated that all the parameters of plastic media blasting had significant effects on the fatigue life of the specimens. Minor changes in the blasting parameters may reveal different results. All fatigue samples were found to

exhibit a general decrease in life of 10 to 46 percent after being subjected to four cycles of paint removal. The samples were cyclically loaded to 20,000 cycles then stripped and repainted four times; 20,000 cycles represents approximately 5 years of life. The initial stress ratio for loading was 0.1 with stresses varying from 20 to 65 ksi. Dissert. Abstr.

N94-29931# Brookhaven National Lab., Upton, NY.
FIRST PRINCIPLES PSEUDOPOTENTIAL CALCULATIONS ON ALUMINUM AND ALUMINUM ALLOYS
J. W. Davenport, N. Chetty, R. B. Marr, S. Narasimhan, J. E. Pasciak, R. F. Peierls, and M. Weinert 1993 10 p Presented at the Fall Meeting of the Minerals, Metals and Materials Society: Physical Metallurgy and Materials, Pittsburgh, PA, 17-21 Oct. 1993
(Contract DE-AC02-76CH-00016)
(DE94-004890; BNL-49718; CONF-931009-18) Avail: CASI HC A02/MF A01

Recent advances in computational techniques have led to the possibility of performing first principles calculations of the energetics of alloy formation on systems involving several hundred atoms. This includes impurity concentrations in the 1% range as well as realistic models of disordered materials (including liquids), vacancies, and grain boundaries. The new techniques involve the use of soft, fully nonlocal pseudopotentials, iterative diagonalization, and parallel computing algorithms. Here the authors give a review of recent results using parallel and serial algorithms on metallic systems including liquid aluminum and liquid sodium and also new results on vacancies in aluminum and on aluminum-magnesium alloys. DOE

N94-29936# Sandia National Labs., Albuquerque, NM.
LOGISTICS FOR THE IMPLEMENTATION OF LEAD-FREE SOLDERS ON ELECTRONIC ASSEMBLIES
P. T. Vianco and I. Artaki 1993 18 p Presented at the International Waste Management Conference, San Juan, Puerto Rico, 28 Apr. - 1 May 1993
(Contract DE-AC04-94AL-85000)
(DE94-004800; SAND-93-0226C; CONF-9304117-6) Avail: CASI HC A03/MF A01

The prospects of legislative and regulatory action aimed at taxing, restricting, or banning lead-bearing materials from manufactured products has prompted the electronics community to examine the implementation of lead-free solders to replace currently used lead-containing alloys in the manufacture of electronic devices and assemblies. The logistics for changing the well established 'tin-lead solder technology' require not only the selection of new compositions but also the qualification of different surface finishes and manufacturing processes. The meniscometer/wetting balance technique was used to evaluate the wettability of several candidate lead-free solders as well as to establish windows on processing parameters so as to facilitate prototype manufacturing. Electroplated and electroless Sn-100 coatings, as well as organic preservatives, were also examined as potential alternative finishes for device leads and terminations as well as circuit board conductor surfaces to replace traditional tin-lead layers. Sandia National Laboratories and AT&T have implemented a program to qualify the manufacturing feasibility of surface mount prototype circuit boards using several commercial lead-free solders by infrared reflow technology. DOE

N94-29946 Selskapet for Industriell og Teknisk Forskning, Trondheim (Norway). Div. of Metallurgy.
ELECTROMAGNETIC EFFECT ON TURBULENT TRANSPORT IN LIQUID METALS AND ELECTROLYTES (BATH)
L. Gu and S. T. Johansen 23 Aug. 1993 36 p
(PB94-138450; STF34-A93169) Avail: Issuing Activity (National Technical Information Service (NTIS))

In order to investigate the effect of an applied magnetic field on the turbulence as well as the heat transfer in the liquid metal flow, the FLUENT computer code has been modified. In addition, a generalized model for the turbulent heat (mass) - flux has been added. Numerical simulations have been carried out in the fluid flow of a channel. It was found that the magnetic field affects the fluid flow by decreasing the turbulent viscosity. The temperature distribution is thus influenced as the turbulent enthalpy transport is decreased by an increased magnetic flux density. In the case of an applied magnetic field a lower turbulent viscosity is computed by the Reynolds stress turbulence model. Thus the heat transfer in the fluid is affected by decreasing the heat loss to the wall. These effects seem to be more pronounced at high magnetic flux density. In the case of aluminum reduction cells a present magnetic field seems to have a modest influence on the turbulent transport. NTIS

N94-29947 Selskapet for Industriell og Teknisk Forskning, Trondheim (Norway). Div. of Metallurgy.
NEW INOCULANTS FOR DUCTILE CAST IRON Progress Report No. 1
A. O. Kluken and O. Grong 5 Jul. 1993 40 p
(PB94-138476; STF34-A93136) Avail: Issuing Activity (National Technical Information Service (NTIS))

The present report summarizes the activities during the project period from January through June 1993. The report is divided into two parts: Part I, Development of Inoculants, and Part II, Evaluation of Inoculation Effect. Four different non-metallic phases (i.e., silicon oxide, SiO2, iron oxide, Fe2O3, calcium silicate, CaOSiO2, and silicon carbide, SiC) were added to the inoculant melts. Foundrisil was chosen as base material for these initial tests due to its relatively high content of reactive trace elements, i.e., calcium and barium. Two of the produced inoculants showed promising oxygen 'yields' (i.e., Foundrisil containing Fe2O3, and CaOSiO2, respectively). In addition to these, pure Foundrisil and Foundrisil containing SiC were used in the foundry experiments. Metallographic examinations of the cast materials revealed that addition of iron oxide to Foundrisil increased the graphite nodule density by 45% in 5 mm section size material and by approximately 30% in 30 mm section size material, compared to pure Foundrisil. However, the increased graphite nodule density was not accompanied by an increased number density of non-metallic inclusions. Consequently, further experiments are required to clarify this inconsistency. NTIS

N94-29997 Selskapet for Industriell og Teknisk Forskning, Trondheim (Norway). Div. for Information Technology.
MELT FLOW DURING ALLOY SOLIDIFICATION: DIMENSIONAL ANALYSIS AND MODEL PROBLEMS
E. Haug and H. J. Thevik 8 Sep. 1993 50 p Sponsored by Royal Norwegian Council for Scientific and Industrial Research, Oslo, Norway
(PB94-138625; STF33-A93019) Avail: Issuing Activity (National Technical Information Service (NTIS))

A set of mechanistic equations describing melt flow during alloy solidification is transformed to a dimensionless form. How to choose appropriate scales are discussed, appropriate dimensionless groups are suggested, and the dominating terms in the equations are identified. Some comments on numerical solution procedures are given. Two classes of simplified model problems are then presented. The first class of problems focuses on the melt flow resulting from solidification shrinkage, and the second class addresses density driven melt transport due to thermal and specie concentration gradients. NTIS

N94-30007# Sandia National Labs., Albuquerque, NM.
THE ORGANOMETALLIC CHEMICAL VAPOR DEPOSITION OF TRANSITION METAL CARBIDES: THE USE OF HOMOLEPTIC ALKYLS
M. D. Healy (Los Alamos National Lab., NM.), D. C. Smith (Los Alamos National Lab., NM.), R. W. Springer (Los Alamos National Lab., NM.), R. R. Rubiano (Massachusetts Inst. of Tech., Cambridge.), and J. E. Parmeter 1993 7 p Presented at the Fall Meeting of the Materials Research Society (MRS), Boston, MA, 29 Nov. - 3 Dec. 1993
(Contract DE-AC04-94AL-85000)
(DE94-005577; SAND-93-4079C; CONF-931108-49) Avail: CASI HC A02/MF A01

The organometallic chemical vapor deposition of transition metal carbides (M = Ti, Zr, Hf, and Cr) from tetraneopentyl-metal precursors has been carried out. Metal carbides can be deposited on Si, Al2O3, and stainless steel substrates from M(CH2C(CH3)3)4 at temperatures in the range of 300 to 750 C and pressures from 10(exp -2) to 10(exp -4) Torr. Thin films have also been grown using a carrier gas (Ar, H2). The effects of variation of the metal center, deposition conditions, and reactor design on the resulting material have been examined by SEM, XPS, XRD, ERD and AES. Hydrocarbon fragments generated in the deposition chamber have been studied by in-situ mass spectrometry. Complementary studies examining the UHV surface decomposition of Zr(CH2C(CH3)3)4 have allowed for a better understanding of the mechanism leading to film growth. DOE

N94-30021# Argonne National Lab., IL.
FATIGUE OF CARBON AND LOW-ALLOY STEELS IN LWR ENVIRONMENTS
O. K. Chopra, W. F. Michaud, and W. J. Shack Oct. 1993 23 p Presented at the Water Reactor Safety Information Meeting, Bethesda, MD, 25-27 Oct. 1993
(Contract W-31-109-eng-38)
(DE94-005116; ANL/ET/CP-80135; CONF-931079-16) Avail: CASI HC A03/MF A01

Fatigue tests have been conducted on A106-Gr B carbon steel and A533-Gr B low-alloy steel to evaluate the effects of an oxygenated-water environment on the fatigue life of these steels. For both steels, environmental effects are modest in PWR water at all strain rates. Fatigue data in oxygenated water confirm the strong dependence of fatigue life on dissolved oxygen (DO) and strain rate. The effect of strain rate on fatigue life saturates at some low value, e.g., between 0.0004 and 0.001%/s in oxygenated water with approximately 0.8 ppm DO. The data suggest that the saturation value of strain rate may vary with DO and sulfur content of the steel. Although the cyclic stress-strain and cyclic-hardening behavior of carbon and low-alloy steels is distinctly different, the degradation of fatigue life of these two steels with comparable sulfur levels is similar. The carbon steel exhibits pronounced dynamic strain aging, whereas strain-aging effects are modest in the low-alloy steel. Environmental effects on nucleation of fatigue crack have also been investigated. The results suggest that the high-temperature oxygenated water has little or no effect on crack nucleation. DOE

N94-30024# Purdue Univ., West Lafayette, IN.
REACTIONS OF METAL IONS AND THEIR CLUSTERS IN THE GAS PHASE USING LASER IONIZATION: FOURIER TRANSFORM MASS SPECTROMETRY
B. S. Freiser Sep. 1993 16 p
(Contract DE-FG02-87ER-13766)
(DE94-006208; DOE/ER-13766/11) Avail: CASI HC A03/MF A01

This report focuses on progress in seven areas: (1) Gas-Phase Reactions of Fe(Benzyne)(sup +) with Simple Alkyl Halides; (2) Photodissociation and Collision-Induced Dissociation of Molecular Ions From Methylphenol and Chloromethylphenol; (3) Isotopomer Differentiation Using Metal Ion Chemical Ionization Reagents; (4) Multiple Excitation Collisional Activation (MECA) in Fourier Transform Mass Spectrometry; (5) Chemistry of Fe(sup +)-Arene Ions with Halobenzenes; (6) Gas-Phase Photodissociation Study of Ag(Benzene)(sup +) and Ag(Toluene)(sup +); and (7) Reactivity of Ti(sup 2+) and V(sup 2+) with Small Alkanes. DOE

N94-30042# Oak Ridge National Lab., TN.
NANOSIZE METAL ALLOY PARTICLE FORMATION IN Ag AND Cu SEQUENTIALLY IMPLANTED SILICA
R. A. Zuhr, R. H. Magruder, III, T. A. Anderson, and J. E. Wittig Dec. 1993 7 p Presented at the Fall Meeting of the Materials Research Society (MRS), Boston, MA, 29 Nov. - 3 Dec. 1993
(Contract DE-AC05-84OR-21400)
(DE94-005592; CONF-931108-50) Avail: CASI HC A02/MF A01

A series of high purity silica samples were sequentially implanted with Ag and Cu ions at energies such that the depth distributions for each of the ions overlap. The samples were characterized by RBS, TEM, and optical spectroscopy. Optical response was found to be dependent on order of sequential implantation as well as relative concentration of implanted elements. The changes in the optical response are attributed to composition changes of the metal colloids that are formed as a result of alloying of the sequentially implanted metal ions, as well as to changes in the size the colloids. DOE

N94-30053# Sandia National Labs., Albuquerque, NM.
NON-CHROMATE TALC CONVERSION COATINGS FOR ALUMINUM
R. G. Buchheit, C. A. Drewien, J. L. Finch, and G. E. Stoner 1994 13 p Presented at the Corrosion 1994: National Association of Corrosion Engineers (NACE) International Annual Conference, Baltimore, MD, 28 Feb. - 4 Mar. 1994
(Contract DE-AC04-94AL-85000)
(DE94-005281; SAND-93-2533C; CONF-940222-10) Avail: CASI HC A03/MF A01

A method was developed for applying an inorganic conversion coating. The process is similar to chromate conversion coating methods; however, this method does not use or involve hazardous/toxic chemicals. The coating forms by precipitation involving Al(3+) Li(+), OH(-), CO3(2-), and possibly other anions. This polycrystalline coating is continuous, conformal, and persistent in aggressive environments. Coating thicknesses range from several tenths to ten micrometers. Although the outer portions of the coating are porous, the pores do not penetrate to the substrate interface. These coatings do not match the levels of performance offered by commercially available chromate conversion coatings, but are capable of meeting many of the corrosion resistance, electrical resistivity, and paint adhesion requirements established in MIL-C-5541E 'Chemical Conversion Coatings on Aluminum and Aluminum Alloys.' In this paper, methods for producing the talc coating on aluminum alloys 1100 and 6061-T6 are described and compared to traditional chromate conversion coating methods. The resulting coating structure and composition are described. Performance data for the talc coatings in MIL-C-5541E required tests are presented along with the data for commercial chromate-based coatings. DOE

N94-30057# Argonne National Lab., IL.
CORROSION PERFORMANCE OF MATERIALS FOR ADVANCED COMBUSTION SYSTEMS
K. Natesan, M. Yanez-Herrero, and C. Fornasieri Dec. 1993 70 p
(Contract W-31-109-eng-38)
(DE94-006726; ANL/FE-93/1) Avail: CASI HC A04/MF A01

Conceptual designs of advanced combustion systems that utilize coal as a feedstock require high-temperature furnaces and heat transfer surfaces capable of operating at more elevated temperatures than those prevalent in current coal-fired power plants. The combination of elevated temperatures and hostile combustion environments necessitates development/application of advanced ceramic materials in these designs. This report characterizes the chemistry of coal-fired combustion environments over the wide temperature range that is of interest in these systems and discusses preliminary experimental results on several materials (alumina, Hexoloy, SiC/SiC, SiC/Si3N4/Si3N4, ZIRCONIA, INCONEL 677 and 617) with potential for application in these systems. DOE

N94-30062# Pacific Northwest Lab., Richland, WA.
INDUCED CRYSTALLIZATION IN CW LASER-IRRADIATED SOL-GEL DEPOSITED TITANIA FILMS
G. J. Exarhos and N. J. Hess 1993 6 p Presented at the Fall Meeting of the Materials Research Society (MRS), Boston, MA, 29 Nov. - 3 Dec. 1993
(Contract DE-AC06-76RL-01830)
(DE94-006527; PNL-SA-22790; CONF-931108-72) Avail: CASI HC A02/MF A01

Isothermal annealing of amorphous TiO2 films deposited from acidic sol-gel precursor solutions results in film densification and concomitant increase in refractive index. Subsequent heating above 300C leads to irreversible transformation to an anatase crystalline phase. Similar phenomena occur when such amorphous films are subjected to focused cw laser irradiation. Controlled variations in laser fluence are used to densify or crystallize selected regions of the film. Low fluence conditioning leads to the evolution of a subtle nanograin-size morphology, evident in AFM images, which appears to retard subsequent film crystallization when such regions are subjected to higher laser fluence. Time-resolved Raman spectroscopy has been used to characterize irradiated regions in order to follow the crystallization kinetics, assess phase homogeneity, and evaluate accompanying changes in residual film stress. DOE

N94-30076 Gosudarstvennyi Komitet po Ispolzovaniyu Atomnoi Energii, Obninsk (USSR).
DEVELOPMENT OF EVALUATED DATA BANK OF PHYSICAL PROPERTIES OF PERSPECTIVE NUCLEAR ENGINEERING STEELS AND ALLOYS
O. V. Sopov and V. A. Solovev 1992 6 p Limited Reproducibility: More than 20% of this document may be affected by microfiche quality
(DE94-607999; FEI-2246) Avail: CASI HC A02 (US Sales Only)

A data bank of physical properties of prospective nuclear engineering steels and alloys is evaluated. The data bank includes the experimental data of the material property investigation by methods of the electric resistance and internal friction determination, of the X-ray structural and metallographic analyses, and also by methods of the hydrostatic weighing,

positron annihilation, neutron diffraction analysis, and Moessbauer spectroscopy. The principal purposes for the data bank and the way in which it was realized were examined. DOE

N94-30090 International Centre for Theoretical Physics, Trieste (Italy).
THERMODYNAMICS OF MOLTEN K-TE ALLOYS
O. Akinlade Aug. 1993 23 p Limited Reproducibility: More than 20% of this document may be affected by microfiche quality
(DE94-608095; IC-93/255) Avail: CASI HC A03 (US Sales Only)

The quasichemical model is used to explain the free energy of mixing, heat of mixing, excess entropy of mixing and chemical short range order parameter for potassium-tellurium as a function of concentration. The study reveals that the constituent metals of these alloys undergo major structural changes in atomic and electronic character on alloying. The concentration dependent behaviour of thermodynamic properties on mixing occurs due to preferential ordering of unlike atoms as nearest neighbors which could simultaneously be understood within the complex formation model. An analysis of the results further suggests that heterocoordination with the formation of K2Te3 is likely to exist in the melt. It is concluded that a reasonable degree of chemical order may exist in the whole concentration range being greatest at about 50 percent at K. DOE

N94-30101# Los Alamos National Lab., NM.
REALTIME STRUCTURAL ELECTROCHEMISTRY OF PLATINUM CLUSTERS USING DISPERSIVE XAFS
P. G. Allen, S. D. Conradson, M. S. Wilson, S. Gottesfeld, and I. D. Raistrick 1993 7 p Presented at the Fall Meeting of the Materials Research Society (MRS), Boston, MA, 29 Nov. - 3 Dec. 1993
(Contract W-7405-eng-36)
(DE94-005093; LA-UR-93-4428; CONF-931108-46) Avail: CASI HC A02/MF A01

Chemical reference tables state that the standard potential for the reaction of Pt with water, Pt + 2H2O yeilds Pt(OH)2 + 2H(+) + 2e(-), is 0.98 V, and electrochemical studies propose that this reaction may occur at potentials as low as 0.8 V. Using dispersive x-ray absorption fine-structure (XAFS) spectroscopy, the authors have directly probed the structural evolution of a Pt catalyst operating in-situ in a polymer electrolyte fuel cell during cyclic voltammetry. The changes in the number of Pt and O nearest-neighbors and the Pt charge demonstrate a close correspondence with features in the voltammogram. Because dispersive XAFS is very sensitive to detecting structural changes, they have been able to detect the presence of chemisorbed oxygen at potentials of 0.6-0.9 V in the anodic sweep. Since double-layer charging is regarded as the only process in this region for bulk Pt, these results may reflect a limitation of previous (indirect) studies on Pt electrochemistry, or they may indicate that these clusters are different from their bulk metal counterparts. Exploiting the time-resolving capability of dispersive XAFS, they also monitored changes in the Pt charge and the number of O and Pt nearest-neighbors during the electrochemical oxidation and reduction of the Pt clusters in real-time. The results are inconsistent with those expected from the place-exchange mechanism for the formation of the surface oxide on bulk Pt electrodes in aqueous solution; Pt(sub red) (k sub 1) yields Pt(submonolayer O) (k sub 2) yields PtO(x) (place exchanged Pt and O atoms: k(sub 1) much greater than k(sub 2)). Their current model for understanding these behaviors is that, relative to bulk Pt, unusual types of surface sites play a major role in determining the reactivity of these clusters. DOE

N94-30108 International Centre for Theoretical Physics, Trieste (Italy).
LOCALIZATION IN PRESENCE OF MAGNETIC FIELD IN 2-D DISORDERED BINARY ALLOYS
A. Brezini and N. Zekri Aug. 1993 14 p Limited Reproducibility: More than 20% of this document may be affected by microfiche quality
(DE94-608093; IC-93/253) Avail: CASI HC A03 (US Sales Only)

The conductance fluctuations in the presence of a magnetic field B for a disordered binary alloy are numerically examined. The Hamiltonian is quite different from the Anderson model. We calculate the participation ration for finite systems in the whole range spectrum to discriminate the nature of eigenstates. We then evaluate the conductivity from the usual Kubo Greenwood formula. The fluctuations are therefore extracted as a function of energy for a given value of B and system size L. The data predict a delocalization of the eigenstates due to the magnetic field and a factor of 2 reduction of the universal conductance fluctuations in agreement with the theory. DOE

N94-30113 Selskapet for Industriell og Teknisk Forskning, Trondheim (Norway). Dept. for Materials Technology.
VOLUME AVERAGED MODEL FOR THE MECHANICS OF ALLOYS SOLIDIFICATION
H. J. Thevik 30 Jun. 1993 40 p Sponsored by Royal Norwegian Council for Scientific and Industrial Research, Oslo, Norway
(PB94-138617; STF28-A93053) Avail: Issuing Activity (National Technical Information Service (NTIS))

A volume averaged mathematical model for macroscopic transport of mass, momentum, energy and species during alloy solidification is established. Details concerning the volume averaging technique are discussed and applied to the one-phase balance and interfacial transfer equations. This yields a macroscopic set of balance equations which constitutes the basis for deriving a simplified model for solidification of a binary alloy in an impermeable two dimensional enclosure. In deriving the equations, constitutive laws, thermodynamic relations, topological, and closure relations are thoroughly discussed. The report concludes with a closed set of transport equations, together with a complete list of the employed simplifications. NTIS

N94-30118 International Centre for Theoretical Physics, Trieste (Italy).
GENERALIZED AUGMENTED SPACE THEOREM FOR CORRELATED DISORDER AND CLUSTER COHERENT POTENTIAL APPROXIMATION
A. Mookerjee and R. Prasad Sep. 1993 15 p Limited Reproducibility: More than 20% of this document may be affected by microfiche quality
(DE94-608110; IC-93/286) Avail: Issuing Activity (Department of Energy (DOE)) (US Sales Only)

We present a method for calculating the electronic structure of disordered alloys with short range order (SRO) which guarantees positive density of states for all values of the SRO parameter. The method is based on the generalized augmented space theorem which is valid for alloys with SRO. This theorem is applied to alloys with SRO in the tight-binding linear muffin-tin orbital (TB-LMTO) framework. This is done by using the augmented space formulation of Mookerjee and cluster coherent potential approximation. As an illustration, the method is applied to a single band mode TB-LMTO Hamiltonian. We find that the SRO can induce substantial changes in the density of states. DOE

N94-30138 British Columbia Univ., Vancouver. Dept. of Metals and Materials Engineering.
PIT INITIATION ON PASSIVATED METAL SURFACES: CRYSTALLOGRAPHIC ORIENTATION AND ENVIRONMENTAL EFFECTS Ph.D. Thesis
Ruijin Guo Sep. 1993 224 p
(ISBN-0-315-85433-2; CTN-94-61159) Copyright Avail: Micromedia Ltd., Technical Information Centre, 240 Catherine Street, Suite 305, Ottawa, Ontario, K2P 2G8, Canada HC/MF

The susceptibility to pitting corrosion of Sn and Zn was found to depend on the crystallographic orientation of the surface in chloride solutions. The critical pitting potentials for Zn and Al were found to be lower in chloride solutions than in bromide solutions. The effects of the solution pH, the presence of buffers, and the halide ion species on the pitting of polycrystalline Ni were investigated in 1-molar halide solutions. It was found that the critical pitting potential (Ecp) was independent of the pH of unbuffered solutions in the 4.5-10.5 pH region. However, Ecp was greatly increased at pH 12.5, and pitting corrosion was totally retarded at pH 14 in 1-molar NaCl solution. Adding Na2CO3/NaHCO3 or Na3PO4/Ha2HPO4 buffer to the pH 10.5 solution raised the critical pitting potential of Ni. Furthermore, Ecp was lower in chloride solution than in bromide solution. Using thermodynamic data for halide complexes, potential-pH and halide concentration /pH diagrams were constructed for H2O- halide- (Sn,Zn,Al,Ni) systems. With increasing halide concentration, the formation of halide complexes is thermodynamically favored and the zone of passivity is diminished. A pitting theory is proposed which emphasizes the change in local solution chemistry and formation of halide complexes during pit initiation. This theory accounts for many effects observed. Author (CISTI)

N94-30146 Manitoba Univ., Winnipeg. Metallurgy Science Lab.
DIRECTIONAL SOLIDIFICATION CHARACTERISTICS OF HYPER-EUTECTIC Al-Cu ALLOYS UNDER VARYING GRAVITY CONDITIONS M.S. Thesis
Hong Yu 1993 191 p
(ISBN-0-315-86108-8; CTN-94-61180) Copyright Avail: Micromedia Ltd., Technical Information Centre, 240 Catherine Street, Suite 305, Ottawa, Ontario, K2P 2G8, Canada HC/MF

A three-zone gradients freeze furnace was specially designed to carry out unidirectional solidification on the ground as well as aboard the space shuttle. The microstructure of Al-Cu alloys was studied and the faceting behavior of the primary Al2Cu theta phase was examined as a function of alloy composition and growth rate. Solidification in microgravity promoted dendrite growth due to lack of convection. The spacings of the primary theta phase and the inter theta phase lamellar eutectic were investigated. It is concluded that the viscous stress due to natural convection disturbs the atoms, not allowing them to incorporate into crystals. Furthermore, the physical motion of nucleation sites due to natural convection may provide more nuclei for growth of theta phase particles. The segregation phenomena of hyper-eutectic Al-Cu alloys was also studied in both vertical and horizontal unidirectional solidification in unit gravity and in microgravity. Lack of convection in microgravity allowed large dendrites to grow, and solidification shrinkage is compensated mostly by deformation of the ingot rather than by interdendritic fluid flow. In ground-based samples, the gravity effect is more pronounced in the case of vertical upwards solidification.
Author (CISTI)

N94-30246# Brookhaven National Lab., Upton, NY.
INCOMMENSURATE MAGNETIC ORDER IN UNi2Al3
J. G. Lussier (McMaster Univ., Hamilton, Ontario.), A. Schroeder (McMaster Univ., Hamilton, Ontario.), B. D. Gaulin (McMaster Univ., Hamilton, Ontario.), J. D. Garrett (McMaster Univ., Hamilton, Ontario.), W. J. L. Buyers (Atomic Energy of Canada Ltd., Chalk River, Ontario.), L. Rebelsky, and S. M. Shapiro 1993 5 p Presented at the International Conference on Strongly Correlated Electron Systems, La Jolla, CA, 16-19 Aug. 1993
(Contract DE-AC02-76CH-00016)
(DE94-005449; BNL-49720; CONF-930865-12) Avail: CASI HC A01/MF A01

Elastic neutron scattering measurements performed on single crystal UNi2Al3 show this heavy fermion superconductor to display long-range incommensurate (IC) magnetic order below T(sub N) = 5.2K. The ordering wavevector is (1/2 (+/-) (tau),0,1/2) with (tau) = 0.110 (+/-) 0.003, and the size of the maximum ordered moment is 0.24 (+/-) 0.1(mu)(sub B)/U.
DOE

N94-30253 Academy of Sciences (USSR), Novosibirsk. Inst. Yadernoj Fiziki.
COMPUTER SIMULATION OF THE INTERACTION OF FAST HYDROGEN ATOMS WITH A MOLYBDENUM CONTAINING SORBED HYDROGEN
A. S. Kupriyanov 1992 36 p Limited Reproducibility: More than 20% of this document may be affected by microfiche quality
(DE94-608419; IYaF-92-23) Avail: CASI HC A03 (US Sales Only)

The general principles of computer program MODA have been described allowing Monte Carlo simulation of an atom-solid interaction for incident energies from 50 eV to 10 keV. It is shown that special selection of some model parameters using experimental data permits the simulation of primary particles, sputtering of metal, and a desorption of adsorbed layers on surfaces. Also report are calculation data of hydrogen reflection and sputtering at an interaction of hydrogen atoms at initial energies from 50 to 500 eV with polycrystalline and amorphous molybdenum, containing adsorbed and penetrated hydrogen.
DOE

N94-30336# Ames Lab., IA.
STUDIES OF HIGH TEMPERATURE TERNARY PHASES IN MIXED-METAL-RICH EARLY TRANSITION METAL SULFIDE AND PHOSPHIDE SYSTEMS Ph.D. Thesis
G. A. Marking Jan. 1994 239 p
(Contract W-7405-eng-82)
(DE94-006034; IS-T-1646) Avail: CASI HC A11/MF A03

Investigations of ternary mixed early transition metal-rich sulfide and phosphide systems resulted in the discovery of new structures and new phases. A new series of Zr and Hf--group V transition metal--sulfur kappa-phases was synthesized and crystallographically characterized. When the group V transition metal was Nb or Ta, the unit cell volume was larger than any previously reported kappa-phase. The presence of adventitious oxygen was determined in two kappa-phases through a combination of neutron scattering and X-ray diffraction experiments. A compound Hf10Ta3S3 was found to crystallize in a new-structure type similar to the known gamma brasses. This structure is unique in that it is the only reported 'stuffed' gamma-brass type structure. The metal components, Hf and Ta, are larger in size and more electropositive than the metals found in normal gamma brasses (e.g. Cu and Zn) and because of the larger metallic radii, sulfur can be incorporated into the structure where it plays an integral role in stabilizing this phase relative to others. X-ray single-crystal, X-ray powder, and neutron powder refinements were performed on this structure. A new structure was found in the ternary Nb-Zr-P system which has characteristics in common with many known early transition metal-rich sulfides, selenides, and phosphides. This structure has the simplest known interconnection of the basic building blocks known for this structural class. Anomalous scattering was a powerful tool for differentiating between Zr and Nb when using Mo K(alpha) X-radiation. The compounds ZrNbP and HfNbP formed in the space group Prima with the simple Co2Si structure which is among the most common structures found for crystalline solid materials. Solid solution compounds in the Ta-Nb-P, Ta-Zr-P, Nb-Zr-P, Hf-Nb-P, and Hf-Zr-S systems were crystallographically characterized. The structural information corroborated ideas about bonding in metal-rich compounds.
DOE

N94-30521 Johns Hopkins Univ., Baltimore, MD.
AN INVESTIGATION OF THE CORROSION PROPERTIES OF ALUMINUM-TANTALUM ALLOYS USING ELECTROCHEMICAL IMPEDANCE SPECTROSCOPY AND LOCAL ELECTROCHEMICAL IMPEDANCE SPECTROSCOPY Ph.D. Thesis
Robert Scott Lillard 1993 119 p
Avail: Univ. Microfilms Order No. DA9313391

An investigation of passivity of single phase Al-Ta alloys and the contribution of the second phase, Al3Ta, to breakdown is presented. In 0.1M NaCl buffered to pH 7 with boric acid and sodium borate the passive current density of pure aluminum was found to be approximately 0.3 microamps/cm(exp 2), the passive current densities of Al 4 at percent Ta, Al 8 at percent Ta were found to be 2.5 and 2.4 microamps/cm(exp 2) respectively while the pitting potentials of these alloys were approximately 500 mV greater than that of pure aluminum. Traditional EIS measurements in 0.5M boric acid 0.05M sodium borate solution found the impedance values of the Al-4Ta and Al-8Ta were found to be 5.6 x 10(exp 4) and 3.1 x 10(exp 4) ohm cm(exp 2) respectively while that of pure aluminum was found to be about 1.2 x 10(exp 5) ohm cm(exp 2). In addition, the thickness of the oxide film on the alloys to be less than that of pure aluminum in all solutions examined. Similar results were obtained for chloride containing solutions. These results indicate that there is no correlation between passive current density and the breakdown potential; that is the passive current density and the breakdown potential are two unrelated phenomena. The results of Local Electrochemical Impedance Spectroscopy (LEIS) experiments on a heat treated Al 1.5 at percent Ta alloy, which contained Al3Ta precipitates, revealed that the capacitance of the film over the precipitate is higher than the capacitance of the film over the aluminum portion of this electrode. This indicates that thickness of the film over the precipitate is thinner than the film over aluminum. This interface, between the oxide over the Al3Ta precipitates and the oxide over the aluminum matrix, is perceived as being incoherent and is interpreted here as a 'residual flaw', as described by the crack/heal mechanism proposed by Wood et al.
Dissert. Abstr.

N94-30690# Iowa State Univ. of Science and Technology, Ames. Ames Lab.
TERFENOL: A STUDY OF THE PHASE EQUILIBRIUM DIAGRAM AND THE SOLIDIFICATION PROCESS Ph.D. Thesis
M. Anderson Dec. 1993 63 p
(Contract W-7405-eng-82)
(DE94-004883; IS-T-1688) Avail: CASI HC A04/MF A01

Terfenol is a rare earth-iron alloy that was first developed at the Naval Ordnance Laboratory because of its rare magnetostrictive properties. Terfenol is composed of terbium and dysprosium combined with iron in a composition Tb(sub x)Dy(sub 1-x)Fe2, where x is approximately 0.3. The

objective of this work was to determine the growth characteristics of Terfenol and its dependence on solidification rate, temperature gradient, and stoichiometry. Specific goals of this work were to verify the phase equilibria that is currently accepted for the systems DyFe2 and TbFe2, and establish the phase equilibria near the composition Tb(sub 0.3)Dy(sub 0.7)Fe2; establish that Terfenol grows directly from the liquid and that the reaction is occurring under metastable conditions; evaluate whether or not Terfenol can be grown under plane front conditions with a new radiofrequency float zone apparatus; and determine whether or not (111) seeded crystals can be grown and (111) single crystals produced by elimination of dendrites employing growth methods capable of achieving high gradient/solidification rate ratios. DOE

N94-30710# California Univ., Berkeley. Lawrence Berkeley Lab.
MICROSTRUCTURAL DEVELOPMENT AND MECHANICAL BEHAVIOR OF EUTECTIC BISMUTH-TIN AND EUTECTIC INDIUM-TIN IN RESPONSE TO HIGH TEMPERATURE DEFORMATION Ph.D. Thesis
J. L. F. Goldstein Nov. 1993 105 p
(Contract DE-AC03-76SF-00098)
(DE94-005202; LBL-34909) Avail: CASI HC A06/MF A02

The mechanical behavior and microstructure of eutectic Bi-Sn and In-Sn solders were studied in parallel in order to better understand high temperature deformation of these alloys. Bi-Sn solder joints were made with Cu substrates, and In-Sn joints were made with either Cu or Ni substrates. The as-cast microstructure of Bi-Sn is complex regular, with the two eutectic phases interconnected in complicated patterns. The as-cast microstructure of In-Sn depends on the substrate. In-Sn on Cu has a nonuniform microstructure caused by diffusion of Cu into the solder during sample preparation, with regions of the Sn-rich (gamma) phase imbedded in a matrix of the In-rich (beta) phase. The microstructure of In-Sn on Ni is uniform and lamellar and the two phases are strongly coupled. The solders deform nonuniformly, with deformation concentrating in a band along the length of the sample for Bi-Sn and In-Sn on Cu, though the deformation is more diffuse in In-Sn than in Bi-Sn. Deformation of In-Sn on Ni spreads throughout the width of the joint. The different deformation patterns affect the shape of the stress-strain curves. Stress-strain curves for Bi-Sn and In-Sn on Cu exhibit sharp decays in the engineering stress after reaching a peak. Most of this stress decay is removed for In-Sn on Ni. The creep behavior of In-Sn also depends on the substrate, with the creep deformation controlled by the soft P phase of the eutectic for In-Sn on Cu and controlled by the harder (gamma) phase for In-Sn on Ni. When In-Sn on Ni samples are aged, the microstructure coarsens and changes to an array of (gamma) phase regions in a matrix of the (beta) phase, and the creep behavior changes to resemble that of In-Sn on Cu. The creep behavior of Bi-Sn changes with temperature. Two independent mechanisms operate at lower temperatures, but there is still some question as to whether one or both of these, or a third mechanism, operates at higher temperatures. DOE

N94-30774# Los Alamos National Lab., NM.
INFLUENCE OF TUNGSTEN ALLOYING ADDITIONS ON THE MECHANICAL PROPERTIES AND TEXTURE OF TANTALUM
G. T. Gray, III, S. R. Bingert, S. I. Wright, and S. R. Chen 1993 7 p Presented at the Fall Meeting of the Materials Research Society (MRS), Boston, MA, 29 Nov. - 3 Dec. 1993
(Contract W-7405-eng-36)
(DE94-004994; LA-UR-93-4231; CONF-931108-32) Avail: CASI HC A02/MF A01

Tantalum, like all bcc metals exhibits deformation behavior substantially influenced by alloying, temperature, and strain rate. Recently, the mechanical response, in particular the high-strain-rate response, of tantalum and tantalum alloys has received increased interest for ballistic applications. In this paper, recent results on the influence of tungsten alloying additions on the mechanical response and starting crystallographic texture of tantalum-tungsten alloys are presented. The stress-strain behavior of three tantalum alloys containing 2.5, 5, and 10 wt. % W has been investigated as a function of loading path, tension and compression, and strain rate, 10(exp -3) to 8000 s(exp -1). The yield strength and work-hardening rate were found to increase with increasing tungsten alloying content compared to unalloyed Ta. Based on measurements of the surface and centerline textures of the Ta-W alloys, no systematic effect of tungsten content on texture was documented. However, due to variations in mechanical behavior between through-thickness and in-plane properties, a need for complete through-thickness texture measurements is indicated. DOE

N94-30776 Los Alamos National Lab., NM.
NATURE OF DISSOLUTION OF BINARY TANTALUM-TITANIUM ALLOYS BY MOLTEN PLUTONIUM
J. D. Cotton, K. M. Axler, P. C. Lopez, J. H. Steele, and J. I. Archuleta 1994 13 p Presented at the International Symposium on Actinides: Processing and Materials, San Francisco, CA, 27 Feb. - 3 Mar. 1994 Limited Reproducibility: More than 20% of this document may be affected by microfiche quality
(Contract W-7405-eng-36)
(DE94-005090; LA-UR-93-4436; CONF-940215-3) Avail: Issuing Activity (Department of Energy (DOE))

Tantalum hardware has often been used for processing molten Pu where ceramics are inappropriate. However, there has only been limited work on the containment of Pu by Ta alloys. In this regard, we have investigated the interaction of Ta-Ti alloys (20, 40, and 60 wt.% Ti) with molten Pu at 850 and 1000 C. Microstructures of Pu/alloy interfaces were characterized chemically and metallographically following various exposures to liquid Pu. Dissolution does not proceed uniformly, but appears to initiate by intergranular attack to a shallow depth and then progress by the formation of a stable mushy zone at the liquid/solid interface. Resistance to dissolution by molten Pu increases with Ta content. DOE

N94-30777# Sandia National Labs., Albuquerque, NM.
A COMPARISON OF THE EVOLUTION OF COLD AND HOT DEFORMATION MICROSTRUCTURES AND TEXTURES IN FCC METALS
D. A. Hughes and N. Hansen 1993 18 p Presented at the TMS Symposium on Advances in Hot Deformation Textures and Microstructures, Pittsburgh, PA, 22 Oct. 1993
(Contract DE-AC04-76DR-00789)
(DE94-005103; SAND-94-8487C; CONF-9310260-1) Avail: CASI HC A03/MF A01

Microstructures and textures which develop during cold deformation are compared to those which develop during hot deformation. This comparison is made using the evolutionary framework of grain subdivision and the formation of low energy dislocation structures. During deformation grains are subdivided into differently deforming regions separated by geometrically necessary dislocation boundaries. These boundaries include dense dislocation walls, microbands, lamellar boundaries, and subgrains. Grain subdivision occurs as a result of the requirement for strain accommodation balanced by energy considerations. This grain subdivision weakens the texture and increases the texture scatter. The tendency for grain subdivision decreases with increasing temperature of deformation with implications for the microstructural evolution and the texture formation. DOE

N94-30796 National Physical Lab., Teddington (England). Materials Metrology Div.
METHOD OF TEST FOR CLEANNESS ASSESSMENT OF METAL ALLOYS: THE PREPARATION OF BUTTON SPECIMENS BY ELECTRON BEAM MELTING AND THE CHARACTERISATION OF RECOVERED INCLUSIONS
P. N. Quested and D. M. Hayes Nov. 1993 28 p Sponsored by Dept. of Trade and Industry
(ISSN 0959-2423)
(NPL-DMM(A)-130; ETN-94-95855) Copyright Avail: Issuing Activity (National Physical Lab., Teddington, Middlesex TW11 0LW, England)

A method for the cleanness assessment of metal alloys in which a metal specimen is electron beam melted into a copper crucible to collect the nonmetallic inclusions present on the specimen into a small area in the top surface of the cast sample known as a button is described. Methods for the examination of the collected inclusions to assess the cleanness of the specimen material with respect to the number, size shape, and approximate composition of the inclusions are also described. ESA

N94-30839# Pittsburgh Univ., PA.
STUDIES OF SUPPORTED MOLYBDENUM AND TUNGSTEN
1993 10 p
(Contract DE-FG02-87ER-13781)
(DE94-006207; DOE/ER-13781/7) Avail: CASI HC A02/MF A01

Work on Mo oxidation state-catalytic activity relations has centered around measuring the distribution of Mo oxidation states on reduced Mo/alumina and Mo/titania catalysts, and correlating catalyst activity with Mo oxidation states. Factor analysis has been developed as a protocol for measuring Mo oxidation state distributions on reduced catalysts. Papers published and submitted are discussed. DOE

N94-30852# Oak Ridge National Lab., TN.
STUDY OF NUCLEATION AND GROWTH IN Al-Zn ALLOYS USING TEM
G. Sundar (Washington State Univ., Pullman.), J. J. Hoyt (Washington State Univ., Pullman.), E. A. Kenik, and S. Spooner 1993 6 p Presented at the Fall Meeting of the Materials Research Society (MRS), Boston, MA, 29 Nov. - 3 Dec. 1993
(Contracts DE-AC05-84OR-21400; DE-AC05-76OR-00033)
(DE94-006312; CONF-931108-75) Avail: CASI HC A02/MF A01

Nucleation and growth studies were conducted on Al-Zn alloys at several temperatures using transmission electron microscopy (TEM) with an in-situ furnace. The value of the critical undercooling was established by noting the lowest temperature at which precipitates were no longer observed, following a quench into the two-phase metastable region. These results were compared with the Langer-Schwartz model of nucleation and growth in which it is predicted that the half-completion time (i.e, the time required for the supersaturation to reach half its initial value) diverges for initial supersaturations which are higher than those predicted by the classical nucleation theory. DOE

N94-30892# Lawrence Livermore National Lab., CA.
APPLICATION OF ALE TECHNIQUES TO METAL FORMING SIMULATIONS
R. Couch, R. Sharp, I. Otero, R. Tipton, and R. McCallen 11 Aug. 1993 8 p Presented at the Annual Winter Meeting of the American Society of Mechanical Engineers, New Orleans, LA, 28 Nov. - 3 Dec. 1993
(Contract W-7405-eng-48)
(DE94-005358; UCRL-JC-114851; CONF-931121-36) Avail: CASI HC A02/MF A01

The utility of the arbitrary Lagrangian-Eulerian (ALE) code format is evaluated in the context of use in simulating metal forming processes. Emphasis is on large deformation processes such as casting, forging and extrusion. The basic point at issue is whether the continual remapping capability inherent in the ALE approach can provide advantages relative to the more standard approach of using a Lagrangian mesh but allowing for isolated remeshing as required. A particular ALE implementation, ALE3D, is used as the basis for the discussion. Pros and cons for this approach are presented along with illustrations of its application to actual forming problems. DOE

N94-29516# National Inst. for Resources and Environment, Ibaraki (Japan). Siliceous Materials Div.
STUDY ON THE FORMATION OF ULTRAFINE PARTICLES OF Sm-Co INTERMETALLIC COMPOUNDS USING RF THERMAL PLASMA [RF NETSU PURAZUMA NI YORU SM-CO KINKOKUKAN KAGOBUTSU CHOBIRYUSHI GOSEI NO KENKYU]
Nobuyuki Kikukawa, Masami Sugasawa, Mikio Kobayashi, Masakazu Nakamura, and Hiroshi Sakamoto *In its* Journal of NIRE, Vol. 2, No. 3 25 May 1993 p 31-46 In JAPANESE (For primary document see N94-29512 08-99)
Avail: CASI HC A03/MF A02

N94-29644*# Hughes Space and Communications Group, El Segundo, CA.
LOW MELTING TEMPERATURE ALLOY DEPLOYMENT MECHANISM AND RECENT EXPERIMENTS
M. J. Madden *In* NASA. Ames Research Center, The 27th Aerospace Mechanisms Symposium May 1993 p 255-266 (For primary document see N94-29627 08-15)
Avail: CASI HC A03/MF A03

N94-30446*# Metafuse Corp., Los Angeles, CA.
METAFUSION: A BREAKTHROUGH IN METALLURGY
Adrian A. Joseph *In* NASA, Washington, Technology 2003: The Fourth National Technology Transfer Conference and Exposition, Volume 1 Feb. 1994 p 60-63 (For primary document see N94-30440 08-99)
Avail: CASI HC A01/MF A04

27 NONMETALLIC MATERIALS

Includes physical, chemical, and mechanical properties of plastics, elastomers, lubricants, polymers, textiles, adhesives, and ceramic materials.

For composite materials see *24 Composite Materials*.

N94-28457# Illinois Univ., Urbana.
MOLECULAR ASPECTS OF TRANSPORT IN THIN FILMS OF CONTROLLED ARCHITECTURE
1993 12 p
(Contract DE-FG02-88ER-13949)
(DE94-004552; DOE/ER-13949/5) Avail: CASI HC A03/MF A01

Work has progressed in two principal areas during the past year: diffusion in swollen polymer films with and without a barrier layer, and molecular aspects of swelling using enhanced Raman spectroscopy. DOE

N94-28516# Ames Lab., IA.
CHEMICALLY MODIFIED POLYMERIC RESINS FOR SEPARATION OF CATIONS, ORGANIC ACIDS, AND SMALL POLAR MOLECULES BY HIGH PERFORMANCE LIQUID CHROMATOGRAPHY Ph.D. Thesis
J. B. Morris Jul. 1993 181 p
(Contract W-7405-eng-82)
(DE94-005548; IS-T-1667) Avail: CASI HC A09/MF A02

This thesis is divided into 4 parts: a review, ion chromatography of metal cations on carboxylic resins, separation of hydrophilic organic acids and small polar compounds on macroporous resin columns, and use of eluent modifiers for liquid chromatographic separation of carboxylic acids using conductivity detection. DOE

N94-28530# Ames Lab., IA.
GEOMETRIC STRUCTURES OF THIN FILM: Pt ON Pd(110) AND NiO ON Ni(100) Ph.D. Thesis
O. L. Warren Jul. 1993 153 p
(Contract W-7405-eng-82)
(DE94-005564; IS-T-1660) Avail: CASI HC A08/MF A02

This thesis is divided into 3 papers: dynamical low-energy electron-diffraction investigation of lateral displacements in topmost layer of Pd(110); determination of (1 x 1) and (1 x 2) structures of Pt thin films on Pd(110) by dynamical low-energy electron-diffraction analysis; and structural determination of a NiO(111) film on Ni(100) by dynamical low-energy electron-diffraction analysis. DOE

N94-28536# Argonne National Lab., IL.
PULL-TEST ADHESION MEASUREMENTS OF DIAMONDLIKE CARBON FILMS ON SILICON CARBIDE, SILICON NITRIDE, ALUMINUM OXIDE, AND ZIRCONIUM OXIDE
R. A. Erck, F. A. Nichols, and J. F. Dierks Oct. 1993 20 p Presented at the 40th National Symposium of the American Vacuum Society, Orlando, FL, 15-19 Nov. 1993
(Contract W-31-109-eng-38)
(DE94-005469; ANL/ET/CP-81579; CONF-9311104-17) Avail: CASI HC A03/MF A01

Hydrogenated amorphous carbon films or diamondlike carbon (DLC) films were formed by ion-beam deposition of 400 eV methane (CH4) ions on several smooth and rough ceramics, as well as on ceramics coated with a layer of Si and Ti. Adhesion was measured by the pin-pull method. Excellent adhesion was measured for smooth SiC and Si3N4, but the adhesion of DLC to Al2O3 and ZrO2 was negligible. The use of a Si bonding interlayer produced good adhesion to all the substrates, but a Ti layer was ineffective because bonding between the DLC film and Ti was poor. The presence of surface roughness appeared to greatly increase the measured adhesion in all cases. Bulk thermodynamic calculations are not directly applicable to bonding at the interface. If the standard enthalpy of formation for reaction between CH4 and substrate is calculated assumpting a carbide or carbon phase is produced, a relation is seen between reaction enthalpy and relative adhesion. Large positive enthalpies are associated with poor adhesion; negative or small positive enthalpies are associated

with good adhesion. This relation between enthalpy and adhesion was also observed for DLC deposited on Si. Lack of adhesion to Ti was attributed to inadvertent formation of a surface oxide layer that rendered the enthalpy for reaction with CH4 strongly positive and similar in magnitude to that for Al2O3 and ZrO2. DOE

N94-28539# Technische Univ., Eindhoven (Netherlands).
ADHESION OF ELECTROLESSLY DEPOSITED Ni(P) ON ALUMINA CERAMIC Ph.D. Thesis
Jan Willem Severin 1993 216 p Prepared in cooperation with Philips Gloielampenfabrieken N.V., Eindhoven, Netherlands
(ETN-94-95358) Avail: CASI HC A10/MF A03

The adhesion of electroless Ni(P) to alumina is addressed. Attention is paid to the procedures and techniques used to study the adhesion, the adhesion strengths obtained and the models proposed to explain the adhesion. The formation of the interface between Ni(P) and alumina is studied. The changes in structure and chemical composition of the substrate surface is analyzed after each successive process step. The adhesion is measured with peel tests and direct pull off tests. Quantitative aspects of both adhesion measurement procedures are highlighted. A fracture mechanics approach is followed for the interpretation of the adhesion measurement results. The metal-ceramic interface and the fracture surfaces are analyzed both on micrometer and on nanometer scale in order to find a relation between the measured adhesion and interface chemistry. The influence of thermal treatments upon the adhesion strength is investigated. Special attention is paid to a distinction between changes in bulk mechanical properties in the metal film and intrinsic adhesion. The influence of substrate surface chemistry upon the adhesion is investigated. Thin metal oxide layers are deposited on the ceramic surfaces. These metal oxide surfaces are metallized and the adhesion and interface chemistry are characterized. Differences in adhesion are tentatively explained in terms of surface chemistry and microroughness. A completely different procedure is followed to apply the Pd catalyst, required to start the electroless deposition process. Pd layers are evaporated instead of the usual wet chemical procedure. A thin titanium layer is applied for improving the adhesion of the Pd nucleation layer on the substrate. The adhesion and the fracture path are determined and a detailed analysis is made of the bonding at the metal-ceramic interface within the first metal monolayers. ESA

N94-28550# Universidad Nacional Autonoma de Mexico, Mexico City.
ELECTRODEPOSITION OF BISMUTH ALLOYS BY THE CONTROLLED POTENTIAL METHOD Ph.D. Thesis
Lopez F. J. Alvarez 1993 129 p
(DE94-605318; INIS-mf-13725) Avail: CASI HC A07/MF A02 (US Sales Only)

We worked with the electrodeposition of three bismuth alloys, the composition of the first electrolyte was: 0.3 g/l Bi; 20 g/l Ni; and the conditions were pH = 5.2 - 5.6; T = 25 Centigrade degrees; current density 0.3 A / dm(sup 2) - 6.6 A / dm(sup 2). Following alloy was between Bi - Pb, composition of the electrolyte was 3.18 g/l Bi (metallic); 31.81 g/l Pb (Pb(NO3)2) pH : 1; T = 20 Centigrade degrees; current density 10.20 A/dm(sup 2) . The third electrolyte was Bi-Cu, its composition was: 20.89 g/l Bi; (metallic) 63.54 g/l Cu (Cu(NO3)2) pH : 1.5 - 1.8; T = 25-30 Centigrade degrees; current density 1-2 A/dm(sup 2) . The best results were obtained with the third electrolyte. The purpose of this work was to experiment with different parameters like temperature, pH and the electrolyte concentration to obtain a bismuth alloy. DOE

N94-28560# Lawrence Livermore National Lab., CA.
HIGH DAMAGE THRESHOLD ANTI-REFLECTORS BY PHYSICAL VAPOR DEPOSITED AMORPHOUS FLUOROPOLYMER
R. Chow, M. K. Spragge, G. E. Loomis, I. M. Thomas, F. Rainer, R. L. Ward, and M. R. Kozlowski Nov. 1993 13 p Presented at the 25th Boulder Damage Symposium: Annual Symposium on Optical Materials for High-Power Lasers, Boulder, CO, 27-29 Oct. 1993
(Contract W-7405-eng-48)
(DE94-004865; UCRL-JC-114841; CONF-931054-2) Avail: CASI HC A03/MF A01

High laser-resistant anti-reflective coatings were made from an amorphous fluoropolymer (Teflon AF2400) material by physical vapor deposition. Single layers of Teflon AF2400 were thermally deposited in a vacuum chamber. Refractive index and adhesion of the coatings were determined as a function of deposition rate (2 to 20 (Angstrom)/s), substrate temperature (20 to 200C), and glow-discharge bias potential (-1500 to 1500 V). An anti-reflective coating of an amorphous fluoropolymer (Teflon AF2400) had a laser resistance of greater than 47 J/cm(exp 2) (1.06 (mu)m, 3-ns pulselength) and is transparent from 200 nm to 1600 nm. The majority of the coatings had a 1.30 refractive index, similar to that of the bulk material. Scanning electron microscopy and preliminary nuclear magnetic resonance observations indicated that morphological changes caused the variations in the refractive index rather than compositional changes. The coatings adhered to fused silica and silicon wafers under normal laboratory handling conditions. Scotch tape with 12.6 gr/mm tension was sufficient to pull off every coating from fused silica substrates. DOE

N94-28641# Naval Command, Control and Ocean Surveillance Center, San Diego, CA. Research, Development, Test and Evaluation Div.
ALUMINA CERAMIC: A COST EFFECTIVE REPLACEMENT FOR TITANIUM IN DEEP SUBMERGENCE PRESSURE HOUSINGS Final Report
Jerry D. Stachiw Sep. 1993 18 p
(AD-A275640; NCCOSC/RDT/E-TD-2582) Avail: CASI HC A03/MF A01

Alumina ceramic's high compressive strength and modulus of elasticity, coupled with its low density, make it feasible to routinely fabricate cylindrical pressure housings with 0.5 weight/displacement ratios for 20,000 ft (6100 m) service. This compares favorably to optimally designed titanium cylindrical housings with 0.86 weight/displacement ratio. This presentation, by J.D. Stachiw, describes past experiences with glass and ceramic pressure housings and presents NCCOSC ceramic housing program objectives, approach, findings, and applications. DTIC

N94-28661# Massachusetts Univ., Amherst. Dept. of Polymer Science and Engineering.
CELLULAR AND MOLECULAR APPROACHES TO POLYMER SYNTHESIS BY BACTERIA Final Report, 1 Jul. 1986 - 28 Feb. 1993
Robert W. Lenz and R. C. Fuller 28 Feb. 1993 6 p
(Contract N00014-90-J-1531)
(AD-A275501) Avail: CASI HC A02/MF A01

A multidisciplinary study of the biosynthesis, regulation, and materials properties of microbial poly beta hydroxy alkanoates (PHA's) was performed. Three principal areas were investigated: the production of new PHA's, the structure and function of proteins associated with the PHA inclusion bodies in the cells, and the enzymatic degradation of PHA's. Derived from text

N94-28725 Ibis Associates, Inc., Wellesley, MA.
ANALYSIS OF COST: CVD DIAMOND DEPOSITION AND FINISHING Quarterly Report No. 2
1993 46 p Limited Reproducibility: More than 20% of this document may be affected by microfiche quality
(Contract N00014-93-C-2044)
(AD-A275586) Avail: CASI HC A03

This report describes several methods for polishing CVD diamond films, which can be applied separately or in conjunction with each other. From industry interviews, IBIS determined that the required surface roughness for the subsequent metallization operation is on the order of 0.1 microns, and polishing operations must be chosen to meet this specification while maximizing material removal rates. According to the experts surveyed, conventional abrasive lapping still remains the prevalent technology for polishing CVD diamond films, although Hot Iron Polishing, Reactive Plasma, and Ion Milling approaches have been considered. The IBIS Technical Cost Model, therefore, assumes only abrasive lapping as the finishing operation, but allows exploration into other technologies. In general, the polishing rate attained with each technology depends greatly on the quality of the deposited diamond films, as measured by the original flatness and surface roughness. The chemical state of the diamond films, with respect to amorphous carbon content and doping levels, can also influence the polishing rate significantly. DTIC

N94-28733# Lawrence Livermore National Lab., CA.
SUPERPLASTICITY IN FINE-GRAINED CERAMICS Final Report, 1 Jul. - 31 Dec. 1993
T. G. Nieh 31 Jan. 1994 42 p

(Contract MIPR-ARO-131-93)
(AD-A275461; UCRL-CR-116116; ARO-31207.1-MS) Avail: CASI HC A03/MF A01

The superplastic deformation behavior of fine-grained, 20% alumina/yttria-stabilized tetragonal zirconia (20%Al2O3NTZP) under conditions of biaxial gas-pressure deformation is described. Sheet specimens were deformed into hemispherical caps at temperatures ranging from 1450 C - 1600 C and at imposed gas pressures of 345 and 690 KPa. For the conditions examined, hemispherical caps were formed at times ranging from 1000 s to 2.1 x 104 s. The correlation between data obtained in uniaxial tensile testing and the behavior observed during the biaxial deformation experiments is discussed. The high-temperature deformation behavior of a SiC whisker-reinforced, yttria-stabilized, tetragonal zirconia polycrystalline composite containing 20 vol % SiC whiskers (SiC/Y-TZP) has also been investigated. Tensile tests were performed in vacuum at temperatures from 1450 C to 1650 C and at strain rates from 10(exp -3) to 10(exp -5) s(exp -1). The material exhibits useful high temperature engineering properties (e.g., approx. 100 MPa and 16% elongation at T = 1550 C and at a strain rate of 10(exp -4) s(exp -1)). The stress exponent was determined to be n=2. Scanning electron microscopy was used to characterize the grain size and morphology of the composites, both before and after deformation. Both dynamic and static grain growth were observed during deformation. The morphology of ceramic reinforcements appears to affect strongly the plastic deformation properties of Y-TZP. A comparison is made between the properties of monolithic Y-TZP, 20 wt.% Al2O3 particulate-reinforced Y-TZP (Al2O3/Y-TZP), and SiCN-TZP composites. Superplasticity deformation processing of ceramics has also been performed. DTIC

N94-28748*# Old Dominion Univ., Norfolk, VA. Dept. of Civil Engineering.
POLYMER INFILTRATION STUDIES Progress Report, 1 Jun. 1993 - 31 Mar. 1994
Joseph M. Marchello Apr. 1994 9 p
(Grant NAG1-1067)
(NASA-CR-195729; NAS 1.26:195729) Avail: CASI HC A02/MF A01

During the past three months, significant progress has been made on the preparation of carbon fiber composites using advanced polymer resins. The results are set forth in recent reports and publications, and will be presented at forthcoming national and international meetings. Current and ongoing research activities reported herein include: textile composites from powder-coated towpreg - role of surface coating in braiding; prepregger hot sled operation in making tape from powder coated tow; ribbonizing powder-impregnated towpreg; textile composites from powder-coated towpreg - role of bulk factor in consolidation; powder curtain prepreg process improvements in doctoring of powder; and hot/cold shoe for ATP open-section part warpage control. Author (revised)

N94-28795 National Physical Lab., Teddington (England). Div. of Electrical Science.
TEMPERATURE DEPENCENCE OF THE FAR INFRARED OPTICAL CONSTANTS OF POLYETHYLENE
J. R. Birch and K. F. Ping 1993 34 p
(PB94-124336; NPL-DES-128) Copyright Avail: Issuing Activity (National Technical Information Service (NTIS))

The optical constants of low density polyethylene in the spectral region from 30 to 120 /cm have been determined at a number of temperatures by the technique of dispersive Fourier transform spectroscopy (DFTS). The temperatures ranged from 6 to 293 K. The results of these studies are presented in both graphical and tabular form. NTIS

N94-28806# New Hampshire Univ., Durham. Dept. of Chemical Engineering.
CORROSION INHIBITION BY ELECTRODEPOSITED CONDUCTIVE-POLYMER FILM Final Report, 15 Aug. 1989 - 30 Jun. 1993
Dale P. Barkey 30 Oct. 1993 9 p
(Contract DAAL03-89-K-0138)
(AD-A275456; ARO-26449.4-MS) Avail: CASI HC A02/MF A01

Conductive polymer coatings were deposited on steel and titanium substrates by electrooxidative polymerization of poly(3-methylthiophene). The properties of the polymer coatings in acidic, basic and chloride containing solutions were evaluated by electroanalytical means, and the effectiveness of the coatings in providing anodic protection of the substrate were evaluated. The polymer contains a reversible couple with an equilibrium potential near 0.4V positive of Ag/AgCl sat'd KCl. It is effective in passivating 430 stainless steel and titanium in sulfuric acid solution at temperatures below 50 C. Excursions of potential negative of -0.3V result in irreversible reduction of the polymer to a nonconductive state. The polymer is also rendered permanently inactive by basic solutions and by chloride. DTIC

N94-28886# New Mexico Univ., Albuquerque. Center for High Technology Materials.
FLOAT POLISHING STUDIES OF FUSED SILICA Final Report, 1 Feb. 1990 - 30 Sep. 1993
K. C. Jungling and C. F. Kranenberg 22 Nov. 1993 44 p
(Grant AF-AFOSR-0145-90)
(AD-A275001; AFOSR-94-0020TR) Avail: CASI HC A03/MF A01

This final report covers all of the efforts and results during the awarded contract period. The format is generally a chronological account of events; however, several projects were performed concurrently. These simultaneous projects are discussed separately rather than chronologically to avoid confusion. An account of the first experiments and results are addressed. The efforts and results from an extensive fused silica grinding and polishing study is given. The bulk of the research performed during the contract period was devoted to the fabrication of optical quality fused silica flats. The results of the optical fabrication of other materials, such as potassium deuterium phosphate (KD*P) and crystalline quartz, are discussed. A list of publications and conference presentations associated with this effort is provided. Derived from text

N94-28922*# National Aeronautics and Space Administration. Lewis Research Center, Cleveland, OH.
SURFACE ENERGY CHANGES PRODUCED BY ULTRAVIOLET-OZONE IRRADIATION OF POLY(METHYLMETHACRYLATE), POLYCARBONE AND POLYTETRAFLUOROETHYLENE
A. B. Ponter (University of Southwestern Louisiana, Lafayette.), W. R. Jones, Jr., and R. H. Jansen Jan. 1994 11 p
(RTOP 505-63-5A)
(NASA-TM-106460; E-7806-1; NAS 1.15:106460) Avail: CASI HC A03/MF A01

Contact angles of water and methylene iodide were measured as a function of UV/O3 treatment time for three polymers: poly(methylmethacrylate) (PMMA), polycarbonate, and polytetrafluoroethylene (PTFE). Surface roughnesses were also measured. Surface free energies were then calculated using relationships developed by Kaelble and Neumann. The surface energy of polycarbonate was found to increase (60 percent) during UV/O3 treatment. However, calculations on PMMA were hampered by the formation of a water soluble surface product. On PTFE surfaces, the UV/O3 treatment etched the surface causing large increases in surface roughness, rendering contact angle measurements impossible. It is concluded that care must be taken in interpreting contact angle measurements and surface energy calculations on UV/O3 treated polymer surfaces. Author (revised)

N94-29031 Helsinki Univ. of Technology, Espoo (Finland). Kemian Tekniikan Laitos.
POLYMER TECHNOLOGY SEMINAR, 1993. KEM-100.600 [KEM-100.600. POLYMEERITEKNOLOGIAN SEMINAARI.]
1993 209 p In FINNISH Seminar was held
(PB94-137593; ISBN-951-22-1707-4) Avail: Issuing Activity (National Technical Information Service (NTIS))

The document contains the papers presented at the Polymer Technology Seminar 1993. Topics include: Copolymerization of ethylene and dienes with metallocene catalysts, Pirjo Pietikainen; Copolymerization of styrene and ethylene, Paivi Aaltonen; Mixing and dispersion in polymer blends, Tommi Vainio; The polymerization of caprolactone with stannous catalyst, Irma Ylikangas; Lactide/caprolactone and lactide/glycolide copolymers, Mari Hiljanen; Properties and polymerization of random, thermotropic copolyesters, Harri Korhonen; Research areas of the multiphase polymer rheology, Juha Tanner; Reaction calorimetry in slurry type chain polymerizations, Mikko Lahti; Weld lines in injection molded components, Taina Tjader; and Crosslinking of polyolefins, Marcus Ahlroth. NTIS

N94-29073# COM:ONE Devices, Inc., San Jose, CA.
A NOVEL APPROACH TO THE FABRICATION OF SiC STRUCTURES OF ARBITRARY SHAPE Final Report, 1 Jul. - 31 Dec. 1993
Martin F. Wolf 31 Dec. 1993 17 p
(Contract DAAH04-93-C-0023)
(AD-A275475; ARO-32129.1-MS-SBI) Avail: CASI HC A03/MF A01

As a result of the phase 1 research, we can reproduce clad silicon carbide films onto graphite rod substrates. During the course of our research, we varied the melt composition, temperature and crucible material. The resultant silicon carbide films were confirmed, independently by Charles Evans Associates using electron microscopy and elemental x-ray analysis. The minimum temperature for silicon carbide formation was determined. The relationship between film thickness and maximum melt temperature was studied. The importance of complete oxygen exclusion was determined. The presence of the proprietary flux was found to be essential in this regard. The thickness and integrity of these films are not yet suitable for commercial applications. It is anticipated that the use of higher temperatures will yield silicon carbide films suitable for extreme environment applications. A new high-efficiency high-temperature furnace was designed with a maximum working temperature of 2000 C. DTIC

N94-29105*# National Aeronautics and Space Administration. Lewis Research Center, Cleveland, OH.
THERMAL EXPANSION AND ELASTIC ANISOTROPY IN SINGLE CRYSTAL Al2O3 AND SiC REINFORCEMENTS
Jonathan A. Salem, Zhuang Li, and Richard C. Bradt Mar. 1994 12 p Presented at the ASME Symposium on Advances in Composite Materials and Structures, Anaheim, CA, 10-12 Dec. 1986; sponsored by ASME
(NASA-TM-106516; E-8635; NAS 1.15:106516) Avail: CASI HC A03/MF A01

In single crystal form, SiC and Al2O3 are attractive reinforcing components for high temperature composites. In this study, the axial coefficients of thermal expansion and single crystal elastic constants of SiC and Al2O3 were used to determine their coefficients of thermal expansion and Young's moduli as a function of crystallographic orientation and temperature. SiC and Al2O3 exhibit a strong variation of Young's modulus with orientation; however, their moduli and anisotropies are weak functions of temperature below 1000 C. The coefficients of thermal expansion exhibit significant temperature dependence, and that of the non-cubic Al2O3 is also a function of crystallographic orientation. Author (revised)

N94-29133# Naval Command, Control and Ocean Surveillance Center, San Diego, CA. Research, Development, Technology and Evaluation Div.
EFFECT OF SURFACE CONDITION ON STRENGTH AND FATIGUE BEHAVIOR OF ALUMINA CERAMIC Final Report
Nov. 1993 90 p
(AD-A275053; NCCOSC/RDT/E-TD-2584) Avail: CASI HC A05/MF A01

The United States Navy is developing deep-water submersible vessels and, in an effort to attain the appropriate strength and buoyancy characteristics, is investigating the suitability of ceramics. The vessels typically consist of cylindrical sections and hemispherical end caps of a ceramic such as aluminum oxide (alumina), which are joined together via metallic rings made of a titanium alloy. Tests of such vessels have shown that fatigue cracks may arise in the alumina during submergence-emergence cycles, which ultimately lead to failure of the vessel. This document presents results from a one-year program designed to develop a fatigue-crack-growth resistant interface between the alumina cylinder sections and the titanium alloy rings. DTIC

N94-29157# Helsinki Univ. of Technology, Espoo (Finland). Dept. of Chemical Engineering.
POLYMER TECHNOLOGY PUBLICATION SERIES NO. 16
P. Pietikaeinen and J. V. Seppaelae 1993 31 p
(ISSN 0785-7144)
(PB94-135522; ISBN-951-22-1712-0) Avail: CASI HC A03/MF A01

Organometallic complexes formed by metallocene/methylalumoxane belong to the most active catalysts for olefin polymerization known today. A general definition of metallocene catalyst used in ethylene co- and terpolymerizations with dienes is given. Cyclopentadienylide catalyst systems using a metallocene complex in conjugation with an alumoxane catalyst or reaction product thereof are suitable for preparing ethylene diene copolymers. The metallocene catalyst may be represented by the general formula (Cp)(sub m)MRnR'(sub n) wherein Cp is a substituted cyclopentadienyl ring; M is a group IVB, VB or VIB transition metal; R and R' are independently selected halogen, hydrocarbyl group, or hydrocarboxyl groups having 1-20 carbon atoms; m = 1-3, n = 0-3, p = 0-3, and the sum of m+n+p equals the oxidation state of M. NTIS

N94-29203 California Inst. of Tech., Pasadena. Seismological Lab.
DYNAMIC RESPONSE OF CERAMICS Final Report, 1 May 1992 - 31 Oct. 1993
Thomas J. Ahrens, Guangging Chen, and James A. Tyburczy 31 Dec. 1993 30 p Limited Reproducibility: More than 20% of this document may be affected by microfiche quality
(Contract DAAL03-92-G-0218)
(AD-A275396; ARO-28884.5-MS) Avail: CASI HC A03

Both solid to gas (CaSO4 + SiO yields SiO3 + SO2 and Si3N4 + 3C (diamond) and 3SiC + 2 N2) can be shock-induced at ballistic velocities. Because of the endothermic nature of the gas-producing reactions, the extent of reactions observed are limited to interfaces. We found the above reactions proceed to a lesser extent than calculation by equilibrium thermodynamic calculations. Reaction products are found to be 0.01 times those calculated for equilibrium. We show that the extent of reaction, rather than limited by the usual diffusion processes, appears to be controlled by dynamic mixing processes arising from Rayleigh-Taylor instabilities at, for example, CaSiO4-SiO2 interfaces. We apply a theory developed by Drucker to account for the observed extent of reaction. DTIC

N94-29359*# National Aeronautics and Space Administration. Langley Research Center, Hampton, VA.
LOW DIELECTRIC POLYIMIDE FIBERS Patent Application
William E. Dorogy, Jr., inventor (to NASA) (Lockheed Corp., Hampton, VA.) and Anne K. St.Clair, inventor (to NASA) 10 Apr. 1992 21 p
(NASA-Case-LAR-14526-1; NAS 1.71:LAR-14526-1;
US-Patent-Appl-SN-870003) Avail: CASI HC A03/MF A01

A high temperature resistant polyimide fiber that has a dielectric constant of less than 3 is presented. The fiber was prepared by first reacting 2,2-bis (4-(4aminophenoxy)phenyl) hexafluoropropane with 2,2-bis (3,4-dicarboxyphenyl) hexafluoropropane dianhydride in an aprotic solvent to form a polyamic acid resin solution. The polyamic acid resin solution is then extruded into a coagulation medium to form polyamic acid fibers. The fibers are thermally cured to their polyimide form. Alternatively, 2,2-bis (4-(4-aminophenoxy)phenyl) hexafluoropropane is reacted with 2,2-bis(3,4-dicarboxyphenyl) hexafluoropropane dianhydride to form a polyamic acid, and the polyamic acid is chemically converted to its polyimide form. The polyimide is then dissolved in a solvent to form a polyimide resin solution, and the polyimide resin is extruded into a coagulation medium to form a polyimide wet gel filament. In order to obtain polyimide fibers of increased tensile properties, the polyimide wet gel filaments are stretched at elevated temperatures. The tensile properties of the fibers were measured and found to be in the range of standard textile fibers. Polyimide fibers obtained by either method will have a dielectric constant similar to that of the corresponding polymer, viz., less than 3 at 10 GHz. NASA

N94-29399*# National Aeronautics and Space Administration. Lewis Research Center, Cleveland, OH.
LUBRICATION OF SPACE SYSTEMS
Robert L. Fusaro Mar. 1994 28 p Proposed for presentation at the Society of Tribologists and Lubrication Engineers Annual Meeting, Pittsburgh, PA, 2-5 May 1994; sponsored by the Society of Tribologists and Lubrication Engineers
(RTOP 506-43-41)
(NASA-TM-106392; E-8217; NAS 1.15:106392) Avail: CASI HC A03/MF A01

NASA has many high-technology programs plannned for the future, such as the space station, Mission to Planet Earth (a series of Earth-observing satellites), space telescopes, and planetary orbiters. These missions will involve advanced mechanical moving components, space mechanisms that will need wear protection and lubrication. The tribology practices used in space today are primarily based on a technology that is more than 20 years old. The question is the following: Is this technology base good enough to meet the needs of these future long-duration NASA missions? This paper examines NASA's future space missions, how

mechanisms are currently lubricated, some of the mechanism and tribology challenges that may be encountered in future missions, and some potential solutions to these future challenges. Author

N94-29424# Aeronautical Research Inst. of Sweden, Stockholm.
EXPERIMENTAL DETERMINATION OF ORTHOTROPIC ELASTIC CONSTANTS
Anders Henriksson Sep. 1993 18 p Sponsored by Foersvarets Materialverk, Stockholm, Sweden
(FFA-TN-1991-35; ETN-94-95525) Avail: CASI HC A03/MF A01

Conventional methods for determining the elastic constants were investigated in order to find a simple method to provide the full stiffness matrix of an orthotropic material. Since the conventional methods were found not to meet these requirements, another method was tried based on the compression of cubic specimens and measurement of the strains using an extensometer designed for this purpose. The elastic parameters E(sub 1), E(sub 2), E(sub 3), G(sub 12), nu(sub 12), nu(sub 23), and nu(sub 31) were measured using this method on only two kinds of specimens. The accuracy was not satisfactory when properties associated with the 1-direction were measured due to the small displacements involved. The properties in the thickness direction were, however, determined successfully. There is a potential to improve the accuracy of the method and achieve better accuracy even for parameters associated with the 1-direction. ESA

N94-29441# Aerospatiale, Bordeaux (France).
IRRADIATION POLYMERIZATION OF BISMALEIMIDE RESINS [POLYMERISATION DES RESINES BISMALEIMIDES SOUS IRRADIATION]
Daniel Beziers, Vincent Denizot, and Marie-Florence Grenier-Loustalot 1993 15 p In FRENCH Presented at Journee Polyimides Structuraux, Arcueil, France, 12 Jan. 1993
(Rept-932-430-105; ETN-94-95463) Avail: CASI HC A03/MF A01

Within research on the polymerization of bismaleimide resins under irradiation, the mechanisms and kinetics of bismaleimide resin polymerization was studied on model systems and industrial prepolymers, taking into account the influence of several parameters such as the concentration of the active diluent, and the nature and strength of the dose (electrons or X-rays). A methodology based on physiochemical studies by infrared absorption spectroscopy and solid C-13 NMR (Nuclear Magnetic Resonance) CP MAS was developed to quantify the chemical species created or residual in the lattice. The results obtained (reaction progress, structure of formed lattice) are correlated with thermal resistant and compared with those obtained by thermal polymerization. ESA

N94-29446*# National Aeronautics and Space Administration. Marshall Space Flight Center, Huntsville, AL.
VACUUM VAPOR DEPOSITION Patent Application
Richard M. Poorman, inventor (to NASA) and Jack L. Weeks, inventor (to NASA) 3 Feb. 1994 13 p
(NASA-Case-MFS-28652-1; NAS 1.71:MFS-28652-1;
US-Patent-Appl-SN-191309) Avail: CASI HC A03/MF A01

A method and apparatus is described for vapor deposition of a thin metallic film utilizing an ionized gas arc directed onto a source material spaced from a substrate to be coated in a substantial vacuum while providing a pressure differential between the source and the substrate so that, as a portion of the source is vaporized, the vapors are carried to the substrate. The apparatus includes a modified tungsten arc welding torch having a hollow electrode through which a gas, preferably inert, flows and an arc is struck between the electrode and the source. The torch, source, and substrate are confined within a chamber within which a vacuum is drawn. When the arc is struck, a portion of the source is vaporized and the vapors flow rapidly toward the substrate. A reflecting shield is positioned about the torch above the electrode and the source to ensure that the arc is struck between the electrode and the source at startup. The electrode and the source may be confined within a vapor guide housing having a duct opening toward the substrate for directing the vapors onto the substrate. NASA

N94-29451*# National Aeronautics and Space Administration. Langley Research Center, Hampton, VA.
POLY(ARYLENE ETHER-CO-IMIDAZOLE)S AS TOUGHNESS MODIFIERS FOR EPOXY RESINS Patent Application
Patricia D. McDaniel, inventor (to NASA) (College of William and Mary, Williamsburg, VA.) and John W. Connell, inventor (to NASA) 18 Jan. 1994 21 p
(NASA-Case-LAR-15229-1-CU; NAS 1.71:LAR-15229-1-CU;
US-Patent-Appl-SN-186054) Avail: CASI HC A03/MF A01

A toughened epoxy was prepared by reacting an epoxy resin with a poly(arylene ether-co-imidazole)s (PAEI). The epoxy resin comprises N,N,N',N'tetraglycidyl-4,4'- methylenebisbenzenamine and 4-aminophenyl sulfone. The PAEI was prepared by reacting an aromatic bisphenol, a bisphenol imidazole, and an activated aromatic dihalide or dinitro compound in the presence of potassium carbonate in a polar aprotic solvent at an elevated temperature. The epoxies which were modified with these particular PAEI's showed a significant increase in toughness with only a 10 weight percent loading of the PAEI into the epoxy. These toughened epoxies were used to prepare composites and molded parts. NASA

N94-29459# Aerospatiale, Suresnes (France). Centre Commun de Recherches Louis-Bleriot.
RULES AND DEFINITION OF THE RANGE OF PAINTS APPLIED ON AERONAUTICAL STRUCTRURAL COMPOSITES [REGLES ET DEFINITION DES GAMMES DE PEINTURES APPLIQUEES SUR LES COMPOSITES AERONAUTIQUES STRUCTURAUX]
P. Michelin and P. Dublineau 1993 13 p In FRENCH
(Rept-932-600-106; ETN-94-95485) Avail: CASI HC A03/MF A01

The advantages of composite materials which have led to their increased use in aeronautical structures are listed. Their major inconveniences--specifically those that must be protected by layers of paint--are addressed. The different types of composites used, the requirements they necessitate in paints, the application of these paints, the treatment of the surfaces before application of the paints, the measurement of the interphase paint/composite cohesion, the fracturing of the protective film, and the choice of paints are addressed. It is concluded that in order to assure perfect adhesion between paint and composite, certain basic rules should be followed: verification of the absorptivity of the surface; a minimal thickness of paint compatible with the esthetic demands; good knowledge of the materials and their surface; and good communication between supplier and client. ESA

N94-29555* National Aeronautics and Space Administration. Langley Research Center, Hampton, VA.
POLYIMIDES CONTAINING PENDENT SILOXANE GROUPS Patent
John W. Connell, inventor (to NASA), Terry L. St.Clair, inventor (to NASA), and Paul M. Hergenrother, inventor (to NASA) 19 Apr. 1994 26 p Filed 2 Nov. 1992
(NASA-Case-LAR-14638-1; US-Patent-5,304,627;
US-Patent-Appl-SN-970755; US-Patent-Class-528-353;
US-Patent-Class-528-22; US-Patent-Class-528-26; US-Patent-Class-528-28;
US-Patent-Class-528-32; US-Patent-Class-528-33; US-Patent-Class-528-34)
Avail: US Patent and Trademark Office

Novel polyimides containing pendent siloxane groups (PISOX) were prepared by the reaction of functionalized siloxane compounds with hydroxy containing polyimides (PIOH). The pendent siloxane groups on the polyimide backbone offer distinct advantages such as lowering the dielectric constant and moisture resistance and enhanced atomic oxygen resistance. The siloxane containing polyimides are potentially useful as protective silicon oxide coatings and are useful for a variety of applications where atomic oxygen resistance is needed.
Official Gazette of the U.S. Patent and Trademark Office

N94-29745 Ohio Univ., Athens.
A PHOTOEMISSION ELECTRON MICROSCOPE INVESTIGATION OF CHEMICAL VAPOR DEPOSITION DIAMOND FILMS AND DIAMOND NUCLEATION Ph.D. Thesis
Congjun Wang 1993 175 p
Avail: Univ. Microfilms Order No. DA9322371

CVD diamond nucleation is investigated using the hot filament technique. The stability of CVD diamond at elevated temperatures in vacuum, O2, and atomic hydrogen environments are studied using photoemission electron microscopy (PEEM) combined with in-vacuo x ray photoelectron spectroscopy (XPS). Dissolution, oxidation, and atomic hydrogen etching processes of CVD diamond are observed in real-time. Low field cold electron emission from CVD diamond films has been observed for the first time by PEEM.

Nucleation density Mo substrates could be increased from 10(exp 4) to 10(exp 8)/cm(exp 2) by polishing. Heating the substrate to 870 C in vacuum prior to deposition, or above 1000 C at the beginning of deposition, reduced nucleation by more than 100-fold. Reduction in nucleation sites is attributed to annealing. Nucleation on Mo2C substrates was found to be very poor (10(exp 4)/cm(exp 2)), which shows carbide alone does not promote nucleation. Carbide formation may remove nucleation sites. CVD diamond was found to dissolve into the Mo substrate in vacuum at about 1200 C. XPS showed formation of Mo2C when the diamond dissolved. Diamond oxidation to gas phase products occurred directly at about 600 C, with no observable participation by the substrate. No detectable etching by atomic hydrogen at a pressure of 1 x 10(exp -4) torr was observed. Boron doped and 'pure' CVD diamond films were found to emit electrons at room temperature under the action of the accelerating electric field of the PEEM (about 30 kV/cm) without photon excitation. The mechanism underlying this phenomenon was investigated with PEEM and by studying the emission current versus voltage characteristics of the CVD diamond films. Morphology and crystalline orientation were found to play only a minor role. Impurities in the CVD diamond structure lowers the potential barrier substantially; tunneling of electrons into the vacuum is facile. The effective work function of the emitting CVD diamond films is measured to be about 0.1 eV. Dissert. Abstr.

N94-29766 Missouri Univ., Rolla.
ANALYSIS OF PRESSURELESS DENSIFICATION OF CERAMIC MATRIX COMPOSITES Ph.D. Thesis
Wei Hong 1993 79 p
Avail: Univ. Microfilms Order No. DA9326595

A finite element method implementing viscoelastic formulations is developed and utilized for analyzing the densification behavior of ceramic matrix composites during a pressureless sintering process. The effort is focused on the investigation of the drastic reduction in densification rates of polycrystalline ceramics reinforced with a second phase of inert, rigid particles or whiskers, compared to that of single phase ceramics. The second phase is relatively rigid inclusions and generally considered to provide a constraint to the sintering matrix. The ceramic matrix is presumed to be viscoelastic. The sintering potential used in the analysis is derived from sintering experiments on the unconstrained matrix, noting that the free strain rate for the constrained matrix is generally different from that of the unconstrained identical matrix. The finite element analysis is performed with several physical and geometric models. The effect of inclusion shape on the densification rates is investigated through a set of geometric models containing a single spherical, a single ellipsoidal and a single cylindrical inclusion, respectively. The densification rates of the sintering matrix are found to be affected significantly by the inclusion shape. The single cylindrical inclusion model serves as an upper bound while the spherical inclusion provides a lower bound for the constraint in these single inclusion models. The single cylindrical inclusion model is also used to study the effects of various constitutive relations. Sintering potential is assumed to depend on the length of sintering time, matrix density and grain size. The interaction among inclusions is investigated using a two dimensional multiple inclusion model. The effect of homogeneous and heterogeneous distribution of initial density is also investigated by accounting for the competition between sintering and pore coarsening. Dissert. Abstr.

N94-29807 Massachusetts Univ., Lowell.
STUDY OF NONLINEAR OPTICAL POLYMERS AND THEIR APPLICATIONS IN OPTICAL WAVEGUIDES Ph.D. Thesis
Yong Ming Chen 1992 143 p
Avail: Univ. Microfilms Order No. DA9305325

This thesis describes the investigations on second-order novel nonlinear optical (NLO) polymeric materials and their applications. The first chapter introduces the subject matter of the dissertation. The second chapter describes parallel plate poling and corona discharge poling to achieve second-order NLO properties. The corona discharge poling provides certain advantages such as higher effective poling field which aligns NLO molecules more efficiently. An existing theoretical model has been used to understand corona poling and to calculate the effective poling field. In the third chapter, the second harmonic generation (SHG) method is discussed and developed to characterize NLO polymeric films. Using SHG measurements, second-order NLO coefficients of polymeric films are determined. Most NLO polymeric films have absorption in the doubled frequency region for a Nd:YAG laser (1.064 micron). The values of second-order NLO coefficients are resonantly enhanced. The derivation of absorption correction of second-order NLO coefficients has been carried out. The absorption corrected d(sub 33) value for poled and crosslinked DGEBA-DO3C film is 31 pm/V. The fourth chapter deals with the stabilization of second-order nonlinearity of polymeric materials. The side chain, photocrosslinked, sol-gel, thermosetting and polyimide systems have been developed to investigate and improve the stability of poled polymeric films. The fifth chapter describes the characterization of linear and quadratic electro-optic (EO) effects of polymers. The linear EO coefficients of poled polymeric films have been characterized by the reflection measurement technique. Using a modified Michelson interferometer, the quadratic EO coefficients have been determined. The sixth chapter reports the investigation of optical waveguides and the waveguide applications. A series of experiments, such as prism coupling and optical loss measurement, have been performed to determine linear properties of waveguides (propagation constant, refractive indices, film thickness, and optical loss). Using these parameters, planar and channel waveguides have been designed and fabricated. Also the SHG in these waveguides have been carried out. The SHG conversion efficiency of a polymeric channel waveguide was 0.1 percent/W. Bright green light was observed even using the Nd:YAG laser in cw mode. Dissert. Abstr.

N94-29830# Sandia National Labs., Albuquerque, NM.
INORGANIC POLYMER-DERIVED CERAMIC MEMBRANES
C. J. Brinker, R. Sehgal, N. Raman, P. R. Schunk, and T. J. Headley 1993 15 p Presented at the Fuels Technology Contractors' Review Meeting, Morgantown, WV, 16-18 Nov. 1993
(Contract DE-AC04-76DP-00789)
(DE94-000082; CONF-931156-25) Avail: CASI HC A03/MF A01

Polymeric silica sols were used to prepare membranes on commercial (gamma)-Al2O3 supports. Aging of the silica sols was shown to be effective to form discrete membrane layers. He/N2 selectivity factors exceeding ideal Knudsen values were observed when the sols were prepared under conditions in which the condensation rate was minimized. It is proposed that the average pore size of the membrane depends on the balance of capillary pressure and modulus during membrane deposition and that the breadth of the pore size distribution might be influenced by the extent of condensation accompanying membrane deposition. The use of organic templates may allow independent control of pore size, pore shape, and pore volume. The membranes are to be used in processing natural gas (gas separation/purification). DOE

N94-29874 Purdue Univ., West Lafayette, IN.
TRANSIENT THERMAL FATIGUE OF CERAMIC COMPOSITES Ph.D. Thesis
Arvind K. Sinha 1992 294 p
Avail: Univ. Microfilms Order No. DA9314079

Ceramic composite materials were developed for use at high temperatures and are subjected to cyclic thermal loads. These loads are an important factor in determining the reliability and mechanical load carrying capability of the composite. Specifically, the effect of cyclic thermal loads is to cause thermal stresses at the interface between the fiber and the matrix and cause debonding between these components. In turn, such debonding results in a change in the mechanical and thermal properties of the composite. Consequently, it is important to understand the mechanics of fiber-matrix interaction under thermal loads in order to optimize the behavior of composites at high temperatures. The changes in stiffness for a Nicalon/CAS-2 unidirectional composite resulting from cyclic heating and cooling were investigated. The experimental measurements were made using an ultrasonic through-transmission method. It is shown that slower cooling rates result in degradation of stiffness mainly in the C22 and C33 direction through interface debonding. For a higher cooling rate, a decrease in C11 is observed due to surface matrix cracks. The behavior of Nicalon/CAS-2 composite under transient thermal load is studied using the various thermomicromechanical models. These models are then used to calculate thermomechanical stresses produced thermal load application. Using three-phase thermomechanical models, it is shown that the behavior of the matrix and the fiber-matrix interface is dependent on the transversely isotropic material surrounding the matrix. The finite element modeling done on the Nicalon/CAS-2 composite verified the results obtained during thermal cycling experiments. To calculate the stiffness degradation, the concept of equivalent homogeneity was applied. The behavior of an interface and a

matrix crack subjected to transient heating and cooling were studied using the single cell fiber-matrix model. Based on this model, the nondimensional strain energy release rate was calculated. Results show that when the critical strain energy release rate for the interface is similar or lower than that of the matrix, the interface crack will propagate before the matrix crack. Dissert. Abstr.

N94-29885 National Physical Lab., Teddington (England). Materials Metrology Div.

THE EFFECT OF TEMPERATURE ON CREEP AND PHYSICAL AGEING OF PVC

P. E. Tomlins, B. E. Read, and G. D. Dean Mar. 1993 28 p Sponsored by Dept. of Trade and Industry, United Kingdom

(ISSN 0959-2423)

(NPL-DMM(A)-93; ETN-94-95504) Copyright Avail: Issuing Activity (National Physical Laboratory, Teddington, Middlesex TW11 0LW, United Kingdom)

Tensile creep data was obtained for PVC at a number of temperatures ranging from 21.5 to 58 C. The results were obtained from specimens of different age characterized by the elapsed time t(sub e) between quenching a sample from 85 C to the test temperature and the start of the creep test. A model for interpreting nonlinear creep data was developed to describe the creep behavior of the material as a function of both age and temperature. The results show that the effect of physical aging is to progressively reduce the level of the relaxed beta compliance and increase the mean retardation time of the glass-rubber alpha relaxation process. The effect of conducting creep tests on specimens of the same age at progressively higher temperatures has the opposite effect; the level of the relaxed beta compliance increases while the mean retardation times of the alpha process decrease. Neither the aging rate nor the shape of the distribution of retardation times are affected by temperature. ESA

N94-29886 National Physical Lab., Teddington (England). Materials Metrology Div.

CREEP AND PHYSICAL AGING OF PVC: DEPENDENCE ON STRESS AND TEMPERATURE

B. E. Read, G. D. Dean, and P. E. Tomlins Jul. 1993 21 p Sponsored by Dept. of Trade and Industry

(ISSN 0959-2423)

(NPL-DMM(A)-115; ETN-94-95507) Copyright Avail: Issuing Activity (National Physical Laboratory, Teddington, Middlesex TW11 0LW, United Kingdom)

On the basis of data obtained for PVC, extensions were made to a model for analyzing the creep compliance curves of glassy, amorphous polymers. Short term data in the alpha region were fitted with a stretched exponential function containing an effective retardation time t(sub 0) which increases with the age of the polymer and decreases with stress and temperature. Physical aging during long term creep gives rise to an increase in t(sub 0) with creep time, the rate of increase depending on stress and temperature. Functions which quantitatively describe these variations in t(sub 0), and which relate the creep compliance to age state, creep time, stress and temperature, were developed. These functions could provide a basis for predicting the creep behavior over wide and continuous ranges of test variables from data acquired in a limited number of tests. ESA

N94-29967 Johns Hopkins Univ., Baltimore, MD.

LUBRICANT RHEOLOGY AT HIGH SHEAR RATES Ph.D. Thesis

Ruqiang Feng 1993 242 p

Avail: Univ. Microfilms Order No. DA9313361

The rheological response of lubricants may become non-Newtonian at high shear rates. The constitutive modeling of such a behavior relies upon the results of high-rate rheological experiments. Substantial viscous heating is always a concern in high-rate rheometry; proper experimental techniques are crucial for obtaining valid measurements of material properties. In this study, a short-time high-rate rheometer is developed using the torsional Kolsky bar technique. A thin layer of lubricant, held between concentric cylinders, is sheared at shear rates up to 4 x 10(exp 4) s(exp -1) for times on the order of 10(exp 2) microsec, and for a range of temperatures. For these short times, the total work done in shearing a lubricant is small; therefore the experimental results are expected to provide constitutive information that is minimally affected by shear heating. Next, a computational scheme is developed to solve the full transient thermo-mechanical problem involved in simple shear rheometry with fully nonlinear constitutive relations and with realistic thermal boundary conditions (including the effect of conduction in the surrounding metal parts). The numerical simulation of the Kolsky bar rheometer suggests that the experimental technique can be used to obtain the rheological properties of lubricants at high shear rates, and that the temperature rise in the lubricant layer can be estimated accurately using the experimental results and adiabatic conditions only. Numerical simulations are also conducted for long-time thin-film rheometry experiments, which provide most of the experimental data that supports the current understanding of the high-rate rheology of lubricants. The computations suggest that, in long-time thin-film rheometry, the commonly used isothermal boundary for the lubricant layer is inadequate, although the temperature rise in the film does decrease significantly with decreasing film thickness. Other critical issues in high-rate rheometry, including the rise time of the boundary velocity, the instability of the shear flow, and the influence of film thickness in short-time rheometry, are studied through numerical simulations. The limitations of wing rheometers to explore high-rate rheology are discussed in the light of the results of these numerical simulations. Dissert. Abstr.

N94-29975 Brown Univ., Providence, RI.

MICROMECHANICS OF THE DYNAMIC RESPONSE OF CERAMICS AND CERAMIC COMPOSITES Ph.D. Thesis

Horacio Dante Espinosa 1992 237 p

Avail: Univ. Microfilms Order No. DA9308802

In this investigation we performed plate impact experiments to study the evolution of damage in ceramics and ceramic composites by subjecting the specimen to stress pulses which are large enough in amplitude to initiate microcracks, but short enough in duration to prevent their coalescence into macrocracks. In the 'soft-recovery' experiment, a star-shaped flyer plate impacts a square specimen which has a square impedance-matching 'momentum trap' behind it. The size and shape of these three plates is such that the central portion of the specimen can be subjected to compressive and tensile stress pulses, which are controllable in magnitude and duration, and which allow the specimen to be recovered for microstructural analyses. Through the use of a laser interferometer, these pulses are monitored and used to determine the validity of proposed models. The recovered specimens are examined using transmission electron microscopy (TEM) and scanning electron microscopy (SEM) to determine the pattern of microcracks for comparison with the predictions of the assumed models. In spite of many contributions to the field of damage induced by compressive waves, lack of consensus on the mechanisms responsible for the measured velocity profiles still remains. Our observations seem to unequivocally point to deformation in the intergranular glassy phase as a major mechanism of inelasticity in ceramics subjected to compressive dynamic loading. The possibility of compressive cracking, an alternative candidate mechanism, is ruled out by the observed absence of retardation of waves traveling through regions of the specimen previously deformed in compression. In addition, the recorded compressive pulse profiles strongly suggest a deformation by 'areal slip' i.e., by interfacial sliding over an expanding area. A detailed finite element analysis of the glass/grain-junction system has revealed that the stress concentration is sufficient to induce plastic flow in the glass under the conditions of our experiments. The numerical simulations demonstrate the ability of the areal slip model to reproduce all the salient features of the experimental record over a wide range of impact velocities. In tension, microcracking is identified as the principal inelastic mechanism. Microcrack growth is modeled using standard relations of dynamic fracture mechanics. Because dynamic crack-tip equations of motion are differential equations of first order in time, the overall response under dynamic tensile loading is of the viscoplastic type. Our simulations demonstrate that the dilute approximation is valid over a wide range of the material response. Dissert. Abstr.

N94-30025# Los Alamos National Lab., NM.

MICROSTRUCTURE AND MECHANICAL PROPERTIES OF NITRIDED MOLYBDENUM SILICIDE COATINGS

J. P. Hirvonen (Technical Research Centre of Finland, Espoo.), I. Suni (Technical Research Centre of Finland, Espoo.), H. Kattelus (Technical Research Centre of Finland, Espoo.), R. Lappalainen (Helsinki Univ., Finland.), P. Torri (Helsinki Univ., Finland.), H. Kung, T. R. Jervis, and M. Nastasi 1993 7 p Presented at the Fall Meeting of the Materials Research Society (MRS), Boston, MA, 29 Nov. - 3 Dec. 1993

(Contract W-7405-eng-36)
(DE94-006249; LA-UR-94-308; CONF-931108-66) Avail: CASI HC A02/MF A01

Mo-Si-N films with a high nitrogen concentration were produced by sputter-deposition in nitrogen plasma. Chemical composition was determined with Rutherford backscattering and nuclear reaction analysis. Ratio of Mo to Si was 1:2 in the coatings with a nitrogen concentration of 50%. Microstructure of the as-deposited coatings on a silicon substrate was amorphous and no crystallization was found after annealing up to 1000 deg C, although some relaxation was observed in X-ray diffraction. This was confirmed by high-resolution TEM. Hardness of Mo-Si-N films was 18.8 GPa as determined with a nanoindenter. This is significantly higher than that of MoSi2 films, 11.2 GPa. Hardness of the Mo-Si-N films increased to 24.4 GPa after annealing at 800 deg C, which is the same as that of the tetragonal phase of MoSi2, 25.5 GPa. Similarly, modulus of as-deposited Mo-Si-N film was higher (257 GPa) than that of MoSi2 film (222 GPa). However, only a slight increase in the modulus of the Mo-Si-N film was found after annealing at 800 deg C, whereas the modulus of the crystallized tetragonal MoSi2 was 382 GPa. No cracking was found in the Mo-Si-N films even after annealing at 1000 deg C. DOE

N94-30036 Manitoba Univ., Winnipeg. Dept. of Electrical and Computer Engineering.
STUDY OF THE ULTRAVIOLET ABSORPTION AND PHOTOCONDUCTION SPECTRA OF POLYIMIDE FILMS FABRICATED AT VARIOUS CURING TEMPERATURES M.S. Thesis
Lin Kan Aug. 1993 84 p
(ISBN-0-315-85923-7; CTN-94-61172) Copyright Avail: Micromedia Ltd., Technical Information Centre, 240 Catherine Street, Suite 305, Ottawa, Ontario, K2P 2G8, Canada HC/MF

The absorption and photoconduction spectra in the ultraviolet region for polyimide films fabricated under various curing temperatures were measured. There are four absorption peaks located at 3.65, 4.35, 5.65, and 6.40 eV in the fully cured polyimide films. The 6.40 eV peak is practically independent of the curing temperature, but the other three peaks increase with increasing curing temperature. These four peaks are due to intra- and intermolecular optical transitions. In the photoconduction quantum efficiency spectra, there are also four peaks in the fully cured polyimide films: 3.55, 4.05, 4.90, and 5.80 eV. Analysis of the photoconduction quantum efficiency spectra yields values of 4.17 and 4.37 eV as the potential barrier heights for photoemission from Au and Ag electrodes to polyimide, respectively. The quantum efficiency increases with increasing applied electric field, following closely the Onsager theory with a thermalization separation 30 Angstroms in the ultraviolet region. The primary yield increases with increasing curing temperature. Author (CISTI)

N94-30066 International Centre for Theoretical Physics, Trieste (Italy).
ABLATION OF POLYMERS BY ULTRAVIOLET PULSED LASER
A. Brezini (Oran Univ., Es-Senia, Algeria.), N. Benharrats, and F. Hamdache Aug. 1993 59 p Limited Reproducibility: More than 20% of this document may be affected by microfiche quality
(DE94-608100; IC-93/264) Avail: CASI HC A04 (US Sales Only)

The surface modifications of different polymers treated by far UV-excimer laser (lambda = 193, 248, and 308 nm) are analyzed by x ray photoelectron spectroscopy. The main feature observed depends strongly on the absorption coefficients. For the high absorbing polymers (e.g., polystyrene, polyimide), the mechanism of the UV-excimer laser interaction appears to be governed by an ablative photodecomposition process (APD) with an APD threshold. In the other limit, i.e. low absorbing polymer, the interaction leads to a photothermal process. DOE

N94-30102 Sandia National Labs., Albuquerque, NM.
NOVEL TECHNIQUES APPLIED TO POLYMER LIFETIME PREDICTIONS
K. T. Gillen, J. Wise, and R. L. Clough 1993 15 p Presented at the 39th International Symposium of the Society for the Advancement of Material and Process Engineering and Exhibition, Anaheim, CA, 11-14 Apr. 1994 Limited Reproducibility: More than 20% of this document may be affected by microfiche quality
(Contract DE-AC04-94AL-85000)
(DE94-005095; SAND-93-1457C; CONF-940412-2) Avail: Issuing Activity (Department of Energy (DOE))

A study aimed at testing the Arrhenius life prediction approach is described. After aging elastomeric materials at several elevated (accelerated) temperatures, a modulus profiling apparatus was used to demonstrate the complicated diffusion-limited oxidation anomalies are typically present under accelerated oven-aging conditions. By using surface modulus results (oxidation less to a monotonic increase in modulus), estimates are made of the true activation energy (E(sub a)) appropriate to the oxidation reactions dominating degradation. Even though macroscopic properties should be influenced by the diffusion-limited oxidation complications, ultimate tensile elongation results were found to be correlated to the true E(sub a). This implies that cracks initiate at the hardened surface of the material and then quickly propagate through the less oxidized interior. If values of E(sub a) obtained from accelerated exposures can be determined and rationalized, another important question involves the Arrhenius assumption that E(sub a) remains constant in the extrapolation region. Preliminary data from two ultra-sensitive techniques (oxygen consumption and microcalorimetry) aimed at testing this fundamental assumption are described. DOE

N94-30104# Ames Lab., IA.
PLASMA ENHANCED CHEMICAL VAPOR DEPOSITION OF ZrO2 THIN FILMS Ph.D. Thesis
K. Saravanan Dec. 1993 129 p
(Contract W-7405-eng-82)
(DE94-006031; IS-T-1424) Avail: CASI HC A07/MF A02

Amorphous ZrO2 thin films were deposited in an inductively coupled PECVD system using a Zr beta-diketonate, Zr(C11H19O2)4, as the precursor. The deposits were air annealed at 900 C for 5 min to get pure, single phase, oriented, polycrystalline alpha-ZrO2. Feasibility of using 2 different types of reactors was investigated. The inductively heated horizontal reactor depositions at 600 C had a lower deposition rate and the films were non-uniform in thickness with a columnar structure. The resistively heated vertical reactor depositions at 350 C had a higher deposition rate and the films were more uniform in thickness with a fine grained microstructure. The statistical design was demonstrated as an effective technique to analyze the effect of process conditions on the rate of deposition and relative (h00) orientation. The factorial design was used to quantify the two responses in terms of the process variables and their mutual interactions. The statistical design for rate of deposition was found to correlate with the trends observed in classical design. DOE

N94-30177*# National Aeronautics and Space Administration. Lewis Research Center, Cleveland, OH.
XPS ANALYSIS OF 440C STEEL SURFACES LUBRICATED WITH PERFLUOROPOLYETHERS UNDER SLIDING CONDITIONS IN HIGH VACUUM
Pilar Herrera-Fierro (Case Western Reserve Univ., Cleveland, OH.), Masabumi Masuko (Tokyo Inst. of Tech., Japan.), William R. Jones, Jr., and Stephen V. Pepper Apr. 1994 22 p
(RTOP 505-63-5A)
(NASA-TM-106548; E-8699; NAS 1.15:106548) Avail: CASI HC A03/MF A01

This work presents the results of the X-Ray Photoelectron Spectroscopy (XPS) analysis of AISI 440C ball surfaces lubricated with perfluoropolyether (PFPE) oils after friction experiments under sliding conditions at high load in air and vacuum environments. The PFPE lubricants tested were Demnum S100, Fomblin Z-25, and Krytox 143AB. It was found that all the PFPE lubricants were degraded by sliding contact causing the formation of inorganic fluorides on the metallic surfaces and a layer of organic decomposition products. KRYTOX 143AB was the least reactive of the three lubricants tested. It was also found that metal fluoride formed at off-scar areas. This suggests the formation of reactive species, such as COF2 or R(sub f)COF, during sliding experiments, which can diffuse through the lubricant film and react with the metallic surfaces away from the contact region. Comparison of reference specimens before sliding with those that had undergone the sliding tests showed that the amount of non-degraded PFPE remaining on the surface of the balls after the sliding experiments was greater than that of the balls without sliding. Author (revised)

N94-30225 Rensselaer Polytechnic Inst., Troy, NY.
EFFECTS OF HYDROGEN ON THE RESISTIVITY OF THIN Au AND Cu FILMS Ph.D. Thesis
Christopher Alan Apblett 1992 239 p
Avail: Univ. Microfilms Order No. DA9314340

The effect of hydrogen on the resistivity of thin (200 nm) gold and copper films has been studied. Hall effect measurements were used to determine if the observed change in resistivity was due to electron density or electron mobility. Measurements of the time dependence of resistivity changes were used to determine the kinetics of the resistivity change caused by hydrogen, and the influence of the substrate on the resistivity change. Measurements of resistivity as a function of hydrogen pressure were used to determine the type of hydrogen adsorption occurring on the surface of the films. Hydrogen was found to raise the mobility of conduction electrons in a metal. The change in the mobility was found to decrease with prior annealing. The kinetics of the resistivity change in vacuum indicated an interface limited reaction, subject to the geometrical constraint of a spherical moving interface. The activation energy for the vacuum annealing was 0.2 +/- 0.1 eV in gold and 0.3 +/- 0.15 eV in copper. In hydrogen annealing, the kinetics were diffusion limited with the same geometry constraint. The activation energy of the hydrogen annealing was 0.06 +/- 0.04 eV in gold and 0.05 +/- 0.04 eV in copper, consistent with the diffusion of hydrogen through a lattice. It was concluded that hydrogen may have assisted in the motion of scattering defects to a grain boundary or free surface. This would increase the mean free path length of the electrons through the metal and lower the resistivity. Hydrogen was found to adsorb as the molecule on gold or copper surfaces and the adsorption followed the Langmuir isotherm. Dissert. Abstr.

N94-30245# Allied-Signal Aerospace Co., Kansas City, MO.
NON-AQUEOUS CLEANING SOLVENT SUBSTITUTION
G. J. Meier Jan. 1994 11 p Presented at the 4th National Technology Transfer Conference and Exposition, Anaheim, CA, 7-9 Dec. 1993
(Contract DE-AC04-76DP-00613)
(DE94-005339; KCP-613-5345; CONF-931244-1) Avail: CASI HC A03/MF A01

A variety of environmental, safety, and health concerns exist over the use of chlorinated and fluorinated cleaning solvents. Sandia National Laboratories, Lawrence Livermore National Laboratories, and the Kansas City Division of Allied Signal have combined efforts to focus on finding alternative cleaning solvents and processes which are effective, environmentally safe, and compliant with local, state, and federal regulations. An alternative solvent has been identified, qualified, and implemented into production of complex electronic assemblies, where aqueous and semi-aqueous cleaning processes are not allowed. Extensive compatibility studies were performed with components, piece-parts, and materials. Electrical testing and accelerated aging were used to screen for detrimental, long-term effects. A terpene, d-limonene, has been selected as the solvent of choice, and has been found to be compatible with the components and materials tested. A brief history of the overall project will be presented, along with representative cleaning efficiency results, compatibility results, and residual solvent data. The electronics industry is constantly searching for proven methods and environmentally safe materials to use in manufacturing processes. The information in this presentation will provide another option to consider on future projects for applications requiring high levels of quality, reliability, and cleanliness from non-aqueous cleaning processes. DOE

N94-30259 Virginia Polytechnic Inst. and State Univ., Blacksburg.
DAMAGE ANALYSIS AND MECHANICAL RESPONSE OF AS-RECEIVED AND HEAT-TREATED NICALON/CAS-2 GLASS-CERAMIC MATRIX COMPOSITES Ph.D. Thesis
Shin Steven Lee 1993 191 p
Avail: Univ. Microfilms Order No. DA9323777

Experimental results of damage development in and mechanical response of heat-treated Nicalon/CAS-2 laminates subjected to monotonic flexure and axial loading and to cyclic tensile loading are reported. The specimens were subjected to post-processing heat treatments at 900, 1000, and 1100 C in air for 100 hours. Changes at the fiber/matrix interface/interphase due to post-processing heat treatments were also characterized. The combined effect of fiber debonding and transverse matrix cracking in both 90 deg and 0 deg plies plays an important role in damage development in (0/90)(sub 4s), Nicalon/CAS-2 laminates, especially in developing the secondary damage modes such as longitudinal matrix cracking and delamination. Frictional wear effects found in cyclically loaded specimens may be responsible for the observed temperature profiles during the intermediate stage of fatigue life. It is also believed that frictional wear is critical to the failure of notch sensitive fibers. Different damage modes such as 'brittle' matrix crack propagation and 'quasi-brittle' matrix crack propagation were observed in heat-treated specimens. Results obtained from microanalysis using an analytical scanning transmission electron microscope equipped with an energy dispersive spectrometer, and microindentation indicated that the changes of damage and failure modes were directly related to the changes of characteristics at the fiber/matrix interface/interphase. Dissert. Abstr.

N94-30263# Sandia National Labs., Albuquerque, NM.
KINETICS OF SURFACE ROUGHENING AND SMOOTHING DURING ION SPUTTERING
E. Chason, T. M. Mayer, and A. J. Howard 1993 12 p Presented at the Fall Meeting of the Materials Research Society (MRS), Boston, MA, 29 Nov. - 3 Dec. 1993
(Contract DE-AC04-76DP-00789)
(DE94-006358; SAND-93-1447C; CONF-931108-64) Avail: CASI HC A03/MF A01

We have measured the kinetics of roughness evolution during low energy ion sputtering of SiO2 surfaces using in situ x-ray reflectivity. Sputtering with heavy ions (Xe) leads to rapid roughening of the surface that can not be explained by a simple random removal process. Subsequent bombardment with light ions (He,H) leads to an exponential decrease in the surface roughness. These kinetics are explained quantitatively by a linear model that contains a balance between smoothing by surface diffusion and viscous flow and roughening by sputter removal of material. A curvature dependent sputter yield leads to amplification of a limited range of spatial frequencies on the surface and the formation of a ripple topography. DOE

N94-30335# Oak Ridge National Lab., TN.
CHARACTERIZATION OF THERMALLY ANNEALED Sb IMPLANTED FUSED SILICA
S. H. Morgan (Fisk Univ., Nashville, TN.), Z. Pan (Fisk Univ., Nashville, TN.), D. O. Henderson (Fisk Univ., Nashville, TN.), S. Y. Park (Vanderbilt Univ., Nashville, TN.), R. A. Weeks (Vanderbilt Univ., Nashville, TN.), R. H. Magruder, III (Vanderbilt Univ., Nashville, TN.), and R. A. Zuhr Dec. 1993 7 p Presented at the Fall Meeting of the Materials Research Society (MRS), Boston, MA, 29 Nov. - 3 Dec. 1993
(Contract DE-AC05-84OR-21400)
(DE94-005464; CONF-931108-44) Avail: CASI HC A02/MF A01

The local environment of the polarizable ion in heavy metal oxide glasses is postulated to strongly influence the nonlinear response of these materials. The authors have previously observed that post-implantation thermal annealing changes the chemical properties of the implanted layer in a different fashion in Pb- and Bi- implanted SiO2. In this paper the authors report the optical behavior of Sb-implanted SiO2 as a function of annealing temperature and atmosphere. High purity fused silica substrates were implanted at room temperature to a dose of 6 x 10(exp 16) ions/cm(exp 2), and subsequently annealed at temperatures from 500 to 1000 C in argon and oxygen atmospheres. RBS, optical absorption (1.8 to 6.2 eV), infrared reflectance (450 to 5000 cm(exp -1)), and nonlinear index of refraction were measured before and after annealing. The results of these measurements indicate that annealing treatment significantly affects the local environment of the implanted Sb ions, and consequently the optical response. DOE

N94-30337# Ames Lab., IA.
CENTRIFUGAL ATOMIZATION OF LANTHANIDE MATERIALS FOR CRYOGENIC COOLERS Ph.D. Thesis
M. G. Osborne Jan. 1994 106 p
(Contract W-7405-eng-82)
(DE94-006035; IS-T-1679) Avail: CASI HC A06/MF A02

Until recently, Pb was the preferred heat exchanger matrix material used in low temperature cryocoolers; however, the heat capacity of Pb drops drastically below approximately 15 K and new matrix materials based on the lanthanide elements were developed. These materials magnetically order at low temperatures and the entropy change associated with ordering contributes to the materials' heat capacities. The drawback to widespread use of lanthanide intermetallic compounds in cryocoolers has been the difficulty in manufacturing high-quality particulates. The purpose of this project was to develop a technique for producing high-quality powders of

lanthanide metals and lanthanide intermetallic compounds for use in cryocooler heat exchangers. A series of atomization experiments was performed using Er3Ni, Nd, Nd3Ni, and (Er(0.5)Nd(0.5))(3)Ni. Atomization of these materials resulted in particles ranging from mostly spherical to extremely flattened. Analyses of size distributions for the experiments indicate that increased atomization disk speed and superheat result in smaller mean particle diameters and narrower size distributions. Chemical analyses of the atomized powders indicate that the CA/RQB technique produces particulate with much lower interstitial contamination than other techniques. The Er3Ni and Nd3Ni powders were predominantly of the desired phase and the (Er(0.5)Nd(0.5))(3)Ni powder had one major and possibly three minor phases. The solidification morphology is typically fine dendritic or cellular with finer microstructure spacings near the particle surfaces. The Er3Ni powders have higher heat capacities than gas atomized powders reported in literature. The heat capacity of Nd3Ni has a peak which does not degrade dramatically with processing. The (Er(0.5)Nd(0.5))(3)Ni material has a higher heat capacity compared to Er3Ni, Nd3Ni, and Nd at temperatures above 10K. DOE

N94-30420 National Aerospace Lab., Amsterdam (Netherlands). Structures and Materials Div.

EVALUATION OF CORROSION PROTECTING PROPERTIES OF MODERN AIRCRAFT PAINT SYSTEMS

W. G. J. tHart and J. A. M. Boogers Dec. 1991 32 p Presented at the Aerospace Corrosion Control Symposium, Amsterdam, Netherlands, 23-25 Mar. 1992 Sponsored by Royal Netherlands Air Force Limited Reproducibility: More than 20% of this document may be affected by microfiche quality

(AD-B179388; NLR-TP-91460-U; ETN-94-95958) Avail: CASI HC A03

The flexibility, adhesion and corrosion protecting properties of several modern paint systems were examined. Since paint cracking around fasteners under operational conditions usually occurs at low temperatures, this was examined by tensile testing of painted metal strips at -50C. After tensile testing the degree of paint delamination (loss of adhesion) was established, and cross sections were made to examine this delamination on a microscopic scale. The corrosion protecting capability of paint systems was determined by exposing specimens with a precracked paint system and crossed scribe lines to an accelerated corrosion test (MASTMAASIS). In this investigation the different paint systems had the same topcoat, Aerodur HF A 132. Since Plastic Media Blasting (PMB) is a potential method for replacing the chemical paint stripping procedure, PMB and various cleaning operations were also considered. ESA

N94-30591 Sandia National Labs., Albuquerque, NM.

PROPERTIES OF CHEMICAL VAPOR INFILTRATION DIAMOND DEPOSITED IN A DIAMOND POWDER MATRIX

J. K. G. Panitz, D. R. Tallant, C. R. Hills, and D. J. Staley 1993 21 p Presented at the 40th National Symposium of the American Vacuum Society (AVS), Orlando, FL, 15-19 Nov. 1993 Limited Reproducibility: More than 20% of this document may be affected by microfiche quality

(Contract DE-AC04-94AL-85000)

(DE94-005429; SAND-93-2594C; CONF-9311104-19) Avail: CASI HC A03

Densifying non-mined diamond powder precursors with diamond produced by chemical vapor infiltration (CVI) is an attractive approach for forming thick diamond deposits that avoids many potential manufacturability problems associated with predominantly chemical vapor deposition (CVD) processes. The authors have developed two techniques: electrophoretic deposition and screen printing, to form non-mined diamond powder precursors on substrates. They then densify these precursors in a hot filament assisted reactor. Analysis indicated that a hot filament assisted chemical vapor infiltration process forms intergranular diamond deposits with properties that are to some degree different from predominantly hot-filament-assisted CVD material. DOE

N94-30692# Air-Conditioning and Refrigeration Technology Inst., Inc., Arlington, VA.

MATERIALS COMPATIBILITY AND LUBRICANTS RESEARCH ON CFC-REFRIGERANT SUBSTITUTES

S. R. Szymurski, G. C. Hourahan, and D. S. Godwin Oct. 1993 44 p

(Contract DE-FG02-91CE-23810)

(DE94-004905; DOE/CE-23810/22) Avail: CASI HC A03/MF A01

The Materials Compatibility and Lubricants Research (MCLR) program supports critical research to accelerate the introduction of CFC and HCFC refrigerant substitutes. The MCLR program addresses refrigerant and lubricant properties and materials compatibility. The primary elements of the work include data collection and dissemination, materials compatibility testing, and methods development. The work is guided by an Advisory Committee consisting of technical experts from the refrigeration and air-conditioning industry and government agencies. The Air-Conditioning and Refrigeration Technology Institute, Inc., (ARTI) manages and contracts multiple research projects and a data collection and dissemination effort. Detailed results from these projects are reported in technical reports prepared by each subcontractor. DOE

N94-30713# Helsinki Univ. of Technology, Espoo (Finland). Dept. of Chemical Engineering.

THE POLYMERIZATION OF EPSILON-CAPROLACTONE WITH STANNOUS CATALYST AND LACTIDE/EPSILON-CAPROLACTONE (LA/EPSILON-CL) AND LACTIDE/GLYCOLIDE (LA/GA) COPOLYMERS. POLYMER TECHNOLOGY PUBLICATION SERIES NO. 15 Literature Review

I. Ylikangas and M. Hiljanen 1993 71 p

(ISSN 0785-7144)

(PB94-137551; ISBN-951-22-1699-X) Avail: CASI HC A04/MF A01

The purpose of the first literature search was to report the published studies on tin catalysts of the polymerization of epsilon-caprolactone (epsilon-CL) monomer. The caprolactone represents an interesting system that can be polymerized with the anionic and coordination catalysts as well as cationic systems. The anionic polymerization of epsilon-CL may be catalyzed by alkoxide catalysts and is complicated by inter- and intramolecular transesterification reactions that give rise to a mixture of linear and cyclic material and broad molecular weight distributions. The second literature study concentrates on lactide/epsilon-CL and lactide/glycolide copolymers obtained by ring polymerization in the presence of stannous octoate as catalyst. Derived from text

N94-30745 Joint Inst. for Nuclear Research, Dubna (USSR). Lab. of High Energy.

NORMAL STATE RESISTIVITY OF MBa2Cu3O(7-x) CERAMICS

C. Sulkowski, N. M. Vladimirova, V. M. Drobin, K. Rogacki, and Z. Damm 1992 7 p Limited Reproducibility: More than 20% of this document may be affected by microfiche quality

(DE94-608456; JINR-R-14-92-65) Avail: CASI HC A02 (US Sales Only)

The precision temperature dependences of resistivity p(T) for ceramic samples MBa2Cu3O(7-x) where M is Y, Er, Eu, Gd, Ho, Dy, Er+Y were measured. The samples with high concentration of oxygen (i.e. with low p) showed clear deviation p(T) from linear dependence below 260-270 K. This deviation (Delta)p is positive and its value decreases with decreasing oxygen concentration and arrives (Delta)p=0 for x=0.2. Another factor decreasing value p appearing below 200 K is fluctuation superconductivity. Its contribution was defined for the sample with (Delta)p=0 and accounted in calculation of normal state resistivity p(sub n)(T). Resulted p(sub n)(T) in the range 120-300 K for samples with oxygen concentration close to 7 is typically metallic and agree with classic Bloch-Crueneisen theory. DOE

N94-30778# Argonne National Lab., IL.

SILICA SCINTILLATING MATERIALS PREPARED BY SOL-GEL METHODS

D. W. Werst, M. C. Sauer, Jr., K. R. Cromack, Y. Lin, E. A. Tartakovsky, and A. D. Trifunac 1993 8 p Presented at the SCIFI 1993 Workshop on Scintillating Fiber Detectors, South Bend, IN, 24-28 Oct. 1993

(Contract W-31-109-eng-38)

(DE94-005123; ANL/CHM/CP-81640; CONF-9310261-2) Avail: CASI HC A02/MF A01

Silica was investigated as a rad-hard alternative to organic polymer hosts for organic scintillators. Silica sol-gels were prepared by hydrolysis of tetramethoxysilane in alcohol solutions. Organic dyes were incorporated into the gels by dissolving in methanol at the sol stage of gel formation. The silica sol-gel matrix is very rad-hard. The radiation stability of silica scintillators prepared by this method is dye-limited. Transient radioluminescence was measured following excitation with 30 ps pulses of 20 MeV electrons. DOE

N94-30797 Colorado Univ., Boulder.
CONTROLLING THE MATERIAL PROPERTIES OF IN VITRO COLLAGEN THROUGH DIRECTED ORIENTATION AND CROSS-LINKING OF FIBRILS Ph.D. Thesis
Todd Edward Bergren 1993 103 p
Avail: Univ. Microfilms Order No. DA9320397

Collagen is a polymeric, fibrillar protein and is the main constituent of all tensile load bearing structures in vivo. Under the proper laboratory conditions, collagen can be dissolved and reassembled into fibers. However, in vitro collagenous constructs have none of the exquisite organization found in in vivo collagen structures. This organization gives in vivo products the propitious material properties (e.g., tensile strength) they exhibit. As a surgical implant material, collagen produced in vitro shows great promise, evincing a low immune response and permitting the infiltration of in vivo collagen. However, in vitro collagenous products lack the material properties of in vivo collagen. It was the purpose of this study to develop methods through which in vitro collagen with more desirable material properties may be produced. Two general methods of increasing the strength of collagen were used, controlling the organization of the in vitro material and increasing the crosslinking of the product. New methods of crosslinking were developed to produce a material with the strength of collagen fixed with glutaraldehyde, but with lower immunogenicity. Collagen strings were extruded from glass tubes into a buffer bath in which the monomers assembled into fibrils. It was believed that the shear gradient of the Poiseuille flow set up in the tubes would force alignment on the collagen molecules in the solution. It was hoped that the final reassembled product would exhibit the longitudinal organization imposed on the molecules in solution. The effects of varying Reynold's number and tube diameter on the final product were tested. The strings were mechanically tested and the material parameters thus obtained (i.e., elastic modulus (Y), ultimate tensile strength (UTS)) analyzed. No significant differences from the controls were found for the fixed samples. Significant increases in Y and UTS were found as Re was increased. An increase in the extrusion tube diameter produced significant decreases in Y and UTS. Scanning electron microscopy supported the conclusion that changes in fibrillar organization were induced by shear flow. An attempt was made to organize collagen during assembly in microgravity through the use of isoelectric focusing of tropocollagen molecules. Histological examination revealed no orientation differences between flight and ground. Dissert. Abstr.

N94-30812 North Dakota State Univ., Fargo.
CROSSLINKING AND SURFACE REACTIONS IN MACROMOLECULES: SPECTROSCOPIC FT-IR STUDIES Ph.D. Thesis
Scott Richard Gaboury 1993 212 p
Avail: Univ. Microfilms Order No. DA9321837

Studies were undertaken to advance our knowledge and to gain new insights about macromolecular crosslinking systems and plasma surface reactions on crosslinked polymers. Analysis of polymeric networks was carried out using Fourier transform infrared (FT-IR) spectroscopic methods, including transmission, photoacoustic (PA), and attenuated, total reflectance (ATR) FT-IR modes of detection. The crosslinking reactions of hydroxyl terminated poly dimethyl siloxane (PDMS) were studied using PA FT-IR spectroscopy and involved the analysis of evolved ethanol. Intensity changes of the ethanol bands were correlated to the viscosity measurements. Transmission FT-IR was found to be insensitive to the crosslinking reactions. PA and transmission FT-IR spectroscopy were also used to elucidate the origin of crosslinking reactions in polyester/styrene (PE/ST). Gelation and vitrification transitions in PE/ST were detected spectroscopically and the formation of atactic polystyrene during crosslinking was revealed. ATR FT-IR spectroscopy was utilized to study the effects of different plasma surface reactions on silicone elastomers. Ammonia plasma reactions of PDMS containing chloro-functional initiators or cleaning solvents resulted in the formation of surface amide groups, but due to the parallel formation of surface ammonium chloride, the amide groups were not chemically bound to the PDMS surface. A novel microwave plasma reactor was developed and used for plasma modification of PDMS elastomer surfaces. Analysis of the ATR spectra revealed the presence of Si-H surface functional groups that were produced by both argon and nitrogen plasmas. The use of a Kramers-Kronig transformation allowed quantitative analysis of the Si-H concentrations. Acrylamide and maleic anhydride solid monomers were microwave plasma reacted onto PDMS elastomers. Plasma reactions, ranging from approximately 5 to 15 seconds, caused maleic anhydride and acrylamide to be chemically bound to the PDMS surface, while the majority of anhydride and amide functionalities were maintained. Quantitative analysis of ATR FT-IR spectra showed that the surface concentrations of solid monomers ranged from 1 to 5 picomole/sq cm. Such functionalized PDMS surfaces can be post plasma reacted using base hydrolysis. The hydrolysis of the amide and anhydride functionalities to carboxylic acid salt groups yielded a 66 percent conversion for acrylamide and a 48 percent conversion for maleic anhydride. Dissert. Abstr.

N94-30826# Minnesota Mining and Mfg. Co., Saint Paul. Corporate Research Labs.
DUAL CURE LOW-VOC COATING PROCESS, PHASE 3
K. E. Kinzer Nov. 1993 20 p
(Contract DE-AC04-88ID-12692)
(DE94-003202; DOE/ID-12692/5-Phase-3) Avail: CASI HC A03/MF A01

The objective of Phase 3 is to complete proof-of-principle testing in full-scale systems of the dual cure photocatalyst technology developed in earlier phases. Phase 3 commercial applications are aerospace topcoats, aerospace primers, and solventless manufacture of tape backings. Progress was made in improving urethane/acrylate formulation for aerospace topcoats, particularly in reverse impact, initial gloss, and loss retention during accelerated weathering. Formulations have now been developed which meet all initial criteria; the formulation was optimized. Aerospace primer formulations based on epoxy/flexibilizer systems were evaluated. Because of cure consistency problems and the increased need for non-chromated primers, work on aerospace primer system was de-emphasized to allow greater effort on development and commercialization of aerospace topcoat. Work on solventless backing saturants for electrical tape backings has been completed; optimal dual cure resin formulations have been used in preparing complete tape constructions. DOE

N94-30829 Lawrence Livermore National Lab., CA.
MATERIAL PROPERTIES AND FRACTURE MECHANICS IN RELATION TO CERAMIC MACHINING
L. V. Griffith 2 Dec. 1993 16 p Limited Reproducibility: More than 20% of this document may be affected by microfiche quality
(Contract W-7405-eng-48)
(DE94-006623; UCRL-ID-115689) Avail: CASI HC A03

Material removal rate, surface finish, and subsurface damage are largely governed by fracture mechanics and plastic deformation, when ceramics are machined using abrasive methods. A recently published model describes many of the most important features of the loose abrasive machining process, for example depth of damage, surface roughness, and material removal rate. Many of the relations in the loose abrasive machining model can be readily discerned from fracture mechanics models, in terms of material properties. By understanding the mechanisms of material removal, from a material properties perspective, a better estimation can be made of how one material will machine in relation to another. Although the fracture mechanics models may have been developed for loose abrasive machining, the principles of crack initiation and propagation are equally valuable for fixed abrasive machining. This report provides a brief review of fracture in brittle materials, the stress distribution induced by abrasives, critical indenter loads, the extension of cracks, and the relation of the fracture process to material removal. DOE

N94-30896# Sandia National Labs., Albuquerque, NM.
SURFACE CHEMISTRY OF BORON-DOPED SiO2 CVD: ENHANCED UPTAKE OF TETRAETHYL ORTHOSILICATE BY HYDROXYL GROUPS BONDED TO BORON
M. E. Bartram and H. K. Moffat 1993 6 p Presented at the Fall Meeting of the Materials Research Society (MRS), Boston, MA, 29 Nov. - 3 Dec. 1993
(Contract DE-AC04-94AL-85000)
(DE94-005428; SAND-93-1497C; CONF-931108-41) Avail: CASI HC A02/MF A01

Insight into how dopants can enhance deposition rates was obtained by comparing reactivities of tetraethyl orthosilicate (TEOS, Si(OCH2)CH3(sub 4)) with silanol and boranol groups on SiO2. This comparison is relevant for boron-doped SiO2 film growth from TEOS and trimethyl borate (TMB, B(OCH3)(sub 3)) sources since boranols and silanols are expected to be

present on surface during CVD. A silica substrate having coadsorbed deuterated silanols (SIOD) and boranols (BOD) was reacted with TEOS in a cold-wall reactor in the mTorr pressure regime at 1000 K. Reactions were followed with Fourier transform infrared spectroscopy. Use of deuterated hydroxyls allowed consumption of hydroxyls by TEOS chemisorption to be distinguished from concurrent formation of SIOH and BOH that results from TEOS decomposition. It was found that TEOS reacts with BOD at twice the rate observed for SIOD demonstrating that hydroxyl groups bonded to boron increase the rate of TEOS chemisorption. Surface ethoxy groups produced by chemisorption of TEOS decompose at a slower rate in the presence of TMB decomposition products. Possible dependencies on reactor geometries and other deposition conditions may determine which of these two competing effects will control deposition rates. This may explain (in part) why the rate enhancement effect is not always observed in boron-doped SiO2 CVD processes. DOE

N94-30900# Sandia National Labs., Albuquerque, NM.
MEASUREMENT OF BULK LONGITUDINAL MODULUS AND CORRECTION FOR EDGE EFFECTS
D. J. Segalman and S. E. Klenke 1993 13 p Presented at the North American Conference on Smart Structures and Materials, Orlando, FL, 13-18 Feb. 1994
(Contract DE-AC04-94AL-85000)
(DE94-005581; SAND-93-2058C; CONF-940206-2) Avail: CASI HC A03/MF A01

Measurement of the bulk longitudinal modulus, M(sup *), of rubbery polymers is a notoriously difficult task. Measurements are traditionally done through a fluid environment in methods that provide M(sup *) over only very narrow frequency ranges. An alternative approach, using a resonant test fixture is presented in this paper. A discussion of some physical limitations is developed. Among them are issues of repeatability and edge effects. A method of data analysis to address edge effects is also presented. DOE

N94-30906# Brookhaven National Lab., Upton, NY.
DEVELOPMENT OF RADIATION RESISTANT ELECTRICAL CABLE INSULATIONS
B. S. Lee, P. Soo, and D. R. MacKenzie 1993 9 p Presented at the 4th National Technology Transfer Conference and Exposition, Anaheim, CA, 7-9 Dec. 1993 See also N94-30480
(Contract DE-AC02-76CH-00016)
(DE94-005189; BNL-49748; CONF-931244-2) Avail: CASI HC A02/MF A01

Two new polyethylene cable insulations have been formulated for nuclear applications, and have been tested under gamma radiation. Both insulations are based on low density polyethylene, one with PbO and the other with Sb2O3 as additives. The test results show that the concept of using inorganic antioxidants to retard radiation initiated oxidation (RIO) is viable. PbO is more effective than Sb2O3 in minimizing RIO. DOE

N94-30909# Sandia National Labs., Albuquerque, NM.
THERMOCHEMICAL DATA FOR CVD MODELING FROM AB INITIO CALCULATIONS
P. Ho and C. F. Melius 1993 9 p Presented at the Fall Meeting of the Materials Research Society (MRS), Boston, MA, 29 Nov. - 3 Dec. 1993
(Contract DE-AC04-94AL-85000)
(DE94-005269; SAND-93-3842C; CONF-931108-39) Avail: CASI HC A02/MF A01

Ab initio electronic-structure calculations are combined with empirical bond-additivity corrections to yield thermochemical properties of gas-phase molecules. A self-consistent set of heats of formation for molecules in the Si-H, Si-H-Cl, Si-H-F, Si-N-H and Si-N-H-F systems is presented, along with preliminary values for some Si-O-C-H species. DOE

N94-30922 Michigan Univ., Ann Arbor.
AN ASYMPTOTIC ANALYSIS FOR COMPRESSIBLE GAS LUBRICATION OF ROUGH SURFACES Ph.D. Thesis
Ki Ook Park 1993 134 p
Avail: Univ. Microfilms Order No. DA9319604

The lubrication of a magnetic head on a rough computer hard disk with compressible gas was modeled by applying an asymptotic analysis. The basic equations were derived from the general conservation equations by means of a perturbation technique using the fluid film thickness-to-length ratio as the small parameter. The analysis focuses on hydrodynamic flow; therefore, elastic deformation of the general bearing surface and even partial asperity contact do not occur. The asymptotic analysis for Reynolds roughness and Stokes roughness uses the continuity and the Navier-Stokes equations. The analysis considers a sufficiently thick gas bearing condition such that air is taken to be a continuous gas but a sufficiently thin film so that roughness effects are significant. Temperature, compressibility, moving-roughness, and Stokes-roughness effects are described. Inertia and temperature effects were found to be not very important. The compressibility effect is presented as the pressure dip at the trailing edge of gas bearing. A deeper pressure dip is detected in the moving roughness models because of the unsteady squeeze effect of moving roughness. The lowest-order equations are reduced to the well-known Reynolds equation and the limit of conventional lubrication analysis can be also seen by the direct comparisons between the zeroth- and second-order solutions.
Dissert. Abstr.

N94-28709*# National Aeronautics and Space Administration. White Sands Test Facility, NM.
FLAMMABILITY, ODOR, OFFGASSING, THERMAL VACUUM STABILITY, AND COMPATIBILITY WITH AEROSPACE FLUIDS OF WIRE INSULATIONS
David Hirsch (Lockheed Engineering and Management Services Co., Inc., Las Cruces, NM.) and Harry Johnson *In* NASA. Lewis Research Center, Second NASA Workshop on Wiring for Space Applications Jan. 1994 p 109-120 (For primary document see N94-28697 08-18)
Avail: CASI HC A03/MF A03; 8 functional color pages

N94-28710*# McDonnell-Douglas Aerospace, Saint Louis, MO.
ELECTRICAL AND MECHANICAL TESTING OF WIRE INSULATION FOR SPACE APPLICATIONS
Linda A. Burkhardt *In* NASA. Lewis Research Center, Second NASA Workshop on Wiring for Space Applications Jan. 1994 p 121-129 (For primary document see N94-28697 08-18)
Avail: CASI HC A02/MF A03; 8 functional color pages

N94-28711*# Sverdrup Technology, Inc., Brook Park, OH.
EVALUATION OF PYROLYSIS AND ARC TRACKING ON CANDIDATE WIRE INSULATION DESIGNS FOR SPACE APPLICATIONS
Thomas J. Stueber and Kenneth Hrovat *In* NASA. Lewis Research Center, Second NASA Workshop on Wiring for Space Applications Jan. 1994 p 131-145 Original contains color illustrations (For primary document see N94-28697 08-18)
Avail: CASI HC A03/MF A03; 8 functional color pages

N94-28712*# National Aeronautics and Space Administration. Lewis Research Center, Cleveland, OH.
WIRE INSULATION DEGRADATION AND FLAMMABILITY IN LOW GRAVITY
Robert Friedman *In its* Second NASA Workshop on Wiring for Space Applications Jan. 1994 p 147-164 Original contains color illustrations (For primary document see N94-28697 08-18)
Avail: CASI HC A03/MF A03; 8 functional color pages

N94-28713*# State Univ. of New York, Buffalo.
BREAKDOWN TESTING OF WIRING INSULATION
Javaid R. Laghari *In* NASA. Lewis Research Center, Second NASA Workshop on Wiring for Space Applications Jan. 1994 p 165-172 (For primary document see N94-28697 08-18)
Avail: CASI HC A02/MF A03; 8 functional color pages

N94-28715*# TRW, Inc., Redondo Beach, CA.
HIGH TEMPERATURE POLYMER DIELECTRIC FILM INSULATION
Robert J. Jones *In* NASA. Lewis Research Center, Second NASA Workshop on Wiring for Space Applications Jan. 1994 p 189-191 (For primary document see N94-28697 08-18)
Avail: CASI HC A01/MF A03; 8 functional color pages

N94-28716*# Foster-Miller Associates, Inc., Waltham, MA.
HIGH TEMPERATURE ARC-TRACK RESISTANT AEROSPACE INSULATION
William Dorogy *In* NASA. Lewis Research Center, Second NASA Workshop on Wiring for Space Applications Jan. 1994 p 193-201 (For primary document see N94-28697 08-18)
Avail: CASI HC A02/MF A03; 8 functional color pages

N94-28717*# Minnesota Mining and Mfg. Co., Saint Paul. Electrical Products Div.
A 3M HIGH TEMPERATURE DIELECTRIC FILM
Edward Hampl, Jr. *In* NASA. Lewis Research Center, Second NASA Workshop on Wiring for Space Applications Jan. 1994 p 203-210 (For primary document see N94-28697 08-18)
Avail: CASI HC A02/MF A03; 8 functional color pages

N94-29513# National Inst. for Resources and Environment, Ibaraki (Japan). Siliceous Materials Div.
LAYERED POLYSILICATE: PROPERTIES AND PERSPECTIVES IN APPLICATIONS [SOJO PORIKEISANEN: SONO TOKUSEI TO SOZAIKA ENO TENBO]
Katsunori Kosuge and Atsumu Tsunashima *In its* Journal of NIRE, Vol. 2, No. 3 25 May 1993 p 1-10 In JAPANESE (For primary document see N94-29512 08-99)
Avail: CASI HC A02/MF A02

N94-29517# National Inst. for Resources and Environment, Ibaraki (Japan). Carbon Materials Div.
PREPARATION OF GRAPHITE FIBERS FROM POLYIMIDE [PORIMIIDO O ZENKUTAI TO SURU KOKESSHOSEI KOKUEN SENI NO SAKUSEI]
Hiroaki Hatori, Yoshio Yamada, Minoru Shiraishi, and Yoshikazu Takahashi *In its* Journal of NIRE, Vol. 2, No. 3 25 May 1993 p 47-55 In JAPANESE (For primary document see N94-29512 08-99)
Avail: CASI HC A02/MF A02

N94-29518# National Inst. for Resources and Environment, Ibaraki (Japan). Carbon Materials Div.
PREPARATION AND STRUCTURE OF AMORPHOUS HYDROGENATED CARBON FILM DEPOSITED WITH RF PLASMA CVD [KOSHUHA PURAZUMA CVD SOCHI NI YORU HISHOSHITSU TANSO(A-C : H) MAKU NO GOSEI TO KOZO KAISEKI]
Noriko Yoshizawa, Yoshio Yamada, and Minoru Shiraishi *In its* Journal of NIRE, Vol. 2, No. 3 25 May 1993 p 57-65 In JAPANESE (For primary document see N94-29512 08-99)
Avail: CASI HC A02/MF A02

N94-29641*# Aerospace Corp., El Segundo, CA. Mechanics and Materials Technology.
THE USE OF SCREENING TESTS IN SPACECRAFT LUBRICANT EVALUATION
Chris Kalogeras, Mike Hilton, David Carre, Stephen Didziulis, and Paul Fleischauer *In* NASA. Ames Research Center, The 27th Aerospace Mechanisms Symposium May 1993 p 197-217 (For primary document see N94-29627 08-15)
(Contract F04701-88-C-0089)
Avail: CASI HC A03/MF A03

N94-30451*# Army Armament Munitions and Chemical Command, Watervliet, NY. Army Research, Development, and Engineering Center.
AN IMPROVED PLATING PROCESS
John C. Askew *In* NASA, Washington, Technology 2003: The Fourth National Technology Transfer Conference and Expositon, Volume 1 Feb. 1994 p 100-107 (For primary document see N94-30440 08-99)
Avail: CASI HC A02/MF A04

N94-30474*# Naval Air Warfare Center, China Lake, CA.
SYNTHESIS AND CHARACTERIZATION OF ADVANCED MATERIALS FOR NAVY APPLICATIONS
J. Covino and I. Lee *In* NASA, Washington, Technology 2003: The Fourth National Technology Transfer Conference and Exposition, Volume 1 Feb. 1994 p 294-306 (For primary document see N94-30440 08-99)
Avail: CASI HC A03/MF A04

N94-30475*# Brookhaven National Lab., Upton, NY. Dept. of Nuclear Energy.
DEPOSITION OF TANTALUM CARBIDE COATINGS ON GRAPHITE BY LASER INTERACTIONS
James Veligdan, D. Branch, P. E. Vanier, and R. E. Barietta *In* NASA, Washington, Technology 2003: The Fourth National Technology Transfer Conference and Exposition, Volume 1 Feb. 1994 p 307-311 (For primary document see N94-30440 08-99)
(Contract DE-AC02-76CH-00016)
Avail: CASI HC A01/MF A04

N94-30476*# USBI Booster Production Co., Titusville, FL.
DEVELOPMENT OF A UNIQUE POLYURETHANE PRIMER/TOPCOAT
Howard L. Novak and James M. Klotz *In* NASA, Washington, Technology 2003: The Fourth National Technology Transfer Conference and Exposition, Volume 1 Feb. 1994 p 312-317 (For primary document see N94-30440 08-99)
Avail: CASI HC A02/MF A04

N94-30477*# Naval Air Warfare Center, China Lake, CA.
HIGH ELONGATION ELASTOMERS
V. L. Brady, R. Reed, L. Merwin, and R. Nissan *In* NASA, Washington, Technology 2003: The Fourth National Technology Transfer Conference and Exposition, Volume 1 Feb. 1994 p 318-336 (For primary document see N94-30440 08-99)
Avail: CASI HC A03/MF A04

N94-30478*# Fluid Polymers, Inc., Las Vegas, NV.
SOLVENTLESS, CURABLE FLUID OLIGOMERIC SYSTEMS FOR HIGH PERFORMANCE MICROWAVE, ACOUSTICAL AND MECHANICAL APPLICATIONS
G. M. LeFave, Leo Stanton, and Jim Foreman *In* NASA, Washington, Technology 2003: The Fourth National Technology Transfer Conference and Exposition, Volume 1 Feb. 1994 p 337-343 (For primary document see N94-30440 08-99)
Avail: CASI HC A02/MF A04

N94-30479*# Sigma Labs., Inc., Tucson, AZ.
PLASMA TREATMENT OF POLYMER DIELECTRIC FILMS TO IMPROVE CAPACITIVE ENERGY STORAGE
A. Yializis, M. Binder, and R. J. Mammone *In* NASA, Washington, Technology 2003: The Fourth National Technology Transfer Conference and Exposition, Volume 1 Feb. 1994 p 344-351 (For primary document see N94-30440 08-99)
Avail: CASI HC A02/MF A04

N94-30480*# Brookhaven National Lab., Upton, NY. Dept. of Advanced Technology.
DEVELOPMENT OF RADIATION RESISTANT ELECTRICAL CABLE INSULATIONS
B. S. Lee, P. Soo, and D. R. MacKenzie *In* NASA, Washington, Technology 2003: The Fourth National Technology Transfer Conference and Exposition, Volume 1 Feb. 1994 p 352-360 (For primary document see N94-30440 08-99)
Avail: CASI HC A02/MF A04

N94-30483*# Axiomatics Corp., Woburn, MA.
IMPROVED CONSTRUCTION MATERIALS FOR POLAR REGIONS USING MICROCELLULAR THERMOPLASTIC FOAMS
Daniel J. Cunningham *In* NASA, Washington, Technology 2003: The Fourth National Technology Transfer Conference and Exposition, Volume 1 Feb. 1994 p 385-391 (For primary document see N94-30440 08-99)
Avail: CASI HC A02/MF A04

28 PROPELLANTS AND FUELS

Includes rocket propellants, igniters, and oxidizers; their storage and handling procedures; and aircraft fuels.

For related information see also *07 Aircraft Propulsion and Power, 20 Spacecraft Propulsion and Power,* and *44 Energy Production and Conversion.*

N94-28502# Southwest Research Inst., San Antonio, TX.
IMPACT STUDY ON THE USE OF BIOMASS-DERIVED FUELS IN GAS TURBINES FOR POWER GENERATION
C. A. Moses and H. Bernstein Jan. 1994 132 p Prepared for Midwest Research Inst., Golden, CO
(Contract DE-AC02-83CH-10093)
(DE94-000261; NREL/TP-430-6085) Avail: CASI HC A07/MF A02

This report evaluates the properties of fuels derived from biomass, both gaseous and liquid, against the fuel requirements of gas turbine systems for generating electrical power. The report attempts to be quantitative rather than merely qualitative to establish the significant variations in the properties of biomass fuels from those of conventional fuels. Three general categories are covered: performance, durability, and storage and handling. DOE

N94-28577# Abacus Technology Corp., Chevy Chase, MD.
ALTERNATIVE FUEL VEHICLES FOR THE STATE FLEETS: RESULTS OF THE 5-YEAR PLANNING PROCESS
May 1993 121 p Sponsored by DOE
(DE94-004709; DOE/EE-0007) Avail: CASI HC A06/MF A02

This report documents the first attempt by the Department of Energy (DOE) to work with states to prepare five-year Alternative Fuel Vehicle (AFV) acquisition plans to identify alternative fuels and vehicles that they are planning on or would like to acquire. The DOE Regional Support Offices (RSO's) met with representatives from the states in their regions and assisted in the preparation of the plans. These plans will be used in conjunction with previously gathered Federal five-year plans to encourage Original Equipment Manufacturers (OEM's) to expand the variety of AFV's produced, reduce the incremental cost of AFV's, and to encourage fuel suppliers to expand the alternative fuel infrastructure and alternative fuel availability. By identifying the needs and requirements of state fleets, DOE can begin to describe the specific nature of the future state fleets, and establish a defined market for OEM's and fuel suppliers. DOE initiated the development and collection of the state five-year plans before the signing of the Energy Policy Act, to raise the awareness of states that they will be required by law to acquire AFV's. As a result, several states that had no AFV acquisition plan when queried have developed or are in the process of developing plans. The DOE and its RSO's are still working with the states to develop and refine acquisition plans, and this report should be treated as documentation of work in progress. DOE

N94-28629 New Energy and Industrial Technology Development Organization, Tokyo (Japan).
FEASIBILITY STUDY ON INTRODUCTION OF A LARGE METHANOL ENGINE POWER GENERATION PLANT
Mar. 1993 116 p In JAPANESE Limited Reproducibility: More than 20% of this document may be affected by microfiche quality
(DE94-732338; NEDO-P-9224) Avail: CASI HC A06

This paper studies a possibility of introducing a 2-cycle methanol diesel engine power generation plant. Since methanol is much in vaporizing latent heat and small in quantity of heat emission per unit weight when using it as fuel, observed are a decline in combustible range temperature and a large decrease in NOx emissions. As for thermal efficiency, generating end efficiency of 46% is expected by heat recovery in the case of 40-50 thousand kW class 2-cycle engines. The methanol engine has such excellent performance characteristics as little lowering of efficiency at middle loads, possible numerical control, short starting time and high load change rate. The construction cost is approximately equal to that of the LNG steam power generation and is lower than that of the LNG combined cycle power generation. The unit power generation cost is lower than those of fuel cells and gas turbines and 2-3 yen/kW higher than those of the combined cycle and the reformed turbines. DOE

N94-28769 Oklahoma State Univ., Stillwater. Dept. of Chemistry.
CHEMICAL DYNAMICS STUDIES OF REACTIONS IN ENERGETIC MATERIALS Final Report, 1989 - 1993
Donald L. Thompson 15 Dec. 1993 19 p Limited Reproducibility: More than 20% of this document may be affected by microfiche quality
(Contract DAAL03-89-K-0052)
(AD-A275607; ARO-26106.23-CH) Avail: CASI HC A03

We have carried out a research program to investigate the chemical dynamics of unimolecular reactions in large polyatomic molecules. The purpose of the studies is an improved understanding of the fundamental behavior of highly excited, reactive molecules, with an emphasis on energetic materials. We have made some significant progress in extending theoretical chemical dynamics calculations to reactions in large molecules, as illustrated by our explicit, full-dimensional classical dynamics study of the unimolecular decomposition of RDX. Leading up to this study of RDX, we performed a long series of dynamics calculations for a variety of molecules to determine the important factors for accurately simulating processes in polyatomic molecules. DTIC

N94-28879# Pennsylvania State Univ., University Park.
A STUDY OF SOLID PROPELLANTS USING A MICROPROBE MASS SPECTROMETER SYSTEM Annual Report No. 1
Thomas A. Litzinger 1993 31 p
(Contract N00014-93-1-0080)
(AD-A275325) Avail: CASI HC A03/MF A01

The objective of this effort is to determine the chemical mechanisms of solid propellant ignition and deflagration with an emphasis on the decomposition of individual propellant ingredients and on the gas phase reactions of the products of decomposition. A quadrupole mass spectrometer system using quartz microprobes measures species profiles above the surface of the sample during CO2 laser induced pyrolysis or during laser assisted deflagration of the sample. In addition microthermocouples are used to measure the surface temperature and gas phase temperatures during testing. To complement the experimental studies, chemical kinetic models produced by other researchers are used to model some of the data obtained. DTIC

N94-28901 Allied-Signal Aerospace Co., Des Plaines, IL. Research and Development.
ADVANCED FUEL PROPERTIES: A COMPUTER PROGRAM FOR ESTIMATING PROPERTY VALUES Final Report, Sep. 1987 - Jan. 1993
C. A. Parker, J. T. Donner, K. R. Squire, R. J. Schofield, and K. R. Kriha
May 1993 175 p Limited Reproducibility: More than 20% of this document may be affected by microfiche quality
(Contract F33615-87-C-2709)
(AD-A275248; WL-TR-93-2086) Avail: CASI HC A08

The U.S. Air Force has seen that in order to develop fuels needed for the high performance aircraft of the future, the ability to design fuels based on the satisfaction of a set needed properties is necessary. This report covers all phases of a project to develop software to accomplish this goal. This report discusses the methods used by the software to obtain the thermochemical properties of organic fuel candidates. Emphasis was placed on describing the methods used to determine the properties of a mixture of compounds, since it is these types of mixtures that are most likely to be found in fuels. DTIC

N94-29092 Materials Research Labs., Ascot Vale (Australia).
CORRELATION OF COOKOFF BEHAVIOR OF ROCKET PROPELLANTS WITH THERMOMECHANICAL AND THERMOCHEMICAL PROPERTIES
Sook Y. Ho, Tony Ferschl, and John Foureu Nov. 1993 33 p Limited Reproducibility: More than 20% of this document may be affected by microfiche quality
(AD-A274983; MRL-TR-93-15; DODA-AR-008-278) Avail: CASI HC A03/MF A01

The fast and slow cookoff behavior of a series of in-service and research composition rocket propellants has been evaluated using the standard small-scale cookoff bomb (SSCB) test (based on the NWC design) as part of a program in Explosives Ordnance Division (EOD) to develop an extensive insensitive munitions technology base. A modified SSCB test methodology, whereby the pressure output can be measured, was developed to enable a more quantitative measure of the reaction violence and to provide further insight into the cookoff mechanism. The temperature

distribution and gradients at various positions and depths in the cylindrical propellant specimen, during fast and slow cookoff, were measured in order to understand the marked difference in the severity of the response shown by some of the propellants when the heating rate was changed. Pressure and heating rate dependent thermochemical properties and thermomechanical properties of the propellants were measured and correlated with cookoff behavior. DTIC

N94-29308# Sandia National Labs., Livermore, CA. Combustion Research Facility.

INSENSITIVE ENERGETIC MATERIALS: THE IMPORTANCE OF PHYSICAL PROPERTIES AND MOLECULAR STRUCTURE Final Report, 17 Apr. 1990 - 30 Sep. 1993

Richard Behrens, Jr. 22 Dec. 1993 11 p

(Contract ARO-MIPR-130-93)

(AD-A275393; ARO-27887.6-CH) Avail: CASI HC A03/MF A01

A summary of the most important findings on the thermal decomposition of five cyclic nitramines is presented. The compounds studied include: octahydro-1,3,5,7- tetranitro-1,3,5,7- tetrazocine (HMX), hexahydro-1,3,5-trinitro-striazine (RDX), hexahydro-l-nitroso-3,5- dinitro-s-triazine (ONDNTA), 1,3,5-trinitro- 1,3,5-triazacycloheptane (TNCHP), and 2-oxo- 1,3,5-trinitro-1,3,5-triazacyclohexane (K6). The thermal decomposition processes were studied using simultaneous thermogravimetric modulated beam mass spectrometry (STMBMS) to identify the decomposition products and to determine their gas formation rates and using mixtures of isotopically labeled analogues of the compounds to track the decomposition mechanisms by analyzing the extent of isotopic scrambling and the deuterium kinetic isotope effect (DKIE). Extensive results on the thermal decomposition of RDX and HMX in the solid and liquid phases show that their decomposition is controlled by several parallel decomposition pathways. One pathway involves the loss of HONO and the formation of oxy-s-triazine (OST) from the RDX ring. The other pathway occurs via the mononitroso intermediate of the parent compound. The decomposition of the mononitroso-RDX intermediate, ONDNTA, has been extensively studied and a summary of the highlights of its decomposition is presented. The results on TNCHP show that it is the only one of the cyclic nitramines studied that is stable in the liquid phase. DTIC

N94-29310# New Orleans Univ., LA. Dept. of Chemistry.

SUPERIOR ENERGETIC MATERIALS THAT CONTAIN CARBOCATIONS AND ANIONS. ENERGETIC MATERIALS RESTRICTED IN COMPOSITION TO C, H, N, AND O ATOMS Final Report, 1 Sep. 1990 - 31 Aug. 1993

Peter Politzer and Joseph H. Boyer 30 Oct. 1993 14 p

(Contract DAAL03-90-G-0205)

(AD-A275449; ARO-28096.7-CH-SAH) Avail: CASI HC A03/MF A01

Energetic compounds restricted in composition to C, H, N, and 0 atoms were synthesized for utilization in formulations for explosives and propellants. Compounds discussed include trinitromethanides, diimidazopyrazines, triazolooxadiazoles, and triazolotriazoles. DTIC

N94-29414# Aerospatiale, Les Mureaux (France). Dept. Equipements et Chaines de Puissances.

THE LASER APPROACH FOR SEQUENTIAL PYROTECHNIC INITIATION SYSTEMS: ENVISAGEABLE CHAIN ARCHITECTURE AND CONCEPTS [SYSTEME SEQUENTIEL D'INITIATION PYROTECHNIQUE PAR LASER: ARCHITECTURE DE CHAINE ET CONCEPTS ENVISAGEABLES]

P. Baraer and J. Masson 1993 24 p In FRENCH Presented at the 7th Institut d'Aeronautique et Spatiale du Canada Conference on Astronautics, Ottawa, Canada, 4-6 Nov. 1992

(Rept-932-430-113; ETN-94-95471) Avail: CASI HC A03/MF A01

The advantages offered by the laser approach for ordnance initiation systems to initiate directly pyrotechnics secondary explosives are described. The basis of light-initiated systems is to develop a unique method that offers the promise of safety in an environment where electromagnetic fields could be a problem. Explosives can be initiated by a wide variety of energy inputs, kinetic energy, electrical discharge, heat, and light. Even if the idea of constructing light initiated systems has been known for 20 years, only recent developments have made their utilization possible. Optical technolgy presents many advantages, most of which concern the optopyrotechnic interface that requires an intense energy which cannot be duplicated by external conditions other than those produced by a specific laser source. Moreover, optical fibers are immune to induced energy from electrical or radio frequency sources, they can survive gamma radiation, and are lighter than metallic cables. The laser ignition program has proved the feasibility of a full chain able to initiate the totality of the pyrotechnic functions in a launcher. The makeup of each component of the pyrotechnic chain is outlined, including the YAG laser, fiber optic distribution system (optomechanical sequencer), and pyrotechnic devices. The characteristics and performances of the ignition device are given. ESA

N94-29429# Aerospatiale Aquitaine, Saint-Medard en Jalles (France).

PYROTECHNIC SHOCK: DEVICES IN PYROTECHNIC ENVIRONMENT QUALIFICATION LOGIC [CHOCS D'ORIGINE PYROTECHNIQUE. LOGIQUE DE QUALIFICATION DES MATERIELS EN ENVIRONNEMENT PYROTECHNIQUE]

J. J. Domenge 1993 11 p In FRENCH

(Rept-932-430-108; ETN-94-95466) Avail: CASI HC A03/MF A01

A qualification logic to check the capacity of spacecraft equipment to withstand pyrotechnic shocks generated by detonating fuses, transmission relays, and explosive bolts, is reported. The following are considered: the characterization of pyrotechnic shock severity; the determination of severity according to the different axes applied to the materials; a qualification logic; and the main damages and effects induced by the pyrotechnic environment. ESA

N94-29490*# National Aeronautics and Space Administration. Pasadena Office, CA.

CATALYTIC IGNITOR FOR REGENERATIVE PROPELLANT GUN Patent Application

Gerald E. Voecks, inventor (to NASA) (Jet Propulsion Lab., California Inst. of Tech., Pasadena.) and Ned W. Ferraro, inventor (to NASA) (Jet Propulsion Lab., California Inst. of Tech., Pasadena.) 17 Feb. 1994 21 p

(Contract NAS7-1260)

(NASA-Case-NPO-18987-1-CU; NAS 1.71:NPO-18987-1-CU;

US-Patent-Appl-SN-200785) Avail: CASI HC A03/MF A01

An ignitor initiates combustion of liquid propellant in a gun by utilizing a heated catalyst onto which the liquid propellant is sprayed in a manner which mitigates the occurrence of undesirable combustion chamber oscillations. The heater heats the catalyst sufficiently to provide the activation necessary to initiate combustion of the liquid propellant sprayed thereonto. Two embodiments of the ignitor and three alternative mountings thereof within the combustion chamber are disclosed. The ignitor may also be utilized to dispose of contaminated, excess, or waste liquid propellant in a safe, controlled, simple, and reliable manner. NASA

N94-30038 Midwest Research Inst., Golden, CO. National Renewable Energy Lab.

BIODIESEL FROM AQUATIC SPECIES

L. M. Brown, S. Sprague, E. E. Jarvis, T. G. Dunahay, P. G. Roessler, and K. G. Zeiler Jan. 1994 33 p Limited Reproducibility: More than 20% of this document may be affected by microfiche quality

(Contract DE-AC02-83CH-10093)

(DE94-000275; NREL/TP-422-5726) Avail: CASI HC A03

Researchers in the Biodiesel/Aquatic Species Project focus on the use of microalgae as a feedstock for producing renewable, high-energy liquid fuels. The program's basic premise is that microalgae, which have been called the most productive biochemical factories in the world, can produce up to 30 times more oil per unit of growth area than land plants. It is estimated that 150 to 400 barrels of oil per acre per year (0.06 to 0.16 million liters/hectar) could be produced with microalgal oil technology. Initial commercialization of this technology is envisioned for the desert Southwest because this area provides high solar radiation and offers flat land that has few competing uses (hence low land costs). Similarly, there are large saline aquifers with few competing uses in the region. This water source could provide a suitable, low-cost medium for the growth of many microalgae. The primary area of research during FY 1993 was the effort to genetically improve microalgae in order to control the timing and magnitude of lipid accumulation. Increased lipid content will have a direct effect on fuel price, and the control of lipid content is a major project goal. The paper describes progress on the following: culture collection; molecular biology of lipid biosynthesis; microalgal transformation; and environmental, safety, and health and quality assurance. DOE

N94-30612# ORTECH International, Mississauga (Ontario).
PROCEEDINGS OF THE 1993 WINDSOR WORKSHOP ON ALTERNATIVE FUELS
Oct. 1993 707 p Workshop held in Toronto, Ontario, 14-16 Jun. 1993 Sponsored by DOE and Energy, Mines and Resources Canada
(DE94-003908; CONF-930696) Avail: CASI HC A99/MF A06

This report contains viewgraph papers on the following topics concerning alternative fuels: availability of alternative fueled engines and vehicles; emerging technologies; overcoming barriers to alternative fuels commercialization; infrastructure issues; and new initiatives in research and development. DOE

N94-30615# Sandia National Labs., Albuquerque, NM.
XCHEM-1D: A HEAT TRANSFER/CHEMICAL KINETICS COMPUTER PROGRAM FOR MULTILAYERED REACTIVE MATERIALS
R. J. Gross, M. R. Baer, and M. L. Hobbs Oct. 1993 61 p
(Contract DE-AC04-94AL-85000)
(DE94-005072; SAND-93-1603) Avail: CASI HC A04/MF A01

An eXplosive CHEMical kinetics code, XCHEM, was developed to solve the reactive diffusion equations associated with the thermal ignition of energetic materials. This method-of-lines code uses stiff numerical methods and adaptive meshing to resolve relevant combustion physics. Solution accuracy is maintained between multilayered materials consisting of blends of reactive components and/or inert materials. Phase change and variable properties are included in one-dimensional slab, cylindrical, and spherical geometries. Temperature-dependent thermal properties were incorporated and the modification of thermal conductivities to include decomposition effects are estimated using solid/gas volume fractions determined by species fractions. Gas transport properties, including high pressure corrections, were also included. Time varying temperature, heat flux, convective and thermal radiation boundary conditions, and layer to layer contact resistances were also implemented. DOE

N94-30708 Massachusetts Univ., Amherst. Dept. of Chemical Engineering.
THEORETICAL STUDIES OF SOLID-FLUID PHASE EQUILIBRIA
P. A. Monson Jun. 1993 21 p Limited Reproducibility: More than 20% of this document may be affected by microfiche quality
(Contract DE-FG02-90ER-14150)
(DE94-006406; DOE/ER-14150/3) Avail: CASI HC A03

Work focused in two directions: understanding the role of anisotropic molecular interactions such as those arising from molecular shape on solid-fluid equilibria and developing a theoretical approach to solid mixtures. A study of the phase diagrams for hard dumbbells (hard sphere dimers), focused especially on the solid-fluid equilibria, was completed; it produced insights into how molecular shape determines the stable crystal structure and solid-fluid equilibria. Results were used to test theoretical predictions from density functional theories and from the cell theory, which were successfully extended to such systems. Results for hard dumbbells provided reference system data for a generalized van der Waals theory of solid-fluid equilibria of nonspherical molecules. This theory provides a basis for understanding trends in experimental solid-fluid equilibrium data, such as reduced triple point temperatures for different substances. A simple extension of this approach to systems with quadrupolar interactions provides a plausible explanation for some features of the phase diagram of CO2 such as its high triple point temperature and large density increase on freezing. The cell theory was extended to mixtures in the solid state. Key development was the incorporation of cell composition fluctuations into the theory. Comparisons with Monte Carlo simulation results for solid-fluid equilibria in hard sphere mixtures show that this theory is the most quantitatively accurate one available and is readily extended to attractive interactions without using a mean field approximation for composition dependence of such interactions. DOE

N94-30761 Midwest Research Inst., Golden, CO.
PROCEEDINGS OF THE LOW COST MATERIALS OF CONSTRUCTION FOR BIOLOGICAL PROCESSES WORKSHOP
13 May 1993 233 p Workshop held in Colorado Springs, CO, 13 May 1993 Limited Reproducibility: More than 20% of this document may be affected by microfiche quality
(Contract DE-AC02-83CH-10093)
(DE94-000218; NREL/CP-420-6032; CONF-9305310) Avail: CASI HC A11

The workshop was held, in May 1993, in conjunction with the 15th Symposium on Biotechnology for Fuels and Chemicals. The purpose of this workshop was to present information on the biomass to ethanol process in the context of materials selection and through presentation and discussion identify promising avenues for future research. Six technical presentations were grouped into two sessions: process assessment and technology assessment. In the process assessment session, the group felt that the pretreatment area would require the most extensive materials research due the complex chemical, physical, and thermal environment. Discussion centered around the possibility of metals being leached into the process stream and their effect on the fermentation mechanics. Linings were a strong option for pretreatment assuming the economics were favorable. Fermentation was considered an important area for research also, due to the unique complex of compounds and dual phases present. Erosion in feedstock handling equipment was identified as a minor concern. In the technology assessment session, methodologies in corrosion analysis were presented in addition to an overview of current coatings/linings technology. Widely practiced testing strategies, including ASTM methods, as well as novel procedures for micro-analysis of corrosion were discussed. Various coatings and linings, including polymers and ceramics, were introduced. The prevailing recommendations for testing included keeping the testing simple until the problem warranted a more detailed approach and developing standardized testing procedures to ensure the data was reproducible and applicable. The need to evaluate currently available materials such as coatings/linings, carbon/stainless steels, or fiberglass reinforced plastic was emphasized. It was agreed that economic evaluation of each material candidate must be an integral part of any research plan. DOE

N94-30818 Midwest Research Inst., Golden, CO.
FUEL CYCLE EVALUATIONS OF BIOMASS-ETHANOL AND REFORMULATED GASOLINE
K. S. Tyson Nov. 1993 130 p Prepared in cooperation with Oak Ridge National Lab., TN Limited Reproducibility: More than 20% of this document may be affected by microfiche quality
(Contract DE-AC02-83CH-10093)
(DE94-000227; NREL/TP-463-4950) Avail: CASI HC A07

The U.S. Department of Energy (DOE) is using the total fuel cycle analysis (TFCA) methodology to evaluate energy choices. The National Energy Strategy (NES) identifies TFCA as a tool to describe and quantify the environmental, social, and economic costs and benefits associated with energy alternatives. A TFCA should quantify inputs and outputs, their impacts on society, and the value of those impacts that occur from each activity involved in producing and using fuels, cradle-to-grave. New fuels and energy technologies can be consistently evaluated and compared using TFCA, providing a sound basis for ranking policy options that expand the fuel choices available to consumers. This study is limited to creating an inventory of inputs and outputs for three transportation fuels: (1) reformulated gasoline (RFG) that meets the standards of the Clean Air Act Amendments of 1990 (CAAA) using methyl tertiary butyl ether (MTBE); (2) gasohol (E10), a mixture of 10% ethanol made from municipal solid waste (MSW) and 90% gasoline; and (3) E95, a mixture of 5% gasoline and 95% ethanol made from energy crops such as grasses and trees. The ethanol referred to in this study is produced from lignocellulosic material--trees, grass, and organic wastes--called biomass. The biomass is converted to ethanol using an experimental technology described in more detail later. Corn-ethanol is not discussed in this report. This study is limited to estimating an inventory of inputs and outputs for each fuel cycle, similar to a mass balance study, for several reasons: (1) to manage the size of the project; (2) to provide the data required for others to conduct site-specific impact analysis on a case-by-case basis; (3) to reduce data requirements associated with projecting future environmental baselines and other variables that require an internally consistent scenario. DOE

N94-30885# Department of Energy, Washington, DC. Assistant Secretary for Policy, Planning and Program Evaluation.
ASSESSMENT OF COSTS AND BENEFITS OF FLEXIBLE AND ALTERNATIVE FUEL USE IN THE US TRANSPORTATION SECTOR
Dec. 1993 40 p
(DE94-006100; DOE/PO-0009) Avail: CASI HC A03/MF A01

As part of the alternative fuels assessment, the Department of Energy

(DOE) is studying the use of derivatives of natural gas, including compressed natural gas and methanol, as alternative transportation fuels. A critical part of this effort is determining potential sources of natural gas and the economics of those sources. This report extends previous analyses to include Alaskan North Slope natural gas that either is not being produced or is being reinjected. The report includes the following: a description of discovered and potential (undiscovered) quantities of natural gas on the Alaskan North Slope, a discussion of proposed alternative uses for Alaskan North Slope natural gas, and a comparison of the economics of the proposed alternative uses for Alaskan North Slope natural gas. The purpose is to illustrate the costs of transporting Alaskan North Slope gas to markets in the lower 48 states as pipeline gas, liquefied natural gas (LNG), or methanol. The information is supplied in sufficient detail to allow incorporation of relevant economic relationships (for example, wellhead gas prices and transportation costs) into the alternative fuels trade model, the analytical framework DOE is using to evaluate various policy options. DOE

N94-29259# Pratt and Whitney Aircraft, West Palm Beach, FL. Fuels and Lubricants Group.
HIGH TEMPERATURE FUEL REQUIREMENTS AND PAYOFFS
Tedd B. Biddle and Bennett M. Croswell *In* AGARD, Fuels and Combustion Technology for Advanced Aircraft Engines Sep. 1993 12 p Sponsored by AFWAL and Naval Air Propulsion Test Center (For primary document see N94-29246 08-25)
Copyright Avail: CASI HC A03/MF A04

N94-29260# Instituto Nacional de Tecnica Aeroespacial, Madrid (Spain). Fuels and Lubricants Lab.
HIGH TEMPERATURE RESISTANT JET FUELS
Luis M. Peloche and Santiago Asensio *In* AGARD, Fuels and Combustion Technology for Advanced Aircraft Engines Sep. 1993 9 p Sponsored by British Petroleum Oil, Inc. (For primary document see N94-29246 08-25)
Copyright Avail: CASI HC A02/MF A04

N94-29261# Wright Lab., Wright-Patterson AFB, OH.
RESEARCH AND DEVELOPMENT OF HIGH THERMAL STABILITY FUELS
T. Edwards, W. M. Roquemore, W. E. Harrison, and S. D. Anderson *In* AGARD, Fuels and Combustion Technology for Advanced Aircraft Engines Sep. 1993 19 p (For primary document see N94-29246 08-25)
Copyright Avail: CASI HC A03/MF A04

N94-29262# Systems Research Labs., Inc., Dayton, OH.
DEVELOPMENT OF GLOBAL/CHEMISTRY MODEL FOR JET-FUEL THERMAL STABILITY BASED ON OBSERVATIONS FROM STATIC AND FLOWING EXPERIMENTS
V. R. Katta, E. G. Jones, and W. M. Roquemore *In* AGARD, Fuels and Combustion Technology for Advanced Aircraft Engines Sep. 1993 11 p (For primary document see N94-29246 08-25)
(Contract F33615-90-C-2033)
Copyright Avail: CASI HC A03/MF A04

N94-29285# Central Inst. of Aviation Motors, Moscow (Russia).
ENDOTHERMIC FUELS FOR HYPERSONIC AVIATION
Leonid S. Ianovski and Clifford Moses *In* AGARD, Fuels and Combustion Technology for Advanced Aircraft Engines Sep. 1993 8 p (For primary document see N94-29246 08-25)
Copyright Avail: CASI HC A02/MF A04

N94-29634*# National Aeronautics and Space Administration. Langley Research Center, Hampton, VA.
INTEGRATION OF PYROTECHNICS INTO AEROSPACE SYSTEMS
Laurence J. Bement and Morry L. Schimmel *In* NASA. Ames Research Center, The 27th Aerospace Mechanisms Symposium May 1993 p 93-106 (For primary document see N94-29627 08-15)
Avail: CASI HC A03/MF A03

N94-30454*# Geo-Centers, Inc., Lake Hopatcong, NJ.
CUBANES: SUPER EXPLOSIVES AND POTENTIAL PHARMACEUTICAL INTERMEDIATES
A. Bashir-Hashemi *In* NASA, Washington, Technology 2003: The Fourth National Technology Transfer Conference and Exposition, Volume 1 Feb. 1994 p 127-130 (For primary document see N94-30440 08-99)
Avail: CASI HC A01/MF A04

29 MATERIALS PROCESSING

Includes space-based development of products and processes for commercial applications.

For biological materials see *55 Space Biology.*

N94-28415*# National Aeronautics and Space Administration, Washington, DC.
MICROGRAVITY SCIENCE AND APPLICATIONS. PROGRAM TASKS AND BIBLIOGRAPHY FOR FY 1993
Washington Mar. 1994 580 p
(NASA-TM-4569; NAS 1.15:4569) Avail: CASI HC A25/MF A06

An annual report published by the Microgravity Science and Applications Division (MSAD) of NASA is presented. It represents a compilation of the Division's currently-funded ground, flight and Advanced Technology Development tasks. An overview and progress report for these tasks, including progress reports by principal investigators selected from the academic, industry and government communities, are provided. The document includes a listing of new bibliographic data provided by the principal investigators to reflect the dissemination of research data during FY 1993 via publications and presentations. The document also includes division research metrics and an index of the funded investigators. The document contains three sections and three appendices: Section 1 includes an introduction and metrics data, Section 2 is a compilation of the task reports in an order representative of its ground, flight or ATD status and the science discipline it represents, and Section 3 is the bibliography. The three appendices, in the order of presentation, are: Appendix A - a microgravity science acronym list, Appendix B - a list of guest investigators associated with a biotechnology task, and Appendix C - an index of the currently funded principal investigators. Author (revised)

N94-28938# Japan Space Utilization Promotion Center, Tokyo.
OVERVIEW OF SPACE ENVIRONMENT UTILIZATION SCIENCE [UCHU KANKYO RIYO NO TENBO]
Mar. 1993 156 p In JAPANESE
(JTN-94-80581) Avail: CASI HC A08/MF A02

The following topics were discussed: microgravity, space environments, low gravity manufacturing, space manufacturing, space processing, spaceborne experiments, vacuum, fluid flow, convection, Marangoni convection, bubbles, liquid drops, fuel combustion, glass processing, furnace, materials processing, electronic devices, amorphous semiconductors, molecular beam graph epitaxy, chemical vapor deposition, physical vapor deposition, protein crystal, crystal growth, enzymes, cell culture, culture apparatus, electric power supplies, solar cells, solar power generator, electric power generator, direct power generation, secondary batteries, fuel cells, and nuclear power generator. For individual titles, see N94-28939 through N94-28945.

N94-28939# Nagaoka Technological Univ., Niigata (Japan). Faculty of Technology.
FLUID AND TRANSPORTATION PHENOMENA UNDER MICROGRAVITY [BISHO JURYOKUKA NI OKERU RYUTAI YUSO GENSHO]
Yasunori Miyata *In* Japan Space Utilization Promotion Center, Overview of Space Environment Utilization Science Mar. 1993 p 1-19 In JAPANESE (For primary document see N94-28938 08-29)
Avail: CASI HC A03/MF A02

Fluid physics under microgravity has been getting much attention because research is possible free from precipitation or natural convection. In order to effectively utilize of this environment, phenomena specific to microgravity must be studied in view of fluid dynamics. Basic research on fluid dynamics in floating zones under microgravity focused on the fluid stability against rotation or vibration and Marangoni convection generated at temperature differences. The size of stable liquid cylinders is determined to minimize the whole liquid energy. Experiments are done on Marangoni convections in rectangular (or cylindrical) vessels in relation to temperature, solute density, minimum surface tension, and chemical waves. Convection effects and contribution on transportation were also studied. Investigation

was also made on utilization of bubbles and liquid drops to transportation, dynamics of vibrating and rotating liquid drops, and quantization of physical constants. Overall, many experiments are being done about cylindrical stability, Marangoni convections, and liquid drop dynamics under microgravity, but there are several inconveniences and problems yet to be solved.
Author (NASDA)

N94-28940# Tokyo Univ. (Japan). Faculty of Engineering.
COMBUSTION STUDIES UNDER MICROGRAVITY [BISHO JURYOKUKA NI OKERU NENSHO KENKYU]
Michikata Kono *In* Japan Space Utilization Promotion Center, Overview of Space Environment Utilization Science Mar. 1993 p 21-42 In JAPANESE (For primary document see N94-28938 08-29)
Avail: CASI HC A03/MF A02

Basically, research was made in the following themes: (1) effects of natural convection, atmospheric pressure and oxygen concentration on combustion of liquid drops; (2) evaporation of fuel liquid drops under hot, high pressure environment; (3) combustion of multi-component fuel liquid drops; (4) self-ignition of fuel liquid drops at high temperature under high pressure; and (5) heat ignition of gas mixture and heat catalysis. The following were found: (1) combustion time was strongly affected by natural convection under normal gravity; (2) natural convection greatly affected evaporation under normal gravity, whereas natural convection was not observed and steam accumulates around liquid drops under microgravity; (3) fuel liquid drops of two components showed three combustion stages under high pressure and microgravity. The critical diameter of liquid drops greatly depended on the initial concentration with higher hexadecane concentration; (4) two-step ignition accompanying cool ignition was observed under low pressure, and ignition time was influenced by natural convection; and (5) under normal gravity, heat was taken away by natural convection, delaying ignition. This effect was more evident if the ignition delay was in large areas. Author (NASDA)

N94-28941# Government Industrial Research Inst., Osaka (Japan). Functional Ceramics Section.
GLASS STUDIES UNDER MICROGRAVITY [BISHO JURYOKU KANKYO O RIYO SHITA GARASU NO KENKYU]
Masaki Makihara *In* Japan Space Utilization Promotion Center, Overview of Space Environment Utilization Science Mar. 1993 p 43-60 In JAPANESE (For primary document see N94-28938 08-29)
Avail: CASI HC A03/MF A02

Floating fusion techniques are important for glass manufacture, and furnaces employing these techniques include sound wave floating furnaces, gas stream sound wave floating furnaces, electromagnetic floating furnaces, electrostatic floating furnaces, and gas film floating furnaces. Glasses generated in microgravity were more uniform, and more tendency for glassification was noted due to vessel-free dissolution. The index of refraction has smaller distribution than that in microgravity. The initial, main objectives of glass studies in microgravity were to: (1) produce glasses with compositions impossible to produce in normal gravity; (2) produce fusing, highly-purified glasses with no vessels; (3) produce hollow glasses to be used for fuel vessels in nuclear reaction experiments; and (4) produce new types of glasses. Although some of them were experimented during Space Shuttle missions, quite a few were discontinued due to lack of equipment or other reasons. There is an opinion to use the sol/gel method to cope with this problem. Another opinion is to employ microgravity environment in glass development and technologies, such as optical fibers with little loss and new glasses for lasers. Author (NASDA)

N94-28942# Osaka Univ., Toyonaka (Japan). Research Center for Extreme Materials.
FABRICATION OF ELECTRONIC MATERIALS IN SPACE [UCHU NI OKERU DENSHI ZAIRYO NO SOSEI]
Yoshihiro Hamakawa *In* Japan Space Utilization Promotion Center, Overview of Space Environment Utilization Science Mar. 1993 p 61-92 In JAPANESE (For primary document see N94-28938 08-29)
Avail: CASI HC A03/MF A02

From a standpoint of new material fabrication, space environment provides five unique characteristics: microgravity, super-high vacuum, abundant solar energy and cosmic rays, good visibility, and vast space. Focusing on the utilization and problems of super-high vacuum environment, the following are phenomena not found on the earth: (1) a phenomenon called 'wake' occurs; (2) metals constantly evaporate from their surfaces, and the evaporation ratio depends on the temperature of the super-high vacuum; (3) metals may adhere each other due to cool deposition; (4) heat is conducted mainly by radiation due to lack of convection in space; (5) discharge is subject to occur; (6) plasma space is generated and potential differences may affect experiments such as electrophoresis; (7) radiation causes some problems such as solar flare being generated, IC's are damaged by radiation, and material may deteriorate by ultraviolet rays; and (8) materials of different specific gravities can be mixed in microgravity. Recently, a new trend is forecasted in view of a technological evolution from the bulk crystalline age to the multilayered thin film age. Possible fabrication and processing for new electronic materials include fabrication of polynary chemical bulk semiconductors and large area thin-film semiconductors as well as oxygen-free vacuum processing. Electronic properties of amorphous semiconductors proved to be far superior to those in normal gravity. Author (NASDA)

N94-28943# Ministry of International Trade and Industry, Tsukuba (Japan). Agency of Industrial Science and Technology.
PROTEIN CRYSTAL GROWTH IN MICROGRAVITY [BISHO JURYOKUKA NI OKERU TANPAKUSHITSU KESSHO SEICHO]
Mitsuo Ataka *In* Japan Space Utilization Promotion Center, Overview of Space Environment Utilization Science Mar. 1993 p 93-114 In ENGLISH and JAPANESE (For primary document see N94-28938 08-29)
Avail: CASI HC A03/MF A02

The crystals generated in space showed approximately 25 percent improvement at the space experiments of protein crystal growth from the USSR's MIR missions. For Space Shuttles, experiments on protein crystal growth were done on 16 missions. Out of 80 types of protein tested in total, 15 showed results clearly benefiting from the microgravity environment. At the experiments conducted in the Swedish rocket, Maser, both types of protein tested showed larger crystals than their earth-grown counterparts. The high resolution obtained was significant enough to perform X-ray structural analysis, and side chains of amino acid revealed to have two types of conformations. Structural analysis with higher resolution was attained by crystals grown in microgravity. At Stanford University, equipment was developed to control nuclear generation during protein crystal growth as well as to control subsequent growth stages independent of nuclear generation by utilizing partial temperature changes. In Wisconsin, a new protein crystallization method was suggested in which water is selectively removed from protein solution, using reverse permeable films.
Author (NASDA)

N94-28944# Tokyo Medical and Dental Univ. (Japan). Faculty of Dentistory.
CELL CULTURE IN SPACE [UCHU NI OKERU SAIBO BAIYO]
Atsushige Sato *In* Japan Space Utilization Promotion Center, Overview of Space Environment Utilization Science Mar. 1993 p 115-130 In JAPANESE (For primary document see N94-28938 08-29)
Avail: CASI HC A03/MF A02

Cell culture is used as a substitute for experiments using animals. Also, cultured cells of animals and plants compose physiological-activation materials useful for medicines, and mass cell culture has been utilized for production of such materials. Cell culture is roughly classified into two types: single-layered culture and floating culture. The former is used for cells with substrate dependency and the latter with no substrate dependency. According to the reports from Skylab Three experiments, multiplication and doubling time of cultured cells were almost the same in space and on the earth. Space experiments conducted by the USSR stated that no changes were noted in shapes, physiological activation or multiplication of cultured cells, but the cells were slightly larger and the division index was higher in space. The production of interferon alpha during flight showed increase by four to eight times compared to the earth counterparts. In summary, cell culture will definitely play an important role as a means to biotechnology as well as animal experiments' substitute and analytical means of physiological mechanism. However, there are things to consider such as secondary effects related to culture environment changes and complex reactions from various factors. The research so far is only in the exploration stage, and it should develop into those of a more mature level.
Author (NASDA)

N94-28945# Ryukoku Univ., Kyoto (Japan). Faculty of Science and Technology.

COSMIC ENERGY EQUIPMENT [UCHU KIKI NO ENERUGI SOCHI]

Kazuyuki Enami *In* Japan Space Utilization Promotion Center, Overview of Space Environment Utilization Science Mar. 1993 p 131-149 In JAPANESE (For primary document see N94-28938 08-29)

Avail: CASI HC A03/MF A01

Cosmic energy equipment has three fundamental factors: primary energy sources, conversion equipment of primary energy to electric energy, and unused energy dumping equipment. The primary energy sources are classified into internal sources which are brought in from the earth, and outer sources such as solar energy and high-frequency, optical-ranged convertible energy. Internal sources are either chemical energy sources (e.g. storage batteries, buffer batteries, fuel batteries, electro-chemical power generators), nuclear energy sources (e.g. isotopes, atomic power generators, nuclear reactors) or electromagnetic energy. Solar batteries, utilizing solar energy, are the basic power supply to near-earth orbits, orbiting stations and automatic cosmic equipment. Isotope energy equipment is used when the efficiency of solar batteries are low. Nuclear energy equipment has an advantage of capabilities to function regardless of orbit positions, time of the day, or distance from the sun. Equipment to convert the primary energy to electric energy includes direct energy convertors and mechanical convertors. Both cooling and radiation devices are quite significant for unused energy dumping equipment, because heat can be expelled only by radiation. Author (NASDA)

N94-29371*# National Aeronautics and Space Administration. Pasadena Office, CA.

PLASMA HEATING FOR CONTAINERLESS AND MICROGRAVITY MATERIALS PROCESSING Patent Application

Emily W. Leung, inventor (to NASA) (Jet Propulsion Lab., California Inst. of Tech., Pasadena.) and Kin F. Man, inventor (to NASA) (Jet Propulsion Lab., California Inst. of Tech., Pasadena.) 15 Nov. 1993 15 p (Contract NAS7-918)

(NASA-Case-NPO-18819-1-CU; NAS 1.71:NPO-18819-1-CU; US-Patent-Appl-SN-153933) Avail: CASI HC A03/MF A01

A method for plasma heating of levitated samples to be used in containerless microgravity processing is disclosed. A sample is levitated by electrostatic, electromagnetic, aerodynamic, or acoustic systems, as is appropriate for the physical properties of the particular sample. The sample is heated by a plasma torch at atmospheric pressure. A ground plate is provided to help direct the plasma towards the sample. In addition, Helmholtz coils are provided to produce a magnetic field that can be used to spiral the plasma around the sample. The plasma heating system is oriented such that it does not interfere with the levitation system. NASA

N94-29996 Selskapet for Industriell og Teknisk Forskning, Trondheim (Norway). Div. of Production Engineering.

MICROGRAVITY COMPATIBLE DRIVE SYSTEM-RIDER. NEW TECHNOLOGIES Technical Note No. 1

H. P. Hildre and T. K. Lien 16 Jun. 1993 57 p Sponsored by European Space Research Organization, Noordwikj, Netherlands

(PB94-138583; STF20-A93105) Avail: Issuing Activity (National Technical Information Service (NTIS))

The report describes the results of a theoretical investigation and analysis of the behavior of reduction gears and linear transmission systems for micro-gravity compatible drive systems. Specific investigations in the area of ultra-low mechanical disturbances are described. The laboratory tests show that the drive system generates unacceptable periodic disturbances. The extreme micro-gravity performance requirements are such that the Traction Reducer becomes an interesting alternative. This alternative will be analyzed and a preliminary design will be presented. NTIS

N94-30145 Manitoba Univ., Winnipeg. Dept. of Mechanical Engineering.

LASER BEAM WELDING OF AISI 316 STAINLESS STEEL IN MICROGRAVITY ENVIRONMENT: EXPERIMENTS ABOARD A KC-135 FLIGHT M.S. Thesis

Guoqing Wang Aug. 1993 96 p

(ISBN-0-315-86095-2; CTN-94-61179) Copyright Avail: Micromedia Ltd., Technical Information Centre, 240 Catherine Street, Suite 305, Ottawa, Ontario, K2P 2G8, Canada HC/MF

Low power (70-watt) continuous wave CO2 laser welding under microgravity conditions was performed during a KC-135 parabolic flight. The welding experiments were conducted on thin stainless steel (American Iron and Steel Institute 316) strips. The welding parameters were first optimized in ground-based tests and then continuous welding was done during the periods of changing gravity level aboard the KC-135. The weld microstructural characteristics were examined using optical and scanning electron microscopy. During the absence of gravity, wider weld width and deeper weld penetration were found to occur. The weld was characterized by dispersed entrapped slag, porosity, and suspended weld particles, which may lead to a weak joint in real space welding. Author (CISTI)

N94-30409 National Aerospace Lab., Amsterdam (Netherlands). Space Div.

MICROGRAVITY FLUID SCIENCE RESEARCH IN EUROPE

J. P. B. Vreeburg 2 Oct. 1992 28 p Presented at Inspace 1992, Sapporo, Japan, 11 Nov.. 1992 Limited Reproducibility: More than 20% of this document may be affected by microfiche quality

(AD-B179178; NLR-TP-93426-U; ETN-94-95962) Avail: Issuing Activity (European Space Agency (ESA))

Activities in Europe related to fluid science research in microgravity are discussed. After a short historical introduction, the general organizational traits and operational modes are described. The available facilities and those under development are surveyed, with the flight opportunities that exist. Fluid science research subjects are introduced under four main headings: molecular physics; thermodynamic properties and transport coefficients; heat and mass transfer processes; mechanics and statics of liquids. A list of research institutes is provided and their main fields of interest are indicated. ESA

N94-30421 National Aerospace Lab., Amsterdam (Netherlands). Space Div.

CONTROL SYSTEM DESIGN FOR A AND R SUPPORTED MICROGRAVITY EXPERIMENTS: AN EXPERIMENT PAYLOAD CONTROL DEVELOPMENT

P. Dieleman 8 Jul. 1992 20 p Presented at the 43rd International Astronautical Federation World Space Congress, Washington, DC, 28 Aug. - 5 Sep. 1992 Limited Reproducibility: More than 20% of this document may be affected by microfiche quality

(AD-B179107; NLR-TP-92327-U; IAF-92-0966; ETN-94-95959) Avail: CASI HC A03

The design of control systems for microgravity experiment payloads, to be integrated into the Columbus infrastructure, for which a comprehensive development methodology is mandatory, is considered. A development model allows structured and formalized development procedures for classes of control systems. A Control Development Methodology (CDM) for Automation and Robotics (A and R) systems, has been proposed by ESA. Ideas to modify and expand this CDM towards a method to develop experiment payload control systems are presented. Such a Payload CDM (PCDM) supports the analysis, design and implementation process of an experiment payload control system. The PCDM consists of engineering guidelines in the form of reference models, standard procedures to support design consistency and traceability, and appropriate tools. ESA

31 ENGINEERING (GENERAL)

Includes vacuum technology; control engineering; display engineering; cryogenics; and fire prevention.

N94-28410# Technical Research Centre of Finland, Tampere. Safety Engineering Lab.

SYSTEMATIC SAFETY CONSIDERATION IN PRODUCT DESIGN Ph.D. Thesis

Markku Reunanen 1993 135 p

(ISSN 1235-0621)

(PB94-132354; VTT/PUB-145; ISBN-951-38-4383-1) Copyright Avail: CASI HC A07/MF A02

Product designers face increasing pressure to improve the level of safety in their designs. To a great extent, the pressure exerted by the regulatory authorities, for example, is currently aimed at product designers. The work was done in order to improve the design process from the point of view of safety. An approach was outlined enabling the inclusion of

safety analyses in the design process in a way that would better reflect the current problems and needs imposed on designers. The basic idea of the approach is that safety analyses are applied in each phase of the design process so that the design is considered during its various levels of maturity. In addition to consideration of the product itself, special attention has been paid to the user instructions needed for safe product operation. The approach was tested in four case studies. NTIS

N94-28563# Calm (James M.), Great Falls, VA.
ARTI REFRIGERANT DATABASE
J. M. Calm 28 Nov. 1993 159 p
(Contract DE-FG02-91CE-23810)
(DE94-004906; DOE/CE-23810/22E) Avail: CASI HC A08/MF A02

The Refrigerant Database consolidates and facilitates access to information to assist industry in developing equipment using alternative refrigerants. The underlying purpose is to accelerate phase out of chemical compounds of environmental concern. The database provides bibliographic citations and abstracts for publications that may be useful in research and design of air-conditioning and refrigeration equipment. The complete documents are not included, though some may be added at a later date. The database identifies sources of specific information on R-32, R-123, R-124, R-125, R-134, R134a, R-141b, R-142b, R-143a, R-152a, R-227ea, R-245ca, R-290 (propane), R-717 (ammonia), ethers, and others as well as azeotropic and zeotropic blends of these fluids. It addresses lubricants including alkylbenzene, polyalkylene glycol, polyol ester, and other synthetics as well as mineral oils. It also references documents addressing compatibility of refrigerants and lubricants with metals, plastics, elastomers, motor insulation, and other materials used in refrigerant circuits. Incomplete citations or abstracts are provided for some documents. They are included to accelerate availability of the information and will be completed or replaced in future updates. DOE

N94-28644 Naval Postgraduate School, Monterey, CA. Dept. of Physics.
ANNUAL SUMMARY OF BASIC RESEARCH THERMOACOUSTIC HEAT TRANSPORT, 1993
Anthony A. Atchley Nov. 1993 26 p Limited Reproducibility: More than 20% of this document may be affected by microfiche quality
(AD-A275751; NPS-PH-94-003) Avail: CASI HC A03

This annual report details progress in basic research in thermoacoustic heat transport made during the period October 1, 1992 through September 30, 1993. Our major research efforts in FY 1993 were concentrated in five areas: (1) an analysis of the initial buildup of oscillations in thermoacoustic prime movers; (2) an investigation of stability curves for a thermoacoustic prime mover; (3) initial measurements of the velocity field in thermoacoustic engines using laser Doppler anemometry; (4) measurements of heat exchanger performance in a thermoacoustic prime mover; and (5) a preliminary investigation of heat driven refrigerators. In addition to these areas, FY 1993 research efforts also included a collaborative experiment on traveling wave thermoacoustic effects. A brief review of the motivation behind these studies and a summary of the important results are contained in this technical report. DTIC

N94-28742# Air Force Inst. of Tech., Wright-Patterson AFB, OH. School of Logistics and Acquisition Management.
THE DEVELOPMENT AND DEMONSTRATION OF THE METRIC ASSESSMENT TOOL M.S. Thesis
Cynthia A. Campbell and Gregory M. Gutterman Sep. 1993 165 p
(AD-A275786; AFIT/GCM/LAS/93S-3) Avail: CASI HC A08/MF A02

This study reflects the development and demonstration of the metric assessment tool. The purpose of the tool was to provide individuals the means to assess metrics and make improvements to the process measurement. The tool was developed using two critical attributes: customer satisfaction and process improvement. Once the tool was developed, a metric assessment process was designed to demonstrate the tool. Two metrics were selected from the Aeronautical Systems Center (ASC) and individuals with a working knowledge of the metric and process were selected for the demonstrations. Using a group support system at Armstrong Laboratory, Wright Patterson AFB, the group was asked to identify behaviors which might be motivated from the metric. Once the behaviors were identified, the group evaluated the behaviors against the critical attributes. From this assessment, behaviors were placed on the metric assessment tool. This tool clearly identified deficient behaviors and how they might distort the process measurement. From this information, the group was asked to generate improvement actions which would serve to eliminate or control deficient behaviors. With the elimination or control of deficient behaviors, the process measurement is improved and the organizational objective is better served. DTIC

N94-29017# Cryogenic Applications F, Inc., Clinton, TN.
ARGON FROST CONTINUOUS CRYOPUMP FOR FUSION APPLICATIONS
C. A. Foster and H. C. McCurdy 1993 5 p Presented at the Symposium on Fusion Engineering, Hyannis, MA, 11-15 Oct. 1993
(Contract DE-FG05-91ER-81236)
(DE94-004478; CONF-931018-74) Avail: CASI HC A01/MF A01

A cryopumping system based on the snail continuous cryopump concept is being developed for fusion applications under a DOE SBIR grant. The primary pump is a liquid helium cooled compound pump designed to continuously pump and fractionate deuterium/tritium and helium. The D/T pumping stage is a 500 mm bore cryocondensation pump with a nominal pumping speed of 45,000 L/s. It will be continuously regenerated by a snail regeneration head every 12 minutes. Continuous regeneration will dramatically reduce the vulnerable tritium inventory in a fusion reactor. Operating at an inlet pressure of 1 millitorr, eight of these pumps could pump the projected D/T flow in the ITER CDA design while reducing the inventory of tritium in the pumping system from 630 to 43 grams. The helium fraction will be pumped in a compound argon frost stage. This stage will also operate continuously with a snail regeneration head. In addition, the argon spray head will be enclosed inside the snail, thereby removing gaseous argon from the process chamber. Since the cryocondensation stage will intercept over 90% of the D/T/H stream, a purified stream from this stage could be directly reinjected into the plasma as gas or pellets, thereby bypassing the isotope separation system and further simplifying the fuel cycle. Experiments were undertaken in phase 1 which demonstrated continuous cryosorption pumping of hydrogen on CO2 and argon frosts. The pumping system and its relevance to fusion reactor pumping will be discussed. DOE

N94-29187# Helsinki Univ. of Technology, Espoo (Finland).
APPLICATION OF HIGH-SPEED MILLING TO THE FINNISH MANUFACTURING INDUSTRY Final Technical Rept
V. Kauppinen, J. Paro, and I. Nieminen 11 Aug. 1993 90 p Prepared for Technical Research Centre of Finland, Espoo
(PB94-135548) Avail: CASI HC A05/MF A01

The aim of the project was to get knowledge of high-speed milling of different materials with commercially available tools and tool materials. In a preliminary project, the machine tool and the materials to be machined were specified in cooperation with Finnish industry. The report is based on the results of a project on high-speed milling which was recently performed in Finland. NTIS

N94-29188 Helsinki Univ. of Technology, Espoo (Finland). Dept. of Industrial Management.
REALIZING THE PRODUCTIVITY POTENTIAL OF EXPEDITIOUS OPERATIONS
J. Holmstroem 1993 86 p Limited Reproducibility: More than 20% of this document may be affected by microfiche quality
(PB94-135555; ISBN-951-22-1773-2) Avail: CASI HC A05

This work addresses the question of how to facilitate sustainable improvements in the operational performance of manufacturing firms. Based on an analysis of international industrial statistics it is argued that there exists a significant productivity potential to be gained from operating expeditiously. Through an analysis of the current discourse in Operations Management it is argued that this productivity potential is based on the improved ability of expeditious firms to deal with uncertainty of the current situation. To realize the potential of expeditious operations a firm must be able to bridge the gap between the reality of words and ideas, and action. Through a case study it is demonstrated how integrative operational structures in combination with enhanced decision making capabilities can facilitate a breakthrough improvement in operational performance. The problem to identifying effective actions to improve the operational performance is approached from a systemic perspective utilizing complementary systems approaches. The utility of a concerted application of statistical, dynamic, and human activity systems approaches is tested in

a case study. Based on the experiences of practical application a systemic framework to implement desirable and feasible actions to improve is constructed. The main contribution of this process model is the inclusion of a human activity systems perspective to deal with the complexity of human affairs. NTIS

N94-29376*# National Aeronautics and Space Administration. John F. Kennedy Space Center, Cocoa Beach, FL.
SI (METRIC) HANDBOOK
Elisa A. Artusa Mar. 1994 240 p
(NASA-TM-109197; KSC-DM-3673; NAS 1.15:109197) Avail: CASI HC A11/MF A03

This guide provides information for an understanding of SI units, symbols, and prefixes; style and usage in documentation in both the US and in the international business community; conversion techniques; limits, fits, and tolerance data; and drawing and technical writing guidelines. Also provided is information of SI usage for specialized applications like data processing and computer programming, science, engineering, and construction. Related information in the appendixes include legislative documents, historical and biographical data, a list of metric documentation, rules for determining significant digits and rounding, conversion factors, shorthand notation, and a unit index. Author

N94-29379*# National Aeronautics and Space Administration. Marshall Space Flight Center, Huntsville, AL.
MANUFACTURING METHODS FOR MACHINING SPRING ENDS PARALLEL AT LOADED LENGTH Patent Application
Patrick Thomas Hinke, inventor (to NASA) (Allied-Signal Corp., Morristown, NJ.), Dwayne M. Benson, inventor (to NASA) (Allied-Signal Corp., Morristown, NJ.), and Donald J. Atkins, inventor (to NASA) (Allied-Signal Corp., Morristown, NJ.) 10 Nov. 1993 9 p
(NASA-Case-MFS-28767-1; NAS 1.71:MFS-28767-1; US-Patent-Appl-SN-149889) Avail: CASI HC A02/MF A01

A first end surface of a coiled compression spring at its relaxed length is machined to a plane transverse to the spring axis. The spring is then placed in a press structure having first and second opposed planar support surfaces, with the machined spring end surface bearing against the first support surface, the unmachined spring end surface bearing against a planar first surface of a lateral force compensation member, and an opposite, generally spherically curved surface of the compensation member bearing against the second press structure support surface. The spring is then compressed generally to its loaded length, and a circumferentially spaced series of marks, lying in a plane parallel to the second press structure support surface, are formed on the spring coil on which the second spring end surface lies. The spring is then removed from the press structure, and the second spring end surface is machined to the mark plane. When the spring is subsequently compressed to its loaded length the precisely parallel relationship between the machined spring end surfaces substantially eliminates undesirable lateral deflection of the spring. NASA

N94-29385*# National Aeronautics and Space Administration. Goddard Space Flight Center, Greenbelt, MD.
MODIS TECHNICAL REPORT SERIES. VOLUME 3: MODIS AIRBORNE SIMULATOR LEVEL 1B DATA USER'S GUIDE
Liam E. Gumley (Applied Research Corp., Landover, MD.), Paul A. Hubanks (Research and Data Systems, Inc., Greenbelt, MD.), and Edward J. Masuoka Apr. 1994 43 p
(NASA-TM-104594; Rept-94B00065; NAS 1.15:104594) Avail: CASI HC A03/MF A01

The purpose of this document is to describe the characteristics of moderate resolution imaging spectroradiometer (MODIS) airborne simulator level 1B data, the calibration and geolocation methods used in processing, the structure and format of the level 1B data files, and methods for accessing the data. The MODIS airborne simulator is a scanning spectrometer which flies on a NASA ER-2 and provides spectral information similar to that which will be provided by the MODIS. Author (revised)

N94-29416# Aerospatiale, Cannes (France).
ISO OVERVIEW: GENERAL PRESENTATION OF THE SATELLITE, CRYOGENIC ASPECTS [ISO: PRESENTATION GENERALE DU SATELLITE, ASPECTS CRYOGENIQUES]
Bernard Collaudin 1993 35 p In FRENCH
(Rept-932-440-102; ETN-94-95473) Avail: CASI HC A03/MF A01

A description of the Infrared Spaced Observatory (ISO), (whose launch is planned for Sep. 1995), is presented. The results of cryogenic tests and the current development status are also presented. The ISO is build up around a 60 cm telescope, cooled down to about 3K from an open helium gas loop. Helium is stored in a tank of 2250 liters at 1.8 K. It evaporates across a phase separator. It is designed for an autonomy of 18 months in orbit, for astronomical observation. The whole satellite is 5.3 m long, 2.5 m wide, and weighs about 2400 kg, including 310 kg for helium. ESA

N94-29477# Aerospatiale Aquitaine, Saint-Medard en Jalles (France).
A NORMATIVE FRAME OF REFERENCE FOR THE METROLOGY FUNCTION [UN REFERENTIEL NORMATIF POUR LA FONCTION METROLOGIE]
Pierre Barbier 1993 5 p In FRENCH
(Rept-932-430-102; ETN-94-95460) Avail: CASI HC A01/MF A01

Metrology is discussed and reasons for the necessity of it being exact, its original appearance in the legal domain, its development up until the use of digital techniques, and existing metrological documentation, are discussed. Exact measurements are necessary since the security of individuals or installations depends on the results of such operations. The incertitude of a measurement is determined through comparisons to standards. The metrological documentation includes information on the metrological obligations of certain industries, and means of assuring quality measurements. This documentation contains the norms supplied by a normative reference frame which serves as an information base to facilitate the installation of metrological functions in industries. ESA

N94-29598# Von Karman Inst. for Fluid Dynamics, Rhode-Saint-Genese (Belgium).
ADVANCED DESIGN OF VENTILATION SYSTEMS
1993 368 p Lecture series held in Rhode-Saint-Genese, Belgium, 7-9 Jun. 1993
(ISSN 0377-8312)
(VKI-LS-1993-07; ETN-94-95488) Copyright Avail: CASI HC A16/MF A03

Fundamental and practical material to conceive, design, and qualify ventilation systems is presented. The indoor air quality and the thermal environment in ventilated or air conditioned spaces are considered, and information on design rules is identified. The principles and criteria of ventilation systems are discussed. Natural and mechanical ventilation and contaminant control methods are covered. Different empirical flow calculations for steady state and time dependent contaminant generation and air flow rate situations are presented. Their application to sizing of air diffusers, local exhausts, filters and air curtains are illustrated in the cases of laboratory fume and biological safety hoods, grinding booths and spray painting rooms. The theory and use of age distribution and N-zone models are described. Design methodology and technology in the field of industrial ventilation are emphasized. For individual titles, see N94-29599 through N94-29612.

N94-29599# Institut National de Recherche et de Securite pour la Prevention des Accidents du Travail et des Maladies Professionnelles, Vandoeuvre (France).
INTRODUCTION TO THE DESIGN OF VENTILATION SYSTEMS
G. Aubertin *In* VKI, Advanced Design of Ventilation Systems 1993 56 p (For primary document see N94-29598 08-31)
Copyright Avail: CASI HC A04/MF A03

The motivations for the installation of a ventilation system are considered: to protect the material or products manufactured at a given site; to eliminate the risk of explosion or dangerous gases or dusts; to reduce the level of pollution and create a healthy atmosphere; and to create comfortable working atmospheres. Additionally, the methods used in their design are described. The methods are all based on the same type of approach and are broken down into three groups which correspond to an empirical, an integral, and a local approach. The empirical approach deals with complex flows with poor or medium accuracy. The local approach deals with the problem of limited range of complexity but with more accuracy and generality. Data available for specific flow configurations such as exhaust devices, jets, and plumes, which to be used for an empirical approach, are given. The integral approach consists of examining a finite volume element of

fluid and integrating the conservation equations over the entire volume. The efficiency of these systems is considered. The local or differential approach consists of determining the characteristics of a fluid at every point in the flow structure. Both viscous and inviscid fluids are considered.
ESA

N94-29600# Technical Univ. of Denmark, Lyngby. Heating and Air Conditioning Lab.
HUMAN REQUIREMENTS TO THE INDOOR AIR QUALITY AND THE THERMAL ENVIRONMENT
P. Ole Fanger *In* VKI, Advanced Design of Ventilation Systems 1993 11 p (For primary document see N94-29598 08-31)
Copyright Avail: CASI HC A03/MF A03

Perceived air quality, general thermal sensation of the occupants and risk of draft, aspects which human comfort in a space depends upon, are reviewed separately based on European Guidelines for Ventilation Requirements in Buildings and on a modified ISO (International Standards Organization) standard 7730 on thermal comfort. The perceived air quality is expressed in decipol or percentage of dissatisfied occupants. The general thermal sensation is expressed by the PMV/PPD indices. The perception of draft is expressed by the model of draft risk. Indoor air quality is mediocre and causes complaints in many buildings. The reason for this is often hidden pollution sources in the building, hitherto ignored in previous ventilation standards. To determine the required ventilation, a method is used in the European Guidelines. The new Guidelines acknowledge all pollution sources in the building, expressed in olfs. The method is based on the desired air quality in the space, the available quality of the outdoor air, the ventilation effectiveness and on the total pollution load in the space. The model of draft risk predicts the percentage of occupants feeling draft as a function of the mean air velocity, the turbulence intensity and the air temperature.
ESA

N94-29601# National Board of Occupational Safety and Health, Stockholm (Sweden).
VENTILATION SYSTEMS
L. Olander *In* VKI, Advanced Design of Ventilation Systems 1993 42 p (For primary document see N94-29598 08-31)
Copyright Avail: CASI HC A03/MF A03

Two different types of ventilation systems and their components are addressed: general ventilation and local or process ventilation. Calculation of the flow rates used in the different systems is addressed. The many different types of flow calculations, how they are used, and some of the computer programs that could be used for these calculations are described. Some calculations start with assumptions regarding air flow rates in rooms and locals. The flow rates can be chosen from rule of thumb or regulations or standards. Thereafter the designer calculates necessary heat and cooling loads, pressure drops, fan effect, etc. The other type of calculation is not very common. By using demands on concentrations, temperatures or air velocities the flow rates are calculated. These calculations include contaminant source generation rates, use of models (physical and theoretical), and computational fluid dynamics. The latter are focused upon.
ESA

N94-29602# Norwegian Building Research Inst., Oslo.
THEORY OF AGE DISTRIBUTION
Eimund Skaaret *In* VKI, Advanced Design of Ventilation Systems 1993 22 p (For primary document see N94-29598 08-31)
Copyright Avail: CASI HC A03/MF A03

The analysis of the age distribution of ventilation air and contaminants is considered with regard to the characterization of the ventilation process. The age distribution functions can be determined using tracer gas or in some cases directly from measurement of the concentration of the actual contaminants. It is important to have in mind that the ventilation air and the contaminants represent different 'populations' and so has to be treated separately. Every air molecule, a member of the 'population' entering the room, spends a certain time there, partly caused by the volume of the space and partly caused by the flow pattern. The residence time varies from molecule to molecule. There is, in other words, a certain characteristic age distribution of the molecules and a characteristic average residence time for the total 'population'. The same can be said about the contaminant molecules.
ESA

N94-29603# Norwegian Building Research Inst., Oslo.
VENTILATION MODELS
Eimund Skaaret *In* VKI, Advanced Design of Ventilation Systems 1993 26 p (For primary document see N94-29598 08-31)
Copyright Avail: CASI HC A03/MF A03

Calculation procedures, used in the design of ventilating systems, which are especially suited for displacement ventilation in addition to linking it to mixing ventilation, are addressed. The two zone flow model is considered and the steady state and transient solutions are addressed. Different methods of supplying air are discussed, and different types of air flow are considered: piston flow, plane flow and radial flow. An evaluation model for ventilation systems is presented.
ESA

N94-29604# Goodfellow Consultants, Inc., Mississauga (Ontario).
INDUSTRIAL VENTILATION
H. D. Goodfellow (Toronto Univ., Ontario.) *In* VKI, Advanced Design of Ventilation Systems 1993 24 p (For primary document see N94-29598 08-31)
Copyright Avail: CASI HC A03/MF A03

Industrial ventilation design methodology, using computers and using fluid dynamic models, is considered. It is noted that the design of a ventilation system must be incorporated into the plant design and layout at the earliest conceptual stage of the project. A checklist of activities concerning the methodology for the design of a ventilation system for a new facility is given. A flow diagram of the computer ventilation model shows a typical input, the initialization and iteration loop, and the output. The application of the fluid dynamic modeling techniques include external and internal flow fields, and individual sources of heat and contaminants. Major activities for a ventilation field test program are also addressed.
ESA

N94-29605# Goodfellow Consultants, Inc., Mississauga (Ontario).
VENTILATION COST AND AIR CLEANING
H. D. Goodfellow (Toronto Univ., Ontario.) *In* VKI, Advanced Design of Ventilation Systems 1993 24 p (For primary document see N94-29598 08-31)
Copyright Avail: CASI HC A03/MF A03

The components associated with the costs of the purchase of pollution control equipment are discussed. These include the capital cost to purchase the equipment and installation, and the costs incurred to operate the control device on an annual basis. Although the capital costs can represent a significant outlay of money, typically these costs are spread out over the life of the equipment. In general, this amortized cost is combined with the operating cost and is referred to as an 'annualized cost'. The annualized cost is a commonly used indicator to demonstrate the actual year to year cost that the equipment and operation will represent. Values and methods used to estimate costs, typical cost indicators, and sources of computerized costing models are presented. A comparison of the capital cost expenditure required for a model case (a cement kiln operation), using three control device alternatives is made.
ESA

N94-29606# Aalborg Univ. (Denmark).
COMPUTATIONAL FLUID DYNAMICS IN VENTILATION. 1: THEORY AND ONE-DIMENSIONAL TEST CASE
Peter V. Nielsen *In* VKI, Advanced Design of Ventilation Systems 1993 30 p (For primary document see N94-29598 08-31)
Copyright Avail: CASI HC A03/MF A03

The important role that the development of computer power has had on the design of ventilation systems is considered. This development has lead to decreasing costs and computational time of Computational Fluid Dynamic (CFD) calculations. CFD is an important tool for the prediction of flow in ventilated spaces and there are research areas where people from the indoor environmental technology should, at least, make a major contribution to the further development. The aim of this lecture is to make people who are involved in indoor environmental technology familiar with a number af statement principles and abbreviations. A basic knowledge of CFD which makes it possible to discuss details of the different commercial programs, to read papers on CFD and to start the process of modifying a standard program, is given. The lecture is based on a single (very simple) example, which can be handled by a desk calculator, a pencil and a piece of paper. This should hopefully make the understanding easy. The example takes into account the following: differential equation for one dimensional

flow; difference equation based on Taylor series formulation; discretization equation based on the control volume method; different schemes for the convection and diffusion terms; iterative solution of the discretization equation. ESA

N94-29607# Aalborg Univ. (Denmark).
COMPUTATIONAL FLUID DYNAMICS IN VENTILATION. 2: THEORY AND CODES
Peter V. Nielsen *In* VKI, Advanced Design of Ventilation Systems 1993 13 p (For primary document see N94-29598 08-31)
Copyright Avail: CASI HC A03/MF A03

Theory and codes for computational fluid dynamic calculations used in the design of ventilation systems are presented as a set of 'overhead graphics'. They include: the equation system for buoyancy affected flow (two dimensional case); wall function for momentum flow; air movement in areas with relaminarization; simulation of displacement ventilation; different types of boundary conditions; simplified conditions of a supply opening; box method; prescribed velocity method; different descriptions of supply opening. ESA

N94-29608# Aalborg Univ. (Denmark).
COMPUTATIONAL FLUID DYNAMICS IN VENTILATION. 3: THE IEA ANNEX 20 WORK
Peter V. Nielsen *In* VKI, Advanced Design of Ventilation Systems 8 p(SEE N94-29598 08-31) 1993 (For primary document see N94-29598 08-31)
Copyright Avail: CASI HC A02/MF A03

The IEA energy conservation in buildings and community systems is considered. The basic aims are to increase energy security, develop alternative energy sources, and develop energy conservation. The annnex 20 subtask 1 involves the prediction of accurate air flow patterns within rooms to obtain energy efficiency. Participating research work included comparative tests of: two Dimensional (2D) Computational Fluid Dynamics (CFD) codes, 3D measurements in full scale rooms, and 3D CFD codes. The calculations of these test cases are presented. ESA

N94-29609# Aalborg Univ. (Denmark).
COMPUTATIONAL FLUID DYNAMICS IN VENTILATION. 4: COMMERCIAL APPLICATION OF CFD IN VENTILATION
Peter V. Nielsen *In* VKI, Advanced Design of Ventilation Systems 5 p(SEE N94-29598 08-31) 1993 (For primary document see N94-29598 08-31)
Copyright Avail: CASI HC A01/MF A03

In considering the commercial applications of Computational Fluid Dynamics (CFD) in ventilation, the following are addressed: typical markets (airport centers, large theaters, atria, shopping malls, etc.); typical problems to be solved (energy flow, draft, ventilation effectiveness, pressure distribution, etc.); and high priority areas, activities and quantities (fast preprocessing, effective visualization software, etc.). It is stated that the commercial application of CFD may be looked upon as an advanced 'zonal' model. The 'zonal' model concept is outlined and CFD with large control volumes is considered. An illustrated example of air flow simulation in a theater is given. ESA

N94-29610# Aalborg Univ. (Denmark).
COMPUTATIONAL FLUID DYNAMICS IN VENTILATION. 5: NEW DEVELOPMENTS IN CFD WITH RELEVANCE TO VENTILATION
Peter V. Nielsen *In* VKI, Advanced Design of Ventilation Systems 7 p(SEE N94-29598 08-31) 1993 (For primary document see N94-29598 08-31)
Copyright Avail: CASI HC A02/MF A03

Overhead graphics illustrating new developments in computational fluid dynamics (CFD) which are relevant to ventilation are presented. They cover: normalized variables in a room with mixing ventilation; penetration of a wall jet into a room; CFD and cooling load calculation; areas with analytical description of flow elements; local grid refinement; and large eddy simulation. ESA

N94-29611# Institut National de Recherche et de Securite pour la Prevention des Accidents du Travail et des Maladies Professionnelles, Vandoeuvre (France).
COMPUTATIONAL FLUID DYNAMICS IN VENTILATION: PRACTICAL APPROACH
J. R. Fontaine *In* VKI, Advanced Design of Ventilation Systems 1993 57 p (For primary document see N94-29598 08-31)
Copyright Avail: CASI HC A04/MF A03

The potential of computation fluid dynamics (CFD) for conceiving ventilation systems is shown through the simulation of five practical cases. The following examples are considered: capture of pollutants on a surface treating tank equipped with a unilateral suction slot in the presence of a disturbing air draft opposed to suction; dispersion of solid aerosols inside fume cupboards; performances comparison of two general ventilation systems in a silkscreen printing workshop; ventilation of a large open painting area; and oil fog removal inside a mechanical engineering workshop. Whereas the two first problems are analyzed through two dimensional numerical simulations, the three other cases require three dimensional modeling. For the surface treating tank case, numerical results are compared to laboratory experiment data. All simulations are carried out using EOL, a CFD software specially devised to deal with air quality problems in industrial ventilated premises. It contains many analysis tools to interpret the results in terms familiar to the industrial hygienist. Much experimental work has been engaged to validate the predictions of EOL for ventilation flows. ESA

N94-29612# Simulog, Valbonne (France).
FINITE ELEMENT METHOD FOR NUMERICAL SIMULATION OF TURBULENT FLOWS. THE N3S CODE
T. Bidot *In* VKI, Advanced Design of Ventilation Systems 1993 40 p (For primary document see N94-29598 08-31)
Copyright Avail: CASI HC A03/MF A03

The N3S thermal hydraulic calculation code which can be fitted to all encountered configurations is considered. It uses the finite element method and so allows local mesh refinements. The aim is to solve the equations of thermal hydraulics, namely Navier-Stokes equations coupled to energy equation in order to take into account thermal convection phenomena, for Reynolds numbers which can vary from several tens to several millions. The constraints which were defined for this code are linked to the industrial environment for which it was developed. It must be able to solve problems of industrial interest with realistic computation times on supercomputers and workstations. The N3S code is used for many industrial applications such as confined flows, thermal hydraulics, turbomachinery, and external flows. The range of application is shown. N3S, with the advantage of tetrahedron for complex three dimensional geometries modeling, expands in the direction of adaptative meshes and moving boundaries, and includes more and more complex physics of fluids. ESA

N94-29701# Ministry of Agriculture, Forestry, and Fisheries, Ibaraki (Japan). National Research Inst. of Fisheries Engineering.
BULLETIN OF NATIONAL RESEARCH INSTITUTE OF FISHERIES ENGINEERING, NO. 13 [SUISAN KOGAKU KENKYUJO KENKYU HOKOKU DAI 13 GO]
Toshibumi Noma, ed., Yasuo Morita, ed., Hiroshi Masuda, ed., Masaaki Yamamoto, ed., Ryutaro Yamamoto, ed., Toshihiko Kawashima, ed., Katsuo Hasegawa, ed., Yoshinari Tsuruta, ed., and Tomonari Akamatsu, ed. et al 5 Mar. 1992 173 p In JAPANESE
(ISSN 0388-9718)
(JTN-94-80596) Avail: CASI HC A08/MF A02

The following topics were discussed: current meters for measuring average water velocities, breakwaters for sea water exchange, shear strength of alluvial soils near fishing port areas, slender-body theory for oscillating ships with finite forward speed, flow fields around bodies with filament covered surfaces, biosonar simulator for dolphin clicks waveforms, and reproduction in the Japanese anchovy as related to population fluctuations. For individual titles, see N94-29702 through N94-29708.

N94-29702# Ministry of Agriculture, Forestry, and Fisheries, Ibaraki (Japan). Systems Analysis of Aquacultural Ground Section.
DEVELOPMENT OF A SIMPLE CURRENT METER USING SOLUTION [YOEKI O MOCHIITA KANI RYOSOKUKEI NO KAIHATSU] **c34**
Shigeru Kawamata *In its* Bulletin of National Research Institute of

Fisheries Engineering, No. 13 5 Mar. 1992 p 1-9 In JAPANESE (For primary document see N94-29701 08-31)
Avail: CASI HC A02/MF A02

A simple method of measuring average water velocity was invented for the field survey of water motion affecting benthic organisms. The method uses a vertical thin pipe, an upper chamber filled up with the neutrally buoyant solution of a substance, and a lower chamber packed with porous media to take in ambient water with little variation of water pressure. When this device is set on the flow bed, the solution in the upper chamber is diluted because the solution is pulled out of the pipe by the moving ambient water while the fresh ambient water comes through the lower chamber. An obtained formula of determining the average water velocity during a measurement needs only to measure the initial and last concentrations of the solute in the upper chamber. Furthermore, experiments using models of this device were conducted to prove the feasibility of this idea. It was shown that the method would be practicable but needed some more improvements, especially enhancement of mixing water in the upper chamber. Author (NASDA)

N94-29703# Ministry of Agriculture, Forestry, and Fisheries, Ibaraki (Japan). Systems Analysis of Aquacultural Ground Section.

DEVELOPMENT OF THE BREAKWATER WITH SUBMERGED MOUND FOR INTERCHANGING SEA WATER [KAISUI DONYU O MOKUTEKI TO SHITA SENTEITSUKI ANAAKI BOHATEI NO KAIHATSU]

Masaaki Yamamoto, Masamitsu Nakaizumi, Motohumi Manabe, and Akihiko Moriguchi *In its* Bulletin of National Research Institute of Fisheries Engineering, No. 13 5 Mar. 1992 p 11-30 In JAPANESE Sponsored by Fisheries Agency, Tokyo, Japan (For primary document see N94-29701 08-31)
Avail: CASI HC A03/MF A02

Recently it has been necessary to purify mooring basin water in fishing ports for a new utilization, such as stock of live fishes or short term breeding. A new method for interchanging sea water was proposed in which fresh sea water is driven into the port by wave energy, raising mean water level through the wave breaking process over a submerged mound. A hydraulic model test was executed to prove this method to be useful for the interchanging. Results present an appropriate profile and plane configuration. Author (NASDA)

N94-29704# Ministry of Agriculture, Forestry, and Fisheries, Ibaraki (Japan). Facilities for Fishing Port Section.

THE UNDRAINED SHEAR STRENGTH CHARACTERISTICS OF UNDISTURBED SOIL FROM FISHING PORT AREAS [GYOKO CHIKU NO SANPURINGUDO NO HI HAISUI KYODO TOKUSEI] **c46**

Seiki Ohmaki, Nobuyuki Horikoshi, Yukio Tsubota, and Ryutaro Yamamoto *In its* Bulletin of National Research Institute of Fisheries Engineering, No. 13 5 Mar. 1992 p 31-56 In JAPANESE (For primary document see N94-29701 08-31)
Avail: CASI HC A03/MF A02

Three types of K0 consolidated undrained compression, extension and isotropically consolidated undrained compression test were carried out on the undisturbed samples from alluvial soil grounds of various fishing port areas in Japan. In these experiments, the values of one to about twenty times effective overburden pressure were used as the axial consolidation pressure. From these experimental results, it is shown that most of the alluvial cohesive soil grounds exhibit the pseudo-overconsolidation property due to secondary compression or cementation effect. The relative relationship of normalized undrained shear strength among three types of experiments conducted here is shown. Using these experimental results, the method of determining the design shear strength for alluvial grounds with a wide range of coarse grain content is proposed. Author (NASDA)

N94-29705# Ministry of Agriculture, Forestry, and Fisheries, Ibaraki (Japan). Ship Performance Section.

AN IMPROVEMENT OF THE SLENDER BODY THEORY FOR OSCILLATING SHIPS WITH FINITE FORWARD SPEED [ZENSHIN SOKUDO O YUSURU FUNE NO DOYO MONDAI NI TAISURU SAICHOSEN RIRON NO KAIRYO]

Toshikazu Masuya *In its* Bulletin of National Research Institute of Fisheries Engineering, No. 13 5 Mar. 1992 p 57-80 In JAPANESE (For primary document see N94-29701 08-31)
Avail: CASI HC A03/MF A02

A slender-body theory for ship motions with finite forward speed is presented. This is an improvement of an earlier interpolation theory. The original theory is unsatisfactory due to the following: three dimensional effects are overestimated for symmetric motions and vanish for antisymmetric motions. The original theory was recasted, and this flaw was removed. The theory is developed for oscillating ships with finite forward speed and expanded to steady motion problems. Author (NASDA)

N94-29706# Ministry of Agriculture, Forestry, and Fisheries, Ibaraki (Japan). Hull Construction Section.

THE FLOW FIELD NEAR THE BODY SURFACE WITH THIN FILAMENTS [KOMITSUDO NO RITSUMO SENI DE OWARETA BUTTAI MAWARI NO NAGAREBA NI KANSURU KENKYU] **c34**

Toshihiko Kawashima, Kumiko Adachi, and Hiroyasu Kato *In its* Bulletin of National Research Institute of Fisheries Engineering, No. 13 5 Mar. 1992 p 81-94 In JAPANESE Prepared in cooperation with National Research Inst. of Aquaculture, Mie, Japan; and Toray Industries, Inc., Shiga, Japan (For primary document see N94-29701 08-31)
Avail: CASI HC A03/MF A02

The hydrodynamic characteristics of a flow-field near a surface that is covered with a special cloth that is vertically woven into many thin filaments are presented. The velocity distribution was measured in order to examine the flow mechanism of the boundary layer on the flat plate with thin filaments. The role that the thin filaments play in increasing the boundary layer is discussed. A new fluid phenomenon, the dead water layer, was discovered. The dead water layer exists on the inside of the boundary layer. The fundamental properties of this layer are indicated. Next, the body surface pressure and flow pattern are examined to analyze the influence of the filaments. This was done by using the cylindrical body with thin filaments and by measuring the change due to thin filaments on the pressure distribution. The separation position and the pressure resistance are pointed out. Additional flow characteristics of bodies combined with thin filaments are discussed. Author (NASDA)

N94-29707# National Research Inst. of Fisheries Engineering, Tokyo (Japan). Ocean Electronics Section.

DESIGN OF THE BIOSONAR SIMULATOR FOR DOLPHIN'S CLICKS WAVEFORM REPRODUCTION [IRUKA NO KURIKKUSU MEION NO SAISEI HOSHA SOCHI: BAIOSONA SHIMYURETA NO SHISAKU] **c35**

Ken Ishii, Tomonari Akamatsu, and Yoshimi Hatakeyama *In its* Bulletin of National Research Institute of Fisheries Engineering, No. 13 5 Mar. 1992 p 95-128 In JAPANESE (For primary document see N94-29701 08-31)
Avail: CASI HC A03/MF A02

The emitted clicks of Dall's porpoises consist of a pulse train of burst signals with an ultrasonic carrier frequency. The authors have designed a biosonar simulator to reproduce the waveforms associated with a dolphin's clicks underwater. The total reproduction system consists of a click signal acquisition block, a waveform analysis block, a memory unit, a click simulator, and a underwater, ultrasonic wave transmitter. In operation, data stored in an EPROM (Erasable Programmable Read Only Memory) are read out sequentially by a fast clock and converted to analog output signals. Then an ultrasonic power amplifier reproduces these signals through a transmitter. The click signal replaying block is referred to as the BSS (Biosonar Simulator). This is what simulates the clicks. The details of the BSS are described in this report. A unit waveform is defined. The waveform is divided into a burst period and a waiting period. Clicks are a sequence based on a unit waveform, and digital data are sequentially read out from an EPROM of waveform data. The basic parameters of the BSS are as follows: (1) reading clock, 100 ns to 25.4 microseconds; (2) number of reading clock, 34 to 1024 times; (3) counter clock in a waiting period, 100 ns to 25.4 microseconds; (4) number of counter clock, zero to 16,777,215 times; (5) number of burst/waiting repetition cycle, one to 128 times; and (6) transmission level adjustment by a programmable attenuator, zero to 86.5 dB. These basic functions enable the BSS to replay clicks of Dall's porpoise precisely. Author (NASDA)

N94-29708# Ministry of Agriculture, Forestry, and Fisheries, Ibaraki (Japan). Analysis of Gear and Methods Section.
REPRODUCTION IN THE JAPANESE ANCHOVY (ENGRAULIS JAPONICA) AS RELATED TO POPULATION FLUCTUATION [KATAKUCHIIWASHI NO SEIJUKU/SANRAN TO SAISEISANRYOKU NO CHOSETSU NI KANSURU KENKYU] **c51**
Yoshinari Tsuruta *In its* Bulletin of National Research Institute of Fisheries Engineering, No. 13 5 Mar. 1992 p 129-168 In JAPANESE (For primary document see N94-29701 08-31)
Avail: CASI HC A03/MF A02

Field surveys and laboratory experiments on the Japanese anchovy, Engraulis japonica, were conducted in order to identify mechanisms which promote stock size stability. Field surveys confirmed the relatively long spawning season, the short time interval between spawning episodes (interspawning interval), and the seasonal change in batch fecundity. In laboratory experiments, long photoperiod and water temperature played a leading role as a trigger of gonad maturation and spawning. A reduction in food resulted in the following: (1) a prolongation of interspawning interval; (2) a reduction in a batch fecundity; and (3) a change in egg size when the food ration was below the level required for body maintenance. The number of eggs spawned per female was reduced at high density even when food for the individual was held constant. On the other hand, growth was better than in a low density tank. Seawater was removed from the high density tank and discharged into the low density tank. This reduced the number of eggs spawned per female in the low-density tank. However this did not apply for sea water from a low-density tank and also a high-density tank without mature fish. Therefore, some unknown organic substance may control gonad maturation. Author (NASDA)

N94-29767*# Jet Propulsion Lab., California Inst. of Tech., Pasadena.
PROCEEDINGS OF THE WORKSHOP ON MICROTECHNOLOGIES AND APPLICATIONS TO SPACE SYSTEMS
B. A. Wilson, ed. 15 Jun. 1993 321 p Workshop held in Pasadena, CA, 27-28 May 1992
(Contract NAS7-918; RTOP 506-49-21)
(NASA-CR-195688; JPL-Publ-93-8; NAS 1.26:195688) Avail: CASI HC A14/MF A03

This volume serves as the Proceedings of this workshop. It contains the manuscripts provided by plenary and parallel session presenters, and summary reports generated from this material and from information presented during the panel discussions. Where manuscripts were not provided, extended abstracts, if available, have been included. The order of the papers follows the original workshop agenda. For individual titles, see N94-29768 through N94-29794.

N94-29768*# Jet Propulsion Lab., California Inst. of Tech., Pasadena.
THE PLUTO FAST FLYBY MISSION: COMPLETING THE RECONNAISSANCE OF THE SOLAR SYSTEM Abstract Only **c91**
Paul K. Henry *In its* Proceedings of the Workshop on Microtechnologies and Applications to Space Systems 15 Jun. 1993 p 13 (For primary document see N94-29767 08-31)
Avail: CASI HC A01/MF A03

The concept of a fast flyby mission to Pluto has been advanced as a means to complete the reconnaissance of the known solar system. In order to acquire data on the Pluto system at the earliest possible time, and within the professional lifetime of investigators now active in the field, concepts are being developed for relatively small spacecraft in the mass range of 70 Kg to 350 Kg with flight times to Pluto of 7 to 13 years. Necessarily, the science complement on such a mission will be very mass and power limited. The challenge will be to define a spacecraft and an instrument package that will maximize the scientific return within these limitations. Cost, of course, will be a major consideration, and funds for new technology development specific to this mission will not be extensive. Consequently, innovative ways to incorporate elegant simplicity into the designs must be found. In order to facilitate exploration of the Pluto-Charon system, fully integrated science payloads must be developed. Two proposed mission designs involving limited mass and power science payloads have been presented to the Outer Planets Science Working Group (OPSWG). These payload mass allocations range from 5 to 30 kilograms with power allocations as low as 5 watts. The drivers behind these low mass and power allocations are that they enable developing missions to fit within the moderate mission cost profile and allow fast flight times to Pluto (7 to 13 years). The OPSWG has prioritized science goals for this class of reconnaissance mission. Three specific science objectives were identified as the highest priority required for the first Pluto mission. These goals were: (1) study of the neutral atmosphere, (2) geology and morphology, and (3) surface compositional mapping. In order to achieve these science goals within the constraints of low mass, power and cost, it may be necessary to combine the functions of 3 conventional instruments (CCD camera, Ultra-Violet Spectrometer, and Infrared Spectrometer) into one fully integrated payload. Where possible, this payload would share optics, mechanisms, electronics and packaging. Author

N94-29769*# Louisiana Tech Univ., Ruston. Institute for Micromanufacturing. I558
MICROMANUFACTURING: RECENT DEVELOPMENTS IN THIS COUNTRY AND ABROAD
Robert O. Warrington, Craig R. Friedrich, Robert X. Gao, and Gang Lin *In* JPL, Proceedings of the Workshop on Microtechnologies and Applications to Space Systems 15 Jun. 1993 p 21-28 (For primary document see N94-29767 08-31)
Avail: CASI HC A02/MF A03

This paper has attempted to summarize some recent activities in this country and overseas. The effort in Louisiana is relatively new and growing. The Russian effort is not well coordinated or documented. A conference on Micro Systems Technologies is scheduled for June of 1993 in St. Petersburg, Russia. Serious consideration should be given to developing a strategy to not only participate in this meeting, but also to spend additional time in Russia assessing the technology. MEMS technologies will eventually affect virtually every aspect of our lives and, at least in the near term, mini-devices with micro-components will probably be the economic drivers for the technology. Author

N94-29770*# Wisconsin Univ., Madison. Dept. of Electrical and Computer Engineering.
MICROACTUATOR PRODUCTION VIA HIGH ASPECT RATIO, HIGH EDGE ACUITY METAL FABRICATION TECHNOLOGY
H. Guckel and T. R. Christenson *In* JPL, Proceedings of the Workshop on Microtechnologies and Applications to Space Systems 15 Jun. 1993 p 35-41 (For primary document see N94-29767 08-31)
(Contract NSF EET-88-15285; SRC-88-MC-507; N00014-91-J-1876; NSF DMR-88-21625)
Avail: CASI HC A02/MF A03

LIGA is a procession sequence which uses x-ray lithography on photoresist layers of several hundred micrometers to produce very high edge acuity photopolymer molds. These plastic molds can be converted to metal molds via electroplating of many different metals and alloys. The end results are high edge acuity metal parts with large structural heights. The LIGA process as originally described by W. Ehrfeld can be extended by adding a surface micromachining phase to produce precision metal parts which can be assembled to form three-dimensional micromechanisms. This process, SLIGA, has been used to fabricate a dynamometer on a chip. The instrument has been fully implemented and will be applied to tribology issues, speed-torque characterization of planar magnetic micromotors and a new family of sensors. Author

N94-29771*# Massachusetts Inst. of Tech., Lexington. Lincoln Lab.
OVERVIEW OF MICROOPTICS: PAST, PRESENT, AND FUTURE **c74**
Wilfrid B. Veldkamp *In* JPL, Proceedings of the Workshop on Microtechnologies and Applications to Space Systems 15 Jun. 1993 p 43-54 (For primary document see N94-29767 08-31)
Avail: CASI HC A03/MF A03

Through advances in semiconductor miniaturization technology, microrelief patterns, with characteristic dimensions as small as the wavelength of light, can now be mass reproduced to form high-quality and low-cost optical components. In a unique example of technology transfer, from electronics to optics, this capability is allowing optics designers to create innovative optical components that promise to solve key problems in optical sensors, optical communication channels, and optical processors. Author

N94-29772*# Jet Propulsion Lab., California Inst. of Tech., Pasadena.
MICRO GUIDANCE AND CONTROL TECHNOLOGY OVERVIEW **c04**
Glen J. Kissel and Fred Y. Hadaegh *In its* Proceedings of the Workshop

on Microtechnologies and Applications to Space Systems 15 Jun. 1993 p 75-81 (For primary document see N94-29767 08-31)
Avail: CASI HC A02/MF A03

This paper gives an overview of micro-guidance and control technologies and in the process previews of the technology/user and systems issues presented in the guidance and control session at the workshop. We first present a discussion of the advantages of using micro-guidance and control components and then detail six micro-guidance and control thrusts that could have a revolutionary impact on space missions and systems. Specific technologies emerging in the micro-guidance and control field will be examined. These technologies fall into two broad categories: micro-attitude determination (inertial and celestial) and micro-actuation, control and sensing. Finally, the scope of the workshop's guidance and control panel are presented. Author

N94-29773*# Jet Propulsion Lab., California Inst. of Tech., Pasadena.
MINIATURIZATION IN X RAY AND GAMMA RAY SPECTROSCOPY **c74**

Jan S. Iwanczyk (XSIRIUS Scientific, Inc., Marina Del Ray, CA.), Yuzhong J. Wang (XSIRIUS Scientific, Inc., Marina Del Ray, CA.), and James G. Bradley *In its* Proceedings of the Workshop on Microtechnologies and Applications to Space Systems 15 Jun. 1993 p 85-94 (For primary document see N94-29767 08-31)
(Contracts NASw-4492; NAS5-33045; NIH-5R01-GM37161)
Avail: CASI HC A02/MF A03

The paper presents advances in two new sensor technologies and a miniaturized associated electronics technology which, when combined, can allow for very significant miniaturization and for the reduction of weight and power consumption in x-ray and gamma-ray spectroscopy systems: (1) Mercuric iodide (HgI2) x-ray technology, which allows for the first time the construction of truly portable, high-energy resolution, non-cryogenic x-ray fluorescence (XRF) elemental analyzer systems, with parameters approaching those of laboratory quality cryogenic instruments; (2) the silicon avalanche photodiode (APD), which is a solid-state light sensitive device with internal amplification, capable of uniquely replacing the vacuum photomultiplier tube in scintillation gamma-ray spectrometer applications, and offering substantial improvements in size, ruggedness, low power operation and energy resolution; and (3) miniaturized (hybridized) low noise, low power amplification and processing electronics, which take full advantage of the favorable properties of these new sensors and allow for the design and fabrication of advanced, highly miniaturized x-ray and gamma-ray spectroscopy systems. The paper also presents experimental results and examples of spectrometric systems currently under construction. The directions for future developments are discussed. Author

N94-29774*# National Aeronautics and Space Administration. Lyndon B. Johnson Space Center, Houston, TX.
BACKSCATTER MOSSBAUER SPECTROMETER (BaMS) FOR EXTRATERRESTRIAL APPLICATIONS **c35**

D. G. Agresti (Alabama Univ., Birmingham.), T. D. Shelfer (Alabama Univ., Birmingham.), M. M. Pimperl (Alabama Univ., Birmingham.), E. L. Wills (Alabama Univ., Birmingham.), M. H. Shen (Alabama Univ., Birmingham.), and R. V. Morris *In* JPL, Proceedings of the Workshop on Microtechnologies and Applications to Space Systems 15 Jun. 1993 p 95-97 (For primary document see N94-29767 08-31)
Avail: CASI HC A01/MF A03

Mossbauer spectroscopy is a nuclear gamma resonance technique particularly well suited to the study of materials that contain iron (Fe-57). It can provide information on the oxidation state of iron as well as the type and proportion of iron-containing mineral species in a sample of interest. Iron Mossbauer spectroscopy (FeMS) has been applied to samples believed to have come from Mars (SNC meteorites) and has been helpful in refining the choice among putative Martian surface materials by suggesting a likely nanophase component of the Martian regolity. FeMS spectrum of a Martial analogue material (Hawaiian palagonite) is shown; it is dominated by ferric-bearing phases and shows evidence of a nanophase component. FeMS has also been applied to lunar materials. It can be used to measure the maturity of lunar surface material and has been proposed as a prospector for lunar ilmenite, an oxygen resource mineral. Several years ago we suggested a backscatter Mossbauer spectrometer (BaMS) for a Mars rover mission. Backscatter design was selected as most appropriate for in-situ application because no sample preparation is required. Since that time, we have continued to develop the BaMS instrument in anticipation that it would eventually find a home on a NASA planetary mission. Gooding proposed BaMS as a geochemistry instrument on MESUR. More recently, an LPI workshop has recommended that BaMS be included in a three-instrument payload on the next (1996?) lunar lander. Author

N94-29775*# Illinois Univ., Chicago. Electrical Engineering and Computer Science Dept.
A SUB-cm MICROMACHINED ELECTRON MICROSCOPE

A. D. Feinerman, D. A. Crewe, D. C. Perng, S. E. Shoaf, and A. V. Crewe *In* JPL, Proceedings of the Workshop on Microtechnologies and Applications to Space Systems 15 Jun. 1993 p 99-120 Repr. from Journal of Vacuum Science Technology A, v. 10, no. 4, pt. 1, Jul.-Aug. 1992 p 611-616 (For primary document see N94-29767 08-31)
(Grant NSF RIA-90-09842)
Avail: CASI HC A03/MF A03

A new approach for fabricating macroscopic (approximately 10x10x10 mm(exp 3)) structures with micron accuracy has been developed. This approach combines the precision of semiconductor processing and fiber optic technologies. A (100) silicon wafer is anisotropically etched to create four orthogonal v-grooves and an aperture on each 10x12 mm die. Precision 308 micron optical fibers are sandwiched between the die to align the v-grooves. The fiber is then anodically bonded to the die above and below it. This procedure is repeated to create thick structures and a stack of 5 or 6 die will be used to create a miniature scanning electron microscope (MSEM). Two die in the structure will have a segmented electrode to deflect the beam and correct for astigmatism. The entire structure is UHV compatible. The performance of an SEM improves as its length is reduced and a sub-cm 2 keV MSEM with a field emission source should have approximately 1 nm resolution. A low voltage high resolution MSEM would be useful for the examination of biological specimens and semiconductors with a minimum of damage. The first MSEM will be tested with existing 6 micron thermionic sources. In the future a micromachined field emission source will be used. The stacking technology presented in this paper can produce an array of MSEMs 1 to 30 mm in length with a 1 mm or larger period. A key question being addressed by this research is the optimum size for a low voltage MSEM which will be determined by the required spatial resolution, field of view, and working distance. Derived from text

N94-29776*# National Aeronautics and Space Administration. Lyndon B. Johnson Space Center, Houston, TX.
DIFFERENTIAL SCANNING CALORIMETRY (DSC) FOR PLANETARY SURFACE EXPLORATION **c35**

James L. Gooding and Douglas W. Ming *In* JPL, Proceedings of the Workshop on Microtechnologies and Applications to Space Systems 15 Jun. 1993 p 121-12 (For primary document see N94-29767 08-31)
Avail: CASI HC A01/MF A03

Differential Scanning Calorimetry (DSC) is the quantitative measurement of the enthalpic response of a material to a systematic change in temperature. In practice, the heat flow into or outward from a sample is measured as the sample is heated or cooled at a carefully controlled rate. DSC superficially resembles, but is not the same as differential thermal analysis (DTA), which is the measurement of temperature differences between a sample and reference material as the pair is heated or cooled. The fundamental properties measured by DSC are enthalpies and temperatures of phase transitions and constant-pressure heat capacities. Depending on instrument design and the nature of the sample, high-quality DSC analyses can be obtained on only a few milligrams of solid materials. DSC requires direct contact with the sample and generally degrades, if not destroys, the sample as a consequence of heating. In laboratory applications, it is common to subject the gaseous effluent from the DSC to analysis by a separate evolved-gas analyzer (EGA). Author

N94-29777*# Jet Propulsion Lab., California Inst. of Tech., Pasadena.
MICRO-SENSORS FOR IN-SITU METEOROLOGICAL MEASUREMENTS **c47**

David Crisp, William J. Kaiser, Thomas R. VanZandt, and James E. Tillman *In its* Proceedings of the Workshop on Microtechnologies and Applications to Space Systems 15 Jun. 1993 p 123-124 (For primary document see N94-29767 08-31)
Avail: CASI HC A01/MF A03

Improved in-situ meteorological measurements are needed for monitoring

the weather and climate of the terrestrial and Martian atmospheres. We have initiated a program to assess the feasibility and utility of micro-sensors for precise in-situ meteorological measurements in these environments. Sensors are being developed for measuring pressure, temperature, wind velocity, humidity, and aerosol amounts. Silicon micro-machining and large scale integration technologies are being used to make sensors that are small, rugged, lightweight, and require very little power. Our long-term goal is to develop very accurate miniaturized sensors that can be incorporated into complete instrument packages or 'micro weather stations,' and deployed on a variety of platforms. If conventional commercially available silicon production techniques can be used to fabricate these sensor packages, it will eventually be possible to mass-produce them at low cost. For studies of the Earth's troposphere and stratosphere, they could be deployed on aircraft, dropsondes, radiosondes, or autonomous surface stations at remote sites. Improved sensor accuracy and reduced sensor cost are the primary challenges for these applications. For studies of the Martian atmosphere, these sensor packages could be incorporated into the small entry probes and surface landers that are being planned for the Mars Environmental SURvey (MESUR) Mission. That decade-long program will deploy a global network of small stations on the Martian surface for monitoring meteorological and geological processes. Low mass, low power, durability, large dynamic range and calibration stability are the principal challenges for this application. Our progress on each of these sensor types is presented. Author

N94-29778*# Jet Propulsion Lab., California Inst. of Tech., Pasadena.
A BROAD-BAND MICROSEISMOMETER FOR PLANETARY OPERATIONS **c35**
W. B. Banerdt, T. VanZandt, W. J. Kaiser, and T. W. Kenny *In its* Proceedings of the Workshop on Microtechnologies and Applications to Space Systems 15 Jun. 1993 p 125-126 (For primary document see N94-29767 08-31)
Avail: CASI HC A01/MF A03

There has recently been renewed interest in the development of instrumentation for making measurements on the surface of Mars. This is due to the Mars Environmental Survey (MESUR) Mission, for which approximately 16 small, long-lived (2-10 years), relatively inexpensive surface stations will be deployed in a planet-wide network. This will allow the investigation of processes (such as seismology and meteorology) which require the simultaneous measurement of phenomena at many widely spaced locations on the surface over a considerable length of time. Due to the large number of vehicles involved, the mass, power, and cost of the payload will be severely constrained. A seismometer has been identified as one of the highest priority instruments in the MESUR straw-man payload. The requirements for an effective seismic experiment on Mars place a number of constraints on any viable sensor design. First, a large number of sensors must be deployed in a long-lived global network in order to be able to locate many events reliably, provide good spatial sampling of the interior, and increase the probability of seismic detection in the event of localized seismicity and/or high attenuation. From a practical standpoint, this means that individual surface stations will necessarily be constrained in terms of cost, mass, and power. Landing and thermal control systems will probably be simple, in order to minimize cost, resulting in large impact accelerations and wide daily and seasonal thermal swings. The level of seismic noise will determine the maximum usable sensitivity for seismometer. Unfortunately, the ambient seismic noise level for Mars is not well known. However lunar seismic noise levels are several orders of magnitude below that of the Earth. Sensitivities on the order of 10(exp -11)g over a bandwidth of .04 to 20 Hz are thought to be necessary to fulfill the science objectives for a seimometer placed on the Martian surface. Silicon micromachined sensor technology offers techniques for the fabrication of monolithic, robust, compact, lower power and mass accelerometers. Conventional micro-machined accelerometers have been developed and are commercially available for high frequency and large acceleration measurements. The new seismometer we are developing incorporates certain principles of conventional silicon micromachined accelerometer technology. However, currently available silicon micromachined sensors offer inadequate sensitivity and bandwidth for the Mars seismometer application. Our implementation of an advanced silicon micromachined seismometer is based on principles recently developed at JPL for high-sensitivity position sensor technology.
Author

N94-29779*# Jet Propulsion Lab., California Inst. of Tech., Pasadena.
IMAGING SPECTROMETRY OF THE EARTH AND OTHER SOLAR SYSTEM BODIES Abstract Only **c35**
Gregg Vane *In its* Proceedings of the Workshop on Microtechnologies and Applications to Space Systems 15 Jun. 1993 p 127 (For primary document see N94-29767 08-31)
Avail: CASI HC A01/MF A03

Imaging spectrometry is a relatively new tool for remote sensing of the Earth and other bodies of the solar system. The technique dates back to the late 1970's and early 1980's. It is a natural extension of the earlier multi-spectral imagers developed for remote sensing that acquire images in a few, usually broad spectral bands. Imaging spectrometers combine aspects of classical spectrometers and imaging systems, making it possible to acquire literally hundreds of images of an object, each image in a separate, narrow spectral band. It is thus possible to perform spectroscopy on a pixel-by-pixel basis with the data acquired with an imaging spectrometer. Two imaging spectrometers have flown in space and several others are planned for future Earth and planetary missions. The French-built Phobos Infrared Spectrometer (ISM) was part of the payload of the Soviet Mars mission in 1988, and the JPL-built Near Infrared Mapping Spectrometer (NIMS) is currently en route to Jupiter aboard the Galileo spacecraft. Several airborne imaging spectrometers have been built in the past decade including the JPL-built Airborne Visible/Infrared Imaging Spectrometer (AVIRIS) which is the only such sensor that covers the full solar reflected portion of the spectrum in narrow, contiguous spectral bands. NASA plans two imaging spectrometers for its Earth Observing System, the Moderate and the High Resolution Imaging Spectrometers (MODIS and HIRIS). A brief overview of the applications of imaging spectrometry to Earth science will be presented to illustrate the value of the tool to remote sensing and indicate the types of measurements that are required. The system design for AVIRS and a planetary imaging spectrometer will be presented to illustrate the engineering considerations and challenges that must be met in building such instruments. Several key sensor technology areas will be discussed in which miniaturization and/or enhanced performance through micromachining and nanofabrication may allow smaller, more robust, and more capable imaging spectrometers to be built in the future. Author

N94-29780*# Jet Propulsion Lab., California Inst. of Tech., Pasadena.
SMART FOCAL-PLANE TECHNOLOGY FOR MICRO-INSTRUMENTS AND MICRO-ROVERS **c63**
Eric R. Fossum *In its* Proceedings of the Workshop on Microtechnologies and Applications to Space Systems 15 Jun. 1993 p 129-130 (For primary document see N94-29767 08-31)
Avail: CASI HC A01/MF A03

It is inevitable that micro-instruments and micro-rovers for space exploration will contain one or more focal-plane arrays for imaging, spectroscopy, or navigation. In this paper, we explore the state-of-the-art in focal-plane technology for visible sensors. Also discussed is present research activity in advanced focal-plane technology with particular emphasis on the development of smart sensors. The paper concludes with a discussion of possible future directions for the advancement of the technology.
Author

N94-29781*# Science Applications International Corp., Santa Barbara, CA.
EVOLUTION OF MINIATURE DETECTORS AND FOCAL PLANE ARRAYS FOR INFRARED SENSORS **c74**
Louis A. Watts *In* JPL, Proceedings of the Workshop on Microtechnologies and Applications to Space Systems 15 Jun. 1993 p 131-14 (For primary document see N94-29767 08-31)
Avail: CASI HC A02/MF A03

Sensors that are sensitive in the infrared spectral region have been under continuous development since the WW2 era. A quest for the military advantage of 'seeing in the dark' has pushed thermal imaging technology toward high spatial and temporal resolution for night vision equipment, fire control, search track, and seeker 'homing' guidance sensing devices. Similarly, scientific applications have pushed spectral resolution for chemical analysis, remote sensing of earth resources, and astronomical exploration applications. As a result of these developments, focal plane arrays (FPA) are now available with sufficient sensitivity for both high spatial and narrow bandwidth spectral resolution imaging over large fields of view. Such devices combined with emerging opto-electronic developments in integrated FPA

data processing techniques can yield miniature sensors capable of imaging reflected sunlight in the near IR and emitted thermal energy in the Mid-wave (MWIR) and longwave (LWIR) IR spectral regions. Robotic space sensors equipped with advanced versions of these FPA's will provide high resolution 'pictures' of their surroundings, perform remote analysis of solid, liquid, and gas matter, or selectively look for 'signatures' of specific objects. Evolutionary trends and projections of future low power micro detector FPA developments for day/night operation or use in adverse viewing conditions are presented in the following test. Author (revised)

N94-29782*# General Electric Co., Schenectady, NY. Corporate Research and Development.

ADVANCED MICROFABRICATION TECHNOLOGIES FOR MICROSPACECRAFT **c18**

M. Ghezzo, B. Bagepalli, S. Kodiyalam, C. Korham, K. Browall, and Norman Alexander *In* JPL, Proceedings of the Workshop on Microtechnologies and Applications to Space Systems 15 Jun. 1993 p 157 (For primary document see N94-29767 08-31)

Avail: CASI HC A01/MF A03

Advanced microfabrication technologies offer the prospect of reducing the weight and size of spacecraft through the use of lighter and stronger materials in conjunction with new mechanical/structural design concepts and design optimization methods. At the same time, electronic components have been scaled down while increasing functional utility. A two-fold benefit is derived for space applications through the use of less expensive components and the lower launch costs associated with lighter components. GE-CRD is actively pursuing research in these key technologies for a wide range of applications including satellites. These key technologies will be reviewed and an update on GE progress will be given. The need to reduce weight and lower cost, while maintaining product quality and reliability are primary drivers in the design of satellites, in general, and microsatellites in particular. For the structural subsystem, these requirements pose a complex design problem unless new mechanical design concepts and computer-aided design optimization methods are employed. Several new concepts, such as battery packs doubling as panel reinforcements and fuel tanks as integral structural members, need to utilized. In addition, new viscoelastic material damping concepts for spacecraft components provide for lighter weight/lower cost designs, while satisfying the structural dynamics requirements. High density interconnect (HDI) technology permits the use of bare IC's on a ceramic substrate with 90 percent active area utilization. A copper/polyimide multilayer structure is the backbone of the technology, which has demonstrated a size/weight reduction of greater than 10x compared to printed circuit board with performance up to the GHz level. HDI modules have exceptional mechanical robustness as evidenced by survival of 180 kg rapid acceleration tests. Microelectromechanical systems (MEMS) are redefining sensors and actuators by miniaturization through micromachining techniques. Sharing many fabrication steps with HDI, we have developed a new technique for surface micromachining of copper/polyimide structures using computer-aided laser patterning. Author (revised)

N94-29783*# Molecular Devices Corp., Menlo Park, CA.

MICROFABRICATED SILICON BIOSENSORS FOR MICROPHYSIOMETRY **c51**

L. J. Bousse, J. M. Libby, and J. W. Parce *In* JPL, Proceedings of the Workshop on Microtechnologies and Applications to Space Systems 15 Jun. 1993 p 163-18 (For primary document see N94-29767 08-31)

(Contract MDA972-92-C-0005)

Avail: CASI HC A03/MF A03

Microphysiometers are biosensor devices that measure the metabolic rate of living cells by detecting the rate of extracellular acidification caused by a small number of cells. The cells are entrapped in a microvolume chamber, whose bottom surface is a silicon sensor chip. In a further miniaturization step, we have recently fabricated multichannel flow-through chips that will allow greater throughput and multiplicity. Microphysiometer technology can be applied to the detection of microorganisms. We describe the sensitive detection of bacteria and yeast. Further applications of microphysiometry to the characterization of microorganisms can be anticipated. Author

N94-29784*# International Business Machines Corp., San Jose, CA. Research Div.

TOWARD MILLI-NEWTON ELECTRO- AND MAGNETO-STATIC MICROACTUATORS **c33**

Long-Sheng Fan *In* JPL, Proceedings of the Workshop on Microtechnologies and Applications to Space Systems 15 Jun. 1993 p 191-20 (For primary document see N94-29767 08-31)

Avail: CASI HC A03/MF A03

Microtechnologies can potentially push integrated electro- and magnetostatic actuators toward the regime where constant forces in the order of milli-Newton (or torques in the order of micro-Newton meter) can be generated with constant inputs within a volume of 1.0 x 1.0 x 0.02 mm with 'conventional' technology. 'Micro' actuators are, by definition, actuators with dimensions confined within a millimeter cube. Integrated microactuators based on electrostatics typically have force/torque in the order of sub-micro-Newton (sub-nano-Newton meter). These devices are capable of moving small objects at MHz frequencies. On the other hand, suppose we want to move a one cubic millimeter object around with 100 G acceleration; a few milli-Newton force will be required. Thus, milli-Newton microactuators are very desirable for some immediate applications, and it challenges micromechanical researchers to develop new process technologies, designs, and materials toward this goal. Author (revised)

N94-29785*# Jet Propulsion Lab., California Inst. of Tech., Pasadena.

MICROMACHINED ELECTRON TUNNELING INFRARED SENSORS **c74**

T. W. Kenny, W. J. Kaiser, J. A. Podosek, H. K. Rockstad, and J. K. Reynolds *In its* Proceedings of the Workshop on Microtechnologies and Applications to Space Systems 15 Jun. 1993 p 205-212 (For primary document see N94-29767 08-31)

Avail: CASI HC A02/MF A03

The development of an improved Golay cell is reported. This new sensor is constructed entirely from micromachined silicon components. A silicon oxynitride (SiO(x)N(y)) membrane is deflected by the thermal expansion of a small volume of trapped gas. To detect the motion of the membrane, an electron tunneling transducer is used. This sensor detects electrons which tunnel through the classically forbidden barrier between a tip and a surface; the electron current is exponentially dependent on the separation between the tip and the surface. The sensitivity of tunneling transducers constructed was typically better than 10(exp -3) A/square root of Hz. Through use of the electron tunneling transducer, the scaling laws which have prevented the miniaturization of the Golay cell are avoided. This detector potentially offers low cost fabrication, compatibility with silicon readout electronics, and operation without cooling. Most importantly, this detector may offer better sensitivity than any other uncooled infrared sensor, with the exception of the original Golay cell. Derived from text

N94-29786*# Louisiana Tech Univ., Ruston. Inst. for Micromanufacturing.

MACRO, MINI, MICRO AND NANO (M(SUP 3)N) TECHNOLOGIES FOR THE FUTURE

Craig R. Friedrich, Robert O. Warrington, Robert X. Gao, and Gang Lin *In* JPL, Proceedings of the Workshop on Microtechnologies and Applications to Space Systems 15 Jun. 1993 p 213-22 (For primary document see N94-29767 08-31)

Avail: CASI HC A02/MF A03

Microelectromechanical systems (MEMS), micro systems technologies (MST), and micromanufacturing are relatively recent phrases or acronyms that have become synonymous with the design, development, and manufacture of 'micro' devices and systems. Micromanufacturing encompasses MEMS or MST and, in addition, includes all of the processes involved in the production of micro things. Integration of mechanical and electrical components, including built-in computers, can be formed into systems which must be connected to the macroworld. Macro, mini, micro, and nano technologies are all a part of MEMS or micromanufacturing. At this point in the development of the technology, it is becoming apparent that mini systems, with micro components, could very well be the economic drivers of the technology for the foreseeable future. Initial research in the fabrication of microdevices using IC processing technology took place over thirty years ago. Anisotropic etching of silicon was used to produce piezoresistive diaphragms. Since the early 60's, there has been gradual progress in MEMS until the early 1980's when worldwide interest in the technology really started to develop. During this time high aspect ratio

micromachining using x rays was started in Germany. In 1987 the concept of a 'silicon micromechanics foundry' was proposed. Since then the interest in the U.S., Germany, and Japan has increased to the point where hundreds of millions of dollars of research monies are being funneled into the technology (at least in Germany and Japan) and the technology has been classified as critical or as a technology or national importance by the U.S. government. Author (revised)

N94-29787*# Jet Propulsion Lab., California Inst. of Tech., Pasadena.
CONTROL OF MICROMACHINED DEFORMABLE MIRRORS **c74**
M. L. Agronin, R. Bartman, F. Y. Hadaegh, W. Kaiser, and P. K. C. Wang *In its* Proceedings of the Workshop on Microtechnologies and Applications to Space Systems 15 Jun. 1993 p 225-246 (For primary document see N94-29767 08-31)
Avail: CASI HC A03/MF A03

A micromachined deformable mirror with pixelated electrostatic actuators is proposed. The paper begins with a physical description of the proposed mirror. Then a mathematical model in the form of a nonlinear partial differential equation describing the mirror surface deformations is derived. This model is used to derive the required voltages for the actuators to achieve a specified static deformation of the mirror surface. This is followed by the derivation of a static nonlinear feedback controller for achieving noninteracting actuation. Then the structure for a complete control system for wavefront correction is proposed. The paper concludes with a discussion of the physical implementation of the proposed control system. Author

N94-29788*# Draper (Charles Stark) Lab., Inc., Cambridge, MA.
EMERGING TECHNOLOGIES IN MICROGUIDANCE AND CONTROL **c04**
Marc S. Weinberg *In* JPL, Proceedings of the Workshop on Microtechnologies and Applications to Space Systems 15 Jun. 1993 p 247-25 (For primary document see N94-29767 08-31)
Avail: CASI HC A02/MF A03

Employing recent advances in microfabrication, the Charles Stark Draper Laboratory has developed inertial guidance instruments of very small size and low cost. Microfabrication employs the batch processing techniques of solid state electronics, such as photolithography, diffusion, and etching, to carve mechanical parts. Within a few years, microfabricated gyroscopes should perform in the 10 to 100 deg/h range. Microfabricated accelerometers have demonstrated performance in the 50 to 500 microgravity range. These instruments will result in not only the redesign of conventional military products, but also new applications that could not exist without small, inexpensive sensors and computing. Draper's microfabricated accelerometers and gyroscopes will be described and test results summarized. Associated electronics and control issues will also be addressed. Gimballed, vibrating gyroscopes and force rebalance accelerometers constructed from bulk silicon, polysilicon surface-machined tuning fork gyroscopes, and quartz resonant accelerometers and gyroscopes are examined. Draper is pursuing several types of devices for the following reasons: to address wide ranges of performance, to realize construction in a flat pack, and to lessen the risks associated with emerging technologies. Author (revised)

N94-29789*# SatCon Technology Corp., Cambridge, MA.
INTEGRATED MICROGYROSCOPE **c35**
Timothy J. Hawkey and Richard P. Torti *In* JPL, Proceedings of the Workshop on Microtechnologies and Applications to Space Systems 15 Jun. 1993 p 257-26 (For primary document see N94-29767 08-31)
Avail: CASI HC A02/MF A03

SalCon Technology Corporation is developing a prototype electrostatically suspended micromechanical gyroscope in the Small Business Innovation Research (SBIR) program under Contracts 19282, and 19585 from NASA Langley Research Center. This paper presents the results of the Phase 1 feasibility study and the plans for fabrication in the upcoming Phase 2 program. Author

N94-29790*# GEC Ferranti, Edinburgh (Scotland).
GEC FERRANTI PIEZO VIBRATORY GYROSCOPE **c35**
J. D. Nuttall *In* JPL, Proceedings of the Workshop on Microtechnologies and Applications to Space Systems 15 Jun. 1993 p 265-27 (For primary document see N94-29767 08-31)
Avail: CASI HC A03/MF A03

Prototypes of a piezo-electric vibratory angular rate transducer (gyroscope) (PVG) have been constructed and evaluated. The construction is on the lines suggested by Burdess. The sensitive element is a cylinder of radially poled piezo-electric ceramic. The cylinder is metallized inside and out, and the outer metallization is divided into eight electrodes. The metallization on the inside is earthed. A phase locked loop, using pairs of the electrodes, causes the cylinder to vibrate in one of its two fundamental, degenerate modes. In the presence of rotation, some of the vibration is coupled into the outer mode. This can be detected, or suppressed with a closed-up technique and provides a measure of rotation rate. The gyroscope provides a number of advantages over rotating mass and optical instruments: low size and mass, lower power consumption, potentially high reliability, potentially good dormancy, low cost and high maximum rate. Author

N94-29791*# National Aeronautics and Space Administration. Lyndon B. Johnson Space Center, Houston, TX.
THE APPLICATION OF MICROMACHINED SENSORS TO MANNED SPACE SYSTEMS **c19**
Aldo Bordano, Gary Havey, Jerry Wald, and Hatem Nasr *In* JPL, Proceedings of the Workshop on Microtechnologies and Applications to Space Systems 15 Jun. 1993 p 279-28 (For primary document see N94-29767 08-31)
Avail: CASI HC A02/MF A03

Micromachined sensors promise significant system advantages to manned space vehicles. Vehicle Health Monitoring (VHM) is a critical need for most future space systems. Micromachined sensors play a significant role in advancing the application of VHM in future space vehicles. This paper addresses the requirements that future VHM systems place on micromachined sensors such as: system integration, performance, size, weight, power, redundancy, reliability and fault tolerance. Current uses of micromachined sensors in commercial, military and space systems are used to document advantages that are gained and lessons learned. Based on these successes, the future use of micromachined sensors in space programs is discussed in terms of future directions and issues that need to be addressed such as how commercial and military sensors can meet future space system requirements. Author

N94-29792*# Jet Propulsion Lab., California Inst. of Tech., Pasadena.
MICRO GUIDANCE AND CONTROL SYNTHESIS: NEW COMPONENTS, ARCHITECTURES, AND CAPABILITIES **c04**
Edward Mettler and Fred Y. Hadaegh *In its* Proceedings of the Workshop on Microtechnologies and Applications to Space Systems 15 Jun. 1993 p 289-304 (For primary document see N94-29767 08-31)
Avail: CASI HC A03/MF A03

New GN&C (guidance, navigation and control) system capabilities are shown to arise from component innovations that involve the synergistic use of microminiature sensors and actuators, microelectronics, and fiber optics. Micro-GN&C system and component concepts are defined that include micro-actuated adaptive optics, micromachined inertial sensors, fiber-optic data nets and light-power transmission, and VLSI microcomputers. The thesis is advanced that these micro-miniaturization products are capable of having a revolutionary impact on space missions and systems, and that GN&C is the pathfinder micro-technology application that can bring that about. Author

N94-29793*# Georgia Inst. of Tech., Atlanta. School of Electrical Engineering.
MICRO-OPTO-MECHANICAL DEVICES AND SYSTEMS USING EPITAXIAL LIFT OFF **c76**
C. Camperi-Ginestet, Young W. Kim, S. Wilkinson, M. Allen, and N. M. Jokerst *In* JPL, Proceedings of the Workshop on Microtechnologies and Applications to Space Systems 15 Jun. 1993 p 305-31 (For primary document see N94-29767 08-31)
Avail: CASI HC A03/MF A03

The integration of high quality, single crystal thin film gallium arsenide (GaAs) and indium phosphide (InP) based photonic and electronic materials and devices with host microstructures fabricated from materials such as silicon (Si), glass, and polymers will enable the fabrication of the next generation of micro-opto-mechanical systems (MOMS) and optoelectronic integrated circuits. Thin film semiconductor devices deposited onto arbitrary host substrates and structures create hybrid (more than one material) near-monolithic integrated systems which can be interconnected electrically using standard inexpensive microfabrication techniques such as vacuum

metallization and photolithography. These integrated systems take advantage of the optical and electronic properties of compound semiconductor devices while still using host substrate materials such as silicon, polysilicon, glass and polymers in the microstructures. This type of materials optimization for specific tasks creates higher performance systems than those systems which must use trade-offs in device performance to integrate all of the function in a single material system. The low weight of these thin film devices also makes them attractive for integration with micromechanical devices which may have difficulty supporting and translating the full weight of a standard device. These thin film devices and integrated systems will be attractive for applications, however, only when the development of low cost, high yield fabrication and integration techniques makes their use economically feasible. In this paper, we discuss methods for alignment, selective deposition, and interconnection of thin film epitaxial GaAs and InP based devices onto host substrates and host microstructures. Author

N94-29794*# OCA Applied Optics, Inc., Garden Grove, CA.
MINIATURE WIDE FIELD-OF-VIEW STAR TRACKERS FOR SPACECRAFT ATTITUDE SENSING AND NAVIGATION **c04**
William McCarty, Eric Curtis, Anthony Hull, and William Morgan *In* JPL, Proceedings of the Workshop on Microtechnologies and Applications to Space Systems 15 Jun. 1993 p 317-32 (For primary document see N94-29767 08-31)
Avail: CASI HC A03/MF A03

Introducing a family of miniature, wide field-of-view star trackers for low cost, high performance spacecraft attitude determination and navigation applications. These devices, derivative of the WFOV Star Tracker Camera developed cooperatively by OCA Applied Optics and the Lawrence Livermore National Laboratory for the Brilliant Pebbles program, offer a suite of options addressing a wide range of spacecraft attitude measurement and control requirements. These sensors employ much wider fields than are customary (ranging between 20 and 60 degrees) to assure enough bright stars for quick and accurate attitude determinations without long integration intervals. The key benefit of this approach are light weight, low power, reduced data processing loads and high information carrier rates for wide ACS bandwidths. Devices described range from the proven OCA/LLNL WFOV Star Tracker Camera (a low-cost, space-qualified star-field imager utilizing the spacecraft's own computer and centroiding and position-finding), to a new autonomous subsystem design featuring dual-redundant cameras and completely self-contained star-field data processing with output quaternion solutions accurate to 100 micro-rad, 3 sigma, for stand-alone applications. Author

N94-29521# National Inst. for Resources and Environment, Ibaraki (Japan). Fire and Explosion Div.
JOINT RESEARCH ACTIVITIES WITH CCMRI (CHINA) [CHUGOKU BAITAN KAGAKU KENKYU SOIN NI OKERU ZAIGAI KENKYU NU GAIYO]
Takeshi Kamai and Makoto Tanaka *In its* Journal of NIRE, Vol. 2, No. 3 25 May 1993 p 81-86 In JAPANESE (For primary document see N94-29512 08-99)
Avail: CASI HC A02/MF A02

N94-30445*# Air Force Systems Command, Wright-Patterson AFB, OH.
A COMBINED ELECTRON BEAM/OPTICAL LITHOGRAPHY PROCESS STEP FOR THE FABRICATION OF SUB-HALF-MICRON-GATE-LENGTH MMIC CHIPS
James S. Sewell and Christopher A. Bozada *In* NASA, Washington, Technology 2003: The Fourth National Technology Transfer Conference and Exposition, Volume 1 Feb. 1994 p 54-59 (For primary document see N94-30440 08-99)
Avail: CASI HC A02/MF A04

N94-30448*# Boeing Defense and Space Group, Philadelphia, PA. Helicopter Div.
COMPOSITE HOT DRAPE FORMING
Thomas Ott *In* NASA, Washington, Technology 2003: The Fourth National Technology Transfer Conference and Exposition, Volume 1 Feb. 1994 p 74-80 (For primary document see N94-30440 08-99)
Avail: CASI HC A02/MF A04

N94-30449*# Lawrence Livermore National Lab., CA.
PRECISION AND MANUFACTURING AT THE LAWRENCE LIVERMORE NATIONAL LABORATORY
Theodore T. Saito, Richard J. Wasley, Irving F. Stowers, Robert R. Donaldson, and Daniel C. Thompson *In* NASA, Washington, Technology 2003: The Fourth National Technology Transfer Conference and Exposition, Volume 1 Feb. 1994 p 81-89 (For primary document see N94-30440 08-99)
(Contract W-7405-eng-48)
Avail: CASI HC A02/MF A04

N94-30467*# National Aeronautics and Space Administration. John F. Kennedy Space Center, Cocoa Beach, FL.
SUPERSONIC GAS-LIQUID CLEANING SYSTEM
Raoul E. B. Caimi and Eric A. Thaxton *In* NASA, Washington, Technology 2003: The Fourth National Technology Transfer Conference and Exposition, Volume 1 Feb. 1994 p 232-240 (For primary document see N94-30440 08-99)
Avail: CASI HC A02/MF A04

N94-30468*# Custom Process Systems and Service Co., Pasadena, TX.
REGENERATING USING AQUEOUS CLEANERS WITH OZONE AND ELECTROLYSIS
Michael P. McGinness *In* NASA, Washington, Technology 2003: The Fourth National Technology Transfer Conference and Exposition, Volume 1 Feb. 1994 p 241-247 (For primary document see N94-30440 08-99)
Avail: CASI HC A02/MF A04

N94-30473*# Pacific Northwest Lab., Richland, WA.
BENCH-SCALE SYNTHESIS OF NANOSCALE MATERIALS
M. F. Buehler, J. G. Darab, D. W. Matson, and J. C. Linehan *In* NASA, Washington, Technology 2003: The Fourth National Technology Transfer Conference and Exposition, Volume 1 Feb. 1994 p 285-292 (For primary document see N94-30440 08-99)
(Contract DE-AC06-76RL-01830)
Avail: CASI HC A02/MF A04

32 COMMUNICATIONS AND RADAR

Includes radar; land and global communications; communications theory; and optical communications.

For related information see also *04 Aircraft Communications and Navigation* and *17 Space Communications, Spacecraft Communications, Command and Tracking.* For search and rescue see *03 Air Transportation and Safety,* and *16 Space Transportation.*

N94-28522# Los Alamos National Lab., NM.
A SPACE-BASED CLASSIFICATION SYSTEM FOR RF TRANSIENTS
K. R. Moore, D. Call, S. Johnson, T. Payne, W. Ford, K. Spencer, J. F. Wilkerson, and C. Baumgart 1993 18 p Presented at the International Workshop on Artificial Intelligence Applications in Solar-Terrestrial Physics, Lund, Sweden, 22-24 Sep. 1993
(Contract W-7405-eng-36)
(DE94-003933; LA-UR-93-4185; CONF-9309289-1) Avail: CASI HC A03/MF A01

The FORTE (Fast On-Orbit Recording of Transient Events) small satellite is scheduled for launch in mid 1995. The mission is to measure and classify VHF (30-300 MHz) electromagnetic pulses, primarily due to lightning, within a high noise environment dominated by continuous wave carriers such as TV and FM stations. The FORTE Event Classifier will use specialized hardware to implement signal processing and neural network algorithms that perform onboard classification of RF transients and carriers. Lightning events will also be characterized with optical data telemetered to the ground. A primary mission science goal is to develop a comprehensive understanding of the correlation between the optical flash and the VHF emissions from lightning. By combining FORTE measurements with ground measurements and/or active transmitters, other science issues can be addressed. Examples include the correlation of global precipitation rates with lightning flash rates and location, the effects of large scale structures within the ionosphere (such as traveling ionospheric disturbances and

horizontal gradients in the total electron content) on the propagation of broad bandwidth RF signals, and various areas of lightning physics. Event classification is a key feature of the FORTE mission. Neural networks are promising candidates for this application. The authors describe the proposed FORTE Event Classifier flight system, which consists of a commercially available digital signal processing board and a custom board, and discuss work on signal processing and neural network algorithms. DOE

N94-28532 Software Kinetics Ltd., Stittsville (Ontario).
DATA FUSION AND CORRELATION TECHNIQUES TESTBED DEVELOPMENT AUDIO PROCESSING STUDY
28 Sep. 1990 28 p Submitted for publication
(SKD-1600-73-014; DSIS-94-00150; CTN-94-61126) Avail: CASI HC A03/MF A01

A study was performed as part of the development of the Data Fusion and Correlation Testbed (DFACT) prototype to investigate the audio processing requirements of the DFACT system. The DFACT system was conceived to provide a testbed for design and implementation of software architectures and communications sensor information, and analysis and correlation algorithms, for land electronic warfare. The base system consists of a number of analyst workstations and intercept operator workstations interconnected through Ethernet. A number of computer controlled intercept receivers along with a communications emitter locating system provide data to DFACT for reduction, correlation, and fusion activities. Intercepted messages are transcribed by the intercept operators and stored in a database for further processing by the analysts. The study examines the basic audio processing capabilities required by DFACT both from a functional and processing perspective. Issues related to throughput, storage capacity, and data retrieval are examined, and a suitable system architecture for a DFACT audio processor is described that satisfies all DFACT system audio processing requirements. Author (CISTI)

N94-28634# Naval Postgraduate School, Monterey, CA. Dept. of Electrical and Computer Engineering.
SPC TOOLBOX: AN INTERACTIVE MATLAB (TM) PACKAGE FOR SIGNAL MODELING, ANALYSIS, AND COMMUNICATIONS
Dennis W. Brown and Monique P. Fargues 15 Oct. 1993 125 p
(AD-A275617; NPS-EC-93-017) Avail: CASI HC A06/MF A02

This report presents the Signal Processing and Communications (SPC) software package. SPC is an interactive package designed to provide the user with a series of data manipulation tools which use MATLAB version 4 graphical interface controls. SPC includes various filtering techniques, AutoRegressive (AR) and linear Moving Average AutoRegressive (ARMA) modeling methods, speech processing, and communication functions. SPC can be used in the classroom to illustrate and to reinforce basic concepts in signal processing and communications. It allows the user to concentrate on the principles presented in class instead of the details related to software usage. It can also be used as a basic analysis and modeling tool for research in signal processing. SPC was designed for Electrical Engineering applications. As a result, it is well suited to reinforce basic concepts presented in the following courses offered at the Naval Postgraduate School: EC 4410: Speech Processing, EC 4420: Modern Spectral Estimation, EC 3420: Statistical Digital Signal Processing, EC 3400: Digital Signal Processing, and EC 2500: Communication Theory. We hope that users will find this package useful, and we welcome any comments and suggestions regarding this software at browndw ece.nps.navy.mil (until 6/94), or fargues ece.nps.navy.mil. DTIC

N94-28745 Army Research Lab., Adelphi, MD.
CHARACTERIZATION OF A DIFFRACTION GRATING AS A SIMULANT OF A SELECTIVE FREQUENCY ANTENNA FOR RADIOMETRIC APPLICATIONS Final Report, Oct. 1991 - Oct. 1992
Thomas J. Pizzillo Jan. 1994 20 p Limited Reproducibility: More than 20% of this document may be affected by microfiche quality
(AD-A275793; ARL-TR-303) Avail: Issuing Activity (Defense Technical Information Center (DTIC))

This report details the study of a blazed diffraction grating as a simulant of a selective frequency antenna for radiometric applications. Specifically, the ability to direct and sweep a beam of millimeter wave (MMW) energy is explored as a potential means of munitions guidance. A grating was designed and built to direct incident energy into the negative first-order peak of the associated diffraction spectrum. A change of 1 GHz in the incident energy frequency is shown to produce a beam displacement of 0.30, a polarization dependence is shown to exist for energy in orders other than zero, and a limited scaling of the optical theory of diffraction to MMW energies is demonstrated to be feasible. DTIC

N94-28755# Martin Marietta Labs., Baltimore, MD.
COLLOCATED TUNABLE WAVENUMBER SENSOR/ACTUATORS FOR SMART STRUCTURES
Lori Jones 7 Feb. 1994 8 p
(Contract N00014-92-C-0214)
(AD-A275872; MML-TM-94-02) Avail: CASI HC A02/MF A01

Two actuator modules have just come out of burnout. This burnout took longer than anticipated due to power outages during January. The measurements on the smaller actuators have been repeated and agreed with the previously reported values within +/- 10%. Measurements made on a glued stack showed stiffening with increasing stress from a modulus of about 4 Mpsi at 1000 psi to 12 Mpsi at 10,000 psi applied stress -- this shows the advantage of the cofired actuator. Derived from text

N94-28762# Harris Corp., Melbourne, FL. Government Communication Systems Div.
PHOTOREFRACTIVE ADAPTIVE ANTENNA ARRAY PROCESSOR Final Report, Dec. 1990 - Jun. 1993
Robert Montgomery, William Beaudet, David Graves, Michael Lange, and Michael Luntz Dec. 1993 90 p
(Contract F30602-91-C-0005)
(AD-A275762; RL-TR-93-245) Avail: CASI HC A05/MF A01

The objective of this contract was to build a laboratory model of a six channel adaptive antenna array processor using acousto-optic delay lines with a photorefractive structure which both computes and applies the adaptive tap weights. The major performance goal of greater than 40 dB suppression for a single narrowband interferer at a fixed frequency in the band was exceeded by 10 dB suppression for narrow band interference. This substantially exceeds that attained by previous optical processors. A goal of greater than 37 dB suppression for a narrow band signal at any frequency in a 20 MHz band was also exceeded. The goal of 20 dB rejection for a signal with 10 MHz instantaneous bandwidth was met with difficulty. To meet this goal, an extensive analysis of the limitations of LMS algorithm processors was required. This analysis indicates that the system was actually performing close to theoretical limits tor this design. The analytic and experimental results are reported here. DTIC

N94-28763# Rome Lab., Hanscom AFB, MA.
RL/ERCT AUTOMATED SWEPT-ANGLE BISTATIC MEASUREMENT SYSTEM Report, Oct. 1985 - Jun. 1989
Marc G. Cote Apr. 1993 121 p
(AF Proj. 4600)
(AD-A275763; RL-TR-93-52) Avail: CASI HC A06/MF A02

A bistatic scattering measurement system well suited to support basic research in target scattering is described. The system can measure bistatic scattering from near backscatter through forward scatter. At X-band frequency, scattering levels of -50 dBsm in the backscattering region and -18 dBsm at forward scatter can be measured to an accuracy of +/-1 dB. This fully automated indoor system fixes the target and direction of illumination and sweeps the receive antenna to collect data as a direct function of bistatic angle. A broadband, coherent, continuous wave radar is used to obtain both amplitude and phase of the component of the total field aligned with the receive antenna polarization. Target scattered fields are derived from the phasor subtraction of target and background measurement runs. We consider the system design, calibration procedure, and measurement accuracy. Example measurements on metal cubes and spheres are presented to demonstrate the system performance. DTIC

N94-28771# Federal Aviation Administration, Atlantic City, NJ. Technical Center.
1.8 GIGAHERTZ (GHz) DIGITAL LOW DENSITY RADIO COMMUNICATIONS LINK (LDRCL) OPERATIONAL TEST AND EVALUATION (OT&E) INTEGRATION AND OT&E OPERATIONAL FINAL TEST REPORT Technical Note
Michael R. Melillo Jan. 1994 35 p
(AD-A275800; DOT/FAA/CT-TN93/41) Avail: CASI HC A03/MF A01

This report contains the results of the Operational Test and Evaluation

(OT&E) Integration and OT&E Operational Testing of the Commercial-Off-The-Shelf (COTS) Low Density Radio Communications Link's (LDRCL) 1.8-gigahertz (GHz) digital radio system. The OT&E testing was accomplished by first testing the LDRCL equipment against its equipment specification (FAA-E-2853) and then performing OT&E testing at the key site (Miami, Florida). These tests proved that the 1.8 GHz LDRCL equipment can fulfill its mission in the National Airspace System (NAS)I, and that, it is suitable and effective. Based on the test results, it is concluded that the 1.8 GHz LDRCL equipment is qualified for operational deployment. DTIC

N94-28812 Naval Postgraduate School, Monterey, CA. Dept. of Electrical and Computer Engineering.

COMMUNICATIONS SUBSYSTEM FOR THE PETITE AMATEUR NAVY SATELLITE (PANSAT) M.S. Thesis

Arnold O. Brown, III Sep. 1993 99 p Limited Reproducibility: More than 20% of this document may be affected by microfiche quality

(AD-A275532) Avail: Issuing Activity (Defense Technical Information Center (DTIC))

This thesis describes a prototype design for a binary phase shift keyed (BPSK) direct sequence spread spectrum (DSSS) communications subsystem intended for use in a small lightweight satellite called the Petite Amateur Navy Satellite (PANSAT). The system was designed using parameters that were established a link analysis. Included as part of this thesis are the link analysis, schematics, and RF board layouts. DTIC

N94-28826*# National Aeronautics and Space Administration. Lewis Research Center, Cleveland, OH.

DEFOCUSSING CHARACTERISTICS OF THE ACTS, T1-VSAT EARTH TERMINAL ANTENNAS

Kevin M. Lambert (Analex Corp., Brook Park, OH.) and Walter M. Strickler Jan. 1994 54 p

(Contract NAS3-25776; RTOP 506-72-1C)

(NASA-TM-106420; E-8257; NAS 1.15:106420) Avail: CASI HC A04/MF A01

This report describes a study, the purpose of which was to determine the characteristics of two reflector antennas, as the reflector feed is moved away from the focus. The antennas are a 1.2 meter and a 2.44 meter reflector that will be used in the T1-VSAT earth terminals for the Advanced Communications Technology Satellite (ACTS). These terminals have been constructed in such a way that is inconvenient to use attenuators to control the gain of the signal that is directed toward the satellite. Feed defocusing was proposed as a simple, convenient way to achieve the required gain control. The study was performed in two parts. In order to determine the feasibility of the technique, a theoretical analysis was performed to obtain the gain, beamwidth and far-field pattern of the antennas, as a function of feed displacement. An experimental investigation followed in which patterns of the 1.2 meter antenna were obtained through measurement in the NASA Lewis Research Center, Near-Field Antenna Test Facility. Results of the theoretical and experimental investigation are presented for both uplink (30 GHz) and downlink (20 GHz) frequencies. Author

N94-28859# Carnegie-Mellon Univ., Pittsburgh, PA. Dept. of Computer Science.

A COGNITIVE MODEL OF DECISION MAKING: CHUNKING AND THE RADAR DETECTION DEVICE

Constantine P. Papageorgiou and Kathleen Carley 13 Dec. 1993 29 p Sponsored by Martin Marietta Corp.

(AD-A275185; CMU-CS-93-228) Avail: CASI HC A03/MF A01

Organizational performance is an issue that pervades many aspects of our society. The value of this subject becomes evident upon realizing that most societal interactions can be regarded as interactions between different organizations. Taking this one step further, the performance of these organizations is of central importance; if bad or incorrect decisions are made most of the time, the organization will fail, whereas making a majority of good or correct decisions leads to the success of the organization. It also becomes obvious that there are many internal and external factors or stressors that can cause the performance of an organization to deteriorate. Thus, organizational performance is, in general, not constant. Training may mitigate the effect of such stressors. Training procedures are of special interest to organizations where performance is more critical than in other organizations. The targeted organizations are those which are involved in certain dangerous or critically important tasks; for example, it is easy to see that more is at stake when designing a training procedure for an agent who is guiding airplanes from a control tower than for one who is separating balls by color at a toy manufacturing plant. As such, there has been much research into identifying different training procedures and the effects of training in improving performance. A significant increase in recent research in this area has been a direct result of an instance of the identify friend or foe task where the incorrect identification of an aircraft resulted in the direct loss of more than 200 civilian lives: the 3 July 1988 tragic shooting of an Iranian passenger plane over the Persian Gulf by the U.S.S. Vincennes. DTIC

N94-28862# Army Engineer Waterways Experiment Station, Vicksburg, MS. Environmental Lab.

ENVIRONMENTAL CHARACTERIZATION FOR TARGET ACQUISITION. ANALYSIS OF THERMAL AND VISIBLE IMAGERY Technical Report No. 2

Bruce M. Sabol and Salvador Rivera, Jr. Nov. 1993 303 p

(AD-A275414; WES/TR/EL-93-9-2) Avail: CASI HC A14/MF A03

Automated/Aided Target Recognition (ATR) systems are being developed for client and next generation attack and reconnaissance helicopters. Part of the development cycle consists of testing and evaluation of the systems at field test facilities within the United States. Preliminary tests of ATR systems have demonstrated a high sensitivity to terrain and environmental conditions. Testers and analysts must therefore have an understanding of the relationship between system performance and terrain/environmental conditions to plan tests and interpret data. To develop an understanding of this relationship, the Environmental Characterization for Target Acquisition (ECTA) Program was initiated. As part of this program, visible and thermal infrared imagery, meteorological data and terrain characterization data were systematically collected from six different U.S. sites for different times of year and times of day. This report describes analysis procedures for evaluating the relationships between the sites' ground-truth measurements and statistical characteristics of resulting imagery. Results of these analyses are presented and discussed. DTIC

N94-28874# Office of the Under Secretary of Defense (Acquisitions), Washington, DC.

DOD ELECTRONIC COMMERCE (EC)/ELECTRONIC DATA INTERCHANGE (EDI) IN CONTRACTING REPORT

20 Dec. 1993 321 p

(AD-A275298) Avail: CASI HC A14/MF A03

Use of Electronic Commerce (EC)/Electronic Data Interchange (EDI) to support Department of Defense (DoD) procurement processes has been under consideration for some time. A 1988 Deputy Secretary of Defense memo calls for maximum use of EDI, based on 10 years of DoD EDI investigation and experiments. In 1990, Defense Management Review Decision 941 stated, 'The strategic goal of DoD's current efforts is to provide the department with the capability to initiate, conduct, and maintain its external business related transactions and internal logistics, contracting, and financial activities without requiring the use of hard copy media.' The EC in Contracting PAT membership reflected a broad cross section of Military Services and Defense Agencies working on a full-time basis for 60 days. The diversity of the EC in Contracting PAT ensured that the needs and concerns of all DoD components were addressed during the creation of the report. The resultant plan, therefore, represents a comprehensive approach for implementing EC throughout the DoD. DTIC

N94-28885 National Defence Research Establishment, Linkoeping (Sweden). Huvudavdelning foer Informationsteknologi.

SYNCHRONIZATION IN MULTISTATIC RADAR [SYNKRONISERING AV MULTISTATISK RADAR]

H. G. Jubrink Aug. 1993 41 p In SWAHILI

(PB94-136975; FOA-C-30727-8.4) Avail: Issuing Activity (National Technical Information Service (NTIS))

This report gives a summary of multistatic radar principles and synchronization methods. Different methods are described using direct and indirect synchronization. The report also presents a general review of synchronization methods for the future. Two LORAN C receivers have been analyzed for use as local reference oscillators in multistatic radar. NTIS

N94-28897# Naval Postgraduate School, Monterey, CA.
SPURS IN DIGITAL RADIO FREQUENCY MEMORY AND APPLICATIONS OF DRFM M.S. Thesis
B. V. Nityananda Sep. 1993 115 p
(AD-A275013) Avail: CASI HC A06/MF A02

A method to calculate the power level of harmonics generated in digital radio frequency memory (DRFM) due to sampling and quantization process is presented. The Fourier series analysis is used for the calculation of the harmonic levels. The quantization process generates the harmonics of the fundamental signal which is folded into the DRFM instantaneous bandwidth by the sampling process. Power level of the harmonics is dependent on the number of quantization bits of the analog to digital converter. It is also dependent on the ratio of signal frequency to sampling frequency. MATLAB programs for computation of harmonic power levels and plots of harmonic power levels of multibit DRFM are included in the thesis. Some applications of the DRFM, such as deception jammer, broadband frequency source, and radar simulator, are also discussed. Author (DTIC)

N94-28898# Naval Postgraduate School, Monterey, CA.
REMOVAL OF COHERENT EXTREMELY LOW FREQUENCY (ELF) BACKGROUND NOISE BY ADAPTIVE NOISE CANCELLATION M.S. Thesis
Samuel J. Strange 23 Sep. 1993 72 p
(AD-A275016) Avail: CASI HC A04/MF A01

The use of the sequential regression algorithm (SER) to coherently remove background noise from an ELF sensor is presented. The SER algorithm is described for a multichannel application in order to cancel coherent portions of reference sensors from a primary sensor. The algorithm adaptively accounts for differences between two parallel array platforms for the purpose of coherent subtraction. A section on likelihood ratio detector schemes for detecting narrowband signals is also presented. This work is in support of a submerged ELF sensor array project run by the Johns Hopkins University Applied Physics Lab. DTIC

N94-28906 National Defence Research Establishment, Linkoeping (Sweden). Huvudavdelning foer Informationsteknologi.
ANALYSIS OF MICROWAVE INDUCED INTERFERENCE IN pn-DIODES [ANALYS AV MIKROVAGSINDUCERADE STOERNINGAR I PN-DIODER]
J. Svedin Aug. 1993 44 p In SWAHILI
(PB94-136983; FOA-C-30720-8.3; FOA-C-30720-3.2) Issuing Activity (National Technical Information Service (NTIS))

Methods for analysis of microwave induced interference in pn-diodes have been evaluated. It has been found that the effects of parasitics may significantly affect the diode susceptibility. This implies that the noise immunity of a given diode depends on the way it is mounted, and on its environment. In this work parasitics have therefore been determined by adapting reflection data to a small signal model. The microwave amplification has then been calculated, both by using a dynamic diode model directly derived from the time-dependent diffusion equation which in principle allows minority carrier recombination times of the same order as the microwave signal period time, but also (for comparison) by using the diode model in SPICE. The agreement between measurements and calculated results concerning change in bias current with a constant bias voltage when the diode is exposed to sinusoidal microwave signals has been found acceptable in regions not to close to the diode knee. Approaches for attacking the practical testing activity have also been discussed. NTIS

N94-28907 National Defence Research Establishment, Linkoeping (Sweden). Huvudavdelning foer Informationsteknologi.
ACTIVE ANTENNAS, A REVIEW [AKTIVA ANTENNER, EN OEVERSIKT]
J. Westerling Sep. 1993 37 p In SWAHILI
(PB94-137445; FOA-C-30722-3.2) Avail: Issuing Activity (National Technical Information Service (NTIS))

The report deals with active antennas for HF-, VHF- and UHF-frequencies. Basic theory and principles of operation of active antennas are presented. Factors that limit the antenna performance are given. A review of the research done up to 1992 is included. An overview of commercially available active antennas is included and examples concerning how one can compare passive and active antenna performance are also given. NTIS

N94-28908 National Defence Research Establishment, Linkoeping (Sweden). Huvudavdelning foer Informationsteknologi.
SYNCHRONIZATION, POSITIONING, AND COMMUNICATION IN MULTISTATIC RADAR SYSTEMS FOR AIR DEFENCE [SYNKRONISERING, POSITIONERING OCH SAMBAND I MULTISTATISKA RADARSYSTEM FOER LUFTBEVAKNING]
A. Alm Jun. 1993 13 p In SWAHILI
(PB94-137478; FOA-A-30082-8.4; FOA-A-30082-3.3) Avail: Issuing Activity (National Technical Information Service (NTIS))

Requirements and possible solutions on synchronization and positioning in a multistatic radar system for air defense are discussed. NTIS

N94-29054# Alabama Univ., University. Bureau of Engineering Research.
ACOUSTIC OR ELECTROMAGNETIC SCATTERING FROM THE PENETRABLE WEDGE Contractor Report, 9 Mar. - 31 Dec. 1992
Robert W. Scarstein 28 Feb. 1993 35 p
(Contract N00014-92-C-6004)
(AD-A275259; BER-583-162; NRL-CR/7181-93-0002) Avail: CASI HC A03/MF A01

The intentional 'or' in the title of this report emphasizes the exact, mathematical equivalence between the acoustic and electromagnetic scattering problems for a two-dimensional, penetrable wedge. A z-directed, time-harmonic line source at the transverse (x,y) position r is external and parallel to the wedge of an infinite wedge of included angle 2 alpha. Both the exterior (region 1) and interior (region 2) are composed of simple media having linear, isotropic, and homogeneous properties. DTIC

N94-29064# Naval Postgraduate School, Monterey, CA.
EVALUATION OF WIRELESS LOCAL AREA NETWORKS M.S. Thesis
Charles L. McBee Sep. 1993 138 p
(AD-A275133) Avail: CASI HC A07/MF A02

This thesis is an in-depth evaluation of the current wireless Local Area Network (LAN) technologies. Wireless LAN's consist of three technologies: they are infrared light, microwave, and spread spectrum. When the first wireless LAN's were introduced, they were unfavorably labeled slow, expensive, and unreliable. The wireless LAN's of today are competitively priced, more secure, easier to install, and provide equal to or greater than the data throughput of unshielded twisted pair cable. Wireless LAN's are best suited for organizations that move office staff frequently, buildings that have historical significance, or buildings that have asbestos. Additionally, an organization may realize a cost savings of between $300 to $1,200 each time a node is moved. Current wireless LAN technologies have a positive effect on LAN standards being developed by the Defense Information System Agency (DISA). DoD as a whole is beginning to focus on wireless LAN's and mobile communications. If system managers want to remain successful, they need to stay abreast of this technology. DTIC

N94-29069# Naval Research Lab., Washington, DC.
PRELIMINARY ANALYSIS OF ASYNCHRONOUS TRANSFER MODE (ATM) OVER MICROWAVE CHANNELS
Christopher C. Yu 15 Dec. 1993 26 p
(AD-A275214; NRL/MR/8121-93-7417) Avail: CASI HC A03/MF A01

Performance of ATM protocol over radio frequency is discussed. Preliminary analysis for various scenarios is presented. The advantages of ATM for microwave communication as well as the challenges are outlined. A simulation of modeling software package, Ptolemy, is demonstrated. DTIC

N94-29072# Northwestern Univ., Evanston, IL.
STABILITY OF DYNAMICAL SYSTEMS IN THE PRESENCE OF NOISE Final Report, 12 Aug. 1991 - 31 Aug. 1993
Mark A. Pinsky and Elton P. Hsu 22 Nov. 1993 2 p
(Contract DAAL03-91-G-0311)
(AD-A275383; Rept-0650-300-L407; ARO-28905.6-MA) Avail: CASI HC A01/MF A01

Pinsky's research is concerned with the exponential growth rate (= Lyapunov exponent) of solutions of stochastic differential equations. In a paper to appear in the Annals of Applied Probability, a formula is obtained for the quadratic Lyapunov exponent of the simple harmonic oscillator in the presence of a finite-state Markov noise process. In case the noise process is reversible, the quadratic Lyapunov exponent is strictly less than

for the corresponding white noise process obtained from the central limit theorem. An example is presented of a non-reversible Markov noise process for which this inequality is reversed. In another article, to appear in the volume 'Stochastic Partial Differential Equations and their Applications' in the Springer Verlag Lecture Notes in Control and Information Sciences (Proceedings of the 1991 Charlotte NC Conference on SPDE, ed. B. Rozovskii), the Lyapunov exponent is computed for the solution of a hyperbolic partial differential equation with damping. In this case, one studies the exponential growth rate of the energy of the solution with Dirichlet boundary conditions. The detailed results depend on the size of the damping constant (overdamped vs. underdamped case). To our knowledge, this is the first study ever of the Lyapunov exponent for a partial differential equation. DTIC

N94-29094# Naval Postgraduate School, Monterey, CA.
ACQUISITION TIME ANALYSIS OF NONCOHERENT PN SEQUENCE ACQUISITION SCHEMES M.S. Thesis
Levent Misirlioglu 23 Sep. 1993 90 p
(AD-A275017) Avail: CASI HC A05/MF A01

In direct-sequence spread-spectrum systems, successful communications require phase synchronization of the incoming pseudonoise (PN) coded waveform with a locally generated replica at the receiver. It has been previously shown that sequential PN code acquisition schemes have the potential to achieve the best performance, but they are the least analyzed because of the analytical difficulties. The acquisition time for a PN code acquisition scheme is an important parameter for system design purposes. This thesis investigates the performance of two acquisition schemes in terms of the acquisition time. A fixed sample size (FSS) test and a truncated sequential probability ratio test (TSPRT) are studied with noncoherent demodulation in a classical additive white Gaussian noise (AWGN) channel and in presence of fading. Optimal selection of desired detection and false alarm probabilities, the effects of penalty time, majority logic verification schemes, and channel signal to noise ratio (SNR) mismatch problems are thoroughly studied using the flow graph technique. Results show that the TSPRT is efficient, robust (against fading), fast, and suitable for real time, low cost implementations. DTIC

N94-29106*# Nebraska Univ., Lincoln.
VIDEO TRANSMISSION ON ATM NETWORKS Ph.D. Thesis
Yun-Chung Chen Dec. 1993 177 p
(Grant NAG5-1612)
(NASA-CR-195124; NAS 1.26:195124) Avail: CASI HC A09/MF A02

The broadband integrated services digital network (B-ISDN) is expected to provide high-speed and flexible multimedia applications. Multimedia includes data, graphics, image, voice, and video. Asynchronous transfer mode (ATM) is the adopted transport techniques for B-ISDN and has the potential for providing a more efficient and integrated environment for multimedia. It is believed that most broadband applications will make heavy use of visual information. The prospect of wide spread use of image and video communication has led to interest in coding algorithms for reducing bandwidth requirements and improving image quality. The major results of a study on the bridging of network transmission performance and video coding are: Using two representative video sequences, several video source models are developed. The fitness of these models are validated through the use of statistical tests and network queuing performance. A dual leaky bucket algorithm is proposed as an effective network policing function. The concept of the dual leaky bucket algorithm can be applied to a prioritized coding approach to achieve transmission efficiency. A mapping of the performance/control parameters at the network level into equivalent parameters at the video coding level is developed. Based on that, a complete set of principles for the design of video codecs for network transmission is proposed. Author (revised)

N94-29109 Rutherford Appleton Lab., Chilton (England).
MODEL-ORIENTED ANALYSIS OF A COMMUNICATIONS PROTOCOL
J. C. Bicarregui Dec. 1993 25 p
(PB94-138146; RAL-93-099) Avail: Issuing Activity (National Technical Information Service (NTIS))

A communications protocol in CCS with value-passing is considered. A data model of the state is given in terms of the type constructors usually found in model-oriented specification. This paper considers some alternative data-models for this system: two abstractions and two reifications of the original specification are given. In particular, strong invariants are used to exclude unreachable values from the state space. VDM is used for the development, and the role of the explicit frames of reference in the operation definitions is examined in some detail. The interaction between read and write frames and invariant is studied, as is the manner by which the information in the frames is propagated during refinement. Also examined is how the use of these frames can be extended and how their use can be combined with operation structuring mechanisms available in other model-oriented methods. The paper concludes with a discussion of some general questions of methodology raised by the example. NTIS

N94-29169 Helsinki Univ. of Technology, Espoo (Finland). Electronic Circuit Design Lab.
THE 19TH CONVENTION ON RADIO SCIENCE: ABSTRACTS OF PAPERS
V. Porra and P. Alinikula Oct. 1993 101 p Conference held in Otaniemi, Finland, 25-26 Oct. 1993 Limited Reproducibility: More than 20% of this document may be affected by microfiche quality
(PB94-136868; ISBN-951-22-1786-4) Avail: Issuing Activity (National Technical Information Service (NTIS))

The 19th Convention on Radio Science was held on 25-26 October, 1993, at the Faculty of Electrical Engineering of Helsinki University of Technology. The topic chosen for this year's meeting is Wireless Communications, Systems and Components--a rapidly evolving field of telecommunications. The keynote presentation of the Convention will be given by Professor Jorgen Bach Andersen, Director of the Center for Personal Communications from Aalborg University, Denmark. Moreover, two contributions from Estonia and several papers by foreign visitors in Finland will give this Convention some international flavor. Instead of the traditional Swedish or Finnish, most of the papers will be delivered in English. In addition to the main topic of the Convention, there is a session on Radio Astronomy elaborating a special field of wireless communication between man and the Universe. NTIS

N94-29176 National Defence Research Establishment, Linkoeping (Sweden). Dept. of Information Technology.
DETECTION METHODS FOR STEALTH RADIO SIGNALS: A LITERATURE SURVEY
G. Andersson Aug. 1993 38 p Limited Reproducibility: More than 20% of this document may be affected by microfiche quality
(ISSN 0347-3708)
(PB94-137452; FOA-C-30724-8.3) Avail: CASI HC A03

In military radio communication systems, a central feature is often the ability to avoid discovery by some hostile interceptor. Therefore, when designing such a stealth radio system, it is naturally important to have knowledge of the different existing signal detection methods, i.e., the threats to a stealth radio system. This report is a literature survey of some of the most interesting methods of detecting different types of digitally modulated radio communication signals. The methods covered are wide-band radiometer detection, optimum detection and cyclic-feature detection. Comparisons between the different methods are also performed. NTIS

N94-29177 National Defence Research Establishment, Stockholm (Sweden). Dept. of Information Technology.
PHOTOCONDUCTIVE SWITCHING FOR HIGH POWER MICROWAVE GENERATION
L. Lundgren Aug. 1993 20 p Limited Reproducibility: More than 20% of this document may be affected by microfiche quality
(ISSN 0347-3708)
(PB94-137460; FOA-C-30719-8.3,3.2,3.3) Avail: CASI HC A03

The possibility to use photoconductive switching for high power microwave radiation is studied. Limitations and simple formulas are derived. The output power of a 1 GHz frozen-wave generator is estimated to 10 MW using silicon technology. Higher output powers could be reached, if the benefits of diamond's hold-off voltage could be utilized in the photoconductive elements. NTIS

N94-29303# Carnegie-Mellon Univ., Pittsburgh, PA. Dept. of Computer Science.
SUBPHONETIC ACOUSTIC MODELING FOR SPEAKER-INDEPENDENT CONTINUOUS SPEECH RECOGNITION Ph.D. Thesis

Mei-Yuh Hwang 17 Dec. 1993 176 p
(Contract N00014-93-1-2005)
(AD-A275217; CMU-CS-93-230) Avail: CASI HC A09/MF A02

To model the acoustics of a large vocabulary well while staying within a reasonable memory capacity, most speech recognition systems use phonetic models to share parameters across different words in the vocabulary. This dissertation investigates the merits of modeling at the subphonetic level. We demonstrate that sharing parameters at the subphonetic level provides more accurate acoustic models than sharing at the phonetic level. The concept of subphonetic parameter sharing can be applied to any class of parametric models. Since the first-order hidden Markov model (HMM) has been overwhelmingly successful in speech recognition, this dissertation bases all its studies and experiments on HMM's. The subphonetic unit we investigate is the state of phonetic HMM's. We develop a system in which similar Markov states of phonetic models share the same Markov parameters. The shared parameter (i.e., the output distribution) associated with a cluster of similar states is called a senone because of its state dependency. The phonetic models that share senones are shared-distribution models or SDM's. Experiments show that SDM's offer more accurate acoustic models than the generalized-triphone model presented by Lee. Senones are next applied to offer accurate models for triphones not experienced in the system training data. In this dissertation, two approaches for modeling unseen triphones are studied - purely decision-tree based senones and a hybrid approach using the concept of Markov state quantization. Both approaches indeed offer a significant error reduction over the previously accepted approach of monophone model substitution. However, the purely decision-tree based senone approach is preferred for its simplicity. DTIC

N94-29311 National Defence Research Establishment, Linkoeping (Sweden). Huvudavdelning for Informationsteknologi.
SIMULATOR FOR MULTISTATIC RADAR [SIMULATOR FOER MULTISTATISK RADAR]
P. Grahn and A. Alm Aug. 1993 48 p In SWAHILI
(PB94-135506; FOA-C-30718-8.4; FOA-C-30718-3.3) Avail: Issuing Activity (National Technical Information Service (NTIS))

This report motivates the need for a simulator directed towards multistatic radar. Requirements on the simulator are defined with its planned use in mind, and its structure is described. A simple simulated scenario is also described and some results are discussed. Also, experiences from the simulator development will be discussed. NTIS

N94-29360*# National Aeronautics and Space Administration. Langley Research Center, Hampton, VA.
DEPLOYABLE REFLECTOR STRUCTURE Patent Application
Martin Mikulas, Jr., inventor (to NASA) and Charles Hoberman, inventor (to NASA) 23 Sep. 1993 27 p
(NASA-Case-LAR-14513-1-SB; NAS 1.71:LAR-14513-1-SB; US-Patent-Appl-SN-126286) Avail: CASI HC A03/MF A01

A deployable reflector structure is presented. The structure has a number of movable reflector panels pivotably supported on rigid arms. Several such arms are pivotably connected to a central structure. The arm can move in starburst fashion from a packaged stage, where all arms are vertical, to a deployed stage, where all arms are horizontal. All of the movable reflector panels are maintained at a predetermined angle to an axis of the reflector structure when the arms are pivoted. The reflector panels are stacked tightly on top of each other in the packaged state of the reflector structure. Simple mechanisms are used for avoiding interference between panels on different arms in the packaged stage and for fitting the movable panels together like tiles in the deployed stage. NASA

N94-29364*# National Aeronautics and Space Administration. Ames Research Center, Moffett Field, CA.
MULTI-CHANNEL SPATIALIZATION SYSTEMS FOR AUDIO SIGNALS Patent Application
Durand R. Begault, inventor (to NASA) (National Academy of Sciences - National Research Council, Washington, DC.) 4 Oct. 1993 26 p
(NASA-Case-ARC-12013-1-CU; NAS 1.71:ARC-12013-1-CU; US-Patent-Appl-SN-130948) Avail: CASI HC A03/MF A01

Synthetic head related transfer functions (HRTF's) for imposing reprogrammable spatial cues to a plurality of audio input signals included, for example, in multiple narrow-band audio communications signals received simultaneously are generated and stored in interchangeable programmable read only memories (PROM's) which store both head related transfer function impulse response data and source positional information for a plurality of desired virtual source locations. The analog inputs of the audio signals are filtered and converted to digital signals from which synthetic head related transfer functions are generated in the form of linear phase finite impulse response filters. The outputs of the impulse response filters are subsequently reconverted to analog signals, filtered, mixed, and fed to a pair of headphones. NASA

N94-29421# Aerospatiale Aquitaine, Saint-Medard en Jalles (France).
DEVELOPMENT OF ELECTROMAGNETIC COMPATIBILITY TESTS [L'EVOLUTION DES ESSAIS DE COMPATIBILITE ELECTROMAGNETIQUE]
B. Raveu 1993 5 p In FRENCH Presented at Astelab, Paris, France, 16 Jun. 1992
(Rept-932-430-110; ETN-94-95468) Avail: CASI HC A01/MF A01

Evolutions in the domain of electromagnetic compatibility tests are addressed. It is reported that there is an increasing demand in the frequency and power domains, and that new conducted signals have been generated. In order to respond to the needs of the users, test facilities show an increase in the frequency domain from 10 to 40 GHz, and an increase in the intensity of the field from 10 to 300 V/m. The test engineers must follow these developments and abide by the different standards. Requirements that concern the surroundings of the objects in test which must be added are considered: for example a clean atmosphere. These new facilities are now set up and they must be used with proceedings that permit traps to be avoided and the results of the equipment tests to be made significant and credible. ESA

N94-29440# Aerospatiale Aquitaine, Saint-Medard en Jalles (France).
RADIOELECTRIC CHARACTERIZATION OF MATERIALS AT 1000 C [CARACTERISATION RADIOELECTRIQUE DE MATERIAUX A 1000 C]
Brigitte Prache 1993 5 p In FRENCH Presented at Journees CMM 92, Arcachon, France, 7-9 Oct. 1992
(Rept-932-430-104; ETN-94-95462) Avail: CASI HC A01/MF A01

A furnace equipped with resistances, in which a waveguide is placed and its electromagnetic properties tested, is described. It satisfies the demands for the 3.3 to 4.9 GHz frequency bands and temperatures up to 1000 C. All the determining factors necessary for measuring the permittivity of materials at high temperatures are satisfied: the control of the heating homogeneity and of the thermal expansions, and the reliability of good radioelectric contacts. Results on a reference material tested at 20 and 1000 C are presented. ESA

N94-29456# Aerospatiale, Cannes (France). Espace et Defense.
THEORETICAL AND EXPERIMENTAL STUDY OF A CYLINDRICAL MICROSTRIP ANTENNA
M. Monaco (Nice Univ., France.), G. Ghio (Nice Univ., France.), E. Cambiaggio (Nice Univ., France.), J. P. Boisset, M. Sauvan, and B. Buralli 1993 5 p
(Rept-932-440-109; ETN-94-95479) Avail: CASI HC A01/MF A01

A low profile microstrip belt antenna concept was developed and tested. The antenna radiation pattern was optimized. The antenna is suitable for optimal air or space based reception of radio localized signals. The antenna, along with a 3.78 bandwidth, offers ripple within +/- 2 dB and 98 percent coverage probability. The system was conceived to receive the global positioning system radio signals beamed from the navigation system by time and range satellite network. The resulting microstrip belt antenna is a low cost, low profile, low weight, and easy integration antenna concept. ESA

N94-29468# Technical Research Centre of Finland, Espoo. Telecommunications Lab.
HIGH THROUGHPUT NETWORK FOR MULTIPROCESSOR INTERCONNECTIONS
Pertti Raatikainen, ed. and Juha Zidbeck, ed. May 1993 74 p Sponsored by Technology Development Center, Finland
(ISSN 1235-0621)
(VTT-PUBS-147; ISBN-951-38-4285-8; ETN-94-95522) Copyright Avail: CASI HC A04/MF A01

Multiprocessor architectures are needed to support modern broadband

applications, since traditional bus structures are not capable of providing high throughput. New bus structures are needed, especially in the area of network components and terminals. A study to find an efficient and cost effective interconnection topology for the future high speed products is presented. The most common bus topologies are introduced, and their characteristics are estimated to decide which one of them offers best performance and lowest implementation cost. The ring topology is chosen to be studied in more detail. Four competing bus access schemes for the high throughput ring are introduced as well as simulation models for each of them. Using transfer delay and throughput results, as well as keeping the implementation point of view in mind, the best candidate is selected to be studied and experimented in the succeeding research project. ESA

N94-29495*# National Aeronautics and Space Administration. Pasadena Office, CA.

EXTENDED HORIZON LIFTING FOR PERIODIC GAIN ADJUSTMENT IN CONTROL SYSTEMS, AND FOR EQUALIZATION OF COMMUNICATION CHANNELS Patent Application

David S. Bayard, inventor (to NASA) (Jet Propulsion Lab., California Inst. of Tech., Pasadena.) 16 Mar. 1994 44 p

(Contract NAS7-1260)

(NASA-Case-NPO-19166-1-CU; NAS 1.71:NPO-19166-1-CU;

US-Patent-Appl-SN-222762) Avail: CASI HC A03/MF A01

Periodic gain adjustment in plants of irreducible order, n, or for equalization of communications channels is effected in such a way that the plant (system) appears to be minimum phase by choosing a horizon time N is greater than n of liftings in periodic input and output windows rho sub u and rho sub y, respectively, where N is an integer chosen to define the extent (length) of each of the windows rho sub u and rho sub y, and n is the order of an irreducible input/output plant. The plant may be an electrical, mechanical, or chemical system, in which case output tracking (OT) is carried out for feedback control or a communication channel, in which case input tracking (IT) is performed. Conditions for OT are distinct from IT in terms of zero annihilation, namely H(sub s)H(sub s)(sup +) = I for OT and H(sub s)H(sub s)(sup +) = I of IT, where the OT conditions are intended for gain adjustments in the control system, and IT conditions are intended for equalization for communication channels.

NASA

N94-29529 Rochester Univ., NY.

AN INVESTIGATION OF DISTRIBUTED COUPLING IN A NONLINEAR SEMICONDUCTOR WAVEGUIDE Ph.D. Thesis

David Floyd Prelewitz 1993 274 p

Avail: Univ. Microfilms Order No. DA9313879

In this thesis, we theoretically and experimentally analyze the nonlinear coupling properties of a model waveguide-grating structure. A planar Si-on-insulator (SOI) structure with a periodic distributed grating coupler is used as the model system. Unlike other optoelectronic materials, Si does not possess a direct band gap or a linear electro-optic effect. However, it may be possible to utilize silicon's large free carrier effect in optoelectronic devices. It may also be possible to integrate Si optical structures with Si based electronic circuits on monolithic substrates. In an experimental study of the SOI structure, a distributed grating input coupler is used to transfer light from a Nd:YAG Q-switched laser (lambda(sub 0) = 1.064 microns) into the guiding region by exciting TE(sub 0) modes. Temporal changes in the waveguide mode pulse profiles are then measured with a digital sampling oscilloscope (DSO). Linear and nonlinear coupling measurements are made using various input conditions in an attempt to characterize the structure. From observations, power dependent optical limiting and damped oscillations are evident in the pulse profiles. By numerically modeling the structure, we attribute the temporal fluctuations in the mode profile to intensity dependent changes in the refractive index of the Si guiding layer. Contributions to the refractive index from both free carrier and thermal changes are considered. Rapid index variations cause the propagation wavevector in the interaction region to be power dependent. As a result, the coherent optical coupling properties of the structure are altered. We have determined that spatial changes in the resonance condition of the coupling structure accounts for most of the limiting effects. Damped oscillations observed in the temporal pulse profile are attributed to interference effects induced by a nonlinear phase shift in the guided mode. The numerical computations indicate that the nonlinear coupling process is dominated by free carrier effects. However, competition between electronic and thermal processes becomes more acute with higher energies. By fully modeling the two dimensional carrier and thermal dynamics, we are able to fully characterize the nonlinear coupling process due to the material and geometric constraints. Dissert. Abstr.

N94-29536 New Mexico Univ., Albuquerque.

AUTOMATIC FOCUS AND REGISTRATION OF SYNTHETIC APERTURE RADAR IMAGES Ph.D. Thesis

Terry Marshall Calloway 1992 235 p

Avail: Univ. Microfilms Order No. DA9315929

A tomographic model explains why aperture phase error produces cross-range blur. New algorithms estimate phase error then correct it to remove blur from a synthetic aperture radar (SAR) image. A new sinusoidal map drift autofocus (SMDA) algorithm removes high-order (greater than five) phase error better than a conventional polynomial map drift autofocus (PMDA) algorithm. A new least squares autofocus (LSA) algorithm focuses an image in fewer iterations than required by a conventional phase gradient autofocus (PGA) algorithm. A new algorithm aligns, or registers, a complex valued SAR image with a reference SAR image. Tests indicate that the algorithm can achieve simultaneously RMS errors of 0.01 degree, 0.03 pixel, and 0.01 percent in rotation, translation, and scale, respectively.

Dissert. Abstr.

N94-29542# Aerospatiale, Cannes (France). Optical Dept.

GLRS-R 2-COLOUR RETROREFLECTOR TARGET DESIGN AND PREDICTED PERFORMANCE

Glenn Lund 1993 17 p See also N94-15615

(Rept-932-440-106; ETN-94-95476) Avail: CASI HC A03/MF A01

The retroreflector ground target design for the GLRS-R spaceborne dual wavelength laser ranging system is described. The passive design flows down from the requirements of high station autonomy, high global field of view, little or no multiple pulse returns, and adequate optical cross section for most ranging geometries. The solution makes use of five hollow cube corner retroreflectors of which one points to the zenith and the remaining four are inclined from the vertical at uniform azimuthal spacings. The need for large retroreflectors is expected to generate narrow diffraction lobes. A good compromise solution is found by spoiling just one of the retroereflector dihedral angles from 90 deg, thus generating two symmetrically oriented diffraction lobes in the return beam. The required spoil angles are found to have little dependance on ground target latitude. Various link budget analyses are presented. They show the influence of such factors as point ahead optimization, turbulence, ranging angle, atmospheric visibility, and ground target thermal deformations. ESA

N94-29589*# National Aeronautics and Space Administration. Lewis Research Center, Cleveland, OH.

NON-ORTHOGONAL SUBBAND/TRANSFORM CODER Patent Application

Daniel R. Glover, inventor (to NASA) 15 Dec. 1993 28 p

(NASA-Case-LEW-15310-1; NAS 1.71:LEW-15310-1;

US-Patent-Appl-SN-167107) Avail: CASI HC A03/MF A01

The present invention is directed to a simplified digital subband coder/decoder. In the present invention a signal is fed into a coder. The coder uses a non-orthogonal algorithm that is simply implemented in the coder hardware. The simple non-orthogonal design is then used in the implementation of the decoder to decode the signal. NASA

N94-29613*# Jet Propulsion Lab., California Inst. of Tech., Pasadena.

THE TELECOMMUNICATIONS AND DATA ACQUISITION REPORT Progress Report, Jan. - Mar. 1991

Edward C. Posner, ed. 15 May 1991 160 p

(Contract NAS7-918)

(NASA-CR-195694; JPL-TDA-PR-42-105; NAS 1.26:195694) Avail: CASI HC A08/MF A02

This quarterly publication provides archival reports on developments in programs managed by JPL's Office of Telecommunications and Data Acquisition (TDA). In space communications, radio navigation, radio science, and ground-based radio and radar astronomy, it reports on activities of the Deep Space Network (DSN). Also included is standards activity at JPL for space data and information systems and reimbursable DSN work performed for other space agencies through NASA. In the search for extraterrestrial intelligence (SETI), 'The TDA Progress Report' reports on implementation and operations for searching the microwave spectrum. In solar system

radar, it reports on the uses of the Goldstone Solar System Radar for scientific exploration of the planets, their rings and satellites, asteroids, and comets. In radio astronomy, the areas of support include spectroscopy, very long baseline interferometry, and astrometry. For individual titles, see N94-29614 through N94-29626.

N94-29614*# Jet Propulsion Lab., California Inst. of Tech., Pasadena.
COMBINING GPS AND VLBI EARTH-ROTATION DATA FOR IMPROVED UNIVERSAL TIME **c04**
A. P. Freedman *In its* The Telecommunications and Data Acquisition Report 15 May 1991 p 1-12 (For primary document see N94-29613 08-32)
(RTOP 310-10-61-87-02)
Avail: CASI HC A03/MF A02

The Deep Space Network (DSN) routinely measures Earth orientation in support of spacecraft tracking and navigation using very long-baseline interferometry (VLBI) with the deep-space tracking antennas. The variability of the most unpredictable Earth-orientation component, Universal Time 1 (UT1), is a major factor in determining the frequency with which the DSN measurements must be made. The installation of advanced Global Positioning System (GPS) receivers at the DSN sites and elsewhere may soon permit routine measurements of UT1 variation with significantly less dependence on the deep-space tracking antennas than is currently required. GPS and VLBI data from the DSN may be combined to generate a precise UT1 series, while simultaneously reducing the time and effort the DSN must spend on platform-parameter calibrations. This combination is not straightforward, however, and a strategy for the optimal combination of these data is presented and evaluated. It appears that, with the aid of GPS, the frequency of required VLBI measurements of Earth orientation could drop from twice weekly to once per month. More stringent real-time Earth orientation requirements possible in the future would demand significant improvements in both VLBI and GPS capabilities, however. Author

N94-29615*# Jet Propulsion Lab., California Inst. of Tech., Pasadena.
COMPUTATION OF VIBRATION MODE ELASTIC-RIGID AND EFFECTIVE WEIGHT COEFFICIENTS FROM FINITE-ELEMENT COMPUTER PROGRAM OUTPUT **c39**
R. Levy *In its* The Telecommunications and Data Acquisition Report 15 May 1991 p 13-20 (For primary document see N94-29613 08-32)
(RTOP 310-20-65-86-04)
Avail: CASI HC A02/MF A02

Post-processing algorithms are given to compute the vibratory elastic-rigid coupling matrices and the modal contributions to the rigid-body mass matrices and to the effective modal inertias and masses. Recomputation of the elastic-rigid coupling matrices for a change in origin is also described. A computational example is included. The algorithms can all be executed by using standard finite-element program eigenvalue analysis output with no changes to existing code or source programs. Author

N94-29616*# Jet Propulsion Lab., California Inst. of Tech., Pasadena.
X-/Ka-BAND DICHROIC PLATE DESIGN AND GRATING LOBE STUDY
J. C. Chen *In its* The Telecommunications and Data Acquisition Report 15 May 1991 p 21-30 (For primary document see N94-29613 08-32)
(RTOP 310-20-64-89-01)
Avail: CASI HC A02/MF A02

An X-/Ka-band dichroic plate is needed for simultaneously receiving X-band and Ka-band in the DSS-13 Beam Waveguide Antenna. The plate is transparent to the allocated Ka-band downlink (31.8-32.3 GHz) and the frequency band for the Mars Observer Ka-band Beacon Link Experiment (KABLE) (33.6-33.8 GHz), while at the same time reflecting the X-band downlink (8.4-8.5 GHz). The design is made using a computer program for dichroic plates with rectangular holes. The theoretical performance of the X-/Ka-band dichroic plate is presented. A study of the grating lobe problem is also included in this article. Author

N94-29617*# Jet Propulsion Lab., California Inst. of Tech., Pasadena.
SITE COMPARISON FOR OPTICAL VISIBILITY STATISTICS IN SOUTHERN CALIFORNIA **c74**
K. Cowles *In its* The Telecommunications and Data Acquisition Report 15 May 1991 p 31-40 (For primary document see N94-29613 08-32)
(RTOP 310-20-67-88-03)
Avail: CASI HC A02/MF A02

Negotiations are under way to locate an atmospheric visibility monitoring (AVM) observatory at Mount Lemmon, just north of Tucson, Arizona. Two more observatories will be located in the southwestern U.S. The observatories are being employed to improve a weather model for deep-space-to-ground optical communications. This article explains the factors considered in choosing a location and recommends Table Mountain Observatory as the location for another AVM facility. Author

N94-29618*# Jet Propulsion Lab., California Inst. of Tech., Pasadena.
MODIFICATIONS OF THE GRIESMER BOUND **c61**
R. J. McEliece (California Inst. of Tech., Pasadena.) and G. Solomon (Solomon, G., Pasadena, CA.) *In its* The Telecommunications and Data Acquisition Report 15 May 1991 p 41-44 (For primary document see N94-29613 08-32)
(RTOP 310-30-71-83-02)
Avail: CASI HC A01/MF A02

The Griesmer bound is a classical technique (developed in 1960) for estimating the minimum length n required for a binary linear code with a given dimension k and minimum distance d. In this article, a unified derivation of the Griesmer bound and two new variations on it are presented. The first variation deals with linear codes which contain the all-ones vector; such codes are quite common and are useful in practice because of their 'transparent' properties. The second variation deals with codes that are constrained to contain a word of weight greater than or equal to M. In both cases these constraints (the all-ones word or a word of high weight) can increase the minimum length of a code with given k and d.
Author (revised)

N94-29619*# Jet Propulsion Lab., California Inst. of Tech., Pasadena.
INTEGER COSINE TRANSFORM FOR IMAGE COMPRESSION **c61**
K.-M. Cheung, F. Pollara, and M. Shahshahani *In its* The Telecommunications and Data Acquisition Report 15 May 1991 p 45-53 (For primary document see N94-29613 08-32)
(RTOP 310-30-71-83-02)
Avail: CASI HC A02/MF A02

This article describes a recently introduced transform algorithm called the integer cosine transform (ICT), which is used in transform-based data compression schemes. The ICT algorithm requires only integer operations on small integers and at the same time gives a rate-distortion performance comparable to that offered by the floating-point discrete cosine transform (DCT). The article addresses the issue of implementation complexity, which is of prime concern for source coding applications of interest in deep-space communications. Complexity reduction in the transform stage of the compression scheme is particularly relevant, since this stage accounts for most (typically over 80 percent) of the computational load. Author

N94-29620*# Jet Propulsion Lab., California Inst. of Tech., Pasadena.
A PORTABLE X-BAND FRONT-END TEST PACKAGE FOR BEAM-WAVEGUIDE ANTENNA PERFORMANCE EVALUATION. PART 2: TESTS ON THE ANTENNA
T. Y. Otoshi, S. R. Stewart, and M. M. Franco *In its* The Telecommunications and Data Acquisition Report 15 May 1991 p 54-68 (For primary document see N94-29613 08-32)
(RTOP 310-30-69-88-04)
Avail: CASI HC A03/MF A02

Results are given for an X-band (8.45 GHz) test package for testing the new 34-m beam-waveguide antenna at Goldstone in an 'on-the-antenna' configuration. Included are X-band zenith noise temperature values and tipping-curve data obtained at the Cassegrain focal point F1 as well as at the pedestal room focal point F3. Subreflector Z-defocus test results for both F1 and F3 are also presented. The X-band test package operated well in all of the different test configurations and exceeded expected performance. Author (revised)

N94-29621*# Jet Propulsion Lab., California Inst. of Tech., Pasadena.
PHASING THE VERY LARGE ARRAY ON GALILEO IN THE PRESENCE OF JUPITER'S STRONG RADIO EMISSION **c17**
J. S. Ulvestad *In its* The Telecommunications and Data Acquisition Report 15 May 1991 p 69-82 (For primary document see N94-29613 08-32)
(RTOP 314-40-31-30-03)
Avail: CASI HC A03/MF A02

Work is in progress to determine the feasibility of using the Very Large Array (VLA) radio telescope to receive telemetry from Galileo during its close encounter with Io on 7 Dec. 1995. The VLA was used previously to receive telemetry from Voyager 2 at Neptune. However, Jupiter's strong radio emission is an additional complication in the case of the Galileo encounter. This article analyzes the effect of Jupiter's radio emission on the phase-adjustment procedure ('autophasing') used to maintain coherence among the 27 VLA antennas. Results of an experiment designed to mimic the Io encounter are presented. As expected, Jupiter's strong radio emission has a considerable effect on the autophasing procedure. A simple emission model is found to give a good approximation to the fringe-visibility plots derived from the VLA data, and that successful model is used to estimate the VLA's ability to autophase on Galileo during the Io encounter. The effect of Jupiter should be small for projected baselines longer than approximately 800 m and completely negligible for projected baselines longer than approximately 1.1 km. The most extended configuration of the VLA (the A configuration) probably can be used successfully for telemetry reception during the Io encounter. Further analysis and testing of the effect of correlated noise from Jupiter is necessary before a final decision can be made about the feasibility of using the second largest (B) configuration of the VLA for reception of Galileo telemetry. Use of the B configuration could simplify the upgrades needed to support the Io encounter. Tests to help choose the preferred VLA configuration could be performed by using the VLA to observe the Magellan spacecraft at Venus during Jul. and Oct. 1991. Examination of the effects of planet noise on the VLA have implications beyond the use of that telescope for supporting the Io encounter. The effects of planet radio emission on spacecraft data received by antenna arrays are relevant to choosing the exact locations of antennas that might be built by the Deep Space Network in coming years. Author (revised)

N94-29622*# Jet Propulsion Lab., California Inst. of Tech., Pasadena.
ELEVATION CONTROL SYSTEM MODEL FOR THE DSS 13 ANTENNA **c37**
W. Gawronski and J. A. Mellstrom *In its* The Telecommunications and Data Acquisition Report 15 May 1991 p 83-108 (For primary document see N94-29613 08-32)
(RTOP 314-40-42-10-40)
Avail: CASI HC A03/MF A02

In order to meet the requirements for precision pointing of 34-m antennas, adequate control design and simulation software have to be developed along with a detailed description of the supporting analytical tools. This article describes a control system model for the elevation drive of the DSS 13 antenna. The model allows one to simulate elevation dynamics, cross-coupled dynamics in azimuth and elevation, and RF pointing error. A modal state-space model of the antenna structure was obtained from its finite-element model with a free rotating tipping structure. Model reduction techniques were applied separately for the antenna model and rate-loop model, thereby reducing the system order to one-third of the original one while preserving its dynamic properties. Extensive simulation results illustrate properties of the model. Author (revised)

N94-29623*# Jet Propulsion Lab., California Inst. of Tech., Pasadena.
RADIO SCIENCE GROUND DATA SYSTEM FOR THE VOYAGER-NEPTUNE ENCOUNTER, PART 1
E. R. Kursinski and S. W. Asmar *In its* The Telecommunications and Data Acquisition Report 15 May 1991 p 109-127 (For primary document see N94-29613 08-32)
(RTOP 314-40-41-10-13)
Avail: CASI HC A03/MF A02

The Voyager radio science experiments at Neptune required the creation of a ground data system array that includes a Deep Space Network complex, the Parkes Radio Observatory, and the Usuda deep space tracking station. The performance requirements were based on experience with the previous Voyager encounters, as well as the scientific goals at Neptune. The requirements were stricter than those of the Uranus encounter because of the need to avoid the phase-stability problems experienced during that encounter and because the spacecraft flyby was faster and closer to the planet than previous encounters. The primary requirement on the instrument was to recover the phase and amplitude of the S- and X-band (2.3 and 8.4 GHz) signals under the dynamic conditions encountered during the occultations. The primary receiver type for the measurements was open loop with high phase-noise and frequency stability performance. The receiver filter bandwidth was predetermined based on the spacecraft's trajectory and frequency uncertainties. Author

N94-29624*# Jet Propulsion Lab., California Inst. of Tech., Pasadena.
GAUSSIAN BEAM AND PHYSICAL OPTICS ITERATION TECHNIQUE FOR WIDEBAND BEAM WAVEGUIDE FEED DESIGN **c74**
W. Veruttipong, J. C. Chen, and D. A. Bathker *In its* The Telecommunications and Data Acquisition Report 15 May 1991 p 128-135 (For primary document see N94-29613 08-32)
(RTOP 314-30-50-12-78)
Avail: CASI HC A02/MF A02

The Gaussian beam technique has become increasingly popular for wideband beam waveguide (BWG) design. However, it is observed that the Gaussian solution is less accurate for smaller mirrors (approximately less than 30 lambda in diameter). Therefore, a high-performance wideband BWG design cannot be achieved by using the Gaussian beam technique alone. This article demonstrates a new design approach by iterating Gaussian beam and BWG parameters simultaneously at various frequencies to obtain a wideband BWG. The result is further improved by comparing it with physical optics results and repeating the iteration. Author

N94-29625*# Jet Propulsion Lab., California Inst. of Tech., Pasadena.
DESIGN AND ANALYSIS OF A LOW-LOSS LINEAR ANALOG PHASE MODULATOR FOR DEEP SPACE SPACECRAFT X-BAND TRANSPONDER APPLICATIONS
N. R. Mysoor and R. O. Mueller *In its* The Telecommunications and Data Acquisition Report 15 May 1991 p 136-145 (For primary document see N94-29613 08-32)
(RTOP 314-30-55-30-01)
Avail: CASI HC A02/MF A02

This article summarizes the design concepts, analyses, and development of an X-band (8145 MHz) transponder low-loss linear phase modulator for deep space spacecraft applications. A single-section breadboard circulator-coupled reflection phase modulator has been analyzed, fabricated, and evaluated. A linear phase deviation of 92 deg with a linearity tolerance of +/- 8 percent was measured for this modulator from 8257 MHz to 8634 MHz over the temperature range -20 to 75 C. The measured insertion loss and the static delay variation with temperature were 2 +/- 0.3 dB and 0.16 psec/ C, respectively. Based on this design, cascaded sections have been modeled, and simulations were performed to provide an X-band deep space transponder (DST) phase modulator with +/- 2.5 radians (+/- 143 deg) of peak phase deviation to accommodate downlink signal modulation with composite telemetry data and ranging, with a deviation linearity tolerance of +/- 8 percent and insertion loss of less than 10 +/- 0.5 dB. A two-section phase modulator using constant gamma hyperabrupt varactors and an efficient modulator driver circuit was breadboarded. The measured results satisfy the DST phase-modulator requirements and show excellent agreement with the predicted results. Author (revised)

N94-29626*# Jet Propulsion Lab., California Inst. of Tech., Pasadena.
ORBITAL DEBRIS RADAR INSTRUMENTATION
Richard M. Goldstein and L. W. Randolph *In its* The Telecommunications and Data Acquisition Report 15 May 1991 p 146-148 (For primary document see N94-29613 08-32)
(RTOP 906-76-40-43-01)
Avail: CASI HC A01/MF A02

In order to increase the usefulness of Goldstone orbital debris observations, several improvements are planned to the experimental Goldstone radar. The first improvement is to add a ranging capability of 1-km accuracy to the radar. This would provide much more detailed information about whatever debris is observed. The second improvement is to widen the bandwidth of the system from 10 kHz to 85 kHz so that particles in more elliptical orbits can be monitored. The two antennas could then also be pointed away from the zenith, say south, where orbits of lesser inclination might also be observed. In any case, the addition of ranging requires a substantial increase of system bandwidth. This article describes the instrumentation necessary to achieve this, together with required signal-processing modifications. Author (revised)

N94-29652*# Jet Propulsion Lab., California Inst. of Tech., Pasadena.
THE TELECOMMUNICATIONS AND DATA ACQUISITION REPORT Progress Report, Oct. - Dec. 1993
Joseph H. Yuen, ed. 15 Feb. 1994 287 p
(Contract NAS7-918)
(NASA-CR-195689; TDA-PR-42-116; NAS 1.26:195689) Avail: CASI HC A13/MF A03

Reports on developments in programs managed by JPL's Office of Telecommunications and Data Acquisition (TDA) are provided. In space communications, radio navigation, radio science, and ground-based radio and radar astronomy, it reports on activities of the Deep Space Network (DSN) in planning, supporting research and technology, implementation, and operations. Also included are standards activity at JPL for space data and information systems and reimbursable DSN work performed for other agencies through NASA. For individual titles, see N94-29653 through N94-29673.

N94-29653*# Jet Propulsion Lab., California Inst. of Tech., Pasadena.
TOWARD ASTROMETRIC TRACKING WITH THE INFRARED SPATIAL INTERFEROMETER **c89**
R. N. Treuhaft, M. Bester, W. C. Danchi, and C. H. Townes *In its* The Telecommunications and Data Acquisition Report 15 Feb. 1994 p 1-9 (For primary document see N94-29652 08-32)
(RTOP 310-10-60-90-03)
Avail: CASI HC A02/MF A03

Infrared interferometric demonstrations with the University of California, Berkeley's infrared spatial interferometer (ISI) on Mt. Wilson explore the potential of infrared and optical astrometry for deep space tracking, reference frame development, and DSN science. Astrometric data taken and analyzed over the last five years from the ISI have shown that instrumental and atmospheric effects limit current demonstrations. The benefits of sensitivity upgrades, which were performed in 1991 and 1992, have been demonstrated by comparing point-to-point phase fluctuations for the fall 1989 and fall 1992 observing epochs. This comparison showed that point-to-point phase fluctuations due to tropospheric and quantum noise, for optimal integration times of 0.2 sec, are approaching the 0.1-cycle level needed to reliably connect the interferometric phase. The increase in sensitivity, coupled with that arising from very recent hardware upgrades, will greatly enhance phase-connection capabilities necessary for astrometry in the presence of atmospheric refractivity fluctuations. The current data set suggests that atmospheric fluctuations on Mt. Wilson during the best seeing are dominated by a low-lying component, approximately 25 m high, which may be minimized with in situ calibration in the future. During poor seeing conditions that currently prohibit the interferometric phase connection necessary for astrometry, fluctuations seem to be generated by atmospheric inhomogeneities at much higher altitudes above Mt. Wilson. Data taken over the last year suggest that the ISI will soon be able to achieve 50- to 100-nrad astrometry in a single observing session, employing current ground-based laser distance interferometer calibrations to minimize atmospheric effects. Author (revised)

N94-29654*# Jet Propulsion Lab., California Inst. of Tech., Pasadena.
LINE-OF-SIGHT TROPOSPHERIC CALIBRATION FROM MEASUREMENTS IN ARBITRARY DIRECTIONS
J. Z. Wilcox *In its* The Telecommunications and Data Acquisition Report 15 Feb. 1994 p 10-23 (For primary document see N94-29652 08-32)
(RTOP 310-10-60-93-01)
Avail: CASI HC A03/MF A03

Tropospheric inhomogeneities limit the accuracy with which a path delay in an arbitrary direction can be estimated from calibration measurements in different directions. This article demonstrates a mathematical procedure that has the potential for minimizing errors in the estimated geometrical and tropospheric path delays. The error is minimized by applying least-squares estimation to a combined set of observables in the calibration directions and the direction to be calibrated. A simulated test of this procedure was conducted using a model set of error-free calibration measurements. In the absence of geometrical delay mismodeling, the simulation yielded delay errors which vary from about 1 mm at zenith to about 1 cm at 10 degrees. The main principles of how this procedure could be applied to improve accuracy of deep space tracking using global positioning system (GPS) data are also discussed. Author (revised)

N94-29655*# Jet Propulsion Lab., California Inst. of Tech., Pasadena.
ENHANCED ORBIT DETERMINATION FILTER SENSITIVITY ANALYSIS: ERROR BUDGET DEVELOPMENT **c13**
J. A. Estefan and P. D. Burkhart *In its* The Telecommunications and Data Acquisition Report 15 Feb. 1994 p 24-36 (For primary document see N94-29652 08-32)
(RTOP 310-10-63-50-00)
Avail: CASI HC A03/MF A03

An error budget analysis is presented which quantifies the effects of different error sources in the orbit determination process when the enhanced orbit determination filter, recently developed, is used to reduce radio metric data. The enhanced filter strategy differs from more traditional filtering methods in that nearly all of the principal ground system calibration errors affecting the data are represented as filter parameters. Error budget computations were performed for a Mars Observer interplanetary cruise scenario for cases in which only X-band (8.4-GHz) Doppler data were used to determine the spacecraft's orbit, X-band ranging data were used exclusively, and a combined set in which the ranging data were used in addition to the Doppler data. In all three cases, the filter model was assumed to be a correct representation of the physical world. Random nongravitational accelerations were found to be the largest source of error contributing to the individual error budgets. Other significant contributors, depending on the data strategy used, were solar-radiation pressure coefficient uncertainty, random earth-orientation calibration errors, and Deep Space Network (DSN) station location uncertainty. Author (revised)

N94-29656*# Jet Propulsion Lab., California Inst. of Tech., Pasadena.
ENHANCED ORBIT DETERMINATION FILTER: INCLUSION OF GROUND SYSTEM ERRORS AS FILTER PARAMETERS **c13**
W. C. Masters, D. J. Scheeres, and S. W. Thurman *In its* The Telecommunications and Data Acquisition Report 15 Feb. 1994 p 37-41 (For primary document see N94-29652 08-32)
(RTOP 310-10-63-50-00)
Avail: CASI HC A01/MF A03

The theoretical aspects of an orbit determination filter that incorporates ground-system error sources as model parameters for use in interplanetary navigation are presented in this article. This filter, which is derived from sequential filtering theory, allows a systematic treatment of errors in calibrations of transmission media, station locations, and earth orientation models associated with ground-based radio metric data, in addition to the modeling of the spacecraft dynamics. The discussion includes a mathematical description of the filter and an analytical comparison of its characteristics with more traditional filtering techniques used in this application. The analysis in this article shows that this filter has the potential to generate navigation products of substantially greater accuracy than more traditional filtering procedures. Author

N94-29657*# Jet Propulsion Lab., California Inst. of Tech., Pasadena.
DETERMINING NOISE TEMPERATURES IN BEAM WAVEGUIDE SYSTEMS
W. Imbriale, W. Veruttipong, T. Otoshi, and M. Franco *In its* The Telecommunications and Data Acquisition Report 15 Feb. 1994 p 42-52 (For primary document see N94-29652 08-32)
(RTOP 310-20-65-86-08)
Avail: CASI HC A03/MF A03

A new 34-m research and development antenna was fabricated and tested as a precursor to introducing beam waveguide (BWG) antennas and Ka-band (32 GHz) frequencies into the NASA/JPL Deep Space Network. For deep space use, system noise temperature is a critical parameter. There are thought to be two major contributors to noise temperature in a BWG system: the spillover past the mirrors, and the conductivity loss in the walls. However, to date, there are no generally accepted methods for computing noise temperatures in a beam waveguide system. An extensive measurement program was undertaken to determine noise temperatures in such a system along with a correspondent effort in analytic prediction. Utilizing a very sensitive radiometer, noise temperature measurements were made at the Cassegrain focus, an intermediate focal point, and the focal point in the basement pedestal room. Several different horn diameters were used to simulate different amounts of spillover past the mirrors. Two analytic procedures were developed for computing noise temperature, one utilizing circular waveguide modes and the other a semiempirical approach.

The results of both prediction methods are compared to the experimental data. Author

N94-29658*# Jet Propulsion Lab., California Inst. of Tech., Pasadena.
A DUAL-CAVITY RUBY MASER FOR THE Ka-BAND LINK EXPERIMENT **c36**
J. Shell and R. B. Quinn *In its* The Telecommunications and Data Acquisition Report 15 Feb. 1994 p 53-70 (For primary document see N94-29652 08-32)
(RTOP 310-20-66-87-02)
Avail: CASI HC A03/MF A03

A 33.68-GHz dual-cavity ruby maser was built to support the Ka-Band Link Experiment (KABLE) conducted with the Mars Observer spacecraft. It has 25 dB of net gain and a 3-dB bandwidth of 85 MHz. Its noise temperature in reference to the cooled feedhorn aperture is 5 K.
Author (revised)

N94-29659*# New Mexico State Univ., Las Cruces.
THE Rb 780-NANOMETER FARADAY ANOMALOUS DISPERSION OPTICAL FILTER: THEORY AND EXPERIMENT **c74**
B. Yin, L. S. Alvarez, and T. M. Shay *In* JPL, The Telecommunications and Data Acquisition Report 15 Feb. 1994 p 71-85 (For primary document see N94-29652 08-32)
(RTOP 310-20-67-92-02)
Avail: CASI HC A03/MF A03

The Faraday anomalous dispersion optical filter may provide ultra-high background noise rejection for free-space laser communications systems. The theoretical model for the filter is reported. The experimental measurements and their comparison with theoretical results are discussed. The results show that the filter can provide a 56-dB solar background noise rejection with about a 2-GHz transmission bandwidth and no image degradation. To further increase the background noise rejection, a composite Zeeman and Faraday anomalous dispersion optical filter is designed and experimentally demonstrated. Author

N94-29660*# Jet Propulsion Lab., California Inst. of Tech., Pasadena.
A DIGITAL COMBINING-WEIGHT ESTIMATION ALGORITHM FOR BROADBAND SOURCES WITH THE ARRAY FEED COMPENSATION SYSTEM
V. A. Vilnrotter and E. R. Rodemich *In its* The Telecommunications and Data Acquisition Report 15 Feb. 1994 p 86-97 (For primary document see N94-29652 08-32)
(RTOP 310-30-70-89-01)
Avail: CASI HC A03/MF A03

An algorithm for estimating the optimum combining weights for the Ka-band (33.7-GHz) array feed compensation system was developed and analyzed. The input signal is assumed to be broadband radiation of thermal origin, generated by a distant radio source. Currently, seven video converters operating in conjunction with the real-time correlator are used to obtain these weight estimates. The algorithm described here requires only simple operations that can be implemented on a PC-based combining system, greatly reducing the amount of hardware. Therefore, system reliability and portability will be improved. Author

N94-29661*# Jet Propulsion Lab., California Inst. of Tech., Pasadena.
DIGITAL COMBINING-WEIGHT ESTIMATION FOR BROADBAND SOURCES USING MAXIMUM-LIKELIHOOD ESTIMATES **c61**
E. R. Rodemich and V. A. Vilnrotter *In its* The Telecommunications and Data Acquisition Report 15 Feb. 1994 p 98-109 (For primary document see N94-29652 08-32)
(RTOP 310-30-70-89-01)
Avail: CASI HC A03/MF A03

An algorithm described for estimating the optimum combining weights for the Ka-band (33.7-GHz) array feed compensation system is compared with the maximum-likelihood estimate. This provides some improvement in performance, with an increase in computational complexity. However, the maximum-likelihood algorithm is simple enough to allow implementation on a PC-based combining system. Author (revised)

N94-29662*# Solomon (G.), Pasadena, CA.
CONVOLUTIONAL ENCODING OF SELF-DUAL CODES **c61**
G. Solomon *In* JPL, The Telecommunications and Data Acquisition Report 15 Feb. 1994 p 110-113 (For primary document see N94-29652 08-32)
(RTOP 310-30-71-83-02)
Avail: CASI HC A01/MF A03

There exist almost complete convolutional encodings of self-dual codes, i.e., block codes of rate 1/2 with weights w, $w = 0 \bmod 4$. The codes are of length 8m with the convolutional portion of length 8m-2 and the nonsystematic information of length 4m-1. The last two bits are parity checks on the two (4m-1) length parity sequences. The final information bit complements one of the extended parity sequences of length 4m. Solomon and van Tilborg have developed algorithms to generate these for the Quadratic Residue (QR) Codes of lengths 48 and beyond. For these codes and reasonable constraint lengths, there are sequential decodings for both hard and soft decisions. There are also possible Viterbi-type decodings that may be simple, as in a convolutional encoding/decoding of the extended Golay Code. In addition, the previously found constraint length $K = 9$ for the QR (48, 24;12) Code is lowered here to $K = 8$.
Author (revised)

N94-29663*# Jet Propulsion Lab., California Inst. of Tech., Pasadena.
OPTIMIZING THE GALILEO SPACE COMMUNICATION LINK
J. I. Statman *In its* The Telecommunications and Data Acquisition Report 15 Feb. 1994 p 114-120 (For primary document see N94-29652 08-32)
(RTOP 314-30-61-02-01)
Avail: CASI HC A02/MF A03

The Galileo mission was originally designed to investigate Jupiter and its moons utilizing a high-rate, X-band (8415 MHz) communication downlink with a maximum rate of 134.4 kb/sec. However, following the failure of the high-gain antenna (HGA) to fully deploy, a completely new communication link design was established that is based on Galileo's S-band (2295 MHz), low-gain antenna (LGA). The new link relies on data compression, local and intercontinental arraying of antennas, a (14,1/4) convolutional code, a (255,M) variable-redundancy Reed-Solomon code, decoding feedback, and techniques to reprocess recorded data to greatly reduce data losses during signal acquisition. The combination of these techniques will enable return of significant science data from the mission. Author (revised)

N94-29664*# Jet Propulsion Lab., California Inst. of Tech., Pasadena.
DECODER SYNCHRONIZATION FOR DEEP SPACE MISSIONS
J. I. Statman, K.-M. Cheung, T. H. Chauvin, J. Rabkin, and M. L. Belongie *In its* The Telecommunications and Data Acquisition Report 15 Feb. 1994 p 121-127 (For primary document see N94-29652 08-32)
(RTOP 314-30-61-02-01)
Avail: CASI HC A02/MF A03

The Consultative Committee for Space Data Standards (CCSDS) recommends that space communication links employ a concatenated, error-correcting, channel-coding system in which the inner code is a convolutional (7,1/2) code and the outer code is a (255,223) Reed-Solomon code. The traditional implementation is to perform the node synchronization for the Viterbi decoder and the frame synchronization for the Reed-Solomon decoder as separate, sequential operations. This article discusses a unified synchronization technique that is required for deep space missions that have data rates and signal-to-noise ratios (SNR's) that are extremely low. This technique combines frame synchronization in the bit and symbol domains and traditional accumulated-metric growth techniques to establish a joint frame and node synchronization. A variation on this technique is used for the Galileo spacecraft on its Jupiter-bound mission.
Derived from text

N94-29665*# Jet Propulsion Lab., California Inst. of Tech., Pasadena.
A COMPARISON OF FULL-SPECTRUM AND COMPLEX-SYMBOL COMBINING TECHNIQUES FOR THE GALILEO S-BAND MISSION
S. Million, B. Shah, and S. Hinedi *In its* The Telecommunications and Data Acquisition Report 15 Feb. 1994 p 128-162 (For primary document see N94-29652 08-32)
(RTOP 314-30-63-03-19)
Avail: CASI HC A03/MF A03

Full-spectrum combining (FSC) and complex-symbol combining (CSC) are two antenna-arraying techniques being considered for the Galileo spacecraft's upcoming encounter with Jupiter. This article describes the performance of these techniques in terms of symbol signal-to-noise ratio

(SNR) degradation and symbol SNR loss. It is shown that both degradation and loss are approximately equal at low values of symbol SNR but diverge at high SNR values. For the Galileo S-band (2.2 to 2.3 GHz) mission, degradation provides a good estimate of performance as the symbol SNR is typically below -5 dB. For the following arrays - two 70-m antennas, one 70-m and one 34-m antenna, one 70-m and two 34-m antennas, and one 70-m and three 34-m antennas - it is shown that FSC has less degradation than CSC when the subcarrier and symbol window-loop bandwidth products are above 3.0, 10.0, 8.5, and 8.2 mHz at the symbol rate of 200 sym/sec, and above 1.2, 4.5, 4.0, and 3.5 mHz at a symbol rate of 400 sym/sec, respectively. Moreover, for an array of four 34-m antennas, FSC has less degradation than CSC when the subcarrier and symbol window-loop bandwidth products are above 0.32 mHz at the symbol rate of 50 sym/sec and above 0.8 mHz at the symbol rate of 25 sym/sec. Author

N94-29666*# Jet Propulsion Lab., California Inst. of Tech., Pasadena.
TOPEX/POSEIDON OPERATIONAL ORBIT DETERMINATION RESULTS USING GLOBAL POSITIONING SATELLITES c13
J. Guinn, J. Jee, P. Wolff, F. Lagattuta, T. Drain, and V. Sierra *In its* The Telecommunications and Data Acquisition Report 15 Feb. 1994 p 163-174 (For primary document see N94-29652 08-32)
(RTOP 314-40-22-42-05)
Avail: CASI HC A03/MF A03

Results of operational orbit determination, performed as part of the TOPEX/POSEIDON (T/P) Global Positioning System (GPS) demonstration experiment, are presented in this article. Elements of this experiment include the GPS satellite constellation, the GPS demonstration receiver on board T/P, six ground GPS receivers, the GPS Data Handling Facility, and the GPS Data Processing Facility (GDPF). Carrier phase and P-code pseudorange measurements from up to 24 GPS satellites to the seven GPS receivers are processed simultaneously with the GDPF software MIRAGE to produce orbit solutions of T/P and the GPS satellites. Daily solutions yield subdecimeter radial accuracies compared to other GPS, LASER, and DORIS precision orbit solutions. Author

N94-29667*# Jet Propulsion Lab., California Inst. of Tech., Pasadena.
DESIGN AND IMPLEMENTATION OF A HYBRID DIGITAL PHASE-LOCKED LOOP WITH A TMS320C25: AN APPLICATION TO A TRANSPONDER RECEIVER BREADBOARD c33
H.-G. Yeh and T. M. Nguyen *In its* The Telecommunications and Data Acquisition Report 15 Feb. 1994 p 175-189 (For primary document see N94-29652 08-32)
(RTOP 315-91-10-13-08)
Avail: CASI HC A03/MF A03

Design, modeling, analysis, and simulation of a phase-locked loop (PLL) with a digital loop filter are presented in this article. A TMS320C25 digital signal processor (DSP) is used to implement this digital loop filter. In order to keep the compatibility, the main design goal was to replace the analog PLL (APLL) of the Deep-Space Transponder (DST) receiver breadboard's loop filter with a digital loop filter without changing anything else. This replacement results in a hybrid digital PLL (HDPLL). Both the original APLL and the designed HDPLL are Type I second-order systems. The real-time performance of the HDPLL and the receiver is provided and evaluated. Author

N94-29668*# Jet Propulsion Lab., California Inst. of Tech., Pasadena.
A 32 GHz MICROSTRIP ARRAY ANTENNA FOR MICROSPACECRAFT APPLICATION
J. Huang *In its* The Telecommunications and Data Acquisition Report 15 Feb. 1994 p 190-203 (For primary document see N94-29652 08-32)
(RTOP 315-91-50-20-04)
Avail: CASI HC A03/MF A03

JPL/NASA is currently developing microspacecraft systems for future deep space applications. One of the frequency bands being investigated for microspacecraft is the Ka-band (32 GHz), which can be used with smaller equipment and provides a larger bandwidth. This article describes the successful development of a circularly polarized microstrip array with 28 dBic of gain at 32 GHz. This antenna, which is thin, flat, and small, can be surface-mounted onto the microspacecraft and, hence, takes very little volume and mass of the spacecraft. The challenges in developing this antenna are minimizing the microstrip antenna's insertion loss and maintaining a reasonable frequency bandwidth. Author

N94-29669*# Jet Propulsion Lab., California Inst. of Tech., Pasadena.
EFFECTS OF LOW SAMPLING RATE IN THE DIGITAL DATA-TRANSITION TRACKING LOOP
A. Mileant, S. Million, and S. Hinedi *In its* The Telecommunications and Data Acquisition Report 15 Feb. 1994 p 204-222 (For primary document see N94-29652 08-32)
(RTOP 314-40-41-11-06)
Avail: CASI HC A03/MF A03

This article describes the performance of the all-digital data-transition tracking loop (DTTL) with coherent and noncoherent sampling using nonlinear theory. The effects of few samples per symbol and of noncommensurate sampling and symbol rates are addressed and analyzed. Their impact on the probability density and variance of the phase error are quantified through computer simulations. It is shown that the performance of the all-digital DTTL approaches its analog counterpart when the sampling and symbol rates are noncommensurate (i.e., the number of samples per symbol is an irrational number). The loop signal-to-noise ratio (SNR) (inverse of phase error variance) degrades when the number of samples per symbol is an odd integer but degrades even further for even integers. Author

N94-29670*# Jet Propulsion Lab., California Inst. of Tech., Pasadena.
AN IMPROVED CONSCAN ALGORITHM BASED ON A KALMAN FILTER c61
D. B. Eldred *In its* The Telecommunications and Data Acquisition Report 15 Feb. 1994 p 223-231 (For primary document see N94-29652 08-32)
(RTOP 314-30-43-10-18)
Avail: CASI HC A02/MF A03

Conscan is commonly used by DSN antennas to allow adaptive tracking of a target whose position is not precisely known. This article describes an algorithm that is based on a Kalman filter and is proposed to replace the existing fast Fourier transform based (FFT-based) algorithm for conscan. Advantages of this algorithm include better pointing accuracy, continuous update information, and accommodation of missing data. Additionally, a strategy for adaptive selection of the conscan radius is proposed. The performance of the algorithm is illustrated through computer simulations and compared to the FFT algorithm. The results show that the Kalman filter algorithm is consistently superior. Author

N94-29671*# Jet Propulsion Lab., California Inst. of Tech., Pasadena.
A COMPLEX SYMBOL SIGNAL-TO-NOISE RATIO ESTIMATOR AND ITS PERFORMANCE
Y. Feria *In its* The Telecommunications and Data Acquisition Report 15 Feb. 1994 p 232-245 (For primary document see N94-29652 08-32)
(RTOP 314-30-61-02-10)
Avail: CASI HC A03/MF A03

This article presents an algorithm for estimating the signal-to-noise ratio (SNR) of signals that contain data on a downconverted suppressed carrier or the first harmonic of a square-wave subcarrier. This algorithm can be used to determine the performance of the full-spectrum combiner for the Galileo S-band (2.2- to 2.3-GHz) mission by measuring the input and output symbol SNR. A performance analysis of the algorithm shows that the estimator can estimate the complex symbol SNR using 10,000 symbols at a true symbol SNR of -5 dB with a mean of -4.9985 dB and a standard deviation of 0.2454 dB, and these analytical results are checked by simulations of 100 runs with a mean of -5.06 dB and a standard deviation of 0.2506 dB. Author

N94-29672*# Jet Propulsion Lab., California Inst. of Tech., Pasadena.
X-BAND ULTRALOW-NOISE MASER AMPLIFIER PERFORMANCE c36
G. W. Glass, G. G. Ortiz, and D. L. Johnson *In its* The Telecommunications and Data Acquisition Report 246-253 (SEE N94-29652 08-32) 15 Feb. 1994 (For primary document see N94-29652 08-32)
(RTOP 310-20-66-53-00)
Avail: CASI HC A02/MF A03

Noise temperature measurements of an 8440-MHz ultralow noise maser amplifier (ULNA) have been performed at subatmospheric, liquid-helium temperatures. The traveling-wave maser was operated while immersed in a

liquid helium bath. The lowest input noise temperature measured was 1.43 +/- 0.16 K at a physical temperature of 1.60 K. At this physical temperature, the observed gain per centimeter of ruby was 4.9 dB/cm. The amplifier had a 3-dB bandwidth of 76 MHz. Author

N94-29673*# Jet Propulsion Lab., California Inst. of Tech., Pasadena.
SIMULATION OF INTERFERENCE BETWEEN EARTH STATIONS AND EARTH-ORBITING SATELLITES
D. F. Bishop *In its* The Telecommunications and Data Acquisition Report 15 Feb. 1994 p 254-270 (For primary document see N94-29652 08-32)
(RTOP 315-90-31-00-02)
Avail: CASI HC A03/MF A03

It is often desirable to determine the potential for radio frequency interference between earth stations and orbiting spacecraft. This information can be used to select frequencies for radio systems to avoid interference or it can be used to determine if coordination between radio systems is necessary. A model is developed that will determine the statistics of interference between earth stations and elliptical orbiting spacecraft. The model uses orbital dynamics, detailed antenna patterns, and spectral characteristics to obtain accurate levels of interference at the victim receiver. The model is programmed into a computer simulation to obtain long-term statistics of interference. Two specific examples are shown to demonstrate the model. The first example is a simulation of interference from a fixed-satellite earth station to an orbiting scatterometer receiver. The second example is a simulation of interference from earth-exploration satellites to a deep-space earth station. Author (revised)

N94-29692# Center for Mathematics and Computer Science, Amsterdam (Netherlands). Dept. of Computer Science/Dept. of Algorithmics and Architecture.
RIPE INTEGRITY PRIMITIVES, PART 1 (RACE INTEGRITY PRIMITIVES EVALUATION) Final Report
B. denBoer (Philips Crypto B.V., Eindhoven, Netherlands.), J. P. Boly (PTT Research, Leidschendam, Netherlands.), A. Bosselaers (Katholieke Univ. te Leuven, Belgium.), J. Brandt (Aarhus Univ., Denmark.), D. Chaum, I. Damgaard, M. Dichtl, W. Fumy, M. vanderHam, and C. J. A. Jansen et al Apr. 1993 111 p Sponsored in part by EEC
(ISSN 0169-118X)
(CWI-CS-R9324-Pt-1; RACE-1040-Pt-1; ETN-94-95437) Copyright Avail: CASI HC A06/MF A02

A manual intended for those seeking to secure information systems by applying modern cryptography is presented. It represents the successful attainment of goals by RIPE (RACE (Research and development of Advanced Communication technology in Europe) Integrity Primitives Evaluation). The recommended portfolio of integrity primitives, which is the main product of the project, forms the heart of the manual. By integrity, is meant the kinds of security that can be achieved through cryptography, apart from keeping messages secret. Thus included are ways to ensure that stored or communicated data is not illicitly modified, that parties exchanging messages are actually present, and that 'signed' electronic messages can be recognized as authentic by anyone. Of particular concern to the project were the high speed requirements of broadband communication. The project also aimed for completeness in its recommendations. As a result, the portfolio contains primitives, that is building blocks, that can meet most of today's perceived needs for integrity. ESA

N94-29693 Center for Mathematics and Computer Science, Amsterdam (Netherlands). Dept. of Computer Science/Dept. of Algorithmics and Architecture.
RIPE INTEGRITY PRIMITIVES, PART 2 (RACE INTEGRITY PRIMITIVES EVALUATION) Final Report
B. denBoer (Philips Crypto B.V., Eindhoven, Netherlands.), J. P. Boly (PTT Research, Leidschendam, Netherlands.), A. Bosselaers (Katholieke Univ. te Leuven, Belgium.), J. Brandt (Aarhus Univ., Denmark.), D. Chaum, I. Damgaard, M. Dichtl, W. Fumy, M. vanderHam, and C. J. A. Jansen et al Apr. 1993 117 p Sponsored in part by EEC Limited Reproducibility: More than 20% of this document may be affected by microfiche quality
(ISSN 0169-118X)
(CWI-CS-R9325-Pt-2; RACE-1040-Pt-2; ETN-94-95438) Copyright Avail: CASI HC A06

A manual intended for those seeking to secure information systems by applying modern cryptography is presented. It represents the successful attainment of goals by RIPE (RACE (Research and development of Advanced Communications technology in Europe) Integrity Primitives Evaluation). The recommended portfolio of integrity primitives, which is the main product of the project, forms the heart of the manual. By integrity, is meant the kinds of security that can be achieved through cryptography, apart from keeping messages secret. Thus included are ways to ensure that stored or communicated data is not illicitly modified, that parties exchanging messages are actually present, and that 'signed' electronic messages can be recognized as authentic by anyone. Of particular concern to the project were the high speed requirements of broadband communication. The project also aimed for completeness in its recommendations. As a result, the portfolio contains primitives, that is building blocks, that can meet most of today's perceived needs for integrity. ESA

N94-29733 Oregon Graduate Inst. of Science and Technology, Beaverton.
EXACT SPHERICAL WAVE SOLUTIONS TO MAXWELL'S EQUATIONS WITH APPLICATIONS Ph.D. Thesis
Guy G. Silvestri 1993 234 p
Avail: Univ. Microfilms Order No. DA9313926

Electromagnetic radiation from bounded sources represent an important class of physical problems that can be solved for exactly. However, available texts on this subject almost always resort to approximate solution techniques that not only obscure the essential features of the problem but also restrict application to limited ranges of observation. This dissertation presents exact solutions for this important class of problems and demonstrates how these solutions can be applied to situations of genuine physical interest, in particular, the design of device structures with prespecified emission characteristics. The strategy employed is to solve Maxwell's equations in the spherical coordinate system. In this system, fundamental parameters such as electric and magnetic multipole moments fall out quite naturally. Expressions for radiated power, force, and torque assume especially illuminating and simple forms when expressed in terms of these multipole moments. All solutions are derived ab initio using first-principles arguments exclusively. Two operator equations that receive particularly detailed treatment are the vector Helmholtz equation for the time-independent potential vector-a and the 'covariant divergence' equation for the energy-momentum-stress tensor T(exp mu nu). An application of classical formulas, as modified by the requirements of statistical mechanics, to the case of heated black bodies leads to inquiries into the foundations of quantum mechanics and their relation to classical field theory. An application of formulas to various emission structures (spherically shaped antennas, surface diffraction gratings, collimated beams) provides a basis upon which to characterize these structures in an exact sense and, ultimately, to elicit clues as to their optimum design. Dissert. Abstr.

N94-29739* National Aeronautics and Space Administration. Goddard Space Flight Center, Greenbelt, MD.
METHOD FOR AMBIGUITY RESOLUTION IN RANGE-DOPPLER MEASUREMENTS Patent
Gerald M. Heymsfield, inventor (to NASA) and Lee S. Miller, inventor (to NASA) 4 Jan. 1994 7 p Filed 2 Feb. 1993
(NASA-Case-GSC-13542-1; US-Patent-5,276,453;
US-Patent-Appl-SN-028091; US-Patent-Class-342-112;
US-Patent-Class-342-116; Int-Patent-Class-G01S-13/58) Avail: US Patent and Trademark Office

A method for resolving range and Doppler target ambiguities when the target has substantial range or has a high relative velocity in which a first signal is generated and a second signal is also generated which is coherent with the first signal but at a slightly different frequency such that there exists a difference in frequency between these two signals of Delta f(sub t). The first and second signals are converted into a dual-frequency pulsed signal, amplified, and the dual-frequency pulsed signal is transmitted towards a target. A reflected dual-frequency signal is received from the target, amplified, and changed to an intermediate dual-frequency signal. The intermediate dual-frequency signal is amplified, with extracting of a shifted difference frequency Delta f(sub r) from the amplified intermediate dual-frequency signal done by a nonlinear detector. The final step is generating two quadrature signals from the difference frequency Delta f(sub t) and the shifted difference frequency Delta f(sub r) and processing the

two quadrature signals to determine range and Doppler information of the target. Official Gazette of the U.S. Patent and Trademark Office

N94-29873*# Michigan Univ., Ann Arbor. Dept. of Electrical Engineering and Computer Science.
RADIATION AND SCATTERING FROM CYLINDRICALLY CONFORMAL PRINTED ANTENNAS Ph.D. Thesis Final Report
Leo C. Kempel (National Aeronautics and Space Administration. Ames Research Center, Moffett Field, CA.) and John L. Volakis (Naval Weapons Center, China Lake, CA.) Apr. 1994 178 p
(Contract NCA2-839)
(NASA-CR-195546; NAS 1.26:195546; UMICH-031173-2T) Avail: CASI HC A09/MF A02

Microstrip patch antennas offer considerable advantages in terms of weight, aerodynamic drag, cost, flexibility, and observables over more conventional protruding antennas. These flat patch antennas were first proposed over thirty years ago by Deschamps in the United States and Gutton and Baisinot in France. Such antennas have been analyzed and developed for planar as well as curved platforms. However, the methods used in these designs employ gross approximations, suffer from extreme computational burden, or require expensive physical experiments. The goal of this thesis is to develop accurate and efficient numerical modeling techniques which represent actual antenna structures mounted on curved surfaces with a high degree of fidelity. In this thesis, the finite element method is extended to cavity-backed conformal antenna arrays embedded in a circular, metallic, infinite cylinder. Both the boundary integral and absorbing boundary mesh closure conditions will be used for terminating the mesh. These two approaches will be contrasted and used to study the scattering and radiation behavior of several useful antenna configurations. An important feature of this study will be to examine the effect of curvature and cavity size on the scattering and radiation properties of wraparound conformal antenna arrays. Derived from text

N94-29882 Northeastern Univ., Boston, MA.
RADAR RETURNS FROM A LOW-FLYING TARGET OVER A ROUGH SEA SURFACE UNDER MULTIPATH AND CLUTTER CONDITIONS Ph.D. Thesis
Feza Coskun 1992 137 p
Avail: Univ. Microfilms Order No. DA9313778

The scattering from surfaces plays an important role in radar operations when the radar beam intercepts the earth surface. Forward scattering gives rise to multipath phenomenon and backward scattering causes clutter returns. These two factors degrade the performance of a radar in its effort to detect a target. In this thesis, a computer simulation program, which traces the electromagnetic pulse in a controlled radar environment and enables us to observe the behavior of various field quantities at different locations, is developed. The program is capable of providing the statistical properties of various parameters such as electromagnetic field values, received voltage waveforms, and normalized radar cross section of the rough surface. It has a modular structure which ensures its flexibility for future extensions and changes. For the particular scenario set given in this thesis, the rough surface is chosen to be the sea surface, the radar antenna has a rectangular aperture, and the target is a flat perfectly conducting rectangular plate. A literature survey on rough surface scattering, multipath, and clutter shows that a single model which combines the effects of all levels of roughness of a surface does not exist. In this work, a composite sea surface model with two scales of roughness is developed. This model along with the antenna and target models is easy and efficient to implement on the computer. Various results on the electromagnetic field from the simulations of different scenarios are provided and compared. The simulation program is used to obtain the ambiguity function of the received time waveform. The received signals, which consist of the returns due to target, clutter, and multipath, are processed by the discrete cross ambiguity function routine and results on both coherent and incoherent processing are provided and discussed. Dissert. Abstr.

N94-29883 University of Central Florida, Orlando.
INTEGRAL EQUATION ANALYSIS OF COMPOSITE BODIES OF REVOLUTION AND ARBITRARY SURFACES WITH APPLICATION TO CAVITY-BACKED ANTENNAS Ph.D. Thesis
Timothy E. Durham 1992 165 p
Avail: Univ. Microfilms Order No. DA9311280

A formulation is developed to treat radiation from structures consisting of conducting and/or dielectric bodies of revolution (BOR) in the presence of multiple arbitrarily shaped three dimensional objects. A set of integral equations is developed on the surfaces of the combined structure using the electromagnetic boundary conditions. The resulting integro-differential equations are solved using the method of moments. On the BOR, harmonic entire domain expansion functions are used for the circumferential dependence, while overlapping subdomain functions are used to model the axial curvature. The arbitrarily shaped portions of the structure are modeled wing triangular surface patch basis functions. The resulting system matrix has a partial block diagonal nature which provides a more economical solution for structures which have some rotational symmetry. The accuracy of the BOR and arbitrary surface formulation is verified using several different approaches. The self-consistency method is used to verify the analysis for both perfectly conducting and dielectrically loaded structures. Special emphasis is placed on a unique cavity-backed antenna that is fed by large aperture patches. Numerical results are presented and compared to radiation pattern measurements performed on these antennas with very good agreement being obtained. An approach for solving the problem of junctions between bodies of revolution and arbitrary surfaces is investigated and shown to be accurate for some cases. Dissert. Abstr.

N94-29894 New Mexico State Univ., Las Cruces.
REMOTE OBSERVATORY ACCESS VIA THE ADVANCED COMMUNICATIONS TECHNOLOGY SATELLITE Ph.D. Thesis
Georghios Andreou Georghiou 1992 141 p
Avail: Univ. Microfilms Order No. DA9313729

The remote access of the Apache Point Observatory (APO) at Sunspot, New Mexico, by using the Advanced Communications Technology Satellite (ACTS) is investigated. This opportunity arose as a result of the announcement by NASA proposing investigations that demonstrate communications techniques and services and verifying technology implementations by using ACTS. An end-to-end simulation testbed has been developed for the underlying satellite communication network, which is composed of the APO's LAN, the remote observer's LAN, and part of the ACTS Low Burst Rate 2 (LBR-2) network which serves as the internetworking medium between the two LAN's. This is accomplished by using COMNET II.5, a communication network oriented tool for designing, developing, and executing simulations within one user interface. Performance tests at different network elements have been performed to measure processing delays. Specifications and/or salient features of network functional subsystems have been used to reach a high degree of accuracy with the real model. Additional features taken into consideration are the traffic model of the telescope, the TDMA frame structure, and the potential protocols for end-to-end delivery of data. Based on the testbed, a detailed output report determines factors in the network, such as access possibilities between APO and major astronomical centers and observatories using the ACTS; latency between the APO and the remote user; TDMA frame capacity requirements to support network data under various conditions; buffer sizes required in various network elements to support data transfer; optimum protocol configurations for end-to-end transport; potential ACTS terminal limitations on the data transport process; identify bottleneck areas and conditions under which they occur in optimizing such a network; and potentials for growth in the APO data source capacity, using the ACTS-type of frame structure. Dissert. Abstr.

N94-29897 Virginia Polytechnic Inst. and State Univ., Blacksburg.
ADAPTIVE POWER CONTROL AS A FADE COUNTERMEASURE ON SATELLITE LINKS Ph.D. Thesis
Dennis Givens Sweeney 1993 169 p
Avail: Univ. Microfilms Order No. DA9312882

Satellite systems in the 20/30 GHz band are very susceptible to outages due to rain-induced fades. In order to reduce the impact of these fades, it has been proposed that the power of the uplink station transmitter be adjusted during the fade to compensate. This dissertation will explore some of the issues involved in implementing this uplink power control (ULPC). Fade slope is examined as a parameter to predict signal strength during a fade. A fade slope model based on fade physics is presented, but it strongly suggests that fade slope is not an appropriate parameter for ULPC. Real time scaling of attenuation from the downlink to the uplink shows more promise for ULPC. Differences in drop size distributions during a rain storm will result is different scaling factors. If the downlink attenuation

is limited to 6 dB at 20 GHz, real time scaling can be accomplished. A scaling type ULPC algorithm driven by downlink attenuation is tested on 66 hours of OLYMPUS 20/30 GHZ fade data. A similar algorithm driven by uplink attenuation is tested and the performance of the two algorithms is presented and compared. Dissert. Abstr.

N94-29929 Lawrence Livermore National Lab., CA.
IMPROVED GROUND-PENETRATING RADAR, BRIDGE DECKS
J. P. Warhus, J. E. Mast, E. M. Johansson, and S. D. Nelson 29 Nov. 1993 8 p Presented at the Structural Materials Non-Destructive Technology Conference, Atlantic City, NJ, 23-25 Feb. 1994 Limited Reproducibility: More than 20% of this document may be affected by microfiche quality
(Contract W-7405-eng-48)
(DE94-004863; UCRL-JC-115463; CONF-940241-1) Avail: CASI HC A02

Inspection of high-value structures, like bridges and buildings, using Ground Penetrating Radar (GPR) is an application of a technology that is growing in importance. In a typical inspection application, inspectors use GPR to locate structural components, like embedded reinforcing bars, to avoid weakening the structure while collecting core samples for detailed inspection. Advanced GPR, integrated with imaging technologies for use as an NDE tool, can provide the capability to quickly locate and characterize construction flaws and wear- or age-induced damage in these structures without resorting to destructive methods. In this paper, we discuss an important inspection application, namely, concrete bridge deck inspection. We describe an advanced bridge deck inspection system concept (Ground Penetrating Imaging Radar, GPIR) and present results from experiments designed to simulate the concept. DOE

N94-29998 Eurocontrol Experimental Centre, Bretigny (France).
INSTALLATION OF EXPERIMENTAL MODE-S DATA LINK IN COMMERCIAL AIRCRAFT
H. P. Englmeier Nov. 1993 27 p
(PB94-138757; EEC/NOTE-18/93) Avail: Issuing Activity (National Technical Information Service (NTIS))

This note describes the experimental Mode-S Data Link chain which has been developed by the EUROCONTROL Experimental Center for installation in commercial aircraft. The status of those installations and the possible use of the existing ground services are presented. NTIS

N94-30031 Ottawa Univ. (Ontario). Dept. of Electrical Engineering.
PARTIALLY COHERENT DETECTION OF PSK SIGNALS IN RICIAN CHANNELS M.S. Thesis
Yasar Tunca 1992 113 p
(ISBN-0-315-85799-4; CTN-94-61167) Copyright Avail: Micromedia Ltd., Technical Information Centre, 240 Catherine Street, Suite 305, Ottawa, Ontario, K2P 2G8, Canada HC/MF

Channel models are developed for noisy phase reference and Rician fading channels, and all the assumptions in the models are explained. After a description of phase shift keying (PSK) signals, their coherent, differential, and multidifferential detection is explained. Analytical expressions are provided for their performance in additive white Gaussian noise and Rician channels. Bit error curves obtained by simulations are plotted and compared with the curves given in the literature. Assuming that partially coherent detection could be an alternative, metric expressions are derived for partially coherent detection of signals in general and applied to PSK signals. The bit error rate performance of partially coherent detection of uncoded binary and quaternary PSK signals obtained through simulation is presented for different signal to noise ratios of carrier recovery loop and direct component power to diffuse component power ratios. The performances obtained are compared to coherent and differential detection performances under the same conditions. Partially coherent detection showed no significant improvement compared to multidifferential detection. It is suggested that partially coherent detection will give significant improvements compared to differential detection for coded systems.
Author (CISTI)

N94-30034 Ottawa Univ. (Ontario). Dept. of Electrical Engineering.
INVESTIGATIONS OF DISPERSION CHARACTERISTICS OF MICROWAVE/OPTICAL GUIDED WAVE STRUCTURES BY USING TRANSMISSION LINE MATRIX METHOD M.S. Thesis
Bing Qiu 1993 123 p
(ISBN-0-315-85856-7; CTN-94-61170) Copyright Avail: Micromedia Ltd., Technical Information Centre, 240 Catherine Street, Suite 305, Ottawa, Ontario, K2P 2G8, Canada HC/MF

A new three dimensional space (3D) condensed node transmission line matrix (TLM) algorithm is presented for the analysis of dispersion characteristics of microwave and optical guided wave structures. The new algorithm requires much less computer memory and computation time than the conventional 3D condensed node TLM. The application of the new algorithm to the modeling of inhomogeneous, lossy, and unbounded guided structures is investigated. More specifically, techniques such as variable mesh size and absorbing boundary conditions are introduced in the algorithm. The error sources, effects due to excitation, and output point location are analyzed, and suggestions are made for more efficient and accurate modeling of complicated geometries. In particular, special treatment is implemented to model curved boundaries accurately. Finally, the dispersion characteristics of various kinds of rectangular and circular guided structures are calculated using the new algorithm. It is found that the results obtained agree fairly well with those observed by theoretical or other proved numerical methods. Author (CISTI)

N94-30035 Lakehead Univ., Port Arthur (Ontario).
THE EFFECTS OF PROPAGATIONAL FACTORS ON QUANTUM WIRES IN CLOSE PARALLEL PROXIMITY M.S. Thesis
David A. Wilson Aug. 1993 52 p
(ISBN-0-315-86157-6; CTN-94-61171) Copyright Avail: Micromedia Ltd., Technical Information Centre, 240 Catherine Street, Suite 305, Ottawa, Ontario, K2P 2G8, Canada HC/MF

The propagation of an electron wave along the length of two coupled quantum wires is investigated theoretically. The quantum nature of the wires arises due to the smallness of their cross sectional area, which is usually of the order of 100 Angstroms in any direction. The wires are defined in terms of two quantum wells such that the electron motion is restricted in the direction transverse to the length of the wire and unrestricted along its length. It is assumed that the wires are sufficiently close to each other that an electron wave introduced in one of the wires is able to tunnel itself into the other. In fact, the wave could oscillate back and forth between the wires at a frequency dependent on the width and depth of the quantum wells and the distance separating the wires. The frequency would also be affected by the effective mass of the electron. It is shown that the motion of the electrons in the parallel and perpendicular directions becomes coupled and that the frequency of oscillations of the electron wave depends on the motion of the wave parallel to the wire. The frequency and the stationary state wave functions for an electron bound to two quantum wires is derived using an approach based on the time dependence of the probability amplitudes of occupancy for the electrons in one wire or the other. Numerical results are obtained and discussed. CISTI

N94-30043# Lawrence Livermore National Lab., CA.
COMMUNICATIONS TECHNOLOGY FOR UNATTENDED SENSORS
D. A. Fuess, D. W. Myers, D. M. Benzel, and J. Baker Aug. 1993 32 p
(Contract W-7405-eng-48)
(DE94-005685; UCRL-ID-114079) Avail: CASI HC A03/MF A01

The objective was to design and demonstrate proof-of-concept communication subsystems for use in unattended sensors. These designs investigated current, advanced technology for frequency synthesis and control, and the use of commercial, highly integrated radio frequency components. The three following subsystems were evaluated: (1) a synthesized (225-400 MHz) exciter/transmitter, (2) a wideband, 100-W, radio-frequency power amplifier (for boosting the level of the exciter/transmitter output), and (3) a command receiver operating in the 240-270 MHz satellite communication band. These subsystems were integrated into a prototype sensor system. Software was written using the Lawrence Livermore National Laboratory's Modular Intelligent Sensor System (MISS) specification for microprocessor control of these communication elements. Operation of the sensor system using these subsystems was demonstrated. DOE

N94-30094* International Centre for Theoretical Physics, Trieste (Italy).
FREQUENCY DEPENDENCE OF POLARIZATION PHASE DIFFERENCE
K. S. Rao, Y. S. Rao, and J. R. Wang Sep. 1993 23 p Sponsored by NASA and DOE Limited Reproducibility: More than 20% of this

document may be affected by microfiche quality
(NASA-TM-109737; NAS 1.15:109737; DE94-608113; IC-93/292) Avail: CASI HC A03 (US Sales Only)

Polarimetric AIRSAR data of July 13, 1990 acquired over Mahatango watershed area was processed for the identification of corn fields and forested areas. Polarization Phase Difference (PPD) values were computed for the corn fields at P-, L- and C- bands and studied as a function of frequency. The results compare well with the model calculations at 24 deg. incidence angle where as the locations of corn fields were computed to be at 35 deg. incidence angle. The discrepancy is attributed to lack of accurate ground truth and the undulating topography of the corn fields. Another study reported here deals with the usefulness of Polarization Index (PI) for the study of vegetation. PI was found to be dependent on frequency for corn fields where as for forest trees no such dependence was noticed. PI(sub HH,HV) is more useful parameter compared to PI(sub HH,VV) even for the study of corn fields. DOE

N94-30105# Oak Ridge National Lab., TN.
THREE-DIMENSIONAL EFFECTS FOR RADIO FREQUENCY ANTENNA MODELING
M. D. Carter, D. B. Batchelor, and D. C. Stallings Sep. 1993 36 p
(Contract DE-AC05-84OR-21400)
(DE94-006102; ORNL/TM-12464) Avail: CASI HC A03/MF A01

Electromagnetic field calculations for radio frequency (RF) antennas in two dimensions (2-D) neglect finite antenna length effects as well as the feeders leading to the main current strap. Comparisons with experiments indicate that these 2-D calculations can overestimate the loading of the antenna and fail to give the correct reactive behavior. To study the validity of the 2-D approximation, the Multiple Antenna Implementation System (MAntIS) has been used to perform 3-D modeling of the power spectrum, plasma loading, and inductance for a relevant loop antenna design. Effects on antenna performance caused by feeders to the main current strap, conducting sidewalls, and finite phase velocity are considered. The plasma impedance matrix for the loading calculation is generated by use of the ORION-1D code. The 3-D model is benchmarked with the 2-D model in the 2-D limit. For finite-length antennas, inductance calculations are found to be in much more reasonable agreement with experiments for 3-D modeling than for the 2-D estimates. The modeling shows that the feeders affect the launched power spectrum in an indirect way by forcing the driven RF current to return in the antenna sidewalls rather than in the plasma as in the 2-D model. Thus, the feeders have much more influence than the plasma on the currents that return in the sidewall. It has also been found that poloidal dependencies in the plasma impedance matrix can reduce the loading from that predicted in the 2-D model. For some plasma parameters, the combined 3-D effects can lead to a reduction in the predicted loading by as much as a factor of 2 from that given by the 2-D model. DOE

N94-30106# Lawrence Livermore National Lab., CA.
A PHYSICAL OPTICS MODEL FOR SCATTERING OF HF RADIATION BY IRREGULAR TERRAIN
G. J. Burke Jan. 1994 8 p Presented at the 10th Annual Review of Progress in Applied Computational Electromagnetics, Monterey, CA, 21-26 Mar. 1994
(Contract W-7405-eng-48)
(DE94-006187; UCRL-JC-115241; CONF-940366-1) Avail: CASI HC A02/MF A01

Physical optics models were developed for scattering of HF radiation by irregular terrain when an antenna is located on or near the scattering surface. The primary interest was in skywave radiation patterns for communication links using the ionosphere. Second-order reflections were included in the solution through an image approximation, and the UTD result for an impedance half-plane was used to reduce reflections due to truncating the current distribution on the surface. Arbitrary 2-D or 3-D terrain profiles can be entered into the codes, and the source can be an antenna with currents generated by the NEC method-of-moments code or a point source. Results were validated by comparing with 2-D integral equation solutions for actual terrain contours. DOE

N94-30153# Aerospatiale Aquitaine, Saint-Medard en Jalles (France). Div. Systemes Balistiques et Spatiaux.
MEASUREMENT BASIS OF NEAR FIELDS IN SPHERICAL COORDINATES IN THE 100 MHz TO 6 GHz BAND [BASE DE MESURE DE CHAMPS PROCHES EN COORDONNEES SPHERIQUES DANS LA BANDE 100 MHZ - 6 GHZ]
G. Cottard (Societe d'Applications Technologiques de l'Imagerie Microone, Les Ulis, France.), P. Berthaud (Societe d'Applications Technologiques de l'Imagerie Microone, Les Ulis, France.), M. Raymond, P. Lahitte, E. Fragonas, J. C. Balomey, and D. Picard 1993 9 p In FRENCH
(Rept-932-430-107; ETN-94-95465) Avail: CASI HC A02/MF A01

The measurement of near fields in spherical coordinates is described. The low part of the band (100 to 450 MHz) is covered by a mechanical displacement probe system. The higher part (1.5 to 6 GHz) is covered by a network of semicircular probes. The feasibility of near fields for the lowest frequencies is considered, the constituent measurement equipment is described, and the first qualification results obtained with the reference antennas are presented. ESA

N94-30172 Academy of Sciences (USSR), Novosibirsk.
ON DETERMINATION OF A MOMENTUM OF ALFVEN WAVE PACKET
V. N. Khudik 1992 14 p In RUSSIAN Limited Reproducibility: More than 20% of this document may be affected by microfiche quality
(DE94-608329; IYaF-92-15) Avail: CASI HC A03 (US Sales Only)

Different determinations of the momentum of a wave disturbance are considered. The determinations correspond the invariance of the Lagrange function relative to different shear transformations in magnetic hydrodynamics. It is shown that the value of the Alfven wave packet momentum, calculated on the base of the used in continuous media electrodynamics determination, does not coincide with the total momentum of medium particles and electrodynamic field in the region of packet localization. DOE

N94-30240 Ottawa Univ. (Ontario). Dept. de Genie Electrique.
DIGITAL PULSE COMPRESSION AND ITS APPLICATION IN REDUCING RADAR INTERFERENCE M.S. Thesis [LA COMPRESSION D'IMPULSION NUMERIQUE ET SON APPLICATION POUR REDUIRE LE BROUILLAGE RADAR]
Martin Blanchette 1992 129 p In FRENCH
(ISBN-0-315-85767-6; CTN-94-61164) Copyright Avail: Micromedia Ltd., Technical Information Centre, 240 Catherine Street, Suite 305, Ottawa, Ontario, K2P 2G8, Canada HC/MF

Pulse compression is a technique which allows improvement in detecting radar targets while preserving a good resolution power at a distance. This technique consists in transmitting a longer coded pulse and receiving it with a filter adapted to the code transmitted. Digital systems of pulse compression can possess a wider variety of codes than analog systems and can use a new code at each transmission. These two advantages are combined to reduce radar noise. The performance of digital pulse compression is evaluated for different types of radar interference. To counter certain types of interference such as replication of code, it is necessary to use a new code at each transmission. Two types of codes are studied: biphase pseudorandom codes and polyphase codes derived from linear frequency modulated signals or chirp. Supplementary methods, such as cumulative detection and coherent integration of a salvo of pulses, are sometimes needed to supress interference residuals. Digital pulse compression was also applied in real time and the results are supported by computer simulations and by tests on an experimental prototype. CISTI

N94-30374 Universiteit Twente, Enschede (Netherlands). Tele-Informatics and Open Systems Group.
PERFORMANCE ISSUES OF SIGNALLING PROTOCOLS FOR BROADBAND ISDN
Xinli Hou and Ignas G. Niemegeers 1993 14 p Sponsored in part by EEC Limited Reproducibility: More than 20% of this document may be affected by microfiche quality
(ISSN 0924-3755)
(Memo-INF-93-30; TIOS-93-18; ETN-94-95602) Copyright Avail: Issuing Activity (European Space Agency (ESA))

The impact of concepts and services of Broadband Integrated Services Digital Networks (B-ISDN) on the definition of performance measures for

signaling systems is addressed. The approach to the development of performance measures is given, followed by the message flow model of signaling in B-ISDN. Proposals on the performance measure definition and ways to include user response times are presented. The potential improvement of resource utilization in B-ISDN, due to the functional separation of the call and bearer control, is studied. ESA

N94-30392 National Aerospace Lab., Amsterdam (Netherlands). Aerodynamics Div.

COMPARISON OF RCS PREDICTION TECHNIQUES, COMPUTATIONS AND MEASUREMENTS

M. G. E. Brand, L. J. vanEwijk, F. Klinker, and H. Schippers 14 Jul. 1992 16 p Presented at the International Conference on Computation in Electromagnetics, London, England, 26-27 Nov. 1991 Sponsored in part by Ministry of Defence Limited Reproducibility: More than 20% of this document may be affected by microfiche quality

(PB94-125515; NLR-TP-92288-U; ETN-94-95590) Avail: CASI HC A03

Three calculation methods to predict radar cross sections (RCS) of three dimensional objects are evaluated by computing the radar cross sections of a generic wing inlet configuration. The following methods are applied: a three dimensional high frequency method, a three dimensional boundary element method, and a two dimensional finite difference time domain method. The results of the computations are compared with the data of measurements. ESA

N94-30398 National Aerospace Lab., Amsterdam (Netherlands). Informatics Div.

LOW FRAME RATE VIDEO CODING FOR SMALL BANDWIDTH REALTIME MULTIMEDIA TELE-EDUCATION SYSTEMS

T. Algra 29 Jun. 1992 11 p Presented at the IEEE Africon 1992 Conference, Swaziland, 22-24 Sep. 1992 Limited Reproducibility: More than 20% of this document may be affected by microfiche quality

(PB94-125531; NLR-TP-92270-U; ETN-94-95587) Avail: CASI HC A03

A Low Frame Rate Video Coding method (LFVC), which was developed as a subsystem for a real time tele-education terminal, is presented. It encompasses a fast and efficient coding scheme, appropriate for software implementation, and aimed at narrow bandwidths. The method applies two level conditional replenishment in combination with Mean Separating Vector Quantizing (MSVQ) and Modified Tunstall Codiding (MTC), (a form of variable to fixed length coding). ESA

N94-30495# Advisory Group for Aerospace Research and Development, Neuilly-Sur-Seine (France).

ATMOSPHERIC PROPAGATION EFFECTS THROUGH NATURAL AND MAN-MADE OBSCURANTS FOR VISIBLE TO MM-WAVE RADIATION [LES EFFETS DES CONDITIONS DEFAVORABLES DE PROPAGATION SUR LES SYSTEMES OPTIQUES, IR ET A ONDES MILLIMETRIQUES]

Nov. 1993 205 p In ENGLISH and FRENCH Presented at the Electromagnetic Wave Propagation Panel Symposium, Palma de Mallorca, Spain, 17-20 May 1993

(AGARD-CP-542; ISBN-92-835-0727-4) Copyright Avail: CASI HC A10/MF A03

This publication reports the papers presented to a specialists' meeting held by the Electromagnetic Wave Propagation Panel at its Spring 1993 meetings. The topics covered include: the effects of natural obscurants (haze, clouds, fog, rain, snow and dust) on system performance; the effects of man-made smokes, battlefield-induced smokes and enhanced scintillation on system performance; atmospheric effects on target and background signatures, and target to background contrast; multispectral camouflage -- weather-related propagation effects on camouflage and obscurants effectiveness and contrast reduction, and theoretical and/or experimental evaluation of camouflage effectiveness; systems mitigation aspects -- methods to mitigate the above-mentioned factors, e.g., image processing, sensor fusion, tactical weather intelligence, and tactical decision aids. For individual titles, see N94-30496 through N94-30514.

N94-30496# Florence Univ. (Italy).

EVALUATION OF DUAL POLARIZATION ATTENUATION OF MILLIMETER FREQUENCIES THROUGH A METEOROLOGICAL RADAR

D. Giuli, L. Baldini, L. Facheris, and P. Mazzetti *In* AGARD, Atmospheric Propagation Effects Through Natural and Man-Made Obscurants for Visible to MM-Wave Radiation Nov. 1993 9 p (For primary document see N94-30495 08-32)

Copyright Avail: CASI HC A02/MF A03

The possibility of exploiting measurements obtained through a C-band dual polarization radar is examined, as an auxiliary tool for the planning of radio relays operating at millimeter frequencies. C-band weather radars, though featuring several advantages related to their cost and reduced size, provide partially attenuated rainfall measurements with respect to their S-band counterparts. However, good reliability of rainfall rates based on C-band dual polarization measurements is achieved after proper processing based on iterative procedures for propagation attenuation due to rain. A simulation program has been utilized to provide synthetic rainfall and C-band dual polarization reflectivity data related to several storms, corresponding to different meteorological conditions. Simulated data, after proper correction of radar data, have been utilized to evaluate path attenuation statistics useful to predict fading at millimeter frequencies and related outage probability. Results show that a C-band radar can be profitably exploited for the purpose, prediction being feasible under different space-time rain patterns. On the other hand, the analysis has shown that differential reflectivity is not so essential for the aforementioned purpose as absolute reflectivity, even if it could be utilized with success in real contexts for the identification of hydrometeors (hail, graupels, wet snow) other than rain, which may be responsible for more pronounced scattering and absorption phenomena. Author (revised)

N94-30497# National Telecommunications and Information Administration, Boulder, CO. Inst. for Telecommunication Sciences.

PROPAGATION MODELING OF MOIST AIR AND SUSPENDED WATER/ICE PARTICLES AT FREQUENCIES BELOW 1000 GHz

H. J. Liebe, G. A. Hufford, and M. G. Cotton *In* AGARD, Atmospheric Propagation Effects Through Natural and Man-Made Obscurants for Visible to MM-Wave Radiation Nov. 1993 11 p (For primary document see N94-30495 08-32)

Copyright Avail: CASI HC A03/MF A03

Propagation characteristics of the atmosphere are modeled for the frequency range from 1 to 1000 GHz (1 THz) by the modular millimeter-wave propagation model MPM. Refractivity spectra of the main natural absorbers (i.e., oxygen, water-vapor, suspended droplets and ice particles) are computed from known meteorological variables. The primary contributions of dry air come from 44 O2 lines. Results from extensive 60-GHz laboratory measurements of the pressure-broadened O3 spectrum were applied to update the line data base. The water-vapor module considers 34 local H2O lines plus continuum contributions from the H2O spectrum above 1 THz, which are formulated as wing response of a pseudo-line centered at 1.8 THz Cloud/fog effects are treated with the Rayleigh approximation employing revised formulations for the permittivities of water and ice. The influence of the Earth's magnetic field on O2 absorption line becomes noticeable at altitudes between 30 and 120 km. Anisotropic medium properties result, which are computed by the Zeema propagation model ZPM. Here the elements of a complex refractivity tensor are determined in the vicinity (plus or minus 10 MHz) of O2 line centers and their effect on the propagation of plane, polarized radiowaves is evaluated. A spherically stratified (0-130 km) atmosphere provides the input for the codes MPM and ZPM in order to analyze transmission and emission properties of radio paths. Height profiles of air and water vapor densities and of the geocoded magnetic field are specified. ZPM predicts polarization- and direction-dependent propagation through the mesosphere. Emission spectra of the 9+ line (61150 plus or minus 3 MHz) for paths with tangential heights ranging from 30 to 125 km are consistent with data measured by the shuttle-based millimeter-wave limb sounder MAS. Author (revised)

N94-30498# Physics and Electronics Lab. TNO, The Hague (Netherlands).

THE INFLUENCE OF THE EVAPORATION DUCT ON THE ANGLE OF ARRIVAL AND AMPLITUDE OF THE BACKSCATTERED SIGNAL FROM TARGETS LOW ABOVE THE SEA

H. Sittrop, H. Gravesteijn, and H. J. M. Heemskerk *In* AGARD, Atmospheric Propagation Effects Through Natural and Man-Made Obscurants for Visible to MM-Wave Radiation Nov. 1993 13 p (For primary document see N94-30495 08-32)

Copyright Avail: CASI HC A03/MF A03

The impact of multipath and atmospheric refractions on the amplitude,

the apparent Radar Cross Section, RCS(sub a), and the Angle of Arrival, AOA, of low altitude target radar backscatter at 9.4 GHz, can be described as typical for 3 ranges, and 3 duct height intervals, i.e., respectively 6, 10, and 19 km, and 10 m, 10-18 m and 18-26 m. The targets are tri-hedrals mounted on poles injected into the sea-bed at the above mentioned ranges. Sensor height is 23 m above normal low sea-tide and the target heights vary from 4.5 m to 8 m depending on the sea-tide. Whereas the RCS(sub a) and the AOA show opposite behavior at 10 km and at 19 km, i.e. and RCS(sub a) decrease and an AOA decrease at 10 km, both for duct heights of 18-26 m, the opposite occurs for duct heights of 10-18 m. However, in this latter case no dramatic differences occur with respect to the AOA. At the 6 km range the RCS(sub a) is persistently larger (4-8 dB) than the free-space RCS(sub o), for duct heights less than 10 m, whereas the AOA is predominantly negative for all recorded duct heights (0-26 m). On the other hand the RCS(sub a) at this range reduces from circa +6 dB to -6 dB relative to RCS(sub 0) for increasing target height and duct heights of 10-26 m. This characteristics target/duct height behavior may introduce misleading information about the type of target. Particularly at long ranges (19 km) and target heights of circa 6 m, the RCS(sub a) may be -20 dB with respect to the free-space RCS(sub o), and the AOA +.6, for duct heights of 10-26 m. Detection probability reduces significantly, and if the target is detected, the height position is entirely wrong, i.e. circa +200 m, whereas the target is only 6 m above sea. At duct heights between 10-18 m the RCS(sub a), and hence the detection probability increases at 19 km. On the other hand this RCS(sub a) can be 10-20 dB lower at 10 km, particularly at target heights between 4-6 m. A lost tract at 10 km may therefore be possible, if detection was just feasible at 19 km at these duct heights. PCPEM predictions and measurements at 5.8 km show in general a fairly comparable trend for target heights between 6-7 m, however, for duct heights of 0-18 m, a too high RCS(sub a) is predicted and for the observed duct heights of 18-25 m a too low RCS(sub a). Within the region of transition from a too high to a too low prediction, comparable values are observed. For target heights between 5.5-6 m PCPEM predicts too large values for all duct heights. Author (revised)

N94-30499# Army Research Lab., White Sands Missle Range, NM. Battlefield Environment Directorate.

MULTISPECTRAL TRANSMITTANCE MEASUREMENTS THROUGH MAN-MADE WATER FOGS

Young P. Yee, Robert A. Sutherland, and James L. Cogan *In* AGARD, Atmospheric Propagation Effects Through Natural and Man-Made Obscurants for Visible to MM-Wave Radiation Nov. 1993 7 p (For primary document see N94-30495 08-32)

Copyright Avail: CASI HC A02/MF A03

A fog system capable of producing water droplets with diameters between 5 and 40 micrometers was used for multispectral transmittance measurements. Measurements were conducted at an arid, desert field location on the White Sands Missile Range, New Mexico. The fog system consists of a supply of local tap water, 50 gallon holding barrels, high pressure hoses and connectors, and an array of specially designed spray nozzles. The spray nozzles have precision made .006-inch diameter orifices. Water under 1000 psi of pressure is forced through the small orifice and impacts onto a curved metal pin causing droplet formation and dispersion. Droplet size distribution of the man-made fog were measured by forward scattering particle-measuring instruments. The advantages of using the fog generation system are low energy requirements, high rates of droplet production, environmentally safe dispersion, and commercial availability. Transmittance measurements were taken by a Multi-Path Transmissometer/Radiometer (MPTR). The MPTR is capable of obtaining transmittances at .4-.7 micron, 1.0-1.1 micron, 3.5-4.8 micron, and 7.9-12.3 micron spectral bands. Results will be presented on transmittance comparisons between the different wavelength bands during varying fog density conditions. The transmittance data from the line of sight were tested for optical depth linearity in the various wavelength bands. Author

N94-30500# Army Research Lab., White Sands Missle Range, NM. Battlefield Environment Directorate.

ESTIMATION OF TRANSMITTANCE FROM SATELLITE IMAGERY

James Cogan and David Williams *In* AGARD, Atmospheric Propagation Effects Through Natural and Man-Made Obscurants for Visible to MM-Wave Radiation Nov. 1993 10 p (For primary document see N94-30495 08-32)

Copyright Avail: CASI HC A02/MF A03

Transmittance in the visible and thermal infrared may be estimated from a variety of in-situ and remote techniques using ground-based or airborne sensors. However, estimation of transmittance in the troposphere from data gathered by sensors on space platforms remains a problem, especially over land surfaces. This paper presents two preliminary methods: one to compute visibility using changes in contrast from a series of luminance images or measuring changes in the nonzero frequency amplitudes from the associated frequency domain images, and the other to calculate thermal infrared transmittance over a horizontal, vertical, or slant path that uses estimates of precipitable water from satellite data, combined with sounding data from satellite or other sources. Author

N94-30501# Arsenal du Materiel Mechanique et de l'Armement, Rocourt (Belgium).

AN EXPERIMENTAL AND COMPREHENSIVE METHOD TO MEASURE EMISSION CHARACTERISTICS [UNE METHODE EXPERIMENTALE ET GLOBALE DE MESURE DE L'EMISSIVITE]

R. Marchal *In* AGARD, Atmospheric Propagation Effects Through Natural and Man-Made Obscurants for Visible to MM-Wave Radiation Nov. 1993 8 p In FRENCH; In FRENCH (For primary document see N94-30495 08-32)

Copyright Avail: CASI HC A02/MF A03

The characteristics of emission may be of thermal infrared multispectral processes: either through direct measurements on the emitted flux, which are compared to a reference black body, or through measurements on reflectivity and application of the Kirchoff laws. Both approaches have advantages and drawbacks according to the type of emission characteristics that are studied. The method which is used in this study uses the first principle: it concerns itself with relatively high levels of emissions (greater than 0.5), which are directional and controlled by a given sensor. In order to maximize the precision of measurements, testing respects the following conditions: (1) lessening of residual parasite flux, through the use of low emission materials and a cooled diaphragm, thus creating a confined enclosure; (2) taking into account the residual parasite flux, through models of radiation exchange within the enclosure; (3) assessment of the homogeneity in temperature of both the sample and the reference materials; and (4) calculations on the confidence levels, in function of the variances in the beginning parameters. This use of models, added to technical advances, make it possible to build a very inexpensive test site, at least as far as specific purchases were concerned. Several comparative measurements showed that the range of measurable emissions goes from 0.5 to 1, with an absolute confidence level of 0.05 to 0.02, according to the material. The best performance was obtained when highly emissive and highly heat conductive materials were used. Transl. by FLS

N94-30502# Physics and Electronics Lab. TNO, The Hague (Netherlands).

EXPERIMENTAL EVALUATION OF CAMOUFLAGE EFFECTIVENESS IN THE THERMAL INFRARED **c74**

Pieter A. M. Jacobs *In* AGARD, Atmospheric Propagation Effects Through Natural and Man-Made Obscurants for Visible to MM-Wave Radiation Nov. 1993 12 p (For primary document see N94-30495 08-32)

Copyright Avail: CASI HC A03/MF A03

The detectability of a target in the infrared spectral region is determined by differences between the radiative signatures of the target and the local background. This implies that both, the difference in surface temperature and emissivity Delta T resp. Delta epsilon and the distribution of these differences over the target area and the background, are of major importance. Therefore camouflage measures have to address both issues in order to achieve maximum signature adaptation to the background. To determine the ability of a camouflage material to follow temperature changes in the background, measurements of camouflage and background temperatures have to be performed under a variety of meteorological conditions. Measurements of representative weather and background conditions are needed to determine those situations, where the camouflage material effectively reduces the target signature. The degree of temperature reduction depends on the required level of protection, that is for detection, recognition and identification. Statistical analyses are given for various camouflage materials in relation to a number of background elements. Camouflage effectiveness is expressed in the percentage of time for which the apparent

temperature contrast between the camouflage material and a background element is 1, 2 or 5 C. Analyses are performed for five consecutive weeks of measurements in summer and winter, using data which were taken during a measurement campaign at Gilze Rijen air force base in 1990.
Author

N94-30503# Ministry of Defence, London (England). Chemical and Biological Defence and Pyrotechnics.
NATO SOCMET TRIALS
C. M. Jenden *In* AGARD, Atmospheric Propagation Effects Through Natural and Man-Made Obscurants for Visible to MM-Wave Radiation Nov. 1993 4 p (For primary document see N94-30495 08-32)
Copyright Avail: CASI HC A01/MF A03

During 1993, Canada, France, Germany and the United Kingdom will be participating in the Smoke and Obscurants Countermeasures Materials Evaluation Tests (SOCMET). The tests will be carried out under the auspices of the NATO Army Armaments Group, AC/225, Panel VI, Sub-Panel 7 whose interests include multispectral smoke screening systems. The tests will comprise two sets of trials; one under cold climate conditions in Quebec, Canada, during February/March 1993 and the other in temperate conditions in Bourges, France during September 1993. This paper provides an insight into the management and aims of SOCMET. The evaluations will be seeking to identify candidate materials which create effective obscurant screens in the visible, infrared and millimetric bands of the electromagnetic spectrum. These materials will be disseminated through a range area dispersal. A key element of the trials will be the evaluation of field test instrumentation which may eventually lead to the development of standardized evaluation techniques. Following the trials, a scientific workshop will be held to review the results. A final report will be presented to NATO which will form the basis of future collaborative developments on multispectral screening systems leading towards standard NATO documentation on smoke and obscurant systems.
Author

N94-30504# Belgian Army, Peutie.
GLOBAL APPROACH TOWARDS THE EVALUATION OF THERMAL INFRARED COUNTERMEASURES **c74**
Patrick Verlinde and Philippe Wilms *In* AGARD, Atmospheric Propagation Effects Through Natural and Man-Made Obscurants for Visible to MM-Wave Radiation Nov. 1993 8 p (For primary document see N94-30495 08-32)
Copyright Avail: CASI HC A02/MF A03

This paper proposes a procedure for the numerical evaluation of the efficiency of countermeasures in the thermal infrared. This procedure consists of three phases. In the first phase the characteristics of different thermal camouflage materials are tested on a lab-scale. These tests comprise measurements of the attenuation of the incident infrared energy and/or of the thermal emissivity factor. With respect to the attenuation measurement, a calibrated infrared sensor is used, to determine the radiation patterns of an object. The comparison of these patterns before and after the application of a camouflage system, gives an absolute measure of its attenuation. The result of this measurement is important since the attenuation is closely related to the contrast between the camouflaged object and its background and thus to the probability of detection. Contrast however, is not the only important feature for the detection of an object in a thermal image. That is why in a second phase the countermeasures under evaluation are tested in a real environment. During this phase, a numerical value is given to the efficiency of the considered camouflage in the thermal infrared, using features selected from those which are known to be important for human vision. These include, besides contrast, other features such as correlation and texture. The third and final phase aims at a verification and a validation of the test results. Indeed, it is of crucial importance to find a link between the performance obtained in the field and the characteristics measured on a lab-scale. It is also necessary to verify that a good correlation exists between the efficiency as determined by human observers and the result of this numerical evaluation procedure. This will be done using a database of thermal images taken with a GEC Avionics TICM II (8 to 12 micron). Those images are then presented as well to human observers as to the machine in a project called 'Psychotest'.
Author

N94-30505# Army Research Lab., Aberdeen Proving Ground, MD.
THE EFFECTS OF MAN-MADE SMOKES AND BATTLEFIELD-INDUCED SMOKES ON THE PROPAGATION OF ELECTROMAGNETIC RADIATION
Anthony VandeWal *In* AGARD, Atmospheric Propagation Effects Through Natural and Man-Made Obscurants for Visible to MM-Wave Radiation Nov. 1993 6 p (For primary document see N94-30495 08-32)
Copyright Avail: CASI HC A02/MF A03

This paper provides an unclassified overview of the U.S. Army program that collects and disseminates information about the effects of battlefied smokes and obscurants on weapon system performance. The primary mechanism for collecting field data is an annual exercise called SMOKE WEEK. In SMOKE WEEK testing, a complete characterization is made of the ambient test conditions, of the electromagnetic radiation propagation in clear and obscured conditions, and of the obscuring cloud that the particles that comprise the cloud. This paper describes the instrumentation and methodology employed to make these field measurements, methods of analysis, and some typical results. The effects of these realistic battlefield environments on weapons system performance are discussed generically.
Author

N94-30506# Defence Research Agency, Malvern (England).
INFRARED POLARIZATION SIGNATURES
D. L. Jordan and G. Lewis *In* AGARD, Atmospheric Propagation Effects Through Natural and Man-Made Obscurants for Visible to MM-Wave Radiation Nov. 1993 6 p (For primary document see N94-30495 08-32)
Copyright Avail: CASI HC A02/MF A03

Target detection using passive electro-optic devices operating in the 8 to 14 micron band is often limited by background clutter. A possible method of overcoming this limitation may be to use the polarization content of the image to discriminate between man-made targets and natural background. Laboratory measurements are presented of the polarization state of 10 to 6 micron radiation reflected from, and emitted by, a range of materials. It is concluded that elliptical polarization is not of primary importance and that measurements of the degree of linear polarization appear to provide useful discrimination between man-made objects and 'natural' ones.
Author (revised)

N94-30507# Centre d'Etudes et de Recherches, Toulouse (France).
MODEL FOR THE SIMULATION OF ATMOSPHERIC EFFECTS ON TARGETS TO BACKGROUND PASSIVE SIGNATURES [MODELE POUR LA SIMULATION DES EFFETS ATMOSPHERIQUES SUR LES SIGNATURES PASSIVES DE CIBLES DANS LEUR ENVIRONNEMENT]
C. Wallez, J. Lemorton, P. F. Combes, and F. Christophe *In* AGARD, Atmospheric Propagation Effects Through Natural and Man-Made Obscurants for Visible to MM-Wave Radiation Nov. 1993 12 p In ENGLISH and FRENCH (For primary document see N94-30495 08-32)
Copyright Avail: CASI HC A03/MF A03

In order to assess very accurately the performances of millimeter wave imaging passive systems, efforts have been made towards the development of a straightforward easy to use computer code. This simulation model has been used to evaluate the influence of meteorological conditions on radiometric contrasts. The following parameters are studied: frequency, terrain emissivity, and radiometer position. A first set of simulations is done in the scatter-free atmosphere assumption. Then scattering by hydrometeors is taken into account. In each case, ground surface discrimination by their radiometric temperature is discussed.
Author (revised)

N94-30508# Defence Research Agency, Malvern (England).
THE EFFECT OF ENHANCED BACKSCATTERING ON TARGET DETECTION
E. Jakeman, J. P. Frank, and G. J. Balmer *In* AGARD, Atmospheric Propagation Effects Through Natural and Man-Made Obscurants for Visible to MM-Wave Radiation Nov. 1993 8 p (For primary document see N94-30495 08-32)
Copyright Avail: CASI HC A02/MF A03

Error probabilities are calculated for the detection of a target illuminated through a random medium in the presence of ambient noise. Comparisons are made between monostatic operation, in which double passage of the radiation leads to an enhanced amplitude and fluctuation of the received

signal, and bistatic operation, where the outward and return radiation paths traverse uncorrelated regions of the intervening random medium. It is shown that although common transmit/receive optics are advantageous in the case of low signal to noise ratios, in normal regimes of operation a bistatic arrangement leads to lower total error probability, particularly when the scattering medium generates strong scintillation in the target plane.
Author (revised)

N94-30509# Massachusetts Univ., Amherst. Microwave Remote Sensing Lab.
POLARIMETRIC BACKSCATTER MEASUREMENTS OF NATURAL SURFACES AT MILLIMETER WAVELENGTHS
James Mead, Paul Chang, and Robert McIntosh *In* AGARD, Atmospheric Propagation Effects Through Natural and Man-Made Obscurants for Visible to MM-Wave Radiation Nov. 1993 10 p (For primary document see N94-30495 08-32)
Copyright Avail: CASI HC A02/MF A03

During the last four years, the Microwave Remote Sensing Laboratory of the University of Massachusetts has studied the polarimetric backscatter response of natural and man-made surfaces at 35, 95, and 225 GHz. These surfaces include grass, asphalt, snowcover, and trees. In addition, ground-based and airborne backscatter measurements of clouds and precipitation were made at 95 GHz. The results of these experiments are summarized by presenting histograms of normalized radar cross section for trees, snowcover, and clouds. The temporal dependence of the normalized radar cross section for snowcover is also presented for 95 and 225 GHz which shows a strong diurnal variation due to melting and refreezing. Also presented is the angular dependence of backscatter from grass and asphalt at 35, 95, and 225 GHz, as well as volume backscattering coefficients for airborne measurements of clouds and precipitation at 96 GHz.
Author (revised)

N94-30510# Michigan Univ., Ann Arbor. Radiation Lab.
A HYBRID ELECTROMAGNETIC-STATISTICAL APPROACH FOR CHARACTERIZING MMW SCATTERING BY TERRAIN
Fawwaz T. Ulaby, Paul Siqueira, and Kamal Sarabandi *In* AGARD, Atmospheric Propagation Effects Through Natural and Man-Made Obscurants for Visible to MM-Wave Radiation Nov. 1993 8 p (For primary document see N94-30495 08-32)
Copyright Avail: CASI HC A02/MF A03

The performance of millimeter wave (MMW) radar systems in target detection, navigation, and other applications depends in part on the scattering characteristics of the terrain background. Two different approaches have been pursued in the literature for characterizing MMW scattering by terrain. The first approach relies on the development of electromagnetic scattering models that relate the backscattering coefficient sigma of a given terrain type (such as bare ground surfaces, snow cover, and vegetation) to the physical properties of the terrain target, and then verifying model predictions though experimental observations conducted under semicontrolled field conditions. The second approach is entirely empirical in nature; it relies on the acquisition of extensive radar data from which statistical distributions are generated. This paper provides an overview of how the hybrid approach can be used to simulate the statistical properties of terrain backscatter at millimeter wavelengths for several types of terrain, including bare soil surfaces, vegetation, and snow cover. The hybrid approach incorporates scintillation effects associated with coherent sensors together with information about the mix of terrain categories present in the scene. Two types of input data (or a merged set of both) can be used as input to the clutter simulation package: measured data that is available in a University of Michigan data base or data generated by electromagnetic models. The data base is available as a handbook that contains MMW scattering observations reported in the literature for certain terrain types and conditions. Alternatively, a set of electromagnetic models can be used for calculating the backscattering coefficient sigma of the specified terrain type. These models, which are semiempirical in form, are based on highly complicated theoretical models that had been tested against experimental observations. With this approach, it is possible to generate a probability density function for the backscatter from a certain type of terrain without the need for a measured clutter data base. This is particularly attractive at millimeter wavelengths because only a limited amount of terrain clutter data is currently available.
Author

N94-30511# Centre d'Etudes et de Recherches, Toulouse (France).
GRANULOMETRY IN ENVIRONMENTS WITH VERY SMALL PARTICLE CONCENTRATIONS [GRANULOMETRIE DE MILIEUX A FAIBLE CONCENTRATION DE PARTICULES]
A. Delfour, B. Guillame, and Alain P. Junchat *In* AGARD, Atmospheric Propagation Effects Through Natural and Man-Made Obscurants for Visible to MM-Wave Radiation Nov. 1993 10 p In FRENCH; In FRENCH (For primary document see N94-30495 08-32)
Copyright Avail: CASI HC A02/MF A03

The principle of granulometry through particle light diffusion in environments with very low levels of concentration was studied. A model was built and its response, when particles were randomly distributed in the measured volume, was numerically simulated. Atmospheric, urban, rural, and seaside conditions were used in models with extended ranges of concentration. Several wavelengths of light were tested. Atmospheric aerosol granulometry is feasible if the concentration per volume is greater than or equal to 10(exp -5) ppm, and if the light wavelength is of the same order as the average size of the particles. The particles' contribution to atmospheric visibility may be measured if a preliminary calibration of the detection system is put into place. Laboratory equipment was used to validate the use of models. In order to simulate the appropriate particles' concentration, a 10 dm(exp 3) test chamber was built. Experiments, conducted with licopode powder (25 to 35 micron in diameter) in known concentration per volume, were correctly reproduced.
Transl. by FLS

N94-30512# Army Research Lab., Adelphi, MD.
RADAR CROSS SECTIONS OF GROUND CLUTTER AT 95 GHz FOR SUMMER AND FALL CONDITIONS
R. J. Wellman, D. R. Hutchins, J. L. Silvious, H. Dropkin, G. Goldman, J. Nemarich, D. A. Wikner, and R. K. Dahlstrom *In* AGARD, Atmospheric Propagation Effects Through Natural and Man-Made Obscurants for Visible to MM-Wave Radiation Nov. 1993 12 p (For primary document see N94-30495 08-32)
Copyright Avail: CASI HC A03/MF A03

Radar cross section (RCS) measurements were made on an extensively instrumented ground-clutter patch over a period of one month from late summer to early fall. The instrumentation allowed collection of a full set of data on meteorological conditions, solar flux, and soil moisture content. The RCS measurements were made using a 95-GHz, polarimetric, monopulse instrumentation radar. The radar is all solid-state, coherent, frequency steppable over a 640-MHz bandwidth, and completely polarimetric for linearly or circularly polarized radiation. The clutter area measured was located in Grayling, Michigan, and consisted of a rectangular patch of ground, 50 by 100 m in area, at a range of about 100 to 250 m from the radar. The clutter patch included areas of bare sandy ground, short grass, low shrubs, evergreen trees, and deciduous trees and was similar to a NATO European environment. A wide range of atmospheric conditions were observed over the measurement period, including a few days of measurable snowfall. The paper describes analysis of the effects of different clutter types and different atmospheric conditions on the measured RCS of the clutter patch.
Author (revised)

N94-30513# Royal Military Academy, Brussels (Belgium). Electrical Engineering Dept.
KNOWLEDGE COMBINATION AND DATA FUSION WITH APPLICATION TO RECOGNITION SYSTEMS **c61**
Christiaan Perneel, Michel deMathelin, and Marc Acheroy *In* AGARD, Atmospheric Propagation Effects Through Natural and Man-Made Obscurants for Visible to MM-Wave Radiation Nov. 1993 10 p (For primary document see N94-30495 08-32)
Copyright Avail: CASI HC A02/MF A03

The fuzzy logic theory is used to derive knowledge combination rules for heuristic search algorithms and data fusion problems. Heuristic search algorithms are especially designed for expert systems which have to explore a large solution space in a limited amount of time. Therefore, search algorithms using heuristic knowledge are designed to limit the exploration of the solution space while preserving some quality in the results. An automatic target recognition expert system was designed using this approach. However, the fuzzy logic approach could be applied to other types of expert systems and to data fusion problems.
Author (revised)

N94-30514# Bilkent Univ., Ankara (Turkey). Dept. of Electrical and Electronics Engineering.
CALCULATION OF TURBULENCE DEGRADED POINT SPREAD FUNCTION OF AN IMAGING SYSTEM
G. Saplakoglu, F. Erden, and A. Altintas *In* AGARD, Atmospheric Propagation Effects Through Natural and Man-Made Obscurants for Visible to MM-Wave Radiation Nov. 1993 7 p (For primary document see N94-30495 08-32)
Copyright Avail: CASI HC A02/MF A03

The point spread function (PSF) of a turbulence degraded imaging system is statistically characterized. In particular, sufficient data and functional fits are given for the calculation of long exposure average PSF and optical transfer function (OTF). Methods are presented for the calculation of second order statistics of PSF. Author (revised)

N94-30518 National Aerospace Lab., Amsterdam (Netherlands). Informatics Div.
END-TO-END DELAY REDUCTION IN NARROW BANDWIDTH REAL-TIME MULTIMEDIA TELE-EDUCATION APPLICATIONS
Theo Algra 23 Feb. 1993 13 p Presented at the EOS/SPIE International Symposium on Fiber Optic Networks and Video Communication, Berlin, Germany, 5-8 Apr. 1993 Limited Reproducibility: More than 20% of this document may be affected by microfiche quality
(AD-B179614; NLR-TP-93069-U; ETN-94-95968) Avail: Issuing Activity (European Space Agency (ESA))

The transmission of multimedia page sequences in real time tele-education presentations via narrowband links results in unacceptable end to end delays. A time shifting method referred to as pretransfer which transfers presentation data in background during the session, without user involvement is proposed. Point to point and multipoint protocols are discussed. For multicast situations an effective page scheduling method is developed. ESA

N94-30520 Universiteit Twente, Enschede (Netherlands). Tele-Informatics and Open Systems Group.
DESIGN AND ANALYSIS OF DYNAMIC LEADER ELECTION PROTOCOLS IN BROADCAST NETWORKS
Jacob Brunekreef (Amsterdam Univ., Netherlands.), Joost-Pieter Katoen, Ron Koymans, and Sjouke Mauw 8 Sep. 1993 79 p Limited Reproducibility: More than 20% of this document may be affected by microfiche quality
(ISSN 0924-3755)
(Memo-INF-93-43; TIOS-93-26; ETN-94-95717) Copyright Avail: CASI HC A05

The problem of leader election in distributed systems is considered in a dynamic context where processes may participate and crash spontaneously. Processes communicate by means of buffered broadcasting as opposed to usual point to point communication. A leader election protocol in such a dynamic system is designed. As the problem at hand is considerably complex, a step wise refinement design method starting from a simple leader election protocol is adopted. In a first refinement a symmetric solution is obtained and eventually a fault tolerant protocol is constructed. This gives rise to three protocols. The worst case message complexity of all protocols is analyzed. A formal approach to the verification of the leader election protocols is adopted. The requirements are specified in a property oriented way and the protocols are denoted by means of extended finite state machines. It is proven using linear time temporal logic that the protocols satisfy their requirements. The protocols are specified in more detail in the process algebra formalism ACP (Algebra of Communicating Processes). ESA

N94-30772 Sandia National Labs., Albuquerque, NM.
MODELING DATA THROUGHPUT ON COMMUNICATION NETWORKS
J. M. Eldridge Nov. 1993 16 p Limited Reproducibility: More than 20% of this document may be affected by poor print
(Contract DE-AC04-94AL-85000)
(DE94-005077; SAND-93-0871) Avail: Issuing Activity (Department of Energy (DOE))

New challenges in high performance computing and communications are driving the need for fast, geographically distributed networks. Applications such as modeling physical phenomena, interactive visualization, large data set transfers, and distributed supercomputing require high performance networking (St89)(Ra92)(Ca92). One measure of a communication network's performance is the time it takes to complete a task -- such as transferring a data file or displaying a graphics image on a remote monitor. Throughput, defined as the ratio of the number of useful data bits transmitted per the time required to transmit those bits, is a useful gauge of how well a communication system meets this performance measure. This paper develops and describes an analytical model of throughput. The model is a tool network designers can use to predict network throughput. It also provides insight into those parts of the network that act as a performance bottleneck. DOE

N94-30785 National Physical Lab., Teddington (England). Electrical Science Div.
FORMULAE FOR THE CALCULATION OF THE MAGNETIC FIELD STRENGTH IN A HELMHOLTZ SYSTEM WITH CIRCULAR COILS
P. Vigoureux Dec. 1993 14 p
(ISSN 0143-7305)
(NPL-DES-130; ETN-94-95848) Copyright Avail: Issuing Activity (National Physical Lab., Teddington, Middlesex TW11 0LW, England)

Formulae for the magnetic field strength H of a Helmholtz system of two circular coils are given. The components of H along and perpendicular to the axis are expressed in series of spherical harmonics which converge rapidly in a region around the center of the system. The formulae are normalized, and thus applicable to systems of any size. The results given are well known; they have been put together for easy reference. ESA

N94-30902# Maryland Univ., College Park. Dept. of Electrical Engineering.
MATHEMATICAL MODELS OF HYSTERESIS
I. D. Mayergoyz Sep. 1993 6 p
(Contract DE-FG05-88ER-13846)
(DE94-005681; DOE/ER-13846/6) Avail: CASI HC A02/MF A01

Progress is reported in 7 areas: development of vector Preisach-type models of hysteresis; modeling of rotational hysteretic losses; experimental testing of generalized vector Preisach models of hysteresis; development of Preisach-type models for after-effect; analytical investigation of penetration of electromagnetic fields into superconductors with gradual resistive transitions; computation of magnetic fields in hysteretic media; and development of new techniques for calculating 3-D eddy current problems. DOE

N94-30940 Politecnico di Milano (Italy). Dipt. di Elettronica e Informazione.
MPEG-2 VIDEO DECODING ARCHITECTURE: ANALYSIS AND DESIGN [UN ARCHITETTURA DI DECODIFICA VIDEO MPEG-2: ANALISI E PROGETTAZIONE]
Luca Mainetti 1993 53 p In ITALIAN
(Rept-93-069; ETN-94-95827) Avail: Issuing Activity (Politecnico di Milano, Piazza Leonardo da Vinci 32, 20133 Milan, Italy)

Analog video, video coding, and the MPEG-2 (Moving Pictures Expert Group) video decoding architecture are addressed. The architecture had to include a multimedia function (personal computer interface) for interactive (hypermedia) use. The MPEG-2 video at 10 Mbit/s bit rate has a competitive quality with professional studio video and at 3 Mbit/s bit rate offers a possibility of memorization identical to that of a casual access videodisc. ESA

N94-28927# Jet Propulsion Lab., California Inst. of Tech., Pasadena.
SYNTHETIC APERTURE RADAR APPLICATIONS: NOW AND IN THE FUTURE [SA DETA DE NANI GA WAKARUKA]
Charles Elachi *In* Earth Resources Satellite Data Analysis Center, Proceedings of the International Symposium on Remote Sensing 30 Mar. 1992 p 41-65 Original contains color illustrations (For primary document see N94-28925 08-43)
Avail: CASI HC A03/MF A03

N94-29566# Shape Technical Center, The Hague (Netherlands).
ACCS SURVEILLANCE EXPLORATORY PROTOTYPE (ASEP)
K. Gaebler *In* AGARD, Machine Intelligence in Air Traffic Management Oct. 1993 18 p (For primary document see N94-29558 08-04)
Copyright Avail: CASI HC A03/MF A04

N94-29631*# Nippon Telegraph and Telephone Public Corp., Yokosuka (Japan). Radio Communication Systems Labs.
A MODULE CONCEPT FOR A CABLE-MESH DEPLOYABLE ANTENNA
Akira Meguro *In* NASA. Ames Research Center, The 27th Aerospace Mechanisms Symposium May 1993 p 51-66 (For primary document see N94-29627 08-15)
Avail: CASI HC A03/MF A03

N94-29632*# Astro Aerospace Corp., Carpinteria, CA.
WAVES IN SPACE PLASMA DIPOLE ANTENNA SUBSYSTEM
Mark Thomson *In* NASA. Ames Research Center, The 27th Aerospace Mechanisms Symposium May 1993 p 67-82 (For primary document see N94-29627 08-15)
Avail: CASI HC A03/MF A03

N94-30673*# Beijing Inst. of Radio Metrology and Measurements (China).
MEASUREMENT OF THE FREQUENCY STABILITY OF RESPONDERS IN AIRCRAFT
Xiaofan Liu *In* NASA. Goddard Space Flight Center, The 25th Annual Precise Time and Time Interval (PTTI) Applications and Planning Meeting May 1994 p 445-456 (For primary document see N94-30639 08-70)
Avail: CASI HC A03/MF A06

N94-30675*# ESE/SEKAI, Santa Fe Springs, CA.
TIME SYNCHRONIZED VIDEO SYSTEMS
Ron Burnett *In* NASA. Goddard Space Flight Center, The 25th Annual Precise Time and Time Interval (PTTI) Applications and Planning Meeting May 1994 p 463-466 (For primary document see N94-30639 08-70)
Avail: CASI HC A01/MF A06

33 ELECTRONICS AND ELECTRICAL ENGINEERING

Includes test equipment and maintainability; components, e.g., tunnel diodes and transistors; microminiaturization; and integrated circuitry.

For related information see also *60 Computer Operations and Hardware* and *76 Solid-State Physics*.

N94-28400# Technical Research Centre of Finland, Espoo. Telecommunications Lab.
FREQUENCY-DOMAIN ANALYSIS OF NONLINEAR MICROWAVE CIRCUITS Ph.D. Thesis
T. Naerhi Jun. 1993 148 p
(PB94-132024; VTT/PUB-148; ISBN-951-38-4386-6) Copyright Avail: CASI HC A07/MF A02

A frequency-domain method is presented for the numerical steady-state analysis of nonlinear microwave circuits. Nonlinear elements are described with Chebyshev expansions or rational functions of Chebyshev expansions and their response is calculated directly in the frequency domain. Since no time-to-frequency conversions are needed, the method is especially suitable for multi-tone problems which are difficult to solve with harmonic-balance methods. Numerically stable recursive procedures allow the use of high-degree expansions for strongly nonlinear devices. The analysis method is coupled with a new measurement-based modeling approach, where the frequency-domain large-signal model is directly constructed through integration from the measured small-signal y-parameters. The resulting model is inherently consistent and allows an accurate representation of the frequency-dependent characteristics of nonlinear devices. The analysis method and modeling approach are experimentally verified by two- and three-tone measurements on a MESFET mixer. NTIS

N94-28487# Argonne National Lab., IL.
PRACTICAL SUPERCONDUCTOR DEVELOPMENT FOR ELECTRICAL POWER APPLICATIONS
Roger B. Poeppel, Kenneth C. Goretta, T. R. Askew, U. Balachandran, Y. S. Cha, J. A. DeLuca, S. E. Dorris, J. T. Dusek, W. A. Ellingson, and J. E. Emerson et al Oct. 1993 58 p
(Contract W-31-109-eng-38)
(DE94-005378; ANL-93/33) Avail: CASI HC A04/MF A01

Development of useful high-critical-temperature superconductors requires synthesis of superconducting compounds; fabrication of wires, tapes, and films from these compounds; production of composite structures that incorporate stabilizers or insulators; and design and testing of efficient components. This report describes technical progress of research and development efforts aimed at producing superconducting components in the Y-Ba-Cu, (Bi,Pb)-Sr-Ca-Cu, (Tl,Pb, Bi)-(Ba,Sr)-Ca-Cu, and Hg-Ba-Ca-Cu-O oxide systems. Topics discussed are synthesis and heat treatment of high-T(sub c) superconductors; formation of monolithic and composite wires, tapes, and coils, characterization of structures and superconducting and mechanical properties; fabrication and properties of films; and development of properties of films; and development of prototype components. Collaborations with industry and academia are documented. DOE

N94-28511*# Southern Colorado State Coll., Pueblo. Dept. of Electronics Engineering.
INVESTIGATION OF ADVANCED FAULT INSERTION AND SIMULATOR METHODS Final Technical Report, Jun. 1984 - Aug. 1986
W. R. Dunn and D. Cottrell 1986 68 p
(Contract NCC2-303)
(NASA-CR-195241; NAS 1.26:195241) Avail: CASI HC A04/MF A01

The cooperative agreement partly supported research leading to the open-literature publication cited. Additional efforts under the agreement included research into fault modeling of semiconductor devices. Results of this research are presented in this report which is summarized in the following paragraphs. As a result of the cited research, it appears that semiconductor failure mechanism data is abundant but of little use in developing pin-level device models. Failure mode data on the other hand does exist but is too sparse to be of any statistical use in developing fault models. What is significant in the failure mode data is that, unlike classical logic, MSI and LSI devices do exhibit more than 'stuck-at' and open/short failure modes. Specifically they are dominated by parametric failures and functional anomalies that can include intermittent faults and multiple-pin failures. The report discusses methods of developing composite pin-level models based on extrapolation of semiconductor device failure mechanisms, failure modes, results of temperature stress testing and functional modeling. Limitations of this model particularly with regard to determination of fault detection coverage and latency time measurement are discussed. Indicated research directions are presented. Author (revised)

N94-28546# California Univ., Berkeley. Lawrence Berkeley Lab.
FABRICATION ISSUES IN OPTIMIZING YBa(2)Cu(3)O(7-x) FLUX TRANSFORMERS FOR LOW I/f NOISE
F. Ludwig, E. Dantsker, D. T. Nemeth, D. Koelle, A. H. Miklich, J. Clarke, S. Knappe, H. Koch, and R. E. Thomson Nov. 1993 15 p Presented at the International Superconductive Electronic Conference, Boulder, CO, 11-14 Aug. 1993
(Contract DE-AC03-76SF-00098)
(DE94-005209; LBL-34878; CONF-930863-3) Avail: CASI HC A03/MF A01

We describe an improved interconnect technology for the fabrication of multiturn flux transformers from YBa(2)Cu(3)O(7-x) - SrTiO(3) - YBa(2)Cu(3)O(7-x) multilayers. The essential improvements are reductions in the thicknesses of the trilayer films, typically to 100 nm 250 nm and 250 mn respectively, and in the deposition rate, to 0.07 nm/laser pulse. This process yields crossovers in which the critical current density in the upper YBa(2)Cu(3)O(7-x) film at 77 K is (2-3) x 10(sup 6) A cm(sup -2). In situ trilayers exhibited 1/f flux noise levels at I Hz below the measurement sensitivity of 15(mu)Phi(sub 0) Hz(sup -1/2), where Phi(sub 0) is the flux quantum. However, the flux noise of trilayers in which each layer had been patterned was significantly higher. The best flip-chip magnetometer had a white noise of 40 fT Hz(sup -1/2) increasing to 340 fT Hz(sup -1/2) at I Hz; the corresponding flux noise levels were 9 (mu)Phi(sub 0) Hz(sup -I/2) and 75 (mu)Phi(sub 0) Hz(sup -I/2), respectively. DOE

N94-28585 Joint Inst. for Nuclear Research, Dubna (USSR).
THE STATIC AND NONSTATIC ELECTRICAL SOLENOIDS
G. N. Afanasev 1992 24 p Limited Reproducibility: More than 20% of this document may be affected by microfiche quality
(DE94-606326; JINR-E-2-92-132) Avail: CASI HC A03 (US Sales Only)

We propose the set of charge and current densities which realize static and nonstatic electrical solenoids. Their properties are discussed. The question on the physical meaning of the electromagnetic potentials outside the solenoids and their experimental verification remains to be opened. DOE

N94-28650 Stanford Univ., CA. Center for Integrated Systems.
LOW VOLTAGE ELECTRON BEAM LITHOGRAPHY Report, Aug. 1993 - Jan. 1994
Aaron Baum and R. F. Pease Jan. 1994 44 p Limited Reproducibility: More than 20% of this document may be affected by microfiche quality
(Contract N00014-92-J-1996)
(AD-A275648) Avail: CASI HC A03

In order to develop a low-energy-spread, high brightness electron source using negative electron affinity technology, it is necessary to survey the effects of cathode structure and activation on energy spread, lateral velocity distribution, peak current, and lifetime. Most research in NEAPC technology has gone into detector applications, to improve photoyield at low light intensity and high wavelength. Intevac is a leader in this area. The scientific understanding and technical expertise developed in this effort are important to achieving our goal of an electron source optimized for low-energy electron applications; however, it will be necessary to investigate other cathode properties (peak brightness, energy spread) under a substantially different operating regime (high light intensity, small emission area, high extraction field). DTIC

N94-28669 California Univ., Los Angeles. Dept. of Electrical Engineering.
PRINTED CIRCUIT ELEMENTS WITH APPLICATIONS TO ANTENNAS, SCATTERING, AND CIRCUITS Final Report, 15 Aug. 1990 - 14 Aug. 1993
N. G. Alexopoulos 14 Oct. 1993 10 p Limited Reproducibility: More than 20% of this document may be affected by microfiche quality
(Contract DAAL03-90-G-0182)
(AD-A275512; ARO-27904.16-EL) Avail: CASI HC A02

The research performed during the duration of this research contract has made an impact on the analysis and design of multiport microstrip and coplanar waveguide function; the design of microstrip corporate feed and electromagnetically coupled microstrip arrays; the characteristics of aperture antennas of arbitrary shape have been extensively studied theoretically and experimentally. The effect of nonreciprocal substrates on printed antenna characteristics has been analyzed. Also, the radar cross-section of printed antennas was studied. DTIC

N94-28687 International Business Machines Corp., Yorktown Heights, NY.
TUNNELLING HOT ELECTRON TRANSFER AMPLIFIERS Final Report
C. J. Kircher 30 Oct. 1993 34 p Limited Reproducibility: More than 20% of this document may be affected by microfiche quality
(Contract N00014-87-C-0709)
(AD-A275529) Avail: CASI HC A03

Significant advances were achieved in tunneling hot electron amplifiers and in the understanding of hot electron transport in the work funded by the contract and carried out by M. Heiblum and his co-workers. The results of this work are described in detail in nine papers that have been published in the open literature. (These papers are listed below as references 1-9 and copies of them are attached.) This report summarizes the principal results. There are three aspects of the work in which the results are particularly noteworthy: the demonstration of the first hot hole tunneling transistor and its use to study hot hole transport in GaAs; the successful fabrication of a hot electron 'THETA' transistor with a pseudomorphic InGaAs base which allowed high transistor gains (beta approx. = 30) to be achieved; and the conception and successful fabrication of a lateral hot electron device and its use to investigate ballistic, hot electron transport in a 2-dimensional electron gas in GaAs. DTIC

N94-28767# Hypres, Inc., Elmsford, NY.
EXPLORATORY RESEARCH FOR A HIGH TEMPERATURE SUPERCONDUCTING INTEGRATED CIRCUIT Final Report, 1 Jul. 1992 - 1 Aug. 1993
E. K. Track, O. Mukhanov, J. N. Eckstein, I. Bozovic, and G. F. Virshup Sep. 1993 42 p Prepared in cooperation with Varian Associates, Palo Alto, CA, and Stanford Univ., CA
(Contract F33615-90-C-1456)
(AD-A275798; WL-TR-93-5031) Avail: CASI HC A03/MF A01

The objective of this effort was the investigation of the molecular beam epitaxy trilayer Josephson junction process under development by Varian Corporation. Under this effort, Stanford University provided fundamental materials characterization to understand and improve the surfaces and interfaces of the thin film structures. HYPRES Inc. provided an independent assessment of the junctions produced by Varian and addressed the possibilities of rapid single fluxquantum (RSFQ) circuit designs. The material system chosen for this investigation was bismuth strontium calcium copper oxide (BSSCO). The Josephson junction character of the devices was confirmed by the observation of microwave induced (Shapior) steps in the I-V curves. Contact resistance was reduced by three orders of magnitude by modulation doping the top few molecular layers of the upper superconductive electrode. The desired properties to warrant RSFQ circuit fabrication were not obtained. A material system with a higher Josephson junction critical temperature and higher critical current is necessary for circuits. DTIC

N94-28805# University of Southern California, Los Angeles. Dept. of Electrical Engineering and Materials Science.
OPTOELECTRONIC INTEGRATED CIRCUITS FABRICATED USING ATOMIC LAYER EPITAXY Final Report, 1 Mar. 1989 - 30 Sep. 1992
P. D. Dapkus Dec. 1993 213 p
(Contract DAAL03-89-K-0072)
(AD-A275454; ARO-26898.1-EL-SDI) Avail: CASI HC A10/MF A03

The interest in monolithic integration of optoelectronic devices based on III-V semiconductors has presented a great challenge to crystal growth and device processing. Laser assisted atomic layer epitaxy (LALE) is attracting increased attention as a candidate to meet the challenge because it offers localized deposition at a control of layer thickness, doping profile, and interface roughness on an atomic scale: This work starts with a detailed study of the gas phase thermal decomposition of trimethylgallium (TMGa) and its relevance to atomic layer epitaxy (ALE) using molecular beam sampling mass spectrometry. The growth of GaAs by LALE is then first studied using triethylgallium (TMGa) and arsine (AsH3) as precursors. The influence of growth chemistry on the carbon contamination in the epilayers is further studied by using combinations of TMGa and tertiarybutylarsine (TBAs) and triethylgallium (TEGa) and AsH3. The device application of the growth technique is demonstrated for the first time through laser diodes with the GaAs QW grown by LALE. DTIC

N94-28842 Naval Postgraduate School, Monterey, CA.
DIGITALLY PROGRAMMABLE COMPOSITE OPERATIONAL AMPLIFIER APPLICATIONS M.S. Thesis
Ronald A. Crowell Sep. 1993 98 p Limited Reproducibility: More than 20% of this document may be affected by microfiche quality
(AD-A275081) Avail: CASI HC A05

In this study, CMOS implementation of composite operational amplifiers onto a single chip is examined. Composite operational amplifiers are realized by interconnecting two or more single operational amplifiers in any one of four high performance circuit topologies. These high performance topologies result in composite operational amplifiers having useful bandwidths that are significantly larger than those associated with their constituent operational amplifiers without sacrificing closed loop gain. Computer simulations using PSPICE are compared with experimental results for performance evaluation. As an application, a multiple feedback bandpass filter implementation is examined. DTIC

N94-28846*# District of Columbia Univ., Washington, DC. Dept. of Electrical Engineering.
HIGH Tc SUPERCONDUCTING BOLOMETRIC AND NONBOLOMETRIC INFRARED (IR) DETECTORS Semiannual Report, Aug. 1993 - Apr. 1994
Samuel Lakeou 1994 9 p
(Grant NAG5-2348)
(NASA-CR-195728; NAS 1.26:195728) Avail: CASI HC A02/MF A01

The original workplan for the first year of the project includes the following: establishment of a pilot superconductivity application laboratory at UDC to support the research component of the project; research on the source of electrical noise in High Tc superconducting films in order to

optimize the film microstructure and lower the NEP; and lay the foundation of an academic support for exposing UDC students to the theory and application of High Tc superconductivity. Attached to this status report are abstracts and the course description for Introduction to Applications of Superconductivity. Derived from text

N94-28913# Wright Lab., Wright-Patterson AFB, OH.
PERFORMANCE EVALUATION OF A 22.5/30 kW 270 VOLTS DIRECT CURRENT GENERATOR SYSTEM Final Report, Jan. 1992 - 1993
John G. Nairus and David A. Criminski Dec. 1993 153 p
(AD-A275106; WL-TR-93-2025) Avail: CASI HC A08/MF A02

This report documents the electrical system performance testing of a 12-pole, wound rotor machine with integral 3:1 speed increaser and recitifer, 22.5/30 kW 270 Vdc generator system. The performance testing was accomplished in the generator test facility of the Aerospace Power Division (WL/POOC-1). This report also documents WL/POOC-I's Data Acquisition System modified for 270 Vdc test and analysis. Generator system parameters measured include transient responses to load applications and removals, ripple voltages, distortion spectrums, and fault currents. Results were compared to electrical system characteristics specified in MIL-STD-704E. DTIC

N94-28915 Raytheon Co., Lexington, MA. Research Div.
RF VACUUM MICROELECTRONICS Quarterly Progress Report No. 8, Sep. - Nov. 1993
7 Jan. 1994 9 p Limited Reproducibility: More than 20% of this document may be affected by microfiche quality
(Contract MDA972-91-C-0032)
(AD-A275221; RAY/RD/S-4955) Avail: Issuing Activity (Defense Technical Information Center (DTIC))

Results concerning several topics are presented: (1) third iteration masks were designed, layed out, and received; (2) new mounting alumina were received; (3) third mounting vacuum flanges were designed and ordered; and (4) on internal funds, cathodes from LETI were procured and evaluated. These results will give direction to this contract. DTIC

N94-28994# General Atomic Co., San Diego, CA.
THE 100 kA, 5000 V SOLID-STATE OPENING SWITCH FOR INDUCTIVE ENERGY STORAGE Technical Report, Apr. 1990 - May 1993
Mark W. Heyse, Joshua Kolawole, Nolan E. Taconi, Jr., and Ed E. Bowles Dec. 1993 11 p
(Contract F08635-90-C-0241)
(AD-A274993; WL-TP-93-005) Avail: CASI HC A03/MF A01

Inductive energy stores have demonstrated higher energy storage densities than capacitive energy stores. A limitation in the use of inductive energy stores has been the availability of adequately rated opening switches. A self commutated solid-state switch has been developed for use as an opening device for an inductive energy store. The switch is rated at 100 kA and 5000 V and is composed of four identical 25 kA switch modules. The charging pulse lengths for the intended application vary from 0.1 to 5 seconds. Efficiency and volumetric power density were optimized. The switch topology is a two stage hybrid consisting of an SCR-FET/SCR-IGBT combination. The switch is designed to charge an inductive energy store and repetitively commutate the current into a railgun load. A 100 kA switch module has been built and successfully tested. The theory of operation, circuit topology, and test results are given in this paper. DTIC

N94-28995# Massachusetts Inst. of Tech., Cambridge. Research Lab. of Electronics.
THREE DIMENSIONAL TRANSIENT ANALYSIS OF MICROSTRIP CIRCUITS IN MULTILAYERED ANISOTROPIC MEDIA Annual Report, 1 Oct. 1992 - 30 Sep. 1993
J. A. Kong 18 Jan. 1994 92 p
(Contract N00014-90-J-1002)
(AD-A274995) Avail: CASI HC A05/MF A01

In high-speed digital circuits, high frequency phenomena affects the characteristics of the interconnections. Physical discontinuities or nonuniformities in the connections may cause severe reflections when they can no longer be considered as conducting wires, but behave as transmission lines and/or waveguides. In multilayered digital circuits, vias constitute one of the most commonly-used class of interconnects. Vias are not good carriers of high-speed signals. They cause signal distortion and reflections as well as severe degradation in the high frequency components. The analysis and modeling of a single via and some quasi-static or quasi-TEM analyses of single via configurations have been carried out previously. To date, the analysis of coupled noise between adjacent vias has received very little attention. The major reasons include the complexity of multi-via structures and the difficulty of modeling and analyzing them accurately over a broad frequency range. DTIC

N94-29025# Sandia National Labs., Albuquerque, NM.
EFFECTS OF OXIDE CHARGE AND SURFACE RECOMBINATION VELOCITY ON THE EXCESS BASE CURRENT OF BJT'S
S. L. Kosier (Arizona Univ., Tucson.), R. D. Schrimpf (Arizona Univ., Tucson.), A. Wei (Arizona Univ., Tucson.), M. DeLaus (Analog Devices, Inc., Woburn, MA.), D. M. Fleetwood, and W. E. Combs 1993 4 p Presented at the Institute of Electrical and Electronics Engineers (IEEE) Bipolar/BiCMOS Circuits and Technology Meeting, Minneapolis, MN, 4-5 Oct. 1993
(Contract DE-AC04-94AL-85000)
(DE94-003711; SAND-93-1870C; CONF-9310238-1) Avail: CASI HC A01/MF A01

The role of net positive oxide trapped charge and surface recombination velocity on excess base current in BJT's is identified. The effects of the two types of damage can be detected by plotting the excess base current versus base-emitter voltage. Differences and similarities between ionizing-radiation-induced and hot electron-induced degradation are discussed. DOE

N94-29028 Rensselaer Polytechnic Inst., Troy, NY.
MODELING THE TOTAL DOSE RADIATION EFFECTS OF Hg(1-x)Cd(x)Te PHOTODIODES USING NUMERICAL DEVICE SIMULATORS Technical Report, 1 Oct. 1992 - 28 Feb. 1993
James C. Petrosky, James W. Howard, Robert C. Block, and Iswara Bhat 1 Jan. 1994 60 p Limited Reproducibility: More than 20% of this document may be affected by microfiche quality
(Contract MIPR-92-501)
(AD-A275235; DNA-TR-93-50) Avail: CASI HC A04

We fabricated high quality MCT diodes using in-situ grown MCT and selective annealing. We used these diodes to benchmark our initial characterization and as a basis for our irradiation modeling. We implemented the models in PISCES-IIB and compared the I-V relationship to measurements. The close match between simulations and measurements demonstrates the applicability of the models. We expanded the simulations to I-V characteristics of irradiated diodes. To do so, we developed models for the induced current mechanisms resulting from radiation interactions. The results confirm the theories concerning the radiation's effect on tunneling in MCT. The simulations also suggest that improvements require knowledge of tunneling currents associated with trap formation in MCT. DTIC

N94-29045# Naval Surface Warfare Center, Silver Spring, MD.
ELECTROSET TECHNOLOGY: ON THE FOREFRONT OF MANUFACTURING
Ronald P. Reitz 1993 4 p
(AD-A275166) Avail: CASI HC A01/MF A01

A newly patented technology is emerging which will help American manufacturers produce goods faster and more affordably. Additionally, manufacturers can use it to diversify their product lines by making complex parts quickly and efficiently. Its called Electroset Technology (EST). With Est, standard casting resins are modified to be electrically semiconductive while they are in their fluid state. Electroset resins are electrically polarizable particles immersed within and suspended throughout casting resins. Because they are semiconductive in their fluid state, electric energy can be applied to and through these resins during cure to do useful work. DTIC

N94-29120 National Physical Lab., Teddington (England). Div. of Materials Metrology.
ELECTRICAL CONDUCTIVITY MEASUREMENTS ON A SiCp/Al ALLOY METAL MATRIX COMPOSITE
E. J. Carman, A. J. Dawson, and B. Roebuck 1993 35 p
(PB94-138310; NPL-DMM(A)85) Copyright Avail: Issuing Activity (National Technical Information Service (NTIS))

Both DC and AC electrical conductivity measurements have been used to assess the homogeneity of several plates and thin sheets of a SiC particulate reinforced aluminum alloy metal matrix composite. The

uncertainties associated with the measurements have been assessed and are compared with the spread in values obtained from measurements on each plate. The AC measurements showed less inherent uncertainty than the DC measurements and revealed some variation from plate to plate and sheet to sheet, probably due to small differences in matrix chemistry. NTIS

N94-29191# Swedish Inst. for Materials Testing, Boras.
UNSCREENED LOW TENSION CABLES SCRAPE ABRASION TESTING. PART 1: AN INTERLABORATORY STUDY ON SCRAPE ABRASION TESTING ACCORDING TO ISO DP 6722-1
L. Spilg 1992 30 p
(ISSN 0284-5172)
(PB94-135605; ISBN-91-7848-335-2) Avail: CASI HC A03/MF A01

A proposal for revision of ISO 6722/1, Road vehicles - Unscreened low tension cables, Part I: General requirements and test methods, specifies a method for scrape abrasion testing. Tests at different laboratories indicate large variations in the results obtained using this method. It is evident that a number of parameters have influence on the results. In an effort to clarify the influence of some of these parameters, the ISO/TC 22/SC3/WG4-Low Tension Cables decided to undertake an interlaboratory test focusing on different equipment, different conductor types and different insulating materials. This report presents the method used and the result of the interlaboratory test. It is concluded that it is not possible to compare data obtained on different equipment although they are made according to standard and that further investigations have to be done before including this method in an international standard. NTIS

N94-29209*# National Aeronautics and Space Administration. Lewis Research Center, Cleveland, OH.
TRANSPORT PROPERTIES OF EPITAXIAL LIFT OFF FILMS
R. A. Mena, S. E. Schacham, P. G. Young, E. J. Haugland, and S. A. Alterovitz May 1993 21 p
(RTOP 506-72-1B)
(NASA-TM-106156; E-7842; NAS 1.15:106156) Avail: CASI HC A03/MF A01

Transport properties of epitaxially lifted-off (ELO) films were characterized using conductivity, Hall, and Shubnikov-de Haas measurements. A 10-15 percent increase in the 2D electron gas concentration was observed in these films as compared with adjacent conventional samples. We believe this result to be caused by a backgating effect produced by a charge build up at the interface of the ELO film and the quartz substrate. This increase results in a substantial decrease in the quantum lifetime in the ELO samples, by 17-30 percent, but without a degradation in carrier mobility. Under persistent photoconductivity, only one subband was populated in the conventional structure, while in the ELO films the population of the second subband was clearly visible. However, the increase of the second subband concentration with increasing excitation is substantially smaller than anticipated due to screening of the backgating effect. Author (revised)

N94-29289# Aerospace Corp., El Segundo, CA. Technology Operations.
SCREENING OF FLEXIBLE CABLES BY NONLINEAR RESISTANCE MEASUREMENTS Technical Report
G. W. Stupian 10 Jan. 1994 29 p
(Contract F04701-88-C-0089)
(AD-A275193; TR-93(3404)-1; SMC-TR-93-56) Avail: CASI HC A03/MF A01

Two traces in flexible cables used in the Milstar agile beam antenna system failed during acceptance testing. The cables, essentially printed circuit boards fabricated on flexible substrates, are composed of copper-foil conductors sandwiched between insulating Kapton layers. The cables carry current pulses used in the steering circuitry for the antenna beam. Upon sectioning and inspection of the suspect cables, substantial thinning of the copper foil conductors at feedthrough connections was noted. Other cables examined also exhibited thinning of metallization. Cables with degraded metallization develop anomalously high electrical resistances or can fail 'open'. The difficulties encountered with these cables resulted from poor workmanship, and the cable manufacturer subsequently lost certification from the Defense Electronics Supply Center. However, a large number of the cables had already been installed in satellites, and the reliability of the cables is critically important to mission success. A considerable effort was, therefore, mounted by the contractors, with the support of Aerospace, to assess the extent of the problem and determine whether a suitable screening procedure could be developed so that only selective, rather than total, replacement of the cables installed on the first Milstar satellite, DFS 1, might be necessary. In the course of this investigation, a screening test based on nonlinearities in cable resistance was developed. This test was originally intended to be applied to the cables in flight hardware. In fact, the application of this test to cables still in stores uncovered additional defective cables and led to a decision to replace all flexible cables with those from another manufacturer. DTIC

N94-29305# Massachusetts Inst. of Tech., Cambridge. Research Lab. of Electronics.
FOCUSED ION BEAM FABRICATION OF MICROELECTRONIC STRUCTURES Final Report, 1 Oct. 1990 - 14 Oct. 1993
John Melngailis 30 Dec. 1993 109 p
(Contract DAAL03-90-G-0223)
(AD-A275384; ARO-28345.5-EL) Avail: CASI HC A06/MF A02

One of the most successful applications of focused ion beams has been the deposition of submicrometer conductors for integrated circuits. Our work has concentrated on demonstrating new materials and on studying the fundamental mechanisms of the deposition and milling processes. One of the important results has been the first demonstration of ion induced copper deposition from a new precursor gas. Copper is being considered a successor to aluminum in integrated circuits, and our copper had the lowest resistivity of any material produced by room temperature focused ion beam deposition. We have also studied the ion induced deposition of gold and tungsten as a function of angle of incidence as well as the milling of Si, SiO2, W, and Au. These processes are also important for the repair of lithography masks. A Monte Carlo model based on collision cascades has been developed for the fundamental mechanism for ion induced deposition and tested against measurements of deposition yield of Au for various ion energies and noble gas Ion species. The deposition appears to be substrate mediated and fits the collision cascade model. The dependent of milling and deposition as a function of ion incidence also appears to fit this model. DTIC

N94-29357*# National Aeronautics and Space Administration. Pasadena Office, CA.
METHOD FOR FORMING THIN COMPOSITE SOLID ELECTROLYTE FILM FOR LITHIUM BATTERIES Patent Application
Ganesan Nagasubramanian, inventor (to NASA) (Jet Propulsion Lab., California Inst. of Tech., Pasadena.) and Alan I. Attia, inventor (to NASA) (Jet Propulsion Lab., California Inst. of Tech., Pasadena.) 19 Jan. 1994 19 p
(Contract NAS7-1260)
(NASA-Case-NPO-18877-1-CU; NAS 1.71:NPO-18877-1-CU; US-Patent-Appl-SN-186183) Avail: CASI HC A03/MF A01

A composite solid electrolyte film is formed by dissolving a lithium salt such as lithium iodide in a mixture of a first solvent which is a co-solvent for the lithium salt and a binder polymer such as polyethylene oxide and a second solvent which is a solvent for the binder polymer and has poor solubility for the lithium salt. Reinforcing filler such as alumina particles are then added to form a suspension followed by the slow addition of binder polymer. The binder polymer does not agglomerate the alumina particles. The suspension is cast into a uniform film. NASA

N94-29372*# National Aeronautics and Space Administration. Marshall Space Flight Center, Huntsville, AL.
MULTI-SPEED MULTI-PHASE RESOLVER CONVERTER Patent Application
Dean Alhorn, inventor (to NASA) and David Howard, inventor (to NASA) 22 Feb. 1994 23 p
(NASA-Case-MFS-28855-1; NAS 1.71:MFS-28855-1; US-Patent-Appl-SN-199924) Avail: CASI HC A03/MF A01

A multiphase converter circuit generates a plurality of sinusoidal outputs of displaced phase and given speed value from the output of an angular resolver system attachable to a motor excited by these multi-phase outputs, the resolver system having a lower speed value than that of the motor. The angular resolver system provides in parallel format sequential digital numbers indicative of the amount of rotation of the shaft of an angular position sensor associated with the angular resolver system. These numbers

are used to excite simultaneously identical addresses of a plurality of addressable memory systems, each memory system having stored therein at sequential addresses sequential values of a sinusoidal wavetrain of a given number of sinusoids. The stored wavetrain values represent sinusoids displaced from each other in phase according to the number of output phases desired. A digital-to-analog converter associated with each memory system converts each accessed word to a corresponding analog value to generate attendant to rotation of the angular resolver a sinusoidal wave of proper phase at each of the plurality of outputs. By properly orienting the angular resolver system with respect to the rotor of the motor, essentially ripple-free torque is supplied to the rotor. The angular resolver system may employ an analog resolver feeding an integrated circuit resolver-to-digital converter to produce the requisite digital values serving as addresses. Alternative versions employing incremental or absolute encoders are also described. NASA

N94-29374*# National Aeronautics and Space Administration. Pasadena Office, CA.

METHOD OF IMPLEMENTING DIGITAL PHASE-LOCKED LOOPS Patent Application

Scott A. Stephens, inventor (to NASA) (Jet Propulsion Lab., California Inst. of Tech., Pasadena.) and Jess Brooks Thomas, Jr., inventor (to NASA) (Jet Propulsion Lab., California Inst. of Tech., Pasadena.) 13 Oct. 1993 89 p

(Contract NAS7-918)

(NASA-Case-NPO-18757-1-CU; NAS 1.71:NPO-18757-1-CU; US-Patent-Appl-SN-141797) Avail: CASI HC A05/MF A01

In a new formulation for digital phase-locked loops, loop-filter constants are determined from loop roots that can each be selectively placed in the s-plane on the basis of a new set of parameters, each with simple and direct physical meaning in terms of loop noise bandwidth, root-specific decay rate, or root-specific damping. Loops of first to fourth order are treated in the continuous-update approximation (BLT yields 0) and in a discrete-update formulation with arbitrary BLT. Deficiencies of the continuous-update approximation in large-BLT applications are avoided in the new discrete-update formulation. A new method for direct, transient-free acquisition with third- and fourth-order loops can improve the versatility and reliability of acquisition with such loops. NASA

N94-29411*# National Aeronautics and Space Administration. Pasadena Office, CA.

DENDRITE PREVENTING SEPARATOR FOR SECONDARY LITHIUM BATTERIES Patent Application

David H. Shen, inventor (to NASA) (Jet Propulsion Lab., California Inst. of Tech., Pasadena.), Subbarao Surampudi, inventor (to NASA) (Jet Propulsion Lab., California Inst. of Tech., Pasadena.), Chen-Kuo Huang, inventor (to NASA) (Jet Propulsion Lab., California Inst. of Tech., Pasadena.), and Gerald Halpert, inventor (to NASA) (Jet Propulsion Lab., California Inst. of Tech., Pasadena.) 17 Nov. 1993 13 p

(Contract NAS7-918)

(NASA-Case-NPO-18585-1-CU; NAS 1.71:NPO-18585-1-CU; US-Patent-Appl-SN-154322) Avail: CASI HC A03/MF A01

Dendrites are prevented from shorting a secondary lithium battery by use of a first porous separator, such as porous polypropylene, adjacent to the lithium anode that is unreactive with lithium and a second porous fluoropolymer separator between the cathode and the first separator, such as polytetrafluoroethylene, that is reactive with lithium. As the tip of a lithium dendrite contacts the second separator, an exothermic reaction occurs locally between the lithium dendrite and the fluoropolymer separator. This results in the prevention of the dendrite propagation to the cathode. NASA

N94-29426* National Aeronautics and Space Administration. Pasadena Office, CA.

NONVOLATILE PROGRAMMABLE NEURAL NETWORK SYNAPTIC ARRAY Patent

Raoul Tawel, inventor (to NASA) (Jet Propulsion Lab., California Inst. of Tech., Pasadena.) 29 Mar. 1994 10 p Filed 8 Jul. 1992 Supersedes N92-30086 (30 - 20, p 3442)

(NASA-Case-NPO-18578-1-CU; US-Patent-5,298,796; US-Patent-Appl-SN-912956; US-Patent-Class-307-201; US-Patent-Class-395-24; US-Patent-Class-395-25; US-Patent-Class-257-323; Int-Patent-Class-H03K-19/08) Avail: US Patent and Trademark Office

A floating-gate metal oxide semiconductor (MOS) transistor is implemented for use as a nonvolatile analog storage element of a synaptic cell used to implement an array of processing synaptic cells. These cells are based on a four-quadrant analog multiplier requiring both X and Y differential inputs, where one Y input is UV programmable. These nonvolatile synaptic cells are disclosed fully connected in a 32 x 32 synaptic cell array using standard very large scale integration (VLSI) complementary MOS (CMOS) technology.

Official Gazette of the U.S. Patent and Trademark Office

N94-29488*# National Aeronautics and Space Administration. Pasadena Office, CA.

MONOLITHIC IN-BASED III-V COMPOUND SEMICONDUCTOR FOCAL PLANE ARRAY CELL WITH SINGLE STAGE CCD OUTPUT Patent Application

Eric R. Fossum, inventor (to NASA) (Jet Propulsion Lab., California Inst. of Tech., Pasadena.), Thomas J. Cunningham, inventor (to NASA) (Jet Propulsion Lab., California Inst. of Tech., Pasadena.), Timothy N. Krabach, inventor (to NASA) (Jet Propulsion Lab., California Inst. of Tech., Pasadena.), and Craig O. Staller, inventor (to NASA) (Jet Propulsion Lab., California Inst. of Tech., Pasadena.) 21 Jan. 1994 15 p

(Contract NAS7-1260)

(NASA-Case-NPO-18978-1-CU; NAS 1.71:NPO-18978-1-CU; US-Patent-Appl-SN-186185) Avail: CASI HC A03/MF A01

A monolithic semiconductor imager includes an indium-based III-V compound semiconductor monolithic active layer of a first conductivity type, an array of plural focal plane cells on the active layer, each of the focal plane cells including a photogate over a top surface of the active layer, a readout circuit dedicated to the focal plane cell including plural transistors formed monolithically with the monolithic active layer and a single-stage charge coupled device formed monolithically with the active layer between the photogate and the readout circuit for transferring photo-generated charge accumulated beneath the photogate during an integration period to the readout circuit. The photogate includes thin epitaxial semiconductor layer of a second conductivity type overlying the active layer and an aperture electrode overlying a peripheral portion of the thin epitaxial semiconductor layer, the aperture electrode being connectable to a photogate bias voltage. NASA

N94-29505* National Aeronautics and Space Administration. Pasadena Office, CA.

ANODE FOR RECHARGEABLE AMBIENT TEMPERATURE LITHIUM CELLS Patent

Chen-Kuo Huang, inventor (to NASA) (Jet Propulsion Lab., California Inst. of Tech., Pasadena.), Subbarao Surampudi, inventor (to NASA) (Jet Propulsion Lab., California Inst. of Tech., Pasadena.), Alan I. Attia, inventor (to NASA) (Jet Propulsion Lab., California Inst. of Tech., Pasadena.), and Gerald Halpert, inventor (to NASA) (Jet Propulsion Lab., California Inst. of Tech., Pasadena.) 15 Mar. 1994 10 p Filed 13 Oct. 1992 Supersedes N93-17278 (31 - 5, p 1150)

(NASA-Case-NPO-18580-1-CU; US-Patent-5,294,503; US-Patent-Appl-SN-959858; US-Patent-Class-429-194; US-Patent-Class-424-218; US-Patent-Class-252-182.1; US-Patent-Class-423-324; Int-Patent-Class-H01M-4/58) Avail: US Patent and Trademark Office

An ambient room temperature, high density, rechargeable lithium battery includes a Li(x)Mg2Si negative anode which intercalates lithium to form a single crystalline phase when x is up to 1.0 and an amorphous phase when x is from 1 to 2.0. The electrode has good reversibility and mechanical strength after cycling.

Official Gazette of the U.S. Patent and Trademark Office

N94-29511# Ramsearch Co., Crofton, MD.

THE INFLUENCE OF TEMPERATURE ON MICROELECTRONIC DEVICE FAILURE MECHANISMS, PHASE 2 Final Report

Michael Pecht 4 Sep. 1993 283 p

(Contract DAAL01-91-C-0142)

(AD-A275029) Avail: CASI HC A13/MF A03

There has been a common belief that reliable electronics can be achieved by lowering temperature. Elevated temperature has in the past been

considered a dominant stress that lowers reliability, so every effort has been made to lower operating temperature until the desired reliability is achieved. The belief in the harmful effects of temperature has woven itself into today's screening and thermal derating processes. High-reliability applications require that the microelectronic device be subjected to high-temperature stress screens, like burn-in, to improve the reliability of the product. Moreover, thermal derating measures for microelectronics often involve lowering temperature. DTIC

N94-29523 Societe des Electriciens et Electroniciens, Paris (France).
ELECTRICAL ENGINEERING AND INDUSTRIAL ELECTRONICS EDUCATION DAYS: CONTROL OF ASYNCHRONOUS GENERATORS [JOURNEES DE L'ENSEIGNEMENT DE L'ELECTROTECHNIQUE ET DE L'ELECTRONIQUE INDUSTRIELLE: COMMANDE DES MACHINES ASYNCHRONES]
Caron, Hautier, Sanhet, Faucher, and Provost Mar. 1993 166 p In FRENCH Sponsored by Direction des Recherches, Etudes et Techniques and Centre de Documentation de l'Armement
(PB94-135514) Avail: Issuing Activity (National Technical Information Service (NTIS))

To advance the teaching of modern electrical engineering, manufacturers, university researchers, and professors involved in technical education at the post-B.S. level organized the first conference on the teaching of electrical and electronic engineering. The topic of the conference was the control of asynchronous generators, and the following seven papers from it are published here: Modeling of steady-state asynchronous generators; Control under high speed; The variable speed of induction generators and the structure of converters and vector control; A few aspects of impulse width modulation; Recent three-phase drive developments at the French National Railway Co.; Applying vector control to electrical drive--cross-channel HST/MF88 subway; Power components for asynchronous generator control. NTIS

N94-29527# Loughborough Univ. of Technology (England). Dept. of Mathematical Sciences.
INVESTIGATION ON APPLICATION OF GENETIC ALGORITHMS TO OPTIMAL REACTIVE POWER DISPATCH OF POWER SYSTEMS
Q. H. Wu and J. T. Ma Sep. 1993 12 p Sponsored by National Grid Co. Plc., United Kingdom
(MATHS-Rept-A-197; ETN-94-95512) Avail: CASI HC A03/MF A01

A primary investigation into application of genetic algorithms in optimal reactive power dispatch and voltage control is presented. The application was achieved, based on (the United Kingdom) National Grid 48 bus network model, using a novel genetic search approach. Simulation results, compared with that obtained using nonlinear programming methods, are included to show the potential of applications of the genetic search methodology in power system economical and secure operations. ESA

N94-29734 Oregon Univ., Eugene.
QUANTUM INTERFERENCE PHENOMENA AND NOVEL SWITCHING IN SPLIT GATE HIGH ELECTRON MOBILITY TRANSISTORS Ph.D. Thesis
Jong-Ching Wu 1992 120 p
Avail: Univ. Microfilms Order No. DA9313325

Nanometer scale electronic channels with and without a discontinuity were made in modulation-doped AlGaAs/GaAs heterojunctions using a split gate technique. Quantum interference phenomena in an electron cavity and fast switching behavior due to hot electron effects in a lateral double potential barrier structure were explored. First, one dimensional channels with a double bend discontinuity were examined in the mK temperature range. Low-field ac-conductance measurements have evidenced quantum waveguide effects: resonant features were observed in the one dimensional conductance plateaus in which the number of peaks was directly related to the geometry of the double bend. Temperature and magnetic field studies, along with a standing wave model, have provided a better understanding of quantum interference phenomena in electron wave guide and cavity structures. Secondly, a structure containing two cascaded double bend discontinuities was studied. The structure behaves as a constricted cavity coupling two point-contacts, in which the depletion by the split gate was used to form and control the lateral double potential barriers. The low temperature source-drain characteristics exhibited a pronounced S-shaped negative differential conductance that can be attributed to a nonlinear electron temperature effect along the conducting path. The data presented show two types of conducting state: electron tunneling in the off state and hot electron conduction (thermionic emission) in the on state. The estimated switching speed of the device could be as fast as 5 ps due to short transit time. Dissert. Abstr.

N94-29805 Texas A&M Univ., College Station.
YIELD AND VARIABILITY OPTIMIZATION OF INTEGRATED CIRCUITS: PRINCIPLES AND PRACTICAL SOLUTIONS Ph.D. Thesis
Jian Cheng Zhang 1992 194 p
Avail: Univ. Microfilms Order No. DA9315171

This dissertation deals with both theoretical and practical aspects of integrated circuits (IC's) statistical design. It stresses and explains that the essential difference between IC statistical design and discrete circuit statistical design lies in basic statistical features of two types of circuits. The main emphasis of the research is placed on principles and practical solutions for performance variability minimization rather than manufacturing yield enhancement alone. A variability gradient formula applicable to a general IC statistical model is first developed, which leads to understanding of the nature of IC variability minimization problem, forms a theoretical basis for the possibility of IC variability minimization, and clarifies the principles of variability minimization and performance tuning. A two-stage strategy, based on separate performance variability minimization and separate performance tuning, is proposed. Practical results show that the two-stage procedure leads to small variability, small 'bias,' and high yield. The use of orthogonal array based design of experiments is advocated for exploring the effects of circuit variables on circuit performances, which aims at eliminating noncritical circuit parameters in order to reduce problem dimension. Several design plans are considered for a variety of applications. The level 3 main effect orthogonal array design approach is used for statistical gradient estimation and applied together with the stochastic approximation method to yield optimization. Taguchi experiments are used to explore the interactions of designable circuit parameters and noise factors, leading to efficient estimation of gradient of variability, and gradient of the mean, in order to identify the parameters essential for variability minimization and performance tuning. The mathematical model corresponding to Taguchi experiments is also studied. The worst-case measure is considered as another measure of performance variability. It is of great importance for digital delay circuits. Mathematical interpretations are provided to bridge the gap between variability minimization and worst-case measure reduction, and make the underlying principles and methods for variability minimization equally applicable to the worst-case measure reduction. The research also goes one step further by using fuzzy set theory as a framework to handle statistical optimization with multiple circuit performances. Dissert. Abstr.

N94-30040 Sandia National Labs., Albuquerque, NM.
CHARGE TRAPPING AND BREAKDOWN IN N2O OXIDES
N. S. Saks (Naval Research Lab., Washington, DC.), D. I. Ma (Naval Research Lab., Washington, DC.), and D. M. Fleetwood 1993 3 p Presented at the International Reliability Physics Symposium, San Jose, CA, 11-14 Apr. 1994 Limited Reproducibility: More than 20% of this document may be affected by microfiche quality
(Contract DE-AC04-94AL-85000)
(DE94-003775; SAND-93-2449C; CONF-940453-1) Avail: CASI HC A01

Nitrided gate oxides have been fabricated by furnace oxidation in N2O with and without prior oxidation in O2. SIMS nitrogen profiles show a sharp peak at the Si-insulator interface for both processes. Improved breakdown characteristics and reduced oxide damage after irradiation and charge injection are obtained. DOE

N94-30055# Sandia National Labs., Albuquerque, NM.
NEARLY TIME-OPTIMAL FEEDBACK CONTROL OF A MAGNETICALLY LEVITATED PHOTOLITHOGRAPHY POSITIONING SYSTEM
J. Redmond 1993 10 p Presented at the North American Conference on Smart Structures and Materials, Orlando, FL, 13-18 Feb. 1994
(Contract DE-AC04-94AL-85000)
(DE94-005288; SAND-93-3984C; CONF-940206-1) Avail: CASI HC A02/MF A01

This paper focuses on the development of an approximate time-optimal feedback strategy for conducting rest-to-rest maneuvers of a magnetically levitated table. Classical switching curves are modified to account for the complexities of magnetic actuation as well as the coupling of the rigid body modes through the control. A smooth blend of time-optimal and

proportional-derivative controls is realized near the destination point to correct for inaccuracies produced by the approximate time-optimal strategy. Detailed computer simulations of the system indicate that this hybrid control strategy provides a significant reduction in settling time as compared to proportional-derivative control alone. DOE

N94-30073 Joint Inst. for Nuclear Research, Dubna (USSR). Lab. of Neutron Physics.
THE BASES FOR THE DEVELOPMENT OF HIGH-TEMPERATURE INTEGRATED SQUID-SYSTEMS
V. N. Polushkin 1992 34 p Limited Reproducibility: More than 20% of this document may be affected by microfiche quality
(DE94-607901; JINR-D-13-92-340) Avail: CASI HC A03 (US Sales Only)

The current state of high-Tc thin film Josephson junction and SQUID development is reviewed. The prospects for application of new devices to supersensitive measurement apparatus are analyzed. It is shown that high T(sub c) SQUID's are able to serve as a basis for the further development of information and measurement engineering. DOE

N94-30092 International Centre for Theoretical Physics, Trieste (Italy).
INTERBAND OPTICAL ABSORPTION IN THE WANNIER-STARK LADDER UNDER THE ELECTRON-LO-PHONON RESONANCE CONDITION
A. O. Govorov Aug. 1993 19 p Limited Reproducibility: More than 20% of this document may be affected by microfiche quality
(DE94-608097; IC-93/258) Avail: CASI HC A03 (US Sales Only)

Interband optical absorption in the Wannier-Stark ladder in the presence of the electron-LO-phonon resonance is investigated theoretically. The electron-LO-phonon resonance occurs when the energy spacing between adjacent Stark-ladder levels coincides with the LO-phonon energy. We propose a model describing the polaron effect in a superlattice. Calculations show that the absorption line shape is strongly modified due to the polaron effect under the electron-LO-phonon resonance condition. We consider optical phenomena in a normal magnetic field that leads to enhancement of polaron effects. DOE

N94-30115 National Physical Lab., Teddington (England). Div. of Electrical Science.
VHF IMPEDANCE MEASUREMENT: A REVIEW
N. M. Ridler Nov. 1993 37 p
(PB94-138682; NPL-DES-127) Copyright Avail: Issuing Activity (National Technical Information Service (NTIS))

This report reviews the current status of top echelon impedance measurement in the UK over the frequency range 30 to 300 MHz (VHF) of the electromagnetic spectrum. The term impedance is used to describe one of the complex electrical properties of one-port passive terminations. Some fundamental concepts of VHF impedance measurement are given along with discussions on the measuring instruments, calibration standards and existing UK national standard capabilities. NTIS

N94-30198*# National Aeronautics and Space Administration. Lewis Research Center, Cleveland, OH.
RADIAL MICROSTRIP SLOTLINE FEED NETWORK FOR CIRCULAR MOBILE COMMUNICATIONS ARRAY
Rainee N. Simons (Sverdrup Technology, Inc., Brook Park, OH.), Eron S. Kelly (Princeton Univ., NJ.), Richard Q. Lee, and Susan R. Taub Apr. 1994 6 p Proposed for presentation at the 1994 IEEE AP-S International Symposium and URSI Radio Science Meeting, Seattle, WA, 19-24 Jun. 1994; sponsored by IEEE
(Contract NAS3-25266; RTOP 506-44-2C)
(NASA-TM-106540; E-8683; NAS 1.15:106540) Avail: CASI HC A02/MF A01

In mobile and satellite communications there is a need for low cost and low profile antennas which have a toroidal pattern. Antennas that have been developed for mobile communications include a L-Band electronically steered stripline phased array, a Ka-Band mechanically steered elliptical reflector antenna and a Ka-Band printed dipole. In addition, a L-Band mechanically steered microstrip array, a L-Band microstrip phased array tracking antenna for mounting on a car roof and an X-Band radial line slotted waveguide antenna have been demonstrated. In the above electronically scanned printed arrays, the individual element radiates normally to the plane of the array and hence require a phase shifter to scan the beam towards the horizon. Scanning in the azimuth is by mechanical or electronic steering. An alternate approach is to mount microstrip patch radiators on the surface of a cone to achieve the required elevation angle. The array then scans in the azimuth by beam switching. Author

N94-30368# Sandia National Labs., Albuquerque, NM.
SELF-STRESSING TEST STRUCTURES USED FOR HIGH-FREQUENCY ELECTROMIGRATION
E. S. Snyder, D. G. Pierce, D. V. Campbell, and S. E. Swanson 1994 7 p Presented at the Institute of Electrical and Electronics Engineers (IEEE) International Conference on Microelectronic Test Structures, San Diego, CA, 22-24 Mar. 1994
(Contract DE-AC04-94AL-85000)
(DE94-006142; SAND-94-0248C; CONF-940369-1) Avail: CASI HC A02/MF A01

We demonstrate high frequency (500 MHz) electromigration at the wafer-level using on-chip, self-stressing test structures. Since the stress temperature, frequency, duty cycle, and current are controlled by DC signals in these structures, we used conventional DC test equipment without any special modifications. This structure significantly reduces the cost of performing realistic high frequency electromigration experiments. DOE

N94-30701 Kansas State Univ., Manhattan.
DOE/KEURP SITE OPERATOR PROGRAM
1993 36 p Limited Reproducibility: More than 20% of this document may be affected by microfiche quality
(Contract DE-FC07-91ID-13074)
(DE94-005832; DOE/ID-13074/T10) Avail: CASI HC A03

Kansas State University, with funding support from federal, state, public, and private companies, is participating in the Department of Energy's Electric Vehicle Site Operator Program. Through participation in this program, Kansas State is displaying, testing, and evaluating electric or hybrid vehicle technology. This participation will provide organizations the opportunity to examine the latest EHV prototypes under actual operating conditions. KSU has purchased several electric cars and proposes to purchase additional electric vehicles. DOE

N94-30711# California Univ., Berkeley. Lawrence Berkeley Lab.
A BIPOLAR ANALOG FRONT-END INTEGRATED CIRCUIT FOR THE SDC SILICON TRACKER
I. Kipnis, H. Spieler, and T. Collins Nov. 1993 9 p Presented at the 1993 IEEE Nuclear Science Symposium and Medical Imaging Conference, San Francisco, CA, 2-5 Nov. 1993
(Contract DE-AC03-76SF-00098)
(DE94-005203; LBL-34864; CONF-931107-32) Avail: CASI HC A02/MF A01

A low noise, low power, high bandwidth, radiation hard, silicon bipolar transistor full-custom integrated circuit (IC) containing 64 channels of analog signal processing has been developed for the SDC silicon tracker. The IC was designed and tested at LBL and was fabricated using CBIC-U2, 4 GHz f(sub T) complementary bipolar technology. Each channel contains the following functions: low noise preamplification, pulse shaping, and threshold discrimination. This is the first iteration of the production analog IC for the SDC silicon tracker. The IC is laid out to directly match the 50 micron pitch double-sided silicon strip detector. The chip measures 6.8 mm by 3.1 mm and contains 3,600 transistors. Three stages of amplification provide 180 mV/fC of gain with a 35 nsec peaking time at the comparator input. For a 14 pF detector capacitance, the equivalent noise charge is 1300 el. rms at a power consumption of 1 mW/channel from a single 3.5 V supply. With the discriminator threshold set to four times the noise level, a 16 nsec time-walk for 1.25 to 10 fC signals is achieved using a time-walk compensation network. Irradiation tests at TRIUMF to a Phi = 10(exp 14) protons/sq cm have been performed on the IC, demonstrating the radiation hardness of the complementary bipolar process. DOE

N94-30716# Los Alamos National Lab., NM.
A TRANSMISSION-LOSS MONITOR USING CURRENT TRANSFORMERS
J. F. Power, J. D. Gilpatrick, and A. J. Jason 1993 7 p Presented at the Beam Instrumentation Workshop, Santa Fe, NM, 20-23 Oct. 1993
(Contract W-7405-eng-36)
(DE94-003974; LA-UR-93-3704; CONF-9310204-13) Avail: CASI HC A02/MF A01

A system for measuring the amount of beam-charge loss in a linear-accelerator structure has been developed that uses a pair of beam-current transformers, otherwise used to monitor the linac beam current. This system is necessary to enable the Ground Test Accelerator (GTA) fast-protect system to shut off the accelerated beam in the event of a beam loss that would deposit sufficient energy to damage the accelerator structure. The present GTA accelerator consists of a 2.5-MeV, H(-) RFQ, an intermediate matching section (IMS) and a single DTL cavity with an output energy of 3.2-MeV and transmitted current of 35 mA. Based on the RFQ output beam, melting of the copper structures will occur when about 40 nC of beam is deposited in a point loss. For a grazing angle of 30 mrad, up to 640 nC may be tolerated. The beam-current-transmission-loss monitor (BCTLM) system in conjunction with the fast-protect system measures the amount of beam loss between two toroidal beam-current monitors and automatically terminates the macropulse when the integrated loss reaches a predetermined set point. The design and operation of the BCTLM system used in the IMS and DTL section of the accelerator is described. DOE

N94-30717# California Univ., Berkeley. Lawrence Berkeley Lab.
A HIGH RATE, LOW NOISE, X RAY SILICON STRIP DETECTOR SYSTEM
B. Ludewigt, J. Jaklevic, I. Kipnis, C. Rossington, and H. Spieler Nov. 1993 5 p Presented at the 1993 IEEE Nuclear Science Symposium and Medical Imaging Conference; IEEE Medical Imaging Conference, San Francisco, CA, 2-5 Nov. 1993
(Contract DE-AC03-76SF-00098)
(DE94-004557; LBL-34060; CONF-931107-23; CONF-9311114-6) Avail: CASI HC A01/MF A01

An x-ray detector system, based on a silicon strip detector wire-bonded to a low noise charge-senstive amplifier integrated circuit, has been developed for synchrotron radiation experiments which require very high count rates and good energy resolution. Noise measurements and x-ray spectra were taken using a 6 mm long, 55 micron pitch strip detector in conjunction with a prototype 16-channel charge-sensitive preamplifier, both fabricated using standard 1.2 micron CMOS technology. The detector system currently achieves an energy resolution of 350 eV FWHM at 5.9 key, 2 microsec peaking time, when cooled to -5 C. DOE

N94-30784 National Physical Lab., Teddington (England). Electrical Science Div.
GUIDANCE ON ELIMINATING INTERFERENCE FROM SENSITIVE ELECTRICAL CIRCUITS
B. P. Kibble and I. A. Robinson Oct. 1993 38 p
(ISSN 0143-7305)
(PB94-139300; NPL-DES-129; ETN-94-95847) Copyright Avail: Issuing Activity (National Physical Lab., Teddington, Middlesex TW11 0LW, England)

The basic principles underlying the elimination of electrical interference from circuits, which is necessary in order that their sensitivities can approach the fundamental Johnson noise limit, are presented. Eliminating all possible sources of extraneous interference is vital for the successful performance of sensitive analog electrical measurements. If interference is present, not only is the resolution of the measurement impaired through degradation of the signal to noise ratio, but rectification of the interference by any of the myriad semiconductor rectifying junctions in electronic signal detectors may well result in systematic error. Focus is on electrical interference, whose elimination depends on applying a very few elementary principles or circuit coupling. ESA

N94-30819 Midwest Research Inst., Golden, CO. National Renewable Energy Lab.
DESIGN OF A VARIABLE-CONDUCTANCE VACUUM INSULATION
D. K. Benson, T. F. Potter, and C. E. Tracy Jan. 1994 8 p Presented at the Society of Automotive Engineers (SAE) Congress and Exposition, Detroit, MI, 28 Feb. - 3 Mar. 1994 Limited Reproducibility: More than 20% of this document may be affected by microfiche quality
(Contract DE-AC02-83CH-10093)
(DE94-000270; NREL/TP-452-5814; CONF-940242-3) Avail: CASI HC A02

This paper describes one approach to the design of variable-conductance vacuum insulation. In this design, the vacuum insulation consists of a permanently sealed, thin sheet steel, evacuated envelope of whatever geometry is required for the application. The steel envelope is supported internally against the atmospheric pressure loads by an array of discrete, low-conductance, ceramic supports, and radiative heat transfer is blocked by layers of thin metal radiation shields. Thermal conductance through this insulation is controlled electronically by changing the temperature of a small metal hydride connected to the vacuum envelope. The hydride reversibly absorbs/desorbs hydrogen to produce a hydrogen pressure typically within the range from less than 10(exp -6) to as much as 1 torr. Design calculations are compared with results from laboratory tests of bench scale samples, and some possible automotive applications for this variable-conductance vacuum insulation are suggested. DOE

N94-30904 Fermi National Accelerator Lab., Batavia, IL.
A MAGNETICALLY COUPLED QUENCH DETECTOR FOR SUPERCONDUCTING MAGNETS
W. Jaskierny, A. Kristalinski, and A. T. Visser Dec. 1993 18 p Limited Reproducibility: More than 20% of this document may be affected by microfiche quality
(Contract DE-AC02-76CH-03000)
(DE94-006040; FNAL-TM-1870) Avail: Issuing Activity (Department of Energy (DOE))

This note describes a low voltage signal detector that is useful for detecting quenches or excessive lead voltages at superconducting magnets. It can also be used for other applications where it is needed to detect low level signals present on high voltage installations. The application of isolated operational amplifiers is often not practical for high voltage applications because of their limited input voltage rating, common mode rejection, and sensitivity. The described detector can withstand 7.5 kV input to ground voltage. It has a typical common mode rejection of -150 dB at 60 Hz and an input sensitivity better than 1 mV. The magnetically coupled quench detector assembly is very sensitive to extremely small (order of 1 micro-Amp) current changes in the sense windings. The detector assembly can therefore also be referred to as a micro current detector. DOE

N94-30907# Brookhaven National Lab., Upton, NY.
AC LOSSES FOR THE SELF FIELD OF AN AC TRANSPORT CURRENT WITH A DC TRANSPORT CURRENT OFFSET IN HIGH T(c) SUPERCONDUCTING MAGNET COILS FOR MagLev APPLICATION
V. F. Koosh Oct. 1993 17 p
(Contract DE-AC02-76CH-00016)
(DE94-005187; BNL-49706) Avail: CASI HC A03/MF A01

Although much research has been conducted concerning the losses of high-T(sub c) superconductors, very little has concentrated on the self-field losses in an actual magnet arrangement. The coils studied in this work were designed for use as actual magnets in an industrial application. Self field loss measurements were made upon tape-wound 2223 superconducting helix coils. The self-field losses were produced by an AC transport current with a DC transport current offset. Losses were taken for single, double and triple tape windings, giving essentially monofilament, dual, and three filament cases. The losses measured here were varied over a range of AC current values for several different DC values, and over a range of frequencies. The currents were all AC sinusoids with a DC offset. All measurements were made at T = 77K. DOE

N94-28698*# European Space Agency. European Space Research and Technology Center, ESTEC, Noordwijk (Netherlands).
ESTEC WIRING TEST PROGRAMME MATERIALS RELATED PROPERTIES
M. D. Judd *In* NASA. Lewis Research Center, Second NASA Workshop on Wiring for Space Applications Jan. 1994 p 15-18 (For primary document see N94-28697 08-18)
Avail: CASI HC A01/MF A03; 8 functional color pages

N94-28699*# Wright Lab., Wright-Patterson AFB, OH.
ROBUST 300 C WIRE INSULATION SYSTEM
John G. Nairus *In* NASA. Lewis Research Center, Second NASA Workshop on Wiring for Space Applications Jan. 1994 p 19-23 (For primary document see N94-28697 08-18)
Avail: CASI HC A01/MF A03; 8 functional color pages

N94-28700*# Sverdrup Technology, Inc., Brook Park, OH.
NASA WIRING PROGRAM: SURVEY OF NASA EXPERIENCES IN WIRING SYSTEM SAFETY
Mark W. Stavnes *In* NASA. Lewis Research Center, Second NASA Workshop on Wiring for Space Applications Jan. 1994 p 27-39 Original contains color illustrations (For primary document see N94-28697 08-18)
Avail: CASI HC A03/MF A03; 8 functional color pages

N94-28701*# National Aeronautics and Space Administration. Lewis Research Center, Cleveland, OH.
SELECTION OF THE SPACE STATION FREEDOM (SSF) FLAT COLLECTOR CIRCUIT (FCC) INSULATION MATERIAL
Dawn Emerson *In its* Second NASA Workshop on Wiring for Space Applications Jan. 1994 p 41-49 (For primary document see N94-28697 08-18)
Avail: CASI HC A02/MF A03; 8 functional color pages

N94-28702*# National Aeronautics and Space Administration. Goddard Space Flight Center, Greenbelt, MD.
NASA PARTS PROGRAM OFFICE RESPONSIBILITIES
Patrick L. Kilroy *In* NASA. Lewis Research Center, Second NASA Workshop on Wiring for Space Applications Jan. 1994 p 51-53 (For primary document see N94-28697 08-18)
Avail: CASI HC A01/MF A03; 8 functional color pages

N94-28703*# Paramax Systems Corp., Lanham, MD.
NASA PARTS PROJECT OFFICE: BASIC GOALS
Jeannette Plante *In* NASA. Lewis Research Center, Second NASA Workshop on Wiring for Space Applications Jan. 1994 p 55-57 (For primary document see N94-28697 08-18)
Avail: CASI HC A01/MF A03; 8 functional color pages

N94-28704*# Naval Air Warfare Center, Indianapolis, IN.
NAVAIR AIRCRAFT WIRING STANDARDIZATION AND QUALIFICATION PROGRAM
Thomas Meiner *In* NASA. Lewis Research Center, Second NASA Workshop on Wiring for Space Applications Jan. 1994 p 59-61 (For primary document see N94-28697 08-18)
Avail: CASI HC A01/MF A03; 8 functional color pages

N94-28705*# Naval Air Warfare Center, Indianapolis, IN.
ORGANIZED WIRING SYSTEMS
Thomas Meiner *In* NASA. Lewis Research Center, Second NASA Workshop on Wiring for Space Applications Jan. 1994 p 63-77 Original contains color illustrations (For primary document see N94-28697 08-18)
Avail: CASI HC A03/MF A03; 8 functional color pages

N94-28706*# National Electrical Mfrs. Association, Washington, DC. Wire and Cable Div.
NEMA WIRE AND CABLE STANDARDS DEVELOPMENT PROGRAMS
Robert W. Baird *In* NASA. Lewis Research Center, Second NASA Workshop on Wiring for Space Applications Jan. 1994 p 79-93 (For primary document see N94-28697 08-18)
Avail: CASI HC A03/MF A03; 8 functional color pages

N94-28707*# National Aeronautics and Space Administration. Marshall Space Flight Center, Huntsville, AL.
MSFC INSPECTIONS OF INSTALLED POLYIMIDE WIRE
Joe C. Landers *In* NASA. Lewis Research Center, Second NASA Workshop on Wiring for Space Applications Jan. 1994 p 95-102 (For primary document see N94-28697 08-18)
Avail: CASI HC A02/MF A03; 8 functional color pages

N94-28708*# Sverdrup Technology, Inc., Cleveland, OH.
WIRING FOR SPACE APPLICATIONS PROGRAM
Ahmad Hammoud *In* NASA. Lewis Research Center, Second NASA Workshop on Wiring for Space Applications Jan. 1994 p 105-108 (For primary document see N94-28697 08-18)
Avail: CASI HC A01/MF A03; 8 functional color pages

N94-28714*# Technische Univ., Darmstadt (Germany).
A NEW TEST METHOD FOR THE ASSESSMENT OF THE ARC TRACKING PROPERTIES OF WIRE INSULATION IN AIR, OXYGEN ENRICHED ATMOSPHERES AND VACUUM
Dieter Koenig *In* NASA. Lewis Research Center, Second NASA Workshop on Wiring for Space Applications Jan. 1994 p 173-188 (For primary document see N94-28697 08-18)
Avail: CASI HC A03/MF A03; 8 functional color pages

N94-29667*# Jet Propulsion Lab., California Inst. of Tech., Pasadena.
DESIGN AND IMPLEMENTATION OF A HYBRID DIGITAL PHASE-LOCKED LOOP WITH A TMS320C25: AN APPLICATION TO A TRANSPONDER RECEIVER BREADBOARD
H.-G. Yeh and T. M. Nguyen *In its* The Telecommunications and Data Acquisition Report 15 Feb. 1994 p 175-189 (For primary document see N94-29652 08-32)
(RTOP 315-91-10-13-08)
Avail: CASI HC A03/MF A03

N94-29784*# International Business Machines Corp., San Jose, CA. Research Div.
TOWARD MILLI-NEWTON ELECTRO- AND MAGNETO-STATIC MICROACTUATORS
Long-Sheng Fan *In* JPL, Proceedings of the Workshop on Microtechnologies and Applications to Space Systems 15 Jun. 1993 p 191-20 (For primary document see N94-29767 08-31)
Avail: CASI HC A03/MF A03

N94-30312 Royal Military Coll. of Canada, Kingston (Ontario). Dept. of Chemistry and Chemical Engineering.
ELECTROCHEMICAL POWER SOURCE (EPS) SELECTION FOR ENERGETICALLY INDEPENDENT ROBOTS (EIR): A SYSTEMATIC APPROACH
P. R. Roberge and K. A. Sosin *In* Defence Research Establishment Suffield, Proceedings of the 3rd Conference on Military Robotic Applications 1991 p 318-326 (For primary document see N94-30275 08-37)
Avail: Issuing Activity (Defence Research Establishment Suffield, P.O. Box 4000, Medicine Hat, AB T1A 8K6 Canada)

34 FLUID MECHANICS AND HEAT TRANSFER

Includes boundary layers; hydrodynamics; fluidics; mass transfer; and ablation cooling.

For related information see also *02 Aerodynamics* and *77 Thermodynamics and Statistical Physics.*

N94-28464# State Univ. of New York, Albany. Atmospheric Sciences Research Center.
THE AUTOMATED ROTATING SHADOWBAND SPECTRORADIOMETER
L. Harrison, M. A. Beik, and J. J. Michalsky 1993 4 p Presented at the Optical Society of America Meeting on Optical Remote Sensing of the Atmosphere, Salt Lake City, UT, 8-12 Mar. 1993
(Contracts DE-FG02-90ER-61072; DE-AC06-76RL-01830)
(DE94-001878; DOE/ER-61072/7; CONF-930346-5) Avail: CASI HC A01/MF A01

We are developing a photodiode array rotating shadowband spectroradiometer (RSS) as part of the Instrument Development Program (IDP) of the Atmospheric Radiation Measurement (ARM) program of the U.S. Department of Energy (DOE). This instrument uses the automated rotating shadowband technique to separate and measure the spectrally resolved direct-normal, total horizontal, and diffuse horizontal irradiances in the 360 to 1060 nm wavelength region. It is intended as an instrument for the central facility of each of the cloud and radiation testbed (CART) sites, and it will complement the array of multi-filter rotating shadowband radiometers (MFRSR) currently being deployed by ARM and other research programs including TOGA/COARE. DOE

N94-28475# Los Alamos National Lab., NM.
MODELING TURBULENCE IN FLOWS WITH A STRONG ROTATIONAL COMPONENT
D. E. Burgess and P. J. ORourke Nov. 1993 27 p
(Contract W-7405-eng-36)
(DE94-003577; LA-12552-MS) Avail: CASI HC A03/MF A01

We consider the effectiveness of various turbulence models in flows with a strong rotational component. To evaluate the models, we implement them into a one-dimensional test code and make comparisons with experimental data for swirling flow in a cylinder. The k-epsilon type turbulence models do poorly in predicting the experimental results. However, we find that the incorporation of a Reynolds stress evolution equation gives good agreement with the experimentally measured mean flow. Modeling the pressure-strain correlation tensor correctly is the key for obtaining good results. A combination of Launder's basic model together with Yakhot's dissipation rate equation works best in predicting both the mean flow and the turbulence intensity. DOE

N94-28476# Lawrence Livermore National Lab., CA.
ANALYSIS OF SPARK-INDUCED BUBBLE EXPERIMENTS USING CALE
S. C. Simonson, III and S. W. McAllister Oct. 1993 69 p
(Contract W-7405-eng-48)
(DE94-003667; UCRL-ID-115283) Avail: CASI HC A04/MF A01

Calculations were made using the 2-D hydrodynamics code CALE of underwater bubble oscillations and collapse for two situations of interest in the development of underwater acoustic sources. The first is the case of a single bubble to which energy is added to prolong oscillations. The second is the case of a three-bubble array, which typifies one end element in a linear array. Comparisons were made with a series of experiments with spark-induced bubbles carried out at Tetra Corp. The bubbles were made at a depth of 64 cm with periods of about 400 micro-s. One dimensional calculations were used to study singlebubbles. The 1-D results showed that energy needs to be added at a precise phase in order to promote bubble re-excitation. The experiments showed evidence of losses caused by interaction with the relatively large electrodes upon collapse, leading to a 50 percent reduction in amplitude and period of the second oscillation. When a second discharge was made at the end of the first oscillation, the next oscillation had 80 percent of the amplitude of the first. This can be interpreted either as formation of a new bubble, or as pumping the previous bubble, both occurring in a disturbed environment. Two-dimensional calculations were used to study the three-bubble array. The 2-D results showed significant interaction between the central and side bubbles, leading to jetting. For the particular combination of size and spacing used, jetting occurred in the third oscillation of the bubbles. DOE

N94-28488# Sandia National Labs., Albuquerque, NM.
SAFSIM THEORY MANUAL: A COMPUTER PROGRAM FOR THE ENGINEERING SIMULATION OF FLOW SYSTEMS
Dean Dobranich Dec. 1993 200 p
(Contract DE-AC04-94AL-85000)
(DE94-005381; SAND-92-0693) Avail: CASI HC A09/MF A03

SAFSIM (System Analysis Flow SIMulator) is a FORTRAN computer program for simulating the integrated performance of complex flow systems. SAFSIM provides sufficient versatility to allow the engineering simulation of almost any system, from a backyard sprinkler system to a clustered nuclear reactor propulsion system. In addition to versatility, speed and robustness are primary SAFSIM development goals. SAFSIM contains three basic physics modules: (1) a fluid mechanics module with flow network capability; (2) a structure heat transfer module with multiple convection and radiation exchange surface capability; and (3) a point reactor dynamics module with reactivity feedback and decay heat capability. Any or all of the physics modules can be implemented, as the problem dictates. SAFSIM can be used for compressible and incompressible, single-phase, multicomponent flow systems. Both the fluid mechanics and structure heat transfer modules employ a one-dimensional finite element modeling approach. This document contains a description of the theory incorporated in SAFSIM, including the governing equations, the numerical methods, and the overall system solution strategies. DOE

N94-28549# Los Alamos National Lab., NM.
LARGE EDDY SIMULATIONS USING LATTICE BOLTZMANN ALGORITHMS
J. D. Serling 28 Sep. 1993 21 p
(Contract W-7405-eng-36)
(DE94-005666; LA-SUB-94-1) Avail: CASI HC A03/MF A01

This report contains the results of a study performed to implement eddy-viscosity models for Large-Eddy-Simulations (LES) into Lattice Boltzmann (LB) algorithms for simulating fluid flows. This implementation requires modification of the LB method of simulating the incompressible Navier-Stokes equations to allow simulation of the filtered Navier-Stokes equations with some subgrid model for the Reynolds stress term. We demonstrate that the LB method can indeed be used for LES by simply locally adjusting the value of the BGK relaxation time to obtain the desired eddy-viscosity. Thus, many forms of eddy-viscosity models including the standard Smagorinsky model or the Dynamic model may be implemented using LB algorithms. Since underresolved LB simulations often lead to instability, the LES model actually serves to stabilize the method. An alternative method of ensuring stability is presented which requires that entropy increase during the collision step of the LB method. Thus, an alternative collision operator is locally applied if the entropy becomes too low. This stable LB method then acts as an LES scheme that effectively introduces its own eddy viscosity to damp short wavelength oscillations. DOE

N94-28665# Ohio State Univ., Columbus. Dept. of Mechanical Engineering.
BOUNDARY LAYERS INDUCED BY THREE-DIMENSIONAL VORTEX LOOPS Final Report, 1 May 1989 - 31 Aug. 1993
A. T. Conlisk, H. Affes, O. R. Burggraf, and Zhenhua Xiao Dec. 1993 278 p
(Contract DAAL03-89-K-0095)
(AD-A275678; RF-767440/722045; ARO-26595.7-EG) Avail: CASI HC A13/MF A03

The flow field generated by a helicopter in flight is extremely complex and it has been recognized that interactions between different components can significantly affect helicopter performance. In particular, the effects of the interaction between the rotor wake and the helicopter fuselage are extremely difficult to predict and pose a challenging problem for researchers and designers in the rotorcraft area. In the present work, a model for the interaction of a rotor-tip-vortex with the airframe of a helicopter is developed. The present report describes the calculation of the motion of the tip-vortex toward the airframe, the calculation of the induced pressure on the airframe, and the calculation of the boundary-layer flow under the vortex during the time period prior to the time when a portion of the tip-vortex collides with the airframe. DTIC

N94-28692# Calspan-Buffalo Univ. Research Center, NY.
DEVELOPMENT OF LASER VELOCIMETRY FOR THE MEASUREMENTS OF TURBULENCE INTENSITY AND FLOW VELOCITY AHEAD OF A NGV ROW IN A FULL-STAGE ROTATING TURBINE Final Report, 1985 - 1993
Sep. 1993 12 p
(Contract F33615-85-C-2566)
(AD-A275712; WL-TR-94-2008) Avail: CASI HC A03/MF A01

This is a letter report which summarizes the six tasks of this effort. It was not possible to complete shock tube measurements as originally planned due to schedule conflicts, equipment failures, and finally an explosion in Calspan's lab. The funding was to expire in 1993, which would have incurred an additional obligation of the government if the effort were to be completed as originally planned. By mutual agreement, in order to prevent incurring any additional cost, the design, fabrication, calibration and installation of heat flux gages on the Advanced High Work turbine hardware was substituted for the only uncompleted task of the effort, that of actually running the shock tube test. The documentation of the delivered hardware's performance will be reported in the appropriate ATARR test report of the Advanced High Work Turbine. The resulting new instrumentation from this modification to the Statement of Work is shown as installed on the Advanced High Work Turbine in photos. DTIC

N94-28724*# Stanford Univ., CA. Joint Inst. for Aeronautics and Acoustics.
A METHOD FOR THE MODELLING OF POROUS AND SOLID WIND TUNNEL WALLS IN COMPUTATIONAL FLUID DYNAMICS CODES
Thomas John Beutner Dec. 1993 124 p

(Contract NCC2-55)
(NASA-CR-195699; NAS 1.26:195699; JIAA-TR-111) Avail: CASI HC A06/MF A02

Porous wall wind tunnels have been used for several decades and have proven effective in reducing wall interference effects in both low speed and transonic testing. They allow for testing through Mach 1, reduce blockage effects and reduce shock wave reflections in the test section. Their usefulness in developing computational fluid dynamics (CFD) codes has been limited, however, by the difficulties associated with modelling the effect of a porous wall in CFD codes. Previous approaches to modelling porous wall effects have depended either upon a simplified linear boundary condition, which has proven inadequate, or upon detailed measurements of the normal velocity near the wall, which require extensive wind tunnel time. The current work was initiated in an effort to find a simple, accurate method of modelling a porous wall boundary condition in CFD codes. The development of such a method would allow data from porous wall wind tunnels to be used more readily in validating CFD codes. This would be beneficial when transonic validations are desired, or when large models are used to achieve high Reynolds numbers in testing. A computational and experimental study was undertaken to investigate a new method of modelling solid and porous wall boundary conditions in CFD codes. The method utilized experimental measurements at the walls to develop a flow field solution based on the method of singularities. This flow field solution was then imposed as a pressure boundary condition in a CFD simulation of the internal flow field. The effectiveness of this method in describing the effect of porosity changes on the wall was investigated. Also, the effectiveness of this method when only sparse experimental measurements were available has been investigated. The current work demonstrated this approach for low speed flows and compared the results with experimental data obtained from a heavily instrumented variable porosity test section. The approach developed was simple, computationally inexpensive, and did not require extensive or intrusive measurements of the boundary conditions during the wind tunnel test. It may be applied to both solid and porous wall wind tunnel tests. Author

N94-28738# Air Force Inst. of Tech., Wright-Patterson AFB, OH.
SPIN-UP IN A RECTANGULAR CYLINDER M.S. Thesis
Dawn L. Stewart Dec. 1993 70 p
(AD-A275465; AFIT/CI/CIA-93-163) Avail: CASI HC A04/MF A01

We examined the spin-up from rest of water in a rectangular cylinder. The presence of corners in the cylinder causes the formation of eddies. We found that the number of eddies, as well as eddy size, position, and rotation rate were dependent on the aspect ratio of the cylinder, the depth of the fluid, and the final angular velocity of the cylinder. Two time scales were found to be important in this experiment: the traditional Ekman number based on depth, which defines the time scale required for spin-up and an additional Ekman number based on the cylinder length which provides some information about the evolution of the fluid pathlines in route to spin-up. This second Eckman number appears to provide an explanation for both the agreement and disagreement of the experimental results herein and previously published results. DTIC

N94-28778# Naval Undersea Warfare Center, Newport, RI.
WALL PRESSURE EVENTS FROM THE DIRECT NUMERICAL SIMULATION OF A TURBULENT WALL-BOUNDED FLOW Final Report
Richard M. Lueptow 6 Dec. 1993 17 p
(AD-A275890; NUWC-NPt-TR-10481) Avail: CASI HC A03/MF A01

Wall pressure events beneath a turbulent wall-bounded flow are related to turbulence-generating events in the flow. The data base for a direct numerical simulation of channel flow allows the analysis of significant pressure events in space and time. Both positive and negative wall pressure events in the data base were detected with a pressure peak conditional sampling technique. The recovered events were ensemble averaged to provide a space and time record of a typical event. Both positive and negative pressure peak events have regions of pressure of the opposite sign just ahead of and just behind them, but the regions of opposite sign do not extend to the sides of the events. Although a positive pressure peak event begins as a double positive pressure hump, the downstream hump eventually dominates and becomes the pressure peak before the event decays. Negative pressure peak events begin as a positive hump leading a negative hump. The negative hump grows to become the peak before decaying. Both positive and negative events begin about 400 wall units upstream of where the maximum pressure occurs and persist to about 400 wall units downstream of the pressure peak. The entire event lasts about 0.4 delta/U Tau. DTIC

N94-28809 Air Force Inst. of Tech., Wright-Patterson AFB, OH.
A FLOW VISUALIZATION STUDY OF ACOUSTICALLY ENHANCED HAIRPIN VORTICES M.S. Thesis
Stephen A. Whyte 1993 66 p Limited Reproducibility: More than 20% of this document may be affected by microfiche quality
(AD-A275467; AFIT/CI/CIA-93-164) Avail: CASI HC A04

For many years the turbulent boundary layer was thought to be composed of totally chaotic and random eddies. However, recent work has shown that a very organized array of structures exists in this regime. These structures, named hairpin, horseshoe, or Lamda-shaped vortices, compose a major portion of the turbulent boundary layer and may be responsible for the increased heat transfer seen in turbulent regimes. The hairpin vortex is a vortex line that has been lifted off of the surface and through mutual induction of its legs forms a loop. This loop is composed of two counter-rotating legs, oriented at 45 degrees to the wall, with a head that joins the two legs together. These legs act like tornados sweeping along the wall. They transport air adjacent to the wall up through the legs and into the head. Research at the University of Washington has shown that this 'tornado effect' increased the heat flux away from the wall. If this capability can be harnessed and enhanced, the effects of film cooling in turbine engines can be dramatically increased. DTIC

N94-28835*# National Aeronautics and Space Administration. Lewis Research Center, Cleveland, OH.
CALCULATION OF PROPULSIVE NOZZLE FLOWFIELDS IN MULTIDIFFUSING CHEMICALLY REACTING ENVIRONMENTS Ph.D. Thesis - Purdue Univ.
Kenneth John Kacynski Apr. 1994 295 p
(RTOP 506-42-72)
(NASA-TM-106532; E-8665; NAS 1.15:106532) Avail: CASI HC A13/MF A03

An advanced engineering model has been developed to aid in the analysis and design of hydrogen/oxygen chemical rocket engines. The complete multispecies, chemically reacting and multidiffusing Navier-Stokes equations are modelled, including the Soret thermal diffusion and the Dufour energy transfer terms. In addition to the spectrum of multispecies aspects developed, the model developed in this study is also conservative in axisymmetric flow for both inviscid and viscous flow environments and the boundary conditions employ a viscous, chemically reacting, reference plane characteristics method. Demonstration cases are presented for a 1030:1 area ratio nozzle, a 25 lbf film cooled nozzle, and a transpiration cooled plug and spool rocket engine. The results indicate that the thrust coefficient predictions of the 1030:1 and the 25 lbf film cooled nozzle are within 0.2 to 0.5 percent, respectively, of experimental measurements when all of the chemical reaction and diffusion terms are considered. Further, the model's predictions agree very well with the heat transfer measurements made in all of the nozzle test cases. The Soret thermal diffusion term is demonstrated to have a significant effect on the predicted mass fraction of hydrogen along the wall of the nozzle in both the laminar flow 1030:1 nozzle and the turbulent flow plug and spool nozzle analysis cases performed. Further, the Soret term was shown to represent an important fraction of the diffusion fluxes occurring in a transpiration cooled rocket engine. Author

N94-29061# Wisconsin Univ., Madison.
[THE MOTION OF DEFORMING BODIES] Progress Report
Athanasios E. Tzavaras 1993 3 p
(Contract N00014-93-1-0015)
(AD-A275224) Avail: CASI HC A01/MF A01

This effort concentrated in the study of self-similar viscous and fluid-dynamic limits. The invariance of hyperbolic systems of conservation laws under dilations of coordinates is a key property underlying much of the current theory. Viscous perturbations introduce an additional parabolic scale and this invariance is lost. Understanding how the two scales interact for small viscosities is an important step in the process of studying viscous limits for general solutions. One illuminating step in that direction is to consider the Riemann problem and to study artificial regularizations, rigged so as to preserve the invariance under dilations of coordinates and the entropy structure of the system. It provides information on how viscosity

regularizes the whole wave fan emerging from Riemann data. At the technical level, it leads to study of singular perturbations for non-autonomous boundary-value problems, and the limiting process involves variation estimates. DTIC

N94-29096*# National Aeronautics and Space Administration. Lewis Research Center, Cleveland, OH.
THEORETICAL STUDY OF THE INCOMPRESSIBLE NAVIER-STOKES EQUATIONS BY THE LEAST-SQUARES METHOD
Bo-Nan Jiang, Ching Y. Loh, and Louis A. Povinelli Mar. 1994 46 p
(Contract NCC3-233; RTOP 505-90-5K)
(NASA-TM-106535; ICOMP-94-04; E-8670; NAS 1.15:106535) Avail: CASI HC A03/MF A01

Usually the theoretical analysis of the Navier-Stokes equations is conducted via the Galerkin method which leads to difficult saddle-point problems. This paper demonstrates that the least-squares method is a useful alternative tool for the theoretical study of partial differential equations since it leads to minimization problems which can often be treated by an elementary technique. The principal part of the Navier-Stokes equations in the first-order velocity-pressure-vorticity formulation consists of two div-curl systems, so the three-dimensional div-curl system is thoroughly studied at first. By introducing a dummy variable and by using the least-squares method, this paper shows that the div-curl system is properly determined and elliptic, and has a unique solution. The same technique then is employed to prove that the Stokes equations are properly determined and elliptic, and that four boundary conditions on a fixed boundary are required for three-dimensional problems. This paper also shows that under four combinations of non-standard boundary conditions the solution of the Stokes equations is unique. This paper emphasizes the application of the least-squares method and the div-curl method to derive a high-order version of differential equations and additional boundary conditions. In this paper, an elementary method (integration by parts) is used to prove Friedrichs' inequalities related to the div and curl operators which play an essential role in the analysis. Author (revised)

N94-29136# Stanford Univ., CA. Dept. of Mechanical Engineering.
ADVANCED DIAGNOSTICS FOR REACTING FLOWS Annual Technical Report, 1 Nov. 1992 - 31 Oct. 1993
R. K. Hanson 24 Nov. 1993 123 p
(Grant AF-AFOSR-0067-89)
(AD-A275057; AFOSR-94-0030TR) Avail: CASI HC A06/MF A02

Progress is reported for the past year of an interdisciplinary program aimed at establishing advanced optical diagnostic techniques applicable to combustion gases and plasmas, with some emphasis on high speed flows. The primary parameters of interest are species concentrations (including electrons), temperature, mass density, pressure, velocity, and quantities derivable from these parameters such as mass flow rate (from the product of density and velocity). The techniques under study are based on laser spectroscopy, particularly laser absorption and laser-induced fluorescence, with the latter capable of providing both single-point and multi-point (2-D and 3-D) measurements. Laser sources include tunable cw lasers (ring dye and semiconductor diode lasers) and tunable pulsed lasers (excimer-pumped dye and narrow-linewidth excimer). The cw lasers are spectrally narrow, allowing study of a new class of techniques based on spectral lineshapes and shifts, while the pulsed lasers provide intense bursts of photons needed for techniques based on light-scattering phenomena. DTIC

N94-29149# Texas Univ., Austin. Applied Research Lab.
INTERACTION OF MULTIPLE SPARK-GENERATED BUBBLES IN A COMPRESSIBLE LIQUID
Jeffrey A. Cook 1 Jun. 1993 160 p
(Contracts N00014-91-J-1366; N00014-93-J-0018)
(AD-A275037; ARL-TR-93-10) Avail: CASI HC A08/MF A02

This dissertation describes the interaction of bubbles generated by underwater electrical discharges. The oscillations of these high temperature vapor and plasma bubbles generate acoustic signatures similar to the signatures generated by air guns, underwater explosions, and combustible sources. Tasks performed by these hydrodynamic sources typically require multiple sources in an array to achieve a directional beam. The properties of a single isolated source can be used to estimate the properties of an array of multiple sources, but in many cases, the acoustic properties of the source change dramatically when several sources are placed near one another. A set of model equations was developed in this report that allowed the time evolution of the bubble generated by a spark discharge to be calculated numerically from a given discharge. A simple interaction scheme was used to couple the model equations for multiple bubbles. The coupled equations were integrated simultaneously to determine the dynamics of the elements. An apparatus containing seven individual spark discharge elements was designed and constructed to test the interaction model experimentally. The model and experimental data agreed over separations down to a few bubble diameters, and the study described when the interaction between bubbles could be neglected. DTIC

N94-29195# Pennsylvania State Univ., University Park. Dept. of Meteorology.
BOUNDARY LAYER COHERENT STRUCTURES Report, 1993
Hampton N. Shirer and George S. Young 1993 5 p
(AD-A275007) Avail: CASI HC A01/MF A01

The correlation dimension D is used commonly to quantify the chaotic structure of an attractor of a smooth dynamical system. The standard algorithm for estimating the value of D is based on finding the mean slope of the curve obtained by plotting ln C(r) versus ln r, where C(r) is the correlation integral and r is the distance between points on the attractor. The alternative, probabilistic method proposed by Takens is based on finding the sample means of the random variable ln(r/p), expressed as the conditional expected value E(ln(r/p):r<p). In this article, this first Takens estimator is extended and generalized. DTIC

N94-29378*# Eloret Corp., Palo Alto, CA.
THEORETICAL INVESTIGATION OF GAS-SURFACE INTERACTIONS Final Technical Report, 1 Sep. 1988 - 31 Jan. 1994
Kenneth G. Dyall 14 Apr. 1994 9 p
(Contract NCC2-552)
(NASA-CR-195755; NAS 1.26:195755) Avail: CASI HC A02/MF A01

The goal of this project was to develop computational tools for the calculation of the electronic structure of molecules containing heavy atoms, and to use these tools in the study of catalytic processes, with the overall objective of gaining an understanding of the catalytic process which could be used to design more efficient catalysts. The main catalytic system of interest was the combustion of hydrogen on platinum surfaces. Under this project, a flexible Dirac-Hartree-Fock (DHF) program has been developed, a code to calculate DHF correlation energies at the second-order Moeller-Plesset perturbation (PP2) level is almost complete, and code to include correlation at the MCSCF and MCSCF/MP2 level is planned. The tools so far developed have been validated and used to calibrate some more approximate methods, and applied to investigate the importance of relativistic effects in the bonding of hydrogen to platinum.
Author (revised)

N94-29381*# Institute for Computer Applications in Science and Engineering, Hampton, VA.
AN ALTERNATIVE ASSESSMENT OF SECOND-ORDER CLOSURE MODELS IN TURBULENT SHEAR FLOWS Final Report
Charles G. Speziale (Boston Univ., MA.) and Thomas B. Gatski Mar. 1994 19 p Submitted for publication
(Contract NAS1-19480; RTOP 505-90-52-01)
(NASA-CR-194881; ICASE-94-10; NAS 1.26:194881) Avail: CASI HC A03/MF A01

The performance of three recently proposed second-order closure models is tested in benchmark turbulent shear flows. Both homogeneous shear flow and the log-layer of an equilibrium turbulent boundary layer are considered for this purpose. An objective analysis of the results leads to an assessment of these models that stands in contrast to that recently published by other authors. A variety of pitfalls in the formulation and testing of second-order closure models are uncovered by this analysis.
Author

N94-29435# Air Force Inst. of Tech., Wright-Patterson AFB, OH.
DETERMINATION OF PRESSURE RESPONSE TIMES FOR GASEOUS FLOW IN A TUBE Ph.D. Thesis
Scott A. Baune 1993 101 p
(AD-A275274; AFIT/CI/CIA-93-1170) Avail: CASI HC A06/MF A02

The motivation for determining the response time for a pressure regulator to adjust the pressure at an area of interest located at the end of a long

tube may be due to several reasons. One of these is the possibility that the regulator cannot be conveniently controlled from a more desirable position closer to the area of interest. Another reason to place to place the regulator a long distance from the area of interest might be to avoid high pressure lines over a prolonged distance. Consider the proposed propulsion system for a microgravity experiment located in the Shuttle car bay. The regulator is controlled electronically so the ability to reduce the amount of electrical wiring will increase system reliability. Furthermore, Shuttle safety requirements demand that high pressure lines be tested for space worthiness, thus placement of the regulator close to the propeliant source may eliminate the presence of these high pressure lines. DTIC

N94-29460*# High Technology Corp., Hampton, VA.
LONG-WAVELENGTH ASYMPTOTICS OF UNSTABLE CROSSFLOW MODES, INCLUDING THE EFFECT OF SURFACE CURVATURE
Meelan Choudhari Apr. 1994 43 p
(Contract NAS1-19299; RTOP 538-05-15-03)
(NASA-CR-4579; NAS 1.26:4579) Avail: CASI HC A03/MF A01

Stationary vortex instabilities with wavelengths significantly larger than the thickness of the underlying three-dimensional boundary layer are studied with asymptotic methods. The long-wavelength Rayleigh modes are locally neutral and are aligned with the direction of the local inviscid streamline. For a spanwise wave number Beta much less than 1, the spatial growth rate of these vortices is O(Beta(exp 3/2)). When Beta becomes O(R(exp -1/7)), the viscous correction associated with a thin sublayer near the surface modifies the inviscid growth rate to the leading order. As Beta is further decreased through this regime, viscous effects assume greater significance and dominate the growth-rate behavior. The spatial growth rate becomes comparable to the real part of the wave number when Beta = O(R(exp -1/4)). At this stage, the disturbance structure becomes fully viscous-inviscid interactive and is described by the triple-deck theory. For even smaller values of Beta, the vortex modes become nearly neutral again and align themselves with the direction of the wall-shear stress. Thus, the study explains the progression of the crossflow-vortex structure from the inflectional upper branch mode to nearly neutral long-wavelength modes that are aligned with the wall-shear direction. Author

N94-29471*# National Aeronautics and Space Administration. Lewis Research Center, Cleveland, OH.
A NEW FLUX-CONSERVING NUMERICAL SCHEME FOR THE STEADY, INCOMPRESSIBLE NAVIER-STOKES EQUATIONS
James R. Scott Apr. 1994 49 p
(RTOP 505-62-52)
(NASA-TM-106520; E-8642; NAS 1.15:106520) Avail: CASI HC A03/MF A01

This paper is concerned with the continued development of a new numerical method, the space-time solution element (STS) method, for solving conservation laws. The present work focuses on the two-dimensional, steady, incompressible Navier-Stokes equations. Using first an integral approach, and then a differential approach, the discrete flux conservation equations presented in a recent paper are rederived. Here a simpler method for determining the flux expressions at cell interfaces is given; a systematic and rigorous derivation of the conditions used to simulate the differential form of the governing conservation law(s) is provided; necessary and sufficient conditions for a discrete approximation to satisfy a conservation law in E2 are derived; and an estimate of the local truncation error is given. A specific scheme is then constructed for the solution of the thin airfoil boundary layer problem. Numerical results are presented which demonstrate the ability of the scheme to accurately resolve the developing boundary layer and wake regions using grids which are much coarser than those employed by other numerical methods. It is shown that ten cells in the cross-stream direction are sufficient to accurately resolve the developing airfoil boundary layer. Author (revised)

N94-29534 Cincinnati Univ., OH.
RNS OPTIMIZATION PROCEDURE FOR THREE-DIMENSIONAL COMPOSITE VELOCITY MULTI-BLOCK APPLICATIONS Ph.D. Thesis
Hussain Mohamed Hasa Almahroos 1992 215 p
Avail: Univ. Microfilms Order No. DA9313812

RNS analysis of the composite velocity formulation has been applied for three dimensional flows. A consistent coupled strongly implicit procedure has been used to solve the coupled system of equations in general nonorthogonal coordinate system. Different forms of contravariant momentum balances have been examined. A multiblock analogy and optimization strategies have been implemented and are presented. Three dimensional subsonic and transonic, viscous-inviscid interacting flows over afterbody configurations have been evaluated. Laminar and turbulent flow solutions, with and without regions of recirculation and shock wave boundary layer interaction, are presented. Three dimensional flows over multiple body configurations are also presented. Dissert. Abstr.

N94-29539* National Aeronautics and Space Administration. Lewis Research Center, Cleveland, OH.
METHOD OF REDUCING HYDRAULIC INSTABILITY Patent
Joseph P. Veres, inventor (to NASA) 15 Feb. 1994 10 p Filed 4 Jan. 1993
(NASA-Case-LEW-15463-1; US-Patent-5,286,162;
US-Patent-Appl-SN-000163; US-Patent-Class-415-115;
US-Patent-Class-415-206; US-Patent-Class-415-914;
Int-Patent-Class-F04D-29/68) Avail: US Patent and Trademark Office

The present invention is directed to a method and apparatus for improving the flow range in centrifugal pumps and compressors. Bleed holes are introduced into a volute tongue of a centrifugal pump or compressor thereby providing a double acting means of boundary layer control at the volute tongue. Official Gazette of the U.S. Patent and Trademark Office

N94-29675 Texas Univ., Austin.
MODELS FOR VIBRATION-DISSOCIATION COUPLING IN HIGH-TEMPERATURE GASES Ph.D. Thesis
David Albert Gonzales 1993 199 p
Avail: Univ. Microfilms Order No. DA9323408

Nonequilibrium conditions are expected in the flowfields about high speed, high altitude research vehicles. These conditions may be found in regions of rapid compression and rapid expansion in the flowfield. The impact of nonequilibrium effects on such quantities as heat transfer rate and pressure distribution is not clear. This is due in part to the lack of reliable theoretical models with which to predict nonequilibrium processes in high temperature gases. Accurate computational chemistry techniques cannot be used for engineering analyses because they are prohibitively expensive. The focus of this research is on the development of engineering models that suitably reproduce the elaborate computational chemistry results with far greater efficiency. Models are presented which represent both microscopic and macroscopic processes. At the microscopic level, the N-state approximation of Rapp and coworkers is extended to compute velocity dependent inelastic and dissociative transition probabilities for atom-diatom and diatom-diatom collisions. Nitrogen atoms and diatoms are considered in this part of the study and an anharmonic model of the diatom is used. Dissociated product states are modeled by dividing the continuum into discrete states. The acceleration scheme of Secrest is applied to the N-state method and preliminary calculations on the simpler H2-He collision system show order of magnitude increases in efficiency. The N-state approximation is seen to be more accurate than currently used first order theories. At the macroscopic level, master equation simulations are performed. A new model for the state-specific dissociative rate coefficient is presented and validated. The present results are compared to published dissociative cross sections for the para-H2-Ar collision system as computed by the quasiclassical trajectory (QCT) technique. In order to make the comparison consistent, all inelastic rate coefficients used in the master equation are scaled to published inelastic QCT results. The present model is seen to reproduce the more sophisticated dissociative QCT cross sections to within a factor of two in general. The master equation results also indicate that the most significant contribution to the average dissociative rate coefficient comes from the low-to-mid vibrational levels. Similar results have been obtained by other researchers from more expensive detailed computations. Dissert. Abstr.

N94-29686 Michigan Univ., Ann Arbor.
EVOLUTION OF THE LARGE-SCALE VORTICES IN TURBULENT MIXING-LAYERS Ph.D. Thesis
Slim Aissi 1992 197 p
Avail: Univ. Microfilms Order No. DA9308260

The evolution of the large-scale vortices in turbulent mixing layers was investigated both theoretically and experimentally. In the theoretical study, a novel approach was used to model the dynamics of the large-scale

vortices. The model accounts for the amalgamation processes as well as the advection of the vortices between the amalgamations. The vortices are characterized by the non-dimensional parameter xi is equivalent to lambda/x at formation, where lambda is the wavelength of the vortex and x is its downstream location at formation. The evolution of xi from one vortex generation to the next was investigated and modeled. The resulting equation could be viewed as the first-return map of a nonlinear dynamical system. Such a deterministic model exhibits a wide range of dynamical behavior and the dynamical states were explored as a function of a defined control parameter a. The value of the parameter a for a turbulent mixing layer was obtained using the statistical theory of the large-scale vortices discussed by Bernal. The picture of the randomization of the large-scale vortices that emerged from the theoretical study is a stable, persistent oscillation of the strengths of the vortices around an equilibrium value. This randomization process was found to increase whenever neighboring vortices of different strengths exist in the mixing layer. Other factors that change the randomization process are also discussed. In order to obtain a better understanding of the evolution of the large-scale vortices during their lifespan an experimental study was performed. This study was based on flow visualization and Particle Image Velocimetry (PIV) measurements. The PIV results showed that small vortices were highly stretched during their lifespan and that their peak core vorticity dropped as they convected. Flow reversal and positive vorticity (with negative vorticity being in the vortex cores) were measured in the neighborhood of the large-scale vortices near the jet exit. In addition, a considerable amount of three-dimensionality in the braid regions was observed at the early stages of a vortex lifespan.

Dissert. Abstr.

N94-29689 California Inst. of Tech., Pasadena.

FORCED GENERATION OF SOLITARY WAVES IN A ROTATING FLUID AND THEIR STABILITY Ph.D. Thesis

Wooyoung Choi 1993 129 p

Avail: Univ. Microfilms Order No. DA9325345

The primary objective of this graduate research is to study forced generation of solitary waves in a rotating fluid and their stability properties. For axisymmetric flow of a non-uniformly rotating fluid within a long cylindrical tube, an analysis is presented to predict the periodic generation of upstream-advancing vortex solitons by axisymmetric disturbance steadily moving with a transcritical velocity as a forcing agent. The phenomenon is simulated using the forced Korteweg-de Vries (fKdV) equation to model the amplitude function of the Stokes stream function for describing this family of rotating flows of an inviscid and incompressible fluid. The numerical results for the weakly nonlinear and weakly dispersive wave motion show that a sequence of well-defined axisymmetrical recirculating eddies is periodically produced and emitted to radiate upstream of the disturbance, soon becoming permanent in the form as a procession of vortex solitons, which we call vortons. Two primary flows, the Rankine vortex and the Burgers vortex, are adopted to exhibit in detail the process of producing the upstream vortons by the critical motion of a slender body moving along the central axis, with the Burgers vortex being found the more effective of the two in the generation of vortons. To investigate the evolution of free or forced waves within a tube of non-uniform radius, a new forced KdV equation is derived which models the variable geometry with variable coefficients. A set of section-mean conservation laws is derived specially for this class of rotational tube flows of an inviscid and incompressible fluid, in both differential and integral forms. A new aspect of stability theory is analyzed for possible instabilities of the axisymmetric solitary waves subject to non-axisymmetric disturbances. The present linear analysis based on the model equation involving the bending mode shows that the axisymmetric solitary wave is neutrally stable with respect to small bending mode disturbances. To study nonlinear interactions between the axisymmetric mode and bending mode, a new model is derived which consists of two coupled equations for disturbances of the two modes. The numerical results of the coupled equations show that the primary axisymmetric soliton appears to maintain its own entity, with some oscillations of its amplitude and an undular tail, inferring an interchange of energy between the two modes, when subject to small non-axisymmetric perturbations. Dissert. Abstr.

N94-29730 California Inst. of Tech., Pasadena.

SPHERICAL MODEL FOR TURBULENCE Ph.D. Thesis

Chung-Yu Mou 1993 133 p

Avail: Univ. Microfilms Order No. DA9325370

A new set of models for homogeneous, isotropic turbulence is considered in which the Navier-Stokes equations for incompressible fluid flow are generalized to a set of N coupled equations in N velocity fields. It is argued that in order to be useful these models must embody a new group of symmetries, and a general formalism is laid out for their construction. The work is motivated by similar techniques that have had extraordinary success in improving the theoretical understanding of equilibrium phase transitions in condensed matter systems. The key result is that these models simplify when N is large. The so-called spherical limit, N approaches infinity, can be solved exactly, yielding a closed pair of nonlinear integral equations for the response and correlation functions. These equations, known as Kraichnan's Direct Interaction Approximation (DIA) equations, are, for the first time, solved fully in the scale-invariant turbulent regime, and the implications of these solutions for real turbulence (N = 1) are discussed. In particular, it is argued that previously applied renormalization group techniques, based on an expansion in the exponent, y, that characterizes the driving spectrum, are incorrect, and that the Kolmogorov exponent zeta has a nontrivial dependence on N, with zeta(N approaches infinity) = 3/2. This value is remarkably close to the experimental result, zeta approximately equals 5/3, which must therefore result from higher order corrections in powers of 1/N. Prospects for calculating these corrections are briefly discussed: though daunting, such a calculation would, for the first time, provide a controlled perturbation expansion for the Kolmogorov, and other exponents. Our techniques may also be applied to other nonequilibrium dynamical problems, such as the KPZ equation for interface growth, and perhaps to turbulence in nonlinear wave systems.

Dissert. Abstr.

N94-29740* National Aeronautics and Space Administration. Lewis Research Center, Cleveland, OH.

METHOD FOR CANCELLING EXPANSION WAVES IN A WAVE ROTOR Patent

Daniel E. Paxson, inventor (to NASA) 29 Mar. 1994 10 p Filed 6 Jul. 1993 Division of US-Patent-Appl-SN-889003, filed 26 May 1992 (NASA-Case-LEW-15218-2; US-Patent-5,297,384; US-Patent-Appl-SN-086581; US-Patent-Appl-SN-889003; US-Patent-Class-60-39.02; Int-Patent-Class-F02C-3/02) Avail: US Patent and Trademark Office

A wave rotor system includes a wave rotor coupled to first and second end plates. Special ports are provided, one in each of the first and second end plates, to cancel expansion waves generated by the release of working fluid from the wave rotor. One of the expansion waves is reflected in the wave rotor from a reflecting portion, and provided to the special port in the second end plate. Fluid present at the special port in the second end plate has a stagnation pressure and mass flow which is substantially the same as that of the cells of the wave rotor communicating with such special port. This allows for cancellation of the expansion wave generated by the release of working fluid from the wave rotor. The special port in the second end plate has a first end corresponding substantially to the head of the expansion wave, and a second end corresponding substantially to the tail of the expansion wave. Also, the special port is configured to continually change along the circumference of the second end plate to affect expansion wave cancellation. An expansion wave generated by a second release of working fluid from the wave rotor is cancelled in a similar manner to that described above using a special port in the first end plate. Preferably the cycle of operation of the wave rotor system is designed so that the stagnation pressure and mass flow of the fluid present at the special ports is the same so that the special ports may be connected by a common duct.

Official Gazette of the U.S. Patent and Trademark Office

N94-29761 Maryland Univ., College Park.

A VORTICITY TRANSPORT CLOSURE METHOD FOR TURBULENT REACTING FLOWS Ph.D. Thesis

Ohbin Kwon 1992 251 p

Avail: Univ. Microfilms Order No. DA9315672

A closure method for variable density turbulent reacting flows is proposed. The vorticity transport theory is herein extended to the case of compressible flows. Specifically, turbulent vorticity and dilatation transport laws have been derived using a Lagrangian analysis of the vorticity transport equation in which velocity-velocity gradient correlations are analyzed keeping compressibility and vortex stretching effects. The complete set of closed

equations includes a new mean dilatation (bar-Theta) transport equation and a turbulent dilatation fluctuation intensity (eta) equation. It is shown that the closure method can also be applied through a primitive variable formulation. In this case, in contrast to the standard eddy viscosity models, the averaged momentum equation has additional terms representing the mechanism of vorticity stretching which is known to be an important boundary layer phenomenon. In addition to the turbulence closure, a turbulent combustion model based on a vorticity dissipation time scale is proposed. To close the turbulent reaction rate expression, a species fluctuation intensity (xi(sub i)) equation is derived as well as species mass balance (bar-Y(sub i)) equation. These equations reflect the rich interaction between turbulence and chemistry. The vorticity transport closure method and the vorticity dissipation combustion model are applied to the internal combustion engine cylinder flow. An implicit finite difference method with full multigrid acceleration is used to solve the governing equations. The calculated results are in good agreement with available experimental data. Dissert. Abstr.

N94-29764 California Inst. of Tech., Pasadena.
FLOW PAST A CIRCULAR CYLINDER WITH A PERMEABLE WAKE SPLITTER PLATE Ph.D. Thesis
Gregory Scott Cardell 1993 227 p
Avail: Univ. Microfilms Order No. DA9325342

Measurements in the near wake region of a circular cylinder in a uniform flow in the Reynolds number range 2.5 x 10(exp 3) approximately less than or equal to Re approximately less than or equal to 1.8 x 10(exp 4) with permeable splitter plates spanning the wake center plane are presented. Permeability is defined by the pressure drop across the plates, and the relationship between permeability and plate solidity is determined for a set of plates constructed from woven wire mesh, permitting unambiguous characterization of the splitter plates by the solidity. The effects of different solidities on the flow in the near wake are investigated using smoke wire flow visualization, hot-wire anemometry, and measurements of the mean pressure at the cylinder surface, and the results are related to cylinder flow without a splitter plate. Flow visualization results demonstrate that the introduction of low solidity splitter plates does not change the basic near wake structure, and that sufficiently high solidity uncouples the large-scale wake instability from the body, with the primary vortex formation occurring downstream of the separation bubble due to instability of the wake profile. Hot-wire and surface pressure measurements confirm and quantify the flow visualization results, showing that the permeable splitter plates reduce the drag and modify the primary wake frequency. When the solidity is high enough that the wake is convectively unstable, the base pressure is independent of the Reynolds number and solidity. For a wide range of solidities, the same asymptotic value of the Strouhal number is reached at high Reynolds numbers. The relationship between the Strouhal number and the base pressure is discussed. Detailed measurements in the separating shear layers with splitter plates moderating the primary vortex formation show that in the mean the development of the separating shear layers is similar to that of the plane mixing layer. The presence of the splitter plates enhances shear layer development, and it is found that for all solidities the instability amplifies a broad frequency band without discrete spectral features. Turbulent transition in the shear layer and its role in the pronounced Reynolds number dependency of the flow in this Reynolds number range is discussed. Acoustic excitation of the separated shear layers confirms the broad band frequency response of the shear layer instability, and the effect of the driven shear layers on the near wake is investigated. Dissert. Abstr.

N94-29809 Illinois Univ., Urbana-Champaign.
DIRECT AND LARGE-EDDY SIMULATIONS OF TURBULENT FLOW IN A SQUARE DUCT Ph.D. Thesis
Ravi Kumar Madabhushi 1993 233 p
Avail: Univ. Microfilms Order No. DA9314909

The fully developed turbulent flow in a square duct has been numerically calculated using both direct (DNS) and largely-eddy (LES) simulation techniques. In the LES calculation, the filtered Navier-Stokes equations were solved using a mixed spectral finite difference procedure in conjunction with a simple eddy viscosity type model for the subgrid stresses. The simulation was conducted at a Reynolds number of 360 based on average friction velocity (5810 based on bulk velocity) and duct width. The simulation was able to predict the existence of turbulence-driven secondary flow and the associated effects on the mean flow and turbulence statistics. The results are in good qualitative agreement with the experimental data available at high Reynolds numbers. The DNS calculation was performed by solving the unsteady, three dimensional Navier-Stokes equations using an efficient and accurate Chebyshev-Fourier collocation procedure. The Reynolds number for this calculation was 260 based on average friction velocity (3850 based on bulk velocity). Distributions of several turbulence statistics (e.g., turbulence stresses, mean-square derivatives, length scales, etc.) in the cross section were computed and discussed in detail. Many of the turbulence statistics along the wall bisector are found to be qualitatively similar to those reported in a channel flow but are generally higher in the square duct flow because of the mean normal velocity along the wall bisector. In the corner region, the characteristics are very different due to the strong influence of the intersecting walls and the secondary flow. A database of instantaneous three dimensional flowfields has been generated and stored for future processing. Dissert. Abstr.

N94-29836 Texas Univ., Austin.
THE h-p ADAPTIVE METHODS FOR INCOMPRESSIBLE VISCOUS FLOW PROBLEMS Ph.D. Thesis
Weihan Robert Wu 1993 222 p
Avail: Univ. Microfilms Order No. DA9323597

The goal of h-p adaptive finite element methods is to obtain the approximate solutions as accurately and quickly as possible and, at the same time, to keep the total cost of computation under control. In this dissertation, we apply h-p adaptive finite element methods to the analysis of complex viscous flow phenomena. These techniques, which are designed to vary simultaneously the mesh size h and the spectral order p of elements, can produce very high resolution of important flow features with relatively small systems of equations and can, under appropriate conditions, deliver exponential rates of convergence. A successful h-p adaptive finite element method requires an efficient data structure, stable incompressible flow solvers for all Reynolds numbers, reliable a posteriori error estimates to measure the accuracy of approximate solutions, and an effective adaptive strategy to seek the best mesh. In this dissertation, we present a family of h-p adaptive finite element methods for solving the time-dependent Navier-Stokes equations in two and three dimensions. We begin by reviewing features of h-p data structures, then discuss the development of stable flow algorithms. An important development presented in this study is a mathematical proof of an a posteriori error estimate for incompressible viscous flows, and an extension of the three-step h-p adaptive strategy to incompressible flow problems. Results indicate that these types of schemes can produce excellent results for incompressible flow simulations at reasonable costs. Dissert. Abstr.

N94-29838 California Inst. of Tech., Pasadena.
NOMINALLY TWO-DIMENSIONAL FLOW ABOUT A NORMAL FLAT PLATE Ph.D. Thesis
Derek Lee Ashton Lisoski 1993 205 p
Avail: Univ. Microfilms Order No. DA9325366

Towing tank and water channel experiments and a vortex element numerical model were used to determine the forces acting on bluff flat plates in nominally two-dimensional flow. Intrinsic (small scale) and extrinsic (large scale) three-dimensional motions in the experimental flow were isolated and their effects studied. Both transient flows starting from rest and steady flow conditions were investigated. A force balance measured unsteady lift and drag while simultaneous LIF flow visualizations imaged the wake structure. Plate aspect ratio, end condition and angle of attack were varied to change large scale three-dimensional motions, while changes in Richardson number (flow stratification) modified three dimensionality intrinsic to the flow. Towing tank experiments indicated that normal plates required sixty to one hundred chord lengths of travel to establish steady vortex shedding. An initial drag peak during acceleration was followed by a drag minimum of C(sub d) approximately equal to 1.3 while the wake was confined to a recirculating bubble. Following the breakdown of this bubble, a region of symmetric flow with C(sub d) approximately equal to 1.6 and no vortex shedding lasted for twenty to thirty chord lengths. During subsequent 'steady-state' shedding, modulation in the vortex shedding amplitude at time scales of five to ten Strouhal periods resulted in a twenty percent fluctuation in the mean level of C(sub d) approximately equal to 2.0. Agreement between three-dimensional experimental and two-dimensional numerical model results was good at early times, indicating experiments were initially two-dimensional. Subsequently, while the wake

was confined to a recirculating bubble, the numerical model gave a drag coefficient C(sub d) approximately equal to 0.9, lower than experiments. Following the breakdown of this closed wake, steady-state drag levels of bar-(C(sub d)) approximately equal to 3.3 were 65 percent higher than experimental values. Dissert. Abstr.

N94-29839 Missouri Univ., Rolla.
LIQUID ATOMIZATION IN SUPERSONIC FLOWS Ph.D. Thesis
Azzedine Missoum 1993 138 p
Avail: Univ. Microfilms Order No. DA9326598

An experimental investigation of the atomization of a round liquid jet by coaxial, costream injection into a supersonic, Mach 1.5 air flow is reported. Extensive flow visualization was conducted using schlieren/shadowgraph, flash photography, and short duration (ns) laser imaging. The finer details of the jet were revealed when viewed under high magnification with the help of a microscope. The liquid and air pressures were varied individually. Photographic evidence indicates the presence of three regions within the liquid jet: a primary region enclosed by the first shock cell where the primary breakup occurs, a secondary region in which the jet is totally broken because of its interaction with the supersonic wave structure, and a third, subsonic region further downstream. It was found that the breakup mechanism of liquid jets in supersonic airstreams is quite complex. The breakup seems to be initiated by the growth of the turbulent structure on the liquid surface and the subsequent detachment of the three-dimensional structure as fine droplets by the intense shear at the liquid-gas interface. This seems to confirm the boundary layer stripping mechanism. The liquid jet expands into a bubble like formation as it interacts with the first set of waves. Higher liquid injection pressures resulted in higher initial spray angles. The liquid jet displayed a geometry strongly dependent on the pressure distribution resulting from the wave structure present in the supersonic jet. Droplet size and velocity distributions were measured by the P/DPA (Phase/Doppler Particle Analyzer) system. The Sauter Mean Diameter (SMD) was measured at several axial and radial locations at various liquid and air pressures. The SMD shows a decrease with increase in both the air-to-liquid mass flow ratio and the Weber number. The drop size decreased towards the outer edges of the jet. The results lead one to conclude that the coaxial, coflowing configuration is very attractive for atomizing scramjet liquid fuels. Dissert. Abstr.

N94-29843 Cincinnati Univ., OH.
NUMERICAL SOLUTION OF 3-D NAVIER-STOKES EQUATIONS IN VORTICITY-VELOCITY FORM FOR INCOMPRESSIBLE FLOWS Ph.D. Thesis
Yong Huang 1992 273 p
Avail: Univ. Microfilms Order No. DA9313817

The three dimensional Navier-Stokes equations are formulated in vorticity-velocity variables for incompressible flows. The attractive features of this formulation are that the pressure is eliminated from the essential part of the governing equations and the form of the equations remains invariant even in noninertial reference frames. The system of equations consists of the vorticity-transport equation and the kinematic velocity problem. The velocity problem is a constrained system of first-order Cauchy-Riemann type equations in three dimensions. Formulated in generalized curvilinear orthogonal coordinates, the equations are discretized using a finite difference method on a staggered grid. The vorticity-transport equation is integrated by an efficient ADI procedure, whereas the velocity problem is solved by a multigrid method. The pressure, if desired, is obtained by solving the pressure Poisson equation, also with a multigrid method. A shear-driven cavity flow is selected for code validation and for a study of the flow itself. Good agreement with available experimental results is obtained. The unsteady structure of the flow is examined in detail. The vorticity-velocity methodology is then applied to the solution of three dimensional flow over an axisymmetric afterbody. A novel analysis is developed for the governing equations at the centerline in the cylindrical coordinate to treat the 'coordinate singularity.' The evolution of streamwise vorticity, its interaction with the wall, and the wake pressure distribution are analyzed in detail. The results show that the streamwise vortices are attenuated significantly at the wall via interaction with the boundary layer. Further, the circumferential vorticity is strengthened by this interaction. The pressure distribution shows that the streamwise vorticity is instrumental in modifying the pressure field. The flow simulation and analysis have shown that the present vorticity-velocity methodology for three dimensional flows is capable of accurately and efficiently predicting the vortex dynamics of complex flows. Dissert. Abstr.

N94-29849 Texas A&M Univ., College Station.
LOCAL HEAT TRANSFER IN AN ENCLOSED COROTATING DISK WITH AXIAL THROUGHFLOW Ph.D. Thesis
Soo Yong Kim 1992 258 p
Avail: Univ. Microfilms Order No. DA9315093

Local heat transfer in an enclosed corotating disk with axial throughflow was investigated. The rotating cavity has two plane disks and a cylindrical rim (shroud). The ratio of the rim span to the disk outer radius is 0.4 and the ratio of the disk inner radius to outer radius is 0.25. The objectives of this study are to investigate the effects of axial coolant flow rate, rotational speed, and disk surface temperature on the local heat transfer coefficient distributions inside the disk cavity. Six disk surface heating conditions (BC1, BC2, BC3, BC4, BC5, and BC6) were tested for the axial flow Reynolds numbers between 2500 and 25,000, the rotational Reynolds numbers between 0 and 5.11 x 10(exp 5), and the rotational Grashof numbers between 1.8 x 10(exp 6) and 2.2 x 10(exp 10), respectively. The results showed that the disk cavity local heat transfer coefficients for the nonrotating cavity increase with increasing axial flow Reynolds number. However, the cavity local heat transfer coefficients decrease with increasing rotational Reynolds number and then increase with further increasing rotational Reynolds number. The downstream disk and rim generally have higher Nusselt numbers than the upstream disk. The Nusselt numbers on the upstream disk for BC 4, BC 5, and BC 6 are respectively lower than BC 1 and the Nusselt numbers on the downstream disk for BC 3, BC 5, and BC 6 are respectively lower than BC 1. However, the uneven disk temperature effect on the local Nusselt numbers decrease with decreasing axial Reynolds number and decrease with low rotational Reynolds number (Re(sub r) = 0 to 3.19 x 10(exp 5)) and increase with high rotational Reynolds number (Re(sub r) = 5.11 x 10(exp 5)). The disk cavity Nusselt numbers for BC 1 and BC 2 are comparable. In general, the modified Nusselt numbers (Nu(sub y)) on the upstream and downstream disks of this study are lower than the flat vertical wall natural convection correlations. The Nusselt numbers for Re(sub z) = 25,000 agree well with that of Farthing et al. (Re(sub z) = 2 x 10(exp 4)) except the present data are higher and lower, respectively, near the disk entrance (Gr(sub y) = 10(exp 10)) and near the rim (Gr(sub y) = 10(exp 7)). The averaged Nusselt numbers on the rim increase with increasing rotational Grashof numbers. However, the present rim data are lower than the natural convection correlation from the face down heated plate. Dissert. Abstr.

N94-29851 Virginia Polytechnic Inst. and State Univ., Blacksburg.
LARGE EDDY SIMULATION OF SUBSONIC MIXING LAYERS Ph.D. Thesis
Shaw-Ching Sheen 1993 161 p
Avail: Univ. Microfilms Order No. DA9312880

Large eddy simulation is used to study the large-scale structures in a low subsonic mixing layer and their breakdown to small scales. For three dimensional simulations, different finite difference and pseudo-spectral schemes are tested. The (2, 4) MacCormack Scheme developed by Gottlieb and Turkel shows the best overall performance. It is very fast and supplies enough but not excessive artificial dissipation. Though slower than the MacCormack scheme, the pseudo-spectral method has its advantage: high resolution of the high-wavenumber range when an adequate de-aliasing scheme is used. When efficient fast Fourier transform routines are available, this method can be a very good alternative to the MacCormack scheme. Most of the simulations use a modified Smagorinsky-type model. The effect of different models and model constants is also studied. It is found that the two subgrid-scale (SGS) models, the Smagorinsky model and the linear combination model, show significant difference even at the low wavenumber range of the spectra. In the study of three dimensional subsonic temporal mixing layers, it is found that the streamwise vortex tubes play an important role in the transition process. The vortex interaction of the streamwise vortex tubes and undulated spanwise vortex structures proves to be the dominant mechanism in the development of three-dimensionality and the subsequent generation of small-scale motions. In the absence of pairing of the spanwise vortex tubes, this vortex interaction causes uneven distribution of vorticity along the span of the spanwise vortex tubes and the breaking of the large structures. Following the breaking of the spanwise vortex tubes, the secondary streamwise vortex tubes become the dominant vortex

structures. In the case involving pairing, it is found that the relative motion of the spanwise vortex tubes in the pre-pairing process creates much stronger strain rate field between the pairing vortex tubes than the case without pairing. The stronger strain rate field leads to the formation of streamwise vortex tubes with very high vorticity and low induced pressure. Author (revised)

N94-29859*# Mississippi State Univ., Mississippi State. Computational Fluid Dynamics Lab.

NUMERICAL SOLUTION OF THE TWO-DIMENSIONAL TIME-DEPENDENT INCOMPRESSIBLE EULER EQUATIONS

David L. Whitfield and Lafayette K. Taylor Apr. 1994 65 p

(Grant NAG3-1157)

(NASA-CR-195775; NAS 1.26:195775) Avail: CASI HC A04/MF A01

A numerical method is presented for solving the artificial compressibility form of the 2D time-dependent incompressible Euler equations. The approach is based on using an approximate Riemann solver for the cell face numerical flux of a finite volume discretization. Characteristic variable boundary conditions are developed and presented for all boundaries and in-flow out-flow situations. The system of algebraic equations is solved using the discretized Newton-relaxation (DNR) implicit method. Numerical results are presented for both steady and unsteady flow. Author

N94-29899 Illinois Univ., Urbana-Champaign.

AN EXPERIMENTAL INVESTIGATION OF FLOW PATTERNS AND LIQUID ENTRAINMENT IN A HORIZONTAL-TUBE EVAPORATOR Ph.D. Thesis

John Steven Barnhart 1993 257 p

Avail: Univ. Microfilms Order No. DA9314839

An experimental study of two-phase flow patterns and droplet entrainment in a horizontal-tube evaporator was conducted. Measurements were made with serpentine aluminum and glass evaporators with geometries typical of those used for domestic refrigeration. The refrigerant in the majority of tests was R134a, which will replace R12 for refrigeration and automotive air-conditioning in 1995. The phenomenon of primary interest was the nonequilibrium transport of droplets within superheated vapor at the evaporator exit. Of particular concern were substantial variations in the liquid rate with time, and corresponding fluctuations in exit temperature. These variations are due to the formation of slugs which rapidly transport a surplus of liquid toward the exit. A flow loop was constructed to circulate oil-free refrigerant through the evaporator under widely varying conditions. Liquid carry over (expressed as a dimensionless entrained mass fraction, EMF) was measured as a function of inlet quality, heat flux, mass flux, and exit superheat. A laser-based phase/Doppler particle analyzer was used to measure droplet diameters and velocities at the evaporator exit. Tests with three refrigerants over wide ranges of operating conditions revealed time-averaged EMF's of no more than 0.1 percent. Analysis of variance showed exit superheat to have the strongest effect, followed by mass flux, inlet quality, and heat flux. Time-averaged EMF's varied with operating conditions by several orders of magnitude, decreasing with increasing superheat level (due to lower entrainment rates near the exit and more rapid droplet vaporization) and mass flux and inlet quality (due to reduced slug formation). The incidence of slug flow and its effect on evaporator exit conditions were documented in time-resolved experiments, using techniques such as auto- and cross-correlation and Fourier transform. Time-resolved EMF's as high as one percent were observed, as well as sharp reductions in exit superheat of as much as 8 degrees C. The distribution of superheat readings was found to follow a Rayleigh probability density function. This finding will facilitate the use of the superheat reading in control strategies, should it become necessary to actively control refrigerant flow rate. Dissert. Abstr.

N94-29902 McGill Univ., Montreal (Quebec).

A NUMERICAL METHOD FOR CONFINED UNSTEADY FLOWS RELATED TO FLUID-STRUCTURE INTERACTIONS Ph.D. Thesis

Francois Belanger 1991 286 p

(ISBN-0-315-74739-0) Avail: Univ. Microfilms Order No. DANN74739

This thesis elaborates three aspects in the field of flow-induced vibrations associated with annular geometries. A method to find the unsteady fluid forces on a cylinder oscillating in annular turbulent flow is developed by considering the superposition of the turbulent fluctuating quantities on potential flow. The theory is compared with experiments. Then, the unsteady fluid forces acting on the vibrating cylinder walls of nonuniform annular configurations are computed by a method which performs the accurate time integration of the Navier-Stokes equations. It is the extension for unsteady flows of the method of artificial compressibility used for steady flows. A time-discretization of the momentum equation using a three-point-backward implicit scheme is introduced, and the addition of pseudo-time derivative terms to the semidiscretized equations, including artificial compressibility in the continuity equation, allows the use of time-marching solution techniques thereafter. Finally, the integration method used for the Navier-Stokes equations is combined with the equation governing the dynamical behavior of a structure in order to perform the fluid-structure stability analysis of this system in the time domain. Dissert. Abstr.

N94-29923# Lawrence Livermore National Lab., CA.

NUMERICAL SIMULATION OF RADIATIVE HEAT LOSS IN AN EXPERIMENTAL BURNER

L. D. Cloutman and L. Brookshaw Sep. 1993 23 p Presented at the Fall Meeting of the Western States Section of the Combustion Institute, Menlo Park, CA, 18-19 Oct. 1993

(Contract W-7405-eng-48)

(DE94-002016; UCRL-JC-115048; CONF-931076-1) Avail: CASI HC A03/MF A01

We describe the numerical algorithm used in the COYOTE two-dimensional, transient, Eulerian hydrodynamics program to allow for radiative heat losses in simulations of reactive flows. The model is intended primarily for simulations of industrial burners, but it is not confined to that application. It assumes that the fluid is optically thin and that photons created by the fluid immediately escape to free space or to the surrounding walls, depending upon the application. The use of the model is illustrated by simulations of a laboratory-scale experimental burner. We find that the radiative heat losses reduce the local temperature of the combustion products by a modest amount, typically on the order of 50 K. However, they have a significant impact on NO(x) production. DOE

N94-29942*# MCAT Inst., San Jose, CA.

ALGORITHM AND CODE DEVELOPMENT FOR UNSTEADY THREE-DIMENSIONAL NAVIER-STOKES EQUATIONS

Shigeru Obayashi Apr. 1994 6 p

(Contract NCC2-605)

(NASA-CR-195774; NAS 1.26:195774; MCAT-94-002) Avail: CASI HC A02/MF A01

Aeroelastic tests require extensive cost and risk. An aeroelastic wind-tunnel experiment is an order of magnitude more expensive than a parallel experiment involving only aerodynamics. By complementing the wind-tunnel experiments with numerical simulations, the overall cost of the development of aircraft can be considerably reduced. In order to accurately compute aeroelastic phenomenon it is necessary to solve the unsteady Euler/Navier-Stokes equations simultaneously with the structural equations of motion. These equations accurately describe the flow phenomena for aeroelastic applications. At ARC a code, ENSAERO, is being developed for computing the unsteady aerodynamics and aeroelasticity of aircraft, and it solves the Euler/Navier-Stokes equations. The purpose of this cooperative agreement was to enhance ENSAERO in both algorithm and geometric capabilities. During the last five years, the algorithms of the code have been enhanced extensively by using high-resolution upwind algorithms and efficient implicit solvers. The zonal capability of the code has been extended from a one-to-one grid interface to a mismatching unsteady zonal interface. The geometric capability of the code has been extended from a single oscillating wing case to a full-span wing-body configuration with oscillating control surfaces. Each time a new capability was added, a proper validation case was simulated, and the capability of the code was demonstrated. Author (revised)

N94-29944 Purdue Univ., West Lafayette, IN.

SPECTRAL ANALYSIS OF WAVE PROPAGATION IN CONNECTED WAVEGUIDES Ph.D. Thesis

Gopalakrishnan Srinivasan 1992 189 p

Avail: Univ. Microfilms Order No. DA9314083

The spectral element method combined with the Fast Fourier Transform (FFT) is a powerful and versatile tool for analysis of wave propagation problems in connected structures. They are formulated entirely in the

frequency domain and use matrix assembly procedures analogous to the finite element method. This thesis extends the approach to connected structures involving non-uniformities and discontinuities. To handle situations involving deep waveguides, spectral elements are formulated based on the higher order waveguide theories of Timoshenko beam and Mindlin-Herrmann rod. Approximate tapered elements (derived using a frequency domain Ritz method) are formulated to handle situations involving member cross-section variations. For waveguides with embedded discontinuities like cracks and holes, the irregular behavior near the discontinuity is isolated by performing Local/Global analysis via the super spectral element concept. Efficient computation of the super element stiffness is the key to the success of the method and it is addressed directly. The formulated element is verified by comparison with the conventional finite element solution. Some interesting problems involving joints, cracks and holes are solved. One of the distinct advantages of the spectral approach is the capability to perform inverse problems. The concept is demonstrated with some illustrative examples involving multiple boundaries. Dissert. Abstr.

N94-29965 Virginia Polytechnic Inst. and State Univ., Blacksburg.
HIGH-RESOLUTION ALGORITHMS FOR THE NAVIER-STOKES EQUATIONS FOR GENERALIZED DISCRETIZATIONS Ph.D. Thesis
Curtis Randall Mitchell 1992 196 p
Avail: Univ. Microfilms Order No. DA9312878

Accurate finite volume solution algorithms for the two dimensional Navier Stokes equations and the three dimensional Euler equations for both structured and unstructured grid topologies are presented. Results for two dimensional quadrilateral and triangular elements and three dimensional tetrahedral elements will be provided. Fundamental to the solution algorithm is a technique for generating multidimensional polynomials which model the spatial variation of the flow variables. Cell averaged data is used to reconstruct pointwise distributions of the dependent variables. The reconstruction errors are evaluated on triangular meshes. The implementation of the algorithm is unique in that three reconstructions are performed for each cell face in the domain. Two of the reconstructions are used to evaluate the inviscid fluxes and correspond to the right and left interface states needed for the solution of a Riemann problem. The third reconstruction is used to evaluate the viscous fluxes. The gradient terms that appear in the viscous fluxes are formed by simply differentiating the polynomial. By selecting the appropriate cell control volumes, centered, upwind and upwind-biased stencils are possible. Numerical calculations in two dimensions include solutions to elliptic boundary value problems, Ringlebs' flow, an inviscid shock reflection, a flat plate boundary layer, and a shock induced separation over a flat plate. Three dimensional results include the ONERA M6 wing. All of the unstructured grids were generated using an advancing front mesh generation procedure. Modifications to the three dimensional grid generator were necessary to discretize the surface grids for bodies with high curvature. In addition, mesh refinement algorithms were implemented to improve the surface grid integrity. Examples include a Glasair fuselage, High Speed Civil Transport, and the ONERA M6 wing. The role of reconstruction as applied to adaptive remeshing is discussed and a new first order error estimator is presented. Numerical examples of the remeshing procedure include both smooth and discontinuous flows.
Dissert. Abstr.

N94-29974 Kansas Univ., Lawrence.
HYDRODYNAMIC STABILITY ANALYSIS OF SWIRLING JETS Ph.D. Thesis
Charles Chengzhi Wu 1992 155 p
Avail: Univ. Microfilms Order No. DA9313200

The present work is fundamental in nature and aims to achieve a better understanding of the instability character of swirling jets. Spatial hydrodynamic instabilities of inviscid swirling jets have been investigated theoretically. The hydrodynamic stability analysis has first been applied to an inviscid, incompressible, top-hat jet, with a swirl distribution of solid body rotation and free vortex in and outside the vortex core, respectively. This velocity profile simulates the mean velocity field near the jet exit. The stability analysis has then been extended to inviscid, incompressible, non-top-hat swirling jets, which describe the mean velocity field downstream. Two types of non-top-hat swirling jets have been studied. Type 1 velocity profile is a trailing-vortex with parallel flow assumption. Type 2 velocity profile is based on analytical-experimental solutions with no parallel flow limitation and, hence, is more realistic. It is found that top-hat jets with swirl distribution of Rankine vortex type are spatially unstable in all the excitation modes examined; i.e., m = 0, +/-1, +/-2, +/-3. Amplification rates of top-hat swirling jets are increased monotonically. Helical-mode excitation has little impact on nonswirling, top-hat jets but has a strong influence on swirling jets. The higher the positive helicity, the less unstable is the behavior; the higher the negative helicity, the more unstable the behavior becomes. It is also found that stronger centrifugal effect makes swirling jets less unstable under positive helical-mode excitation, and makes them more unstable under negative helical-mode excitation. Non-top-hat swirling jets are only unstable under excitation modes m = 0, -1, -2, -3 and under small frequency excitations. They become stable as frequency increases. Their amplification rates behave differently than those of top-hat swirling jets with a 'hump' distribution. The trends of helical-mode excitation and centrifugal effect are similar to those of 'top-hat swirling jets.' In general, non-top-hat swirling jets are less unstable than top-hat swirling jets. Combining the results of these two parts, the overall instability character of swirling jets is captured in the stream wise direction. Two comparisons are made between the experimental data and theoretical results for a low intensity swirling jet. The initial growth trend of the fundamental instability wave in the near field is captured. The comparisons also show the limitation of linear, inviscid stability theory. Dissert. Abstr.

N94-29976 Stanford Univ., CA.
THE INSTANTANEOUS CONCENTRATION FIELD IN THE SELF-SIMILAR REGION OF A HIGH SCHMIDT NUMBER ROUND JET Ph.D. Thesis
Minami Yoda 1993 175 p
Avail: Univ. Microfilms Order No. DA9309689

The aim of this work is to characterize the far-field structure of the nearly and fully turbulent (Reynolds number less than or = 5000) round water (high Schmidt number) jet. This thesis describes the acquisition and analysis of three-dimensional concentration data using a laser-induced fluorescence technique. Isoconcentration surfaces are used to deduce the large-scale structure and modal composition of the jet. The evolution of two-dimensional (x-y-t) axial concentration fields in fully turbulent natural, circularly and axially excited water jets is visualized. Large-scale structure is found in the form of 'ridges' on the x-y-t isoconcentration surfaces; they are common and robust, or long-lived. Assuming that these structures correspond to the instability modes predicted by linear theory, and that symmetry arguments can be used to distinguish these modes, cross correlation techniques are used to determine whether these structures are in the axisymmetric and helical modes. Both symmetric (axisymmetric mode) and antisymmetric (helical mode) structures are found in the natural jet; only antisymmetric structures are found in both types of excited jets. The instantaneous three-dimensional (x-y-z) concentration fields of nearly and fully turbulent (Reynolds numbers 1000, 2000 and 4000) natural and circularly excited jets are measured. Large-scale structure, which appears to be present only in fully turbulent jets, is found in the form of axisymmetric 'clumps' of higher concentration jet fluid along the flow direction x. These structures are of a downstream extent approximately equal to the local jet diameter. The antisymmetric two-dimensional images previously thought to be 'slices' of a spiral in three dimensions turn out instead to be slices of a simple sinusoid. This result suggests that the helical instability mode, if present, is in the form of a pair of counter rotating spiral vortex filaments. The local structure of the concentration gradient field is analyzed using critical point concepts. The concentration field is shown to consist of axisymmetric filamentary structures stretched along the axis of symmetry, which tends to be inclined at an angle of +/- 135 deg to x, or the expected intermediate (extensive) strain direction. These results and results from direct numerical simulations suggest that the small-scale flow consists of intense vortex filaments aligned with this direction; these filaments draw in and 'swirl' the passive scalar around their axis, while the strain stretches the scalar along the filament axis. Finally, the scalar dissipation is calculated and visualized. It is shown that much of the mixing in the flow is taking place in a small fraction of the flow volume, in regions that geometrically appear to be convoluted and sheetlike. Dissert. Abstr.

N94-29977*# Foster-Miller Associates, Inc., Waltham, MA.
LUNAR BASE HEAT PUMP, PHASE 1 DRAFT Final Report
Jeffrey H. Goldman, A. Harvey, T. Lovell, and David H. Walker Apr. 1994 67 p

(Contract NAS9-18819; FMI Proj. NAS-9614)
(NASA-CR-195211; NAS 1.26:195211; NAS-8819-FM-9614-820) Avail: CASI HC A04/MF A01

This report describes the Phase 1 process and analysis used to select a refrigerant and thermodynamic cycle as the basis of a vapor compression heat pump requiring a high temperature lift, then to perform a preliminary design to implement the selected concept, including major component selection. Use of a vapor compression heat pump versus other types was based on prior work performed for the Electric Power Research Institute. A high lift heat pump is needed to enable a thermal control system to remove heat down to 275K from a habitable volume when the external thermal environment is severe. For example, a long-term lunar base habitat will reject heat from a space radiator to a 325K environment. The first step in the selection process was to perform an optimization trade study, quantifying the effect of radiator operating temperature and heat pump efficiency on total system mass; then, select the radiator operating temperature corresponding to the lowest system mass. Total system mass included radiators, all heat pump components and the power supply system. The study showed that lunar night operation, with no temperature lift, dictated the radiator size. To operate otherwise would require a high mass penalty to store power. With the defined radiation surface, and heat pump performances assumed to be from 40 percent to 60 percent of the Carnot ideal, the optimum heat rejection temperature ranged from 387K to 377K, as a function of heat pump performance. Refrigerant and thermodynamic cycles were then selected to best meet the previously determined design conditions. The system was then adapted as a ground-based prototype lifting temperature to 360K (versus 385K for flight unit) and using readily available commercial-grade components. Over 40 refrigerants, separated into wet and dry compression behavioral types, were considered in the selection process. Refrigerants were initially screened for acceptable critical temperature. The acceptable refrigerants were analyzed in ideal single and two-stage thermodynamic cycles. Top candidates were analyzed assuming realistic component limits and system pressure drops, and were evaluated for other considerations such as safety, environmental impact and commercial availability. A maximum coefficient of performance (COP) of 56 percent of the Carnot ideal was achievable for a three-stage CFC-11 cycle operating under the flight conditions above. The program was completed by defining a control scheme and by researching and selecting the major components, compressor and heat exchangers, that could be used to implement the thermodynamic cycle selected. Special attention was paid to using similar technologies for the SIRF and flight heat pumps resulting in the commercially available equivalent of the flight unit. A package concept was generated for the components selected and mass and volume estimated. Author

N94-29999 Selskapet for Industriell og Teknisk Forskning, Trondheim (Norway). Div. of Refrigeration Engineering.
LARGE HEAT PUMPS USING CO2 REFRIGERANT
G. Lorentzen 17 Feb. 1993 10 p
(PB94-138773; STF11-A93017) Avail: Issuing Activity (National Technical Information Service (NTIS))

It has been demonstrated in previous reports that carbon dioxide (CO2) is a near ideal refrigerant in every respect, provided that a suitable thermodynamic process to give a competitively low power consumption can be designed. Such a process has been proposed for the use in large heat pumps, where the output has to be supplied to a gliding temperature sink, typically a district heating system. Also CO2 lends itself to the effective recovery of expansion work. It is possible to improve the efficiency and COP of district heating systems with at least 20-25 percent over conventional technology. NTIS

N94-30003 New York Univ., New York.
COMPUTATIONAL FLUID AND COMBUSTION DYNAMICS
M. J. Berger 1993 3 p Limited Reproducibility: More than 20% of this document may be affected by microfiche quality
(Contract DE-FG02-92ER-25139)
(DE94-006596; DOE/ER-25139/1) Avail: CASI HC A01

Research efforts this year concentrated on automatic geometry definition for Cartesian grid calculations in 3D, including a CAD interface, and development of a parallel compressible adaptive AMR in a data parallel environment also in 3D. Effort is still on conservative interface conditions for overlapping meshes. DOE

N94-30020 Argonne National Lab., IL.
TWO-PHASE POWER-LAW MODELING OF PIPE FLOWS DISPLAYING SHEAR-THINNING PHENOMENA
Jianmin Ding, R. W. Lyczkowski, and W. T. Sha 1993 11 p Presented at the 5th Joint DOE/NSF Workshop on Flow of Particulates, Ithaca, NY, 29 Sep. - 1 Oct. 1993 Limited Reproducibility: More than 20% of this document may be affected by microfiche quality
(Contract W-31-109-eng-38)
(DE94-005115; ANL/ET/CP-80624; CONF-9309310-1) Avail: Issuing Activity (Department of Energy (DOE))

This paper describes work in modeling concentrated liquid-solids flows in pipes. COMMIX-M, a three-dimensional transient and steady-state computer program developed at Argonne National Laboratory, was used to compute velocities and concentrations. Based on the authors' previous analyses, some concentrated liquid-solids suspension flows display shear-thinning rather than Newtonian phenomena. Therefore, they developed a two-phase non-Newtonian power-law model that includes the effect of solids concentration on solids viscosity. With this new two-phase, power-law, solids-viscosity model, and with constitutive relationships for interfacial drag, virtual mass effect, shear lift force, and solids partial-slip boundary conditions at the pipe walls, COMMIX-M is capable of analyzing concentrated three-dimensional liquid-solids flows. DOE

N94-30147*# National Aeronautics and Space Administration. Lewis Research Center, Cleveland, OH.
NUMERICAL COMPARISON OF CONVECTIVE HEAT TRANSFER AUGMENTATION DEVICES USED IN COOLING CHANNELS OF HYPERSONIC VEHICLES
Jaime J. Maldonado Apr. 1994 28 p
(RTOP 505-70-69)
(NASA-TM-106546; E-8695; NAS 1.15:106546) Avail: CASI HC A03/MF A01

Hypersonic vehicles are exposed to extreme thermal conditions compared to subsonic aircraft; therefore, some level of thermal management is required to protect the materials used. Normally, hypersonic vehicles experience the highest temperatures in the nozzle throat, and aircraft and propulsion system leading edges. Convective heat transfer augmentation techniques can be used in the thermal management system to increase heat transfer of the cooling channels in those areas. The techniques studied in this report are pin-fin, offset-fin, ribbed and straight roughened channel. A smooth straight channel is used as the baseline for comparing the techniques. SINDA '85, a lumped parameter finite difference thermal analyzer, is used to model the channels. Subroutines are added to model the fluid flow assuming steady one dimensional compressible flow with heat addition and friction. Correlations for convective heat transfer and friction are used in conjunction with the fluid flow analysis mentioned. As expected, the pin-fin arrangement has the highest heat transfer coefficient and the largest pressure drop. All the other devices fall in between the pin-fin and smooth straight channel. The selection of the best heat augmentation method depends on the design requirements. A good approach may be a channel using a combination of the techniques. For instance, several rows of pin-fins may be located at the region of highest heat flux, surrounded by some of the other techniques. Thus, the heat transfer coefficient is maximized at the region of highest heat flux while the pressure drop is not excessive. Author

N94-30224 Alabama Univ., Tuscaloosa.
UNSTRUCTURED SPACE-TIME FINITE ELEMENT METHOD OF HEAT CONDUCTION Ph.D. Thesis
Chi-Kyung Kim 1992 115 p
Avail: Univ. Microfilms Order No. DA9313053

A space-time finite element method is presented for solving heat transfer involving a moving heat source so that small time steps can be used in areas of large time rates of change of temperature. The weighted residual process is used to formulate a finite element method in a space-time domain based upon the discontinuous Galerkin method. Most of the early works on the discontinuous Galerkin method for ordinary differential equations have been mathematically oriented. Based on the numerical success of the time-discontinuous Galerkin method for ordinary differential equations, this research extends the method to problems involving second-order parabolic equations, e.g. transient heat conduction. The focus is on adaptively controlling the time step in a one-dimensional moving

heat source simulation. Utilizing the efficiency of finite elements by choosing a finite element mesh in the space-time domain, the finite element mesh has been adjusted to steep gradients of the solution with respect to the space and time variables. Dissert. Abstr.

N94-30228 Vanderbilt Univ., Nashville, TN.
PREDICTION OF FLUID FLOW AND HEAT TRANSFER IN INTERNALLY FINNED TUBES Ph.D. Thesis
Mohammed Youssef Al-Hashem 1993 113 p
Avail: Univ. Microfilms Order No. DA9324418

Fully developed fluid flow and heat transfer characteristics in internally finned tubes were investigated. Both laminar and turbulent flows were considered. Longitudinal fins of trapezoidal profile integrally attached to the tube wall are equally spaced circumferentially in the tube. The assumption of axially constant heat flux per unit length was applied. The tube wall temperature was assumed to be circumferentially uniform at any cross section but varies axially with the change of the bulk temperature. With a fin of finite conductivity, the temperature varies along the fin height. The influence of the ratio of the fin to fluid thermal conductivity ratio, K(sub fin)/K(sub fluid), was investigated for both laminar and turbulent flows. Results for laminar flow case were presented for a fin height to tube radius ratio H/R, ranging from 0.2 to 0.9; the number of fins, NFIN, was varied from 6 to 30; and fin half angles, beta, were varied from 1.5 to 3 degrees. It was found that for any specified geometry the Nusselt number is influenced by a single parameter, K(sub fin)/K(sub fluid). A mixing length model developed by Ivanovic and Patankar was used to predict the results for turbulent fluid flow. Results were presented for a range of fin height to tube radius, H/R, which was varied from 0.2 to 0.4; NFIN ranged from 6 to 22; beta was selected as 1.5 and 3 degrees; and Reynolds number, Re, varied from 10,000 to 100,000. Predicted results for isothermal fins were shown to be in agreement with other researchers. The results provide extensive information on the influence of the fin to fluid thermal conductivities ratio. It is evident from the results that the assumption of isothermal fins is an inaccurate one, especially at high Reynolds number and either high H/R or low K(sub fin)/K(sub fluid) ratio. Dissert. Abstr.

N94-30229 City Univ. of New York, NY.
THREE-DIMENSIONAL FLOW CHARACTERISTICS DOWNSTREAM OF A BLADE ENDWALL CORNER Ph.D. Thesis
AbdulKarim A. J. Abd Altaii 1993 231 p
Avail: Univ. Microfilms Order No. DA9325064

The flow downstream of the corner formed by an airfoil and a flat plate was investigated experimentally. The region for this study was simulated by attaching two uncambered, unswept NACA 65-015 airfoils on either side of a flat plate. The airfoils had a semicircular leading edge. The initial 7 cm of the leading edge of the flat plate was artificially roughened by gluing a strip of sand paper to promote a thicker turbulent boundary layer. Free stream turbulence of the order of 1.5 percent was introduced, by inserting a combination of two grids, to avoid a separation bubble on the airfoil. Measurement techniques employed in this investigation were: surface flow visualization, conventional pitot-static probe, the Preston tube, and the five hole probe. Surface flow visualization defined the boundaries of the vortex system and provided information on the direction and the magnitude of the wall shear stress. Local wall shear stress was measured using specially constructed Preston tubes. The characteristics of the Preston tube were also investigated. Total and static pressure distribution measurements, including the flat plate surface, were made using a pitot-static probe. The five hole probe was used, in the seminulling mode, to collect data on the three components of mean velocity. The measurements were carried out at eight axial stations downstream of the trailing edge of the airfoil. At every axial location downstream of the trailing edge of the airfoil forming the corner with a flat plate, a single dominant horseshoe vortex was identified which persisted more than one chord length downstream. A smaller and weaker corner vortex was also identified. It dissipated and ceased to exist by a downstream axial location of approximately 0.2C. There was no evidence of stress induced vortices in the region of this investigation. The secondary flow system redistributes the mean flow momentum and distorts total pressure profiles and contours. In planes parallel to the flat plate, total pressure profiles were found to be higher than the undisturbed two dimensional boundary layer at that height. Surface static pressure was found to be at its maximum at the airfoil trailing edge location and it decreased in both the downstream and transverse directions. There was no significant static pressure variation in the spanwise direction. Dissert. Abstr.

N94-30272 Illinois Univ., Urbana-Champaign.
THE EFFECT OF A WAVY BOUNDARY ON TURBULENT FLOW Ph.D. Thesis
John Dale Hudson 1993 195 p
Avail: Univ. Microfilms Order No. DA9329065

Two-component velocity measurements were obtained near a solid wavy boundary. The resulting database includes a variety of flow conditions including two wave steepnesses and a large range of flow rates. Detailed analyses of one of these flows are given. These serve as a reference point for determining the effects of wave steepness and flow rate. The contributions of this study of the effect of a wavy boundary on turbulent flow are fourfold. First, the outer flow is found to be insensitive to the method of turbulence generation near the wavy surface. Second, the turbulence in the near wall region is found to originate from shear layers which separate from the wave crests. The turbulent stresses and turbulent energy production of the flow are, largely, associated with these layers. Third, detailed information on the Reynolds stress is provided which should help in understanding important flow systems and should provide a challenge of current general methods for computing turbulent fields. Finally, velocity measurements were used to map out the pressure field within the flowing system. Dissert. Abstr.

N94-30352 Arizona Univ., Tucson.
A SINGLE-FLUID, SELF-CONSISTENT FORMULATION OF PARTICLE TRANSPORT AND FLUID DYNAMICS Ph.D. Thesis
Lance Lee Williams 1993 138 p
Avail: Univ. Microfilms Order No. DA9328566

I present a formulation of fluid dynamics that is consistent with particle transport and acceleration. This formulation consists of two parts: a transport equation that describes the evolution of a particle distribution function in terms of a fluid velocity in which the distribution is embedded, and an equation for the fluid velocity that involves integrals of the distribution function. The motivation for this work is to provide a formalism for calculating the effect of particle acceleration on the flows of typical astrophysical plasmas. It is shown that the equation to be solved simultaneously with the transport equation is just the momentum equation for the system, and that the number and energy equations are implicit in the transport equation. There is no restriction on the energies of particles constituting such systems. Connections are made to the cosmic-ray transport equation, two-fluid models of cosmic ray/thermal gas interaction, and self-consistent Monte Carlo models of particle acceleration at parallel shocks. The formalism is developed for non-relativistic flow speeds. It is assumed that particle distributions are nearly isotropic in the fluid frame, an assumption that is generally valid in space plasmas. It is assumed that particle scattering mean-free-paths are much less than the length scales associated with changes in the fluid velocity or particle distribution. Dissert. Abstr.

N94-30487 Pennsylvania State Univ., University Park.
THE ENHANCEMENT OF COMPRESSIBLE TURBULENT MIXING VIA STREAMWISE VORTICITY Ph.D. Thesis
Jonathan Wayne Naughton 1993 257 p
Avail: Univ. Microfilms Order No. DA9326911

Compressible turbulent mixing layers have been studied in great detail in an attempt to understand and control the mechanisms governing them. Although much has been learned from these studies, attempts to significantly increase the mixing of the two component streams have been largely unsuccessful. Based upon promising results from subsonic swirling-jet studies, the present work was initiated to demonstrate conclusively the effect of streamwise vorticity on the mixing of co-flowing supersonic streams. A vortex injector was designed in order to produce a supersonic vortical primary stream along the axis of the wind tunnel test section. These flowfields are imaged by the planar laser scattering (PLS) technique, while the vortices' strengths are quantified using intrusive probes and laser Doppler velocimetry (LDV). In addition, the PLS seed particles are shown to represent faithfully the dynamics of the turbulent swirling flow. The results of analyzing the PLS images indicate that an enhancement in mixing rate of up to 60% for the present test cases is possible through the addition of streamwise vorticity. Furthermore, the degree of mixing enhancement scales with the

vortex strength and appears to be independent of the degree of compressibility of the mixing layer. Analysis of the instantaneous turbulent structure suggests that the observed increase in mixing is due to a modification of large-scale turbulent structures in the mixing layer.
Dissert. Abstr.

N94-30494 Michigan Univ., Ann Arbor.
A NEW ORTHOGONAL DECOMPOSITION METHOD FOR TURBULENT FLOWS Ph.D. Thesis
Ali Kodal 1993 159 p
Avail: Univ. Microfilms Order No. DA9319564

This thesis deals with the decomposition of general turbulent flow variables into their mean, organized, and turbulent parts. After decomposition, equations of fluid motion can then be devised for each component of flow. While numerous techniques have been proposed for identifying organization in fluid motion, they are typically statistical rather than physical and do not necessarily provide desirable properties such as orthogonality between decomposed components. The aim of this thesis is to explore a new technique for identifying organization in turbulent fluid flow which incorporates physical information, makes efficient use of measured data, and can be applied to turbulent flows with complexities such as nonstationarity and inhomogeneity. In this study, attributes of stationary steady and unsteady turbulent flows are first considered. A new frequency domain filtering technique is then developed to make an orthogonal decomposition of turbulent flow into organized and residual turbulent components. The technique is then adapted for applications of nonstationary and inhomogeneous data series in one and two dimensions. Performance evaluations and comparisons between this new technique and existing ones are made. From these evaluations, this new technique is shown to give better performance than existing ones for stationary and selected nonstationary turbulent flow data series and shows promise as an adaptive tool for identifying organization in turbulence. Dissert. Abstr.

N94-30519 Case Western Reserve Univ., Cleveland, OH.
THREE DIMENSIONAL COMPRESSIBLE TURBULENT FLOW COMPUTATIONS FOR A DIFFUSING S-DUCT WITH/WITHOUT VORTEX GENERATORS Ph.D. Thesis
Soo Yong Cho 1993 216 p
Avail: Univ. Microfilms Order No. DA9321875

Numerical investigations on a diffusing S-duct with/without vortex generators and a straight duct with vortex generators are presented. The investigation consists of solving the full 3-D unsteady compressible mass averaged Navier-Stokes equations. An implicit finite volume lower-upper time marching code (RPLUS3D) has been employed and modified. A 3-D Baldwin-Lomax turbulence model has been modified in conjunction with the flow physics. A model for the analysis of vortex generators in a fully viscous subsonic internal flow is evaluated. A vortical structure for modeling the shed vortex is used as a source term in the computation domain. The injected vortex paths in the straight duct are compared with the analysis by two kinds of prediction models. The flow structures by the vortex generators are investigated along the duct. Computed results of the flow in a circular diffusing S-duct provide an understanding of the flow structure within a typical engine inlet system. These are compared with the experimental wall static-pressure, static-, and total-pressure field, and secondary velocity profiles. Additionally, boundary layer thickness, skin friction values, and velocity profiles in wall coordinates are presented. In order to investigate The effect of vortex generators, various vortex strengths are examined. The total-pressure recovery and distortion coefficients are obtained at the exit of the S-duct. The numerical results clearly depict the interaction between the low velocity flow by the flow separation and the injected vortices. Dissert. Abstr.

N94-30600 Lawrence Livermore National Lab., CA.
DESIGN OF AN ELECTROMAGNETIC ACCELERATOR FOR TURBULENT HYDRODYNAMIC MIX STUDIES
A. R. Susoeff, R. S. Hawke, J. J. Morrison, G. Dimonte, and B. A. Remington Dec. 1993 16 p Presented at the 7th Symposium on Electromagnetic Launch Technology, San Diego, CA, 20-24 Apr. 1994 Limited Reproducibility: More than 20% of this document may be affected by microfiche quality
(Contract W-7405-eng-48)
(DE94-005821; UCRL-JC-114805; CONF-940481-2) Avail: CASI HC A03

An electromagnetic accelerator in the form of a linear electric motor (LEM) has been designed to achieve controlled acceleration profiles of a carriage containing hydrodynamically unstable fluids for the investigation of the development of turbulent mix. The Rayleigh-Taylor instability is investigated by accelerating two dissimilar density fluids using the LEM to achieve a wide variety of acceleration and deceleration profiles. The acceleration profiles are achieved by independent control of rail and augmentation currents. A variety of acceleration-time profiles are possible including: (1) constant, (2) impulsive and (3) shaped. The LEM and support structure are a robust design in order to withstand high loads with deflections and to mitigate operational vibration. Vibration of the carriage during acceleration could create artifacts in the data which would interfere with the intended study of the Rayleigh-Taylor instability. The design allows clear access for diagnostic techniques such as laser induced fluorescence radiography, shadowgraphs and particle imaging velocimetry. Electromagnetic modeling codes were used to optimize the rail and augmentation coil positions within the support structure framework. Results of contemporary studies for non-arcing sliding contact of solid armatures are used for the design of the driving armature and the dynamic electromagnetic braking system. A 0.6MJ electrolytic capacitor bank is used for energy storage to drive the LEM. This report will discuss a LEM design which will accelerate masses of up to 3kg to a maximum of about 3000g(sub o), where g(sub o) is accelerated due to gravity. DOE

N94-30743 National Aerospace Lab., Amsterdam (Netherlands). Informatics Div.
EIGENVALUE ANALYSIS OF THE CONVERGENCE BEHAVIOUR OF AN EULER METHOD
W. Cazemier (Groningen Rijksuniv., Netherlands.), J. I. vandenBerg, and A. E. P. Veldman 1 Jun. 1992 13 p Presented at the 1st European Computational Fluid Dynamics Conference, Brussels, Belgium, 7-11 Sep. 1992 Limited Reproducibility: More than 20% of this document may be affected by microfiche quality
(PB94-1255722-U; NLR-TP-92222-U; ETN-94-95583) Avail: CASI HC A03

An eigenvalue analysis is developed for a Euler method, using cell centered central differences and a Runge-Kutta time integration method, and applied to a quasi one-dimensional nozzle flow. An accurate estimation of the convergence behavior is made, based on the largest amplification factor of all eigenvalues of the Jacobian. This analysis method is used to investigate the influence of boundary conditions and numerical parameters on the convergence behavior. ESA

N94-30756 National Aerospace Lab., Amsterdam (Netherlands). Informatics Div.
EULER RESULTS OF THE ISNaS COMPRESSIBLE MULTI-BLOCK FLOW SOLVER
W. Wagenaar and M. E. S. Vogels 30 Oct. 1992 24 p Presented at the 5th ISNaS Symposium, Twente, Netherlands, 5-6 Nov. 1992 Sponsored by Ministry of Education and Sciences, and Ministry of Transport and Public Works Limited Reproducibility: More than 20% of this document may be affected by microfiche quality
(AD-B179299; NLR-TP-92443-U; ETN-94-95963) Avail: CASI HC A03

The development of a multizone multiblock Navier-Stokes flow solver, directed towards the multielement airfoil application, for the ISNaS, an Information System for flow simulation based on the Reynolds averaged Navier-Stokes equations, is addressed. In the pipeline of the flow solver special editors support the input preparation. The development and test approach for the Euler computational kernel are described. Euler results for the flow solver are discussed to the level of verification. It is demonstrated that the flow solver gives flow results for the multielement airfoil application. The starting point of the validation of the flow solver was reached. Further development will involve validation, performance acceleration, and addition of new models, algorithms, and boundary types. ESA

N94-30763 National Aerospace Lab., Amsterdam (Netherlands). Informatics Div.
INFORMATION SYSTEM FOR FLOW SIMULATION BASED ON THE NAVIER-STOKES EQUATIONS VECTORIZATION
P. A. vanMourik 26 Feb. 1993 38 p Presented at Negende Supercomputer-Gebruikersdag, Amsterdam, Netherlands, 17 Dec. 1992

Limited Reproducibility: More than 20% of this document may be affected by microfiche quality
(AD-B179293; NLR-TP-93082-U; ETN-94-95969) Avail: CASI HC A03

The vectorization of a multiblock Navier-Stokes solver on the NEC SX-3 supercomputer is described. The flow solver under consideration was developed in a project, resulting in ISNaS, an Information System for flow simulation based on the Reynolds averaged Navier-Stokes equations, of which the flow solver is a part. With this solver it is possible to calculate three dimensional flows around multielement airfoil geometries with extended flaps and slats. ESA

N94-30791 Illinois Univ., Urbana-Champaign.
DEVELOPMENT AND APPLICATION OF PARTICLE IMAGE VELOCIMETRY IN HIGH-SPEED SEPARATED FLOW: TWO-DIMENSIONAL BASE CAVITIES Ph.D. Thesis
Michael Joseph Molezzi 1993 197 p
Avail: Univ. Microfilms Order No. DA9329114

A new particle image velocimetry (PIV) system has been developed to obtain two-dimensional instantaneous velocity data over a planar region in high-speed separated flows for the quantitative analysis of turbulent and unsteady flow structures. This PIV system is the first of its type to incorporate sub-micron seed particles and birefringent image shifting for the resolution of flow velocity in separated regions. The system was also developed with improved in-plane spatial resolution over previous high-speed flow PIV applications by using a 1.0 sq mm interrogation region (in flowfield dimensions) for each independent velocity measurement. The system has been proven in preliminary experiments using a simple low-speed round jet flow and had been validated for accuracy with both known-displacement simulated PIV photographs and uniform flow experiments at Mach 0.5 (170 m/s) for comparison to pressure and laser Doppler velocimeter (LDV) data. The PIV system was also used in a study of the near-wake structure of a two-dimensional base in subsonic flow. This application was chosen in order to determine the fluid dynamic mechanism of the observed base drag reduction in the presence of a base cavity. Experiments were done over a range of freestream Mach numbers up to 0.8, including local flowfield velocities up to 300 m/s. Effects of the base cavity on the von Karman vortex street wake were found to be related to the expansion and diffusion of vortices near the cavity, although the effects are of small magnitude and no significant change of the vortex formation location or path was observed. The base cavity effects are also less significant at higher freestream velocities due to the formation of vortices further downstream from the base. The base cavity drag reduction was found to be mainly due to the displacement of the base surface to a location upstream of the low-pressure wake vortices, with only a slight modification in the vortex street itself. Dissert. Abstr.

N94-30807 California Univ., Davis.
THE EFFECT OF PRESSURE GRADIENT ON THE STRUCTURE OF AN EQUILIBRIUM TURBULENT BOUNDARY LAYER Ph.D. Thesis
Ting-Kwo Lei 1993 157 p
Avail: Univ. Microfilms Order No. DA9328854

Hot-wire anemometry was used to study the effect of adverse pressure gradient on the large-scale structures of equilibrium turbulent boundary layers. A previously existing zero-pressure gradient wind tunnel was modified into an adverse-pressure gradient wind tunnel, which had the capability of creating designated adverse-pressure gradient equilibrium turbulent boundary layer flows. The range of the equilibrium parameter beta was from 0.0 to 1.8 along a 1.50 m long test section of the wind tunnel. Computer programs were developed to predict the geometric shape of the test section for an equilibrium adverse-pressure gradient turbulent boundary layer flow. The numerical prediction of the test section geometry was found to be satisfactory and a substantial effort was saved in the establishment of an equilibrium boundary layer. Three equilibrium boundary layer flows at values of beta = 0.0, 0.8, and 1.8, which respectively represents zero, mild, and strong adverse pressure gradient, were established and were found to be suitable for turbulence structure measurements. Space-time correlation measurements were carried out to determine the convection velocities and inclination angles of the large-scale structures for the three different pressure gradient cases. The convection velocity measurements were performed at various heights which ranged form y(sup +) = 225 to 525 for each beta value. It was found that, within the range of height of the measurements, the convection velocity was independent of height In the case of the strong adverse-pressure gradient flow, the convection velocity was observed to be much lower than the convection velocity observed in the case of zero-pressure gradient. In the case of the mild-pressure gradient flow, it was observed that the pressure gradient effect on the convection velocity was negligible as compared to the zero-pressure gradient case. The inclination angle in the case of strong-pressure gradient case was found to be much greater than that observed in the case of zero-pressure gradient case. The pressure gradient effect on the inclination angle was observed to be negligible in the case of mild ad verse-pressure gradient case.
Dissert. Abstr.

N94-30816 California Univ., Los Angeles.
MIXED EULERIAN-LAGRANGIAN FINITE ELEMENT SOLUTIONS OF UNSTEADY FLOW AND FLUTTER IN TRANSONIC CASCADE Ph.D. Thesis
Chingteng Hsiao 1993 212 p
Avail: Univ. Microfilms Order No. DA9319918

Unsteady flow and flutter phenomena of turbomachinery cascades operating in the transonic regime are explored by a new numerical approach. The two dimensional unsteady Euler equations are used to model the transonic cascade flows, and the cascade blades are modeled as thin plates. To minimize the discretization incompatibility, both the fluid and the solid domains are discretized using finite element procedures. The Rayleigh-Ritz finite element formulations are employed in the structural discretization while the Galerkin finite element procedure is used in the fluid discretization. As is customary, the discretized equations of the cascade blades are described in purely Lagrangian coordinates. However, in order to take care of the time-varying boundary conditions effectively, the mixed Lagrangian-Eulerian description is used in the fluid domain. The fluid and the structural models are coupled by introducing a channel theory, which is equivalent to a strip theory in the classical sense. In this procedure several two dimensional aerodynamic solvers are combined with one three dimensional structural solver to form a quasi three dimensional aeroelastic system. The whole system is marched toward in time using an explicit four-stage Runge-Kutta scheme to obtain the time domain solutions. Steady and unsteady transonic flow results are both presented. The current finite element Euler solutions show very good agreement with available finite volume Euler solutions. Free vibration analyses of nonrotating and rotating blades using the present finite element model with 80 degrees of freedom have been carried out. The computed natural frequencies and mode shapes are comparable to other finite element and Rayleigh-Ritz results. Aeroelastic responses of several cascade configurations in different transonic flow fields are investigated using either a typical section model or the present quasi three dimensional model. These analyses demonstrate that the current full blade structure formulation can handle flutters involving higher modes and hence have a better estimation of the flutter boundary.
Dissert. Abstr.

N94-30855 National Aerospace Lab., Amsterdam (Netherlands). Informatics Div.
NUMERICAL SIMULATION OF A CONDENSER IN TWO-PHASE HEAT TRANSPORT SYSTEMS: A FEASIBILITY STUDY
A. A. tenDam and J. I. vandeBerg 30 Apr. 1992 38 p Limited Reproducibility: More than 20% of this document may be affected by microfiche quality
(AD-B173650; NLR-TP-92081-U; ETN-94-95572) Avail: CASI HC A03

The numerical simulation of a mathematical model of a condenser is discussed. This mathematical model is part of an approach to model and scale two phase heat transport systems. The model of the condenser is reformulated to a model that is suitable for a numerical discussion. The result is a model that is represented by an implicit nonlinear differential/algebraic equation. One numerical solution procedure is discussed. Test cases are defined and simulation studies are conducted with several working fluids and under varying gravity conditions. The simulation results show that the approach taken is suitable to obtain the behavior of a condenser. ESA

N94-30953 Notre Dame Univ., IN.
AN EXPERIMENTAL STUDY OF NONLINEAR WAVE COUPLING AND ENERGY TRANSFER CHARACTERIZING THE TRANSITION OF A PLANAR JET SHEAR LAYER Ph.D. Thesis

Huan Chang Chu 1993 282 p
Avail: Univ. Microfilms Order No. DA9319299

An experimental study of the nonlinear spectral development associated with the transition of an initially laminar planar jet shear layer is presented. The local shear layer spectral dynamics are modeled as a nonlinear system containing both linear and two quadratically nonlinear system elements. The experimental technique motivated by the related governing equation for the flow is based upon the 'wave coupling equation' which results from a temporal Fourier transform of the incompressible Navier-Stokes equation. A novel digital signal processing technique is applied which allows the local spectral dynamics to be estimated directly from time-series velocity fluctuations. From the linear coupling coefficient, the local spectral growth rate and dispersion relation can be estimated. Of particular interest is the associated wave coupling coefficients which provides a measure of the efficiency of local nonlinear wave-wave interactions. These show that the jet shear layer exhibits a strong preference for difference mode interactions. Particular emphasis is placed upon discerning the mechanism which gives rise to subharmonic resonance with the fundamental instability. Results show that the amplification of the subharmonic instability is largely due to a 'parametric resonance' with the fundamental rather than by direct fundamental-subharmonic interaction. Based upon the result of the dual-input/single-output nonlinear system model, it is surprising to note that u-v nonlinear interaction (i.e., f(sub e) at u + f(sub e) at v yields 2f(sub e) at u) plays a primary role in the amplification of the harmonic 2f(sub e) at u while the contribution from self-interaction of the fundamental f(sub e) (i.e., f(sub e) at u + f(sub e) at u yields 2f(sub e) at u) relatively small in the jet shear layer transition. Dissert. Abstr.

N94-30954 Colorado Univ., Boulder.
LOCAL TWO-PHASE FLOW SIMULATIONS INCLUDING INTERFACE TRACKING WITH MASS TRANSFER Ph.D. Thesis
Samuel Williamson Jo Welch 1993 180 p
Avail: Univ. Microfilms Order No. DA9320490

The purpose of this work is to develop a code to perform local simulations of fundamental two-phase fluid flows in two dimensions. We consider flows in which there is mass transfer across a phase interface separating the vapor and liquid phases. Calculation of the flow field near the interface requires that we track the location of the interface as part of the solution procedure. This work is an attempt to provide a tool to be used in understanding basic flow phenomenon near interfaces heretofore not considered in engineering two-phase flow calculations. Current practice in two-phase flow simulations is to use volume averaged equations which require engineering correlations for closure. This approach does not attempt to resolve the physics near phase interfaces. The physical phenomena near interfaces is instead approximated in subgrid models similar to the approach used in turbulence modeling. The liquid and vapor phases are considered as viscous, conducting, compressible fluids with different state equations. The interface is modeled as lines embedded in the two dimensional region. The interface is considered to have significant surface tension along with significant surface energy and entropy. The interface is nonmaterial due to the mass transfer across it. The numerical method is a finite volume method on a collocated moving mesh. The mesh motion is neither Lagrangian nor Eulerian, but rather is specified by the motion of the nonmaterial phase interface. The basic philosophy in designing the numerical method was to create a simple first order scheme allowing us to concentrate on the problems associated with the interface and the mesh motion. The basic capabilities of the scheme are illustrated in simulations both with and without mass transfer. The simulations without mass transfer are chosen to test the code against known results. The simulations with mass transfer are fundamental local simulations in two-phase flow chosen because of the simple physical insight contained within them. Dissert. Abstr.

N94-30955 Worcester Polytechnic Inst., MA.
GENERALIZED EULERIAN-LAGRANGIAN FORMULATIONS IN FREE AND MOVING BOUNDARY PROBLEMS: PROCESSING OF VISCOELASTIC POLYMERS AND FIBER SUSPENSIONS Ph.D. Thesis
Alauddin Ahmed 1993 205 p
Avail: Univ. Microfilms Order No. DA9320564

The thrust of this dissertation is to develop methods of analysis of processes associated with the manufacturing of fiber reinforced composites. The manufacturing processes are characterized by flows in complex geometries with apriori unknown free and moving boundaries. In addition, the materials are characterized by constitutive relations ranging from simple differential to complex integro-differential models. Improved and efficient mathematical formulations and numerical techniques are, therefore, required to successfully solve these complicated flow problems. The generalized Eulerian-Lagrangian (GEL) formulation provides an excellent opportunity to address some of the difficulties associated with these problems. The processes are modeled using the complete unsteady form of the conservation equations and solved using a classical mixed Galerkin finite element method coupled with Newton-Raphson iterations. In the analysis of injection and compression molding of viscoelastic polymers, the White-Metzner model is used to describe the stress state and the components of the stress tensor are treated as independent variables. The unsteady flow of dilute fiber suspensions is analyzed using the transversely isotropic fluid approach. The orientation state of the fibers is expressed in terms of orientation tensors and the development of fiber orientation is described by means of evolution equations. The model is completed using a second order quadratic closure approximation. The resulting flow field and implied fiber orientation agree well with the available experimental results. In the analysis of the semiconcentrated fiber suspensions, the Dinh-Armstrong integral constitutive equation is used to describe the stress and fiber orientation state. The Currie approximation is used to express the integral equation in the form of algebraic equations involving the finite deformation tensors and their invariants. These tensors are expressed in terms of the flow kinematics through a semi-implicit finite difference scheme. The accuracy of the scheme is tested on a radially diverging source flow for which the analytical solutions are obtained. The method is used in the analysis of the filling of simple injection and compression molding cavities. The flow pattern and fiber orientation agree well with the available experimental results. Dissert. Abstr.

N94-30958 Washington Univ., Seattle.
TRANSITION TO TURBULENCE IN CONFINED COMPRESSIBLE MIXING LAYERS Ph.D. Thesis
Ho-Shuenn Huang 1992 270 p
Avail: Univ. Microfilms Order No. DA9312686

Four different numerical schemes have been tested at a subsonic convective Mach number: a spectral method, a fourth-order compact scheme, a second-order TVD/MacCormack scheme, and a TVD method. A spectral numerical method is chosen as the numerical scheme to investigate mixing layers from subsonic to supersonic convective Mach numbers. Two types of initial conditions are involved. One comes from linear stability theory; the other uses finite, broadband white noise. Results of the simulations reveal that, in a mixing layer subjected to perturbations consisting of finite, broadband white noise, the perturbations will grow in the linear regime close to the predictions of normal-mode analysis. There are modes which grow algebraically at early times. The three dimensional effects developing from oblique Kelvin-Helmholtz (K-H) instabilities and streamwise minus modes are also important when the flow becomes strongly nonlinear. Mushroom structures form owing to the effects of such three dimensional instabilities. Mixing is governed by the evolution of both two and three dimensional K-H instabilities. If the Reynolds number is low enough viscous shocks are likely to form during the nonlinear development. Complicated mushroom structures are observed in the evolution of the mixing interface as the mixing layers become strongly nonlinear; such succeeding development of entangling mushroom structures is believed to be the key mechanism leading to the transition to turbulence. Mixing is dominated by the three dimensional evolution of the mixing layers, e.g., oblique K-H instabilities and streamwise minus modes. For the supersonic convective Mach number, the mixing layers are dominated in the transitional regime by the development of two dimensional, confined supersonic modes. Viscous shocks interact with other unstable modes and develop in a three dimensional manner. Mixing is governed mainly by the development of two dimensional confined supersonic instabilities. The energy transfer among various modes is examined in two ways for subsonic, transonic, and supersonic convective Mach numbers. In one method a mode of potential importance is suppressed, and the resulting effect on other modes of interest is examined. A second method employs Fourier decomposition and examines the modal energy transfer rate due to triad interaction. Dissert. Abstr.

N94-30967 GKSS-Forschungszentrum Geesthacht (Germany). Inst. fuer Anlagentechnik.
TURBULENCE MODELS AND THEIR APPLICATION IN IMPLOSION ANALYSES WITH TWO-PHASE FLOW
J. G. Chen (Jiaotong Univ., Shanghai, China.) and R. A. Dietrich 26 Oct. 1992 22 p Sponsored by BMFT Limited Reproducibility: More than 20% of this document may be affected by microfiche quality
(ISSN 0344-9629)
(GKSS-92/E/98; ETN-94-95956) Avail: CASI HC A03

A general review of existing mathematical models describing the turbulent flow is given. These models are classified and their merits and limitations are presented. Special attention is paid to the developed turbulence models and their application in implosion problems with two phase flows. Some known research results are summarized. ESA

N94-30968 GKSS-Forschungszentrum Geesthacht (Germany). Inst. fuer Anlagentechnik.
NUMERICAL SIMULATION AND PREDICTION OF IMPLOSION PHENOMENA
J. Chen (Jiaotong Univ., Shanghai, China.) and R. A. Dietrich 26 Oct. 1992 53 p Sponsored by BMFT Limited Reproducibility: More than 20% of this document may be affected by microfiche quality
(ISSN 0344-9629)
(GKSS-92/E/99; ETN-94-95957) Copyright Avail: CASI HC A04

Using gas-liquid two phase flow theory, a modified mathematical model based on the computational fluid dynamics method SIMPLE (Semi Implicit Method for Pressure Linked Equations) is introduced to investigate implosion phenomena in high pressure chambers. For a characteristic physical model, the numerical results are obtained and analyzed, without referring to experimental data. Extensive calculations to predict the highest pressure on the chamber wall are performed under varying conditions such as the implosion pressure, the dimensions of the test models, and the height of the upper air layer. The efficiency of different highest pressure reduction methods is analyzed. The results of these simulations and predictions are shown in a series of plots. ESA

N94-28948# National Aerospace Lab., Tokyo (Japan).
MONTE CARLO SIMULATION OR NORMAL SHOCK WAVE. PART 2: VHS MODEL AND VSS MODEL [SHOGEKIHA NO MONTE KARURO SHIMYURESHON. 2: VHS MODERU TO VSS MODERU]
Hiroaki Matsumoto and Katsuhisa Koura *In its* Proceedings of the 10th NAL Symposium on Aircraft Computational Aerodynamics Dec. 1992 p 7-10 In JAPANESE (For primary document see N94-28946 08-02)
Avail: CASI HC A01/MF A03

N94-28949# National Aerospace Lab., Tokyo (Japan). Aerodynamics Div.
VARIABLE SOFT SPHERE MOLECULAR MODEL IN THE MONTE CARLO SIMULATION OF AIR SPECIES [KUKI BUNSHI NO MONTE KARURO SHIMYURESHON NIOKERU VSS BUNSHI MODERU]
Katsuhisa Koura, Hiroaki Matsumoto, and Mikinari Takahira *In its* Proceedings of the 10th NAL Symposium on Aircraft Computational Aerodynamics Dec. 1992 p 11-15 In JAPANESE (For primary document see N94-28946 08-02)
Avail: CASI HC A01/MF A03

N94-28956# National Aerospace Lab., Amsterdam (Netherlands).
ENGRID: A GRAPHICAL INTERACTIVE CODE FOR THE COMPUTATION OF STRUCTURED GRIDS FOR BLOCKED FLOW DOMAINS
S. P. Spekreijse *In its* Proceedings of the 10th NAL Symposium on Aircraft Computational Aerodynamics Dec. 1992 p 51-56 Prepared in cooperation with Alenia, Rome, Italy Sponsored by Netherlands Agency for Aerospace Programs, Delft, Netherlands (For primary document see N94-28946 08-02)
Avail: CASI HC A02/MF A03

N94-28964# Kawasaki Heavy Industries Ltd., Gifu (Japan).
ROLE OF COMPUTATIONAL FLUID DYNAMICS IN AERONAUTICAL ENGINEERING. PART 10: NUMERICAL ANALYSIS OF FLOW AROUND 2-D MULTI-ELEMENT HLD [SEKKEI NICKERU SUCHI KAISEKI NO KATSUYO NITSUITE. SONO 10: 2 JIGEN TAYOKUSO MAWARI NAGARE NO SUCHI KAISEKI]
Koichi Egami, Eiji Shima, Kanichi Amano, and Shingo Nakamura *In* NAL, Proceedings of the 10th NAL Symposium on Aircraft Computational Aerodynamics Dec. 1992 p 99-104 In JAPANESE (For primary document see N94-28946 08-02)
Avail: CASI HC A02/MF A03

N94-28968# Toyota Motor Co., Aichi (Japan).
NUMERICAL ANALYSIS OF INCOMPRESSIBLE VISCOUS FLOW AROUND A BUBBLE [HENKEI WO TOMANAU KIHO MAWARI NO NAGARE NO SUCHI KAISEKI]
Minoru Sugano, Ryuji Ishii, and Shigeki Morioka *In* NAL, Proceedings of the 10th NAL Symposium on Aircraft Computational Aerodynamics Dec. 1992 p 121-126 In JAPANESE Prepared in cooperation with Kyoto University, Kyoto, Japan (For primary document see N94-28946 08-02)
Avail: CASI HC A02/MF A03

N94-28970# Shimizu Corp. (Japan).
STUDY OF MODELING OF TURBULENCE OF RENORMALIZATION GROUP ANALYSIS [KURIKOMIGUN NIYORU RANRYU MODERU NO ICHI KOSATSU]
Wako Takanashi *In* NAL, Proceedings of the 10th NAL Symposium on Aircraft Computational Aerodynamics Dec. 1992 p 133-134 In JAPANESE (For primary document see N94-28946 08-02)
Avail: CASI HC A01/MF A03

N94-28971# Nagoya Univ. (Japan). Dept. of Aeronautical Engineering.
THE UPSILON-q METHOD AND THE PSI-q METHOD FOR INCOMPRESSIBLE FLOWS [HIASSHUKUSEI RYU NITAISURU UPUSHIRON-Q HO TO PUSAI-Q HO]
Wei Jia and Yoshiaki Nakamura *In* NAL, Proceedings of the 10th NAL Symposium on Aircraft Computational Aerodynamics Dec. 1992 p 135-140 In JAPANESE (For primary document see N94-28946 08-02)
Avail: CASI HC A02/MF A03

N94-28972# National Aerospace Lab., Tokyo (Japan).
ON THE NUMERICAL ANALYSIS OF SHEAR FLOWS [SENDANRYU NO SUCHI KAISEKI NITSUITE]
Satoru Ogawa and Yoko Takakura *In its* Proceedings of the 10th NAL Symposium on Aircraft Computational Aerodynamics Dec. 1992 p 141-144 In JAPANESE (For primary document see N94-28946 08-02)
Avail: CASI HC A01/MF A03

N94-28973# National Aerospace Lab., Tokyo (Japan). Computational Sciences Div.
ON APPROXIMATE RIEMANN SOLVERS: IMPROVEMENT OF HLLEM SCHEME AND ITS GENERALIZATION FOR CHEMICALLY REACTING FLOWS [KINJI RIMAN KAIHO NITSUITE: HLLEM SUKIMO NO KAIRYO TO HANNOURYU ENO KAKUCHO]
Yasuhiro Wada *In its* Proceedings of the 10th NAL Symposium on Aircraft Computational Aerodynamics Dec. 1992 p 145-152 In JAPANESE (For primary document see N94-28946 08-02)
Avail: CASI HC A02/MF A03

N94-28976# Kawasaki Heavy Industries Ltd., Tokyo (Japan).
VERIFICATION OF A THREE-DIMENSIONAL VISCOUS FLOW ANALYSIS FOR A SINGLE STAGE COMPRESSOR [NS KAISEKI NIYORU TANDAN ASSHUKUKI YOKURETSU NAGARE NO KENSHO]
Akinori Matsuoka, Keisuke Hashimoto, Osamu Nozaki, Kazuo Kikuchi, Masahiro Fukuda, and Atsuhiro Tamura *In* NAL, Proceedings of the 10th NAL Symposium on Aircraft Computational Aerodynamics Dec. 1992 p 163-168 In JAPANESE (For primary document see N94-28946 08-02)
Avail: CASI HC A02/MF A03

N94-28979# Osaka Prefecture Univ., Sakai (Japan). Dept. of Aeronautical Engineering.
THREE-DIMENSIONAL EXTERNAL FLOW COMPUTATIONS USING PRISMATIC GRID [PURIZUMU KOSHI NIYORU SANJIG EN GAIBURYU NO SUICHI KEISAN]
Kazuhiro Nakahashi *In* NAL, Proceedings of the 10th NAL Symposium on Aircraft Computational Aerodynamics Dec. 1992 p 181-186 In JAPANESE (For primary document see N94-28946 08-02)
Avail: CASI HC A02/MF A03

N94-28982# SofTek Systems, Inc., Tokyo (Japan).
UPWIND METHOD USING LOCAL INTERPOLATION [KYOKUSHOTEKINA HOKAN O MOCHIITA KAZAKAMIHO NITSUITE]
Susumu Shirayama *In* NAL, Proceedings of the 10th NAL Symposium on Aircraft Computational Aerodynamics Dec. 1992 p 199-204 In JAPANESE (For primary document see N94-28946 08-02)
Avail: CASI HC A02/MF A03

N94-28983# Kyushu Univ., Fukuoka (Japan). Dept. of Mechanical Engineering for Power.
AN IMPLICIT UPWIND SCHEME FOR THE THREE-DIMENSIONAL EULER EQUATIONS USING A POINTWISE RELAXATION METHOD [TEN KANWAHO O MOCHIITA SANJIGEN OIRA HOTEISHIKI NO INTEKI KAZAKAMI KAIHO]
Masato Furukawa, Seiichi Ibaraki, Eito Matsuo, and Masahiro Inoue *In* NAL, Proceedings of the 10th NAL Symposium on Aircraft Computational Aerodynamics Dec. 1992 p 205-210 In JAPANESE (For primary document see N94-28946 08-02)
Avail: CASI HC A02/MF A03

N94-28984# National Aerospace Lab., Kakuda (Japan).
FLOW AND HEAT TRANSFER IN A ROTATING SQUARE SECTIONED U-BEND [KAITENSURU U-BENDO NAI NO NAGARE TO NETSUDENTATSU]
Hiroshi Tamura and Hiroshi Ishigaki *In its* Proceedings of the 10th NAL Symposium on Aircraft Computational Aerodynamics Dec. 1992 p 211-214 In JAPANESE (For primary document see N94-28946 08-02)
Avail: CASI HC A01/MF A03

N94-28985# Tokyo Inst. of Tech. (Japan). Dept. of Energy Sciences.
TRANSONIC EXPANDING FLOW THROUGH AXIALLY SYMMETRIC ORIFICES [JIKU TAISHO ORIFISU O TORU SENONSOKU BOCHORYU]
Yuminobu Igarashi and Hisashi Mikami *In* NAL, Proceedings of the 10th NAL Symposium on Aircraft Computational Aerodynamics Dec. 1992 p 215-220 In JAPANESE (For primary document see N94-28946 08-02)
Avail: CASI HC A02/MF A03

N94-28986# National Aerospace Lab., Kakuda (Japan).
SIMILARITY BETWEEN TURBULENT FLOWS THROUGH CURVED PIPE AND ORTHOGONAL ROTATING PIPE [NIJI NAGARE O TOMONAU KANNAI RANRYU NO SOJISEI]
Hiroshi Ishigaki *In its* Proceedings of the 10th NAL Symposium on Aircraft Computational Aerodynamics Dec. 1992 p 221-224 In JAPANESE (For primary document see N94-28946 08-02)
Avail: CASI HC A01/MF A03

N94-28987# National Aerospace Lab., Kakuda (Japan).
NUMERICAL ANALYSIS OF LAMINAR FLOW IN S-CURVED SQUARE DUCT WITH INLET AND OUTLET STRAIGHT REGION [S-GATA BENDO NO NAGARE NO SUCHI KAISEKEI]
Hitoshi Yamada, Hiroshi Ishigaki, and Munekazu Mochizuki *In its* Proceedings of the 10th NAL Symposium on Aircraft Computational Aerodynamics Dec. 1992 p 225-228 In JAPANESE (For primary document see N94-28946 08-02)
Avail: CASI HC A01/MF A03

N94-28988# National Aerospace Lab., Kakuda (Japan).
DEVELOPMENT OF BUOYANCY AFFECTED LAMINAR FLOW IN A HEATED PIPE [FURYOKU GA SAYOSURU KANETSU KANNAI NAGARE NO HATTATSU]
Munekazu Mochizuki and Hiroshi Ishigaki *In its* Proceedings of the 10th NAL Symposium on Aircraft Computational Aerodynamics Dec. 1992 p 229-233 In JAPANESE (For primary document see N94-28946 08-02)
Avail: CASI HC A01/MF A03

N94-28989# National Aerospace Lab., Kakuda (Japan).
MUTUAL SIMILARITY OF DEVELOPING LAMINAR FLOWS WITH SECONDARY STREAMS IN DUCTS: CURVED PIPE FLOW AND ORTHOGONAL ROTATING PIPE FLOW [NIJI NAGARE O TOMANAU KANNAI SORYU JOSO NAGARE NO SOJISEI: KYOKKAN TO CHOKKO KAITENKAN]
Hiroshi Ishigaki *In its* Proceedings of the 10th NAL Symposium on Aircraft Computational Aerodynamics Dec. 1992 p 235-239 In JAPANESE (For primary document see N94-28946 08-02)
Avail: CASI HC A01/MF A03

N94-29280*# National Aeronautics and Space Administration. Lewis Research Center, Cleveland, OH.
EXPERIMENTAL STUDIES ON EFFERVESCENT ATOMIZERS WITH WIDE SPRAY ANGLES
J. D. Whitlow (Purdue Univ., West Lafayette, IN.), A. H. Lefebvre (Purdue Univ., West Lafayette, IN.), and R. J. Rollbuhler *In* AGARD, Fuels and Combustion Technology for Advanced Aircraft Engines Sep. 1993 11 p (For primary document see N94-29246 08-25)
Copyright Avail: CASI HC A03/MF A04

N94-29282# Deutsche Forschungs- und Versuchsanstalt fuer Luft- und Raumfahrt, Cologne (Germany). Inst. for Propulsion Technology.
INVESTIGATION OF THE TWO-PHASE FLOW IN A RESEARCH COMBUSTOR UNDER REACTING AND NON-REACTING CONDITIONS
C. Hassa, A. Deick, and H. Eickhoff *In* AGARD, Fuels and Combustion Technology for Advanced Aircraft Engines Sep. 1993 12 p Sponsored by TECFLAM (For primary document see N94-29246 08-25)
Copyright Avail: CASI HC A03/MF A04

N94-29283# Karlsruhe Univ. (Germany). Lehrstuhl und Inst. fuer Thermische Stroemungsmaschinen.
TIME-RESOLVED MEASUREMENTS IN A THREE DIMENSIONAL MODEL COMBUSTOR
R. Jeckel and S. Wittig *In* AGARD, Fuels and Combustion Technology for Advanced Aircraft Engines Sep. 1993 15 p Sponsored by Arbeitsgemeinschaft Hochtemperatur Gasturbine and BMFT (For primary document see N94-29246 08-25)
Copyright Avail: CASI HC A03/MF A04

N94-29702# Ministry of Agriculture, Forestry, and Fisheries, Ibaraki (Japan). Systems Analysis of Aquacultural Ground Section.
DEVELOPMENT OF A SIMPLE CURRENT METER USING SOLUTION [YOEKI O MOCHIITA KANI RYOSOKUKEI NO KAIHATSU]
Shigeru Kawamata *In its* Bulletin of National Research Institute of Fisheries Engineering, No. 13 5 Mar. 1992 p 1-9 In JAPANESE (For primary document see N94-29701 08-31)
Avail: CASI HC A02/MF A02

N94-29706# Ministry of Agriculture, Forestry, and Fisheries, Ibaraki (Japan). Hull Construction Section.
THE FLOW FIELD NEAR THE BODY SURFACE WITH THIN FILAMENTS [KOMITSUDO NO RITSUMO SENI DE OWARETA BUTTAI MAWARI NO NAGAREBA NI KANSURU KENKYU]
Toshihiko Kawashima, Kumiko Adachi, and Hiroyasu Kato *In its* Bulletin of National Research Institute of Fisheries Engineering, No. 13 5 Mar. 1992 p 81-94 In JAPANESE Prepared in cooperation with National Research Inst. of Aquaculture, Mie, Japan; and Toray Industries, Inc., Shiga, Japan (For primary document see N94-29701 08-31)
Avail: CASI HC A03/MF A02

N94-30450*# Argonne National Lab., Idaho Falls, ID. Energy Technology Div.
POTENTIAL CAPABILITIES OF REYNOLDS STRESS TURBULENCE MODEL IN THE COMMIX-RSM CODE
F. C. Chang and M. Bottoni *In* NASA, Washington, Technology 2003:

The Fourth National Technology Transfer Conference and Exposition, Volume 1 90-99 (SEE N94-30440 08-99) Feb. 1994 (For primary document see N94-30440 08-99)
Avail: CASI HC A02/MF A04

35 INSTRUMENTATION AND PHOTOGRAPHY

Includes remote sensors; measuring instruments and gages; detectors; cameras and photographic supplies; and holography.

For aerial photography see *43 Earth Resources and Remote Sensing*. For related information see also *06 Aircraft Instrumentation*, and *19 Spacecraft Instrumentation*.

N94-28466# Sandia National Labs., Albuquerque, NM.
HOLOGRAPHIC INTERFEROMETRY: A USER'S GUIDE
D. Griggs Oct. 1993 31 p
(Contract DE-AC04-94AL-85000)
(DE94-003136; SAND-92-2909) Avail: CASI HC A03/MF A01

This manual describes the procedures and components necessary to produce a holographic interferogram of a flow field in the Sandia National Laboratories hypersonic wind tunnel. In contrast to classical interferometry, holographic interferometry records the amplitude and phase distribution of a lightwave passing through the flow field at some instant of time. This information can then be reconstructed outside the wind tunnel for visual analysis and digital processing. This yields precise characterizations of aerodynamic phenomena. The reconstruction and subsequent hologram image storage process is discussed, with particular attention paid to the digital image processor and the data reduction technique. DOE

N94-28553# Joint Inst. for Nuclear Research, Dubna (USSR).
THE COMPUTER-AIDED SYSTEM FOR THE HIGH RESOLUTION SQUID-MAGNETOMETER
E. I. Litvinenko, Yu. V. Obukhov, V. N. Shatokhin, and N. A. Yakovenko 1992 23 p In RUSSIAN
(DE94-606138; JINR-R-10-92-188) Avail: CASI HC A03/MF A01 (US Sales Only)

The described computer-aided system for the high resolution SQUID-magnetometer permits one to regulate the thermostat temperature, vary the working magnetic field, change the sample position and allow acquisition and processing of signal from a SQUID. A brief description of electronics and the principal program algorithms is proposed. DOE

N94-28824*# Virginia Polytechnic Inst. and State Univ., Blacksburg. Dept. of Mechanical Engineering.
HEAT FLUX INSTRUMENTATION FOR HYFLITE THERMAL PROTECTION SYSTEM Final Report, 13 Aug. 1993 - 13 Jan. 1994
T. E. Diller 1994 29 p
(Grant NAG1-1538)
(NASA-CR-195731; NAS 1.26:195731; NLPN-93-428) Avail: CASI HC A03/MF A01

Using Thermal Protection Tile core samples supplied by NASA, the surface characteristics of the FRCI, TUFI, and RCG coatings were evaluated. Based on these results, appropriate methods of surface preparation were determined and tested for the required sputtering processes. Sample sensors were fabricated on the RCG coating and adhesion was acceptable. Based on these encouraging results, complete Heat Flux Microsensors were fabricated on the RCG coating. The issue of lead attachment was addressed with the annnealing and welding methods developed at NASA Lewis. Parallel gap welding appears to be the best method of lead attachment with prior heat treatment of the sputtered pads. Sample Heat Flux Microsensors were submitted for testing in the NASA Ames arc jet facility. Details of the project are contained in two attached reports. One additional item of interest is contained in the attached AIAA paper, which gives details of the transient response of a Heat Flux Microsensors in a shock tube facility at Virginia Tech. The response of the heat flux sensor was measured to be faster than 10 micro-s. Author (revised)

N94-28831 Army Engineer Waterways Experiment Station, Vicksburg, MS. Environmental Lab.
DEVELOPMENT AND APPLICATION OF A THERMISTOR CURRENT METER Final Report
Carl M. Way, Albert J. Burky, and Christine A. Miller-Way Jan. 1994 35 p Limited Reproducibility: More than 20% of this document may be affected by microfiche quality
(AD-A275816; WES/TR-EL-94-1) Avail: CASI HC A03

This report provides details for the construction of a hot-bead thermistor current meter which is capable of measuring water velocities on a millimeter spatial scale and for the construction of a compact and accurate calibration system. Hot-bead thermistor current meters can be built with response times of 200 ms capable of measuring velocities between 0.1 and 80 cm/s. The construction of a sturdy probe for application in lotic systems such as high gradient Hawaiian streams was achieved by the use of heavy-duty acrylic tubing, small stainless steel gas-chromatography tubing, and flexible Tygon spaghetti tubing. An acrylic handle anchors the electrical cable at one end and the thermistors at the other. The following criteria were central to the development of the calibration system: (1) accurate calibration; (2) compact unit for storage and use in limited laboratory space; (3) leak-proof system; (4) inexpensive design requirement for readily available materials; and (5) construction requirements for the use of hand tools. The thermistor current meter has been used to measure velocities in the water column and around various substrate features in riverine habitats. More detailed spatial velocity measurements were made in streams by dividing a habitat into small grid cells. With fine spatial scales (e.g., grid sizes of 200 to 300 sq cm or less) and repetitive sampling under varying water flow conditions, insights into relationships between various spatial and temporal characteristics of microhabitat velocities were made. The current meter has been used to determine ambient velocity profiles around a variety of benthic streams. DTIC

N94-29000*# National Aeronautics and Space Administration. Lewis Research Center, Cleveland, OH.
CRYOGENIC PROBE STATION FOR USE IN AUTOMATED MICROWAVE AND NOISE FIGURE MEASUREMENTS
Susan R. Taub, Samuel A. Alterovitz, Paul G. Young, Ben T. Ebihara, and Robert R. Romanofsky Mar. 1994 11 p Proposed for presentation at the Automated RF Techniques Group Meeting, San Diego, CA, 27 May 1994; sponsored by IEEE, MTIS and ARFTG
(RTOP 235-01-0B)
(NASA-TM-106560; E-8726; NAS 1.15:106560) Avail: CASI HC A03/MF A01

A cryogenic measurement system capable of performing on-wafer RF testing of semiconductor devices and circuits has been developed. This 'CryoProbe Station' can wafer-probe devices and circuits at cryogenic temperatures, thus eliminating the need for wire bonds. The system operates under vacuum created by a sorption pump. It uses an open cycle cooling system that can be cooled with either liquid nitrogen or liquid helium. Presently, it can reach temperatures, as low as 80 K and 37 K for each of the coolants, respectively. The temperature can be raised using a heater and it is stabilized to within 0.2 K by use of a temperature controller. The CryoProbe Station features a 1 by 2 inch stage that can hold large circuits and calibration standards simultaneously. The system is used with a Hewlett Packard 8510C Automatic Network Analyzer (ANA) to obtain S-parameter data over the frequency range 0.045-26.5 GHz. S-parameter data on HEMT (high electron mobility transistors) devices has been obtained with this station. With the use of DEEMBED software from NIST, detailed transmission line studies have been performed. Although the CryoProbe Station is designed for frequencies up to 26.5 GHz, useful transmission line data has been obtained for frequencies as high as 40 GHz. The CryoProbe station has also been used with the ATN noise figure measurement system to perform automatic, temperature dependent noise figure measurements. Author

N94-29113 Rutherford Appleton Lab., Chilton (England).
DOUBLE-CRYSTAL ANALYSER SYSTEM FOR THE PRISMA SPECTROMETER: TEST OF A PROTOTYPE
C. Petrillo, F. Sacchetti, M. Hagen, and U. Steigenberger Nov. 1993 44 p Prepared in cooperation with Istituto Nazionale di Fisica Nucleare, Frascati, Italy and Keele Univ., England
(PB94-138245; RAL-93-091) Avail: Issuing Activity (National Technical Information Service (NTIS))

A prototype of a double-analyzer system has been tested at the ISIS pulsed neutron source in order to determine the performance of such an analyzing device in the low energy transfer region. The performance of

such a system has been found satisfactory in terms of reflectivity and energy resolution as well as alignment procedures. Based on our test results, we propose the construction of a second arm for the PRISMA spectrometer at ISIS. This new arm would enable us to perform measurements with much improved energy resolution and to extend the wavevector transfer range to much smaller values, thus improving the instrument performance significantly for magnetic scattering experiments. The new, modular approach of the upgrade will also strengthen the flexibility of the instrument and open up the opportunity for further instrumental developments, for example the introduction of a polarization option. NTIS

N94-29199*# National Aeronautics and Space Administration. Langley Research Center, Hampton, VA.

ABSOLUTE CALIBRATION TECHNIQUE FOR BROADBAND ULTRASONIC TRANSDUCERS Patent Application

William T. Yost, inventor (to NASA) and John H. Cantrell, inventor (to NASA) 31 Aug. 1993 15 p

(NASA-Case-LAR-14672-1; NAS 1.71:LAR-14672-1;

US-Patent-Appl-SN-117511) Avail: CASI HC A03/MF A01

Calibrating an ultrasonic transducer can be performed with a reduced number of calculations and testing. A wide-band pulser is connected to an ultrasonic transducer under test to generate ultrasonic waves in a liquid. A single frequency is transmitted to the electrostatic acoustic transducer (ESAT) and the voltage change produced is monitored. Then a broadband ultrasonic pulse is generated by the ultrasonic transducer and received by the ESAT. The output of the ESAT is amplified and input to a digitized oscilloscope for fast Fourier transform. The resulting plot is normalized with the monitored signal from the single frequency pulse. The plot is then corrected for characteristics of the membrane and diffraction effects. The transfer function of the final plot is determined. The transfer function gives the final sensitivity of the ultrasonic transducer as a function of frequency. The advantage of the system is the speed of calibrating the transducer by a reduced number of measurements and removal of the membrane and diffraction effects.

NASA

N94-29358*# National Aeronautics and Space Administration. Marshall Space Flight Center, Huntsville, AL.

SUSPENSION SYSTEM FOR GIMBAL SUPPORTED SCANNING PAYLOADS Patent Application

Michael E. Polites, inventor (to NASA) 15 Sep. 1993 22 p

(NASA-Case-MFS-28817-1; NAS 1.71:MFS-28817-1;

US-Patent-Appl-SN-123629) Avail: CASI HC A03/MF A01

Gimballed scanning devices or instruments are the subject of this invention. Scanning is an important aspect of space science. To achieve a scan pattern some means must be provided which impart to the payload an oscillatory motion. Various forms of machines have been employed for controllably conferring on scanning instruments predetermined scan patterns. They include control moment gyroscopes, reaction wheels, torque motors, reaction control systems, and the like. But rotating unbalanced mass (RUM) devices are a new and efficient way to generate scans in gimballed payloads. RUM devices are superior to previous scanning apparatus, but they require power consuming and frequently complex auxiliary control systems to position and reposition the particular scan pattern relative to a target or a number of targets. Herein the control system is simplified. The most frequently employed method for achieving the various scan patterns is to gimbal the scanning device. Gimbals are suspended in such a way that they can be activated to generate the scan pattern. The suspension means described is for payloads supported in gimbals wherein the payload rotation is restricted by a flex pivot so that the payload oscillates, thereby moving in a scan pattern.

NASA

N94-29361*# National Aeronautics and Space Administration. Ames Research Center, Moffett Field, CA.

SYSTEM FOR IMPROVING MEASUREMENT ACCURACY OF TRANSDUCER BY MEASURING TRANSDUCER TEMPERATURE AND RESISTANCE CHANGE USING THERMOELECTRIC VOLTAGES Patent Application

Karl F. Anderson, inventor (to NASA) and Allen R. Parker, Jr., inventor (to NASA) 24 Sep. 1993 19 p

(NASA-Case-ARC-12014-1; NAS 1.71:ARC-12014-1;

US-Patent-Appl-SN-125888) Avail: CASI HC A03/MF A01

A constant current loop measuring system measures a property including the temperature of a sensor responsive to an external condition being measured. The measuring system includes thermocouple conductors connected to the sensor, sensing first and second induced voltages responsive to the external condition. In addition, the measuring system includes a current generator and reverser generating a constant current, and supplying the constant current to the thermocouple conductors in forward and reverse directions generating first and second measured voltages, and a determining unit receiving the first and second measured voltages from the current generator and reverser, and determining the temperature of the sensor responsive to the first and second measured voltages.

NASA

N94-29368*# National Aeronautics and Space Administration. Langley Research Center, Hampton, VA.

OPTICAL FLAMEOUT DETECTOR Patent Application

Stephen E. Borg, inventor (to NASA), James W. West, inventor (to NASA), Robert M. Lawrence, inventor (to NASA), Samuel E. Harper, Jr., inventor (to NASA), and David W. Alderfer, inventor (to NASA) 19 Oct. 1993 12 p

(NASA-Case-LAR-14997-1; NAS 1.71:LAR-14997-1;

US-Patent-Appl-SN-141294) Avail: CASI HC A03/MF A01

A device has been developed which monitors the presence of a flame within a combustion chamber. The optical flameout detection system responds to gross changes in combustor light intensity, which is monitored in two spectral bands. A photomultiplier tube makes optical measurements in the ultraviolet portion of the spectrum, and a silicon photodiode covers the visible region. The detectors, located outside the combustion chamber, receive the light energy radiated from the combustion process through fiber optic probes designed to operate in a high pressure environment. The optical fibers are aimed diagonally through the center of the injector at the combustion chamber wall downstream of the injector. The probes observe events occurring within a narrow conical-shaped field of view so that the system can quickly detect longitudinal movement of the flame front away from the injector. If a change in intensity of the flame is detected, the fuel supply to the combustion chamber is shut off, limiting the amount of unburned fuel in the combustion chamber which could reignite.

NASA

N94-29373*# National Aeronautics and Space Administration. Pasadena Office, CA.

DIGITAL CAMERA WITH APPARATUS FOR AUTHENTICATION OF IMAGES PRODUCED FROM AN IMAGE FILE Patent Application

Gary L. Friedman, inventor (to NASA) (Jet Propulsion Lab., California Inst. of Tech., Pasadena.) 24 Nov. 1993 22 p

(Contract NAS7-918)

(NASA-Case-NPO-19108-1-CU; NAS 1.71:NPO-19108-1-CU;

US-Patent-Appl-SN-159980) Avail: CASI HC A03/MF A01

A digital camera equipped with a processor for authentication of images produced from an image file taken by the digital camera is provided. The digital camera processor has embedded therein a private key unique to it, and the camera housing has a public key that is so uniquely based upon the private key that digital data encrypted with the private key by the processor may be decrypted using the public key. The digital camera processor comprises means for calculating a hash of the image file using a predetermined algorithm, and second means for encrypting the image hash with the private key, thereby producing a digital signature. The image file and the digital signature are stored in suitable recording means so they will be available together. Apparatus for authenticating at any time the image file as being free of any alteration uses the public key for decrypting the digital signature, thereby deriving a secure image hash identical to the image hash produced by the digital camera and used to produce the digital signature. The apparatus calculates from the image file an image hash using the same algorithm as before. By comparing this last image hash with the secure image hash, authenticity of the image file is determined if they match, since even one bit change in the image hash will cause the image hash to be totally different from the secure hash.

NASA

N94-29400*# Foster-Miller Associates, Inc., Waltham, MA.

CONTROLLED THERMAL EXPANSION PRINTED WIRING BOARDS BASED ON LIQUID CRYSTAL POLYMER DIELECTRICS

Thomas E. Knoll, Kent Blizard, K. Jayaraj, and Leslie S. Rubin Apr. 1994

11 p
(Contract NAS5-31996)
(NASA-CR-189338; NAS 1.26:189338) Avail: CASI HC A03/MF A01

Dielectric materials based on innovative Liquid Crystal Polymers (LCP's) have been used to fabricate surface mount printed wiring boards (PWB's) with a coefficient of thermal expansion matched to leadless ceramic chip carriers. Proprietary and patented polymer processing technology has resulted in self reinforcing material with balanced in-plane mechanical properties. In addition, LCP's possess excellent electrical properties, including a low dielectric constant (less than 2.9) and very low moisture absorption (less than 0.02%). LCP-based multilayer boards processed with conventional drilling and plating processes show improved performance over other materials because they eliminate the surface flatness problems of glass or aramid reinforcements. Laser drilling of blind vias in the LCP dielectric provides a very high density for use in direct chip attach and area array packages. The material is ideally suited for MCM-L and PCMCIA applications fabricated with very thin dielectric layers of the liquid crystal polymer.
Author (revised)

N94-29437# Army Topographic Engineering Center, Fort Belvoir, VA.
THE USE OF DIGITAL STEREO PHOTOGRAMMETRIC METHODS IN HISTORICAL PHOTO ANALYSIS
Glenn Frano, Daniel Edwards, Mitchell Pierson, Maurits Roos, and Michael Barwick Jan. 1994 11 p
(AD-A275287) Avail: CASI HC A02/MF A01

A historical, temporal photointerpretation method is presented for combining the use of a current digital stereo photogrammetric system with manual photointerpretation techniques. The U.S. Army Topographic Engineering Center was tasked to provide products showing the current three-dimensional position of certain features present on a 1918 photomosaic. This mosaic is over a former chemical munitions test area in Washington, D.C.. In order to provide this data, aerial photography from 1918, 1927, 1991 and 1993 was used in the process. This paper will discuss the front end research and collection of textual and photographic data, the manual photo interpretation process, the photogrammetric process and its accuracies, the problems encountered, the digital mapping process and the final products. DTIC

N94-29484*# National Aeronautics and Space Administration. Langley Research Center, Hampton, VA.
METHOD FOR MAKING A DYNAMIC PRESSURE SENSOR AND A PRESSURE SENSOR MADE ACCORDING TO THE METHOD Patent Application
Allan J. Zuckerwar, inventor (to NASA), William E. Robbins, inventor (to NASA), and Glenn M. Robins, inventor (to NASA) 7 Oct. 1993 16 p
(NASA-Case-LAR-14029-1; NAS 1.71:LAR-14029-1;
US-Patent-Appl-SN-138046) Avail: CASI HC A03/MF A01

A method for providing a perfectly flat top with a sharp edge on a dynamic pressure sensor using a cup-shaped stretched membrane as a sensing element is described. First, metal is deposited on the membrane and surrounding areas. Next, the side wall of the pressure sensor with the deposited metal is machined to a predetermined size. Finally, deposited metal is removed from the top of the membrane in small steps, by machining or lapping while the pressure sensor is mounted in a jig or the wall of a test object, until the true top surface of the membrane appears. A thin indicator layer having a color contrasting with the color of the membrane may be applied to the top of the membrane before metal is deposited to facilitate the determination of when to stop metal removal from the top surface of the membrane. NASA

N94-29497*# National Aeronautics and Space Administration. Pasadena Office, CA.
AN ALTERNATE METHOD FOR ACHIEVING TEMPERATURE CONTROL IN THE -160 TO +90 C RANGE Patent Application
Kenneth R. Johnson, inventor (to NASA) (Jet Propulsion Lab., California Inst. of Tech., Pasadena.) 4 Nov. 1993 34 p
(Contract NAS7-918)
(NASA-Case-NPO-18995-1-CU; NAS 1.71:NPO-18995-1-CU;
US-Patent-Appl-SN-152631) Avail: CASI HC A03/MF A01

A single-pass method for accurate and precise temperature control in the -160 to +90 C range is discussed. The method exhibited minimal set-point overshoot during temperature transitions. Control to +/-2 C with transitions between set-points of 7 C per minute were achieved. The method uses commercially available temperature controllers and a gaseous nitrogen/liquid nitrogen mixer to dampen the amplitude of cold temperature spikes caused by liquid nitrogen pulsing. NASA

N94-29538* National Aeronautics and Space Administration. Goddard Space Flight Center, Greenbelt, MD.
BOLT AND NUT EVALUATOR Patent
James J. Kerley, inventor (to NASA), Raymond Burkhardt, inventor (to NASA), and Steven White, inventor (to NASA) 22 Feb. 1994 23 p Filed 19 May 1992
(NASA-Case-GSC-13468-1; US-Patent-5,287,747;
US-Patent-Appl-SN-885697; US-Patent-Class-73-761;
US-Patent-Class-73-789; Int-Patent-Class-G01D-7/02) Avail: US Patent and Trademark Office

A device for testing fasteners such as nuts and bolts is described which consists of a fixed base plate having a number of threaded and unthreaded holes of varying size for receiving the fasteners to be tested, a torque marking paper taped on top the fixed base plate for marking torque-angle indicia, a torque wrench for applying torque to the fasteners being tested, and an indicator for showing the torque applied to the fastener. These elements provide a low cost, nondestructive device for verifying the strength of bolts and nuts.
Official Gazette of the U.S. Patent and Trademark Office

N94-29699 Department of the Navy, Washington, DC.
THREE-AXIS FIBER OPTIC VECTOR MAGNETOMETER Patent
Kee P. Koo, inventor (to Navy), George H. Sigel, Jr., inventor (to Navy), and Frank Bucholtz, inventor (to Navy) 7 Sep. 1993 7 p Filed 30 Sep. 1991
(AD-D016016; US-Patent-5,243,403; US-Patent-Appl-SN-767955) Avail: US Patent and Trademark Office

This patent discloses a three-axis fiber optic vector magnetometer which is provided for measuring both the direction and magnitude of a DC or low frequency magnetic field. The magnetometer includes an optical interferometer system including a sensing fiber arm disposed with three respective sensing portions perpendicular to one another and attached to a unidirectional sensor material. The interferometer system also includes a reference fiber arm and a laser light source for generating and introducing a laser light into both of the arms. Respective biasing devices generate a reference AC magnetic bias and a respective reference frequency in the three sensing portions. A detecting device detects a reference light signal from the reference fiber arm and the magnetically altered sensing light signal from the sensing fiber arm and forms an interferometer output signal. Respective separating devices then separate the respective magnetically induced interferometer signals at respective ones of the frequencies and produce a respective output signal indicative thereof. DTIC

N94-29726* National Aeronautics and Space Administration. Goddard Space Flight Center, Greenbelt, MD.
SIX-DEGREE-OF-FREEDOM PARALLEL MINIMANIPULATOR WITH THREE INEXTENSIBLE LIMBS Patent
Farhad Tahmasebi, inventor (to NASA) and Lung-Wen Tsai, inventor (to NASA) 18 Jan. 1994 13 p Filed 20 Jul. 1992
(NASA-Case-GSC-13485-1; US-Patent-5,279,176;
US-Patent-Appl-SN-915567; US-Patent-Class-74-479B;
US-Patent-Class-74-479PF; US-Patent-Class-901-14;
US-Patent-Class-901-19; Int-Patent-Class-G05G-11/00;
Int-Patent-Class-B25J-11/00) Avail: US Patent and Trademark Office

A Six-Degree-of-Freedom Parallel-Manipulator having three inextensible limbs for manipulating a platform is described. The three inextensible limbs are attached via universal joints to the platform at non-collinear points. Each of the inextensible limbs is also attached via universal joints to a two-degree-of-freedom parallel driver such as a five-bar linkage, a pantograph, or a bidirectional linear stepper motor. The drivers move the lower ends of the limbs parallel to a fixed base and thereby provide manipulation of the platform. The actuators are mounted on the fixed base without using any power transmission devices such as gears or belts.
Official Gazette of the U.S. Patent and Trademark Office

N94-29742*# Akron Univ., OH. Dept. of Mechanical Engineering.
STEREO IMAGING BASED PARTICLE VELOCIMETER Final Technical Report
Celal Batur 16 Apr. 1994 22 p
(Contract NCC3-231)
(NASA-CR-195800; NAS 1.26:195800) Avail: CASI HC A03/MF A01

Three dimensional coordinates of an object are determined from it's two dimensional images for a class of points on the object. Two dimensional images are first filtered by a Laplacian of Gaussian (LOG) filter in order to detect a set of feature points on the object. The feature points on the left and the right images are then matched using a Hopfield type optimization network. The performance index of the Hopfield network contains both local and global properties of the images. Parallel computing in stereo matching can be achieved by the proposed methodology. Author

N94-29824 Virginia Polytechnic Inst. and State Univ., Blacksburg.
AN ACTIVELY COOLED FLOATING ELEMENT SKIN FRICTION BALANCE FOR DIRECT MEASUREMENT IN HIGH ENTHALPY SUPERSONIC FLOWS Ph.D. Thesis
Kenneth Michael Chadwick 1992 178 p
Avail: Univ. Microfilms Order No. DA9312871

An investigation was conducted to design instruments to directly measure skin friction along the chamber walls of supersonic combustor models. Measurements were made in a combustor at the General Applied Science Laboratory (GASL) and in the Direct Connect Arcjet Facility (DCAF) supersonic combustor at the NASA AMES Research Center. Flow conditions in the high enthalpy combustor models ranged from total pressures of 275-800 psia (1900-5550 kPa) and total temperatures from 5800-8400 R (3222-4667 K). This gives enthalpies in the range of 1700-3300 BTU/lb(sub m) (3950-7660 KJ/kg) and simulated flight Mach number from 9 to 13. A direct force measurement device was used to measure the small tangential shear force resulting from the flow passing over a non-intrusive floating element. The floating head is mounted to a stiff cantilever beam arrangement with deflection due to the shear force on the order of 0.0005 in (0.0125 mm). This small deflection allows the balance to be a non-nulling type. Several measurements were conducted in cold supersonic flows to verify the concept and establish accuracy and repeatability. This balance design includes actively controlled cooling of the floating sensor head temperature through an internal cooling system to eliminate non-uniform temperature effects between the head and the surrounding chamber wall. This enabled the device to be suitable for shear force measurement in very hot flows. The key to this device is the use of a quartz tube cantilever with strain gages bonded at orthogonal positions directly on the surface at the base. A symmetric fluid flow was developed inside the quartz tube to provide cooling to the backside of the floating head. Bench tests showed that this did not influence the force measurement. Numerical heat transfer calculations were conducted for design feasibility and analysis, and to determine the effectiveness of the active cooling of the floating head. Analysis of the measurement uncertainty in cold supersonic flow tests show that uncertainty under 8 percent is achievable, but variations in the balance cooling during a particular test raised uncertainty up to 20 percent in these very hot flows during the early tests. Improvements to the strain gages and balance cooling reduced uncertainty for the later tests to under 15 percent.
Dissert. Abstr.

N94-29872*# Space Optics Research Labs., Inc., Chelmsford, MA. Intergraph Div.
DEFORMED ELLIPSOIDAL DIFFRACTION GRATING BLANK Final Report
Alan E. DeCew, Jr. Mar. 1994 113 p
(Contract NAS5-31790)
(NASA-CR-189334; NAS 1.26:189334) Avail: CASI HC A06/MF A02

The Deformed Ellipsoidal Grating Blank (DEGB) is the primary component in an ultraviolet spectrometer. Since one of the major concerns for these instruments is throughput, significant efforts are made to reduce the number of components and subsequently reflections. Each reflection results in losses through absorption and scattering. It is these two sources of photon loss that dictated the requirements for the DEGB. The first goal is to shape the DEGB in such a way that the energy at the entrance slit is focused as well as possible on the exit slit. The second goal is to produce a surface smooth enough to minimize the photon loss due to scattering. The program was accomplished in three phases. The first phase was the fabrication planning. The second phase was the actual fabrication and initial testing. The last phase was the final testing of the completed DEGB. Author

N94-29907*# California Univ., Berkeley. Space Sciences Lab.
A SOUNDING ROCKET PROGRAM IN EXTREME AND FAR ULTRAVIOLET INTERFEROMETRY Final Technical Report
S. Chakrabarti 29 Apr. 1994 2 p
(Grant NAG5-675)
(NASA-CR-195114; NAS 1.26:195114) Avail: CASI HC A01/MF A01

A self-compensating, all reflection interferometric (SCARI) spectrometer was developed that can provide high resolution measurements of spectral features at any wavelength. Several mechanical components were developed that aid the instrument's performance at the short wavelength range. Examples include an optical bench and modular removable precision mechanisms for alignment. Upon alignment and lock down of the interferometer with the latter, the device is removed to minimize weight. A ray-trace code was developed to simulate the instrument's performance. Interference patterns were obtained at the shortest wavelength: the hydrogen Lyman alpha (1216 A). A laboratory instrument was developed that will be flown aboard a Black Brant sounding rocket to study the very local interstellar medium. Derived from text

N94-29927# Sandia National Labs., Albuquerque, NM.
A NON-CONTACTING VERTICAL ALIGNMENT SYSTEM FOR MASS PROPERTIES MEASURING INSTRUMENTS
G. H. James, III, J. E. Suazo, and R. C. Varga Nov. 1993 79 p
(Contract DE-AC04-94AL-85000)
(DE94-004680; SAND-93-1425) Avail: CASI HC A05/MF A01

A non-contact system for the alignment of objects on mass properties measuring instruments is described. Test parts can be aligned to within the capabilities of the user and the fixture to make the adjustments. The current implementation can align objects to less than .001 inches at two points with final requested adjustments of a few ten-thousands of an inch. The non-contact capability allows the alignment of objects which are too compliant or fragile for traditional contacting measurement methods. Also, this system allows the definition of a reference axis for objects which are not perfectly symmetric. The reference axis is defined at the top of the object by an appropriate marker and defined at the bottom by a best fit circle through the surface at a specified height. A general description of the hardware, procedures, and results are presented for the non-user. Appendices which contain a complete description of the software, usage, and mathematical implementation are provided for the reader who is interested in using or further developing the system. DOE

N94-30027# California Univ., Berkeley. Lawrence Berkeley Lab.
PHOTOELECTRON DIFFRACTION AND HOLOGRAPHY: SOME NEW DIRECTIONS
C. S. Fadley (California Univ., Davis.) Aug. 1993 26 p Presented at the 4th International Conference on the Structure of Surfaces, Shanghai, China, 16-19 Aug. 1993
(Contract DE-AC03-76SF-00098)
(DE94-006297; LBL-35051; CONF-9308154-3) Avail: CASI HC A03/MF A01

Photoelectron diffraction has by now become a versatile and powerful technique for studying surface structures, with special capabilities for resolving chemical and magnetic states of atoms and deriving direct structural information from both forward scattering along bond directions and back-scattering path length differences. Further fitting experiment to theory can lead to structural accuracies in the +/- 0.03 Angstrom range. Holographic inversions of such diffraction data also show considerable promise for deriving local three-dimensional structures around a given emitter with accuracies of +/- 0.2-0.3 Angstrom. Resolving the photoelectron spin in some way and using circularly polarized radiation for excitation provide added dimensions for the study of magnetic systems and chiral experimental geometries. Synchrotron radiation with the highest brightness and energy resolution, as well as variable polarization, is crucial to the full exploitation of these techniques. DOE

N94-30059 Lawrence Livermore National Lab., CA.
MICROWAVE MICHELSON INTERFEROMETER SYSTEM REPORT OF FIRST USE ON A RAILGUN, GREEN FARM, SAN DIEGO, CA

R. S. Hawke, D. Greenwood, J. Morrison, and F. Schildmeyer 20 Oct. 1993 10 p Limited Reproducibility: More than 20% of this document may be affected by microfiche quality
(Contract W-7405-eng-48)
(DE94-005294; UCRL-ID-115694) Avail: CASI HC A02

This report summarizes the successful first attempt to use a Michelson microwave interferometer to measure the position of a projectile throughout its acceleration by a railgun. The test was performed at the DNA Green Farm facility operated by Maxwell Labs Inc. The test was performed using the ARDEC-ACB gun to accelerate a 1.1 kg polycarbonate projectile to about 2.5 km/s. The projectile had an initial injection velocity of about 490 m/s. DOE

N94-30148 Joint Inst. for Nuclear Research, Dubna (USSR). Lab. of Nuclear Problems.

MESO-OPTICAL FOURIER TRANSFORM MICROSCOPE WITH DOUBLE FOCUSING

Yu. A. Batusov, L. M. Soroko, and V. V. Tereshchenko 1992 11 p Limited Reproducibility: More than 20% of this document may be affected by microfiche quality
(DE94-607851; JINR-E-13-92-179) Avail: CASI HC A03 (US Sales Only)

The meso-optical Fourier transform microscope (MFTM) with double focusing for particle tracks of low ionization level in the nuclear emulsion is described. It is shown experimentally that this device enables one to get high concentration of information about the position of the particle track in the nuclear emulsion and thus to increase the signal-to-noise ratio. It is shown that spreading of the meso-optical image of the particle track in the sagittal section of the MFTM can be eliminated completely in the frame of the diffraction limit. The number of the additional degrees of freedom in this new MFTM system along depth coordinate is equal to 20 in comparison to single degree of freedom in the Fourier transform microscope of the direct observation. DOE

N94-30199*# National Aeronautics and Space Administration. Marshall Space Flight Center, Huntsville, AL.

AMPOULE FAILURE SENSOR TIME RESPONSE TESTING: EXPERIMENT 1

M. L. Johnson and D. A. Watring Apr. 1994 15 p
(NASA-TM-108449; NAS 1.15:108449) Avail: CASI HC A03/MF A01

The response time of an ampoule failure sensor exposed to a liquid or vapor gallium-arsenide (GaAs) is investigated. The experimental configuration represents the sample/ampoule cartridge assembly used in NASA's Crystal Growth Furnace (CGF). The sensor is a chemical fuse made from a metal with which the semiconductor material reacts more rapidly than it does with the containing cartridge. For the III-IV compound of GaAs, a platinum metal was chosen based on the reaction of platinum and arsenic at elevated temperatures which forms a low melting eutectic. Ampoule failure is indicated by a step change in resistance of the failure sensor on the order of megohms. The sensors will increase the safety of crystal growth experiments by providing an indication that an ampoule has failed. Experimental results indicate that the response times (after a known ampoule failure) for the 0.003 and 0.010 inch ampoule failure sensors are 2.4 and 3.6 minutes, respectively. This ampoule failure sensor will be utilized in the CGF during the second United States Microgravity Laboratory Mission (USML-2) and is the subject of a NASA patent application.
Author

N94-30232 Laval Univ. (Quebec). Dept. des Sciences Geodesiques et de Teledetection.

CALIBRATION OF CHARGE COUPLED DEVICE DIGITAL CAMERAS M.S. Thesis [CALIBRAGE DE CAMERAS NUMERIQUES CCD]

Martin Brindamour Oct. 1993 115 p In FRENCH
(ISBN-0-315-85539-8; CTN-94-61147) Copyright Avail: Micromedia Ltd., Technical Information Centre, 240 Catherine Street, Suite 305, Ottawa, Ontario, K2P 2G8, Canada HC/MF

The arrival of charge coupled device (CCD) cameras has revolutionized short-range photogrammetry. A prototype system of measurement and representation of small objects (METRICAN), based on use of CCD cameras, was developed at Laval University. Since the cameras used are non-metrical cameras, calibration of their internal geometry must be carried out before taking measurements. A study was conducted to verify whether adding polynomials modelling the distortions to the mathematical model of calibration could improve the metrical precision of the system. It is shown that it is important to consider the radial distortion in calibration. The tangential distortion can be ignored due to its small contribution. The effects of adding an infrared filter to faces parallel to the different distortion components were also examined. The presence of the infrared filter, which facilitates the automatic reconnaissance of the measuring points, does not significantly modify the value of the interior orientation parameters. CISTI

N94-30254 Johns Hopkins Univ., Baltimore, MD.

TIME-RESOLVED HOLOGRAPHY FOR THE MICROSCOPIC STUDY OF CRACK-TIP MOTION IN DYNAMIC FRACTURE Ph.D. Thesis

John Scott Steckenrider 1993 188 p
Avail: Univ. Microfilms Order No. DA9313436

A novel laser system has been designed and developed for the time-resolved holographic analysis of dynamic crack propagation with a frame-to-frame resolution of from 28.3 to 161.6 ns. Average velocities of approximately 1300 m/s were measured in macroscopic (1.2 mm thick) glass specimens, and velocities of 1200 m/s were measured in microscopic (0.15 mm thick) glass specimens. Holographic analyses were conducted using both diffuse and direct laser illumination, demonstrating a broad range of applicability for this method. Normalized crack length versus time plots were generated for a series of specimens with pre-crack lengths of from 3.5 to 10.5 mm wing various pre-load levels and initiating explosive sizes. All specimens exhibited similar dynamic fracture behavior, particularly those outside of the region of shock of the initiating explosive (those of the longer pre-crack set). A best-fit to the theoretical prediction for mode I crack growth revealed a good match to the case for a specimen overloaded by 64 percent. However, no variation with applied load was evident, indicating that an immediate acceleration to a velocity of approximately 1200 m/s (near the empirically determined terminal velocity) was the more plausible fit. Since the terminal velocity was approximately the same for all specimens, this investigation also demonstrated that the terminal velocity is independent of crack-tip stresses, even for the most extreme explosive pulses. In addition, a different loading configuration was attempted in which the specimen was shielded from the explosive shock. The resulting crack growth behavior displayed a velocity well below the aforementioned terminal velocity, indicating an acceleration was present. However, owing to the lack of reproducibility in this method of loading, repeated experiments were not possible. Finally, applications of the described laser system for use in laser ultrasonics were investigated, and these results are included.
Dissert. Abstr.

N94-30742 National Aerospace Lab., Amsterdam (Netherlands). Space Div.

DETERMINATION OF ACCELERATION FIELD PARAMETERS WITH LINEAR ACCELEROMETERS

J. P. B. Vreeburg 29 Apr. 1992 15 p Submitted for publication Limited Reproducibility: More than 20% of this document may be affected by microfiche quality
(PB94-125606; NLR-TP-92184-U; ETN-94-95580) Avail: CASI HC A03

The ballistometer carried on the Wet Satellite Model (WSM), whose output provides the WSM motional parameters, is described. From these data and knowledge of the ten inertial parameters of the solid part of the WSM, it is possible to determine the force and torque exerted by liquid carried in an onboard tank. These data are needed for the verification of capillary liquid slosh models. The linear and angular motions of a rigid body induce an acceleration field that is described in a coordinate system fixed to the body. The response of a linear accelerometer to this field depends on the magnitude and direction of the motional parameters, and on this configuration, that is, its location and the direction of the sensitive axis. Combination of the signals from an arrangement of accelerometers allows reconstitution of the linear and angular acceleration, and the angular rate vectors of the body. Formulas for the analysis of arbitrary arrangements of three, six and nine accelerometers are given. Substitution of the Newton and the Euler equations in the formula for the force field expresses the acceleration as a function of force and torque and the ten inertial parameters of the body. Possible applications are indicated. ESA

N94-30782 National Physical Lab., Teddington (England). Radiation Science and Acoustics Div.

THE USE OF THERMISTORS IN THE NPL ELECTRON-BEAM CALORIMETER

M. R. McEwen, D. T. Burns, and A. J. Williams Mar. 1993 18 p
(ISSN 0955-9655)
(PB94-139334; NPL-RSA(Ext)-41; ETN-94-95849) Copyright Avail: Issuing Activity (National Physical Lab., Teddington, Middlesex TW11 0LW, England)

The system developed for calibrating thermistors, which have been employed in the primary standard electron beam graphite calorimeter for several years, and the results of investigations into self-heating and dose response are described. The overall uncertainty in measuring temperature rises is estimated to be +/- 0.1 percent at the 95 percent confidence level. The self-heating of the thermistor type used in the calorimeter was determined to be constant over the temperature range 14 to 29 C. The same thermistor type showed no change in response within the uncertainties to an accumulated dose up to 3000 kGy. A second type of thermistor (to be used in a new calorimeter) showed no change in sensitivity although there was a change in absolute resistance of approximately 0.1 percent per MGy. ESA

N94-30930 Politecnico di Milano (Italy). Dipt. di Elettronica e Informazione.
A LOW NOISE SILICON DETECTOR PREAMPLIFIER SYSTEM FOR ROOM TEMPERATURE X RAY SPECTROSCOPY
A. Pullia 1993 8 p
(Rept-93-058; ETN-94-95820) Avail: Issuing Activity (Politecnico di Milano, Piazza Leonardo da Vinci 32, 20133 Milan, Italy)

The design and performances of a system for high resolution x-ray spectroscopy are presented. The detector is a low capacitance diode built on high resistivity silicon. The signal preamplification is made by means of an ultra-low noise charge amplifier. The system exhibits an equivalent noise charge of 61 root mean square electrons at 297K and 32 root mean square electrons at 223K. It is shown how an improvement down to 30 root mean square electrons at room temperature is expected employing an integrated transistor on the detector chip. ESA

N94-30979 Ecole Nationale Superieure des Telecommunications, Paris (France).
NOISE REDUCTION TECHNIQUES FOR THE RESTORATION OF MUSICAL RECORDINGS Ph.D. Thesis [TECHNIQUES DE REDUCTION DE BRUIT POUR LA RESTAURATION D'ENREGISTREMENTS MUSICAUX]
Olivier Cappe 1993 214 p In FRENCH Limited Reproducibility: More than 20% of this document may be affected by microfiche quality
(ISSN 0751-1353)
(TELECOM-93-E-019; ETN-94-95983) Avail: CASI HC A10

The evaluation of short time spectral attenuation techniques using a simplified model of standard noise suppression rules and with elementary test signals is assessed. Signal distortions induced by the restoration process are evaluated analytically, and their audibility is addressed by use of classic psychoacoustics results. Phenomena observed experimentally in previous studies, such as the modification of timbre, the appearance of modulations, and the spreading of transients, are brought to light. Drawing from these results, a noise reduction technique intended for enhancing musical signals is described. In the first step, the noisy signal is analyzed by use of a medium frequency resolution short time transform. The restoration then takes place in each subband in two different ways according to the nature of the subband signal: the processing is carried out block by block when steady signal components are detected, or locally otherwise. This approach was successfully applied to several musical recordings yielding promising results. ESA

N94-29707# National Research Inst. of Fisheries Engineering, Tokyo (Japan). Ocean Electronics Section.
DESIGN OF THE BIOSONAR SIMULATOR FOR DOLPHIN'S CLICKS WAVEFORM REPRODUCTION [IRUKA NO KURIKKUSU MEION NO SAISEI HOSHA SOCHI: BAIOSONA SHIMYURETA NO SHISAKU]
Ken Ishii, Tomonari Akamatsu, and Yoshimi Hatakeyama *In its* Bulletin of National Research Institute of Fisheries Engineering, No. 13 5 Mar. 1992 p 95-128 In JAPANESE (For primary document see N94-29701 08-31)
Avail: CASI HC A03/MF A02

N94-29774*# National Aeronautics and Space Administration. Lyndon B. Johnson Space Center, Houston, TX.
BACKSCATTER MOSSBAUER SPECTROMETER (BaMS) FOR EXTRATERRESTRIAL APPLICATIONS
D. G. Agresti (Alabama Univ., Birmingham.), T. D. Shelfer (Alabama Univ., Birmingham.), M. M. Pimperl (Alabama Univ., Birmingham.), E. L. Wills (Alabama Univ., Birmingham.), M. H. Shen (Alabama Univ., Birmingham.), and R. V. Morris *In* JPL, Proceedings of the Workshop on Microtechnologies and Applications to Space Systems 15 Jun. 1993 p 95-97 (For primary document see N94-29767 08-31)
Avail: CASI HC A01/MF A03

N94-29776*# National Aeronautics and Space Administration. Lyndon B. Johnson Space Center, Houston, TX.
DIFFERENTIAL SCANNING CALORIMETRY (DSC) FOR PLANETARY SURFACE EXPLORATION
James L. Gooding and Douglas W. Ming *In* JPL, Proceedings of the Workshop on Microtechnologies and Applications to Space Systems 15 Jun. 1993 p 121-12 (For primary document see N94-29767 08-31)
Avail: CASI HC A01/MF A03

N94-29778*# Jet Propulsion Lab., California Inst. of Tech., Pasadena.
A BROAD-BAND MICROSEISMOMETER FOR PLANETARY OPERATIONS
W. B. Banerdt, T. VanZandt, W. J. Kaiser, and T. W. Kenny *In its* Proceedings of the Workshop on Microtechnologies and Applications to Space Systems 15 Jun. 1993 p 125-126 (For primary document see N94-29767 08-31)
Avail: CASI HC A01/MF A03

N94-29779*# Jet Propulsion Lab., California Inst. of Tech., Pasadena.
IMAGING SPECTROMETRY OF THE EARTH AND OTHER SOLAR SYSTEM BODIES Abstract Only
Gregg Vane *In its* Proceedings of the Workshop on Microtechnologies and Applications to Space Systems 15 Jun. 1993 p 127 (For primary document see N94-29767 08-31)
Avail: CASI HC A01/MF A03

N94-29789*# SatCon Technology Corp., Cambridge, MA.
INTEGRATED MICROGYROSCOPE
Timothy J. Hawkey and Richard P. Torti *In* JPL, Proceedings of the Workshop on Microtechnologies and Applications to Space Systems 15 Jun. 1993 p 257-26 (For primary document see N94-29767 08-31)
Avail: CASI HC A02/MF A03

N94-29790*# GEC Ferranti, Edinburgh (Scotland).
GEC FERRANTI PIEZO VIBRATORY GYROSCOPE
J. D. Nuttall *In* JPL, Proceedings of the Workshop on Microtechnologies and Applications to Space Systems 15 Jun. 1993 p 265-27 (For primary document see N94-29767 08-31)
Avail: CASI HC A03/MF A03

N94-30216 Bubble Technology Industries, Inc., Chalk River (Ontario).
ADAPTION OF THE BUBBLE DETECTOR FOR USE AS A LET SPECTROMETER
H. Ing, R. Noulty, and T. Cousins *In* Defence Research Establishment, Proceedings of the 1991 Single Event Upset Symposium 1991 14 p (For primary document see N94-30211 08-73)
Avail: Issuing Activity (Defence Research Establishment, Ottawa, ON K1A 0Z4 Canada)

N94-30218 Defence Research Establishment, Ottawa (Ontario).
ADVANCED DEVELOPMENT OF THE SPECTRUM SCIENCES MODEL 5005-TF, SINGLE EVENT TEST FIXTURE
M. R. Ackermann, J. S. Browning, B. W. Hughlock, G. K. Lum, W. C. Tsacoyeanes, and M. D. Weeks *In its* Proceedings of the 1991 Single Event Upset Symposium 1991 12 p (For primary document see N94-30211 08-73)
Avail: Issuing Activity (Defence Research Establishment, Ottawa, ON K1A 0Z4 Canada)

36 LASERS AND MASERS

Includes parametric amplifiers.
For related information see also *76 Solid-State Physics.*

N94-28478# California Univ., Berkeley. Lawrence Berkeley Lab.
LASER-MATERIAL INTERACTIONS: A STUDY OF LASER ENERGY COUPLING WITH SOLIDS Ph.D. Thesis
Mark Alan Shannon Nov. 1993 212 p
(Contract DE-AC03-76SF-00098)
(DE94-005212; LBL-34889) Avail: CASI HC A10/MF A03

This study of laser light interactions with solid materials ranges from low temperature heating to explosive, plasma-forming reactions. Contained are works concerning laser-energy coupling: laser heating and melting monitored using a mirage effect technique, the mechanical stress-power generated during high powered laser ablation, and plasma shielding. First, a photothermal deflection (PTD) technique is presented for monitoring heat transfer during modulated laser heating of opaque solids that have not undergone phase change. Of main interest is the physical significance of the shape, magnitude, and phase for the temporal profile of the deflection signal. Considered are the effects that thermophysical properties, boundary conditions, and geometry of the target and optical probe-beam have on the deflection response. PTD is shown to monitor spatial and temporal changes in heat flux leaving the surface due to changes in laser energy coupling. The PTD technique is then extended to detect phase change at the surface of a solid target. Experimental data shows the onset of melt for indium and tin targets. The conditions for which melt can be detected by PTD is analyzed in terms of geometry, incident power and pulse length, and thermophysical properties of the target and surroundings. Next, monitoring high powered laser ablation of materials with stress-power is introduced. The motivation for considering stress-power is given, followed by a theoretical discussion of stress-power and how it is determined experimentally. Experiments are presented for the ablation of aluminum targets as a function of energy and intensity. The stress-power response is analyzed for its physical significance. Lastly, the influence of plasma shielding during high powered pulsed laser-material interactions is considered. Crater size, emission, and stress-power are measured to determine the role that the gas medium and laser pulse length have on plasma shielding. DOE

N94-28481# Stanford Linear Accelerator Center, CA.
LINAC COHERENT LIGHT SOURCE (LCLS) AT 2-4 nm USING THE SLAC LINAC
J. T. Seeman, K. Bane, R. Boyce, G. Loew, P. Morton, H. D. Nuhn, J. Paterson, P. Pianetta, T. Raubenheimer, and R. Tatchyn et al Aug. 1993 10 p Presented at the Annual Meeting of the Society of Photo-Optical Instrumentation Engineers (SPIE), San Diego, CA, 11-16 Jul. 1993
(Contract DE-AC03-76SF-00515)
(DE94-005235; SU-SLAC-PUB-6312; LBL-33456; CONF-930722-56) Avail: CASI HC A02/MF A01

The authors describe the possible use of the SLAC linac to drive a unique, powerful, short wavelength Linac Coherent Light Source (LCLS). Using the FEL principle, lasing is achieved in a single pass of a high peak current electron beam through a long undulator by self-amplified spontaneous-emission (SASE). The main components are a high-brightness electron RF gun with a photocathode, two electron bunch length compressors, the existing SLAC linac, beam diagnostics, and a long undulator combined with a FODO quadrupole focusing system. The RF gun, to be installed about 1 km from the end of the SLAC linac, would produce a single bunch of 6 x 10(exp 9) electrons with an invariant emittance of about 3 mm-mrad and a bunch length of about 500 (mu)m. That bunch is then accelerated to 100 MeV and compressed to a length of about 200 (mu)m. The main SLAC linac accelerates the bunch to 2 GeV were a second bunch compressor reduces the length to 30-40 (mu)m and produces a peak current of 2-3 kA. The bunch is then accelerated to 7-8 GeV and transported to a 50-70 m long undulator. Using electrons below 8 GeV, the undulator could operate at wavelengths down to 2 nm, producing about 10 GW peak power in sub-ps light pulses. At a linac repetition rate of 120 Hz, the average power is about 1 W. Linac operation at lower beam energies provides longer wavelength radiation. After the undulator, the beam is deposited in a dump. The LCLS light pulses are then distributed to multiple user stations using grazing incident mirrors. Length compression, emittance control, phase stability, FEL design criteria, and parameter tolerances are discussed. A demonstration experiment is also described which uses the SLAC linac and (possibly) the PALADIN undulator to study SASE to power saturation at wavelengths of 40-360 nm. DOE

N94-28482# Sandia National Labs., Albuquerque, NM.
REACTOR-PUMPED LASER EXPERIMENTAL RESULTS
G. A. Hebner and G. N. Hays 1994 11 p Presented at the International Symposium on Optoelectronic and Microwave Engineering, Los Angeles, CA, 22-28 Jan. 1994
(Contract DE-AC04-94AL-85000)
(DE94-005247; SAND-93-3993C; CONF-940114-1) Avail: CASI HC A03/MF A01

Reactor pumped lasers have the potential to be scaled to multi-megawatt power levels with long run times. In proposed designs, the laser will be capable of output powers of several megawatts of power for run times of several hours. Such a laser would have many diverse applications such as material processing, space debris removal and power beaming to geosynchronous satellites or the moon. However, before such systems can be designed, fundamental laser parameters such as small signal gain, saturation intensity and efficiency must be determined over a wide operational parameter space. We have recently measured fundamental laser parameters for a selection of nuclear pumped visible and near IR laser transitions in atomic neon, argon and xenon. An overview of the results of this investigation will be presented. DOE

N94-28635 Electro-Optical Sciences, Inc., Irvington, NY.
INNOVATIVE DIRECT DETECTION RANGE-DOPPLER LASER RADAR Progress Report No. 2
31 Oct. 1993 2 p Limited Reproducibility: More than 20% of this document may be affected by microfiche quality
(Contract N00014-93-C-0147)
(AD-A275619) Avail: CASI HC A01

During this Phase of our research program, EOS completed the Laser Radar preliminary design effort discussed below. In addition, we initiated the evaluation of new applications of the high efficiency Multi Beam Fizeau Interferometer (MBFI) for dual-use DOD and commerical applications. This commercialization study effort appears very promising and will be reported on in the next Progress Report. DTIC

N94-28765# Spire Corp., Bedford, MA.
LASER BEAM STEERING WITH SEMICONDUCTOR WAVEGUIDE Progress Report No. 3, 17 Mar. - 29 Aug. 1993
29 Aug. 1993 11 p
(AD-A275775) Avail: CASI HC A03/MF A01

The ability to rapidly and randomly steer a laser beam is critical to the success of free-space satellite-based laser radar systems for missile defense and target tracking. By applying waveguide technology, we will demonstrate multi-dimensional, all-electronic laser beam steering. Parallel arrays of electronically phase-modulated waveguide structures are being fabricated, and a metal grating was designed to spatially dissect an incident coherent planar waveform, emitted at 1059 nm by a Nd:YAG laser. The rotation of the output light-beam will occur through constructive interference effects in the far field. A two dimensional array of phase-control channels would allow scanning the beam over the entire image plane. Initial efforts in Phase 1 are being focused on fabrication and testing of a two channel, vertically situated set of buried waveguides. The implementation of a double-buried semiconductor structure with two GaAs cores and Al(x)Ga(1-x)As cladding was analyzed in detail to determine materials parameters that would allow us to demonstrate the highly novel concept of high speed, electronic laser steering of a laser beam in the vertical direction. The GaAs waveguide is being grown to contain a pn junction, while the cladding consists of Al(0.08)Ga(0.92)As, with the lower cladding doped n-type, and the upper cladding doped p-type. For a 2 micron thick waveguide, only the fundamental mode and perhaps the first harmonic can be supported, which should allow demonstration of optical interference in the far field. DTIC

N94-28770 North Carolina State Univ., Raleigh. Dept. of Electrical and Computer Engineering.
FUSION OF RANGE AND LUMINANCE DATA FROM LASER RADAR SYSTEMS Final Report, 1 May 1990 - 30 Jul. 1993

Griff L. Bilbro 7 Nov. 1993 11 p Limited Reproducibility: More than 20% of this document may be affected by microfiche quality
(Contract DAAL03-89-D-0003)
(AD-A275608; ARO-28099.2-EL) Avail: CASI HC A03

In this project, a technique was developed for computing the optimal description of some physical scene by using global optimization and Bayesian techniques to combine correlated outputs of diverse nonlinear sensors. Two laser range/intensity imagers were considered, but the major application was to obtain the best known restorations of very noisy PD-, TI-, and T2-weighted Magnetic Resonance Images by fusing the information in all the input images. DTIC

N94-28786# Nauchno-Issledovatelskii Inst. Ehlekt- Rofizicheskoj Apparatury, Leningrad (USSR).
RADIATION TRANSPORT AND FOCUSING SYSTEMS FOR POWER INDUSTRIAL LASERS
I. A. Alekseev, G. A. Baranov, and A. K. Zinchenko 1992 19 p In RUSSIAN
(DE94-606817; NIIEFA-P-0908) Avail: CASI HC A03/MF A01 (US Sales Only)

Basic principles of setting up multiposted systems of radiation transport and focusing are discussed. Development of certain unified units, from which various systems of transport and focusing are composed, is reported and their main performances are given. Standard units, including stationary revolving mirrors, optical switches for one or two beams, universal posts, etc., permit assembly and flexible rearrangement of radiation transport systems of several powerful lasers to a number of technological posts. DOE

N94-28839*# Computer Sciences Corp., Hampton, VA.
LASER VELOCIMETER DATA ACQUISITION SYSTEM FOR THE LANGLEY 14- BY 22-FOOT SUBSONIC TUNNEL. SOFTWARE REFERENCE GUIDE VERSION 3.3
Judith K. Jumper Feb. 1994 74 p
(Contract NAS1-20048; RTOP 505-59-36-01)
(NASA-CR-191606; NAS 1.26:191606) Avail: CASI HC A04/MF A01

The Laser Velocimeter Data Acquisition System (LVDAS) in the Langley 14- by 22-Foot Tunnel is controlled by a comprehensive software package. The software package was designed to control the data acquisition process during wind tunnel tests which employ a laser velocimeter measurement system. This report provides detailed explanations on how to configure and operate the LVDAS system to acquire laser velocimeter and static wind tunnel data. Author (revised)

N94-28919# Air Force Inst. of Tech., Wright-Patterson AFB, OH.
VISIBLE VERTICAL CAVITY SURFACE EMITTING LASERS Ph.D. Thesis
James A. Lott 1993 270 p
(AD-A275334; AFIT/CI/CIA-93-23D) Avail: CASI HC A12/MF A03

This dissertation explores the design, fabrication, and characterization of visible (620 to 690 nm) vertical cavity surface emitting lasers (VCSEL's), consisting of a strained quantum well optical cavity active region, surrounded by distributed Bragg reflectors (DBR's). The lattice-matched device structures are grown on GaAs substrates by metalorganic vapor phase epitaxy (MOVPE). The key design and fabrication issues are reviewed and contrasted with conventional near infrared (IR) VCSEL's. Design trade-offs and quantum well gain characteristics are examined by studying optically pumped structures. Device fabrication techniques are developed, and the first electrically injected visible AlGaInP VCSEL's are demonstrated. Prototype devices operate with pulsed current excitation at room temperature with a maximum output power of 3.38 mW at a lasing emission wavelength of 650 nm with threshold current densities of about 4.2 kA/sq. cm and threshold voltages of about 2.7 V. Due to cavity losses and unoptimized gain layer design, lasing is only achieved with significant gain contributions from the second (n=2) quantized quantum well state. With several design improvements, pulsed room temperature (23 deg C) lasing is achieved over the very broad range 629.6 to 691.4 nm, where the lasing emission above 650 nm is due primarily to gain contributions from the first (n=1) quantized quantum well state. DTIC

N94-29179 Michigan Univ., Ann Arbor. Dept. of Electrical Engineering and Computer Science.
ELECTRON BEAM ANALYSIS FOR CYCLOTRON HARMONIC AND FREE-ELECTRON LASER DEVICES Final Technical Report No. 6, 1 Oct. 1989 - 31 Dec. 1992
Ward D. Getty 21 Jan. 1994 32 p Limited Reproducibility: More than 20% of this document may be affected by microfiche quality
(Contract N00014-90-J-1065)
(AD-A275070) Avail: Issuing Activity (Defense Technical Information Center (DTIC))

Two separate experiments are described. The first was on the velocity distribution analysis of a gyrating electron beam. A retarding potential analyzer was developed which operated at 75 kV and accepted gyrating electrons with large Larmo radii. Velocity distributions were compared with simulation results. The second experiment explored the possibility of forming a large-area electron beam from polycrystalline diamond film. Diamond, a negative electron affinity material in the crystalline group of zone axes (111) direction, has been observed to emit electrons into vacuum in certain configurations, but this effort was unsuccessful in obtaining emission. DTIC

N94-29309# Stanford Univ., CA. Physics Lab.
HIGH-POWER CW DIODE-LASER-ARRAY-PUMPED SOLID-STATE LASERS AND EFFICIENT NONLINEAR OPTICAL FREQUENCY Final Report
Robert J. Shine and Robert L. Byer 3 Jan. 1994 9 p
(Contract DAAL03-93-G-0415)
(AD-A275394; GL-5130; ARO-32311.1-PH) Avail: CASI HC A02/MF A01

During the interim period of this bridging contract, we have continued to work on the development of high-power cw diode-laser-array-pumped solid-state lasers. Towards that end, we have built lower power lasers in order to test individual components needed for the high-power laser, specifically we have built a 1 watt ring laser and a 5 watt slab laser. The 1 watt laser was used to study the injection locking process while assembling all the necessary electronics. We have demonstrated that it is possible to injection lock a diode-pumped laser using a single piezo-mounted mirror due to the lower intrinsic laser noise compared to an arc-lamp-pumped system. This allows us to optimize the injection locking servo loop and build a more stable locking system. The 5 watt laser was used as a test bed to find a practical way to mount the slab laser while minimizing the losses that occur at the total internal reflection (TIR) points in the slab. After trying many different means of protecting the TIR surfaces, we found that a new product from DuPont, Teflon AF 1600, has all the properties needed to provide a low loss protective coating. Using this material, the laser had a cavity loss of below 2%, which allowed for efficient operation of the laser in a side-pumped design. This laser produced 5 watts of output power with a slope efficiency near 20%. DTIC

N94-29493*# National Aeronautics and Space Administration. Pasadena Office, CA.
LASERCOM SYSTEM ARCHITECTURE WITH REDUCED COMPLEXITY Patent Application
James R. Lesh, inventor (to NASA) (Jet Propulsion Lab., California Inst. of Tech., Pasadena.), Chien-Chung Chen, inventor (to NASA) (Jet Propulsion Lab., California Inst. of Tech., Pasadena.), and Homayoon Ansari, inventor (to NASA) (Jet Propulsion Lab., California Inst. of Tech., Pasadena.) 31 Mar. 1994 28 p
(Contract NAS7-1260)
(NASA-Case-NPO-19069-1-CU; NAS 1.71:NPO-19069-1-CU; US-Patent-Appl-SN-223938) Avail: CASI HC A03/MF A01

Spatial acquisition and precision beam pointing functions are critical to spaceborne laser communication systems. In the present invention, a single high bandwidth CCD detector is used to perform both spatial acquisition and tracking functions. Compared to previous lasercom hardware design, the array tracking concept offers reduced system complexity by reducing the number of optical elements in the design. Specifically, the design requires only one detector and one beam steering mechanism. It also provides the means to optically close the point-ahead control loop. The technology required for high bandwidth array tracking was examined and shown to be consistent with current state of the art. The single detector

design can lead to a significantly reduced system complexity and a lower system cost. NASA

N94-29531 Columbia Univ., New York, NY.
NEAR-ULTRAVIOLET LASER PHOTOEMISSION: SCANNING MICROSCOPY, BURIED INTERFACES AND IMAGE-POTENTIAL STATES Ph.D. Thesis
Bertrand Olivier Mar Quiniou 1992 118 p
Avail: Univ. Microfilms Order No. DA9313663

This work reports the use of near-ultraviolet laser radiation, through the photoelectric effect, in the development of probes for surfaces. This effect offers the advantage of being contactless and nondestructive even at photon fluences at which nonlinear effects, such as two-photon photoemission processes, are observed. The probing of the energy band parameters at insulator/semiconductor buried interfaces is demonstrated. A study of the sensitivity of image-potential induced states upon temperature changes and atomic adsorption is presented, which leads to the uncovering of a new method to measure the temperature dependence of work functions on most metallic surfaces. Finally, a new, simple, photoemission scanning microscope is developed, which circumvents the need for energy-resolved techniques, for the mapping of doped regions on semiconductor surfaces. Dissert. Abstr.

N94-29551 Georgia Inst. of Tech., Atlanta.
DYNAMICS OF A COUPLED SOLID STATE LASER ARRAY Ph.D. Thesis
Larry Fabiny 1992 348 p
Avail: Univ. Microfilms Order No. DA9315875

The results of an investigation of the dynamic behavior of coupled solid state laser arrays are reported. Experimental results are compared with numerical simulations and analytic theory. Cavity designs for uncoupled and coupled arrays of Nd:YAG lasers are developed and experimental realizations of the arrays are fabricated. Spatially coupled Nd:YAG lasers are found to operate in stable phase-locked configurations, a result which is drastically different from the chaotic output present in semiconductor laser arrays. The phase-locking angle between adjacent lasers is observed to be pi radians, except when this angle is not possible for all nearest-neighbor pairs in the array. In that case, adjacent lasers phase lock with the relative angle nearest to pi that produces a self-consistent solution for the entire array. An analysis of the model rate equations for a coupled solid state laser array shows that stable phase-locked solutions for the Nd:YAG array are present for most values of the coupling coefficient. The same phase-locked solutions are unstable for semiconductor laser arrays, resulting in chaotic power fluctuations from individual lasing elements. The critical difference between semiconductor laser arrays and Nd:YAG laser arrays is the linewidth enhancement factor, which is significant only for the semiconductor lasers. The phase dynamics and mutual coherence of two spatially coupled Nd:YAG lasers are examined. A sharp transition from independent lasing to phase-locked out-of-phase lasing is observed as the separation distance between the lasers is reduced. The mutual coherence of the lasers is revealed by measuring the interference fringes formed by overlapping the output beams. A theoretical model that includes the relative frequency detuning of the two lasers makes predictions regarding the phase dynamics that are in excellent agreement with the experimental results. A nine-element Nd:YAG laser array coupled through diffractive feedback is fabricated. Self-feedback is observed to destabilize the output of a single Nd:YAG laser, thereby generating chaotic intensity fluctuations. When all nine lasers are operational, correlations between the intensity fluctuations of the lasers are seen. Small adjustments to the array cavity are sufficient to change the correlation from positive to negative. Dissert. Abstr.

N94-29590 Rochester Univ., NY.
LONGITUDINAL EFFECTS AND INTENSITY-PHASE COUPLING IN DISTRIBUTED FEEDBACK SEMICONDUCTOR LASERS Ph.D. Thesis
Lars Magnus Olofsson 1993 115 p
Avail: Univ. Microfilms Order No. DA9313874

The phenomenon of intensity-phase coupling in semiconductor lasers is investigated theoretically as well as experimentally for distributed feedback lasers. In addition, conditions for a uniform intensity profile are identified for such lasers. The theoretical study of intensity-phase coupling examines the importance of the longitudinal laser structure for this coupling exploiting a near threshold model. For the case of uniform gain and carrier density, no effect is expected from a periodic or quasi-periodic corrugation. On the other hand, when the gain-layer is corrugated or a gain-coupling mechanism is otherwise implemented, the influence may be considerable. It is shown that the degree of gain-coupling relative to index-coupling between right- and left-travelling waves and the specific mechanism by which variations in the carrier density influence this coupling are of key importance. We find that depending on the degree and nature of the gain-coupling, the strength of the intensity-phase coupling may be considerably reduced or enhanced. An interferometric method is wed to measure the coupling between intensity- and phase-modulation for 1.551 micron distributed feedback lasers for different bias and modulation frequency under small-signal modulation of the injection current. The strength of the measured intensity-phase coupling is quantified in terms of an effective chirp factor. We find this factor to increase monotonically and nearly double as the modulation frequency increases from below to above the resonance frequency of the relaxation oscillation. Our results contradict the commonly held view of the chirp factor as a constant parameter for a given laser structure. Simple conditions for a uniform intensity profile are presented for two kinds of center frequency DFB lasers. For a purely gain-coupled DFB laser the envelope of the intensity distribution is shown to be uniform when the spatially averaged gain constant is equal to zero. A second-order index-coupled laser structure with no second harmonic in its Fourier spectrum is predicted to lase precisely at the Bragg resonance and is shown to have a similar uniformity condition. For the special case of lasers with zero facet reflectivities, the condition is satisfied for both lasers when the product of the magnitude of the coupling constant and the length of the resonator is an odd integer multiple of pi/2. Dissert. Abstr.

N94-29914*# American Univ., Washington, DC.
SOLID STATE LASER SYSTEMS FOR SPACE APPLICATION Annual Report, Jan. 1994
Richard B. Kay 1994 9 p
(Grant NAG5-1319)
(NASA-CR-195777; NAS 1.26:195777) Avail: CASI HC A02/MF A01

Since the last report several things have happened to effect the research effort. In laser metrology, measurements using Michelson type interferometers with an FM modulated diode laser source have been performed. The discrete Fourier transform technique has been implemented. Problems associated with this technique as well as the overall FM scheme were identified. The accuracy of the technique is not at the level we would expect at this point. We are now investigating the effect of various types of noise on the accuracy as well as making changes to the system. One problem can be addressed by modifying the original optical layout. Our research effort was also expanded to include the assembly and testing of a diode pumpedNd:YAG laser pumpedTi sapphire laser for possible use in sounding rocket applications. At this stage, the diode pumped Nd:YAG laser has been assembled and made operational. Author (revised)

N94-29934# Los Alamos National Lab., NM.
ADVANCES IN TUNABLE POWERFUL LASERS: THE ADVANCED FREE-ELECTRON LASER
S. Singer and R. Sheffield 1993 22 p Presented at the 11th International Workshop on Laser Interaction and Related Plasma Phenomena, Monterey, CA, 25-29 Oct. 1993
(Contract W-7405-eng-36)
(DE94-004997; LA-UR-93-4410; CONF-931048-2) Avail: CASI HC A03/MF A01

In the past several decades, remarkable progress in laser science and technology has made it possible to obtain laser light from the ultra-violet to the far infra-red from a variety of laser types and at power levels from milliwatts to kilowatts (and, some day, megawatts). However, the availabiiity of tunable lasers at 'high' power (above a few tens of watts) is more limited. An assessment of the availability of tunable lasers shows the covered range to be about 400 to 2000 nanometers. A variety of dye lasers cover the visible and near infrared, each one of which is tunable over approximately a 10% range. In the same region, the TI:sapphire laser is adjustable over a 20 to 25% range. And finally, optical parametric oscillators can cover the range from about 400 nanometers out to about 2000 nm (even farther at reduced energy output). The typical output energy per pulse may vary from a few to one hundred millijoules, and since repetition rates of 10 to 100 Hertz are generally attainable, average output

powers of tens of watts are possible. In recent years, a new approach to powerful tunable lasers--the Free-Electron Laser (FEL)--has emerged. In this paper we will discuss advances in FEL technology which not only enable tunability at high average power over a very broad range of wavelengths, but also make this device more usable. At present, that range is about one micron to the far infrared; with extensions of existing technology, it should be extendable to the vacuum ultraviolet region. DOE

N94-30060# Lawrence Livermore National Lab., CA.
ENHANCED COHERENCE X RAY LASER EXPERIMENTS AND SIMULATIONS
A. S. Wan, S. B. Libby, and J. C. Moreno Oct. 1993 6 p Presented at the 11th International Workshop on Laser Interaction and Related Plasma Phenomena, Monterey, CA, 25-29 Oct. 1993
(Contract W-7405-eng-48)
(DE94-005367; UCRL-JC-114832; CONF-931048-4) Avail: CASI HC A02/MF A01

Bright, spatially coherent x-ray lasers (XRL's) have applications in areas such as holography, interferometric imaging, and non-linear optics. Nominally, the authors can improve XRL coherence by either increasing the length or by reducing the aperture. Length can be increased by coupling multiple stages of XRL's or by using multilayer optics, but the effective gain length of an XRL is limited by refractive propagation and multilayer damages. The laser aperture is typically limited by the best-focused configuration defined by the driving optical lasers. Design of XRL's produced in exploding foil or slab configuration is further complicated by large spatial gain and n(sub e) inhomogeneities. This paper explores a new XRL design that uses the concept of adaptive spatial filtering by geometric shaping to improve the transverse coherence. One example of such shaped XRL's is a bowtie. The authors present here computational and experimental characterization of shaped XRL's during laser plasma expansion by studying their hydrodynamic behaviors, ionization histories, and laser output intensities. DOE

N94-30186# National Inst. for Fusion Science, Nagoya (Japan).
DEVELOPMENT OF HIGH TIME-RESOLUTION LASER FLASH EQUIPMENT FOR THERMAL DIFFUSIVITY MEASUREMENTS USING MINIATURE-SIZE SPECIMENS
Tatsuo Shikama (Tohoku Univ., Oarai, Japan.), Chusei Namba, Michinori Kosuda, and Yukio Maeda Jan. 1994 18 p Submitted for publication
(ISSN 0915-633X)
(NIFS-268) Avail: CASI HC A03/MF A01

For measurements of thermal diffusivity of miniature-size specimens heavily irradiated by neutrons, a new Q-switched laser-flash instrument was developed. In the present instrument the time resolution was improved to 0.1 ms by using a laser-pulse width of 25 ns. The realization of high time-resolution made it possible to measure the thermal diffusivity of thin specimens. It is expected that copper of 0.7mm thick, and SUS 304 of 0.1 mm could be used for the measurements. In case of ATJ graphite, 0.5mm thick specimen could be used for the reliable measurement in the temperature range of 300-1300K. Author

N94-30265# Sandia National Labs., Albuquerque, NM.
REACTOR-PUMPED LASER FACILITY AT DOE'S NEVADA TEST SITE
R. J. Lipinski 1994 8 p Presented at the OE/LASE 1994: Conference on Optics, Electro-Optics, and Laser Applications in Science and Engineering, Los Angeles, CA, 22-29 Jan. 1994
(Contract DE-AC04-94AL-85000)
(DE94-006371; SAND-94-0074C; CONF-940142-12) Avail: CASI HC A02/MF A01

The Nevada Test Site (NTS) is one excellent possibility for a laser power beaming site. It is in the low latitudes of the U.S., is in an exceptionally cloud-free area of the southwest, is already an area of restricted access (which enhances safety considerations), and possesses a highly-skilled technical team with extensive engineering and research capabilities from underground testing of our nation's nuclear deterrence. The average availability of cloud-free clear line of site to a given point in space is about 84%. With a beaming angle of +/- 60 degrees from the zenith, about 52 geostationary-orbit (GEO) satellites could be accessed continuously from NTS. In addition, the site would provide an average view factor of about 10% for orbital transfer from low earth orbit to GEO. One of the major candidates for a long-duration, high-power laser is a reactor-pumped laser being developed by DOE. The extensive nuclear expertise at NTS makes this site a prime candidate for utilizing the capabilities of a reactor pumped laser for power beaming. The site then could be used for many dual-use roles such as industrial material processing research, defense testing, and removing space debris. DOE

N94-30367# Sandia National Labs., Albuquerque, NM.
FISSION-ACTIVATED LASER AS PRIMARY POWER FOR CW LASER PROPULSION
D. K. Monroe 1993 8 p Presented at the OE/LASE 1994: Conference on Optics, Electro-Optics, and Laser Applications in Science and Engineering, Los Angeles, CA, 22-29 Jan. 1994
(Contract DE-AC04-94AL-85000)
(DE94-006138; SAND-93-1524C; CONF-940142-5) Avail: CASI HC A02/MF A01

Recent advances in the development of reactor-pumped lasers (RPL's) have stimulated renewed interest in the concept of laser-powered propulsion. This paper surveys a number of laser propulsion concepts and identifies the one that is most promising from the standpoint of practicality. It is proposed that a ground-based FALCON (fission-activated laser concept) RPL can provide primary power for this launch vehicle design. The laser vehicle system could launch small payloads into low earth orbit (LEO) with high repetition rates and at low costs per kilogram. For the favored design, thruster efficiencies are currently estimated to be about 50 percent, with 80 percent being seen as a potentially realizable goal after further design refinements. Laser launch system simulations indicate that with a buy-in laser power of 10 MW, it will be possible to obtain specific impulses in the range of 600 to 800 seconds and payload-to-power ratios of 1 to 3 kg/MW. DOE

N94-30595 Michigan Univ., Ann Arbor. Intense Energy Beam Interaction Lab.
INVESTIGATIONS OF LARGE AREA ELECTRON BEAM DIODES FOR EXCIMER LASERS
1993 91 p Prepared for Los Alamos National Lab., NM Limited Reproducibility: More than 20% of this document may be affected by microfiche quality
(Contract W-7405-eng-36)
(DE94-005670; LA-Sub-93-207) Avail: CASI HC A05

This report summarizes the results of a one year research program at the University of Michigan to investigate the physics and technology of microsecond electron beam diodes. These experiments were performed on the Michigan Electron Long Beam Accelerator (MELBA) at parameters: Voltage equals -0.65 to -0.9 MV, current equals 1 to 50 kA, and pulselength equals 0.5 to 5 microseconds. Major accomplishments include: (1) the first two-wavelength (CO2 and HeNe) laser deflection measurements of diode plasma and neutrals; (2) measurements of the effects on magnetic field gradient on microsecond diode closure; (3) demonstration of good fidelity of processed x-ray signals as a diagnostic of beam voltage; (4) extended-pulselength scaling of electron beam diode arcing and diode closure; and (5) innovative Cerenkov plate diagnostics of e-beam dynamics. DOE

N94-30598 Lawrence Livermore National Lab., CA.
NONLINEAR ABSORPTION IN HIGH REFLECTOR MULTILAYERS
C. J. Stolz, T. G. Sarginson, and J. R. Taylor Nov. 1993 12 p Presented at the 25th Boulder Damage Symposium: Annual Symposium on Optical Materials for High-Power Lasers, Boulder, CO, 27-29 Oct. 1993 Limited Reproducibility: More than 20% of this document may be affected by microfiche quality
(Contract W-7405-eng-48)
(DE94-005818; UCRL-JC-114983; CONF-931054-6) Avail: Issuing Activity (Department of Energy (DOE))

Low absorption coatings were examined using a high repetition rate copper vapor laser to study the surface temperature as a function of incident power. Nonlinear absorption was observed in some of the coatings as a result of increased incident power. A variety of commercial coating vendors using common dielectric oxide material combinations were surveyed. Wavelength, coating material, and coating vendor were varied to study their effects on the linearity of the absorption. The films were deposited

by electron beam or ion beam sputtering technologies. Changes in the film characteristics were observed after exposure to high incident power. The nature of these changes and their permanency were also examined. DOE

N94-30614 Missouri Univ., Columbia. Dept. of Nuclear Engineering.
REMOTE PUMPING OF SOLID STATE LASERS WITH NUCLEAR DRIVEN FLUORESCERS
M. A. Prelas 30 Nov. 1993 33 p Limited Reproducibility: More than 20% of this document may be affected by microfiche quality
(Contract DE-FG02-90ER-13029)
(DE94-004846; DOE/ER-13029/T3) Avail: CASI HC A03

Development of an electron density model, microwave propagation model, and power density model was completed for various visible excimer gas media including the xenon oxide excimer (XeO*). In addition, a heat transfer model was developed. Optimization of a microwave pumped excimer lamp has begun and the results indicate that high frequency modes can be excited efficiently. A model for power density in the cavity has been developed and indicates that 111 modes appear to be the most uniform. A He3 excited nuclear 'pumped' lamp was built to take spectra of gas mixtures in a reactor environment. The effects of nuclear radiation on optical materials was examined from 350 nm to 950 nm. The results demonstrated that radiation effects are nonlinear with power. Additionally, radiation damage was strongest in the UV bandwidth. Studies were also made of radiation induced fluorescence. A method was developed to subtract radiation induced fluorescence from the fluorescence signal in the lamp. Using the results of radiation induced absorption and radiation induced fluorescence, a technique for determining absolutely calibrated spectra from the lamp was developed. Absolutely calibrated spectra from He, He-Ar, He-Xe, and He-Kr were taken. The results from this study were compared to electrically driven flashlamps. A heat pipe for a reactor experimentation with alkali metals was developed. Several experiments were run using the heat pipe filled with 5 grams of sodium. Radiation from the violet bands of sodium at around 436 nm was expected. Indeed observations of emission at 436 nm were made. The overall results of this work were: (1) development of a microwave excitation system which approximated nuclear 'pumping'; (2) development of methods to compensate for radiation induced absorption and radiation induced fluorescence in optical systems in high radiation environments; and (3) development of methods to obtain absolutely calibrated spectra from light. DOE

N94-30688# Brookhaven National Lab., Upton, NY.
TOWARDS SHORT WAVELENGTHS FELs WORKSHOP
I. Ben-Zvi and H. Winick 1993 98 p Workshop held in Upton, NY, 21-22 May 1993
(Contract DE-AC02-76CH-00016)
(DE94-004346; BNL-49651; CONF-9305307) Avail: CASI HC A05/MF A02

This workshop was caged because of the growing perception in the FEL source community that recent advances have made it possible to extend FEL operation to wavelengths about two orders of magnitude shorter than the 240 nm that has been achieved to date. In addition short wavelength FEL's offer the possibilities of extremely high peak power (several gigawatts) and very short pulses (of the order of 100 fs). Several groups in the USA are developing plans for such short wavelength FEL facilities. However, reviewers of these plans have pointed out that it would be highly desirable to first carry out proof-of-principle experiments at longer wavelengths to increase confidence that the shorter wavelength devices will indeed perform as calculated. The need for such experiments has now been broadly accepted by the FEL community. Such experiments were the main focus of this workshop as described in the following objectives distributed to attendees: (1) Define measurements needed to gain confidence that short wavelength FEL's will perform as calculated. (2) List possible hardware that could be used to carry out these measurements in the near term. (3) Define a prioritized FEL physics experimental program and suggested timetable. (4) Form collaborative teams to carry out this program. DOE

N94-30801 Guelph Univ. (Ontario).
THE DEVELOPMENT AND EVALUATION OF A TUNABLE DIODE LASER TRACE GAS SENSOR FOR THE MEASUREMENT OF N2O AND CH4 FLUXES USING MICROMETEOROLOGICAL TECHNIQUES Ph.D. Thesis
Grant Carleton Edwards 1992 123 p
(ISBN-0-315-78975-1) Avail: Univ. Microfilms Order No. DANN78975

A sensitive fast response fieldworthy trace gas sensor, based on tunable diode laser absorption spectroscopy, has been successfully developed for the measurement of the exchange of methane or nitrous oxide between a surface and the atmosphere using micrometeorological techniques. The instrument has been proven to be suitable for the reliable continuous measurement of the flux of methane or nitrous oxide. This development is a significant advance over other techniques for the measurement of the fluxes of trace gases. The instrument developed has a total system noise of less than 5 ppbv rms for CH4 and better than 2 ppbv rms for N2O with an effective bandwidth of 0.001 to 1.6 Hz. The system sampling rate of 10 Hz, was determined by a 0.18 data point averaging time. The instrument was developed through extensive field testing involving the continuous measurement of nitrous oxide and methane fluxes in forest and wetland ecosystems respectively. Measurements of N2O fluxes from a deciduous forest were made with a first generation instrument using a tower based eddy correlation approach. Instrument performance was sufficient to obtain a limited data set on the emission of N2O from a deciduous forest during an 'Indian Summer' event during the fall of 1989. These data showed an average daytime emission of 119 ng m(exp -2)/s of N2O. On average, measured values fell below the estimated detection limit of 40 ng m(exp -2)/s during the evening. The data suggested that the forest can be a significant natural source of N2O. The results emphasizes the need for continuous high time resolution data on N2O emission from natural ecosystems before rational global budgets can be constructed. Based on the operating experience during this field study, improvements to the optical, electronic and digital signal processing systems were implemented. With a second generation TDL sensor, tower based eddy correlation measurements of the methane fluxes were made above a wetland. Approximately 900 half hour average methane flux measurements were obtained during a 30 day period in July, 1990. Fluxes averaged over the study period showed an overall methane emission of 16 mg m(exp -2)/d with a daytime average of 20 mg m(exp -2)/d and a nighttime average of 9 mg m(exp -2)/d. The effect of heterogeneous surface emissions were evident in the data. A strong relationship between the daily average methane flux and wet bog temperature at 20 cm depth was observed.
Dissert. Abstr.

N94-30830# Lawrence Livermore National Lab., CA.
DIODE-PUMPED SOLID-STATE-LASER DRIVERS AND THE COMPETITIVENESS OF INERTIAL FUSION ENERGY
C. D. Orth Dec. 1993 12 p Presented at the 11th International Workshop on Laser Interaction and Related Plasma Phenomena, Monterey, CA, 25-29 Oct. 1993
(Contract W-7405-eng-48)
(DE94-006654; UCRL-JC-114902; CONF-931048-5) Avail: CASI HC A03/MF A01

Based on five technical advances at LLNL and a new systems-analysis code, we present conceptual designs for diode-pumped solid state laser (DPSSL) drivers for inertial fusion energy (IFE) power plants. Such designs are based on detailed physics calculations for the drive and on generic scaling relationships for the reactor and balance of plant (BOP). We describe the performance and economics of such power plants, show how sensitive these results are to changes in the major parameters, and indicate how technological improvements can make DPSSL-driven IFE plants more competitive. DOE

N94-30908# Ames Lab., IA.
INVESTIGATIONS INTO ULTRAVIOLET MATRIX-ASSISTED LASER DESORPTION Ph.D. Thesis
T. W. Heise Jul. 1993 105 p
(Contract W-7405-eng-82)
(DE94-005265; IS-T-1657) Avail: CASI HC A06/MF A02

Matrix-assisted laser desorption (MALD) is a technique for converting large biomolecules into gas phase ions. Some characteristics of the commonly used uv matrices are determined. Solubilities in methanol range from 0.1 to 0.5 M. Solid phase absorption spectra are found to be similar to solution, but slightly red-shifted. Acoustic and quartz crystal microbalance signals are investigated as possible means of uv-MALD quantitation. Evidence for the existence of desorption thresholds is presented. Threshold values are determined to be in the range of 2 to 3 MW/sq cm. A transient

imaging technique based on laser-excited fluorescence for monitoring MALD plumes is described. Sensitivity is well within the levels required for studying matrix-assisted laser desorption, where analyte concentrations are significantly lower than those in conventional laser desorption. Results showing the effect of film morphology, particularly film thickness, on plume dynamics are presented. In particular, MALD plumes from thicker films tend to exhibit higher axial velocities. Fluorescent labeling of protein and of DNA is used to allow imaging of their uv-MALD generated plumes. Integrated concentrations are available with respect to time, making it possible to assess the rate of fragmentation. The spatial and temporal distributions are important for the design of secondary ionization schemes to enhance ion yields and for the optimization of ion collection in time-of-flight MS instruments to maximize resolution. Such information could also provide insight into whether ionization is closely associated with the desorption step or whether it is a result of subsequent collisions with the matrix gas (e.g., proton transfer). Although the present study involves plumes in a normal atmosphere, adaptation to measurements in vacuum (e.g., inside a mass spectrometer) should be straightforward. DOE

N94-29658*# Jet Propulsion Lab., California Inst. of Tech., Pasadena.
A DUAL-CAVITY RUBY MASER FOR THE Ka-BAND LINK EXPERIMENT
J. Shell and R. B. Quinn *In its* The Telecommunications and Data Acquisition Report 15 Feb. 1994 p 53-70 (For primary document see N94-29652 08-32)
(RTOP 310-20-66-87-02)
Avail: CASI HC A03/MF A03

N94-29672*# Jet Propulsion Lab., California Inst. of Tech., Pasadena.
X-BAND ULTRALOW-NOISE MASER AMPLIFIER PERFORMANCE
G. W. Glass, G. G. Ortiz, and D. L. Johnson *In its* The Telecommunications and Data Acquisition Report 246-253 (SEE N94-29652 08-32) 15 Feb. 1994 (For primary document see N94-29652 08-32)
(RTOP 310-20-66-53-00)
Avail: CASI HC A02/MF A03

N94-30664*# National Research Council of Canada, Ottawa (Ontario).
HYDROGEN MASERS AND CESIUM FOUNTAINS AT NRC
J.-S. Boulanger, D. Morris, R. J. Douglas, and M.-C. Gagne *In* NASA. Goddard Space Flight Center, The 25th Annual Precise Time and Time Interval (PTTI) Applications and Planning Meeting May 1994 p 345-356 (For primary document see N94-30639 08-70)
Avail: CASI HC A03/MF A06

N94-30666*# Observatoire de la Cote d'Azur, Grasse (France).
LASSO EXPERIMENT: INTERCALIBRATIONS OF THE LASSO RANGING STATIONS
J. Gaignebet, J.-L. Hatat, J. F. Mangin, J. M. Torre, William J. Klepczynski, L. McCubin, J. Wiant, and R. Rickefs *In* NASA. Goddard Space Flight Center, The 25th Annual Precise Time and Time Interval (PTTI) Applications and Planning Meeting May 1994 p 367-378 (For primary document see N94-30639 08-70)
Avail: CASI HC A03/MF A06

N94-30670*# NeoComm Systems, Inc., La Canada-Flintridge, CA.
PROVIDING HYDROGEN MASER TIMING STABILITY TO ORBITING VLBI RADIO TELESCOPE OBSERVATIONS BY POST-MEASUREMENT COMPENSATION OF LINKED FREQUENCY STANDARD IMPERFECTIONS
James C. Springett *In* NASA. Goddard Space Flight Center, The 25th Annual Precise Time and Time Interval (PTTI) Applications and Planning Meeting May 1994 p 413-424 (For primary document see N94-30639 08-70)
Avail: CASI HC A03/MF A06

37 MECHANICAL ENGINEERING

Includes auxiliary systems (nonpower); machine elements and processes; and mechanical equipment.

N94-28399 Technische Univ., Delft (Netherlands).
JOINING SILICON CARBIDE TO AUSTENITIC STAINLESS STEEL THROUGH DIFFUSION WELDING Ph.D. Thesis
J. P. H. M. Krugers 19 Jan. 1993 186 p Limited Reproducibility: More than 20% of this document may be affected by microfiche quality
(PB94-126331) Avail: CASI HC A09

In the thesis, the results are presented of a study dealing with joining silicon carbide to austenitic stainless steel AISI316 by means of diffusion welding. Welding experiments were carried out with and without the use of a metallic intermediate, like copper, nickel, and copper-nickel alloys at various conditions of process temperature, process time, mechanical pressure, and interlayer thickness. Most experiments were carried out in high vacuum. For reasons of comparison, however, some experiments were also carried out in a gas shielded environment of 95% vol. Ar and 5% vol. H2. NTIS

N94-28419*# Sverdrup Technology, Inc., Huntsville, AL. MSFC Group.
MECHANICAL FLEXIBLE JOINT DESIGN DOCUMENT
Vic Daily 22 Oct. 1993 108 p
(Contract NAS8-37814)
(NASA-CR-193941; NAS 1.26:193941; Rept-324-005-93-041) Avail: CASI HC A06/MF A02

The purpose of this report is to document the status of the Mechanical Flexible Joint (MFJ) Design Subtask with the intent of halting work on the design. Recommendations for future work is included in the case that the task is to be resumed. The MFJ is designed to eliminate two failure points from the current flex joint configuration, the inner 'tripod configuration' and the outer containment jacket. The MFJ will also be designed to flex 13.5 degrees and have three degrees of freedom. By having three degrees of freedom, the MFJ will allow the Low Pressure Fuel Duct to twist and remove the necessity to angulate the full 11 degrees currently required. The current flex joints are very labor intensive and very costly and a simple alternative is being sought. The MFJ is designed with a greater angular displacement, with three degrees of freedom, to reside in the same overall envelope, to meet weight constraints of the current bellows, to be compatible with cryogenic fuel and oxidizers, and also to be man-rated. Derived from text

N94-28461# Argonne National Lab., IL.
CURRENT LEADS AND MAGNETIC BEARINGS
J. R. Hull 1993 6 p Presented at the 6th US-Japan Workshop on Superconductivity, Houston, TX, 6-7 Dec. 1993
(Contract W-31-109-eng-38)
(DE94-004607; ANL/ET/CP-81504; CONF-931238-2) Avail: CASI HC A02/MF A01

Since the discovery of high temperature superconductors (HTS's), Argonne National Laboratory (ANL) has been active in a broad spectrum of activities in developing these materials for applications. Work at every stage of development has involved industrial collaboration in order to accelerate commercialization. While most of the development work has been devoted to improving the properties of current-carrying wires, some effort has been devoted to applications that can utilize HTS's with properties available now or in the near future. In this paper, advances made in the area of current leads and magnetic bearings are discussed. DOE

N94-28485# Clemson Univ., SC.
ADVANCED GAS TURBINE SYSTEMS RESEARCH
1993 6 p
(Contract DE-FC21-92MC-29061)
(DE94-005303; DOE/MC-29061/3566) Avail: CASI HC A02/MF A01

The responses to the first Request for Proposals issued by AGTSR in March were received and evaluated by the industrial Review Board. Ten were selected for subcontract awards, which are presently being negotiated. The number of Performing Member universities has increased by six, to 56, since the last report. Two additional members are pending. DOE

N94-28838*# National Aeronautics and Space Administration. Lewis Research Center, Cleveland, OH.
DEVELOPMENT OF BRAIDED ROPE ENGINE SEALS
Frank K. Ko (Drexel Univ., Philadelphia, PA.), Zhong Cai (Drexel Univ., Philadelphia, PA.), Rajakkannu Mutharasan (Drexel Univ., Philadelphia, PA.), and Bruce M. Steinetz Feb. 1994 16 p Presented at the 39th International SAMPE Symposium and Exhibition, Anaheim, CA, 11-14 Apr. 1994; sponsored by the Advancement of Materials and Process Engineering
(RTOP 763-22-2J)
(NASA-TM-105902; E-8639; NAS 1.15:105902) Avail: CASI HC A03/MF A01

In this study, after reviewing current seal design concepts, the potential of textile structures for seal design is examined from the material, structural, and fabrication points of view. Braided structures are identified as potential candidates for hypersonic seal structures because of their conformability and design flexibility. A large family of braided structures using 2-D and 3-D architecture can be designed using well established methods to produce a wide range of braiding yarn orientation for wear resistance as well as seal porosity control. As a first demonstration of the approach, 2-D braided fiberglass seals were fabricated according to a factorial design experiment by varying braiding angles, fractional longitudinal fibers, and preload pressure levels. Factorial diagrams and response surfaces were constructed to elucidate the inter-relationship of the braiding parameters as well as the effect of preload pressures on leakage resistance of the seal. It was found that seal resistance is a strong function of fractional longitudinal fiber content. As braiding angle increases, seal leakage resistance increases, especially at high preload pressures and in seals having high proportion of longitudinal fibers. Author (revised)

N94-28894# Air Force Inst. of Tech., Wright-Patterson AFB, OH. School of Engineering.
DESIGN AND CONSTRUCTION OF THE AEROBOT ROBOTIC MANIPULATOR (ARM) M.S. Thesis
William L. Cochran Dec. 1993 118 p
(AD-A275362; AFIT/GA/ENY-93D-2) Avail: CASI HC A06/MF A02

This thesis designed, constructed, and tested a robotic arm for the Aerobot (Aerial Robot). The main purpose of the ARM is to enable the Aerobot to retrieve objects during an annual robotics competition. Design of the ARM involved synthesizing the characteristics of simplicity, weight, strength, and size. The result was a three-degree-of-freedom manipulator that uses electric motors, cable linkages, and telescoping tubes to access a work space below the Aerobot. Forward and inverse kinematics were investigated to enable automation of the ARM. Data was collected from infrared sensors to validate the model. Manipulation of the ARM is presently under open loop control (joy stick) which demonstrates the use of tele-robotics and its capabilities. DTIC

N94-29290# Ohio State Univ., Columbus. Dept. of Mechanical Engineering.
ATOMIC-SCALE FRICTION MEASUREMENTS USING FRICTION FORCE MICROSCOPY. PART 2: APPLICATION TO MAGNETIC MEDIA
Bharat Bhushan and Ju-Ai Ruan 3 May 1993 39 p
(AD-A275202) Avail: CASI HC A03/MF A01

Atomic Force/Friction Force Microscopes (AFM/FFM) were used to study tribological properties of metal-particle tapes with two roughnesses, Co-gamma Fe2O3 tapes (unwiped and wiped), and unlubricated and lubricated thin-film magnetic rigid disks (as-polished and standard textured). Nanoindentation studies showed that the hardness of the tapes through the magnetic coating is not uniform. These results are consistent with the fact that the tape surface is a composite and is not homogeneous. Nanoscratch experiments performed on magnetic tapes using silicon nitride tips revealed that deformation and displacement of tape surface material occurred after one pass under light loads (approx. 100 nN). A comparison between friction force profiles and the corresponding surface roughness profiles of all samples tested shows a poor correlation between localized values of friction and surface roughness. Detailed studies of friction and surface profiles demonstrate an excellent correlation between localized variation of the slope of the surface roughness along the sliding direction and the localized variation of friction. Atomic-scale friction in magnetic media and natural diamond appears to be due to adhesive and ratchet (roughness) mechanisms. Directionality in the local variation of atomic-scale friction data was observed as the samples were scanned in either direction, resulting from the scanning direction and the anisotropy in the surface topography. Atomic-scale coefficient of friction is generally found to be smaller than the macrocoefficient of friction as there may be less ploughing contribution in atomic-scale measurements. DTIC

N94-29351*# National Aeronautics and Space Administration. Marshall Space Flight Center, Huntsville, AL.
PLASMA ARC WELDING TORCH HAVING MEANS FOR VORTEXING PLASMA FOR EXITING THE WELDING TORCH Patent Application
Daniel J. Rybicki, inventor (to NASA) (Martin Marietta Space Systems, Inc., Huntsville, AL.) and William F. McGee, inventor (to NASA) (Martin Marietta Space Systems, Inc., Huntsville, AL.) 29 Nov. 1993 13 p
(NASA-Case-MFS-28828-1; NAS 1.71:MFS-28828-1;
US-Patent-Appl-SN-158327) Avail: CASI HC A03/MF A01

A plasma arc welding torch is described wherein a plasma gas is directed through the body of the welding torch and out of the body across the tip of the welding electrode disposed at the forward end of the body. The plasma gas is provided with a vortexing motion prior to exiting the body by a vortex motion imparting member which is mounted in an orifice housing member and carried in the forward portion of the torch body. The orifice housing member is provided with an orifice of an predetermined diameter through which the electric arc and the plasma gas exits. NASA

N94-29352*# National Aeronautics and Space Administration. Marshall Space Flight Center, Huntsville, AL.
METAL INERT GAS WELDING SYSTEM FOR USE IN VACUUM Patent Application
Charles D. Stocks, inventor (to NASA) 20 Sep. 1993 18 p
(NASA-Case-MFS-28808-1; NAS 1.71:MFS-28808-1;
US-Patent-Appl-SN-123945) Avail: CASI HC A03/MF A01

Disclosed are a device and a method for inert gas plasma welding in a low pressure or vacuum environment. The device comprises: a pre-plasma cavity having a first opening therein capable of accepting an inert gas into the pre-plasma cavity, first and second electrodes within the pre-plasma cavity capable of applying an electromagnetic field to the inert gas to thereby convert the inert gas into a plasma and a second opening capable of allowing the plasma to exit the pre-plasma cavity and a structure capable of directing the plasma from the second opening of the pre-plasma cavity to an arc welding cavity adjacent to the second opening, the arc welding cavity capable of being placed adjacent to a working surface, the arc welding cavity further capable of accepting a welding material therein, the plasma impinging on the working surface and the welding material, the directing means focusing the plasma within the arc welding cavity to thereby increase a rate of heat transfer between the plasma and the working surface and the welding material. The present invention allows welding to be done in a vacuum by preventing the vacuum from prematurely dispersing the plasma. NASA

N94-29353*# National Aeronautics and Space Administration. Marshall Space Flight Center, Huntsville, AL.
TUNED MASS DAMPER FOR INTEGRALLY BLADED TURBINE ROTOR Patent Application
John J. Marra, inventor (to NASA) (Pratt and Whitney Aircraft, West Palm Beach, FL.) 12 Oct. 1993 12 p
(NASA-Case-MFS-28697-1; NAS 1.71:MFS-28697-1;
US-Patent-Appl-SN-134443) Avail: CASI HC A03/MF A01

The invention is directed to a damper ring for damping the natural vibration of the rotor blades of an integrally bladed rocket turbine rotor. The invention consists of an integral damper ring which is fixed to the underside of the rotor blade platform of a turbine rotor. The damper ring includes integral supports which extend radially outwardly therefrom. The supports are located adjacent to the base portion and directly under each blade of the rotor. Vibration damping is accomplished by action of tuned mass damper beams attached at each end to the supports. These beams vibrate at a predetermined frequency during operation. The vibration of the beams enforce a local node of zero vibratory amplitude at the interface between the supports and the beam. The vibration of the beams create forces upon the supports which forces are transmitted through the rotor blade mounting platform to the base of each rotor blade. When these forces attain a predetermined design frequency and magnitude and are

directed to the base of the rotor blades, vibration of the rotor blades is effectively counteracted. NASA

N94-29354*# Florida State Univ., Tallahassee. Coll. of Engineering.
LUNAR SURFACE OPERATIONS. VOLUME 1: LUNAR SURFACE EMERGENCY SHELTER Annual Report
William Shields, Salah Feteih, and Patrick Hollis Jul. 1993 174 p
(Contract NASw-4435)
(NASA-CR-195551; NAS 1.26:195551) Avail: CASI HC A08/MF A02

The lunar surface emergency shelter (LSES) is designed to provide survival-level accommodations for up to four astronauts for a maximum of five days. It would be used by astronauts who were caught out in the open during a large solar event. The habitable section consists of an aluminum pressure shell with an inner diameter of 6 ft. and a length of 12.2 ft. Access is through a 4 in. thick aluminum airlock door mounted at the rear of the shelter. Shielding is provided by a 14.9 in. thick layer of lunar regolith contained within a second, outer aluminum shell. This provides protection against a 200 MeV event, based on a 15 REM maximum dose. The shelter is self-contained with a maximum range of 1000 km. Power is supplied by a primary fuel cell which occupies 70.7 cu ft. of the interior volume. Mobility is achieved by towing the shelter behind existing lunar vehicles. It was assumed that a fully operational, independent lunar base was available to provide communication support and tools for set-up and maintenance. Transportation to the moon would be provided by the proposed heavy lift launch vehicle. Major design considerations for the LSES were safety, reliability, and minimal use of earth materials. Author (revised)

N94-29365*# National Aeronautics and Space Administration. Marshall Space Flight Center, Huntsville, AL.
APPARATUS FOR TESTING HIGH PRESSURE INJECTOR ELEMENTS Patent Application
William Neill Myers, inventor (to NASA), Ewell M. Scott, inventor (to NASA), John C. Forbes, inventor (to NASA), and Michael D. Shadoan, inventor (to NASA) 7 Sep. 1993 19 p
(NASA-Case-MFS-28773-1; NAS 1.71:MFS-28773-1;
US-Patent-Appl-SN-117587) Avail: CASI HC A03/MF A01

An apparatus for testing and evaluating the spray pattern of high pressure fuel injector elements for use in supplying fuel to combustion engines is presented. Prior art fuel injector elements were normally tested by use of low pressure apparatuses which did not provide a purge to prevent mist from obscuring the injector element or to prevent frosting of the view windows; could utilize only one fluid during each test; and had their viewing ports positioned one hundred eighty (180 deg) apart, thus preventing optimum use of laser diagnostics. The high pressure fluid injector test apparatus includes an upper hub, an upper weldment or housing, a first clamp and stud/nut assembly for securing the upper hub to the upper weldment, a standoff assembly within the upper weldment, a pair of window housings having view glasses within the upper weldment, an injector block assembly and purge plate within the upper weldment for holding an injector element to be tested and evaluated, a lower weldment or housing, a second clamp and stud/nut assembly for securing the lower weldment to the upper weldment, a lower hub, a third clamp and stud/nut assembly for securing the lower hub to the lower weldment, mechanisms for introducing fluid under high pressure for testing an injector element, and mechanisms for purging the apparatus to prevent frosting of view glasses within the window housings and to permit unobstructed viewing of the injector element. NASA

N94-29367*# National Aeronautics and Space Administration. Marshall Space Flight Center, Huntsville, AL.
COLLAPSIBLE MECHANICAL JOINT Patent Application
Glen A. Robertson, inventor (to NASA) 1 Nov. 1993 8 p
(NASA-Case-MFS-28765-1; NAS 1.71:MFS-28765-1;
US-Patent-Appl-SN-143601) Avail: CASI HC A02/MF A01

A mechanical joint that can be configured to be either flexible or rigid is presented. The mechanical joint comprises three members which are flexibly attached to each other with a cable. When the cable is tightened, the three members come together to form a rigid joint capable of withstanding structural loads. NASA

N94-29370*# National Aeronautics and Space Administration. Lyndon B. Johnson Space Center, Houston, TX.
ROTARY BLOOD PUMP Patent Application
Richard J. Bozeman, inventor (to NASA), James W. Akkerman, inventor (to NASA), Greg S. Aber, inventor (to NASA), George A. VanDamm, inventor (to NASA), James W. Bacak, inventor (to NASA), Paul A. Svejkovsky, inventor (to NASA), and Robert J. Benkowski, inventor (to NASA) 10 Nov. 1993 33 p
(NASA-Case-MSC-22424-1; NAS 1.71:MSC-22424-1;
US-Patent-Appl-SN-153595) Avail: CASI HC A03/MF A01

A rotary blood pump is presented. The pump includes a pump housing for receiving a flow straightener, a rotor mounted on rotor bearings and having an inducer portion and an impeller portion, and a diffuser. The entrance angle, outlet angle, axial, and radial clearances of the blades associated with the flow straightener, inducer portion, impeller portion, and diffuser are optimized to minimize hemolysis while maintaining pump efficiency. The rotor bearing includes a bearing chamber that is filled with crosslinked blood or other bio-compatible material. A back emf integrated circuit regulates rotor operation and a microcomputer may be used to control one or more back emf integrated circuits. A plurality of magnets are disposed in each of a plurality of impeller blades with a small air gap. A stator may be axially adjusted on the pump housing to absorb bearing load and maximize pump efficiency. NASA

N94-29386*# Florida State Univ., Tallahassee. Coll. of Engineering.
LUNAR SURFACE OPERATIONS. VOLUME 4: LUNAR ROVER TRAILER Annual Report
William Shields, Salah Feteih, and Patrick Hollis Jul. 1993 77 p
(Contract NASw-4435)
(NASA-CR-195554; NAS 1.26:195554) Avail: CASI HC A05/MF A01

The purpose of the project was to design a lunar rover trailer for exploration missions. The trailer was designed to carry cargo such as lunar geological samples, mining equipment and personnel. It is designed to operate in both day and night lunar environments. It is also designed to operate with a maximum load of 7000 kilograms. The trailer has a ground clearance of 1.0 meters and can travel over obstacles 0.75 meters high at an incline of 45 degrees. It can be transported to the moon fully assembled using any heavy lift vehicle with a storage compartment diameter of 5.0 meters. The trailer has been designed to meet or exceed the performance of any perceivable lunar vehicle. Author

N94-29409*# Old Dominion Univ., Norfolk, VA. Dept. of Mechanical Engineering and Mechanics.
THE 1992-1993 ADVANCED DESIGN PROGRAM. PART 1: THE MARS METHANE ENGINE PROJECT. PART 2: THE MARS OXYGEN PROCESSOR NEW FURNACE Final Report
Stephen Lauer, Scott Hoover, Lori Lawrence, Christos Paparistodemou, and Doug Taylor 21 Apr. 1993 173 p
(Contract NASw-4435)
(NASA-CR-195513; NAS 1.26:195513) Avail: CASI HC A08/MF A02

Three constituents of the Martian atmosphere, methane, carbon dioxide, and oxygen, can be used for internal combustion in engines utilized for future space exploration on Mars. These three gases, considered as the test case in this research, will be examined to determine required flow rates needed for combustion and optimization of engine performance. Results of the test case are examined in relation to a base case of methane and air for comparative purposes. Testing of exhaust temperatures, cylinder pressure, and exhaust gas analysis were performed for the base case and test case. Also described is a study utilizing a zirconia cell to convert carbon dioxide into usable oxygen to help support future Mars missions. Derived from text

N94-29420*# National Aeronautics and Space Administration. Pasadena Office, CA.
AN EMERGENCY RESPONSE MOBILE ROBOT FOR OPERATIONS IN COMBUSTIBLE ATMOSPHERES Patent Application
Henry W. Stone, inventor (to NASA) (Jet Propulsion Lab., California Inst. of Tech., Pasadena.) and Timothy R. Ohm, inventor (to NASA) (Jet Propulsion Lab., California Inst. of Tech., Pasadena.) 15 Nov. 1993 21 p
(Contract NAS7-918)
(NASA-Case-NPO-19020-1-CU; NAS 1.71:NPO-19020-1-CU;
US-Patent-Appl-SN-153934) Avail: CASI HC A03/MF A01

A mobile, self-powered, self-contained, and remote-controlled robot is presented. The robot is capable of safely operating in a combustible atmosphere and providing information about the atmosphere to the operator. The robot includes non-sparking and non-arcing electro-mechanical and electronic components designed to prevent the robot from igniting the combustible atmosphere. The robot also includes positively pressurized enclosures that house the electromechanical and electronic components of the robot and prevent intrusion of the combustible atmosphere into the enclosures. The enclosures are interconnected such that a pressurized gas injected into any one of the enclosures is routed to all the other enclosures through the interconnections. It is preferred that one or more sealed internal channels through structures intervening between the enclosures be employed. Pressure transducers for detecting if the pressure within the enclosures falls below a predetermined level are included. The robot also has a sensing device for determining the types of combustible substances in the surrounding atmosphere, as well as the concentrations of each type of substance relative to a pre-determined lower explosive limit (LEL). In addition, the sensing device can determine the percent level of oxygen present in the surrounding atmosphere. NASA

N94-29427* National Aeronautics and Space Administration. Lewis Research Center, Cleveland, OH.

SYSTEM FOR THE INSTALLATION AND REPLACEMENT OF COMPONENTS IN HOSTILE ENVIRONMENTS Patent

Andrew L. Gordan, inventor (to NASA) and James L. Dolce, inventor (to NASA) 1 Mar. 1994 11 p Filed 28 May 1992 Supersedes N93-12203 (31 - 2, p 329)
(NASA-Case-LEW-14906-1-SB; US-Patent-5,290,121;
US-Patent-Appl-SN-889572; US-Patent-Class-403-322;
US-Patent-Class-24-513; US-Patent-Class-74-89.15;
US-Patent-Class-74-436; US-Patent-Class-269-94; US-Patent-Class-269-238;
US-Patent-Class-269-242) Avail: US Patent and Trademark Office

Service equipment for use in hostile environments is presented. The equipment includes a detachable service unit secured to a stationary service unit. The detachable service unit includes a housing with an exterior plate, a power control interface for connection to an exterior power source, locating pins located in said exterior plate, an electrical connector in the exterior plate electrically coupled to said power control interface, and a pair of clamping receptacles formed in the exterior plate and located on adjacent opposite edges of the exterior plate. The stationary unit includes an electrical connector for connection to the electrical connector of the detachable service unit, a clamping apparatus for clamping and unclamping the detachable service unit from the stationary unit, a base clamp assembly for mounting the clamping apparatus onto the stationary unit, and locating pin holes for receiving the locating pins and aligning the detachable service unit onto the stationary unit. The detachable service unit have mating scalloped faces which aid in alignment and provide a mechanism for heat dissipation. Official Gazette of the U.S. Patent and Trademark Office

N94-29428* National Aeronautics and Space Administration. Lyndon B. Johnson Space Center, Houston, TX.

EXTRA-VEHICULAR ACTIVITY TRANSLATION TOOL Patent

Leslie S. Hartz, inventor (to NASA) 1 Mar. 1994 10 p Filed 21 Aug. 1992 Supersedes N93-14842 (31 - 4, p 891)
(NASA-Case-MSC-21955-1; US-Patent-5,289,614;
US-Patent-Appl-SN-931468; US-Patent-Class-16-114R;
US-Patent-Class-16-125; US-Patent-Class-294-1.1;
US-Patent-Class-248-205.3; Int-Patent-Class-E05B-1/00) Avail: US Patent and Trademark Office

A portable hand-grip device for use during extravehicular activity is described. The device has a base member overlaid by a flexible pad having its opposite end releasably secured to the base. The pad includes an adhesive-covered surface which may be attached to a flat surface. A plurality of closely-spaced elongated rigid members are arranged side-by-side across the back of the flexible sheet to reinforce the flexible pad. The ends of these reinforcing members project beyond the opposite sides of the base and flexible pad. A selectively-operable mechanism on the base member releasably captures the outer end of the reinforcing members and secures them when the pad member is attached to a flat surface and provides a load path between a handle on the base and the flexible pad. The selectively-operable mechanism is further arranged to selectively release the reinforcing members so that the device may be progressively peeled away from a wall surface.

Official Gazette of the U.S. Patent and Trademark Office

N94-29448*# National Aeronautics and Space Administration. Lyndon B. Johnson Space Center, Houston, TX.

LANDING GEAR ENERGY ABSORPTION SYSTEM Patent Application

Christopher P. Hansen, inventor (to NASA) 1 Dec. 1993 17 p
(NASA-Case-MSC-22277-1; NAS 1.71:MSC-22277-1;
US-Patent-Appl-SN-159606) Avail: CASI HC A03/MF A01

A landing pad system is described for absorbing horizontal and vertical impact forces upon engagement with a landing surface where circumferentially arranged landing struts respectively have a clevis which receives a slidable rod member and where the upper portion of a slidable rod member is coupled to the clevis by friction washers which are force fit onto the rod member to provide for controlled constant force energy absorption when the rod member moves relative to the clevis. The lower end of the friction rod is pivotally attached by a ball and socket to a support plate where the support plate is arranged to slide in a transverse direction relative to a housing which contains an energy absorption material for absorbing energy in a transverse direction. NASA

N94-29486*# National Aeronautics and Space Administration. Marshall Space Flight Center, Huntsville, AL.

QUICK CONNECT FASTENER Patent Application

Bruce Weddendorf, inventor (to NASA) 27 Jan. 1994 16 p
(NASA-Case-MFS-28829-1; NAS 1.71:MFS-28829-1;
US-Patent-Appl-SN-187032) Avail: CASI HC A03/MF A01

A quick connect fastener and method of use is presented wherein the quick connect fastener is suitable for replacing available bolts and screws, the quick connect fastener being capable of installation by simply pushing a threaded portion of the connector into a member receptacle hole, the inventive apparatus being comprised of an externally threaded fastener having a threaded portion slidably mounted upon a stud or bolt shaft, wherein the externally threaded fastener portion is expandable by a preloaded spring member. The fastener, upon contact with the member receptacle hole, has the capacity of presenting cylindrical threads of a reduced diameter for insertion purposes and once inserted into the receiving threads of the receptacle member hole, are expandable for engagement of the receptacle hole threads forming a quick connect of the fastener and the member to be fastened, the quick connect fastener can be further secured by rotation after insertion, even to the point of locking engagement, the quick connect fastener being disengagable only by reverse rotation of the mated thread engagement. NASA

N94-29506* National Aeronautics and Space Administration. Marshall Space Flight Center, Huntsville, AL.

WELDING WIRE PRESSURE SENSOR ASSEMBLY Patent

Timothy B. Morris, inventor (to NASA), Peter F. Milly, Sr., inventor (to NASA), and J. Kevin White, inventor (to NASA) 12 Apr. 1994 6 p Filed 27 May 1993 Supersedes N93-28951 (31 - 11, p 3442)
(NASA-Case-MFS-26216-1-SB; US-Patent-5,302,805;
US-Patent-Appl-SN-070132; US-Patent-Class-219-137.71;
Int-Patent-Class-B23K-9/12) Avail: US Patent and Trademark Office

The present invention relates to a device which is used to monitor the position of a filler wire relative to a base material being welded as the filler wire is added to a welding pool. The device is applicable to automated welding systems wherein nonconsumable electrode arc welding processes are utilized in conjunction with a filler wire which is added to a weld pool created by the electrode arc. The invention senses pressure deviations from a predetermined pressure between the filler wire and the base material, and provides electrical signals responsive to the deviations for actuating control mechanisms in an automatic welding apparatus so as to minimize the pressure deviation and to prevent disengagement of the contact between the filler wire and the base material.

Official Gazette of the U.S. Patent and Trademark Office

N94-29550*# Scientific Research Associates, Inc., Glastonbury, CT.

CFD ANALYSES FOR ADVANCED PUMP DESIGN Final Report

F. J. deJong, S.-K. Choi, and T. R. Govindan Apr. 1994 57 p Original contains color illustrations

(Contract NAS8-38866)
(NASA-CR-194866; NAS 1.26:194866; R94-9081-F) Avail: CASI HC A04/MF A01; 23 functional color pages

As one of the activities of the NASA/MSFC Pump Stage Technology Team, the present effort was focused on using CFD in the design and analysis of high performance rocket engine pumps. Under this effort, a three-dimensional Navier-Stokes code was used for various inducer and impeller flow field calculations. An existing algebraic grid generation procedure was-extended to allow for nonzero blade thickness, splitter blades, and hub/shroud cavities upstream or downstream of the (main) blades. This resulted in a fast, robust inducer/impeller geometry/grid generation package. Problems associated with running a compressible flow code to simulate an incompressible flow were resolved; related aspects of the numerical algorithm (viz., the matrix preconditioning, the artificial dissipation, and the treatment of low Mach number flows) were addressed. As shown by the calculations performed under the present effort, the resulting code, in conjunction with the grid generation package, is an effective tool for the rapid solution of three-dimensional viscous inducer and impeller flows.

Author (revised)

N94-29552*# Kentucky Univ., Lexington.
EXPERIMENTAL VALIDATION OF FINITE ELEMENT AND BOUNDARY ELEMENT METHODS FOR PREDICTING STRUCTURAL VIBRATION AND RADIATED NOISE Final Report
A. F. Seybert, T. W. Wu, and X. F. Wu Jan. 1994 94 p Original contains color illustrations
(Grant NAG3-912; DA Proj. 1L1-62211-A-47A; RTOP 505-62-10)
(NASA-CR-4561; ARL-CR-109; E-8264; NAS 1.26:4561) Avail: CASI HC A05/MF A01; 3 functional color pages

This research report is presented in three parts. In the first part, acoustical analyses were performed on modes of vibration of the housing of a transmission of a gear test rig developed by NASA. The modes of vibration of the transmission housing were measured using experimental modal analysis. The boundary element method (BEM) was used to calculate the sound pressure and sound intensity on the surface of the housing and the radiation efficiency of each mode. The radiation efficiency of each of the transmission housing modes was then compared to theoretical results for a finite baffled plate. In the second part, analytical and experimental validation of methods to predict structural vibration and radiated noise are presented. A rectangular box excited by a mechanical shaker was used as a vibrating structure. Combined finite element method (FEM) and boundary element method (BEM) models of the apparatus were used to predict the noise level radiated from the box. The FEM was used to predict the vibration, while the BEM was used to predict the sound intensity and total radiated sound power using surface vibration as the input data. Vibration predicted by the FEM model was validated by experimental modal analysis; noise predicted by the BEM was validated by measurements of sound intensity. Three types of results are presented for the total radiated sound power: sound power predicted by the BEM model using vibration data measured on the surface of the box; sound power predicted by the FEM/BEM model; and sound power measured by an acoustic intensity scan. In the third part, the structure used in part two was modified. A rib was attached to the top plate of the structure. The FEM and BEM were then used to predict structural vibration and radiated noise respectively. The predicted vibration and radiated noise were then validated through experimentation.

Author (revised)

N94-29556* National Aeronautics and Space Administration. Goddard Space Flight Center, Greenbelt, MD.
SIMPLIFIED AND SYMMETRICAL FIVE-BAR LINKAGE DRIVER FOR MANIPULATING A SIX-DEGREE-OF-FREEDOM PARALLEL MINIMANIPULATOR WITH THREE INEXTENSIBLE LIMBS Patent
Farhad Tahmasebi, inventor (to NASA) and Lung-Wen Tsai, inventor (to NASA) 12 Apr. 1994 15 p Filed 20 Aug. 1993 Division of US-Patent-Appl-SN-915567, filed 20 Jul. 1992
(NASA-Case-GSC-13485-2; US-Patent-5,301,566;
US-Patent-Appl-SN-110181; US-Patent-Appl-SN-915567;
US-Patent-Class-74-479B; US-Patent-Class-74-469;
US-Patent-Class-74-479PP; US-Patent-Class-901-14;
US-Patent-Class-901-19; Int-Patent-Class-G05G-11/00) Avail: US Patent and Trademark Office

A six degree of freedom parallel manipulator having three inextensible limbs for manipulating a platform is described in which the three inextensible limbs are attached via universal joints to the platform at noncollinear points. Each of the inextensible limbs is also attached via universal joints to a two degree of freedom parallel driver such as a five-bar linkage, a pantograph, or a bidirectional linear stepper motor. The drivers move the lower ends of the limbs parallel to a fixed base and thereby provide manipulation of the platform. The actuators are mounted on the fixed base without using any power transmission devices such as gears or belts.

Official Gazette of the U.S. Patent and Trademark Office

N94-29557* National Aeronautics and Space Administration. Lewis Research Center, Cleveland, OH.
FUSION WELDING WITH SELF-GENERATED FILLER METAL Patent
Thomas J. Moore, inventor (to NASA) and Joseph M. Kalinowski, inventor (to NASA) 8 Feb. 1994 10 p Filed 23 Apr. 1993
(NASA-Case-LEW-15671-1; US-Patent-5,284,290;
US-Patent-Appl-SN-063222; US-Patent-Class-228-211;
US-Patent-Class-228-203; US-Patent-Class-228-232;
US-Patent-Class-428-610; US-Patent-Class-148-512;
Int-Patent-Class-B23K-31/02) Avail: US Patent and Trademark Office

NiAl is preheated to a temperature between 1530 and 1638 C causing some of the aluminum to evaporate along the faying surfaces, thereby forming a glazed layer of nickel rich self-generated filler metal. The glazed faying surfaces are placed in contact, heated to 1530 to 1570 C, and pressed together to form a fusion weld.

Official Gazette of the U.S. Patent and Trademark Office

N94-29679 Helsinki Univ. of Technology, Espoo (Finland).
COMBUSTION AND HEAT TRANSFER IN A HIGH SPEED DIESEL ENGINE OPERATING WITH RAPE SEED OIL METHYL ESTER FUEL
R. Turunen 1994 68 p Limited Reproducibility: More than 20% of this document may be affected by microfiche quality
(PB94-137536; ISBN-951-22-1710-4) Avail: CASI HC A04

The properties of RME (rape seed oil methyl ester) as a fuel for a diesel engine have been investigated theoretically and experimentally. The experiments were made with a turbocharged high-speed DI engine. During experiments the specific fuel consumption, exhaust gas emissions, heat release rate, flame temperature and the temperatures of the combustion chamber walls were measured. A test was also made using the measured flame temperature as an initial value for a two-zone combustion model. The theoretical investigations show that it is possible to achieve with RME approximately the same power as with ordinary diesel fuel from the same cylinder volume. The fuels give very similar theoretical (ideal) working cycles and also the efficiencies of the cycles are very near to each other. NTIS

N94-29847 Columbia Univ., New York, NY.
KINEMATIC REPRESENTATIONS, WORKSPACE ANALYSIS, AND GRASP STABILITY IN ROBOT ARMS AND MULTI-FINGERED HANDS Ph.D. Thesis
Fu-Hua Jen 1992 123 p
Avail: Univ. Microfilms Order No. DA9313618

This work studies three related aspects of robotics: the set of possible kinematic representations of robot motion, the range of all possible robot positions, i.e., the workspace, and the designing of stable grasps with a multifingered end-effector. A survey of alternatives to the homogeneous transformation to represent robot coordinate translations and rotations is given. The advantages and disadvantages of each are discussed, and their computational complexities are compared, giving the number of arithmetic operations required by the different methods. In viewing rigid body motions, two aspects are considered: point transformations, which result in matrix-based transformations, and line transformations, which result in screw-based transformations. Algebraic expressions for the robot workspace are helpful in the design of robots. Here, a complete methodology is developed to obtain algebraic expressions to aid robot workspace construction, based on the analysis of Jacobian matrices. Reduction of the complexity of the workspace analysis is achieved by choice of the coordinate system used in the representation. It is shown that, in the worst case 2 x 2 submatrices of the Jacobian need to be checked, and with some specific kinematic structures, it is sufficient to examine only a set of scalar expressions. Examples of using algebraic expressions to generate workspace without mechanical limitations are given. The third part of this work represents the first application of Liapunov stability theory of differential equations to

the problem of generating stable grasps of an object with a multifingered hand. The analysis of grasp stability where finger forces are maintained constant is considered, as well as certain modified force control laws that introduce damping. In the robotics community there is considerable research emphasis related to the use of force control methods rather than the usual position control, and this motivates the study. Stability theory for nonlinear differential equations is applied to establish the conditions on finger locations and grasp force directions that are associated with Liapunov stability, with asymptotic stability, and with instability of grasps. Relationships are given between these mathematical concepts and various desirable properties of grasp that have previously been used in defining various concepts of stable grasp. A geometrical representation of the stability condition is given which assists the synthesis of the grasp, and examples in two and three dimensions are given. Dissert. Abstr.

N94-29870 Texas A&M Univ., College Station.
A DESIGN METHODOLOGY FOR SYNTHESIZING LOW-ORDER ROBUST CONTROLLERS FOR FLEXIBLE STRUCTURES Ph.D. Thesis
Byung-Keun Song 1992 204 p
Avail: Univ. Microfilms Order No. DA9315147

A design methodology is developed for realizing low order robust controllers for flexible structures modelled as partial differential equations (PDE's). The efficacy of the methodology is illustrated by synthesizing robust controllers for a free-free beam system and a flexible robot link system. The performance of these controllers is evaluated in simulations and in actual implementation on a flexible robot link set up. Reduced (finite) order models are frequently used in designing controllers for flexible structures due to their simplicity. They often lead to control spillover effects which tend to degrade the performance or even destabilize. The control spillover can be completely removed only by designing a controller based on a full (infinite) order model. Recently, full order models have been used for designing controllers by modern robust control design techniques such as H(sub infinity) and H(sub 2). However, the resulting controllers from these techniques typically have excessively high orders since the optimization involved calls for a systematic cancellation of the stable poles and zeros of the plant. The design methodology proposed here is an outgrowth of the standard quantitative feedback theory (QFT) and utilizes the closed form irrational transfer function obtained from an infinite-dimensional model described by hyperbolic PDE's. Although standard QFT has many attractive features such as its capacity to deal with parametric plant uncertainty and cost of feedback, the loop-shaping procedure is not necessarily straightforward. Hence when the standard QFT procedure is applied to these infinite order plants, the loop-shaping procedure becomes even more difficult. The proposed methodology alleviates this by converting the loop-shaping procedure for an infinite order plant into that of a finite order plant by introducing a finite order quasi-nominal plant. In spite of the challenging loop-shaping task, the method provides enough transparency for one to customize the controllers by trading off some design specifications to achieve more practical or realizable controllers. Dissert. Abstr.

N94-29884 Purdue Univ., West Lafayette, IN.
COLLISION AVOIDANCE AND CONTROL OF MULTIPLE REVOLUTE MANIPULATORS Ph.D. Thesis
Zohreh Erfan 1992 120 p
Avail: Univ. Microfilms Order No. DA9313979

In Chapter 1, a survey on collision avoidance for multirobot systems is presented. In Chapter 2, the problem of path planning for a revolute two-link arm, operating in a workspace filled with obstacles whose boundaries are enveloped by circles or possibly any other shape, is addressed. The path planning approach presented in this chapter is developed in the manipulator joint space and consists of two strategies. The first strategy is used in tightly packed free spaces located between the workspace obstacles; this approach relies on constrained optimization. The second strategy is used whenever the manipulator is operating in any free space region far from the workspace obstacles; this strategy does not use optimization but relies on a global but safe approximation of the free regions of the joint space. This division of the path planning approach reduces the chances that the manipulator will get stuck in a geometrical local minimum during the planning procedure, compared to what would likely happen if the first strategy is used throughout the entire path planning procedure. With the approach taken here, the chance of finding a path for the manipulator from its given start point to its desired goal point in an automated manner is high in comparison to one which uses just one of the two approaches. In Chapter 3, the problem of path planning and control of multiple robots operating in a common workspace is addressed. The developments in this chapter merge the control and trajectory planning issues for obstacle avoidance into one. An on-line control law has been determined which avoids collisions between the arms while guiding the end-effectors from their respective starting positions S to their respective desired goal positions G, if such a collision free trajectory exists. The control law is determined from a Lyapunov function based on the total system energy. Simulation results are presented which show that the control scheme developed in this chapter is able to guide two manipulators working in a common workspace avoid collisions with each other as they reach their goal points. No off-line path planning involving geometric analysis is necessary for this scheme to work if a collision free trajectory is feasible. Dissert. Abstr.

N94-29916 Texas A&M Univ., College Station.
ROTORDYNAMIC ANALYSIS OF ANNULAR HONEYCOMB-STATOR TURBULENT GAS SEALS USING A NEW FRICTION-FACTOR MODEL BASED ON FLAT PLATE TESTS Ph.D. Thesis
Tae Woong Ha 1992 193 p
Avail: Univ. Microfilms Order No. DA9315067

A flat plate tester with various honeycomb geometries has been extended to develop a better understanding of the friction-factor behavior of honeycomb surfaces. The friction-factor-jump phenomenon, which is characterized by the dramatic drop and then rise of the friction-factor with increasing Reynolds number, has been explained by acoustic excitation of a large scale coherent flow structure from pressure fluctuation measurements inside the honeycomb cavities. A new friction-factor model based on the flat-plate-test results has been developed as a function of Mach number, dimensionless pressure, and honeycomb geometry variables. A rotordynamic analysis has been developed for centered, turbulent-annular honeycomb-stator seals incorporating the new empirical friction-factor model for honeycomb-stator surfaces. The validity of the new analysis in predicting the rotordynamic and leakage characteristics has been compared to Moody's friction-factor model analysis and experimental data for a short (L/D = 1/6, 25.4 mm long) seal and a longer (L/D = 1/3, 50.8 mm long) seal. The comparisons show that the new honeycomb friction-factor model greatly improves the predictions of leakage and rotordynamic coefficients compared to Moody's friction-factor model for both the short and longer seal, especially, for direct stiffness and cross-coupled stiffness. The new honeycomb friction-factor model predicts leakage and rotordynamic coefficients better for the short than the longer seals. Dissert. Abstr.

N94-29922# Midwest Research Inst., Golden, CO. National Renewable Energy Lab.
ANALYSIS OF DATA FROM ELECTRIC AND HYBRID ELECTRIC VEHICLE STUDENT COMPETITIONS
K. B. Wipke, N. Hill, and R. P. Larsen Jan. 1994 13 p Presented at the Society of Automotive Engineers (SAE) Congress and Exposition, Detroit, MI, 28 Feb. - 3 Mar. 1994
(Contract DE-AC02-83CH-10093)
(DE94-000269; NREL/TP-473-6227; CONF-940242-1) Avail: CASI HC A03/MF A01

The U.S. Department of Energy sponsored several student engineering competitions in 1993 that provided useful information on electric and hybrid electric vehicles. The electrical energy usage from these competitions has been recorded with a custom-built digital meter installed in every vehicle and used under controlled conditions. When combined with other factors, such as vehicle mass, speed, distance traveled, battery type, and type of components, this information provides useful insight into the performance characteristics of electrics and hybrids. All the vehicles tested were either electric vehicles or hybrid vehicles in electric-only mode, and had an average energy economy of 7.0 km/kwh. Based on the performance of the 'ground-up' hybrid electric vehicles in the 1993 Hybrid Electric Vehicle Challenge, data revealed a 1 km/kwh energy economy benefit for every 133 kg decrease in vehicle mass. By running all the electric vehicles at a competition in Atlanta at several different constant speeds, the effects of rolling resistance and aerodynamic drag were evaluated. On average, these vehicles were 32% more energy efficient at 40 km/h than at 72 km/h. The results of the competition data analysis confirm that these engineering competitions not only provide an educational experience for the students,

but also show technology performance and improvements in electric and hybrid vehicles by setting benchmarks and revealing trends. DOE

N94-29966 Illinois Univ., Urbana-Champaign.
STOCHASTIC STABILITY AND NONLINEAR CONTROL IN MECHANICAL SYSTEMS Ph.D. Thesis
Sanjiv Talwar 1993 209 p
Avail: Univ. Microfilms Order No. DA9314948

Almost-sure asymptotic stability of 3 and 4 dimensional co-dimension two dynamical systems under small intensity stochastic excitations is investigated. The method of stochastic averaging is used to derive a set of approximate Ito equations which are then examined to obtain the almost-sure stability conditions. The sample properties of the process are based on the boundary behavior of the associated scalar diffusion process of the amplitude Ito equations. This method is then applied to a linear, gyroscopic problem of a rotating shaft with a random loading demonstrating the conservative nature of mean square stability. In addition to stochastic excitations, many systems also undergo harmonic loading. The almost-sure stability of two degree-of-freedom systems subjected to both random and harmonic excitation is then investigated. In this analysis, stochastic averaging followed by a perturbation theoretic approximation is used to facilitate the solution of the multi-dimensional diffusive Markov process. The emerging field of nonlinear control theory has attempted to alleviate the problem associated with applying linear control theory to nonlinear problems. A segment of nonlinear control theory, called exact feedback linearization, has proven useful in a class of problems satisfying certain controllability and integrability constraints. Approximate feedback linearization has enlarged this class by weakening the integrability conditions, but application of both these techniques remains limited to problems in which a series of linear partial differential equations can easily be solved. By use of the idea of normal forms, from dynamical systems theory, a method of obtaining the necessary coordinate transformation and nonlinear feedback rules is given. This method, algebraic in nature, is valid for any dimensional system and any order nonlinearity provided it meets the approximate feedback linearization conditions. Dissert. Abstr.

N94-30019# National Research Council of Canada, Ottawa (Ontario). Tribology and Mechanics Lab.
SLIDING FRICTION AND WEAR BETWEEN TITANIUM NITRIDE, M50 STEEL AND SILICON NITRIDE (ROUND 3 OF VAMAS WEAR TEST PROGRAM)
S. K. Yick and H. M. Hawthorne Feb. 1994 42 p
(IMR-TM-TR-003; CTN-94-61134) Avail: CASI HC A03/MF A01

As a continuation of the Versailles Project on Advanced Materials and Standards (VAMAS) wear test program, a series of wear tests was conducted on common source specimens of M50 steel, TiN coating, and Si3N4. The objective of the program is to obtain reliable information on the reproducibility of test results for establishing internationally agreed-to wear test methodology. Results of the unlubricated sliding wear tests of three material pair combinations performed on a pin-on-disc tribometer using new test procedures are reported. The friction and wear behavior of each material pair is discussed in relation to the morphology of the wear debris generated on the worn specimen surfaces. The unworn TiN coatings on the disc specimens are characterized by surface profilometry and ultra micro indentation. The three material combinations are ranked, with regard to both friction and wear, in the order M50/TiN - Si3N4/TiN - TiN/TiN. Author (CISTI)

N94-30135 British Columbia Univ., Vancouver. Dept. of Mechanical Engineering.
A STUDY OF THE FLEXIBLE SPACE PLATFORM BASED DEPLOYABLE MANIPULATOR Ph.D. Thesis
Itshak Marom Jul. 1993 196 p
(ISBN-0-315-85410-3; CTN-94-61156) Copyright Avail: Micromedia Ltd., Technical Information Centre, 240 Catherine Street, Suite 305, Ottawa, Ontario, K2P 2G8, Canada HC/MF

A relatively general formulation is presented for studying the nonlinear dynamics and control of a flexible space-based mobile deployable manipulator. The formulation is applicable to a two-link deployable manipulator translating along a flexible space platform. The manipulator's revolute and prismatic joints are flexible with finite gear ratio and rotor inertia. The nonlinear nonautonomous and coupled equations of motion are presented in compact form, and validity of the formulation and computer code were established through checks on conservation of system energy and comparison with test cases. Results of the dynamical analysis clearly show that under critical combinations of parameters, the system can become unstable. An inverse kinematic technique, accounting for the linear and angular displacements of the flexible platform, has been developed to meet the desired position and orientation requirement of the end effector with respect to the chosen reference frame. A nonlinear control strategy based on the feedback linearization technique was developed to ensure accurate tracking of a desired trajectory in presence of system libration as well as the base translations and vibrations. Closed loop simulation results show that a desired degree of system stability and high tracking accuracy can be achieved. Author (CISTI)

N94-30173*# National Aeronautics and Space Administration. Marshall Space Flight Center, Huntsville, AL.
TERNARY ARC GAS PLASMA WELDING TORCH Patent Application
Daniel J. Rybicki, inventor (to NASA) (Martin Marietta Corp., Huntsville, AL.), William F. McGee, inventor (to NASA) (Martin Marietta Corp., Huntsville, AL.), and Douglas J. Waldron, inventor (to NASA) (Waldron, Douglas J..) 27 Dec. 1993 12 p
(NASA-Case-MFS-28857-1; NAS 1.71:MFS-28857-1; US-Patent-Appl-SN-172961) Avail: CASI HC A03/MF A01

A plasma arc welding torch wherein a first plasma gas is directed through the body of the welding torch and out of the body across the tip of a welding electrode disposed at the forward end of the body. A second plasma gas is disposed for flow through a longitudinal bore in the electrode. The second plasma gas enters one end of the electrode and exits the electrode at the tip thereof for co-acting with the electric welding arc to produce the desired weld. A shield gas is directed through the torch body for circulating around the head of the torch adjacent to the electrode tip. NASA

N94-30205*# Illinois Univ., Chicago.
GENERATION OF GEAR TOOTH SURFACES BY APPLICATION OF CNC MACHINES Final Report
F. L. Litvin and N. X. Chen Apr. 1994 84 p
(Grant NAG3-1263; DA Proj. 1L1-62211-A-47-A; RTOP 505-62-36)
(NASA-CR-195306; E-8712; NAS 1.26:195306; ARL-CR-145) Avail: CASI HC A05/MF A01

This study will demonstrate the importance of application of computer numerically controlled (CNC) machines in generation of gear tooth surfaces with new topology. This topology decreases gear vibration and will extend the gear capacity and service life. A preliminary investigation by a tooth contact analysis (TCA) program has shown that gear tooth surfaces in line contact (for instance, involute helical gears with parallel axes, worm gear drives with cylindrical worms, etc.) are very sensitive to angular errors of misalignment that cause edge contact and an unfavorable shape of transmission errors and vibration. The new topology of gear tooth surfaces is based on the localization of bearing contact, and the synthesis of a predesigned parabolic function of transmission errors that is able to absorb a piecewise linear function of transmission errors caused by gear misalignment. The report will describe the following topics: description of kinematics of CNC machines with six degrees of freedom that can be applied for generation of gear tooth surfaces with new topology. A new method for grinding of gear tooth surfaces by a cone surface or surface of revolution based on application of CNC machines is described. This method provides an optimal approximation of the ground surface to the given one. This method is especially beneficial when undeveloped ruled surfaces are to be ground. Execution of motions of the CNC machine is also described. The solution to this problem can be applied as well for the transfer of machine tool settings from a conventional generator to the CNC machine. The developed theory required the derivation of a modified equation of meshing based on application of the concept of space curves, space curves represented on surfaces, geodesic curvature, surface torsion, etc. Condensed information on these topics of differential geometry is provided as well. Author (revised)

N94-30227*# National Aeronautics and Space Administration. Lewis Research Center, Cleveland, OH.
SURFACE FATIGUE LIFE OF HIGH TEMPERATURE GEAR MATERIALS
Dennis P. Townsend Apr. 1994 12 p Proposed for presentation at

the 30th Joint Propulsion Conference, Indianapolis, IN, 27-29 Jun. 1994; sponsored by AIAA, ASME, SAE, and ASEE
(DA Proj. 1L1-62211-A-47-A; RTOP 505-62-36)
(NASA-TM-106562; E-8738; NAS 1.15:106562; ARL-TR-401; AIAA Paper 94-3078) Avail: CASI HC A03/MF A01

Three high temperature gear materials were evaluated using spur gear surface fatigue tests. These materials were, VASCO max 350, VASCO matrix 2, and nitralloy N and were evaluated for possible use in high temperature gear applications. The fatigue life of the three high temperature gear materials were compared with the life of the standard AISI 9310 aircraft gear material. Surface fatigue tests were conducted at a lubricant inlet temperature of 321 K (120 F), a lubricant outlet temperature of 350 K (170 F), a maximum Hertz stress of 1.71 GPa (248 ksi), a speed of 10,000 rpm, and with a synthetic paraffinic lubricant. The life of the nitralloy N was approximately the same as the AISI 9310, the life of the VASCO max 350 was much less than the AISI 9310 while the life of the VASCO matrix 2 was several times the life of the AISI 9310. The VASCO max 350 also showed very low fracture toughness with approximately half of the gears failed by tooth fracture through the fatigue spall. The VASCO matrix 2 had approximately 10-percent fracture failure through the fatigue spalls indicating moderate to good fracture toughness. Author (revised)

N94-30230 Texas Technological Univ., Lubbock.
NUMERICAL PREDICTION OF MIXING PROCESS IN A METHANE-FUELED ENGINE Ph.D. Thesis
Mehmet Emin Arici 1993 179 p
Avail: Univ. Microfilms Order No. DA9325771

One of the most important factors controlling the combustion process within internal combustion engines is the charge mixing. The charge mixing process in a gaseous fueled engine is different than that in a liquid fueled engine. In a conventional liquid fueled engine, the liquid fuel goes through the process of vaporization before the gaseous mixing takes place. Gaseous fuels, on the other hand, are already in a vapor form and do not go through the vaporization process. Among the gaseous fuels, natural gas, which consists of about 90 percent methane, is gaining acceptance because of its low emission levels and alternative energy source concerns. Introducing methane into the conventional spark ignition engine intake system causes about a 10 percent engine power loss contributed by low density of the fuel. By introducing natural gas directly into the engine cylinder, this power loss can be reduced. The present work concerns numerical prediction of in-cylinder methane/air mixing preparation. A computer-based solution procedure, which employs a finite difference solution of general conservation equations of motion in a piston/cylinder assembly, has been developed to predict the fuel/air mixing characteristics. This solution procedure has been used as a predictive tool to investigate the dependence of charge mixing characteristics on the flow field in the absence of combustion. Computational results show that the flow field has a great effect on charge mixing. The fuel/air mixing characteristics at the time of initiation of combustion are satisfactorily close to the mixing requirements when the fuel charging is prescribed properly. Dissert. Abstr.

N94-30238 British Columbia Univ., Vancouver. Dept. of Electrical Engineering.
EXPERIMENTAL SLIDING MODE CONTROL OF A FLEXIBLE SINGLE LINK MANIPULATOR Ph.D. Thesis
Timothy Wei Tie Qian Sep. 1993 215 p
(ISBN-0-315-85466-9; CTN-94-61161) Copyright Avail: Micromedia Ltd., Technical Information Centre, 240 Catherine Street, Suite 305, Ottawa, Ontario, K2P 2G8, Canada HC/MF

A study was conducted to explore and develop practical controller designs for a flexible manipulator based on the variable structure (VS) system and sliding mode (SM) theory. A new control design method is first proposed based on the continuous time VSSM theory, which can significantly simplify the VS system design process. Moreover, the variables concerned can be assigned separate gains. Direct application of the VSSM control system to the flexible arm, however, has limitations due to the inherent properties of the system. To solve this problem, facilitate digital implementation, and eliminate undesirable chattering in conventional VS system control, the discrete time quasi sliding mode control (DQSMC) is developed. Two control algorithms are derived satisfying the conditions for existence of discrete time sliding hypersurfaces. It is proven that the DQSMC design is equivalent to a full state feedback with its steady state motion constrained to the sliding hypersurfaces, and that DQSMC provides a general structure unifying the three different kinds of discrete time SM control. Experimental testing of the DQSMC controller showed good results, which compared favorably to the linear quadratic Gaussian controller under the same load variations. A novel approach was then devised to realize the proposed new controller designs. Author (CISTI)

N94-30269# New Energy and Industrial Technology Development Organization, Tokyo (Japan).
TECHNICAL ANALYSIS OF ALTERNATIVE FUELED VEHICLES
Mar. 1993 10 p
(DE94-744238; ETDE/JP-MF-94744238) Avail: CASI HC A02/MF A01

The current status of alternative fueled vehicles, such as methanol fueled, compressed natural gas (CNG) fueled, and electric vehicles, that have feasibility to take the place of oil fueled ones is analyzed from the viewpoints of environmental pollution control, energy resources conservation, and economic performances. As for environmental pollution control, these three vehicles are compared by such items as nitrogen oxides, photochemical reactivity, adaptability to future regulations, earth warming substances, and toxicity. As for practical applicability, the following items are compared: power density (torque, power, acceleration performance), energy density, range, energy consumption, vehicle initial costs, energy costs, freight transportation energy costs (yen/ton/km), and energy supply suitability. Conclusions include: methanol vehicles have the problem of fueling stations to be arranged; since CNG vehicles are considered to be loaded with CNG fuel tanks on the top of vehicles, safety must be ensured; electric vehicles still have many problems in spite of their many advantages. DOE

N94-30275 Defence Research Establishment Suffield, Medicine Hat (Alberta).
PROCEEDINGS OF THE 3RD CONFERENCE ON MILITARY ROBOTIC APPLICATIONS
David J. Mackay, ed. 1991 349 p Conference held in Medicine Hat, Alberta, 9-12 Sep. 1991 Prepared in cooperation with Alberta Research Council, Edmonton
(DRES-SP-149; CTN-94-61130) Avail: Issuing Activity (Defence Research Establishment Suffield, P.O. Box 4000, Medicine Hat, AB T1A 8K6 Canada)

A conference on military robotics focused on developments in intelligent robotic systems for military applications and on advances in component technologies. The objective of the conference was to provide a forum for representatives from government, industry, and universities to meet and discuss advances in the field of intelligent robotic systems. Papers were presented on battlefield robotics, guidance and navigation, robotic arm control, robotic sensing, supervisory control, and unmanned vehicles. Separate abstracts have been prepared for 37 papers from this conference. For individual titles, see N94-30276 through N94-30312.

N94-30276 Robotic Technology, Inc., Potomac, MD.
AUTONOMOUS INTELLIGENT MILITARY ROBOTS: ARMY ANTS, KILLER BEES, AND CYBERNETIC SOLDIERS
Robert Finkelstein *In* Defence Research Establishment Suffield, Proceedings of the 3rd Conference on Military Robotic Applications 1991 p 4-11 (For primary document see N94-30275 08-37)
Avail: Issuing Activity (Defence Research Establishment Suffield, P.O. Box 4000, Medicine Hat, AB T1A 8K6 Canada)

The rationale for developing autonomous intelligent robots in the military is to render conventional warfare systems ineffective and indefensible. The Desert Storm operation demonstrated the effectiveness of such systems as unmanned air and ground vehicles and indicated the future possibilities of robotic technology. Robotic military vehicles would have the advantages of expendability, low cost, lower complexity compared to manned systems, survivability, maneuverability, and a capability to share in instantaneous communication and distributed processing of combat information. Basic characteristics of intelligent systems and hierarchical control systems with sensor inputs are described. Genetic algorithms are seen as a means of achieving appropriate levels of intelligence in a robotic system. Potential impacts of robotic technology in the military are outlined. Author (CISTI)

N94-30277 Department of National Defence, Ottawa (Ontario).
ROBOTICS AND THE BATTLEFIELD OF THE FUTURE

Erik Solem *In* Defence Research Establishment Suffield, Proceedings of the 3rd Conference on Military Robotic Applications 1991 p 19-25 (For primary document see N94-30275 08-37)
Avail: Issuing Activity (Defence Research Establishment Suffield, P.O. Box 4000, Medicine Hat, AB T1A 8K6 Canada)

The possible future roles for robotics are discussed from a military and strategic point of view. The future battlefield itself is then examined along with some of the anticipated changes which may take place. Robotics is likely to play a major role in future military operations. Robotic equipment will be increasingly used on the battlefield, aboard ships, on land, in the air, and in space applications. Potential application areas extend beyond such important operations as minefield clearing, reconnaissance, ammunition handling, and construction tasks. The future battlefield itself will change with the introduction of new forms and factors of combat. There will be qualitatively different forms of conflict in which robotics may play specific and important roles, such as masked clashes, anti-terrorist activities, and anti-industrial sabotage operations. The battlefield itself will widen and include new strategic factors of increasing importance. Our understanding and use of robotics will also change. Nonconventional strategies are needed as are new and different conflict scenarios, some of which are examined.
Author (CISTI)

N94-30278 Defence Research Establishment Valcartier (Quebec).
DREV ACTIVITIES RELATED TO MILITARY VEHICLES ROBOTIZATION
B. Montminy *In* Defence Research Establishment Suffield, Proceedings of the 3rd Conference on Military Robotic Applications 1991 p 37-41 (For primary document see N94-30275 08-37)
Avail: Issuing Activity (Defence Research Establishment Suffield, P.O. Box 4000, Medicine Hat, AB T1A 8K6 Canada)

The Defence Research Establishment Valcartier (DREV) is involved in a number of activities aimed at improving the performance of systems installed aboard military vehicles, automating functions normally carried out by human operators, and adding new functions that become essential to cope with new scenarios and threats. These activities relate to the development of sensors that sense the surrounding environment, processors that interpret the sensor data, and actuators that perform various robotic actions. DREV research related to those activities is reviewed as they relate to robotics which continues to increase the portion of vehicular function that is carried out autonomously. Of special interest is the CF aircraft robotization project which aims to develop an autonomous integrated aircraft protection system to detect and counter threats without any human intervention. This research involves development of means for passive surveillance of the surrounding environment, processing of multisensor data, triggering of sensing-aid devices, and actuation of countermeasures that modify the environment.
Author (CISTI)

N94-30279 International Submarine Engineering Ltd., Port Coquitlam (British Columbia).
AUTONOMOUS ROBOTIC REFUELING SYSTEM (ARRS) FOR RAPID AIRCRAFT TURNAROUND
O. R. Williams, E. Jackson, K. Rueb, B. Thompson, and K. Powell *In* Defence Research Establishment Suffield, Proceedings of the 3rd Conference on Military Robotic Applications 1991 p 42-46 (For primary document see N94-30275 08-37)
Avail: Issuing Activity (Defence Research Establishment Suffield, P.O. Box 4000, Medicine Hat, AB T1A 8K6 Canada)

An autonomous robotic refuelling system is being developed to achieve rapid aircraft turnaround, notably during combat operations. The proposed system includes a gantry positioner with sufficient reach to position a robotic arm that performs the refuelling tasks; a six degree of freedom manipulator equipped with a remote center of compliance, torque sensor, and a gripper that can handle standard tools; a computer vision system to locate and guide the refuelling nozzle, inspect the nozzle, and avoid collisions; and an operator interface with video and graphics display. The control system software will include components designed for trajectory planning and generation, collision detection, sensor interfacing, sensory processing, and human interfacing. The robotic system will be designed so that upgrading to perform additional tasks will be relatively straightforward.
Author (CISTI)

N94-30280 National Research Council of Canada, Ottawa (Ontario). Autonomous Systems Lab.
THE NRC MOBILE ROBOT PROJECT
Ramiro Liscano, David Green, Allan Manz, Larry Korba, and Sherman Lang *In* Defence Research Establishment Suffield, Proceedings of the 3rd Conference on Military Robotic Applications 1991 p 47-53 (For primary document see N94-30275 08-37)
Avail: Issuing Activity (Defence Research Establishment Suffield, P.O. Box 4000, Medicine Hat, AB T1A 8K6 Canada)

An overview is presented of the autonomous mobile robot project being conducted at the National Research Council of Canada. The main area of investigation is autonomous navigation of a vehicle in an indoor environment. A brief outline is given of a line-of-sight path planning algorithm which uses line representations of data from a laser range scanner to compute a collision-free path through a cluttered environment. This is followed by a description of a reflexive collision avoidance algorithm based on a histogram representation of ultrasound sensor data extracted from a certainty grid. Implementation details of these two collision avoidance methods on an autonomous platform is also described. The research is aimed at eventually designing a system to navigate in an indoor environment autonomously and to be robust enough to do this reliably.
Author (CISTI)

N94-30281 University of Western Ontario, London.
EXTENDED OCCUPANCY GRID METHOD FOR MODELLING UNKNOWN DYNAMIC ENVIRONMENTS **c04**
Robert E. Webber and Yue-Feng Zhang *In* Defence Research Establishment Suffield, Proceedings of the 3rd Conference on Military Robotic Applications 1991 p 54-60 (For primary document see N94-30275 08-37)
Avail: Issuing Activity (Defence Research Establishment Suffield, P.O. Box 4000, Medicine Hat, AB T1A 8K6 Canada)

The occupancy grid method represents a region to be navigated as a grid of cells. Within each cell, there is an associated probability that the cell is occupied given a robot's knowledge coming from sensor readings. The behavior of the sensors is modelled conceptually by an array of probabilities. A Bayesian updating procedure allows each sensor reading to be combined with existing knowledge to produce a new worldview. Path planning can then be performed directly on the grid information without additional scene analysis processing. The occupancy grid method was developed for handling a world where the robot was the only moving object, thus it lacks the ability to predict the location of a moving obstacle at some future time. An approach has been developed for extending the method to handle obstacles moving at constant velocity. The two dimensional grid representation is extended to be a four dimensional representation of location and velocity combinations. Each grid cell stores the probability that there is not an obstacle at time t at location x,y moving with velocity Vx,Vy. Experiments with a number of rules for combining the sensor information with grid values to produce new grid values are reported and evaluated.
Author (CISTI)

N94-30282* National Aeronautics and Space Administration, Washington, DC.
NAVIGATION OF MILITARY AND SPACE UNMANNED GROUND VEHICLES IN UNSTRUCTURED TERRAINS **c04**
Paul Lescoe (Army Tank-Automotive Command, Warren, MI.), David Lavery, and Roger Bedard *In* Defence Research Establishment Suffield, Proceedings of the 3rd Conference on Military Robotic Applications 1991 p 61-67 (For primary document see N94-30275 08-37)
Avail: Issuing Activity (Defence Research Establishment Suffield, P.O. Box 4000, Medicine Hat, AB T1A 8K6 Canada)

Development of unmanned vehicles for local navigation in terrains unstructured by humans is reviewed. Modes of navigation include teleoperation or remote control, computer assisted remote driving (CARD), and semiautonomous navigation (SAN). A first implementation of a CARD system was successfully tested using the Robotic Technology Test Vehicle developed by Jet Propulsion Laboratory. Stereo pictures were transmitted to a remotely located human operator, who performed the sensing, perception, and planning functions of navigation. A computer provided range and angle measurements and the path plan was transmitted to the vehicle which autonomously executed the path. This implementation is to be enhanced by providing passive stereo vision and a reflex control system for autonomously stopping the vehicle if blocked by an obstacle. SAN

achievements include implementation of a navigation testbed on a six wheel, three-body articulated rover vehicle, development of SAN algorithms and code, integration of SAN software onto the vehicle, and a successful feasibility demonstration that represents a step forward towards the technology required for long-range exploration of the lunar or Martian surface. The vehicle includes a passive stereo vision system with real-time area-based stereo image correlation, a terrain matcher, a path planner, and a path execution planner. Author (CISTI)

N94-30283 Defence Research Establishment Suffield, Medicine Hat (Alberta).
A GENERIC SEMI-AUTONOMOUS GROUND VEHICLE CONTROL SYSTEM **c63**
Ron Eirich and Alan Kramer *In its* Proceedings of the 3rd Conference on Military Robotic Applications 1991 p 68-73 (For primary document see N94-30275 08-37)
Avail: Issuing Activity (Defence Research Establishment Suffield, P.O. Box 4000, Medicine Hat, AB T1A 8K6 Canada)

A generic control system has been developed which is capable of piloting virtually any surface vehicle and navigating semi autonomously to deliver a payload. The system permits an incremental approach to autonomy, since software and hardware modules can be easily added as developments occur. The modular nature of the system also enables quick repair and allows it to be easily installed on any ground vehicle just by redesigning a personality module for that vehicle. The first phases of development involved extensive system definition and construction of hardware to enable tele-operated control. The second phase added semiautonomous operation utilizing global positioning system information. Subsequent phases will add obstacle detection and avoidance, multiple vehicle control, and route planning. Field trials have shown the system to operate reliably over long distances. The system's vehicle electronics package and control station are described and some operational roles in both military and civilian applications are outlined. Author (CISTI)

N94-30284 Combustion Dynamics Ltd., Medicine Hat (Alberta).
PAYLOAD CENTRAL CONTROL FOR UNMANNED AIRCRAFT **c08**
D. R. Weiler, M. G. Henders, R. H. Chesney, and D. Ehman *In* Defence Research Establishment Suffield, Proceedings of the 3rd Conference on Military Robotic Applications 1991 p 74-80 (For primary document see N94-30275 08-37)
Avail: Issuing Activity (Defence Research Establishment Suffield, P.O. Box 4000, Medicine Hat, AB T1A 8K6 Canada)

A control system concept is being developed for use in unmanned surveillance aircraft to control the aircraft automatically in response to the imagin g sensor payload requirement. The implementation of such a control system is discussed and results of simulation tests are presented. Author (CISTI)

N94-30285 Defence Research Establishment Suffield, Medicine Hat (Alberta).
THE USE OF LOW COST DIFFERENTIAL MODE GPS RECEIVERS IN UNMANNED VEHICLES **c04**
Thomas E. Ollevier *In its* Proceedings of the 3rd Conference on Military Robotic Applications 1991 p 81-85 (For primary document see N94-30275 08-37)
Avail: Issuing Activity (Defence Research Establishment Suffield, P.O. Box 4000, Medicine Hat, AB T1A 8K6 Canada)

A critical component of the guidance and control system of an unmanned vehicle is the position and attitude determination system. This system determines the accuracy with which the unmanned vehicle system can determine the position of the behicle and hence the position of the object in the vehicle's sensor field of view. Author (CISTI)

N94-30286 Ottawa Univ. (Ontario). Dept. of Electrical Engineering.
ENCODING TECHNIQUE FOR AUTOMATED GUIDED VEHICLE POSE RECOVERY IN A STRUCTURED ENVIRONMENT **c04**
E. Petriu, T. Bieseman, N. Trif, W. S. McMath, and S. K. Yeung *In* Defence Research Establishment Suffield, Proceedings of the 3rd Conference on Military Robotic Applications 1991 p 86-92 (For primary document see N94-30275 08-37)
Avail: Issuing Activity (Defence Research Establishment Suffield, P.O. Box 4000, Medicine Hat, AB T1A 8K6 Canada)

A new position orientation and scaling estimation (POSE) recovery method is presented for a free-ranging automated guided vehicle (AGV) moving in an encoded environment using vision. The environment is structured by permanently encoding the floor with the terms, marked by distinct graphical symbols, of a pseudo random binary array (PBRA) requiring only one bit of code per quantization interval, independent of the desired resolution. The PRBA-based two-dimensional encoding method is discussed and results of its application in an experimental AGV for absolute position recovery are described. The proposed PRBA-based POSE recovery technique is restricted in applicability to controllable environments such as nuclear plants and space stations which allow for object encoding and a-priori mapping of all encoded surfaces in a geometric data base. The experiments validated the performance and practical value of the encoding method presented. Author (CISTI)

N94-30287 Royal Military Coll. of Canada, Kingston (Ontario). Dept. of Electrical and Computer Engineering.
AN OPTIMAL OBSTACLE AVOIDANCE PATH PLANNING ALGORITHM FOR THE EXCALIBUR ROBOT **c63**
V. Banerjee, C. Earl, T. D. Looke, and M. Farooq *In* Defence Research Establishment Suffield, Proceedings of the 3rd Conference on Military Robotic Applications 1991 p 93-98 (For primary document see N94-30275 08-37)
Avail: Issuing Activity (Defence Research Establishment Suffield, P.O. Box 4000, Medicine Hat, AB T1A 8K6 Canada)

An algorithm was developed using a heuristic approach to solve the problem of obstacle avoidance of a robot arm and payload moving among cylindrical obstacles. The algorithm is optimized with respect to minimum distance and minimum joint rotation criteria. The strategy was implemented and tested on a laboratory Excalibur robot using Automatix's RAIL programming language on a Macintosh IIx. The algorithm is described in its six steps: obstacle identification, obstacle prioritization, feasible path set creation, optimal path selection, optimal path execution, and position update. The algorithm is iterative; once all the obstacles have been identified and prioritized, the last four steps of the algorithm are accomplished for each obstacle separately in order of priority. A more in-depth strategy is provided for critical situations when an object is in the line of sight between the base coordinate system and the desired manipulator position, or when each of the avoidance paths is found to be non-feasible. The path planning obstacle avoiding algorithm is a simple and effective solution to the problem of moving the Excalibur robot arm in a restricted workspace. Author (CISTI)

N94-30288 National Research Council of Canada, Ottawa (Ontario). Inst. for Information Technology.
MAESTRO: AN OPEN SYSTEM ARCHITECTURE FOR MULTI-ROBOT CONTROL **c63**
Shadia Elgazzar and Arthur Castonguay *In* Defence Research Establishment Suffield, Proceedings of the 3rd Conference on Military Robotic Applications 1991 p 99-106 (For primary document see N94-30275 08-37)
Avail: Issuing Activity (Defence Research Establishment Suffield, P.O. Box 4000, Medicine Hat, AB T1A 8K6 Canada)

Replacing the robot controller supplied by the manufacturer with a multiprocessor system based on an industry standard microcomputer system bus and an object based software architecture results in a flexible open system architecture for single/multiple robot control. This architecture allows the integration of sensors and other peripherals in an effective and simple way, and is able to meet the realtime requirements of the system. The controller has been named Maestro to complement Harmony, the name of the operating system, and to convey the idea of conducting multiple robots. The hardware implementation and software functionality of Maestro is presented along with the available robot system environments and robot programming levels. The task structure for Maestro and the method used for communication and synchronization are also detailed. An object-oriented software design has allowed extraction of inherent parallelism in the controller, which was then exploited using the available hardware architecture and operating system. Author (CISTI)

N94-30289 Thomson-CSF Systems Canada, Inc., Ottawa (Ontario).
COORDINATED CONTROL OF MULTIPLE ROBOT MANIPULATORS
S. Kalaycioglu and D. S. Necsulescu *In* Defence Research Establishment

Suffield, Proceedings of the 3rd Conference on Military Robotic Applications 1991 p 107-113 (For primary document see N94-30275 08-37)
Avail: Issuing Activity (Defence Research Establishment Suffield, P.O. Box 4000, Medicine Hat, AB T1A 8K6 Canada)

The coordination of multiple robots is achieved by the control of each arm in a nonconflicting way as the robots control the position of an object being handled. An analysis of the load distribution problems for coordinating robots handling a single payload is carried out and an optimal load sharing algorithm is applied to a possible task. The minimum (norm) joint torques and minimum contact forces are obtained by the minimization of a quadratic function associated with the joint torques and the force vectors of multiple robot arms with the constraints of the robot system equations. The applied algorithm is not computationally intensive compared with existing algorithms described in the literature and is therefore very attractive for real-time applications. The effectiveness of the control strategy for coordinated motion of the robots performing different tasks is checked by digital simulation. It is noted that the control strategy is very effective and the investigated control architecture is well suited for a distributed computer architecture. Author (CISTI)

N94-30290 Defence Research Establishment Pacific, Victoria (British Columbia).
THREE METHODS TO IMPROVE THE ACCURACY OF A PUMA 560 ROBOT **c63**
G. R. Hardy *In* Defence Research Establishment Suffield, Proceedings of the 3rd Conference on Military Robotic Applications 1991 p 114-121 (For primary document see N94-30275 08-37)
Avail: Issuing Activity (Defence Research Establishment Suffield, P.O. Box 4000, Medicine Hat, AB T1A 8K6 Canada)

It is planned to use the PUMA 560 six-axis robotic arm to scan surface areas of CF-18 aircraft with an ultrasonic scanner to detect delaminations in composite materials. A problem with using a robot to perform repeatable scans on a CF-18 is accuracy. Although the calibration method is accurate enough at the present time, it is complex to implement and requires a very fast computer to correct errors in realtime. Three simple methods to improve scanning accuracy are compared. One method uses an ultrasonic positioning system to continuously correct position. The second uses the positioning system to correct only the endpoints of the scan lines. The third method, a modified calibration technique, corrects six of the 24 parameters defining the manipulator. Both methods using the positioning system reduce errors to an acceptable level as long as there is a clear line of sight between the transmitter mounted on the arm and the receivers. However, large errors occur when a direct path is blocked and the system responds to a reflected signal. The third method is robust and reliable, but not as accurate as the other two. Author (CISTI)

N94-30291 Alberta Research Council, Edmonton. Dept. of Advanced Computing and Engineering.
FORCE CONTROL TECHNIQUES FOR ROBOT MANIPULATORS AND THEIR MILITARY APPLICATIONS
P. Wojcik and K. Chrystall *In* Defence Research Establishment Suffield, Proceedings of the 3rd Conference on Military Robotic Applications 1991 p 122-128 (For primary document see N94-30275 08-37)
Avail: Issuing Activity (Defence Research Establishment Suffield, P.O. Box 4000, Medicine Hat, AB T1A 8K6 Canada)

An overview is presented of existing techniques for providing compliant motion control to robot manipulators. Active compliance of robot manipulators can be achieved by using either logic branching feedback or continuous feedback methods, but the latter has a broader range of potential applications. The theoretical background, working principles, and advantages and drawbacks of two continuous feedback approaches are discussed. These approaches are hybrid position/force control, which integrates explicit force control and pure position control concepts, and impedance control, in which a specific mechanical impedance is achieved at the manipulator end-effector. The requirements of compliant motion control (force control) for military robotics are outlined and three scenarios of force control applications are presented: ordnance handling, refuelling of vehicles, and mine field clearing. Author (CISTI)

N94-30292 Defence Research Establishment Pacific, Victoria (British Columbia).
AN INVERSE KINEMATICS ALGORITHM FOR THE DREP/PHILIPS REAL-TIME RADIOGRAPHIC MANIPULATOR SYSTEM **c63**
K. K. Yeung *In* Defence Research Establishment Suffield, Proceedings of the 3rd Conference on Military Robotic Applications 1991 p 129-135 (For primary document see N94-30275 08-37)
Avail: Issuing Activity (Defence Research Establishment Suffield, P.O. Box 4000, Medicine Hat, AB T1A 8K6 Canada)

A gantry-type robotic manipulator was installed in a real-time radiography research facility to develop automated radiographic inspection procedures for large-area aircraft structures. The original position controller of the manipulator system is a set of three joysticks designed only for manual operations. Numerical control capability has been added to allow direct control of the scanning motion from an external computer. In order to move the radiographic imaging end-effector to a given location in the world coordinate system, an inverse algorithm is required to compute the joint variables for the desired end-effector location. A closed-form inverse kinematics algorithm is presented for the manipulator system. The algorithm was implemented in a C language program. Robot modelling and simulation techniques were used to facilitate the development and verify the functionality of the program. Using the CIMSTATION robot simulation software, it was possible to simulate the inspection operation performed by the manipulator on a disassembled leading edge flap of the CF-18 aircraft. Author (CISTI)

N94-30293 Defence Research Establishment Suffield, Ralston (Alberta).
HATT-X: A HIGH PERFORMANCE FLYING LABORATORY FOR AUTONOMOUS UNMANNED AIRCRAFT RESEARCH AND DEVELOPMENT **c05**
Alex B. Markov and Robert W. Herring *In its* Proceedings of the 3rd Conference on Military Robotic Applications 1991 p 136-142 (For primary document see N94-30275 08-37)
Avail: Issuing Activity (Defence Research Establishment Suffield, P.O. Box 4000, Medicine Hat, AB T1A 8K6 Canada)

An experimental flight vehicle has been developed by the Canadian Forces to serve as a flying platform on which to investigate and demonstrate a variety of emerging technologies. This vehicle is the High-speed Aeronautical Technologies Testbed (HATT-X), a high subsonic speed rocket powered drone that has evolved from the ROBOT-X aerial target drone. HATT-X is a highly maneuverable platform that is capable of autonomous and semiautonomous flight. It is currently being used to investigate a number of drone technologies. Capabilities that are being pursued include highly agile evasive maneuvering, the ability to take intelligent actions to counter defensive measures, and supersonic flight. Current capabilities of HATT-X and ongoing research and development are reviewed. Planned enhancements that will facilitate a number of advanced configurations are also discussed. Author (CISTI)

N94-30294 Royal Military Coll. of Canada, Kingston (Ontario). Dept. of Mechanical Engineering.
SIMULATION OF LIGHTWEIGHT ROBOTS AND THEIR CONTROLLERS
J.-C. Piedboeuf and R. J. Ferguson *In* Defence Research Establishment Suffield, Proceedings of the 3rd Conference on Military Robotic Applications 1991 p 143-149 (For primary document see N94-30275 08-37)
Avail: Issuing Activity (Defence Research Establishment Suffield, P.O. Box 4000, Medicine Hat, AB T1A 8K6 Canada)

The development of a simulator for a n-degree of freedom robot with elastic joints and flexible links is described. The model of the robot is derived using d'Alembert's principle and takes into account both the stiffening effect and the angular momentum of the rotors in the robot motors. A closed kinematic loop is allowed for between the endpoint of the manipulator and the working plane. These kinematic loops are handled using Lagrange multipliers. A general formulation for the Jacobian derivative for any rigid or flexible robot was also developed and implemented. The control problem is discussed for flexible robots, in which the endpoint and not the joint has to be controlled. The suite of programs used for developing the simulator has modules for model generation, model simulation, and system analysis. The first two modules are written in Fortran while the core of the third is the MATLAB commercial software package. Author (CISTI)

N94-30295 Royal Military Coll. of Canada, Kingston (Ontario). Dept. of Electrical and Computer Engineering.
THE RESPONSE OF FLEXIBLE MANIPULATORS TO A NEW COMPUTED TORQUE CONTROL STRATEGY: SIMULATION RESULTS
T. D. Looke, M. M. Bayoumi, and M. Farooq *In* Defence Research Establishment Suffield, Proceedings of the 3rd Conference on Military Robotic Applications 1991 p 150-156 (For primary document see N94-30275 08-37)
Avail: Issuing Activity (Defence Research Establishment Suffield, P.O. Box 4000, Medicine Hat, AB T1A 8K6 Canada)

The need for faster and lighter autonomous and teleoperated robots, especially in military land, undersea, and space applications, requires control algorithms which account for the elastic response of lightweight, flexible structures. The numerical analysis and testing of these control algorithms further requires accurate simulation techniques. The finite element simulation method generally yields very accurate predictions of the transient dynamic response of flexible structures to applied loads. It is shown that a standard finite element simulation package (ANSYS) may be used to test computed torque and adaptive feedback control algorithms for multi-link flexible manipulators. The response of one- and two-link, planar and non-planar flexible manipulators to computed torque algorithms is illustrated. The results demonstrate the usefulness of the new computed torque approach.
Author (CISTI)

N94-30296 Alberta Univ., Calgary. Dept. of Mechanical Engineering.
SYMBOLIC GENERATION OF DYNAMICS EQUATIONS FOR MANIPULATORS MOUNTED ON MOVING BASES **c63**
R. W. Toogood, L. El-Rayyes, and D. J. Mackay *In* Defence Research Establishment Suffield, Proceedings of the 3rd Conference on Military Robotic Applications 1991 p 157-164 (For primary document see N94-30275 08-37)
Avail: Issuing Activity (Defence Research Establishment Suffield, P.O. Box 4000, Medicine Hat, AB T1A 8K6 Canada)

With the growing interest in lightweight and high-speed robots, the effects of link flexibility have been included in dynamic models of robots. Generally, such models concern robots mounted on a fixed base and under the influence of gravity. This is not the case, however, with robots mounted on space vehicles, on moving earthbound vehicles, or for small manipulators mounted on the end of a larger robot arm. A number of programs have therefore been implemented for the symbolic generation of computer code for the inverse and direct dynamic analysis of serial link robots mounted on moving bases. A review of these programs is presented, including the implemented dynamics algorithms, the major features of the symbolic generation procedures, and the computational efficiency of the generated code. The added computational load from including the base motion is shown. Some dynamics simulation results are described for a three link rigid manipulator mounted on an oscillating base, which graphically illustrates the effect of the base movement on the manipulator dynamics.
Author (CISTI)

N94-30297 Imago Mfg. Ltd., Ottawa (Ontario).
ACTIVITIES IN MACHINE VISION AT IMAGO MANUFACTURING LTD. **c63**
Roy Ball, Terry Folinsbee, and Lionel Pelkowitz *In* Defence Research Establishment Suffield, Proceedings of the 3rd Conference on Military Robotic Applications 1991 p 165-168 (For primary document see N94-30275 08-37)
Avail: Issuing Activity (Defence Research Establishment Suffield, P.O. Box 4000, Medicine Hat, AB T1A 8K6 Canada)

An overview is presented of machine vision research and development at Imago in the areas of robotic control, target tracking, image stabilization, and image registration. Applications are aimed at real-world scenarios which present the machine vision system with various combinations of low contrast, noise, variable illumination, cluttered background, and partial obscuration of the objects of interest. A powerful near-realtime software development system has been built featuring a wide range of algorithms and a software architecture that quickly determines the best combinations of algorithms for a given application. The software is designed for easy migration to more powerful and/or cost-effective platforms as necessary.
Author (CISTI)

N94-30298 Alberta Univ., Edmonton. Dept. of Computing Science.
VARIABLE-RESOLUTION STEREO MATCHING **c63**
Anup Basu *In* Defence Research Establishment Suffield, Proceedings of the 3rd Conference on Military Robotic Applications 1991 p 169-176 (For primary document see N94-30275 08-37)
Avail: Issuing Activity (Defence Research Establishment Suffield, P.O. Box 4000, Medicine Hat, AB T1A 8K6 Canada)

The human visual system can be characterized as a variable resolution system. Foveal information is processed at very high spatial resolution while peripheral information is processed at low spatial resolution. Although the quantitative aspects of this variable resolution processing are known quite precisely, it is unclear what computational advantages it has over uniform resolution processing. It is demonstrated that variable resolution visual processing can indeed be useful in stereo matching and vergence control. A method is presented for controlling vergence movements using a variable resolution representation of the input image. The method relies on a very simple scheme for matching edges of the left and right views, ignoring any constraints that might be used for eliminating false edge alignments. It is shown that this approach generates a matching function, with disparity as a free variable, which increases to a peak corresponding to the correct match and then decreases. The shape of the matching function helps in obtaining rapid and reliably correct vergence with respect to a given object.
Author (CISTI)

N94-30299 Defence Research Establishment Suffield, Medicine Hat (Alberta).
MOTION AND STRUCTURE FROM PLANAR MOTION IN NOISY MONOCULAR IMAGE SEQUENCES **c74**
V. C. Aitken and H. M. Schwartz *In its* Proceedings of the 3rd Conference on Military Robotic Applications 1991 p 177-184 (For primary document see N94-30275 08-37)
Avail: Issuing Activity (Defence Research Establishment Suffield, P.O. Box 4000, Medicine Hat, AB T1A 8K6 Canada)

Linear motion and structural models are proposed for a rigid object which is constrained to lie on a known planar surface, and a nonlinear measurement model which describes noisy monocular perspective projection observations from an arbitrary position above the known plane. Absolute motion and structural parameters are recovered with discrete time extended Kalman filtering in the presence of feature point occlusion. Comparison of Monte Carlo simulation results with approximate Cramer-Rao bounds demonstrates algorithm performance. In the planar motion problem, all feature points lie at constant heights relative to the plane of motion. A fundamental assumption of the proposed technique is that the height of one feature point from the plane is known or approximated. Another limitation is that the systems as formulated are not observable for zero angular velocity. Filter performance can be seriously degraded as rotational rates become very small.
Author (CISTI)

N94-30300 Central and Technical Establishment for Armament, Arcueil (France).
THERMAL IMAGING FOR A MOBILE ROBOT **c74**
Claude Caillas *In* Defence Research Establishment Suffield, Proceedings of the 3rd Conference on Military Robotic Applications 1991 p 191-197 (For primary document see N94-30275 08-37)
Avail: Issuing Activity (Defence Research Establishment Suffield, P.O. Box 4000, Medicine Hat, AB T1A 8K6 Canada)

A novel model is presented that uses thermal imaging for identifying different types of materials in outdoor scenes. The thermal imaging model is described, showing that it is possible to calculate body temperatures as a function of time and thermal inertia. From the model and from experiments measuring temperature of sand and rock, it is shown that the thermal inertia can be derived as a function of temperature and time. This should allow determination of the type of material, since thermal inertia is a characteristic of materials. The application envisaged for this materials identification technique is exploration of the surface of Mars using an autonomous robot. The infrared sensing requirements for Mars are summarized and the problems of determining grain size of the material, choosing footfall positions for the robot, and selecting sites for material collection are described. The thermal imaging technique is thought to be able to distinguish between dust, sand, and rock, allowing the robot to infer soil features such as load-bearing capacity and coefficient of friction.

Distinguishing between varieties of sand is theoretically possible.
Author (CISTI)

N94-30301 McGill Univ., Montreal (Quebec). Research Center for Intelligent Machines.
SONAR SENSING AND OBSTABLE DETECTION **c63**
Gregory Dudek, Michael Jenkin, Evangelos Milios, and David Wilkes *In* Defence Research Establishment Suffield, Proceedings of the 3rd Conference on Military Robotic Applications 1991 p 198-205 (For primary document see N94-30275 08-37)
Avail: Issuing Activity (Defence Research Establishment Suffield, P.O. Box 4000, Medicine Hat, AB T1A 8K6 Canada)

The problems of sensor error modeling and the exploration of unknown environments are considered in the context of mapping an unknown closed environment with a sonar sensor. The sensor characteristics are modeled, unavoidable anomalies in the data obtained are taken into account, and a long-term representation of the environment is constructed. Algorithms are presented for extracting obstacle contours from sonar data. The model of sonar range sensing for robot navigation accounts for multiple reflections of the sonar signal between transmission and reception. This controlled data acquisition methodology can be subsequently used to compare techniques for the interpretation of the acquired data. From this model of sonar sensing itself, a new model for inferring coherent reflecting surfaces is developed, based on an assumption of coherent smooth surfaces in the world. This is accomplished by using an energy based minimization algorithm to reject sonar measurements that are not consistent with an a-priori world model. Finally, a representation for large-scale structure of the environment is discussed which is based only on the topological interrelation between places of interest and the paths crossing them. Author (CISTI)

N94-30302 British Columbia Univ., Vancouver. Dept. of Electrical Engineering.
OBSTACLE DETECTION FOR AN AUTONOMOUS VEHICLE **c63**
R. Neil Braithwaite and M. P. Beddoes *In* Defence Research Establishment Suffield, Proceedings of the 3rd Conference on Military Robotic Applications 1991 p 206-213 (For primary document see N94-30275 08-37)
Avail: Issuing Activity (Defence Research Establishment Suffield, P.O. Box 4000, Medicine Hat, AB T1A 8K6 Canada)

The most primitive module in a navigational control system of an autonomous vehicle is discussed. The task performed by this module is the detection of moving and stationary obstacles from a vehicle undergoing predominantly rectilinear motion. Stereo cameras provide image flow and depth estimates from which properties of the obstacles and vehicle are extracted. Localized changes in the depth and image flow fields provide information on the position and velocity of the obstacles. Global changes in the image flow fields provide the translational and rotational velocity of the vehicle. The vehicle rotation is required to stabilize the stereo image sequence so that obstacle and vehicle motion can be estimated using pure translation Kalman filters. Important obstacle parameters, such as how close the vehicle will be as it passes the obstacle and how long before it passes, are predicted using the estimated vehicle and obstacle motions. The basis of this method is the Gabor filter whose phase response is used to extract normal image velocity and depth from the stereo image sequence. Simple experiments illustrate the potential of this method for detecting obstacles. Author (CISTI)

N94-30303 Alberta Research Council, Edmonton. Dept. of Advanced Computing and Engineering.
ELEMENTS OF SUPERVISORY CONTROL FOR MILITARY ROBOTIC APPLICATIONS **c63**
A. Dagnino, P. Feighan, and K. Chrystall *In* Defence Research Establishment Suffield, Proceedings of the 3rd Conference on Military Robotic Applications 1991 p 214-219 (For primary document see N94-30275 08-37)
Avail: Issuing Activity (Defence Research Establishment Suffield, P.O. Box 4000, Medicine Hat, AB T1A 8K6 Canada)

Supervisory control for robots can be viewed as a spectrum ranging from teleoperated devices on one extreme to fully autonomous systems on the other. At any point along this spectrum, there is a shared responsibility of control between the human operator and the robotic device. The basic elements needed to attain a significant degree of supervisory control beyond teleoperation are reviewed. Sensor systems allow the robot's operational status and its working environment to be perceived both by the robot and the human operator. Actuator systems allow the robot to move and bring about changes in its environment. Workspace models are computer representations of the robotic system and its immediate environment, and are used to provide the information required by the machine-based planning element to generate sequences of robot activities. The machine-based planning system must be designed for a dynamic environment, reasoning with uncertainty, an ability to trace its line of reasoning, knowledge representation, and user interfacing. A supervisory control architecture, such as the NASREM hierarchical architecture, provides the means of integrating these elements into a coherent system. The application of supervisory control to military use such as aircraft refueling is discussed and future areas of research are recommended. Author (CISTI)

N94-30304 Alberta Research Council, Edmonton. Dept. of Advanced Computing and Engineering.
ASPECTS OF THE OPERATOR INTERFACE FOR MILITARY ROBOTIC APPLICATIONS IN UNSTRUCTURED ENVIRONMENTS **c54**
P. Feighan, P. Wojcik, and K. Chrystall *In* Defence Research Establishment Suffield, Proceedings of the 3rd Conference on Military Robotic Applications 1991 p 220-226 (For primary document see N94-30275 08-37)
Avail: Issuing Activity (Defence Research Establishment Suffield, P.O. Box 4000, Medicine Hat, AB T1A 8K6 Canada)

The major challenges facing a designer of a military robotics operator interface are discussed. These include operating in unstructured environments, coping with restricted communications between operator and remote robotic system, defining the level of autonomy of the robotic system, and monitoring system health. Currently available operator interface technologies for remote robotic systems are reviewed which have been developed and tested in industrial or research laboratories. This overview includes discussion of the level of autonomy of telerobotic systems and its impact on the operator interface design, as well as description of the best ways of displaying information from the remote system and of inputting necessary commands and controls for telerobots. The concepts of military robotics operator interfaces are then introduced, based on two scenarios: simple teleoperation and remote control of a semiautonomous robotic system. Both use synthetic graphics to help the operator understand the work environment. This technology has recently been found very useful and its importance in operating remote robotic systems is expanding. Further areas of research are recommended. Author (CISTI)

N94-30305 Kinetic Sciences, Inc., Vancouver (British Columbia).
SUPERVISED AUTONOMOUS CONTROL FOR SPACE STATION SPECIAL PURPOSE DEXTROUS MANIPULATOR (SPDM) ROBOT
Guy Immega *In* Defence Research Establishment Suffield, Proceedings of the 3rd Conference on Military Robotic Applications 1991 p 227-232 (For primary document see N94-30275 08-37)
Avail: Issuing Activity (Defence Research Establishment Suffield, P.O. Box 4000, Medicine Hat, AB T1A 8K6 Canada)

The Special Purpose Dextrous Manipulator (SPDM) robot is intended to be built as part of Canada's contribution to Space Station Freedom. The SPDM will help to reduce astronaut workload and instead of providing closer coupling of the operator to the robot through telepresence, the robot control system will be upgraded with the ability to function autonomously under operator supervision. For supervised autonomous operation of the SPDM to be successful, new technologies must be integrated into a system design to accommodate the task requirements, the inherent limitations of the SPDM manipulators, and the demands made on the human operators. Innovative technologies are being developed for the SPDM project, and are reviewed in the areas of system conceptual design, operator interface, task planning and execution, database design, modeling of the SPDM configuration and the immediate work region, and vision system processing. Author (CISTI)

N94-30306 International Submarine Engineering Ltd., Port Coquitlam (British Columbia).
A TESTBED FOR THE DEVELOPMENT OF GROUND-BASED CONTROL OF SPACE-BASED MANIPULATORS
E. Jackson, K. Buchan, D. Eddy, G. Springle, K. Chrystall, P. Feighan, and A. Dagnino *In* Defence Research Establishment Suffield, Proceedings of

the 3rd Conference on Military Robotic Applications 1991 p 233-241 (For primary document see N94-30275 08-37)
Avail: Issuing Activity (Defence Research Establishment Suffield, P.O. Box 4000, Medicine Hat, AB T1A 8K6 Canada)

A project is under way to develop ground-based control technologies for space-based robots. This is a critical step in the development of autonomous control capabilities for space-based robots such as on the Space Station Freedom. Fundamental requirements for autonomous control are described in the areas of inputs and outputs, planning capability, workspace modeling, impedance control, and goal seeking behavior. To understand the tasks that the space based robot is to perform, hardware simulation of the work tasks must be performed. This requires a hardware simulation facility to allow testing of proposed robotic work task scenarios. Such a facility is being designed in the form of a testbed that will include components to emulate both ground and space based equipment, including the robotic manipulator. The integrated testbed system is reviewed, including the operator interface, planning system, manipulator control coordinator, workspace modeling computer, low level control system, vision system, and testbed manipulator. Author (CISTI)

N94-30307 International Submarine Engineering Ltd., Port Coquitlam (British Columbia).
ACHIEVING ROBOT AUTONOMY **c63**
Eric Jackson, Owen Williams, and Keir Buchan *In* Defence Research Establishment Suffield, Proceedings of the 3rd Conference on Military Robotic Applications 1991 p 242-248 (For primary document see N94-30275 08-37)
Avail: Issuing Activity (Defence Research Establishment Suffield, P.O. Box 4000, Medicine Hat, AB T1A 8K6 Canada)

Autonomy is defined as a measure of supervision and is quantified in terms of communication bandwidth. The need for increased autonomy is established and the driving and opposing factors are identified. The close relationship between increased autonomy and reduced bandwidth of a robot control channel and its data channel is established. The command channel bandwidth can be reduced by decreasing the performance requirements in the work task and by offloading the high frequency, high resolution, and high degree of freedom tasks to the robot. Reduction of the data channel bandwidth may be achieved by adding the appropriate data processing capabilities to the robot, by adding actuators or effectors to allow the robot to act on the data, by increasing the capability of the robot to handle complexity, and by reducing the risk of the robot acting on the data. Increases in robot autonomy result in increases in their responsibility to interpret their environment and act as desired. Health monitoring and fault tolerance become significant issues. Finally, several requirements for autonomous robotic control systems are presented. Author (CISTI)

N94-30308 Royal Military Coll. of Canada, Kingston (Ontario). Dept. of Electrical and Computer Engineering.
IMPROVING THE EXECUTION SPEED OF ROBOT CONTROL COMPUTATIONS: AN ALLOCATION SCHEME FOR HETEROGENEOUS MULTIPROCESSORS **c63**
M. McKay, M. Farooq, and C. Wortley *In* Defence Research Establishment Suffield, Proceedings of the 3rd Conference on Military Robotic Applications 1991 p 249-254 (For primary document see N94-30275 08-37)
Avail: Issuing Activity (Defence Research Establishment Suffield, P.O. Box 4000, Medicine Hat, AB T1A 8K6 Canada)

As the environment in which a robot operates and the autonomy of its operation increases in complexity, the computers used to control the robot often become inadequate. If a multiprocessor is used as a controller, affordable increases in processing power can be made one board at a time. The resulting heterogeneous multiprocessor requires special task allocation routines to ensure optimum utilization and minimum real-time delay. A method is proposed for heterogeneous multiprocessor pre-runtime task allocation which attempts to minimize the execution time of an acyclic sequence of tasks with precedence constraints on a given heterogeneous multiprocessor. The multiprocessor is assumed to be tightly coupled with shared memory. The method involves a branch and bound heuristic search which finds a good initial solution to the allocation problem and then tries to improve the solution through exhaustive search. Author (CISTI)

N94-30309 Ottawa Univ. (Ontario). Dept. of Mechanical Engineering.
MOTION CONTROL OF MOBILE ROBOTS **c63**
D. S. Necsulescu and S. Kalaycloglu *In* Defence Research Establishment Suffield, Proceedings of the 3rd Conference on Military Robotic Applications 1991 p 255-260 (For primary document see N94-30275 08-37)
Avail: Issuing Activity (Defence Research Establishment Suffield, P.O. Box 4000, Medicine Hat, AB T1A 8K6 Canada)

For most military applications, or for dealing with unstructured tasks in unstructured or uncertain environments, controllers for mobile robots and automatic guided vehicles require a suitable robot model in order to interact with the environment as well as to perform a collision-free motion incorporating sensory information about the environment. The artificial impedance approach is used for developing the high level controller of a mobile robot. The kinematic and dynamic models of a three-wheel mobile robot are first described. The control of the mobile robot is formulated so that the robot behaves like a linear virtual impedance linking the center of mass of the mobile robot and the destination point. Simulation results for obstacle-free work volumes are presented. The performance of the impedance controller for obstacle avoidance is also discussed. The major advantage of the proposed impedance control for the motion of a mobile vehicle is that the trajectory is generated rather than preplanned and is corrected to avoid obstacles in real time. Author (CISTI)

N94-30310 Defence and Civil Inst. of Environmental Medicine, Toronto (Ontario).
A MULTIPLEXED TWO-WAY SOLID COMMUNICATIONS LINK FOR TELEOPERATED ROBOTS **c63**
J. J. Grodski and D. Stampe *In* Defence Research Establishment Suffield, Proceedings of the 3rd Conference on Military Robotic Applications 1991 p 266-271 (For primary document see N94-30275 08-37)
Avail: Issuing Activity (Defence Research Establishment Suffield, P.O. Box 4000, Medicine Hat, AB T1A 8K6 Canada)

Remote mobile investigator robots used by the Canadian Forces in explosive ordnance disposal tasks comprise a remote unit and a control station. In the system's original version, the control station and the remote unit were linked by an 80-m heavy electrical cable spooled at the control station. This cable provides the control, video, and audio communications link between the two units. A new multiplexer and demultiplexer system was developed to reduce the size of the cable, extend the range of the communication link, and minimize the cost of the link. The link uses a single 75-ohm coaxial cable to carry multiplexed audio and control signals to the remote unit and video and audio back to the control station. Critical design features and characteristics of the system are described. Preliminary tests of the system indicate that performance is very good. The link will be proposed for implementation in the remote mobile investigator or other explosive ordnance disposal systems requiring a solid communications link. The link can also be readily adapted to other teleoperated systems with similar communications requirements. Author (CISTI)

N94-30311 Defence Research Establishment Suffield, Medicine Hat (Alberta).
UNMANNED VEHICLE MOBILITY: LIMITS OF AUTONOMOUS NAVIGATION
A. W. McCormac, D. M. Hanna, and J. McFee *In its* Proceedings of the 3rd Conference on Military Robotic Applications 1991 p 301-310 (For primary document see N94-30275 08-37)
Avail: Issuing Activity (Defence Research Establishment Suffield, P.O. Box 4000, Medicine Hat, AB T1A 8K6 Canada)

Considerable research is being conducted on the development of unmanned vehicles for military and civilian applications, particularly for hostile environments. It is desirable to produce a vehicle which can select its own route, not requiring remote navigation, but then it would be required to sense its surroundings. Although imaging systems and modern computers make this possible, the extreme data processing demands usually make it impractical. It is suggested that an inverse relationship exists between vehicle mobility and the complexity of the autonomous navigation system required for an unmanned vehicle. An overview of vehicle navigation is presented which shows the degree to which navigation is affected by increasing inherent mobility. If the inherent mobility of a vehicle is greatly enhanced, the scene image processing requirements and navigational

computations are greatly simplified. This means the vehicle path selection and speed and steering adjustments may be made more quickly, resulting in higher vehicle speeds whenever possible. Combined with reduced deviation from the intended path, this would greatly increase the speed of the vehicle from one given point to another, suggesting that high speed autonomous navigation may be feasible. Author (CISTI)

N94-30312 Royal Military Coll. of Canada, Kingston (Ontario). Dept. of Chemistry and Chemical Engineering.
ELECTROCHEMICAL POWER SOURCE (EPS) SELECTION FOR ENERGETICALLY INDEPENDENT ROBOTS (EIR): A SYSTEMATIC APPROACH c33
P. R. Roberge and K. A. Sosin *In* Defence Research Establishment Suffield, Proceedings of the 3rd Conference on Military Robotic Applications 1991 p 318-326 (For primary document see N94-30275 08-37)
Avail: Issuing Activity (Defence Research Establishment Suffield, P.O. Box 4000, Medicine Hat, AB T1A 8K6 Canada)

The term energetically independent robots (EIR) is used for robots that can perform a mission while depending only on energy stored and carried by themselves. In the case of long missions, periodical refuelling or recharging is admissible. The selection of electrochemical power sources for EIRs constitutes a serious engineering challenge. The selection process is a compromise between various and contradictory requirements. A structured approach to the selection process is introduced. The key selection factors considered in this approach are mission duration and environment, total energy demand, power profile, acceptable weight and size, and reliability. A critical analysis of existing electrochemical power sources with respect to these considerations is presented, revealing the applicability of fuel cells for a wide range of EIR's. Contemporary fuel cell technology offers lightweight electrochemical power sources capable of delivering large amounts of energy at relatively high power rates. Those sources can be combined with others, demonstrating high resistance to overloading, thus creating hybrid power supplies potentially better than classic internal combustion engines. Advantages of those sources are quietness and low heat emission. Author (CISTI)

N94-30391 National Aerospace Lab., Amsterdam (Netherlands). Space Div.
DEVELOPMENT AND VALIDATION OF A LINEAR RECURSIVE ORDER-N ALGORITHM FOR THE SIMULATION OF FLEXIBLE SPACE MANIPULATORS DYNAMICS
P. T. L. M. vanWoerkom and A. deBoer 30 Jun. 1992 20 p Presented at the International Astronautical Federation 43rd Congress, Washington, DC, 31 Aug. - 4 Sep. 1992 Limited Reproducibility: More than 20% of this document may be affected by microfiche quality
(Contract NIVR-02506N)
(AD-B173557; NLR-TP-92284-U; IAF-Paper-92-0030; ETN-94-95589)
Copyright Avail: Issuing Activity (European Space Agency (ESA))

The development and validation of an advanced algorithm for the simulation of the dynamics of flexible spacecraft/space manipulator systems are outlined. The requirements imposed during the development of the present prototype dynamics simulator led to the modification and implementation of an existing linear recursive algorithm ('order-N' algorithm), which requires a computational effort proportional to the number of component bodies in the system. Starting with the Lagrange form of the d'Alembert principle, a parametric form which is found to yield, among others, the basic forms of the Newton-Euler, the d'Alembert, and the Gauss dynamics principles was deduced. It is shown how the application of each of the latter three principles can be made to lead graciously to be desired order-N agorithm for the flexible multibody system. ESA

N94-30596 Sandia National Labs., Livermore, CA.
IN-CYLINDER GAS VELOCITY MEASUREMENTS COMPARING CRANKCASE AND BLOWER SCAVENGING IN A FIRED TWO-STROKE CYCLE ENGINE
P. C. Miles, R. M. Green, and P. O. Witze 1994 20 p Presented at the Society of Automotive Engineers (SAE) Congress and Exposition, Detroit, MI, 28 Feb. - 3 Mar. 1994 Limited Reproducibility: More than 20% of this document may be affected by microfiche quality
(Contract DE-AC04-76DP-00789)
(DE94-005752; SAND-94-8521C; CONF-940242-2) Avail: CASI HC A03

The in-cylinder flow field of a Schnuerle (loop) scavenged two-stroke engine has been examined under conditions simulating both blower and crankcase driven scavenging. Measurements of the radial component of velocity were obtained along the cylinder centerline during fired operation at delivery ratios of 0.4, 0.6, and 0.8. Both mean velocity profiles and root mean square velocity fluctuations near top center show a strong dependence on the scavenging method. Complementary in-cylinder pressure measurements indicate that combustion performance is better under blower driven scavenging for the engine geometry studied. DOE

N94-30703 Argonne National Lab., IL.
TCM EXEMPTIONS TO PROMOTE ALTERNATIVE-FUEL VEHICLES: THE GOOD, THE BAD, AND THE UGLY
M. Mintz 1994 15 p Presented at the Transportation Research Board Annual Meeting, Washington, DC, Jan. 1994 Limited Reproducibility: More than 20% of this document may be affected by microfiche quality
(Contract W-31-109-eng-38)
(DE94-005924; ANL/ES/VU-81732; CONF-940128-5-Vugraphs) Avail: CASI HC A03

Viewgraphs from a presentation on transportation control measures (TCM) to facilitate the use of alternative-fuel vehicles (AFV) are given. Types of TCM's that pertain to AFV exemptions are: parking fees and restrictions, high occupancy vehicle lanes, fuel taxes, and possibly congestion pricing and time of day and day of week restrictions. The degree to which these measures will impact AFV production by the year 2010 is predicted. DOE

N94-30792 Texas A&M Univ., College Station.
PARAMETER IDENTIFICATION OF THE ROTORDYNAMIC COEFFICIENTS OF HIGH-REYNOLDS-NUMBER HYDROSTATIC BEARINGS Ph.D. Thesis
Constantinos Rouvas 1993 87 p
Avail: Univ. Microfilms Order No. DA9328796

The research presented here concentrates on experimental and analytical methods to identify the twelve rotordynamic coefficients of high-Reynolds-number hydrostatic bearings. Fluid-flow-induced noise (turbulence, cavitation) presents a significant problem in testing these bearings, since this noise exists in the same frequency range as the test signals. This common frequency range eliminates the possibility of rejecting the noise through filtering. A frequency-domain analysis method has been developed to extract the rotordynamic coefficients from data obtained by multi-frequency sequential excitation testing. Power-spectral-density estimates are used to reject noise that is independent of the applied excitation. The method is verified experimentally by single-frequency excitation, and repeatability tests. A second power-spectral-density based identification method has been developed and applied to simultaneous excitation test data. Here, two independent random excitations are applied simultaneously to the bearing, and their effects are separated by computing appropriate power-spectral-density estimates, while, at the same time, maintaining excellent noise rejection properties. This method yields results identical to the sequential excitation procedure, and reduces the actual test and analysis times by one half. Last, an analysis method in the time domain has been developed and implemented. In essence it is a direct application of least squares to the bearing housing equations of motion. For this method, it is shown that for the low-frequency noise present in the measurements, differentiation of the signals is acceptable, and preferable over integration. The twelve rotordynamic coefficients are obtained from a recursive formulation of least squares, and the results are shown to have acceptable convergence. Also, the coefficients extracted from this method are found to reconstruct the bearing response more accurately than the coefficients extracted from the power-spectral-density methods.
Dissert. Abstr.

N94-30793 Toronto Univ. (Ontario).
KINEMATIC ANALYSIS OF PLATFORM-TYPE ROBOTIC MANIPULATORS Ph.D. Thesis
Xiaolun Shi 1993 302 p
(ISBN-0-315-78703-1) Avail: Univ. Microfilms Order No. DANN78703

New methods are developed for the kinematic analysis of serial and platform-type parallel robotic manipulators, including forward and inverse kinematic solutions, singularity identifications and workspace evaluation. Differences between serial and platform-type parallel manipulators, which can provide substantially improved end-point rigidity compared with the

conventional serial robotic arms, are addressed. The problem of determining the screw parameters of rigid body motion from initial and final position data is discussed, as a basis to search for a general and efficient procedure to solve the complex forward kinematics problem of platform-type manipulators. Several Screw-Theory based approaches for solving the inverse instantaneous problem of 6 DOF serial manipulators are studied and compared in terms of their computational efficiency, accuracy, sensitivity to data error and capability of dealing with singularities. A modified Vector Decomposition method is then proposed for solving the IIK problem and for singularity analysis of serial kinematic chains, the method is especially effective when applied to the wrist partitioned serial manipulators, which are essential components to any platform-type parallel manipulators. By using the data of three point positions, velocities, and accelerations of the end effector a general method is developed for solving the forward kinematics problem, including position, velocity and acceleration kinematics, of platform-type manipulators. The solution procedure can be applied to a wide variety of platform-type manipulators such as the 6 DOF Steward Platform manipulator and other models. It is found that while the solution for the forward position kinematics of a platform-type manipulator can be obtained by solving a non-linear system of equations, the closed-form solutions for forward rate and acceleration kinematics can be found by solving a system of linear equations. Based on the proposed kinematic formulations, an algorithm for detecting the boundaries of reachable workspace of platform-type manipulators is introduced, using a new concept of the Geometric Envelope. As the algorithm is based on the relatively simple inverse kinematic solution of platform-type manipulators, it is, in general, more efficient and easier to implement than any other existing methods for this purpose. Singular configurations of platform-type manipulators are discussed and a general analytical condition for configuration singularity is derived, based on the forward rate kinematics of platform-type manipulators. It is believed that this is one of the most general analytical expressions so far for singular configurations of a platform-type parallel manipulator. Dissert. Abstr.

N94-30809 Texas A&M Univ., College Station.
ROTOR INSTABILITY INDUCED BY DEAD BAND CLEARANCE IN BEARING SUPPORTS Ph.D. Thesis
Yao-Qun Lin 1993 203 p
Avail: Univ. Microfilms Order No. DA9328763

Rotor instability, or rotor nonsynchronous natural frequency vibration, is of major concern in the rotor dynamics field. Efforts have been made continuously to explain this phenomenon since it was identified more than seventy years ago. To date, rotor instability vibration has been almost ascribed to two mechanisms, i.e., internal friction effects and fluid actions. It has been predicted by some investigations that dead band clearance in bearing supports can induce only sub and/or super harmonics tracking the synchronous speed and does not cause the nonsynchronous (non-harmonic) natural frequency vibration. It is shown, however, in this dissertation that dead band clearance in ball bearing supports can induce rotor nonsynchronous natural frequency vibration. The computer simulations show that in a limited speed range, the ball-bearing outer race of an unbalanced rotor may leave (tight-loose) then touch (loose-tight) the housing surface and induce an internal impact. Internal impacts will excite the natural frequency vibration of the rotor, which is independent of the rotor synchronous vibration and will reach a limit cycle due to system's damping. Beyond the speed range, the nonsynchronous natural frequency disappears. Half-frequency vibration is also predicted by the computer simulations. It is shown that the half-frequency vibration is induced by the nonlinear coupling between the equations of motion due to dead band clearance. Experiments with a rotor supported on ball bearings with dead band clearance are conducted. The experimental results agree well with the theoretical predictions. The nonsynchronous natural frequency vibration of ball-bearing supported rotors (without seals) has been traditionally explained as internal friction induced rotor instability. The classical internal friction theory is discussed in this dissertation. It is claimed here that what is predicted by the classical linear theory on internal friction is a divergent (Liapunov unstable) response and hence is unmeasurable. But rotor instability vibration, which has two significant components at the synchronous and the natural frequencies, is measurable and hence is Liapunov stable. Dissert. Abstr.

N94-30831 New Energy and Industrial Technology Development Organization, Tokyo (Japan).
INVESTIGATION OF THE TECHNOLOGY DEVELOPMENT STATUS OF ALTERNATE FUEL VEHICLES
Mar. 1993 73 p In JAPANESE Limited Reproducibility: More than 20% of this document may be affected by microfiche quality
(DE94-744237; ETDE/JP-MF-94744237) Avail: CASI HC A04

The main purpose of the introduction of alternate fuel vehicles is to contribute to the reduction of pollution, the alternate energy for petroleum, and the energy savings. This report describes the development status of methanol, natural gas, and electric vehicles, which have high potential as alternate fuel vehicles. Characteristics of alternate fuel vehicles are compared by using the same factors on the basis of technological data. Outlines of individual alternate fuel vehicles are illustrated. Then, practicabilities of the alternate fuel vehicles are compared with each other, as for the output and energy densities, maximum output and torque of motors, power performance, specific consumption of energy, driving distance, initial cost, running cost and life cycle cost, convenience of fuel and energy supply, low pollution, and health effects. DOE

N94-30866 Massachusetts Inst. of Tech., Cambridge.
INTEGRATED STRUCTURE/CONTROL DESIGN OF NONRIGID ROBOT ARMS FOR HIGH-SPEED MANIPULATION Ph.D. Thesis
Jahng-Hyon Park 1992
Avail: Issuing Activity (MIT Libraries, Rm. 14-0551, Cambridge, MA 02139-4307)

In assembly of PC boards and VLSI's, there is a great need for ultrahigh speed robots that can significantly reduce the cycle time and thereby increase productivity. To meet this demand, a technical breakthrough is necessary for arm design, which substantially departs from the traditional design paradigm. Traditionally, arm linkage and drive mechanisms are designed first followed by control design. Structure design, while it is optimal with respect to kinematics and statics, is not always optimal from the control standpoint. There exists intricate interactions between mechanisms and controls, which must be taken into account in designing the system. To achieve high performance, a cohesive and comprehensive design method that integrates both structure and control design is necessary. First, flexibility of arm links is included in the model to consider the dynamic deflections in high speed manipulation. An actuator relocation method for improving flexible arm dynamics is presented. The endpoint control of a flexible arm has been known as a nonminimum phase system due to the noncollocated sensor and actuator. By relocating the actuator near the endpoint, the system can be changed to a minimum phase system. Pole-zero locations of a single-link flexible arm are obtained for the actuator types (force and torque) and the actuator locations. Pole-zero configurations and their effect on control are analyzed with regard to the location of the actuation point. The guidelines for the actuator locations are developed with respect to the operation bandwidth, stability, and controllability. An integrated approach to the concurrent design of arm structure and control is presented. To achieve high speed positioning, a technique is developed in which comprehensive design parameters describing arm link geometry, actuator locations, and feedback gains are optimized with respect to the settling time of the system. A two-link, nonrigid arm is analyzed and a simple dynamic model representing rapid positioning processes is obtained. Optimal feedback gains minimizing the settling times are obtained as functions of structural parameters involved in the dynamic model. The structural parameters are then optimized using a nonlinear programming technique in order to obtain an overall optimal performance. The resultant arm design shows an outstanding performance, which is otherwise unattainable if one designs the structure and control separately. Dissert. Abstr.

N94-30878 Urban Consortium for Technology Initiatives. Energy Task Force.
COMPRESSED NATURAL GAS FUELED VEHICLES: THE HOUSTON EXPERIENCE
1993 141 p Limited Reproducibility: More than 20% of this document may be affected by microfiche quality
(Contract DE-FG02-90CE-27504)
(DE94-005804; DOE/CE-27504/T11) Avail: CASI HC A07

Houston's experience in defining the compressed natural gas fueled vehicle research scope and issues is described. It details the ways in which the project met initial expectations and how the project scope,

focus, and duration were adjusted in response to unanticipated results. It provides examples of real world successes and failures in efforts to commercialize basic research in adapting a proven technology (natural gas) to a noncommercially proven application (vehicles). Phase one of the demonstration study investigates, develops, documents, and disseminates information regarding the economic, operational, and environmental implications of utilizing compressed natural gas (CNG) in various truck fueling applications. The four truck classes investigated are light duty gasoline trucks, medium duty gasoline trucks, medium duty diesel trucks, and heavy duty diesel trucks. The project researches aftermarket CNG conversions for the first three vehicle classes and original equipment manufactured (OEM) CNG vehicles for light duty gasoline and heavy duty diesel classes. In phase two of the demonstration project, critical issues are identified and assessed with respect to implementing use of CNG fueled vehicles in a large vehicle fleet. These issues include defining changes in local, state, and industry CNG fueled vehicle related codes and standards; addressing vehicle fuel storage limitations; using standardized vehicle emission testing procedures and results; and resolving CNG refueling infrastructure implementation issues and related cost factors. The report identifies which CNG vehicle fueling options were tried and failed and which were tried and succeeded, with and without modifications. The conclusions include a caution regarding overly optimistic assessments of CNG vehicle technology at the initiation of the project. DOE

N94-30937 Politecnico di Milano (Italy). Dipt. di Elettronica e Informazione.
IDENTIFICATION OF THE DAMPING RATIO RELATIONSHIP OF AN AUTOVEHICLE SUSPENSION [IDENTIFICAZIONE DEL RAPPORTO DI SMORZAMENTO DELLE SOSPENSIONI DI UN AUTOVEICOLO]
Cesare Alippi Oct. 1993 29 p In ITALIAN
(Rept-93-063; ETN-94-95824) Avail: Issuing Activity (Politecnico di Milano, Piazza Leonardo da Vinci 32, 20133 Milan, Italy)

The damping ratio of automobile shock absorbers is studied. The inadequacy of a first order model for an automobile shock absorption system is demonstrated and a wheel shock absorption model is considered. From analysis of the frequency response, and from the phase diagram in particular, the relation sought between damping ratio and critical car parameters is obtained. ESA

N94-30952 Toronto Univ. (Ontario).
A CONTROL METHOD FOR BILATERAL TELEOPERATING SYSTEMS Ph.D. Thesis
Yesayahu Strassberg 1992 263 p
(ISBN-0-315-78705-8) Avail: Univ. Microfilms Order No. DANN78705

The thesis focuses on control of bilateral master-slave teleoperators. The bilateral control issue of teleoperators is studied and a new scheme that overcomes basic unsolved problems is proposed. A performance measure, based on the multiport modeling method, is introduced in order to evaluate and understand the limitations of earlier published bilateral control laws. Based on the study evaluating the different methods, the objective of the thesis is stated. The proposed control law is then introduced, its ideal performance is demonstrated, and conditions for stability and robustness are derived. It is shown that stability, desired performance, and robustness can be obtained under the assumption that the deviation of the model from the actual system satisfies certain norm inequalities and the measurement uncertainties are bounded. The proposed scheme is validated by numerical simulation. The simulated system is based on the configuration of the RAL (Robotics and Automation Laboratory) telerobot. From the simulation results it is shown that good tracking performance can be obtained. In order to verify the performance of the proposed scheme when applied to a real hardware system, an experimental setup of a three degree of freedom master-slave teleoperator (i.e. three degree of freedom master and three degree of freedom slave robot) was built. Three basic experiments were conducted to verify the performance of the proposed control scheme. The first experiment verified the master control law and its contribution to the robustness and performance of the entire system. The second experiment demonstrated the actual performance of the system while performing a free motion teleoperating task. From the experimental results, it is shown that the control law has good performance and is robust to uncertainties in the models of the master and slave.
Dissert. Abstr.

N94-30957 Catholic Univ. of America, Washington, DC.
KINEMATICS AND FORCE ANALYSIS OF A ROBOT HAND BASED ON AN ARTIFICIAL BIOLOGICAL CONTROL SCHEME Ph.D. Thesis
Man Guen Kim 1993 263 p
Avail: Univ. Microfilms Order No. DA9320188

An artificial biological control scheme (ABCS) is used to study the kinematics and statics of a multifingered hand with a view to developing an efficient control scheme for grasping. The ABCS is based on observation of human grasping, intuitively taking it as the optimum model for robotic grasping. A final chapter proposes several grasping measures to be applied to the design and control of a robot hand. The ABCS leads to the definition of two modes of the grasping action: natural grasping (NG), which is the human motion to grasp the object without any special task command, and forced grasping (FG), which is the motion with a specific task. The grasping direction line (GDL) is defined to determine the position and orientation of the object in the hand. The kinematic model of a redundant robot arm and hand is developed by reconstructing the human upper extremity and using anthropometric measurement data. The inverse kinematic analyses of various types of precision and power grasping are studied by replacing the three-link with one virtual link and using the GDL. The static force analysis for grasping with fingertips is studied by applying the ABCS. A measure of grasping stability, that maintains the positions of contacts as well as the configurations of the redundant fingers, is derived. The grasping stability measure (GSM), a measure of how well the hand maintains grasping under the existence of external disturbance, is derived by the torque vector of the hand calculated from the external force applied to the object. The grasping manipulability measure (GMM), a measure of how well the hand manipulates the object for the task, is derived by the joint velocity vector of the hand calculated from the object velocity. The grasping performance measure (GPM) is defined by the sum of the directional components of the GSM and the GMM. Finally, a planar redundant hand with two fingers is examined in order to study the various postures of the hand performing pinch grasping by applying the GSM and the GMM. Dissert. Abstr.

N94-29622*# Jet Propulsion Lab., California Inst. of Tech., Pasadena.
ELEVATION CONTROL SYSTEM MODEL FOR THE DSS 13 ANTENNA
W. Gawronski and J. A. Mellstrom *In its* The Telecommunications and Data Acquisition Report 15 May 1991 p 83-108 (For primary document see N94-29613 08-32)
(RTOP 314-40-42-10-40)
Avail: CASI HC A03/MF A02

N94-29629*# National Aeronautics and Space Administration. Lewis Research Center, Cleveland, OH.
A COMPACT ROLLER-GEAR PITCH-YAW JOINT MODULE: DESIGN AND CONTROL ISSUES
Mark E. Dohring (Case Western Reserve Univ., Cleveland, OH.), William J. Anderson (NASTEC, Inc., Cleveland, OH.), Wyatt S. Newman (Case Western Reserve Univ., Cleveland, OH.), and Douglas A. Rohn *In* NASA. Ames Research Center, The 27th Aerospace Mechanisms Symposium May 1993 p 21-36 (For primary document see N94-29627 08-15)
Avail: CASI HC A03/MF A03

N94-29630*# Jet Propulsion Lab., California Inst. of Tech., Pasadena.
MARS ROVER MECHANISMS DESIGNED FOR ROCKY 4
Tommaso P. Rivellini *In* NASA. Ames Research Center, The 27th Aerospace Mechanisms Symposium May 1993 p 37-49 (For primary document see N94-29627 08-15)
Avail: CASI HC A03/MF A03

N94-29633*# National Aeronautics and Space Administration. Langley Research Center, Hampton, VA.
DESIGN AND TESTING OF THE LITE VARIABLE FIELD STOP MECHANISM
Robert A. Dillman *In* NASA. Ames Research Center, The 27th Aerospace Mechanisms Symposium May 1993 p 83-92 (For primary document see N94-29627 08-15)
Avail: CASI HC A02/MF A03

N94-29635*# Space Industries, Inc., League City, TX.
RETENTION LATCH MECHANISM FOR THE WAKE SHIELD FACILITY
Timothy G. Vendrely *In* NASA. Ames Research Center, The 27th

Aerospace Mechanisms Symposium May 1993 p 107-120 (For primary document see N94-29627 08-15)
Avail: CASI HC A03/MF A03

N94-29637*# Starsys Research Corp., Boulder, CO.
METAL BAND DRIVES IN SPACECRAFT MECHANISMS
Daryl Maus *In* NASA. Ames Research Center, The 27th Aerospace Mechanisms Symposium May 1993 p 137-146 (For primary document see N94-29627 08-15)
Avail: CASI HC A02/MF A03

N94-29638*# Jet Propulsion Lab., California Inst. of Tech., Pasadena.
POINTING MECHANISMS FOR THE SHUTTLE RADAR LABORATORY
Gerald W. Lilienthal, Argelio M. Olivera, and Lori R. Shiraishi *In* NASA. Ames Research Center, The 27th Aerospace Mechanisms Symposium May 1993 p 147-164 (For primary document see N94-29627 08-15)
Avail: CASI HC A03/MF A03

N94-29642*# Lockheed Missiles and Space Co., Palo Alto, CA.
THREE HIGH DUTY CYCLE, SPACE-QUALIFIED MECHANISMS
David Akin, Ralph Horber, and Jake Wolfson *In* NASA. Ames Research Center, The 27th Aerospace Mechanisms Symposium May 1993 p 219-236 (For primary document see N94-29627 08-15)
(Contracts NAS5-30386; NAS5-26813; NAS8-37334)
Avail: CASI HC A03/MF A03

N94-29646*# Lockheed Missiles and Space Co., Sunnyvale, CA.
LOCK-UP FAILURE OF A FOUR-BAR LINKAGE DEPLOYMENT MECHANISM
Michael Zinn *In* NASA. Ames Research Center, The 27th Aerospace Mechanisms Symposium May 1993 p 283-298 (For primary document see N94-29627 08-15)
Avail: CASI HC A03/MF A03

N94-29647*# National Aeronautics and Space Administration. Langley Research Center, Hampton, VA.
MINIATURE LINEAR-TO-ROTARY MOTION ACTUATOR
Michael R. Sorokach, Jr. *In* NASA. Ames Research Center, The 27th Aerospace Mechanisms Symposium May 1993 p 299-314 (For primary document see N94-29627 08-15)
Avail: CASI HC A03/MF A03

N94-29650*# National Aeronautics and Space Administration. Marshall Space Flight Center, Huntsville, AL.
DESIGN AND TEST OF ELECTROMECHANICAL ACTUATORS FOR THRUST VECTOR CONTROL
J. R. Cowan and Rae Ann Weir *In* NASA. Ames Research Center, The 27th Aerospace Mechanisms Symposium May 1993 p 349-366 (For primary document see N94-29627 08-15)
Avail: CASI HC A03/MF A03

N94-29981# National Inst. of Polar Research, Tokyo (Japan).
A NEWLY DEVELOPED SNOW VEHICLE (SM100S) FOR ANTARCTICA. PART 1: NECESSITY AND PROCESS OF THE DEVELOPMENT [NANKYOKU OGATA SETSUJOSHA (SM100S) NO KAIHATSU. 1: HITSUYOSEI TO KAIHATSU KEII]
Sadao Takeuchi, Atsushi Kino, Masayuki Hosoya, Jiro Yoshida, and Kenji Ishizawa *In its* Antarctic Record, Vol. 36, no. 3 30 Nov. 1992 p 363-375 In JAPANESE (For primary document see N94-29978 08-46)
Avail: CASI HC A03/MF A02

N94-29982# Ohara Corp., Nagaoka (Japan).
A NEWLY DEVELOPED SNOW VEHICLE (SM100S) FOR ANTARCTICA. PART 2: DESIGN OF THE SYSTEM [NSNKYOKU OGATA SETSUJOSHA (SM100S) NO KAIHATSU. 2: SHISUTEMU DEZAIN]
Masashi Nakajima and Masayuki Hosoya *In* National Inst. of Polar Research, Antarctic Record, Vol. 36, No. 3 30 Nov. 1992 p 376-392 In JAPANESE (For primary document see N94-29978 08-46)
Avail: CASI HC A03/MF A02

N94-29984# Bando Chemical Industries Ltd., Kobe (Japan).
A NEWLY DEVELOPED SNOW VEHICLE (SM100S) FOR ANTARCTICA. PART 4: LOW TEMPERATURE PROPERTIES OF CRAWLER BELT [NANKYOKU OGATA SETSUJOSHA (SM100S) NO KAIHATSU. 4: GOMU RITAI NO TEION TOKUSEI]
Etsuji Maekawa and Yoshihide Terayama *In* National Inst. of Polar Research, Antarctic Record, Vol. 36, No. 3 30 Nov. 1992 p 398-409 In JAPANESE (For primary document see N94-29978 08-46)
Avail: CASI HC A03/MF A02

N94-29985# Ohara Corp., Nagaoka (Japan).
A NEWLY DEVELOPED SNOW VEHICLE (SM100S) FOR ANTARCTICA. PART 5: RESULT OF GENERAL PERFORMANCE TESTS [NANKYOKU OGATA SETSUJOSHA (SM100S) NO KAIHATSU. 5: SEINO SHIKEN]
Mitsuru Saito, Tsuyoshi Seki, and Masayuki Hosoya *In* National Inst. of Polar Research, Antarctic Record, Vol. 36, No. 3 30 Nov. 1992 p 410-440 In JAPANESE (For primary document see N94-29978 08-46)
Avail: CASI HC A03/MF A02

N94-30441*# Jet Propulsion Lab., California Inst. of Tech., Pasadena.
A FORCE-CONTROLLABLE MACRO-MICRO MANIPULATOR AND ITS APPLICATION TO MEDICAL ROBOTS
Neville I. Marzwell, Darrin R. Uecker, and Yulun Wang *In* NASA, Washington, Technology 2003: The Fourth National Technology Transfer Conference and Exposition, Volume 1 Feb. 1994 p 3-16 (For primary document see N94-30440 08-99)
(Contract NAS7-1149)
Avail: CASI HC A03/MF A04

N94-30442*# Jet Propulsion Lab., California Inst. of Tech., Pasadena.
THE USE OF INTERACTIVE COMPUTER VISION AND ROBOT HAND CONTROLLERS FOR ENHANCING MANUFACTURING SAFETY
Neville I. Marzwell, Charles J. Jacobus, Thomas M. Peurach, and Brian T. Mitchell *In* NASA, Washington, Technology 2003: The Fourth National Technology Transfer Conference and Exposition, Volume 1 Feb. 1994 p 17-31 (For primary document see N94-30440 08-99)
(Contract NAS7-1189)
Avail: CASI HC A03/MF A04

N94-30443*# Babcock and Wilcox Co., Lynchburg, VA. CIM Systems.
PROGRAMMABLE AUTOMATED WELDING SYSTEM (PAWS): CONTROL OF WELDING THROUGH SOFTWARE AND HARDWARE
Martin D. Kline and Thomas E. Doyle *In* NASA, Washington, Technology 2003: The Fourth National Technology Transfer Conference and Exposition, Volume 1 Feb. 1994 p 32-37 (For primary document see N94-30440 08-99)
Avail: CASI HC A02/MF A04

N94-30444*# Idaho National Engineering Lab., Idaho Falls.
SENSING THE GAS METAL ARC WELDING PROCESS
N. M. Carlson, J. A. Johnson, H. B. Smartt, A. D. Watkins, E. D. Larsen, P. L. Taylor, and M. A. Waddoups *In* NASA, Washington, Technology 2003: The Fourth National Technology Transfer Conference and Exposition, Volume 1 Feb. 1994 p 38-53 (For primary document see N94-30440 08-99)
(Contract DE-AC07-76ID-01570)
Avail: CASI HC A03/MF A04

N94-30484*# Wright Lab., Wright-Patterson AFB, OH.
USE OF MAGNETIC COMPRESSION TO SUPPORT TURBINE ENGINE ROTORS
Chris J. Pomfret *In* NASA, Washington, Technology 2003: The Fourth National Technology Transfer Conference and Exposition, Volume 1 Feb. 1994 p 395-410 (For primary document see N94-30440 08-99)
Avail: CASI HC A03/MF A04

38 QUALITY ASSURANCE AND RELIABILITY

Includes product sampling procedures and techniques; and quality control.

N94-28503# Sandia National Labs., Albuquerque, NM.
IDENTIFICATION OF COMPONENTS TO OPTIMIZE IMPROVEMENT IN SYSTEM RELIABILITY
L. Painton (Carnegie-Mellon Univ., Pittsburgh, PA.) and J. Campbell 1993 6 p Presented at the 2nd Probabilistic Safety Assessment and Management Conference (PSAM), San Diego, CA , 20-24 Mar. 1994
(Contract DE-AC04-94AL-85000)
(DE94-001601; SAND-93-2420C; CONF-940312-22) Avail: CASI HC A02/MF A01

The fields of reliability analysis and risk assessment have grown dramatically since the 1970's. There are now bodies of literature and standard practices which cover quantitative aspects of system analysis such as failure rate and repair models, fault and event tree generation, minimal cut sets, classical and Bayesian analysis of reliability, component and system testing techniques, and decomposition methods. In spite of the growth in the sophistication of reliability models, however, little has been done to integrate optimization models within a reliability analysis framework. That is, often reliability models focus on characterization of system structure in terms of topology and failure/availability characteristics of components. A number of approaches have been proposed to help identify the components of a system that have the largest influence on overall system reliability. While this may help rank order the components, it does not necessarily help a system design team identify which components they should improve to optimize overall reliability (it may be cheaper and more effective to focus on improving two or three components of smaller importance than one component of larger importance). In this paper, we present an optimization model that identifies the components to be improved to maximize the increase in system MTBF, subject to a fixed budget constraint. A dual formulation of the model is to minimize cost, subject to achieving a certain level of system reliability. DOE

N94-28646# Instron Corp., Canton, MA.
DEVELOPMENT OF ALTERNATING CURRENT POTENTIAL DROP (ACPD) PROCEDURES FOR CRACK DETECTION IN ALUMINUM AIRCRAFT PANELS Final Report, May - Dec. 1990
D. A. Jablonski Dec. 1993 108 p
(Contract DTRS57-89-D-00007)
(AD-A275755; DOT-VNTSC-FAA-93-9; DOT/FAA/CT-93/76) Avail: CASI HC A06/MF A02

The Alternating Current Potential Drop (ACPD) method is investigated as a means of making measurements in laboratory experiments on the initiation and growth of multiple site damage (MSD) cracks in a common aluminum alloy used for aircraft construction. Procedures for instrumenting MSD test specimens are recommended. The ACPD method is found to be capable of the following: (1) detecting crack initiation at a crack length of the order of 1 mm; (2) monitoring crack propagation at a resolution of the order of 5 micrometers; and (3) providing an indirect measurement of crack extension in R-curve type tests of fastener hole details. DTIC

N94-29020# Sandia National Labs., Albuquerque, NM. Manufacturing Systems Reliability.
ALGORITHMS FOR TREATING REDUNDANCY IN REPAIRABLE AND NON-REPAIRABLE SYSTEMS
James E. Campbell, Dennis E. Longsine, and Joel Atkins Oct. 1993 75 p
(Contract DE-AC04-94AL-85000)
(DE94-005289; SAND-93-1822) Avail: CASI HC A04/MF A01

This report presents equations and computational algorithms for analyzing the reliability of several forms of redundancy in repairable and non-repairable systems. For repairable systems, active, standby, and R of N redundancy with and without repair are treated. For non-repairable systems, active, standby, and R of N redundancy are addressed. These equations can be used to calculate mean time between failures, mean time to repair, and reliability for complex systems involving redundancy. DOE

N94-29366*# National Aeronautics and Space Administration. Langley Research Center, Hampton, VA.
FLUX-FOCUSING EDDY CURRENT PROBE AND METHOD FOR FLAW DETECTION Patent Application
John W. Simpson, inventor (to NASA) (Lockheed Engineering and Sciences Co., Hampton, VA.) and C. Gerald Clendenin, inventor (to NASA) 12 Oct. 1993 24 p
(NASA-Case-LAR-15046-1; NAS 1.71:LAR-15046-1;
US-Patent-Appl-SN-134444) Avail: CASI HC A03/MF A01

A flux-focusing electromagnetic sensor which uses a ferromagnetic flux-focusing lens simplifies inspections and increases detectability of fatigue cracks and material loss in high conductivity material is presented. The unique feature of the device is the ferrous shield isolating a high-turn pick-up coil from an excitation coil. The use of the magnetic shield is shown to produce a null voltage output across the receiving coil in the presence of an unflawed sample. A redistribution of the current flow in the sample caused by the presence of flaws, however, eliminates the shielding condition and a large output voltage is produced, yielding a clear unambiguous flaw signal. The maximum sensor output is obtained when positioned symmetrically above the crack. Hence, by obtaining the position of the maximum sensor output, it is possible to track the fault and locate the area surrounding its tip. The accuracy of tip location is enhanced by two unique features of the sensor; a very high signal-to-noise ratio of the probe's output which results in an extremely smooth signal peak across the fault, and a rapidly decaying sensor output outside a small area surrounding the crack tip which enables the region for searching to be clearly defined. Under low frequency operation, material thinning due to corrosion damage causes an incomplete shielding of the pick-up coil. The low frequency output voltage of the probe is therefore a direct indicator of the thickness of the test sample. NASA

N94-29474# Aerospatiale, Suresnes (France). Centre Commun de Recherches Louis-Bleriot.
AUTOMATION OF THE NDT DIAGNOSTIC USING NEURAL NETS. APPLICATION: INSPECTION OF AIRBUS LONGITUDINAL JOINTS DURING MAINTENANCE [AUTOMATISATION DU DIAGNOSTIC EN CND PAR L'UTILISATION DE RESEAUX NEURONAUX. APPLICATION: INSPECTION EN MAINTENANCE DES LIAISONS LONGITUDINALES AIRBUS]
Christine Brousset and Gilles Baudrillard 1993 11 p In FRENCH
(Rept-932-600-104; ETN-94-95483) Avail: CASI HC A03/MF A01

A neural network tool was developed to automate the Non Destructive Testing (NDT) of aeronautical structures carried out with the SIAM system. The SIAM system is used to reveal splits in longitudinal metal joints on the Airbus fuselage. The integration of the neural net tool within the SIAM control system is considered possible. The automatic diagnostic should provide the operator with an aid which will permit a greater reliability of maintenance control. The diagnostic performed with this tool would be rapid;: the control of 30,000 rivets on the Airbus fuselage would take approximately 45 minutes. ESA

N94-29548* National Aeronautics and Space Administration. Langley Research Center, Hampton, VA.
METHOD AND APPARATUS FOR INDICATING DISBONDS IN JOINT REGIONS Patent
Eric I. Madaras, inventor (to NASA) 25 Jan. 1994 8 p Filed 29 Aug. 1991 Supersedes N92-17859 (30 - 8, p 1309)
(NASA-Case-LAR-14626-1; US-Patent-5,280,722;
US-Patent-Appl-SN-751489; US-Patent-Class-73-588;
US-Patent-Class-73-644; Int-Patent-Class-G01N-29/10;
Int-Patent-Class-G01N-29/28) Avail: US Patent and Trademark Office

A method for indicating disbonds in joint regions is discussed. A critical bondline region is located between a first material and a second material having a higher acoustic impedance than the first material. A form member having an acoustic impedance which is substantially similar to the first material has a first face which is form fitted to a surface of the first material opposite to and non-parallel with the critical bondline region. The form member has an opposite second face which is shaped to be parallel to the critical bondline region. Transducers are acoustically coupled to the second face of the form member to generate an ultrasonic tone burst through the acoustically similar form member and first material which is reflected by the critical bondline region. This reflected tone burst is received

and a resulting signal is compared with a normal signal for no disbond to determine the presence of an unacceptable disbond.
Official Gazette of the U.S. Patent and Trademark Office

N94-29724*# Alabama Univ., Huntsville. Research Inst.
FIELD METHODS TO MEASURE SURFACE DISPLACEMENT AND STRAIN WITH THE VIDEO IMAGE CORRELATION METHOD Final Technical Report, 15 Jun. 1993 - 31 Mar. 1994
Gary A. Maddux, Charles M. Horton, Stephen R. McNeill, and Matthew D. Lansing 31 Mar. 1994 38 p
(Contract NAS8-38609)
(NASA-CR-195796; NAS 1.26:195796; UAH-5-33282) Avail: CASI HC A03/MF A01

The objective of this project was to develop methods and application procedures to measure displacement and strain fields during the structural testing of aerospace components using paint speckle in conjunction with the Video Image Correlation (VIC) system. Author (revised)

N94-30235 Laval Univ. (Quebec). Dept. de Genie Electrique.
STUDY OF THE PROBLEMS OF NONUNIFORMITY OF HEATING IN INFRARED VISION APPLIED TO THE INSPECTION OF MATERIALS HAVING NON-PLANAR RELIEF M.S. Thesis [ETUDE DES PROBLEMES DE NON UNIFORMITE DE CHAUFFAGE EN VISION INFRAROUGE APPLIQUEE A L'INSPECTION DES MATERIAUX AU RELIEF NON PLAN]
Louis Fortin Jul. 1993 72 p In FRENCH
(ISBN-0-315-85637-8; CTN-94-61150) Copyright Avail: Micromedia Ltd., Technical Information Centre, 240 Catherine Street, Suite 305, Ottawa, Ontario, K2P 2G8, Canada HC/MF

Infrared thermography is a relatively new technique for nondestructive inspection of parts and components. It allows detection of the presence of subsurface defects such as debonding, delaminations, and inclusions. Nevertheless, certain problems must be resolved before this material inspection technique can be made universal. One of these problems concerns the deposition of energy on the surface of the samples being analyzed. In effect, it is not easy to find an inexpensive and powerful source which also achieves a uniform deposition of energy. Laser sweeping might be possible, but at a prohibitive cost. Special 1000-W bulbs can be used if a calibration of the spatial distribution of energy in the measurement zone is carried out. This latter approach has been followed in a study of spatial calibration of the deposition of thermal energy (read by the infrared camera) and modelling of internal heat transfer, so that the response of the analyzed parts could be characterized a-priori. A simple finite difference model was used in the theoretical part of the study. The experimental and theoretical results obtained are promising and open up other interesting applications for thermography. CISTI

39 STRUCTURAL MECHANICS

Includes structural element design and weight analysis; fatigue; and thermal stress.

For applications see *05 Aircraft Design, Testing and Performance* and *18 Spacecraft Design, Testing and Performance.*

N94-28402# Technical Research Centre of Finland, Espoo. Metallilaboratorio.
SINGLE SPECIMEN FRACTURE TOUGHNESS DETERMINATION PROCEDURE USING INSTRUMENTED IMPACT TEST Ph.D. Thesis
Rauno Rintamaa 1993 163 p
(ISSN 1235-0621)
(PB94-132040; VTT/PUB-140; ISBN-951-38-4258-4) Copyright Avail: CASI HC A08/MF A02

The focus of the work is aimed at two scientific issues. The primary emphasis is directed to development of a method which enables the detection of ductile crack initiation, and hence, the energy-based fracture toughness, by applying an optical crack opening displacement (COD) measuring device. It is claimed that the Double Displacement Ratio (DDR), i.e., the ratio of crack opening displacement vs. specimen displacement, indicates the onset of ductile crack growth initiation in a way which is easy and reliable enough to apply in transition and upper shelf regions of a fracture toughness transition temperature curve. The method is extensively verified by experimental and analytical investigations, and compared with other single specimen methods used for dynamic fracture toughness determination. NTIS

N94-28404# Technical Research Centre of Finland, Espoo. Instrument Lab.
CHARACTERIZATION OF STRUCTURAL VIBRATION: FIELD DESCRIPTORS BASED ON ENERGY DENSITY AND INTENSITY
Jukka Linjama 1993 35 p
(ISSN 1235-0621)
(PB94-132230; VTT/PUB-152; ISBN-951-38-4390-4) Copyright Avail: CASI HC A03/MF A01

Measurement of energy flow in acoustical and vibrational fields is usually based on the detection of one linear field quantity (e.g. sound pressure) and its spatial gradient, two transducers being used for the measurement. This report first reviews the quantities which can be obtained from the measurement of acoustical intensity with a two-microphone probe: intensity and the energy densities. A set of 'field descriptors', relative quantities giving a measure of propagating (active) character of the waves in the sound field, is proposed. These energetic quantities are based entirely on the transversal velocity measured and the gradient of that velocity, and are available when the two-transducer method of bending wave intensity is used. Examples of the energy densities and field descriptors measured in an aluminum plate are presented, and proposals for further work are given. NTIS

N94-28409# Technical Research Centre of Finland, Espoo. Metals Lab.
VISCOUS AND ELASTIC-PLASTIC MATERIAL MODEL IN THE ABAQUS
Kari Santaoja 1993 54 p
(PB94-132347; VTT/PUB-144; ISBN-951-38-4382-3) Copyright Avail: CASI HC A04/MF A01

The implementation of constitutive equations into a structural analysis computer program is investigated. The material model under consideration describes pure linear elastic, elastic-plastic, and viscous deformation mechanisms. The elastic-plastic material model assumes isotropic hardening and the uniaxial stress-strain curve is bilinear. The von Mises yield condition is applied. Viscous deformation is described by the equation proposed by Le Gac and Duval. This model is coded into the ABAQUS finite element method program. The time integration is carried out by the Euler forward method. The computed examples show that the implementation is carried out successfully. NTIS

N94-28508*# Rockwell International Corp., Canoga Park, CA. Rocketdyne Div.
COMPOSITE LOAD SPECTRA FOR SELECT SPACE PROPULSION STRUCTURAL COMPONENTS Final Report
Hing W. Ho and James F. Newell Mar. 1994 269 p
(Contract NAS3-26371; RTOP 584-03-11)
(NASA-CR-194476; E-8621; NAS 1.26:194476) Avail: CASI HC A12/MF A03

Generic load models are described with multiple levels of progressive sophistication to simulate the composite (combined) load spectra (CLS) that are induced in space propulsion system components, representative of Space Shuttle Main Engines (SSME), such as transfer ducts, turbine blades and liquid oxygen (LOX) posts. These generic (coupled) models combine the deterministic models for composite load dynamic, acoustic, high-pressure and high rotational speed, etc., load simulation using statistically varying coefficients. These coefficients are then determined using advanced probabilistic simulation methods with and without strategically selected experimental data. The entire simulation process is included in a CLS computer code. Applications of the computer code to various components in conjunction with the PSAM (Probabilistic Structural Analysis Method) to perform probabilistic load evaluation and life prediction evaluations are also described to illustrate the effectiveness of the coupled model approach. Author

N94-28726 Acoustical Society of America, New York, NY.
MINUTES: ACCREDITED STANDARDS COMMITTEE ON MECHANICAL VIBRATION AND SHOCK, S2. US TAG FOR ISO/TC 108 MECHANICAL VIBRATION AND SHOCK
6 Oct. 1993 57 p Meeting held in Ottawa, Ontario, 19 May 1993
Limited Reproducibility: More than 20% of this document may be affected

by microfiche quality
(AD-A275591) Avail: Issuing Activity (Defense Technical Information Center (DTIC))

Topics include: approval of minutes of Ottawa, Canada meeting, held 19 May 1993; organization; standards approved by ANSI in 1992/1993 and published (or being published) by ASA; organizational matters and reports on working groups, including reports on letter ballots and international matters; International Organization for Standardization (ISO); International Electrotechnical Commission (IEC); review of standards more than five years in existence; new international standards available from ANSI; documents from other organizations submitted to S2 for vote and/or comment; procedural ballots; other business; future meetings; and adjournment. CASI

N94-28761# Washington Univ., Seattle. Dept. of Mechanical Engineering.
PLANE STRESS STABLE CRACK GROWTH AND J-INTEGRAL/HRR FIELD
G. B. May and A. S. Kobayashi Dec. 1993 40 p
(Contract N00014-89-J-1276)
(AD-A275761; UWA/DME/TR-93-74) Avail: CASI HC A03/MF A01

Moire interferometry with line densities of 1200 and 40 lines per mm was used to determine the two orthogonal displacements surrounding a stably extending crack in a 2024-T3 aluminum alloy, single edge-cracked specimen. The test protocol consisted of using the fine moire grating prior to and up to the onset of crack extension and the coarse moire grating for the ensuing crack extension up to delta(a) = 6 mm. The displacement fields were used to compute the J-integrals for various contours during crack tip blunting and crack extension. As expected, the far-field J-integral value prior to stable crack growth coincided with the LEFM strain energy release rate, G, and validated the experimental procedure. However, the J values obtained from the near tip contour increased slowly while the far field J values increased rapidly with increasing stable crack growth. The HRR displacement field was computed from the experimentally determined far field J. The HRR displacement field agreed with the measured displacement field prior to stable crack growth since J = G. However, the HRR horizontal displacement field progressively deviated from the measured values with crack extension. DTIC

N94-28801*# Virginia Polytechnic Inst. and State Univ., Blacksburg. Dept. of Engineering Science and Mechanics.
NUMERICAL AND EXPERIMENTAL INVESTIGATION OF THE BENDING RESPONSE OF THIN-WALLED COMPOSITE CYLINDERS Interim Report No. 95, Aug. 1988 - Sep. 1993
J. P. Fuchs, M. W. Hyer, and J. H. Starnes, Jr. Sep. 1993 193 p
(Grant NAG1-343)
(NASA-CR-195730; NAS 1.26:195730; CCMS-93-19; VPI-E-93-11) Avail: CASI HC A09/MF A03

A numerical and experimental investigation of the bending behavior of six eight-ply graphite-epoxy circular cylinders is presented. Bending is induced by applying a known end-rotation to each end of the cylinders, analogous to a beam in bending. The cylinders have a nominal radius of 6 inches, a length-to-radius ratio of 2 and 5, and a radius-to-thickness ratio of approximately 160. A (+/- 45/0/90)S quasi-isotropic layup and two orthotropic layups, (+/- 45/0 sub 2)S and (+/- 45/90 sub 2)S, are studied. A geometrically nonlinear special-purpose analysis, based on Donnell's nonlinear shell equations, is developed to study the prebuckling responses and gain insight into the effects of non-ideal boundary conditions and initial geometric imperfections. A geometrically nonlinear finite element analysis is utilized to compare with the prebuckling solutions of the special-purpose analysis and to study the buckling and post buckling responses of both geometrically perfect and imperfect cylinders. The imperfect cylinder geometries are represented by an analytical approximation of the measured shape imperfections. Extensive experimental data are obtained from quasi-static tests of the cylinders using a test fixture specifically designed for the present investigation. A description of the test fixture is included. The experimental data are compared to predictions for both perfect and imperfect cylinder geometries. Prebuckling results are presented in the form of displacement and strain profiles. Buckling end-rotations, moments, and strains are reported, and predicted mode shapes are presented. Observed and predicted moment vs. end-rotation relations, deflection patterns, and strain profiles are illustrated for the post buckling responses. It is found that a geometrically nonlinear boundary layer behavior characterizes the prebuckling responses. The boundary layer behavior is sensitive to laminate orthotropy, cylinder geometry, initial geometric imperfections, applied end-rotation, and non-ideal boundary conditions. Buckling end-rotations, strains, and moments are influenced by laminate orthotropy and initial geometric imperfections. Measured buckling results correlate well with predictions for the geometrically imperfect specimens. The postbuckling analyses predict equilibrium paths with a number of scallop-shaped branches that correspond to unique deflection patterns. The observed postbuckling deflection patterns and measured strain profiles show striking similarities to the predictions in some cases. Ultimate failure of the cylinders is attributed to an interlaminar shear failure mode along the nodal lines of the postbuckling deflection patterns. Author

N94-28811 Pennsylvania State Univ., University Park. Dept. of Materials Science and Engineering.
A MODELING STUDY OF THE EFFECT OF STRESS STATE ON VOID LINKING DURING DUCTILE FRACTURE
A. B. Geltmacher, D. A. Koss, P. Matic, and M. G. Stout 28 Jan. 1994 34 p Limited Reproducibility: More than 20% of this document may be affected by microfiche quality
(Contract N00014-91-J-1414)
(AD-A275505; TR-8) Avail: CASI HC A03

Specimens containing arrays of through-thickness holes are used to model aspects of void linking during ductile, microvoid fracture. Specifically, the contrasting deformation and fracture behavior of sheet specimens containing either pairs or pseudo-random arrays of equi-sized holes is examined in both uniaxial and equal-biaxial tension utilizing experiment as well as computer simulation. Our results show for this plane-stress situation that hole linking is always caused by flow localization within the ligaments between neighboring holes. The imposed strains to initiate flow localization and subsequent ligament failure are sensitive to stress state (uniaxial versus biaxial), strain hardening, and the location of the neighboring hole(s). A significant observation is the influence of stress state on the multidirectionality of hole linking paths. As a result, increasing the biaxial component of the stress-state increases the number of holes that can participate in a hole linking process increases. A related and subtle implication to microvoid fracture is that the strain range over which void linking occurs decreases with increasing triaxiality of the stress state; in effect, after the initiation of void linking, its propagation is accelerated under biaxial or triaxial tension. DTIC

N94-28815*# Pratt and Whitney Aircraft, East Hartford, CT.
THERMAL/STRUCTURAL TAILORING OF ENGINE BLADES (T/SEAEBL). THEORETICAL MANUAL Final Report
K. W. Brown and W. B. Clevenger Mar. 1994 40 p
(Contract NAS3-22525; RTOP 505-63-5B)
(NASA-CR-194462; E-8495; NAS 1.26:194462) Avail: CASI HC A03/MF A01

The Thermal/Structural Tailoring of Engine Blades (T/STAEBL) system is a family of computer programs executed by a control program. The T/STAEBL system performs design optimizations of cooled, hollow turbine blades and vanes. This manual describes the T/STAEBL data block structure and system organization. The approximate analysis and optimization modules are detailed, and a validation test case is provided. Author

N94-28819*# National Aeronautics and Space Administration. Lewis Research Center, Cleveland, OH.
AN ANALYSIS OF ISOTHERMAL, BITHERMAL, AND THERMOMECHANICAL FATIGUE DATA OF HAYNES 188 AND B1900+Hf BY ENERGY CONSIDERATIONS
V. M. Radhakrishnan (Indian Inst. of Tech., Madras.), Sreeramesh Kalluri (Sverdrup Technology, Inc., Brook Park, OH.), and Gary R. Halford Sep. 1993 25 p
(Contract NAS3-25266; RTOP 505-63-5B)
(NASA-TM-106359; E-8153; NAS 1.15:106359) Avail: CASI HC A03/MF A01

The low-cycle fatigue behavior of Haynes 188 and B1900+Hf under isothermal, bithermal, and thermomechanical loading conditions has been analyzed on the basis of the total hysteresis energy expended per cycle. It has been observed that in the case of isothermal fatigue the total hysteresis energy correlates well with the fatigue life. In the case of bithermal

'high rate' fatigue, for a given total hysteresis energy per cycle, the fatigue life is equal to or greater than the isothermal fatigue life at the maximum bithermal temperature. This observation could be used to establish a lower bound on life for design purposes. In one case of bithermal creep-fatigue and in thermomechanical fatigue, the life is shorter than that corresponding to the isothermal life at the maximum temperature. The energy supplied, per se, may not always give a systematic correlation with the fatigue life in the cases where time-dependent creep and environmental effects are encountered. Thus, in bithermal creep-fatigue and thermomechanical fatigue, the role of creep and environment and their dependence on the energy supplied have to be properly accounted for before the energy term can be used for life prediction. Author (revised)

N94-28821*# Akron Univ., OH.
AN ANISOTROPIC EXTENSION OF BODNER'S MODEL OF VISCOPLASTICITY: MODEL DEVELOPMENT Final Report
David N. Robinson Mar. 1994 17 p
(Grant NAG3-379; RTOP 505-63-12)
(NASA-CR-195289; E-8649; NAS 1.26:195289) Avail: CASI HC A03/MF A01

An anisotropic viscoplasticity model is developed as an extension of the well known Bodner model. The extension is made by replacing the effective stress of the isotropic Bodner model by one involving invariants for transverse isotropy. The resulting model retains the simplicity of Bodner's in the ease with which the material constants are determined experimentally. It allows a representation of strong initial anisotropy yet is based on the scalar state variable under the assertion that induced anisotropy is negligible relative to the strong initial anisotropy. Temperature dependence is taken as in the original Bodner theory. Account is made of fiber volume fraction through nonlinear rules of mixture applied to the stress history and anisotropy parameters. Focus is on the theoretical development of the model, however, application to a W/Cu composite is in progress and will be reported as a sequel to this report. Author

N94-28840*# Texas Univ., San Antonio. Dept. of Mechanical Engineering.
PROBABILISTIC MATERIAL STRENGTH DEGRADATION MODEL FOR INCONEL 718 COMPONENTS SUBJECTED TO HIGH TEMPERATURE, MECHANICAL FATIGUE, CREEP AND THERMAL FATIGUE EFFECTS Final Report
Callie Corinne Schei Bast Mar. 1994 75 p
(Grant NAG3-867; RTOP 584-03-11)
(NASA-CR-195284; E-8629; NAS 1.26:195284) Avail: CASI HC A04/MF A01

This thesis presents the on-going development of methodology for a probabilistic material strength degradation model. The probabilistic model, in the form of a postulated randomized multifactor equation, provides for quantification of uncertainty in the lifetime material strength of aerospace propulsion system components subjected to a number of diverse random effects. This model is embodied in the computer program entitled PROMISS, which can include up to eighteen different effects. Presently, the model includes four effects that typically reduce lifetime strength: high temperature, mechanical fatigue, creep, and thermal fatigue. Statistical analysis was conducted on experimental Inconel 718 data obtained from the open literature. This analysis provided regression parameters for use as the model's empirical material constants, thus calibrating the model specifically for Inconel 718. Model calibration was carried out for four variables, namely, high temperature, mechanical fatigue, creep, and thermal fatigue. Methodology to estimate standard deviations of these material constants for input into the probabilistic material strength model was developed. Using the current version of PROMISS, entitled PROMISS93, a sensitivity study for the combined effects of mechanical fatigue, creep, and thermal fatigue was performed. Results, in the form of cumulative distribution functions, illustrated the sensitivity of lifetime strength to any current value of an effect. In addition, verification studies comparing a combination of mechanical fatigue and high temperature effects by model to the combination by experiment were conducted. Thus, for Inconel 718, the basic model assumption of independence between effects was evaluated. Results from this limited verification study strongly supported this assumption. Author (revised)

N94-28841 National Physical Lab., Teddington (England). Div. of Materials Metrology.
MEASUREMENT AND MODELLING OF BOLTED JOINT STRESS RELAXATION IN PLASTICS
A. Cook, D. Dawson, and B. C. Duncan Jul. 1993 49 p
(PB94-124849; DMM(A)-109) Avail: Issuing Activity (National Technical Information Service (NTIS))

The loss of joint integrity caused by viscoelastic stress relaxation limits the service life of plastic components bolted to dissimilar materials. A technique, which incorporates an integral load cell, to measure the stress relaxation properties of bolted polymer components over extended time periods at temperatures of up to 150 C was developed. Models were developed to extrapolate the measured stress relaxation, thus providing an estimate of the service life. At elevated temperatures, isothermal shrinkage of the polymer can have a significant impact on the load, contrary to what was believed previously. Phenolic thermostat housings undergoing the standard post-cure (seven hours at 170 C) should have service lives of 3 years at operating temperatures of up to 100 C. NTIS

N94-29057# Lynntech, Inc., College Station, TX.
PORTABLE ELECTRONICALLY BASED METHOD FOR THE NONDESTRUCTIVE REMOTE SENSING OF CREVICE CORROSION Final Report, 27 Apr. - 31 Oct. 1993
D. Hodko, M. Novak, C. C. Andrews, O. J. Murphy, and G. D. Hitchens 31 Oct. 1993 30 p
(Contract N00014-93-C-0067)
(AD-A275403) Avail: CASI HC A03/MF A01

Corrosion in the crevices of gasketed joints in the presence of sea-water has been particularly troublesome for the Navy in pipelines. Some of the existing non-destructive techniques can be used without entering the pipeline system but most of them suffer from low signal-to-noise ratios due to spurious signals caused by scattering on rough-pitted surfaces. The main advantages of four-point probe pulsed current resistance measurements, the innovative approach described in this report, are that the sensing probe can be easily adapted for inspection of different sizes of flanges and the costs for development and application of this technique will be very low. Significant conclusions from the research included: (1) the results fully demonstrated the feasibility of using the pulsed current resistance technique for the non-destructive detection of crevice corrosion in flanges; (2) resistance measurements based on current pulsing are more sensitive than measurements made using constant DC currents; (3) the pulsed current resistance measurement technique can be easily automated and computerized, which can provide high resolution three-dimensional images of flange damage. The key research and development area for follow-on work is full development of an automated, portable, flange crevice corrosion detection system, consisting of: (1) resistance probes of appropriate size; and (2) a computerized resistance meter based on high amplitude pulsed currents/low voltage sensing system. DTIC

N94-29091 Aeronautical Research Labs., Melbourne (Australia).
COLD EXPANSION AND INTERFERENCE FOR EXTENDING THE FATIGUE LIFE OF MULTI-LAYER METAL JOINTS
J. M. Finney Oct. 1993 34 p Limited Reproducibility: More than 20% of this document may be affected by microfiche quality
(AD-A274982; ARL-RR-17; DODA-AR-008-369) Avail: CASI HC A03

The influences of both hole cold expansion and interference-fit fasteners for extending the fatigue life of multilayer aluminum alloy joint specimens under variable amplitude loading have been examined experimentally. Improvements in fatigue life were markedly dependent on the degree of load transfer in the specimen joint. The cold expansion of fastener holes enhanced fatigue life in low load transfer joints but not in 100% load transfer joints. The use of interference-fit fasteners, especially at high degrees of interference, was an effective means of life improvement irrespective of proportion of load transfer. Interfacial fretting limited the improvement in fatigue life of low load transfer joints to a factor of about six, and, although some fretting occurred in 100% load transfer joints, it was not determinative, and a 40-fold increase in fatigue life was obtained with a combination of hole cold expansion and interference-fit fastener. DTIC

N94-29104*# Sverdrup Technology, Inc., Brook Park, OH.
TURBOMACHINERY FORCED RESPONSE PREDICTION SYSTEM (FREPS): USER'S MANUAL Final Report
M. R. Morel and D. V. Murthy Mar. 1994 115 p
(Contract NAS3-25266; NAG3-1669; RTOP 505-63-5B; RTOP 232-01-0B)
(NASA-CR-194465; E-8518; NAS 1.26:194465) Avail: CASI HC A06/MF A02

The turbomachinery forced response prediction system (FREPS), version 1.2, is capable of predicting the aeroelastic behavior of axial-flow turbomachinery blades. This document is meant to serve as a guide in the use of the FREPS code with specific emphasis on its use at NASA Lewis Research Center (LeRC). A detailed explanation of the aeroelastic analysis and its development is beyond the scope of this document, and may be found in the references. FREPS has been developed by the NASA LeRC Structural Dynamics Branch. The manual is divided into three major parts: an introduction, the preparation of input, and the procedure to execute FREPS. Part 1 includes a brief background on the necessity of FREPS, a description of the FREPS system, the steps needed to be taken before FREPS is executed, an example input file with instructions, presentation of the geometric conventions used, and the input/output files employed and produced by FREPS. Part 2 contains a detailed description of the command names needed to create the primary input file that is required to execute the FREPS code. Also, Part 2 has an example data file to aid the user in creating their own input files. Part 3 explains the procedures required to execute the FREPS code on the Cray Y-MP, a computer system available at the NASA LeRC. Derived from text

N94-29121 National Physical Lab., Teddington (England). Div. of Materials Metrology.
MODELLING AND ANALYSIS OF CREEP DEFORMATION AND FRACTURE IN A 1 Cr 1/2 Mo FERRITIC STEEL
B. F. Dyson and D. Osgerby 1993 47 p
(PB94-138328; NPL-DMM(A)-116) Copyright Avail: Issuing Activity (National Technical Information Service (NTIS))

A quantitative model, based upon a proposed new mechanism of creep deformation in particle-hardened alloys, has been validated by analysis of creep data from a 13CrMo 4 4 (1Cr 1/2 Mo) material tested under a range of stresses and temperatures. The methodology that has been used to extract the model parameters quantifies, as a first approximation, only the main degradation (damage) processes - in the case of the 1CR 1/2 Mo steel, these are considered to be the parallel operation of particle-coarsening and a progressively increasing stress due to a constant-load boundary condition. These 'global' model parameters can then be modified (only slightly) as required to obtain a detailed description and 'fit' to the rupture lifetime and strain/time trajectory of any individual test. The global model parameter approach may be thought of as predicting average behavior and the detailed fits as taking account of uncertainties (scatter) due to variability in the material. Using the global parameter dataset, predictions have also been made of behavior under biaxial stressing; constant straining rate; constant total strain (stress relaxation) and the likely success or otherwise of metallographic and mechanical remanent lifetime procedures. NTIS

N94-29384*# National Aeronautics and Space Administration. Lewis Research Center, Cleveland, OH.
A METHOD FOR THE PROBABILISTIC DESIGN ASSESSMENT OF COMPOSITE STRUCTURES
Michael C. Shiao (Sverdrup Technology, Inc., Brook Park, OH.), Surendra N. Singhal (Sverdrup Technology, Inc., Brook Park, OH.), and Christos C. Chamis Mar. 1994 16 p Presented at the 24th International SAMPE Technical Conference, Toronto, Ontario, 20-22 Oct. 1992; sponsored by the Society for the Advancement of Materials and Process Engineering
(RTOP 510-02-12)
(NASA-TM-106384; E-8204; NAS 1.15:106384) Avail: CASI HC A03/MF A01

A formal procedure for the probabilistic design assessment of a composite structure is described. The uncertainties in all aspects of a composite structure (constituent material properties, fabrication variables, structural geometry, service environments, etc.), which result in the uncertain behavior in the composite structural responses, are included in the assessment. The probabilistic assessment consists of design criteria, modeling of composite structures and uncertainties, simulation methods, and the decision making process. A sample case is presented to illustrate the formal procedure and to demonstrate that composite structural designs can be probabilistically assessed with accuracy and efficiency. Author (revised)

N94-29406*# National Aeronautics and Space Administration. Lewis Research Center, Cleveland, OH.
STIFFNESS-GENERATED RIGID-BODY MODE SHAPES FOR LANCZOS EIGENSOLUTION WITH SUPORT DOF BY WAY OF A MSC/NASTRAN DMAP ALTER
Ayman A. Abdallah (Analex Corp., Brook Park, OH.), Alan R. Barnett (Analex Corp., Brook Park, OH.), Timothy W. Widrick (Analex Corp., Brook Park, OH.), Richard T. Manella, and Robert P. Miller Mar. 1994 18 p Proposed for presentation at the 1994 MSC World Users' Conference, Orlando, FL, 20-24 Jun. 1994; sponsored by the MacNeal-Schwendler Corp.
(Contract NAS3-25776)
(NASA-TM-106537; E-8676; NAS 1.15:106537) Avail: CASI HC A03/MF A01

When using all MSC/NASTRAN eigensolution methods except Lanczos, the analyst can replace the coupled system rigid-body modes calculated within DMAP module READ with mass orthogonalized and normalized rigid-body modes generated from the system stiffness. This option is invoked by defining MSC/NASTRAN r-set degrees of freedom via the SUPORT bulk data card. The newly calculated modes are required if the rigid-body modes calculated by the eigensolver are not 'clean' due to numerical roundoffs in the solution. When performing transient structural dynamic load analysis, the numerical roundoffs can result in inaccurate rigid-body accelerations which affect steady-state responses. Unfortunately, when using the Lanczos method and defining r-set degrees of freedom, the rigid-body modes calculated within DMAP module REIGL are retained. To overcome this limitation and to allow MSC/NASTRAN to handle SUPORT degrees of freedom identically for all eigensolvers, a DMAP Alter has been written which replaces Lanczos-calculated rigid-body modes with stiffness-generated rigid-body modes. The newly generated rigid-body modes are normalized with respect to the system mass and orthogonalized using the Gram-Schmidt technique. This algorithm has been implemented as an enhancement to an existing coupled loads methodology. Author (revised)

N94-29433# Auburn Univ., AL. Dept. of Civil Engineering.
NUMERICAL ANALYSIS OF DYNAMIC DIRECT TENSION AND DIRECT COMPRESSION TESTS Final Report, Feb. 1990 - Apr. 1991
Joseph W. Tedesco, Mary L. Hughes, and Brian P. ONeil Jan. 1993 379 p
(AD-A275255; AFCESA/ESL-TR-91-41) Avail: CASI HC A17/MF A03

This report summarizes the results of a comprehensive numerical analysis of direct tension and direct compression tests of plain concrete performed at strain rates between 1 and 10 to the 2nd power on a Split Hopkinson Pressure Bar (SHPB). The objective of this study was to investigate failure mechanisms in plain concrete specimens at high strain rates. Both an elastic and inelastic concrete material model were employed in all numerical analyses. The modes of failure predicted by the numerical analyses are consistent with those observed in experimental studies. In all instances, the mode of failure was significantly influenced by the rate of loading. DTIC

N94-29469*# National Aeronautics and Space Administration. Lewis Research Center, Cleveland, OH.
TRANSIENT ANALYSIS MODE PARTICIPATION FOR MODAL SURVEY TARGET MODE SELECTION USING MSC/NASTRAN DMAP
Alan R. Barnett (Analex Corp., Brook Park, OH.), Omar M. Ibrahim (Analex Corp., Brook Park, OH.), Timothy L. Sullivan (Analex Corp., Brook Park, OH.), and Thomas W. Goodnight Mar. 1994 21 p Proposed for presentation at the 1994 MSC World Users' Conference, Orlando, FL, 20-24 Jun. 1994; sponsored by the MacNeal-Schwendler Corp.
(Contract NAS3-25776)
(NASA-TM-106536; E-8674; NAS 1.15:106536) Avail: CASI HC A03/MF A01

Many methods have been developed to aid analysts in identifying component modes which contribute significantly to component responses. These modes, typically targeted for dynamic model correlation via a modal survey, are known as target modes. Most methods used to identify target modes are based on component global dynamic behavior. It is sometimes

unclear if these methods identify all modes contributing to responses important to the analyst. These responses are usually those in areas of hardware design concerns. One method used to check the completeness of target mode sets and identify modes contributing significantly to important component responses is mode participation. With this method, the participation of component modes in dynamic responses is quantified. Those modes which have high participation are likely modal survey target modes. Mode participation is most beneficial when it is used with responses from analyses simulating actual flight events. For spacecraft, these responses are generated via a structural dynamic coupled loads analysis. Using MSC/NASTRAN DMAP, a method has been developed for calculating mode participation based on transient coupled loads analysis results. The algorithm has been implemented to be compatible with an existing coupled loads methodology and has been used successfully to develop a set of modal survey target modes. Author

N94-29681# Swedish Inst. for Materials Testing, Boras.
MODELLING SOFT IMPACTS FOR VIBRATIONAL EXCITATION OF CIVIL ENGINEERING STRUCTURES
L. Agardh 1993 50 p
(PB94-137619; SP-RAPP-1993:50) Avail: CASI HC A03/MF A01

Experimental modal analyses of civil engineering structures are performed for various reasons. One is to assess the condition of the structure. Another is to verify the behavior of the structure under dynamic loads. An accurate method to excitate the structure is to use vibrators and random noise. For large structures in field conditions this may be quite expensive, and requires heavy equipment. Excitation by impact is often an effective alternative. In the report an impact equipment consisting of a striker and a mobile 'lift and drop' arrangement is used and some problems with impact excitation are discussed. The striker consists of a falling weight, a damper and a load cell. A soft interface between the load cell and the surface of the structure is used to prolong the contact time and filter out high frequency components. The contact force history is measured for 'soft' impacts on a stiff floor, for various choices of the mass and initial velocity of the striker. The floor is considered to be at rest during the impact event. Under these assumptions an analytical model of the contact force history is fitted to the measurements and used to solve a differential equation governing the striker system. From the solution the nonlinear stiffness of the striker system is estimated. NTIS

N94-29688 Missouri Univ., Rolla.
FINITE ELEMENT ANALYSIS OF AXISYMMETRIC DEFORMATIONS OF THICK THERMOVISCOPLASTIC TARGETS Ph.D. Thesis
Xingju Chen 1993 175 p
Avail: Univ. Microfilms Order No. DA9326587

The dissertation consists of four parts. We first conduct an approximate analysis of steady state axisymmetric deformations of a viscoplastic target being penetrated by a hemispherical nosed rigid penetrator. A kinematically admissible velocity field is presumed, and the unknown parameters are determined by minimizing the error in satisfying the balance of linear momentum. The solution so obtained is found to be very close to the finite element solution of the problem. In the second part, we postulate a velocity dependent expression for the frictional force on the target/penetrator interface. The values of the two constants in the expression for the frictional force are determined by comparing the distribution of the tangential traction on the penetrator nose surface as obtained from a finite element solution of the problem with that obtained by modeling the target material as a viscous fluid. The computed results show that the frictional force affects noticeably the tangential speed and the strain-rate on the penetrator nose surface, but minimally the normal traction there. Finally, we simulate numerically the penetration of a hemispherical nosed rigid rod into a thick thermoviscoplastic target and employ the aforestated expression for the frictional force. The finite element mesh is refined adaptively whenever one of its elements has been severely distorted. The computed results reveal that depth of penetration correlates well with the test value, the consideration of thermal softening of the target material influences strongly its deformations and the frictional force at the target/penetrator interface reduces the penetration depth by about 12 percent. Dissert. Abstr.

N94-29690 South Carolina Univ., Columbia.
ANALYSES OF STATIONARY AND GROWING CRACK TIP DEFORMATION BY DIGITAL IMAGE PROCESSING Ph.D. Thesis
Gang Han 1993 173 p
Avail: Univ. Microfilms Order No. DA9321959

Computer vision technique was applied to study crack tip deformation for a stationary crack and a stable growing crack in single edge cracked (SEC) specimens made by elastic and elastic-plastic material. The in-plane displacement and strain distributions in the vicinity of the crack tip before and after the crack initiation were obtained and compared with theoretical predictions. Results indicate that (1) the HRR solution can be used to quantify deformation field only in the region plastic strain strongly dominates the elastic strain, (2) for elastic-plastic materials, U has neither a elastic nor HRR singularity, V agrees with the HRR prediction in a large region. This suggests that higher order terms will be needed to accurately predict the deformation, (3) after the crack initiation crack tip deformation fields are controlled by J when w factor was smaller than 10.0, and (4) for small amounts of crack growth, the crack tip deformation fields seem to confirm the Quasi-static growing crack tip fields, predicted by the Gao-Hwang theory. In addition, the elastic unloading phenomenon for a growing crack was also investigated. In order to study the crack initiation and stable growth, the J-integral, crack tip opening displacement (CTOD) and crack tip opening angle (CTOA) were investigated to determine if they can be used as fracture parameters for thin specimens. Results indicate that the J resistance (J(sub R)), CTOD resistance and CTOA resistance curves were found to be independent of specimen size and a/w ratios; and CTOA are attained constant value when crack growth is larger than specimen thickness. However, the results for J-integral are dependent on the loading conditions. It was determined that J-integral value obtained of using displacement controlled condition was significantly lower relative to a load controlled condition for single edge cracked specimens having longer crack.
Dissert. Abstr.

N94-29765 Notre Dame Univ., IN.
THE IMPACT OF ELECTRICALLY CHARGED MICROSPHERES WITH PLANAR SURFACES UNDER VACUUM CONDITIONS Ph.D. Thesis
Michael Joseph Caylor 1993 166 p
Avail: Univ. Microfilms Order No. DA9325913

The normal and oblique impact of electrically charged microspheres with planar surfaces under vacuum conditions is examined experimentally. The experimental methods and results are presented. An analytical model for the normal impact case is used to examine the empirical results. The impact experiments were performed in a vacuum test cell maintained at pressures near 1 x 10(exp -4) Torr. Three types of microspheres (approximately 1 to 50 microns diameter) were used including silver-coated glass, stainless steel and nickel. The particles were impacted against a set of five planar, target surfaces including three metallic surfaces, a polymer surface and a glass-coated surface. The particles were electrostatically charged by induction (from approximately 0.1 to 10 fC) and dispensed using an electrostatic particle dispenser. The particle velocities were controlled to provide the desired range of incident velocities (approximately 1 to 20 m/s). A one-component Phase Doppler Particle Analyzer (PDPA), which also provided a particle sizing capability, was used to measure incident and rebound velocities for the normal impact experiments. A particle trajectory imaging system (PTIS) was developed and used for velocity measurements for the oblique impact tests. Average particle electrostatic charge was determined using a charge sensitive amplifier and from electrometer current measurements. This unique experimental approach permitted the examination of individual impact events. The coefficient of restitution, e, was determined by a matching algorithm that paired corresponding incident and rebound velocities. Average values of e ranged from 0.45 to 0.85. The data demonstrated the presence of adhesion effects at low incident velocities (below 2 m/s). An analytical model of this type of impact process showed that the magnitude of van der Waals force was dependent on the amount of elastic deformation during impact. For the particle charge levels of approximately 0.5 fC, the contribution of the electrostatic image force to the total adhesion force was found to be negligible. Electron micrographs of the impact surface verified the occurrence of permanent deformation for some microsphere impacts. Impulse ratios, mu, determined from oblique impact tests also showed that the microspheres can not be considered as point masses in these impact experiments.
Dissert. Abstr.

N94-29808 California Inst. of Tech., Pasadena.
MECHANISMS AND EFFECTS OF HEAT GENERATION AT THE TIPS OF DYNAMIC CRACKS AND NOTCHES IN METALS Ph.D. Thesis
James Joseph Mason 1993 168 p
Avail: Univ. Microfilms Order No. DA9325369

It is known that plastic work in metals is converted mostly to heat. Under dynamic plastic deformation conditions there is not enough time for conductive, convective or radiative cooling to prevent the generated heat from raising the temperature of the material. The resulting temperature rise can significantly alter the material properties and influence the failure behavior of the material. Several experiments have been performed using a high speed InSb infrared (IR) detector array to examine the mechanisms and effects of heat generation at the tip of a dynamic notch or crack. First, dynamically propagating cracks are investigated. It is seen that adiabatic conditions exist at the crack tip resulting in a simple relationship between the active plastic work zone and the temperature field and that, consequently, no effects of hyperbolic heat condition are observed. The dependence of the dynamically propagating crack tip temperature field upon crack speed and material parameters is reported. Next, the dependence of the rate of conversion of plastic work to heat upon strain and strain rate are examined. Using the split Hopkinson bar several materials were tested and compared to simple theories in the literature. It is seen that the materials do not always behave as expected, and that further investigation is necessary. Last, asymmetrically impact loaded, stationary notches are investigated with special attention paid to the formation of adiabatic shear bands at the notch tip. A new interferometer, the coherent gradient sensor (CGS), is used in conjunction with high speed photography to record the deformation field around the crack tip. The recorded field is shown to agree with a model of the deformation for low velocity impact of PMMA. For high velocity impact of C300 steel, shear bands are formed and a Dugdale model is used to produce measurements of the shear stress on the shear band from the recorded fringe patterns. Dissert. Abstr.

N94-29812 McGill Univ., Montreal (Quebec).
ON FATIGUE CRACK CLOSURE: ANALYSIS AND MEASUREMENT Ph.D. Thesis
Majid Mirzaei 1991 195 p
(ISBN-0-315-74873-7) Avail: Univ. Microfilms Order No. DANN74873

This thesis describes a novel approach to the analysis of fatigue crack closure phenomena. Based on the proposed model, the combined effect of residual plastic stretch, asperity mismatch, and corrosion debris on the closure behavior of a fatigue crack can be simulated by a hypothetical rigid insert located in an ideal crack wake. Accordingly, the crack closing period can be modeled by a gradual contact between the ideal crack faces and the rigid insert. The formulation of the model results in a set of equations which can predict the closure load as well as the load-CMOD characteristics using the residual CMOD at zero load as a unique experimental input. Based on the initial model, the final form of the derived equations are either logarithmic or quadratic. While the latter can be solved directly for the closure load, the former requires a numerical solution. The model qualitatively predicts the effect of gradual crack wake removal on the crack closure load level and the load-CMOD behavior. It also accounts for the response of a cracked component to an anomalous crack wake formed by single or block overloads. The model is verified, both qualitatively and quantitatively, using specifically designed experimental techniques, a variety of specimen sizes, and two different alloys. Dissert. Abstr.

N94-29829 South Carolina Univ., Columbia.
HIGHER ORDER ASYMPTOTIC CRACK TIP FIELDS IN A POWER-LAW HARDENING MATERIAL Ph.D. Thesis
Shaorui Yang 1993 102 p
Avail: Univ. Microfilms Order No. DA9322011

In this work, a method for determining a series of the higher order terms in the asymptotic expansion of the elastic-plastic crack-tip fields is developed. Based on the small strain formulation and the J(sub 2) deformation plasticity theory with power-law hardening, the governing equations for the higher order terms, which include the second, third and fourth order terms, are derived for both mode I and mode II loadings under either plane strain or plane stress conditions. Solutions for several higher order terms are presented. A comparison of the asymptotic expansion to finite element results indicates that the expansion can accurately predict the stress distribution for all angles within a substantial distance from the crack tip. For the mode I plane strain crack problem, it is found that, for the values of the hardening exponent n greater than or equal to 4 the four-terms asymptotic expansion with three independent amplitudes is controlled by plasticity; when n is greater than or equal to 3, the three-term expansion with two independent amplitudes is controlled by plasticity, and can be characterized by J and a second parameter A(sub 2) which is the dimensionless amplitude of the second order term. The effect of elasticity enters the second term at n = 1.5, the third term at n = 2, and the fourth term at n = 3. It is further demonstrated that the three-term expansion controlled by two parameters (J and A(sub 2)) can be used to describe the elastic-plastic crack-tip stress fields over a microscopically significant scale (1 less than (r-bar)/(J/sigma(sub o)) less than 5) for a variety of plane strain specimens at small to large scale yielding. The value of A(sub 2) can directly predict the stress triaxiality and the effect of geometry. It should be noted that, in general, the two-term expansion is not enough to predict the crack-tip field over the scale, because the effect of the third order term can not be neglected over the scale. For mode II case, two parameters (J and another parameter) control at least the first three terms for n less than or equal to 10 for both plane strain and plane stress problems. Dissert. Abstr.

N94-29951# Lawrence Livermore National Lab., CA.
LARGE-SCALE COMPUTATIONS IN ANALYSIS OF STRUCTURES
D. B. McCallen and G. L. Goudreau Sep. 1993 12 p Presented at the American Society of Civil Engineers (ASCE) Structures Congress, Atlanta, GA, Apr. 1994
(Contract W-7405-eng-48)
(DE94-004022; UCRL-JC-115223; CONF-940466-2) Avail: CASI HC A03/MF A01

Computer hardware and numerical analysis algorithms have progressed to a point where many engineering organizations and universities can perform nonlinear analyses on a routine basis. Though much remains to be done in terms of advancement of nonlinear analysis techniques and characterization on nonlinear material constitutive behavior, the technology exists today to perform useful nonlinear analysis for many structural systems. In the current paper, a survey on nonlinear analysis technologies developed and employed for many years on programmatic defense work at the Lawrence Livermore National Laboratory is provided, and ongoing nonlinear numerical simulation projects relevant to the civil engineering field are described. DOE

N94-30018# National Research Council of Canada, Ottawa (Ontario). Tribology and Mechanics Lab.
THEORETICAL PREDICTION OF THE INFLUENCE COEFFICIENTS ON DAMPED SIMPLE FLEXIBLE ROTORS USING THE TRANSFER MATRIX METHOD
Oh-Sung Jun (Korea Research Inst. of Standards and Science, Taejon, Republic of Korea.) and Paul Y. Kim Feb. 1994 60 p
(IMR-TM-TR-002; CTN-94-61133) Avail: CASI HC A04/MF A01

The influence coefficients for undamped flexible rotors are analytically derived and then compared and discussed for various damping coefficients. The concept of the transfer matrix method is partially adapted in the formulation. Single-disk and single cylinder rotor models are used for one- and two-plane balancing models, respectively. The gyroscopic effect of the disk or cylinder, which has been included in the formulation, is proved important through a simplified example rotor model. Taking the gyroscopic effect into account when calculating the influence coefficient is especially important near the resonant and antiresonant frequencies of the rotor. The simplified model also shows that an increase in damping reduces the sharpness of magnitude curve of influence coefficients and smoothens the change of phase at around the resonant and antiresonant frequencies.
Author (CISTI)

N94-30033 Ottawa Univ. (Ontario). Dept. de Genie Mecanique.
POSITION CONTROL OF A FLEXIBLE BEAM WITH ACTIVE DAMPING OF VIBRATIONS M.S. Thesis [REGLAGE DE POSITION D'UNE POUTRE FLEXIBLE AVEC AMORTISSEMENT ACTIF DES VIBRATIONS]
Jean De Carufel 1992 166 p In FRENCH
(ISBN-0-315-85841-9; CTN-94-61169) Copyright Avail: Micromedia Ltd., Technical Information Centre, 240 Catherine Street, Suite 305, Ottawa, Ontario, K2P 2G8, Canada HC/MF

A theoretical and experimental study was conducted on the active

damping of vibrations in a flexible beam having one free end and the other attached to the axis of a motor. Two methods for controlling the position of flexible structures are studied and are applied to the Euler-Bernoulli beam. The first is an active impedance dynamic gain method in the frequency domain. The second is a more complex method of feedback control by filtered states. A transfer function and a state model are also presented. The experimental work was conducted using a flexible beam, a direct current motor, and a digital controller. The experimental results were used to establish numerical models used for synthesizing the proposed controllers and for simulating the performance of these controllers. A good agreement was observed between the analytically evaluated natural frequencies and those obtained experimentally. Simulation and experimental results of application of the proposed control methods show that the active impedance dynamic gain method is advantageous for flexible structures of great modal complexity. CISTI

N94-30114 National Physical Lab., Teddington (England). Div. of Materials Metrology.

ESTIMATION OF WEIBULL MODULUS FROM DYNAMIC AND STATIC FATIGUE EXPERIMENTS

M. J. Reece, J. M. Cox, R. Morrell, and M. R. Phillips Mar. 1993 29 p
(PB94-138641; NPL-DMM(A)-108) Copyright Avail: Issuing Activity (National Technical Information Service (NTIS))

In the statistical analysis of strength data on brittle materials, it is useful to estimate the range of uncertainties in the calculation of parameters which characterize strength distributions, such that the reliability of subsequent use of the parameters can be judged. This has been performed for simple short-term strength distributions before, but in this report we develop a method for analyzing static and dynamic fatigue data and evaluate it using a Monte Carlo simulation based on a single Weibull distribution of flaw sizes and hence inert strengths. It is shown that the technique is appropriate for analyzing 50 dynamic fatigue results over four decades of stressing rate, and gives a Weibull modulus with a confidence level similar to that for a randomly chosen set of simple strength test specimens. Similar results were obtained with an analysis of static fatigue tests. The method was applied to real experimental data for soda-lime glass and provided a reasonable match between the Weibull modulus for conventional strength testing and those for static and dynamic fatigue. NTIS

N94-30206*# National Aeronautics and Space Administration. Marshall Space Flight Center, Huntsville, AL.

ROOT-SUM-SQUARE STRUCTURAL STRENGTH VERIFICATION APPROACH

Henry M. Lee Apr. 1994 48 p
(NASA-TM-108453; NAS 1.15:108453) Avail: CASI HC A03/MF A01

Utilizing a proposed fixture design or some variation thereof, this report presents a verification approach to strength test space flight payload components, electronics boxes, mechanisms, lines, fittings, etc., which traditionally do not lend themselves to classical static loading. The fixture, through use of ordered Euler rotation angles derived herein, can be mounted on existing vibration shakers and can provide an innovative method of applying single axis flight load vectors. The versatile fixture effectively loads protoflight or prototype components in all three axes simultaneously by use of a sinusoidal burst of desired magnitude at less than one-third the first resonant frequency. Cost savings along with improved hardware confidence are shown. The end product is an efficient way to verify experiment hardware for both random vibration and strength. Author (revised)

N94-30226 Maryland Univ., College Park.

THE ROLE OF PLASTIC DEFORMATION IN BRITTLE AND NEAR-BRITTLE CRACKING BEHAVIOR Ph.D. Thesis

Hyungjae Shin 1992 186 p
Avail: Univ. Microfilms Order No. DA9315726

New measurements are reported for the ambient temperature indentation behavior of silicon crystals, involving several types of indentation systems and indenter shapes. Analysis of these and previously reported measurements on either a force-indentation of size related ductile-brittle transition description or a hardness stress-strain basis leads to the conclusion that crack initiation in silicon is facilitated by Cottrell-type dislocation reactions. The occurrence of an undetected phase transformation is concluded to be, at most, a secondary factor. Nanoindentation test results obtained at the National Institute of Standards and Technology on carbon-ion implanted silicon material, produced at the Naval Research Laboratory, show that hardening of the silicon surface layer has occurred, particularly for the case of SiC being formed by high temperature implantation. Measurement of the orientations of (100) cleavage facets, presumably initiated by the Cottrell dislocation reaction mechanism, on split and transverse fractured steel materials has led to an interpreted influence of polycrystal texture on the ductile-brittle transition properties of the material. Dissert. Abstr.

N94-30258 Texas Univ., Arlington.

CLOSED FORM EXPRESSIONS FOR A CONSISTENT STRESS MATERIAL NONLINEAR FINITE ELEMENT Ph.D. Thesis

Richard Lee Knipe 1993 101 p
Avail: Univ. Microfilms Order No. DA9328489

Finite element expressions for two dimensional elasto-plasticity problems were implemented in closed form. These closed form expressions are based upon a distribution of the elasto-plastic constitutive relationship that is consistent with the interpolating functions used for the displacement. Closed form expressions for the element tangent stiffness matrix and initial stress nodal load vector were developed for the non hierarchic constant, linear, and quadratic strain triangle. Decreased solution times were obtained when using the closed form expressions instead of expressions based on numerical integration. The quality of the solutions obtained from the closed form expressions was measured against published solutions for two dimensional elasto-plasticity problems. Dissert. Abstr.

N94-30354 Ohio State Univ., Columbus.

PLANE STRAIN FINITE ELEMENT ANALYSIS OF SHEET FORMING OPERATIONS INCLUDING BENDING EFFECTS Ph.D. Thesis

Uk Youn Cho 1993 191 p
Avail: Univ. Microfilms Order No. DA9325477

An improved finite element method suitable for the plane-strain analysis of sheet metal forming operations is presented. The method incorporates a computationally efficient shell model and a consistent frictional contact algorithm through an implicit updated Lagrangian formulation. The workpiece material model is rigid-viscoplastic with a choice of power law hardening and plastic normal anisotropy and is capable of modeling a wide variety of sheet metals. A simplified nonlinear incremental shell theory is employed along with an optional reduced integration through the thickness for computational efficiency, while retaining the advantages of the kinematic model containing the bending effects. Complex tool geometry can be handled by discrete data points, by primitives (lines and arcs), or by analytical functions. The capabilities of the method are demonstrated through verification problems and comparisons with experimental data, benchmark results, and published data for several practical problems of the sheet metal forming industry. The problems include stretching and/or deep drawing operations, simulation of automobile panel section, and brake bending operation. As an independent investigation from the first portion of the dissertation, measured data from a set of simple bending experiments of two types of aluminum are presented and analyzed. Generated data from the experiments include strain histories (loading and unloading), spring back information (spring back angle and strains), and friction coefficients. As a by-product, a simple way of estimating the friction coefficient (Coulomb's law) during a bending operation is proposed and demonstrated. Dissert. Abstr.

N94-30523 National Physical Lab., Teddington (England). Materials Metrology Div.

APPROXIMATE ESTIMATION OF THE EFFECTS OF ASYMMETRY ON THE TESTING OF TENSILE SPECIMENS

D. H. Ferriss and G. F. Miller Aug. 1993 36 p
(ISSN 0959-2423)
(NPL-DMM(A)-117; ETN-94-95839) Copyright Avail: Issuing Activity (National Physical Lab., Teddington, Middlesex TW11 0LW, England)

An analysis of the plane stress problem represensting the tensile testing of rectangular orthotropic material specimens is made. The effects of various geometric nonsymmetries are considered and some approximate polynomial solutions are obtained and tabulated. Comparisons of the theory with specific finite element calculations show good general agreement. ESA

N94-30689 Oak Ridge National Lab., TN.
EXPERIMENTAL AND ANALYTICAL COMPARISON OF CONSTRAINT EFFECTS DUE TO BIAXIAL LOADING AND SHALLOW-FLAWS
T. J. Theiss, B. R. Bass, and J. W. Bryson 1993 56 p Presented at the 2nd Symposium on Constraint Effects in Fracture, Fort Worth, TX, 17-18 Nov. 1993 Limited Reproducibility: More than 20% of this document may be affected by microfiche quality
(Contract DE-AC05-84OR-21400)
(DE94-004794; CONF-931118-1) Avail: CASI HC A04

A program to develop and evaluate fracture methodologies for the assessment of crack-tip constraint effects on fracture toughness of reactor pressure vessel (RPV) steels has been initiated in the Heavy-Section Steel Technology (HSST) Program. The focus of studies described herein is on the evaluation of a micromechanical scaling model based on critical stressed volumes for quantifying crack-tip constraint through applications to experimental data. Data were utilized from single-edge notch bend (SENB) specimens and HSST-developed cruciform beam specimens that were tested in HSST shallow-crack and biaxial testing programs. Shallow-crack effects and far-field tensile out-of-plane biaxial loading have been identified as constraint issues that influence both fracture toughness and the extent of the toughness scatter band. Results from applications indicate that the micromechanical scaling model can be used successfully to interpret experimental data from the shallow- and deep-crack SENB specimen tests. When applied to the uniaxially and biaxially loaded cruciform specimens, the two methodologies showed some promising features, but also raised several questions concerning the interpretation of constraint conditions in the specimen based on near-tip stress fields. Crack-tip constraint analyses of the shallow-crack cruciform specimen subjected to uniaxial or biaxial loading conditions are shown to represent a significant challenge for these methodologies. Unresolved issues identified from these analyses require resolution as part of a validation process for biaxial loading applications.
DOE

N94-30813 Iowa State Univ. of Science and Technology, Ames.
DYNAMIC MODELING OF MULTIBODY FLEXIBLE STRUCTURES Ph.D. Thesis
Jiechi Xu 1993 336 p
Avail: Univ. Microfilms Order No. DA9321229

The dynamic modeling of a three dimensional, multibody, flexible, structural system with mutually coupled multicoordinates of unknown large overall rigid body motion is discussed. The study includes theory development and mathematical modeling, time integration numerical technique investigation, computer simulation and results, and experimental measurements and verification. The specific structure under consideration is characterized as an open loop system with spherical unconstrained chains capable of three dimensional rotation motion. The elastic deflections and rotations change the instantaneous body shape and energy level of each individual flexible member and consequently affect the rigid body motion of the system. In return, rigid body motion induces passive inertial forces resulting from tangential, centrifugal, and Coriolis accelerations and therefore influence the elastic deformation. In addition, an elastic-to-elastic coupling phenomenon, an effect of elastic deformation in succeeding links on the current link, is also involved during the motion of the system. All of these strongly nonlinear coupling terms are accounted for and are derived exactly in the dynamic modeling of the structure. The Lagrangian approach associated with a conventional stiffness finite element method is adopted in the derivation of the dynamic equations of motion and in the space discretization of the flexible members. Some hypotheses are made in the modeling of three dimensional elastic deformations using finite element analysis in order to reduce the total elastic degrees of freedom and to simplify the procedure of space discretization with only minor loss of exactness. A special numerical technique, a sequential implicit-explicit time integration method with predictor-corrector schemes, is developed to solve a second-order, nonlinear, ordinary differential equation system with time-varying coefficient matrices. The numerical algorithms are capable of handling the dynamic equation systems with inherent characteristics involving the variables of large overall nonlinear rigid body motion and the variables of small linear vibration. A general purpose computer code is developed with the implementation of the numerical technique presented in this work. Multiple finite elements of beam type are selected for each flexible member in order to increase accuracy where concerned. Extensive computer simulation of the dynamic response of the system is performed for several cases with different conditions and numerical parameters. The measurement instrumentation and computerized data acquisition system are set up to measure structural deflections at different locations. The most significant deformation, the overall deflection at the end of the chain accounting for all the possible elastic deflections and rotations preceding that location, is also calculated and the result is compared with experimental data. Good agreement between the analytical and experimental results in terms of overall radial deflection at the tank center is achieved. Dissert. Abstr.

N94-30814 Oklahoma Univ., Norman.
AN INVESTIGATION OF FATIGUE CRACK PROPAGATION UNDER MODE 1 AND MIXED MODE 1/2 LOADINGS Ph.D. Thesis
Tapan Kumar Paul 1993 174 p
Avail: Univ. Microfilms Order No. DA9315794

An investigation on fatigue crack propagation under mode 1 and mixed mode (1 and 2) loadings has been performed. Fatigue crack growth data in the case of plane strain mode 1 have been obtained by performing experiments on compact tension specimens of 4340 steel for increasing Delta-K(sub 1), decreasing Delta-K(sub 1), and constant Delta-K(sub 1) loading conditions. Under mixed mode plane stress condition, the fatigue crack growth trajectory has been determined by performing experiments on the center cracked thin disk specimen of aluminum 2024. With two mixed mode loading ratios, the subsequent propagation of the main crack has been performed by producing a series of kinks and forks. For practical applications such as the case of a flaw or a crack in aircraft or ship structure in which the loading axis (with respect to the crack) frequently changes, a zig-zag or complicated crack trajectory is very important in both experimental and theoretical studies. In order to apply any specific crack growth criterion for the analysis of the experimental results, a detailed analysis for the stresses near the crack front and the extent of yielding is necessary. A full field solution, based on small deformation, three dimensional elastic-plastic finite element analysis of the centrally cracked thin disk under mode 1 loading has been performed. The solution for the stresses under small-scale yielding and locally fully plastic state has been compared with the HRR plane stress solution. At the outside of the three dimensional zone, within a distance of r sigma(sub 0)/J = 18, HRR dominance is maintained in the presence of a significant amount of compressive stress along the crack flanks. Ahead of this region, the HRR field overestimate the stresses. These results demonstrate a completely reversed state of stress in the near crack front compared to that in the plane strain case. The combined effect of geometry and finite thickness of the specimen on elastic-plastic crack tip stress field has been explored. Under mixed mode loading, the dominance of the elastic K-field outside the elastic-plastic region has been demonstrated at the load level at which the crack extension experiment has been performed in the thin disk. The complex crack trajectory has been analyzed on the basis of the strain energy density criterion for the prediction of propagated crack path under subsequent changes in orientation of the crack to the loading axis or, equivalently, the changes in loading direction with respect to the crack. Dissert. Abstr.

N94-30815 Colorado Univ., Boulder.
SECOND-ORDER STRUCTURAL IDENTIFICATION VIA STATE SPACE-BASED SYSTEM REALIZATIONS Ph.D. Thesis
Kenneth F. Alvin 1993 216 p
Avail: Univ. Microfilms Order No. DA9320384

The present study has focused on the estimation of normal modes and their mode shapes from experimental data. The determination of accurate undamped modal parameters from experimental data in the presence of damping is critical for the construction or reconciliation of structural dynamics models, in which the physical mass and stiffness properties are isolated from the dissipative effects of damping. The response functions measured from experimental data are generally approximated by finite-dimensional first-order difference equations in the time domain using algorithms such as ERA. Such models, or realizations, do not directly determine the mass and stiffness matrices, except under special restrictions. This thesis develops a family of transformation-based methods for the construction of second-order structural dynamic models from first-order system realizations of experimental data. Transformations to a second-order canonical basis are effective for the systematic extraction of the normal modes from the first-order realizations. Two separate transformations are developed: the common basis normalized structural identification (CBSI)

procedure and the uncoupled nonproportional damping (UNDAMP) procedure. CBSI transforms the first-order state space realizations to the well-known form of second-order proportionally damped equations of motion. The resulting structural dynamics models are shown not only to yield the accurate normal modes for proportionally damped cases, but also improved estimates of the normal mode shapes in the presence of nonproportional damping as compared to existing methods. The UNDAMP algorithm extends the CBSI method to a global transformation spanning up to the full space of the damped modes. As such, UNDAMP is capable of filtering out the contaminating attributes of nonproportional damping from the CBSI-determined normal modal parameters. Furthermore, UNDAMP is applicable to the extracting of nonproportional damping when the number of measured sensors is less than the number of identified modes. Using normal modal parameters determined by CBSI or UNDAMP a method for determining minimal-order mass and stiffness matrices is presented. The resultant model is an alternative second-order realization with measured physical variables as degrees of freedom, and the derived mass and stiffness matrices are shown to have asymptotic equivalence to Guyan-reduced and/or Craig-Bampton synthesized structural models. The efficiency and accuracy of the present transformation methods are demonstrated through simulated numerical examples and experimental data. In particular, the present methods are used to reconstruct frequency response functions and applied to damage detection in truss structures. Finally, the implications of these analytical techniques for structural system identification and directions for future research are also discussed. Dissert. Abstr.

N94-30872 National Aerospace Lab., Amsterdam (Netherlands). Structures and Materials Div.
WISPER AND WISPERX: FINAL DEFINITION OF TWO STANDARDISED FATIGUE LOADING SEQUENCES FOR WIND TURBINE BLADES
A. A. tenHave 23 Sep. 1992 84 p Sponsored by Netherlands Agency for Energy and Environment Limited Reproducibility: More than 20% of this document may be affected by microfiche quality
(AD-B175835; NLR-TP-91476-U; ETN-94-95569) Avail: CASI HC A05

Relevant information used to develop WISPER (Wind turbine reference Spectrum) and WISPERX, standardized variable amplitude test loading histories for use in the fatigue design of horizontal axis wind turbine blades, is presented. WISPER and WISPERX are based on flap load service measurements on nine different horizontal axis wind turbines, covering a wide range of materials, rotor diameters and geographical locations. Their backgrounds are reported, basic data and associated data handling procedures are described, and quantitative data analysis results and statistical information on both standards are presented. The information given will enable fatigue specialists to judge whether the standard will suit their test objectives and to check for correct application of the load sequences on their test equipment. ESA

N94-30920 Illinois Univ., Urbana-Champaign.
THIN-WALLED ORTHOTROPIC LAMINATED BEAM THEORY Ph.D. Thesis
Gerry Darren Pollock 1993 164 p
Avail: Univ. Microfilms Order No. DA9329139

A refined beam theory is developed for thin-walled, orthotropic, laminated elastic beams. The motivation for the formulation is the necessity of accounting for deformations brought about by coupling induced shear strains in open section beams. The engineering formulation allows for completely arbitrary section geometry and lay-ups. The present theory and a related closed section theory are validated by comparisons with experimental, finite element, and other analytical methods. The results show the necessity of incorporating shear strain produced deformations for open sections. In general, both the open section and closed section results agree to within 10 to 15 percent of either experimental or finite element data for a broad range of section geometries, lay-ups and loadings. The present open and closed section formulations reduce, as required, to their classical isotropic counterparts when isotropic properties are invoked. Shear center concepts for anisotropic beams are investigated as well. For arbitrary ply lay-ups, it is impossible to find a point (shear center) at which applied shear loads simultaneously satisfy conditions of zero twist and zero resultant moment. The method of determining isotropic shear centers leads to moment balancing of resultant shear load and shear stresses about some point. A completely analogous procedure can be arrived at for anisotropic beams, and hence the condition of zero resultant torque is deemed the more natural condition to satisfy. The consequence is that the beam twists despite the fact that the shear load passes through the shear center. Anisotropic shear centers are found to be functions of material properties. Dissert. Abstr.

N94-29615*# Jet Propulsion Lab., California Inst. of Tech., Pasadena.
COMPUTATION OF VIBRATION MODE ELASTIC-RIGID AND EFFECTIVE WEIGHT COEFFICIENTS FROM FINITE-ELEMENT COMPUTER PROGRAM OUTPUT
R. Levy *In its* The Telecommunications and Data Acquisition Report 15 May 1991 p 13-20 (For primary document see N94-29613 08-32)
(RTOP 310-20-65-86-04)
Avail: CASI HC A02/MF A02

42 GEOSCIENCES (GENERAL)

N94-28693# Meteorological Research Inst., Tsukuba (Japan).
PAPERS IN METEOROLOGY AND GEOPHYSICS, VOL. 44, NO.1 [KISHO KENKYUJO KENKYU HOKOKU, DAI 44 KAN DAI 1 GO]
Koji Shigehara, Isao Takano, Shinji Nakagawa, Masahiro Hara, Toru Sasaki, Takahisa Kobayashi, Hiroshi Nirasawa, Toshikazu Odaka, Katsunobu Nishiyama, and Yoshimi Suzuki et al 31 Mar. 1993 41 p
(ISSN 0031-126X)
(JTN-94-80585) Avail: CASI HC A03/MF A01

The following topics were discussed: water circulation, proper water, water flow, ocean temperature, temperature distribution, salinity, salinity distribution, atmospheric flow, barotropic flow, turbulent flow, turbulent boundary layer, Ekman boundary layer, atmospheric blocking, flow stability, solitary waves, planetary waves, Verkley's modon, Liapunov stability, mathematical model, numerical simulation, schemes, and the Sea of Japan. For individual titles, see N94-28694 through N94-28696.

N94-28694# Meteorological Research Inst., Tsukuba (Japan).
THE JAPAN SEA PROPER WATER AND WATER CIRCULATION IN THE JAPAN SEA [NIHONKAI KOYUSUI NO SEISEI TO NIHONKAI NO KAISUI JUNKAN] **c48**
Katsunobu Nishiyama, Masaru Inagawa, and Takanori Mizuno *In its* Papers in Meteorology and Geophysics, Vol. 44, No. 1 31 Mar. 1993 p 1-10 (For primary document see N94-28693 08-42)
Avail: CASI HC A02/MF A01

Water circulation in the Sea of Japan is characterized as a formation of the Sea of Japan proper water from the data observed in 1969 by research vessels belonging to the Japan Meteorological Agency. Below 500 m depth in the Sea of Japan, salinity is relatively high in the northern part and low in the southern. This is opposite to the conditions in the surface layer, where the northern part is generally the cold current region and the southern part the warm current region. In the southern part of the eastern Japan Basin of the northern Sea of Japan anticyclonic circulation occurs and sea waters sink towards the bottom. In the western Japan Basin and in the Yamato Basin, sea waters flow upward, in contrast to the southern part of the eastern Japan Basin. Therefore, vertical water circulation generates in the deep layer of the Sea of Japan, that is, downwelling appears in the southern part of the eastern Japan Basin, and upwelling occurs in the western Japan Basin and in the Yamato Basin.
Author (NASDA)

N94-28695# Meteorological Research Inst., Tsukuba (Japan).
ON THE LINEAR STABILITY OF VERKLEY'S MODONS [BAKUREI MODON NO SENKEI ANTEISEI] **c46**
Hirotada Kanehisa *In its* Papers in Meteorology and Geophysics, Vol. 44, No. 1 31 Mar. 1993 p 11-16 (For primary document see N94-28693 08-42)
Avail: CASI HC A02/MF A01

Verkley (1987, 1990) constructed modons on a sphere as models of atmospheric blocking phenomena. These are exact solitary wave solutions to the barotropic potential vorticity equation on a sphere. In this report, the linear Liapunov stability of Verkley's 1987 modons is proved by means of Arnol'd's invariant, and moreover it is shown that Verkley's 1990 modons are linearly spectrally stable. In spite of the fact that Arnol'd's invariant

does not exist for the 1990 modon, it is still possible for the 1990 modon to be proved linearly spectrally stable because of the fact that the 1990 modon is a limiting case of the 1987 modon. Author (NASDA)

N94-28696# Meteorological Research Inst., Tsukuba (Japan).
STRUCTURE OF NEUTRALLY STRATIFIED TURBULENT EKMAN LAYER AS PREDICTED BY CLOSURE MODELS WITH PROGNOSTIC EQUATION FOR MASTER LENGTH SCALE **c46**
Nobuyuki Kinoshita *In its* Papers in Meteorology and Geophysics, Vol. 44, No. 1 31 Mar. 1993 p 17-28 (For primary document see N94-28693 08-42)
Avail: CASI HC A03/MF A01

The turbulent Ekman boundary layer in a neutral atmosphere is studied by means of a second order turbulence closure model incorporated with a prognostic equation for the master length scale and those of a one-and-a-half order closure model. The results of the second order closure model are compared with those of a second order closure model incorporated with an equation for the dissipation rate, an E-epsilon model and a direct numerical simulation. It is shown that the height of the Ekman layer simulated by the present model is higher than those by the other closure models and that the turbulence kinetic energy and turbulent momentum fluxes in the upper part of the boundary layer are larger. These differences result from the fact that the length scale predicted by the present model is longer than those by the other closure models. The structure of the Ekman boundary layer simulated by the present second order closure model is close to that by a direct numerical simulation. The results of the one-and-a-half order closure model coincide with the present results, though it is found that the growth of the boundary layer is a little slower than that of the present second order closure model. Author (NASDA)

43 EARTH RESOURCES AND REMOTE SENSING

Includes remote sensing of earth resources by aircraft and spacecraft; photogrammetry; and aerial photography.

For instrumentation see *35 Instrumentation and Photography.*

N94-28808# Army Topographic Engineering Center, Fort Belvoir, VA.
EXPLOITATION OF STEREOPHOTOGRAMMETRICALLY DERIVED 3-D WIREFRAME MODELS TO PRODUCE URBAN SIMULATIONS Scientific Paper
Tom Witte Feb. 1994 7 p
(AD-A275459; TEC-R-214) Avail: CASI HC A02/MF A01

The U.S. Army Topographic Engineering Center (TEC) is investigating methods to incorporate photogrammetrically derived 3-D models of urban features into terrain visualization software, to facilitate the photorealistic simulation of urban environments. Ideally, cultural features such as buildings will be extracted automatically from digital imagery as 3-D wireframe models. Coordinates representing the vertices of the models are to be input to terrain visualization software running on a Unix workstation. Phototexture is to be applied to the models and to the underlying digital terrain elevation data in order to create photorealistic, 3-D urban environments for simulated fly-throughs. DTIC

N94-28849 Army Cold Regions Research and Engineering Lab., Hanover, NH.
THERMAL VARIATION IN VEGETATED OR SNOW-COVERED BACKGROUND SCENES AND ITS EFFECT ON PASSIVE INFRARED SYSTEMS
Lindamae Peck Nov. 1993 22 p Limited Reproducibility: More than 20% of this document may be affected by microfiche quality
(DA Proj. 4A7-62784-AT-42)
(AD-A275174; CRREL-93-22) Avail: CASI HC A03

The diurnal and seasonal variations in the magnitude of and rate of change of surface temperature were investigated for vegetated and snow-covered ground under winter, summer, and transitional weather conditions at a site in Vermont. The variability in thermal radiance is evident as changes in the proximity-to-alarm status of passive infrared detection systems. A midwinter snow cover is the most favorable background because its associated thermal radiance changes are less dynamic than are the radiance changes of uniform grass covers in summer or mixed backgrounds of grass, thatch, and soil following winter. Grass, thatch, and soil backgrounds typically experience a larger diurnal range in temperature (from nighttime low to daytime high) and greater spatial variability in thermal radiance than do the uniform grass covers. The summer grass is more likely to be long enough to blow in the wind, thereby causing a change in thermal radiance as variously the sun-warmed, upper portion of the grass blades or the shaded (and therefore cooler) basal portion of the grass blades, and perhaps the sheltered soil, are momentarily exposed to the passive infrared system. DTIC

N94-28863# Army Topographic Engineering Center, Fort Belvoir, VA.
FEATURE MAPPING IN A PHOTOGRAMMETRIC GIS
Roger O. Brown Jan. 1994 9 p
(AD-A275418; TEC-R-211) Avail: CASI HC A02/MF A01

The U.S. Army Corps of Engineers Topographic Engineering Center (TEC) has assembled a Terrain Information Extraction System (TIES). The TIES uses photogrammetric Geographic Information System (GIS) technology for digital image-based mapping (Brown, 1991). The TIES is a modular system for generating digital terrain data (Desmond, Edwards, 1990). Components of the TIES exchange Digital Topographic Data (DTD) by a Feature Map Exchange Format (FMEF). DTIC

N94-28881# Washington Univ., Seattle.
PHYSICAL PROCESSES IN SNOWPACKS DURING RAIN OR MELT EVENTS Final Report, 15 May 1991 - 14 Nov. 1993
H. Conway 10 Jan. 1994 28 p
(Contract DAAL03-91-G-0143)
(AD-A275445; ARO-28344.1-GS) Avail: CASI HC A03/MF A01

Observations during rain-on-snow indicate three evolutionary regimes of snow behavior, immediate avalanching, delayed avalanching, and a return to stability. Immediate avalanching occurs within minutes of the onset of rain. This is important information for avalanche control technicians; the avalanches release several hours before, liquid water has penetrated to the sliding layer. Delayed avalanches release several hours after rain has started. The delay varies depending on the rate of increasing stress associated with additional precipitation, and the time taken for water to penetrate and weaken the snowpack. Avalanche activity is rare after continuation of rain for 15 hours or more. This return to stability occurs after a drainage system has been established. Infiltration is not uniform and water penetrates through localized channels that often occupy less than 50% of the total volume of the snowpack. Runoff starts much sooner than would be predicted if wetting was homogeneous. In situ measurements of deformation indicate that the strain rate in low density snow often increases without increased normal loading. Forces other than gravity must contribute to the deformation. This important finding is supported by measurements on slopes that show that the usual assumption that snow behaves as a linear, isotropic, viscous material is incorrect. A new theory involving thermodynamically induced strain is suggested. DTIC

N94-28925# Earth Resources Satellite Data Analysis Center, Tokyo (Japan).
PROCEEDINGS OF THE INTERNATIONAL SYMPOSIUM ON REMOTE SENSING [KOKUSAI SHINPOJIUMU: JERS-1, NIJUISSEIKI ENO KAKEHASHI, KOENSHU]
30 Mar. 1992 294 p In ENGLISH and JAPANESE Symposium held in Tokyo, Japan, 21-22 Nov. 1991 Sponsored by Ministry of International Trade and Industry, Tokyo, Japan; Science and Technology Agency, Tokyo, Japan; National Space Development Agency of Japan, Tokyo, Japan; Japan Resources Observation System Organization, Tokyo, Japan
(JTN-94-80578) Avail: CASI HC A13/MF A03

The following topics are discussed: remote sensing, earth observation, earth resources management, earth resources sounding, environmental monitoring, disaster prevention, hurricanes, floods, change detection, forest management, deforestation, geological surveys, image analysis, image processing, data systems, data processing, data management, ground support stations, ocean surface observation, sea ice monitoring, ice mapping, wind velocity, wave height, remote sensors, radiometers, scatterometers, synthetic aperture radar (SAR), optical sensors (OPS), advanced very high resolution radiometer (AVHRR), Japanese Earth Resources Satellite-1 (JERS-1), ERS-1, LANDSAT satellites, and NOAA satellites. For individual titles, see N94-28926 through N94-28937.

N94-28926# Tokyo Univ. (Japan).
KEYNOTE ADDRESS [KICHO KOEN]
Shigeburni Saito *In* Earth Resources Satellite Data Analysis Center, Proceedings of the International Symposium on Remote Sensing 30 Mar. 1992 p 11-39 In ENGLISH and JAPANESE Original contains color illustrations (For primary document see N94-28925 08-43)
Avail: CASI HC A03/MF A03

More importance has been placed nowadays on remote sensing, a new field ranging in many professional areas, while global environment issues are getting much public attention. In order to promote the development of various types of satellites for earth observation and their sensors, Japan should focus on the following: an organization must be established where basic studies and research and development on remote sensing can entirely be conducted; aircraft for remote sensing experiments and observations should be prepared for sensor development, data collection and accumulation by new sensors, and practical observations; and observation satellites should be continued in sequence - many of the satellites were not continued for the second or third versions, and thus continuous data are not available, inconveniencing data users. Although these three items cannot be achieved immediately, it is strongly hoped that Japan will grow in joining the advanced countries in the field of remote sensing satellites. Author (NASDA)

N94-28927# Jet Propulsion Lab., California Inst. of Tech., Pasadena.
SYNTHETIC APERTURE RADAR APPLICATIONS: NOW AND IN THE FUTURE [SA DETA DE NANI GA WAKARUKA] **c32**
Charles Elachi *In* Earth Resources Satellite Data Analysis Center, Proceedings of the International Symposium on Remote Sensing 30 Mar. 1992 p 41-65 Original contains color illustrations (For primary document see N94-28925 08-43)
Avail: CASI HC A03/MF A03

The future will see a major increase in the utilization of spaceborne imaging radars in earth sciences and applications. ERS-1 and ERS-2 as well as RADARSAT will provide extensive amounts of coverage and large scale monitoring. Imaging radars have been used for geologic mapping of planetary surfaces, mapping of surface morphologic texture and roughness, mapping or the polar ice cover and ocean surface features, and monitoring of land use changes. Future potential applications will capitalize on the ability of the radar signal to sense volumetric information and to measure surface moisture. Three new techniques have the potential for major advances in the field of spaceborne radar remote sensing: radar polarimetry, radar interferometry, and bistatic imaging. The power of the radar data will be significantly enhanced when the advanced capabilities using these three techniques become widely available and when the synergism of visible infrared and microwave system is fully exploited. Author (NASDA)

N94-28928# Tokyo Univ. (Japan). Inst. of Industrial Science.
RESEARCH TRENDS ON REMOTE SENSING AT RESEARCH FACILITIES IN JAPAN: THE PRIORITY AREA PROGRAMME ON BETTER UNDERSTANDING OF EARTH ENVIRONMENT VIA SATELLITE [NIHON NO KENKYU KIKAN NI OKERU RIMOTO SENSHINGU KENKYU NO TORENDU: MONBUSHO KAGAKU KENKYUHI JUTEN RYOIKI KENKYU EISEI NI YORU CHIKYU KANKYO NO KAIMEI]
Mikio Takagi *In* Earth Resources Satellite Data Analysis Center, Proceedings of the International Symposium on Remote Sensing 30 Mar. 1992 p 67-128 In ENGLISH and JAPANESE Sponsored by Ministry of Education (For primary document see N94-28925 08-43)
Avail: CASI HC A04/MF A03

Since 1989, a focused area study 'Exploration of Earth Environment by Satellites' funded by the Ministry of Education is ongoing as a three-year program. The objectives of the program is, by utilizing the information on earth observed from space, to establish observation techniques for various earth environments and to conduct basic researches so as to understand the mechanism of environmental changes, utilizing the information on earth observed from space. Understanding earth phenomena ranging in atmosphere, geosphere, and hydrosphere requires an earth observation technique by satellites allowing collection of information covering large areas in a short time as well as multiple observation of the same areas. Applications of this technique, remote sensing, are expected to see significant increase. Japan is still behind in the basic studies to utilize data from satellites to academic studies of global environments covering air, ocean and land. The program was established to cope with these problems with an intention to catch up with Europe and the USA. With close cooperation between scientists and engineers, this program aims for effective researches featuring boundary area studies between atmosphere and geosphere, atmosphere and hydrophere, and geosphere and hydrosphere, for example. Author (NASDA)

N94-28929# Geosat Committee, Inc., Norman, OK.
EVALUATION OF SIMULATED JERS-1 DATA FOR GEOLOGIC MAPPING AT DRUM MOUNTAINS, UTAH, SILVER BELL, ARIZONA, AND WIND RIVER, WYOMING UNDER THE GEOSAT-ERSDAC/JAPEX/JGI/RESTEC JOINT STUDIES [SHIMYURESHON DETA NI YORU JERS-1 DETA RIYO NO KENTO]
Frederic B. Henderson, III, I. W. Bill Ginsberg, William Malila, Amy Collins, David A. Cole, and Lyle Burgess *In* Earth Resources Satellite Data Analysis Center, Proceedings of the International Symposium on Remote Sensing 30 Mar. 1992 p 129-143 Original contains color illustrations (For primary document see N94-28925 08-43)
Avail: CASI HC A03/MF A03

Optical Sensor (OPS) and Synthetic Aperture Radar (SAR) simulation studies were made in 1989 and 1990 at test sites in the U.S. The main purpose was to jointly understand and develop applications of simulated Japanese Earth Resources Satellite-1 (JERS-1) electro-OPS and SAR remote sensing technology to petroleum and mineral geological mapping problems before the scheduled launch of the Japanese JERS-1 satellite in 1992. The studies at various sites demonstrated that the JERS-1 data would be superior to other satellite remote sensing data for many geologic mapping applications, and that the data could be expected to effectively map major rock and alteration types, and better discriminate between hydroxyl-bearing rocks. Moreover, the JERS-1 data will improve the mapping of subtle lithologic variations regionally within sedimentary sequences of rocks. These capabilities for better mineral, alteration, and rock facies discrimination will contribute significantly to geological remote sensing worldwide. The JERS-1 data will provide new and improved spectral information for mapping and understanding earth's land and ocean surfaces for global resource development and better global environmental management.
Author (NASDA)

N94-28930# Commonwealth Scientific and Industrial Research Organization, Parkside (Australia).
IMAGE PROCESSING FOR HYPERSPECTRAL DATA Abstract Only [CHO TABANDO DETA NO GAZO SHORI]
Andrew A. Green, M. Berman, and M. Craig *In* Earth Resources Satellite Data Analysis Center, Proceedings of the International Symposium on Remote Sensing 30 Mar. 1992 p 145-147 (For primary document see N94-28925 08-43)
Avail: CASI HC A01/MF A03

A number of methods, including expert system methods, were examined for the interpretation of very high dimensional remote sensing data. Many of them were thought to be too cumbersome for dealing with spectra which were a mixture of several components. Among these expert system methods, the most persuasive argument was the clear advantages of unmixing techniques, which seemed to be the best way to proceed in the analysis of high dimensional data sets. The main reason was that despite the very large number of bands acquired, the fundamental dimensionality of the data was usually much less. It became clear that the data variability is determined by the linear mixing of the radiance properties of relatively few spectally distinct materials, called endmembers. Inconveniences of principal components analysis led to the development of a new coordinate transformation which produces new components that separate the signal and noise as much as possible. It was found that band-to-band misregistration could cause serious problems in the unmixing process. Not only does it invalidate the assumptions made in the mixing model, it gives the data extra dimensionality by simulating false endmembers. The selection of endmembers in high dimensional data is difficult because of our weak capability to visualize the data distributions. Author (NASDA)

N94-28931# Remote Sensing Technology Center, Tokyo (Japan).
JERS-1 DATA ACQUISITION AND DISTRIBUTION [JERS-1 DETA NO SHUTOKU HAIFU NI TSUITE]
Hiroshi Ishigami *In* Earth Resources Satellite Data Analysis Center, Proceedings of the International Symposium on Remote Sensing 30 Mar. 1992 p 149-187 In ENGLISH and JAPANESE (For primary document

see N94-28925 08-43)
Avail: CASI HC A03/MF A03

The Japanese Earth Resources Satellite-1 (JERS-1) system consists of a space segment (the satellite itself) and a ground segment. The satellite has two sections: a bus section with basic functions of communication data processing and power supply, and a mission section. The mission section includes the following: (1) Synthetic Aperture Radar (SAR) which provides means to obtain information of objects by measuring scattering coefficients; (2) an Optical Sensor (OPS) which gathers lights (both forward and directly below the satellite) to be filtered and converted later to electric signals; (3) a mission data transmitter which transmits SAR, OPS, and Mission Data Recorder (MDR) data to ground; and (4) a mission MDR which records, reproduces and outputs SAR and OPS data to ground stations. The ground segment consists of: (1) tracking and control functions; (2) data acquisition and processing functions responsible for data receiving, recording, processing, inspection, evaluation, storage, retrieval and distribution; and (3) Mission Management Organization (MMO) which coordinates various requests and transmits mission operation requests, operation plans and orbit information, and performs the primary evaluation of mission instruments. Author (NASDA)

N94-28932# Earth Resources Satellite Data Analysis Center, Tokyo (Japan).
JERS-1 DATA AND INFORMATION SYSTEM FOR RESOURCES EXPLORATION [SHIGEN TANSA NO TAMENO JERS-1 KANSOKU DETA RIYO SHISUTEMU NI TSUITE]
In its Proceedings of the International Symposium on Remote Sensing 30 Mar. 1992 p 189-204 In ENGLISH and JAPANESE Original contains color illustrations (For primary document see N94-28925 08-43)
Avail: CASI HC A03/MF A03

The Japanese Earth Resources Satellite-1 (JERS-1), scheduled to be launched in February 1992, was jointly developed by the Ministry of International Trade and Industry (MITI) and the National Space Development Agency of Japan (NASDA). JERS-1 has two mission sensors: an L-band synthetic aperture radar, and an optical sensor which gathers reflected sunlight from the earth in the regions between visible, near infrared to short-wavelength infrared lights. JERS-1 has been getting much attention not only from those conducting resources exploration but also from various users both domestic and abroad for forestry, fishery, agriculture, and environmental management. The Earth Resources Satellite Data Analysis Center (ERSDAC) engages in promotion of research and development of remote sensing technologies, application to resources exploration, and collection of ground truth data. With guidance from the MITI and cooperation with relevant organizations, the ERSDAC has started to develop JERS-1 Data and Information System (ERSDIS) to effectively utilize observation data from JERS-1. The operation is expected to start in the middle of 1992, and international users will be accepted if conditions allow. The distribution policy of JERS-1 observation data is expected to be settled at the start of ERSDIS's operation at the latest. By taking users' advice and opinions into account, ERSDIS will be further improved and refined.
Author (NASDA)

N94-28933# European Space Research Inst., Frascati (Italy). Earthnet Programme Office.
OBSERVATIONS BY ERS-1 START [KANSOKU GA HAJIMATTA ERS-1]
Gianmaria M. Pinna *In* Earth Resources Satellite Data Analysis Center, Proceedings of the International Symposium on Remote Sensing 30 Mar. 1992 p 205-245 Original contains color illustrations (For primary document see N94-28925 08-43)
Avail: CASI HC A03/MF A03

The European Remote Sensing Program is designed as an end-to-end system to serve a large variety of users with a wide range of response-time and applications requirements. The first ERS (European Remote Sensing Satellite) mission, built around the launch of ERS-1, was expected to demonstrate the ability of remote sensing systems to provide valuable earth-observation data from space platforms. The performance of various sensors onboard ERS-1 (apart from the PRARE (Precise Range and Range Rate Experiment) instrument) has been very promising. All LBR (Low Bit Rate) sensors showed a behavior well beyond the more optimistic expectations. The wind scatterometer gave very good results, and the radar altimeter clearly showed its ability to generate the global wind and wave pattern fields in the ocean/atmosphere system. Both instruments will be extremely powerful tools for meteorologists. The SAR (Synthetic Aperture Radar) image revealed astonishing performance. The SAR showed an incredible amount of information extremely useful for several categories of scientists and applications studies including land processes monitoring, disaster accessment, and coastal and off-shore applications. The fast delivery processor showed results that were very promising for users that wish receive the data in near real time. Author (NASDA)

N94-28934# Canada Centre for Remote Sensing, Ottawa (Ontario).
SEA ICE AND OCEANS APPLICATIONS OF SAR [SA NI YORU KAIYO KANSOKU] **c48**
Michael J. Manore, Paris W. Vachon, and Marie-Catherine Mouchot *In* Earth Resources Satellite Data Analysis Center, Proceedings of the International Symposium on Remote Sensing 30 Mar. 1992 p 247-271 Original contains color illustrations (For primary document see N94-28925 08-43)
Avail: CASI HC A03/MF A03

This paper will examine the use of remote sensing technologies, specifically Synthetic Aperture Radar (SAR), for sea ice and ocean applications. The emphasis on SAR is made because of the large volume of such data expected for the first time in the 1990's from a number of different satellite platforms (e.g., ERS-1, Japanese Earth Resources Satellite-1 (JERS-1), and RADARSAT). In addition, the all-weather capability of microwave sensors is particularly well suited to ice and oceans applications because the regions of interest are often affected by poor conditions for optical imaging (i.e., cloud, fog, darkness). Overall, SAR is an excellent sensor for ice applications because it is capable of distinguishing open water from ice and discriminating among different types of ice. This information is used operationally for ship navigation. For oceans applications, the technical complexity of imaging the moving ocean surface makes the reliable extraction of wave information difficult, especially from satellite sensors. However, SAR is capable of imaging oceanographic features such as current fronts, eddies, and large scale waves under low-wind conditions. The applications of SAR described in this paper will be highlighted with examples of recent Canadian activities. Author (NASDA)

N94-28935# Instituto de Pesquisas Espaciais, Sao Jose dos Campos (Brazil).
AMAZONIA: REMOTE SENSING TEST SITE AND SURVEY [AMAZON NI OKERU SEIKATSUIKI NO KAKUDAI TO SHINRIN NO HOZEN]
Roberto PereiradaCunha *In* Earth Resources Satellite Data Analysis Center, Proceedings of the International Symposium on Remote Sensing 30 Mar. 1992 p 273 (For primary document see N94-28925 08-43)
Avail: CASI HC A01/MF A03

Microwave remote sensing has been a promising tool since early seventies when SAR (Synthetic Aperture Radar) airborne campaigns began worldwide. The nineties reached the microwave remote sensing satellite era: ERS-1; JERS-1 (Japanese Earth Resources Satellite-1); and RADARSAT. To a large extent, the user community has been exposed to isolated examples of application of microwave remote sensing for test areas. Now, the time has come when one has the opportunity to use the full coverage provided by systematically orbiting, microwave remote sensing satellites. Amazonia has been envisaged as a test site or calibration site for the last ten years, even though several other forested areas may serve for the same purposes. Today, in some cases, much of expertise needed is for the ability to work with very large areas where an enormous amount of data have to be handled. The paper and presentation will focus on recent studies done for deforestation evaluation of the Amazonia based on wall to wall satellite coverage. These studies previously done to the ERS-1 and JERS-1 will allow comparisons with SAR coverage. Other environmental issues such as mining will also be addressed. Author (NASDA)

N94-28936# National Research Council, Bangkok (Thailand).
UTILIZATION OF REMOTE SENSING DATA IN SOUTHEAST ASIA [TONAN AJIA NI OKERU RIMOTO SENSHINGU DETA NO RIYO]
Suvit Vibulsresth *In* Earth Resources Satellite Data Analysis Center, Proceedings of the International Symposium on Remote Sensing 30 Mar. 1992 p 275-291 Original contains color illustrations (For primary document see N94-28925 08-43)
Avail: CASI HC A01/MF A03

In Southeast Asia, the problems of soil erosion due to deforestation,

land degradation due to salt accumulation, and desertification are approaching an alarming scale. Most countries also depend on the export of natural resources. In the past the reserve and the distribution of natural resources in Southeast Asia had not been sufficiently mapped and the management of natural resources on a national scale had been deficient. By focusing on the synoptic, temporal and uniformity of satellite imagery, the countries in Southeast Asia can utilize the remote sensing data for better management of their natural resources. Some examples are shown to highlight the applications. The role of remote sensing in policy-making of natural resources development projects is clearly stated. In Southeast Asia, a feedback management system is strongly needed whereby the gaps between the management goal as determined by policy-makers and the actual situation are constantly monitored on a seasonal or annual basis by remote sensing and fed back to the decision-making process.

Author (NASDA)

N94-28937# Hiroshima Inst. of Tech. (Japan).
REMOTE SENSING AND GLOBAL MANAGEMENT [RIMOTO SENSHINGU TO CHIKYU NO SOGOTEKI MANEJIMENTO]
Katsuya Nakayama, Yoshinori Ishii, Kazuhiko Otake, Tadami Katahira, Toshibumi Sakata, F. B. Henderson, III, G. M. Pinna, and Suvit Vibulsresth *In* Earth Resources Satellite Data Analysis Center, Proceedings of the International Symposium on Remote Sensing 30 Mar. 1992 p 293-343 In JAPANESE Original contains color illustrations (For primary document see N94-28925 08-43)
Avail: CASI HC A03/MF A03

Remote sensing is utilized in many fields. It is a very effective means for mineral explorations. In lithology, rocks can be discriminated by images in high resolution and spectral characteristics. Visual images from satellites are useful for environmental monitoring. The simultaneity and wide coverage of remote sensing are considered quite beneficial for obtaining single year's information of the whole country of Japan, for instance, to study its land utilization. Remote sensing can also be applied to archaeology to discover ruins. Satellites contribute to the protection against natural disasters such as hurricanes, floods, and fires, or even to the capture of illegal wood cutters. However, in Southeast Asia including Bangladesh, an organization is not yet established to utilize the data from remote sensing, which could reduce damages from disasters. In Japan, projects related to hardware like computers are quite generously funded by the government, but software-related funding such as data analysis and utilization is less than 1/500 of the funding for hardware, and this could result in satellites just orbiting for nothing. International cooperation is vital in selecting and effectively utilizing remote sensing data with limited manpower and budget. It is also important to continue remote sensing, and extract, organize and systematize abundant data available. Consensus and cooperation are the two key words for the future in remote sensing. Author (NASDA)

N94-29036# National Space Development Agency, Tokyo (Japan).
PROCEEDINGS OF THE 15TH EARTH OBSERVATION SYMPOSIUM [DAI 15 KAI CHIKYU KANSOKU SHINPOJIUMU SHIRYO]
9 Sep. 1993 43 p In JAPANESE Symposium held in Miyagi, Japan, Sep. 1993 Prepared in cooperation with Tohoku Aerospace Development Promotion Association, Miyagi, Japan, and Remote Sensing Technology Center, Tokyo, Japan Original contains color illustrations
(JTN-94-80607) Avail: CASI HC A03/MF A01

The following topics were discussed: trends, trend analysis, satellite observation, satellite sounding, satellite imagery, remote sensing, remote sensors, radiometers, environmental monitoring, earth resources management, land management, land use, forest management, vegetative index, weather information, marine observation, NOAA, LANDSAT, SPOT, TRMM (Tropical Rainfall Measuring Mission) satellite, JERS-1 (Japanese Earth Resources Satellite-1), ERS-1, ADEOS (Advanced Earth Observing Satellite), NASDA (National Space Development Agency of Japan), earth observation system, data management, data system, data acquisition, and Japan. For individual titles, see N94-29037 through N94-29041.

N94-29037# Remote Sensing Technology Center, Tokyo (Japan).
PRINCIPLES AND APPLICATION TENDENCY OF REMOTE SENSING: ITS PRINCIPLE, FUNCTION AND UTILIZATION [RIMOTO SENSHINGU NO GENRI TO RIYO DOKO: GENRI SHIKUMI RIYO]
Kaname Takeda *In* NASDA, Proceedings of the 15th Earth Observation Symposium 9 Sep. 1993 p 1-15 In JAPANESE (For primary document see N94-29036 08-43)
Avail: CASI HC A03/MF A01

An overview of the fundamental system structure, principles, data collection and distribution, and distribution data formats by related organizations of remote sensing in Japan is presented. Applicability (merit and demerit), geometrical resolution, spectral (wavelength) characteristics (visible and near infrared radiometer, thermal infrared radiometer, microwave radiometer, synthetic aperture radar, and total ozone mapping spectrometer and their suitable application) and time periods between observations of satellite remote sensing are outlined. Remote sensing data application tendency are discussed in the following aspects: (1) utilization from global view points such as world wheat crop prediction, elucidation of El Nino, hydrological survey for desertification prevention, and so on; and (2) utilization from regional view point, especially by local self-governing bodies in such areas as land utilization, forest survey, disaster prevention, environmental survey, and fishery survey. Author (NASDA)

N94-29038# National Space Development Agency, Ohashi (Japan). Earth Observation Center.
STATUS AND TENDENCY OF EARTH OBSERVATION SYSTEM [UCHU KARA NO CHIKYU KANSOKU SHITUTEMO NO GENJO OYOBI DOKO NI TSUITE]
Takehiro Iida *In* NASDA, Proceedings of the 15th Earth Observation Symposium 9 Sep. 1993 p 16-24 In JAPANESE (For primary document see N94-29036 08-43)
Avail: CASI HC A02/MF A01

This article describes the status and future equipment plan of Japanese earth observation system. The function of the NASDA (National Space Development Agency of Japan) EOC (Earth Observation Center) is explained. Outlines of world satellites such as MOS-1 (Marine Observation Satellite-1), JERS-1 (Japanese Earth Resources Satellite-1), LANDSAT, SPOT, and ERS-1, which data are now received and utilized in EOC, are also described. Projects of Japanese earth observation system including ADEOS (Advanced Earth Observing Satellite) and TRMM (Tropical Rainfall Measuring Mission) satellite projects and information system design are outlined.

Author (NASDA)

N94-29039# Tokai Univ., Tokyo (Japan).
PERSPECTIVES OF EARTH OBSERVING TECHNIQUES: EXPECTATION OF EARTH OBSERVATION IN SPACE DEVELOPMENT HISTORY [CHIKYU KANSOKU GIJUTSU NO SHORAI TENBO: UCHU KAIHATSU NO AYUMI NI MIRU CHIKYU KANSOKU ENO KITAI]
Toshibumi Sakata *In* NASDA, Proceedings of the 15th Earth Observation Symposium 9 Sep. 1993 p 25-28 In JAPANESE (For primary document see N94-29036 08-43)
Avail: CASI HC A01/MF A01

This article explains the overview of the space development history and its future perspectives. Transition of the space technology development including rocket design, satellite design and remote sensing fields is reviewed in relation to the social background. Based on the above review, perspectives of the space development is described laying emphasis on the earth observation. Author (NASDA)

N94-29040# Tohoku Univ., Sendai (Japan).
OCEANIC SURVEY UTILIZING SATELLITES [JINKO EISEI KARA UMI O SHIRABERU]
Yoshiaki Toba *In* NASDA, Proceedings of the 15th Earth Observation Symposium 9 Sep. 1993 p 29-35 In JAPANESE Original contains color illustrations (For primary document see N94-29036 08-43)
Avail: CASI HC A02/MF A01

Marine observation technologies utilizing satellite remote sensors are explained. Oceanographic and meteorological parameters which can be obtained from the satellite data are introduced. Examples of the data extracted from the satellite imageries such as ocean current, sea surface temperature, ocean wave, wind profiles, and biomass are shown.

Author (NASDA)

N94-29041# Iwate Univ., Morioka (Japan). Computer Science.
TOHOKU DISTRICT OBSERVED BY ARTIFICIAL SATELLITES [JINKO EISEI KARA MITA TOHOKU]
Ryuzo Yokoyama *In* NASDA, Proceedings of the 15th Earth Observation

Symposium 9 Sep. 1993 p 36-40 In JAPANESE (For primary document see N94-29036 08-43)
Avail: CASI HC A01/MF A01

This article outlines the remote sensing technology utilizing the satellite data. Examples of satellite observation data for land management, forest management, and environmental monitoring around the north of Japan are explained. Author (NASDA)

N94-29095# Naval Postgraduate School, Monterey, CA.
SPECTRAL AND POLARIMETRIC ANALYSIS OF HYPERSPECTRAL DATA COLLECTED BY AN ACOUSTO-OPTIC TUNABLE FILTER SYSTEM M.S. Thesis
Melissa A. Sturgeon 23 Sep. 1993 148 p
(AD-A275076) Avail: CASI HC A07/MF A02

Analysis of data collected during a ground-based experiment of an acousto-optic tunable filter (AOTF) hyperspectral imaging system illustrates the utility of this technology for military applications. The unique ability of an AOTF system to simultaneously acquire two orthogonally polarized images allows both spectral and polarimetric characterization of targets. The data images selected for analysis contain camouflaged military equipment deployed in a desert background. After geometric and atmospheric correction, spectral analysis is accomplished using two different methods. Comparing images created by the difference between polarizations for each band provides the basis for polarimetric analysis of the data. An algorithm developed to combine the information provided by spectral and polarimetric analysis shows how features within a scene can be distinguished from the background. Results show that AOTF hyperspectral technology has potential to enhance current military intelligence collection capabilities. DTIC

N94-29098*# Old Dominion Univ., Norfolk, VA. Research Foundation.
CONCEPTUAL RADIOMETER DESIGN STUDIES FOR EARTH OBSERVATIONS FROM LOW EARTH ORBIT
Richard F. Harrington Apr. 1994 44 p
(Contract NAS1-18584; RTOP 233-01-03-22)
(NASA-CR-4588; NAS 1.26:4588) Avail: CASI HC A03/MF A01

A conceptual radiometer design study was performed to determine the optimum design approach for spaceborne radiometers in low Earth orbit. Radiometric system configurations which included total power radiometers, unbalanced Dicke radiometers, and balanced Dicke, or as known as noise injection, radiometers were studied. Radiometer receiver configurations which were analyzed included the direct detection radiometer receiver, the double sideband homodyne radiometer receiver, and the single sideband heterodyne radiometer receiver. Radiometer system performance was also studied. This included radiometric sensitivity analysis of the three different radiometer system configurations studied. Both external and internal calibration techniques were analyzed. An accuracy analysis with and without mismatch losses was performed. It was determined that the balanced Dicke radiometer system configuration with direct detection receivers and external calibrations was optimum where frequent calibration such as once per minute were not feasible. Author

N94-29107 Rutherford Appleton Lab., Chilton (England).
ROLE OF SATELLITE OBSERVATIONS OF SEA-SURFACE TEMPERATURE IN THE DETECTION OF GLOBAL CHANGE
M. R. Allen 28 Nov. 1993 51 p
(PB94-138120; RAL-93-095) Avail: Issuing Activity (National Technical Information Service (NTIS))

The report presents the scientific case for the development of a 10-12 year data-set of consistent, accurate, global observations of sea surface temperature (SST) from the Along-Track Scanning Radiometer (ATSR) and its successors, the ATSR-2 and AATSR. The case focuses on the role such data will play in detecting and quantifying evidence for anthropogenic climatic change. Four key areas in which data from the ATSR series can play a useful role are identified. They are: providing high spatial and temporal resolution data for the validation of climate models; providing independent corroboration of in situ observations of SST; providing direct evidence of global changes taking place; and allowing the detection of global patterns of change extending into the Southern Hemisphere extra-tropical regions. NTIS

N94-29173# Helsinki Univ. of Technology, Espoo (Finland). Lab. of Hydrology and Water Resources Management.
MODEL-ORIENTED DATA ANALYSIS WITH APPLICATIONS TO LAKE AND SOIL WATER SIMULATION Ph.D. Thesis
J. Kettunen 5 Nov. 1993 99 p
(PB94-136942; ISBN-951-221762-7) Avail: CASI HC A05/MF A02

The general aim of all water resources modelling is to cover the broadest possible range of empirical facts with the smallest possible set of hypotheses. The study, which summarizes eight earlier publications, undertook to investigate practical techniques to attain the goal. The aims of the study were to develop methods for structural characterization, optimal observational design and for choice of the best model structure from among rival candidates. The problems were analyzed using the theory of optimal experimental design. A method to detect and identify non-linear dependency among model parameters was suggested. The method is based on the logarithmic transformation of parameter space and the principal component analysis of the Fisher information matrix. The technique can also be used to approximate the admissible level of the observational error. The non-linear D-optimal design of observations was studied. NTIS

N94-29213 Army Topographic Engineering Center, Fort Belvoir, VA.
THE IMAGE DIGITIZING SYSTEM (IDS) Scientific Paper
Maurits Roos Jan. 1994 13 p Limited Reproducibility: More than 20% of this document may be affected by microfiche quality
(AD-A275341; TEC-R-209) Avail: CASI HC A03

The conversion of mapping technology in the DOD community from analog- to digital-based technology, which started in the 1980's required precise equipment to convert aerial photographs to digital data (pixels). These are referred to as image scanners or digitizers. This paper describes the recent development of a precise image scanner by the Topographic Engineering Center (TEC) (formerly ETL). A contractor successfully developed this scanner, called the Image Digitizing System (IDS). This paper describes the general design and operation of the system, and many of its unique characteristics. The paper also describes several test results, that verify the high-geometric and high-photometric characteristics of the IDS. DTIC

N94-29217# Earth Resources Satellite Data Analysis Center, Tokyo (Japan).
PROCEEDINGS OF THE 3RD INTERNATIONAL SYMPOSIUM: JERS-1 AND REMOTE SENSING IN THE FUTURE [DAI 3 KAI KOKUSAI SHINPOJIUMU: JERS-1 TO KONGO NO RIMOTO SENSHINGU KOENSHU]
29 Mar. 1991 222 p In ENGLISH and JAPANESE Symposium held in Tokyo, Japan, 17-18 Jan. 1991 Sponsored by Japan Motorcycle Racing Organization, Tokyo, Japan Original contains color illustrations
(JTN-94-80597) Avail: CASI HC A10/MF A03

The following topics were discussed: remote sensing, earth observation, Earth Observing System (EOS), environmental monitoring, earth resources, resources management, resources survey, land management, forest management, disaster prevention, agriculture, remote sensors, infrared scanners, multispectral band scanners, Optical Sensor (OPS), Synthetic Aperture Radar (SAR), Advanced Spaceborne Thermal Emission and Reflection Radiometer (ASTER), radar imagery, satellite imagery, image processing, image analysis, data processing, data reduction, data acquisition, data transmission, transmission networks, geological survey, Japanese Earth Resources Satellite-1 (JERS-1), petroleum detection, European Space Agency (ESA), agriculture, and ecological system. For individual titles, see N94-29218 through N94-29232.

N94-29218# Tokyo Univ. (Japan). Mineral Development Engineering.
REMOTE SENSING AND THE EARTH [RIMOTO SENSHINGU TO CHIKYU]
Yoshinori Ishii *In* Earth Resources Satellite Data Analysis Center, Proceedings of the 3rd International Symposium: JERS-1 and Remote Sensing in the Future 29 Mar. 1991 p 9-40 In JAPANESE Original contains color illustrations (For primary document see N94-29217 08-43)
Avail: CASI HC A03/MF A03

Recent global problems consist of three factors which are related to one another; population, natural resources and environment. For example, increase of population enlarges energy consumption which leads to burning

of a mass of petroleum, which would result in environmental disruption and global warming. In human history, energy is closely associated with civilization; in the early stage, woods were the only energy source, then coal, petroleum, and nuclear energy is used today. Most of such earth resources produce carbon dioxide which causes global warming by the greenhouse effect. Therefore new energy sources are proposed to protect the environment, such as sunlight, agricultural wastes, hydropower, wind and geothermal energy. However, a more direct and easier method is to improve the energy efficiency. Recently, interest has been focused on remote sensing as a method to resolve these problems by observing the Earth from a macro and global viewpoint. For more practical applications, future satellites will be small systems which require low cost and short development period. We also require a new science that can integrate human and earth science and can regard the Earth as one system.

Author (NASDA)

N94-29219# Tokai Univ., Tokyo (Japan). Research and Information Center.

A NEW INFORMATION SYSTEM: SATELLITE OBSERVATION [ATARASHII JOHO SHISUTEMU: EISEI KANSOKU]

Toshibumi Sakata *In* Earth Resources Satellite Data Analysis Center, Proceedings of the 3rd International Symposium: JERS-1 and Remote Sensing in the Future 29 Mar. 1991 p 41-64 In JAPANESE Original contains color illustrations (For primary document see N94-29217 08-43)

Avail: CASI HC A03/MF A03

Today, several countries launched satellites for geophysical observation, which includes stationary satellites and polar satellites. By combination of these satellites, it is possible to observe the entire Earth. The low resolution and wide swath data can be used for global observation, such as meteorology, oceanic survey, forestry and disaster observation, while high resolution and narrow swath data can be used for regional observation such as land usage and survey of plant ecology and natural resources. To realize the application of remote sensing data, it is necessary to build a sufficient number of receiving stations. When enough stations are linked by relay satellites, a network to observe the whole Earth will be completed. Japan is planning to build automatic receiving stations to cover all over Japan, and collect the data at the image processing center. These data will be used for resolving global issues including desertification, natural disaster and oceanic survey, and the accumulation of the results should contribute to social activities and have the second usage for general users.

Author (NASDA)

N94-29220# National Space Development Agency, Tokyo (Japan). Earth Observation Satellite Group.

OUTLINE OF JERS-1 SYSTEM [JERS-1 SHISUTEMU NO GAIYO]

Takashi Suzuki *In* Earth Resources Satellite Data Analysis Center, Proceedings of the 3rd International Symposium: JERS-1 and Remote Sensing in the Future 29 Mar. 1991 p 65-71 In JAPANESE (For primary document see N94-29217 08-43)

Avail: CASI HC A02/MF A03

Japanese Earth Resources Satellite-1 (JERS-1) is a geophysical observatory satellite developed for survey of natural resources as well as for observation of landscapes and disasters. It is a joint project of the National Space Development Agency and the Ministry of International Trade and Industry; the former takes charge of development of the satellite structure, system tests, launching, tracking control, and data receiving, and the latter develops mission devices. The satellite utilizes synthetic aperture radar (SAR) using L band, optical sensor (OPS) for short wave infrared observation, and a mission data recorder (MDR), all of which will show unique characteristics in global coverage, especially for lithologic mapping. The satellite structure has a system for energy supply and thermal and attitude control which is an accumulation of the latest techniques. The JERS-1 is scheduled to be launched in February 1992. The development was started in 1986 and the prototype was completed on the basis of several system development tests. At present, the flight tests are being performed using the prototype, in addition to simultaneous preparation for launch and operation in orbit.

Author (NASDA)

N94-29221# Japan Resources Observation System Organization.

OBSERVATORY SYSTEM OF EARTH RESOURCES SATELLITE-1 Abstract Only [CHIKYU SHIGEN EISEI 1 GO (ERS-1) KANSOKU SHISUTEMU NI TSUITE]

Mitsuru Takei *In* Earth Resources Satellite Data Analysis Center, Proceedings of the 3rd International Symposium: JERS-1 and Remote Sensing in the Future 29 Mar. 1991 p 73 In JAPANESE (For primary document see N94-29217 08-43)

Avail: CASI HC A01/MF A03

The Japanese Earth Resources Satellite-1 (JERS-1) has been developed as a joint project of the National Space Development Agency (NASDA) and the Ministry of International Trade and Industry dominantly for survey of natural resources, as well as for observation of landscape and environmental change, oceanic survey, monitoring of disaster, and reconnaissance of coastline. The observatory system consists of Synthetic Aperture Radar (SAR), Optical Sensor (OPS), Mission Data Recorder (MDR) and Mission Data Transmitter (MDT). The SAR is an active sensor using L band which enables all-weather observation, and the data will be used for lithologic survey. The OPS includes Visible and Near Infrared Radiometer (VNIR) and Short Wave Infrared Radiometer (SWIR). The VNIR can collect three-dimensional geographical data, and SWIR will be used to identify rocks. Having completed flight tests using the prototype, the observatory system was delivered from March to September 1990 to NASDA which takes charge of development of the satellite body. The JERS-1 is scheduled to be launched in winter 1992, and to collect observatory data for two years.

Author (NASDA)

N94-29222# Geological Survey of Japan, Ibaraki.

APPLICATION OF JERS-1 DATA TO GEOLOGIC ANALYSES [CHISHITSU KOZO KAISEKI ENO JERS-1 DETA NO RIYO]

Yasushi Yamaguchi *In* Earth Resources Satellite Data Analysis Center, Proceedings of the 3rd International Symposium: JERS-1 and Remote Sensing in the Future 29 Mar. 1991 p 75-95 In JAPANESE (For primary document see N94-29217 08-43)

Avail: CASI HC A03/MF A03

The Japanese Earth Resources Satellite-1 (JERS-1) is an orbiting geophysical observatory satellite unique in loading Synthetic Aperture Radar (SAR) and Optical Sensor (OPS). This report discusses predictable JERS-1 data from the viewpoint of an end-user who deals with remote sensing as a geologist. The first characteristic of SAR data is the ability of transmittance. Since SAR scans the Earth surface with microwaves which can pass through clouds and fog, observation will be possible anytime in any weather. Although JERS-1 uses L band that can penetrate deeper than X band used in previous observation, it is difficult to observe soil and rocks over plants. The second characteristic is off-nadir angle which is set at 35 deg in JERS-1; in general, large off-nadir angle lessen geographical distortion, while small angle is excellent in distinguishing surface substances. From the standpoint of a user, it is ideal to have a changeable off-nadir angle. For the same reason, a changeable SAR parameter will improve the ability to distinguish and identify the surface changes multidisciplinarily. So far, both can be realized by comparing data of the same region among satellites with different parameters or off-nadir angles. It is expected in JERS-1 that application of four bands in short wave infrared region makes it possible to distinguish rock phases in detail, and that stereo observation will also be realized by the OPS. These functions will improve lithologic data.

Author (NASDA)

N94-29223# JAPEX Geoscience Inst., Tokyo (Japan).

APPLICATION OF OPTICAL SENSOR DATA TO RESOURCE SURVEY [KOGAKU SENSA DETA NO SHIGEN TANSA ENO OYO]

Hiroshi Watanabe *In* Earth Resources Satellite Data Analysis Center, Proceedings of the 3rd International Symposium: JERS-1 and Remote Sensing in the Future 29 Mar. 1991 p 97-102 In JAPANESE Original contains color illustrations (For primary document see N94-29217 08-43)

Avail: CASI HC A02/MF A03

Advance of sensors makes it possible to obtain various kinds of remote sensing data, most of which have been applied for natural resource survey. Remote sensing includes an optical sensor and microwave sensor. Latest optical sensors used in geophysical observatory tend to have high-resolution and multi-band function, and they can collect a huge volume of data. It is planned that a sensor of short wave infrared will be applied in a satellite

observation, which will also improve natural resource survey. The remote sensing data is used for resource survey by the following three methods: (1) structural geological analysis using a small-scale image of large area; (2) structural geological analysis using a large-scale image of small area, which also makes a spectral observation possible when using multi-band sensor; and (3) collection of general information on land surface of a candidate site. The software to analyze remote sensing data has not reached a fully practical usage, however, systems to analyze the images and to identify the objective rocks are being developed. Author (NASDA)

N94-29224# Canada Centre for Remote Sensing, Ottawa (Ontario).
RADAR APPLICATIONS AT THE CANADA CENTRE FOR REMOTE SENSING
V. R. Slaney *In* Earth Resources Satellite Data Analysis Center, Proceedings of the 3rd International Symposium: JERS-1 and Remote Sensing in the Future 29 Mar. 1991 p 103-107 (For primary document see N94-29217 08-43)
Avail: CASI HC A01/MF A03

The Canada Centre for Remote Sensing (CCRS) is a Branch of the Department of Energy, Mines and Resources of the government of Canada. The CCRS was formed to support remote sensing technology in Canada by operating satellite receiving stations and facilities for processing and disseminating satellite data. These ground receiving stations are now processing LANDSAT, SPOT and AVHRR (Advanced Very High Resolution Radiometer) data routinely, and will be prepared to receive data from ERS-1, the Japan Earth Resource Satellite-1 (JERS-1) and RADARSAT. CCRS scientists are grouped into five Divisions; Applications, Methodology, User Services, Satellite Operations and Airborne Operations. The Applications Division is mainly concerned with developing and demonstrating practical ways to apply remotely sensed data to the management of Canada's natural resources. Studies are presently carried out in forestry, agriculture, hydrology, geology, oceanography, ice and, most recently, in monitoring global change. This report provides outline of investigation and operation of CCRS according to each field. Author (NASDA)

N94-29225# Lemigas Research and Development Centre for Oil and Gas Technology, Jakarta (Indonesia).
APPLICATION OF REMOTE SENSING TECHNIQUES IN PETROLEUM EXPLORATION: THE INDONESIAN EXPERIENCE
B. Situmorang *In* Earth Resources Satellite Data Analysis Center, Proceedings of the 3rd International Symposium: JERS-1 and Remote Sensing in the Future 29 Mar. 1991 p 109-125 (For primary document see N94-29217 08-43)
Avail: CASI HC A03/MF A03

The extensive application of remote sensing techniques used in petroleum exploration for a general geological mapping and hydrocarbon exploration in Indonesia is presented. The Japanese Earth Resources Satellite-1 (JERS-1), which will be launched in early 1992, appears to have some advantages over the U.S. Landsat and French SPOT, especially for Indonesia. They are: high spatial resolution will permit more detailed mapping as in the case of SPOT; the availability of a long wavelength synthetic aperture radar (SAR) will permit penetration of cloud cover and dense vegetation; the stereoscopic capability of JERS-1 (as in SPOT) will be very useful in structural interpretation, making possible the recognition of the structural framework of basinal areas; and short wave infrared bands will enable the differentiation of clay minerals, which are very useful in studying the hydrothermal alteration zones. It appears that various advantages that have been provided by Landsat, SPOT, and radar are integrated in JERS-1. With the setting up of the Image Processing Laboratory for Oil and Gas Study at Lemigas, which is funded by the government of Japan, it shall be possible to develop image processing and analytical techniques to obtain optimum geological information for hydrocarbon exploration.
Author (NASDA)

N94-29226# Geological Survey of Japan, Ibaraki.
EOS PROJECT AND ASTER (ITIR)
Hiroji Tsu *In* Earth Resources Satellite Data Analysis Center, Proceedings of the 3rd International Symposium: JERS-1 and Remote Sensing in the Future 29 Mar. 1991 p 127-153 (For primary document see N94-29217 08-43)
Avail: CASI HC A03/MF A03

The Earth Observing System (EOS) project is a plan to understand global changes using satellite observatory data, mainly under the direction of NASA. The scientific mission of EOS aims at collecting data to enlarge knowledge of relevant academic fields and multidisciplinary intervention, and to recognize how the earth system is changing. It has been decided that nine sensors are planned for EOS-A, one of which is the advanced spaceborne thermal emission and reflection radiometer (ASTER) (intermediate thermal infrared radiometer (ITIR)) proposed by the Ministry of International Trade and Industry, Japan. ASTER is a unified imaging system that can detect visible through thermal infrared spectra, and can make images with both high spatial and spectral resolutions. This scientific mission will be performed with close collaboration between Japanese and U.S. ASTER science teams. The ASTER project is managed by the Ministry of International Trade and Industry, under which Japan Resources Observation System Organization (JARO) takes charge in development of sensors, and Earth Resource Satellite Data Analysis Center (ERSDAC) is responsible for processing and analyses of the data and user services.
Author (NASDA)

N94-29227# European Space Research Inst., Frascati (Italy). Earthnet Programme Office.
EARTH-OBSERVATION PLAN IN EUROPE
G. Triebnig *In* Earth Resources Satellite Data Analysis Center, Proceedings of the 3rd International Symposium: JERS-1 and Remote Sensing in the Future 29 Mar. 1991 p 155-162 (For primary document see N94-29217 08-43)
Avail: CASI HC A02/MF A03

It has become increasingly obvious that humans are faced with a number of potentially major environmental problems (e. g. climatic change due to the greenhouse effect, ozone depletion). Observation of the Earth from space is one of the keys to a better understanding of the Earth as a system and is vital to achieving a comprehensive assessment of the influence of man's activities on the environment. Observation of the Earth and its environment has been part of the European Space Agency's (ESA) programs since the advent of the METEOSAT program in the early 1970's. The all-weather satellite ERS-1 will provide a new perspective in the early 1990's for better understanding and monitoring the Earth and its environment. Future plans of the Agency include the following: ERS-2, a follow-on mission to ERS-1; a solid Earth gravity mission; a second generation METEOSAT with improved capabilities; and a series of polar-orbit missions to provide a wide range of observations of the Earth which are particularly important for monitoring and understanding the environment. Author (NASDA)

N94-29228# Jet Propulsion Lab., California Inst. of Tech., Pasadena.
ROCK IDENTIFICATION USING THERMAL INFRARED DATA
Anne B. Kahle *In* Earth Resources Satellite Data Analysis Center, Proceedings of the 3rd International Symposium: JERS-1 and Remote Sensing in the Future 29 Mar. 1991 p 163-174 Original contains color illustrations (For primary document see N94-29217 08-43)
Avail: CASI HC A03/MF A03

The Advanced Spaceborne Thermal Emission and Reflection Radiometer (ASTER) instrument will be the first spaceborne multispectral thermal infrared instrument with spatial and spectral resolution adequate for geologic applications. From thermal data one can derive both surface temperature and surface spectral emissivity. The primary application of the emissivity is for surface lithologic mapping. The temperature data can be used for studies of thermal inertia of surface materials and for studies of thermal processes related to volcanism and hydrology. This report describes the theoretical background and examples of the use of multispectral thermal data. From theoretical and experimental framework, the ASTER instrument will allow mapping and identification of most terrestrial rocks, such as silicates, iron oxides, carbonates, and clay minerals. The importance of multispectral thermal data was demonstrated by NASA's Airborne Thermal Infrared Multispectral Scanner (TIMS) which clearly imaged rocks and temperature, especially for mineral survey. Author (NASDA)

N94-29229# National Inst. of Agro-Environmental Science, Ibaraki (Japan). Div. of Information Analysis.
JERS-1 AND FUTURE REMOTE SENSING: APPLICATION OF REMOTE SENSING DATA TO AGROECOLOGICAL PROBLEMS [JERS-1 TO KONGO NO RIMOTO SENSHINGU: NOGYO KANKYO MONDAI NI OKERU RIMOTO SENSHINGU DETA NO RIYO]
Tsuyoshi Akiyama *In* Earth Resources Satellite Data Analysis Center,

Proceedings of the 3rd International Symposium: JERS-1 and Remote Sensing in the Future 29 Mar. 1991 p 175-184 In JAPANESE (For primary document see N94-29217 08-43)
Avail: CASI HC A02/MF A03

Although global environmental change is closely related with agriculture, the influence of environmental change on agriculture and environmental disruption by agricultural production have not been analyzed quantitatively. The amount and change of factors in a global ecological system should be determined in a global scale for grasping agroecological problems. This is difficult to do by conventional methods, but remote sensing is expected to be able to collect these data accurately and promptly. In industrialized countries, environmental change is a concern due to global warming and depletion of the ozone layer by increases in the use of chemical products and by the burning of petroleum products. Water pollution by toxic substances and acid rain have been spreading. On the other hand, in developing countries, rapid increases in population promote desertification and degeneration of soil and tropical rain forests. There are also problems with pollution that are similar to those of the industrialized countries. In order to cope with these problems, a sensor with high spatial and spectral resolution is necessary. For these reasons, it is essential to develop a technique to process remote sensing data to obtain detailed and practical information for agroecology. Author (NASDA)

N94-29230# National Research Inst. for Earth Science and Disaster Prevention, Tsukuba (Japan).
APPLICATION OF REMOTE SENSING IN PREVENTION OF DISASTERS [BOSAI BUNYA NI OKERU RIMOTO SENSHINGU DETA NO RIYO]
Shigetsugu Uehara *In* Earth Resources Satellite Data Analysis Center, Proceedings of the 3rd International Symposium: JERS-1 and Remote Sensing in the Future 29 Mar. 1991 p 185-193 In JAPANESE Original contains color illustrations (For primary document see N94-29217 08-43)
Avail: CASI HC A02/MF A03

The expectation of applying remote sensing in monitoring disasters has increased recently. To prevent disasters, it is necessary to obtain the most recent information on natural and social changes; rapid analysis, advice, and cooperation by specialists are important. Remote sensing is excellent for monitoring disasters for a long-term periodically, and sudden occurrences will be able to be monitored when an all-weather and all-day sensor, Synthetic Aperture Radar (SAR), is applied. Improvement of communication and transmission systems is also necessary to cope with disasters quickly and effectively. Today, the remote sensing is applied in prevention of disasters in various fields (such as floods, landslides, volcano eruptions, and earthquakes) and has provided useful information worldwide. Future disasters are considered to be closely associated with global environmental changes, so that the emphasis on remote sensing and international cooperation should be increased to resolve these problems.
Author (NASDA)

N94-29231# Government Industrial Research Inst., Chugoku (Japan).
FUTURE EXPECTATION OF REMOTE SENSING TECHNOLOGY [RIMOTO SENSHINGU GIJUTSU ENO KONGO NO KITAI]
Katsuya Nakayama, Higashi Iijima, Yoshinori Ishii, Toshibumi Sakata, Nobuhiko Kodaira, and Yasuaki Ishiwada *In* Earth Resources Satellite Data Analysis Center, Proceedings of the 3rd International Symposium: JERS-1 and Remote Sensing in the Future 29 Mar. 1991 p 195-218 In JAPANESE (For primary document see N94-29217 08-43)
Avail: CASI HC A03/MF A03

This panel discussion focused on the future of remote sensing. The participants were specialists of various scientific fields associated with remote sensing. Possible applications to geographical study and natural resources surveys, predictable data collected by Synthetic Aperture Radar (SAR) and Optical Sensors (OPS) to be loaded in Japanese Earth Resources Satellite-1 (JERS-1), expectations of the international society of remote sensing, practical and low-cost applications of remote sensing data, international evaluation of JERS-1 especially with respect to the SAR sensor, and the desired function of a future sensor are main topics. Comparison of development of remote sensing among Europe, the USA and Japan, and what should be done in the next decade was also discussed. Emphasis is made on the use of remote sensing data not only for Japan but on a global scale. Author (NASDA)

N94-29232# National Space Development Agency, Tokyo (Japan). Earth Observation Program Office.
JAPAN'S EARTH OBSERVATION SATELLITE PROGRAMS
Yukio Haruyama *In* Earth Resources Satellite Data Analysis Center, Proceedings of the 3rd International Symposium: JERS-1 and Remote Sensing in the Future 29 Mar. 1991 p 219-226 (For primary document see N94-29217 08-43)
Avail: CASI HC A02/MF A03

This program was formed by the National Space Development Agency of Japan (NASDA), and presents the following: (1) basic plans for research and development on earth science and technology based on the report by the Council for Science and Technology which emphasizes the comprehensive and systematic development of satellite sensor technology, information system, and network technology, are recognized as key subjects; (2) Japan's earth observation satellite program (schedule and outline of Marine Observation Satellite-1 (MOS-1), MOS-1b, Japanese Earth Resources Satellite-1 (JERS-1), Advanced Earth Observing Satellite (ADEOS), Tropical Rainfall Measuring Mission (TRMM), Japanese Polar Orbiting Platform (JPOP) and relevant meetings held in Japan); (3) earth observation satellite programs in the world (time table of operation, development and plan/research phase of Japan, the U.S., European Space Agency (ESA), France, and other countries' satellites); (4) status of each program (MOS-1b, JERS-1, ADEOS, TRMM); (5) geostationary meteorological satellites programs (launch, orbit, weight and phase of Geostationary Meteorological Satellite (GMS), GMS-2, GMS-3, GMS-4 and GMS-5); and (6) JERS-1 (main characteristics and mission equipments of JERS-1). Author (NASDA)

N94-29288 Army Cold Regions Research and Engineering Lab., Hanover, NH.
ON THE TEMPERATURE DISTRIBUTION NEAR A COLD SURFACE
Yin-Chao Yen Oct. 1993 29 p Limited Reproducibility: More than 20% of this document may be affected by microfiche quality
(AD-A275162; CRREL-93-19) Avail: CASI HC A03

Temperature profiles were taken during the 1991-92 season at an experimental site on CRREL's grounds; however, they were rather limited because of the unusual lack of snowfall and the location of the site, which was small and had elevated sides (especially in the direction of the prevailing wind). Nevertheless, some unusual features have been observed for the first time. The profiles show the existence of a double-reversal in temperature structure close to the snow surface when the snow temperature is much lower than its melting point, in contrast to a persistent raised maximum temperature over a melting snowpack. This indicates that the micro-heat transport process is complicated by the presence of a non-isothermal lower boundary. Over frozen or partially frozen ground without snow, and with air temperature either above or below the melting point of ice, a thin, nearly isothermal air layer on the order of 2 to 3 cm in thickness at varying heights was observed for the first time. With very few exceptions, in general, the temperature decreases as height increases, but the extent is less pronounced over a snow cover (where conditions are nearly isothermal) than over cold ground. On the basis of limited measurements, the overall temperature gradient over the bare ground is about twice that over snow-covered ground. DTIC

N94-29417# Aerospatiale, Cannes (France).
AN EARTH OBSERVATION TELESCOPE REFOCUSING MECHANISM
M. Lavadoux (Societe d'Applications Generales d'Electricite et de Mecanique, Cergy-Pontoise, France.) and J. F. Patin 1993 6 p
(Rept-932-440-103; ETN-94-95474) Avail: CASI HC A02/MF A01

The development, requirements, and testing of the refocusing mechanism of a space telescope are reported. The refocusing mechanism that was developed holds the focus lens in the nominal flight position throughout the launch phase, and acquires and maintains the focus lens position during observation to compensate for dimensional variations in the telescope in orbit. The refocusing mechanism developed for this observation satellite is particularly interesting because of its high precision characteristics. Its two innovating originalities are essentially its translatory motion guidance device using two parallel deformable leaves and its linear actuator, which is highly efficient for its characteristics of precision, life time, and environmental ability. To date, this mechanism has been validated by several elementary tests that have enabled qualification of the technologies and components: stepper motor, coupling belows, linear actuator, ball bearings, guidance device, locking device, and transmission arm. ESA

N94-29528# Loughborough Univ. of Technology (England). Dept. of Mathematical Sciences.
FRONTS AT THE CONFLUENCES OF SPRING-FED STREAMS WITH JOEKULSA A FJOELLUM: POSSIBLY THERMAL BARS?
Anthony Kay Oct. 1993 12 p Original contains color illustrations
(MATHS-Rept-A-198; ETN-94-95513) Avail: CASI HC A03/MF A01

Remarkably sharp fronts observed where spring water streams flow into the glacial river Jokulsa a Fjollum, which flows northwards from the ice cap Vatnajoekuli to the north coast of Iceland. Reasons for speculating that these fronts are thermal bars resulting from the temperatures of the river water and the spring water being on opposite sides of the temperature of maximum density are given. It is suggested that measurements of temperature and flow profiles across the fronts are to be made in order to determine whether this is indeed the correct explanation. Ideas for future research are given. ESA

N94-29540 Texas A&M Univ., College Station.
AUTOMATING GEOGRAPHICALLY REFERENCED DIGITAL MOSAICS FROM AERIAL VIDEOGRAPHY WITH AREA-BASED FEATURE MATCHING Ph.D Thesis
Douglas Frank Wunneburger 1992 121 p
Avail: Univ. Microfilms Order No. DA9315164

Resource managers are frequently in need of high resolution imagery within short turn-around periods. Videography provides a source for such data. Current videographic capabilities are limited by the narrow field of view of the sensor and the lack of geographic reference. However through automated processing, digital mosaics overcome videography's narrow field of view while maintaining high resolution and large scale. Aerial videography has several advantages over conventional photographic and satellite remote sensing data. Photographic processing costs and time are virtually eliminated, and unlike pushbroom type scanners, stereo coverage is achieved in each single flight line. Using dynamic GPS (global positioning system) locators with videography, it is possible to generate geo-referenced images. Upon capturing these images in digital form, machine vision area matching procedures provide the capability to generate automated digital mosaics with multiple geo-referenced anchor points. The project integrates aerial videography, geographic referencing systems, and area based feature matching to produce a system able to generate referenced mosaics of contiguous videographic images. Dissert. Abstr.

N94-29553*# National Aeronautics and Space Administration. Marshall Space Flight Center, Huntsville, AL.
INTER-COMPARISON OF WILDFIRE AND HIGH-RESOLUTION INTERFEROMETER SOUNDER (HIS) DATA FROM STORM-FEST: AN INVESTIGATION OF WILDFIRE SPECTRAL CHANNEL DISCREPANCIES
G. J. Jedlovec and G. S. Carlson Mar. 1994 31 p
(NASA-TM-108439; NAS 1.15:108439) Avail: CASI HC A03/MF A01

This simultaneous collection of HIS spectral measurements aboard the ER-2 during STORM-FEST provided a means to explore calibration problems in the infrared bands of the Wildfire instrument. Large discrepancies in brightness temperatures were noted in Wildfire bands designed to sample the 'wings' of the strong ozone absorption band centered at 9.6 microns, where the atmospheric transmittance changes rapidly with wavelength. Examination of interchannel relationships in Wildfire data and subsequent comparison to Wildfire data synthesized from the HIS measurements suggests that a wavelength shift in the channel spectral response from those determined in the laboratory may have occurred. Based on comparisons from several flights, this spectral shift has been empirically determined to be about 0.15 micron. It is speculated that this problem resulted from a slight misalignment of the spectrometer grating or other optical elements, or was a result of extreme range in temperatures experienced by the instrument throughout the course of an ER-2 flight. A consequence of this temperature fluctuation may be a change in a position of the grating in the optical path and could result in the variations in channel spectral response during flight. These findings for Wildfire may have significant bearing on future use of the MAS because of the similarities to the original Wildfire configuration. Author (revised)

N94-29762 Texas Univ., Austin.
A SIMULATION STUDY OF HIGH DEGREE AND ORDER GEOPOTENTIAL DETERMINATION USING SATELLITE GRAVITY GRADIOMETRY Ph.D. Thesis
Srinivas Viswanath Bettadpur 1993 172 p
Avail: Univ. Microfilms Order No. DA9323340

For several applications in oceanography and geophysics, there is an evident need for the determination of high resolution global geopotential fields to a great accuracy. The problem of estimation of high degree and order spherical harmonic expansions of the geopotential from satellite measurements of gravity gradients has been studied in the framework of a numerical simulation study of the Aristoteles gravity gradiometer mission. Computational issues in high speed spherical harmonic synthesis and large least squares estimation are discussed in detail. The focus has been on the development of highly vectorized and parallelized algorithms for these computations. The resulting estimation software is seen to sustain 90 percent of peak performance on a CRAY Y-MP, facilitating simulations for large gravity fields with reasonable computer expenses. Appropriate noise models for the gravity gradients measured in the ESA Aristoteles mission scenario have been developed. Detailed analysis is presented of the instrument colored and white noise. The spectral and spatial distribution of the drag errors in the presence of density and wind perturbations in the atmosphere has been studied. The resulting error gradient models include effects due to the instrument noise, drag residuals and angular velocity errors. From the simulated measurements of the radial gravity gradients, the coefficients of a degree and order 100 model of the geopotential have been estimated. A comparison of the estimates made using a dense and a sparse linear system method from the literature is also given. The results indicate that the largest errors in the geopotential are caused by drag, with the instrument, attitude and orbit errors being of secondary importance. The sparse system method is seen to be inadequate in comparison to the dense linear system simulations. It is concluded that for gradiometer data analysis, dense linear system methods are a viable option, even though computationally expensive. The results from these simulations indicate that the long wavelength geopotential cannot be determined with any significant accuracy in the assumed Aristoteles mission and error scenario, requiring possible augmentation with other data types. At higher frequencies, however, the geoid errors appear acceptably low, indicating that such a mission might provide significant improvements in the knowledge of the high frequency geopotential. Dissert. Abstr.

N94-29958 City Univ. of New York, NY.
THE USES AND LIMITATIONS OF FRACTAL GEOMETRY IN DIGITAL TERRAIN MODELLING Ph.D. Thesis
Zong-Guo Xia 1993 263 p
Avail: Univ. Microfilms Order No. DA9315515

In this study, fractal concepts and techniques are tested using nearly 200 DEM's (digital elevation models) produced by the USGS. The specific objectives include (1) an examination of statistical self-similarity of topographic data; (2) an evaluation of three most commonly used methods for estimating the fractal dimension of topographic surfaces; (3) a preliminary test of using fractal parameters to characterize various landforms and to delineate landform regions; and (4) an examination of the relationships between fractal parameters and geomorphic variables affecting landform characteristics. The analysis of the computational results has led to the following conclusions: (1) the fractal model fits certain types of terrain surface better than others, and topography is only self-similar within quite limited scale ranges and in certain direction(s); (2) the fractal dimension of landforms varies within a wide range, the fractal dimension used to produce realistic-looking synthetic terrain ($D = 2.2$) only represents some special type of terrain surface, and a D value of 2.5 obtained by some early researchers is merely a result of artificial agglomeration of diversified terrain surfaces; (3) most DEM's from the mountain regions can be easily separated from those of plains or plateaus, and the fractal parameters of adjacent physiographic provinces are significantly different so that fractal segmentation of landform regions appears possible; (4) fractal parameters reflect well the effects of lithology, geological structure, and the stage of landform evolution on landform characteristics, but no clear relationship between fractal parameters and climate was identified possibly due to the relatively coarse resolution of the data; and (5) the variogram method is the most suitable method for estimating the fractal dimension of topographic profiles or surfaces, the box-counting method also produces reasonable results when careful consideration is given to the selection of the maximum cell

size, the contour interval and the minimum r-squared value, and the walking dividers method can not be easily applied to self-affine fractals such as topographic profiles. Dissert. Abstr.

N94-29959 Texas A&M Univ., College Station.
EXTRAPOLATION OF POINT DATA FOR RESOURCE MAPPING Ph.D. Thesis
David William Long 1992 103 p
Avail: Univ. Microfilms Order No. DA9315359

Since the early seventies, the usefulness of satellite imagery for producing vegetation maps has been well known. Even small scale imagery such as advanced very high resolution radiometer (AVHRR) has been applied to continental vegetation mapping. Much has been written about how remote sensing can provide this kind of data for a GIS (Geographic Information System), however, little attention has been placed on the role of GIS for supplying data to automate the image classification process. Large data bases such as the USDA SCS National Resources Inventory (NRI) now being constructed have a potential for filling this role. The NRI has a potential for contributing to the improvement of vegetation mapping in at least three ways: Automated classification of imagery using NRI sample points to create training sets, classification verification through use of NRI sample points as field verification points, and automated map generation directly from the NRI data base through use of Thiessen polygons. Classification accuracy of a TM scene classified using NRI data to produce training sets was fair (43.6 percent overall classification accuracy) considering the process was completely automated with no human judgment involved. Adding ancillary data and temporal image information should improve this figure. Classification accuracy was tested for training sets of various sized polygons constructed around the NRI points. It was found that the smallest polygon (3 x 3 box) around each point resulted in a training set that produced the most accurate classification. Land use/land cover maps can be easily generated from the NRI data base using the Thiessen polygon process. They provide a good overview of the conditions for a large area such as a state, however, for a county sized map, there are too few NRI data points to allow a reasonable depiction of the true conditions. Thiessen polygon maps do not depict accurate boundaries due to the process used for polygon generation, however, with the large number of sample points in the NRI, they provide a quick approximation of the conditions and have a potential for displaying land use/land cover change as the NRI is updated every five years. Dissert. Abstr.

N94-29970 Maryland Univ., College Park.
SATELLITE ESTIMATION OF THE GLOBAL DISTRIBUTION AND INTERANNUAL VARIABILITY OF PHOTOSYNTHETICALLY ACTIVE RADIATION Ph.D. Thesis
Dennis Gene Dye 1992 196 p
Avail: Univ. Microfilms Order No. DA9315635

Photosynthetically active radiation (PAR) (400-700 nm) is a fundamental resource for global primary production, but existing data sources have been insufficient to provide a reliable, quantitative account of global PAR distribution and variability. The objectives of this research were as follows: (1) evaluate the accuracy of a new satellite remote sensing method for estimating and monitoring incident PAR on a global basis; and (2) evaluate the magnitude, distribution, and interannual variability of global incident PAR to determine its potential significance as a factor contributing to variability in global patterns of vegetation-absorbed PAR (APAR) and primary production. The method employs ultraviolet (370 nm) reflectance data from the Nimbus-7 Total Ozone Mapping Spectrometer (TOMS) with a maximum spatial resolution of 1 deg x 1.25 deg. The study covers the 11-year period between Jan. 1979 and Dec. 1989 and latitudes between 66 deg N and 66 deg S. Validation of monthly PAR estimates at sample points produced coefficients of determination (r2) between .863 and .996 and RMS differences between 2.8 and 16.1 percent. Possible sources of error in both the satellite estimates and reference data are identified. The global analysis identified distinct regions of substantial inter annual variability in incident PAR. Coefficients of variation (CV) as high as 18-24 percent for the growing season months and 4-7 percent for annual PAR were observed in Europe, China, Southeast Brazil, and Northern Australia, among other regions. CV's as high as 20 percent for monthly PAR and 8 percent for annual PAR in the western tropical Pacific Ocean region may be associated with El Nino-Southern Oscillation (ENSO) conditions. Deviations in global average PAR observed in 1982 suggest possible global-scale effects of the El Chichon volcanic eruption and/or ENSO. The results from the study confirmed that many regions of the globe are subject to substantial interannual variations in monthly and annual amounts of PAR received. Based on understanding from current physical models and evidence from recent field investigations, this variability represents a significant, potential source of variability in vegetation-absorbed PAR (APAR) and primary production. Dissert. Abstr.

N94-30022# Argonne National Lab., IL.
USE OF SATELLITE DATA TO IMPROVE PARAMETERIZATION OF SPATIAL AND TEMPORAL VARIATIONS OF GASEOUS DRY DEPOSITION IN REGIONAL-SCALE MODELS
Wei-Gang Gao and M. L. Wesely 1994 8 p Presented at the 74th American Meteorological Society Annual Meeting, Nashville, TN, 23-28 Jan. 1994
(Contract W-31-109-eng-38)
(DE94-005110; ANL/ER/CP-80787; CONF-940115-20) Avail: CASI HC A02/MF A01

The removal of gaseous substances from the atmosphere by dry deposition represents an important sink in the atmospheric budget for many trace gases. Hence, the surface removal rate needs to be described quantitatively in modeling atmospheric transport and chemistry with regional- and global-scale models. Because the uptake capability of a terrestrial surface is strongly influenced by the type and condition of its vegetation, the seasonal and spatial changes in vegetation should be described in considerable detail in large-scale models. The objective of the present study is to develop a model that links remote sensing data from satellites with the RADM dry deposition module to provide a parameterization of dry deposition over large scales with improved temporal and spatial coverage. This paper briefly discusses the modeling methods and initial results obtained by applying the improved dry deposition module to a tallgrass prairie, for which measurements of O3 dry deposition and simultaneously obtained satellite remote sensing data are available. DOE

N94-30037 Manitoba Univ., Winnipeg. Dept. of Geological Sciences.
APPLICATION OF REMOTE SENSING TECHNIQUES FOR THE SEISMO-TECTONIC STUDY OF NAHANNI EARTHQUAKE AREA M.S. Thesis
Bo Li Aug. 1993 247 p
(ISBN-0-315-85942-3; CTN-94-61173) Copyright Avail: Micromedia Ltd., Technical Information Centre, 240 Catherine Street, Suite 305, Ottawa, Ontario, K2P 2G8, Canada HC/MF

Three major earthquakes occurred in 1985 and 1988 near the south branch of the North Nahanni River, Northwest Territories. A detailed investigation is presented of the local earthquake tectonic activities, using remote sensing images, earthquake data, and other relevant information. An integrated data processing approach is applied to the analysis, including the integration of different remote sensing data sets. Multispectral satellite images from the Landsat MSS and SPOT, as well as airborne C-band synthetic aperture radar images, are geometrically corrected and enhanced for linear feature interpretation. The Hough transform is implemented and tested for automatic mapping of linear features from remote sensing images. Digital seismograms are utilized to obtain focal parameters of the main shocks and aftershocks of the Nahanni earthquakes. The mapped linear features and focal parameters are then correlated to study the structural geological mechanisms and faulting processes associated with the three main events. Both remote sensing images and earthquake data indicate that the west-dipping thrust faulting is active in the earthquake processes, particularly where it meets the new east-west striking faults. Several linear patterns mapped provided additional information about the tectonic setting and local geological structures related to the earthquakes. Author (CISTI)

N94-30236 Laval Univ. (Quebec). Faculte de Foresterie et de Geomatique.
THE EXTRACTION AND REPRESENTATION OF FOREST INVENTORY INFORMATION USING CONTINUOUS DENSITY SURFACES M.S. Thesis
Norman R. Eldridge Nov. 1993 162 p
(ISBN-0-315-85658-0; CTN-94-61151) Copyright Avail: Micromedia Ltd., Technical Information Centre, 240 Catherine Street, Suite 305, Ottawa, Ontario, K2P 2G8, Canada HC/MF

Standard image analysis methods developed for satellite based remotely sensed images do not appear to be appropriate for high resolution digital

images from airborne systems. A new approach to the analysis of the latter type of image is presented. This approach, combined with a new approach to the cartographic representation of the image analysis results, is seen as potentially more appropriate for the needs of operational forestry and other uses. A study was conducted of a region within an Ontario forest. Mature trees of three conifer species were examined in detail, and a simple technique using local image maxima was employed to isolate individual trees. A new method of computing tree density using the Voronoi diagram and individual tree positions was investigated. Continuous density surfaces were computed for each species distribution using an interpolation method based on the Voronoi diagram. The results were then validated from inventories based on individual tree positions. The resulting stem estimates agreed relatively well with the ground information, and appeared to reproduce the local variations in stem density distribution of each species. Author (CISTI)

N94-30594 Lawrence Livermore National Lab., CA.
AIR-DEPLOYABLE GEOPHYSICS PACKAGE
S. L. Hunter and P. E. Harben Nov. 1993 13 p Limited Reproducibility: More than 20% of this document may be affected by microfiche quality
(Contract W-7405-eng-48)
(DE94-005651; UCRL-ID-115370) Avail: CASI HC A03

We are using Lawrence Livermore National Laboratory's (LLNL's) diverse expertise to develop a geophysical monitoring system that can survive being dropped into place by a helicopter or airplane. Such an air-deployable system could significantly decrease the time and effort needed to set up such instruments in remote locations following a major earthquake or volcanic eruption. Most currently available geophysical monitoring and survey systems, such as seismic monitoring stations, use sensitive, fragile instrumentation that requires personnel trained and experienced in data acquisition and field setup. Rapid deployment of such equipment can be difficult or impossible. Recent developments in low-power electronics, new materials, and sensors that are resistant to severe impacts have made it possible to develop low-cost geophysical monitoring packages for rapid deployment missions. Our strategy was to focus on low-cost battery-powered systems that would have a relatively long (several months) operational lifetime. We concentrated on the conceptual design and engineering of a single-component seismic system that could survive an air-deployment into an earth material, such as alluvium. Actual implementation of such a system is a goal of future work on this concept. For this project, we drew on LLNL's Earth Sciences Department, Radio Shop, Plastics Shop, and Weapons Program. The military has had several programs to develop air-deployed and cannon-deployed seismometers. Recently, a sonobuoy manufacturer has offered an air-deployable geophone designed to make relatively soft landings. DOE

N94-30610# Los Alamos National Lab., NM.
A MONOTONICITY CONJECTURE FOR REAL CUBIC MAPS
S. P. Dawson, R. Galeeva, J. Milnor, and C. Tresser 1993 18 p Presented at the NATO/ASI Meeting on Real and Complex Dynamical Systems, Hillerod, NJ, Jun. 1993
(Contract W-7405-eng-36)
(DE94-003969; LA-UR-93-3844; CONF-9306286-1) Avail: CASI HC A03/MF A01

This will be an outline of work in progress. We study the conjecture that the topological entropy of a real cubic map depends 'monotonely' on its parameters, in the sense that each locus of constant entropy in parameter space is a connected set. This material will be presented in more detail in a later paper. DOE

N94-30759 National Aerospace Lab., Amsterdam (Netherlands). Space Div.
FAME: A FOREST ASSESSMENT AND MONITORING ENVIRONMENT SCENARIO
Wim J. Looyen, Frank O. Zeppenfeldt, Jan Cees Venema, Gert vandenBurg, Dirk H. Hoekman, Joost J. vanderSanden, Paul G. Reichert, and Eduard Westinga 26 Feb. 1993 17 p Presented at the International Symposium on Operationalization of Remote Sensing, Enschede, Netherlands, 19-23 Apr. 1993 Limited Reproducibility: More than 20% of this document may be affected by microfiche quality
(AD-B179106; NLR-TP-93047-U; ETN-94-95967) Avail: Issuing Activity (European Space Agency (ESA))

A feasibility study on a global operational forest cover monitoring network using satellite remote sensing data within the framework of the Tropical Forestry Action Plan is addressed. The study indicates that the use of remote sensing data for global forest cover monitoring is of great importance. To enable this, provisions are required to allow operational preprocessing of remote sensing data to well defined and standardized products. A scenario for the development of a Forest Assessment and Monitoring Environment (FAME) is presented. Firstly, Pilot FAME (PFAME) is developed, aiming at providing a suitable infrastructure for forest management using satellite remote sensing data to compile information on global forests. Secondly, PFAME, is upgraded to improve its functionality and to introduce forest management systems. Thirdly, PFAME is extended by introducing remote sensing data from other newly launched sensors. By introducing this three step approach, uniform and validated remote sensing end products will become available for use in sustainable forest management providing information on the state, extent and distribution of tropical forests. ESA

N94-30919 Delaware Univ., Newark.
STATISTICAL ANALYSIS OF A SATELLITE IMAGERY TIME SERIES: IMPLICATIONS FOR THE STUDY OF COASTAL AND ESTUARINE CIRCULATION Ph.D. Thesis
Anna Maria Matteoda 1992 213 p
Avail: Univ. Microfilms Order No. DA9319093

Empirical Orthogonal Functions analysis of a thirteen month AVHRR imagery time series was performed to assess the temporal and spatial variability of turbidity patterns in Delaware Bay and the coastal area to the south. The statistical results were interpreted in light of existing knowledge of the coastal and estuarine circulation in the study area, and compared to data sets of wind and river discharge for the concurrent period of time. Several analyses, including eigenvector rotation for the EOF modes and cluster analysis, were run on different subsets of the imagery data, normalized to tidal cycle or to wind strength as well as to location within and outside the estuary. The results produced spatial patterns of variability and plots of temporal modulation of such variability over subtidal time scales; tidal cycle normalization allowed a separate examination of the variability due to tidal forcing, the dominant circulation driving force, which was inadequately sampled in the original series. The estuarine turbidity maximum variability was captured by the dominant EOF modes and corresponded to variability in the river discharge records. Analysis of the turbidity signal along the coastal zone to the south of Delaware Bay revealed a spatial pattern that is entirely consistent with the presence of a buoyant coastal current flowing out of the Delaware Estuary and hugging the coast in a southward flow, as reported recently by Garvine and Munchow. Tidal variability analysis produced ambiguous results which suggest that further study is needed in this area. The main source of error was the occasional presence of localized clouds, but it did not affect the dominant first EOF mode, because of the random nature of such error. The techniques developed for this study can be useful as a data reduction tool in the management of the large volumes of operational satellite-derived data, since the first few EOF modes summarize the variability of the data set. Dissert. Abstr.

N94-30942# National Aerospace Lab., Amsterdam (Netherlands). Remote Sensing Div.
MULTITEMPORAL ANALYSIS OF A BRAIDING RIVER: THE ADVANCED STUDY OF 1992
H. H. S. Noorbergen 15 May 1993 20 p Presented at the International Symposium on Operationalization of Remote Sensing, Enschede, Netherlands, 19-93 Apr. 1993
(NLR-TP-93100-U; ETN-94-95971) Avail: CASI HC A03/MF A01

A project which used satellite imagery for the monitoring and forecasting of the erosion of the Jamuna river banks in Bangladesh is presented. For the remote sensing analysis fifteen satellite images collected between 1973 and 1992 were processed. These images were obtained by the LANDSAT multispectral scanner, LANDSAT Thematic Mapper, and the Marine Observation Satellite (MOS-MESSR). An important criterion was to select only images from seasons with comparable low water levels in the main channels. From each year a user defined classification was made into the four categories water, sand, vegetation and bare soil. By combining the classification results of the separate years several products can be made, such as difference images between any two years, successive river courses and number of water occurrences. ESA

N94-30944# Stockholm Univ. (Sweden). Dept. of Meteorology.
CHEMICAL COMPOSITION OF INSOLUBLE PARTICLES IN SUPERIMPOSED ICE ON STOROEYA, SVALBARD (SWEDEN)
Margareta E. Hansson, Hans-Christen Hansson, Stig Jonsson, and Jost Heintzenberg Sep. 1993 22 p Sponsored by Swedish Natural Science Research Council
(ISSN 0280-445X)
(CM-82; ETN-94-95851) Avail: CASI HC A03/MF A01

The chemical composition of the insoluble impurities in a seven meter long ice core of superimposed ice from the Storoeya ice cap is examined. The concentrations of fourteen elements were determined by PIXE (Particle Induced X-ray Emission) and soot photometer analyses. Si is the mass dominating element, making up 49% of the mass of determined elements, followed by elemental carbon forming 26%. Fe, K, Ca and Ti, in descending order, account for 24% while Mn, Zn, Ga, As, Rb, Sr, Zr and Pb together constitute less than 1% of the mass. Size separation by filtration, multivariate statistical analyses and calculation of enrichment factors are used to reveal the origin of the impurities. A crustal source, most likely local, is found to dominate. A second comparatively weak source, possibly anthropogenic, is suggested to contribute to 15 to 100% of the concentrations of elemental carbon, Zn, As and Pb. ESA

N94-30965 Aerospatiale, Cannes (France). Optical Dept.
NEW PERSPECTIVES FOR HIGH ACCURACY SLR WITH SECOND GENERATION GEODESIC SATELLITES
Glenn Lund 1993 10 p Limited Reproducibility: More than 20% of this document may be affected by microfiche quality
(Rept-932-440-105; ETN-94-95953) Avail: CASI HC A02

It was shown from link budget analyses that, when coupled with an appropriate satellite configuration, realistic single retroreflector dimensions could enable millimetric absolute accuracies to be achieved with the 2-color SLR (Satellite Laser Ranger), through the removal of center of mass uncertainties in the range determination. The engineering of retroreflector velocity aberration corrections is an important factor in the design of a geodesic satellite and in the link budget performance to be expected from the complete ranging system. Two approaches to the design of second generation geodesic satellites were suggested. Although these might imply the use of nonspherical orbiting bodies, with consequently higher atmospheric drag and solar radiation pressure imbalances than for existing satellites, they could nevertheless enable excellent geometric mode (short arc) range determinations to be achieved, and they could be expected to provide very good long arc performance for high altitude orbits. ESA

44 ENERGY PRODUCTION AND CONVERSION

Includes specific energy conversion systems, e.g., fuel cells; global sources of energy; geophysical conversion; and windpower.

For related information see also *07 Aircraft Propulsion and Power, 20 Spacecraft Propulsion and Power,* and *28 Propellants and Fuels.*

N94-28472 Courtesy Associates, Inc., Washington, DC.
FUEL CELL SEMINAR, 1992: PROGRAM AND ABSTRACTS
1992 677 p Presented at the Fuel Cell Seminar, Tucson, AZ, 29 Nov. - 2 Dec. 1992 Limited Reproducibility: More than 20% of this document may be affected by poor print
(DE94-003882; CONF-921114) Avail: Issuing Activity (Department of Energy (DOE))

This year's theme, 'Fuel Cells: Realizing the Potential,' focuses on progress being made toward commercial manufacture and use of fuel cell products. Fuel cell power plants are competing for market share in some applications and demonstrations of market entry power plants are proceeding for additional applications. Development activity on fuel cells for transportation is also increasing; fuel cell products have potential in energy and transportation industries, with very favorable environmental impacts. This Seminar has the purpose of fostering communication by providing a forum for the international community interested in development, application, and business opportunities related fuel cells. Over 190 technical papers are included, the majority being processed for the data base. DOE

N94-28489# Sandia National Labs., Albuquerque, NM.
BATTERY ENERGY AND SUPERCONDUCTING MAGNETIC ENERGY STORAGE FOR UTILITY APPLICATIONS: A QUALITATIVE ANALYSIS
A. A. Akhil, P. Butler, and T. C. Bickel Nov. 1993 21 p
(Contract DE-AC04-94AL-85000)
(DE94-005382; SAND-93-2477) Avail: CASI HC A03/MF A01

This report was prepared at the request of the US Department of Energy's Office of Energy Management for an objective comparison of the merits of battery energy storage with superconducting magnetic energy storage technology for utility applications. Conclusions are drawn regarding the best match of each technology with these utility application requirements. Staff from the Utility Battery Storage Systems Program and the superconductivity Programs at Sandia National contributed to this effort. DOE

N94-28499# Morgantown Technology Center, WV.
PROCEEDINGS OF THE JOINT CONTRACTORS MEETING: FE/EE ADVANCED TURBINE SYSTEMS CONFERENCE FE FUEL CELLS AND COAL-FIRED HEAT ENGINES CONFERENCE
D. W. Geiling, ed. Aug. 1993 499 p Meeting held in Morgantown, WV, 3-5 Aug. 1993
(DE93-011308; DOE/METC-93-6132; CONF-930893) Avail: CASI HC A21/MF A04

The joint contractors meeting--the FE/EE Advanced Turbine Systems Conference and the FEE Fuel Cells and Coal-Fired Heat Engines Conference--was sponsored by the U.S. Department of Energy Office of Fossil Energy, and it was held at the Morgantown Energy Technology Center on 3-5 Aug. 1993. The individual papers were entered separately. DOE

N94-28500# Springborn Labs., Inc., Enfield, CT.
ADVANCED DEVELOPMENT OF PV ENCAPSULENTS Semiannual Technical Progress Report
W. H. Holley Dec. 1993 67 p Prepared for Midwest Research Inst., Golden, CO
(Contract DE-AC02-83CH-10093)
(DE94-000219; NREL/TP-411-5800) Avail: CASI HC A04/MF A01

This report describes the results of the literature search, interviews, and site visits conducted during the first six months of this subcontract. This survey was conducted to establish a baseline of information about thermal and photothermal degradation of EVA and case history surveys on discoloration (yellowing/browning) of EVA-based encapsulants in fielded flat-plate PV modules. The literature search revealed that EVA will undergo thermolysis of the acetate groups at temperatures of 130 C to 150 C and above leading to formation of double bonds in the backbone of the copolymer. The survey of case histories of EVA-based encapsulant discoloration in fielded modules in the United States revealed that the problem is limited to those areas of the west and southwest that have comparatively high solar insolation and ambient temperature. It is clear that the discoloration problem is not limited to the modules of any one manufacturer. Discoloration in the EVA encapsulant was experienced in fielded modules from all major U.S. module producers. DOE

N94-28501# Astropower, Inc., Newark, DE.
SILICON-FILM (TM) PHOTOVOLTAIC MANUFACTURING TECHNOLOGY
W. R. Bottenberg Jan. 1994 34 p Prepared for Midwest Research Inst., Golden, CO
(Contract DE-AC02-83CH-10093)
(DE94-000258; NREL/TP-411-6110) Avail: CASI HC A03/MF A01

AstroPower is in the second phase of a 3-year, phased effort to upgrade its facility to produce 1.22-sq m Silicon-Film(trademark) PV modules with an output of 170 W(sub p). Productivity improvements of the Silicon-Film(trademark) machine were accomplished during the second phase. Improvements were made in solar cell performance while decreasing materials consumption, integrating and mechanizing the fabrication process for solar cells, and scaling-up solar cell and module equipment for fabricating larger cells. AstroPower is continuing work on separating out effects due to impurities and effects due to defects. Analytical tools were developed for measuring area-based response based on EBIC and LBIC methods. The Kauffman source for hydrogen ion implantation was used to map out the process space for Silicon-Film(trademark) solar cell improvement. Progress was made on improving short-circuit current. Areas of focus include

developing tools to quickly assess material quality; developing a hydrogen implantation process; increasing material quality on large-area, high-throughput wafers; and studying potential processes for improving solar cell power output during cell fabrication. A method to improve current collection in a solar cell after contact formation is under development. DOE

N94-28627 New Energy and Industrial Technology Development Organization, Tokyo (Japan).
FISCAL 1991 GEOTHERMAL DEVELOPMENT PROMOTION ENERGY
Feb. 1993 119 p In JAPANESE Limited Reproducibility: More than 20% of this document may be affected by microfiche quality
(DE94-732332; ETDE/JP-mf-94732332) Avail: CASI HC A06

The paper surveys the spouting of geothermal fluids in test boring wells, the well logging, and the status of geothermal fluids, as a part of the geothermal development promotion survey in the Mizuwake-Toge south area. In the spouting test of N3-MW-6 well, the 53rd swabbing led successfully to spouting. The spouting amounted to 3.6 tons/h in steam and geothermal water, but stopped spontaneously in 100 minutes. Results of the logging are hardly different between before and after the spouting indicating a maximum temperature of 200 C, barometric pressure of 75, and water levels of a 250-300m section. The geothermal water is a neutral Cl deep-area type. N2-MW-2 well spouted immediately after the 10th swabbing, indicating steam of 3 tons/h at the stable time, geothermal water of 7.3 tons/h, pH9, Cl of 1500ppm, and the total spouting time of 4029 minutes. The place where the geothermal fluid flows in is 635m deep, and when the well head pressure was 1.7-3.9 barometric pressure, the spouted fluid temperature was 199-198 C. The geothermal water is a Cl-HCO3 type. In both wells geothermal water is ground water originated from meteoric water which reacted with peripheral rocks by volcanic heating and was formed in the deep area. DOE

N94-28628# New Energy and Industrial Technology Development Organization, Tokyo (Japan).
FISCAL 1990 GEOTHERMAL DEVELOPMENT PROMOTION SURVEY
Mar. 1992 366 p
(DE94-732333; ETDE/JP-mf-94732333) Avail: CASI HC A16/MF A03

The development of a geothermal reservoir evaluation method is mentioned for the purpose of reducing the risk of the geothermal development and drawing up an appropriate power generation plan. As for simulators, a geothermal reservoir simulator (SING-I,II) and a geothermal well two-phase simulator (WENG) are developed. For SING-II, an evaluation is made of fracture effects in the pressure interference test, production predicting simulation using fracture models, development of a multicomponent gas-liquid two-phase simulator and a tracer simulation function. As to WENG, verification on fluids containing CO2 and survey on fluids containing NaCl are made. In the Mori area which is a model field, continued observation on reservoir pressure is conducted as well as temperature/pressure logging and chemical analysis of spouted fluids. By three-dimensional grid models of reservoirs, reappearance of natural conditions of temperature/pressure distribution and discharge into the ground surface can roughly be made, and history matching is tried to be made. Newly also in Oguni area, reappearance of natural conditions is simulated using SING-I. DOE

N94-28631# New Energy and Industrial Technology Development Organization, Tokyo (Japan).
REPORT OF FEASIBILITY STUDY ON INTERNATIONAL-COOPERATION IN HIGH EFFICIENT ENERGY CONVERSION TECHNOLOGY
Mar. 1993 250 p
(DE94-732340; NEDO-P-9255) Avail: CASI HC A11/MF A03

With regard to accelerated introduction of high efficient energy conversion technology to developing countries, the paper investigates the countries' thoughts of the introduction of the technology and the status of the introduction bases. The countries for survey are the Philippines, Indonesia, Malaysia and Thailand. The Philippine government expects to develop cogeneration as well as large power sources and to widen effective use of natural energy. In Indonesia, they largely expect effective use of biomass energy using Stirling engines by international cooperation and the promoted local electrification using standalone distributed fuel cells. In Malaysia, they have great expectations of the introduction of air conditioning facilities using Stirling engines and the use of standalone distributed fuel cells for promotion of local electrification. Thailand hopes for the use of Stirling engines to air conditioning systems, and the development of solar Stirling generators with solar energy as a heat source and electric vehicles. DOE

N94-28909 National Defence Research Establishment, Linkoeping (Sweden). Huvudavdelning foer Informationsteknologi.
QUALITY AND EFFICIENCY OF SOLAR COLLECTORS IN SWEDEN [SOLFANGARES KVALITET OCH BESTAENDIGHET I SVERIGE. DEL 2. KONVEKTIONSHINDER AV FEP-FILM-SKADEUTREDNING]
H. Wennerholm 1993 99 p In SWAHILI
(PB94-137486; SP-RAPP-1993:17) Avail: Issuing Activity (National Technical Information Service (NTIS))

Transparent or translucent insulation materials (TIM's) represent a new class of materials with a high potential for increasing the efficiency of solar thermal conversion systems. A large number of materials have been subjected to theoretical and experimental investigation. If materials that suppress heat losses are transparent to solar radiation, vacuum, certain gases, convection barriers, etc., then they can be regarded as TIM's. Exploratory field and laboratory studies of degraded FEP-film convection barriers in flat plate thermal solar collectors are described. The study related to collectors that had been operating in Sweden for periods of one year to ten years. Both physical, functional (thermal) and chemical aspects of degradation were considered. The report identifies the mistakes made so that they need not be repeated by the solar collector manufacturers in the future. NTIS

N94-29018# Sandia National Labs., Albuquerque, NM.
PERFORMANCE OF THE SOUTHERN CALIFORNIA EDISON COMPANY STIRLING DISH
C. W. Lopez (Southern California Edison Co., Rosemead.) and K. W. Stone (Mako Enterprises, Huntington, CA.) Oct. 1993 211 p
(Contract DE-AC04-94AL-85000)
(DE94-004676; SAND-93-7098) Avail: CASI HC A10/MF A03

McDonnell Douglas Astronautics Company (MDAC) and United Stirling AB of Sweden (USAB) formed a joint venture in 1982 to develop and produce a Stirling dish solar generating system. In this report, the six year development and testing program continued by the Southern California Edison Company (SCE) is described. Each Stirling dish module consists of a sun tracking dish concentrator developed by the MDAC and a Stirling engine driven power conversion unit (PCU) developed by USAB. The Stirling dish system demonstrated twice the peak and daily solar-to-electric conversion efficiency of any other system then under development. This system continues to set the performance standard for solar to electric systems being developed in the early 1990's. Test data are presented and used to estimate the performance of a commercial system. DOE

N94-29033# Krug Life Sciences, Inc., San Antonio, TX.
METHANE CHALLENGE OF HIGH PERFORMANCE MOLECULAR SIEVE OXYGEN CONCENTRATOR Interim Report, period ending Nov. 1992
Aaron M. Shakocius and George W. Miller Nov. 1993 8 p
(Contract F33615-92-C-0018)
(AD-A275155; AL/CF-PC-1993-0045) Avail: CASI HC A02/MF A01

The purpose of this work was to determine the ability of a high performance molecular sieve oxygen concentrator (MSOC) to remove methane while operating at high oxygen purity levels. This work was accomplished using a laboratory scale, four-bed, high performance MSOC which consisted of two primary beds containing OXYSIV-5 zeolite molecular sieve and two secondary beds containing Takeda 3A carbon molecular sieve. The concentrator operated at an inlet air pressure of 45 psia, a cycle time of 14 seconds, and a product flow rate of one standard liter per minute. Methane was injected into the MSOC inlet gas stream at levels up to approximately 5000 parts per million by volume (ppmv). Contaminant levels were allowed to reach steady-state and measured in the MSOC inlet, product, and exhaust gases with a Beckman model 402 hydrocarbon analyzer. The experimental results indicate the contaminant introduced into the MSOC inlet gas was separated and carried out with the exhaust gas. The injected methane was not detected in the product gas. The results indicate the high performance MSOC may be more capable of removing contaminants from the inlet gas stream than standard MSOC's, i.e., those containing only zeolite molecular sieve. Further experimental work with other contaminants is planned. DTIC

N94-29953# Department of Energy, Washington, DC. Office of Energy Research.

FOSSIL ENERGY BIOTECHNOLOGY: A RESEARCH NEEDS ASSESSMENT

Nov. 1993 302 p

(Contract DE-AC01-91ER-30156)

(DE94-004239; DOE/ER-30156/H1) Avail: CASI HC A14/MF A03

The Office of Program Analysis of the U.S. Department of Energy commissioned this study to evaluate and prioritize research needs in fossil energy biotechnology. The objectives were to identify research initiatives in biotechnology that offer timely and strategic options for the more efficient and effective uses of the Nation's fossil resource base, particularly the early identification of new and novel applications of biotechnology for the use or conversion of domestic fossil fuels. Fossil energy biotechnology consists of a number of diverse and distinct technologies, all related by the common denominator -- biocatalysis. The expert panel organized 14 technical subjects into three interrelated biotechnology programs: (1) upgrading the fuel value of fossil fuels; (2) bioconversion of fossil feedstocks and refined products to added value chemicals; and (3) the development of environmental management strategies to minimize and mitigate the release of toxic and hazardous petrochemical wastes. DOE

N94-29955# Lawrence Livermore National Lab., CA.

ENERGY AND TECHNOLOGY REVIEW

W. J. Quirk, ed. Aug. 1993 17 p

(Contract W-7405-eng-48)

(DE94-004472; UCRL-52000-93-8) Avail: CASI HC A03/MF A01

The Lawrence Livermore National Laboratory was established in 1952 to do research on nuclear weapons and magnetic fusion energy. Since then, other major programs have been added including laser fusion, and laser isotope separation, biomedical and environmental science, strategic defense and applied energy technology. These programs, in turn, require research in basic scientific disciplines, including chemistry and materials science, computer science and technology, engineering and physics. In this issue, Herald Brown, the Laboratory's third director and now counselor at the Center for Strategic and International Studies, reminisces about his years at Livermore and comments about the Laboratory's role in the future. Also an article on visualizing dynamic systems in three dimensions is presented. Researchers can use our interactive algorithms to translate massive quantities of numerical data into visual form and can assign the visual markers of their choice to represent three-dimensional phenomena in a two-dimensional setting, such as a monitor screen. Major work has been done in the visualization of climate modeling, but the algorithms can be used for visualizing virtually any phenomena. DOE

N94-30048# Morgantown Technology Center, WV.

FUNDAMENTAL STACK AND SYSTEM ISSUES IN MOLTEN CARBONATE FUEL CELL DEVELOPMENT

M. C. Williams, E. L. Parsons, Jr., and M. J. Mayfield 1993 9 p Presented at the Annual Meeting of the American Institute of Chemical Engineers, St. Louis, MO, 7-12 Nov. 1993

(DE94-005960; DOE/METC-C/94/7118; CONF-931164-7) Avail: CASI HC A02/MF A01

Stack research and system issues in molten carbonate fuel cell (MCFC) technology development and commercialization are discussed within context of status of MCFC development and commercialization in US. Status of MCFC development is addressed. Major known fundamental stack research issues remaining for the MCFC technology are identified and discussed. The cathode remains a focal point of performance improvement and cost reduction. The various aspects of MCFC power plant network and systems issues are also addressed and discussed. These include cost, heat loss management, startup and shutdown modes, dynamic response, footprint, packaging and integration, parasitic power losses, pressurization, and reforming. Potential of MCFC networks is discussed. With the initial demonstration of full-area, full-height 250-kW to 2-MW MCFC power plants, the spatial configuration of the MCFC stacks into networks in the fuel cell power plant takes on importance for the first time. DOE

N94-30196*# National Aeronautics and Space Administration. Lewis Research Center, Cleveland, OH.

THE VIABILITY OF PHOTOVOLTAICS ON THE MARTIAN SURFACE

James R. Gaier and Marla E. Perez-Davis Mar. 1994 18 p Presented at the Case for Mars V Conference, Boulder, CO, 26-29 May 1993; sponsored by the Boulder Center for Science and Policy

(RTOP 583-02-21)

(NASA-TM-106478; E-8407; NAS 1.15:106478) Avail: CASI HC A03/MF A01

The viability of photovoltaics (PV) on the Martian surface may be determined by their ability to withstand significant degradation in the Martian environment. Probably the greatest threat is posed by fine dust particles which are continually blown about the surface of the planet. In an effort to determine the extent of the threat, and to investigate some abatement strategies, a series of experiments were conducted in the Martian Surface Wind Tunnel (MARSWIT) at NASA Ames Research Center. The effects of dust composition, particle size, wind velocity, angle of attack, and protective coatings on the transmittance of light through PV coverglass were determined. Both initially clear and initially dusted samples were subjected both to clear winds and simulated dust storms in the MARSWIT. It was found that wind velocity, particle size, and angle of attack are important parameters affecting occlusion of PV surfaces, while dust composition and protective coatings were not. Neither induced turbulence nor direct current biasing up to 200 volts were effective abatement techniques. Abrasion diffused the light impinging on the PV cells, but did not reduce total coverglass transmittance by more than a few percent. Author

N94-30313# Morgantown Technology Center, WV.

CONFIGURATION AND PERFORMANCE OF THE INDIRECT-FIRED FUEL CELL BOTTOMED TURBINE CYCLE

P. L. Micheli, M. C. Williams, and E. L. Parsons, Jr. 1993 17 p Presented at the Annual Meeting of the American Institute of Chemical Engineers, St. Louis, MO, 7-12 Nov. 1993

(DE94-005961; DOE/METC-C/94/7117; CONF-931164-6) Avail: CASI HC A03/MF A01

The natural gas, indirect-fired fuel cell bottomed turbine cycle (NG-IFFC) is introduced as a novel power plant system for the distributed power and on-site markets in the 20-200 megawatt (MW) size range. The novel indirect-fired carbonate fuel cell bottomed turbine cycle (NG-IFCFC) power plant system configures the ambient pressure carbonate fuel cell with a gas turbine, air compressor, combustor, and ceramic heat exchanger. Performance calculations from ASPEN simulations present material and energy balances with expected power output. The results indicate efficiencies and heat rates for the NG-IFCFC are comparable to conventionally bottomed carbonate fuel cell steam bottomed cycles, but with smaller and less expensive components. DOE

N94-30328 National Aerospace Lab., Amsterdam (Netherlands). Informatics Div.

MODAL ANALYSIS OF SOLAR PANELS USING BOUNDARY INTEGRAL EQUATIONS

H. T. Koelink, H. Schippers, J. J. Heijstek, and J. J. Derksen 3 Jul. 1992 16 p Presented at the Boundary Element International Conference, Seville, Spain, 3-6 Nov. 1992 Limited Reproducibility: More than 20% of this document may be affected by microfiche quality

(Contract NIVR-02003N)

(NLT-TP-92218-U; ETN-94-95582) Avail: Issuing Activity (European Space Agency (ESA))

The acoustic effects of the surrounding air on a harmonically vibrating solar panel in a test room are investigated. The dynamics of the solar panel are modeled by a differential equation for a harmonically vibrating plate. The force acting on the plate is caused by the jump in the acoustic pressure. The sound pressure is modeled by a boundary integral ansatz and these models are coupled by the acoustic coupling equation. This results in a perturbed eigenvalue problem which is solved approximately with respect to the perturbation parameter. The perturbation parameter is the ratio of the density of the air and the density of the solar panel. This analysis involves the solution of a hypersingular integral equation representing the pressure jump over the solar panel. The hypersingular integral equation is rewritten as a singular equation, which is numerically solved by a boundary element method. It involves the numerical evaluation of weakly singular and nearly weakly singular integrals. For an application the first and second order approximation is calculated (with respect to the perturbation parameter) for the eigenfrequency of the first bending mode of a solar panel in air. The second order approximation is in correspondence with the measured test room eigenfrequency. ESA

N94-30601# Midwest Research Inst., Golden, CO.
PHOTOVOLTAIC PERFORMANCE AND RELIABILITY WORKSHOP
L. Mrig, ed. 1993 504 p Presented at the Photovoltaic Performance and Reliability Workshop, Golden, CO, 8-10 Sep. 1993
(Contract DE-AC02-83CH-10093)
(DE94-000236; NREL/CP-410-6033; CONF-9309188) Avail: CASI HC A22/MF A04

This workshop was the sixth in a series of workshops sponsored by NREL/DOE under the general subject of photovoltaic testing and reliability during the period 1986-1993. PV performance and PV reliability are at least as important as PV cost, if not more. In the U.S., PV manufacturers, DOE laboratories, electric utilities, and others are engaged in the photovoltaic reliability research and testing. This group of researchers and others interested in the field were brought together to exchange the technical knowledge and field experience as related to current information in this evolving field of PV reliability. The papers presented here reflect this effort since the last workshop held in September, 1992. The topics covered include: cell and module characterization, module and system testing, durability and reliability, system field experience, and standards and codes. DOE

N94-30602# Midwest Research Inst., Golden, CO.
INTERNATIONAL COLLABORATIVE RESEARCH IN WIND TURBINE ROTOR AERODYNAMICS
D. A. Simms and C. P. Butterfield Dec. 1993 4 p Presented at the 13th Energy-Sources Technology Conference and Exhibition (ETCE) on Wind Energy, New Orleans, LA, 23-26 Jan. 1994
(Contract DE-AC02-83CH-10093)
(DE94-000244; NREL/TP-441-5810; CONF-940113-6) Avail: CASI HC A01/MF A01

Five organizations from four countries are collaborating to conduct detailed wind turbine aerodynamic test programs. Fullscale atmospheric testing will be conducted on turbines configured to measure aerodynamic forces on rotating airfoils. The purpose of these test programs is to come to a better understanding of the steady and unsteady aerodynamic behavior of wind turbine rotors, and provide information needed to build accurate aerodynamic models for design codes. Stall, dynamic inflow, yaw conditions, and tower effects all contribute to unknown aerodynamic responses. These unknown responses make it extremely difficult to produce cost-effective wind turbine designs. Turbines behave unexpectedly, experiencing power surges and higher fatigue loads than predicted. In order to evolve state-of-the-art wind turbine designs, these aerodynamic effects must be quantified and understood. This paper describes a coordinated international research effort that is underway to accelerate this key research area, and help develop a more thorough understanding of wind turbine aerodynamics. DOE

N94-30603# Midwest Research Inst., Golden, CO.
PV Cz SILICON MANUFACTURING TECHNOLOGY IMPROVEMENTS
T. Jester (Siemens Solar Industries, Camarillo, CA.) Jan. 1994 50 p
(Contract DE-AC02-83CH-10093)
(DE94-000248; NREL/TP-411-6010) Avail: CASI HC A03/MF A01

This report describes work performed under a 3-year contract to demonstrate significant cost reductions and improvements in manufacturing technology. The work focused on near-term projects for implementation in the Siemens Solar Industries Czochralski (Cz) manufacturing facility in Camarillo, California. The work was undertaken to increase the commercial viability and volume of photovoltaic manufacturing by evaluating the most significant cost categories and then lowering the cost of each item through experimentation, materials refinement, and better industrial engineering. The initial phase of the program concentrated on the areas of crystal growth; wafer technology; and environmental, safety, and health issues. DOE

N94-30604# Midwest Research Inst., Golden, CO.
LARGE-AREA TRIPLE-JUNCTION a-Si ALLOY PRODUCTION SCALE UP
R. Oswald (Solarex Corp., Newtown, PA.) and J. ODowd (Solarex Corp., Newtown, PA.) Jan. 1994 51 p
(Contract DE-AC02-83CH-10093)
(DE94-000249; NREL/TP-411-6047) Avail: CASI HC A04/MF A01

The objective of this subcontract over its three-year duration is to advance Solarex's photovoltaic manufacturing technologies, reduce its a-Si:H module production costs, increase module performance and expand the Solarex commercial production capacity. Solarex shall meet these objectives by improving the deposition and quality of the transparent front contact; optimizing the laser patterning process; scaling up the semiconductor deposition process; improving the back contact deposition; and scaling up and improving the encapsulation and testing of its a-Si:H modules. In the Phase 1 portion of this subcontract Solarex focused on scaling up components of the chemical vapor deposition system for deposition of the front contact; scaling up laser scribing techniques; triple-junction recipes for module production; and metal oxide back contacts. These efforts resulted in adopting portions of the manufacturing line to handle substrates larger than 0.37 sq m. DOE

N94-30605 Midwest Research Inst., Golden, CO.
THIN EFG OCTAGONS
J. P. Kalejs (Mobil Tyco Solar Energy Corp., Billerica, MA.) Jan. 1994 34 p Limited Reproducibility: More than 20% of this document may be affected by poor print
(Contract DE-AC02-83CH-10093)
(DE94-000257; NREL/TP-411-6046) Avail: Issuing Activity (Department of Energy (DOE))

Mobil Solar Energy Corporation currently practices a unique crystal growth technology for producing crystalline silicon sheet, which is then cut with lasers into wafers. The wafers are processed into solar cells and incorporated into modules for photovoltaic applications. The silicon sheet is produced using a method known as Edge-defined Film-fed growth (EFG), in the form of hollow eight-sided polygons (octagons) with 10 cm faces. These are grown to lengths of 5 meters and thickness of 300 microns, with continuous melt replenishment, in compact furnaces designed to operate at a high sheet area production area of 135 sq cm/min. The present Photovoltaic Manufacturing Technology (PVMaT) three-year program seeks to advance the manufacturing line capabilities of the Mobil Solar crystal growth and cutting technologies. If successful, these advancements will provide significant reductions in already low silicon raw material usage, improve process productivity, laser cutting throughput and yield, and so lower both individual wafer cost and the cost of module production. This report summarizes the significant technical improvements in EFG technology achieved in Phase 1 of this program. Technical results are reported for each of the three main program areas: (1) thin octagon growth (crystal growth) -- to reduce the thickness of the octagon to an interim goal of 250 microns during Phase 1, with an ultimate goal of achieving 200 micron thicknesses; (2) laser cutting -- to improve the laser cutting process, so as to produce wafers with decreased laser cutting damage at increased wafer throughput rates; and (3) process control and product specification -- to implement advanced strategies in crystal growth process control and productivity designed to increase wafer yields. DOE

N94-30606# Midwest Research Inst., Golden, CO.
THE DIRECT OBSERVATION OF ALKALI VAPOR SPECIES IN BIOMASS COMBUSTION AND GASIFICATION
R. J. French, D. C. Dayton, and T. A. Milne Jan. 1994 89 p
(Contract DE-AC02-83CH-10093)
(DE94-000262; NREL/TP-430-5597) Avail: CASI HC A05/MF A01

This report summarizes new data from screening various feedstocks for alkali vapor release under combustion conditions. The successful development of a laboratory flow reactor and molecular beam, mass spectrometer interface is detailed. Its application to several herbaceous and woody feedstocks, as well as a fast-pyrolysis oil, under 800 and 1100 C batch combustion, is documented. Chlorine seems to play a large role in the facile mobilization of potassium. Included in the report is a discussion of relevant literature on the alkali problem in combustors and turbines. Highlighted are the phenomena identified in studies on coal and methods that have been applied to alkali speciation. The nature of binding of alkali in coal versus biomass is discussed, together with the implications for the ease of release. Herbaceous species and many agricultural residues appear to pose significant problems in release of alkali species to the vapor at typical combustor temperatures. These problems could be especially acute in direct combustion fired turbines, but may be ameliorated in integrated gasification combined cycles. DOE

N94-30609# Sandia National Labs., Albuquerque, NM.
CRYSTALLINE-SILICON SOLAR CELL DEVELOPMENT SPONSORED BY THE US DEPARTMENT OF ENERGY
P. A. Basore 1993 4 p Presented at the 6th Sunshine Workshop on Crystalline Silicon Solar Cells, Tokyo, Japan, 18 Nov. 1993
(Contract DE-AC04-94AL-85000)
(DE94-003783; SAND-93-2744C; CONF-9311134-1) Avail: CASI HC A01/MF A01

Activities planned for the current fiscal year at Sandia National Laboratories include investigation of specific industrial cell processing issues using Sandia's Photovoltaic Device Processing Laboratory (PDFL), as well as several processing issues of general interest to companies using multicrystalline silicon. A significant and difficult goal for Sandia this year will be the fabrication of a 15% efficient prototype module using large-area multicrystalline cells. Sandia also provides primary funding for the University Center of Excellence in Photovoltaic Research and Education at the Georgia Institute of Technology. The National Renewable Energy Laboratory's (NREL's) plans for c-Si this fiscal year include continuation of the University Silicon Materials Research Program, which funds research at six universities to study the effect of cell processing on the properties of silicon materials. As the lead DOS laboratory for thin film technologies, NREL supports the development of thin film silicon cells by providing both funding and expertise. NREL also provides substantial funding to the PV industry through the PV Manufacturing Technology (PVMaT) initiative, some of which supports the development of c-Si cell technology either directly or indirectly. DOE

N94-30700 Oregon Inst. of Tech., Klamath Falls. Geo-Heat Center.
GEOTHERMAL DIRECT-HEAT UTILIZATION ASSISTANCE
1993 22 p Limited Reproducibility: More than 20% of this document may be affected by microfiche quality
(Contract DE-FG07-90ID-13040)
(DE94-005831; DOE/ID-13040/T21) Avail: CASI HC A03

This report consists of brief summaries of the activities of the Geo-Heat Center during the report period. Technical assistance was given to requests from 20 states in the following applications: space and district heating; geothermal heat pumps; greenhouses; aquaculture; industrial plants; electric power; resource/well; equipment; and resort/spa. Research and development activities progressed on compilation of data on low temperature resources and evaluation of groundwater versus ground-coupled heat pumps. Also summarized are technology transfer activities and geothermal progress monitoring activities. DOE

N94-30820# Midwest Research Inst., Golden, CO. National Renewable Energy Lab.
NREL PHOTOVOLTAIC PROGRAM FY 1993 BIBLIOGRAPHY
L. Pohle, ed. Jan. 1994 16 p
(Contract DE-AC02-83CH-10093)
(DE94-000272; NREL/TP-411-6270) Avail: CASI HC A03/MF A01

This report lists all published documents of the Photovoltaic Program for FY 1993. Documents include conference papers, journal articles, book chapters, etc. DOE

N94-30833# Horizon Data Corp., Reston, VA.
INTERAGENCY ADVANCED POWER GROUP: SOLAR WORKING GROUP Meeting Minutes
14 Oct. 1993 9 p Meeting held in Denver, CO, 18 Oct. 1993
(Contract DE-AC01-90CE-90053)
(DE94-004953; CONF-9310251-Summ) Avail: CASI HC A02/MF A01

This report is the minutes of the Solar Working Group. The meeting was prompted by the Steering Group's desire to resolve issues of the Solar Working Group. DOE

N94-30843 Sandia National Labs., Albuquerque, NM.
SOLAR PHOTOVOLTAICS FOR DEVELOPMENT APPLICATIONS
L. W. Shepperd (Florida Solar Energy Center, Cape Canaveral.) and E. H. Richards Aug. 1993 45 p Limited Reproducibility: More than 20% of this document may be affected by microfiche quality
(Contract DE-AC04-94AL-85000)
(DE94-006116; SAND-93-1642) Avail: CASI HC A03

This document introduces photovoltaic technology to individuals and groups specializing in development activities. Examples of actual installations illustrate the many services supplied by photovoltaic systems in development applications including water pumping, lighting, health care, refrigeration, communications, and a variety of productive uses. The various aspects of the technology are explored to help potential users evaluate whether photovoltaics can assist them in achieving their organizational goals. Basic system design, financing techniques, and the importance of infrastructure are included, along with additional sources of information and major U.S. photovoltaic system suppliers. DOE

N94-30879# Arkansas Univ., Fayetteville.
BIOLOGICAL CONVERSION OF SYNTHESIS GAS
R. Basu, K. T. Klasson, M. Takriff, E. C. Clausen, and J. L. Gaddy Sep. 1993 98 p
(Contract DE-FG21-90MC-27225)
(DE94-005815; DOE/MC-27225/3602) Avail: CASI HC A05/MF A02

The purpose of this research is to develop a technically and economically feasible process for biologically producing H2 from synthesis gas while, at the same time, removing harmful sulfur gas compounds. Six major tasks are being studied: culture development, where the best cultures are selected and conditions optimized for simultaneous hydrogen production and sulfur gas removal; mass transfer and kinetic studies in which equations necessary for process design are developed; bioreactor design studies, where the cultures chosen in the first task are utilized in continuous reaction vessels to demonstrate process feasibility and define operating conditions; evaluation of biological synthetic gas conversion under limiting conditions in preparation for industrial demonstration studies; process scale-up where laboratory data are scaled to larger-size units in preparation for process demonstration in a pilot-scale unit; and economic evaluation, where process simulations are used to project process economics and identify high cost areas during sensitivity analyses. DOE

N94-30945# Aeronautical Research Inst. of Sweden, Stockholm.
THE EXECUTION OF WIND ENERGY PROJECTS 1986 - 1992 BETWEEN CHINA AERODYNAMICS RESEARCH AND DEVELOPMENT CENTRE (CARDC) AND THE AERONAUTICAL RESEARCH INSTITUTE OF SWEDEN (FFA)
He Dexin and Sven-Erik Thor Jun. 1993 35 p Sponsored by Swedish Board for Industrial and Technical Development
(FFA-TN-1993-19; ETN-94-95856) Avail: CASI HC A03/MF A01

The execution of the first phase agreement on wind energy projects, covering the period from 1986 to 1992, is summarized. The following are addressed: wind tunnel tests of a 2.2 m and 2.8 m diameter turbine, a 5.35 m turbine in stationary yaw operation, pressure measurements, wall interference correction, a 5.35 m diameter turbine under yaw control, visualization of the flow on the rotating blade. It was concluded that the yaw characteristics (including aerodynamic performance and control characteristics) and three dimensional flow of the wind turbine chosen as cooperation items have significant engineering application background and academic value. The results are applicable for medium as well as large size wind turbines and has a positive effect on the development of wind energy technology. ESA

N94-30946# Aeronautical Research Inst. of Sweden, Stockholm.
WIND TUNNEL TESTS OF A 5.3 M DIAMETER YAW CONTROLLED TURBINE
Eskil Ulen Sep. 1993 130 p Sponsored by Swedish Board for Industrial and Technical Development Prepared in cooperation with Chinese Aerodynamic Research and Development Center
(FFA-TN-1993-20; ETN-94-95857) Avail: CASI HC A07/MF A02

In order to meet the need for accurate wind turbine operating data from a variety of situations, a wind turbine was designed, built and tested. A description of the equipment and test results are given from a control point of view. The intention of the tests was to get a better understanding of the performance of a wind power station which from a system point of view is characterized by: two blades with fixed pitch angle, variable speed, yaw control of max rotor speed, hub with teeter, and induction generator. Some tests in stall region were also included. The intention was to get practical experiences by performing tests in a wind tunnel as realistically as possible. Of special interest are the following points: the load and aerodynamic torque of the blades with realistic values of rotor speed and yaw rate and angles; magnitude of teeter angle under yaw control; the required yaw motor torque; the coupling between yaw movements and tower lateral resonance ('fish tail' movement); disturbances, especially around

yaw axis caused by blade rotation; and the performance of a hub with teeter in stall region. A small complete wind power station with a realistic yaw servo was used. ESA

N94-30465*# Naval Surface Warfare Center, Panama City, FL. Coastal Systems Station.
PHOTOVOLTAIC POWER WITHOUT BATTERIES FOR CONTINUOUS CATHODIC PROTECTION
W. W. Muehl, Sr. *In* NASA, Washington, Technology 2003: The Fourth National Technology Transfer Conference and Exposition, Volume 1 Feb. 1994 p 219-222 (For primary document see N94-30440 08-99)
Avail: CASI HC A01/MF A04

N94-30486*# Midwest Research Inst., Golden, CO.
FIBER OPTICAL SOLAR SIMULATOR
Bhushan L. Sopori and Craig Marshall *In* NASA, Washington, Technology 2003: The Fourth National Technology Transfer Conference and Exposition, Volume 1 Feb. 1994 p 421-428 (For primary document see N94-30440 08-99)
(Contract DE-AC02-83CH-10093)
Avail: CASI HC A02/MF A04

45 ENVIRONMENT POLLUTION

Includes atmospheric, noise, thermal, and water pollution.

N94-28412# Technical Research Centre of Finland, Espoo. Reactor Lab.
SPECIATION IN WATER AND SOIL: A LITERATURE REVIEW
Torbojorn Carlsson Mar. 1993 72 p
(ISSN 1235-0605)
(PB94-132388; VTT/RN-1455; ISBN-951-38-4348-3) Copyright Avail: CASI HC A04/MF A01

It is well known by now that the study of environmental pollution should be focused on the chemical forms of pollutants rather than on total concentrations. The need for more research on elemental speciation increases as pollutants are constantly released into the air, water, and soil. The work focuses mainly on heavy metal pollution in Finnish soil/water systems. The following topics are dealt with: (1) The geology and geochemistry of Finland, (2) pollution, (3) chemical time bombs (CTB's), (4) computer modeling, and (5) speciation. NTIS

N94-28454# Pacific Northwest Lab., Richland, WA.
USER-CENTERED GUIDELINES FOR ENVIRONMENTAL MANAGEMENT
D. R. Eike, J. A. Fox, and R. Dailey Aug. 1993 7 p Presented at the 5th International Conference on Human-Computer Interaction, Orlando, FL, 8-13 Aug. 1993
(Contract DE-AC06-76RL-01830)
(DE94-004313; PNL-SA-22420; CONF-9308124-2) Avail: CASI HC A02/MF A01

Environmental management requirements facing U.S. Department of Energy (DOE) facilities are detailed, complex, and often subject to rapid change. DOE's Office of Environmental Guidance, RCRA/CERCLA Division (EH-231), is responsible for developing and issuing guidance to assist DOE facilities in interpreting and complying with federal, state, and local requirements. Recognizing the potential for computerization of the guidance, EH-231 requested that Pacific Northwest Laboratory (PNL) develop an approach for preparing automated guidance. The approach developed by PNL, termed 'user-centered guidance,' combines participatory design and traditional rapid prototyping techniques to produce a new form of environmental guidance that emphasizes the user's needs. This paper describes the objectives, processes, and current status of this effort. DOE

N94-28463# North Dakota Univ., Grand Forks. Energy and Environmental Research Center.
CATALYTIC FABRIC FILTRATION FOR SIMULTANEOUS NO(x) AND PARTICULATE CONTROL
G. F. Weber, S. R. Ness, D. L. Laudal, and G. E. Dunham Aug. 1993 20 p
(Contract DE-AC22-90PC-90361)
(DE94-001660; DOE/PC-90361/T11) Avail: CASI HC A03/MF A01

The University of North Dakota Energy and Environmental Research Center (EERC), Owens-Corning Fiberglas Corporation (OCF), and Raytheon Engineers and Constructors (RE&C), are conducting research to develop a catalytic fabric filter (CFF) for simultaneous NO(x) and particulate control. Advances at OCF have shown that a high-activity catalyst can be applied to a high-temperature woven glass cloth resulting in a fabric filter material that can operate at temperatures higher than commercially available, coated glass fabric. The NO(x) is removed by catalytic reduction with ammonia to form nitrogen and water. The catalyst employed at this time is vanadium/titanium, but the exact catalyst composition and the unique method of applying the catalyst to high-temperature glass fabric are the property of OCF. Other catalyst options are being evaluated by OCF in order to improve catalyst performance and minimize catalyst cost. Bench-scale experimental results have shown that over 90% NO(x) removal can be achieved, that the catalyst/fabric has promising self-abrasion characteristics, and that the potential exists for substantially reduced cost compared to conventional SCR/fabric filtration technology. However, development of the technology requires further evaluation of air-to-cloth ratio effects, ammonia slip, SO2 oxidation to SO3, temperature cycling, catalyst-coated fabric preparation, fuel impacts, fabric cleaning (reverse-gas versus pulse-jet), catalyst life (poisoning and resistance to erosion), and filter performance/life (particulate control, differential pressure, and durability). DOE

N94-28465# Carnegie-Mellon Univ., Pittsburgh, PA. Center for Energy and Environmental Studies.
DEVELOPMENT OF THE INTEGRATED ENVIRONMENTAL CONTROL MODEL: PERFORMANCE MODELS OF SELECTIVE CATALYTIC REDUCTION NO(x) CONTROL SYSTEMS
H. C. Frey Jul. 1993 50 p
(Contract DE-AC22-92PC-91346)
(DE94-002151; DOE/PC-91346/3) Avail: CASI HC A03/MF A01

This report concerns the Integrated Environmental Control Model (IECM) created and enhanced by Carnegie Mellon University (CMU) for the US Department of Energy's Pittsburgh Energy Technology Center (DOE/PETC). The IECM provides a capability to model various conventional and advanced processes for controlling air pollutant emissions from coal-fired power plants before, during, or after combustion. The principal purpose of the model is to calculate the performance, emissions, and cost of power plant configurations employing alternative environmental control methods. The model consists of various control technology modules, which may be integrated into a complete utility plant in any desired combination. In contrast to conventional deterministic models, the IECM offers the unique capability to assign probabilistic values to all model input parameters, and to obtain probabilistic outputs in the form of cumulative distribution functions indicating the likelihood of different costs and performance results. DOE

N94-28473# Department of Energy, Washington, DC. Office of Energy Research.
GLOBAL CHANGE RESEARCH: SUMMARIES OF RESEARCH IN FY 1993
Oct. 1993 230 p
(DE94-003150; DOE/ER-0597T) Avail: CASI HC A11/MF A03

This document describes the activities and products of the Global Research Program in FY 1993. This publication describes all of the projects funded by the Environmental Sciences Division of DOE under annual contracts, grants, and interagency agreements in FY 1993. Each description contains the project's title; its 3-year funding history (in thousands of dollars); the period over which the funding applies; the name(s) of the principal investigator(s); the institution(s) conducting the projects; and the project's objectives, products, approach, and results to date (for most projects older than 1 year). Project descriptions are categorized within the report according to program areas: climate modeling, quantitative links, global carbon cycle, vegetation research, ocean research, economics of global climate change, education, information and integration, and NIGEC. Within these categories, the descriptions are grouped alphabetically by principal investigator. Each program area is preceded by a brief text that defines the program area, states its goals and objectives, lists principal research questions, and identifies program managers. DOE

N94-28521# Los Alamos National Lab., NM.
GLOBAL ATMOSPHERIC AND OCEAN MODELING ON THE CONNECTION MACHINE
S. R. Atlas (Thinking Machines Corp., Cambridge, MA.) 1993 12 p Presented at the North Atlantic Treaty Organization/Advanced Study Institute (NATO/ASI) Workshop in High Performance Computing in Geosciences, Chamouix, France, 21-25 Jun. 1993
(Contract W-7405-eng-36)
(DE94-003930; LA-UR-93-4224; CONF-9306285-1) Avail: CASI HC A03/MF A01

This paper describes the high-level architecture of two parallel global climate models: an atmospheric model based on the Geophysical Fluid Dynamics Laboratory (GFDL) SKYHI model, and an ocean model descended from the Bryan-Cox-Semtner ocean general circulation model. These parallel models are being developed as part of a long-term research collaboration between Los Alamos National Laboratory (LANL) and the GFDL. The goal of this collaboration is to develop parallel global climate models which are modular in structure, portable across a wide variety of machine architectures and programming paradigms, and provide an appropriate starting point for a fully coupled model. Several design considerations have emerged as central to achieving these goals. These include the expression of the models in terms of mathematical primitives such as stencil operators, to facilitate performance optimization on different computational platforms; the isolation of communication from computation to allow flexible implementation of a single code under message-passing or data parallel programming paradigms; and judicious memory management to achieve modularity without memory explosion costs. DOE

N94-28523# Brookhaven National Lab., Upton, NY.
OZONE PRODUCTION AT A RURAL SITE IN GEORGIA DURING THE SUMMER 1992 SOS CAMPAIGN
L. I. Kleinman, Yin-Nan Lee, and S. R. Springston et al Jun. 1993 7 p Presented at the 74th American Meteorological Society Annual Meeting, Nashville, TN, 23-28 Jan. 1994
(Contract DE-AC02-76CH-00016)
(DE94-003989; BNL-49231; CONF-940115-13) Avail: CASI HC A02/MF A01

As part of the Southern Oxidant Study (SOS) (UCAR, 1990), Brookhaven National Laboratory operated a SENIOR (South Eastern Network for Intensive Ozone Research) measurement site on a campaign basis during parts of the summers of 1991 and 1992. Measurements were made for the purpose of understanding the pervasive high levels of O3 observed in the southeastern U.S. In this article, the authors focus on the 1992 observations of O3 and the predication of O3 formation rates based on a radical budget calculation and based on the photostationary state. DOE

N94-28587*# SRI International Corp., Menlo Park, CA.
LOCAL MEASUREMENT OF TROPOSPHERIC HO(x) Final Report
David R. Crosley Hampton, VA NASA Feb. 1994 79 p Sponsored by NASA. Langley Research Center and NSF
(RTOP 464-54-03-70)
(NASA-CP-3245; L-17370; NAS 1.55:3245) Avail: CASI HC A05/MF A01

In March of 1992 a workshop sponsored by NASA and NSF was held at SRI International to assess the current ability to measure atmospheric OH and HO2. The measurement techniques reviewed during the workshop for detection of OH included five laser-induced fluorescence schemes, five laser-based adsorption techniques, and four non-laser methods. Six instruments or instrument concepts for HO2 detection, including chemical amplification, conversion to OH with subsequent OH detection, or direct spectroscopic detection of the HO2 were also discussed. The conclusions from the workshop identify several measurement techniques for OH and HO2 that are ready for field tests. These have the ability to measure the radicals with sufficient sensitivity and accuracy to form meaningful comparison with atmospheric model predictions. The workshop conclusions also include recommendations for informal and formal intercomparison protocols. For individual titles, see N94-28588 through N94-28608.

N94-28588*# Georgia Inst. of Tech., Atlanta. School of Earth and Atmospheric Sciences.
TWO-PHOTON/LASER-INDUCED FLUORESCENCE (TP/LIF) SENSOR Abstract Only
John D. Bradshaw *In* SRI International Corp., Local Measurement of Tropospheric HO(x) Feb. 1994 1 p (For primary document see N94-28587 08-45)
Avail: CASI HC A01/MF A01

The Two-Photon/Laser-Induced Fluorescence (TP/LIF) technique is based on the stepwise excitation of the OH transitions, X(exp 2)II, v(exp '') = 0 yields X(exp 2)II, v(exp '') = 1 (lambda = 2.9 microns) and X(exp 2)II v(exp '') = 1 yields A(exp2)Sigma, v' = 0 (lambda = 345 nm) with background free fluorescence monitoring of the A(exp 2)Sigma, v' = 0 yields X(exp 2)II, v(exp '') = 0 transition near 309 nm. This technique has awaited the advent of a suitable mid-infrared (2.9 microns) laser source. Turnable mid-IR lasers now exist that are capable of meeting the specifications required of a high sensitivity TP/LIF OH sensor. Author

N94-28589*# Pennsylvania State Univ., University Park. Dept. of Meteorology.
IN SITU DETECTION OF TROPOSPHERIC OH AND HO2 BY LASER-INDUCED FLUORESCENCE IN A DETECTION CHAMBER AT LOW PRESSURE Abstract Only
William H. Brune, Philip S. Stevens, and James Mather *In* SRI International Corp., Local Measurement of Tropospheric HO(x) Feb. 1994 1 p (For primary document see N94-28587 08-45)
Avail: CASI HC A01/MF A01

Just as in the method of Hard and O'Brien, ambient air is pulled through an approximately 1 mm diameter inlet into a detection chamber that is maintained at a pressure of 2.4 torr. The ambient air stream travels through the detection chamber with a velocity of greater than 100 m sec(exp -1) in a narrow stream, constrained by the addition of an inert gas flow (0.4 torr). The OH molecule is both excited and detected in the A(exp 2)Sigma (v' = 0) yields X(exp 2)II (v'' = 0) transition at 308 nm. Light from a copper vapor-pumped dye laser (rep. rate = 10kHz; pulse length = 20 ns; linewidth = .1 cm(exp -1), and average power = 15 mW), resonant with the Q(sub 1)(3) transition, is multipassed through a White cell and intercepts the air stream as 24 non-overlapping 2mm by 5mm beams. A fast microchannel plate detector is turned off during the laser pulse to prevent saturation of the detector due to Rayleigh and chamber scattering. It is turned on 30-100 nsec after the end of the laser pulse for 300 ns to collect resonance fluorescence from OH. HO2 is detected by chemical conversion to OH by reaction with reagent NO, followed by OH detection. Both the detection sensitivity and the inlet characteristics must be understood for any in situ instrument. For the calibration of the detection sensitivity, OH is produced quantitatively by the fast H + NO2 yields OH + NO reaction in a low pressure, flowing discharge tube connected to the detection chamber. The inlet transmission of OH inlet is calibrated separately. Derived from text

N94-28590*# Portland State Univ., OR. Dept. of Chemistry.
TROPOSPHERIC HO DETERMINATION BY FAGE Abstract Only
Thomas M. Hard, L. A. George, and Robert J. OBrien *In* SRI International Corp., Local Measurement of Tropospheric HO(x) Feb. 1994 1 p (For primary document see N94-28587 08-45)
Avail: CASI HC A01/MF A01

In the measurement of tropospheric HO we have employed three low-pressure laser-excited fluorescence (LEF) experimental systems. These instruments operate by expanding the ambient air flow via a nozzle, followed by transit down a flowtube through a detection region traversed by the excitation laser beam. This sampling method we named FAGE (fluorescence assay with gas expansion). The instruments employed a hydrocarbon reagent, added below the nozzle, to remove HO for background measurement. In the second and third instruments, air sampling via parallel nozzles and tubes, with reagent addition alternating between two channels, permitted continuous signal measurement with simultaneous measurement of background. The first two instruments (FAGE1 and FAGE2) used 282 nm HO excitation by frequency-doubled tunable dye lasers, pumped by pulsed Nd:YAG lasers at 10-30 Hz repetition rate. The third instrument (FAGE3) uses 308 nm excitation in which the dye laser is pumped by a copper vapor laser, pulsed at 5600 Hz. Author

N94-28591*# Forschungszentrum Juelich G.m.b.H. (Germany). Inst. fuer Atmospheric Chemistry.

DETECTION OF TROPOSPHERIC OH AND HO2 BY LASER-INDUCED FLUORESCENCE AT LOW PRESSURE USING THE 308nm EXCITATION OF OH Abstract Only

Andreas Hofzumahaus and Frank Holland *In* SRI International Corp., Local Measurement of Tropospheric HO(x) Feb. 1994 1 p (For primary document see N94-28587 08-45)

Avail: CASI HC A01/MF A01

Laser-induced fluorescence (LIF) spectroscopy is a highly sensitive method for the direct in situ measurement of hydroxyl concentrations in the atmosphere. Its sensitivity and selectivity relies on the intense discrete UV-absorption lines of OH which are strongest around 282nm and 308nm. We have developed a LIF-instrument based on the low-pressure experiment (FAGE). However, we use 308nm instead of 282nm as excitation wavelength for OH, a concept that is also pursued by other groups. One advantage of the longer excitation wavelength is the higher detection sensitivity due to the about 6 times larger effective OH-fluorescence cross-section. Moreover, the O3/H2O-interference (OH self-generation by the laser) is about a factor of 200 smaller at 308nm than at 282nm. This keeps the interference level well below the projected detection limit of 10(exp 5) OH/cm(exp 3). Atmospheric HO2-radicals are detected by chemical conversion of HO2 into OH with NO. Author

N94-28592*# Harvard Univ., Cambridge, MA. Dept. of Earth and Planetary Sciences.

HARVARD ER-2 OH LASER-INDUCED FLUORESCENCE INSTRUMENT Abstract Only

Paul O. Wennberg and James G. Anderson *In* SRI International Corp., Local Measurement of Tropospheric HO(x) Feb. 1994 1 p (For primary document see N94-28587 08-45)

Avail: CASI HC A01/MF A01

The Harvard ER-2 OH instrument is scheduled to be integrated into the NASA ER-2 high altitude aircraft ozone payload in August 1992. Design and fabrication is presently underway. This experiment is a descendant of a balloon borne instrument designed and built in the mid-1980s. The ER-2 instrument is being designed to measure OH and HO2 as part of the NASA ozone payload for the investigation of processes controlling the concentration of stratospheric ozone. Although not specifically designed to do so, it is hoped that valid measurements of OH and HO2 can be made in the remote free troposphere with this instrument. Author

N94-28593*# Jet Propulsion Lab., California Inst. of Tech., Pasadena.

JPL FOURIER TRANSFORM ULTRAVIOLET SPECTROMETER Abstract Only

R. P. Cageao, R. R. Friedl, Stanley P. Sander, and Y. L. Yung *In* SRI International Corp., Local Measurement of Tropospheric HO(x) Feb. 1994 1 p (For primary document see N94-28587 08-45)

Avail: CASI HC A01/MF A01

The Fourier Transform Ultraviolet Spectrometer (FTUVS) is a new high resolution interferometric spectrometer for multiple-species detection in the UV, visible and near-IR. As an OH sensor, measurements can be carried out by remote sensing (limb emission and column absorption), or in-situ sensing (long-path absorption or laser-induced fluorescence). As a high resolution detector in a high repetition rate (greater than 10 kHz) LIF system, OH fluorescence can be discriminated against non-resonant background emission and laser scatter, permitting (0, 0) excitation.

Author (revised)

N94-28594*# Johann-Wolfgang-Goethe-Univ., Frankfurt am Main (Germany). Inst. fuer Physikalische und Theoretische Chemie.

ABSOLUTE DETERMINATION OF LOCAL TROPOSPHERIC OH CONCENTRATIONS Abstract Only

Wolfgang Armerding and Franz-Josef Comes *In* SRI International Corp., Local Measurement of Tropospheric HO(x) Feb. 1994 1 p (For primary document see N94-28587 08-45)

Avail: CASI HC A01/MF A01

Long path absorption (LPA) according to Lambert Beer's law is a method to determine absolute concentrations of trace gases such as tropospheric OH. We have developed a LPA instrument which is based on a rapid tuning of the light source which is a frequency doubled dye laser. The laser is tuned across two or three OH absorption features around 308 nm with a scanning speed of 0.07 cm(exp -1)/microsecond and a repetition rate of 1.3 kHz. This high scanning speed greatly reduces the fluctuation of the light intensity caused by the atmosphere. To obtain the required high sensitivity the laser output power is additionally made constant and stabilized by an electro-optical modulator. The present sensitivity is of the order of a few times 10(exp 5) OH per cm(exp 3) for an acquisition time of a minute and an absorption path length of only 1200 meters so that a folding of the optical path in a multireflection cell was possible leading to a lateral dimension of the cell of a few meters. This allows local measurements to be made. Tropospheric measurements have been carried out in 1991 resulting in the determination of OH diurnal variation at specific days in late summer. Comparison with model calculations have been made. Interferences are mainly due to SO2 absorption. The problem of OH self generation in the multireflection cell is of minor extent. This could be shown by using different experimental methods. The minimum-maximum signal to noise ratio is about 8 x 10(exp -4) for a single scan. Due to the small size of the absorption cell the realization of an open air laboratory is possible in which by use of an additional UV light source or by additional fluxes of trace gases the chemistry can be changed under controlled conditions allowing kinetic studies of tropospheric photochemistry to be made in open air. Author

N94-28595*# Forschungszentrum Juelich G.m.b.H. (Germany). Inst. for Atmospheric Chemistry.

UV LASER LONG-PATH ABSORPTION SPECTROSCOPY Abstract Only

Hans-Peter Dorn, Theo Brauers, and Rudolf Neuroth *In* SRI International Corp., Local Measurement of Tropospheric HO(x) Feb. 1994 1 p (For primary document see N94-28587 08-45)

Avail: CASI HC A01/MF A01

Long path Differential Optical Absorption Spectroscopy (DOAS) using a picosecond UV laser as a light source was developed in our institute. Tropospheric OH radicals are measured by their rotational absorption lines around 308 nm. The spectra are obtained using a high resolution spectrograph. The detection system has been improved over the formerly used optomechanical scanning device by application of a photodiode array which increased the observed spectral range by a factor of 6 and which utilizes the light much more effectively leading to a considerable reduction of the measurement time. This technique provides direct measurements of OH because the signal is given by the product of the absorption coefficient and the OH concentration along the light path according to Lambert-Beers law. No calibration is needed. Since the integrated absorption coefficient is well known the accuracy of the measurement essentially depends on the extent to which the OH absorption pattern can be detected in the spectra. No interference by self generated OH radicals in the detection lightpath has been observed. The large bandwidth (greater than 0.15 nm) and the high spectral resolution (1.5 pm) allows absolute determination of interferences by other trace gas absorptions. The measurement error is directly accessible from the absorption-signal to baseline-noise ratio in the spectra. The applicability of the method strongly depends on visibility. Elevated concentrations of aerosols lead to considerable attenuation of the laser light which reduces the S/N-ratio. In the moderately polluted air of Julich, where we performed a number of OH measurement spectra. In addition absorption features of unidentified species were frequently detected. A quantitative deconvolution even of the known species is not easy to achieve and can leave residual structures in the spectra. Thus interferences usually increase the noise and deteriorate the OH detection sensitivity. Using diode arrays for sensitive absorption measurements some specific problems of those detectors have to be solved experimentally (i.e. fixed pattern noise, dark signal noise, nonuniform efficiency of individual elements, spatial sensitivity variations). In order to improve the low spatial resolution we performed laboratory studies using a multiple reflection cell to convert the long path technique to a real in situ point measurement. Under the conditions of field experiments in Julich residual absorbance signals at present are about 1.5x10(exp -4) corresponding to an OH detection sensitivity of 2x10(exp 6) OH/cm(exp 3) using a light path of 5.8 km. Total integration times for one measurement point vary between a few minutes and an hour. Author

N94-28596*# Max-Planck-Inst. fuer Chemie, Mainz (Germany). Abteilung Chemie der Atmosphaere.

MEASUREMENT OF TROPOSPHERIC OH BY LASER LONG-PATH ABSORPTION SPECTROSCOPY Abstract Only

Michael Kraft and D. Perner *In* SRI International Corp., Local Measurement of Tropospheric HO(x) Feb. 1994 1 p (For primary document see N94-28587 08-45)
Avail: CASI HC A01/MF A01

OH-radicals are measured by laser long-path absorption spectroscopy. A tunable Nd:YAG/dye laser system provides broadbanded light at 308 nm. The beam is expanded to 0.3 m and pointed to an array of retroreflectors placed at a distance of 2800 m. The returning beam is separated from the outgoing beam and focused into a spectrometer of 0.3 pm resolution. A 1024 element diode array is used as a detector. The signal is digitized by a 14 bit analog to digital converter. The ultimate aim is a detection limit of 10(exp 5) molecules cm(exp -3) of OH. However the measurements in 1991 allowed only the recognition of OH absorptions corresponding to 3 x 10(exp 6) OH cm(exp -3) with a signal to noise ratio of two. Improvements of the instrument are under way. The advantages of the DOAS method are: the accuracy of detection is guaranteed because loss of OH radicals within the device is avoided, the rate of OH production by the device is negligible, and absorptions of other trace gases could be corrected for; and the calibration procedure for the device is fast and easy. The disadvantages of the system are: time resolution is about minutes because about ten spectra had to be added to keep the noise level down, the OH concentration is averaged along the whole light path, weight (500 kg) and size (4x4 m) of the device; and approximately 10 l/min of coolant and supply of 8 kW electrical power are necessary. Author (revised)

N94-28597*# Aerodyne Research, Inc., Billerica, MA.
ON THE POSSIBILITY OF MEASURING ATMOSPHERIC OH USING INTRACAVITY LASER SPECTROSCOPY Abstract Only
J. Barry McManus and C. E. Kolb *In* SRI International Corp., Local Measurement of Tropospheric HO(x) Feb. 1994 1 p (For primary document see N94-28587 08-45)
Avail: CASI HC A01/MF A01

Intracavity laser spectroscopy (ILS) has been demonstrated to be useful for measuring extremely weak absorption produced by gases in air. ILS is based on the observation that when there are spectrally narrow losses within the cavity of a broadband laser, the laser output has corresponding spectral holes where the laser oscillation is partially quenched. The depth of the laser output dips can be enhanced by a factor of 10(exp 5) over the depth of the initial cavity loss, and absorptivities of 10(exp -8) cm(exp -1) have been measured in lasers only one meter long. With ILS, one can achieve in a compact space a spectral contrast that would otherwise require kilometers of pathlength. ILS systems typically use quasi-continuous wave dye lasers operating close to threshold. The pump laser is modulated from just below to just above the threshold level for the dye laser, and the dye laser output is spectroscopically observed during a well defined time interval after the onset of lasing (the generation time). The spectral contrast of an intracavity absorber is equivalent to that produced by absorption through a path length equal to the generation time multiplied by the speed of light (assuming the cavity is completely filed with the absorber) up to some limiting time. Thus, if one measures the spectrum after 33 microseconds, the effective path length is 10,000 meters.
Derived from text

N94-28598*# National Oceanic and Atmospheric Administration, Boulder, CO. Aeronomy Lab.
NOAA AERONOMY LABORATORY LONG-PATH OH EXPERIMENT, FRITZ PEAK OBSERVATORY, COLORADO Abstract Only
George H. Mount *In* SRI International Corp., Local Measurement of Tropospheric HO(x) Feb. 1994 1 p (For primary document see N94-28587 08-45)
Avail: CASI HC A01/MF A01

Long path absorption of laser light over a 20.6 km path at Fritz Peak Observatory 17 km west of Boulder is described: elevation 2800 m, average beam height above terrain approximately 250 m, and operational since March 1991. System runs at maximum signal to noise with integration times longer than 64 seconds. Most of the data obtained to date are 15-minute averages due to the lengthy data analysis required.
Derived from text

N94-28599*# Arizona Univ., Tucson. Dept. of Atmospheric Sciences.
MEASUREMENT OF ATMOSPHERIC OH BY TITRATION OF NEAR-IR FLUORESCENT DYES Abstract Only
Eric A. Betterton and Karl Gast *In* SRI International Corp., Local Measurement of Tropospheric HO(x) Feb. 1994 1 p (For primary document see N94-28587 08-45)
(EPRI Proj. 8004-11)
Avail: CASI HC A01/MF A01

Recent research has shown that certain polymethine dyes can be detected at ultratrace levels (greater than or equal to 6x10(exp -14) M) in solution by fluorimetry. These detection limits are possible because of the inherent sensitivity of fluorescence techniques, because the dyes fluoresce in the near infrared region where background interference is negligible, and because powerful infrared diode lasers are now available to improve the signal to noise ratio. Other work has shown that the hydroxyl radical destroys the ability of polymethine dyes to fluoresce. These observations form the basis for a new hydroxyl radical detector that is essentially a fluorometric titrator. Theoretically, the detector should show an acceptable sensitivity and response time. Assuming that the atmospheric HO concentration is about 10(exp -11) moles m(exp -3) (i.e. 10(exp 6) molecules cm(exp -3)), then 10 L of air 'titrated' with 20 mL of 10(exp -11) M dye solution (an easily detected concentration) should result in a drop in the fluorescent signal of 50 percent - a readily detectable change. At a flow rate of 3 L min(exp -1) the sampling time would be 3 minutes. The biggest potential problem is selectivity: other oxidants may also cause the fluorescence signal to be lost. The chemistry of polymethine dyes has not been studied in detail and so no quantitative data are available. However, a survey of the literature suggests that in general HO should react up to six orders of magnitude faster than HO2 and other radicals such as RO2 and RO. It should also react much more rapidly than H2O2 and O3. Thus it may be possible to discriminate kinetically against potential interfering substances. It was shown in the laboratory that 10(exp -4) M H2O2 has little effect on the absorption spectrum of the dye IR125 over a period of hours but that the band at 780 nm is slowly lost in water over a period of days even under argon in the dark. By contrast, DMSO solutions of IR125 are stable. Author

N94-28600*# Washington State Univ., Pullman. Dept. of Civil and Environmental Engineering.
THE RADIOCARBON HYDROXYL TECHNIQUE Abstract Only
Malcolm J. Campbell and John C. Sheppard *In* SRI International Corp., Local Measurement of Tropospheric HO(x) Feb. 1994 1 p (For primary document see N94-28587 08-45)
Avail: CASI HC A01/MF A01

The Radiocarbon Technique depends upon measuring the rate of oxidation of CO in an essentially unperturbed sample of air. The airborne technique is slightly different. Hydroxyl concentrations can be calculated directly; peroxyl concentrations can be obtained by NO doping. Author

N94-28601*# Georgia Inst. of Tech., Atlanta. Physical Sciences Lab.
ION-ASSISTED TROPOSPHERIC OH MEASUREMENT TECHNIQUE Abstract Only
Fred L. Eisele *In* SRI International Corp., Local Measurement of Tropospheric HO(x) Feb. 1994 1 p (For primary document see N94-28587 08-45)
Avail: CASI HC A01/MF A01

The present technique measures atmospheric OH concentrations by first titrating OH into isotopically labeled H2(exp 34)SO4 by a series of gas phase reactions in an effectively wall-less flow tube reactor on a time-scale which is short in comparison to the OH lifetime. The gas phase H2SO4 concentration is then determined by reacting it with NO3(-)(center dot)HNO3 ions in a flow tube, and subsequently measuring the resulting (HSO4(-))/(NO3(-)) ion ratio. Since the determination of H2SO4 concentration does not depend on the measurement of an absolute photon flux or chemical concentration but rather only on the relative concentration measurement of two fairly similar mass ions in conjunction with a fixed reaction time and reaction rate coefficient, no in-field calibration technique should be required. The ion-assisted OH measurement technique provides a concentration measurement about once each 10 to 20 seconds and had a detection sensitivity less than or equal to 1 x 10(exp 5) molecules/cu cm (2 standard deviations) with an integration time of 5 minutes during the past field study. Typically, the total background signal level is in the low 10(exp 6) molecule/cu cm range with the scatter in this background (or background noise in 5 minutes) in the mid 10(exp 4) molecules/cu cm range. Author (revised)

N94-28602*# Massachusetts Inst. of Tech., Cambridge. Dept. of Earth, Atmospheric and Planetary Sciences.

THE ACTIVE TITRATION METHOD FOR MEASURING LOCAL HYDROXYL RADICAL CONCENTRATION Abstract Only

Michele Sprengnether and Ronald G. Prinn *In* SRI International Corp., Local Measurement of Tropospheric HO(x) Feb. 1994 1 p (For primary document see N94-28587 08-45)

Avail: CASI HC A01/MF A01

We are developing a method for measuring ambient OH by monitoring its rate of reaction with a chemical species. Our technique involves the local, instantaneous release of a mixture of saturated cyclic hydrocarbons (titrants) and perfluorocarbons (dispersants). These species must not normally be present in ambient air above the part per trillion concentration. We then track the mixture downwind using a real-time portable ECD tracer instrument. We collect air samples in canisters every few minutes for roughly one hour. We then return to the laboratory and analyze our air samples to determine the ratios of the titrant to dispersant concentrations. The trends in these ratios give us the ambient OH concentration from the relation: dlnR/dt = -k(OH). A successful measurement of OH requires that the trends in these ratios be measureable. We must not perturb ambient OH concentrations. The titrant to dispersant ratio must be spatially invariant. Finally, heterogeneous reactions of our titrant and dispersant species must be negligible relative to the titrant reaction with OH. We have conducted laboratory studies of our ability to measure the titrant to dispersant ratios as a function of concentration down to the few part per trillion concentration. We have subsequently used these results in a gaussian puff model to estimate our expected uncertainty in a field measurement of OH. Our results indicate that under a range of atmospheric conditions we expect to be able to measure OH with a sensitivity of 3x10(exp 5) cm(exp -3). In our most optimistic scenarios, we obtain a sensitivity of 1x10(exp 5) cm(exp -3). These sensitivity values reflect our anticipated ability to measure the ratio trends. However, because we are also using a rate constant to obtain our (OH) from this ratio trend, our accuracy cannot be better than that of the rate constant, which we expect to be about 20 percent.

Author (revised)

N94-28603*# National Center for Atmospheric Research, Boulder, CO. Atmospheric Chemistry Div.

PEROXY RADICAL MEASUREMENTS WITH NCAR'S CHEMICAL AMPLIFIER Abstract Only

Christopher Cantrell, Richard Shetter, and Jack G. Calvert *In* SRI International Corp., Local Measurement of Tropospheric HO(x) Feb. 1994 1 p (For primary document see N94-28587 08-45)

Avail: CASI HC A01/MF A01

The present NCAR instrument for HO2/RO2 measurements has been described previously. It is based on the reactions involving HO2, RO2, and HO radicals with CO and NO. Since (HO2) + (RO2) + (HO) is much greater than (HO) for most atmospheres, it is useful as a peroxy radical detector. Operation of the instrument depends on the creation of a chemical chain reaction which is initiated as HO2 and RO2 radicals in ambient air encounter added NO gas; this forms an NO2 molecule and an HO or RO radical: HO2(RO2) + NO yields HO(RO) + NO2. RO radicals react relatively efficiently with O2 to form an HO2 radical, and subsequently an HO-radical, by reaction with NO. CO gas added to the reaction chamber during part of the operating cycle, recycles the HO to HO2; HO + CO (+O2) yields HO2 + CO2. The reaction sequence may form several hundred NO2 molecules per HO2 (RO2) originally present, before chain termination occurs. The added CO is replaced by N2 addition periodically so that the chain reaction is suppressed, and a 'blank' signal resulting from NO2, O3 and possibly other NO2-forming species (non-chain processes) in ambient air is recorded. The difference between the signal with and without CO is proportional to the peroxy radical concentration. The NO2 produced is monitored using a sensitive luminol chemiluminescence detector system. In the NCAR instrument the length of the amplification chain is determined using a stable source of HO2 radicals (H2O2 thermal decomposition); the ratio of the signal seen with CO present to that with N2 present gives the sensitivity of the instrument to HO2 (molecules of NO2 formed/peroxy radical). The instrument is automated to carry out in hourly repeated cycles: (1) chain length determination; (2) NO2 calibration; and (3) linearity check on the response of signals. One minute averages of signals are normally recorded. The sensitivity of the instrument to detect peroxy radicals is in the pptv range. The present instrument has operated continuously (24 hr/day) in the field studies which extended over a period of several weeks. The major advantages of this instrument are as follows: (1) its relative simplicity; (2) low power requirements; and (3) its rapid response to all types of peroxy radicals--HO2, CH3O2 and the higher alkyl and acyl peroxy radicals; however not all RO2 species generate HO2 radicals with perfect efficiency and hence have somewhat lower response/molecule than HO2 radicals.

Author

N94-28604*# York Univ. (Ontario).

THE RADICAL AMPLIFIER Abstract Only

D. R. Hastie *In* SRI International Corp., Local Measurement of Tropospheric HO(x) Feb. 1994 1 p (For primary document see N94-28587 08-45)

Avail: CASI HC A01/MF A01

The radical amplifier as a method for measuring radical concentrations in the atmosphere has received renewed attention lately. In principle, it can measure the total concentration of HO(x) and RO(x) radicals by reacting ambient air with high concentrations of CO (3-10 percent) and NO (2-6 pprnv), and measuring the NO2 produced.

Author

N94-28605*# SRI International Corp., Menlo Park, CA.

AN IMPROVED METHOD OF MEASURING TROPOSPHERIC NO2, NO3, HO2, AND RO2 BY MATRIX ISOLATION AND ELECTRONIC SPIN RESONANCE (MIESR) Abstract Only

In its Local Measurement of Tropospheric HO(x) 1 p(SEE N94-28587 08-45) Feb. 1994 (For primary document see N94-28587 08-45)

Avail: CASI HC A01/MF A01

The MIESR method consists of two steps (1) collection of the radicals present in the ambient air at 77K in a polycrystalline D2O matrix and (2) identification and quantification of the different radicals in the laboratory by Electron Spin Resonance spectroscopy. In step (1), the sampling efficiency for sampling NO2 and RO2 was determined to be greater than or equal to 95 percent, with a measured accuracy of plus or minus 5 percent. In step (2), after collection, the samples are maintained at 77 K and spectra are recorded in the laboratory using a standard 9.5 GHz ESR system (Varian E-line). About 50 individual scans of each spectrum are recorded and digitally averaged in order to improve the signal-to-noise ratio. The ESR-spectra are analyzed with a recently developed numerical procedure which was demonstrated to allow speciation of NO2, NO3, HO2, CH3C(O)O2, and the sum of the alkylperoxy radicals. The detection limit is 5ppt for HO2, RO2, and NO2 and 3ppt for NO3 due to its narrower ESR-linewidth.

Author

N94-28606*# Portland State Univ., OR. Dept. of Chemistry.

TROPOSPHERIC HO2 DETERMINATION BY FAGE Abstract Only

Thomas M. Hard, L. A. George, and Robert J. OBrien *In* SRI International Corp., Local Measurement of Tropospheric HO(x) Feb. 1994 1 p (For primary document see N94-28587 08-45)

Avail: CASI HC A01/MF A01

In the present work, HO2 is determined by FAGE, a method which employs low-pressure laser-excited fluorescence to observe the hydroxyl radical HO, using chemical modulation to distinguish the desired signal from the background. In the HO2 determination mode, NO is added to the low-pressure flowing sample, converting HO2 to HO.

Author

N94-28607*# Southwest Sciences, Inc., Santa Fe, NM.

NEAR-IR DIODE LASER ABSORPTION FOR MEASUREMENT OF TROPOSPHERIC HO2 Abstract Only

Alan C. Stanton *In* SRI International Corp., Local Measurement of Tropospheric HO(x) Feb. 1994 1 p (For primary document see N94-28587 08-45)

Avail: CASI HC A01/MF A01

The possibility of using tunable lead salt diode lasers in the infrared for measurement of tropospheric HO2 has been frequently considered. Although the sensitivity of diode laser absorption has been improved through the use of high frequency detection techniques, nature has been unkind in that the HO2 absorption cross sections are weak. Even using the most optimistic assumptions about attainable path length and detectable absorbance, measurement of tropospheric HO2 by diode laser absorption in the mid-IR appears marginal. A possible alternative method for measuring HO2 is by absorption at near-infrared wavelengths. Several absorption

bands of HO2 occur in the wavelength region between 1.2 and 1.6 micron due to electronic transitions and overtones of the fundamental vibrational modes. InGaAsP diode lasers operate in this wavelength region and can be used for high resolution spectroscopy in a manner analogous to the lead salt lasers. A diode laser system in the near-IR offers some advantages. Author

N94-28608*# Aerodyne Research, Inc., Billerica, MA.
HO2 DETECTION BY NEAR INFRARED ABSORPTION USING TUNABLE DIODE LASERS Abstract Only
David Nelson and Mark S. Zahniser *In* SRI International Corp., Local Measurement of Tropospheric HO(x) Feb. 1994 1 p (For primary document see N94-28587 08-45)
Avail: CASI HC A01/MF A01

The strongest absorption lines are in the v sub 2 vibrational band around 1400/cm; several near-coincident line pairs in this region provide max linestrengths of 1.2 x 10 exp -20 sq. cm/(molecule*cm). High Frequency wavelength modulation coupled with sweep integration were used to minimize noise and maintain spectral discrimination. Reduced pressure sampling was performed using supersonic nozzle and an aerodynamic flow cell to minimize residence time and wall losses of radicals. The astigmatic mirror design provides pathlengths up to 200 m in volume of 3 liters with minimal optical interference fringes; longer pathlengths are possible. The detection limit depends on pathlength and minimum fractional absorptions.
Derived from text

N94-28630# New Energy and Industrial Technology Development Organization, Tokyo (Japan).
SURVEY ON EFFECTS OF PETROLEUM SUBSTITUTION ENERGY UTILIZATION ON THE GLOBAL ENVIRONMENT
Mar. 1993 199 p
(DE94-732339; NEDO-P-9228) Avail: CASI HC A09/MF A03

Investigations/analyses are conducted on objectives, policies and measures of the world's major countries in relation to the Framework Convention on Climate Change, particularly CO2 emission. The problem on climate change is a global issue, and the CO2 emission control is directly connected with energy consumption closely related to national economies. Therefore, interests conflict between the north and the south, and among the developed countries. The U.S. Clinton administration is beginning to show a more positive attitude than before, and aims to take the most realistic measures such as the proposed new Btu tax in the developed countries. As for EC, whether or not CO2 stabilization targeted in 2000 is made possible depends on how much Germany can achieve the target. British strong opposition attitude toward the carbon/energy taxes presents a question to the target to be attained by 2000. Hereafter, tie-ups jointly taken for CO2 control measures between developed countries and developing countries are expected to be a matter of increasing importance. DOE

N94-28722 Army Construction Engineering Research Lab., Champaign, IL.
ENVIRONMENTAL COMPLIANCE ASSESSMENT SYSTEM (ECAS) Final Report
David A. Krooks and Tina M. Hurt Dec. 1993 226 p Limited Reproducibility: More than 20% of this document may be affected by microfiche quality
(AD-A275549; CERL-SR-EC-94/04) Avail: CASI HC A11

The U.S. Army has adopted an environmental compliance program that identifies compliance problems before they are cited as violations by the U.S. Environmental Protection Agency (USEPA). Major Army Commands (MACOM's) must conduct comprehensive environmental assessments at all installations on a 4-year cycle and conduct a mid-cycle internal assessment. Because each MACOM developed a separate system, the Army mandated a unified, Army-wide assessment mechanism, which combines Federal, Department of Defense (DOD), and Army environmental regulations; good management practices; and risk-management issues into a series of checklists that show requirements and specific items or operations to review. Each protocol lists a point of contact to help assessors review checklist items. The Worldwide Environmental Compliance Assessment System (ECAS) manual incorporates checklists from USEPA and from private industry. It integrates information from the Overseas Environmental Baseline Guidance Document (OEBGD). Worldwide ECAS includes pertinent information from Army Regulations and DOD Directives and Instructions and cites management practices for an overall environmental review. The ECAS JAPAN supplement incorporates Japanese legislation, regulations, and suggested management practices. It was developed for use in conjunction with the Worldwide ECAS manuals (USACERL SR-EC-93/03) and is updated continually to address changes in Japanese laws and regulations. DTIC

N94-28727 Army Construction Engineering Research Lab., Champaign, IL.
ENVIRONMENTAL COMPLIANCE ASSESSMENT AND MANAGEMENT SYSTEM PROGRAM (ECAMP). US AIR FORCE EUROPEAN ECONOMIC COMMUNITY (EEC) Final Report
Donna J. Schell and Tina M. Beckler Sep. 1993 290 p Limited Reproducibility: More than 20% of this document may be affected by microfiche quality
(AF Proj. 9201)
(AD-A275593; CERL-SR-EC-93/12) Avail: Issuing Activity (Defense Technical Information Center (DTIC))

In response to the growing number of environmental laws and regulations worldwide, the Air Force adopted an environmental compliance program that identifies compliance problems before they are cited as violations by the U.S. Environmental Protection Agency (USEPA). Beginning in 1984, the U.S. Army Construction Engineering Research Laboratories, in cooperation with the Air Force Engineering and Services Center, began research on ECAMP. Federal, Department of Defense (DOD), and Air Force environmental regulations, along with documentation of good management practices and risk-management information, were integrated into a series of checklists that show (1) legal requirements, and (2) specify items or operations to review. Assessment protocols list a point of contact to help assessors review the checklists as effectively as possible. The Worldwide ECAMP incorporates existing USEPA and private industry checklists, and integrates the DOD Overseas Environmental Baseline Guidance Document (OEBGD), published in October 1992. Additionally, Worldwide ECAMP includes pertinent information from Air Force Regulations, DOD Directives and Instructions, and cited good management practices for overall environmental review. The EEC manual supplements Worldwide ECAMP with existing EEC directives, regulations, and decisions and suggested management practices. The program was tested at Aviano Air Force Bass (AFB), Italy in November 1992 and Soesterberg AFB, Netherlands in June 1993. DTIC

N94-28774# Army Construction Engineering Research Lab., Champaign, IL.
ENVIRONMENTAL REVIEW GUIDE FOR OPERATIONS (ERGO) Final Report
Donna J. Schell and Tina M. Beckler Apr. 1993 810 p
(AD-A275611; CERL-SR-EC-93/10) Avail: CASI HC A99/MF A10

In response to the growing number of environmental laws and regulations worldwide, the Corps of Engineers adopted an environmental compliance program that identifies compliance problems before they are cited as violations by the U.S. Environmental Protection Agency (USEPA). Beginning in 1989, the U.S. Army Construction Engineering Research Laboratories, in cooperation with a Steering Committee representing the Corps of Engineers, began research on ERGO. The concept was to combine Code of Federal Regulations (CFR's) and Engineering Regulations, along with good management practices and risk-management information, into a series of checklists that show (1) legal requirements and (2) which specific items or operations to review. Each assessment protocol lists a point of contact to help assessors review the checklists as effectively as possible. The ERGO manual incorporates CFR's and Engineering Regulations as well as suggested management practices. The manual was tested at Nashville, Tennessee in 1990. After this evaluation, the first ERGO manual was printed and distributed to the environmental coordinators at Army Corps of Engineers' Facilities located in the United States. Since this initial printing, the ERGO manual has been updated and revised annually. The manual is continually updated to address new environmental compliance laws and regulations. DTIC

N94-28844# Air Force Inst. of Tech., Wright-Patterson AFB, OH.
THE EUROPEAN COMMUNITY DIRECTIVE: AN ALTERNATIVE ENVIRONMENTAL IMPACT ASSESSMENT PROCEDURE AFTER MASSEY? M.S. Thesis
Paul D. McHugh 30 Sep. 1993 100 p
(AD-A275550) Avail: CASI HC A05/MF A02

The similarities and differences between the 'father' of environmental impact assessment (EIA) legislation, the United States' National Environmental Policy Act (NEPA), and one of its important progeny, the 1985 European Community directive requiring member nations to assess the environmental effects of major projects, both private and public, are examined. Both NEPA's and the EC directive's policies and objectives are discussed. The background and procedures of the regulations implementing environmental impact assessment requirements, and opportunities for public participation, are examined. A discussion of the international problems associated with their application is presented. CASI

N94-29023# Aerospace Corp., El Segundo, CA. Technology Operations.
SYSTEM REQUIREMENTS REVIEW FOR THE HIGH-RESOLUTION OZONE IMAGER (HIROIG) Technical Report
D. L. McKenzie, D. J. Gutierrez, J. H. Hecht, D. J. Mabry, and M. N. Ross 15 Sep. 1993 80 p
(Contract F04701-88-C-0089)
(AD-A275151; TR-93(3231)-2; SMC-TR-93-62) Avail: CASI HC A05/MF A01

The HIROIG System Requirements Review was held on 17 Feb. 1993 at The Aerospace Corporation. The purpose of the review was to demonstrate the way in which the requirements for a spaceborne ozone imaging experiment are derived from the fundamental goal of the program, which is to measure how space-vehicle launches affect the ozone layer of the atmosphere. The review included, towards the end, short presentations on the experiment team's approaches to meeting the program requirements. This report is a compilation of the briefing charts that were presented at the review. DTIC

N94-29099*# Bionetics Corp., Cocoa Beach, FL.
DEVELOPMENT AND IMPLEMENTATION OF A SCRUB HABITAT COMPENSATION PLAN FOR KENNEDY SPACE CENTER
Paul A. Schmalzer, David R. Breininger, Frederic W. Adrian, Ron Schaub, and Brean W. Duncan Jan. 1994 55 p
(Contract NAS10-11624)
(NASA-TM-109202; NAS 1.15:109202) Avail: CASI HC A04/MF A01

Kennedy Space Center (KSC), located on Merritt Island on the east coast of central Florida, is one of three remaining major populations of the Florida Scrub Jay (Aphelocoma coerulescens coerulescens), listed as threatened by the U.S. Fish and Wildlife Service (USFWS) since 1987. Construction of new facilities by the National Aeronautics and Space Administration (NASA) on KSC over the next five years has the potential to impact up to 193 ac (78.1 ha) of Scrub Jay habitat. Under an early consultation process with the Endangered Species Office of the USFWS, NASA agreed to a compensation plan for loss of Scrub Jay habitat. The compensation plan required NASA to restore or create scrub on KSC at a 2:1 ratio for that lost. The compensation plan emphasized restoration of scrub habitat that is of marginal or declining suitability to Scrub Jays because it has remained unburned. Although prescribed burning has been conducted by the USFWS Merritt Island National Wildlife Refuge (MINWR) for more than ten years, significant areas of scrub remain unburned because they have been excluded from fire management units or because landscape fragmentation and a period of fire suppression allowed scrub to reach heights and diameters that are fire resistant. For such areas, mechanical cutting followed by prescribed burning was recommended for restoration. A second part of the restoration plan is an experimental study of scrub reestablishment (i.e., creation) on abandoned, well drained agricultural sites by planting scrub oaks and other scrub plants. The compensation plan identified 260 ac (105 ha) of scrub restoration in four areas and a 40 ac (16 ha) scrub creation site. Monitoring of restoration sites required under the plan included: establishing permanent vegetation sample transects before treatment and resampling annually for ten years after treatment, and color banding Scrub Jays to determine territories prior to treatment followed by monitoring reproductive success and survival for ten years after treatment. Monitoring scrub creation sites included determining survival of planted material for five years and establishing permanent transects to follow vegetation development for ten years after planting. Scrub Jay monitoring of creation sites is incorporated with that of adjacent restoration sites. Author

N94-29158 National Defence Research Establishment, Umea (Sweden). ABC Research Dept.
CAESIUM-137 IN A BOREAL FOREST ECOSYSTEM: ASPECTS ON THE LONG-TERM BEHAVIOR
R. Bergman, T. Nylen, P. Nelin, and T. Palo Nov. 1993 30 p Limited Reproducibility: More than 20% of this document may be affected by microfiche quality
(ISSN 0347-2124)
(PB94-137809; FOA-C-40284-4.3) Avail: Issuing Activity (National Technical Information Service (NTIS))

Cycling of radioactive cesium, particularly the isotope Cs-137, is studied in boreal forest biotopes mainly located at the Vindeln experimental forest, 60 km NW of Umea, Sweden. The distribution of radioactive cesium in this forest ecosystem, prior to and in different periods after the Chernobyl accident, reflects the existence of fast changes particularly at an early stage after the deposition, superimposed on slow redistribution over long time periods. The definite causes to this complex dynamic behavior are not yet unambigously established. In the work, the authors use the specific results from local field studies as a basis to describe the general pattern and time dependence of Cs-137 redistribution in a boreal forest. NTIS

N94-29192# Acurex Corp., Research Triangle Park, NC.
CHARACTERIZATION OF AIR EMISSIONS FROM THE SIMULATED OPEN COMBUSTION OF FIBERGLASS MATERIALS Final Report, 1 Jan. - Aug. 1993
C. C. Lutes and J. V. Ryan Dec. 1993 99 p See also PB91-227967 and PB92-115286
(Contract EPA-68-DO-0141)
(PB94-136231; EPA/600/R-93/239) Avail: CASI HC A05/MF A02

The exposure of persons to fiberglass combustion emissions from structural fires, fires at waste landfills, and fires at demolition sites has become an issue of increasing concern. The study identifies and quantifies a broad range of pollutants that are discharged during small-scale, simulated, open combustion of fiberglass and reports these emissions relative to the mass of fiberglass material combusted. Two types of fiberglass materials (representing the boating and building materials industries) were combusted in a controlled outbuilding designed to simulate open burning. Volatile, semivolatile, and particulate-bound organics were collected and analyzed by gas chromatography/mass spectrometry (GC/MS). NTIS

N94-29452# European Space Agency, Paris (France).
GOME: GLOBAL OZONE MONITORING EXPERIMENT Interim Science Report
T. D. Guyenne, ed. and C. Readings, ed. Sep. 1993 57 p Original contains color illustrations
(ESA-SP-1151; ISBN-92-9092-041-6; ETN-94-95458) Avail: CASI HC A04/MF A01

A review of the scientifc objectives and capabilities of the Global Ozone Monitoring Experiment (GOME), to be carried on the payload of the ERS-2 satellite, to monitor absorption by trace gases in the solar spectrum, is presented. Its actual capabilities are also assessed and some of the calculations underlying the assessment are contained in the annexes. Topics such as calibration and data processing are considered and other experiments (intended to study the chemical composition of the atmosphere) which are planned to fly before the end of the century, are reviewed. This serves to set the GOME into the overall context of atmospheric chemistry studies. ESA

N94-29549*# Aerodyne Research, Inc., Billerica, MA. Center for Chemical and Environmental Physics.
LABORATORY STUDIES OF CHEMICAL AND PHOTOCHEMICAL PROCESSES RELEVANT TO STRATOSPHERIC OZONE Annual Report No. 2, May 1993 - Apr. 1994
Mark S. Zahniser, David D. Nelson, Douglas R. Worsnop, and Charles E. Kolb Apr. 1994 15 p
(Contract NAS5-31847)
(NASA-CR-195779; NAS 1.26:195779; ARI-RR-1072) Avail: CASI HC A03/MF A01

The purpose of this project is to reduce the uncertainty in several key gas-phase kinetic processes which impact our understanding of stratospheric ozone. The main emphasis of this work is on measuring rate coefficients and product channels for reactions of HO(sub x) and NO(sub x) species in the temperature range 200 K to 240 K relevant to the lower stratosphere. Other areas of study have included infrared spectroscopic studies of the HO2 radical, measurements of OH radical reactions with alternative fluorocarbons, and determination of the vapor pressures of nitric acid hydrates under stratospheric conditions. The results of these studies will improve models of stratospheric ozone chemistry and predictions of perturbations due to human influences. In this annual report, we focus on our recent accomplishments in the quantitative spectroscopy of the HO2 radical. This report details the measurements of the broadening coefficients for the v(sub 2) vibrational band. Further measurements of the vapor pressures of nitric acid hydrates relevant to the polar stratospheric cloud formation indicate the importance of metastable crystalline phases of H2SO4, HNO3, and H2O. Large particles produced from these metastable phases may provide a removal mechanism for HNO3 in the polar stratosphere.
Author (revised)

N94-29749 Maryland Univ., College Park.
GCM STUDIES OF THE INFLUENCE OF VEGETATION ON THE GENERAL CIRCULATION: THE ROLE OF ALBEDO IN MODULATING CLIMATE CHANGE Ph.D. Thesis
Paul Alan Dirmeyer 1992 242 p
Avail: Univ. Microfilms Order No. DA9315631

An atmospheric general circulation model (GCM) coupled to a simple biosphere model is used to examine the role of vegetation change on climate. Various biomes are substituted to simulate degradation of vegetation. It is found that albedo change plays a distinct role in the local decrease of rainfall. Changes in vegetation morphology and physiology do not cause catastrophic decreases in precipitation. Simulations of Amazon deforestation show that the climatic response is very dependent on the amount of change in albedo between rain forest and degraded grass. Precipitation drops as albedo increases. The change in plant physiology decreases evapotranspiration, but moisture convergence increases to offset the drying. This compensation is a result of cloud feedback in this model, and does not occur when cloudiness is prescribed. Experiments with idealized boundary conditions show a similar dependence of rainfall on albedo in cases of tropical deforestation, subtropical desertification, and mid-latitude deforestation. In the tropics, rainfall decreases over land only when reflectivity is increased, even when the rain forest is left intact. The monsoon precipitation of the subtropical experiment fails when savannah is replaced by high-albedo desert. When low-albedo desert is used, the decrease in summer rainfall is small. When mid-latitude forest is replaced by grassland, precipitation patterns shift, but net rainfall remains unchanged. Additional simulations of mid-latitude drought show that low soil moisture leads to moderate spring and summer droughts, but dry soil combined with dormant vegetation produces extremely severe droughts. Soil moisture deficits were more persistent when vegetation did not go dormant. Dissert. Abstr.

N94-29750 California Univ., Davis.
OPTICAL MODELING OF VISIBILITY AND VISIBILITY INSTRUMENTATION USING STRATIFIED MIE THEORY Ph.D. Thesis
Ronald Robert Rickards 1992 255 p
Avail: Univ. Microfilms Order No. DA9313523

A new method of matching stratified Mie theory to size-time-composition resolved impactor data is developed and applied to rural data. The new model is free of theoretical systematic errors which exist in the standard approach and also includes the effect of relative humidity in an alternate and improved format. A physical description based on the volume Mie coefficients is emphasized and a corresponding lognormal parameterization scheme is introduced. Both theoretical and experimental results indicate that aerosols in D(sub p) less than 2.5 micron dichotomous sampling protocols are not adequate to predict visible or ultraviolet extinction. Further, to the extent that size shifts occur within the accumulation mode, the experimental results also indicate a limited correlation between those aerosols responsible for visibility reduction and those that extinguish ultraviolet. Hence, in order to better understand and monitor the effect of anthropogenic aerosols on atmospheric visibility and ground level ultraviolet fluxes, we must routinely combine impactor data sets in discrete highly resolved size ranges with stratified Mie theory. In addition, highly instructional computer-generated three dimensional surface plots are presented which convey the global theoretical characteristics of the Mie parameters, including extensions well into the strong absorption region. Dissert. Abstr.

N94-29800 Princeton Univ., NJ.
SENSITIVITY AND FEEDBACKS ASSOCIATED WITH VEGETATION-RELATED LAND SURFACE PARAMETERS IN A GENERAL CIRCULATION MODEL Ph.D. Thesis
Brent Melvin Lofgren 1993 214 p
Avail: Univ. Microfilms Order No. DA9316092

A series of general circulation model (GCM) experiments were run to investigate the effects on climate of surface albedo, surface roughness, and field capacity. When decreased surface albedo is prescribed, at low latitudes, precipitation and soil moisture are increased, because of the increased upward motion resulting from additional atmospheric heating. At midlatitudes, the precipitation is insensitive to decreased surface albedo, but soil moisture is decreased. A prescribed decrease in land surface roughness causes a general decrease in evaporation from land and water vapor flux convergence over land, and consequently also in precipitation. In particular, precipitation is reduced along coasts with shoreward winds, where decreased surface roughness results in decreased low-level convergence. In another experiment, land surface albedo was interactive with the GCM climate, using the climate to determine the vegetative cover. When compared to a control case with constant surface albedo over all land, tropical rain forests have increased precipitation and soil moisture. This promotes more growth of vegetation, causing positive feedback within the system. Subtropical deserts have decreased precipitation and soil moisture, again a positive feedback, and there is evidence of a southward shift in the Sahara. Midlatitudes again have little response in precipitation, but have soil moisture responses which imply negative feedback. When surface roughness is interactively predicted, low-latitude forests have increased precipitation, primarily along coasts where there are shoreward winds. This leads to increased vegetation and greater surface roughness, making it a positive feedback. At midlatitudes, particularly in eastern North America, the roughness of the forests causes enhanced Ekman convergence, resulting in increased precipitation. This is also a positive feedback. Interactive field capacity was found to have little or no systematic effect. With its inclusion, neither the pattern of changes in precipitation nor of changes in soil moisture as a fraction of field capacity is clearly correlated to the distribution of initially predicted field capacity. When all three parameters are made interactive simultaneously, the precipitation and soil moisture responses are found to be approximately the sum of the responses to individual parameters, except where more than one parameter produced a large response. Dissert. Abstr.

N94-29901 Miami Univ., Coral Gables, FL.
ANALYSIS AND MODELING OF ENVIRONMENTAL AND ECONOMIC IMPACTS OF THE SOLAR HYDROGEN ENERGY SYSTEM Ph.D. Thesis
Frano Barbir 1992 189 p
Avail: Univ. Microfilms Order No. DA9314507

The solar hydrogen energy system has been designed as a replacement of the present energy system based mainly on fossil fuels. Such a system has been found to be technically feasible. A method for analysis of environmental damage and estimation of associated external costs of fossil fuels has been developed. The analysis indicates that the solar hydrogen energy system might provide the same energy services as fossil fuels, but at lower societal costs, if the costs of environmental damage are taken into account. An analysis of the solar hydrogen energy system and its components has found no insurmountable physical obstacles for its introduction. A model of global energy / environment / economy interactions has been developed using energy circuit language to study the transition to the solar hydrogen energy system. The results of the model simulation indicate that timely transition might benefit the economy and the environment. The solar hydrogen energy system would stop carbon dioxide build up in the atmosphere and might provide energy for human civilization practically forever. Dissert. Abstr.

N94-29926# Pennsylvania State Univ., University Park.
BRIEF SUMMARY OF ACCOMPLISHMENTS SINCE OUR DOE-SPONSORED RADON PROJECT COMMENCED
1993 16 p

(Contract DE-FG02-88ER-60668)
(DE94-004643; DOE/ER-60668/7) Avail: CASI HC A03/MF A01

We have focused on determining the thermomechanical and kinetic properties that are involved in the interactions of common atmospheric molecules and indoor pollutants. In view of the fact that a large fraction of the progeny ions are thought to be in the singly charged state, we have directed our attention to the evolving chemistry of these species. Emphasis has been placed on acquiring fundamental thermochemical information which will provide a basis for modeling studies. The studies are requisite in obtaining a more complete picture of growth, attachment to aerosols, and ultimately transport to the bioreceptor. DOE

N94-29932# Allied-Signal Aerospace Co., Kansas City, MO.
PRACTICAL APPLICATIONS OF PLASMA SURFACE MODIFICATION
M. D. Smith Dec. 1993 17 p Presented at the International Symposium on Polymer Surface Modification: Relevance to Adhesion, Las Vegas, NV, 3-5 Nov. 1993
(Contract DE-AC04-76DP-00613)
(DE94-004892; KCP-613-5331; CONF-9311164-1) Avail: CASI HC A03/MF A01

Radio frequency activated gas plasma is an environmentally conscious manufacturing process which provides surface treatments for improved product quality. Plasma processing offers significant potential for reducing the use of solvents and other wet processing chemicals now used in surface treatments such as cleaning, activation for bonding, and moisture removal. Plasma treatments are generally accomplished without creating hazardous waste streams to dispose of. Plasma process development and application are ongoing at Allied Signal Inc., Kansas City Division. DOE

N94-29954# Lawrence Livermore National Lab., CA.
IMPACT OF BIOMASS BURNING ON THE ATMOSPHERE
J. Dignon Mar. 1993 16 p Presented at the North Atlantic Treaty Organization (NATO) Advanced Research Workshop on Ice Core Studies of Global Biogeochemical Cycles, Annecy, France, 26-31 Mar. 1993
(Contract W-7405-eng-48)
(DE94-004333; UCRL-JC-115082; CONF-9303250-1) Avail: CASI HC A03/MF A01

Fire has played an important part in biogeochemical cycling throughout most of the history of our planet. Ice core studies have been very beneficial in paleoclimate studies and constraining the budgets of biogeochemical cycles through the past 160,000 years of the Vostok ice core. Although to date there has been no way of determining cause and effect, concentration of greenhouse gases directly correlates with temperature in ice core analyses. Recent ice core studies on Greenland have shown that significant climate change can be very rapid on the order of a decade. This chapter addresses the coupled evolution of our planet's atmospheric composition and biomass burning. Special attention is paid to the chemical and climatic impacts of biomass burning on the atmosphere throughout the last century, specifically looking at the cycles of carbon, nitrogen, and sulfur. Information from ice core measurements may be useful in understanding the history of fire and its historic affect on the composition of the atmosphere and climate. DOE

N94-30023 Argonne National Lab., IL.
THE SUITABILITY OF LOW-COST URBAN AIRSHED MODELING IN THE CHICAGO AREA
M. E. Fernau, W. J. Makofske, and D. W. South 1994 4 p Presented at the 74th American Meteorological Society Annual Meeting, Nashville, TN, 23-28 Jan. 1994 Limited Reproducibility: More than 20% of this document may be affected by microfiche quality
(Contract W-31-109-eng-38)
(DE94-005114; ANL/DIS/CP-81382; CONF-940115-21) Avail: CASI HC A01

The interesting composition of the utility mix in the Chicago region and the potential for electric vehicle use in that area make it an interesting candidate for emissions sensitivity and scenario studies. However, it is difficult to apply the Urban Airshed Model (UAM) to the Chicago region because of the complex meteorology associated with Lake Michigan. The Lake Michigan Air Directors consortium (LADCO) has developed, at considerable expense, an improved version with nested grids and embedded plumes (UAM-V) for application in the Lake Michigan Ozone Study (LMOS) and for regulatory use. The complexity of the LMOS modeling system makes it costly and time-consuming to implement. In this study, the authors apply UAM-4 in its simple 'PLANR (Practice for Low-cost Application in Nonattainment Regions)' mode to the Chicago region to study various interesting scenarios in a rapid and low-cost manner. The details of the data sets, methods, and results of this study are summarized here. In addition, the authors comment on the usefulness of this type of limited-data study as compared to more complex modeling systems and data inputs. DOE

N94-30044# Lawrence Livermore National Lab., CA.
INTERMEDIA TRANSFER FACTORS FOR FIFTEEN TOXIC POLLUTANTS RELEASED TO AIR BASINS IN CALIFORNIA
T. E. McKone, J. I. Daniels, F. F. Chiao, and D. P. H. Hsieh Oct. 1993 247 p
(Contract W-7405-eng-48)
(DE94-005699; UCRL-CR-115620) Avail: CASI HC A11/MF A03

This report provides a summary definition of the intermedia-transfer factors (ITF's). Methods are discussed for estimating these parameters in the absence of measured values, and the estimation errors inherent in these estimation methods are considered. A detailed summary is provided of measured and estimated ITF values for fifteen air contaminants. They include: 1,3 butadiene; cadmium; cellosolve; cellosolve acetate; chloroform; di-2-ethylhexylphthalate; 1,4-dioxame; hexachlorobenzene; inorganic arsenic; inorganic lead; nickel; tetrachloroethylene; toluene; toluene-2,4-diisocyanate; and 1,3-xylene. Recommendations are made regarding the expected value and variance in these values for use in exposure models. DOE

N94-30046# Pennsylvania State Univ., University Park. Environmental Resources Research Inst.
A COUPLED APPROACH TO SPATIALLY DERIVED PARAMETERS NECESSARY FOR ECOSYSTEM MODELING ON THE NORTH SLOPE OF ALASKA: APPENDIX A
G. W. Petersen, R. L. Day, and J. Pollack Dec. 1993 44 p
(Contract DE-FG02-89ER-60760)
(DE94-005853; DOE/ER-60760/5-App-A) Avail: CASI HC A03/MF A01

This study concerned an investigation of ecosystem dynamics in several small study sites in the North Slope region of Alaska. The scope of the proposed research is to quantitatively determine spatial interrelationships between landform geometry within these study areas and such ecologically important factors as vegetation type, depth-to-permafrost, hydraulic conductivity and incoming solar radiation. Extrapolation techniques developed and terrain-related data generated as a result of this research will augment R4D Phase 2 goals which relate to running the General Arctic Simulac (GAS) model (and associated ecosystem models) at different locations on the North Slope. In particular, Penn State has contributed significantly to extrapolation efforts by developing techniques which can be used to initialize conditions for model input either through direct measurement (e.g., slope and aspect) and GIS-based simulation models (e.g., drainage basin characterization). As stated in the R4D Phase 2 Research Plan, the long-term objectives of this program are: (1) to determine effects and to develop models based on ecosystem disturbances commonly created by energy development so that appropriate, cost-effective measures can be utilized to minimize deleterious disturbances; and (2) to extend the results to other arctic and alpine areas which are important because of likely impact from energy development. It is this second long-term objective which relates most directly to Penn State's work. DOE

N94-30047# SRI International Corp., Menlo Park, CA.
NOVEL MASS SPECTROMETRIC INSTRUMENT FOR GASEOUS AND PARTICULATE CHARACTERIZATION AND MONITORING
M. J. Coggiola Jul. 1993 17 p
(Contract DE-AC21-92MC-29116)
(DE94-005896; DOE/MC-29116/3575) Avail: CASI HC A03/MF A01

A mass spectrometric (MS) instrument is being developed for real-time (less than 1 min) analysis of gaseous and particulate pollutants from DOE waste cleanup activities. The pollutants will include volatile organic compounds, PAHs, heavy metals, and transuranics. Design has been completed for the sampler and its vacuum interface with ion trap detectors and fabrication started. Design, fabrication, and testing of pyrolysis filament for particulate analysis is under way. DOE

N94-30116 Argonne National Lab., IL. Mathematics and Computer Science Div.

PCCM2: A GCM ADAPTED FOR SCALABLE PARALLEL COMPUTERS

J. Drake, B. D. Semeraro, P. Worley, I. Foster, J. Michalakes, B. Toonen, J. J. Hack, and D. L. Williamson 1994 8 p Presented at the 5th Annual Symposium on Global Change Studies, Nashville, TN, 24-28 Jan. 1994 Limited Reproducibility: More than 20% of this document may be affected by microfiche quality

(Contract W-31-109-eng-38)

(DE94-005113; ANL/MCS/CP-81098; CONF-940131-3) Avail: Issuing Activity (Department of Energy (DOE))

The Computer Hardware, Advanced Mathematics, and Model Physics (CHAMMP) program seeks to provide climate researchers with an advanced modeling capability for the study of global change issues. One of the more ambitious projects being undertaken in the CHAMMP program is the development of PCCM2, an adaptation of the Community Climate Model (CCM2) for scalable parallel computers. PCCM2 uses a message-passing, domain-decomposition approach, in which each processor is allocated responsibility for computation on one part of the computational grid, and messages are generated to communicate data between processors. Much of the research effort associated with development of a parallel code of this sort is concerned with identifying efficient decomposition and communication strategies. In PCCM2, this task is complicated by the need to support both semi-Lagrangian transport and spectral transport. Load balancing and parallel I/O techniques are also required. In this paper, the authors review the various parallel algorithms used in PCCM2 and the work done to arrive at a validated model. DOE

N94-30613# Lawrence Livermore National Lab., CA.

RADIATIVE FLUX CALCULATIONS AT UV AND VISIBLE WAVELENGTHS

A. S. Grossman, K. E. Grant, and D. J. Wuebbles Oct. 1993 7 p

(Contract W-7405-eng-48)

(DE94-004278; UCRL-ID-115336) Avail: CASI HC A02/MF A01

A radiative transfer model to calculate the short wavelength fluxes at altitudes between 0 and 80 km was developed at LLNL. The wavelength range extends from 175-735 nm. This spectral range covers the UV-B wavelength region, 250-350 nm, with sufficient resolution to allow comparison of UV-B measurements with theoretical predictions. Validation studies for the model were made for both UV-B ground radiation calculations and tropospheric solar radiative forcing calculations for various ozone distributions. These studies indicate that the model produces results which agree well with respect to existing UV calculations from other published models. DOE

N94-30616*# University Corp. for Atmospheric Research, Boulder, CO. Office for Interdisciplinary Earth Studies.

MODELING THE EARTH SYSTEM, VOLUME 3

Dennis Ojima, ed. 1992 485 p The Third Global Change Inst. on Earth System Modeling was held in Snowmass, CO, 16-27 Jul. 1990 Sponsored by NASA, Washington; DOE; EPA; Geological Survey; NOAA; and NSF

(NASA-CR-194256; NAS 1.26:194256) Avail: CASI HC A21/MF A04

The topics covered fall under the following headings: critical gaps in the Earth system conceptual framework; development needs for simplified models; and validating Earth system models and their subcomponents. For individual titles, see N94-30617 through N94-30638.

N94-30617*# Massachusetts Inst. of Tech., Cambridge. Dept. of Earth, Atmospheric and Planetary Sciences.

ATMOSPHERE, OCEAN, AND LAND: CRITICAL GAPS IN EARTH SYSTEM MODELS

Ronald G. Prinn and Dana Hartley *In* University Corp. for Atmospheric Research, Modeling the Earth System, Volume 3 1992 p 9-38 Sponsored in part by NSF (For primary document see N94-30616 08-45)

Avail: CASI HC A03/MF A04

We briefly review current knowledge and pinpoint some of the major areas of uncertainty for the following fundamental processes: (1) convection, condensation nuclei, and cloud formation; (2) oceanic circulation and its coupling to the atmosphere and cryosphere; (3) land surface hydrology and hydrology-vegetation coupling; (4) biogeochemistry of greenhouse gases; and (5) upper atmospheric chemistry and circulation. Derived from text

N94-30618*# Commonwealth Scientific and Industrial Research Organization, Hobart (Australia). Div. of Oceanography.

TOWARDS COUPLED PHYSICAL-BIOGEOCHEMICAL MODELS OF THE OCEAN CARBON CYCLE

Stephen R. Rintoul *In* University Corp. for Atmospheric Research, Modeling the Earth System, Volume 3 1992 p 39-75 Prepared in cooperation with Princeton Univ., NJ (For primary document see N94-30616 08-45)

Avail: CASI HC A03/MF A04

The purpose of this review is to discuss the critical gaps in our knowledge of ocean dynamics and biogeochemical cycles. It is assumed that the ultimate goal is the design of a model of the earth system that can predict the response to changes in the external forces driving climate.

Derived from text

N94-30619*# Lamont-Doherty Geological Observatory, Palisades, NY.

DYNAMIC CONSTRAINTS ON CO2 UPTAKE BY AN IRON-FERTILIZED ANTARCTIC

Tsung-Hung Peng, Wallace S. Broecker, and H. G. Oestlund *In* University Corp. for Atmospheric Research, Modeling the Earth System, Volume 3 1992 p 77-105 Sponsored in part by Exxon Corp. (For primary document see N94-30616 08-45)

(Contract DE-AC05-84OR-21400)

Avail: CASI HC A03/MF A04

The topics covered include the following: tracer distribution and dynamics in the Antarctic Ocean; a model of Antarctic and Non-Antarctic Oceans; effects on an anthropogenically affected atmosphere; effects of seasonal iron fertilization; and implications of the South Atlantic Ventilation Experiment C-14 results. CASI

N94-30620*# Dartmouth Coll., Hanover, NH. School of Engineering.

THE ROLE OF SEA ICE DYNAMICS IN GLOBAL CLIMATE CHANGE

William D. Hibler, III *In* University Corp. for Atmospheric Research, Modeling the Earth System, Volume 3 1992 p 107-130 (For primary document see N94-30616 08-45)

Avail: CASI HC A03/MF A04

The topics covered include the following: general characteristics of sea ice drift; sea ice rheology; ice thickness distribution; sea ice thermodynamic models; equilibrium thermodynamic models; effect of internal brine pockets and snow cover; model simulations of Arctic Sea ice; and sensitivity of sea ice models to climate change. CASI

N94-30621*# Arizona Univ., Tucson. Inst. for Atmospheric Physics.

LAND SURFACE INTERACTION

Robert E. Dickinson *In* University Corp. for Atmospheric Research, Modeling the Earth System, Volume 3 1992 p 131-150 Sponsored by NSF (For primary document see N94-30616 08-45)

Avail: CASI HC A03/MF A04

The topics covered include the following: land and climate modeling; sensitivity studies; the process of a land model; model-specific parameterizations; water stress; within-canopy resistances; partial vegetation; canopy temperature; and present experience with a land model coupled to a general circulation model. CASI

N94-30622*# National Aeronautics and Space Administration. Goddard Inst. for Space Studies, New York, NY.

THE CARBON CYCLE REVISITED

Bert Bolin and Inez Fung *In* University Corp. for Atmospheric Research, Modeling the Earth System, Volume 3 1992 p 151-164 (For primary document see N94-30616 08-45)

Avail: CASI HC A03/MF A04

Discussions during the Global Change Institute indicated a need to present, in some detail and as accurately as possible, our present knowledge about the carbon cycle, the uncertainties in this knowledge, and the reasons for these uncertainties. We discuss basic issues of internal consistency within the carbon cycle, and end by summarizing the key unknowns.

Derived from text

N94-30623*# Commonwealth Scientific and Industrial Research Organization, Hobart (Australia). Div. of Oceanography.

OCEAN-ATMOSPHERIC LINKAGES

Stephen R. Rintoul *In* University Corp. for Atmospheric Research, Modeling

the Earth System, Volume 3 1992 p 165-180 (For primary document see N94-30616 08-45)
Avail: CASI HC A03/MF A04

This chapter focuses on the role of the ocean in the global carbon cycle on the time scale of decades to centuries. The input rate of CO2 to the atmosphere due to fossil fuel burning and deforestation has continued to increase over the last century. To balance the global carbon budget, a sink is required whose magnitude is changing on similar time scales. We have sought to identify aspects of the ocean system that are capable of responding on decadal time scales, to examine our present ability to model such changes, and to pinpoint ways in which this ability could be improved. Many other important aspects of the ocean's role in global change are not addressed, including the importance of oceanic heat transport and thermal inertia to the climate system, biogeochemical cycling of elements other than carbon, and the importance of the ocean as a source or sink of trace gases. Derived from text

N94-30624*# National Aeronautics and Space Administration. Goddard Inst. for Space Studies, New York, NY.
LINKAGES BETWEEN TERRESTRIAL ECOSYSTEMS AND THE ATMOSPHERE
Francis Bretherton (Wisconsin Univ., Madison.), Robert E. Dickinson (Arizona Univ., Tucson.), Inez Fung, Berrien Moore, III, Michael Prather, Steven W. Running, and Holm Tiessen *In* University Corp. for Atmospheric Research, Modeling the Earth System, Volume 3 1992 p 181-196 (For primary document see N94-30616 08-45)
Avail: CASI HC A03/MF A04

The primary research issue in understanding the role of terrestrial ecosystems in global change is analyzing the coupling between processes with vastly differing rates of change, from photosynthesis to community change. Representing this coupling in models is the central challenge to modeling the terrestrial biosphere as part of the earth system. Terrestrial ecosystems participate in climate and in the biogeochemical cycles on several temporal scales. Some of the carbon fixed by photosynthesis is incorporated into plant tissue and is delayed from returning to the atmosphere until it is oxidized by decomposition or fire. This slower (i.e., days to months) carbon loop through the terrestrial component of the carbon cycle, which is matched by cycles of nutrients required by plants and decomposers, affects the increasing trend in atmospheric CO2 concentration and imposes a seasonal cycle on that trend. Moreover, this cycle includes key controls over biogenic trace gas production. The structure of terrestrial ecosystems, which responds on even longer time scales (annual to century), is the integrated response to the biogeochemical and environmental constraints that develop over the intermediate time scale. The loop is closed back to the climate system since it is the structure of ecosystems, including species composition, that sets the terrestrial boundary condition in the climate system through modification of surface roughness, albedo, and, to a great extent, latent heat exchange. These separate temporal scales contain explicit feedback loops which may modify ecosystem dynamics and linkages between ecosystems and the atmosphere. The long-term change in climate, resulting from increased atmospheric concentrations of greenhouse gases (e.g., CO2, CH4, and nitrous oxide (N2O)) will further modify the global environment and potentially induce further ecosystem change. Modeling these interactions requires coupling successional models to biogeochemical models to physiological models that describe the exchange of water, energy, and biogenic trace gases between the vegetation and the atmosphere at fine time scales. There does not appear to be any obvious way to allow direct reciprocal coupling of atmospheric general circulation models (GCM's), which inherently run with fine time steps, to ecosystem or successional models, which have coarse temporal resolution, without the interposition of physiological canopy models. This is equally true for biogeochemical models of the exchange of carbon dioxide and trace gases. This coupling across time scales is nontrivial and sets the focus for the modeling strategy.
Derived from text

N94-30625*# New Hampshire Univ., Durham. Inst. for the Study of Earth, Oceans and Space.
FOUR SIMPLE OCEAN CARBON MODELS
Berrien Moore, III *In* University Corp. for Atmospheric Research, Modeling the Earth System, Volume 3 1992 p 197-223 (For primary document see N94-30616 08-45)
Avail: CASI HC A03/MF A04

This paper briefly reviews the key processes that determine oceanic CO2 uptake and sets this description within the context of four simple ocean carbon models. These models capture, in varying degrees, these key processes and establish a clear foundation for more realistic models that incorporate more directly the underlying physics and biology of the ocean rather than relying on simple parametric schemes. The purpose of this paper is more pedagogical than purely scientific. The problems encountered by current attempts to understand the global carbon cycle not only require our efforts but set a demand for a new generation of scientist, and it is hoped that this paper and the text in which it appears will help in this development. Derived from text

N94-30626*# Puget Sound Univ., Tacoma, WA. Dept. of Physics. **c48**
A TOY MODEL OF SEA ICE GROWTH
Alan S. Thorndike *In* University Corp. for Atmospheric Research, Modeling the Earth System, Volume 3 1992 p 225-238 (For primary document see N94-30616 08-45)
Avail: CASI HC A03/MF A04

My purpose here is to present a simplified treatment of the growth of sea ice. By ignoring many details, it is possible to obtain several results that help to clarify the ways in which the sea ice cover will respond to climate change. Three models are discussed. The first deals with the growth of sea ice during the cold season. The second describes the cycle of growth and melting for perennial ice. The third model extends the second to account for the possibility that the ice melts away entirely in the summer. In each case, the objective is to understand what physical processes are most important, what ice properties determine the ice behavior, and to which climate variables the system is most sensitive.
Derived from text

N94-30627*# National Aeronautics and Space Administration. Goddard Inst. for Space Studies, New York, NY.
A TOY MODEL FOR ESTIMATING N2O EMISSIONS FROM NATURAL SOILS
Inez Fung *In* University Corp. for Atmospheric Research, Modeling the Earth System, Volume 3 1992 p 239-262 (For primary document see N94-30616 08-45)
Avail: CASI HC A03/MF A04

A model of N2O emissions from natural soils, whose ultimate objective is to evaluate what contribution natural ecosystems make to the global N2O budget and how the contribution would change with global change, is presented. Topics covered include carbon and nitrogen available in the soil, delivery of nitrifiable N, soil water and oxygen status, soil water budget model, effects of drainage, nitrification and denitrification potentials, soil fertility, N2O production, and a model evaluation. A major implication of the toy model is that the tropics account for more than 80 percent of global emission. CASI

N94-30628*# Montana Univ., Missoula. School of Forestry.
A BOTTOM-UP EVOLUTION OF TERRESTRIAL ECOSYSTEM MODELING THEORY, AND IDEAS TOWARD GLOBAL VEGETATION MODELING
Steven W. Running *In* University Corp. for Atmospheric Research, Modeling the Earth System, Volume 3 1992 p 263-280 (For primary document see N94-30616 08-45)
(Contract NAS5-30920; NAGw-252; NSF BSR-88-17965)
Avail: CASI HC A03/MF A04

A primary purpose of this review is to convey lessons learned in the development of a forest ecosystem modeling approach, from it origins in 1973 as a single-tree water balance model to the current regional applications. The second intent is to use this accumulated experience to offer ideas of how terrestrial ecosystem modeling can be taken to the global scale: earth systems modeling. A logic is suggested where mechanistic ecosystem models are not themselves operated globally, but rather are used to 'calibrate' much simplified models, primarily driven by remote sensing, that could be implemented in a semiautomated way globally, and in principle could interface with atmospheric general circulation models (GCM's).
Derived from text

N94-30629*# Colorado State Univ., Fort Collins. Natural Resources Environmental Lab.

DEVELOPMENT OF SIMPLIFIED ECOSYSTEM MODELS FOR APPLICATIONS IN EARTH SYSTEM STUDIES: THE CENTURY EXPERIENCE

William J. Parton, Dennis S. Ojima, David S. Schimel, and Timothy G. F. Kittel *In* University Corp. for Atmospheric Research, Modeling the Earth System, Volume 3 1992 p 281-302 (For primary document see N94-30616 08-45)

Avail: CASI HC A03/MF A04

During the past decade, a growing need to conduct regional assessments of long-term trends of ecosystem behavior and the technology to meet this need have converged. The Century model is the product of research efforts initially intended to develop a general model of plant-soil ecosystem dynamics for the North American central grasslands. This model is now being used to simulate plant production, nutrient cycling, and soil organic matter dynamics for grassland, crop, forest, and shrub ecosystems in various regions of the world, including temperate and tropical ecosystems. This paper will focus on the philosophical approach used to develop the structure of Century. The steps included were model simplification, parameterization, and testing. In addition, the importance of acquiring regional data bases for model testing and the present regional application of Century in the Great Plains, which focus on regional ecosystem dynamics and the effect of altering environmental conditions, are discussed. Derived from text

N94-30630*# Colorado State Univ., Fort Collins. Natural Resources Environmental Lab.

A TOY TERRESTRIAL CARBON FLOW MODEL

William J. Parton, Steven W. Running, and Brian Walker *In* University Corp. for Atmospheric Research, Modeling the Earth System, Volume 3 1992 p 303-314 (For primary document see N94-30616 08-45)

Avail: CASI HC A03/MF A04

A generalized carbon flow model for the major terrestrial ecosystems of the world is reported. The model is a simplification of the Century model and the Forest-Biogeochemical model. Topics covered include plant production, decomposition and nutrient cycling, biomes, the utility of the carbon flow model for predicting carbon dynamics under global change, and possible applications to state-and-transition models and environmentally driven global vegetation models. CASI

N94-30631*# Stanford Univ., CA. Dept. of Biological Sciences.

CARBON CYCLING IN HIGH-LATITUDE ECOSYSTEMS

Alan Townsend, Stephen Frolking, and Elizabeth Holland *In* University Corp. for Atmospheric Research, Modeling the Earth System, Volume 3 1992 p 315-326 (For primary document see N94-30616 08-45)

Avail: CASI HC A03/MF A04

The carbon-rich soils and peatlands of high-latitude ecosystems could substantially influence atmospheric concentrations of CO2 and CH4 in a changing climate. Currently, cold, often waterlogged conditions retard decomposition, and release of carbon back to the atmosphere may be further slowed by physical protection of organic matter in permafrost. As a result, many northern ecosystems accumulate carbon over time (Billings et al., 1982; Poole and Miller, 1982), and although such rates of accumulation are low, thousands of years of development have left Arctic ecosystems with an extremely high soil carbon content; Schlesinger's (1984) average value of 20.4 kg C/m(sup 2) leads to a global estimate of 163 x 10(exp 15) g C. All GCM simulations of a doubled CO2 climate predict the greatest warming to occur in the polar regions (Dickinson, 1986; Mitchell, 1989). Given the extensive northern carbon pools and the strong sensitivity of decomposition processes to temperature, even a slight warming of the soil could dramatically alter the carbon balance of Arctic ecosystems. If warming accelerates rates of decomposition more than rates of primary production, a sizeable additional accumulation of CO2 in the atmosphere could occur. Furthermore, CH4 produced in anaerobic soils and peatlands of the Arctic already composes a good percentage of the global efflux (Cicerone and Oremlund, 1988); if northern soils become warmer and wetter as a whole, CH4 emissions could dramatically rise. A robust understanding of the primary controls of carbon fluxes in Arctic ecosystems is critical. As a framework for a systematic examination of these controls, we discussed a conceptual model of regional-scale Arctic carbon turnover, including CH4 production, and based upon the Century soil organic matter model. Derived from text

N94-30632*# Dartmouth Coll., Hanover, NH. School of Engineering.

CRYOSPHERE AND CLIMATE

William D. Hibler, III and Alan S. Thorndike *In* University Corp. for Atmospheric Research, Modeling the Earth System, Volume 3 1992 p 327-333 (For primary document see N94-30616 08-45)

Avail: CASI HC A02/MF A04

This chapter will discuss two main issues related to the cryosphere and climate. One is the effect of sea ice and salinity gradients on ocean circulation, and in particular the possible role of sea ice transport on the ocean conveyer belt. The other is the effect of the cryosphere on climate, and in particular in high-latitude warming under increased CO2. In understanding the role of the cryosphere in both cases, it is useful to elucidate two types of toy sea ice models. Neither of these represents reality, but both are useful for illustrating the archetypal features of sea ice that control much of its large-scale behavior. The first model is a simple slab thermodynamic sea ice model as presented by Thorndike. In this model there are no dynamical effects and the thickness of ice is determined by surface heat budget and oceanic heat flux considerations, with the thickness of the ice critically affecting the effective conductivity whereby heat is transferred from the bottom ice boundary to the upper ice boundary. In this model all of the sea ice characteristics are controlled by the vertical heat fluxes from the atmosphere and ocean into the ice. The thickness is controlled by the ice's becoming an effective insulator as it thickens, thus reducing conductive heat loss to the atmosphere. A second model emphasizes the effects of dynamics. It considers the ice pack to be a collection of floes moving in response to synoptic wind fields and ocean currents. These motions create semipermanent leads (open areas) over which ice can grow rapidly. Derived from text

N94-30633*# Weizmann Inst. of Science, Rehovoth (Israel). Dept. of Isotopes.

METHODS OF TESTING PARAMETERIZATIONS: VERTICAL OCEAN MIXING

Eli Tziperman *In* University Corp. for Atmospheric Research, Modeling the Earth System, Volume 3 1992 p 335-358 (For primary document see N94-30616 08-45)

Avail: CASI HC A03/MF A04

The ocean's velocity field is characterized by an exceptional variety of scales. While the small-scale oceanic turbulence responsible for the vertical mixing in the ocean is of scales a few centimeters and smaller, the oceanic general circulation is characterized by horizontal scales of thousands of kilometers. In oceanic general circulation models that are typically run today, the vertical structure of the ocean is represented by a few tens of discrete grid points. Such models cannot explicitly model the small-scale mixing processes, and must, therefore, find ways to parameterize them in terms of the larger-scale fields. Finding a parameterization that is both reliable and plausible to use in ocean models is not a simple task. Vertical mixing in the ocean is the combined result of many complex processes, and, in fact, mixing is one of the less known and less understood aspects of the oceanic circulation. In present models of the oceanic circulation, the many complex processes responsible for vertical mixing are often parameterized in an oversimplified manner. Yet, finding an adequate parameterization of vertical ocean mixing is crucial to the successful application of ocean models to climate studies. The results of general circulation models for quantities that are of particular interest to climate studies, such as the meridional heat flux carried by the ocean, are quite sensitive to the strength of the vertical mixing. We try to examine the difficulties in choosing an appropriate vertical mixing parameterization, and the methods that are available for validating different parameterizations by comparing model results to oceanographic data. First, some of the physical processes responsible for vertically mixing the ocean are briefly mentioned, and some possible approaches to the parameterization of these processes in oceanographic general circulation models are described in the following section. We then discuss the role of the vertical mixing in the physics of the large-scale ocean circulation, and examine methods of validating mixing parameterizations using large-scale ocean models. Derived from text

N94-30634*# Lawrence Livermore National Lab., CA.

THE CHALLENGE OF IDENTIFYING GREENHOUSE GAS-INDUCED CLIMATIC CHANGE

Michael C. MacCracken *In* University Corp. for Atmospheric Research, Modeling the Earth System, Volume 3 1992 p 359-376 (For primary

document see N94-30616 08-45)
(Contract W-7405-eng-48)
Avail: CASI HC A03/MF A04

Meeting the challenge of identifying greenhouse gas-induced climatic change involves three steps. First, observations of critical variables must be assembled, evaluated, and analyzed to determine that there has been a statistically significant change. Second, reliable theoretical (model) calculations must be conducted to provide a definitive set of changes for which to search. Third, a quantitative and statistically significant association must be made between the projected and observed changes to exclude the possibility that the changes are due to natural variability or other factors. This paper provides a qualitative overview of scientific progress in successfully fulfilling these three steps. Derived from text

N94-30635*# Wisconsin Univ., Madison. Center for Climatic Research.
MODELING EARTH SYSTEM CHANGES OF THE PAST
John E. Kutzbach *In* University Corp. for Atmospheric Research, Modeling the Earth System, Volume 3 1992 p 377-404 (For primary document see N94-30616 08-45)
Avail: CASI HC A03/MF A04

This review outlines some of the challenging problems to be faced in understanding the causes and mechanisms of large climatic changes and gives examples of initial studies of these problems with climate models. The review covers climatic changes in three main periods of earth history: (1) the past several centuries; (2) the past several glacial-interglacial cycles; and (3) the past several million years. The review will concentrate on studies of climate but, where possible, will mention broader aspects of the earth system. Author (revised)

N94-30636*# National Center for Atmospheric Research, Boulder, CO. Climate Systems Modeling Program.
MODELS OF ATMOSPHERE-ECOSYSTEM-HYDROLOGY INTERACTIONS: APPROACHES AND TESTING
David S. Schimel *In* University Corp. for Atmospheric Research, Modeling the Earth System, Volume 3 1992 p 405-421 (For primary document see N94-30616 08-45)
Avail: CASI HC A03/MF A04

Interactions among the atmosphere, terrestrial ecosystems, and the hydrological cycle have been the subject of investigation for many years, although most of the research has had a regional focus. The topic is broad, including the effects of climate and hydrology on vegetation, the effects of vegetation on hydrology, the effects of the hydrological cycle on the atmosphere, and interactions of the cycles via material flux such as solutes and trace gases. The intent of this paper is to identify areas of critical uncertainty, discuss modeling approaches to resolving those problems, and then propose techniques for testing. I consider several interactions specifically to illustrate the range of problems. These areas are as follows: (1) cloud parameterizations and the land surface, (2) soil moisture, and (3) the terrestrial carbon cycle. Author (revised)

N94-30637*# Georgia Univ., Athens. Dept. of Botany.
EVALUATING MODELS OF CLIMATE AND FOREST VEGETATION
James S. Clark *In* University Corp. for Atmospheric Research, Modeling the Earth System, Volume 3 1992 p 423-440 (For primary document see N94-30616 08-45)
Avail: CASI HC A03/MF A04

Understanding how the biosphere may respond to increasing trace gas concentrations in the atmosphere requires models that contain vegetation responses to regional climate. Most of the processes ecologists study in forests, including trophic interactions, nutrient cycling, and disturbance regimes, and vital components of the world economy, such as forest products and agriculture, will be influenced in potentially unexpected ways by changing climate. These vegetation changes affect climate in the following ways: changing C, N, and S pools; trace gases; albedo; and water balance. The complexity of the indirect interactions among variables that depend on climate, together with the range of different space/time scales that best describe these processes, make the problems of modeling and prediction enormously difficult. These problems of predicting vegetation response to climate warming and potential ways of testing model predictions are the subjects of this chapter. Author (revised)

N94-30638*# Carnegie Institution of Washington, Stanford, CA.
COMPREHENSIVE SYSTEM MODELS: STRATEGIES FOR EVALUATION
Christopher Field, John E. Kutzbach, V. Ramanathan, and Michael C. MacCracken *In* University Corp. for Atmospheric Research, Modeling the Earth System, Volume 3 1992 p 441-462 (For primary document see N94-30616 08-45)
Avail: CASI HC A03/MF A04

The task of evaluating comprehensive earth system models is vast involving validations of every model component at every scale of organization, as well as tests of all the individual linkages. Even the most detailed evaluation of each of the component processes and the individual links among them should not, however, engender confidence in the performance of the whole. The integrated earth system is so rich with complex feedback loops, often involving components of the atmosphere, oceans, biosphere, and cryosphere, that it is certain to exhibit emergent properties very difficult to predict from the perspective of a narrow focus on any individual component of the system. Therefore, a substantial share of the task of evaluating comprehensive earth system models must reside at the level of whole system evaluations. Since complete, integrated atmosphere/ ocean/ biosphere/ hydrology models are not yet operational, questions of evaluation must be addressed at the level of the kinds of earth system processes that the models should be competent to simulate, rather than at the level of specific performance criteria. Here, we have tried to identify examples of earth system processes that are difficult to simulate with existing models and that involve a rich enough suite of feedbacks that they are unlikely to be satisfactorily described by highly simplified or toy models. Our purpose is not to specify a checklist of evaluation criteria but to introduce characteristics of the earth system that may present useful opportunities for model testing and, of course, improvement. Author (revised)

N94-30715# Association of Energy Engineers, Atlanta, GA.
INTERNATIONAL ENERGY AND ENVIRONMENTAL CONGRESS: PROCEEDINGS
1993 266 p Presented at the International Energy and Environmental Congress, Minneapolis, MN, 4-5 Aug. 1993 Prepared in cooperation with Cogeneration and Competitive Power Inst., Demand-Side Management Society, and Environmental Engineers and Managers' Inst.
(DE93-040609; CONF-930895) Avail: CASI HC A12/MF A03

Symposiums of the 1993 proceedings included demand-side management strategic directions, federal energy management, corporate energy management, and pollution control technologies. DOE

N94-30729# Center for Mathematics and Computer Science, Amsterdam (Netherlands). Dept. of Numerical Mathematics.
AN EVALUATION OF EXPLICIT PSEUDO-STEADY-STATE APPROXIMATION SCHEMES FOR STIFF ODE SYSTEMS FROM CHEMICAL KINETICS
J. G. Verwer and M. vanLoon Jul. 1993 16 p Sponsored by Rijksinst. voor Volksgezondheit en Milieuhygieene
(ISSN 0169-0388)
(CWI-NM-R9312; ETN-94-95669) Copyright Avail: CASI HC A03/MF A01

A pseudo steady state approximation approach for solving chemical kinetics equations in reactive flows is discussed. For a set of three example problems from atmospheric chemistry a comparison is presented between an explicit pseudo steady state solver and the two implicit state of the art solvers RADAU5 and DASSL from the numerically stiff ODE (Ordinary Differential Equation) field. ESA

N94-30757# Department of Energy, Portland, OR. Bonneville Power Administration.
ELECTRIC POWER LINES: QUESTIONS AND ANSWERS ON RESEARCH INTO HEALTH EFFECTS
Nov. 1993 48 p
(DE94-005637; DOE/BP-2081) Avail: CASI HC A03/MF A01

Most people know that electric power lines, like the wiring in our homes, can cause serious electric shocks if we're not careful. Many people also want to know whether the electric and magnetic fields (EMF) produced by power lines and other electrical devices cause health effects. The purpose of this pamphlet is to answer some common questions that the Bonneville Power Administration (BPA) receives about the possible effects of power

lines on health. (BPA is the Pacific Northwest's Federal electric power marketing agency.) First, some basic electrical terms are defined, and electric and magnetic fields are described. Next, answers are given to several questions about recent scientific studies. We then describe how BPA is addressing public concerns raised by these studies. Some important information about electrical safety follows. The last section tells you how to obtain more detailed information about the health and safety issues summarized in this pamphlet. DOE

N94-30822# Lawrence Livermore National Lab., CA.
COMPLEX SOURCE RATE ESTIMATION FOR ATMOSPHERIC TRANSPORT AND DISPERSION MODELS
L. L. Edwards 13 Sep. 1993 34 p
(Contract W-7405-eng-48)
(DE94-000958; UCRL-ID-115264) Avail: CASI HC A03/MF A01

The accuracy associated with assessing the environmental consequences of an accidental atmospheric release of radioactivity is highly dependent on our knowledge of the source release rate. This paper reports on a technique that integrates the radiological measurements with atmospheric dispersion modeling for more accurate source term estimation. We construct a minimum least squares methodology for solving the inverse problem with no a priori information about the source rate. DOE

N94-29086# National Inst. of Polar Research, Tokyo (Japan).
PROTOCOL ON ENVIRONMENTAL PROTECTION TO THE ANTARCTIC TREATY AND ITS ANNEXES: INTERNATIONAL AGREEMENT ON THE COMPREHENSIVE MEASURES FOR THE PROTECTION OF ANTARCTIC ENVIRONMENT AND ECOSYSTEMS [NANKYOKU JOYAKU NI TAISURU KANKYO HOGO GITEISHO OYOBI SONO FUZOKUSHO NANKYOKU NO KANKYO TO SEITAIKEI NO HOGO NO TAMENO HOKATSUTEKI SOCHI NI KANSURU KOKUSAI GOI]
Yoshio Yoshida *In its* Antarctic Record, Volume 36, No. 1 30 Mar. 1992 p 116-161 In ENGLISH and JAPANESE (For primary document see N94-29078 08-46)
Avail: CASI HC A03/MF A02

N94-29247# Deutsche Forschungsanstalt fuer Luft- und Raumfahrt, Oberpfaffenhofen (Germany). Inst. fuer Physik der Atmosphaere.
ON THE EFFECT OF EMISSIONS FROM AIRCRAFT ENGINES ON THE STATE OF THE ATMOSPHERE
U. Schumann *In* AGARD, Fuels and Combustion Technology for Advanced Aircraft Engines Sep. 1993 19 p Sponsored by DFG; BMFT; and Commision of the European Communities (For primary document see N94-29246 08-25)
Copyright Avail: CASI HC A03/MF A04

N94-29522# National Inst. for Resources and Environment, Ibaraki (Japan).
SECOND JAPAN-U.S. WORKSHOP ON GLOBAL CHANGE: ENVIRONMENTAL RESPONSE TECHNOLOGIES FOR GLOBAL CHANGE (MITIGATION AND ADAPTATION) [CHIKYU KANKYO HENDO NO KEIGEN OYOBI TEKIO NO KENKYU SENRYAKU NI KANSURU NICHIBEI WAKU SHOPPU NO HOKOKU: DAI 2 KAI KAIGO]
Tateki Mizuno *In its* Journal of NIRE, Vol. 2, No. 3 25 May 1993 p 87-95 In JAPANESE (For primary document see N94-29512 08-99)
Avail: CASI HC A02/MF A02

N94-30463*# National Aeronautics and Space Administration. Marshall Space Flight Center, Huntsville, AL.
COMPUTERIZED IN VITRO TEST FOR CHEMICAL TOXICITY BASED ON TETRAHYMENA SWIMMING PATTERNS
David A. Noever, Helen C. Matsos, Raymond J. Cronise, Loren L. Looger, Rachna A. Relwani, and Jacqueline U. Johnson *In* NASA, Washington, Technology 2003: The Fourth National Technology Transfer Conference and Exposition, Volume 1 Feb. 1994 p 196-208 (For primary document see N94-30440 08-99)
Avail: CASI HC A03/MF A04

N94-30464*# Idaho National Engineering Lab., Idaho Falls.
A MODULAR APPROACH FOR AUTOMATED SAMPLE PREPARATION AND CHEMICAL ANALYSIS
Michael L. Clark, Terry D. Turner, Kerry M. Klingler, and Randolph Pacetti *In* NASA, Washignton, Technology 2003: The Fourth National Technology Transfer Conference and Exposition, Volume 1 Feb. 1994 p 209-218 (For primary document see N94-30440 08-99)
Avail: CASI HC A02/MF A04

N94-30466*# Allied-Signal Corp., Kansas City, MO.
NON-AQUEOUS CLEANING SOLVENT SUBSTITUTION
Gerald J. Meier *In* NASA, Washington, Technology 2003: The Fourth National Technology Transfer Conference and Exposition, Volume 1 Feb. 1994 p 223-231 (For primary document see N94-30440 08-99)
(Contract DE-AC04-76DP-00613)
Avail: CASI HC A02/MF A04

N94-30469*# McDonnell-Douglas Corp., Huntington Beach, CA.
GAS STREAM PURIFIER
Steven J. Adam *In* NASA, Washington, Technology 2003: The Fourth National Technology Transfer Conference and Exposition, Volume 1 Feb. 1994 p 248-257 (For primary document see N94-30440 08-99)
Avail: CASI HC A02/MF A04

N94-30470*# National Aeronautics and Space Administration. Lyndon B. Johnson Space Center, Houston, TX.
USING SPACECRAFT TRACE CONTAMINANT CONTROL SYSTEMS TO CURE SICK BUILDING SYNDROME
John C. Graf *In* NASA, Washington, Technology 2003: The Fourth National Technology Transfer Conference and Exposition, Volume 1 Feb. 1994 p 258-265 (For primary document see N94-30440 08-99)
Avail: CASI HC A02/MF A04

N94-30471*# National Aeronautics and Space Administration. Lewis Research Center, Cleveland, OH.
A NEW MATERIAL FOR REMOVING HEAVY METALS FROM WATER
Warren H. Philipp, Jr. and Kenneth W. Street, Jr. *In* NASA, Washington, Technology 2003: The Fourth National Technology Transfer Conference and Exposition, Volume 1 Feb. 1994 p 266-272 (For primary document see N94-30440 08-99)
Avail: CASI HC A02/MF A04

N94-30472*# Bureau of Mines, Tuscaloosa, AL.
DEWATERING OF CONTAMINATED RIVER SEDIMENTS
Ronald H. Church, Carl W. Smith, and Bernard J. Scheiner *In* NASA, Washington, Technology 2003: The Fourth National Technology Transfer Conference and Exposition, Volume 1 Feb. 1994 p 273-282 (For primary document see N94-30440 08-99)
Avail: CASI HC A02/MF A04

46 GEOPHYSICS

Includes aeronomy; upper and lower atmosphere studies; ionospheric and magnetospheric physics; and geomagnetism.

For space radiation see *93 Space Radiation.*

N94-28416*# Lunar and Planetary Inst., Houston, TX.
FIELD GUIDE TO CRETACEOUS-TERTIARY BOUNDARY SECTIONS IN NORTHEASTERN MEXICO
Gerta Keller (Princeton Univ., NJ.), Wolfgang Stinnesbeck (Universidad Nacional Autonoma de Mexico, Mexico City.), Thierry Adatte (Neuchatel Univ., Switzerland.), Norman MacLeod (Princeton Univ., NJ.), and Donald R. Lowe (Stanford Univ., CA.) 1994 122 p Conference on New Developments Regarding the KT Event and Other Catastrophes in Earth History, held in Houston, TX, 5-8 Feb. 1994 Prepared in cooperation with Houston Univ., Clear Lake, TX
(Contract NASw-4574)
(NASA-CR-195719; NAS 1.26:195719; LPI-Contrib-827) Avail: CASI HC A06/MF A02

This guide was prepared for the field trip to the KT elastic sequence of northeastern Mexico, 5-8 February 1994, in conjunction with the Conference on New Developments Regarding the KT Event and Other Catastrophes in Earth History, held in Houston, Texas. The four-day excursion offers an invaluable opportunity to visit three key outcrops: Arroyo El Mimbral, La Lajilla, and El Pinon. These and other outcrops of this sequence have

recently been interpreted as tsunami deposits produced by the meteorite impact event that produced the 200 to 300-km Chicxulub basin in Yucatan, and distributed ejecta around the world approximately 65 m.y. ago that today is recorded as a thin clay layer found at the K/T boundary. The impact tsunami interpretation for these rocks has not gone unchallenged, and others examining the outcrops arrive at quite different conclusions: not tsunami deposits but turbidites; not KT at all but 'upper Cretaceous.' Indeed, it is in hopes of resolving this debate through field discussion, outcrop evaluation, and sampling that led the organizers of the conference to sanction this field trip. This field guide provides participants with background information on the KT clastic sequence outcrops and is divided into two sections. The first section provides regional and logistical context for the outcrops and a description of the clastic sequence. The second section presents three representative interpretations of the outcrops by their advocates. There is clearly no way that these models can be reconciled and so two, if not all three, must be fundamentally wrong. Readers of this guide should keep in mind that many basic outcrop observations that these models are based upon remain unresolved. While great measures were taken to ensure that the information in the description section was as objective as possible, many observations are rooted in interpretations and the emphasis placed on certain observations depends to some degree upon the perspective of the author. Derived from text

N94-28538# Los Alamos National Lab., NM.
DISLOCATION THEORY OF MELTING FOR IRON, REVISITED
J. P. Poirier (Institut de Physique du Globe, Paris, France.) and T. J. Shankland 1993 5 p Presented at the 14th International Conference of the International Association for the Advancement of High Pressure Science and Technology, Colorado Springs, CO, 27 Jun. - 2 Jul. 1993
(Contract W-7405-eng-36)
(DE94-002715; LA-UR-93-3658; CONF-930676-63) Avail: CASI HC A01/MF A01

Melting point T(sub m) of iron at conditions of the Earth's inner core boundary (ICB) has been calculated from dislocation theory of melting in metals. Monte Carlo calculations were used to estimate uncertainties introduced by uncertainty in the geophysical parameters that are used in the calculations. These calculations take into account the effects of pressure at ICB conditions and of possible freezing point depression resulting from dilution of pure iron in the outer core. With this approach T(sub m) of pure (var epsilon)-Fe at a pressure of 330 GPa and without freezing point depression is 6160 (+/-) 250 K; for a 1000 K freezing point depression it is 6110 K. T(sub m) of pure (gamma)-Fe is 6060 K, a value that is not significantly different. A possible (alpha)' phase would melt at 5600 K. These values agree with calculated shock wave determinations of T(sub m). Although calculated T(sub m) of the pure phase is little affected by assumptions about the extent of freezing point depression, the estimated temperature of the inner core boundary is lower by the freezing point depression, perhaps 500 - 1000 K less than T(sub m) of a pure phase. DOE

N94-28558 Department of Energy, Washington, DC. Office of Energy Reseach.
SUMMARIES OF FY 1993 GEOSCIENCES RESEARCH
Dec. 1993 155 p Limited Reproducibility: More than 20% of this document may be affected by microfiche quality
(DE94-004710; DOE/ER-0597P) Avail: CASI HC A08

The Department of Energy supports research in the geosciences in order to provide a sound foundation of fundamental knowledge in those areas of the geosciences that are germane to the DOE's many missions. The Geosciences Research Program is supported by the Office of Energy Research. The participants in this program include DOE laboratories, academic institutions, and other governmental agencies. These activities are formalized by a contract or grant between the DOE and the organization performing the work, providing funds for salaries, equipment, research materials, and overhead. The summaries in this document, prepared by the investigators, describe the scope of the individual programs. The Geosciences Research Program includes research in geophysics, geochemistry, resource evaluation, solar-terrestrial interactions, and their subdivisions including earth dynamics, properties of earth materials, rock mechanics, underground imaging, rock-fluid interactions, continental scientific drilling, geochemical transport, solar-atmospheric physics, and modeling, with emphasis on the interdisciplinary areas. DOE

N94-28684# Naval Postgraduate School, Monterey, CA.
ELECTRON BEAMS AT GEOSYNCHRONOUS ORBIT M.S. Thesis
Raymond C. Gaw Sep. 1993 102 p
(AD-A275471) Avail: CASI HC A06/MF A02

This thesis surveys electron and ion measurements collected by the geosynchronous satellite 1989-046. In particular, this survey focuses on a phenomenon known as electron beams, which are attributed to the sudden acceleration of electrons along the earth's magnetic field lines. Observations over a twelve day period reveal electron beam occurrences during the first few minutes of hot plasma injection associated with a magnetospheric substorm. Analysis of distribution functions show these beams have a characteristic peak. These distributions can be approximately fitted as Maxwellians, providing a means of characterizing the temperature, density, and potential drop associated with the beam. Plots of the differential flux also show a general diffusion of the beam into neighboring pitch angles. Theories on the source of the acceleration and diffusion are presented. DTIC

N94-28685# Naval Research Lab., Bay Saint Louis, MS.
UPDATED DEEP-TOW ACOUSTICS/GEOPHYSICS SYSTEM COMPRESSIONAL VELOCITY DATABASE Final Report
Mary M. Rowe and Joseph F. Gettrust 12 Jan. 1994 21 p
(AD-A275477; NRL/MR/7432-93-7081) Avail: CASI HC A03/MF A01

This memorandum report describes the deep-tow acoustics/geophysics system (DTAGS) compressional velocity database, a compilation of compressional velocity-layer thickness functions derived from DTAGS deep-tow multichannel seismic data. Geologic environments represented by the velocity functions included in this database include thick turbidite deposits, thick sediment basin deposits, sediment containing methane hydrate, and thin sediments overlying young basement. Horizontal sampling frequency (distance between velocity profiles) of the database ranges from 45 to 230 m. Vertical sampling frequency (layer thickness) ranges from 5 to 300 m. These compressional velocity-layer thickness profiles were determined from DTAGS multichannel seismic data using standard semblance velocity analysis procedures. DTIC

N94-28728# Gifford (F. A.), Oak Ridge, TN.
A FRACTAL ANALYSIS OF NEAR-FIELD ATMOSPHERIC CONCENTRATION DATA Final Report, 1 Nov. 1992 - 31 Oct. 1993
Franklin A. Gifford 25 Nov. 1993 48 p
(Contract DAAH04-93-C-0002)
(AD-A275460; ARO-29192.1-GS-S) Avail: CASI HC A03/MF A01

A previous study showed that regional and large scale atmospheric motions have Hurst exponents on the order of .4 to .5. The Hurst exponent, H, equals 2-D, where D is the fractal dimension, for a time series. These numbers characterize the degree of irregularity of the time-series. Hurst exponents were calculated for a large number of concentration-time series from several sources, whose sampling times ranged from 6 seconds to 1 hour. Hurst exponents for these data ranged from about .2 to .4. Such values indicate that the small-scale, near-field turbulent eddies differ qualitively from the larger-scale motions, for which H approaches the value .5, the value for Brownian motion. Since models in effect assume the value H = .5 in turbulence parameterizations, these results suggest that smaller, realistic H-values, appropriate to planetary boundary layer turbulence, should be used to parameterize turbulence. DTIC

N94-28737# Naval Research Lab., Bay Saint Louis, MS.
A PROGRAM FOR RAPID COMPUTATION OF MULTIOFFSET VERTICAL SEISMIC PROFILE SYNTHETIC SEISMOGRAMS FOR LAYERED MEDIA Final Report
Dennis Lindwall and Subhashis Mallick 4 Jan. 1994 43 p
(NR Proj. 032-02)
(AD-A275464; NRL/MR/7432-93-7022) Avail: CASI HC A03/MF A01

PNSEB is a set of FORTRAN programs for calculating the response of a layered elastic medium using the reflectivity method as described in Mallick and Frazer (Practical Aspects of Reflectivity Modeling, Geophysics 52, 1355-1364, 1987; Rapid Computation of Multi-offset VSP Synthetic Seismograms for Layered Media, Geophysics 53, 479-491, 1988). PNSEB consists of two basic modules, each of which consists of more than one major option. The first module, PNSN, calculates the earth's response (Green's function) in frequency-wavenumber (omega-p) space. Using the proper option, the program can calculate the response at very small or

very large offsets. No lateral variability or anisotropy are allowed, but the full response including interface waves is calculated. The second module, PNSYN, in its main form converts the output from PNSN to time-distance (t-x) space, which can then be plotted by the VSPLT module or by other plotting packages. The program has been written and optimized for vector computers, such as a Cray or Convex, but also runs well on scalar computers such as Sun workstations. DTIC

N94-28791# Naval Research Lab., Bay Saint Louis, MS.
BROAD GEOACOUSTIC ASSESSMENT OF SOME REGIONAL AREAS Final Report
James K. Fulford 17 Dec. 1993 26 p
(NR Proj. H12-92)
(AD-A275504; NRL/MR/7175-93-7055) Avail: CASI HC A03/MF A01

A broad geoacoustic assessment of three regional shallow-water areas has been made. The geoacoustic properties within each region are mapped into three geoacoustic models representing low (sand-sift-clay), moderate (clayey-sift), and high (silty-clay) bottom loss. Representative extreme sound speed profiles are used to generate a cone of launch angles where the loss is less than a specified amount per bounce. In general, only regions of low loss have good propagation characteristics for each extreme of sound speed. DTIC

N94-28803# Joint Inst. for Nuclear Research, Dubna (USSR).
THE KLEIN-FOCK EQUATION, MINIMAL SURFACES AND GRAVITATIONAL FIELDS
F. I. Fedorov and N. S. Shavokhina 1992 12 p
(DE94-606340; JINR-E-2-92-377) Avail: CASI HC A03/MF A01 (US Sales Only)

A nonlinear scalar field of the Born-Infeld type is considered whose linear analog is the scalar field obeying the Klein-Fock equation. It is shown that if the initial scalar field is massless, a nonlinear field of the Born-Infeld type corresponding to it is described by the equations of minimal surfaces in pseudo-Euclidean spaces with the coordinates ct, x, and b phi. The coordinate phi may have both space-like and time-like nature. If the initial field is massive, the corresponding field of the Born-Infeld type is described by the equations of minimal surfaces in curved spaces with the same coordinates ct, x, and b phi. Massive fields of the Born-Infeld type are extended sources of the gravitational fields. DOE

N94-28843# Naval Postgraduate School, Monterey, CA.
FAR ULTRAVIOLET IMAGES OF THE NIGHTTIME IONOSPHERE M.S. Thesis
Thomas P. Hekman 23 Sep. 1993 66 p
(AD-A275083) Avail: CASI HC A04/MF A01

The Naval Research Laboratory's Far Ultraviolet Cameras Experiment is part of an ongoing project to develop a means for real time space based monitoring of the upper atmosphere. A method by which useable data can be extracted from the images obtained from the cameras is developed. The required output is an intensity profile of the light in the band of the camera as a function of observation zenith angle. From this data future analysis can be done to determine the spatial distribution and density of the upper atmosphere. The long term application of this project is to develop a method for using space based imaging of the ionosphere to provide real time radio frequency propagation analysis. DTIC

N94-28868# Royal Norwegian Council for Scientific and Industrial Research, Kjeller.
THE NORWEGIAN SEISMIC ARRAY (NORSAR), PHASE 3 Semiannual Technical Summary, 1 Oct. 1992 - 31 Mar. 1993
Jul. 1993 150 p
(AD-A275440; Rept-2-92/93) Avail: CASI HC A07/MF A02

This Semiannual Technical Summary describes the operation, maintenance and research activities at the Norwegian Seismic Array (NORSAR), the Norwegian Regional Seismic Array (NORESS), the Arctic Regional Seismic Array (ARCESS) and the experimental Spitsbergen regional array for the period 1 October 1992 - 31 March 1993. Statistics are also presented for additional seismic stations, which through cooperative agreements with institutions in the host countries provide continuous data to the NORSAR Data Processing Center (NPDC). These stations comprise the Finnish Experimental Seismic Array (FINESA), the German Experimental Seismic Array (GERESS), and an experimental regional seismic array in Apatity, Russia. DTIC

N94-28869# Aerospace Corp., El Segundo, CA. Technology Operations.
SPACE-TIME STRUCTURE OF THE MORNING AURORA INFERRED FROM COINCIDENT DMSP-F6, -F8, AND SONDRESTROM INCOHERENT SCATTER RADAR OBSERVATIONS
J. Watermann, O. DeLaBeaujardiere, and H. E. Spence 1 Oct. 1993 16 p
(Contract F04701-88-C-0089)
(AD-A275442; TR-92(2940)-4; SMC-TR-93-63) Avail: CASI HC A03/MF A01

On rare occasions, observations from the DMSP-F6 and -F8 spacecraft and the Sondrestrom incoherent scatter radar coincide in space. Such coincidence offers a unique opportunity to study temporal vs spatial variations on a small scale. We discuss data from one of those occasions, with observations made in the dawn sector in the presence of moderate auroral precipitation during a magnetically quiet period. The DMSP satellites measured vertical electron and ion flux and cross-track plasma drift while the radar measured the ionospheric electron density distribution and line-of-sight plasma velocities. We combine these data sets to construct a two-dimensional map of a possible auroral pattern above Sondrestrom. It is characterized by the following properties. No difference is seen between the gross precipitation patterns measured along the DMSP-F6 and -F8 trajectories (separated by 32 km in magnetic east-west direction and some 4 s in travel time in magnetic north-south direction), except that they are not exactly aligned with the L shells. However, F6 and F8 observed minor differences in the small-scale structures. More significant differences are found between small-scale features in the DMSP precipitation measurements and in radar observations of the E-region plasma density distribution. These measurements are separated by 74 km, equivalent to 2.4 deg, in magnetic longitude, and 0-40 s in time along the spacecraft trajectories (varying with magnetic latitude). Large-scale magnetospheric-ionospheric surfaces such as plasma flow reversal, poleward boundary of the keV ion and electron precipitation, and poleward boundary of E-region ionization, coincide. DTIC

N94-28882# Purdue Univ., West Lafayette, IN. Research Foundation.
TOWARD A MOLECULAR SCALE UNDERSTANDING OF FROST HEAVING, PHASE 1 Final Report, 15 Apr. 1990 - 30 Sep. 1993
John H. Cushman 13 Dec. 1993 15 p
(Contract DAAL03-90-G-0074)
(AD-A275446; ARO-27316.7-GS) Avail: CASI HC A03/MF A01

A fundamental understanding of the physical and chemical basis for frost heaving is of utmost importance for improving the design of structures for use in cold regions. The research reported here represents a multidisciplinary effort to develop a molecular-scale understanding of this cold region phenomena. Propagation of the molecular-scale information to a field scale is also important and the scale-up problem has also been addressed. A multiphase, multicomponent hybrid theory of mixtures approach was used to scale up information. Equilibrium and nonequilibrium statistical mechanical tools were developed and employed to examine nonlocal diffusion and dispersion. Phase transitions were studied with MC and MD methods. New techniques were developed to compute the chemical potential of the vicinal phase. Interfacial tension was studied using GCEMC. Anomalous diffusion in monolayer films was analyzed via MD, scaling arguments and fractal Brown motion. DTIC

N94-28891 Boston Univ., MA. Center for Space Physics.
THE EFFECTS OF MAGNETIC STORM PHASES ON F-LAYER IRREGULARITIES FROM AURORAL TO EQUATORIAL LATITUDES Quarterly Report, 1 Oct. - 31 Dec. 1993
Jules Aarons and Michael Mendillo 31 Dec. 1993 4 p Limited Reproducibility: More than 20% of this document may be affected by microfiche quality
(Contract N00014-89-J-1754)
(AD-A275203) Avail: CASI HC A01

During this quarter, an extensive review of the literature on middle latitude irregularities was started. In earlier reports we have noted the levels of irregularities at latitudes above the equatorial anomaly region (within 15 deg of the magnetic equator) thru our analysis of a few examples of raw data from Osan, Korea. We then began to reduce and analyze

data from Puerto Rico and Hawaii using 136 MHz scintillation data taken during both high and low solar flux years. At the levels that can be noted (peak to peak excursions of 15-20 dB) there is considerable activity.
DTIC

N94-28893 Phillips Lab., Hanscom AFB, MA.
SHARC, A MODEL FOR CALCULATING ATMOSPHERIC AND INFRARED RADIATION UNDER NON-EQUILIBRIUM CONDITIONS
R. L. Sundberg, J. W. Duff, J. H. Gruninger, L. S. Bernstein, and R. D. Sharma 24 Jan. 1994 18 p Limited Reproducibility: More than 20% of this document may be affected by microfiche quality
(AD-A275207; PL-TR-94-2010) Avail: CASI HC A03

A new computer model, SHARC, has been developed by the Air Force for calculating high-altitude atmospheric IR radiance and transmittance spectra with a resolution of better than 1/cm. Comprehensive coverage of the 2 to 40 microns (250/cm to 5,000/cm) wavelength region is provided for arbitrary lines of sight in the 50-300 km altitude regime. SHARC accounts for the deviation from local thermodynamic equilibrium (LTE) in vibrational state populations by explicitly modeling the detailed production, loss, and energy transfer process among the important molecular vibrational states. The calculated vibrational populations are found to be similar to those obtained from other non-LTE codes. The radiation transport algorithm is based on a single-line equivalent width approximation along with a statistical correction for line overlap. This approach is reasonably accurate for most applications and is roughly two orders of magnitude faster than the traditional LBL methods which explicitly integrate over individual line shapes. In addition to quiescent atmospheric processes, this model calculates the auroral production and excitation of CO2, NO, and NO(+) in localized regions of the atmosphere. Illustrative comparisons of SHARC predictions to other models and to data from the CIRRIS, SPIRE, and FWI field experiments are presented.
DTIC

N94-29062# Naval Research Lab., Bay Saint Louis, MS.
THE EFFECTS OF ALTIMETER SAMPLING CHARACTERISTICS: SOME GEOSAT EXAMPLES Contract Report
Michael E. Parke and George Born 6 Apr. 1993 29 p
(Contract N00014-92-J-6004)
(AD-A275225; NRL-CR/7320-93-0002) Avail: CASI HC A03/MF A01

Altimetric satellites have characteristic sampling patterns in both space and time. This paper looks at the distortions of oceanographic and atmospheric signals as seen in Geosat altimeter data. Because of the pattern of ground tracks lain down by Geosat, measurements of oceanographic and atmospheric phenomena can be distorted spatially as well as temporally. As a result, phenomena measured by altimetric measurements can appear as propagating waves with both wavelength and wavenumber different from the original phenomena. These changes, if not understood, can result in misinterpretation of results from altimeter data. Also, in some parts of the world, distorted signals satisfy the dispersion relation of other oceanographic waves, or two phenomena can both have the same distorted dispersion relations. The use of multiple satellites to resolve these problems will be discussed in a follow-on paper.
DTIC

N94-29070# Army Cold Regions Research and Engineering Lab., Hanover, NH.
GROWTH CONDITION OF AN ICE LAYER IN FREEZING SOILS UNDER APPLIED LOADS. PART 1: EXPERIMENT
Kazuo Takeda and Yoshisuke Nakano Nov. 1993 73 p
(DA Proj. 4A1-61102-AT-24)
(AD-A275215; CRREL-93-21) Avail: CASI HC A04/MF A01

A series of freezing tests on Kanto loam were conducted under various overburden pressures to find the steady growth condition of a segregated ice layer. The steady growth condition was found to be determined by the absolute value of the temperature gradient of the unfrozen part of the soil a sub u near the 0 C isotherm and that of the frozen part of the soil alpha sub f near the warmest end of an ice layer under given hydraulic conditions and applied effective pressure sigma. This is the first of a two-part presentation on the subject; the analytical aspects of the study are presented in a second report.
DTIC

N94-29078# National Inst. of Polar Research, Tokyo (Japan).
ANTARCTIC RECORD, VOLUME 36, NO. 1 [NANKYOKU SHIRYO, VOLUME 36, NO. 1]
Takao Hoshiai, ed., Masaki Ejiri, ed., Takeo Hirasawa, ed., Yoshikuni Hiroi, ed., Katsutada Kaminuma, ed., Sadao Kawaguchi, ed., Katsuhiro Kikuchi, ed., Susumu Kokubun, ed., Yasuhiko Naito, ed., and Nobuo Ono, ed. et al 30 Mar. 1992 167 p In ENGLISH and JAPANESE Original contains color illustrations
(ISSN 0085-7289)
(Rept-106-Vol-36-No-1; JTN-94-80589) Avail: CASI HC A08/MF A02

The following topics were discussed: Antarctic regions, Showa station, Japan Antarctic Research Expedition, Pc5 pulsation, geomagnetic conjugate points, mathematical models, numerical analysis, Soar-Rondane mountain, geographic surveys, geological surveys, land ice, maps, moss, photosynthesis, respiratory rate, regression analysis, zooplankton, copepods, ionospheric sounding, magnetospheric sounding, ecological survey, ozonosphere, seismometers, project management, research facilities management, waste treatment, auroras, air-water-ice interactions, low temperature effects, physiological effects, communication, snow damage, environmental protection, environmental monitoring, international agreement, and laws. For individual titles, see N94-29079 through N94-29086.

N94-29079# Tokai Univ., Hiratsuka (Japan). Dept. of Aeronautics and Astronautics.
ESTIMATION OF GEOMAGNETIC CONJUGATE POINTS BY USING Pc5 PULSATIONS [PC5 MYAKUDO O MOCHIITA CHIJIKI KYOEKITEN NO SUITEI]
Ken-Ichi Kato, Yutaka Tonegawa, and Natsuo Sato *In* National Inst. of Polar Research, Antarctic Record, Volume 36, No. 1 30 Mar. 1992 p 1-14 In JAPANESE (For primary document see N94-29078 08-46)
Avail: CASI HC A03/MF A02

In this report, an attempt was made to estimate the geomagnetic conjugate points by using the Pc5 geomagnetic pulsation data obtained simultaneously at three stations in Iceland and at three stations in Antarctica (including Showa Station) during the period of Mar. and May in 1988. It is assumed in the estimation that Pc5 pulsations are odd mode standing oscillations of the field line and have linear phase variations among the stations in the horizontal plane. The result shows that conjugate points of Showa Station estimated from Pc5 events are concentrated around the point calculated from the magnetic field model, within the range of +/- 3 deg in the longitude, i.e., less than 1/5 wave length, and +/-0.5 deg in the latitude.
Author (NASDA)

N94-29080# National Inst. of Polar Research, Tokyo (Japan).
GLACIAL LANDFORMS AND LATE CENOZOIC HISTORY OF THE WESTERN SOER-RONDANE MOUNTAINS [SERU RONDANE SANCHI SEIBU NO CHIKEI TO KOKI SHINSEIDAI NO HYOSHO HENDO]
Kiichi Moriwaki and Kazuomi Hirakawa *In its* Antarctic Record, Volume 36, No. 1 30 Mar. 1992 p 15-48 In JAPANESE Original contains color illustrations (For primary document see N94-29078 08-46)
Avail: CASI HC A03/MF A02

The western Soer-Rondane Mountains were once covered by the ice sheet. The mountains are in some places covered with tills weathered in various degrees. Heavily weathered ground including Pliocene till is found on flat-topped surfaces of the mountains and glacial benches about 100 m higher than the present ice surface. Heavily weathered ground is found also in ice-free valley, bottom of which is lower than surrounding ice surface. Tills of the early to middle Pleistocene are small in quantity and form only small lateral moraines on the mountain flanks about 100 m higher than the present ice surface. The Pliocene temperate ice sheet produced, transported, and deposited a large quantity of tills and eroded the valley systems. The ice sheet shrank and the most part of the mountains emerged from ice by the latest Pliocene. The lowest level of the ice sheet during this deglaciation was probably lower than that of the present day. The temperate ice sheet changed into cold one in early Pliocene and re-advanced up to about 100 m higher than the present ice surface. Subsequently, the ice sheet retreated again to about 10 m higher than the present level by tens of thousands of years ago. Then, notable fluctuation of the ice level has not occurred. A warmer environment is suggested by large crystals of gypsum grown in lakes during the last deglaciation period.
Author (NASDA)

N94-29081# Waseda Univ., Tokyo (Japan). School of Education.
ESTIMATION OF THE NET PRODUCTION OF MOSS COMMUNITY AT LANGHOVDE, EAST ANTARCTICA [HIGASHI NANKYOKU RANGUHOBUDE NI OKERU SENRUI NO JUN SEISANRYO NO SUITEI] **c51**

Yoshio Ino *In* National Inst. of Polar Research, Antarctic Record, Volume 36, No. 1 30 Mar. 1992 p 49-59 Sponsored by National Inst. of Polar Research (For primary document see N94-29078 08-46)
Avail: CASI HC A03/MF A02

Field measurements of net photosynthesis and dark respiration (CO2 exchange) of moss colonies were carried out at Langhovde, East Antarctica, 17 Jan. 1988. Each colony growing at the Yukidori Valley, Langhovde was composed of Grimmia lawiana, Bryum pseudotriquetrum or the mixture of Ceratodon purpureus and B. pseudotriquetrum. Microclimatic data (photo-synthetic photon flux density and moss temperature) in the assimilation chamber were recorded at the same time. A simple model to estimate the net photosynthetic rate and dark respiration rate on the basis of the microclimatic data was developed on Kappen's model. Net primary production of these moss colonies was calculated with the microclimatic data recorded separately at the Yukidori Valley Jan. 1988 - Jan. 1989. The estimated net production rates of moss colonies growing in the upper reaches of the Yukidori Valley ranged from 8.8 to 11.3 mol CO2 m(exp -2)y(exp -1), or from 230 to 296 gdw m(exp -2)y(exp -1). Author (NASDA)

N94-29082# Aichi Fisheries Research Inst., Minato (Japan).
COPEPODS COLLECTED ALONG 33.5 DEG E LONGITUDE OF THE ANTARCTIC OCEAN IN THE 1976 SUMMER [1976 NEN KAKI, NANKYOKUKAI INDOYOKU NO TOKEI 33.5 DO SEN NI SOTTE ERARETA KAIASHIRUI SHIRYO] **c51**

Satoshi Yamada, Atsushi Tanimura, and Takashi Minoda *In* National Inst. of Polar Research, Antarctic Record, Volume 36, No. 1 30 Mar. 1992 p 60-64 (For primary document see N94-29078 08-46)
Avail: CASI HC A01/MF A02

Zooplankton samplings were conducted at six stations along 33.5 deg E in the Indian sector of the Antarctic Ocean 25 Feb. - 2 Mar. 1976 by the 17th Japanese Antarctic Research Expedition. Vertical hauls from a depth of 200 m to the surface with a Norpac net (45 cm in diameter, 0.33 mm mesh openings) were performed. Copepoda occupied more than 85 percent of the total individual numbers of zooplankton at all stations. The species composition and abundance of copepods were investigated. A total of 18 species except for Oncaeidae were identified. Calanus propinquus, Calanoides acutus, Rhincalanus gigas, Ctenocalanus vanus, Scolecithricella glacialis, and Oithona similis were found commonly at almost all stations. Miclocalanus pygmaeus, Lucicutia sp., Haloptilus ocellatus, Haloptilus oxycephalus and Metridia gerlachei occurred south of 60 deg S and Calanus simillimus, Clausocalanus laticeps, Metridia lucens and Oithona frigida occurred north of 60 deg S. Euchaeta antarctica, Racovitzanus antarcticus and Heterorhabdus austrinus occurred sporadically and/or in small number. Author (NASDA)

N94-29083# National Inst. of Polar Research, Tokyo (Japan).
ACTIVITIES OF THE WINTERING PARTY AT SHOWA STATION BY THE 31ST JAPANESE ANTARCTIC RESEARCH EXPEDITION IN 1990 [DAI 31 JI NANKYOKU CHIIKI KANSOKUTAI SHOWA KICHI ETTI (1990) HOKOKU]

Yasuhiko Naito *In its* Antarctic Record, Volume 36, No. 1 30 Mar. 1992 p 65-82 In JAPANESE (For primary document see N94-29078 08-46)
Avail: CASI HC A03/MF A02

JARE (Japanese Antarctic Research Expedition) dispatched two wintering parties to Showa and Asuka Stations in Antarctica. The report describes the activities of the JARE-31 wintering party at Showa Station. A total of 30 members, including 15 scientists and 15 logistics, had stayed at the station 1 Feb. 1990 - 31 Jan. 1991. The major tasks assigned to the wintering party by the JARE headquarters were to conduct more than 60 items of the observation including launching of the ozone sonde and total ozone observation as a routine meteorological observation, STS (Space Transportation System) earthquake observation, and field experiments of ACR (Active Cavity Radiometer) program with major focus on the interaction between sea ice and atmosphere. EXOS-D (Exospheric Satellite-D) and MOS-1 (Marine Observation Satellite-1) observation and the experiments on penguin foraging ecology were also important programs. All these scientific experiments were performed successfully. The particular success of the field experiments of ACR was partly due to the better sea ice condition that guaranteed safe activities on sea ice throughout the year. Regarding the maintenance of the station, a new program on the waste disposal has started in relation to the conservation of the Antarctic environment. A large amount of the disposed waste was brought back to the country. Author (NASDA)

N94-29084# National Inst. of Polar Research, Tokyo (Japan).
ACTIVITIES OF THE FOURTH WINTERING PARTY AT ASUKA STATION BY THE 31ST JAPANESE ANTARCTIC RESEARCH EXPEDITION IN 1990 [DAI 31 JI NANKYOKU CHIIKI KANSOKUTAI ASUKA KANSOKU KYOTEN ETTO (1990) HOKOKU]

Kazuyuki Shiraishi *In its* Antarctic Record, Volume 36, No. 1 30 Mar. 1992 p 83-10 In JAPANESE (For primary document see N94-29078 08-46)
Avail: CASI HC A03/MF A02

The wintering party at Asuka Station (71 deg 31 min 34 sec S, 24 deg 8 min 17 sec E, 30 m a.s.l.) by the 31st Japanese Antarctic Research Expedition-31 (JARE-31), consisting of eight personnel, maintained Asuka Station continuously 25 Dec. 1989 - 26 Dec. 1990. The main scientific programs of the party were the meteorological observation and studies of upper atmosphere physics. Other programs comprised geological investigation and search for meteorites in the Soer Rondane Mountains, and medical-biological studies, glaciological studies and logistic survey of the housing at Asuka Station and its vicinity. During the 1989/1990 summer season, Asuka Station was used as the base camp for the helicopter operation in the Soer Rondane Mountains. All programs were carried out successfully during the wintering and the Station was succeeded by JARE-32. Author (NASDA)

N94-29085# National Inst. of Polar Research, Tokyo (Japan).
JAPAN-CHINA COLLABORATION RESEARCH PROGRAM ON TERRESTRIAL BIOLOGY AT GREAT WALL STATION IN KING GEORGE ISLAND, IN THE SUMMER OF 1990/1991 [1990/1991 NEN KAKI, KINGU JOJITO CHOJO KICHI NI OKERU NICCHU KYODO KANSOKU (DAN 3 NENJI)] **c51**

Shuji Otani and Takayuki Nakatsubo *In its* Antarctic Record, Volume 36, No. 1 30 Mar. 1992 p 109-115 In JAPANESE (For primary document see N94-29078 08-46)
Avail: CASI HC A02/MF A02

The collaboration between Japanese and Chinese biologists started in the 1988/1989 season with a three-year program at Great Wall Station, King George Island. For the third year of the program (1990/1991), two Japanese botanists carried out the field survey on freshwater algae and bryophytes in the 7th Chinese National Antarctic Expedition (CHINARE-7). Taxonomic study of freshwater algae was carried out at the Fildes Peninsula. About 110 taxa were recognized in the samples collected from a variety of freshwater habitats. Distribution of snow algae was studied with reference to micro-habitat and snow properties as a cooperative study with a Chinese scientist. The microclimate and photosynthetic activities of moss colonies around Great Wall Station were studied. Vertical cross-sections of moss colonies were examined to study the structure and dynamics of moss colonies. Author (NASDA)

N94-29086# National Inst. of Polar Research, Tokyo (Japan).
PROTOCOL ON ENVIRONMENTAL PROTECTION TO THE ANTARCTIC TREATY AND ITS ANNEXES: INTERNATIONAL AGREEMENT ON THE COMPREHENSIVE MEASURES FOR THE PROTECTION OF ANTARCTIC ENVIRONMENT AND ECOSYSTEMS [NANKYOKU JOYAKU NI TAISURU KANKYO HOGO GITEISHO OYOBI SONO FUZOKUSHO NANKYOKU NO KANKYO TO SEITAIKEI NO HOGO NO TAMENO HOKATSUTEKI SOCHI NI KANSURU KOKUSAI GOI] **c45**

Yoshio Yoshida *In its* Antarctic Record, Volume 36, No. 1 30 Mar. 1992 p 116-161 In ENGLISH and JAPANESE (For primary document see N94-29078 08-46)
Avail: CASI HC A03/MF A02

According to the Recommendation 15-1 adopted at the 15th Antarctic Treaty Consultative Meeting in October 1989, the elaboration of the Comprehensive Measures for the Protection of the Antarctic Environment and Dependent and Associated Ecosystems was undertaken by the ATCP (Antarctic Treaty Consultative Parties) at Vina del Mar in Chile in Nov.

1990. The five meetings, one at Vina del Mar and four at Madrid, were held as the 11th Antarctic Treaty Special Consultative Meeting. The meetings were attended also by non-Consultative Antarctic Treaty Parties and intergovernmental and non-governmental organizations such as CCAMLR (Convention on the Conservation of Antarctic Marine Living Resources), IOC (Intergovernmental Oeanographic Commission), SCAR (Scientific Committee on Antarctic Research), IUCN (International Union for the Conservation of Nature and Natural Resources), ASOC (Antarctica and Southern Ocean Coalition), etc., as observers. The Protocol on Environmental Protection to the Antarctic Treaty and its four annexes were adopted by the ATCP on 4 Oct. 1991. Part of the process of negotiations and the background of the adopted instruments are reported. The authentic texts of Protocol and its Annexes in English and their provisional Japanese translation are appended. Author (NASDA)

N94-29137# Science Applications International Corp., San Diego, CA.
INITIAL WAVE-TYPE IDENTIFICATION WITH NEURAL NETWORKS AND ITS CONTRIBUTION TO AUTOMATED PROCESSING IN IMS VERSION 3.0 Technical Report, Nov. 1992 - Dec. 1993
Thomas J. Sereno, Jr. and Gagan B. Patnaik 10 Dec. 1993 48 p
(Contract MDA972-92-C-0026; ARPA Order 6266)
(AD-A275058; SAIC-93/1219) Avail: CASI HC A03/MF A01

This report describes a new 4-class neural network for automated identification of initial wave type (Teleseism, Regional P, Regional S, or Noise) for data recorded by 3-component stations or arrays. This is an extension of the 2-class (P or S) neural network that we developed for 3-component stations. The input data are dominant period, polarization attributes, contextual information (e.g., measurements related to a group of arrivals), a spectral representation of the horizontal-to-vertical power ratio, and the slowness determined by f-k analysis for array stations. We used a three-staged approach, and each stage consists of a 2-class neural network. The first stage separates signal from noise. The signals are passed to the second stage which separates regional S phases from regional P phases and teleseisms. The regional P phases and teleseisms are passed to the final stage which separates them into two distinct classes. A three-layer backpropagation neural network is used at each stage. Neural networks were trained for six 3-component IRIS/IDA stations in the CIS, and a 4-element micro-array in Kislovodsk. The identification accuracy of the neural networks is greater than 90% for most of the stations that we tested. The neural network module was integrated into the Intelligent Monitoring System (IMS), and it was applied to the 3-component IRIS/IDA data under simulated operational conditions. The result was a reduction in the number of false-alarms produced by the automated processing and interpretation system by about 60%. DTIC

N94-29233# National Inst. of Polar Research, Tokyo (Japan).
PROCEEDINGS OF THE NIPR SYMPOSIUM ON UPPER ATMOSPHERE PHYSICS, NO. 6
Hisao Yamagishi, Masaki Ejiri, Takeo Hirasawa, Susumu Kokubun, and Natsuo Sato et al Feb. 1993 143 p Presented at the 15th Symposium on Coordinated Observations of the Ionosphere and the Magnetosphere in the Polar Regions, Tokyo, Japan, 28-29 Jan. 1992 Original contains color illustrations
(ISSN 0914-5613)
(JTN-94-80593) Avail: CASI HC A07/MF A02

The following topics were discussed: earth atmosphere, upper atmosphere, stratosphere, earth ionosphere, earth magnetosphere, earth magnetosphere-ionosphere coupling, geomagnetic fields, auroras, auroral irradiation, ionospheric radiation, radio emission, Very Low Frequencies (VLF), Extremely Low Frequencies (ULF), electric current, electric potential, plasmas, magnetohydrodynamic stability, magnetohydrodynamic waves, magnetohydrodynamic oscillation, magnetohydrodynamic flow, Hall effects, stereoscopic observation, Polar Patrol Balloon (PPB), solar wind, solar activity effects, polar regions, Antarctic regions, polar cusps, numerical analysis, finite element method, mathematical models, HF (High Frequency) radar, doppler radar, riometers, magnetometer, and computerized simulation. For individual titles, see N94-29234 through N94-29245.

N94-29234# Kyoto Univ., Sakyoku (Japan). Dept. of Electrical Engineering.
AURORA STEREO OBSERVATION IN ICELAND
Takehiko Aso, Masaki Ejiri, Hiroshi Miyaoka, Takayuki Ono, Takeshi Hashimoto, Tetsuro Yabu, and Minoru Abe *In* National Inst. of Polar Research, Proceedings of the NIPR Symposium on Upper Atmosphere Physics, No. 6 Feb. 1993 p 1-14 Sponsored by Ministry of Education, Science and Culture, Tokyo, Japan (For primary document see N94-29233 08-46)
Avail: CASI HC A03/MF A02

Aurora stereoscopic observation for the monochromatic regime has been carried out in Iceland from November to December, 1991. A distance between two observation sites, Husafell and Efri-Brunna, is about 0 km in the magnetic meridian plane. The aim is to obtain stereo image data with longer baseline for the detailed study of inverse algorithm and to clarify three-dimensional luminous structures of aurora at typical wavelengths. This report gives a brief description of the observation and some provisional results of data analysis. Author (NASDA)

N94-29235# Tokai Univ., Hiratsuka (Japan).
OBSERVATIONS OF THE GEOMAGNETIC FIELD BY POLAR PATROL BALLOON (PPB) EXPERIMENT IN ANTARCTICA
Fumio Toyama, Ryoichi Fujii, Masaki Ejiri, and Nobuyuki Yajima *In* National Inst. of Polar Research, Proceedings of the NIPR Symposium on Upper Atmosphere Physics, No. 6 Feb. 1993 p 15-24 (For primary document see N94-29233 08-46)
Avail: CASI HC A02/MF A02

Two scientific balloon experiments of the Polar Patrol Balloon (PPB) project were performed by the 32nd Japanese Antarctic Research Expedition in December 1990 to January 1991. Proton precession magnetometers were used to measure the total intensity of the geomagnetic field for studying the underground magnetic structure by detecting magnetic anomalies and geomagnetic variations like pulsations. The first balloon (PPB-1) showed a trajectory through the center of the Magnetic South Pole with a circumpolar trajectory. The total intensity of the geomagnetic field as obtained by the ARGOS data transmission system every 30 s with an accuracy of 1 nT during the flight of 22 days. A new proton precession magnetometer system that had a wide dynamical measurement range for the PPB observation was developed. This paper reports magnetometry, data processing system, and some preliminary results. Author (NASDA)

N94-29236# British Antarctic Survey, Cambridge (England).
SIGNATURES OF DAYSIDE SOLAR WIND/MAGNETOSPHERE/IONOSPHERE COUPLING AS REVEALED BY THE PACE HF RADARS AND ASSOCIATED EXPERIMENTS
J. R. Dudeney *In* National Inst. of Polar Research, Proceedings of the NIPR Symposium on Upper Atmosphere Physics, No. 6 Feb. 1993 p 25-35 Original contains color illustrations (For primary document see N94-29233 08-46)
Avail: CASI HC A03/MF A02

The nature of the coupling between the solar wind and magnetosphere on the dayside of the Earth, and the response of the ionosphere to this coupling are currently topics of considerable interest and debate. This paper summarizes recent studies of some ionospheric signatures of such coupling processes for a range of spatial and temporal scales, utilizing the unique combination of the two PACE (Polar Anglo-American Conjugate Experiment) HF (High Frequency) radars (at conjugate locations in the Arctic and Antarctic), the IMP-8 (Interplanetary Monitoring Platform-8) and DMSP-F9 (Defense Meteorological Satellite Program-F9) spacecraft, and ground-based experiments at South Pole. Author (NASDA)

N94-29237# Ministry of Posts and Telecommunications, Tokyo (Japan). Communications Research Lab.
LONG TERM VARIATIONS OF RADIO AURORAL ACTIVITY
Kazuhiro Otaka and Takashi Tanaka *In* National Inst. of Polar Research, Proceedings of the NIPR Symposium on Upper Atmosphere Physics, No. 6 Feb. 1993 p 36-41 (For primary document see N94-29233 08-46)
Avail: CASI HC A02/MF A02

Long term variations of radio auroral activity are investigated from auroral radar data obtained at Showa Station during 1978-1990. The diurnal variation of radio auroral activity shows a maximum in the post-midnight period with a small peak in the evening. Similar to the case of magnetic activity, the occurrence rate of radio aurora shows semi-annual variations with summer (December) and winter (June) time minimums. For post-midnight radio aurora, summer minimums are more pronounced than winter minimums. The magnetic activity controls the occurrence of evening time radio aurora

more notably than post-midnight radio aurora. For the solar cycle variation, a double-peaked modulation is seen during an 11-year sunspot cycle, with a major peak in the declining phase of the sunspot cycle and a secondary peak in the increasing phase. Author (NASDA)

N94-29238# Ministry of Posts and Telecommunications, Tokyo (Japan). Communications Research Lab.

NEW-TYPE ECHOES OBSERVED WITH THE 50 MHz AURORAL DOPPLER RADAR AT SHOWA STATION Abstract Only

Manabu Kunitake, Takashi Tanaka, Kiyoshi Igarashi, Shinichi Yamamoto, Hideo Maeno, and Tadahiko Ogawa *In* National Inst. of Polar Research, Proceedings of the NIPR Symposium on Upper Atmosphere Physics, No. 6 Feb. 1993 p 42-46 (For primary document see N94-29233 08-46)
Avail: CASI HC A01/MF A02

VHF Doppler radars have been used for the study of auroral E-region irregularities. The Doppler spectra of radar echoes, which give important information for investigating the plasma instabilities responsible for irregularities, are categorized into type 1 - 4. This report presents a new type of aurora echoes detected by the 50 MHz auroral Doppler radar at Showa Station. Preliminary statistical analyses indicate that these echoes (almost appearing at nearest radar ranges) have narrow spectral peaks located at the frequencies less than the range between plus and minus 20 MHz, and occur in the morning with the durations of a few tens of seconds to a few tens of minutes. The diurnal occurrence rate is very different from that of usual radar echoes. The new-type echoes do not seem to belong to any of echo types (type 1 - 4). At this stage, the mechanisms causing these new echoes are supposed to be some electrostatic waves existing between 0 and 110 km altitudes, or specular back-scatter reflection. More analytical and theoretical work is required to understand the new-type echoes. Author (NASDA)

N94-29239# Nagoya Univ., Toyokawa (Japan). Solar-Terrestrial Environment Lab.

INITIAL OBSERVATION RESULTS WITH IMAGING RIOMETER AT NY-ALESUND (L IS EQUAL TO 16)

Masanori Nishino, Yoshihito Tanaka, Takasi Oguti, Hisao Yamagishi, and Jan A. Holtet *In* National Inst. of Polar Research, Proceedings of the NIPR Symposium on Upper Atmosphere Physics, No. 6 Feb. 1993 p 47-61 Original contains color illustrations (For primary document see N94-29233 08-46)
Avail: CASI HC A03/MF A02

An imaging riometer was installed at Ny-Alesund (invariant latitude, 75.6 deg) for observations of spatial structure and motion of auroral absorption regions. The antenna consists of a two-dimensional dipole array with 64 elements, and a phasing matrix that produces 64 pencil beams viewing an ionospheric area of about 200 km square at 0 km altitude. The instrument provides with a two-dimensional image of enhanced absorption at 30 MHz with spatial resolution of 20 km and time resolution of 1 s by using an eight-channel radio receiver. With the aid of a personal computer, the absorption images are able to be monitored in real time by using a quiet day curve produced from daily variations of cosmic radio noise intensity during initial 10 days. Three examples of the absorption images are presented for events that occurred in daytime, evening, and night time.
Author (NASDA)

N94-29240# Tokyo Univ. (Japan). Dept. of Earth and Planetary Physics and Inst. of Industrial Science.

A THEORY OF CURRENT GENERATOR IN THE MAGNETOSPHERE-IONOSPHERE COUPLING

Takashi Yamamoto and Masao Ozaki *In* National Inst. of Polar Research, Proceedings of the NIPR Symposium on Upper Atmosphere Physics, No. 6 Feb. 1993 p 62-69 (For primary document see N94-29233 08-46)
Avail: CASI HC A02/MF A02

A theoretical model for generation of a pair of region 1 and region 2 Field-Aligned Currents (FAC's) is presented. From the observed pattern of auroras, the existence of a Hot Plasma Torus (HPT) in the magnetosphere can be assumed. An HPT is defined as a hot plasma contained in the magnetic shell which is connected to two ovals of diffuse auroras on the northern and southern polar ionospheres. It is proposed that region 1/region 2 FAC's can be generated as a result of natural distortion of the HPT under the influence of the solar wind convection. Author (NASDA)

N94-29241# Ehime Univ., Matsuyama (Japan). Dept. of Computer Science.

COMPUTER SIMULATIONS ON DEVELOPMENT OF THE FAST RECONNECTION MECHANISM Abstract Only

Masayuki Ugai *In* National Inst. of Polar Research, Proceedings of the NIPR Symposium on Upper Atmosphere Physics, No. 6 Feb. 1993 p 70-75 (For primary document see N94-29233 08-46)
Avail: CASI HC A02/MF A02

In space plasma, large dissipative events, such as solar flares and geomagnetic substorms, occur by drastic release of critically stored magnetic energy in a current sheet system resulting from electrical resistivity or switch-off shocks. The fast reconnection mechanism is a process in which magnetic reconnection rapidly proceeds in the local-diffusing region to retain the switch-off shocks in the system. This study examined why the fast reconnection mechanism occurs and is maintained in actual system, using two-dimensional Magnetohydrodynamic (MHD) simulations by a computer. Spontaneous growth of magnetic reconnection in a large-scale current sheet system was simulated, varying resistivity without special boundary conditions. As a result, it is demonstrated that the reconnection process is strongly controlled by the resistivity models. For a suitable anomalous resistivity model, the quasi-steady fast reconnection mechanism, involving standing switch-off shocks, can be spontaneously established from the current sheet, and the boundaries enclosing the quasi-steady region are not physical boundaries, but must be determined only by the self-consistent development of the fast reconnection process. Author (NASDA)

N94-29242# Ministry of Transportation, Chiba (Japan). Meteorological College.

COUPLED MAGNETOHYDRODYNAMIC OSCILLATIONS IN THE MAGNETOSPHERE-IONOSPHERE SYSTEM: HALL CURRENT EFFECT

Shigeru Fujita *In* National Inst. of Polar Research, Proceedings of the NIPR Symposium on Upper Atmosphere Physics, No. 6 Feb. 1993 p 76-89 (For primary document see N94-29233 08-46)
Avail: CASI HC A03/MF A02

As the first step to a quantitative study of the magnetohydrodynamic coupled oscillations for the magnetosphere-ionosphere system, the basic equations are revised into a suitable form for computer calculations by means of the finite element method. Numerical analysis is performed by using a simple box model, taking account of the anisotropically conducting ionosphere and the insulating atmosphere. Owing to limited capacity of a computer, the effect of the ionospheric Hall current is discussed. The following results were obtained: (1) the mode conversion effect due to the Hall current gives rise to resonant coupling when the azimuthal wave number is zero (the azimuthal direction is referred to the direction perpendicular to the plane of the box model); and (2) the Alfven mode perturbation is enhanced along the resonant field line but in the case of the fast magnetosonic mode the enhancement does not occur.
Author (NASDA)

N94-29243*# National Aeronautics and Space Administration. Goddard Space Flight Center, Greenbelt, MD.

SCALE-LENGTH DEPENDENCE OF THE RATIO BETWEEN THE MAGNETIC AND ELECTRIC FIELD PERTURBATIONS IN THE IONOSPHERIC FIELD-ALIGNED CURRENT REGION

Mamoru Ishii, Masahisa Sugiura, Toshihiko Iemori, and James A. Slavin *In* National Inst. of Polar Research, Proceedings of the NIPR Symposium on Upper Atmosphere Physics, No. 6 Feb. 1993 p 90-102 Sponsored by Ministry of Education, Science and Culture (For primary document see N94-29233 08-46)
Avail: CASI HC A03/MF A02

There is generally high correlation between the orthogonal magnetic and electric field perturbations on the ionospheric field-aligned current region based on observations by polar orbiting satellites. The ratio between the magnetic and electric field perturbations, delta B(sub z)/mu(sub 0)E(sub x), has a scale-length dependence: the ratio delta B(sub z)/mu(sub 0)E(sub x) decreases with decreasing scale length. B. Forget et al. explained this scale-length dependence using a static model. In this report, the ratio delta B(sub z)/mu(sub 0)E(sub x) observed by the DE-2 (Dynamics Explorer-2) satellite for various spatial scales was compared with the effective Pedersen conductivity Sigma(sub P, eff) calculated by the method of Forget et al. The results show that in many cases this model can adequately explain the observed scale-length dependence. However, cases exist in

which the difference, delta B(sub z)/mu(sub 0)E(sub x)-Sigma(sub P, eff), decreases at about 0.25 - 1.0 s in temporal scales (2 - 8 km in spatial scales). This behavior is explained as being due to Alfven waves.
Author (NASDA)

N94-29244# Tokai Univ., Hiratsuka (Japan).
ULF WAVES AND MAGNETIC FIELD CHARACTERISTICS IN THE POLAR CUSP OBSERVED AT GODHAVN
Toru Sakurai, Yutaka Tonegawa, Kenichi Kato, Kazuo Makita, Masaki Ejiri, Hisao Yamagishi, and Natsuo Sato *In* National Inst. of Polar Research, Proceedings of the NIPR Symposium on Upper Atmosphere Physics, No. 6 Feb. 1993 p 103-116 (For primary document see N94-29233 08-46)
Avail: CASI HC A03/MF A02

For the intrusion of the solar energy into the magnetosphere the polar cusp has been believed to be the most important region in the magnetosphere. By using magnetometer data obtained in November 1989 at Godhavn in Greenland located in the polar cusp, the dayside enhancement of Ultra Low Frequency (ULF) wave activity is studied in relation to both variations of the ground magnetic field and the interplanetary magnetic field. Godhavn is found to be one of the appropriate stations for studying magnetic field variations and ULF waves in the polar cusp, i.e., the normal-run magnetograms show negative H component excursion during the day time, sometimes sporadically and in the other time gradually. The ULF waves enhance their activity closely associated with these negative field variations. These field variations might be considered to occur when the station passes under the westward current flowing in the cusp ionosphere. By comparing the ground magnetic activities with the interplanetary magnetic field, the ground magnetic activities occur in association with high frequency fluctuations of the Interplanetary Magnetic Field (IMF). A comparison of spectral power of the ULF wave at Godhavn (cusp latitude) with those at Showa (auroral latitude) showed more enhanced magnetic power and more resonance-like oscillation of ULF waves at the auroral latitude.
Author (NASDA)

N94-29245# University of Electro-Communications, Chofu (Japan).
STUDY OF GENERATION MECHANISMS OF MAGNETOSPHERIC VLF/ELF EMISSIONS BASED ON THE DIRECTION FINDINGS
Masashi Hayakawa *In* National Inst. of Polar Research, Proceedings of the NIPR Symposium on Upper Atmosphere Physics, No. 6 Feb. 1993 p 117-133 (For primary document see N94-29233 08-46)
Avail: CASI HC A03/MF A02

The purpose of this report is to review the studies on the generation and propagation mechanisms of magnetospheric VLF (Very Low Frequency)/ELF (Extremely Low Frequency) emissions based on the direction finding measurements on board spacecrafts in order to demonstrate the potential use of the direction finding measurements in plasma wave studies. The plasma waves treated in this report are: (1) half-gyrofrequency VLF emissions; (2) ELF hiss in detached plasma regions of the magnetosphere; (3) plasmaspheric ELF hiss; (4) VLF/ELF chorus; and (5) hiss-triggered chorus.
Author (NASDA)

N94-29286# Army Cold Regions Research and Engineering Lab., Hanover, NH.
GLACIOHYDROLOGIC AND GLACIOHYDRAULIC EFFECTS ON RUNOFF AND SEDIMENT YIELD IN GLACIERIZED BASINS
Daniel E. Lawson Nov. 1993 121 p
(AD-A275134; CRREL-MONO93-2) Avail: CASI HC A06/MF A02

Glaciers exert significant control on runoff and sediment yield of partly glacierized basins, such basins being inherently more complex than non-glacierized basins. Glaciohydraulic and glaciohydrologic processes and factors determine the characteristics of runoff and of sediment discharge of rivers draining glacierized catchments. Significant problems develop in predicting both short- and long-term variations in water and sediment discharge because of the complicating effects of these processes and factors. Predictions are necessary for effective management of a basin or watershed's water resources. These processes and factors must therefore be incorporated to improve predictive models of runoff and develop models for sediment yield. In this monograph, the current state of knowledge on the nature of runoff and sediment yield in rivers originating in partly glacierized basins is reviewed and integrated into analyzing the glaciohydrologic and glaciohydraulic processes and factors determining basin characteristics. Current statistical and physical models for predicting runoff and sediment yield in glacierized basins are reviewed and, based upon an assessment of both the state of knowledge and modeling techniques, future research or application of existing knowledge to improve predictions are recommended.
DTIC

N94-29393# Teledyne Geotechnical, Alexandria, VA. Alexandria Lab.
STATISTICAL CHARACTERIZATION OF RUGGED PROPAGATION PATHS WITH APPLICATION TO Rg SCATTERING STUDY Semiannual Report
Rong-Song Jih 5 Nov. 1993 186 p
(Contract F29601-91-C-DB23)
(AD-A275237; TGAL-93-07) Avail: CASI HC A09/MF A02

Motivated by many observations of correlation between the free-surface topography and the coda generation at teleseismic and regional distances, seven simple statistics have been tested whether they can fully characterize the roughness of an arbitrary rugged free-surface topography. Based on 2-dimensional finite-difference simulations, the normalized arc length and Durbin-Watson number are identified as the best and the poorest, respectively, roughness measures, in terms of correlating with the propagation behavior of Rg. The numerical experiments show that rougher topography causes stronger attenuation (as expected), that reflection is an efficient process, and that the bulk of the energy which is not transmitted across the topography is either converted to body waves or reflected back. The scattered P and S waves are radiated as coda to teleseismic distances and some P-SV energy could be trapped in the crustal waveguide. The scattered body waves appear to radiate from the changes in slope and to first order can be visualized as from point diffractors along the rugged free-surface. Rg-to-S conversion is more efficient than that of Rg-to-P. The spatial Q values associated with rough topographic profiles range from 15 to 80, which are in excellent agreement with Q(Beta) of the uppermost crust in many places of the world. The attenuation coefficient, gamma, and the scattering loss can be asymptotically represented as linear functions of the roughness parameters. This work offers a promising approach to quantify effects of scattering by topography and heterogeneity upon other regional phases.
DTIC

N94-29430# Air Force Inst. of Tech., Wright-Patterson AFB, OH.
MESOPAUSE WINDS AND OH INTENSITIES AT MID-LATITUDES-FABRY-PEROT INTERFEROMETER OBSERVATIONS OF THE OH EMISSION AT 8430 A FROM BEAR LAKE OBSERVATORY M.S. Thesis
Carolyn M. Vadnais 1993 202 p
(AD-A275246; AFIT/CI/CIA-93-157) Avail: CASI HC A10/MF A03

Observations were made from Bear Lake Observatory using an Imaging-Fabry-Perot Interferometer. Neutral winds were derived from the Doppler shift to the emission line, and relative intensity was also analyzed. Results presented are from the period between December 1991 and March 1992. The 8430 A OH data showed remarkable day-to-day variability in the wind pattern. Diurnal, semidiurnal, and terdiurnal tidal components all appeared at some point during the observing period with no consistent regularity. The OH intensities showed the presence of gravity wave activity with discernible period down to approximately 3 hours. The 6300 A O(1D) wind and intensity observations showed a high degree of magnetic activity which correlated positively with Kp and Ap indices. We noted a definite presence of auroral and SAR-arc activity almost nightly on nights when the 6300 A O(1D) emission was observed.
DTIC

N94-29588*# McDonnell-Douglas Space Systems Co., Houston, TX.
FAST GRAVITY, GRAVITY PARTIALS, NORMALIZED GRAVITY, GRAVITY GRADIENT TORQUE AND MAGNETIC FIELD: DERIVATION, CODE AND DATA
Robert G. Gottlieb Feb. 1993 64 p
(Contract NAS9-17885)
(NASA-CR-188243; NAS 1.26:188243) Avail: CASI HC A04/MF A01

Derivation of first and second partials of the gravitational potential is given in both normalized and unnormalized form. Two different recursion formulas are considered. Derivation of a general gravity gradient torque algorithm which uses the second partial of the gravitational potential is given. Derivation of the geomagnetic field vector is given in a form that closely mimics the gravitational algorithm. Ada code for all algorithms that precomputes all possible data is given. Test cases comparing the new

algorithms with previous data are given, as well as speed comparisons showing the relative efficiencies of the new algorithms. Author

N94-29743 Clemson Univ., SC.
A STUDY OF THE THERMOSPHERIC DYNAMICS OF THE HIGH-LATITUDE E REGION USING A SPECTRAL THERMOSPHERIC GENERAL CIRCULATION MODEL Ph.D. Thesis
James Phillip Gundlach 1993 151 p
Avail: Univ. Microfilms Order No. DA9323876

The E region of the thermosphere suffers from a paucity of data due to the difficulty of obtaining E region measurements. Theoretical modeling studies of the region are therefore of great importance. This study examines the dynamics of the E region using a three dimensional, time dependent, spectral thermospheric general circulation model (STGCM) developed at the Danish Meteorological Institute. The model is nonlinear and includes specifications for the solar heating, auroral forcing, and upward propagating tides. The method of analysis included an examination of the horizontal and vertical wind fields, the vertical momentum fluxes, and the momentum flux-induced accelerations, all of which were obtained as a function of spatial location and universal time. The results obtained for study were from a simulation of two chemical release experiments done in Alaska in 1978 under disturbed conditions and opposite configuration of the IMF B(sub y) component. The model results are shown to adequately reproduce the salient features of the observed wind profiles. A comparison of a steady-state solution, used as the initial condition for the model runs, demonstrate the superiority of the spectral model over the finite difference models for high-latitude studies. The momentum flux is shown to be controlled by the vertical circulation which, in turn, is shown to be controlled by proximity to the high-latitude double-vortex wind system. Consequently, the largest vertical velocities are seen to occur in regions characterized by magnetospheric forcing; minimal vertical velocities occur both outside and within the center of the neutral wind vortices. Significantly, the vertical velocities generally reverse direction around 140 to 150 km. They also reverse directions from upward in the dayside inflow region to downward in the nightside exit flow region. In the F region, they have the same reversal in direction when going from the dawn side to the dusk side. The convergence of the momentum flux with height is seen to imply accelerations with a vertical variation that indicates strong vertical coupling in the upper E region. Dissert. Abstr.

N94-29752 State Univ. of New York, Albany.
DEVELOPING A DIODE ARRAY SPECTROMETER FOR TROPOSPHERIC CHEMISTRY STUDIES Ph.D. Thesis
Thomas Robert Lanni 1992 201 p
Avail: Univ. Microfilms Order No. DA9323723

The vital role of experimental probes in expanding the horizons of our knowledge of atmospheric chemistry has long been recognized. Application of the growing constellation of spectroscopic techniques to the study of trace gas photochemistry has constituted a new paradigm and contributed in many ways to our understanding of the troposphere. We present a novel technique, Long-Path Diode Array Differential Optical Absorption Spectroscopy (LPDA DOAS), to monitor trace gases in the troposphere. The technique is based on the multiplex advantage of the diode array and the principle of a 'differential' optical absorption cross-section. It enjoys the distinction of being an ambient measurement and hence avoids the pitfalls arising due to sampling biases and wall effects. The use of a diode array permits the dynamic and simultaneous acquisition of constituent spectra, rapid signal averaging, and enhanced dynamic range and signal-to-noise ratio. We show that the technique is sensitive, rapid, and lends itself to a straightforward analysis of species concentration and related photochemical parameters. Furthermore, the use of long optical paths makes this technique useful in relatively clean environments and allows for intercomparison with computer models of the troposphere. Dissert. Abstr.

N94-29909 Purdue Univ., West Lafayette, IN.
A STUDY OF THE CONVERGENCE OF SPHERICAL HARMONIC EXPANSIONS OF GRAVITY USING DISTRIBUTED POINT-MASS EARTH MODELS Ph.D. Thesis
William Danny Braswell 1992 195 p
Avail: Univ. Microfilms Order No. DA9313956

A new Earth model consisting of flattened concentric ellipsoidal layers overlaid by a distribution of point masses is developed and used to study convergence of spherical harmonic expansions of gravity in the vicinity of the smallest sphere bounding all the mass. The ellipsoidal layers are formed by 'flattening' the spherical layers from the Preliminary Reference Earth Model (PREM). Cases are examined in which the point masses are distributed uniformly and randomly, with the majority of the masses placed within 5 km of the surface. The masses of the point sources are determined by a least squares fit of the new model to NASA's experimentally derived GEMT1 gravity model. Closed form expressions for gravity external to the model and for the expansion coefficients are derived allowing convergence analysis to arbitrary accuracy to be performed. Results indicate that while spherical harmonic expansions of gravity do converge exterior to the bounding sphere, as theory indicates, when very close to the bounding sphere they may do so only after an initial period of divergence which can continue for several hundred or more terms and during which significant measurable errors can occur. Dissert. Abstr.

N94-29935 Moscow State Univ. (Russia). Nauchno-Issledovatelskij Inst.
QUASI-ADIABATIC MOTION OF ENERGETIC PARTICLES IN A DIPOLE MAGNETIC FIELD
V. D. Ilin, S. N. Kuznetsov, and B. Yu. Yushkov 1992 15 p Limited Reproducibility: More than 20% of this document may be affected by microfiche quality
(DE94-607322; NIIYaF-MGU-92-23-272) Avail: Issuing Activity (Department of Energy (DOE)) (US Sales Only)

A moving coordinate system for a dipole magnetic field in which reversible variations of magnetic moment for the range of obvious violations of adiabatic conditions are absent and the description of magnetic moment violations is relatively simple is considered. Constructing of a coordinate system, features of the central trajectory, determining its motion, the application range, the main application field, and consequences are discussed. DOE

N94-29939 Purdue Univ., West Lafayette, IN.
MOTION AND DEVELOPMENT OF THE PACIFIC PLATE FROM THE MIDDLE JURASSIC TO THE LATE CRETACEOUS Ph.D. Thesis
Brian Paul Wallick 1992 250 p
Avail: Univ. Microfilms Order No. DA9314094

Aspects of the early history of the Pacific plate were studied using the techniques of rock magnetism and paleomagnetism on samples retrieved from the presumed oldest portion of the Pacific plate. The magnetic properties of 51 basalt samples from Hole 801C were analyzed to study the reason for the magnetic quiescence in the presumed oldest portion of the Pacific plate. The results indicate magnetizations which are not atypical of other younger sites and which are very similar in several respects to Jurassic basalts from the Atlantic. The identification of five inclination zones within the basalt pile are interpreted to be the result of rapid change in polarity of the Earth's magnetic field and suggest a possible reason for the apparent magnetic quiescence. Paleomagnetic analysis of 25 Cretaceous basalts recovered from the Jurassic Quiet Zone region (ODP Site 802) yielded a useful paleolatitude approximation of approximately 19 deg S. Similarities between this estimate and that calculated for the basalts of Site 462, in addition to age similarities and geochemical data, suggest that these may be related as part of an episode of mid-Cretaceous spreading. Finally, the paleomagnetic analysis of sediments from five sites produced reliable paleolatitude estimates from the Bathonian-Callovian to the Campanian-Maestrichtian. The principal results from these paleolatitude estimates outline a general northward migration of the plate for much of its history; however, a period of anomalous south motion was observed for the period of time from approximately 150 to 125 Ma. A period of counter-clockwise rotation of 41 deg calculated from a combination of sediment structural data and FMS images is thought to be responsible for the apparent south motion. Dissert. Abstr.

N94-29940 Columbia Univ., New York, NY.
STUDIES IN JURASSIC AND CRETACEOUS NORTH AMERICAN APPARENT POLAR WANDER Ph.D. Thesis
Mickey Charles VanFossen 1992 220 p
Avail: Univ. Microfilms Order No. DA9313701

An alternative middle Jurassic through mid-Cretaceous North American apparent polar wander path is presented based on pole position studies of middle Jurassic plutons, volcanics and mid-Cretaceous plutons in New England (White Mountains Magma Series), the late Jurassic Morrison Formation in central Colorado, and the latest Jurassic-early Cretaceous

kimberlite dikes in New York State. Isolation of magnetizations on which the pole position data are based is achieved through laboratory decomposition of natural remanent magnetization (NRM) via detailed thermal and alternating field demagnetization experiments. Magnetization stability is evaluated through the application of field tests (e.g., bedding-tilt, reversal, baked contact, and glacial boulder tests). The results suggest an interval of middle Jurassic (approximately 166 Ma) apparent polar wander at 82 deg N, 090 deg E which differs greatly from previous interpretations. Together the new poles break up the latter half of the Mesozoic North American apparent polar wander path into two segments, each about 20 million years long (166 to 143 Ma, and 143 to 124 Ma). The path runs a general easterly course from 82 deg N, 090 deg E to about 58 deg N, 203 deg E during the late Jurassic and early Cretaceous, followed by an abrupt turn north to the mid-Cretaceous pole at 71 deg N, 194 deg E. The implications of this alternative North American apparent polar wander path to plate tectonic studies and to previous analyses of apparent polar wander are discussed. Dissert. Abstr.

N94-29941 Connecticut Univ., Storrs.
EFFECTS AND IMPLICATIONS OF FAULT ZONE HETEROGENEITY AND ANISOTROPY ON EARTHQUAKE STRONG GROUND MOTION Ph.D. Thesis
Wei-Jou Su 1992 170 p
Avail: Univ. Microfilms Order No. DA9315399

This thesis consists of two parts. Part one is concerned with the effect of fault zone heterogeneity on the strong ground motion of the Loma Preita earthquake. Part two is concerned with the effect of the effective hexagonal anisotropy of a fault zone on strong ground motion. A superposition of Gaussian beams is used to analyze these problems because it can account for both the rupture history of the fault plane and the fault zone heterogeneity. We also extend this method to investigate the combined effects of the rupture process on a fault plane and medium anisotropy on the synthetic seismograms. The strong ground motion of the Loma Prieta Earthquake is synthesized using a known three-dimensional crustal model of the region, a rupture model determined under the assumption of laterally homogeneous structure, and Green's functions computed by superposition of Gaussian beams. Compared to results obtained assuming a laterally homogeneous crust, stations lying to the northeast of the rupture zone are predicted to be defocused, while stations lying to the west of the fault trace are predicted to be focused. The defocusing is caused by a zone of high velocity material between the San Andreas and Sargent faults, and the focusing is caused by a region of low velocity lying between the Zayantes and San Andreas faults. If lateral homogeneity is assumed, the net effect of the predicted focusing and defocusing is to bias estimates of the relative slip of two high slip regions found in inversions of local and teleseismic body waves. These biases are similar in magnitude to those estimated for waveform inversions from the effects of using different subsets of data and/or different misfit functions and are similar in magnitude to the effects predicted for non-linear site responses. Dissert. Abstr.

N94-29969 Columbia Univ., New York, NY.
THE RUPTURE PROCESS OF LARGE EARTHQUAKES ALONG CONVERGENT MARGINS: CAST STUDIES FROM ALASKA AND ARMENIA Ph.D. Thesis
Charles Hershey Estabrook 1992 271 p
Avail: Univ. Microfilms Order No. DA9313589

This thesis focuses on the varied nature of earthquake ruptures in regions of convergent tectonics. Several modern and historical earthquakes along the Alaska-Aleutian arc and in Armenia are investigated using body and surface waves. The 1979 St. Elias, Alaska earthquake is analyzed because of unresolved questions about its depth, focal mechanism, seismic moment, and location in a seismic gap. Source mechanisms and locations of the two distinct mainshock subevents and aftershock locations define a shallow dipping surface at the eastern edge of the Pacific plate. The amount of strike-slip motion increases with time in the mainshock implying that a change from thrusting to strike-slip faulting occurs along the plate interface. Aftershock relocation suggests that the main plate boundary may be offset as a result of collision and subduction of the Yakutat terrane. Seismic waves from the 1988 Armenia earthquake are best fit with a source model that includes three subevents. Rupture apparently initiated as a shallow reverse fault at a point of maximum bending on a right-lateral strike-slip fault and then extended bilaterally towards the southeast and west. The largest events along the Alaska Peninsula and Shumagin Islands segments of the Aleutian arc since 1917 are studied to understand the likely modes of rupture in the next sequence of large and great events and to delineate the plate interface geometry. Results from body and surface wave modeling suggest that the 1917 earthquake was smaller than previously thought and was restricted to the eastern-most portion of the gap. Seismic moment and gross rupture characteristics of the great 1938 earthquake along the Alaska Peninsula are estimated using teleseismic body and surface waves. Dissert. Abstr.

N94-29978# National Inst. of Polar Research, Tokyo (Japan).
ANTARCTIC RECORD, VOL. 36, NO. 3 [NANKYOKU SHIRYU VOL. 36, NO. 3]
Takao Hoshiai, ed., Masaki Ejiri, ed., Takeo Hirasawa, ed., Yoshikuni Hiroi, ed., Katsutada Kaminuma, ed., Sadao Kawaguchi, ed., Shunichi Kobayashi, ed., Susumu Kokubun, ed., and Yasuhiko Naito, ed. et al 30 Nov. 1992 146 p In ENGLISH and JAPANESE
(ISSN 0085-7289)
(Rept-108; JTN-94-80591) Avail: CASI HC A07/MF A02

The following topics were discussed: Antarctica, antarctic regions, earth observation, atmospheric sounding, earth stratosphere, earth ionosphere, earth magnetosphere, geomagnetism, magnetic disturbance, upper atmosphere, meteorological observation, atmospheric radiation, precipitation, climate change, air sea ice interaction, radar observation, Polar Patrol Balloon (PPB), argos system, data transmission, satellite transmission, snow vehicle, crawler tractors, temperature effects, low temperature environment, physiological effects, crawler belt, welded joints, joint strength, snow vehicle performance, vertical pointing radar, annual variation, auroras, and Showa station. For individual titles, see N94-29979 through N94-29986.

N94-29979# National Inst. of Polar Research, Tokyo (Japan).
A STUDY OF PRECIPITATION IN THE COASTAL AREA OF ANTARCTICA AS OBSERVED AT SYOWA STATION USING A VERTICAL POINTING RADAR [NANKYOKU ENGANIKI SHOWA KICHI DE NO SUICHOKU REDA O MOCHIITA KOSUIRYO NO KENKYU] **c47**
Makoto Wada and Hiroyuki Konishi *In its* Antarctic Record, Vol. 36, No. 3 30 Nov. 1992 p 341-349 (For primary document see N94-29978 08-46)
Avail: CASI HC A02/MF A02

A new vertical pointing radar was installed at Showa Station in 1988 for observing precipitation and clouds in Antarctic Climate Research project started in 1987. The precipitation of 1988 was approximately half of that of 1989. The total precipitation was estimated at about 200 mm from February 23, 1988 to February 22, 1989 and about 390 mm form February 1 to November 30, 1989. The tendency of little snow accumulation in 1988 can be seen in the year-to-year data of the maximum snow depth measured on the sea ice near Showa Station and in the annual data of snow accumulation around the coastal area of the continent near Showa Station. The small precipitation of 1988 at Showa Station seems to be mainly due to small precipitation in winter and spring of 1988, compared with that of 1989. Author (NASDA)

N94-29980# National Inst. of Polar Research, Tokyo (Japan).
DATA TRANSFER SYSTEM USING A MULTI-ID ARGOS TRANSMITTER FOR THE ANTARCTIC POLAR PATROL BALLOON EXPERIMENT [NANKTOKU SHUKAI KIKYU (PIPIBI) NI OKERU MARUCHI AIDI ARUGOSU SHISUTEMU O MOCHIITA DETA DENSO]
Ryoichi Fujii, Kazuhiko Ono, and Shigeo Ota *In its* Antarctic Record, Vol. 36, No. 3 30 Nov. 1992 p 350-362 In JAPANESE (For primary document see N94-29978 08-46)
Avail: CASI HC A03/MF A02

A newly developed multi-ID (Identification) ARGOS data transfer system for the PPB (Polar Patrol Balloon) experiment (1990-1993) is described. This system on board the PPBs with a main processor continuously transferred data of about 2 kB/h with great reliability during the entire observation periods (longer than one month). This brief report describes the principle and specifications of the system. Author (NASDA)

N94-29981# National Inst. of Polar Research, Tokyo (Japan).
A NEWLY DEVELOPED SNOW VEHICLE (SM100S) FOR ANTARCTICA. PART 1: NECESSITY AND PROCESS OF THE DEVELOPMENT [NANKYOKU OGATA SETSUJOSHA (SM100S) NO KAIHATSU. 1: HITSUYOSEI TO KAIHATSU KEII] **c37**
Sadao Takeuchi, Atsushi Kino, Masayuki Hosoya, Jiro Yoshida, and Kenji Ishizawa *In its* Antarctic Record, Vol. 36, no. 3 30 Nov. 1992 p 363-375 In JAPANESE (For primary document see N94-29978 08-46)
Avail: CASI HC A03/MF A02

Four types of snow vehicles have so far been employed in the Japanese Antarctic Research Expedition. These snow vehicles are mainly used on the inland ice sheet and on the sea ice. As for the inland traverses, the SM50S-type snow vehicle has been used, but the research area is now expanding to the much colder area, and the deep ice coring project at Dome Fuji, East Antarctica, has recently been proposed. Therefore, a committee for the design of a new snow vehicle was organized in the special committee on logistics of the National Institute of Polar Research. The committee made the design of a new snow vehicle capable of operating under very cold and low pressure conditions. The newly developed snow vehicle was operated on the Antarctic ice sheet in the winter of 1992, and the performance was almost just as expected. Author (NASDA)

N94-29982# Ohara Corp., Nagaoka (Japan).
A NEWLY DEVELOPED SNOW VEHICLE (SM100S) FOR ANTARCTICA. PART 2: DESIGN OF THE SYSTEM [NSNKYOKU OGATA SETSUJOSHA (SM100S) NO KAIHATSU. 2: SHISUTEMU DEZAIN] **c37**
Masashi Nakajima and Masayuki Hosoya *In* National Inst. of Polar Research, Antarctic Record, Vol. 36, No. 3 30 Nov. 1992 p 376-392 In JAPANESE (For primary document see N94-29978 08-46)
Avail: CASI HC A03/MF A02

This report describes the design of the systems of a newly developed snow vehicle, which will be used for the deep ice coring project at Dome Fuji, East Antarctica. This vehicle is a cab-over full-track type, in which the accommodations for two persons are prepared. The vehicle is 11,500 kg in gross weight and traverses at 5 to 8 km/h pulling seven wooden type sledges each of which is 2.6 t in loaded weight. The vehicle operates at low temperature down to -60 C on the Antarctic ice sheet from the plain up to the high plateau of 4,000 m in altitude. In addition, the preservation of the vehicle is possible under the severe environment as cold as -0 C. In the process of the development, the requested performance was analyzed first, and then the structure, configuration, and dimensions of the vehicle were estimated. Problems from other snow vehicles operated before in Antarctica were extracted and then were solved by means of experiments and researches to make use of the results for the design.
Author (NASDA)

N94-29983# Nippon Kokan K. K., Kawasaki (Japan).
A NEWLY DEVELOPED SNOW VEHICLE (SM100S) FOR ANTARCTICA. PART 3: LOW TEMPERATURE TOUGHNESS OF THE WELDED JOINTS OF THE STRUCTURAL STEEL [NANKYOKU OGATA SETSUJOSHA (SM100S) NO KAIHATSU. 3: SHATAI ZAIRYO NO YOSETSUBU TEION JINSEI] **c76**
Shin Sakui and Masashi Nakajima *In* National Inst. of Polar Research, Antarctic Record, Vol. 36, No. 3 30 Nov. 1992 p 393-397 In JAPANESE (For primary document see N94-29978 08-46)
Avail: CASI HC A01/MF A02

For the purpose of developing a new snow vehicle (common use at temperature about -50 C) for the deep ice coring project at Dome Fuji, East Antarctica, the low temperature toughness of the welded joints of structural steel was investigated. It is empirically well known that in case of vehicles employed in a cold air temperature of about -50 C, the low temperature brittle fracture of the structural members does not take place, if one uses semi-killed or killed steel, for which 50 percent FATT's (fracture appearance transition temperature) of the Charpy impact test is about -50 C and Charpy impact values at -50 C are 20 to 29 J/sq cm. In the present report, the Charpy impact test has been performed for both single pass SMAW (shield metal arc welding) and CO2 arc welded joints of JIS (Japan Industrial Standards) steels of SS400, SL2N255, STPL380, and STPL450. The test results show that the JIS steels of SL2N255 and STPL450 can be used for the new vehicle, considering their toughness.
Author (NASDA)

N94-29984# Bando Chemical Industries Ltd., Kobe (Japan).
A NEWLY DEVELOPED SNOW VEHICLE (SM100S) FOR ANTARCTICA. PART 4: LOW TEMPERATURE PROPERTIES OF CRAWLER BELT [NANKYOKU OGATA SETSUJOSHA (SM100S) NO KAIHATSU. 4: GOMU RITAI NO TEION TOKUSEI] **c37**
Etsuji Maekawa and Yoshihide Terayama *In* National Inst. of Polar Research, Antarctic Record, Vol. 36, No. 3 30 Nov. 1992 p 398-409 In JAPANESE (For primary document see N94-29978 08-46)
Avail: CASI HC A03/MF A02

In order to discover a high cold-resistance material for use in the crawler belt of snow vehicles, the physical properties at very low temperatures of a recently developed material, isoprene/butadiene (70/30) random copolymer filled with carbon black, was investigated in comparison with a blended rubber NR (Natural Rubber) / BR (Butadiene Rubber) (65/35) as well as a currently used NR. It has been found that this material can keep rubber elasticity even at low temperatures below - 70 C, though it is somewhat inferior to the other two materials as to strengths such as stress-at-break and tear; and hence, it is considered as quite worthy of a practical test for a snow vehicle in the Antarctic area.
Author (NASDA)

N94-29985# Ohara Corp., Nagaoka (Japan).
A NEWLY DEVELOPED SNOW VEHICLE (SM100S) FOR ANTARCTICA. PART 5: RESULT OF GENERAL PERFORMANCE TESTS [NANKYOKU OGATA SETSUJOSHA (SM100S) NO KAIHATSU. 5: SEINO SHIKEN] **c37**
Mitsuru Saito, Tsuyoshi Seki, and Masayuki Hosoya *In* National Inst. of Polar Research, Antarctic Record, Vol. 36, No. 3 30 Nov. 1992 p 410-440 In JAPANESE (For primary document see N94-29978 08-46)
Avail: CASI HC A03/MF A02

This report describes the results of the fundamental and the general performance tests for a newly developed snow vehicle, which will be used for the deep ice coring project at Dome Fuji, East Antarctica. The result of the tests showed that the vehicle generally satisfied the expected performance and the purpose of the systems design, but was partially unsatisfactory in its structure. The tests were carried out on the concrete pavement where its reproducibility is capable of comparing with the performance of similar vehicles and on the compacted snow surface which has the simulated hardness of the Antarctic snow. Author (NASDA)

N94-29986# National Inst. of Polar Research, Tokyo (Japan).
ACTIVITIES OF THE WINTERING PARTY AT SYOWA STATION BY THE 32ND JAPANESE ANTARCTIC RESEARCH EXPEDITION IN 1991 [DAI 32 JI NANKYOKU CHIIKI KANSOKUTAI SHOWA KICHIETTO (1991) HOKOKU]
Yoshiyuki Fujii *In its* Antarctic Record, Vol. 36, No. 3 30 Nov. 1992 p 441-472 In JAPANESE (For primary document see N94-29978 08-46)
Avail: CASI HC A03/MF A02

The winter party of the 32nd Japanese Antarctic Research Expedition performed its activities at two wintering sites 1991-1992, consisting of 31 members at Showa Station (69 deg 00 min S, 39 deg 35 min E) and eight members at Asuka Station (71 deg 31.5 min S, 24 deg 8 min E). Wintering activities at Asuka Station will be reported separately. The main scientific research programs at Showa Station were as follows: (1) studies on ocean-atmosphere interaction in the sea ice area part of the Antarctic Climate Research Program (ACR); (2) environmental science studies; (3) polar patrol balloon experiment; and (4) life science studies. Various airborne observations and inland glaciological traverses were carried out.
Author (NASDA)

N94-30014*# Alabama Univ., Huntsville.
[ACCURATE MODELING OF F-REGION ELECTRON DENSITIES] Annual Progress Report, 1993-1994
1994 8 p
(Grant NAGw-996)
(NASA-CR-195781; NAS 1.26:195781) Avail: CASI HC A02/MF A01

In the past year, we have made considerable progress in a number of areas including algorithm development, completion of two major case studies, and the development of a new EUV flux model. As a result, there has been a major improvement in our ability to model global emissions in

support of NASA's imaging plans. Activity highlights include the following: developed a new algorithm to allow physical models to reproduce observed NmF2; investigated the relationship between NmF2 and F10.7 at Millstone Hill during 1990; developed a new solar EUV flux model; statistical survey of anomalously high nighttime electron T(sub e) at Millstone Hill; conducted a case study of the March 1990 magnetic storm; and conducted a comparison between theory and data of magnetically quiet behavior of the winter ionosphere at Millstone Hill. Derived from text

N94-30093 International Centre for Theoretical Physics, Trieste (Italy).
EXTENSION OF LOVE WAVE TRANSFORMATION THEORY TO LATERALLY HETEROGENEOUS STRUCTURES
F. Romanelli and G. F. Panza Aug. 1993 20 p Limited Reproducibility: More than 20% of this document may be affected by microfiche quality
(DE94-608098; IC-93/259) Avail: CASI HC A03 (US Sales Only)

By means of the spherical-to-flat transformations for torsional waves, all the flat-transformed components of motion (two for displacement and five for stress) have been derived. This provides the formal basis necessary to treat the propagation of torsional waves in spherical 3-D structures, by using the existing flat-structure computational techniques. DOE

N94-30107 Moscow State Univ. (Russia). Nauchno-Issledovatelskij Inst.
SIMULATION OF SPACE-ENERGY DISTRIBUTIONS OF HOT PLASMA ON A GEOSTATIONARY ORBIT
A. S. Kovtyukh and M. I. Panasyuk 1992 41 p Limited Reproducibility: More than 20% of this document may be affected by microfiche quality
(DE94-607324; NIIYaF-MGU-92-28-277) Avail: CASI HC A03 (US Sales Only)

A review is presented of known empirical models for space-energy distributions of particles (electrons and ions) of hot plasma in the region of a geostationary orbit of a satellite. For magnetically quiet periods are developed practically completed models both for ions, and for electrons. The stationary models have simple analytical expressions. DOE

N94-30134 British Columbia Univ., Vancouver. Dept. of Mathematics.
LARGE EDDY SIMULATION OF THE UPPER ATMOSPHERIC SURFACE LAYER Ph.D. Thesis
Xiaoming Cai Jul. 1993 208 p
(ISBN-0-315-85393-X; CTN-94-61155) Copyright Avail: Micromedia Ltd., Technical Information Centre, 240 Catherine Street, Suite 305, Ottawa, Ontario, K2P 2G8, Canada HC/MF

Three dimensional large eddy simulation (LES) is adopted to simulate turbulence in the atmospheric boundary layer (ABL), with a fine resolution in the atmospheric surface layer, so that an a-priori value of the von Karman constant and the Monin Obukhov similarity formulas can be derived from the resolved scale turbulence in the upper surface layer (USL). Smagorinsky's sub-grid scale (SGS) model is adopted. The Smagorinsky model Reynolds number ReS is proposed for a LES adopting the Smagorinsky SGS model. This number is shown to be an independent model parameter which determines the statistics of the resolved scale (RS) turbulence in the USL. If ReS is smaller than a critical value, RS fields are damped out, thereby establishing a criterion for a LES adopting the Smagorinsky SGS model. For a neutral static stability ABL, grid spacings are used which fall within the inertial subrange of the USL turbulence in order to follow the assumption of the Smagorinsky SGS model. The average of the velocity fields yields a logarithmic velocity profile in the USL from which the von Karman constant can be derived. The value of this constant and other quantities in the USL exhibit a strong dependence on ReS. For an unstable ASL, profiles of the mean velocity in the USL yield a Monin Obukhov similarity formula for the dimensionless momentum flux.
Author (CISTI)

N94-30223 Moscow State Univ. (Russia). Nauchno-Issledovatelskij Inst.
VARIATIONS OF ELECTRON FLUXES, LOW-FREQUENCY RADIATIONS AND PLASMA DENSITY DURING THE GEOMAGNETIC STORM ON 9-12 MARCH, 1979 ACCORDING TO DATA OF THE INTERKOSMOS-19 SATELLITES
A. A. Gusev, Yu. V. Mineev, M. G. Nikiforova, G. I. Pugacheva, E. D. Tolstaya, and V. I. Larkina 1992 38 p Limited Reproducibility: More than 20% of this document may be affected by microfiche quality
(DE94-607323; NIIYaF-MGU-92-24-273) Avail: CASI HC A03 (US Sales Only)

During the geomagnetic storm on 9-12 March, 1979 simultaneous data were obtained on the field intensity (electronic and magnetic components) of low-frequency radiations (0,1-20 kHz), energetic electron flux density at E(sub e)=0.04-2.0 MeV and protons at E(sub p)=1-30 MeV and thermal plasma density (10(sup 1) - 2x10(sup 6) cm(sup -3)). Correlation dependences of VLF radiation intensity with the plasma parameters and energetic particle variations are established. DOE

N94-30608# Utah Univ., Salt Lake City. Dept. of Meteorology.
CLOUD AND AEROSOL CHARACTERIZATION FOR THE ARM CENTRAL FACILITY: MULTIPLE REMOTE SENSOR TECHNIQUES DEVELOPMENT
K. Sassen 1 Nov. 1993 13 p
(Contract DE-FG02-90ER-61059)
(DE94-003523; DOE/ER-61059/2) Avail: CASI HC A03/MF A01

In support of the initial phase of the Instrument Development Program (IDP) of the Atmospheric Radiation Measurement (ARM) program, the authors have researched the means by which multiple remote sensing techniques could be best applied to characterizing the cloudy atmosphere. This research has directly supported the short-term goal of aiding in the selection of the most appropriate instrumentation for ARM Clouds and Radiation Testbed (CART) sites, but also has more long-term consequences for the application of remote sensing for measuring cloud properties of crucial concern to general circulation and climate models. To accomplish the goals they have (1) developed a mobile, state-of-the-art, scanning polarization diversity lidar (PDL) to test a variety of techniques for cloud remote sensing, including simultaneous dual-wavelength and dual-polarization, and high-speed variable field-of-view operations; (2) successfully participated in field projects using the PDL along with other remote sensors and instrumented aircraft to obtain detailed datasets for the testing of instrument techniques; and (3) in collaboration with researchers at the NOAA Wave Propagation Laboratory, used numerical cloud modeling and empirical studies to develop and refine remote sensing approaches for cloud property retrieval. DOE

N94-30789 California Univ., Los Angeles.
GENERATION MECHANISMS OF QUASI-STATIONARY WAVES IN THE SOUTHERN HEMISPHERE Ph.D. Thesis
Ignacio-Arturo Quintanar 1993 162 p
Avail: Univ. Microfilms Order No. DA9317893

The effect of Antarctic elevations, the rest of the world orography and thermal forcing from lower latitudes on the atmospheric circulation of the Southern Hemisphere is investigated by following an approach based on the comparison of simulations using the UCLA General Circulation Model (GCM) with different prescribed surface boundary conditions. With the GCM we have started by performing an extended control simulation and a systematic series of hypothesis-testing simulations in which orographic and surface conditions were artificially modified. In high latitudes, GCM simulations without the Antarctic orography or even with the Antarctic orography rotated 180 deg around the South Pole show a QS-wave 1 with substantial amplitude and approximately the same phase as in the control simulation with full orography. At polar latitudes, on the other hand, the local maximum in QS-wave 1 that is present in the observational data is only obtained in the control simulation, although the experiment where the Antarctic elevations are rotated 180 deg also produces large values. The GCM simulation with all orographic elevations removed shows QS-wave 1 with an amplitude about 40 percent smaller than that found in the control simulation. Thus QS-wave 1 in the Southern Hemisphere is not primarily generated by the Antarctic elevations. Other contributors to the generation of QS-wave 1 are the rest of the world orography, thermal forcing from lower latitudes and forcing by transient eddies. The results also suggest that zonal asymmetries in sea surface temperature (SST) and sea-ice south of 46 deg S are closely linked to the phase of a zonal wavenumber 2 component (QS-wave 2) at upper levels at high and polar latitudes of the Southern Hemisphere. Previous studies with simpler models suggest that the Antarctic orography can generate a stationary wave field at high and middle latitudes that has substantial pattern similarities with the observed. This is verified by using a barotropic model with both idealized and realistic representation of the Antarctic orography forced by relaxation to the October zonal mean climatology. Nevertheless, to obtain a realistic amplitude of the waves with the barotropic model requires a somewhat arbitrary specification of the magnitude of the forcing. The results of the GCM

simulation suggest, however, that realistic forcings would produce amplitudes of the quasi-stationary wave field that are significantly weaker than the observed. Dissert. Abstr.

N94-30802 Illinois Univ., Urbana-Champaign.
THEORY AND OBSERVATIONS OF HORIZONTAL AND VERTICAL STRUCTURE OF GRAVITY WAVE PERTURBATIONS IN THE MIDDLE ATMOSPHERE Ph.D. Thesis
Chris Alan Hostetler 1993 142 p
Avail: Univ. Microfilms Order No. DA9329061

Gravity wave models for the horizontal wave number spectra of atmospheric velocity and density fluctuations are derived by assuming that both saturated and unsaturated waves obey the polarization and dispersion relations and that the joint (m,w) spectrum is separable. The models show that the joint (k,l,m) and (k,l,w) spectra are not separable. The one-dimensional horizontal wave number spectra models are consistent with existing observations of horizontal wave number spectra in the lower stratosphere and upper mesosphere. The gravity wave models are used to analyze the effects of Doppler shifting caused by the mean wind field on the separability of gravity wave spectra. If the intrinsic joint (m,w) spectrum is separable, Doppler effects associated with even small mean winds will destroy separability of the observed joint (m,w(sub o)) spectrum, particularly at high vertical wave numbers. Vertical and horizontal wave number spectra of density perturbations in the upper stratosphere (25-40 km) and the upper mesosphere (approximately 80-105 km) measured during the ALOHA-90 campaign are presented. The spectra were inferred from approximately 45 h of airborne Na/Rayleigh lidar observations in the vicinity of Hawaii. Density variances, vertical shear variances, Richardson's numbers, characteristic vertical and horizontal wave numbers, and power law slopes of the vertical and horizontal wave number spectra are computed and discussed. The observed m-spectra contradict the predictions of the linear instability theory of Dewan and Good, and the scale-dependent diffusive filtering theory of Gardner, and appear to be compatible with the Doppler spreading theory of Hines, the scale-dependent diffusion theory of Weinstock, the scale-independent diffusive filtering theory of Gardner, and the similitude model of Dewan. In the stratosphere, the m-spectra exhibit significant energy at low wave numbers less than the values expected for m(sub *). The source of this energy is believed to be geostrophic adjustment of the jet stream. Dissert. Abstr.

N94-30805 Alaska Univ., Fairbanks.
RADIATION TRANSPORT IN CLOUDY AND AEROSOL LOADED ATMOSPHERES Ph.D. Thesis
Arve Kylling 1992 179 p
Avail: Univ. Microfilms Order No. DA9325174

The equation for radiation transport in vertical inhomogeneous absorbing, scattering, and emitting atmospheres is derived from first principles. It is cast in a form amenable to solution, and solved using the discrete ordinate method. Based on the discrete ordinate solution a new computationally efficient and stable two-stream algorithm which accounts for spherical geometry is developed. The absorption and scattering properties of atmospheric molecules and particulate matter is discussed. The absorption cross sections of the principal absorbers in the atmosphere, H2O, CO2 and O3, vary erratically and rapidly with wavelength. To account for this variation, the correlated-k distribution method is employed to simplify the integration over wavelength necessary for calculation of warming/cooling rates. The radiation model, utilizing appropriate absorption and scattering cross sections, is compared with ultraviolet radiation measurements. The comparison suggests that further experiments are required. Ultraviolet (UV) and photosynthetically active radiation (PAR) is computed for high and low latitudes for clear and cloudy skies under different ozone concentrations. An ozone depletion increases UV-B radiation detrimental to life. Water clouds diminish UV-B, UV-A and PAR for low surface albedos and increase them for high albedos. The relative amount of harmful UV-B increases on overcast days. The daily radiation doses exhibit small monthly variations at low latitudes but vary by a factor of 3 at high latitudes. Photodissociation and warming/cooling rates are calculated for clear skies, aerosol loaded atmospheres, and atmospheres with cirrus and water clouds. After major volcanic explosions aerosols change O3 and NO2 photodissociation rates by 20 percent. Both aged aerosols and cirrus clouds have little effect on photodissociation rates. Water clouds increase (approximately 100 percent) photodissociation rates that are sensitive to visible radiation above the cloud. Solar warming rates vary by 50 percent in the stratosphere due to changing surface albedo. Water clouds have a similar effect. The net effect of cirrus clouds is to warm the troposphere and the stratosphere. Only extreme volcanic aerosol loadings affect the terrestrial warming rate, causing warming below the aerosol layer and cooling above it. Aerosols give increased solar warming above the aerosol layer and cooling below. Dissert. Abstr.

N94-30808 Harvard Univ., Cambridge, MA.
ELECTROMAGNETIC CORE-MANTLE COUPLING Ph.D. Thesis
Jeffrey James Love 1993 144 p
Avail: Univ. Microfilms Order No. DA9318678

Due to exchanges of angular momentum between the earth's fluid outer core and the overlying solid mantle, the earth's rotational rate fluctuates on periods of a few years to a few decades. However, the mechanism which allows the exchange of angular momentum is not understood. Here we examine the possibility that core-mantle coupling is predominantly electromagnetic and thus responsible for the decadal length of day variations. The electromagnetic couple may be divided into poloidal, advective, and leakage couples. The poloidal couple results entirely from the interaction of the poloidal field with currents induced by its time variation. The advective couple results from the dragging of poloidal field lines through a conducting mantle. The leakage couple results from the diffusion of toroidal magnetic field from the core's interior into the mantle. The poloidal and advective couples can be calculated by using models of the downward continued poloidal field and models of the core velocity field deduced from the secular variation of the poloidal field. On the other hand, the leakage field requires knowledge of the toroidal field, which cannot be obtained directly from surface observations. By treating the determination of the toroidal field at the core-mantle boundary as an inverse problem, we find that toroidal field models consistent with both advection in the core and the decadal length of day variations have a complex structure and are not simply quadrupolar, as assumed by other investigators. Moreover these toroidal field models are too strong according to dynamo theory, produce electric fields at the earth's surface which are stronger than measured values, and produce ohmic heating which either exceeds or contributes an unacceptably large fraction of the earth's surface heat flow. Therefore, we conclude that core-mantle coupling is not predominantly electromagnetic. We also investigate the effect of lateral variations in mantle conductivity on our interpretation of processes occurring in the core and find that the effect is negligible. Dissert. Abstr.

N94-30867 Rhode Island Univ., Kingston.
THE LONG-RANGE TRANSPORT OF AEROSOL PARTICLES OVER THE NORTH ATLANTIC OCEAN Ph.D. Thesis
William Grenville Ellis, Jr. 1992 217 p
Avail: Univ. Microfilms Order No. DA9316591

As part of the Atmosphere/Ocean Chemistry Experiment (AEROCE), daily aerosol samples were collected at Bermuda and Barbados. In addition, gas-phase (222)Rn concentrations were analyzed hourly from July 1991 to June 1992. Isentropic analyses, isentropic trajectories, and non-isentropic trajectories were used to understand the long-range transport of these substances. In particular, the sources of selenium (Se) at Bermuda and Barbados, the transport of aluminum (Al) at Barbados, and the effect of atmospheric stability on radionuclides at Bermuda, were investigated. At Bermuda, approximately 55 percent of the aerosol Se came from anthropogenic sources located in North America, while the remainder appeared to be from a marine biogenic source. At Barbados, 60-80 percent of the Se was attributed to marine biogenic sources. At Barbados, the transport of Al from northern Africa to Barbados was modelled using a vertical interpolation of wind fields. Stokes's law of gravitational settling was used to parameterize the vertical motion. The trajectories using Stokes's law more accurately predicted the source region of the Al compared to low-level isentropic trajectories. The affect of tropospheric stability on the concentrations of (222)Rn, (210)Pb and (7)Be sampled at Bermuda was investigated. (7)Be has an upper tropospheric source, while (222)Rn and (210)Pb both have a continental source. The stability of the lower troposphere was calculated based on the relative separation of isentropic surfaces over North America. The results showed that this measure of stability was able to resolve the seasonal effect of stability on these radionuclides, but was not a quantitative predictor. Dissert. Abstr.

N94-30869 Colorado Univ., Boulder.
THEORY AND APPLICATION OF A RADIO-ACOUSTIC SOUNDING SYSTEM (RASS) Ph.D. Thesis
Richard Joseph Lataitis 1992 222 p
Avail: Univ. Microfilms Order No. DA9318108

The speed of sound in air is proportional to the square root of the virtual temperature. A conventional Doppler wind-profiler radar can measure the speed of a sound wave, emitted from a nearby acoustic source, at various heights, from which a virtual temperature profile can be inferred. This thesis examines the effect of various environmental factors on the performance of such a Radio-Acoustic Sounding System (RASS). A simple expression for the RASS echo power in the form of a radar equation has been derived. The effects of horizontal winds, turbulence, vertical temperature gradients, and a displacement of the acoustic source from the radar have been included. Previous developments considered only pieces of the total problem. The development here unifies and extends earlier work. A RASS comprising a monostatic pulsed Doppler radar and a band-limited acoustic source was analyzed theoretically for the first time. Previous results based on uniform turbulence profiles were extended to include realistic profiles. The effect of a vertical temperature gradient, which was studied only numerically in the past, is described analytically here. The accuracy of the RASS temperature retrievals was also theoretically examined. An analytic expression for the temperature error that includes all of the above effects was developed. The contribution of turbulence to this error was identified and quantified for the first time. Multiple acoustic sources are often used in RASS to enhance the height coverage. No analytic description of such systems had previously existed. The development was extended to include multiple acoustic sources and the expected enhancement was theoretically confirmed. The effect of multiple acoustic sources on the error in the temperature retrieval was also investigated. The ability of a wind-profiler/RASS to measure mean winds and temperatures is well documented. In contrast there have been few studies investigating how well such a system can measure wind and temperature variances, and fluxes. Vertical wind and temperature spectra and heat flux cospectra, obtained from sonic anemometer and windprofiler/RASS time series were compared. The agreement was poor suggesting the need for more comparative studies to identify sources of error. Dissert. Abstr.

N94-30876# Lawrence Livermore National Lab., CA.
TROPOSPHERIC RADIATIVE FORCING OF O3 FOR THE 1994 IPCC REPORT
A. S. Grossman, K. E. Grant, and D. J. Wuebbles 22 Sep. 1993 9 p
(Contract W-7405-eng-48)
(DE94-005698; UCRL-ID-115827) Avail: CASI HC A02/MF A01

We have determined the tropospheric radiative forcing of O3 in the 175 to 735 nm (UV-visible) wavelength range plus the 500 to 1650 cm(exp -1) (infrared) wavenumber range in accordance with a set of IPCC test cases provided to all interested modeling groups. The atmospheric test cases involved perturbed ozone scenarios in a McClatchey midlatitude summer, clear sky, model atmosphere. A new short wave radiative transfer code has been developed to calculate the radiative forcing in the 175 to 735 nm wavelength range. The IR radiative forcing was calculated using a correlated k-distribution transmission model. The tropospheric radiative forcing values obtained for the IR spectral region and the UV-visible spectral region lie in the middle of the range of preliminary values submitted from all of the models used in the IPCC test calculations. DOE

N94-30883 Morgantown Technology Center, WV.
ANALYSIS OF DEEP SEISMIC REFLECTION AND OTHER DATA FROM THE SOUTHERN WASHINGTON CASCADES Quarterly Report, 1 Mar. - 31 May 1993
W. D. Stanley (Geological Survey, Reston, VA.) 1994 8 p Limited Reproducibility: More than 20% of this document may be affected by microfiche quality
(Contract DE-AT21-92MC-29267)
(DE94-005915; DOE/MC-29267/3523) Avail: CASI HC A02

This report covers the period 1 Mar. - 31 May 1993. The overall goals of the program task are to provide a final synthesis of six deep seismic reflection profiles and other geological and geophysical data from the southern Washington Cascades region where a probable extensive deep sedimentary basin has been discovered. This deep sedimentary basin is hypothesized from geological, regional magnetotelluric (MT), gravity, magnetic, and seismic reflection data. This report analyzed three seismic reflection profiles acquired by the Morgantown Energy Technology Centers in combination with the extensive MT and other data to outline a probable geological model for a thick conductive section of rocks in the southern Washington Cascades (called the Southern Washington Cascades conductor, SWCC). Earlier MT models suggested that the section consisted of an east-dipping package that extended to depths of as much as 20 km but appeared to surface in the Bear Canyon area near Morton, Washington, and along the axis of the Carbon River and Morton anticlines. Interpretation of the first three DOE seismic reflections approximately confirmed the MT interpretation and added new information on anticlinal structures and detailed stratigraphy. In this quarterly report, we summarize the progress over the first two quarters of the program for FY93, and project the possible findings during the remainder of the project. DOE

N94-30917 Massachusetts Inst. of Tech., Cambridge.
GEOCHEMICAL AND FLUID DYNAMIC INVESTIGATIONS INTO THE NATURE OF CHEMICAL VARIABILITY IN THE EARTH'S MANTLE Ph.D. Thesis
Erik Harold Hauri 1992
Avail: Issuing Activity (MIT Libraries, Rm. 14-0551, Cambridge, MA 02139-4307)

This dissertation examines the trace element and isotope geochemistry of mantle peridotites and oceanic island basalts, and studies aspects of the flow of viscous fluids driven by thermal buoyancy. The trace element and isotopic systematics of peridotites and associated mafic layers from the Ronda Ultramafic Complex, southern Spain (Chapter 2), provides information bearing on the geochemical behavior of the highly incompatible elements U, Th, and Pb in the mantle, and on the length scales of geochemical variability in a well exposed peridotite massif. The isotopic evolution of Ronda is consistent with an origin as ancient (3 Ga) MORB source mantle which experienced a partial melting event at 1.3 Ga ago, and was subsequently incorporated into the subcontinental lithosphere. An investigation of the trace element and isotopic compositions of clinopyroxenes in peridotite xenoliths from Savaii, Western Samoa and Tubuai, Austral Islands (Chapter 3) reveals geochemical signatures which are not present in basalts from these islands, due to the inherent averaging of melting processes. The data indicate similarities in the melting and melt segregation processes beneath these isotopically extreme islands. A large majority of the xenolith clinopyroxenes from both Savaii and Tubuai are LREE enriched to varying degrees, and many samples display significant intergrain trace element heterogeneity. This highly variable yet systematic heterogeneity was the result of metasomatism by percolating melts undergoing chromatographic trace element fractionation. The Re-Os isotope systematics of oceanic island basalts from Rarotonga, Savaii, Tahaa, Rurutu, Tubuai, and Mangaia are examined (Chapter 4). Results indicate that the low-temperature alteration signature of altered oceanic crust may be largely removed during subduction, and that oceanic crust was recycled into the lower mantle source of the Macdonald hotspot plume. A fluid dynamic model for mantle plumes is developed (Chapter 5) by examining a vertical, axisymmetric boundary layer originating from a point source of heat, and incorporating experimentally constrained rheological and physical properties of the mantle. Examination of the global isotopic database for oceanic island basalts reveals the presence of a mantle component (FOZO), common to many hotspots worldwide, characterized by depleted (87)Sr/(86)Sr and (143)Nd/(144)Nd, radiogenic (206, 207, 208)Pb/(204)Pb and high (3)He/(4)He. This component is isotopically distinct from the source of MORB; thus, with the exception of ridge centered hotspots such as Iceland and the Galapagos, upper mantle does not appear to be a component in most hotspots, in agreement with entrainment theory. Dissert. Abstr.

N94-30921 North Carolina State Univ., Raleigh.
A LABORATORY SIMULATION OF URBAN HEAT-ISLAND-INDUCED CIRCULATION IN A STRATIFIED ENVIRONMENT Ph.D. Thesis
Jie Lu 1993 190 p
Avail: Univ. Microfilms Order No. DA9317117

A three-dimensional heat-island model is established in the convection tank of the Fluid Modeling Facility, U.S. Environmental Protection Agency. Water is used as the working fluid. The model is capable of simulating the temperature and velocity fields induced by a low-aspect-ratio heat island in a calm and stably stratified environment. The convective circulation is turbulent and the Froude number is found to be the controlling parameter

when Reynolds number independence holds. The differences between low- and high-aspect-ratio plumes are discussed and two analytical models, the bulk convective model and the hydrostatic model, are developed for low-aspect-ratio plumes to predict the plume heights, heat-island intensities, and velocity distributions. An extensive and systematic study is conducted to study the heat-island-induced flow with different underlying surface heating rates, heat-island sizes, and different ambient temperature gradients. Different parameterizations and scalings for the heating process, stability effects, velocity fields, and turbulent characteristics are studied, as well as the limitations of the experimental technique. The experimental results are compared with field observations from several cities, previous numerical simulations, and predictions of the analytical models. Good agreement is found with proper convective scalings. The experimental results in their non-dimensional forms, including the thermal plume height, equilibrium height, flow-reversal height, heat-island intensity, the mean horizontal and vertical velocity distributions, and the statistics of temperature and velocity fluctuations, may be applied to any low-aspect-ratio thermal plumes.

Dissert. Abstr.

N94-28695# Meteorological Research Inst., Tsukuba (Japan).
ON THE LINEAR STABILITY OF VERKLEY'S MODONS [BAKUREI MODON NO SENKEI ANTEISEI]
Hirotada Kanehisa *In its* Papers in Meteorology and Geophysics, Vol. 44, No. 1 31 Mar. 1993 p 11-16 (For primary document see N94-28693 08-42)
Avail: CASI HC A02/MF A01

N94-28696# Meteorological Research Inst., Tsukuba (Japan).
STRUCTURE OF NEUTRALLY STRATIFIED TURBULENT EKMAN LAYER AS PREDICTED BY CLOSURE MODELS WITH PROGNOSTIC EQUATION FOR MASTER LENGTH SCALE
Nobuyuki Kinoshita *In its* Papers in Meteorology and Geophysics, Vol. 44, No. 1 31 Mar. 1993 p 17-28 (For primary document see N94-28693 08-42)
Avail: CASI HC A03/MF A01

N94-29520# National Inst. for Resources and Environment, Ibaraki (Japan). Mining System Engineering Div.
INFLUENCE OF CLEARANCE AND RAKE ANGLES ON THE CUTTING FORCE OF ROCK [GANSEKI NO SESSAKU TEIKO NI OYOBOSU NIGEKAKU TO SUKUIKAKU NO EIKYO]
Tetsuji Ono, Hirokazu Karasawa, and Shigeo Misawa *In its* Journal of NIRE, Vol. 2, No. 3 25 May 1993 p 73-80 In JAPANESE (For primary document see N94-29512 08-99)
Avail: CASI HC A02/MF A02

N94-29704# Ministry of Agriculture, Forestry, and Fisheries, Ibaraki (Japan). Facilities for Fishing Port Section.
THE UNDRAINED SHEAR STRENGTH CHARACTERISTICS OF UNDISTURBED SOIL FROM FISHING PORT AREAS [GYOKO CHIKU NO SANPURINGUDO NO HI HAISUI KYODO TOKUSEI]
Seiki Ohmaki, Nobuyuki Horikoshi, Yukio Tsubota, and Ryutaro Yamamoto *In its* Bulletin of National Research Institute of Fisheries Engineering, No. 13 5 Mar. 1992 p 31-56 In JAPANESE (For primary document see N94-29701 08-31)
Avail: CASI HC A03/MF A02

47 METEOROLOGY AND CLIMATOLOGY

Includes weather forecasting and modification.

N94-28455# Pacific Northwest Lab., Richland, WA.
NEW PARAMETERS FOR CHARACTERIZING TURBULENCE AT A POTENTIAL WIND SITE
L. L. Wendell, J. C. Barnard, and V. R. Morris Jul. 1993 11 p Presented at the Windpower 1993, San Francisco, CA , 12-16 Jul. 1993
(Contract DE-AC06-76RL-01830)
(DE94-004355; PNL-SA-22124; CONF-930726-7) Avail: CASI HC A03/MF A01

The most widely used parameter for characterizing turbulence at a potential wind turbine site has been the quantity called 'turbulence intensity' (TI). Analyses of data from several sites in the US Department of Energy's Turbulence Characterization Project show that this parameter can sometimes be seriously misleading. This project has produced a data base of three-component wind turbulence at four strategic locations over a rotor disk in different types of complex terrain. The 0.2-s sampling interval of the data from the four anemometers makes it possible to compute a composite wind over the rotor disk, as well as the wind experienced at a point on a rotating wind turbine blade. From considerations of specialized plots of these wind data, the authors have introduced engulfing gust (TEG) and fluctuating shear (TFS) turbulence parameters and compared their behavior with TI over a range of wind speeds at sites with different terrain configurations. The comparisons showed TEG and TFS to be somewhat more discriminating than TI of the nature of the turbulence at different sites. To obtain a more complete understanding of the nature of the turbulence and its relationship to upwind terrain features, shaded relief and cross-section analyses were applied to provide an overview of the upwind fetch. Using these analyses, along with the time-series plots of wind speed, allowed us to detect eddies being shed from an upwind feature at one site, and to detect a subtle difference in ridge configuration between two sites that resulted in flow separation at one site, but not at the other.

DOE

N94-28568# Argonne National Lab., IL.
ON EDDY ACCUMULATION WITH LIMITED CONDITIONAL SAMPLING TO MEASURE AIR-SURFACE EXCHANGE
M. L. Wesely and R. L. Hart 1994 5 p Presented at the 74th American Meteorological Society Annual Meeting, Nashville, TN, 23-28 Jan. 1994
(Contract W-31-109-eng-38)
(DE94-005112; ANL/ER/CP-80341; CONF-940115-19) Avail: CASI HC A01/MF A01

An analysis of turbulence data collected at a height of 12.3 m above grasslands was carried out to illustrate some of the limitations and possible improvements in methods to compute vertical fluxes of trace substances by the eddy accumulation technique with conditional sampling. The empirical coefficient used in the technique has a slight dependence on atmospheric stability, which can be minimized by using a threshold vertical velocity equal to approximately 0.75 sigma(sub w), below which chemical sampling is suspended. This protocol results in a smaller chemical sample but increases the differences in concentrations by approximately 70%. For effective conditional sampling when mass is being accumulated in a trap or reservoir, the time of sampling during updrafts versus downdrafts should be measured and used to adjust estimates of the mean concentrations.

DOE

N94-28638# Air Force Environmental Technical Applications Center, Scott AFB, IL.
CATALOG OF AIR FORCE WEATHER TECHNICAL PUBLICATIONS 1992-1993
Jan. 1994 38 p
(AD-A275635; USAFETAC/TC-94/001) Avail: CASI HC A03/MF A01

This catalog lists unclassified technical publications produced by HQ Air Weather Service (AWS) and its three centers from Jan. 1992 through Dec. 1993. It supplements, but does not supersede AWS/TC-91/001, which lists technical documents produced by or for AWS and its subordinate units from 1941 through 1991. Documents listed in this catalog include technical reports, technical notes, data summaries, project reports, forecaster memos, interactive training programs, microcomputer programs, and subject bibliographies.

DTIC

N94-28652# Air Force Environmental Technical Applications Center, Scott AFB, IL.
CAPABILITIES, PRODUCTS, AND SERVICES OF USAFETAC (USAF ENVIRONMENTAL TECHNICAL APPLICATIONS CENTER)
Jan. 1994 35 p
(AD-A275654; USAFETAC/TN-94/0001) Avail: CASI HC A03/MF A01

This document describes the capabilities, products, and services of the USAF Environmental Technical Applications Center (USAFETAC), an agency that creates, maintains, and applies the Air Force's environmental climatological database. It describes USAFETAC products and services and tells how to request them. It describes the climatic database and

USAFETAC computer assets. It discusses USAFETAC mission and organization. Appendices provide request formats, Dial-In applications, and a history of USAFETAC and military climatology. DTIC

N94-28663 Atmospheric and Environmental Research, Inc., Cambridge, MA.
A GLOBAL FORECAST MODEL COMPARISON STUDY - YEAR 1
Thomas Nehrkorn, Mark Mickelson, Lawrence W. Knowlton, and Marina Zivkovic 15 Sep. 1993 46 p Limited Reproducibility: More than 20% of this document may be affected by microfiche quality
(Contract F19628-92-C-0092)
(AD-A275674; PL-TR-93-2203) Avail: CASI HC A03

This report describes the results of the first 15 months of a two-year effort aimed at evaluating the advanced physics global spectral model (APGSM) developed by the Phillips Laboratory, in comparison with the currently operational GSM at Global Weather Central (GWC). Preliminary results from the verification of forecasts from the GWC GSM and APGSM, using the GWC analyses as a reference, are presented. The compaction and analysis of RTNEPH cloud data in preparation for generating and verifying cloud forecasts from the APGSM are described. The development of a cloud forecast scheme based on an application of the cloud curve algorithm to synoptically defined weather regimes is described. DTIC

N94-28847 Colorado Univ., Boulder. Dept. of Astrophysical Planetary and Atmospheric Sciences.
US NATIONAL WEATHER EXPERIMENT STORM-FEST: WAVES AND TURBULENCE IN FRONTAL ZONES Final Report, 1 Jan. 1992 - 31 Dec. 1993
William Blumen 23 Dec. 1993 5 p Limited Reproducibility: More than 20% of this document may be affected by microfiche quality
(Contract F49620-92-J-0137)
(AD-A275084; AFOSR-94-0004TR) Avail: CASI HC A01

A high density of surface and upper air observations, including aircraft observations, were accumulated during the STORM-FEST field campaign in the central United States (1 February - 13 March 1992). These data were analyzed to identify significant internal gravity wave and turbulent activity that occurred in association with low-level frontal passages through the boundary layer. The principal analysis method was local decomposition using wavelets as basis functions. These functions provided information on both scale and translation of coherent events, and were well-suited for frontal and boundary layer analyses. Dissipation of kinetic energy in frontal zones was determined using data obtained during STORM-FEST. This information was used to interpret some of the physical processes in low-level frontal zones, but specific models of the observed events were not constructed. DTIC

N94-28873# Air Force Inst. of Tech., Wright-Patterson AFB, OH.
NUMERICAL SIMULATIONS OF A MOUNTAIN THUNDERSTORM. A COMPARISON WITH DOPPLER RADAR OBSERVATIONS M.S. Thesis
Mark E. Raffensberger 4 Nov. 1993 236 p
(AD-A275296; AFIT/CI/CIA-93-155) Avail: CASI HC A11/MF A03

A two-dimensional, non-hydrostatic cloud model was used to isolate the processes and initial conditions most important in the initiation and development of a small mountain thunderstorm. Six numerical simulations were conducted -- one control and five experiments. The control simulation was conducted with realistic initial conditions and physical processes. The simulation's accuracy was evaluated by comparison to multiple-Doppler radar analyses of a storm that occurred on 31 July, 1984 near Langmuir Laboratory, New Mexico and to a microphysical retrieval conducted for a different, but similar storm. The other five simulations were conducted to test the sensitivity of the simulated storms to the initial wind profile, the lack of solar heating, restriction to warm rain processes, and the initial moisture profile. Comparison of the evolution of the control's simulated storm with observation sand with the microphysical retrieval show that the simulation accurately captured the major features observed by the radars and accurately depicted the microphysical evolution of the storm cells. The results of the numerical experiments showed the following conditions and processes to be most important (in descending order) to the development and maintenance of the storm: solar heating, ice phase microphysical processes, environmental wind profile, and low-level moisture profile. The environmental wind profile was the single most important factor in the convective initiation location. DTIC

N94-29011# Air Force Inst. of Tech., Wright-Patterson AFB, OH.
ON THE ORIGINS OF LOW-LEVEL TORNADIC CIRCULATIONS WITHIN THE REMNANTS OF HURRICANE ANDREWS M.S. Thesis
Steven T. Fiorino Sep. 1993 78 p
(AD-A275373; AFIT/CI/CIA-93-148) Avail: CASI HC A05/MF A01

A literature review establishes a key characteristic of tornadic hurricane environments to be the highly sheared lowest 1500 m. The thesis proposes that the shear-produced horizontal vorticity is turned vertical mainly via vertical velocities induced by mass convergence in boundary layer wind-shift zones, rather than by buoyant updrafts. A two dimensional mass continuity and convective available potential energy analysis is performed on data from a profiler and acoustic sounder exposed to Hurricane Andrew's tornadic remnants. This analysis suggests the presence of a convergence-produced 5 m/s updraft at a wind-shift in the thermodynamically stable boundary layer of a tornadic rainband. DTIC

N94-29067# Arizona State Univ., Tempe. Dept. of Mechanical Engineering.
HYDRODYNAMICS OF CONVECTION UNDER WINTER POLAR LEADS Final Report, 1 Oct. 1991 - 30 Sep. 1993
H. J. Fernando 30 Sep. 1993 17 p
(Contract N00014-90-J-1045)
(AD-A275182) Avail: CASI HC A03/MF A01

Because of large space and time scales involved, oceanic convective motions (which may take the form of plumes and thermals) are expected to be influenced by the background rotation. These rotational effects may arise either due to the earth's rotation or due to the presence of a parent cyclone. Thus, the understanding of oceanic convection requires a good knowledge on the influence of rotation on convection from isolated sources. DTIC

N94-29183 Air Force Inst. of Tech., Wright-Patterson AFB, OH.
ERROR GROWTH IN POOR ECMWF FORECASTS OVER THE CONTIGUOUS UNITED STATES M.S. Thesis
Norman R. Modlin 9 Dec. 1993 93 p Limited Reproducibility: More than 20% of this document may be affected by microfiche quality
(AD-A275297; AFIT/CI/CIA-93-154) Avail: CASI HC A05

Successive improvements to the European Center for Medium-range Weather Forecasting model have resulted in improved forecast performance over the contiguous United States (CONUS). While the overall performance of the model in this region was found to have improved during the period of the 1981-1990 winter seasons, the number of poor forecasts increased over this time. This study uses the root mean square (RMS) error to measure the performance of five-day 500 mb winter forecasts over the CONUS. Poor and good forecasts were defined in terms of the 10-year distribution of the RMS values between the 1981 and 1990 winter seasons. Subjective analysis of a subset of poor forecasts yielded no obvious patterns of error growth, location, or propagation in the evolution of poor forecasts. A tendency was noted for in situ amplification of forecast errors. Additionally, successive forecasts verifying on the same day were found to have similar error patterns, with increased amplitudes at longer forecast lengths. This implies that the initial conditions are not a significant source of the error in poor forecasts. DTIC

N94-29194 Air Force Inst. of Tech., Wright-Patterson AFB, OH.
PROTOTYPE TERMINAL AERODROME FORECASTS USING A MESOSCALE MODEL M.S. Thesis
Benjamin I. Edwards, II 1993 73 p Limited Reproducibility: More than 20% of this document may be affected by microfiche quality
(AD-A275308; AFIT/CI/CIA-93-156) Avail: CASI HC A04

The purpose of this study is to evaluate the potential of the Regional Atmospheric Modeling System (RAMS) in this configuration to develop a prototype terminal aerodrome forecast (TAF). RAMS was developed at Colorado State University and is being used to simulate convection over central Florida using a nested grid model where the smallest grid has a horizontal spacing of five kilometers. To obtain meaningful results a 2.5w cumulus parameterization scheme was used which is different than the traditional schemes. The model performed a 12 hour simulation. The coarse grid had a horizontal grid spacing of 80 kilometers and covered the southeastern United States. The second grid has a horizontal grid spacing of 20 kilometers. The third grid was centered over the Kennedy Space Center, Florida. The placement and size of the third grid was used to

evaluate the usefulness of producing model-aided TAF's. One of the problems facing the forecasting community is how to prepare a TAF, the aviation communities forecast, with the current numerical weather prediction products. The NGM parameterizes convection on this scale while the 2.5w parameterization can explicitly resolve features on the five kilometer scale. This increased resolution will greatly aid in the production of aviation forecast. As a demonstration the RAMS model output will be used to produce a TAF for Kennedy Space Center. DTIC

N94-29394# Air Force Systems Command, Wright-Patterson AFB, OH. Foreign Aerospace Science and Technology Center.

STUDY OF DYNAMIC CHARACTERISTICS OF A MONSOON CIRCULATION TUBE

Xu Xiangde and Yin Shuxin 10 Dec. 1993 22 p Transl. into ENGLISH from Jifeng Liuguan Donglixue Tezheng Yanjiu, Qixiang (Meteorology), v 49, no. 1, Feb. 1991 p 108-115

(AD-A275238; FASTC-ID(RS)T-0332-93) Avail: CASI HC A03/MF A01

In China with a prevailing summer monsoon, there is often on mainland China a shear line with east-to-west trend, or a quasistationary rainfall belt on the northern side of a subtropical high pressure. There is ascending movement along the rainfall belt; however, there is a subtropical high ridge line with east-to-west trend to the south of the shear line or the quasistationary front rain belt. Between the shear line and ridge line, there is a meridian circulation system with ascending movement in the north and descending movement in the south. The structure of this (more than 1000 kilometers long, in an east-to-west direction) secondary vertical circulation system is like a tube with east-to-west trend. In this article, the tubular secondary meridionally vertical circulation system (along the east-to-west trend shear line or quasistationary front cloud and rain belt) in summer on mainland China is called the monsoon circulation tube. Its characteristics reveal the configuration relationship and mutual correlation of easterly and westerly air currents, as well as subtropical high systems in the East Asia monsoon zone. DTIC

N94-29408*# National Aeronautics and Space Administration. Goddard Space Flight Center, Greenbelt, MD.

ON THE RELATION BETWEEN SMMR 37-GHz POLARIZATION DIFFERENCE AND THE RAINFALL OVER AFRICA AND AUSTRALIA

Bhaskar J. Choudhury and Nicolo E. DiGirolamo Mar. 1994 82 p

(NASA-TM-104598; Rept-94B00049; NAS 1.15:104598) Avail: CASI HC A05/MF A01

A major difficulty in interpreting coarse resolution satellite data in terms of land surface characteristics is unavailability of spatially and temporally representative ground observations. Under certain conditions rainfall has been found to provide a proxy measure for surface characteristics, and thus a relation between satellite observations and rainfall might provide an indirect approach for relating satellite data to these characteristics. Relationship between rainfall over Africa and Australia and 7-year average (1979-1985) polarization difference (PD) at 37 GHz from scanning multichannel microwave radiometer (SMMR) on board the Nimbus-7 satellite is studied in this paper. Quantitative methods have been used to screen (accept or reject) PD data considering antenna pattern, geolocation uncertainty, water contamination, surface roughness, and adverse effect of drought on the relation between rainfall and surface characteristics. The rainfall data used in the present analysis are climatologic averages and also 1979-1985 averages, and no screening has been applied to this data. The PD data has been screened considering only the location of rainfall stations, without any regard to rainfall amounts. The present analysis confirms a non-linear relation between rainfall and PD published previously. Author

N94-29423# International Meteorological Inst., Stockholm (Sweden). Arrhenius Lab.

[ACTIVITIES REPORT OF THE INTERNATIONAL METEOROLOGICAL INSTITUTE] Annual Report, Jul. 1992 - Jun. 1993

Aug. 1993 69 p

(ISSN 0349-0068)

(ETN-94-95524) Avail: CASI HC A04/MF A01

The annual report of the International Meteorological Institute of Sweden which conducts research in meteorology and associated fields and promotes international scientific cooperation within meteorology is presented. The following are covered: international activities; research activities; visiting scientists; staff members, finances; and publications and reports. Four research areas are covered: dynamic meteorology (mesoscale circulation and synoptic large scale dynamics); chemical meteorology (precipitation chemistry, trace gas exchange between the atmosphere and the underlying surfaces, modeling of tropospheric chemistry, and the global carbon cycle); atmospheric physics (minor constituents, airglow studies, studies of the mesopause region, and stratospheric composition studies); and atmospheric aerosol science (airborne particles and CO2, cloud physics and chemistry, and ice core research). ESA

N94-29455*# National Aeronautics and Space Administration. Langley Research Center, Hampton, VA.

TIME SERIES COMPARISONS OF SATELLITE AND ROCKETSONDE TEMPERATURES IN 1978-1979

Ellis E. Remsberg, Praful P. Bhatt, and Francis J. Schmidlin Apr. 1994 139 p

(RTOP 579-21-44-70)

(NASA-TP-3409; L-17250; NAS 1.60:3409) Avail: CASI HC A07/MF A02

The Limb Infrared Monitor of the Stratosphere (LIMS) experiment on Nimbus 7 yielded temperature-versus-pressure (T(p)) profiles for each radiance scan. The present report describes time series comparisons between LIMS and rocketsonde T(p) values at rocketsonde station locations. Sample size has increased up to 665 by this new approach, leading to better statistics for a T(p) validation. The results indicate no clearly significant bias for LIMS versus Datasonde from 10 kPa at low and mid latitudes. There is a positive LIMS bias of 2 to 3 K in the upper stratosphere at high latitudes for the Northern Hemisphere in both winter and spring. LIMS is progressively colder than Datasonde from 0.4 kPa (about -3 K) to 0.1 kPa (about -9 K) at all latitudes. A similar comparison between LIMS and the more accurate falling sphere measurements reveals an equivalent mid-latitude LIMS bias at 0.4 kPa but a much smaller bias at 0.1 kPa (-4.6 K). Because the biases do not vary noticeably with season, it is concluded that they are not a function of atmospheric state. This result confirms the robustness of the LIMS temperature retrieval technique. Author

N94-29697 Clemson Univ., SC.

RADAR ESTIMATIONS OF ATMOSPHERIC WINDS IN THE TROPOSPHERE AND LOWER STRATOSPHERE Ph.D. Thesis

Emory Lamar Sheppard 1992 88 p

Avail: Univ. Microfilms Order No. DA9323828

This dissertation deals with the estimation of atmospheric flow field parameters using the spaced antenna (SA) and spatial interferometer (SI) methods. In the first section, a computer simulation of scattering from inhomogeneities in the refractive index is used to compare the SA and SI methods for measuring winds in clear air both with and without turbulent fading. The results show that the SA analysis which is carried out in the time domain and the SI analysis which is carried out in the frequency domain are equivalent in terms of the information that the two methods yield. A data analysis method equivalent to full correlation analysis, which can be carried out in the frequency domain, is presented. The method is applied to model-generated data in order to extract the typical full correlation analysis output parameters such as the apparent and true velocities. The results obtained are consistent with the model input parameters. In the second section a statistical comparison of the SA and SI methods for estimating horizontal winds in the troposphere and the lower stratosphere is presented. The data analyzed were obtained with the Middle and Upper (MU) atmosphere radar from 1910 LT on June 29, 1990, through 0950 LT on July 2, 1990. At all heights, velocity estimates based on frequency domain data are within 4 percent of those based on time domain data. We conclude that frequency domain techniques provide an alternate method for estimating true horizontal velocity. Nevertheless, it is not clear that they offer any significant advantage over time domain methods. In fact, the results obtained indicate that the SI method for estimating horizontal velocity may be slightly more difficult to apply in practice. The final section presents an analytical evaluation of SA-based instrumental setups with the potential for estimating the vertical component of atmospheric vorticity from a single-radar location. Methods considered are the oblique spaced antenna (OAS) method and a modified SA system employing four vertically-pointed receiving antennas. Analogies are drawn between the Doppler and SA methods, and it is concluded that the two systems gather the same information when atmospheric turbulence is small and the

reflectivity is uniform. Furthermore, it is concluded that under normal conditions measurement uncertainties will preclude the estimation of atmospheric vorticity from a single-radar location. Dissert. Abstr.

N94-29741 Maryland Univ., College Park.
THE DYNAMICS OF TROPICAL INTRASEASONAL VARIABILITY Ph.D. Thesis
Benjamin Paul Kirtman 1992 302 p
Avail: Univ. Microfilms Order No. DA9315666

The dynamics of tropical intraseasonal variability is theoretically examined with a hierarchy of numerical and analytical models. We investigated the relative roles of conditional instability of the second kind (CISK), the evaporation-wind (E-W) feedback, positive only heating, and nonlinear dynamics. The two problems that plague our understanding of the 30 to 60 day oscillation is the predominance of the planetary scales and the slow phase speed of propagation. Current observation evidence indicates that moist Kelvin wave dynamics may address these problems. A linear analytical twelve-layer model is developed that, for the first time, considers the destabilization of Kelvin waves due to both CISK and the E-W feedback simultaneously. A surface easterly E-W feedback excites modes that are deeper and faster than their CISK counterparts. Numerical calculations with a quasilinear model (positive only heating) shows that the E-W feedback serves as a catalyst in exciting wave-CISK modes that would otherwise be damped. The conceptual model of the E-W feedback is modified to reflect the fact that a surface easterly (westerly) E-W feedback increases (decreases) the phase speeds of the wave-CISK modes. Scale selection experiments with the quasilinear model indicate that in the case of CISK only any horizontal scale can dominate but the global mode is the most unstable. In the case of a strong surface easterly E-W feedback only a global mode can be supported. A fully nonlinear model is presented that incorporates both the wave-CISK and E-W feedback mechanisms. Two regimes are identified: one that behaves similarly to the quasilinear model and the second that is highly nonlinear. In the second regime the propagation speeds are very fast (10 day period) and a wave number one eastward propagation modulates multiple precipitation events along the equator. In either regime regardless of the initial condition the solution always cascades to a wavenumber one dominated solution. Finally, an 'aqua-planet' model is presented in which both nonlinear regimes can be identified. The effects of the E-W feedback enhance the wave-CISK mechanism and nonlinear dynamics coupled with positive only heating leads to the wavenumber one dominance. Dissert. Abstr.

N94-29744 Utah Univ., Salt Lake City.
EVALUATION OF THE NATIONAL METEOROLOGICAL CENTER MESOSCALE MODEL FOR PREDICTION OF SEVERE CONVECTION OVER CENTRAL ARIZONA Ph.D. Thesis
Lawrence Bennet Dunn 1993 160 p
Avail: Univ. Microfilms Order No. DA9322404

The utility of numerical model guidance produced by the National Meteorological Center has been evaluated for the forecast of convection over central Arizona during the summer monsoon season. Model output from the nested grid model (NGM) and ETA model has been compared to observations taken during the 1990 field experiment referred to as the Southwest Area Monsoon Project (SWAMP). The NGM precipitation forecasts showed little skill for events in which heavy precipitation was observed over Phoenix, Arizona. Synoptic-scale rising motion associated with the heavy rain events was best identified in gridded model output in terms of differential advection of absolute vorticity between 300 and 500 mb, but the NGM correctly predicted these fields only 50 percent of the time. Selected events during the SWAMP period were simulated using the ETA model. Qualitative comparisons of the ETA model's precipitation forecasts with lightning data and satellite imagery suggest that the model has skill in predicting precipitation 12 to 24 hours in advance in areas to the east of the Rockies and over Mexico. However, precipitation forecasts from the ETA model showed little skill over central Arizona as a result of inaccurate lower tropospheric moisture fields and the model's inability to trigger convection. The moisture field over southern Arizona was inaccurately forecast since the model generated an unrealistically strong sea-breeze circulation in the vicinity of the Gulf of California. Insufficient moisture in the lower troposphere over Arizona inhibited the development in the model of the strong convective instability observed prior to the onset of convection. However, in some cases, the ETA model correctly predicted the vertical profile of temperature and moisture observed over central Arizona just prior to the outbreak of severe convection, but was still unable to predict any precipitation. The convective parameterization used in the ETA model was not able to generate precipitation in the arid environment over Arizona in which the relative humidity rarely exceeds 80 percent in the lower troposphere prior to the onset of convection. It is theorized that the lack of evaporative cooling processes in the model prohibits the development of colliding outflow boundaries that may initiate the severe convection in this region. Dissert. Abstr.

N94-29747# Sterling Software, Inc., Bellevue, NE. Information Technology Div.
AFGWC DIAL-IN SUBSYSTEM (AFDIS) SOFTWARE USERS MANUAL, VERSION 2.2 Technical Note
Oct. 1993 148 p
(Contract F11623-92-D-0003)
(AD-A275844; AFGWC-TN-93/001) Avail: CASI HC A07/MF A02

This technical note describes the Air Force Global Weather Central's (AFGWC's) Dial-In Subsystem (AFDIS) Remote User Software (AFRUS) that allows remote access (by small computer and modem) to certain applications of AFGWC's Satellite Data Handling System (SDHS). It provides users step-by-step instructions for installing and using the software required for access to SDHS. DTIC

N94-29751 McGill Univ., Montreal (Quebec).
PHYSICAL PROCESSES ASSOCIATED WITH VARIABILITY IN SUCCESSIVE OPERATIONAL MODEL FORECASTS OF CYCLOGENESIS Ph.D. Thesis
Paul J. Roebber 1991 209 p
(ISBN-0-315-74753-6) Avail: Univ. Microfilms Order No. DANN74753

Cyclogenesis is examined based on the principle that development can be viewed as an interaction between upper and lower cyclonic disturbances, and that the surface response is related to the magnitude of both disturbances. It is shown that variability in successive operational model forecasts results from variations in the representation of the features at both levels, but that particular predictions can be sufficiently realistic for diagnostic purposes. The variability in two successive forecasts of a specific case is explained as a moist baroclinic response modulated by the growth of low-level cyclonic vorticity prior to the period of rapid deepening. This antecedent vorticity growth came about through a self-development mechanism involving an interaction between quasigeostrophic processes, surface energy fluxes, and warm-frontal latent heat release. In order to define the preconditioning for this case, it is necessary to resolve these processes, interacting on both meso and synoptic scales. Dissert. Abstr.

N94-29753 Oklahoma Univ., Norman.
DYNAMICS OF TORNADO-LIKE VORTICES Ph.D. Thesis
Litao Deng 1993 326 p
Avail: Univ. Microfilms Order No. DA9323659

Several important processes related to the tornado-like vortex are studied. Those are vortex breakdown, turbulence with rotation and helicity, vortex stability, generation of tornado-like vortices and nondimensional parameters. Both axisymmetric and three-dimensional vortex breakdown are simulated numerically. A mechanism for the breakdown is proposed after unsuccessful applications of existed theories. An investigation of vortex stability shows that the vortex jet under the breakdown point is unstable to asymmetric disturbances. The most unstable wavenumber is 1. The oscillation of the breakdown point observed in laboratory is explained consequently. The effects of rotation and helicity on turbulence decay is studied as an attempt to provide guidance on tornado dynamics in a turbulent environment. Tornado genesis is investigated by simulating and extending the Rothfusz-Lilly experiment. The role of downdraft introduced by secondary circulation is emphasized. The nondimensional parameters governing the laboratory vortex flow is discussed. A new definition for the swirl ratio is proposed and tested. Also, a treatment of the corner point in staggered grids and a nesting method to simulate the core flow are provided in the description of various numerical models developed in the thesis. Dissert. Abstr.

N94-29763 Hawaii Univ., Honolulu.
ON THE ANNUAL CYCLE OF THE TROPICAL PACIFIC ATMOSPHERE

AND OCEAN Ph.D. Thesis
Tianming Li 1993 135 p
Avail: Univ. Microfilms Order No. DA9325038

A simple climate model is proposed for studying the key parameters of the coupled ocean-atmosphere system, monthly mean surface winds and precipitation. In this model, sea-level pressure is thermodynamically determined from sea surface temperature (SST) through a vertically integrated hydrostatic equation in which the vertical mean lapse rate is a function of SST plus a time-independent correction. The surface wind are then computed from the sea-level pressure gradients through a linear surface momentum balance with the anisotropic and latitude-dependent Rayleigh friction coefficients. The precipitation is calculated from a moisture budget by taking into account the effect of SST on convective instability. This model is capable of simulating a realistic annual cycle of the surface winds, sea-level pressure, and precipitation over the tropical Pacific. The response of the tropical atmosphere to symmetric and antisymmetric SST forcing is examined using the simple model. It is found that the annual variation of the symmetric SST mode results in the westward propagation of the surface zonal wind, sea-level pressure, and precipitation along the equator and the antisymmetric SST variation causes the seasonal oscillation of monsoonal circulations and rainfall. The mechanisms of annual variations of the tropical Pacific sea surface temperature are investigated using a reduced-gravity ocean model. It is found that the westward propagation of the equatorial SST anomaly is due to wind-related dynamic processes. Therefore, the westward propagation of atmospheric and oceanic quantities is a manifestation of coupled air-sea interaction. The initiation of anomalous warming or cooling in the eastern Pacific, however, is primarily due to the northward propagation of the SST anomaly in response to solar radiation forcing. As a result, the annual variation of the Pacific SST can be regarded as an interplay between coupled air-sea interaction and solar radiation forcing. The remote forcing of anomalous winds in the western Pacific also shows contribution on the SST variation in the eastern Pacific. The annual variation of cloudiness has effects on the change of SST in the western Pacific and the northeastern Pacific monsoon region.

Dissert. Abstr.

N94-29796 Princeton Univ., NJ.
DOWNSTREAM DEVELOPMENT OF BAROCLINIC WAVES Ph.D. Thesis
Edmund Kar-Man Chang 1993 279 p
Avail: Univ. Microfilms Order No. DA9316091

Downstream development of baroclinic waves is studied using models and observations. Localized perturbations in a baroclinic basic state spread out towards the downstream (and upstream) direction by radiation of energy via ageostrophic geopotential fluxes. The energy budget of these perturbations is examined, and it is found that their growth is triggered by the convergence of ageostrophic geopotential fluxes radiated from upstream (downstream) disturbances, while their decay stage is dominated by downstream (upstream) radiation of energy, with baroclinic and barotropic conversion playing only secondary roles. Such a behavior is different from the traditional baroclinic growth/barotropic decay life-cycle propounded in studies of waves which grow from the most unstable linear normal mode. A variable Coriolis parameter and surface friction both act to favor downstream over upstream development. Downstream development of baroclinic waves in zonally inhomogenous environments are studied to understand the energetics and maintenance of storm tracks. In experiments with zonally varying baroclinicity introduced by zonal variations in heating, it is found that eddies grow due to baroclinic conversion over regions with high baroclinicity and then form coherent wave groups through downstream development. These wave groups propagate into regions with weak baroclinicity and extend the storm track deep into such regions. An eddy kinetic energy equation is derived using simple parametrizations of the various sources and sinks to diagnose the zonal distribution of eddy kinetic energy in a storm track. The effects of mountains on eddy distribution is examined briefly. Apart from generating stationary waves which modulate the baroclinicity of the atmosphere, it is found that mountains may directly affect eddies by reducing their vertical phase tilt, making them less efficient in extracting energy from the mean flow and producing a minimum in eddy activity directly over the mountain. Atmospheric observations analyzed by the European Centre for Medium Range Weather Forecasting are examined. Synoptic scale waves in the Northern Hemisphere storm track regions are found to display a clear signal of downstream development, and their energy budgets are very similar to those found in modeling studies.

Dissert. Abstr.

N94-29802 Florida Univ., Gainesville.
A STUDY OF CLOUD-TO-GROUND LIGHTNING PROCESSES WITH EMPHASIS ON DATA ANALYSIS AND MODELING OF THE RETURN STROKE Ph.D. Thesis
Rajeev Thottappillil 1992 255 p
Avail: Univ. Microfilms Order No. DA9314302

Properties of cloud-to-ground lightning are determined from electric field and optical records of natural lightning flashes and from electric field, current, and optical records of triggered-lightning flashes. Some of these results are used to compare existing return stroke models, develop two new return stroke models, and model continuing currents and M-components. Analysis of electric field records of natural lightning in conjunction with multiple station TV images of the lightning channel has yielded new properties of natural lightning which impact lightning protection standards. Lightning return stroke current parameters and other flash current parameters have been determined from the currents recorded at the base of the channel during triggered-lightning experiments. Current pulses during continuing current have been correlated with the corresponding optical events in streak camera records showing that these current pulses, named M-current pulses, are associated with optical M-components. Properties of M-current pulses are given. Existing return stroke current models are compared by using simultaneous measurements of channel base currents, return stroke speeds, and remote electric fields from triggered lightning. The influence of the wave shape of the channel-base current on the model predictions are discussed. Measured return stroke currents having a maximum rate of rise occurring near the peak current tend to be associated with remotely measured electric fields having a very narrow spike at the field peak, while a maximum current rate-of-rise occurring earlier does not produce a remote field with such a spike. The Diendorfer-Uman model is generalized to include a varying upward return stroke speed with height and a varying downward discharge current speed with height. A new return stroke model is proposed which allows the calculation of spatial and temporal distribution of current along the channel for a specified current at the channel base and for any specified upward return stroke speed, downward discharge current speed, and discharge time constant, each as a different and arbitrary function of height. A model for continuing currents and M-components is developed. From the model it is inferred that the M-component wavefront travels from cloud to ground and not from ground to cloud.

Dissert. Abstr.

N94-29813 Iowa State Univ. of Science and Technology, Ames.
AN OBSERVATIONAL AND NUMERICAL STUDY OF SEA/LAND-BREEZE CIRCULATIONS IN AN AREA OF COMPLEX COASTAL HEATING Ph.D. Thesis
Shiyuan Zhong 1992 162 p
Avail: Univ. Microfilms Order No. DA9311547

This dissertation presents an observational and a numerical study of sea/land-breeze circulations as well as a theoretical study on the boundary layer turbulence parameterization. Data from the Kennedy Space Center Atmospheric Boundary Layer Experiment have been used to examine the three dimensional structure of the mesoscale Atlantic sea/land-breeze and small-scale river-breeze circulations frequently occur over the area of Kennedy Space Center/Cape Canaveral (KSC/CC) where there exists irregular topographic features such as rivers and lagoons. Detailed characteristic features over a diurnal cycle of the circulation onset time, strength, depth, propagation speed, and both seaward and landward extensions are documented. Some boundary layer characteristics related to atmospheric diffusion including atmospheric stability, depth of the thermal internal boundary layer and its evolution with time, and turbulence mixing are also discussed. A three dimensional numerical mesoscale model is used to study the effects of synoptic forcing on the sea/land-breeze circulation at KSC/CC area. The sensitivity of mesoscale features to the large-scale background flow is explored by examining the low-level convergence field location, strength, and timing of maximum vertical motion; diurnal variation of depth of inflow layer and the thermal internal boundary layer; and the rotation of wind vector. Both of these studies may lead to not only an improved forecast of local weather and atmospheric diffusion of rocket exhausts at KSC/CC area, but also to a better understanding of

the physical mechanism of the thermally induced circulations, such as their dependence on the three dimensional coastal effects and the synoptic forcing. A new scheme for parameterizing the turbulent stress in terms of the mean wind profile is also presented in this dissertation. This new parameterization scheme is based on the balance of turbulence kinetic energy and is valid in a deeper layer than the constant-flux layer where the previous schemes all fail because of the violation of the fundamental assumption of constant turbulent fluxes. This new scheme may have direct impact on boundary layer and mesoscale modeling because it may improve the accuracy of solutions and also reduce the computation time by allowing a minimum number of vertical nodes needed to capture the sharp gradients near the low boundary. Dissert. Abstr.

N94-29814 Oklahoma Univ., Norman.
THE INCORPORATION AND INITIALIZATION OF CLOUD WATER/ICE IN AN OPERATIONAL FORECAST MODEL Ph.D. Thesis
Qingyun Zhao 1993 215 p
Avail: Univ. Microfilms Order No. DA9323630

Quantitative precipitation forecasts have been one of the weakest aspects of numerical weather prediction models. Theoretical studies show that the errors in precipitation calculation can arise from three sources: errors in the large-scale forecasts of primary variables, errors in the crude treatment of condensation/evaporation and precipitation processes, and errors in the model initial conditions. A new precipitation parameterization scheme has been developed to investigate the forecast value of improved precipitation physics via the introduction of cloud water and cloud ice into a numerical prediction model. The main feature of this scheme is the explicit calculation of cloud water and cloud ice in both the convective and stratiform precipitation parameterization. This scheme has been applied to the eta model at the National Meteorological Center. Four extensive tests have been performed. The statistical results show a significant improvement in the model precipitation forecasts. Diagnostic studies suggest that the inclusion of cloud ice is important in transferring water vapor to precipitation and in the enhancement of latent heat release; the latter subsequently affects the vertical motion field significantly. Since three dimensional cloud data is absent from the analysis/assimilation system for most numerical models, a method has been proposed to incorporate observed precipitation and nephanalysis data into the data assimilation system to obtain the initial cloud field for the eta model. In this scheme, the initial moisture and vertical motion fields are also improved at the same time as cloud initialization. The physical initialization is performed in a dynamical initialization framework that uses the Newtonian dynamical relaxation method to nudge the model's wind and mass fields toward analyses during a 12-hour data assimilation period. Results from a case study showed that a realistic cloud field was produced by this method at the end of the data assimilation period. Precipitation forecasts have been significantly improved as a result of the improved initial cloud, moisture, and vertical motion fields. Dissert. Abstr.

N94-29817# Westinghouse Savannah River Co., Aiken, SC.
COMPARISON OF SAVANNAH RIVER SITE'S METEOROLOGICAL DATABASES
A. H. Weber Jul. 1993 125 p
(Contract DE-AC09-89SR-18035)
(DE94-001751; WSRC-RP-93-269) Avail: CASI HC A06/MF A02

A five-year meteorological database from the 61-meter, H-Area tower for the period 1987-1991 was compared to an earlier database for the period 1982-1986. The amount of invalid data for the newer 87-91 database was one third that for the earlier database. The data recovery percentage for the last four years of the 87-91 database was well above 90%. Considerable effort was necessary to fill in for missing data periods for the newer database for the H-Area tower. Therefore, additional databases that have been prepared for the remaining SRS meteorological towers have had missing and erroneous data flagged, but not replaced. The F-Area tower's database was used for cross-comparison purposes because of its proximity to H Area. The primary purpose of this report is to compare the H-Tower databases for 82-86 and 87-91. Statistical methods enable the use of probability statements to be made concerning the hypothesis of no differences between the distributions of the two time periods, assuming each database is a random sample from its respective distribution. This assumption is required for the statistical tests to be valid. A number of statistical comparisons can be made between the two data sets, even though the 82-86 database exist only as distributions of frequency and mean speed. DOE

N94-29908 McGill Univ., Montreal (Quebec).
INTERANNUAL TEMPERATURE VARIABILITY AND CYCLONE FREQUENCY OVER EASTERN CANADA AND THE NEW ENGLAND STATES. A CASE STUDY: WINTER SEASONS 1931-1932 TO 1984-1985 Ph.D. Thesis
Mario Daoust 1992 212 p
(ISBN-0-315-74841-9) Avail: Univ. Microfilms Order No. DANN74841

Interannual variability of temperature and cyclone frequencies for Eastern Canada and the New England States have been investigated for the winter seasons 1931-32 to 1984-85. Seasonal analyses have revealed that cyclone frequency has decreased by 21 percent over the research area; the highest losses occurring over the Maritimes and the New England States (30 percent) and in the southern Quebec-southwestern Ontario region (31 percent). The seasonal average temperature has remained fairly stable during the research period. However, the Temperature Variability Index (TVI) suggests that the interannual variability of temperature has been through some changes since 1931-32. The latest shift indicates that, since the early seventies, the temperature variability appears to be increasing during the winter season. Half-month periods were analyzed which revealed some features of the climatic variability during the winter season since 1931-32. The average temperature for the first 15 days of January recorded a significant decrease over the last 54 years. On the other hand, the last half of February presented a general increase in temperature. Parallel to that, the last half of January and the first 15 days of February have recorded substantial decreases in cyclone frequency. Thus, these half-month periods reveal trends which indicate that the overall winter season of the mid-seventies-early eighties differs from the prevailing winter climatic conditions of the thirties and forties. Dissert. Abstr.

N94-29962 Columbia Univ., New York, NY.
INTERANNUAL-DECADAL VARIABILITY IN TROPICAL CLIMATE SYSTEMS: STABLE ISOTOPE RECORDS AND GENERAL CIRCULATION MODEL EXPERIMENTS Ph.D. Thesis
Julia Ellen Cole 1992 324 p
Avail: Univ. Microfilms Order No. DA9313573

A thorough understanding of natural climate variability requires characterizing the patterns and causes of interannual-decadal climate change. The El Nino/Southern Oscillation (ENSO) system of the tropical Pacific imparts interannual variability to climate worldwide, but its past behavior remains poorly documented. Oxygen isotope records from corals that grew at Tarawa Atoll (1 N, 172 E) monitor regional rainfall variability driven by ENSO extremes, providing the ability to track past migrations of the Indonesian Low convective system. A 96-year coral delta(sup 18)O record correlates highly with large-scale ENSO indices, yielding a monthly-resolution ENSO record of comparable quality to measurements confirm the link between rainfall and seawater delta(sup 18)O at Tarawa. Ice-core isotopic records, though commonly interpreted as temperature proxies, incorporate the isotopic content of precipitation, which also depends on amount and seasonality of precipitation, conditions of water vapor evaporation and transport, and air mass mixing and stability. A 180-year record of delta D from the Dunde ice cap (Tibet) lacks consistent seasonality but displays large interannual changes. The delta D record does not show the trend to heavier values observed in a nearby core and interpreted as regional trace-gas-induced warming. The difference between cores and the disappearance of delta D seasonality imply that post-depositional processes dictate recent isotopic variability at Dunde. Alteration of the primary isotopic signal likely occurs by diffusion or wind scour, which would preferentially remove isotopically lighter species. General circulation models that include isotopic tracers in the hydrologic cycle may clarify the isotopic response to climatic change and improve paleoclimatic interpretation. Simulations of ENSO-related climate variability suggest that interannual temperature variations often occur via adjective changes. Changing advection alters the sources and transport of water vapor as well as local temperature and precipitation, complicating the isotopic response to climatic factors. In the tropics, simulated rainfall amount determines isotopic variability, in quantitative agreement with observations. Dissert. Abstr.

N94-29963 Alaska Univ., Fairbanks.
ON INTERANNUAL VARIABILITY AND CLIMATE CHANGE IN THE NORTH PACIFIC Ph.D. Thesis
David Kurt Salmon 1992 229 p
Avail: Univ. Microfilms Order No. DA9303404

Long term changes in the atmospheric and oceanic environment of the North Pacific were investigated for the period 1946-1991. A climatology of North Pacific wind stress curl was developed because of the relevance of changes in wind stress curl to both oceanic and atmospheric variability. The dominant scales of spatial and temporal wind stress curl variability were determined and examined within the context of observed changes in North Pacific air temperature, sea surface temperature (SST), sea ice cover, oceanic mass transport, and the occurrence of blocking anticyclones. Relationships between these variables and indices of tropical Pacific variability were also determined on interannual time scales. During 1976-1988, phase relationships were very strong between long term mean anomalies of wind stress curl, SST, air temperature, sea ice cover, the Pacific North American Index, the Southern Oscillation Index (SOI), and tropical Pacific SST. Long term mean anomalies of these parameters did not change sign during 1976-88. These strong phase relationships did not occur amongst these variables during any other period of the record. The 1976-1988 period is characterized by intensified storminess, the decreased occurrence of blocking anticyclones, and decreased sea ice cover in the subarctic North Pacific. Intensified atmospheric circulation also occurred in the western Pacific subtropical anticyclone. Anomalously low SST occurred across the central and western North Pacific during this period while anomalously high SST was present in the eastern North Pacific adjacent to North America. Changes in the sign of the long term mean anomalies of wind stress curl, central North Pacific SST, and the SOI suggest that this climate regime ended or relaxed after 1988. After 1975, long term changes in anomalies of the Southern Oscillation Index, tropical Atlantic wind stress, Sahel rainfall, and Greenland Sea ice cover have characteristics similar to those observed in the North Pacific. It is suggested that the climate anomalies observed in the North Pacific during 1976-1988 occurred as part of a hemispheric or global scale climate regime. Dissert. Abstr.

N94-29972 Columbia Univ., New York, NY.
GLOBAL PATTERNS OF CLOUD OPTICAL THICKNESS VARIATION WITH TEMPERATURE AND THE IMPLICATIONS FOR CLIMATE CHANGE Ph.D. Thesis
George Tselioudis 1992 155 p
Avail: Univ. Microfilms Order No. DA9313699

This thesis presents a correlative analysis of cloud optical thickness and cloud temperature in large space and time scales. The analysis is designed to document and explain the patterns of cloud optical thickness variation with temperature, and to produce an understanding of cloud optical property feedbacks on climate change. The results of the global correlations between cloud optical thickness and temperature are presented in Chapter 1. The analysis focuses on low clouds to limit variations in cloud vertical extent, particle size and water phase. Coherent patterns of change are observed on several time and space scales. On the planetary and the seasonal scales, clouds in the colder latitudes and seasons are found to be optically thicker than clouds in the warmer latitudes and seasons. The seasonal, latitudinal and day-to-day variations of this relation show that in cold continental clouds optical thickness increases with temperature consistent with the temperature variation of the adiabatic cloud water content, but in warm continental and in most maritime clouds optical thickness decreases with temperature. In Chapter 2, a number of case studies are presented that attempt to identify the cloud parameters responsible for the optical thickness changes and to resolve the atmospheric processes that produce those changes. It is found that the temperature variation of low cloud optical thickness primarily reflect changes in the liquid water content of the clouds, and that changes in cloud particle size and vertical extent play a secondary role. In continental clouds, the optical thickness temperature relation changes from a positive to a negative slope at the same temperature range that the percentage of precipitating clouds shows a marked increase. It is proposed that an increase in the efficiency of formation of warm rain at higher temperatures relative to condensation, raises the probability of occurrence of optically thin clouds at warmer temperatures and produces the observed negative optical thickness slopes. In Chapter 3, a two dimensional radiative convective model is used to estimate the magnitude and sign of the feedback that the observed cloud optical thickness changes would produce in a climate warming scenario. A positive feedback is derived that increases the predicted 2 x CO2 warming by 1.5 C in the subtropics and by 0.5 C in the mid latitudes of the Northern Hemisphere. The latitudinal contrast in the strength of the feedback acts to negate the high latitude amplification of the greenhouse warming. Dissert. Abstr.

N94-30187*# Gerber Scientific, Inc., Reston, VA.
TEST OF PROTOTYPE LIQUID-WATER-CONTENT METER FOR AIRCRAFT USE Final Report
Hermann E. Gerber 12 Mar. 1993 99 p Sponsored in part by NASA. Goddard Space Flight Center
(Grant NSF ATM-92-07345; GSFC Proj. 913-44468)
(NASA-CR-189304; NAS 1.26:189304) Avail: CASI HC A05/MF A02

This report describes the effort undertaken to meet the objectives of National Science Foundation Grant ATM-9207345 titled 'Test of Prototype Liquid-Water-Content Meter for Aircraft Use.' Three activities were proposed for testing the new aircraft instrument, PVM-100A: (1) Calibrate the PVM-100A in a facility where the liquid-water-content (LWC) channel, and the integrated surface area channel (PSA) could be compared to standard means for LWC and PSA measurements. Scaling constant for the channels were to be determined in this facility. The fog/wind tunnel at ECN, Petten, The Netherlands was judged the most suitable facility for this effort. (2) Expose the PVM-100A to high wind speeds similar to those expected on research aircraft, and test the anti-icing heaters on the PVM-100A under typical icing conditions expected in atmospheric clouds. The high-speed icing tunnel at NRC, Ottawa, Canada was to be utilized. (3) Operate the PVM-100A on an aircraft during cloud penetrations to determine its stability and practicality for such measurements. The C-131A aircraft of the University of Washington was the aircraft of opportunity for these-tests, which were to be conducted during the 4-week Atlantic Stratocumulus Transition Experiment (ASTEX) in June of 1992. Derived from text

N94-30587# Pacific Northwest Lab., Richland, WA.
APPLICABILITY OF DIGITAL TERRAIN ANALYSES TO WIND ENERGY PROSPECTING AND SITING
L. L. Wendell, G. L. Gower, M. B. Birn, and C. C. Castellano Jul. 1993 8 p Presented at the Windpower 1993 Conference, San Francisco, CA, 12-16 Jul. 1993
(Contract DE-AC06-76RL-01830)
(DE94-004363; PNL-SA-22117; CONF-930726-6) Avail: CASI HC A02/MF A01

The recent publication of the Digital Elevation Model (DEM) database by the U.S. Geological Survey (USGS) has provided a unique opportunity for the development of cost-effective wind energy prospecting technology. This database contains terrain elevation values on a Latitude-Longitude grid with a resolution of 3 arc-seconds (about 90 m) for the contiguous United States, Hawaii, and Puerto Rico. This database has been coupled with software that will produce shaded-relief maps on a laser printer in a format compatible with the state wind power maps in the U.S. wind energy atlas. By providing a much higher resolution of the terrain features than was possible when the U.S. atlas was prepared, these maps can be useful in general wind prospecting activities. As highly resolved as the 90-m DEM data seem to be when compared to the atlas grid, they still appear to be too coarse to resolve terrain features in the detail required for local wind flow characterization and wind plant layout. Gridded terrain data at about 10-m resolution are available from the USGS for some areas of the United States. In areas where these data are unavailable, they may be generated by digitizing and gridding the contours from a 1:24,000-scale USGS map over the area of interest. Comparisons of terrain profiles from cross sections of the 10-m and 90-m data provide an indication of the effect of resolution on the reliability of terrain feature representation. Oblique views of the terrain in shaded-relief format provide a dramatic enhancement of the shape and relative position of features of interest. DOE

N94-30810 Delaware Univ., Newark.
SPATIAL INTERPOLATION, NETWORK BIAS, AND TERRESTRIAL AIR TEMPERATURE VARIABILITY Ph.D. Thesis
Scott Michael Robeson 1992 103 p
Avail: Univ. Microfilms Order No. DA9319059

Variations in air temperature have profound impacts on our planetary

environment. Estimating air temperature variability, therefore, is of considerable importance not only for environmental analyses, but for assessing social and economic impacts as well. Although a variety of approaches (e.g., mathematical modeling, analysis of satellite and paleoclimatic data) are used to analyze air temperature variability, estimates made from observational station networks still are considered the most reliable. Estimates of air temperature change made from station data, nonetheless, are subject to several types of error. While observational errors have been identified at station locations, errors related to using sparse and highly irregular spatial and temporal distributions of stations (i.e., network bias) have not been assessed adequately. Since irregularly spaced data usually are interpolated to obtain a terrestrial average, methods of spatial analysis clearly play a role in determining estimates of air temperature change. Through graphical and statistical analysis, several spherically-based interpolation methods - inverse distance-weighting, triangular surface patches, and smoothing by functional minimization - are evaluated and compared. Analysis of spatial interpolation errors also provides information about the strengths and weaknesses of the station network. Cross validation and other resampling methods are used to evaluate interpolation methods and the station network for both air temperature anomalies and raw air temperatures. Cross validation analysis of air temperature anomalies suggests that errors are nontrivial and, for some years, interpolation error may be as large as estimates of temperature trends over the last century. Resampling from the station network also suggests substantial network induced variability in estimates of global change. By removing spatial variability, reducing air temperatures to anomalies from a station mean does reduce interpolation error relative to raw air temperatures. At the same time, however, valuable information needed for physically based studies (e.g., radiative emission, phase changes of water, etc.) is removed. To obtain reliable air temperature space-time series, information from a high-resolution climatology is incorporated to reduce interpolation error. Dissert. Abstr.

N94-30863 Texas A&M Univ., College Station.
ATMOSPHERIC MOISTURE FIELDS DERIVED BY SATELLITE OBSERVATIONS OVER THE TROPICAL PACIFIC OCEAN Ph.D. Thesis
Hyosang Chung 1993 182 p
Avail: Univ. Microfilms Order No. DA9328703

Values of precipitable water are retrieved over the tropical and subtropical Pacific Ocean from TOVS infrared and microwave channel brightness temperature and OLR observations by means of stepwise linear regression. The most useful temperature and moisture sensing channels are pre-selected from sensitivity tests of a radiative transfer model. Numerous models are developed and tested against collocated radiosonde observations and Nimbus-7 SMMR precipitable water estimates. For RAOB comparisons, the best estimator used 15 TOVS predictors and captured 71.1 percent of the variance (+/- 0.62 g cm(exp -2) standard error) for column precipitable water; for precipitable water of 700-500 mb bulk layer, these values were 71.7 percent and +/- 0.17 g cm(exp -2). Little skill of estimated precipitable water was obtained for moisture above 500 mb. Regressions were less skillful against SMMR, unless collocation parameters were tightly controlled; SMMR was less acceptable than RAOB's because of observational drift and errors. Generally, the most skillful predictors were boundary layer brightness temperatures of TOVS channels and satellite estimated stability indices. 'Moisture channels' were hardly useful except for estimating middle and upper tropospheric moisture. Additional regression models were constructed testing the sensitivity to different observational and meteorological characteristics. Models which used some in situ observations, surface observations or stabilities calculated from RAOB, were the most successful. The best of these explained 87.5 percent of the variance, but the regression selected almost no TOVS channels, relying instead on conventional RAOB and surface observations. A set of four regression models were developed, stratifying atmospheric characteristics on the basis of collocated OLR values. These models improved the variance explained by 5.0 percent; the model associated with the highest OLR values (275 W m(exp -2) less than or equal to OLR; that is, no cloud) showed only marginal skill. Precipitable water fields were generated from the best TOVS-only model for seven days in January 1983 and compared with SMMR-estimated fields, OLR fields and ECMWF precipitable water analysis. The TVOS regression model compared favorably to the SMMR analysis in amplitudes and features. It revealed more evolving synoptic signal than the ECMWF analysis. In synoptically active regions, it differed with respect to the OLR analysis, primarily because of actual differences in the vertical distribution of water vapor. Dissert. Abstr.

N94-30868 California Univ., Los Angeles.
MODELING STUDIES OF FRONTOGENESIS IN THE UPPER AND MIDDLE TROPOSPHERE Ph.D. Thesis
Celal Sukru Konor 1992 280 p
Avail: Univ. Microfilms Order No. DA9317496

This research addresses fundamental questions associated with upper-level frontogenesis during the evolution of a mid-latitude disturbance in the framework of three-dimensional primitive-equation model simulations on a beta-plane. Simulations are performed by using two different models based on pressure and isentropic vertical coordinates starting with similar initial conditions in a nearly adiabatic atmosphere. The performance of the models is evaluated by using different spatial resolutions for various initial conditions to select the most realistic upper-level frontogenesis simulation. Dynamical processes involved in upper-level frontogenesis are analyzed separately in selected pressure and isentropic coordinate model simulations. Analyses reveal many similarities as well as differences in the process of simulated frontogenesis and tropopause folding with these models. The isentropic coordinate model produces stronger and very narrow upper-level fronts and deep tropopause foldings compared to the pressure coordinate model. Analyses suggest that this difference in the isentropic model simulation is a result of the existence of a positive-feedback mechanism suggested by Mudrick acting during the upper-level frontogenesis. With this feedback, as isentropic surfaces are tilted vertically in the upper-level fronts to enhance the horizontal temperature gradients, stratospheric air with high potential vorticity penetrates into the troposphere. Local increases in the static stability enhances vertical tilting further which leads to very local and narrow frontal developments. Difficulties resulting from intersection of isentropic surfaces with lower boundary with isentropic coordinate model remain unsolved. Consequently, near the lower boundary, potential vorticity and temperature fields are unrealistic. Therefore, combining isentropic coordinate with a sigma-coordinate, which follows the terrain, appears very attractive. However, there are many technical difficulties associated with such a general coordinate system. In this study, a method to design such a hybrid coordinate system is discussed in detail. Dissert. Abstr.

N94-30870 British Columbia Univ., Vancouver.
ATMOSPHERIC TURBULENCE WITHIN AND ABOVE A CONIFEROUS FOREST Ph.D. Thesis
Xuhui Lee 1992 214 p
(ISBN-0-315-75468-0) Avail: Univ. Microfilms Order No. DANN75468

An experiment to study the exchange processes within and above an extensive coniferous forest of Douglas fir trees was conducted on Vancouver Island during a two-week rainless period in July and August 1990. The stand, which was planted in 1962, thinned and pruned uniformly in 1988, had a (projected) leaf area index of 5.4 and a height of h = 16.7 m. The experimental site was located on a 5 degree gentle slope. The primary instrumentation included two eddy correlation units which were operated in the daytime to measure the fluctuations in the three velocity components, air temperature and water vapor density. One unit was mounted permanently at a height of 23.0 m (z/h = 1.38) and the other at various heights of (z/h) 2.0 (0.12), 7.0 (0.42), 10.0 (0.60), and 16.7 m (1.00) with three 8-hour periods of measurement at each level. Profiles of wind speed and air temperature were measured continuously during the experimental period at heights of 0.9, 2.0, 4.6, 7.0, 10.0, 12.7, 16.7 and 23.0 m using sensitive cup anemometers and fine wire thermocouples, respectively. Radiation regimes and air humidity were measured both above and beneath the overstory of the stand. The vertical structure of the stand affected, to a great extent, the vertical distributions of the velocity statistics (wind speed, variance, turbulence intensity, Reynolds stress, skewness, and kurtosis), air temperature, sensible and latent heat fluxes. The effect was also evident in the quadrant representation of the fluxes of momentum, sensible heat and water vapor. Negative Reynolds stress persistently occurred at the lower heights of the stand (z/h = 0.12 and 0.42). The negative values were related to the local wind speed gradients and it is believed that the longitudinal pressure gradient due to land-sea/upslope-downslope circulations was the main factor responsible for the upward transport of the momentum at these heights. Energy budget was examined both above and beneath the overstory of the stand. The sum of sensible and latent

heat fluxes above the stand accounted for, on average, 83 percent of the available energy flux. Beneath the overstory, the corresponding figure was 74 percent. On some days, energy budget closure was far better than on others. Counter-gradient flux of sensible heat constantly occurred at the canopy base (z/h = 0.42), invalidating the conventional gradient-diffusion relationship of K-theory at this height. Near the forest floor, however, K-theory with a far-field eddy diffusivity appeared to work satisfactorily. The daytime profiles of the dimensionless potential temperature Delta(theta)/theta(sub x), where the characteristic temperature, theta(sub x), was defined as the ratio of the kinematic sensible heat flux to the square root of the vertical velocity variance both measured above the stand (z/h = 1.38), were found to be well stratified by H(sub g)/H(sub T), the ratio of the sensible heat flux measured near the forest floor (z/h = 0.12) to that measured above the stand (z/h = 1.38). The profile of Delta(theta)/theta(sub x) was simulated by combining the random flight technique for the dispersion of sensible heat from the elevated canopy source and the gradient-diffusion model with a far-field diffusivity for the dispersion from the ground-level source. The simulated profile agreed reasonably well with the measured one. The simulation results suggested that the profile of Delta(theta)/theta(sub x) was not sensitive to the shape of the wind speed profile. Dissert. Abstr.

N94-30966 Stockholm Univ. (Sweden). Dept. of Meteorology.
MULTIPLE WEATHER REGIMES AND BAROCLINICALLY FORCED SPHERICAL RESONANCE
Shuting Yang 22 Oct. 1993 26 p Limited Reproducibility: More than 20% of this document may be affected by microfiche quality
(ISSN 0349-0467)
(DM-65; ETN-94-95954) Avail: CASI HC A03

Systematically recurrent, geographically fixed weather regimes forced by a single isolated mountain in a two layer, high resolution, quasi geostrophic model modified for the sphere are found to be robust phenomena. While the climatological stationary wave is often confined to the region just downstream of the orography, giving the appearance of a wave train propagating into the tropics, the regional maximum center of low frequency variance appears around the hemisphere, giving the appearance of zonal resonance or some type of zonally confined propagation. This result is not anticipated in light of Rossby wave dispersion theory on the sphere. On the other hand, baroclinic disturbances developing on a meridional temperature gradient of finite extent force subtropical and polar easterlies as well as a sharpened midlatitude westerly jet, which provide a powerful zonal waveguide (by refraction and/or reflection) for the Rossby waves. These conditions are favorable for the establishment of multiple weather regimes. The baroclinicity of the atmosphere is then continuously forcing a mean state which favors forced zonal propagation counteracting the meridional dispersion generated by the spherical geometry alone. ESA

N94-29777*# Jet Propulsion Lab., California Inst. of Tech., Pasadena.
MICRO-SENSORS FOR IN-SITU METEOROLOGICAL MEASUREMENTS
David Crisp, William J. Kaiser, Thomas R. VanZandt, and James E. Tillman *In its* Proceedings of the Workshop on Microtechnologies and Applications to Space Systems 15 Jun. 1993 p 123-124 (For primary document see N94-29767 08-31)
Avail: CASI HC A01/MF A03

N94-29979# National Inst. of Polar Research, Tokyo (Japan).
A STUDY OF PRECIPITATION IN THE COASTAL AREA OF ANTARCTICA AS OBSERVED AT SYOWA STATION USING A VERTICAL POINTING RADAR [NANKYOKU ENGANIKI SHOWA KICHI DE NO SUICHOKU REDA O MOCHIITA KOSUIRYO NO KENKYU]
Makoto Wada and Hiroyuki Konishi *In its* Antarctic Record, Vol. 36, No. 3 30 Nov. 1992 p 341-349 (For primary document see N94-29978 08-46)
Avail: CASI HC A02/MF A02

48 OCEANOGRAPHY

Includes biological, dynamic, and physical oceanography; and marine resources.

For related information see also *43 Earth Resources and Remote Sensing.*

N94-28642# Naval Postgraduate School, Monterey, CA. Dept. of Oceanography.
OBJECTIVE ANALYSIS OF A COASTAL OCEAN EDDY USING SATELLITE AVHRR AND IN SITU HYDROGRAPHIC DATA M.S. Thesis
Rogerio P. Chumbinho 23 Sep. 1993 51 p
(AD-A275715) Avail: CASI HC A04/MF A01

A common characteristic of the interaction between the coastal topography and eastern boundary currents (EBC) is the appearance of cold filaments and mesoscale eddies. Hydrographic and satellite temperature data obtained during a cruise on board R/V Point Sur off Point Arena, California, in May 1993, were analyzed to study a particular eddy field in this area. The hydrographic data was first used to verify the remotely sensed surface temperature field, using three dimensional data visualization. Selected vertical levels from each hydrographic station were then interpolated into a broader, finer resolution grid domain in preparation for an eventual model initialization, using multiquadric interpolation. The results verify the existence of the eddy and show its signature in the vertical to about 300 meters depth. A sensitivity study of interpolation parameters was performed to evaluate approximately the optimal set of parameters, showing that the multiquadric interpolation resolves very well the temperature field in the upper levels and introduces small amplitude, small scale noise in the deeper levels. This noise can be eliminated by a more thorough parameter sensitivity study. DTIC

N94-28690# Naval Postgraduate School, Monterey, CA.
THE VELOCITY FIELD IN THE NORTHEAST ATLANTIC FROM SATELLITE-TRACKED DRIFTING BUOYS M.S. Thesis
Paolo Giannetti Sep. 1993 82 p
(AD-A275704) Avail: CASI HC A05/MF A01

Data from 36 surface drifters (Holey Socks) were collected for a period of 23 months from July 1991 to May 1993 in the Northeast Atlantic Ocean between the Azores Islands and the Canary Islands as a part of the SUBDUCTION experiment. The position information from those drifters is analyzed in this study to obtain horizontal velocity statistics at the drogue level (15m). Mean currents in the area are found to be less than 2 cm/sec except in the vicinity of the Azores Front where the 2-year mean eastward currents measure 3.9+/-1.7 cm/sec. Zonally-averaged northward currents are divergent over most of the area in contrast to the convergent surface currents expected in the region due to convergence of the climatological Ekman transport. It is shown, however, that array bias due to the nonuniform distribution of particles in the presence of an eddy field can account for this result. The mean eddy kinetic energy level is 103/sq cm/sq sec and the mean diffusivity is 5.0 x 10(exp 7)/sq cm/sec. These values are in line with results from previous drifter studies. Mean Lagrangian integral time and length scales are 5.7 days and 48 km, respectively and, in all cases, east-west scales are greater than north-south scales. In general, this long data set is still dominated by the effects of mesoscale eddies. An objective method to select eddy portions of drifter trajectories is presented that may help to characterize the eddy field in future studies. DTIC

N94-28740# Woods Hole Oceanographic Inst., MA.
GLOBAL ACOUSTIC MAPPING OF OCEAN TEMPERATURES (GAMOT) Quarterly Progress Report, Oct. - Dec. 1993
Dec. 1993 63 p
(Contract MDA972-93-1-0004)
(AD-A275777) Avail: CASI HC A04/MF A01

Work performed on global acoustic mapping of ocean temperatures (GAMOT) tasks is described. Task A involves the acoustic thermometry data taken in 1987 along fifteen basin scale sections in the northeast Pacific, the development of a signal processing package for the surface suspended acoustic receiver (SSAR), and the computation of travel times of rays through ocean models of the Pacific. Task B involves simulation of the northeast Pacific Ocean for 1961-1991 driven by equatorial Kelvin waves and real winds. Task C covers development of the SSAR. Task D

describes the procurement of a 70 Hz source which can be moored autonomously. CASI

N94-28877# Colorado Univ., Boulder. Div. of Cryospheric and Polar Processes.
LEAD DETECTION AND MAPPING WITH REFERENCE TO RELATIONSHIPS BETWEEN SCALE, SENSOR CHARACTERISTICS, SURFACE CONDITIONS AND ATMOSPHERIC PROPERTIES Final Report, 15 Apr. 1991 - 31 Oct. 1993
J. Key, J. A. Maslanik, and R. S. Stone 31 Oct. 1993 138 p
(Contract N00014-90-J-1840)
(AD-A275321) Avail: CASI HC A07/MF A02

During the three project years, empirical studies of scale relationships in the retrieval of sea ice lead statistics have been undertaken, as have modeling investigations of atmospheric influences on the satellite signal. Additionally, we have developed statistical models that describe the scaling properties of leads. The empirical studies have been based primarily on comparisons within and between Landsat and AVHRR imagery, while the atmospheric models have been specific to the AVHRR. Submarine sonar data have been used in the statistical model development. Specific accomplishments include: atmospheric temperature and humidity profiles for the Arctic have been constructed from Soviet ice island data and were used in the construction of three-season imagery, and nearest-neighbor resampling has been shown to be the most effective in maintaining the spectral characteristics of leads while spatial interpolation (e.g., bilinear) retains their spatial structure; empirical relationship between pixel size and lead width have been determined; procedures for the retrieval of lead statistics have been developed and applied to Landsat and ERS-1 SAR data; and the relationship between 'apparent' lead widths measured along a transect. DTIC

N94-29128# Washington Univ., Seattle. Dept. of Atmospheric Sciences.
STUDIES OF MARINE AEROSOLS AND THEIR EVOLUTION IN THE EASTERN NORTH ATLANTIC Annual Report
Peter V. Hobbs 1993 20 p
(Contract N00014-92-J-1587)
(AD-A275011) Avail: CASI HC A03/MF A01

Abstracts are provided for papers, technical reports, and book titles generated by the research, including: aerosol size distributions in the cloudy atmospheric boundary layer of the North Atlantic Ocean; light scattering and cloud condensation nucleus activity of sulfate aerosol measured over the northeast Atlantic Ocean; the structure of frontal weather systems in western Europe; aerosol-cloud-climate interactions; recent field studies of sulfur gases, particles, and cloud in clean marine air and their significance with respect to the DMS-cloud-climate hypothesis; and recent field studies of aerosol and cloud processes relevant to climate. DTIC

N94-29164# Naval Postgraduate School, Monterey, CA.
A MODEL ANALYSIS OF POTENTIAL VORTICITY ON ISOPYCNAL SURFACES FOR THE GLOBAL OCEAN M.S. Thesis
Douglas C. Marble Sep. 1993 81 p
(AD-A275047) Avail: CASI HC A05/MF A01

Charts of potential vorticity (q) within four different density layers, calculated from an eddy resolving global ocean general circulation model, are presented for the Atlantic, Pacific, and Indian Ocean Basins. Potential Vorticity is evaluated as q = (f/p)(delta(sigma)/delta(z)), a formulation that is valid for large, slow scales and allows it to be readily calculated from model output. Here, f is Coriolis, p in situ density, sigma the potential density referred to the sea surface, and z the vertical coordinate. The model is shown to represent oceanic density structure with reasonable accuracy. The most significant departure from observations are the steep density gradients on the northern boundary of the Antarctic Circumpolar Current. This may be due to model convective adjustment parameterizations and the extent of the smoothing in the cataloged data, which may be greater in the southern oceans due to relatively scarce observations. Model derived values of potential vorticity correspond well with those calculated from observations. In the middle and lower layers, the three basins tend toward homogenization, representing unventilated layers. Gyres of q in the upper layers of the northern Atlantic and Pacific Oceans, with their northern boundaries anchored in the outcrop region, illustrate the ventilation of these layers. DTIC

N94-29204 Naval Research Lab., Bay Saint Louis, MS.
SEAFLOOR CHARACTERIZATION USING TEXTURE Final Report
Suresh Subramaniam, Herb Barad, Andrew B. Martinez, and Brian S. Bourgeois 1993 9 p Limited Reproducibility: More than 20% of this document may be affected by microfiche quality
(AD-A275399; NRL/PP/7441-93-0013) Avail: CASI HC A02

Texture analysis is performed on multibeam sonar imagery. A set of fourteen texture features is computed using co-occurrence matrices to form the feature space. The dimensionality of the feature space is reduced by extracting the principal components from the original feature space. Classification of the image is performed on the principal components using K-Means algorithm. Results indicate that seafloor bottom types can be characterized by analyzing the texture of the bathymetric sonar images. DTIC

N94-29432# Naval Research Lab., Bay Saint Louis, MS.
TIDAL ATLAS SOFTWARE DEVELOPMENT Final Report
Y. L. Hsu, Juan F. Reynaud, and Ernst W. Schwiderski 7 Dec. 1993 50 p
(AD-A275251; NRL/MR/7442-93-7060) Avail: CASI HC A03/MF A01

Tidal atlas software has been developed for naval hydrographic survey operations. The software displays an integrated database of tides, bathymetry, and coastlines. It is a menu-driven PC/WINDOWS program. The tidal databases include the tidal constituent bank from the International Hydrographic Organization and Schwiderski's global tidal data. The bathymetry uses the 5-minute ETOPO5 database and the coastlines use the world vector shoreline database. The software can display tidal stations and tidal constituents for a user-specified area. The software also provides other functions including tidal height plot, tidal zone plot, cotidal, and corange plots. DTIC

N94-29436# Pennsylvania State Univ., University Park. Dept. of Meteorology.
SAR-RELATED STRESS VARIABILITY IN THE MARINE ATMOSPHERIC BOUNDARY LAYER (MABL) Report, 1 Oct. 1992 - 30 Sep. 1993
Hampton N. Shirer and George S. Young 30 Sep. 1993 9 p
(Contract N00014-90-J-4012)
(AD-A275275) Avail: CASI HC A02/MF A01

By variably stressing the sea surface, secondary circulations within the marine atmospheric boundary layer (MABL) can modulate the sea-surface wave field and so can produce discernible signatures on SAR images of the ocean. Indeed, at the Fall '93 ARI workshop, Robert Beal showed ERS-I images illustrating the ubiquity of these signatures during the second HIGH-RES cruise in June 1993. Among the resulting signatures, the quasi-linear and cellular microscale patterns still require adequate explanation. The ubiquitous MABL two- and three-dimensional convective circulations provide promising candidates for the forcing phenomena producing these signatures. These microscale circulations have horizontal wavelengths on the order of one to ten times the boundary layer depth, or approximately one to ten km, and temporal scales on the order of one to ten hours. Thus, they produce stress variations on the spatial and temporal scales of the quasi-linear and cellular SAR signatures. Similarly the frequent occurrence of two-dimensional mesoscale atmospheric circulations in response to the SST gradient along the northwest wall of the Gulf Stream adds an atmospheric component to Gulf Stream signatures on SAR images on cross-stream scales of 1 to 50 km. DTIC

N94-29595# Japan Marine Science and Technology Center, Tokyo.
RESEARCH REPORT ON THE POTENTIAL OF OCEAN DEVELOPMENT SUITABLE FOR AREA CHARACTERISTICS [CHIIKI TOKUSEI O IKASHITA KAIYO KAIHATSU NO KANOSEI NI KANSURU CHOSA KENKYU HOKOKUSHO]
Toshitsugu Sako, Shin Kisugi, Tsune Kusakawa, Yoshiharu Kon, Hideaki Nakada, Hitoshi Nishimura, Norihisa Yokouchi, Hiizu Isa, Hisashi Soma, and Norihiko Kaneko et al Mar. 1993 149 p In JAPANESE
(JTN-94-80587) Avail: CASI HC A07/MF A02

Technologies required for ocean development were explored by conducting case studies at two model sites: at a spacious site with much reserved nature which can be utilized for development, and at a close, densely populated site with shallow depth of water, requiring much environmental improvement before development. After investigation of characteristics of each site, development conception and plans were set

up conforming to the characteristics of the sites. Then ocean technologies to realize the plans were selected by evaluating technical, sociological and environmental factors. Based on the evaluation results, important technologies for future coast development were reviewed, and eleven were selected as science and technology fields for future research and development. In 1990 and 1991, development of coast/ocean was studied focusing on the three items: (1) 'waterfront' project was investigated as a measure for densely populated areas; (2) ecology along the shallow coasts was evaluated to study influences to ecological environments; and (3) the possibility of adopting 'mitigation', an environmental compensation, was reviewed. Author (NASDA)

N94-29815 Hawaii Univ., Honolulu.
MODELING DEEP EQUATORIAL CIRCULATION Ph.D. Thesis
Dailin Wang 1993 176 p
Avail: Univ. Microfilms Order No. DA9325058

Observations show that there are significant zonal currents near the equator below the thermocline, the so called equatorial deep jets. The dynamics of these currents are unknown. In this study, the origin of the equatorial deep jets is explored through a series of numerical experiments. High resolution thermohaline spin up experiments were undertaken to investigate the thermohaline hypothesis of equatorial deep jets. It is found that the deep circulation strongly depends on the deep stratification. If this is unrealistically weak, an alternating jet structure and strong deep upwelling near the equator can be generated. This strong upwelling can result in an extra meridional overturning cell near the equator in the meridional mass transport stream function. The lack of stratification in the deep ocean is a generic deficiency of large scale circulation models which employ insulating bottom boundary conditions. The deep stratification can be improved greatly by using a Newtonian bottom boundary condition for temperature. The resulting stream function is more realistic and the deep equatorial overturning cell and alternating jets disappeared. It is the bottom boundary condition rather than the size of the vertical diffusion coefficient that is more important in determining the deep stratification and deep equatorial flow. Even though we cannot completely rule out the thermohaline forcing hypothesis of the equatorial deep jets (because thermohaline spinup experiments with very low explicit diffusion have not been carried out to investigate the dynamics of thermohaline circulation in a low diffusive regime), it is improbable that the deep jets are purely thermohaline in origin. High resolution, low diffusion wind-forced equatorial models were next run to investigate whether subthermocline mean equatorial currents can be generated via instabilities of the surface currents and wave-wave interactions. It is found that if eddy diffusion coefficients for momentum and heat are low enough, there are significant subthermocline time-mean currents. These currents are connected to low latitude western and eastern boundary subsurface currents. The eddy processes (Reynolds stress divergence) are found to be as important as the parameterized subgrid processes (explicit diffusion). Dissert. Abstr.

N94-30002 Selskapet for Industriell og Teknisk Forskning, Trondheim (Norway). Div. for Information Technology.
SPLINES AND OCEAN WAVE MODELLING
E. Mehlum 19 May 1993 44 p
(PB94-139409; STF82-595-7759-3) Avail: Issuing Activity (National Technical Information Service (NTIS))

The report introduces spline functions as approximants in the solution of differential equations. The differential equations are taken from the fully nonlinear theory for ocean waves. Worked examples as well as computer output are presented. NTIS

N94-30714# Technische Univ., Delft (Netherlands). Faculty of Geodetic Engineering.
ALTIMETER DATA PROCESSING FROM SEA SURFACE TOPOGRAPHY TO HORIZONTAL EDDY MOMENTUM FLUXES Thesis
A. Bollweg Aug. 1993 93 p See also PB90-149907
(PB94-147550) Avail: CASI HC A05/MF A01

Before the launch of the first radar altimeter satellites, large parts of the ocean surface remained unexplored. The idea of remotely sensing the ocean surface was realized in 1973. Analyzing recordings of the ocean surface at different epochs resulted in information on specific tidal components, ocean currents, and the geoid. The time variability of the sea surface of the oceans between +60 degrees and -60 degrees is investigated. NTIS

N94-30790 California Univ., Santa Barbara.
ON THE NONLINEAR DYNAMICS OF OCEAN WAVE SYSTEMS Ph.D. Thesis
Jiyue J. Li 1992 204 p
Avail: Univ. Microfilms Order No. DA9317181

The thesis is composed of three subjects, independent yet interrelated. The first part deals with the surface wave breaking problem, in which a mechanism of wave-breaking through intrinsic hydrodynamic instability is discovered. The second part is a general theory for nonlinear evolution of three-dimensional resonant wide-band wave systems. In part three, dynamics of nonlinear wave systems is generalized for non-conservative systems, and applied to model energetic ocean wave systems by taking the real effects into account of wind and dissipation due to nonlinear breaking and large scale diffusion at sea. In Part I, a physical picture, how waves deform and break, is presented by employing energy approaches, where both inter- and intra-wave interactions within the wide-band wave system are distinguished, and corresponding energy transfer through inter- and intra-wave interactions is demonstrated. It is shown that the result of inter-wave interaction is directly related to the instability of the Benjamin-Feir type; and the consequence of intra-wave interaction is principally responsible for the asymmetric deformation of a wave profile which leads to wave-breaking. In Part II, a general theory by a united approach is schematized for any resonant or near-resonant three-dimensional side-band multi-wave systems. A set of parabolic evolution equations is derived for the case n = 2, which includes the Benjamin-Feir system as a special case. Based on the new evolution equations, analytic results are developed for instability and temporal evolution of the system; also a global picture of its dynamics and bifurcation in a phase space is provided. Finally, bifurcation of planar wave solutions into 3-d non-interactive solutions of permanent form is studied. In Part III, modeling of energetic ocean wind-waves as a dynamical system is developed, in the light of the Kahma's wind-wave growth formulation relevant to the most energetic part in the Kitaigorodskii-Toba spectrum, and Toba's observational law. Based on the resulting equation of complex Ginzburg-Landau type, combined effects of pumping and damping on the modulational instability and temporal evolution of the side-band system are investigated. It is shown, over certain ranges of the parameters, that the asymptotic wave solutions could be either (1) a stable limiting cycle or (2) a pair of equilibria, or (3) a new discovered complex attractor in the phase space; they correspond respectively to (1) periodic, (2) stationary, or (3) chaotic modulation of waves in physical space. The results suggest that wind forcing and dissipation play a key role in contributing to the observed stochastic nature of wind-waves at sea. Finally, we discuss the formation of solitary wind-wave groups and their stability, and the theory is in good agreement with ocean observations of energetic wave groups. In addition, existence of ocean wave envelope front solutions is also discussed. Dissert. Abstr.

N94-30823# Lawrence Livermore National Lab., CA.
THE VALIDATION OF OCEAN SURFACE HEAT FLUXES IN AMIP
P. J. Gleckler and D. A. Randall Sep. 1993 6 p Presented at the 74th American Meteorological Society Annual Meeting, Nashville, TN, 23-28 Jan. 1994
(Contract W-7405-eng-48)
(DE94-001539; UCRL-JC-114684; CONF-940115-5) Avail: CASI HC A02/MF A01

Recent intercomparisons of Atmospheric General Circulation Models (AGCM's) constrained with sea-surface temperatures have shown that while there are substantial differences among various models (with each other and available observations), overall the differences between them have been decreasing. The primary goal of AMIP is to enable a systematic intercomparison and validation of state-of-the-art AGCM's by supporting in-depth diagnosis of and interpretation of the model results. Official AMIP simulations are 10 years long, using monthly mean Sea-Surface Temperatures (SST's) and sea ice conditions which are representative of the 1979-1988 decade. Some model properties are also dictated by the design of AMIP such as the solar constant, the atmospheric CO2 concentration, and the approximate horizontal resolution. In this paper, some of the preliminary results of AMIP Subproject No. 5 will be summarized. The focus will be on the intercomparison and validation of ocean surface heat fluxes of the AMIP simulations available thus far. DOE

N94-28694# Meteorological Research Inst., Tsukuba (Japan).
THE JAPAN SEA PROPER WATER AND WATER CIRCULATION IN THE JAPAN SEA [NIHONKAI KOYUSUI NO SEISEI TO NIHONKAI NO KAISUI JUNKAN]
Katsunobu Nishiyama, Masaru Inagawa, and Takanori Mizuno *In its* Papers in Meteorology and Geophysics, Vol. 44, No. 1 31 Mar. 1993 p 1-10 (For primary document see N94-28693 08-42)
Avail: CASI HC A02/MF A01

N94-28934# Canada Centre for Remote Sensing, Ottawa (Ontario).
SEA ICE AND OCEANS APPLICATIONS OF SAR [SA NI YORU KAIYO KANSOKU]
Michael J. Manore, Paris W. Vachon, and Marie-Catherine Mouchot *In* Earth Resources Satellite Data Analysis Center, Proceedings of the International Symposium on Remote Sensing 30 Mar. 1992 p 247-271 Original contains color illustrations (For primary document see N94-28925 08-43)
Avail: CASI HC A03/MF A03

N94-30626*# Puget Sound Univ., Tacoma, WA. Dept. of Physics.
A TOY MODEL OF SEA ICE GROWTH
Alan S. Thorndike *In* University Corp. for Atmospheric Research, Modeling the Earth System, Volume 3 1992 p 225-238 (For primary document see N94-30616 08-45)
Avail: CASI HC A03/MF A04

51 LIFE SCIENCES (GENERAL)

N94-28408 Technical Research Centre of Finland, Espoo. Biotekniikan Lab.
BARLEY CELL CULTURE AS A PRODUCER OF HETEROLOGOUS PROTEIN Ph.D. Thesis
L. Mannonen 1993 77 p Limited Reproducibility: More than 20% of this document may be affected by microfiche quality
(PB94-132339; VTT/PUB-138) Copyright Avail: CASI HC A05

The purpose of the present study was to demonstrate the possibility of using the stable cell culture of barley (Hordeum vulgare var. Pokko) established in our laboratory, in the production of heterologous proteins. Production of a cellulolytic enzyme, heat stable endoglucanase EGI from the filamentous fungi Trichoderma reesei, was chosen as an example.
NTIS

N94-28420# Advisory Group for Aerospace Research and Development, Neuilly-Sur-Seine (France). Aerospace Medical Panel.
THE SUPPORT OF AIR OPERATIONS UNDER EXTREME HOT AND COLD WEATHER CONDITIONS [LES OPERATIONS AERIENNES EN ENVIRONNEMENT EXTREME CHAUD/FROID]
Oct. 1993 312 p In ENGLISH and FRENCH Symposium held in Victoria, British Columbia, 17-21 May 1993
(AGARD-CP-540; ISBN-92-835-0721-5) Copyright Avail: CASI HC A14/MF A03

Extreme temperatures, both hot and cold, can severely restrict the ability of aircrew and support personnel to accomplish their missions. Under emergency conditions of bail-out, ejection, and ditching of fixed or rotary-wing aircraft on land or in water, the survival rate of aircrew and passengers is also affected by the intensity of thermal stress experienced and the duration of exposure to the thermal stress. This has all recently been borne out by the experience of intense air operations in the Gulf War. This symposium reviewed the operational conditions experienced under extreme hot and cold weather. The papers presented at this symposium highlighted recent advances in thermal physiology, clothing sciences, personal flying equipment, and microclimate cooling. Emphasis was placed on the potential applications of these advances in situations where thermal stress may confound the efficient achievement of mission objectives. For individual titles, see N94-28421 through N94-28453.

N94-28421# Robert Gordon's Inst. of Tech., Aberdeen (Scotland).
MEDICAL SUPPORT FOR BRITISH OPERATIONS IN THE ANTARCTIC **c52**
S. R. K. Coleshaw and J. N. Norman *In* AGARD, The Support of Air Operations under Extreme Hot and Cold Weather Conditions Oct. 1993 5 p (For primary document see N94-28420 08-51)
Copyright Avail: CASI HC A01/MF A03

This paper presents an overview of the work undertaken and support given to members of the British Antarctic Survey, discussing some of the environmental hazards to which the personnel are exposed.
Derived from text

N94-28422# Norwegian Transarctic Expedition, His.
EVALUATION OF LIFE SUPPORT EQUIPMENT DURING AN UNSUPPORTED NORTH POLE EXPEDITION **c54**
W. Gautvik, J. O. Owe, and T. A. Oftedal *In* AGARD, The Support of Air Operations under Extreme Hot and Cold Weather Conditions Oct. 1993 6 p (For primary document see N94-28420 08-51)
Copyright Avail: CASI HC A02/MF A03

This paper presents practical experience with the following life support equipment used during an unsupported North Pole expedition in 1992: clothing, sleeping bag with vapor barrier inner liner, a high efficiency cooking gear for melting water, and freeze dried food with 70 percent of the energy from fat.
Derived from text

N94-28423# Royal Air Force, Farnborough (England). Inst. of Aviation Medicine.
PREDICTION OF SURVIVAL TIMES ON LAND IN A COLD CLIMATE **c52**
G. Maidment *In* AGARD, The Support of Air Operations under Extreme Hot and Cold Weather Conditions Oct. 1993 12 p (For primary document see N94-28420 08-51)
Copyright Avail: CASI HC A03/MF A03

Eight subjects were exposed to three different combinations of air temperature and wind speed for two hours in a climatic chamber. Changes in core temperature, surface temperatures and heat flux, and metabolic rate were recorded during the exposure. The results obtained were compared with the predictions derived from a sophisticated computer model of human thermoregulation and heat exchange. Conclusions about the factors responsible for the rate of body cooling in air and the causes of the wide range of variability observed are discussed. The problems of predicting survival times on land for a diverse population are considered, and possible solutions are suggested.
Author (revised)

N94-28424# Naval Aviation HQ, Yeovil (England).
THE CONCEPT OF ROYAL NAVY AIR OPERATIONS UNDER EXTREME ENVIRONMENTAL CONDITIONS **c66**
A. P. Steele-Perkins *In* AGARD, The Support of Air Operations under Extreme Hot and Cold Weather Conditions Oct. 1993 11 p (For primary document see N94-28420 08-51)
Copyright Avail: CASI HC A03/MF A03

The Fleet Air Arm of the Royal Navy has always operated on a worldwide basis, with environmental extremes and therefore the accompanying stressors. Its procedures and essential support, including equipment and aviation medicine, have evolved to ensure a safe and efficient modus operandi. The post cold war concept of operations has proved the original philosophy. Recent events are discussed together with the aviation medicine implications.
Author

N94-28425# Survival Systems Ltd., Dartmouth (Nova Scotia).
EFFECT OF SEASICKNESS ON AIRCREW STUDENT SURVIVOR ABILITY AFTER DITCHING IN COLD WATER **c52**
Albert Bohemier *In* AGARD, The Support of Air Operations under Extreme Hot and Cold Weather Conditions Oct. 1993 7 p (For primary document see N94-28420 08-51)
Copyright Avail: CASI HC A02/MF A03

It is suggested that immediate, effective biochemical seasickness treatment for ditched aircrew does not exist, in addition to the fact that the severity of the problem in cold water survival is not currently documented, and therefore not sufficiently recognized.
Author (revised)

N94-28426# Defence and Civil Inst. of Environmental Medicine, North York (Ontario). Environmental Physiology Section.
FUELLING SHIVERING IN HUMANS DURING COLD WATER IMMERSION **c52**

I. Jacobs *In* AGARD, The Support of Air Operations under Extreme Hot and Cold Weather Conditions Oct. 1993 3 p (For primary document see N94-28420 08-51)
Copyright Avail: CASI HC A01/MF A03

Military cold survival research has traditionally concentrated on ways of conserving body heat. In contrast, this paper will describe recent investigations of metabolic heat production during cold exposure. In humans, increased heat production in the cold is achieved by increased shivering, i.e. involuntary intermittent skeletal muscle contractions, which must be fuelled. This research has focused on the thermoregulatory effects of manipulating the availability of specific fuel substrates to the shivering musculature. Using procedures such as muscle biopsies to quantify intramuscular substrate utilization, venous blood sampling to quantify circulating substrates, and continuous monitoring of metabolic rates and rectal temperatures during cold exposure, the importance of skeletal muscle carbohydrates stores has been demonstrated for the ability to maintain heat production and delay the onset of hypothermia during cold water immersions. Acute reductions in muscle carbohydrate stores were associated with significant reductions in heat production by the body during shivering, and a more rapid decrease in rectal temperature. In contrast, another series of studies induced acute reductions in circulating fat stores, but there was no effect on body temperature regulation. The availability of sufficient carbohydrate stores to the shivering musculature seems to be critical for the body's ability to delay hypothermia during acute cold stress.
Author (revised)

N94-28427# Defence and Civil Inst. of Environmental Medicine, North York (Ontario). Environmental Physiology Section.
BIOCHEMICAL ENHANCEMENT OF COLD TOLERANCE **c52**
A. L. Vallerand *In* AGARD, The Support of Air Operations under Extreme Hot and Cold Weather Conditions Oct. 1993 8 p (For primary document see N94-28420 08-51)
Copyright Avail: CASI HC A02/MF A03

It is well established that humans have a poor resistance to cold. Once the insulation provided by the microclimate and by peripheral vasoconstriction has been maximized, the last line of defense against the cold resides in an increase in metabolic heat production (M-dot). Several techniques have been used to further enhance M-dot in the cold, but it is a pharmacological approach that has received the most support. To that effect, recent experiments in cold-exposed subjects have shown that the ingestion of ephedrine (E; a decongestant) and caffeine (C; a methylxanthine) improves M-dot, heat debt (body heat deficit), and the drop in body core (rectal) temperature T(sub re), (P less than 0.05). The ingestion of an E, C, and theophylline (T; a bronchodilator) capsule produced about the same beneficial effect (P less than 0.05). Although some authors have reported that T alone reduces the drop in T(sub re) (i.e. warmer T(sub re)), these improvements require further clarification since M-dot and mean skin temperature T(sub sk)-bar practically did not change. A theobromine-based (another xanthine) Recreation and Sports bar (Cold Buster) is purported to reduce the drop in T(sub re) and thus delay the onset of hypothermia. However, such claims could not be confirmed in two different studies performed in our lab. Despite an increase in M-dot in some studies, C alone did not alter T(sub re) in the cold. It is concluded that ephedrine/xanthine mixtures represent at the moment, one of the best and safe pharmacological agents to enhance heat production and cold resistance.
Author

N94-28428# Manitoba Univ., Winnipeg. Lab. for Exercise and Environmental Medicine.
TREATMENT OF MILD IMMERSION HYPOTHERMIA BY BODY-TO-BODY AND FORCED-AIR WARMING **c52**
Gordon G. Giesbrecht, Igor B. Mekjavic, Daniel I. Sessler, Marc Schroeder, and Gerald K. Bristow *In* AGARD, The Support of Air Operations under Extreme Hot and Cold Weather Conditions Oct. 1993 2 p (For primary document see N94-28420 08-51)
Copyright Avail: CASI HC A01/MF A03

The purpose of these studies was to test two methods (one traditional, one recent) for treating mild immersion hypothermia.
Derived from text

N94-28429# Army Research Inst. of Environmental Medicine, Natick, MA. Military Health Div.
NUTRITION AND HYDRATION STATUS OF AIRCREW MEMBERS CONSUMING AN IMPROVED SURVIVAL RATION DURING A SIMULATED SURVIVAL SCENARIO **c52**
Tanya E. Jones, Susan H. Mutter, Judy M. Aylward, and Eldon W. Askew *In* AGARD, The Support of Air Operations under Extreme Hot and Cold Weather Conditions Oct. 1993 14 p Prepared in cooperation with Army Natick Research and Development Command (For primary document see N94-28420 08-51)
Copyright Avail: CASI HC A03/MF A03

Adequate nutrition and hydration can be crucial to the survival of downed aircrews. To determine the nutritional adequacy and palatability of an improved, all-purpose, all-environment survival packet (GP-I) compared to the old survival packet (GP), a field test was conducted using combat survival school students. During a five day survival exercise, 41 aircrew members ate the GP-I and 57 ate the GP. Nutrition/hydration status were assessed from food/fluid intake records as well as changes in body weight. Water turnover was measured in a subset of subjects (n=30) using deuterium oxide. Pre- and post-test hemoglobin, hematocrit, plasma osmolality, urine specific gravity (SG) and ketones were also measured. Acceptability of the two rations was evaluated. Subjects eating the GP-I consumed more calories; GP-I 774 +/- 436 versus GP 642 +/- 408 kcal/d. Carbohydrate and protein consumption were similar but the GP-I group ate significantly more fat, 35 +/- 21 versus 24 +/- 18 g/d. Mean fluid intake was similar for both groups (GP-I 4.3 +/- 1.7, GP 4.4 +/- 1.9 L/d). Sodium intakes were 1.1 g/d. Weight decreased significantly for the GP-I and GP groups (2.9 +/- 1.4, 3.4 +/- 1.7 kg, respectively); changes were similar between groups. Water turnover data indicated subjects maintained adequate hydration as did hemoglobin, hematocrit, and plasma osmolality. Mean post-test urine SG was 1.024 +/- 0.007 and moderate amounts of ketones were detected in urine. Both rations received favorable ratings, but the greater variety of the GP-I ration resulted in higher acceptability ratings. Either ration is adequate; however, the GP-I is more desirable and palatable than the GP.
Author

N94-28430# Guelph Univ. (Ontario). School of Engineering.
THE POTENTIAL OF NEW TEXTILES IN IMPROVING SURVIVAL PROSPECTS **c54**
K. Slater *In* AGARD, The Support of Air Operations under Extreme Hot and Cold Weather Conditions Oct. 1993 13 p (For primary document see N94-28420 08-51)
Copyright Avail: CASI HC A03/MF A03

The paper surveys briefly the role of textile materials in enhancing comfort and survival prospects, in both cold and hot climates, identifying the fiber, fabric and textile construction factors of critical importance. An examination of the interaction between these factors, showing how they enhance or interfere with one another, is also carried out in outline. Selected new textile fibers and fabric construction or finishing techniques are then analyzed to determine how their novel characteristics can improve their cold- or hot-weather performance, with a prediction in each case of how the advantages derived from their incorporation may potentially be of use in improving aircrew or ground support staff clothing applications.
Derived from text

N94-28431# META Research, Inc., Richmond (British Columbia).
FIRE-RESISTANT WATER VAPOUR PERMEABLE BUOYANT INSULATION **c54**
Wendell Uglene and Brian Farnworth *In* AGARD, The Support of Air Operations under Extreme Hot and Cold Weather Conditions Oct. 1993 8 p Sponsored by Mustang Survival and British Columbia Research Council (For primary document see N94-28420 08-51)
Copyright Avail: CASI HC A02/MF A03

Compared to closed cell foam, constant wear garments designed with this material provide added comfort due to increased heat losses during sweating, shortened drying times after sweating, and added flexibility. Although introducing water vapor permeability causes a degradation to the material's cold water immersion protection, the integrity of its fire protection and buoyancy remains unaltered.
Author

N94-28432# Gore (W. L.) and Associates, Inc., Elkton, MD.
DEVELOPMENT OF A NEW CHEMICAL WARFARE AGENT PROTECTIVE MATERIAL **c54**
S. Nicholas Allen, Robert J. Bender, and Terri L. Kelly *In* AGARD, The Support of Air Operations under Extreme Hot and Cold Weather Conditions Oct. 1993 8 p (For primary document see N94-28420 08-51)
Copyright Avail: CASI HC A02/MF A03

In 1976 W. L. Gore & Associates, Inc. invented GORE-TEX fabric utilizing expanded polytetra-fluoroethylene (ePTFE). This was the first truly waterproof and moisture vapor permeable fabric laminate. In 1980 the company began to develop products for military applications. Since that time, Gore has supplied GORE-TEX fabric for, and assisted in the development of, some of the military's most technically sophisticated apparel: the U. S. Army's Extended Cold Weather Clothing System (ECWCS), the U. S. Navy's Over Water Flight Suit (OWFS), and the U. S. Air Force's Security Police Jacket being but a few examples. All of these garments provide the user with increased levels of protection from harsh environments and have proved themselves to be very durable. GORE-TEX fabric laminate has consistently proven itself to be technically superior to any other material. This paper details the development by Gore of a new chemical warfare protective material based on proven ePTFE technology combined with a new highly activated polymer system (APS). Author

N94-28433# Alberta Univ., Edmonton. Dept. of Human Ecology.
THERMAL PROTECTIVE PERFORMANCE AND INSTRUMENTED MANNEQUIN EVALUATION OF MULTI-LAYER GARMENT SYSTEMS **c54**
E. M. Crown, M. Y. Ackerman, J. D. Dale, and K. B. Rigakis *In* AGARD, The Support of Air Operations under Extreme Hot and Cold Weather Conditions Oct. 1993 8 p Sponsored by Canadian Petroleum Association and Defence Research Establishment (For primary document see N94-28420 08-51)
Copyright Avail: CASI HC A02/MF A03

The purpose of this research was to evaluate the relative effectiveness of different clothing systems in their contribution to protection against exposure to high heat flux flash fires. All systems were exposed to controlled simulated flash fires (80 or 84 kW/sq m) on a thermally instrumented mannequin. The percentage of the mannequin surface reaching second and third degree burn criteria was recorded. In addition, the multiple layers of fabrics which were used together in each of the garment systems were tested according to a standard thermal protective performance (TPP) test. The protection provided by multiple layered garment systems was significantly greater than would be expected from the additive effects of the layers used singly. The outer layer of a garment system must be flame retardant, however; wearing a flammable garment over a flame retardant one clearly negates the benefits of the FR layer. While it cannot be concluded for certain that undergarments must also be flame retardant, results demonstrate that FR undergarments offer more protection than non-FR ones, especially when worn under the relatively light-weight fabrics which may be used for military flightsuits. Only in one experiment with garment systems comprising all-FR layers did small-scale TPP tests indicate the relative protection provided by the systems. The TPP test did not indicate the potential hazard of systems in which the outer layer is non-FR. Nor did it differentiate among the three different flight suit fabrics or demonstrate the relative protective performance of different underwear materials. Author (revised)

N94-28434# Institute for Perception RVO-TNO, Soesterberg (Netherlands).
DETERIORATION OF MANUAL PERFORMANCE IN COLD AND WINDY CLIMATES **c52**
H. A. M. Daanen *In* AGARD, The Support of Air Operations under Extreme Hot and Cold Weather Conditions Oct. 1993 10 p (For primary document see N94-28420 08-51)
Copyright Avail: CASI HC A02/MF A03

Manual performance during work in cold and windy climates is severely hampered by decreased dexterity. In this study, the quantitative performance decrease is investigated as a function of climatic factors. The decrease in finger and hand dexterity and grip force was quantified for nine combinations of ambient temperature (-20, -10, and 0 C) and wind speeds (0.2, 4, and 8 ms(exp -1)), controlled in a climatic chamber. Finger dexterity was determined by the Purdue pegboard test, hand dexterity by the Minnesota manual dexterity test, and grip force by a hand dynamometer. Twelve subjects with average to low fat percentage were exposed to cold air for one hour with and without extra insulation by a parka. The subjects were clothed in standard work clothing of the Royal Netherlands Air Force for cold conditions. Extra insulation did affect cold sensation but not manual performance. The deterioration (in percent) in performance is strongly dependent upon Wind Chill Equivalent Temperature (C), and exposure time (min). In a computer program, the performance decreases and freezing risk is indicated for variable climatic conditions. Derived from text

N94-28435# German Air Force, Fuerstenfeldbruk (Germany). Inst. of Aviation Medicine.
EFFECTIVENESS OF PROTECTION CLOTHING FOR COLD WEATHER CONDITIONS AFTER EJECTION OVER SEA: A CASE REPORT **c54**
B. Mayr and M. Kraemer *In* AGARD, The Support of Air Operations under Extreme Hot and Cold Weather Conditions Oct. 1993 8 p (For primary document see N94-28420 08-51)
Copyright Avail: CASI HC A02/MF A03

During a night formation mission including an approach without establishing a connection to the tanker aircraft a collision of both aircrafts, Typ PA 200 Tornado occurred. The four aircrew members performed an ejection. The site of the accident is located over the baltic sea in the Skagerrak region. At the time of accident, the air temperature was noted with 6 C, the water temperature with 11 C, and the sea with waves of 4 to 4.5 m height with a frequency of 8 waves per minute. The time of rescue ranged from 1 hour 28 minutes to 2 hours 14 minutes. This document reports on clothing and personal equipment, on the clinical findings, and on statements of the crew members. The crew member who was recovered after 2 hours and 14 minutes did not survive. This accident shows that with the ordered clothing, a survival under these conditions is supported, yet with incomplete equipment, it must be reckoned with a fatal outcome. Further details are discussed. Derived from text

N94-28436# Shark Group of Companies, Morpeth (England).
ADVANCED INTEGRATED COLD PROTECTION FOR AIRCREW **c54**
E. Bramham and M. J. Tipton *In* AGARD, The Support of Air Operations under Extreme Hot and Cold Weather Conditions Oct. 1993 8 p (For primary document see N94-28420 08-51)
Copyright Avail: CASI HC A02/MF A03

In this paper, the concept of an Advanced Integrated Survival System is introduced and discussed in relation to the Helicopter Crew Member and Passengers, although the principles are equally applicable to many other types of user and circumstances requiring specialized protective clothing. The fundamental principles behind the concept are firstly that the wearer should be given protection against all of the hazardous responses associated with immersion in cold water and secondly, that the individual components which make up the integrated survival system (ISS) must be compatible and complementary. They may also be interdependent. Derived from text

N94-28437# Surrey Univ., Guildford (England).
EMERGENCY UNDERWATER BREATHING AIDS FOR HELICOPTER PASSENGERS AND CREW **c54**
M. J. Tipton (Institute of Naval Medicine, Alverstoke, England.), E. Bramham (Shark Group of Companies, Morpeth, England.), and D. H. Elliott *In* AGARD, The Support of Air Operations under Extreme Hot and Cold Weather Conditions Oct. 1993 8 p Sponsored by Shell Research Ltd. and Esso Research Center (For primary document see N94-28420 08-51)
Copyright Avail: CASI HC A02/MF A03

In this paper, the rationale for the provision of some form of helicopter emergency underwater breathing aid (HEUBA) for helicopter passengers and crew is briefly discussed and the thoughts and work which resulted in the production of a new aid, 'Air Pocket', is reviewed. Derived from text

N94-28438# Royal Danish Navy, Gentofte. Health Services.
THERMOREGULATION IN THE EXTREME COLD ENVIRONMENT **c52**
Leif Vanggaard *In* AGARD, The Support of Air Operations under Extreme Hot and Cold Weather Conditions Oct. 1993 5 p (For primary document see N94-28420 08-51)
Copyright Avail: CASI HC A01/MF A03

Thermoregulation is normally viewed as the physiological responses aimed towards keeping the deep body temperature constant and high. For

this work, this viewpoint is changed, and the human thermoregulation is viewed as those physiological mechanisms that keep the body at an optimal functional state. Here, the extremities and their thermal state is of the highest importance. In the extremities, the arteriovenous anastomoses (AVA's) determine the local temperatures, and by their action also define the thermoregulatory state of the body. The AVA's are centrally regulated, they determine the heat exchange with the environment, and they are the main determinants of the average skin temperature. By following their reactions, man's thermoregulatory state can be ascertained. In the treatment of hyperthermia and hypothermia, these functions are highly relevant. The role of the AVA's place them as a specific thermoregulatory organ responsible for the maintenance of optimal extremity temperatures.
Derived from text

N94-28439# Erlangen-Nuremberg Univ. Childrens Hospital (Germany). Inst. of Forensic Medicine.
PHYSIOLOGICAL INVESTIGATIONS OF THE ISOLATED RAT'S LIVER IN HYPOTHERMIA AND HYPOXIA AND THEIR RELEVANCE IN AIRCRAFT INCIDENTS ABOVE THE SEA
T. Dumser, M. Kraemer, and J. Hoeper *In* AGARD, The Support of Air Operations under Extreme Hot and Cold Weather Conditions Oct. 1993 11 p (For primary document see N94-28420 08-51)
Copyright Avail: CASI HC A03/MF A03

Animals have two main methods of adjusting their body temperature. Poikilothermic animals adjust it to the existing ambient temperature, temperature, whereas homoiothermic animals keep temperature at a relatively constant value which is frequently above the ambient temperature; thus, temperature; thus, they able to stay in contrast to poikilothermic animals whose metabolic processes slow down increasingly due to van't Hoff's rule when ambient temperatures are when ambient temperatures are low, rendering sometimes even resulting in low-temperature rigidity. This, however, enables them to survive for a longer period of time in case of a lack of food and/or cold spells. Hibernating animals are something in between. In times of food shortage and in the period of cold weather, they reduce their metabolic processes and lower their body temperature. Without a doubt, man is part of the group of homoiothermic organisms. However, when having a closer look at homoiothermic organisms, it becomes obvious that their body temperature is only constant as far as the body core and the vital organs are concerned - there are fluctuations in the temperature of the extremities, i.e., the outer parts of the body, which are mainly induced by the environment. Consequently, the tissue of these regions of the body is subject to changes in temperature which may be considerable without resulting in permanent damage. Findings, mainly obtained from transplantation medicine, have shown that the organs of the body core need not be damaged irreversibly either, if their temperature is lowered for several hours - on the contrary, they can even be preserved this way for a limited period. Derived from text

N94-28440# Institute of Aviation Medicine, Fuerstenfeldbruck (Germany).
AEROPATHOLOGICAL DIAGNOSIS OF LETHAL HYPOTHERMIA c52
M. Kraemer *In* AGARD, The Support of Air Operations under Extreme Hot and Cold Weather Conditions Oct. 1993 6 p (For primary document see N94-28420 08-51)
Copyright Avail: CASI HC A02/MF A03

The decrease of central body temperature by warmth withdrawal leads in most cases to pathological changes of signal devices as the energy metabolism. The central body temperature may be lowered to 28 to 26 C without irreversible disturbances of life functions occurring. Not earlier as below 26 C rectal temperature life sustaining becomes critical. With continued exposure to cold and missing therapy, hypothermia passes several phases. Below 26 C rectal temperature in a phase of paralysis death occurs with cardiac disturbances like cardiac oscillation and disorders of atrio-ventricular conduction. Findings on the corpses of persons dying by cold exposure are discussed. Findings of a crew member dying after ejection and immersion in cold water are demonstrated and weighted by means of differential diagnosis. Author (revised)

N94-28441# Naval Health Research Center, San Diego, CA.
REWARMING METHODOLOGIES IN THE FIELD c52
R. S. Pozos, R. L. Hesslink, J. Reading, P. Kincaid, and S. Feith *In* AGARD, The Support of Air Operations under Extreme Hot and Cold Weather Conditions Oct. 1993 8 p (For primary document see N94-28420 08-51)
Copyright Avail: CASI HC A02/MF A03

Hypothermia may occur with prolonged exposure to cold air or water. Recovery from hypothermia involves removing the individual from the cold environment and utilizing a rewarming strategy. Three major rewarming strategies include the following: passive rewarming, active external heating, and active internal heating. Controversy continues regarding the best rewarming procedure for use in the field. Author (revised)

N94-28442# Royal Naval Hospital, Haslar (England). Dept. of Accident and Emergency Medicine.
A COMPARISON OF FOUR METHODS OF REWARMING INDIVIDUALS COOLED BY IMMERSION IN COLD WATER c52
C. J. Cahill, P. J. Balmi, and M. J. Tipton *In* AGARD, The Support of Air Operations under Extreme Hot and Cold Weather Conditions Oct. 1993 8 p (For primary document see N94-28420 08-51)
Copyright Avail: CASI HC A02/MF A03

It has been suggested that hypothermia individuals could be actively rewarmed in the field by immersion of only the extremities (hands and feet) in hot water. If successful this technique would have enormous potential in the pre-hospital and hospital care of the victims of accidental hypothermia. The theory is that local heat to the extremities results in opening of the arteriovenous anastomoses with return of warmed blood directly to the core, via the superficial veins bypassing the intervening cold peripheral tissues. A comparison of four techniques for rewarming subjects with lowered core temperatures has been undertaken. The techniques examined were: immersion to the neck in water at 40 C; immersion of one hand in water at 40 C; immersion of two hands plus forearms in water at 42 C; and passive rewarming. During rewarming, core and skin temperatures, heart rate, blood pressure, oxygen consumption, and peripheral blood flow were measured at frequent intervals. No significant difference, in the ability to raise the core temperature, was found among the techniques. It is concluded that hand rewarming, although theoretically attractive, does not work in practice and may even be detrimental in some circumstances, by suppressing intrinsic heat production. Author (revised)

N94-28443# Aerospace Medical Research Labs., Brooks AFB, TX.
AEROMEDICAL SUPPORT FOR CASUALTIES IN EXTREMELY HOT CLIMATES c54
S. A. Nunneley and R. U. Bisson *In* AGARD, The Support of Air Operations under Extreme Hot and Cold Weather Conditions Oct. 1993 7 p (For primary document see N94-28420 08-51)
Copyright Avail: CASI HC A02/MF A03

Aeromedical support for operations in hot climates involves exposure to acute heat injury and chronic heat stress which are unfamiliar to many medical personnel in NATO nations. Preparation for deployment to a hot climate should include review of climatic data for the site, appropriate adjustment to supplies and equipment needed to handle predicted numbers of heat casualties, and education of all air base personnel regarding methods of preventing heat illness. Medical facilities at the remote site may include local buildings or air transportable units. Special care is required with respect to housekeeping and provision of safe food and water in hot climates. Casualties arriving from remote sites should be assumed to suffer from heat stress and dehydration; those with elevated temperatures or disturbed consciousness must be treated as heat stroke cases until proven otherwise. Oral rehydration mixtures should be used whenever possible, reserving intravenous fluids for severe cases. Plans for air evacuation of all patients should attempt to minimize heat stress during loading and allow for continued rehydration in flight. Author

N94-28444# Spanish Air Force, Talavera AFB.
WORK CONDITIONS ASSESSMENT IN PILOTS AND GROUND PERSONNEL UNDER HIGH WEATHER TEMPERATURES c54
J. L. GarciaAlcon and J. M. MorenoVazquez *In* AGARD, The Support of Air Operations under Extreme Hot and Cold Weather Conditions Oct. 1993 9 p (For primary document see N94-28420 08-51)
Copyright Avail: CASI HC A02/MF A03

Humans and animals often exhibit a remarkable ability to adapt to harsh or rapidly changing environmental conditions. One obvious means of adaptation is to move to where the environmental stresses are less severe. The body also has a great physiological capacity for adaptation. There

exists ample literature on adaptative mechanisms and processes. When a person becomes acclimatized, the hypothalamus and other body control organs and systems settle into cooperative equilibrium, with certain chemical or hormonal levels that are appropriate for that particular season. The present study, describes how simple dietary rules can prevent involuntary dehydration brought about by sweating. Author (revised)

N94-28445# Royal Air Force, Farnborough (England). Inst. of Aviation Medicine.

THERMAL STRAIN GENERATED BY AN ENHANCED ANTI-G PROTECTION SYSTEM IN A HOT CLIMATE **c54**

P. J. Sowood and E. M. OConnor *In* AGARD, The Support of Air Operations under Extreme Hot and Cold Weather Conditions Oct. 1993 13 p (For primary document see N94-28420 08-51)

Copyright Avail: CASI HC A03/MF A03

A flight trial was conducted at RAF Akrotiri to assess the level of thermal strain associated with, and the G protection provided by, the prototype European Fighter Aircraft (EFA) interim aircrew equipment assembly (AEA) in a warm climate. Six subjects flew a standardized sortie four times in the RAF IAM Hawk aircraft: two while wearing the EFA AEA, and two wearing standard Hawk Summer AEA. The sortie profile included simulated air combat and four high G turns. Cockpit temperatures, rectal and skin temperatures, heart rate, and sweat rate were recorded. Subjective thermal comfort, fatigue, and G tolerance were also assessed. Skin temperatures at the chest, back, and upper thigh sites and mean skin temperatures were greater in flight, and sweat rate was increased when the EFA AEA was worn. However, rectal temperature and heart rate did not differ significantly when the EFA AEA was worn indicating that homeostasis was maintained by thermoregulatory mechanisms. Superior G protection was provided by the EFA AEA. Taken as 8 whole, these findings suggest that wearing the EFA AEA in a warm climate is associated with an increased but not unacceptable level of thermal stress while offering greater G protection. These results may not generalize to conditions where ambient temperatures are higher or where more insulative protective clothing is required. Author (revised)

N94-28446# Royal Air Force, Farnborough (England). Inst. of Aviation Medicine.

IMPLICATIONS OF CLIMATIC EXTREMES IN AIRCREW NBC OPERATIONS **c54**

A. J. F. Macmillan *In* AGARD, The Support of Air Operations under Extreme Hot and Cold Weather Conditions Oct. 1993 6 p (For primary document see N94-28420 08-51)

Copyright Avail: CASI HC A02/MF A03

The NBC protective equipment and facilities in service with UK forces must be used when an appropriate threat exists irrespective of climate. Modifications to the individual assemblies, including provision of heated ventilating air to the aircrew respirator and additional insulation in cold conditions together with means to increase loss of body heat in hot climates and combined with changes to procedures and adaptation of concepts of use, can minimize the impedance to effective air operations which may occur from the additive effects of wearing NBC protective equipment in climatic extremes. Author (revised)

N94-28447# Army Research Inst. of Environmental Medicine, Natick, MA. Military Performance and Neuroscience Div.

THE ENVIRONMENTAL SYMPTOMS QUESTIONNAIRE: ASSESSING REACTIONS TO ENVIRONMENTAL EXTREMES IN MILITARY OPERATIONS **c54**

John L. Kobrick, James B. Sampson, and Richard F. Johnson *In* AGARD, The Support of Air Operations under Extreme Hot and Cold Weather Conditions Oct. 1993 8 p (For primary document see N94-28420 08-51)

Copyright Avail: CASI HC A02/MF A03

The environmental symptoms questionnaire (ESQ) was developed to aid in the standardized assessment of symptoms experienced by individuals exposed to environmental extremes. It was used initially to delineate the symptoms of acute mountain sickness, but has since evolved into a more comprehensive tool for assessing subjective reactions to ambient heat and cold, to diet, physical exercise, and medications. The ESQ has also been made more reliable and user friendly by revision, addition and removal of certain items, and by compression of the initial scale values. Factor analysis of responses has identified several meaningful symptom clusters, and has provided a useful technique for scoring those clusters under both laboratory and field conditions. Studies utilizing the ESQ under various environmental extremes are summarized and reviewed. Current administration and scoring methods are presented. Author (revised)

N94-28448# Naval Aerospace Medical Research Lab., Pensacola, FL. Environmental Physiology Div.

EFFECTS OF THREE HYDRATION BEVERAGES ON EXERCISE PERFORMANCE DURING 60 HOURS OF SIMULATED DESERT EXPOSURE **c52**

L. G. Meyer, D. J. Horrigan, Jr., H. M. Neisler, and W. G. Lotz *In* AGARD, The Support of Air Operations under Extreme Hot and Cold Weather Conditions Oct. 1993 10 p (For primary document see N94-28420 08-51)

Copyright Avail: CASI HC A02/MF A03

Without adequate hydration, profound heat stress and dehydration can occur in military forces operating in hot environments. The purpose was to evaluate the effectiveness of three beverages on temperature regulation, cardiovascular response, and work performance during prolonged heat exposure. Nine male subjects, attired in standard military combat uniforms, lived in a climatic chamber for 3 days (60 h) in simulated desert conditions varying from 25 to 45 C, 20 percent relative humidity. Three submaximal treadmill exercise bouts (40 min at 4.8 km/h, 0 percent grade) were performed at 4-h intervals each day. Subjects randomly consumed three beverages: a water placebo of water, citric acid, and aspartame (WP); a 5 percent carbohydrate drink containing water, citric acid, sucrose, fructose, and electrolytes (CE); and a 4 percent carbohydrate drink containing water, citric acid, sucrose, glucose, electrolytes, pyruvate, and 1 percent glycerol (CEG). Subjects drank only one of the three beverages ad libitum during the 60 h but were encouraged to drink every 15 min during exercise. Each subject tested all three beverages in a double blind, repeated-measures experimental design. Sweat rate (SR), core (rectal) temperature (Tre), average skin temperature (Tsk), heart rate (HR), oxygen consumption (VO2), and subjective ratings of perceived exertion (RPE) were recorded during exercise. Body temperatures and metabolic parameters remained within expected physiologic limits during 60 h of simulated desert conditions. During exercise, RPE and HR were similar for all beverages, but VO2, Tre, Tsk, and SR differed among beverages. During the 3rd exercise session on all days, VO2 was higher for CE than CEG and WP; CEG tests had the lowest VO2 on the 2nd and 3rd days. Rectal temperature was lower with CE and CEG than with WP on the 2nd and 3rd exercise periods of each day. Skin temperatures were different during the second exercise period on all three days. Exercise sessions with CEG produced the highest SR. It was concluded that carbohydrate-electrolyte beverages, preferably with a small amount of glycerol, may provide beneficial physiological responses during exercise in hot-dry conditions during the first 24 h of exposure. However, water alone appears to provide adequate hydration for working in desert conditions over extended periods of time.

Author (revised)

N94-28449# Defence and Civil Inst. of Environmental Medicine, North York (Ontario).

ALLEVIATION OF THERMAL STRAIN IN THE CF: KEEPING OUR COOL DURING THE GULF CONFLICT **c52**

J. Frim, L. L. Bossi, K. C. Glass, and M. J. Ballantyne *In* AGARD, The Support of Air Operations under Extreme Hot and Cold Weather Conditions Oct. 1993 10 p (For primary document see N94-28420 08-51)

Copyright Avail: CASI HC A02/MF A03

Thermal stress can be a serious problem for military personnel. This is largely because the measures employed to reduce such stress under normal working conditions are impractical under operational circumstances. For example, the specialized clothing worn by soldiers cannot generally be removed to reduce insulation and facilitate cooling. Similarly, operations are often conducted in hostile environments where ambient conditions, even inside vehicles, cannot be altered substantially. While reductions in work rate are feasible during peacetime, they have little place in combat as they compromise objectives and may still not be adequate to reduce thermal strain to acceptable levels. When operationally feasible, the provision of personal cooling can assist the body with heat dissipation and thermoregulation, often to the point that work can be continued at a near-normal rate with only slight to moderate thermal strain. An overview

of personal cooling technology studies conducted at DCIEM within the last decade is presented. It outlines the problems of thermal stress in operations and its effects on performance, examines various solutions to the problem, and summarizes the R&D efforts that culminated in the integration of personal cooling into the CH124 Sea King helicopters during Op Friction. This was to our knowledge the world's first use of air crew personal cooling garments during combat and it enabled the Canadian Forces (CF) to conduct their Sea King helicopter operations without being time-limited due to thermal physiological strain. Author

N94-28450# Laboratoire de Medecine Aerospatiale, Bretigny-sur-Orge (France). Centre d'Essais en Vol.
EXPERIMENTAL EVALUATION OF TWO SYSTEMS OF INDIVIDUAL AIR-CONDITIONING [EVALUATION EXPERIMENTALE DE DEUX SYSTEMES DE CLIMATISATION INDIVIDUELLE] **c52**
D. Lejeune, J. M. Clere, M. Beaumont, and M. Loncle *In* AGARD, The Support of Air Operations under Extreme Hot and Cold Weather Conditions Oct. 1993 8 p In FRENCH (For primary document see N94-28420 08-51)
Copyright Avail: CASI HC A02/MF A03

The thermal stress in military aeronautics can involve a drop in physical and psychomotor performances; in particular the tolerance for accelerations is decreased. The use of a system of individual air-conditioning is likely to decrease the storage of heat and to thus allow the prolongation of missions. Two techniques are possible: a circulation of cooled fluid in contact with the body or a ventilation of cooled air inside the suit. Two systems were tested, one using a cooled water circulation, the other a circulation of air saturated with 20 C water vapor. The fluid, air, or water circulating in contact with the body is cooled using thermoelectric modules. The tests carried out on voluntary human subjects, in a hot environment going from 40 to 50 C, made it possible to highlight a clear improvement in thermal comfort. Each system has advantages and disadvantages. They must undergo technological improvements in order to allow their use on board combat aircraft. Author

N94-28451# Exotemp Systems, Inc., Stittsville (Ontario).
RECENT CANADIAN ADVANCES IN ACTIVE THERMAL PROTECTION **c54**
P. A. Browne *In* AGARD, The Support of Air Operations under Extreme Hot and Cold Weather Conditions Oct. 1993 9 p (For primary document see N94-28420 08-51)
Copyright Avail: CASI HC A02/MF A03

The Gulf war created an unusual incentive to the rapid development and deployment of active cooling systems for defense personnel. One of the most successful efforts in this respect concerned a liquid-circulating system which departed from prior art in a number of significant ways. The system was deployed first by Canadian aircrew, and then by their British counterparts in the later stages of the conflict. The systems used by these forces are described, with an account of their physical and thermal characteristics, and an account of their performance in the field. Very recent developments in electrically powered cooling units for microclimate use are also described. These new devices offer very real advantages in terms of power and space consumption. The impact they will have on air operations in extreme heat is discussed. Author

N94-28452# Institute of Aviation Medicine, Manching (Germany).
TEST OF A NEW PROTECTION SUIT IN A CLIMATIC CHAMBER **c54**
H. Pongratz, M. Harre, B. Karmann, A. Rieck, and H. Vaic *In* AGARD, The Support of Air Operations under Extreme Hot and Cold Weather Conditions Oct. 1993 4 p (For primary document see N94-28420 08-51)
Copyright Avail: CASI HC A01/MF A03

Within the framework of the research and technology program, a whole-body protection suit with integrated helmet was developed by the Dornier Company. The thermophysiological capabilities of this suit were tested by Division IV Ergonomics of the German Air Force Institute of Aviation Medicine. Ambient temperatures higher than those normally to be expected in the cockpit were chosen intentionally. In spite of this fact, pulse rates remained below the limiting value and the average rise in core temperature was insignificant. Loss of weight through sweating amounted to approximately 1% of body weight. It proved possible to remove 82% of this sweat by means of ventilation. Based on the results of the questionnaires on subjective sensibility, no prejudice to well-being and no negative effects in respect of the capability to act were established with regard to the testing of the whole-body protection suit under laboratory conditions. Author (revised)

N94-28453# Army Aeromedical Research Lab., Fort Rucker, AL.
THE USE OF LIQUID AND AIR MICROCLIMATE CONDITIONING SYSTEMS TO ALLEVIATE HEAT STRESS IN HELICOPTER NBC OPERATIONS **c54**
Robert Thornton, J. Lynn Caldwell, and Frank Guardiani *In* AGARD, The Support of Air Operations under Extreme Hot and Cold Weather Conditions Oct. 1993 23 p (For primary document see N94-28420 08-51)
Copyright Avail: CASI HC A03/MF A03

The effects of microclimate cooling on aviator performance and physiology in Nuclear, Biological, and Chemical (NBC) Individual Protective Equipment (IPE) were evaluated in the USAARL UH-60 research flight simulator. Sixteen male aviators flew the simulator in two temperature conditions, 35 C and 41 C, both at 50% relative humidity (RH). Two thermoelectric conditioning units were used, one providing cooled blown air, the other cooled water to the aviators. At each temperature they flew for up to six hours in NBC IPE with no cooling, air cooling, and liquid cooling. Author (revised)

N94-28667 Kent State Univ., OH.
DEVELOPMENT OF NOVEL SWITCHABLE PROTEIN SURFACES Final Report, 15 Mar. 1990 - 31 Jul. 1993
Roger K. Gilpin Dec. 1993 11 p Limited Reproducibility: More than 20% of this document may be affected by microfiche quality
(Contract DAAL03-90-G-0061)
(AD-A275510; ARO-27695.21-CH-SM) Avail: CASI HC A03

The objective of the proposed work was to develop a range of new separation and purification media based on ligand imprinting techniques to generate ligand binding sites on silica-immobilized proteins for specifically targeted compounds. Ligand imprinting take advantage of our ability to manipulate the dynamical properties of proteins using water as a plasticizer. DTIC

N94-28829 Louisiana State Univ., Baton Rouge.
EFFECTS OF PRESSURE ON MEMBRANE-ASSOCIATED RECEPTORS AND EFFECTOR ELEMENTS Final Report, 1 Jun. - 30 Nov. 1993
Joseph F. Siebenaller 30 Nov. 1993 2 p Limited Reproducibility: More than 20% of this document may be affected by microfiche quality
(Contract N00014-89-J-1865)
(AD-A275813) Avail: CASI HC A01

To identify the effects of moderate hydrostatic pressure on receptor and effector elements involved in transmembrane signal transduction, we examined the A1 adenosine receptor - inhibitory G protein (G) - adenylylcyclase signal transduction complex. Our experiments were designed to identify and define at the molecular level pressure effects on system components in isolation and on the entire functional complex. DTIC

N94-28884# Connecticut Univ., Farmington. Health Center.
STUDIES ON BACTERIAL SPORE ULTRAVIOLET LIGHT RESISTANCE AND REGULATION OF THE ACTIVITY OF A SPORE PROTEASE Final Report, 1 May 1990 - 31 Oct. 1993
Peter Setlow 10 Dec. 1993 6 p
(Contract DAAL03-90-G-0110)
(AD-A275448; Rept-31522-LS; ARO-27956.17-LS) Avail: CASI HC A02/MF A01

Highlights of the most significant research finding in the last few years are: (1) alpha/beta-type SASP have been shown in vitro to be a novel group of non-specific, double-strand DNA binding proteins which slow DNA depurination, block hydroxyl-radical cleavage of the backbone, and block UV induced pyrimidine dimer formation, while promoting spore photoproduct formation; (2) the effects of alpha/beta-type SASP in vitro are also exerted in vivo as these proteins are important factors in spore heat and hydrogen peroxide resistance, and the major cause of spore UV resistance; (3) studies of the regulation and processing of the SASP specific protease have strongly suggested that the processing of the zymogen form of this enzyme during sporulation is an autocatalyzed event triggered by changes in the forespore (very likely dehydration) which will block attack of the

active enzyme on SASP. In the first minutes of spore germination spore core rehydration then allows rapid SASP degradation. DTIC

N94-29156# Sveriges Lantbruksuniv., Uppsala. Dept. of Microbiology.
STABLE RNA SEQUENCES AS A TOOL FOR DNA PROBES AND PHYLOGENETIC STUDIES
J. Mattsson 1993 175 p See also PB93-201895
(ISSN 0348-4041)
(PB94-135423; SLU-MIKRO-R-57-SE; ISBN-95-576-4755-0) Copyright Avail: CASI HC A08/MF A02

In the work, several different detection systems based on 16S rRNA sequences were studied. The rRNA sequences were also used to infer phylogenetic relationships. The catalytic RNA from RNase P was studied as a potential alternative to rRNA sequences. Species-specific rDNA probes for Mycoplasma agalactiae, Mycoplasma bovis, Mycoplasma hyopneumoniae and Renibacterium salmoninarum were designed. The different probes were specific and could be used to identify their respective targets in clinical samples. It was observed that unexpected cross-hybridization of a probe to a non-target organism may depend on the type of mismatch. M. agalactiae is the closest relative to M. bovis, as was concluded from phylogenetic analysis. Group-specific rDNA probes for the detection of mycoplasma contaminated cell cultures was developed and tested on a large number of samples. NTIS

N94-29189 Helsinki Univ. of Technology, Espoo (Finland). Dept. of Chemical Engineering.
PLANT-MICROBE INTERACTIONS: PLANT HORMONE PRODUCTION BY PHYLLOPLANE FUNGI
T. Tuomi, J. Ilvesoksa, and H. Rosenqvist 23 Jun. 1993 16 p Limited Reproducibility: More than 20% of this document may be affected by microfiche quality
(PB94-135563; ISBN-951-22-1671-X) Avail: CASI HC A03

The molds Botrytis cinerea, Cladosporium cladosporioides and the yeast Aureobasidium pullulans, isolated from the leaves of three short-rotation Salix clones, were found to produce indole-3-acetic acid (a growth promoter of plants). Abscisic acid (a growth inhibitor of plants) production was detected in B. cinerea. The contents of indole-3-acetic acid and abscisic acid in the leaves of the Salix clones and the amounts of fungal propagules in these leaves were also measured, in order to evaluate whether the amounts of plant growth regulators produced by the fungi would make a significant contribution to the hormonal quantities of the leaves. The content of abscisic acid, and to a lesser degree that of indole-3-acetic acid, showed a positive correlation with the frequency of infection by the hormone producing organisms. The amounts of hormone producing fungi on leaves that bore visible colonies were, however, not sufficiently high to support the argument that neither the fungal production of abscisic nor indole-3-acetic acid would to a significant degree contribute to the hormonal contents of the leaves of the Salix clones. NTIS

N94-29190 Helsinki Univ. of Technology, Espoo (Finland). Dept. of Chemical Engineering.
PHYSIOLOGY AND MOLECULAR-GENETICS OF THERMUS AND BACILLUS
K. M. Nordstroem Apr. 1993 15 p See also PB93-226363 Limited Reproducibility: More than 20% of this document may be affected by microfiche quality
(PB94-135571; ISBN-951-22-1633-7) Avail: CASI HC A03

The use of the API 20 NE system for the identification of Thermus was evaluated and compared with results obtained for conventional microbiological identification tests. Five Thermus strains were studied, including T. thermophilus DSM 579, T. flavus DSM 674 and three wild strains originating from hot springs in Iceland. The results for the API 20 NE system were in accord with conventional tests with reference to nitrate reduction, beta-galactosidase production, and the absence of indole and urease production. Furthermore, acid was not produced from glucose. Thus the API 20 NE kit provides a convenient tool for the characterization of Thermus strains, although gelatinase and aesculin hydrolysis must be verified using conventional methodology. NTIS

N94-29401*# National Aeronautics and Space Administration. Ames Research Center, Moffett Field, CA.
LEG MUSCLE VOLUME DURING 30-DAY 6-DEGREE HEAD-DOWN BED REST WITH ISOTONIC AND ISOKINETIC EXERCISE TRAINING
J. E. Greenleaf, P. L. Lee, S. Ellis, R. H. Selzer, and D. A. Ortendahl Mar. 1994 11 p
(RTOP 199-18-12-07)
(NASA-TM-4580; A-94054; NAS 1.15:4580) Avail: CASI HC A03/MF A01

Magnetic resonance imaging (MRI) was used to compare the effect of two modes of lower-extremity exercise training on the mass (volume) of posterior leg group (PLG) muscles (soleus, flexor hallucis longus, tibialis posterior, lateral and medial gastrocnemius, and flexor digitorum longus) on 19 men (ages 32-42 years) subjected to intense dynamic-isotonic (ITE, cycle ergometer, number of subjects (N) = 7), isokinetic (IKE, torque egrometer, N = 7), and no exercise (NOE, N = 5) training for 60 min/day during head-down bed rest (HDBR). Total volume of the PLG muscles decreased (p less than 0.05) similarly: ITE = 4.3 +/- SE 1.6%, IKE = 7.7 +/- 1.6%, and NOE = 6.3 +/- 0.8%; combined volume (N = 19) loss was 6.1 +/- 0.9%. Ranges of volume changes were 2.6% to -9.0% (ITE), -2.1% to -14.9% (IKE), and -3.4% to -8/1% (NOE). Correlation coefficients (r) of muscle volume versus thickness measured with ultrasonography were: ITE r + 0.79 (p less than 0.05), IKE r = 0.27 (not significant (NS)), and NOE r = 0.63 (NS). Leg-muscle volume and thickness were highly correlated (r = 0.79) when plasma volume was maintained during HDBR with ITE. Thus, neither intensive lower extremity ITE nor IKE training influence the normal non-exercised posterior leg muscle atrophy during HDBR. The relationship of muscle volume and thickness may depend on the mode of exercise training associated with the maintenance of plasma volume. Author

N94-29943*# Ohio State Univ., Columbus. Dept. of Plant Biology.
CELLULAR POLARITY AND INTERACTIONS IN PLANT GRAVIPERCEPTION Final Report, 1 Jun. 1991 - 17 Jun. 1993
Fred D. Sack 1993 4 p
(Grant NAG10-0085)
(NASA-CR-195261; NAS 1.26:195261; OSURF-724742) Avail: CASI HC A01/MF A01

Presented are results of studies on the mechanisms of gravitropic sensing in higher and lower plants. Gravitropic roots of the aquatic angiosperm, Limnobium, were found to have sedimented amyloplasts in their elongation zone but not in their rootcap; nuclei were found to sediment in the elongation zone as well. Another study attempted to understand how plastid sedimentation occurs in vertical Ceratodon cells and how this sedimentation is regulated. To determine whether the cytoskeleton restricts plastid sedimentation, the effects of amiprophos-methyl (APM) and cytochalasin (CD) on plastid position were qualified. Results suggest that microtubules restrict the sedimentation of plastids along the length of the cell and that microtubules are load-bearing for all the plastids in the apical cell, demonstrating the importance of the cytoskeleton in maintaining organelle position and cell organization against the force of gravity. Physcomitrella and Funaria were also studied. Results suggest that gravitropism may be relatively common in moss protonemata and reinforce the idea that amyloplast mass functions in gravitropic sensing. CASI

N94-29968*# East Carolina Univ., Greenville, NC. Anatomy and Cell Biology School of Medicine.
PHYSIOLOGICAL ANATOMICAL RODENT EXPERIMENT (PARE) .04 FEASIBILITY TEST 2
Hubert W. Burden 11 Apr. 1994 85 p
(Contract NCC2-810)
(NASA-CR-195210; NAS 1.26:195210) Avail: CASI HC A05/MF A01

The objective of this feasibility study was to subject pregnant rats of the same age, strain, and size that will be utilized in a shuttle flight experiment to all flight conditions except the unique microgravity of space flight and determine the feasibility of the proposed experimental design to meet the experimental objectives. The study utilized facilities at NASA, Ames Research Center, Moffett Field, CA to subject the rats to the gravitational stresses of a simulated shuttle launch and simulated shuttle landing. One hundred pregnant rats were received on gestation day (G) 2 (day 1 = day of vaginal sperm) and on G7, eighty rats were laparotomized to determine the condition of pregnancy and allow assignment to test

groups. The five test groups (N=10 each group) were as follows: Group 1, Nominal Flight; Group 2, Laparotomy Control; Group 3, Hysterectomy Control; Group 4, Vivarium Control; Group 5, Delayed Recovery. On G9, animals in groups 1,2,3, and 5 were subjected to a shuttle launch simulation. On G18, groups 1,2, and 3 were subjected to a shuttle landing simulation and on this same day groups 1 and 2 were subjected to unilateral hysterectomy to obtain fetuses and placentas for evaluation. Fetal crown-rump length and fetal weight of the Nominal Flight group was significantly less than the Laparotomy Control group, but placentas were similar. On G20, group 5 was subjected to a shuttle landing simulation and on this day this group received a unilateral hysterectomy and fetuses and placentas were weighed. Animals in all groups were allowed to go to term and all animals delivered between 06:00 hours G22 and 18:00 hours G23. After delivery, a blood sample was taken from each experimental dam, and they were euthanized and the thymus and adrenal glands weighed. The thymus weight from all experimental group dams was decreased relative to the Vivarium Control group but adrenal glands and hormone values in dam plasma was similar in all groups. Pups from experimental groups were tattooed for identification, the anogenital distance of male pups was measured, and all pups placed with foster dams and litter sizes were standardized to 10. There was no difference in anogenital distances between male pups from different test groups. Pups delivered from Delayed Recovery animals were smaller than pups delivered from Nominal Flight animals. On neonatal day 7, all pups were euthanized and pup adrenal glands and thymus weighed. There was no difference in weights of thymus and adrenal glands in pups euthanized at neonatal day 7. Collectively, these data confirm the feasibility of the experimental design to meet objectives of the studies proposed for shuttle flight. Author

N94-30180 Michigan Biotechnology Inst., Lansing.
ONE CARBON METABOLISM IN ANAEROBIC BACTERIA: REGULATION OF CARBON AND ELECTRON FLOW DURING ORGANIC ACID PRODUCTION
J. G. Zeikus and M. Jain 1993 8 p Limited Reproducibility: More than 20% of this document may be affected by microfiche quality
(Contract DE-FG02-87ER-13719)
(DE94-004852; DOE/ER-13719/5) Avail: CASI HC A02

The project deals with understanding the fundamental biochemical mechanisms that physiologically control and regulate carbon and electron flow in anaerobic chemosynthetic bacteria that couple metabolism of single carbon compounds and hydrogen to the production of organic acids (formic, acetic, butyric, and succinic) or methane. The authors compare the regulation of carbon dioxide and hydrogen metabolism by fermentation, enzyme, and electron carrier analysis using Butyribacterium methylotrophicum, Anaeroblospirillum succiniciproducens, Methanosarcina barkeri, and a newly isolated triculture composed of a syntrophic butyrate degrader strain IB, Methanosarcina mazei, and Methanobacterium formicicum as model systems. To understand the regulation of hydrogen metabolism during butyrate production or acetate degradation, hydrogenase activity in B. methylotrophicum or M. barkeri is measured in relation to growth substrate and pH; hydrogenase is purified and characterized to investigate number of hydrogenases and their localization and functions; and their sequences are determined. To understand the mechanism for catabolic CO2 fixation to succinate the PEP carboxykinase enzyme and gene of A. succiniciproducens are purified and characterized. Genetically engineered strains of Escherichia coli containing the phosphoenol pyruvate (PEP) carboxykinase gene are examined for their ability to produce succinate in high yield. To understand the mechanism of fatty acid degradation by syntrophic acetogens during mixed culture methanogenesis formate and hydrogen production are characterized by radio tracer studies. It is intended that these studies provide strategies to improve anaerobic fermentations used for the production of organic acids or methane and new basic understanding on catabolic CO2 fixation mechanisms and on the function of hydrogenase in anaerobic bacteria. DOE

N94-30607# Department of Energy, Washington, DC. Office of Energy Research.
ANNUAL REPORT AND SUMMARIES OF FY 1993 ACTIVITIES: DIVISION OF ENERGY BIOSCIENCES
Sep. 1993 140 p
(DE94-001723; DOE/ER-0602P) Avail: CASI HC A07/MF A02

The mission of the Energy Biosciences program is to generate fundamental information about plants and non-health related microorganisms that will constitute the base for new biotechnologies as well as supply information to improve usages of such organisms in their current form. The collective aims are totally consistent with the Department of Energy's objectives of developing alternate energy sources, replacements for otherwise fossil energy derived products and providing critical fundamental information for the preservation and restoration of environmental conditions affected by energy related activities. The EB program takes full advantage of its organizational locale in the Office of Basic Energy Sciences to directly interact with such disciplines as Materials Sciences, Chemistry, Engineering and Geosciences to promote cross-disciplinary research and planning activities. One of the major specific objectives of the EB program is to probe the enormous capabilities of the specified organisms to carry out biochemical conversions. The limitation to realization of entirely new products and processes via biotechnology is the lack of basic understanding of natural processes. Such knowledge will then afford the advantage of developing procedures to the benefit of people and their society in providing new products along with providing new employment possibilities. This document consists of abstracts of projects supported in FY 1993. DOE

N94-30895 Michigan Univ., Ann Arbor.
ROLE OF X RAY-INDUCED TRANSCRIPTS IN ADAPTIVE RESPONSES FOLLOWING X RAYS Progress Report No. 2
D. A. Boothman 1993 18 p Limited Reproducibility: More than 20% of this document may be affected by microfiche quality
(Contract DE-FG02-91ER-61256)
(DE94-005412; DOE/ER-61256/T2) Avail: Issuing Activity (Department of Energy (DOE))

The overall goal of this proposal is to clone low dose X-ray-induced genes via molecular biology cloning techniques. From previous data, certain human cells can clearly carry out adaptive survival responses (ASR's) following ionizing radiation. Research goals are to better understand how some human cells can establish ASR's, and why other cells fail to do so. The author has been successful at identifying several genes whose expressions are altered during the establishment of, and actual processes occurring in, the adaptive response of U1-Mel cells. He will, in the next year or so, investigate the kinetics of expression of these genes, and whether or not other environmental stresses affect the expressions of these genes via Northern blot analyses. Finally, he will begin to investigate the function(s) of these genes within the cell, either under normal conditions of growth or following X-irradiation, using antisense expression technologies. Antisense RNA analyses and DNA repair endpoints (i.e., survival recovery, alkaline/neutral filter elutions, and PFGE) will be combined to examine the effects of specific gene 'knock out' experiments on ASR's in those human cells which demonstrate this response. The author is constructing mammalian expression vectors containing cyclin A, cyclin B, p53, or xip5, and xip12 (when full-length cDNA's are available) in the 'sense' orientation to overexpress these genes in human cells which did not demonstrate ASR's, such as HTB-152 or a variety of other human fibroblasts. Since many of the xips identified by 2-D gel electrophoresis were cell cycle regulated, the factors turning them on or off within a normal cell cycle may be clearly related to the events occurring in human cells following a genetic insult. DOE

N94-28853# Nihon Univ., Tokyo (Japan). Dept. of Hygiene.
EFFECT OF CHRONIC CENTRIFUGATION ON IN VITRO FERTILIZATION AND EARLY DEVELOPMENT IN MICE OVA [MAUSU RANSHI NO JUSEI TO SHOKI HASSEI NI OYOBOSU JI FUKA NO EIKYO]
Masao Ito, Ruriko Maru, Takashi Maeda, Ester Sanada, Takaichi Mano, Shinichi Horigome, Kenichi Iwasaki, Yuichi Kameyama, Yoshiro Ishijima, and Kazuyoshi Yajima *In* Japan Society of Aerospace and Environmental Medicine, Japanese Journal of Aerospace and Environmental Medicine, Volume 30, No. 1 1 Mar. 1993 p 19-25 In JAPANESE See also A93-49179 (For primary document see N94-28850 08-52)
Avail: CASI HC A02/MF A01

N94-29081# Waseda Univ., Tokyo (Japan). School of Education.
ESTIMATION OF THE NET PRODUCTION OF MOSS COMMUNITY AT LANGHOVDE, EAST ANTARCTICA [HIGASHI NANKYOKU RANGUHOBUDE NI OKERU SENRUI NO JUN SEISANRYO NO SUITEI]
Yoshio Ino *In* National Inst. of Polar Research, Antarctic Record, Volume

36, No. 1 30 Mar. 1992 p 49-59 Sponsored by National Inst. of Polar Research (For primary document see N94-29078 08-46)
Avail: CASI HC A03/MF A02

N94-29082# Aichi Fisheries Research Inst., Minato (Japan).
COPEPODS COLLECTED ALONG 33.5 DEG E LONGITUDE OF THE ANTARCTIC OCEAN IN THE 1976 SUMMER [1976 NEN KAKI, NANKYOKUKAI INDOYOKU NO TOKEI 33.5 DO SEN NI SOTTE ERARETA KAIASHIRUI SHIRYO]
Satoshi Yamada, Atsushi Tanimura, and Takashi Minoda *In* National Inst. of Polar Research, Antarctic Record, Volume 36, No. 1 30 Mar. 1992 p 60-64 (For primary document see N94-29078 08-46)
Avail: CASI HC A01/MF A02

N94-29085# National Inst. of Polar Research, Tokyo (Japan).
JAPAN-CHINA COLLABORATION RESEARCH PROGRAM ON TERRESTRIAL BIOLOGY AT GREAT WALL STATION IN KING GEORGE ISLAND, IN THE SUMMER OF 1990/1991 [1990/1991 NEN KAKI, KINGU JOJITO CHOJO KICHI NI OKERU NICCHU KYODO KANSOKU (DAN 3 NENJI)]
Shuji Otani and Takayuki Nakatsubo *In its* Antarctic Record, Volume 36, No. 1 30 Mar. 1992 p 109-115 In JAPANESE (For primary document see N94-29078 08-46)
Avail: CASI HC A02/MF A02

N94-29519# National Inst. for Resources and Environment, Ibaraki (Japan). Biomass Div.
GROWTH OF HYDROCARBON-RICH MICROALGA BOTRYOCOCCUS BRAUNII IN SECONDARILY TREATED SEWAGE AND ITS CONSUMPTION OF NITRATE ION AND PHOSPHATE ION [GESUI SHORISUI NI OKERU BOTRYOCOCCUS BRAUNII NO ZOSHOKU TO CHISSO OYOBI RIN NO SHOHI NI TSUITE]
Shigeki Sawayama, Seiichi Inoue, Tomoaki Minowa, and Yutaka Dote *In its* Journal of NIRE, Vol. 2, No. 3 25 May 1993 p 67-71 In JAPANESE (For primary document see N94-29512 08-99)
Avail: CASI HC A01/MF A02

N94-29648*# National Aeronautics and Space Administration. Ames Research Center, Moffett Field, CA.
PORTABLE LINEAR SLED (PLS) FOR BIOMEDICAL RESEARCH
Will Vallotton (Sverdrup Technology, Inc., Moffett Field, CA.), Dennis Matsuhiro, Tom Wynn, and John Temple *In its* The 27th Aerospace Mechanisms Symposium May 1993 p 315-331 (For primary document see N94-29627 08-15)
(RTOP 199-16-12-17; RTOP 199-16-12-19; RTOP 199-90-63-20)
Avail: CASI HC A03/MF A03

N94-29708# Ministry of Agriculture, Forestry, and Fisheries, Ibaraki (Japan). Analysis of Gear and Methods Section.
REPRODUCTION IN THE JAPANESE ANCHOVY (ENGRAULIS JAPONICA) AS RELATED TO POPULATION FLUCTUATION [KATAKUCHIIWASHI NO SEIJUKU/SANRAN TO SAISEISANRYOKU NO CHOSETSU NI KANSURU KENKYU]
Yoshinari Tsuruta *In its* Bulletin of National Research Institute of Fisheries Engineering, No. 13 5 Mar. 1992 p 129-168 In JAPANESE (For primary document see N94-29701 08-31)
Avail: CASI HC A03/MF A02

N94-29711# Hamamatsu Univ., Shizuoka (Japan).
SPACE MOVEMENT OF TRICHINELLA SPIRALIS UNDER MICROGRAVITY [SENMOCHU NO BISHO JURYOKU NI TAISURU YUEI HANNO]
Akira Murakami, Kenjiro Yoshimura, and Keiichi Takahashi *In* Society of Medical Research for Space Station, The MERSS 5th Symposium on Space Medicine: Medical and Physiological Experiment Utilizing Parabolic Flight Mar. 1993 p 9-13 In JAPANESE (For primary document see N94-29709 08-52)
Avail: CASI HC A01/MF A01

N94-29712# Fujita Health Univ., Toyohashi (Japan). School of Hygiene.
POSTURE CONTROL OF GOLDFISHES UNDER MICROGRAVITY [BISHO JURYOKUKA NI OKERU KINGYO NO SHISEI SEIGYO]
Akira Takabayashi *In* Society of Medical Research for Space Station, The MERSS 5th Symposium on Space Medicine: Medical and Physiological Experiment Utilizing Parabolic Flight Mar. 1993 p 14-18 In JAPANESE (For primary document see N94-29709 08-52)
Avail: CASI HC A01/MF A01

N94-29713# Tokyo Univ. (Japan).
BEHAVIOR AND VISUAL CONTROL OF CYPRINODONTS UNDER MICROGRAVITY [BISHO JURYOKUKA NI OKERU MEDAKA NO KYODO TO SHIKAKU NI YORU SEIGYO]
Kenichi Ijiri, Hoshio Eguchi, Yasuko Taguchi, Shunji Nagaoka, Masamichi Yamashita, and Akemi Kurotani *In* Society of Medical Research for Space Station, The MERSS 5th Symposium on Space Medicine: Medical and Physiological Experiment Utilizing Parabolic Flight Mar. 1993 p 19-25 In JAPANESE (For primary document see N94-29709 08-52)
Avail: CASI HC A02/MF A01

N94-29783*# Molecular Devices Corp., Menlo Park, CA.
MICROFABRICATED SILICON BIOSENSORS FOR MICROPHYSIOMETRY
L. J. Bousse, J. M. Libby, and J. W. Parce *In* JPL, Proceedings of the Workshop on Microtechnologies and Applications to Space Systems 15 Jun. 1993 p 163-18 (For primary document see N94-29767 08-31)
(Contract MDA972-92-C-0005)
Avail: CASI HC A03/MF A03

N94-29866# Saint Marianna Univ., Kawasaki (Japan). Dept. of Physiology.
SHORTENING VELOCITY AND CALCIUM SENSITIVITY OF SINGLE FIBERS FROM HINDLIMB SUSPENDED MUSCLE IN RATS [RATTO HAIYOSEI ISHUKU KINSENI NO TANSHUKU SOKUDO TO KARUSHIUMU KANJUSEI]
Katsumasa Yamashita and Toshitada Yoshioka *In* Japan Society of Aerospace and Environmental Medicine, Japanese Journal of Aerospace and Environmental Medicine, Vol. 30, No. 2 1 Jun. 1993 p 71-80 In JAPANESE See also A93-55329 (For primary document see N94-29863 08-52)
Avail: CASI HC A02/MF A01

N94-30461*# Department of Agriculture, Starkville, MS. Forest Service.
SEED VIABILITY DETECTION USING COMPUTERIZED FALSE-COLOR RADIOGRAPHIC IMAGE ENHANCEMENT
J. A. Vozzo and Michael Marko *In* NASA, Washington, Technology 2003: The Fourth National Technology Transfer Conference and Exposition, Volume 1 Feb. 1994 p 179-187 (For primary document see N94-30440 08-99)
Avail: CASI HC A02/MF A04

52 AEROSPACE MEDICINE

Includes physiological factors; biological effects of radiation; and effects of weightlessness on man and animals.

N94-28495# Japan Society of Aerospace and Environmental Medicine, Tokyo.
JAPANESE JOURNAL OF AEROSPACE AND ENVIRONMENTAL MEDICINE, VOL. 30, NO. 3 [UCHU KOKU KANKYO IGAKU DAI 30 KAN DAI 3 GO]
Makoto Masuda, Masamitsu Oshima, Kenichi Takagi, Sakae Yokobori, Mitsuo Sasaki, Ichiro Asukata, Sachio Ikawa, Yukiko Kakimoto, Hiroshi Kansaku, and Tadaaki Mano et al Sep. 1993 45 p In JAPANESE
(ISSN 0387-0723)
(JTN-94-80606) Avail: CASI HC A03/MF A01

The following topics were discussed: hypobaric hypoxia, electrolyte metabolism, endocrine responses, physical exercise effects, low oxygen, high altitude environments, heat rate, urination, Antidiuretic Hormone (ADH), Adrenocorticotropic Hormone (ACTH), Aldosterone (Aldo), Plasma Renin Activity (PRA), Atrial Natriuretic Peptide (ANP), space foods, space flight, feeding, eating, taste, astronauts, aerospace environment, microgravity, Head Down Tilt (HDT), gravitational effects, physiological effects, psychological

effects, stress, and nutritional requirements. For individual titles, see N94-28496 through N94-28498.

N94-28496# Tsukuba Univ., Ibaraki (Japan). Lab. of Exercise Physiology.

STUDIES ON WATER ELECTROLYTE METABOLISM AND ENDOCRINE RESPONSES AT REST AND DURING SUBMAXIMAL EXERCISE AT 6,000 m SIMULATED ALTITUDE [6,000 M SOTO KOTO NI OKERU ANSEI OYOBI SAIDAIKA UNDOJI NO MIZU/DENKAISHITSU TAISHA TO NAIBUNPI OTO]

Isao Suganuma, Koh Mizuno, Yasuhito Kumazaki, and Katsumi Asano *In* Japan Society of Aerospace and Environmental Medicine, Japanese Journal of Aerospace and Environmental Medicine, Vol. 30, No. 3 Sep. 1993 p 109-116 In JAPANESE See also A94-12178 (For primary document see N94-28495 08-52)

Avail: CASI HC A02/MF A01

Five healthy male climbers were investigated in a hypobaric simulator to elucidate the effect of hypobaric exposure on water-electrolyte metabolism and endocrine responses at rest and during exercise. After urination, the subjects drank water and rested for 30 minutes. Then blood and urine were taken and the simulator was decompressed to a simulated altitude of 6,000 m. They drank water again on arrival to 6,000 m, and blood and urine were taken after 30 minutes rest, and they conducted pedaling exercise. Heart Rate (HR) was monitored every 5 minutes during the exercise. After exercise, blood and urine were collected. Control experiment was done on another day by the same protocol at sea level. HR during exercise was about 120 beats/min at the simulated altitude, while the value at sea level was about 90 beats/min. A significant increase in blood cortisol and increasing tendencies in blood adrenocorticotropic hormone, aldosterone, etc. were observed after exercise at the simulated altitude, while blood atrial natriuretic peptide and urine volume did not show remarkable change. Because the subjects had experienced climbing above 6,000 m, it seemed that the endocrine responses of stress, sodium retention and antidiuresis were relatively mild. Urine and endocrine responses after exercise at 6,000 m became highly variant among the subjects. Endocrine responses of stress, sodium retention and antidiuresis after exercise at 6,000 m would be suggested to correlate with vulnerability to acute motion sickness during actual mountaineering. Author (NASDA)

N94-28497# Tsukuba Univ., Ibaraki (Japan). Lab. of Exercise Physiology.

EFFECTS OF TRAINING AT SIMULATED ALTITUDE OF 6,000 m ON ENDOCRINE RESPONSES AT REST AND DURING EXERCISE AT THE SAME ALTITUDE [6,000 M SOTO KOSHO JUNNO TORENINGU NO TOKOSHO NI OKERU ANSEI OYOBI UNDOJI NAIBUNPITSU OTO NI OYOBOSU EIKYO]

Koh Mizuno, Isao Suganuma, Yasuhito Kumazaki, and Katsumi Asano *In* Japan Society of Aerospace and Environmental Medicine, Japanese Journal of Aerospace and Environmental Medicine, Vol. 30, No. 3 1 Sep. 1993 p 117-125 In JAPANESE See also A94-12179 (For primary document see N94-28495 08-52)

Avail: CASI HC A02/MF A01

A study was conducted to elucidate the effect of intermittent hypobaric training on response of endocrine at rest and during exercise under hypobaric hypoxia at a simulated altitude of 6,000 m. Two male subjects; elite climber aged 35 years who had arrived over 7,000 m altitude (Testee 1), and beginner climber aged 27 years who had climbed only in comparatively low altitude mountains (Testee 2), trained in the hypobaric simulator for 8 times during 3.5 months. Simulated altitude, temperature, and relative humidity in the simulator were 6,000 m (354 Torr), 20 C, and 60 percent respectively. Training intensity was 30 minutes pedaling exercise under normoxia. At the first, fifth, and last training session, blood samples were taken before and after exercise at the 6,000 m simulated altitude. Heart Rate (HR) during exercise was monitored at all training sessions. Testee 2 showed remarkable increase of blood Adrenocorticotropic Hormone (ACTH), Antidiuresis Hormone (ADH), aldosterone, and Plasma Resin Activity (PRA) after exercise at the first training session, which tended to decrease as training progressed. Testee 1 showed almost no change of these hormones after exercise during all training sessions. Testee 2 showed about 20 to 30 beats/min decrease of HR during exercise with training progress. It might be concluded that intermittent hypobaric training cause the attenuation of stress and antidiuretic responses during exercise under hypobaric hypoxia for beginner climber and that elite climber should acquire attenuated responses of those hormones as a result of experience of severe hypoxia during actual mountaineering. Author (NASDA)

N94-28498# Kawasaki Heavy Industries Ltd., Tokyo (Japan).

SOME ISSUES ON JAPAN'S SPACE FOOD DEVELOPMENT AND RELATING PRELIMINARY EXPERIMENTAL STUDY [WAGAKUNI NO UCHUSHOKU KAIHATSU NI OKERU KADAI TO KISOTEKI JIKKEN]

c54

Shuji Kanda, Shizuko Yamaguchi, Chiharu Sekiguchi, Sei Yumikura, Makoto Doi, Masao Ito, Akira Miyamoto, and Kazuyoshi Yajima *In* Japan Society of Aerospace and Environmental Medicine, Japanese Journal of Aerospace and Environmental Medicine, Vol. 30, No. 3 1 Sep. 1993 p 127-133 In JAPANESE See also A94-12180 (For primary document see N94-28495 08-52)

Avail: CASI HC A02/MF A01

Space food is an important subject of the manned space technology and some kinds of space food have been developed in USA and Russia. Although they meet the basic requirements, such as nutrition and preservation, some problems still remain from the viewpoint of crew comfort like hedonic acceptability. In this report, some investigations are made on the necessity of Japan's space food concerning physiological and psychological issues. These investigations are based on the hypothesis that the food having good acceptability on the ground (1 G) might have also good acceptability under the microgravity condition of space. As the first step to verify the hypothesis, a taste sensitivity test was carried out under the bed rest condition of HDT (Head Down Tilt), as a simulated microgravity condition. From the test results, no significant change of taste sensitivity is found between upright and HDT conditions. Therefore, the aforementioned hypothesis is supported on the universality of the food acceptance of humans under 1 G gravity and microgravity conditions. Author (NASDA)

N94-28756# Naval Aerospace Medical Research Lab., Pensacola, FL.

NAVAL AVIATION VISION STANDARDS RESEARCH AT THE NAVAL AEROSPACE MEDICAL RESEARCH LABORATORY: THE LONG VIEW Special Report

Leonard A. Temme Apr. 1993 20 p

(AD-A275885; NAMRL-SR-93-2) Avail: CASI HC A03/MF A01

The Naval Aerospace Medical Research Laboratory (NAMRL) has been pursuing a research program to develop easily administered tests of vision skills that are valid, practical tools for the selection of personnel likely to be successful in the naval aviation arena. From 1980 to 1985, NAMRL maintained a data collection effort measuring the vision of U.S. Navy fighter pilots assigned to the air-to-air combat training range (NAS Oceana, VA). Both operational performance and vision test data were collected from the pilots. This report presents (1) the underlying theoretical orientation that guided that research effort, (2) a summary of the research results to date, and (3) the ideas guiding the design of the research strategy projected for the future. For convenience, abstracts of the principle publications describing this work are assembled in the appendix. DTIC

N94-28757# Army Aeromedical Research Lab., Fort Rucker, AL.

AVIATION EPIDEMIOLOGY DATA REGISTER: AGE DISTRIBUTION OF U.S. ARMY AVIATORS STRATIFIED BY GENDER AND COMPONENT OF SERVICE Final Report

Kevin T. Mason and S. G. Shannon Jan. 1994 26 p

(DA Proj. 3M1-62787-A-879)

(AD-A275901; USAARL-94-4) Avail: CASI HC A03/MF A01

The U.S. Army Aviation Epidemiology Data Register (AEDR) contains information on the history and physical parameters of Army aircrew members. As a reference for AEDR users and customers, the age distribution of Army aviators was extracted. The data were tabulated by age, gender, and component of service for calendar years 1986 through 1992. AEDR researchers can use the tables to calculate annual incidence rates, annual period prevalence rates, and other rates based on aviator-years of occupational exposure stratified by age, gender, and/or component. Aeromedical resource, policy and standards managers can use the tables for planning and funding aviator health care programs. DTIC

N94-28797# Navy Personnel Research and Development Center, San Diego, CA.

MARKOV CHAINS FOR RANDOM URINALYSIS 3: DAILY MODEL AND DRUG KINETICS Final Report, Oct. 1992 - Sep. 1993

Theodore J. Thompson and James P. Boyle Jan. 1994 20 p

(AD-A275540; NPRDC-TN-94-12) Avail: CASI HC A03/MF A01

This is the third in a series of reports on the use of Markov chains for the analysis of random urinalysis programs. A Markov model for random drug urinalysis testing that allows for daily variations in testing probabilities was developed. The formulation allows for any fixed length cycle (e.g., week, month). Drug kinetics and drug user gaming are incorporated into the Markov model via conditional probabilities. The Markov chain provides estimates of the distribution of time to detection and mean time to detection. The analyses have shown that time to detection varies dramatically with varying (observed) daily testing rates. Unequal daily testing rates provide opportunities for gaming drug users to extend the mean time to detection. Gaming is not possible with equal probabilities of testing across days. DTIC

N94-28810# Air Force Inst. of Tech., Wright-Patterson AFB, OH.

DIGITAL TRACKING AND CONTROL OF RETINAL IMAGES M.S. Thesis

Steven F. Barrett 1993 17 p

(AD-A275469; AFIT/CI/CIA-93-28D) Avail: CASI HC A03/MF A01

Laser induced retinal lesions are used to treat a variety of eye diseases such as diabetic retinopathy and retinal tears or breaks. Both the location and size of the retinal lesions are critical for effective treatment and minimal complications. Currently, once an irradiation is begun, no attempt is made to alter the laser beam location on the retina. However, adjustments are desirable to correct for patient eye movements. Lesions form in much less than one second and typical treatment for a disease such as diabetic retinopathy requires as many as 2000 lesions per eye. This type of tedious task is ideally suited for computer implementation. A system has been developed to track a specific lesion coordinate on the retinal surface and provide corrective signals to maintain laser position on the coordinate. Six distinct retinal landmarks are tracked on a high contrast retinal image using two-dimensional blood vessel templates. Use of therapeutic lesions as tracking algorithm landmarks is also investigated. An x and y laser correction signal is derived from the landmark tracking information and provided to a pair of galvanometer steered mirrors to maintain the laser on a prescribed location. Once the laser position has been corrected, a function checks the terminal laser position for minor corrections. A development speed tracking algorithm has been implemented and tested using both vessel and lesion templates. Closed loop feedback control of laser position is demonstrated with calibrated retinal velocities and in vivo testing of the development system. Trade-off analysis of parameters affecting tracking system performance is used to specify requirements and implementation details for a real time system. DTIC

N94-28850# Japan Society of Aerospace and Environmental Medicine, Tokyo.

JAPANESE JOURNAL OF AEROSPACE AND ENVIRONMENTAL MEDICINE, VOLUME 30, NO. 1 [UCHU KOKU KANKYO IGAKU DAI 30 KAN DAI 1 GO]

Makoto Masuda, ed., Masamitsu Oshima, ed., Kanichi Takagi, ed., Sakae Yokobori, ed., Mitsuo Sasaki, ed., Ichiro Asukata, ed., Sachio Ikawa, ed., Yukiko Kakimoto, ed., Hiroshi Kansaku, ed., and Tadaaki Mano, ed. et al 1 Mar. 1993 58 p In ENGLISH and JAPANESE

(ISSN 0387-0723)

(JTN-94-80598) Avail: CASI HC A04/MF A01

The following topics were discussed: humans, mice, gravitational effects, acceleration tolerance, microgravity, artificial gravity, physiological effects, arteries, spine, blood, oxygen saturation, ova, fertilization, embryos, early development, growth, food, meal ingestion, vasomotor response, nervous system, oculomotor nerves, head-up tilt, cardiovascular system, blood flow, blood vessel, motion sickness, space motion sickness, space adaptation syndrome, space perception, vertigo, dizziness, aircraft pilots, astronauts, flight, nystagmus, ADH (Antidiuretic Hormone), and electronystagmography. For individual titles, see N94-28851 through N94-28858.

N94-28851# Kanagawa Prefectual Coll. (Japan). Dept. of Oral and Maxillofacial Radiology.

IMAGE TECHNOLOGY AND INFORMATION ANALYSIS OF BONE CHANGE WITH GRAVITATIONAL EXPOSURE

Kosuke Nishimura *In* Japan Society of Aerospace and Environmental Medicine, Japanese Journal of Aerospace and Environmental Medicine, Volume 30, No. 1 1 Mar. 1993 p 1-10 See also A93-49177 (For primary document see N94-28850 08-52)

Avail: CASI HC A02/MF A01

The influences of gravitational changes (microgravity approximately equals 0 G, control: 1 G, hypergravity: 2 G) on the bone were analyzed from the point of view of imaging technology using a microfocus tube and a highly sensitive x-ray image sensor with the photostimulable phosphor. Gravitational changes markedly affected the spongy bone of the posterior vertebral joint, with bone resorption occurring at approximately equals 0 G and enhancement of bone formation at 2 G. Such changes were larger in the posterior vertebral joints that bear more weight. In the seventh posterior vertebral joint, which showed the largest bone changes, the photostimulated luminescence level increased by about 19 percent and decreased by about 4 percent at approximately equals 0 G and 2 G, respectively, compared with 1 G. These bone changes resemble those occurring during the aging process of mandibular bone trabeculae on earth. Author (NASDA)

N94-28852# Nihon Univ., Tokyo (Japan). Dept. of Anesthesiology.

ARTERIAL OXYGEN SATURATION DURING +Gz ACCELERATION BY SHORT-RADIUS CENTRIFUGE [KOGATA ENSHINKI NI YORU JINKO JURYOKU FUKACHU NO DOMYAKUKETSU SANSO HOWADO NO HENKA]

Kenichi Iwasaki, Hajime Suzuki, Masao Ito, Takaichi Mano, Chikako Saeki, and Kazuyoshi Yajima *In* Japan Society of Aerospace and Environmental Medicine, Japanese Journal of Aerospace and Environmental Medicine, Volume 30, No. 1 1 Mar. 1993 p 11-17 In JAPANESE See also A93-49178 (For primary document see N94-28850 08-52)

Avail: CASI HC A02/MF A01

Artificial gravity has been proposed to prevent the problems of physiological deconditioning in space. When Ground-based studies to make an artificial gravity with short-radius centrifuge were intended, it has been reported that decreases of the arterial Oxygen Saturation (SaO2) caused by a ventilation/perfusion mismatch in human lung and a decrease in central blood volume were observed at +3 Gz or above it. However, the duration of centrifuge was only a few minutes. SaO2 was measured during 60 min +Gz acceleration by a pulse oximeter. Seven men were studied at 1.4 G, 1.7 G, and 2.0 G. Significant decreases of SaO2 occurred at 1.7 G from 10 min to 30 min and at 2.0 G from 10 min to 40 min. SaO2 were improved after 35 min (1.7 G) and 45 min (2.0 G). Increases in heart rate, blood pressure, and tidal volume improved the decreases of SaO2 during +Gz acceleration. Author (NASDA)

N94-28853# Nihon Univ., Tokyo (Japan). Dept. of Hygiene.

EFFECT OF CHRONIC CENTRIFUGATION ON IN VITRO FERTILIZATION AND EARLY DEVELOPMENT IN MICE OVA [MAUSU RANSHI NO JUSEI TO SHOKI HASSEI NI OYOBOSU JI FUKA NO EIKYO] **c51**

Masao Ito, Ruriko Maru, Takashi Maeda, Ester Sanada, Takaichi Mano, Shinichi Horigome, Kenichi Iwasaki, Yuichi Kameyama, Yoshiro Ishijima, and Kazuyoshi Yajima *In* Japan Society of Aerospace and Environmental Medicine, Japanese Journal of Aerospace and Environmental Medicine, Volume 30, No. 1 1 Mar. 1993 p 19-25 In JAPANESE See also A93-49179 (For primary document see N94-28850 08-52)

Avail: CASI HC A02/MF A01

The effect of chronic centrifugation on in vitro fertilization and early development in mice ova was investigated. The results of the study on the effect of acceleration on fertilization and early development is discussed. The fertilization rate was lower for the ova receiving 0.6 to 1.2 G and those receiving 1.8 G and over. The mechanism for the impairment of fertilization, was apparently different between two ranges. The unfertilized ova that had been subjected to 0.6 to 1.2 G of acceleration ceased to grow mostly at Metaphase 2 and sperms penetration were prevented. In the ova receiving 1.8 G and over, sperms had penetrated the ovular cytoplasm and the nucleus had reached the Anaphase or Telophase. Polyspermy and other abnormalities were frequent while normally fertilized ova were limited in number. It was noted that centrifugation at 2 G or less

had no effect on the in vitro growth of 2-cell ova into blastcysts. Cell number of embryos thus produced was significantly smaller compared to the control. In the 2-cell ova receiving 3.6 or 4.0 G, most of them do not grow into blastocysts and if they do, the cell number of these blastocysts is smaller than 60. This finding suggested a delay in embryo growth and a subsequent increase in embryo mortality. Author (NASDA)

N94-28854# Kanazawa Woman's Junior Coll. (Japan).
EFFECT OF FOOD INTAKE ON SKIN VASOMOTOR RESPONSES TO HEAD-UP TILT IN HUMANS
Atsuo Hirai, Yoshie Uketa, Minoru Tanabe, and Sotaro Sakurada *In* Japan Society of Aerospace and Environmental Medicine, Japanese Journal of Aerospace and Environmental Medicine, Volume 30, No. 1 1 Mar. 1993 p 27-29 See also A93-49180 (For primary document see N94-28850 08-52)
Avail: CASI HC A01/MF A01

Cardiovascular responses to a 10 min head-up tilt at 60 deg were investigated in seven subjects before and after meal ingestion. The tilt increased heart rate and body core temperature, and decreased blood pressure, mean skin temperature (calculated from forehead, trunk, forearm, finger, thigh, calf and foot temperatures), and finger blood flow regardless of feeding conditions. However, finger temperature at the end of the tilt was significantly higher after food ingestion than before, which was not the case in other sites of the skin. Furthermore, the amount of reduction in finger blood flow was significantly reduced by food ingestion. These results suggest that vasoconstrictor drive to skin vessels is suppressed by food ingestion only in the fingers. Author (NASDA)

N94-28855# Nagoya City Univ. (Japan). Dept. of Otorhinolaryngology.
BASIC UNDERSTANDING OF VERTIGO [MEMAI NO KISO]
Motoyuki Hashiba *In* Japan Society of Aerospace and Environmental Medicine, Japanese Journal of Aerospace and Environmental Medicine, Volume 30, No. 1 1 Mar. 1993 p 34-37 In JAPANESE Presented at the Symposium of the 38th Annual Meeting of Japan Society of Aerospace and Environmental Medicine, Tokyo, Japan, 3 Oct. 1992 (For primary document see N94-28850 08-52)
Avail: CASI HC A01/MF A01

Human kinesthesia is largely dependent on visual sense, vestibular sense, and somatic sense, and unbalance of these senses causes failure of integration, which may result in vertigo. Abnormal vertigo often occurs when the right and left vestibule senses different information. For example, when rotated, endolymphatic fluid in semicircular canals flows in the opposite direction in right and left, so that nerve activity is stimulated in one organ while suppressed in the other. For vertigo without rotation, a disorder must occur in one vestibular system to cause unbalanced nerve impulses. Physiological vertigo often occurs after rotation; that is, endolymphatic fluid flows by inertia after rotation, which keeps stimulating hairy cells, although visual and somatic nerves transmit contradictory information. In addition, the velocity storage mechanism in the semicircular canals may also prolong stimulation of hair cells. For other physiological vertigo, it was reported that caloric stimulation of the internal acoustic meatus causes vertigo. This phenomenon was explained by convection of endolymphatic fluid, however, in the experiment of caloric stimulation in outer space, vertigo occurred under weightless condition. Therefore, there may be mechanisms other than convection. In addition, it was known that vertigo was caused by visual stimulation alone. In studying vertigo, it is necessary to evaluate the subjective symptom by objective kinesthesia responses, however, such responses may be affected more or less by the central nervous system. Author (NASDA)

N94-28856# Japan Air Lines Co. Ltd., Tokyo. Dept. of Otorhinolaryngology.
DISTURBANCE OF EQUILIBRIUM ON JAL FLIGHT CREW [UNKO JOMUIN NI OKERU MEMAI]
Takakuni Kato *In* Japan Society of Aerospace and Environmental Medicine, Japanese Journal of Aerospace and Environmental Medicine, Volume 30, No. 1 1 Mar. 1993 p 38-40 In JAPANESE Presented at the Symposium of the 38th Annual Meeting of Japan Society of Aerospace and Environmental Medicine, Tokyo, Japan, 3 Oct. 1992 (For primary document see N94-28850 08-52)
Avail: CASI HC A01/MF A01

Flight crew are obliged to undergo flight physical examination periodically by the Ministry of Transport. This examination must follow the flight physical examination manual that regulates standards of diagnosis for each organ disease, including acoustic and equilibrium sense. This article discusses the cases with disturbance of equilibrium and nystagmus. The subjects were 47 Japan Airlines (JAL) flight crew who were found to have either statoacoustic disorder or anamnesis in the physical examination. As a result, 19 cases were asymptomatic, and, in the other 28 cases, symptoms were recognized regardless of flight in most cases, although it happened during and after flight in some cases. A total of 8 cases were asymptomatic nystagmus. According to the standard of flight physical examination, flight crew who are found to exhibit a statoacoustic disorder must be scrutinized by electronystagmography (ENG), and if nystagmus is identified, the license will be suspended. However, it is a big loss of man-power to suspend from flight these crew who have no subjective symptoms and able to spend normal life. Author (NASDA)

N94-28857# Jikei Univ., Tokyo (Japan). Dept. of Otorhinolaryngology.
SPACE AND VERTIGO: IN RELATION TO SPACE MOTION SICKNESS [UCHU TO MEMAI: UCHUYOI TONO KANREN NI TSUITE]
Masanori Ishii *In* Japan Society of Aerospace and Environmental Medicine, Japanese Journal of Aerospace and Environmental Medicine, Volume 30, No. 1 1 Mar. 1993 p 41-45 In JAPANESE Presented at the Symposium of the 38th Annual Meeting of Japan Society of Aerospace and Environmental Medicine, Tokyo, Japan, 3 Oct. 1992 (For primary document see N94-28850 08-52)
Avail: CASI HC A01/MF A01

When a man goes to outer space, he will be exposed to weightless condition, so that the sense of space must be modified to adapt himself the new situation. The space motion sickness is considered to be a process to adapt oneself to weightless condition. However, the disease causes not only nausea and vomiting, but also disorder of equilibrium sense and illusion, which may degenerate operation ability of payload specialists. In fact, several missions had to be changed due to space motion sickness. This disease occurs immediately after coming to weightless condition, peaks at one to two day, and then gradually disappears in many cases. The cause may be disintegration of senses because input to the labyrinthus system and semicircular canal could be changed under weightless condition. To examine this theory, Occular Counter Rolling (OCR) has been used as an objective index of labyrinthus function, and it was proposed that difference between right and left OCR may be associated with space motion sickness. On the other hand, although in the same weightless condition, the disease did not occur in about one third of crew, and the incidence was affected by frequency of flight or physical conditions. Therefore, space motion sickness may result from not only disintegration of senses, but also from other factors such as effects of Antidiuretic Hormone (ADH) and enkephalin, which are associated with long term memory and is necessary for adaptation to a new environment. Author (NASDA)

N94-28858# Tokyo Medical and Dental Univ. (Japan). Dept. of Otolaryngology.
EQUILIBRIUM DYSFUNCTION IN THE CLINICAL FIELD [RINSHO NI OKERU MEMAI]
Jin Okubo *In* Japan Society of Aerospace and Environmental Medicine, Japanese Journal of Aerospace and Environmental Medicine, Volume 30, No. 1 1 Mar. 1993 p 46-49 In JAPANESE Presented at the Symposium of the 38th Annual Meeting of Japan Society of Aerospace and Environmental Medicine, Tokyo, Japan, 3 Oct. 1992 (For primary document see N94-28850 08-52)
Avail: CASI HC A01/MF A01

This article presents symptoms and diagnosis of equilibrium dysfunction in the clinical field. In general, equilibrium dysfunction is a subjective symptom so that it is difficult to objectively diagnose. It is problematic to confirm diagnosis by only nystagmus test because not only vestibular disorders but also also visual and somatid disorders may cause equilibrium dysfunction. In fact, nystagmus is not always observed in equilibrium dysfunction patients. The equilibrium dysfunction can be classified into vertigo, dizziness and blackout, and this classification is important in diagnosis to identify the causal sites. For nystagmus tests, voluntary and involuntary occular movement is examined, however, there are a few outpatients who showed nystagnus in diagnosis. Induction and duration of nystagmus are also useful to identify the dysfunctional sites. In addition, accessory symptoms should be considered for diagnosis. It is interesting that the direction of nystagmus

is related to head position. Nystagmus by caloric stimulation changes in duration or development according to the head position. These phenomena suggest that gravity may intervene in the occurrence of nystagmus.
Author (NASDA)

N94-28892 Krug Life Sciences, Inc., San Antonio, TX.
RELAXED TOLERANCE FOLLOWING HSG, HIGH SUSTAINED +Gz Interim Report, Nov. 1992 - Nov. 1993
Robert M. Shaffstaff Nov. 1993 5 p Limited Reproducibility: More than 20% of this document may be affected by microfiche quality
(Contract F33615-92-C-0018)
(AD-A275204; AL/CF-PC-1993-0042) Avail: CASI HC A01

Changes in relaxed +G(sub z) tolerance impact the support required from G protective measures and may affect the capability of the aircrew to reengage following exposure to HSG. During and post-HSG, simultaneous physiological events which could increase or decrease G-tolerance are activated. This study exposed 6 male centrifuge subjects to a GOR(Gradual Onset Rate = 0.067 G/second) acceleration to their subjective G-tolerance limit. Following a rest period, the subjects were exposed to a 7+G(sub z) ROR (Rapid Onset Rate = 1.0 G/second) acceleration for 60 seconds. Immediately after the ROR the subjects were reexposed to the GOR and taken to their relaxed tolerance limit. RESULTS. The subjects relaxed tolerance on the first GOR (pre-HSG) was 5.4+G(sub z)+/-0.7 (X+/-SD) and their second GOR tolerance (post-HSG) was 4.5+/-0.6. Statistical significance via Student's T Test (2 tailed) was p=0.065, but 5 of 6 subjects had a reduction in post-HSi tolerance. Electrocardiogram and heart rate evaluations provided an indicator of the cardiovascular response. This study suggests that relaxed +G(sub z) tolerance is lowered following a high G exposure. Such a post-HSG reduction in relaxed tolerance would place a greater burden on the pilot's G protective systems thereby limiting one's ability to fully utilize the capability of the aircraft. DTIC

N94-28912# Naval Health Research Center, San Diego, CA.
PHYSIOLOGICAL RESPONSES DURING SHIPBOARD FIREFIGHTING Final Report
Brad L. Bennett, R. D. Hagan, G. Banta, and F. Williams Jul. 1993 24 p
(AD-A275104; NHRC-93-9) Avail: CASI HC A03/MF A01

The findings from previous studies of men wearing firefighting clothing suggest a high potential for individual heat strain associated with firefighting. However, no study has determined the level of heat strain during actual firefighting conditions. Thus, the objective of this study was to determine the level of heat strain experienced by U.S. Navy personnel while combating fires aboard a fire research ship. Subject volunteers (n=9) were recorded for rectal and mean skin temperatures and heart rate during three fire test days. Air temperatures in the compartment containing the fire to be extinguished averaged 470 + or - 170 c, while air temperatures in the compartment from which the fire was fought ranged from 40 to 125 C. Peak values for rectal temperature averaged 39.2 + or - 1.0 C, while peak mean skin temperature averaged 39.5 + or + 0.9 C. Peak body heat storage averaged 2.02 + or - 0.77 kcal.kg-1 and peak heart rate averaged 186 + or - 13 bpm. Our findings indicate that shipboard firefighting is associated with a remarkable level of individual heat strain. These findings have applications to operational training programs, generation of exposure guidelines, and development of heat strain countermeasures. DTIC

N94-29049# Defence and Civil Inst. of Environmental Medicine, Downsview (Ontario).
EFFECTS OF ENDURANCE TRAINING ON HEAT-EXERCISE TOLERANCE IN MEN WEARING NBC PROTECTIVE CLOTHING Research Report
Yukitoshi Aoyagi, Tom M. McLellan, and Roy J. Shephard Aug. 1993 37 p
(AD-A275176; DCIEM-93-46) Avail: CASI HC A03/MF A01

Protective clothing imposes significant physiological and psychological stresses on the human body and may limit work tolerance, especially in hot environments. The additional strains imposed by protective clothing arise mainly because it is difficult for sweat to evaporate through relatively impermeable fabrics. Endurance training is a commonly adopted tactic to improve tolerance times when individuals must work in the heat. Potential benefits include improved physical fitness, increased sweating, and expanded plasma volume. However, it is unclear whether such responses develop and/or are helpful when wearing protective garments with limited vapor permeability. The purpose of this study was therefore to examine the influence of endurance training on exercise tolerance in a hot environment when subjects were wearing either normal light combat clothing or clothing offering protection against nuclear, biological, and/or chemical (NBC) agents. DTIC

N94-29071 Krug Life Sciences, Inc., San Antonio, TX.
DECOMPRESSION SICKNESS RISK VERSUS TIME AND ALTITUDE Interim Report, Nov. 1992 - 1993
James T. Webb and Andrew A. Pilmanis Nov. 1993 6 p Limited Reproducibility: More than 20% of this document may be affected by microfiche quality
(Contract F33615-92-C-0018)
(AD-A275261; AL/CF-PC-1993-0039) Avail: Issuing Activity (Defense Technical Information Center (DTIC))

To predict altitude decompression sickness (DCS) risk with any degree of accuracy, one must weigh variables such as prebreathe time, rate of ascent/descent, time at altitude, altitude, mixed breathing gas (dependent upon altitude), and profiles with multiple ascents and descents. The length of research chamber exposures is fixed. Therefore, risk assessment is based on DCS incidence after this fixed period at simulated altitude. From an operational standpoint, variable time at altitude complicates any predictive capability, although a computer model to handle all of these variables is in development. In the interim, a retrospective study from the Armstrong Laboratory Decompression Sickness Research Database has produced risk curves which can be used to predict DCS or venous gas emboli (VGE) incidence as a function of time at various altitudes. We limited the data to: (1) zero-prebreathe exposures to less than 20,000 ft breathing 50% O2, 50% N2; (2) zero-prebreathe exposures to less than 20,000 ft breathing 100% O2; and (3) 1-h prebreathe exposures to greater than 20,000 ft breathing 100% O2. Using the curves, one can select a time/altitude of exposure and estimate the DCS and VGE percentage. DTIC

N94-29116# Army Medical Center, Aurora, CO. Dept. of Clinical Investigation.
CLINICAL INVESTIGATION PROGRAM Annual Progress Report No. 29, FY 1993
Kenneth E. Sherman 30 Sep. 1993 524 p
(AD-A275025) Avail: CASI HC A22/MF A04

This report identifies those individuals who are conducting investigative protocols at Fitzsimons Army Medical. An abstract of each protocol--which gives abbreviated technical approach, objectives, and progress--is presented. DTIC

N94-29150# Edgerton, Germeshausen and Grier, Inc., Albuquerque, NM.
BLAST OVERPRESSURE STUDIES WITH ANIMALS AND MAN
Daniel L. Johnson, John T. Yelverton, William Hicks, and Roy Doyal 31 Oct. 1993 245 p
(Contract DAMD17-88-C-8141)
(AD-A275038) Avail: CASI HC A11/MF A03

Anesthetized sheep were exposed to explosions generated by the detonation of various weights of C-4 ranging in size from 57 to 1361 g in three different enclosures. The dimensions of the enclosures were 3.05 x 1.52 x 2.44 m, 3.05 x 2.44 x 2.44 m, and 4.88 x 3.05 x 2.44 m or 11.3, 18.2, and 36.3 cu m, respectively. The results from these experiments were used to establish an injury prediction curve using severity of injury indices and smoothed peak pressure. It appears to be an adequate model for the data collected and correlates well with previously reported injury prediction curves. It was determined that quasi-static pressure per se doesn't influence non-auditory injury to any appreciable degree. However, changes in the quasi-static pressure can affect the reverberant nature of the complex wave which seems to have a role in solid intra-abdominal response. There was also a simple relationship between lung injury and loading density demonstrated. As loading density increases, lung injury increases. DTIC

N94-29211 Air Force Inst. of Tech., Wright-Patterson AFB, OH.
EVALUATION OF MONITORING AUDIOMETRY IN THE UNITED STATES AIR FORCE HEARING CONSERVATION PROGRAM Ph.D. Thesis
Theresa Y. Schulz 1993 27 p Limited Reproducibility: More than

20% of this document may be affected by microfiche quality
(AD-A275309; AFIT/CI/CIA-93-24D) Avail: CASI HC A03

The purpose of this study is to evaluate the effectiveness and efficiency of the methods and procedures of audiometric monitoring as used in the United States Air Force (USAF) Hearing Conservation Program (HCP). These program elements are common to HCP's both in the other military services (U.S. Army and Navy) and in civilian industry. However, there are a multitude of variations in implementing these common elements of a HCP. DTIC

N94-29431# Army Armament Research, Development and Engineering Center, Watervliet, NY. Benet Lab.

SYNAPTOGENESIS, SELECTIVE STABILIZATION, AND FREE ASSOCIATION Final Report

Mark A. Johnson and Raymond D. Scanlon Nov. 1993 20 p
(AD-A275250; ARCCB-TR-93039) Avail: CASI HC A03/MF A01

This report describes the material aspects of learning through the processes of synaptogenesis, transient redundancy, and selective stabilization. Synapses are potentiated during these processes and provide channels for incoming signal energy en route to nominate motor responses. They form codons that represent the activity of a large assemblage of neurons in various cortical regions. Codons are active during a state of dynamic instability in the neocortex when the thalamus blocks sensory input. They may also alter the gating cycle of the thalamus through interaction with the thalamic reticular nucleus. A computer simulation of these processes illustrates these concepts. DTIC

N94-29709# Society of Medical Reseacrh for Space Station, Nagoya (Japan).

THE MERSS 5TH SYMPOSIUM ON SPACE MEDICINE: MEDICAL AND PHYSIOLOGICAL EXPERIMENT UTILIZING PARABOLIC FLIGHT Report No. 8 [DAI 5 KAI UCHU IGAKU SHINPOJIUMU: PARABORIKKU FURAITO NI OKERU IGAKU SEIRIGAKU JIKKEN]

Mar. 1993 71 p In JAPANESE Symposium held in Aichi, Japan, 28 Nov. 1992
(JTN-94-80588) Avail: CASI HC A04/MF A01

The following topics were discussed: parabolic flight, flight control, aircraft control, aircraft performance, aircraft equipment, fuel system, hydraulic system, engine oil system, safety management, Paramecium, microgravity, gravitational effects, gold fish, attitude control, sailing, vestibules, Cyprinodontidae, visual perception, behavior, cardiovascular system, eye movement, head movement, sensory match, information processing, autonomic nervous system, pupillary reflex, heart rate, blood pressure, blood volume, respiration rate, stomach, emesis, electrogastrogram, motion sickness, physiological effects, physiological factors, space adaptation syndrome, space commercialization, space tour, manned space flight, safety management, and economic factor. For individual titles, see N94-29710 through N94-29718.

N94-29710# Diamond Air Service, Inc. (Japan).

MICROGRAVITY BY PARABOLIC FLIGHT WITH MU-300 AIRCRAFT [MU-300 BIJINESU JETTOKI NI YORU MAIKURO G FURAITO] **c54**

Mitsuo Sato *In* Society of Medical Research for Space Station, The MERSS 5th Symposium on Space Medicine: Medical and Physiological Experiment Utilizing Parabolic Flight Mar. 1993 p 1-8 In JAPANESE (For primary document see N94-29709 08-52)
Avail: CASI HC A02/MF A01

Parabolic flight has an advantage to achieve microgravity with ease and at a low-cost, as well as to enable the performance of science experiments by payload specialists themselves. This report summarizes results of a simulation study and actual flight for microgravity. Model flight pattern was determined on the basis of the most appropriate values for recovery gravity, maximum rising degree, maximum descending degree and pull-up gravity which were obtained by results of simulating calculation and test flights measuring gravity every 5 deg during chandelling and nose driving. In the test flights, the plane was controlled by manual steering, assuming that the stabilater trim was out of order. As a result, 1/100 to 5/100 G was achieved for an average of 20 seconds, maximum 24 seconds. The safety was confirmed in simulation calculation, determination of flight pattern, and structure and checking of the airframe. The microgravity experiments have been utilized for various fields, such as life science, material engineering, and physics. Author (NASDA)

N94-29711# Hamamatsu Univ., Shizuoka (Japan).

SPACE MOVEMENT OF TRICHINELLA SPIRALIS UNDER MICROGRAVITY [SENMOCHU NO BISHO JURYOKU NI TAISURU YUEI HANNO] **c51**

Akira Murakami, Kenjiro Yoshimura, and Keiichi Takahashi *In* Society of Medical Research for Space Station, The MERSS 5th Symposium on Space Medicine: Medical and Physiological Experiment Utilizing Parabolic Flight Mar. 1993 p 9-13 In JAPANESE (For primary document see N94-29709 08-52)
Avail: CASI HC A01/MF A01

Under microgravity, Trichinell speralis, including a Paramecium, increases pace of cytokinesis, probably because disappearance of space movement reaction against gravity decreases energy consumption. If this hypothesis is true, gravity may affect various phases of fundamental activity of this microorganism. On the other hand, it is known that a Paramecium moves in the opposite direction of gravity under 1 G. This negative gravitaxis may be associated with not only a physical mechanism based on gravity, but also some physiological mechanisms. The purpose of this study is to clarify the effect of gravity on Parameciums by analyzing space movement under microgravity. In previous studies, the microgravity effect on movement of Paramecium was examined during free falling. Despite short period, the findings revealed that not only gravity but also some other effects may participate in the special movement under microgravity. This study examined the movement for longer period of microgravity using parabolic flight, in which microgravity could be achieved after hypergravity conditions. As a result, the Parameciums showed diphasic movement pace which increased under hypergravity, then decreased during change of gravity, and increased again under microgravity. This phenomenon cannot be explained by only a physical mechanism, therefore some physiological mechanisms, such as Ca ion or K ion participation, may affect the movement under microgravity. Author (NASDA)

N94-29712# Fujita Health Univ., Toyohashi (Japan). School of Hygiene.

POSTURE CONTROL OF GOLDFISHES UNDER MICROGRAVITY [BISHO JURYOKUKA NI OKERU KINGYO NO SHISEI SEIGYO] **c51**

Akira Takabayashi *In* Society of Medical Research for Space Station, The MERSS 5th Symposium on Space Medicine: Medical and Physiological Experiment Utilizing Parabolic Flight Mar. 1993 p 14-18 In JAPANESE (For primary document see N94-29709 08-52)
Avail: CASI HC A01/MF A01

Microgravity may cause several functional disorders mainly due to a lack of stimulation of labyrinthus. This may result in Space Adaptation Syndrome (SAS) observed during exposure to a weightless condition. The purpose of this study was to examine the effect of microgravity on statokinetic system using goldfish with or without labyrinthectomy or excision of eye balls. It is known that fish control their posture by stimulation of light and gravity; i.e. they keep the back to the direction of light and the ventral side to the direction of gravity. As a result, labyrinthectomized goldfish could adapt themselves under 1 G condition, although it took several months. Under microgravity, normal goldfish controlled their posture by light direction. While hemilateral labyrinthectomized ones showed a tendency to incline to the labyrinthectomized side, those with hemilateral and bilateral labyrinthectomy controlled their posture by the direction of light. Goldfish with excision of eye balls could keep normal posture under 1 G, however, when labyrinthectomized goldfish were exposed to microgravity in the dark, looping behavior was observed. These results suggest that in labyrinthectomized fish's gravireceptors other than labyrinthus may function under 1 G, however, they cannot work under microgravity, which may cause unstable posture under microgravity. Author (NASDA)

N94-29713# Tokyo Univ. (Japan).

BEHAVIOR AND VISUAL CONTROL OF CYPRINODONTS UNDER MICROGRAVITY [BISHO JURYOKUKA NI OKERU MEDAKA NO KYODO TO SHIKAKU NI YORU SEIGYO] **c51**

Kenichi Ijiri, Hoshio Eguchi, Yasuko Taguchi, Shunji Nagaoka, Masamichi Yamashita, and Akemi Kurotani *In* Society of Medical Research for Space Station, The MERSS 5th Symposium on Space Medicine: Medical and Physiological Experiment Utilizing Parabolic Flight Mar. 1993 p 19-25 In JAPANESE (For primary document see N94-29709 08-52)
Avail: CASI HC A02/MF A01

In order to collect fundamental data for the experiments under microgravity in IML-2 (International Microgravity Laboratory-2), behavior of

cyprinodonts was observed under microgravity, as well as with visual stimulation. Microgravity condition was achieved by parabolic flight, and cyprinodonts showed looping behavior with some twist as turning the ventral side to inside. There was a difference in looping pattern by strains of cyprinodonts in the light, while every strain of cyptinodonts showed looping behavior in the dark. This suggests that visual stimulation may be related with posture control under microgravity. For this reason, visual stimulation was given by rotating a cylinder with black and white stripes around a tank of cyprinodonts under 1 G. As a result, all strains of cyprinodonts followed the stripes, and among them, the strain with less looping behavior under microgravity showed the most remarkable ability to follow them. This suggests that the strain tolerant of microgravity have high sensitivity to visual stimulation. Author (NASDA)

N94-29714# Ministry of Education, Science and Culture, Sagamihara (Japan).

START OF SPACE TOURISM [SUPESU TSURIZUMU KENKYU KOTOHAJIME] **c16**

Makoto Nagatomo *In* Society of Medical Research for Space Station, The MERSS 5th Symposium on Space Medicine: Medical and Physiological Experiment Utilizing Parabolic Flight Mar. 1993 p 26-33 In JAPANESE (For primary document see N94-29709 08-52)

Avail: CASI HC A02/MF A01

Space tourism means commercialization of manned space flight. From the early stage of space development, space commercialization is a profound theme in multidisciplinary fields, on the basis of a principle that the outcomes of advanced technique developed by tax should be returned to citizens. In these days, space satellite system in which users pay a fee for utilization has succeeded commercially in business such as communication network or broadcasting, and an attempt has been made to observe the earth from outer space to resolve global problems, such as environmental destruction. There is also an increasing interest in space tourism, however, many obstacles should be overcome for the realization, especially the medical problems such as effect of acceleration, cosmic ray, noise or weightless condition. In addition, the space flight business should be managed on the commercial base so that reasonable cost and large number of passengers are essential. It is necessary to design rockets suitable for tourism. For attractive design, the policy of space tourism should be clarified. Author (NASDA)

N94-29715# Nagoya Univ. (Japan). Space Medicine Research Center.

A DISCUSSION OF EYE-HEAD COORDINATIVE MOVEMENT UNDER MICROGRAVITY DURING PARABOLIC FLIGHT [PARABORIKKU FURAITO NI YORU TEI JURYOKU KANKYOKA DENO HITO NO TOBU/GANKYU KYOUOU UNDO NO KENTO] **c53**

Kazuo Koga *In* Society of Medical Research for Space Station, The MERSS 5th Symposium on Space Medicine: Medical and Physiological Experiment Utilizing Parabolic Flight Mar. 1993 p 34-41 In JAPANESE (For primary document see N94-29709 08-52)

Avail: CASI HC A02/MF A01

The labyrinthus can sense gravity as a mechanical stimulation of statoliths. In addition, some muscles which are always forced to be strained against gravity, baroreceptor and tactor on skin surface, and deep sensitivity of arthrosis can also sense gravity as a secondary information. There is a possibility that visual information may be indirectly related with sensing gravity. This multi-modal sensory is integrated in normal condition, however, the integration may be lost when environment is changed, such as in weightless condition. Therefore, it is meaningful to study man's adaptation to the microgravity by using visually up-down reversing mirror, and to study impression of a person he meets, with up-down position with or without the up-down reversing mirror. It can be predicted that the up-down reversing and front-back reversing have more eccentric cue other than visual sense so that the adaptation will be achieved more smoothly, than right-left reversing. For these reasons, eye-head coordination is going to be examined under microgravity achieved by parabolic flight. The measurement devices necessary for such experiment was discussed. This report explained the potential of parabolic flight, and measuring instrument of head movement, such as miniaturized three-axis acceleration sensor and optical position sensor. Author (NASDA)

N94-29716# Toyohashi Univ. of Technology, Aichi (Japan). Information and Computer Sciences.

ANALYSIS OF VARIOUS BIOLOGICAL ACTIVITY PARAMETERS DURING PARABOLIC FLIGHT [PARABORIKKU FURAITO NI OKERU KAKUSHU SEITAI SHINGO NO KAISEKI] **c53**

Shiro Usui and Yutaka Hirata *In* Society of Medical Research for Space Station, The MERSS 5th Symposium on Space Medicine: Medical and Physiological Experiment Utilizing Parabolic Flight Mar. 1993 p 42-47 In JAPANESE Prepared in cooperation with NASDA, Tokyo, Japan; the Research Inst. of Environmental Medicine, Nagoya Univ., Aichi, Japan; and Nihon Univ., Tokyo, Japan (For primary document see N94-29709 08-52)

Avail: CASI HC A02/MF A01

Whether a man can keep vital activity in weightless condition largely depends on homeostasis, and the homeostasis is controlled by autonomic nervous system. Because pupillary response is also related with autonomic nervous system, it has been used as an index of autonomic nervous activity. In this study, the pupillary response as well as other biological activity parameters were measured in order to examine whether the response is useful for monitoring autonomic nervous activity during microgravity achieved by parabolic flight. As a result, heart rate, blood pressure and spirogram changed according to the change of gravity, and psychogalvanic response showed mental tension during parabolic flight. For pupillary response, diameter of the pupil, degree of miosis, delay of response time, maximum miosis velocity and maximum mydriasis velocity were determined as parameters. All of these parameters were changed according to change of gravity, which implies that these parameters can indicate autonomic nervous activity under microgravity. Author (NASDA)

N94-29717# National Space Development Agency, Tokyo (Japan).

HEMODYNAMIC MEASUREMENT DURING PARABOLIC FLIGHT [PARABORIKKU FURAITO NI OKERU JUNKAN DOTAI NO KEISOKU]

Akira Miyamoto, Shunji Nagaoka, and Seizo Ishikura *In* Society of Medical Research for Space Station, The MERSS 5th Symposium on Space Medicine: Medical and Physiological Experiment Utilizing Parabolic Flight Mar. 1993 p 48-54 In JAPANESE (For primary document see N94-29709 08-52)

Avail: CASI HC A02/MF A01

Under microgravity such as in outer space, several changes may occur in the human body by movement of fluid. To examine the hemodynamic effect, microgravity condition was simulated by parabolic flight, and the change of hemodynamics was measured. During parabolic flight, the subject, a 28 year old healthy volunteer, experienced hypergravity of approximately 2.3 g prior to microgravity. The flight was performed from 9 to 11 times a day for six days. As a result, the measurements of blood pressure, heart rate, and stroke volume changed under microgravity. In addition, such changes were affected by time and sitting position; that is, when sitting up straight (90 deg), the change of gravity affected the heart rate and stroke volume more than when sitting in the halfway up (45 deg) position. Comparing heart rates between the first three days and later three days, the change decreased as time passed. These results suggest that hemodynamics may be affected by hypergravity and posture, as well as by experience, at least under microgravity by parabolic flight. Author (NASDA)

N94-29718# Nagoya Univ. (Japan). Dept. of Equilibrium Adaptation Research.

MOTION SICKNESS IN PARABOLIC FLIGHT: POSSIBILITY OF ELECTROGASTROGRAPHY AS AN OBJECTIVE INDEX [PARABORIKKU FURAITO NI OKERU MOSHON SHIKKUNESU: TAKAKUTEKI KYAKKANTEKI SHIHYO TO SHITENO IDENZU NO KANOSEI]

Hiroyuki Suzuki, Yoshiro Wada, and Satoru Watanabe *In* Society of Medical Research for Space Station, The MERSS 5th Symposium on Space Medicine: Medical and Physiological Experiment Utilizing Parabolic Flight Mar. 1993 p 55-63 In JAPANESE Sponsored by Science and Technology Agency, Tokyo, Japan (For primary document see N94-29709 08-52)

Avail: CASI HC A02/MF A01

Motion sickness is a disease that causes autonomic nervous symptoms such as vomiting or nausea by vestibular stimulation in weightless condition, linear acceleration, or by visual sense. Interest is focused on the disease from the point of space sickness. The purpose of this study was to discuss the effectiveness of electrogastrography as an objective index of

motion sickness under microgravity achieved by parabolic flight. The electrogastrogram obtained during parabolic flight was examined to determine if it is capable of being used as an objective index of motion sickness, whether it can predict vomiting, and whether it can reflect the change of gravity. As a result, there was a correlation between amplitude of electrogastrogram and motion sickness. In addition, electrogastrogram showed particular patterns before and during vomiting, although physiological events which are supposed to be reflected by this pattern are unknown yet. Electrogastrogram also showed changes of each pattern when gravity was changed. Author (NASDA)

N94-29863# Japan Society of Aerospace and Environmental Medicine, Tokyo.

JAPANESE JOURNAL OF AEROSPACE AND ENVIRONMENTAL MEDICINE, VOL. 30, NO. 2 [UCHU KOKU KANKYO IGAKU DAI 30 KAN DAI 2 GO]

Makoto Masuda, Masamitsu Oshima, Kanichi Takagi, Sakae Yokobori, Mitsuo Sasaki, Ichiro Asukata, Sachio Ikawa, Yukiko Kakimoto, Hiroshi Kansaku, and Tadaaki Mano et al 1 Jun. 1993 59 p In JAPANESE
(ISSN 0387-0723)
(JTN-94-80599) Avail: CASI HC A04/MF A01

The following topics were discussed: brain, thermoregulation, regulatory mechanisms, temperature control, blood flow, facial skin, make-up, heat transfer, body temperature, muscles, musculoskeletal system, muscle atrophy, sympathetic nerve response, gravitational effects, microgravity, physiological effects, physiological factors, psychological factors, water immersion, tail suspension, skinned fiber, shortening velocity, calcium sensitivity, aircraft pilots, pilot performance, visual perception, perceptual errors, visual discrimination, dot target, target detection, aircraft structures, response time, tachistoscopes, electroencephalography, rats, and human beings. For individual titles, see N94-29864 through N94-29867.

N94-29864# Kanazawa Woman's Junior Coll. (Japan).

EFFECTS OF MAKE-UP ON THE HEAT TRANSFER FROM THE HEAD IN HYPERTHERMIC CONDITIONS [MUFU KOON KANKYO DE TOBU NO NETSU IDO NI OYOBOSU KESHO NO EIKYO]

Atsuo Hirai, Kozo Hirata, Masami Hirashita, and Tetsuo Nagasaka *In* Japan Society of Aerospace and Environmental Medicine, Japanese Journal of Aerospace and Environmental Medicine, Vol. 30, No. 2 1 Jun. 1993 p 55-62 In JAPANESE Sponsored by the Ministry of Education, Science and Culture, Tokyo, Japan; the Decente and Ishimoto Memorial Foundation for the Promotion of Sports Science, Osaka, Japan; and Kao Co. Ltd., Tokyo, Japan (For primary document see N94-29863 08-52)
Avail: CASI HC A02/MF A01

This study was performed to verify whether the make-up disturbs selective brain cooling in hyperthermic conditions. Seven male volunteers were subjected to passive body warming in a climatic chamber (air temperature, 25 C; relative humidity, 40 percent). Body warming was made for about 40 min by placing the subjects in a box-shaped body warming unit, enclosing all but the subject's head. When Esophageal Temperature (T(sub es)) reached a level 0.5 C higher than the prewarming temperature, Hand-Grip exercise (HG) at 20 percent of maximal strength commenced and continued until exhaustion. In subjects with make-up (Hyperthermia Cosmetic (HC)), increases in forehead skin blood flow and temperature were significantly less than compared with the control group (Hyperthermia Non-Cosmetic (HNC)). However, local thermal sensation of the face was significantly higher in HC than in HNC. Tympanic Temperature (T(sub ty)) was always higher than T(sub es) before body warming, but the relationship reversed about 30 min after the start of body warming. Compared with that in HNC, the difference between T(sub es) and T(sub ty) 30 min after the start of body warming became less in HC (HC: 0.05 C versus HNC: 0.09 C). There was no significant difference in blood pressure, heart rate, T(sub es), and T(sub ty) between the two groups. Endurance time for HG was also not different between the two groups. From these results, it is concluded that the make-up can disturb selective brain cooling during body warming, although the extent is small. Author (NASDA)

N94-29865# Toyota Coll. of Technology (Japan). Lab. of Applied Physiology.

EFFECT OF WATER IMMERSION ON MUSCLE SYMPATHETIC NERVE RESPONSE DURING STATIC MUSCLE CONTRACTION [UNDOJI NO KIN KOKAN SHINKEI HANNO NI OYOBOSU SUISHIN NO KOKA]

Mitsuru Saito, Tadaaki Mano, Satoshi Iwase, Kazuo Koga, Chihiro Miwa, and Kinsaku Inamura *In* Japan Society of Aerospace and Environmental Medicine, Japanese Journal of Aerospace and Environmental Medicine, Vol. 30, No. 2 1 Jun. 1993 p 63-69 In JAPANESE See also A93-55328 (For primary document see N94-29863 08-52)
Avail: CASI HC A02/MF A01

To clarify the effects of microgravity on sympathetic nerve response to muscular exercise, Muscle Sympathetic nerve Activity (MSA) was recorded from the tibial or peroneal nerve microneurographically during Static Handgrip (SHG) exercise in a subject with a 20 degree head up tilt position under weightlessness simulated by water immersion (WET) and during dry condition (DRY). At the resting condition, MSA burst rate, which was .4 bursts/min in DRY, was strongly suppressed by 38 percent (3.6 bursts/min) of DRY under WET. This change was significant. Static handgrip increased MSA burst rate, 10.3 bursts/min in DRY and 10.7 bursts/min in WET at the second minute of SHG, while it showed insignificant change at the first minute period of SHG (-1.2 bursts/min in DRY and -1.7 in WET). The difference in delta in MSA burst rate during SHG between DRY and WET was insignificant. However, an absolute value of MSA burst rate during the second minute of SHG was higher in DRY (19.7 bursts/min) than that in WET (14.3 bursts/min). These results indicated that the MSA responsiveness to static muscle contraction was not altered under simulated weightlessness condition, but the level of MSA was significantly suppressed at resting condition and during muscular contraction. Thus the strong suppression of sympathetic outflow to the skeletal muscle under microgravity may be related, at least in part, to reduced adaptation of skeletal muscle function and the mechanism of muscular atrophy under microgravity.
Author (NASDA)

N94-29866# Saint Marianna Univ., Kawasaki (Japan). Dept. of Physiology.

SHORTENING VELOCITY AND CALCIUM SENSITIVITY OF SINGLE FIBERS FROM HINDLIMB SUSPENDED MUSCLE IN RATS [RATTO HAIYOSEI ISHUKU KINSENI NO TANSHUKU SOKUDO TO KARUSHIUMU KANJUSEI] **c51**

Katsumasa Yamashita and Toshitada Yoshioka *In* Japan Society of Aerospace and Environmental Medicine, Japanese Journal of Aerospace and Environmental Medicine, Vol. 30, No. 2 1 Jun. 1993 p 71-80 In JAPANESE See also A93-55329 (For primary document see N94-29863 08-52)
Avail: CASI HC A02/MF A01

The effect of suspension hypokinesia on the maximal shortening velocity (Vmax) and the calcium (Ca(2+)) sensitivity (pCa(sub 50)) of slow and fast skinned muscle fibers in rats after two-week-tail-suspension and recovery for two weeks (two-week-recovery) was examined. Maximal tension in the fiber dissected from Extensor Digitorum Longus (EDL) muscle was significantly lower (p is less than 0.01), but that in the fiber dissected from soleus muscle not different from the cage control. The Vmax in soleus and EDL and Ca(2+) sensitivity (pCa(sub 50)) in EDL increased following suspension. The maximal tension in EDL, Vmax and Ca(2+) sensitivity (pCa(sub 50)) in soleus and EDL were normalized after two weeks of recovery. The results demonstrate that the rate constant of cross-bridge cycle is altered during hypokinesia and the altered muscle function during hypokinesia recovered to the control level when the rats were released from suspension for the same period as tail suspension. Author (NASDA)

N94-29867# Kyorin Univ., Tokyo (Japan). Dept. of Physiology.

PSYCHOPHYSIOLOGICAL STUDY ON THE EFFECTS OF CO-EXISTENCE OF LINES FOR DETECTING DOT TARGET [TEN SHIHYO NO SHININSEI NI OYOBOSU KINBO SENBUN NO EIKYO NI KANSURU SHINRI SEIRIGAKUTEKI KENKYU] **c53**

Kiyoshi Mizumoto *In* Japan Society of Aerospace and Environmental Medicine, Japanese Journal of Aerospace and Environmental Medicine, Vol. 30, No. 2 1 Jun. 1993 p 81-91 In JAPANESE See also A93-55330 (For primary document see N94-29863 08-52)
Avail: CASI HC A03/MF A01

The following two experiments were carried out in normal subjects to verify the difficulty to detect the small target near the frame of windshield in the airplane: (1) using a tachistoscope, small black dot stimulus was exposed for 10, 30, 50, 70 and 0 msec at either side of and at either of 1.83, 2.24 and 2.65 degrees from the central fixation point with or without a pair of vertical lines. Nine subjects pushed a key to answer the side of

the dot exposed. The correct response rates increased while the reaction time decreased with the exposure time. Detectability of the dot stimulus near lines was poorer than that in the white background, especially for 0 msec stimulus exposure time; and (2) visual event-related potentials in response to the dot stimuli exposed for 0 msec were recorded from six scalp electrode sites in eight subjects. Two dots were exposed simultaneously at both sides of the fixation point with or without lines. The position of dots was 1.83 and 2.65 degrees and lines 1.32 and 3.15 degrees apart from the fixation point respectively. Dots were exposed 128 times (50 percent) randomly per each condition. Subjects were directed to count the number of the exposure with dots. The difference of the amplitude of P300 components between dot exposure and no-exposure was largest when the dots were exposed without lines. These results suggest the difficulty to detect targets near the frame of aircraft windshield.

Author (NASDA)

N94-29919# Federal Aviation Administration, Oklahoma City, OK. Civil Aeromedical Inst.

TOXICITY OF CARBON MONOXIDE-HYDROGEN CYANIDE GAS MIXTURES: EXPOSURE CONCENTRATION, TIME-TO-INCAPACITATION, CARBOXYHEMOGLOBIN, AND BLOOD CYANIDE PARAMETERS Final Report

Donald C. Sanders, Arvind K. Chaturvedi, Boyd R. Endecott, Roxane M. Ritter, and Ngocoanh Vu Apr. 1994 13 p

(DOT/FAA/AM-94/7) Avail: CASI HC A03/MF A01

During aircraft interior fires, carbon monoxide (CO) and hydrogen cyanide (HCN) are produced in sufficient amounts to cause incapacitation and death. Time-to-incapacitation (t(sub i)) is a practical parameter for estimating escape time in fire environments. Exposures to CO-HCN mixtures have demonstrated that these gases have additive effects (producing shorter times to incapacitation), but the resulting concentrations of carboxyhemoglobin (COHb) and blood cyanide (CN(sup -)) at incapacitation are not well defined. These undefined relationships between COHb and blood CN(sup -) levels and the onset of incapacitation make the interpretation of postmortem levels difficult for medical accident investigators. To explore these relationships, t(sub i) was determined in laboratory rats exposed to 2 CO-HCN mixtures consisting of CO and HCN concentrations that produce 5- and 35-min t(sub i) in individual gas exposures; COHb and blood CN(sup -) concentrations were determined at incapacitation. In the high concentration CO-HCN mixture, the resultant t(sub i) was shortened from 5 min to 2.6 min; COHb dropped from 81 percent to 55 percent and CN(sup -) from 2.3 mu g/mL to 1.1 mu g/mL. At the lower concentration CO-HCN mixture, where the resultant t(sub i) was reduced from 35 min to 11.1 min, COHb dropped from 71 percent to 61 percent and blood CN(sup -) decreased from 4.2 mu g/mL to 1.1 mu g/mL. Comparison of the COHb and blood CN(sup -) values with the values from our singie gas exposure studies indicated that any alteration of the uptake of either gas in blood by the presence of the other was minimal. These findings suggest that changes in COHb and blood CN(sup -) may not be directly correlated with the onset of incapacitation and that postmortem blood levels should be carefully evaluated, particularly when both gases are present in fire victims. Author

N94-30028# Grenoble-1 Univ. (France). Techniques de l'Imagerie, de la Modelisation et de la Cognition.

COMPUTER ASSISTED MEDICAL INTERVENTIONS: APPLICATION TO CONFORMAL RADIOTHERAPY

L. Brunie, P. Cinquin, L. Desbat, N. Laieb, Y. Menguy, S. Lavallee, J. Troccaz, P. Vassal, M. Bolla, and A. Dusserre et al Jun. 1993 30 p

(RR-912-I; ETN-94-95000) Avail: CASI HC A03/MF A01

Requirements and results of conformal external radiotherapy of prostatic carcinoma are presented. A system which achieves a high overall accuracy in the delivery of the prostatic boost is described. This system is based on the use of '2.5D' ultrasonic images for measuring the actual position of the prostate just before irradiation. Since these images are registrated with preoperative (computer tomography (CT) or magnetic resonance imaging) images, the position and orientation of the planning target volume is computed with respect to the irradiation system, and can be corrected accordingly. A second paper refers to the accurate repositioning of a patient with respect to CT images, which is essential for high precision radiotherapy. It is shown the intraradiotherapy portable imaging devices images may be automatically registered with three dimensional presession examinations, thus enabling an automatic adjustment of positioning. For individual titles, see N94-30029 through N94-30030.

N94-30029# Grenoble-1 Univ. (France). Techniques de l'Imagerie, de la Modelisation et de la Cognition.

CONFORMAL EXTERNAL RADIOTHERAPY OF PROSTATIC CARCINOMA: REQUIREMENTS AND PRELIMINARY RESULTS

J. Troccaz, Y. Menguy, M. Bolla, P. Cinquin, P. Vassal, N. Laieb, L. Desbat, A. Dusserre, and S. DalSoglio *In its* Computer Assisted Medical Interventions: Application to Conformal Radiotherapy Jun. 1993 13 p Sponsored by Digital Equipment Corp., and Siemens (For primary document see N94-30028 08-52)

Avail: CASI HC A03/MF A01

The aim of conformal radiotherapy is to deliver with a high precision a specific dose (which may be a high dose) to a planning target volume, while concurrently irradiating as little as possible healthy tissue and organs at risks. Radiation therapy may suffer from a number of problems that result in both over or undersizing the irradiation fields, simplifying the irradiation ballistics, and delivering an insufficient tumoral dose (to spare critical organs and reduce toxicity). One of these problems lies in the accurate positioning of the planning target volume with respect to the irradiation system, thence in the correct execution of the ballistics. A system aiming at achieving a higher overall accuracy in the delivery of prostatic boost for carcinoma of the prostate is described. The system is based on the use of '2.5D' ultrasonic images for measuring the actual position of the prostate just before the irradiation. Since these images are registrated with preoperative (computed tomography or magnetic resonance imaging) images, the position and orientation of the planning target volume is computed with respect to the irradiation system, and can be corrected accordingly. ESA

N94-30030# Grenoble-1 Univ. (France). Techniques de l'Imagerie, de la Modelisation et de la Cognition.

PRE- AND INTRA-RADIOTHERAPY MULTIMODAL IMAGE REGISTRATION: PRINCIPLES AND FIRST EXPERIMENTS

Lionel Brunie, Stephane Lavallee, Jocelyne Troccaz, Philippe Cinquin, and Michel Bolla *In its* Computer Assisted Medical Interventions: Application to Conformal Radiotherapy Jun. 1993 16 p Sponsored by Digital Equipment Corp., and Safir-Groupe SEM (For primary document see N94-30028 08-52)

Avail: CASI HC A03/MF A01

Accurate repositioning of the patient with respect to computer tomography (CT) images is essential for high precision radiotherapy. It is shown that intraradiotherapy portable imaging device images may be automatically registered with three dimensional presession examinations (typically morphological images like CT or magnetic resonance images), thus enabling an automatic adjustment of the planned strategy to the actual positioning of the patient. Based on computer vision techniques, the principles of this new method of multimodal image registration is presented, and the first experiments with a model are analyzed. ESA

N94-30185# Weizmann Inst. of Science, Rehovoth (Israel). Dept. of Physics.

CHARACTERISTICS OF SECONDARY ELECTRON EMISSION FROM CsI INDUCED BY X RAYS WITH ENERGIES UP TO 100 keV

A. Gibrekhterman, A. Akkerman, A. Breskin, and R. Chechik Jul. 1993 16 p

(DE94-608422; WIS-PH-93-60) Avail: CASI HC A03/MF A01 (US Sales Only)

Our microscopic model for low energy electron interaction in alkali-halides was used to simulate secondary electron emission from CsI, induced by X-rays of energies up to 100 keV. The integral 'current' and 'pulse' yields were calculated as a function of the X-ray energy, CsI convertor thickness and angle of incidence. We observed a decrease in true low energy (less than 50 eV) secondary electron yields at increasing X-ray energies and discuss the effectiveness of CsI convertors coupled to gaseous electron multipliers developed for fast, high resolution X-ray imaging. DOE

N94-30970# Ecole Nationale Superieure des Telecommunications, Paris (France). Groupe Image.

USE OF SNAKES TO LINK EDGE POINTS TO CREATE LEFT VENTRICULAR BOUNDARIES IN ECHOCARDIOGRAPHIC IMAGES

Iain Hunter (Strathclyde Univ., Glasgow, Scotland.) and Henri Maitre 23 Sep. 1993 37 p
(Grant SERC-92314900) (ISSN 0751-1345)
(TELECOM-93-D-016; ETN-94-95976) Avail: CASI HC A03/MF A01

The use of snakes to link edge points in left ventricular echocardiographic images to create the epicardial and endocardial boundaries is described. The edge points are created by an artificial neural network based radial search algorithm. This acts as a preprocessing stage for the snake and greatly reduces the size and complexity of the snake's external energy map. The edge points are given in terms of their polar coordinates, and the snake is used to interpolate where no edge points are present and to select the correct edge points for that boundary. The minimization of the snake's energy function by both simulated annealing and dynamic programming is studied, with dynamic programming giving better performance both in terms of accuracy and speed. ESA

N94-30978 Ecole Nationale Superieure des Telecommunications, Paris (France). Dept. Images.
ELEMENTS FOR THE RECOGNITION OF THREE DIMENSIONAL DEFORMABLE SHAPES: APPLICATION TO BIOMEDICAL IMAGERY Ph.D. Thesis [ELEMENTS POUR LA RECONNAISSANCE DE FORMES TRIDIMENSIONNELLES DEFORMABLES: APPLICATION A L'IMAGERIE BIOMEDICALE]
Nicolas Rougon 1993 248 p In FRENCH Limited Reproducibility: More than 20% of this document may be affected by microfiche quality
(ISSN 0751-1353)
(TELECOM-93-E-006; ETN-94-95981) Avail: CASI HC A11

The kinematics of closed nonsingular deformable manifolds with a codimension of one when their local instantaneous evolution obeys a first order dynamics is presented. A mathematical characterization of the complex phenomena modifying differential and integral properties of nonsingular manifolds during an arbitrary deformation is given. In particular, reactive diffusive propagative processes controlling the evolution of curvature features along the manifold are identified. A multidimensional deformable model, called a membrane/thin plate stabilizer under pressure or g-snake, is developed. Dealing with 2D (two dimensional) sequences or 3D images consisting of parallel slices, a model of 2D coupled g-snakes which preserves the intrinsic geometry of data is developed. To extend the scope of g-snakes to highly noisy imaging, a cooperation between deformable manifolds and regional filtering processes is introduced; the concept of 'deformable marker' for segmentation, focused on the 'interaction' process between a deformable model and image data. Exploiting controlled morphological techniques developed in mathematical morphology, a specific interaction process based on numerical geodesic reconstruction and automated initialization procedures is proposed. To increase segmentation accuracy, the 2D g-snake model is further generalized resulting in a fully adaptive deformable model which is invariant with respect to rigid transformations within the image space. The models were applied to segmentation and global tracking of deformable anatomical structures in medical images from various modalities within the framework of quantitative functional studies. ESA

N94-28421# Robert Gordon's Inst. of Tech., Aberdeen (Scotland).
MEDICAL SUPPORT FOR BRITISH OPERATIONS IN THE ANTARCTIC
S. R. K. Coleshaw and J. N. Norman *In* AGARD, The Support of Air Operations under Extreme Hot and Cold Weather Conditions Oct. 1993 5 p (For primary document see N94-28420 08-51)
Copyright Avail: CASI HC A01/MF A03

N94-28423# Royal Air Force, Farnborough (England). Inst. of Aviation Medicine.
PREDICTION OF SURVIVAL TIMES ON LAND IN A COLD CLIMATE
G. Maidment *In* AGARD, The Support of Air Operations under Extreme Hot and Cold Weather Conditions Oct. 1993 12 p (For primary document see N94-28420 08-51)
Copyright Avail: CASI HC A03/MF A03

N94-28425# Survival Systems Ltd., Dartmouth (Nova Scotia).
EFFECT OF SEASICKNESS ON AIRCREW STUDENT SURVIVOR ABILITY AFTER DITCHING IN COLD WATER
Albert Bohemier *In* AGARD, The Support of Air Operations under Extreme Hot and Cold Weather Conditions Oct. 1993 7 p (For primary document see N94-28420 08-51)
Copyright Avail: CASI HC A02/MF A03

N94-28426# Defence and Civil Inst. of Environmental Medicine, North York (Ontario). Environmental Physiology Section.
FUELLING SHIVERING IN HUMANS DURING COLD WATER IMMERSION
I. Jacobs *In* AGARD, The Support of Air Operations under Extreme Hot and Cold Weather Conditions Oct. 1993 3 p (For primary document see N94-28420 08-51)
Copyright Avail: CASI HC A01/MF A03

N94-28427# Defence and Civil Inst. of Environmental Medicine, North York (Ontario). Environmental Physiology Section.
BIOCHEMICAL ENHANCEMENT OF COLD TOLERANCE
A. L. Vallerand *In* AGARD, The Support of Air Operations under Extreme Hot and Cold Weather Conditions Oct. 1993 8 p (For primary document see N94-28420 08-51)
Copyright Avail: CASI HC A02/MF A03

N94-28428# Manitoba Univ., Winnipeg. Lab. for Exercise and Environmental Medicine.
TREATMENT OF MILD IMMERSION HYPOTHERMIA BY BODY-TO-BODY AND FORCED-AIR WARMING
Gordon G. Giesbrecht, Igor B. Mekjavic, Daniel I. Sessler, Marc Schroeder, and Gerald K. Bristow *In* AGARD, The Support of Air Operations under Extreme Hot and Cold Weather Conditions Oct. 1993 2 p (For primary document see N94-28420 08-51)
Copyright Avail: CASI HC A01/MF A03

N94-28429# Army Research Inst. of Environmental Medicine, Natick, MA. Military Health Div.
NUTRITION AND HYDRATION STATUS OF AIRCREW MEMBERS CONSUMING AN IMPROVED SURVIVAL RATION DURING A SIMULATED SURVIVAL SCENARIO
Tanya E. Jones, Susan H. Mutter, Judy M. Aylward, and Eldon W. Askew *In* AGARD, The Support of Air Operations under Extreme Hot and Cold Weather Conditions Oct. 1993 14 p Prepared in cooperation with Army Natick Research and Development Command (For primary document see N94-28420 08-51)
Copyright Avail: CASI HC A03/MF A03

N94-28434# Institute for Perception RVO-TNO, Soesterberg (Netherlands).
DETERIORATION OF MANUAL PERFORMANCE IN COLD AND WINDY CLIMATES
H. A. M. Daanen *In* AGARD, The Support of Air Operations under Extreme Hot and Cold Weather Conditions Oct. 1993 10 p (For primary document see N94-28420 08-51)
Copyright Avail: CASI HC A02/MF A03

N94-28438# Royal Danish Navy, Gentofte. Health Services.
THERMOREGULATION IN THE EXTREME COLD ENVIRONMENT
Leif Vanggaard *In* AGARD, The Support of Air Operations under Extreme Hot and Cold Weather Conditions Oct. 1993 5 p (For primary document see N94-28420 08-51)
Copyright Avail: CASI HC A01/MF A03

N94-28440# Institute of Aviation Medicine, Fuerstenfeldbruck (Germany).
AEROPATHOLOGICAL DIAGNOSIS OF LETHAL HYPOTHERMIA
M. Kraemer *In* AGARD, The Support of Air Operations under Extreme Hot and Cold Weather Conditions Oct. 1993 6 p (For primary document see N94-28420 08-51)
Copyright Avail: CASI HC A02/MF A03

N94-28441# Naval Health Research Center, San Diego, CA.
REWARMING METHODOLOGIES IN THE FIELD
R. S. Pozos, R. L. Hesslink, J. Reading, P. Kincaid, and S. Feith *In* AGARD, The Support of Air Operations under Extreme Hot and Cold Weather Conditions Oct. 1993 8 p (For primary document see N94-28420 08-51)
Copyright Avail: CASI HC A02/MF A03

N94-28442# Royal Naval Hospital, Haslar (England). Dept. of Accident and Emergency Medicine.
A COMPARISON OF FOUR METHODS OF REWARMING INDIVIDUALS COOLED BY IMMERSION IN COLD WATER
C. J. Cahill, P. J. Balmi, and M. J. Tipton *In* AGARD, The Support of Air Operations under Extreme Hot and Cold Weather Conditions Oct. 1993 8 p (For primary document see N94-28420 08-51)
Copyright Avail: CASI HC A02/MF A03

N94-28448# Naval Aerospace Medical Research Lab., Pensacola, FL. Environmental Physiology Div.
EFFECTS OF THREE HYDRATION BEVERAGES ON EXERCISE PERFORMANCE DURING 60 HOURS OF SIMULATED DESERT EXPOSURE
L. G. Meyer, D. J. Horrigan, Jr., H. M. Neisler, and W. G. Lotz *In* AGARD, The Support of Air Operations under Extreme Hot and Cold Weather Conditions Oct. 1993 10 p (For primary document see N94-28420 08-51)
Copyright Avail: CASI HC A02/MF A03

N94-28449# Defence and Civil Inst. of Environmental Medicine, North York (Ontario).
ALLEVIATION OF THERMAL STRAIN IN THE CF: KEEPING OUR COOL DURING THE GULF CONFLICT
J. Frim, L. L. Bossi, K. C. Glass, and M. J. Ballantyne *In* AGARD, The Support of Air Operations under Extreme Hot and Cold Weather Conditions Oct. 1993 10 p (For primary document see N94-28420 08-51)
Copyright Avail: CASI HC A02/MF A03

N94-28450# Laboratoire de Medecine Aerospatiale, Bretigny-sur-Orge (France). Centre d'Essais en Vol.
EXPERIMENTAL EVALUATION OF TWO SYSTEMS OF INDIVIDUAL AIR-CONDITIONING [EVALUATION EXPERIMENTALE DE DEUX SYSTEMES DE CLIMATISATION INDIVIDUELLE]
D. Lejeune, J. M. Clere, M. Beaumont, and M. Loncle *In* AGARD, The Support of Air Operations under Extreme Hot and Cold Weather Conditions Oct. 1993 8 p In FRENCH (For primary document see N94-28420 08-51)
Copyright Avail: CASI HC A02/MF A03

N94-30453*# National Aeronautics and Space Administration. Lyndon B. Johnson Space Center, Houston, TX.
MICROENCAPSULATION OF ANTI-TUMOR, ANTIBIOTIC AND THROMBOLYTIC DRUGS IN MICROGRAVITY
Dennis R. Morrison, Benjamin Mosier, and John Cassanto *In* NASA, Washington, Technology 2003: The Fourth National Technology Transfer Conference and Exposition, Volume 1 Feb. 1994 p 117-126 (For primary document see N94-30440 08-99)
Avail: CASI HC A02/MF A04

N94-30455*# National Aeronautics and Space Administration. Lyndon B. Johnson Space Center, Houston, TX.
DUAL USE OF IMAGE BASED TRACKING TECHNIQUES: LASER EYE SURGERY AND LOW VISION PROSTHESIS
Richard D. Juday *In* NASA, Washington, Technology 2003: The Fourth National Technology Transfer Conference and Exposition, Volume 1 Feb. 1994 p 131-137 (For primary document see N94-30440 08-99)
Avail: CASI HC A02/MF A04

N94-30456*# Jet Propulsion Lab., California Inst. of Tech., Pasadena.
ANALYSIS AND AN IMAGE RECOVERY ALGORITHM FOR ULTRASONIC TOMOGRAPHY SYSTEM
Michael Y. Jin *In* NASA, Washington, Technology 2003: The Fourth National Technology Transfer Conference and Exposition, Volume 1 Feb. 1994 p 138-145 (For primary document see N94-30440 08-99)
Avail: CASI HC A02/MF A04

N94-30457*# National Aeronautics and Space Administration. Marshall Space Flight Center, Huntsville, AL.
COMPOSITE REDESIGN OF OBSTETRICAL FORCEPS
Seth W. Lawson and Stan S. Smeltzer *In* NASA, Washington, Technology 2003: The Fourth National Technology Transfer Conference and Exposition, Volume 1 Feb. 1994 p 146-150 (For primary document see N94-30440 08-99)
Avail: CASI HC A01/MF A04

N94-30458*# National Aeronautics and Space Administration. Lyndon B. Johnson Space Center, Houston, TX.
DEVELOPMENT OF THE NASA/BAYLOR VAD
G. S. Aber, J. W. Akkerman, R. J. Bozeman, Jr., D. R. Saucier, J. W. Bacak, P. A. Svejkovsky, G. A. Damm, K. Mizuguchi, G. P. Noon, and Y. Nose et al *In* NASA, Washington, Technology 2003: The Fourth National Technology Transfer Conference and Exposition, Volume 1 Feb. 1994 p 151-157 (For primary document see N94-30440 08-99)
Avail: CASI HC A02/MF A04

N94-30459*# Jet Propulsion Lab., California Inst. of Tech., Pasadena.
A FUZZY LOGIC CONTROLLER FOR HORMONE ADMINISTRATION USING AN IMPLANTABLE PUMP
L. Stephen Coles and George H. Wells, Jr. *In* NASA, Washington, Technology 2003: The Fourth National Technology Transfer Conference and Exposition, Volume 1 Feb. 1994 p 158-167 (For primary document see N94-30440 08-99)
Avail: CASI HC A02/MF A04

N94-30460*# Army Armament Research, Development and Engineering Center, Watervliet, NY. Benet Labs.
MONITOR FOR STATUS EPILEPTICUS SEIZURES
Mark Johnson and Thomas Simkins *In* NASA, Washington, Technology 2003: The Fourth National Technology Transfer Conference and Exposition, Volume 1 Feb. 1994 p 168-175 (For primary document see N94-30440 08-99)
Avail: CASI HC A02/MF A04

53 BEHAVIORAL SCIENCES

Includes psychological factors; individual and group behavior; crew training and evaluation; and psychiatric research.

N94-28754# Naval Aerospace Medical Research Lab., Pensacola, FL.
AN EVALUATION OF PERSONALITY TESTING AND THE FIVE-FACTOR MODEL IN THE SELECTION OF LANDING CRAFT AIR CUSHION VEHICLE CREW MEMBERS
D. R. Street, Jr., K. T. Helton, and T. Nontasak 30 Jul. 1993 21 p (AD-A275869; NAMRL-1385) Avail: CASI HC A03/MF A01

The purpose of our investigation was to determine if personality testing and a five-factor model could improve the selection of Landing Craft Air Cushion (LCAC) vehicle crew members. Vehicle crew members for the LCAC are currently selected on the basis of their performance on a computer-based psychomotor selection system. The various psychomotor tests in the selection system have demonstrated predictive validity in LCAC crew training. Certain personality characteristics may also be involved in the LCAC vehicle crew training success. In fact, various researchers have found that personality testing may improve the selection of Navy/Marine Corps aviators. There is increasing evidence that a five-factor model may be useful in describing the personality characteristics involved in training success. We believe that a five-factor model may improve the selection system used for LCAC vehicle crew members. A principal component analysis with varimax rotation was conducted to determine the underlying structure of the Adult Personality Inventory (API) with 168 LCAC crew candidates. The resulting factor scores were then analyzed using advanced statistical techniques to determine the relation of the personality factor scores and the performance-based test to an underway grade in training criterion. The results indicated that one personality factor, openness, significantly improved predictions of the criterion (p less than 0.05). Based on these results, we believe that personality testing would improve the selection of LCAC vehicle crew members. DTIC

N94-28860# Carnegie-Mellon Univ., Pittsburgh, PA. Dept. of Computer Science.
NON-INTRUSIVE GAZE TRACKING USING ARTIFICIAL NEURAL NETWORKS

Shumeet Baluja and Dean Pomerleau 5 Jan. 1994 14 p
(Contract N00014-93-1-0806)
(AD-A275186; CMU-CS-94-102) Avail: CASI HC A03/MF A01

An artificial neural network based gaze tracking system which can be customized to individual users was developed. A three layer feedforward network, trained with standard error back propagation, is used to determine the position of a user's gaze from the appearance of the user's eye. Unlike other gaze trackers, which normally require the user to wear cumbersome headgear or to use a chin rest to ensure head mobility, the system is entirely nonintrusive. Currently, the best intrusive gaze tracking systems are accurate to approximately 0.75 degrees. An accuracy of 1.5 degrees was achieved with the nonintrusive system, while allowing head mobility. In its current implementation, the system works at 15 Hz. An empirical analysis of the performance of a large number of artificial neural network architectures is presented. Suggestions for further explorations for neurally based gaze trackers are provided, and are related to other similar artificial neural network applications such as autonomous road following.
DTIC

N94-28887# Air Force Test Pilot School, Edwards AFB, CA.
HUMAN PILOT RESPONSE DURING SINGLE- AND MULTI-AXIS TRACKING TASKS Final Report, 8-11 Oct. 1993
Craig R. Edkins, Benjamin J. Coffey, John Kruzinauskas, Jr., Darcy Granley, and Mary McNeely Dec. 1993 193 p
(AD-A275080; AFFTC-TLR-93-41) Avail: CASI HC A09/MF A03

This report presents the results of a limited evaluation of human pilot response during single and multiaxis tracking tasks. A five member team from the USAF Test Pilot School conducted this evaluation at Buffalo, New York, from 8-11 October 1993. Five sorties totalling 7.6 hours were flown in the Calspan variable stability Lear 2 aircraft. Ground simulations in Lear 2 were also performed. Four different pitch and four different roll dynamics were evaluated using three different single and multiaxis tracking tasks. For each set of dynamics, primary pilot response parameters were recorded and examined using Fourier transform analysis in an attempt to provide a data base for pilot model development and validation. Pilot comments and Cooper-Harper ratings were also recorded. This report serves as a guide for flight test data and gives an initial look at the test results.
DTIC

N94-29027 Massachusetts Inst. of Tech., Cambridge.
STRATEGIES TO SUSTAIN AND ENHANCE PERFORMANCE IN STRESSFUL ENVIRONMENTS Final Report, 15 Dec. 1990 - 15 Dec. 1992
Richard J. Wurtman, Andrew B. Dollins, Harris B. Lieberman, and Harry J. Lynch 14 Dec. 1993 83 p Limited Reproducibility: More than 20% of this document may be affected by microfiche quality
(Grant AF-AFOSR-0125-90)
(AD-A275223; AFOSR-94-0038-TR) Avail: CASI HC A05

This report contains the five manuscripts (one published, two in-press, one in-review, and one in-preparation) and six published abstracts completed during the three year grant period. These include descriptions of the four original research projects completed during the grant period. STUDY 1 was designed to test the effects of illumination on human nocturnal serum melatonin levels and performance. Results indicate that overnight exposure to 300, 1500, or 3000 lux of light significantly diminished serum melatonin levels in a dose-dependent manner. Performance on vigilance, reaction time, and other tasks deteriorated throughout the night, consistent with known circadian variations in these parameters, but independent of ambient light intensity and circulating melatonin levels.
DTIC

N94-29154# City Univ. of New York, NY.
TEMPORAL AND QUALITATIVE DECOMPOSITION OF PLAUSIBLE REASONING Final Technical Report, 15 Mar. 1991 - 15 Jun. 1993
David A. Swinney and Edward E. Smith 15 Dec. 1993 12 p
(Grant AF-AFOSR-0225-91)
(AD-A275073; AFOSR-94-0002TR) Avail: CASI HC A03/MF A01

The goal of this work is to detail the temporal course of information integration during plausible reasoning, with a focus on: (1) the component processes in terms of their time-courses and information content; (2) the degree to which reasoning consists of 'modular' (autonomous, independent, informationally encapsulated) stages of processing; and (3) how components of reasoning are drawn together to eventuate in a single answer to a reasoning problem. This work has involved three relevant lines of inquiry: (1) Conceptual Combination. The set of studies in this area demonstrated that claims by Springer and Murphy to the effect that conceptual combination takes place such that initial components of the combination are not activated and processed separately, are not supported. (2) Reasoning and Categorization. These studies have demonstrated that evidence from Rips that categorization can take place based on reasoning as well as on similarity, seems to be true, but only under conditions where the informational basis for categorization is quite sparse and when the subject is aware that his/her basis for the categorization must be defended. (3) Modularity and Discourse. A claim by Marslen-Wilson and Tyler purporting to demonstrate an important lack of modularity of processing during discourse/sentence comprehension was examined in detail utilizing a more sensitive task. It was demonstrated that modularity between semantic and syntactic information was maintained during this (particularly critical) stage of language processing. (4) Reasoning and Cognition in Neurologically Involved Populations. A series of studies focussing on the role of language in plausible reasoning, studied the degree to which early modular processes are disrupted by brain damage and aging. It was demonstrated that the early cognitive/language processing is robustly modular.
DTIC

N94-29313# Carnegie-Mellon Univ., Pittsburgh, PA. Dept. of Computer Science.
AN ARCHITECTURALLY-BASED THEORY OF HUMAN SENTENCE COMPREHENSION Ph.D. Thesis
Richard L. Lewis 18 Dec. 1993 259 p
(Contract F33615-93-1-1330)
(AD-A275380; CMU-CS-93-226) Avail: CASI HC A12/MF A03

This thesis presents NL-Soar, a detailed computational model of human sentence comprehension that accounts for a broad range of psycholinguistic phenomena. NL-Soar provides in-depth accounts of structural ambiguity resolution, garden path effects, unproblematic ambiguities, parsing breakdown on difficult embeddings, acceptable embeddings, immediacy of interpretation, and the time course of comprehension. The model explains a variety of both modular and interactive effects, and shows how learning can affect ambiguity resolution behavior. In addition to accounting for the qualitative phenomena surrounding parsing breakdown and garden path effects, NL-Soar explains a wide range of contrasts between garden paths and unproblematic ambiguities, and difficult and acceptable embeddings: the theory has been applied in detail to over 100 types of structures representing these contrasts, with a success rate of about 90%. The account of real-time immediacy includes predictions about the time course of comprehension and a zero-parameter prediction about the average rate of skilled comprehension. Finally, the theory has been successfully applied to a suggestive range of cross-linguistic examples, including constructions from head-final languages such as Japanese.
DTIC

N94-29918# Federal Aviation Administration, Oklahoma City, OK. Civil Aeromedical Inst.
SCANNING AND MONITORING PERFORMANCE: EFFECTS OF THE REINFORCEMENT VALUES OF THE EVENTS BEING MONITORED Final Report
P. G. Rasmussen and A. M. Revzin Apr. 1994 9 p
(DOT/FAA/AM-94/8) Avail: CASI HC A02/MF A01

We formulated a hypothesis suggesting that operators could make scanning and monitoring errors if they tended to concentrate on a 'high-value' display sub-area while ignoring 'low-value' problems elsewhere on the display. Such 'data' would have application to Air Traffic Control Specialist (ATCS) jobs. We tested the hypothesis in an experiment rewarding good performance in a laboratory task. Subjects monitored two visual display 'work areas' with defined task difficulty. In the high-value work area, each error cost the subjects four or ten times as much as in the low-value work area. The data obtained suggest that differing task error penalties, or reinforcement values, can induce a greater than usual frequency of errors in some subjects. Rewarding good performance in two-work area tests without differing error penalties did not induce significant error rate differences, nor did such rewards significantly affect total task performance levels. This was true even in tests where such differential attention could benefit the subject's overall performance score, thereby increasing subject's performance bonus. However, about 15 percent of our subjects showed a marked tendency to concentrate their attention on a display sub-area having

high-value events while periodically ignoring events elsewhere on the display. Such information may be useful in reducing the frequency of scanning errors by revising training protocols or personnel selection criteria. Author

N94-30969 National Aerospace Lab., Amsterdam (Netherlands). Flight Div.
SPECTRAL ANALYSIS OF HEART RATE AND PSYCHOLOGICAL STATE: A REVIEW OF ITS VALIDITY AS A WORKLOAD INDEX
P. G. A. M. Jorna (Institute for Perception RVO-TNO, Soesterberg, Netherlands.) 25 Feb. 1993 25 p Submitted for publication Limited Reproducibility: More than 20% of this document may be affected by microfiche quality
(AD-B179387; NLR-TP-93034-U; ETN-94-95975) Avail: CASI HC A03

Background information on concepts of mental workload and stress and the possibility of indexing them by means of spectral analysis of heart rate is presented. A literature review of practical implementations of the technique in laboratory and field studies is provided with the purpose of evaluating its utility as a tool in the study of mental workload and stress. ESA

N94-29715# Nagoya Univ. (Japan). Space Medicine Research Center.
A DISCUSSION OF EYE-HEAD COORDINATIVE MOVEMENT UNDER MICROGRAVITY DURING PARABOLIC FLIGHT [PARABORIKKU FURAITO NI YORU TEI JURYOKU KANKYOKA DENO HITO NO TOBU/GANKYU KYOUOU UNDO NO KENTO]
Kazuo Koga *In* Society of Medical Research for Space Station, The MERSS 5th Symposium on Space Medicine: Medical and Physiological Experiment Utilizing Parabolic Flight Mar. 1993 p 34-41 In JAPANESE (For primary document see N94-29709 08-52)
Avail: CASI HC A02/MF A01

N94-29716# Toyohashi Univ. of Technology, Aichi (Japan). Information and Computer Sciences.
ANALYSIS OF VARIOUS BIOLOGICAL ACTIVITY PARAMETERS DURING PARABOLIC FLIGHT [PARABORIKKU FURAITO NI OKERU KAKUSHU SEITAI SHINGO NO KAISEKI]
Shiro Usui and Yutaka Hirata *In* Society of Medical Research for Space Station, The MERSS 5th Symposium on Space Medicine: Medical and Physiological Experiment Utilizing Parabolic Flight Mar. 1993 p 42-47 In JAPANESE Prepared in cooperation with NASDA, Tokyo, Japan; the Research Inst. of Environmental Medicine, Nagoya Univ., Aichi, Japan; and Nihon Univ., Tokyo, Japan (For primary document see N94-29709 08-52)
Avail: CASI HC A02/MF A01

N94-29867# Kyorin Univ., Tokyo (Japan). Dept. of Physiology.
PSYCHOPHYSIOLOGICAL STUDY ON THE EFFECTS OF CO-EXISTENCE OF LINES FOR DETECTING DOT TARGET [TEN SHIHYO NO SHININSEI NI OYOBOSU KINBO SENBUN NO EIKYO NI KANSURU SHINRI SEIRIGAKUTEKI KENKYU]
Kiyoshi Mizumoto *In* Japan Society of Aerospace and Environmental Medicine, Japanese Journal of Aerospace and Environmental Medicine, Vol. 30, No. 2 1 Jun. 1993 p 81-91 In JAPANESE See also A93-55330 (For primary document see N94-29863 08-52)
Avail: CASI HC A03/MF A01

54 MAN/SYSTEM TECHNOLOGY AND LIFE SUPPORT

Includes human engineering; biotechnology; and space suits and protective clothing.

For related information see also *16 Space Transportation.*

N94-28406# Technical Research Centre of Finland, Tampere. Regional Inst. of Occupational Health.
SIMULATION OF THE EFFECT OF WIND ON CLOTHING BY MEASUREMENTS AND CALCULATIONS
Hannu Anttonen, Esa Hiltunen, and Ralf Oesterlund 1993 49 p
(ISSN 1235-0621)
(PB94-132289; VTT/PUB-133; ISBN-951-38-4251-7) Copyright Avail: CASI HC A03/MF A01

The conventional measuring methods of thermal resistance R(ct) and water vapor resistance R(et), do not give enough information about the function of winter clothing in different conditions. In the study, two self-constructed cylinders were used, with diameters of 300 and 200 mm, both 500 mm in height. The cylinder was placed in a wind-tunnel in the climatic chamber where ambient temperature (-15 to +5 C) and wind velocity (1 to 8 m/s) were adjustable. Skin temperature and sweating level of the cylinder were controlled by a computer. The development of measuring method, the theory, and the clothing models are under progress, but is is obvious that cylinder measurements are suitable especially in windy conditions. NTIS

N94-28649# Federal Aviation Administration, Cambridge, MA. National Transportation Systems Center.
KEY COGNITIVE ISSUES IN THE DESIGN OF ELECTRONIC DISPLAYS OF INSTRUMENT APPROACH PROCEDURE CHARTS Final Report, Nov. 1992 - Jul. 1993
Melanie C. Clay Nov. 1993 111 p
(AD-A275647; DOT-VNTSC-FAA-93-18; DOT/FAA/RD-93/39) Avail: CASI HC A06/MF A02

This report provides a general introduction to the field of cognitive psychology and the application of well researched cognitive issues to the design of electronic instrument approach procedures (EIAP) displays. It presents 46 cognitive issues and 108 design principles. Its basic premise is a recognition of the need for the pilot to get unambiguous information as quickly and easily as possible in such a way that it can be remembered until the time that it must be used. Recognition and discriminability of patterns, stress resulting from heavy workload, the effects of divided attention, and the need to take account of the pilot's expectations are discussed. The merits of color and size, paper and electronic display, and temporary removal of nonessential information are examined. Among the conclusions made by the report are recommendations for more investigation in the following areas: symbol design, grouping and coding of information, orientation and scaling of information, control of clutter, and ways of overcoming the harmful effect of interruptions to attention or to performance of sequential actions. DTIC

N94-28766# Krug Life Sciences, Inc., San Antonio, TX.
A RELIABLE AND REPEATABLE METHOD FOR VOLUME CALCULATION OF PRESSURIZED GARMENTS Interim Report, May - Nov. 1993
Ricardo Perez, III, John H. Ohlhausen, and Philip J. Preen Nov. 1993 5 p
(Contract F33615-92-C-0018)
(AD-A275600; AL/CF-PC-1993-0051) Avail: CASI HC A01/MF A01

A rapid, accurate and efficient method to conduct inflation, volume and leak tests on pressure containing personal protective garments was developed and validated. The new system consists of a computer data acquisition and process control system that integrates flow rate over time to calculate volume. Validation of the new test system was accomplished by comparing the volumes calculated by the computer with volumes actually measured via a wet spirometer. Results from the validation study showed that the computerized system was highly accurate. In addition, the computerized system allows suits to be rapidly and effectively evaluated. DTIC

N94-28861# Klein Assoiciates, Inc., Fairborn, OH.
DESIGNING FOR PERFORMANCE: A COGNITIVE SYSTEMS ENGINEERING APPROACH TO MODIFYING AN AWACS HUMAN COMPUTER INTERFACE Final Report, Jan. 1991 - Feb. 1993
David W. Klinger, Stephen J. Andriole, Laura G. Militello, Leonard Adelman, and Gary Klein Mar. 1993 109 p
(Contract F33615-90-C-0533)
(AD-A275187; AL/CF-TR-1993-0093) Avail: CASI HC A06/MF A02

Cognitive systems engineering (CSE) is primarily a blend of technological opportunities, findings from cognitive research, and cognitive task analysis. Using CSE, we were able to produce an efficient and effective redesign of the AWACS weapons director (WD) station. The revised WD station was tested using 17 WD's. These WD's performed defensive counter air missions with both the current interface and the revised interface. The training of

the participants on the revised interface was quite brief (4.5 hours). As a result, the WD's did not achieve the same degree of familiarity or automation with the revised interface that they have with the current interface. Yet, when WD's were using the revised system, their performance improved. This is indicated by an increase in performance for a number of process and outcome measures. Also, a skilled WD provided blind ratings of WD performance. These global ratings were significantly higher for the revised interface. The effectiveness of the revised interface suggests that it is possible to pinpoint cognitive task requirements and to make these the driving factors in a design effort. The use of CSE ray be a feasible aspect of the design process, enabling system developers to achieve a much stronger effectiveness at relatively low cost. DTIC

N94-28902# Naval Health Research Center, San Diego, CA.
COMPARISON OF TWO COOL VESTS ON HEAT-STRAIN REDUCTION WHILE WEARING A FIREFIGHTING ENSEMBLE IN A HOT/HUMID ENVIRONMENT Final Report
Brad L. Bennett, R. D. Hagan, K. A. Huey, C. Minson, and D. Cain Jul. 1993 27 p
(AD-A275103; NHRC-93-10) Avail: CASI HC A03/MF A01

Understanding the impact of heat strain on the performance of naval personnel has important application to shipboard fire-suppression activities. Firefighting is associated with heat strain as demonstrated by large increases in skin and core temperatures and near maximal heart rates (Duncan et al., 1979; Romet and Frim, 1987; Bennett et al., 1992). These responses can attribute to body heat production caused by wearing 30 to 40 pounds of personnel protection equipment, the physical effort associated with carrying equipment (e.g., fire hose, ventilation fans), and the heat gain due to exposure to high ambient temperature and humidity. DTIC

N94-28918# Air Force Inst. of Tech., Wright-Patterson AFB, OH.
AN INVESTIGATION OF STEREOPSIS WITH AN/AVS-6 NIGHT VISION GOGGLES AT VARYING LEVELS OF ILLUMINANCE AND CONTRAST M.S. Thesis
Jeffrey J. Armentrout 1993 81 p
(AD-A275332; AFIT/CI/CIA-93-160) Avail: CASI HC A05/MF A01

The increased reliance on night operations by the military over the last few decades has led to the development of various night imaging devices. Night vision goggles (NVG's) are one device which have gained widespread use in nighttime helicopter operations. However, rotorcraft accident data have indicated an increased occurrence of 'pilot error' type accidents when NVG's are in use. NVG related accidents often can be linked to extremely poor ambient lighting and contrast conditions during nighttime operations as well as the imaging limitations of the NVG's. Research has shown that NVG's reduce visual acuity and depth perception when compared to unaided daylight viewing conditions. In this study the effects of illumination and contrast on stereoscopic vision with and without AN/AVS-6 goggles were investigated. Stereoacuity was measured using a modified Howard-Dolman apparatus with four levels of illumination and three levels of contrast. DTIC

N94-28996# Aerospace Medical Research Labs., Brooks AFB, TX. Crew Systems Directorate.
COMPARATIVE CENTRIFUGE EVALUATION OF THE AIR FORCE ADVANCED TECHNOLOGY ANTI-G SUIT (ATAGS) AND THE NAVY ENHANCED ANTI-G LOWER ENSEMBLE (EAGLE) Final Report, Sep. 1992 - Dec. 1993
John W. Burns and Ronald C. Hill 30 Dec. 1993 6 p
(AD-A275348; AL/CF-PC-1993-0052) Avail: CASI HC A02/MF A01

The centrifuge evaluation of the ATAGS and EAGLE was undertaken to determine which extended coverage anti-G suit would enter engineering and manufacturing development for joint service use. Eight male centrifuge subjects were used. The subjects were wearing either an ATAGS, with or without pressure socks, or an EAGLE. Pressure breathing during G (COMBAT EDGE) was used with all three combinations. The combinations were randomized to eliminate any order effect. The arms of all subjects were wrapped from the wrist to the axilla with 3 in. wide elastic bandage to reduce the possibility that subjects might stop the +G(sub z) exposure for arm pain rather than for fatigue or light loss. GOR, ROR, and 5-9 SACM +G(sub z) profiles were used to compare the suits. Although not significantly different, the average number of 9G plateaus completed for the ATAGS with socks, the ATAGS without socks, and the EAGLE were 8.0, 7.8, and 6.5, respectively. Subject HR, while wearing the ATAGS with pressure socks, was significantly ($p = .03$) lower than HR while wearing the EAGLE during the 5G plateaus of the 5-9 +G(sub z) SACM. The perceived effort involved in the straining maneuver during the 5-9 SACM with the EAGLE was consistently, but not significantly, greater across the 9G plateaus compared to the ATAGS with pressure socks. However, there was a significant ($p = .032$) suit/time interaction between the ATAGS with pressure socks and the EAGLE. There was no significant difference in subject HR or +G(sub z) tolerance between the three G-suit combinations during the GOR or ROR +G(sub z) exposures. DTIC

N94-28997# Krug Life Sciences, Inc., San Antonio, TX.
PROCEDURES AND METRICS FOR ANTI-G SUIT EVALUATIONS Interim Report, Nov. 1992 - Nov. 1993
Grady L. Ripley, Richardo Perez, III, and Daniel H. Bauer Nov. 1993 5 p
(Contract F33615-92-C-0018)
(AD-A275349; AL/CF-PC-1993-0043) Avail: CASI HC A01/MF A01

The ATAGS (Advanced Technology Anti-G Suit) design process initially relied on comments made by human test subjects to subjectively evaluate the effects of design changes on inflation characteristics. A standardized test method was needed to objectively quantify the effects of the design changes and also to compare the inflation characteristics of other anti-G suits. Therefore, a test was designed to measure the filling characteristics of different anti-G suits fitted to a standard mannikin. Several factors had to be considered in developing a test method that was both operationally significant and provided consistently valid data. The factors considered were as follows: don/doff requirements, the effects of evacuation of the anti-G suits prior to testing, mannikin position, and additional life support equipment worn with the anti-G suit. Parameters measured to assess the inflation characteristics were flow rate, fill times, and differential pressures in the suit. DTIC

N94-29029 Southeastern Center for Electrical Engineering Education, Inc., Saint Cloud, FL.
REMOTE CONTROL OF TRANSCRANIAL DOPPLER (TCD) PROBE DURING CENTRIFUGE EXPOSURES UP TO 9 +Gz Final Report, Oct. 1987 - Dec. 1993
Ulf I. Baldwin, Paul Werchan, and Travis Eddy Jan. 1994 6 p Limited Reproducibility: More than 20% of this document may be affected by microfiche quality
(Contract F33615-87-D-0609)
(AD-A275253; AL/CF-PC-1993-0046) Avail: CASI HC A02

TCD systems have been successfully used in clinical practice for estimating cerebral perfusion by registering blood flow velocity in the middle cerebral artery. However, when used in centrifuges, probe movement during high +Gz have resulted in the loss of Doppler signal making interpretations of data very difficult. To solve this problem, the Doppler probe and three electrical motors were mounted on a tightly fitted helmet. Remote control of these motors allows precise tilting and sliding of the probe during G exposures. Vertical movement of the probe is recorded when a good flow velocity signal is achieved. On succeeding G-exposures, the probe is moved to the predicted positions for different G-loads when the G-load changes. A computer program to automate this process is currently under development. With this device, blood flow velocity in the middle cerebral artery can be registered at G-loads up to 9 +Gz with increased accuracy. DTIC

N94-29034# Air Force Systems Command, Wright-Patterson AFB, OH. Crew Systems Directorate.
STRESS AND ERGONOMIC DESIGN AND EVALUATION OF PERSON-MACHINE SYSTEMS Final Report, Jan. 1992 - May 1993
Herschel C. Self May 1993 35 p
(AF Proj. 7184)
(AD-A275156; AL/CF-SR-1993-0008) Avail: CASI HC A03/MF A01

This report was written to make system designers and developers more stress-conscious and more alert to sources of potentially harmful operator stress. They are then more capable of designing person-machine systems in which stress is optimized, in which equipment and operating procedures are a good fit to system operators. In such systems, worker morale and performance are maintained, and the lifecycle system costs are less. Despite careful design efforts aided by preproduction tests and

evaluations, person-machine systems often come into wide use with unanticipated and potentially harmful stress-related operator problems. How this can happen is made evident by examining stress in general and stress in and out of the workplace. Examples of stress and strain are given. Stress from inadequate visual conditions is given special emphasis. The presentation is from ergonomic or application viewpoint. A stress checklist is given in the appendix. DTIC

N94-29093 Materials Research Labs., Ascot Vale (Australia).
PORTABLE VENTILATORY RESUSCITATION SYSTEMS
Wai-Man Lau and Margaret Dowling Nov. 1993 15 p Limited Reproducibility: More than 20% of this document may be affected by microfiche quality
(AD-A274984; MRL-TN-649; DODA-AR-008-575) Avail: Issuing Activity (Defense Technical Information Center (DTIC))

A review on the commonly used resuscitators in Australia was conducted. Their specifications, capability, and limitations are examined and discussed. Some products are modified for operations in chemically contaminated environments and one of them will soon undergo clinical trials. DTIC

N94-29184 Navy Experimental Diving Unit, Panama City, FL.
ADVANCED SEAL DELIVERY SYSTEM LIFE SUPPORT PARAMETERS Technical Report, May - Dec. 1993
M. E. Knafelc Dec. 1993 14 p Limited Reproducibility: More than 20% of this document may be affected by microfiche quality
(AD-A275304; NEDU-2-94) Avail: CASI HC A03

The purpose of this document is to provide a guideline to the technical evaluation board when reviewing the proposals for the Advanced SEAL Delivery System (ASDS). These guidelines are based upon a design that consists of at least two habitable compartments. The pilot and navigator will occupy one compartment, and its internal pressure will be maintained at 1 ATA. Another habitable compartment will hold the divers, and its inside pressure can be adjusted to permit controlled compression and decompression, or be maintained at a constant 1 ATA. The habitable chambers will be kept dry. Because of safety, environmental, and human factors' considerations, it is desirable for the lock-out chamber to be separate from the habitable compartments. DTIC

N94-29302# Defence and Civil Inst. of Environmental Medicine, Downsview (Ontario).
INSULATIVE PROPERTIES OF TWO THERMO-METAL NEOPRENES Research Report
Michael B. Ducharme and John Frim Dec. 1993 17 p
(AD-A275209; DCIEM-93-53) Avail: CASI HC A03/MF A01

The objective of the present study was to compare the thermal resistance of two thermo-metal neoprenes (titanium and stainless steel coated) to the current Canadian Forces Arctic diving suit neoprene (CF-N) in dry and wet environment. The test in the dry environment were conducted using a Rapid-k thermal conductivity instrument, and in the wet environment using a custom-made apparatus. The dry tests were conducted at 1 atmosphere in the laboratory, and the wet tests were done in a hyperbaric water chamber maintained at 5 C and at depths of 0, 10, 25, 50, and 100 m. Pre- and post-dive tests were performed on the same samples to investigate the effects of two dives on the thermal resistance of the neoprenes. It was found that the thermal insulation of the two thermo-metal neoprenes tested was significantly higher than that of the CF-N in both the dry and the wet environments. The best thermo-metal neoprene, the stainless steel coated neoprene, averaged an improvement of 53% in the dry and 60% in the wet environment (ranging from 70% at 0 m to 34% at 100 m). The insulative properties of the thermo-metal neoprenes were affected, however, by the dives, decreasing by about 12% after two dives. It was concluded that the stainless steel thermo-metal neoprene could be a potential alternative to the current CF Arctic diving suit neoprene but further testing is needed on the long term effects of dives and aging on the insulative properties of the material. DTIC

N94-29729 Vanderbilt Univ., Nashville, TN.
EVA GLOVE EVALUATION METHODOLOGY AND TEST PROTOCOL Ph.D. Thesis
Elaine Marie Hinman-Sweeney 1993 244 p
Avail: Univ. Microfilms Order No. DA9324440

One of the most critical components of a spacesuit is the gloves, yet gloves have traditionally presented significant design challenges. With the continued and varied efforts at glove development, a method for evaluating glove performance is needed. This dissertation presents a pressure glove evaluation protocol. A brief history of extra-vehicular activity (EVA) glove development and test procedures is given. A description of this evaluation protocol, and its development is provided. The protocol allows comparison of one glove design to another, or any one design to bare handed performance. Gloves for higher pressure suits may be evaluated at current and future design pressures to drive out differences in performance due to pressure effects. Using this protocol, gloves may be evaluated during design to drive out design problems and determine areas for improvement or fully mature designs may be evaluated with respect to mission requirements. Several different test configurations are presented to handle these cases. A glovebox, set of tasks, and a methodology to evaluate glove performance was developed. Evaluating comfort has been a difficulty in glove testing. A technique for quantifying comfort data is presented. This protocol was run on a prototype glove. The prototype was evaluated at two operating pressures and in the unpressurized state, with results compared to bare-handed performance. Results and analysis from this test series are provided, as is a description of the test configuration used for this test . Dissert. Abstr.

N94-29950 Selskapet for Industriell og Teknisk Forskning, Trondheim (Norway). Div. of Applied Thermodynamics.
MAINTAINING ACCEPTABLE THERMAL COMFORT WITH A LOW AIR TEMPERATURE BY MEANS OF LOCAL HEATING
R. Soerlie 13 Jul. 1993 11 p See also DE85750802
(PB94-138526; STF15-A93053) Avail: Issuing Activity (National Technical Information Service (NTIS))

The main objective was to assess (1) the lower room temperature for acceptable thermal comfort of the person seated at the desk, and (2) to assess the energy-saving qualities of the local heater. During the experiments various temperatures, air velocity, radiant flux and thermal asymmetry were all measured. The thermal mannequin was used in order to verify the level of thermal comfort and was constructed in such a way as to be thermally equivalent to a human. The local heater creates a local microclimate with satisfactory thermal comfort for the person seated at the desk, while the temperature in the rest of the room can be as low as 17-18 C. Supplementary thermal simulations carried out on computer showed that it is possible to save heating energy by reducing the general room temperature. NTIS

N94-30000 Selskapet for Industriell og Teknisk Forskning, Trondheim (Norway). Div. of Refrigeration Engineering.
CONTROL OF HEATING, VENTILATION AND AIR CONDITIONING (HVAC) SYSTEMS
M. C. Svensson 11 Aug. 1993 40 p
(PB94-138807; STF11-A93056) Avail: Issuing Activity (National Technical Information Service (NTIS))

The report contains the English version of chapter 9 in a new book which will be published in German (Bauverlag). Chapter 9 discusses different aspects regarding control of heating, ventilation, and air-conditioning (HVAC) systems. The book project coordinator is Dring S. Nowotny, and the preliminary book title is: Technische Gebaudeausrustungen. NTIS

N94-30122*# George Washington Univ., Washington, DC. Science Communication Studies.
PUBLICATIONS OF THE NASA CONTROLLED ECOLOGICAL LIFE SUPPORT SYSTEM (CELSS) PROGRAM 1989-1992
Janet V. Powers Mar. 1994 46 p
(Contract NASw-4324)
(NASA-CR-4603; NAS 1.26:4603) Avail: CASI HC A03/MF A01

Publications of research sponsored by the NASA Controlled Ecological Life Support System (CELSS) program are listed. The CELSS program encompasses research and technology with the goal of developing an autonomous bioregenerative life support system, which is based upon the integration of biological and physical/chemical processes, that will produce nutritious and palatable food, potable and hygienic water, and a breathable atmosphere by recycling metabolic and other wastes. This research and technology development is being performed in the areas of biomass production/food processing, waste management, and systems management and control. The bibliography follows these divisions. Principal investigators whose research tasks resulted in publication are identified by an asterisk.

Publications are identified by a record number corresponding with their entry in the Life Sciences Bibliographic Database, maintained at the George Washington University. Author (revised)

N94-30132# Defence and Civil Inst. of Environmental Medicine, Downsview (Ontario).

THE USE OF TASK NETWORK SIMULATION IN WORKLOAD PREDICTION

Mary Margaret Schuck and Keith C. Hendy 1992 7 p

(DCIEM-92-32; CTN-94-61138) Avail: CASI HC A02/MF A01

As aviation systems become increasingly complex, it becomes more important to design these systems within the capabilities and limitations of their operators. Practical workload and performance prediction techniques are thus required for the design of systems. One technique which has proven useful is task network simulation. This approach produces a simulated task timeline for the given mission, but must be linked with some model of human information processing in order to make workload or performance predictions. The use of task network simulation within the Canadian Department of National Defence for the prediction of workload during the early design of complex man-machine systems is reviewed. The measures of workload used within the simulation are detailed, with particular emphasis on the use of task rating scales and task conflict matrices. The modifications to these two tools made at the Defence and Civil Institute of Environmental Medicine are presented as well as their present and future applications. Author (CISTI)

N94-30186*# Rush-Presbyterian-Saint Luke's Medical Center, Chicago, IL.

CIRCADIAN COUNTERMEASURES FOR SHIFTWORKERS DURING USMP-2: A REPORT TO MISSION MANAGEMENT Final Report

Karen T. Stewart and Julie Hayes Apr. 1994 30 p

(NASA Order H-13012-D)

(NASA-CR-195260; NAS 1.26:195260) Avail: CASI HC A03/MF A01

People who must work at night experience a number of physiological and psychological difficulties. These include sleepiness and fatigue at work, poor daytime sleep, gastrointestinal distress, impaired concentration and performance, disturbed mood, and increased health complaints and risk of disease. These difficulties arise because nocturnal work and daytime sleep take place at inappropriate phases of the body's circadian rhythms. Intense artificial light can shift the phase of human circadian rhythms, and can thus be used to promote adaptation to shifted work schedules. The first attempts to investigate the efficacy of light treatment for MSFC POCC shiftworkers took place during USML-1 and ATLAS-2. The findings from these studies led to the development of a Circadian Countermeasures Program that was implemented during USMP-2. Light treatment and other circadian countermeasures were employed to promote adjustment to mission shiftwork in POCC cadre volunteers. Treatment protocols were designed and customized for each volunteer's work hours and personal preferences. Treatment protocols included some or all of the following: scheduled self-administration of intense light, scheduled avoidance or attenuation of sunlight at other times, and sleep schedules. Data from post-mission questionnaires indicated that volunteers found the program to be effective, convenient, and beneficial. Author

N94-30210*# National Aeronautics and Space Administration. Lyndon B. Johnson Space Center, Houston, TX.

TACTILITY AS A FUNCTION OF GRASP FORCE: EFFECTS OF GLOVE, ORIENTATION, PRESSURE, LOAD, AND HANDLE

Ram R. Bishu (Nebraska Univ., Lincoln.), Lisa A. Bronkema (Nebraska Univ., Lincoln.), Dishayne Garcia (Wichita State Univ., KS.), Glenn Klute, and Sudhakar Rajulu May 1994 23 p

(NASA-TP-3474; S-761; NAS 1.60:3474) Avail: CASI HC A03/MF A01

One of the reasons for reduction in performance when gloves are donned is the lack of tactile sensitivity. It was argued that grasping force for a weight to be grasped will be a function of the weight to be lifted and the hand conditions. It was further reasoned that the differences in grasping force for various hand conditions will be a correlate of the tactile sensitivity of the corresponding hand conditions. The objective of this experiment, therefore, was to determine the effects of glove type, pressure, and weight of load on the initial grasping force and stable grasping force. It was hypothesized that when a person grasps an object, he/she grasps very firmly initially and then releases the grasp slightly after realizing what force is needed to maintain a steady grasp. This would seem to be particularly true when a person is wearing a glove and has lost some tactile sensitivity and force feedback during the grasp. Therefore, the ratio of initial force and stable force and the stable force itself would represent the amount of tactile adjustment that is made when picking up an object, and this adjustment should vary with the use of gloves. A dynamometer was fabricated to measure the grasping force; the tests were performed inside a glove box. Four female and four male subjects participated in the study, which measured the effects of four variables: load effect, gender effect, glove type, and pressure variance. The only significant effects on the peak and stable force were caused by gender and the weight of the load lifted. Neither gloves nor pressure altered these forces when compared to a bare-handed condition, as was suspected before the test. It is possible that gloves facilitate in holding due to coefficient of friction while they deter in peak grasp strength. Author (revised)

N94-30320 Center for Mathematics and Computer Science, Amsterdam (Netherlands). Dept. of Algorithmics and Architecture.

THE ERGONOMICS OF COMPUTER INTERFACES: DESIGNING A SYSTEM FOR HUMAN USE

Lambert G. L. T. Meertens and Steven Pemberton Dec. 1992 29 p

Limited Reproducibility: More than 20% of this document may be affected by microfiche quality

(ISSN 0169-118X)

(CWI-CS-R9258; ETN-94-95540) Copyright Avail: CASI HC A03

A discussion on the ergonomic problems with currently available software products and what in general is necessary in order to make an application pleasant to use is presented. The application of these principles to an open architecture user interface system, Views, is described. ESA

N94-30390 National Aerospace Lab., Amsterdam (Netherlands). Informatics Div.

AIDING THE OPERATOR IN THE MANUAL CONTROL OF A SPACE MANIPULATOR

J. F. T. Bos, H. G. Stassen, and A. vanLunteren 29 Jun. 1992 11 p

Presented at the 5th IFAC/IFIP/IFORS/IEA Symposium on Analysis, Design and Evaluation of Man-Machine Systems, The Hague, Netherlands, 9-11 Jun. 1992 Sponsored by Netherlands Technology Foundation Prepared in cooperation with Fokker Space and Systems Limited Reproducibility: More than 20% of this document may be affected by microfiche quality

(PB94-125549; NLR-TP-92261-U; ETN-94-95586) Avail: Issuing Activity (European Space Agency (ESA))

Three problems faced by an operator when controlling a space manipulator manually were investigated: lack of direct vision, up to six degrees of freedom to be controlled, and slow and complex dynamics. The results showed that reference lines enhance the three dimensional perception; further automation of the insert task led to a more efficient task execution; the display of the stopping configuration can lead to a faster and safer task execution. The display of the predicted trajectory led to less energy consumption due to a more calm control behavior. The length of the prediction horizon should equal half of the stopping time. ESA

N94-30422 National Aerospace Lab., Amsterdam (Netherlands). Flight Div.

SAMPLING BEHAVIOUR IN A FOUR INSTRUMENT MONITORING TASK: EFFECTS OF SIGNAL BANDWIDTH AND NUMBER OF EVENTS PER SIGNAL

H. G. M. Bohnen, M. A. M. Leermakers, and P. J. Venemans 31 Dec. 1992 35 p Submitted for publication Sponsored by the Co-Operation Centre of Tilburg and Eindhoven Universities Limited Reproducibility: More than 20% of this document may be affected by microfiche quality

(AD-B179613; NLR-TP-92386-U; ETN-94-95960) Avail: CASI HC A03

The effect of global signal characteristics, such as bandwidth and number of events on human sampling behavior, is investigated. Whether or not the influence of these characteristics on sampling strategy is affected by local (actually observed) signal features, such as the degree with which a sampled signal value falls short of an event region and the rate of change, is examined. Four independent, numerically displayed signals were used; two different bandwidths and two different event numbers were chosen. To take a sample, subjects had to use a mouse. The mouse key responses were used as an index of sampling. It was demonstrated that both bandwidth

and number of events equally affected the distribution of samples over signals. In addition, it was shown that global signal characteristics determine sampling behavior less prominently when the attentional demands brought about by the local features become of greater importance. This indicates that not predictability as governed by global signal characteristics as such, but rather predictability given certain local signal features is a crucial factor in determining sampling behavior. ESA

N94-30799 Vanderbilt Univ., Nashville, TN.
ANALYSIS AND DESIGN OF INFLATABLE AEROSPACE STRUCTURES Ph.D. Thesis
John Alan Main 1993 227 p
Avail: Univ. Microfilms Order No. DA9324454

This dissertation presents a new structural model for the bending behavior of inflated cylindrical fabric structures that are used as beams. The goal of this investigation was twofold: to perform a fundamental investigation into the static and dynamic bending behavior of the inflated fabric beam and to apply the results to practical problems faced in the design of aerospace inflated structures. Fundamental work was done in development of a model for the static and dynamic bending behavior of the inflated beam. The bending analysis of the inflated beam resulted in a differential equation of bending for the unwrinkled regions of the beam that is identical to the Euler Bernoulli solution. A more complex differential equation was found when the fabric wrinkled due to the applied moments. Experimental work was performed to verify the bending model for the inflated beam. Excellent agreement was found between the model and experimental results in static bending tests of a number of inflated cantilever beams. Dynamic tests were performed and mode shapes, natural frequencies, and damping mechanisms for the inflated beam examined. A series of dynamic tests were also performed on the NASA KC-135 Low Gravity Simulator aircraft to determine the sensitivity of the dynamics of inflated beam structures to changes in gravitation level. Large changes in structural damping were found to occur across G level. This basic research was used to predict the dynamics of a complex inflated structure, a mockup of an inflated solar concentrator. Structural modeling was performed using a finite element software package and the lower modes of vibration of the inflated structure were accurately predicted by the finite element model. The inflated beam bending model also proved itself immediately useful in aerospace applications since many of the current space suit components are essentially fabric tubes. Recommendations for improving space suit flexibility that have arisen from this research include reducing the modulus and increasing the Poisson's ratio of the fabric. A series of experiments were performed to prove these concepts. The results of those tests and the space suit glove design recommendations arising from them are included in this work. Dissert. Abstr.

N94-28422# Norwegian Transarctic Expedition, His.
EVALUATION OF LIFE SUPPORT EQUIPMENT DURING AN UNSUPPORTED NORTH POLE EXPEDITION
W. Gautvik, J. O. Owe, and T. A. Oftedal *In* AGARD, The Support of Air Operations under Extreme Hot and Cold Weather Conditions Oct. 1993 6 p (For primary document see N94-28420 08-51)
Copyright Avail: CASI HC A02/MF A03

N94-28430# Guelph Univ. (Ontario). School of Engineering.
THE POTENTIAL OF NEW TEXTILES IN IMPROVING SURVIVAL PROSPECTS
K. Slater *In* AGARD, The Support of Air Operations under Extreme Hot and Cold Weather Conditions Oct. 1993 13 p (For primary document see N94-28420 08-51)
Copyright Avail: CASI HC A03/MF A03

N94-28431# META Research, Inc., Richmond (British Columbia).
FIRE-RESISTANT WATER VAPOUR PERMEABLE BUOYANT INSULATION
Wendell Uglene and Brian Farnworth *In* AGARD, The Support of Air Operations under Extreme Hot and Cold Weather Conditions Oct. 1993 8 p Sponsored by Mustang Survival and British Columbia Research Council (For primary document see N94-28420 08-51)
Copyright Avail: CASI HC A02/MF A03

N94-28432# Gore (W. L.) and Associates, Inc., Elkton, MD.
DEVELOPMENT OF A NEW CHEMICAL WARFARE AGENT PROTECTIVE MATERIAL
S. Nicholas Allen, Robert J. Bender, and Terri L. Kelly *In* AGARD, The Support of Air Operations under Extreme Hot and Cold Weather Conditions Oct. 1993 8 p (For primary document see N94-28420 08-51)
Copyright Avail: CASI HC A02/MF A03

N94-28433# Alberta Univ., Edmonton. Dept. of Human Ecology.
THERMAL PROTECTIVE PERFORMANCE AND INSTRUMENTED MANNEQUIN EVALUATION OF MULTI-LAYER GARMENT SYSTEMS
E. M. Crown, M. Y. Ackerman, J. D. Dale, and K. B. Rigakis *In* AGARD, The Support of Air Operations under Extreme Hot and Cold Weather Conditions Oct. 1993 8 p Sponsored by Canadian Petroleum Association and Defence Research Establishment (For primary document see N94-28420 08-51)
Copyright Avail: CASI HC A02/MF A03

N94-28435# German Air Force, Fuerstenfeldbruk (Germany). Inst. of Aviation Medicine.
EFFECTIVENESS OF PROTECTION CLOTHING FOR COLD WEATHER CONDITIONS AFTER EJECTION OVER SEA: A CASE REPORT
B. Mayr and M. Kraemer *In* AGARD, The Support of Air Operations under Extreme Hot and Cold Weather Conditions Oct. 1993 8 p (For primary document see N94-28420 08-51)
Copyright Avail: CASI HC A02/MF A03

N94-28436# Shark Group of Companies, Morpeth (England).
ADVANCED INTEGRATED COLD PROTECTION FOR AIRCREW
E. Bramham and M. J. Tipton *In* AGARD, The Support of Air Operations under Extreme Hot and Cold Weather Conditions Oct. 1993 8 p (For primary document see N94-28420 08-51)
Copyright Avail: CASI HC A02/MF A03

N94-28437# Surrey Univ., Guildford (England).
EMERGENCY UNDERWATER BREATHING AIDS FOR HELICOPTER PASSENGERS AND CREW
M. J. Tipton (Institute of Naval Medicine, Alverstoke, England.), E. Bramham (Shark Group of Companies, Morpeth, England.), and D. H. Elliott *In* AGARD, The Support of Air Operations under Extreme Hot and Cold Weather Conditions Oct. 1993 8 p Sponsored by Shell Research Ltd. and Esso Research Center (For primary document see N94-28420 08-51)
Copyright Avail: CASI HC A02/MF A03

N94-28443# Aerospace Medical Research Labs., Brooks AFB, TX.
AEROMEDICAL SUPPORT FOR CASUALTIES IN EXTREMELY HOT CLIMATES
S. A. Nunneley and R. U. Bisson *In* AGARD, The Support of Air Operations under Extreme Hot and Cold Weather Conditions Oct. 1993 7 p (For primary document see N94-28420 08-51)
Copyright Avail: CASI HC A02/MF A03

N94-28444# Spanish Air Force, Talavera AFB.
WORK CONDITIONS ASSESSMENT IN PILOTS AND GROUND PERSONNEL UNDER HIGH WEATHER TEMPERATURES
J. L. GarciaAlcon and J. M. MorenoVazquez *In* AGARD, The Support of Air Operations under Extreme Hot and Cold Weather Conditions Oct. 1993 9 p (For primary document see N94-28420 08-51)
Copyright Avail: CASI HC A02/MF A03

N94-28445# Royal Air Force, Farnborough (England). Inst. of Aviation Medicine.
THERMAL STRAIN GENERATED BY AN ENHANCED ANTI-G PROTECTION SYSTEM IN A HOT CLIMATE
P. J. Sowood and E. M. OConnor *In* AGARD, The Support of Air Operations under Extreme Hot and Cold Weather Conditions Oct. 1993 13 p (For primary document see N94-28420 08-51)
Copyright Avail: CASI HC A03/MF A03

N94-28446# Royal Air Force, Farnborough (England). Inst. of Aviation Medicine.
IMPLICATIONS OF CLIMATIC EXTREMES IN AIRCREW NBC OPERATIONS
A. J. F. Macmillan *In* AGARD, The Support of Air Operations under Extreme Hot and Cold Weather Conditions Oct. 1993 6 p (For primary document see N94-28420 08-51)
Copyright Avail: CASI HC A02/MF A03

N94-28447# Army Research Inst. of Environmental Medicine, Natick, MA. Military Performance and Neuroscience Div.
THE ENVIRONMENTAL SYMPTOMS QUESTIONNAIRE: ASSESSING REACTIONS TO ENVIRONMENTAL EXTREMES IN MILITARY OPERATIONS
John L. Kobrick, James B. Sampson, and Richard F. Johnson *In* AGARD, The Support of Air Operations under Extreme Hot and Cold Weather Conditions Oct. 1993 8 p (For primary document see N94-28420 08-51)
Copyright Avail: CASI HC A02/MF A03

N94-28451# Exotemp Systems, Inc., Stittsville (Ontario).
RECENT CANADIAN ADVANCES IN ACTIVE THERMAL PROTECTION
P. A. Browne *In* AGARD, The Support of Air Operations under Extreme Hot and Cold Weather Conditions Oct. 1993 9 p (For primary document see N94-28420 08-51)
Copyright Avail: CASI HC A02/MF A03

N94-28452# Institute of Aviation Medicine, Manching (Germany).
TEST OF A NEW PROTECTION SUIT IN A CLIMATIC CHAMBER
H. Pongratz, M. Harre, B. Karmann, A. Rieck, and H. Vaic *In* AGARD, The Support of Air Operations under Extreme Hot and Cold Weather Conditions Oct. 1993 4 p (For primary document see N94-28420 08-51)
Copyright Avail: CASI HC A01/MF A03

N94-28453# Army Aeromedical Research Lab., Fort Rucker, AL.
THE USE OF LIQUID AND AIR MICROCLIMATE CONDITIONING SYSTEMS TO ALLEVIATE HEAT STRESS IN HELICOPTER NBC OPERATIONS
Robert Thornton, J. Lynn Caldwell, and Frank Guardiani *In* AGARD, The Support of Air Operations under Extreme Hot and Cold Weather Conditions Oct. 1993 23 p (For primary document see N94-28420 08-51)
Copyright Avail: CASI HC A03/MF A03

N94-28498# Kawasaki Heavy Industries Ltd., Tokyo (Japan).
SOME ISSUES ON JAPAN'S SPACE FOOD DEVELOPMENT AND RELATING PRELIMINARY EXPERIMENTAL STUDY [WAGAKUNI NO UCHUSHOKU KAIHATSU NI OKERU KADAI TO KISOTEKI JIKKEN]
Shuji Kanda, Shizuko Yamaguchi, Chiharu Sekiguchi, Sei Yumikura, Makoto Doi, Masao Ito, Akira Miyamoto, and Kazuyoshi Yajima *In* Japan Society of Aerospace and Environmental Medicine, Japanese Journal of Aerospace and Environmental Medicine, Vol. 30, No. 3 1 Sep. 1993 p 127-133 In JAPANESE See also A94-12180 (For primary document see N94-28495 08-52)
Avail: CASI HC A02/MF A01

N94-29710# Diamond Air Service, Inc. (Japan).
MICROGRAVITY BY PARABOLIC FLIGHT WITH MU-300 AIRCRAFT [MU-300 BIJINESU JETTOKI NI YORU MAIKURO G FURAITO]
Mitsuo Sato *In* Society of Medical Research for Space Station, The MERSS 5th Symposium on Space Medicine: Medical and Physiological Experiment Utilizing Parabolic Flight Mar. 1993 p 1-8 In JAPANESE (For primary document see N94-29709 08-52)
Avail: CASI HC A02/MF A01

N94-30304 Alberta Research Council, Edmonton. Dept. of Advanced Computing and Engineering.
ASPECTS OF THE OPERATOR INTERFACE FOR MILITARY ROBOTIC APPLICATIONS IN UNSTRUCTURED ENVIRONMENTS
P. Feighan, P. Wojcik, and K. Chrystall *In* Defence Research Establishment Suffield, Proceedings of the 3rd Conference on Military Robotic Applications 1991 p 220-226 (For primary document see N94-30275 08-37)
Avail: Issuing Activity (Defence Research Establishment Suffield, P.O. Box 4000, Medicine Hat, AB T1A 8K6 Canada)

55 SPACE BIOLOGY

Includes exobiology; planetary biology; and extraterrestrial life.

No abstracts in this category.

59 MATHEMATICAL AND COMPUTER SCIENCES (GENERAL)

No abstracts in this category.

60 COMPUTER OPERATIONS AND HARDWARE

Includes hardware for computer graphics, firmware, and data processing.

For components see *33 Electronics and Electrical Engineering.*

N94-28505# Lawrence Livermore National Lab., CA.
THE HIGH PERFORMANCE STORAGE SYSTEM
R. A. Coyne (IBM Federal Systems Div., Houston, TX.), H. Hulen (IBM Federal Systems Div., Houston, TX.), and R. Watson Sep. 1993 12 p Presented at the Supercomputing Conference on High Performance Computing and Communications, Portland, OR, 15-19 Nov. 1993 Revised
(Contract W-7405-eng-48)
(DE94-004350; UCRL-JC-115318-Rev-1; CONF-931115-13-Rev-1) Avail: CASI HC A03/MF A01

The National Storage Laboratory (NSL) was organized to develop, demonstrate, and commercialize technology for the storage systems that will be the future repositories for our national information assets. Within the NSL, four Department of Energy laboratories and the IBM Federal Systems Company, have pooled their resources to develop an entirely new High Performance Storage System (HPSS). The HPSS project concentrates on scalable parallel storage systems for highly parallel computers as well as traditional supercomputers and workstation clusters. Concentrating on meeting the high end of storage system and data management requirements, HPSS is designed using network-connected storage devices to transfer data at rates of 100 million bytes per second and beyond and to handle storage capacities measured in petabytes. The resulting products will be portable to many vendor's platforms. The three year project is targeted to be complete in 1995. This paper provides an overview of the requirements, design issues, and architecture of HPSS, as well as a description of the distributed, multi-organization, industry and national laboratory HPSS project. DOE

N94-28517# Ames Lab., IA.
PERFORMANCE ANALYSIS OF MEMORY HIERACHIES IN HIGH PERFORMANCE SYSTEMS Ph.D. Thesis
A. Yogesh Jul. 1993 53 p
(Contract W-7405-eng-82)
(DE94-005549; IS-T-1673) Avail: CASI HC A04/MF A01

This thesis studies memory bandwidth as a performance predictor of programs. The focus of this work is on computationally intensive programs. These programs are the most likely to access large amounts of data, stressing the memory system. Computationally intensive programs are also likely to use highly optimizing compilers to produce the fastest executables possible. Methods to reduce the amount of data traffic by increasing the average number of references to each item while it resides in the cache

are explored. Increasing the average number of references to each cache item reduces the number of memory requests. Chapter 2 describes the DLX architecture. This is the architecture on which all the experiments were performed. Chapter 3 studies memory moves as a performance predictor for a group of application programs. Chapter 4 introduces a model to study the performance of programs in the presence of memory hierarchies. Chapter 5 explores some compiler optimizations that can help increase the references to each item while it resides in the cache. DOE

N94-28533 Software Kinetics Ltd., Stittsville (Ontario).
DATA FUSION AND CORRELATION TECHNIQUES TESTBED DEVELOPMENT. PHASE 1: INTERIM REPORT
28 Sep. 1990 37 p Submitted for publication
(SKD-1600-73-015; DSIS-94-00233; CTN-94-61128) Avail: CASI HC A03/MF A01

The Data Fusion and Correlation Testbed (DFACT) prototype system was conceived to provide a prototype platform for design, development, and implementation of software architectures and communications sensor information analysis and correlation algorithms suitable for a multiprocessor computer system. Achievements and lessons learned from the first phase of DFACT prototype development are summarized. The first phase involves development of a baseline system that will provide a demonstration platform to enable potential users of the system to evaluate it and provide feedback for further development. Four areas of investigation are reviewed: the intercept operator workstation, the analyst workstation, the data simulator, and system integration. In addition, results of the audio processing study performed for this phase is included, as well as a discussion of issues pertinent to the development environment. Author (CISTI)

N94-28764# California Univ., Berkeley.
CONSTRUCTION OF A CONNECTIONIST NETWORK SUPERCOMPUTER Technical Progress Report, 1 Nov. 1993 - 1 Feb. 1994
1 Feb. 1994 4 p
(Contract N00014-92-J-1617)
(AD-A275765) Avail: CASI HC A01/MF A01

Significant efforts continue in the VLSI implementations of the first Torrent processor, TO, and CNS-1 network interface chip, Hydrant. Several novel board level technologies for the CNS-1 have been verified. We have made progress in the development of support software for the Torrent processor. Work continued in CNS-1 performance evaluation and architecture refinement. We have worked on adapting speech algorithms for the CNS-1, and we have reached a significant milestone in the use of analog preprocessors for speech recognition. DTIC

N94-28798 California Univ., San Diego, La Jolla.
DESIGN AND PACKAGING OF FAULT TOLERANT OPTOELECTRONIC MULTIPROCESSOR COMPUTING SYSTEM Annual Progress Report, 15 Dec. 1992 - 14 Dec. 1993
Sing H. Lee 14 Dec. 1993 27 p Limited Reproducibility: More than 20% of this document may be affected by microfiche quality
(Contract N00014-91-J-1988)
(AD-A275896) Avail: CASI HC A03

There is considerable interest in developing optical interconnects for multi-chip modules (MCM). As a consequence, there is the basic need to develop a methodology for partitioning the system for effective utilization of the optical and electronic technologies. For the given system design, the key question to be answered is concerned with where to use optical interconnections. This paper introduces the Computer Aided Design (CAD) approach for partitioning opto-electronic systems into Opto-Electronic Multichip Modules (OE MCM). We will first discuss the design tradeoff issues in optoelectronic system design including speed, power dissipation, area, and diffraction limits for free space optics. We will then define a formulation for OE MCM partitioning and describe new algorithms for optimizing this partitioning based on the minimization of the power dissipation. The models for the algorithms are discussed in detail and an example of a multistage interconnect network is given. Different results, with the number and size of chips being variable, are presented where improvement for the system packaging has been observed when the partitioning algorithms are applied. DTIC

N94-28845*# Jet Propulsion Lab., California Inst. of Tech., Pasadena.
NSC 800, 8-BIT CMOS MICROPROCESSOR
S. F. Suszko Mar. 1984 98 p
(NASA-CR-195736; NAS 1.26:195736; JPL-D-1272) Avail: CASI HC A05/MF A02

The NSC 800 is an 8-bit CMOS microprocessor manufactured by National Semiconductor Corp., Santa Clara, California. The 8-bit microprocessor chip with 40-pad pin-terminals has eight address buffers (A8-A15), eight data address – I/O buffers (AD(sub 0)-AD(sub 7)), six interrupt controls and sixteen timing controls with a chip clock generator and an 8-bit dynamic RAM refresh circuit. The 22 internal registers have the capability of addressing 64K bytes of memory and 256 I/O devices. The chip is fabricated on N-type (100) silicon using self-aligned polysilicon gates and local oxidation process technology. The chip interconnect consists of four levels: Aluminum, Polysi 2, Polysi 1, and P(+) and N(+) diffusions. The four levels, except for contact interface, are isolated by interlevel oxide. The chip is packaged in a 40-pin dual-in-line (DIP), side brazed, hermetically sealed, ceramic package with a metal lid. The operating voltage for the device is 5 V. It is available in three operating temperature ranges: 0 to +70 C, -40 to +85 C, and -55 to +125 C. Two devices were submitted for product evaluation by F. Stott, MTS, JPL Microprocessor Specialist. The devices were pencil-marked and photographed for identification. Derived from text

N94-28916 Carnegie-Mellon Univ., Pittsburgh, PA. School of Computer Science.
BASIC RESEARCH IN COMPUTER SCIENCE Final Report, 1 Aug. 1990 - 2 Aug. 1993
S. Shafer, R. Bryant, J. Wing, B. Myers, and J. Reynolds Oct. 1993 150 p Limited Reproducibility: More than 20% of this document may be affected by microfiche quality
(Contract F33615-90-C-1465)
(AD-A275222; WL-TR-93-1142) Avail: Issuing Activity (Defense Technical Information Center (DTIC))

This report documents a broad program of basic and applied information processing research conducted by Carnegie Mellon's School of Computer Science. The Information Processing Technology Office of the Advanced Projects Agency (ARPA) supported this work during the period 1 Aug. 1990 through 2 Aug. 1993. Chapters 1 through 6 present in detail the six major research areas: Image Understanding, VLSI, Object Management, Integrated Architectures for Intelligent Systems, Creating Graphical Applications, and Types in Programming. Each chapter briefly describes the significant results of one research area and provides references for more detailed descriptions in the published literature. DTIC

N94-29110 Rutherford Appleton Lab., Chilton (England).
INVARIANTS, FRAMES AND POSTCONDITIONS: A COMPARISON OF TWO FORMAL SPECIFICATION NOTATIONS
J. Bicarregui and B. Ritchie Dec. 1993 31 p
(PB94-138153; RAL-93-100) Avail: Issuing Activity (National Technical Information Service (NTIS))

VDM and B are two 'model-oriented' formal methods. Each gives a notation for the specification of systems as state machines in terms of a set of states with operations defined as relations on that set. Each has a notion of refinement of data and operations based on the principles of reduction of non-determinism and increase in definedness. This paper makes a comparison of the two notations through an example of a communications protocol previously formalized. Two abstractions and two reifications of the original specification are given. Particular attention is paid to three areas where the notations differ: to the use of postconditions that assume the invariant as opposed to postconditions that enforce it; to the explicit 'framing' of operations as opposed to the 'minimal frame' approach; and to the use of relational postconditions as opposed to generalized substitutions. NTIS

N94-29181# Carnegie-Mellon Univ., Pittsburgh, PA. Dept. of Computer Science.
BASIC RESEARCH IN COMPUTER SCIENCE Final Report, 1990 - 1993
Dale A. James and C. R. Taylor 22 Dec. 1993 147 p
(Contract F33615-90-C-1465; ARPA Order 7597)
(AD-A275184; CMU-CS-93-229) Avail: CASI HC A07/MF A02

This report documents a broad program of basic and applied information processing research conducted by Carnegie Mellon's School of Computer Science. The Information Processing Technology Office of the Advanced Research Projects Agency (ARPA) supported this work during the period 1

August 1990 - 2 August 1993. Chapters 1 through 6 present in detail the six major research areas: image understanding, VLSI, object management, integrated architectures for intelligent systems, creating graphical applications, and types in programming. Each chapter briefly describes the significant results of one research area and provides references for more detailed descriptions in the published literature. DTIC

N94-29375*# National Aeronautics and Space Administration. Ames Research Center, Moffett Field, CA.
IMAGE-ADAPTED VISUALLY WEIGHTED QUANTIZATION MATRICES FOR DIGITAL IMAGE COMPRESSION Patent Application
Andrew B. Watson, inventor (to NASA) 25 Jan. 1994 28 p
(NASA-Case-ARC-12015-1; NAS 1.71:ARC-12015-1;
US-Patent-Appl-SN-186366) Avail: CASI HC A03/MF A01

A method for performing image compression that eliminates redundant and invisible image components is presented. The image compression uses a Discrete Cosine Transform (DCT) and each DCT coefficient yielded by the transform is quantized by an entry in a quantization matrix which determines the perceived image quality and the bit rate of the image being compressed. The present invention adapts or customizes the quantization matrix to the image being compressed. The quantization matrix comprises visual masking by luminance and contrast techniques and by an error pooling technique all resulting in a minimum perceptual error for any given bit rate, or minimum bit rate for a given perceptual error. NASA

N94-29695*# Illinois Univ., Urbana-Champaign. Coordinated Science Lab.
A STUDY OF THE RELATIONSHIP BETWEEN THE PERFORMANCE AND DEPENDABILITY OF A FAULT-TOLERANT COMPUTER
Kumar K. Goswami Feb. 1994 42 p
(Contracts NAG1-613; N00014-91-J-1116; CSC-468969)
(NASA-CR-195758; NAS 1.26:195758; UILU-ENG-94-2205; CRHC-94-04)
Avail: CASI HC A03/MF A01

This thesis studies the relationship by creating a tool (FTAPE) that integrates a high stress workload generator with fault injection and by using the tool to evaluate system performance under error conditions. The workloads are comprised of processes which are formed from atomic components that represent CPU, memory, and I/O activity. The fault injector is software-implemented and is capable of injecting any memory addressable location, including special registers and caches. This tool has been used to study a Tandem Integrity S2 Computer. Workloads with varying numbers of processes and varying compositions of CPU, memory, and I/O activity are first characterized in terms of performance. Then faults are injected into these workloads. The results show that as the number of concurrent processes increases, the mean fault latency initially increases due to increased contention for the CPU. However, for even higher numbers of processes (less than 3 processes), the mean latency decreases because long latency faults are paged out before they can be activated. Author

N94-30004# Ames Lab., IA.
RECENT RESULTS FROM TESTING FAST ADCs
W. T. Meyer, H. B. Crawley, R. L. McKay, E. I. Rosenberg, and W. D. Thomas 1993 8 p Presented at the Electronics for Future Colliders, Chestnut Ridge, NY, 4-5 May 1993
(Contract W-7405-eng-82)
(DE94-005565; IS-M-752; CONF-9305276-2) Avail: CASI HC A02/MF A01

We present results of tests of 8, 10, and 12 bit ADC's that operates in the range of 10 to 120 megasamples per second (MSPS). Tests include measurements of differential non-linearity, integral non-linearity, the effective number of bits, and the word error rate. Because the tests are performed on all devices with the same signal sources and the same software, direct comparisons between devices can be made. We also present results from testing a radiation hardened ADC at ionizing radiation exposures up to 81 MRad. DOE

N94-30008# Sandia National Labs., Albuquerque, NM.
POLYNOMIAL MODELING OF ANALOG-TO-DIGITAL CONVERTERS
O. M. Solomon, Jr. 1994 10 p Presented at the 1994 Measurement Science Conference, Pasadena, CA, 27-28 Jan. 1994
(Contract DE-AC04-76DP-00789)
(DE94-005579; SAND-94-0011C; CONF-940151-1) Avail: CASI HC A02/MF A01

Analog-to-digital converters are frequently modeled as a linear polynomial plus a random process. The parameters of the linear polynomial are the familiar gain and offset of the analog-to-digital converter. The output of the random process is uniformly distributed on plus or minus the least significant bit of the analog-to-digital converter. In this paper, the transfer function of an analog-to-digital converter is modeled as a nonlinear polynomial plus a random process. This model can explain the generation of harmonics by the analog-to-digital converter, but the simpler linear model cannot. The parameters of the nonlinear polynomial are estimated from the response to the analog-to-digital converter to a sine wave. The model parameters are used to estimate the nonlinear part of the transfer function of the analog-to-digital converter. DOE

N94-30074 Joint Inst. for Nuclear Research, Dubna (USSR). Lab. of Neutron Physics.
DIGITAL FILTER
V. A. Ermakov and Kim Hyong Do 1992 8 p Limited Reproducibility: More than 20% of this document may be affected by microfiche quality
(DE94-607902; JINR-R-13-92-112) Avail: CASI HC A02 (US Sales Only)

A device which was designed to reduce unimportant information being recorded on carriers during a multiparameter experiment is discussed. The device was also developed to enable a computer to form one- and two-dimensional spectra for the control of real time experiments at high information flows. DOE

N94-30081 Joint Inst. for Nuclear Research, Dubna (USSR). Lab. of Computing Techniques and Automation.
PAW USING UNDER MS DOS
O. G. Smirnova, T. A. Strizh, and V. Eh. Fajn 1992 38 p Limited Reproducibility: More than 20% of this document may be affected by microfiche quality
(DE94-608012; JINR-R-11-92-416) Avail: Issuing Activity (Department of Energy (DOE)) (US Sales Only)

The Physics Analysis Workstation (PAW) and the special features of its MS DOS implementation are presented. To show the PAW system facilities, some examples are performed. This is an addition to the original CERN PAW User Guide. DOE

N94-30727 Utrecht State Univ. (Netherlands). Dept. of Computer Science.
DYNAMIC MICROSETS FOR RAMs
J. A. LaPoutre Jul. 1993 13 p Sponsored in part by Royal Netherlands Academy of Arts and Sciences Limited Reproducibility: More than 20% of this document may be affected by microfiche quality
(Contract EC-7141) (ISSN 0924-3275)
(RUU-CS-93-22; ETN-94-95659) Avail: CASI HC A03

A generalization of the concept of Gabow and Tarjan's microsets to dynamic microsets is presented. The dynamic microsets allow the use of direct addressing in a RAM (Random Access Machine) for incremental problems that can be partitioned into subproblems which are merged from time to time. A sequence of operations on dynamic microsets can be performed in O(n + m.alpha(m, n)) time, where n is the size of the problem and m is the number of queries. ESA

61 COMPUTER PROGRAMMING AND SOFTWARE

Includes computer programs, routines, alogorithms, and specific applications, e.g., CAD/CAM.

N94-28401# Technical Research Centre of Finland, Espoo. Lab. for Information Processing.
WORK-ORIENTED DEVELOPMENT OF INTERACTIVE SOFTWARE TOOLS: UNDERSTANDING THE WORK OF SOFTWARE MAINTAINERS AND MAKING AN INTERACTIVE SOFTWARE TOOL FOR THEM Thesis
Risto Suitiala 1993 186 p

(ISSN 1235-0621)
(PB94-132032; VTT/PUB-139; ISBN-951-38-4257-6) Copyright Avail: CASI HC A09/MF A02

Contents: Introduction; A Methodological Review; Development in Work; Theories of Software Development; Software Maintenance as Work; Where is Programming Knowledge: An Empirical Study; The Interactivity of Programming Tools; The Work-Oriented Development Cycle; Conclusions; and Use of the Browser Illustrated. NTIS

N94-28403# Technical Research Centre of Finland, Oulu. Computer Technology Lab.
OBJECT-BASED DESIGN OF EMBEDDED SOFTWARE Thesis
Pekka Pesonen 1993 84 p
(PB94-132073; VTT/PUB-143) Copyright Avail: CASI HC A05/MF A01

This thesis demonstrates how results of object-oriented analysis for embedded software can be mapped into designs using the real-time operating system. The special features of embedded software and the main principles of the object-oriented methods are highlighted. Guidelines for an object-based design method of embedded software are presented. This design method is based on the graphical description of software taking into account the special features of embedded software. The use of the proposed design method is illustrated by some examples. NTIS

N94-28411# Technical Research Centre of Finland, Espoo. Rakennetekniikan Lab.
OBJECT-ORIENTED CAD TOOL IMPLEMENTATIONS FOR THE CONSTRUCTION INDUSTRY [TIETOKONEYHDENNETYN RAKENTAMISEN OLIOPOHJAINEN SOVELLUSKEHITYS]
Karl-Johan Seren, Matti Hannus, Kari Karstila, Markku Kihlman, and Jukka Pellosniemi 1993 97 p In FINNISH
(ISSN 1235-0605)
(PB94-132370; VTT/TIED-1460; ISBN-951-38-4354-8) Copyright Avail: CASI HC A05/MF A02

The objective of the project described in the report - the OOCAD project - was to further refine and develop previous work in the Finnish construction industry concerning computerized methods for describing and designing buildings as product models. The work included the development of a formal generic product model on a conceptual level (the OOCAD model) based on object-oriented concepts and the definition of a neutral data exchange file format (the OXF-format) mapping the model as closely as possible. The model is based on a hierarchical composition of objects with part-of relationships where the data of real world entities, such as buildings, consist of two kinds of objects: types and instances. This dualism was introduced to avoid redundant data: the type objects describe the common data of one or several identical objects, such as shape and material, whereas the instance objects describe occurrence-specific data, such as position. NTIS

N94-28506# California Univ., Berkeley. Lawrence Berkeley Lab. Dept. of Computing Resources.
ANALYTIC RENDERING OF CURVILINEAR VOLUME DATA
Wes Bethel Mar. 1993 11 p
(Contract DE-AC03-76SF-00098)
(DE94-004934; LBL-33808) Avail: CASI HC A03/MF A01

A technique is presented for analytically rendering volume data from curvilinear grids. The method employs analytic techniques for manipulating and rendering curvilinear voxels. A curvilinear voxel is represented using a cubic triparametric solid formulation. The control points defining the cubic triparametric voxel are computed from the original curvilinear grid using the Catmull-Rom formulation, and subsequently rendered using a three dimensional forward difference operator. The primary benefit from using such a representation is the fact the voxel shape and data values are C1-continuous across voxel boundaries. The issue of voxel opacity, both at the subvoxel and supervoxel levels, is investigated. The use of both tricubic representation and rendering, along with the new approach to managing voxel opacity, results in images which are markedly different from those presented in previous work. DOE

N94-28622 Joint Inst. for Nuclear Research, Dubna (USSR).
VARIATIONAL CALCULATION OF THE EIGENPOTENTIAL FOR H(SUP -)-SYSTEM
V. B. Belyaev, O. I. Kartavtsev, and V. I. Kochkin 1992 6 p In RUSSIAN Limited Reproducibility: More than 20% of this document may be affected by microfiche quality
(DE94-606269; JINR-R-4-92-297) Avail: CASI HC A02 (US Sales Only)

The variational approach is applied for the calculation of the eigenfunctions and eigenvalues of the surface function equation which arises in the solution of the two-electron atom problem in hyperspherical variables. The variational ansatz matches with the asynmptotic behaviour at small and large values of the hyperradius. DOE

N94-28633 Carnegie-Mellon Univ., Pittsburgh, PA. Software Engineering Inst.
TECHNOLOGY TRANSITION PUSH. PART 1: A CASE STUDY OF RATE MONOTONIC ANALYSIS Final Report
Priscilla Fowler and Linda Levine Dec. 1993 57 p Limited Reproducibility: More than 20% of this document may be affected by microfiche quality
(Contract F19628-90-C-0003)
(AD-A275616; CMU/SEI-93-TR-29; ESC-TR-93-203) Avail: CASI HC A04

This case study reports on efforts to transform rate monotonic scheduling theory from an academic theory into a practical analytical technique and to transition that technique into routine practice among developers and maintainers of software embedded in real-time systems. DTIC

N94-28639# Carnegie-Mellon Univ., Pittsburgh, PA. Software Engineering Inst.
A CONCEPTUAL FRAMEWORK FOR SOFTWARE TECHNOLOGY TRANSITION Final Report
Priscilla Fowler and Linda Levine Dec. 1993 35 p
(Contract F19628-90-C-0003)
(AD-A275637; CMU/SEI-93-TR-31; ESC-TR-93-317) Avail: CASI HC A03/MF A01

We present a conceptual framework that integrates and describes the intersections of three life cycles of software technology transition: research and development; new product development; and adoption and implementation in organizations. We then apply the framework to the technology transition experiences of the Software Engineering Institute. DTIC

N94-28648# Carnegie-Mellon Univ., Pittsburgh, PA. Software Engineering Inst.
PROCESS GUIDE FOR THE DOMAIN-SPECIFIC SOFTWARE ARCHITECTURES (DSSA) PROCESS LIFE CYCLE Final Report
James W. Armitage Dec. 1993 45 p
(Contract F19628-90-C-0003)
(AD-A275642; CMU/SEI-93-SR-21) Avail: CASI HC A03/MF A01

This document describes the prototype domain-specific software architecture (DSSA) process life cycle developed by GTE as part of the ARPA, formerly DARPA DSSA program. It is a high-level process description and represents a snapshot of the process as it was in the fall of 1992. DTIC

N94-28664# IBM Federal Systems Div., Gaithersburg, MD.
SOFTWARE TECHNOLOGY FOR ADAPTABLE, RELIABLE SYSTEMS (STARS) PROGRAM Final Report
James A. Whittaker, Ara Kouchakdjian, and Richard H. Cobb 31 Jul. 1993 33 p
(Contract F19628-88-D-0032)
(AD-A275675; Rept-05503-004) Avail: CASI HC A03/MF A01

This document presents the final evaluation results gathered from the STARS Technology Transfer Demonstration Project for the U.S. Army. The intent of this demonstration project is to evaluate comparative measures of effectiveness in developing software by using Cleanroom Engineering versus the current software development approaches presently used at Picatinny Arsenal, a DoD software support activity. DTIC

N94-28691# Defense Information Systems Agency, Arlington, VA. Center for Information Management.
SOFTWARE SYSTEMS REENGINEERING PROCESS MODEL, VERSION 1.0
1993 43 p
(AD-A275711) Avail: CASI HC A03/MF A01

The Center for Information Management (CIM) Software Systems

Reengineering Process Model provides guidance for applying software reengineering technology for the development and modernization of automated information systems (AIS's) within the Department of Defense (DoD). The CIM is chartered to support the Director of Defense Information by providing information management technical services to the DoD community. The services are an integral part of the Corporate Information Management program, a DoD-wide effort to streamline business operations and processes which will help improve the design of cost-effective, standard information systems. This paper defines the CIM software reengineering process composed of activities for creating AIS's to support current business needs. The purpose of the CIM Software Systems Reengineering Process Model is to capture the essence of software reengineering as it applies in the DoD Information Management (IM) community. The activities described in the Model compose the software reengineering process, including Define Project (initial project planning), Reverse Engineer, and Forward Engineer. The Model is represented using the IDEFO Activity Modeling technique, the DoD standard for process modeling. DTIC

N94-28760# New Jersey Inst. of Tech., Newark.
THE BOOTSTRAPPED ALGORITHM: A FAST ALGORITHM FOR BLIND SIGNAL SEPARATION Final Report, Apr. 1992 - Jun. 1993
Yeheskel Bar-Ness, Abdulkadir Dinc, Hagit Messer-Yaron, Zoran Siveski, and Raafat Kamel Dec. 1993 157 p
(Contract F30602-88-D-0025)
(AD-A275759; RL-TR-93-236) Avail: CASI HC A08/MF A02

The bootstrapped algorithm was introduced in a previous report, RL-TR-93-24, dated April 1993. The different structures were proposed and shown to be suitable for blind signal separation and interference cancellation. It was demonstrated that the speed of convergence of these algorithms is much faster than other algorithms. Unlike other algorithms, the speed of convergence does not depend on the signals' power ratios and, hence, does not depend on the eigenvalue spread of the input correlation matrix. Further studies of these algorithms are reported in this section, which includes questions related to bandwidth, complexity, and dynamic studies for real-time control. Also reported are studies of spatial separation and direction-of-arrival estimation of wideband signals as well as application of the algorithm for broadband interference cancellation. Some preliminary results on applications to the blind decision feedback equalizer and separation of CDMA signals are also included. DTIC

N94-28784 Rome Lab., Griffiss AFB, NY.
GUIDE TO THE ENVIRONMENTAL-LANGUAGE In-House Report, Jun. - Aug. 1993
Jason Hamshar Dec. 1993 46 p Limited Reproducibility: More than 20% of this document may be affected by microfiche quality
(AF Proj. 5581)
(AD-A275849; RL-TR-93-203) Avail: CASI HC A03

The Environmental-Language (E-L) was designed and developed by Dr. Mike Karr of Software Options Inc., and Harvard University. The software performs most of the functions of a Configuration Management system and an Activity Coordination system. It is constructed on top of the Emacs text editor (Emacs is part of GNU and copyrighted 1985, 1986) using the ELSP programming language embedded in Emacs. Configuration Management is the process which monitors multiple programmers working on a project and provides the capability to document each others work without over-writing others. All changes are tracked and recorded. In lieu of working with files, E-L operates on artifacts, which differ in that they are: In theory, never deleted; Alterations are handled by creating new artifacts; By saving previous versions, the user can rollback in the event of problems; Typed, such as Unix-programs, C-modules, C-source, or Lisp-modules, rather than by extension conventions. Activity Coordination manages activations, which are formalized by transaction graphs. With E-L servers running on multiple hosts, an activity (known as a process) will execute in parallel across these member sites distributed according to each system's utilization and uninhibited by the host's architecture and operating system. DTIC

N94-28790# California Univ., Los Angeles. Dept. of Chemistry and Biochemistry.
POLYANILINE MEMBRANES FOR GAS AND LIQUID SEPARATION Abstract Only
Jeanine A. Conklin, Shu-Chuan Huang, and Richard B. Kaner 7 Feb. 1994 2 p
(Contract N00014-93-1-1307)
(AD-A275851) Avail: CASI HC A01/MF A01

Membrane separation systems have gained attention recently as low cost energy-saving methods of purification. Mixtures are separated based on chemical or physical interactions with the polymer membrane. Current membrane systems are limited by the difficulty involved in predicting polymer morphology prior to synthesis and in modifying of the polymer's morphology after film formation. However, polyaniline membranes can be tailored after film formation through the doping and undoping process. In this report we discuss the utility of polyaniline as liquid and gas separation membranes. Morphological changes to the polyaniline membrane and the effect these changes have on separations are explored. DTIC

N94-28794# Cornell Univ., Ithaca, NY. Dept. of Computer Science.
REASONING ABOUT PROGRAMS BY EXPLOITING THE ENVIRONMENT Interim Report
Limor Fix and Fred B. Schneider 2 Feb. 1994 44 p
(Contract N00014-91-J-1219)
(AD-A275852) Avail: CASI HC A03/MF A01

A method for making aspects of a computational model explicit in the formulas of a programming logic is given. The method is based on a new notion of environment--an environment augments the state transitions defined by a program's atomic actions rather than being interleaved with them. Two simple semantic principles are presented for extending a programming logic in order to reason about executions feasible in various environments. The approach is illustrated (1) discussing a new way to reason in TLA and Hoare-style programming logics about real-time and by (2) deriving the first TLA and Hoare-style proof rules for reasoning about schedulers. DTIC

N94-28818*# Computer Sciences Corp., Hampton, VA. Applied Technology Div.
TRANSFERABLE OUTPUT ASCII DATA (TOAD) EDITOR VERSION 1.0 USER'S GUIDE
Bradford D. Bingel, Anne L. Shea, and Alicia S. Hofler Feb. 1991 145 p
(Contract NAS1-19038; RTOP 505-59-10-03)
(NASA-CR-187507; NAS 1.26:187507) Avail: CASI HC A07/MF A02

The Transferable Output ASCII Data (TOAD) editor is an interactive software tool for manipulating the contents of TOAD files. The TOAD editor is specifically designed to work with tabular data. Selected subsets of data may be displayed to the user's screen, sorted, exchanged, duplicated, removed, replaced, inserted, or transferred to and from external files. It also offers a number of useful features including on-line help, macros, a command history, an 'undo' option, variables, and a full compliment of mathematical functions and conversion factors. Written in ANSI FORTRAN 77 and completely self-contained, the TOAD editor is very portable and has already been installed on SUN, SGI/IRIS, and CONVEX hosts.
Author (revised)

N94-28825*# Old Dominion Univ., Norfolk, VA. Dept. of Electrical and Computer Engineering.
A NEW METHOD FOR RECOGNIZING QUADRIC SURFACES FROM RANGE DATA AND ITS APPLICATION TO TELEROBOTICS AND AUTOMATION, FINAL PHASE Final Report, period ending 28 Feb. 1994
Roland Mielke, Ivan DCunha, and Nicolas Alvertos Mar. 1994 61 p Original contains color illustrations
(Grant NAG1-1223)
(NASA-CR-195733; NAS 1.26:195733) Avail: CASI HC A04/MF A01; 1 functional color page

In the final phase of the proposed research a complete top to down three dimensional object recognition scheme has been proposed. The various three dimensional objects included spheres, cones, cylinders, ellipsoids, paraboloids, and hyperboloids. Utilizing a newly developed blob determination technique, a given range scene with several non-cluttered quadric surfaces is segmented. Next, using the earlier (phase 1) developed alignment scheme, each of the segmented objects are then aligned in a desired coordinate system. For each of the quadric surfaces based upon their intersections with certain pre-determined planes, a set of distinct features (curves) are obtained. A database with entities such as the equations of the planes and angular bounds of these planes has been created for each of the

quadric surfaces. Real range data of spheres, cones, cylinders, and parallelpipeds have been utilized for the recognition process. The developed algorithm gave excellent results for the real data as well as for several sets of simulated range data. Author

N94-28866# Army Topographic Engineering Center, Fort Belvoir, VA.
AN EFFICIENT ALGORITHM FOR 3D CONNECT-THE-DOTS
John Kim Jan. 1994 11 p
(AD-A275431; TEC-R-210) Avail: CASI HC A03/MF A01

This paper proposes an efficient algorithm to solve the problem. In the algorithm, piecewise cubic Bezier curves will have a tangential continuity at the end points of each piece, so that the whole curve is continuous and differentiable everywhere. The curvature around a given point and the shape of the whole curve are controllable with user parameters. This paper analyzes the effects of the user parameters on the whole curve and will discuss the implementation of the algorithm in an efficient way using matrix operations. DTIC

N94-28878# Institute for Defense Analyses, Alexandria, VA.
COMPARING Ada AND FORTRAN LINES OF CODE: SOME EXPERIMENTAL RESULTS Final Report, Apr. - Nov. 1993
Thomas P. Frazier, John W. Bailey, and Melissa L. Young Nov. 1993 46 p
(AD-A275322; AD-E501740; IDA-P-2899; IDA/HQ-93-044552) Avail: CASI HC A03/MF A01

This paper presents the results of an experiment in rewriting four FORTRAN programs in the Ada computer language. We counted and compared the numbers of lines of code in both languages. We found Ada programs to be larger than their functionally equivalent FORTRAN counterparts. However, we observed that the overhead for Ada diminishes as the program size is increased. Our limited data suggested that there may even be a cross-over point beyond which the size of an Ada program is smaller than a functionally equivalent FORTRAN program. DTIC

N94-28895# BRTRC, Inc., Vienna, VA.
BUSINESS PLANNING MODEL USER'S GUIDE
Dec. 1993 17 p
(Contract DAAK70-92-D-0003)
(AD-A274978) Avail: CASI HC A03/MF A01

The Belvoir Business Planning Model (BPM) was developed to provide an efficient means of collecting and analyzing data concerning future revenue projections and spending plans. The overall idea of this model is to balance the estimated costs against the available revenue. This balancing is available at any appropriate level of analysis: at the FOE/function level, at the laboratory/directorate level, and at the center level. In general, the model tries to estimate most nonsalary personnel related expenses, based upon the amount of the government payroll. It uses multiplier factors for such things as travel and transportation costs rather than having the user input these costs specifically. This frees the user from having to estimate them manually and enhances the ability to perform rapid 'what if' analyses. Changes in related expenses due to simple changes in revenue or personnel projections can be quickly recalculated rather than having to completely reevaluate and reenter the other costs. DTIC

N94-28896 Naval Postgraduate School, Monterey, CA. Dept. of Computer Science.
AUTOMATED INTERFACE FOR RETRIEVING REUSABLE SOFTWARE COMPONENTS M.S. Thesis
Scott J. Dolgoff Sep. 1993 410 p Limited Reproducibility: More than 20% of this document may be affected by microfiche quality
(AD-A275004) Avail: CASI HC A18

The Computer Aided Prototyping System (CAPS) software base contains software components described by formal specifications written in the Prototype System Description Language (PSDL). One problem addressed is the development of a retrieval mechanism for extracting components that match user-provided PSDL specifications. Another problem addressed is the integration of a retrieved component into a software prototype. The approach taken was to match specifications by comparing operations and parameter types to include indirect subtype relations. Integrating a selected software base component required generating mappings to account for different operation and parameter orderings and, for generic components, automatic instantiation. The result was a tool which implements automated assistance for finding reusable components in a large software repository. Methods were developed for parameter and operator mapping, parameter type matching, and ensuring instantiation of a generic was possible. Upon receipt of a PSDL specification query, these methods are employed to automate the retrieval of all matching components and the integration of the selected component into the software prototype. This has been fully implemented for operator components and partially implemented for type components. The retrieval mechanism, a potential processing bottleneck, is extremely accurate and reasonably fast. A query on a 1,000 component repository retrieved all 50 possible matches in under three minutes. DTIC

N94-28910# Eagle Technology, Inc., Winter Park, FL.
APPLICATION OF DIGITAL VIDEO TO HYPERMEDIA TRAINING SYSTEMS Final Report, Jan. 1991 - Mar. 1993
Lee Lacy, Richard Braby, De Pass Smith, Mike Slaven, and Kevin Glass Nov. 1993 34 p
(Contract F33615-91-C-0003)
(AD-A274989; Rept-879.01.4; AL/HR-TR-1993-0132) Avail: CASI HC A03/MF A01

A research effort was conducted to analyze the potential for using autoauthoring training hypermedia in teaching students to perform procedures. In this effort, autoauthoring involved automating the creation of training material from a description of a procedure rather than using traditional methods such as flowcharting and programming. The Prototype Animated Training Hypermedia System (PATHS) was the computer program developed to perform this process. Sample applications were produced using PATHS, demonstrating the feasibility of this concept for procedural training. PATHS rapidly generates training hypermedia. A prototype, PATHS, needs further testing and development before it can become an operational system. DTIC

N94-28917# Carnegie-Mellon Univ., Pittsburgh, PA. Management Sciences Research Group.
WEIGHTED AND UNWEIGHTED MAXIMUM CLIQUE ALGORITHMS WITH UPPER BOUNDS FROM FRACTIONAL COLORING
Egon Balas and Jue Xue Apr. 1993 23 p
(Contract N00014-85-K-0198; NSF DDM-92-01340)
(AD-A275328; MSRR-590) Avail: CASI HC A03/MF A01

The linear programming relaxation of the minimum vertex coloring problem, called the fractional coloring problem, is NP-hard. We describe efficient approximation procedures for both the weighted and unweighted versions of the problem. These fractional coloring procedures are then used for generating upper bounds for the (weighted or unweighted) maximum clique problem in the framework of a branch and bound procedure. Extensive computational testing shows that replacing the standard upper bounding procedures based on various integer coloring heuristics with the somewhat more expensive fractional coloring procedure results in improvements of the bound by up to one fourth in the unweighted and up to one fifth in the weighted case, accompanied by a decrease in the size of the search tree by a factor of almost two. DTIC

N94-28920# Case Western Reserve Univ., Cleveland, OH. Dept. of Electrical Engineering and Applied Physics.
INTELLIGENT AUTOMATED PROCESS PLANNING AND CODE GENERATION FOR COMPUTER-CONTROLLED INSPECTION Final Report, Aug. 1991 - Jan. 1993
Steven M. Ruegsegger Jan. 1994 149 p
(Contract F33615-87-C-5250)
(AD-A275346; WL-TR-94-4002) Avail: CASI HC A07/MF A02

Requirements for greater precision and reduced rejection rates demand improved inspection methods that can be provided by implementing increased automation into the process. This thesis discusses the implementation of an automated intelligent inspection planner and its integration into a feature-based concurrent engineering system. The approach utilizes features as the common language of the individual modules that promote ideas of geometry, functionality, and design intent throughout the system by feature translation among the modules. An artificial neural network optimizes the sequence of inspection points based on inspection rule criteria. A collision avoidance algorithm ensures the safety of automated inspection in a computationally efficient manner. The goal of the inspection planner is to output instruction code that will be executed on a computer-controlled

coordinate measurement machine (CMM) to properly, efficiently, and safely measure and evaluate the tolerances of the manufactured product. DTIC

N94-29006# Carnegie-Mellon Univ., Pittsburgh, PA. Dept. of Computer Science.

TINKERTOY(TM) TRANSACTIONS

Nicholas Haines, Darrell Kindred, J. G. Morrisett, Scott M. Nettles, and Jeannette M. Wing Dec. 1993 20 p

(Contract F33615-93-1-1330)

(AD-A275271; CMU-CS-93-202) Avail: CASI HC A03/MF A01

This document describes the design of a transaction facility for a language that supports higher-order functions. We factor transactions into four separable features: persistence, undoability, locking, and threads. Then, relying on function composition, we show how we can put them together again. Our 'Tinkertoy' approach towards building transactions enables us to construct a model of concurrent, nested, multi-threaded transactions, as well as other non-traditional models where not all natures of transactions are present. Key to our approach is the use of higher-order functions to make transactions first-class. Not only do we get clean composability of transactional features, but also we avoid the need to introduce special control and block-structured constructs as done in more traditional transactional systems. We implemented our design in Standard ML of New Jersey. DTIC

N94-29007# Carnegie-Mellon Univ., Pittsburgh, PA. Dept. of Computer Science.

ADVANCED LANGUAGES FOR SYSTEMS SOFTWARE

Robert Harper and Peter Lee Jan. 1994 27 p

(Contract F19628-91-C-0168; ARPA Order 8313)

(AD-A275272; CMU-CS-94-104) Avail: CASI HC A03/MF A01

It has been amply demonstrated in recent years that careful attention to the structure of systems software can lead to greater flexibility, reliability, and ease of implementation, without incurring an undue penalty in performance. It is our contention that advanced programming languages-particularly languages with a mathematically rigorous semantics, and featuring higher-order functions, polymorphic types, first-class continuations, and a useful and powerful module system-are ideally suited to expressing such structure. Indeed, our previous research has shown that the use of an advanced programming language can have a fundamental effect on system design, leading naturally to system architectures that are highly modular, efficient, and allow re-use of code. We are thus working to demonstrate the viability and benefits of advanced languages for programming real-world systems. To achieve this, we have organized our research into the three areas of language design, compiler technology, and systems building. This report describes the current plans for this effort, which we refer to as the Fox project. DTIC

N94-29019# California Univ., Berkeley. Lawrence Berkeley Lab. Energy and Environment Div.

WINDOW 4.0: DOCUMENTATION OF CALCULATION PROCEDURES

E. U. Finlayson, D. K. Arasteh, C. Huizenga, M. D. Rubin, and M. S. Reilly Jul. 1993 45 p

(Contract DE-AC03-76SF-00098)

(DE94-004935; LBL-33943; TA-309) Avail: CASI HC A03/MF A01

WINDOW 4.0 is a publicly available IBM PC compatible computer program developed by the Building Technologies Group at the Lawrence Berkeley Laboratory for calculating the thermal and optical properties necessary for heat transfer analyses of fenestration products. This report explains the calculation methods used in WINDOW 4.0 and is meant as a tool for those interested in understanding the procedures contained in WINDOW 4.0. All the calculations are discussed in the International System of units (SI). WINDOW 4.0 is the latest in a series of programs released by the Lawrence Berkeley Laboratory. The WINDOW program has its roots in a paper detailing a method for calculating heat transfer through windows. WINDOW 4.0 replaces the widely used 3.1 version. Although WINDOW 4.0 is a major revision, many of the algorithms used in WINDOW 4.0 build upon those previously documented. This report documents the calculations that are unchanged from WINDOW 3.1, as well as those calculations that are new to WINDOW 4.0. This report uses the organization of the WINDOW 4.0 program. Results displayed on a WINDOW 4.0 screen are discussed in a section describing that screen. In the conclusion the aspects of the calculation method currently slated for revision are discussed. A glossary of variables used throughout the report is found in Section 11. DOE

N94-29068# Carnegie-Mellon Univ., Pittsburgh, PA. Software Engineering Inst.

REFERENCE MODEL FOR PROJECT SUPPORT ENVIRONMENTS, VERSION 2.0 Final Report

Alan Brown, David Carney, Patricia Oberndorf, and Marvin Zelkowitz Nov. 1993 125 p

(Contract F19628-90-C-0003)

(AD-A275191; CMU/SEI-93-TR-23; ESC-TR-93-199) Avail: CASI HC A06/MF A02

The U.S. Navy has embarked on the next Generation Computer Resources (NGCR) program to fulfill its need for standard computing resources. The program revolves around the selection of interface standards in six areas. The interface standards will be based on existing industry standards with multi-vendor support. The objective is to restructure the Navy's approach to take better advantage of commercial advances and to reduce cost and duplication of computer resources. This document is part of the NGCR program. DTIC

N94-29088# BRTRC, Inc., Vienna, VA.

FINANCIAL RESOURCE REVIEW MODEL USER'S GUIDE

Dec. 1993 44 p

(Contract DAAK70-92-D-0003)

(AD-A274979) Avail: CASI HC A03/MF A01

The Belvoir Financial Resource Review Model (FRRM) was developed to provide an efficient means of assembling data for the zero quarter and quarterly execution year reviews and preparation of presentation graphics. In the zero quarter reviews, management is concerned with the spending plans for the upcoming year. In particular, they are looking at the plan for spending money outside the center (on contracts to industry and transfers to other government agencies), added to the plan for spending money in-house (on salaries and related internal costs). Taken together, these plans should match goals set for spending which have been established by AMC as targets. These goals are heavily front loaded. Since in-house costs tend to be uniform throughout the year, this implies that the external costs should be planned for early in the fiscal year. DTIC

N94-29115# Naval Postgraduate School, Monterey, CA.

A CONCURRENT, OBJECT-BASED IMPLEMENTATION FOR THE TACTICAL LEVEL OF THE RATIONAL BEHAVIOR MODEL M.S. Thesis

Frederick P. Thornton, Jr. Sep. 1993 142 p

(AD-A275024) Avail: CASI HC A07/MF A02

The middle, or Tactical, level of the Rational Behavior Model (RBM) is the essential bridge linking the top and bottom levels of the model together. To insure an autonomous vehicle maintains control and thus exhibits rational behavior during such time-consuming tasks as search, homing, and route replanning, the Tactical level must be able to handle concurrency. Until now, this level has been implemented in only a limited way using an object-oriented language and sequential operations. The objective of this thesis is to construct an implementation model that represents the concurrency inherent in the Tactical level within the framework of the design model already developed. The method for building this implementation is to use the Ada task construct for concurrency to represent the objects of the design model and their communication with each other. This research creates a Tactical level implementation in Ada for the NPS Autonomous Underwater Vehicle (AUV) simulator that successfully executes a mission scenario involving transit, search, task, and return phases and the same mission scenario with route replanning. This work thus provides a foundation for future development of concurrent implementations of this level of RBM. DTIC

N94-29152# Naval Postgraduate School, Monterey, CA.

HYPER-NPSNET: EMBEDDED MULTIMEDIA IN A 3D VIRTUAL WORLD M.S. Thesis

Charles P. Lombardo Sep. 1993 73 p

(AD-A275063) Avail: CASI HC A04/MF A01

As virtual world systems continue to evolve, the need exists to embed multimedia information into the world so users can query objects for additional information while maintaining frame rates greater than 15 frames per second. The need also exists for software tools to aid in the creation of multimedia

documents intended for virtual worlds. This thesis addresses the problems of how to attach/query multimedia information to/from 3D locations in a virtual world and the design of a Graphical User Interface (GUI) to facilitate the creation of multimedia documents. The method chosen is to attach the multimedia information files to fixed 3D locations called Anchors. The anchors can be queried by the user and the multimedia information retrieved. Through the same interface, users can create multimedia documents by creating and/or editing anchor properties. The approach used differs from previous work in that navigation through the virtual world is unconstrained and a variety of information types may be attached to a single anchor. With video running and fully interactive navigation underway, the implementation presented gives rendering performance greater than 15 frames per second for high-end graphics workstations. DTIC

N94-29159 Swedish Inst. for Materials Testing, Boras. Physics and Electrotechnics.

MICROCOMPUTER-BASED PROTECTIVE FUNCTIONS IN INDUSTRIAL PRODUCTION SYSTEMS: ASSESSMENT METHOD

P. Bremer, A. Hallden, and J. Jacobson 1993 67 p Limited Reproducibility: More than 20% of this document may be affected by microfiche quality
(ISSN 0284-5172)
(PB94-137817; SP-RAPP-1993:51; ISBN-91-7848-437-5) Avail: CASI HC A04

An assessment method to verify adequate safety of microprocessor-based protective functions used in industrial production systems is presented. The assessment is divided into seven steps: identification, analysis on system level, functional testing, analysis below system level, testing below system level, environmental stress testing, and testing of user faults. Safety requirements and verification methods for microprocessor-based protective functions are introduced both on system level and below system level. Detailed measures are presented in appendices. They shall be used in addition to the commonly used requirements for safety devices based on conventional electronics without microprocessors. The described assessment method makes it possible to verify adequate safety for a microprocessor-based device to be used in safety critical applications according to the European standards draft prEN954-1 category 4 or 2. NTIS

N94-29180 Naval Undersea Warfare Center, Newport, RI.

PROPAGATION OF EVIDENCE THROUGH FUZZY RULES Final Report

P. R. Kersten 1 Sep. 1993 38 p Limited Reproducibility: More than 20% of this document may be affected by microfiche quality
(AD-A275071; NUWC-NPt-TR-10222) Avail: Issuing Activity (Defense Technical Information Center (DTIC))

Propagation of evidence through fuzzy rules is discussed and illustrated for three different certainty representations. The first certainty representation is single-valued using a real number to represent the certainty for both the premise and the conclusion. This single-valued representation is often found in fuzzy expert system shells. The second certainty representation is interval-valued and is useful in expert system applications. Finally, the third certainty representation is functional-valued and is the most general and the most complex. DTIC

N94-29193 Helsinki Univ. of Technology, Espoo (Finland). Dept. of Computer Science.

EXTdesign. VERSION 1.0: REFERENCE MANUAL

T. Laakko and M. Maentylae 1993 152 p Limited Reproducibility: More than 20% of this document may be affected by microfiche quality
(PB94-136827; TKO-C63) Copyright Avail: Issuing Activity (National Technical Information Service (NTIS))

A feature modeling system which implements a hybrid of feature-based design and feature recognition in a single framework is described. Solid and feature-based modeling operations can be utilized in parallel during the design process of a part. The modeling operations consist of design-by-features type operations and basic solid modeling operations combined with incremental feature recognition. (Copyright (c) 1993 Product Modelling and Realisation Group Helsinki University of Technology.) NTIS

N94-29201 Kutztown State Coll., PA.

Ada, OBJECT-ORIENTED TECHNIQUES, AND CONCURRENCY IN TEACHING DATA STRUCTURES AND FILE MANAGEMENT Final Report, 25 Sep. 1992 - 24 Sep. 1993

Henry G. Gordon 19 Nov. 1993 9 p Limited Reproducibility: More than 20% of this document may be affected by microfiche quality
(Contract DAAL03-92-G-0413)
(AD-A275385; ARO-30995.1-MA) Avail: CASI HC A02

This project examined the use of Ada in teaching Data Structures and File Management. The object-based features of Ada, its packaging mechanism, and its generic capabilities were used to develop reusable packages for a variety of data and file structures. These packages were used in software applications to illustrate software development for already existing code. Developed packages included singly and doubly-linked list; stacks; queues; general binary search trees; AVL-trees; directed, weighted graphs with traversal; random files; B-tree files; B+-tree files; and hash files. DTIC

N94-29202 Naval Surface Warfare Center, Dahlgren, VA.

STATISTICAL MODELING AND ESTIMATION OF RELIABILITY FUNCTIONS FOR SOFTWARE (SMERFS) USER'S GUIDE, REVISION 3 Final Report

William H. Farr and Oliver D. Smith Sep. 1993 177 p Supersedes NAVSWC-TR-84-373 dated Mar. 1991 Limited Reproducibility: More than 20% of this document may be affected by microfiche quality
(AD-A275390; NSWCDD-TR-84-373-Rev-3; NAVSWC-TR-84-373) Avail: CASI HC A09

This is the third in a series of Naval Surface Warfare Center Dahlgren Division (NSWCDD) technical reports concerning software reliability. The first report, 'A Survey of Software Reliability Modeling and Estimation,' NSWC TR 82-171, discusses various approaches advocated for reliability estimation; reviews various models proposed for this estimation process; provides model assumptions, estimates of reliability, and the precision of those estimates; and provides the data required for the models' implementation. Eight software reliability models were selected to form the basis of a library. This library also contains data edit, transformation, general statistics, and Goodness-of-Fit functions. The original Statistical Modeling and Estimation of Reliability Functions for Software (SMERFS) Library was described in the SMERFS Library Access Guide, NSWC TR 84-371. The enhanced library, which now contains 11 models and model applicability analyses, is explained in NSWCDD TR 84-371, Revision 3. The execution of this more powerful library, through the new SMERFS driver, is explained herein. DTIC

N94-29207 Naval Surface Warfare Center, Dahlgren, VA.

STATISTICAL MODELING AND ESTIMATION OF RELIABILITY FUNCTIONS FOR SOFTWARE (SMERFS) LIBRARY ACCESS GUIDE, REVISION 3

William H. Farr and Oliver D. Smith Sep. 1993 146 p Supersedes NAVSWC-TR-84-371-REV-2 dated Mar. 1991 Limited Reproducibility: More than 20% of this document may be affected by microfiche quality
(AD-A275405; NSWCDD/TR-84-371-Rev-3; NAVSWC/TR-84-371-Rev-2)
Avail: CASI HC A07

This is the second in a series of Naval Surface Warfare Center Dahlgren Division (NSWCDD) technical reports concerning software reliability. The first report, 'A Survey of Software Reliability Modeling and Estimation,' NSWC TR 82-171, discusses various approaches advocated for reliability estimation; reviews various models proposed for this estimation process; provides model assumptions, estimates of reliability, and the precision of those estimates; and provides the data required for the models' implementation. Eight software reliability models were selected to form the basis of a library. This library also contains data edit, transformation, general statistics, and Goodness-of-Fit functions. The original Statistical Modeling and Estimation of Reliability Functions for Software (SMERFS) Library was described in the 1985 version of this report. The enhanced library, which now contains 11 models and model applicability analyses, is explained herein. The SMERFS User's Guide, NSWCDD TR 84-373, Revision 3, explains the execution of the new SMERFS driver. DTIC

N94-29214 Pennsylvania Univ., Philadelphia.

NORTH AMERICAN JUMELAGE 'TYPE SYSTEMS' Final Report, 15 Oct. 1992 - 14 Oct. 1993

Andre Scedrov 20 Oct. 1993 30 p Limited Reproducibility: More than 20% of this document may be affected by microfiche quality
(Contract N00014-93-1-0102)
(AD-A275342) Avail: CASI HC A03

The methods of classical denotational semantics provide a number of valuable tools to designers of sequential Algol-like programming languages. In particular, Algol-like languages can be described by recursive domain equations and semantic clauses. It is rather difficult to solve such equations from first principles. Fortunately for language designers, the metatheory of denotational semantics shows that every set of recursive domain equations has a solution. Indeed, the metatheory is so powerful that programming language designers can use the theory naively and be guaranteed that no foundational problems will arise. However, the theory that has been so successful for Algol-like languages is less appropriate for concurrency. The approach to language definition that seems most effective so far is structural operational semantics (SOS). To date, most uses of SOS for language definitions have been ad-hoc. We sketch the outlines of a metatheory of SOS's as used to define concurrent languages, and in particular the discipline of process algebras. DTIC

N94-29287# Georgia Inst. of Tech., Atlanta.
EMPIRICAL STUDIES OF THE VALUE OF ALGORITHM ANIMATION IN ALGORITHM UNDERSTANDING Ph.D. Thesis
Andrea W. Lawrence Aug. 1993 178 p
(AD-A275135) Avail: CASI HC A09/MF A02

A series of studies is presented using algorithm animation to teach computer algorithms. These studies are organized into three components: eliciting students' preferences, developing algorithm animation guidelines, and evaluating the effects of using algorithm animation in the classroom. Many systems for creating computer animations have been designed. These systems reflect the designers' confidence that visual representation is a valuable technique for conveying conceptual knowledge. Little formal experimentation has been carried out to determine whether such animations are beneficial in teaching the algorithms presented. Also, formal guidelines have not been developed for either design or use of these animations. This work addresses both concerns. Student preference for animation does not predict student performance on a post-test to measure learning. Several types of labeling (data, steps, actions) were examined and a variety of effects were found. One of these effects was that a text description of the algorithm increased accuracy on conceptual questions. Also, students are more accurate on a post-test if they are allowed to design their own data sets than if they use experimenter-defined data sets. Finally, use of the animations was evaluated in a classroom-type setting. All students were given a lecture on an algorithm. Adding a laboratory in which the subject controlled the animation and data sets led to more accurate performance than a lecture only or than a lecture with experimenter-preprepared data sets. This work has implications for the design and use of animated algorithms in teaching computer algorithms and for the design of laboratory experiences for beginning computer science courses. DTIC

N94-29315# Advisory Group for Aerospace Research and Development, Neuilly-Sur-Seine (France). Avionics Panel.
AEROSPACE SOFTWARE ENGINEERING FOR ADVANCED SYSTEMS ARCHITECTURES [L'INGENIERIE DES LOGICIELS POUR LES ARCHITECTURES DES SYSTEMES AEROSPATIAUX]
Nov. 1993 333 p In ENGLISH and FRENCH Symposium held in Paris, France, 10-13 May 1993
(AGARD-CP-545; ISBN-92-835-0725-8) Copyright Avail: CASI HC A15/MF A03

During the past decade, many avionics functions which have traditionally been accomplished with analogue hardware technology are now being accomplished by software residing in digital computers. The purpose of this Symposium was to bring together military aerospace software experts from all NATO countries to share the results of their software research and development and virtually every aspect of software was considered with the following representing a partial set of topics: Aerospace Electronics Software Specification, Software Design, Programming Practices and Techniques, Software Validation and Testing, Software Management and Software Environments. For individual titles, see N94-29316 through N94-29349.

N94-29316# Aerospatiale, Toulouse (France).
HOW TO CONTROL THE INCREASE IN THE COMPLEXITY OF CIVIL AIRCRAFT ON-BOARD SYSTEMS **c06**
P. Chanet and V. Cassigneul *In* AGARD, Aerospace Software Engineering for Advanced Systems Architectures Nov. 1993 10 p (For primary document see N94-29315 08-61)
Copyright Avail: CASI HC A02/MF A03

After showing how the complexity of digital systems is doubling about every five years, and evoking the difficulties caused by this evolution, a methodological approach is described called the 'Systems Development Workshop' aiming to gain mastery of this evolution. Among design, production and validation stages, the importance of the design process is emphasized. The most acute problems of system development are generally described, and examples are given of the power and benefits that can be expected from computer design tools. System architecture design and functional specification are expanded somewhat, to show what benefits can be expected from an integrated approach. Through the SAO example, all development stages are evoked. A rough outline of the necessary capacities for a common work environment is drawn. Finally, it is noted that the increasing necessity of international cooperation in civil aviation consolidates the proposed approach. Author

N94-29317# Societe de Fabrication d'Instruments de Mesure, Massy (France). Industries Groupe Avionique.
PERFORMING SPECIFICATIONS FOR COMPLEX SYSTEMS' SOFTWARE [SPECIFICATIONS EXECUTABLES DES LOGICIELS DES SYSTEMES COMPLEXES] **c08**
F. Delhaye and D. Paquot *In* AGARD, Aerospace Software Engineering for Advanced Systems Architectures Nov. 1993 14 p In FRENCH (For primary document see N94-29315 08-61)
Copyright Avail: CASI HC A03/MF A03

The role played by numerical technologies has increased with each generation of flight control systems. Most of the functions of these systems are now assumed by integrated software and to industrialize the production of these software systems is rapidly becoming a necessity. The SFIM Industries have created a system which can successfully address each phase of the life cycle. Helicopter operating is intrinsically complex and any redundancy in the control systems increases this complexity. To create specifications for such systems is difficult but it is critical, as errors in specifications are often detected in the final phases of development, resulting in costly corrections. It is thus necessary to verify the precision and the justification of the specifications as early as possible. Within its Research and Development activities in avionics, SFIM evaluated the specifications' techniques in the cycle of complex systems' development. Several techniques have been studied (structural analysis, synchronized languages, expert systems) and two of them were tested in experiments. These techniques made it possible to create and validate some of the specifications, with varying degrees of success. The positive aspect of these techniques was clearly shown, they are significant elements in the cost management program of complex systems' software. Author

N94-29318# Shape Technical Center, The Hague (Netherlands).
DESIGNING AND MAINTAINING DECISION-MAKING PROCESSES
Andrew Borden *In* AGARD, Aerospace Software Engineering for Advanced Systems Architectures Nov. 1993 6 p (For primary document see N94-29315 08-61)
Copyright Avail: CASI HC A02/MF A03

The design of the optimal strategy for decision making is intractably difficult when information sources (sensors) provide different amounts of information and have different costs associated with their use. This paper describes a sub-optimal design algorithm which can be further simplified if the user specifies some parts of the decision process to be executed at run-time. The design algorithm is provided with diagnostics so that the result can be compared with accuracy and response time requirements, and a learning module which enables new information to be incorporated into the knowledge base. The complexity of this algorithm is compared to that of the optimal design algorithm. Author

N94-29319# Thomson-CSF, Malakoff (France).
EMBEDDED EXPERT SYSTEM: FROM THE MOCK-UP TO THE REAL WORLD
Frederic Cagnache *In* AGARD, Aerospace Software Engineering for

Advanced Systems Architectures Nov. 1993 7 p (For primary document see N94-29315 08-61)
Copyright Avail: CASI HC A02/MF A03

This paper is presenting a methodology for the integration of an expert system in an embedded real time software running the VRTX operating system. We define the 'Expert Unit' concept and its life cycle referring to a real experimentation. The production of operational embedded expert system becomes a reality because of the use of efficient tools and an original methodology for its integration. This paper is showing how software engineering techniques and methods (Life-Cycle definition, identification of generic configuration items) can help an embedded expert system development to be more efficient and controllable than by using the Boehm's spiral model. This Life-Cycle is compatible with military quality standards (GAM T17 and DOD 2167a). Derived from text

N94-29320# Dassault-Breguet Aviation, Saint Cloud (France). Div. des Etudes Avancees.
FLIGHT COMMAND SOFTWARE DEVELOPMENT: RAFALE STUDIES [LE DEVELOPPEMENT DES LOGICIELS DE COMMANDES DE VOL, L'EXPERIENCE RAFALE]
D. Beurrier, F. Vergnol, and Ph. Bourdais *In* AGARD, Aerospace Software Engineering for Advanced Systems Architectures Nov. 1993 13 p In FRENCH (For primary document see N94-29315 08-61)
Copyright Avail: CASI HC A03/MF A03

After the introduction of the RAFALE's Flight Command System (Systeme de Commande de Vol: SCV). DASSAULT Aviation presents its studies on software applications to critical safety systems, with an emphasis on the following: (1) The methodology used in the development. It includes a phase for the formalization of the software specifications, its objective being to improve on the dialogue between two distinct entities: the automaticians on one hand and the computer programmers on the other hand. (2) The key support systems used in this methodology: GISELE: specification tool using a formal language whose testing and automatic prototype potential guarantee a descriptive quality, and VALIRAF: validation tool which automatically compares the results of the system to the models obtained during the studies on specifications. It manages the testing process and evaluates its level of reliability. An assessment of the results and a presentation of future programs of study are also included.
Author (revised)

N94-29321# Alenia Spazio S.p.A., Turin (Italy).
OBJECT VERSUS FUNCTIONAL ORIENTED DESIGN
P. Occelli *In* AGARD, Aerospace Software Engineering for Advanced Systems Architectures Nov. 1993 9 p (For primary document see N94-29315 08-61)
Copyright Avail: CASI HC A02/MF A03

Since the early Eighties the Object Oriented approach to software system development was proposed as a possible solution of the so called 'software crisis'. The claimed benefits were that Object Oriented Design (OOD) had the potential to improve software quality by making possible a direct and natural correspondence between the real world and its model. Many variants of the original approach were proposed and the new trend was spread across the Software Engineering community. The 'traditional' functional oriented methods were suddenly considered out of date and not appropriate to support development of large real time systems. There were, of course, some drawbacks but they were always attributed to method immaturity and poor tool support, two self-solving problems as time passed. Ten years or more have gone since then and OOD methods have been widely adopted for the development of large distributed real time systems. Are the lessons learnt from such projects according to the expectations? Are Functional Oriented methods still able to support software projects of the size required by the Aerospace industry in the years leading to the 2000? This paper proposes a possible answer to these questions comparing the pro and cons of both methods. This comparison will be carried out on issues like transition from requirements to design and to Ada code, traceability from requirements to design, software safety, software maintainability, software testing and relationship with DOD-STD-2167.
Derived from text

N94-29322# Steria Mediterranee, Vitrolles (France).
HIERARCHICAL OBJECT ORIENTED DESIGN (HOOD): POSSIBILITIES, LIMITATIONS, AND CHALLENGES
Patrice M. Micouin and Daniel J. Ubeaud *In* AGARD, Aerospace Software Engineering for Advanced Systems Architectures Nov. 1993 8 p (For primary document see N94-29315 08-61)
Copyright Avail: CASI HC A02/MF A03

The goal of this article is to sketch a first evaluation after almost four year usage of the Hood methodology in the context of Ada real time software systems. For this purpose, it is made up of four parts: First, we will give a brief outline of Hood methodology. Secondly we quickly sketch out four years of Hood usage. Thirdly, we will summarize the main lessons learned throughout this experience. Fourthly, we will outline some directions useful to follow-up in the future. Author

N94-29323# Wright Lab., Wright-Patterson AFB, OH.
OBJECT ORIENTED DESIGN OF THE AUTONOMOUS FIXTAKING MANAGEMENT SYSTEM **c04**
Joseph Diemunsch and John Hancock *In* AGARD, Aerospace Software Engineering for Advanced Systems Architectures Nov. 1993 14 p (For primary document see N94-29315 08-61)
Copyright Avail: CASI HC A03/MF A03

The Air Force Avionics Laboratory has sponsored several efforts to increase the accuracy of aircraft navigation functions while decreasing crew workload through the application of intelligent systems. Two such efforts were the Adaptive Tactical Navigation (ATN) System and the Autonomous Fixtaking Management (AFM) system, which were both awarded to The Analytic Sciences Corporation (TASC). An intelligent system to aid the pilot with navigation functions was developed under the ATN program. This system incorporated real-time knowledge base software to manage the tactical navigation moding, fault tolerance, and pilot aiding to provide a robust navigation prototype for the next generation fighter aircraft. The ATN program highlighted the aircraft weapons officer's heavy workload associated with the location and identification of fixpoints to update and verify the accuracy of the navigation system. With this problem in mind, it was determined that an intelligent system was needed to automatically locate, image, and identify fixpoints and update the navigation solution. The AFM System was developed to prove the feasibility of automated navigation updates using tactical sensors and existing mission data processing systems. Several technologies developed under ATN were incorporated into the AFM system including a proven simulation of the navigation sensors, controllers, and mission planning and management software. Automation of human fix taking activity required integration of several emerging technologies including a real-time data fusion architecture, neural network and heuristic automatic recognition algorithms, and associative memories to retrieve fix points from on-board databases. Integration of these diverse technologies was simplified by the employment of an object-oriented software development approach and real-time control system. Derived from text

N94-29324# National Aerospace Lab., Amsterdam (Netherlands).
THE DEVELOPMENT PROCEDURES AND TOOLS APPLIED FOR THE ATTITUDE CONTROL SOFTWARE OF THE ITALIAN SATELLITE SAX **c18**
G. J. Hameetman and G. J. Dekker *In* AGARD, Aerospace Software Engineering for Advanced Systems Architectures Nov. 1993 8 p (For primary document see N94-29315 08-61)
Copyright Avail: CASI HC A02/MF A03

The Italian satellite (with a large Dutch contribution) SAX is a scientific satellite which has the mission to study roentgen sources. One main requirement for the Attitude and Orbit Control Subsystem (AOCS) is to achieve and maintain a stable pointing accuracy with a limit cycle of less than 90 arcsec during pointings of maximal 28 hours. The main SAX instrument, the Narrow Field Instrument, is highly sensitive to (indirect) radiation coming from the Sun. This sensitivity leads to another main requirement that under no circumstances the safe attitude domain may be left. The paper describes the application software in relation with the overall SAX AOCS subsystem, the CASE tools that have been used during the development, some advantages and disadvantages of the use of these tools, the measures taken to meet the more or less conflicting requirements of reliability and flexibility, and the lessons learned during development. The quality of the approach to the development has proven the (separately executed) hardware/software integration tests. During these tests, a neglectible number of software errors has been detected in the application software. Derived from text

N94-29325# Electronic System G.m.b.H., Munich (Germany). Elektroniksystem-und Logistik.

EXPERIENCES WITH THE HOOD DESIGN METHOD ON AVIONICS SOFTWARE DEVELOPMENT

W. Mala and E. Grandi *In* AGARD, Aerospace Software Engineering for Advanced Systems Architectures Nov. 1993 12 p (For primary document see N94-29315 08-61)

Copyright Avail: CASI HC A03/MF A03

HOOD represents one of the most interesting approaches of the recent years to support an object oriented SW design for large embedded systems written in Ada. This paper reports about experiences gained by the authors in the context of a current large European avionic development project, where the Ada SW design has been performed using HOOD Version 3.0. A simplified example describes the approach taken in the project for SW architectural design. A critical evaluation of the HOOD method follows, where advantages and disadvantages are discussed and some hints are given to overcome some identified weak areas. The paper concludes with the recognition of HOOD as a promising approach and encourages further discussion to remove the weak areas. Derived from text

N94-29326# Aerospatiale Etablissement des Mureaux (France). Espace and Defense.

SOFTWARE ENGINEERING METHODS IN THE HERMES ON-BOARD SOFTWARE

Philippe Lacan and Paolo Colangeli *In* AGARD, Aerospace Software Engineering for Advanced Systems Architectures Nov. 1993 12 p (For primary document see N94-29315 08-61)

Copyright Avail: CASI HC A03/MF A03

The HERMES On-board Software is executed in a complex multi-processor environment composed of two segregated computers pools. It provides all services to control the trajectory and the attitude of the space plane and its configuration. It also provides aids to the On-board Crew and the Ground Facilities in the Mission and Space Vehicle management. Being highly 'Safety Critical', the attitude control functions are foreseen to be supported by a quad-computers pool in hot redundancy, running in parallel and tightly synchronized. To support 'Mission Critical' functions, as mission and vehicle management, a dual-computers pool in cold redundancy is the baseline. This paper describes how the use of HOOD methodology has been experienced in the HERMES On-board Software Mock-Up framework, from now onwards designated for the sake of brevity as MU. In this technical survey of MU, a number of figures characterizing application size, specification and design complexity of the developed software along with a technical balance of the experienced methods are given. Derived from text

N94-29327# Thomson-CSF, Boulogne-Billancourt (France). CNI Div.

REACTIVE SYSTEM SOFTWARE CONCEPT WITH AUTOMATION USING THE LDS LANGUAGE [CONCEPTION LOGICIELLE DE SYSTEME REACTIF AVEC UNE METHODOLOGIE D'AUTOMATES UTILISANT LE LANGAGE LDS]

J. J. Bosc *In* AGARD, Aerospace Software Engineering for Advanced Systems Architectures Nov. 1993 7 p In FRENCH (For primary document see N94-29315 08-61)

Copyright Avail: CASI HC A02/MF A03

The phase of conception of a reactive system is the most important step, as the paths that are chosen will only be validated when the software is integrated with the material and when the real time conditions are tested and verified. Thus, a very strict method has to be adopted, which takes into account the specifics of the problems to be solved. The question is to assess how far the LDS language can be taken and what associated coding techniques can be used. Transl. by FLS

N94-29328# Rome Lab., Griffiss AFB, NY. Knowledge Engineering Branch.

ARTIFICIAL INTELLIGENCE TECHNOLOGY PROGRAM AT ROME LABORATORY **c63**

Robert N. Ruberti and Louis J. Hoebel *In* AGARD, Aerospace Software Engineering for Advanced Systems Architectures Nov. 1993 11 p (For primary document see N94-29315 08-61)

Copyright Avail: CASI HC A03/MF A03

This paper provides an overview of the Artificial Intelligence (AI) Program at Rome Laboratory. The three major thrusts of the program are described. The Knowledge-Based Planning Program seeks to develop the next generation of AI planning and scheduling tools. The engineering of knowledge-based systems focuses on the development and demonstration of technology to support large-scale, real-time systems of knowledge-based components. The knowledge-based software assistant program seeks to develop a new programming paradigm in which the full life-cycle of software activities are machine mediated. Author (revised)

N94-29329# Alenia, Nerviano (Italy).

POTENTIAL SOFTWARE FAILURES METHODOLOGY ANALYSIS

M. Nogarino, D. Coppola, and L. Contrastano *In* AGARD, Aerospace Software Engineering for Advanced Systems Architectures Nov. 1993 7 p (For primary document see N94-29315 08-61)

Copyright Avail: CASI HC A02/MF A03

Nerviano Plant is mainly involved in the development of complex avionic systems, of which software is essential component, often presenting safety critical features. The traditional techniques and methods imposed to support them with additional refinement tools to build the product safety during developing phases are inadequate. The paper describes a methodological approach for the systematic identification and classification of the effects caused by potential software failures. The potential software failures are identified evaluating the effects that would be produced by incorrect outputs on the other software parts and on the external environment. Furthermore, the proposed approach allows us to evaluate the necessity of introducing fault tolerance, recovery and backup procedures, and to define the adequate quantity and typology of testing and quality activities. Derived from text

N94-29330# Rome Lab., Griffiss AFB, NY.

ROME LABORATORY SOFTWARE ENGINEERING TECHNOLOGY PROGRAM

Elizabeth S. Kean *In* AGARD, Aerospace Software Engineering for Advanced Systems Architectures Nov. 1993 7 p (For primary document see N94-29315 08-61)

Copyright Avail: CASI HC A02/MF A03

This paper highlights the technology recently developed or under development in the US Air Force's Rome Laboratory Software Engineering Technology Branch. This program is generic in nature and is focused around the development and support of large, mission critical and embedded software systems, and thus, is very relevant to the development and support of avionics systems. Further, when a technology is programming language sensitive or a demonstration vehicle requires selection of a specific language, the program language selected is always Ada. Finally, this program has four major thrusts. One thrust emphasizes system definition technology and is concerned with development and validation of requirements and specifications. A second thrust explores and builds technology for integrated software and system engineering environments, with emphasis on tools, process support and enforcement, and support to development and acquisition managers. New explorations in this area include certification methodologies and tools for reusable software components, and software fault-tolerance (robustness). A third thrust deals with the specification, prediction, and assessment of software quality. Rome Lab has a framework for dealing with all aspects of software quality that has proven itself in Japan. The newest thrust is on software engineering for high performance computing. This unique program is evaluating and developing generic software methods and tools for using high performance, massively parallel computers in embedded and other mission critical applications.

Derived from text

N94-29331# Wright Lab., Wright-Patterson AFB, OH.

A COMMON Ada RUN-TIME SYSTEM FOR AVIONICS SOFTWARE **c06**

Clive L. Benjamin, Marc J. Pitarys, Eliezer N. Solomon, and Steve Sedrel *In* AGARD, Aerospace Software Engineering for Advanced Systems Architectures Nov. 1993 11 p (For primary document see N94-29315 08-61)

Copyright Avail: CASI HC A03/MF A03

The United States Air Force (USAF) requires the use of the Ada programming language in the development of new weapon system software. Each Ada compilation system uses a Run-Time System (RTS) for executive services such as tasking, memory management, and system initialization. Implementing and using custom RTS services in each software development activity inhibits avionics software reuse and portability. In addition, the USAF must support many Ada compilers over the operational life of the

weapon system. Finally, extensive testing and knowledge is required for each RTS. In 1990 the USAF began defining a Common Ada Run-Time System (CARTS) for real-time avionics applications. A contract was awarded to Westinghouse Electric Corporation (WEC) with subcontracts issued to compiler vendors DDC-I, Inc. and Tartan, Inc. A specification for the CARTS was completed in 1991 and coding of selected CARTS features was undertaken. The specification defined common interfaces between the application software and the RTS, and between the Ada compiler and the RTS. Incremental coding of the CARTS prototype is being done by DDC-I for the MIPS R3000 processor, and by Tartan for the Intel 80960 MC processor. Several prototypes have been developed and tested. This paper covers the significant CARTS features and services offered to avionics software engineers. The paper provides the results of performance testing of the CARTS features. Finally, this paper provides information on the appropriate use of the CARTS by avionics software engineers.

Derived from text

N94-29332# Alsys, Inc., Saint Cloud (France).

Ada RUN TIME SYSTEM CERTIFICATION FOR AVIONICS APPLICATIONS **c06**

Jacques Brygier and Marc Richard-Foy *In* AGARD, Aerospace Software Engineering for Advanced Systems Architectures Nov. 1993 9 p (For primary document see N94-29315 08-61)

Copyright Avail: CASI HC A02/MF A03

The certification procedures apply to a fully developed system including both hardware and software components. The issue is that the equipment supplier must integrate various components coming from separate sources. In particular, the Ada Run Time System is embedded in the equipment like any other application component. This leads to two major requirements: the Ada Run Time System must be a glass box, and unused run-time services must be eliminated from the embedded components. The first requirement comes from the civil aviation procedures DO 178A, and the second is a consequence of the need to proof the system. This can lead to the elimination of some unpredictable or unsafe Ada language features. The criticality of the system consists of three levels: critical, essential, and non-essential. The report ARINC 613 (from the Airlines Electronic Engineering Committee) surveys the Ada language and provides a list of features not to be used in avionics embedded software, at least for the first two levels.

Author (revised)

N94-29333# National Research Council of Canada, Ottawa (Ontario). Software Engineering Lab.

DESIGN OF A THINWIRE REAL-TIME MULTIPROCESSOR OPERATING SYSTEM **c62**

Charles Gauthier *In* AGARD, Aerospace Software Engineering for Advanced Systems Architectures Nov. 1993 11 p (For primary document see N94-29315 08-61)

Copyright Avail: CASI HC A03/MF A03

As more and more capabilities are added to avionics and other real-time or embedded systems, it becomes necessary to increase the processing power of the underlying executors. At any point, technology imposes limits on the available performance of individual processors. Increasing the computing power beyond those limits requires the use of multiple processors. This paper presents an implementation of a multiprocessor multitasking real-time operating system on difficult architectures. The development of applications on this operating system does not require any special software development tools such as special compilers. Furthermore, the applications can be ported to a very wide range of multiprocessor architectures. The principles of operation of the operating system can be applied to the implementation of an Ada runtime environment, if some restrictions are observed.

Author (revised)

N94-29334# Alenia, Torino (Italy).

ON GROUND SYSTEM INTEGRATION AND TESTING: A MODERN APPROACH **c06**

B. DiGiandomenico *In* AGARD, Aerospace Software Engineering for Advanced Systems Architectures Nov. 1993 7 p (For primary document see N94-29315 08-61)

Copyright Avail: CASI HC A02/MF A03

Modern aircraft, military or civil, incorporate the most up-to-date technology from all fields of research and development. There is an increasing tendency to develop digital control systems to replace analog control systems in all areas: engine control, power generation, fuel control, and environmental control. Digital systems are felt to be irreplaceable in avionics, and they are quickly approaching this level in flight control systems. Indeed, digital systems are responsible for the increased sophistication of modern aircraft and for the success of avionics as it now exists. The net result is that, while in the first generation of jet planes there were no onboard computers, modern aircraft may have more than twenty--with single or multiple 32 bit microprocessors, multiple megabytes of RAM, and sophisticated real time operating systems.

Author (revised)

N94-29335# Alenia, Torino (Italy).

SOFTWARE TESTING PRACTICES AND THEIR EVOLUTION FOR THE 1990'S

Patrizia DiCarlo *In* AGARD, Aerospace Software Engineering for Advanced Systems Architectures Nov. 1993 9 p (For primary document see N94-29315 08-61)

Copyright Avail: CASI HC A02/MF A03

The experiences of an aerospace company in solving specific problems associated with the host testing of embedded software is described. Operational applicability and exploitation of off-the-shelf tools, solutions for the management of both process and testing information, and the impact of the possible use of formal methods for the automatic generation of test cases are investigated and assessed from the user's point of view. The driving topics are the analysis of the effects of the assessed solutions on the current working practices together with their transfer to operational divisions.

Author (revised)

N94-29336# Wright Lab., Wright-Patterson AFB, OH. Avionics Logistics Branch.

VALIDATION AND TEST OF COMPLEX WEAPON SYSTEMS **c06**

Mark M. Stephenson *In* AGARD, Aerospace Software Engineering for Advanced Systems Architectures Nov. 1993 12 p (For primary document see N94-29315 08-61)

Copyright Avail: CASI HC A03/MF A03

As avionics software complexity increases, traditional techniques for avionics software validation and testing become time consuming, expensive, and ultimately unworkable. New test issues arise with the development and maintenance of complex 'super federated' systems like that of the B-2 and highly integrated systems like that of the F-22. Upgrades to existing weapon systems that produce a blend of federated and integrated architectures further complicate the problem. This paper discusses the limitations of current approaches, equipment, and software. It defines a next generation of avionics software validation and test procedures, along with the hardware and software components that are required to make the process work. The central goals of the process and components are to reduce development and maintenance costs, to minimize womanpower requirements, to decrease the time required to perform the testing, and to insure the quality of the final product. The process is composed of unit test, component test, configuration item test, subsystem test, integration test, avionics-system test, and weapon-system test. Some of the topics covered are as follows: automated testing of avionics software, real-time monitoring of avionics equipment, nonreal-time and real-time avionics emulation, and real-time simulation. This paper is based upon several years of experience in the following areas: (1) research and development of new technologies to improve the supportability of weapon-system software; and (2) design and implementation of facilities for the development, enhancement, and test of avionics software.

Author (revised)

N94-29337# Wright Lab., Wright-Patterson AFB, OH. Avionics Logistics Branch.

TESTING OPERATIONAL FLIGHT PROGRAMS (OFPs)

Charles P. Satterthwaite *In* AGARD, Aerospace Software Engineering for Advanced Systems Architectures Nov. 1993 10 p (For primary document see N94-29315 08-61)

Copyright Avail: CASI HC A02/MF A03

The ability to accurately test a system is a highly desirable feature in the engineering design process. The ability to model your system's environment and to exercise your system, in that environment, is also highly desirable. Operational Flight Programs are the software programs of avionics embedded computer systems. Not only is it desirable to be able to test and model Operational Flight Programs, it is essential. The consequences of not performing accurate Operational Flight Program testing

can be devastating. Some of these include premature weapons release, erroneous flight instrument displays, and complete system failure. In order to test Operational Flight Programs, there are several things one must know about the Operational Flight Program, its weapons system host, its support environment, and how to generate and perform its test. This paper will address these issues as it develops a strategy to test an Operational Flight Program. Author (revised)

N94-29338# TA Consultancy Services Ltd., Farnham (England).
INTEGRATED FORMAL VERIFICATION AND VALIDATION OF SAFETY CRITICAL SOFTWARE
N. J. Ward *In* AGARD, Aerospace Software Engineering for Advanced Systems Architectures Nov. 1993 11 p (For primary document see N94-29315 08-61)
Copyright Avail: CASI HC A03/MF A03

Embedded software providing the functionality for a flight vehicle self destruct system was judged to be safety critical and required the highest level of assurance in its correctness. In order to achieve this a program of independent verification and validation was initiated which involved the definition of a formal specification of the software combined with static analysis and dynamic testing. The formal specification, written in an Object Oriented form of Z, was used to clarify the requirements and to provide a definition against which the code could be formally verified. A range of static analyses were performed culminating in Compliance analysis which effectively provided a proof of the code against low level mathematical specifications that were refined down from the Z specification. The dynamic test sets were chosen partly from the requirements specification and partly from the static analysis results so that complete path coverage through every module was achieved. The work revealed a number of errors within the code and its specifications, which were corrected. Through its rigor and the identification of errors, the analysis has given a very high degree of confidence in the correctness of the software. Author (revised)

N94-29339# Air Force Systems Command, Wright-Patterson AFB, OH.
A DISCIPLINED APPROACH TO SOFTWARE TEST AND EVALUATION
J. Lea Gordon *In* AGARD, Aerospace Software Engineering for Advanced Systems Architectures Nov. 1993 8 p (For primary document see N94-29315 08-61)
Copyright Avail: CASI HC A02/MF A03

This paper discusses the impact DOD development standards and Integrated Product Teams have had on influencing F-22 cockpit Controls and Displays software test and evaluation. Author

N94-29340# Defence Research Agency, Portland (England). Sonar Signal and Data Processing Div.
THE UNICON APPROACH TO THROUGH-LIFE SUPPORT AND EVOLUTION OF SOFTWARE-INTENSIVE SYSTEMS
Donald Nairn *In* AGARD, Aerospace Software Engineering for Advanced Systems Architectures Nov. 1993 11 p (For primary document see N94-29315 08-61)
Copyright Avail: CASI HC A03/MF A03

A new approach is presented to the through-life support and evolution of software-intensive systems. The new approach involves a sequence of development contractors. The problems addressed have to do with the avoidance of a 'through-life dependency' on any of the development contractors, and of achieving a unified engineering system description without imposing undue restrictions on the use of evolving software methodologies. The UNICON approach is to vest the through-life continuity in a unified engineering description held in a new type of Project Support Database. This scheme now views the development contractors as having a 'jobbing' role. The technical feasibility of this approach was held to depend on achieving a much more complete engineering description--from the Statement of Requirement, through to the mapping of the software onto the hardware (variants)--than any yet available. This led to the development of the UNICON system description language, based on extensions to the familiar ENTITY/RELATION/ATTRIBUTE notation. Details are presented of a reverse engineering experiment. Author (revised)

N94-29341# Electronic System G.m.b.H., Munich (Germany). Elektroniksystem- und Logistik.
A GENERALIZATION OF THE SOFTWARE ENGINEERING MATURITY MODEL
Karl G. Brammer and James H. Brill *In* AGARD, Aerospace Software Engineering for Advanced Systems Architectures Nov. 1993 9 p (For primary document see N94-29315 08-61)
Copyright Avail: CASI HC A02/MF A03

The software process consists of the methods, practices, and tools used to generate a software product. The Software Engineering Institute at Carnegie Mellon University has developed a capability maturity model (CMM) which defines five levels of maturity for the software process. Also included are sets of criteria that allow the specific assessment of actual software engineering maturity in given projects or organizations. In aerospace projects, software engineering very often is coupled with or embedded in systems engineering. It is therefore desirable to know if and how the CMM can be extended to systems engineering. The paper shows that this approach is feasible. After a brief summary of the original capability maturity model, an overview and comparison of software and systems engineering disciplines is provided. Differences between software and systems engineering are highlighted and modifications are proposed to adapt and generalize the CMM accordingly. Finally, the framework for a systems engineering maturity model is presented. This model is intended as a reference scale for systems engineering capability, in a similar way as the CMM applies to the software process. Author (revised)

N94-29342# Alenia Spazio S.p.A., Rome (Italy).
APPLICATION OF INFORMATION MANAGEMENT METHODOLOGIES FOR PROJECT QUALITY IMPROVEMENT IN A CHANGING ENVIRONMENT **c82**
Fabrizio Sandrelli *In* AGARD, Aerospace Software Engineering for Advanced Systems Architectures Nov. 1993 6 p (For primary document see N94-29315 08-61)
Copyright Avail: CASI HC A02/MF A03

In the technologically advanced field of avionics, quality is required both by the market and the engineers. This means that quality is not only a goal to reach new customers, but is a different way of working which aims to reach a higher and more satisfactory working environment. The attention has been focused on the technical information produced during the development of the project and its diffusion through the technical and managerial environment. The goal is to improve the quality of the whole development process where the quality of the final products improves as a consequence. A methodology experienced in the last few years in ALENIA (Pomezia Plant) to plan, achieve, and manage a more flexible and advanced way of working, through the strong involvement of all who contribute to the realization of the product, is described. Attention was focused both on the organizational aspect of the project and the product configuration. These two aspects are self related and result in a correct management of the project. Author (revised)

N94-29343# Naval Air Warfare Center, Warminster, PA. Software and Computer Technology Div.
THE DISCIPLINE OF DEFINING THE SOFTWARE PRODUCT
John K. Bergey *In* AGARD, Aerospace Software Engineering for Advanced Systems Architectures Nov. 1993 13 p (For primary document see N94-29315 08-61)
Copyright Avail: CASI HC A03/MF A03

An initiative was undertaken to establish a de facto project standard for a 'software product' for mission critical computer resources (MCCR). This effort is an outgrowth of a risk reduction approach to improving the MCCR software development and acquisition process based on Deming's quality principles. While defining a 'software product' might appear to be rudimentary, the hypothesis is put forth that the software product itself, which has been inexplicably neglected by the software engineering community, is the key element and focal point for understanding and improving the software development and acquisition process. A model of a 'software product' is described that was developed to promote uniform software product nomenclature, serve as a reference point for software process improvement, provide a basis for developing a more cost-effective software documentation standard, and provide a more rigorous means of specifying software deliverables for MCCR. Other potential benefits of the software product model include providing a convenient and effective means to uniformly baseline diverse software products, establish software configuration management and control, ensure the capture of all software components required for regeneration, provide a natural mechanism for the collection of software product metrics, and facilitate the on-line sharing

and reuse of software programs, documents, and data. The software product model that has been developed is referred to as SPORE, which stands for software product organization and enumeration. SPORE is a graphical, hierarchical model that provides a complete and logical decomposition and description of a software product for MCCR. Author (revised)

N94-29344# British Aerospace Defence Ltd., Preston (England). Military Aircraft Div.

SDE's FOR THE YEAR 2000 AND BEYOND: AN EF PERSPECTIVE

D. J. Goodwin *In* AGARD, Aerospace Software Engineering for Advanced Systems Architectures Nov. 1993 8 p (For primary document see N94-29315 08-61)

Copyright Avail: CASI HC A02/MF A03

The process of selecting a software development environment for the embedded software of a large, complex military aircraft project can be long and costly. The process adopted on the European Fighter Aircraft (EFA) project by British Aerospace (BAe) is described, from the initial research and prototyping exercises performed in the seventies to the demonstration of the technology on the experimental aircraft project and finally leading to the collaboration with the Eurofighter partner companies (EPC's), building on European software experience to specify, procure, and release the EFA software development environment (EFA SDE). Issues arising within the EF forum that could influence the development of SDE's for future military aircraft projects are described. Author (revised)

N94-29345# Centre d'Etudes et de Recherches, Toulouse (France). Dept. d'Etudes et de Recherches en Informatique.

DISTRIBUTED APPLICATIONS AND FAILURE TOLERANCE PROGRAMS USING A RECONFIGURABLE PARALLEL ARCHITECTURE [UN ENVIRONNEMENT DE PROGRAMMATION D'APPLICATIONS DISTRIBUEES ET TOLERANTES AUX PANNES SUR UNE ARCHITECTURE PARALLELE RECONFIGURABLE]

Ch. Fraboul and P. Siron *In* AGARD, Aerospace Software Engineering for Advanced Systems Architectures Nov. 1993 7 p In FRENCH (For primary document see N94-29315 08-61)

Copyright Avail: CASI HC A02/MF A03

The studies conducted within the MODULOR project were centered on the necessary specifications for the creation of a modular parallel machine whose dynamics could be reconfigured. The software tools needed for reconfiguration during the development of parallel applications were also studied. The functional architectural reconfiguration was first considered, in view of automatically adapting the interconnective topology as efficiently as possible for a given application. Adding reconfiguration capabilities to the interconnective systems, in order to ensure a tolerance of the parallel architecture against processing systems failure, was treated in the second part of the study. The studies stress the importance of the complementary reconfiguring systems ('functional' and 'in case of failure') and define the architecture which guarantees the maximum efficiency in real time communications, in spite of the failure of some of the components of the system. Transl. by FLS

N94-29346# Alenia, Torino (Italy).

A COMMON APPROACH FOR AN AEROSPACE SOFTWARE ENVIRONMENT

F. D. Cheratzu *In* AGARD, Aerospace Software Engineering for Advanced Systems Architectures Nov. 1993 6 p (For primary document see N94-29315 08-61)

Copyright Avail: CASI HC A02/MF A03

AIMS is a European industrial research project which focuses on the process for the development and maintenance of embedded computing systems which are an integral part of high technology aerospace products. It is a user driven project which uses a problem oriented approach to solve the difficulties encountered in the production of such systems. The relevance of the proposed solutions to the problems is ensured by involving aerospace engineers, who work on the development and maintenance of embedded systems. This involvement ensures that new technologies, or improved practices, can be rapidly introduced into operational projects. Author (revised)

N94-29347# Defence Research Agency, Farnborough (England). Flight Systems.

A DISTRIBUTED OBJECT-BASED ENVIRONMENT IN Ada

M. J. Corbin, G. F. Butler, P. R. Birkett, and D. F. Crush *In* AGARD, Aerospace Software Engineering for Advanced Systems Architectures Nov. 1993 6 p Sponsored by Ministry of Defence (For primary document see N94-29315 08-61)

Copyright Avail: CASI HC A02/MF A03

An object-based environment for implementing distributed systems is described. This can be used to create worlds of interacting objects, operating over a network of processors. The precise manner of the distribution is transparent to the objects within the environment. A prototype of this environment is being implemented in Ada, augmented by support for object-oriented constructs. This is intended for use in real-time simulations of combat missions and will be known as Multi-sim. Author

N94-29348# International Business Machines Corp., Owego, NY.

DSSA-ADAGE: AN ENVIRONMENT FOR ARCHITECTURE-BASED AVIONICS DEVELOPMENT **c06**

Louis H. Coglianese and Raymond Szymanski *In* AGARD, Aerospace Software Engineering for Advanced Systems Architectures Nov. 1993 8 p Sponsored in part by DARPA (For primary document see N94-29315 08-61)

Copyright Avail: CASI HC A02/MF A03

This paper describes the domain-specific software architectures avionics development application generation environment (DSSA-ADAGE) under development for the United States' Defense Advanced Research Projects Agency (DARPA) and the USAF's Wright Laboratory. It introduces the goals of the project, recent results in the development of a reusable software architecture for integrated avionics, a description of the process used to develop the architecture, and an overview of the ADAGE development environment. The remainder of the paper is devoted to presenting the formal languages that describe the problem, solution, and implementation views of the avionics architecture. Derived from text

N94-29349# Entreprise 2 Software, Saint-Cloud (France).

ENTREPRISE 2: A PCTE INTEGRATED PROJECT SUPPORT ENVIRONMENT

Gerard Olivier *In* AGARD, Aerospace Software Engineering for Advanced Systems Architectures Nov. 1993 9 p (For primary document see N94-29315 08-61)

Copyright Avail: CASI HC A02/MF A03

Entreprise 2 users are in the technical and scientific software industry and include members of software development and maintenance teams at all levels: administrators, project managers, project leaders, those in charge of subprojects or tasks, developers, and maintenance staff. Entreprise 2 is also designed for software tool editors, who need an integrated CASE tools environment in which they can develop and distribute their own tools. Developers of software systems face numerous problems directly related to software development, upkeep, and maintenance. Entreprise 2 provides a solution to these problems, at both organizational and technical levels. Derived from text

N94-29390# Georgia Inst. of Tech., Atlanta.

A CASE-BASED APPROACH TO CREATIVE DESIGN Annual Report, 1 Oct. 1992 - 30 Sep. 1993

Janet L. Kolodner and Ashok Goel 5 Oct. 1993 49 p

(Contract N00014-92-J-1234)

(AD-A275229) Avail: CASI HC A03/MF A01

We are studying and modeling creative design processes. Our goals are two-fold. One is to make intelligent, computer-based design assistants more creative (e.g., able to suggest unusual but useful solutions and to bring up important issues that might not have been considered otherwise). The other is to build computational models that help us understand human creativity. This will have implications for design education and suggest ways of enhancing the creativity of human designers DTIC

N94-29392# Army Research Lab., Aberdeen Proving Ground, MD.

ANIMATION TECHNIQUES IN BRL-CAD Final Report

Lee A. Butler and Christine Murdza Dec. 1993 39 p

(DA Proj. 1L1-62618-AH-80)

(AD-A275232; ARL-TR-313) Avail: CASI HC A03/MF A01

Complex model systems can be difficult to depict using static images. Some phenomena are not apparent when viewed at a single instance in time. Many such things become much clearer, easier to detect and

understand when they can be presented as moving, changing, evolving entities. For this reason, a set of tools have been created to help users generate motion picture sequences of systems modeled with BRL-CAD. Raytracing is a fundamental analysis and rendering technique within BRL-CAD. Most users of BRL-CAD are acquainted with the use of the program 'rt' for creating still images. A relative few understand how to utilize its capabilities for generating animation sequences or 'movies.' This paper introduces some of the tools and techniques available for creating animation sequences with 'rt.' A basic knowledge of BRL-CAD, the geometry editor 'mged' and image creation using 'rt' is assumed. DTIC

N94-29404*# Illinois Univ., Urbana-Champaign. Coordinated Science Lab.

REDUNDANT DISK ARRAYS IN TRANSACTION PROCESSING SYSTEMS Ph.D. Thesis, 1993

Antoine Nagib Mourad 8 Feb. 1994 128 p

(Contract NAG1-613; N00014-91-J-1283)

(NASA-CR-195759; NAS 1.26:195759; UILU-ENG-94-2208; CRHC-94-07)

Avail: CASI HC A07/MF A02

We address various issues dealing with the use of disk arrays in transaction processing environments. We look at the problem of transaction undo recovery and propose a scheme for using the redundancy in disk arrays to support undo recovery. The scheme uses twin page storage for the parity information in the array. It speeds up transaction processing by eliminating the need for undo logging for most transactions. The use of redundant arrays of distributed disks to provide recovery from disasters as well as temporary site failures and disk crashes is also studied. We investigate the problem of assigning the sites of a distributed storage system to redundant arrays in such a way that a cost of maintaining the redundant parity information is minimized. Heuristic algorithms for solving the site partitioning problem are proposed and their performance is evaluated using simulation. We also develop a heuristic for which an upper bound on the deviation from the optimal solution can be established. Author

N94-29418# Aerospatiale, Cannes (France).

AID TO Ada COMPONENT REUSE AT AEROSPATIALE CANNES (FRANCE) [CANNES ADA: AIDE A LA REUTILISATION DE COMPOSANTS ADA A AEROSPATIALE CANNES]

D. DeGabai 1993 8 p In FRENCH

(Rept-932-440-102; ETN-94-95475) Avail: CASI HC A02/MF A01

Software tools designed to improve productivity and reliability of Ada programmed simulation codes are described. The Cannes-Ada software designed to assist users in identifying requirements is summarized. The aim of the study is promoting reuse of existing codes. Code reuse is economically very important. In order to achieve the objectives, the user requirements and their adequate resources must be known. Component evolution in order to adapt the system to new requirements must not affect the existing software. ESA

N94-29434# Carnegie-Mellon Univ., Pittsburgh, PA. Dept. of Computer Science.

CONSTRAINED OBJECTS Ph.D. Thesis

Bruce Horn 28 Nov. 1993 192 p

(Contract F33615-90-C-1465; ARPA Order 7597)

(AD-A275273; CMU-CS-93-154) Avail: CASI HC A09/MF A02

Object-oriented programming has shown to be a suitable paradigm for implementing a wide variety of systems. The concepts of encapsulation and inheritance are powerful and useful features, providing flexibility in an understandable and extensible framework. Most object-oriented programming languages, however, are complicated; in providing these features, they present a bewildering array of mechanisms for describing programs, such as classes, metaclasses, methods, class variables, and various control structures. Even more importantly, object-oriented languages do not provide explicit support for maintaining the consistency of internal object states; it is up to the programmer to code methods that respect an implicit set of consistency requirements for the object as a whole. This thesis presents a new model of programming, called constrained objects, in which algebraic constraints are used as a foundation for object-oriented programming. In this model, objects are encapsulated constraint systems that communicate with each other via a message-passing mechanism. Each object maintains a consistent state under perturbation from messages sent by other objects using a constraint satisfaction process. One object may inherit from another; the set of constraints from the first object is conjoined with the set of constraints from the second, and the subsequent satisfaction of the combined constraints ensures the semantic consistency of the derived object. DTIC

N94-29449 Center for Mathematics and Computer Science, Amsterdam (Netherlands). Dept. of Computer Science/Dept. of Algorithmics and Architecture.

GRAPHICS FOR ABC

Jaap Zwaan (IHBO de Maere, Enschede, Netherlands.) and Rolf Zwart (IHBO de Maere, Enschede, Netherlands.) Dec. 1992 23 p Limited Reproducibility: More than 20% of this document may be affected by microfiche quality

(ISSN 0168-118X)

(CWI-CS-R9255; ETN-94-95537) Copyright Avail: CASI HC A03

Steps towards developing a graphical facility for the programming language ABC are reported. A discussion on which features are to be included as primitives in a graphical extension to the language and the way pictures could be represented is given. Current trends towards an implementation are given. ESA

N94-29479# Aerospatiale, Suresnes (France). Dept. Industrialisation et Productique.

NUMERICAL SIMULATION OF INDUSTRIAL WORKPIECE SUPERPLASTIC FORMING [SIMULATION NUMERIQUE DU FORMAGE SUPERPLASTIQUE DE PIECES INDUSTRIELLES]

Valerie Donal 1993 9 p In FRENCH

(Rept-932-600-102; ETN-94-95481) Avail: CASI HC A02/MF A01

A finite element method based code (SUPFORM3), which was developed for modeling superplastic forming processes, is described. The purpose of the computer code is to provide an improved process control tool for aerospace industries. The mechanical description is based on the model of a membrane under plane stress for a material allowing isotropic strains. The Newton-Raphson calculation and the viscoplastic description law are used. The friction between the workpiece and the tool is taken into account and the pressure cycle is optimized. The simulation is carried out in three steps: data file generation, numerical calculation, and color graphic visualizations. The simulation is performed by using four titanium alloy circular sheets. ESA

N94-29487 Center for Mathematics and Computer Science, Amsterdam (Netherlands). Dept. of Computer Science/Dept. of Algorithmics and Architecture.

THE ABC STRUCTURE EDITOR: STRUCTURE-BASED EDITING FOR THE ABC PROGRAMMING ENVIRONMENT

Lambert G. L. T. Meertens, Steven Pemberton, and Guido vanRossum Dec. 1992 22 p Limited Reproducibility: More than 20% of this document may be affected by microfiche quality

(ISSN 0169-118X)

(CWI-CS-R9256; ETN-94-95538) Copyright Avail: CASI HC A03

ABC is an interactive programming language where both ease of learning and ease of use stood high amongst its principle design aims. The language is embedded in a dedicated environment that includes a structure based editor. To fit in with the design aims, the editor had to be easy to learn, demanding a small command set, and easy to use, demanding a powerful command set and strong support for the user in composing programs, without enforcing a computer science understanding of issues of syntax and the like. Some novel design rules have led to an interesting editor, where the user may enter and edit text either structurally or nonstructurally, without having to use different 'modes'. ESA

N94-29503 Center for Mathematics and Computer Science, Amsterdam (Netherlands). Dept. of Computer Science/Dept. of Software Technology.

ANIMATORS AND ERROR REPORTERS FOR GENERATED PROGRAMMING ENVIRONMENTS

T. B. Dinesh and F. Tip Dec. 1992 100 p Sponsored in part by EEC Limited Reproducibility: More than 20% of this document may be affected by microfiche quality

(ISSN 0169-118X)

(CWI-CS-R9253; ETN-94-95535) Copyright Avail: CASI HC A05

Animators and error reporters for generated programming environments are studied. An 'error reporter' is a tool for indicating the exact position of a type-error in the source text. An 'animator' visualizes program execution;

typically, it highlights the statement that is currently executing. Applications of both tools are mainly to be found in the areas of debugging and tutoring. Instead of explicitly extending language specifications with these facilities, it is claimed that error reporters and animators can be generated from existing specifications for type-checkers and interpreters with little effort; to this end, a simple pattern matching mechanism is used in conjunction with origin tracking, a generic tracing technique. The claim is discussed, and the limitations and deficiencies of origin tracking are investigated. The techniques are illustrated using an example language named CLaX, a Pascal relative. The full specifications of the CLaX syntax, type-checker and interpreter are included. ESA

N94-29678# UniView Systems, Mountain View, CA.
FORMAL SPECIFICATION AND VERIFICATION OF REAL-TIME SEQUENTIAL CONTROL SYSTEMS
Armen Gabrielian 1994 12 p
(Contract N00014-93-C-0100)
(AD-A275776) Avail: CASI HC A03/MF A01

A variety of methods have been employed for specifying the behavior of sequential control systems that, e.g., can be implemented by programmable logic controllers (PLC's). In dealing with real-time issues, timed Petri nets and other popular formalisms provide limited capabilities with respect to both specification and analysis of behavior. At the same time, many of the formal methods that have been reported in the literature are not readily applicable to the area of sequential control. In this paper, we explore the application of a formal method for real-time systems based on hierarchical multi-state (HMS) machines to the specification and verification of sequential control systems. Verification in this context goes beyond simulation and testing by attempting to provide mathematical proofs for correctness of behavior with respect to general safety properties. HMS machines, which were originally introduced in 1988, consist of parallel and hierarchical automata in which multiple states are true and multiple transitions can fire simultaneously. The temporal behavior of an HMS machine is defined in terms of an interval-based temporal logic. Examples of applications of HMS machines to sequential control problems and an overview of verification approaches are presented. DTIC

N94-29680 Helsinki Univ. of Technology, Espoo (Finland). Lab. of Computer and Information Science.
NONLINEAR PCA: ALGORITHMS AND APPLICATIONS
E. Oja and J. Karhumen Sep. 1993 26 p Limited Reproducibility: More than 20% of this document may be affected by microfiche quality
(PB94-137544; ISBN-951-22-1716-3) Avail: CASI HC A03

Many neural approaches have lately been proposed for performing standard PCA (Principal Component Analysis) of the input data. PCA networks provide an optimal solution to some information processing problems, but their generality is limited by the linearity of the input-output mapping. Recently the present authors suggested a class of nonlinear PCA networks for more complex tasks, especially robust PCA, and showed how they are derived from constrained Hebbian learning. This work is reviewed here. Some of these networks have been successfully used for sinusoidal signal detection in colored noise. The algorithms are related to nonlinear statistical optimization criteria, which typically involve a nonlinear expansion of the input vector in terms of the neuron weight vectors. The nonlinearities implicitly take into account higher-order moments in computing the optimal solution. Another variation of the basic neural network is the nonlinear Minor Component Analysis (MCA) network, which can solve a robust least squares problem and can be applied to robust curve and surface fitting with good results. NTIS

N94-29727*# National Aeronautics and Space Administration. Goddard Space Flight Center, Greenbelt, MD.
SOFTWARE MANAGEMENT ENVIRONMENT (SME) CONCEPTS AND ARCHITECTURE, REVISION 1
Robert Hendrick (Computer Sciences Corp., Beltsville, MD.), David Kistler (Computer Sciences Corp., Beltsville, MD.), and Jon Valett Sep. 1992 84 p
(NASA-CR-189293; NAS 1.26:189293; SEL-89-103-Rev-1) Avail: CASI HC A05/MF A01

This document presents the concepts and architecture of the Software Management Environment (SME), developed for the Software Engineering Branch of the Flight Dynamic Division (FDD) of GSFC. The SME provides an integrated set of experience-based management tools that can assist software development managers in managing and planning flight dynamics software development projects. This document provides a high-level description of the types of information required to implement such an automated management tool. Author (revised)

N94-29746# Naval Air Warfare Center, Orlando, FL.
ENGINEERING SPECIFICATION EDITING TOOLS Final Report
John T. Oriel Dec. 1993 64 p
(AD-A275116; NAWCTSD-TR-93-022) Avail: CASI HC A04/MF A01

The techniques described are intended to help writers and reviewers of specifications identify weaknesses in their drafts more quickly, thoroughly, and accurately than in the past. There were two parts to the effort that went into their development. The first involved the 'knowledge-engineering' needed in order to learn more about what makes specifications good or bad, so that the computer might be programmed to flag significant sources of potential error. The second part was experimentation with software techniques for automating the examination process. It was centered around the development of a small-scale natural language parser intended for parsing sentences that are typical in training systems specifications and statements of work. Surprisingly, for such an important subject as it is, relatively little organized knowledge was found about how to write and edit specifications. Most of the material used was borrowed from other fields. DTIC

N94-29797# Software Productivity Consortium, Herndon, VA.
USING RDD-100 WITH CoRE. VERSION 01.00.03 Final Report
Richard A. Kirk and Haywood S. Osborne 19 Jan. 1994 90 p Prepared for Virginia Center of Excellance for Software Software Reuse and Technology Transfer, Herndon
(Contract MDA972-92-J-1018)
(AD-A275336; SPC-93099-CMC) Avail: CASI HC A05/MF A01

This technical report describes how to develop a specification of software requirements using the Software Productivity Consortium's CoRE software requirements method from a system requirements and design specification developed using Ascent Logic Corporation's RDD-100. Specifically, this report describes the transition from system design to software requirements analysis when: (1) RDD-100 has been used to create system requirements and design specifications, or: (2) the software requirements analysis activity is to be performed according to the CoRE method. RDD-100 is the implementation of the Requirements Driven Design (RDD) system design and engineering method, wherein the system design is driven by the customer's expectations of system behavior. CoRE is the Software Productivity Consortium's software requirements engineering method. Created to support the development of precise, testable specifications that are demonstrably complete and consistent. An RDD-100 system model contains all of the information needed to begin building a CoRE software requirements specification. DTIC

N94-29816# Los Alamos National Lab., NM.
PERFORMANCE OF MCNP4A ON SEVEN COMPUTING PLATFORMS
J. S. Hendricks and R. C. Brockhoff 1994 6 p Presented at the 8th International Conference on Radiation Shielding, Arlington, TX, 24-27 Apr. 1994
(Contract W-7405-eng-36)
(DE93-040101; LA-UR-93-2968; CONF-940424-1) Avail: CASI HC A02/MF A01

The performance of seven computer platforms has been evaluated with the MCNP4A Monte Carlo radiation transport code. For the first time, we report timing results using MCNP4A and its new test set and libraries. Comparisons are made on platforms not available to us in previous MCNP timing studies. By using MCNP4A and its 325-problem test set, a widely-used and readily-available physics production code is used; the timing comparison is not limited to a single 'typical' problem, demonstrating the problem dependence of timing results; the results are reproducible at the more than 100 installations around the world using MCNP; comparison of performance of other computer platforms to the ones tested in this study is possible because we present raw data rather than normalized results; and a measure of the increase in performance of computer hardware and software over the past two years is possible. The computer platforms reported are the Cray-YMP 8/64, IBM RS/6000-560, Sun Sparc10, Sun Sparc2, HP/9000-735, 4 processor 100 MHz Silicon Graphics ONYX, and

Gateway 2000 model 4DX2-66V PC. In 1991 a timing study of MCNP4, the predecessor to MCNP4A, was conducted using ENDF/B-V cross-section libraries, which are export protected. The new study is based upon the new MCNP 25-problem test set which utilizes internationally available data. MCNP4A, its test problems and the test data library are available from the Radiation Shielding and Information Center in Oak Ridge, Tennessee, or from the NEA Data Bank in Saclay, France. Anyone with the same workstation and compiler can get the same test problem sets, the same library files, and the same MCNP4A code from RSIC or NEA and replicate our results. And, because we report raw data, comparison of the performance of other compute platforms and compilers can be made. DOE

N94-29844# Sandia National Labs., Albuquerque, NM.
EXTENDING THE X WINDOW SYSTEM
J. P. Brenkosh 23 Dec. 1993 58 p
(Contract DE-AC04-94AL-85000)
(DE94-006496; SAND-93-4100) Avail: CASI HC A04/MF A01

The X Window System was originally developed in 1984 at Massachusetts Institute of Technology. It provides client-server computing functionality and also facilitates the establishment of a distributed computing environment. Since its inception, the X Window System has undergone many enhancements. Despite these enhancements there will always be a functionality desired in the standard released version of X that is not supported or commercially or academically available. The developers of the X Window System have designed it in such a way that it is possible to add functionality that is not included in the standard release. This is called an extension. Extensions are one method used to develop a customized version of the X Window System to support a specialized application. This report presents the mechanics of adding an extension and examines a particular extension that was developed at Sandia National Laboratories to support data compression in X Windows which was one aspect of the Desktop Video and Collaborative Engineering Laboratory Directed Research and Development (LDRD). DOE

N94-29890*# Illinois Univ., Urbana-Champaign. Coordinated Science Lab.
DESIGN FOR DEPENDABILITY: A SIMULATION-BASED APPROACH Ph.D. Thesis, 1993
Kumar K. Goswami 2 Feb. 1994 149 p
(Contract NAG1-613; N00014-91-J-1116)
(NASA-CR-195757; NAS 1.26:195757; UILU-ENG-94-2204; CRHC-94-03)
Copyright Avail: CASI HC A07/MF A02

This research addresses issues in simulation-based system level dependability analysis of fault-tolerant computer systems. The issues and difficulties of providing a general simulation-based approach for system level analysis are discussed and a methodology that address and tackle these issues is presented. The proposed methodology is designed to permit the study of a wide variety of architectures under various fault conditions. It permits detailed functional modeling of architectural features such as sparing policies, repair schemes, routing algorithms as well as other fault-tolerant mechanisms, and it allows the execution of actual application software. One key benefit of this approach is that the behavior of a system under faults does not have to be pre-defined as it is normally done. Instead, a system can be simulated in detail and injected with faults to determine its failure modes. The thesis describes how object-oriented design is used to incorporate this methodology into a general purpose design and fault injection package called DEPEND. A software model is presented that uses abstractions of application programs to study the behavior and effect of software on hardware faults in the early design stage when actual code is not available. Finally, an acceleration technique that combines hierarchical simulation, time acceleration algorithms and hybrid simulation to reduce simulation time is introduced. Author

N94-29906*# Illinois Univ., Urbana-Champaign. Coordinated Science Lab.
SPACE RECLAMATION FOR UNCOORDINATED CHECKPOINTING IN MESSAGE-PASSING SYSTEMS Ph.D. Thesis
Yi-Min Wang 19 Nov. 1993 118 p
(Grant NAG1-613)
(NASA-CR-195761; NAS 1.26:195761; UILU-ENG-93-2251; CRHC-93-24)
Avail: CASI HC A06/MF A02

Checkpointing and rollback recovery are techniques that can provide efficient recovery from transient process failures. In a message-passing system, the rollback of a message sender may cause the rollback of the corresponding receiver, and the system needs to roll back to a consistent set of checkpoints called recovery line. If the processes are allowed to take uncoordinated checkpoints, the above rollback propagation may result in the domino effect which prevents recovery line progression. Traditionally, only obsolete checkpoints before the global recovery line can be discarded, and the necessary and sufficient condition for identifying all garbage checkpoints has remained an open problem. A necessary and sufficient condition for achieving optimal garbage collection is derived and it is proved that the number of useful checkpoints is bounded by $N(N+1)/2$, where N is the number of processes. The approach is based on the maximum-sized antichain model of consistent global checkpoints and the technique of recovery line transformation and decomposition. It is also shown that, for systems requiring message logging to record in-transit messages, the same approach can be used to achieve optimal message log reclamation. As a final topic, a unifying framework is described by considering checkpoint coordination and exploiting piecewise determinism as mechanisms for bounding rollback propagation, and the applicability of the optimal garbage collection algorithm to domino-free recovery protocols is demonstrated.
Author (revised)

N94-29945*# Loral Space Information Systems, Houston, TX.
ANALYSIS OF EDP PERFORMANCE Final Report
4 Apr. 1994 30 p Revised
(Contract NAS2-13758)
(NASA-CR-195726; NAS 1.26:195726) Avail: CASI HC A03/MF A01

The objective of this contract was the investigation of the potential performance gains that would result from an upgrade of the Space Station Freedom (SSF) Data Management System (DMS) Embedded Data Processor (EDP) '386' design with the Intel Pentium (registered trade-mark of Intel Corp.) '586' microprocessor. The Pentium ('586') is the latest member of the industry standard Intel X86 family of CISC (Complex Instruction Set Computer) microprocessors. This contract was scheduled to run in parallel with an internal IBM Federal Systems Company (FSC) Internal Research and Development (IR&D) task that had the goal to generate a baseline flight design for an upgraded EDP using the Pentium. This final report summarizes the activities performed in support of Contract NAS2-13758. Our plan was to baseline performance analyses and measurements on the latest state-of-the-art commercially available Pentium processor, representative of the proposed space station design, and then phase to an IBM capital funded breadboard version of the flight design (if available from IR&D and Space Station work) for additional evaluation of results. Unfortunately, the phase-over to the flight design breadboard did not take place, since the IBM Data Management System (DMS) for the Space Station Freedom was terminated by NASA before the referenced capital funded EDP breadboard could be completed. The baseline performance analyses and measurements, however, were successfully completed, as planned, on the commercial Pentium hardware. The results of those analyses, evaluations, and measurements are presented in this final report.
Derived from text

N94-29949 Selskapet for Industriell og Teknisk Forskning, Trondheim (Norway). Div. for Information Technology.
STRATEGY FOR THE APPROXIMATION OF LARGE SCATTERED DATA SETS
E. Arge, M. Daehlen, and A. Tveito 29 Jun. 1993 20 p See also AD-A129595
(PB94-138518; STF33-A93015) Avail: Issuing Activity (National Technical Information Service (NTIS))

The authors present a three-stage scheme for constructing smooth function approximations to data defined over scattered point sets in R(sup s). The scheme is useful for dealing with huge and irregularly scattered data sets, particularly when the data is subject to some noise. NTIS

N94-30056# Lawrence Livermore National Lab., CA.
PROCEEDINGS: SISAL 1993
J. T. Feo, ed. Oct. 1993 200 p Meeting held in San Diego, CA, 3-5 Oct. 1993
(Contract W-7405-eng-48)
(DE94-006641; CONF-9310206) Avail: CASI HC A09/MF A03

This report contain papers on: programmability and performance issues;

the case of an iterative partial differential equation solver; implementing the kernal of the Australian Region Weather Prediction Model in Sisal; even and quarter-even prime length symmetric FFT's and their Sisal Implementations; top-down thread generation for Sisal; overlapping communications and computations on NUMA architechtures; compiling technique based on dataflow analysis for functional programming language Valid; copy elimination for true multidimensional arrays in Sisal 2.0; increasing parallelism for an optimization that reduces copying in IF2 graphs; caching in on Sisal; cache performance of Sisal Vs. FORTRAN; FFT algorithms on a shared-memory multiprocessor; a parallel implementation of nonnumeric search problems in Sisal; computer vision algorithms in Sisal; compilation of Sisal for a high-performance data driven vector processor; Sisal on distributed memory machines; a virtual shared addressing system for distributed memory Sisal; developing a high-performance FFT algorithm in Sisal for a vector supercomputer; implementation issues for IF2 on a static data-flow architecture; and systematic control of parallelism in array-based data-flow computation. Selected papers have been indexed separately for inclusion in the Energy Science and Technology Database. DOE

N94-30077 Joint Inst. for Nuclear Research, Dubna (USSR).
COMPLICATED PROBLEM SOLUTION TECHNIQUES IN OPTIMAL PARAMETER SEARCHING
V. P. Gergel (Moscow State Univ., Russia.), V. A. Grishagin (Moscow State Univ., Russia.), E. A. Rogatneva (Moscow State Univ., Russia.), R. G. Strongin (Moscow State Univ., Russia.), I. N. Vysotskaya (Moscow State Univ., Russia.), and V. V. Kukhtin 1992 18 p Limited Reproducibility: More than 20% of this document may be affected by microfiche quality
(DE94-608007; JINR-E-11-92-218) Avail: CASI HC A03 (US Sales Only)

An algorithm is presented of a global search for the numerical solution of multidimensional, multiextremal, multicriteria optimization problems with complicated constraints. A boundedness of object characteristic changes is assumed at restricted changes of its parameters (Lipschitz condition). The algorithm was realized as a computer code. The program was used to solve applied optimization problems. DOE

N94-30080 Gosudarstvennyi Komitet po Ispolzovaniyu Atomnoi Energii, Obninsk (USSR).
FAST PRECISE ALGORITHM FOR SIMULATION OF IONIZATION ENERGY LOSSES
S. I. Striganov 1992 6 p Limited Reproducibility: More than 20% of this document may be affected by microfiche quality
(DE94-608010; IHEP-OEIUNK-92-80) Avail: CASI HC A02 (US Sales Only)

Methods of simulating ionization fluctuation are discussed. A new algorithm combining the advantages of the standard approaches is presented. DOE

N94-30083 Joint Inst. for Nuclear Research, Dubna (USSR).
ALGORITHM AND PROGRAM ORANGE FOR MAGNETIC FIELD SIMULATION OF MAGNETIC SYSTEM SPECTROMETER STORS
E. P. Zhidkov, R. S. Egikyan, L. A. Merkulov, Eh. G. Nikonov, A. D. Solovev, and I. P. Yudin 1992 4 p Limited Reproducibility: More than 20% of this document may be affected by microfiche quality
(DE94-608013; JINR-R-11-92-488) Avail: Issuing Activity (Department of Energy (DOE)) (US Sales Only)

Presented is a description of an algorithm and program ORANGE for magnetic field calculation of superconducting air-core toroidal spectrometer STORS. Special attention has been given to field calculation from bends with rectangular cross sections. Gauss-Legander method is very effective choice for calculation of corresponding integrals. Design time of magnetic field has been reduced 8-9 times. Magnetic field calculation has been made with relative accuracy about 3 x 10(sup -4). DOE

N94-30117 Lawrence Livermore National Lab., CA.
GENETIC ALGORITHMS AT UC DAVIS/LLNL
V. R. Vemuri, comp. 1993 74 p Limited Reproducibility: More than 20% of this document may be affected by microfiche quality
(Contract W-7405-eng-48)
(DE94-006625; UCRL-ID-115982) Avail: CASI HC A04

A tutorial introduction to genetic algorithms is given. This brief tutorial should serve the purpose of introducing the subject to the novice. The tutorial is followed by a brief commentary on the term project reports that follow. DOE

N94-30136 British Columbia Univ., Vancouver. Dept. of Mathematics.
COMPUTATIONAL METHODS FOR THE SHAPE SHADING PROBLEM Ph.D. Thesis
Paul M. Carter Jul. 1993 175 p
(ISBN-0-315-85430-8; CTN-94-61157) Copyright Avail: Micromedia Ltd., Technical Information Centre, 240 Catherine Street, Suite 305, Ottawa, Ontario, K2P 2G8, Canada HC/MF

Computational methods for the shape from shading problem as formulated through the image irradiance equation are explored. Three approaches are considered in developing robust, efficient methods and in testing the resulting algorithms on synthetic images. The first revises the method of characteristic strips with more stable integration schemes. Although the effects of noise are reduced, the solution is deemed unsatisfactory. The second approach considers Horn's variational technique as a basis for producing a fast solver. A discretization technique is devised and coupled with a special continuation multigrid method. Given multiple image data, excellent results are obtained even in the presence of discontinuities. The third approach examines a class of solution techniques based on fluid flow. A regularization of the generally ill-posed formulation is proposed and it is observed that the algorithm is prone to producing spurious results due to the non-random accumulation of errors in the computed solution. The variational method yields the most promising results of the three approaches considered. Efficient, good quality reconstructions are obtained, especially when data from more than one image are available. Author (CISTI)

N94-30155# Office of Research Analyses, Ottawa (Ontario).
ADDENDUM TO THE FINAL REPORT FOR THE INVESTIGATION OF PROOF TECHNIQUES WITHIN THE EVES VERIFICATION TECHNOLOGY
Mark Saaltink, Sentot Kromodimoeljo, and Bill Pase Dec. 1993 20 p
(TR-93-5451-03; CTN-94-61139) Copyright Avail: CASI HC A03/MF A01

An addendum is provided to work which investigated and experimented with various approaches for enhancing the capabilities of the theorem prover NEVER and the overall effectiveness of EVES, a software tool for the development of verified software. The addendum discusses two further tasks. The first is an improved understanding of how to use NEVER's forward chaining mechanisms to write complete rulesets, thereby, implementing decision procedures for various kinds of mathematical theories. In particular, based on ongoing work, it will record either a specific means for writing such procedures along with a mathematical justification for the approach, or the difficulties in achieving a general approach. The second task is an attempt to integrate the separate prototype Knuth-Bendix algorithm into EVES. The shortcomings of the present implementation are noted and several possible solutions are enumerated. A simple user interface to the algorithm was successfully completed, having a single command for initialization and execution. Example results are displayed. CISTI

N94-30174*# National Aeronautics and Space Administration. Lewis Research Center, Cleveland, OH.
AN INTERACTIVE, DESIGN AND EDUCATIONAL TOOL FOR SUPERSONIC EXTERNAL-COMPRESSION INLETS
Thomas J. Benson May 1994 15 p Proposed for presentation at the 30th Joint Propulsion Conference, Indianapolis, IN, 27-29 Jun. 1994; sponsored by AIAA, ASME, SAE, and ASEE
(RTOP 505-62-52)
(NASA-TM-106581; E-8841; NAS 1.15:106581) Avail: CASI HC A03/MF A01

A workstation-based interactive design tool called VU-INLET was developed for the inviscid flow in rectangular, supersonic, external-compression inlets. VU-INLET solves for the flow conditions from free stream, through the supersonic compression ramps, across the terminal normal shock region and the subsonic diffuser to the engine face. It calculates the shock locations, the capture streamtube, and the additive drag of the inlet. The inlet geometry can be modified using a graphical user interface and the new flow conditions recalculated interactively. Free stream conditions and engine airflow can also be interactively varied and off-design performance evaluated. Flow results from VU-INLET can be

saved to a file for a permanent record, and a series of help screens make the simulator easy to learn and use. This paper will detail the underlying assumptions of the models and the numerical methods used in the simulator. Author (revised)

N94-30175*# National Aeronautics and Space Administration. Lewis Research Center, Cleveland, OH.
AN INTERACTIVE EDUCATIONAL TOOL FOR COMPRESSIBLE AERODYNAMICS
Thomas J. Benson Apr. 1994 14 p
(RTOP 505-62-52)
(NASA-TM-106568; E-8768; NAS 1.15:106568) Avail: CASI HC A03/MF A01

A workstation-based interactive educational tool was developed to aid in the teaching of undergraduate compressible aerodynamics. The tool solves for the supersonic flow past a wedge using the equations found in NACA 1135. The student varies the geometry or flow conditions through a graphical user interface and the new conditions are calculated immediately. Various graphical formats present the variation of flow results to the student. One such format leads the student to the generation of some of the graphs found in NACA-1135. The tool includes interactive questions and answers to aid in both the use of the tool and to develop an understanding of some of the complexities of compressible aerodynamics. A series of help screens make the simulator easy to learn and use. This paper will detail the numerical methods used in the tool and describe how it can be used and modified. Author (revised)

N94-30197*# Jet Propulsion Lab., California inst. of Tech., Pasadena.
COMMON SPACEBORNE MULTICOMPUTER OPERATING SYSTEM AND DEVELOPMENT ENVIRONMENT
L. G. Craymer, B. F. Lewis, P. J. Hayes, and R. L. Jones Feb. 1994 34 p
(RTOP 233-01-03)
(NASA-TM-109092; JPL-D-11525; NAS 1.15:109092) Avail: CASI HC A03/MF A01

A preliminary technical specification for a multicomputer operating system is developed. The operating system is targeted for spaceborne flight missions and provides a broad range of real-time functionality, dynamic remote code-patching capability, and system fault tolerance and long-term survivability features. Dataflow concepts are used for representing application algorithms. Functional features are included to ensure real-time predictability for a class of algorithms which require data-driven execution on an iterative steady state basis. The development environment supports the development of algorithm code, design of control parameters, performance analysis, simulation of real-time dataflow applications, and compiling and downloading of the resulting application. Author

N94-30251# Lawrence Livermore National Lab., CA.
GNU DEBUGGER INTERNAL ARCHITECTURE
P. Miller, ed. and D. Nessett, ed. 16 Dec. 1993 36 p
(Contract W-7405-eng-48)
(DE94-006665; UCRL-MA-115656) Avail: CASI HC A03/MF A01

This document describes the internal and architecture and implementation of the GNU debugger, gdb. Topics include inferior process management, command execution, symbol table management and remote debugging. Call graphs for specific functions are supplied. This document is not a complete description but offers a developer an overview which is the place to start before modification. DOE

N94-30273*# Computer Software Management and Information Center, Athens, GA.
COSMIC MONTHLY PROGRESS REPORT
Apr. 1994 31 p
(Contract NASw-4670)
(NASA-CR-195809; NAS 1.26:195809) Avail: CASI HC A03/MF A01

Activities of the Computer Software Management and Information Center (COSMIC) are summarized for the month of April 1994. Tables showing the current inventory of programs available from COSMIC are presented and program processing and evaluation activities are summarized. Five articles were prepared for publication in the NASA Tech Brief Journal. These articles (included in this report) describe the following software items: GAP 1.0 - Groove Analysis Program, Version 1.0; SUBTRANS - Subband/Transform MATLAB Functions for Image Processing; CSDM - COLD-SAT Dynamic Model; CASRE - Computer Aided Software Reliability Estimation; and XOPPS - OEL Project Planner/Scheduler Tool. Activities in the areas of marketing, customer service, benefits identification, maintenance and support, and disseminations are also described along with a budget summary. CASI

N94-30314 National Aerospace Lab., Amsterdam (Netherlands). Informatics Div.
SOFTWARE ENGINEERING AND SOFTWARE MANAGEMENT IN A DISTRIBUTED UNIX ENVIRONMENT
S. deJong and E. H. Baalbergen 1 Apr. 1992 22 p Presented at the 4th ISNaS Symposium, Delft, Netherlands, 23-24 Apr. 1992 Limited Reproducibility: More than 20% of this document may be affected by microfiche quality
(NLR-TP-92233-U; ETN-94-95591) Avail: Issuing Activity (European Space Agency (ESA))

A method for software engineering and a software management environment that supports the method are described. The main features of the software engineering method include cooperation between specialists of various disciplines, separation of the user interface of a system from the rest of the system, and support for reuse of information. The main goals of the software management environment are to support the software engineering method and to use the network of computer systems (running the UNIX operating system) effectively. ESA

N94-30318 Amsterdam Univ. (Netherlands). Dept. of Mathematics and Computer Science.
PARALLEL QUANTIFICATION
Martijn Spaan 22 Feb. 1993 27 p Submitted for publication Limited Reproducibility: More than 20% of this document may be affected by microfiche quality
(ISSN 0928-3307)
(LP-93-01; ETN-94-95559) Avail: CASI HC A03

Forms of paralliel quantification are investigated both from a linguistic and a logical point of view. In particular, interest is in finding a general branching definition. The natural language examples suggest strong connections between parallel and collective readings. In fact, confusion seems to exist between the two classes of readings. Following the intuitions of G. Sher's 'ways of branching quantifiers', the effects of various notions of maximality are investigated. In the logical treatment, starting from basic intuitions of globality and parallelism, various semantic principles that parallel definition schemes should satisfy are introduced. These strongly suggest that the three parallel definition schemes eventually found, are in fact the only ones. Notions concerning quantifiers that may be applicable to other parts of generalized quantifier theory as well are introduced throughout. ESA

N94-30321 Center for Mathematics and Computer Science, Amsterdam (Netherlands). Dept. of Algorithmics and Architecture.
PROGRAMMING ASPECTS OF VIEWS: AN OPEN-ARCHITECTURE APPLICATION ENVIRONMENT
Steven Pemberton Dec. 1992 17 p Limited Reproducibility: More than 20% of this document may be affected by microfiche quality
(ISSN 0169-118X)
(CWI-CS-R9259; ETN-94-95541) Copyright Avail: CASI HC A03

Views is an open architecture application environment that offers a consistent user interface across applications, interoperability between them, much less programming to produce an application, and the ability to add and modify applications on the fly. The system kernel contains a user interface layer and a persistent data storage layer, so that applications only have to implement the true functionality. Objects contain no information on how they are to be displayed, so the presentation of documents can be changed easily, even on the fly. The main implementation technique is the use of invariants between objects which are automatically made two-way by the system. Aspects of programming for Views are described. ESA

N94-30322 Center for Mathematics and Computer Science, Amsterdam (Netherlands). Dept. of Algorithmics and Architecture.
GRAPHICS IN THE VIEWS SYSTEM
Lon G. Barfield Dec. 1992 25 p Limited Reproducibility: More than

20% of this document may be affected by microfiche quality
(ISSN 0169-118X)
(CWI-CS-R9260; ETN-94-95542) Copyright Avail: CASI HC A03

The Views system is a computing environment currently under development. One of its many facets is a graphics facility enabling structured picture objects to be easily entered and manipulated. Such pictures can be included as illustrations in text, as icons in the user interface and ultimately as the specification of all the visible aspects of the system; menus, scroll-bars, windows and so on. Views graphics objects can also be linked to other Views objects with invariants, resulting in pictures that automatically react to changes within other parts of the system. The Views system is outlined, and some of the design and implementation issues of the graphics facilities are described. ESA

N94-30323 Center for Mathematics and Computer Science, Amsterdam (Netherlands). Dept. of Algorithmics and Architecture.
MODELLING INTERACTION TOOLS IN THE VIEWS ARCHITECTURE
Eddy D. G. Boeve Dec. 1992 14 p Limited Reproducibility: More than 20% of this document may be affected by microfiche quality
(ISSN 0169-118X)
(CWI-CS-R9261; ETN-94-95543) Copyright Avail: Issuing Activity (European Space Agency (ESA))

Views is a user interface system in which the user interface is a layer above the applications guaranteeing consistency of the interface. Additionally, the data layer implements external object representation allowing an exchange of objects between applications without loss of structure. Although Views offers an architecture to deal with user interface aspects on a high level, it is shown that low level interaction can be modeled with the architecture provided. ESA

N94-30324 Center for Mathematics and Computer Science, Amsterdam (Netherlands). Dept. of Algorithmics and Architecture.
MAINTAINING PRESENTATION INVARIANTS IN THE VIEWS SYSTEM
Job Ganzevoort Dec. 1992 49 p Limited Reproducibility: More than 20% of this document may be affected by microfiche quality
(ISSN 0169-118X)
(CWI-CS-R9262; ETN-94-95544) Copyright Avail: Issuing Activity (European Space Agency (ESA))

The Views system is an open application integration environment in which the data layer and user interface layer are supplied by the system. Objects in this environment can be linked through invariants; when the value of either of the objects changes, the other is updated to match the invariant. The invariant mechanism is also used for the presentations of objects on screen. If an object changes, the presentation is updated. Additonally, the inverse is true: if the presentation changes, for example by an edit action, the structure of the object should be updated incrementally to match the presentation. An incremental implementation of some functional list operators (map, reduce, filter) is presented, and using these operators, a general parsing algorithm is described. The resulting parser is therefore automatically incremental, without any attention being paid to incrementality in the algorithm. ESA

N94-30331 Nijmegen Univ. (Netherlands). Research Inst. for Declarative Systems.
THE BEAUTY AND THE BEAST
Peter Achten and Rinus Plasmeijer Mar. 1993 11 p Limited Reproducibility: More than 20% of this document may be affected by microfiche quality
(TR-93-03; ETN-94-95622) Avail: CASI HC A03

A method for programming window-based I/O (Input/Output) in a pure functional language is presented. This method enables the programmer to specify interactions at a very high level of abstraction. It employs a machine independent declarative specification of devices such as windows, dialogues and menus. These devices are specified via predefined algebraic data types containing event handlers (user defined higher order functions). All low level handling is hidden from the programmer. The event stream is handled by a library function that takes the algebraic specification of the devices and applies recursively the appropriate event handler for each event. The system is implemented for the lazy functional language Concurrent Clean. It was used successfully for the implementation of large interactive applications such as a window based editor and a relational database. Due to the use of uniqueness types (that make it possible to define functions that perform updates without violating the functional semantics) applications run as efficiently as their imperative counterparts: they can be actually used in practice. The presented method is felt to turn I/O handling into one of the strengths of functional languages. ESA

N94-30332 Nijmegen Univ. (Netherlands). Dept. of Computer Science.
INCREASING THE APPLICABILITY OF LR PARSING
Mark-Jan Nederhof and Janos J. Sarbo Mar. 1993 20 p Limited Reproducibility: More than 20% of this document may be affected by microfiche quality
(Grant NWO-00-62-518)
(TR-93-06; ETN-94-95623) Avail: CASI HC A03

A phenomenon present in some context free grammars, called 'hidden left recursion', is described. It is shown that ordinary LR (Left Right) parsing according to hidden left recursive grammars is not possible, and a range of solutions to this problem are indicated. One of these solutions proposes a new parsing technique, which is a variant of traditional LR parsing. This parsing technique can be used both with and without lookahead and also to define a variant of Tomita parsing. A derivation of the parsing technique is shown and the static space requirements are discussed. ESA

N94-30341 Center for Mathematics and Computer Science, Amsterdam (Netherlands). Dept. of Algorithmics and Architecture.
THE VIEWS APPLICATION ENVIRONMENT
Steven Pemberton Dec. 1992 13 p Limited Reproducibility: More than 20% of this document may be affected by microfiche quality
(ISSN 0169-118X)
(CWI-CS-R9257; ETN-94-95539) Copyright Avail: Issuing Activity (European Space Agency (ESA))

There are a number of problems associated with current windowing environments: a lack of consistency both within and between applications, the poor integration between applications, little or no interoperability, 'hard wired' and inflexible interfaces, and the enormous cost of producing applications. These problems are examined, and a unified approach that addresses them is presented. ESA

N94-30344# Nijmegen Univ. (Netherlands). Dept. of Informations Systems.
A CONCEPTUAL LANGUAGE FOR THE DESCRIPTION AND MANIPULATION OF COMPLEX INFORMATION MODELS
A. H. M. terHofstede (Utrecht State Univ., Netherlands.), H. A. Proper, and T. P. vanderWeide Dec. 1992 15 p Sponsored by Software Engineering Research Centre; and Netherlands Organization for Scientific Research
(TR-92-34; ETN-94-95619) Avail: CASI HC A03/MF A01

Conceptual data modeling techniques aim at the representation of data at a high level of abstraction. This implies that conceptual data modeling techniques should not only be capable of naturally representing complex structures, but also the rules (constraints) that must hold for these structures. Contemporary data modeling techniques however, do not provide a language, which on the one hand has a formal semantics and on the other hand leads to natural looking expressions, for formulating these constraints. An informal introduction to such a language (LISA-D) for the data modeling technique (PSM (Predicator Set Model)), is presented. PSM is a generalization of object-role models (such as ER and NIAM). The semantics of LISA-D are discussed. ESA

N94-30345 Utrecht State Univ. (Netherlands). Dept. of Computer Science.
TWO ALGORITHMS FOR FINDING RECTANGULAR DUALS OF PLANAR GRAPHS
Goos Kant and Xin He Dec. 1992 19 p Limited Reproducibility: More than 20% of this document may be affected by microfiche quality
(Contract EC-7141; NSF CCR-90-11214) (ISSN 0924-3275)
(RUU-CS-92-41; ETN-94-95631) Avail: CASI HC A03

Two linear time algorithms for computing a regular edge labeling of 4-connected planar triangular graphs are presented. This labeling is used to compute in linear time a rectangular dual of this class of planar graphs. The two algorithms are based on totally different frameworks, and both are conceptually simpler than the previous known algorithm and are of independent interests. The first algorithm is based on edge contraction. The second algorithm is based on the canonical ordering. This ordering

can also be used to compute more compact visibility representations for this class of planar graphs. ESA

N94-30347 Utrecht State Univ. (Netherlands). Dept. of Computer Science.

ON BLOCKS: LOCALITY AND ASYNCHRONOUS COMMUNICATION (EXTENDED ABSTRACT)

F. S. deBoer (Technische Univ., Eindhoven, Netherlands.), J. N. Kok, C. Palamidessi, and J. J. M. M. Rutten Dec. 1992 19 p Limited Reproducibility: More than 20% of this document may be affected by microfiche quality

(ISSN 0924-3275)

(RUU-CS-92-44; ETN-94-95634) Avail: CASI HC A03

A general construct for locality in languages based on asynchronous communication is introduced. The construct allows a uniform semantic description of such seemingly different notions of locality as the hiding of local variables in imperative shared variable languages and the existantial quantification of logical variables in concurrent constraint languages. The compositional model is fully abstract with respect to the operational one. ESA

N94-30348 Utrecht State Univ. (Netherlands). Dept. of Computer Science.

A DETERMINISTIC ALGORITHM FOR THE THREE-DIMENSIONAL DIAMETER PROBLEM

Jiri Matousek and Otfried Schwarzkopf Dec. 1992 13 p Sponsored in part by Netherlands Organization for Scientific Research; EEC; and Alexander von Humboldt Foundation Limited Reproducibility: More than 20% of this document may be affected by microfiche quality

(ISSN 0924-3275)

(RUU-CS-92-45; ETN-94-95635) Avail: CASI HC A03

The following problem is considered: given an n point set P in three dimensional space, compute its diameter diam(P), defined as the maximum distance between a pair of points in P. This problem was solved by Clarkson and Shor by a randomized algorithm with optimal expected running time O(n log n). However, it seems quite difficult to construct a deterministic algorithm with a comparable asymptotic efficiency. Chazelle et al. applied Megiddo's parametric search in connection with the Clarkson-Shor algorithm and further techniques and obtained a deterministic O(n(sup 1 + epsilon)) algorithm, where epsilon greater than 0 is an arbitrarily small constant. This study improves this running time to O(n polylog n), where polylog n is used as a generic notation for a function of the form (log n)(sup c), c greater than 0 a constant). ESA

N94-30364 Utrecht State Univ. (Netherlands). Dept. of Computer Science.

GENERALIZED HIDDEN SURFACE REMOVAL

Mark deBerg Feb. 1993 22 p Sponsored by Netherlands Organization for Scientific Research, and EEC Limited Reproducibility: More than 20% of this document may be affected by microfiche quality

(ISSN 0924-3275)

(RUU-CS-93-05; ETN-94-95642) Avail: CASI HC A03

The following generalization of the classical hidden surface removal problem is studied: given a set S of objects, a view point and a point light source, compute which parts of the objects in S are visible, subdivided into parts that are lit and parts that are not lit. Tight bounds on the maximum combinatorial complexity of such views are proved and efficient output sensitive algorithms to compute the views for three cases are given: S consists of non intersecting triangles; S consists of horizontal axis parallel rectangles; S is the set of faces of a polyhedral terrain. ESA

N94-30371# Amsterdam Univ. (Netherlands). Dept. of Mathematics and Computer Science.

LOGIC OF TRANSITION SYSTEMS

Johan vanBenthem and Jan Bergstra Mar. 1993 40 p

(ISSN 0928-3323)

(CT-93-03; ETN-94-95557) Avail: CASI HC A03/MF A01

A study which shows how labeled transition systems, which are key structures for modeling computation, lend themselves to ordinary logical analysis (without any special new formalisms), by introducing their standard first order theory, is presented. This perspective enables several basic model theoretic questions of definability, axiomatization and preservation for various notions of process equivalence found in the computational literature to be raised, and answered using well known logical techniques (including the Compactness theorem, Saturation and Ehrenfeucht games). Consideration is given as to what happens to this general theory when attention is restricted to special classes of transition systems (in particular, finite ones), as well as extended logical languages (in particular, infinitary first order logic). It is hoped that this puts standard logical formalisms on the map as a serious option for a theory of computational processes. As a side benefit, the approach increases comparability with several other existing formalisms over labeled transition systems (such as process algebra or modal logic). Pointers to this effect are provided. ESA

N94-30379 Utrecht State Univ. (Netherlands). Dept. of Computer Science.

SELF-STABILIZING l-EXCLUSION ALGORITHMS

Mitchell Flatebo (Nevada Univ., Las Vegas.), Ajoy Kumar Datta (Nevada Univ., Las Vegas.), and Anneke A. Schoone Jan. 1993 25 p Sponsored in part by EEC Limited Reproducibility: More than 20% of this document may be affected by microfiche quality

(Contract NF-62-376) (ISSN 0924-3275)

(RUU-CS-93-01; ETN-94-95638) Avail: CASI HC A03

A distributed system consists of a set of loosely connected machines that do not share a global memory. The system is self stabilizing if it can be started in any global state and achieves its consistency all by itself. This also means that the system can deal with infrequent errors. Self stabilizing l-exclusion algorithms are presented. The l-exclusion problem is a generalization of the mutual exclusion problem (where l = 1). The algorithms presented are generalizations of a self stabilizing mutual exclusion algorithm by Dijkstra. The first algorithm serves to illustrate the underlying ideas but uses unbounded numbers. The second algorithm is adapted to the use of bounded numbers, while the third algorithm overcomes a disadvantage of the first two algorithms. ESA

N94-30386# Amsterdam Univ. (Netherlands). Dept. of Mathematics and Computer Science.

THE VANILLA META-INTERPRETER FOR DEFINITE LOGIC PROGRAMS AND AMBIVALENT SYNTAX

Marianne Kalsbeek Jan. 1993 25 p Sponsored by Netherlands Organization for Scientific Research

(ISSN 0928-3323)

(CT-93-01; ETN-94-95555) Avail: CASI HC A03/MF A01

Syntax and semantics for the Vanilla meta-interpreter are presented. The Vanilla meta-interpreter is a definite logic program which consists of two parts: a general part consisting of an intensional formalization of derivability by SLD resolution from definite object programs; an object program specific part consisting of a metalevel description of the clauses of an object program. Ambivalent syntax, which is characterized by the occurrence of formulas as terms, is discussed, and a suitable semantics is provided. Ambivalent syntax is shown to be appropriate for the Vanilla meta-interpreter. Correctness of the Vanilla meta-interpreter is proved for definite programs. ESA

N94-30400 National Aerospace Lab., Amsterdam (Netherlands). Informatics Div.

FAST AND EFFICIENT VARIABLE-TO-FIXED-LENGTH CODING ALGORITHM

T. Algra 27 Aug. 1992 12 p Repr. from Electronics Letters, v. 28, no. 15, 16 Jul. 1992 Limited Reproducibility: More than 20% of this document may be affected by microfiche quality

(PB94-125465; NLR-TP-92353-U; ETN-94-95593) Avail: Issuing Activity (European Space Agency (ESA))

Variable to fixed length coding implementations, according to the algorithm of Tunstall, are shown to be significantly less complex than fixed to variable length coding schemes such as the Huffman scheme. In a variable to fixed length coding situation, the encoder chops the source outputs sequence into segments of about the same probability. To inform the decoder, the encoder sends it the lexicographical index of the segments. The segments belong to a segment set S with cardinality T. Tunstall developed the construction algorithm for the segment set to derive a proper and complete code; the performance of such a coder converges to the source entropy as T approaches infinity. A modified version of the

Tunstall algorithm is proposed with improved coding efficiency. It is shown that high speed, software based decoding can be implemented, with significantly lower complexity than Huffman schemes. ESA

N94-30414 Center for Mathematics and Computer Science, Amsterdam (Netherlands). Dept. of Computer Science.
HIGHER ORDER RECURSIVE PROGRAM SCHEMES ARE TURING INCOMPLETE
Zurab Khasidashvili Jul. 1993 21 p Limited Reproducibility: More than 20% of this document may be affected by microfiche quality
(ISSN 0169-118X)
(CWI-CS-R9348; ETN-94-95691) Copyright Avail: Issuing Activity (European Space Agency (ESA))

Higher Order Recursive Program Schemes (HRPS's) are defined by allowing metasubstitutions (as in the lambda calculus) in right hand sides of function and quantifier definitions. To study reductions in a HRPS, it is split into 'first order part' and 'pure substitution part'. A study of pure substitutions and several kinds of 'similarity' of redexes makes it possible to lift properties of (first order) RPS's to the higher order case. The crucial properties are that corresponding arguments of 'essentially similar' redexes are either both essential or both inessential, and that essentially similar redexes create essentially similar redexes. The main result is the decidability of weak normalization in HRPS's, which immediately implies that HRPS's do not have full computational power. The structural properties of HRPS's are analyzed, and several kinds of 'persistent' higher order rewrite systems that enjoy similar properties are introduced. For 'uniformly' persistent systems, an efficient optimal sequential normalizing strategy is designed. ESA

N94-30415 Center for Mathematics and Computer Science, Amsterdam (Netherlands). Dept. of Computer Science.
COMPARING CURRIED AND UNCURRIED REWRITING
J. Richard Kennaway (East Anglia Univ., Norwich, England.), Jan Willem Klop, M. Ronan Sleep, and Fer-Jan deVries Jul. 1993 28 p Revised Sponsored in part by EEC Limited Reproducibility: More than 20% of this document may be affected by microfiche quality
(Grant SERC-GR/F-91582) (ISSN 0169-118X)
(CWI-CS-R9350; ETN-94-95692) Copyright Avail: CASI HC A03

The properties of WN (Weak Normalization), SN (Strong Normalization), WCR (Weak Church-Rosser) and completeness of functional term rewriting systems are preserved if systems are curried into applicative term rewriting systems. Under the condition of left linearity, the properties CR (Church-Rosser or Confluence), NF (Normal Form), UN and UN(forward arrow) (two properties concerning unique normal forms), and semi completeness, are also preserved by currying. By a counterexample, it is shown that the latter set of properties, with the possible exception of semi completeness, are in general not preserved for non left linear systems. ESA

N94-30416 Universiteit Twente, Enschede (Netherlands). Tele-Informatics and Open Systems Group.
MODELING SYSTEMS BY PROBABILISTIC PROCESS ALGEBRA: AN EVENT STRUCTURES APPROACH
Joost-Pieter Katoen, Rom Langerak, and Diego Latalla 1993 24 p Revised Sponsored in part by CNR-NATO Advanced Fellowships Program Limited Reproducibility: More than 20% of this document may be affected by microfiche quality
(ISSN 0924-3755)
(Memo-INF-93-29-Rev; TIOS-93-17; ETN-94-95714) Copyright Avail: CASI HC A03

A probabilistic version of a subset of the process algebra LOTOS (Language of Temporal Ordering Specification) is addressed. It incorporates a probabilistic choice assigning a probability of occurrence to each of its alternatives. Opposed to the traditional interleaving semantics used for existing probabilistic process algebras the presented language is based on a true concurrency semantics. This enables a distinction to be made between non determinism and parallelism, the state explosion problem to be reduced and part of the system to be analyzed without considering other (irrelevant) parts. The language is presented and the formal semantics is defined by using an extension of bundle event structures. Two examples illustrate the novelties of the language and link the langauge to stochastic analysis based on semi Markov chains. ESA

N94-30417 Universiteit Twente, Enschede (Netherlands). Dept. of Computer Science.
DTL: A DEDUCTIVE AND TYPED OBJECT-ORIENTED LANGUAGE
C. M. Rene Bal and Herman Balsters Aug. 1993 26 p Limited Reproducibility: More than 20% of this document may be affected by microfiche quality
(ISSN 0924-3755)
(Memo-INF-93-41; ETN-94-95715) Copyright Avail: CASI HC A03

A logical query language extended with object oriented typing facilities is introduced. This language, called DTL (from DataTypeLog), can be seen as an extension of Datalog equipped with complex objects, object identities, and multiple inheritance based on Cardelli type theory. The language also incorporates a very general notion of sets as first class objects. An evaluation strategy and a denotational semantics for DTL programs, are offered. ESA

N94-30426 Utrecht State Univ. (Netherlands). Dept. of Computer Science.
A MORE COMPACT VISIBILITY REPRESENTATION
Goos Kant Aug. 1993 18 p Sponsored in party by EEC Limited Reproducibility: More than 20% of this document may be affected by microfiche quality
(ISSN 0924-3275)
(RUU-CS-93-26; ETN-94-95663) Avail: CASI HC A03

A linear time and space algorithm for constructing a visibility representation of a planar graph on an ((3/2)n - 3) by (n - 1) grid, thereby improving the previous bound of (2n - 5) by (n - 1), is presented. To this end, the four-block tree of a triangulated planar graph is built in linear time. ESA

N94-30428 Center for Mathematics and Computer Science, Amsterdam (Netherlands). Dept. of Computer Science.
MANIFOLD VERSION 1.0 PROGRAMMING: PROGRAMS AND PROBLEMS
Kees L. Blom Jun. 1993 42 p Limited Reproducibility: More than 20% of this document may be affected by microfiche quality
(ISSN 0169-118X)
(CWI-CS-R9334; ETN-94-95676) Copyright Avail: CASI HC A03

MANIFOLD is a programming language designed to control multiple concurrent activities by managing the communications among a number of active communicating entities. The present initial version of the MANIFOLD language is a minimal language attempting solely to implement a conceptual model of asynchronously communicating processes, called the MANIFOLD model. Such a model can be useful in an implementation environment where processes and interprocess communication are fast and amply available (for example massive parallelism). A tutorial introduction to the first experimental version of the MANIFOLD language (using listings of simple working example programs) is presented, followed by four larger working programs. The detailed operation of each of these latter four programs is described with the help of illustrations, and a number of language features and problems are explained. The MANIFOLD conceptual model and language are both concluded to be implementable and to actually work, and in their initial first experimental versions, they have some imperfections which must be taken into account in the design and implementation of the next version of the MANIFOLD system. ESA

N94-30432# Center for Mathematics and Computer Science, Amsterdam (Netherlands). Dept. of Computer Science.
TOPOLOGICAL MODELS FOR HIGHER ORDER CONTROL FLOW
J. W. deBakker (Vrije Univ., Amsterdam, Netherlands.) and F. vanBreugel (Vrije Univ., Amsterdam, Netherlands.) Jun. 1993 22 p Presented at the 9th Conference on the Mathematical Foundations of Programming Semantics, New Orleans, LA, 7-10 Apr. 1993 Submitted for publication Sponsored in part by Netherlands Nationale Faciliteit Informatica Programme
(ISSN 0169-118X)
(CWI-CS-R9340; ETN-94-95682) Copyright Avail: CASI HC A03/MF A01

Semantic models for two simple imperative languages with higher order constructs are presented. In the first language the interesting notion is that of second order assignment x:= s, for x a procedure variable and s a statement. The second language extends this idea by a form of higher

order communication, with statements c! and c?x, for c a channel. perational and denotational models are developed for both languages and their relationships are studied. Both in the definitions and the comparisons of the semantic models, convenient use is made of some tools from (metric) topology. The operational models are based on (SOS style) transition systems; the denotational definitions use domains specified as solutions of domain equations in a category of 1 bounded complete ultrametric spaces. In establishing the connection between the two kinds of models, fruitful use is made of Rutten's 'processes as terms' technique. Another tool consists of the use of 'metric' transition systems, with a metric defined on the configurations of the system. In addition to higher order programming notions, higher order definition techniques are used, for example in defining the semantic mappings as fixed points of (contractive) higher order operators. By Banach's theorem, such fixed points are unique, yielding another important proof principle. ESA

N94-30434 Center for Mathematics and Computer Science, Amsterdam (Netherlands). Dept. of Computer Science.

THE BOLTZMANN ENTROPY AND RANDOMNESS TESTS

Peter Gacs (Boston Univ., MA.) Jun. 1993 31 p Limited Reproducibility: More than 20% of this document may be affected by microfiche quality

(Contract NF-62-376; NSF CCR-90-02614) (ISSN 0169-118X)

(CWI-CS-R9342; ETN-94-95684) Copyright Avail: CASI HC A03

Descriptional (Kolmogorov) complexity has a certain well understood relation to the information theoretical entropy introduced by Shannon. The latter is, by its form, related to the Gibbs entropy of statistical mechanics. Entropy in physics has several different definitions, and a history of philosophical controversy concerning the related notion of irreversibility. The necessary concepts of thermodynamics, complexity and randomness tests are introduced, and some of the connections to physics are developed by introducing a notion called 'algorithmic entropy'. This, on the one hand, is in a simple relation to randomness tests (of Martin-Lof and others), and on the other hand, is a connecting link between description complexity, Gibbs entropy and Boltzmann entropy. Its coarse grained approximation is shown to have the desirable properties of Boltzmann entropy on a somewhat wider range of systems, including those of interest in the 'thermodynamics of computation'. It is hoped that eventually these concepts will prove helpful not only for computer science but also for physics and dynamical system theory, by extending thermodynamical reasoning to some new classes of systems. ESA

N94-30435 Center for Mathematics and Computer Science, Amsterdam (Netherlands). Dept. of Computer Science.

A USER'S GUIDE TO THE SOFTWARE TESTPILOT

M. L. Kersten and F. Kwakkel Jun. 1993 22 p Sponsored by EEC Limited Reproducibility: More than 20% of this document may be affected by microfiche quality

(ISSN 0169-118X)

(CWI-CS-R9343; ETN-94-95685) Copyright Avail: Issuing Activity (European Space Agency (ESA))

The Software Testpilot is a performance assessment tool for software systems, in particular, database management systems. A user's guide to the Testpilot is presented, and the Testsuite Specification Language (TSL) concepts are described. An introduction to designing a TSL program using the Wisconsin Benchmark as a case study is provided. An illustration of a session using the graphical user interface is given. ESA

N94-30437 Center for Mathematics and Computer Science, Amsterdam (Netherlands). Dept. of Computer Science.

PERPETUAL REDUCTIONS AND STRONG NORMALIZATION IN ORTHOGONAL TERM REWRITING SYSTEMS

Zurab Khasidashvili Jul. 1993 15 p Limited Reproducibility: More than 20% of this document may be affected by microfiche quality

(ISSN 0169-118X)

(CWI-CS-R9345; ETN-94-95687) Copyright Avail: CASI HC A03

A strategy that, for any given term t in an Orthogonal Term Rewriting System (OTRS), constructs a longest reduction starting from t if it is strongly normalizable, and constructs an infinite reduction otherwise, is designed. Classes of OTRS's for which the strategy is easily computable are defined. A method for finding the least upper bound of lengths of reductions starting from a strongly normalizable term is developed and applications of the results are given. ESA

N94-30488 Utrecht State Univ. (Netherlands). Dept. of Computer Science.

EFFICIENT AND CONSTRUCTIVE ALGORITHMS FOR THE PATHWIDTH AND TREEWIDTH OF GRAPHS

Hans L. Bodlaender and Ton Kloks Sep. 1993 42 p Sponsored in part the Netherlands Foundation for Computer Science Limited Reproducibility: More than 20% of this document may be affected by microfiche quality

(Contract EC-3075) (ISSN 0924-3275)

(RUU-CS-93-27; ETN-94-95664) Avail: Issuing Activity (European Space Agency (ESA))

For all constants k, l, explicit algorithms are presented, that given a graph G = (V, E) with a tree decomposition of G with treewidth at most l, decide whether the treewidth (or pathwidth) of G is at most k, and if so, find a tree decomposition (path decomposition) of G of width at most k and that uses O(absolute value of V) time. In contrast with previous solutions, the algorithms do not rely on nonconstructive reasoning and are single exponential in k and l. This result can be combined with a result of Reed, yielding explicit O(n log n) algorithms for the problem, given a graph G, to determine whether the treewidth of G is at most k, and if so, to find a tree decomposition of width at most k (k constant). It is also shown that for all constants k, there exists a polynomial time algorithm that, when given a graph G = (V, E) with treewidth less than or equal to k, computes the pathwidth of G and a path decomposition of G of minimum width. ESA

N94-30489 Utrecht State Univ. (Netherlands). Dept. of Computer Science.

EFFICIENT BOUNDED TIMESTAMPING USING TRACEABLE USE ABSTRACTION: IS WRITER'S GUESSING BETTER THAN READER'S TELLING?

S. Haldar Sep. 1993 25 p Limited Reproducibility: More than 20% of this document may be affected by microfiche quality

(Contract NF-62-376) (ISSN 0924-3275)

(RUU-CS-93-28; ETN-94-95665) Avail: CASI HC A03

'Traceable use' is a helpful abstraction to recycling values in bounded wait-free systems. Several researchers have demonstrated the power of the traceable use abstraction in constructing concurrent timestamping systems, snapshot variables, and bounded round numbers. An efficient implementation technique of the traceable use abstraction, which is used in developing a new construction of concurrent timestamping systems, is presented. This new construction is simpler than the other traceable use abstraction based construction in the literature. The new implementation exhibits that sometimes writer's guessing is better than reader's explicit telling. ESA

N94-30490 Utrecht State Univ. (Netherlands). Dept. of Computer Science.

THE SECRETS OF CAUSALITY

F. Rietman Sep. 1993 71 p Limited Reproducibility: More than 20% of this document may be affected by microfiche quality

(Contract NF-62-518) (ISSN 0924-3275)

(RUU-CS-93-29; ETN-94-95666) Avail: Issuing Activity (European Space Agency (ESA))

A model for a relational calculus for distributed program design is introduced. The distributed programs are compositions of so called 'processes.' The construction of the model is guided by desired properties for several forms of composition of processes, such as sequential composition and feedback. Functionality (determinism) and totality of processes are defined. After the observation that functionality and totality are not preserved by the feedback operator, the class of 'causal' processes is introduced. Causality is shown to guarantee the preservation by the feedback of functionality and totality. ESA

N94-30491 Center for Mathematics and Computer Science, Amsterdam (Netherlands). Dept. of Computer Science.

COMPARATIVE SEMANTICS FOR LINEAR ARRAYS OF COMMUNICATING PROCESSES

J. W. deBakker (Vrije Univ., Amsterdam, Netherlands.), F. vanBreugel (Vrije Univ., Amsterdam, Netherlands.), and A. deBruin (Erasmus Univ., Rotterdam, Netherlands.) Jun. 1993 17 p Presented at the 18th International Symposium on Mathematical Foundations of Computer Science, Gdansk,

Poland, 30 Aug. - 3 Sep. 1993 Submitted for publication Sponsored in part by Netherlands Nationale Faciliteit Informatica Programme Limited Reproducibility: More than 20% of this document may be affected by microfiche quality
(ISSN 0169-118X)
(CWI-CS-R9336; ETN-94-95678) Copyright Avail: CASI HC A03

Operational (O) and Denotational (D) semantic models are designed for a language incorporating a version of the UNIX fork and pipe commands. Taking a simple imperative language as starting point, a number of programming constructs are added which achieve that a program can generate a dynamically evolving linear array of processes connected by channels. Over these channels sequences of values ('streams') are transmitted. Both O and D are defined as (unique) fixed point of a contractive higher order operator. This allows a smooth proof that O and D are equivalent. Additional features are the use of hiatons, and the closely related syntactic resumptions and semantic continuations. ESA

N94-30585# Universiteit Twente, Enschede (Netherlands). Dept. of Applied Mathematics.
THE TRANSIENT PERIOD OF A CYCLIC PROCESS: AN HORIZON THEOREM
W. M. Nawijn Jul. 1993 15 p
(ISSN 0169-2960)
(MEMO-1149; ETN-94-95723) Avail: CASI HC A03/MF A01

Necessary and sufficient conditions are presented for the existence of an integer N such that the process x(sub i)(r) = max (j greater than or equal to 1 and less than or equal to n) (a(sub ij) + x(sub j)(r-1)), i greater than or equal to 1 and less than or equal to n, r greater than or equal to 1, satisfies x(sub i)(r + 1) = c + x(sub i)(r) for all r greater than or equal to N and all initial conditions x(sub i)(0). If such an integer N exists the property can be interpreted as a horizon theorem for a finite state space deterministic decision process with unbounded horizon. ESA

N94-30590 Westinghouse Hanford Co., Richland, WA.
NUMERICAL PRECISION AND ROUNDOFF CONSIDERATIONS CONCERNING COMPUTER CODE MIGRATION
K. N. Schwinkendorf Dec. 1993 9 p Presented at the Simulation Multi Conference, San Diego, CA, 11-15 Apr. 1994 Limited Reproducibility: More than 20% of this document may be affected by microfiche quality
(Contract DE-AC06-87RL-10930)
(DE94-005421; WHC-SA-2178; CONF-940456-6) Avail: CASI HC A02

Code conversion between different computer platforms may not be as straightforward or as simple as some people might think. When migrating computer codes between different computers, thought must be given to the importance of numerical precision. Some applications require greater numerical precision than others. Cray architecture treats floating-point numbers and operations as double precision compared to most other platforms, many of which are based on a 32-bit architecture. In some systems, only 32-bit compilers are available, even though the hardware is 64 bit. The default floating-point representation on the Cray is 15-place accuracy, as compared to 8 places on most workstations. Some applications do not inherently require accuracy to the 15th decimal place. Examples in nuclear engineering include Monte Carlo simulations, where numerical round-off error generated in the tracking of one neutron does not propagate seriously to neutrons in succeeding generations. Other applications, particularly time-dependent simulations, are susceptible to the cumulative effects of round-off errors. In addition, multidimensional transient simulations require an iterative solution methodology, whether the simulation is of groundwater contamination, space-time nuclear kinetics, fluid flow, or chemical migration. This paper will at least partially address the concerns of numerical precision by illustrating by example what differences in precision can do to the running of a simulation. DOE

N94-30705 Los Alamos National Lab., NM.
USE OF BAD TRAINING DATA FOR BETTER PREDICTIONS
T. Grossman and A. Lapedes 1994 9 p Presented at the Neural Information Processing Systems (NIPS) Conference, Denver, CO, 30 Nov. - 2 Dec. 1993 Limited Reproducibility: More than 20% of this document may be affected by microfiche quality
(Contract W-7405-eng-36)
(DE94-006233; LA-UR-94-111; CONF-9311171-1) Avail: CASI HC A02

We show how randomly scrambling the output classes of various fractions of the training data may be used to improve predictive accuracy of a classification algorithm. We present a method for calculating the 'noise sensitivity signature' of a learning algorithm which is based on scrambling the output classes. This signature can be used to indicate a good match between the complexity of the classifier and the complexity of the data. Use of noise sensitivity signatures is distinctly different from other schemes to avoid overtraining, such as cross-validation, which uses only part of the training data, or various penalty functions, which are not data-adaptive. Noise sensitivity signature methods use all of the training data and are manifestly data-adaptive and nonparametric. They are well suited for situations with limited training data. DOE

N94-30725 Utrecht State Univ. (Netherlands). Dept. of Computer Science.
PLACING REGISTRATION MARKS
Anil S. Rao and Kenneth Y. Goldberg Jun. 1993 24 p Sponsored in part by EEC; National Inst. for Standards and Technology; Institute for Manufacturing and Automation Research; and Adept Technology, Inc. Limited Reproducibility: More than 20% of this document may be affected by microfiche quality
(Grant NSF IRI-91-23747) (ISSN 0924-3275)
(RUU-CS-93-21; ETN-94-95658) Avail: Issuing Activity (European Space Agency (ESA))

In industrial assembly, a registration mark can be placed on parts to aid a computer vision system in determining the position and orientation of the parts. However, when sensor noise and limits on resolution introduce errors in the measured location of the registration mark, these errors can propagate into the measurement of part pose. A definition of the registration mark problem is given: given an n sided rigid planar polygonal part and a set of k poses for the part, locate a point on the surface of the part that maximizes the minimum distance between transformed points. A registration mark at this point will be maximally robust to sensor imperfections. An O((n log n) + (k(exp 4)(log k log(star)k) time algorithm to solve this planar problem using a result from Schwartz and Sharir is given and the algorithm is demonstrated using a commercial vision system. The results extend to classes of curved planar parts and polyhedral parts. ESA

N94-30732 Center for Mathematics and Computer Science, Amsterdam (Netherlands). Dept. of Computer Science/Dept. of Algorithmics and Architecture.
RELATIONS BETWEEN VARIETIES OF KOLMOGOROV COMPLEXITIES
Vladimir A. Uspensky (Moscow M. V. Lomonosov Inst. of the Technology of Fine Chemicals, USSR.) and Alexander Shen (Moscow M. V. Lomonosov Inst. of the Technology of Fine Chemicals, USSR.) Apr. 1993 41 p Sponsored by Netherlands Organization for Scientifc Research Limited Reproducibility: More than 20% of this document may be affected by microfiche quality
(ISSN 0169-118X)
(CWI-CS-R9329; ETN-94-95672) Copyright Avail: CASI HC A03

There are several sorts of Kolmogorov complexities: decision complexity, simple complexity, prefix complexity, monotonic complexity, and a priori complexity. The last three can and the first two cannot be used for defining randomness of an infinite binary sequence. All five versions of Kolmogorov complexity were previously considered from a unified point of view. Upper and lower bounds for those complexities and also for their differences were announced without proofs. Proofs for those bounds are presented. The word 'entropy' (not in a physical sense) is used instead of 'complexity', which is a Moscow tradition suggested by A.N. Kolmogorov himself. By this tradition the term 'complexity' relates to any mode of description and 'entropy' is the complexity related to an optimal mode (that is, to a mode that, roughly speaking, gives the shortest descriptions). ESA

N94-30733 Center for Mathematics and Computer Science, Amsterdam (Netherlands). Dept. of Computer Science/Dept. of Software Technology.
ON THE UNIFICATION FREE PROLOG PROGRAMS
Krysztof R. Apt (Amsterdam Univ., Netherlands.) and Sandro Etalle (Padua Univ., Italy.) May 1993 19 p Submitted for publication Sponsored in part by EEC Limited Reproducibility: More than 20% of this document may be affected by microfiche quality
(ISSN 0169-118X)
(CWI-CS-R9331; ETN-94-95673) Copyright Avail: CASI HC A03

Simple conditions which allow the conclusion that in the case of several

well known PROLOG programs the unification algorithm can be replaced by iterated matching are provided. The main tools used are types and generic expressions for types. Such a replacement offers a possibility of improving the efficiency of the program's execution. ESA

N94-30734 Center for Mathematics and Computer Science, Amsterdam (Netherlands). Dept. of Computer Science/Dept. of Software Technology.

MORE PROBLEMS ON REWRITING

Nachum Dershowitz (Illinois Univ., Urbana.), Jean-Pierre Jouannaud (Paris-Sud Univ., Orsay, France.), and Jan Willem Klop (Vrije Univ., Amsterdam, Netherlands.) May 1993 22 p Sponsored in part by Weizmann Inst. of Science, and EEC Limited Reproducibility: More than 20% of this document may be affected by microfiche quality

(Grants NSF CCR-90-07195; NSF CCR-90-24271) (ISSN 0169-118X)

(CWI-CS-R9332; ETN-94-95674) Copyright Avail: Issuing Activity (European Space Agency (ESA))

An update of the list of open problems in the theory of rewriting is presented. Old problems for which progress can be reported are repeated and new problems since RTA-91 are included. Research areas are described. ESA

N94-30739 National Aerospace Lab., Amsterdam (Netherlands). Informatics Div.

ENGINEERING OF SYSTEMS FOR APPLICATION OF SCIENTIFIC COMPUTING IN INDUSTRY WP PROJECT MANAGEMENT ISNaS 9209099

W. Loeve 9 Sep. 1992 34 p Presented at the Effective Concurrent Engineering in Aerospace Industry Seminar, Paris, France, 8-10 Apr. 1992, and IFIP WG5.2, WG5.2 CATE TF Workshop on Manufacturing in the ERA of Concurrent Engineering, Tel-Aviv, Israel, 13-15 Apr. 1992 Submitted for publication Limited Reproducibility: More than 20% of this document may be affected by microfiche quality

(PB94-126232; NLR-TP-126232; ETN-94-95557) Avail: CASI HC A03

A method for development and production of mathematics software is presented. The aim of the method is to produce software that can be applied for simulation purposes in industry. It is argued that mathematics software for applications in industry can be realized only if various specialists contribute to the development and production process. For this reason, the method is designed in such a way that it supports cooperative engineering preocesses. The method has organizational and technical aspects. Both aspects need equal attention for the method to be effective. The quality of the result of application of the method depends on the skills and the attitude of the specialists that are involved in the development and production process. ESA

N94-30746 Utrecht State Univ. (Netherlands). Dept. of Computer Science.

MAPPING OBJECTS TO FILES: A UNIX FILE SYSTEM INTERFACE TO AN OBJECT MANAGEMENT SYSTEM

Gert Florijn, Leo Soepenberg, and Atze Dijkstra Feb. 1993 19 p Limited Reproducibility: More than 20% of this document may be affected by microfiche quality

(ISSN 0924-3275)

(RUU-CS-93-08; ETN-94-95645) Avail: CASI HC A03

The design of a UNIX file system interface for the Camera Object Management System (OMS), an extensible, fully object oriented environment comparable to Smalltalk, is described. The interface was developed to let the UNIX system act as a user interface to the OMS, and to be able to run existing UNIX tools from within the OMS. Via the interface, users are presented with a file tree which in actual fact is generated from objects and attributes stored in the OMS. Manipulating the tree implies sending messages to OMS objects. The design uses the NFS (Network File System) protocol for client-server communication and is based on a user level NFS server that connects to multiple OMS processes. Essential in the architecture is that one particular mapping is not imposed from OMS concepts (objects, etc.) to a file tree. Instead, a multiple of such mappings (or views) can be defined within each OMS. Furthermore, it is possible to switch dynamically between views. The design goals are discussed, the major components of the system are described and examples of how object oriented concepts in the OMS can be accommodated in a UNIX file tree are given, by describing some of the sample views. ESA

N94-30749 Utrecht State Univ. (Netherlands). Dept. of Computer Science.

UNRAVELLING NONDETERMINISM: ON HAVING THE ABILITY TO CHOOSE

W. vanderHoek, B. vanLinder, and J. J. C. Meyer Sep. 1993 37 p Sponsored in part by EEC; Vrije Univ.; and Katholieke Univ. Limited Reproducibility: More than 20% of this document may be affected by microfiche quality

(ISSN 0924-3275)

(RUU-CS-93-30; ETN-94-95667) Avail: CASI HC A03

Ways to incorporate nondeterminism in a system designed to formalize the reasoning of agents concerning their abilities and the results of the actions that they may perform are demonstrated. A distinction is made between two kinds of nondeterministic choice operators: one that expresses an internal choice, in which the agent decides what action to take, and one that expresses an external choice, which cannot be influenced by the agent. The presence of abilities in the system is the reason why the usual approaches towards nondeterminism cannot be used. The semantics defined for nondeterministic actions is based on the idea that composite actions are unravelled in the strings of atomic actions and tests that constitute them. The main notions used in defining this semantics are finite computation sequences and finite computation runs of actions. The results obtained meet intuitions regarding events and abilities in the presence of nondeterminism. ESA

N94-30754# Argonne National Lab., IL.

PARALLEL LANGUAGE CONSTRUCTS FOR PARADIGM INTEGRATION AND DETERMINISTIC COMPUTATIONS

K. M. Chandy and I. T. Foster 1993 10 p Presented at the Parallel Computing 1993 Conference, Grenoble, France, 7-10 Sep. 1993

(Contract W-31-109-eng-38)

(DE94-005119; ANL/MCS/CP-81591; CONF-9309319-1) Avail: CASI HC A02/MF A01

We describe parallel extensions of sequential programming languages for writing programs that integrate different programming paradigms and that execute in heterogeneous environments comprising both distributed and shared memory. The extensions can be used to write programs with dynamic process and communication structures. Programs can use shared-memory, message passing, and data parallel programming paradigms, and can be written in a way that permits the compiler and run-time system to verify that they are deterministic. The extensions also provide the programmer with control over how data and processes are mapped to processors, and hence how computational resources are allocated to different parts of a program. A subset of these ideas has been incorporated in an extension to Fortran called Fortran M. However, the underlying sequential notation is not central to the ideas. DOE

N94-30764 National Aerospace Lab., Amsterdam (Netherlands). Flight Div.

SYSTEMATIC ERROR ESTIMATION IN MULTISENSOR FUSION SYSTEMS

B. A. vanDoorn and H. A. P. Blom 3 Mar. 1993 18 p Presented at the SPIE Conference on Signal and Data Processing of Small Targets, Orlando, FL, 12-16 Apr. 1993 Limited Reproducibility: More than 20% of this document may be affected by microfiche quality

(AD-B179298; NLR-TP-93094-U; ETN-94-95970) Avail: CASI HC A03

An algorithm to estimate the systematic macro errors in multisensor fusion systems is evaluated. For abruptly changing macro errors this requires dynamic estimation of these macro errors, online with the maintenance of tracks. The problem with this dynamic estimation is that, in theory, their filter equations are coupled to the track maintenance equations for the individual tracks. Hence, to keep things manageable, an approach to decouple filter equations for macro error estimation from the track maintenance filter equations is developed. The result is a Kalman-like filter, called the macro filter. For this macro filter, experimental results are presented to illustrate its effectiveness. The problem is formulated by means of a system equation and an observation equation. For this problem, the exact Kalman filter equations are given and the approach for the decoupling of the macro filter equations from the track maintenance filter is derived. This is networked out for a single sensor situation and it is extended to multiple sensors of different type. The results of some experiments for the macro filter are described. ESA

N94-30765# Universiteit Twente, Enschede (Netherlands). Dept. of Computer Science.

A NEW PROGRAMMING METHODOLOGY FOR LAZY FUNCTIONAL LANGUAGES

F. A. vanGilst and P. M. vandenBroek Sep. 1993 18 p

(ISSN 0924-3755)

(Memo-INF-93-44; ETN-94-95718) Copyright Avail: CASI HC A03/MF A01

A programming methodology for lazy functional programming languages is presented. It is based on divide and conquer: the division of problems into subproblems. Such a division is represented by a call graph. A class of program schemes, which implement call graphs, is derived based on Johnsson's approach to attribute evaluation in attribute grammars. The key idea is to consider the passing of arguments to functions and the return of results by functions in a call graph as the propagation of inherited and synthesized attributes respectively in an attribute grammar. The methodology is illustrated by examples and a case study: the design and implementation of a compiler generator. Author

N94-30840 Argonne National Lab., IL.

EARLY EXPERIENCES WITH THE IBM SP1 AND THE HIGH-PERFORMANCE SWITCH

W. Gropp, ed. Nov. 1993 28 p Limited Reproducibility: More than 20% of this document may be affected by microfiche quality

(Contract W-31-109-eng-38)

(DE94-006261; ANL-93/41) Avail: CASI HC A03

The IBM SP1 is IBM's newest parallel distributed-memory computer. As part of a joint project with IBM, Argonne took delivery of an early system in order to evaluate the software environment and to begin porting programming packages and applications to this machine. This report discusses the results of those efforts once the high-performance switch was installed. An earlier report (ANL/MCS-TM-177) emphasized software usability and the initial ports to the SP1. This report contains performance results and discusses some applications and tools not covered in TM 177. DOE

N94-30912 National Aerospace Lab., Amsterdam (Netherlands). Informatics Div.

VALIDATION EXPERIMENTS WITH AN ETHERNET MODEL USING THE SIMULATION TOOL 'PROMISE'

G. Wedzinga 25 May 1989 28 p Presented at the 1989 European Computer Simulation Conference, Edinburgh, Scotland, 5-8 Sep. 1989 Limited Reproducibility: More than 20% of this document may be affected by microfiche quality

(AD-B174795; NLR-TP-89191-U; ETN-94-95563) Avail: CASI HC A03

The validation of an Ethernet simulation model with the aid of the PROMISE simulation tool is described. PROMISE is a general computer based simulation tool for studying systems consisting of concurrent processes. Ethernet is a packet switching, broadcast, multiaccess local area network, using carrier sense and collision detection as access procedure. The Ethernet simulation model consists of two interconnected submodels, that is, a controller submodel and a channel submodel. Both submodels are fully parametrized, allowing all Ethernet parameters to be varied and giving a free choice of the network configuration. The Ethernet model is validated using measurements of Ethernet performance by Boggs, Mogul and Kent. The results of the simulation show good agreement with the measurements. ESA

N94-30924 Politecnico di Milano (Italy). Dipt. di Elettronica e Informazione.

THEORETICAL AND EXPERIMENTAL ANALYSIS OF A NEW ALGORITHM FOR THE EUCLIDEAN 1-CENTER PROBLEM

Giovanni Righini Jun. 1993 9 p Sponsored in part by Ministry of University and Scientific and Technological Research

(Rept-93-045; ETN-94-95813) Avail: Issuing Activity (Politecnico di Milano, Piazza Leonardo da Vinci 32, 20133 Milan, Italy)

A geometrical algorithm for the euclidean 1-center problem is addressed. Its time complexity was previously conjectured to be linear in the number of points. Such conjecture is now proven to be false by a counter-example. Nevertheless experimental analysis of the algorithm behavior on random generated instances shows that the amount of computing time grows linearly with the number of points both in the weighted and in the unweighted cases. ESA

N94-30925 Politecnico di Milano (Italy). Dipt. di Elettronica e Informazione.

HEURISTIC ALGORITHMS FOR STATIC AND DYNAMIC PROBLEMS OF LOCATING THE CENTER AND THE BARYCENTER OF A GRAPH

Giovanni Righini Jul. 1993 19 p Sponsored in part by Ministry of University and Scientific and Technological Research

(Rept-93-050; ETN-94-95815) Avail: Issuing Activity (Politecnico di Milano, Piazza Leonardo da Vinci 32, 20133 Milan, Italy)

Given a graph with weights on the vertices as well as on the edges, two location problems are considered: locating the absolute center and the absolute barycenter of the graph. The dynamic version of the problems is also considered. Iterative approximated algorithms are proposed: they use as a subroutine the exact algorithm for finding the optimal location on a tree. A local search procedure which makes such algorithms much more robust is presented. The algorithms do not require the calculation of the shortest distance for every pair of vertices. ESA

N94-30928 Politecnico di Milano (Italy). Dipt. di Elettronica e Informazione.

FEDERAL GRAMMARS AND MODULAR COMPILERS

Stefano Crespi-Reghizzi and Giuseppe Psaila Sep. 1993 97 p Sponsored in part by EEC; Politecnico di Milano, and CNR-CSISEI

(Rept-93-054; ETN-94-95818) Avail: Issuing Activity (Politecnico di Milano, Piazza Leonardo da Vinci 32, 20133 Milan, Italy)

The process of designing a large language at the same time as its compiler causes repeated changes to the latter. The cost of changes is compounded with team coordination overhead for large projects. In order to confine changes, the notions of syntax module and of federal grammar as a set of modules are introduced. Deterministic LL(1) parsing conditions are defined for federal grammars. Modularity is defined for semantic evaluation based on attribute grammars. A set of tools was implemented for federal grammar design within the ATELIER Grammatica environment. The proposed approach and tools were used for the design of the deductive, active, object oriented DB language Chimera. The method is also potentially useful for embedding one language into another. ESA

N94-30931 Politecnico di Milano (Italy). Dipt. di Elettronica e Informazione.

AN UIO-BASED METHOD FOR PROTOCOL CONFORMANCE TESTING

Franco Fummi Oct. 1993 19 p

(Rept-93-060; ETN-94-95822) Avail: Issuing Activity (Politecnico di Milano, Piazza Leonardo da Vinci 32, 20133 Milan, Italy)

An improved UIO (Unique Input/Output) based algorithm for functional test generation of the communication protocols is introduced. The control portion of these protocols is examined by assuming a finite state machine description of its functionality. UIO sequences definition is extended in order to deal with finite state machines with states that do not have an UIO sequence. Both algorithms for efficient extended UIO sequence identification and for optimal test sequence generation are presented, together with the achieved results. ESA

N94-30936 Politecnico di Milano (Italy). Dipt. di Elettronica e Informazione.

REALIZATION OF FUNCTION LOGICS BY MEANS OF TRANSMISSION GATE [REALIZZAZIONE DI FUNZIONI LOGICHE MEDIANTE TRANSMISSION GATE]

Fabio Salice Oct. 1993 19 p In ITALIAN

(Rept-93-061; ETN-94-95823) Avail: Issuing Activity (Politecnico di Milano, Piazza Leonardo da Vinci 32, 20133 Milan, Italy)

A synthesis technique with transmission gate which can be automized and integrated in a CAD (Computer Aided Design) instrument for ASIC (Application Specific Integrated Circuit) design is presented. As an example, the synthesis of a full adder is reported: electrical simulation of the transmission chain of the reports and the related functional model are also reported. ESA

N94-30973 Amsterdam Univ. (Netherlands). Dept. of Mathematics and Computer Science.
THE STRUCTURE OF EXPONENTIALS: UNCOVERING THE DYNAMICS OF LINEAR LOGIC PROOFS
Vincent Danos (Paris VII Univ., France.), Jean-Baptiste Joinet (Paris VII Univ., France.), and Harold Schellinx May 1993 23 p Sponsored in part by EEC Limited Reproducibility: More than 20% of this document may be affected by microfiche quality
(ISSN 0928-3315)
(ML-93-10; ETN-94-95986) Avail: CASI HC A03

The exponential graph of proof pi in (second order) linear logic, an artefact that displays the interdependencies of exponentials, is constructed. Within this graph superfluous exponentials are defined, the removal of which is shown to yield a correct proof pi(sup triangle pointing to the right) with essentially the same set of reductions. Applications to intuitionistic and classical logic are obtained by means of reduction preserving embeddings: a given proof is embedded into linear logic, then the removal procedure is applied to it, resulting in a least, (that is, optimally) exponentiated linearization of the original proof. Things are then put the other way round, and families of linear logics in which exponential dependencies are ruled by a given graph are defined. ESA

N94-28947# National Aerospace Lab., Amsterdam (Netherlands).
ENGINEERING OF SYSTEMS FOR APPLICATION OF SCIENTIFIC COMPUTING IN INDUSTRY
W. Loeve *In* NAL, Proceedings of the 10th NAL Symposium on Aircraft Computational Aerodynamics Dec. 1992 p 1-5 (For primary document see N94-28946 08-02)
Avail: CASI HC A01/MF A03

N94-29618*# Jet Propulsion Lab., California Inst. of Tech., Pasadena.
MODIFICATIONS OF THE GRIESMER BOUND
R. J. McEliece (California Inst. of Tech., Pasadena.) and G. Solomon (Solomon, G., Pasadena, CA.) *In its* The Telecommunications and Data Acquisition Report 15 May 1991 p 41-44 (For primary document see N94-29613 08-32)
(RTOP 310-30-71-83-02)
Avail: CASI HC A01/MF A02

N94-29619*# Jet Propulsion Lab., California Inst. of Tech., Pasadena.
INTEGER COSINE TRANSFORM FOR IMAGE COMPRESSION
K.-M. Cheung, F. Pollara, and M. Shahshahani *In its* The Telecommunications and Data Acquisition Report 15 May 1991 p 45-53 (For primary document see N94-29613 08-32)
(RTOP 310-30-71-83-02)
Avail: CASI HC A02/MF A02

N94-29661*# Jet Propulsion Lab., California Inst. of Tech., Pasadena.
DIGITAL COMBINING-WEIGHT ESTIMATION FOR BROADBAND SOURCES USING MAXIMUM-LIKELIHOOD ESTIMATES
E. R. Rodemich and V. A. Vilnrotter *In its* The Telecommunications and Data Acquisition Report 15 Feb. 1994 p 98-109 (For primary document see N94-29652 08-32)
(RTOP 310-30-70-89-01)
Avail: CASI HC A03/MF A03

N94-29662*# Solomon (G.), Pasadena, CA.
CONVOLUTIONAL ENCODING OF SELF-DUAL CODES
G. Solomon *In* JPL, The Telecommunications and Data Acquisition Report 15 Feb. 1994 p 110-113 (For primary document see N94-29652 08-32)
(RTOP 310-30-71-83-02)
Avail: CASI HC A01/MF A03

N94-29670*# Jet Propulsion Lab., California Inst. of Tech., Pasadena.
AN IMPROVED CONSCAN ALGORITHM BASED ON A KALMAN FILTER
D. B. Eldred *In its* The Telecommunications and Data Acquisition Report 15 Feb. 1994 p 223-231 (For primary document see N94-29652 08-32)
(RTOP 314-30-43-10-18)
Avail: CASI HC A02/MF A03

N94-30513# Royal Military Academy, Brussels (Belgium). Electrical Engineering Dept.
KNOWLEDGE COMBINATION AND DATA FUSION WITH APPLICATION TO RECOGNITION SYSTEMS
Christiaan Perneel, Michel deMathelin, and Marc Acheroy *In* AGARD, Atmospheric Propagation Effects Through Natural and Man-Made Obscurants for Visible to MM-Wave Radiation Nov. 1993 10 p (For primary document see N94-30495 08-32)
Copyright Avail: CASI HC A02/MF A03

62 COMPUTER SYSTEMS

Includes computer networks and special application computer systems.

N94-28659# California Univ., Berkeley. Dept. of Electrical Engineering and Computer Science.
DESIGN OF PARALLEL SYSTEMS FOR SIGNAL PROCESSING
Edward A. Lee 3 Sep. 1993 18 p
(AD-A275490) Avail: CASI HC A03/MF A01

This report concludes phase 1 of the project. Two significant accomplishments are reported, the first relating to the design of heterogeneous parallel systems, and the second related to the synthesis of a parallel program for the CM-5 from Thinking Machines. A methodology for design and evaluation of parallel architectures with heterogeneous components has been developed. Specifically, the communicating processes (CP) domain in Ptolemy has been used to model heterogeneous parallel hardware systems. The first demonstration design uses the alternative low-level primitive structures (ALPS) concept. The CP domain in Ptolemy has a multitasking kernel managing concurrent processes. A process, or thread, is created for each computational and communications system resource in a particular design. The CP model of computation makes it easy to write and interconnect a variety of computational resources and simulate the execution of an application to evaluate the particular architectural configuration. DTIC

N94-28781# Alabama Univ., Huntsville. Center for Applied Optics.
A/GATECH DOSP FABRICATION Final Technical Report, Apr. 1991 - Apr. 1992
H. J. Caulfield and Steven Kupiec Nov. 1993 110 p
(Contract F30602-88-D-0025)
(AD-A275848; RL-TR-93-224) Avail: CASI HC A06/MF A02

The beginning of a true massively parallel processor based on holographic technology is presented. The theory, algorithms, and initial research are set forth and explored. Preliminary research results show great possibility for this architecture in areas of large-scale interconnects, and low-energy processing. Future research efforts, as well as possible applications, are also discussed. DTIC

N94-29050# Air Force Inst. of Tech., Wright-Patterson AFB, OH.
INVESTIGATION INTO FORMALIZATION OF DOMAIN-ORIENTED PARALLEL SOFTWARE DEVELOPMENT M.S. Thesis
Daniel P. King 15 Dec. 1993 240 p
(AD-A275177; AFIT/GCE/ENG/93D-08) Avail: CASI HC A11/MF A03

This research investigates the conceptual design of a semi-automated platform for parallel software development. The proposed semi-automated environment applies transformational techniques and domain-specific knowledge to a parallel software development process. Domain-specific and software design knowledge interact within the transformational development process in the creation of a software application. The underlying parallel specification language requires a set of parallel composition operators in order to capture an application's concurrent properties. A set of parallel composition operators is proposed that consists of parallel composition, parallel enumeration, nondeterministic choice, and sequential composition; specific communication and synchronization variable types are also proposed. A semi-automated environment based on this set of composition operators is considered and presented. DTIC

N94-29051 Defense Technical Information Center, Alexandria, VA.
LEARNING ABOUT THE INTERNET BIBLIOGRAPHY AND BEGINNERS' GUIDE Final Report

Phyllis L. Ovsiew Jan. 1994 57 p Supersedes AD-A268847 Limited Reproducibility: More than 20% of this document may be affected by microfiche quality
(AD-A275205; DTIC/TR-94-4) Avail: CASI HC A04

This documentation briefly describes and explores the basic functionality of using the Internet computer network for e-mail, ftp (file transfer protocol), and telenet. In addition, once these basics are mastered, the user is provided with a bibliography of sources available on the Internet and in traditional print sources. This is a beginners guide and is intended to help the novice user begin using the Internet. Navigational tools such as Gopher, WAIS (wide area information servers), and World Wide Web (WWW) are mentioned. Also included are a guide to Netiquette and Internet Sources of Government Information. DTIC

N94-29127# Wisconsin Univ., Madison. Dept. of Computer Sciences.
CENTER FOR PARALLEL OPTIMIZATION Final Report, 1 Jun. 1989 - 30 Sep. 1993
Olvi L. Mangasarian 30 Sep. 1993 52 p
(Grant AF-AFOSR-0410-89)
(AD-A274988; AFOSR-94-0017TR) Avail: CASI HC A04/MF A01

A strategy has been developed for the distribution of the constraint of large linear programs among parallel processors. New parallel algorithms for multicommodity flows problems have been developed. DTIC

N94-29396# Elizabeth City State Univ., NC.
ECSU HOME-INSTITUTION SUPPORT PROGRAM (1993) Quarterly Report No. 4
Linda Hayden 31 Jan. 1994 14 p
(Contract N00014-91-J-1308)
(AD-A275244) Avail: CASI HC A03/MF A01

This program, entitled 'Nurturing ECSU Research Talent in Parallel Processing and Computer Visualization' focuses on undergraduate education and undergraduate research experiences in computer science. Nurturing these young researchers will be our primary concern. Highest priority will be given to providing them with the guidance and skills to insure their entrance and success in graduate school. Further, each student in our program will learn the fundamentals of scientific research as they conduct investigations in parallel processing and computer visualization. Student development activities will include the following: (1) Recruitment of 20 high ability minority students; (2) Providing a summer program for recruited students; (3) Providing research experiences in computer visualization and parallel processing; (4) Providing a mentor, graduate school counseling and GRE preparation; (5) Providing financial support for students in the form of research scholarships; and (6) Providing funds for student travel. We are also proposing to strengthen the infrastructure of the Mathematics and Computer Science Department of ECSU. Activities proposed are: (1) Enhancement of current computer graphics and operating systems courses; (2) Development of two new courses in parallel processing and computer visualization (PPCV); (3) Acquisition of computer equipment appropriate to support PPCV research; (4) Establishing a visiting lecture series in computer science; and (5) Hiring a UNIX network manager. This project will build on the lessons learned and resources acquired during the 1991-93 ONR pilot program at ECSU. DTIC

N94-29494*# National Aeronautics and Space Administration. Langley Research Center, Hampton, VA.
ASSIST INTERNALS REFERENCE MANUAL
Sally C. Johnson and David P. Boerschlein Apr. 1994 101 p
(RTOP 505-64-10-07)
(NASA-TM-109102; NAS 1.15:109102) Avail: CASI HC A06/MF A02

The Abstract Semi-Markov Specification Interface to the SURE Tool (ASSIST) program was developed at NASA LaRC in order to analyze the reliability of virtually any fault-tolerant system. A user manual was developed to detail its use. Certain technical specifics are of no concern to the end user, yet are of importance to those who must maintain and/or verify the correctness of the tool. This document takes a detailed look into these technical issues. Author (revised)

N94-29846*# Illinois Univ., Urbana-Champaign. Coordinated Science Lab.
DEPENDABILITY ANALYSIS OF PARALLEL SYSTEMS USING A SIMULATION-BASED APPROACH M.S. Thesis
Darren Charles Sawyer 2 Feb. 1994 70 p
(Contract NAG1-613; N00014-91-J-1116)
(NASA-CR-195762; NAS 1.26:195762; UILU-ENG-94-2203; CRHC-94-02)
Avail: CASI HC A04/MF A01

The analysis of dependability in large, complex, parallel systems executing real applications or workloads is examined in this thesis. To effectively demonstrate the wide range of dependability problems that can be analyzed through simulation, the analysis of three case studies is presented. For each case, the organization of the simulation model used is outlined, and the results from simulated fault injection experiments are explained, showing the usefulness of this method in dependability modeling of large parallel systems. The simulation models are constructed using DEPEND and C++. Where possible, methods to increase dependability are derived from the experimental results. Another interesting facet of all three cases is the presence of some kind of workload of application executing in the simulation while faults are injected. This provides a completely new dimension to this type of study, not possible to model accurately with analytical approaches. Author

N94-29869*# Illinois Univ., Urbana-Champaign. Coordinated Science Lab.
CHECKPOINT-BASED FORWARD RECOVERY USING LOOKAHEAD EXECUTION AND ROLLBACK VALIDATION IN PARALLEL AND DISTRIBUTED SYSTEMS Ph.D. Thesis, 1992
Junsheng Long 28 Jan. 1994 166 p
(Contract NAG1-613; N00014-91-J-1283)
(NASA-CR-195760; NAS 1.26:195760; UILU-ENG-94-2201; CRHC-94-01)
Avail: CASI HC A08/MF A02

This thesis studies a forward recovery strategy using checkpointing and optimistic execution in parallel and distributed systems. The approach uses replicated tasks executing on different processors for forwared recovery and checkpoint comparison for error detection. To reduce overall redundancy, this approach employs a lower static redundancy in the common error-free situation to detect error than the standard N Module Redundancy scheme (NMR) does to mask off errors. For the rare occurrence of an error, this approach uses some extra redundancy for recovery. To reduce the run-time recovery overhead, look-ahead processes are used to advance computation speculatively and a rollback process is used to produce a diagnosis for correct look-ahead processes without rollback of the whole system. Both analytical and experimental evaluation have shown that this strategy can provide a nearly error-free execution time even under faults with a lower average redundancy than NMR. Author (revised)

N94-29952# Lawrence Livermore National Lab., CA.
MANAGEMENT OF PEM PUBLIC KEY CERTIFICATES USING X.500 DIRECTORY SERVICE: SOME PROBLEMS AND SOLUTIONS
Terry C. Cheung Aug. 1993 9 p Presented at the ISOC Symposium on Network and Distributed System Security, San Diego, CA, 3-4 Feb. 1994
(Contract W-7405-eng-48)
(DE94-004200; UCRL-JC-114374; CONF-940240-1) Avail: CASI HC A02/MF A01

Internet Privacy Enhanced Mail (PEM) provides security services to users of Internet electronic mail. While the prevalent PEM implementation uses a public key certificate-based strategy, certificates are mostly distributed via e-mail exchanges, which raises several security and performance issues. This paper discusses some problems with this strategy, explores the relevant issues, and develops an approach to address them. DOE

N94-29995 Selskapet for Industriell og Teknisk Forskning, Trondheim (Norway). Div. of Industrial Mathematics.
PROGRESS REPORT FOR THE PTUF PROJECT-93 Q1 AND Q2
T. H. Hansen 5 Sep. 1993 22 p Prepared in cooperation with Norges Tekniske Hoegskole, Trondheim, and Norske Data A.S., Oslow, Norway
(PB94-138591; STF10-A93015) Avail: Issuing Activity (National Technical Information Service (NTIS))

This report describes the research activities related to the PTUF project (Parallel Technology in Research and Education at NTH, SINTEF and Statoil) and the results achieved throughout the first six months of 1993. The PTUF project was initiated in 1992. The main objective of the project is to establish competence and experience on application of Massively

Parallel Programming (MPP) technology. The 56 node Intel Paragon XP/S parallel supercomputer purchased for the project was installed in December 1992. The report refers to the early experiences with Intel Paragon. Encouraging results have been achieved in areas like computational fluid dynamics, weather forecasting, and molecular dynamics. Research plans for the project and software update plans for the Paragon for Q3 and Q4 of 1993 are also included. NTIS

N94-30100 Los Alamos National Lab., NM.
COMPUTATIONAL BALANCE IN REAL-TIME CYCLIC SPECTRAL ANALYSIS
R. S. Roberts and H. H. Loomis, Jr. 1993 4 p Presented at the International Acoustics, Speech and Signal Processing Conference, Adelaide, Australia, 19-22 Apr. 1994 Limited Reproducibility: More than 20% of this document may be affected by microfiche quality
(Contract W-7405-eng-36)
(DE94-005091; LA-UR-93-4435; CONF-940476-1) Avail: CASI HC A01

Real-time cyclic spectral analysis is useful in many applications, but is difficult to achieve because of its computational complexity. This paper studies the distribution of complex multipliers in multiprocessor cyclic spectrum analyzers, with the objective of obtaining computational balance. Computationally balanced implementations efficiently use hardware so that computational bottlenecks are reduced and a smooth flow of data between computational sections of the analyzer is maintained. Tables are presented that give the number of complex multipliers required in each section of the analyzer to obtain computational balance. DOE

N94-30140 Manitoba Univ., Winnipeg. Dept. of Electrical and Computer Enginnering.
UNSUPERVISED LEARNING IN ANALOG NETWORKS M.S. Thesis
Dean Kevin McNeill 1993 60 p
(ISBN-0-315-85959-8; CTN-94-61174) Copyright Avail: Micromedia Ltd., Technical Information Centre, 240 Catherine Street, Suite 305, Ottawa, Ontario, K2P 2G8, Canada HC/MF

Artificial neural networks have shown their usefulness in the solution of a number of complex problems such as pattern recognition and associative memories. These networks are typically simulated on serial computers or using expensive vector processors. Several issues are examined which are important to the implementation of unsupervised learning algorithms in compact dedicated analog structures. Two algorithms known as coherence based unsupervised learning (CBUL) and competitive learning are discussed in detail. A fully custom analog implementation of CBUL is presented and test circuitry implemented in 3-micrometer complementary metal oxide semiconductor (CMOS). These circuits make extensive use of a CMOS version of the Gilbert multiplier to perform most of the neural computations. A complete implementation of the coherence based network, with capacitive weight storage, would consist of about 20 neurons and 400 synapses when fabricated on a 1-cm silicon die. The effect of inherent device fabrication variations are examined in terms of their effects on construction of analog circuits for competitive learning. Simulations are conducted involving a number of modelled hardware effects. The results show that competitive learning is tolerant of most expected fabrication variations except for multiplier zero-crossing offset errors. Author (CISTI)

N94-30143 Manitoba Univ., Winnipeg. Dept. of Electrical and Computer Engineering.
A LOCALLY SYNCHRONOUS GLOBALLY ASYNCHRONOUS VERTEX-8 PROCESSING ELEMENT FOR IMAGE RECONSTRUCTION ON A MESH M.S. Thesis
Jeffrey W. Fitchett Jul. 1993 125 p
(ISBN-0-315-86005-7; CTN-94-61177) Copyright Avail: Micromedia Ltd., Technical Information Centre, 240 Catherine Street, Suite 305, Ottawa, Ontario, K2P 2G8, Canada HC/MF

Image or field reconstruction problems from non-invasive measurements are a class of signal processing applications that demand parallel processing to achieve real-time operation. Image reconstruction from parallel beam projections, such as computerized tomography scans, falls within this class. A novel architecture is presented which is suitable for wafer scale integration (WSI) on which cyclic image processing algorithms could be embedded, namely the mesh of vertex-8 processors. Mapping of iterative reconstruction algorithms onto a fine-grained mesh of custom processors is illustrated, allowing inference of mappings for other image transform (such as the Hough transform) and pattern recognition problems. The focus is on the hardware design of a locally synchronous globally asynchronous vertex-8 processing element (PE) that is suitable for implementation in a WSI array with one PE per pixel. The PE has several unique features, including self-timed handshaking elements for interprocessor communications and a novel asynchronous scan test structure. Test chips have been sent for fabrication. Author (CISTI)

N94-30160*# National Aeronautics and Space Administration. Langley Research Center, Hampton, VA.
TOTAL USER MANUAL
Sally C. Johnson and David P. Boerschlein Apr. 1994 74 p
(RTOP 505-64-10-07)
(NASA-TM-109101; NAS 1.15:109101) Avail: CASI HC A04/MF A01

Semi-Markov models can be used to analyze the reliability of virtually any fault-tolerant system. However, the process of delineating all of the states and transitions in the model of a complex system can be devastatingly tedious and error-prone. Even with tools such as the Abstract Semi-Markov Specification Interface to the SURE Tool (ASSIST), the user must describe a system by specifying the rules governing the behavior of the system in order to generate the model. With the Table Oriented Translator to the ASSIST Language (TOTAL), the user can specify the components of a typical system and their attributes in the form of a table. The conditions that lead to system failure are also listed in a tabular form. The user can also abstractly specify dependencies with causes and effects. The level of information required is appropriate for system designers with little or no background in the details of reliability calculations. A menu-driven interface guides the user through the system description process, and the program updates the tables as new information is entered. The TOTAL program automatically generates an ASSIST input description to match the system description. Author

N94-30356 Nijmegen Univ. (Netherlands). Dept. of Informatics.
GENERALIZED LEFT-CORNER PARSING
Mark-Jan Nederhof Aug. 1992 11 p Limited Reproducibility: More than 20% of this document may be affected by microfiche quality
(Grant NWO-00-62-518)
(TR-92-21; ETN-94-95610) Avail: CASI HC A03

A study showing how techniques known from generalized LR (Left Right) parsing can be applied to left corner parsing is presented. The resulting parsing algorithm for context free grammars has some advantages over generalized LR parsing: the sizes and generation times of the parsers are smaller, the produced output is more compact, and the basic parsing technique can be more easily be adapted to arbitrary context free grammars. ESA

N94-30363 Nijmegen Univ. (Netherlands). Dept. of Informatics.
PARSING IN ISBES
Eerke A. Boiten Dec. 1992 15 p Limited Reproducibility: More than 20% of this document may be affected by microfiche quality
(Grant NF-63/62-518)
(TR-92-32; ETN-94-95618) Avail: CASI HC A03

A study which shows how parsing can be described as a problem from the class ISBES (Intersection of a Set and a Bag Extended Substructures) defined in a referenced study on 'bag comprehension,' that is using intersections of sets and bags of extended substructures, is presented. The resulting description is shown to be a good starting point for the transformational derivation of the Cocke-Kasami-Younger (CKY) tabular parsing algorithm. ESA

N94-30411 Utrecht State Univ. (Netherlands). Dept. of Computer Science.
AN ALL PAIRS SHORTEST PATHS DISTRIBUTED ALGORITHM USING 2n(EXP 2) MESSAGES
S. Haldar May 1993 20 p Sponsored in part by EEC Limited Reproducibility: More than 20% of this document may be affected by microfiche quality
(Contract NF-62-376) (ISSN 0924-3275)
(RUU-CS-93-19; ETN-94-95656) Avail: CASI HC A03

An investigation into the efficient building of a routing table for an arbitrary network is presented. In an execution of a distributed program, processes communicate among themselves by exchanging messages. The

execution speed of the program could be expedited by a faster message delivery system, transmitting messages to their destinations through their respective shortest paths. Some distributed algorithms were proposed in recent years for determining all pairs shortest paths for an arbitrary computer network. The best known algorithm uses O(n(exp 2) log n) messages, where n is the number of computers in the network. A distributed algorithm for the same problem using 2n(exp 2) messages in the worst case is presented. This algorithm uses a strategy quite different from those of the other algorithms for the same problem. ESA

N94-30429 Center for Mathematics and Computer Science, Amsterdam (Netherlands). Dept. of Computer Science.

MANRAY: A REPLICATED WORKERS PROGRAM IN MANIFOLD

P. Spilling and F. Arbab Jun. 1993 29 p Limited Reproducibility: More than 20% of this document may be affected by microfiche quality

(ISSN 0169-118X)

(CWI-CS-R9337; ETN-94-95679) Copyright Avail: Issuing Activity (European Space Agency (ESA))

Management of the communications among a set of concurrent processes arises in many applications and is a central concern in parallel computing. MANIFOLD is a coordination language whose sole purpose is to describe and manage complex interconnections among independent, concurrent processes. In the underlying paradigm of this language, the primary concern is not with what functionality the individual processes in a parallel system provide. Instead, the emphasis is on that these processes are inter-connected and how their interaction patterns change during the execution life of the system. The language is described, and as an example of the application of MANIFOLD, it is shown how a replicated workers program can be implemented in MANIFOLD. The concern is to show the expressiveness of MANIFOLD, and its usefulness in practice. ESA

N94-30431 Center for Mathematics and Computer Science, Amsterdam (Netherlands). Dept. of Computer Science.

RELATING STATE TRANSFORMATION SEMANTICS AND PREDICATE TRANSFORMER SEMANTICS FOR PARALLEL PROGRAMS

Franck vanBruegel (Vrije Univ., Amsterdam, Netherlands.) Jun. 1993 23 p Sponsored in part by Netherlands Nationale Programme Faciliteit Informatica Limited Reproducibility: More than 20% of this document may be affected by microfiche quality

(ISSN 0169-118X)

(CWI-CS-R9339; ETN-94-95681) Copyright Avail: CASI HC A03

A state transformation semantics and a predicate transformer semantics for programs built from atomic actions, sequential composition, nondeterministic choice, parallel composition, atomization, and a recursion are presented. Both semantic models are derived from some SOS style labeled transition systems. The state transformation semantics and the predicate transformer semantics are shown to be isomorphic extending results of Plotkin and Best. ESA

N94-30720 Utrecht State Univ. (Netherlands). Dept. of Computer Science.

ON THE RELATION BETWEEN UNITY PROPERTIES AND SEQUENCES OF STATES

R. T. Udink and J. N. Kok Feb. 1993 20 p Limited Reproducibility: More than 20% of this document may be affected by microfiche quality

(Contract SION-612-317-107) (ISSN 0924-3275)

(RUU-CS-93-07; ETN-94-95644) Avail: CASI HC A03

Stepwise refinement of programs has proven to be a suitable method for developing parallel and distributed programs. Different notions of program refinement for Unity are examined and compared. Two of these notions are based on execution sequences. Refinement corresponds to the reduction of the set of execution sequences, that is, reducing the amount of nondeterminism. The other refinement notions are based on Unity properties as introduced by Chandy and Misra. The Unity approach is to refine specifications. Although it has proven a suitable formalism for deriving algorithms, it seems less suitable for handling implementation details. Following Sanders and Singh, program refinement is formalized in the Unity framework as the preservation of Unity properties. Unity properties are shown to be not powerful enough to characterize execution sequences. As a consequence, the notion of property preserving refinement differs from the notion of reducing the set of execution sequences. ESA

N94-30730 Center for Mathematics and Computer Science, Amsterdam (Netherlands). Dept. of Numerical Mathematics.

PARALLEL ITERATION ACROSS THE STEPS OF HIGH ORDER RUNGE-KUTTA METHODS FOR NONSTIFF INITIAL VALUE PROBLEMS

P. J. vanderHouwen, B. P. Sommeijer, and W. A. vanderVeen Aug. 1993 18 p Sponsored in part by Netherlands Foundation for the Technical Sciences Limited Reproducibility: More than 20% of this document may be affected by microfiche quality

(ISSN 0169-0388)

(CWI-NM-R9313; ETN-94-95670) Copyright Avail: CASI HC A03

For the parallel integration of nonstiff Initial Value Problems (IVP's), three main approaches can be distinguished: approaches based on 'parallelism across the problem,' 'parallelism across the method,' and on 'parallelism cross the steps'. The first type of parallelism does not require special integration methods and can be exploited within any available IVP solver. The method parallelism approach received much attention, particularly within the class of explicit Runge-Kutta methods originating from fixed point iteration of implicit Runge-Kutta methods of Gaussian type. The construction and implementation on a parallel machine of such methods is extremely simple. Since the computational work per processor is modest with respect to the number of data to be exchanged between the various processors, this type of parallelism is most suitable for shared memory systems. The required number of processors is roughly half the order of the generating Runge-Kutta method, and the speed up with respect to a good sequential IVP solver is about a factor 2. The third type of parallelism (step parallelism) can be achieved in any IVP solver based on predictor corrector iteration and requires the processors to communicate after each full iteration. If the iterations have sufficient computational volume, then the step parallel approach may be suitable for implementation on distributed memory systems. Most step parallel methods proposed so far employ a large number of processors, but they lack the property of robustness due to a poor convergence behavior in the iteration process. Hence, the effective speed up is rather poor. The dynamic step parallel iteration process proposed is less massively parallel, but turns out to be sufficiently robust to achieve speed up factors up to 15. ESA

N94-30913 National Aerospace Lab., Amsterdam (Netherlands). Informatics Div.

SUPERCOMPUTING HAS TO BE PART OF AN ORGANIZATION-WIDE AUTOMATION CONCEPT

W. Loeve 11 Nov. 1990 15 p Presented at the Singapore Supercomputing Conference, 11-12 Dec. 1990 Limited Reproducibility: More than 20% of this document may be affected by microfiche quality

(AD-B174654; NLR-TP-90376-U; ETN-94-95564) Avail: CASI HC A03

The procedures and methods which have to be defined to support cooperation of specialists in development and application of digital simulation methods are described. It is concluded that supercomputers for development and application of advanced digital simulation methods have to be supplemented by workstations, mainframes and possibly minicomputers. The additional systems are needed for pre- and postprocessing and management of information in the form of enhanced data and software. The computer systems have to be connected via a network to form an infrastructure that can serve as a central nerve system of the organization. This has to enable specialists of different kinds to exchange information in cooperative execution of complicated tasks that are related to development of digital simulation methods and to application of these methods in computer aided engineering. In view of this, supercomputers shall support general communication standards. A high quality support organization is needed to keep the computer network and the implemented information in adequate condition. To this computer sciences specialists as well as application specialists shall contribute. ESA

N94-28990# National Aerospace Lab., Tokyo (Japan).

PARALLELIZATION TECHNIQUES FOR HIGHLY PARALLEL VECTOR COMPUTER [KOHEIRETSU BEKUTORU KEISANKI NIOKERU HEIRETSUKA GIHO]

Kinuyo Nakamura, Noriyuki Ando, and Naoki Nishi *In its* Proceedings of the 10th NAL Symposium on Aircraft Computational Aerodynamics Dec. 1992 p 241-246 In JAPANESE (For primary document see N94-28946 08-02)

Avail: CASI HC A02/MF A03

N94-28991# National Aerospace Lab., Tokyo (Japan).
PARALLEL FORTRAN PROGRAMMING FOR NWT [NWT MUKE HEIRETSU FORTRAN PUROGURAMINGU NITSUITE]
Masahiro Yoshida, Takashi Nakamura, Masahiro Fukuda, Shin Okada, and Shuichi Nakamura *In its* Proceedings of the 10th NAL Symposium on Aircraft Computational Aerodynamics Dec. 1992 p 247-252 In JAPANESE Prepared in cooperation with Fujitsu Ltd., Tokyo, Japan (For primary document see N94-28946 08-02)
Avail: CASI HC A02/MF A03

N94-28992# National Aerospace Lab., Tokyo (Japan).
PERFORMANCE EVALUATION OF THE NWT WITH PARALLEL FORTRAN [NWT HEIRETSU FORTRAN NI MOTODUKU HEIRETSU HYOKA]
Takashi Nakamura, Masahiro Yoshida, Masahiro Fukuda, Shuichi Nakamura, Takeo Murase, and Tatsuya Matsuzaki *In its* Proceedings of the 10th NAL Symposium on Aircraft Computational Aerodynamics Dec. 1992 p 253-258 In JAPANESE Prepared in cooperation with Fujitsu Ltd., Tokyo, Japan (For primary document see N94-28946 08-02)
Avail: CASI HC A02/MF A03

N94-28993# National Aerospace Lab., Tokyo (Japan).
A METHOD OF USER INTERFACE FOR NWT [NWT NO YUZA INTAFEISU JITSUGEN HOSHIKI]
Masako Tsuchiya, Kazuyo Suematsu, Shunji Suematsu, Haruo Hatama, Hiroshi Morishige, Yasushi Yamaguchi, and Yukihiro Karube *In its* Proceedings of the 10th NAL Symposium on Aircraft Computational Aerodynamics Dec. 1992 p 259-264 In JAPANESE (For primary document see N94-28946 08-02)
Avail: CASI HC A02/MF A03

N94-29333# National Research Council of Canada, Ottawa (Ontario). Software Engineering Lab.
DESIGN OF A THINWIRE REAL-TIME MULTIPROCESSOR OPERATING SYSTEM
Charles Gauthier *In* AGARD, Aerospace Software Engineering for Advanced Systems Architectures Nov. 1993 11 p (For primary document see N94-29315 08-61)
Copyright Avail: CASI HC A03/MF A03

63 CYBERNETICS

Includes feedback and control theory, artificial intelligence, robotics and expert systems.

For related information see also *54 Man/System Technology and Life Support.*

N94-28613 Joint Inst. for Nuclear Research, Dubna (USSR).
TRACK FILTERING BY ROBUST NEURAL NETWORK
S. A. Baginyan, I. V. Kisel, E. V. Konotopskaya, and G. A. Ososkov 1993 11 p Limited Reproducibility: More than 20% of this document may be affected by microfiche quality
(DE94-606067; JINR-E-10-93-86) Avail: Issuing Activity (Department of Energy (DOE)) (US Sales Only)

In the present paper we study the following problems of track information extraction by the artificial neural network (ANN) rotor model: providing initial ANN configuration by an algorithm general enough to be applicable for any discrete detector in or out of a magnetic field; robustness to heavy contaminated raw data (up to 100% signal-to-noise ratio); and stability to the growing event multiplicity. These problems were carried out by corresponding innovations of our model, namely: by a special one-dimensional histogramming, by multiplying weights by a specially designed robust multiplier, and by replacing the simulated annealing schedule by ANN dynamics with an optimally fixed temperature. Our approach is valid for both circular and straight (non-magnetic) tracks and tested on 2D simulated data contaminated by 100% noise points distributed uniformly. To be closer to some reality in our simulation, we keep parameters of the cylindrical spectrometer ARES. DOE

N94-28672 Naval Postgraduate School, Monterey, CA.
THE STATE TRANSITION DIAGRAM WITH PATH PRIORITY AND IT'S APPLICATIONS M.S. Thesis
Thomas Scholz Sep. 1993 100 p Limited Reproducibility: More than 20% of this document may be affected by microfiche quality
(AD-A275524) Avail: CASI HC A05

The overall software structure of the Naval Postgraduate School Autonomous Underwater Vehicle (NPS AUV) is the Rational Behavior Model (RBM), a tri-level, multilingual software architecture which is based on three levels of abstraction called the strategic, tactical, and execution level. In this study, interests were focused on the implementation of the strategic level in CLIPS such that it exhibits the same behavior as the already existing implementation written in Prolog. As a tool for translating a backward chaining version of the Strategic level software (like Prolog) to a forward chaining one (like CLIPS), the State Transition Diagram With Path Priority (STDWP) was introduced in this study. Specifically, STDWP allows graphical translation between backward and forward chaining versions of the strategic level. This research shows empirically that the translation is always possible and that the two versions hold logical and behavioral equivalence. Thus, STDWP bridges two approaches in robot control which are based on forward and backward chaining. DTIC

N94-29013# Air Force Inst. of Tech., Wright-Patterson AFB, OH.
EXPERIMENTAL EVALUATION OF FUZZY LOGIC CONTROL OF A FLEXIBLE ARM MANIPULATOR Ph.D. Thesis
Joel Jackson 9 Dec. 1993 87 p
(AD-A275375; AFIT/CI/CIA/93-167) Avail: CASI HC A05/MF A01

The purpose of the research reported in this thesis was to explore fuzzy logic control of a single link, flexible robot arm. The performance and stability robustness properties of fuzzy logic control were evaluated in simulation and with hardware in the loop in the University of Washington Control Systems Laboratory. The plant model and the Integrated System, Inc., AC100-C30 real time control prototyping system were first validated using a PID controller, which was also used as a comparison for the performance of various fuzzy logic controllers. The control objective was to slew the arm rapidly to commanded positions while minimizing the excitation of the link's flexible modes. The available sensor was a hub angle sensor (no tip position or tip rate information was used for the controllers). The stability robustness of the PID controller and the fuzzy logic controller were evaluated in hardware for mismodeled system parameters. Tests were conducted for increased tip mass relative to the design condition controller as well as for a significantly more flexible link than the design condition. The fuzzy controller was found to be stable for all test conditions, while the PID controller was unstable for one of the off-design conditions. DTIC

N94-29026 Florida Atlantic Univ., Boca Raton.
PARTIAL SUPPORT FOR THE SECOND INTERNATIONAL SYMPOSIUM ON ARTIFICIAL INTELLIGENCE AND MATHEMATICS Final Report, 1 Jan. 1992 - 30 Apr. 1993
Frederick Hoffman 30 Apr. 1993 3 p Second Symposium held in Boca Raton, FL, 5-8 Jan. 1992 Limited Reproducibility: More than 20% of this document may be affected by microfiche quality
(Contract F49620-92-J-0120)
(AD-A275199; AFOSR-94-0029-TR) Avail: CASI HC A01

For the Second Symposium, the invited speakers were Zolar Manna (Standford) 'Modular Temporal Reasoning,' Heinz-Otto Peitgen (Bremen and Florida Atlantic University, 'Cellular Automata, Fractals, and Attractors,' K. Ebcioglu (IBM Yorktown Heights), 'A logic Programming System for Chorale Harmonization,' and J. C. Latombe (Stanford), 'Geometry and Search in Motion Planning.' The program Committee accepted 52 papers and had speakers from 16 countries. The sessions were on logic, non-monotonic logic, theorem proving, logic programming, constraints, learning, reasoning, neutral networks, and genetic algorithms. Additionally, there was one session on applications and one general session. There was also a somewhat autonomous 'Autonomous Control Workshop', organized by Anil Nerode, and held concurrently with the Symposium. Sunday morning's session and the invited talks were plenary; there were two concurrent sessions the rest of the three and one-half days. DTIC

N94-29044# Naval Postgraduate School, Monterey, CA.
FEEDBACK CONTROL OF A THREE-LINK PLANAR UNDER-ACTUATED MANIPULATOR USING A SURGE VELOCITY M.S. Thesis
Pernell A. Jordan 23 Sep. 1993 46 p
(AD-A275159) Avail: CASI HC A03/MF A01

An under-actuated robot manipulator is one that has fewer joint actuators than the number of degrees of freedom of the manipulator. Such manipulators are studied with the objective of developing smarter mechanical systems; ones that can provide low-cost automation and enable design simplification. While in space these manipulators can afford to have any kind of mechanical structure, on earth they need to be strictly planar to be feasible. In this paper, we develop a control scheme for a three link planar robot manipulator with two actuators such that it can reach any joint configuration from any other. We assume that the first joint of the robot is passive and is provided with a brake and a rotary dashpot. We show that our control is robust to the variations in certain parameters and unmodelled dynamics like stiction. DTIC

N94-29198 Army Topographic Engineering Center, Fort Belvoir, VA.
NEURAL NETWORK SOLUTIONS TO LOGIC PROGRAMS WITH GEOMETRIC CONSTRAINTS Scientific Paper
Jo A. Parikh, Anne Werkheiser, and V. S. Subrahamanian Jan. 1994 15 p Limited Reproducibility: More than 20% of this document may be affected by microfiche quality
(AD-A275419; TEC-R-206) Avail: CASI HC A03

Hybrid knowledge bases (HKB's), proposed by Nerode and Subrahmanian, provide a uniform theoretical framework for dealing with the mixed data types and multiple reasoning modes required for solving logical deployment problems. Algorithms based on mixed integer linear programming techniques have been developed for the syntactic subset of HKB's corresponding to function-free Prolog-like logic programs. In this study, we examine the ability of neural networks to solve a more comprehensive set of problems expressed within the hybrid knowledge base framework. The objective of this research is to design and implement a nonlinear optimization procedure for solving extended logic programs with neural networks. We focus upon two types of extensions which are typically required in the formulation of logical deployment problems. The first type of extension, which we shall refer to as a Type I extension, consists of embedding numerical and geometric constraints into logic programs. The second type of extension, which we shall call a Type II extension, consists of incorporating optimization problems into logic clauses. DTIC

N94-29465* National Aeronautics and Space Administration. Pasadena Office, CA.
HIGH LEVEL LANGUAGE-BASED ROBOTIC CONTROL SYSTEM Patent
Guillermo Rodriguez, inventor (to NASA) (Jet Propulsion Lab., California Inst. of Tech., Pasadena.), Kenneth K. Kreutz, inventor (to NASA) (Jet Propulsion Lab., California Inst. of Tech., Pasadena.), and Abhinandan Jain, inventor (to NASA) (Jet Propulsion Lab., California Inst. of Tech., Pasadena.) 12 Apr. 1994 34 p Filed 1 Nov. 1991 Supersedes N92-17895 (30 - 8, p 1349) Continuation-in-part of US-Patent-Appl-SN-459438, filed 2 Jan. 1990
(NASA-Case-NPO-17918-2-CU; US-Patent-5,303,384;
US-Patent-Appl-SN-786499; US-Patent-Appl-SN-459438;
US-Patent-Class-395-99; US-Patent-Class-395-80; US-Patent-Class-395-89;
Int-Patent-Class-G05B-19/00) Avail: US Patent and Trademark Office

This invention is a robot control system based on a high level language implementing a spatial operator algebra. There are two high level languages included within the system. At the highest level, applications programs can be written in a robot-oriented applications language including broad operators such as MOVE and GRASP. The robot-oriented applications language statements are translated into statements in the spatial operator algebra language. Programming can also take place using the spatial operator algebra language. The statements in the spatial operator algebra language from either source are then translated into machine language statements for execution by a digital control computer. The system also includes the capability of executing the control code sequences in a simulation mode before actual execution to assure proper action at execution time. The robot's environment is checked as part of the process and dynamic reconfiguration is also possible. The languages and system allow the programming and control of multiple arms and the use of inward/outward spatial recursions in which every computational step can be related to a transformation from one point in the mechanical robot to another point to name two major advantages.
Official Gazette of the U.S. Patent and Trademark Office

N94-29466* National Aeronautics and Space Administration. Lyndon B. Johnson Space Center, Houston, TX.
MEASURAND TRANSIENT SIGNAL SUPPRESSOR Patent
Richard J. Bozeman, Jr., inventor (to NASA) 22 Mar. 1994 8 p Filed 2 Oct. 1992 Supersedes N93-17056 (31-5, p 1261)
(NASA-Case-MSC-22027-1; US-Patent-5,296,750;
US-Patent-Appl-SN-955801; US-Patent-Class-307-308;
US-Patent-Class-307-118; US-Patent-Class-307-234;
US-Patent-Class-307-542.1; US-Patent-Class-328-1;
US-Patent-Class-340-309.15; US-Patent-Class-340-507) Avail: US Patent and Trademark Office

A transient signal suppressor for use in a controls system which is adapted to respond to a change in a physical parameter whenever it crosses a predetermined threshold value in a selected direction of increasing or decreasing values with respect to the threshold value and is sustained for a selected discrete time interval is presented. The suppressor includes a sensor transducer for sensing the physical parameter and generating an electrical input signal whenever the sensed physical parameter crosses the threshold level in the selected direction. A manually operated switch is provided for adapting the suppressor to produce an output drive signal whenever the physical parameter crosses the threshold value in the selected direction of increasing or decreasing values. A time delay circuit is selectively adjustable for suppressing the transducer input signal for a preselected one of a plurality of available discrete suppression time and producing an output signal only if the input signal is sustained for a time greater than the selected suppression time. An electronic gate is coupled to receive the transducer input signal and the timer output signal and produce an output drive signal for energizing a control relay whenever the transducer input is a non-transient signal which is sustained beyond the selected time interval. Official Gazette of the U.S. Patent and Trademark Office

N94-29480# Aerospatiale, Suresnes (France).
INTEGRATION OF A PATH GENERATION ALGORITHM INTO OFF-LINE PROGRAMMING OF AIRBUS PANELS
L. Graux, P. Millies, P. L. Kociemba, and B. Langlois 1993 9 p
(Rept-932-600-103; ETN-94-95482) Avail: CASI HC A02/MF A01

A method for programming robot motions in an industrial environment is described. The purpose of this study was the offline programming automation of riveting machines for Airbus (A320-A340) panels and subassemblies. Providing the initial and goal configuration of the robot on the Airbus part, the method determines a collision free path taking into account computer aided design models of both the robot and Airbus parts. This method, based on the attractive potential field concept and the random motion technique was implemented on a robotic simulation software. The results obtained in planning trajectories for the industrial robot in a complex environment shows that the random motion method can be applied. The factors which limit the path planning performance are the time required for smoothing and the large number of anticollision tests required. The method can deal with all Airbus panels and subassemblies, and this approach could be extended to high degree of freedom industrial robots. ESA

N94-29492*# National Aeronautics and Space Administration. Pasadena Office, CA.
A NEURAL NETWORK WITH MODULAR HIERARCHICAL LEARNING Patent Application
Pierre F. Baldi, inventor (to NASA) (Jet Propulsion Lab., California Inst. of Tech., Pasadena.) and Nikzad Toomarian, inventor (to NASA) (Jet Propulsion Lab., California Inst. of Tech., Pasadena.) 24 Mar. 1994 23 p
(Contract NAS7-1260)
(NASA-Case-NPO-19077-1-CU; NAS 1.71:NPO-19077-1-CU;
US-Patent-Appl-SN-223953) Avail: CASI HC A03/MF A01

This invention provides a new hierarchical approach for supervised neural learning of time dependent trajectories. The modular hierarchical methodology leads to architectures which are more structured than fully interconnected networks. The networks utilize a general feedforward flow of information and sparse recurrent connections to achieve dynamic effects. The advantages include the sparsity of units and connections, the modular

organization. A further advantage is that the learning is much more circumscribed learning than in fully interconnected systems. The present invention is embodied by a neural network including a plurality of neural modules each having a pre-established performance capability wherein each neural module has an output outputting present results of the performance capability and an input for changing the present results of the performance capabilitiy. For pattern recognition applications, the performance capability may be an oscillation capability producing a repeating wave pattern as the present results. In the preferred embodiment, each of the plurality of neural modules includes a pre-established capability portion and a performance adjustment portion connected to control the pre-established capability portion. NASA

N94-29504* National Aeronautics and Space Administration. Pasadena Office, CA.

KINEMATIC FUNCTIONS FOR REDUNDANCY RESOLUTION USING CONFIGURATION CONTROL Patent

Homayoun Seraji, inventor (to NASA) 15 Mar. 1994 29 p Filed 27 Oct. 1992 Supersedes N93-17275 (31 - 5, p 1261)
(NASA-Case-NPO-18608-1-CU; US-Patent-5,294,873;
US-Patent-Appl-SN-967083; US-Patent-Class-318-568.1;
US-Patent-Class-318-561; US-Patent-Class-318-646;
US-Patent-Class-318-628; US-Patent-Class-395-95; US-Patent-Class-901-9;
Int-Patent-Class-G05B-19/42) Avail: US Patent and Trademark Office

The invention fulfills new goals for redundancy resolution based on manipulator dynamics and end-effector characteristics. These goals are accomplished by employing the recently developed configuration control approach. Redundancy resolution is achieved by controlling the joint inertia matrix of the end-effector mass matrix that affect the inertial torques or by reducing the joint torques due to gravity loading and payload. The manipulator mechanical-advantage and velocity-ratio are also used as performance measures to be improved by proper utilization of redundancy. Furthermore, end-effector compliance, sensitivity, and impulsive force at impact are introduced as redundancy resolution criteria. The new goals for redundancy resolution allow a more efficient utilization of the redundant joints based on the desired task requirements.
Official Gazette of the U.S. Patent and Trademark Office

N94-29526# Loughborough Univ. of Technology (England). Dept. of Mathematical Sciences.

ON-LINE SEARCH FOR OPTIMAL CONTROLLER PARAMETERS USING INTERCONNECTED LEARNING AUTOMATA

Q. H. Wu Sep. 1993 19 p
(MATHS-Rept-A-196; ETN-94-95511) Avail: CASI HC A03/MF A01

The application of interconnected learning automata to control of unknown stochastic dynamic systems is addressed. A method of using N learning automata and subsets of actions to search controller parameters according to a given performance index is presented. Simulation results of evaluation on this method for control of an unknown turbogenerator system are included. The results demonstrated potential for control of unknown stochastic dynamic systems. ESA

N94-29720 Texas Univ., Austin.

PULSE RESPONSE BASED MINIMUM TIME CONTROL OF FLEXIBLE STRUCTURES Ph.D. Thesis

Shih-Hsiao Mark Chang 1993 128 p
Avail: Univ. Microfilms Order No. DA9323361

A pulse response based control method is presented for solving minimum time flexible maneuver problems on the basis of the measured response to pulses applied in control inputs. Once the response of the structure to pulses in control inputs has been measured, the numerical optimization problem is solved to find the smallest number of time steps for which a control history exists that consists of a train of bounded pulses and results in desired outputs at the end of the control task. This method has the advantage that identification requirements are greatly reduced, because very little explicit knowledge of the system is needed. In fact, linear behavior of the structure is represented without modal truncation in terms of the pulse response measurements. However, for maneuver problems, nonlinear effects associated with rapid large-angle rotation are significant, but only in a few modes. These nonlinear effects are taken into account by explicitly modeling the response in a few of the lowest modes, so that the model order required for explicitly representing significant nonlinear behavior of the structure is much lower using this approach than if all linear behavior must be represented explicitly. The effect of actuator dynamics does not have to be modeled, because it is naturally represented in the measured pulse response. An efficient algorithm employing a quadratic programming code is developed to find the minimum time control of the structure. The effect of measurement noise on the accuracy of the pulse response based control method is investigated. Precise response of an example model which consists of a rigid hub with four identical uniform flexible appendages and tip masses is simulated by analytically separating the rigid body and flexible components of response. Then, the model is used to demonstrate the application of pulse response based control method to nonlinear large angle maneuver problems. A near minimum time pulse response based control method which requires virtually no real time computation is presented. A stable feedback control scheme which takes into account both nonlinear rotational stiffening effects and bounds on control inputs is also presented. The methods developed are demonstrated with numerical examples.
Dissert. Abstr.

N94-29756* National Aeronautics and Space Administration. Pasadena Office, CA.

NEURAL NETWORK WITH DYNAMICALLY ADAPTABLE NEURONS Patent

Raoul Tawel, inventor (to NASA) (Jet Propulsion Lab., California Inst. of Tech., Pasadena.) 29 Mar. 1994 13 p Filed 27 May 1993 Continuation of abandoned US-Patent-Appl-SN-905061, filed 24 Jun. 1992 which is a continuation of abandoned US-Patent-Appl-SN-473024, filed 31 Jan. 1992
(NASA-Case-NPO-17803-1-CU; US-Patent-5,299,285;
US-Patent-Appl-SN-071206; US-Patent-Appl-SN-905061;
US-Patent-Appl-SN-473024; US-Patent-Class-395-24;
US-Patent-Class-395-23; Int-Patent-Class-G06F-15/18;
Int-Patent-Class-G06G-7/19) Avail: US Patent and Trademark Office

This invention is an adaptive neuron for use in neural network processors. The adaptive neuron participates in the supervised learning phase of operation on a co-equal basis with the synapse matrix elements by adaptively changing its gain in a similar manner to the change of weights in the synapse IO elements. In this manner, training time is decreased by as much as three orders of magnitude.
Official Gazette of the U.S. Patent and Trademark Office

N94-29835 California Inst. of Tech., Pasadena.

ROBOTIC HAND-EYE MOTOR LEARNING Ph.D. Thesis

Carl Frederick Ruoff 1993 223 p
Avail: Univ. Microfilms Order No. DA9325386

This thesis investigates the use of neural networks and nonlinear estimation in robotic motor learning. It presents a detailed experimental investigation of the performance and parametric sensitivity of resource-allocating neural networks along with a new learning algorithm that offers rapid adaptation and excellent accuracy. It also includes an appendix that relates feedforward neural networks to familiar mathematical ideas. In addition, it presents two learning hand-eye calibration systems, one based on neural networks and the other on nonlinear estimation. The network-based system learns to correct robot positioning errors arising from the use of nominal system kinematics, while the estimation-based system identifies the robot's kinematic parameters. Both systems employ the same two-link robot with stereo vision, and include noise and various other error sources. The network-based system is robust to all error sources considered, though noise naturally limits performance. The estimation-based system has significantly better performance when the robot and vision systems are well modeled, but is extremely sensitive to unmodeled error sources and noise. Finally, it presents a robot control system based on neural networks that learns to catch balls perfectly without requiring explicit programming or conventional controllers. It uses only feedforward pursuit motions learned through practice, and is initially incapable of even moving its arm in response to external stimuli. It learns to identify and control its pursuit movements, to identify and predict ball behavior, and, with the aid of advice from a critic, to modify its movement commands to improve catching success. The system, which incorporates information from visual, arm state, and drive force sensors, characterizes control situations using input/response pairs. This allows it to learn and respond to plant variations without requiring parametric models or parameter identification. It achieves robust execution by comparing predicted and observed behavior, using inconsistencies to trigger learning and behavioral change. Dissert. Abstr.

N94-29840 Cleveland State Univ., OH.
NEURAL NETWORK APPLICATION TO PARTICLE IMPACT NOISE DETECTION Ph.D. Thesis
Lois Jean Scaglione 1993 133 p
Avail: Univ. Microfilms Order No. DA9324929

Particle Impact Noise Detection (PIND) is a NASA developed test to determine the presence of loose particles inside the cavity of electronic parts. The loose particles may cause failures during launch conditions or in zero gravity. PIND testing analysis currently relies on audio static detection, visual interpretation of fluctuating oscilloscope signals, or a threshold detector which cannot distinguish between PIND failures and electric line transients. As a result, PIND testing is limited by human senses and is a subjective test with an accuracy level of less than 50 percent. In this research project, the PIND test is standardized and automated by digitizing the analog noise signal obtained from a PIND tester and analyzing the data using neural networks. Two types of neural networks were successfully trained and tested on the PIND data within 1 percent accuracy. A mathematical model of PIND testing was used to study the important characteristics of PIND testing and verified MIL-STD-883C Notice 8 Method 2020.7 and Method 2052. A validity study verified that particles were present in the electronic parts cavity when indicated by the PIND test. The results of this study indicate a significant improvement in the quality, reliability, and cost associated with PIND testing. Dissert. Abstr.

N94-29853 Carnegie-Mellon Univ., Pittsburgh, PA.
REINFORCEMENT LEARNING FOR ROBOTS USING NEURAL NETWORKS Ph.D. Thesis
Long-Ji Lin 1992 160 p
Avail: Univ. Microfilms Order No. DA9322750

Reinforcement learning agents are adaptive, reactive, and self-supervised. The aim of this dissertation is to extend the state of the art of reinforcement learning and enable its applications to complex robot learning problems. In particular, it focuses on two issues. First, learning from sparse and delayed reinforcement signals is hard and in general a slow process. Techniques for reducing learning time must be devised. Second, most existing reinforcement learning methods assume that the world is a Markov decision process. This assumption is too strong for many robot tasks of interest. This dissertation demonstrates how we can possibly overcome the slow learning problem and tackle non-Markovian environments, making reinforcement learning more practical for realistic robot tasks. Reinforcement learning can be naturally integrated with artificial neural networks to obtain high-quality generalization, resulting in a significant learning speedup. Neural networks are used in this dissertation, and they generalize effectively even in the presence of noise and a large number of binary and real-valued inputs. Reinforcement learning agents can save many learning trials by using an action model, which can be learned on-line. With a model, an agent can mentally experience the effects of its actions without actually executing them. Experience replay is a simple technique that implements this idea, and is shown to be effective in reducing the number of action executions required. Reinforcement learning agents can take advantage of instructive training instances provided by human teachers, resulting in a significant learning speedup. Teaching can also help learning agents avoid local optima during the search for optimal control. Simulation experiments indicate that even a small amount of teaching can save agents many learning trials. Reinforcement learning agents can significantly reduce learning time by hierarchical learning: they first solve elementary learning problems and then combine solutions to the elementary problems to solve a complex problem. Simulation experiments indicate that a robot with hierarchical learning can solve a complex problem, which otherwise is hardly solvable within a reasonable time. Reinforcement learning agents can deal with a wide range of non-Markovian environments by having a memory of their past. Three memory architectures are discussed. They work reasonably well for a variety of simple problems. One of them is also successfully applied to a nontrivial non-Markovian robot task. The results of this dissertation rely on computer simulation, including an agent operating in a dynamic and hostile environment and a mobile robot operating in a noisy and non-Markovian environment. The robot simulator is physically realistic. This dissertation concludes that it is possible to build artificial agents than can acquire complex control policies effectively by reinforcement learning. Dissert. Abstr.

N94-29895 Illinois Univ., Urbana-Champaign.
ROBUST ADAPTIVE CONTROL AND FILTERING Ph.D. Thesis
Sanjeev Manubhai Naik 1992 173 p
Avail: Univ. Microfilms Order No. DA9305630

This thesis examines the robustness properties of various adaptive systems for control, filtering, and identification. These include the uniform boundedness or mean square boundedness of all closed-loop signals (robust boundedness, robust ultimate boundedness) and the closed-loop system tracking error performance in the presence (robust performance) and absence (nominal performance) of unmodeled dynamics, disturbances, and parameter time variations. The thesis is divided into three main parts. The first part considers the robustness of continuous-time adaptive control, the second part is concerned with robust adaptive control of discrete-time plants with time-varying parameters, and the third part deals with the robustness of stochastic adaptive algorithms that include parallel model adaptation problems such as output error identification, adaptive IIR filtering, adaptive feedforward control, and adaptive noise canceling, and ELS (extended least squares)-based adaptive control. In the first part, a continuous-time direct model reference adaptive controller (MRAC) using a gradient adaptation law based on parameter projection and 'extended regressor' normalization is proposed. Based on this, boundedness of all closed-loop signals is established for a continuous-time plant of arbitrary positive relative degree, in the presence of persistent bounded disturbances and small unmodeled dynamics that depend on both input and output, in possibly nonlinear or time-varying fashion. The deterioration of output tracking error performance is shown to be a continuous function of the sizes of the disturbance and unmodeled dynamics. In the second part, a discrete-time indirect adaptive pole-zero placement controller using a gradient adaptation law based on parameter projection and 'extended regressor' normalization is proposed for adaptive control of a discrete-time plant with time-varying parameters. Based on this, closed-loop boundedness and performance are established in the presence of disturbances, small unmodeled dynamics, and slow-in-the-mean parameter variations. In the third part, we consider the robustness of parameter projection-based parallel adaptation (output error-based) problems such as output error identification, adaptive IIR filtering, adaptive feedforward control, and adaptive noise canceling to unmodeled dynamics and to violation of statistical assumptions on the noise. We analyze vanishing gain algorithms. In the case of output error identification/adaptive IIR filtering, we also consider nonvanishing gain algorithms. It is found that the commonly imposed strict positive realness (SPR) condition can be relaxed in certain cases. We also consider the robustness of ELS-based adaptive control, which is an equation error-based approach. Dissert. Abstr.

N94-30250# Sandia National Labs., Albuquerque, NM.
NEURAL NETWORK BASED TIME-OPTIMAL CONTROL OF A MAGNETICALLY LEVITATED PRECISION POSITIONING SYSTEM
J. Redmond and S. Tucker 1994 9 p Presented at the 35th American Institute of Aeronautics and Astronautics (AIAA) Structures, Structural Dynamics and Materials Conference, Hilton Head, SC, 18-22 Apr. 1994
(Contract DE-AC04-94AL-85000)
(DE94-006573; SAND-94-0417C; CONF-940432-1) Avail: CASI HC A02/MF A01

This paper describes an application of artificial neural networks to the problem of time-optimal control of a magnetically levitated platen. The system of interest is a candidate technology for advanced photolithography machines used in the manufacturing of integrated circuits. The nonlinearities associated with magnetic levitation actuators preclude the direct application of classical time-optimal control methodologies for determining optimal rest-to-rest maneuver strategies. Instead, a computer simulation of the platen system is manipulated to provide a training set for an artificial neural network. The trained network provides optimal switching times for conducting one dimensional rest-to-rest maneuvers of the platen that incorporate the full nonlinear effects of the magnetic levitation actuators. Sample problems illustrate the effectiveness of the neural network based control as compared to traditional proportional-derivative control. DOE

N94-30255 British Columbia Univ., Vancouver. Dept. of Mathematics.
SECOND ORDER NECESSARY CONDITIONS IN OPTIMAL CONTROL Ph.D. Thesis
Harry Huiheng Zheng May 1993 110 p

(ISBN-0-315-85443-X; CTN-94-61160) Copyright Avail: Micromedia Ltd., Technical Information Centre, 240 Catherine Street, Suite 305, Ottawa, Ontario, K2P 2G8, Canada HC/MF

Second order necessary conditions for the standard deterministic optimal control problem are presented, without conventional regularity assumptions. Three different advances in second-order theory are reported. In a study of conjugate points in smooth optimal control, a set of conditions is described under which the second variation along an external trajectory is certain to be negative. When these are satisfied, they identify a certain point in the basic interval as a generalized conjugate point (GCP). GCP's include all conjugate points in the classical sense and all points where the Legendre condition is violated. GCP's were also found in many problems left unresolved in the literature, and it is deduced that the associated extremals are not optimal. A second order tangent set is then used to predict second order variations along a trajectory to a different inclusion. A generalized form is obtained of the statement that the second variation associated with a minimum point is nonnegative. Finally, Rockafellar's theory of epi differentiability is applied to integral functionals. Using Attouch's theorem, it is shown that certain nonconvex integral functionals of interest in optimal control are twice epi differentiable. From this the necessary conditions of optimality are deduced for problems without endpoint constraints.

Author (CISTI)

N94-30334 Utrecht State Univ. (Netherlands). Cognitive Artificial Intelligence.

A LATERAL INHIBITION NEURAL NETWORK THAT EMULATES A WINNER-TAKES-ALL ALGORITHM

B. Krekelberg and J. N. Kok Dec. 1992 8 p Limited Reproducibility: More than 20% of this document may be affected by microfiche quality

(ISSN 0924-3275)
(RUU-CS-92-46; ETN-94-95636) Avail: CASI HC A02

The conditions under which a lateral inhibition type network with binary neurons selects a unit which receives the maximal input are determined. It is shown that the lateral interaction between two neurons needs to be tuned to a critical value. The resulting neural network is a local implementation of the first phase of the Kohonen learning algorithm. ESA

N94-30349 Utrecht State Univ. (Netherlands). Dept. of Computer Science.

A MULTISCALE APPROACH TO IMAGE SEGMENTATION USING KOHONEN NETWORKS

S. Haring, M. A. Viergever, and J. N. Kok Feb. 1993 16 p Limited Reproducibility: More than 20% of this document may be affected by microfiche quality

(RUU-CS-93-06; ETN-94-95643) Avail: CASI HC A03

An approach to multiscale image segmentation, based on pixel classification by means of a Kohonen network, is developed. An image is described by assigning a feature pattern to each pixel, consisting of a scaled family of differential geometrical invariant features. The invariant feature pattern representation of a training image is input to a Kohonen network, in order to obtain a description of the feature space in terms of so called prototypical feature patterns (the weight vectors of the network). Supervised labeling of these prototypical feature patterns may be accomplished using classes derived from an a priori segmentation of the training image. Any image similar to the training image can be segmented by comparing the feature pattern representation of each pixel with all weight vectors, and assigning each pixel the class of the best matching weight vector. The benefit of applying features at multiple scales, and the effects of first and second order information on the results, were evaluated. ESA

N94-30373 Universiteit Twente, Enschede (Netherlands). Tele-Informatics and Open Systems Group.

PERFORMANCE EVALUATION OF INTELLIGENT NETWORK SERVICES

P. J. E. Leever (PTT Research, Leidschendam, Netherlands.), G. S. Vermeer (PTT Research, Leidschendam, Netherlands.), R. A. J. Reijmerink (PTT Research, Leidschendam, Netherlands.), L. J. N. Franken (PTT Research, Leidschendam, Netherlands.), and B. R. Haverkort 1993 12 p Presented at the 10th United Kingdom Teletraffic Symposium, Ipswich, England, 14-16 Apr. 1993 Limited Reproducibility: More than 20% of this document may be affected by microfiche quality

(ISSN 0924-3755)
(Memo-INF-93-20; TIOS-93-11; ETN-94-95596) Copyright Avail: Issuing Activity (European Space Agency (ESA))

A model to determine performance metrics for an intelligent network (IN) is presented. The model was constructed using queueing network theory. The model can be solved for a certain configuration by either simulation or analytical calculation. A simulation model was built using the SIMSCRIPT language. The simulation model was verified by analytical calculations. This verification indicates that the simulation model was correct. The simulation model provides, besides performance metrics like utilization and average response times, estimations of response time distributions. These distributions may be very useful in order to assure a certain quality of service towards PTT customers. Using the model it is possible to get some hands on experience for capacities needed in the IN, guaranteeing a good quality of service. With simulation it is possible to get online experience with the parametrizing of the IN. The effect of adding a new service or installing new equipment can be shown. ESA

N94-30375 Universiteit Twente, Enschede (Netherlands). Tele-Informatics and Open Systems Group.

CUSTOMER CREATION AND COMBINATION IN QUEUEING NETWORKS

Geert Heijenk, Magda ElZarki, and Ignas Niemegeers 1993 32 p Submitted for publication Sponsored by Netherlands Organization for Scientific Research Limited Reproducibility: More than 20% of this document may be affected by microfiche quality

(ISSN 0924-3755)
(Memo-INF-93-35; TIOS-93-25; ETN-94-95604) Copyright Avail: CASI HC A03

Constraints are relaxed and the analysis of the class of open queueing networks are extended with general arrival processes and general service time distributions, considered in Queueing Network Analyzer (QNA) software package. In order to allow for the modeling of, for example, segmentation and reassembly processes in communication networks, two new types of nodes are introduced. A customer creation node generated a certain number of departing customers upon arrival of one single customer. A customer combination node combines a certain number of arriving customers into one departing customer, which departs as soon as all the originating customers have arrived. Both the numbers of customers to be created and the number of customers to be combined are random variables. The analysis of the nodes are presented in the context of QNA. The feasibility and the accuracy of the extension is illustrated by example queueing networks. ESA

N94-30410 Utrecht State Univ. (Netherlands). Dept. of Computer Science.

A PROBABILISTIC APPROACH TO MOTION PLANNING FOR CAR-LIKE ROBOTS

Petr Svestka Apr. 1993 88 p Sponsored in part by EEC, and Netherlands Organization for Scientific Research Limited Reproducibility: More than 20% of this document may be affected by microfiche quality

(ISSN 0924-3275)
(RUU-CS-93-18; ETN-94-95655) Avail: CASI HC A05

A study aimed at finding a collision free path in an environment containing some obstacles for a given robot from start configuration to goal configuration is presented. Solid robots which move in a planar environment are addressed; the technique described can be applied to other robot types. Two versions of the random motion planning method are described: one based on an undirected graph, and one based on a directed one. An explanation as to how the constraints of the robot prescribe whether the underlying graph should be directed or not is given. Attention is paid to the way in which edges should be added to the underlying graph, and how to prevent adding useless edges. A number of heuristic techniques for adding via-points in a smarter way then just fully randomly are described. Two methods for smoothing the paths generated by the basic algorithm are given. Formal definitions of car-like robots and paths respecting their nonholonomic constraints are given and the described techniques are applied to them. ESA

N94-30517 Washington Univ., Seattle.

A DIRECT DIGITAL CONTROL-LAW SYNTHESIS IN THE w-DOMAIN:

W-SYNTHESIS METHODOLOGY Ph.D. Thesis
Cheolkeun Ha 1993 206 p
Avail: Univ. Microfilms Order No. DA9326360

In this dissertation, a new framework for direct digital control-law synthesis of a typical single-rate sampled-data system is presented. The synthesis procedure is conducted in the w-domain for design and analysis of sampled-data systems. A general procedure of direct digital controller synthesis in the w-domain is proposed and it is called the W-synthesis procedure. In the synthesis procedure, a generalized root-locus method in the w-domain is presented. Based on the W-synthesis procedure, an optimal W-synthesis method is developed to solve the general class of H2 optimal control problems for sampled-data systems using a numerical search algorithm applied to continuous-time optimal control problems. The H2 optimal control problem is extended to address computation time-delay at the control action. A (s,w)-hybrid method for frequency response analysis is developed that takes into account aliasing frequency components. An extended-optimal W-synthesis (EOW-synthesis) method is developed to allow a convenient design of discrete-time controller defined in the z-domain. To synthesize robust digital control-laws to plant parameter variations, the EOW-synthesis procedure makes use of a multi-objective criterion in the setting of multiple plant conditions. The EOW-synthesis method is implemented in the numerical search algorithm 'Wsandy' which is a modification of the algorithm SANDY developed for continuous-time H2 optimal control problems. The optimal W-synthesis methods have been applied to a pitch augmentation design of B767 airplane, a benchmark problem of a two-mass-spring system with computation time-delay and the control of a flexible two-link robot manipulator. Dissert. Abstr.

N94-30526*# National Aeronautics and Space Administration. Lyndon B. Johnson Space Center, Houston, TX.
CONFERENCE ON INTELLIGENT ROBOTICS IN FIELD, FACTORY, SERVICE, AND SPACE (CIRFFSS 1994), VOLUME 1
Jon D. Erickson, ed. Mar. 1994 472 p Conference held in Houston, TX, 21-24 Mar. 1994; sponsored by NASA, Johnson Space Center, AIAA, IEEE Robotics and Automation Society, NSRA, RIA, SOIE, and ISA
(NASA-CP-3251; S-754-Vol-1; NAS 1.55:3251) Avail: CASI HC A20/MF A04

The AIAA/NASA Conference on Intelligent Robotics in Field, Factory, Service, and Space (CIRFFSS '94) was originally proposed because of the strong belief that America's problems of global economic competitiveness and job creation and preservation can partly be solved by the use of intelligent robotics, which are also required for human space exploration missions. Individual sessions addressed nuclear industry, agile manufacturing, security/building monitoring, on-orbit applications, vision and sensing technologies, situated control and low-level control, robotic systems architecture, environmental restoration and waste management, robotic remanufacturing, and healthcare applications. For individual titles, see N94-30527 through N94-30584.

N94-30527*# National Aeronautics and Space Administration. Lyndon B. Johnson Space Center, Houston, TX.
INTELLIGENT ROBOTICS CAN BOOST AMERICA'S ECONOMIC GROWTH
Jon D. Erickson *In its* Conference on Intelligent Robotics in Field, Factory, Service, and Space (CIRFFSS 1994), Volume 1 Mar. 1994 p 1-7 (For primary document see N94-30526 08-63)
(AIAA Paper 94-1301-CP) Avail: CASI HC A02/MF A04

A case is made for strategic investment in intelligent robotics as a part of the solution to the problem of improved global competitiveness for U.S. manufacturing, a critical industrial sector. Similar cases are made for strategic investments in intelligent robotics for field applications, construction, and service industries such as health care. The scope of the country's problems and needs is beyond the capability of the private sector alone, government alone, or academia alone to solve independently of the others. National cooperative programs in intelligent robotics are needed with the private sector supplying leadership direction and aerospace and non-aerospace industries conducting the development. Some necessary elements of such programs are outlined. The National Aeronautics and Space Administration (NASA) and the Lyndon B. Johnson Space Center (JSC) can be key players in such national cooperative programs in intelligent robotics for several reasons: (1) human space exploration missions require supervised intelligent robotics as enabling tools and, hence must develop supervised intelligent robotic systems; (2) intelligent robotic technology is being developed for space applications at JSC (but has a strong crosscutting or generic flavor) that is advancing the state of the art and is producing both skilled personnel and adaptable developmental infrastructure such as integrated testbeds; and (3) a NASA JSC Technology Investment Program in Robotics has been proposed based on commercial partnerships and collaborations for precompetitive, dual-use developments. Author

N94-30528*# TECHNIKA, Saint Petersburg (Russia).
TELEOPERATED SYSTEMS FOR NUCLEAR REACTORS: INSPECTION AND MAINTENANCE
V. P. Dorokhov, D. V. Dorokhov, and A. P. Eperin *In* NASA. Johnson Space Center, Conference on Intelligent Robotics in Field, Factory, Service, and Space (CIRFFSS 1994), Volume 1 Mar. 1994 p 8-11 (For primary document see N94-30526 08-63)
(AIAA Paper 94-1176-CP) Avail: CASI HC A01/MF A04

The present paper describes author's work in the field of teleoperated equipment for inspection and maintenance of the RBML technological channels and graphite laying, emergency operations. New technological and design solutions of teleoperated robotic systems developed for Leningradsky Power Plant are discussed. Author

N94-30529*# Institut de Recherche de l'Hydro-Ontario, Toronto.
ARK: AUTONOMOUS MOBILE ROBOT IN AN INDUSTRIAL ENVIRONMENT
S. B. Nickerson, P. Jasiobedzki, M. Jenkin, A. Jepson, E. Milios, B. Down, J. R. R. Service, D. Terzopoulos, J. Tsotsos, and D. Wilkes et al *In* NASA. Johnson Space Center, Conference on Intelligent Robotics in Field, Factory, Service, and Space (CIRFFSS 1994), Volume 1 Mar. 1994 p 12-20 (For primary document see N94-30526 08-63)
(AIAA Paper 94-1177-CP) Avail: CASI HC A02/MF A04

This paper describes research on the ARK (Autonomous Mobile Robot in a Known Environment) project. The technical objective of the project is to build a robot that can navigate in a complex industrial environment using maps with permanent structures. The environment is not altered in any way by adding easily identifiable beacons and the robot relies on naturally occurring objects to use as visual landmarks for navigation. The robot is equipped with various sensors that can detect unmapped obstacles, landmarks and objects. In this paper we describe the robot's industrial environment, it's architecture, a novel combined range and vision sensor and our recent results in controlling the robot in the real-time detection of objects using their color and in the processing of the robot's range and vision sensor data for navigation. Author

N94-30530*# Case Western Reserve Univ., Cleveland, OH. Dept. of Mechanical and Aerospace Engineering.
BIOLOGICALLY-INSPIRED HEXAPOD ROBOT DESIGN AND SIMULATION
Kenneth S. Espenschied and Roger D. Quinn *In* NASA. Johnson Space Center, Conference on Intelligent Robotics in Field, Factory, Service, and Space (CIRFFSS 1994), Volume 1 Mar. 1994 p 21-28 (For primary document see N94-30526 08-63)
(AIAA Paper 94-1178-CP) Avail: CASI HC A02/MF A04

The design and construction of a biologically-inspired hexapod robot is presented. A previously developed simulation is modified to include models of the DC drive motors, the motor driver circuits and their transmissions. The application of this simulation to the design and development of the robot is discussed. The mechanisms thought to be responsible for the leg coordination of the walking stick insect were previously applied to control the straight-line locomotion of a robot. We generalized these rules for a robot walking on a plane. This biologically-inspired control strategy is used to control the robot in simulation. Numerical results show that the general body motion and performance of the simulated robot is similar to that of the robot based on our preliminary experimental results. Author

N94-30531*# Binghamton Univ., NY. AIAA Lab.
ODYSSEUS AUTONOMOUS WALKING ROBOT: THE LEG/ARM DESIGN
N. G. Bourbakis, M. Maas, A. Tascillo, and C. Vandewinckel *In* NASA. Johnson Space Center, Conference on Intelligent Robotics in Field, Factory, Service, and Space (CIRFFSS 1994), Volume 1 Mar. 1994 p 29-36 (For primary document see N94-30526 08-63)
(AIAA Paper 94-1180-CP) Avail: CASI HC A02/MF A04

ODYSSEUS is an autonomous walking robot, which makes use of three wheels and three legs for its movement in the free navigation space. More specifically, it makes use of its autonomous wheels to move around in an environment where the surface is smooth and not uneven. However, in the case that there are small height obstacles, stairs, or small height unevenness in the navigation environment, the robot makes use of both wheels and legs to travel efficiently. In this paper we present the detailed hardware design and the simulated behavior of the extended leg/arm part of the robot, since it plays a very significant role in the robot actions (movements, selection of objects, etc.). In particular, the leg/arm consists of three major parts: The first part is a pipe attached to the robot base with a flexible 3-D joint. This pipe has a rotated bar as an extended part, which terminates in a 3-D flexible joint. The second part of the leg/arm is also a pipe similar to the first. The extended bar of the second part ends at a 2-D joint. The last part of the leg/arm is a clip-hand. It is used for selecting several small weight and size objects, and when it is in a 'closed' mode, it is used as a supporting part of the robot leg. The entire leg/arm part is controlled and synchronized by a microcontroller (68CH11) attached to the robot base. Author

N94-30532*# Grumman Aerospace Corp., Bethpage, NY.
VAS: A VISION ADVISOR SYSTEM COMBINING AGENTS AND OBJECT-ORIENTED DATABASES
James L. Eilbert, William Lim, Jay Mendelsohn, Ron Braun, and Michael Yearwood *In* NASA. Johnson Space Center, Conference on Intelligent Robotics in Field, Factory, Service, and Space (CIRFFSS 1994), Volume 1 Mar. 1994 p 37-46 (For primary document see N94-30526 08-63)
(AIAA Paper 94-1181-CP) Avail: CASI HC A02/MF A04

A model-based approach to identifying and finding the orientation of non-overlapping parts on a tray has been developed. The part models contain both exact and fuzzy descriptions of part features, and are stored in an object-oriented database. Full identification of the parts involves several interacting tasks each of which is handled by a distinct agent. Using fuzzy information stored in the model allowed part features that were essentially at the noise level to be extracted and used for identification. This was done by focusing attention on the portion of the part where the feature must be found if the current hypothesis of the part ID is correct. In going from one set of parts to another the only thing that needs to be changed is the database of part models. This work is part of an effort in developing a Vision Advisor System (VAS) that combines agents and objected-oriented databases. Author

N94-30533*# Tufts Univ., Medford, MA. Dept. of Mechanical Engineering.
APPLICATION OF THE MODULAR AUTOMATED RECONFIGURABLE ASSEMBLY SYSTEM (MARAS) CONCEPT TO ADAPTABLE VISION GAUGING AND PARTS FEEDING
Andre Bernard By, Ken Caron, Michael Rothenberg, and Vic Sales *In* NASA. Johnson Space Center, Conference on Intelligent Robotics in Field, Factory, Service, and Space (CIRFFSS 1994), Volume 1 Mar. 1994 p 47-55 (For primary document see N94-30526 08-63)
(AIAA Paper 94-1182-CP) Avail: CASI HC A02/MF A04

This paper presents the first phase results of a collaborative effort between university researchers and a flexible assembly systems integrator to implement a comprehensive modular approach to flexible assembly automation. This approach, named MARAS (Modular Automated Reconfigurable Assembly System), has been structured to support multiple levels of modularity in terms of both physical components and system control functions. The initial focus of the MARAS development has been on parts gauging and feeding operations for cylinder lock assembly. This phase is nearing completion and has resulted in the development of a highly configurable system for vision gauging functions on a wide range of small components (2 mm to 100 mm in size). The reconfigurable concepts implemented in this adaptive Vision Gauging Module (VGM) are now being extended to applicable aspects of the singulating, selecting, and orienting functions required for the flexible feeding of similar mechanical components and assemblies. Author

N94-30534*# Ford Motor Co., Dearborn, MI. Alpha Simultaneous Engineering.
AGILE MANUFACTURING: THE FACTORY OF THE FUTURE
Joseph M. Loibl and Terry A. Bossieux *In* NASA. Johnson Space Center, Conference on Intelligent Robotics in Field, Factory, Service, and Space (CIRFFSS 1994), Volume 1 Mar. 1994 p 56-62 (For primary document see N94-30526 08-63)
(AIAA Paper 94-1184-CP) Avail: CASI HC A02/MF A04

The factory of the future will require an operating methodology which effectively utilizes all of the elements of product design, manufacturing and delivery. The process must respond rapidly to changes in product demand, product mix, design changes or changes in the raw materials. To achieve agility in a manufacturing operation, the design and development of the manufacturing processes must focus on customer satisfaction. Achieving greatest results requires that the manufacturing process be considered from product concept through sales. This provides the best opportunity to build a quality product for the customer at a reasonable rate. The primary elements of a manufacturing system include people, equipment, materials, methods and the environment. The most significant and most agile element in any process is the human resource. Only with a highly trained, knowledgeable work force can the proper methods be applied to efficiently process materials with machinery which is predictable, reliable and flexible. This paper discusses the affect of each element on the development of agile manufacturing systems. Author

N94-30535*# Boeing Co., Seattle, WA. Commercial Airplane Group.
CONFESSIONS OF A ROBOT LOBOTOMIST
R. Marc Gottshall *In* NASA. Johnson Space Center, Conference on Intelligent Robotics in Field, Factory, Service, and Space (CIRFFSS 1994), Volume 1 Mar. 1994 p 63-72 (For primary document see N94-30526 08-63)
(AIAA Paper 94-1185-CP) Avail: CASI HC A02/MF A04

Since its inception, numerically controlled (NC) machining methods have been used throughout the aerospace industry to mill, drill, and turn complex shapes by sequentially stepping through motion programs. However, the recent demand for more precision, faster feeds, exotic sensors, and branching execution have existing computer numerical control (CNC) and distributed numerical control (DNC) systems running at maximum controller capacity. Typical disadvantages of current CNC's include fixed memory capacities, limited communication ports, and the use of multiple control languages. The need to tailor CNC's to meet specific applications, whether it be expanded memory, additional communications, or integrated vision, often requires replacing the original controller supplied with the commercial machine tool with a more powerful and capable system. This paper briefly describes the process and equipment requirements for new controllers and their evolutionary implementation in an aerospace environment. The process of controller retrofit with currently available machines is examined, along with several case studies and their computational and architectural implications. Author

N94-30536*# Ford Motor Co., Dearborn, MI. Alpha Manufacturing Technologies Applications Center.
INTEGRATION OF VISION AND ROBOTIC WORKCELL
T. A. Bossieux *In* NASA. Johnson Space Center, Conference on Intelligent Robotics in Field, Factory, Service, and Space (CIRFFSS 1994), Volume 1 Mar. 1994 p 73-77 (For primary document see N94-30526 08-63)
(AIAA Paper 94-1186-CP) Avail: CASI HC A01/MF A04

The paper discusses the incorporation of vision into a robotic cell to obtain cell status information and use this information to influence the robot operation. It discusses both mechanical and informational solutions to the operational issues which are present. The cell uses a machine vision system to determine information about part presence in the shipping tray, part location in the tray, and tray orientation. The vision system's edge detector algorithm is used to identify the orientation of the packing trays. In addition, different vision tools are used to determine if parts are present in the trays based on the unique configuration of the individual parts. The mechanical solutions discuss the handling of medium weight (10 - 25 lb.) parts at an average cycle time of 3.1 seconds per part. The robot gripper must handle 33 different models, three identical parts at a time. This is accomplished by using stacks of rotary actuators and slides between the stacks. Author

N94-30537*# Cyberomotion, Inc., Salem, VA.
MEETING THE CHALLENGES OF INSTALLING A MOBILE ROBOTIC SYSTEM
Celeste DeCorte *In* NASA. Johnson Space Center, Conference on

Intelligent Robotics in Field, Factory, Service, and Space (CIRFFSS 1994), Volume 1 Mar. 1994 p 78-81 (For primary document see N94-30526 08-63)
(AIAA Paper 94-1187-CP) Avail: CASI HC A01/MF A04

The challenges of integrating a mobile robotic system into an application environment are many. Most problems inherent to installing the mobile robotic system fall into one of three categories: (1) the physical environment - location(s) where, and conditions under which, the mobile robotic system will work; (2) the technological environment - external equipment with which the mobile robotic system will interact; and (3) the human environment - personnel who will operate and interact with the mobile robotic system. The successful integration of a mobile robotic system into these three types of application environment requires more than a good pair of pliers. The tools for this job include: careful planning, accurate measurement data (as-built drawings), complete technical data of systems to be interfaced, sufficient time and attention of key personnel for training on how to operate and program the robot, on-site access during installation, and a thorough understanding and appreciation - by all concerned - of the mobile robotic system's role in the security mission at the site, as well as the machine's capabilities and limitations. Patience, luck, and a sense of humor are also useful tools to keep handy during a mobile robotic system installation. This paper will discuss some specific examples of problems in each of three categories, and explore approaches to solving these problems. The discussion will draw from the author's experience with on-site installations of mobile robotic systems in various applications. Most of the information discussed in this paper has come directly from knowledge learned during installations of Cybermotion's SR2 security robots. A large part of the discussion will apply to any vehicle with a drive system, collision avoidance, and navigation sensors, which is, of course, what makes a vehicle autonomous. And it is with these sensors and a drive system that the installer must become familiar in order to foresee potential trouble areas in the physical, technical, and human environment. Author

N94-30538*# Robotic Systems Technology, Westminster, MD.
DESIGN OF AN AUTONOMOUS EXTERIOR SECURITY ROBOT
Scott D. Myers *In* NASA. Johnson Space Center, Conference on Intelligent Robotics in Field, Factory, Service, and Space (CIRFFSS 1994), Volume 1 Mar. 1994 p 82-87 (For primary document see N94-30526 08-63)
(AIAA Paper 94-1188-CP) Avail: CASI HC A02/MF A04

This paper discusses the requirements and preliminary design of robotic vehicle designed for performing autonomous exterior perimeter security patrols around warehouse areas, ammunition supply depots, and industrial parks for the U.S. Department of Defense. The preliminary design allows for the operation of up to eight vehicles in a six kilometer by six kilometer zone with autonomous navigation and obstacle avoidance. In addition to detection of crawling intruders at 100 meters, the system must perform real-time inventory checking and database comparisons using a microwave tags system. Author

N94-30539*# Oak Ridge National Lab., TN. Center for Engineering Systems Advanced Research.
TASK AUTOMATION IN A SUCCESSFUL INDUSTRIAL TELEROBOT
Philip F. Spelt and Sammy L. Jones *In* NASA. Johnson Space Center, Conference on Intelligent Robotics in Field, Factory, Service, and Space (CIRFFSS 1994), Volume 1 Mar. 1994 p 88-92 (For primary document see N94-30526 08-63)
(Contract DE-AC05-84OR-21400)
(AIAA Paper 94-1189-CP) Avail: CASI HC A01/MF A04

In this paper, we discuss cooperative work by Oak Ridge National Laboratory and Remotec, Inc., to automate components of the operator's workload using Remotec's Andros telerobot, thereby providing an enhanced user interface which can be retrofit to existing fielded units as well as being incorporated into new production units. Remotec's Andros robots are presently used by numerous electric utilities to perform tasks in reactors where substantial exposure to radiation exists, as well as by the armed forces and numerous law enforcement agencies. The automation of task components, as well as the video graphics display of the robot's position in the environment, will enhance all tasks performed by these users, as well as enabling performance in terrain where the robots cannot presently perform due to lack of knowledge about, for instance, the degree of tilt of the robot. Enhanced performance of a successful industrial mobile robot leads to increased safety and efficiency of performance in hazardous environments. The addition of these capabilities will greatly enhance the utility of the robot, as well as its marketability. Author

N94-30540*# Naval Command, Control and Ocean Surveillance Center, San Diego, CA. RDT&E Div.
CONTROLLING MULTIPLE SECURITY ROBOTS IN A WAREHOUSE ENVIRONMENT
H. R. Everett, G. A. Gilbreath, T. A. Heath-Pastore, and R. T. Laird *In* NASA. Johnson Space Center, Conference on Intelligent Robotics in Field, Factory, Service, and Space (CIRFFSS 1994), Volume 1 Mar. 1994 p 93-102 (For primary document see N94-30526 08-63)
(AIAA Paper 94-1300-CP) Avail: CASI HC A02/MF A04

The Naval Command Control and Ocean Surveillance Center (NCCOSC) has developed an architecture to provide coordinated control of multiple autonomous vehicles from a single host console. The multiple robot host architecture (MRHA) is a distributed multiprocessing system that can be expanded to accommodate as many as 32 robots. The initial application will employ eight Cybermotion K2A Navmaster robots configured as remote security platforms in support of the Mobile Detection Assessment and Response System (MDARS) Program. This paper discusses developmental testing of the MRHA in an operational warehouse environment, with two actual and four simulated robotic platforms. Author (revised)

N94-30541*# National Aeronautics and Space Administration. Lyndon B. Johnson Space Center, Houston, TX.
TECHNOLOGY TRANSFER AND EVALUATION FOR SPACE STATION TELEROBOTICS
Charles R. Price, LeBarian Stokes, and Myron A. Diftler *In its* Conference on Intelligent Robotics in Field, Factory, Service, and Space (CIRFFSS 1994), Volume 1 Mar. 1994 p 103-111 (For primary document see N94-30526 08-63)
(AIAA Paper 94-1190-CP) Avail: CASI HC A02/MF A04

The international space station (SS) must take advantage of advanced telerobotics in order to maximize productivity and safety and to reduce maintenance costs. The Automation and Robotics Division at the NASA Lyndon B. Johnson Space Center (JSC) has designed, developed, and constructed the Automated Robotics Maintenance of Space Station (ARMSS) facility for the purpose of transferring and evaluating robotic technology that will reduce SS operation costs. Additionally, JSC had developed a process for expediting the transfer of technology from NASA research centers and evaluating these technologies in SS applications. Software and hardware system developed at the research centers and NASA sponsored universities are currently being transferred to JSC and integrated into the ARMSS for flight crew personnel testing. These technologies will be assessed relative to the SS baseline, and, after refinements, those technologies that provide significant performance improvements will be recommended as upgrades to the SS. Proximity sensors, vision algorithms, and manipulator controllers are among the systems scheduled for evaluation. Author (revised)

N94-30542*# National Aeronautics and Space Administration. Lyndon B. Johnson Space Center, Houston, TX.
SPACE FLIGHT MANIPULATOR TECHNOLOGIES AND REQUIREMENTS FOR THE NASA FLIGHT TELEROBOTIC SERVICER (FTS)
John T. Chladek and William M. Craver *In its* Conference on Intelligent Robotics in Field, Factory, Service, and Space (CIRFFSS 1994), Volume 1 Mar. 1994 p 112-122 (For primary document see N94-30526 08-63)
(AIAA Paper 94-1191-CP) Avail: CASI HC A03/MF A04

NASA Headquarters' Office of Advanced Concepts and Technology (OACT) joined efforts with Johnson Space Center's (JSC) Automation and Robotics Division and Langley Research Center's (LaRC) Information Systems Division to capture the technologies developed during the cancelled NASA Flight Telerobotic Servicer (FTS) program planned for use on Space Station Freedom. The recent FTS technology capture effort completed the build and testing of one flight qualifiable FTS manipulator, deliverable to JSC's Automation & Robotics Division for environmental testing. The many robotic technologies developed to meet the 30 year space environment design requirements are discussed in this paper. The manipulator properties were to allow positioning control to one thousandths of an inch, with zero actuator backlash over a temperature range of -50 to +95 C, and were to include impedance control and inertial decoupling. Safety and reliability

requirements are discussed that were developed to allow a thirty year life in space with minimum maintenance. The system had to meet the safety requirements for hazardous payloads for operation in the shuttle payload bay during demonstration test flights prior to station use. A brief description is contained on an orbiter based robotic experiment and operational application using the dexterous FTS manipulator operating on the end of the shuttle remote manipulator systems (SRMS) from ground control.
Author (revised)

N94-30543*# Carnegie-Mellon Univ., Pittsburgh, PA. The Robotics Inst.
A SPACE STATION ROBOT WALKER AND ITS SHARED CONTROL SOFTWARE
Yangsheng Xu, Ben Brown, Shigeru Aoki, and Tetsuji Yoshida *In* NASA. Johnson Space Center, Conference on Intelligent Robotics in Field, Factory, Service, and Space (CIRFFSS 1994), Volume 1 Mar. 1994 p 123-130 (For primary document see N94-30526 08-63)
(AIAA Paper 94-1192-CP) Avail: CASI HC A02/MF A04

In this paper, we first briefly overview the update of the self-mobile space manipulator (SMSM) configuration and testbed. The new robot is capable of projecting cameras anywhere interior or exterior of the Space Station Freedom (SSF), and will be an ideal tool for inspecting connectors, structures, and other facilities on SSF. Experiments have been performed under two gravity compensation systems and a full-scale model of a segment of SSF. This paper presents a real-time shared control architecture that enables the robot to coordinate autonomous locomotion and teleoperation input for reliable walking on SSF. Autonomous locomotion can be executed based on a CAD model and off-line trajectory planning, or can be guided by a vision system with neural network identification. Teleoperation control can be specified by a real-time graphical interface and a free-flying hand controller. SMSM will be a valuable assistant for astronauts in inspection and other EVA missions. Author (revised)

N94-30544*# Jet Propulsion Lab., California Inst. of Tech., Pasadena.
TECHNOLOGY FOR ROBOTIC SURFACE INSPECTION IN SPACE
Richard Volpe and J. Balaram *In* NASA. Johnson Space Center, Conference on Intelligent Robotics in Field, Factory, Service, and Space (CIRFFSS 1994), Volume 1 Mar. 1994 p 131-141 (For primary document see N94-30526 08-63)
(AIAA Paper 94-1193-CP) Avail: CASI HC A03/MF A04

This paper presents on-going research in robotic inspection of space platforms. Three main areas of investigation are discussed: machine vision inspection techniques, an integrated sensor end-effector, and an orbital environment laboratory simulation. Machine vision inspection utilizes automatic comparison of new and reference images to detect on-orbit induced damage such as micrometeorite impacts. The cameras and lighting used for this inspection are housed in a multisensor end-effector, which also contains a suite of sensors for detection of temperature, gas leaks, proximity, and forces. To fully test all of these sensors, a realistic space platform mock-up has been created, complete with visual, temperature, and gas anomalies. Further, changing orbital lighting conditions are effectively mimicked by a robotic solar simulator. In the paper, each of these technology components will be discussed, and experimental results are provided.
Author (revised)

N94-30545*# Jet Propulsion Lab., California Inst. of Tech., Pasadena.
A HIGHLY REDUNDANT ROBOT SYSTEM FOR INSPECTION
Thomas S. Lee, Tim Ohms, and Samad Hayati *In* NASA. Johnson Space Center, Conference on Intelligent Robotics in Field, Factory, Service, and Space (CIRFFSS 1994), Volume 1 Mar. 1994 p 142-148 (For primary document see N94-30526 08-63)
(AIAA Paper 94-1194-CP) Avail: CASI HC A02/MF A04

The work on the serpentine inspection system at JPL is described. The configuration of the inspection system consists of 20 degrees of freedom in total. In particular, the design and development of the serpentine micromanipulator end-effector tool which has 12 degrees of freedom is described. The inspection system is used for application in JPL's Remote Surface Inspection project and as a research tool in redundant manipulator control. Author (revised)

N94-30546*# Ohio Univ., Athens. Dept. of Mechanical Engineering.
FREE-FLOATING DUAL-ARM ROBOTS FOR SPACE ASSEMBLY
Sunil Kumar Agrawal and M. Y. Chen *In* NASA. Johnson Space Center, Conference on Intelligent Robotics in Field, Factory, Service, and Space (CIRFFSS 1994), Volume 1 Mar. 1994 p 149-157 (For primary document see N94-30526 08-63)
(AIAA Paper 94-1195-CP) Avail: CASI HC A02/MF A04

Freely moving systems in space conserve linear and angular momentum. As moving systems collide, the velocities get altered due to transfer of momentum. The development of strategies for assembly in a free-floating work environment requires a good understanding of primitives such as self motion of the robot, propulsion of the robot due to onboard thrusters, docking of the robot, retrieval of an object from a collection of objects, and release of an object in an object pool. The analytics of such assemblies involve not only kinematics and rigid body dynamics but also collision and impact dynamics of multibody systems. In an effort to understand such assemblies in zero gravity space environment, we are currently developing at Ohio University a free-floating assembly facility with a dual-arm planar robot equipped with thrusters, a free-floating material table, and a free-floating assembly table. The objective is to pick up workpieces from the material table and combine them into prespecified assemblies. This paper presents analytical models of assembly primitives and strategies for overall assembly. A computer simulation of an assembly is developed using the analytical models. The experiment facility will be used to verify the theoretical predictions. Author (revised)

N94-30547*# Arizona Univ., Tucson. Dept. of Electrical and Computer Engineering.
DESIGN AND CONTROL OF ACTIVE VISION BASED MECHANISMS FOR INTELLIGENT ROBOTS
Liwei Wu and Michael M. Marefat *In* NASA. Johnson Space Center, Conference on Intelligent Robotics in Field, Factory, Service, and Space (CIRFFSS 1994), Volume 1 Mar. 1994 p 158-167 (For primary document see N94-30526 08-63)
(Grants NSF DDM-93-19208; NSF DDM-92-10018)
(AIAA Paper 94-1196-CP) Avail: CASI HC A02/MF A04

In this paper, we propose a design of an active vision system for intelligent robot application purposes. The system has the degrees of freedom of pan, tilt, vergence, camera height adjustment, and baseline adjustment with a hierarchical control system structure. Based on this vision system, we discuss two problems involved in the binocular gaze stabilization process: fixation point selection and vergence disparity extraction. A hierarchical approach to determining point of fixation from potential gaze targets using evaluation function representing human visual behavior to outside stimuli is suggested. We also characterize different visual tasks in two cameras for vergence control purposes, and a phase-based method based on binarized images to extract vergence disparity for vergence control is presented. A control algorithm for vergence control is discussed. Author (revised)

N94-30548*# Michigan Univ., Ann Arbor. Artificial Intelligence Lab.
VISION BASED OBJECT POSE ESTIMATION FOR MOBILE ROBOTS
Annie Wu, Clint Bidlack, Arun Katkere, Roy Feague, and Terry Weymouth *In* NASA. Johnson Space Center, Conference on Intelligent Robotics in Field, Factory, Service, and Space (CIRFFSS 1994), Volume 1 Mar. 1994 p 168-174 (For primary document see N94-30526 08-63)
(AIAA Paper 94-1197-CP) Avail: CASI HC A02/MF A04

Mobile robot navigation using visual sensors requires that a robot be able to detect landmarks and obtain pose information from a camera image. This paper presents a vision system for finding man-made markers of known size and calculating the pose of these markers. The algorithm detects and identifies the markers using a weighted pattern matching template. Geometric constraints are then used to calculate the position of the markers relative to the robot. The selection of geometric constraints comes from the typical pose of most man-made signs, such as the sign standing vertical and the dimensions of known size. This system has been tested successfully on a wide range of real images. Marker detection is reliable, even in cluttered environments, and under certain marker orientations, estimation of the orientation has proven accurate to within 2 degrees, and distance estimation to within 0.3 meters. Author (revised)

N94-30549*# Italian Space Agency, Matera. Center for Space Geodesy.
UNSUPERVISED TEXTURE IMAGE SEGMENTATION BY IMPROVED NEURAL NETWORK ART2
Zhiling Wang, G. Sylos Labini, R. Mugnuolo, and Marco DeSario *In*

NASA. Johnson Space Center, Conference on Intelligent Robotics in Field, Factory, Service, and Space (CIRFFSS 1994), Volume 1 Mar. 1994 p 175-180 (For primary document see N94-30526 08-63)
(AIAA Paper 94-1199-CP) Avail: CASI HC A02/MF A04

We here propose a segmentation algorithm of texture image for a computer vision system on a space robot. An improved adaptive resonance theory (ART2) for analog input patterns is adapted to classify the image based on a set of texture image features extracted by a fast spatial gray level dependence method (SGLDM). The nonlinear thresholding functions in input layer of the neural network have been constructed by two parts: firstly, to reduce the effects of image noises on the features, a set of sigmoid functions is chosen depending on the types of the feature; secondly, to enhance the contrast of the features, we adopt fuzzy mapping functions. The cluster number in output layer can be increased by an autogrowing mechanism constantly when a new pattern happens. Experimental results and original or segmented pictures are shown, including the comparison between this approach and K-means algorithm. The system written in C language is performed on a SUN-4/330 sparc-station with an image board IT-150 and a CCD camera. Author (revised)

N94-30550*# Lockheed Sanders, Inc., Nashua, NH.
MICROWAVE VISION FOR ROBOTS
Leon Lewandowski and Keith Struckman *In* NASA. Johnson Space Center, Conference on Intelligent Robotics in Field, Factory, Service, and Space (CIRFFSS 1994), Volume 1 Mar. 1994 p 181-189 (For primary document see N94-30526 08-63)
(AIAA Paper 94-0887-CP) Avail: CASI HC A02/MF A04

Microwave Vision (MV), a concept originally developed in 1985, could play a significant role in the solution to robotic vision problems. Originally our Microwave Vision concept was based on a pattern matching approach employing computer based stored replica correlation processing. Artificial Neural Network (ANN) processor technology offers an attractive alternative to the correlation processing approach, namely the ability to learn and to adapt to changing environments. This paper describes the Microwave Vision concept, some initial ANN-MV experiments, and the design of an ANN-MV system that has led to a second patent disclosure in the robotic vision field. Author

N94-30551*# Bureau of Mines, Pittsburgh, PA.
AN ELECTROMAGNETIC NONCONTACTING SENSOR FOR THICKNESS MEASUREMENT IN A DISPERSIVE MEDIUM
Robert L. Chufo *In* NASA. Johnson Space Center, Conference on Intelligent Robotics in Field, Factory, Service, and Space (CIRFFSS 1994), Volume 1 Mar. 1994 p 190-194 (For primary document see N94-30526 08-63)
(AIAA Paper 94-1200-CP) Avail: CASI HC A01/MF A04

This paper describes a general purpose imaging technology developed by the U.S. Bureau of Mines (USBM) that, when fully implemented, will solve the general problem of 'seeing into the earth.' A first-generation radar coal thickness sensor, the RCTS-1, has been developed and field-tested in both underground and highwall mines. The noncontacting electromagnetic technique uses spatial modulation created by moving a simple sensor antenna in a direction along each axis to be measured while the complex reflection coefficient is measured at multiple frequencies over a two-to-one bandwidth. The antenna motion imparts spatial modulation to the data that enables signal processing to solve the problems of media, target, and antenna dispersion. Knowledge of the dielectric constant of the media is not necessary because the electrical properties of the media are determined automatically along with the distance to the target and thickness of each layer of the target. The sensor was developed as a navigation guidance sensor to accurately detect the coal/noncoal interface required for the USBM computer-assisted mining machine program. Other mining applications include the location of rock fractures, water-filled voids, and abandoned gas wells. These hazards can be detected in advance of the mining operation. This initiating technology is being expanded into a full three-dimensional (3-D) imaging system that will have applications in both the underground and surface environment. Author

N94-30552*# Centre National de la Recherche Scientifique, Toulouse (France).
PERCEPTION SYSTEM AND FUNCTIONS FOR AUTONOMOUS NAVIGATION IN A NATURAL ENVIRONMENT
Raja Chatila, Michel Devy, Simon Lacroix, and Matthieu Herrb *In* NASA. Johnson Space Center, Conference on Intelligent Robotics in Field, Factory, Service, and Space (CIRFFSS 1994), Volume 1 Mar. 1994 p 195-205 (For primary document see N94-30526 08-63)
(AIAA Paper 94-1201-CP) Avail: CASI HC A03/MF A04

This paper presents the approach, algorithms, and processes we developed for the perception system of a cross-country autonomous robot. After a presentation of the tele-programming context we favor for intervention robots, we introduce an adaptive navigation approach, well suited for the characteristics of complex natural environments. This approach lead us to develop a heterogeneous perception system that manages several different terrain representatives. The perception functionalities required during navigation are listed, along with the corresponding representations we consider. The main perception processes we developed are presented. They are integrated within an on-board control architecture we developed. First results of an ambitious experiment currently underway at LAAS are then presented. Author

N94-30553*# Houston Univ., TX. College of Technology.
FUZZY LOGIC BASED ROBOTIC CONTROLLER
F. Attia and M. Upadhyaya *In* NASA. Johnson Space Center, Conference on Intelligent Robotics in Field, Factory, Service, and Space (CIRFFSS 1994), Volume 1 Mar. 1994 p 206-211 (For primary document see N94-30526 08-63)
(AIAA Paper 94-1202-CP) Avail: CASI HC A02/MF A04

Existing Proportional-Integral-Derivative (PID) robotic controllers rely on an inverse kinematic model to convert user-specified cartesian trajectory coordinates to joint variables. These joints experience friction, stiction, and gear backlash effects. Due to lack of proper linearization of these effects, modern control theory based on state space methods cannot provide adequate control for robotic systems. In the presence of loads, the dynamic behavior of robotic systems is complex and nonlinear, especially where mathematical modeling is evaluated for real-time operators. Fuzzy Logic Control is a fast emerging alternative to conventional control systems in situations where it may not be feasible to formulate an analytical model of the complex system. Fuzzy logic techniques track a user-defined trajectory without having the host computer to explicitly solve the nonlinear inverse kinematic equations. The goal is to provide a rule-based approach, which is closer to human reasoning. The approach used expresses end-point error, location of manipulator joints, and proximity to obstacles as fuzzy variables. The resulting decisions are based upon linguistic and non-numerical information. This paper presents a solution to the conventional robot controller which is independent of computationally intensive kinematic equations. Computer simulation results of this approach as obtained from software implementation are also discussed. Author

N94-30554*# University of Southern California, Los Angeles. Dept. of Electrical Engineering.
VEHICLE FOLLOWING CONTROLLER DESIGN FOR AUTONOMOUS INTELLIGENT VEHICLES
C. C. Chien, M. C. Lai, and R. Mayr *In* NASA. Johnson Space Center, Conference on Intelligent Robotics in Field, Factory, Service, and Space (CIRFFSS 1994), Volume 1 Mar. 1994 p 212-222 (For primary document see N94-30526 08-63)
(AIAA Paper 94-1203-CP) Avail: CASI HC A03/MF A04

A new vehicle following controller is proposed for autonomous intelligent vehicles. The proposed vehicle following controller not only provides smooth transient maneuvers for unavoidable nonzero initial conditions but also guarantees the asymptotic platoon stability without the availability of feedforward information. Furthermore, the achieved asymptotic platoon stability is shown to be robust to sensor delays and an upper bound for the allowable sensor delays is also provided in this paper. Author

N94-30555*# Stanford Univ., CA. Dept. of Computer Science.
THE REAL-WORLD NAVIGATOR
Marko Balabanovic, Craig Becker, Sarah K. Morse, and Illah R. Nourbakhsh *In* NASA. Johnson Space Center, Conference on Intelligent Robotics in Field, Factory, Service, and Space (CIRFFSS 1994), Volume 1 Mar. 1994 p 223-232 (For primary document see N94-30526 08-63)
(Contracts NAG2-581; N00014-92-J-1809; N00014-90-J-1533)
(AIAA Paper 94-1204-CP) Avail: CASI HC A02/MF A04

The success of every mobile robot application hinges on the ability to

navigate robustly in the real world. The problem of robust navigation is separable from the challenges faced by any particular robot application. We offer the Real-World Navigator as a solution architecture that includes a path planner, a map-based localizer, and a motion control loop that combines reactive avoidance modules with deliberate goal-based motion. Our architecture achieves a high degree of reliability by maintaining and reasoning about an explicit description of positional uncertainty. We provide two implementations of real-world robot systems that incorporate the Real-World Navigator. The Vagabond Project culminated in a robot that successfully navigated a portion of the Stanford University campus. The Scimmer project developed successful entries for the AIAA 1993 Robotics Competition, placing first in one of the two contests entered. Author

N94-30556*# Mitre Corp., McLean, VA. Washington AI Technical Center.

A STREAMLINED SOFTWARE ENVIRONMENT FOR SITUATED SKILLS

Sophia T. Yu, Marc G. Slack, and David P. Miller *In* NASA. Johnson Space Center, Conference on Intelligent Robotics in Field, Factory, Service, and Space (CIRFFSS 1994), Volume 1 Mar. 1994 p 233-239 (For primary document see N94-30526 08-63)

(AIAA Paper 94-1205-CP) Avail: CASI HC A02/MF A04

This paper documents a powerful set of software tools used for developing situated skills. These situated skills form the reactive level of a three-tiered intelligent agent architecture. The architecture is designed to allow these skills to be manipulated by a task level engine which is monitoring the current situation and selecting skills necessary for the current task. The idea is to coordinate the dynamic activations and deactivations of these situated skills in order to configure the reactive layer for the task at hand. The heart of the skills environment is a data flow mechanism which pipelines the currently active skills for execution. A front end graphical interface serves as a debugging facility during skill development and testing. We are able to integrate skills developed in different languages into the skills environment. The power of the skills environment lies in the amount of time it saves for the programmer to develop code for the reactive layer of a robot. Author

N94-30557*# Texas A&M Univ., College Station. Dept. of Computer Science.

SITUATIONAL REACTION AND PLANNING

John Yen and Nathan Pfluger *In* NASA. Johnson Space Center, Conference on Intelligent Robotics in Field, Factory, Service, and Space (CIRFFSS 1994), Volume 1 Mar. 1994 p 240-245 (For primary document see N94-30526 08-63)

(AIAA Paper 94-1206-CP) Avail: CASI HC A02/MF A04

One problem faced in designing an autonomous mobile robot system is that there are many parameters of the system to define and optimize. While these parameters can be obtained for any given situation determining what the parameters should be in all situations is difficult. The usual solution is to give the system general parameters that work in all situations, but this does not help the robot to perform its best in a dynamic environment. Our approach is to develop a higher level situation analysis module that adjusts the parameters by analyzing the goals and history of sensor readings. By allowing the robot to change the system parameters based on its judgement of the situation, the robot will be able to better adapt to a wider set of possible situations. We use fuzzy logic in our implementation to reduce the number of basic situations the controller has to recognize. For example, a situation may be 60 percent open and 40 percent corridor, causing the optimal parameters to be somewhere between the optimal settings for the two extreme situations. Author

N94-30558*# University of Southern California, Los Angeles. Computer Science Dept.

AUTONOMOUS MOBILE ROBOT TEAMS

Arvin Agah and George A. Bekey *In* NASA. Johnson Space Center, Conference on Intelligent Robotics in Field, Factory, Service, and Space (CIRFFSS 1994), Volume 1 Mar. 1994 p 246-252 (For primary document see N94-30526 08-63)

(AIAA Paper 94-1207-CP) Avail: CASI HC A02/MF A04

This paper describes autonomous mobile robot teams performing tasks in unstructured environments. The behavior and the intelligence of the group is distributed, and the system does not include a central command base or leader. The novel concept of the Tropism-Based Cognitive Architecture is introduced, which is used by the robots in order to produce behavior transforming their sensory information to proper action. The results of a number of simulation experiments are presented. These experiments include worlds where the robot teams must locate, decompose, and gather objects, and defend themselves against hostile predators, while navigating around stationary and mobile obstacles. Author

N94-30559*# Massachusetts Inst. of Tech., Cambridge. Artificial Intelligence Lab.

BUILDING BRAINS FOR BODIES

Rodney Allen Brooks and Lynn Andrea Stein *In* NASA. Johnson Space Center, Conference on Intelligent Robotics in Field, Factory, Service, and Space (CIRFFSS 1994), Volume 1 Mar. 1994 p 253-263 (For primary document see N94-30526 08-63)

(AIAA Paper 94-1208-CP) Avail: CASI HC A03/MF A04

We describe a project to capitalize on newly available levels of computational resources in order to understand human cognition. We will build an integrated physical system including vision, sound input and output, and dextrous manipulation, all controlled by a continuously operating large scale parallel MIMD computer. The resulting system will learn to 'think' by building on its bodily experiences to accomplish progressively more abstract tasks. Past experience suggests that in attempting to build such an integrated system we will have to fundamentally change the way artificial intelligence, cognitive science, linguistics, and philosophy think about the organization of intelligence. We expect to be able to better reconcile the theories that will be developed with current work in neuroscience. Author

N94-30560*# Stanford Univ., CA. Aerospace Robotics Lab.

OBJECT-BASED TASK-LEVEL CONTROL: A HIERARCHICAL CONTROL ARCHITECTURE FOR REMOTE OPERATION OF SPACE ROBOTS

H. D. Stevens, E. S. Miles, S. J. Rock, and R. H. Cannon *In* NASA. Johnson Space Center, Conference on Intelligent Robotics in Field, Factory, Service, and Space (CIRFFSS 1994), Volume 1 Mar. 1994 p 264-273 (For primary document see N94-30526 08-63)

(AIAA Paper 94-1209-CP) Avail: CASI HC A02/MF A04

Expanding man's presence in space requires capable, dexterous robots capable of being controlled from the Earth. Traditional 'hand-in-glove' control paradigms require the human operator to directly control virtually every aspect of the robot's operation. While the human provides excellent judgment and perception, human interaction is limited by low bandwidth, delayed communications. These delays make 'hand-in-glove' operation from Earth impractical. In order to alleviate many of the problems inherent to remote operation, Stanford University's Aerospace Robotics Laboratory (ARL) has developed the Object-Based Task-Level Control architecture. Object-Based Task-Level Control (OBTLC) removes the burden of teleoperation from the human operator and enables execution of tasks not possible with current techniques. OBTLC is a hierarchical approach to control where the human operator is able to specify high-level, object-related tasks through an intuitive graphical user interface. Infrequent task-level command replace constant joystick operations, eliminating communications bandwidth and time delay problems. The details of robot control and task execution are handled entirely by the robot and computer control system. The ARL has implemented the OBTLC architecture on a set of Free-Flying Space Robots. The capability of the OBTLC architecture has been demonstrated by controlling the ARL Free-Flying Space Robots from NASA Ames Research Center. Author

N94-30561*# Carnegie-Mellon Univ., Pittsburgh, PA. School of Computer Science.

TASK-LEVEL CONTROL FOR AUTONOMOUS ROBOTS

Reid Simmons *In* NASA. Johnson Space Center, Conference on Intelligent Robotics in Field, Factory, Service, and Space (CIRFFSS 1994), Volume 1 Mar. 1994 p 275-281 (For primary document see N94-30526 08-63)

(Contract NAGW-1175; F08635-92-C-0019)

(AIAA Paper 94-1210-CP) Avail: CASI HC A02/MF A04

Task-level control refers to the integration and coordination of planning, perception, and real-time control to achieve given high-level goals. Autonomous mobile robots need task-level control to effectively achieve complex tasks in uncertain, dynamic environments. This paper describes the Task Control Architecture (TCA), an implemented system that provides commonly needed constructs for task-level control. Facilities provided by TCA include distributed communication, task decomposition and sequencing, resource management, monitoring and exception handling. TCA supports a

design methodology in which robot systems are developed incrementally, starting first with deliberative plans that work in nominal situations, and then layering them with reactive behaviors that monitor plan execution and handle exceptions. To further support this approach, design and analysis tools are under development to provide ways of graphically viewing the system and validating its behavior. Author

N94-30562*# Rice Univ., Houston, TX. Dept. of Electrical and Computer Engineering.

A SURVEY OF NASA AND MILITARY STANDARDS ON FAULT TOLERANCE AND RELIABILITY APPLIED TO ROBOTICS

Joseph R. Cavallaro and Ian D. Walker *In* NASA. Johnson Space Center, Conference on Intelligent Robotics in Field, Factory, Service, and Space (CIRFFSS 1994), Volume 1 Mar. 1994 p 282-286 (For primary document see N94-30526 08-63)

(AIAA Paper 94-1211-CP) Avail: CASI HC A01/MF A04

There is currently increasing interest and activity in the area of reliability and fault tolerance for robotics. This paper discusses the application of Standards in robot reliability, and surveys the literature of relevant existing standards. A bibliography of relevant Military and NASA standards for reliability and fault tolerance is included. Author

N94-30563*# Rensselaer Polytechnic Inst., Troy, NY. Electrical, Computer, and Systems Engineering Dept.

A PERFORMANCE ANALYSIS METHOD FOR DISTRIBUTED REAL-TIME ROBOTIC SYSTEMS: A CASE STUDY OF REMOTE TELEOPERATION

D. R. Lefebvre and A. C. Sanderson *In* NASA. Johnson Space Center, Conference on Intelligent Robotics in Field, Factory, Service, and Space (CIRFFSS 1994), Volume 1 Mar. 1994 p 287-297 (For primary document see N94-30526 08-63)

(Grants NGT-10000; NAGw-1333)

(AIAA Paper 94-1212-CP) Avail: CASI HC A03/MF A04

Robot coordination and control systems for remote teleoperation applications are by necessity implemented on distributed computers. Modeling and performance analysis of these distributed robotic systems is difficult, but important for economic system design. Performance analysis methods originally developed for conventional distributed computer systems are often unsatisfactory for evaluating real-time systems. The paper introduces a formal model of distributed robotic control systems; and a performance analysis method, based on scheduling theory, which can handle concurrent hard-real-time response specifications. Use of the method is illustrated by a case of remote teleoperation which assesses the effect of communication delays and the allocation of robot control functions on control system hardware requirements. Author

N94-30564*# Maryland Univ., College Park. Inst. for Advanced Computer Studies.

PREDICTIVE SUFFICIENCY AND THE USE OF STORED INTERNAL STATE

David J. Musliner, Edmund H. Durfee, and Kang G. Shin *In* NASA. Johnson Space Center, Conference on Intelligent Robotics in Field, Factory, Service, and Space (CIRFFSS 1994), Volume 1 Mar. 1994 p 298-305 (For primary document see N94-30526 08-63)

(Grants NSF IRI-92-09031; NSF IRI-91-58473)

(AIAA Paper 94-1213-CP) Avail: CASI HC A02/MF A04

In all embedded computing systems, some delay exists between sensing and acting. By choosing an action based on sensed data, a system is essentially predicting that there will be no significant changes in the world during this delay. However, the dynamic and uncertain nature of the real world can make these predictions incorrect, and thus, a system may execute inappropriate actions. Making systems more reactive by decreasing the gap between sensing and action leaves less time for predictions to err, but still provides no principled assurance that they will be correct. Using the concept of predictive sufficiency described in this paper, a system can prove that its predictions are valid, and that it will never execute inappropriate actions. In the context of our CIRCA system, we also show how predictive sufficiency allows a system to guarantee worst-case response times to changes in its environment. Using predictive sufficiency, CIRCA is able to build real-time reactive control plans which provide a sound basis for performance guarantees that are unavailable with other reactive systems. Author

N94-30565*# Sandia National Labs., Albuquerque, NM.

USING GENERIC TOOL KITS TO BUILD INTELLIGENT SYSTEMS

David J. Miller *In* NASA. Johnson Space Center, Conference on Intelligent Robotics in Field, Factory, Service, and Space (CIRFFSS 1994), Volume 1 Mar. 1994 p 306-314 (For primary document see N94-30526 08-63)

(Contract DE-AC04-94AL-85000)

(AIAA Paper 94-1214-CP) Avail: CASI HC A02/MF A04

The Intelligent Systems and Robots Center at Sandia National Laboratories is developing technologies for the automation of processes associated with environmental remediation and information-driven manufacturing. These technologies, which focus on automated planning and programming and sensor-based and model-based control, are used to build intelligent systems which are able to generate plans of action, program the necessary devices, and use sensors to react to changes in the environment. By automating tasks through the use of programmable devices tied to computer models which are augmented by sensing, requirements for faster, safer, and cheaper systems are being satisfied. However, because of the need for rapid cost-effect prototyping and multi-laboratory teaming, it is also necessary to define a consistent approach to the construction of controllers for such systems. As a result, the Generic Intelligent System Controller (GISC) concept has been developed. This concept promotes the philosophy of producing generic tool kits which can be used and reused to build intelligent control systems. Author

N94-30566*# Carnegie-Mellon Univ., Pittsburgh, PA. The Robotics Inst.

A REACTIVE SYSTEM FOR OPEN TERRAIN NAVIGATION: PERFORMANCE AND LIMITATIONS

D. Langer, J. Rosenblatt, and M. Hebert *In* NASA. Johnson Space Center, Conference on Intelligent Robotics in Field, Factory, Service, and Space (CIRFFSS 1994), Volume 1 Mar. 1994 p 315-321 (For primary document see N94-30526 08-63)

(Contracts DACA76-89-C-0014; DAAE07-90-C-R059; NSF BCS-91-20655)

(AIAA Paper 94-1218-CP) Avail: CASI HC A02/MF A04

We describe a core system for autonomous navigation in outdoor natural terrain. The system consists of three parts: a perception module which processes range images to identify untraversable regions of the terrain, a local map management module which maintains a representation of the environment in the vicinity of the vehicle, and a planning module which issues commands to the vehicle controller. Our approach is to use the concept of 'early traversability evaluation', and on the use of reactive planning for generating commands to drive the vehicle. We argue that our approach leads to a robust and efficient navigation system. We illustrate our approach by an experiment in which a vehicle travelled autonomously for one kilometer through unmapped cross-country terrain. Author

N94-30567*# Universidade Nova de Lisboa (Portugal).

THE ROAD PLAN MODEL: INFORMATION MODEL FOR PLANNING ROAD BUILDING ACTIVITIES

Rafaela K. Azinhal and Fernando Moura-Pires *In* NASA. Johnson Space Center, Conference on Intelligent Robotics in Field, Factory, Service, and Space (CIRFFSS 1994), Volume 1 Mar. 1994 p 322-332 (For primary document see N94-30526 08-63)

(AIAA Paper 94-1219-CP) Avail: CASI HC A03/MF A04

The general building contractor is presented with an information model as an approach for deriving a high-level work plan of construction activities applied to road building. Road construction activities are represented in a Road Plan Model (RPM), which is modeled in the ISO standard STEP/EXPRESS and adopts various concepts from the GARM notation. The integration with the preceding road design stage and the succeeding phase of resource scheduling is discussed within the framework of a Road Construction Model. Construction knowledge is applied to the road design and the terrain model of the surrounding road infrastructure for the instantiation of the RPM. Issues regarding the implementation of a road planner application supporting the RPM are discussed. Author

N94-30568*# Lockheed Engineering and Sciences Co., Houston, TX. Automation and Robotics Dept.

DESIGN REUSE EXPERIENCE OF SPACE AND HAZARDOUS OPERATIONS ROBOTS

P. Graham ONeil *In* NASA. Johnson Space Center, Conference on Intelligent Robotics in Field, Factory, Service, and Space (CIRFFSS 1994),

Volume 1 Mar. 1994 p 333-338 (For primary document see N94-30526 08-63)
(AIAA Paper 94-1220-CP) Avail: CASI HC A02/MF A04

A comparison of design drivers for space and hazardous nuclear waste operating robots details similarities and differences in operations, performance and environmental parameters for these critical environments. The similarities are exploited to provide low risk system components based on reuse principles and design knowledge. Risk reduction techniques are used for bridging areas of significant differences. As an example, risk reduction of a new sensor design for nuclear environment operations is employed to provide upgradeable replacement units in a reusable architecture for significantly higher levels of radiation. Author

N94-30569*# McDonnell-Douglas Corp., Houston, TX.
A MULTI-MODE MANIPULATOR DISPLAY SYSTEM FOR CONTROLLING REMOTE ROBOTIC SYSTEMS
Michael J. Massimino, Michael F. Meschler, and Alberto A. Rodriguez *In* NASA. Johnson Space Center, Conference on Intelligent Robotics in Field, Factory, Service, and Space (CIRFFSS 1994), Volume 1 Mar. 1994 p 339-347 (For primary document see N94-30526 08-63)
(AIAA Paper 94-0888-CP) Avail: CASI HC A02/MF A04

The objective and contribution of the research presented in this paper is to provide a Multi-Mode Manipulator Display System (MMDS) to assist a human operator with the control of remote manipulator systems. Such systems include space based manipulators such as the space shuttle remote manipulator system (SRMS) and future ground controlled teleoperated and telescience space systems. The MMDS contains a number of display modes and submodes which display position control cues position data in graphical formats, based primarily on manipulator position and joint angle data. Therefore the MMDS is not dependent on visual information for input and can assist the operator especially when visual feedback is inadequate. This paper provides descriptions of the new modes and experiment results to date. Author

N94-30570*# Babcock and Wilcox Co., Lynchburg, VA. CIM Systems.
PROGRAMMABLE AUTOMATED WELDING SYSTEM (PAWS)
Martin D. Kline *In* NASA. Johnson Space Center, Conference on Intelligent Robotics in Field, Factory, Service, and Space (CIRFFSS 1994), Volume 1 Mar. 1994 p 348-353 (For primary document see N94-30526 08-63)
(AIAA Paper 94-1221-CP) Avail: CASI HC A02/MF A04

An ambitious project to develop an advanced, automated welding system is being funded as part of the Navy Joining Center with Babcock & Wilcox as the prime integrator. This program, the Programmable Automated Welding System (PAWS), involves the integration of both planning and real-time control activities. Planning functions include the development of a graphical decision support system within a standard, portable environment. Real-time control functions include the development of a modular, intelligent, real-time control system and the integration of a number of welding process sensors. This paper presents each of these components of the PAWS and discusses how they can be utilized to automate the welding operation. Author

N94-30571*# Babcock and Wilcox Co., Lynchburg, VA. CIM Systems.
ROBOTIC NDE INSPECTION OF ADVANCED SOLID ROCKET MOTOR CASINGS
Glenn E. McNeelege and Chris Sarantos *In* NASA. Johnson Space Center, Conference on Intelligent Robotics in Field, Factory, Service, and Space (CIRFFSS 1994), Volume 1 Mar. 1994 p 354-366 (For primary document see N94-30526 08-63)
(AIAA Paper 94-1222-CP) Avail: CASI HC A03/MF A04

The Advanced Solid Rocket Motor program determined the need to inspect ASRM forgings and segments for potentially catastrophic defects. To minimize costs, an automated eddy current inspection system was designed and manufactured for inspection of ASRM forgings in the initial phases of production. This system utilizes custom manipulators and motion control algorithms and integrated six channel eddy current data acquisition and analysis hardware and software. Total system integration is through a personal computer based workcell controller. Segment inspection demands the use of a gantry robot for the EMAT/ET inspection system. The EMAT/ET system utilized similar mechanical compliancy and software logic to accommodate complex part geometries. EMAT provides volumetric inspection capability while eddy current is limited to surface and near surface inspection. Each aspect of the systems are applicable to other industries, such as, inspection of pressure vessels, weld inspection, and traditional ultrasonic inspection applications. Author

N94-30572*# Carnegie-Mellon Univ., Pittsburgh, PA.
AUTOMATION FOR NONDESTRUCTIVE INSPECTION OF AIRCRAFT
M. W. Siegel *In* NASA. Johnson Space Center, Conference on Intelligent Robotics in Field, Factory, Service, and Space (CIRFFSS 1994), Volume 1 Mar. 1994 p 367-377 (For primary document see N94-30526 08-63)
(Contract MDA972-92-J-1010)
(AIAA Paper 94-1223-CP) Avail: CASI HC A03/MF A04

We discuss the motivation and an architectural framework for using small mobile robots as automated aids to operators of nondestructive inspection (NDI) equipment. We review the need for aircraft skin inspection, and identify the constraints in commercial airlines operations that make small mobile robots the most attractive alternative for automated aids for NDI procedures. We describe the design and performance of the robot (ANDI) that we designed, built, and are testing for deployment of eddy current probes in prescribed commercial aircraft inspections. We discuss recent work aimed at also providing robotic aids for visual inspection. Author

N94-30573*# National Aeronautics and Space Administration. Marshall Space Flight Center, Huntsville, AL.
GRAPHICAL SIMULATION FOR AEROSPACE MANUFACTURING
Majid Babai and Christopher Bien *In* NASA. Johnson Space Center, Conference on Intelligent Robotics in Field, Factory, Service, and Space (CIRFFSS 1994), Volume 1 Mar. 1994 p 378-380 (For primary document see N94-30526 08-63)
(AIAA Paper 94-1224-CP) Avail: CASI HC A01/MF A04

Simulation software has become a key technological enabler for integrating flexible manufacturing systems and streamlining the overall aerospace manufacturing process. In particular, robot simulation and offline programming software is being credited for reducing down time and labor cost, while boosting quality and significantly increasing productivity. Author

N94-30574*# Mercer Univ., Macon, GA. Mercer Engineering Research Center.
THE AUTOMATED AIRCRAFT REWORK SYSTEM (AARS): A SYSTEM INTEGRATION APPROACH
Michael J. Benoit *In* NASA. Johnson Space Center, Conference on Intelligent Robotics in Field, Factory, Service, and Space (CIRFFSS 1994), Volume 1 Mar. 1994 p 381-392 (For primary document see N94-30526 08-63)
(AIAA Paper 94-1225-CP) Avail: CASI HC A03/MF A04

The Mercer Engineering Research Center (MERC), under contract to the United States Air Force (USAF) since 1989, has been actively involved in providing the Warner Robins Air Logistics Center (WR-ALC) with a robotic workcell designed to perform rework automated defastening and hole location/transfer operations on F-15 wings. This paper describes the activities required to develop and implement this workcell, known as the Automated Aircraft Rework System (AARS). AARS is scheduled to be completely installed and in operation at WR-ALC by September 1994. Author

N94-30575*# Environmental Research Inst. of Michigan, Ann Arbor.
AUTOMATED INSPECTION OF TURBINE BLADES: CHALLENGES AND OPPORTUNITIES
Manish Mehta, Joseph C. Marron, Robert E. Sampson, and George M. Peace *In* NASA. Johnson Space Center, Conference on Intelligent Robotics in Field, Factory, Service, and Space (CIRFFSS 1994), Volume 1 Mar. 1994 p 393-398 (For primary document see N94-30526 08-63)
(AIAA Paper 94-1226-CP) Avail: CASI HC A02/MF A04

Current inspection methods for complex shapes and contours exemplified by aircraft engine turbine blades are expensive, time-consuming and labor intensive. The logistics support of new manufacturing paradigms such as integrated product-process development (IPPD) for current and future engine technology development necessitates high speed, automated inspection of forged and cast jet engine blades, combined with a capability of retaining and retrieving metrology data for process improvements upstream (designer-level) and downstream (end-user facilities) at commercial and

military installations. The paper presents the opportunities emerging from a feasibility study conducted using 3-D holographic laser radar in blade inspection. Requisite developments in computing technologies for systems integration of blade inspection in production are also discussed. Author

N94-30576*# Transition Research, Inc., Danbury, CT.
TRC RESEARCH PRODUCTS: COMPONENTS FOR SERVICE ROBOTS
W. Stuart Lob *In* NASA. Johnson Space Center, Conference on Intelligent Robotics in Field, Factory, Service, and Space (CIRFFSS 1994), Volume 1 Mar. 1994 p 399-404 (For primary document see N94-30526 08-63)
(AIAA Paper 94-1227-CP) Avail: CASI HC A02/MF A04

Transitions Research Corporation has developed a variety of technologies to accomplish its central mission: the creation of commercially viable robots for the service industry. Collectively, these technologies comprise the TRC 'robot tool kit.' The company started by developing a robot base that serves as a foundation for mobile robot research and development, both within TRC and at customer sites around the world. A diverse collection of sensing techniques evolved more recently, many of which have been made available to the international mobile robot research community as commercial products. These 'tool-kit' research products are described in this paper. The largest component of TRC's commercial operation is a product called HelpMate for material transport and delivery in health care institutions. Author

N94-30577*# Cyberotics, Inc., Waltham, MA
AN UPDATE ON LAB ROVER: A HOSPITAL MATERIAL TRANSPORTER
Paul Mattaboni *In* NASA. Johnson Space Center, Conference on Intelligent Robotics in Field, Factory, Service, and Space (CIRFFSS 1994), Volume 1 Mar. 1994 p 405-406 (For primary document see N94-30526 08-63)
(AIAA Paper 94-1228-CP) Avail: CASI HC A01/MF A04

The development of a hospital material transporter, 'Lab Rover', is described. Conventional material transport now utilizes people power, push carts, pneumatic tubes and tracked vehicles. Hospitals are faced with enormous pressure to reduce operating costs. Cyberotics, Inc. developed an Autonomous Intelligent Vehicle (AIV). This battery operated service robot was designed specifically for health care institutions. Applications for the AIV include distribution of clinical lab samples, pharmacy drugs, administrative records, x-ray distribution, meal tray delivery, and certain emergency room applications. The first AIV was installed at Lahey Clinic in Burlington, Mass. Lab Rover was beta tested for one year and has been 'on line' for an additional 2 years. Author (revised)

N94-30578*# KISS Inst. for Practical Robotics, Reston, VA.
A ROBOTIC WHEELCHAIR
David P. Miller and Edward Grant *In* NASA. Johnson Space Center, Conference on Intelligent Robotics in Field, Factory, Service, and Space (CIRFFSS 1994), Volume 1 Mar. 1994 p 407-411 (For primary document see N94-30526 08-63)
(AIAA Paper 94-1229-CP) Avail: CASI HC A01/MF A04

Many people who are mobility impaired are incapable, for a variety of reasons, of using an ordinary wheelchair. These people must rely on either a power wheelchair, which they control, or another person to push and guide them while they are in an ordinary or power wheelchair. Power wheelchairs can be difficult to operate. If a person has additional disabilities, either in perception or fine motor control of their hands, a power chair can be difficult or impossible for them to use safely. Having one person push and guide a person who is mobility impaired is very expensive, and if the disabled person is otherwise independent, very inefficient and frustrating. This paper describes a low-cost robotic addition to a power wheelchair that assists the rider of the chair in avoiding obstacles, going to pre-designated places, and maneuvering through doorways and other narrow or crowded areas. This system can be interfaced to a variety of input devices, and can give the operator as much or as little moment by moment control of the chair as they wish. Author

N94-30579*# Micro-Dexterity Systems, Inc., Memphis, TN.
DEXTERITY ENHANCEMENT IN MICROSURGERY USING TELEMICRO-ROBOTICS Abstract Only
Steve Charles *In* NASA. Johnson Space Center, Conference on Intelligent Robotics in Field, Factory, Service, and Space (CIRFFSS 1994), Volume 1 Mar. 1994 p 412 (For primary document see N94-30526 08-63)
(AIAA Paper 94-1230-CP) Avail: CASI HC A01/MF A04

The presentation will focus on finding the spectrum of dexterity performance while performing microsurgery in various specialties. It will be noted that individuals vary markedly in their performance in the position, velocity, stability, and force domains. There are surgeons who have a tremor who otherwise move very slowly and carefully while there are other surgeons who apply excessive force, but never have a tremor or move excessively fast. There are yet other surgeons who move excessively fast, yet they do not have a tremor. Dexterity enhancement includes position down scaling, tremor filtering, fatigue elimination, and other second-order issues such as confining the work space, velocities, accelerations, or forces. It will be described that the hand's position performance is degraded when it is asked to actuate the tools and that remote actuation alone increases the positioning capabilities. It will be noted that rotary and telescopic functions are far more difficult than writing or engraving-like motions. The safety issues concerning velocities and forces will be discussed and the need for impedance control pointed out. Simplistically, the devices should be made with variable compliance so that they can function rigidly as a robot would or compliantly as a human would, depending on the setting of this parameter. Tool interfaces will be discussed with an emphasis on the overall performance of the position, end effector, and tool as a unit. Space constraints, force, and velocity requirements will be discussed in this section as well. Referencing the coordinate system to pre- or inter-operative imaging systems will be discussed as well as an emphasis on the system architecture. Author

N94-30580*# Vanderbilt Univ., Nashville, TN. Center for Intelligent Systems.
AN INTELLIGENT ROBOTIC AID SYSTEM FOR HUMAN SERVICES
K. Kawamura, S. Bagchi, M. Iskarous, R. T. Pack, and A. Saad *In* NASA. Johnson Space Center, Conference on Intelligent Robotics in Field, Factory, Service, and Space (CIRFFSS 1994), Volume 1 Mar. 1994 p 413-420 (For primary document see N94-30526 08-63)
(AIAA Paper 94-1232-CP) Avail: CASI HC A02/MF A04

The long term goal of our research at the Intelligent Robotic Laboratory at Vanderbilt University is to develop advanced intelligent robotic aid systems for human services. As a first step toward our goal, the current thrusts of our R&D are centered on the development of an intelligent robotic aid called the ISAC (Intelligent Soft Arm Control). In this paper, we describe the overall system architecture and current activities in intelligent control, adaptive/interactive control and task learning. Author

N94-30581*# National Aeronautics and Space Administration. Lyndon B. Johnson Space Center, Houston, TX.
AN INTELLIGENT ROBOT FOR HELPING ASTRONAUTS
J. D. Erickson, K. A. Grimm, and T. W. Pendleton *In its* Conference on Intelligent Robotics in Field, Factory, Service, and Space (CIRFFSS 1994), Volume 1 Mar. 1994 p 421-433 (For primary document see N94-30526 08-63)
(AIAA Paper 94-1233-CP) Avail: CASI HC A03/MF A04

This paper describes the development status of a prototype supervised intelligent robot for space application for purposes of (1) helping the crew of a spacecraft such as the Space Station with various tasks, such as holding objects and retrieving/replacing tools and other objects from/into storage, and (2) for purposes of retrieving detached objects, such as equipment or crew, that have become separated from their spacecraft. In addition to this set of tasks in this low-Earth-orbiting spacecraft environment, it is argued that certain aspects of the technology can be viewed as generic in approach, thereby offering insight into intelligent robots for other tasks and environments. Candidate software architectures and their key technical issues which enable real work in real environments to be accomplished safely and robustly are addressed. Results of computer simulations of grasping floating objects are presented. Also described are characterization results on the usable reduced gravity environment in an aircraft flying parabola (to simulate weightlessness) and results on hardware performance there. These results show it is feasible to use that environment for evaluative testing of dexterous grasping based on real-time vision of freely rotating and translating objects. Author

N94-30582*# National Aeronautics and Space Administration, Washington, DC.

TERRESTRIAL APPLICATIONS OF NASA SPACE TELEROBOTICS TECHNOLOGIES

Dave Lavery *In* NASA. Johnson Space Center, Conference on Intelligent Robotics in Field, Factory, Service, and Space (CIRFFSS 1994), Volume 1 Mar. 1994 p 434-440 (For primary document see N94-30526 08-63)

(AIAA Paper 94-1235-CP) Avail: CASI HC A02/MF A04

In 1985 the National Aeronautics and Space Administration (NASA) instituted a research program in telerobotics to develop and provide the technology for applications of telerobotics to the United States space program. The activities of the program are intended to most effectively utilize limited astronaut time by facilitating tasks such as inspection, assembly, repair, and servicing, as well as providing extended capability for remotely conducting planetary surface operations. As the program matured, it also developed a strong heritage of working with government and industry to directly transfer the developed technology into industrial applications. Author

N94-30583*# Spar Aerospace Ltd., Brampton (Ontario). Advanced Technology Systems Group.

ON-ORBIT SPACECRAFT SERVICING: AN ELEMENT IN THE EVOLUTION OF SPACE ROBOTICS APPLICATIONS

Carl J. Anders and Claude H. Roy *In* NASA. Johnson Space Center, Conference on Intelligent Robotics in Field, Factory, Service, and Space (CIRFFSS 1994), Volume 1 Mar. 1994 p 441-450 (For primary document see N94-30526 08-63)

(AIAA Paper 94-1236-CP) Avail: CASI HC A02/MF A04

This paper addresses the renewed interest in on-orbit spacecraft servicing (OSS), and how it fits into the evolution of space applications for intelligent robots. Investment in the development of space robotics and associated technologies is growing as nations recognize that it is a critical component of the exploration and commercial development of space. At the same time, changes in world conditions have generated a renewal of the interest in OSS. This is reflected in the level of activity in the U.S., Japan and Europe in the form of studies and technology demonstration programs. OSS is becoming widely accepted as an opportunity in the evolution of space robotics applications. Importantly, it is a feasible proposition with current technologies and the direction of ongoing research and development activities. Interest in OSS dates back more than two decades, and several programs have been initiated, but no operational system has come on line, arguably with the Shuttle as the exception. With new opportunities arising, however, a fresh look at the feasibility of OSS is warranted. This involves the resolution of complex market, technical and political issues, through market studies, economic analyses, mission requirement definitions, trade studies, concept designs and technology demonstrations. System architectures for OSS are strongly dependent on target spacecraft design and launch delivery systems. Performance and cost factors are currently forcing significant changes in these areas. This presents both challenges and opportunities in the provision of OSS services. In conclusion, there is no question OSS will become a reality, but only when the technical feasibility is combined with either economic viability or political will. In the evolution of space robotics satellite servicing can become the next step towards its eventual role in support of planetary exploration and human beings' journey out into the universe. Author

N94-30584*# New Technology, Inc., Huntsville, AL.

A MODULAR ARTIFICIAL INTELLIGENCE INFERENCE ENGINE SYSTEM (MAIS) FOR SUPPORT OF ON ORBIT EXPERIMENTS

Thomas M. Hancock, III *In* NASA. Johnson Space Center, Conference on Intelligent Robotics in Field, Factory, Service, and Space (CIRFFSS 1994), Volume 1 Mar. 1994 p 451-455 (For primary document see N94-30526 08-63)

(AIAA Paper 94-1237-CP) Avail: CASI HC A01/MF A04

This paper describes a Modular Artificial Intelligence Inference Engine System (MAIS) support tool that would provide health and status monitoring, cognitive replanning, analysis and support of on-orbit Space Station, Spacelab experiments and systems. Author

N94-30731 Center for Mathematics and Computer Science, Amsterdam (Netherlands). Dept. of Computer Science/Dept. of Software Technology.

SERVICE INDEPENDENT BUILDING BLOCKS-1: CONCEPTS, EXAMPLES AND FORMAL SPECIFICATIONS

A. Steven Klusener, Bas vanVlijmen, and Arjan vanWaveren Apr. 1993 66 p Sponsored in part by EEC Limited Reproducibility: More than 20% of this document may be affected by microfiche quality

(ISSN 0169-118X)

(CWI-CS-R9326; ETN-94-95671) Copyright Avail: CASI HC A04

Descriptions of some Service Independent Building Blocks (SIBB's) and related concepts like Global Service Logic, which form part of the conceptual model for Intelligent Networks are presented. These descriptions correspond with the formal specifications given, but differ slightly from the definitions in the CCITT recommendation. The differences occur at points at which the recommendation was not clear and are discussed. A formal specification is useful for a thorough understanding of the SIBB's. It enables simulation of services and can serve as a basis for studies of the correctness of implementations. ESA

N94-30741 National Aerospace Lab., Amsterdam (Netherlands). Informatics Div.

MULTI-SENSOR DATA FUSION AND THE USE OF ARTIFICIAL INTELLIGENCE

Rene G. Zuidgeest 22 Apr. 1992 18 p Presented at the 12th Conference on Artificial Intelligence, Avignon, France, 1-6 Jun. 1992 Limited Reproducibility: More than 20% of this document may be affected by microfiche quality

(Contract MOD-01689029811)

(PB94-126216; NLR-TP-92174-U; ETN-94-95579) Avail: CASI HC A03

The potential use of artificial intelligence in Multi-Sensor Data Fusion (MSDF) is shown. A general functional architecture of an MSDF system based on a command and control model, applied to battlefield surveillance, is given. Battlefield surveillance is considered as the continuous observation of the battlefield area to provide timely information for command and control functions. In TA-10, a project from which the results were generalized and are presented, battlefield surveillance was chosen as primary domain. The presented results are valid for application to other domains. A global description of the world model that includes MSDF and knowledge about the observed world is given. A specific set of artificial intelligence (AI) techniques for representation of that knowledge and reasoning with it is discussed. These techniques emerge from knowledge based systems (KBS); neural networks are not considered. KBS techniques were preferred because of their relative maturity, their ability to explain their reasoning process in a comprehensive manner (might be important in order to convince the operator), and the ease with which explicitly represented knowledge can be modified. A global distributed architecture for MSDF is described in which different KBS are identified. Conclusions are drawn. ESA

N94-30803 Maryland Univ., College Park.

ASPECTS OF VISION AND PLANNING IN A DYNAMIC, UNCERTAIN ENVIRONMENT Ph.D. Thesis

Rajeev Sharma 1993 183 p

Avail: Univ. Microfilms Order No. DA9327493

Autonomous visual navigation involves the challenge of developing vision and planning algorithms for dealing with an uncertain and changing environment. Traditional approaches to visual navigation assume that a 3-D description of the scene is necessary for planning and that it is possible to extract such a description from a sequence of images. This typically leads to the development of vision and planning modules that do not work well together. An alternative is to use abstractions that adequately describe the interaction between the robot and its dynamic environment without relying on a 3-D description of the dynamic scene. This helps in posing simpler vision problems and in reducing the computational burden on the dynamic motion planning algorithms. An important step in sensing a dynamic environment is the detection of moving objects in the scene. We present an active vision technique for motion detection which is based on exploration strategies that can be dynamically adjusted to suit the current goal or purpose of the overall system. A theoretical analysis establishes conditions that are necessary and sufficient to guarantee motion detection at a point. The technique uses the spatio-temporal gradients of the image sequence, hence is implementable in real time and is robust compared to approaches that require the computation of optical flow. For

motion planning in a dynamic, uncertain environment, one of the main problems is that of modeling the situation so that a meaningful criterion can be applied to evaluate alternate plans. We propose a probabilistic model based on 'discrete events' that would effect the robot's behavior in response to the unknown component of the dynamic environment. The resulting framework makes it possible to design and evaluate motion planning strategies that consider both the known portion of the environment and the portion that is unknown but satisfies a probability distribution. We give a few instances of the general model which can be used for developing motion planning algorithms as a function of parameters representing a robot's environment and its behavior with respect to unexpected events detected by visual and other sensors. Detailed solutions are developed for a local path optimization problem and for motion planning in a hazardous environment. Dissert. Abstr.

N94-30806 Delaware Univ., Newark.
ROBUST ADAPTIVE CONTROL OF A MECHANICAL MANIPULATOR Ph.D. Thesis
Zanyu Yan 1992 248 p
Avail: Univ. Microfilms Order No. DA9319114

This dissertation concerns an active topic: robust adaptive control of a mechanical manipulator. The contributions of the dissertation are mainly in two areas: a robust control design method has been analyzed and a practical robust adaptive control scheme has been proposed to deal with real systems in the presence of not only structured but also unstructured uncertainties. In addition, an application of the proposed robust adaptive control scheme for a mechanical manipulator has been developed and numerically demonstrated. Based on small gain theorem and averaging method, the analysis explains that instabilities in adaptive control schemes are mainly due to high frequency infinite gain and inaccurate parameter estimation. Also, based on the control design principal of high gain in the low frequency range and low gain in the high frequency range, we clearly divide the entire frequency range into three frequency ranges: a low frequency range, a high frequency range, and an interconnect frequency range. Thus, we propose second-order desired dynamics with damping factor zeta = 1, a prefilter design, and a suitable sampling period. This will ensure dominant low frequency characteristics and robustness of the control system. The combination of robust control and accurate parameter estimation ensures robustness of the entire adaptive control system. The simulation for a two-link mechanical manipulator shows that this proposed method results in a robot system which is very robust to structured and unstructured uncertainties. The simulation for a more realistic six degree of freedom PUMA 560 demonstrates that the proposed approach may result in better performance when compared with other methods. Dissert. Abstr.

N94-30923 Politecnico di Milano (Italy). Artificial Intelligence and Robotics Project.
ELF: LEARNING INCOMPLETE FUZZY RULE SETS FOR AN AUTONOMOUS ROBOT
Andrea Bonarini Jun. 1993 9 p
(Rept-93-043; ETN-94-95812) Avail: Issuing Activity (Politecnico di Milano, Piazza Leonardo da Vinci 32, 20133 Milan, Italy)

Experience in learning fuzzy rules using Evolutionary Algorithms (EA's) is presented. The application is a mobile robot, FAMOUSE (Fuzzy AutonoMOUSE), which has to do reactive tasks in an unknown environment. The characteristic feature of the learning algorithm, ELF (Evolutionary Learning of Fuzzy rules), is that, in contrast to most of the other approaches based on genetic algorithms, it is to learn a set of rules smaller than that needed to cover completely the combinations of all the values of all the antecedents (complete rulebase). ELF can also generate and maintain in the rule population rules for situations where the evaluation function does not evaluate uniformly all the rules. ESA

N94-30939 Politecnico di Milano (Italy). Artificial Intelligence and Robotics Project.
SOME METHODOLOGICAL ISSUES ABOUT DESIGNING AUTONOMOUS AGENTS WHICH LEARN THEIR BEHAVIORS: THE ELF EXPERIENCE
Andrea Bonarini Oct. 1993 10 p Sponsored in part by Ministry of University and Scientific and Technological Research
(Rept-93-068; ETN-94-95826) Avail: Issuing Activity (Politecnico di Milano, Piazza Leonardo da Vinci 32, 20133 Milan, Italy)

Experience in developing behavior based autonomous agents is presented. Focus is on methodological aspects of 'behavior engineering', a branch of engineering whose aim is to design and implement behavior based agents. Once a behavior is defined, it must be decided whether to implement it by programming the agent, or to make the agent learn its behavior. Results obtained with a machine learning algorithm (ELF (Evolutionary Learning of Fuzzy Systems)) learning behaviors described as sets of fuzzy rules are reported. The characteristic features of ELF are that it can learn the only rules it needs to achieve its task, it is resistant to biased evaluation functions, and it can learn generalizations. ESA

N94-30941 Politecnico di Milano (Italy). Dipt. di Elettronica e Informazione.
A NEURAL NETWORK-BASED TECHNIQUE FOR STRUCTURAL IDENTIFICATION OF SISO SYSTEMS
Alberto Leva and Luigi Piroddi 1993 11 p Sponsored in part by Ministry of University and Scientific and Technological Research, and CNR
(Rept-93-076; ETN-94-95828) Avail: Issuing Activity (Politecnico di Milano, Piazza Leonardo da Vinci 32, 20133 Milan, Italy)

A technique for the structural identification of SISO systems based on the use of a neural network is presented. The network is trained to recognize some significant features of the process dynamics starting from a simplified representation of its unit step response which in turn is obtained by a convenient input/output experiment. In addition, the network classifies the process with respect to a convenient set of possible model structures, which represent the most common situations arising when a process model needs to be identified for control purposes. ESA

N94-30962 Politecnico di Milano (Italy). Artificial Intelligence and Robotics Project.
ITERATIVE REMOVAL OF BOUNDARY MINIMA OF HARMONIC POTENTIAL FUNCTION FOR MOBILE ROBOT NAVIGATION
Giuseppe Borghi 1993 7 p
(Rept-93-059; ETN-94-95821) Avail: Issuing Activity (Politecnico di Milano, Piazza Leonardo da Vinci 32, 20133 Milan, Italy)

An algorithm for real time obstacle avoidance for mobile robots with a navigation task is presented. The method, based on harmonic potential function and real time world modeling, allows unexpected obstacles to be detected and avoided without any need to stop the robot. The algorithm, overcoming limitations of local minima, can face unknown cluttered environment composed of arbitrarily shaped obstacles. The use of harmonic potential functions eliminates local minima in the free space (only unstable minima are present). The algorithm, starting from a given path to be followed, makes local replanning of it, based on sonar sensor data. This approach allows unexpected obstacles to be avoided, integrating information provided by global path planner. A grid type world model is used, building on it a harmonic potential function. A method to compute in real time the potential function and to manage its boundary minima, is presented. The proposed algorithm can face arbitrarily shaped obstacles (for example concave obstacles), narrow passages (for example doorway) and slow moving obstacles (for example persons). The method was tested on a mobile robot having 24 sonar sensors in an indoor environment. ESA

N94-30963 Universiteit Twente, Enschede (Netherlands). Dept. of Applied Mathematics.
ROBUST CONTROL OF ROBOTS VIA LINEAR ESTIMATED STATE-FEEDBACK
Harry Berghuis and Henk Nijmeijer Aug. 1993 14 p Sponsored by Netherlands Technology Foundation Limited Reproducibility: More than 20% of this document may be affected by microfiche quality
(ISSN 0169-2690)
(MEMO-1153; ETN-94-95727) Avail: CASI HC A03

A robust tracking controller for robots that requires only position measurements is proposed. The controller consists of two parts: a linear observer part that generates an estimated error state from the error on the position, and a linear feedback part that utilizes this estimated state. It is shown that this computationally efficient controller yields uniform ultimate boundedness of the tracking error. An interesting feature of the controller is that it straightforwardly extends recent results on robust control of robots by linear state feedback to linear estimated state feedback. ESA

N94-28980# Kyoto Univ., Sakyoku (Japan).
APPLICATION OF DIGITAL CONTROL THEORY TO ADAPTIVE GRID GENERATION [SAITEKI SEIGYO O MOCHIITA TEKIO KOSHI SEISEIHO]
Makoto Kobayakawa and Eitaro Yamada *In* NAL, Proceedings of the 10th NAL Symposium on Aircraft Computational Aerodynamics Dec. 1992 p 187-192 In JAPANESE (For primary document see N94-28946 08-02)
Avail: CASI HC A02/MF A03

N94-29328# Rome Lab., Griffiss AFB, NY. Knowledge Engineering Branch.
ARTIFICIAL INTELLIGENCE TECHNOLOGY PROGRAM AT ROME LABORATORY
Robert N. Ruberti and Louis J. Hoebel *In* AGARD, Aerospace Software Engineering for Advanced Systems Architectures Nov. 1993 11 p (For primary document see N94-29315 08-61)
Copyright Avail: CASI HC A03/MF A03

N94-29780*# Jet Propulsion Lab., California Inst. of Tech., Pasadena.
SMART FOCAL-PLANE TECHNOLOGY FOR MICRO-INSTRUMENTS AND MICRO-ROVERS
Eric R. Fossum *In its* Proceedings of the Workshop on Microtechnologies and Applications to Space Systems 15 Jun. 1993 p 129-130 (For primary document see N94-29767 08-31)
Avail: CASI HC A01/MF A03

N94-30283 Defence Research Establishment Suffield, Medicine Hat (Alberta).
A GENERIC SEMI-AUTONOMOUS GROUND VEHICLE CONTROL SYSTEM
Ron Eirich and Alan Kramer *In its* Proceedings of the 3rd Conference on Military Robotic Applications 1991 p 68-73 (For primary document see N94-30275 08-37)
Avail: Issuing Activity (Defence Research Establishment Suffield, P.O. Box 4000, Medicine Hat, AB T1A 8K6 Canada)

N94-30287 Royal Military Coll. of Canada, Kingston (Ontario). Dept. of Electrical and Computer Engineering.
AN OPTIMAL OBSTACLE AVOIDANCE PATH PLANNING ALGORITHM FOR THE EXCALIBUR ROBOT
V. Banerjee, C. Earl, T. D. Looke, and M. Farooq *In* Defence Research Establishment Suffield, Proceedings of the 3rd Conference on Military Robotic Applications 1991 p 93-98 (For primary document see N94-30275 08-37)
Avail: Issuing Activity (Defence Research Establishment Suffield, P.O. Box 4000, Medicine Hat, AB T1A 8K6 Canada)

N94-30288 National Research Council of Canada, Ottawa (Ontario). Inst. for Information Technology.
MAESTRO: AN OPEN SYSTEM ARCHITECTURE FOR MULTI-ROBOT CONTROL
Shadia Elgazzar and Arthur Castonguay *In* Defence Research Establishment Suffield, Proceedings of the 3rd Conference on Military Robotic Applications 1991 p 99-106 (For primary document see N94-30275 08-37)
Avail: Issuing Activity (Defence Research Establishment Suffield, P.O. Box 4000, Medicine Hat, AB T1A 8K6 Canada)

N94-30290 Defence Research Establishment Pacific, Victoria (British Columbia).
THREE METHODS TO IMPROVE THE ACCURACY OF A PUMA 560 ROBOT
G. R. Hardy *In* Defence Research Establishment Suffield, Proceedings of the 3rd Conference on Military Robotic Applications 1991 p 114-121 (For primary document see N94-30275 08-37)
Avail: Issuing Activity (Defence Research Establishment Suffield, P.O. Box 4000, Medicine Hat, AB T1A 8K6 Canada)

N94-30292 Defence Research Establishment Pacific, Victoria (British Columbia).
AN INVERSE KINEMATICS ALGORITHM FOR THE DREP/PHILIPS REAL-TIME RADIOGRAPHIC MANIPULATOR SYSTEM
K. K. Yeung *In* Defence Research Establishment Suffield, Proceedings of the 3rd Conference on Military Robotic Applications 1991 p 129-135 (For primary document see N94-30275 08-37)
Avail: Issuing Activity (Defence Research Establishment Suffield, P.O. Box 4000, Medicine Hat, AB T1A 8K6 Canada)

N94-30296 Alberta Univ., Calgary. Dept. of Mechanical Engineering.
SYMBOLIC GENERATION OF DYNAMICS EQUATIONS FOR MANIPULATORS MOUNTED ON MOVING BASES
R. W. Toogood, L. El-Rayyes, and D. J. Mackay *In* Defence Research Establishment Suffield, Proceedings of the 3rd Conference on Military Robotic Applications 1991 p 157-164 (For primary document see N94-30275 08-37)
Avail: Issuing Activity (Defence Research Establishment Suffield, P.O. Box 4000, Medicine Hat, AB T1A 8K6 Canada)

N94-30297 Imago Mfg. Ltd., Ottawa (Ontario).
ACTIVITIES IN MACHINE VISION AT IMAGO MANUFACTURING LTD.
Roy Bail, Terry Folinsbee, and Lionel Pelkowitz *In* Defence Research Establishment Suffield, Proceedings of the 3rd Conference on Military Robotic Applications 1991 p 165-168 (For primary document see N94-30275 08-37)
Avail: Issuing Activity (Defence Research Establishment Suffield, P.O. Box 4000, Medicine Hat, AB T1A 8K6 Canada)

N94-30298 Alberta Univ., Edmonton. Dept. of Computing Science.
VARIABLE-RESOLUTION STEREO MATCHING
Anup Basu *In* Defence Research Establishment Suffield, Proceedings of the 3rd Conference on Military Robotic Applications 1991 p 169-176 (For primary document see N94-30275 08-37)
Avail: Issuing Activity (Defence Research Establishment Suffield, P.O. Box 4000, Medicine Hat, AB T1A 8K6 Canada)

N94-30301 McGill Univ., Montreal (Quebec). Research Center for Intelligent Machines.
SONAR SENSING AND OBSTABLE DETECTION
Gregory Dudek, Michael Jenkin, Evangelos Milios, and David Wilkes *In* Defence Research Establishment Suffield, Proceedings of the 3rd Conference on Military Robotic Applications 1991 p 198-205 (For primary document see N94-30275 08-37)
Avail: Issuing Activity (Defence Research Establishment Suffield, P.O. Box 4000, Medicine Hat, AB T1A 8K6 Canada)

N94-30302 British Columbia Univ., Vancouver. Dept. of Electrical Engineering.
OBSTACLE DETECTION FOR AN AUTONOMOUS VEHICLE
R. Neil Braithwaite and M. P. Beddoes *In* Defence Research Establishment Suffield, Proceedings of the 3rd Conference on Military Robotic Applications 1991 p 206-213 (For primary document see N94-30275 08-37)
Avail: Issuing Activity (Defence Research Establishment Suffield, P.O. Box 4000, Medicine Hat, AB T1A 8K6 Canada)

N94-30303 Alberta Research Council, Edmonton. Dept. of Advanced Computing and Engineering.
ELEMENTS OF SUPERVISORY CONTROL FOR MILITARY ROBOTIC APPLICATIONS
A. Dagnino, P. Feighan, and K. Chrystall *In* Defence Research Establishment Suffield, Proceedings of the 3rd Conference on Military Robotic Applications 1991 p 214-219 (For primary document see N94-30275 08-37)
Avail: Issuing Activity (Defence Research Establishment Suffield, P.O. Box 4000, Medicine Hat, AB T1A 8K6 Canada)

N94-30307 International Submarine Engineering Ltd., Port Coquitlam (British Columbia).
ACHIEVING ROBOT AUTONOMY
Eric Jackson, Owen Williams, and Keir Buchan *In* Defence Research

Establishment Suffield, Proceedings of the 3rd Conference on Military Robotic Applications 1991 p 242-248 (For primary document see N94-30275 08-37)
Avail: Issuing Activity (Defence Research Establishment Suffield, P.O. Box 4000, Medicine Hat, AB T1A 8K6 Canada)

N94-30308 Royal Military Coll. of Canada, Kingston (Ontario). Dept. of Electrical and Computer Engineering.
IMPROVING THE EXECUTION SPEED OF ROBOT CONTROL COMPUTATIONS: AN ALLOCATION SCHEME FOR HETEROGENEOUS MULTIPROCESSORS
M. McKay, M. Farooq, and C. Wortley *In* Defence Research Establishment Suffield, Proceedings of the 3rd Conference on Military Robotic Applications 1991 p 249-254 (For primary document see N94-30275 08-37)
Avail: Issuing Activity (Defence Research Establishment Suffield, P.O. Box 4000, Medicine Hat, AB T1A 8K6 Canada)

N94-30309 Ottawa Univ. (Ontario). Dept. of Mechanical Engineering.
MOTION CONTROL OF MOBILE ROBOTS
D. S. Necsulescu and S. Kalaycioglu *In* Defence Research Establishment Suffield, Proceedings of the 3rd Conference on Military Robotic Applications 1991 p 255-260 (For primary document see N94-30275 08-37)
Avail: Issuing Activity (Defence Research Establishment Suffield, P.O. Box 4000, Medicine Hat, AB T1A 8K6 Canada)

N94-30310 Defence and Civil Inst. of Environmental Medicine, Toronto (Ontario).
A MULTIPLEXED TWO-WAY SOLID COMMUNICATIONS LINK FOR TELEOPERATED ROBOTS
J. J. Grodski and D. Stampe *In* Defence Research Establishment Suffield, Proceedings of the 3rd Conference on Military Robotic Applications 1991 p 266-271 (For primary document see N94-30275 08-37)
Avail: Issuing Activity (Defence Research Establishment Suffield, P.O. Box 4000, Medicine Hat, AB T1A 8K6 Canada)

64 NUMERICAL ANALYSIS

Includes iteration, difference equations, and numerical approximation.

N94-28571# New York Univ., New York. Inst. of Mathematical Sciences.
APPLIED ANALYSIS/COMPUTATIONAL MATHEMATICS
P. Lax and M. Berger Dec. 1993 22 p
(Contract DE-FG02-88ER-25053)
(DE94-005133; DOE/ER-25053/T2) Avail: CASI HC A03/MF A01
This is the final report for the Courant Mathematics and Computing Laboratory (CMCL) research program for the years 1991-1993. Our research efforts encompass the formulation of physical problems in terms of mathematical models (both old and new), the mathematical analysis of such models, and their numerical resolution. This last step involves the development and implementation of efficient methods for large scale computation. Our analytic and numerical work often go hand in hand; new theoretical approaches often have numerical counterparts, while numerical experimentation often suggests avenues for analytical investigation. DOE

N94-28651# Colorado Univ., Denver.
A CHARACTERIZATION OF GRAPHS WITH INTERVAL TWO-STEP GRAPHS Technical Report, Apr. - Jul. 1993
J. R. Lundgren, Sarah K. Merz, John S. Maybee, and Craig W. Rasmussen 14 Oct. 1993 20 p
(Contract N00014-91-J-1145)
(AD-A275652; NPS-MA-93-021) Avail: CASI HC A03/MF A01
One of the intriguing open problems on competition graphs is determining what digraphs have interval competition graphs. In this paper we consider this problem for the class of loopless symmetric digraphs. Here we first consider forbidden subgraph characterizations of graphs with interval two-step graphs. We then characterize a large class of graphs with interval two-step graphs, using the Fulkerson-Gross characterization of interval graphs. DTIC

N94-28723# Cincinnati Univ., OH. Dept. of Mathematical Sciences.
NUMERICAL ANALYSIS AND COMPUTATION OF NONLINEAR PARTIAL DIFFERENTIAL EQUATIONS FROM APPLIED MATHEMATICS Final Report, 1 Jan. 1991 - 30 Sep. 1993
Donald A. French 30 Nov. 1993 4 p
(Contract DAAL03-91-G-0010)
(AD-A275582; ARO-28535.7-MA) Avail: CASI HC A01/MF A01
This report gives a brief discussion of the different problem areas under which research papers have been published during the term of the grant as well as a short description of the main results. In this research finite element methods were applied to a simple model of shear band formation. They were also used for elliptic and parabolic problems that arise in optimal control and for equations that simulate phase transitions. These finite element schemes were analyzed and implemented. Also, studies of space-time schemes where the Galerkin technique is used to discretize time as well as space were the focus of several papers. Finally, a last paper contains a thorough analysis of an adaptive time discretization technique. DTIC

N94-28739 Pacific Northwest Lab., Richland, WA.
FREQUENCY-DOMAIN TRANSFER-FUNCTION IDENTIFICATION USING CHEBYSHEV POLYNOMIALS
J. M. Johnson and D. J. Trudnowski Dec. 1993 3 p Presented at the 32nd IEEE Conference on Decision and Control, San Antonio, TX, Dec. 1993 Limited Reproducibility: More than 20% of this document may be affected by microfiche quality
(Contracts DE-AC06-76RL-01830; DE-FG06-89ER-75522)
(DE94-004777; PNL-SA-22915; CONF-931233-3) Avail: CASI HC A01
An approach is proposed for identifying a linear single-input single-output model from the frequency response of a system with unknown order. The approach involves representing the transfer function as the ratio of linearly-combined Chebyshev polynomials and solving an over-determined linear equation set. The method is compared with two other previously proposed techniques and shown to perform very well under noisy data conditions. DOE

N94-28783# Joint Inst. for Nuclear Research, Dubna (USSR).
THE SOLVING OF THE RELATIVISTIC TWO-BODY PROBLEM WITH A NONLINEAR DEPENDENCE UPON A SPECTRUM PARAMETER
E. P. Zhidkov, N. B. Skachkov, B. N. Khoromskij, M. M. Gregus, and T. M. Makarenko 1992 7 p In RUSSIAN
(DE94-606343; JINR-R-11-92-142) Avail: CASI HC A02/MF A01 (US Sales Only)
An approach to the numerical investigation of the quasipotential integral equation describing the coupled two-particle system in momentum space is proposed for the case when the integral operator contain the nonlinear dependence on the eigenvalue mu, connected with total mass of system M by the correlation mu = M/m. The results of numerical calculations for some potentials are given. DOE

N94-28792# North Carolina Agricultural and Technical State Univ., Greensboro. Dept. of Mathematics.
COMPUTATIONAL METHODS IN CONTINUUM MECHANICS Final Report, 1 Nov. 1990 - 31 Oct. 1993
Bolindra N. Borah, Robert E. White, A. Kyrillidis, S. Shankarlingham, and Y. Ji 30 Nov. 1993 84 p
(Contract DAAL03-90-G-0216)
(AD-A275560; ARO-28186.9-MA) Avail: CASI HC A05/MF A01
The primary objectives of this research are the development of algorithms which are applicable to non-linear continuum mechanic problems, especially to Stefan's Problems and Fluid Flows in Porous Media (Richard's Equation). We have studied 2-D and 3-D related problems. The codes are written in Cray Fortran and vectorization are done on the Cray Y-MP. The results obtained by Compact ADI, Finite Difference SOR and ADI are compared. It is seen that Compact ADI is superior. Six scientific research Papers have been presented/published in various conferences and journals in the last two years. All of the papers are attached in the appendix as attachments. Two senior faculty members worked in this project. Bolindra N. Borah

(P.I.), Professor, North Carolina A&T State University, Robert E. White (Co-P.I.), Professor, North Carolina State University are the principal researchers. Besides, four graduate students participated in this project. Two have already completed the M.S. in Applied Mathematics while the other two are completing in the Spring Semester 1994. DTIC

N94-28864# Army Research Lab., Aberdeen Proving Ground, MD.
LEAST-SQUARES DETERMINATION OF BURST-POINT COORDINATES Final Report, Jan. 1992 - Sep. 1993
Aivars Celmins and Miguel Andriolo Dec. 1993 30 p
(DA Proj. 1L1-62618-AH-80)
(AD-A275423; ARL-TR-321) Avail: CASI HC A03/MF A01

This report describes the determination of burst-point coordinates from azimuth and elevation measurements by the method of least squares. The observations are made from a number of observation towers and observed are angles of azimuth and elevation. Both angles are treated as regression variables, and the burst-point coordinates are determined by minimizing the sum of the correction squares of all observations. Two numerical solution methods are presented, both producing identical results. Methods for the detection of outliers in burst-point observations are briefly discussed. The presented coordinate determination is based on the concept of least-squares regression and differs from another algorithm that has been recently proposed in the Ballistic Research Laboratory Report BRL-MR-3894. DTIC

N94-28883# North Carolina State Univ., Raleigh.
A NUMERICAL SOLVER FOR INITIAL AND BOUNDARY VALUE PROBLEMS IN DIFFERENTIAL-ALGEBRAIC SYSTEMS Final Report, 1 Apr. 1990 - 15 Oct. 1993
Stephen L. Campbell and Kenneth D. Clark 15 Oct. 1993 15 p
(Contract DAAL03-89-D-0003)
(AD-A275447; ARO-27786.20-MA) Avail: CASI HC A03/MF A01

Differential algebraic equations arise in many applications including constrained mechanical systems. This project has investigated both their numerical solution and analytic properties. Among the many contributions has been the creation, analysis, and partial development of the first numerical method for general nonstructured solvable DAE's. DTIC

N94-29016# Air Force Inst. of Tech., Wright-Patterson AFB, OH.
STABILITY PROPERTIES OF INCLUSIVE CONNECTIVITY FOR GRAPHS Ph.D. Thesis
David W. Cribb Dec. 1993 141 p
(AD-A275360; AFIT/CI/CIA-93-29D) Avail: CASI HC A07/MF A02

This dissertation is an investigation of inclusive connectivity which is a localization of connectivity defined for each vertex and each edge of a graph. The inclusive edge (vertex, mixed) connectivity of a vertex v is the minimum number of edges (vertices, graph elements) whose removal yields a subgraph in which v is a cut vertex. All possible combinations of these three parameters with regard to edge addition stability, in which the value of the parameter will remain unchanged after the addition of any edge, are studied along with other various properties including a relationship between the stability of inclusive connectivity and global connectivity. A similar study in the stability for inclusive connectivity for edge deletion is conducted. Final topics include neutral edges, where a neutral edge is one whose removal does not change the respective inclusive connectivity value of any vertex, and inclusive connectivity stable graphs, where the sum of the respective inclusive connectivity values for all vertices remains the same no matter what edge is deleted. DTIC

N94-29063# Army Topographic Engineering Center, Fort Belvoir, VA.
INCORPORATING GEOMETRIC CONSTRAINTS INTO RULE-BASED SYSTEMS USING NONLINEAR OPTIMIZATION Scientific Paper
Jo Ann Parikh and Anne Werkheiser Jan. 1994 8 p
(Grant NSF IRI-91-08638)
(AD-A275093; TEC-R-204) Avail: CASI HC A02/MF A01

A transformation procedure is presented for converting rule-based systems with nonlinear constraints into nonlinear optimization problems. The transformation procedure is then applied to an illustrative site identification system. Nonlinear optimization problems are constructed both for the subset of rules consisting only of logical predicates and for the complete system. Experimental results obtained by solving the nonlinear optimization problems for the site identification system yield a complete description of valid variable bindings for all rules in the system. This procedure was developed in response to the need to solve logical deployment problems for the U.S. Army. In this application domain, numerical, geometric, and geographic constraints must be incorporated with logical constraints in a uniform framework as in human inference. Rules in the system must be able to express various types of relationships, including relationships in the form of nonlinear constraints. Modeling rule-based systems as nonlinear optimization problems provides a powerful, uniform framework with the flexibility to handle mixed data types and numerical and geometric relationships. DTIC

N94-29111 Rutherford Appleton Lab., Chilton (England). Central Computing Dept.
SOLUTION OF AUGMENTED SYSTEMS
I. S. Duff 1 Nov. 1993 19 p
(PB94-138211; RAL-93-084) Avail: Issuing Activity (National Technical Information Service (NTIS))

We examine the solution of sets of linear equations for which the coefficient matrix has the form--first row: H A; second row (beneath first row): A(sup T) 0, where the matrix H is symmetric. We are interested in the case when the matrices H and A are sparse. These augmented systems occur in many application areas, for example in the solution of linear programming problems, structural analysis, magnetostatics, differential algebraic systems, constrained optimization, electrical networks, and computational fluid dynamics. We discuss in some detail how they arise in the last three of these applications and consider particular characteristics and methods of solution. We then concentrate on direct methods of solution. We examine issues related to conditioning and scaling, and discuss the design and performance of a code for solving these systems. NTIS

N94-29118# Institut des Hautes Etudes Scientifiques, Bures-sur-Yvette (France).
REIDEMEISTER NUMBERS OF EQUIVARIANT MAPS
A. Felshtyn, R. Hill, and P. Wong Dec. 1993 18 p
(PB94-138286; IHES/M/93/64) Avail: CASI HC A03/MF A01

In this note, we generalize the arithmetic congruence relations among the Reidemeister numbers of iterates of maps to similar congruences for equivariant maps. NTIS

N94-29148 Institut des Hautes Etudes Scientifiques, Bures-sur-Yvette (France).
APPROXIMATION OF SOLUTIONS OF THE CUBIC NLSE BY FINITE DIMENSIONAL EQUATIONS AND NON-SQUEEZING PROPERTIES
J. Bourgain Nov. 1993 12 p Limited Reproducibility: More than 20% of this document may be affected by microfiche quality
(PB94-138294; IHES/M/93/61) Avail: CASI HC A03

We prove a non-squeezing result for the cubic non-linear Schrodinger equation (NLSE), extending to the NLSE some recent work of S. Kuksin. The main feature of this situation is that the flow map is not a compact perturbation of a linear map. The method consists in a direct reduction of the problem to a finite dimensional model where the symplectic capacity preservation holds. This is achieved by elaborating some of the techniques of other papers by the author. The precise form of the non-linearity is of importance in this argument. NTIS

N94-29171# Helsinki Univ. of Technology, Espoo (Finland). Dept. of Computer Science.
SOME EFFICIENT PROCEDURES FOR CORRECTING TRIANGULATED MODELS
I. Maekelae and A. Dolenc Jul. 1993 17 p
(PB94-136926; TKO-B108) Avail: CASI HC A03/MF A01

This paper describes methods for handling efficiently a large class of problems encountered when dealing with 3D models represented by a collection of triangles in STL format. In spite of its drawbacks, the STL format has become a de facto industrial standard for transferring models to manufacturing processes generally known as Rapid Prototyping Techniques (RPT) or Solid Freeform Fabrication (SF2). As the accuracy and size of the workspace of such processes increases, so does the size of the models one wishes to manufacture. Therefore, the efficiency of application programs is an important consideration. Previous published work has focused on the problem of eliminating gaps in triangulated models. In addition to efficiency, this paper describes methods for dealing with other

problems such as overlapping triangles and intersecting triangles. The algorithms have been implemented and tested in industry. The underlying data structures based on adaptive space subdivision also allow the development of other efficient tools such as slicing. NTIS

N94-29174 National Defence Research Establishment, Linkoeping (Sweden). Huvudavdelning foer Informationsteknologi.
CODES ON THE UNIT SPHERE
G. Hedby Sep. 1993 26 p Limited Reproducibility: More than 20% of this document may be affected by microfiche quality
(PB94-136991; FOA-C-30728-3.5) Avail: CASI HC A03

We consider the problem of packing as many equally sized spheres as possible into a given volume. The report is an overview summarizing some of the methods proposed. Included are lattice constructions, group codes, permutation modulation and a construction starting with code concatenation. The constructions are compared to known bounds on the maximal number of points that is possible to put on the n-dimensional sphere which all at least at distance square root of rho from each other. NTIS

N94-29304# Carnegie-Mellon Univ., Pittsburgh, PA. Dept. of Computer Science.
PROGRAM DERIVATION BY PROOF TRANSFORMATION Ph.D. Thesis
Penny Anderson Oct. 1993 189 p
(Contract F33615-90-C-1465; ARPA Order 7597)
(AD-A275260; CMU-CS-93-206) Avail: CASI HC A09/MF A02

In the proofs-as-programs methodology, verified programs are developed through theorem-proving a constructive logic. Under this approach, the theorem-proving process can be regarded as a program derivation process. The merits of this approach to programming are twofold. First, working with proofs instead of programs concentrates the developer's effort on the intellectually difficult part of the development process: understanding, solving, and explaining the solution to a mathematical problem. Second, the proof provides a formal and trustworthy basis for an explanation of the program. This thesis investigates the use of proof transformation as a way to address important concerns in program derivation that are not addressed by theorem-proving alone. One difficulty with the proofs-as-programs strategy arises from the conflict between elegance and efficiency. A simple, elegant proof may lead to an inefficient program. A more complex proof that corresponds to a more efficient program may be difficult to invent or understand. With proof transformations, a developer can start with an elegant proof that is easy to understand, and incrementally derive a more complex proof and thus, a more efficient program. Another problem comes from the need for adaptation and reuse. With current automated support for theorem-proving, it is difficult to re-use previous work other than by re-using lemmas from a library. This kind of reuse is analogous to the use of subroutine libraries in ordinary programming, and does not directly, support adaptation. Proof transformations provide a way of adapting a proof to a new context. DTIC

N94-29439# Helsinki Univ. of Technology, Espoo (Finland). Dept. of Industrial Management.
SOME REMARKABLE SINE AND COSINE FUNCTIONS
P. Lindqvist (Norges Tekniske Hoegskole, Trondheim.) Jun. 1993 23 p
(PB94-137759; ISBN-951-22-1594-2) Avail: CASI HC A03/MF A01

Some special functions akin to the familiar trigonometric and hyperbolic functions are described. A surprisingly rich structure is revealed. NTIS

N94-29476 National Defence Research Establishment, Stockholm (Sweden). Dept. of Weapon Systems, Effects and Protection.
COMPOUND MATRIX METHOD FOR MULTI-POINT BOUNDARY-VALUE PROBLEMS
S. Ivansson Oct. 1993 36 p Limited Reproducibility: More than 20% of this document may be affected by microfiche quality
(ISSN 0347-3694)
(PB94-137791; FOA-C-20948-2.2) Avail: CASI HC A03

The compound matrix method is generalized to handle multi-point boundary-value problems for ordinary differential equation (ODE) systems. A general treatment is given, covering all orders of the linear ODE system and all distributions of the linear boundary conditions in a unified way. Certain quadratic relations for the minors are derived. An appropriate adjoint problem is defined for the multi-point case. In the applications, it frequently happens that a family of boundary-value problems has to be considered that depends analytically on some parameter. We show how a characteristic function and eigensolutions can be computed in this case. An explicit formula is derived for the excitation coefficients of the eigensolutions (the residue contributions). It is given in terms of the solution to the adjoint problem and hence, it does not involve compound entities. Applications to wave propagation computations for range-independent fluid-solid media are presented in a companion paper. NTIS

N94-29889 Center for Mathematics and Computer Science, Amsterdam (Netherlands). Dept. of Computer Science.
SECOND-ORDER ALGEBRAIC SPECIFICATION OF STATE SEMANTICS
Jan Heering Dec. 1992 19 p Sponsored in part by EEC Limited Reproducibility: More than 20% of this document may be affected by microfiche quality
(ISSN 0169-118X)
(CWI-CS-R9254; ETN-94-95536) Avail: CASI HC A03

Higher order algebraic specification is a synthesis of first order algebraic specification and higher order functional programming which is both logically appealing as well as considerably more expressive than its two predecessors. To illustrate this, the static semantics of a simple block structured programming language using second order equations in addition to first order ones are described. The specification has a highly nondeterministic character and does not use a type environment. It supports error recovery and early detection of errors in incomplete programs. ESA

N94-30078 Joint Inst. for Nuclear Research, Dubna (USSR). Lab. of Theoretical Physics.
ITERATIVE PROCEDURE AS EQUATION OF MOTION
V. I. Yukalov and E. P. Yukalova 1992 15 p Limited Reproducibility: More than 20% of this document may be affected by microfiche quality
(DE94-608008; JINR-E-5-92-428) Avail: CASI HC A03 (US Sales Only)

It is shown that any iterative procedure can be treated as an equation of motion corresponding to an autonomous dynamical system. Iterative cascades and flows are defined. The sequence of iterative terms composes a trajectory whose form is governed by a set of governing functions. The latter are given by fixed point conditions. The sought limit of the iterative procedure plays the role of an attractor. DOE

N94-30091 International Centre for Theoretical Physics, Trieste (Italy).
PERIODIC ORBITS OF n-BODY TYPE PROBLEMS: THE FIXED PERIOD CASE
H. Riahi Aug. 1993 23 p Limited Reproducibility: More than 20% of this document may be affected by microfiche quality
(DE94-608096; IC-93/256) Avail: CASI HC A03 (US Sales Only)

This paper gives a proof of the existence and multiplicity of periodic solutions to Hamiltonian systems. The proof is based on the study of the critical points at infinity done by the author in a previous paper and generalizes the topological arguments used by A. Bahri and P. Rabinowitz in their study of the 3-body problem. It uses a recent result of E. Fadell and S. Husseini on the homology of free loop spaces on configuration spaces. The detailed proof is given for the 4-body problem then generalized to the n-body problem. DOE

N94-30119 International Centre for Theoretical Physics, Trieste (Italy).
HOMOGENEOUS POISSON STRUCTURES
A. ShafeiDehAbad and F. Malek Sep. 1993 9 p Limited Reproducibility: More than 20% of this document may be affected by microfiche quality
(DE94-608112; IC-93/291) Avail: CASI HC A02 (US Sales Only)

The authors provide an algebraic definition for the Schouten product and give a decomposition for any homogeneous Poisson structure in any n-dimensional vector space. A large class of n-homogeneous Poisson structures in R(sup k) is also characterized. DOE

N94-30139 Ottawa Univ. (Ontario). Dept. of Electrical Engineering.
M-INTERFERENCE QUEUE ANALYSIS BY DECOMPOSITION METHOD M.S. Thesis
Xiao-Xiong Yao 1992 136 p
(ISBN-0-315-85795-1; CTN-94-61166) Copyright Avail: Micromedia Ltd., Technical Information Centre, 240 Catherine Street, Suite 305, Ottawa, Ontario, K2P 2G8, Canada HC/MF

The M-interference queueing problem in shared channel communication networks is studied. An effective approach called the decomposition method

is proposed, which decomposes the interaction of M-interference stations into a set of simple queues. The performance of the symmetric shared channel communication networks can be evaluated through analysis of the queueing behavior of only one station using queueing theory. Three examples are used to illustrate this approach. Simulation programs were also developed and run to verify the analytical results. For the time division multiple access system, analytical results for both the packet delay performance and message delay performance were obtained. The analytical results were found to match the existing and simulation results exactly, indicating that the system is decomposable. For the token ring system, results show that the token ring network can be decomposed in an exhaustive service policy and can be approximated as a decomposable system in a single service policy. For a slotted ALOHA system with a finite number of stations, each with an infinite buffer, delay performance values obtained by the decomposition approach were in good agreement with the simulation results. The overall results indicate that the decomposition method is feasible for the analysis of the M-interference queueing problem. Author (CISTI)

N94-30207*# Institute for Computer Applications in Science and Engineering, Hampton, VA.

A SPECTRAL BOUNDARY INTEGRAL EQUATION METHOD FOR THE 2-D HELMHOLTZ EQUATION Final Report

Fang Q. Hu (Old Dominion Univ., Norfolk, VA.) Mar. 1994 24 p Submitted for publication

(Contract NAS1-19480; RTOP 505-90-52-01)

(NASA-CR-194890; NAS 1.26:194890; ICASE-94-15) Avail: CASI HC A03/MF A01

In this paper, we present a new numerical formulation of solving the boundary integral equations reformulated from the Helmholtz equation. The boundaries of the problems are assumed to be smooth closed contours. The solution on the boundary is treated as a periodic function, which is in turn approximated by a truncated Fourier series. A Fourier collocation method is followed in which the boundary integral equation is transformed into a system of algebraic equations. It is shown that in order to achieve spectral accuracy for the numerical formulation, the nonsmoothness of the integral kernels, associated with the Helmholtz equation, must be carefully removed. The emphasis of the paper is on investigating the essential elements of removing the nonsmoothness of the integral kernels in the spectral implementation. The present method is robust for a general boundary contour. Aspects of efficient implementation of the method using FFT are also discussed. A numerical example of wave scattering is given in which the exponential accuracy of the present numerical method is demonstrated. Author (revised)

N94-30208*# Institute for Computer Applications in Science and Engineering, Hampton, VA.

CANONICAL-VARIABLES MULTIGRID METHOD FOR STEADY-STATE EULER EQUATIONS

Shlomo Taasan (Weizmann Inst. of Science, Rehovoth, Israel.) Mar. 1994 14 p Proposed for presentation at the 14th International Conference on Numerical Methods in Fluid Dynamics, Bangalore, India, Jul. 1994

(Contract NAS1-19480; RTOP 505-90-52-01)

(NASA-CR-194888; NAS 1.26:194888; ICASE-94-14) Avail: CASI HC A03/MF A01

A novel approach for the solution of inviscid flow problems for subsonic compressible flows is described. The approach is based on canonical forms of the equations, in which subsystems governed by hyperbolic operators are separated from those governed by elliptic ones. The discretizations used as well as the iterative techniques for the different subsystems are inherently different. Hyperbolic parts, which describe, in general, propagation phenomena, are discretized using upwind schemes and are solved by marching techniques. Elliptic parts, which are directionally unbiased, are discretized using h-elliptic central discretizations, and are solved by pointwise relaxations together with coarse grid acceleration. The resulting discretization schemes introduce artificial viscosity only for the hyperbolic parts of the system; thus a smaller total artificial viscosity is used, while the multigrid solvers used are much more efficient. Solutions of the subsonic compressible Euler equations are achieved at the same efficiency as the full potential equation. Author (revised)

N94-30209*# Institute for Computer Applications in Science and Engineering, Hampton, VA.

ACCURATE FINITE DIFFERENCE METHODS FOR TIME-HARMONIC WAVE PROPAGATION Final Report

Isaac Harari (Tel-Aviv Univ., Israel.) and Eli Turkel (Tel-Aviv Univ., Israel.) Mar. 1994 41 p Submitted for publication

(Contract NAS1-19480; RTOP 505-90-52-01)

(NASA-CR-194887; NAS 1.26:194887; ICASE-94-13) Avail: CASI HC A03/MF A01

Finite difference methods for solving problems of time-harmonic acoustics are developed and analyzed. Multidimensional inhomogeneous problems with variable, possibly discontinuous, coefficients are considered, accounting for the effects of employing nonuniform grids. A weighted-average representation is less sensitive to transition in wave resolution (due to variable wave numbers or nonuniform grids) than the standard pointwise representation. Further enhancement in method performance is obtained by basing the stencils on generalizations of Pade approximation, or generalized definitions of the derivative, reducing spurious dispersion, anisotropy and reflection, and by improving the representation of source terms. The resulting schemes have fourth-order accurate local truncation error on uniform grids and third order in the nonuniform case. Guidelines for discretization pertaining to grid orientation and resolution are presented. Author (revised)

N94-30241 Ottawa Univ. (Ontario).

FORMULAS OF THE RUNGE-KUTTA-NYSTROEM TYPE M.S. Thesis [FORMULES DE TYPE RUNGE-KUTTA-NYSTROEM]

Fadi Malek 1992 56 p In FRENCH

(ISBN-0-315-85774-9; CTN-94-61165) Copyright Avail: Micromedia Ltd., Technical Information Centre, 240 Catherine Street, Suite 305, Ottawa, Ontario, K2P 2G8, Canada HC/MF

Explicit Runge Kutta Nystroem pairs, which solve directly second order initial value problems of the form $y'' = f(x,y)$ with the first derivative y' absent, are considered. Pairs consisting of formulae of order p-1 and p, respectively, can be designed to control the local error in y, in y', or in y and y'. They may also advance the numerical approximations using the lower order formulae or the higher order formulae. These two sets of choices lead to five types of pairs. The minimum number of stages required to form the five types of pairs are established for $p=2$ to 6 by producing an existing pair and disproving the existence of a similar pair with fewer stages. Notions of Nystroem methods and Nystroem trees are recalled along with the order conditions for these methods. Author (CISTI)

N94-30317# Oak Ridge National Lab., TN.

LARGE-SCALE 3-D SOLUTIONS OF THE TIME-DEPENDENT DIRAC EQUATION

A. S. Umar (Vanderbilt Univ., Nashville, TN.), J. C. Wells (Vanderbilt Univ., Nashville, TN.), V. E. Oberacker (Vanderbilt Univ., Nashville, TN.), and M. R. Strayer 1993 9 p Presented at the 2nd International Conference on Computational Physics, Beijing, China, 13-17 Sep. 1993

(Contract DE-AC05-84OR-21400)

(DE94-005591; CONF-9309176-4) Avail: CASI HC A02/MF A01

The authors present the numerical approach used in solving the time-dependent Dirac equation on a three-dimensional Cartesian lattice. Discretization is achieved through the lattice basis-spline collocation method, in which quantum-state vectors and coordinate-space operators are expressed in terms of basis-spline functions on a spatial lattice. All numerical procedures reduce to a series of matrix-vector operations which are performed on the Intel iPSC/860 hypercube, making full use of parallelism. The authors discuss their solutions to the problems of limited node memory and node-to-node communication overhead inherent in using distributed-memory. DOE

N94-30319# Amsterdam Univ. (Netherlands). Inst. for Logic, Language and Computation.

DYNAMIC GENERALIZED QUANTIFIERS AND MONOTONICITY

Makoto Kanazawa (Stanford Univ., CA.) Mar. 1993 31 p

(Contract NF-102/62-356) (ISSN 0928-3307)

(LP-93-02; ETN-94-95560) Avail: CASI HC A03/MF A01

The system of DPL (Dynamic Predicate Logic) augmented with Generalized Quantifiers (GQ's) is addressed. This can be seen as a refinement of first order logic with GQ's, just as DPL is a refinement of

first order logic. The GQ of interest is what Groenendijk and Stokhof would call 'internally dynamic' GQ's. They allow an indirect binding relation to obtain between dynamic existential quantifiers in their first argument and corresponding variables in their second argument. An empirical motivation for studying such GQ's comes from donkey sentences with relative clauses. ESA

N94-30325 Amsterdam Univ. (Netherlands). Dept. of Mathematics and Computer Science.
A SMART CHILD OF PEANO'S
V. Y. Shavrukov 8 Dec. 1992 28 p Limited Reproducibility: More than 20% of this document may be affected by microfiche quality
(ISSN 0928-3315)
(ML-92-10; ETN-94-95545) Avail: Issuing Activity (European Space Agency (ESA))

The provability logic of a special form of the Feferman provability predicate together with the usual provability predicate of Peano Arithmetic (PA) is calculated. In other words, a bimodal system is constructed with the intended interpretation of the expression square phi being as usual the formalization of 'phi is provable in PA' and the new modal operator triangle standing, when applied to phi, for 'there exists an x s.t. l(summation(sub x)) is consistent and proves phi.' The new system is called LF. A Kripke semantics for LF is constructed, and the arithmetical completeness theorem for this system is proved. A small number of other issues concerning the Feferman predicate, such as uniqueness of goedelsentences for the triangle, are considered. ESA

N94-30326 Amsterdam Univ. (Netherlands). Inst. for Logic, Language and Computation.
COMPLETENESS OF THE LAMBEK CALCULUS WITH RESPECT TO RELATIVIZED RELATIONAL SEMANTICS
Nikolai Pankratev (Moscow State Univ., Russia.) 11 Mar. 1993 15 p Limited Reproducibility: More than 20% of this document may be affected by microfiche quality
(ISSN 0928-3307)
(LP-93-03; ETN-94-95561) Avail: Issuing Activity (European Space Agency (ESA))

It was shown that many substructural logics including Lambek calculus L are complete with respect to relativized relational semantics. A proof that it is sufficient for L to consider a relativization to the relation 'x divides y' in some fixed semigroup G is presented. ESA

N94-30327 Amsterdam Univ. (Netherlands). Dept. of Philosophy.
IDENTITY: QUARRELLING WITH AN UNPROBLEMATIC NOTION
Jacques vanLeeuwen Mar. 1993 36 p Limited Reproducibility: More than 20% of this document may be affected by microfiche quality
(ISSN 0928-3307)
(LP-93-04; ETN-94-95562) Avail: CASI HC A03

A progressive series of questions about identity is answered. The questions, and where possible answers, are: are there genuine questions of identity (yes); why can there be problems of identity if identity is such a simple and unproblematic relation; how can it be guaranteed that in each specific identity statement the relevant criterion of identity is co-satisfiable with the general structural properties of identity (especially the principle of indiscernibility); does the fact that there are incompatible criteria of identity imply that the basic properties of identity must be denied for the corresponding identity relations (no). The treatment of identity in possible world semantics is also addressed. The interplay between identity, reference, quantification and intensional operators has been frequently discussed in the literature on possible world semantics. It is hoped to shed light on these discussions with the help of the philosophical insights exposed. Concentration is thereby on the opposite approaches of Kripke and Hintikka in their treatment of cross-world identity. A critical study of the philosophical motivations of these writers is given. It is considered that the use of alternative 'world lines' in Hintikka's approach is important for the purpose of knowledge representation. It is proposed to use world lines in order to represent the identifications of a subject of knowledge, including cases of misidentification. In this way a drawback of Kripke's approach is overcome. ESA

N94-30333 Utrecht State Univ. (Netherlands). Dept. of Computer Science.
ONLY FEW GRAPHS HAVE BOUNDED TREEWIDTH
T. Kloks and H. Bolaender Nov. 1992 15 p Sponsored by Netherlands Foundation for Computer Science Limited Reproducibility: More than 20% of this document may be affected by microfiche quality
(ISSN 0924-3275)
(RUU-CS-92-35; ETN-94-95625) Avail: CASI HC A03

The treewidth of random graphs is studied. Let delta be greater than 1 and epsilon less than (delta - 1)/(delta + 1). Then almost all graphs with n vertices and with at least delta(n) edges have treewidth greater than or equal to n to the power epsilon. It is also shown that almost all graphs with n vertices and delta(n) edges have treewidth greater than b(sub delta)(n), where b(sub delta) is strictly positive if delta is greater than 1.18. It is shown that for every b greater than 0 and less than 1, there exists a delta(sub b), such that almost all graphs with at least delta(sub b)(n) edges have treewidth greater than bn. The methods, together with recent results on minor theory, also show the following. Let delta be greater than or equal to 1.18. There exists a positive constant c(sub delta), such that a.e. graph G(sub n, m) with m greater than or equal to delta(n) has a clique minor K(sub s) with s greater than or equal to (C(sub delta)n to the 1/3 power). This extends earlier results of Bollobas et al. The following is shown. Let G be a minor closed class of graphs (for example the class of planar graphs). For all delta greater than or equal to 1.18, if m is greater than or equal to delta(n) then a.e. graph with m edges is not in G. ESA

N94-30346 Utrecht State Univ. (Netherlands). Dept. of Computer Science.
DERIVATION LENGTHS IN TERM REWRITING FROM INTERPRETATIONS IN THE NATURALS
V. C. S. Meeussen and H. Zantema Dec. 1992 15 p Limited Reproducibility: More than 20% of this document may be affected by microfiche quality
(ISSN 0924-3275)
(RUU-CS-92-43; ETN-94-95633) Avail: CASI HC A03

Monotone interpretations in the natural numbers provide a useful technique for proving termination of Term Rewriting Systems (TRS). Termination proofs of this shape imply upper bounds on derivation lengths expressed in bounds on the interpretations. For a hierarchy of classes of interpretations, a description of these upper bounds, among which the doubly exponential upper bound for polynomial interpretations, found by Hofbauer and Lautemann, is given. By examples of term rewriting systems it is shown that all of these upper bounds are sharp in a natural sense. In particular, all Ackermann functions are found as sharp upper bounds on derivation lengths exhausting primitive recursive functions. ESA

N94-30353 Pennsylvania State Univ., University Park.
FOUR-DIMENSIONAL DATA ASSIMILATION USING THE ADJOINT METHOD Ph.D. Thesis
Jian-Wen Bao 1993 167 p
Avail: Univ. Microfilms Order No. DA9326808

The calculus of variations is used to confirm that variational four-dimensional data assimilation (FDDA) using the adjoint method can be implemented when the numerical model equations have a finite number of first-order discontinuous points. These points represent the on/off switches associated with physical processes, for which the Jacobian matrix of the model equation does not exist. Numerical evidence suggests that, in some situations when the adjoint method is used for FDDA, the temperature field retrieved using horizontal wind data is numerically not unique. A physical interpretation of this type of non-uniqueness of the retrieval is proposed in terms of energetics. The adjoint equations of a numerical model can also be used for model-parameter estimation. A general computational procedure is developed to determine the size and distribution of any internal model parameter. The procedure is then applied to a one-dimensional shallow fluid model in the context of analysis-nudging FDDA; the weighting coefficients used by the Newtonian nudging technique are determined. The sensitivity of these nudging coefficients to the optimal objectives and constraints is investigated. Experiments of FDDA using the adjoint method are conducted using the dry version of the hydrostatic Penn State/NCAR mesoscale model (MM4) and its adjoint. The minimization procedure

converges and the initialization experiment is successful. Temperature-retrieval experiments involving an assimilation of the horizontal wind are also carried out using the adjoint of MM4. Dissert. Abstr.

N94-30370# Amsterdam Univ. (Netherlands). Dept. of Mathematics and Computer Science.

A NOTE ON THE COMPLEXITY OF LOCAL SEARCH PROBLEMS

Sophie Fischer Mar. 1993 15 p Sponsored by Netherlands Organization for Scientific Research

(ISSN 0928-3323)

(CT-93-02; ETN-94-95556) Avail: CASI HC A03/MF A01

The complexity of finding a local optimum in combinatorial optimization problems is studied. For many optimization problems derived from NP complete decision problems, for example MAXCLIQUE, a locally optimal solution starting from a given solution can be found in (deterministic) polynomial time. It is not known, however, whether this is a property shared by all these problems. In particular, the class of PLS complete problems seems to form an exception. Several problems for which the question, whether for a given solution a local optimum 'exists' within a polynomial of PLS steps, is NP complete, are presented. ESA

N94-30372# Amsterdam Univ. (Netherlands). Dept. of Philosophy.

INTERROGATIVES AND ADVERBS OF QUANTIFICATION

Jeroen Groenendijk and Martin Stokhof Dec. 1992 31 p Submitted for publication

(ISSN 0928-3307)

(LP-92-14; ETN-94-95558) Avail: CASI HC A03/MF A01

A topic in the semantics of interrogatives is studied. It is a modified and extended version of a note on interrogatives and quantification, taking into consideration remarks by U. Lahiri. An aim is to show that, appearances notwithstanding, quantificational variability can be accounted for in an approach which complies with strong exhaustiveness. The implementation of the semantic analysis of interrogatives is outlined, and the challenge that Berman's proposals form for this analysis is discussed. The meeting of this challenge, making use of insights from dynamic semantics, is shown. Addressing of some of Lahiri's examples is outlined. ESA

N94-30377# Utrecht State Univ. (Netherlands). Dept. of Computer Science.

THE EXACT FITTING PROBLEM IN HIGHER DIMENSIONS

Jean-Marc Robert (Quebec Univ., Chicoutimi.), Leonidas J. Guibas (Stanford Univ., CA.), and Mark H. Overmars Nov. 1992 20 p Sponsored in part by Netherlands Organization for Scientific Research, and EEC

(ISSN 0924-3275)

(RUU-CS-92-37; ETN-94-95627) Avail: CASI HC A03/MF A01

Let S be a family of n points in E(sup d). The 'exact fitting' problem asks for finding a hyperplane containing the maximum number of points of S. An O(min((n(sup d))/(m(sup d - 1))log n/m, n(sub d)) time algorithm where m denoted the number of points on the hyperplane is presented. This algorithm is based on upper bounds on the maximum number of incidences between families of points and families of hyperplanes in E(sup d) and on an algorithm to compute these incidences. It is also shown how the upper bound on the maximum number of incidences between families of points and families of hyperplanes can be used to derive new bounds on some well known problems in discrete geometry. ESA

N94-30378 Utrecht State Univ. (Netherlands). Dept. of Computer Science.

PEARL'S BELIEF PROPAGATION: THE PROOFS

Linda vanderGaag Dec. 1992 28 p Limited Reproducibility: More than 20% of this document may be affected by microfiche quality

(ISSN 0924-3275)

(RUU-CS-92-47; ETN-94-95637) Avail: Issuing Activity (European Space Agency (ESA))

The belief network framework for plausible reasoning provides both a formalism for representing knowledge concerning a joint probability distribution on a problem domain and a set of algorithms for efficiently propagating evidence and computing probabilities of interest. A review of the set of algorithms for belief propagation proposed by J. Pearl, including full proofs, is presented. ESA

N94-30380 Amsterdam Univ. (Netherlands). Dept. of Mathematics and Computer Science.

BOUNDED CONTRACTION AND MANY-VALUED SEMANTICS

Andreja Prijatelj Feb. 1993 24 p Limited Reproducibility: More than 20% of this document may be affected by microfiche quality

(ISSN 0928-3315)

(ML-93-04; ETN-94-95549) Avail: CASI HC A03

A Gentzen style propositional logic with n bounded contraction (n greater than or equal to 2), a version of the contraction rule where n + 1 occurrences of a formula may be contracted to n occurrences, is considered. In particular, expansions of the linear models for n valued Lukasiewicz logic as models of n bounded contraction are studied. A proof of the finite axiomatizability of these logics, with the resulting axiomatizations in the form of a Gentzen sequent calculus with additional axioms, is presented. ESA

N94-30381 Amsterdam Univ. (Netherlands). Dept. of Mathematics and Computer Science.

MODELS OF THE UNTYPED LAMBDA-CALCULUS IN SEMI CARTESIAN CLOSED CATEGORIES

Raymond Hoofman and Harold Schellinx Feb. 1993 15 p Limited Reproducibility: More than 20% of this document may be affected by microfiche quality

(ISSN 0928-3315)

(ML-93-05; ETN-94-95550) Avail: Issuing Activity (European Space Agency (ESA))

Soundness and completeness of two classes of category theoretical models for the untyped lambda-beta calculus, classes that are distinguished from (but closely related to) the traditional class of categorical models consisting of reflexive objects in cartesian closed categories, are shown. ESA

N94-30382 Amsterdam Univ. (Netherlands). Inst. for Logic, Language and Computation.

CATEGORIAL GENERALIZATION OF ALGEBRAIC RECURSION THEORY

J. Zashev (Sofia Univ., Bulgaria.) Mar. 1993 47 p Limited Reproducibility: More than 20% of this document may be affected by microfiche quality

(Contract I-32-91) (ISSN 0928-3315)

(ML-93-06; ETN-94-95551) Avail: Issuing Activity (European Space Agency (ESA))

A generalization of recursion theory which seems to be interesting also from a purely categorial point of view and arises in a natural way from a well established and point free algebraic generalization of recursion theory is presented. A special kind of enriched categories called DM categories are addressed and a notion of iterative DM category is introduced. The notion is a generalization of a possible version of the concept of iterativity for operative spaces. The question of what can be expected from properly categorial models of the theory of DM categories is addressed by three examples. ESA

N94-30383 Amsterdam Univ. (Netherlands). Inst. for Logic, Language and Computation.

ALGORITHMIC PROBLEMS CONCERNING FIRST-ORDER DEFINABILITY OF MODAL FORMULAS ON THE CLASS OF ALL FINITE FRAMES

A. V. Chagrov (Tver State Univ., Russia.) and L. A. Chagrova (Tver State Univ., Russia.) Mar. 1993 23 p Limited Reproducibility: More than 20% of this document may be affected by microfiche quality

(ISSN 0928-3315)

(ML-93-07; ETN-94-95552) Avail: Issuing Activity (European Space Agency (ESA))

The problem of describing the 'behavior' of modal, or other propositional intensional formulas on the class of finite frames seems rather natural. Almost all modal logics resulting from formulation of substantial ideas have turned out to have the finite model property. Moreover, different semantic constructions in the finite case are effectively intertranslatable (there is no incompleteness effect). A result on the undecidability of semantic consequence for finite GL-frames and some generalizations thereof are proved. The main technical lemma shows how to reduce the halting problem for Minsky machines to the finite frame consequence problem. Technical facts about first order definability of modal formulas are proved. Formulas

closely connected with the constructions are presented, which have no first order equivalents on the class of finite frames. Results are combined to obtain short proofs of the undecidability of various problems connected with first order definability on the class of finite frames. Two notions of first order definability are considered, a 'local' one and a 'global' one. A problem concerning the difference between global and local definability on the class of all transitive frames is decided. ESA

N94-30384 Amsterdam Univ. (Netherlands). Dept. of Mathematics and Computer Science.

REMARKS ON THE THEORY OF SEMI-FUNCTORS

Raymond Hoofman and Ieke Moerdijk Mar. 1993 14 p Limited Reproducibility: More than 20% of this document may be affected by microfiche quality

(ISSN 0928-3315)

(ML-93-08; ETN-94-95553) Avail: CASI HC A03

By establishing an appropriate equivalence, it is shown that the theory of semi-functors can be fully embedded in the theory of (ordinary) functors. As a result, standard properties and constructions on functors extend automatically to semi-functors. ESA

N94-30385 Amsterdam Univ. (Netherlands). Dept. of Mathematics and Computer Science.

NATURAL DEDUCTION FOR INTUITIONISTIC LINEAR LOGIC

A. S. Troelstra 14 Apr. 1993 30 p Limited Reproducibility: More than 20% of this document may be affected by microfiche quality

(ISSN 0928-3315)

(ML-93-09; ETN-94-95554) Avail: CASI HC A03

Two versions of the fragment with unit, tensor, linear implication and storage operator (the exponential) of intuitionistic linear logic, are addressed. The first version, ILL, appears in a paper by Benton, Bierman, Hyland and de Paiva; the second one, ILL+, is described. ILL has a contraction rule and an introduction rule ! for the exponential; in ILL+, instead of a contraction rule, multiple occurrences of labels for assumptions are permitted under certain conditions; moreover, there is a different introduction rule for the exponential, ! +, which is closer in spirit to the necessitation rule for the normalizable version of S4 discussed by Prawitz in his monograph 'Natural deduction'. t is relatively easy to adapt Prawitz's treatment of natural deduction for intuitionistic logic to ILL+; in particular, a notion of strong validity permitting a proof of strong normalization can be formulated. The conversion rules for ILL explicitly mentioned in the paper by Benton et al. do not suffice for normal forms with subformula property, but it can be shown that this can be remedied by addition of a single conversion rule. ILL+ also suggests the study of a class of categorical models, more special than the class introduced by Benton et al. ESA

N94-30393 Utrecht State Univ. (Netherlands). Dept. of Computer Science.

A NOTE ON THE SMYTH POWERDOMAIN CONSTRUCTION

Peter Knijnenburg Jan. 1993 9 p Limited Reproducibility: More than 20% of this document may be affected by microfiche quality

(ISSN 0924-3275)

(RUU-CS-93-02; ETN-94-95639) Avail: CASI HC A02

A representation for the Smyth powerdomain is defined, using minimal representatives, rather than maximal ones. A review of domain theory and the chain completion method is given and the method is used to define the Smyth powerdomain. The construction immediately gives rise to a collection of subsets of the underlying domain which are again Smyth pre-ordered. This is not trivial: in the Plotkin powerdomain construction the Egli-Milner order on the finite elements 'becomes' the Plotkin order on the infinite ones. Minimal representatives for the equivalence classes for the pre-order are defined, and it is shown how continuous functions on the underlying domain lift to continuous functions on the Smyth powerdomain. ESA

N94-30394 Utrecht State Univ. (Netherlands). Dept. of Computer Science.

ALGEBRAIC DOMAINS, CHAIN COMPLETION, AND THE PLOTKIN POWERDOMAIN CONSTRUCTION

Peter Knijnenburg Jan. 1993 33 p Limited Reproducibility: More than 20% of this document may be affected by microfiche quality

(ISSN 0924-3275)

(RUU-CS-93-03; ETN-94-95640) Avail: Issuing Activity (European Space Agency (ESA))

A review of the Plotkin powerdomain construction over algebraic cpo's is given. Algebraic cpo's are cpo's that are completely determined by their collection of finite elements. It is shown how an algebraic cpo can be built out of any preordered set using the method of chain completion. This method is applied to define the powerdomain over an algebraic cpo. It is shown how to interpret this powerdomain as a subset of the powerset of the base domain together with a suitable ordering relation. This ordering relation is the Plotkin order and it extends the Egli-Milner order. A necessary and sufficient condition on the base domain to ensure that the Plotkin order and the Egli-Milner order coincide is given. It is shown how to construct continuous functions between powerdomains out of functions between the underlying base domains. It follows that the powerdomain construction is a continuous functor on the category of algebraic cpo's. ESA

N94-30395 Amsterdam Univ. (Netherlands). Inst. for Logic, Language and Computation.

COMMUTATIVE LAMBEK CATEGORIAL GRAMMARS

Maciej Kandulski (Adam Mickiewicz Univ., Poznan, Poland.) Jan. 1993 23 p Limited Reproducibility: More than 20% of this document may be affected by microfiche quality

(ISSN 0928-3315)

(ML-93-01; ETN-94-95546) Avail: CASI HC A03

The problem of establishing the generative power of Categorical Grammars (CG's) based on the Nonassociative and Commutative Lambek calculus with product (NCL) is addressed. It is proved that the class of languages generated by CG's based on NCL coincides with the class of CF languages of finite degree whose rules are closed with respect to permutation (CF(bar) languages). To establish the inclusion of the class of NCL languages in the class of CF(bar) languages, the notion of normal form of derivation which already proved useful in investigations concerning generative power of categorial grammars is employed. The proof of the converse inclusion makes use of an algebraic characterization of phrase languages generated by classical (Ajdukiewicz) CG's and CF grammars. ESA

N94-30396 Amsterdam Univ. (Netherlands). Dept. of Mathematics and Computer Science.

MODAL QUANTIFICATION OVER STRUCTURED DOMAINS

Johan vanBenthem and Natasha Alechina 5 Jan. 1993 30 p Limited Reproducibility: More than 20% of this document may be affected by microfiche quality

(ISSN 0928-3315)

(ML-93-02; ETN-94-95547) Avail: Issuing Activity (European Space Agency (ESA))

Generalized quantifiers as modal operators are addressed. A basic deductive calculus for the modal quantifier logic is developed. The semantic properties of modal quantifiers are illustrated; an analog to the basic model theoretic invariance relation of modal logic is considered. Frame correspondence is addressed. A Sahlqvist theorem is proved. Limitative results are given. ESA

N94-30397 Amsterdam Univ. (Netherlands). Inst. for Logic, Language and Computation.

THE CONJOINABILITY RELATION IN LAMBEK CALCULUS IN LINEAR LOGIC

Mati Pentus (Moscow State Univ., Russia.) Feb. 1993 22 p Limited Reproducibility: More than 20% of this document may be affected by microfiche quality

(Contract NF-102/62-356) (ISSN 0928-3315)

(ML-93-03; ETN-94-95548) Avail: Issuing Activity (European Space Agency (ESA))

In 1958 J. Lambek introduced a calculus L of syntactic types and defined an equivalence relation on types: 'x is equivalent to y means that there exists a sequence x = x(sub 1),..., x(sub n) = y (n greater than or equal to 1), such that x(sub i) implies x(sub i + 1) or x(sub i + 1) implies x(sub i) (i greater than or equal to 1 and less than n).' He pointed out that x is equivalent to y if and only if there is join z such that x implies z and y implies z. An effective characterization of this equivalence for the

Lambek calculi L and LP, and for the multiplicative fragments of Girard's and Yetter's linear logics, is given. For the non directed Lambek calculus LP and the multiplicative fragment of Girard's linear logic, linear time algorithms deciding whether two types are equal, and finding a join for them if they are, are presented. ESA

N94-30402 National Aerospace Lab., Amsterdam (Netherlands). Informatics Div.

REPRESENTATIONS OF DYNAMICAL SYSTEMS DESCRIBED BY BEHAVIORAL INEQUALITIES

A. A. tenDam 12 Oct. 1992 14 p Presented at the European Control Conference, Groningen, Netherlands, 28 Jun. - 1 Jul. 1993 Limited Reproducibility: More than 20% of this document may be affected by microfiche quality

(AD-B173649; NLR-TP-92408-U; ETN-94-95595) Avail: CASI HC A03

Dynamical systems described by inequalities are considered from a behavioral point of view. The notions convex, conical, and polyhedral are introduced for the manifest behavior. Systems described by difference inequalities are introduced and redundancy, implicit equalities, and minimal representations are discussed. The class of unimodular polynomical matrices for systems described by difference inequalities is introduced. ESA

N94-30403 Utrecht State Univ. (Netherlands). Dept. of Computer Science.

ISOMORPHISMS BETWEEN PREDICATE AND STATE TRANSFORMERS

Marcello Bonsangue (Center for Mathematics and Computer Science, Amsterdam, Netherlands.) and Joost N. Kok Mar. 1993 26 p Limited Reproducibility: More than 20% of this document may be affected by microfiche quality

(Grant CNR-203.15.3) (ISSN 0924-3275)

(RUU-CS-93-09; ETN-94-95646) Avail: CASI HC A03

The relation between state transformers based on directed complete partial orders and predicate transformers is studied. Concepts like 'predicate,' 'liveness,' 'safety,' and 'predicate transformers' are formulated in a topological setting. State transformers based on the Hoare, Smyth, and Plotkin powerdomains are addressed and continuous, monotonic, and unrestricted functions are considered. The transformers are related by isomorphisms thereby extending and completing earlier results and giving a complete picture of all the relationships. ESA

N94-30404# Utrecht State Univ. (Netherlands). Dept. of Computer Science.

MINIMUM FILL-IN FOR CHORDAL BIPARTITE GRAPHS

T. Kloks Mar. 1993 12 p Sponsored by Netherlands Foundation for Computer Science

(ISSN 0924-3275)

(RUU-CS-93-11; ETN-94-95648) Avail: CASI HC A03/MF A01

Chordal bipartite graphs are exactly those bipartite graphs in which every cycle of length at least six has a chord. The 'minimum fill-in' problem is the problem of finding a chordal embedding of the graph with a minimum number of edges. A polynomial time algorithm for the exact computation of the minimum fill-in for all chordal bipartite graphs is presented. ESA

N94-30405# Utrecht State Univ. (Netherlands). Dept. of Computer Science.

TREEWIDTH OF CIRCLE GRAPHS

T. Kloks Mar. 1993 13 p Sponsored by Netherlands Foundation for Computer Science

(ISSN 0924-3275)

(RUU-CS-93-12; ETN-94-95649) Avail: CASI HC A03/MF A01

A study showing that the treewidth of a circle graph can be computed in polynomial time is presented. A circle graph is a graph that is isomorphic to the intersection graph of a finite collection of chords of a circle. The treewidth problem can be viewed upon as the problem of finding a chordal embedding of the graph that minimizes the maximum clique size. The algorithm to determine the treewidth of a circle graph can be implemented to run in O(n cubed) time, where n is the number of vertices of the graph. ESA

N94-30406 Utrecht State Univ. (Netherlands). Dept. of Computer Science.

L(SUB)p OPTIMAL d DIMENSIONAL TRIANGULATIONS FOR PIECEWISE LINEAR INTERPOLATION: A NEW RESULT ON DATA DEPENDENT TRIANGULATIONS

Elefterios A. Melissaratos Apr. 1993 19 p Sponsored by Netherlands Organization for Scientific Research, and EEC Limited Reproducibility: More than 20% of this document may be affected by microfiche quality

(ISSN 0924-3275)

(RUU-CS-93-13; ETN-94-95650) Avail: CASI HC A03

The problem of optimum piecewise linear approximation of general quadratic functions in R(sup d) for d greater than or equal to 2 is addressed. In particular the problem is posed as follows: given a quadratic function f : R(sup d) to R of the form f(x) = x(sup tau)Ax + b(sup tau)x + c, where matrix A symmetric and positive definite and x is a member of R(sup d). Let X (x(sub 1), x(sub 2), ..., x(sub n)) a set of n points in R(sup d) and let F = (f(sub 1), f(sub 2), ..., f(sub n)) the set of values of function f at each of the points in the set X (i.e., f(x(sub i)) = f(sub i) for i = 1, 2, ..., n). For each triangulation T of the convex hull CH(X) of X and for each set of corresponding values F there exists a unique piecewise linear funciton pi(sub F)(sup T) : R(sup d) to R wich approximates function f. The problem of finding a triangulation T(sub 0) of CH(X) is addressed such that pi(sub F)(sup T(sub 0)) best approximates f with respect to the L(sub p) error in any finite dimension d. ESA

N94-30407 Utrecht State Univ. (Netherlands). Dept. of Computer Science.

SHAPE FROM DIAMETER: NEGATIVE RESULTS

Anil S. Rao and Kenneth Y. Goldberg Apr. 1993 25 p Sponsored in part by EEC Limited Reproducibility: More than 20% of this document may be affected by microfiche quality

(Grant NSF IRI-91-23747) (ISSN 0924-3275)

(RUU-CS-93-16; ETN-94-95653) Avail: Issuing Activity (European Space Agency (ESA))

A study with the objective to automatically recognize parts in a structured environment (such as a factory) using inexpensive and widely available hardware is presented. The planar problem of determining the convex shape of a polygonal part from a sequence of projections is considered. Projecting the part onto an axis in the plane of the part produces a scalar measure, the diameter, which is a function of the angle of projection. The diameter of a part at a particular angle can be measured using an instrumented parallel-jaw gripper. The negative result that shape cannot be uniquely recovered is presented: for a given set of diameter measurements, there is an (uncountably) infinite set of polygonal shapes consistent with these measurements. Since most of these shapes have parallel edges of varying lengths, the related problem of identifying a representative polygon with no parallel edges is also considered. It is shown that given a diameter function, deciding whether such a polygon exists is NP complete. ESA

N94-30408 Utrecht State Univ. (Netherlands). Dept. of Computer Science.

SHAPE FROM DIAMETER: POSITIVE RESULTS

Anil S. Rao and Kenneth Y. Goldberg Apr. 1993 25 p Sponsored in part by EEC Limited Reproducibility: More than 20% of this document may be affected by microfiche quality

(Grant NSF IRI-91-23747) (ISSN 0924-3275)

(RUU-CS-93-17; ETN-94-95654) Avail: CASI HC A03

A study with the objective to automatically recognize parts in a structured environment (such as a factory) using inexpensive and widely available hardware is presented. The planar problem of determining the convex shape of a polygonal part from a sequence of projections is considered. Projecting the part onto an axis in the plane of the part produces a scalar measure, the diameter, which is a function of the angle of projection. The diameter of a part at a particular angle can be measured using an instrumented parallel-jaw gripper. Previously presented negative results motivate consideration to the problem of recognizing a part from a known (finite) set of parts. Given a set of polygonal parts with a total of N faces, can the shortest sensing plan for disambiguating the parts be found. Only diameters at n less than or equal to N stable faces can be measured. An internal representation of these stable diameters in O(N + (n cubed)) time is constructed, and two planning algorithms are given: one constructs an

optimal sensing plan in time O(n(exp 4) 2(exp n)), the other constructs a suboptimal sensing plan in time O((n squared) log n). Neither plan requires more than n measurements. ESA

N94-30412 Center for Mathematics and Computer Science, Amsterdam (Netherlands). Dept. of Computer Science.
EVENT STRUCTURES AND ORTHOGONAL TERM GRAPH REWRITING
J. R. Kennaway (East Anglia Univ., Norwich, England.), J. W. Klop, M. R. Sleep, and F. J. deVries Jul. 1993 22 p Sponsored in part by EEC Limited Reproducibility: More than 20% of this document may be affected by microfiche quality
(Grant SERC-GR/F-91582) (ISSN 0169-118X)
(CWI-CS-R9347; ETN-94-95689) Copyright Avail: CASI HC A03

For every normalizable term in an orthogonal term graph rewrite system, an elementary event structure is constructed. Its events are the essentially different redexes which must be reduced to reach the normal form of the term. The associated state domain is the set of Levy equivalence classes of needed reduction sequences starting from the term. Various properties of the event structure and state domain are related to properties of the term. The problems arising in extending this work to term rewrite systems and non orthogonal rewrite systems are also discussed. ESA

N94-30413 Center for Mathematics and Computer Science, Amsterdam (Netherlands). Dept. of Computer Science.
PERPETUAL REDUCTIONS IN ORTHOGONAL COMBINATORY REDUCTION SYSTEMS
Zurab Khasidashvili Jul. 1993 22 p Limited Reproducibility: More than 20% of this document may be affected by microfiche quality
(ISSN 0169-118X)
(CWI-CS-R9349; ETN-94-95690) Copyright Avail: CASI HC A03

A strategy that, for any given term t in an Orthogonal Combinatory Reduction System (OCRS) (that is, a term rewriting system with bound variables and substitutions), constructs a longest reduction starting from t if t is strongly normalizable, and constructs an infinite reduction otherwise, is designed. A method for finding the least upper bound of lengths of reductions starting from a strongly normalizable term is developed. Properties of pure substitutions and several kinds of similarity of redexes are studied. These results are applied to construct an algorithm for finding lengths of longest reductions in 'strongly persistent' OCRS's. As a corollary, there is an algorithm for finding lengths of longest developments in orthogonal CRS's. ESA

N94-30424 Utrecht State Univ. (Netherlands). Dept. of Computer Science.
TERMINATION OF TERM REWRITING BY SEMANTIC LABELLING
H. Zantema Jul. 1993 19 p Revised Limited Reproducibility: More than 20% of this document may be affected by microfiche quality
(ISSN 0924-3275)
(RUU-CS-93-24; RUU-CS-92-38; ETN-94-95661) Avail: Issuing Activity (European Space Agency (ESA))

A transformation of TRS (term rewriting system) is proposed, depending on a choice for a model for the TRS. The labeled TRS is obtained from the original one by labeling operation symbols, possibly creating extra copies of some rules. This construction has the remarkable property that the labeled TRS is terminating if and only if the original TRS is terminating. Although the labeled version has more operation symbols and may have more rules (sometimes infinitely many), termination is often easier to prove for the labeled TRS than for the original one. This provides a technique for proving termination, making classical techniques like RPO (recursive path order) and polynomial interpretations applicable for nonsimplifying TRS. ESA

N94-30425 Utrecht State Univ. (Netherlands). Dept. of Computer Science.
RECTILINEAR DECOMPOSITIONS WITH LOW STABBING NUMBER
Mark deBerg and Marc vanKreveld Jul. 1993 13 p Sponsored by Netherlands Organization for Scientific Research; EEC; and Natural Sciences and Engineering Research Council, Canada Limited Reproducibility: More than 20% of this document may be affected by microfiche quality
(ISSN 0924-3275)
(RUU-CS-93-25; ETN-94-95662) Avail: Issuing Activity (European Space Agency (ESA))

Let P be a rectilinear polygon. The stabbing number of a decomposition of P into rectangles is the maximum number of rectangles intersected by any axis parallel segment that lies completely inside P. A proof that any simple rectilinear polygon with n vertices admits a decomposition with stabbing number O(log n) and an example of a simple rectilinear polygon for which any decomposition has stabbing number Omega(log n) are given. It is shown that any rectilinear polygon with k greater than or equal to 1 rectilinear holes and n vertices in total admits a decomposition with stabbing number O((square root of k)(log n)). When the holes are rectangles, then a decomposition exists with stabbing number O((square root of k) + (log n)), which is shown to be tight. All the above decompositions consist of O(n) rectangles. ESA

N94-30427 Center for Mathematics and Computer Science, Amsterdam (Netherlands). Dept. of Computer Science.
THREE METRIC DOMAINS OF PROCESSES FOR BISIMULATION
Franck vanBreugel (Vrije Univ., Amsterdam, Netherlands.) Jun. 1993 20 p Presented at the 9th Conference on the Mathematical Foundations of Programming Semantics, New Orleans, LA, 7-10 Apr. 1993 Submitted for publication Sponsored in part by Netherlands Nationale Faciliteit InformaticaPro gramme Limited Reproducibility: More than 20% of this document may be affected by microfiche quality
(ISSN 0169-118X)
(CWI-CS-R9335; ETN-94-95677) Copyright Avail: CASI HC A03

A metric domain of processes is presented. This domain is located in between two metric process domains introduced by De Bakker and Zucker. The process domain characterizes the collection of image finite processes. This domain has as advantages over the other process domains that no complications arise in the definitions of operators like sequential composition and parallel composition, and that image finite language constructions like random assignment can be modeled in an elementary way. As in the other domains, bisimilarity and equality coincide in this domain. The three domains are obtained as unique (up to isometry) solutions of equations in a category of 1 bounded complete metric spaces. In the case the action set is finite, the three domains are shown to be equal (up to isometry). For infinite action sets, for example equipollent to the set of natural or real numbers, the process domains are proved not to be isometric. ESA

N94-30430 Center for Mathematics and Computer Science, Amsterdam (Netherlands). Dept. of Computer Science.
ISOMORPHISMS BETWEEN PREDICATE AND STATE TRANSFORMERS
Marcello Bonsangue and Joost N. Kok Jun. 1993 33 p Limited Reproducibility: More than 20% of this document may be affected by microfiche quality
(Grant CNR-203.15.3) (ISSN 0169-118X)
(CWI-CS-R9338; ETN-94-95680) Copyright Avail: CASI HC A03

The relation between state transformers based on directed complete partial orders and predicate transformers are studied. Concepts like 'predicate', 'liveness', 'safety' and 'predicate transformers' are formulated in a topological setting. State transformers based on the Hoare, Smyth, and Plotkin powerdomains are addressed, and continuous, monotonic, and unrestricted functions are considered. The transformers are related by isomorphisms, thereby, extending and completing earlier results and giving a complete picture of all the relationships. ESA

N94-30436 Center for Mathematics and Computer Science, Amsterdam (Netherlands). Dept. of Computer Science.
HOMOMORPHISM PRESERVING ALGEBRAIC SPECIFICATIONS REQUIRE HIDDEN SORTS
J. A. Bergstra (Amsterdam Univ., Netherlands.) and J. Heering Jul. 1993 15 p Sponsored in part by EEC Limited Reproducibility: More than 20% of this document may be affected by microfiche quality
(ISSN 0169-118X)
(CWI-CS-R9344; ETN-94-95686) Copyright Avail: CASI HC A03

Although every computable data type has an initial algebra specification with hidden functions, it may happen that some of the homomorphic images of the data type are not models of the specification. The latter are reducts of algebras that would be models of the specification if all its functions were visible, whereas the homomorphic images of the data type are independent of the specification and need not be compatible with the hidden functions used in it. A hidden function specification that does not exclude any of the homomorphic images of its initial model from its model

class is termed homomorphism preserving. It turns out that, unlike unrestricted initial algebra specification, homomorphism preserving initial algebra specification of computable data types requires both hidden sorts and hidden functions. ESA

N94-30515 Ohio State Univ., Columbus.
FURTHER INVESTIGATION OF CURVE VEERING PHENOMENA Ph.D. Thesis
Jeenhuei Tsai 1993 246 p
Avail: Univ. Microfilms Order No. DA9325602

For an eigenvalue problem, if loci are plotted by eigenvalue versus certain system parameters, the phenomenon of curve veering, which is characterized by the continuous alternation of eigenfunctions associated with the continuous variation of eigenvalues, may show. One dimensional (string and beam), two-dimensional (rectangular membrane and plate), and three-dimensional (thick circular plate and solid cylinder) problems are considered. The Galerkin method, the finite difference method, and the three-dimensional Ritz method are used for approximate solutions. Exact closed form solutions are also available in some problems. Unlike previous studies, not all approximate methods would generate this kind of occurrence. The finite difference method is a typical example. On the other hand, the problems with closed form solutions also exhibit curve veering. More importantly, the existence of curve veering in three-dimensional problems, which require no kinematic assumptions, may prove it to be in reality. The theory by Perkins and Mote is examined and found to be applicable to some problems only. Dissert. Abstr.

N94-30721 Utrecht State Univ. (Netherlands). Dept. of Computer Science.
PIECEWISE LINEAR PATHS AMONG CONVEX OBSTACLES
Mark deBerg, Jiri Matousek, and Otfried Schwarzkopf May 1993 26 p Sponsored in part by Netherlands Organization for Applied Scientific Research; Commission of the European Communities; and Alexander van Humboldt Foundation Limited Reproducibility: More than 20% of this document may be affected by microfiche quality
(ISSN 0924-3275)
(RUU-CS-93-20; ETN-94-95657) Avail: CASI HC A03

Let B be a set of n arbitrary (possibly intersecting) convex obstacles in R(sup d). It is shown that any two points which can be connected by a path avoiding the obstacles can also be connected by a path consisting of O(n(sup d - 1)(sup d/2 + 1)) segments. The bound cannot be improved below Omega(n(sup d)), thus in R cubed, the answer is between n cubed and n to the 4th power. For open disjoint convex obstacles, a Theta(n) bound is proved. By a well known reduction, the general case result also upper bounds the complexity for a translational motion of an arbitrary convex robot among convex obstacles. In the planar case, asymptotically tight bounds and efficient algorithms are given. ESA

N94-30726 Joint Inst. for Nuclear Research, Dubna (USSR). Lab. of Theoretical Physics.
GL(SUB q)(N)-COVARIANT QUANTUM ALGEBRAS AND COVARIANT DIFFERENTIAL CALCULUS
A. P. Isaev and P. N. Pyatov 1992 12 p Limited Reproducibility: More than 20% of this document may be affected by microfiche quality
(DE94-608072; JINR-E-2-92-477) Avail: CASI HC A03 (US Sales Only)

GL(sub q)(N)-covariant quantum algebras with generators satisfying quadratic polynomial relations are considered. It is that, up to some inessential arbitrariness, there are only two kinds of such quantum algebras, namely, the algebras with q-deformed commutation and q-deformed anticommutation relations. DOE

N94-30728 Utrecht State Univ. (Netherlands). Dept. of Computer Science.
PERFECT BINARY SPACE PARTITIONS
Mark deBerg, Marko deGroot, and Mark H. Overmars Jul. 1993 15 p Sponsored in part by Netherlands Organization for Scientific Research Limited Reproducibility: More than 20% of this document may be affected by microfiche quality
(Contract EC-7141) (ISSN 0924-3275)
(RUU-CS-93-23; ETN-94-95660) Avail: CASI HC A03

Results on perfect binary space partitions on sets of nonintersecting line segments in two dimensions are discussed. A binary space partition is a scheme for recursively dividing a configuration of objects by hyperplanes until all objects are separated. A binary space partition is called perfect when none of the objects is cut by the hyperplanes used by the binary space partition. Given a set of n nonintersecting line segments, the method constructs a perfect binary space partition, or decides that no perfect binary space partition exists for the arrangement of line segments, in O((n squared)(log n)) time. ESA

N94-30735 Center for Mathematics and Computer Science, Amsterdam (Netherlands). Dept. of Computer Science/Dept. of Software Technology.
BISIMULATIONS AND PREDICATE LOGIC
R. Tim P. Fernando May 1993 18 p Limited Reproducibility: More than 20% of this document may be affected by microfiche quality
(Contract NF-102/62-356) (ISSN 0169-118X)
(CWI-CS-R9333; ETN-94-95675) Copyright Avail: CASI HC A03

Elementary (first order) and non-elementary (set theoretic) aspects of the largest bisimulation are considered with a view towards analyzing operational semantics from the perspective of predicate logic. The notion of a bisimulation is employed in two distinct ways: as an extensional notion of equivalence on programs (or processes) generalizing input/output equivalence (at a cost exceeding Pi(sub 1)(sup 1) over certain transition predicates computable in log space); and as a tool for analyzing the dependence of transitions on data (which can be shown to be elementary or non-elementary, depending on the formulation of the transitions). These ways contrast not only in the logical dependence they uncover, but also in their use of sets as abstractions describing mechanical computation. ESA

N94-30736 Universiteit Twente, Enschede (Netherlands). Dept. of Applied Mathematics.
GRADED FROELICHER-NIJENHUIS BRACKETS AND THE THEORY OF RECURSION OPERATORS FOR SUPER DIFFERENTIAL EQUATIONS
P. H. M. Kersten and I. S. Krasilshchik Jul. 1993 58 p Sponsored in part by Univ. Twente, and Netherlands Organization for Scientific Research Limited Reproducibility: More than 20% of this document may be affected by microfiche quality
(ISSN 0169-2690)
(MEMO-1147; ETN-94-95721) Avail: CASI HC A04

A theory of Froelicher-Nijenhuis brackets for n-graded commutative algebras is developed. Based on this theory, deformations and recursion operators are defined, both in local and nonlocal cases. New recursion operators are computed for super versions of Korteweg de Vries, nonlinear Schroedinger, and Boussinesq equations. These operators are shown to generate new series of symmetries for these equations. ESA

N94-30738 Universiteit Twente, Enschede (Netherlands). Dept. of Applied Mathematics.
DISSIPATION IN HAMILTONIAN SYSTEMS: DECAYING CNOIDAL WAVES
G. L. A. Derks and E. W. C. vanGroesen 30 Jul. 1993 24 p Sponsored by Netherlands Organization for Scientific Research Limited Reproducibility: More than 20% of this document may be affected by microfiche quality
(ISSN 0169-2690)
(MEMO-1151; ETN-94-95725) Avail: CASI HC A03

A perturbed Hamiltonian system is investigated by using the family of relative equilibria of the unperturbed Hamiltonian system. Solutions of a Hamiltonian system with dissipation, starting near a relative equilibrium, are approximated with the relative equilibria. The approximation for the Hamiltonian system with dissipation consists of a quasistatic succession of relative equilibria. A main subject is the investigation of the conditions for which the quasistatic approximation can be justified, even in case the eventual deviation from the initial state, caused by the small perturbation, is large. These general ideas are illustrated for the specific example of the uniformly damped Korteweg de Vries equation with periodic boundary conditions. The relative equilibria of the Korteweg de Vries equation are space periodic soliton-like waves, known as cnoidal waves. It is shown that the difference in shape of a solution and a quasistatic approximation is at each instant of the order of the damping rate times the norm of the cnoidal wave. ESA

N94-30744 Utrecht State Univ. (Netherlands). Dept. of Computer Science.
TOTAL TERMINATION OF TERM REWRITING

M. C. F. Ferreira and H. Zantema Dec. 1992 26 p Limited Reproducibility: More than 20% of this document may be affected by microfiche quality
(ISSN 0924-3275)
(RUU-CS-92-42; ETN-94-95632) Avail: CASI HC A03

An investigation on proving termination of term rewriting systems (TRS) by interpretation of terms in a compositional way in a total well founded order is presented. This kind of termination is called total termination. On one hand it is more restrictive than simple termination, on the other it generalizes most of the usual techniques for proving termination. For total termination it turns out that below epsilon(sub 0) the only orders of interest are built from the natural numbers by lexicographic product and the multiset construction. By examples, both constructions are shown to be essential. For a wide class of term rewriting systems, total termination is proved to be a modular property. Most of the techniques are based on ordinal arithmetic. ESA

N94-30747 Utrecht State Univ. (Netherlands). Dept. of Computer Science.
THE (n SQUARED)-HARD PROBLEMS IN COMPUTATIONAL GEOMETRY
Anka Gajentaan and Mark H. Overmars Apr. 1993 25 p Sponsored in part by EEC, and Netherlands Organization for Scientific Research Limited Reproducibility: More than 20% of this document may be affected by microfiche quality
(ISSN 0924-3275)
(RUU-CS-93-15; ETN-94-95652) Avail: CASI HC A03

There are many problems in computational geometry for which the best known algorithms take time Theta(n squared) (or more) in the worst case, while only very low lower bounds are known. A large class of so called n squared hard problems for which it is proved that they are all at least as difficult as the following base problem is described: given a set S of n integers, are there three elements of S that sum up to 0. The best known algorithm for this base problem takes Theta(n squared) time. The class includes problems like: given a set of lines in the plane, are there three that meet in a point; or given a set of triangles in the plane, does their union have a hole. Also certain visibility and motion planning problems are n squared hard. Although this does not prove a lower bound for these problems, there is no hope of obtaining omicron(n squared) solutions for them unless the solution for the base problem can be improved. ESA

N94-30751 Center for Mathematics and Computer Science, Amsterdam (Netherlands). Dept. of Numerical Mathematics.
EVALUATION OF DISCRETIZATION SCHEMES FOR ADVECTION-DIFFUSION EQUATIONS
B. Koren and C. B. Vreugdenhil Jul. 1993 24 p Limited Reproducibility: More than 20% of this document may be affected by microfiche quality
(ISSN 0924-3275)
(CWI-NM-R9311; ETN-94-95668) Copyright Avail: Issuing Activity (European Space Agency (ESA))

A comparative study is made of accuracy, monotonicity, conservation, and computational efficiency, for a wide variety of advection diffusion schemes. The evaluation is based on a set of scalar test problems with known exact solutions: an unsteady, linear one dimensional advection diffusion problem; a steady, linear one dimensional advection diffusion problem with source term; an unsteady, nonlinear one dimensional advection problem (with and without discontinuity); and an unsteady, linear two dimensional advection problem. ESA

N94-30753 Center for Mathematics and Computer Science, Amsterdam (Netherlands). Dept. of Computer Science/Dept. of Software Technology.
A STRUCTURAL CO-INDUCTION THEOREM
J. J. M. M. Rutten Jul. 1993 20 p Presented at the 9th Conference on the Mathematical Foundations of Programming Semantics, New Orleans, LA, 7-10 Apr. 1993 Submitted for publication Limited Reproducibility: More than 20% of this document may be affected by microfiche quality
(ISSN 0169-118X)
(CWI-CS-R9346; ETN-94-95688) Copyright Avail: CASI HC A03

The structural induction theorem (Lehmann and Smyth; Plotkin) characterizes initial F algebra's of locally continuous functors F on the category of CPO's with strict and continuous maps. A dual of that theorem is presented, giving a number of equivalent characterizations of final coalgebras of such functors. In particular, final coalgebras are order strongly extensional (sometimes called internal full abstractness): the order is the union of all (ordered) F bisimulations. (Since the initial fixed point for locally continuous functors is also final, both theorems apply). A similar co-induction theorem is given for a category of complete metric spaces and locally contracting functors. ESA

N94-30758# Oak Ridge National Lab., TN.
ON SOME GENERAL PROPERTIES OF PARABOLIC CONSERVATION EQUATIONS
L. Dresner Oct. 1993 56 p
(Contract DE-AC05-84OR-21400)
(DE94-006101; ORNL/TM-12509) Avail: CASI HC A04/MF A01

This report deals with certain general properties of partial differential equations of the form S(c)c(sub t) + q(sub z) = Q(c), where t may thought of as time, z as distance, c as an intensive quantity (e.g., temperature), q is its flux (e.g., heat flux), and where q depends on both c and c(sub z). Six topics are studied: mMaximum and minimum principles; ordering of solutions; invariance to stretching (affine) groups; stability of steady states; comparability of solutions; and traveling wave solutions. Illustrative examples are given from the field of nonlinear diffusion, applied superconductivity, and helium cryogenics. DOE

N94-30766 Universiteit Twente, Enschede (Netherlands). Dept. of Applied Mathematics.
RELATIVE LENGTH OF LONG PATHS AND CYCLES IN GRAPHS WITH LARGE DEGREE SUMS
Hikoe Enomoto (Keio Univ., Yokahama, Japan.), Jan P. M. vandenHeuvel, Atsushi Kaneko, and Akira Saito Jul. 1993 15 p Limited Reproducibility: More than 20% of this document may be affected by microfiche quality
(ISSN 0169-2690)
(MEMO-1145; ETN-94-95719) Avail: CASI HC A03

For a graph G, p(G) denotes the order of a longest path in G and c(G) the order of a longest cycle. It is shown that if G is a connected graph on n greater than or equal to 3 vertices such that d(u) + d(v) + d(w) is greater than or equal to n for all triples u, v, w of independent vertices, then G satisfies c(G) greater than or equal to p(G) - 1, or G is in one of six families of exceptional graphs. This generalizes results in Bondy, and in Bauer, Morgana, Schmeichel and Veldman. ESA

N94-30767 Universiteit Twente, Enschede (Netherlands). Dept. of Applied Mathematics.
PANCYCLICITY OF HAMILTONIAN LINE GRAPHS
E. vanBlanken, J. P. M. vandenHeuvel, and H. J. Veldman Jul. 1993 13 p Limited Reproducibility: More than 20% of this document may be affected by microfiche quality
(ISSN 0169-2690)
(MEMO-1146; ETN-94-95720) Avail: CASI HC A03

Let f(n) be the smallest integer such that for every graph G of order n with minimum degree delta(G) greater than f(n), the line graph L(G) of G is pancyclic whenever L(G) is hamiltonian. Results showing that f(n) = Theta(n(sup 1/3)) are proved. ESA

N94-30817# Oak Ridge National Lab., TN.
USING THE LOG-NORMAL DISTRIBUTION IN ANALYZING AEROSOLS: THE MATHEMATICAL REASONING UNDERLYING THE VARIOUS DIAMETERS USED AND THE PLOTTING PROCEDURE
M. L. Tobias Dec. 1993 19 p
(Contract DE-AC05-84OR-21400)
(DE94-006459; ORNL/TM-12669) Avail: CASI HC A03/MF A01

This paper is intended to clarify the use of terminology and notation used in the analysis of aerosol particle sizing on the basis of the log-normal distribution. The connection between log-normal distribution and the normal distribution is shown; the mathematical basis for the various diameters used in the literature is developed, and the reasoning behind the graphical presentation on so-called 'log-normal' graph paper is presented. DOE

N94-30821# Los Alamos National Lab., NM.
SELECTING MODEL COMPLEXITY IN LEARNING PROBLEMS
K. L. Buescher and P. R. Kumar 1993 9 p Presented at the 32nd Institute of Electrical and Electronic Engineers (IEEE) Conference on Decision and Control, San Antonio, TX, Dec. 1993

(Contract W-7405-eng-36)
(DE94-000764; LA-UR-93-3381; CONF-931233-1) Avail: CASI HC A02/MF A01

To learn (or generalize) from noisy data, one must resist the temptation to pick a model for the underlying process that overfits the data. Many existing techniques solve this problem at the expense of requiring the evaluation of an absolute, a priori measure of each model's complexity. We present a method that does not. Instead, it uses a natural, relative measure of each model's complexity. This method first creates a pool of 'simple' candidate models using part of the data and then selects from among these by using the rest of the data. DOE

N94-30849# Sandia National Labs., Albuquerque, NM.
FUZZY-ALGEBRA UNCERTAINTY ANALYSIS FOR ABNORMAL-ENVIRONMENT SAFETY ASSESSMENT
J. A. Cooper Jan. 1994 33 p
(Contract DE-AC04-94AL-85000)
(DE94-006257; SAND-93-2665) Avail: CASI HC A03/MF A01

Many safety (risk) analyses depend on uncertain inputs and on mathematical models chosen from various alternatives, but give fixed results (implying no uncertainty). Conventional uncertainty analyses help, but are also based on assumptions and models, the accuracy of which may be difficult to assure. Some of the models and assumptions that on cursory examination seem reasonable can be misleading. As a result, quantitative assessments, even those accompanied by uncertainty measures, can give unwarranted impressions of accuracy. Since analysis results can be a major contributor to a safety-measure decision process, risk management depends on relating uncertainty to only the information available. The uncertainties due to abnormal environments are even more challenging than those in normal-environment safety assessments, and therefore require an even more cautious approach. A fuzzy algebra analysis is proposed in this report that has the potential to appropriately reflect the information available and portray uncertainties well, especially for abnormal environments. DOE

N94-30859 Utrecht State Univ. (Netherlands). Dept. of Computer Science.
TERMINATION OF TERM REWRITING BY SEMANTIC LABELLING
H. Zantema Dec. 1992 16 p Limited Reproducibility: More than 20% of this document may be affected by microfiche quality
(ISSN 0924-3275)
(RUU-CS-92-38; ETN-94-95628) Avail: CASI HC A03

A kind of transformation of TRS (Term Rewriting System(s)) is proposed, depending on a choice for a model for the TRS. The labelled TRS is obtained from the original one by labelling operation symbols, possibly creating extra copies of some rules. This construction has the remarkable property that the labelled TRS is terminating if and only if the original TRS is terminating. Although the labelled version has more operation symbols and may have more rules (sometimes infinitely many), termination is often easier to prove for the labelled TRS than for the original one. This provides a new technique for proving termination, making classical techniques like RPO (Recursive Path Order) and polynomial interpretations applicable for nonsimplifying simplifying TRS. ESA

N94-30860# Utrecht State Univ. (Netherlands). Dept. of Computer Science.
OPTIMAL SIZE FINITE ELEMENT MESHES WITHOUT OBTUSE AND SMALL ANGLES
Elefterios A. Melissaratos (Rutgers Univ., New Brunswick, NJ.) Dec. 1992 47 p Sponsored in part by Netherlands Organization for Scientific Research, and EEC
(Grants NSF CCR-88-03549; NSF CCR-91-0473; NSF STC-88-09648)
(ISSN 0924-3275)
(RUU-CS-92-39; ETN-94-95629) Avail: CASI HC A03/MF A01

An algorithm which produces 'quality' triangulations of polygonal domains with holes, for the Finite Element Method (FEM), is introduced. Quality triangulation is used to mean satisfaction of both of the following conditions: (1) no obtuse angles; (2) no 'small' angles. Triangulations satisfying only (1) are termed as 'non obtuse'; those satisfying only (2) are termed as 'non-small angle'; and those which satisfy both conditions are termed as 'nice'. The main contributions of the study are: new techniques to produce nice triangulations of polygonal domains with holes using nonuniform (quadtree) underline square grid; it is shown that the asymptotic size of a nice triangulation is the same as for a non-small angle triangulation. In other words, achieving both non-obtuse and non-small angle condition at the same time is not more expensive than achieving only the non-small angle condition. ESA

N94-30889 Institut des Hautes Etudes Scientifiques, Bures-sur-Yvette (France).
NON-COMMUTATIVE GEOMETRY
A. Connes Oct. 1993 523 p See also PB93-215499
(PB94-139342; IHES/M-93/54) Avail: Issuing Activity (National Technical Information Service (NTIS))

The correspondence between geometric spaces and commutative algebras is a familiar and basic idea of algebraic geometry. The purpose of this book is to extend this correspondence to the non-commutative case in the framework of real analysis. The theory, called non-commutative geometry, rests on two essential points: (1) The existence of many natural spaces for which the classical set theoretic tools of analysis, such as measure theory, topology, calculus, and metric ideas lose their pertinence but which correspond very naturally to a non-commutative algebra. Such spaces arise both in mathematics and in quantum physics, and we shall discuss them in more detail below. Moreover, even for classical spaces, which correspond to a commutative algebra, the new point of view will give new tools and results, for instance for the Julia sets of iteration theory. (2) The extension of the classical tools--measure theory, topology, differential calculus and Riemannian geometry, to the non-commutative situation--is also presented. This extension involves an algebraic reformulation of the above tools but passing from the commutative to the non-commutative case is never straightforward. NTIS

N94-30964 Universiteit Twente, Enschede (Netherlands). Dept. of Applied Mathematics.
AN INTRINSIC HAMILTONIAN FORMULATION OF THE DYNAMICS OF LC-CIRCUITS
B. M. Maschke (Conservatoire National des Arts et Metiers, Paris, France.), A. J. vanderSchaft, and P. C. Breedveld Aug. 1993 23 p Limited Reproducibility: More than 20% of this document may be affected by microfiche quality
(ISSN 0169-2690)
(MEMO-1154; ETN-95728) Avail: CASI HC A03

The dynamics of LC circuits is formulated as a Hamiltonian system with respect to a Poisson structure which may be degenerate, that is, non symplectic. This Poisson structure is deduced from the network graph of the circuit and captures the dynamic invariants due to Kirchhoff's laws. The antisymmetric relation defining the Poisson structure is realized as a physical network using the gyrator element and partially dualizing the network graph constraints. From the network realization of the Poisson structure, the reduced symplectic Hamiltonian system and the realization of the embedding symplectic Hamiltonian system are deduced. ESA

N94-30971 Ecole Nationale Superieure des Telecommunications, Paris (France). Dept. Signal.
THE STROEMBERG WAVELET ON THE INTERVAL AND THE FRANKLIN SYSTEM
K. Drouiche and D. Kateb 28 Apr. 1993 19 p Submitted for publication Limited Reproducibility: More than 20% of this document may be affected by microfiche quality
(ISSN 0751-1337)
(TELECOM-93-C-002; ETN-94-95977) Avail: CASI HC A03

Tha Franklin system is an orthonormal basis of interval L(sup 2)(0,1). A multiresolution analysis of interval L(sup 2)(0,1) is given, and it is shown how this system can be interpreted as a special basis of Stroemberg wavelets on the interval (0,1). A fast algorithm which enables a given signal on an interval to be analyzed and synthesized is derived. Special considerations are held near the edges, where the extension of the interval is no longer needed (zero padding method, etc.). The error term, due to the edge effects, is calculated and injected in the reconstruction formulas to recover the exact original signal. Numerical simulations are provided to emphasize the performance of the results. ESA

N94-30974 Amsterdam Univ. (Netherlands). Dept. of Mathematics and Computer Science.
INVENTORY OF FRAGMENTS AND EXACT MODELS IN INTUITIONISTIC PROPORTIONAL LOGIC
Lex Hendriks 2 Jul. 1993 66 p Limited Reproducibility: More than 20% of this document may be affected by microfiche quality
(ISSN 0928-3315)
(ML-93-11; ETN-94-95987) Avail: CASI HC A04

The semantic structure of fragments of Intuitionistic propositional Logic (IpL) is addressed. It is demonstrated that in some of the fragments there is subordering of the Lindenbaum algebra of the fragment F which not only reflects its structural properties but also is, or can be extended to, a Kripke model which is complete for the fragment. ESA

N94-30975 Amsterdam Univ. (Netherlands). Dept. of Mathematics and Computer Science.
REMARKS ON UNIFORMLY FINITELY PRECOMPLETE POSITIVE EQUIVALENCES
V. Y. Shavrukov 1 Aug. 1993 25 p Limited Reproducibility: More than 20% of this document may be affected by microfiche quality
(ISSN 0928-3315)
(ML-93-12; ETN-94-95988) Avail: Issuing Activity (European Space Agency (ESA))

Miscellaneous results and observations on three classes of equivalences are documented. The necessary definitions and notations are introduced and an exposition of earlier results to be built on is given. Partial isomorphisms (that is, isomorphisms of domains of proper subobjects) between e and between precomplete equivalences are addressed. These partial isomorphisms are shown to enjoy strong, and, in a way, complementary extendability properties. A property that singles out the e and the precomplete positive equivalences among all the uniformly, finitely precomplete ones is formulated. The effort spent was not objectless in that there exist uniformly finitely positive equivalences that are neither e nor precomplete. Sets of fixed points of endomorphisms of uniformly finitely precomplete positive equivalences are described. ESA

N94-30976 Amsterdam Univ. (Netherlands). Dept. of Mathematics and Computer Science.
UNDECIDABILITY IN DIAGONALIZABLE ALGEBRAS
V. Y. Shavrukov 13 Sep. 1993 41 p Limited Reproducibility: More than 20% of this document may be affected by microfiche quality
(ISSN 0928-3315)
(ML-93-13; ETN-94-95989) Avail: CASI HC A03

If a formal theory T is able to reason about its own syntax, then the diagonizable algebra of a formal theory T is defined as its Lindenbaum sentence algebra endowed with a unary operator (square) which sends a sentence phi to the sentence (square)(sub phi) asserting the provability of phi in T. A proof that the elementary theories of diagonizable algebras of a wide class of theories are undecidable is presented and related results are established. ESA

N94-30977 Amsterdam Univ. (Netherlands). Dept. of Mathematics and Computer Science.
EMBEDDINGS OF HEYTING ALGEBRAS
Dick deJongh and Albert Visser Sep. 1993 31 p Limited Reproducibility: More than 20% of this document may be affected by microfiche quality
(ISSN 0928-3315)
(ML-93-14; ETN-94-95990) Avail: CASI HC A03

Embeddings of Heyting algebras are studied. It is pointed out that such embeddings are naturally connected with derived rules. The Heyting algebras embeddable in the Heyting algebra of the Intuitionistic Propositional Calculus (IPC), that is, the free Heyting algebra on countably, infinitely many generators, and those embeddable in the Heyting algebra of Heyting's Arithmetic (HA), are compared. A partial result is obtained. Every recursively enumerable prime Heyting algebra is shown to be embeddable in the Heyting Algebra of HA(*) a 'natural' extension of HA. ESA

65 STATISTICS AND PROBABILITY

Includes data sampling and smoothing; Monte Carlo method; and stochastic processes.

N94-28548# Los Alamos National Lab., NM.
RESEARCH ACTIVITIES OF MARTIN C. CASDAGLI AT SFI SEPTEMBER 1989--MAY 1991
1993 3 p
(Contract W-7405-eng-36)
(DE94-005655; LA-SUB-93-223) Avail: CASI HC A01/MF A01

My research over this period has focused on the theory and application of nonlinear time series forecasting. The purpose of time series forecasting is to predict apparently random behavior about which we have little or no knowledge. A time series is a set of values that change in time, for example, daily stock market prices for a given set of firms, or the volume of the polar ice caps over the last two million years. Recent developments in the understanding of chaotic dynamical systems have stimulated new approaches to time series analysis. These results raise the possibility that apparently random behavior may essentially be the consequence of chaotic behavior of deterministic equations with a small number of variables. My main research effort has been to develop a theory of nonlinear time series forecasting which applies to chaotic time series with low levels of observational noise. I have also developed a new algorithm for analyzing experimental time series data in order to determine whether a nonlinear deterministic, as opposed to nonlinear stochastic model is an appropriate description of the data, and have applied this algorithm to a wide range of time series data. In addition to involvement in these and other research activities, I have helped organize a conference on nonlinear modeling and forecasting, jointly sponsored by NATO and SFI. I describe the above projects in more detail in the following paragraphs. Several of these projects benefited greatly fro the excellent computer facilities available at SFI. DOE

N94-28670 Mitre Corp., Bedford, MA.
A FAMILY OF JOINT PROBABILITY MODELS FOR COST AND SCHEDULE UNCERTAINTIES
Paul R. Garvey Sep. 1993 47 p Presented at the 27th Annual DOD Cost Analysis Symposium Limited Reproducibility: More than 20% of this document may be affected by microfiche quality
(AD-A275513) Avail: CASI HC A03

This paper discusses a family of analytical models from which the joint probability of total program cost and schedule can be calculated, analyzed, and presented to decision-makers. Specifically, the classical bivariate normal and two lesser known joint distributions, the normal-lognormal and the bivariate lognormal distributions are discussed. Experiences from Monte Carlo simulations suggest that this family of bivariate distributions are candidate models for computing joint and conditional cost and schedule probabilities. In particular, the discussion on the normal-lognormal distribution as a joint cost-schedule probability model extends research on the applicability of the bivariate lognormal presented last year. DTIC

N94-28759# Naval Undersea Warfare Center, New London, CT.
OUTPUT STATISTICS OF THE SALFAS FM NORMALIZER SMOOTHING/PREDICTION FUNCTION
Fyzodeen Khan and Carl J. Wenk 2 Apr. 1993 19 p
(AD-A275758; NUWC-NL-TM-931139) Avail: CASI HC A03/MF A01

An analytic performance evaluation methodology for the determination of the expected value and variance of the noise mean estimate of the smoothing/prediction function of the SALFAS FM normalizer is presented. These statistics are necessary for the determination of the output Receiver Operating Characteristic (ROC) curves of the normalizer. DTIC

N94-28768 Naval Postgraduate School, Monterey, CA.
USING MULTIPLE SEARCHERS TO LOCATE A RANDOMLY MOVING TARGET M.S. Thesis
Almir G. Santos 23 Sep. 1993 56 p Limited Reproducibility: More than 20% of this document may be affected by microfiche quality
(AD-A275602) Avail: CASI HC A04

The need to search effectively for objects presents itself in many civilian and military applications. This thesis develops and tests six heuristics and an optimal branch and bound procedure to solve the heretofore

uninvestigated problem of searching for a Markovian moving target using multiple searchers. For more than one searcher, the time needed to guarantee an optimal solution for the problems considered is prohibitive. The heuristics represent a wide variety of approaches and consist of two based on the expected number of detections, two genetic algorithm implementations, one based on solving partial problems optimally, and local search. A heuristic based on the expected number of detections obtains solutions within two percent of the best known solution for each one, two, and three searcher test problem considered. For one and two searcher problems, the same heuristic's solution time is less than that of other heuristics considered. A genetic algorithm implementation performs acceptably for one and two searcher problems and highlights its ability, effectively solving three searcher problems in as little as 20% of other heuristic run-times. DTIC

N94-28876# Stanford Univ., CA. Dept. of Statistics.
TESTING FOR A SIGNAL WITH UNKNOWN LOCATION AND SCALE IN A STATIONARY GAUSSIAN RANDOM FIELD
David O. Siegmund and Keith J. Worsley 7 Jan. 1994 40 p
(Contract N00014-92-J-1264; NSF DMS-91-04432)
(AD-A275320; TR-477) Avail: CASI HC A03/MF A01

We suppose that our observations can be decomposed into a fixed signal plus random noise, where the noise is modelled as a particular stationary Gaussian random field in N-dimensional Euclidean space. The signal has the form of a known function centered at an unknown location and multiplied by an unknown amplitude, and we are primarily interested in a test to detect such a signal. There are many examples where the signal scale or width is assumed known, and the test is based on maximizing a Gaussian random field over all locations in a subset of N-dimensional Euclidean space. The novel feature of this work is that the width of the signal is also unknown and the test is based on maximizing a Gaussian width. Two convergent approaches are used to approximate the null distribution: one based on the method of Knowles and Siegmund (1989), which uses a version of Weyl's (1939) tube (1993b), which uses the Hadwiger characteristic of excursion sets as introduced by Adler (1981). Finally we compared the power of our method with one based on a fixed but perhaps incorrect signal width. DTIC

N94-29014# Stanford Univ., CA. Dept. of Statistics.
THE MODIFIED CRAMER-VON MISES GOODNESS-OF-FIT CRITERION FOR TIME SERIES
T. W. Anderson and M. A. Stephens 17 Jan. 1994 18 p
(Contract N00014-92-J-1264; NSF DMS-91-04432)
(AD-A275377; TR-478) Avail: CASI HC A03/MF A01

In this paper we consider somewhat analogous quadratic forms in normal variables when the dimensionality is infinite. Then the quadratic forms are distributed infinite weighted sums of X2-variables. These come about as goodness-of-fit criteria for a hypothesis that a cumulative distribution function is a specified one or that two cdf's are the same. Such criteria also arise for goodness-of-fit tests for standardized spectral distributions. As examples, we give tables of the distribution of the criterion for testing the hypothesis that a stationary stochastic process is a given moving average process order 1 and for testing the hypothesis that it is a specified autoregressive process order 1. Two methods are described for calculating the distribution. Either method is appropriate for calculating the distribution of the criterion for testing the hypothesis that a process is a stationary process whose standardized spectral density of distribution is a specified one. DTIC

N94-29030 Helsinki Univ. of Technology, Espoo (Finland). Inst. of Mathematics.
DYNAMICS OF DEFECT ENSEMBLES IN ONE-DIMENSIONAL CELLULAR AUTOMATA
K. Eloranta Jun. 1993 24 p Sponsored by Suomen Akatemia
(PB94-136819; ISBN-951-22-1636-1) Avail: Issuing Activity (National Technical Information Service (NTIS))

We investigate the dynamics of ensembles of defects in one-dimensional deterministic cellular automata. In individual confinement the motions from disordered initial state are perfect random walks as shown in a 1992 paper by the author. Here we give a natural condition guaranteeing this also in the presence of other defects. Simple branching and birth mechanisms are introduced, and prototype classes of weakly interacting walks capable of annihilation and coalescence are studied. Their equilibrium behavior is also characterized. The design principles of cellular automata with desired diffusive interaction properties becomes transparent from this analysis. NTIS

N94-29129# California Univ., Santa Barbara.
U-STATISTICS OF RANDOM-SIZE SAMPLES AND LIMIT THEOREMS FOR SYSTEMS OF MARKOVIAN PARTICLES WITH NON-POISSON INITIAL DISTRIBUTIONS
Raisa E. Feldman and Svetlozar Rachev 1994 21 p
(Contract N00014-89-J-1870; NSF DMS-91-03452)
(AD-A275018) Avail: CASI HC A03/MF A01

Limiting distributions of square-integrable infinite order U-statistics are extended to the case of non-Poisson random sample size. Multiple integrals of non-Gaussian generalized fields are constructed to identify the limiting distributions. An invariance principle is also established. These results are used to study the limiting distribution of the amount of charge left in some set by an infinite system of signed Markovian particles when the initial particle density goes to infinity. By selecting the initial particle distribution, we determine the limiting distribution of charge, constructing different non-Gaussian generalized random fields, including Laplace, alpha-stable, and their multiple integrals. DTIC

N94-29178 Institut des Hautes Etudes Scientifiques, Bures-sur-Yvette (France).
HIERARCHICAL STRUCTURES AND ASYMMETRIC STOCHASTIC PROCESSES ON p-ADICS AND ADELES
W. Warwowski (Wroclaw Univ., Poland.) and R. V. Mendes Dec. 1993 19 p Limited Reproducibility: More than 20% of this document may be affected by microfiche quality
(PB94-138203; IHES/M/93/65) Avail: CASI HC A03

The space of states of some phenomena, in physics and other sciences, displays a hierarchical structure. When that is the case, it is natural to label the states by a p-adic number field. Both the classification of the states and their relationships are then based on a notion of distance with ultrametric properties. The dynamics of the phenomena, that is the transition between different states, is also a function of the p-adic distance d(sub p). However, because the distance is a symmetric function, probabilistic processes which depend only on d(sub p) have a uniform invariant probability measure, that is, all states are equally probable at large times. This being a severe limitation for cases of physical interest, we have studied processes with asymmetric transition functions. In addition to the dependence on the ultrametric distance, the asymmetric transition functions are allowed to depend also on the probability of the target state, leading to any desired invariant probability measure. When each state of a physical system is associated to several distinct hierarchical structures or parametrizations, an appropriate labeling set is the ring of adeles. We also construct stochastic processes on the adeles. NTIS

N94-29450 Utrecht State Univ. (Netherlands). Dept. of Computer Science.
CONDITIONAL DEPENDENCE IN PROBABILISTIC NETWORKS
Remco R. Bouckaert 1990 14 p Submitted for publication Limited Reproducibility: More than 20% of this document may be affected by microfiche quality
(ISSN 0924-3275)
(RUU-CS-92-34; ETN-94-95624) Avail: Issuing Activity (European Space Agency (ESA))

Conditional independence and its relation with probabilistic networks are reviewed. A probabilistic network is in general considered a representation of a set of conditional independency statements. However, probabilistic networks also represent dependencies. An axiomatic characterization of conditional dependence is given. A criterion to read conditional dependencies from a probabilistic network is given. ESA

N94-29482# Loughborough Univ. of Technology (England). Dept. of Mathematical Sciences.
A NOTE ON THE POISSON BRACKETS ASSOCIATED WITH LAX OPERATORS
W. Oevel Sep. 1993 12 p
(MATHS-Rept-A-195; ETN-94-95510) Avail: CASI HC A03/MF A01

Modifications of the standard Poisson brackets associated with differential scattering operators are considered. A linear bracket originates from a

non-standard r matrix on the algebra of pseudodifferential operators. Two quadratic brackets which provide Hamiltonian formulations for various reductions of the modified KP hierarchy are investigated. ESA

N94-29925# Edgerton, Germeshausen and Grier, Inc., Idaho Falls, ID.
ACCEPTANCE SAMPLING METHODS FOR SAMPLE RESULTS VERIFICATION
C. A. Jesse Jun. 1993 42 p
(Contract DE-AC07-76ID-01570)
(DE94-002882; EGG-ER-10792) Avail: CASI HC A03/MF A01

This report proposes a statistical sampling method for use during the sample results verification portion of the validation of data packages. In particular, this method was derived specifically for the validation of data packages for metals target analyte analysis performed under United States Environmental Protection Agency Contract Laboratory Program protocols, where sample results verification can be quite time consuming. The purpose of such a statistical method is to provide options in addition to the 'all or nothing' options that currently exist for sample results verification. The proposed method allows the amount of data validated during the sample results verification process to be based on a balance between risks and the cost of inspection. DOE

N94-30154# Technical Research Centre of Finland, Espoo. Electrical and Automation Engineering Lab.
RISK MEASURES IN LIVING PROBABILISTIC SAFETY ASSESSMENT
Jan Holmberg, Gunnar Johanson, and Ilkka Niemelae May 1993 73 p
(ISSN 1235-0621)
(VTT-PUBS-146; ISBN-951-38-4384-X; ETN-94-95521) Copyright Avail: CASI HC A04/MF A01

By Probabilistic Safety Assessment (PSA), nuclear power plants are assessed with respect to the likelihood of accidents. PSA provides a structured and logical procedure for the identification of credible accident sequences and for the assessment of their corresponding likelihood. To increase the availability of PSA for the operational safety management, the model as well as the whole PSA program should be developed to a more dynamic tool. The process, to update the PSA model to represent the current or planned configuration and to use the model to evaluate and direct the changes in the configuration, is called the 'living' PSA program. Risk measures needed in the living use of PSA are defined and used in the presentation of the results of the applications to end users who are the plant safety management, operational management maintenance planning personnel, designers and authorities. By proper risk measures, PSA can be better integrated with other safety management methods. Operational or design alternatives can be compared in a more understandable way, and a more effective support can be gained to react to gradual or sudden changes in the operational safety status of the plant. ESA

N94-30358 Nijmegen Univ. (Netherlands). Dept. of Informatics.
INDEX EXPRESSION BELIEF NETWORKS FOR INFORMATION DISCLOSURE
P. D. Bruza and L. C. vanderGaag Aug. 1992 25 p Sponsored in part by EEC Limited Reproducibility: More than 20% of this document may be affected by microfiche quality
(TR-92-23; ETN-94-95612) Avail: Issuing Activity (European Space Agency (ESA))

It is widely accepted that to extend the effectiveness of information disclosure beyond the limitations of current empirically based retrieval systems, some notion of document semantics has to be incorporated onto the retrieval mechanism. An approach to bringing semantics into play is to find information retrieval on the notion of logical inference. This approach is built on, and a promising mechanism for information disclosure, called the Refinement Machine, is described. The Refinement Machine features the index expressions as a language for characterizing information objects and a deduction mechanism driven by rules of inference. Two types of inference rule are distinguished. The rules of strict inference follow the line of traditional logical deduction. As the characterizations of objects are incomplete and requests are typically partial descriptions of the information need, the rules of strict inference are supplemented with a rule of plausible inference. This rule of plausible inference is motivated by work in the area of plausible reasoning in knowledge based systems and, in particular, is derived from the work on belief networks. Details of the Refinement Machine are given and preliminary experimental results are presented. ESA

N94-30366# Los Alamos National Lab., NM.
TEN NEW CHECKS TO ASSESS THE STATISTICAL QUALITY OF MONTE CARLO SOLUTIONS IN MCNP
R. A. Forster, T. E. Booth, and S. P. Pederson 1994 10 p Presented at the 8th International Conference on Radiation Shielding, Arlington, TX, 24-27 Apr. 1994
(Contract W-7405-eng-36)
(DE94-006137; LA-UR-94-227; CONF-940424-8) Avail: CASI HC A02/MF A01

The central limit theorem can be applied to a Monte Carlo solution if the random variable x has a finite mean and a finite variance and the number N of independent observations grows large. When these two conditions are satisfied, a confidence interval based on the normal distribution with a specified coverage probability can be formed. The first requirement is generally satisfied by the knowledge of the type of Monte Carlo tally being used. The Monte Carlo practitioner has only a limited number of marginally quantifiable methods to assess the fulfillment of the second requirement. Ten new statistical checks have been created and added to MCNP4A to assist with this assessment. The checks examine the mean, relative error, figure of merit, and two new quantities: the relative variance of the variance and the empirical history score probability density function f(x). The two new quantities are described. The underlying f(x) for Monte Carlo tallies is calculated for routine inspection and automated analysis. The ten statistical checks are defined, followed by the results from a statistical study on analytic Monte Carlo and other realistic f(x)s to validate their values and uses in MCNP. Passing all ten checks is a reasonable indicator that f(x) has been adequately sampled, N has become large, and valid confidence intervals can be formed. Additional experience with these checks is required to determine their effectiveness in assessing the fulfillment of the central limit theorem requirements for a wide variety of MCNP Monte Carlo solutions. Passing all ten checks does not guarantee a valid confidence interval because there is no guarantee that the entire f(x) has been sampled. DOE

N94-30376 Utrecht State Univ. (Netherlands). Dept. of Computer Science.
BAYESIAN BELIEF NETWORKS AND CONDITIONAL INDEPENDENCIES
Remco R. Bouckaert 1992 26 p Limited Reproducibility: More than 20% of this document may be affected by microfiche quality
(ISSN 0924-3275)
(RUU-CS-92-36; ETN-94-95626) Avail: CASI HC A03

The preliminaries for the development of a theory for Bayesian Belief Networks (BBN) construction using conditional independencies are presented. An overview of the work done in constructing BBN's using conditional independencies, and a uniform formalization of this work including full proofs of claims made about this work, are offered. ESA

N94-30696 Oak Ridge National Lab., TN.
PREDICTION AND STANDARD ERROR ESTIMATION FOR A FINITE UNIVERSE TOTAL WHEN A STRATUM IS NOT SAMPLED
T. Wright Jan. 1994 37 p Limited Reproducibility: More than 20% of this document may be affected by poor print
(Contract DE-AC05-84OR-21400)
(DE94-004929; ORNL/TM-12379) Avail: Issuing Activity (Department of Energy (DOE))

In the context of a universe of trucks operating in the United States in 1990, this paper presents statistical methodology for estimating a finite universe total on a second occasion when a part of the universe is sampled and the remainder of the universe is not sampled. Prediction is used to compensate for the lack of data from the unsampled portion of the universe. The sample is assumed to be a subsample of an earlier sample where stratification is used on both occasions before sample selection. Accounting for births and deaths in the universe between the two points in time, the detailed sampling plan, estimator, standard error, and optimal sample allocation are presented with a focus on the second occasion. If prior auxiliary information is available, the methodology is also applicable to a first occasion. DOE

66 SYSTEMS ANALYSIS

Includes mathematical modeling; network analysis; and operations research.

N94-28888 Georgia Inst. of Tech., Atlanta.
SUMMER INTERN PROGRAM Final Report, Jun. - Jul. 1993
William Appelbe 14 Jan. 1994 16 p Limited Reproducibility: More than 20% of this document may be affected by microfiche quality
(Contract N00014-92-J-1828)
(AD-A275194) Avail: CASI HC A03

This report summarizes this summer's internship program. The report describes the work undertaken by the students, results of the program, and future plans. Overall, the internship program was a complete success. Every one of the seven students in the program completed a significant research project under supervision of a faculty member and rated their experience highly. DTIC

N94-29489*# National Aeronautics and Space Administration. Langley Research Center, Hampton, VA.
THERMAL ENCLOSURE SYSTEM FUNCTIONAL SIMULATION USER'S MANUAL
A. Terry Morris Mar. 1994 55 p
(RTOP 233-03-03-03)
(NASA-TM-109094; NAS 1.15:109094) Avail: CASI HC A04/MF A01

A form and function simulation of the thermal enclosure system (TES) for a microgravity protein crystal growth experiment has been developed as part of an investigation of the benefits and limitations of intravehicular telerobotics to aid in microgravity science and production. A user can specify the time, temperature, and sample rate profile for a given experiment, and menu options and status are presented on an LCD display. This report describes the features and operational procedures for the functional simulation. Author

N94-30586# Lawrence Livermore National Lab., CA.
MISSILE LAUNCH DETECTION ELECTRIC FIELD PERTURBATION EXPERIMENT
R. J. Kane and T. M. Rynne 28 Apr. 1993 45 p
(Contract W-7405-eng-48)
(DE94-004224; UCRL-ID-114322) Avail: CASI HC A03/MF A01

The Lawrence Livermore National Laboratory and SARA Inc. participated in the ATMD missile launch activities that occurred at WSMR during January 1993. LLNL and SARA deployed sensors for monitoring of basic phenomena. An attempt was made to measure perturbations of the earth geo-potential during the launch of a Lance missile. The occurrence of the perturbation is expected from the conducting body of the missile and the exhaust plume. A set of voltage-probe antennas were used to monitor the local electric field perturbation from the launch at ranges of approximately 1 km. Examination of the data acquired during the launch period failed to show identifiable correlation of the field variations with the launch event. Three reasons are ascribed to this lack of event data: (1) The electric field potential variations have a limited spatial correlation length - the fields measured in one region have little correlation to measurements made at distances of a kilometer away. The potential variations are related to localized atmospheric disturbances and are generally unpredictable. A value for the spatial correlation length is also not known. (2) The conductivity of the plume and missile body are not adequate to produce a field perturbation of adequate magnitude. Phenomena related to the exhaust plume and missile may exist and be outside of the collection range of the equipment employed for these measurements. (3) The presence of 60 Hz power line noise was of sufficient magnitude to irreversibly contaminate measurements. DOE

N94-30737 Universiteit Twente, Enschede (Netherlands). Dept. of Applied Mathematics.
SET GAMES
H. F. M. Aarts, Y. Funaki, and C. Hoede Jul. 1993 17 p Limited Reproducibility: More than 20% of this document may be affected by microfiche quality
(ISSN 0169-2960)
(MEMO-1148; ETN-94-95722) Avail: Issuing Activity (European Space Agency (ESA))

A type of cooperative games in characteristic function form (called set games) is introduced. In a set game, the worth of a coalition is expressed by a set instead of a real number. For this class of games, the notion of value is defined, being a solution concept and also several axioms. Values for set games that satisfy the so called additivity axiom which is the analog of the additivity axiom of the Shapley value are studied. ESA

N94-28424# Naval Aviation HQ, Yeovil (England).
THE CONCEPT OF ROYAL NAVY AIR OPERATIONS UNDER EXTREME ENVIRONMENTAL CONDITIONS
A. P. Steele-Perkins *In* AGARD, The Support of Air Operations under Extreme Hot and Cold Weather Conditions Oct. 1993 11 p (For primary document see N94-28420 08-51)
Copyright Avail: CASI HC A03/MF A03

67 THEORETICAL MATHEMATICS

Includes topology and number theory.

N94-28467 International Centre for Theoretical Physics, Trieste (Italy).
SOME CONSTRAINTS AND SOLUTIONS OF THE KADOMTSEV-PETVIASHVILI EQUATION
Tian Chou Jul. 1993 15 p Limited Reproducibility: More than 20% of this document may be affected by poor print
(DE93-634355; IC-93/172) Avail: Issuing Activity (Department of Energy (DOE)) (US Sales Only)

The relations among the symmetry, invariant group, and constraint for a differential equation are illustrated. Applied to the Kadomtsev-Petviashvili equation, some constraints and solutions are given. In particular, the associate equation to the KP equation and the symmetry (sigma) are introduced and discussed. DOE

N94-28785# Joint Inst. for Nuclear Research, Dubna (USSR).
PATH INTEGRAL FOR COHERENT STATES OF THE DYNAMICAL U(SUB 2) GROUP AND U(SUB 2/1) SUPERGROUP
E. A. Kochetov 1992 14 p
(DE94-606382; JINR-E-17-92-412) Avail: CASI HC A03/MF A01 (US Sales Only)

A part-integral formulation in the representation of coherent states for the unitary U(sub 2) group and U(sub 2/1) supergroup is introduced. U(sub 2) and U(sub 2/1) path integrals are shown to be defined on the coset spaces U(sub 2)/U(sub 1)xU(sub 1) and U(sub 2/1)/U(sub 1/1)xU(sub 1), respectively. These coset appears as curved classical phase spaces. Partition functions are expressed as path integrals over these spaces. In the case when U(sub 2) and U(sub 2/1) are the dynamical groups, the corresponding path integrals are evaluated with the help of linear fractional transformations that appear as the group (supergroup) action in the coset space (superspace). Possible applications for quantum models are discussed. DOE

N94-28807 Santa Fe Inst., NM.
THE LECTURES IN COMPLEX SYSTEMS, VOLUME 5 Final Report, 1 Apr. 1992 - 31 Mar. 1993
Lynn Nadel and Daniel L. Stein 11 May 1993 701 p Limited Reproducibility: More than 20% of this document may be affected by microfiche quality
(Contract N00014-92-J-1455)
(AD-A275458) Avail: Issuing Activity (Defense Technical Information Center (DTIC))

The Complex Systems Summer School focuses on developing techniques for measuring and analyzing complex behavior, and applying these techniques to the study of a limited number of specific mathematical, physical, and living systems. The 1992 summer school consisted of approximately twelve short courses together with a number of seminars on selected topics, and took place over a period of four weeks. Topics covered include chaos, computational and algorithmic complexity, neural nets and computational neurobiology, parallel models in cognition, stochastic processes in physical and biological systems and pattern formation in biological systems. An important component of the schools is the publication

of the complete set of lecture notes in book form, the purpose of which is to provide students and researchers in the general scientific community with an overview of the emerging concepts of complex behavior, and their applications to specific systems. DTIC

N94-29147 Institut des Hautes Etudes Scientifiques, Bures-sur-Yvette (France).
REMARKS ON GALOIS SYMMETRY IN RCFT
A. Coste (Ecole Polytechnique, Palaiseau, France.) and T. Gannon Oct. 1993 13 p Limited Reproducibility: More than 20% of this document may be affected by microfiche quality
(PB94-138179; IHES/M/93/57) Avail: Issuing Activity (National Technical Information Service (NTIS))

We show that a recently discovered Galois symmetry is present in the torus partition function of any rational conformal field theory (RCFT), as well as in chiral fusion rings. S matrix elements are linear combinations over Q of roots of unity. An example of su(2) Wess-Zumino-Novikov-Witten (WZNW) theory is discussed. NTIS

N94-29162 Institut des Hautes Etudes Scientifiques, Bures-sur-Yvette (France).
METHOD OF CHABAUTY-COLEMAN AND THE SECOND CASE OF FERMAT'S LAST THEOREM FOR REGULAR PRIMES
W. G. McCallum Nov. 1993 34 p Prepared for NSF, Washington, DC Limited Reproducibility: More than 20% of this document may be affected by microfiche quality
(Grant NSF DMS-90-02095)
(PB94-138187; IHES/M/93/62) Avail: Issuing Activity (National Technical Information Service (NTIS))

Let C be a curve of genus g = or greater than 2, defined over a number field K, and let J be the Jacobian of C. Colemen, following Chabauty, has shown how to obtain good bounds on the cardinality of C(K) if the rank r of the Mordell-Weil group J(K) is less than g. The key to the method is to construct a logarithm on J(K sub v), for some valuation v of K, whose kernel contains J(K), and whose restriction to C(K sub v) is represented explicitly as the integral of a differential. This paper is an attempt to make the case, through a detailed examination of the case of Fermat curves, that this method can be fashioned into a quite precise tool for bounding rational points on curves. In particular, we will present an explicit description of the logarithm in question, given the existence of certain elements in a Selmer group attached to J. NTIS

N94-29163 Institut des Hautes Etudes Scientifiques, Bures-sur-Yvette (France).
TRACE FORMULAS AND DYNAMICAL ZETA FUNCTIONS IN THE NIELSEN THEORY
A. Felshtyn and R. Hill Dec. 1993 37 p Limited Reproducibility: More than 20% of this document may be affected by microfiche quality
(PB94-138195; IHES/M/93/67) Avail: Issuing Activity (National Technical Information Service (NTIS))

In this paper, we prove the trace formulas for the Reidemeister numbers of group endomorphisms in the following cases: the group is finitely generated and an endomorphism is eventually commutative; the group is finite; the group is a direct sum of a finite group and a finitely generated free abelian group; the group is finitely generated, nilpotent and torsion free. These results had previously been known only for the finitely generated free abelian group. As a consequence, we obtain under the same conditions on the fundamental group of a compact polyhedron, the trace formulas for the Reidemeister numbers of a continuous map and under suitable conditions the trace formulas for the Nielsen numbers of a continuous map. The trace formula for the Reidemeister numbers implies the rationality of the Reidemeister zeta function. We prove the rationality and functional equation for the Reidemeister zeta function of an endomorphism of a finitely generated torsion free nilpotent group and of a direct sum of a finite group and a finitely generated free abelian group. NTIS

N94-29910 New Mexico State Univ., Las Cruces.
SIGNIFICANT FIGURES AND LYAPUNOV EXPONENTS IN CHAOS AND CONSTRAINED DIVERGENCE OF CHAOTIC ORBITS Ph.D. Thesis
Robert Hal Dalling 1992 190 p
Avail: Univ. Microfilms Order No. DA9313723

A numerical technique is developed which can determine the maximum Lyapunov exponent in n-dimensional systems. This exponent can be calculated from the rate at which the number of valid figures in a solution decreases. The advantages of this technique over existing methods are described. Chaos is shown to be independent of the number of significant figures used in measurements and in calculations. The existence of restricted error growth regions is shown. For orbits in these regions the magnitude of the exponentially growing error is less than the maximum difference in orbital values, that is, the chaotic orbit is constrained throughout time to a subset of the phase space covered by the orbit. These regions are anomalous in that the Lyapunov exponent is positive in the region, but the magnitude of the exponentially growing error is limited to a finite value. This means that long-term prediction can still be possible, within limits, at certain parameter values of a chaotic system. Dissert. Abstr.

N94-30065 International Centre for Theoretical Physics, Trieste (Italy).
APPROXIMATION METHODS FOR NONLINEAR OPERATOR EQUATIONS OF THE m-ACCRETIVE TYPE
C. E. Chidume and M. O. Osilike Aug. 1993 13 p Limited Reproducibility: More than 20% of this document may be affected by microfiche quality
(DE94-608099; IC-93/260) Avail: CASI HC A03 (US Sales Only)

Let E be a real Banach space which is both uniformly convex and uniformly smooth. Let T: D(T) is included in E yields E be m-accretive, where the domain of T, D(T), is a proper subset of E. For any f is an element of E, approximation methods are constructed which converge strongly to a solution of the operator equation chi + T chi = f. Explicit error estimates are obtained. A related result deals with operator equations of the dissipative type. DOE

N94-30088 International Centre for Theoretical Physics, Trieste (Italy).
FRACTAL APPROACH TO COMPUTER-ANALYTICAL MODELLING OF TREE CROWN
F. S. Berezovskaya, G. P. Karev, O. F. Kisliuk, R. G. Khlebopros, and Yu. L. Tcelniker Sep. 1993 12 p Limited Reproducibility: More than 20% of this document may be affected by microfiche quality
(DE94-608089; IC-92/267) Avail: CASI HC A03 (US Sales Only)

In this paper we discuss three approaches to the modeling of a tree crown development. These approaches are experimental (i.e. regressive), theoretical (i.e. analytical) and simulation (i.e. computer) modeling. The common assumption of these is that a tree can be regarded as one of the fractal objects which is the collection of semi-similar objects and combines the properties of two- and three-dimensional bodies. We show that a fractal measure of crown can be used as the link between the mathematical models of crown growth and light propagation through canopy. The computer approach gives the possibility to visualize a crown development and to calibrate the model on experimental data. In the paper different stages of the above-mentioned approaches are described. The experimental data for spruce, the description of computer system for modeling and the variant of computer model are presented. DOE

N94-30166 International Centre for Theoretical Physics, Trieste (Italy).
SYMPLECTIC TOPOLOGY OF INTEGRABLE HAMILTONIAN SYSTEMS
Nguyen Tien Zung Aug. 1993 78 p Limited Reproducibility: More than 20% of this document may be affected by microfiche quality
(DE94-608120; IC-93/305) Avail: CASI HC A05 (US Sales Only)

We study the topology of integrable Hamiltonian systems, giving the main attention to the affine structure of their orbit spaces. In particular, we develop some aspects of Fomenko's theory about topological classification of integrable non-degenerate systems, and consider some relations between such systems and 'pure' contact and symplectic geometry. We give a notion of integrable surgery and use it to obtain some interesting symplectic structures. DOE

N94-30202 International Centre for Theoretical Physics, Trieste (Italy).
IS IT POSSIBLE TO EXTEND THE DEFORMED WEYL ALGEBRA W(SUB q)(n) TO A HOPF ALGEBRA?
T. D. Palev Jul. 1993 6 p Limited Reproducibility: More than 20% of this document may be affected by microfiche quality
(DE94-608092; IC-93/163) Avail: CASI HC A02 (US Sales Only)

We argue that the algebra W(sub q)(n), generated by n pairs of deformed q-bosons, does not allow a Hopf algebra structure. To this end we show that it is impossible to define a comultiplication even for the usual,

nondeformed case. We indicate how the co-multiplication on U(sub q)(osp(1/2n)) can be used in order to construct representations of deformed (not necessarily Hopf) algebra in tensor products of Fock spaces. DOE

70 PHYSICS (GENERAL)

For precision time and time interval (PTTI) see *35 Instrumentation and Photography;* for geophysics, astrophysics or solar physics see *46 Geophysics, 90 Astrophysics,* or *92 Solar Physics.*

N94-28459# Argonne National Lab., IL.
THREE-DIMENSIONAL FINITE ELEMENT MODELING OF A MAGNET ARRAY SPINNING ABOVE A CONDUCTOR
W. L. Lorimer (California Univ., Berkeley.), D. K. Lieu (California Univ., Berkeley.), J. R. Hull, T. M. Mulcahy, and T. D. Rossing 1993 5 p Presented at the Conference on Computation of Electromagnetic Fields, Miami, FL, 31 Oct. - 4 Nov. 1993
(Contract W-31-109-eng-38)
(DE94-004573; ANL/ET/CP-81277; CONF-931013-3) Avail: CASI HC A01/MF A01

Drag forces due to eddy currents induced by the relative motion of a conductor and a magnetic field occur in many practical devices: motors, brakes, magnetic bearings, and magnetically levitated vehicles. Recently, finite element codes have included solvers for three dimensional eddy current geometries and have the potential to be very useful in the design and analysis of these devices. In this paper, numerical results from three dimensional modeling of a magnet array spinning above a conductor are compared to experimental results in order to assess the capabilities of these codes. DOE

N94-28720# Joint Inst. for Nuclear Research, Dubna (USSR).
ON THE EKL-EFFECT
V. N. Streltsov 1992 3 p
(DE94-606325; JINR-D-2-92-196) Avail: CASI HC A01/MF A01 (US Sales Only)

An investigation of the electric field around a neutral conductor after steady conduction current excitation was carried out in the experiments of Edwards et al. The calculations performed on the basis of Lienard-Wiechert's potential and taking into account retardation show that the electric field must not arise in experiments of a similar type. DOE

N94-30026# California Univ., Berkeley. Lawrence Berkeley Lab.
ESTIMATING THE COST OF LARGE SUPERCONDUCTING THIN SOLENOID MAGNETS
M. A. Green and S. J. St.Lorant Jul. 1993 6 p Presented at the International Cryogenic Engineering Conference and International Cryogenic Materials Conference, Albuquerque, NM, 12-16 Jul. 1993
(Contract DE-AC03-76SF-00098)
(DE94-006289; LBL-35002; CONF-930703-42) Avail: CASI HC A02/MF A01

The cost of thin superconducting solenoid magnets can be estimated if one knows the magnet stored energy, the magnetic field volume product or the overall mass of the superconducting coil and its cryostat. This report shows cost data collected since 1979 for large superconducting solenoid magnets used in high energy physics. These magnets are characterized in most cases by the use of indirect two phase helium cooling and a superconductor stabilizer of very pure aluminum. This correlation can be used for making a preliminary cost estimate of proposed one of a kind superconducting magnets. The magnet costs quoted include the power supply and quench protection system but the cost of the helium refrigerator and helium distribution system is not included in the estimated cost. DOE

N94-30110 International Centre for Theoretical Physics, Trieste (Italy).
SOME RESULTS ON THE PHASE DIAGRAM OF THE ANTIFERROMAGNETIC POTTS MODEL IN AN EXTERNAL MAGNETIC FIELD
A. Benyoussef (Mohammed V Univ., Rabat, Morocco.) and H. Ez-Zahraouy Sep. 1993 21 p Limited Reproducibility: More than 20% of this document may be affected by microfiche quality
(DE94-608115; IC-93/299) Avail: CASI HC A03 (US Sales Only)

Phase diagram of the q state antiferromagnetic Potts model on a square lattice is investigated in a neighborhood of the critical point h = 4, T = 0. Using a constructive criterion of uniqueness introduced by Dobrushin, Kolafa, and Shlosman, for the antiferromagnetic Ising model, we show that the activity, a(sub c)(q) greater than 1/(q - 1) and the slope increases from zero (q = 2) to infinity (q = is proportional). The phase diagram bulges near the mentioned critical point for 2 less than q less than is proportional. DOE

N94-30639*# National Aeronautics and Space Administration. Goddard Space Flight Center, Greenbelt, MD.
THE 25TH ANNUAL PRECISE TIME AND TIME INTERVAL (PTTI) APPLICATIONS AND PLANNING MEETING
Richard L. Sydnor, ed. (Jet Propulsion Lab., California Inst. of Tech., Pasadena.) Washington May 1994 583 p Meeting held in Marina Del Rey, CA, 29 Nov. - 2 Dec. 1993; sponsored by NASA, U.S. Naval Observatory, JPL, Space and Naval Warfare Systems Command, NRL, U.S. Army Research Lab., and AFOSR
(Contract NAS5-31000)
(NASA-CP-3267; Rept-94B00063; NAS 1.55:3267) Avail: CASI HC A25/MF A06

Papers in the following categories are presented: recent developments in rubidium, cesium, and hydrogen-based frequency standards, and in cryogenic and trapped-ion technology; international and transnational applications of precise time and time interval (PTTI) technology with emphasis on satellite laser tracking networks, GLONASS timing, intercomparison of national time scales and international telecommunication; applications of PTTI technology to the telecommunications, power distribution, platform positioning, and geophysical survey industries; application of PTTI technology to evolving military communications and navigation systems; and dissemination of precise time and frequency by means of GPS, GLONASS, MILSTAR, LORAN, and synchronous communications satellites. For individual titles, see N94-30640 through N94-30684.

N94-30640*# Jet Propulsion Lab., California Inst. of Tech., Pasadena.
STATUS OF FREQUENCY AND TIME SUPPORT FOR NASA SYSTEMS
Paul F. Kuhnle, Paul J. Kushmeider, and S. Clark Wardrip *In* NASA. Goddard Space Flight Center, The 25th Annual Precise Time and Time Interval (PTTI) Applications and Planning Meeting May 1994 p 21-32 (For primary document see N94-30639 08-70)
Avail: CASI HC A03/MF A06

NASA has frequency and timing systems at many facilities and centers. Timing systems with specifications tighter than several microseconds are covered. These ground based systems support scientific experiments and spacecraft tracking for the following programs; NASA Satellite Laser Ranging (NSLR); Network Mission Operations Support (NMOS); Kennedy Space Center (KSC); Very Long Baseline Interferometry (VLBI); Tracking Data Relay Satellite System (TDRSS) Ground Terminal Network; and the Deep Space Network (DSN). Major equipment assemblies, specifications, performance, and requirements, both present and future, are presented.
Author (revised)

N94-30641*# National Inst. of Standards and Technology, Boulder, CO.
TIME AND FREQUENCY TECHNOLOGY AT NIST
D. B. Sullivan *In* NASA. Goddard Space Flight Center, The 25th Annual Precise Time and Time Interval (PTTI) Applications and Planning Meeting May 1994 p 33-38 (For primary document see N94-30639 08-70)
Avail: CASI HC A02/MF A06

The state of development of advanced timing systems at NIST is described. The work on cesium and rubidium frequency standards, stored-ion frequency standards, diode lasers used to pump such standards, time transfer, and methods for characterizing clocks, oscillators, and time distribution systems is presented. The emphasis is on NIST-developed technology rather than the general state of the art in this field.
Author (revised)

N94-30642*# Istituto Elettrotecnico Nazionale, Turin (Italy).
EUROPEAN PTTI REPORT
Franco Cordara, Sabrina Grimaldi, and Sigfrido Leschiutta *In* NASA. Goddard Space Flight Center, The 25th Annual Precise Time and Time Interval (PTTI) Applications and Planning Meeting May 1994 p 39-56

(For primary document see N94-30639 08-70)
Avail: CASI HC A03/MF A06

Time and frequency metrology in Europe presents some peculiar features in its three main components: research on clocks, comparisons and dissemination methods, and dissemination services. Apart from the usual activities of the national metrological laboratories, an increasing number of cooperation between the European countries are promoted inside some European organizations, such as the ECC, EFTA, EUROMET, and WECC. Cooperation between these organizations is covered. The present, evolving situation will be further influenced by the recent political changes in Eastern Europe. Author (revised)

N94-30643*# Air Force Systems Command, Falcon AFB, CO.
AN OPERATIONAL CONTROL SEGMENT (OCS) UPDATE ON GPS CONSTELLATION STATUS AND FUTURE PROGRAM DIRECTIONS **c04**

Harrison C. Freer *In* NASA. Goddard Space Flight Center, The 25th Annual Precise Time and Time Interval (PTTI) Applications and Planning Meeting May 1994 p 65-78 (For primary document see N94-30639 08-70)
Avail: CASI HC A03/MF A06

An update on what is going on with the Global Positioning System (GPS) is presented. The performance of the GPS is covered, and the Federal Radionavigation Plan is discussed. Derived from text

N94-30644*# Coast Guard, Washington, DC.
LORAN-C TIME MANAGEMENT **c04**

Charles Justice, Norm Mason, and Doug Taggart *In* NASA. Goddard Space Flight Center, The 25th Annual Precise Time and Time Interval (PTTI) Applications and Planning Meeting May 1994 p 79-92 (For primary document see N94-30639 08-70)
Avail: CASI HC A03/MF A06

As of 1 Oct. 1993, the US Coast Guard (USCG) supports and operates fifteen Loran-C chains. With the introduction of the Global Positioning Systems (GPS) and the termination of the Department of Defense (DOD) overseas need for Loran-C, the USCG will cease operating the three remaining overseas chains by 31 Dec. 1994. Following this date, the USCG Loran-C system will consist of twelve chains. Since 1971, management of time synchronization of the Loran-C system has been conducted under a Memorandum of Agreement between the US Naval Observatory (USNO) and the USCG. The requirement to maintain synchronization with Coordinated Universal Time (UTC) was initially specified as +/- 25 microseconds. This tolerance was rapidly lowered to +/- 2.5 microseconds in 1974. To manage this synchronization requirement, the USCG incorporated administrative practices which kept the USNO appraised of all aspects of the master timing path. This included procedures for responding to timing path failures, timing adjustments, and time steps. Conducting these aspects of time synchronization depended on message traffic between the various master stations and the USNO. To determine clock adjustment the USCG relied upon the USNO's Series 4 and 100 updates so that the characteristics of the master clock could be plotted and controls appropriately applied. In 1987, Public Law 100-223, under the Airport and Airway Improvement Act Amendment, reduced the synchronization tolerance to approximately 100 nanoseconds for chains serving the National Airspace System (NAS). This action caused changes in the previous administrative procedures and techniques. The actions taken by the USCG to meet the requirements of this law are presented. Author (revised)

N94-30645*# Ministry of Defence, London (England).
REPORT ON NATO PTTI

J. Bishop *In* NASA. Goddard Space Flight Center, The 25th Annual Precise Time and Time Interval (PTTI) Applications and Planning Meeting May 1994 p 93-100 (For primary document see N94-30639 08-70)
Avail: CASI HC A02/MF A06

The work of the NATO Working Group on precise time and frequency (AC302/SG4/WG4), since its inception in 1988 to the end of 1993, is covered. The aim of the group was to produce STANAG 4430 detailing a standard interface for the transfer of precise time and frequency to assist the interoperability of NATO forces. The design of the interface is outlined together with the concepts leading to the design. The problem of providing and maintaining a traceable UTC in military user systems is described. Author (revised)

N94-30646*# National Service of Metrology, Delft (Netherlands). NMi Van Swinden Laboratorium.
TWO-WAY SATELLITE TIME TRANSFER: OVERVIEW AND RECENT DEVELOPMENTS

Gerrit deJong *In* NASA. Goddard Space Flight Center, The 25th Annual Precise Time and Time Interval (PTTI) Applications and Planning Meeting May 1994 p 101-118 (For primary document see N94-30639 08-70)
Avail: CASI HC A03/MF A06

The experiment using small earth stations for transatlantic two-way satellite time transfer between the USA and Germany has had its 10th anniversary this year. Pseudo-random noise coded time signals were phase modulated and demodulated at each station using a modem. Recently, during the last two weeks of Aug. 1993, six European time laboratories have used the INTELSAT 307E satellite for line-up tests and preliminary time transfer sessions using the same type of MITREX modem. The need for a uniform format for the exchange of data was felt heavily after these sessions. This problem was foreseen and addressed in international working parties. During Apr. 1993, in Task Group 7/2 of the ITU Radiocommunication Sector, a very intense discussion has taken place about what procedure should be recommended for TWSTFT and what items the header and data lines of the resulting data fields should contain. A difficulty is that two different methods of calibration of the earth station delays exist which result in different sets of delay data to be exchanged. Further study and discussions are necessary. Also, a meeting of the CCDS Working Group on TWSTFT addressed this in Oct. 1993. The outcome of the discussions and the prospect for future developments are presented. Author (revised)

N94-30647*# Observatoire de la Cote d'Azur, Grasse (France).
OPTICAL TECHNIQUES FOR TIME AND FREQUENCY TRANSFER **c74**

Francoise Baumont and Jean Gaignebet *In* NASA. Goddard Space Flight Center, The 25th Annual Precise Time and Time Interval (PTTI) Applications and Planning Meeting May 1994 p 119-132 (For primary document see N94-30639 08-70)
Avail: CASI HC A03/MF A06

Light has been used as a means for time synchronization for a long time. The flight time was supposed to be negligible. The first scientific determination of the velocity of the light was done by measuring a round trip flight time on a given distance. The well known flying clock experiment leading to Einstein's General Relativity is another example. The advent of lasers, particularly short pulse and modulated ones, as well as the improvements of the timing equipments have led to new concepts for time and frequency transfer. We describe some experiments using different techniques and configurations which have been proposed and tested in this field since the beginning of the space age. Added to that, we set out advantages, drawbacks, and performances achieved in the different cases. Author (revised)

N94-30648*# Bureau International des Poids et Mesures, Sevres (France).
GPS COMMON-VIEW TIME TRANSFER **c04**

W. Lewandowski *In* NASA. Goddard Space Flight Center, The 25th Annual Precise Time and Time Interval (PTTI) Applications and Planning Meeting May 1994 p 133-148 (For primary document see N94-30639 08-70)
Avail: CASI HC A03/MF A06

The introduction of the GPS common-view method at the beginning of the 1980's led to an immediate and dramatic improvement of international time comparisons. Since then, further progress brought the precision and accuracy of GPS common-view intercontinental time transfer from tens of nanoseconds to a few nanoseconds, even with SA activated. This achievement was made possible by the use of the following: ultra-precise ground antenna coordinates, post-processed precise ephemerides, double-frequency measurements of ionosphere, and appropriate international coordination and standardization. This paper reviews developments and applications of the GPS common-view method during the last decade and comments on possible future improvements whose objective is to attain sub-nanosecond uncertainty. Author (revised)

N94-30649*# Telecom Solutions Ltd., San Jose, CA.
CASCADED CLOCKS MEASUREMENT AND SIMULATION FINDINGS

Don Chislow and George Zampetti *In* NASA. Goddard Space Flight Center, The 25th Annual Precise Time and Time Interval (PTTI) Applications

and Planning Meeting May 1994 p 149-168 (For primary document see N94-30639 08-70)
Avail: CASI HC A03/MF A06

This paper will examine aspects related to network synchronization distribution and the cascading of timing elements. Methods of timing distribution have become a much debated topic in standards forums and among network service providers (both domestically and internationally). Essentially these concerns focus on the need to migrate their existing network synchronization plans (and capabilities) to those required for the next generation of transport technologies (namely, the Synchronous Digital Hierarchy (SDH), Synchronous Optical Networks (SONET), and Asynchronous Transfer Mode (ATM). The particular choices for synchronization distribution network architectures are now being evaluated and are demonstrating that they can indeed have a profound effect on the overall service performance levels that will be delivered to the customer. The salient aspects of these concerns reduce to the following: (1) identifying that the devil is in the details of the timing element specifications and the distribution of timing information (i.e., small design choices can have a large performance impact); (2) developing a standardized method of performance verification that will yield unambiguous results; and (3) presentation of those results. Specifically, this will be done for two general cases: an ideal input, and a noisy input to a cascaded chain of slave clocks. Author (revised)

N94-30650*# Jet Propulsion Lab., California Inst. of Tech., Pasadena.
TIME AND POSITION ACCURACY USING CODELESS GPS c04
C. E. Dunn, D. C. Jefferson, S. M. Lichten, J. B. Thomas, Y. Vigue, and L. E. Young *In* NASA. Goddard Space Flight Center, The 25th Annual Precise Time and Time Interval (PTTI) Applications and Planning Meeting May 1994 p 169-182 (For primary document see N94-30639 08-70)
Avail: CASI HC A03/MF A06

The Global Positioning System has allowed scientists and engineers to make measurements having accuracy far beyond the original 15 meter goal of the system. Using global networks of P-Code capable receivers and extensive post-processing, geodesists have achieved baseline precision of a few parts per billion, and clock offsets have been measured at the nanosecond level over intercontinental distances. A cloud hangs over this picture, however. The Department of Defense plans to encrypt the P-Code (called Anti-Spoofing, or AS) in the fall of 1993. After this event, geodetic and time measurements will have to be made using codeless GPS receivers. However, there appears to be a silver lining to the cloud. In response to the anticipated encryption of the P-Code, the geodetic and GPS receiver community has developed some remarkably effective means of coping with AS without classified information. We will discuss various codeless techniques currently available and the data noise resulting from each. We will review some geodetic results obtained using only codeless data, and discuss the implications for time measurements. Finally, we will present the status of GPS research at JPL in relation to codeless clock measurements. Author (revised)

N94-30651*# Bureau International des Poids et Mesures, Sevres (France).
THE USE OF THE AOA TTR-4P GPS RECEIVER IN OPERATION AT THE BIPM FOR REAL-TIME RESTITUTION OF GPS TIME c04
Claudine Thomas *In* NASA. Goddard Space Flight Center, The 25th Annual Precise Time and Time Interval (PTTI) Applications and Planning Meeting May 1994 p 183-196 (For primary document see N94-30639 08-70)
Avail: CASI HC A03/MF A06

The Global Positioning System is an outstanding tool for the dissemination of time. Using mono-channel C/A-code GPS time receivers, the restitution of GPS time through the satellite constellation presents a peak-to-peak discrepancy of several tens of nanoseconds without SA but may be as high as several hundreds of nanoseconds with SA. As a consequence, civil users are more and more interested in implementing hardware and software methods for efficient restitution of GPS time, especially in the framework of the project of a real-time prediction of UTC (UTCp) which could be available in the form of time differences (UTCp - GPS time). Previous work, for improving the real-time restitution of GPS time with SA, to the level obtained without SA, focused on the implementation of a Kalman filter based on past data and updated at each new observation. An alternative solution relies upon the statistical features of the noise brought about by SA; it has already been shown that the SA noise is efficiently reduced by averaging data from numerous satellites observed simultaneously over a sufficiently long time. This method was successfully applied to data from a GPS time receiver, model AOA TTR-4P, connected to the cesium clock kept at the BIPM. This device, a multi-channel, dual frequency, P-code GPS time receiver, is one of the first TTR-4P units in operation in a civil laboratory. Preliminary comparative studies of this new equipment with conventional GPS time receivers are described in this paper. The results of an experimental restitution of GPS time, obtained in June 1993, are also detailed: 3 to 6 satellites were observed simultaneously with a sample interval of 15 s, an efficient smoothing of SA noise was realized by averaging data on all observed satellites over more than 1 hour. When the GPS system is complete in 1994, 8 satellites will be observable continuously from anywhere in the world and the same level of uncertainty will be obtained using a shorter averaging time.
Author (revised)

N94-30652*# Hydro-Electric Power Commission, Burnaby (British Columbia).
DEVELOPMENT OF AN ACCURATE TRANSMISSION LINE FAULT LOCATOR USING THE GLOBAL POSITIONING SYSTEM SATELLITES c04
Harry Lee *In* NASA. Goddard Space Flight Center, The 25th Annual Precise Time and Time Interval (PTTI) Applications and Planning Meeting May 1994 p 197-204 (For primary document see N94-30639 08-70)
Avail: CASI HC A02/MF A06

A highly accurate transmission line fault locator based on the traveling-wave principle was developed and successfully operated within B.C. Hydro. A transmission line fault produces a fast-risetime traveling wave at the fault point which propagates along the transmission line. This fault locator system consists of traveling wave detectors located at key substations which detect and time tag the leading edge of the fault-generated traveling wave as if passes through. A master station gathers the time-tagged information from the remote detectors and determines the location of the fault. Precise time is a key element to the success of this system. This fault locator system derives its timing from the Global Positioning System (GPS) satellites. System tests confirmed the accuracy of locating faults to within the design objective of +/-300 meters. Author (revised)

N94-30653*# Bureau International des Poids et Mesures, Sevres (France).
RELATIVISTIC THEORY FOR PICOSECOND TIME TRANSFER IN THE VICINITY OF EARTH
G. Petit and P. Wolf *In* NASA. Goddard Space Flight Center, The 25th Annual Precise Time and Time Interval (PTTI) Applications and Planning Meeting May 1994 p 205-216 (For primary document see N94-30639 08-70)
Avail: CASI HC A03/MF A06

The problem of light propagation is treated in a geocentric reference system with the goal of ensuring picosecond accuracy for time transfer techniques using electromagnetic signals in the vicinity of the Earth. We give an explicit formula for a one way time transfer, to be applied when the spatial coordinates of the time transfer stations are known in a geocentric reference system rotating with the Earth. This expression is extended, at the same accuracy level of one picosecond, to the special cases of two way and LASSO time transfers via geostationary satellites.
Author (revised)

N94-30654*# Bureau International des Poids et Mesures, Sevres (France).
A REAL-TIME PREDICTION OF UTC
Claudine Thomas and David W. Allan *In* NASA. Goddard Space Flight Center, The 25th Annual Precise Time and Time Interval (PTTI) Applications and Planning Meeting May 1994 p 217-230 (For primary document see N94-30639 08-70)
Avail: CASI HC A03/MF A06

The reference time scale for all scientific and technologic applications on the Earth, the Universal Coordinated Time (UTC), must be as stable, reliable, and accurate as possible. With this in view the BIPM and before it the BIH, have always calculated and then disseminated UTC with a delay of about 80 days. There are three fundamental reasons for doing this: (1) It takes some weeks for data, gathered from some 200 clocks

spread world-wide, to be collected and for errors to be eliminated; (2) changes in clock rates can only be measured with high precision well after the fact; and (3) the measurement noise originating in time links, in particular using Loran-C, is smoothed out only when averaging over an extended period. Until mid-1992, the ultimate stability of UTC was reached at averaging times of about 100 days and corresponded to an Allan deviation sigma(sub y)(tau) of about 1,5x10(exp -14) then compared to the best primary clock in the world, the PTB CS2. For several years now, a predicted UTC has been computed by the USNO through an extrapolation of the values as published in deferred time by the BIPM. This is made available through the USNO Series 4, through the USNO Automated Data Service, and through GPS signals. Due to the instability of UTC, the poor predictability of the available clocks, and the intentional SA degradation of GPS signals, the real-time access to this extrapolated UTC has represented the true deferred-time UTC only to within several hundreds of nanoseconds.

Author (revised)

N94-30655*# Graz Univ. (Austria).

TROPOSPHERIC CORRECTIONS TO GPS MEASUREMENTS USING LOCALLY MEASURED METEOROLOGICAL PARAMETERS COMPARED WITH GENERAL TROPOSPHERIC CORRECTIONS **c04**

D. Kirchner, C. Lentz, and H. Ressler *In* NASA. Goddard Space Flight Center, The 25th Annual Precise Time and Time Interval (PTTI) Applications and Planning Meeting May 1994 p 231-248 (For primary document see N94-30639 08-70)

Avail: CASI HC A03/MF A06

At the Technical University Graz (TUG), Austria, the Global Positioning System (GPS) has been used for time transfer purposes since the early 80's and from that time on local meteorological parameters have been recorded together with each measurement (satellite track). The paper compares the tropospheric corrections (delays) obtained from models usually employed in GPS receivers and those using locally measured meteorological parameters.

Author (revised)

N94-30656*# National Research Council of Canada, Ottawa (Ontario).

ACCURACY METRICS FOR JUDGING TIME SCALE ALGORITHMS

R. J. Douglas, J.-S. Boulanger, and C. Jacques *In* NASA. Goddard Space Flight Center, The 25th Annual Precise Time and Time Interval (PTTI) Applications and Planning Meeting May 1994 p 249-266 (For primary document see N94-30639 08-70)

Avail: CASI HC A03/MF A06

Time scales have been constructed in different ways to meet the many demands placed upon them for time accuracy, frequency accuracy, long-term stability, and robustness. Usually, no single time scale is optimum for all purposes. In the context of the impending availability of high-accuracy intermittently-operated cesium fountains, we reconsider the question of evaluating the accuracy of time scales which use an algorithm to span interruptions of the primary standard. We consider a broad class of calibration algorithms that can be evaluated and compared quantitatively for their accuracy in the presence of frequency drift and a full noise model (a mixture of white PM, flicker PM, white FM, flicker FM, and random walk FM noise). We present the analytic techniques for computing the standard uncertainty for the full noise model and this class of calibration algorithms. The simplest algorithm is evaluated to find the average-frequency uncertainty arising from the noise of the cesium fountain's local oscillator and from the noise of a hydrogen maser transfer-standard. This algorithm and known noise sources are shown to permit interlaboratory frequency transfer with a standard uncertainty of less than 10(exp -15) for periods of 30-100 days.

Author (revised)

N94-30657*# Observatoire de Besancon (France).

TIME TRANSFER USING GEOSTATIONARY SATELLITES: IMPLEMENTATION OF A KALMAN FILTER

F. Meyer *In* NASA. Goddard Space Flight Center, The 25th Annual Precise Time and Time Interval (PTTI) Applications and Planning Meeting May 1994 p 267-276 (For primary document see N94-30639 08-70)

Avail: CASI HC A02/MF A06

Since 1988, various experiments have shown that the TV signals transmitted by direct TV satellites may easily be used to perform time transfers at the level of a few tens of nanoseconds, the main source of error being the uncertainty on the satellite position. We first present the two methods used in our experiment to reduce the effects of the satellite residual motion: the first one consists in estimating the longitude variations of the satellite and then using this information to improve other measurements. This allows reducing the uncertainty to values between 9 and 50 nanoseconds according to the position of the involved stations. In the second method we determine the satellite position by using the data collected by three calibrated stations. Time transfer between each of these stations and a fourth one has been shown to be achievable at the precision level of ten nanoseconds. A new approach based on the use of a Kalman filter is proposed in order to take into account the dynamics of the geostationary satellite. The precisions on orbital elements and clock differences and rates determination given by the first simulated applications of the Kalman filter are presented and compared to those obtained by the other methods.

Author

N94-30658*# Shaanxi Astronomical Observatory, Lintong (China).

THE TWO-WAY TIME SYNCHRONIZATION SYSTEM VIA A SATELLITE VOICE CHANNEL

Zheng Heng-Qiu, Zhang Ren-Huan, and Hu Yong-Hui *In* NASA. Goddard Space Flight Center, The 25th Annual Precise Time and Time Interval (PTTI) Applications and Planning Meeting May 1994 p 277-284 (For primary document see N94-30639 08-70)

Avail: CASI HC A02/MF A06

A newly developed two-way time synchronization system is described in this paper. The system uses one voice channel at a SCPC satellite digital communication earth station, whose bandwidth is only 45 kHz, thus saving satellite resources greatly. The system is composed of one master station and one or several, up to sixty-two, secondary stations. The master and secondary stations are equipped with the same equipment, including a set of timing equipment, a synthetic data terminal for time synchronizing, and a interface unit between the data terminal and the satellite earth station. The synthetic data terminal for time synchronization also has an IRIG-B code generator and a translator. The data terminal of master station is the key part of whole system. The system synchronization process is full automatic, which is controlled by the master station. Employing an autoscanning technique and conversational mode, the system accomplishes the following tasks: linking up liaison with each secondary station in turn, establishing a coarse time synchronization, calibrating date (years, months, days) and time of day (hours, minutes, seconds), precisely measuring the time difference between local station and the opposite station, exchanging measurement data, statistically processing the data, rejecting error terms, printing the data, calculating the clock difference and correcting the phase, thus realizing real-time synchronization from one point to multiple points. We also designed an adaptive phase circuit to eliminate the phase ambiguity of the PSK demodulator. The experiments have shown that the time synchronization accuracy is better than 2 mu S. The system has been put into regular operation.

Author

N94-30659*# Naval Observatory, Washington, DC.

REMOTE CLOCKS LINKED BY A FULLY CALIBRATED TWO-WAY TIMING LINK

James A. DeYoung and Ronald J. Andrukitis *In* NASA. Goddard Space Flight Center, The 25th Annual Precise Time and Time Interval (PTTI) Applications and Planning Meeting May 1994 p 285-292 (For primary document see N94-30639 08-70)

Avail: CASI HC A02/MF A06

Fully calibrated two-way time transfers between the U.S. Naval Observatory (USNO) and the U.S. Naval Observatory Time Service Substation (NOTSS) have become operational. The calibration method employed was the co-located Earth station method. Results concerning timing, stability, comparison of two-way and Global Positioning System (GPS) timing links, and remote clock contribution to local time scale computation will be presented.

Author

N94-30660*# National Inst. of Standards and Technology, Boulder, CO. Time and Frequency Div.

A COMPARISON OF GPS BROADCAST AND DMA PRECISE EPHEMERIDES **c04**

Marc A. Weiss, Gerard Petit, and Steve Shattil *In* NASA. Goddard Space Flight Center, The 25th Annual Precise Time and Time Interval (PTTI) Applications and Planning Meeting May 1994 p 293-306 (For primary document see N94-30639 08-70)

Avail: CASI HC A03/MF A06

We compare the broadcast ephemerides from Global Positioning Satellites (GPS) to the postprocessed ephemerides from the Defense Mapping Agency (DMA). We find significant energy in the spectrum of the residuals at 1 cycle/day and higher multiples. We estimate the time variance of the residuals and show that the short term residuals, from 15 min, exhibit power law processes with greater low frequency perturbations than white phase modulation. We discuss the significance of these results for the performance of the GPS Kalman filter which estimates the broadcast orbits. Author

N94-30661*# Beijing Inst. of Radio Metrology and Measurements (China).

SOME APPLICATIONS OF GPS TIMING INFORMATION **c04**

Yinbai Zhang *In* NASA. Goddard Space Flight Center, The 25th Annual Precise Time and Time Interval (PTTI) Applications and Planning Meeting May 1994 p 307-315 (For primary document see N94-30639 08-70)

Avail: CASI HC A02/MF A06

GPS Satellites transmit two independent signals. One is C/A code (course acquisition signal) which could be utilized by all civilian users. This service is called a Standard Positioning Service (SPS). Another is P code (precise signal) that could be only accessed by those authorized users. The service is called a precise positioning service (PPS). SPS C/A code users can navigate with accuracy of approximately 100 m and timing accuracy of about 250-300 ns (1 sigma). Such timing accuracy is not enough for precision time and frequency value transfer. For this reason we must do some research work to improve the SPS C/A code accuracy which SPS users can get. This paper presents our recent progress on timing information analysis, its data processing and its timing and frequency measurement applications. Derived from text

N94-30662*# Naval Observatory, Washington, DC.

A COMPARISON OF SEVERAL GPS DATA REDUCTION METHODS **c04**

H. Chadsey *In* NASA. Goddard Space Flight Center, The 25th Annual Precise Time and Time Interval (PTTI) Applications and Planning Meeting May 1994 p 317-328 (For primary document see N94-30639 08-70)

Avail: CASI HC A03/MF A06

For several years, discussions have been ongoing about how to analyze GPS time information in order to get the most accurate and precise time comparison between two locations. Many similar studies were done several years ago before the constellation was dominated by Block II satellites. With the Block II satellites and the use of Selective Availability (S/A), time comparisons have lost some precision and accuracy. This paper presents the results of research that was performed to find not only the best of several time comparison methods, but also to determine to what degree precision and accuracy have declined due to S/A. Author

N94-30663*# Rockwell International Corp., Colorado Springs, CO.

CESIUM AND RUBIDIUM FREQUENCY STANDARDS STATUS AND PERFORMANCE ON THE GPS PROGRAM **c04**

M. J. VanMelle *In* NASA. Goddard Space Flight Center, The 25th Annual Precise Time and Time Interval (PTTI) Applications and Planning Meeting May 1994 p 329-344 (For primary document see N94-30639 08-70)

Avail: CASI HC A03/MF A06

This paper is an update of the on-orbit operational performance of the frequency standards on the Block I GPS 8 to 11 Navstar satellites, the Block II GPS 13 to 21 Navstar satellites and the Block IIA GPS 22 to 40 Navstar satellites. A brief history of the frequency standards depicting improvements incorporated in the GPS Program with corresponding results will be presented. The frequency standards configurations from the start to the present, including the various Block IIA clock configurations will be discussed. Topics such as clock observations and long term trending analysis which could enhance on-orbit performance analysis will be covered. Author

N94-30664*# National Research Council of Canada, Ottawa (Ontario).

HYDROGEN MASERS AND CESIUM FOUNTAINS AT NRC **c36**

J.-S. Boulanger, D. Morris, R. J. Douglas, and M.-C. Gagne *In* NASA. Goddard Space Flight Center, The 25th Annual Precise Time and Time Interval (PTTI) Applications and Planning Meeting May 1994 p 345-356 (For primary document see N94-30639 08-70)

Avail: CASI HC A03/MF A06

The NRC masers H-3 and H-4 have been operating since June 1993 with cavity servo control. These low-flux active H masers are showing stabilities of about 10(exp -15) from 1 hour to several days. Stability results are presented, and the current and planned uses of the masers are discussed. A cesium fountain primary frequency standard project has been started at NRC. Trapping and launching experiments with the goal of 7 m/s launches are beginning. We discuss our plans for a local oscillator and servo that exploit the pulsed aspect of cesium fountain standards, and meet the challenge of 10(exp -14) tau(exp -1/2) stability without requiring masers. At best, we expect to run this frequency standard initially for periods of hours each working day rather than continuously for years, and so frequency transfer to outside laboratories has been carefully considered. We conclude that masers (or other even better secondary clocks) are required to exploit this potential accuracy of the cesium fountain. We present and discuss our conclusion that it is feasible to transfer frequency in this way with a transfer-induced uncertainty of less than 10(exp -15), even in the presence of maser frequency drift and random walk noise. Author

N94-30665*# Bureau International des Poids et Mesures, Sevres (France).

COMPARISON OF LASSO AND GPS TIME TRANSFERS **c04**

W. Lewandowski, G. Petit, F. Baumont, P. Fridelance, J. Gaignebet, P. Grudler, C. Veillet, J. Wiant, and W. J. Klepczynski *In* NASA. Goddard Space Flight Center, The 25th Annual Precise Time and Time Interval (PTTI) Applications and Planning Meeting May 1994 p 357-366 (For primary document see N94-30639 08-70)

Avail: CASI HC A02/MF A06

The LASSO is a technique which should allow the comparison of remote atomic clocks with sub-nanosecond precision and accuracy. The first successful time transfer using LASSO has been carried out between the Observatoire de la Cote d'Azur in France and the McDonald Observatory in Texas, United States. This paper presents a preliminary comparison of LASSO time transfer with GPS common-view time transfer. Author

N94-30666*# Observatoire de la Cote d'Azur, Grasse (France).

LASSO EXPERIMENT: INTERCALIBRATIONS OF THE LASSO RANGING STATIONS **c36**

J. Gaignebet, J.-L. Hatat, J. F. Mangin, J. M. Torre, William J. Klepczynski, L. McCubin, J. Wiant, and R. Rickefs *In* NASA. Goddard Space Flight Center, The 25th Annual Precise Time and Time Interval (PTTI) Applications and Planning Meeting May 1994 p 367-378 (For primary document see N94-30639 08-70)

Avail: CASI HC A03/MF A06

Presented are equations for time synchronization of laser ranging stations. The system consists of a satellite fitted with laser retroreflectors associated to a light detector and an event timer and two laser ranging stations with their own event timers. Methods of determining the Lasso intercalibration constant are given. CASI

N94-30667*# Observatoire de Besancon (France).

NOISE AND DRIFT ANALYSIS OF NON-EQUALLY SPACED TIMING DATA

F. Vernotte, G. Zalamansky, and E. Lantz *In* NASA. Goddard Space Flight Center, The 25th Annual Precise Time and Time Interval (PTTI) Applications and Planning Meeting May 1994 p 379-388 (For primary document see N94-30639 08-70)

Avail: CASI HC A02/MF A06

Generally, it is possible to obtain equally spaced timing data from oscillators. The measurement of the drifts and noises affecting oscillators is then performed by using a variance (Allan variance, modified Allan variance, or time variance) or a system of several variances (multivariance method). However, in some cases, several samples, or even several sets of samples, are missing. In the case of millisecond pulsar timing data, for instance, observations are quite irregularly spaced in time. Nevertheless, since some observations are very close together (one minute) and since the timing data sequence is very long (more than ten years), information on both short-term and long-term stability is available. Unfortunately, a direct variance analysis is not possible without interpolating missing data. Different interpolation algorithms (linear interpolation, cubic spline) are used

to calculate variances in order to verify that they neither lose information nor add erroneous information. A comparison of the results of the different algorithms is given. Finally, the multivariance method was adapted to the measurement sequence of the millisecond pulsar timing data: the responses of each variance of the system are calculated for each type of noise and drift, with the same missing samples as in the pulsar timing sequence. An estimation of precision, dynamics, and separability of this method is given.
Author (revised)

N94-30668*# Istituto Elettrotecnico Nazionale (Galileo Ferraris), Turin (Itlay).
AN ALGORITHM FOR THE ITALIAN ATOMIC TIME SCALE
F. Cordara, G. Vizio, P. Tavella, and V. Pettiti *In* NASA. Goddard Space Flight Center, The 25th Annual Precise Time and Time Interval (PTTI) Applications and Planning Meeting May 1994 p 389-400 (For primary document see N94-30639 08-70)
Avail: CASI HC A03/MF A06

During the past twenty years, the time scale at the IEN has been realized by a commercial cesium clock, selected from an ensemble of five, whose rate has been continuously steered towards UTC to maintain a long term agreement within 3 x 10(exp -13). A time scale algorithm, suitable for a small clock ensemble and capable of improving the medium and long term stability of the IEN time scale, has been recently designed taking care of reducing the effects of the seasonal variations and the sudden frequency anomalies of the single cesium clocks. The new time scale, TA(IEN), is obtained as a weighted average of the clock ensemble computed once a day from the time comparisons between the local reference UTC(IEN) and the single clocks. It is foreseen to include in the computation also ten cesium clocks maintained in other Italian laboratories to further improve its reliability and its long term stability. To implement this algorithm, a personal computer program in Quick Basic has been prepared and it has been tested at the IEN time and frequency laboratory. Results obtained using this algorithm on the real clocks data relative to a period of about two years are presented. Author (revised)

N94-30669*# Naval Observatory, Washington, DC.
A COMPARATIVE STUDY OF CLOCK RATE AND DRIFT ESTIMATION
Lee A. Breakiron *In* NASA. Goddard Space Flight Center, The 25th Annual Precise Time and Time Interval (PTTI) Applications and Planning Meeting May 1994 p 401-412 (For primary document see N94-30639 08-70)
Avail: CASI HC A03/MF A06

Five different methods of drift determination and four different methods of rate determination were compared using months of hourly phase and frequency data from a sample of cesium clocks and active hydrogen masers. Linear least squares on frequency is selected as the optimal method of determining both drift and rate, more on the basis of parameter parsimony and confidence measures than on random and systematic errors. Author

N94-30670*# NeoComm Systems, Inc., La Canada-Flintridge, CA.
PROVIDING HYDROGEN MASER TIMING STABILITY TO ORBITING VLBI RADIO TELESCOPE OBSERVATIONS BY POST-MEASUREMENT COMPENSATION OF LINKED FREQUENCY STANDARD IMPERFECTIONS **c36**
James C. Springett *In* NASA. Goddard Space Flight Center, The 25th Annual Precise Time and Time Interval (PTTI) Applications and Planning Meeting May 1994 p 413-424 (For primary document see N94-30639 08-70)
Avail: CASI HC A03/MF A06

Orbiting VLBI (OVLBI) astronomical observations are based upon measurements acquired simultaneously from ground-based and earth-orbiting radio telescopes. By the mid-1990s, two orbiting VLBI observatories, Russia's Radioastron and Japan's VSOP, will augment the worldwide VLBI network, providing baselines to earth radio telescopes as large as 80,000 km. The challenge for OVLBI is to effectuate space to ground radio telescope data cross-correlation (the observation) to a level of integrity currently achieved between ground radio telescopes. VLBI radio telescopes require ultrastable frequency and timing references in order that long term observations may be made without serious cross-correlation loss due to frequency source drift and phase noise. For this reason, such instruments make use of hydrogen maser frequency standards. Unfortunately, space-qualified hydrogen maser oscillators are currently not available for use on OVLBI satellites. Thus, the necessary long-term stability needed by the orbiting radio telescope may only be obtained by microwave uplinking a ground-based hydrogen maser derived frequency to the satellite. Although the idea of uplinking the frequency standard intrinsically seems simple, there are many 'contaminations' which degrade both the long and short term stability of the transmitted reference. Factors which corrupt frequency and timing accuracy include additive radio and electronic circuit thermal noise, slow or systematic phase migration due to changes of electronic circuit temporal operating conditions (especially temperature), ionosphere and troposphere induced scintillations, residual Doppler-incited components, and microwave signal multipath propagation. What is important, though, is to realize that ultimate stability does not have to be achieved in real-time. Instead, information needed to produce a high degree of coherence in the subsequent cross-correlation operation may be derived from a two-way coherent radio link, recorded and later introduced as compensations adjunct to the VLBI correlation process. Accordingly, this paper examines the technique for stable frequency/time transfer within the OVLBI system, together with a critique of the types of link degradation components which must be compensated, and the figures of merit known as coherence factors.
Author (revised)

N94-30671*# Beijing Inst. of Radio Metrology and Measurements (China).
PRECISION FREQUENCY SYNTHESIZING SOURCES WITH EXCELLENT TIME/FREQUENCY PERFORMANCES
Liren Zhou and Hai Lin *In* NASA. Goddard Space Flight Center, The 25th Annual Precise Time and Time Interval (PTTI) Applications and Planning Meeting May 1994 p 425-432 (For primary document see N94-30639 08-70)
Avail: CASI HC A02/MF A06

Precision frequency synthesizing sources are needed in the time / frequency measuring system, atomic frequency standards, telemetry, communication, and radar systems. This kind of frequency synthesizing source possesses high frequency accuracy and excellent long term and short term frequency stability. Several precision frequency synthesizing sources developed by Beijing Institute of Radio Metrology and Measurement (BIRMM) which have been successfully applied to the time / frequency measuring system, atomic frequency standards system, and radar system are described. In addition, the working principle, implementation approach, and the main technical specifications of the frequency synthesizing sources are also given. Author (revised)

N94-30672*# Johns Hopkins Univ., Columbia, MD. Applied Physics Lab.
TIME MAINTENANCE SYSTEM FOR THE BMDO MSX SPACECRAFT **c18**
Martin J. Hermes *In* NASA. Goddard Space Flight Center, The 25th Annual Precise Time and Time Interval (PTTI) Applications and Planning Meeting May 1994 p 433-444 (For primary document see N94-30639 08-70)
Avail: CASI HC A03/MF A06

The Johns Hopkins University Applied Physics Laboratory (APL) is responsible for designing and implementing a clock maintenance system for the Ballistic Missile Defense Organizations (BMDO) Midcourse Space Experiment (MSX) spacecraft. The MSX spacecraft has an on-board clock that will be used to control execution of time-dependent commands and to time tag all science and housekeeping data received from the spacecraft. MSX mission objectives have dictated that this spacecraft time, UTC(MSX), maintain a required accuracy with respect to UTC(USNO) of +/- 10 ms with a +/- 1 ms desired accuracy. APL's atomic time standards and the downlinked spacecraft time were used to develop a time maintenance system that will estimate the current MSX clock time offset during an APL pass and make estimates of the clock's drift and aging using the offset estimates from many passes. Using this information, the clock's accuracy will be maintained by uplinking periodic clock correction commands. The resulting time maintenance system is a combination of offset measurement, command/telemetry, and mission planning hardware and computing assets. All assets provide necessary inputs for deciding when corrections to the MSX spacecraft clock must be made to maintain its required accuracy without inhibiting other mission objectives. The MSX time maintenance system is described as a whole and the clock offset measurement subsystem, a unique combination of precision time maintenance and

measurement hardware controlled by a Macintosh computer, is detailed. Simulations show that the system estimates the MSX clock offset to less than +/- 33 microseconds. Author (revised)

N94-30673*# Beijing Inst. of Radio Metrology and Measurements (China).
MEASUREMENT OF THE FREQUENCY STABILITY OF RESPONDERS IN AIRCRAFT **c32**
Xiaofan Liu *In* NASA. Goddard Space Flight Center, The 25th Annual Precise Time and Time Interval (PTTI) Applications and Planning Meeting May 1994 p 445-456 (For primary document see N94-30639 08-70)
Avail: CASI HC A03/MF A06

Measurement on an aircraft orbit, such as a satellite launching orbit, is made by the responder in the aircraft along with several remote track stations on the ground. During the launching, the system is required to have precise time synchronization and frequency accuracy. At the same time, accurate measurement of aircraft velocity requires high frequency stability of the system. However, atomic frequency standards in the ground stations supply time and frequency reference standard with excellent long term and short term frequency stability for the above-mentioned goals. The stability of responder is also an important factor affecting the performance of the system and there are more requirements for the corresponding time/frequency measurements. In the system, the responders do not use continuous wave (CW) but narrow pulse modulated wave; consequently, the characterization theory of their stability is more complicated and the measurement technique is more difficult for pulsed wave than that for CW. A systematic characterization theory of the frequency stability for pulsed wave is demonstrated and the measuring methods are discussed. The measurement systems, which have been set up in Beijing Institute of Radio Metrology and Measurement (BIRMM) and can be used to test the frequency stability of pulse coherent responders in time domain and frequency domain with high sensitivity and accuracy, are described. Using these measurement systems, successful measurements for the responders were made with which the satellite launching orbits were precisely obtained and tracked. Author (revised)

N94-30674*# Johns Hopkins Univ., Columbia, MD. Applied Physics Lab.
GROUND CONTROL SYSTEM FOR THE MIDCOURSE SPACE EXPERIMENT UTC CLOCK
Richard Dragonette *In* NASA. Goddard Space Flight Center, The 25th Annual Precise Time and Time Interval (PTTI) Applications and Planning Meeting May 1994 p 457-462 (For primary document see N94-30639 08-70)
Avail: CASI HC A02/MF A06

One goal of the Midcourse Space Experiment (MSX) spacecraft Operations Planning Center is to maintain the onboard satellite UTC clock (UTC(MSX)) to within 1 millisecond of UTC(APL) (the program requirement is 10 msec). The UTC(MSX) clock employs as its time base an APL built 5 MHz quartz oscillator, which is expected to have frequency instabilities (aging rate + drift rate + frequency offset) that will cause the clock to drift approximately two to ten milliseconds per day. The UTC(MSX) clock can be advanced or retarded by the APL MSX satellite ground control center by integer multiples of 1 millisecond. The MSX Operations Planning Center is developing software which records the drift of UTC(MSX) relative to UTC(APL) and which schedules the time of day and magnitude of UTC(MSX) clock updates up to 48 hours in advance. Because of the manner in which MSX spacecraft activities are scheduled, MSX clock updates are planned 24 to 48 hours in advance, and stored in the satellite's computer controller for later execution. Data will be collected on the drift of UTC(MSX) relative to UTC(APL) over a three to five day period. Approximately six times per day, the time offset between UTC(MSX) and UTC(APL) will be measured by APL with a resolution of less than 100 microseconds. From this data a second order analytical model of the clock's drift will be derived. This model will be used to extrapolate the offset of the MSX clock in time from the present to 48 hours in the future. MSX clock updates will be placed on the spacecraft's daily schedule whenever the predicted clock offset exceeds 0.5 milliseconds. The paper includes a discussion of how the empirical model of the MSX clock is derived from satellite telemetry data, as well as the algorithm used to schedule MSX clock updates based on the model. Author (revised)

N94-30675*# ESE/SEKAI, Santa Fe Springs, CA.
TIME SYNCHRONIZED VIDEO SYSTEMS **c32**
Ron Burnett *In* NASA. Goddard Space Flight Center, The 25th Annual Precise Time and Time Interval (PTTI) Applications and Planning Meeting May 1994 p 463-466 (For primary document see N94-30639 08-70)
Avail: CASI HC A01/MF A06

The idea of synchronizing multiple video recordings to some type of 'range' time has been tried to varying degrees of success in the past. Combining this requirement with existing time code standards (SMPTE) and the new innovations in desktop multimedia however, have afforded an opportunity to increase the flexibility and usefulness of such efforts without adding costs over the traditional data recording and reduction systems. The concept described can use IRIG, GPS or a battery backed internal clock as the master time source. By converting that time source to Vertical Interval Time Code or Longitudinal Time Code, both in accordance with the SMPTE standards, the user will obtain a tape that contains machine/computer readable time code suitable for use with editing equipment that is available off-the-shelf. Accuracy on playback is then determined by the playback system chosen by the user. Accuracies of +/- 2 frames are common among inexpensive systems and complete frame accuracy is more a matter of the users' budget than the capability of the recording system. Author

N94-30676*# Cantonal Observatory, Neuchatel (Switzerland).
HYDROGEN MASER CLOCKS IN SPACE FOR SOLID-EARTH RESEARCH AND TIME-TRANSFER APPLICATIONS: EXPERIMENT OVERVIEW AND EVALUATION OF RUSSIAN MINIATURE SAPPHIRE LOADED CAVITY
G. Busca, L. G. Bernier, P. Silvestrin, S. Feltham, B. A. Gaygerov, and V. M. Tatarenkov *In* NASA. Goddard Space Flight Center, The 25th Annual Precise Time and Time Interval (PTTI) Applications and Planning Meeting May 1994 p 467-480 (For primary document see N94-30639 08-70)
Avail: CASI HC A03/MF A06

The Observatoire Cantonal de Neuchatel (ON) is developing for ESTEC a compact H-maser for space use based upon a miniature sapphire loaded microwave cavity, a technique pioneered at VNIIFTRI. Various contacts between West-European parties, headed by ESA, and the Russian parties, headed by ESA, led to the proposal for flying two H-masers on Meteor 3M, a Russian meteorology satellite in low polar orbit. The experiment will include two masers, one provided by ON and the other by VNIIFTRI. T/F transfer and precise positioning will be performed by both a microwave link, using PRARE equipment, and an optical link, using LASSO-like equipment. The main objectives of the experiment are precise orbit determination and point positioning for geodetic/geophysical research, ultra-accurate time comparison and dissemination as well as in-orbit demonstration of operation and performance of H-masers. Within the scope of a preliminary space H-maser development phase performed for ESTEC at ON in preparation to the joint experiment, a Russian miniature sapphire loaded microwave cavity, on loan from VNIIFTRI, was evaluated in a full-size EFOS hydrogen maser built by ON. The experimental evaluation confirmed the theoretical expectation that with a hydrogen storage volume of only 0.65 liter an atomic quality factor of 1.5 x 10(exp 9) can be obtained for a -105 dBm output power. This represents a theoretical Allan deviation of 1.7 x 10(exp -15) averaged on a 1000 s time interval. From a full-size design to a compact one, therefore, the sacrifice in performance due to the reduction of the storage volume is very small. Author

N94-30677*# Osborne (Allen) Associates, Westlake Village, CA.
IONOSPHERIC CORRECTIONS TO PRECISE TIME TRANSFER USING GPS **c04**
Robert W. Snow, Allen W. Osborne, III, John A. Klobuchar, and Patricia H. Doherty *In* NASA. Goddard Space Flight Center, The 25th Annual Precise Time and Time Interval (PTTI) Applications and Planning Meeting May 1994 p 495-504 (For primary document see N94-30639 08-70)
Avail: CASI HC A02/MF A06

The free electrons in the earth's ionosphere can retard the time of reception of GPS signals received at a ground station, compared to their time in free space, by many tens of nanoseconds, thus limiting the accuracy of time transfer by GPS. The amount of the ionospheric time delay is proportional to the total number of electrons encountered by the wave on its path from each GPS satellite to a receiver. This integrated number of electrons is called Total Electron Content, or TEC. Dual frequency GPS

receivers designed by Allen Osborne Associates, Inc. (AOA) directly measure both the ionospheric differential group delay and the differential carrier phase advance for the two GPS frequencies and derive from this the TEC between the receiver and each GPS satellite in track. The group delay information is mainly used to provide an absolute calibration to the relative differential carrier phase, which is an extremely precise measure of relative TEC. The AOA Mini-Rogue ICS-4Z and the AOA TurboRogue ICS-4000Z receivers normally operate using the GPS P code, when available, and switch to cross-correlation signal processing when the GPS satellites are in the Anti-Spoofing (A-S) mode and the P code is encrypted. An AOA ICS-Z receiver has been operated continuously for over a year at Hanscom AFB, MA to determine the statistics of the variability of the TEC parameter using signals from up to four different directions simultaneously. The 4-channel ICS-4Z and the 8-channel ICS-4000Z, have proven capabilities to make precise, well calibrated, measurements of the ionosphere in several directions simultaneously. In addition to providing ionospheric corrections for precise time transfer via satellite, this dual frequency design allows full code and automatic codeless operation of both the differential group delay and differential carrier phase for numerous ionospheric experiments being conducted. Statistical results of the data collected from the ICS-4Z during the initial year of ionospheric time delay in the northeastern U.S., and initial results with the ICS-4000Z, will be presented. Author

N94-30678*# Joint Inst. for Lab. Astrophysics, Boulder, CO.

THE NIST INTERNET TIME SERVICE

Judah Levine *In* NASA. Goddard Space Flight Center, The 25th Annual Precise Time and Time Interval (PTTI) Applications and Planning Meeting May 1994 p 505-514 Prepared in cooperation with National Inst. of Standards and Technology, and Colorado Univ. (For primary document see N94-30639 08-70)

(Grant NSF NCR-91-15055)

Avail: CASI HC A02/MF A06

We will describe the NIST Network Time Service which provides time and frequency information over the Internet. Our first time server is located in Boulder, Colorado, a second backup server is under construction there, and we plan to install a third server on the East Coast later this year. The servers are synchronized to UTC(NIST) with an uncertainty of about 0.8 ms RMS and they will respond to time requests from any client on the Internet in several different formats including the DAYTIME, TIME and NTP protocols. The DAYTIME and TIME protocols are the easiest to use and are suitable for providing time to PC's and other small computers. In addition to UTC(NIST), the DAYTIME message provides advance notice of leap seconds and of the transitions to and from Daylight Saving Time. The Daylight Saving Time notice is based on the US transition dates of the first Sunday in April and the last one in October. The NTP is a more complex protocol that is suitable for larger machines; it is normally run as a 'daemon' process in the background and can keep the time of the client to within a few milliseconds of UTC(NIST). We will describe the operating principles of various kinds of client software ranging from a simple program that queries the server once and sets the local clock to more complex 'daemon' processes (such as NTP) that continuously correct the time of the local clock based on periodic calibrations. Author

N94-30679*# All-Union Research Inst. for Physical and Radiotechnical Measurements, Mendeleevo (USSR). Inst. of Metrology for Time and Space.

RUSSIAN NATIONAL TIME SCALE LONG-TERM STABILITY

A. P. Alshina, B. A. Gaigerov, N. B. Koshelyaevsky, and S. B. Pushkin *In* NASA. Goddard Space Flight Center, The 25th Annual Precise Time and Time Interval (PTTI) Applications and Planning Meeting May 1994 p 523-532 (For primary document see N94-30639 08-70)

Avail: CASI HC A02/MF A06

The Institute of Metrology for Time and Space NPO 'VNIIFTRI' generates the National Time Scale (NTS) of Russia -- one of the most stable time scales in the world. Its striking feature is that it is based on a free ensemble of H-masers only. During last two years the estimations of NTS longterm stability based only on H-maser intercomparison data gives a flicker floor of about (2 to 3) x 10(exp -15) for averaging times from 1 day to 1 month. Perhaps the most significant feature for a time laboratory is an extremely low possible frequency drift -- it is too difficult to estimate it reliably. The other estimations, free from possible inside the ensemble correlation phenomena, are available based on the time comparison of NTS relative to the stable enough time scale of outer laboratories. The data on NTS comparison relative to the time scale of secondary time and frequency standards at Golitzino and Irkutsk in Russia and relative to NIST, PTB and USNO using GLONASS and GPS time transfer links gives stability estimations which are close to that based on H-maser intercomparisons. Author (revised)

N94-30680*# Russian Inst. of Radionavigation and Time, Saint Petersburg.

USING GLONASS SIGNAL FOR CLOCK SYNCHRONIZATION

Yuri G. Gouzhva, Arvid G. Gevorkyan, Pyotr P. Bogdanov, and Vitaly V. Ovchinnikov *In* NASA. Goddard Space Flight Center, The 25th Annual Precise Time and Time Interval (PTTI) Applications and Planning Meeting May 1994 p 533-540 (For primary document see N94-30639 08-70)

Avail: CASI HC A02/MF A06

Although in accuracy parameters GLONASS is correlated with GPS, using GLONASS signals for high-precision clock synchronization was, up to the recent time, of limited utility due to the lack of specialized time receivers. In order to improve this situation, in late 1992 the Russian Institute of Radionavigation and Time (RMT) began to develop a GLONASS time receiver using as a basis the airborne ASN-16 receiver. This paper presents results of estimating user clock synchronization accuracy via GLONASS signals using ASN-16 receiver in the direct synchronization and common-view modes. Author

N94-30681*# Air Force Office of Scientific Research, Bolling AFB, Washington, DC.

A LOOK INTO THE CRYSTAL BALL: THE NEXT 25 YEARS

Helmut Hellwig *In* NASA. Goddard Space Flight Center, The 25th Annual Precise Time and Time Interval (PTTI) Applications and Planning Meeting May 1994 p 541-548 (For primary document see N94-30639 08-70)

Avail: CASI HC A02/MF A06

The PTTI Planning Meeting was born at about the same time as the atomic definition of the unit of time, the second. This use of the cesium resonance was made possible by advances in quantum electronics during the preceding decade which resulted in commercial availability of cesium, rubidium, and hydrogen clocks and frequency standards. Twenty-five years later these types of clocks still are the backbone of time and frequency applications; together with a variety of crystal oscillators, transmitters, and receivers, as well as signal distribution, conditioning and switching systems, atomic clocks are an essential part of the infrastructure of modern navigation and communication technology. The next 25 years undoubtedly will see a pervasive expansion of PTTI into the infrastructure that supports and leverages industrial, social, environmental, defense, and even individual human activities. Speculation as to what capabilities, services, and personal conveniences may become available will be limited by two factors: the degree to which existing device concepts can be made more affordable and reliable, and the ability to miniaturize for purposes of compatibility with electronic integration. With regard to the latter, history teaches us that the required technological breakthrough is unlikely to originate in existing technology; thus, we may expect a paradigm shift in PTTI device concepts not unlike the shift in the 1960s from vacuum tubes to semiconductors. Author

N94-30682*# Jet Propulsion Lab., California Inst. of Tech., Pasadena.

FREQUENCY STANDARDS FROM GOVERNMENT LABORATORIES OVER THE NEXT 25 YEARS

L. Maleki *In* NASA. Goddard Space Flight Center, The 25th Annual Precise Time and Time Interval (PTTI) Applications and Planning Meeting May 1994 p 549-560 (For primary document see N94-30639 08-70)

Avail: CASI HC A03/MF A06

Based on a number of considerations including projected needs, current status, future trends, and status of key technologies, an attempt is made to project the future of government supported frequency standards development in the next 25 years. Author

N94-30683*# Hewlett-Packard Labs., Palo Alto, CA.

FREQUENCY STANDARDS FROM INDUSTRY OVER THE NEXT 25 YEARS

Leonard S. Cutler *In* NASA. Goddard Space Flight Center, The 25th Annual Precise Time and Time Interval (PTTI) Applications and Planning

Meeting May 1994 p 561-572 (For primary document see N94-30639 08-70)
Avail: CASI HC A03/MF A06

Present and possible future performance for many of the existing and new commercial frequency standards is presented here. Recent progress in the gas cell atomic standards with regards to size and cost is significant and considerable improvement is expected. Cesium beam standards will benefit in stability and accuracy from optical pumping. Cooled hydrogen masers will offer extremely good stability. Advances in trapped ion and cesium fountain technologies make them good high performance candidates for the future. The quartz oscillator field is more mature and consequently performance improvements for the future are going to be less spectacular. Oscillators stabilized to GPS will have many applications. Recent performance of cooled microwave dielectric resonator oscillators is very good and they offer the promise of serving as flywheel oscillators for advanced performance atomic standards. Author

N94-30684*# National Inst. of Standards and Technology, Boulder, CO.
THE FUTURE OF TIME AND FREQUENCY DISSEMINATION
Judah Levine *In* NASA. Goddard Space Flight Center, The 25th Annual Precise Time and Time Interval (PTTI) Applications and Planning Meeting May 1994 p 573-578 (For primary document see N94-30639 08-70)
Avail: CASI HC A02/MF A06

I will try to extrapolate the changes in the dissemination of time and frequency information that have taken place during the last 25 years to predict the future developments both in the methods of disseminating time and frequency and in the kinds of customers we will be asked to serve. Two important developments are likely to play pivotal roles in driving the evolution of dissemination. The first is the commercial availability of very high quality clocks -- devices whose performance may eventually rival that of the current generation of primary frequency standards. The widespread use of these devices may blur the traditional distinction between client and server, and may replace it with a more symmetrical interchange of data among peers. The second is the increasing demand for digital time and frequency information driven by the increasing sophistication of everything from traffic lights to electric power meters. The needs of these individual users may not tax the state of the art of primary frequency standards in principle, but their large numbers and wide geographical distribution present a technological challenge that is difficult to meet at a reasonable price using existing methods. Some of these problems may be solved (or at least addressed) using developments in communications and consumer electronics such as the increasing use of fiber-optic telephone circuits and the increasing bandwidth and sophistication of the cable network used to transmit television pictures. To be useful, these advances in hardware must stimulate parallel advances in software algorithms and methods. These advances are more difficult to predict with great confidence, but the developments of the last few years will be examined to provide some indications of the future. Author

N94-30780 National Physical Lab., Teddington (England). Electrical Science Div.
GUIDANCE NOTES FOR USE WITH NPL LOW PERMEABILITY REFERENCE MATERIALS
C. I. Ager and A. E. Drake Aug. 1993 12 p
(ISSN 0143-7305)
(NPL-DES-121; ETN-94-95844) Copyright Avail: Issuing Activity
(National Physical Lab. Teddington, Middlesex TW11 0LW, England)

Guidelines prepared to assist users of low permeability measuring equipment who wish to calibrate their instruments using certain reference materials are presented. There are three main types of commercial instruments which could be calibrated using the considered reference materials. There is the magnetic balance type, which compares the attraction of a magnet to a series of reference inserts and its attraction to the specimen under test. This instrument indicates the range of permeability in which the test sample lies. The two other types of instruments, which give a continuous scale reading, utilize a permanent magnet and either strain gauge or fluxgate elements to measure the effect of test materials in contact with their probes. The last two types usually have a number of ranges and their linearity over these ranges is not good. The instruments, therefore, need to be calibrated using a material of permeability close in value to that under test. The magnetic field strength at the tip of the probe of each type of instrument was found to be significantly different. The magnetic field strength at the tip of a particular probe can be conveniently measured using a Hall effect probe and Gaussmeter. ESA

N94-30781 National Physical Lab., Teddington (England). Electrical Science Div.
RF AND MICROWAVE DIELECTRIC MEASUREMENTS UPON LAYERED MATERIALS USING REFLECTOMETRIC COAXIAL SENSOR
A. P. Gregory, R. N. Clarke, T. E. Hodgetts, and G. T. Symm Mar. 1993 87 p
(ISSN 0143-7305)
(NPL-DES-125; ETN-94-95845) Copyright Avail: Issuing Activity
(National Physical Lab., Teddington, Middlesex TW11 0LW, England)

Progress on the application of coaxial reflectometric sensors to the measurement of Radio Frequency (RF) and microwave dielectric properties of laminated materials is described. Measurements were performed in the range 300 MHz to 3 GHz, but the findings can be applied over the whole of the RF and microwave range. As a result of the work described, both high and low loss materials can be measured by coaxial sensors. Suitable specimens of one, two, and three dielectric layers can be characterized. A cell attachment was constructed for a 14 mm diameter sensor which allows circular specimens to be measured more accurately. The cell also allows liquid immersion measurements to be performed, which affords greatly improved uncertainties. Three independent computer programs were written to analyze multilayer laminar specimens. The programs were intercompared and were shown to agree numerically to well within expected measurement uncertainties. Measurements upon liquid and solid materials of known permittivity were compared with the program predictions and shown to agree sufficiently well to allow the system to be used for traceable measurements within the national measurement system. ESA

N94-30783 National Physical Lab., Teddington (England). Electrical Science Div.
REPORT ON THE DEVELOPMENT OF LOW MAGNETIC PERMEABILITY REFERENCE MATERIALS
A. E. Drake and C. I. Ager Aug. 1993 17 p
(ISSN 0143-7305)
(NPL-DES-119; ETN-94-95843) Copyright Avail: Issuing Activity
(National Physical Lab., Teddington, Middlesex TW11 0LW, England)

A study to select suitable reference materials for the calibration of magnetic permeability measuring instruments over their normal working range of relative magnetic permeability of 1.0025 to 1.4 was performed. With the exception of some of the rare Earth elements, the permeability of the elements is below the lower limit of this range. It was necessary, therefore, to investigate metallic alloys and composites. As a result, three magnetic alloys were selected on grounds of their stability and uniformity of composition: 1.0025 to 1.007 stainless steel type American Iron and Steel Institute (AISI) 316; 1.03 to 1.07 high tensile brass; and 1.2 to 1.4 aluminum nickel bronze. ESA

N94-30841# California Univ., Berkeley. Lawrence Berkeley Lab.
STUDIES OF INTERFACES AND VAPORS WITH OPTICAL SECOND HARMONIC GENERATION Ph.D. Thesis
C. S. Mullin (California Univ., Berkeley.) Dec. 1993 131 p
(Contract DE-AC03-76SF-00098)
(DE94-006295; LBL-35028) Avail: CASI HC A07/MF A02

Optical Second Harmonic Generation (SHG) has been applied to the study of soap-like molecules adsorbed to the water-air interface. By calibrating the signal from a soluble monolayer with that of an insoluble homolog, absolute measurements of the surface density could be obtained and related to the bulk concentration and surface tension. We could then demonstrate that the soluble surfactant forms a single monolayer at the interface. Furthermore, it deviates significantly from the ideal case in that its activity coefficients are far from 1, yet those coefficients remain constant over a broad range of surface pressures. We present evidence of a first-order phase transition taking place during the adsorption of this soluble monolayer. We consider the effects of the non-ideal behavior and the phase transition on the microscopic model of adsorption, and formulate an alternative to the Langmuir picture of adsorption which is just as simple, yet it can more easily allow for non-ideal behavior. The second half of this thesis considers the problem of SHG in bulk metal vapors. The symmetry of the vapor forbids SHG, yet it has been observed. We consider several models whereby

the symmetry of the vapor is broken by the presence of the laser and compare their predictions to new observations we have made using a few-picosecond laser pulse. The two-lobed output beam profile shows that it is the vapor-plus-beam combination whose symmetry is important. The dependence on vapor pressure demonstrates the coherent nature of the radiation, while the dependence on buffer gas pressure hints at a change of the symmetry in time. The time-dependence is measured directly with a preliminary pump-probe measurement. The magnitude and intensity dependence of the signal are also measured. All but one of the models are eliminated by this comparison. DOE

N94-30873# Argonne National Lab., IL.
NON-MARKOVIAN QUANTUM BROWNIAN MOTION OF A HARMONIC OSCILLATOR
J. Tang 1994 15 p
(Contract W-31-109-eng-38)
(DE94-005922; ANL/CHM/PP-79434) Avail: CASI HC A03/MF A01

We apply the density-matrix method to the study of the quantum Brownian motion of a harmonic oscillator coupled to a heat bath. This is a system investigated previously by Caldeira and Leggett using a different method. Unlike the earlier work, in our derivation of the master equation the non-Markovian terms are maintained. Although the same model of interaction is used, discrepancy is found between their results and our equation in the Markovian limit. We also point out that the particular interaction model used by both works cannot lead to the phenomenological generalized Langevin theory of Kubo. DOE

71 ACOUSTICS

Includes sound generation, transmission and attenuation.
For noise pollution see *45 Environmental Pollution.*

N94-28636# Acoustical Society of America, New York, NY.
MINUTES. ACCREDITED STANDARDS COMMITTEE ON NOISE, S12. US TAG FOR ISO/TC 43/SC1 NOISE AND ISO/TC 94/SC12 HEARING PROTECTION
7 Oct. 1993 72 p Meeting held in Denver, CO, 7 Oct. 1993
(AD-A275622) Avail: CASI HC A04/MF A01

Standards approved by ANSI in 1992/1993 and published include the following: (1) quantities and procedures for description and measurement of outdoor environmental sound; (2) engineering methods for the determination of sound power levels of noise sources using sound intensity; (3) methods for the field measurement of the sound output of audible public warning devices installed at fixed locations outdoors; (4) acoustics-portable electric power tools, stationary and fixed electric power tools, and gardening appliances and measurement of sound emitted; and (5) guidelines for the specification of noise of new machinery. DTIC

N94-28689# Acoustical Society of America, New York, NY.
MINUTES. ACCREDITED STANDARDS COMMITTEE ON ACOUSTICS, S1. US TAG FOR ISO/TC 43 ACOUSTICS AND IEC/TC 29 ELECTROACOUSTICS
7 Oct. 1993 81 p Meeting held in Denver, CO, 7 Oct. 1993
(Contract N00014-93-I-G019)
(AD-A275702) Avail: CASI HC A05/MF A01

The following items were discussed: approval of the minutes of the Ottawa, Canada meeting held 20 May 1993; organization; standards approved by ANSI in 1992/1993 and published (or being published) by ASA; organizational matters and reports on working groups, including reports on letter ballots and international matters; work items without working groups; international matters; review of standards more than five years in existence; new international standards available; procedural ballots; other business; new business; future meetings; and adjournment. CASI

N94-28904# Scientific Research Associates, Inc., Glastonbury, CT.
FLUID DYNAMIC NOISE IN A CENTRIFUGAL PUMP Final Report
D. G. Tse and J. H. Whitelaw Aug. 1993 110 p
(Contract N00014-91-C-0172)
(AD-A275264; R93-9245-F) Avail: CASI HC A06/MF A02

Pressure distributions and frequency spectra have been obtained in a centrifugal pump having flow rates between the design point and near shut-down. The pump was comprised of a radial flow impeller with four backswept blades and a single volute. Measurements were obtained at the design flow rate and at off-design conditions to advance understanding of noise generation, to quantify the contribution of tonal, narrowband and broadband components to the overall noise and to develop strategies for suppressing fluid dynamic noise by flow control and active control. Fluid dynamic noise was generated by the unsteady conditions encountered by the impeller blade. Unsteady conditions originated from non-uniformities at the inlet and the impeller outlet at design and off-design conditions. Inlet flow non-uniformity was induced by separation regions. Flow separations are inherent in turbomachinery because of growth of the boundary layer and the disturbance effect of the rotating impeller. Flow non-uniformity at the impeller outlet stemmed from inlet flow non-uniformities in the inlet, from propagation of pressure waves in a vaneless diffuser, and from scroll effects. DTIC

N94-29003# Naval Postgraduate School, Monterey, CA.
QUADRUPLET EXPANSION OF THE ACOUSTIC PRESSURE FIELD IN A WEDGE SHAPED OCEAN M.S. Thesis
Michael D. Joyce Sep. 1993 40 p
(AD-A275121) Avail: CASI HC A03/MF A01

In a wedge shaped ocean, the method of images is used to develop an analytical approximation of the acoustic pressure field. Contemporary work develops acoustic doublets from a combination of the source and surface reflection image using simple dipole theory. The method of images is then used to sum the dipole images. This thesis matches dipole pairs to achieve a quadruplet expansion. A computer program using the derived quadruplet equation is then created to verify the results by comparing them with the URTEXT program. DTIC

N94-29117# Naval Postgraduate School, Monterey, CA.
A COMPARISON OF TWO COMPUTER MODELS OF SOUND PROPAGATION FOR A WEDGE SHAPED OCEAN OVER A PENETRABLE BOTTOM M.S. Thesis
Charles C. Meisenheimer Sep. 1993 67 p
(AD-A275031) Avail: CASI HC A04/MF A01

The problem of determining the acoustic pressure in a wedge shaped wave guide is examined. Two computer models, one using the method of images, the other using coupled normal modes, are compared. This comparison is over the benchmark wedge of the Acoustic Society of America. Three scenarios were examined: isovelocity water over a pressure release bottom; isovelocity water over a penetrable, lossless bottom; and isovelocity water over a penetrable, lossy bottom. In all cases good agreement was seen between both models, with some differences due to a rigid subbottom in the normal mode model. The strengths and weaknesses of each model are examined. An analytic solution in normal modes of the waveguide with a pressure release surface, rigid bottom and a discontinuous speed of sound profile are presented. A brief history of research into the wedge problem is included in the introduction. DTIC

N94-29175# Swedish Inst. for Materials Testing, Boras.
DETERMINATION OF SOUND POWER LEVELS OF AIR TERMINAL UNITS ACCORDING TO ISO 5135-NORDIC INTER-LABORATORY TESTS, NORDTEST PROJECT NO. 968-91 Technical Report No. 214
G. Andresen and H. G. Jonasson 1993 46 p
(PB94-137411; SP-RAPP-1993-43) Avail: CASI HC A03/MF A01

An inter-laboratory test program to determine the sound power level of air terminal units was carried out. The measurements were performed in accordance with ISO 5135. Four laboratories participated, each carrying out measurements on six test objects: two non-adjustable air terminal units, two adjustable air terminal units and two dampers. The diameters of the chosen units were 125 and 250 mm. The statistical basis for firm conclusions has not been satisfactory. One of the participating laboratories was unable to measure on such low flow rates as those used for the test objects chosen for this investigation and two of the test objects were damaged during the transportation between the participating laboratories. NTIS

N94-29186 Helsinki Univ. of Technology, Espoo (Finland). Low Temperature Lab.
ACOUSTIC AND OPTICAL INVESTIGATIONS OF SUPERFLUID (3)HE

A. Manninen 1993 61 p See also PB93-224889 Limited Reproducibility: More than 20% of this document may be affected by microfiche quality
(PB94-135415) Avail: CASI HC A04

The thesis is an experimental survey of properties of rotating and stationary superfluid (3)He. Two techniques, acoustics and optics, were used. Ultrasound, together with NMR, has provided most of the present experimental knowledge about the superfluid phases of (3)He. The author applied acoustics for the first time to study rotating (3)He. The main result was the discovery of a new vortex in (3)He-A when the magnetic field is low. New phenomena were observed in stationary (3)He as well. Most importantly, one of the collective modes, the real squashing (rsq) mode, of (3)He-B could be excited by means of two-phonon absorption. Superfluid (3)He was studied optically for the first time. No one has previously seen (3)He in the superfluid state. The principal achievement was developing techniques which facilitate optical experiments at temperatures below 1 mK, required to study superfluid (3)He. Optical fibers were used to transmit light between room temperature and the cold parts of the cryostat. Before these investigations, photography had not been done below 10 mK. The usefulness of optics as a probe of the superfluid phases of (3)He was demonstrated by studying the macroscopic shape of the free surface of rotating (3)He-B. The classical parabolic meniscus was observed, which is indicative of the equilibrium density of vortices. The supporting proofs, along with the thesis, is also available. NTIS

N94-29206 Naval Research Lab., Bay Saint Louis, MS.
CONSIDERATIONS IN THE MODELLING OF SEAFLOOR ACOUSTIC BACKSCATTER Final Report
Rebecca M. Gott, Andrew B. Martinez, and Brian S. Bourgeois 1993 8 p Limited Reproducibility: More than 20% of this document may be affected by microfiche quality
(AD-A275404; NRL/PP/7441-92-0002) Avail: CASI HC A02

The modelling of acoustic backscatter has long been of interest to the U.S. Navy because the application of these models offers the possibility of remote characterization of the seafloor. Basic scattering mechanisms and empirical studies of seafloor backscatter are reviewed in this paper. The Rayleigh criterion offers a means of classifying a rough surface. The Rayleigh parameter, a measure of vertical roughness, and the Rayleigh reflection coefficient, a measure of reflection loss between boundaries, are reviewed. The task of modelling the scattering from a surface with two scales of roughness is approached using a combination of two scattering approximations, one valid for small-scale roughness and one valid for large-scale roughness. The method of small perturbation is used for small-scale roughness, and the method of tangent plane, or Kirchoff approximation, is used for large-scale roughness. DTIC

N94-29314# Army Cold Regions Research and Engineering Lab., Hanover, NH.
ATTENUATION OF OUTDOOR SOUND PROPAGATION LEVELS BY A SNOW COVER
Donald G. Albert Nov. 1993 111 p
(DA Proj. 4A7-62730-AT-24; DA Proj. 4A7-62730-AT-42)
(AD-A275387; CRREL-93-20) Avail: CASI HC A06/MF A02

The absorption of sound energy by the ground has been studied extensively because of its importance in understanding noise propagation through the atmosphere. This report investigates the attenuative effect of snow on sound propagation, and provides, quantitative measurements and an accurate model for predicting these effects. Summer and winter experiments were conducted at a site in northern Vermont to investigate the effect of a snow cover on low energy sound propagation in the 5- to 500-Hz frequency band for propagation distances between 1 and 274 m. Pistol shots were used as the source of the acoustic waves, with geophones and microphones serving as the receivers. A comparison of the summer and winter recordings revealed a number of effects caused by the introduction of a 0.25-m-thick snow cover. The peak amplitude of the air wave was more strongly attenuated in the winter, with a decay rate proportional to r(exp 1.6) versus r(exp 1.2) in the summer, corresponding to an order of magnitude difference in the signal levels after 100 m of propagation. The waveforms were also markedly changed, with broadened pulses and greatly enhanced low frequencies appearing in the winter recordings. The pulse broadening and peak amplitude decay rates of the acoustic waveforms were successfully predicted theoretically using a layered, rigid, porous model of the snow, with an assumed surface effective flow resistivity of 20 kN s/m to the 4th. Calculations of ground motion induced by the atmospheric sound waves were made using a viscoelastic model of the ground and the wavenumber integration technique. DTIC

N94-29362*# National Aeronautics and Space Administration. Ames Research Center, Moffett Field, CA.
BOUNDARY LAYER CONTROL DEVICE FOR DUCT SILENCERS Patent Application
Fredric H. Schmitz, inventor (to NASA) and Paul T. Soderman, inventor (to NASA) 15 Nov. 1993 12 p
(NASA-Case-ARC-12030-1; NAS 1.71:ARC-12030-1;
US-Patent-Appl-SN-151690) Avail: CASI HC A03/MF A01

A boundary layer control device includes a porous cover plate, an acoustic absorber disposed under the porous cover plate, and a porous flow resistive membrane interposed between the porous cover plate and the acoustic absorber. The porous flow resistive membrane has a flow resistance low enough to permit sound to enter the acoustic absorber and high enough to damp unsteady flow oscillations. NASA

N94-29363*# National Aeronautics and Space Administration. Ames Research Center, Moffett Field, CA.
IMPROVED IN-FLOW ACOUSTIC SENSOR Patent Application
Christopher S. Allen, inventor (to NASA) (Sterling Software, Inc., Moffett Field, CA.) 10 Nov. 1993 22 p
(Contract NAS2-13210)
(NASA-Case-ARC-12001-1; NAS 1.71:ARC-12001-1;
US-Patent-Appl-SN-149896) Avail: CASI HC A03/MF A01

An acoustic sensor for measuring acoustic waves contained in fluid flowing over the sensor is described. The acoustic sensor reduces any unwanted self-noise associated with the flowing fluid by providing a nose cone having proper aerodynamic properties and by positioning the diaphragm of a microphone of the sensor at a location where any unwanted noise is at a relatively low level. The nose cone has a rounded, blunt or even sharp tip, neither of which creates any major disturbances in the flowing fluid which it intercepts. NASA

N94-29382*# National Aeronautics and Space Administration. Langley Research Center, Hampton, VA.
A NON-LOCAL COMPUTATIONAL BOUNDARY CONDITION FOR DUCT ACOUSTICS
William E. Zorumski, Willie R. Watson, and Steve L. Hodge Mar. 1994 35 p
(RTOP 505-59-52)
(NASA-TM-109091; NAS 1.15:109091) Avail: CASI HC A03/MF A01

A non-local boundary condition is formulated for acoustic waves in ducts without flow. The ducts are two dimensional with constant area, but with variable impedance wall lining. Extension of the formulation to three dimensional and variable area ducts is straightforward in principle, but requires significantly more computation. The boundary condition simulates a nonreflecting wave field in an infinite duct. It is implemented by a constant matrix operator which is applied at the boundary of the computational domain. An efficient computational solution scheme is developed which allows calculations for high frequencies and long duct lengths. This computational solution utilizes the boundary condition to limit the computational space while preserving the radiation boundary condition. The boundary condition is tested for several sources. It is demonstrated that the boundary condition can be applied close to the sound sources, rendering the computational domain small. Computational solutions with the new non-local boundary condition are shown to be consistent with the known solutions for nonreflecting wavefields in an infinite uniform duct.
Author (revised)

N94-29388# Pennsylvania State Univ., University Park.
A REVIEW OF SIGNAL DETECTION USING THE BISPECTRUM WITH APPLICATIONS IN UNDERWATER ACOUSTICS
G. L. Morella Jan. 1994 93 p
(Contract N00039-92-C-0100)
(AD-A275227; PSU/ARL-TR-94-03) Avail: CASI HC A05/MF A01

This paper reviews attempts at signal detection in Gaussian noise using a higher order statistical (Higher Order Spectra (HOS) or polyspectra) technique. Examples comparing power spectral and bispectral analysis include the following topics: the identification of signals generated by a

system of coupled nonlinear differential equations, radar backscatter processing and target identification, and a statistical treatment of the detection of narrowband harmonic components resulting in a Receiver Operating Characteristic (ROC) curve. The critical signal and noise probability density function (pdf) assumptions from polyspectra theory which must be met for more effective noise suppression relative to classical second order power spectral methods are: (1) discussed in relation to detection results as reported in the literature review; and (2) illustrated via examples using both direct and indirect nonparametric Discrete Fourier Transform (DFT) bispectrums employing Fast Fourier Transforms (FFT) for both simulated and real data. The signal set consisted of pure tones and a hop code used in active sonar. DTIC

N94-29407*# Old Dominion Univ., Norfolk, VA.
REVIEW OF SONIC FATIGUE TECHNOLOGY
B. L. Clarkson (University Coll. of Swansea, Wales.) Apr. 1994 75 p
(Grant NAG1-363; RTOP 763-23-45-70)
(NASA-CR-4587; NAS 1.26:4587) Avail: CASI HC A04/MF A01

From the early-1960s until the mid-1980s, there was very little theoretical development for sonic fatigue prediction. Design nomographs based on simple theoretical models and results of specially designed tests were developed for most common aircraft structures. The use of advanced composites in the 1980s, however, generated an increased interest in development of more sophisticated theoretical models because of the possibilities for a much wider range of structural designs. The purpose of this report is to review sonic fatigue technology and, in particular, to assess recent developments. It also suggests a plan for a coordinated program of theoretical and experimental work to meet the anticipated needs of future aerospace vehicles. Author

N94-29461*# National Aeronautics and Space Administration. Langley Research Center, Hampton, VA.
FREE VIBRATION OF THERMALLY LOADED PANELS INCLUDING INITIAL IMPERFECTIONS AND POST-BUCKLING EFFECTS
K. D. Murphy (Duke Univ., Durham, NC.), L. N. Virgin (Duke Univ., Durham, NC.), and S. A. Rizzi Apr. 1994 13 p Proposed for presentation at the Fifth International Conference on Recent Advances in Structural Dynamics, Southampton, England, 18-21 Jul. 1994
(RTOP 505-63-50-10)
(NASA-TM-109097; NAS 1.15:109097) Avail: CASI HC A03/MF A01

A combined theoretical and experimental approach is developed to consider the small amplitude free vibration characteristics of fully clamped panels under the influence of uniform heating. Included in this study are the effects of higher modes, in-plane boundary elasticity, initial imperfections, and post-buckling. Comparisons between theory and experiment reveal excellent agreement. Author (revised)

N94-29464*# National Aeronautics and Space Administration. Langley Research Center, Hampton, VA.
SUBJECTIVE RESPONSE TO SONIC BOOMS HAVING DIFFERENT SHAPES, RISE TIMES, AND DURATIONS
David A. McCurdy Mar. 1994 44 p
(RTOP 537-03-21-03)
(NASA-TM-109090; NAS 1.15:109090) Avail: CASI HC A03/MF A01

Two laboratory experiments were conducted to quantify the subjective response of people to simulated outdoor sonic booms having different pressure signatures. The specific objectives of the experiments were to compare subjective response to sonic booms when described in terms of 'loudness' and 'annoyance'; to determine the ability of various noise metrics to predict subjective response to sonic booms; to determine the effects on subjective response of rise time, duration, and level; and to compare the subjective response to 'N-wave' sonic boom signatures with the subjective response to 'minimized' sonic boom signatures. The experiments were conducted in a computer-controlled, man-rated sonic boom simulator capable of reproducing user-specified pressure signatures for a wide range of sonic boom parameters. One hundred and fifty sonic booms representing different combinations of two wave shapes, four rise times, seven durations, and three peak overpressures were presented to 36 test subjects in each experiment. The test subjects in the first experiment made judgments of 'loudness' while the test subjects in the second experiment judged 'annoyance.' Subjective response to sonic booms was the same whether expressed in terms of loudness or in terms of annoyance. Analyses of several different noise metrics indicated that A-weighted sound exposure level and Perceived Level were the best predictors of subjective response. Further analyses indicated that, of these two noise metrics, only Perceived Level completely accounted for the effects of wave shape, rise time, and peak overpressure. Neither metric fully accounted for the effect of duration. However, the magnitude of the duration effect was small over the very wide range of durations considered. Author

N94-29597# National Inst. for Resources and Environment, Ibaraki (Japan). System Safety Div.
REPORT OF NATIONAL INSTITUTE FOR RESOURCES AND ENVIRONMENT. NO. 8: RESEARCH ON BLASTING SOUND RELATED TO IT'S MEASUREMENT, PROPAGATION PREDICTION, CONTROL AND EVALUATION [SHIGEN KANKYO GIJUTSU SOGO KENKYUSHO HOKOKU SAI 8 GO: HAPPAON NO KEISOKU OYOBI DENPAN YOSOKU SEIGYO HYOKA NI KANSURU KENKYU]
Takehiro Isei, Sunao Kunimatsu, Hiroyuki Imaizumi, Makoto Tanaka, Michiaki Kinoshita, Yuji Ogata, Masazumi Shiota, Hidenobu Uchida, Hiroyuki Obara, and Yoshio Nakayama et al 28 Jun. 1993 144 p In JAPANESE Prepared in cooperation with Tobishima Corp., Tokyo, Japan and Japan Machinery and Metals Inspection Inst., Tokyo, Japan Original contains color illustrations
(ISSN 0916-9989)
(JTN-94-80605) Avail: CASI HC A07/MF A02

Measuring methods, propagation prediction, evaluation and control method of blasting sound are investigated from both theoretical and experimental aspects. Special features of blasting sound are compared with the properties of audible noise and low frequency sound. Problems on the measuring method and the frequency analysis of blasting sound are discussed. Relation between the properties of conventional sound level meter and its output signals are also investigated in relation to the measurement of blasting sound. Limitation on the time resolution and frequency resolution of digital filter and Fourier transform technique is also indicated. Analyzed results by wavelet transform show better time and frequency resolution and better understanding than Wigner-Ville analysis from the comparison of those results. Two methods to predict the time-sound pressures at a receiver are investigated. A control method of blasting sound is discussed theoretically. Possibilities of control of the sound pressure level and the frequency component at a receiver are discussed. Discussion on the evaluation of blasting sound is conducted from two aspects of human perception and response of building fittings. In case of blasting noise, quite high correlation is found between the sound exposure level (SLOW) and the pressure level measured by the 'SLOW' time weighting. Author (NASDA)

N94-29856*# National Aeronautics and Space Administration. Langley Research Center, Hampton, VA.
DYNAMIC FRACTURE MECHANICS ANALYSIS FOR AN EDGE DELAMINATION CRACK
Stephen A. Rizzi and James F. Doyle Apr. 1994 13 p Proposed for presentation at the Fifth International Conference on Recent Advances in Structural Dynamics, Southampton, England, 18-21 Jul. 1994
(RTOP 505-63-50-10)
(NASA-TM-109106; NAS 1.15:109106) Avail: CASI HC A03/MF A01

A global/local analysis is applied to the problem of a panel with an edge delamination crack subject to an impulse loading to ascertain the dynamic J integral. The approach uses the spectral element method to obtain the global dynamic response and local resultants to obtain the J integral. The variation of J integral along the crack front is shown. The crack behavior is mixed mode (Mode 2 and Mode 3), but is dominated by the Mode 2 behavior. Author

N94-29988 Washington State Univ., Pullman.
INTERACTION OF SOUND WITH SOUND BY NOVEL MECHANISMS: ULTRASONIC FOUR-WAVE MIXING MEDIATED BY A SUSPENSION AND ULTRASONIC THREE-WAVE MIXING AT A FREE SURFACE Ph.D. Thesis
Harry Jay Simpson 1992 317 p
Avail: Univ. Microfilms Order No. DA9309082

Two mechanisms of sound interacting with sound are experimentally and theoretically investigated. Ultrasonic four-wave mixing in a dilute particle suspension, analogous to optical four-wave mixing in photorefractive

materials, involves the interaction of three ultrasonic wavefields that produces a fourth scattered wavefield. The experimental configuration consists of two ultrasonic (800 kHz) pump waves that are used to produce a grating in a suspension of 25 micron diameter polymer particles in salt water. The pump waves are counter-propagating, which form a standing wavefield in the suspension and the less compressible particles are attracted to the pressure nodes in response to the time averaged radiation pressure. A higher frequency (2 to 10 MHz) ultrasonic wavefield is used to probe the resulting grating. The ultrasonic Bragg scattering is then measured. The scattering depends strongly on the response to the pump wave and is an unusual class of acoustical nonlinearity. Investigation of very small amplitude gratings are done by studying the temporal response of the Bragg scattering to a sudden turn on of a moderate amplitude pump wavefield in a previously homogeneous particle suspension. The Bragg scattering has been verified experimentally and is modeled for early-time grating formations using a sinusoidal grating. The larger amplitude gratings are studied in equilibrium and are modeled using an Epstein layer approximation. Ultrasonic three-wave mixing at a free surface involves the interaction of a high amplitude 400 kHz plane wavefield incident at 33 degrees on a water-air interface with a normally incident high frequency (4.6 MHz) focused wavefield. The 400 kHz 'pump' wavefield reflects from the surface and produces an oscillating surface displacement that forms a local traveling phase grating. Simultaneously the 4.6 MHz 'probe' wavefield is reflected from the free surface. The grating scatters the focused probe wavefield and produces (or contributes to) spatially and Doppler shifted foci relative to the main focus. Dissert. Abstr.

N94-30098# Los Alamos National Lab., NM.
RESONANT ULTRASOUND SPECTROSCOPY FOR ELASTIC CONSTANT MEASUREMENTS
R. D. Dixon, A. Migliori, and L. H. Roe 1993 10 p Presented at the American Welding Society International Conference on Modeling and Control of Joining Processes, Orlando, FL, 8 Dec. 1993
(Contract W-7405-eng-36)
(DE94-005016; LA-UR-93-4477; CONF-931234-5) Avail: CASI HC A02/MF A01

All objects exhibit vibrational resonances when mechanically excited. These resonant frequencies are determined by density, geometry, and elastic moduli. Resonant ultrasound spectroscopy (RUS) takes advantage of the known relationship between the parameters. In particular, for a freely suspended object, with three of the four parameters (vibrational spectra, density, geometry, or elastic moduli) known the remaining one can be calculated. From a materials characterization standpoint it is straight-forward to measure density and geometry but less so to measure all the elastic moduli. It has recently become possible to quickly and accurately measure vibrational spectra, and using code written at Los Alamos, calculate all the elastic moduli simultaneously. This is done to an accuracy of better than one percent for compression and 0.1 percent for shear. RUS provides rapid acquisition of materials information here-to-fore obtainable only with difficulty. It will greatly facilitate the use of real materials properties in models and thus make possible more realistic modeling results. The technique is sensitive to phase changes and microstructure. This offers a change to input real data into microstructure and phase change models. It will also enable measurement of moduli at locations in and about a weld thus providing information for a validating coupled thermomechanical calculations. DOE

N94-30274*# Continuum Dynamics, Inc., Princeton, NJ.
COMPUTATIONAL ANALYSIS OF HIGH RESOLUTION UNSTEADY AIRLOADS FOR ROTOR AEROACOUSTICS
Todd R. Quackenbush, C.-M. Gordon Lam, Daniel A. Wachspress, and Donald B. Bliss May 1994 120 p
(Contract NAS1-19303; SBIR-02.09-9282; RTOP 324-02-03)
(NASA-CR-194894; NAS 1.26:194894; CDI-93-12) Avail: CASI HC A06/MF A02

The study of helicopter aerodynamic loading for acoustics applications requires the application of efficient yet accurate simulations of the velocity field induced by the rotor's vortex wake. This report summarizes work to date on the development of such an analysis, which builds on the Constant Vorticity Contour (CVC) free wake model, previously implemented for the study of vibratory loading in the RotorCRAFT computer code. The present effort has focused on implementation of an airload reconstruction approach that computes high resolution airload solutions of rotor/rotor-wake interactions required for acoustics computations. Supplementary efforts on the development of improved vortex core modeling, unsteady aerodynamic effects, higher spatial resolution of rotor loading, and fast vortex wake implementations have substantially enhanced the capabilities of the resulting software, denoted RotorCRAFT/AA (AeroAcoustics). Results of validation calculations using recently acquired model rotor data show that by employing airload reconstruction it is possible to apply the CVC wake analysis with temporal and spatial resolution suitable for acoustics applications while reducing the computation time required by one to two orders of magnitude relative to that required by direct calculations. Promising correlation with this body of airload and noise data has been obtained for a variety of rotor configurations and operating conditions. Author (revised)

N94-30786 National Physical Lab., Teddington (England). Radiation Science and Acoustics Div.
INDEX OF NPL ACOUSTICS PUBLICATIONS 1981-1990
J. Kane and M. S. Shipton May 1993 77 p
(ISSN 0955-9655)
(NPL-RSA(Ext)-0044; ETN-94-95853) Copyright Avail: Issuing Activity (National Physical Lab., Teddington, Middlesex TW11 0LW, England)

The title, abstract, and name of the author of 148 publications published from 1981 to 1990 and related to acoustics, are presented. If appropriate, the details of the conference at which the paper was presented are given. The index list includes the following: aircraft; audiometry, beam calibrator, calibration, characterization, earphones, environment, hearing, hydrophone, laser interferometer, and medical ultrasonic equipment; microphone; and nonlinear propagation, protectors, speech, standardization, standards, thresholds, tissue, traffic, and vibration. Addresses from which the publications can be obtained are given. ESA

N94-30804 Pennsylvania State Univ., University Park.
EXPERIMENTS ON THE AERODYNAMIC GENERATION OF NOISE IN CENTRIFUGAL TURBOMACHINERY Ph.D. Thesis
Paul Henry Bent 1993 299 p
Avail: Univ. Microfilms Order No. DA9326811

An experimental investigation has been made to identify the aerodynamic sources of noise in centrifugal turbomachinery. Emphasis was placed on the generation of noise at frequencies other than the blade passage frequency and harmonics. Experiments were performed on a centrifugal water pump impeller with seven highly backswept blades running in air. Identification of the acoustic sources was made by measurement of the mean and unsteady flow fields and the radiated noise. Two distinct noise generation mechanisms have been identified. The first is the interaction of the impeller with a highly coherent fluid dynamic instability pattern that forms in the discharge of the impeller. This rotating diffuser stall-like instability pattern rotates around the impeller at a fraction of the impeller speed and is comprised of a series of distinct azimuthal modes. The flow field associated with these modes has been modelled as a rotating vorticity sheet of sinusoidally varying strength. It is hypothesized that due to a potential flow type of interaction, the discharge instability pattern causes the loading on the impeller blades to fluctuate and generate noise. Noise generated by this mechanism is narrow-band in character and occurs at frequencies proportional to the relative rotational speed of the discharge instability and the impeller. Significant constructive interference of the sound occurs when the azimuthal mode order is equal to an integer multiple of the number of impeller blades. The second noise generation mechanism is scattering of sound by the interaction of the discharge flow field turbulence with the trailing edges of the impeller blades. The turbulence convecting in the impeller discharge was found to be comprised of a broad range of length scales. To varying degrees, depending on flow rate, the pressure field associated with the discharge turbulence retains some coherence between the surfaces of adjacent impeller blades close to the trailing edge. When the turbulence is coherent, the resulting noise spectra are comprised of a series of harmonically related broad humps. The turbulent length scales corresponding to the center frequencies of the humps in the noise spectra are equal to integer fractions of the blade spacing. Dissert. Abstr.

N94-30972# Ecole Nationale Superieure des Telecommunications, Paris (France). Groupe Acoustique.
NUMERICAL SIMULATIONS OF PIANO STRINGS. PART 1: A PHYSICAL MODEL FOR A STRUCK STRING USING FINITE DIFFERENCE METHODS
Antoine Chaigne and Anders Askenfelt 27 Apr. 1993 29 p Submitted for publication Sponsored by CNRS; Swedish Natural Research Council; Swedish Council for Research in the Humanities and Social Sciences; Bank of Sweden Tercentenary Foundation; and Wenner-Gren Center Foundation
(ISSN 0751-1337)
(TELECOM-93-C-003; ETN-94-95978) Avail: CASI HC A03/MF A01

An improvement to the numerical approach and the underlying physical model made by Hiller and Ruiz in their attempt to generate musical sounds by solving the equations of vibrating strings by means of Finite Difference Methods (FDM) in order to simulate the notion of the piano string with a high degree of realism, is shown. Starting from the fundamental equations of a damped, stiff string interacting with a nonlinear hammer, a numerical finite difference scheme is derived, from which the time histories of string displacement and velocity for each point of the string are computed in the time domain. The interacting force between hammer and string, and the force acting on the bridge, are given by the same scheme. The performance of the model is illustrated by examples of simulated string waveforms. Aspects of numerical stability and dispersion are discussed with reference to the proper choice of sampling parameters. ESA

N94-28974# Science Univ. of Tokyo (Japan). Faculty of Science.
ANALYSIS OF 3-D ACOUSTIC PROBLEMS USING BOUNDARY ELEMENT METHOD [KYOKAI YOSOHO NIYORU SANJIGEN ONKYO KAISEKI]
Mitsunori Yanagizawa *In* NAL, Proceedings of the 10th NAL Symposium on Aircraft Computational Aerodynamics Dec. 1992 p 153-156 In JAPANESE (For primary document see N94-28946 08-02)
Avail: CASI HC A01/MF A03

72 ATOMIC AND MOLECULAR PHYSICS

Includes atomic structure, electron properties, and molecular spectra.

N94-28462# Argonne National Lab., IL.
REPORT OF THE SUBGROUP ON THE TOP QUARK
C. P. Yuan (Michigan State Univ., East Lansing.), L. Nodulman, and H. Baer 1993 6 p Presented at the Workshop on Physics At Current Accelerators and the Supercollider, Argonne, IL, 2-5 Jun. 1993
(Contract W-31-109-eng-38)
(DE94-004624; ANL-HEP-CP-93-94; CONF-9306176-20) Avail: CASI HC A02/MF A01

The top group studied discovery issues as well as measurements to be made at the Tevatron, the LHC, and the SSC. Topics addressed include how to produce top quarks, polarization of top quarks, how top quarks decay, how to detect top quarks, measuring the top quark mass and width, cp violation in top quarks, top quark couplings, and top quark decays as backgrounds. DOE

N94-28468 International Centre for Theoretical Physics, Trieste (Italy).
EMISSION OF SUPERSYMMETRIC NEUTRON PAIR BY CHARGED LEPTON IN MAGNETIC FIELD
Elena V. Arbuzova (Moscow State Univ., Russia.) and A. I. Studenikin Jul. 1993 9 p Limited Reproducibility: More than 20% of this document may be affected by poor print
(DE93-634365; IC-93/169) Avail: Issuing Activity (Department of Energy (DOE)) (US Sales Only)

The emission of a supersymmetric neutrino (sneutrino) pair by a charged lepton in a strong magnetic field is investigated. On this base the supersymmetric (mu)-decay and the emission of a sneutrino pair by an electron in a magnetic field are studied in detail. It is shown that the probability of the process with sneutrino can exceed the probability of the analogous process (with neutrino) of the Standard Model. DOE

N94-28469 International Centre for Theoretical Physics, Trieste (Italy).
EFFECT OF PHONON DISPERSION ON PROPERTIES OF EXCITON IN MAGNETIC FIELD
Gu Shi Wei (Shanghai Polytechnic Univ., China.), Fu Xin Yong, and Hu Qi Tu Mar. 1993 6 p Limited Reproducibility: More than 20% of this document may be affected by poor print
(DE93-634756; IC-93/44) Avail: Issuing Activity (Department of Energy (DOE)) (US Sales Only)

The properties of exciton in magnetic field, taking into account the dispersion of LO phonons is discussed. The effective Hamiltonian in such a case is derived, and the effect of the phonon dispersion on the self-trapping energy of exciton, as well as on the triple-coupling energy of exciton-phonon-magnetic field is discussed. DOE

N94-28470 International Centre for Theoretical Physics, Trieste (Italy).
EXTENDED NONABELIAN SYMMETRIES FOR FREE FERMIONIC MODEL
R. P. Zaikov Aug. 1993 18 p Limited Reproducibility: More than 20% of this document may be affected by poor print
(DE94-601554; IC-93/237) Avail: Issuing Activity (Department of Energy (DOE)) (US Sales Only)

The higher spin symmetry for both Dirac and Majorana massless free fermionic field models are considered. An infinite Lie algebra which is a linear realization of the higher spin extension of the cross products of the Virasoro and affine Kac-Moody algebras is obtained. The corresponding current algebra is closed which is not the case of analogous current algebra in the WZNW model. The gauging procedure for the higher spin symmetry is also given. DOE

N94-28471 Melbourne Univ., Parkville (Australia). School of Physics.
DISCRETE QUARK-LEPTON SYMMETRY NEED NOT POSE A COSMOLOGICAL DOMAIN WALL PROBLEM
H. Lew and R. R. Volkas 1992 35 p Limited Reproducibility: More than 20% of this document may be affected by poor print
(DE94-601606; UM-P-92/70; PURD-TH-92/10; OZ-92/22) Avail: Issuing Activity (Department of Energy (DOE)) (US Sales Only)

Quarks and leptons may be related to each other through a spontaneously broken discrete symmetry. Models with acceptable and interesting collider phenomenology have been constructed which incorporate this idea. However, the standard Hot Big Bang model of cosmology is generally considered to eschew spontaneously broken discrete symmetries because they often lead to the formation of unacceptably massive domain walls. It is pointed out that there are a number of plausible quark-lepton symmetric models in nature which do not produce cosmologically troublesome domain walls. DOE

N94-28491# Rochester Univ., NY.
LOW ENERGY ION-MOLECULE REACTIONS AND CHEMIIONIZATION KINETICS
James M. Farrar 26 Jul. 1993 20 p
(Contract DE-FG02-88ER-13849)
(DE94-005414; DOE/ER-13849/6) Avail: CASI HC A03/MF A01

Work over the past 3 years was directed toward the dynamics of elementary gas phase proton transfer reactions, particularly those of the O(sup -) ion. Such reactions are important in flames. Published work over the past 30 months was concerned with dynamics of reactions of O(sup -) with H2O, NH3, and HF. Results are enumerated here. DOE

N94-28492# State Univ. of New York, Binghamton. Dept. of Physics.
ASYMPTOTIC COHERENCE OF GLUONS AND OF q-BOSONS
C. A. Nelson 1993 10 p Presented at the Coherent States: Past Present and Future, Oak Ridge, TN, 14-17 Jun. 1993
(Contract DE-FG02-86ER-40291)
(DE94-005417; DOE/ER-40291/20; CONF-9306140-2) Avail: CASI HC A02/MF A01

In theoretical physics one of the most important aspects of coherent states is that they can often be simply and reliably used to investigate the quantum coherence and correlation properties of new dynamical, quantum field theories. First, this paper reviews the coherent/degenerate state treatment of the infra-red dynamics of perturbative QCD. This based on the asymptotic behavior of the Hamiltonian operator as (vert bar)t(vert bar) yields infinity in the interaction representation. Second, the paper reviews

the usage of q-analogue coherent states (vert bar)z greater than (sub q) to deduce coherence and uncertainty properties of the q-analogue quantized radiation field in the (vert bar)z greater than (sub q) 'classical limit' where (vert bar)z(vert bar) is large. Third, for future applications, a new 'projector' definition of the usual coherent states and of the squeezed states is reported. DOE

N94-28493# Stanford Linear Accelerator Center, CA.
A MEASUREMENT OF THE LMP EFFECT
S. R. Klein (California Univ., Santa Cruz.), P. Anthony (Lawrence Livermore National Lab., CA.), R. Becker-Szendy (Stanford Univ., CA.), P. E. Bosted (American Univ., Washington, DC.), M. Cavalli-Sforza (California Univ., Santa Cruz.), L. P. Keller (Stanford Univ., CA.), L. A. Kelley (California Univ., Santa Cruz.), G. Niemi (Stanford Univ., CA.), M. L. Perl (Stanford Univ., CA.), and L. S. Rochester (Stanford Univ., CA.) et al Nov. 1993 16 p Presented at the 16th International Symposium on Lepton and Photon Interactions, Ithaca, NY, 10-15 Aug. 1993
(Contracts DE-AC03-76SF-00515; W-7405-eng-48)
(DE94-005225; SU-SLAC-PUB-6378; CONF-930823-18) Avail: CASI HC A03/MF A01

We have performed an experiment to measure accurately the Landau-Pomeranchuk-Migdal (LPM) effect in the production of 5 to 500 MeV photons due to bremsstrahlung of 8 and 25 GeV electron beams traversing thin (2 to 6% X(sub 0)) targets of varying densities. Our measurements confirm that the LPM effect exists and that the Migdal calculations are accurate. We see that, for thin targets, LPM suppression disappears leaving a Bethe-Heitler spectrum, as predicted by theory. For intermediate target thicknesses, we lack an acceptable theory, but have measured energy spectra for targets of differing thickness. We have also measured the production rate of 500 keV to 5 MeV photons at the same electron energies, to study dielectric suppression. We see qualitative agreement with the theory of Ter-Mikaelian; more work is needed before we can make quantitative comparisons. DOE

N94-28494# Stanford Linear Accelerator Center, CA.
ENERGY DISTRIBUTION OF THE LEPTONS IN TOP DECAY TO CHARGED HIGGS
A. Pomarol and C. R. Schmidt Sep. 1993 3 p Presented at the Workshop on Physics at Current Accelerators and the Supercollider, Argonne, IL, 2-5 Jun. 1993
(Contract DE-AC03-76SF-00515)
(DE94-005231; SU-SLAC-PUB-6354; CONF-9306176-22) Avail: CASI HC A01/MF A01

The energy, distribution of the leptons coming from the top decay t yields bH(+), bW(+) yields bl(+)v was analyzed. The correlation between the lepton energy distribution and the top spin may be useful for distinguishing the H(+) signature from the W background. Such a correlation can also be useful for disentangling the two different H(+)(bar t)b couplings and determining the experimental value of tan (beta). DOE

N94-28504# Tennessee Univ., Knoxville. Dept. of Physics and Astronomy.
ELEMENTARY PARTICLE INTERACTIONS
W. M. Bugg, G. T. Condo, T. Handler, E. L. Hart, K. Read, and B. F. L. Ward Oct. 1993 124 p
(Contract DE-FG05-91ER-40627)
(DE94-004238; DOE/ER-40627/3) Avail: CASI HC A06/MF A02

This report discusses: Fermilab E782-E745; GEM; L3 experiment; fixed target photoproduction; SLD; E144 at SLAC; and silicon detectors - radiation hardness program. DOE

N94-28509# Argonne National Lab., IL.
THE GENERALIZED SPIN-BOSON MODEL FOR ELECTRON-TRANSFER REACTIONS INVOLVING TWO HARMONIC POTENTIALS WITH A DIFFERENT FORCE CONSTANT
J. Tang 1994 23 p
(Contract W-31-109-eng-38)
(DE94-005470; ANL/CHM/PP-80389) Avail: CASI HC A03/MF A01

The generalized spin-model is employed to analyze the electron-transfer reactions involving two harmonic potentials with a different force constant. An analytical expression for the nonadiabatic rate constant is derived with fill consideration of the effects of quantum modes. For a single dominant solvent mode at low frequency, the result of the high temperature regime is reduced to the formula derived earlier based on the stochastic Liouville theory. For multiple soft solvent modes, the rate constant is a convoluted integral of a rate function for each individual single mode. DOE

N94-28518# Ames Lab., IA.
QUENCHING OF THE EXCITED STATE OF HYDRATED EUROPIUM(3) IONS BY ELECTRON TRANSFER Ph.D. Thesis
K. Christensen Aug. 1993 38 p
(Contract W-7405-eng-82)
(DE94-005553; IS-T-1674) Avail: CASI HC A03/MF A01

This thesis explores the oxidation-reduction chemistry of the excited state of Eu(III) ions, *Eu(sub aq)(sup 3+), in aqueous solutions. Evidence is presented for the quenching of *Eu(sup 3+) by reductive electron transfer. It is concluded that *Eu(sup 3+) is not a strong energy transfer reagent. The reactivity of *Eu(sub aq)(sup 3+) is compared with that of *UO(sub 2)(sup 2+). DOE

N94-28520# Ames Lab., IA.
A MEASUREMENT OF THE TAU POLARIZATION AT THE RESONANCE WITH THE DELPHI DETECTOR AT LEP Ph.D. Thesis
Antonio Wong Chan Jul. 1993 148 p
(Contract W-7405-eng-82)
(DE94-005557; IS-T-1654) Avail: CASI HC A07/MF A02

The polarization of tau leptons produced in the reaction e(sup +)e(sup -) yields tau(sup +)(tau)(sup -) near the peak of the Z degree resonance has been measured using a sample of 24,904 tau(sup +)(tau)(sup -) events, with an estimated background of 1.5%. We have selected 4562 tau yields e(nu)(bar nu) 2218 (tau) yields (pi)(nu) and 5133 tau yields (rho)(nu) candidates. The mean value obtained is P(sub tau) = -0.176 +/- 0.029. This corresponds to a ratio of the neutral current vector to the axial-vector coupling constants of the tau lepton of g(sub V)(sup tau)/g(sub A)(sup tau) = 0.088 +/- 0.014. This leads to a value of the electroweak mixing angle of sin(exp 2)(theta)(sub W) = 0.2280 +/- 0.0036. This result is in good agreement with previous measurements of the weak mixing angle from the study of the Z degree lineshape and the forward-backward asymmetries in the processes Z degree yields l(sup +)l(sup -) and Z degree yields q(bar q). DOE

N94-28524# California Univ., Berkeley. Lawrence Berkeley Lab.
PROPERTIES OF W + JET EVENTS IN PROTON-ANTIPROTON COLLISIONS AT 1.8 TeV Ph.D. Thesis
R. B. Drucker (California Univ., Berkeley.) 22 Nov. 1993 189 p
(Contract DE-AC03-76SF-00098)
(DE94-004002; LBL-34738) Avail: CASI HC A09/MF A02

W boson + QCD jet events, produced in 1.8 TeV proton-antiproton collisions and measured by the Collider Detector at Fermilab (CDF), were used to measure the center-of-mass production angle of the W + jet system, and were also used to place limits on the production of excited quark states. The center-of-mass production angular distribution agrees well with leading order and next-to-leading order QCD predictions. Excited quark states were searched for in the reaction q + g yields q* yields q + W. Upper limits on the q* cross section, as a function of the q* mass, are shown. Comparison with a theoretical prediction for q* production excludes excited quark states with a mass in the range 150-530 GeV/c(exp 2), at 95% confidence. DOE

N94-28531# Wisconsin Univ., Madison.
PROPERTIES OF EVENTS CONTAINING A PHOTON AND SEVERAL JETS SEEN IN P(BAR P) COLLISIONS AT (RADICAL)S = 1.8 TeV Ph.D. Thesis
P. A. Maas 1993 172 p
(Contract DE-AC02-76ER-00881)
(DE94-005596; DOE/ER-00881/T5) Avail: CASI HC A08/MF A02

The CDF detector is used to investigate the properties of events containing a photon and two jets. The rate of photon +2 jet production is higher than the theoretical calculation, but the shape of the events agrees with QCD predictions. DOE

N94-28541# Stanford Linear Accelerator Center, CA.
RESULTS ON STRUCTURE FUNCTIONS FROM FIXED-TARGET EXPERIMENTS

E. Hughes Sep. 1993 11 p Presented at the Conference on Physics in Collision, Heidelberg, Germany, 16-18 Jun. 1993
(Contract DE-AC03-76SF-00515)
(DE94-005233; SU-SLAC-PUB-6347; CONF-9306251-2) Avail: CASI HC A03/MF A01

A review of proton and neutron structure function measurements from fixed-target experiments is presented. Results on unpolarized structure functions have stabilized for (chi) greater than 0.1, and new results on lower (chi) measurements are appearing. Recent results on the measurement of the neutron spin structure function are given and discussed in relation to previous surprising results from the proton spin structure function measurement. DOE

N94-28542# Stanford Linear Accelerator Center, CA.
DETERMINATION OF THE NEUTRON SPIN-STRUCTURE FUNCTION
G. G. Petratos Oct. 1993 3 p Presented at the 13th International Conference on Particles and Nuclei, Perugia, Italy, 27 Jun. - 3 Jul. 1993
(Contract DE-AC03-76SF-00515)
(DE94-005234; SU-SLAC-PUB-6329; CONF-930637-13) Avail: CASI HC A01/MF A01

The neutron spin-structure function g(sub 1)(sup n) was determined by measuring the asymmetry in deep inelastic scattering of polarized electrons off a polarized He-3 target. The results are interpreted in the quark-parton model and used, in conjuction with earlier proton results, to test the Bjorken sum rule. DOE

N94-28552# Joint Inst. for Nuclear Research, Dubna (USSR). Lab. of Neutron Physics.
ENERGY LOSSES OF FAST CHARGED PARTICLES IN THIN SILICON DETECTORS
K. Yu. Akimov and V. V. Ivanov 1993 6 p In RUSSIAN
(DE94-606065; JINR-E-1-93-115) Avail: CASI HC A02/MF A01 (US Sales Only)

The Monte Carlo method for the calculation of fast charged particle ionization losses in thin silicon layers for the range of thicknesses from 1 to 100 microns, is developed. The dependence of the energy-loss distribution on the thickness of a layer is investigated and the calculation results are compared with the existing experimental data and analytical results. DOE

N94-28554# Joint Inst. for Nuclear Research, Dubna (USSR).
SIMULATION OF EXPERIMENTS ON DEEP INELASTIC SCATTERING OF MUONS ON SUPERCONDUCTING MAGNETIC TOROIDAL SPECTROMETER STORS
A. Yu. Bonyushkina, V. I. Genchev, and I. M. Ivanchenko et al 1992 16 p In RUSSIAN
(DE94-606267; JINR-R-10-92-370) Avail: CASI HC A03/MF A01 (US Sales Only)

Methods and results of precision estimate of kinematic parameter calculations of deep inelastic scattering of muons are analyzed for a choice configuration of the set-up. The suggested method for calculating track parameters takes into account nonlinear effects that depend on the motion of high energy particles in complicated magnetic fields, energy losses, multiple scattering and measurement errors. A calculation experiment shows high precision of the method. Summary estimate is approximately 1% for realistic conditions of the experiment. DOE

N94-28559# Oak Ridge National Lab., TN.
DENSITY REDUCTION: A MECHANISM FOR AMORPHIZATION AT HIGH ION DOSES
E. D. Specht, S. J. Zinkle, and D. A. Walko 1993 6 p Presented at the Materials Research Society Meeting, Pittsburgh, PA, 29 Nov. - 3 Dec. 1993
(Contract DE-AC05-84OR-21400)
(DE94-004793; CONF-9311153-1) Avail: CASI HC A02/MF A01

At cryogenic temperatures, the accumulation of vacancy-interstitial pairs in AlO3 from atomic displacements associated with ion implantation produces amorphization. At room temperature, these pairs recombine, and amorphization occurs only at high doses. X-ray reflectivity measurements show that amorphization of the surface of Al2O3 implanted at room temperature with 160 keV Cr(+) ions is preceded by a progressive reduction in near-surface density. Monte Carlo simulations show that this density reduction can be accounted for by high-energy-transfer collisions which knock atoms deep into the target, leaving widely separated vacancies and interstitials, which do not recombine. Electron microscopy shows that at least some of these vacancies condense into voids. We propose that this reduction in near-surface density can lead to amorphization at high doses. We present simple approximations for the density reduction expected for different ions and targets. DOE

N94-28565# Brookhaven National Lab., Upton, NY.
DERIVATION OF A FOKKER-PLANCK EQUATION FOR BUNCHED BEAMS
Alessandro G. Ruggiero Nov. 1993 5 p Presented at the CERN Workshop on Beam Cooling and Related Topics, Geneva, Switzerland, 4-8 Oct. 1993
(Contract DE-AC02-76CH-00016)
(DE94-004950; BNL-49554-Rev; CONF-9310193-10-Rev) Avail: CASI HC A01/MF A01

This report investigates the derivation of the Fokker-Planck equation which is used to evaluate the evolution with time of an ensemble of particles under the effect of external RF forces, cooling, and forces of stochastic nature. The conventional approach based on the classical work by Chandrasekhar is outlined; the phase angle and the momentum error of the particles are used. The method is then extended to the case where the distribution function is expressed in terms of the amplitude of motion. To avoid a singularity behavior, the new Fokker-Planck equation is obtained with an averaging process over the phase distribution instead of the time-averaging. The beam lifetime in the presence of the separatrix of the RF buckets is determined. Finally, the numerical estimates are applied to the Relativistic Heavy Ion Collider (RHIC). DOE

N94-28566# Illinois Univ., Urbana. Dept. of Physics.
RESEARCH ON ELEMENTARY PARTICLE PHYSICS. TASK P: STUDIES IN THEORY AND PHENOMENOLOGY OF ELEMENTARY PHYSICS
Annual Progress Report
L. E. Holloway and T. A. OHalloran May 1993 14 p
(Contract DE-FG02-91ER-40677)
(DE94-004955; DOE/ER-40677/2-Pt-1) Avail: CASI HC A03/MF A01

Continued progress has been made in isolating the variables needed to completely specify a quark or gluon jet, independent of the process in which it is created. We have evidence of a slow, but statistically significant, dependence on the sub-energy of the hard process in which the jet arises. Once this is taken into account, jets from e(+)e(-) are consistent with those created in p(bar p). Neural network jet identification studies will be based on this expanded set of variables. Work on the new type of Dirac equation for a relativistic oscillator was presented at the International Conference on High Energy Physics in Dallas and will be published in the Proceedings of the Conference. Theoretical studies involving jet signals for theoretically predicted (but as yet undiscovered) particles are underway. DOE

N94-28569# Argonne National Lab., IL.
PHYSICS AT HERA
M. Derrick 1993 18 p Presented at the 23rd International Symposium on Multiparticle Dynamics, Aspen, CO, 13-17 Sep. 1993
(Contract W-31-109-eng-38)
(DE94-005117; ANL-HEP-CP-93-105; CONF-9309297-2) Avail: CASI HC A03/MF A01

HERA is the first electron-proton colliding beam facility and the big news about it is that it works, despite concerns both about the reproducibility of the magnetic field in the proton ring magnets at injection and about the e-p beam-beam interaction. It is, however, a complex accelerator facility that will take a few years to bring up to full and efficient operation. With the present center of mass energy of 296 GeV, it extends the energy range for photoproduction studies by an order of magnitude over fixed target experiments and deep-inelastic e-p scattering up to momentum transfer values approaching 10(sup 5) GeV(sup 2) in both neutral and charged current interactions. At reasonable Q(sup 2), and so with the present luminosity, events with Bjorken x down to a few times 10(sup -5) are being studied. Two powerful general-purpose detectors -- H1 and ZEUS -- have been constructed to address these physics challenges and both collaborations have made new and interesting measurements as presented at this and other recent HEP conferences. The experimental program started

in July 1992 and we are on a steep learning curve both with HERA and with the detectors. DOE

N94-28573# Fermi National Accelerator Lab., Batavia, IL.
SEARCH FOR EXCITED QUARKS IN p(BAR p) COLLISIONS AT THE SQUARE ROOT OF s = 1.8 TeV
R. D. Kephart Nov. 1993 8 p Presented at the 9th Workshop on Proton-Antiproton Collider Physics, Tsukuba, Japan, 18-22 Oct. 1993
(Contract DE-AC02-76CH-03000)
(DE94-004658; FNAL/C-93/347-E; CONF-9310247-1) Avail: CASI HC A02/MF A01

If quarks are composite particles then excited states are expected. We have searched in p(bar p) collisions for excited quarks (q*) which decay to common quarks by emitting a W boson (q* yields qW) or a photon (q* yields q(gamma)). The simplest model of excited quarks has been excluded for mass M* less than 540 GeV/c(sup 2) at 95% confidence level. DOE

N94-28574# Fermi National Accelerator Lab., Batavia, IL.
B PRODUCTION AND B(0)(BAR B)(0) MIXING AT DO
D. Denisov (Superconducting Super Collider Lab., Dallas, TX.) Nov. 1993 11 p Presented at the Advanced Study Conference on Heavy Flavours, Pavia, Italy, 3-7 Sep. 1993
(Contract DE-AC02-76CH-03000)
(DE94-004664; FNAL/C-93/352-E; CONF-9309292-2) Avail: CASI HC A03/MF A01

Preliminary results on B physics studies from the D0 experiment at the Fermilab collider are presented. Single and dimuon events produced in p(bar p) collisions at (radical)s = 1.8 TeV were used in the analysis. Inclusive single muon and J/(Psi) differential cross sections are shown. The results of a measurement of the time averaged B(sup 0)(bar B)(sup 0) to mixing parameter are presented. DOE

N94-28576# Columbia Univ., New York, NY.
RELATIVISTIC HEAVY ION RESEARCH Progress Report
S. Nagamiya 1993 5 p
(Contract DE-FG02-86ER-40281)
(DE94-004701; DOE/ER-40281/8) Avail: CASI HC A01/MF A01

This progress report describes the participation of members of the Nevis group in different experiments during the FY93 period. There was major involvement in: BNL/AGS experiment E802/859/866; BNL RHIC experiment PHENIX; and CERN/SPS experiment NA44. The group was also involved in the small scale experiment E858/878 at BNL/AGS. For the BNL/AGS experiment data collection is now complete, and the group is involved in data analysis. Contributions to systematic procedures for measuring and maintaining the high calibration of the time-of-flight system, along with the previously developed trigger system have been significant contributions to the physics which is beginning to emerge from this heavy ion experiment. The CERN experiment has published first results on S-Pb collisions, with emphasis on two particle correlations. The group has been actively involved in data collection this year. Emphasis is being placed on proton-proton interactions in S-Pb and proton-Pb collisions. The PHENIX experiment is aimed at measuring signatures of quark-gluon plasma. The Nevis group has been actively involved in this experiment from design of the time-of-flight and trigger system, to acting as experiment spokesman. DOE

N94-28578# Princeton Univ., NJ.
SURFACE STRUCTURE AND STEREOCHEMICAL PROPERTIES OF SELF-ASSEMBLED MONOLAYER MATERIALS
Dec. 1993 6 p
(Contract DE-FG02-93ER-45503)
(DE94-004960; DOE/ER-45503/1) Avail: CASI HC A02/MF A01

This document reports the progress made in support of a proposal to generate well-characterized, well-ordered organic surfaces and to impinge upon the array of oriented organic molecules a well-collimated beam of radical atoms at a well-defined angle of incidence. Using the intensity of helium atom diffraction from the organic surface as a measure of the number of unreacted molecules at the surface, the rate of the reaction is measured. The angle of incidence of the reactive atom beam is varied and the measurement is repeated. In this manner the reactivity of the molecules on the surface is mapped out as a function of the angle of incidence of the reactive moiety. To carry out this experiment requires that two fields of research be brought together: molecular beam technology and the science/art of growing well-ordered organic surfaces. The first half of this report describes recent helium diffraction results from molecular beam deposited organic monolayers (structural layer characterization work). The second half reports progress in constructing and characterizing the reactive atom (oxygen) beam source. DOE

N94-28584 Joint Inst. for Nuclear Research, Dubna (USSR).
QUASIPOTENTIAL IN THE FOURTH ORDER OF PERTURBATION THEORY
N. A. Bojkova, V. V. Dvoeglazov, Yu. N. Tyukhtyaev, and R. N. Faustov 1992 6 p Limited Reproducibility: More than 20% of this document may be affected by microfiche quality
(DE94-606299; JINR-E-2-92-440) Avail: CASI HC A02 (US Sales Only)

The quasipotential in the fourth order of perturbation theory is calculated in the Coulomb gauge for the unequal mass particles. It could be used for the future calculations of energy spectra in two-body systems. DOE

N94-28610 Joint Inst. for Nuclear Research, Dubna (USSR).
DEEP INELASTIC LEPTON SCATTERING ON NUCLEI: OPERATOR PRODUCT EXPANSION AND MESON-NUCLEON THEORY
L. P. Kaptari and A. Yu. Umnikov 1992 26 p Limited Reproducibility: More than 20% of this document may be affected by microfiche quality
(DE94-606442; JINR-E-2-92-388) Avail: CASI HC A03 (US Sales Only)

A novel point of view on the x-rescaling model in lepton-nucleus deep inelastic scattering is suggested. Using the operator product expansion method within the effective meson-nucleon theory, a rigorous consideration of the scattering on the deuteron is presented. It is demonstrated that with the contributions interpreter as the Fermi motion corrections, the x-rescaling idea is exactly reproduced. The diagrams of scattering of bound nucleons have also been computed numerically. An example of application of the method, viz. the problem of extraction of the neutron structure function from the combined proton-deuteron data, is considered. DOE

N94-28611 Joint Inst. for Nuclear Research, Dubna (USSR).
MASSES AND MIXING OF LEPTONS AND QUARKS (DIRAC PARTICLES)
Kh. M. Beshtoev 1993 6 p In RUSSIAN Limited Reproducibility: More than 20% of this document may be affected by microfiche quality
(DE94-606446; JINR-R-2-93-44) Avail: CASI HC A02 (US Sales Only)

The work is devoted to the discussion of the question on influence of different types of interactions on the mass matrix of leptons and quarks. The conclusion is made that electromagnetic and strong interactions do not influence on nondiagonal elements of the mass matrix of leptons and quarks. It is shown, for specific (left) character of weak interaction, the interaction does not contribute to the mass matrix of leptons and quarks and so does not lead to the mixing of leptons and quarks due to the masses. DOE

N94-28614 Gosudarstvennyi Komitet po Ispolzovaniyu Atomnoi Energii, Obninsk (USSR).
SOLUTION OF CHARGED PARTICLE TRANSPORT EQUATION BY MONTE-CARLO METHOD IN THE BRANDZ CODE SYSTEM
S. N. Artamonov, P. A. Androsenko, and A. A. Androsenko 1992 25 p In RUSSIAN Limited Reproducibility: More than 20% of this document may be affected by microfiche quality
(DE94-606270; FEI-2244) Avail: Issuing Activity (Department of Energy (DOE)) (US Sales Only)

Consideration is given to the issues of Monte-Carlo employment for the solution of charged particle transport equation and its implementation in the BRANDZ code system under the conditions of real 3D geometry and all the data available on radiation-to-matter interaction in multicomponent and multilayer targets. For the solution of implantation problem the results of BRANDZ data comparison with the experiments and calculations by other codes in complex systems are presented. The results of direct nuclear pumping process simulation for laser-active media by a proton beam are also included. DOE

N94-28619 Joint Inst. for Nuclear Research, Dubna (USSR).
NUMERICAL SOLUTION OF THE MULTICHANNEL SCATTERING PROBLEM
V. I. Korobov 1992 10 p Limited Reproducibility: More than 20% of

this document may be affected by microfiche quality
(DE94-606297; JINR-E-11-92-357) Avail: Issuing Activity (Department of Energy (DOE)) (US Sales Only)

A numerical algorithm for solving the multichannel elastic and inelastic scattering problem is proposed. The starting point is the system of radial Schroedinger equations with linear boundary conditions imposed at some point R = R(sub m) placed somewhere in asymptotic region. It is discussed how the obtained linear equation can be split into a zero-order operator and its perturbative part. It is shown that Lentini - Pereyra variable order finite-difference method appears to be very suitable for solving that kind of problems. The derived procedure is applied to d(mu)+t yields t(mu)+d inelastic scattering in the framework of the adiabatic multichannel approach. DOE

N94-28621 Joint Inst. for Nuclear Research, Dubna (USSR).
SPECIALIZED DATA BASE MANAGEMENT SYSTEM FOR DATA PROCESSING IN THE EXPERIMENTS AT LOW ENERGIES
A. N. Andreev, D. V. Vakatov, M. Veselsky, S. M. Maltseva, V. F. Nikitin, and V. I. Nikitina 1993 10 p In RUSSIAN Limited Reproducibility: More than 20% of this document may be affected by microfiche quality
(DE94-606268; JINR-R-10-93-15) Avail: Issuing Activity (Department of Energy (DOE)) (US Sales Only)

The work contains a description of a data base management system (DBMS) which was designed for automating the experiments being performed by a kinematic separator of recoil nuclei, VASILISA. However, the wide spectrum of possibilities built into the system makes possible its application to other low energy experiments. It is a closed-type system with a three-level architecture which is oriented to abstract data types. It has many third generation DBMS features. DOE

N94-28624# Tokyo Univ. (Japan).
PROCEEDINGS OF THE WORKSHOP ON QUARK AND LEPTON MASS MATRICES
Yoshio Koide, ed. Mar. 1993 107 p Workshop held in Tanashi, Japan, 1-2 Dec. 1992
(DE94-707692; INS-J-176; CONF-921296) Avail: CASI HC A06/MF A02

This issue is the collection of the papers presented at the title workshop. The 8 of the presented papers are indexed individually. DOE

N94-28625 Joint Inst. for Nuclear Research, Dubna (USSR).
PROJECT OF THE EXPERIMENT TO TEST THE HYPOTHESIS ON EXISTENCE OF WHITE AND BLACK p(MU)-ATOMS
V. B. Brudanin, V. M. Bystritskij, and J. Wawryscuk et al 1992 10 p Limited Reproducibility: More than 20% of this document may be affected by microfiche quality
(DE94-606751; JINR-D-15-92-327) Avail: CASI HC A02 (US Sales Only)

This article is dedicated to the analysis of the experiment on the investigation of the muon transfer from p(mu)-atom to oxygen and sulphur nuclei in the H2 + SO2 mixture performed to Swiss group on the meson factory PSI. The conclusion of the authors of the considered article about existence of the different types of p(mu)-atoms ('colored') because they didn't take into account a number of the accompanying physical processes which imitate the observed effect have doubt. With the purpose of the checking the hypothesis of the existence of 'colored' p(mu)-atoms the experiment in which the influence of the accompanying processes is minimal is proposed. DOE

N94-28668 Nebraska Univ., Lincoln.
EXPERIMENTAL AND THEORETICAL STUDIES OF MOLECULAR SOLIDS Final Report, May 1990 - Sep. 1993
John R. Hardy and Frank G. Ullman 1 Nov. 1993 13 p Limited Reproducibility: More than 20% of this document may be affected by microfiche quality
(Contract DAAL03-90-G-0112)
(AD-A275511; ARO-27780.18-PH) Avail: CASI HC A03

Work over a three year period on the optical and dielectric properties of a sequence of ionic molecular solids such as K2SeO4, KNO, and NaNO2 is described. This work had both experimental and theoretical components. Principally, the experiments used light scattering and birefringence to monitor structural and optical changes associated with solid-solid phase transitions. Theoretical studies concentrated on developing a unified theory of the ionic interactions in these systems which resulted in parameter free molecular dynamics simulations which closely reproduced the observed transition and structural behavior of these increasingly complex systems. DTIC

N94-28718# Joint Inst. for Nuclear Research, Dubna (USSR).
MODEL OF POLYLINEAR BOSE- AND FERMI-LIKE OSCILLATOR
R. M. Yamaleev 1992 14 p In RUSSIAN
(DE94-606303; JINR-R-2-92-66) Avail: CASI HC A03/MF A01 (US Sales Only)

A model of a polylinear bose- and fermi-like oscillator, the Hamiltonian of which has a polylinear dependence of generators, is suggested. The rules of operation of fermi- and bose-type generators in the discrete Hilbert space of Hamiltonians are defined. It is proved, N-linear oscillator model may be used for the description of the process of creation and annihilation of the N particles which are related to each other similar to particles and antiparticles. The supersymmetric model of a polylinear oscillator is built. DOE

N94-28741# Brookhaven National Lab., Upton, NY.
ENHANCED ION DISSOCIATION OF LiCF3SO3 BY NEW CARBONATE PLASTICIZERS: RAMAN AND IR STUDIES
L. K. Hanson, H. S. Lee, X. Q. Yang, and J. McBreen 1993 8 p Presented at the 184th Meeting of the Electrochemical Society, New Orleans, LA, 10-15 Oct. 1993
(Contract DE-AC02-76CH-00016)
(DE94-005448; BNL-48999; CONF-931024-7) Avail: CASI HC A02/MF A01

The extent of ion dissociation of LiCF3SO3 in propylene carbonate (PC) and new, modified carbonates (MC-3, MC-5) prepared in our laboratory has been determined by Raman spectroscopy. In the modified carbonates the polyether groups -CH2(OCH2CH2) (sub n)OCH3 (n = 3 for MC-3 and n = 5 for MC-5) replace the 4-CH3 substituent of PC. The spectra clearly show that both MC-3 and MC-5 promote ion dissociation of the Li triflate salt relative to PC. Furthermore, MC-5 solutions contain more free ions than MC-3 solutions, and are less affected by concentration changes. Infrared spectra demonstrate that Li(+) cations associate less with the carbonyl of the modified carbonates than with the carbonyl of PC. These results suggest that the enhanced ion dissociation of Li triflate in MC-3 and MC-5 arises from complexation of the Li(+) to the oxygens of the polyether sidechains, and that MC-5 with its six ether oxygens forms the more stable complex. DOE

N94-28758# Joint Inst. for Nuclear Research, Dubna (USSR).
THE SMALL-X BEHAVIOUR OF PARTON DISTRIBUTION FUNCTIONS
A. V. Kotikov 1992 15 p
(DE94-606414; JINR-E-2-92-361) Avail: CASI HC A03/MF A01 (US Sales Only)

The analysis of parton distributions for the small-x region Bjorken variables is given. It is shown how the inclusion of the next-to-leading corrections to the anomalous dimensions of the Wilson operators changes the behavior of Q(sup 2)-evolution of parton distributions. For 'conventional' (nonsingular for x approaches zero) choice of parton distributions this change is determined by the values of anomalous dimensions. DOE

N94-28788# Japan Atomic Energy Research Inst., Tokyo.
ANALYTIC CROSS SECTIONS FOR COLLISIONS OF H, H2, He AND Li ATOMS AND IONS WITH ATOMS AND MOLECULES
Rinsuke Ito, Tatsuo Tabata, Toshizo Shirai, and R. A. Phaneuf Jun. 1993 96 p
(DE94-707686; JAERI-M-93-117) Avail: CASI HC A05/MF A01

Analytic expressions fitted to Barnett's recommended data are given for the cross sections of the following reactions: electron capture by H, H(+), H(2)(+), He(+), and He(2+) colliding with atoms, molecules, and ions, and electron capture into excited states by H(+), He(+), and He(2+) colliding with atoms and molecules. The latter category includes cross sections for photon emission due to electron capture. The expressions use the semiempirical functional forms proposed by Green and McNeal and some modified forms to make it possible not only to interpolate but also to extrapolate the recommended data. DOE

N94-29021# Dartmouth Coll., Hanover, NH. Thayer School of Engineering.
STRUCTURE OF ORDINARY ICE I(SUB h). PART 1: IDEAL STRUCTURE OF ICE Special Report
Victor F. Petrenko Oct. 1993 30 p
(Contract DAAL03-91-G-0164)
(AD-A275149; CRREL-SR-93-25) Avail: CASI HC A03/MF A01

This report examines the defect-free structure of ordinary I(sub h), reviewing experimental results and theoretical models of the arrangement of oxygen and hydrogen atoms and the electronic structure of ice. Special attention is given to the results of studies from the last two decades. Among the experimental techniques under consideration are X-ray diffraction, optical absorption, X-ray photoelectron spectroscopy and ultraviolet optical spectroscopy, nuclear magnetic resonance, and electron spin resonance. The main subjects discussed are the chemical content of ice, the structure and properties of water molecules, hydrogen bonds, phase transitions, protonic disorder, and electron energy spectrum of ice. DTIC

N94-29032# California Univ., Santa Barbara.
THE EFFECTS OF MOLECULAR ORIENTATION GEOMETRY AND SURFACE ANISOTROPY UPON ETCHING Final Report, 15 Jan. 1992 - 14 Jan. 1994
Andrew C. Kummel Dec. 1993 3 p
(Grant AF-AFOSR-0390-89)
(AD-A275154; AFOSR-94-0039TR) Avail: CASI HC A01/MF A01

Sticking probabilities have been measured for molecular chlorine upon the GaAs (100) Ga-rich c(8x2), GaAs(100) As-rich c(2.8), and GaAs(110) stoichiometric (1x1) surfaces. The sticking probability was measured as a function of incident translational energy (0.038 to 0.66 eV), surface temperature (150-835 K), angle of incidence (0 to 37 deg), and surface chlorine coverage. Our data indicate the presence of both precursor and direct activated chemisorption mechanisms on all three surfaces. Total energy scaling is observed on both the GaAs(100) Ga-rich c(8x2) surface and the stoichiometric (1x1) surface for both precursor mediated and direct activated chemisorption indicating a highly corrugated gas-surface interaction potential. DTIC

N94-29060# Utah Univ., Salt Lake City. Dept. of Chemistry.
HALOGEN CHEMISORPTION ON SILVER(111): SCANNING TUNNELING MICROSCOPY OF COADSORBED HALOGEN ATOMS
Joachim H. Schott and Henry S. White 20 Jan. 1994 26 p
(Contract N00014-91-J-1927)
(AD-A275219) Avail: CASI HC A03/MF A01

The structures of halogen monolayers (I, Br, Cl, and F) and mixed halogen monolayers on Ag(111) surfaces are measured by scanning tunneling microscopy (STM). Adatom radii determined from nearest-neighbor bond distances are in excellent agreement with literature values of the radii of halides, indicating that the adsorbed halogen atoms have an essentially ionic character and are adsorbed as a surface Ag-halide complex. STM images of mixed halogen adlayers comprised of either coadsorbed I and Cl, I and F, or Cl and F, exhibit several structural features, e.g. a low frequency moire pattern and a large atom vacancy density, that are not observed in single-atom adlayers and that are ascribed to coulombic forces within the ionic adlayer. STM has also been used to monitor variations in adlayer structures following ion exchange of chemically distinct halogen species. STM images and data obtained from Auger electron spectroscopy indicate that the chemical stability of the surface Ag halide complexes in aqueous solutions decreases with increasing halogen electronegativity. The results suggest that the energy of solvation of the halide ions determines the relative stability of the Ag-halide surface bond similar to that observed for bulk Ag halide crystals. DTIC

N94-29087# Princeton Univ., NJ. Dept. of Chemical Engineering.
COMPUTER SIMULATION OF MOLECULAR INTERACTIONS IN SUPERCRITICAL SOLVENTS Technical Report, 1 Dec. 1992 - 30 Nov. 1993
P. G. Debenedetti 30 Nov. 1993 27 p
(Contract F49620-93-I-0040)
(AD-A274977; AFOSR-94-0036TR) Avail: CASI HC A03/MF A01

Integral equation calculations were performed on two model supercritical mixtures: naphthalene in carbon dioxide (nonvolatile solute; attractive mixture) and neon in xenon (volatile solute; repulsive mixture). Both systems were studied at high dilution, at supercritical temperature, and over a broad range of densities. The attractive system exhibited significant short-ranged solvent enrichment around the solute. The difference between the solvent density averaged over three solvation shells, and the bulk solvent density was found to be more pronounced between 50 and 80% of the solvent's critical density. In contrast, the repulsive system exhibited local solvent depletion near the solvent's critical point. The extent of the solvation region responsible for determining the solute's chemical potential varies between three and five solvent diameters for the attractive mixture, with the maximum occurring near the solvent's critical density. At 60% of the solvent's critical density, the local concentration of naphthalene molecules around each other is almost ten times higher than in the bulk. Dynamic simulations of pyrene in carbon dioxide revealed insignificant solute-solute aggregation. The mean lifetime of transient solute dimers, roughly 0.8 picoseconds, was found not to change even when the bulk density was varied by a factor of four. DTIC

N94-29112 Rutherford Appleton Lab., Chilton (England).
ISSUES IN LIGHT HADRON SPECTROSCOPY
D. Morgan Oct. 1993 32 p
(PB94-138229; RAL-93-078) Avail: Issuing Activity (National Technical Information Service (NTIS))

A high priority in light hadron spectroscopy is to seek out and characterize various types of non-(Q,Q bar) meson. The large quantity of new data now appearing will present a great opportunity. To identify the non-(Q,Q bar) intruders one needs to know the regular (Q,Q bar) pattern well; whole meson families thus become a target for close investigation. A powerful discovery strategy is to observe the same meson in a variety of reactions. Because mesons appear as resonances, other dynamics can distort the signal in a particular decay channel. Unitarity is the master principle for co-ordinating various sightings of the same resonance. Much of the new spectroscopic information in prospect will come from inferring two-body dynamics from three-body final states. Conventional methods of analysis via the isobar model use approximations to unitarity that need validation. Of all the meson families, the scalars should be a prime hunting ground for non-(Q,Q bar)'s. Even before the advent of the new results, some revisions of the 'official' classifications are urged. NTIS

N94-29131# Duke Univ., Durham, NC. Dept. of Chemistry.
SYNTHESIS AND MOLECULAR STRUCTURES OF R(Me3CCH2)2In-E(SiMe3) (R = Me3CCH2, E = P OR As; R = Me, E = P)
Mark F. Self, Andrew T. McPhail, Leonidas J. Jones, III, and Richard D. Wells 18 Jan. 1994 25 p
(Contract N00014-89-J-1545)
(AD-A275020; DU/DC/TR-37) Avail: CASI HC A03/MF A01

Combining P(SiMe3)3 or As(SiMe3)3 with (Me3CCH2)3In in a 1:1 mole ratio yields simple adducts (Me3CCH2)3In P(SiMe3)3 (1) and (Me3CCH2)3In As(SiMe3)3 (2), respectively. Addition of (Me3CCH2)2InCl to a diethyl ether solution of LiP(SiMe3)2 results in the formation of Me(Me3CCH2)2In P(SiMe3)3 (3). Isomorphous 1 and 2 crystallize in the trigonal system, space group P3(C3), with a = b = 16.278(1), c = 11.496(1) A, V = 2638(1) A(exp 3), Z = 3, D(sub calc.) = 1.093 g/cu cm for 1, and a = b = 16.304(1), c = 11.579(1) A, V = 2665.6(6) A(exp 3), Z=3, D(sub calc.) = 1.164 g/cu cm for 2 . Full-matrix least squares refinement based on 2859 (1) and 2920 (2) reflections with I greater than 3 sigma(I), respectively, converged at R = 0.049 (R(sub w) = 0.065) and R = 0.042 (R(sub w) = 0.055), respectively. Monoclinic crystals of 3 belong to space group P2(sub 1)/c(C(2h)(exp 5)), with a = 16.047(2), b = 12.641(2), c = 31.576(4) A, Beta = 102.92(1) degrees, V = 6243(3) A(exp 3), Z = 8, D(sub calc.) = 1.112 g/cu cm. Full-matrix least squares refinement converged at R = 0.069 (R(sub w) = 0.087) over 4611 reflections with I greater than 3 sigma(I). DTIC

N94-29143 Rutherford Appleton Lab., Chilton (England).
WEAK DECAYS OF CHARGED K-MESONS AND CHARM PARTICLES
G. E. Kalmus Nov. 1993 20 p
(PB94-138062; RAL-93-087) Copyright Avail: Issuing Activity (National Technical Information Service (NTIS))

In the first part of the paper, the contribution of the bubble chamber in the early and mid 1960's to the understanding of the strangeness changing weak interaction is discussed by means of selected examples in charged

K decay. In the second part of the paper, the extension of the technique in the late 1970's and early 1980's needed to investigate charm particle properties is briefly discussed. Selected results from bubble chamber experiments are compared with theoretical predictions and with the present experimental information. NTIS

N94-29145 Rutherford Appleton Lab., Chilton (England).
ONE-LOOP QCD MASS EFFECTS IN THE PRODUCTION OF POLARIZED BOTTOM AND TOP QUARKS
J. G. Koerner, A. Pilaftsis, and M. M. Tung Dec. 1993 19 p Sponsored by Mainz Univ. and BMFT
(PB94-138104; RAL/93-81) Avail: Issuing Activity (National Technical Information Service (NTIS))

The analytic expressions for the production cross sections of polarized bottom and top quarks in e(+)e(-) annihilation are explicitly derived at the one-loop order of strong interactions. Chirality-violating mass effects will reduce the longitudinal spin polarization for the light quark pairs by an amount of 3%, when one properly considers the massless limit for the final quarks. Numerical estimates of longitudinal spin polarization effects in the processes e(+)e(-) greater than or equal to b(b bar)(g) and e(+)e(-) greater than or equal to t(t bar)(g) are presented. NTIS

N94-29161 Rutherford Appleton Lab., Chilton (England).
IMPROVED QCD SUM RULE ESTIMATES OF THE HIGHER TWIST CONTRIBUTIONS TO POLARISED AND UNPOLARISED NUCLEON STRUCTURE FUNCTIONS
G. G. Ross and R. G. Roberts Dec. 1993 14 p Prepared in cooperation with Oxford Univ., Englan d
(PB94-138112; RAL-93-092) Avail: Issuing Activity (National Technical Information Service (NTIS))

We re-examine the estimates of the higher twist contributions to the integral of g(sub 1), the polarized structure function of the nucleon, based on QCD sum rules. By including corrections both to the perturbative contribution and to the low energy contribution, we find that the matrix elements of the relevant operators are more stable to variations of the Borel parameter M(sup 2), allowing for a meaningful estimate of the matrix elements. We find that these matrix elements are typically twice as large as previous estimates. However, inserting these new estimates into the recently corrected expressions for the first moments of g(sub 1) leads to corrections too small to affect the phenomenological analysis. For the unpolarized case, the higher twist corrections to the GLS and Bjorken sum rules are substantial, and bring the estimate of Lambda(sub QCD) from the former into good agreement with that obtained from the Q(sup 2) dependence of deep inelastic data. NTIS

N94-29500 International Centre for Theoretical Physics, Trieste (Italy).
THERMOMECHANICAL PROPERTIES OF 3-D TRANSITION METALS
B. Karaoglu (Sultan Qaboos Univ., Muscat, Oman.) and S. M. MujiburRahman (Sultan Qaboos Univ., Muscat, Oman.) Jul. 1993 17 p Limited Reproducibility: More than 20% of this document may be affected by microfiche quality
(DE94-604015; IC-93/229) Avail: CASI HC A03 (US Sales Only)

We have investigated the density variation of the Einstein temperatures and elastic constants of the 3-D transition metals. In this respect we have employed the transition metal (TM) pair potentials involving the sp contribution with an appropriate exchange and correlation function, the d-band broadening contribution and the d-band hybridization term. These calculations are aimed at testing the TM pair potentials in generating the aforesaid quasilocal and local thermomechanical properties. DOE

N94-29502# Joint Inst. for Nuclear Research, Dubna (USSR).
SEMILEPTONIC HEAVY-TO-LIGHT DECAYS OF BARYONS
G. V. Efimov, M. A. Ivanov, N. B. Kulimanova, and V. E. Lyubovitskij 1992 24 p
(DE94-606481; JINR-E-2-92-106) Avail: CASI HC A03/MF A01 (US Sales Only)

The results about semileptonic decays of baryons with only heavy quark into light baryons are reported. These processes are considered in the framework of the quark confinement model. Weak form factors, decay rates and differential distributions of semileptonic heavy-to-light baryon decays are calculated. The limit m(sub Q) yields infinity is examined. DOE

N94-29683 Helsinki Univ. of Technology, Espoo (Finland). Nuclear Engineering Lab.
KNOWLEDGE BASED SYSTEM FOR IDENTIFICATION OF GAMMA SOURCES
T. T. Hakulinen 3 Jun. 1993 151 p Limited Reproducibility: More than 20% of this document may be affected by microfiche quality
(PB94-137742; TKK-F-B147) Avail: CASI HC A08

SHAMAN is an expert system for the qualitative identification of radionuclides in the measured gamma spectrum. The goal of SHAMAN is to correctly identify all radionuclides in the sample and to quantitatively determine their activities and all related parameters. This report documents the SHAMAN system starting from the algorithmic level and ending with programming issues. The first three chapters give an overview of the initial problem of radionuclide identification and expert system concepts in general. Chapters 4 and 5 present the special programming interface of SHAMAN. The entire methodology of SHAMAN system ranging from fundamental algorithms to data processing is contained in chapters 6-10. The last chapter of the report is devoted to performance issues and conclusions presenting some test results. NTIS

N94-29700# Superconducting Super Collider Lab., Dallas, TX.
SOME REMARKS ABOUT PSEUDO-HAMILTONIAN
N. Malitsky, G. Bourianoff, and Yu. Severgin Nov. 1993 13 p
(Contract DE-AC35-89ER-40486)
(DE94-003273; SSCL-648) Avail: CASI HC A03/MF A01

For the many applied tasks of accelerator physics, the four dimensional single particle pseudo-Hamiltonian may be presented as the Hamiltonian of the near-integrable system consisting of integrable and perturbed terms. The KAM theorem states that for sufficiently small perturbation the invariant surfaces continue to exist and, for the systems with two degrees of freedom, completely isolate the thin stochastic layers. As the perturbation strength increases, a transition can occur in which these surfaces disappear and the stochastic layers connect, resulting in globally stochastic motion. One of the important problems is to determine this 'boundary' invariant surface. There are several approaches that may be used to describe the regular trajectories in the small limited region. The most powerful method is the perturbation theory which allows us to study the combined influence of the different multipoles. The inclusion of Lie operators improved this method and developed it up to high order perturbation. But the perturbation theory failed to describe the change in topology and since the regular trajectories depend discontinuously on choice of initial coordinates, it cannot be used in the whole region of the stable motion. The authors suggest limiting attention to the study of the 'boundary' invariant and implementation of the additional 'local' transformation. The authors briefly review the well known theories, their advantages and imperfections, and the necessity of the 'local' transformation. They present the comparison of the map tracking with the invariants determined by the perturbation methods. DOE

N94-29841# Brookhaven National Lab., Upton, NY.
PERFORMANCE OF CVD AND CVR COATED CARBON-CARBON IN HIGH TEMPERATURE HYDROGEN
J. W. Adams, R. E. Barletta, J. Svandrlik, and P. E. Vanier 1993 6 p Presented at the Fall Meeting of the Materials Research Society (MRS), Boston, MA, 29 Nov. - 3 Dec. 1993
(Contract DE-AC02-76CH-00016)
(DE94-005451; BNL-49299; CONF-931108-44) Avail: CASI HC A02/MF A01 (US Sales Only)

As a part of the component development process for the particle bed reactor (PBR), it is necessary to develop coatings which will be time and temperature stable at extremely high temperatures in flowing hydrogen. These coatings must protect the underlying carbon structure from attack by the hydrogen coolant. Degradation which causes small changes in the reactor component, e.g. hole diameter in the hot frit, can have a profound effect on operation. The ability of a component to withstand repeated temperature cycles is also a coating development issue. Coatings which crack or spall under these conditions would be unacceptable. While refractory carbides appear to be the coating material of choice for carbon substrates being used in PBR components, the method of applying these coatings can have a large effect on their performance. Two deposition processes for these refractory carbides, chemical vapor deposition (CVD) and chemical vapor reaction (CVR), have been evaluated. Screening tests for these coatings consisted of testing of coated 2-D and 3-D weave carbon-carbon

in flowing hot hydrogen at one atmosphere. Carbon loss from these samples was measured as a function of time. Exposure temperatures up to 3,000 K were used, and samples were exposed in a cyclical fashion cooling to room temperature between exposures. The results of these measurements are presented along with an evaluation of the relative merits of CVR and CVD coatings for this application. DOE

N94-29845# Lawrence Livermore National Lab., CA.
OPTICAL FIELD IONIZATION OF ATOMS AND IONS USING ULTRASHORT LASER PULSES Ph.D. Thesis
D. N. Fittinghoff Dec. 1993 156 p
(Contract W-7405-eng-48)
(DE94-006643; UCRL-LR-115496) Avail: CASI HC A08/MF A02

This dissertation research is an investigation of the strong optical field ionization of atoms and ions by 120-fs, 614-run laser pulses and 130-fs, 800-nm laser pulses. The experiments have shown ionization that is enhanced above the predictions of sequential tunneling models for He(+2), Ne(+2), and Ar(+2). The ion yields for He(+1), Ne(sup +1) and Ar(sup +1) agree well with the theoretical predictions of optical tunneling models. Investigation of the polarization dependence of the ionization indicates that the enhancements are consistent with a nonsequential ionization mechanism in which the linearly polarized field drives the electron wavefunction back toward the ion core and causes double ionization through inelastic e-2e scattering. These investigations have initiated a number of other studies by other groups and are of current scientific interest in the fields of high-irradiance laser-matter interactions and production of high-density plasmas. This work involved the following: (1) Understanding the characteristic nature of the ion yields produced by tunneling ionization through investigation of analytic solutions for tunneling at optical frequencies. (2) Extensive characterization of the pulses produced by 614-nm and 800-ran ultrashort pulse lasers. Absolute calibration of the irradiance scale produced shows the practicality of the inverse problem--measuring peak laser irradiance using ion yields. (3) Measuring the ion yields for three noble gases using linear, circular and elliptical polarizations of laser pulses at 614-nm and 800-nm. The measurements are some of the first measurements for pulse widths as low as 120-fs. DOE

N94-29903 Columbia Univ., New York, NY.
EFFECTS OF DIFFUSION AND INERTIA ON CHAOTIC MIXING: A COMPUTATIONAL AND EXPERIMENTAL STUDY Ph.D. Thesis
Pradip Dutta 1992 191 p
Avail: Univ. Microfilms Order No. DA9313586

The role of molecular diffusion and transient velocities in the overall mixing of particles by chaotic advection produced in a periodic journal-bearing flow is studied numerically and experimentally. For the numerical study, the Lagrangian description of diffusing particles is modeled by the use of the Langevin equation, in which the effective velocity of a diffusing particle is expressed as the sum of the deterministic velocity (as a result of the flow solution) and a stochastic component arising out of the Brownian motion of the molecules. The stochastic component is modelled as a Gaussian process with zero mean and variance proportional to the diffusivity, D. Two separate cases are considered in obtaining the deterministic velocity. In the first case, the flow solution is obtained analytically by making Stokes approximation. Numerical experiments are performed by stirring a blob of particles for a few cycles and then reversing the flow. It is observed that the mean square separation (after flow reversal) of the diffusing particles initialized in chaotic regions are a few times greater than those initialized in regular regions. The main causes of enhancement of separation are identified to be stretching and folding of material lines. Corresponding experimental observations are made by taking photographs of blobs of dye before and after stirring, and by analyzing the pictures by digital image processing. For a few cycles, there is a good agreement between the numerical results and the experimental observations. But, for longer stirring, the final distribution of particles after flow reversal predicted numerically deviates from the corresponding experimental results. The cause of this deviation is believed to be the omission of the transient terms from the governing momentum equation. Hence, in the second case, the effect of diffusion is studied in the presence of transient velocities. The flow solution is obtained for the transient Navier-Stokes equation in the eccentric annulus geometry by a finite difference method using the stream function-vorticity formulation and ADI method in a curvilinear coordinate system. On including the effects of transient velocities in the numerical model, there is a striking agreement with experimental observations even for higher numbers of cycles of stirring. The transient effects, however, are not significant if the advection is not chaotic. Dissert. Abstr.

N94-29930 Oklahoma Univ., Norman.
A TEVATRON COLLIDER BEAUTY FACTORY
1992 57 p Limited Reproducibility: More than 20% of this document may be affected by microfiche quality
(Contract DE-AS05-80ER-10629)
(DE94-004879; DOE/ER-10629/T9) Avail: CASI HC A04

This document which is labeled a final report consists of several different items. The first is a proposal for a detector to be developed for beauty physics. The detector is proposed for the Fermilab Tevatron and would be designed to measure mixing reactions, rare decay modes, and even CP violation in hadron collider beauty production. The general outline of the work proposed is given, and an estimate of the time to actually design the detector is presented, along with proposed changes to the Tevatron to accommodate the system. A preliminary report on an experiment to verify a reported observation of a 17 keV neutrino in tritium decay is presented. The present results in the decay spectra actually showing a depression below expected levels, which is not consistent with a massive neutrino. Additional interest has been shown in finishing an electrostatic beta spectrometer which was started several years previously. The instrument uses hemispherical electrostatic electric fields to retard electrons emitted in tritium decay allowing measurement of integral spectra. The design goal has a 5 eV energy resolution, which may be achievable. A new PhD student is pursuing this experiment. Also the report contains a proposal for additional work in the field of non-perturbative quantum field theory by the theoretical group at OU. The work which is proposed will be applied to electroweak and strong interactions, as well as to quantum gravitational phenomena. DOE

N94-30039 Los Alamos National Lab., NM.
COMPARISON OF 14 MeV ISOMER PRODUCTION OF Hf-178m1 AND Hf-179m2 USING FESHBACH-KERMAN-KOONIN AND EXCITON PREEQUILIBRIUM MODELS
M. B. Chadwick (Lawrence Livermore National Lab., CA.) and P. G. Young 1993 12 p Presented at the 2nd International Atomic Energy Authority/Coordinated Research Program (IAEA/CRP) Meeting on Activation Cross Sections for the Generation of Long-Lived Radionuclides, San Diego, CA, 29-30 Apr. 1994 Limited Reproducibility: More than 20% of this document may be affected by microfiche quality
(Contract W-7405-eng-36)
(DE94-002640; LA-UR-93-3632; CONF-940459-2) Avail: CASI HC A03

The Hf-178m2(16+) isomeric state has a 31-yr half life and could pose serious radioactive problems in nuclear fusion reactors if its production in 14 MeV neutron-induced reactions is significant. We present statistical/pre-equilibrium model calculations for the production of this isomer in the Hf-179(n, 2n) Hf-178m2 reaction, as well as the 25-days 12.5(-) isomer in the Hf-179(n,n')Hf-179m2 reaction, using two different preequilibrium models: the exciton model and the Feshbach-Kerman-Koonin (FKK) theory. Our calculations which use the exciton model agree well with measurements, but those with the FKK theory underestimate measurements. Our calculations are the first to probe angular momentum transfer effects in the FKK theory and suggest that, as it is presently applied, high spin-transfer reactions are underestimated. We suggest modifications to the FKK statistical averaging procedure which may result in an improved agreement with experiment. DOE

N94-30049# Fermi National Accelerator Lab., Batavia, IL.
INCLUSIVE JET AND DIRECT PHOTON PRODUCTION AT THE D0 EXPERIMENT
J. Kotcher (Superconducting Super Collider Lab., Dallas, TX.) Dec. 1993 9 p Presented at the 9th Workshop on Proton-Antiproton Collider Physics, Tsukuba, Japan, 18-22 Oct. 1993
(Contract DE-AC02-76CH-03000)
(DE94-006001; FNAL/C-93/387-E; CONF-9310247-9) Avail: CASI HC A02/MF A01

Preliminary measurements of the inclusive jet and single photon production cross sections in p(bar p) collisions at sq. root of delta = 1.8 TeV by the D0 experiment at the Fermilab Tevatron are reported. The inclusive jet cross sections in various pseudorapidity ranges covering (vert

bar)(eta)(vert bar) less than 3 are presented, along with comparisons to next-to-leading order QCD predictions. The single photon cross section in the central region ((vert bar)(eta)(vert bar) less than 0.9) is also presented, as is a description of the conversion method used to determine the background contamination. The single photon cross section is compared to a recent next-to-leading logarithm QCD calculation. DOE

N94-30050 Gosudarstvennyi Komitet po Ispolzovaniyu Atomnoi Energii, Serpukhov (USSR).
ON POSSIBILITY TO CREATE THE SCINTILLATION TRIGGER FOR LIQUID-ARGON NEUTRINO DETECTOR
S. V. Belikov, S. N. Gurzhiev, V. I. Kochetkov, and V. S. Startsev 1992 15 p Limited Reproducibility: More than 20% of this document may be affected by microfiche quality
(DE94-607844; IFVE-ONF-92-24) Avail: Issuing Activity (Department of Energy (DOE)) (US Sales Only)

Different methods of the trigger organization for the liquid argon neutrino detector of the Tagged Neutrino Facility are discussed and the construction of the fast scintillating trigger using polymethylmethacrylate as the base of the scintillator is proposed. As a result of experimental investigations, photomultiplier PM-84-3 with a standard devider was choosen. Characteristics for the scintillator and the wavelength shifter, which are required for creating a highly efficient (90%) fast less than or equal to 5 ns trigger suitable for a liquid argon under increased pressure (P less than or equal to 3 atm) were defined. DOE

N94-30051 Joint Inst. for Nuclear Research, Dubna (USSR). Lab. of High Energy.
EXPERIMENTAL SETUP FOR STUDY OF HADRON AND HARD PHOTON PRODUCTION IN NUCLEUS-NUCLEUS COLLISIONS
V. I. Yurevich, R. M. Yakovlev, V. G. Lyapin, I. O. Tsvetkov, and A. V. Daniehl 1992 14 p Limited Reproducibility: More than 20% of this document may be affected by microfiche quality
(DE94-607849; JINR-E-1-92-249) Avail: CASI HC A03 (US Sales Only)

The tandem of the (Delta)E-E and t-E spectrometers has been made at an external heavy-ion beam channel of the JINR synchrophasotron for an experimental study of short-lived extreme nuclear matter states by inclusive measurements of double differential cross sections of hadron and hard photon production in central nucleus-nucleus collisions. The possibilities and characteristics of this setup are discussed. DOE

N94-30052 Joint Inst. for Nuclear Research, Dubna (USSR). Lab. of High Energy.
EXPERIMENTAL SETUPS AND METHODS TO OBTAIN NEW NUCLEAR DATA AT INTERMEDIATE AND HIGH ENERGIES
A. D. Kovalenko, Yu. A. Panebratsev, S. S. Shimanskiij, V. I. Yurevich, and R. M. Yakovlev 1992 18 p Limited Reproducibility: More than 20% of this document may be affected by microfiche quality
(DE94-607850; JINR-E-1-92-250) Avail: CASI HC A03 (US Sales Only)

A short description of new experimental setup designed for a comprehensive study of the production process of secondary hadrons, neutrons and hard photons in proton- and nucleus-nucleus collisions and also for obtaining nuclear data at intermediate and high energy beams of the Dubna synchrophasotron is given. Nuclear data needed for different applications can be obtained at available beams with (0.3-3.6)A GeV energy of incident nucleus with A less than or equal to 28. The possibilities of setups will be substantially expanded after putting the new superconducting synchrotron, the Nuclotron, into operation. DOE

N94-30061# Massachusetts Inst. of Tech., Cambridge. Dept. of Chemistry.
SPECTROSCOPIC AND DYNAMICAL STUDIES OF HIGHLY ENERGIZED SMALL POLYATOMIC MOLECULES
R. W. Field and R. J. Silbey 1993 11 p
(Contract DE-FG02-87ER-13671)
(DE94-006509; DOE/ER-13671/7) Avail: CASI HC A03/MF A01

Stimulated emission pumping was used to determine molecular constants and linewidths of vibrational levels of HCO (tilde X)(sup 2)A' state in an energy region. Some of the results of the initial study of the HCO (tilde B)(left arrow)(tilde X) transition were the subject of ab initio calculations. A paper was written which provides a lineshape and linestrength theory for Frequency Modulation (FM) enhanced Magnetic Rotation Spectroscopy (free radical spectroscopy). Pulsed dye amplification does not degrade the sensitivity of FM spectroscopy; a pulsed amplified FM spectrometer is being set up. A superpolyad model is being tested and extended for acetylene states. An ICCD-DF (intensified change-coupled detector-dispersed fluorescence) scheme is being set up. DOE

N94-30085 Joint Inst. for Nuclear Research, Dubna (USSR).
ON RELATIVITY PRINCIPLE VIOLATION IN LOCAL MEASUREMENTS OF SPIN PRECESSION OF MOVING PARTICLES
B. S. Neganov 1992 28 p Limited Reproducibility: More than 20% of this document may be affected by microfiche quality
(DE94-608067; JINR-D-2-92-446) Avail: CASI HC A03 (US Sales Only)

The repeated analysis of spin precession phenomenon of relativistic charged particles was performed. The inevitability of the relativity principle violation on local measurements of spin precession was shown while particle moving along a curvilinear trajectory due to the Thomas precession. The simplest deduction of spin equations of motion has been received in the fixed and reference frames. The possibility to determine the Earth's absolute velocity by means of measuring the azimuthal asymmetry of spin precession was shown. Besides, Lorentz's etheric conception is being developed as a more fundamental theory, which establishes the limits of existing phenomenological method of the conventional isotropic description of the phenomena in moving reference frames within the limits of the special relativity theory. DOE

N94-30095 Joint Inst. for Nuclear Research, Dubna (USSR).
SEARCH FOR HEAVY NEUTRINOS AT THE IHEP-JINR NEUTRINO DETECTOR
S. A. Baranov, Yu. A. Batusov, and A. A. Borisov 1992 12 p In RUSSIAN Limited Reproducibility: More than 20% of this document may be affected by microfiche quality
(DE94-608175; JINR-R-1-92-494) Avail: CASI HC A03 (US Sales Only)

Data from a proton beam-dump experiment at the 70 GeV Serpukhov accelerator were analyzed to search for the heavy neutrino decay nu(sub H) yields e(+) e(-) nu(sub e) at the IHEP-JINR Neutrino Detector. No signal over background was found. The upper limits on the elements of a mixing matrix absolute value of U(sub eH) squared in the mass range 5 MeV less than M(sub nu(sub H)) less than 493 MeV and absolute value of U(sub eH) times absolute value of U(sub mu H) in the mass range 3 MeV less than m(sub nu(sub H)) less than 388 MeV were established at 90 percent CL. DOE

N94-30096 Academy of Sciences (USSR), Leningrad.
OBSERVATION OF THE PHASE SHIFT OF THE WAVE FUNCTION OF THE NEUTRON UNDER TOTAL REFLECTION
N. K. Pleshanov May 1991 19 p In RUSSIAN Limited Reproducibility: More than 20% of this document may be affected by microfiche quality
(DE94-608244; LIYaF-1691) Avail: Issuing Activity (Department of Energy (DOE)) (US Sales Only)

By means of a thin semitransparent film as an interference element, the phase shift of the wave function of a massive particle, the neutron, under total reflection has been observed. This effect may turn out to be useful in the study of magnetic properties and other details of the structure of thin films and the surface of solids. By reflection of polarized neutrons, the magnetization (10,200 +/- 350 Gs) and the roughness of the upper boundary (51 +/- 5 A) of a thermally sputtered 5000 A thick iron film as well as the roughness of the glass substrate (10 +/- 4 A) have been found. DOE

N94-30097 International Centre for Theoretical Physics, Trieste (Italy).
NUCLEON AND NUCLEI AT FINITE TEMPERATURE, AS A PHENOMENOLOGICAL TEST OF THE ENTROPY BOUND
M. Dey, S. Chakrabarty, and J. Dey Aug. 1993 13 p Limited Reproducibility: More than 20% of this document may be affected by microfiche quality
(DE94-608094; IC-93/254) Avail: Issuing Activity (Department of Energy (DOE)) (US Sales Only)

Using the Bekenstein's entropy bound, the stability of a nucleon and nuclei have been investigated in simple models like 'bag model' for the nuclear and mean field model of Serot and Walecka for nuclei. DOE

N94-30103# Fermi National Accelerator Lab., Batavia, IL.
MEASUREMENT OF THE W MASS IN THE D0 DETECTOR
Qiang Zhu (New York Univ., New York.) Dec. 1993 12 p Presented at the 9th Workshop on Proton-Antiproton Collider Physics, Tsukuba, Japan, 18-22 Oct. 1993
(Contract DE-AC02-76CH-03000)
(DE94-006002; FNAL/C-93/396-E; CONF-9310247-8) Avail: CASI HC A03/MF A01

We report the results of a preliminary analysis of the W yields e(nu) decays observed in 14 pb(-1) of data taken during the Fermilab Tevatron Run I(a). After normalizing the mass scale to the Z mass measured at LEP, we find a value for the W mass of 79.86 +/- 0.16(stat) +/- 0.20(syst) +/- 0.31(scale) GeV. The method for extracting the W mass and the details of the error analysis are presented and discusses. DOE

N94-30112 Joint Inst. for Nuclear Research, Dubna (USSR).
STATISTICAL DESCRIPTION OF HOT AND DENSE CLUSTERING MATTER
A. A. Shanenko, E. P. Yukalova, and V. I. Yukalov 1992 15 p Limited Reproducibility: More than 20% of this document may be affected by microfiche quality
(DE94-608155; JINR-E-2-92-378) Avail: CASI HC A03 (US Sales Only)

A statistical model is constructed by treating hadrons as clusters of elementary objects, gluons and quarks. The basis of the model is an effective cluster Hamiltonian. The principle of thermodynamic equivalence for Hamiltonians is formulated, which makes it possible to describe all the thermodynamics of the system with an effective Hamiltonian in a completely correct way. To check the accuracy of the model, detailed calculations for the region of zero baryon density have been made for which computer simulations on the lattice are known. The results are found to be in good agreement with the lattice numerical data. DOE

N94-30120 Joint Inst. for Nuclear Research, Dubna (USSR).
MODELLING OF MULTIPARTICLE PRODUCTION BY DYNAMICAL SEMIGROUP METHOD
B. F. Kostenko 1992 19 p In RUSSIAN Limited Reproducibility: More than 20% of this document may be affected by microfiche quality
(DE94-608132; JINR-R-2-92-580) Avail: CASI HC A03 (US Sales Only)

The clan description of multiparticle production process suggested by Giovannini and Van Hove is discussed on the base of quantum master equations for open systems. It is shown that the Poisson distribution of fragments created on the first hard stage is model independent to a great extent and can be obtained from rather general assertions of the theory of open systems. The second stage or development of the avalanche is characterized by self-organizing critical behavior. The stage of hadronization can be satisfactorily described with the help of the model of two-level sources and reminds of the laser operation under the coherent threshold. A possible cause of deviation of multiplicity distributions from the NB regularity and the hypothesis of local parton-hadron duality is also discussed. DOE

N94-30141 Manitoba Univ., Winnipeg. Dept. of Physics.
GLUON AND FERMION DAMPING IN HOT QCD Ph.D. Thesis
Kin Wah Mak Jul. 1993 110 p
(ISBN-0-315-85982-2; CTN-94-61175) Copyright Avail: Micromedia Ltd., Technical Information Centre, 240 Catherine Street, Suite 305, Ottawa, Ontario, K2P 2G8, Canada HC/MF

The basic formal content of field theories at non-zero temperature is presented, with application to the stability of quark-gluon plasma. Linear response theory is used to express the positions of the physical poles in the finite temperature gluon propagator in terms of the components of the proper self-energy. The formalism is then applied to the calculation at the one-loop level of the bare plasma parameters and of Landau ghosts in two classes of gauges: the covariant gauge and a one-parameter family of non covariant gauges interpolating between the static temporal gauge and the Coulomb gauge. The requirement of gauge invariance leads to searching a self-consistent expansion scheme instead of the usual loop expansion. In particular, one such scheme recently developed which incorporates all relevant higher-loop diagrams in terms of the hard thermal loops has been used to calculate the fermion damping rate in the long wavelength limit. Both a heavy and a massless fermion are considered. Ward identities between the effective propagators and vertices are used in formal proof of the gauge fixing independence of the damping rate to this order in a wide class of gauges. Finally, the gauge fixing dependence problem of the damping rate is revisited through the consideration of the exact cancellation of the infrared divergences in the two-loop photon polarization tensor.
Author (CISTI)

N94-30182 Joint Inst. for Nuclear Research, Dubna (USSR). Lab. of Neutron Physics.
ON THE STRUCTURE AND ATOMIC MOTIONS IN LIQUID SODIUM
I. Padureanu (Institutul de Fizica Atomica, Bucharest, Romania.), Gh. Rotarescu (Institutul de Fizica Atomica, Bucharest, Romania.), I. Popescu (Institutul de Fizica Atomica, Bucharest, Romania.), O. E. Kudryashov (Latvian P. Stuchka State Univ., Riga.), and I. E. Ovchinnikov (Latvian P. Stuchka State Univ., Riga.) 1992 12 p Limited Reproducibility: More than 20% of this document may be affected by microfiche quality
(DE94-608386; JINR-E-14-92-79) Avail: CASI HC A03 (US Sales Only)

The microscopic structure function for liquid Na in the temperature range T = 100 - 600 C from the hard sphere approach and neutron diffraction data at the low momentum transfer measurements are obtained. These data are used within the mean field, viscoelastic, and memory function approach theories to derive the self and effective current longitudinal correlation function and its spectral function. DOE

N94-30184 Gosudarstvennyi Komitet po Ispolzovaniyu Atomnoi Energii, Obninsk (USSR).
DISTRIBUTION FUNCTIONS OF ELECTRONS WITHIN ALUMINIUM OXIDE THIN FILMS
P. P. Dyachenko and V. A. Rykov 1992 9 p Limited Reproducibility: More than 20% of this document may be affected by microfiche quality
(DE94-608418; FEI-2255) Avail: CASI HC A02 (US Sales Only)

In this work the electron spectrum in Al2O3 is presented. Experimental electron spectrum after passage of fission fragments through thin Al2O3 film is measured by time-of-flight technique. Electron spectrum withinthe target is calculated by the surface barrier model. DOE

N94-30234 Laval Univ. (Quebec). Dept. de Physique.
GLUEBALL AND MESON DISPERSION AND DIFFUSION RELATIONS IN COMPACT U(1)(2+1) GAUGE THEORY Ph.D. Thesis [RELATIONS DE DISPERSION ET DIFFUSION DES GLUEBALLS ET DES MESONS DANS LA THEORIE DU JAUGE U(1)(2+1) COMPACTE]
El Mouez Ahmed Chaara May 1993 152 p In FRENCH
(ISBN-0-315-85577-0; CTN-94-61149) Copyright Avail: Micromedia Ltd., Technical Information Centre, 240 Catherine Street, Suite 305, Ottawa, Ontario, K2P 2G8, Canada HC/MF

The dispersion and diffusion relations of glueballs and mesons in the compact U(1)(2+1) model were studied. This model has been often used as a simple model of quantum chromodynamics (QCD) since it possesses the property of confinement as well as the states of glueballs. However, its mathematical structure is much more simple than QCD. The method used for studying the dispersion relations consisted in diagonalizing the Hamiltonian of that model in an appropriate base. All calculations were carried out on a 5 by 5 lattice. For diffusion, the time dependent method was employed to calculate the S matrix and the effective diffusion section of the glueballs and mesons. The various results obtained appear to be in agreement with previous work by Hakim (1981), Alessandrini et al. (1980-82), and Irving et al (1983), who used the theory of strongly coupled perturbations and worked on a space-time lattice. CISTI

N94-30262# Valparaiso Univ., IN. Dept. of Physics and Astronomy.
HIGH SENSITIVITY TESTS OF THE STANDARD MODEL FOR ELECTROWEAK INTERACTIONS
1994 8 p
(Contract DE-FG02-88ER-40416)
(DE94-005415; DOE/ER-40416/6) Avail: CASI HC A02/MF A01

The work done on this project focused on two LAMPF experiments. The MEGA experiment is a high-sensitivity search for the lepton family number violating decay mu yields e(gamma) to a sensitivity which, measured in terms of the branching ratio, BR = (mu yields e(gamma))/(mu e(nu)(sub mu)(nu)(sub e)) approximately 10(exp -13), will be over two orders of magnitude better than previously reported values. The second is a precision measurement of the Michel (rho) parameter from the positron energy spectrum of mu yields e(nu)(sub mu)(nu)(sub e) to test the predictions V-A

theory of weak interactions. In this experiment, the uncertainty in the measurement of the Michel (rho) parameter is expected to be a factor of three lower than the present reported value. The detectors are operational, and data taking has begun. DOE

N94-30369# Wisconsin Univ., Madison.
DIRECT ANTI-b b PRODUCTION IN ANTI-pp COLLISIONS AT THE SQUARE ROOT OF s = 1.8 TeV Ph.D. Thesis
J. Lamoureux 1993 244 p
(Contract DE-AC02-76ER-00881)
(DE94-006167; DOE/ER-00881/T6) Avail: CASI HC A11/MF A03

The first measurement of bottom quark production in the forward detector at CDF is presented in this thesis. Events from the 1988/89 Fermilab collider run were selected with forward muons with nearby jets to form a bottom quark tag. The efficiency and acceptance of the detector are then taken into account and the number of events is turned into a cross section: sigma(p(sub t)(sup b) greater than 20 GeV, 1.9 less than the absolute value of eta(sup b) less than 2.5) = 124 +/- 35 +/- 76 nb. The contribution from direct bottom quarks is sigma(p(sub t)(sup b) greater than 20 GeV, p(sub t)(sup anti-b) greater than 15 GeV, 1.9 less than the absolute value of eta(sup b) less than 2.5) = 100 +/- 30(sub -31)(sup +30) nb. DOE

N94-30685# Institute for Advanced Study, Princeton, NJ.
PROBLEMS IN PARTICLE THEORY
S. L. Adler and F. Wilczek Nov. 1993 19 p
(Contract DE-FG02-90ER-40542)
(DE94-003665; DOE/ER-40542/88) Avail: CASI HC A03/MF A01

Areas of emphasis include acceleration algorithms for the Monte Carlo analysis of lattice field and gauge theories, quaternionic generalizations of complex quantum mechanics and field theory, application of the renormalization group to the QCD phase transition, the quantum Hall effect, and black holes. Other work involved string theory, statistical properties of energy levels in integrable quantum systems, baryon asymmetry and the electroweak phase transition, anisotropies of the cosmic microwave background, and theory of superconductors. DOE

N94-30686# Columbia Univ., New York, NY.
THEORY OF ULTRA DENSE MATTER AND THE DYNAMICS OF HIGH ENERGY INTERACTIONS INVOLVING NUCLEI
M. Gyulassy 15 Sep. 1993 13 p
(Contract DE-FG02-93ER-40764)
(DE94-004178; DOE/ER-40764/1) Avail: CASI HC A03/MF A01

Progress in the areas of pQCD radiative processes in dense matter, QCD transport theories to describe the evolution of nonequilibrium phenomena in dense matter, and the development and testing of phenomenological models of high-energy nuclear collisions is summarized. The evolution of the total energy density of quarks and gluons with minijet initial conditions at RHIC energy is shown for Au+Au. DOE

N94-30695 Pacific Northwest Lab., Richland, WA.
PRELIMINARY DETECTOR DESIGN ST862-PROTOTYPE NEUTRON DETECTOR
S. D. Miller, J. D. Affinito, and D. R. Sisk Dec. 1993 22 p Limited Reproducibility: More than 20% of this document may be affected by poor print
(Contract DE-AC06-76RL-01830)
(DE94-004714; PNL-8957) Avail: Issuing Activity (Department of Energy (DOE))

The detection of fast neutrons has been accomplished with commercially available liquid scintillators in detectors. Liquid scintillators discriminate fast neutrons from gamma radiation by discarding pulses with short decay constants. However, pulse-timing methods require expensive, bulky equipment and a high degree of technical sophistication in the user. Researchers at Pacific Northwest Laboratory have developed a new class of scintillating material, polymerizing crystals of CaF2Eu and liquid acrylate monomers with matched indexes of refraction. The new detectors avoid the pulse-timing methods of liquid detectors and allow detectors to be large and relatively light. Fast neutrons can be discriminated from gamma radiation solely on the basis of pulse height (i.e., energy deposition). Using these detectors, a hand-held neutron detection instrument is proposed that can operate on battery power for 8 to 12 hours and be easily used in field conditions for surveying vehicles and structures. DOE

N94-30702# Massachusetts Univ., Amherst.
EXPERIMENT STUDIES OF ELECTRON-POSITRON INTERACTIONS AT THE STANFORD LINEAR ACCELERATOR CENTER
S. S. Hertzbach and R. R. Kofler 1993 10 p
(Contract DE-FG02-92ER-40715)
(DE94-005877; DOE/ER-40715/2) Avail: CASI HC A02/MF A01

The High Energy Physics group at the University of Massachusetts has continued its program of experimental studies of electron-positron interactions at the Stanford Linear Accelerator Center (SLAC). The group activities, including analysis of data taken between 1982 and 1990 with the TPC detector at the PEP facility, continuing data collection and data analysis using the SLC/SLD facility, planning for the newly approved B-factory at SLAC, and participation in design studies for future high energy linear colliders, are briefly summarized. DOE

N94-30709# California Univ., Berkeley. Lawrence Berkeley Lab.
OPERATOR ANALYSIS FOR QUARK AND LEPTON MASSES IN SO(10)
L. J. Hall 1 Nov. 1993 16 p Presented at the 16th Meeting on Elementary Particle Physics, Kazimierz, Poland, 24-28 May 1993
(Contract DE-AC03-76SF-00098)
(DE94-005201; LBL-34797; CONF-9305309-2) Avail: CASI HC A03/MF A01

A sequence of simple assumptions leads to a supersymmetric SO(10) theory with eight predictions in addition to (sin theta)(exp 2): tan beta, m(sub t), V(sub cb), m(sub s), m(sub s)/m(sub d), m(sub u)/m(sub d), V(sub ub), and the amount of CP violation J. These predictions are presented, together with experiments which test them. DOE

N94-30719# Fermi National Accelerator Lab., Batavia, IL.
HEAVY FLAVOR PRODUCTION AT FIXED TARGET PHOTO- AND HADROPRODUCTION
S. Kwan Nov. 1993 9 p Presented at the Advanced Study Conference on Heavy Flavours, Pavia, Italy, 3-7 Sep. 1993
(Contract DE-AC02-76CH-03000)
(DE94-004651; FNAL/C-93/333; CONF-9309292-3) Avail: CASI HC A02/MF A01

Recent results on photo- and hadro-production of heavy flavor particles from fixed target experiments at CERN and Fermilab are presented. These include results on production characteristics, cross-section, and pair correlation for both charm and beauty mesons. DOE

N94-30722# Fermi National Accelerator Lab., Batavia, IL.
A SEARCH FOR RAPIDITY GAP EVENTS IN p(BAR p) COLLISIONS AT D(0)
K. T. Streets (Maryland Univ., College Park.) Nov. 1993 4 p Presented at the International Europhysics Conference on High-energy Physics, Marseille, France, 22-28 Jul. 1993
(Contract DE-AC02-76CH-03000)
(DE94-004654; FNAL/C-93/349-E; CONF-930761-6) Avail: CASI HC A01/MF A01

Preliminary results from a search for jet events with rapidity gaps are presented. These events were produced in p(bar p) interactions at sq. root of s = 1.8 TeV and measured with the D(0) detector at Fermilab. The fraction of events with a rapidity gap is measured as a function of the pseudo-rapidity difference between the cone edges of the two leading jets ((Delta)(eta)(sub c)). An upper limit on the fraction of events with no particles between jets is measured at 0.0093 at a 90% confidence level for events with (Delta)(eta)(sub c) greater than 3 and jet transverse energies greater than 30 GeV. DOE

N94-30762# Louisiana State Univ., Baton Rouge.
RESEARCH IN ELEMENTARY PARTICLE PHYSICS
Lai-Him Chan, R. Haymaker, R. Imlay, R. McNeil, W. Metcalf, and R. Svoboda 1993 141 p
(Contract DE-FG05-91ER-40617)
(DE94-001657; DOE/ER-40617/158) Avail: CASI HC A07/MF A02

Theoretical work on effective action expansion, low-energy models of hadrons, and lattice gauge theories is reported. The progress on the

electron-proton experiment ZEUS in Germany, the LSND neutrino experiment at LAMPF, the Dumand experiment in Hawaii, and the Super Kamiokande experiment in Japan is described. Results from IMB are described. DOE

N94-30775# Los Alamos National Lab., NM.
SCALING IN HEAVY-FERMION SYSTEMS
J. D. Thompson, Z. Fisk, and J. M. Lawrence 1993 36 p Presented at the Workshop on Cuprate and Heavy-fermion Superconductors, Cologne, Germany, 21-30 Sep. 1993
(Contract W-7405-eng-36)
(DE94-005002; LA-UR-93-4344; CONF-9309321-1) Avail: CASI HC A03/MF A01

Ambient pressure characteristics of heavy-fermion compounds, such as the ratio of the low temperature magnetic susceptibility to the electronic specific heat coefficient (gamma) and a simple relationship between the T(exp 2)-coefficient of resistivity and gamma(exp 2), suggest that a single-energy scale T(sub o) dictates the physics of these materials. Such is the case for Kondo-impurity systems to which heavy-fermions are related. We consider the consequences of assuming that the electronic free energy is given by a universal function of T/T(sub 0)(V) where V is the molar volume. We show that volume-dependent magnetic susceptibility, specific heat and electrical resistivity of some heavy-fermion compounds scale as T/T(sub 0)(V), at least over a range in pressures and temperatures. A further consequence of the principle assumption is that Gruneisen parameters defined as - (partial derivative)lnX/(partial derivative)lnV, where X is some physical property, should be identical for all properties and equal to that determined from electronic contributions to the volume-thermal expansion coefficient and specific heat. In several materials, this equality holds, at least approximately. Although evidence is found for single-energy scaling in heavy-fermion materials, we cannot conclude unambiguously that the basic assumption is correct in detail. DOE

N94-30779# Fermi National Accelerator Lab., Batavia, IL.
SEARCH FOR THE TOP QUARK IN THE ELECTRON-ELECTRON AND ELECTRON-MUON CHANNELS AT D0
M. Fatyga (Brookhaven National Lab., Upton, NY.) 3 Dec. 1993 12 p Presented at the 9th Workshop on Proton-Antiproton Collider Physics, Tsukuba, Japan, 18-22 Oct. 1993
(Contract DE-AC02-76CH-03000)
(DE94-006174; FNAL/C-93/385-E; CONF-9310247-5) Avail: CASI HC A03/MF A01

We discuss preliminary results of a search for top quarks using their decays in two di-lepton, with the D0 detector at Fermilab. The present analysis has been optimized to search for a top with mass near 100(GeV/sq. c), consistent with published limits. In the event sample corresponding to an integrated luminosity of 15pb(exp -1) we observe two events passing all selection cuts. The number of events observed is consistent with the expected number of background events. Consequently, we do not claim the observation of a top decay in the present event sample. We note, however, that the kinematic properties of one of the events appear to be far removed from known backgrounds. We discuss the event and show results of the mass likelihood analysis when applied to this event. DOE

N94-30795 National Physical Lab., Teddington (England). Radiation Science and Acoustics Div.
DETERMINATION OF PHOTON FLUENCE SPECTRA FROM THE NPL MOBALTRON Co-60 UNIT
D. R. Shipley and S. Duane Jan. 1994 15 p
(ISSN 0955-9655)
(NPL-RSA(EXT)-46; ETN-94-95854) Copyright Avail: Issuing Activity (National Physical Lab., Teddington, Middlesex TW11 0LW, England)

Absorbed dose to water calibrations of secondary standard hospital dosemeters are carried out in both x-radiation from 4 to 19 MV and in Co-60 gamma radiation. Measurements are performed using the primary standard graphite calorimeter and by inserting the secondary standard and working standard chambers at a reference depth in either a water or graphite phantom. Details of the dose distributions and the responses of these chambers in each phantom for the Co-60 radiation quality are, however, unknown. A knowledge of the photon fluence spectra produced by the Co-60 unit is therefore required to enable this analysis to be carried out. Work undertaken to determine the photon fluence spectra incident on the front face of the water and graphite phantoms under standard measurement conditions is described. The spectra were validated by comparing calculated tissue phantom ratios with recent experimental values. The calculated tissue phantom ratio (TPR) values were found to agree with measurements to within 1 to 2 sigma (total uncertainty), and also with independent estimates obtained using the program AVERMV. The observed discrepancies were primarily systematic in nature with the largest source of uncertainty being the change in beam quality, and hence chamber calibration factor, with depth in the phantom. ESA

N94-30834 New York Univ., New York.
SUPERDIFFUSION
G. M. Zaslavsky Oct. 1993 41 p Limited Reproducibility: More than 20% of this document may be affected by microfiche quality
(Contract DE-FG02-92ER-54184)
(DE94-002333; DOE/ER-54184/1) Avail: CASI HC A03

A new approach to the problem of anomalous transport is developed, which is based on an understanding of the phase space topological properties of incomplete dynamical chaos of magnetic surfaces and particles. General concepts are reviewed, self-similar behavior is established for a force-free model, and the presence of super-diffusion in toroidal geometry is confirmed for appropriate conditions. Manipulation with control parameters can be effectively used to change the rate of diffusion and the characteristic exponent of the transport. As an additional example of the anomalous transport, chaotic instability induced by computer simulation is demonstrated. This is important in preparing of codes and simulation programs. DOE

N94-30836 Purdue Univ., West Lafayette, IN.
DEEXCITATION PROCESSES IN NUCLEAR REACTIONS: THE STUDY OF HOT HADRONIC MATTER
N. T. Porile 1993 35 p Limited Reproducibility: More than 20% of this document may be affected by microfiche quality
(Contract DE-FG02-88ER-40408)
(DE94-003396; DOE/ER-40408/8) Avail: CASI HC A03

The research program involved continuing analysis of Fermilab E-735--search for quark-gluon plasma (QGP) in (bar p)-p collisions; experiments on multi-fragmentation using reverse kinematics at the Bevalac; continuing study of target fragments produced in the interaction of copper with intermediate-energy heavy ions; and detector R&D for the STAR detector at RHIC. DOE

N94-30837# Kansas State Univ., Manhattan.
ATOMIC PHYSICS WITH HIGHLY CHARGED IONS
P. Richard Oct. 1993 22 p
(Contract DE-FG02-86ER-13491)
(DE94-003397; DOE/ER-13491/641) Avail: CASI HC A03/MF A01

The past year has been a busy one for all three accelerators: the LINAC, EBIS, and the tandem. The EBIS continues to deliver beams of highly charged ions around the clock for the study of low energy collisions with gases and surfaces. The electron beam energy was upgraded to 10 keV, and intensities of highly charged species such as Xe(44+) were greatly increased. The tandem, the traditional source of highly charged binary encounter electron production at zero degrees were studied for medium Z (Si,Cl,Cu) projectiles. Recoil momentum spectroscopy has been used to separate the contributions to collisional ionization of one-electron ions (C(5+), O(7+), F(8+)) from the nucleus and the electrons of a He target. Marked structure in the binary encounter electron spectra for Cu(sup q+) on H2 targets was measured for moderate velocity projectiles. Electron capture by slow multiply charged (EBIS) projectiles from laser excited targets has been carried out. Cross sections for capture from Na(3s) and Na*(3p) were measured for velocities between 0.1 and 1 au. The extension of these experiments to laser excited Rydberg targets is proceeding. Electron capture cross sections and average Q values for Ar(16+) on He at velocities between 0.23 and 1.67 au were measured. The charge state distribution of the He recoils following large angle scattering of C(4+) and C(6+) ions at 7.5 keV/u has been measured. Cross sections have been measured for up to sextuple capture from C60 (buckminsterfullerene) by highly charged slow projectiles. Coupled channel calculations for double capture from He by slow multicharge ions were carried out. DOE

N94-30838# Maryland Univ., College Park. Dept. of Physics.
THEORETICAL STUDIES IN HADRONIC AND NUCLEAR PHYSICS

J. J. Griffin and T. D. Cohen Jul. 1993 51 p
(Contract DE-FG02-93ER-40762)
(DE94-003524; DOE/ER-40762/010) Avail: CASI HC A04/MF A01

Research in the Maryland Nuclear Theory Group focusses on problems in four basic areas of current relevance. The section on Hadrons in Nuclei reports research into the ways in which the properties of nucleons and the mesons which play a role in the nuclear force are modified in the nuclear medium. QCD sum rules supply a new insight into the decrease of the nucleon's mass in the nuclear medium. The quark condensate decreases in nuclear matter, and this is responsible for the decrease of the nucleon's mass. The section on the Structure of Hadrons reports progress in understanding the structure of the nucleon. These results cover widely different approaches: lattice gauge calculations, QCD sum rules, quark-meson models with confinement, and other hedgehog models. Progress in Relativistic Nuclear Physics is reported on electromagnetic interactions in a relativistic bound state formalism, with applications to elastic electron scattering by deuterium, and on application of a two-body quasipotential equation to calculate the spectrum of mesons formed as bound states of a quark and antiquark. A Lorentz-invariant description of the nuclear force suggests a decrease of the nucleon's mass in the nuclear medium similar to that found from QCD sum rules. Calculations of three-body bound states with simple forms of relativistic dynamics are also discussed. The section on Heavy Ion Dynamics and Related Processes describes progress on the (e(+)e(-)) problem and heavy-on dynamics. In particular, the sharp electrons observed in (beta)(+) irradiation of heavy atoms have recently been subsumed into the 'Composite Particle Scenario,' generalizing the '(e(+)e(-))-Puzzle' of the pairs from heavy ion collisions to the 'Sharp Lepton Problem.' DOE

N94-30874# Argonne National Lab., IL.
THEORY FOR ELECTRON-TRANSFER REACTIONS INVOLVING TWO MARCUS SURFACES WITH A DIFFERENT FORCE CONSTANT
Jau Tang 1994 17 p
(Contract W-31-109-eng-38)
(DE94-005925; ANL/CHM/PP-80227) Avail: CASI HC A03/MF A01

A theory concerning electron-transfer reactions at high temperature involving two Marcus parabolic surfaces with a different force constant is presented. The dynamic solvent effects are also considered using the stochastic Liouville equation assuming an overdamped Debye solvent. An analytical expression for the adiabatic/nonadiabatic electron-transfer rate constant is derived. DOE

N94-30881# Massachusetts Inst. of Tech., Cambridge. Plasma Fusion Center.
SELF-SIMILAR VARIABLES AND THE PROBLEM OF NONLOCAL ELECTRON HEAT CONDUCTIVITY
S. I. Krasheninnikov and O. G. Bakunin Oct. 1993 31 p
(Contract DE-FG02-91ER-54109)
(DE94-005826; PFC/RR-93-4) Avail: CASI HC A03/MF A01

Self-similar solutions of the collisional electron kinetic equation are obtained for the plasmas with one and three dimensional plasma parameter inhomogeneities and arbitrary Z(sub eff). For the plasma parameter profiles characterized by the ratio of the mean free path of thermal electrons with respect to electron-electron collisions, lambda(sub T), to the scale length of electron temperature variation, L, one obtains a criterion for determining the effect that tail particles with motion of the nondiffusive type have on the electron heat conductivity. For these conditions it is shown that the use of a 'symmetrized' kinetic equation for the investigation of the strong nonlocal effect of suprathermal electrons on the electron heat conductivity is only possible at sufficiently high Z(sub eff) (Z(sub eff) greater than or equal to (L/lambda(sub T))(exp 1/2). In the case of three dimensional inhomogeneous plasma (spherical symmetry), the effect of the tail electrons on the heat transport is less pronounced since they are spread across the radius r. DOE

N94-30886# Fermi National Accelerator Lab., Batavia, IL.
CHARMONIUM AND BOTTOMONIUM IN (-p)p INTERACTIONS
S. Pordes Dec. 1993 13 p Presented at the Advanced Study Conference on Heavy Flavours, Pavia, Italy, 3-7 Sep. 1993
(Contract DE-AC02-76CH-03000)
(DE94-006173; FNAL/C-93/383; CONF-9309292-4) Avail: CASI HC A03/MF A01

Some examples of data from the CDF collaboration on J/psi, chi, psi-prime, and Gamma production are presented. Such data are used to test models of production dynamics and for the understanding of rates for b quark production. As a complement to this data from the highest energy accelerator experiment, operating at square root of s = 1.8 TeV, data from Fermilab experiment E760 on masses, widths, states and branching ratios in the Charmonium system, obtained by studying resonant formation of c(bar c) states in p(bar p) annihilation at square root of s = m(c(bar c)), is also shown. DOE

N94-30887# Fermi National Accelerator Lab., Batavia, IL.
INCLUSIVE SINGLE MUON PRODUCTION IN D0
A. K. A. Maciel (Centro Brasileiro de Pesquisas Fisicas, Rio de Janeiro.) Dec. 1993 9 p Presented at the 9th Workshop on Proton-Antiproton Collider Physics, Tsukuba, Japan, 18-22 Oct. 1993
(Contract DE-AC02-76CH-03000)
(DE94-006175; FNAL/C-93/395-E; CONF-9310247-6) Avail: CASI HC A02/MF A01

Preliminary cross section measurements from the D0 experiment at Fermilab for the inclusive production of single muons in proton-antiproton collisions at square root of s = 1.8 TeV are presented. It is found that the experimental results are consistent with those obtained from a Monte Carlo simulation using NLO calculations from ISAJET. DOE

N94-30891# Lawrence Livermore National Lab., CA.
DISSOCIATIVE RECOMBINATION OF H3(+)
A. E. Orel (California Univ., Davis.), K. C. Kulander, and B. H. Lengsfield, III Dec. 1993 9 p Presented at the Physical Chemistry of Molecules and Grains in Space, Mount Saint-Odile, France, 6-10 Sep. 1993
(Contract W-7405-eng-48)
(DE94-005356; UCRL-JC-114022; CONF-9309317-1) Avail: CASI HC A02/MF A01

Recent experiments by Larsson et al. have confirmed the prediction of a high energy (approximately 9.5 eV) peak in cross section for dissociative recombination of H3(+). This peak is caused by four doubly excited resonance states of H3. Electron scattering calculations using the complex Kohn method provide resonance positions and widths as functions of the internuclear geometry. This information was used as input to a wave packet calculation for the dissociation dynamics on a fit to the resonant state potential energy surfaces. The resulting cross sections agree well with this experiment. DOE

N94-30893# Argonne National Lab., IL.
NEUTRONICS OF A D-Li NEUTRON SOURCE: AN OVERVIEW
I. C. Gomes and D. L. Smith Nov. 1993 23 p Presented at the 6th International Conference on Fusion Reactor Materials, Stresa, Italy, 27 Sep. - 1 Oct. 1993 Revised
(Contract W-31-109-eng-38)
(DE94-005372; ANL/EP/CP-79739-Rev; CONF-930928-6-Rev) Avail: CASI HC A03/MF A01

The importance of having a high energy (14 MeV) neutron source for fusion materials testing is widely recognized. The availability of a test volume with easy accessibility, with a radiation environment similar to the one expected for a fusion reactor, and with dimensions large enough to accommodate several small samples or a small blanket mock-up are requirements impossible to meet with the existing reactors and irradiation facilities. A D-Li neutron source meets the above mentioned requirements and can be built today with well known technology. This paper describes some relevant topics related to beam target configuration, neutron flux spectrum, and nuclear responses for a D-Li neutron source. The target-beam configuration is analyzed for different beam cross sectional areas and trade-offs between the area of the beam and related quantities such as available volume for testing, peak fluxes, and flux or nuclear responses gradient are presented. The conclusion is that the D-Li neutron source has the necessary characteristics to be the option of choice for IFMIF. DOE

N94-30903# Argonne National Lab., IL.
THEORY FOR ELECTRON-TRANSFER REACTIONS IN A THREE-COMPONENT SYSTEM: THE DEGENERATE REGIME
J. Tang 1994 17 p
(Contract W-31-109-eng-38)
(DE94-005919; ANL/CHM/PP-79990) Avail: CASI HC A03/MF A01

Theory for nonadiabatic electron-transfer reactions at high temperature is presented for a three-component system: a donor, an acceptor, and a bridging intermediate. Only the 'degenerate' regime of triple energy-level crossing is considered assuming three Marcus parabolas cross at the same point and the direct free energy gap vanishes. Because the ordinary second-order perturbation theory fails, the nonperturbative stochastic Liouville approach of Zusman is used in deriving analytical expressions for the superexchange and the sequential electron-transfer rate constants. DOE

N94-30980 Stockholm Univ. (Sweden). Dept. of Physics.
CALCULATION OF INELASTIC MEAN FREE PATH AND STOPPING POWER FOR ELECTRONS IN SOLIDS FROM AN OPTICAL-DATA MODEL
J. M. Fernandez-Varea (Universidad Autonoma de Barcelona, Bellaterra, Spain.), D. Liljequist, R. Mayol, and F. Salvat Nov. 1992 28 p Limited Reproducibility: More than 20% of this document may be affected by microfiche quality
(USIP-92-06; ETN-94-95984) Avail: CASI HC A03

The numerical calculation of electron inelastic mean free path and stopping power from an optical data model recently proposed by Fernandez-Varea et al. is described. Explicit expressions for the one electron total cross sections of the two modes model of the free electron gas and the delta oscillator are derived. The inelastic mean free path and the stopping power are obtained as integrals of these one electron total cross sections weighted by the optical oscillator strength. The integrals can be easily evaluated, with a selected accuracy, by using the FORTRAN 77 subroutine GABQ described, which implements a 20 point Gauss Adaptive Bipartition Quadrature method. Source listings of FORTRAN 77 subroutines to compute the one electron total cross sections are also given. ESA

N94-30485*# Greenville Coll., IL. Dept. of Physics.
A FUTURE, INTENSE SOURCE OF NEGATIVE HYDROGEN IONS
Hugh Siefken and Charles Stein *In* NASA, Washington, Technology 2003: The Fourth National Technology Transfer Conference and Exposition, Volume 1 Feb. 1994 p 411-420 (For primary document see N94-30440 08-99)
Avail: CASI HC A02/MF A04

73 NUCLEAR AND HIGH-ENERGY PHYSICS

Includes elementary and nuclear particles; and reactor theory. For space radiation see *93 Space Radiation.*

N94-28486# Department of Energy, Washington, DC. Office of High Energy and Nuclear Physics.
US/JAPAN COOPERATION IN HIGH ENERGY PHYSICS
16 Nov. 1993 148 p
(DE94-005376; DOE/ER-0607T) Avail: CASI HC A07/MF A02

The objective of the Implementing Arrangement was to further the energy programs of both countries by establishing a framework for cooperation in the field of high energy physics, including research, accelerator and detector instrumentation research and development, the fabrication and subsequent use of new experimental devices and facilities, and related joint efforts as may be mutually agreed. Over the years, this cooperation has been very effective and has strengthened the overall collaborative efforts and the understanding between our nations and their citizens. It has demonstrated to the world our ability to work together to attack difficult problems. High Energy Physics goes across national borders; the bond is clearly intellectual and common ground is shared for the benefit of all in a most effective manner. This review covers the activities conducted under the aegis of the US/Japan Committee for Cooperation in High Energy Physics during the past five years (1988-1993). This was the second such US review of the US/Japan cooperative activities; the first was held in 1987. DOE

N94-28507# California Univ., Berkeley. Lawrence Berkeley Lab.
THE INDUCTION APPROACH TO HEAVY ION INERTIAL FUSION: ACCELERATOR AND TARGET CONSIDERATIONS
R. O. Bangerter Aug. 1993 21 p Presented at the International Symposium on Heavy Ion Fusion, Frascati, Italy, 25-28 May 1993
(Contract DE-AC03-76SF-00098)
(DE94-005216; LBL-33798; HIFAN-577; CONF-9305136-16) Avail: CASI HC A03/MF A01

Induction acceleration is one of two principal approaches for producing ion beam for heavy-ion inertial fusion. This approach was first suggested by the late Denis Keefe of Lawrence Berkeley Laboratory and is the main approach of the U.S. heavy-ion-fusion program. Induction accelerators have the ability to handle high beam currents; therefore, accumulation rings or storage rings are not required. The target and accelerator considerations that are important for the design of induction accelerators for fusion are reviewed. These considerations, including some important assumptions, have led to a standard induction accelerator concept; however, a careful examination of the assumptions and considerations shows that many of them are not truly fundamental. Through improvements in technology, changes in design, and alternate ways of focusing beams, it appears possible to circumvent or relax the constraints imposed by the standard orthodoxy. If it is possible, it will lead to induction accelerators that are more efficient and less costly than the standard concept. DOE

N94-28612 Joint Inst. for Nuclear Research, Dubna (USSR).
POSSIBLE EXPLANATION OF THE INTERACTION CROSS-SECTION GROWTH AT HIGH ENERGIES
V. A. Belyakov and V. N. Streltsov 1992 4 p Limited Reproducibility: More than 20% of this document may be affected by microfiche quality
(DE94-606457; JINR-E-2-92-368) Avail: CASI HC A01 (US Sales Only)

On the basis of the relativized Yukawa potential it is shown that the mowing hadron transverse size grows with increasing its energy approximately (ln(gamma))(exp 0.8) (gamma is the Lorentz factor). The opinion is expressed that the known growth of the interaction cross section at high energies is due to the indicated reason. DOE

N94-28623 Technical Research Centre of Finland, Espoo.
NUCLEAR ENERGY RELATED RESEARCH
R. Rintamaa, ed. May 1992 55 p Limited Reproducibility: More than 20% of this document may be affected by microfiche quality
(DE94-606286; VTT-EKA-B-9) Avail: CASI HC A04

The annual Research Program Plan describes publicly funded nuclear energy related research to be carried out mainly at the Technical Research Center of Finland (VTT) in 1992. The research is financed primarily by the Ministry of Trade and Industry (KTM), the Finnish Center for Radiation and Nuclear Safety (STUK), and VTT itself. Other research institutes, utilities, and industry also contribute to many projects. DOE

N94-29065 Aerospace Corp., El Segundo, CA. Technology Operations.
ADVANTAGES OF THE LBL 88-INCH CYCLOTRON ION BEAM FOR SEP STUDIES
Rocky Koga and Steven D. Pinkerton 15 Sep. 1993 23 p Limited Reproducibility: More than 20% of this document may be affected by microfiche quality
(Contract F04701-88-C-0089)
(AD-A275142; TR-0091(6940-05)-4; SMC-TR-93-59) Avail: CASI HC A03

The Lawrence Berkeley Laboratory 88-inch cyclotron has been widely used for single-event phenomena (SEP) studies. The advantages and disadvantages of using ions at this facility are compared with those for other accelerator facilities in the U.S. One major advantage of the 88-inch cyclotron is that several ion species, with varying stopping powers, can be made available in a matter of seconds by simply adjusting the cyclotron frequency. The importance of this capability is illustrated via test results for a high-density SRAM and an EEPROM device type. DTIC

N94-29422# Nationaal Inst. voor Kernfysica en Hoge Energiefysica, Amsterdam (Netherlands).
TUNING OF AmPS
R. Maas and Y. Wu Jul. 1993 22 p
(NIKHEF-K-AmPS-93-01; ETN-94-95517) Avail: CASI HC A03/MF A01

Experience in the tuning of the AmPS (Amsterdam Pulse Stretcher) is reported. Documentation on ring components is described and the control system nomenclature is explained. Tuning of the AmPS is described for storage mode and stretcher mode. ESA

N94-29467# Nationaal Inst. voor Kernfysica en Hoge Energiefysica, Amsterdam (Netherlands).
BPM901N MONITOR ELECTRONICS FOR THE DETERMINATION OF THE BUNDLE PROFILE IN THE EXTRACTION LINE OF AmPS [BPM901N MONITOR ELEKTRONICA VOOR BEPALING VAN HET BUNDELPROFIEL IN DE EXTRACTIELIJN VAN AmPS]
H. Verkooijen 24 Jun. 1993 21 p In DUTCH
(DIGEL-1993-9; ETN-94-95516) Avail: CASI HC A03/MF A01

The Bundle Profile Monitor 901N (BPM901N) was developed to determine the bundle profile of the electron bundle in the AmPS (Amsterdam Pulse Stretcher) storage ring. The extracted bundle and the outer side of the circulating bundle are measured. The current detected by the monitor is converted into a voltage and integrated during an adjustable time, such that the output signal gives the charge. The monitor electronics consists of an amplifier, an integrator, and a computer interface. The current range of the amplifier is between 1 pA and 1 microA. The integration time ranges between 10 ms and 100 ms. The charge signal is digitized and then processed by the computer. ESA

N94-29596# Tokyo Univ., Tanashi (Japan). Synchrotron Radiation Lab.
ACTIVITY REPORT OF SYNCHROTRON RADIATION LABORATORY 1992
Katsuaki Sato, Masami Fujisawa, Koji Tsuzukiyama, Yuji Togami, Koki Takanashi, Hiroyasu Fujimori, Toshiaki Osaka, Kimihiro Ishii, Toshinobu Kanai, and Tsutomu Tsutaya et al Mar. 1993 103 p
(JTN-94-80600) Avail: CASI HC A06/MF A02

This report describes the scientific activity of the Synchrotron Radiation Laboratory of the Institute for Solid State Physics (SRL-ISSP), the University of Tokyo. The central experimental facility is SOR-RING, a 380 MeV electron storage ring with six experimental stations dedicated to synchrotron radiation science. Reports on the performance of SOR-RING and related accelerator science are also included along with the activity of the Branch Laboratory of SRL-ISSP located at the Photon Factory of the National Laboratory for High Energy Physics (PF-KEK). In 1992, active experiments were carried out on solid state spectroscopy and radiation effects on biological materials, optical absorption and reflection spectroscopy mainly for unoccupied conduction states, and photoemission, especially resonant photoemission to identify energy levels of localized electrons. Major actions were improving the monochromator slit system, replacing the electron energy analyzer with a double-stage Cylindrical Mirror Analyzer (CMA), which enables photoelectron EDC's (Energy Distribution Curve) of better quality and photoemission experiments using monochromatic light from a modified Wadsworth monochromator. Author (NASDA)

N94-29888# Nationaal Inst. voor Kernfysica en Hoge Energiefysica, Amsterdam (Netherlands).
STRIPLINE MONITOR ELECTRONICS FOR THE BUNDLE POSITION DETERMINATION IN AmPS [STRIPLINE MONITOR ELEKTRONICA VOOR DE BUNDELPOSITIE BEPALING BIJ AMPS]
H. Verkooijen 11 May 1993 37 p In DUTCH
(DIGEL-1993-8; ETN-94-95515) Avail: CASI HC A03/MF A01

A stripline monitor was developed to measure the current and the position of the bundle in the AmPS (Amsterdam Pulse Stretcher) storage ring. The monitor consists of four strips of a quarter wavelength (the accelerator frequency is 2856 MHz). The signals from the strips are processed by stripline monitor electronics using a converter. The electronics delivers two output signals depending on the bundle position, and a signal depending on the bundle current. The system has a 15 MHz bandwidth, allowing the detection of 20 nS position and intensity changes. ESA

N94-29924# Oak Ridge National Lab., TN.
OVERVIEW OF SHIELDING ANALYSES FOR THE MHTGR FROM 1986 TO 1991
J. A. Bucholz 1993 5 p Presented at the 8th International Conference on Radiation Shielding, Arlington, TX, 24-27 Apr. 1994
(Contract DE-AC05-84OR-21400)
(DE94-002448; CONF-940424-5) Avail: CASI HC A01/MF A01

This paper provides an historical overview of the shielding analyses performed at ORNL for the Modular High Temperature Gas-Cooled Reactor (MHTGR) between late 1985 and early 1992. While the present commercial MHTGR design has evolved considerably and is different in many respects from the 1988/1989 reference design discussed in this paper, the analytical techniques used to address several key areas of concern are still in use today. This paper highlights some of those areas of concern and traces the evolution of the analytical techniques used to address them over a 6 or 7 year period. DOE

N94-30211 Defence Research Establishment, Ottawa (Ontario).
PROCEEDINGS OF THE 1991 SINGLE EVENT UPSET SYMPOSIUM
1991 406 p Symposium held in Ottawa, Ontario, 30 Apr. - 2 May 1991
(DSIS-92-00652; CTN-94-61129) Avail: Issuing Activity (Defence Research Establishment, Ottawa, ON K1A 0Z4 Canada)

A symposium was held to provide a forum for exchange of scientific results of research into single event upsets (SEU's). Papers were presented on SEU and latchup measurements, proton upset measurements, SEU's in various microelectronic devices, SEU research programs, space radiation, SEU-related test facilities and procedures, SEU modelling and basic physics, and detectors. For individual titles, see N94-30212 through N94-30222.

N94-30212 Massachusetts Inst. of Tech., Lexington. Lincoln Lab.
SINGLE EVENT UPSET AND LATCHUP MEASUREMENTS AT BROOKHAVEN NATIONAL LABORATORY
V. J. Sterrino *In* Defence Research Establishment, Proceedings of the 1991 Single Event Upset Symposium 1991 22 p (For primary document see N94-30211 08-73)
Avail: Issuing Activity (Defence Research Establishment, Ottawa, ON K1A 0Z4 Canada)

Single event upset (SEU) and single event latchup (SEL) tests were conducted on a large number of digital and analog devices intended for use in the Mid-course Space Experiment satellite. Seven different heavy ion beams were utilized in the tests, conducted in the Heavy Ion Test Facility at Brookhaven National Laboratory. The ions included C-12, F-19, Si-28, Ni-59, Br-80, I-127, and Au-197. The linear energy transfer (LET) for these particles ranged from 1.43 to 163.4 MEV cm squared/Mg. SEL is a phenomenon occurring when a single high-energy particle triggers the normal operating point of a device to a new stable state, where it can remain latched if the power supply supplies sufficient current. Generally, all the memory devices tested showed some latchup tendency. For devices having both epitaxial and non-epitaxial versions, the non-epitaxial version latched but the epitaxial did not, even at the highest tested LET value. All of the Motorola DSP56001 (the central processor element in the satellite's signal processor) were latchup sensitive. Those devices that showed evidence of SEL had a mean time to latchup of 2,500 to 25,000 powered days. For the DSP56001, mean time to SEU of any memory segment varied from 25 to 50 days. Memory devices showed mean time to SEU of .033 days. Implications of these results for the software and processor design are discussed. Author (CISTI)

N94-30213 Clarkson Univ., Potsdam, NY. Dept. of Physics.
ENERGETIC HEAVY-ION TRACKS IN MICRON SITES Abstract Only
J. F. Dicello and M. Zaider *In* Defence Research Establishment, Proceedings of the 1991 Single Event Upset Symposium 1991 1 p (For primary document see N94-30211 08-73)
Avail: Issuing Activity (Defence Research Establishment, Ottawa, ON K1A 0Z4 Canada)

As sensitive volumes increase, energy deposition patterns from energetic heavy ions (those ions heavier than He) exhibit unique and perhaps surprising characteristics. In comparison with low-energy heavy ions of the same linear energy transfer, the mean energy deposited per event in sites of micrometer dimensions can be significantly lowered by atomic interactions. Similarly, nuclear interactions, which tend to increase the mean energy deposited by protons and neutrons, actually tend to lower the energy deposited by high-energy heavy ions, such as Fe irons in the GeV range. Measurements of energy deposition patterns in plastics for energetic heavy ion beams, including microdosimetric spectra, illustrate these effects. Author (CISTI)

N94-30214 Aerospace Corp., El Segundo, CA.
SINGLE EVENT UPSET SUSCEPTIBILITIES OF LATCHUP IMMUNE CMOS PROCESS PROGRAMMABLE GATE ARRAYS
R. Koga, W. R. Crain, K. B. Crawford, S. J. Hansel, D. D. Lau, and T. K. Tsubota *In* Defence Research Establishment, Proceedings of the 1991 Single Event Upset Symposium 1991 12 p (For primary document

see N94-30211 08-73)
Avail: Issuing Activity (Defence Research Establishment, Ottawa, ON K1A 0Z4 Canada)

Single event upsets (SEU) and latchup susceptibilities of complementary metal oxide semiconductor programmable gate arrays (CMOS PPGA's) were measured at the Lawrence Berkeley Laboratory 88-in. cyclotron facility with Xe (603 MeV), Cu (290 MeV), and Ar (180 MeV) ion beams. The PPGA devices tested were those which may be used in space. Most of the SEU measurements were taken with a newly constructed tester called the Bus Access Storage and Comparison System (BASACS) operating via a Macintosh II computer. When BASACS finds that an output does not match a prerecorded pattern, the state of all outputs, position in the test cycle, and other necessary information is transmitted and stored in the Macintosh. The upset rate was kept between 1 and 3 per second. After a sufficient number of errors are stored, the test is stopped and the total fluence of particles and total errors are recorded. The device power supply current was closely monitored to check for occurrence of latchup. Results of the tests are presented, indicating that some of the PPGA's are good candidates for selected space applications. Author (CISTI)

N94-30215* National Aeronautics and Space Administration. Goddard Space Flight Center, Greenbelt, MD.
MULTIPLE SINGLE EVENT UPSETS IN CMOS STATIC RAMS Abstract Only
E. G. Stassinopoulos and G. J. Brucker *In* Defence Research Establishment, Proceedings of the 1991 Single Event Upset Symposium 1991 1 p (For primary document see N94-30211 08-73)
Avail: Issuing Activity (Defence Research Establishment, Ottawa, ON K1A 0Z4 Canada)

The occurrence of multiple upset errors during ground tests can contaminate the data and lead to error cross sections which are too high. In space, multiple errors may produce higher upsets than predicted and if they occur in single words they can defeat error detection and correction hardware. This investigation involves data which were taken during an experimental study of dose imprint effects in static memories. The results show that multiple errors occurred mainly for heavy ions with high linear energy transfers and with the majority of these in the soft upset sections of the dose-imprinted memory samples. The percentages of the total number of errors which were singles, doubles, and triplets, were determined as a function of LET, dose, and soft or hard section of the devices. The experimental observations are compared to the predictions of simple binomial statistics. Author (CISTI)

N94-30216 Bubble Technology Industries, Inc., Chalk River (Ontario).
ADAPTION OF THE BUBBLE DETECTOR FOR USE AS A LET SPECTROMETER **c35**
H. Ing, R. Noulty, and T. Cousins *In* Defence Research Establishment, Proceedings of the 1991 Single Event Upset Symposium 1991 14 p (For primary document see N94-30211 08-73)
Avail: Issuing Activity (Defence Research Establishment, Ottawa, ON K1A 0Z4 Canada)

A new family of radiation detectors has been developed over the last few years whose principle is closely related to the concept of linear energy transfer (LET). These detectors, called bubble detectors, consist of a dispersion of superheated liquid droplets in an elastic medium. When radiation enters the detector, it imparts energy to a liquid droplet. If the energy exceeds a critical value, the droplet will boil and a bubble is formed. These detectors have been used in biological dosimetry, but their use for space related applications requires modifications imposed by the nature of the radiation of interest. For instance, certain heavy ions in space which pose no hazard to biological systems could still cause severe damage to electronics. The elastic medium in a biological dosimeter would shield the charged particles of low penetrability, so a new bubble detector configuration is being developed which eliminates use of the normal elastic medium. By using various types of bubble detector layers, it should be possible to measure the LET distributions appropriate for electronic components. Author (CISTI)

N94-30217 Defence Research Establishment, Ottawa (Ontario).
MCMASTER ACCELERATOR FACILITY
J. W. Stark, T. Cousins, and J. A. Davies *In its* Proceedings of the 1991 Single Event Upset Symposium 1991 3 p (For primary document see N94-30211 08-73)
Avail: Issuing Activity (Defence Research Establishment, Ottawa, ON K1A 0Z4 Canada)

The McMaster model FN tandem accelerator is useful for producing particle beams for the single event upset test facility. Ions are produced by a universal negative ion source and accelerated by potential differences toward the van de Graaff accelerator. The particles will acquire an energy equal to the potential on the high voltage terminal, where the low- and high-energy acceleration tubes are connected by an electron stripper canal. Carbon stripper foils in the canal strip the ion beam of its negative charge, producing a positive beam of particles. A gas stripper is used for heavy ions. At the end of the high energy acceleration tube, an analyzing magnet deflects the ion beam for a final mass selection. The target facility is a scattering chamber which has many benefits for single event upset operation. New additions to the target facility include a Faraday cup at the zero degree scattering chamber entrance and a multi-device automated holder that allows simultaneous installation of two devices under test (DUT), along with a surface barrier detector coaxial with the DUT. Second and third barrier detectors can be added to allow direct measurements of energy and fluence while the DUT is under bombardment. An associated facility has two evaporators used for preparing targets. Author (CISTI)

N94-30218 Defence Research Establishment, Ottawa (Ontario).
ADVANCED DEVELOPMENT OF THE SPECTRUM SCIENCES MODEL 5005-TF, SINGLE EVENT TEST FIXTURE **c35**
M. R. Ackermann, J. S. Browning, B. W. Hughlock, G. K. Lum, W. C. Tsacoyeanes, and M. D. Weeks *In its* Proceedings of the 1991 Single Event Upset Symposium 1991 12 p (For primary document see N94-30211 08-73)
Avail: Issuing Activity (Defence Research Establishment, Ottawa, ON K1A 0Z4 Canada)

A commercial application of particle identification methods commonly used in high-energy physics research has been developed for single-event testing of microelectronics. The Model 5005-TF single event test fixture can be used to substantially reduce the parts qualification testing costs for many space satellite systems. The 5005-TF includes a californium source, photomultiplier tubes, ultra thin film scintillation detectors, mountings, a vacuum chamber and related controls, and electronics for processing time-of-flight (TOF) signals. Tests were conducted to examine how well the TOF parameter identified the fission fragment (atomic number, mass, kinetic energy). For the lighter fragments, the TOF parameter has a maximum error of about 30 atomic mass units, which is inadequate for particle identification. Since light output of thin-film scintillators was known to correlate with average velocity of a fission fragment passing through the scintillator, it was decided to use the light output in conjunction with TOF to improve particle identification. This dual-parameter method was implemented in the 5005-TF and test results show favorable comparison with results from an ion beam facility. Author (CISTI)

N94-30219 Rensselaer Polytechnic Inst., Troy, NY.
USING Cf-252 FOR SINGLE EVENT UPSET TESTING
J. W. Howard, R. Chen, R. C. Block, M. Becker, A. G. Costantine, L. S. Smith, G. A. Soli, and M. C. Stauber *In* Defence Research Establishment, Proceedings of the 1991 Single Event Upset Symposium 1991 8 p (For primary document see N94-30211 08-73)
Avail: Issuing Activity (Defence Research Establishment, Ottawa, ON K1A 0Z4 Canada)

An improved system using Cf-252 and associated nuclear instrumentation has been used to determine single event upset (SEU) cross section versus linear energy transfer (LET) curve for several static random access memory (SRAM) devices. Through the use of a thin-film scintillator, providing energy information on each fission fragment, individual SEU's and ion energy can be associated to calculate the cross section curves. Results are presented from tests of several SRAM's over the 17-43 MeV-cm squared/mg LET range. Values obtained for SEU cross sections and LET thresholds are in good agreement with the results from accelerator testing. The equipment is described, the theory of thin-film scintillation detector response is summarized, experimental procedures are reviewed, and the test results are discussed. Author (CISTI)

N94-30220 Clemson Univ., SC. Dept. of Physics and Astronomy.
CHARGE COLLECTION SPECTROSCOPY APPLIED TO MOS RAM'S
c25

P. J. McNulty, D. R. Roth, W. J. Beauvais, and W. G. Abdel-Kader *In* Defence Research Establishment, Proceedings of the 1991 Single Event Upset Symposium 1991 13 p (For primary document see N94-30211 08-73)
Avail: Issuing Activity (Defence Research Establishment, Ottawa, ON K1A 0Z4 Canada)

Pulse-height analysis of signals observed on the powerlines of metal oxide semiconductor static random access memory (MOS SRAM) devices provide useful information regarding the devices' potential sensitivity to single event upsets (SEU's) in space, including the dimensions of the sensitive volume. It is also useful to test model dependent assumptions regarding the increase in charge collection at the junction with increasing angle of incidence and the corresponding decrease in the number of particles traversing the junction. Experimental charge collection measurements were made across the powerlines of a functional device, but not while it was functioning, using the standard equipment used for pulse height spectroscopy with solid state detectors. A typical pulse-height spectrum for a MOS SRAM shows three peaks dominated by events in the memory array. Data for the peaks are consistent with the charge collected being proportional to the product of the linear energy transfer and the secant of the angle of incidence. The number of events falls off with the cosine of the angle of incidence. Author (CISTI)

N94-30221 McMaster Univ., Hamilton (Ontario).
PULSE HEIGHT RESPONSE OF Si SURFACE BARRIER DETECTORS
c76

D. Comedi and J. Davies *In* Defence Research Establishment, Proceedings of the 1991 Single Event Upset Symposium 1991 14 p (For primary document see N94-30211 08-73)
Avail: Issuing Activity (Defence Research Establishment, Ottawa, ON K1A 0Z4 Canada)

An extensive series of pulse height measurements was made in partially depleted 50-mm square ORTEC surface barrier detectors, using various heavy ions (Li, B, C, and Cl) at energies between 5 and 60 MeV. An Am-241 radioactive source was used for calibration purposes. By varying the angle of incidence and the detector bias, it was established that the charge collection efficiency is close to 100 percent in all cases. These angle of incidence studies also provide experimental values for the correction for the small energy loss in traversing the Au surface barrier layer. After correcting for this window loss and for the residual nuclear stopping, the resulting pulse heights per MeV for the various heavy ions were found to be up to 3 percent larger than for the Am-241 alpha particle. This increase, although significant, is considerably smaller than had been anticipated from an extrapolation of an earlier study of H, He, and Li by Lennard et al (1986). The dependence of the detector resolution on the energy and atomic number of the particle was also measured to provide a suitable data base for selecting the optimum ion beams for various backscattering analysis problems. Author (CISTI)

N94-30222 Hughes Aircraft Co., Los Angeles, CA.
DETERMINATION OF COSMIC RAY LATCHUP RATE IN CMOS DEVICES
c93

M. A. Shoga and E. C. Smith *In* Defence Research Establishment, Proceedings of the 1991 Single Event Upset Symposium 1991 7 p (For primary document see N94-30211 08-73)
Avail: Issuing Activity (Defence Research Establishment, Ottawa, ON K1A 0Z4 Canada)

Unlike single event upsets, an acceptable method to determine the single event latchup (SEL) rate does not exist. Such a method is very important, since SEL rates can be compared with reliability failure rates where latchup may induce failure. For complementary metal oxide semiconductor (CMOS) devices, cyclotron measurements of latchup cross section and the critical threshold are not sufficient to determine the latchup rate. A method is described for determining the latchable areas in a CMOS device. The dimensions of the sensitive volume were determined by a combination of cyclotron data and micrographic observation of delidded devices. The critical charge is determined from the linear energy transfer measurements with the cyclotron and from capacitance voltage measurements. Latchup rates were calculated using a version of the CRIER computer program. The environment assumed was that calculated from the Adams model for solar minimum, which corresponds to the maximum galactic cosmic ray flux. Mean time between latchups was found to be 11 to 4,100 years for the three devices tested. Author (CISTI)

N94-30588# Brookhaven National Lab., Upton, NY.
SMALL LOW MASS ADVANCED PBR'S FOR PROPULSION

J. R. Powell, M. Todosow, and H. Ludewig 1 Oct. 1993 8 p Presented at the 11th Symposium on Space Nuclear Power Systems, Albuquerque, NM, 9-13 Jan. 1994
(Contract DE-AC02-76CH-00016)
(DE94-005142; BNL-49696; CONF-940101-30) Avail: CASI HC A02/MF A01 (US Sales Only)

The advanced Particle Bed Reactor (PBR) to be described in this paper is characterized by relatively low power, and low cost, while still maintaining competition values for thrust/weight, specific impulse and operating times. In order to retain competitive values for the thrust/weight ratio while reducing the reactor size, it is necessary to change the basic reactor layout, by incorporating new concepts. The new reactor design concept is termed SIRIUS (Small Lightweight Reactor Integral Propulsion System). The following modifications are proposed for the reactor design to be discussed in this paper: Pre-heater (U-235 included in Moderator); Hy-C (Hydride/De-hydride for Reactor Control); Afterburner (U-235 impregnated into Hot Frit); and Hy-S (Hydride Spike Inside Hot Frit). Each of the modifications will be briefly discussed below, with benefits, technical issues, design approach, and risk levels addressed. The paper discusses conceptual assumptions, feasibility analysis, mass estimates, and information needs. DOE

N94-30712# Stanford Linear Accelerator Center, CA.
QUANTUM-MECHANICAL SUPPRESSION OF BREMSSTRAHLUNG

R. Becker-Szendy, P. Anthony, P. Bosted, M. Cavalli-Sforza, L. Keller, L. Kelley, S. Klein, G. Niemi, M. Perl, and L. Rochester et al Dec. 1993 15 p Presented at the 21st Annual SLAC Summer Institute on Particle Physics: Spin Structure in High-Energy Processes; 23rd International Symposium on Multiparticle Dynamics, Stanford, CA; Aspen, CO, 26 Jul. - 6 Aug. 1993
(Contracts DE-AC03-76SF-00515; W-7405-eng-48)
(DE94-005223; SLAC-PUB-6400; CONF-930767-1; CONF-9309297-3)
Avail: CASI HC A03/MF A01

We have studied quantum mechanical suppression of bremsstrahlung of low energy 1-500 MeV photons from high energy 25 GeV electrons. We measured the LPM effect, where multiple scattering of the radiating electron destroys coherence required for the emission of low energy photons, and the dielectric effect, where the emitted photon traveling in the radiator medium interferes with itself. For the experiment, the collaboration developed a novel method of extracting a parasitic low-intensity high-energy electron beam into the fixed target area during normal SLC operation of the accelerator. The results agree quantitatively with Migdal's calculation of the LPM effect. Surface effects, for which there is no satisfactory theoretical prediction, are visible at low photon energies. For very thin targets, the suppression disappears, as expected. Preliminary results on dielectric suppression of bremsstrahlung are in qualitative agreement with the expectation. DOE

N94-30825# Los Alamos National Lab., NM.
INTERCOMPARISON OF THEORETICAL CALCULATIONS OF IMPORTANT ACTIVATION CROSS SECTIONS FOR FUSION REACTOR TECHNOLOGY

M. B. Chadwick (Lawrence Livermore National Lab., CA.), M. Gardner (Lawrence Livermore National Lab., CA.), D. Gardner (Lawrence Livermore National Lab., CA.), O. T. Grudzevich (Institute of Physics and Power Engineering, Obninsk, USSR.), A. V. Ignatyuk (Institute of Physics and Power Engineering, Obninsk, USSR.), and J. W. Meadows 1993 10 p Presented at the 2nd IAEA/CRP Meeting on Activation Cross Sections for the Generation of Long-Lived Radionuclides, San Diego, CA, 29-30 Apr. 1994
(Contracts W-7405-eng-36; W-7405-eng-48)
(DE94-002642; LA-UR-93-3633; UCRL-JC-115239; CONF-940459-1; CONF-9304181-4) Avail: CASI HC A02/MF A01

Various theoretical calculations of radionuclides in the reactions Mo-94(n,p)Nb-94, Ag-109(n,2n)Ag-108(m), Eu-151(n,2n)Eu-150(m),

Eu-153(n,2n)Eu-152(g+m2), Tb-159(n,2n)Tb-158, Re-187(n,2n)Re-186(m), Hf-179(n,2n)Hf- 178(m2), Ir-193(n,2n)Ir-192(m2) are compared. We normalize the theoretical results to the evaluated experimental data at 14.5 MeV and take their average. This yields averaged theoretical excitation functions for the production of the various radionuclides at neutron energies ranging from threshold to 14.5 MeV. We discuss differences between the various theoretical results and between theory and data where they exist. Our theoretical results may be used in conjunction with experimental data to produce evaluated radionuclide production cross sections for neutron energies lower than 14.5 MeV. DOE

N94-30846 Los Alamos National Lab., NM.
TOPAZ 2 SYSTEM DESCRIPTION
S. S. Voss 1994 12 p Presented at the Space 1994: International Conference and Exposition on Engineering, Construction, and Operations in Space, Albuquerque, NM, 26 Feb. - 3 Mar. 1994 Limited Reproducibility: More than 20% of this document may be affected by microfiche quality
(Contract W-7405-eng-36)
(DE94-006230; LA-UR-94-4; CONF-940214-7) Avail: CASI HC A03

The TOPAZ 2 single-cell thermionic space reactor power system was designed, built, and tested by the former Soviet Union (Russia). It was purchased by the United States (U.S.) for technology transfer, testing, and the possible integration and launch with a U.S. satellite. To support the program, ground facilities consisting primarily of Russian hardware, have been built in Albuquerque, New Mexico to perform non-nuclear ground testing of the system. The purpose of this paper is to provide a brief overview of the Russian TOPAZ 2 system. DOE

N94-30847# Los Alamos National Lab., NM.
THE TOPAZ 2 SPACE REACTOR RESPONSE UNDER ACCIDENT CONDITIONS
S. S. Voss 1993 10 p Presented at the International Topical Meeting on the Safety of Advanced Reactors, Pittsburgh, PA, 18-20 Apr. 1994
(Contract W-7405-eng-36)
(DE94-004998; LA-UR-93-4409; CONF-940402-2) Avail: CASI HC A02/MF A01

The TOPAZ 2 is a single-cell thermionic space reactor power system developed by the U.S.S.R. during the period of time from approximately 1969 to 1989. The TOPAZ 2 was never flight demonstrated, but the system was extensively tested on the ground. As part of the development and test program, the response of the TOPAZ 2 under accident conditions was analyzed and characterized. The U.S. TOPAZ 2 team has been working closely with the Russian specialists to understand the TOPAZ 2 system, its operational characteristics, and its response under potential accident conditions. The purpose of the technical exchange is to enable a potential launch of a TOPAZ 2 by the U.S. The information is required to integrate the system with a U.S. spacecraft and to support the safety review process. The purpose of this paper is to provide a brief overview of the system and its response under actual and postulated accident conditions. DOE

N94-29651*# General Electric Co., San Jose, CA.
SP-100 CONTROL DRIVE ASSEMBLY DEVELOPMENT
Thomas Gleason, A. Richard Gilchrist, and Gary Schuster *In* NASA. Ames Research Center, The 27th Aerospace Mechanisms Symposium May 1993 p 367-375 (For primary document see N94-29627 08-15)
Avail: CASI HC A02/MF A03

74 OPTICS

Includes light phenomena; and optical devices.
For lasers see *36 Lasers and Masers.*

N94-28534# Wisconsin Univ., Madison. Dept. of Physics.
BROADBAND EUV SURVEY SPECTROMETER FOR SHORT-TIMESCALE EXPERIMENTS
B. E. Chapman, D. J. Den Hartog, and R. J. Fonck Nov. 1993 13 p
(Contract DE-FG02-85ER-53198)
(DE94-005459; DOE/ER-53198/229) Avail: CASI HC A03/MF A01

A fast and inexpensive spectrometer system has been developed to record EUV impurity spectra in a magnetic fusion research device. To simplify the vacuum system, light is passed out of the spectrometer's vacuum to the detector using a sodium-salicylate-coated fiber optic coupler. This coupler is positioned such that the focal field is nearly flat over its aperture. The system's detector is a microchannel-plate-intensified, linear, self-scanning photodiode array. The 1024-pixel array covers a bandwidth of over 80 nm and is read out once every millisecond. The readout, which is four times faster than the manufacturer's maximum rating, is fully synchronized to the experiment using a locally-designed control circuit. DOE

N94-28656# Boeing Defense and Space Group, Seattle, WA.
ADVANCED OPTICAL A/D CONVERTER Final Report, 29 Apr. 1988 - 30 Nov. 1992
M. C. Hamilton, J. A. Bell, D. A. Leep, and J. P. Lin 1 May 1993 59 p
(Contract N00014-88-C-0285; ARPA Order 9537)
(AD-A275663) Avail: CASI HC A04/MF A01

This program demonstrated the potential of optical techniques for superior wideband analog-to-digital (A/D) conversion. The key performance goals were a signal bandwidth of at least 1.5 GHz with precision of more than 4 bits. The approach should have potential for eventual significant extension beyond these performance levels. Signal bandwidths of more than 10 GHz, with precision of 8 bits, were long term goals. To summarize the final results, an experimental simulation of a four-channel optical analog-to-digital converter (ADC) operating at 4 GS/s with 2-GHz bandwidth was conducted. The precision obtained in the bandpass sampling mode (near 10 GHz) was 3.8 bits. For baseband signals of up to 2 GHz, the measured precision was 4.6 bits. This performance exceeded the original program goals and constitutes the best known performance obtained with an optics-based ADC approach. The optical ADC technique developed offers potential performance of 10 GHz bandwidth, 20 gigasamples/sec (GS/s) sampling rate, and precision of 6 bits or more. A secondary result from the testing was the development of a data reduction methodology that revealed a previously unreported correlation between jitter and pulse-energy fluctuations. The calculated jitter was twice as small as that derived using a commonly used power spectral density analysis that assumes no correlation between these quantities. DTIC

N94-28780 North Carolina State Univ., Raleigh. Dept. of Electrical and Computer Engineering.
MODELING, ANALYSIS, AND SIMULATION OF AN OPTICAL TIME-DIVISION MULTIPLE-ACCESS NETWORK ARCHITECTURE Final Report
Michael Devetsikiotis, Quing G. Zhou, Gavin R. Cato, J. K. Townsend, and Robert M. Kolbas Nov. 1993 52 p Limited Reproducibility: More than 20% of this document may be affected by microfiche quality
(Contract F30602-92-C-0016)
(AD-A275847; RL-TR-93-225) Avail: CASI HC A04

An optical time-division multiple-access (OTDMA) network architecture has been proposed which has the potential of avoiding electronic processing of signals at the aggregate network bandwidth. New specifications for the optical components used in this OTDMA network architecture will be required before a practical system is realized. In this report, we present a model of the OTDMA architecture that relates parameters at the device level such as carrier mobility, physical geometry, charge trapping, and carrier-concentration to system-level performance measures such as bit error rate and noise margin. We present mathematical models of the devices in the system. These models are interconnected into a system-level Monte Carlo simulation model of the OTDMA architecture. DTIC

N94-28804 Rome Lab., Griffiss AFB, NY.
PHOTONIC DEVICES AND SYSTEMS FOR OPTICAL SIGNAL PROCESSING In-House Report, Apr. 1989 - Sep. 1991
Michael A. Parker, Paul D. Swanson, and Stuart I. Libby Aug. 1993 146 p Prepared in cooperation with Cornell University, Ithaca, New York Limited Reproducibility: More than 20% of this document may be affected by microfiche quality
(AD-A275818; RL-TR-93-157) Avail: CASI HC A07

This report is a compilation of the preliminary designs, fabrication, and test results for multiquantum well optical amplifiers, stripe and square broad area lasers, mode switched optical memory elements, optical RS flip flops, NOR gates, photodetectors, and acousto-optic switches. DTIC

N94-28813# California Univ., Irvine.
A NEW GUIDED WAVE LENS STRUCTURE AND ITS APPLICATION Final Report, 15 Jul. 1991 - 30 Jun. 1993
Chin C. Lee 8 Oct. 1993 15 p
(Contract MIPR-ARO-132-91)
(AD-A275541; ARO-28587.1-PH) Avail: CASI HC A03/MF A01

A low-index, lens shaped waveguide is embedded in a high-index Ga(.72)Al(.28)/Ga(.59)Al(.41)As host waveguide with an anti-reflection layer incorporated at the lens boundaries to reduce reflections. An improvement factor of 1.25 in the throughput efficiency of the lens is achieved by the inclusion of AR layer. At an f-number of 1.8 and a wavelength of 1.152 microns, a focal spot size of 2.1 microns and a sidelobe level of -13 dB were measured. The angular field of view measured in the host waveguide is 11 deg. A quadri-level photomasking technique was developed for the fabrication of the new lens structure. This technique can be applied to various integrated optics structures where reflection reduction is required between low-index and high-index waveguide regions. DTIC

N94-28848# Rhode Island Univ., Kingston.
GORDON RESEARCH CONFERENCE ON OPTICAL SIGNAL PROCESSING AND HOLOGRAPHY Final Report, 1 Jun. - 30 Nov. 1993
Alexander Cruickshank 17 Dec. 1993 4 p Conference held in University Park, PA, 27 Jun. - 2 Jul. 1992
(Contract F49620-93-I-0348)
(AD-A275092; AFOSR-94-0026TR) Avail: CASI HC A01/MF A01

Topics discussed included: digital optical computing; optical neural networks; novel transform techniques; optical memories; pseudodeep holography: bacterio rhodopsin thin films: photorefractive material; electro-optic devices; and photopolymer holography. DTIC

N94-28875# Air Force Inst. of Tech., Wright-Patterson AFB, OH.
ABERRATED POINT-SPREAD FUNCTIONS AND BEAM QUALITY FOR OPTICAL SYSTEMS WITH ANNULAR PUPILS M.S. Thesis
Carl F. Maes Dec. 1993 124 p
(AD-A275311; AFIT/CI/CIA-93-150) Avail: CASI HC A06/MF A02

The effect of the central obscuration of an annular pupil of an incoherent optical imaging system on its aberrated point-spread function (PSF) is discussed. A simple model is presented which approximates the aberrated PSF by an aberration-free PSF scaled by its Strehl ratio. The approximation of a PSF with rotationally symmetric aberration by an aberration-free PSF scaled by the Strehl ratio improves as the obscuration of the pupil increases. Specifically, as the obscuration approached the outer radius, the PSF of the optical systems with rotationally symmetric aberations. For the rotationally nonsymmetric aberrations of astigmatism, balanced astigmatism, and coma the aberrated PSF in its central region can also be approximated by the scaled aberration-free PSF but for large Strehl ratios. For rotationally nonsymmetric aberrations, the region or spot sizes are given for which the aberration-free encircled energy without scaling by the Strehl ratio provides better agreement with the actual aberrated encircled energy than the aberration-free encircled energy scaled by the Strehl ratio. DTIC

N94-29009# Air Force Inst. of Tech., Wright-Patterson AFB, OH.
SYNTHETIC IMAGE GENERATOR MODEL; APPLICATION OF VIEW ANGLE DEPENDENT REFLECTIVITY COMPONENTS AND PERFORMANCE EVALUATION IN THE VISIBLE REGION M.S. Thesis
Richard B. Stark Feb. 1993 68 p
(AD-A275365; AFIT/CI/CIA-93-158) Avail: CASI HC A04/MF A01

This proposal focuses on operation of the RIT Digital and Remote Sensing Lab's synthetic image generation (DIRSIG) software model within the 0.4 to 1.0 micrometer wavelength region. The approach to this study is two-fold. First, an improved method is established for modeling reflectivity effects. This will include generating the associated reflectivity database. Currently, DIRSIG permits only ideal specular or ideal diffuse behavior. In a real scene, most objects actually exhibit some mixture of specular and diffuse behavior. The proposed treatment will essentially separate the reflectance characteristics into specular and diffuse components which vary as a function of view angle. Second, the performance of DIRSIG in the visible region using the improved technique must be evaluated. This will be accomplished by collecting truth data from an actual scene and comparing it to data from a synthetically generated image of the same scene. This evaluation will also serve as a first overall assessment of the model's performance in this wavelength region. DTIC

N94-29059# Carnegie-Mellon Univ., Pittsburgh, PA. Dept. of Computer Science.
OPTIMIZING RAY TRACING WITH VISUAL COHERENCE
Nathan Loofbourrow and Steven A. Shafer 8 Dec. 1993 20 p
(Contract F33615-90-C-1465; ARPA Order 7597)
(AD-A275218; CMU-CS-93-209) Avail: CASI HC A03/MF A01

We present a method that directs sampling and reconstruction for image generation. This method reduces the cost of the sampling stage, allows a reconstruction of the scene to be progressively refined during the sampling process, and produces a representation of the scene that permits flexibility in the generation of images. The method employs a set of region estimators to model and evaluate the samples that are taken of the image. These models describe coherent regions of the image plane. The region estimators are used to direct the sampling process and to provide a description of the scene for reconstruction. The use of region estimators removes the dependence of the reconstruction process upon the sampling process by providing a compact and accurate representation of the sampled data. This representation permits the resolution and filter kernel to be chosen at reconstruction. An algorithm is presented to perform this reconstruction efficiently. DTIC

N94-29114# Arizona State Univ., Tempe. Dept. of Electrical and Computer Engineering.
SPATIAL LIGHT MODULATORS WITH ARBITRARY QUANTUM WELLS PROFILES Final Technical Report, 15 Jan. 1992 - 14 Jul. 1993
George N. Maracas and Krishan K. Bajaj 27 Sep. 1993 69 p
(Grant AF-AFOSR-0118-90)
(AD-A275023; DWA-1764; AFOSR-94-0019TR) Avail: CASI HC A04/MF A01

This is the final technical report for the University Research Initiative (URI) program 'Spatial Light Modulators with Arbitrary Quantum Well Profiles.' This program explored the use of quantum wells having arbitrary shapes for optical modulators and lasers. This comprehensive effort addressed MBE growth of compositionally graded wells and dielectric mirrors, accurate measurements of absorption coefficient in free-standing membranes, comparison of different active region optical properties, device fabrication, and the theory of excitons in the presence of applied electric and magnetic fields. DTIC

N94-29491*# National Aeronautics and Space Administration. Pasadena Office, CA.
RECONFIGURABLE OPTICAL INTERCONNECTIONS VIA DYNAMIC COMPUTER-GENERATED HOLOGRAMS Patent Application
Hua-Kuang Liu, inventor (to NASA) (Jet Propulsion Lab., California Inst. of Tech., Pasadena.) and Shaomin Zhou, inventor (to NASA) (Jet Propulsion Lab., California Inst. of Tech., Pasadena.) 27 Jan. 1994 26 p
(Contract NAS7-1260)
(NASA-Case-NPO-19039-1-CU; NAS 1.71:NPO-19039-1-CU; US-Patent-Appl-SN-192476) Avail: CASI HC A03/MF A01

A system is proposed for optically providing one-to-many irregular interconnections, and strength-adjustable many-to-many irregular interconnections which may be provided with strengths (weights) w(sub ij) using multiple laser beams which address multiple holograms and means for combining the beams modified by the holograms to form multiple interconnections, such as a cross-bar switching network. The optical means for interconnection is based on entering a series of complex computer-generated holograms on an electrically addressed spatial light modulator for real-time reconfigurations, thus providing flexibility for interconnection networks for largescale practical use. By employing multiple sources and holograms, the number of interconnection patterns achieved is increased greatly. NASA

N94-29694# Defense Forecasts, Inc., Washington, DC.
DUAL-USE APPLICATIONS OF INFRARED SENSITIVE MATERIALS Final Report
Barry M. Blechman and Scott C. Lush Jun. 1993 165 p
(Contract MDA972-91-C-0046)
(AD-A275140) Avail: CASI HC A08/MF A02

High performance infrared focal plane arrays made from sensitive materials such as mercury cadmium telluride grown on a substrate of cadmium zinc telluride have been proposed for use in an extensive variety

of military equipment for over a decade. The proposed uses have ranged from early-warning satellites to missile seekers. In this report, we describe and quantify the potential dual-use markets for such detectors. DTIC

N94-29759 Maryland Univ., College Park.
OPTICAL PROPERTIES OF CADMIUM SULFIDE, ZINC SELENIDE, AND ZINC MANGANESE SELENIDE SEMICONDUCTOR FILMS Ph.D. Thesis
Rachid Dahmani 1992 203 p
Avail: Univ. Microfilms Order No. DA9315627

Optical properties of CdS, ZnSe, and (ZnMn)Se semiconductor films were investigated in the vicinity of their main absorption edge. Experimental transmission spectra of thin CdS platelets of thickness 1.2 micron were theoretically fitted using a Fabry-Perot cavity and the source of the A(sub n=1) excitonic polariton damping dispersion was identified for temperatures between 2 and 180 K. It was found that for a given temperature the damping constant Gamma(omega) is independent of frequency below the resonance frequency while it is detuning-dependent above the resonance. Below 70 K, Gamma was found to be constant below resonance due to the scattering of polaritons with defects and impurities, and increased linearly above resonance because of the scattering of polaritons with acoustical phonons. Above 70 K, the damping parameter increased exponentially both below and above resonance where it is dominated by the scattering of polaritons by optical phonons. The optical phonon and room temperature gap energies were found to be equal to 38.01 MeV and 2.451 eV, respectively. The dielectric function and the lattice misfit induced strain in ZnSe and (ZnMn)Se films grown on (001) GaAs were also investigated by room temperature spectroscopic ellipsometry. The bulk-like dielectric function of unstrained ZnSe films was first determined for energies between 1.5 and 4.5 eV. This dielectric constant was then used to study the effects of strain on the top valence band at the origin of the Brillouin zone in thin ZnSe films. It was found that because of the tetragonal deformation of the cubic lattice in the plane of the film-substrate interface the top valence band splits into light and heavy hole bands and these subbands and the spin-orbit band shift towards lower energies. The coupling between the light hole and spin-orbit band induces an additional shift and broadening of the critical points. In (ZnMn)Se films the critical thickness is smaller than that of ZnSe, and the strain becomes tensile for film thicknesses above 0.5 micron because of the difference in the thermal expansion coefficients between GaAs and (ZnMn)Se. In this case, the shift of the various bands is towards higher energies. Furthermore, the ZnSe/GaAs interface was identified as a 9 A layer of Ga2Se3. Dissert. Abstr.

N94-29799# Midwest Research Inst., Golden, CO. National Renewable Energy Lab.
AN OUTDOOR EXPOSURE TESTING PROGRAM FOR OPTICAL MATERIALS USED IN SOLAR THERMAL ELECTRIC TECHNOLOGIES
T. Wendelin and G. Jorgensen Jan. 1994 6 p Presented at the American Society of Mechanical Engineers (ASME) International Solar Energy Conference, San Francisco, CA, 27-30 Mar. 1994
(Contract DE-AC02-83CH-10093)
(DE94-000265; NREL/TP-471-5865; CONF-940326-8) Avail: CASI HC A02/MF A01

Developing low cost, durable advanced optical materials is important for making solar thermal energy technologies viable for electricity production. The objectives of a new outdoor testing program recently initiated by the National Renewable Energy Laboratory (NREL) are to determine the expected lifetimes of candidate reflector materials and demonstrate their optical durability in real-world service conditions. NREL is working with both utilities and industry in a collaborative effort to achieve these objectives. To date, simulated/accelerated exposure testing of these materials has not been correlated with actual outdoor exposure testing. Such a correlation is desirable to provide confidence in lifetime predictions based upon accelerated weathering results. This outdoor testing program will allow outdoor exposure data to be obtained for realistic environments and will establish a data base for correlating simulated/accelerated outdoor exposure data with actual outdoor exposure data. In this program, candidate reflector materials are subjected to various outdoor exposure conditions in a network of sites across the southwestern United States. Important meteorological data are continuously recorded at these sites; these data will be analyzed for possible correlations with material optical performance. Weathered samples are characterized on a regular basis using a series of optical tests. These tests provide the basis for tracking material performance and durability with exposure time in the various outdoor environments. This paper describes the outdoor testing program in more detail including meteorological monitoring capabilities and the optical tests that are performed on these materials. DOE

N94-29928 Oak Ridge National Lab., TN.
ISSUES ARISING WITH THE APPLICATION OF OPTICAL FIBER TRANSMISSION IN CLASS 1E SYSTEMS IN NUCLEAR POWER PLANTS
K. Korsah and C. Antonescu 1993 12 p Presented at the Water Reactor Safety Information Meeting, Bethesda, MD, 25-27 Oct. 1993 Limited Reproducibility: More than 20% of this document may be affected by microfiche quality
(Contract DE-AC05-84OR-21400)
(DE94-004743; CONF-931079-15) Avail: Issuing Activity (Department of Energy (DOE))

The application of fiber optic links and networks in safety-critical systems in the next generation of nuclear power plants, as well as in some digital upgrades in present-day plants, will mean that these links must be highly reliable and able to withstand the effect of environmental stressors present at the installation location. This paper discusses the failure modes and age-related mechanisms of fiber optic transmission components and identifies environmental stressors that could adversely affect their reliability over the long term. Some of the standards that could be used in their qualification for safety-critical applications are also discussed briefly. DOE

N94-30075 Joint Inst. for Nuclear Research, Dubna (USSR). Lab. of Nuclear Problems.
MICROSECOND FIBER OPTIC DELAY LINE
V. G. Zinov, S. V. Medved, A. I. Rudenko, A. N. Grigorev, V. S. Mazur, I. Ya. Tsybin, and V. N. Tochilov 1992 3 p Limited Reproducibility: More than 20% of this document may be affected by microfiche quality
(DE94-607903; JINR-R-13-92-489) Avail: CASI HC A01 (US Sales Only)

The description of an analog delay line for fiber optic digital signals is given. The time delay is 5 mcs, and the broadband is 50 MHz. DOE

N94-30084 Joint Inst. for Nuclear Research, Dubna (USSR).
THIRD-ORDER BEAM OPTICS OF REAL SOLENOID MAGNETIC LENS
V. V. Andreev and I. P. Yudin 1992 19 p Limited Reproducibility: More than 20% of this document may be affected by microfiche quality
(DE94-608014; JINR-R-9-92-53) Avail: CASI HC A03 (US Sales Only)

The dynamics of charge particle beam in a solenoid with a real distribution of magnetic field, is under consideration in this paper. In cylindrical geometry the power series expansions truncated after r(sup 3) for magnetic field component Br and Bz, is taken into account with axial field distribution B(z) either rectangular or any other type. The nonlinear equation of motion with a respect matrix formalism the chromatic and spherical aberration coefficients have been determined. The described method is realized in the code of a TRANSPORT-type program. Particle simulation, carried out with some solenoid lenses has shown full agreement with results obtained on a numerical differential method (Runge-Kutta method). Physical effects of a beam focusing and a current density distribution have been investigated. DOE

N94-30233 Laval Univ. (Quebec). Dept. de Genie Electrique.
SYNCHRONIZATION OF MICROWAVE OSCILLATORS BY DIRECT OPTICAL INJECTION M.S. Thesis [SYNCHRONISATION D'OSCILLATEURS MICRO-ONDES PAR INJECTION OPTIQUE DIRECTE]
Christian Beaulieu Sep. 1993 113 p In FRENCH
(ISBN-0-315-85546-0; CTN-94-61148) Copyright Avail: Micromedia Ltd., Technical Information Centre, 240 Catherine Street, Suite 305, Ottawa, Ontario, K2P 2G8, Canada HC/MF

Optical methods have promise for generating a defined radiation pattern in a phased array antenna made of a plurality of small radiating elements. The technique of synchronizing microwave oscillators by direct optical injection was examined in a study of the use of field effect transistors (MESFET's) as fast photodetectors. A variable frequency microwave oscillator was designed and then synchronized by an intensity modulated optical signal. The maximum phase-following band of 5.4 MHz was measured while the reference signal was injected at the oscillator fundamental frequency of 1.7, 1.1, and 0.9 MHz respectively for the 2nd, 3rd, and 5th subharmonics. In addition, supplementary measures show that it is possible

to control the phase of the signal at the output of the oscillator over a range greater than 180 deg simply by varying the voltage at the terminals of the varactor included in the oscillator circuit. The frequency stability of the synchronized oscillator was evaluated in the time and frequency domains. At 100 kHz of the carrier, a noise to carrier ratio of -97 dBc/Hz was obtained, or an improvement of -32 dB compared to the non synchronized oscillator. CISTI

N94-30252# Georgia Univ., Athens. Dept. of Physics and Astronomy.
OPTICAL STUDIES OF DYNAMICAL PROCESSES IN DISORDERED SYSTEMS
W. M. Yen 1993 8 p
(Contract DE-FG09-87ER-45291)
(DE94-006751; DOE/ER-45291/6) Avail: CASI HC A02/MF A01

Focus continues to be on dynamical processes such as relaxation and energy diffusion which affect the structure and optical properties of disordered and amorphous materials, particularly glasses which are luminescent in the near infrared and their efficiency. Elementary excitations in amorphous materials are also under study. DOE

N94-30261# Sandia National Labs., Albuquerque, NM.
OPTOELECTRONIC PACKAGING ACTIVITIES AT SANDIA NATIONAL LABORATORIES
R. F. Carson, M. G. Armendariz, and P. K. Seigal 1993 5 p Presented at the DOD Fiber Optics Conference 1994, McLean, VA, 22-24 Mar. 1994
(Contract DE-AC04-94AL-85000)
(DE94-005287; SAND-93-4029C; CONF-940363-1) Avail: CASI HC A01/MF A01 (US Sales Only)

Optoelectronics and photonics hold great potential for high data-rate communication and computing. Wide use in computing applications was limited first by device technologies and now suffers due to the need for high-precision, mass-produced packaging. The use of photons as a medium of communication and control implies a unique set of packaging constraints that was not present in traditional telecommunications application. At Sandia National Laboratories, state-of-the-art optoelectronic packaging activities are increasingly being driven by microelectronic techniques that have potential for low cost and high volume manufacturing. DOE

N94-30418# European Space Agency, Paris (France).
HYBRID OPTICS FOR SPACE APPLICATIONS Ph.D. Thesis - Neuchatel Univ.
Reinhard H. Czichy and Michael A. Perry Jul. 1993 185 p Sponsored by ESA
(ESA-CP-1158; ISBN-9-29-092069-6; ETN-94-95798) Copyright Avail: CASI HC A09/MF A02; ESA, EPD, ESTEC, Noordwijk, Netherlands, HC

The theoretical foundations for hybrid optics, the combination of diffractive optical elements with conventional optics (refractive and reflective elements), are discussed. The application of this theory to practical cases in several design examples, exploring also the use of computer aided optimization routines is illustrated. Particular attention is given to the correction of lens aberrations. The transfer of computer generated design information into the manufacturing of the hybrid elements is described and it is shown why the techniques such as photolithography and ion beam etching, which are already established in the semiconductor industry, may be used with excellent results. Measurement techniques appropriate to testing and characterizing the imaging performance of hybrid optic elements are described, and the results obtained by evaluating prototype samples by these techniques are presented and assessed. The material presented in the text illustrates the cross fertilization of ideas taken from existing and new fields of technology which, together with the efficient combination of resources, has logically lead to the development of hybrid optics. The future of this new optical technology, both for space and ground based applications, is both clear and promising. ESA

N94-30522 National Physical Lab., Teddington (England). Materials Metrology Div.
THE PERFORMANCE OF GLOSS METERS ON CURVING SURFACES
A. Cook and B. C. Duncan Jul. 1993 18 p
(ISSN 0959-2423)
(NPL-DMM(A)-111; ETN-94-95835) Copyright Avail: Issuing Activity (National Physical Lab., Teddington, Middlesex TW11 0LW, England)

Models for calculating the performance of gloss meters on cylindrical surfaces to correct for the geometry of the sample are presented. It is noted that although quantitative measurements of surface gloss can be made easily on flat surface using commercial gloss meters, the measurement of gloss on curved plastic mouldings is inaccurate due to the divergence of light caused by the geometrical effects. The predictions of the models are compared with the actual performance of several meters. In the appropriate orientation, no change in performance occurs from the flat surface behavior provided that the radius of curvature of the cylinder is greater than a critical value. ESA

N94-30599 Lawrence Livermore National Lab., CA.
CHARACTERIZATION OF DEFECT GEOMETRIES IN MULTILAYER OPTICAL COATINGS
R. J. Tench, R. Chow, and M. R. Kozlowski Dec. 1993 11 p Presented at the 25th Boulder Damage Symposium: Annual Symposium on Optical Materials for High-Power Lasers, Boulder, CO, 27-29 Oct. 1993 Limited Reproducibility: More than 20% of this document may be affected by microfiche quality
(Contract W-7405-eng-48)
(DE94-005820; UCRL-JC-114999; CONF-931054-4) Avail: CASI HC A03

Laser-induced damage in optical coatings is generally associated with micrometer-scale defects. A simple geometric model for nodule-shaped defects is commonly used to describe defects in optical coatings. No systematic study has been done, however, to prove the applicability of that model to standard optical coating deposition. Some defects are known not to have a classic nodule geometry. The present study uses atomic force microscopy (AFM) and scanning electron microscopy to characterize the topography of coating defects in a HfO2/SiO2 multilayer mirror system. Focused ion-beam cross-sectioning is then used to study the underlying defect structure. This work develops a model for defect shape such that the overall geometry of a coating defect, particularly seed size and depth, can be inferred from non-destructive evaluation measurements such as AFM. The relative mechanical stabilities of nodular defects can be deduced based on the nodule's geometry. Auger analysis showed that the seed material that causes nodular defects in HfO2/SiO2 multilayers is a hafnia oxide. Such characterization capabilities are needed for understanding the enhanced susceptibility of particular defects to laser damage and for developing improved techniques for depositing low-defect density coatings. DOE

N94-30828 Sandia National Labs., Albuquerque, NM.
PHOTONICS AT SANDIA NATIONAL LABORATORIES: FROM RESEARCH TO APPLICATIONS
J. Meyer, A. Owyoung, T. E. Zipperian, J. Y. Tsao, and D. R. Myers 1994 4 p Presented at the DOD Fiber Optics Conference 1994, McLean, VA, 22-24 Mar. 1994 Limited Reproducibility: More than 20% of this document may be affected by microfiche quality
(Contract DE-AC04-94AL-85000)
(DE94-006463; SAND-94-0132C; CONF-940363-2) Avail: CASI HC A01

Photonics activities at Sandia National Laboratories (SNL) are founded on a strong materials research program. The advent of the Compound Semiconductor Research Laboratory (CSRL) in 1988 accelerated device and materials research and development. Recently, industrial competitiveness has been added as a major mission of the labs. Photonics projects have expanded towards applications-driven programs requiring device and subsystem prototype deliveries and demonstrations. This evolution has resulted in a full range of photonics programs from materials synthesis and device fabrication to subsystem packaging and testing. DOE

N94-30910 Sandia National Labs., Albuquerque, NM.
STANDARD TESTING PROCEDURES FOR OPTICAL FIBER AND UNSHIELDED TWISTED PAIR AT SANDIA NATIONAL LABORATORIES
R. L. Adams Nov. 1993 32 p Limited Reproducibility: More than 20% of this document may be affected by microfiche quality
(Contract DE-AC04-94AL-85000)
(DE94-005315; SAND-93-1076) Avail: CASI HC A03

This document will establish a working standard for testing optical fiber and unshielded twisted pair cables included in the Lab-wide telecommunications cabling system. The purpose of these standard testing procedures is to deliver to all Sandians a reliable, low-maintenance,

state-of-the-art, ubiquitous telecommunications cabling infrastructure capable of satisfying all current and future telecommunication needs. DOE

N94-29617*# Jet Propulsion Lab., California Inst. of Tech., Pasadena.
SITE COMPARISON FOR OPTICAL VISIBILITY STATISTICS IN SOUTHERN CALIFORNIA
K. Cowles *In its* The Telecommunications and Data Acquisition Report 15 May 1991 p 31-40 (For primary document see N94-29613 08-32)
(RTOP 310-20-67-88-03)
Avail: CASI HC A02/MF A02

N94-29624*# Jet Propulsion Lab., California Inst. of Tech., Pasadena.
GAUSSIAN BEAM AND PHYSICAL OPTICS ITERATION TECHNIQUE FOR WIDEBAND BEAM WAVEGUIDE FEED DESIGN
W. Veruttipong, J. C. Chen, and D. A. Bathker *In its* The Telecommunications and Data Acquisition Report 15 May 1991 p 128-135 (For primary document see N94-29613 08-32)
(RTOP 314-30-50-12-78)
Avail: CASI HC A02/MF A02

N94-29639*# Honeywell, Inc., Glendale, AZ. Satellite Systems Operation.
OPTICAL CHOPPER ASSEMBLY FOR THE MARS OBSERVER
Terry Allen *In* NASA. Ames Research Center, The 27th Aerospace Mechanisms Symposium May 1993 p 165-180 (For primary document see N94-29627 08-15)
Avail: CASI HC A03/MF A03

N94-29659*# New Mexico State Univ., Las Cruces.
THE Rb 780-NANOMETER FARADAY ANOMALOUS DISPERSION OPTICAL FILTER: THEORY AND EXPERIMENT
B. Yin, L. S. Alvarez, and T. M. Shay *In* JPL, The Telecommunications and Data Acquisition Report 15 Feb. 1994 p 71-85 (For primary document see N94-29652 08-32)
(RTOP 310-20-67-92-02)
Avail: CASI HC A03/MF A03

N94-29771*# Massachusetts Inst. of Tech., Lexington. Lincoln Lab.
OVERVIEW OF MICROOPTICS: PAST, PRESENT, AND FUTURE
Wilfrid B. Veldkamp *In* JPL, Proceedings of the Workshop on Microtechnologies and Applications to Space Systems 15 Jun. 1993 p 43-54 (For primary document see N94-29767 08-31)
Avail: CASI HC A03/MF A03

N94-29773*# Jet Propulsion Lab., California Inst. of Tech., Pasadena.
MINIATURIZATION IN X RAY AND GAMMA RAY SPECTROSCOPY
Jan S. Iwanczyk (XSIRIUS Scientific, Inc., Marina Del Ray, CA.), Yuzhong J. Wang (XSIRIUS Scientific, Inc., Marina Del Ray, CA.), and James G. Bradley *In its* Proceedings of the Workshop on Microtechnologies and Applications to Space Systems 15 Jun. 1993 p 85-94 (For primary document see N94-29767 08-31)
(Contracts NASw-4492; NAS5-33045; NIH-5R01-GM37161)
Avail: CASI HC A02/MF A03

N94-29781*# Science Applications International Corp., Santa Barbara, CA.
EVOLUTION OF MINIATURE DETECTORS AND FOCAL PLANE ARRAYS FOR INFRARED SENSORS
Louis A. Watts *In* JPL, Proceedings of the Workshop on Microtechnologies and Applications to Space Systems 15 Jun. 1993 p 131-14 (For primary document see N94-29767 08-31)
Avail: CASI HC A02/MF A03

N94-29785*# Jet Propulsion Lab., California Inst. of Tech., Pasadena.
MICROMACHINED ELECTRON TUNNELING INFRARED SENSORS
T. W. Kenny, W. J. Kaiser, J. A. Podosek, H. K. Rockstad, and J. K. Reynolds *In its* Proceedings of the Workshop on Microtechnologies and Applications to Space Systems 15 Jun. 1993 p 205-212 (For primary document see N94-29767 08-31)
Avail: CASI HC A02/MF A03

N94-29787*# Jet Propulsion Lab., California Inst. of Tech., Pasadena.
CONTROL OF MICROMACHINED DEFORMABLE MIRRORS
M. L. Agronin, R. Bartman, F. Y. Hadaegh, W. Kaiser, and P. K. C. Wang *In its* Proceedings of the Workshop on Microtechnologies and Applications to Space Systems 15 Jun. 1993 p 225-246 (For primary document see N94-29767 08-31)
Avail: CASI HC A03/MF A03

N94-30299 Defence Research Establishment Suffield, Medicine Hat (Alberta).
MOTION AND STRUCTURE FROM PLANAR MOTION IN NOISY MONOCULAR IMAGE SEQUENCES
V. C. Aitken and H. M. Schwartz *In its* Proceedings of the 3rd Conference on Military Robotic Applications 1991 p 177-184 (For primary document see N94-30275 08-37)
Avail: Issuing Activity (Defence Research Establishment Suffield, P.O. Box 4000, Medicine Hat, AB T1A 8K6 Canada)

N94-30300 Central and Technical Establishment for Armament, Arcueil (France).
THERMAL IMAGING FOR A MOBILE ROBOT
Claude Caillas *In* Defence Research Establishment Suffield, Proceedings of the 3rd Conference on Military Robotic Applications 1991 p 191-197 (For primary document see N94-30275 08-37)
Avail: Issuing Activity (Defence Research Establishment Suffield, P.O. Box 4000, Medicine Hat, AB T1A 8K6 Canada)

N94-30462*# Purus, Inc., San Jose, CA.
A COMMERCIALIZED, CONTINUOUS FLOW FIBER OPTIC SENSOR FOR TRICHLOROETHYLENE AND HALOFORMS
James C. Wells and Mark D. Johnson *In* NASA, Washington, Technology 2003: The Fourth National Technology Transfer Conference and Exposition, Volume 1 Feb. 1994 p 188-195 (For primary document see N94-30440 08-99)
Avail: CASI HC A02/MF A04

N94-30502# Physics and Electronics Lab. TNO, The Hague (Netherlands).
EXPERIMENTAL EVALUATION OF CAMOUFLAGE EFFECTIVENESS IN THE THERMAL INFRARED
Pieter A. M. Jacobs *In* AGARD, Atmospheric Propagation Effects Through Natural and Man-Made Obscurants for Visible to MM-Wave Radiation Nov. 1993 12 p (For primary document see N94-30495 08-32)
Copyright Avail: CASI HC A03/MF A03

N94-30504# Belgian Army, Peutie.
GLOBAL APPROACH TOWARDS THE EVALUATION OF THERMAL INFRARED COUNTERMEASURES
Patrick Verlinde and Philippe Wilms *In* AGARD, Atmospheric Propagation Effects Through Natural and Man-Made Obscurants for Visible to MM-Wave Radiation Nov. 1993 8 p (For primary document see N94-30495 08-32)
Copyright Avail: CASI HC A02/MF A03

N94-30647*# Observatoire de la Cote d'Azur, Grasse (France).
OPTICAL TECHNIQUES FOR TIME AND FREQUENCY TRANSFER
Francoise Baumont and Jean Gaignebet *In* NASA. Goddard Space Flight Center, The 25th Annual Precise Time and Time Interval (PTTI) Applications and Planning Meeting May 1994 p 119-132 (For primary document see N94-30639 08-70)
Avail: CASI HC A03/MF A06

75 PLASMA PHYSICS

Includes magnetohydrodynamics and plasma fusion.

For ionospheric plasmas see *46 Geophysics*. For space plasmas see *90 Astrophysics*.

N94-28458# George Washington Univ., Washington, DC. Office of Sponsored Research.

NEW HIGH TEMPERATURE PLASMAS AND SAMPLE INTRODUCTION SYSTEMS FOR ANALYTICAL ATOMIC EMISSION AND MASS SPECTROMETRY

A. Montaser 1993 9 p

(Contract DE-FG02-93ER-14320)

(DE94-004564; DOE/ER-14320/1) Avail: CASI HC A02/MF A01

In this research, new high-temperature plasmas and new sample introduction systems are explored for rapid elemental and isotopic analysis of gases, solutions, and solids using mass spectrometry and atomic emission spectrometry. During the period January - December 1993, emphasis was placed on: analytical investigations of atmospheric-pressure helium inductively coupled plasmas (He ICP) that are suitable for atomization, excitation, and ionization of elements possessing high excitation and ionization energies; simulation and computer modeling of plasma sources to predict their structure and fundamental and analytical properties without incurring the enormous cost of experimental studies; spectroscopic imaging and diagnostic studies of high-temperature plasmas; fundamental studies of He ICP discharges and argon-nitrogen plasma by high-resolution Fourier transform spectrometry; and fundamental and analytical investigation of new, low-cost devices as sample introduction systems for atomic spectrometry and examination of new diagnostic techniques for probing aerosols. Only the most important achievements are included in this report to illustrate progress and obstacles. Detailed descriptions of the authors' investigations are outlined in the reprints and preprints that accompany this report. The technical progress expected next year is briefly described at the end of this report. DOE

N94-28490# Wisconsin Univ., Madison.

THEORETICAL REVERSED FIELD PINCH AND TOKAMAK STUDIES

1993 4 p

(Contract DE-FG02-85ER-53212)

(DE94-005409; DOE/ER-53212/T2) Avail: CASI HC A01/MF A01

This report discusses the following topics: fluctuation suppression by electrostatic current injection; pulsed poloidal current drive; effect of current drive on fluctuations; RF current drive in the RFP; development of a hyper-dissipation algorithms; and interacting magnetic islands. DOE

N94-28513# National Inst. for Fusion Science, Nagoya (Japan).

PROCEEDINGS OF JAPAN-US WORKSHOP P-196 ON HIGH HEAT FLUX COMPONENTS AND PLASMA SURFACE INTERACTIONS FOR NEXT DEVICES

K. N. Wilson, ed. and T. Yamashina, ed. Mar. 1993 323 p Proceedings held in Kasuga, Japan, 17-19 Nov. 1992

(DE94-701164; NIFS-PROC-12; CONF-9211262; AD-B173696L) Avail: CASI HC A14/MF A03

The Japan-US Workshop P-196 was successfully carried out at Kyushu University, Chikushi Campus, from 17-19 Nov. The major concern was on the research and development required for the International Thermonuclear Experimental Reactor (ITER) and the Large Helical Device (LHD). Most of the discussion items were similar to that of the last workshop: PFC and PSI in the Large Device; High Heat Flux Components; Laboratory Studies; and Neutron Damage. The greatest number of presentations were concerned with the High Heat Flux Component. DOE

N94-28514# Wisconsin Univ., Madison. Dept. of Plasma Physics.

FLUCTUATION AND TRANSPORT REDUCTION IN A REVERSED FIELD PINCH BY INDUCTIVE POLOIDAL CURRENT DRIVE

J. S. Sarff, S. A. Hokin, H. Ji, S. C. Prager, and C. R. Sovinec Dec. 1993 15 p

(Contract DE-FG02-85ER-53198)

(DE94-005542; DOE/ER-53198/231) Avail: CASI HC A03/MF A01

An auxiliary poloidal inductive electric field applied to a reversed field pinch plasma reduces the current density gradient, slows the growth of m=1 tearing fluctuations, suppresses their associated sawteeth, and doubles the energy confinement time. Small sawteeth occur in the improved state but with m=0 precursors. By requiring a change of toroidal flux embedding the plasma, inductive poloidal current profile drive is transient, but the improvement encourages the program of RFP transport suppression using current profile control. DOE

N94-28515# Wisconsin Univ., Madison. Dept. of Plasma Physics.

PHOTON COUNTING SPECTROSCOPY AS DONE WITH A THOMSON SCATTERING DIAGNOSTIC

D. J. DenHartog and D. E. Ruppert Nov. 1993 48 p

(Contract DE-FG02-85ER-53198)

(DE94-005543; DOE/ER-53198/230) Avail: CASI HC A03/MF A01

The measurement and reduction of photon counting spectral data is demonstrated within the context of a Thomson scattering diagnostic. This diagnostic contains a microchannel plate (MCP) photomultiplier tube (PMT) as the photon sensing device. The MCP PMT is not an ideal photon sensor, the loss of photoelectrons at the MCP input and the broad charge pulse distribution at the output add to the uncertainty in recorded data. Computer simulations are used to demonstrate an approach to quantification of this added uncertainty and to develop an understanding of its source; the methodology may be applicable to the development of an understanding of photon detectors other than an MCP PMT. Emphasis is placed on the Poisson statistical character of the data, because the assumption that a Gaussian probability distribution is a reasonable statistical description of photon counting data is often questionable. When the count rate is low, the product of the possible number of photon counts and the probability of measurement of a single photon is usually not sufficiently large to justify Gaussian statistics. Rather, because probabilities of measurement are so low, the Poisson probability distribution best quantifies the inherent statistical fluctuations in such counting measurements. The method of maximum likelihood is applied to derive the Poisson statistics equivalent of chi(exp 2). A Poisson statistics based data fitting code is implemented using the Newton-Raphson method of multi-dimensional root finding; we also demonstrate an algorithm to estimate the uncertainties in derived quantities. DOE

N94-28547# Dartmouth Coll., Hanover, NH.

NONLINEAR MAGNETOHYDRODYNAMICS

1994 12 p

(Contract DE-FG02-85ER-53194)

(DE94-005654; DOE/ER-53194/6) Avail: CASI HC A03/MF A01

Resistive MHD equilibrium, even for small resistivity, differs greatly from ideal equilibrium, as do the dynamical consequences of its instabilities. The requirement, imposed by Faraday's law, that time independent magnetic fields imply curl-free electric fields, greatly restricts the electric fields allowed inside a finite-resistivity plasma. If there is no flow and the implications of the Ohm's law are taken into account (and they need not be, for ideal equilibria), the electric field must equal the resistivity times the current density. The vanishing of the divergence of the current density then provides a partial differential equation which, together with boundary conditions, uniquely determines the scalar potential, the electric field, and the current density, for any given resistivity profile. The situation parallels closely that of driven shear flows in hydrodynamics, in that while dissipative steady states are somewhat more complex than ideal ones, there are vastly fewer of them to consider. Seen in this light, the vast majority of ideal MHD equilibria are just irrelevant, incapable of being set up in the first place. The steady state whose stability thresholds and nonlinear behavior needs to be investigated ceases to be an arbitrary ad hoc exercise dependent upon the whim of the investigator, but is determined by boundary conditions and choice of resistivity profile. DOE

N94-28555 Japan Atomic Energy Research Inst., Tokyo.

ELECTRON BEAM IRRADIATION EXPERIMENTS OF MONOBLOCK DIVERTOR MOCK-UP

Kazuyoshi Satoh, Masato Akiba, Masanori Araki, Satoshi Suzuki, Kenji Yokoyama, I. Smid, A. Cardella, R. Duwe, and E. DiPietro Mar. 1993 27 p Limited Reproducibility: More than 20% of this document may be affected by microfiche quality

(DE94-707497; JAERI-M-93-058) Avail: CASI HC A03

It is one of the key issues for ITER to develop the divertor plate. Electron beam irradiation tests were carried out on a NET divertor mock-up using JEBIS at JAERI under a collaboration between the NET team, JAERI,

and KFA Juelich. Screening tests (maximum heat flux of 23 MW/sq m) and thermal cycling tests (18 MW/sq m, 30 s, 1000 cycles) were carried out. As a result of the screening tests, the erosion caused by sublimation of C/C was observed on the surface of armor tile. No serious damage such as cracks or detachments, however, were found. As a result of the thermal cycling tests, no major damage was detected on the C/C surface. However, the cooling time constant of the divertor mock-up increased over 600 cycles. Therefore it implies that some defects would occur at the brazing interface of the divertor mock-up. DOE

N94-28556 Japan Atomic Energy Research Inst., Tokyo.
EXPERIMENTAL AND ANALYTICAL STUDIES OF HIGH HEAT FLUX COMPONENTS FOR FUSION EXPERIMENTAL REACTOR
Masanori Araki Mar. 1993 142 p Limited Reproducibility: More than 20% of this document may be affected by microfiche quality
(DE94-707671; JAERI-M-93-073) Avail: CASI HC A07

In this report, the experimental and analytical results concerning the development of plasma facing components of ITER are described. With respect to developing high heat removal structures for the divertor plates, an externally-finned swirl tube was developed based on the results of critical heat flux (CHF) experiments on various tube structures. As the result, the burnout heat flux, which also indicates incident CHF, of 41 (+/-) 1 MW/sq m was achieved in the externally-finned swirl tube. The applicability of existing CHF correlations based on uniform heating conditions was evaluated by comparing the CHF experimental data with the smooth and the externally-finned tubes under one-sided heating condition. As the results, experimentally determined CHF data for straight tube show good agreement, for the externally-finned tube, no existing correlations are available for prediction of the CHF. With respect to the evaluation of the bonds between carbon-based material and heat sink metal, results of brazing tests were compared with the analytical results by three dimensional model with temperature-dependent thermal and mechanical properties. Analytical results showed that residual stresses from brazing can be estimated by the analytical three directional stress values instead of the equivalent stress value applied. In the analytical study on the separatrix sweeping for effectively reducing surface heat fluxes on the divertor plate, thermal response of the divertor plate was analyzed under ITER relevant heat flux conditions and has been tested. As the result, it has been demonstrated that application of the sweeping technique is very effective for improvement in the power handling capability of the divertor plate and that the divertor mock-up has withstood a large number of additional cyclic heat loads. DOE

N94-28564# Academy of Sciences of the Armenian SSR, Erivan. Physics Inst.
COULOMB FIELD EFFECT ON PLASMA FOCUSING AND WAKE FIELD ACCELERATION
A. Ts. Amatuni, S. S. Elbakian, and E. V. Sekhpossian Nov. 1993 29 p Prepared for LBL
(Contract DE-AC03-76SF-00098)
(DE94-004937; LBL-34836) Avail: CASI HC A03/MF A01

It is shown that the fields generated by relativistic electron (positron) bunches moving in overdense cold plasma have two components: wake and Coulomb. The existence of the Coulomb component is caused by the absence of the Debay screening of the charge moving in plasma with the velocity greater than the thermal velocity of the plasma electrons. It is shown that at some conditions the contribution of the Coulomb component to focusing and self-focusing of the electron (positron) bunches and wake field generation could be essential. This conclusion is valid for different descriptions of cold plasma-relativistic electron bunch system. DOE

N94-28575# Wisconsin Univ., Madison. Dept. of Electrical and Computer Engineering.
TFTR ION CYCLOTRON RANGE OF FREQUENCIES (ICRF) EXPERIMENTAL DATA ANALYSIS COLLABORATION
J. E. Scharer Dec. 1993 13 p
(Contract DE-FG02-93ER-54196)
(DE94-004699; DOE/ER-54196/1) Avail: CASI HC A03/MF A01

The research performed under this grant during the past year has been concentrated on two TFTR tokamak ICRF (Ion Cyclotron Range of Frequencies) coupling, and heating issues. This includes a '3-D' coupling analysis of the TFTR ICRF cavity-backed coil antennas to plasma edge profiles including the Faraday shield blade angle and fast wave coupling for heating and current drive; TFTR ICRF full-wave field solutions, heating analyses for the D-T supershot; and the effects of fusion alpha particle and ion tail populations on the ICRF absorption. Research progress, publications, and conference presentations are summarized in this report. DOE

N94-28686 Kings Coll., London (England).
CONTROLLING CHAOS IN PLASMA FILLED DIODES Final Report, 15 May 1992 - 14 Nov. 1993
P. A. Lindsay, J. Watkins, and X. Chen 14 Jan. 1994 104 p Limited Reproducibility: More than 20% of this document may be affected by microfiche quality
(Contract F49620-92-J-0219)
(AD-A275525; EOARD-TR-94-02) Avail: Issuing Activity (Defense Technical Information Center (DTIC))

This report covers the first eighteen months of our investigations. Following a brief introduction, the report discusses in some detail the mathematical model of the system, the methods used in solving the corresponding differential equations, and the various ways of presentation of the results. The effect of an external load is then discussed in some detail. The report ends with suggestions for future work based on the results obtained so far. DTIC

N94-28776# Research Triangle Inst., Research Triangle Park, NC.
DEVELOPMENT OF LARGE AREA RF INDUCTION PLASMA FOR COST EFFECTIVE DIAMOND Quarterly Report No. 1, 20 Oct. - 20 Dec. 1993
R. A. Rudder and R. C. Hendry Oct. 1993 15 p
(Contract N00014-94-C-0030)
(AD-A275888; RTI-83U-5676) Avail: CASI HC A03/MF A01

Progress continues on the development of a large area RF induction plasma system. An early problem with a hole in the deposition pattern has been assigned to poor gas distribution. The injection port has been modified to eliminate the hole. New 30 micron films on quartz substrates were fabricated. Plasma modeling and gas modeling were initiated. A downstream process gas monitor was proven. A smaller scale system for evaluating RF power vs. rate data is under construction. Additionally, a data acquisition and process control package was identified and ordered from National Instruments. DTIC

N94-28828# California Univ., Los Angeles. Inst. of Geophysics and Planetary Physics.
ACTIVE ELECTRON AND ION BEAM EXPERIMENTS IN SPACE Final Report, 18 Feb. 1988 - 31 Dec. 1992
M. Ashour-Abdalla, P. L. Pritchett, and D. Schriver Feb. 1993 50 p
(Contract F19628-88-K-0011)
(AD-A275570; PL-TR-93-2112; AD-E201743) Avail: CASI HC A03/MF A01

The basic physical processes that occur during the active electron beam experiments in the ionosphere are examined using multi-dimensional particle simulations. A three-dimensional isolated-system, electrostatic model is used to establish the characteristic time scales associated with injection and to investigate the processes of spacecraft charging and the loss of coherence during beam propagation. Two-dimensional electromagnetic simulations indicate that the beam-plasma interaction leads to the formation of a current structure which acts like an antenna and emits whistler waves in a coherent manner. An ion emitter instrument which injects indium ions will be used during the Geotail and Cluster satellite missions to control the spacecraft potential to be near that of the ambient plasma. To understand the beam-plasma interaction that can occur due to the ejection of the ion beam into various regions of the Earth's magnetosphere, a linear theory study is presented to see whether particular combinations of ambient plasma parameters and ion beam emission modes exist, such that plasma instabilities may be excited. DTIC

N94-29055# Boston Coll., Chestnut Hill, MA. Dept. of Physics.
TOWARDS EXPERIMENTAL VERIFICATION AND DEVICE APPLICATIONS OF CURRENT DRIVEN PLASMA INSTABILITIES IN SOLID STATE SYSTEMS Final Report, 15 May 1991 - 14 May 1993
P. Bakshi and K. Kempa Nov. 1993 8 p
(Contract DAAL03-91-G-0121)
(AD-A275395; ARO-28652.4-PH) Avail: CASI HC A02/MF A01

In this program, we have identified theoretically the most promising

candidate for current driven plasma instabilities (CDPI) in semiconductor based systems: the modulated lower dimensional systems. We also investigated the effects of a grating coupler and a strong magnetic field on CDPI in uniform two-dimensional electron gases. Significant progress was made in pursuing the goal of experimental verification of this phenomenon in superconductor based systems. DTIC

N94-29074# Institute of Plasma Physics, Prague (Czechoslovakia).
PROGRESS IN Z-PINCH RESEARCH
May 1992 23 p
(IPPCZ-321) Avail: CASI HC A03/MF A01

The contributions of the Z-pinch research that were made to the 9th International Conference on High-Power Particle Beams and the 19th IEEE International Conference on Plasma Science are included. These papers are: 'Investigation of Intense XUV Emission of Nitrogen-puff Z-Pinch with Small Energy Input' (preliminary results), 'Multichannel X-ray Spectral Measurement of Hot Plasma Evolution in Nitrogen-puff Z-Pinch,' and 'X-ray Emission Scaling and Energy Balance of Small Gas-puff Z-Pinch.' For individual titles, see N94-29075 through N94-29077.

N94-29075# Institute of Plasma Physics, Prague (Czechoslovakia).
INVESTIGATION OF INTENSE XUV EMISSION OF NITROGEN-PUFF Z-PINCH WITH SMALL ENERGY INPUT
J. Raus, Ales Krejci, and V. Piffl *In its* Progress in Z-Pinch Research May 1992 p 2-7 Presented at the 9th International Conference on High-Power Particle Beams, Washington, DC, 25-29 May 1992 Sponsored by Czechoslovakian Academy of Sciences Grant Agency (For primary document see N94-29074 08-75)
(PH-23) Avail: CASI HC A02/MF A01

Light elements like nitrogen or carbon are suggested as optimum working media for small Z-pinches (several kJ energy input). It is shown that such elements can be ionized up to K-shell ionization stages not only in hot-spots, but also in the bulk plasma. The yield of nitrogen K-shell radiation (about 10 J/shot) is therefore substantially higher than that of traditionally used neon. Besides the pinch physics and radiation dynamics, such radiation could be of interest for applications in 'water window' spectral region. Author

N94-29076# Institute of Plasma Physics, Prague (Czechoslovakia).
MULTICHANNEL X RAY SPECTRAL MEASUREMENT OF HOT PLASMA EVOLUTION IN NITROGEN-PUFF Z-PINCH
Ales Krejci, J. Raus, V. Piffl, A. V. Golubev, Yu. Ya. Platonov, E. Krousky, and O. Renner *In its* Progress in Z-Pinch Research May 1992 p 8-13 Presented at the 9th International Conference on High-Power Particle Beams, Washington, DC, 25-29 May 1992 (For primary document see N94-29074 08-75)
(PH-24) Avail: CASI HC A02/MF A01

Soft x-ray emission from nitrogen plasma of gas-puff Z-pinch device (with energy input 4.3 kJ and current 160 kA) has been studied. Multilayer mirror polychromator with time-resolved registration by PIN diodes was installed and its relatively narrow spectral windows were aligned to the important parts of nitrogen spectrum between 390 and 710 eV. The Te evolution (approximately 400 eV in hot spots) was measured from a slope of recomb. continuum of He-like N. The T(sub e) of bulk plasma (approximately 100 eV) is compared with T(sub e) calculated from yields of K-shell lines. Moreover, pinhole cameras were used for better understanding the radiation phase of the pinch. Time sequences of peaks in x-ray signals corresponding to a number of bright spots on photographs, are presented. Author

N94-29077# Institute of Plasma Physics, Prague (Czechoslovakia).
X RAY EMISSION SCALING AND ENERGY BALANCE OF SMALL GAS-PUFF Z-PINCH
Ales Krejci *In its* Progress in Z-Pinch Research May 1992 p 14-20 Presented at the 19th IEEE International Conference on Plasma Science, Tampa, FL, 1-3 Jun. 1992 Sponsored by Czechoslovakian Academy of Sciences Grant Agency (For primary document see N94-29074 08-75)
Avail: CASI HC A02/MF A01

Gas-puff Z-pinch is discussed as an intensive pulsed source of soft x-rays. Measurements of total x-ray yield Y(sub T) and the yield Y(sub K) from K-shells of highly-ionized atoms of argon, neon, and nitrogen are presented. The radiation produced by small (4.3 kJ) gas-puff Z-pinch confirmed the Y(sub K) approximately equal to I(sup 4) scaling (well-known from large devices) also for pinch currents I = 120 - 200 kA. The yield Y(sub T) scales as I(exp 2). Some basic considerations about energy balance of Z-pinch as well as similarities between terawatt and gigawatt devices are expressed. Author

N94-29134# Washington Univ., Seattle. Aerospace and Energetics Research Program.
TRANSIENT INTERNAL PROBE Final Technical Report, 15 Sep. 1990 - 15 Oct. 1993
Thomas R. Jarboe and Arthur T. Mattick 15 Dec. 1993 58 p
(Grant AF-AFOSR-0345-90)
(AD-A275054; AFOSR-94-0022TR) Avail: CASI HC A04/MF A01

The Transient Internal Probe (TIP) diagnostic is a novel method for probing the interior of hot magnetic fusion plasmas that are inaccessible with ordinary stationary probes. A small probe of magneto-optic (Verdet) material is fired through a plasma at speeds of several km/sec, illuminated by a laser beam. The beam's polarization is rotated in the probe by the local magnetic field and retroreflection back to a polarimetry detector allows determination of the B-field profile across the diameter of a plasma at a spatial resolution of better than 1-cm and an absolute B-field resolution of a few tens of Gauss. The principal components of a TIP diagnostic system were developed and tested. A two-stage light gas gun was constructed that accelerates 30-caliber projectiles to 3 km/sec, and methods were examined for stripping a lexan sabot from a probe prior to entry into a plasma. Probes of CdMnTe and FR-5 Verdet glass were fabricated, and a polarimetry system was constructed for resolving polarization to within 0.25 deg. The diagnostic was validated by measuring a static B-field with a moving (dropped) TIP probe, and finding agreement with Hall-probe measurements to within experimental accuracy (40 Gauss). DTIC

N94-29397# National Inst. for Fusion Science, Nagoya (Japan).
A 6MeV HEAVY ION BEAM PROBE FOR THE LARGE HELICAL DEVICE
A. Fujisawa, H. Iguchi, A. Taniike, M. Sasao, and Y. Hamada Feb. 1994 33 p Submitted for publication
(ISSN 0915-633X)
(NIFS-272) Avail: CASI HC A03/MF A01

A 6 MeV heavy ion beam probe (HIBP) is designed for potential measurements on the Large Helical Device (LHD). The article describes a method to control the 3-D probing beam trajectories in the helical magnetic field, an estimate of beam attenuation and energy reduction arising from the long paths in the plasma, and a cylindrical analyzer as a candidate of the energy analyzer. Author (revised)

N94-29398# National Inst. for Fusion Science, Nagoya (Japan).
THE EFFECT OF MAGNETIC FIELD CONFIGURATION ON PARTICLE PINCH VELOCITY IN COMPACT HELICAL SYSTEM (CHS)
H. Iguchi, K. Ida, H. Yamada, K. Itoh, S.-I. Itoh, K. Matsuoka, S. Okamura, H. Sanuki, I. Yamada, and H. Takenaga et al Jan. 1994 20 p Submitted for publication
(ISSN 0915-633X)
(NIFS-267) Avail: CASI HC A03/MF A01

Radial particle transport has been experimentally studied in the low-aspect-ratio heliotron/torsatron device, CHS. A non-diffusive outward particle flow (inverse pinch) is observed in the magnetic configuration with the magnetic axis shifter inward. This change in the direction of anomalous particle flow is not due to the reversal of temperature gradient nor the radial electric field. The observation suggests that the particle pinch velocity is sensitive to the magnetic field structure. Author

N94-29483# National Inst. for Fusion Science, Nagoya (Japan).
FORMATION AND SELF-HEALING OF MAGNETIC ISLANDS IN FINITE-BETA HELIAS EQUILIBRIA
T. Hayashi, T. Sato, P. Merkel, J. Nuehrenberg, and U. Schwenn Jan. 1994 23 p Submitted for publication
(ISSN 0915-633X)
(NIFS-269) Avail: CASI HC A03/MF A01

The behavior of finite pressure induced magnetic islands is numerically analyzed for three dimensional magnetohydrodynamic equilibria of the Helias configuration by using a three dimensional equilibrium code. It is found that an island chain is generated on the 5/6 rational surface, when such a

surface appears in the plasma region of the finite-beta equilibrium. The island chain, however, is not so dangerous as to destroy the plasma confinement even if it appears in a vanishingly small shear region. Thus, a high beta equilibrium with clear magnetic surfaces can be realized. Moreover, it is definitely confirmed that the finite pressure effect sometimes exhibits an unexpectedly good aspect, namely, that the vacuum islands are removed as beta increases, which can be called 'self-healing' of islands. This property can be explained by the numerically discovered fact that the phases of islands induced by the finite pressure effect are always locked in the same phase regardless of beta. Author (revised)

N94-29499# National Inst. for Fusion Science, Nagoya (Japan).
EFFICIENCIES OF THE ICRF MINORITY HEATING IN THE CHS AND LHD PLASMAS
S. Murakami, M. Okamoto, N. Nakajima, and T. Mutoh Jan. 1994 26 p
(ISSN 0915-633X)
(NIFS-270) Avail: CASI HC A03/MF A01

ICRF minority heatings are investigated in the plasmas of the Compact Helical System (CHS) and the Large Helical Device (LHD) by means of the orbit following Monte Carlo simulation. It is found that the heating efficiency decreases with increase in the absorption power by minority ions and depends strongly on the magnetic field strength and the field configuration. Author

N94-29510# Argonne National Lab., IL.
LIQUID METAL MHD AND HEAT TRANSFER IN A TOKAMAK BLANKET SLOTTED COOLANT CHANNEL
C. B. Reed, T. Q. Hua, D. B. Black, I. R. Kirillov, S. I. Sidorenkov, A. M. Shapiro, and I. A. Evtushenko 1993 10 p Presented at the Symposium on Fusion Engineering, Hyannis, MA, 11-15 Oct. 1993
(Contract W-31-109-eng-38)
(DE94-004622; ANL/EP/CP-79904; CONF-931018-73) Avail: CASI HC A02/MF A01

A liquid metal MHD (Magnetohydrodynamic)/heat transfer test was conducted at the ALEX (Argonne Liquid Metal Experiment) facility of ANL (Argonne National Laboratory), jointly between ANL and NIIEFA (Efremov Institute). The test section was a rectangular slotted channel geometry (meaning the channel has a high aspect ratio, in this case 10:1, and the long side is parallel to the applied magnetic field). Isothermal and heat transfer data were collected. A heat flux of approximately 9 W/sq cm was applied to the top horizontal surface (the long side) of the test section. Hartmann Numbers to 1050 (2 Tesla), interaction parameters to 9 x 10(exp 3), Peclet numbers of 10-200, based on the half-width of the small dimension (7 mm), and velocities of 1-75 cm/sec. were achieved. The working fluid was NaK (sodium potassium eutectic). All four interior walls were bare, 300-series stainless steel, conducting walls. DOE

N94-29547# National Inst. for Fusion Science, Nagoya (Japan).
LARGE AMPLITUDE LANGMUIR AND ION-ACOUSTIC WAVES IN A RELATIVISTIC TWO-FLUID PLASMA
Y. Nejoh (Hachinohe Inst. of Tech., Japan.) and H. Sanuki Feb. 1994 69 p Submitted for publication
(ISSN 0915-633X)
(NIFS-271) Avail: CASI HC A04/MF A01

Large amplitude Langmuir and ion-acoustic waves in a relativistic two-fluid plasma are analyzed by the pseudo-potential method. The existence conditions for relativistic nonlinear Langmuir waves depend on the relativistic effect, the particular energy, and the ion mass to electron mass ratio. The allowable range of the normalized potential depends on the relativistic effect. It is shown that the Mach number has the significant effect for the formation of relativistic nonlinear ion-acoustic waves rather than the ratio of the ion-acoustic velocity to the velocity of light. The allowable range of the normalized potential depends on the Mach number. The present investigation predicts new findings of relativistic nonlinear Langmuir and ion-acoustic waves in plasmas in which high-speed electrons and ions coexist. Author (revised)

N94-29822 Maryland Univ., College Park.
NONLINEAR WAVE PACKET EVOLUTION IN A DISPERSIVE PLASMA: APPLICATION TO ROTATIONAL DISCONTINUITIES Ph.D. Thesis
Bernard John Vasquez 1992 228 p
Avail: Univ. Microfilms Order No. DA9315737

This dissertation examines low frequency (approximately less than ion gyrofrequency) wave packets and rotational discontinuities (RD's) in a dispersive two-fluid plasma. A one dimensional numerical hybrid code with ion simulation particles and a massless electron fluid is used. The evolution, speed, and structure of strongly modulated wave packets, which propagate parallel to an external magnetic field, are investigated as a function of helicity, amplitude, beta(defined equal to 8 pi P/B(exp 2)), and beta(sub i)/beta(sub e) (= T(sub i)/T(sub e)). Gradients of the wave envelope are found to have a substantial influence on wave speeds and other properties. Weakly nonlinear packets show wave coupling with structuring that qualitatively resembles wave solutions of the derivative nonlinear Schrodinger (DNLS) equation for all beta and beta(sub i)/beta(sub e). Nonlinearity has its greatest impact on evolution when the initial packet speed and the linear sound speed of the plasma are equal. Strongly nonlinear Alfven (ion sense of helicity) wave packets do not undergo wave collapse, but do steepen for beta approximately less than 1 and form substantial fast (electron sense of helicity) wave regions on their leading sides. This evolution is shown to differ qualitatively from DNLS wave solutions. An extensive parameter variation on the evolution of RDs is perfromed with particular emphasis on beta, beta(sub i)/beta(sub e), theta(sub B) (the angle between the normal and total magnetic field), and the helicity of the RD. The RD structure is shown to have features in common with the evolution of both strongly modulated, nonlinear wave packets and linear dispersive wave propagation in oblique magnetic fields. For moderate theta(sub B) (approximately less than 45 deg), nonlinearity is important and strong coupling to a compressional (sonic) component can occur in the main current layer. When beta(sub i) = 0, there is a critical value of beta(sub e)(=beta(sub *)) when the intermediate wavetrain moves from the downstream side of the RD to the upstream, and is replaced on the downstream side by slow modes. This is reflected in the hodograms by a change of the wave polarization on both sides. As beta(sub i)/beta(sub e) increases, the spreading rate of the current layer increases for moderate theta(sub B). For large theta(sub B) (approximately greater than 45 deg), RDs with electron (ion) sense of rotation show increased (decreased) spreading with increasing beta(sub i)/beta(sub e). These results are applied to RDs observed in the solar wind and at the magnetopause.
Dissert. Abstr.

N94-29831# Israel Academy of Sciences and Humanities, Jerusalem.
THE SEVENTH INTERNATIONAL BEER SHEVA SEMINAR ON MHD FLOWS AND TURBULENCE
Feb. 1993 168 p Seminar held in Jerusalem, Israel, 14-18 Feb. 1993
(DE94-607211; INIS-MF-13737; CONF-930216) Avail: CASI HC A08/MF A02 (US Sales Only)

Fluid flows, two-phase flows, turbulent flows and magnetohydrodynamics of plasmas and liquid metals are discussed. Flows in MHD generators and MHD channel instabilities are discussed too. DOE

N94-30045# Massachusetts Inst. of Tech., Cambridge. Plasma Fusion Center.
CONCEPTUAL STUDY OF MODERATELY COUPLED PLASMAS AND EXPERIMENTAL COMPARISON OF LABORATORY X RAY SOURCES Ph.D. Thesis
C. Li Dec. 1993 223 p
(Contracts DE-FG02-91ER-54109; W-7405-eng-48)
(DE94-005828; PFC/RR-93-6) Avail: CASI HC A10/MF A03

In this thesis the fundamental concepts of moderately coupled plasmas, for which 2 approximately less than ln(lambda(sub b) approximately less than 10, are, for the first time, presented. This investigation is motivated because neither the conventional Fokker-Planck approximation (for weakly coupled plasmas (ln(lambda)(sub b) approximately less than 10) nor the theory of dielectric response with correlations for strongly coupled plasmas (ln(lambda)(sub b) approximately less than 1) has satisfactorily addressed this regime. Specifically, the standard Fokker-Planck operator for Coulomb collisions has been modified to include neglected terms that are directly associated with large-angle scattering. In addition, a reduced electron-ion collision operator has been calculated that, for the first time, manifests 1/ln(lambda)(sub b) corrections. Precise calculations of some relaxation rates and crude calculations of electron transport coefficients have been made. As one of major applications of the modified Fokker-Planck equation, the stopping powers and (rho)R have been calculated for charged fusion products (alpha's, H-3, He-3) and hot electrons interacting with plasmas

relevant to inertial confinement fusion. In the second major topic of this thesis, advances made in the area of laboratory x-ray sources are presented. First, and most importantly, through the use a Cockcroft-Walton linear accelerator, a charged particle induced x-ray emission (PIXE) source has been developed. Intense line x radiation (including K-, L-, M-, and N-lines) with wavelengths from 0.5 A to 111 A have been successfully produced. Second, a new high intensity electron-beam x-ray generator has also been developed, and it has been used with advantage in the soft x-ray region (less than 3 keV). Finally, a direct comparisons of both sources (PIXE and electron-beam x-ray sources) to a commercially available radioactive (alpha) fluorescent x-ray source has been made. DOE

N94-30071 International Centre for Theoretical Physics, Trieste (Italy).
A RELATIVISTIC SOLITARY WAVE IN ELECTRON POSITRON PLASMA
V. I. Berezhiani, V. Skarka, and S. Mahajan Sep. 1993 12 p Limited Reproducibility: More than 20% of this document may be affected by microfiche quality
(DE94-608107; IC-93/282) Avail: Issuing Activity (Department of Energy (DOE)) (US Sales Only)

The relativistic solitary wave propagation is studied in cold electron-positron plasma embedded in an external arbitrary strong magnetic field. The exact, analytical soliton-like solution corresponding to a localized, purely electromagnetic pulse with arbitrary big amplitude is found. DOE

N94-30126*# Lockheed Missiles and Space Co., Palo Alto, CA. Research and Development Div.
A STUDY OF THE FORMATION AND DYNAMICS OF THE EARTH'S PLASMA SHEET USING ION COMPOSITION DATA Final Report, 10 Apr. 1991 - 9 May 1994
O. W. Lennartsson 20 Apr. 1994 74 p
(Contract NAS5-31209)
(NASA-CR-195119; NAS 1.26:195119; F254278) Avail: CASI HC A04/MF A01

Over two years of data from the Lockheed Plasma Composition Experiment on the ISEE 1 spacecraft, covering ion energies between 100 eV/e and about 16 keV/e, have been analyzed in an attempt to extract new information about three geophysical issues: (1) solar wind penetration of the Earth's magnetic tail; (2) relationship between plasma sheet and tail lobe ion composition; and (3) possible effects of heavy terrestrial ions on plasma sheet stability. For individual titles, see N94-30127 through N94-30128.

N94-30127*# Lockheed Missiles and Space Co., Palo Alto, CA. Research and Development Div.
TAIL LOBE ION COMPOSITION AT ENERGIES OF 0.1 TO 16 keV/e: EVIDENCE FOR MASS-DEPENDENT DENSITY GRADIENTS
O. W. Lennartsson *In its* A Study of the Formation and Dynamics of the Earth's Plasma Sheet Using Ion Composition Data 20 Apr. 1994 15 p Repr. from Journal of Geophysical Research, v. 99, no. A2, 1 Feb. 1994 p 2387-2401 (For primary document see N94-30126 08-75)
(Contract NAS5-33047) (ISSN 0148-0227)
(Paper-93JA03201) Copyright Avail: CASI HC A03/MF A01

A large set of energetic (0.1 to 16 keV/e) ion composition data from the central magnetotail, obtained by the ISEE 1 spacecraft between 10 and 23R(sub E) from Earth, is sorted according to measured total ion beta value, in order to investigate whether bulk properties of different ions vary in different ways between plasma sheets and lobes, as suggested by a comparison of certain experimental and theoretical results in the literature. Despite inevitable difficulties with extracting statistically valid data at very low beta (10(exp -2) or lower), the results seem to support a recent theoretical model suggesting that lighter ions have a steeper density gradient than heavier ions, especially when comparing H(+) ions with O(+) ions. The results also indicate that ion velocity distributions are fairly isotropic even at low beta, at least those of H(+) ions, although field-aligned flows are common. The results are evaluated in the context of plasma transport and are found to lend some support to the notion that tail lobe convection may be directed inward from the dawn and dusk flanks. Author (revised)

N94-30128*# Lockheed Missiles and Space Co., Palo Alto, CA. Research and Development Div.
EXPERIMENTAL INVESTIGATION OF POSSIBLE GEOMAGNETIC FEEDBACK FROM ENERGETIC (0.1 TO 16 keV) TERRESTRIAL O(+) IONS IN THE MAGNETOTAIL CURRENT SHEET
O. W. Lennartsson, D. M. Klumpar, E. G. Shelley, and J. M. Quinn *In its* A Study of the Formation and Dynamics of the Earth's Plasma Sheet Using Ion Composition Data 20 Apr. 1994 12 p Repr. from Journal of Geophysical Research, v. 98, no. A11, 1 Nov. 1993 p 19443-19454 (For primary document see N94-30126 08-75)
(Contracts NAS5-30565; NAS5-33047) (ISSN 0148-0227)
(Paper-93JA01991) Copyright Avail: CASI HC A03/MF A01

Data from energetic ion mass spectrometers on the ISEE 1 and AMPTE/CCE spacecraft are combined with geomagnetic and solar indices to investigate, in a statistical fashion, whether energized O(+) ions of terrestrial origin constitute a source of feedback which triggers or amplifies geomagnetic activity as has been suggested in the literature, by contributing a destabilizing mass increase in the magnetotail current sheet. The ISEE 1 data (0.1-16 keV/e) provide in situ observations of the O(+) concentration in the central plasma sheet, inside of 23 R(sub E), during the rising and maximum phases of solar cycle 21, as well as inner magnetosphere data from same period. The CCE data (0.1-17 keV/e) taken during the subsequent solar minimum all within 9 R(sub E). provide a reference for long-term variations in the magnetosphere O(+) content. Statistical correlations between the ion data and the indices, and between different indices. all point in the same direction: there is probably no feedback specific to the O(+) ions, in spite of the fact that they often contribute most of the ion mass density in the tail current sheet. Author (revised)

N94-30156# Saskatchewan Univ., Saskatoon. Plasma Physics Lab.
HIGHER ORDER COLLISIONLESS BALLOONING MODE IN TOKAMAKS
A. Hirose and L. Zhang Feb. 1994 12 p
(PPL-143; CTN-94-61140) Avail: CASI HC A03/MF A01

Kinetic stability analysis of general electromagnetic modes in tokamaks has revealed the existence of a higher order ballooning mode which is not subject to second stabilization. This collisionless mode is characterized by broad eigenfunctions in the ballooning space. The first stability boundary revealed from the kinetic analysis is significantly smaller than predicted from the ideal magneto hydrodynamic analysis. In particular, at large shear, the threshold for electromagnetic modes vanishes, and the modes are expected to be unstable in the region well below the ideal magneto hydrodynamic limit. The ion temperature gradient provides the dominant destabilization mechanism. Author (CISTI)

N94-30157# Texas Technological Univ., Lubbock. Dept. of Electrical Engineering.
PLASMA TURBULENT BREMSSTRAHLUNG
Osamu Ishihara and Akira Hirose Feb. 1994 9 p
(PPL-144; CTN-94-61141) Avail: CASI HC A02/MF A01

Turbulent bremsstrahlung is a radiation mechanism of high frequency plasma modes produced by the scattered electrons due to the effective turbulent collisions associated with low frequency fluctuations. The mechanism of turbulent bremsstrahlung is examined, taking into account quasilinear effects. A collisionless, unmagnetized plasma is considered in which low frequency ion acoustic fluctuations are excited by, for example, current driven instability. A simple dispersion relation for the ion acoustic mode is assumed, and a test Langmuir wave is launched in the model analysis. It is shown that if the spontaneous emission term is retained in the quasilinear evolution of the distribution function, the test Langmuir waves become unstable in the presence of ion acoustic turbulence. Electrons resonating with ion acoustic waves are scattered by the low frequency fluctuations and emit Langmuir waves. The upconversion of the low frequency ion acoustic modes to high frequency Langmuir modes may occur in a collisionless plasma even when the system is closed. The proposed theory of turbulent bremsstrahlung seems to explain various plasma phenomena both in the laboratory and in space, such as the generation of long wavelength Langmuir waves by low frequency magnetospheric turbulence and the pulsed acceleration of electrons in solar flares. Author (CISTI)

N94-30158# Saskatchewan Univ., Saskatoon. Plasma Physics Lab.
EIGENMODE ANALYSIS OF THE DESTABILIZED ION ACOUSTIC MODE

IN TOKAMAKS

A. Hirose and L. Zhang Jan. 1994 12 p
(PPL-142; CTN-94-61142) Avail: CASI HC A03/MF A01

Ballooning eigenmode analysis is presented of the destabilized ion acoustic mode (or long wavelength drift mode) in tokamaks. Destabilization of the ion acoustic transit mode previously predicted within local or semi-local approximation has been confirmed. The eigenfunction resembles the trial function used in the semi-local analysis and thus supports the eigenvalues obtained from the same approximation. The absence of ion Landau damping prevails, particularly in the long wavelength region. Author (CISTI)

N94-30159# Saskatchewan Univ., Saskatoon. Plasma Physics Lab.
BETA ENHANCEMENT OF THERMAL DIFFUSIVITY IN TOKAMAKS

A. Hirose and A. I. Smolyakov Aug. 1993 12 p
(PPL-141; CTN-94-61143) Avail: CASI HC A03/MF A01

Electromagnetic corrections to the quasilinear anomalous thermal diffusivity due to long wavelength electrostatic modes in tokamaks are investigated in terms of the semi-local kinetic dispersion relation. The diffusivity increases with beta (the ratio of plasma to magnetic pressure) almost linearly, even though the dispersion relation and thus the field polarization remain predominantly electrostatic. The enhancement in thermal conduction is largely due to resonant interaction of untrapped electrons with a fluctuating magnetic field. Author (CISTI)

N94-30171 Academy of Sciences (USSR), Novosibirsk.
RESISTIVE BALLOONING MODE IN A GAS-DYNAMIC TRAP

Yu. A. Tsidulko 1992 22 p In RUSSIAN Limited Reproducibility: More than 20% of this document may be affected by microfiche quality
(DE94-608328; IYaF-92-10) Avail: CASI HC A03 (US Sales Only)

MGD instability (resistive ballooning mode) is considered, which is developed in a gas-dynamic trap due to: plasma finite conductivity. The consideration is carried out with the account for resonance effects. Two varieties of the resistive ballooning mode (fast and slow) are determined. The first one appears only in the case when the plasma conductivity in the mirror range is less some threshold value. The slow resistive mode has a positive increment at any high conductivity. A qualitative comparison with experimental data is fulfilled. DOE

N94-30191 Academy of Sciences (USSR), Novosibirsk.
LANGMUIR WAVES IN THE ELECTRON-POSITRON PLASMA

N. S. Buchelnikova and E. P. Matochkin 1992 31 p In RUSSIAN Limited Reproducibility: More than 20% of this document may be affected by microfiche quality
(DE94-608330; IYaF-92-27) Avail: CASI HC A03 (US Sales Only)

The numerical experiments (PIC-method) were made to study the evolution of the travelling Langmuir waves in the one-dimensional nonrelativistic electron-positron plasma. If the initial wave amplitudes are not high the main process is the selfconversion of the wave. This process leads to the generation of the modes and to the development of the modulational instability as a secondary process. The damping of the electric field is due to the trapping of the electrons and positrons and to the development of the large-scale stochasticity. If the initial wave amplitudes are high the essential role plays the electron and positron nonlinearity and the trapping of the electrons and positrons by the main wave ('kinetic' effect) and the steapening and the breaking of the wave ('hydrodynamic' effect). The electron-positron plasma can be considered as a model of the equal mass positive and negative ions plasma. DOE

N94-30192 Israel Atomic Energy Commission, Yavneh.
MAGNETIC FIELD GENERATION BY CIRCULARLY POLARIZED LASER LIGHT AND INERTIAL PLASMA CONFINEMENT IN A MINIATURE MAGNETIC BOTTLE INDUCED BY CIRCULARLY POLARIZED LASER LIGHT Ph.D. Thesis

E. Kolka Jul. 1993 71 p In HEBREW Limited Reproducibility: More than 20% of this document may be affected by microfiche quality
(DE94-608353; IA-1480) Avail: Issuing Activity (Department of Energy (DOE)) (US Sales Only)

A new concept of hot plasma confinement in a miniature magnetic bottle induced by circularly polarized laser light is suggested in this work. Magnetic fields generated by circularly polarized laser light may be of the order of a megagauss. In this configuration, the circularly polarized laser light is used to get confinement of a plasma contained in a good conductor vessel. The poloidal magnetic field induced by the circularly polarized laser and the efficiency of laser absorption by the plasma are calculated in this work. The confinement in this scheme is supported by the magnetic forces and the Lawson criterion for a DT plasma might be achieved for number density n = 5*10(exp 21)cm(exp -3) and confinement time tau = 20 nsec. The laser and the plasma parameters required to get an energetic gain are calculated. DOE

N94-30193 Academy of Sciences (USSR), Novosibirsk.
EXPERIMENTS ON THE TWO-STAGE DENSE PLASMA HEATING ON THE GOL-3 DEVICE

A. V. Burdakov, S. G. Voropaev, and A. F. Guber et al 1992 56 p In RUSSIAN Limited Reproducibility: More than 20% of this document may be affected by microfiche quality
(DE94-608356; IYaF-92-12) Avail: CASI HC A04 (US Sales Only)

The experimental results on heating of a dense plasma by electron beam (1 MeV, 40 kA, 4 micro-sec) on the GOL-3 device are presented. The relativistic electron beam is injected into a (7-meter long plasma column of a mirror machine). The beam deposits about 20-30% of its energy into 'hot' (1-10 keV) plasma electrons in the homogeneous part of plasma (n - 10(exp 15) cm(exp -3), T approximately = 1 keV). These electrons are slowed down in a 0.5-3 meter long gas cloud of a density of 10(exp 16)-10(exp 17)cm(exp -3) (so-called two-stage heating scheme). The 'hot' electrons ionize the cloud, create a plasma which is heated due to binary collisions. The resulting total energy of the cloud is 2-4 times greater than the instantaneous energy content of the lower density homogeneous plasma. The shock waves were observed in the plasma. Temperature distribution along the plasma cloud was measured and was used to estimate the average energy of 'hot' electrons. The experiment demonstrates a high efficiency of the two-stage scheme of a dense plasma heating. DOE

N94-30194 Academy of Sciences (USSR), Novosibirsk. Inst. Yadernoj Fiziki.
PECULIARITIES OF HEAT TRANSFER IN THE EXPERIMENTS OF BEAM INJECTION HEATING OF A PLASMA AT THE GOL-3 DEVICE

A. V. Burdakov and V. V. Postupaev 1992 23 p Limited Reproducibility: More than 20% of this document may be affected by microfiche quality
(DE94-608357; IYaF-92-9) Avail: CASI HC A03 (US Sales Only)

The dynamics is discussed of the heat redistribution in plasma, heated by microsecond relativistic electron beam in the GOL-3 facility. The electron temperature dependence on time and distance up to beam injection point are compared with heat transfer calculations. At the stage of plasma cooling, the time dependence of the plasma temperature is well described by the classical electron heat conduction on the facility buttends. At the same time, the dynamics of the observed electron temperature increase and its distribution in the facility length during beam injection time can not be explained by the classical electron heat conduction. DOE

N94-30339# Oak Ridge National Lab., TN.
OVERVIEW OF THE US STELLARATOR REACTOR STUDY

J. F. Lyon, K. Gulec, R. L. Miller, and L. El-Guebaly 1993 7 p Presented at the Symposium on Fusion Engineering, Hyannis, MA, 11-15 Oct. 1993
(Contract DE-AC05-84OR-21400)
(DE94-006042; CONF-931018-78) Avail: CASI HC A02/MF A01

This study, which uses a cost-minimization code that incorporates the ARIES costing and reactor component models with a 1-D energy transport calculation, shows that a torsatron reactor could be competitive with a tokamak reactor. DOE

N94-30365# Oak Ridge National Lab., TN.
IRRADIATION-INDUCED STRUCTURE AND PROPERTY CHANGES IN TOKAMAK PLASMA-FACING, CARBON-CARBON COMPOSITES

T. D. Burchell 1994 14 p Presented at the 39th International Symposium of the Society for the Advancement of Material and Process Engineering and Exhibition, Anaheim, CA, 11-14 Apr. 1994
(Contract DE-AC05-84OR-21400)
(DE94-006046; CONF-940412-3) Avail: CASI HC A03/MF A01

Carbon-carbon composites are an attractive choice for fusion reactor plasma-facing components because of their low atomic number, superior thermal shock resistance, and low neutron activation. Next generation plasma fusion reactors, such as the International Thermonuclear Experimental

Reactor (ITER), will require advanced carbon-carbon composite materials possessing high thermal conductivity to manage the anticipated severe heat loads. Moreover, ignition machines such as ITER will produce large neutron fluxes. Consequently, the influence of neutron damage on the structure and properties of carbon-carbon composite materials must be evaluated. Data from two irradiation experiments are reported and discussed here. Carbon-carbon composite materials were irradiated in target capsules in the High Flux Isotope Reactor (HFIR) at Oak Ridge National Laboratory (ORNL). A peak damage dose of 4.7 displacements per atom (dpa) at 600 C was attained. The carbon materials irradiated included unidirectional, two-directional, and three-directional carbon-carbon composites. Dimensional changes are reported for the composite materials and are related to single crystal dimensional changes through fiber and composite structural models. Moreover, the irradiation-induced dimensional changes are reported and discussed in terms of their architecture, fiber type, and graphitization temperature. The effect of neutron irradiation on thermal conductivity of two three-directional, carbon-carbon composites is reported and the recovery of thermal conductivity due to thermal annealing is discussed. DOE

N94-30597 Lawrence Livermore National Lab., CA.
A REVIEW OF THE ABLATIVE STABILIZATION OF THE RAYLEIGH-TAYLOR INSTABILITY IN REGIMES RELEVANT TO ICF
J. D. Kilkenny, S. G. Glendinning, S. W. Haan, B. A. Hammel, J. D. Lindl, D. Munro, B. A. Remington, S. V. Weber, J. P. Knauer, and C. P. Verdon Dec. 1993 34 p Presented at the Fall Meeting of the Plasma Physics Division of the American Physical Society, St. Louis, MO, 1-5 Nov. 1993 Limited Reproducibility: More than 20% of this document may be affected by microfiche quality
(Contract W-7405-eng-48)
(DE94-005809; UCRL-JC-115537; CONF-931132-1) Avail: CASI HC A03

It has been recognized for many years that the most significant limitation of ICF is the Rayleigh-Taylor (R-T) instability. It limits the distance an ablatively driven shell can be moved to several times its initial thickness. Fortunately material flow through the unstable region at velocity v(sub A) reduces the growth rate to the square root of (kg/1+kL) minus (beta)kv(sub A) with (beta) from 2-3. In recent years experiments using both x-ray drive and smoothed laser drive to accelerate foils have confirmed our understanding of the R-T instability. The growth of small initial modulations on the foils is measured for growth factors up to 60 for direct drive and 80 for indirect drive. For x-ray drive large stabilization is evident. After some growth, the instability enters the non-linear phase when mode coupling and saturation are also seen and compare well with modeling. Normalized growth rates for direct drive are measured to be higher, but strategies for reduction by raising the isentrope are being investigated. For direct drive, high spatial frequencies are imprinted from the laser beam and amplified by the R-T instability. Modeling shows an understanding of this laser imprinting. DOE

N94-30697 Argonne National Lab., IL.
MODELLING EROSION DAMAGE FROM LOW-ENERGY PLASMA GUN SIMULATIONS OF DISRUPTIONS
D. A. Ehst and A. Hassanein Oct. 1993 41 p Limited Reproducibility: More than 20% of this document may be affected by poor print
(Contract W-31-109-eng-38)
(DE94-005196; ANL/FPP/TM-268) Avail: Issuing Activity (Department of Energy (DOE))

Energy transfer to material surfaces is dominated by photon radiation through low temperature plasma vapors if tokamak disruptions are due to low kinetic energy particles (approximately less than 100 eV). Simple models of radiation transport are derived and incorporated into a fast-running computer routine to model this process. The results of simulations are in good agreement with plasma gun erosion tests on several metal targets. DOE

N94-30752# Los Alamos National Lab., NM.
MOLECULAR DYNAMICS SIMULATIONS OF DENSE PLASMAS
L. A. Collins, J. D. Kress, I. Kwon, D. L. Lynch, and N. Troullier 1993 11 p Presented at the American Physical Society Conference, San Antonio, TX, Sep. 1993
(Contract W-7405-eng-36)
(DE94-005082; LA-UR-93-4474; CONF-9309320-1) Avail: CASI HC A03/MF A01

We have performed quantum molecular dynamics simulations of hot, dense plasmas of hydrogen over a range of temperatures (0.1 to 5 eV) and densities (0.0625 to 5 g/cc). We determine the forces quantum mechanically from density functional, extended Huckel, and tight binding techniques and move the nuclei according to the classical equations of motion. We determine pair-correlation functions, diffusion coefficients, and electrical conductivities. We find that many-body effects predominate in this regime. We begin to obtain agreement with the OCP and Thomas-Fermi models only at the higher temperatures and densities. DOE

N94-30755# Naval Research Lab., Washington, DC.
THE INVESTIGATION OF ELECTRON-ION RADIATIVE AND DIELECTRONIC RECOMBINATION IN HIGH-TEMPERATURE PLASMAS
V. L. Jacobs 1993 42 p
(Contract DE-AI05-89ER-53281)
(DE94-005150; DOE/ER-53281/T3) Avail: CASI HC A03/MF A01

This paper describes progress in the following six areas: unified description of radiative and dielectronic recombination; calculations of specific dielectronic satellite transitions; modeling of K(sub alpha) dielectronic satellite spectra; effects of electron collisions and electric fields; density-sensitive dielectronic satellite lines; and polarization of atomic radiative emission in crossed electric and magnetic fields. Also discussed are proposed investigations and coordination with current tokamak observations. DOE

N94-30760# Oak Ridge National Lab., TN.
THE IMPACT OF IMPROVED PHYSICS ON COMMERCIAL TOKAMAK REACTORS
J. D. Galambos, L. J. Perkins, S. Haney, and J. Mandrekas Jan. 1994 51 p
(Contract DE-AC05-84OR-21400)
(DE94-006103; ORNL/TM-12483) Avail: CASI HC A04/MF A01

Improvements in the confinement and beta capability of tokamak devices have long been a goal of the fusion program. We examine the impact of improvements in present day confinement and beta capabilities on commercial tokamak reactors. We characterize confinement with the achievable enhancement factor (H) over the ITER89 Power scaling confinement time and beta by the Troyon coefficient g. A surprisingly narrow range of plasma confinement and beta are found to be useful in minimizing the cost of electricity for a tokamak reactor. Improvements in only one of these quantities is not useful beyond some point, without accompanying improvements in the other. For the plasma beta limited by a Troyon coefficient (g) near 4.3 (%mT/MA), confinement levels characterized by H factor enhancements of only 2 are useful for our nominal steady-state driven tokamak. These confinement levels are similar to those observed in present day experiments. If the permissible Troyon beta coefficient is near 6, the useful H factor confinement range increases to 2.5, still close to present day confinement levels. Inductively driven, pulsed reactors have somewhat increased useful ranges of confinement, relative to the steady-state cases. For a Troyon beta limit coefficient g near 4.3, H factors up to 2.5 are useful, and for g near 6, H factors up to 3 are useful. DOE

N94-30768# Lawrence Livermore National Lab., CA.
ADVANCED STEADY-STATE OPERATING SCENARIOS
W. M. Nevins, R. H. Bulmer, L. D. Pearlstein, S. W. Haney, and J. Manickam 2 Dec. 1993 8 p
(Contract W-7405-eng-48)
(DE94-004810; UCRL-ID-115904) Avail: CASI HC A02/MF A01

The goal for advanced steady-state operation in ITER should be to demonstrate the operation of the plasma core for a steady-state fusion reactor. To accomplish this the authors must develop steady-state operating scenarios at high beta for high fusion power density, low auxiliary power requirements (Q(sub CD) greater than or = 25, where Q(sub CD) congruent to P fusion/P(sub CD) and P(sub DC) is the power required for sustaining the plasma current) for low recirculating power requirements, and at moderate safety factor (q(sub psi)) less than or = 4.5) to minimize the cost for the tokamak core of a steady-state demonstration power reactor based on the operating modes demonstrated in ITER. The key to achieving steady-state operation at high fusion power in ITER will be the development of operating scenarios with very high bootstrap current fractions (f(sub BS) greater than or = 90%) in which the radial profile of the bootstrap current density is well aligned with that of the total plasma current density, and for which

the MHD beta-limit exceeds beta(sub n)(sup *) = 0.05 T - m/MA. They are in the process of developing such operating modes for ITER. In section 1, they propose two advanced steady-state operating points: a preliminary operating point that was the basis for the MHD studies reported in section 2, and a second operating point that has been optimized based on the authors studies to date. In section 2 they present calculations indicating that the initial operating point is stable to MHD ballooning and low-n kink modes (with a conducting wall at r = 1.25a) up to beta(sub n)(sup *) approximately = 6 x 10(exp -2) T - m/MA. In section 3, they present a free-boundary MHD equilibrium, and show that advanced steady-state operating modes are compatible with the ITER poloidal field system and diverter. DOE

N94-30832# General Atomics Technologies Corp., San Diego, CA.
APPLICATION OF DIVERTOR CRYOPUMPING TO H-MODE DENSITY CONTROL IN DIII-D
M. A. Mahdavi, J. R. Ferron, A. W. Hyatt, R. J. LaHaye, G. L. Laughon, M. Leh, R. Maingi, M. M. Menon, P. K. Mioduszewski, and K. M. Schuabel et al Nov. 1993 7 p Presented at the Symposium on Fusion Engineering, Hyannis, MA, 11-15 Oct. 1993
(Contracts DE-AC03-89ER-51114; DE-AC05-84OR-21400)
(DE94-004859; GA-A-21501; CONF-931018-75) Avail: CASI HC A02/MF A01

In this paper, we describe the method and the results of experiments where a unique in-vessel cryopump-baffle system was used to control density of H-mode plasmas. We were able to independently regulate current and density of ELMing H-mode plasmas, each over a range of factor two, and measure the H-mode confinement scaling with plasma density and current. With a modest pumping speed of approximately 40 kl/s, particle exhaust rates as high as 2 x 10(exp 22) atom/s(exp -1) have been observed. DOE

N94-30875# Lawrence Livermore National Lab., CA.
INERTIAL CONFINEMENT FUSION
R. A. Sacks, ed., P. W. Murphy, ed., and D. P. Schleich, ed. 1993 59 p
(Contract W-7405-eng-48)
(DE94-005957; UCRL-LR-105821-93-4) Avail: CASI HC A04/MF A01

This report discusses the following research: a diode-pumped solid-state laser driver for inertial fusion energy power plants; longitudinal beam dynamics in heavy ion fusion accelerators; design of the ion sources for heavy ion fusion; measurement of electron density in laser-produced plasma with a soft x-ray moire deflectometer; and analysis of weakly nonlinear three-dimensional Rayleigh-Taylor instability growth. DOE

N94-30882# Massachusetts Inst. of Tech., Cambridge. Plasma Fusion Center.
MAGNETIC FLUX RECONSTRUCTION METHODS FOR SHAPED TOKAMAKS Ph.D. Thesis
Chi-Wa Tsui Dec. 1993 173 p
(Contract DE-AC02-78ET-51013)
(DE94-005827; PFC/RR-93-05; DOE/ET-51013/304) Avail: CASI HC A08/MF A02

The use of a variational method permits the Grad-Shafranov (GS) equation to be solved by reducing the problem of solving the two dimensional nonlinear partial differential equation to the problem of minimizing a function of several variables. This high speed algorithm approximately solves the GS equation given a parameterization of the plasma boundary and the current profile (p' and FF' functions). The current profile parameters are treated as unknowns. The goal is to reconstruct the internal magnetic flux surfaces of a tokamak plasma and the toroidal current density profile from the external magnetic measurements. This is a classic problem of inverse equilibrium determination. The current profile parameters can be evaluated by several different matching procedures. Matching of magnetic flux and field at the probe locations using the Biot-Savart law and magnetic Green's function provides a robust method of magnetic reconstruction. The matching of poloidal magnetic field on the plasma surface provides a unique method of identifying the plasma current profile. However, the power of this method is greatly compromised by the experimental errors of the magnetic signals. The Casing principle provides a very fast way to evaluate the plasma contribution to the magnetic signals. It has the potential of being a fast matching method. The performance of this method is hindered by the accuracy of the poloidal magnetic field computed from the equilibrium solver. A flux reconstruction package has been implemented which integrates a vacuum field solver using a filament model for the plasma, a multilayer perception neural network as an interface, and the volume integration of plasma current density using Green's functions as a matching method for the current profile parameters. The flux reconstruction package is applied to compare with the ASEQ and EFIT data. DOE

76 SOLID-STATE PHYSICS

Includes superconductivity.

For related information, see also *33 Electronics and Electrical Engineering* and *36 Lasers and Masers.*

N94-28484# Sandia National Labs., Albuquerque, NM.
RESPONSE OF GaAs CHARGE STORAGE DEVICES TO TRANSIENT IONIZING RADIATION
D. L. Hetherington, J. F. Klem, R. C. Hughes, and H. T. Weaver 1993 5 p Presented at the International Semiconductor Device Research Symposium, Charlottesville, VA, 5-8 Dec. 1993
(Contract DE-AC04-94AL-85000)
(DE94-005273; SAND-93-2311C; CONF-931230-1) Avail: CASI HC A01/MF A01

Charge storage devices in which non-equilibrium depletion regions represent stored charge are sensitive to ionizing radiation. This results since the radiation generates electron-hole pairs that neutralize excess ionized dopant charge. Silicon structures, such as dynamic RAM or CCD cells are particularly sensitive to radiation since carrier diffusion lengths in this material are often much longer than the depletion width, allowing collection of significant quantities of charge from quasi-neutral sections of the device. For GaAs the situation is somewhat different in that minority carrier diffusion lengths are shorter than in silicon, and although mobilities are higher, we expect a reduction of radiation sensitivity as suggested by observations of reduced quantum efficiency in GaAs solar cells. Dynamic memory cells in GaAs have potential increased retention times. In this paper, we report the response of a novel GaAs dynamic memory element to transient ionizing radiation. The charge readout technique is nondestructive over a reasonable applied voltage range and is more sensitive to stored charge than a simple capacitor. DOE

N94-28512# Brookhaven National Lab., Upton, NY.
LOW FREQUENCY DYNAMICS OF CO/Cu-BREAKDOWN OF BORN-OPPENHEIMER APPROXIMATION
C. Hirschmugl (Yale Univ., New Haven, CT.), G. P. Williams, and Y. J. Chabal 1993 14 p Presented at the 40th National Symposium of the American Vacuum Society, Orlando, FL, 15-19 Nov. 1993
(Contract DE-AC02-76CH-00016)
(DE94-005508; BNL-49777; CONF-9311104-16) Avail: CASI HC A03/MF A01

Synchrotron infrared studies of adsorbates on surfaces offer the possibility of probing low frequency vibrational modes and dynamics at high resolution (1 cm(exp -1), 125 (mu)eV). Extensive experiments have been performed for ordered submonolayers of CO on low index Cu surfaces (((radical)3 x (radical)3)R30 degree CO/Cu(111), c(2 x 2) CO/Cu(100) and (1 x 2) CO/Cu(110)), in the 100-2500 cm(exp -1) (approximately 12.5-312.5 MeV) range. These are the first IR experiments to directly probe the adsorbate-substrate vibrations for this system. In addition, however, several surprising features are observed including the dipole-forbidden hindered rotation and an unexpected broadband absorption. Two theories have been motivated by this work, and will be compared to our experimental results. The first theory is a cluster calculation by Head-Gordon and Tully, which takes into account the breakdown of the Born-Oppenheimer approximation and predicts lifetimes and frequencies of the vibrational modes for CO/Cu(100). Another Drude-based theory, proposed by Persson, considers the coupling of the conduction electron current to the vibrations of the adsorbates, accounting for the observation of both the broad-band absorption and dipole-forbidden peak. DOE

N94-28529# Ames Lab., IA.
SYNTHESIS AND CHARACTERIZATION OF NOVEL TERNARY AND QUATERNARY REDUCED MOLYBDENUM OXIDES Ph.D. Thesis

G. L. Schimek Jul. 1993 321 p
(Contract W-7405-eng-82)
(DE94-005563; IS-T-1651) Avail: CASI HC A14/MF A03

This thesis is divided into 8 sections: synthesis and characterization (char.) of Ba3Mo18O28 (an oligomer with four traps edge-sharing Mo octahedra); synthesis and char. of K(x)M(y)Mo14O22 (M=Sn, Pb, Sr) (oligomers with three traps edge-sharing Mo octahedra); synthesis and char. of K(0.19Ba(3.81)Mo22O34 (an oligomer with five traps edge-sharing Mo octahedra); synthesis and char. of Ti(0.31)Fe(1.69)Mo4O7 (a material containing closest-packing of infinite chains of octahedral Mo clusters); synthesis and char. of K(x)M(2-x)Mo10O16 (M=Ca, Sr, Gd) (oligomers with two traps edge-sharing Mo octahedra); synthesis and char. of the RE4Mo4O11 series; synthesis and char. of Pb(0.31WO3 (a tetragonal tungsten bronze containing lead); and examination of superstructure in Fe(1.89)Mo(4.11)O7, Sn(0.9)Mo4O6, InMo4O 6, and Mn(1. 5)Mo8O11 by electron microscopy. DOE

N94-28535# Oak Ridge National Lab., TN.
ON THE PREDICTION OF HAZ GRAIN SIZE USING MONTE CARLO SIMULATION
B. Radhakrishnan and T. Zacharia 1993 9 p Presented at the American Welding Society International Conference on Modeling and Control of Joining Processes, Orlando, FL, 8 Dec. 1993
(Contract DE-AC05-84OR-21400)
(DE94-005465; CONF-931234-4) Avail: CASI HC A02/MF A01

The Monte Carlo (MC) technique has been widely used to simulate the evolution of grain structures during recrystallization and curvature-driven grain growth processes. However, one of the drawbacks of the simulations is that a one-to-one correlation between the simulated and the experimental results of grain structures cannot be obtained. This is because the two important quantities, grain size and time, have been represented in the simulations as dimensionless quantities. The paper outlines a methodology by which a one-to-one correlation can be obtained between the simulated and experimental measures of grain size and time, so that the technique can be readily applied to quantitatively predict the microstructural evolution in real materials when they are subjected to complicated thermal cycles, such as in welding. DOE

N94-28570# Argonne National Lab., IL.
ENERGY GAP STRUCTURE OF LAYERED SUPERCONDUCTORS
S. H. Liu (Oak Ridge National Lab., TN.) and R. A. Klemm Nov. 1993 17 p Presented at the Superconducting Superlattices and Multilayers and Oxide Superconductory Physics and Nanoengineering, Los Angeles, CA, 23-28 Jan. 1994
(Contracts W-31-109-eng-38; DE-AC05-84OR-21400)
(DE94-005132; ANL/MSD/CP-80230; CONF-940121-1) Avail: CASI HC A03/MF A01

We report the energy gap structure and density-of-states (DOS) of a model layered superconductor with one superconducting layer and one normal layer in a unit cell along the c-axis. In the physically interesting parameter range where the interlayer hopping strengths of the quasiparticles are comparable to the critical temperature, the peaks in the DOS curve do not correspond to the order parameter (OP) of the superconducting layer, but depend on the OP and the band dispersion in the c-direction in a complex manner. In contrast to a BCS superconductor, the DOS of layered systems have logarithmic singularities. Our simulated tunneling characteristics bear close resemblance to experimental results. DOE

N94-28626 Joint Inst. for Nuclear Research, Dubna (USSR).
HYSTERESIS PHENOMENA AT SPIN-FLOP TRANSITION INDUCED BY THE PULSED MAGNETIC FIELD
D. Georgiev, V. V. Nitts, and A. P. Sirotin 1992 8 p In JAPANESE Limited Reproducibility: More than 20% of this document may be affected by microfiche quality
(DE94-606851; JINR-R-14-92-401) Avail: CASI HC A02 (US Sales Only)

The experimental results of neutron diffraction on single crystals of Cr2O3 and alpha-Fe2O3 in which spin-flop transition is induced by the pulsed magnetic field are presented. The dynamic hysteresis arises in the measurements of the dependence of neutron scattering intensity on a field value; it is connected with the fact that the process of reaching equilibrium for sublattices magnetizations lags behind the change of the magnetic field. At a relatively high amplitude of field pulses, providing high rate of change of the field at phase transition, the hysteresis loop takes a limiting value and form. The dependences of phase reorientation on sample temperature correspond to the distinctions of phase diagrams of these substances. DOE

N94-28734# Florida Univ., Gainesville.
DEVELOPMENT OF ULTRA-LOW NOISE, HIGH PERFORMANCE 3 -5 QUANTUM WELL INFRARED PHOTODETECTORS (QWIPs) FOR FOCAL PLANE ARRAY STARING IMAGE SENSOR SYSTEMS Quarterly Progress Report, 1 Nov. 1993 - 31 Jan. 1994
Sheng S. Li 6 Feb. 1994 55 p
(AD-A275745) Avail: CASI HC A04/MF A01

During this reporting period (11-01-93 to 01-31-94) we have continued to make significant progress towards the program goals. We have developed a new normal incidence p-type strained-layer InGaAs/InAlAs quantum well infrared photodetectors (QWIP's) grown on InP by MBE. This PSL QWIP has achieved an ultra-low dark current and very high detectivity at 8.1 micrometers and 77 K. The detector is under background limited performance (BLIP) for T less than 100 K, which is the highest BLIP temperature ever reported for a QWIP. A dark current density of 7x10(exp -8) A/sq cm and BLIP detectivity of 5.9x10(exp 10) Jones were obtained for this QWIP at 77 K. Other tasks performed during this period include: (1) Design, fabrication and characterization of a new two-color stacked BTM and BTC QWIP for 3-5 and 8-12 micrometers IR detection, (2) design and fabrication and characterization of a normal incidence p-type compressive strained-layer InGaAs/GaAs QWIP grown on GaAs, and (3) theoretical and experimental studies of parameter optimization for an InGaAs BTM QWIP. Detailed results and accomplishments are described in this report. DTIC

N94-28750# Japan Atomic Energy Research Inst., Tokyo.
CRYSTAL STRUCTURE OF La(2-x)Ba(x)CuO4
Susumu Katano, Satoru Funahashi, J. A. Fernandez-Baca, Nobuo Mori, Yutaka Ueda, and Kei-ichi Koga Jul. 1993 50 p
(DE94-707688; JAERI-M-93-131) Avail: CASI HC A03/MF A01

The crystal structure of La(2-x)Ba(x)CuO4 (0.03 less than or equal to x less than or equal to 0.24) have been studied at 115 K and 15 K by high-resolution neutron powder diffraction experiments. The variations in the Cu-O bond lengths refined by profile analysis suggest importance of the apical O(2) as well as that of the planar O(1) for the charge transfer. The compound with x = 0.125 at 15 K exhibits changes of the Cu-O bonds accompanied by the structural phase transition to the low-temperature tetragonal (LTT) phase. These results are discussed in terms of correlations with the superconducting properties of the system. Furthermore, to clarify a correlation between structural phase transitions and superconductivity, the crystal structure of the compound with x = 0.125 has been investigated under pressures up to 0.7 GPa. The transition to the LTT phase, observed at around 80 K at ambient pressure, decreases greatly at the rate of about -135 K/GPa. The bulk superconductivity, on the other hand, enhances under high pressure when the LTT phase disappears. These results show a strong relationship between the crystal structure and superconductivity in this system. DOE

N94-28773 Cornell Univ., Ithaca, NY. Dept. of Electrical Engineering.
INNOVATIVE OPTOELECTRONIC MATERIALS AND STRUCTURES USING OMVPE Annual Report, 1 Jan. - 31 Dec. 1993
James R. Shealy 14 Feb. 1994 18 p Limited Reproducibility: More than 20% of this document may be affected by microfiche quality
(Contract N00014-89-J-1311)
(AD-A275811) Avail: CASI HC A03

An advanced organo-metallic vapor phase epitaxy (OMVPE) process is being developed for the deposition of 3-5 semiconductor materials and structures. There are important optoelectronic device structures which cannot be realized be conventional means. The new OMVPE apparatus combines the multichamber reaction cell with deep UV photo-assisted growth and modulation flow epitaxial techniques. Using a combination of such processes, the-growth temperature requirements for 3-5 alloys can be substantially reduced. Selective growth on a sub-micron scale will be attempted with in-situ interference holography. The materials and techniques developed in this research program will result in significant simplifications to the fabrication sequence required to realize complex integrated optoelectronic circuits. DTIC

N94-28775 Pennsylvania State Univ., University Park. Dept. of Chemistry.
SPUTTERING OF SINGLE CRYSTALS: EXPERIMENTAL EVIDENCE OF THE EJECTION PROCESS
N. Winograd Feb. 1994 34 p Limited Reproducibility: More than 20% of this document may be affected by microfiche quality
(Contract N00014-91-J-1410)
(AD-A275819; TR-70) Avail: CASI HC A03

The objective of this review is to summarize recent experimental evidence of the sputtering of atoms from single crystal targets. The information is extracted primarily from literature published within the last 10 years and is meant to compliment other recent reviews on single crystal sputtering. The emphasis of the discussion is on experiments that are performed on well characterized surfaces obtained under low-dose conditions. Because of this restriction, most of the experiments utilized laser post-ionization as the detection scheme. The discussion of experimental results is focused mainly toward comparison with results of molecular dynamics computer simulations. The review includes a discussion of experimental techniques, a sampling of results obtained at normal incidence with keV Ar(+) ions, and others obtained at variable incident angles. In addition, energy and angular distributions of ground-state and excited-state sputtered atoms are compared in detail. DTIC

N94-28787# Joint Inst. for Nuclear Research, Dubna (USSR).
ION CHANNELING PECULIARITIES IN YBa2Cu3 O7 MONOCRYSTAL
A. S. Borovik, A. A. Epifanov, V. S. Malyshevskij, and D. A. Korneev 1992 18 p In RUSSIAN
(DE94-606885; JINR-R-14-92-396) Avail: CASI HC A03/MF A01 (US Sales Only)

The approach was developed in the frame of the diffusion model. It permits the description of the fast light ions channeling process for the near-surface region of multicomponent low-symmetry crystals. Theoretical analysis of channeling in a thin film monocrystal YBa2Cu3O7 showed that the given structure has peculiarities of angle-dependent yield of scattered ions which is not specific for one-component crystals. The developed approach permits increasing the abilities of an experimental data interpretation, the aim of which is to extract details of the depth dependence of structural and dynamical properties of a thin monocrystal film of YBaCuO. DOE

N94-28871# Northwestern Univ., Evanston, IL. Dept. of Electrical Engineering and Computer Science.
MOCVD GROWTH OF GaN, AlN AND AlGaN FOR UV PHOTODETECTOR APPLICATIONS
Manijeh Razeghi 1993 144 p
(Contract N00014-93-1-0235)
(AD-A275078) Avail: CASI HC A07/MF A02

For the growth of III-V nitrides, three main problems hinder the production of device quality materials. They are large lattice mismatch between nitride films and substrates, high n-type background concentration, and difficulty in p-type doping. In the past year, we focused on the first problem, the lattice mismatch. Different substrates and different orientations of the substrates have been used in order to find a suitable substrate for the nitride growth. An atmospheric horizontal-type metalorganic chemical vapor deposition (MOCVD) reactor was used for the growth of aluminum nitride, gallium nitride and ternary Al(x)Ga(1-x)N. DTIC

N94-28872# Northwestern Univ., Evanston, IL. Dept. of Electrical Engineering and Computer Science.
InTlSb FOR LONG-WAVELENGTH INFRARED PHOTODETECTORS AND ARRAYS Annual Report
Manijeh Razeghi 1993 23 p
(Contracts N00014-92-J-1951; N00014-93-1-0409)
(AD-A275079) Avail: CASI HC A03/MF A01

The objective of this research program is to grow InTlSb alloys by low-pressure metalorganic chemical vapor deposition and to investigate their physical properties, in order to demonstrate the feasibility of long-wavelength infrared detectors based on these materials. Ab initio theoretical calculations indicate that InTlSb is a potential alternative to HgCdTe, with the added metallurgical and processing advantages offered by III-V technology. TlSb has been predicted to be a semimetal with a bandgap of -1.5 eV. Therefore, it should be possible to cover the whole infrared spectrum by alloying InSb with TlSb. In addition, TlSb is expected to remain lattice-matched to InSb within two percent, which is an advantage for the growth of device-quality InTlSb alloys. Even though TlSb was expected to favor the Cs-Cl-type structure, InTlSb alloy was estimated to exhibit a stable zinc-blend structure up to 15 to 20 percent Tl. DTIC

N94-28880# North Carolina State Univ., Raleigh.
CARRIER COLLECTION AND SCATTERING IN QUANTUM WELL AND SUPERLATTICE DEVICES Final Report, 1 May 1990 - 31 Oct. 1993
Robert M. Kolbas 16 Dec. 1993 93 p
(Contract DAAL03-90-G-0118)
(AD-A275443; ARO-28070.1-EL-SDI) Avail: CASI HC A05/MF A01

The objective of this experimental program is to define the regimes in which scattering and carrier collection dominate the performance of quantum well and superlattice devices. The program consists of five thrusts: (1) materials growth; (2) carrier collection experiments; (3) utilization of ultra-thin monolayer thick quantum wells; (4) the understanding, control and utilization of dissipative mechanisms for new device concepts, and; (5) the demonstration of devices. The results obtained are applicable to monolithic photonic devices and high speed optical interconnect technology. A new device called a Bias Induced Color-Tuned Emitter (BICE) based on the selective collection of carriers in a quantum well was demonstrated for the first time. DTIC

N94-28889 Arizona State Univ., Tempe. Dept. of Chemical and Bioengineering.
SILICON GERMANIUM CARBON HETEROEPITAXIAL GROWTH ON SILICON Final Technical Report, 15 Jul. 1992 - 14 Oct. 1993
James W. Mayer 14 Oct. 1993 7 p Limited Reproducibility: More than 20% of this document may be affected by microfiche quality
(Contract F49620-92-J-0420)
(AD-A275197; AFOSR-94-0028TR) Avail: CASI HC A02

This project represents the initiation of band-gap engineering of Si-based devices at Arizona State University by James W. Mayer. While at Cornell, he directed the Microscience and Technology program supported by the Semiconductor Research Corporation. His Work on heteoepitaxy of SiGe on silicon convinced him that heteroepitaxy on Si was a viable technique for forming smaller band gap layers on silicon but the requirement was for larger energy-gap materials. In the fall of 1991, James Mayer visited Tom Picraux of Sandia National Laboratories and Clarence Tracy of Motorola Semiconductor Products to discuss the possibility of a joint program to investigate Silicon Germanium Carbon Heteroepitaxial Growth on Silicon. This represented a new research and development initiate for band gap engineering. DTIC

N94-28890 Massachusetts Inst. of Tech., Cambridge. Research Lab. of Electronics.
ELECTRONIC STRUCTURE AND MECHANICAL PROPERTIES OF GRAIN BOUNDARIES Final Report, 15 May 1990 - 14 May 1993
John D. Joannopoulos 17 Aug. 1993 12 p Limited Reproducibility: More than 20% of this document may be affected by microfiche quality
(Grant AF-AFOSR-0276-90)
(AD-A275198; AFOSR-94-0021-TR) Avail: CASI HC A03

Our ab-initio quantum mechanical calculations on grain boundaries have progressed beautifully. We have succeeded in obtaining some interesting and new results for both clean and doped gain boundary systems. For the clean Ge(Sigma 5)(310) tilt boundary, the ideal atomic configuration is as shown. This occurs along the 130 axis. The 310 grain boundary plane is perpendicular to the plane and passes through the atoms. The horizontal direction is 001. On either side of the boundary plane, There are atoms from the two grains. DTIC

N94-29101*# Clemson Univ., SC. Dept. of Ceramic Engineering.
NONAQUEOUS SLIP CASTING OF YBa2Cu3O(7-x) SUPERCONDUCTIVE CERAMICS Ph.D. Thesis - 1993
Matthew W. Hooker and Theodore D. Taylor Mar. 1994 114 p
(Grant NGT-50548; RTOP 142-20-14-02)
(NASA-CR-4575; NAS 1.26:4575) Avail: CASI HC A06/MF A02

This study investigates the slip casting of YBa2Cu3O(7-x) powders using nonaqueous carrier liquids and fired ceramic molds. The parameters of the process examined here include the rheological properties of YBa2Cu3O(7-x) powder dispersed in various solvent/dispersant systems, the combination

of nonaqueous slips with fired ceramic molds to form the superconductive ceramics, the process-property relationships using a four-factor factorial experiment, and the applicability of magnetic fields to align the YBa2Cu3O(7-x) grains during the casting process. Author

N94-29125# Carnegie-Mellon Univ., Pittsburgh, PA.
HIGH RESISTIVITY BUFFER LAYERS BY OXYGEN DOPING Final Report, 1 Sep. 1991 - 31 Aug. 1993
Marek Skowronski 31 Oct. 1993 52 p
(Grant AF-AFOSR-0373-91)
(AD-A274986; AFOSR-94-0023TR) Avail: CASI HC A04/MF A01

The goal of this project was to study the effects of GaAs doping with dimethyl aluminum methoxide (DMAIMO) during OMVPE growth. Incorporation of both aluminum and oxygen was analyzed as a function of growth conditions (growth temperature, V/III ratio, reactor pressure, growth rate, and DMAIMO mole fraction) by secondary ion mass spectroscopy. The aluminum content changed only slightly with deposition parameters but oxygen incorporation exhibited thermally activated behavior with the activation energy of 2.0 eV. At temperatures below 500 C oxygen content approached that of aluminum indicating that Al-O is incorporated as a pair into GaAs. The oxygen concentrations were as high as 5 x 10(exp 19)/cu cm without degrading surface morphology. Layers with high oxygen content exhibited short carrier lifetime (very weak near-band-edge photoluminescence) and high resistivity as determined by C-V profiles and Hall effect measurements. Localized vibrational mode spectroscopy proved that aluminum and oxygen atoms remain bonded as pairs in the volume of the epilayer. DTIC

N94-29130# Duke Univ., Durham, NC. Dept. of Chemistry.
PREPARATION, CHARACTERIZATION, AND FACILE THERMOLYSIS OF (X2GaP(SiMe3)2) (X = Br, I) AND (Cl3Ga2P)n; NEW PRECURSORS TO NANOCRYSTALLINE GALLIUM PHOSPHIDE
Steven R. Aubuchon, Andrew T. McPhail, Richard L. Wells, Julia A. Giambra, and James R. Bowser 18 Jan. 1994 25 p
(Contract N00014-89-J-1545)
(AD-A275019; DU/DC/TR-38) Avail: CASI HC A03/MF A01

(Br2GaP(SiMe3)2)2 and (I2GaP(SiMe3)2)2 were prepared by the 1:1 mole ratio reaction of the corresponding gallium(III) halide with (Me3Si)3P. Direct introduction probe mass spectrometry indicates that the former product is dimeric in the gas phase; single crystal x ray analysis reveals that it is also dimeric in the solid state and it is isostructural with (Cl2GaP(SiMe3)2)2, but the crystals are not isomorphous. (Br2GaP(SiMe3)2)2 crystallizes in the orthorhombic system, space group Pbca, with a = 13.803(2), b = 16.652(2), c = 13.636(2) A, V = 3134(1) A(exp 3), and D(sub calc) = 1.725 g/cu cm for Z = 4; the mean Ga-P bond length in the planar Ga-P-Ga-P core is 2.386 A. Also described is the synthesis of (Cl3Ga2P)(n) via the 2:1 mole ratio reaction of GaCl3 and (Me3Si)3P. All of the title compounds undergo thermolysis at relatively low temperature to yield nanocrystalline GaP. Thermolysis has been studied by thermal gravimetric analysis, and the resultant air-stable powders have been characterized by x ray diffraction and elemental analysis. DTIC

N94-29155# Duke Univ., Durham, NC. Dept. of Chemistry.
X RAY CRYSTAL STRUCTURES OF ((Me3SiCH2)2InCl)2 AND ((Me3SiCH2)InCl2)
Mark F. Self, Andrew T. McPhail, Leonidas J. Jones, III, and Richard L. Wells 18 Jan. 1994 14 p
(Contract N00014-89-J-1545)
(AD-A275074; DU/DC/TR-36) Avail: CASI HC A03/MF A01

The use of alternative group 13 and group 15 compounds to fabricate traditional 13-15 materials has received great attention over the past decade. Indeed, fundamental chemistry involving the structure, bonding, and reactivity of such species has been of primary concern in our laboratory for some time. It is our belief, that through these investigations a better understanding can be obtained as to the factors that influence and dictate the reactivity of these species. Herein we report the solid-state structures of (Me3SiCH2)2InCl2 (I) and (Me3SiCH2)InCl2 (infinity) (II) which have been found to be dimeric and polymeric, respectively. DTIC

N94-29210# Joint Inst. for Nuclear Research, Dubna (USSR).
ATOMIC AND MAGNETIC STRUCTURE OF YBa2(Cu(1-x)Fe(x))3O(6+y) AT 0.05 LESS THAN OR EQUAL TO x LESS THAN OR EQUAL TO 0.30, y IS APPROXIMATELY EQUAL TO 1 AND y IS APPROXIMATELY EQUAL TO 0.5
A. M. Balagurov and I. S. Lyubutin 1992 24 p In RUSSIAN
(DE94-606852; JINR-R-14-92-579) Avail: CASI HC A03/MF A01 (US Sales Only)

The system YBa2Cu(1-x)Fe(x)3O(6+y) was studied by neutron diffraction and Mossbauer spectroscopy in the wide interval of iron concentration, 0.05 less than or = x less than or = 0.30, in both oxygen saturated, y approx. = 1, and oxygen deficient, y approx. = 0.5, compositions. The very detailed data about the atomic structure and magnetic state were obtained for all the samples and compared with the Y123-Cu/Co system. A marked difference in magnetic phase diagrams of Fe and Co systems was established. DOE

N94-29215 Cornell Univ., Ithaca, NY. Dept. of Chemistry.
X RAY STANDING WAVE STUDIES OF UNDERPOTENTIALLY DEPOSITED METAL MONOLAYERS
G. M. Bommarito, D. Acevedo, J. F. Rodriguez, H. D. Abruna, and T. Gog 1992 21 p Limited Reproducibility: More than 20% of this document may be affected by microfiche quality
(AD-A275409) Avail: CASI HC A03

The x-ray standing wave technique has been employed in the study of the structure of underpotentially deposited (UPD) copper on an iodine covered platinum surface and of copper on a Au(100) single crystal electrode. For Cu UPD on Pt, surface coverage isotherms derived from both electrochemical and x-ray measurements are compared. The growth mode of the copper ad-layer appears to be strongly influenced by the electrode's surface morphology. For Cu UPD on Au(100), the coherence of the adlayer is strongly dependent on the mode of deposition. DTIC

N94-29501* National Aeronautics and Space Administration. Pasadena Office, CA.
EPITAXIAL HETEROJUNCTIONS OF OXIDE SEMICONDUCTORS AND METALS ON HIGH TEMPERATURE SUPERCONDUCTORS Patent
Richard P. Vasquez, inventor (to NASA) (Jet Propulsion Lab., California Inst. of Tech., Pasadena.), Brian D. Hunt, inventor (to NASA) (Jet Propulsion Lab., California Inst. of Tech., Pasadena.), and Marc C. Foote, inventor (to NASA) (Jet Propulsion Lab., California Inst. of Tech., Pasadena.) 19 Apr. 1994 8 p Filed 11 Mar. 1992 Supersedes N93-15151 (31 - 4, p 994) Prepared in cooperation with Jet Propulsion Lab., California Inst. of Tech., Pasadena.
(NASA-Case-NPO-18483-1-CU; US-Patent-5,304,538;
US-Patent-Appl-SN-852620; US-Patent-Class-505-190;
US-Patent-Class-257-35; US-Patent-Class-257-33; US-Patent-Class-505-702;
US-Patent-Class-505-785; US-Patent-Class-427-62;
Int-Patent-Class-H01L-39/22) Avail: US Patent and Trademark Office

Epitaxial heterojunctions formed between high temperature superconductors and metallic or semiconducting oxide barrier layers are provided. Metallic perovskites such as LaTiO3, CaVO3, and SrVO3 are grown on electron-type high temperature superconductors such as Nd(1.85)Ce(0.15)CuO(4-x). Alternatively, transition metal bronzes of the form A(x)MO(3) are epitaxially grown on electron-type high temperature superconductors. Also, semiconducting oxides of perovskite-related crystal structures such as WO3 are grown on either hole-type or electron-type high temperature superconductors.
Official Gazette of the U.S. Patent and Trademark Office

N94-29530 Rensselaer Polytechnic Inst., Troy, NY.
NONADIABATIC EFFECTS IN THE QUANTUM HALL REGIME Ph.D. Thesis
Douglas Arthur Page 1992 319 p
Avail: Univ. Microfilms Order No. DA9314373

In considering the effect of uniform external fields on the behavior of independent electrons in a two dimensional crystal, the relationship of transport properties to Berry's phase, in the limit of weak electric field, is examined. A numerical algorithm, based on the effective Hamiltonian formalism, is developed to study the magnetic subbands corresponding to an isolated Bloch band. This algorithm involves a matrix diagonalization at only three points in the magnetic Brillouin zone, and allows the effects of

varying bandstructure to be included. Results for the spectrum and quantized Hall conductivities are presented for two simple forms of band dispersion, over a range of magnetic field strengths. The effects of a finite electric field are treated in a time dependent formalism, in which the electric and magnetic fields appear symmetrically. In addition to a wave vector k, the states are characterized by a frequency omega specifying their behavior under time translations through a fundamental period. The effective Hamiltonian formalism is again employed to obtain concrete results. An isolated Bloch band is found to break up into 'frequency' subbands, each characterized by a frequency dispersion omega(k). A method of obtaining the transport properties of the system is outlined. This method is shown to be consistent with known results for the weak field limit, as well as a more conventional approach in the time independent gauge. Numerical results for a model system are presented over a range of electric field strengths. A transition between strong and weak field regimes is seen, with level repulsions between the frequencies playing an important role. These results show how the magnetic subband structure and the corresponding integer Hall conductivities emerge as the electric field becomes weaker. In this regime, the behavior can be understood by comparison to the predictions of the adiabatic approximation. The origin of deviations from the weak field predictions is identified. Dissert. Abstr.

N94-29691 Universidad Autonoma del Estado de Mexico, Toluca.
STUDY OF IRON EXCHANGED ZEOLITES BY MOESSBAUER EFFECT AND ELECTRON SPIN RESONANCE SPECTROSCOPY Ph.D. Thesis [ESTUDIO DE ZEOLITAS DE HIERRO POR EL EFECTO MOESSBAER Y LA RESONANCIA PARAMAGNETICA ELECTRONICA]
C. E. AguirreCampuzano 1993 76 p In SPANISH Limited Reproducibility: More than 20% of this document may be affected by microfiche quality
(DE94-605138; INIS-mf-13718) Avail: CASI HC A05 (US Sales Only)

Crystalline iron exchanged NaY zeolites, prepared from aqueous solutions and calcined at atmospheric conditions, have been studied and characterized by XRD, Moessbauer and EPR spectroscopies and TGA analysis. Three iron sites are clearly distinguished from Moessbauer and EPR measurements. Firstly, characteristic Moessbauer and EPR spectra may arise from framework sites, suggesting that Fe has substituted Al. It is also found that their spectroscopic signals are not intensity affected by thermal treatments. Secondly, a Moessbauer doublet which may arise from octahedral sites in the large cavity of the zeolite, shows however, that this doublet and its EPR signal are intensity temperature affected. An additional line broadening is observed on the low velocity line of this doublet. Thirdly, characteristic Moessbauer and EPR signals, which are also intensity temperature dependent have been associated to accluded material, where the Moessbauer doublet presents the line broadening effect before mentioned. Such line broadening effect may be due to perturbing signals from iron ions in tetrahedral sites. Finally, it has been observed that during calcination of the FeY zeolites, the three characteristic EPR signals for the three iron sites, do not increase at the expenses of the other. A result that may suggest a strong bonding between Fe-site of the Y zeolite, irrespective of the iron source. DOE

N94-29801# Midwest Research Inst., Golden, CO. National Renewable Energy Lab.
PRODUCTION OF FULLERENES WITH CONCENTRATED SOLAR FLUX
M. J. Hale, C. Fields, A. Lewandowski, C. Bingham, and R. Pitts Jan. 1994 9 p Presented at the American Society of Mechanical Engineers (ASME) International Solar Energy Conference, San Francisco, CA, 27-30 Mar. 1994
(Contract DE-AC02-83CH-10093)
(DE94-000266; NREL/TP-471-5864; CONF-940326-7) Avail: CASI HC A02/MF A01

Research at the National Renewable Energy Laboratory (NREL) has demonstrated that fullerenes can be produced using highly concentrated sunlight from a solar furnace. Since they were first synthesized in 1989, fullerenes have been the subject of intense research. They show considerable commercial potential in advanced materials and have potential applications that include semiconductors, superconductors, high-performance metals, and medical technologies. The most common fullerene is C60, which is a molecule with a geometry resembling a soccer ball. Graphite vaporization methods such as pulsed-laser vaporization, resistive heating, and carbon arc have been used to produce fullerenes. None of these, however, seems capable of producing fullerenes economically on a large scale. The use of concentrated sunlight may help avoid the scale-up limitations inherent in more established production processes. Recently, researchers at NREL made fullerenes in NREL's 10 kW high flux solar furnace (HFSF) with a vacuum reaction chamber designed to deliver a solar flux of 1200 W/sq cm to a graphite pellet. Analysis of the resulting carbon soot by mass spectrometry and high pressure liquid chromatography confirmed the existence of fullerenes. This paper presents the method, experimental apparatus, and results of fullerene production research performed with the HFSF. DOE

N94-29818# Los Alamos National Lab., NM.
A POT-POURRI OF RESULTS IN QCD FROM LARGE LATTICE SIMULATIONS ON THE CM5
T. Bhattacharya and R. Gupta 1993 6 p Presented at the LATTICE 1993: International Symposium on Lattice Field Theory, Dallas, TX, 12-17 Oct. 1993
(Contract W-7405-eng-36)
(DE94-005084; LA-UR-93-4459; CONF-9310250-5) Avail: CASI HC A02/MF A01

A status report on simulations being done on 32(exp 3) (times) 64 lattices at beta = 6.0 using quenched Wilson fermions is presented. Results for the spectrum, decay constants, the kaon B-parameter B(sub K), and semi-leptonic form factors are given based on the current statistical sample of 28 configuration. These Grand Challenge calculations are being done on the CM5 at Los Alamos in collaboration with G. Kilcup, S. Sharpe and P. Tamayo. They end with a brief statement of code performance. DOE

N94-29915 Johns Hopkins Univ., Baltimore, MD.
NANODISLOCATION STRUCTURES GENERATED IN SHOCKED CRYSTALS Ph.D. Thesis
Faris Afif Bandak 1993 172 p
Avail: Univ. Microfilms Order No. DA9313332

Dislocation structures proposed to model plastic deformation at a shock front are analyzed. The creation and glide movement of the dislocations are considered. Glide-type movement violates the condition of one-dimensional strain except if dislocation dipoles with Burgers vectors parallel and antiparallel to the shock propagation direction are directly generated by alternating shear stresses as in a punching action. The stress, strain and dilatation characteristics are presented for a dislocation structure originally proposed by Armstrong, Miller and Sandusky (AMS) to give a residual one-dimensional strain state. The AMS dislocation structure is related to independent results from a molecular dynamics description of shear displacements in a shocked triangular lattice and is used as a basis for estimating the extent of post-shock strengthening levels. The shock strengthening predictions are in reasonable agreement with post-shock deformation measurements. Molecular dynamics calculations are conducted to investigate several aspects of the AMS dislocation model. The evolution of dislocations from the shock compression of a vacancy cluster in a body centered cubic lattice is studied using molecular dynamics. Detailed calculations have revealed the atomic displacements by which the clustered vacancies collapse. The energetics of the process were also monitored in detail. Stable (100) and (111) Burgers vector dislocations have been identified in dipole configurations. The post-shock stability of the AMS dipole nanostructure was also evaluated on a molecular dynamics basis and the stress/strain behaviors of the crystal for the pre- and post-shock compression conditions were compared. Dissert. Abstr.

N94-30001 Pacific Northwest Lab., Richland, WA.
THE MSRC AB INITIO METHODS BENCHMARK SUITE: A MEASUREMENT OF HARDWARE AND SOFTWARE PERFORMANCE IN THE AREA OF ELECTRONIC STRUCTURE METHODS
D. F. Feller Jul. 1993 90 p Limited Reproducibility: More than 20% of this document may be affected by microfiche quality
(Contract DE-AC06-76RL-01830)
(DE94-006428; PNL-8670) Avail: CASI HC A05

This collection of benchmark timings represents a snapshot of the hardware and software capabilities available for ab initio quantum chemical calculations at Pacific Northwest Laboratory's Molecular Science Research Center in late 1992 and early 1993. The 'snapshot' nature of these results should not be underestimated, because of the speed with which both hardware and software are changing. Even during the brief period of this study, we were presented with newer, faster versions of several of the

codes. However, the deadline for completing this edition of the benchmarks precluded updating all the relevant entries in the tables. As will be discussed below, a similar situation occurred with the hardware. The timing data included in this report are subject to all the normal failures, omissions, and errors that accompany any human activity. In an attempt to mimic the manner in which calculations are typically performed, we have run the calculations with the maximum number of defaults provided by each program and a near minimum amount of memory. This approach may not produce the fastest performance that a particular code can deliver. It is not known to what extent improved timings could be obtained for each code by varying the run parameters. If sufficient interest exists, it might be possible to compile a second list of timing data corresponding to the fastest observed performance from each application, using an unrestricted set of input parameters. Improvements in I/O might have been possible by fine tuning the Unix kernel, but we resisted the temptation to make changes to the operating system. Due to the large number of possible variations in levels of operating system, compilers, speed of disks and memory, versions of applications, etc., readers of this report may not be able to exactly reproduce the times indicated. Copies of the output files from individual runs are available if questions arise about a particular set of timings. DOE

N94-30005 International Centre for Theoretical Physics, Trieste (Italy).
AGGREGATION EQUILIBRIA IN ARSENIC DOPED SILICON
M. Derdour, G. Furlan, and D. Nobili Aug. 1993 9 p Limited Reproducibility: More than 20% of this document may be affected by microfiche quality
(DE94-607269; IC-93/265) Avail: CASI HC A02 (US Sales Only)

Carrier density profile determinations are reported which confirm that a mass action relation holds between the ionized and the inactive mobile As in silicon. Experiments were performed under equilibrium conditions at temperatures in the range 780-885 C. The carrier density n vs. the dopant concentration N(sub T) exhibits a very pronounced saturation behavior which is compared with the one expected in well known cluster models. These results complement the recent finding that the inactive As can exist in equilibrium with the monoclinic SiAs. From this information and previous SAXS, TEM, and EXAFS results one can conclude that a pre-precipitation phenomenon, with its inherent cluster distribution, is responsible for the inactive As. DOE

N94-30006# Sandia National Labs., Albuquerque, NM.
ECR PLASMA SYNTHESIS OF SILICON NITRIDE FILMS ON GaAs AND InSb
J. C. Barbour, M. L. Lovejoy, C. I. H. Ashby, A. J. Howard, J. S. Custer, and R. J. Shul 1993 6 p Presented at the Fall Meeting of the Materials Research Society (MRS), Boston, MA, 29 Nov. - 3 Dec. 1993
(Contract DE-AC04-94AL-85000)
(DE94-005575; SAND-93-1662C; CONF-931108-47) Avail: CASI HC A02/MF A01

Growth of high-quality dielectric films from Electron Cyclotron Resonance (ECR) plasmas provides for low-temperature surface passivation of compound semiconductors. Silicon nitride (SiN(x)) films were grown at temperatures from 30 to 250 C on GaAs substrates. Stress in films was measured as a function of bias applied during growth (varied from 0 to 200 V), and of sample annealing treatments. Composition profiles of the samples were measured using ion beam analysis. The GaAs photoluminescence (PL) signal after SiN(x) growth without an applied bias (ion energy congruent to 30 eV) was twice as large as the PL signal from the cleaned GaAs substrate. The PL signal from samples biased at -50 and -100 V indicated that damage degraded the passivation quality, while atomic force microscopy of these samples showed a threefold increase in rms surface roughness relative to unbiased samples. The sample grown with a bias of -200 V showed the largest reduction in film stress but also the smallest PL signal. DOE

N94-30009 California Univ., Berkeley. Lawrence Berkeley Lab.
PICOSECOND RESPONSE OF THE QUASIPARTICLE CURRENT IN SUPERCONDUCTING TUNNEL JUNCTIONS
S. Verghese, C. Karadi, J. O. Orenstein, J. O. Mearst, P. L. Richards, and A. T. Bartknecht Aug. 1993 2 p Presented at the Conference of the International Union of Pure and Applied Physics on Low Temperature Physics (LT 20), Eugene, OR, 1-11 Aug. 1993 Limited Reproducibility: More than 20% of this document may be affected by microfiche quality
(Contract DE-AC03-76SF-00098)
(DE94-006300; LBL-35035; CONF-930801-13) Avail: CASI HC A01

We have investigated the response of the quasiparticle tunneling currents in superconductor-insulator-superconductor (SIS) junctions to picosecond electrical pulses. DOE

N94-30015*# Alabama Univ., Huntsville. Center for Microgravity and Materials Research.
CONVECTIVE FLOW EFFECTS ON PROTEIN CRYSTAL GROWTH
Semiannual Progress Report No. 2, 1 Aug. 1993 - 31 Jan. 1994
Franz Rosenberger and Lisa A. Monaco 31 Jan. 1994 34 p
(Grant NAG8-950)
(NASA-CR-195785; NAS 1.26:195785) Avail: CASI HC A03/MF A01

The long-term stability of the interferometric setup for the monitoring of protein morphologies has been improved. Growth or dissolution of a crystal on a 100 A scale can now be clearly distinguished from dimensional changes occurring within the optical path of the interferometer. This capability of simultaneously monitoring the local interfacial displacement at several widely-spaced positions on the crystal surface with high local depth resolution, has already yielded novel results. We found with lysozyme that (1) the normal growth rate is oscillatory, and (2) the mean growth step density is greater at the periphery of a facet than in its center. The repartitioning of Na(+) and Cl(-) ions between lysozyme solutions and crystals was studied for a wide range of crystallization conditions. A nucleation-growth-repartitioning model was developed to interpret the large body of data in a unified way. The results strongly suggests that (1) the ion to lysozyme ratio in the crystal depends mostly on kinetic rather than crystallographic parameters, and (2) lysozyme crystals possess a salt-rich core with a diameter on the order of 10 microns. The computational model for diffusive-convective transport in protein crystallization (see the First Report) has been applied to a realistic growth cell geometry, taking into account the findings of the above repartitioning studies. These results show that some elements of a moving boundary problem must be incorporated into the model in order to obtain a more realistic description. Our experimental setup for light scattering investigations of aggregation and nucleation in protein solutions has been extensively tested. Scattering intensity measurements with a true Rayleigh scatterer produced systematically increased forward scattering, indicating problems with glare. These have been resolved. Preliminary measurements with supersaturated lysozyme solutions revealed that the scatterers grow with time. Work has begun on a computer program for the unified evaluation of simultaneously obtained, multi-angle static and dynamic light scattering data. Author

N94-30032 Ottawa Univ. (Ontario). Dept. of Physics.
NEW EVIDENCE FOR FLUX CUTTING IN TYPE II SUPERCONDUCTORS M.S. Thesis
David Leblanc 1992 75 p
(ISBN-0-315-85830-3; CTN-94-61168) Copyright Avail: Micromedia Ltd., Technical Information Centre, 240 Catherine Street, Suite 305, Ottawa, Ontario, K2P 2G8, Canada HC/MF

New evidence is presented for cross flow and cutting of nonparallel flux lines in type-II superconductors. A dramatic reversal is observed in the evolution of the axial flux density in the cavity of a hollow cylinder when the magnitude of a helical magnetic field is increased or decreased along the cylinder surfaces. Measurements of the concurrent evolution of the axial flux density threading the cylinder wall complement the above data. These two phenomena are explained, based on the ideas of two way traffic of sublattices of nonparallel flux lines traversing each other via flux line cutting processes. The classical critical state concept is reviewed and the essential features of the flux cutting process, cross traversal of flux line sheets, and attendant breathing modes are outlined. A generalized critical state model incorporating a phenomenological framework based on Maxwell's equations, standard physical constraints, and two separate energy dissipation mechanisms is summarized. Data curves are presented and it is shown in qualitative detail that the observed behavior demonstrates that flux line cutting occurs and associated breathing in and out of nonparallel flux lines takes places across the surface of type-II superconductors subjected to a varying helical magnetic field. Author (CISTI)

N94-30054# Lawrence Livermore National Lab., CA.
INFLUENCE OF DOPING ON THE ELECTRONIC STRUCTURE OF (La, Sr)2CuO4
R. H. Howell, M. J. Fluss, P. A. Sterne, and J. H. Kaiser 23 Aug. 1993 15 p Presented at the Physics and Chemistry of Molecular and Oxide Superconductors, Eugene, OR, 27-31 Jul. 1993
(Contract W-7405-eng-48)
(DE94-006383; UCRL-JC-114155; CONF-930710-5) Avail: CASI HC A03/MF A01

High statistics, (greater than 4 x 10(exp 8) counts), room temperature measurements of the electron-positron momentum density of La(2-x)Sr(x)CuO4 have been performed for samples with Sr concentrations of x - 0.0, 0.1, 0.13 and 0.2. These spectra have been analyzed in conjunction with theoretical calculations of the electron-positron momentum density. The metallic samples show features consistent with the presence of a Fermi surface, but its evolution with increasing Sr concentration does not follow the predictions of band theory. These results may indicate the effects of electron-electron correlation on the electron momentum distribution in the Cu-O plane. DOE

N94-30063# Oak Ridge National Lab., TN.
STRUCTURAL CHARACTERIZATION OF SEMICONDUCTOR HETEROSTRUCTURES BY ATOMIC RESOLUTION Z-CONTRAST IMAGING AT 300 kV
A. J. McGibbon, S. J. Pennycook, and Z. Wasilewski Dec. 1993 7 p Presented at the Fall Meeting of the Materials Research Society (MRS), Boston, MA, 29 Nov. - 3 Dec. 1993
(Contract DE-AC05-84OR-21400)
(DE94-006561; CONF-931108-68) Avail: CASI HC A02/MF A01

By applying Z-contrast imaging to study of a GaAs/AlGaAs multilayer using a newly developed 300kV scanning transmission electron microscope, we show that it is possible to directly observe the interlocking group III and group V sub-lattices on a column-by-column level. In addition to direct observation of structural polarity in the (110) orientation, we show that, by using a maximum entropy approach to image processing, the experimentally acquired data can provide direct information on interface structures at atomic resolution. DOE

N94-30064# Oak Ridge National Lab., TN.
ATOMIC-SCALE STRUCTURE AND CHEMISTRY OF INTERFACES BY Z-CONTRAST IMAGING AND ELECTRON ENERGY LOSS SPECTROSCOPY IN THE STEM
M. M. McGibbon, N. D. Browning, M. F. Chisholm, S. J. Pennycook, V. Ravikumar, and V. P. Dravid Dec. 1993 6 p Presented at the Fall Meeting of the Materials Research Society (MRS), Boston, MA, 29 Nov. - 3 Dec. 1993
(Contract DE-AC05-84OR-21400)
(DE94-006563; CONF-931108-69) Avail: CASI HC A02/MF A01

The macroscopic properties of many materials are controlled by the structure and chemistry at grain boundaries. A basic understanding of the structure-property relationship requires a technique which probes both composition and chemical bonding on an atomic scale. The high-resolution Z-contrast imaging technique in the scanning transmission electron microscope (STEM) forms an incoherent image in which changes in atomic structure and composition can be interpreted intuitively. This direct image allows the electron probe to be positioned over individual atomic columns for parallel detection electron energy loss spectroscopy (EELS) at a spatial resolution approaching 0.22nm. In this paper we have combined the structural information available in the Z-contrast images with the bonding information obtained from the fine structure within the EELS edges to determine the grain boundary structure in a SrTi3 bicrystal. DOE

N94-30067 International Centre for Theoretical Physics, Trieste (Italy).
STRONG OVERLAP AND TRANSMISSION IN TRIPLE BARRIER RESONANT STRUCTURES
R. Romo (Centro de Investigacion Cientifica y de Educacion Superior de Ensenada, Mexico.) and G. Garcia-Calderon Aug. 1993 22 p Limited Reproducibility: More than 20% of this document may be affected by microfiche quality
(DE94-608103; IC-93/274) Avail: CASI HC A03 (US Sales Only)

The transition from two unity peaks into a single under-unity peak in the transmission coefficient T in symmetrical triple barrier resonant structures, as the width of the central barrier is increased, is analyzed in terms of a resonance formalism in a Breit-Wigner fashion to show that the above situation is due to strong overlap between the two resonance states of the corresponding miniband, i.e., T = T(sub 1) + T(sub 2) + T(sub 12). Results contradict a recent claim that the under-unity transmission peak corresponds to a singlet resonance state. We discuss the implications of strong overlap on the current-voltage characteristics of these triple barrier structures. DOE

N94-30068 International Centre for Theoretical Physics, Trieste (Italy).
ELECTRONIC STRUCTURE OF Zn-BASED QUANTUM WELLS
B. A. Camacho Aug. 1993 17 p Limited Reproducibility: More than 20% of this document may be affected by microfiche quality
(DE94-608104; IC-93/279) Avail: CASI HC A03 (US Sales Only)

The electronic structure of recently demonstrated laser active heterostructures based on ZnSe quantum wells has been calculated within a tight-binding framework. A Green function method, appropriate to consider layered systems, is applied to obtain the main features of energy spectrum and density of states and spatial probability distribution of valence states. The formalism allows strain effects to be taken into account in a very natural way. In addition, atomic orbital composition of the uppermost valence bands as a function of the quantum well width are easily obtained. Hopping parameters are scaled according to Harrison's d(exp 2) law. Since the quantum well itself is a ternary compound, we describe it within the virtual crystal approximation (VCA). A systematic study of the effects of well width in these structures is presented. DOE

N94-30069 International Centre for Theoretical Physics, Trieste (Italy).
VIBRATIONAL PROPERTIES OF HOMOPOLAR AND HETEROPOLAR SURFACES AND INTERFACES OF THE CdTe/HgTe SYSTEM
R. Rey-Gonzales, B. A. Camacho, and L. Quiroga Aug. 1993 13 p Limited Reproducibility: More than 20% of this document may be affected by microfiche quality
(DE94-608105; IC-93/280) Avail: CASI HC A03 (US Sales Only)

We present results of calculations for the density of vibrational modes for (001) and (111) homopolar as well as for (011) heteropolar free surfaces of CdTe and HgTe. A rigid-ion model with a dynamical matrix parametrization including force constants up to second neighbors is used. We report on the existence of highly localized surface resonant modes at the top of the acoustic branch for CdTe and the bottom of the optical branch for HgTe. A different behavior in the three directions analyzed is found. The interface atomic planes show themselves as phonon gapless layers. The contribution of in-plane and out-of-plane vibration is analyzed for both the surface and interface cases. DOE

N94-30070 International Centre for Theoretical Physics, Trieste (Italy).
II-VI WIDE BAND GAP SEMICONDUCTORS UNDER HYDROSTATIC PRESSURE
R. Baquero, R. DeCoss, and D. Olguin Aug. 1993 13 p Limited Reproducibility: More than 20% of this document may be affected by microfiche quality
(DE94-608106; IC-93/281) Avail: Issuing Activity (Department of Energy (DOE)) (US Sales Only)

We set an analytical expression for the gap as a function of hydrostatic deformation, E(sub g)(epsilon), by diagonalizing in Gamma the corresponding empirical tight-binding Hamiltonian (ETBH). In the ETBH we use the well known d(exp -2) Harrison scaling law (HSL) to adjust the TB parameter (TBP) to the changes in interatomic distances. We do not consider cation-anion charge transfer. We calculate E(sub g)(epsilon) for wide band gap II-VI semiconductors with zincblende crystal structure for deformations under pressure up to -5 percent. Results are in good agreement with experiment for the compounds of lower ionicity but deviate as the ionicity of the compound increases. This is due to the neglect of charge transfer which should be included self-consistently. Within the approximation we always find a positive second derivative of E(sub g)(epsilon) with respect to epsilon, independent of the material. Furthermore, the inclusion of deviations from HSL appear to be unimportant to this problem. DOE

N94-30072 International Centre for Theoretical Physics, Trieste (Italy).
BAND STRUCTURE OF SUPERLATTICE WITH (DELTA)-LIKE POTENTIAL
N. F. Gashimzade, F. M. Gashimzade, and A. T. Hajiev Aug. 1993 7 p

Limited Reproducibility: More than 20% of this document may be affected by microfiche quality
(DE94-608108; IC-93/283) Avail: CASI HC A02 (US Sales Only)

Band structure of superlattice with delta-like potential has been calculated taking into account interaction of carriers of different kinds. Superlattices of semiconductors with degenerated valence band and zero-gap semiconductors have been considered. For the latter, semimetal-semiconductor transition has been obtained. DOE

N94-30082 Joint Inst. for Nuclear Research, Dubna (USSR). Lab. of Neutron Physics.
THE BASES FOR THE DEVELOPMENT OF HIGH-TEMPERATURE INTEGRATED SQUID-SYSTEMS
V. N. Polushkin 1992 23 p Limited Reproducibility: More than 20% of this document may be affected by microfiche quality
(DE94-608462; JINR-D-13-92-339) Avail: Issuing Activity (Department of Energy (DOE)) (US Sales Only)

The current state of high-T(sub c) thin-film Josephson junction and SQUID development is reviewed. The prospects for applying the new devices in supersensitive measurement apparatus are analyzed. It is shown that high T(sub c) SQUID's can facilitate the further development of information and measurement engineering. DOE

N94-30109 International Centre for Theoretical Physics, Trieste (Italy).
MAGNETIC PROPERTIES OF A QUANTUM TRANSVERSE SPIN-1 BLUME-EMERY-GRIFFITHS MODEL
H. Ez-Zahraouy Sep. 1993 23 p Limited Reproducibility: More than 20% of this document may be affected by microfiche quality
(DE94-608114; IC-93/298) Avail: CASI HC A03 (US Sales Only)

Using an expansion technique for cluster identities of spin-1 localized spin systems, we study the magnetic properties of a quantum transverse spin-1 Blume-Emery-Griffiths model. The longitudinal and transverse magnetizations and the quadrupolar moments are calculated. General formula applicable to structures with arbitrary coordination number are given. DOE

N94-30165 International Centre for Theoretical Physics, Trieste (Italy).
MAGNETIC PROPERTIES OF A TRANSVERSE SPIN-1 ISING MODEL WITH LONGITUDINAL CRYSTAL FIELD INTERACTIONS
A. Benyoussef (Mohammed V Univ., Rabat, Morocco.) and H. Ez-Zahraouy Sep. 1993 20 p Limited Reproducibility: More than 20% of this document may be affected by microfiche quality
(DE94-608118; IC-93/302) Avail: Issuing Activity (Department of Energy (DOE)) (US Sales Only)

The three dimensional spin-1 Ising model with crystal field interactions exhibit tri-critical behavior. Using an expansion technique for cluster identities of spin-1 localized spin systems, we study the influence of transverse magnetic field on this behavior. Temperature-crystal-field phase diagrams is investigated for different values of transverse field. The longitudinal and transverse magnetizations, the quadrupolar moments are calculated. General formulae, applicable to structures with arbitrary coordination number N, are given. DOE

N94-30181 International Centre for Theoretical Physics, Trieste (Italy).
MAGNETIC PROPERTIES OF A TRANSVERSE SPIN-1 ISING MODEL WITH RANDOM CRYSTAL FIELD INTERACTIONS
A. Benyoussef (Mohammed V Univ., Rabat, Morocco.) and H. Ez-Zahraouy Sep. 1993 19 p Limited Reproducibility: More than 20% of this document may be affected by microfiche quality
(DE94-608117; IC-93/301) Avail: CASI HC A03 (US Sales Only)

We study the phase diagram and magnetic properties of a transverse spin-1 Ising model with random longitudinal crystal field interactions within an expansion technique for cluster identities of spin-1 localized spin systems. The partially ordered phases appear for a particular two valued distribution P(D(sub i)) = 1/2((delta)(D(sub i) - (1+alpha)D) + (delta)(D(sub i) - (1-alpha)D)), and for sufficiently small transverse field Omega. The longitudinal and transverse magnetizations, the quadrupolar moments are calculated. General formulae applicable to structures with arbitrary coordination number, are given. DOE

N94-30183 Joint Inst. for Nuclear Research, Dubna (USSR). Lab. of Theoretical Physics.
OVERLAP OF METAL CLUSTERS AND NUCLEAR STRUCTURE PHYSICS
V. O. Nesterenko 1992 11 p Limited Reproducibility: More than 20% of this document may be affected by microfiche quality
(DE94-608387; JINR-E-4-92-529) Avail: CASI HC A03 (US Sales Only)

The properties of metal cluster (MC) are discussed. The MC representing the bound systems of atoms of some metals have recently been discovered to possess shells of the same type as in atoms and nuclei. Subsequent investigation has shown the striking similarities of many features of MC and nuclei: shells, quadrupole deformation, fission, and giant resonances. As a result, a lot of ideas and methods (first of all the theoretical ones) of nuclear structure may be applied after some modification in the MC field. MC have also their own very specific properties, such as supershells, the opportunity to form very large clusters with the number of atoms up to 20000, mixed clusters and etc. DOE

N94-30195 Joint Inst. for Nuclear Research, Dubna (USSR). Lab. of Nuclear Problems.
ON THE (MU)SR ACTIVITY AT LNP JINR PHASOTRON
I. I. Gurevich (Kurchatov, I. V. Inst. of Atomic Energy, Moscow, USSR.), V. N. Duginov (Kurchatov, I. V. Inst. of Atomic Energy, Moscow, USSR.), V. G. Firsov (Institute of Engineering Physics, Moscow, USSR.), V. G. Grebinnik (Kurchatov, I. V. Inst. of Atomic Energy, Moscow, USSR.), E. P. Krasnoperov (Kurchatov, I. V. Inst. of Atomic Energy, Moscow, USSR.), T. N. Mamedov (Kurchatov, I. V. Inst. of Atomic Energy, Moscow, USSR.), B. A. Nikolsky (Kurchatov, I. V. Inst. of Atomic Energy, Moscow, USSR.), V. G. Olshevsky (Kurchatov, I. V. Inst. of Atomic Energy, Moscow, USSR.), V. Yu. Pomjakushin (Kurchatov, I. V. Inst. of Atomic Energy, Moscow, USSR.), and A. N. Ponomarev (Kurchatov, I. V. Inst. of Atomic Energy, Moscow, USSR.) et al 1992 26 p Limited Reproducibility: More than 20% of this document may be affected by microfiche quality
(DE94-608385; JINR-E-14-92-574) Avail: CASI HC A03 (US Sales Only)

The current state of muon spin rotation activity at LNR JINR phasotron is presented, including short description of experimental facilities. The possible trends of muon spin rotation investigation for future work are outlined. The list of main publications (1967-1992) is included. DOE

N94-30201# Los Alamos National Lab., NM.
DISLOCATION LOOPS IN SPINEL CRYSTALS IRRADIATED SUCCESSIVELY WITH DEEP AND SHALLOW ION IMPLANTS
Rebecca X. Ai, Elizabeth A. Cooper, Kurt E. Sickafus, Michael Nastasi, Nicole Bordes, and R. C. Ewing 1993 6 p Presented at the Fall Meeting of the Materials Research Society, Boston, MA, 29 Nov. - 3 Dec. 1993
(Contract W-7405-eng-36)
(DE94-005083; LA-UR-93-4464; CONF-931108-34) Avail: CASI HC A02/MF A01

This study examines the influence of microstructural defects on irradiation damage accumulation in the oxide spinel. Single crystals of the compound MgAl2O4 with surface normal (111) were irradiated under cryogenic temperature (100 K) either with 50 keV Ne ions (fluence 5.0 x 10(sup 12)/cm(sup 2)), 400 keV Ne ions (fluence 6.7 x 10(sup 13)/cm(sup 2)) or successively with 400 keV Ne ions followed by 50 keV Ne ions. The projected range of 50 keV Ne ions in spinel is approximately 50 mn ('shallow') while the projected range of 400 keV Ne ions is (approximately)500 mn ('deep'). Transmission electron microscopy (TEM) was used to examine dislocation loops/defect clusters formed by the implantation process. Measurements of the dislocation loop size were made using weak-beam imaging technique on cross-sectional TEM ion-implanted specimens. Defect clusters were observed in both deep and shallow implanted specimens, while dislocation loops were observed in the shallow implanted sample that was previously irradiated by 400 keV Ne ions. Cluster size was seen to increase for shallow implants in crystals irradiated with a deep implant (size approximately 8.5 nm) as compared to crystals treated only to a shallow implant (size approximately 3.1 nm). DOE

N94-30203 British Columbia Univ., Vancouver. Dept. of Physics.
MuSR MEASUREMENT OF THE MAGNETIC PENETRATION DEPTH AND COHERENCE LENGTH IN THE HIGH-Tc SUPERCONDUCTOR YBa2Cu3O(6.95) Ph.D. Thesis

Tanya Maria Riseman May 1993 248 p
(ISBN-0-315-85385-9; CTN-94-61154) Copyright Avail: Micromedia Ltd., Technical Information Centre, 240 Catherine Street, Suite 305, Ottawa, Ontario, K2P 2G8, Canada HC/MF

The temperature dependence and anisotropy of the magnetic penetration depth L and the Ginzburg Landau parameter K in a high temperature Y-Ba-Cu-O superconductor was studied using muon spin rotation (MSR) measurements of the local field inhomogeneity produced by the vortex state. The anisotropy of L leads to variation in the measured field inhomogeneity as a function of the angle between the applied field and the c-axis of the crystal. If the applied field is not parallel to one of the superconductor's principal axes, an attractive force between vortices along one direction arises when the superconductor is cooled in a constant and low field. When the net intervortex repulsion exceeds the forces pinning the vortices in place, the aspect ratio of the isoceles triangle defining the vortex lattice will change. The degree of disorder makes it impossible to determine the low temperature aspect ratio of the Y-Ba-Cu-O superconductor using MSR. In the vortex lattice, the maximum field is reached at the vortex core. In the low and moderate field regimes, the core occupies a very small percentage of the lattice's unit cell, so the maximum field is not observable by MSR. In the high field regime, the core results in a high field cutoff in the distribution of local fields, which can be observed directly in the Fourier transform of MSR data. Author (CISTI)

N94-30239 Ottawa Univ. (Ontario). Dept. of Physics.
PHOTOELECTRONIC STUDY OF GaAs EPILAYERS AND In(x)Ga(1-x)As/GaAs QUANTUM WELLS M.S. Thesis
Ye Wang 1992 165 p
(ISBN-0-315-85756-0; CTN-94-61162) Copyright Avail: Micromedia Ltd., Technical Information Centre, 240 Catherine Street, Suite 305, Ottawa, Ontario, K2P 2G8, Canada HC/MF

The photo electromagnetic (PEM) effect was used to perform experiments on photocarrier transport properties in GaAs substrates and epitaxial layers. For the undoped semi-insulating substrate, the carrier mobility at 77 K was measured by the PEM effect method, giving a value of 40,000 sq cm/volt/second. It was found that the carrier diffusion length is 0.27 micrometers at 300 K and 0.44 micrometers at 77 K. For the 3.4 micrometer thick epitaxial layer grown by metal organic chemical vapor deposition, the carrier diffusion length was measured to be 2.6 micrometers at 300 K, 3.1 micrometers at 77 K, and 3.5 micrometers at 5 K. A photocurrent spectroscopy study of In(x)Ga(1-x)As/GaAs quantum wells on Cr-doped and undoped substrates was also performed. Several well-resolved structures related to inter-subband transitions are observed in the photo conductivity spectra at both 300 K and 77 K, and they are in good agreement with calculations taking into account the strain induced splitting of the bands. Both Cr-doped and undoped substrates have been found to influence the results, as shown by optical quenching techniques.
Author (CISTI)

N94-30247# Sandia National Labs., Albuquerque, NM.
ELECTROOPTICAL AND OPTICAL EVALUATION OF Pb(Zr,Ti)O3 THIN FILMS USING WAVEGUIDE REFRACTOMETRY
B. G. Potter, Jr., M. B. Sinclair, D. Dimos, B. A. Tuttle, and R. W. Schwartz 1993 21 p Presented at the 1st Meeting of the Pacific Rim Ceramic Societies, Honolulu, HI, 7-10 Nov. 1993
(Contract DE-AC04-94AL-85000)
(DE94-006374; SAND-93-0974C; CONF-931142-7) Avail: CASI HC A03/MF A01

Prism-coupled, waveguide refractometry was utilized to independently monitor electric field-induced changes in the extraordinary and ordinary refractive indices of a Pb(Zr(0.53)Ti(0.47))O3(PZT 53/47) thin film. Under an electric field, applied normal to the film plane and corresponding to saturation of the electric polarization, ratio of the extraordinary to ordinary refractive index change ((Delta)n(sub e)/(Delta)n(sub o)) is found to be (minus)4/1, contributing to a net birefringence change ((Delta)n(sub e)-n(sub o)) of -0.021. The technique, thus, accesses both diagonal and off-diagonal elements of the electrooptic response tensor describing the macroscopic behavior of the polycrystalline film. In addition, the widths of waveguide mode reflectivity minima were sensitive to variation in the microstructure of several PZT (40/60) films, indicating that the refractometry technique can provide information helpful in evaluating optical quality in these films.
DOE

N94-30249# Oak Ridge National Lab., TN.
THE INFLUENCE OF AN IN-SITU ELECTRIC FIELD ON H(+) AND He(+) IMPLANTATION INDUCED DEFECTS INSIL ICON
J. Ravi (North Carolina State Univ., Raleigh.), Y. N. Erokhin (North Carolina State Univ., Raleigh.), S. Koveshnikov (North Carolina State Univ., Raleigh.), G. A. Rozgonyi (North Carolina State Univ., Raleigh.), and C. W. White Dec. 1993 7 p Presented at the Fall Meeting of the Materials Research Society (MRS), Boston, MA, 29 Nov. - 3 Dec. 1993
(Contract DE-AC05-84OR-21400)
(DE94-006553; CONF-931108-71) Avail: CASI HC A02/MF A01

The influence of in-situ electronic perturbations on defect generation during 150-keV proton implantation into biased silicon p-n junctions has been investigated. The concentration and spatial distribution of the deep traps were characterized using a modification of the double corRelation deep level transient spectroscopy technique (D-DLTS). With the in-situ electric field applied, a decrease in concentration of vacancy-related, as well as H-related, traps was observed. 500 keV He(+) implantation was also performed to supplement the above studies and to differentiate any passivation effects due to hydrogen. A model based on the charge states of hydrogen and vacancies was used to explain the observed behavior.
DOE

N94-30315# Sandia National Labs., Albuquerque, NM.
DENSIFICATION AND CRYSTALLIZATION OF ZIRCONIA THIN FILMS PREPARED BY SOL-GEL PROCESSING
R. W. Schwartz, J. A. Voigt, C. D. Buchheit, and T. J. Boyle 1993 28 p Presented at the 1st Meeting of the Pacific Rim Ceramic Societies, Honolulu, HI, 7-10 Nov. 1993
(Contract DE-AC04-94AL-85000)
(DE94-005573; SAND-93-0975C; CONF-931142-5) Avail: CASI HC A03/MF A01

We have investigated the effects of precursor nature and heat treatment schedule on the densification and crystallization behavior of sol-gel derived zirconia thin films. Precursor solutions were prepared from n-propanol, zirconium (IV) n-propoxide, and either acetic acid, or 2,4-pentanedione (acac) and water additions. By controlling the ligand type and ligand-to-metal ratio, we were able to prepare films which displayed significant differences in densification behavior. We attribute the dissimilarity in densification to variations in the nature of the as-deposited films, as influenced by ligand type and concentration. While the acac-derived film was a physical gel, (i.e., a physical aggregation of the oligomeric species), the acetic acid-derived film, which exhibited less consolidation, was a chemical gel that could not be redissolved in the parent solvent. Films prepared with large acac/metal ratios and small water additions exhibited minimal crosslinking at 25 C, displayed the greatest consolidation (approximately 86% shrinkage) and the highest refractive index (n = 2.071) when heat treated. These results indicate the importance that M-O-M bonds (crosslinks) formed at low temperature can have on densification behavior. We also report on the effects of heat-treatment schedules and ramp rates on densification behavior. All of the films of the present study crystallized into the cubic phase, at temperatures ranging from approximately 400 C to greater than 700 C, depending on the heating rate.
DOE

N94-30316# Sandia National Labs., Albuquerque, NM.
THE GROWTH OF InAsSb/InGaAs STRAINED-LAYER SUPERLATTICES BY METAL-ORGANIC CHEMICAL VAPOR DEPOSITION
R. M. Biefeld, K. C. Baucom, S. R. Kurtz, and D. M. Follstaedt 1993 5 p Presented at the Fall Meeting of the Materials Research Society (MRS), Boston, MA, 29 Nov. - 3 Dec. 1993
(Contract DE-AC04-94AL-85000)
(DE94-005576; SAND-93-1483C; CONF-931108-48) Avail: CASI HC A01/MF A01

We have grown InAs(1-x)Sb(x)/In(1-y)Ga(y)As strained-layer superlattice (SLS) semiconductors lattice matched to InAs using a variety of conditions by metal-organic chemical vapor deposition. The V/III ratio was varied from 2.5 to 10 at 475 C, at pressures of 200 to 660 torr and growth rates of 3-5 angstrom/s and layer thicknesses ranging from 55 to 152 angstrom. Composition of InAsSb ternary can be predicted from the input gas molar flow rates using a thermodynamic model. At lower temperatures, the thermodynamic model must be modified to take account of the incomplete decomposition of arsine and trimethylantimony. Diodes have been prepared using Zn as the p-type dopant and undoped SLS as the n-type material.

The diode was found to emit at 3.56 (mu)m. These layers have been characterized by optical microscopy, SIMS, x-ray diffraction, and transmission electron diffraction. The optical properties of these SLS's were determined by infrared photoluminescence and absorption measurements. DOE

N94-30338# Ames Lab., IA.
BUTTERFLY AND SCALING LAW IN YBa2Cu4O8
Ming Xu, D. K. Finnemore, K. Zhang, B. Dabrowski, G. W. Crabtree, and D. G. Hinks 1994 4 p Presented at the 7th IWCC International Workshop on Critical Currents in Superconductors, Alpbach, Austria, 24-27 Jan. 1994
(Contracts W-7405-eng-82; W-31-109-eng-38)
(DE94-006037; IS-M-779; CONF-940122-1) Avail: CASI HC A01/MF A01

Magnetization hysteresis loops have been studied over a wide range of field and temperature for a single crystal of Y-124 in order to look for scaling in characteristic fields of the loops. A multivalued magnetization curve in the shape of 'butterfly' is observed with characteristic minimum fields, H(sub min), and maximum fields, H(sub max), that change systematically with temperature. H(sub max) varies as (1-T/T(sub c))(exp alpha) where alpha is close to 1.5. On a reduced scale, H(sub max) for this Y-124 sample is very similar to several Y-123 samples, suggesting that the origin of this effect is the same in these two systems. H(sub min) is exponential in temperature. DOE

N94-30592 Sandia National Labs., Albuquerque, NM.
STRAIN RELAXATION AND SURFACE ROUGHNESS AS A FUNCTION OF GROWTH TEMPERATURE IN LINEARLY GRADED In(x)Al(1-x)As (x = 0.05 TO 0.25) BUFFERS
J. A. Olsen (California Univ., Santa Barbara.), E. L. Hu (California Univ., Santa Barbara.), S. R. Lee, I. J. Fritz, A. J. Howard, B. E. Hammons, and J. Y. Tsao 1993 7 p Presented at the Fall Meeting of the Materials Research Society (MRS), Boston, MA, 29 Nov. - 3 Dec. 1993 Limited Reproducibility: More than 20% of this document may be affected by microfiche quality
(Contract DE-AC04-94AL-85000)
(DE94-005430; SAND-93-1462C; CONF-931108-57) Avail: CASI HC A02

The relation of relaxation to surface morphology in linearly-graded InAlAs was examined as a function of growth temperature using x-ray diffraction and atomic force microscopy (AFM). Samples were grown at temperatures ranging from 370 to 550C. Weak diffraction features for samples grown at 370 and 420C limited determination of the extent of their relaxation. The fractional relaxation of samples grown between 470 to 550C was essentially identical (approximately 77%) and symmetric in orthogonal (110) directions. The character of the surface morphology changed from random small scale roughness to a roughness more periodic in nature as the growth temperature increased. Although no asymmetry was observed in the relaxation, the roughness developed an asymmetry at higher growth temperatures with more prominent ridges along (-1 1 0) - (1 -1 0). DOE

N94-30611# Oak Ridge National Lab., TN.
RESEARCH ON THE ATOMIC LAYER-BY-LAYER GROWTH OF HIGH-TEMPERATURE SUPERCONDUCTOR THIN FILMS AT THE INSTITUTE OF SCIENTIFIC AND INDUSTRIAL RESEARCH, JAPAN
R. Feenstra 24 Nov. 1993 9 p
(Contract DE-AC05-84OR-21400)
(DE94-003739; ORNL/FTR-4840) Avail: CASI HC A02/MF A01 (US Sales Only)

A collaborative research project on the layer-by-layer growth of HTSC oxide thin films was continued. The equipment available for research at the host institute includes a laser molecular beam epitaxy vacuum deposition system. Such a system is currently also under consideration for construction at ORNL. Essential new research was performed to test ideas which resulted from the previous assignment. Technical discussions with staff members and students were held concerning preparation of a joint scientific publication. DOE

N94-30691 Iowa State Univ. of Science and Technology, Ames. Ames Lab.
INVESTIGATION OF THE PHASE EQUILIBRIA AND PHASE TRANSFORMATIONS ASSOCIATED WITH THE Bi2Sr2CaCu2O(y) SUPERCONDUCTOR Ph.D. Thesis
T. Holesinger Dec. 1993 172 p Limited Reproducibility: More than 20% of this document may be affected by microfiche quality
(Contract W-7405-eng-82)
(DE94-004889; IS-T-1631) Avail: CASI HC A08

The solid solution region and reaction kinetics of the Bi2Sr2CaCu2O(sub y) (2212) superconductor were examined as a function of temperature and oxygen partial pressure. Crystallization studies from the glassy and molten states were undertaken to determine the phase transformation and kinetics associated with the formation of 2212 and other competing phases. Crystallization of nominal 2212 glasses was found to proceed in two steps with the formation of Bi2Sr(sub 2-x)Ca(sub x)CuO(sub y) (2201) and Cu2O followed by Bi2Sr(sub 3-x)Ca(sub x)O(sub y), CaO, and SrO. The 2212 phase converts from the 2201 phase with increasing temperatures. However, its formation below 800 C was kinetically limited. At 800 C and above, a nearly full conversion to the 2212 phase was achieved after only one minute although considerably longer anneal times were necessary for the system to reach equilibrium. In low oxygen partial pressures, the solidus is reduced to approximately 750 C. Solidification studies revealed an eutectic structure separating the incongruently melting 2212/2201 phases at high oxygen partial pressures from the congruently melting Bi2Sr(sub 3-x)Ca(sub x)O(sub y) (23x) and Bi2Sr(sub 2-x)Ca(sub x)O(sub y) (22x) phases present at low oxygen partial pressures. During solidification in various oxygen partial pressures, the separation of CaO in the melt and the initial crystallization of alkaline-earth cuprates leaves behind a Bi-rich liquid from which it is impossible to form single-phase 2212. Hence, significant amounts of 2201 were also present in these samples. These problems could be reduced by melt processing in inert atmospheres. Bulk 2212 material produced in this manner was found to possess high transition temperatures, high intergranular critical current densities below 20K, and modest critical current densities at 77K. DOE

N94-30707 California Univ., Berkeley. Lawrence Berkeley Lab.
GIANT MAGNETORESISTANCE AND MICROSTRUCTURAL CHARACTERISTICS OF EPITAXIAL Fe-Ag AND Co-Ag GRANULAR THIN FILMS
N. Thangaraj, C. Echer, K. M. Krishnan, R. F. C. Farrow, R. F. Marks, and S. S. P. Parkin Oct. 1993 14 p Presented at the 38th Annual Conference on Magnetism and Magnetic Materials, Minneapolis, MN, 15-18 Nov. 1993 Limited Reproducibility: More than 20% of this document may be affected by microfiche quality
(Contract DE-AC03-76SF-00098)
(DE94-006287; LBL-34587; CONF-931133-7) Avail: CASI HC A03

The microstructure and magnetic properties of phase-separated Fe-Ag and Co-Ag granular alloy films, grown epitaxially on NaCl (001) substrates and exhibiting giant magnetoresistance (GMR), have been investigated. Surprisingly, two Fe-Ag films of similar composition grown under identical conditions are found to have substantially different microstructures yet display similar GMR. The microstructure of these films is characterized by Fe-rich or Co-rich regions respectively, 350 to 700 nm in extent, surrounded by a Ag-rich matrix. Within the Ag-rich regions, the Fe concentration varies from 20 to 25 atomic percent and the Co concentration is approximately equal to 16 atomic percent. Within these regions essentially pure fcc Co particles and bcc Fe particles are in parallel and rotated epitaxial alignment respectively with the fcc silver matrix. The Co and Fe particles are approximately 15 to 25 A in diameter. It is these small particles which most likely account for the giant magnetoresistance exhibited by these alloys. This suggests that a size distribution of magnetic particles, sharply peaked at the optimum size with limited bulk segregation, might give rise to larger GMR values. DOE

N94-30718# Argonne National Lab., IL.
FULLERENES AS PRECURSORS FOR DIAMOND FILM GROWTH WITHOUT HYDROGEN OR OXYGEN ADDITIONS
D. M. Gruen, S. Liu, A. R. Krauss, J. Luo, and X. Pan Oct. 1993 14 p
(Contract W-31-109-eng-38)
(DE94-004582; ANL/CHM/PP-81072) Avail: CASI HC A03/MF A01

Diamond films are predominantly grown using one percent or so of a hydrocarbon precursor in hydrogen gas. Hydrogen is generally believed to be necessary for the diamond thin film growth process. However, hydrogen in varying amounts is inevitably incorporated in the growing diamond lattice, leading to structural defects. The authors report here for the first time the successful growth of diamond films using fullerene precursors in an argon

microwave plasma, a unique development achieved without the addition of hydrogen or oxygen. It is speculated that collisional fragmentation of C60 to give C2 could be responsible for the high growth rate of the very fine grained diamond films. DOE

N94-30724# Oak Ridge National Lab., TN.
THERMAL CONDUCTIVITIES, ELECTRICAL RESISTIVITIES, AND SEEBECK COEFFICIENTS OF YBa2Cu3O(7-x) SUPERCONDUCTORS FROM 80 TO 300 K
D. W. Yarbrough, R. K. Williams, and D. R. Shockley 1993 15 p Presented at the 22nd International Thermal Conductivity Conference, Tempe, AZ, 7-10 Nov. 1993
(Contract DE-AC05-84OR-21400)
(DE94-004796; CONF-9311131-2) Avail: CASI HC A03/MF A01

Thermal conductivities, electrical resistivities, and Seebeck coefficients of three polycrystalline YBa2Cu3O(7-x) specimens have been measured over the temperature range 80 to 300 K in a longitudinal-heat-flow apparatus. Smoothed values for thermal conductivity, and electrical resistivity have been obtained for temperatures above the superconducting transition temperature of 90 K. The thermal conductivity values decreased as the temperature was increased, a trend which is inconsistent with the results of some other investigators. The thermal conductivities were less than previously published values and it is suggested that these differences are due to radiative heat loss in the published values. This effect is especially important for linear heat flow measurements on low thermal conductivity materials. The electrical and thermal conductivities of the specimens varied with Ba content and this variation was used to separate the thermal conductivity into lattice and electronic components are significant. The phonon component exhibits the expected temperature variation and an analysis indicates that the electron-phonon interaction is unusually strong. DOE

N94-30773# Oak Ridge National Lab., TN.
IONIC CONDUCTION MECHANISMS IN CaF2 AND CaF2-Al2O3 NANOCOMPOSITE FILMS ON Al2O3 SUBSTRATES
F. A. Modine, D. Lubben, and J. B. Bates Nov. 1993 7 p Presented at the Fall Meeting of the Materials Research Society (MRS), Boston, MA, 29 Nov. - 3 Dec. 1993
(Contract DE-AC05-84OR-21400)
(DE94-004792; CONF-931108-40) Avail: CASI HC A02/MF A01

Thin films of pure CaF2 and nanocomposite mixtures of Al2O3 with CaF2 were sublimated on Al2O3 substrates. Interdigital electrodes allowed in situ measurements of the electrical conduction vs thickness, deposition rate, composition, time, and temperature. Conductivity in pure CaF2 adjacent to an Al2O3 interface sometimes exceeded the bulk CaF2 conductivity (i.e., value at more than 50 nm distance) by as much as a factor of 6700 at 200 C. The high conductivity is characterized by an activation energy of 0.6 +/- 0.1 eV, significantly lower than about 1.0 eV for bulk conduction. However, this high conductivity is thermally unstable and diminishes in time. A high but stable conductivity was obtained in CaF2 films containing about 10 mole percent Al2O3 as a dispersed second phase. At 200 C, a 2-phase film gave a factor of 360 enhancement over the measured bulk CaF2 conductivity and a factor of 7 improvement over the best previously reported conductivity for CaF2-Al2O3 composite materials. The origin of enhanced conduction in CaF2 is attributed to ion transport along dislocations. Dislocations anneal with a characteristic log of time dependence that is recognizable in the annealing behavior of the electrical conductivity. Presumably, the addition of a dispersed second phase of Al2O3 to CaF2 serves both to generate and to pin dislocations; the electrical conductance is thereby enhanced and stabilized. DOE

N94-30835# California Univ., Berkeley. Lawrence Berkeley Lab.
NONLINEAR OPTICS RESPONSE OF SEMICONDUCTOR QUANTUM WELLS UNDER HIGH MAGNETIC FIELDS
D. S. Chemla Jul. 1993 28 p Presented at the International School of Physics Enrico Fermi Conference, Varenna, Italy, 20-30 Jul. 1993
(Contract DE-AC03-76SF-00098)
(DE94-003244; LBL-34434; CONF-9307156-1) Avail: CASI HC A03/MF A01

Recent investigations on the nonlinear optical response of semiconductor quantum wells (QW's) in a strong perpendicular magnetic field, H, are reviewed. After some introductory material, the evolution of the linear optical properties of GaAs QW's as a function of H is discussed; an examination is made of how the magneto-excitons (MX) extrapolate continuously between quasi-2D QW excitons (X) when H = 0, and pairs of Landau levels (LL) when H (yields) (infinity). Next, femtosecond time resolved investigations of their nonlinear optical response are presented; the evolution of MX-MX interactions with increasing H is stressed. Finally, as the dimensionality is reduced by application of H, the number of scattering channels is limited and relaxation of electron-hole pairs is affected. How nonlinear optical spectroscopy can be exploited to access the relaxation of angular momentum within magneto-excitons is also discussed. DOE

N94-30842# California Univ., Berkeley. Lawrence Berkeley Lab.
NUCLEAR MAGNETIC RELAXATION STUDIES OF SEMICONDUCTOR NANOCRYSTALS AND SOLIDS Ph.D. Thesis
J. R. Sachleben (California Univ., Berkeley.) Sep. 1993 145 p
(Contract DE-AC03-76SF-00098)
(DE94-006301; LBL-34884) Avail: CASI HC A07/MF A02

Semiconductor nanocrystals, small biomolecules, and C-13 enriched solids were studied through the relaxation in NMR spectra. Surface structure of semiconductor nanocrystals (CdS) was deduced from high resolution H-1 and C-13 liquid state spectra of thiophenol ligands on the nanocrystal surfaces. The surface coverage by thiophenol was found to be low, being 5.6 and 26% for nanocrystal radii of 11.8 and 19.2 angstrom. Internal motion is estimated to be slow with a correlation time greater than 10(exp -8) s(exp -1). The surface thiophenol ligands react to form a dithiophenol when the nanocrystals were subjected to O2 and ultraviolet. A method for measuring (N-14)-(H-1) J-couplings is demonstrated on pyridine and the peptide oxytocin; selective 2D T(sub 1) and T(sub 2) experiments are presented for measuring relaxation times in crowded spectra with overlapping peaks in 1D, but relaxation effects interfere. Possibility of carbon-carbon cross relaxation in C-13 enriched solids is demonstrated by experiments on zinc acetate and L-alanine. DOE

N94-30848# Los Alamos National Lab., NM.
MAGNETOTRANSPORT MEASUREMENTS IN MAGNETIC FIELDS UP TO 50T IN SmB6 AND FeSi
A. Lacerda, T. Graf, J. L. Sarrao, D. Mandrus, M. F. Hundley, J. D. Thompson, Z. Fisk, and L. VanBockstal 31 Dec. 1993 9 p Presented at the Strongly Correlated Electron Materials, Los Alamos, NM, 15-18 Dec. 1993
(Contract W-7405-eng-36)
(DE94-006227; LA-UR-94-40; CONF-931247-6) Avail: CASI HC A02/MF A01

We have measured the transverse magnetoresistance in high-quality single-crystalline samples of SmB6 and FeSi at 4K in applied magnetic fields to 50T and in the temperature range 4K less than T less than 150K in magnetic fields to 18T. The magnetoresistance in SmB6 at 4K decreases quadratically and reaches about -45% at 50T. The compound FeSi reveals three distinct features in the magnetoresistance: a negative magnetoresistance for fields below 5T, a kink at around 10T, and a broad maximum near 30T. DOE

N94-30850# California Univ., Berkeley. Lawrence Berkeley Lab.
CALCULATING THE J(c), B, T SURFACE FOR COMMERCIAL NIOBIUM TIN CONDUCTORS USING A REDUCED STATE MODEL
M. A. Green Jul. 1993 7 p Presented at the International Cryogenic Engineering Conference and International Cryogenic Materials Conference, Albuquerque, NM, 12-16 Jul. 1993
(Contract DE-AC03-76SF-00098)
(DE94-006296; LBL-35001; CONF-930703-44) Avail: CASI HC A02/MF A01

This report presents a method for calculating the J(sub c), B, T critical surface for commercial grade niobium tin given an effective (Tc) and B(sub c2) and J(sub c) over a range of magnetic inductions B. Given the effective (Tc) and B(sub c2) and J(sub c), one can estimate the J(sub c) over a range of magnetic inductions from 0.1 T to 0.8 times effective B(sub c2) and a range of temperatures from 1.5 K to about 14 K. The effects of conductor strain can also be estimated using the method. A comparison between calculated values of J(sub c) and measurements is illustrated for a number of cases. The method presented in this report can be used to estimate the performance of niobium tin in magnets at temperatures different

from those where measured data is available. The method of calculating the J(sub c) can also be used to estimate the effects of superconductor magnetization on the field quality at low fields. DOE

N94-30851# Oak Ridge National Lab., TN.
SYNTHESIS OF (SiC)3N4 THIN FILMS BY ION IMPLANTATION
C. Uslu, D. H. Lee, Y. Berta, B. Park, N. N. Thadhani, and D. B. Poker 1993 6 p Presented at the Fall Meeting of the Materials Research Society (MRS), Boston, MA, 29 Nov. - 3 Dec. 1993
(Contract DE-AC05-84OR-21400)
(DE94-006311; CONF-931108-74) Avail: CASI HC A02/MF A01

We have investigated the synthesis of carbon-silicon-nitride compounds by ion implantation. In these experiments, 100 keV nitrogen ions were implanted into polycrystalline (beta)-SiC (cubic phase) at various substrate temperatures and ion doses. These thin films were characterized by x-ray diffraction with a position-sensitive detector, transmission electron microscopy with chemical analysis, and Rutherford backscattering spectroscopy. The as-implanted samples show a buried amorphous layer at a depth of 170 nm. Peak concentration of nitrogen saturates at approximately 45 at. % with doses above approximately 9.0 times 10(sup 17) N/sq cm at 860 C. These results suggest formation of a new phase by nitrogen implantation into (beta)-SiC. DOE

N94-30888 International Centre for Theoretical Physics, Trieste (Italy).
A SOLID-ON-SOLID INVASION PERCOLATION MODEL FOR SELF-AFFINE INTERFACES
C. M. Arizmendi (La Plata Univ., Argentina.), H. O. Martin, and J. R. Sanchez Aug. 1993 10 p Limited Reproducibility: More than 20% of this document may be affected by microfiche quality
(DE94-608102; IC-93/273) Avail: CASI HC A02 (US Sales Only)

The scaling properties of the interface of a new growth model are studied. The model is based on the standard invasion percolation without trapping in which the solid-on-solid condition is imposed. The local correlation between points of the interface can be controlled through a parameter. The self-affine properties of the interface show strong dependence on the existence of the local correlation. The dependence of the relevant exponents of the interface with the correlation is analyzed. DOE

N94-30894 Argonne National Lab., IL.
ION DAMAGE STUDIES IN GaAs/Al(0.6)Ga(0.4)As/GaA LCS HETEROSTRUCTURES
B. A. Turkot (Illinois Univ., Urbana.), D. V. Forbes (Illinois Univ., Urbana.), H. Xiao (Illinois Univ., Urbana.), I. M. Robertson (Illinois Univ., Urbana.), J. J. Coleman (Illinois Univ., Urbana.), M. A. Kirk, L. E. Rehn, and P. Baldo Dec. 1993 7 p Presented at the Fall Meeting of the Materials Research Society (MRS), Boston, MA, 29 Nov. - 3 Dec. 1993 Limited Reproducibility: More than 20% of this document may be affected by microfiche quality
(Contracts DE-FG02-91ER-45439; W-31-109-eng-38)
(DE94-005384; ANL/MSD/CP-80260; CONF-931108-42) Avail: CASI HC A02

Development of damage structure produced in (100) GaAs/Al(0.6)Ga(0.4)As/GaAs by 1 MeV Kr(+) ion irradiation at 77 and 293 K was investigated by RBS channeling and cross-sectional high-resolution TEM techniques. Following an implantation to a dose of 10(exp 14) ions CM(sup -2) at 77 K, RBS channeling spectra indicate that the Al(0.6)Ga(0.4)AS layer contained a high defect density and was possibly amorphous. Warming to room temperature resulted in a change in the channeling spectrum, which indicated that the damage in the Al(0.6)Ga(0.4)As layer had partially recovered. The degree of recovery was greatest at the GaAs/Al(0.6)Ga(0.4)As interface, and decreased with increasing depth. TEM observations show the damage in the Al(0.6)Ga(0.4)As to be comprised of planar defects, the density of which increases with depth, and an amorphous layer at the bottom interface. This difference in the damage distribution is consistent with the asymmetry in the channeling spectrum. A model based on the depth variation of cascade density is proposed to account for the observations. DOE

N94-30897# Argonne National Lab., IL.
ROTATOR PHASES IN NARROW-GAP SEMICONDUCTORS
D. L. Price, M. L. Saboungi, J. Fortner, J. W. Richardson, and W. S. Howells Dec. 1993 13 p Presented at the 2nd International Conference on Quasielastic Neutron Scattering, San Sebastian, Spain, 27-28 Sep. 1993
(Contract W-31-109-eng-38)
(DE94-005472; ANL/MSD/CP-79750; CONF-9309318-1) Avail: CASI HC A03/MF A01

Zintl compounds of lead and tin with the heavier alkali metals are semiconductors with surprising and unusual properties in both solid and liquid states. These are ascribed to the formation of tetrahedral complex anions arising from charge transfer and covalent bonding around the polyvalent metal ions. The tetrahedra exhibit both rotational and translational order, leading to a variety of complex dynamical behaviors in both solid and liquid phases. The changes in order have dramatic effects on electrical transport properties. DOE

N94-30898# Argonne National Lab., IL.
INTRA- VERSUS INTERLAYER PAIRING IN THE COPPER OXIDE SUPERCONDUCTORS: RESPONSE TO A MAGNETIC FIELD
R. A. Klemm and Samuel H. Liu Jan. 1994 14 p Presented at the Superconducting Superlattices and Multilayers and Oxide Superconductory Physics and Nanoengineering, Los Angeles, CA, 23-28 Jan. 1994
(Contracts W-31-109-eng-38; DE-AC05-84OR-21400)
(DE94-005475; ANL/MSD/CP-78012; CONF-940121-2) Avail: CASI HC A03/MF A01

We have investigated the response of layered superconductors to an external magnetic field using the semiclassical phase approximation. The linearized-gap equations have been derived, and solved numerically to calculate the upper critical field H(sub c2)(T) for layered superconductors with one or two layers per unit cell for both s-wave and interlayer BCS-like pairing mechanisms. In the weak-hopping limit the equations reduce to the Lawrence-Doniach form, and for general hopping the appropriate gap equations are derived and numerically analyzed. One encounters the familiar dimensional crossover in the H(sub c2)(parallel)(T) curve for weak hopping. A different type of dimensional crossover can occur in the two-layer case with unequal intralayer or interlayer coupling strengths, such that at the dimensional crossover temperature, the magnetic field suppresses the superconductivity in the weakly coupled layers while leaving the strongly coupled layers superconducting. The effect is enhanced by unequal hopping strengths. The flux lattice consists of alternating superconducting and normal layers. DOE

N94-30899# Ames Lab., IA.
RHEED STUDIES OF THE NUCLEATION, GROWTH, AND MOBILITY OF Ag ATOMS ON THE Si(111)7 X 7 SURFACE Ph.D. Thesis
K. R. Roos Jul. 1993 98 p
(Contract W-7405-eng-82)
(DE94-005551; IS-T-1664) Avail: CASI HC A05/MF A02

The low temperature and flux dependent growth of ultrathin Ag films on the Si(111)7x7 surface is studied with Reflection High-Energy Electron Diffraction (RHEED). The grazing incidence geometry of RHEED allows for an incident molecular beam normal to the surface and makes it an ideal surface probe for studying ultrathin film growth in real time. Short-lived oscillations in the diffracted intensity are observed during Ag deposition at 150 K, indicating quasi-layer-by-layer growth mediated by adatom mobility. When the 150 K growth is performed over a wide range of deposition rates F, the peak intensity is observed to scale, i.e. I(Ft) depends only on the total amount deposited, which implies thermally activated diffusion is absent at 150 K. Scaling is not obeyed at higher temperatures (T greater than or equal to 473 K) for the growth of the particular superstructure. Testing for scaling of the diffracted intensity constitutes a new experimental method which can be applied generally to determine if thermal diffusion is active at a particular temperature. Scaling is consistent with a constant diffusion length R(sub 0), independent of substrate temperature and deposition rate. The presence of a non-thermal diffusion mechanism is confirmed by monitoring the flux dependence of the (radical)3 superstructure growth during deposition at T greater than or equal to 473 K. At these temperatures the total diffusion length R is given by R = R(sub 0)+(4Dt)(sup 1/2), where (4Dt)(sup 1/2) is the thermal component. A non-zero intercept R(sub 0) is found by plotting the peak intensity I(sub p)(exp 1/2) vs. deposition rate F(exp -1/2) (F(exp -1) is proportional to the available diffusion time). From the FWHM of a low coverage (0.2 ML) (radical)3 spot, an estimation of 50 (angstrom) is made for a lower bound of the magnitude of R(sub 0). DOE

N94-30901# Virginia Polytechnic Inst. and State Univ., Blacksburg. Dept. of Chemical Engineering.
INFLUENCE OF SURFACE DEFECTS AND LOCAL STRUCTURE ON OXYGENATE REACTION PATHWAYS OVER METAL OXIDE SURFACES
D. F. Cox Jul. 1993 10 p
(Contract DE-FG05-90ER-14129)
(DE94-005680; DOE/ER-14129/3) Avail: CASI HC A02/MF A01

Complete thermal desorption and photoemission studies of seven molecules (methanol, formaldehyde, formic acid, isopropanol, acetone, water, and carbon monoxide) were completed on four different SnO2(110) surfaces (stoichiometric, reduced, slightly-defective, and highly-defective). Initial thermal desorption studies of acetic acid and propene were also done. Results indicate that different initial surface conditions can dramatically affect: (1) probability for heterolytic dissociation of Bronsted acids, (2) reaction kinetics for unimolecular decomposition of oxygenated surface intermediates, and (3) product selectivity. DOE

N94-29515# National Inst. for Resources and Environment, Ibaraki (Japan). Siliceous Materials Div.
SYNTHESIS OF DIAMOND IN A HYDROGEN PLASMA JET: SIMULATIONS OF XRD PATTERNS OF DIAMOND POLYTYPES AND BOUNDARY LAYER ON A SUBSTRATE [SUISO PURAZUMA JETTO NI YORU DAIYAMONDO GOSEI: ROPPOSHO DAIYAMONDO PORITAIPU NO XRD PATAN OYOBI KIBANJO KYOKAISO NO SHIMYURESHON]
Nobuyuki Kikukawa, Mitsuo Makino, Katsuhisa Maruyama, and Minoru Shiraishi *In its* Journal of NIRE, Vol. 2, No. 3 25 May 1993 p 21-29 In JAPANESE (For primary document see N94-29512 08-99)
Avail: CASI HC A02/MF A02

N94-29793*# Georgia Inst. of Tech., Atlanta. School of Electrical Engineering.
MICRO-OPTO-MECHANICAL DEVICES AND SYSTEMS USING EPITAXIAL LIFT OFF
C. Camperi-Ginestet, Young W. Kim, S. Wilkinson, M. Allen, and N. M. Jokerst *In* JPL, Proceedings of the Workshop on Microtechnologies and Applications to Space Systems 15 Jun. 1993 p 305-31 (For primary document see N94-29767 08-31)
Avail: CASI HC A03/MF A03

N94-29983# Nippon Kokan K. K., Kawasaki (Japan).
A NEWLY DEVELOPED SNOW VEHICLE (SM100S) FOR ANTARCTICA. PART 3: LOW TEMPERATURE TOUGHNESS OF THE WELDED JOINTS OF THE STRUCTURAL STEEL [NANKYOKU OGATA SETSUJOSHA (SM100S) NO KAIHATSU. 3: SHATAI ZAIRYO NO YOSETSUBU TEION JINSEI]
Shin Sakui and Masashi Nakajima *In* National Inst. of Polar Research, Antarctic Record, Vol. 36, No. 3 30 Nov. 1992 p 393-397 In JAPANESE (For primary document see N94-29978 08-46)
Avail: CASI HC A01/MF A02

N94-30221 McMaster Univ., Hamilton (Ontario).
PULSE HEIGHT RESPONSE OF Si SURFACE BARRIER DETECTORS
D. Comedi and J. Davies *In* Defence Research Establishment, Proceedings of the 1991 Single Event Upset Symposium 1991 14 p (For primary document see N94-30211 08-73)
Avail: Issuing Activity (Defence Research Establishment, Ottawa, ON K1A 0Z4 Canada)

77 THERMODYNAMICS AND STATISTICAL PHYSICS

Includes quantum mechanics; theoretical physics; and Bose and Fermi statistics.

For related information see also *25 Inorganic and Physical Chemistry* and *34 Fluid Mechanics and Heat Transfer.*

N94-28543# Los Alamos National Lab., NM.
THE (j,0) + (0,j) REPRESENTATION SPACE: MAJORNA-LIKE CONSTRUCT
D. V. Ahluwalia, T. Goldman, and M. B. Johnson 1993 11 p Presented at the 17th International School of Theoretical Physics Meeting on Standard Model and Beyond, Krakow, Poland, Sep. 1993
(Contract W-7405-eng-36)
(DE94-005010; LA-UR-93-4316; CONF-9309304-1) Avail: CASI HC A03/MF A01

This is second of the two invited lectures presented at the '17th International School of Theoretical Physics: Standard Model and Beyond 93.' The text is essentially based on a recent publication by the present authors. Here, after briefly reviewing the (j, 0) + (0, j) Dirac-like construct in the front form, we present a detailed construction of the (j, 0) + (0, j) Majorana-like fields. DOE

N94-28572# Los Alamos National Lab., NM.
THE (j,0) + (0,j) REPRESENTATION SPACE: DIRAC-LIKE CONSTRUCT
D. V. Ahluwalia, M. B. Johnson, and T. Goldman 1993 9 p Presented at the 17th International School of Theoretical Physics Meeting on Standard Model and Beyond, Krakow, Poland, Sep. 1993
(Contract W-7405-eng-36)
(DE94-005011; LA-UR-93-4315; CONF-9309304-2) Avail: CASI HC A02/MF A01

This is first of the two invited lectures presented at the '17th International School of Theoretical Physics: Standard Model and Beyond 1993.' The text is essentially based on a recent publication by the present authors. Here we show that the Dirac-like construct in the (j,0)(circle +)(0,j) representation space support a Bargmann-Wightman-Wigner type quantum field theory. DOE

N94-28582# Joint Inst. for Nuclear Research, Dubna (USSR).
CALCULATION OF EIGENVALUES OF SCHROEDINGER OPERATORS FOR ARBITRARY COUPLING
E. P. Yukalova and V. I. Yukalov 1992 14 p In RUSSIAN
(DE94-606302; JINR-E-5-92-202) Avail: CASI HC A03/MF A01 (US Sales Only)

The method of self-similar approximations is applied for calculating the eigenvalues of Schroedinger operators. In this method the self-similar approximation is treated as a fixed-point of a self-similar mapping. DOE

N94-28586 Joint Inst. for Nuclear Research, Dubna (USSR).
APPARENT UNAMBIGUOUSNESS OF RELATIVISTIC TIME DILATION
V. N. Streltsov 1992 4 p Limited Reproducibility: More than 20% of this document may be affected by microfiche quality
(DE94-606328; JINR-D-2-92-114) Avail: CASI HC A01 (US Sales Only)

It is indicated on the definite analogy between the dependence of visible sizes of relativistic objects and period of the wave, emitted by the moving source from the observation conditions ('retradition factor'). It is noted that the definition of time for moving extended objects, led to relativistic dilation, corresponds to the definition of the relativistic (radar) length led to the 'elongation formula'. DOE

N94-28609 Joint Inst. for Nuclear Research, Dubna (USSR).
ON INVARIANT MEASURES FOR SOME INFINITE-DIMENSIONAL DYNAMICAL SYSTEMS
P. E. Zhidkov 1992 14 p Limited Reproducibility: More than 20% of this document may be affected by microfiche quality
(DE94-606342; JINR-E-5-92-395) Avail: CASI HC A03 (US Sales Only)

An abstract infinite-dimensional Hamiltonian system recently introduced by M. Grillakis, J. Shatah and W.A. Strauss is considered. A lot of nonlinear evolution equations of the mathematical physics may be represented in that form. The aim of the paper is the construction of an invariant measure for this system. This measure has many applications in the theory of dynamical systems. In particular, the conditions for the finiteness of the constructed measure are presented. It makes it possible to apply the Poincare recurrence theorem which explains the well-known Fermi-Past-Ulam phenomenon of the return of any solution to its initial data with time with an arbitrary accuracy. DOE

N94-28616 Gosudarstvennyi Komitet po Ispolzovaniyu Atomnoi Energii, Obninsk (USSR).
MILN EQUATION FOR THE CALCULATION OF THE PHASES AND AMPLITUDES OF WAVE FUNCTIONS FOR CONTINUUM SPECTRUM OF COULOMB TWO-CENTER PROBLEM
V. I. Puzynin 1992 14 p Limited Reproducibility: More than 20% of

this document may be affected by microfiche quality
(DE94-606292; IFVE-OMVT-92-119) Avail: CASI HC A03 (US Sales Only)

A statement of boundary problem is proposed for solving the quantum mechanics two-center problem for continuum spectrum. The solution of the Schroedinger radial equation is based as the solution to the Miln equation. An effective algorithm and its program realization is given for quick and accurate calculation of the wave function phases and for a continuum spectrum. The results of numerical computations are presented for some parameters and compared with other analogous results. DOE

N94-28617 Moscow State Univ. (Russia).
DISSIPATIVE QUANTUM DYNAMICS AND NONLINEAR SIGMA-MODEL
V. E. Tarasov 1992 24 p Limited Reproducibility: More than 20% of this document may be affected by microfiche quality
(DE94-606295; INP-MSU-92-33-282; NIIYAF-MGU-92-33-282) Avail: Issuing Activity (Department of Energy (DOE))

Sedov variational principle which is the generalization of the least action principle for the dissipative and irreversible processes and the classical dissipative mechanics in the phase space is considered. Quantum dynamics for the dissipative and irreversible processes is constructed. As an example of the dissipative quantum theory the nonlinear two-dimensional sigma-model is considered. The conformal anomaly of the energy momentum tensor trace for closed bosonic string on the affine-metric manifold is investigated. The two-loop metric beta-function for nonlinear dissipative sigma-model was calculated. The results are compared with the ultraviolet two-loop conterterms for affine-metric sigma model. DOE

N94-28618 Joint Inst. for Nuclear Research, Dubna (USSR).
RETARDED DISTANCES AND THE DOPPLER EFFECT
V. N. Streltsov 1992 6 p Limited Reproducibility: More than 20% of this document may be affected by microfiche quality
(DE94-606296; JINR-D-2-92-147) Avail: Issuing Activity (Department of Energy (DOE)) (US Sales Only)

A relativistic transformation of the retarded distance is presented. Arguments of general nature in favor of the concept of the relativistic (radar) length leading to this formula are presented. DOE

N94-28620 Joint Inst. for Nuclear Research, Dubna (USSR).
ON THE IMPORTANCE OF THE MICHELSON-MORLEY EXPERIMENT
V. N. Streltsov 1992 8 p Limited Reproducibility: More than 20% of this document may be affected by microfiche quality
(DE94-606298; JINR-E-2-92-160) Avail: Issuing Activity (Department of Energy (DOE)) (US Sales Only)

The opinion of an important role of the Michelson-Morley experiment in the establishment of the pronciple of the light velocity constancy is expressed. It is stressed that the radar length used for the treatment of the Michelson-Morley experiment leads to the elongation formulas for the longitudinal arm of an interferometer. DOE

N94-28662# Naval Postgraduate School, Monterey, CA.
THE INFLUENCE OF WALL CONDUCTIVITY OF FILM CONDENSATION WITH INTEGRAL FIN TUBES M.S. Thesis
Robert L. Cobb 23 Sep. 1993 263 p
(AD-A275503) Avail: CASI HC A12/MF A03

Heat transfer performance of steam condensing on horizontal finned tubes made of copper, aluminum, copper nickel (90/10), and stainless steel (316) was studied using a condenser test rig at both vacuum and atmospheric conditions. Integral fin tubes included conventional rectangular shaped fins as well as rectangular fins having a radiussed root geometry (i.e., a fillet radius equal to half the fin spacing). All finned tubes had inner and outer diameters of 12.70 mm and 15.88 mm respectively, and had a fin thickness of 1.0 mm and a fin spacing of 1.5 mm. The overall heat transfer coefficient, U(sub o), was determined experimentally and the outside heat transfer coefficient, h(sub o), was obtained utilizing a modified Wilson plot procedure. Results indicate that the performance of a finned tube was strongly dependent on the tube material and weakly dependent on fin geometry. Radiussing the fin root to remove condensate between fins in the unflooded portion (i.e., top portion) of a finned tube reduced the heat transfer performance compared to a conventional rectangular shaped integral fin. Experimental data were compared to the models of Beatty and Katz as well as to a modified model of Rose. DTIC

N94-28719# Joint Inst. for Nuclear Research, Dubna (USSR).
CLASSICAL INTERPRETATION OF QUANTUM MECHANICS
V. K. Ignatovich 1992 15 p In RUSSIAN
(DE94-606304; JINR-R-4-92-389) Avail: CASI HC A03/MF A01 (US Sales Only)

The wave-function is considered to be a classical field with the particle as a source. The behavior of a particle is determined by the interaction of its field with surrounding objects. An experiment, permitting to estimate the wave composition of a particle field is considered. DOE

N94-28721# Joint Inst. for Nuclear Research, Dubna (USSR).
ON A DIRECT EXPERIMENTAL VERIFICATION OF THE ELONGATION FORMULA
V. N. Streltsov 1992 3 p
(DE94-606329; JINR-D-2-92-70) Avail: CASI HC A01/MF A01 (US Sales Only)

It is noted that experiments on studying the transverse Doppler effect are the direct evidence in favor of the 'elongation formula' following from the concept of the relativistic length. This concept is the base of the radar formulation of the relativity. DOE

N94-28751# Joint Inst. for Nuclear Research, Dubna (USSR).
THE PROPER FIELD OF CHARGES AND GAUGE-INVARIANT VARIABLES IN ELECTRODYNAMICS
S. V. Shabanov 1992 18 p
(DE94-606405; JINR-E-2-92-136) Avail: CASI HC A03/MF A01 (US Sales Only)

According to Dirac it follows from the gauge invariance requirement for physical dynamical variables in electrodynamics that charges are created and annihilated together with their proper (Coulomb) field that induces the static (Coulomb) interaction of charges. It is shown that in electrodynamics there is an infinite number of ways to determine gauge-invariant variables. The proper field configuration of charges depends on the choice of these variables and may differ from the Coulomb one. DOE

N94-28782# Joint Inst. for Nuclear Research, Dubna (USSR).
THREE FORMS OF RELATIVITY
V. N. Streltsov 1992 6 p
(DE94-606338; JINR-D-2-92-63) Avail: CASI HC A02/MF A01 (US Sales Only)

The physical sense of three forms of relativity is discussed. The first, instant form, corresponds to the traditional approach based on the concept of instant distance. The normal form corresponds to the radar formulation which is based on the light or retarded distances. The front form in the special case is characterized by 'observable' variables, and the known method of k-coefficient is its obvious expression. DOE

N94-28802# Joint Inst. for Nuclear Research, Dubna (USSR).
TWISTOR-LIKE TYPE 2 SUPERSTRING AND BOSONIC STRING
V. V. Chikalov and A. I. Pashnev 1992 11 p
(DE94-606339; JINR-E-2-92-337) Avail: CASI HC A03/MF A01

The superfield formulation of type 2 Green-Schwarz superstring with n = (1,0) world-sheet supersymmetry is constructed. It is shown that the inclusion of the second spinor coordinate in the target superspace leads to the possibility of the reparametrization invariant description of the superstring in the absence of any field from the two-dimensional supergravity multiplet. The twistor-like action of Chern-Simons type for bosonic string in D = 3, 4, 6, 10 is deduced from the superstring action. DOE

N94-29146 Institut des Hautes Etudes Scientifiques, Bures-sur-Yvette (France).
EXISTENCE OF QUANTUM CHARACTERISTIC EXPONENTS
R. V. Mendes Nov. 1993 6 p Limited Reproducibility: More than 20% of this document may be affected by microfiche quality
(PB94-138161; IHES/M/93/58) Avail: CASI HC A02

The Lyapunov characteristic exponents provide a rigorous characterization of the notion of chaos in classical mechanics. Similar quantities have been proposed as a characterization of quantum chaos. In this note, we find the conditions under which the existence of quantum characteristic exponents can be proved. NTIS

N94-29481# Imperial Coll. of Science and Technology, London (England). Dept. of Aeronautics.

THE MAXIMUM ENTROPY APPROACH APPLIED TO ENERGY EXCHANGE, CHEMICAL REACTIONS AND IONISATION IN THE DIRECT SIMULATION MONTE CARLO METHOD FOR RAREFIED HYPERSONIC FLOWS

Michael A. Gallis and John K. Harvey Jul. 1993 28 p
(ISSN 0308-7247)
(IC-Aero-93-01; ETN-94-95508) Avail: CASI HC A03/MF A01

The Maximum Entropy (ME) method, pioneered for use by chemists, was applied to the direct simulation Monte Carlo method for rarefied hypersonic ionized flow. The method was used to model the reaction rates and the disposal of post collision energy for the predominant reactions occurring in a nitrogen/oxygen flow. Unlike the commonly used Borgnakke and Larsen approach the ME method does not assume equilibrium for the distribution of energy states before or after the collisions but it calculates the most probable distribution based on the entropy associated with each distribution. Two flow field examples are presented: a plane shock wave and the axisymmetric flow about spherically blunted cone. These examples illustrate the application of the ME model for reaction between neutral and ionized species in situations of high chemical and thermodynamic nonequilibrium. ESA

N94-29498 International Centre for Theoretical Physics, Trieste (Italy).

COHERENT STATES OF SU(L,1) GROUPS

D. M. Gitman (Sao Paulo Univ., Brazil.) and A. L. Shelepin (MIRA, Moscow, Russia.) Jul. 1993 25 p Limited Reproducibility: More than 20% of this document may be affected by microfiche quality
(DE94-603654; IC-93/212) Avail: CASI HC A03 (US Sales Only)

This work can be considered as a continuation of our previous one (J. Phys., 26 (1993) 313), in which an explicit form of coherent states (CS) for all SU(N) groups was constructed by means of representations on polynomials. Here we extend that approach to any SU(l,1) group and construct explicitly corresponding CS. The CS are parametrized by dots of a coset space, which is, in that particular case, the open complex ball CD(sup l). This space together with the projective space CP(sup l), which parametrizes CS of the SU(l + 1) group, exhaust all complex spaces of constant curvature. Thus, both sets of CS provide a possibility for an explicit analysis of the quantization problem on all the spaces of constant curvature. That is a reason why CS of the SU(N) and SU(l,1) groups are of importance in connection with the quantization theory. The CS constructed form an overcompleted system in the representation space and, as quantum states, possess of a minimum uncertainty, they minimize an invariant dispersion of the quadratic Casimir operator. The classical limit is investigated in terms of symbols of operators; the limit of the so called star commutator of the symbols generates the Poisson bracket in CD(sup l), the latter plays the role of the phase space for the corresponding classical mechanics. DOE

N94-29911 Yale Univ., New Haven, CT.

ANOMALOUS ALGEBRAIC STRUCTURES IN QUANTUM FIELD THEORIES Ph.D. Thesis

Wen-Xin Jiang 1992 84 p
Avail: Univ. Microfilms Order No. DA9315219

In this thesis we will investigate the anomalous algebraic structures (the Schwinger terms and their equivalents) in quantum field theories, especially those with higher than two space time dimensions. The universal behavior of the c-number Schwinger terms in higher than two dimensional conformal field theories are discussed, for both the current algebra and the stress-energy tensor algebra. Operational extensions for spatial diffeomorphisms and gauge transformations in the physical space time are also discussed. We also use the anomalous Ward identities to establish a relation between the consistent gravitational anomaly and the Schwinger terms for the gravitational constraint algebras. Dissert. Abstr.

N94-29987 Maryland Univ., College Park.

A SEMICLASSICAL STUDY OF QUANTUM MAPS Ph.D. Thesis

Yin Guo 1992 127 p
Avail: Univ. Microfilms Order No. DA9315647

The study of the behavior of quantum systems whose classical limit exhibits chaos defines the problem of quantum chaos. Because of some strongly contrasting properties exhibited by classical and quantum theories, one would naturally ask how quantum mechanics approaches the classical limit h = 0, and how the chaotic motion in classical systems manifests itself in the corresponding quantum counterparts. Semiclassical mechanics is the bridge between these two fundamental frameworks: quantum mechanics and classical mechanics. For studying the quantum mechanics corresponding to generic classical motion it is desirable to use the simplest possible model. The model system we use is the kicked rotator, which is one of the most studied model systems due to its simplicity and generic features. Detailed computations of both classical and quantum mechanics are feasible for this system. The relationship between invariant classical phase space structures and quantum eigenfunctions has been the focus of recent semiclassical studies. We study the eigenstates of the quantum standard map associated with both integrable and nonintegrable regions in classical phase space. The coherent-state representation is used to make the correspondence between the quantum eigenstates and the classical phase space structure. The importance of periodic orbits in the quantum eigenstates of classically chaotic Hamiltonians has become a popular topic in study of semiclassical limits of the systems. It is well known that periodic orbits arise without any assumption in the trace formula developed by Gutzwiller. We calculate the semiclassical coherent-state propagator. Since computing all the complex stationary orbits is not practical, we make a further assumption which we call the periodic point dominance (PPD). We present arguments and evidence to show that the PPD approximation works well in hard chaos regions where the full semiclassical approximation is not practical to use. The method fails in some boundary regions where both stable and unstable points are present, but the full semiclassical approximation is not a much better method than the PPD in many of this kind of situations. Dissert. Abstr.

N94-30086 International Centre for Theoretical Physics, Trieste (Italy).

ON CHAOS IN QUANTUM MECHANICS: THE TWO MEANINGS OF SENSITIVE DEPENDENCE

R. L. Ingraham (New Mexico State Univ., Las Cruces.) and G. A. Luna-Acosta Aug. 1993 9 p Limited Reproducibility: More than 20% of this document may be affected by microfiche quality
(DE94-608069; IC-93/270) Avail: CASI HC A02 (US Sales Only)

Sensitive dependence on initial conditions, the most important signature of chaos, can mean failure of Lyapunov stability, the primary meaning adopted in dynamical systems theory, or the presence of positive Lyapunov exponents, the meaning favored in physics. These are not equivalent in general. We show that there is sensitive dependence in quantum mechanics in the sense of violation of Lyapunov stability for maps of the state vector like /A/ involving unbounded operators A. This is true even for bounded quantum systems, where the corresponding Lyapunov exponents are all zero. Experiments to reveal this sensitive dependence, a definite though unfamiliar prediction of quantum mechanics, should be devised. It may also invalidate the usual assumption of linear response theory in quantum statistical mechanics in some cases. DOE

N94-30087 Joint Inst. for Nuclear Research, Dubna (USSR). Lab. of Theoretical Physics.

RECONSTRUCTION OF SPECTRA IN THE DISCRETE QUANTUM MECHANICS (NEW ELEMENTS OF THE LATTICE QUANTUM ENGINEERING)

B. N. Zakharev and S. I. Serdyukova 1992 14 p Limited Reproducibility: More than 20% of this document may be affected by microfiche quality
(DE94-608075; JINR-R-4-92-10) Avail: CASI HC A03 (US Sales Only)

It is shown what perturbation is required to variate the normalizing constants of the chosen levels and to shift separate energy levels in the rectangular well for the finite-difference Schroedinger eq. Peculiarities are found of the discrete case in comparison with the equation of motion with the continuous coordinate. The ordinary potential parameters v(sub n) (diagonal) determine the shape of the lower boundary of the allowed zone, and the u(sub n) on the neighbor diagonals determine the width of the zone. The different influence of v(sub n) and u(sub n) on the shifts of the energy levels in the rectangular well is clarified. The v pushes in one direction the levels symmetrically posed according to the middle of the spectrum, and u(sub n) pushes them in opposite directions. DOE

N94-30089 International Centre for Theoretical Physics, Trieste (Italy).

DISCRETE SYMMETRIES, STRONG CP PROBLEM AND GRAVITY

G. Senjanovic May 1993 5 p Limited Reproducibility: More than 20%

of this document may be affected by microfiche quality
(DE94-608091; IC-93/113) Avail: Issuing Activity (Department of Energy (DOE)) (US Sales Only)

Spontaneous breaking of parity or time reversal invariance offers a solution to the strong CP problem, the stability of which under quantum gravitational effects provides an upper limit on the scale of symmetry breaking. Even more important, these Planck scale effects may provide a simple and natural way out of the resulting domain wall problem. DOE

N94-30121 Weizmann Inst. of Science, Rehovoth (Israel). Dept. of Physics.
EXCLUSIVE MANY-PARTICLE DIFFUSION IN DISORDERED MEDIA AND CORRELATION FUNCTIONS FOR RANDOM VERTEX MODELS
G. Schuetz and S. Sandow May 1993 32 p Limited Reproducibility: More than 20% of this document may be affected by microfiche quality
(DE94-608134; WIS-PH-93-46) Avail: CASI HC A03 (US Sales Only)

We consider systems of particles hopping stochastically on d-dimensional lattices with space-dependent probabilities. We map the master equation in a Fock space where the dynamics are given by a quantum Hamiltonian (continuous time) or a transfer matrix (discrete time). We show that under certain conditions the time-dependent two-point density correlation function in N-particle steady state can be computed from the probability distribution of a single particle moving in the same environment. Focusing on exclusion models where the lattice site can be occupied by at most one particle, we discuss as an example for such a stochastic process a generalized Heisenberg antiferromagnet where the strength of the spin-spin coupling is space-dependent. In discrete time one obtains for one dimensional systems the diagonal-to-diagonal transfer matrix of the two dimensional six vertex model with space dependent vertex weights. For a random distribution of the vertex weights one obtains a version of the random barrier model describing diffusion of particles in disordered media. We derive exact expressions for the average two-point density correlation function in the presence of weak, correlated disorder. DOE

N94-30142 Manitoba Univ., Winnipeg. Dept. of Physics.
CURVED-SPACE QUANTIZATION, AND DIRAC VERSUS REDUCED QUANTIZATION OF POINCARE GAUGE THEORIES Ph.D. Thesis
Richard J. Epp Nov. 1993 161 p
(ISBN-0-315-85990-3; CTN-94-61176) Copyright Avail: Micromedia Ltd., Technical Information Centre, 240 Catherine Street, Suite 305, Ottawa, Ontario, K2P 2G8, Canada HC/MF

It is well known that the difference between Dirac and reduced quantization of gauge theories can be understood in terms of factor ordering ambiguities. The presence of symmetries such as Poincare invariance leads to restrictions on the possible factor orderings. Scalar electrodynamics is considered: its reduced field space is curved, which amplifies the van Hove obstructions and obscures the correct factor ordering of the Poincare generators. In Dirac quantization, however, the initial field space on which the quantum operators are defined, is flat. It is shown that the natural factor ordering automatically realizes the Poincare algebra on physical states. This result is generalized to a broader class of observables and gauge theories. Kaluza Klein-like geometric methods are applied to determine what if anything makes the Dirac factor ordering special. Unlike reduced quantization, remarkable similarities are discovered between Dirac quantization on the physical state space and other curved space quantization schemes. Nevertheless, the Dirac factor ordering retains some dependence on the gauge structure of the theory; it could not have been guessed working strictly within the classical reduced theory. This sheds new light on the Dirac versus reduced quantization debate, as well as curved space quantization in general. Author (CISTI)

N94-30164 International Centre for Theoretical Physics, Trieste (Italy).
MAGNETIC PROPERTIES OF THE THREE DIMENSIONAL ISING MODEL WITH INTERFACE SINGLE-ION ANISOTROPY
A. Benyoussef (Mohammed V Univ., Rabat, Morocco.), A. ElKenz (Mohammed V Univ., Rabat, Morocco.), H. Ez-Zahraouy, and T. Kaneyoshi Sep. 1993 25 p Limited Reproducibility: More than 20% of this document may be affected by microfiche quality
(DE94-608116; IC-93/300) Avail: CASI HC A03 (US Sales Only)

Within the framework of effective-field theory, we investigate the effects of an interface single-ion anisotropy on the magnetic properties in the simple cubic spin-1/2 Ising model. We find a new tricritical behavior of the interface magnetization depending on the strength of the ferromagnetic perpendicular exchange interaction the spin between the spins at the interface and their neighbors in the next layers in the right and left sides. The magnetic behavior of an interface coupled antiferromagnetically to the two sides is also examined. DOE

N94-30167 International Centre for Theoretical Physics, Trieste (Italy).
THE BOND DILUTED SPIN-1 BLUME-EMERY-GRIFFITHS MODEL IN A TRANSVERSE FIELD
H. Ez-Zahraouy Sep. 1993 26 p Limited Reproducibility: More than 20% of this document may be affected by microfiche quality
(DE94-608121; IC-93/306) Avail: CASI HC A03 (US Sales Only)

The effect of Bond-dilution on the magnetic properties of a quantum transverse spin-1 Blume-Emery-Griffiths model is investigated within an expansion technique for cluster identities of a spin-1 localized spin system. The longitudinal and transverse magnetizations and quadrupolar moments are studied for several values of the bond concentration. A general formula, applicable to structures with arbitrary coordination number N, is given. DOE

N94-30169 Joint Inst. for Nuclear Research, Dubna (USSR).
THEORY OF FUNDAMENTAL INTERACTIONS
A. B. Pestov 1992 52 p Limited Reproducibility: More than 20% of this document may be affected by microfiche quality
(DE94-608126; JINR-E-2-92-537) Avail: CASI HC A04 (US Sales Only)

The theory of fundamental interactions is derived in a systematic way from the first principles. In the developed theory, there is no separation between space-time and internal gauge space. Main equations for basic fields are derived. In is shown that the theory satisfies the correspondence principle and gives rise to new notions in the considered region. In particular, the conclusion is made about the existence of particles which are characterized not only by the mass, spin, charge but also by the moment of inertia. These are rotating particles, the particles which represent the notion of the rigid body on the microscopical level and give the key for understanding strong interactions. The main concepts and dynamical laws for these particles are formulated. The basic principles of the theory may be examined experimentally not in the distant future. DOE

N94-30170 International Centre for Theoretical Physics, Trieste (Italy).
PERIODIC ELECTROMAGNETIC VACUUM IN THE TWO-DIMENSIONAL YANG-MILLS THEORY WITH THE CHERN-SIMONS MASS
V. V. Skalozub, S. A. Vilensky, and A. Yu. Zaslavsky Jun. 1993 7 p Limited Reproducibility: More than 20% of this document may be affected by microfiche quality
(DE94-608128; IC-93/171) Avail: CASI HC A02 (US Sales Only)

The periodic vacuum structure formed from magnetic and electric fields is derived in the two-dimensional Yang-Mills theory with the Chern-Simons term. It is shown that both the magnetic flux quantization in the fundamental sell and conductivity quantization inherent to the vacuum. Hence, the quantum Hall effect gets its natural explanation. DOE

N94-30244 Ottawa Univ. (Ontario). Dept. of Physics.
PROCEDURES FOR BASIC INVERSE PROBLEMS: BLACK BODY RADIATION PROBLEM AND PHONON DENSITY OF STATES PROBLEM M.S. Thesis
Lixin Dou 1992 96 p
(ISBN-0-315-85757-9; CTN-94-61163) Copyright Avail: Micromedia Ltd., Technical Information Centre, 240 Catherine Street, Suite 305, Ottawa, Ontario, K2P 2G8, Canada HC/MF

The regularization method and the maximum entropy method are investigated and developed to solve some basic inverse problems in theoretical physics. Both of these numerical procedures are applied to the inverse black body radiation problem, concerned with the determination of the area temperature distribution of a black body source from spectral measurements of its radiation, and the inverse phonon density of states problem, which is defined to be the determination of the phonon density of states function from the measured lattice specific heat function at constant volume. These problems are ill-posed and can be expressed as a Fredholm integral equation of the first kind. It appears that both the regularization method and the maximum entropy method are successful in solving the two ill-posed problems. Generally, the two procedures can be applied to any inverse problem which belongs to the class of the Fredholm integral

equation of the first kind. A comparison with the two procedures to the Laplace transform method demonstrates the superiority of the regularization and maximum entropy methods. Author (CISTI)

N94-30433 Center for Mathematics and Computer Science, Amsterdam (Netherlands). Dept. of Computer Science.
THERMODYNAMICS OF COMPUTATION AND INFORMATION DISTANCE
Charles H. Bennett (International Business Machines Corp., Yorktown Heights, NY.), Peter Gacs (Boston Univ., MA.), Ming Li (Waterloo Univ., Ontario.), Paul M. R. B. Vitanyi (Amsterdam Univ., Netherlands.), and Wojciech H. Zurek (Los Alamos National Lab., NM.) Jun. 1993 18 p Limited Reproducibility: More than 20% of this document may be affected by microfiche quality
(Contract NF-62-376; NSF CCR-90-02614; NSERC-OGP-046506; NSERC-ISE-0046203) (ISSN 0169-118X)
(CWI-CS-R9341; ETN-94-95683) Copyright Avail: CASI HC A03

Intuitively, the minimal information distance between x and y is the length of the shortest program for a universal computer to transform x into y and y into x. This measure is shown to be, up to a logarithmic additive term, equal to the maximum of the conditional Kolmogorov complexities E(sub 1)(x,y) = max(K(y/x), K(x/y)). Any reasonable distance to measure similarity of pictures should be an effectively approximable, symmetric, positive function of x and y satisfying a reasonable normalization condition and obeying the triangle inequality. It turns out that E(sub 1) is minimal up to an additive constant among all such distances. Hence it is a universal 'picture distance', which accounts for any effective similarity between pictures. A third information distance, based on the ideal that the aim should be for dissipationless computations, and hence for reversible ones, is given by the length E(sub 2)(x,y) = KR(y/x) = KR(x/y) of the shortest reversible program that transforms x into y and y into x on a universal reversible computer. It is shown that also E(sub 2) = E(sub 1), up to a logarithmic additive term. It is remarkable that three so differently motivated definitions turn out to define one and the same notion. Another information distance, E(sub 3), is obtained by minimizing the total amount of information flowing in and out during a reversible computation in which the program is not retained, in other words the number of extra bits (apart from x) that must be irreversibly supplied at the beginning, plus the number of garbage bits (apart from y) that must be irreversibly erased at the end of the computation to obtain a 'clean' y. This distance is within a logarithmic additive term of the sum of the conditional complexities, E(sub 3)(x, y) = K(y/x) + K(x/y). Using the physical theory of reversible computation, the simple difference K(x) - K(y) is shown to be an appropriate (universal, antisymmetric, and transitive) measure of the amount of thermodynamic work required to transform string x into string y by the most efficient process. ESA

N94-30750# Los Alamos National Lab., NM.
SPACE-TIME SYMMETRIES: P AND CP VIOLATION
D. V. Ahluwalia, M. B. Johnson, and T. Goldman 1993 4 p Presented at the 3rd International Wigner Symposium, Oxford, England, Sep. 1993
(Contract W-7405-eng-36)
(DE94-005012; LA-UR-93-4314; CONF-9309322-1) Avail: CASI HC A01/MF A01

We begin with a few remarks on an explicit construction of a Bargmann - Wightman - Wigner-type quantum field theory in which bosons and antibosons have opposite relative intrinsic parities. We then construct (1,0) circle plus (0,1) Majorana (CP self conjugate) and Majorana-like (C Gamma(sup 5) self conjugate, Gamma(sup 5) = chirality operator) fields. We point out that this new structure in the space time symmetries may be relevant to P and CP violation. DOE

N94-30950 North Carolina State Univ., Raleigh.
AN INVESTIGATION INTO CERTAIN GEOMETRICAL AND VARIATIONAL PROPERTIES OF THE P(4) THEORY OF GRAVITATION AND ELECTROMAGNETISM Ph.D. Thesis
Jimmie Herbert Chilton 1993 140 p
Avail: Univ. Microfilms Order No. DA9326983

We propose a Lagrangian for the P(4) theory of gravitation and electromagnetism which is a straightforward generalization of the Einstein Lagrangian of general relativity. A constrained Palatini variation of this Lagrangian yields the Einstein-Maxwell affine field equations. The Lagrangian is extended to account for electric, magnetic and matter sources. Also examined are the conservation laws arising from the invariance properties of the Lagrangian. A generalization of this Lagrangian of the Born-Infeld type is proposed with the goal of producing a P(4) theory of the classical electron which avoids the infinite self-energy problem. The attempt is successful but in the process the analogy between the electromagnetic and gravitational sectors of the Lagrangian is weakened and a mild restriction is placed on the assumption that classical charged particles follow affine 4-momentum geodesics. The Bianchi identities for the P(4) theory are decomposed into the standard O(1, 3) Riemannian Bianchi identity plus an additional R(sup 4*) component. When combined with the Einstein-Maxwell affine field equations the R(sup 4*) component implies conservation of magnetic charge and the standard wave equation for the Maxwell field strength in a curved space time. We show that our development is the analog of the manner in which the Riemannian Bianchi identity when combined with Einstein's field equation imply conservation of stress-energy-momentum and the wave equation for the Lanczos H-tensor. The analog between the Lanczos H-tensor and the Maxwell field strength is examined in more detail by the P(4) generalization of the variational principle from which the Lancros H-tensor first arose. We construct by analogy additional terms for the Lanczos Lagrangian which are thought of as comprising the electromagnetic sector of the total Lagrangian. Variation of the total Lagrangian leads to simultaneous creation of alternative potential structures for both the gravitational and electromagnetic sectors in terms of the Lagrange multipliers which multiply the constraints to the O(1, 3) and R(sup 4*) components of the P(4) Bianchi identity. Dissert. Abstr.

80 SOCIAL SCIENCES (GENERAL)

Includes educational matters.

N94-28746*# Michigan State Univ., East Lansing. Dept. of Physics and Astronomy.
THE SEVENTH ANNUAL NATIONAL CONFERENCE OF BLACK PHYSICS STUDENTS Summary Report
Gerard M. Crawley 1993 44 p Conference held in East Lansing, MI, 12-13 Feb. 1993
(Grant NAGw-3214)
(NASA-CR-195735; NAS 1.26:195735) Avail: CASI HC A03/MF A01

The National Conference of Black Physics Students began in 1986 when several Black physics graduate students at MIT and Harvard decided to address the 'pipeline problem' of African Americans in physics by organizing a conference for Black physics undergraduates. The goals of the conference were: (1) to develop a network within the Black physics community, (2) to make Black students in physics, particularly at graduate level, aware of academic and professional opportunities and (3) to bring important issues and developments in the field to the attention of these students. We are pleased to announce the Seventh Annual National Conference of Black Physics Students held February 12 and 13, 1993 served the largest population of students so far. The largest conference previous to this one hosted 150 students. We registered and prepared for 240 students with 210 actually attenting. We received so many qualified abstracts for technical talks by students that instead of NCBPS's tradition of 3-4 student presentations, we ran 4 parallel sessions in different rooms with 4-5 presentations in each room. In response to comments from previous conferences, the program contained 3 workshop/discussion sessions. The topics for the interactive discussion workshops were: 'Getting Ready for Graduate School,' 'How to Succeed in Graduate School,' and 'Issues Facing Black Scientists.' Derived from text

81 ADMINISTRATION AND MANAGEMENT

Includes management planning and research.

N94-28474# Lawrence Livermore National Lab., CA.
RISK-BASED PRIORITIZATION: A COMPARISON OF APPROACHES
R. S. Strait Oct. 1993 6 p Presented at the 2nd Probabilistic Safety Assessment and Management Conference (PSAM), San Diego, CA, 20-24 Mar. 1994

(Contract W-7405-eng-48)
(DE94-003368; UCRL-JC-115244; CONF-940312-47) Avail: CASI HC A02/MF A01

The use of analytical techniques for risk-based prioritization, both quantitative and non-quantitative, is becoming much more wide spread and organizations are tailoring analytical techniques for risk management to their particular needs. This has led to the use of different techniques for different applications within the same organization, and correspondingly, the need for management to reconcile the process and results of different risk-based prioritization approaches. Different risk-based prioritization methods may be used to prioritize different types of activities, but eventually these prioritizations may need to be integrated to allocate organizational resources at a higher level or to develop an overall organizational budget. This paper focuses on comparing and contrasting the different risk-based approaches. The objective is to help management understand the different approaches, choose the best approach for their needs, and reconcile different approaches. DOE

N94-28779# Naval Surface Warfare Center, Dahlgren, VA.
SOLID-STATE, ACTIVE-PHASED ARRAYS: SOME ASPECTS OF RECEIVER DESIGN Final Report
Joseph D. Harrop Feb. 1994 142 p
(AD-A275893; NSWCDD/TR-93249) Avail: CASI HC A07/MF A02

The Navy's use of solid-state transmitter technology has been limited to communication equipment or other uses requiring relatively low power, low frequency, or both. It has now become necessary to address some of the issues and tradeoffs involved in the design of transmit/receive modules so that active phased-array characteristics can be fully understood. The analytical work performed here determines the general relationship among the system noise figure and the third-order intercept requirements of phased-array receivers and the effect on noise figure of adding receive-attenuation to implement weighting (taper) of the array elements. DTIC

N94-28796# University of Central Florida, Orlando.
EFFECTS OF WORKLOAD ON COMMUNICATION PROCESSES IN DECISION MAKING TEAMS Final Report
Julie M. Urban, Clint A. Bowers, Ben B. Morgan, Jr., and Susan D. Monday 14 Dec. 1993 90 p
(AD-A275894; TR-93-01) Avail: CASI HC A05/MF A01

This report is a continuation of the research first described by Bowers and his colleagues and attempts to investigate those variables which, according to a broad model of team performance, might contribute to a more thorough understanding of team decision making. While the goal of the previous study was to determine the relative effects of two different team structures and two workload levels on team processes and performance, the current investigation incorporated a third structure into the previously employed design. The team structure that was simulated in the current study is a structure that is prevalent in organizations and operational environments, and hence, enhances generalizability to operational teams. Therefore, this report describes the evaluation of the relative performance effectiveness of these three structures under two levels of workload, as well as the identification of team coordination processes associated with effective decision making within these groups. DTIC

N94-28905# Naval Postgraduate School, Monterey, CA.
THE MANAGEMENT ISSUES OF IMPLEMENTING TELECOMMUTING: A CASE STUDY M.S. Thesis
Chuck H. Bane, Jr. Sep. 1993 95 p
(AD-A275267) Avail: CASI HC A05/MF A01

This thesis is a case study of the implementation of telecommuting by CalComp at the Telecommuting Workcenter of Riverside County and is a real life example of the management issues that surround telecommuting. The issues brought forth in this study will enable those responsible for implementing a telecommuting program to better understand the impact of this change on their organization and how a telecommuting center may be used in their program. Using this study as background, the military use of telecommuting for U.S. Navy detailers will be developed. Developing a peace time telecommuting program could help train Navy personnel to function as a remote staff member for a Battle Group or Joint Commander. A conceptual application of telecommuting for the Department of the Navy (DON) could be to allow selected officer and enlisted detailers to telecommute up to three days a week. This insight, properly used, will help program managers avoid problems that other programs have experienced during their transition to telecommuting. This insight, properly used, will help the program managers avoid problems other programs have had during the transition to telecommuting. Recommendations for further research and use of telecommuting for the Department of the Navy are provided. DTIC

N94-29153# Naval Postgraduate School, Monterey, CA.
EVALUATING THE ANALYTIC HIERARCHY PROCESS AND RECOMMENDED MODIFICATIONS FOR ITS USE IN MULTI-ATTRIBUTE DECISION MAKING M.S. Thesis
William H. McQuail Sep. 1993 80 p
(AD-A275065) Avail: CASI HC A05/MF A01

The Combined Arms Analysis Directorate of the Training and Doctrine Analysis Command (TRAC) uses the Analytic Hierarchy Process (AHP) to evaluate the contribution of modernization initiatives to U.S. Army capabilities. This thesis identifies several problems with using AHP. Most significantly, AHP can cause rank reversal of alternatives if a new alternative is considered, even if the new alternative has the same attribute levels as one of the previous alternatives. This thesis proposes several modifications that would improve results when AHP is used. It contains a different method of weight fitting that appears to provide alternative weights that are more accurate than the traditional AHP eigenvalue method. This thesis has two proposals for improving the nine point integer scale by which pairwise comparisons are made. Most significantly, this thesis proposes a modification to AHP that will maintain a ratio scale and avoid rank reversals. This last improvement requires the decision maker to establish and maintain units of measurement. Additionally, the decision maker must make comparisons of attributes to establish a meaningful scale not sensitive to the abundance or lack of alternatives considered. If units are maintained and the decision maker is consistent in the pairwise comparisons, there will be no rank reversals. DTIC

N94-30041 Pacific Northwest Lab., Richland, WA.
TRIPLE DIAGONAL MODELING: A MECHANISM TO FOCUS PRODUCTIVITY IMPROVEMENT FOR BUSINESS SUCCESS
L. O. Levine and L. D. Villareal Sep. 1993 7 p Presented at the 2nd International Symposium on Productive and Quality Improvement with a Focus on Government, Washington, DC, 8-10 Sep. 1993 Limited Reproducibility: More than 20% of this document may be affected by microfiche quality
(Contract DE-AC06-76RL-01830)
(DE94-004309; PNL-SA-21413; CONF-9309168-2) Avail: Issuing Activity (Department of Energy (DOE))

Triple Diagonal (M) modeling is a technique to help quickly diagnose an organization's existing production system and to identify significant improvement opportunities in executing, controlling, and planning operations. TD modeling is derived from ICAM Definition Language (IDEF 0)-also known as Structured Analysis and Design Technique. It has been used successfully at several Department of Defense remanufacturing facilities trying to accomplish significant production system modernization. TD has several advantages over other modeling techniques. First, it quickly does 'As-Is' analysis and then moves on to identify improvements. Second, creating one large diagram makes it easier to share the TD model throughout an organization, rather than the many linked 8 1/2 x 11 inch drawings used in traditional decomposition approaches. Third, it acts as a communication mechanism to share understanding about improvement opportunities that may cross existing functional/organizational boundaries. Finally, TD acts as a vehicle to build a consensus on a prioritized list of improvement efforts that hangs together as an agenda for systemic changes in the production system and the improved integration of support functions. DOE

N94-30698# Edgerton, Germeshausen and Grier, Inc., Idaho Falls, ID.
WHY TQM FAILS (AND WHAT YOU CAN DO ABOUT IT)
R. K. Smith 1993 7 p Presented at the 6th National Quality Management Conference, New Orleans, LA, 26-28 Jan. 1994
(Contract DE-AC07-76ID-01570)
(DE93-018945; EGG-M-93253; CONF-940127-1) Avail: CASI HC A02/MF A01

This report describes pit-falls of total quality management programs and provides suggestions towards getting started in a successful program.
DOE

N94-30824 Department of Energy, Washington, DC. Assistant Secretary for Environmental Restoration and Waste Management.
BENCHMARKING FOR COST IMPROVEMENT
Sep. 1993 88 p Limited Reproducibility: More than 20% of this document may be affected by microfiche quality
(DE94-002276; DOE/EM-0106P) Avail: CASI HC A05

The U.S. Department of Energy's (DOE) Office of Environmental Restoration and Waste Management (EM) conducted the Benchmarking for Cost Improvement initiative with three objectives: pilot test benchmarking as an EM cost improvement tool; identify areas for cost improvement and recommend actions to address these areas; and provide a framework for future cost improvement. The benchmarking initiative featured the use of four principal methods (program classification, nationwide cost improvement survey, paired cost comparison, and component benchmarking). Interested parties contributed during both the design and execution phases. The benchmarking initiative was conducted on an accelerated basis. Of necessity, it considered only a limited set of data that may not be fully representative of the diverse and complex conditions found at the many DOE installations. The initiative generated preliminary data about cost differences and it found a high degree of convergence on several issues. Based on this convergence, the report recommends cost improvement strategies and actions. This report describes the steps taken as part of the benchmarking initiative and discusses the findings and recommended actions for achieving cost improvement. The results and summary recommendations, reported below, are organized by the study objectives.
DOE

N94-30934# Advisory Group for Aerospace Research and Development, Neuilly-Sur-Seine (France). Technical Information Panel.
MARKETING TOOLS FOR INCREASING PROACTIVITY IN TECHNICAL INFORMATION CENTERS [LES OUTILS DE MARKETING DANS LA STIMULATION DE LA PROACTIVITE AU SEIN DES INFOCENTRES]
Christine A. Olson (Olson, Christine A. and Associates, Arnold, MD.) Feb. 1994 47 p
(AGARD-AR-326; ISBN-92-835-0737-1) Copyright Avail: CASI HC A03/MF A01

This publication is based on a presentation to the Technical Information Panel of AGARD given in April 1993 in Rome, Italy. It discusses the 'marketing' of library and information services, necessary even for services which do not charge their users, from a number of different aspects such as the need for a marketing information system, market research, positioning, products, pricing, placement, promotion, public relations, planning and auditing.
Author

82 DOCUMENTATION AND INFORMATION SCIENCE

Includes information management; information storage and retrieval technology; technical writing; graphic arts; and micrography.

For computer documentation see *61 Computer Programming and Software*.

N94-28414*# National Aeronautics and Space Administration. Goddard Space Flight Center, Greenbelt, MD.
NASA SPACE AND EARTH SCIENCE DATA ON CD-ROM
Syed S. Towheed Aug. 1993 29 p
(NASA-TM-109709; NAS 1.15:109790; NSSDC-WDC-A-R/S-93-27) Avail: CASI HC A03/MF A01

The National Space Science Data Center (NSSDC) is very interested in facilitating the widest possible use of the scientific data acquired through NASA spaceflight missions. Therefore, NSSDC has participated with projects and data management elements throughout the NASA science environment in the creation, archiving, and dissemination of data using Compact Disk-Read Only Memory (CD-ROM). This CD-ROM technology has the potential to enable the dissemination of very large data volumes at very low prices to a great many researchers, students and their teachers, and others. This catalog identifies and describes the scientific CD-ROM's now available from NSSDC including the following data sets: Einstein Observatory CD-ROM, Galileo Cruise Imaging on CD-ROM, International Halley Watch, IRAS Sky Survey Atlas, Infrared Thermal Mapper (IRTM), Magellan (MIDR), Magellan (ARCDR's), Magellan (GxDR's), Mars Digital Image Map (MDIM), Outer Planets Fields & Particles Data, Pre-Magellan, Selected Astronomical Catalogs, TOMS Gridded Ozone Data, TOMS Ozone Image Data, TOMS Update, Viking Orbiter Images of Mars, and Voyager Image.
Derived from text

N94-28615 Joint Inst. for Nuclear Research, Dubna (USSR).
THE PROGRAM FOR CATALOGIZATION OF MAGNETIC TAPES IN EXCHARM EXPERIMENT
A. F. Kamburyan and Yu. K. Potrebenikov 1993 7 p In RUSSIAN Limited Reproducibility: More than 20% of this document may be affected by microfiche quality
(DE94-606271; JINR-R-10-93-40) Avail: CASI HC A02 (US Sales Only)

The features of catalogization program created in frames of database management system CLARION are described. The simplicity of the program organization, its updatability and extendability allow one to use it for analogue purposes in other experiments.
DOE

N94-28637# Army Research Inst. for the Behavioral and Social Sciences, Alexandria, VA.
SIMULATION NETWORKING/TRAINING REQUIREMENTS RELATIONAL DATABASE: USER'S GUIDE Final Report, Aug. 1990 - Mar. 1993
Larry L. Meliza Nov. 1993 53 p
(AD-A275634; ARI-RP-94-01) Avail: CASI HC A04/MF A01

The Simulation Networking/Training Requirements Relational Database was developed to support analyses and training research projects for applying networked simulators to collective training. The collective tasks, subtasks, and standards described in armor platoon-, company team-, and battalion task force-level Mission Training Plan (MTP) documents form the core of the database. This core is supplemented with three types of data on each of over five thousand collective performance standards. The first type of data rates the extent to which the unit can perform the activities associated with each standard in the current simulation networking (SIMNET) environment. The second type of data provides information on how each of 41 potential enhancements to SIMNET would change the extent to which units can perform activities associated with each standard. This type of data ensures the utility of the database as new generations of network simulators are fielded. The third type of data identifies the source or sources of the data required to assess whether a unit meets performance standards in the networked simulator training environment. These data sources include data broadcast over the simulation network, unit plans for performing the mission, terrain data, tactical communications, and direct observation of behavior.
DTIC

N94-28640 Naval Postgraduate School, Monterey, CA.
SECURITY ASPECTS OF COMPUTER SUPPORTED COLLABORATIVE WORK M.S. Thesis
George V. Haroutunian, Jr. Sep. 1993 88 p Limited Reproducibility: More than 20% of this document may be affected by microfiche quality
(AD-A275638) Avail: CASI HC A05

Computer Supported Collaborative Work (CSCW) is a topic of considerable academic inquiry and rapid commercial development. Meeting Room Systems, Conferencing Systems, Co-authoring and Argumentation Systems, Message Systems, and Autonomous Agents which support group collaboration currently exist; however, Department of Defense (DoD) computer security requirements, as they impact CSCW system design, have received little attention. This thesis describes CSCW systems and relates group dynamic issues to predict the form of the sophisticated CSCW which will probably become commonplace in the future. Next the Trusted Computer Security Evaluation Criteria (TCSEC), with which all DoD systems must comply, are synopsized. An extension of the Bell-LaPadula model underlying the TCSEC requirements is proposed which would allow 'Functionally Trusted CSCW' (FT-CSCW), CSCW which would meet many but not all of the TCSEC requirements. Possible first order (efficiency) effects of FT-CSCW, including the effect of sparse group domains, the breakdown of compartmentation, and organizational stratification are discussed. Second order (social) effects are also discussed, as are possible FT-CSCW problems (unstable group membership, attempts to implement

Quality Improvement Circles, inter-group CSCW and the effect of visitors). Finally, some suggestions are made for future FT-CSCW research. DTIC

N94-28645 Purdue Univ., West Lafayette, IN. School of Industrial Engineering.
TOWARD A MODEL OF EXPERT KNOWLEDGE STRUCTURE AND THEIR ROLE IN COGNITIVE TASK PERFORMANCE Final Report, Nov. 1989 - Jun. 1993
Richard Koubek 1 Nov. 1993 90 p Limited Reproducibility: More than 20% of this document may be affected by microfiche quality
(Contract N00014-92-J-1153)
(AD-A275641) Avail: CASI HC A05

This project addressed the role of knowledge structure in skilled cognitive task performance. In particular, efforts focused on four areas: identification of attributes affecting the development of knowledge structures, derivation of theoretical dimensions for the knowledge structure construct, mapping the impact of knowledge structure on task performance, and derivation of automated knowledge structure measures. This project has provided information useful for the selection and training of personnel suggesting a focus on selecting and training individuals to develop the appropriate knowledge structure. Both the type of knowledge structures and examples of effective training methods are provided. Key unanswered questions include the following: (1) the development of a comprehensive matching algorithm between particular task features and the type of knowledge structure which is best suited for these task attributes, and (2) identification of individual difference characteristics which influence the type of knowledge structure developed. DTIC

N94-28820*# National Aeronautics and Space Administration. Marshall Space Flight Center, Huntsville, AL.
A SURVEY OF GEOGRAPHICAL INFORMATION SYSTEMS APPLICATIONS FOR THE EARTH SCIENCE AND APPLICATIONS DIVISION, SPACE SCIENCES LABORATORY, MARSHALL SPACE FLIGHT CENTER
D. Rickman, K. A. Butler, and C. A. Laymon Feb. 1994 40 p
(NASA-TM-108438; NAS 1.15:108438) Avail: CASI HC A03/MF A01

The purpose of this document is to introduce Geographical Information System (GIS) terminology and summarize interviews conducted with scientists in the Earth Science and Applications Division (ESAD). There is a growing need in ESAD for GIS technology. With many different data sources available to the scientists comes the need to be able to process and view these data in an efficient manner. Since most of these data are stored in vastly different formats, specialized software and hardware are needed. Several ESAD scientists have been using a GIS, specifically the Man-computer Interactive Data Access System (MCIDAS). MCIDAS can solve many of the research problems that arise, but there are areas of research that need more powerful tools; one such example is the multispectral image analysis which is described in this document. Given the strong need for GIS in ESAD, we recommend that a requirements analysis and implementation plan be developed using this document as a basis for further investigation. Author

N94-28903# Army Training and Doctrine Command, Fort Monroe, VA.
TRADOC LIBRARY AND INFORMATION NETWORK (TRALINET). UNION LIST OF PERIODICALS (TULIP) Final Report
Edwin B. Burgess, John W. Shields, David B. Conlin, and Russell P. Rafferty Dec. 1993 604 p Supersedes AD-A258935
(AD-A275263) Avail: CASI HC A99/MF A06

This is the sixth edition of the TRADOC Library and Information Network (TRALINET) union list of periodicals. It is a composite of the fifth edition and all changes submitted by TRADOC libraries. DTIC

N94-28911 Defense Technical Information Center, Alexandria, VA.
DEFENSE TECHNICAL INFORMATION CENTER CATALOGING GUIDELINES
Loretta Brown, comp., Claudine Long, comp, Sara Best, comp., Joyce Keith, comp., and Charles Reed, comp. Feb. 1994 155 p Supersedes DTIC/TR-91/5 dated Jan. 1992, AD-A246500 Limited Reproducibility: More than 20% of this document may be affected by microfiche quality
(AD-A275100; DTIC/TR-94/3; DTIC/TR-91/5) Avail: CASI HC A08

The guidelines for descriptive cataloging is a procedure manual published by the Defense Technical Information Center (DTIC) . It outlines the cataloging information to be included in the data fields for online input of technical publications. The text is arranged numerically, by field number, and includes Appendices A through N, with separate sections on special handling and search procedures for duplicate checking. Changes to the security classifications fields have been added to implement DoD 5200.1-R, Information Security Program Regulation. An enhanced version of this guideline for remote input is available as the Shared Bibliographic Input Manual. DTIC

N94-29053# Naval Postgraduate School, Monterey, CA. Dept. of Computer Science.
A PORTING METHODOLOGY FOR PARALLEL DATABASE SYSTEMS M.S. Thesis
Stanley H. Watkins Sep. 1993 97 p
(AD-A275256) Avail: CASI HC A05/MF A02

The Multibackend Database Supercomputer (MDBS) pioneered in the Naval Postgraduate School Laboratory for Database Systems Research offers an elegant solution to the four most pressing problems associated with the traditional approach to very large database management systems: capacity growth, performance improvement, data sharing, and resource consolidation. The purpose of this thesis is to develop a theory of system software portability for this large and complex network application which will facilitate others in the installation and utilization of MDBS. The first challenge is the almost total lack of documentation about MDBS software of use to system porters. A second set of issues revolves around the use of hardware by MDBS, particularly the use of mass storage devices for the storage and manipulation of base- and meta-data. A third challenge concerns the portability of system calls, shell programs, and the C language implementation. A final set of portability issues arises from the extensive use of inter-process and inter-machine communications by MDBS. DTIC

N94-29066# Naval Postgraduate School, Monterey, CA.
AN EVALUATION OF TECHNIQUES FOR RANKING ACADEMIC INFORMATION SYSTEMS JOURNALS M.S. Thesis
TeddiAnn S. Hayes and Winnie L. Huskey 23 Sep. 1993 68 p
(AD-A275179) Avail: CASI HC A04/MF A01

In an evolution from academic journal prestige ranking procedures used in economics, marketing, sociology and previous efforts in information systems (IS), this study developed prestige weights for IS journals based on a probability sample of 400 IS faculty in the United States and Canada. The weights are derived from subjective rankings by survey questionnaire. In addition to developing a master schedule of journal prestige weights, differences in prestige ranking are examined according to location of respondents' employing school, respondents' academic specialties within IS, types of degrees held by the respondents, and years in which respondents earned terminal degree at a graduate school with a national ranking. Characteristics of respondents are compared to nonrespondents to test the hypothesis the respondents are representative of the sample frame. Implications of the procedure developed here are discussed in terms of its application to evaluation of research productivity in DOD laboratories. DTIC

N94-29108 Rutherford Appleton Lab., Chilton (England).
OPERATION SEMANTICS WITH READ AND WRITE FRAMES
J. C. Bicarregui Dec. 1993 21 p
(PB94-138138; RAL-93-098) Avail: Issuing Activity (National Technical Information Service (NTIS))

The read and write 'externals' clauses in VDM implicit operation definitions play two distinct roles. On the one hand, they bind the free variables that appear in the preconditions and postconditions, whilst on the other hand, they can be understood to indicate the sets of state variables that an implementation of the operation can be permitted to 'read' and 'write'. However, in the case of the read frame, existing semantic models for VDM give no formal interpretation to this latter role. This paper investigates an extension to the denotational model of operations which captures this informal understanding of the read frame. It interprets the read frame via an extra constraint on the semantics of operations which formalizes the idea that the behavior of an operation should not depend on the variables outside the read frame. This semantics is shown to justify a new formalization of the satisfiability obligation and to yield a property of non-interference between operations with sufficiently disjoint frames.

However, some difficulties remain with this approach as a means of justifying algorithm refinement with read frames the resolution of which would require more substantial changes to the semantic model. NTIS

N94-29138# Naval Postgraduate School, Monterey, CA.
TOWARDS AN INFORMATION MODEL AND MECHANISMS FOR DESIGN RATIONALE CAPTURE AND USE M.S. Thesis
Debra A. Morris and Tina M. Paco Sep. 1993 89 p
(AD-A275060) Avail: CASI HC A05/MF A01

Every year the Department of Defense's (DoD) expenditures on software alone amount to almost ten billion dollars, with maintenance costs comprising the majority of this figure. Recent studies have indicated that an effective solution to help curtail the large maintenance cost is by capturing the rationale which was used to create the systems requirements and designs and using this information throughout the life cycle. However, various models proposed by current research for capture of design rationale address only some specific aspects of the design process rather than the entire design process. This thesis identifies the important components of a comprehensive design rationale information model, proposes mechanisms to facilitate their capture, and identifies the generic functionalities of a design rationale management tool to use the rationale in various systems development activities. DTIC

N94-29139# Naval Postgraduate School, Monterey, CA. Dept. of Computer Science.
NPSNET: INTEGRATION OF DISTRIBUTED INTERACTIVE SIMULATION (DIS) PROTOCOL FOR COMMUNICATION ARCHITECTURE AND INFORMATION INTERCHANGE M.S. Thesis
Steven R. Zeswitz Sep. 1993 79 p
(AD-A275061) Avail: CASI HC A05/MF A01

The Computer Science Department at the Naval Postgraduate School in Monterey, California has developed a low-cost, real-time interactive network based simulation system, known as NPSNET, that uses Silicon Graphics workstations. NPSNET has used non-standard protocols which constrains its participation in distributed simulation. DIS specifies standard protocols and is emerging as the international standard for distributed simulation. This research focused on the development of a robust, high-performance implementation of the DIS Version 2.0.3 protocol to support graphic simulation systems (e.g. NPSNET). The challenge was to comply with the standard and minimize network latency thereby maintaining the time and space coherence of distributed simulations. The resulting DIS Network Library consists of an application program interface (API) to low level network routines, a host of network utilities, and a network harness that takes advantage of multiprocessor workstations. The library was successfully tested on our local network and two configurations of a T-I based internet, the Defense Simulation Internet (DSI), with the Air Force Institute of Technology and Advanced Research Projects Agency. The testing confirmed that the semantics and syntax of the DIS protocol is properly implemented and the latency incurred by the network does not adversely effect the simulation application. DTIC

N94-29141# Helsinki Univ. of Technology, Espoo (Finland). Lab. of Graphic Arts Technology.
FUNDAMENTALS OF PRINTING TECHNOLOGY
H. J. Saarelma and P. T. Oittinen 1994 250 p
(PB94-132602; ISBN-951-22-1692-2) Avail: CASI HC A11/MF A03

The book has been written to fill the needs of course material at the basic course in printing technology given in the Laboratory of Graphic Arts Technology at Helsinki University of Technology. Depending on the extension of the course and its orientation at any given time, the material presented in the book can be covered to different depths. As is characteristic of basic courses, a lot of the subject matter deals with concepts, definitions, and principles. In addition to teaching students the basic vocabulary, the book tries to provide an overall framework of printing technology and to explain some of the key principles employed. NTIS

N94-29165# Naval Postgraduate School, Monterey, CA.
THE COVERING PROPERTY OF THE OBJECT-ORIENTED DATA MODEL: DESIGN AND IMPLEMENTATION ISSUES M.S. Thesis
Todd G. Estes and Eric M. Mueller Sep. 1993 120 p
(AD-A275048) Avail: CASI HC A06/MF A02

Inheritance is a necessary condition for construction of an object-oriented data model (OODM), but it is not sufficient. This is because inheritance applies to only one hierarchy. The covering construct meets this deficiency because covering maps an object in one hierarchy to a class of objects in another hierarchy. To date, covering has not been implemented into an existing OODM application. This thesis implements the covering construct into a functioning object-oriented database environment. Implementation was achieved through modification of data constructs and the creation of a user-defined relation linking two or more hierarchies. Using the Multi-model Multi-lingual Database Supercomputer (MDBS), a sample, working application is described illustrating real world applications. The results of this thesis show that the covering property can be implemented into an existing OODM without sacrificing the integrity of the data model. The cross-hierarchical mapping afforded by covering is a powerful construct that expands the capabilities of the model beyond pure inheritance. This makes the OODM suitable for a far wider range of applications. Together, inheritance and covering meet the necessary and sufficient conditions of the OODM. DTIC

N94-29167# Helsinki Univ. of Technology, Espoo (Finland). Dept. of Computer Science.
BATCH UPDATES AND CONCURRENCY IN B-TREES
K. Pollari-Malmi, E. Soisalon-Soininen, and T. Yloenen 1993 19 p Prepared for Suomen Akatemja, Helsinki
(PB94-136835; TKO-B106) Avail: CASI HC A03/MF A01

In many applications it is important to be able to insert (or delete) keys into a B-tree as a batch, instead of inserting them one by one. Moreover, it may be necessary to search the B-tree concurrently with the batch update. An example of this is a text database system supporting a newspaper house: all words (keys) of each article obtained from a news agency should be inserted at once, and, at the same time, searches should be allowed as efficiently as possible. We have designed two solutions to the problem of concurrent batch update. The first solution--implemented in our commercial text database system--optimizes the speed of the batch update, and the second solution optimizes the average search time during the batch update. NTIS

N94-29172 Helsinki Univ. of Technology, Espoo (Finland). Dept. of Computer Science.
ENGINEERING DOCUMENT MANAGEMENT SYSTEM
H. Peltonen, T. Maennistoe, K. Alho, and R. Sulonen 1993 19 p Limited Reproducibility: More than 20% of this document may be affected by microfiche quality
(PB94-136934; TKO-B109) Avail: CASI HC A03

The implementation of an engineering document management system (EDMS) is described. The system models CAD drawings and other engineering documents as objects, which can be composed of subdocuments and have multiple versions and representations. Documents contain user-defined attributes and the actual data for separate CAD tools. The documents are accessed with a server program, which stores document contents and attributes in a repository built on top of a relational database. The server accepts service requests from various client programs, including a graphical user interface. Document approval and release procedures can be described by means of user-defined state graphs. Access rights are controlled in a flexible manner with an authorization program. Attributes can be treated as active data by means of procedures which enforce dependencies between attribute values. NTIS

N94-29182 Tera Computer Co., Seattle, WA.
I/O ON THE TERA FILE SYSTEM
5 Feb. 1993 8 p Limited Reproducibility: More than 20% of this document may be affected by microfiche quality
(AD-A275278) Avail: CASI HC A02

This document describes the mechanism for performing input and output on the Tera File System. In particular, we discuss the functional characteristics of the read(), write(), mmap(), and munmap() system calls as they are implemented on Tera. DTIC

N94-29533 Union Coll., Schenectady, NY.
INFORMATION ENGINEERING IMPLEMENTATION AND ACCEPTANCE Ph.D. Thesis
Michael Abellera Sobremonte 1992 81 p
Avail: Univ. Microfilms Order No. DA9311966

The purpose of this study is to determine if difficulties in Information Engineering (IE) implementation and its acceptance in an Information Systems (IS) environment are a result of inaccurate expenditure reporting, lack of top-level management support, and ineffective personnel culture change. In addition, the study aims to provide an in-depth review of the IE approach, its methodology, techniques, and tools. According to the study, inaccurate expenditure reporting is not a problem that contributes to the difficulties in implementing IE. Lack of top-level management support hinders IE implementation and acceptance indicated by 81 percent of the respondents. Culture change, or lack thereof, contributes to the difficulty in implementing IE as indicated by 94 percent of the sample population. In addition, most of the respondents from all categories have indicated their interest to train and participate in future IE workshops, seminars, and forums. Respondents acknowledged that IE is a disciplined approach to Information Systems design and development, based on stable data models and structures. IE aims to ensure correct user requirements identification at all levels of an organization and to guarantee that these requirements can be implemented in an integrated, cost-justified system. IE provides concepts that can be applied both at the corporate level to support long-range information systems planning and at the systems architecture level to develop effective computer-based systems. These IE concepts and principles make IE an effective Information Systems development approach. The in-depth IE review may help project managers better explain the IE approach to top-level management -- the risk involved, the initial high cost of investment, and the potential benefits for implementing IE. The study stresses the importance of strong and on-going high level management support and the need for adequate culture change from end users in order to support an effective and successful IE implementation. The findings may assist IS practitioners and IE experts in developing new strategies for implementing IE more effectively. Ultimately, the study may lead to a wider acceptance of IE in the IS environment. Dissert. Abstr.

N94-29535 Georgia Inst. of Tech., Atlanta.
ON CONCEPTUAL DESIGN OF ACTIVE DATABASES Ph.D. Thesis
Asterio Kiyoshi Tanaka 1992 182 p
Avail: Univ. Microfilms Order No. DA9315916

An active database management system (DBMS) is a system with full database functionality plus the additional capabilities of monitoring the state of the database and executing some predefined actions when appropriate events are detected. Although this is a well-established research area, and a few commercial relational DBMS's already support some active capabilities, no support for conceptual modeling and design of active database behavior is currently provided to take advantage of the new capabilities. The current database design methodology forces the user to defer major modeling decisions concerning the active behavior of the database to late stages of the design process, where the semantics of the real-world situations are obscured by the intricacies of the implementation model. This research addresses the conceptual design problem by incorporating active database behavior into the Entity-Relationship (ER) model, in the form of events and rules. The resulting Entity-Relationship Event-Rule (ER)(exp 2) model provides an extended architecture of tools for assisting the database designer in the task of specifying, analyzing, and translating active behavior into executable data definition statements in specific relational DBMS's. Meta-behaviors are identified that automatically enforce invariant properties of the model, along with user-defined integrity constraints. A high-level Petri net, e/r-net, whose places are events, transitions are rules, and net inscriptions are (ER)(exp 2) schema definitions is proposed as an analysis tool for validating the active behavior design. A prototype implementation of the extended architecture is described that takes advantage of the meta-data about the design process generated during the schema translation. The following benefits result from the extended data modeling and database design methodology: reduced database design and application development effort with the automatic generation of meta-behavior and translation of active behavior into executable DBMS language constructs; better control of the development of database applications by introducing precision in the specification of active behavior; and better quality of the overall design, with an interactive environment capturing the knowledge of application experts and automatically dealing with the DBMS constraints.

Dissert. Abstr.

N94-29537 Georgia Inst. of Tech., Atlanta.
THE EFFECTS OF INHERITANCE ON THE PROPERTIES OF PHYSICAL STORAGE MODELS IN OBJECT-ORIENTED DATABASES Ph.D. Thesis
Mary Jane Willshire 1992 132 p
Avail: Univ. Microfilms Order No. DA9315922

An important aspect of OODB is the concept of inheritance of properties down the class hierarchy. This thesis is the first to originate and name four data storage models for inherited instance variables: the repeat class, RC, implementing the logical view; the home class, HC, storing the data only once; the split instance, SI, splitting instances based on the class of origin; and the value triple, VT, using value triples and string pairs. We create a simulation and also generate a formal mathematical analysis to measure the performance of the models. For any set of parameter values, the numerical results are identical whether obtained from the simulation or by calculation. RC duplicates data which facilitates retrievals but is shown to result in high storage overhead and expensive writes. Thus RC is suitable for stable applications where space is not an issue. HC is a horizontal partitioning of the database and has no duplication. This facilitates write operations and reduces storage but complicates retrievals. This thesis shows that HC should be a good choice for a dynamic, general purpose application. SI is a vertical partitioning of the database with minor duplication. It is shown to have higher storage overhead than HC and the retrieval and write algorithms are more complicated because multiple classes are involved. Nevertheless, SI is also a good general purpose model. VT does not partition the database. VT requires the generation and storage of multiple identifiers and thus higher storage overhead. If clustering is enforced, then VT has good performance. But without clustering, this model is the worst of the four and should only be used in limited applications. In a parallel execution environment both HC and SI are shown to exhibit good speedup. However, HC is more limited and will not scale. SI maintains speedup over the range tested and will scale better than HC. We generated data allocation methods and parallel transaction algorithms, then tested the models under a mixed transaction load. This research provides the foundation for an OODB benchmark and demonstrates parallel execution benefits for an OODBMS.

Dissert. Abstr.

N94-29591 Texas A&M Univ., College Station.
DESIGN AND ANALYSIS OF CONCURRENCY CONTROL SCHEMES FOR HETEROGENEOUS DATABASE SYSTEMS Ph.D. Thesis
Heon Young Yeom 1992 125 p
Avail: Univ. Microfilms Order No. DA9315168

In Heterogeneous Database Systems (HDBS), concurrency control presents a new problem since serializability at the local level does not guarantee serializability at the global level. Several approaches have been proposed to solve the concurrency control problem in HDBS. However, most of the approaches either require some modification of the existing DBMS or put some restrictions on execution of the global transactions. The performance of these schemes are not studied very well. We propose a new scheme based on two phase processing of global transactions. In the first phase, the global transaction obtains all the locks for the data items to be accessed. The actual processing is performed in the second phase. Global locking is wed to resolve direct conflicts between the global transactions and indirect conflicts are handled by controlling the subtransactions using static locking for all the locking sites. Subtransactions are submitted to the timestamping sites only when other subtransactions for the locking site get all necessary locks. When lock predeclaration is possible, our scheme shows superior performance compared to other schemes. Even for the cases when locks cannot be predeclared, our scheme shows better performance if the DBMS provides enough database cache space. In addition to a detailed simulation model for the concurrency control performance, we present an analytic model for our scheme.

Dissert. Abstr.

N94-29677 Oregon Graduate Inst. of Science and Technology, Beaverton.
OBJECT-ORIENTED DATABASE SUPPORT FOR SCIENTIFIC DATA MANAGEMENT: A SYSTEM FOR EXPERIMENTATION Ph.D. Thesis
Hitomi Ohkawa 1993 210 p
Avail: Univ. Microfilms Order No. DA9320330

Scientific data management has recently become a critical research issue due to computerization and automation of scientific research procedures and the resulting explosion of electronic data. For proper

management of scientific data, adequate data types must be provided for representing the semantics of scientific data directly. Issues such as large data volume and data evolution are common among scientific applications, so traditional database support, such as storage management, are also beneficial to them. Current approaches such as standardized data formats and adoption of traditional databases do not accommodate the data support requirements of existing scientific applications well. Object-oriented databases, on the other hand, seem to hold promise, by combining flexible data models with traditional database support. In this dissertation, we constructed an experimental platform for exploring the design space for a scientific data management system. With this experimental approach, we could dynamically examine possible architectures for data support against actual instances of scientific data and typical operations executed on them. As many of the dynamic features of existing scientific applications, such as data access patterns, are yet to be discovered, the platform also provides an opportunity to explore such features. Based on the observed potential of object-oriented databases for scientific data management, the GemStone object-oriented database management system was chosen for the baseline data management architecture of the platform. Among scientific applications where better data support is desired, a scientific persistent language and data analysis environment called 'NewS' and applications using it were selected as a target for the study. Connecting NewS with GemStone provided a cost effective experimental platform where we could investigate a variety of scientific applications with single implementation. We incorporated GemStone into the NewS environment in such a manner that we could use existing NewS applications without modifications for experiments. We describe the design and implementation of our platform, GemStone-based NewS, and experiments performed on the platform. At the end, we describe primary contributions of the work, and assess whether or not our approach was a productive initial step toward improved scientific data management. Dissert. Abstr.

N94-29682# Helsinki Univ. of Technology, Espoo (Finland). Library System.

EVALUATION OF THE RESOURCE LIBRARY SYSTEM IN FINLAND

E. Toernudd 1993 60 p

(PB94-137734; OTA-KIRJASTO-A17) Avail: CASI HC A04/MF A01

The Finnish Council for Scientific Information and Research Libraries decided at its meeting on April 24, 1991 to have an inquiry made of the resource library system. The study was to examine the goals formulated for the system and their accomplishment with special reference to the use of the findings in the system of operating cost budgeting and in the development of LINNEA, the national network of research libraries using the American Virginia Tech Library System (VTLS) automation system. The integrated automated data processing system adopted by all major research libraries in the country greatly improves the opportunities to utilize the resource libraries. NTIS

N94-29803 Indiana Univ., Bloomington.

SCIENTIFIC AND TECHNICAL INFORMATION TRANSFER: PROMOTING INFORMATION ACQUISITION IN THE SAUDI ARABIAN INDUSTRIAL SECTOR Ph.D. Thesis

Sulaiman Ibn Saleh Alogla 1993 240 p

Avail: Univ. Microfilms Order No. DA9323225

The availability of scientific and technical information (STI) resulting from adequate information acquisition on as broad a scale as possible is indispensable to maintaining the vitality and international competitiveness of industry. This study therefore investigates the current status of STI transfer to the industrial sector in Saudi Arabia. The study has both a broad and an immediate purpose: The study's broad purpose is to contribute to efforts made by Saudi scholars in planning for development of a comprehensive national Saudi network system for STI; and its immediate purpose is to propose a methodology based on the concept of information transfer that can aid in transmitting information quickly and efficiently from information producers to ultimate users in Saudi industry. In order to accomplish the above purposes, the study examined the general characteristics of STI flow to Saudi industrial companies, acquisition patterns among various industries, and factors affecting information flow to the industrial sector. The study's variables were examined using a self-administered mail questionnaire supplemented by field visits to Saudi industries. A purposive sample of Saudi industries was taken by selecting those industries possessing libraries or information centers. Descriptive statistics were used for the study's data analysis. Based on the study's findings, it was found that Saudi industries acquired a large amount of information in one year, 1991. In acquiring information, Saudi industries used original producer nodes for domestic information and distributor nodes for foreign resources. Information most often was transferred directly from originating sources to industrial information centers, and the second most common means of transfer was through the use of one intermediary. Also based on the study's findings, there appeared to be many barriers affecting information transfer in the Saudi industrial sector, for instance, shortage of skilled Saudi information specialists, absence of acquisition tools, absence of professional industrial information centers, lack of cooperation between the public and industrial sectors, and lack of scientific impact on the highest levels of industrial management. These barriers can be minimized by the study's proposed information transfer system. The system presents ways in which Saudi industrial companies acquire information quickly and efficiently from foreign and domestic sources, and thus links information producers to ultimate users in Saudi industries. The system can be used by Saudi industries to improve and facilitate information service to their community users. Dissert. Abstr.

N94-29804 North Carolina Univ., Chapel Hill.

HUMAN AND INSTITUTIONAL FACTORS IN GIS IMPLEMENTATION BY LOCAL GOVERNMENTS Ph.D. Thesis

Zorica D. Budic 1993 391 p

Avail: Univ. Microfilms Order No. DA9324002

Large numbers of local governments in the U.S. engage in acquisition and implementation of geographic information systems (GIS). Among other factors, the human and the institutional factors appear as major obstacles to successful implementation of GIS technology and thus are very important determinants of adoption of the technology. Influence of personal and institutional factors on the adoption of GIS technology in local governments is the main focus of this research. It examines the process of GIS diffusion in local government and GIS management as it affects the implementation of GIS technology. The research employs case study and survey methodology. A multiple case study was conducted on four agencies in a county government setting. A mail survey was administered in 140 local government agencies located in North Carolina, on a sample of 627 employees, with 55.7 percent return rate. The research has dual units of analysis, local government agencies and individual employees within those agencies. It studies the relationship between people, organizations, and technology as the prime determinant of GIS implementation success. Founded on the theory of diffusion of innovations and research on organizational computing, this research achieves three objectives. First, it tests propositions that advance the perceptions, experience, attitudes, and communication behavior of current and prospective GIS users as they affect the employees' decisions to adopt or reject the GIS technology. Perceived relative advantage from using the technology and computer experience are found to strongly impact the adoption. Secondly, it isolates the major elements of GIS management, organizational environment, and organizational internal context which foster or impede the adoption of GIS technology in local government settings. Among those factors, provision of incentives for prospective users, GIS training, political support for GIS, organizational conflicts, stability of organizational internal environment, availability of resources, and motivation for incorporation of the technology are found to exert significant influence on the success of GIS implementation. And thirdly, it gains considerable insight into the process of diffusion of GIS technology within local governments. Complexity, dynamism, and idiosyncrasy are three major attributes that describe the process.

Dissert. Abstr.

N94-29806 North Carolina Univ., Chapel Hill.

ENHANCING PERFORMANCE OF FULL-TEXT RETRIEVAL SYSTEMS USING RELEVANCE FEEDBACK Ph.D. Thesis

Sung Been Moon 1993 208 p

Avail: Univ. Microfilms Order No. DA9324078

The primary purpose of the study is to improve the low precision often found in full-text retrieval systems. In order to enhance the low precision of full-text retrieval while retaining its high recall, relevance feedback mechanisms based on probabilistic retrieval models (binary independence model and two-Poisson independence model) were employed. This study investigates the performance of full-text retrieval systems before and after the incorporation of relevance feedback. Main effects and interaction effects

of three independent variables ((A) types of document representation, (B) term distribution models, and (C) incorporating relevance feedback) were examined using three repeated measures of ANOVA. It was observed that the tests of the main effect on A and C were significant, but the test of the main effect on B was not significant. There was no significant three-way interaction, but there were two-way interactions between the variables. The pattern of the interaction (between A and B) revealed that the retrieval effectiveness of using abstracts and titles deteriorated when moving from the BI model to the TPI model, while the retrieval effectiveness of full-texts improved. The pattern of the interaction (between B and C) indicated that the incorporation of relevance feedback gained more with the TPI model than the BI model. The analysis of the overall performance (average precision at 0.25, .50, and 0.75 recall levels), averaged over all 83 queries, showed that retrieval using abstracts and titles with the BI model outperformed the others, both with and without relevance feedback. On the other hand, it was found that retrieval performance of full-texts significantly improved after the incorporation of relevance feedback. In particular, the analysis of the retrieval performance of the seven queries having large numbers of relevant documents, after the incorporation of relevance feedback, revealed that the precision at relatively high recall levels of full-text retrieval exceeded that of retrieval using abstracts and titles. The findings of this study suggest that the use of abstracts/titles is better for retrieval than full-texts, and that relevance feedback be incorporated in full-text retrieval systems to enhance the low precision. Dissert. Abstr.

N94-29811 University of Southwestern Louisiana, Lafayette.
A UNIFIED FRAMEWORK FOR RETRIEVAL IN IMAGE DATABASES Ph.D. Thesis
Venkat Naidu Gudivada 1993 170 p
Avail: Univ. Microfilms Order No. DA9324600

Image Retrieval (IR) problem is concerned with retrieving images that are relevant to users' requests from a large collection of images, referred to as the image database. Since the image database application areas are very diverse, the features of the existing image database systems have essentially evolved from domain specific considerations. In order to provide a generic approach to the IR problem, we have introduced a unified framework for retrieval in image databases. The framework supports four generic retrieval types: Retrieval by Browsing (RBR), Retrieval by Non-semantic Attributes (RNA), Retrieval by Spatial Constraints (RSC), and Retrieval by Semantic Attributes (RSA). To support these generic retrieval types, we have proposed an image data model referred to as AIR. AIR data model employs multiple logical representations. The logical representations can be viewed as abstractions of physical images at various levels and help toward achieving domain independence. We identify and provide solutions to the following three major research issues that arise in the context of AIR data model: algorithms for processing RSC queries, methods for the identification of semantic attributes, and algorithms for processing RSA queries. An algorithm, referred to as SIM(sub R), is developed for processing RSC queries. SIM(sub R) is robust in the sense that it can deal with translation, scale, and rotation variances in images. Personal Construct Theory (PCT) from clinical psychology is introduced as a knowledge elicitation tool for systematically deriving semantic attributes to support RSA. Also, an algorithm for RSA (based on the knowledge elicited from a domain expert using PCT) is developed. This algorithm incorporates user relevance judgments in the form of preference relations and incrementally improves retrieval quality. Dissert. Abstr.

N94-29855 State Univ. of New York, Binghamton.
INFORMATION CENTER ASSESSMENT Ph.D. Thesis
Joan E. Hoopes 1993 256 p
Avail: Univ. Microfilms Order No. DA9326072

Information centers (IC's) need to justify their existence to general management. Although the IC is an accepted part of the organization, management needs an accounting of what the IC provides to the organization. Several assessment methods can be used. Critical success factors and end user satisfaction are two methods studied in this thesis. The objectives of this research are to provide IC managers with information regarding IC assessment practices and a set of practical assessment measures and tools that they can use, and to provide information for IC researchers about IC assessment that has been sorely lacking. These objectives were fulfilled by developing an assessment framework from the IC and assessment literature, two survey instruments to determine IC performance ratings and importance rankings of critical success factors (CSFs) by IC personnel and end users, and a usable end-user satisfaction questionnaire. The research findings indicate that assessment does take place in industry and that the most widely used and recommended assessment measure is end-user satisfaction. Critical success factors (CSF's) are a good indicator of IC health and can be used to determine its success. IC managers can monitor the CSF's to ensure the health of the IC. The proposed end-user satisfaction questionnaire is a useful measurement tool and can be used to help IC's achieve success. Dissert. Abstr.

N94-29921 Selskapet for Industriell og Teknisk Forskning, Trondheim (Norway).
HYPRA/TR: A TUPLE ORIENTED RECOVERY METHOD FOR A CONTINUOUSLY AVAILABLE DISTRIBUTED DBMS ON A SHARED NOTHING MULTI-COMPUTER
S. Hvasshovd 6 Jul. 1993 279 p Prepared in cooperation with DELAB, Trondheim, Norway
(PB94-141264; STF40-A93085) Avail: Issuing Activity (National Technical Information Service (NTIS))

The relational data base management system (DBMS) technology is a success in the commercial market place with respect to business data processing and related applications. This success is a result of cost effective application development combined with high data consistency. The success has led to the use of relational DBMS technology in other application environments requesting its traditional virtues, and at the same time adding new requirements. For example, the integration of relational DBMS technology with telecommunications has led to such requirements as transaction rates of 50,000 TPC-B equivalent transactions per second, transaction service availability of certain transaction classes of 99.9996%, and transaction response time under 10 milliseconds. The current trends in hardware price/performance and parallel technology make relational DBMS's which support very high transaction rates, very high availability, and soft real-time transaction response a cost effective possibility. This thesis describes a recovery method supporting the traditional high DBMS data consistency while offering very high transaction rates, continuous availability, and soft real-time transaction response. NTIS

N94-29948 Selskapet for Industriell og Teknisk Forskning, Trondheim (Norway).
SECURE NETWORK DATABASES: SURVEY AND ANALYSIS
S. O. Hvasshovd and S. Haug 22 Jun. 1993 77 p See also AD-A225528
(PB94-138492; STF40-A93074) Avail: Issuing Activity (National Technical Information Service (NTIS))

This report presents a survey and an analysis of multilevel secure database management systems (DBMS). The DBMS is assumed applied in network databases. Secure databases become of vital concern when customers are allowed to access mission critical telecommunication network databases. The report gives an overview of the major concerns of database security: Secrecy, consistency, and availability. The focus has been on the two first items. A survey and analysis of different architectural and policy approaches to mandatory and discretionary access control policies are given. Multilevel security affects a number of the internal mechanisms of a DBMS such as concurrency control and recovery. It is vital to choose policies that avoid covert channels. We have in the report developed a new concurrency control policy called advanced orange locking. A recovery method that goes with the advanced orange locking policy is developed. The recovery method is based on the ARIES recovery method. The report gives a survey of multilevel secure distributed DBMS's. We have in particular focused on management of cryptography keys as this is of particular concern in a secure DBMS. A scheme supporting mode autonomy with respect to cryptography key is proposed. NTIS

N94-29960 Maryland Univ., College Park.
PAUSING BEHAVIOR OF END-USERS IN ONLINE SEARCHING Ph.D. Thesis
Mu-Hsuan Huang 1992 270 p
Avail: Univ. Microfilms Order No. DA9315656

This research used an information processing approach to analyze the behavior of end-users in searching online bibliographic databases, emphasizing their pausing behavior. It is based on viewing the search as a

series of actions and pauses (rests). The end-users are 41 students and 3 faculty. After instruction, subjects searched throughout the semester, doing 79 searches. Nineteen did multiple searches. Pausing behavior was related to time as a measure of growing experience. Six hypotheses were supported by the results of ANOVA and t-tests: The searchers paused less frequently and for shorter periods as they progressed through searches. With more experience and practice, searchers moved more smoothly online, and the ratio of pausing to online time decreased over time. Over a series of searches or cycles within long searches, searchers gradually began to chunk more information between pauses, both in amount of time and in number of elements. Pauses related to syntax decreased over time. This study identified 250 reasons for pausing (e.g. to verify a set number, to choose appropriate term operator, to consider alternative terms) and 6 types of searches on the basis of pausing behavior. The six types of searches were highly associated with search fluency and the construction of a mental model. Types 1 and 2 describe gradations of fluent searches and Types 3 to 6 describe various slow searches. Type 1 and 2 searches were conducted by subjects who had more knowledge about the search topic and more experience in the search language and in CD-Rom searching. They generated fewer pauses and chunked more information online. They paused for shorter times and had a lower hesitation rate. The other types were conducted by subjects with less experience in the search language, in CD-Rom searching, and in the search topic. They made more syntax-related pauses (especially in the beginning of the searches), generated more and longer pauses, chunked less information online, and had a higher hesitation rate. Finally, as searchers gained more experience, they increased their search proficiency and became more fluent online. The changes of search level in multiple searches showed most searchers moved toward greater fluency. Dissert. Abstr.

N94-29961 Alabama Univ., Huntsville.
COMPUTER-BASED LINKING OF THESAURI Ph.D. Thesis
Amba Sanjeevi 1992 160 p
Avail: Univ. Microfilms Order No. DA9313069

Studies on database searching indicate that searching of multiple databases is on the increase. This searching requires the use of multiple thesauri, when a controlled vocabulary search is carried out. The use of multiple thesauri involves identification of terms in the different thesauri. The terms should be analogous to each other and substitutable for one another. The problem could be stated as: For each term in Thesaurus 1, associate a set of terms in Thesaurus 2, such that the retrieval based on the set of terms from Thesaurus 2 is as effective as the retrieval using the original term from Thesaurus 1. The study examined the feasibility of the vector-space model. The cluster-based approach was used to link terms from two thesauri, 'The Thesaurus of ERIC Descriptors' and the 'Thesaurus of Psychological Index Terms.' A set of documents, indexed by terms from the two thesauri, was identified and these common documents formed the basis of the study. Co-occurrences of ERIC and Psyc descriptors in the set of common documents were used to form clusters using the Single Link Method. The clusters contained both ERIC and Psyc terms to ensure linking at the time of clustering itself. Effectiveness of linking was checked by validating each cluster on the basis of pre-established criteria using Precision and Recall, two standard measures in information retrieval. The clusters generated were tested further on another set of documents common to both databases. It was demonstrated that the procedures developed can be used to link thesauri. The advantages of this approach are: linking is done on the basis of the thesaurus terms assigned as descriptors; flexibility in cluster formation is possible; changes in terminology or indexing policies will not affect the basic procedures developed; and problems of reconciling incompatibility among thesauri are circumvented. It was also found that (1) terms which are in a cluster or co-occur do not always exhibit thesaural relationships; (2) a term from one thesaurus is not always linked to only one term from the second thesaurus; and (3) lexically equivalent terms do not always co-occur. Dissert. Abstr.

N94-30079 Joint Inst. for Nuclear Research, Dubna (USSR).
PROGRAM SCREEN FOR ACQUISITION, VISUALIZATION, PROCESSING AND OUTPUT OF EXPERIMENTAL DATA
A. V. Rashevskij and B. Yu. Semenov 1992 15 p Limited Reproducibility: More than 20% of this document may be affected by microfiche quality
(DE94-608009; JINR-R-10-92-220) Avail: CASI HC A03 (US Sales Only)

The SCREEN program is intended for acquisition, visualization, processing, and output of experimental data for systems based on the IBM PC computer. The program provides for the two dimensional representation of data placed in data buffer on the display screen taking into account user-defined initial values and scales over the abscissa and ordinate axes. Data concerning the program speed are given. The program is written in TURBO PASCAL 6.0, and the executive module occupies 54 Kbytes including data buffers. DOE

N94-30099# Sandia National Labs., Albuquerque, NM.
SMART DOCUMENT SYSTEM (SDS) USED IN MANAGING DOE ORDER'S WITH ELECTRONIC ENGINEERING PROCEDURES
R. Graham and D. Robbins Dec. 1993 66 p
(Contract DE-AC04-94AL-85000)
(DE94-005076; SAND-92-2926) Avail: CASI HC A04/MF A01

The Microsoft (MS) Windows product is widely available for PC's. There exists many thousands of them at Sandia. All of the MS applications in Windows have a Help file. This help file informs the user 'how to' use and run that application. It is an 'on-line' manual. The 'Help Compiler' was obtained from Microsoft. Use of this compiler enables one to insert text in a form the MS 'Help Engine' recognizes. This means all of the features of the Help file, hypertext (hot links), browsing, searching, indexing, bookmarks, annotation, are available for your text. This turns a document into a 'Smart Document.' The use of this Smart Document System (SDS) for Engineering Procedures (EP's) is described. DOE

N94-30149*# National Aeronautics and Space Administration. Langley Research Center, Hampton, VA.
NASA/DOD AEROSPACE KNOWLEDGE DIFFUSION RESEARCH PROJECT. REPORT 23: THE COMMUNICATIONS PRACTICES OF US AEROSPACE ENGINEERING FACULTY AND STUDENTS: RESULTS OF THE PHASE 3 SURVEY
Thomas E. Pinelli, Rebecca O. Barclay, and John M. Kennedy Apr. 1994 56 p
(RTOP 505-90-00)
(NASA-TM-109085; NAS 1.15:109085) Avail: CASI HC A04/MF A01

The U.S. government technical report is a primary means by which the results of federally funded research and development (R&D) are transferred to the U.S. aerospace industry. However, little is known about this information product in terms of its actual use, importance, and value in the transfer of federally funded R&D. To help establish a body of knowledge, the U.S. government technical report is being investigated as part of the NASA/DOD Aerospace Knowledge Diffusion Research Project. In this report, we summarize the literature on technical reports and provide a model that depicts the transfer of federally funded aerospace R&D via the U.S. government technical report. We present results from our investigation of aerospace knowledge diffusion vis-a-vis the U.S. government technical report, and present the results of research that investigated aerospace knowledge diffusion vis-a-vis U.S. aerospace engineering faculty and students.
Author

N94-30150*# National Aeronautics and Space Administration. Langley Research Center, Hampton, VA.
NASA/DOD AEROSPACE KNOWLEDGE DIFFUSION RESEARCH PROJECT. REPORT 22: US ACADEMIC LIBRARIANS AND TECHNICAL INFORMATION SPECIALISTS AS INFORMATION INTERMEDIARIES: RESULTS OF THE PHASE 3 SURVEY
Thomas E. Pinelli, Rebecca O. Barclay, and John M. Kennedy Mar. 1994 62 p
(RTOP 505-90-00)
(NASA-TM-109067; NAS 1.15:109067) Avail: CASI HC A04/MF A01

The U.S. government technical report is a primary means by which the results of federally funded research and development (R&D) are transferred to the U.S. aerospace industry. However, little is known about this information product in terms of its actual use, importance, and value in the transfer of federally funded R&D. To help establish a body of knowledge, the U.S. government technical report is being investigated as part of the NASA/DOD Aerospace Knowledge Diffusion Research Project. In this report, we summarize the literature on technical reports and provide a model that depicts the transfer of federally funded aerospace R&D via the U.S. government technical report. We present results from our investigation of aerospace knowledge diffusion vis-a-vis the U.S. government technical report,

and present the results of research that investigated aerospace knowledge diffusion vis-a-vis U.S. academic librarians and technical information specialists as information intermediaries. Author

N94-30179# TRW Environmental Services, Las Vegas, NV.
THE EVOLUTION OF INFORMATION MANAGEMENT
E. Moak (Southern Services, Inc., Birmingham, AL.) and T. Reding 1993 12 p Presented at the Nuclear Information and Records Management Association Meeting, Augusta, GA, 2 Sep. 1993
(Contract DE-AC01-91RW-00134)
(DE94-004173; CONF-9309293-1) Avail: CASI HC A03/MF A01

Historical problems faced by records managers and data managers are described. Differences between the two roles are delineated. Future impacts of new technology on the two groups are discussed. Coordination efforts that could be made are outlined. DOE

N94-30329 Nijmegen Univ. (Netherlands). Dept. of Informatics.
MODELLING THE EVOLUTION OF INFORMATION SYSTEMS
J. L. H. Oei, H. A. Proper, and E. D. Falkenberg 20 Dec. 1992 24 p Sponsored by Netherlands Organization for Scientific Research Limited Reproducibility: More than 20% of this document may be affected by microfiche quality
(TR-92-36; ETN-94-95620) Avail: CASI HC A03

The need for information systems capable of evolving to the same extent as organization systems is addressed. A set of requirements for evolving information systems is presented, implying the importance of the time concept in these systems. On the basis of these requirements an architecture and a conceptual framework for evolving information systems is proposed. In the conceptual framework for update, distinction is made between recording, correction and forgetting. State transitions are considered on three different levels of abstraction: the event level, the recording level and the correction level. A formal specification of the transformation process between user update requests, primitive update requests, and the three level model for update is provided. ESA

N94-30330 Nijmegen Univ. (Netherlands). Dept. of Informations Systems.
GENETIC ALGORITHMS FOR OPTIMAL DATABASE DESIGN
P. vanBommel, C. B. Lucasius, and T. P. vanderWeide Feb. 1993 12 p Limited Reproducibility: More than 20% of this document may be affected by microfiche quality
(TR-93-01; ETN-94-95621) Avail: CASI HC A03

A genetic algorithm for the optimization of (internal) database structures, using a multicriterion objective function, is presented. This function expresses conflicting objectives, reflecting the well known time/space tradeoff. It is shown how the solution space of the algorithm can be set up in the form of tree structures (forests), and how these are encoded as fixed length strings. Genetic operators defined in terms of strings behave as if they manipulate tree structures. ESA

N94-30357 Nijmegen Univ. (Netherlands). Dept. of Information Systems.
TOWARDS A GENERAL THEORY FOR THE EVOLUTION OF APPLICATION DOMAINS
H. A. Proper and T. P. vanderWeide 31 Aug. 1992 11 p Sponsored by Netherlands Organization for Scientific Research Limited Reproducibility: More than 20% of this document may be affected by microfiche quality
(TR-92-22; ETN-94-95611) Avail: CASI HC A03

A study on evolving information systems is presented. A delimitation of the concept of evolution is discussed. The main result is a first attempt to a general theory for such evolution. In this theory, the underlying data model is a parameter, making the theory applicable for a wide range of modeling techniques. ESA

N94-30359 Nijmegen Univ. (Netherlands). Dept. of Information Systems.
EVOLVING INFORMATION SYSTEMS: MEETING THE EVER-CHANGING ENVIRONMENT
J. L. H. Oei, H. A. Proper, and E. D. Falkenberg 9 Oct. 1992 18 p Sponsored by Netherlands Organization for Scientific Research Limited Reproducibility: More than 20% of this document may be affected by microfiche quality
(TR-92-24; ETN-94-95613) Avail: Issuing Activity (European Space Agency (ESA))

To meet the demands of organizations and their ever changing environment, information systems are required which are capable of evolving to the same extent as organizations do. Such a system has to support changes of all time and application dependent aspects. Requirements and a conceptual framework for evolving information systems are presented. This framework includes an architecture for such systems, and a revision of the traditional notion of update. Based on this evolutionary notion of update (recording, correction, and forgetting) a state transition oriented model on three levels of abstraction (event level, recording level, correction level) is introduced. A running example is provided to illustrate the conceptual framework for evolving information systems. ESA

N94-30360 Nijmegen Univ. (Netherlands). Dept. of Information Systems.
A GENERAL THEORY FOR THE EVOLUTION OF APPLICATION DOMAINS
H. A. Proper and T. P. vanderWeide 3 Nov. 1992 25 p Sponsored by Netherlands Organization for Scientific Research Limited Reproducibility: More than 20% of this document may be affected by microfiche quality
(TR-92-26; ETN-94-95614) Avail: CASI HC A03

A study on evolving information systems is presented. A delimitation of the concept of evolution is discussed. The main results are a first attempt to a general theory for such evolutions, and a general study on the issue of type relatedness of object types. In this theory, the underlying data model is a parameter, making the theory applicable for a wide range of modeling techniques. ESA

N94-30361 Nijmegen Univ. (Netherlands). Dept. of Information Systems.
A FRAMEWORK FOR COMPARING CONCEPTUAL MODELLING LANGUAGES
T. A. Halpin (Queensland Univ., Brisbane, Australia.) and J. L. H. Oei Nov. 1992 12 p Limited Reproducibility: More than 20% of this document may be affected by microfiche quality
(TR-92-29; ETN-94-95616) Avail: Issuing Activity (European Space Agency (ESA))

In practice various methods are used for the conceptual modeling phase of information systems design. For a given application, a single method or even a mix of method components may be more appropriate. To judiciously select methods it is necessary to have some appreciation of their strengths and weaknesses. In some cases (for example re-engineering, or large scale schema integration) it may be necessary to translate between different modeling approaches. A framework for comparing conceptual modeling methods, from the viewpoints of expressive power and practicality (with respect to convenience, efficiency and learnability), is discussed. The general ideas are illustrated by comparing two popular methods (entity-relationship modeling and object-role modeling), with the formal comparison being presented at the metalevel. Extensions are suggested to widen the scope of the framework. ESA

N94-30362 Nijmegen Univ. (Netherlands). Dept. of Informatics.
A NOTE ON SCHEMA EQUIVALENCE
A. H. M. terHofstede, H. A. Proper, and T. P. vanderWeide Nov. 1992 7 p Limited Reproducibility: More than 20% of this document may be affected by microfiche quality
(TR-92-30; ETN-94-95617) Avail: CASI HC A02

Terminology for comparing the expressiveness of conceptual data modeling techniques, such as ER, NIAM, and PM, that are finitely bounded by their underlying domains, is introduced. Schema equivalence is considered, and effects of the sizes of the underlying domains are discussed. This leads to the introduction of the concept of finite equivalence. Examples of finite equivalence and inequivalence in the context of PM are given. ESA

N94-30699# Department of Energy, Oak Ridge, TN. Office of Scientific and Technical Information.
DOE NEW TECHNOLOGY: SHARING NEW FRONTIERS, APRIL 1, 1993 - SEPTEMBER 30, 1993
A. T. Tamura, ed. and D. M. Henline, ed. Dec. 1993 98 p
(DE93-041289; DOE/ER-0535P-3) Avail: CASI HC A05/MF A02

The purpose of DOE New Technology is to provide information on how to access specific technologies developed through research sponsored by DOE and performed by DOE laboratories or by DOE-contracted researchers.

This document describes technologies identified as having potential for commercial applications in addition to a catalog of current patent applications and patents available for licensing from DOE and DOE contractors. DOE

N94-30706 Los Alamos National Lab., NM.
USING STEREOSCOPIC IMAGING FOR VISUALIZATION APPLICATIONS
S. J. Adelson 1994 13 p Presented at the IS and T/Society of Photo-Optical Instrumentation Engineers (SPIE) Meeting on Electronic Imaging Science and Technology, San Jose, CA, 6-10 Feb. 1994 Limited Reproducibility: More than 20% of this document may be affected by microfiche quality
(Contract W-7405-eng-36)
(DE94-006247; LA-UR-94-0116; CONF-940247-1) Avail: CASI HC A03

The purpose of scientific visualization is to simplify the analysis of numerical data by rendering the information as an image. Even when the image is familiar, as in the case of terrain data, preconceptions about what the image should look like and deceptive image artifacts can create misconceptions about what information is actually contained in the scene. One way of aiding the development of unambiguous visualizations is to add stereoscopic depth to the image. Despite the recent proliferation of affordable stereoscopic viewing equipment, few researchers are at this time taking advantage of stereo in their visualizations. It is generally perceived that the rendering time will have to be doubled in order to generate the pair, and so stereoscopic viewing is sacrificed in the name of expedient rendering. We show that this perception is often invalid. The second half of a stereoscopic image can be generated from the first half for a fraction of the computational cost of complete rendering, usually no more than 50 percent of the cost and in many cases as little as 5 percent. Using the techniques presented here, the benefits of stereoscopy can be added to existing visualization systems for only a small cost over current single-frame rendering methods. DOE

N94-30918 Maryland Univ., College Park.
INFORMATION-SEEKING IN HYPERTEXT: MULTIPLE ACCESS METHODS IN A FULL-TEXT HYPERTEXT DATABASE Ph.D. Thesis
Peter Liebscher 1993 267 p
Avail: Univ. Microfilms Order No. DA9327456

This study focussed on the interaction between users, the system, and tasks during information retrieval in a full-text hypertext system. It drew on mental model theory to examine the users' views of information retrieval systems and how these views affected their information seeking behavior in a hypertext system offering multiple access methods. The access methods provided for this study were an alphabetical index, an hierarchical subject index, Boolean string search, and a network browser. Eleven undergraduate participants and one expert in hypertext systems were given a number of tasks and were observed intensively and individually over five sessions, each lasting approximately 2 to 2.5 hours. Access methods were used individually for the first four sessions. For the final session, all four access methods were available. Participants were given a total of 22 information retrieval tasks. Because the study was exploratory, no hypothesis testing was done. Eleven research questions served to guide the design of the protocols and the observations themselves. Results indicate that undergraduate users of new hypertext information systems use elements of existing mental models for information systems as they interact with the new system. Benefits are quick learnability of system syntax and the ability to apply known information-seeking strategies in the new environment. Drawbacks are inefficient or failed searches due to misapplication of mental models for familiar systems. String search proved to be the overwhelming choice of access method for hands-on retrieval tasks. Selection of string search was independent of task. Principal reasons for selection of string search were a desire to do word rather than conceptual searches and to minimize the amount of text scanned/read. Hypertext features, such as text embedded highlighted links, were also used to minimize reading. User characteristics, such as subject knowledge, computer experience, and gender, rather than task characteristics, were factors in selection of access method. Overall, participants were successful in their retrieval tasks, but more successful using string search and the network browser than using the indexes. However, success was often attained through serendipitous browsing which indicates that the relatively small size of the database was also a factor. Dissert. Abstr.

N94-30927 Politecnico di Milano (Italy). Dipt. di Elettronica e Informazione.
VIEW INTEGRATION: A SURVEY OF CURRENT DEVELOPMENTS
C. Francalanci and B. Pernici Jul. 1993 85 p Sponsored in part by CNR, and EEC
(Rept-93-053; ETN-94-95817) Avail: Issuing Activity (Politecnico di Milano, Piazza Leonardo da Vinci 32, 20133 Milan, Italy)

Past study of view integration has resulted in the standardization of the terminology and of the steps of the integration process. Nevertheless, the issues left open by past research and the evolution of database technology has originated a reconsideration of the problems related with view integration. This has happened not only in the database design context, but in other areas as well, such as artificial intelligence applications, repository design and maintenance, software requirement elicitation, yielding new approaches, new techniques and new tools for performing view integration. However, researchers in different fields have selected and studied the subset of integration problems that is related to the purposes of the specific context, so causing a proliferation of proposals isolating and investigating single problems. The set of integration problems separately studied in different contexts can be the basis of a framework for the comparative analysis of the different contributions. A classification of the integration problems studied in recent research work is proposed, and available results for each of them are illustrated, highlighting agreements and disagreements among solutions proposed in different contexts and under different hypotheses. ESA

N94-30929 Politecnico di Milano (Italy). Dipt. di Elettronica e Informazione.
MEASURING THE IMPACT OF INVESTMENTS IN INFORMATION TECHNOLOGIES ON BUSINESS PERFORMANCE
C. Francalanci and P. Maggiolini Sep. 1993 24 p
(Rept-93-056; ETN-94-95819) Avail: Issuing Activity (Politecnico di Milano, Piazza Leonardo da Vinci 32, 20133 Milan, Italy)

The relationship between performance and investments in information technologies are analyzed. The research is conducted by investigating the correlation between the aggregate annual expense in information technology and two indexes of firm performance, which are defined and justified. In the literature, this research stream is not particularly active, especially due to the failure of traditional business performance indicators; nevertheless, the positive results of some research works and the generally high interest of firms, especially within the current crisis context, inspired the study. A theory explaining the role of information technology in the organizations as a basis for the definition of the indexes of firm performance and for experience on the business data collected is presented. Results of experimentation are presented, illustrating trends confirming theoretical hypotheses and discussing possible causes motivating opposite trends. ESA

N94-29342# Alenia Spazio S.p.A., Rome (Italy).
APPLICATION OF INFORMATION MANAGEMENT METHODOLOGIES FOR PROJECT QUALITY IMPROVEMENT IN A CHANGING ENVIRONMENT
Fabrizio Sandrelli *In* AGARD, Aerospace Software Engineering for Advanced Systems Architectures Nov. 1993 6 p (For primary document see N94-29315 08-61)
Copyright Avail: CASI HC A02/MF A03

83 ECONOMICS AND COST ANALYSIS

Includes cost effectiveness studies.

N94-29144 Sussex Univ., Brighton (England). Inst. of Manpower Studies.
DEVELOPMENT CENTRES: ASSESSING OR DEVELOPING PEOPLE
C. Jackson and J. Yeates 1993 51 p
(PB94-138070; IMS-261) Copyright Avail: Issuing Activity (National Technical Information Service (NTIS))

The purpose of this research was to explore in detail the ways that companies were experimenting with using assessment centers for development purposes. Ten case study organizations were visited in the course of the research for this study. They were chosen for their varying

experience in the use of development centers. This report is intended as a summary of the main issues which arose during the case study visits. It is written for practitioners within organizations and focuses, in particular, on the issues concerned with the use of development centers. It is concerned with how information from a development center is used to foster individual career development within organizations, rather than on technical issues concerned with assessment methods. NTIS

84 LAW, POLITICAL SCIENCE AND SPACE POLICY

Includes NASA appropriation hearings; aviation law; space law and policy; international law; international cooperation; and patent policy.

N94-28540# Congress of the United States, Washington, DC.
OMNIBUS BUDGET RECONCILIATION ACT OF 1990
Washington GPO 5 Nov. 1990 632 p S. 3209 enacted into law by the 101st Congress, 5 Nov. 1990
(Pub-Law-101-508) Avail: CASI HC A99/MF A06; Subcommittee on Technology and Competitiveness, House of Representatives, Washington DC 20515 HC

The following topics are covered: agriculture and related programs; banking, housing, and related programs; student loans and labor provisions; medicare, medicaid, and other health-related programs; income security, human resources, and related programs; energy and environmental programs; civil service and postal service programs; veterans' programs; transportation; miscellaneous user fees and other provisions; revenue provisions; pensions; and budget enforcement. Author (revised)

85 URBAN TECHNOLOGY AND TRANSPORTATION

Includes applications of space technology to urban problems; technology transfer; technology assessment; and surface and mass transportation.

For related information see also *03 Air Transportation and Safety, 16 Space Transportation,* and *44 Energy Production and Conversion.*

N94-28405# Technical Research Centre of Finland, Espoo. Group of Technology Studies.
SPIN-OFF COMPANIES AS AGENTS OF TECHNOLOGY TRANSFER: AN EMPIRICAL STUDY OF THE SPIN-OFF COMPANIES OF THE TECHNICAL RESEARCH CENTRE OF FINLAND
Erkko Autio 1993 158 p
(ISSN 1235-0621)
(PB94-132248; VTT/PUB-151; ISBN-951-38-4389-0) Copyright Avail: CASI HC A08/MF A02

Spin-off companies constitute one important technology transfer channel between technical research institutes and their environment. Such companies thus constitute an important element of national systems of innovation. The technology transfer effects of companies spun off from technological research have only rarely been systematically analyzed. The present study expands the scope of analysis over the early life cycle of a new, technology-based company. For this purpose, a three stage model depicting the technology transfer effects of new, technology-based companies is developed. The empirical sample of the present study consists of 35 companies spun off from the Technical Research Center of Finland. The empirical data is gathered in personal interviews of the founders of the companies. In the interviews, structured questionnaires are used. NTIS

N94-29168 Helsinki Univ. of Technology, Espoo (Finland). Centre for Urban and Regional Studies.
CITIES FOR TOMORROW: DIRECTIONS FOR CHANGE
A. Haila 1993 103 p Limited Reproducibility: More than 20% of this document may be affected by microfiche quality
(PB94-136850; ISBN-951-22-1698-1) Avail: CASI HC A06

Contents: The Landscape of the Recession; Urban Land Policy, Ethics and Planning: A Finnish Point of View; The Change of Planning in Finland - and Its Cognitive Mapping; Future Challenges for Finnish Housing Policy; The Reaction of Finnish Localities to Restructuration Gateway - A Common Ground for Development of Helsinki; Lost Utopia - Thoughts on the Dilemma of the Modern City; Real Planning; Environmental Impact Assessment in Finland. NTIS

N94-29350*# National Aeronautics and Space Administration. Lewis Research Center, Cleveland, OH.
THICK THERMAL BARRIER COATINGS FOR DIESEL COMPONENTS Final Report
T. M. Yonushonis Aug. 1991 131 p Sponsored by DOE, Washington, DC Original contains color illustrations
(Contracts DEN3-331; DE-AI01-86CE-50162)
(NASA-CR-187111; NAS 1.26:187111; DOE/NASA/0331-1) Avail: CASI HC A07/MF A02; 1 functional color page

An engineered thick thermal barrier coating consisting of multiple layers of zirconia and CoCrAlY with a zirconia top layer and having a system thermal conductance less than 410 w/m(exp 2)K exceeded the 100 hour engine durability goals set forth in this program. The thermal barrier coatings were intact at the test conclusion. Back to back single cylinder research engine tests were conducted with watercooled, metal hardware and oil-cooled, thermal barrier coating insulated hardware to determine apparent heat release and fuel economy. Apparent heat release data revealed that the insulated engine had a shorter ignition delay and a longer combustion duration than the metal engine. The insulated engine fuel economy was approximately two percent worse on average for this series of tests. There was no attempt to optimize engine efficiency of the insulated engine by modifying the engine timing, coating, or other techniques. Author

N94-29410*# Alabama Univ., Huntsville.
TECHNOLOGY TRANSFER INITIATIVES Final Report, Apr. - Dec. 1993
Wayne McCain, Bernard J. Schroer, and M. Carl Ziemke Jan. 1994 92 p
(Contract NCC8-18)
(NASA-CR-195151; NAS 1.26:195151; CAR-94-02) Avail: CASI HC A05/MF A01

This report summarizes the University of Alabama in Huntsville (UAH) technology transfer activities with the Marshall Space Flight Center (MSFC) for the period of April 1993 through December 1993. Early in 1993, the MSFC/TUO and UAH conceived of the concept of developing stand-alone, integrated data packages on MSFC technology that would serve industrial needs previously determined to be critical. Furthermore, after reviewing over 500 problem statements received by MSFC, it became obvious that many of these requests could be satisfied by a standard type of response. As a result, UAH has developed two critical area response (CAR) packages: CFC (chlorofluorocarbon) replacements and modular manufacturing and simulation. Publicity included news releases, seminars, articles and conference papers. The Huntsville Chamber of Commerce established the Technology Transfer Subcommittee with the charge to identify approaches for the Chamber to assist its members, as well as non-members, access to the technologies at the federal laboratories in North Alabama. The Birmingham Chamber of Commerce has expressed interest in establishing a similar technology transfer program. This report concludes with a section containing a tabulation of the problem statements, including CAR packages, submitted to MSFC from January 1992 through December 1993.
Derived from text

N94-30926 Politecnico di Milano (Italy). Dipt. di Elettronica e Informazione.
OPTIMIZATION TECHNIQUES FOR A DIAL-A-RIDE TRANSPORTATION SYSTEM IN URBAN ENVIRONMENT
A. Colorni and G. Righini Jul. 1993 18 p Presented at the 6th Workshop on Scheduling of Public Transport, Lisbon, Portugal, 1993 Sponsored in part by CNR
(Rept-93-051; ETN-94-95816) Avail: Issuing Activity (Politecnico di Milano, Piazza Leonardo da Vinci 32, 20133 Milan, Italy)

The optimization of a dial-a-ride transportation system in urban environment presents a double combinatorial aspect: allocating customers to vehicles and routing every vehicle. The problem has two different versions: the static one, in which all requests for service are known in advance, and the dynamic one, in which the requests come at run time. Due to the

complexity of the problem it is necessary to design approximate algorithms, especially for the dynamic problem where tight bounds on the computing time must be satisfied. The problem is faced from two viewpoints: the model is defined, and in particular an objective function different from those usually mentioned in the literature and more coherent with the viewpoint of customers is proposed; an allocation routing algorithm, in which the allocation phase is performed with annealing techniques, while the routing phase takes some ideas from genetic algorithms, is proposed. Open research questions which will lead to future developments are indicated. ESA

88 SPACE SCIENCES (GENERAL)

No abstracts in this category.

89 ASTRONOMY

Includes radio, gamma-ray, and infrared astronomy, and astrometry.

N94-28671# Mission Research Corp., Nashua, NH.
CBSD: THE CELESTIAL BACKGROUND SCENE DESCRIPTOR Final Report, Apr. 1988 - Jan. 1993
J. P. Kennealy, P. V. Noah, E. F. Tedesco, R. M. Cutri, and S. F. Dermott Jan. 1993 257 p
(Contract F19628-88-C-0014)
(AD-A275521; PL-TR-93-2215) Avail: CASI HC A12/MF A03

This report documents the Celestial Background Scene Descriptor (CBSD) program which is a suite of models to simulate the radiance of astronomical sources. The model simulate the contribution of the celestial background in the wavelength regime 2 to 30 micrometers with a positional accuracy of 2 arcseconds. The output of the models are tables and images suitable for use in sensor simulation. The CBAMP model calculates the thermal radiance and scattered light for the solar system objects including the Sun, Moon, the planets, the Galilean Satellites, 4559 numbered asteroids, and 9643 unnumbered asteroids. The solar system dust cloud (Zodiacal light model CBZODY) uses a Lorentzian out of the plane dust density distribution to derive a number density from which the emitted and scattered radiances are computed. The stellar point sources model, CBPNTS, is a 'fast' running scene generator version of the Air Force/NASA/Ames statistical point source model, SKY. The sky is divided into 899 regions with size inversely proportional to stellar density. In addition, there are 87 different spectral classes, including 82 classes of stars, two classes each of planetary and reflection nebulae, and one of compact H2 regions. The nature of the galactic infrared cirrus is discussed. DTIC

N94-29001*# Lockheed Aircraft Corp., Palo Alto, CA. Research Lab.
X RAY STUDIES OF THE HYADES CLUSTER Final Report
Robert A. Stern 8 Oct. 1993 22 p
(Contract NAS5-32070)
(NASA-CR-189325; NAS 1.26:189325) Avail: CASI HC A03/MF A01

The Hyades cluster occupies a unique position in both the history of astronomy and at the frontiers of contemporary astronomical research. At a distance of only 45 pc, the Hyades is the nearest star cluster in the Galaxy which is localized in the sky: the UMa cluster, which is closer, but much sparser, essentially surrounds the Solar neighborhood. The Hyades is the prototype cluster for distance determination using the 'moving-cluster' method, and thus serves to define the zero-age main sequence from which the cosmic distance scale is essentially bootstrapped. The Hyades age (0.6-0.7 Gyr), nearly 8 times younger than the Sun, guarantees the Hyades critical importance to studies of stellar evolution. The results of a complete survey of the Hyades cluster using the ROSAT All Sky Survey (RASS) are reported. Author

N94-29170 Helsinki Univ. of Technology, Kylmaelae (Finland). Radio Research Station.
FINNISH ASTRONOMY DAYS, 1992-1993. PROCEEDINGS OF THE FINNISH ASTRONOMICAL SOCIETY
S. Pohjolainen, ed. and K. Lehtinen, ed. 1993 20 p Limited Reproducibility: More than 20% of this document may be affected by microfiche quality
(ISSN 0783-8751)
(PB94-136892; ISBN-951-22-1725-2) Avail: Issuing Activity (National Technical Information Service (NTIS))

Contents: Some new results of the strongest water maser source in our galaxy; Recent outburst in Markarian 421; Electronic communication in scientific work--short overview; SN 1993J in M81. NTIS

N94-29732 Yale Univ., New Haven, CT.
GLOBULAR CLUSTER PHOTOMETRY NEAR THE TURNOFF: BLUE STRAGGLERS, RELATIVE AGES, AND THE HORIZONTAL BRANCH Ph.D. Thesis
Ata Sarajedini 1992 360 p
Avail: Univ. Microfilms Order No. DA9315242

Using CCD color-magnitude diagrams of Galactic globular clusters in the B and V filter bands, we focus on the main sequence turnoff region and its usefulness in studying blue straggler stars, relative cluster ages, and the luminosity of the horizontal branch. In addition, we have measured several basic photometric parameters for the clusters in our program; these include NGC 288, NGC 3201, NGC 4372, NGC 4590 (M68), IC 4499, NGC 5897, NGC 6101, NGC 6171 (M107), NGC 6496, NGC 6584, NGC 6723, NGC 6809 (M55), NGC 6934, and NGC 6981 (M72). Of the 14 globular clusters in our sample, 11 appear to have definite blue straggler sequences. In the majority of cases, the blue stragglers are found to be more centrally concentrated and therefore more massive than the subgiant branch stars. Furthermore, the characteristics of the clusters which contain blue stragglers span practically the entire observed range for Galactic globular clusters. It therefore seems that all such systems must contain blue stragglers. The HR diagram of the blue stragglers reveals that all of these stars occupy the same general region of this diagram, but the mean location of the individual cluster sequences do scale with metal abundance in the expected fashion. Finally, the luminosity function indicates the possible identification of blue stragglers which have evolved away from their initial positions. There exists a range in age among the Galactic globular clusters of 3 to 5 gigayears. Such a range suggests a relatively slow formation timescale for the Galactic halo. In addition, from the variation of age as a function of horizontal branch type, we conclude that age is the 'second parameter' which, along with metallicity, governs the behavior of the horizontal branch. Finally, we derive a simple algebraic expression that describes the slope of the horizontal branch luminosity-metallicity relation in terms of three relative cluster parameters. Using available values of these quantities in 8 globular clusters, we compute a slope of 0.15 +/- 0.05 for the variation of horizontal branch luminosity with metallicity.
Dissert. Abstr.

N94-29795 Rochester Univ., NY.
ON OBSERVING NEUTRON STAR OSCILLATIONS Ph.D. Thesis
Tod E. Strohmayer 1992 258 p
Avail: Univ. Microfilms Order No. DA9304794

To investigate detecting and identifying neutron star oscillations in x ray sources, a technique for computing the light curves produced from polar cap hotspots on rotating, oscillating neutron stars is developed. The calculations include the effects of general relativity on the photon trajectories and allow for anisotropic beaming of radiation from the polar caps. A simple model, based on stellar oscillation, for the subpulse drift phenomenon observed in some radio pulsars is also described. Simulations of x ray observations of both x ray bursters and x ray pulsars using parameters appropriate to XTE and AXAF are investigated in order to assess the likelihood of detecting neutron star oscillations in these sources. To examine theoretically whether or not oscillations of neutron stars can modulate pulsar radio emission, a cylindrical model for the polar cap region of pulsars is investigated. An argument based on relativistic beaming allows estimation of the surface oscillation amplitude required to produce potentially observable variations in the beaming angle. For this model, short period modes require smaller surface displacements, and therefore less energy, to excite potentially observable variations. To investigate the hypothesis

that neutron star oscillations may be present in the radio emission from pulsars, radio pulsar data are analyzed for the presence of coherent periodicities. The analysis technique described here allows measurement of the coherence properties of pulsar signals. To test this method and interpret results from pulsar data several simulated pulsar models are constructed and analyzed. An analysis of 2000 consecutive pulses from PSR 2016 + 28 yields the following conclusions: The micropulse coherence time at 430 MHz is much less than the spin period of this object. This result could be consistent with a coherent model if the random phase jitter in such a model were greater than or equal to 35 percent of the micropulse quasiperiodicity. The subpulse separation, P(sub 2) approximately equals 10 ms, is coherent across four to five pulse periods, suggesting a higher Q-value for this process than for the micropulses. This coherence level is reasonably consistent with a model of subpulse drift that allows for random variation about some mean drift rate. Additional analysis of data from two other pulsars, PSR 1133 + 16 and PSR 0950 + 08, reveals no evidence for coherent oscillations in these objects as well.

Dissert. Abstr.

N94-29819 Dartmouth Coll., Hanover, NH.

THE CATACLYSMIC VARIABLES FROM THE PALOMAR-GREEN SURVEY Ph.D. Thesis

F. A. Ringwald 1993 299 p

Avail: Univ. Microfilms Order No. DA9322598

This thesis explores the cataclysmic variables (CV's) found by the Palomar-Green (PG) survey. This is the first compilation of a statistically complete sample of CV's found by ultraviolet color excess, and not outburst behavior. Blue and red follow-up spectrophotometry suggests that 22 of 68 objects classified originally as CV's are hot subdwarfs. Cool companions may be mimicking CVs' flat energy distributions, although the possibility remains that some are face-on CV's. Spectra taken with the International Ultraviolet Explorer prove useful for distinguishing difficult cases. With the CV sample defined, the orbital periods for eleven systems are investigated with radial velocity studies. At 16th magnitude, CV number counts increase by 2.3 mag(exp -1), although this may level off. The luminosity function is examined for the first time, and a trend toward higher space density at low luminosity is suspected. Outburst properties are compiled, and low-luminosity dwarf novae inflate the total space density to 6 x 10(exp -6) pc(exp -3). I describe all the PG CV's and candidate objects, and show spectra for most. This sample should be useful for population studies, such as measuring the space density with trigonometric parallaxes, or finding the fraction of eclipsing CV's. A new class of nova-likes, the SW Sextans stars, is characterized by absorption events of the emission lines at spectroscopic phase 0.5, accompanied by large phase lags between the lightcurves and the radial velocity curves and strong high-excitation emission. There are at least six such CV's in this sample of 33, so this mysterious behavior must be common and not peculiar, as previously thought. Five of these six objects eclipse. Serendipitous results for individual CV's include finding low-frequency quasi-periodic variations in the radial velocity curve of the dwarf nova BZ Ursa Majoris. While erratic from epoch to epoch, these are too coherent to be pure noise. Another dwarf nova, HX Pegasi, is caught with time-resolved spectrophotometry on the rise to outburst. This is the second-ever such observation, and the first with red spectra. HX Pegasi is also confirmed as having a novel subdwarf-K red star.

Dissert. Abstr.

N94-29820# Washington Univ., Seattle.

ABUNDANCE PATTERNS IN RED-GIANT CH STARS Ph.D. Thesis

Andrew Douglas Vanture 1992 172 p

Avail: Univ. Microfilms Order No. DA9312755

A detailed abundance analysis of seven red-giant CH stars has been conducted. Using high resolution echelle and coude spectrographic data and modern analysis techniques involving model stellar atmospheres and computer codes which model LTE radiative transfer, the abundances of carbon, nitrogen, and oxygen, the carbon isotope ratios, and the abundances of the s-process elements have been determined. The carbon isotope ratios are found to break the red-giant CH stars into two groups: those with C-12/C-13 greater than or equal to 20 and those with C-12/C-13 approximately equal to 4 (a value associated with equilibrium burning of the CN cycle). In addition, carbon and nitrogen abundances are found to be greatly enhanced, (C + N/Fe) approximately equal to +1.0. Lastly, it is found that the red-giant CH stars show large enhancements of the s-process elements with the enhancements of the heavy s-process peak elements (Ba through Sm) being larger than the light s-process peak elements (Sr, Y, and Zr) by a factor of approximately six. Taken with the orbital data available for the red-giant CH stars, these abundances are consistent with a picture in which carbon and s-process elements were dumped onto the incipient red-giant CH star from an AGB star in which the C-13(alpha,n)O-16 reaction was the source of neutrons for the s-process. In addition, the abundance patterns in the globular cluster CH star, M22 III-106, have been analyzed. It is found to have an abnormally large carbon abundance, but the C/O ratio is much less than unity and the star shows no evidence for enhanced abundances of the s-process elements. Therefore, M22 III-106 is most likely not a CH star in the sense that term is applied to galactic CH stars. The most probable explanation for the carbon overabundance in M22 III-106 is that CN processing has not been as complete in this star as in other giants of similar composition in M22.

Dissert. Abstr.

N94-29821 Texas Univ., Austin.

A MULTI WAVELENGTH OBSERVATIONAL STUDY OF THE CARTWHEEL RING GALAXY Ph.D. Thesis

James Lloyd Higdon 1993 254 p

Avail: Univ. Microfilms Order No. DA9323424

Ring galaxies are examples of extended starbursts triggered by a collisionally induced ring density wave. Because of their highly extended rings, high rates of inferred star formation, and the simplicity of the density wave, they offer advantages for the study of the starburst phenomenon. This work presents an observational investigation of the Cartwheel, a large and gas rich ring galaxy. CCD imagery in the H alpha, H beta, and (OIII) lambda 5007 emission lines is used to map the distribution and intensity of massive star formation and to determine properties in the HII regions. Off-line imagery is used to map the continuum intensity and color variations and to probe the stellar populations. VLA observations in the 21 cm line of hydrogen are used to measure the distribution and kinematics of the neutral atomic gas in the ring galaxy and its companions. Radio continuum mapping at 20 cm and 6 cm provides independent and extinction free tracers of massive star formation. Finally, (12)CO(1-0) observations are presented that constrain the mass of molecular gas in the starburst. The main conclusions of this study are: The Cartwheel's outer ring is experiencing a moderate starburst, though massive star formation is not measured anywhere else in the galaxy. A large radial color gradient spans the Cartwheel's disk, a fact consistent with a propagating starburst leaving large numbers of young massive stars in its wake. The observations are consistent with the outer ring triggering the first major episode of star formation. Moreover, the IMF appears biased towards massive star formation in the starburst. While 80 percent of the HI in the Cartwheel is organized into the outer ring, a low surface density distribution fills the interior. Noncircular motions are evident in the Cartwheel's HI velocity field, which are attributed to the infall of gas. Regions not experiencing massive star formation are characterized by low gas surface density, suggesting a threshold effect. Only the Cartwheel's outer ring is above the critical density for the growth of gravitational perturbations. The (12)CO(1-0) upper limit implies that the ISM of the Cartwheel is dominated by atomic gas on large scales.

Dissert. Abstr.

N94-29825 California Inst. of Tech., Pasadena.

A STUDY OF RECYCLED PULSARS IN GLOBULAR CLUSTERS Ph.D. Thesis

Stuart Bruce Anderson 1993 106 p

Avail: Univ. Microfilms Order No. DA9325333

We have performed a search for radio pulsars in 11 globular clusters visible from the 305 m Arecibo radio telescope. We have found 11 pulsars in the four clusters: M53, M13, NGC 6760, and M15; each containing one binary pulsar: 1310+18A, 1639+36B, 1908+00A, and 2127+11C, respectively; as well as a total of seven isolated pulsars: 1639+36A, 2127+11B, 2127+11D, 2127+11E, 2127+11F, 2127+11G, and 2127+11H. In this thesis we present the various search strategies employed and discuss the results of pulse time of arrival analysis for the seven isolated pulsars and the binary pulsar 2127+11C, as well as initial Doppler orbits for the binary pulsars 1310+18A and 1639+36B. The remaining pulsar 1908+00A is the subject of current research. The binary pulsar 2127+11C has been found to be in an 8 hour orbit about another degenerate star. The detection of a relativistic precession of the orbit and time dilation

effects constrain the pulsar and companion star masses to be m(sub p) = 1.34 +/- .23 solar mass and m(sub c) = 1.37 +/- .23 solar mass. Study of the radial positions and anomalous spin period derivatives of the seven isolated pulsars in M15 has revealed otherwise unobtainable information on the structure of this post core collapsed globular cluster. From the observed spatial pulsar distribution of n(sub p) varies as r(exp -3), it is inferred that the mass of isolated pulsars in M15 is approximately 1.4 solar mass. From the negative period derivative of PSR 2127+11A,D, it is inferred that the central mass-to-light ratio is greater than 1.9 solar mass/solar luminosity(sub U) and the central mass density is greater than 2.7 x 10(exp 6) solar mass pc(exp -3). From the observed isolated pulsar luminosity function in M15, Phi(L) varies as L(exp -0.93), and an assumed minimum luminosity of 1.0 mJy kpc(exp 2), it is inferred that the current population of observable isolated pulsars in M15 is O(100). The observed dispersion measures towards the eight pulsars in M15 and their relative spatial positions indicate that the spectrum of inhomogeneities in the interstellar medium observed at smaller length scales extends up to 10(exp 17) cm. Dissert. Abstr.

N94-29833 Johns Hopkins Univ., Baltimore, MD.
A MULTIWAVELENGTH STUDY OF TWO PROTOTYPICAL SUPERNOVA REMNANTS Ph.D. Thesis
Olaf Vancura 1993 222 p
Avail: Univ. Microfilms Order No. DA9313447

Multiwavelength observations are an important tool in the study of supernova remnants (SNR's) on large and small scales. In this thesis, we perform a detailed analysis of two SNR's, the Cygnus Loop and N49. We have used the Voyager 1 and 2 Ultraviolet Spectrometers to study the far-ultraviolet (FUV) emission from the Cygnus Loop. We find widespread emission from O VI lambda lambda 1032, 1038, and C III lambda 977 and we estimate total luminosities in these lines. We create the first FUV images of this remnant. Nonradiative and incomplete shocks contribute substantially to the FUV emission. We find that shocks with velocities greater than or equal to 160 km/s must be widespread even in the optically bright regions. We present a detailed imaging and spectroscopic study of N49 and find that most of the ultraviolet and optical emission emanates from shocks with velocities less than or equal to 140 km/s. However, O VI emission arises behind shocks with velocities approximately 200 km/s. A power-law shock velocity distribution corresponding to 40 km/s less than or equal to V(sub s) less than or equal to 270 km/s provides a good match to the data. We derive improved abundances for N49 and conclude by discussing implications for the interstellar medium surrounding the SNR. We develop a model invoking a Sedov solution in which the main blast wave also encounters large interstellar clouds. For this model, we demonstrate that the energies of N49's evolution as a whole and blast wave/cloud interactions on a smaller scale are self-consistent. Finally, we have constructed models that for the first time predict the dynamic evolution and emission properties of grains behind nonradiative shock waves. We predict observable IR grain and x ray plasma emissions, and we study the effects of varying the preshock density and shock velocity. Our predictions compare favorably to observations of the Cygnus Loop primary shock at IR and x ray energies. Dissert. Abstr.

N94-29957*# Arizona Univ., Tucson.
HIGH REDSHIFT QSOs AND THE X RAY BACKGROUND Final Report, 15 Feb. - 31 Oct. 1993
Chris Impey 1993 26 p
(Grant NAG5-1867)
(NASA-CR-195112; NAS 1.26:195112) Avail: CASI HC A03/MF A01

ROSAT pointed observations were made of 9 QSO's from the Large Bright Quasar Survey (LBQS). The LBQS is based on machine measurement of objective prism plates taken with the UK Schmidt Telescope. Software has been used to select QSO's by both color and by the presence of spectral features and continuum breaks. The probability of detection can be calculated as a function of magnitude, redshift and spectral features, and the completeness of the survey can be accurately estimated. Nine out of 1040 QSO's in the LBQS have z greater than 3. The observations will provide an important data point in the X-ray luminosity function of QSO's at high redshift. The QSO's with z greater than 3 span less than a magnitude in M(sub B), so can be combined as a homogeneous sample. This analysis is only possible with a sample drawn from a large and complete catalog such as the LBQS. Four of the 9 QSO's that were observed with the ROSAT PSPC for this proposal were detected, including one of the most luminous X-ray sources ever observed. The April 1992 version of the PROS DETECT package was used to reduce the data. The results have been used to search for evolution of the X-ray properties of QSO's in redshift. The 9 QSO's lie in the range -28.7 less than M(sub B) less than -27.8. When combined with data for 16 QSO's in a similar luminosity range at lower redshift correlations with luminosity and redshift can be separated out. The LBQS sample also yields a new constraint on the contribution of high redshift QSO's to the X-ray background. An initial requirement is knowledge of the X-ray properties (alpha(sub OX)) as a function of redshift. Integration over the evolving luminosity function of the LBQS then gives the QSO contribution to the source counts.

Author (revised)

N94-29971 Washington Univ., Seattle.
A NEAR-INFRARED SURVEY OF THE STAR FORMING REGION NGC 2264 Ph.D. Thesis
Francois Piche 1992 341 p
Avail: Univ. Microfilms Order No. DA9312731

We present the results of a large scale near infrared (J, H, K) survey of the star forming region NGC 2264. The survey covers 48' (Dec) x 27' (RA) with a completeness limit of 15.5, 14.5 and 14 magnitudes at J, H, and K respectively. Complementary observations of NGC 2023, NGC 2068, and NGC 7023 are also discussed. Young stars in NGC 2264 are concentrated in two clusters. The northern cluster is highlighted by the bright star S Mon. The infrared source NGC 2264 IRS, the molecular outflow NGC 2264D and the Cone Nebula are associated with the southern cluster. The northern cluster is divided into two subclusters, the southern cluster has three subclusters. The luminosity functions (LF's) of NGC 2264 subclusters have slopes in the range 0.28-0.30. This is also case for NGC 2068. NGC 2023's LF is shallower (0.21). There is a break in the LF of NGC 7023 around K = 10.5 magnitudes. All LF's are consistent with a Salpeter IMF and a Miller-Scalo IMF. For NGC 7023, we obtain a better agreement with a Miller-Scalo IMF. The differences in LF can be attributed to cluster ages. NGC 2023 is approximately one million years old. NGC 7023 is old enough for its LF to be consistent with a cluster of main sequence stars. The NGC 2264 clusters and NGC 2068 have ages intermediate between NGC 2023 and NGC 7023. A large fraction of LF's have turn-offs at their faint end. These can be interpreted as turn-offs at the low mass end of the corresponding initial mass function. We present a new optical-infrared color-color diagram (V - J vs J - K) that is more efficient at detecting stars with infrared excesses than the infrared color-color diagram (J - H vs H - K). The luminosity function of infrared excess stars in NGC 2264 peaks around K = 11 magnitudes. Finally, we report the detection of a pedestal stellar population in NGC 2264. Dissipation of the main clusters could explain the properties of this stellar population.

Dissert. Abstr.

N94-29990 Illinois Univ., Urbana-Champaign.
PHYSICS, ASTRONOMY, AND ASTROPHYSICS: A NUMERICAL STUDY OF THE BLACK HOLE PLUS BRILL WAVE SPACETIME Ph.D. Thesis
David Harold Bernstein 1993 356 p
Avail: Univ. Microfilms Order No. DA9314846

We investigate solutions of the vacuum Einstein equations in space-times containing a single Einstein-Rosen bridge. The physical and geometrical content of the Schwarzschild solution is analyzed in a number of different spacetime coordinate systems, some well known and some new. In addition, the accuracy of numerical schemes for solving the evolution equations is studied. The same numerical methods are then used to construct axisymmetric solutions which correspond to a Schwarzschild black hole in the presence of time symmetric gravitational radiation (which we call 'Brill waves'). The initial data, evolution of perturbations, and evolution of large amplitude waves are discussed in detail. The initial data is found to display some of the properties of similar data sets studied in the past. The perturbation solutions are shown to agree with known black hole perturbation theory results to within a few percent. Some new results about the apparent horizon in the perturbed Schwarzschild solution are displayed (e.g., the apparent horizon undergoes oscillations similar to that of a damped harmonic oscillator). In addition, traditional radiative variables used in numerical relativity are matched against the known radiative variables of perturbation theory and good agreement is reached in most cases. The large amplitude wave space times are then studied by examining the behavior of the

apparent horizon and by investigating the nature of the waveforms as the amplitude is increased into the 'nonlinear' regime. It is found that the apparent horizon may undergo severe distortions by collision with a large amplitude wave. The total mass loss in radiation is studied and it is shown that in some cases a large amount of the initial radiation may escape to null infinity. Dissert. Abstr.

N94-29994 Maryland Univ., College Park.
INFRARED OBSERVATIONS OF COMETARY DUST BY COBE Ph.D. Thesis
Carey Michael Lisse 1992 345 p
Avail: Univ. Microfilms Order No. DA9315684

The COBE/Diffuse Infrared Background Experiment (DIRBE) is a 0.7 degree x 0.7 degree broadband absolute photometer covering the wavelength range 1 to 240 micrometers. During its November 1989-September 1990 all-sky survey, DIRBE detected the comets C/Okazaki-Levy-Rudenko (C/OLR), C/Austin, P/ Schwassmann-Wachmann 3 (P/SW-3), and C/Levy, providing unique near to far infrared photometry and large-scale images for these comets. The observations of C/Austin were the most detailed, as the comet exhibited an approximately 7 degree long, highly structured dust tail at 12 and 25 micrometers. The lack of a similar visible tail, the results of dynamical modeling of the tail morphology, and the near-greybody behavior of the observed spectra suggest a dust particle surface area distribution dominated by large particles. Compared to visible estimates, a relatively large dust mass loss rate is found for C/Austin. C/OLR and C/Levy were detected only as line sources extended approximately 2 degrees in the antisolar direction, but exhibited interesting infrared spectra. The spectra of C/OLR were very similar to C/Austin. The spectra of C/Levy were very different, exhibiting an elevated color temperature, a fall-off in grain emissivity at long wavelength, and a particle size distribution dominated by small particles. Interestingly, C/Levy was the only one of the four comets found by other observers to have a pronounced light curve and significant activity. P/SW-3 was detected only as a low S/N point source. The mere detection of the comet is interesting, as four other visibly brighter comets were not detected by DIRBE. This suggests an enhancement of the infrared flux of this comet, possibly due to the presence of a dust trail. Comparison of the DIRBE data for these comets suggests that the observed differences are due to particle size effects, not compositional variations. Cometary dust emission is found to be an important source of the zodiacal cloud if the mass emission rate for C/Austin is typical for all gassy comets. The estimated lower limit for the dust/gas ratio of these comets is 0.1 to 0.5. Dissert. Abstr.

N94-30133 British Columbia Univ., Vancouver. Dept. of Electrical Engineering.
RECONSTRUCTION OF STELLAR IMAGES FROM CORRELATIONS Ph.D. Thesis
Xiaotian Shi Sep. 1993 149 p
(ISBN-0-315-85382-4; CTN-94-61153) Copyright Avail: Micromedia Ltd., Technical Information Centre, 240 Catherine Street, Suite 305, Ottawa, Ontario, K2P 2G8, Canada HC/MF

The problem of object reconstruction from a series of short exposure astronomical data observed by ground-based telescopes is addressed. An approach using the self cross correlation is proposed and implemented. This is defined as the cross correlation between an image observation and a truncated part of it. The relation among the phase of the cross spectrum, the phase of the object, and the edges in the object are established. Based on these relations, some efficient and effective algorithms for retrieving the unknown phase of the object and its modulus are developed. These algorithms are found to be insensitive to noise. The phasor image (the inverse Fourier transform (FT) of the phasor part of the FT) of the self cross correlation is shown to preserve the edges of the unknown object. If all the stars and sub-objects in the object have edges, a phase retrieval method based on the iterative FT method is proposed. If some of those objects have edges, a non-iterative phase retrieval method is developed, and if none have edges, a modified version is used to retrieve the object phase. The approach can be extended to reconstruct an object under anisoplanatic atmospheric turbulence. A comparison of signal to noise ratios obtained using the proposed method and existing reconstruction methods demonstrates the superiority of the proposed method.
Author (CISTI)

N94-30231 Laval Univ. (Quebec). Faculte des Sciences et de Genie.
STUDY OF THE STELLAR POPULATIONS OF THE FORNAX DWARF SPHEROIDAL GALAXY M.S. Thesis [ETUDE DES POPULATIONS STELLAIRES DE LA GALAXIE SPHEROIDALE NAINE FORNAX]
Dominique Beauchamp Jun. 1993 132 p In FRENCH
(ISBN-0-315-85526-6; CTN-94-61146) Copyright Avail: Micromedia Ltd., Technical Information Centre, 240 Catherine Street, Suite 305, Ottawa, Ontario, K2P 2G8, Canada HC/MF

A study was conducted to verify the presence of intermediate age stars within the field of the Fornax dwarf galaxy and to attempt to confirm the very large metallicity interval among the various globular clusters which this galaxy contains. If this interval is found to be real, it would be then possible to make use of it to calibrate the Sandage Oosterhoff effect which links the metallicity of an old population to the luminosity of its horizontal branch. Color magnitude diagrams are produced of the different regions observed in order to determine, using isochronous curves, the different parameters of the stellar populations in question. It is concluded that the Fornax field is populated with intermediate age stars of which the youngest have about 1 Ga. The absence of a blue horizontal branch indicates that there are no old stars (greater than 10 Ga). This population of the field also shows a large metallicity interval, Fe/H less than -1 and greater than -2. As for the clusters, they are probably very old (presence of a blue horizontal branch) and poor in metals. The metallicity interval among them is perhaps not as large as believed. CISTI

N94-30270 Missouri Univ., Columbia.
MULTICOLOR PHOTOMETRY OF BARRED SPIRAL GALAXIES Ph.D. Thesis
William Douglas Horst 1992 196 p
Avail: Univ. Microfilms Order No. DA9327834

We present BVRI surface photometry for six barred spiral galaxies. B-V and R-I color maps are used to investigate stellar populations of the bar and nucleus. Results suggest a difference between the nucleus and bar populations, albeit minor. Nuclear and bar populations correspond roughly to integrated spectral types of early K-type and late G-type giants, respectively. In all galaxies, surface brightness profiles suggest star formation activity is occurring near the ends of the bar. In addition, color indices in the central regions of all but one galaxy suggest active star formation within the nucleus. Within the central 5 arc seconds of all but one galaxy, both B-V and R-I color indices become bluer than surrounding regions. Examination of 2-color diagrams strongly suggests the effect of interstellar extinction is uniform along the bar and nucleus. Dissert. Abstr.

N94-30800 Virginia Univ., Charlottesville.
OPTICAL DEPTH EFFECTS IN CLUSTER COOLING FLOWS Ph.D. Thesis
Michael Wayne Wise 1992 258 p
Avail: Univ. Microfilms Order No. DA9324889

In this thesis, we focus on several sources of opacity in cluster cooling flows and examine how they affect both what we see and what we interpret from these objects. In Chapter 2, we derive a technique for obtaining distances to cluster cooling flows using observations of electron scattered light. The majority of cluster cooling flows contain a centrally dominant galaxy at the center of the flow, and many of these galaxies contain active galactic nuclei (AGN). Typically 1 percent of the radiation from this central source will be scattered into our line of sight by hot electrons in the surrounding cooling flow. Observations of this electron scattered radiation may be used in combination with the X-ray surface brightness to determine an independent distance to the cluster. In Chapter 3, we discuss how this scattered radiation can provide information on the cluster environment and the central AGN. Specifically, we consider inhomogeneous gas distributions or situations where the central AGN varies with time, exhibits beaming, or emits polarized radiation. The remainder of this thesis addresses the effects of photoionization and resonant line opacity on the X-ray properties of cluster cooling flows. In Chapter 4, we calculate X-ray luminosities, surface brightness profiles, spectra, and line profiles, both spectral and spatial, several model cooling flows. These models serve as a useful comparison point for models including the effects of X-ray opacity. As we show in Chapter 4, the assumptions one makes concerning how the gas cools out of the intracluster medium can produce drastic differences in many of the observed X-ray properties for these objects. Finally in Chapter 5, we recalculate the X-ray properties for the models

discussed in Chapter 4 including the effects of the radiative transfer through the ICM. The numerical technique employed to solve the transfer equation is discussed in some detail in Appendix D. Dissert. Abstr.

N94-30861 Maryland Univ., College Park.
PUSHING THE LIMIT: PRECISION RADIAL VELOCITIES, TECHNIQUES, AND APPLICATIONS Ph.D. Thesis
Robert Paul Butler 1993 121 p
Avail: Univ. Microfilms Order No. DA9327393

A description is given of an instrument that makes use of an iodine absorption cell, a coude echelle spectrograph, and a sophisticated software analysis package to reduce relative radial velocity errors by two orders of magnitude. Short and long term errors have been reduced to 5 and 20 m/s respectively. Work continues on new software techniques to reduce long term errors to less than 10 m/s. A method of deducing the instrumental point spread function directly from observation is also introduced. Three applications of this technique are covered. Perhaps the most exciting application is the search for sub-stellar companions to solar type stars. The presence of a Jupiter-like planet can be indirectly detected in orbit about a solar type star from the reflex motion of the star. For example, Jupiter induces a 13 m/s velocity on the Sun. Marcy and Butler have been monitoring about 100 solar type stars over a 5 year period. Historically it has not been possible to search for small amplitude variable stars by means of radial velocity change because of measurement error. Using an iodine cell, the accuracy of radial velocity measurements surpasses that of photometric techniques. A survey is being made of stars previously thought to be stable that lie in or near the Cepheid instability strip. This survey has uncovered the smallest amplitude Cepheid yet known. The iodine cell has been used to obtain radial velocity curves from several hundred optical absorption lines in four bright Cepheid variable stars. Differential velocities between various classes of lines reveal detail about the atmospheric structure of Cepheids and provide the raw information needed to construct detailed physical models. As a first order correction to the Barnes-Evans/Baade-Wesselink method, it is suggested that the amplitude of radial velocity curves be reduced by 10 percent to better match the motion of the continuum forming region. With the exception of the Na D lines, these observations reveal no unambigous examples of line splitting. The shape and amplitude of the radial velocity curve of delta Cep is shown to have been extremely constant over most of the last century.
Dissert. Abstr.

N94-30862 Maryland Univ., College Park.
SPECTRAL AND TEMPORAL BEHAVIOR OF LOW MASS X RAY BINARIES OBSERVED WITH THE EINSTEIN SSS AND MPC, AND THE BROAD BAND X RAY TELESCOPE Ph.D. Thesis
Damian Joseph Christian 1993 300 p
Avail: Univ. Microfilms Order No. DA9327400

An extensive survey of 50 low mass X-ray binaries was carried out using the HEAO-2 Einstein Solid State Spectrometer data (0.5-4.5 keV) with the Monitor Proportional Counter data (1.2-20.0 keV). The SSS provided 160 eV resolution below 4.5 keV with about 200 sq cm of area, 100 times that of grating instruments on Einstein and EXOSAT. Additional observations were obtained with the Broad Band X-Ray Telescope (0.5-12 keV). Although LMXRB are some of the most luminous X-ray sources and include one of the first X-ray sources discovered, the nature of their emission regions has remained uncertain. Spectra were selected on the basis of intensity and fit with a set of simple and complex spectral models. For all the subclasses, including Eddington-limited bulge sources, bursters, dippers, the soft spectrum black hole candidates, and a few transients in decline, the spectra could be fit acceptably with combinations of thermal bremsstrahlung and blackbody spectra or a Comptonized spectrum and a blackbody. The results rule out optically thick disk models for the bright Z sources and power law models for bursters. The results suggest a progression of spectra as a function of X-ray luminosity for the bursters, Atoll, and Z sources, in which there are separate emission regions, one optically thin to scattering. The optically thick component that appears for higher luminosity may be due to a boundary layer or to high optical depth to scattering in the flow. A lower temperature blackbody indicated in some cases could be an expected contribution from the accretion disk. The soft spectrum sources are dominated by blackbody spectra, but for two, low effective area of emission is a problem for the black hole interpretation. There did not appear to be any clear selection between models for the sources with high binary orbit inclinations. Column densities for absorption by cold gas were determined simultaneously with the fits. They give distance estimates for the galactic bulge sources on the basis of a galactic disk model. The strongest of previously reported low energy X-ray lines due to OVIII or Fe L transitions are confirmed. Similar line emission is seen for several other sources. The source X0614+091 exhibited a large emission feature consistent with being due to OVIII, showing that a low luminosity disk accretor can have a disk corona. For Cyg X-2 a broadened emission line centered on 6.7 keV was measured with BBXRT. It has been interpreted as K lines from Fe XXV emitted and scattered in the photoionized gas in the inner part of an accretion disk corona photoionized by the central X-ray source. Upper limits for line emission were obtained for X0614+091 and M15 which are consistent with the coronal model. Dissert. Abstr.

N94-29653*# Jet Propulsion Lab., California Inst. of Tech., Pasadena.
TOWARD ASTROMETRIC TRACKING WITH THE INFRARED SPATIAL INTERFEROMETER
R. N. Treuhaft, M. Bester, W. C. Danchi, and C. H. Townes *In its* The Telecommunications and Data Acquisition Report 15 Feb. 1994 p 1-9
(For primary document see N94-29652 08-32)
(RTOP 310-10-60-90-03)
Avail: CASI HC A02/MF A03

90 ASTROPHYSICS

Includes cosmology; celestial mechanics; space plasmas; and interstellar and interplanetary gases and dust.

For related information see also *75 Plasma Physics.*

N94-28480# California Univ., Berkeley. Lawrence Berkeley Lab.
EQUATION OF STATE OF NEUTRON STAR MATTER, LIMITING ROTATIONAL PERIODS OF FAST PULSARS, AND THE PROPERTIES OF STRANGE STARS
F. Weber (Technische Univ., Munich, Germany.) and N. K. Glendenning 25 Oct. 1993 15 p Presented at the NATO Advanced Study Institute on Hot and Dense Nuclear Matter, Bodrum, Turkey, 26 Sept. - 9 Oct. 1993
(Contract DE-AC03-76SF-00098)
(DE94-005214; LBL-34783; CONF-930999-4) Avail: CASI HC A03/MF A01

The present status of dense nuclear matter calculations and constraints on the behavior of the associated equation of state at high densities from data on rapidly rotating pulsars is reviewed. Recent finding of the likely existence of a mixed phase of baryons and quarks forming a coulomb lattice in the dense cores of neutron stars is discussed. A review of important findings of recently performed calculations of rapidly rotating compact stars is given. These are constructed in the framework of general relativity theory for a representative collection of realistic nuclear equations of state. The minimum possible rotational periods of gravitationally bound neutron stars and self-bound strange stars are established. Its knowledge is of fundamental importance for the decision between pulsars that can be understood as rotating neutron stars and those that cannot (signature of hypothetical self-bound matter of which strange stars are the likely stellar candidates). The properties of sequences of strange stars are investigated. Specifically, the question of whether such objects can give rise to the observed phenomena of pulsar glitches is answered, which is at the present time the only astrophysical test of the strange quark matter hypothesis.
DOE

N94-28526# Lawrence Livermore National Lab., CA.
EQUATION OF STATE OF STELLAR PLASMAS
F. J. Rogers Jun. 1993 29 p Presented at the Equation of State in Astrophysics Workshop, Saint-Malo, France, 14-18 Jun. 1993
(Contract W-7405-eng-48)
(DE94-004186; UCRL-JC-115702; CONF-9306287-1) Avail: CASI HC A03/MF A01

The equation of state (EOS) of astrophysical plasmas is, for a wide range of stars, nearly ideal; with only small non-ideal Coulomb corrections. Calculating the EOS of an ionizing plasma from a ground state ion, ideal gas model is easy, whereas, fundamental methods to include the small Coulomb corrections are difficult. Attempts to include excited bound states

are also complicated by plasma screening and microfield phenomena that weaken and broaden these states. Nevertheless, the high quality of current observational data, particularly seismic, dictates that the best possible models should be used. The present article discusses these issues and describes how they are resolved by fundamental many-body quantum statistical methods. Particular emphasis is placed on the activity expansion method that is the basis of the OPAL opacity code. Some comparisons with standard methods are given. DOE

N94-28545# Los Alamos National Lab., NM.
PRODUCTION RATES OF TERRESTRIAL IN-SITU-PRODUCED COSMOGENIC NUCLIDES
R. C. Reedy, C. Tuniz, and D. Fink 1993 7 p Presented at the 6th International Conference on Accelerator Mass Spectrometry, Canberra, Australia, 17 Sep - 1 Oct. 1993
(Contract W-7405-eng-36)
(DE94-005156; LA-UR-93-4397; CONF-930960-7) Avail: CASI HC A02/MF A01

Production rates of cosmogenic nuclides made in situ in terrestrial samples and how they are applied to the interpretation of measured radionuclide concentrations were discussed at a one-day Workshop held 2 October 1993 in Sydney, Australia. The status of terrestrial in-situ studies using the long-lived radionuclides Be-10, C-14, Al-26, Cl-36, and Ca-41 and of various modeling and related studies were presented. The relative uncertainties in the various factors that go into the interpretation of these terrestrial in-situ cosmogenic nuclides were discussed. The magnitudes of the errors for these factors were estimated and none dominated the final uncertainty. DOE

N94-29696*# Sao Paulo Univ. (Brazil). Inst. Astronomico e Geofisico.
DUST IN THE SMALL MAGELLANIC CLOUD Progress Report, 1 Nov. 1993 - 15 Apr. 1994
Antonio Mario Magalhaes 27 Apr. 1994 5 p
(Grant NAG5-1463)
(NASA-CR-195764; NAS 1.26:195764) Avail: CASI HC A01/MF A01

Observations of reddened stars in the Small Magellanic Cloud (SMC) indicate that the interstellar grains in that galaxy may show distinct optical properties from those in the galaxy. The ultimate aim of this research is to determine the extinction law in the direction of these three objects, correlating the results with polarimetric data and building dust models that fit both extinction and polarization. UV extinction and optical polarization data suggest that stars with the 'typical' SMC extinction, i.e., with no bump at bluer wavelengths than the galaxy, have wavelengths of maximum polarization smaller than the galactic average. This shows that the carbon abundance is not the only parameter distinguishing the dust properties for the galaxy and the SMC, the grain size distribution being another distinguishing factor. Derived from text

N94-29698 Arizona Univ., Tucson.
THE THERMAL CONSEQUENCES OF GIANT IMPACTS IN THE EARLY SOLAR SYSTEM Ph.D. Thesis
William Brian Tonks 1993 298 p
Avail: Univ. Microfilms Order No. DA9322636

Recent advances in understanding planetary formation indicate that mass and energy accumulation are dominated the impact of objects containing up to several percent of the protoplanet's mass. This work examines consequences of such 'giant' impacts, including the initiation of core formation and the development and subsequent evolution of deep magma oceans. Large, high speed impacts on silicate planets with masses greater than approximately 10(exp 23) kg result in formation of intact melt regions. Iron rapidly settles to the melt region's base, forming a negatively buoyant mass. If the differential stress generated by this mass is too large, it overcomes the elastic strength of the mantle beneath and rapidly forms a core. The same process might also trigger differentiation of the largest known icy bodies. A melting model based on the Hugoniot equations empirical particle velocity-distance, and linear shock-particle velocity relationships was developed. Impact-induced core formation occurs in silicate planets with masses between 1-6 x 10(exp 23) kg. Thus, the largest planetesimals that accreted to form the Earth were already differentiated. Impact-induced core formation may occur in icy bodies as small as Triton, if an intact melt region forms on bodies that small. If the icy bodies accreted high speed, heliocentric particles, core formation can be triggered in somewhat smaller bodies. Giant impacts do not explain whole-body differentiation of asteroid sized bodies. Giant impacts on large terrestrial planets can form magma oceans 1000-2000 km deep. It is widely assumed that such a magma ocean necessarily differentiates by fractional crystallization. Scientists making this assumption have not accounted for the possibility that crystal suspension in a planetary scale convecting system may prevent crystal-magma separation. It is shown that crystals less than 1-2 cm in diameter are suspended from the onset of cooling. Surprisingly, the ability of a magma ocean to suspend crystals is only weakly dependent on gravity and depth. The difference in magma ocean evolution between the Earth and Moon may be due to gravity's effect on the solidus, liquidus, and adiabatic temperature profiles. Dissert. Abstr.

N94-29719 Drexel Univ., Philadelphia, PA.
BINARY-SINGLE STAR SCATTERING: AN INVESTIGATION OF A REALISTIC CHAOTIC SCATTERING SYSTEM Ph.D. Thesis
Patricia Therese Boyd 1993 232 p
Avail: Univ. Microfilms Order No. DA9319724

The scattering interaction between a bound pair of stars (a binary) and a single star plays an important role in the evolution of globular star clusters. We investigate binary-single-star scattering as an example of a realistic chaotic scattering encounter, concentrating on the character of the space of initial values onto which exit parameters are mapped. In this space, regions of simple behavior -- ejection of one of the stars after a single close approach of the incoming star -- are separated from each other by regions of resonance, in which a temporarily bound triple system is formed. We present a number of distinct slices of initial-value space and discuss the evolution of the resonance regions as a function of the total energy of the system and of the mass ratios of the stars. In addition, statistical properties are studied as a function of these parameters. The initial-value space boundaries between regions of simple ejection and resonance are found to be smooth, and an explanation is given for why this is so. In the direction perpendicular to these smooth boundaries, the structure of the resonance regions is discontinuous, composed of a nested structure of smooth bands separated from one another by random-looking bands. This structure persists to arbitrary scales. The bands are found to be distributed in a Cantor-set-like way, and are associated with the number of bound excursions described by the three particles before eventual ejection. Based on a straightforward dynamical argument, we derive an expression for the scaling of the bands. The fractal properties of the resonance regions are investigated as a function of the total energy and of the mass ratios. The fractal dimension is found to be insensitive to the total energy of the system, and sensitive to the mass ratio of the incoming star. We explain this in terms of each star's probability of escaping from the system once bound, which is also a function of mass ratio. The dynamics of some long-lived interactions is investigated by studying the total kinetic energy as a function of time. This scalar function is found to contain a wealth of information about the interaction, and based upon this information, we apply a symbolic dynamics to the orbits. This is found to be useful in determining which orbital resonances, defined for our purposes in terms of the ratios of the two orbital frequencies, the system stays near.
Dissert. Abstr.

N94-29722 Washington Univ., Seattle.
PHYSICAL CONDITIONS IN CLASSICAL H2 REGIONS IN THE MAGELLANIC CLOUDS Ph.D. Thesis
Eric Matthew Wilcots 1992 370 p
Avail: Univ. Microfilms Order No. DA9312761

Presented is an analysis of the physical properties of a sample of classical H2 regions in the Magellanic Clouds. The morphology, H(alpha) luminosity, flux of Lyman continuum photons, spectral type of ionizing source(s), electron temperature, electron density, and dust content, the primary parameters upon which H2 regions can be compared, are considered. The results presented here show that H2 regions in the clouds bear a close resemblance to similar Galactic H2 regions such as Orion. The primary exception to this is that the electron temperatures in this sample of H2 regions are systematically higher than those found in similar Galactic H2 regions. These classical H2 regions are found to be primarily ionized by a single massive star; in the brighter H2 regions the source of ionization tends to be of spectral type O5-O7, while the fainter H2 regions are primarily ionized by a B0-O9 star. In most cases the main ionizing source is accompanied by several other stars of equal or later spectral type. The

data also shows that the amount of interstellar extinction varies from one star-forming region to the next and suggests that the dust distribution is clumpy and internal to the H2 regions. In addition to these general trends, evidence for the presence of low-velocity shocks exists in at least one H2 region. Four of the H2 regions in this sample are dominated by bright, compact cores, and the data suggests that these are unevolved H2 regions. Given the observational results of this thesis, the optical spectra of these H2 regions are well fit by the standard H2 region models. Taken together, a wide array of observational data and the theoretical models provide a detailed description of the physical conditions within H2 regions.

Dissert. Abstr.

N94-29723 Alabama Univ., Huntsville.

THE STRUCTURE OF SOLAR MAGNETIC FIELDS AND THEIR ASSOCIATED ELECTRIC CURRENTS Ph.D. Thesis

Ladye Kathryn Wilkinson 1992 136 p

Avail: Univ. Microfilms Order No. DA9312026

The threads of magnetic flux which permeate the solar atmosphere are known to play several important roles in the activity of the Sun. Most notably, it is the excess energy stored in these magnetic fields which powers the violent eruptions known as flares. The presence of free energy in active regions of magnetic flux is evidenced by observations of 'magnetic shear' and of electric currents present in the regions. This dissertation considers several topics related to the structure of active region magnetic fields, observations of magnetic shear, and measurements of electric currents flowing in the magnetic fields of active regions. First, we consider the problem of modeling the structure of the loops of magnetic flux. We find solutions to the force-free equation for slightly bent, thin flux tubes and evidence that the effects of curvature on force-free flux tubes may in fact contribute to their stability. The implication is that the critical twist of flux tubes may be higher than previously thought and thus that greater amounts of energy may be stored within these loops. Our second endeavor is to find reasonable limits under which the evaluation of magnetic shear may be made using the observed photospheric magnetic field of active regions. The calculation of magnetic shear relies upon simplifying assumptions to overcome the problem of noise in magnetic field data. Under these assumptions, the calculation of magnetic shear is subject to projection effects which become significant for regions located away from the center of the solar disk. We demonstrate, using an analytical force-free field model, that the calculation of shear is valid only for regions within 15 deg of disk center. Lastly, we concern ourselves with the measurement of electric currents flowing in active regions. We demonstrate that previously used methods of measuring current densities from magnetic field measurements using the differential form of Ampere's law are highly vulnerable to the high noise levels of magnetic field data. We propose, instead, an integral method, arguing that it is less susceptible to the noise levels. Our aim is to demonstrate the great need for reliable measurements of the electric currents flowing in active region magnetic fields.

Dissert. Abstr.

N94-29725 Virginia Univ., Charlottesville.

NUMERICAL SIMULATIONS OF CLUSTER COOLING FLOWS Ph.D. Thesis

Eric Andrew Lufkin 1992 170 p

Avail: Univ. Microfilms Order No. DA9237501

Time-dependent effects for cluster cooling flows are examined in the cases of 1-D spherical symmetry and 2-D axisymmetry. Physical effects included in the simulations are radiative cooling, mass deposition and time-dependent gravitational potentials. The gravitational potential is assumed generally to be due to three sources: a smooth cluster distribution, a massive central galaxy, and in the 2-D case, a perturbing galaxy on a radial orbit. A 2-D axisymmetric finite difference code is developed and tested for these applications. At modest resolution, the code is accurate to one tenth of one percent in the fundamental fluid variables, making it a good tool for observing wave phenomena and departures from spherical symmetry. In the 1-D case, flows with mass deposition reach a steady state after an initial central cooling time. The mass accretion rate generally remains nearly constant thereafter. The spatial structure of the flow agrees in detail with previous steady-state models. Even if the cluster potential is allowed to deepen with time, it is found that adiabatic compression delays neither the cooling of the gas nor the onset of steady-state flow. On the other hand, flows for which the self-gravity of the gas is dynamically important are shown to be unstable to collapse on a hydrodynamic timescale. Despite the relative success of the spherical model, there is considerable observational evidence that the cooling accretion takes place preferentially in clumps rather than uniformly. Recent ROSAT images also indicate that the gas in clusters is nonuniformly distributed. We therefore investigate the formation and evolution of finite-amplitude and finite-wavelength disturbances through axisymmetric numerical simulations of cluster cooling flows perturbed by a single galaxy orbiting along the symmetry axis. Dissert. Abstr.

N94-29731 Oregon Univ., Eugene.

A STUDY OF WHITE DWARF RADIATIVE ACCRETION SHOCKS Ph.D. Thesis

Hussain Yousef Rashed 1992 319 p

Avail: Univ. Microfilms Order No. DA9313313

Quasi-periodic oscillations (QPO's) of period of 1-3 seconds, with root mean square amplitude 1-3 percent have been discovered in the optical emission from four AM Her objects, AN UMa, V834 Cen, VV Pup, and EF Eri. Middleditch (1982) suggested that the QPO's were due to the oscillatory instability of radiative shocks discovered by Langer, Chanmugam, and Shaviv (1981). If the QPO's are due to shock oscillations then the QPO's can be used to constrain several fundamental parameters of the AM Her QPO systems such as the mass and magnetic field strength of the white dwarf. Unfortunately, it is not clear if the QPO's are due to the oscillatory instability. The QPO's are found only in the optical portion of the spectrum and, thus, presumably, are due to variations in the cyclotron luminosity of the shock. Prior to this work, no detailed calculations of the cyclotron (optical) emission from accreting white dwarfs have been performed. Chanmugam et al. (1985) presented calculations for the cyclotron emission of white dwarf shocks, but they did not self-consistently solve the radiative transfer and hydrodynamic equations. This work provides theoretical results for the stability properties and the optical spectra of white dwarf radiative accretion shocks for the weak cyclotron case thought to apply to the AM Her objects. Comparison of these results with observations of the AM Her QPO sources suggests that the properties of the shock oscillation model, in its current form, are not compatible with observations. Namely, radiative shocks with parameters typical of the AM Her QPO sources probably cannot sustain limit cycle oscillations due to strong cyclotron emission and/or electron thermal conduction. However, because several aspects of the observations are naturally explained as shock oscillations, it may turn-out that shock oscillations, in some guise, are responsible for the QPO's.

Dissert. Abstr.

N94-29738 California Inst. of Tech., Pasadena.

THE KINEMATICS OF MOLECULAR GAS AND DUST IN THE NEARBY GALAXIES CENTAURUS A AND M82 Ph.D. Thesis

Alice C. Quillen 1993 139 p

Avail: Univ. Microfilms Order No. DA9325382

This thesis presents a kinematical study of the molecular gas and dust in the nearby radio galaxy Centaurus A (NGC 5128) and the nearby starburst M82. The CO (2-1) emission along the inner dust lane of Centaurus A, shows the molecular gas to be in a thin disk, with a low velocity dispersion. The profile shapes are inconsistent with planar circular and noncircular motion. However, a warped disk in a prolate potential provides a good fit to the profile shapes. Near infrared images of Cen A (NGC 5128) in the J, H, and K bands are presented. The infrared morphology is primarily determined by the presence of a thin absorptive warped disk. By integrating the light of the underlying prolate galaxy through such a disk, we construct models which are compared to infrared and X-ray data. A scenario is proposed where a small gas rich galaxy infalling under the force of dynamical friction is tidally stripped. Stripping occurs at different times during its infall. The orientation of the resulting gas disk depends upon the angular momentum of the infalling galaxy. We find that the resulting precession angle of the disk is well described by the precession model, but that the inclination angle may vary as a function of radius. We propose an orbit for the infalling galaxy that is consistent with the geometry of the warped disk needed to fit our infrared data, and rotation observed in the outer part of the galaxy. The kinematics of the molecular gas in the nearly edge-on disk in M82 are modeled by considering velocity and surface density perturbations caused by a possible rotating kpc long bar. A model with a bar fits the molecular observations of the inner torus remarkably well. The clouds have a low cloud-cloud velocity dispersion implying that the disk is unstable to short timescale axisymmetric perturbations. This is

consistent with the hypothesis that the high star formation efficiencies in starbursts are due to the short timescales of gravitational instability. It is likely that the bar has mediated the starburst. Dissert. Abstr.

N94-29755 Alabama Univ., Huntsville.
THE ROLE OF CLOUD COLLISIONS IN N-BODY SIMULATIONS OF DISK GALAXIES Ph.D. Thesis
Mario Klaric 1993 243 p
Avail: Univ. Microfilms Order No. DA9325203

I have created a cloud collision recipe for use in N-body, polar grid, 3-d code. As a result of collisions two clouds can undergo one of four major processes: coalescence, fragmentation, star formation, and dynamical disturbance. I tested my recipe in simulations of disk galaxies, both isolated and interacting. In cases of isolated disks, I have found that cloud collisions play a key role in bulge formation by scattering stars out of the disk plane, which then end up forming a bulge. I have also shown that cloud collisions turn an initially uniform cloud size spectrum into an exponential size spectrum, agreeing very well with observations by Solomon and Rivolo (1989). In addition, I have shown that a disk needs to have a stellar component to form a bar. The bar then often has blobs at its ends, primarily composed of older stars. As a case of interacting disks, I have studied NGC 2535/6, and found that it seems the primary stayed relatively isolated for a few rotation periods, and consequently relaxed to some degree. Then the companion started tidally interacting with the primary, changing its morphology, intensifying cloud collision rates, and bringing about an earlier onset of star formation, which does not reach the same maximum value as in comparable isolated disk. Dissert. Abstr.

N94-29827 New Mexico State Univ., University Park.
SURFACE DIFFERENTIAL ROTATION IN A SAMPLE OF COOL DWARF STARS Ph.D. Thesis
Robert Andrew Donahue 1993 231 p
Avail: Univ. Microfilms Order No. DA9323939

A study of rotation in lower main-sequence stars has been progressing at Mount Wilson Observatory since 1980. The rotation program is part of a long-term study of stellar activity cycles, akin to the 11-year sunspot cycle. This dissertation uses the available time series of Ca II H and K chromospheric data in an attempt to uncover information on surface differential rotation in a sample of stars (including the Sun) based upon frequent and reliable measurements of rotation. A method is developed to diagnose the potential contribution of active region growth and decay within an observing season. The existence of surface differential rotation is perceived and analyzed for 37 stars. For some stars, patterns of rotation versus level of mean activity are apparent, and are interpreted to indicate the existence of migrating dynamo waves. The evolution of surface differential rotation is suggested from results based on stars of different ages. Specific results include: (1) there is a power-law relationship between rotation and fractional differential rotation with exponent 3/4; (2) there appears to be an abrupt change in differential rotation morphology and dynamo number which occurs at P(sub rot) approximately equals 10 days. One of these morphologies coincides with stars bordering the Vaughan-Preston Gap; (3) For fast-rotating stars, active regions appear to prefer high-latitude belts, as inferred from the shape of their seasonal time series; and (4) some slowly-rotating stars do show the same equatorward migration pattern over the activity cycle as the Sun. However, an equal number of slowly-rotating stars show poleward (anti-solar) migration. It remains to be seen whether this is caused by some physical difference between these stars or is time-dependent. A model for time series fitting is examined, and its limitations are discussed. The problem of determining the chromospheric contrast is outlined using high-resolution spectroscopy of the Ca II K line of the Sun and stars. Dissert. Abstr.

N94-29832 Johns Hopkins Univ., Baltimore, MD.
INFRARED PROPERTIES OF OBSCURING DUST TORI IN ACTIVE GALACTIC NUCLEI Ph.D. Thesis
Edward A. Pier 1993 118 p
Avail: Univ. Microfilms Order No. DA9313416

A new algorithm for radiative transfer in axisymmetric geometries is presented, and it is applied to the optically thick, compact, dust tori which are thought to surround many active galactic nuclei. The general trends exhibited by the spectra of these tori are discussed and compared with observations of active galactic nuclei. Also, the radiation pressure within the torus and its role in supporting the torus are investigated. The spectra emitted by compact tori are basically 'bumps' which are consistently about 50 percent wider than blackbodies and peak in the mid infrared. They radiate anisotropically throughout the infrared, and their infrared color temperatures vary with viewing angle by approximately 100 K. The 10 micron silicate feature often associated with dust can appear in absorption, emission, or not at all. A comparison with observations reveals a good correspondence between the model predictions and the following: the continuum and near IR size of the nucleus of NGC 1068, the 3.5 to 10.5 micron colors of type 2 Seyferts, the 10 micron silicate feature as well as the 8 to 13 micron spectral index in both types of Seyferts, and the anisotropy of the emission from active galactic nuclei. Furthermore, the effective temperature of the nuclear radiation on the inner edge of the torus is about 600 K, and tori typically cover about 86 percent of the solid angle around the nucleus. In type 1 Seyferts and quasars the observed 3.5 micron fluxes are often a factor of a few larger than predicted by the models. This is explained by a small amount of low angular momentum material which approaches much closer to the central engine than the bulk of the torus and radiates near 3 microns. This hot dust is obscured by the torus in narrow line active galactic nuclei. The radiation force within the torus is likely to be comparable to the gravity of the central engine. It may therefore alleviate a theoretical problem of the compact torus model by supporting its geometrical thickness. It may do this both directly and by driving the random motions of the clouds in the torus. Dissert. Abstr.

N94-29834 Wisconsin Univ., Madison.
THE STABILITY OF PERFECT ELLIPTIC DISKS Ph.D. Thesis
Stephen E. Levine 1992 80 p
Avail: Univ. Microfilms Order No. DA9306467

Two dimensional perfect elliptic disk models with maximum streaming were tested for stability by N-body integration. The perfect elliptic disks are the two dimensional limiting case of the perfect ellipsoids, integrable triaxial potentials with the density stratified on concentric ellipsoids, which could be viewed as models for both galactic bars and elliptical galaxies. To obtain a discrete representation of each model suitable for testing by N-body methods, we used simulated annealing to choose a set of orbits which sampled the distribution function. Quiet start techniques were developed to place particles on these orbits uniformly on the torus in action-angle space, which makes the initial conditions as smooth as possible. We found that the nearly axisymmetric models exhibited spiral instabilities similar to those seen in cold disks; the most elliptical models showed bending instabilities. Between these extremes, there is a range of axial ratios from b/a = 0.715 to 0.250 for which these models appear to be stable. All of our methods can easily be extended to three dimensions. On the basis of these experiments, we expect that the moderately triaxial perfect ellipsoids should also be stable. Dissert. Abstr.

N94-29861*# Lockheed Missiles and Space Co., Palo Alto, CA. Research Lab.
CORONAL TEMPERATURES OF UNUSUALLY ACTIVE K-DWARF BINARY SYSTEMS
Robert A. Stern 1 Mar. 1994 10 p
(Contract NAS5-32079)
(NASA-CR-189335; NAS 1.26:189335) Avail: CASI HC A02/MF A01

We report the results of a ROSAT pointed study of 4 BY Dra systems. Good quality pulse-height spectra are available from all four systems. Except for a required interstellar absorption component in HD 319139, the four systems have remarkably similar x-ray spectra; the two systems BD +22deg.669 and BD +23deg.635 look virtually identical in x rays. Analysis of the 4 x-ray spectra reveals that, in all cases, a single-temperature hot plasma (RS or Mewe) spectra is inadequate to fit the data, and two temperatures are required. We present examples of fitted pulse-height spectra and chi squared contours in kT(sub 1)-kT(sub 2) space.
Author (revised)

N94-29871*# Applied Research Corp., Landover, MD.
SPATIALLY RESOLVED SPECTROSCOPY OF AG CARINAE, AND DIRECT EVIDENCE FOR STELLAR EVOLUTION: THE CENTRAL STAR OF NGC 2392 Final Report, 8 Jun. 1992 - 7 Jun. 1993
Bruce Altner and Steven N. Shore 9 Jun. 1993 9 p
(Contract NAS5-31838)

(NASA-CR-189291; NAS 1.26:189291; ARC-R93-207) Avail: CASI HC A02/MF A01

We have performed spatially-resolved low dispersion long-slit spectroscopy for the circumstellar shell of the luminous blue variable AG Carinae with IUE between lambda lambda 1200 - 3200 A. At all positions a strong dust-scattered stellar continuum is detected. Only a few emission lines, FE II 2600 and O I (?) 1304, have been detected; the emission is stronger on the southern side of the shell. The UV surface brightness and derived dust properties are completely consistent with the groundbased and KAO FIR observations: the grains are large (0.1 - 1 micron), warm (45 - 100 K depending on composition), highly reflecting (C(sub sca)/C(sub abs) approximately equal to 1), and tie up about 10(exp -4) to 10(exp -3) solar mass of material. We also observe similarities of the results for HR Car and LBV's to those reported here. Author

N94-29905*# Arizona Univ., Tucson.
COSMOGENIC C-14 IN ANTARCTIC AND NON-ANTARCTIC METEORITES AND LUNAR SAMPLES Final Technical Report, 1 Jun. 1987 - 31 May 1994
A. J. Timothy Jull, D. J. Donahue, and G. S. Burr 1994 4 p
(Grant NAG9-233)
(NASA-CR-195795; NAS 1.26:195795) Avail: CASI HC A01/MF A01

We were able to develop measurements of C-14 in meteorites as a useful tool for estimates of terrestrial age. Prior to this accomplishment, only a few measurements of C-14 terrestrial ages had been made. The sample sizes were larger, and there had been no systematic study of the various parameters affecting production of C-14, such as depth dependence, and the production cross sections for C-14 from spallation amounted to a few data points. Presently, C-14 ages are an accepted terrestrial age estimate in the meteorite community, whereas before this work the few data available were difficult to interpret. We have obtained terrestrial ages not only on groups of meteorites from different geographic areas but also information on unique meteorites from particularly interesting groups, such as meteorites originating from the Moon, or SNC meteorites, which many researchers believe are derived from Mars. Author (revised)

N94-29912 Yale Univ., New Haven, CT.
ON DYONIC BLACK HOLES AND COSMIC CENSORSHIP Ph.D. Thesis
Ibrahim Semiz 1992 63 p
Avail: Univ. Microfilms Order No. DA9315258

In this thesis, we construct two thought experiments to test the Cosmic Censorship Conjecture attempting to overcharge and/or overspin a critical four-parameter (the usual three of mass, electric charge, and angular momentum plus magnetic charge) black hole. The first is a generalization of a previous thought experiment where Wald tried to give the critical black hole extra charge and/or angular momentum by letting it swallow particles. We generalize this thought experiment to cover the possibility of magnetic charge, both on the particle and the black hole. The second is a new thought experiment where we feed charge and/or angular momentum to the black hole via a Klein-Gordon field. In both cases, we find that the Cosmic Censorship Conjecture cannot be violated. To be able to do the calculations for the second thought experiment, we separate the Klein-Gordon Equation on this black hole metric. We also separate the Dirac Equation and investigate the effects of the black hole's magnetic charge on the ergosphere and on superradiance. Dissert. Abstr.

N94-29913 Yale Univ., New Haven, CT.
CONVECTIVE TURBULENCE AND TRANSPORT IN STARS Ph.D. Thesis
Miguel Perez-Saborid 1992 161 p
Avail: Univ. Microfilms Order No. DA9315230

This work treats the convection zone of a slowly rotating, weakly magnetic star. It assumes that the turbulence is weak, short scale-length, and sound-wave-like in character, that the mean pressure and density in the convection zone are linked by the condition of marginal stability against convection, and that the statistics of the turbulence is axisymmetric about the axis of rotation. In these circumstances one obtains limited information about the turbulence, namely the average radial velocity and the turbulent mass flux, in terms of quantities determined by standard, spherically symmetric, stellar evolution calculations independently of any assumptions about the character of the turbulence. The theory is illustrated numerically for the sun. It is demonstrated that under the assumptions made, the average acoustic energy flux is to the lowest order equal to the average turbulent energy flux determined by conventional stellar evolution. With the purpose of using this result to predict features of the statistics of the oscillations which can be compared with existing solar observations, the average acoustic energy flux is expressed in terms of the spatial eigenfunctions associated with the acoustic modes. After an approximate analysis, which assumes that the oscillations are excited by a broadband random source (white noise) and damped according to a linear damping mechanism, one obtains an expression for the acoustic energy flux that contains partial information about the statistics of the mode amplitudes. Dissert. Abstr.

N94-29991 Illinois Univ., Urbana-Champaign.
NEAR-CRITICAL SPHERICALLY SYMMETRIC ACCRETION BY NEUTRON STARS Ph.D. Thesis
Brand Irving Fortner 1993 145 p
Avail: Univ. Microfilms Order No. DA9314869

The luminous, low-mass x ray binary systems are thought to contain neutron stars with luminosities comparable to the Eddington critical luminosity L(sub E) at which the outward force of radiation balances gravity. A subset of these systems, called Z sources, show three distinct spectral states and quasiperiodic intensity oscillations. In a recently proposed unified model of this behavior, mass accretes not only through a disk but also approximately radially from the inner disk. This thesis reports the results of an investigation of the structure and stability of the radial flow when the luminosity of the star is near-critical. It is shown that when the luminosity of the star is comparable to L(sub E), radiation drag creates a significant, approximately radial inflow from the inner disk corona to the star. A simplified model of this flow and the time-dependent radiation hydrocode used to simulate it are described. As expected, the simulated flow has an outer region where the inflow velocity increases with decreasing radius, a middle region where the velocity is roughly constant, and an inner region where the velocity decreases toward the star. The simulations show that the radial flow becomes over-stable (that is, the flow oscillates with increasing amplitude) when the luminosity rises to within a few percent of L(sub E). If the radial inflow begins approximately 300 km from the neutron star (as expected), the frequency of the oscillations is approximately 5 to 10 Hz, comparable to the frequency of one class of quasiperiodic oscillations observed in the Z sources. The variation in optical depth is substantial, whereas the variation in luminosity is relatively small. Calculations of the amplitudes and phases of the resulting oscillations in the x ray intensity agree with the observed properties of this class of quasiperiodic oscillations. Dissert. Abstr.

N94-29992 Florida Univ., Gainesville.
CORRELATION ANALYSIS ON OPTICAL AND RADIO LIGHT CURVES FOR A LARGE SAMPLE OF ACTIVE GALACTIC NUCLEI Ph.D. Thesis
Sandra Denise Clements 1992 220 p
Avail: Univ. Microfilms Order No. DA9314209

Long-term optical and radio light curves for a large sample of active galactic nuclei were investigated in order to examine the relationship between the two emission regions. Correlation analysis using the discrete correlation function was performed to determine if radio events are correlated with optical events, and, if so, to determine the lag times between them. In addition, similar analysis was performed to determine lag times between events at 14.5 GHz, 8.0 GHz, and 4.8 GHz. A total of forty-six objects were examined. Nine showed correlated optical and radio events with optical leading the radio in every case. Six of these were BL Lacertids, all having lag times of less than 6 months. The one QSO which showed correlated optical and radio events had a longer lag time, on the order of a year. No difference between BL Lacs and QSO's is seen in the results of correlation analysis on two radio frequencies. Lag times between 14.5 GHz and 8.0 GHz radio data are less than 5 months in almost every case. The same is true for lag times between 8.0 GHz and 4.8 GHz data. An additional nine objects showed no correlated behavior in their optical and radio light curves. Seven of these objects were QSO's. The rest of the objects either did not have light curves with adequate temporal coverage for reliable correlation analysis, or the analysis was confused by the number and spacing of events in one or both light curves. This analysis was seriously hampered by inadequate temporal coverage in the optical light curves. Some variability timescales in the optical are very short, making frequent observations necessary in order to resolve events. Unavoidable constraints on ground-based observations due to the weather, the sun,

and the moon make it impossible to obtain the frequent, uninterrupted observations that are necessary to obtain a light curve without yearly gaps and with well-resolved short-term events. Dissert. Abstr.

N94-29993 Maryland Univ., College Park.
THE EFFECTS OF RELATIVISTIC NEUTRONS ON NONTHERMAL MODELS OF ACTIVE GALACTIC NUCLEI Ph.D. Thesis
Peter Michael Giovanoni 1992 176 p
Avail: Univ. Microfilms Order No. DA9315644

Active galactic nuclei produce large amounts of radiation from relatively small regions. How this energy is generated is one of the main topics of research on active galaxies. This work emphasizes the effects of relativistic neutrons on the observed spectrum and on the variability properties of active galactic nuclei. The energy emitted as radiation is initially injected into the system as relativistic protons from a static shock front. The shape of the energy distribution function of the protons is assumed to be a power law form. Through inelastic hadronic collisions the energy in the protons is put into neutrinos, positrons, electrons, and neutrons. The emitted radiation from roughly the near infrared to gamma rays of a few MeV energy is due to emission in the core near the shock front. The neutrons that are sufficiently energetic escape the core and, when they decay, they transfer their energy to charged particles in outer regions that are orders of magnitude larger in size than the core. In this thesis the effects of this energy transport on steady-state and time-dependent active nuclei are studied. When matter falls into the core at roughly the Eddington mass accretion rate the neutron energy transport gives rise to radio-loud and gamma ray loud objects. Both the radio and the gamma ray photons in these objects come from the regions farthest from the central core. A small increase in the infalling medium's density prevents the neutrons from reaching these distances and such models yield radio and gamma ray quiet objects; that is, one sees only the radiation from the core. When the luminosity varies with time, one may expect the radiation from the core to vary on a shorter timescale than radiation from the outer regions. The main parameters in the model are varied in order to determine the relative importance of synchrotron, inverse Compton, and photon-photon interactions. In the time-dependent model, the response of the system to three types of pulses in the proton injection rate were studied. The three forms were a delta function, a step function, and a top-hat function. Two timescales control the observable changes in the radiation, the proton collision timescale and the light travel time to the radiating region for each frequency. The response was mostly as expected from the steady-state model. The proton collision timescale tends to be the dominant timescale. There was both rapid and longer term variability in the gamma ray emission, with the short term variability being strongest in the lower gamma ray frequencies. The radio variations were usually very weak in the models. Dissert. Abstr.

N94-30010 Arizona State Univ., Tempe.
THE ANGULAR TWO-POINT CORRELATION FUNCTION OF GALAXIES DOWN TO 25TH MAG Ph.D. Thesis
Lyman Wade Neuschaefer 1992 226 p
Avail: Univ. Microfilms Order No. DA9307122

This dissertation examines the evolution of galaxy clustering from deep CCD exposures. The deep images obtained for this work are from two widely separated (b(sup II) approximately greater than 30 degrees) fields imaged in Gunn gri pass bands, both approximately equal to 0.5 degree in extent. More than 90 percent of the galaxies brighter than g approximately equal to 24.5 mag are detected, with more than 23,000 galaxies found in each field, in each passband. The precision of the zero-points is approximately less than 0.1 mag for all frames and the overall precision of the CCD astrometric solutions is approximately less than 0.5(sup II). Galaxy angular two-point correlation functions are measured and interpreted in terms of sample completeness, evolution in galaxy spectra, evolution in clustering, and the overall matter density in the universe. The observed galaxies undergo a moderate bluing trend with increasing sample depth. Given the most recent measured faint galaxy redshift distributions, this suggests that a significant fraction of medium redshift galaxies (0.2 approximately less than z approximately less than 0.8) either undergo mild episodic bursts of star formation or are a new class of dwarf galaxies unobservable at the present epoch, or a combination thereof. Two trends in the correlation function, w(theta) varies as theta(sup delta), are observed as a function of increasing survey depth: The amplitude of w(theta) steadily decreases (but levels off beyond the 90 percent completeness limit), and is lower at a given apparent magnitude than expected for a flat universe containing galaxies with nonevolving spectra; the slope in w(theta) is observed to mildly flatten, from delta approximately equal to -0.8 locally to delta approximately equal to -0.4 at g(sub mcd) = 25 mag. These results suggest one or a combination of the following explanations: the slope, delta(z), of w(theta) grows steeper with cosmological time, consistent with galaxy clusters forming before individual galaxies; galaxy clustering evolves in amplitude, expressed by a relatively large value of the clustering exponent epsilon approximately less than 0 (epsilon = 0 (-1.2) corresponds to galaxy cluster sizes fixed in proper (comoving) coordinates); and field galaxies have undergone mild spectral evolution out to redshifts z approximately less than 1. Although the results are somewhat insensitive to space curvature, they are consistent with a flat (Omega(sub 0) = 1) universe, with mild evolution in galaxy spectra, correlation slope, and correlation amplitude since z is approximately less than 1. Dissert. Abstr.

N94-30011 Texas Univ., Austin.
THEORETICAL ASTEROSEISMOLOGY OF WHITE DWARF STARS: THE ENCYCLOPEDIA SEISMOLOGICA Ph.D. Thesis
Paul Andrew Bradley 1993 312 p
Avail: Univ. Microfilms Order No. DA9323347

White dwarfs represent the most common fate suffered by stars as they exhaust their supply of nuclear fuel and cool to oblivion. According to conventional wisdom, these objects have degenerate carbon/oxygen cores overlain by a pure helium mantle (DB white dwarfs); in many cases, a thin veneer of hydrogen lies on the surface (DA white dwarfs). The PG1159 stars are pre-white dwarfs that hold clues to their previous evolution through the planetary nebula stage; about half of these stars pulsate. My goal is to understand the internal structure of these stars by applying the tools of asteroseismology. I present parametric grids of evolutionary pre-white dwarf, DB, and DA models and develop the theoretical tools necessary to determine the internal structure of these stars. I use the nearly continuous photometric data provided by the Whole Earth Telescope on the pre-white dwarf PG1159-035, and the DBV white dwarfs GD358 and PG1115+158 to determine their internal structure in detail. The mass of PG1159-035 is 0.59 +/- 0.01 solar mass, GD358 has a mass of 0.61 +/- 0.03 solar mass, and the mass of PG1115+158 is 0.62 +/- 0.06 solar mass; all three masses are similar to the mean masses of white dwarfs in general. The He/C/O surface layer mass of PG1159-035 is 3.9 x 10(exp -3)M*, which can be duplicated by stellar evolution models, although they cannot duplicate the observed surface abundance, suggesting that our knowledge of mass loss is incomplete. The helium layer mass of GD358 is 1.5 x 10(exp -6)M*, and is less than 10(exp -4)M(sub *) for PG1115+158. These helium layers are vastly thinner than suggested by stellar evolution theory and present problems for current evolutionary models of DB white dwarfs. If these helium layer masses are correct, then we must revise our thinking on how convective dredge up works in the presence of diffusion. I also present preliminary assessments of the structure of several pulsating DA white dwarf (DAV) stars. In spite of the relatively small number of observable modes in the DAV white dwarfs, several of them appear to have thick hydrogen layer masses (approx. 10(exp -(5-6))M(sub *)), based on existing stellar mass estimates and assumptions about the identity of the observed modes. Finally, I describe how my structure determinations and recent spectroscopic observations may help to clarify our picture of white dwarf evolution. Dissert. Abstr.

N94-30012 Maryland Univ., College Park.
ENERGETIC EVENTS IN THE EARLY UNIVERSE Ph.D. Thesis
Biman Bihari Nath 1992 117 p
Avail: Univ. Microfilms Order No. DA9315706

Various forms of energy inputs at high redshifts and their measurable effects are considered. Distortions in the microwave background radiation from various energetic phenomena are calculated. Radiation in the x ray and UV from the diffuse gas in collapsing galaxies is investigated from the point of view of their discovery with present-day detectors. In the first chapter, it is shown that, for a nontrivial radiative decay channel of the 17-keV neutrino, the photons would distort the microwave background radiation through ionization of the universe. The constraint on the branching ratio of such decays from COBE measurements is found to be more stringent than that from SN 1987A. We then derive analytical formulae for the optical depths of a radiation-dominated universe and find that if the universe were radiation-dominated at redshifts z approximately greater than

10(exp 2) to 10(exp 3), it would be optically thin in soft gamma rays up to redshifts of z approximately 10(exp 4). This is larger by an order of magnitude than for the matter-dominated universe. In chapter 3, general similarity solutions are obtained for spherical, cooling blast waves in an Omega(sub b) much less than Omega = 1 universe, given an energy input that is some power of time. The distortion of the microwave background is calculated in terms of the present-day peculiar velocities and the present-day voids in the velocity space caused by the explosions. The predicted distortion is found to be marginally consistent with the present-day observations and could provide a test of the model in the near future. Next, the diffuse emission from galaxies during their initial collapse is considered. It is shown that large galaxies could be seen and spatially resolved in the x ray, if they form at z approximately 1 to 5, by AXAF and ROSAT. UV cameras could discover such objects if much of their radiation emerges in the He(+) Lyman alpha. An estimate is made for the sensitivity of the x ray luminosity to the baryon mass while the baryons are still diffuse. The possibility of using the x ray observations as a diagnostic for the dominant mass component in the protogalaxy is discussed. Finally, the possibility of detecting protogalaxies in UV band is pointed out, assuming galaxy formation occurred at z approximately 5. It is shown that the diffuse gas in collapsing galaxy sized objects with temperatures approximately 10(exp 6 +/- 0.5) K, and with a modest amount of metallicity, should copiously produce emission lines from highly ionized iron atoms. The predicted luminosities from different models of galaxy formation are compared with the sensitivity of HST.
Dissert. Abstr.

N94-30058 Montreal Univ. (Quebec). Dept. de Physique.
INHOMOGENEITIES IN THE WIND FROM WOLF-RAYET STARS Ph.D. Thesis [INHOMOGENEITES DANS LE VENT DES ETOILES WOLF-RAYET]
Carmelle Robert Dec. 1991 396 p In FRENCH
(ISBN-0-315-85893-1; CTN-94-61132) Copyright Avail: Micromedia Ltd., Technical Information Centre, 240 Catherine Street, Suite 305, Ottawa, Ontario, K2P 2G8, Canada HC/MF

Spectroscopic measurements on nine Wolf-Rayet stars have shown the existence of perturbated regions of motion in their stellar winds. The presence of the perturbations is signalled by numerous small variable structures superposed on the profile of the emission lines formed in the stellar wind. A study of the global variations of the lines and an examination of individual microstructures have allowed description of various characteristics of the perturbations. Among others, significant correlations are observed between the level of variability of the lines and certain stellar parameters which confirm that the phenomenon of variability is intrinsic to the stellar wind. It is also concluded that the perturbated regions have a finite extent with respect to the stellar envelope. It is proposed to represent the perturbations by a model of discrete inhomogeneities in expansion within the wind. A correlation is obtained between the number of detected inhomogeneities and the terminal velocity. It is estimated that the loss in mass due to detectable inhomogeneities corresponds to 10 percent of the mass loss of the whole wind. The structures observed in the Wolf-Rayet spectra have very similar characteristics to those of O type stars, and it is thus proposed that the perturbations observed in those two types of stars have the same origin.
CISTI

N94-30163 International Centre for Theoretical Physics, Trieste (Italy).
A THEORY APPROACH FOR CREATION OF THE MATTER OF UNIVERSE
Duong Van Phi and Duong Anh Duc Aug. 1993 21 p Limited Reproducibility: More than 20% of this document may be affected by microfiche quality
(DE94-608109; IC-93/284) Avail: CASI HC A03 (US Sales Only)

We shall represent an approach for the creation of the matter of Universe in the framework of a quantum theory, established in an 8-dimensional space. The primitive matter was being created from the Primary Vacuum and it consisted of the deuterons atoms, neutrinos and photons. From these neutral elements the attractive centers were formed and in the final stage an extremely high mass density Universe was built, and successively, the Big-Bang occurred. The problems of particle dominance, of excess of the deuterons and of magnitude of the numbers of neutrinos, etc. are discussed.
DOE

N94-30271 Stevens Inst. of Tech., Hoboken, NJ.
A NUMERICAL STUDY OF GRAVITATIONAL COLLAPSE Ph.D. Thesis
Shang-Wen Sun 1993 176 p
Avail: Univ. Microfilms Order No. DA9328529

The Einstein equations coupled with the scalar wave equation are studied as an initial value problem within the restriction of spherical symmetry. A spherical shell of the scalar field sandwiched between the flat and the Schwarzschild geometry is evolved using various numerical techniques. Two drastically distinct fates can be met for this initial scalar field depending on a certain criterion. In one case, the scalar field eventually dispersed to infinity; in the other case, the scalar field collapses to form a black hole. In most coordinate systems, the motion of the scalar field inside event horizon appears to freeze when a black hole starts to form. A special coordinate system is chosen to study the dynamical evolution inside the event horizon and the criterion that determines the fate of a given initial scalar field.
Dissert. Abstr.

N94-30340 Illinois Univ., Urbana-Champaign.
STELLAR AND GAS DYNAMICS OF INTERACTING RING GALAXIES Ph.D. Thesis
Richard Alan Gerber 1993 217 p
Avail: Univ. Microfilms Order No. DA9329038

The development of ring and arc structures due to the collision of a spherical galaxy normal to the plane of a disk galaxy is studied with analytic and numerical models. In the numerical model, the disk contains one-tenth of its mass in gas and the hydrodynamics equations are solved using the method of Smoothed Particle Hydrodynamics. It is found that axisymmetric collisions between equal mass galaxies produce a strong expanding ring with a complex three-dimensional structure. Density and velocity profiles for the disk are given. Off-center collisions produce greater gas density enhancements in the nonnuclear portion of the disk when compared to the axisymmetric case. Strong gas interactions in the off-center collisions cause the stellar and gaseous flows to follow separate trajectories. If star formation is associated with the strongest gas shocks and greatest gas densities, the morphology of ring galaxies is strongly dependent on a proper treatment of gas dynamical processes. A Rayleigh-Taylor instability is believed to be present in the strong shock regions, which could contribute to the knotty structure observed in ring galaxies.
Dissert. Abstr.

N94-30694# Los Alamos National Lab., NM.
THE SECOND COMING OF COLD DARK MATTER?
W. H. Zurek, M. S. Warren, P. J. Quinn, and J. K. Salmon 1993 11 p Presented at the Cosmic Velocity Fields Conference, Paris, France, Nov. 1993
(Contract W-7405-eng-36)
(DE94-004992; LA-UR-93-4240; CONF-9311156-1) Avail: CASI HC A03/MF A01

In recent years standard cold dark matter (CDM) theory, which enjoyed a large following throughout much of the past decade, has been abandoned by virtually all of its early supporters. The most serious argument against CDM was the incompatibility between the relatively high value of the pairwise radial velocity dispersion between galaxies, sigma(sub v), inferred from numerical simulation with the much lower observational estimates. We reexamine this argument in the light of our new, high-resolution, COBE-normalized simulations and conclude that sigma(sub v) is significantly overestimated in simulations which do not have sufficient resolution (i.e., which have masses of galaxies comparable to the mass of N-body particles) and that it is also difficult to reliably estimate sigma(sub v) from the observational catalogues used for this purpose. We conclude that inflationary cosmology and CDM are not -- contrary to the presently prevailing prejudice -- incompatible with the observations of small scale peculiar velocities, as characterized, for example, by sigma(sub v).
DOE

N94-30951 Minnesota Univ., Minneapolis.
SUBSTRUCTURE, DYNAMICS AND EVOLUTION IN CLUSTERS OF GALAXIES Ph.D. Thesis
Christina Marie Bird 1993 240 p
Avail: Univ. Microfilms Order No. DA9328326

Most models for the formation of large scale structure imply that clusters of galaxies are currently forming. Because the Hubble time is on the order of a few dynamical timescales for clusters, there is some hope that their structure will retain signatures of their formation and initial

conditions. In order to objectively identify the different sorts of substructure which may exist in clusters of galaxies at the present time, I present a variety of statistical diagnostics which measure deviations of cluster galaxy velocities and positions from those expected in a relaxed system. These tests are applied to a database of rich clusters with at least 50 measured redshifts, depending on the diagnostic considered. 30-70 percent of all well-studied clusters possess significant substructure. Only one system in the cluster database, A496, does not have any significant deviations from the structure expected for a relaxed, dynamically-evolved cluster. Once the importance of substructure in any particular cluster has been assessed, a maximum likelihood technique is used to assign individual galaxies to their host subclusters. These statistical techniques are applied to the study of central galaxy peculiar velocities. Formation models for central dominant galaxies require them to be preferentially located at the bottom of their cluster potential well. Without correcting for substructure, 50 percent of the cD-type systems in the cluster database have central galaxies which are displaced from their potential minimum (as defined by the cluster average velocity). These systems are much more likely to exhibit correlations between galaxy velocities and positions than clusters in which the central galaxy is at rest, providing evidence that substructure may be responsible for the high velocity offsets. If dynamical models which include subcluster assignments are used to determine the peculiar velocities, only 20 percent of the cD-type clusters have significant velocity offsets. Dissert. Abstr.

N94-29628*# European Space Agency. European Space Research and Technology Center, ESTEC, Noordwijk (Netherlands).

COLLECTING COMETARY SOIL SAMPLES? DEVELOPMENT OF THE ROSETTA SAMPLE ACQUISITION SYSTEM

P. A. Coste, M. Fenzi, and Michael Eiden *In* NASA. Ames Research Center, The 27th Aerospace Mechanisms Symposium May 1993 p 1-19 (For primary document see N94-29627 08-15)
Avail: CASI HC A03/MF A03

91 LUNAR AND PLANETARY EXPLORATION

Includes planetology; and manned and unmanned flights.

For spacecraft design or space stations see *18 Spacecraft Design, Testing and Performance.*

N94-28418*# Michigan Univ., Ann Arbor. Dept. of Atmospheric, Oceanic and Space Sciences.

MUADEE: MARS UPPER ATMOSPHERE DYNAMICS, ENERGETICS, AND EVOLUTION DISCOVERY MISSION. EXECUTIVE SUMMARY VOLUME Final Report

Timothy L. Killeen 15 Mar. 1994 100 p
(Grant NAG5-2250)
(NASA-CR-195732; NAS 1.26:195732) Avail: CASI HC A05/MF A02

This document is the final report of the MAUDEE (Mars Upper Atmosphere Dynamics, Energetics, and Evolution) consortium. It describes a low cost Discovery mission to investigate the upper atmosphere of Mars and to understand the manner in which Mars has evolved over geologic time. In keeping with the innovative philosophy permeating the Discovery Program and in order to minimize the burden of reading an extensive prose exposition, a new presentation format has been adopted. The format involves a series of view graphs with facing text. The view graphs form the basis of a complete oral presentation of the MAUDEE mission and the facing text provides more detailed, but still brief, explanatory descriptions. Readers can scan the view graphs and/or read the facing text at their discretion. The oral presentation of this study was given to code SL personnel at NASA Headquarters on February 23, 1994. MAUDEE is an essential component of the Mars Exploration Program. It provides the information required to understand the evolution of the planet via the escape of volatiles. It provides the key measurements needed to understand the upper atmosphere of the last of the three terrestrial planets to be so studied. It connects and supplements investigations based on other Mars missions: Mars Surveyor, Planet-B and Mars-96. The MAUDEE mission plan involves a combination of remote and in-situ sensors, housed in three instrument packages. The sensors make measurements of the atmospheric regions between 60-200 km. These instruments are based on extensive heritage from Earth explorers and Pioneer Venus. The mission scenario has several phases and employs aerobraking maneuvers to lower initial apoapsis, thereby reducing fuel requirements. The spacecraft has body-mounted solar cells, enabling deep diving into the Martian atmosphere. The orbital inclination allows for pole-to-pole latitudinal sweeps in an initial elliptical phase, followed by a circular phase affording detailed diurnal measurements. The nominal mission duration at Mars is one Mars year. Derived from text

N94-28816*# SRI International Corp., Menlo Park, CA. Molecular Physics Lab.

PREDISSOCIATION IN N2(C'4, 1 SIGMA u +) AND OTHER N2 STATES AND ITS IMPORTANCE IN THE ATMOSPHERES OF TITAN AND TRITON Annual Report

Tom G. Slanger and Richard A. Copeland Apr. 1994 6 p
(Grant NAGw-3581; SRI Proj. 4725)
(NASA-CR-195727; NAS 1.26:195727) Avail: CASI HC A02/MF A01

The objectives of this program are to further the understanding of the upper atmospheres of Titan, Triton, and the Earth in terms of the observed emissions of the 13-14 eV states of N2. These states are generated at quite high rates, yet very little emission is observed from them. The reasons are complex, involving resonance trapping and predissociation, and it is desired to quantify the effects of predissociation, particularly on the c(sub 4)' 1 Sigma(sub u),(sup +) state of N2. Earlier experiments had indicated that predissociation of the c(sub 4)' state was of little importance, yet over the last two years a growing body of evidence has shown that for levels above v = 2, predissociation is in fact a major process. It is the v = 0 level for which production by electron bombardment and photoexcitation is highest, and so it has been most important to evaluate the effects of predissociation on this particular level. The goal has been to target c(sub 4)' (v = 0) for a thorough analysis, in which both the extent of predissociation as a function of rotational level and the atomic product branching ratio, where the only possible products are N(4S) + N(4S) and N(2D) + N(4S), are determined. For the first year of funding, the intention was to demonstrate two-photon excitation of the intermediate N2(a(sup 1) Pi(sub g)) state, so that the gap to the 13 eV energy region could be bridged, and then use a second laser to reach the c(sub 4)' state itself. Derived from text

N94-29102*# Lunar and Planetary Inst., Houston, TX. Center for Information and Research Services.

VENUS DATA ANALYSIS PROGRAM: DIRECTORY OF RESEARCH PROJECTS (1993-1994)

11 Apr. 1994 99 p
(Contract NASw-4574)
(NASA-CR-195742; NAS 1.26:195742; LPI-TR-94-01) Avail: CASI HC A05/MF A02

This directory provides information about the scientific investigations funded by the NASA Venus Data Analysis Program (VDAP) during fiscal year 1993. The VDAP Directory consists of summary sheets from the proposals that were selected by NASA for funding in FY 93. Each summary sheet indicates the title, principal investigator, institution of the investigation, and information related to the objectives of the research activities proposed for FY 93. The objective of the VDAP Program is to advance our understanding of the nature and evolution of Venus. VDAP supports scientific investigation using data obtained from the Magellan, Pioneer Venus, and other Venus missions, as well as earth-based observations that contribute to understanding the physical and evolutionary properties of Venus. The program intends to enhance the scientific return from these missions by broadening the participation in the analysis of Venus data. Categories of research funded by VDAP are atmosphere, ionosphere, geology, geophysics, and mapping. The directory is intended to provide the science community with an overview of the research projects supported by this program. Research activities identified in this directory were selected for funding in FY 93 on the basis of scientific peer review conducted by the VDAP Review Panel. Derived from text

N94-29737*# Woods Hole Oceanographic Inst., MA. Dept. of Geology and Geophysics.

ANALYSIS OF CRUSTAL STRUCTURE OF VENUS UTILIZING RESIDUAL LINE-OF-SIGHT (LOS) GRAVITY ACCELERATION AND SURFACE TOPOGRAPHY DATA. A TRIAL OF GLOBAL MODELING OF VENUS GRAVITY FIELD USING HARMONIC SPLINE METHOD Final Technical Report

Ming Fang and Carl Bowin 1992 9 p

(Grant NAG2-768)
(NASA-CR-195799; NAS 1.26:195799) Avail: CASI HC A02/MF A01

To construct Venus' gravity disturbance field (or gravity anomaly) with the spacecraft-observer line of site (LOS) acceleration perturbation data, both a global and a local approach can be used. The global approach, e.g., spherical harmonic coefficients, and the local approach, e.g., the integral operator method, based on geodetic techniques are generally not the same, so that they must be used separately for mapping long wavelength features and short wavelength features. Harmonic spline, as an interpolation and extrapolation technique, is intrinsically flexible to both global and local mapping of a potential field. Theoretically, it preserves the information of the potential field up to the bound by sampling theorem regardless of whether it is global or local mapping, and is never bothered with truncation errors. The improvement of harmonic spline methodology for global mapping is reported. New basis functions, a singular value decomposition (SVD) based modification to Parker & Shure's numerical procedure, and preliminary results are presented. Derived from text

N94-29892*# San Jose State Univ., CA.
CORRELATION STUDIES OF PIONEER VENUS IMAGERY OBTAINED FROM PV EXPERIMENTS WITH NEAR IR IMAGERY OBTAINED FROM GROUND-BASED OBSERVATIONS DURING VENUS INFERIOR CONJUNCTION Final Report
Boris Ragent Oct. 1993 55 p
(Grant NAG2-681)
(NASA-CR-195772; NAS 1.26:195772) Avail: CASI HC A04/MF A01

The purpose of this study is to attempt to find correlations between data taken by experiments aboard the Pioneer-Venus Orbiter (PVO) and those obtained from Earth-based near-infrared (NIR) measurements of Venus during periods near inferior conjunction. Since the NIR measurements have been found to provide data on the middle atmosphere cloud morphology and motion, it is assumed that any correlations will also indicate that the PVO experiments are also documenting cloud behavior. If such correlations are found, then a further task is to attempt to study the long term behavior of the cloud features implied by the correlations. Many PVO data have been obtained over an extended period extending from 1978 until the PV demise in 1992. There exists a long, somewhat ill-conditioned time series of data that may contain valuable information on the long time, as well as short term behavior of the clouds, and, derivatively from cloud motion, atmospheric dynamics and wave activity in the Venus atmosphere. For example, determination of the zonal velocities of any OCPP (Cloud Photopolarimeter) 0.935 micron features could then be used for comparisons with data from other sources to attempt to fix the altitude region in which such features existed. A further task of this study is to attempt to correlate any features found in simultaneously obtained data, for example, the OCPP 0.365 and 0.935 micron data. The existence of such correlations may imply that data was obtained in overlapping altitude regions of the atmosphere. Derived from text

N94-30798 Michigan Univ., Ann Arbor.
OBSERVATION OF JOVIAN AURORAL LY-ALPHA LINE PROFILE AND EMISSION VARIABILITY WITH A SOUNDING ROCKET AND THE IUE ARCHIVES Ph.D. Thesis
Walter Michael Harris 1993 229 p
Avail: Univ. Microfilms Order No. DA9319535

The Jovian auroral system provides an excellent laboratory for the study of the interaction of a planetary atmosphere and magnetosphere. The plasma population in the Jovian magnetosphere is dominated by an internal source (Io) and the dynamics of this plasma are controlled by its corotation with the Jovian magnetic field. Observations of the Jovian aurora indicate an energy budget two to three orders of magnitude greater than the earth. These characteristics, combined with the decrease in solar flux and solar wind at 5 AU, make this internally driven auroral system a valuable model from which to expand our understanding of the more complex terrestrial aurora. This research focuses on determining the characteristics of auroral H Ly-alpha emission. Ly-alpha is a powerful diagnostic of the Jovian aurora because it is the only far ultraviolet (FUV) emission feature which may be observed for both line profile information and integrated intensity, and because FUV emission probes the altitudes of greatest auroral energy deposition. The research presented here was approached from two directions. First, a high resolution spectrograph has been constructed to study the Ly-alpha line profile for information regarding the dynamical properties of the auroral atmosphere, the identity of the auroral progenitor particles, and the type and altitude distribution of the contributing emission processes. In the second phase of this research, the archive of IUE auroral spectra is examined for the integrated intensity of auroral Ly-alpha, particularly as it relates to variability in solar Ly-alpha, as well as the altitude, longitude distribution, and variability of auroral H2 band emission. The result of this study indicates no evidence of a link between auroral and solar Ly-alpha. However, a link is established in both the longitude distribution and the optical depth to hydrocarbon absorption of Ly-alpha and H2 emission. The detection of hydrocarbon attenuation in the Ly-alpha emission implies a complex radiative transfer solution in which the effects of resonant scattering must be included. This study concludes with a preliminary examination of these effects on both the intensity of the emission and the shape of the observed line profile. Dissert. Abstr.

N94-29768*# Jet Propulsion Lab., California Inst. of Tech., Pasadena.
THE PLUTO FAST FLYBY MISSION: COMPLETING THE RECONNAISSANCE OF THE SOLAR SYSTEM Abstract Only
Paul K. Henry *In its* Proceedings of the Workshop on Microtechnologies and Applications to Space Systems 15 Jun. 1993 p 13 (For primary document see N94-29767 08-31)
Avail: CASI HC A01/MF A03

92 SOLAR PHYSICS

Includes solar activity, solar flares, solar radiation and sunspots. For related information see *93 Space Radiation.*

N94-29122# National Geophysical Data Center, Boulder, CO.
SOLAR-GEOPHYSICAL DATA NUMBER 591, NOVEMBER 1993. PART 1: PROMPT REPORTS. DATA FOR SEPTEMBER, OCTOBER 1993 AND LATE DATA
H. E. Coffey Nov. 1993 125 p See also PB94-125903
(PB94-140548; SGD-591-Pt-1) Avail: CASI HC A06/MF A02

Contents include the following: Data for October 1993: Solar-Terrestrial Environment; IUWDS Alert Periods (Advance and Worldwide); Solar Activity Indices; Solar Flares; Solar Radio Emission; Stanford Mean Solar Magnetic Field; Data for September 1993: Solar Active Regions; Sudden Ionospheric Disturbances; Solar Radio Spectral Observations; Solar Radioheliograph - 164 MHz - Nancay; Cosmic Ray Measurements by Neutron Monitor; and Geomagnetic Indices. NTIS

N94-29123 National Geophysical Data Center, Boulder, CO.
SOLAR-GEOPHYSICAL DATA NUMBER 592, DECEMBER 1993. PART 1: PROMPT REPORTS. DATA FOR OCTOBER, NOVEMBER 1993 AND LATE DATA
H. E. Coffey Dec. 1993 149 p See also PB94-140548 and PB94-142148 Limited Reproducibility: More than 20% of this document may be affected by microfiche quality
(PB94-142130; SGD-592-Pt-1) Avail: CASI HC A07

Contents include the following: Solar-Terrestrial Environment; IUWDS Alert Periods (Advance and Worldwide); Solar Activity Indices; Solar Flares; Solar Radio Emission; and Stanford Mean Solar Magnetic Field. NTIS

N94-29124 National Geophysical Data Center, Boulder, CO.
SOLAR-GEOPHYSICAL DATA NUMBER 592, DECEMBER 1993. PART 2: COMPREHENSIVE REPORTS. DATA FOR JUNE 1993 AND MISCELLANEOUS
H. E. Coffey Dec. 1993 56 p See also PB94-134830 and PB94-142130 Limited Reproducibility: More than 20% of this document may be affected by microfiche quality
(PB94-142148; SGD-592-Pt-2) Avail: CASI HC A04

Contents include the following: Solar Flares; Solar Radio Bursts at Fixed Frequencies; Solar X-ray Radiation from GOES Satellite Graphs; Mass Ejections from the Sun; Active Prominences and Filaments; Solar Irradiance (Unavailable at time of publication); and IMP-8 Solar Wind Plot (Unavailable at time of publication). NTIS

N94-29132# California Univ., San Diego, La Jolla.
REMOTE SENSING OF INNER HELIOSPHERIC PLASMAS Final Technical Report, 15 Nov. 1990 - 14 Nov. 1993

Bernard V. Jackson 14 Nov. 1993 24 p
(Grant AF-AFOSR-0091-91)
(AD-A275021; AFOSR-94-0004TR) Avail: CASI HC A03/MF A01

Solar disturbances produce major effects on the corona, the solar wind, the interplanetary medium, and the earth along with its magnetosphere. We have developed new techniques for studying plasma disturbances in the inner heliosphere by remotely sensing them. These techniques use data from the HELIOS spacecraft zodiacal light photometers and in situ data, the ISEE-3 spacecraft in situ and kilometer radio wave experiments, and a variety of other spacecraft and ground-based instruments. We use interplanetary scintillation (IPS) data from the Cambridge, England, radio telescope. The zodiacal-light photometers on board the two HELIOS spacecraft (data coverage from 1974 to 1986) provide the first reliable information about the heliospheric masses and shapes of propagating disturbances. DTIC

N94-29212 Air Force Inst. of Tech., Wright-Patterson AFB, OH.
THE APPEARANCE OF THE SUN AND MOON SEEN THROUGH CLOUDS M.S. Thesis
Jeffrey R. Linskens Dec. 1993 66 p Limited Reproducibility: More than 20% of this document may be affected by microfiche quality
(AD-A275338; AFIT/CI/CIA-93-147) Avail: CASI HC A04

The sun occasionally appears fuzzy through altostratus because altostratus is composed of larger particles than other clouds, and is of the necessary optical thickness. Experimental results indicate that the range of optical thicknesses of a cloud at which a fuzzy sun is seen increases with the size of the particles. This relationship is caused by an increase in the attenuation of contrast at high spatial frequencies relative to that at low spatial frequencies when the size of cloud particles increases. The increase in the size of cloud particles is caused by the presence of raindrops and crystals in the cloud. DTIC

N94-29453*# Applied Research Corp., Landover, MD.
CORRELATIVE ANALYSIS OF HARD AND SOFT X RAY OBSERVATIONS OF SOLAR FLARES Final Report
Dominic M. Zarro 21 Jan. 1994 9 p
(Contract NAS5-32064)
(NASA-CR-189329; NAS 1.26:189329) Avail: CASI HC A02/MF A01

We have developed a promising new technique for jointly analyzing BATSE hard X-ray observations of solar flares with simultaneous soft X-ray observations. The technique is based upon a model in which electric currents and associated electric fields are responsible for the respective heating and particle acceleration that occur in solar flares. A useful by-product of this technique is the strength and evolution of the coronal electric field. The latter permits one to derive important flare parameters such as the current density, the number of current filaments composing the loop, and ultimately the hard X-ray spectrum produced by the runaway electrons. We are continuing to explore the technique by applying it to additional flares for which we have joint BATSE/Yohkoh observations. A central assumption of our analysis is the constant of proportionality alpha relating the hard X-ray flux above 50 keV and the rate of electron acceleration. For a thick-target model of hard X-ray production, it can be shown that cv is in fact related to the spectral index and low-energy cutoff of precipitating electrons. The next step in our analysis is to place observational constraints on the latter parameters using the joint BATSE/Yohkoh data. Derived from text

N94-29858*# Lockheed Missiles and Space Co., Palo Alto, CA. Research Lab.
CORONAL ABUNDANCES AND THEIR VARIATION Semiannual Report
Julia L. R. Saba 15 Apr. 1994 20 p
(Contract NASw-4814)
(NASA-CR-195767; NAS 1.26:195767) Avail: CASI HC A03/MF A01

This contract supports the investigation of elemental abundances in the solar corona, principally through analysis of high-resolution soft x-ray spectra from the Flat Crystal Spectrometer (FCS) on the Solar Maximum Mission. The goals of the study are a characterization of the mean values of relative abundances of elements accessible in the FCS data, and information on the extent and circumstances of their variability. This report is a summation of the data analysis and reporting activities which occurred during the first ten months of the contract, 15 Jun. 1993 to 15 Apr. 1994. Author (revised)

N94-30845 Los Alamos National Lab., NM.
RECENT RESULTS FROM SAGE
V. N. Gavrin (Academy of Sciences, USSR, Moscow.), E. L. Faizov (Academy of Sciences, USSR, Moscow.), and A. V. Kalikhov (Academy of Sciences, USSR, Moscow.) 1993 7 p Presented at the Theory and Phenomenology in Astroparticle and Underground Physics Conference, Gran Sasso, Italy, 19-23 Sep. 1993 Limited Reproducibility: More than 20% of this document may be affected by microfiche quality
(Contract W-7405-eng-36)
(DE94-006229; LA-UR-94-25; CONF-9309296-2) Avail: CASI HC A02

A radiochemical Ga-71-Ge-71 experiment to determine the primary flux of neutrinos from the Sun began measurements of the solar neutrino flux at the Baksan Neutrino Observatory in 1990. The number of Ge-71 atoms extracted from initially 30 and later 57 tons of metallic gallium was measured in fifteen runs during the period of Jan. 1990 to May 1992. The observed capture rate is 70 +/- 19 (stat) +/- 10 (syst) SNU. This is to be compared with 132 SNU predicted by the Standard Solar Model. DOE

N94-30884# Brookhaven National Lab., Upton, NY.
SOLAR NEUTRINO EXPERIMENTS: AN UPDATE
R. L. Hahn 1993 23 p Presented at the 14th International Workshop on Weak Interactions and Neutrinos, Seoul, Republic of Korea, 19-24 Jul. 1993
(Contract DE-AC02-76CH-00016)
(DE94-006061; BNL-49971; CONF-9307114-2) Avail: CASI HC A03/MF A01

The situation in solar neutrino physics has changed drastically in the past few years, so that now there are four neutrino experiments in operation, using different methods to look at different regions of the solar neutrino energy spectrum. These experiments are the radiochemical Cl-37 Homestake detector, the realtime Kamiokande detector, and the different forms of radiochemical Ga-71 detectors used in the GALLEX and SAGE projects. It is noteworthy that all of these experiments report a deficit of observed neutrinos relative to the predictions of standard solar models (although in the case of the gallium detectors, the statistical errors are still relatively large). This paper reviews the basic principles of operation of these neutrino detectors, reports their latest results, and discusses some theoretical interpretations. The progress of three real-time neutrino detectors that are currently under construction, SuperKamiok, SNO, and Borexino, is also discussed. DOE

N94-30948*# National Center for Atmospheric Research, Boulder, CO. High Altitude Observatory.
[SOLAR MEASUREMENTS FROM THE AIRGLOW-SOLAR SPECTROMETER INSTRUMENT (ASSI) ON THE SAN MARCO 5 SATELLITE] Final Report
Thomas N. Woods 26 Apr. 1994 39 p Sponsored in part by NSF
(NASA Order S-97242-E)
(NASA-CR-193815; NAS 1.26:193815) Avail: CASI HC A03/MF A01

The analysis of the solar spectral irradiance from the Airglow-Solar Spectrometer Instrument (ASSI) on the San Marco 5 satellite is the focus for this research grant. A pre-print copy of the paper describing the calibrations of and results from the San Marco ASSI is attached to this report. The calibration of the ASSI included (1) transfer of photometric calibration from a rocket experiment and the Solar Mesosphere Explorer (SME), (2) use of the on-board radioactive calibration sources, (3) validation of the ASSI sensitivity over its field of view, and (4) determining the degradation of the spectrometers. We have determined that the absolute values for the solar irradiance needs adjustment in the current proxy models of the solar UV irradiance, and the amount of solar variability from the proxy models are in reasonable agreement with the ASSI measurements. This research grant also has supported the development of a new solar EUV irradiance proxy model. We expected that the magnetic flux is responsible for most of the heating, via Alfen waves, in the chromosphere, transition region, and corona. From examining time series of solar irradiance data and magnetic fields at different levels, we did indeed find that the chromospheric emissions correlate best with the large magnetic field levels. Derived from text

93 SPACE RADIATION

Includes cosmic radiation; and inner and outer earth's radiation belts.

For biological effects of radiation see *52 Aerospace Medicine.* For theory see *73 Nuclear and High-Energy Physics.*

N94-28580# Los Alamos National Lab., NM.
ACCELERATION IN ASTROPHYSICS
Stirling A. Colgate 1993 21 p Presented at the International Workshop on Acceleration and Radiation Generation in Space and Laboratory Plasmas, Kardmall, Greece, 10 Aug. - 4 Sep. 1993 Submitted for publication
(Contract W-7405-eng-36)
(DE94-004986; LA-UR-93-4262; CONF-9308206-1) Avail: CASI HC A03/MF A01

The origin of cosmic rays and applicable laboratory experiments are discussed. Some of the problems of shock acceleration for the production of cosmic rays are discussed in the context of astrophysical conditions. These are: The presumed unique explanation of the power law spectrum is shown instead to be a universal property of all lossy accelerators; the extraordinary isotropy of cosmic rays and the limited diffusion distances implied by supernova induced shock acceleration require a more frequent and space-filling source than supernovae; the near perfect adiabaticity of strong hydromagnetic turbulence necessary for reflecting the accelerated particles each doubling in energy roughly 10(exp 5) to 10(exp 6) scatterings with negligible energy loss seems most unlikely; the evidence for acceleration due to quasiparallel heliosphere shocks is weak (there is small evidence for the expected strong hydromagnetic turbulence and, instead, only a small number of particles accelerate after only a few shock traversals); and the acceleration of electrons in the same collisionless shock that accelerates ions is difficult to reconcile with the theoretical picture of strong hydromagnetic turbulence that reflects the ions. The hydromagnetic turbulence will appear adiabatic to the electrons at their much higher Larmor frequency and so the electrons should not be scattered incoherently as they must be for acceleration. Therefore the electrons must be accelerated by a different mechanism. This is unsatisfactory, because wherever electrons are accelerated, these sites, observed in radio emission, may accelerate ions more favorably. The acceleration is coherent provided the reconnection is coherent, in which case the total flux, as for example of collimated radio sources, predicts single charge accelerated energies much greater than observed. DOE

N94-29046# Aerospace Corp., El Segundo, CA. Technology Operations.
IDENTIFICATION OF AN UNEXPECTED SPACE RADIATION HAZARD
J. B. Blake, M. S. Gussenhoven, E. G. Mullen, and R. W. Fillius 1 Nov. 1993 8 p
(Contract F04701-88-C-0089)
(AD-A275170; TR-92(2940)-12; SMC-TR-93-60) Avail: CASI HC A02/MF A01

A new radiation belt was formed on 24 Mar. 1991 by the interaction of a strong shock in the solar wind with the Earth's magnetosphere. This brief report describes observations of the moment of creation by sensors aboard the CRRES (Combined Release and Radiation Effects Satellite). DTIC

N94-29687 California Inst. of Tech., Pasadena.
A STUDY OF THE ULTRAHIGH-ENERGY COSMIC RAY MASS COMPOSITION WITH THE MACRO AND EAS-TOP EXPERIMENTS Ph.D. Thesis
Stephane Coutu 1993 200 p
Avail: Univ. Microfilms Order No. DA9325348

Two components of cosmic-ray-induced air showers are measured simultaneously at the Gran Sasso Laboratory: the electromagnetic shower at the ground surface by the EAS-TOP extensive air shower array, and the deep-underground muons by the MACRO experiment. The two independent data sets collected during 96.3 days of simultaneous running are combined, and underground muon multiplicity distributions are obtained for anticoincident events (no surface trigger) and high-energy, coincident events. These categories correspond to ranges in primary energy from about 2 x 10(exp 3) GeV to a few times 10(exp 5) GeV, and from about 1.5 x 10(exp 5) GeV to about 10(exp 7) GeV, respectively. The experimental shower size and muon multiplicity distributions, as well as the distribution of mean muon multiplicity as a function of shower size (N-bar(sub mu) -- log(N(sub e)) relation), are compared to the ones obtained with detailed Monte Carlo calculations (with a generator based on recent hadronic accelerator data) using various trial compositions as input. This is done in an effort to discriminate between these models of primary cosmic-ray mass composition at and above the 'kneel' in the all-particle spectrum, where contradictory experimental evidence exists and where a knowledge of the composition would bear upon possible mechanisms for cosmic-ray acceleration and propagation. Detailed studies of simulated anticoincident event rates (which arise from a region of primary energy where the composition has been measured directly by satellite and balloon experiments) uncover problems with the generator used, with between 25 and 40 percent too few high-energy muons created. This, combined with the dependence of absolute event rates on the assumed differential primary energy spectra, hampers the interpretation in terms of composition of underground muon or surface air shower data taken separately. However, the N-bar(sub mu) -- log(N(sub e)) relation is independent of the spectra or overall Monte Carlo normalization problems. The simulated N-bar(sub mu) -- log(N(sub e)) relation for coincident events is found to be inconsistent with the possibility that the cosmic ray flux becomes proton-dominated at and above the knee. Dissert. Abstr.

N94-29823 California Univ., Irvine.
A STUDY OF ULTRA HIGH-ENERGY RADIATION ASSOCIATED WITH HERCULES X-1 Ph.D. Thesis
Steven Douglas Biller 1992 274 p
Avail: Univ. Microfilms Order No. DA9323904

Data from the CYGNUS experiment has been used to examine ultra high energy (UHE) radiation associated with the x ray binary star system Hercules X-1. A search for both pulsed and unpulsed emission over time scales ranging from minutes to years has failed to yield a result of comparable significance to that of the previously published observation of 24 July 1986. A reassessment of this result in light of the number of hypotheses that have been examined for Hercules X-1 yields a probability estimate of 0.44 percent that the data is consistent with background fluctuations. If the number of independent source hypotheses is also accounted for, an overall chance probability of 1.8 percent is assessed for the observations of the CYGNUS experiment. The extensive air showers corresponding to the episode of 24 July 1986 contain a substantial muon content, in contradiction with traditional predictions for primary gamma rays. No satisfactory theory has yet been put forward to explain this phenomenon. A further analysis of shower characteristics for events associated with this episode indicates a steeper radial dependence of the shower-front timing width at a chance probability level of 0.16 percent. This property might be explained by a model that invokes a forward-peaked and/or a deeply interacting component of the hadronic interaction in the atmosphere. The potential importance of UHE observations of Hercules X-1 is great; however, the evidence is not yet compelling. Dissert. Abstr.

N94-29989 Columbia Univ., New York, NY.
BROAD H ALPHA PROFILES OF RADIO-LOUD ACTIVE GALACTIC NUCLEI AND RAPID PROFILE VARIABILITY IN SEYFERT AND RADIO GALAXIES Ph.D. Thesis
Michael Eracleous 1992 114 p
Avail: Univ. Microfilms Order No. DA9313588

This thesis is a study of the shapes and variability of the broad H alpha emission lines of radio-loud active galactic nuclei (AGN's). We present the results of a comprehensive search for double-peaked H alpha profiles among moderate redshift radio galaxies and radio-loud quasars. We find seven new double-peaked H alpha profiles which can be fitted with a simple, relativistic, Keplerian disk model, bringing the total number of such profiles known to 11. Disk-like profiles (12 percent of all the objects we have considered) have noticeably larger full widths at half maximum. This confirms, and possibly explains, the results of previous studies which concluded that radio-loud AGN's have wider and more complex profiles than optically selected objects. In the (radio-loud) objects of our collection, the broad H alpha lines are preferentially redshifted with respect to the frame defined by the narrow lines, in contrast to optically selected samples where blueshifts and redshifts are equally common. In disk-like emitters the continuum in the vicinity of H alpha is dominated by starlight, and the low-excitation, forbidden lines are unusually strong. These trends can be understood in the context of a physical model in which the lines originate

in the outer parts of the accretion disk and are driven by illumination from the inner disk. Alternative models for the origin of double-peaked emission lines include supermassive binary black holes and biconical radial flow. We also present the results of a search for rapid variability (on time scales of hours to days) in the H alpha profiles of eight nearby Seyfert and radio galaxies. The purpose of the search was to look for specific evidence for reverberation from an accretion disk in response to flaring of the source of ionizing radiation. The results are largely negative in that they reveal no profile variability in the H alpha profiles of any of the target objects at the one percent level on time scales of a few days or less. We do, however, find long term variability in some Seyfert galaxies of a type which suggests that the broad H alpha lines may consist of several components that do not vary in concert. Dissert. Abstr.

N94-30248# EG and G Energy Measurements, Inc., Los Alamos, NM.
TAXONOMY OF GAMMA RAY BURSTER DATA USING A SELF-ORGANIZING NEURAL NETWORK
C. W. Baumgart 1993 26 p Presented at the 16th SPIE Thermosense: International Conference on Thermal Sensing and Imaging and Diagnostic Applications, Orlando, FL, 4-8 Apr. 1994
(Contract DE-AC08-93NV-11265)
(DE94-006480; EGG-11265-5012; CONF-940483-3) Avail: CASI HC A03/MF A01

This paper summarizes the results of a signal taxonomy study of gamma ray burst (GRB) data acquired with sensors on-board the Pioneer-Venus Orbiter (PVO) spacecraft. GRB events produce large fluxes of gamma rays with durations of seconds to minutes and have been observed since the early 1970's. The true nature of GRB's is still unknown, and several competing theories exist. A fundamental point of contention among such theories is whether or not different types of GRB exist. If different types of GRB's are discovered in the existing PVO data base, the differences may correlate with their position or source characteristics. Hence, the goal of this project was to use artificial neural networks to perform signal taxonomy on the GRB data base to determine if unique classes or types of GRB's exist. A total of 26 signal features were identified, some of which can be associated directly with some characteristic of the GRB, such as duration, peak count rate, and gamma ray spectrum hardness. Additional features that were selected included the number of zero crossings in the wavelet transform and the fractal dimension of each signal. A self organizing neural network was used with the signal features to search for correlations among the signals contained in the database. The results of this analysis revealed an intrinsic dimensionality of 2 or 3 in the database. That is, it appears as though 2 or 3 distinct types of GRB may exist. In particular, two of the classes contain roughly 90% of the signals in the database of GRB signals we had to work with. These two classes are similar in characteristics but are still sufficiently distinct from one another to form separate categories. The third class of GRB is definitely distinct from the first two. DOE

N94-30351 Princeton Univ., NJ.
AN ABSOLUTE MEASUREMENT OF THE COSMIC BACKGROUND RADIATION TEMPERATURE AT 1.4 GHz Ph.D. Thesis
Suzanne Therese Staggs 1993 160 p
Avail: Univ. Microfilms Order No. DA9328063

A ground-based radiometer is used to measure the absolute temperature of the cosmic background radiation (CBR) at a frequency of 1.4 GHz. The instrument comprises a corrugated horn antenna coupled to a cryogenic correlation receiver. Accurate gain calibrations are made every few minutes; the zero-level is calibrated at the beginning and the end of the observing season. Tip scans are made to measure the atmospheric emission. We find T(sub atm) = 1550 +/- 170 mK for a pencil beam measured from an elevation of 836 m. The galactic foreground emission is removed by extrapolation from a lower-frequency map. Cold loads are used to measure the instrumental emission. The ability to sample narrow (5 MHz) frequency bins across a 5 percent band pass provides a powerful tool for studying systematic effects. The systematic errors are described in detail. For the absolute temperature of the CBR, we find T(sub CBR) = 2.65 (+.33)(-.30) K. This result is in agreement with recent very accurate measurements at higher frequencies. However, the result reported here does not conflict with a low value of T(sub CBR) at 1.4 GHz which has also been reported. Dissert. Abstr.

N94-30222 Hughes Aircraft Co., Los Angeles, CA.
DETERMINATION OF COSMIC RAY LATCHUP RATE IN CMOS DEVICES
M. A. Shoga and E. C. Smith *In* Defence Research Establishment, Proceedings of the 1991 Single Event Upset Symposium 1991 7 p (For primary document see N94-30211 08-73)
Avail: Issuing Activity (Defence Research Establishment, Ottawa, ON K1A 0Z4 Canada)

99 GENERAL

N94-29512# National Inst. for Resources and Environment, Ibaraki (Japan).
JOURNAL OF NIRE, VOL. 2, NO. 3 [SHIGEN TO KANKYO, VOL. 2, NO. 3]
Takeshi Usami, Yoshihiro Ogisu, Masahiro Saito, Nobuo Kido, Koichi Mizuno, Akira Miyazaki, Hiroaki Kondo, Yoshio Yamada, Mikio Kobayashi, and Katsuya Tsurusaki et al 25 May 1993 99 p In JAPANESE
(ISSN 0916-9997)
(JTN-94-80553) Avail: CASI HC A05/MF A02

The following topics were discussed: layered polysilicate, rare metals, rare earth metals, monodispersed fine particles, diamond synthesis, RF (Radio Frequency) plasma, plasma processing, CVD (Chemical Vapor Deposition), plasma jets, gas flow, samarium-cobalt intermetallics, polyimides, graphite fibers, amorphous hydrogenated carbon film, waste water, water treatment, microorganisms, algae, Botryococcus braunii, limestone, andesite, cutter blades, coal mining, coal dust, methane, research facility, international cooperation, earth environment, global warming, green house effect gases, carbon dioxide, and mitigation. For individual titles, see N94-29513 through N94-29522.

N94-29513# National Inst. for Resources and Environment, Ibaraki (Japan). Siliceous Materials Div.
LAYERED POLYSILICATE: PROPERTIES AND PERSPECTIVES IN APPLICATIONS [SOJO PORIKEISANEN: SONO TOKUSEI TO SOZAIKA ENO TENBO] **c27**
Katsunori Kosuge and Atsumu Tsunashima *In its* Journal of NIRE, Vol. 2, No. 3 25 May 1993 p 1-10 In JAPANESE (For primary document see N94-29512 08-99)
Avail: CASI HC A02/MF A02

This report reviews studies on the properties and applications of layered polysilicates. These compounds consist of silica as a major constituent and alkali ions and water molecules. The internal and external surfaces carry silanol group. From these points, layered polysilicates are different from clay minerals and are expected to provide high reactivity in the interlayer space. Particular attention is directed to the potential of these polysilicates for applications relating to their properties such as chemical composition, layered structure, thermal stability, cation exchange, dispersion of particles, gas adsorption and intercalation. An idea to prepare new materials from layered polysilicates by intercalation is also considered.
Author (NASDA)

N94-29514# National Inst. for Resources and Environment, Ibaraki (Japan). Rare Metals Div.
PREPARATION OF MONODISPERSED FINE PARTICLES CONTAINING RARE METALS AND RARE EARTHS [EKISOHO NI YORU REAMETARU REAASU KEI TANBUNSAN BIRYUSHI NO GOSEI] **c25**
Mikio Kobayashi and Yoshihiro Nishisu *In its* Journal of NIRE, Vol. 2, No. 3 25 May 1993 p 11-20 In JAPANESE (For primary document see N94-29512 08-99)
Avail: CASI HC A02/MF A02

The preparation of monodispersed fine particles containing rare metals and rare earths is indispensable to the production of highly functional materials and their performance. The homogeneous nucleation and separation of nucleation stage and growth stage are essential to the preparation of the monodispersed fine particles. The homogeneous precipitation method, hydrolysis method and microemulsion method, which are probably adequate for these purposes, are mainly reviewed.
Author (NASDA)

N94-29515# National Inst. for Resources and Environment, Ibaraki (Japan). Siliceous Materials Div.

SYNTHESIS OF DIAMOND IN A HYDROGEN PLASMA JET: SIMULATIONS OF XRD PATTERNS OF DIAMOND POLYTYPES AND BOUNDARY LAYER ON A SUBSTRATE [SUISO PURAZUMA JETTO NI YORU DAIYAMONDO GOSEI: ROPPOSHO DAIYAMONDO PORITAIPU NO XRD PATAN OYOBI KIBANJO KYOKAISO NO SHIMYURESHON] **c76**

Nobuyuki Kikukawa, Mitsuo Makino, Katsuhisa Maruyama, and Minoru Shiraishi *In its* Journal of NIRE, Vol. 2, No. 3 25 May 1993 p 21-29 In JAPANESE (For primary document see N94-29512 08-99)

Avail: CASI HC A02/MF A02

Two kinds of diamond film were obtained by synthesizing diamond film on Mo substrates in a hydrogen plasma jet. One (type A) was random oriented cubic diamond film with clear habit planes. The other (type B) was film with no habit plane. It was inferred that the majority of type B film consisted of oriented hexagonal diamond polytypes. In order to confirm this fact, XRD (x ray diffraction) patterns of the polytypes was simulated. From the results of the simulated XRD patterns and the analysis of SAD (selected area diffraction) patterns, it can be concluded that type B film consists mainly of a mixture of many kinds of higher hexagonal diamond polytypes, and that these polytypes show a strong bracket 110 bracket orientation in the growth direction; that is, a direction vertical to the substrate surface. The flow and temperature field just above the substrate were simulated to find growth conditions for hexagonal diamond polytypes. It was found that the polytypes could be synthesized when the temperature gradient of boundary layer is greater than the gradient at which cubic diamond is synthesized. Author (NASDA)

N94-29516# National Inst. for Resources and Environment, Ibaraki (Japan). Siliceous Materials Div.

STUDY ON THE FORMATION OF ULTRAFINE PARTICLES OF Sm-Co INTERMETALLIC COMPOUNDS USING RF THERMAL PLASMA [RF NETSU PURAZUMA NI YORU SM-CO KINKOKUKAN KAGOBUTSU CHOBIRYUSHI GOSEI NO KENKYU] **c26**

Nobuyuki Kikukawa, Masami Sugasawa, Mikio Kobayashi, Masakazu Nakamura, and Hiroshi Sakamoto *In its* Journal of NIRE, Vol. 2, No. 3 25 May 1993 p 31-46 In JAPANESE (For primary document see N94-29512 08-99)

Avail: CASI HC A03/MF A02

Alloy ultrafine particles have been successfully synthesized using RF (radio frequency) thermal plasma only in cases in which all constituent elements have essentially the same physical properties such as melting point and vapor pressure. For the Sm - Co system, the difference between the vapor pressures around 2000 K is as much as the factor of 10(exp 4). Moreover, samarium has great affinity toward oxygen. Ultrafine particles of Sm - Co intermetallic compounds such as SmCo5 and Sm2Co17 thus have not been studied. For their preparation, various new techniques were applied such as quenching/sampling by water-cooled probe, holding effluent gas at high temperature by quartz tube, feeding raw materials as mist of organic solutions, and collecting ultrafine particles as colloidal suspension. The products mainly consisted of ultrafine particles of Co and monoclinic Sm2O3. When finely ground alloy powder was used as raw material, intermetallic compounds may possibly have been formed as several ten nanometer particles. The shortcomings and merits of these new techniques were also discussed. Author (NASDA)

N94-29517# National Inst. for Resources and Environment, Ibaraki (Japan). Carbon Materials Div.

PREPARATION OF GRAPHITE FIBERS FROM POLYIMIDE [PORIMIIDO O ZENKUTAI TO SURU KOKESSHOSEI KOKUEN SENI NO SAKUSEI] **c27**

Hiroaki Hatori, Yoshio Yamada, Minoru Shiraishi, and Yoshikazu Takahashi *In its* Journal of NIRE, Vol. 2, No. 3 25 May 1993 p 47-55 In JAPANESE (For primary document see N94-29512 08-99)

Avail: CASI HC A02/MF A02

An in-plane oriented film of Kapton-type polyimide gives a graphite film with high crystallinity after high temperature heat treatment. In-plane orientation is readily brought about when the polyamic acid film, i.e., precursor of the polyimide film, is imidized on a substrate. Through application of this feature, graphite fibers expected to have high conductivity and high strength were prepared. A polyacrylonitrile (PAN) based carbon fiber served as the fibrous substrate and was coated with a polyimide layer, in which molecules were aligned along the fiber surface, was well graphitized after heat treatment up to 2800 C, though the core fiber was nongraphitic. Polyimide coated Kevlar fibers also gave graphite fibers with high crystallinity. In this case, however, the core fibers changed from nongraphitizable to graphitizable by complexing with polyimide. Author (NASDA)

N94-29518# National Inst. for Resources and Environment, Ibaraki (Japan). Carbon Materials Div.

PREPARATION AND STRUCTURE OF AMORPHOUS HYDROGENATED CARBON FILM DEPOSITED WITH RF PLASMA CVD [KOSHUHA PURAZUMA CVD SOCHI NI YORU HISHOSHITSU TANSO(A-C : H) MAKU NO GOSEI TO KOZO KAISEKI] **c27**

Noriko Yoshizawa, Yoshio Yamada, and Minoru Shiraishi *In its* Journal of NIRE, Vol. 2, No. 3 25 May 1993 p 57-65 In JAPANESE (For primary document see N94-29512 08-99)

Avail: CASI HC A02/MF A02

An a-C:H (Amorphous Hydrogenated Carbon) film was prepared from RF (radio frequency) plasma CVD (Chemical Vapor Desposition), and the structure was investigated by means of FT (Fourier Transform)-IR (Infrared), TEM (Transmission Electron Microscope), and EELS (Electron Energy-Loss Spectrometry). The proportion among aromatic, aliphatic sp(sup 2)-, and sp(sup 3)-coordinated carbons were determined to be 1:4:10 by curve-separation technique of FT-IR absorption peaks. The diameters of the hexagonal planes and the cluster of sp(sup 3)-coordinated carbons were determined to be about 7 A with the electron diffraction pattern of the a-C:H. The low elergy-loss region of the EELS spectrum for the a-C:H was analyzed by the use of the elergy-loss function and separated into a pi plasmon peak and two plasmon peaks. These are assigned as aromatic sp(sup 2)-coordinated carbon, aliphatic sp(sup 2)-coordinated carbon, and sp(sup 3)-coordinated carbon, respectively. The ratio of electrons contributing to the peaks was calculated using the theory of the effective number of electrons. The sigma electrons associated with the peak by sp(sup 2)-coordinated carbons(sigma(sub g)) were successfully distinguished from those with sp(sup 3)-coordinated carbons(sigma(sub d)). Considering the pi electrons (pi), the relative numbers of electrons were estimated to be pi:sigma(sub g):sigma(sub d) = 1:6:4. A possible structure for the a-C:H used was exemplified on the basis of these quantitative data.

Author (NASDA)

N94-29519# National Inst. for Resources and Environment, Ibaraki (Japan). Biomass Div.

GROWTH OF HYDROCARBON-RICH MICROALGA BOTRYOCOCCUS BRAUNII IN SECONDARILY TREATED SEWAGE AND ITS CONSUMPTION OF NITRATE ION AND PHOSPHATE ION [GESUI SHORISUI NI OKERU BOTRYOCOCCUS BRAUNII NO ZOSHOKU TO CHISSO OYOBI RIN NO SHOHI NI TSUITE] **c51**

Shigeki Sawayama, Seiichi Inoue, Tomoaki Minowa, and Yutaka Dote *In its* Journal of NIRE, Vol. 2, No. 3 25 May 1993 p 67-71 In JAPANESE (For primary document see N94-29512 08-99)

Avail: CASI HC A01/MF A02

Secondarily Treated Sewage (STS) was used as the growing medium of the green micro-alga, B. (Botryococcus) braunii, which produces hydrocarbon as 50 percent of its dry weight. Algal growth in STS from domestic wastewater was good in a batch system, and hydrocarbon contents of the alga grown in two types of STS were sufficiently high at 53 and 40 percent compared with 58 percent for the Chu 13 medium. B. braunii consumed the nitrate ions in STS, thereby causing a reduction from 7.67 and 4.48 N mg/l to a level below detection (0.01 N mg/l). Phosphate ions were also consumed by B. braunii from 0.02 and 0.29 P mg/l to a level below detection (0.01 P mg/l). Using STS as the growth medium of B. braunii could facilitate the removal of nitrate and phosphate from STS by algal consumption. Author (NASDA)

N94-29520# National Inst. for Resources and Environment, Ibaraki (Japan). Mining System Engineering Div.

INFLUENCE OF CLEARANCE AND RAKE ANGLES ON THE CUTTING FORCE OF ROCK [GANSEKI NO SESSAKU TEIKO NI OYOBOSU NIGEKAKU TO SUKUIKAKU NO EIKYO] **c46**

Tetsuji Ono, Hirokazu Karasawa, and Shigeo Misawa *In its* Journal of NIRE, Vol. 2, No. 3 25 May 1993 p 73-80 In JAPANESE (For

primary document see N94-29512 08-99)
Avail: CASI HC A02/MF A02

Fundamental rock cutting tests for several types of rock were conducted to determine the influence of clearance and rake angles on cutting force (the horizontal and vertical forces). Bits used in the tests had rake angles of -20, 0, 20 deg., and clearance angles were changed from 0 to 12.5 deg. at each rake angle. Oya tuff, Akiyoshi marble and Sanjome andesite (the uniaxial compressive strength is 110, 740, and 1100 kgf/sq cm, respectively) were cut using each bit at a cutting depth of 0.5 to 2.0 mm and cutting speed of 5m/min. The following results were obtained: (1) minimum clearance angle not affecting cutting force was between 2.5 and 5 deg. for Sanjome andesite and Akiyoshi marble, and between 0 and 1 deg. for Oya tuff; (2) rake angle affected cutting force significantly. For example, the cutting force of the bit with a -20 deg. rake angle decreased about 30 - 80 percent, compared to that of the bit with a -20 deg. rake angle; and (3) increase in cutting force with cutting depth became lower with increase in rake angle. Drag bit performance is shown to improve considerably when the rake and clearance angles are set appropriately based on rock formation conditions. Author (NASDA)

N94-29521# National Inst. for Resources and Environment, Ibaraki (Japan). Fire and Explosion Div.
JOINT RESEARCH ACTIVITIES WITH CCMRI (CHINA) [CHUGOKU BAITAN KAGAKU KENKYU SOIN NI OKERU ZAIGAI KENKYU NU GAIYO] **c31**
Takeshi Kamai and Makoto Tanaka *In its* Journal of NIRE, Vol. 2, No. 3 25 May 1993 p 81-86 In JAPANESE (For primary document see N94-29512 08-99)
Avail: CASI HC A02/MF A02

Joint research was made with the Coal Research Institute in China (CCMRI (Central Coal Mining Research Institute)) at their site. The study was conducted as a part of a program called 'Measures against ignition sources of gas and coal dust in coal mines' which focused on abnormal combustion resulting from electrical/frictional sparks and explosives. Safety of coal mine explosives was discussed. Explosion techniques, details, and related experiments were studied. Then detonation properties of explosives were reviewed, followed by experiments on exploding rate measurement and its analysis. The institute has been investigating experiments to study properties of explosions by gas/coal dust and fires in coal mines. Two basic experiments were made at a branch of the Institute: (1) detonation properties of methane-coal dust mixture; and (2) ignition properties of light alloys by frictional sparks. In the first experiment, higher coal dust concentration showed higher explosion pressure, and this was especially evident with high methane gas concentration. In the second experiment, both Japanese and Chinese aluminum alloys revealed to have quite similar ignition properties. Overall, the research produced new discoveries and information on safety and detonation properties of coal mine explosives as well as ignition properties of gas/coal dust by frictional sparks, and they are expected to serve as fundamental data for improvement in ignition sources reduction. Author (NASDA)

N94-29522# National Inst. for Resources and Environment, Ibaraki (Japan).
SECOND JAPAN-U.S. WORKSHOP ON GLOBAL CHANGE: ENVIRONMENTAL RESPONSE TECHNOLOGIES FOR GLOBAL CHANGE (MITIGATION AND ADAPTATION) [CHIKYU KANKYO HENDO NO KEIGEN OYOBI TEKIO NO KENKYU SENRYAKU NI KANSURU NICHIBEI WAKU SHOPPU NO HOKOKU: DAI 2 KAI KAIGO] **c45**
Tateki Mizuno *In its* Journal of NIRE, Vol. 2, No. 3 25 May 1993 p 87-95 In JAPANESE (For primary document see N94-29512 08-99)
Avail: CASI HC A02/MF A02

The second Japan-U.S. Workshop on Global Change: Environmental Response Technologies was held in Hawaii on February 1-3, 1993. Over fifty leading scientists from two countries attended this workshop to examine present technology and decide on research required for the development of new technologies, for mitigation and adaptation to global change. The workshop was organized around three areas of research: (1) capture, fixation/utilization, and disposal of CO2; (2) energy production and conservation technologies to reduce CO2; and (3) adaptation technologies. Priorities for joint research in each of these areas were discussed. Author (NASDA)

N94-29798 Ishikawajima-Harima Heavy Industries Co. Ltd., Tokyo (Japan).
[ACTIVITIES OF ISHIKAWAJIMA-HARIMA HEAVY INDUSTRIES CO. LTD.]
1993 97 p In JAPANESE
(PB94-137981) Copyright Avail: Issuing Activity (National Technical Information Service (NTIS))

Contents include the following: Aircraft Experiment of Six Degrees of Freedom Vibration Isolation System for Microgravity Environments; Robust Control of Jet Engines; Control System for Experimental Equipment on SFU; Neural Network Controller for Underwater Work ROV; Auto-Evaluation of Training for Ship Maneuvering Simulator; pH Fuzzy Control for Pharmaceutical Manufacture; Dynamic Characteristics of Molten Carbonate Fuel Cell Power Plant; Computer Simulation for Rolling Process; Development of Synthesized Control System for Fluidized-Bed Incinerator; Expertizing Diagnosis System and Operation Supporting System for Boiler Plant; and Enhanced In-Service Inspection System for BWR Plant. NTIS

N94-29891*# National Aeronautics and Space Administration. Ames Research Center, Moffett Field, CA.
RESEARCH AND TECHNOLOGY, 1992
Nov. 1993 317 p Original contains color illustrations
(NASA-TM-103996; A-93030; NAS 1.15:103996) Avail: CASI HC A14/MF A03; 7 functional color pages

Selected research and technology activities at Ames Research Center, including the Moffett Field site and the Dryden Flight Research Facility, are summarized. These activities exemplify the Center's varied and productive research efforts for 1992. Author

N94-30168 Israel Atomic Energy Commission, Tel Aviv.
RESEARCH LABORATORIES ANNUAL REPORT 1992
Jul. 1993 279 p Limited Reproducibility: More than 20% of this document may be affected by microfiche quality
(DE94-608124; IA-1481) Avail: CASI HC A13 (US Sales Only)

The report book presents the various research activities within the Israel Atomic Energy Commission, during 1992 calendar year. The discipline reported here are (by chapters): theoretical physics and theoretical chemistry, optics and lasers, solid states and nuclear physics, material sciences, chemistry, radiopharmaceuticals, labelled compounds and environmental studies, radiation effects, dosimetry and protection, and instrumentation and techniques. DOE

N94-30440*# National Aeronautics and Space Administration, Washington, DC.
TECHNOLOGY 2003: THE FOURTH NATIONAL TECHNOLOGY TRANSFER CONFERENCE AND EXPOSITION, VOLUME 1
Michael Hackett, comp. Feb. 1994 460 p Conference held in Anaheim, CA, 7-9 Dec. 1993
(NASA-CP-3249; NAS 1.55:3249) Avail: CASI HC A20/MF A04

Proceedings from symposia of the Technology 2003 Conference and Exposition, December 7-9, 1993, Anaheim, CA, was discussed. Volume 1 features the Plenary Session and the Plenary Workshop, plus papers presented in Advanced Manufacturing, Biotechnology/Medical Technology, Environmental Technology, Materials Science, and Power and Energy. For individual titles, see N94-30441 through N94-30486.

N94-30441*# Jet Propulsion Lab., California Inst. of Tech., Pasadena.
A FORCE-CONTROLLABLE MACRO-MICRO MANIPULATOR AND ITS APPLICATION TO MEDICAL ROBOTS **c37**
Neville I. Marzwell, Darrin R. Uecker, and Yulun Wang *In* NASA, Washington, Technology 2003: The Fourth National Technology Transfer Conference and Exposition, Volume 1 Feb. 1994 p 3-16 (For primary document see N94-30440 08-99)
(Contract NAS7-1149)
Avail: CASI HC A03/MF A04

This paper describes an 8-degrees-of-freedom macro-micro robot. This robot is capable of performing tasks that require accurate force control, such as polishing, finishing, grinding, deburring, and cleaning. The design of the macro-micro mechanism, the control algorithms, and the hardware/software implementation of the algorithms are described in this paper. Initial experimental results are reported. In addition, this paper includes a discussion of medical surgery and the role that force control may play.

We introduce a new class of robotic systems collectively called Robotic Enhancement Technology (RET). RET systems introduce the combination of robotic manipulation with human control to perform manipulation tasks beyond the individual capability of either human or machine. The RET class of robotic systems offers new challenges in mechanism design, control-law development, and man/machine interface design. We believe force-controllable mechanisms such as the macro-micro structure we have developed are a necessary part of RET. Work in progress in the area of RET systems and their application to minimally invasive surgery is presented, along with future research directions. Author

N94-30442*# Jet Propulsion Lab., California Inst. of Tech., Pasadena.
THE USE OF INTERACTIVE COMPUTER VISION AND ROBOT HAND CONTROLLERS FOR ENHANCING MANUFACTURING SAFETY **c37**
Neville I. Marzwell, Charles J. Jacobus, Thomas M. Peurach, and Brian T. Mitchell *In* NASA, Washington, Technology 2003: The Fourth National Technology Transfer Conference and Exposition, Volume 1 Feb. 1994 p 17-31 (For primary document see N94-30440 08-99)
(Contract NAS7-1189)
Avail: CASI HC A03/MF A04

Current available robotic systems provide limited support for CAD-based model-driven visualization, sensing algorithm development and integration, and automated graphical planning systems. This paper describes ongoing work which provides the functionality necessary to apply advanced robotics to automated manufacturing and assembly operations. An interface has been built which incorporates 6-DOF tactile manipulation, displays for three dimensional graphical models, and automated tracking functions which depend on automated machine vision. A set of tools for single and multiple focal plane sensor image processing and understanding has been demonstrated which utilizes object recognition models. The resulting tool will enable sensing and planning from computationally simple graphical objects. A synergistic interplay between human and operator vision is created from programmable feedback received from the controller. This approach can be used as the basis for implementing enhanced safety in automated robotics manufacturing, assembly, repair and inspection tasks in both ground and space applications. Thus, an interactive capability has been developed to match the modeled environment to the real task environment for safe and predictable task execution. Author

N94-30443*# Babcock and Wilcox Co., Lynchburg, VA. CIM Systems.
PROGRAMMABLE AUTOMATED WELDING SYSTEM (PAWS): CONTROL OF WELDING THROUGH SOFTWARE AND HARDWARE **c37**
Martin D. Kline and Thomas E. Doyle *In* NASA, Washington, Technology 2003: The Fourth National Technology Transfer Conference and Exposition, Volume 1 Feb. 1994 p 32-37 (For primary document see N94-30440 08-99)
Avail: CASI HC A02/MF A04

The ATD phase of the PAWS program ended in November 1992 and the follow-on ManTech program was started in September 1993. The system will be industrially hardened during the first year of this program. Follow-on years will focus upon the transition into specific end-user sites. These implementations will also expand the system into other welding processes (e.g. FCAW, GTAW, PAW). In addition, the architecture is being developed for application to other non-welding robotic processes (e.g. inspection, surface finishing). Future development is anticipated to encompass hardening for extreme environments, expanded exception handling techniques, and application to a range of manipulators. Author

N94-30444*# Idaho National Engineering Lab., Idaho Falls.
SENSING THE GAS METAL ARC WELDING PROCESS **c37**
N. M. Carlson, J. A. Johnson, H. B. Smartt, A. D. Watkins, E. D. Larsen, P. L. Taylor, and M. A. Waddoups *In* NASA, Washington, Technology 2003: The Fourth National Technology Transfer Conference and Exposition, Volume 1 Feb. 1994 p 38-53 (For primary document see N94-30440 08-99)
(Contract DE-AC07-76ID-01570)
Avail: CASI HC A03/MF A04

Control of gas metal arc welding (GMAW) requires real-time sensing of the process. Three sensing techniques for GMAW are being developed at the Idaho National Engineering Laboratory (INEL). These are (1) noncontacting ultrasonic sensing using a laser/EMAT (electromagnetic acoustic transducer) to detect defects in the solidified weld on a pass-by-pass basis, (2) integrated optical sensing using a CCD camera and a laser stripe to obtain cooling rate and weld bead geometry information, and (3) monitoring fluctuations in digitized welding voltage data to detect the mode of metal droplet transfer and assure that the desired mass input is achieved. Author

N94-30445*# Air Force Systems Command, Wright-Patterson AFB, OH.
A COMBINED ELECTRON BEAM/OPTICAL LITHOGRAPHY PROCESS STEP FOR THE FABRICATION OF SUB-HALF-MICRON-GATE-LENGTH MMIC CHIPS **c31**
James S. Sewell and Christopher A. Bozada *In* NASA, Washington, Technology 2003: The Fourth National Technology Transfer Conference and Exposition, Volume 1 Feb. 1994 p 54-59 (For primary document see N94-30440 08-99)
Avail: CASI HC A02/MF A04

Advanced radar and communication systems rely heavily on state-of-the-art microelectronics. Systems such as the phased-array radar require many transmit/receive (T/R) modules which are made up of many millimeter wave - microwave integrated circuits (MMIC's). The heart of a MMIC chip is the Gallium Arsenide (GaAs) field-effect transistor (FET). The transistor gate length is the critical feature that determines the operating frequency of the radar system. A smaller gate length will typically result in a higher frequency. In order to make a phased array radar system economically feasible, manufacturers must be capable of producing very large quantities of small-gate-length MMIC chips at a relatively low cost per chip. This requires the processing of a large number of wafers with a large number of chips per wafer, minimum processing time, and a very high chip yield. One of the bottlenecks in the fabrication of MIMIC chips is the transistor gate definition. The definition of sub-half-micron gates for GaAs-based field-effect transistors is generally performed by direct-write electron beam lithography (EBL). Because of the throughput limitations of EBL, the gate-layer fabrication is conventionally divided into two lithographic processes where EBL is used to generate the gate fingers and optical lithography is used to generate the large-area gate pads and interconnects. As a result, two complete sequences of resist application, exposure, development, metallization and lift-off are required for the entire gate structure. We have baselined a hybrid process, referred to as EBOL (electron beam/optical lithography), in which a single application of a multi-level resist is used for both exposures. The entire gate structure, (gate fingers, interconnects and pads), is then formed with a single metallization and lift-off process. The EBOL process thus retains the advantages of the high-resolution E-beam lithography and the high throughput of optical lithography while essentially eliminating an entire lithography/metallization/lift-off process sequence. This technique has been proven to be reliable for both trapezoidal and mushroom gates and has been successfully applied to metal-semiconductor and high-electron-mobility field-effect transistor (MESFET and HEMT) wafers containing devices with gate lengths down to 0.10 micron and 75 x 75 micron gate pads. The yields and throughput of these wafers have been very high with no loss in device performance. We will discuss the entire EBOL process technology including the multilayer resist structure, exposure conditions, process sensitivities, metal edge definition, device results, comparison to the standard gate-layer process, and its suitability for manufacturing. Author

N94-30446*# Metafuse Corp., Los Angeles, CA.
METAFUSION: A BREAKTHROUGH IN METALLURGY **c26**
Adrian A. Joseph *In* NASA, Washington, Technology 2003: The Fourth National Technology Transfer Conference and Exposition, Volume 1 Feb. 1994 p 60-63 (For primary document see N94-30440 08-99)
Avail: CASI HC A01/MF A04

The Metafuse Process is a patented development in the field of thin film coatings utilizing cold fusion which results in a true inter-dispersion of dissimilar materials along a gradual transition gradient through a boundary of several hundred atomic layers. The process is performed at ambient temperatures and pressures requiring relatively little energy and creating little or no heat. The process permits a remarkable range of material combinations and joining of materials which are normally incompatible. Initial applications include titanium carbide into and onto the copper resistance welding electrodes and tungsten carbide onto the cutting edges of tool steel blades. The process is achieved through application of an RF

signal of low power and is based on the theory of vacancy fusion. Author

N94-30447*# Idaho National Engineering Lab., Idaho Falls.
NEAR-NET-SHAPE MANUFACTURING: SPRAY-FORMED METAL MATRIX COMPOSITES AND TOOLING **c24**
Kevin M. McHugh *In* NASA, Washington, Technology 2003: The Fourth National Technology Transfer Conference and Exposition, Volume 1 Feb. 1994 p 64-73 (For primary document see N94-30440 08-99)
(Contract DE-AC07-76ID-01570)
Avail: CASI HC A02/MF A04

Spray forming is a materials processing technology in which a bulk liquid metal is converted to a spray of fine droplets and deposited onto a substrate or pattern to form a near-net-shape solid. The technology offers unique opportunities for simplifying materials processing without sacrificing, and oftentimes substantially improving, product quality. Spray forming can be performed with a wide range of metals and nonmetals, and offers property improvements resulting from rapid solidification (e.g. refined microstructures, extended solid solubilities and reduced segregation). Economic benefits result from process simplification and the elimination of unit operations. The Idaho National Engineering Laboratory is developing a unique spray-forming method, the Controlled Aspiration Process (CAP), to produce near-net-shape solids and coatings of metals, polymers, and composite materials. Results from two spray-accompanying technical and economic benefits. These programs involved spray forming aluminum strip reinforced with SiC particulate, and the production of tooling, such as injection molds and dies, using low-melting-point metals. Author

N94-30448*# Boeing Defense and Space Group, Philadelphia, PA. Helicopter Div.
COMPOSITE HOT DRAPE FORMING **c31**
Thomas Ott *In* NASA, Washington, Technology 2003: The Fourth National Technology Transfer Conference and Exposition, Volume 1 Feb. 1994 p 74-80 (For primary document see N94-30440 08-99)
Avail: CASI HC A02/MF A04

This program was initiated to replace labor-intensive ply-by-ply layup of composite I-beam posts and angle stiffeners used in the Space Station Freedom (SSF) rack structure. Hot drape forming (HDF) has been successfully implemented by BCAG for 777 composite I-stringers and by Bell Helicopter/Textron for the V-22 I-stingers. The two companies utilize two vastly different approaches to the I-beam fabrication process. A drape down process is used by Bell Helicopter where the compacted ply charge is placed on top of a forming mandrel and heated. When the heated ply charge reached a set temperature, vacuum pressure is applied and the plies are formed over the mandrel. The BCAG 777 process utilizes an inverted forming process where the ply stack is placed on a forming table and the mandrel is inverted and placed upon the ply stack. A heating and vacuum bladder underneath the ply stack form the play stack up onto the mandrels after reaching the temperature setpoint. Both methods have their advantages, but the drape down process was selected for SSF because it was more versatile and could be fabricated from readily available components. Author

N94-30449*# Lawrence Livermore National Lab., CA.
PRECISION AND MANUFACTURING AT THE LAWRENCE LIVERMORE NATIONAL LABORATORY **c31**
Theodore T. Saito, Richard J. Wasley, Irving F. Stowers, Robert R. Donaldson, and Daniel C. Thompson *In* NASA, Washington, Technology 2003: The Fourth National Technology Transfer Conference and Exposition, Volume 1 Feb. 1994 p 81-89 (For primary document see N94-30440 08-99)
(Contract W-7405-eng-48)
Avail: CASI HC A02/MF A04

Precision Engineering is one of the Lawrence Livermore National Laboratory's core strengths. This paper discusses the past and present current technology transfer efforts of LLNL's Precision Engineering program and the Livermore Center for Advanced Manufacturing and Productivity (LCAMP). More than a year ago the Precision Machine Commercialization project embodied several successful methods of transferring high technology from the National Laboratories to industry. Currently, LCAMP has already demonstrated successful technology transfer and is involved in a broad spectrum of current programs. In addition, this paper discusses other technologies ripe for future transition including the Large Optics Diamond Turning Machine. Author

N94-30450*# Argonne National Lab., Idaho Falls, ID. Energy Technology Div.
POTENTIAL CAPABILITIES OF REYNOLDS STRESS TURBULENCE MODEL IN THE COMMIX-RSM CODE **c34**
F. C. Chang and M. Bottoni *In* NASA, Washington, Technology 2003: The Fourth National Technology Transfer Conference and Exposition, Volume 1 90-99 (SEE N94-30440 08-99) Feb. 1994 (For primary document see N94-30440 08-99)
Avail: CASI HC A02/MF A04

A Reynolds stress turbulence model has been implemented in the COMMIX code, together with transport equations describing turbulent heat fluxes, variance of temperature fluctuations, and dissipation of turbulence kinetic energy. The model has been verified partially by simulating homogeneous turbulent shear flow, and stable and unstable stratified shear flows with strong buoyancy-suppressing or enhancing turbulence. This article outlines the model, explains the verifications performed thus far, and discusses potential applications of the COMMIX-RSM code in several domains, including, but not limited to, analysis of thermal striping in engineering systems, simulation of turbulence in combustors, and predictions of bubbly and particulate flows. Author

N94-30451*# Army Armament Munitions and Chemical Command, Watervliet, NY. Army Research, Deveiopment, and Engineering Center.
AN IMPROVED PLATING PROCESS **c27**
John C. Askew *In* NASA, Washington, Technology 2003: The Fourth National Technology Transfer Conference and Expositttion, Volume 1 Feb. 1994 p 100-107 (For primary document see N94-30440 08-99)
Avail: CASI HC A02/MF A04

An alternative to the immersion process for the electrodeposition of chromium from aqueous solutions on the inside diameter (ID) of long tubes is described. The Vessel Plating Process eliminates the need for deep processing tanks, large volumes of solutions, and associated safety and environmental concerns. Vessel Plating allows the process to be monitored and controlled by computer thus increasing reliability, flexibility and quality. Elimination of the trivalent chromium accumulation normally associated with ID plating is intrinsic to the Vessel Plating Process. The construction and operation of a prototype Vessel Plating Facility with emphasis on materials of construction, engineered and operational safety and a unique system for rinse water recovery are described. Author

N94-30452*# Phillips Lab., Edwards AFB, CA.
THE UNIVERSAL APPLICATIONS OF MICROTUBES AND MICROTUBE COMPOSITES **c24**
Wesley P. Hoffman and Kamleshwar Upadhya *In* NASA, Washignton, Technology 2003: The Fourth National Technology Transfer Conference and Exposition, Volume 1 Feb. 1994 p 108-113 (For primary document see N94-30440 08-99)
Avail: CASI HC A02/MF A04

Microtubes are a basic component for a myriad of potential products. They are very small tubes (hundreds can fit in a human hair) that can be made from practically any material. Tubes larger than 1 micron diameter can be made with any cross-sectional shape desired. The significance of microtubes and microtube composites is that they provide the opportunity to miniaturize (even to the nanoscale) numerous products and devices that are currently in existence as well as allowing the fabrication of products that have to date been impossible to produce. Author

N94-30453*# National Aeronautics and Space Administration. Lyndon B. Johnson Space Center, Houston, TX.
MICROENCAPSULATION OF ANTI-TUMOR, ANTIBIOTIC AND THROMBOLYTIC DRUGS IN MICROGRAVITY **c52**
Dennis R. Morrison, Benjamin Mosier, and John Cassanto *In* NASA, Washington, Technology 2003: The Fourth National Technology Transfer Conference and Exposition, Volume 1 Feb. 1994 p 117-126 (For primary document see N94-30440 08-99)
Avail: CASI HC A02/MF A04

Encapsulation of cytotoxic or labile drugs enables targeted delivery and sustained release kinetics that are not available with intravenous

injection. A new liquid-liquid diffusion process has been developed for forming unique microcapsules that contain both aqueous and hydrocarbon soluble drugs. Microgravity experiments, on sounding rockets (1989-92) and Shuttle missions STS-52 (1992) and STS-56 (1993) using an automated Materials Dispersion Apparatus, produced multi-lamellar microcapsules containing both Cis-platinum (anti-tumor drug) and iodinated poppy seed oil (a radiocontrast medium), surrounded by a polyglyceride skin. Microcapsules formed with amoxicillin (antibiotic) or urokinase (a clot dissolving enzyme), co-encapsulated with IPO, are still intact after two years. Microcapsules were formed with the drug so concentrated that crystals formed inside. Multi-layered microspheres, with both hydrophobic drug compartments, can enable diffusion of complementary drugs from the same microcapsule, e.g. antibiotics and immuno-stimulants to treat resistant infections or multiple fibrinolytic drugs to dissolve emboli. Co-encapsulation of enough radio-contrast medium enables oncologists to monitor the delivery of anti-tumor microcapsules to target tumors using computerized tomography and radiography that would track the distribution of microcapsules after release from the intra-arterial catheter. These microcapsules could have important applications in chemotheraphy of certain liver, kidney, brain and other tumors. Author

N94-30454*# Geo-Centers, Inc., Lake Hopatcong, NJ.
CUBANES: SUPER EXPLOSIVES AND POTENTIAL PHARMACEUTICAL INTERMEDIATES **c28**
A. Bashir-Hashemi *In* NASA, Washington, Technology 2003: The Fourth National Technology Transfer Conference and Exposition, Volume 1 Feb. 1994 p 127-130 (For primary document see N94-30440 08-99)
Avail: CASI HC A01/MF A04

The cubane molecule, in which eight carbon atoms are locked in a cubic framework, shows great potential for both military and pharmaceutical applications. Octanitrocubane, with a predicted density of 2.1 g/cc and strain energy of more than 165 kcal/mol, is considered to be the 'super-explosive', while cubane derivatives submitted to the National Institutes of Health for preliminary biological activity screening have displayed promising anti-cancer and anti-HIV activity. Author

N94-30455*# National Aeronautics and Space Administration. Lyndon B. Johnson Space Center, Houston, TX.
DUAL USE OF IMAGE BASED TRACKING TECHNIQUES: LASER EYE SURGERY AND LOW VISION PROSTHESIS **c52**
Richard D. Juday *In* NASA, Washington, Technology 2003: The Fourth National Technology Transfer Conference and Exposition, Volume 1 Feb. 1994 p 131-137 (For primary document see N94-30440 08-99)
Avail: CASI HC A02/MF A04

With a concentration on Fourier optics pattern recognition, we have developed several methods of tracking objects in dynamic imagery to automate certain space applications such as orbital rendezvous and spacecraft capture, or planetary landing. We are developing two of these techniques for Earth applications in real-time medical image processing. The first is warping of a video image, developed to evoke shift invariance to scale and rotation in correlation pattern recognition. The technology is being applied to compensation for certain field defects in low vision humans. The second is using the optical joint Fourier transform to track the translation of unmodeled scenes. Developed as an image fixation tool to assist in calculating shape from motion, it is being applied to tracking motions of the eyeball quickly enough to keep a laser photocoagulation spot fixed on the retina, thus avoiding collateral damage. Author

N94-30456*# Jet Propulsion Lab., California Inst. of Tech., Pasadena.
ANALYSIS AND AN IMAGE RECOVERY ALGORITHM FOR ULTRASONIC TOMOGRAPHY SYSTEM **c52**
Michael Y. Jin *In* NASA, Washington, Technology 2003: The Fourth National Technology Transfer Conference and Exposition, Volume 1 Feb. 1994 p 138-145 (For primary document see N94-30440 08-99)
Avail: CASI HC A02/MF A04

The problem of an ultrasonic reflectivity tomography is similar to that of a spotlight-mode aircraft Synthetic Aperture Radar (SAR) system. The analysis for a circular path spotlight mode SAR in this paper leads to the insight of the system characteristics. It indicates that such a system when operated in a wide bandwidth is capable of achieving the ultimate resolution; one quarter of the wavelength of the carrier frequency. An efficient processing algorithm based on the exact two dimensional spectrum is presented. The results of simulation indicate that the impulse responses meet the predicted resolution performance. Compared to an algorithm previously developed for the ultrasonic reflectivity tomography, the throughput rate of this algorithm is about ten times higher. Author

N94-30457*# National Aeronautics and Space Administration. Marshall Space Flight Center, Huntsville, AL.
COMPOSITE REDESIGN OF OBSTETRICAL FORCEPS **c52**
Seth W. Lawson and Stan S. Smeltzer *In* NASA, Washington, Technology 2003: The Fourth National Technology Transfer Conference and Exposition, Volume 1 Feb. 1994 p 146-150 (For primary document see N94-30440 08-99)
Avail: CASI HC A01/MF A04

Due to the increase in the number of children being born recently, medical technology has struggled to keep pace in certain areas. In these areas, particular needs have arisen to which the subject of this paper is directed. In the area of obstetrics, the forceps design and function has remained relatively unchanged for a number of years. In an effort to advance the technology, NASA Marshall Space Flight Center has been asked by the obstetrical community to help in a redesign of the obstetric forceps. Traditionally the forceps design has been of tubular stainless steel, constructed in two halves which interlock and hinge to provide the gripping force necessary to aid in the delivery of an infant. The stainless steel material was used to provide for ease of cleaning and sterilization. However, one of the drawbacks of the non-flexible steel design is that excessive force can be placed upon an infants head which could result in damage or injury to the infant. The redesign of this particular obstetric tool involves applying NASA's knowledge of advanced materials and state of the art instrumentation to create a tool which can be used freely throughout the obstetrics community without the fear of injury to an infant being delivered. Author

N94-30458*# National Aeronautics and Space Administration. Lyndon B. Johnson Space Center, Houston, TX.
DEVELOPMENT OF THE NASA/BAYLOR VAD **c52**
G. S. Aber, J. W. Akkerman, R. J. Bozeman, Jr., D. R. Saucler, J. W. Bacak, P. A. Svejkovsky, G. A. Damm, K. Mizuguchi, G. P. Noon, and Y. Nose et al *In* NASA, Washington, Technology 2003: The Fourth National Technology Transfer Conference and Exposition, Volume 1 Feb. 1994 p 151-157 (For primary document see N94-30440 08-99)
Avail: CASI HC A02/MF A04

A cooperative effort between the NASA/Johnson Space Center (JSC) and the Baylor College of Medicine (BCM) has been underway since 1988 to develop a long-term implantable Ventricular Assist Device (VAD). The VAD is intended to boost the cardiac output of patients with deteriorated cardiac function. For many of these patients, the best alternative is heart transplantation. Heart transplantation is a complex and expensive procedure and usually requires a long waiting period for a donor heart. The condition of the patient often deteriorates during this waiting period which complicates the pre and post-operative care. Because of these factors, the need for a long-term implantable VAD for use as a bridge-to-transplant device or as a permanent assist device has become the focus of much research. The need for a VAD has been estimated at 50,000 to 60,000 patients per year in the United States alone. A device which satisfies all the system performance and reliability requirements has yet to be achieved. However, the development of the NASA/Baylor VAD has progressed to a state in which commercial viability can being to be considered. The device is small, simple, efficient and reliable which meets all requirements for a totally implantable VAD. Author

N94-30459*# Jet Propulsion Lab., California Inst. of Tech., Pasadena.
A FUZZY LOGIC CONTROLLER FOR HORMONE ADMINISTRATION USING AN IMPLANTABLE PUMP **c52**
L. Stephen Coles and George H. Wells, Jr. *In* NASA, Washington, Technology 2003: The Fourth National Technology Transfer Conference and Exposition, Volume 1 Feb. 1994 p 158-167 (For primary document see N94-30440 08-99)
Avail: CASI HC A02/MF A04

This paper describes the requirements for a Fuzzy Logic Controller for the physiologic administration of hormones by means of a FDA-approved surgically implantable infusion pump. Results of a LabVIEW computer simulation for the administration of insulin for diabetic adult patients as

well as human growth hormone for pediatric patients are presented. A VHS video tape of the simulation in action has been prepared and is available for viewing. Author

N94-30460*# Army Armament Research, Development and Engineering Center, Watervliet, NY. Benet Labs.

MONITOR FOR STATUS EPILEPTICUS SEIZURES c52

Mark Johnson and Thomas Simkins *In* NASA, Washington, Technology 2003: The Fourth National Technology Transfer Conference and Exposition, Volume 1 Feb. 1994 p 168-175 (For primary document see N94-30440 08-99)

Avail: CASI HC A02/MF A04

This paper describes the sensor technology and associated electronics of a monitor designed to detect the onset of a seizure disorder called status epilepticus. It is a condition that affects approximately 3-5 percent of those individuals suffering from epilepsy. This form of epilepsy does not follow the typical cycle of start-peak-end. The convulsions continue until medically interrupted and are life threatening. The mortality rate is high without prompt medical treatment at a suitable facility. The paper describes the details of a monitor design that provides an inexpensive solution to the needs of those responsible for the care of individuals afflicted with this disorder. The monitor has been designed as a cooperative research and development effort involving the United States Army Armament Research, Development, and Engineering Center's Benet Laboratories (Benet) and the Cerebral Palsy Center for the Disabled (Center), in association with the Department of Neurology at Albany Medical College (AMC). Benet has delivered a working prototype of the device for field testing, in collaboration with Albany Medical College. The Center has identified several children in need of special monitoring and has agreed to pursue commercialization of the device. Author

N94-30461*# Department of Agriculture, Starkville, MS. Forest Service.

SEED VIABILITY DETECTION USING COMPUTERIZED FALSE-COLOR RADIOGRAPHIC IMAGE ENHANCEMENT c51

J. A. Vozzo and Michael Marko *In* NASA, Washington, Technology 2003: The Fourth National Technology Transfer Conference and Exposition, Volume 1 Feb. 1994 p 179-187 (For primary document see N94-30440 08-99)

Avail: CASI HC A02/MF A04

Seed radiographs are divided into density zones which are related to seed germination. The seeds which germinate have densities relating to false-color red. In turn, a seed sorter may be designed which rejects those seeds not having sufficient red to activate a gate along a moving belt containing the seed source. This results in separating only seeds with the preselected densities representing biological viability lending to germination. These selected seeds demand a higher market value. Actual false-coloring isn't required for a computer to distinguish the significant gray-zone range. This range can be predetermined and screened without the necessity of red imaging. Applying false-color enhancement is a means of emphasizing differences in densities of gray within any subject from photographic, radiographic, or video imaging. Within the 0-255 range of gray levels, colors can be assigned to any single level or group of gray levels. Densitometric values then become easily recognized colors which relate to the image density. Choosing a color to identify any given density allows separation by morphology or composition (form or function). Additionally, relative areas of each color are readily available for determining distribution of that density by comparison with other densities within the image. Author (revised)

N94-30462*# Purus, Inc., San Jose, CA.

A COMMERCIALIZED, CONTINUOUS FLOW FIBER OPTIC SENSOR FOR TRICHLOROETHYLENE AND HALOFORMS c74

James C. Wells and Mark D. Johnson *In* NASA, Washington, Technology 2003: The Fourth National Technology Transfer Conference and Exposition, Volume 1 Feb. 1994 p 188-195 (For primary document see N94-30440 08-99)

Avail: CASI HC A02/MF A04

Purus, Inc. has commercialized a fiber optic chemical sensor using technology developed by Lawrence Livermore National Laboratory and licensed from The University of California. The basis for the sensor is the development of color within a reagent when exposed to an analyte. The sensor consists of an optrode, reagent delivery and recover system, fiber optic transmitter-receiver, controller, and display. Reagent is pumped through the optrode. Analyte diffuses across a gas permeable membrane and reacts with the reagent to form a colored product. The colored product is detected by measuring the absorbance of light from a 568 nm diode. Reagents are currently available for TCE and trihalomethanes. Initial reagent chemistry is based on the Fujiwara alkaline pyridine reaction. The optrode contacts only gas streams, but the volatility of the current analytes also allows measurements of aqueous streams, without being affected by aqueous interferents that are non-volatile. Sensitivity of the sensor has been demonstrated to 5 ppb aqueous solutions and 0.1 ppmv in flowing gas streams. Author

N94-30463*# National Aeronautics and Space Administration. Marshall Space Flight Center, Huntsville, AL.

COMPUTERIZED IN VITRO TEST FOR CHEMICAL TOXICITY BASED ON TETRAHYMENA SWIMMING PATTERNS c45

David A. Noever, Helen C. Matsos, Raymond J. Cronise, Loren L. Looger, Rachna A. Relwani, and Jacqueline U. Johnson *In* NASA, Washington, Technology 2003: The Fourth National Technology Transfer Conference and Exposition, Volume 1 Feb. 1994 p 196-208 (For primary document see N94-30440 08-99)

Avail: CASI HC A03/MF A04

An apparatus and method for rapidly determining chemical toxicity was evaluated. The toxicity monitor includes an automated scoring of how motile biological cells (Tetrahymena pyriformis) slow down or otherwise change their swimming patterns in a hostile chemical environment. The device, called the Motility Assay Apparatus (MAA) is tested for 30 second determination of chemical toxicity in 20 aqueous samples containing trace organics and salts. With equal or better detection limits, results compare favorably to in vivo animal tests of eye irritancy, in addition to agreeing for all chemicals with previous manual evaluations of single cell motility. Author (revised)

N94-30464*# Idaho National Engineering Lab., Idaho Falls.

A MODULAR APPROACH FOR AUTOMATED SAMPLE PREPARATION AND CHEMICAL ANALYSIS c45

Michael L. Clark, Terry D. Turner, Kerry M. Klingler, and Randolph Pacetti *In* NASA, Washignton, Technology 2003: The Fourth National Technology Transfer Conference and Exposition, Volume 1 Feb. 1994 p 209-218 (For primary document see N94-30440 08-99)

Avail: CASI HC A02/MF A04

Changes in international relations, especially within the past several years, have dramatically affected the programmatic thrusts of the U.S. Department of Energy (DOE). The DOE now is addressing the environmental cleanup required as a result of 50 years of nuclear arms research and production. One major obstacle in the remediation of these areas is the chemical determination of potentially contaminated material using currently acceptable practices. Process bottlenecks and exposure to hazardous conditions pose problems for the DOE. One proposed solution is the application of modular automated chemistry using Standard Laboratory Modules (SLM) to perform Standard Analysis Methods (SAM). The Contaminant Analysis Automation (CAA) Program has developed standards and prototype equipment that will accelerate the development of modular chemistry technology and is transferring this technology to private industry. Author

N94-30465*# Naval Surface Warfare Center, Panama City, FL. Coastal Systems Station.

PHOTOVOLTAIC POWER WITHOUT BATTERIES FOR CONTINUOUS CATHODIC PROTECTION c44

W. W. Muehl, Sr. *In* NASA, Washington, Technology 2003: The Fourth National Technology Transfer Conference and Exposition, Volume 1 Feb. 1994 p 219-222 (For primary document see N94-30440 08-99)

Avail: CASI HC A01/MF A04

The COASTSYSTA designed, installed, and started up on 20 Jan. 1990, a state-of-the-art stand alone photovoltaic powered impressed current cathodic protection system (PVCPSYS) not requiring any auxiliary/battery backup power for steel and iron submerged structures. The PVCPSYS installed on 775' of steel sheet piling of a Navy bulkhead is continuing to provide complete, continuous corrosion protection. This has been well documented by COASTSYSTA and verified on-site by the U.S. Army Civil Engineering Research Laboratory, Champaign, Illinois and the Navy Energy

Program Office-Photovoltaic Programs, China Lake, California. The Department of Defense (DoD) Photovoltaic Review Committee and Sandia National Laboratories consider this successful and cost effective system a major advance in the application of photovoltaic power. The PVCPSYS uses only renewable energy and is environmentally clean. A patent is pending on the new technology. Other possible PVCPSYS applications are mothballed ships, docks, dams, locks, bridges, marinas, offshore structures, and pipelines. The initial cost savings by installing a PVCPSYS vs. a conventional CP system was in excess of $46,000.00. Author

N94-30466*# Allied-Signal Corp., Kansas City, MO.
NON-AQUEOUS CLEANING SOLVENT SUBSTITUTION c45
Gerald J. Meier *In* NASA, Washington, Technology 2003: The Fourth National Technology Transfer Conference and Exposition, Volume 1 Feb. 1994 p 223-231 (For primary document see N94-30440 08-99)
(Contract DE-AC04-76DP-00613)
Avail: CASI HC A02/MF A04

A variety of environmental, safety, and health concerns exist over use of chlorinated and fluorinated cleaning solvents. Sandia National Laboratories, Lawrence Livermore National Laboratories, and the Kansas City Division of AlliedSignal have combined efforts to focus on finding alternative cleaning solvents and processes which are effective, environmentally safe, and compliant with local, state, and federal regulations. An alternative solvent has been identified, qualified, and implemented into production of complex electronic assemblies, where aqueous and semi-aqueous cleaning processes are not allowed. Extensive compatibility studies were performed with components, piece-parts, and materials. Electrical testing and accelerated aging were used to screen for detrimental, long-term effects. A terpene, d-limonene, was selected as the solvent of choice, and it was found to be compatible with the components and materials tested. A brief history of the overall project will be presented, along with representative cleaning efficiency results, compatibility results, and residual solvent data. The electronics industry is constantly searching for proven methods and environmentally-safe materials to use in manufacturing processes. The information in this presentation will provide another option to consider on future projects for applications requiring high levels of quality, reliability, and cleanliness from non-aqueous cleaning processes. Author (revised)

N94-30467*# National Aeronautics and Space Administration. John F. Kennedy Space Center, Cocoa Beach, FL.
SUPERSONIC GAS-LIQUID CLEANING SYSTEM c31
Raoul E. B. Caimi and Eric A. Thaxton *In* NASA, Washington, Technology 2003: The Fourth National Technology Transfer Conference and Exposition, Volume 1 Feb. 1994 p 232-240 (For primary document see N94-30440 08-99)
Avail: CASI HC A02/MF A04

A system to perform cleaning and cleanliness verification is being developed to replace solvent flush methods using CFC 113 for fluid system components. The system is designed for two purposes: internal and external cleaning and verification. External cleaning is performed with the nozzle mounted at the end of a wand similar to a conventional pressure washer. Internal cleaning is performed with a variety of fixtures designed for specific applications. Internal cleaning includes tubes, pipes, flex hoses, and active fluid components such as valves and regulators. The system uses gas-liquid supersonic nozzles to generate high impingement velocities at the surface of the object to be cleaned. Compressed air or any inert gas may be used to provide the conveying medium for the liquid. The converging-diverging nozzles accelerate the gas-liquid mixture to supersonic velocities. The liquid being accelerated may be any solvent including water. This system may be used commercially to replace CFC and other solvent cleaning methods widely used to remove dust, dirt, flux, and lubricants. In addition, cleanliness verification can be performed without the solvents which are typically involved. This paper will present the technical details of the system, the results achieved during testing at KSC, and future applications for this system. Author (revised)

N94-30468*# Custom Process Systems and Service Co., Pasadena, TX.
REGENERATING USING AQUEOUS CLEANERS WITH OZONE AND ELECTROLYSIS c31
Michael P. McGinness *In* NASA, Washington, Technology 2003: The Fourth National Technology Transfer Conference and Exposition, Volume 1 Feb. 1994 p 241-247 (For primary document see N94-30440 08-99)
Avail: CASI HC A02/MF A04

A new process converts organic oil and grease contaminates in used water based cleaners into synthetic surfactants. This permits the continued use of a cleaning solution long after it would have been dumped using previously known methods. Since the organic soils are converted from contaminates to cleaning compounds the need for frequent bath dumps is totally eliminated. When cleaning solutions used in aqueous cleaning systems are exhausted and ready for disposal, they will always contain the contaminates removed from the cleaned parts and drag-in from prior cleaning steps. Even when the cleaner is biodegradable these contaminants will frequently cause the waste cleaning solution to be a hazardous waste. Chlorinated solvents are rapidly being replaced by aqueous cleaners to avoid the new ozone-depletion product-labeling-law. Many industry standard halocarbon based solvents are being completely phased out of production, and their prices have nearly tripled. Waste disposal costs and cradle-to-grave liability are also major concerns for industry today. This new process reduces the amount of water and chemicals needed to maintain the cleaning process. The cost of waste disposal is eliminated because the water and cleaning compounds are reused. Energy savings result by eliminating the need for energy currently used to produce and deliver fresh water and chemicals as well as the energy used to treat and destroy the waste from the existing cleaning processes. This process also allows the cleaning bath to be maintained at the peak performance of a new bath resulting in decreased cycle times and decreased energy consumption needed to clean the parts. This results in a more efficient and cost effective cleaning process. Author (revised)

N94-30469*# McDonnell-Douglas Corp., Huntington Beach, CA.
GAS STREAM PURIFIER c45
Steven J. Adam *In* NASA, Washington, Technology 2003: The Fourth National Technology Transfer Conference and Exposition, Volume 1 Feb. 1994 p 248-257 (For primary document see N94-30440 08-99)
Avail: CASI HC A02/MF A04

A gas stream purifier has been developed that is capable of removing corrosive acid, base, solvent, organic, inorganic, and water vapors as well as particulates from an inert mixed gas stream using only solid scrubbing agents. This small, lightweight purifier has demonstrated the ability to remove contaminants from an inert gas stream with a greater than 99 percent removal efficiency. The Gas Stream Purifier has outstanding market and sales potential in manufacturing, laboratory and science industries, medical, automotive, or any commercial industry where pollution, contamination, or gas stream purification is a concern. The purifier was developed under NASA contract NAS9-18200 Schedule A for use in the international Space Station. A patent application for the Gas Stream Purifier is currently on file with the United States Patent and Trademark Office. Author

N94-30470*# National Aeronautics and Space Administration. Lyndon B. Johnson Space Center, Houston, TX.
USING SPACECRAFT TRACE CONTAMINANT CONTROL SYSTEMS TO CURE SICK BUILDING SYNDROME c45
John C. Graf *In* NASA, Washington, Technology 2003: The Fourth National Technology Transfer Conference and Exposition, Volume 1 Feb. 1994 p 258-265 (For primary document see N94-30440 08-99)
Avail: CASI HC A02/MF A04

Many residential and commercial buildings with centralized, recirculating, heating ventilation and air conditioning systems suffer from 'Sick Building Syndrome.' Ventilation rates are reduced to save energy costs, synthetic building materials off-gas contaminants, and unsafe levels of volatile organic compounds (VOC's) accumulate. These unsafe levels of contaminants can cause irritation of eyes and throat, fatigue and dizziness to building occupants. Increased ventilation, the primary method of treating Sick Building Syndrome is expensive (due to increased energy costs) and recently, the effectiveness of increased ventilation has been questioned. On spacecraft venting is not allowed, so the primary methods of air quality control are; source control, active filtering, and destruction of VOC's. Four non-venting contaminant removal technologies; strict material selection to provide source control, ambient temperature catalytic oxidation, photocatalytic oxidation, and uptake by higher plants, may have potential application for indoor air quality control. Author

N94-30471*# National Aeronautics and Space Administration. Lewis Research Center, Cleveland, OH.
A NEW MATERIAL FOR REMOVING HEAVY METALS FROM WATER **c45**
Warren H. Philipp, Jr. and Kenneth W. Street, Jr. *In* NASA, Washington, Technology 2003: The Fourth National Technology Transfer Conference and Exposition, Volume 1 Feb. 1994 p 266-272 (For primary document see N94-30440 08-99)
Avail: CASI HC A02/MF A04

The NASA Lewis Research Center developed and is patenting a new high capacity ion exchange material (IEM) that removes toxic metals from contaminated water in laboratory tests. The IEM can be made into many forms, such as thin films, coatings, pellets, and fibers. As a result, it can be adapted to many applications to purify contaminated water wherever it is found, be it in waste water treatment systems, lakes, ponds, industrial plants, or in homes. Laboratory tests have been conducted on aqueous solutions containing only one of the following metal cations: lead, copper, mercury, cadmium, silver, chromium (III), nickel, zinc, and yttrium. Tests were also conducted with: (1) calcium present to determine its effects on the uptake of cadmium and copper, and (2) uranium and lanthanides which are stand-ins for other radioactive elements, (3) drinking water for the removal of copper and lead, and (3) others compositions. The results revealed that the IEM removes all these cations, even in the presence of the calcium. Of particular interest are the results of the tests with the drinking water: the lead concentration was reduced from 142 ppb down to 2.8 ppb (well below the accepted EPA standard). Author

N94-30472*# Bureau of Mines, Tuscaloosa, AL.
DEWATERING OF CONTAMINATED RIVER SEDIMENTS **c45**
Ronald H. Church, Carl W. Smith, and Bernard J. Scheiner *In* NASA, Washington, Technology 2003: The Fourth National Technology Transfer Conference and Exposition, Volume 1 Feb. 1994 p 273-282 (For primary document see N94-30440 08-99)
Avail: CASI HC A02/MF A04

Dewatering of slurries has been successfully accomplished by the proper use of polymers in flocculating the fine particulate matter suspended in mineral processing streams. The U.S. Bureau of Mines (USBM) entered into a cooperative research effort with the U.S. Army Corps of Engineers (Corps) for the purpose of testing and demonstrating the applicability of mining flocculation technology to dredging activities associated with the removal of sediments from navigable waterways. The Corps has the responsibility for maintaining the navigable waterways in the United States. Current technology relies primarily on dredging operations which excavate the material from the bottom of waterways. The Corps is testing new dredging technology which may reduce resuspension of sediments by the dredging operation. Pilot plant dredging equipment was tested by the Corps which generated larger quantities of water when compared to conventional equipment, such as the clam shell. The transportation of this 'excess' water adds to the cost of sediment removal. The process developed by the USBM consists of feed material from the barge being pumped through a 4-in line by a centrifugal pump and exiting through a 4-in PVC delivery system. A 1,000-gal fiberglass tank was used to mix the polymer concentrate. The polymer was pumped through a 1-in line using a variable speed progressive cavity pump and introduced to the 4-in feed line prior to passing through a 6-in by 2-ft static mixer. The polymer/feed slurry travels to the clarifying tank where the flocculated material settled to the bottom and allowed 'clean' water to exit the overflow. A pilot scale flocculation unit was operated on-site at the Corps' 'Confined Disposal Facility' in Buffalo, NY. Author

N94-30473*# Pacific Northwest Lab., Richland, WA.
BENCH-SCALE SYNTHESIS OF NANOSCALE MATERIALS **c31**
M. F. Buehler, J. G. Darab, D. W. Matson, and J. C. Linehan *In* NASA, Washington, Technology 2003: The Fourth National Technology Transfer Conference and Exposition, Volume 1 Feb. 1994 p 285-292 (For primary document see N94-30440 08-99)
(Contract DE-AC06-76RL-01830)
Avail: CASI HC A02/MF A04

A novel flow-through hydrothermal method used to synthesize nanoscale powders is introduced by Pacific Northwest Laboratory. The process, Rapid Thermal Decomposition of precursors in Solution (RTDS), uniquely combines high-pressure and high-temperature conditions to rapidly form nanoscale particles. The RTDS process was initially demonstrated on a laboratory scale and was subsequently scaled up to accommodate production rates attractive to industry. The process is able to produce a wide variety of metal oxides and oxyhydroxides. The powders are characterized by scanning and transmission electron microscopic methods, surface-area measurements, and x-ray diffraction. Typical crystallite sizes are less than 20 nanometers, with BET surface areas ranging from 100 to 400 sq m/g. A description of the RTDS process is presented along with powder characterization results. In addition, data on the sintering of nanoscale ZrO2 produced by RTDS are included. Author

N94-30474*# Naval Air Warfare Center, China Lake, CA.
SYNTHESIS AND CHARACTERIZATION OF ADVANCED MATERIALS FOR NAVY APPLICATIONS **c27**
J. Covino and I. Lee *In* NASA, Washington, Technology 2003: The Fourth National Technology Transfer Conference and Exposition, Volume 1 Feb. 1994 p 294-306 (For primary document see N94-30440 08-99)
Avail: CASI HC A03/MF A04

The synthesis of ceramics and ceramic coatings through the sol-gel process has extensive application with the United States Navy and a broad range of potential commercial applications as well. This paper surveys seven specific applications for which the Navy is investigating these advanced materials. For each area, the synthetic process is described and the characteristics of the materials are discussed. Author

N94-30475*# Brookhaven National Lab., Upton, NY. Dept. of Nuclear Energy.
DEPOSITION OF TANTALUM CARBIDE COATINGS ON GRAPHITE BY LASER INTERACTIONS **c27**
James Veligdan, D. Branch, P. E. Vanier, and R. E. Barietta *In* NASA, Washington, Technology 2003: The Fourth National Technology Transfer Conference and Exposition, Volume 1 Feb. 1994 p 307-311 (For primary document see N94-30440 08-99)
(Contract DE-AC02-76CH-00016)
Avail: CASI HC A01/MF A04

Graphite surfaces can be hardened and protected from erosion by hydrogen at high temperatures by refractory metal carbide coatings, which are usually prepared by chemical vapor deposition (CVD) or chemical vapor reaction (CVR) methods. These techniques rely on heating the substrate to a temperature where a volatile metal halide decomposes and reacts with either a hydrocarbon gas or with carbon from the substrate. For CVR techniques, deposition temperatures must be in excess of 2000 C in order to achieve favorable deposition kinetics. In an effort to lower the bulk substrate deposition temperature, the use of laser interactions with both the substrate and the metal halide deposition gas has been employed. Initial testing involved the use of a CO2 laser to heat the surface of a graphite substrate and a KrF excimer laser to accomplish a photodecomposition of TaCl5 gas near the substrate. The results of preliminary experiments using these techniques are described. Author

N94-30476*# USBI Booster Production Co., Titusville, FL.
DEVELOPMENT OF A UNIQUE POLYURETHANE PRIMER/TOPCOAT **c27**
Howard L. Novak and James M. Klotz *In* NASA, Washington, Technology 2003: The Fourth National Technology Transfer Conference and Exposition, Volume 1 Feb. 1994 p 312-317 (For primary document see N94-30440 08-99)
Avail: CASI HC A02/MF A04

USBI Company, a Division of Pratt & Whitney Government Engines and Space Propulsion, is involved in corrosion and environmental research and development activities both at their headquarters in Huntsville, Alabama and their Florida Operations at Kennedy Space Center, Florida. The programs involve the development of environmentally compatible materials that improve the corrosion protection of expensive Solid Rocket Boosters (SRB) that are part of the Space Shuttle systems developed and managed by Marshall Space Flight Center in Huntsville, Alabama. Coatings For Industry, a paint manufacturer in Souderton, PA helped formulate and produce the first lot of BOOSTERCOAT paint. High strength aluminum aerospace flight hardware exposed to harsh seacoast environments and seawater immersion presently uses high volatile organic compound (VOC) chromated and lead bearing primers and epoxy topcoats for corrosion protection. Epoxy paint tends to be brittle and has relatively low ultraviolet (UV) exposure resistance. A

unique, environmentally compatible, non-leaded/non-chromated, low VOC polyurethane single coat (primer/topcoat) trade named BOOSTERCOAT has been developed for excellent corrosion protection, flexibility, adhesion, chemical and solvent resistance properties. This report will discuss the development of BOOSTERCOAT and the potential opportunities for commercial use in the energy, transportation, chemical, maritime, structural fields. Author

N94-30477*# Naval Air Warfare Center, China Lake, CA.
HIGH ELONGATION ELASTOMERS **c27**
V. L. Brady, R. Reed, L. Merwin, and R. Nissan *In* NASA, Washington, Technology 2003: The Fourth National Technology Transfer Conference and Exposition, Volume 1 Feb. 1994 p 318-336 (For primary document see N94-30440 08-99)
Avail: CASI HC A03/MF A04

A new class of liquid curable elastomers with unusual strength and elasticity has been developed at the Naval Air Warfare Center Weapons Division, China Lake. Over the years, studies have been conducted on polymer structure and its influence on the mechanical properties of the ensuing composites. Different tools, including nuclear magnetic resonance, have been used. This paper presents a summary of the factors controlling the mechanical behavior of composites produced with the new liquid curable elastomers, including the effects of plasticizers. It also provides an overview of the nuclear magnetic resonance study on polymer structure, the composition and properties of some live and inert formulations produced at China Lake, and some possible peace-time applications for these new elastomeric materials. Author

N94-30478*# Fluid Polymers, Inc., Las Vegas, NV.
SOLVENTLESS, CURABLE FLUID OLIGOMERIC SYSTEMS FOR HIGH PERFORMANCE MICROWAVE, ACOUSTICAL AND MECHANICAL APPLICATIONS **c27**
G. M. LeFave, Leo Stanton, and Jim Foreman *In* NASA, Washington, Technology 2003: The Fourth National Technology Transfer Conference and Exposition, Volume 1 Feb. 1994 p 337-343 (For primary document see N94-30440 08-99)
Avail: CASI HC A02/MF A04

While establishing the basis for a 'Technology 2000' product plan several years ago we plugged in the usual factors contributing toward product success: price/performance justifiable; profitable, warranting high quality maintenance, enhancement, and specific property improvement; narrow inventory requirements; and raw material integrable backwards with easily variable properties (molecular weight, functionality, and isomer control). We resolved this by selecting radical functional, low molecular weight polybutadiene liquid polymers. Encouraged by the need for solid rocket binders, several companies embarked on various perceptions of binder performance requirements over four decades ago. Initially dominated by progress of liquid polysulfides, soon a few settled primarily upon polybutadiene based binders. Such an approach in a few instances was exploited quite viably with a series of functional group terminated liquid polybutadienes: hydroxyl, mercaptan, carboxyl, vinyl, and amine. Good results are obtained for oligomers, liquid polymers, and their hybrids. The only significant limits on compounded products has been solvent resistance and oxidative sensitivity, unless sufficient proportion of sulfide or nitrile moiety is incorporated. For convenience, they have been grouped under the trademarks Nylane, Seamax, Oligomax, and Castomax.
Author (revised)

N94-30479*# Sigma Labs., Inc., Tucson, AZ.
PLASMA TREATMENT OF POLYMER DIELECTRIC FILMS TO IMPROVE CAPACITIVE ENERGY STORAGE **c27**
A. Yializis, M. Binder, and R. J. Mammone *In* NASA, Washington, Technology 2003: The Fourth National Technology Transfer Conference and Exposition, Volume 1 Feb. 1994 p 344-351 (For primary document see N94-30440 08-99)
Avail: CASI HC A02/MF A04

Demand for compact instrumentation, portable field equipment, and new electromagnetic weapons is creating a need for new dielectric materials with higher energy storage capabilities. Recognizing the need for higher energy storage capacitors, the Army Research Lab at Fort Monmouth, NJ, initiated a program a year ago to investigate potential methods for increasing the dielectric strength of polyvinylidene difluoride (PVDF) film, which is the highest energy density material commercially available today. Treatment of small area PVDF films in a CF4/O2 plasma showed that the dielectric strength of PVDF films can be increased by as much as 20 percent when treated in a 96 percent CF4/4 percent O2 plasma. This 44 percent increase in energy storage of a PVDF capacitor is significant considering that the treatment can be implemented in a conventional metallizing chamber, with minimum capital investment. The data shows that improved breakdown strength may be unique to PVDF film and the particular CF4/O2 gas mixture, because PVDF film treated with 100 percent CF4, 100 percent O2, Ar gas plasma, and electron irradiation shows no improvement in breakdown strength. Other data presented includes dissipation factor, dielectric constant, and surface tension measurements. Author (revised)

N94-30480*# Brookhaven National Lab., Upton, NY. Dept. of Advanced Technology.
DEVELOPMENT OF RADIATION RESISTANT ELECTRICAL CABLE INSULATIONS **c27**
B. S. Lee, P. Soo, and D. R. MacKenzie *In* NASA, Washington, Technology 2003: The Fourth National Technology Transfer Conference and Exposition, Volume 1 Feb. 1994 p 352-360 (For primary document see N94-30440 08-99)
Avail: CASI HC A02/MF A04

Two new polyethylene cable insulations have been formulated for nuclear applications and have been tested under gamma radiation. Both insulations are based on low density polyethylene, one with PbO and the other with Sb2O3 as additives. The test results show that the concept of using inorganic antioxidants to retard radiation initiated oxidation (RIO) is viable. PbO is more effective than Sb2O3 in minimizing RIO. Author (revised)

N94-30481*# National Aeronautics and Space Administration. Langley Research Center, Hampton, VA.
FOUR ADVANCES IN CARBON-CARBON MATERIALS TECHNOLOGY **c24**
Howard G. Maahs, Wallace L. Vaughn, and Witold Kowbel *In* NASA, Washington, Technology 2003: The Fourth National Technology Transfer Conference and Exposition, Volume 1 Feb. 1994 p 361-370 (For primary document see N94-30440 08-99)
Avail: CASI HC A02/MF A04

Carbon-carbon composites are a specialty class of materials having many unique properties making these composites attractive for a variety of demanding engineering applications. Chief among these properties are exceptional retention of mechanical properties at temperatures as high as 4000 F, excellent creep resistance, and low density (1.6 to 1.8 g/cu cm). Although carbon-carbon composites are currently in service in a variety of applications, much development work remains to be accomplished before these materials can be considered to be fully mature, realizing their full potential. Four recent technology advances holding particular promise for overcoming current barriers to the wide-spread commercialization of carbon-carbon composites are described. These advances are: markedly improved interlaminar strengths (more than doubled) of two dimensional composites achieved by whiskerization of the fabric reinforcing plies, simultaneously improved oxidation resistance and mechanical properties achieved by the incorporation of matrix-phase oxidation inhibitors based on carborane chemistry, improved oxidation resistance achieved by compositionally graded oxidation protective coatings, and markedly reduced processing times (hours as opposed to weeks or months) accomplished through a novel process of carbon infiltration and coatings deposition based on the use of liquid-phase precursor materials. Author (revised)

N94-30482*# National Aeronautics and Space Administration. Marshall Space Flight Center, Huntsville, AL.
CASTING OF WELDABLE GRAPHITE/MAGNESIUM METAL MATRIX COMPOSITES WITH BUILT-IN METALLIC INSERTS **c24**
Jonathan A. Lee, Uday Kashalikar, and Patricia Majkowski *In* NASA, Washington, Technology 2003: The Fourth National Technology Transfer Conference and Exposition, Volume 1 Feb. 1994 p 371-376 (For primary document see N94-30440 08-99)
Avail: CASI HC A02/MF A04

Technology innovations directed at the advanced development of a potentially low cost and weldable graphite/magnesium metal matrix composites (MMC) through near net shape pressure casting are described. These MMC components uniquely have built-in metallic inserts to provide

an innovative approach for joining or connecting other MMC components through conventional joining techniques such as welding, brazing, mechanical fasteners, etc. Moreover, the metallic inserts trapped within the MMC components can be made to transfer the imposed load efficiently to the continuous graphite fiber reinforcement thus producing stronger, stiffer, and more reliable MMC components. The use of low pressure near net shape casting is economical compared to other MMC fabrication processes. These castable and potentially weldable MMC components can provide great payoffs in terms of high strength, high stiffness, low thermal expansion, lightweight, and easily joinable MMC components for several future NASA space structural, industrial, and commercial applications. Author (revised)

N94-30483*# Axiomatics Corp., Woburn, MA.
IMPROVED CONSTRUCTION MATERIALS FOR POLAR REGIONS USING MICROCELLULAR THERMOPLASTIC FOAMS **c27**
Daniel J. Cunningham *In* NASA, Washington, Technology 2003: The Fourth National Technology Transfer Conference and Exposition, Volume 1 Feb. 1994 p 385-391 (For primary document see N94-30440 08-99)
Avail: CASI HC A02/MF A04

Microcellular polymer foams (MCF) are thermoplastic foams with very small cell diameters, less than 10 microns, and very large cell densities, 10(exp 9) to 10(exp 15) cells per cubic centimeter of unfoamed material. The concept of foaming polymers with microcellular voids was conceived to reduce the amount of material used for mass-produced items without compromising the mechanical properties. The reasoning behind this concept was that if voids smaller than the critical flaw size pre-existing in polymers were introduced into the matrix, they would not affect the overall strength of the product. MCF polycarbonate (PC), polystyrene (PS), and polyvinyl chloride (PVC) were examined to determine the effects of the microstructure towards the mechanical properties of the materials at room and arctic temperatures. Batch process parameters were discovered for these materials and foamed samples of three densities were produced for each material. To quantify the toughness and strength of these polymers, the tensile yield strength, tensile toughness, and impact resistance were measured at room and arctic temperatures. The feasibility of MCF polymers has been demonstrated by the consistent and repeatable MCF microstructures formed, but the improvements in the mechanical properties were not conclusive. Therefore the usefulness of the MCF polymers to replace other materials in arctic environments is questionable. Author (revised)

N94-30484*# Wright Lab., Wright-Patterson AFB, OH.
USE OF MAGNETIC COMPRESSION TO SUPPORT TURBINE ENGINE ROTORS **c37**
Chris J. Pomfret *In* NASA, Washington, Technology 2003: The Fourth National Technology Transfer Conference and Exposition, Volume 1 Feb. 1994 p 395-410 (For primary document see N94-30440 08-99)
Avail: CASI HC A03/MF A04

Ever since the advent of gas turbine engines, their rotating disks have been designed with sufficient size and weight to withstand the centrifugal forces generated when the engine is operating. Unfortunately, this requirement has always been a life and performance limiting feature of gas turbine engines and, as manufacturers strive to meet operator demands for more performance without increasing weight, the need for innovative technology has become more important. This has prompted engineers to consider a fundamental and radical breakaway from the traditional design of turbine and compressor disks which have been in use since the first jet engine was flown 50 years ago. Magnetic compression aims to counteract, by direct opposition rather than restraint, the centrifugal forces generated within the engine. A magnetic coupling is created between a rotating disk and a stationary superconducting coil to create a massive inwardly-directed magnetic force. With the centrifugal forces opposed by an equal and opposite magnetic force, the large heavy disks could be dispensed with and replaced with a torque tube to hold the blades. The proof of this concept has been demonstrated and the thermal management of such a system studied in detail; this aspect, especially in the hot end of a gas turbine engine, remains a stiff but not impossible challenge. The potential payoffs in both military and commercial aviation and in the power generation industry are sufficient to warrant further serious studies for its application and optimization. Author (revised)

N94-30485*# Greenville Coll., IL. Dept. of Physics.
A FUTURE, INTENSE SOURCE OF NEGATIVE HYDROGEN IONS **c72**
Hugh Siefken and Charles Stein *In* NASA, Washington, Technology 2003: The Fourth National Technology Transfer Conference and Exposition, Volume 1 Feb. 1994 p 411-420 (For primary document see N94-30440 08-99)
Avail: CASI HC A02/MF A04

By directly heating lithium hydride in a vacuum, up to 18 micro-A/sq cm of negative hydrogen has been obtained from the crystal lattice. The amount of ion current extracted and analyzed is closely related to the temperature of the sample and to the rate at which the temperature is changed. The ion current appears to be emission limited and saturates with extraction voltage. For a fixed extraction voltage, the ion current could be maximized by placing a grid between the sample surface and the extraction electrode. Electrons accompanying the negative ions were removed by a magnetic trap. A Wein velocity filter was designed and built to provide definitive mass analysis of the extracted ion species. This technique when applied to other alkali hydrides may produce even higher intensity beams possessing low values of emittance. Author (revised)

N94-30486*# Midwest Research Inst., Golden, CO.
FIBER OPTICAL SOLAR SIMULATOR **c44**
Bhushan L. Sopori and Craig Marshall *In* NASA, Washington, Technology 2003: The Fourth National Technology Transfer Conference and Exposition, Volume 1 Feb. 1994 p 421-428 (For primary document see N94-30440 08-99)
(Contract DE-AC02-83CH-10093)
Avail: CASI HC A02/MF A04

A new solar simulator is described whose output closely matches a desired solar spectrum for testing photovoltaic cells. The accurate simulation of the spectrum is attained by combining three light beams, each tailored to have suitable spectral content. The three light beams, derived from two sources, are filtered and 'mixed' by means of a trifurcated, randomized fiber cable so that when superimposed they add up to the desired solar spectrum. The fiber optic solar simulator (FOSS) simplifies solar cell testing by greatly reducing measurement time, obviating need for spectral mismatch corrections, and improving the accuracy of measurement. Other applications of FOSS are also described. Author (revised)

N94-30844 Lawrence Livermore National Lab., CA.
COMPUTING AT THE LEADING EDGE: RESEARCH IN THE ENERGY SCIENCES
A. A. Mirin, ed. and P. T. VanDyke, ed. 1994 98 p Limited Reproducibility: More than 20% of this document may be affected by microfiche quality
(Contract W-7405-eng-48)
(DE94-006121; UCRL-TB-111084) Avail: CASI HC A05

The purpose of this publication is to highlight selected scientific challenges that have been undertaken by the DOE Energy Research community. The high quality of the research reflected in these contributions underscores the growing importance both to the Grand Challenge scientific efforts sponsored by DOE and of the related supporting technologies that the National Energy Research Supercomputer Center (NERSC) and other facilities are able to provide. The continued improvement of the computing resources available to DOE scientists is prerequisite to ensuring their future progress in solving the Grand Challenges. Titles of articles included in this publication include: the numerical tokamak project; static and animated molecular views of a tumorigenic chemical bound to DNA; toward a high-performance climate systems model; modeling molecular processes in the environment; lattice Boltzmann models for flow in porous media; parallel algorithms for modeling superconductors; parallel computing at the Superconducting Super Collider Laboratory; the advanced combustion modeling environment; adaptive methodologies for computational fluid dynamics; lattice simulations of quantum chromodynamics; simulating high-intensity charged-particle beams for the design of high-power accelerators; and electronic structure and phase stability of random alloys. DOE

SUBJECT INDEX

Typical Subject Index Listing

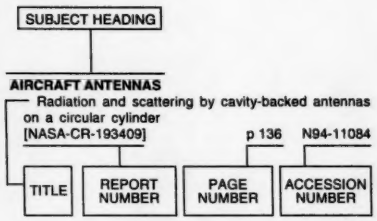

The subject heading is a key to the subject content of the document. Titles, report numbers, and accession numbers of pertinent documents are provided under each subject heading. When the title is insufficiently descriptive of the document content, a title extension is added, separated from the title by three hyphens. The report number helps to indicate the type of document cited (e.g., NASA report, NASA translation, NASA contractor report). The accession number is the number by which the document abstracts are arranged in this journal and by which the document is sold or requested. The page number helps you locate the citation in the abstract section. The titles, with title extensions if present, are arranged under each subject heading in ascending accession number order. The subject headings have been selected from the latest revision of the *NASA Thesaurus*.

A

A STARS
Equation of state of stellar plasmas
[DE94-004186] p 3542 N94-28526
Pushing the limit: Precision radial velocities, techniques, and applications p 3542 N94-30861
ABEL FUNCTION
Trace formulas and dynamical zeta functions in the Nielsen theory
[PB94-138195] p 3467 N94-29163
ABERRATION
Potential hazards of magnetic resonance imagers to emergency medical service helicopter operations
[DOT/FAA/RD-92/15] p 3135 N94-29862
ABLATION
A review of the ablative stabilization of the Rayleigh-Taylor instability in regimes relevant to ICF
[DE94-005809] p 3509 N94-30597
Modelling erosion damage from low-energy plasma gun simulations of disruptions
[DE94-005196] p 3509 N94-30697
ABRASION
Unscreened low tension cables scrape abrasion testing. Part 1: An interlaboratory study on scrape abrasion testing according to ISO DP 6722-1
[PB94-135605] p 3264 N94-29191
The effect of mechanical paint stripping on the fatigue and fracture of thin aluminum airplane skin
p 3205 N94-29900
Material properties and fracture mechanics in relation to ceramic machining
[DE94-006623] p 3221 N94-30829
ABSORBENTS
Methane challenge of high performance molecular sieve oxygen concentrator
[AD-A275155] p 3337 N94-29033
ABSORBERS (MATERIALS)
Boundary layer control device for duct silencers
[NASA-CASE-ARC-12030-1] p 3478 N94-29362
ABSORPTION CROSS SECTIONS
Radiation transport in cloudy and aerosol loaded atmospheres p 3366 N94-30805
ABSORPTION SPECTRA
Absolute determination of local tropospheric OH concentrations p 3343 N94-28594
Template synthesized nanoscopic gold particles: Optical spectra and the effects of particle size and shape
[AD-A275378] p 3197 N94-29312
Nanosize metal alloy particle formation in Ag and Cu sequentially implanted silica
[DE94-005592] p 3207 N94-30042
The far-infrared absorption spectrum of low temperature hydrogen gas
[ISBN-0-315-85432-4] p 3199 N94-30137
ABSORPTION SPECTROSCOPY
UV laser long-path absorption spectroscopy
p 3343 N94-28595
Measurement of tropospheric OH by laser long-path absorption spectroscopy p 3343 N94-28596
NOAA Aeronomy Laboratory long-path OH experiment, Fritz Peak Observatory, Colorado p 3344 N94-28598
Near-IR diode laser absorption for measurement of tropospheric HO2 p 3345 N94-28607
Structure of ordinary ice I(sub h). Part 1: Ideal structure of ice
[AD-A275149] p 3486 N94-29021
Advanced diagnostics for reacting flows
[AD-A275057] p 3272 N94-29136
Developing a diode array spectrometer for tropospheric chemistry studies p 3362 N94-29752
Realtime structural electrochemistry of platinum clusters using dispersive XAFS
[DE94-005093] p 3208 N94-30101
The far-infrared absorption spectrum of low temperature hydrogen gas
[ISBN-0-315-85432-4] p 3199 N94-30137
Magnetic field generation by circularly polarized laser light and inertial plasma confinement in a miniature magnetic bottle induced by circularly polarized laser light
[DE94-608353] p 3508 N94-30192
ABSTRACTS
ARTI Refrigerant Database
[DE94-004906] p 3230 N94-28563
Catalog of Air Force weather technical publications 1992-1993
[AD-A275635] p 3368 N94-28638
Clinical investigation program
[AD-A275025] p 3391 N94-29116
ABUNDANCE
Abundance patterns in red-giant CH stars
p 3539 N94-29820
Coronal abundances and their variation
[NASA-CR-195767] p 3551 N94-29858
ACCELERATED LIFE TESTS
Safety enhancement of composites via periodic proof testing
[AD-A275662] p 3176 N94-28655
ACCELERATION (PHYSICS)
Determination of acceleration field parameters with linear accelerometers
[PB94-125606] p 3290 N94-30742
ACCELERATION PROTECTION
Comparative centrifuge evaluation of the Air Force Advanced Technology Anti-G Suit (ATAGS) and the Navy Enhanced Anti-G Lower Ensemble (EAGLE)
[AD-A275348] p 3400 N94-28996
Procedures and metrics for anti-G suit evaluations
[AD-A275349] p 3400 N94-28997
ACCELERATION STRESSES (PHYSIOLOGY)
Comparative centrifuge evaluation of the Air Force Advanced Technology Anti-G Suit (ATAGS) and the Navy Enhanced Anti-G Lower Ensemble (EAGLE)
[AD-A275348] p 3400 N94-28996
ACCELEROMETERS
Summary report of mission acceleration measurements for Spacehab-01, STS-57 launched 21 June 1993
[NASA-TM-106514] p 3168 N94-29757
A broad-band microseismometer for planetary operations p 3237 N94-29778
Emerging technologies in microguidance and control
p 3144 N94-29788
Air-deployable geophysics package
[DE94-005651] p 3335 N94-30594
Determination of acceleration field parameters with linear accelerometers
[PB94-125606] p 3290 N94-30742
ACCEPTOR MATERIALS
Photochemistry in constrained spaces: Zeolites and layered double metal hydroxides
[DE94-004958] p 3200 N94-30769
Theory for electron-transfer reactions in a three-component system: The degenerate regime
[DE94-005919] p 3493 N94-30903
ACCESS CONTROL
Secure network databases: Survey and analysis
[PB94-138492] p 3533 N94-29948
ACCIDENT PREVENTION
Systematic safety consideration in product design
[PB94-132354] p 3229 N94-28410
ACCIDENTS
A comparison of four methods of rewarming individuals cooled by immersion in cold water p 3382 N94-28442
Caesium-137 in a boreal forest ecosystem: Aspects on the long-term behavior
[PB94-137809] p 3347 N94-29158
Aircraft accident/incident summary report: In-flight loss of control, leading to forced landing and runway overrun, Continental Express, Inc., N24706 Embraer EMB-120 RT, Pine Bluff, Arkansas, 29 April 1993
[PB94-910404] p 3135 N94-29402
Risk measures in living probabilistic safety assessment
[VTT-PUBS-146] p 3465 N94-30154
Complex source rate estimation for atmospheric transport and dispersion models
[DE94-000958] p 3354 N94-30822
ACCRETION DISKS
Broad H alpha profiles of radio-loud active galactic nuclei and rapid profile variability in Seyfert and radio galaxies
p 3552 N94-29989
ACCURACY
Report on NATO PTTI p 3469 N94-30645
Relativistic theory for picosecond time transfer in the vicinity of Earth p 3470 N94-30653
New perspectives for high accuracy SLR with second generation geodesic satellites
[REPT-932-440-105] p 3336 N94-30965
ACETONE
Ab initio study of vibrational frequency shift upon the 1:1 acetone-iodine complex formation
p 3188 N94-28681
ACETYLENE
Spectroscopic and dynamical studies of highly energized small polyatomic molecules
[DE94-006509] p 3489 N94-30061
ACOUSTIC ATTENUATION
Attenuation of outdoor sound propagation levels by a snow cover
[AD-A275387] p 3478 N94-29314
Noise reduction techniques for the restoration of musical recordings
[TELECOM-93-E-019] p 3291 N94-30979
ACOUSTIC COUPLING
An experimental study of nonlinear wave coupling and energy transfer characterizing the transition of a planar jet shear layer p 3282 N94-30953
ACOUSTIC DUCTS
A non-local computational boundary condition for duct acoustics
[NASA-TM-109091] p 3478 N94-29382
ACOUSTIC EMISSION
Convective turbulence and transport in stars
p 3546 N94-29913
Enhanced fatigue crack detection in aging aircraft using continuous acoustic emission monitoring
[DREP-93-16] p 3148 N94-30131

ACOUSTIC EXCITATION
Temperature and combustion analysis of combustor with acoustically controlled primary zone air-jet mixing p 3196 N94-29284
Method and apparatus for indicating disbonds in joint regions
[NASA-CASE-LAR-14626-1] p 3315 N94-29548
Rotordynamic analysis of annular honeycomb-stator turbulent gas seals using a new friction-factor model based on flat plate tests p 3302 N94-29916
Evaluation of flip-flop jet nozzles for use as practical excitation devices
[NASA-TM-106377] p 3135 N94-30949
ACOUSTIC FATIGUE
Review of sonic fatigue technology
[NASA-CR-4587] p 3479 N94-29407
ACOUSTIC IMPEDANCE
Method and apparatus for indicating disbonds in joint regions
[NASA-CASE-LAR-14626-1] p 3315 N94-29548
Measurement of bulk longitudinal modulus and correction for edge effects
[DE94-005581] p 3222 N94-30900
ACOUSTIC MEASUREMENT
Characterization of structural vibration: Field descriptors based on energy density and intensity
[PB94-132230] p 3316 N94-28404
Analysis of spark-induced bubble experiments using CALE
[DE94-003667] p 3270 N94-28476
Minutes. Accredited Standards Committee on Noise, S12. US tag for ISO/TC 43/SC1 noise and ISO/TC 94/SC12 hearing protection
[AD-A275622] p 3477 N94-28636
The nozzle acoustic test rig: An acoustic and aerodynamic free-jet facility
[NASA-TM-106495] p 3156 N94-28749
Determination of sound power levels of air terminal units according to ISO 5135-Nordic inter-laboratory tests, Nordtest project no. 968-91
[PB94-137411] p 3477 N94-29175
Acoustic and optical investigations of superfluid (3)He
[PB94-135415] p 3477 N94-29186
Improved in-flow acoustic sensor
[NASA-CASE-ARC-12001-1] p 3478 N94-29363
Resonant ultrasound spectroscopy for elastic constant measurements
[DE94-005016] p 3480 N94-30098
Acoustic emission monitoring of aging aircraft structures
[DREP-93-17] p 3148 N94-30129
Enhanced fatigue crack detection in aging aircraft using continuous acoustic emission monitoring
[DREP-93-16] p 3148 N94-30131
ACOUSTIC PROPERTIES
Characterization of structural vibration: Field descriptors based on energy density and intensity
[PB94-132230] p 3316 N94-28404
Broad geoacoustic assessment of some regional areas
[AD-A275504] p 3356 N94-28791
A comparison of two computer models of sound propagation for a wedge shaped ocean over a penetrable bottom
[AD-A275031] p 3477 N94-29117
Interaction of multiple spark-generated bubbles in a compressible liquid
[AD-A275037] p 3272 N94-29149
Seafloor characterization using texture
[AD-A275399] p 3377 N94-29204
Subphonetic acoustic modeling for speaker-independent continuous speech recognition
[AD-A275217] p 3244 N94-29303
An investigation of the reacting vortex structures associated with pulse combustion p 3200 N94-30911
ACOUSTIC SCATTERING
Acoustic or electromagnetic scattering from the penetrable wedge
[AD-A275259] p 3243 N94-29054
Considerations in the modelling of seafloor acoustic backscatter
[AD-A275404] p 3478 N94-29206
Experiments on the aerodynamic generation of noise in centrifugal turbomachinery p 3480 N94-30804
ACOUSTIC SOUNDING
Theory and application of a Radio-Acoustic Sounding System (RASS) p 3367 N94-30869
Remote sensor observations during WISP91: The use of microwave radiometers, RASS, and lidar ceilometers for detection of aircraft icing conditions
[PB94-142106] p 3136 N94-30890
ACOUSTIC VELOCITY
Updated deep-tow acoustics/geophysics system compressional velocity database
[AD-A275477] p 3355 N94-28685
Broad geoacoustic assessment of some regional areas
[AD-A275504] p 3356 N94-28791
Quadrupiet expansion of the acoustic pressure field in a wedge shaped ocean
[AD-A275121] p 3477 N94-29003
A comparison of two computer models of sound propagation for a wedge shaped ocean over a penetrable bottom
[AD-A275031] p 3477 N94-29117
Nonlinear wave packet evolution in a dispersive plasma: Application to rotational discontinuities p 3506 N94-29822
Theory and application of a Radio-Acoustic Sounding System (RASS) p 3367 N94-30869
ACOUSTICS
Updated deep-tow acoustics/geophysics system compressional velocity database
[AD-A275477] p 3355 N94-28685
Minutes. Accredited Standards Committee on Acoustics, S1. US tag for ISO/TC 43 acoustics and IEC/TC 29 electroacoustics
[AD-A275702] p 3477 N94-28689
Analysis of 3-D acoustic problems using boundary element method p 3127 N94-28974
Subphonetic acoustic modeling for speaker-independent continuous speech recognition
[AD-A275217] p 3244 N94-29303
Accurate finite difference methods for time-harmonic wave propagation
[NASA-CR-194887] p 3454 N94-30209
Computational analysis of high resolution unsteady airloads for rotor aeroacoustics
[NASA-CR-194894] p 3480 N94-30274
Index of NPL acoustics publications 1981-1990
[NPL-RSA(EXT)-0044] p 3480 N94-30786
ACOUSTO-OPTICS
Photorefractive adaptive antenna array processor
[AD-A275762] p 3241 N94-28762
Spectral and polarimetric analysis of hyperspectral data collected by an acousto-optic tunable filter system
[AD-A275076] p 3329 N94-29095
ACQUISITION
Acquisition time analysis of noncoherent PN sequence acquisition schemes
[AD-A275017] p 3244 N94-29094
ACRYLIC RESINS
A new material for removing heavy metals from water p 3354 N94-30471
ACRYLONITRILES
Ballistic performance of polycarbonate/polyester and polycarbonate/styrene- acrylonitrile microlayer sheets
[AD-A275462] p 3177 N94-28735
ACTIVATION
Study of activation data of metal samples from LDEF-1 and Spacelab-2
[NASA-CR-195802] p 3205 N94-29736
ACTIVATION ENERGY
Novel techniques applied to polymer lifetime predictions
[DE94-005095] p 3218 N94-30102
Ionic conduction mechanisms in CaF2 and CaF2-Al2O3 nanocomposite films on Al2O3 substrates
[DE94-004792] p 3520 N94-30773
ACTIVE CONTROL
Integrated active and passive control design methodology for the LaRC CSI evolutionary model
[NASA-CR-4580] p 3164 N94-28417
Fluid dynamic noise in a centrifugal pump
[AD-A275264] p 3477 N94-28904
Active control of delaminations in smart composite structures p 3181 N94-29593
Miniature linear-to-rotary motion actuator p 3163 N94-29647
An actively cooled floating element skin friction balance for direct measurement in high enthalpy supersonic flows p 3289 N94-29824
Position control of a flexible beam with active damping of vibrations
[ISBN-0-315-85841-9] p 3321 N94-30033
Design and control of active vision based mechanisms for intelligent robots
[AIAA PAPER 94-1196-CP] p 3442 N94-30547
A performance analysis method for distributed real-time robotic systems: A case study of remote teleoperation
[AIAA PAPER 94-1212-CP] p 3445 N94-30563
ACTIVE GALACTIC NUCLEI
Infrared properties of obscuring dust tori in active galactic nuclei p 3545 N94-29832
Broad H alpha profiles of radio-loud active galactic nuclei and rapid profile variability in Seyfert and radio galaxies p 3552 N94-29989
Correlation analysis on optical and radio light curves for a large sample of active galactic nuclei p 3546 N94-29992
The effects of relativistic neutrons on nonthermal models of active galactic nuclei p 3547 N94-29993
Optical depth effects in cluster cooling flows p 3541 N94-30800
ACTIVITY
Study of activation data of metal samples from LDEF-1 and Spacelab-2
[NASA-CR-195802] p 3205 N94-29736
ACTIVITY (BIOLOGY)
The MSRC ab initio methods benchmark suite: A measurement of hardware and software performance in the area of electronic structure methods
[DE94-006428] p 3514 N94-30001
ACTIVITY CYCLES (BIOLOGY)
Surface differential rotation in a sample of cool dwarf stars p 3545 N94-29827
Circadian countermeasures for shiftworkers during USMP-2: A report to mission management
[NASA-CR-195260] p 3402 N94-30188
ACTS
Remote observatory access via the advanced communications technology satellite p 3253 N94-29894
ACTUATORS
Collocated tunable wavenumber sensor/actuators for smart structures
[AD-A275872] p 3241 N94-28755
Feedback control of a three-link planar under-actuated manipulator using a surge velocity
[AD-A275159] p 3435 N94-29044
Rotary actuator
[NASA-CASE-MFS-28581-1] p 3205 N94-29447
The 27th Aerospace Mechanisms Symposium
[NASA-CP-3205] p 3160 N94-29627
A gimbaled low noise momentum wheel p 3162 N94-29640
Low melting temperature alloy deployment mechanism and recent experiments p 3163 N94-29644
Miniature linear-to-rotary motion actuator p 3163 N94-29647
Design and test of electromechanical actuators for thrust vector control p 3163 N94-29650
SP-100 control drive assembly development p 3163 N94-29651
Toward milli-Newton electro- and magneto-static microactuators p 3238 N94-29784
Control of micromachined deformable mirrors p 3239 N94-29787
On possibility to create the scintillation trigger for liquid-argon neutrino detector
[DE94-607844] p 3489 N94-30050
Nearly time-optimal feedback control of a magnetically levitated photolithography positioning system
[DE94-005288] p 3266 N94-30055
Damage identification in composites using built-in piezoelectrics p 3184 N94-30355
Local interaction control for space construction p 3170 N94-30960
ACUITY
Microactuator production via high aspect ratio, high edge acuity metal fabrication technology p 3235 N94-29770
ACYLATION
Group transfer and electron transfer reactions of organometallic complexes: Summary of research accomplished in 1993
[DE94-004963] p 3200 N94-30770
ADA (PROGRAMMING LANGUAGE)
Comparing Ada and FORTRAN lines of code: Some experimental results
[AD-A275322] p 3409 N94-28878
Ada, object-oriented techniques, and concurrency in teaching data structures and file management
[AD-A275385] p 3411 N94-29201
A common Ada run-time system for avionics software p 3150 N94-29331
Ada run time system certification for avionics applications p 3150 N94-29332
The UNICON approach to through-life support and evolution of software-intensive systems p 3416 N94-29340
Aid to Ada component reuse at Aerospatiale Cannes (France)
[REPT-932-440-102] p 3418 N94-29418
ADAPTATION
Work conditions assessment in pilots and ground personnel under high weather temperatures p 3382 N94-28444
Photorefractive adaptive antenna array processor
[AD-A275762] p 3241 N94-28762
Circadian countermeasures for shiftworkers during USMP-2: A report to mission management
[NASA-CR-195260] p 3402 N94-30188
ADAPTIVE CONTROL
Application of digital control theory to adaptive grid generation p 3127 N94-28980

Robust adaptive control and filtering
p 3437 N94-29895
Adaptive power control as a fade countermeasure on satellite links p 3253 N94-29897
Robust adaptive control of a mechanical manipulator
p 3449 N94-30806

ADAPTIVE FILTERS
Removal of coherent Extremely Low Frequency (ELF) background noise by adaptive noise cancellation
[AD-A275016] p 3243 N94-28898
Robust adaptive control and filtering
p 3437 N94-29895

ADDING CIRCUITS
Realization of function logics by means of transmission gate
[REPT-93-061] p 3429 N94-30936

ADDITIVES
High resistivity buffer layers by oxygen doping
[AD-A274986] p 3513 N94-29125
Research and development of high thermal stability fuels p 3192 N94-29261

ADDUCTS
Synthesis and molecular structures of R(Me3CCH2)2In-E(SiMe3) (R = Me3CCH2, E = P or As; R = Me, E = P)
[AD-A275020] p 3486 N94-29131

ADHESION
Pull-test adhesion measurements of diamondlike carbon films on silicon carbide, silicon nitride, aluminum oxide, and zirconium oxide
[DE94-005469] p 3211 N94-28536
Adhesion of electrolessly deposited Ni(P) on alumina ceramic
[ETN-94-95358] p 3212 N94-28539
High damage threshold anti-reflectors by physical vapor deposited amorphous fluoropolymer
[DE94-004865] p 3212 N94-28560
Rules and definition of the range of paints applied on aeronautical structrural composites
[REPT-932-600-106] p 3215 N94-29459

ADHESION TESTS
Pull-test adhesion measurements of diamondlike carbon films on silicon carbide, silicon nitride, aluminum oxide, and zirconium oxide
[DE94-005469] p 3211 N94-28536
Adhesion of electrolessly deposited Ni(P) on alumina ceramic
[ETN-94-95358] p 3212 N94-28539

ADHESIVE BONDING
Composite panel failure analysis and improvement plan
[AD-A275655] p 3176 N94-28653
Preliminary evaluation of hybrid titanium composite laminates
[NASA-TM-109095] p 3180 N94-29472

ADHESIVES
Solventless, curable fluid oligomeric systems for high performance microwave, acoustical and mechanical applications p 3223 N94-30478

ADIABATIC CONDITIONS
Quasi-adiabatic motion of energetic particles in a dipole magnetic field
[DE94-607322] p 3362 N94-29935

ADSORBENTS
Low frequency dynamics of CO/Cu-breakdown of Born-Oppenheimer approximation
[DE94-005508] p 3510 N94-28512
Journal of NIRE, Vol. 2, No. 2
[JTN-94-80552] p 3187 N94-28675
Properties of adsorbents for collection and analysis of trace amount of chlorofluorocarbons in air
p 3188 N94-28680

ADSORPTION
Low frequency dynamics of CO/Cu-breakdown of Born-Oppenheimer approximation
[DE94-005508] p 3510 N94-28512
Fundamental studies of hydrogen interaction with supported meta and bimetallic catalysts
[DE94-004887] p 3202 N94-28562
Nuclear magnetic relaxation studies of semiconductor nanocrystals and solids
[DE94-006301] p 3520 N94-30842
Influence of surface defects and local structure on oxygenate reaction pathways over metal oxide surfaces
[DE94-005680] p 3522 N94-30901

ADVANCED SOLID ROCKET MOTOR (STS)
Robotic NDE inspection of advanced solid rocket motor casings
[AIAA PAPER 94-1222-CP] p 3446 N94-30571

ADVANCED VERY HIGH RESOLUTION RADIOMETER
Objective analysis of a coastal ocean eddy using satellite AVHRR and in situ hydrographic data
[AD-A275715] p 3376 N94-28642

ADVECTION
Evolution of the large-scale vortices in turbulent mixing-layers p 3273 N94-29686
Effects of diffusion and inertia on chaotic mixing: A computational and experimental study
p 3488 N94-29903
Evaluation of discretization schemes for advection-diffusion equations
[CWI-NM-R9311] p 3461 N94-30751

AERIAL PHOTOGRAPHY
The Image Digitizing System (IDS)
[AD-A275341] p 3329 N94-29213
The use of digital stereo photogrammetric methods in historical photo analysis
[AD-A275287] p 3288 N94-29437
The extraction and representation of forest inventory information using continuous density surfaces
[ISBN-0-315-85658-0] p 3334 N94-30236

AERIAL RECONNAISSANCE
MODIS technical report series. Volume 3: MODIS airborne simulator level 1B data user's guide
[NASA-TM-104594] p 3231 N94-29385
Cockpit video: A low cost BDA source
[AD-A275228] p 3150 N94-29389
Payload central control for unmanned aircraft
p 3155 N94-30284

AEROACOUSTICS
A non-local computational boundary condition for duct acoustics
[NASA-TM-109091] p 3478 N94-29382
Aeroacoustic sensitivity analysis and optimal aeroacoustic design of turbomachinery blades
[NASA-CR-195786] p 3153 N94-30013
Computational analysis of high resolution unsteady airloads for rotor aeroacoustics
[NASA-CR-194894] p 3480 N94-30274

AEROBRAKING
Particle kinetic simulation of high altitude hypervelocity flight
[NASA-CR-194535] p 3131 N94-29893

AERODYNAMIC CHARACTERISTICS
Holographic interferometry: A user's guide
[DE94-003136] p 3286 N94-28466
Exploring QDES as a tool for determining limits of achievable performance in aircraft design
[AD-A275359] p 3146 N94-28998
Study of bridge design and technology
[PB94-137916] p 3121 N94-29160
Low-speed longitudinal aerodynamic characteristics of a flat-plate planform model of an advanced fighter configuration
[NASA-TM-109045] p 3130 N94-29443
An experimental and theoretical study of the aerodynamic characteristics of some generic missile concepts at Mach numbers from 2 to 6.8
[NASA-TM-109110] p 3130 N94-29473
Algorithm and code development for unsteady three-dimensional Navier-Stokes equations
[NASA-CR-195774] p 3277 N94-29942
Aircraft aerodynamics with deflected jets in ground effect p 3132 N94-29973
Expanding the waverider design space using arbitrary generating flowfields p 3148 N94-30516
International collaborative research in wind turbine rotor aerodynamics
[DE94-000244] p 3339 N94-30602

AERODYNAMIC CONFIGURATIONS
An experimental investigation of the effect of leading edge extensions on directional stability and the effectiveness of forebody nose strakes
p 3155 N94-29728
Three-dimensional flow characteristics downstream of a blade endwall corner p 3280 N94-30229
The design of a system of codes for industrial calculations of flows around aircraft and other complex aerodynamic configurations
[PB94-125598] p 3133 N94-30387
Calculus of variations applied to 2D multi-point airfoil design
[PB94-125457] p 3133 N94-30401

AERODYNAMIC DRAG
Unsteady aerodynamic computations around NACA0012 at high angles of attack
p 3126 N94-28969
Nominally two-dimensional flow about a normal flat plate p 3275 N94-29838
Aerodynamic characteristics of a propeller-powered high-lift semispan wing
[NASA-TM-4541] p 3132 N94-29937
Potential of the ramjet engine for hypersonic flight speeds p 3153 N94-30935

AERODYNAMIC INTERFERENCE
Experimental studies of transonic flow field near a longitudinally slotted wind tunnel wall
[NASA-TP-3392] p 3130 N94-29545
Prospects of time-linearized unsteady calculation methods for exponentially diverging motions in aeroelasticity
[PB94-126224] p 3134 N94-30740
Aerodynamic analysis of slipstream/wing/nacelle interference for preliminary design of aircraft configurations
[AD-B173651] p 3135 N94-30916

AERODYNAMIC LOADS
Structural/aerodynamic blade analyzer (SAB) user's guide, version 1.0
[NASA-CR-194460] p 3151 N94-29103
Aeroacoustic sensitivity analysis and optimal aeroacoustic design of turbomachinery blades
[NASA-CR-195786] p 3153 N94-30013
Computational analysis of high resolution unsteady airloads for rotor aeroacoustics
[NASA-CR-194894] p 3480 N94-30274
A modernised HST of NLR
[AD-B179220] p 3158 N94-30423
International collaborative research in wind turbine rotor aerodynamics
[DE94-000244] p 3339 N94-30602
Prospects of time-linearized unsteady calculation methods for exponentially diverging motions in aeroelasticity
[PB94-126224] p 3134 N94-30740

AERODYNAMIC NOISE
Determination of sound power levels of air terminal units according to ISO 5135-Nordic inter-laboratory tests, Nordtest project no. 968-91
[PB94-137411] p 3477 N94-29175
Experiments on the aerodynamic generation of noise in centrifugal turbomachinery p 3480 N94-30804

AERODYNAMIC STABILITY
Closed loop vibrational control: Theory and applications
[AD-A275451] p 3154 N94-28632
Exploring QDES as a tool for determining limits of achievable performance in aircraft design
[AD-A275359] p 3146 N94-28998
Study of bridge design and technology
[PB94-137916] p 3121 N94-29160

AERODYNAMIC STALLING
A free-wake Euler and Navier-Stokes CFD method and its application to helicopter rotors including dynamic stall
[AD-A275416] p 3129 N94-29197

AERODYNAMICS
Aeronautical engineering: A cumulative index to a continuing bibliography (supplement 300)
[NASA-SP-7037(300)] p 3121 N94-28537
Aerodynamic design using parallel processors
[AD-A275470] p 3122 N94-28674
Experimental investigation of three-dimensional vortex-airfoil interaction in a supersonic stream
[AD-A275107] p 3122 N94-28899
Proceedings of the 10th NAL Symposium on Aircraft Computational Aerodynamics
[NAL-SP-19] p 3123 N94-28946
ENGRID: A graphical interactive code for the computation of structured grids for blocked flow domains
p 3124 N94-28956
Aerothermochemical calculations in afterburners
p 3154 N94-29258
Algorithm and code development for unsteady three-dimensional Navier-Stokes equations
[NASA-CR-195774] p 3277 N94-29942
An experimental study of the aerodynamics of a swept and unswept semispan wing with a simulated glaze ice accretion
[NASA-CR-195330] p 3133 N94-30152
An interactive educational tool for compressible aerodynamics
[NASA-TM-106568] p 3422 N94-30175

AEROELASTICITY
Turbomachinery forced response prediction system (FREPS): User's manual
[NASA-CR-194465] p 3319 N94-29104
Time-marching aeroelastic and spatial adaptation procedures on triangular and tetrahedral meshes using an unstructured-grid Euler method p 3131 N94-29877
Algorithm and code development for unsteady three-dimensional Navier-Stokes equations
[NASA-CR-195774] p 3277 N94-29942
Development of a method to predict transonic limit cycle oscillation characteristics of fighter aircraft (continued)
[NLR-TP-92156-U] p 3148 N94-30342
Sensitivity analysis of the static aeroelastic response of a wing p 3134 N94-30525
Prospects of time-linearized unsteady calculation methods for exponentially diverging motions in aeroelasticity
[PB94-126224] p 3134 N94-30740

AEROEMBOLISM
Decompression sickness risk versus time and altitude
[AD-A275261] p 3391 N94-29071

AEROGELS
Alkylene-bridged polygerm- and polygermsilsesqui-oxanes: New hybrid organic-inorganic materials
[DE94-005096] p 3174 N94-28557

AERONAUTICAL ENGINEERING
Aeronautical engineering: A cumulative index to a continuing bibliography (supplement 300)
[NASA-SP-7037(300)] p 3121 N94-28537
Proceedings of the 10th NAL Symposium on Aircraft Computational Aerodynamics
[NAL-SP-19] p 3123 N94-28946
Engineering of systems for application of scientific computing in industry p 3123 N94-28947
Monte Carlo simulation or normal shock wave. Part 2: VHS model and VSS model p 3123 N94-28948
Variable soft sphere molecular model in the Monte Carlo simulation of air species p 3123 N94-28949
Rarefied gas numerical wind tunnel. Part 8: HOPE p 3123 N94-28950
Numerical simulation of arc heated wind tunnel flow p 3123 N94-28951
Numerical simulation of unsteady aerodynamic heating induced by shock reflections p 3123 N94-28952
Numerical simulation of steady Mach reflection by shock capturing schemes p 3123 N94-28953
Higher-order accurate numerical simulation of 3D supersonic mixing layers p 3124 N94-28954
Numerical simulation of aerothermodynamic heating of hypersonic space transportation vehicles p 3124 N94-28955
Transonic expanding flow through axially symmetric orifices p 3128 N94-28985
Similarity between turbulent flows through curved pipe and orthogonal rotating pipe p 3128 N94-28986
Fishermans Bend: A centre of Australian aviation
[AD-A274981] p 3121 N94-29090

AERONAUTICS
Research and technology, 1992
[NASA-TM-103996] p 3555 N94-29891

AERONOMY
NOAA Aeronomy Laboratory long-path OH experiment, Fritz Peak Observatory, Colorado p 3344 N94-28598

AEROSOLS
Measurement of elemental speciation by liquid chromatography: Inductively coupled plasma mass spectrometry (LC-ICP-MS) with the Direct Injection Nebulizer (DIN)
[DE94-005261] p 3187 N94-28483
Studies of marine aerosols and their evolution in the eastern North Atlantic
[AD-A275011] p 3377 N94-29128
Activities report of the International Meteorological Institute
[ETN-94-95524] p 3370 N94-29423
Optical modeling of visibility and visibility instrumentation using stratified Mie theory p 3348 N94-29750
Micro-sensors for in-situ meteorological measurements p 3236 N94-29777
Brief summary of accomplishments since our DOE-sponsored radon project commenced
[DE94-004643] p 3348 N94-29926
Granulometry in environments with very small particle concentrations p 3259 N94-30511
Cloud and aerosol characterization for the ARM central facility: Multiple remote sensor techniques development
[DE94-003523] p 3365 N94-30608
Radiation transport in cloudy and aerosol loaded atmospheres p 3366 N94-30805
Using the log-normal distribution in analyzing aerosols: The mathematical reasoning underlying the various diameters used and the plotting procedure
[DE94-006459] p 3461 N94-30817
The long-range transport of aerosol particles over the North Atlantic Ocean p 3366 N94-30867

AEROSPACE ENGINEERING
Aerospace Software Engineering for Advanced Systems Architectures
[AGARD-CP-545] p 3412 N94-29315
Lubrication of space systems
[NASA-TM-106392] p 3214 N94-29399
The 27th Aerospace Mechanisms Symposium
[NASA-CP-3205] p 3160 N94-29627
NASA/DOD Aerospace Knowledge Diffusion Research Project. Report 23: The communications practices of US aerospace engineering faculty and students: Results of the phase 3 survey
[NASA-TM-109085] p 3534 N94-30149
NASA/DOD Aerospace Knowledge Diffusion Research Project. Report 22: US academic librarians and technical information specialists as information intermediaries: Results of the phase 3 survey
[NASA-TM-109067] p 3534 N94-30150

AEROSPACE ENVIRONMENTS
Japanese Journal of Aerospace and Environmental Medicine, vol. 30, no. 3
[JTN-94-80606] p 3387 N94-28495
Some issues on Japan's space food development and relating preliminary experimental study p 3388 N94-28498
Fluid and transportation phenomena under microgravity p 3227 N94-28939
Glass studies under microgravity p 3228 N94-28941
Fabrication of electronic materials in space p 3228 N94-28942
Protein crystal growth in microgravity p 3228 N94-28943
Cell culture in space p 3228 N94-28944
Cosmic energy equipment p 3229 N94-28945

AEROSPACE INDUSTRY
Retention latch mechanism for the Wake Shield Facility p 3161 N94-29635
Confessions of a robot lobotomist
[AIAA PAPER 94-1185-CP] p 3440 N94-30535
Graphical simulation for aerospace manufacturing
[AIAA PAPER 94-1224-CP] p 3446 N94-30573

AEROSPACE MEDICINE
The Support of Air Operations under Extreme Hot and Cold Weather Conditions
[AGARD-CP-540] p 3379 N94-28420
The concept of Royal Navy air operations under extreme environmental conditions p 3379 N94-28424
Aeromedical support for casualties in extremely hot climates p 3382 N94-28443
Work conditions assessment in pilots and ground personnel under high weather temperatures p 3382 N94-28444
Test of a new protection suit in a climatic chamber p 3384 N94-28452
Japanese Journal of Aerospace and Environmental Medicine, vol. 30, no. 3
[JTN-94-80606] p 3387 N94-28495
The MERSS 5th Symposium on Space Medicine: Medical and Physiological Experiment Utilizing Parabolic Flight
[JTN-94-80588] p 3392 N94-29709
Hemodynamic measurement during parabolic flight p 3393 N94-29717
Motion sickness in parabolic flight: Possibility of electrogastrography as an objective index p 3393 N94-29718
Shortening velocity and calcium sensitivity of single fibers from hindlimb suspended muscle in rats p 3387 N94-29866

AEROSPACE PLANES
Numerical simulation of supersonic flow around space plane with engine installed p 3125 N94-28961
Some problems of scramjet propulsion for aerospace planes. Part 1: Scramjet: Aims and features p 3151 N94-29295
Some problems of scramjet propulsion for aerospace planes. Part 2: Scramjet: Development and test problems p 3152 N94-29301

AEROSPACE SAFETY
Second NASA Workshop on Wiring for Space Applications
[NASA-CP-3244] p 3165 N94-28697
NASA wiring program: Survey of NASA experiences in wiring system safety p 3165 N94-28700
Wire insulation degradation and flammability in low gravity p 3166 N94-28712
Vulnerability of manned spacecraft to crew loss from orbital debris penetration
[NASA-TM-108452] p 3169 N94-30161

AEROSPACE SYSTEMS
Second NASA Workshop on Wiring for Space Applications
[NASA-CP-3244] p 3165 N94-28697
Wiring for space applications program p 3166 N94-28708
High temperature arc-track resistant aerospace insulation p 3167 N94-28716
General theory and algorithms for the non-casual inversion, slewing and control of space-based articulated structures
[AD-A275118] p 3167 N94-29002
A generalization of the software engineering maturity model p 3416 N94-29341
Lubrication of space systems
[NASA-TM-106392] p 3214 N94-29399
Integration of pyrotechnics into aerospace systems p 3161 N94-29634
Advanced vehicle concepts systems and design analysis studies
[NASA-CR-195115] p 3147 N94-29721
Proceedings of the Workshop on Microtechnologies and Applications to Space Systems
[NASA-CR-195688] p 3235 N94-29767
The application of micromachined sensors to manned space systems p 3171 N94-29791
A study of the flexible space platform based deployable manipulator
[ISBN-0-315-85410-3] p 3303 N94-30135
Object-based task-level control: A hierarchical control architecture for remote operation of space robots
[AIAA PAPER 94-1209-CP] p 3444 N94-30560
An intelligent robot for helping astronauts
[AIAA PAPER 94-1233-CP] p 3447 N94-30581
Dual cure low-VOC coating process, phase 3
[DE94-003202] p 3221 N94-30826

AEROSPACE TECHNOLOGY TRANSFER
NASA/DOD Aerospace Knowledge Diffusion Research Project. Report 23: The communications practices of US aerospace engineering faculty and students: Results of the phase 3 survey
[NASA-TM-109085] p 3534 N94-30149
NASA/DOD Aerospace Knowledge Diffusion Research Project. Report 22: US academic librarians and technical information specialists as information intermediaries: Results of the phase 3 survey
[NASA-TM-109067] p 3534 N94-30150
Terrestrial applications of NASA space telerobotics technologies
[AIAA PAPER 94-1235-CP] p 3448 N94-30582

AEROSPACE VEHICLES
Second NASA Workshop on Wiring for Space Applications
[NASA-CP-3244] p 3165 N94-28697
NASA wiring program: Survey of NASA experiences in wiring system safety p 3165 N94-28700
Variable soft sphere molecular model in the Monte Carlo simulation of air species p 3123 N94-28949
Rarefied gas numerical wind tunnel. Part 8: HOPE p 3123 N94-28950
Numerical simulation of aerothermodynamic heating of hypersonic space transportation vehicles p 3124 N94-28955
Code development for hypersonic real-gas flow simulations toward the design of space vehicles, part 2 p 3125 N94-28966
Review of sonic fatigue technology
[NASA-CR-4587] p 3479 N94-29407

AEROTHERMOCHEMISTRY
Numerical simulation of arc heated wind tunnel flow p 3123 N94-28951
Aerothermochemical calculations in afterburners p 3154 N94-29258
Models for vibration-dissociation coupling in high-temperature gases p 3273 N94-29675
A study of low emissions gas turbine combustions
[NASA-CR-195763] p 3152 N94-29860

AEROTHERMODYNAMICS
Ducted kerosene spray flames p 3195 N94-29276

AFTERBURNING
Aerothermochemical calculations in afterburners p 3154 N94-29258
Technology rigs: A tool for afterburner development p 3154 N94-29270

AGING (BIOLOGY)
Aviation epidemiology data register: Age distribution of U.S. Army aviators stratified by gender and component of service
[AD-A275901] p 3388 N94-28757

AGING (MATERIALS)
Aircraft age impacts on maintenance requirements
[AD-A275701] p 3121 N94-28666
Correlation between wet ageing, humidity absorption and properties on composite materials based on different resins family
[REPT-932-600-107] p 3179 N94-29462
Effects of physical aging on long-term creep of polymers and polymer matrix composites
[NASA-TM-109081] p 3181 N94-29541
The effect of temperature on creep and physical ageing of PVC
[NPL-DMM(A)-93] p 3217 N94-29885
Creep and physical aging of PVC: Dependence on stress and temperature
[NPL-DMM(A)-115] p 3217 N94-29886
Novel techniques applied to polymer lifetime predictions
[DE94-005095] p 3218 N94-30102

AGING (METALLURGY)
Low temperature behavior of virgin martensite
[PB94-132925] p 3204 N94-29142

AGREEMENTS
Protocol on environmental protection to the Antarctic Treaty and its annexes: International agreement on the comprehensive measures for the protection of Antarctic environment and ecosystems p 3354 N94-29086

AGRICULTURE
JERS-1 and future remote sensing: Application of remote sensing data to agroecological problems p 3331 N94-29229

AIR BREATHING ENGINES
Research and development of ramjets/ramrockets. Part 1: Integral solid propellant ramrockets p 3151 N94-29294

AIR CONDITIONING
Experimental evaluation of two systems of individual air-conditioning p 3384 N94-28450
ARTI Refrigerant Database [DE94-004906] p 3230 N94-28563
Ventilation cost and air cleaning p 3232 N94-29605
Control of heating, ventilation and air conditioning (HVAC) systems [PB94-138807] p 3401 N94-30000
Using spacecraft trace contaminant control systems to cure sick building syndrome p 3354 N94-30470

AIR CONDITIONING EQUIPMENT
The use of liquid and air microclimate conditioning systems to alleviate heat stress in helicopter NBC operations p 3384 N94-28453
Ventilation cost and air cleaning p 3232 N94-29605
Control of heating, ventilation and air conditioning (HVAC) systems [PB94-138807] p 3401 N94-30000

AIR COOLING
The use of liquid and air microclimate conditioning systems to alleviate heat stress in helicopter NBC operations p 3384 N94-28453
Acquisition, design modification, assembly, and ground test of NPS Hummingbird remotely piloted helicopter [AD-A275546] p 3146 N94-28837
Chambers of turboreactors with variable geometry: A response to the matrix of pollution in cycles at high temperature, high pressure p 3194 N94-29273

AIR CURRENTS
Objective analysis of a coastal ocean eddy using satellite AVHRR and in situ hydrographic data [AD-A275715] p 3376 N94-28642
A laboratory simulation of urban heat-island-induced circulation in a stratified environment p 3367 N94-30921

AIR CUSHION LANDING SYSTEMS
An evaluation of personality testing and the five-factor model in the selection of landing craft air cushion vehicle crew members [AD-A275869] p 3397 N94-28754

AIR DEFENSE
Synchronization, positioning, and communication in multistatic radar systems for air defence [PB94-137478] p 3243 N94-28908

AIR DROP OPERATIONS
Air-depioyable geophysics package [DE94-005651] p 3335 N94-30594

AIR FILTERS
Using spacecraft trace contaminant control systems to cure sick building syndrome p 3354 N94-30470

AIR FLOW
Papers in meteorology and geophysics, vol. 44, no.1 [JTN-94-80585] p 3324 N94-28693
On the linear stability of Verkley's modons p 3324 N94-28695
Structure of neutrally stratified turbulent Ekman layer as predicted by closure models with prognostic equation for master length scale p 3325 N94-28696
Evaluation of the transient operation of advanced gas turbine combustors p 3154 N94-29269
Chambers of turboreactors with variable geometry: A response to the matrix of pollution in cycles at high temperature, high pressure p 3194 N94-29273
The influence of air distribution on homogeneity and pollutant formation in the primary zone of a tubular combustor p 3194 N94-29274
Advanced Design of Ventilation Systems [VKI-LS-1993-07] p 3231 N94-29598
Introduction to the design of ventilation systems p 3231 N94-29599
Ventilation systems p 3232 N94-29601
Theory of age distribution p 3232 N94-29602
Computational fluid dynamics in ventilation. 1: Theory and one-dimensional test case p 3232 N94-29606
Computational fluid dynamics in ventilation. 2: Theory and codes p 3233 N94-29607
Computational fluid dynamics in ventilation. 3: The IEA annex 20 work p 3233 N94-29608
Computational fluid dynamics in ventilation. 4: Commercial application of CFD in ventilation p 3233 N94-29609
Computational fluid dynamics in ventilation. 5: New developments in CFD with relevance to ventilation p 3233 N94-29610
Computational fluid dynamics in ventilation: Practical approach p 3233 N94-29611

AIR JETS
The mixing process in the quenching zone of the rich-lean-combustion concept p 3196 N94-29281
Temperature and combustion analysis of combustor with acoustically controlled primary zone air-jet mixing p 3196 N94-29284
Computational fluid dynamics in ventilation. 5: New developments in CFD with relevance to ventilation p 3233 N94-29610

AIR LAND INTERACTIONS
On eddy accumulation with limited conditional sampling to measure air-surface exchange [DE94-005112] p 3368 N94-28568
Modeling the Earth System, volume 3 [NASA-CR-194256] p 3350 N94-30616
Atmosphere, ocean, and land: Critical gaps in Earth system models p 3350 N94-30617
Land surface interaction p 3350 N94-30621
A toy model for estimating N2O emissions from natural soils p 3351 N94-30627
A bottom-up evolution of terrestrial ecosystem modeling theory, and ideas toward global vegetation modeling p 3351 N94-30628
A laboratory simulation of urban heat-island-induced circulation in a stratified environment p 3367 N94-30921

AIR NAVIGATION
Object oriented design of the autonomous fixtaking management system p 3143 N94-29323
Ground independent landing system p 3137 N94-29564
GPS/GNSS for ATM p 3138 N94-29565
Simulation of fully automated air traffic control concepts p 3139 N94-29569
Interactive analysis and planning tools for air traffic and airspace management p 3139 N94-29573
ARC2000: Automatic radar control p 3141 N94-29583

AIR POLLUTION
Measurement of volatile metal species at elevated temperatures [PB94-132321] p 3186 N94-28407
Development of the integrated environmental control model: Performance models of selective catalytic reduction NO(x) control systems [DE94-002151] p 3341 N94-28465
An improved method of measuring tropospheric NO2, NO3, HO2, and RO2 by Matrix Isolation and Electronic Spin Resonance (MIESR) p 3345 N94-28605
Feasibility study on introduction of a large methanol engine power generation plant [DE94-732338] p 3224 N94-28629
Studies of marine aerosols and their evolution in the eastern North Atlantic [AD-A275011] p 3377 N94-29128
Characterization of air emissions from the simulated open combustion of fiberglass materials [PB94-136231] p 3347 N94-29192
On the effect of emissions from aircraft engines on the state of the atmosphere p 3189 N94-29247
Pollutant emissions from and within a model gas turbine combustor at elevated pressures and temperatures p 3194 N94-29271
Reduction of NO(x) by fuel-staging in gas turbine engines: A commitment to the future p 3194 N94-29272
The influence of air distribution on homogeneity and pollutant formation in the primary zone of a tubular combustor p 3194 N94-29274
Introduction to the design of ventilation systems p 3231 N94-29599
The suitability of low-cost urban airshed modeling in the Chicago area [DE94-005114] p 3349 N94-30023
Intermedia transfer factors for fifteen toxic pollutants released to air basins in California [DE94-005699] p 3349 N94-30044
Novel mass spectrometric instrument for gaseous and particulate characterization and monitoring [DE94-005896] p 3349 N94-30047
Granulometry in environments with very small particle concentrations p 3259 N94-30511
An evaluation of explicit pseudo-steady-state approximation schemes for stiff ODE systems from chemical kinetics [CWI-NM-R9312] p 3353 N94-30729

AIR PURIFICATION
Using spacecraft trace contaminant control systems to cure sick building syndrome p 3354 N94-30470

AIR QUALITY
Advanced Design of Ventilation Systems [VKI-LS-1993-07] p 3231 N94-29598
Human requirements to the indoor air quality and the thermal environment p 3232 N94-29600
Computational fluid dynamics in ventilation: Practical approach p 3233 N94-29611
The suitability of low-cost urban airshed modeling in the Chicago area [DE94-005114] p 3349 N94-30023
Using spacecraft trace contaminant control systems to cure sick building syndrome p 3354 N94-30470
Fuel cycle evaluations of biomass-ethanol and reformulated gasoline [DE94-000227] p 3226 N94-30818

AIR SAMPLING
Measurement of volatile metal species at elevated temperatures [PB94-132321] p 3186 N94-28407
On eddy accumulation with limited conditional sampling to measure air-surface exchange [DE94-005112] p 3368 N94-28568
Tropospheric HO determination by FAGE p 3342 N94-28590
The active titration method for measuring local hydroxyl radical concentration p 3345 N94-28602
An improved method of measuring tropospheric NO2, NO3, HO2, and RO2 by Matrix Isolation and Electronic Spin Resonance (MIESR) p 3345 N94-28605
Tropospheric HO2 determination by FAGE p 3345 N94-28606
HO2 detection by near infrared absorption using tunable diode lasers p 3346 N94-28608
Properties of adsorbents for collection and analysis of trace amount of chlorofluorocarbons in air p 3188 N94-28680
A study of low emissions gas turbine combustions [NASA-CR-195763] p 3152 N94-29860
The long-range transport of aerosol particles over the North Atlantic Ocean p 3366 N94-30867

AIR SEA ICE INTERACTIONS
Antarctic Record, volume 36, no. 1 [REPT-106-VOL-36-NO-1] p 3357 N94-29078
Activities of the wintering party at Showa Station by the 31st Japanese Antarctic Research Expedition in 1990 p 3358 N94-29083
A toy model of sea ice growth p 3351 N94-30626
Cryosphere and climate p 3352 N94-30632

AIR TRAFFIC
Machine Intelligence in Air Traffic Management [AGARD-CP-538] p 3136 N94-29558
Ground independent landing system p 3137 N94-29564
GPS/GNSS for ATM p 3138 N94-29565
Contributions of DLR to air traffic capacity enhancement within a terminal area p 3138 N94-29567
Simulation of fully automated air traffic control concepts p 3139 N94-29569
DLR's ATM demonstration programme p 3140 N94-29575

AIR TRAFFIC CONTROL
Machine Intelligence in Air Traffic Management [AGARD-CP-538] p 3136 N94-29558
Advances in development capabilities for intelligent air traffic management systems p 3137 N94-29559
Intelligent systems for air space control and management p 3137 N94-29560
Use of advanced technologies in ATM (air traffic management) domain p 3137 N94-29561
Air traffic management as principled negotiation between intelligent agents p 3137 N94-29562
Use of GPS in automated air traffic control p 3137 N94-29563
Ground independent landing system p 3137 N94-29564
GPS/GNSS for ATM p 3138 N94-29565
ACCS Surveillance Exploratory Prototype (ASEP) p 3138 N94-29566
Contributions of DLR to air traffic capacity enhancement within a terminal area p 3138 N94-29567
Design of Center-TRACON Automation System p 3138 N94-29568
Simulation of fully automated air traffic control concepts p 3139 N94-29569
Decision Making Aids (DMA) in on-line ATC systems p 3139 N94-29570
Cognitive approach to specifications on air traffic controllers' decision assistance systems p 3139 N94-29571
Considerations on graphical user interfaces for intelligent ATM support systems p 3139 N94-29572
Interactive analysis and planning tools for air traffic and airspace management p 3139 N94-29573
DAISY: A decision aid for an air situation interpretation system p 3139 N94-29574
DLR's ATM demonstration programme p 3140 N94-29575
Advanced air traffic control and flight management system concepts p 3140 N94-29576
Opportunities for integrating the aircraft FMS, aeronautical operational control centers, and future air traffic management systems in oceanic airspace p 3140 N94-29577
Profile negotiation: An air/ground automation integration concept for managing arrival traffic p 3140 N94-29578

Air-ground integration of the ATM system in PHARE p 3141 N94-29579
Experimental flight management system p 3141 N94-29580
The PHARE advanced tools p 3141 N94-29581
The Common Modular Simulator (CMS): An architecture test bed for future advanced ATM systems p 3141 N94-29582
ARC2000: Automatic radar control p 3141 N94-29583
A novel near-range radar network for airport surface control p 3142 N94-29586
Development of precision runway monitor system for increasing capacity of parallel runway operations p 3142 N94-29587
Scanning and monitoring performance: Effects of the reinforcement values of the events being monitored [DOT/FAA/AM-94/8] p 3398 N94-29918
Installation of experimental mode-S data link in commercial aircraft [PB94-136757] p 3254 N94-29998
A simulator for multi-radar analysis for realistic traffic [AD-B179099] p 3142 N94-30439
A stochastic control approach to flight path monitoring [AD-B174630] p 3143 N94-30853
Maintaining vigilance on a simulated ATC monitoring task across repeated sessions [DOT/FAA/AM-94/6] p 3143 N94-30933
The experimental flight management system: An air traffic management research tool [NLR-TP-92253-U] p 3143 N94-30943

AIR TRAFFIC CONTROLLERS (PERSONNEL)
Decision Making Aids (DMA) in on-line ATC systems p 3139 N94-29570
Cognitive approach to specifications on air traffic controllers' decision assistance systems p 3139 N94-29571
Considerations on graphical user interfaces for intelligent ATM support systems p 3139 N94-29572
Interactive analysis and planning tools for air traffic and airspace management p 3139 N94-29573
DAISY: A decision aid for an air situation interpretation system p 3139 N94-29574
Scanning and monitoring performance: Effects of the reinforcement values of the events being monitored [DOT/FAA/AM-94/8] p 3398 N94-29918
Maintaining vigilance on a simulated ATC monitoring task across repeated sessions [DOT/FAA/AM-94/6] p 3143 N94-30933

AIR TRANSPORTATION
National Transportation Safety Board annual review of aircraft accident data. US general aviation, 1990 [PB94-126869] p 3135 N94-29185
A capacity planning model for Canadian military airlift requests [ISBN-0-315-86079-0] p 3136 N94-30144

AIR WATER INTERACTIONS
Research trends on remote sensing at research facilities in Japan: The priority area programme on better understanding of earth environment via satellite p 3326 N94-28928
SAR-related stress variability in the Marine Atmospheric Boundary Layer (MABL) [AD-A275275] p 3377 N94-29436
The dynamics of tropical intraseasonal variability p 3371 N94-29741
On the annual cycle of the tropical Pacific atmosphere and ocean p 3371 N94-29763
Modeling the Earth System, volume 3 [NASA-CR-194256] p 3350 N94-30616
Atmosphere, ocean, and land: Critical gaps in Earth system models p 3350 N94-30617
Ocean-atmospheric linkages p 3350 N94-30623
Four simple ocean carbon models p 3351 N94-30625
Studies of interfaces and vapors with Optical Second Harmonic Generation [DE94-006295] p 3476 N94-30841
The long-range transport of aerosol particles over the North Atlantic Ocean p 3366 N94-30867

AIRBORNE RADAR
Ground independent landing system p 3137 N94-29564

AIRBORNE/SPACEBORNE COMPUTERS
Software engineering methods in the Hermes on-board software p 3414 N94-29326
Ada run time system certification for avionics applications p 3150 N94-29332
On ground system integration and testing: A modern approach p 3150 N94-29334
Testing Operational Flight Programs (OFPs) p 3415 N94-29337
Future manned systems advanced avionics study [NASA-CR-188277] p 3150 N94-29377

AIRCRAFT ACCIDENT INVESTIGATION
Aircraft accident/incident summary report: In-flight loss of control, leading to forced landing and runway overrun, Continental Express, Inc., N24706 Embraer EMB-120 RT, Pine Bluff, Arkansas, 29 April 1993 [PB94-910404] p 3135 N94-29402

AIRCRAFT ACCIDENTS
Physiological investigations of the isolated rat's liver in hypothermia and hypoxia and their relevance in aircraft incidents above the sea p 3382 N94-28439
Crashworthiness analysis of commuter aircraft seats [AD-A275889] p 3135 N94-28799
National Transportation Safety Board annual review of aircraft accident data. US general aviation, 1990 [PB94-126869] p 3135 N94-29185
Fire behavior of aeronautical materials [REPT-932-600-105] p 3197 N94-29457

AIRCRAFT APPROACH SPACING
Contributions of DLR to air traffic capacity enhancement within a terminal area p 3138 N94-29567
Design of Center-TRACON Automation System p 3138 N94-29568
Profile negotiation: An air/ground automation integration concept for managing arrival traffic p 3140 N94-29578
ARC2000: Automatic radar control p 3141 N94-29583
Development of precision runway monitor system for increasing capacity of parallel runway operations p 3142 N94-29587

AIRCRAFT COMPARTMENTS
Aircraft evacuations: The effect of a cabin water spray system upon evacuation rates and behaviour [CAA-PAPER-93008] p 3148 N94-29887

AIRCRAFT CONFIGURATIONS
Three-dimensional external flow computations using prismatic grid p 3127 N94-28979
Expanding the waverider design space using arbitrary generating flowfields p 3148 N94-30516
Nonlinear multibody formulation for rotorcraft analysis p 3149 N94-30787
Aerodynamic analysis of slipstream/wing/nacelle interference for preliminary design of aircraft configurations [AD-B173651] p 3135 N94-30916

AIRCRAFT CONSTRUCTION MATERIALS
Service life prediction of composite structures through fiber testing [AD-A275661] p 3176 N94-28654
Full-scale testing and analysis of curved aircraft fuselage panels [AD-A275666] p 3145 N94-28657
NAVAIR aircraft wiring standardization and qualification program p 3166 N94-28704
Role of microstructure on the fatigue durability of aluminum aircraft alloys [AD-A275814] p 3202 N94-28830
Fire behavior of aeronautical materials [REPT-932-600-105] p 3197 N94-29457
Rules and definition of the range of paints applied on aeronautical structrural composites [REPT-932-600-106] p 3215 N94-29459
The machining of fiber metal laminates. Part 1: An inventory of forming processes [LR-710-PT-1] p 3184 N94-30343
Composite hot drape forming p 3240 N94-30448

AIRCRAFT CONTROL
An experimental and theoretical study of the aerodynamic characteristics of some generic missile concepts at Mach numbers from 2 to 6.8 [NASA-TM-109110] p 3130 N94-29473
Opportunities for integrating the aircraft FMS, aeronautical operational control centers, and future air traffic management systems in oceanic airspace p 3140 N94-29577
Decoupled flight control system design using the singular perturbation method p 3155 N94-29850
Payload central control for unmanned aircraft p 3155 N94-30284

AIRCRAFT DESIGN
Organized wiring systems p 3166 N94-28705
Modification of ACSYNT aircraft computer program for preliminary design [NASA-CR-195737] p 3145 N94-28817
Exploring QDES as a tool for determining limits of achievable performance in aircraft design [AD-A275359] p 3146 N94-28998
Information presentation for expert systems in future fighter aircraft [AD-A275126] p 3149 N94-29005
Spray combustion experiments and numerical predictions p 3195 N94-29277
Low-speed longitudinal aerodynamic characteristics of a flat-plate planform model of an advanced fighter configuration [NASA-TM-109045] p 3130 N94-29443

AIRCRAFT ENGINES
Fuels and Combustion Technology for Advanced Aircraft Engines [AGARD-CP-536] p 3189 N94-29246
On the effect of emissions from aircraft engines on the state of the atmosphere p 3189 N94-29247
Combustion technology needs for advanced high pressure cycle engines p 3190 N94-29248
Combustion for future supersonic transport propulsion p 3190 N94-29249
Flowfield prediction of NO(x) and smoke production in aircraft engines p 3191 N94-29252
High temperature fuel requirements and payoffs p 3192 N94-29259
Design aspects in small aircraft gas turbine fuel injectors p 3154 N94-29264
Technology rigs: A tool for afterburner development p 3154 N94-29270
Reduction of NO(x) by fuel-staging in gas turbine engines: A commitment to the future p 3194 N94-29272
The influence of air distribution on homogeneity and pollutant formation in the primary zone of a tubular combustor p 3194 N94-29274
Effects of hydrogen addition on pollutant emissions in a gas turbine combustor p 3195 N94-29275
Ducted kerosene spray flames p 3195 N94-29276
Spray combustion experiments and numerical predictions p 3195 N94-29277
Some problems of scramjet propulsion for aerospace planes. Part 2: Scramjet: Development and test problems p 3152 N94-29301
Automated inspection of turbine blades: Challenges and opportunities [AIAA PAPER 94-1226-CP] p 3446 N94-30575

AIRCRAFT EQUIPMENT
Thermal strain generated by an enhanced anti-G protection system in a hot climate p 3383 N94-28445
Cockpit video: A low cost BDA source [AD-A275228] p 3150 N94-29389

AIRCRAFT FUELS
Advanced fuel properties: A computer program for estimating property values [AD-A275248] p 3224 N94-28901
Fuels combustion research [AD-A275122] p 3189 N94-29004
Fuels and Combustion Technology for Advanced Aircraft Engines [AGARD-CP-536] p 3189 N94-29246
High temperature resistant jet fuels p 3192 N94-29260

AIRCRAFT GUIDANCE
Opportunities for integrating the aircraft FMS, aeronautical operational control centers, and future air traffic management systems in oceanic airspace p 3140 N94-29577
Profile negotiation: An air/ground automation integration concept for managing arrival traffic p 3140 N94-29578
Air-ground integration of the ATM system in PHARE p 3141 N94-29579
Experimental flight management system p 3141 N94-29580
The PHARE advanced tools p 3141 N94-29581
Automatic control steps for aircraft taxi guidance p 3141 N94-29584
A novel near-range radar network for airport surface control p 3142 N94-29586
Development of precision runway monitor system for increasing capacity of parallel runway operations p 3142 N94-29587
A stochastic control approach to flight path monitoring [AD-B174630] p 3143 N94-30853
Flight simulator evaluation of advanced MLS procedures [AD-B174270] p 3143 N94-30915

AIRCRAFT ICING
An experimental study of the flowfield on a semispan rectangular wing with a simulated glaze ice accretion p 3130 N94-29674
The 3-D LDV measurements on a 30-degree swept wing with a simulated ice accretion [NASA-CR-195327] p 3132 N94-30124
An experimental study of the aerodynamics of a swept and unswept semispan wing with a simulated glaze ice accretion [NASA-CR-195330] p 3133 N94-30152
Test of prototype liquid-water-content meter for aircraft use [NASA-CR-189304] p 3374 N94-30187
Remote sensor observations during WISP91: The use of microwave radiometers, RASS, and lidar ceilometers for detection of aircraft icing conditions [PB94-142106] p 3136 N94-30890

AIRCRAFT INDUSTRY
Fishermans Bend: A centre of Australian aviation
[AD-A274981] p 3121 N94-29090
AIRCRAFT INSTRUMENTS
GPS/GNSS for ATM p 3138 N94-29565
Installation of experimental mode-S data link in commercial aircraft
[PB94-138757] p 3254 N94-29998
Test of prototype liquid-water-content meter for aircraft use
[NASA-CR-189304] p 3374 N94-30187
AIRCRAFT MAINTENANCE
Effects of repair on structural integrity
[AD-A275756] p 3145 N94-28647
Aircraft age impacts on maintenance requirements
[AD-A275701] p 3121 N94-28666
Organized wiring systems p 3166 N94-28705
Aircraft age impact on individual operating and support cost elements
[AD-A275739] p 3121 N94-28732
Evaluation of access/navigational features of a graphical-user interface installed on a portable maintenance aid
[AD-A275791] p 3136 N94-28744
Role of microstructure on the fatigue durability of aluminum aircraft alloys
[AD-A275814] p 3202 N94-28830
A time reasoning system based on the event calculus for scheduling in aeronautic maintenance
[REPT-932-710-101] p 3122 N94-29463
The effect of mechanical paint stripping on the fatigue and fracture of thin aluminum airplane skin
p 3205 N94-29900
The Automated Aircraft Rework System (AARS): A system integration approach
[AIAA PAPER 94-1225-CP] p 3446 N94-30574
AIRCRAFT MODELS
Modification of ACSYNT aircraft computer program for preliminary design
[NASA-CR-195737] p 3145 N94-28817
A non-linear simulation for an autonomous unmanned air vehicle
[AD-A275062] p 3146 N94-29200
Miniature linear-to-rotary motion actuator
p 3163 N94-29647
Sensitivity analysis of the static aeroelastic response of a wing p 3134 N94-30525
AIRCRAFT NOISE
Experimental validation of finite element and boundary element methods for predicting structural vibration and radiated noise
[NASA-CR-4561] p 3301 N94-29552
AIRCRAFT PERFORMANCE
Exploring QDES as a tool for determining limits of achievable performance in aircraft design
[AD-A275359] p 3146 N94-28998
AIRCRAFT PILOTS
Effects of repair on structural integrity
[AD-A275756] p 3145 N94-28647
Naval aviation vision standards research at the naval aerospace medical research laboratory: The long view
[AD-A275885] p 3388 N94-28756
Aviation epidemiology data register: Age distribution of U.S. Army aviators stratified by gender and component of service
[AD-A275901] p 3388 N94-28757
Disturbance of equilibrium on JAL flight crew
p 3390 N94-28856
AIRCRAFT PRODUCTION
Fishermans Bend: A centre of Australian aviation
[AD-A274981] p 3121 N94-29090
AIRCRAFT RELIABILITY
Automation for nondestructive inspection of aircraft
[AIAA PAPER 94-1223-CP] p 3446 N94-30572
AIRCRAFT SAFETY
Full-scale testing and analysis of curved aircraft fuselage panels
[AD-A275666] p 3145 N94-28657
Crashworthiness analysis of commuter aircraft seats
[AD-A275889] p 3135 N94-28799
National Transportation Safety Board annual review of aircraft accident data. US general aviation, 1990
[PB94-126869] p 3135 N94-29185
Fire behavior of aeronautical materials
[REPT-932-600-105] p 3197 N94-29457
Aircraft evacuations: The effect of a cabin water spray system upon evacuation rates and behaviour
[CAA-PAPER-93008] p 3148 N94-29887
Remote sensor observations during WISP91: The use of microwave radiometers, RASS, and lidar ceilometers for detection of aircraft icing conditions
[PB94-142106] p 3136 N94-30890
Analysis concerning the inspection threshold for multi-site damage
[PB94-142429] p 3149 N94-30905
AIRCRAFT STRUCTURES
Development of Alternating Current Potential Drop (ACPD) procedures for crack detection in aluminum aircraft panels
[AD-A275755] p 3315 N94-28646
Effects of repair on structural integrity
[AD-A275756] p 3145 N94-28647
Full-scale testing and analysis of curved aircraft fuselage panels
[AD-A275666] p 3145 N94-28657
A moment plotting method for characterizing aircraft fatigue data population distributions
[AD-A275500] p 3145 N94-28660
Crashworthiness analysis of commuter aircraft seats
[AD-A275889] p 3135 N94-28799
Fuels combustion research
[AD-A275122] p 3189 N94-29004
Backscatter haze device for measurement of haze in aircraft transparencies
[AD-A275127] p 3146 N94-29042
Cold expansion and interference for extending the fatigue life of multi-layer metal joints
[AD-A274982] p 3318 N94-29091
Review of sonic fatigue technology
[NASA-CR-4587] p 3479 N94-29407
Automation of the NDT diagnostic using neural nets. Application: Inspection of Airbus longitudinal joints during maintenance
[REPT-932-600-104] p 3315 N94-29474
Dual-Band Infrared (DBIR) imaging inspections of Boeing 737 and KC-135 aircraft panels
[DE94-005700] p 3122 N94-29842
Dynamic fracture mechanics analysis for an edge delamination crack
[NASA-TM-109106] p 3479 N94-29856
Rotorcraft airframe structural optimization for vibration and dynamic stress reduction including damping treatment p 3147 N94-29878
Acoustic emission monitoring of aging aircraft structures
[DREP-93-17] p 3148 N94-30129
Enhanced fatigue crack detection in aging aircraft using continuous acoustic emission monitoring
[DREP-93-16] p 3148 N94-30131
Automation for nondestructive inspection of aircraft
[AIAA PAPER 94-1223-CP] p 3446 N94-30572
Dual-band infrared imaging for quantitative corrosion detection in aging aircraft
[DE94-004187] p 3149 N94-30687
Prospects of time-linearized unsteady calculation methods for exponentially diverging motions in aeroelasticity
[PB94-126224] p 3134 N94-30740
Analysis concerning the inspection threshold for multi-site damage
[PB94-142429] p 3149 N94-30905
AIRFIELD SURFACE MOVEMENTS
Automatic control steps for aircraft taxi guidance
p 3141 N94-29584
Airside ground movements surveillance
p 3141 N94-29585
A novel near-range radar network for airport surface control p 3142 N94-29586
AIRFOIL PROFILES
A design of third-generation airfoils for helicopter rotor blades using Navier-Stokes p 3124 N94-28957
Numerical analysis of airfoil for helicopter blade at high angle of attack using Navier-Stokes code
p 3124 N94-28958
Unsteady aerodynamic computations around NACA0012 at high angles of attack
p 3126 N94-28969
Application of digital control theory to adaptive grid generation p 3127 N94-28980
Helicopter mission and rotor performance optimization with quasi-linear inflow theory p 3147 N94-29594
A residual correction method applied to 2D multi-point airfoil design and 3D single-point wing design
[NLR-TP-92524-U] p 3134 N94-30493
Hopf bifurcation in viscous, low-speed flows about an airfoil with structural coupling p 3134 N94-30865
AIRFOILS
Aerodynamic design using parallel processors
[AD-A275470] p 3122 N94-28674
Proceedings of the 10th NAL Symposium on Aircraft Computational Aerodynamics
[NAL-SP-19] p 3123 N94-28946
Application of flow field simulation to turbine vane design p 3127 N94-28978
Time-marching aeroelastic and spatial adaptation procedures on triangular and tetrahedral meshes using an unstructured-grid Euler method p 3131 N94-29877
Calculus of variations applied to 2D multi-point airfoil design
[PB94-125457] p 3133 N94-30401
A residual correction method applied to 2D multi-point airfoil design and 3D single-point wing design
[NLR-TP-92524-U] p 3134 N94-30493
Euler results of the ISNaS compressible multi-block flow solver
[AD-B179299] p 3281 N94-30756
Grid adaption in computational aerodynamics
[PB94-126240] p 3134 N94-30858
AIRFRAMES
An analytical study of unsteady rotor/fuselage interaction in hover and forward flight
p 3131 N94-29826
Integrated propulsion-airframe dynamics and control
p 3147 N94-29854
Rotorcraft airframe structural optimization for vibration and dynamic stress reduction including damping treatment p 3147 N94-29878
Fatigue management and verification of airframes
[FFA-TN-1993-55] p 3149 N94-30947
AIRGLOW
Solar measurements from the Airglow-Solar Spectrometer Instrument (ASSI) on the San Marco 5 satellite
[NASA-CR-193815] p 3551 N94-30948
AIRLINE OPERATIONS
Effects of repair on structural integrity
[AD-A275756] p 3145 N94-28647
Design of Center-TRACON Automation System
p 3138 N94-29568
DLR's ATM demonstration programme
p 3140 N94-29575
AIRPORTS
Los Angeles international airport instrument landing system approach data collection and reduction, phase 1
[AD-A275115] p 3136 N94-28914
Contributions of DLR to air traffic capacity enhancement within a terminal area p 3138 N94-29567
Design of Center-TRACON Automation System
p 3138 N94-29568
DLR's ATM demonstration programme
p 3140 N94-29575
Development of precision runway monitor system for increasing capacity of parallel runway operations
p 3142 N94-29587
AIRSPACE
Contributions of DLR to air traffic capacity enhancement within a terminal area p 3138 N94-29567
Interactive analysis and planning tools for air traffic and airspace management p 3139 N94-29573
ALASKA
A coupled approach to spatially derived parameters necessary for ecosystem modeling on the North Slope of Alaska: Appendix A
[DE94-005853] p 3349 N94-30046
Assessment of costs and benefits of flexible and alternative fuel use in the US transportation sector
[DE94-006100] p 3226 N94-30885
ALBEDO
GCM studies of the influence of vegetation on the general circulation: The role of albedo in modulating climate change p 3348 N94-29749
Sensitivity and feedbacks associated with vegetation-related land surface parameters in a general circulation model p 3348 N94-29800
ALERTNESS
Strategies to sustain and enhance performance in stressful environments
[AD-A275223] p 3398 N94-29027
Maintaining vigilance on a simulated ATC monitoring task across repeated sessions
[DOT/FAA/AM-94/6] p 3143 N94-30933
ALEUTIAN ISLANDS (US)
The rupture process of large earthquakes along convergent margins: Cast studies from Alaska and Armenia p 3363 N94-29969
ALGAE
Japan-China collaboration research program on terrestrial biology at Great Wall Station in King George Island, in the summer of 1990/1991
p 3358 N94-29085
Growth of hydrocarbon-rich microalga Botryococcus braunii in secondarily treated sewage and its consumption of nitrate ion and phosphate ion p 3387 N94-29519
Biodiesel from aquatic species
[DE94-000275] p 3225 N94-30038
ALGEBRA
Remarks on Galois symmetry in RCFT
[PB94-138179] p 3467 N94-29147
High level language-based robotic control system
[NASA-CASE-NPO-17918-2-CU] p 3435 N94-29465
Second-order algebraic specification of state semantics
[CWI-CS-R9254] p 3453 N94-29889
Is it possible to extend the deformed Weyl algebra W(sub q)(n) to a Hopf algebra?
[DE94-608092] p 3467 N94-30202

Categorial generalization of algebraic recursion theory
[ML-93-06] p 3456 N94-30382
Algebraic domains, chain completion, and the Plotkin powerdomain construction
[RUU-CS-93-03] p 3457 N94-30394
Homomorphism preserving algebraic specifications require hidden sorts
[CWI-CS-R9344] p 3459 N94-30436
The transient period of a cyclic process: An horizon theorem
[MEMO-1149] p 3427 N94-30585
GL(sub q)(N)-covariant quantum algebras and covariant differential calculus
[DE94-608072] p 3460 N94-30726
Graded Froelicher-Nijenhuis brackets and the theory of recursion operators for super differential equations
[MEMO-1147] p 3460 N94-30736
A structural co-induction theorem
[CWI-CS-R9346] p 3461 N94-30753
Fuzzy-algebra uncertainty analysis for abnormal-environment safety assessment
[DE94-006257] p 3462 N94-30849
Non-commutative geometry
[PB94-139342] p 3462 N94-30889
Undecidability in diagonalizable algebras
[ML-93-13] p 3463 N94-30976
Embeddings of Heyting algebras
[ML-93-14] p 3463 N94-30977

ALGOL

North American jumelage 'type systems'
[AD-A275342] p 3411 N94-29214

ALGORITHMS

Identification of components to optimize improvement in system reliability
[DE94-001601] p 3315 N94-28503
Large eddy simulations using lattice Boltzmann algorithms
[DE94-005666] p 3270 N94-28549
Applied analysis/computational mathematics
[DE94-005133] p 3451 N94-28571
Track filtering by robust neural network
[DE94-606067] p 3434 N94-28613
Frequency-domain transfer-function identification using Chebyshev polynomials
[DE94-004777] p 3451 N94-28739
The bootstrapped algorithm: A fast algorithm for blind signal separation
[AD-A275759] p 3408 N94-28760
Photorefractive adaptive antenna array processor
[AD-A275762] p 3241 N94-28762
Construction of a connectionist network supercomputer
[AD-A275765] p 3405 N94-28764
Design and packaging of fault tolerant optoelectronic multiprocessor computing system
[AD-A275896] p 3405 N94-28798
An efficient algorithm for 3D connect-the-dots
[AD-A275431] p 3409 N94-28866
Removal of coherent Extremely Low Frequency (ELF) background noise by adaptive noise cancellation
[AD-A275016] p 3243 N94-28898
Weighted and unweighted maximum clique algorithms with upper bounds from fractional coloring
[AD-A275328] p 3409 N94-28917
General theory and algorithms for the non-casual inversion, slewing and control of space-based articulated structures
[AD-A275118] p 3167 N94-29002
Algorithms for treating redundancy in repairable and non-repairable systems
[DE94-005289] p 3315 N94-29020
Center for Parallel Optimization
[AD-A274988] p 3431 N94-29127
Empirical studies of the value of algorithm animation in algorithm understanding
[AD-A275135] p 3412 N94-29287
Automatic focus and registration of synthetic aperture radar images p 3246 N94-29536
A digital combining-weight estimation algorithm for broadband sources with the array feed compensation system p 3250 N94-29660
Convolutional encoding of self-dual codes p 3250 N94-29662
An improved conscan algorithm based on a Kalman filter p 3251 N94-29670
Infrared properties of obscuring dust tori in active galactic nuclei p 3545 N94-29832
First principles pseudopotential calculations on aluminum and aluminum alloys
[DE94-004890] p 3206 N94-29931
Algorithm and code development for unsteady three-dimensional Navier-Stokes equations
[NASA-CR-195774] p 3277 N94-29942
High-resolution algorithms for the Navier-Stokes equations for generalized discretizations p 3278 N94-29965
Investigations of dispersion characteristics of microwave/optical guided wave structures by using transmission line matrix method
[ISBN-0-315-85856-7] p 3254 N94-30034
Complicated problem solution techniques in optimal parameter searching
[DE94-608007] p 3421 N94-30077
Fast precise algorithm for simulation of ionization energy losses
[DE94-608010] p 3421 N94-30080
Algorithm and program ORANGE for magnetic field simulation of magnetic system spectrometer STORS
[DE94-608013] p 3421 N94-30083
A lateral inhibition neural network that emulates a winner-takes-all algorithm
[RUU-CS-92-46] p 3438 N94-30334
Two algorithms for finding rectangular duals of planar graphs
[RUU-CS-92-41] p 3423 N94-30345
A deterministic algorithm for the three-dimensional diameter problem
[RUU-CS-92-45] p 3424 N94-30348
The exact fitting problem in higher dimensions
[RUU-CS-92-37] p 3456 N94-30377
Pearl's belief propagation: The proofs
[RUU-CS-92-47] p 3456 N94-30378
Self-stabilizing l-exclusion algorithms
[RUU-CS-93-01] p 3424 N94-30379
Development and validation of a linear recursive order-N algorithm for the simulation of flexible space manipulators dynamics
[AD-B173557] p 3311 N94-30391
The conjoinability relation in Lambek calculus in linear logic
[ML-93-03] p 3457 N94-30397
Fast and efficient variable-to-fixed-length coding algorithm
[PB94-125465] p 3424 N94-30400
Minimum fill-in for chordal bipartite graphs
[RUU-CS-93-11] p 3458 N94-30404
Treewidth of circle graphs
[RUU-CS-93-12] p 3458 N94-30405
Shape from diameter: Positive results
[RUU-CS-93-17] p 3458 N94-30408
A probabilistic approach to motion planning for car-like robots
[RUU-CS-93-18] p 3438 N94-30410
An all pairs shortest paths distributed algorithm using 2n(exp 2) messages
[RUU-CS-93-19] p 3432 N94-30411
A more compact visibility representation
[RUU-CS-93-26] p 3425 N94-30426
Thermodynamics of computation and information distance
[CWI-CS-R9341] p 3526 N94-30433
The Boltzmann entropy and randomness tests
[CWI-CS-R9342] p 3426 N94-30434
Analysis and an image recovery algorithm for ultrasonic tomography system p 3397 N94-30456
Efficient and constructive algorithms for the pathwidth and treewidth of graphs
[RUU-CS-93-27] p 3426 N94-30488
Unsupervised texture image segmentation by improved neural network ART2
[AIAA PAPER 94-1199-CP] p 3442 N94-30549
Perception system and functions for autonomous navigation in a natural environment
[AIAA PAPER 94-1201-CP] p 3443 N94-30552
Accuracy metrics for judging time scale algorithms p 3471 N94-30656
An algorithm for the Italian atomic time scale p 3473 N94-30868
Placing registration marks
[RUU-CS-93-21] p 3427 N94-30725
Dynamic microsets for RAMs
[RUU-CS-93-22] p 3406 N94-30727
Perfect binary space partitions
[RUU-CS-93-23] p 3460 N94-30728
Relations between varieties of Kolmogorov complexities
[CWI-CS-R9329] p 3427 N94-30732
On the unification free PROLOG programs
[CWI-CS-R9331] p 3427 N94-30733
The (n squared)-hard problems in computational geometry
[RUU-CS-93-15] p 3461 N94-30747
Systematic error estimation in multisensor fusion systems
[AD-B179298] p 3428 N94-30764
Computing at the leading edge: Research in the energy sciences
[DE94-006121] p 3563 N94-30844
Optimal size finite element meshes without obtuse and small angles
[RUU-CS-92-39] p 3462 N94-30860
ELF: Learning incomplete fuzzy rule sets for an autonomous robot
[REPT-93-043] p 3449 N94-30923
Theoretical and experimental analysis of a new algorithm for the Euclidean 1-center problem
[REPT-93-045] p 3429 N94-30924
Heuristic algorithms for static and dynamic problems of locating the center and the barycenter of a graph
[REPT-93-050] p 3429 N94-30925
Optimization techniques for a dial-a-ride transportation system in urban environment
[REPT-93-051] p 3537 N94-30926
Use of snakes to link edge points to create left ventricular boundaries in echocardiographic images
[TELECOM-93-D-016] p 3395 N94-30970
The Stroemberg wavelet on the interval and the Franklin system
[TELECOM-93-C-002] p 3462 N94-30971

ALIGNMENT

A non-contacting vertical alignment system for mass properties measuring instruments
[DE94-004680] p 3289 N94-29927

ALIPHATIC HYDROCARBONS

Structural changes during carbonization and oxidation of coal p 3187 N94-28678

ALKALI METALS

Synthesis and neutron diffraction study of Na3WN3 and Na3MoN3
[AD-A275158] p 3203 N94-29043
The direct observation of alkali vapor species in biomass combustion and gasification
[DE94-000262] p 3339 N94-30606
Rotator phases in narrow-gap semiconductors
[DE94-005472] p 3521 N94-30897

ALKANES

The active titration method for measuring local hydroxyl radical concentration p 3345 N94-28602

ALKYL COMPOUNDS

Group transfer and electron transfer reactions of organometallic complexes: Summary of research accomplished in 1993
[DE94-004963] p 3200 N94-30770

ALLOYING

Low temperature behavior of virgin martensite
[PB94-132925] p 3204 N94-29142
Mechanical alloying processing with application to structural materials: ASSERT supplement
[AD-A275400] p 3204 N94-29205
Nanosize metal alloy particle formation in Ag and Cu sequentially implanted silica
[DE94-005592] p 3207 N94-30042
Studies on the optimization of deformation processed metal-metal matrix composites
[DE94-006033] p 3185 N94-30704
Influence of tungsten alloying additions on the mechanical properties and texture of tantalum
[DE94-004994] p 3210 N94-30774
Method of test for cleanness assessment of metal alloys: The preparation of button specimens by electron beam melting and the characterisation of recovered inclusions
[NPL-DMM(A)-130] p 3210 N94-30796

ALLOYS

Generalized augmented space theorem for correlated disorder and cluster coherent potential approximation
[DE94-608110] p 3208 N94-30118

ALOHA SYSTEM

M-interference queue analysis by decomposition method
[ISBN-0-315-85795-1] p 3453 N94-30139

ALTERNATING CURRENT

Development of Alternating Current Potential Drop (ACPD) procedures for crack detection in aluminum aircraft panels
[AD-A275755] p 3315 N94-28646

ALTERNATING DIRECTION IMPLICIT METHODS

Unsteady aerodynamic computations around NACA0012 at high angles of attack p 3126 N94-28969

ALTITUDE SIMULATION

Decompression sickness risk versus time and altitude
[AD-A275261] p 3391 N94-29071

ALTITUDE TOLERANCE

Japanese Journal of Aerospace and Environmental Medicine, vol. 30, no. 3
[JTN-94-80606] p 3387 N94-28495

ALUMINIDES

Directional solidification studies in Ni-Al alloys
[DE94-005562] p 3201 N94-28527
Fusion welding with self-generated filler metal
[NASA-CASE-LEW-15671-1] p 3301 N94-29557
Thermodynamic analysis of chemical compatibility of several compounds with Fe-Cr-Al alloys
[NASA-CR-191166] p 3181 N94-29684

ALUMINUM

High resistivity buffer layers by oxygen doping
[AD-A274986] p 3513 N94-29125

Pit initiation on passivated metal surfaces: Crystallographic orientation and environmental effects
[ISBN-0-315-85433-2] p 3208 N94-30138
The long-range transport of aerosol particles over the North Atlantic Ocean p 3366 N94-30867

ALUMINUM ALLOYS
Directional solidification studies in Ni-Al alloys
[DE94-005562] p 3201 N94-28527
Failures to model the development of a cube texture during the high temperature compression of Al-Mg alloys
[DE94-005013] p 3201 N94-28544
Development of Alternating Current Potential Drop (ACPD) procedures for crack detection in aluminum aircraft panels
[AD-A275755] p 3315 N94-28646
Role of microstructure on the fatigue durability of aluminum aircraft alloys
[AD-A275814] p 3202 N94-28830
Cold expansion and interference for extending the fatigue life of multi-layer metal joints
[AD-A274982] p 3318 N94-29091
Electrical conductivity measurements on a SiCp/Al alloy metal matrix composite
[PB94-138310] p 3263 N94-29120
Electrochemical behavior and surface chemistry of nonequilibrium aluminum alloys: Passivity mechanism and fabrication methods
[AD-A275401] p 3204 N94-29196
The effect of various metallurgical parameters on the flow and fracture behavior of polycrystalline NiAl near the brittle-to-ductile transition
[NASA-TM-106534] p 3205 N94-29758
The effect of mechanical paint stripping on the fatigue and fracture of thin aluminum airplane skin p 3205 N94-29900
First principles pseudopotential calculations on aluminum and aluminum alloys
[DE94-004890] p 3206 N94-29931
Non-chromate talc conversion coatings for aluminum
[DE94-005281] p 3207 N94-30053
Directional solidification characteristics of hyper-eutectic Al-Cu alloys under varying gravity conditions
[ISBN-0-315-86108-8] p 3209 N94-30146
Incommensurate magnetic order in UNi2Al3
[DE94-005449] p 3209 N94-30246
An investigation of the corrosion properties of aluminum-tantalum alloys using electrochemical impedance spectroscopy and local electrochemical impedance spectroscopy p 3209 N94-30521
Study of nucleation and growth in Al-Zn alloys using TEM
[DE94-006312] p 3211 N94-30852

ALUMINUM ARSENIDES
Structural characterization of semiconductor heterostructures by atomic resolution Z-contrast imaging at 300 kV
[DE94-006561] p 3516 N94-30063
Strain relaxation and surface roughness as a function of growth temperature in linearly graded In(x)Al(1-x)As (x = 0.05 to 0.25) buffers
[DE94-005430] p 3519 N94-30592
Ion damage studies in GaAs/Al(0.6)Ga(0.4)As/GaAs heterostructures
[DE94-005384] p 3521 N94-30894

ALUMINUM COATINGS
Composite flexible blanket insulation
[NASA-CASE-ARC-11955-1-CU] p 3180 N94-29509

ALUMINUM GALLIUM ARSENIDES
Quantum interference phenomena and novel switching in split gate high electron mobility transistors p 3266 N94-29734

ALUMINUM NITRIDES
MOCVD growth of GaN, AlN and AlGaN for UV photodetector applications
[AD-A275078] p 3512 N94-28871

ALUMINUM OXIDES
Pull-test adhesion measurements of diamondlike carbon films on silicon carbide, silicon nitride, aluminum oxide, and zirconium oxide
[DE94-005469] p 3211 N94-28536
Adhesion of electrolessly deposited Ni(P) on alumina ceramic
[ETN-94-95358] p 3212 N94-28539
Density reduction: A mechanism for amorphization at high ion doses
[DE94-004793] p 3483 N94-28559
Fabrication and testing of plasma-spray formed MoSi2 and MoSi2 composite tubes
[DE94-004995] p 3175 N94-28581
Alumina ceramic: A cost effective replacement for titanium in deep submergence pressure housings
[AD-A275640] p 3212 N94-28641
Superplasticity in fine-grained ceramics
[AD-A275461] p 3212 N94-28733
Effect of surface condition on strength and fatigue behavior of alumina ceramic
[AD-A275053] p 3214 N94-29133
Interface engineering in alumina fiber/glass composites p 3182 N94-29852
Distribution functions of electrons within aluminium oxide thin films
[DE94-608418] p 3490 N94-30184
Ionic conduction mechanisms in CaF2 and CaF2-Al2O3 nanocomposite films on Al2O3 substrates
[DE94-004792] p 3520 N94-30773

ALUMINUM SILICATES
Fatigue behavior of a cross-ply ceramic matrix composite at elevated temperatures under tension-tension loading
[AD-A275466] p 3176 N94-28673

AMAZON REGION (SOUTH AMERICA)
Amazonia: Remote sensing test site and survey p 3327 N94-28935

AMBIENT TEMPERATURE
Deterioration of manual performance in cold and windy climates p 3381 N94-28434
Anode for rechargeable ambient temperature lithium cells
[NASA-CASE-NPO-18580-1-CU] p 3265 N94-29505
Particulate metal matrix composites: Draft procedure for tensile tests at ambient temperature
[NPL-DMM(A)-100] p 3184 N94-30419

AMBIGUITY
Method for ambiguity resolution in range-Doppler measurements
[NASA-CASE-GSC-13542-1] p 3252 N94-29739

AMMONIA
Low energy ion-molecule reactions and chemiionization kinetics
[DE94-005414] p 3481 N94-28491
A study of low emissions gas turbine combustions
[NASA-CR-195763] p 3152 N94-29860
Direct measurement of the reactivity of NH and OH on a silicon nitride surface
[DE94-005286] p 3199 N94-30260

AMMONIUM PERCHLORATES
Correlation of cookoff behavior of rocket propellants with thermomechanical and thermochemical properties
[AD-A274983] p 3224 N94-29092

AMORPHOUS MATERIALS
Pull-test adhesion measurements of diamondlike carbon films on silicon carbide, silicon nitride, aluminum oxide, and zirconium oxide
[DE94-005469] p 3211 N94-28536
Density reduction: A mechanism for amorphization at high ion doses
[DE94-004793] p 3483 N94-28559
High damage threshold anti-reflectors by physical vapor deposited amorphous fluoropolymer
[DE94-004865] p 3212 N94-28560
Anode for rechargeable ambient temperature lithium cells
[NASA-CASE-NPO-18580-1-CU] p 3265 N94-29505
Preparation and structure of amorphous hydrogenated carbon film deposited with RF plasma CVD p 3223 N94-29518
Creep and physical aging of PVC: Dependence on stress and temperature
[NPL-DMM(A)-115] p 3217 N94-29886
Induced crystallization in CW laser-irradiated sol-gel deposited titania films
[DE94-006527] p 3207 N94-30062
Plasma enhanced chemical vapor deposition of ZrO2 thin films
[DE94-006031] p 3218 N94-30104
Optical studies of dynamical processes in disordered systems
[DE94-006751] p 3501 N94-30252
Structural analysis of amorphous phosphates using high performance liquid chromatography
[DE94-004791] p 3199 N94-30723

AMORPHOUS SILICON
Survey report of JSUP Space Environment Utilization Research Committee in fiscal year 1992: Functional New Materials Session
[JTN-94-80582] p 3159 N94-30162

AMPLIFIER DESIGN
Tunnelling hot electron transfer amplifiers
[AD-A275529] p 3262 N94-28687

AMPLIFIERS
Tunnelling hot electron transfer amplifiers
[AD-A275529] p 3262 N94-28687

AMPOULES
Ampoule failure sensor time response testing: Experiment 1
[NASA-TM-108449] p 3290 N94-30199

ANAEROBES
One carbon metabolism in anaerobic bacteria: Regulation of carbon and electron flow during organic acid production
[DE94-004852] p 3386 N94-30180

ANALOG CIRCUITS
Nonvolatile programmable neural network synaptic array
[NASA-CASE-NPO-18578-1-CU] p 3265 N94-29426
Design and analysis of a low-loss linear analog phase modulator for deep space spacecraft X-band transponder applications p 3248 N94-29625
Unsupervised learning in analog networks
[ISBN-0-315-85959-8] p 3432 N94-30140
A bipolar analog front-end integrated circuit for the SDC silicon tracker
[DE94-005203] p 3267 N94-30711

ANALOG DATA
MPEG-2 video decoding architecture: Analysis and design
[REPT-93-069] p 3260 N94-30940

ANALOG TO DIGITAL CONVERTERS
Advanced optical A/D converter
[AD-A275663] p 3498 N94-28656
Spurs in digital radio frequency memory and applications of DRFM
[AD-A275013] p 3243 N94-28897
Recent results from testing fast ADCs
[DE94-005565] p 3406 N94-30004
Polynomial modeling of analog-to-digital converters
[DE94-005579] p 3406 N94-30008

ANALYSIS OF VARIANCE
Noise and drift analysis of non-equally spaced timing data p 3472 N94-30667

ANALYTIC FUNCTIONS
Some remarkable sine and cosine functions
[PB94-137759] p 3453 N94-29439

ANATOMY
Elements for the recognition of three dimensional deformable shapes: Application to biomedical imagery
[TELECOM-93-E-006] p 3396 N94-30978

ANDESITE
Influence of clearance and rake angles on the cutting force of rock p 3368 N94-29520

ANGIOSPERMS
Cellular polarity and interactions in plant graviperception
[NASA-CR-195261] p 3385 N94-29943

ANGLE OF ATTACK
Numerical analysis of airfoil for helicopter blade at high angle of attack using Navier-Stokes code p 3124 N94-28958
An experimental study of the flowfield on a semispan rectangular wing with a simulated glaze ice accretion p 3130 N94-29674
Aerodynamic characteristics of a propeller-powered high-lift semispan wing
[NASA-TM-4541] p 3132 N94-29937
The viability of photovoltaics on the Martian surface
[NASA-TM-106478] p 3338 N94-30196

ANGLES (GEOMETRY)
Influence of clearance and rake angles on the cutting force of rock p 3368 N94-29520

ANGULAR CORRELATION
The angular two-point correlation function of galaxies down to 25th mag p 3547 N94-30010

ANGULAR MOMENTUM
A gimbaled low noise momentum wheel p 3162 N94-29640

ANHYDRIDES
Low dielectric polyimide fibers
[NASA-CASE-LAR-14526-1] p 3214 N94-29359

ANIONS
Measurement of elemental speciation by liquid chromatography: Inductively coupled plasma mass spectrometry (LC-ICP-MS) with the Direct Injection Nebulizer (DIN)
[DE94-005261] p 3187 N94-28483
Rotator phases in narrow-gap semiconductors
[DE94-005472] p 3521 N94-30897

ANISOTROPIC MEDIA
Three dimensional transient analysis of microstrip circuits in multilayered anisotropic media
[AD-A274995] p 3283 N94-28995

ANISOTROPY
Practical superconductor development for electrical power applications
[DE94-005378] p 3261 N94-28487
An anisotropic extension of Bodner's model of viscoplasticity: Model development
[NASA-CR-195289] p 3318 N94-28821
The effects of molecular orientation geometry and surface anisotropy upon etching
[AD-A275154] p 3486 N94-29032
Effects and implications of fault zone heterogeneity and anisotropy on earthquake strong ground motion p 3363 N94-29941
Magnetic properties of the three dimensional Ising model with interface single-ion anisotropy
[DE94-608116] p 3525 N94-30164

ANNEALING
Modeling the total dose radiation effects of Hg(1-x)Cd(x)Te photodiodes using numerical device simulators
[AD-A275235] p 3263 N94-29028
An analysis of the microstructure and reinforcement distribution of an extruded particle-reinforced Al 6061-10 volume percent Al2O3 metal matrix composite
[AD-A275050] p 3178 N94-29166
ECR plasma synthesis of silicon nitride films on GaAs and InSb
[DE94-005575] p 3515 N94-30006
Microstructure and mechanical properties of nitrided molybdenum silicide coatings
[DE94-006249] p 3217 N94-30025
Plasma enhanced chemical vapor deposition of ZrO2 thin films
[DE94-006031] p 3218 N94-30104
Characterization of thermally annealed Sb implanted fused silica
[DE94-005464] p 3219 N94-30335
Ionic conduction mechanisms in CaF2 and CaF2-Al2O3 nanocomposite films on Al2O3 substrates
[DE94-004792] p 3520 N94-30773

ANNIHILATION REACTIONS
Path integral for coherent states of the dynamical U(sub 2) group and U(sub 2/1) supergroup
[DE94-606382] p 3466 N94-28785
One-loop QCD mass effects in the production of polarized bottom and top quarks
[PB94-138104] p 3467 N94-29145
Direct anti-b b production in anti-pp collisions at the square root of s = 1.8 TeV
[DE94-006167] p 3491 N94-30369
Charmonium and bottomonium in (-p)p interactions
[DE94-006173] p 3493 N94-30886
Inclusive single muon production in D0
[DE94-006175] p 3493 N94-30887

ANNUAL VARIATIONS
Thermal variation in vegetated or snow-covered background scenes and its effect on passive infrared systems
[AD-A275174] p 3325 N94-28849
On the annual cycle of the tropical Pacific atmosphere and ocean p 3371 N94-29763
A study of precipitation in the coastal area of Antarctica as observed at Syowa Station using a vertical pointing radar p 3363 N94-29979
A toy model of sea ice growth p 3351 N94-30626

ANNULAR FLOW
A numerical method for confined unsteady flows related to fluid-structure interactions
[ISBN-0-315-74739-0] p 3277 N94-29902

ANODES
Dendrite preventing separator for secondary lithium batteries
[NASA-CASE-NPO-18585-1-CU] p 3265 N94-29411
Anode for rechargeable ambient temperature lithium cells
[NASA-CASE-NPO-18580-1-CU] p 3265 N94-29505

ANODIZING
Anodization of copper in chloride media
[AD-A275565] p 3202 N94-28793
An analysis of the microstructure and reinforcement distribution of an extruded particle-reinforced Al 6061-10 volume percent Al2O3 metal matrix composite
[AD-A275050] p 3178 N94-29166

ANTARCTIC OCEAN
Dynamic constraints on CO2 uptake by an iron-fertilized Antarctic p 3350 N94-30619

ANTARCTIC REGIONS
Medical support for British operations in the Antarctic p 3379 N94-28421
Antarctic Record, volume 36, no. 1
[REPT-106-VOL-36-NO-1] p 3357 N94-29078
Estimation of geomagnetic conjugate points by using Pc5 pulsations p 3357 N94-29079
Activities of the wintering party at Showa Station by the 31st Japanese Antarctic Research Expedition in 1990 p 3358 N94-29083
Activities of the fourth wintering party at Asuka Station by the 31st Japanese Antarctic Research Expedition in 1990 p 3358 N94-29084
Japan-China collaboration research program on terrestrial biology at Great Wall Station in King George Island, in the summer of 1990/1991 p 3358 N94-29085
Protocol on environmental protection to the Antarctic Treaty and its annexes: International agreement on the comprehensive measures for the protection of Antarctic environment and ecosystems p 3354 N94-29086
Observations of the geomagnetic field by Polar Patrol Balloon (PPB) experiment in Antarctica p 3359 N94-29235
Long term variations of radio auroral activity p 3359 N94-29237
New-type echoes observed with the 50 MHz auroral Doppler radar at Showa Station p 3360 N94-29238
Initial observation results with imaging riometer at NY-Alesund (L is equal to 16) p 3360 N94-29239
A theory of current generator in the magnetosphere-ionosphere coupling p 3360 N94-29240
Cosmogenic C-14 in Antarctic and non-Antarctic meteorites and lunar samples
[NASA-CR-195795] p 3546 N94-29905
Antarctic Record, vol. 36, no. 3
[REPT-108] p 3363 N94-29978
A study of precipitation in the coastal area of Antarctica as observed at Syowa Station using a vertical pointing radar p 3363 N94-29979
Data transfer system using a multi-ID ARGOS transmitter for the Antarctic polar patrol balloon experiment p 3363 N94-29980
Activities of the wintering party at Syowa Station by the 32nd Japanese Antarctic Research Expedition in 1991 p 3364 N94-29986

ANTENNA ARRAYS
Photorefractive adaptive antenna array processor
[AD-A275762] p 3241 N94-28762
Solid-state, active-phased arrays: Some aspects of receiver design
[AD-A275893] p 3527 N94-28779
Pointing mechanisms for the Shuttle Radar Laboratory p 3162 N94-29638
A digital combining-weight estimation algorithm for broadband sources with the array feed compensation system p 3250 N94-29660
Digital combining-weight estimation for broadband sources using maximum-likelihood estimates p 3250 N94-29661
A comparison of full-spectrum and complex-symbol combining techniques for the Galileo S-band mission p 3250 N94-29665
A 32 GHz microstrip array antenna for microspacecraft application p 3251 N94-29668
Radiation and scattering from cylindrically conformal printed antennas
[NASA-CR-195546] p 3253 N94-29873
Radial microstrip slotline feed network for circular mobile communications array
[NASA-TM-106540] p 3267 N94-30198
Synchronization of microwave oscillators by direct optical injection
[ISBN-0-315-85546-0] p 3500 N94-30233

ANTENNA DESIGN
Defocussing characteristics of the ACTS, T1-VSAT Earth terminal antennas
[NASA-TM-106420] p 3242 N94-28826
Beam scanning offset Cassegrain reflector antennas by subreflector movement
[NASA-CR-191604] p 3160 N94-28836
Active antennas, a review
[PB94-137445] p 3243 N94-28907
Screening of flexible cables by nonlinear resistance measurements
[AD-A275193] p 3264 N94-29289
Theoretical and experimental study of a cylindrical microstrip antenna
[REPT-932-440-109] p 3245 N94-29456
Elevation control system model for the DSS 13 antenna p 3248 N94-29622
A module concept for a cable-mesh deployable antenna p 3161 N94-29631
Waves in space plasma dipole antenna subsystem p 3161 N94-29632
A 32 GHz microstrip array antenna for microspacecraft application p 3251 N94-29668
Radiation and scattering from cylindrically conformal printed antennas
[NASA-CR-195546] p 3253 N94-29873
Three-dimensional effects for radio frequency antenna modeling
[DE94-006102] p 3255 N94-30105

ANTENNA FEEDS
Defocussing characteristics of the ACTS, T1-VSAT Earth terminal antennas
[NASA-TM-106420] p 3242 N94-28826
A dual-cavity ruby maser for the Ka-band link experiment p 3250 N94-29658

ANTENNA RADIATION PATTERNS
Defocussing characteristics of the ACTS, T1-VSAT Earth terminal antennas
[NASA-TM-106420] p 3242 N94-28826
Screening of flexible cables by nonlinear resistance measurements
[AD-A275193] p 3264 N94-29289
Theoretical and experimental study of a cylindrical microstrip antenna
[REPT-932-440-109] p 3245 N94-29456
Radiation and scattering from cylindrically conformal printed antennas
[NASA-CR-195546] p 3253 N94-29873
Integral equation analysis of composite bodies of revolution and arbitrary surfaces with application to cavity-backed antennas p 3253 N94-29883
Three-dimensional effects for radio frequency antenna modeling
[DE94-006102] p 3255 N94-30105
A physical optics model for scattering of HF radiation by irregular terrain
[DE94-006187] p 3255 N94-30106

ANTIBIOTICS
Microencapsulation of anti-tumor, antibiotic and thrombolytic drugs in microgravity p 3397 N94-30453

ANTIBODIES
Effects of pressure on membrane-associated receptors and effector elements
[AD-A275813] p 3384 N94-28829

ANTICYCLONES
On interannual variability and climate change in the North Pacific p 3374 N94-29963

ANTIFERROMAGNETISM
Some results on the phase diagram of the antiferromagnetic Potts model in an external magnetic field
[DE94-608115] p 3468 N94-30110
Magnetic properties of the three dimensional Ising model with interface single-ion anisotropy
[DE94-608116] p 3525 N94-30164

ANTIMISSILE DEFENSE
Dual-use applications of infrared sensitive materials
[AD-A275140] p 3499 N94-29694
TacSats for NATO
[AGARD-AR-322] p 3169 N94-30350

ANTIOXIDANTS
Development of radiation resistant electrical cable insulations p 3223 N94-30480
Development of radiation resistant electrical cable insulations
[DE94-005189] p 3222 N94-30906

ANTIPROTONS
Properties of W + jet events in proton-antiproton collisions at 1.8 TeV
[DE94-004002] p 3482 N94-28524
Properties of events containing a photon and several jets seen in p(bar p) collisions at (radical)s = 1.8 TeV
[DE94-005596] p 3482 N94-28531
Inclusive jet and direct photon production at the D0 experiment
[DE94-006001] p 3488 N94-30049
A search for rapidity gap events in p(bar p) collisions at D(0)
[DE94-004654] p 3491 N94-30722

ANTIREFLECTION COATINGS
High damage threshold anti-reflectors by physical vapor deposited amorphous fluoropolymer
[DE94-004865] p 3212 N94-28560
A new guided wave lens structure and its application
[AD-A275541] p 3499 N94-28813

ANTISUBMARINE WARFARE
Quadruplet expansion of the acoustic pressure field in a wedge shaped ocean
[AD-A275121] p 3477 N94-29003

APERTURES
Printed circuit elements with applications to antennas, scattering, and circuits
[AD-A275512] p 3262 N94-28669
Design and testing of the LITE Variable Field Stop mechanism p 3161 N94-29633
Enhanced coherence x ray laser experiments and simulations
[DE94-005367] p 3295 N94-30060

APEXES
Stability properties of inclusive connectivity for graphs
[AD-A275360] p 3452 N94-29016

APPLICATION SPECIFIC INTEGRATED CIRCUITS
Realization of function logics by means of transmission gate
[REPT-93-061] p 3429 N94-30936

APPLICATIONS PROGRAMS (COMPUTERS)
SPC toolbox: An interactive MATLAB (tm) package for signal modeling, analysis, and communications
[AD-A275617] p 3241 N94-28634
A program for rapid computation of multioffset vertical seismic profile synthetic seismograms for layered media
[AD-A275464] p 3355 N94-28737
Comparing Ada and FORTRAN lines of code: Some experimental results
[AD-A275322] p 3409 N94-28878
Quadruplet expansion of the acoustic pressure field in a wedge shaped ocean
[AD-A275121] p 3477 N94-29003
WINDOW 4.0: Documentation of calculation procedures
[DE94-004935] p 3410 N94-29019

Preliminary analysis of Asynchronous Transfer Mode (ATM) over microwave channels
[AD-A275214] p 3243 N94-29069
Solution of augmented systems
[PB94-138211] p 3452 N94-29111
EXTdesign. Version 1.0: Reference manual
[PB94-136827] p 3411 N94-29193
Flight command software development: RAFALE studies p 3413 N94-29320
The development procedures and tools applied for the attitude control software of the Italian satellite SAX p 3170 N94-29324
A common Ada run-time system for avionics software p 3150 N94-29331
Distributed applications and failure tolerance programs using a reconfigurable parallel architecture p 3417 N94-29345
Tidal atlas software development
[AD-A275251] p 3377 N94-29432
High level language-based robotic control system
[NASA-CASE-NPO-17918-2-CU] p 3435 N94-29465
Considerations on graphical user interfaces for intelligent ATM support systems p 3139 N94-29572
Finite element method for numerical simulation of turbulent flows. The N3S code p 3233 N94-29612
A pot-pourri of results in QCD from large lattice simulations on the CM5
[DE94-005084] p 3514 N94-29818
Abundance patterns in red-giant CH stars p 3539 N94-29820
Splines and ocean wave modelling
[PB94-139409] p 3378 N94-30002
Smart Document System (SDS) used in managing DOE order's with electronic Engineering Procedures
[DE94-005076] p 3534 N94-30099
An interactive, design and educational tool for supersonic external-compression inlets
[NASA-TM-106581] p 3421 N94-30174
An interactive educational tool for compressible aerodynamics
[NASA-TM-106568] p 3422 N94-30175
The ergonomics of computer interfaces: Designing a system for human use
[CWI-CS-R9258] p 3402 N94-30320
Programming aspects of Views: An open-architecture application environment
[CWI-CS-R9259] p 3422 N94-30321
Modelling interaction tools in the Views architecture
[CWI-CS-R9261] p 3423 N94-30323
The Views application environment
[CWI-CS-R9257] p 3423 N94-30341
Potential capabilities of Reynolds stress turbulence model in the COMMIX-RSM code p 3285 N94-30450

APPROACH

Los Angeles international airport instrument landing system approach data collection and reduction, phase 1
[AD-A275115] p 3136 N94-28914
Extremely Low Visibility IFR Rotorcraft Approach (ELVIRA) operational concept development. Volume 1: Executive Summary
[DOT/FAA/RD-94/1,I] p 3142 N94-30189

APPROACH CONTROL

Advanced air traffic control and flight management system concepts p 3140 N94-29576
Profile negotiation: An air/ground automation integration concept for managing arrival traffic p 3140 N94-29578
Experimental flight management system p 3141 N94-29580
Extremely Low Visibility IFR Rotorcraft Approach (ELVIRA) operational concept development. Volume 1: Executive Summary
[DOT/FAA/RD-94/1,I] p 3142 N94-30189
Flight simulator evaluation of advanced MLS procedures
[AD-B174270] p 3143 N94-30915

APPROACH INDICATORS

Key cognitive issues in the design of electronic displays of instrument approach procedure charts
[AD-A275647] p 3399 N94-28649

APPROXIMATION

Approximation of solutions of the cubic NLSE by finite dimensional equations and non-squeezing properties
[PB94-138294] p 3452 N94-29148
Strategy for the approximation of large scattered data sets
[PB94-138518] p 3420 N94-29949
Splines and ocean wave modelling
[PB94-139409] p 3378 N94-30002
Approximation methods for nonlinear operator equations of the m-accretive type
[DE94-608099] p 3467 N94-30065
Generalized augmented space theorem for correlated disorder and cluster coherent potential approximation
[DE94-608110] p 3208 N94-30118
L(sub)p optimal d dimensional triangulations for piecewise linear interpolation: A new result on data dependent triangulations
[RUU-CS-93-13] p 3458 N94-30406
Optimization techniques for a dial-a-ride transportation system in urban environment
[REPT-93-051] p 3537 N94-30926

AQUEOUS SOLUTIONS

Quenching of the excited state of hydrated Europium(3) ions by electron transfer
[DE94-005553] p 3482 N94-28518

AQUICULTURE

Bulletin of National Research Institute of Fisheries Engineering, No. 13
[JTN-94-80596] p 3233 N94-29701
Reproduction in the Japanese anchovy (Engraulis japonica) as related to population fluctuation p 3235 N94-29708

ARC DISCHARGES

Evaluation of pyrolysis and arc tracking on candidate wire insulation designs for space applications p 3166 N94-28711
A new test method for the assessment of the arc tracking properties of wire insulation in air, oxygen enriched atmospheres and vacuum p 3167 N94-28714
Non-isolated 30 kW class arcjet PCU
[NASA-CR-189148] p 3173 N94-29444

ARC HEATING

Numerical simulation of arc heated wind tunnel flow p 3123 N94-28951

ARC JET ENGINES

Arcjet system integration development
[NASA-CR-187147] p 3171 N94-28736
Non-isolated 30 kW class arcjet PCU
[NASA-CR-189148] p 3173 N94-29444

ARC SPRAYING

Direct measurement of the reactivity of NH and OH on a silicon nitride surface
[DE94-005286] p 3199 N94-30260

ARC WELDING

Welding wire pressure sensor assembly
[NASA-CASE-MFS-26216-1-SB] p 3300 N94-29506
Programmable Automated Welding System (PAWS): Control of welding through software and hardware p 3314 N94-30443
Sensing the gas metal arc welding process p 3314 N94-30444

ARCHITECTURE (COMPUTERS)

Performance analysis of memory hierachies in high performance systems
[DE94-005549] p 3404 N94-28517
Data fusion and correlation techniques testbed development audio processing study
[SKD-1600-73-014] p 3241 N94-28532
Process guide for the Domain-Specific Software Architectures (DSSA) process life cycle
[AD-A275642] p 3407 N94-28648
Design of parallel systems for signal processing
[AD-A275490] p 3430 N94-28659
The state transition diagram with path priority and it's applications
[AD-A275524] p 3434 N94-28672
Construction of a connectionist network supercomputer
[AD-A275765] p 3405 N94-28764
A/GATECH DOSP fabrication --- optical programmable logic array
[AD-A275848] p 3430 N94-28781
Advanced languages for systems software
[AD-A275272] p 3410 N94-29007
How to control the increase in the complexity of civil aircraft on-board systems p 3150 N94-29316
Hierarchical Object Oriented Design (HOOD): Possibilities, limitations, and challenges p 3413 N94-29322
Distributed applications and failure tolerance programs using a reconfigurable parallel architecture p 3417 N94-29345
Future manned systems advanced avionics study
[NASA-CR-188277] p 3150 N94-29377
Lasercom system architecture with reduced complexity
[NASA-CASE-NPO-19069-1-CU] p 3293 N94-29493
Software Management Environment (SME) concepts and architecture, revision 1
[NASA-CR-189293] p 3419 N94-29727
Design for dependability: A simulation-based approach
[NASA-CR-195757] p 3420 N94-29890
The MSRC ab initio methods benchmark suite: A measurement of hardware and software performance in the area of electronic structure methods
[DE94-006428] p 3514 N94-30001
A locally synchronous globally asynchronous Vertex-8 processing element for image reconstruction on a mesh
[ISBN-0-315-86005-7] p 3432 N94-30143
Maestro: An open system architecture for multi-robot control p 3306 N94-30288
Modelling the evolution of information systems
[TR-92-36] p 3535 N94-30329
Evolving information systems: Meeting the ever-changing environment
[TR-92-24] p 3535 N94-30359
Object-based task-level control: A hierarchical control architecture for remote operation of space robots
[AIAA PAPER 94-1209-CP] p 3444 N94-30560
MPEG-2 video decoding architecture: Analysis and design
[REPT-93-069] p 3260 N94-30940
The experimental flight management system: An air traffic management research tool
[NLR-TP-92253-U] p 3143 N94-30943

ARCTIC OCEAN

The role of sea ice dynamics in global climate change p 3350 N94-30620

ARCTIC REGIONS

Evaluation of life support equipment during an unsupported North Pole expedition p 3379 N94-28422
A coupled approach to spatially derived parameters necessary for ecosystem modeling on the North Slope of Alaska: Appendix A
[DE94-005853] p 3349 N94-30046
Carbon cycling in high-latitude ecosystems p 3352 N94-30631

ARGON

Argon frost continuous cryopump for fusion applications
[DE94-004478] p 3230 N94-29017
Optical field ionization of atoms and ions using ultrashort laser pulses
[DE94-006643] p 3488 N94-29845
On possibility to create the scintillation trigger for liquid-argon neutrino detector
[DE94-607844] p 3489 N94-30050

ARGON PLASMA

Fullerenes as precursors for diamond film growth without hydrogen or oxygen additions
[DE94-004582] p 3519 N94-30718

ARGOS SYSTEM

Data transfer system using a multi-ID ARGOS transmitter for the Antarctic polar patrol balloon experiment p 3363 N94-29980

ARITHMETIC

A smart child of Peano's
[ML-92-10] p 3455 N94-30325
Embeddings of Heyting algebras
[ML-93-14] p 3463 N94-30977

ARIZONA

Evaluation of the National Meteorological Center mesoscale model for prediction of severe convection over Central Arizona p 3371 N94-29744

ARMED FORCES (UNITED STATES)

Evaluation of monitoring audiometry in the United States Air Force Hearing Conservation Program
[AD-A275309] p 3391 N94-29211

ARMENIA

The rupture process of large earthquakes along convergent margins: Cast studies from Alaska and Armenia p 3363 N94-29969

ARMOR

Simulation Networking/Training Requirements Relational Database: User's guide
[AD-A275634] p 3528 N94-28637
3-D braided, continuous fiber ceramic composites produced by chemical vapor infiltration
[AD-A275192] p 3178 N94-29024

AROMATIC COMPOUNDS

Structural changes during carbonization and oxidation of coal p 3187 N94-28678

ARSENIC

Aggregation equilibria in arsenic doped silicon
[DE94-607269] p 3515 N94-30005

ARSENIC COMPOUNDS

Measurement of elemental speciation by liquid chromatography: Inductively coupled plasma mass spectrometry (LC-ICP-MS) with the Direct Injection Nebulizer (DIN)
[DE94-005261] p 3187 N94-28483
Synthesis and molecular structures of R(Me3CCH2)2In-E(SiMe3) (R = Me3CCH2, E = P or As; R = Me, E = P)
[AD-A275020] p 3486 N94-29131

ARSENIDES

Tris(trimethylsily)arsine and lithium bis(trimethylsily)arsenide
[AD-A275075] p 3189 N94-29140

ARTERIES

Arterial oxygen saturation during +Gz acceleration by short-radius centrifuge p 3389 N94-28852

Remote control of transcranial Doppler (TCD) probe during centrifuge exposures up to 9 +Gz
[AD-A275253] p 3400 N94-29029

ARTIFICIAL INTELLIGENCE

Track filtering by robust neural network
[DE94-606067] p 3434 N94-28613
The state transition diagram with path priority and it's applications
[AD-A275524] p 3434 N94-28672
Information presentation for expert systems in future fighter aircraft
[AD-A275126] p 3149 N94-29005
Partial support for the Second International Symposium on Artificial Intelligence and Mathematics
[AD-A275199] p 3434 N94-29026
Basic research in computer science
[AD-A275184] p 3405 N94-29181
An architecturally-based theory of human sentence comprehension
[AD-A275380] p 3398 N94-29313
Object oriented design of the autonomous fixtaking management system p 3143 N94-29323
Artificial intelligence technology program at Rome Laboratory p 3414 N94-29328
A case-based approach to creative design
[AD-A275229] p 3417 N94-29390
Machine Intelligence in Air Traffic Management
[AGARD-CP-538] p 3136 N94-29558
Advances in development capabilities for intelligent air traffic management systems p 3137 N94-29559
Intelligent systems for air space control and management p 3137 N94-29560
Reinforcement learning for robots using neural networks p 3437 N94-29853
Proceedings of the 3rd Conference on Military Robotic Applications
[DRES-SP-149] p 3304 N94-30275
Autonomous intelligent military robots: Army ants, killer bees, and cybernetic soldiers p 3304 N94-30276
Performance evaluation of intelligent network services
[MEMO-INF-93-20] p 3438 N94-30373
Algorithmic problems concerning first-order definability of modal formulas on the class of all finite frames
[ML-93-07] p 3456 N94-30383
VAS: A Vision Advisor System combining agents and object-oriented databases
[AIAA PAPER 94-1181-CP] p 3440 N94-30532
Building brains for bodies
[AIAA PAPER 94-1208-CP] p 3444 N94-30559
Predictive sufficiency and the use of stored internal state
[AIAA PAPER 94-1213-CP] p 3445 N94-30564
Using generic tool kits to build intelligent systems
[AIAA PAPER 94-1214-CP] p 3445 N94-30565
The road plan model: Information model for planning road building activities
[AIAA PAPER 94-1219-CP] p 3445 N94-30567
An intelligent robotic aid system for human services
[AIAA PAPER 94-1232-CP] p 3447 N94-30580
A Modular Artificial Intelligence Inference Engine System (MAIS) for support of on orbit experiments
[AIAA PAPER 94-1237-CP] p 3448 N94-30584
Service independent building blocks-1: Concepts, examples and formal specifications
[CWI-CS-R9326] p 3448 N94-30731
Multi-sensor data fusion and the use of artificial intelligence
[PB94-126216] p 3448 N94-30741

ARTIFICIAL SATELLITES

Communications subsystem for the Petite Amateur Navy Satellite (PANSAT)
[AD-A275532] p 3242 N94-28812
Satellites: Reliability and operation security
[REPT-932-440-108] p 3168 N94-29419

ASPHALT

Asphaltic concrete performance under heavy fighter aircraft loading
[AD-A275046] p 3157 N94-29151

ASSAYING

Tropospheric HO determination by FAGE p 3342 N94-28590
Computerized in vitro test for chemical toxicity based on tetrahymena swimming patterns p 3354 N94-30463

ASSEMBLING

Integration of a path generation algorithm into off-line programming of airbus panels
[REPT-932-600-103] p 3435 N94-29480

ASSEMBLY

Application of the Modular Automated Reconfigurable Assembly System (MARAS) concept to adaptable vision gauging and parts feeding
[AIAA PAPER 94-1182-CP] p 3440 N94-30533

ASSESSMENTS

Identification of components to optimize improvement in system reliability
[DE94-001601] p 3315 N94-28503

ASSIMILATION

Four-dimensional data assimilation using the adjoint method p 3455 N94-30353

ASTIGMATISM

Aberrated point-spread functions and beam quality for optical systems with annular pupils
[AD-A275311] p 3499 N94-28875

ASTROMETRY

Toward astrometric tracking with the infrared spatial interferometer p 3249 N94-29653
The angular two-point correlation function of galaxies down to 25th mag p 3547 N94-30010

ASTRONAUT PERFORMANCE

Space and vertigo: In relation to space motion sickness p 3390 N94-28857
Tactility as a function of grasp force: Effects of glove, orientation, pressure, load, and handle
[NASA-TP-3474] p 3402 N94-30210

ASTRONOMICAL INTERFEROMETRY

A sounding rocket program in extreme and far ultraviolet interferometry
[NASA-CR-195114] p 3289 N94-29907

ASTRONOMICAL MODELS

The role of cloud collisions in N-body simulations of disk galaxies p 3545 N94-29755
The effects of relativistic neutrons on nonthermal models of active galactic nuclei p 3547 N94-29993
The second coming of cold dark matter?
[DE94-004992] p 3548 N94-30694

ASTRONOMICAL OBSERVATORIES

Remote observatory access via the advanced communications technology satellite p 3253 N94-29894

ASTRONOMICAL PHOTOGRAPHY

Reconstruction of stellar images from correlations
[ISBN-0-315-85382-4] p 3541 N94-30133

ASTRONOMICAL PHOTOMETRY

Globular cluster photometry near the turnoff: Blue stragglers, relative ages, and the horizontal branch p 3536 N94-29732
The cataclysmic variables from the Palomar-Green survey p 3539 N94-29819

ASTRONOMICAL SPECTROSCOPY

Backscatter Mossbauer Spectrometer (BaMS) for extraterrestrial applications p 3236 N94-29774
Camera artifacts in IUE spectra
[NASA-CR-189337] p 3198 N94-29857
Coronal abundances and their variation
[NASA-CR-195767] p 3551 N94-29858
Spatially resolved spectroscopy of AG Carinae, and direct evidence for stellar evolution: The central star of NGC 2392
[NASA-CR-189291] p 3545 N94-29871
Pushing the limit: Precision radial velocities, techniques, and applications p 3542 N94-30861

ASTRONOMY

CBSD: The celestial background scene descriptor
[AD-A275521] p 3538 N94-28671
Finnish astronomy days, 1992-1993. Proceedings of the Finnish Astronomical Society
[PB94-136892] p 3538 N94-29170

ASTROPHYSICS

Physics, astronomy, and astrophysics: A numerical study of the black hole plus Brill wave spacetime p 3540 N94-29990

ASYMMETRY

Hierarchical structures and asymmetric stochastic processes on p-adics and adeles
[PB94-138203] p 3464 N94-29178

ASYMPTOTIC GIANT BRANCH STARS

Abundance patterns in red-giant CH stars p 3539 N94-29820

ASYMPTOTIC METHODS

Numerical solution of the multichannel scattering problem
[DE94-606297] p 3484 N94-28619
Long-wavelength asymptotics of unstable crossflow modes, including the effect of surface curvature
[NASA-CR-4579] p 3273 N94-29460
An asymptotic analysis for compressible gas lubrication of rough surfaces p 3222 N94-30922

ASYMPTOTIC PROPERTIES

Asymptotic coherence of gluons and of q-bosons
[DE94-005417] p 3481 N94-28492
Stochastic stability and nonlinear control in mechanical systems p 3303 N94-29966
Dissipation in Hamiltonian systems: Decaying cnoidal waves
[MEMO-1151] p 3460 N94-30738

ASYMPTOTIC SERIES

Higher order asymptotic crack tip fields in a power-law hardening material p 3321 N94-29829

ASYNCHRONOUS MOTORS

Electrical engineering and industrial electronics education days: Control of asynchronous generators
[PB94-135514] p 3266 N94-29523

ATLANTIC OCEAN

The velocity field in the Northeast Atlantic from satellite-tracked drifting buoys
[AD-A275704] p 3376 N94-28690
Studies of marine aerosols and their evolution in the eastern North Atlantic
[AD-A275011] p 3377 N94-29128

ATMOSPHERIC ATTENUATION

Optical modeling of visibility and visibility instrumentation using stratified Mie theory p 3348 N94-29750
Adaptive power control as a fade countermeasure on satellite links p 3253 N94-29897
Atmospheric Propagation Effects Through Natural and Man-Made Obscurants for Visible to MM-Wave Radiation
[AGARD-CP-542] p 3256 N94-30495
Evaluation of dual polarization attenuation of millimeter frequencies through a meteorological radar p 3256 N94-30496
Propagation modeling of moist air and suspended water/ice particles at frequencies below 1000 GHz p 3256 N94-30497
Multispectral transmittance measurements through man-made water fogs p 3257 N94-30499

ATMOSPHERIC BOUNDARY LAYER

Papers in meteorology and geophysics, vol. 44, no.1
[JTN-94-80585] p 3324 N94-28693
Structure of neutrally stratified turbulent Ekman layer as predicted by closure models with prognostic equation for master length scale p 3325 N94-28696
US National Weather experiment STORM-FEST: Waves and turbulence in frontal zones
[AD-A275084] p 3369 N94-28847
SAR-related stress variability in the Marine Atmospheric Boundary Layer (MABL)
[AD-A275275] p 3377 N94-29436
An observational and numerical study of sea/land-breeze circulations in an area of complex coastal heating p 3372 N94-29813
Large eddy simulation of the upper atmospheric surface layer
[ISBN-0-315-85393-X] p 3365 N94-30134

ATMOSPHERIC CHEMISTRY

Ozone production at a rural site in Georgia during the summer 1992 SOS campaign
[DE94-003989] p 3342 N94-28523
Local Measurement of Tropospheric HO(x)
[NASA-CP-3245] p 3342 N94-28587
Two-Photon/Laser-Induced Fluorescence (TP/LIF) sensor p 3342 N94-28588
In situ detection of tropospheric OH and HO2 by laser-induced fluorescence in a detection chamber at low pressure p 3342 N94-28589
Tropospheric HO determination by FAGE p 3342 N94-28590
The radical amplifier p 3345 N94-28604
Lead detection and mapping with reference to relationships between scale, sensor characteristics, surface conditions and atmospheric properties
[AD-A275321] p 3377 N94-28877
Activities report of the International Meteorological Institute
[ETN-94-95524] p 3370 N94-29423
Developing a diode array spectrometer for tropospheric chemistry studies p 3362 N94-29752
Brief summary of accomplishments since our DOE-sponsored radon project commenced
[DE94-004643] p 3348 N94-29926
Impact of biomass burning on the atmosphere
[DE94-004333] p 3349 N94-29954
Atmosphere, ocean, and land: Critical gaps in Earth system models p 3350 N94-30617

ATMOSPHERIC CIRCULATION

Papers in meteorology and geophysics, vol. 44, no.1
[JTN-94-80585] p 3324 N94-28693
US National Weather experiment STORM-FEST: Waves and turbulence in frontal zones
[AD-A275084] p 3369 N94-28847
On the origins of low-level tornadic circulations within the remnants of hurricane Andrews
[AD-A275373] p 3369 N94-29011
Hydrodynamics of convection under winter polar leads
[AD-A275182] p 3369 N94-29067
Boundary layer coherent structures
[AD-A275007] p 3272 N94-29195
Study of dynamic characteristics of a monsoon circulation tube
[AD-A275238] p 3370 N94-29394
Activities report of the International Meteorological Institute
[ETN-94-95524] p 3370 N94-29423

Radar estimations of atmospheric winds in the troposphere and lower stratosphere
p 3370 N94-29697
A study of the thermospheric dynamics of the high-latitude E region using a spectral thermospheric general circulation model p 3362 N94-29743
GCM studies of the influence of vegetation on the general circulation: The role of albedo in modulating climate change p 3348 N94-29749
Downstream development of baroclinic waves
p 3372 N94-29796
An observational and numerical study of sea/land-breeze circulations in an area of complex coastal heating p 3372 N94-29813
On interannual variability and climate change in the North Pacific p 3374 N94-29963
Use of satellite data to improve parameterization of spatial and temporal variations of gaseous dry deposition in regional-scale models
[DE94-005110] p 3334 N94-30022
Generation mechanisms of quasi-stationary waves in the Southern Hemisphere p 3365 N94-30789
Complex source rate estimation for atmospheric transport and dispersion models
[DE94-000958] p 3354 N94-30822
Multiple weather regimes and baroclinically forced spherical resonance
[DM-65] p 3376 N94-30966

ATMOSPHERIC COMPOSITION
On eddy accumulation with limited conditional sampling to measure air-surface exchange
[DE94-005112] p 3368 N94-28568
Detection of tropospheric OH and HO2 by laser-induced fluorescence at low pressure using the 308nm excitation of OH p 3343 N94-28591
Harvard ER-2 OH laser-induced fluorescence instrument p 3343 N94-28592
JPL Fourier transform ultraviolet spectrometer
p 3343 N94-28593
Absolute determination of local tropospheric OH concentrations p 3343 N94-28594
UV laser long-path absorption spectroscopy
p 3343 N94-28595
Measurement of tropospheric OH by laser long-path absorption spectroscopy p 3343 N94-28596
On the possibility of measuring atmospheric OH using intracavity laser spectroscopy p 3344 N94-28597
Measurement of atmospheric OH by titration of near-IR fluorescent dyes p 3344 N94-28599
The radiocarbon hydroxyl technique
p 3344 N94-28600
Ion-assisted tropospheric OH measurement technique
p 3344 N94-28601
Tropospheric HO2 determination by FAGE
p 3345 N94-28606
A fractal analysis of near-field atmospheric concentration data
[AD-A275460] p 3355 N94-28728
On the effect of emissions from aircraft engines on the state of the atmosphere p 3189 N94-29247
GOME: Global Ozone Monitoring Experiment
[ESA-SP-1151] p 3347 N94-29452
Laboratory studies of chemical and photochemical processes relevant to stratospheric ozone
[NASA-CR-195779] p 3347 N94-29549
Developing a diode array spectrometer for tropospheric chemistry studies p 3362 N94-29752
Use of satellite data to improve parameterization of spatial and temporal variations of gaseous dry deposition in regional-scale models
[DE94-005110] p 3334 N94-30022
The far-infrared absorption spectrum of low temperature hydrogen gas
[ISBN-0-315-85432-4] p 3199 N94-30137
The carbon cycle revisited p 3350 N94-30622
Ocean-atmospheric linkages p 3350 N94-30623
Linkages between terrestrial ecosystems and the atmosphere p 3351 N94-30624
Carbon cycling in high-latitude ecosystems
p 3352 N94-30631
Models of atmosphere-ecosystem-hydrology interactions: Approaches and testing
p 3353 N94-30636
Evaluating models of climate and forest vegetation
p 3353 N94-30637
The development and evaluation of a tunable diode laser trace gas sensor for the measurement of N2O and CH4 fluxes using micrometeorological techniques
[ISBN-0-315-78975-1] p 3296 N94-30801
The validation of ocean surface heat fluxes in AMIP
[DE94-001539] p 3378 N94-30823
The long-range transport of aerosol particles over the North Atlantic Ocean p 3366 N94-30867

ATMOSPHERIC CORRECTION
Spectral and polarimetric analysis of hyperspectral data collected by an acousto-optic tunable filter system
[AD-A275076] p 3329 N94-29095
Tropospheric corrections to GPS measurements using locally measured meteorological parameters compared with general tropospheric corrections
p 3144 N94-30655
Ionospheric corrections to precise time transfer using GPS p 3145 N94-30677
New perspectives for high accuracy SLR with second generation geodesic satellites
[REPT-932-440-105] p 3336 N94-30965

ATMOSPHERIC DIFFUSION
A fractal analysis of near-field atmospheric concentration data
[AD-A275460] p 3355 N94-28728

ATMOSPHERIC EFFECTS
Line-of-sight tropospheric calibration from measurements in arbitrary directions
p 3249 N94-29654
Atmospheric Propagation Effects Through Natural and Man-Made Obscurants for Visible to MM-Wave Radiation
[AGARD-CP-542] p 3256 N94-30495
Model for the simulation of atmospheric effects on targets to background passive signatures
p 3258 N94-30507
The carbon cycle revisited p 3350 N94-30622

ATMOSPHERIC ELECTRICITY
A study of cloud-to-ground lightning processes with emphasis on data analysis and modeling of the return stroke p 3372 N94-29802

ATMOSPHERIC ENTRY
Parachute Swivel Mechanism for planetary entry
p 3162 N94-29643

ATMOSPHERIC GENERAL CIRCULATION MODELS
Global atmospheric and ocean modeling on the connection machine
[DE94-003930] p 3342 N94-28521
A study of the thermospheric dynamics of the high-latitude E region using a spectral thermospheric general circulation model p 3362 N94-29743
GCM studies of the influence of vegetation on the general circulation: The role of albedo in modulating climate change p 3348 N94-29749
Sensitivity and feedbacks associated with vegetation-related land surface parameters in a general circulation model p 3348 N94-29800
PCCM2: A GCM adapted for scalable parallel computers
[DE94-005113] p 3350 N94-30116
Generation mechanisms of quasi-stationary waves in the Southern Hemisphere p 3365 N94-30789
The validation of ocean surface heat fluxes in AMIP
[DE94-001539] p 3378 N94-30823

ATMOSPHERIC HEATING
Cryosphere and climate p 3352 N94-30632
The challenge of identifying greenhouse gas-induced climatic change p 3352 N94-30634

ATMOSPHERIC MODELS
Global change research: Summaries of research in FY 1993
[DE94-003150] p 3341 N94-28473
Global atmospheric and ocean modeling on the connection machine
[DE94-003930] p 3342 N94-28521
The active titration method for measuring local hydroxyl radical concentration p 3345 N94-28602
A global forecast model comparison study - year 1
[AD-A275674] p 3369 N94-28663
CBSD: The celestial background scene descriptor
[AD-A275521] p 3538 N94-28671
Structure of neutrally stratified turbulent Ekman layer as predicted by closure models with prognostic equation for master length scale p 3325 N94-28696
A fractal analysis of near-field atmospheric concentration data
[AD-A275460] p 3355 N94-28728
Numerical simulations of a mountain thunderstorm. A comparison with Doppler radar observations
[AD-A275296] p 3369 N94-28873
Lead detection and mapping with reference to relationships between scale, sensor characteristics, surface conditions and atmospheric properties
[AD-A275321] p 3377 N94-28877
SHARC, a model for calculating atmospheric and infrared radiation under non-equilibrium conditions
[AD-A275207] p 3357 N94-28893
Monte Carlo simulation or normal shock wave. Part 2: VHS model and VSS model p 3123 N94-28948
Variable soft sphere molecular model in the Monte Carlo simulation of air species p 3123 N94-28949
Rarefied gas numerical wind tunnel. Part 8: HOPE
p 3123 N94-28950
Role of satellite observations of sea-surface temperature in the detection of global change
[PB94-138120] p 3329 N94-29107
Error growth in poor ECMWF forecasts over the contiguous United States
[AD-A275297] p 3369 N94-29183
Prototype terminal aerodrome forecasts using a mesoscale model
[AD-A275308] p 3369 N94-29194
Proceedings of the NIPR Symposium on Upper Atmosphere Physics, no. 6
[JTN-94-80593] p 3359 N94-29233
A theory of current generator in the magnetosphere-ionosphere coupling
p 3360 N94-29240
Evaluation of the National Meteorological Center mesoscale model for prediction of severe convection over Central Arizona p 3371 N94-29744
Physical processes associated with variability in successive operational model forecasts of cyclogenesis
[ISBN-0-315-74753-6] p 3371 N94-29751
On the annual cycle of the tropical Pacific atmosphere and ocean p 3371 N94-29763
A study of cloud-to-ground lightning processes with emphasis on data analysis and modeling of the return stroke p 3372 N94-29802
The incorporation and initialization of cloud water/ice in an operational forecast model p 3373 N94-29814
Large eddy simulation of the upper atmospheric surface layer
[ISBN-0-315-85393-X] p 3365 N94-30134
Modeling the Earth System, volume 3
[NASA-CR-194256] p 3350 N94-30616
Atmosphere, ocean, and land: Critical gaps in Earth system models p 3350 N94-30617
Land surface interaction p 3350 N94-30621
Modeling Earth system changes of the past
p 3353 N94-30635
Comprehensive system models: Strategies for evaluation p 3353 N94-30638
Complex source rate estimation for atmospheric transport and dispersion models
[DE94-000958] p 3354 N94-30822
Computing at the leading edge: Research in the energy sciences
[DE94-006121] p 3563 N94-30844
Modeling studies of frontogenesis in the upper and middle troposphere p 3375 N94-30868
Tropospheric radiative forcing of O3 for the 1994 IPCC report
[DE94-005698] p 3367 N94-30876
Multiple weather regimes and baroclinically forced spherical resonance
[DM-65] p 3376 N94-30966

ATMOSPHERIC MOISTURE
Test of prototype liquid-water-content meter for aircraft use
[NASA-CR-189304] p 3374 N94-30187
Propagation modeling of moist air and suspended water/ice particles at frequencies below 1000 GHz
p 3256 N94-30497
The influence of the evaporation duct on the angle of arrival and amplitude of the backscattered signal from targets low above the sea p 3256 N94-30498
Multispectral transmittance measurements through man-made water fogs p 3257 N94-30499
Radiation transport in cloudy and aerosol loaded atmospheres p 3366 N94-30805
Atmospheric moisture fields derived by satellite observations over the tropical Pacific Ocean
p 3375 N94-30863
Atmospheric turbulence within and above a coniferous forest
[ISBN-0-315-75468-0] p 3375 N94-30870

ATMOSPHERIC OPTICS
The appearance of the Sun and Moon seen through clouds
[AD-A275336] p 3551 N94-29212
Toward astrometric tracking with the infrared spatial interferometer p 3249 N94-29653
Optical modeling of visibility and visibility instrumentation using stratified Mie theory p 3348 N94-29750
Atmospheric Propagation Effects Through Natural and Man-Made Obscurants for Visible to MM-Wave Radiation
[AGARD-CP-542] p 3256 N94-30495
Estimation of transmittance from satellite imagery
p 3257 N94-30500

ATMOSPHERIC PHYSICS
Proceedings of the NIPR Symposium on Upper Atmosphere Physics, no. 6
[JTN-94-80593] p 3359 N94-29233
A theory of current generator in the magnetosphere-ionosphere coupling
p 3360 N94-29240

Study of generation mechanisms of magnetospheric VLF/ELF emissions based on the direction findings p 3361 N94-29245
Activities report of the International Meteorological Institute
[ETN-94-95524] p 3370 N94-29423
Physical processes associated with variability in successive operational model forecasts of cyclogenesis
[ISBN-0-315-74753-6] p 3371 N94-29751

ATMOSPHERIC PRESSURE
Synthesis and neutron diffraction study of Na3WN3 and Na3MoN3
[AD-A275158] p 3203 N94-29043
Plasma heating for containerless and microgravity materials processing
[NASA-CASE-NPO-18819-1-CU] p 3229 N94-29371
Micro-sensors for in-situ meteorological measurements p 3236 N94-29777

ATMOSPHERIC RADIATION
The automated rotating shadowband spectroradiometer
[DE94-001878] p 3269 N94-28464
Proceedings of the NIPR Symposium on Upper Atmosphere Physics, no. 6
[JTN-94-80593] p 3359 N94-29233
ULF waves and magnetic field characteristics in the polar cusp observed at Godhavn p 3361 N94-29244
Atmospheric moisture fields derived by satellite observations over the tropical Pacific Ocean p 3375 N94-30863

ATMOSPHERIC REFRACTION
The influence of the evaporation duct on the angle of arrival and amplitude of the backscattered signal from targets low above the sea p 3256 N94-30498

ATMOSPHERIC SCATTERING
Atmospheric Propagation Effects Through Natural and Man-Made Obscurants for Visible to MM-Wave Radiation
[AGARD-CP-542] p 3256 N94-30495
The influence of the evaporation duct on the angle of arrival and amplitude of the backscattered signal from targets low above the sea p 3256 N94-30498
Radiation transport in cloudy and aerosol loaded atmospheres p 3366 N94-30805

ATMOSPHERIC SOUNDING
On the possibility of measuring atmospheric OH using intracavity laser spectroscopy p 3344 N94-28597
An improved method of measuring tropospheric NO2, NO3, HO2, and RO2 by Matrix Isolation and Electronic Spin Resonance (MIESR) p 3345 N94-28605
Near-IR diode laser absorption for measurement of tropospheric HO2 p 3345 N94-28607
Research trends on remote sensing at research facilities in Japan: The priority area programme on better understanding of earth environment via satellite p 3326 N94-28928
Activities of the wintering party at Showa Station by the 31st Japanese Antarctic Research Expedition in 1990 p 3358 N94-29083
Activities of the fourth wintering party at Asuka Station by the 31st Japanese Antarctic Research Expedition in 1990 p 3358 N94-29084
Proceedings of the NIPR Symposium on Upper Atmosphere Physics, no. 6
[JTN-94-80593] p 3359 N94-29233
Time series comparisons of satellite and rocketsonde temperatures in 1978-1979
[NASA-TP-3409] p 3370 N94-29455
Inter-comparison of Wildfire and High-resolution Interferometer Sounder (HIS) data from STORM-FEST: An investigation of wildfire spectral channel discrepancies
[NASA-TM-108439] p 3333 N94-29553
Data transfer system using a multi-ID ARGOS transmitter for the Antarctic polar patrol balloon experiment p 3363 N94-29980
Remote sensor observations during WISP91: The use of microwave radiometers, RASS, and lidar ceilometers for detection of aircraft icing conditions
[PB94-142106] p 3136 N94-30890

ATMOSPHERIC STRATIFICATION
Structure of neutrally stratified turbulent Ekman layer as predicted by closure models with prognostic equation for master length scale p 3325 N94-28696

ATMOSPHERIC TEMPERATURE
Prediction of survival times on land in a cold climate p 3379 N94-28423
Objective analysis of a coastal ocean eddy using satellite AVHRR and in situ hydrographic data
[AD-A275715] p 3376 N94-28642
SHARC, a model for calculating atmospheric and infrared radiation under non-equilibrium conditions
[AD-A275207] p 3357 N94-28893
On the temperature distribution near a cold surface
[AD-A275162] p 3332 N94-29288
Time series comparisons of satellite and rocketsonde temperatures in 1978-1979
[NASA-TP-3409] p 3370 N94-29455
Second Japan-U.S. Workshop on Global Change: Environmental Response Technologies for Global Change (Mitigation and Adaptation) p 3354 N94-29522
Global patterns of cloud optical thickness variation with temperature and the implications for climate change p 3374 N94-29972
The challenge of identifying greenhouse gas-induced climatic change p 3352 N94-30634
Spatial interpolation, network bias, and terrestrial air temperature variability p 3374 N94-30810
Atmospheric turbulence within and above a coniferous forest
[ISBN-0-315-75468-0] p 3375 N94-30870

ATMOSPHERIC TURBULENCE
New parameters for characterizing turbulence at a potential wind site
[DE94-004355] p 3368 N94-28455
On eddy accumulation with limited conditional sampling to measure air-surface exchange
[DE94-005112] p 3368 N94-28568
A fractal analysis of near-field atmospheric concentration data
[AD-A275460] p 3355 N94-28728
US National Weather experiment STORM-FEST: Waves and turbulence in frontal zones
[AD-A275084] p 3369 N94-28847
An observational and numerical study of sea/land-breeze circulations in an area of complex coastal heating p 3372 N94-29813
Calculation of turbulence degraded point spread function of an imaging system p 3260 N94-30514
Modeling studies of frontogenesis in the upper and middle troposphere p 3375 N94-30868
Atmospheric turbulence within and above a coniferous forest
[ISBN-0-315-75468-0] p 3375 N94-30870

ATOMIC BEAMS
Surface structure and stereochemical properties of self-assembled monolayer materials
[DE94-004960] p 3484 N94-28578
Computer simulation of the interaction of fast hydrogen atoms with a molybdenum containing sorbed hydrogen
[DE94-608419] p 3209 N94-30253

ATOMIC CLOCKS
The 25th Annual Precise Time and Time Interval (PTTI) Applications and Planning Meeting
[NASA-CP-3267] p 3468 N94-30639
Two-way satellite time transfer: Overview and recent developments p 3469 N94-30646
Optical techniques for time and frequency transfer p 3469 N94-30647
GPS common-view time transfer p 3144 N94-30648
A real-time prediction of UTC p 3470 N94-30654
Accuracy metrics for judging time scale algorithms p 3471 N94-30656
Comparison of LASSO and GPS time transfers p 3145 N94-30665
An algorithm for the Italian atomic time scale p 3473 N94-30668
A comparative study of clock rate and drift estimation p 3473 N94-30669
A look into the crystal ball: The next 25 years p 3475 N94-30681

ATOMIC EXCITATIONS
Asymptotic coherence of gluons and of q-bosons
[DE94-005417] p 3481 N94-28492

ATOMIC FORCE MICROSCOPY
Atomic-scale friction measurements using friction force microscopy. Part 2: Application to magnetic media
[AD-A275202] p 3298 N94-29290

ATOMIC PHYSICS
Atomic physics with highly charged ions
[DE94-003397] p 3492 N94-30837

ATOMIC STRUCTURE
Electronic structure and mechanical properties of grain boundaries
[AD-A275198] p 3512 N94-28890
Structure of ordinary ice I(sub h). Part 1: Ideal structure of ice
[AD-A275149] p 3486 N94-29021
Halogen chemisorption on silver(111): Scanning tunneling microscopy of coadsorbed halogen atoms
[AD-A275219] p 3486 N94-29060
Atomic and magnetic structure of YBa2(Cu(1-x)Fe(x))3O(6+y) at 0.05 less than or equal to x less than or equal to 0.30, y is approximately equal to 1 and y is approximately equal to 0.5
[DE94-606852] p 3513 N94-29210
Theoretical investigation of gas-surface interactions
[NASA-CR-195755] p 3272 N94-29378
The MSRC ab initio methods benchmark suite: A measurement of hardware and software performance in the area of electronic structure methods
[DE94-006428] p 3514 N94-30001
Influence of doping on the electronic structure of (La, Sr)2CuO4
[DE94-006383] p 3516 N94-30054
Electronic structure of Zn-based quantum wells
[DE94-608104] p 3516 N94-30068
Generalized augmented space theorem for correlated disorder and cluster coherent potential approximation
[DE94-608110] p 3208 N94-30118
On the structure and atomic motions in liquid sodium
[DE94-608386] p 3490 N94-30182
Overlap of metal clusters and nuclear structure physics
[DE94-608387] p 3517 N94-30183
Nonlinear optics response of semiconductor quantum wells under high magnetic fields
[DE94-003244] p 3520 N94-30835
RHEED studies of the nucleation, growth, and mobility of Ag atoms on the Si(111)7 x 7 surface
[DE94-005551] p 3521 N94-30899
Thermochemical data for CVD modeling from ab initio calculations
[DE94-005269] p 3222 N94-30909

ATOMIZERS
Experimental studies on effervescent atomizers with wide spray angles p 3196 N94-29280
Investigation of the two-phase flow in a research combustor under reacting and non-reacting conditions p 3196 N94-29282

ATOMIZING
Experimental studies on effervescent atomizers with wide spray angles p 3196 N94-29280
Centrifugal atomization of lanthanide materials for cryogenic coolers
[DE94-006035] p 3219 N94-30337

ATOMS
On the structure and atomic motions in liquid sodium
[DE94-608386] p 3490 N94-30182
Research on the atomic layer-by-layer growth of high-temperature superconductor thin films at the Institute of Scientific and Industrial Research, Japan
[DE94-003739] p 3519 N94-30611

ATROPHY
Leg muscle volume during 30-day 6-degree head-down bed rest with isotonic and isokinetic exercise training
[NASA-TM-4580] p 3385 N94-29401
Shortening velocity and calcium sensitivity of single fibers from hindlimb suspended muscle in rats p 3387 N94-29866

ATTENTION
Maintaining vigilance on a simulated ATC monitoring task across repeated sessions
[DOT/FAA/AM-94/6] p 3143 N94-30933

ATTITUDE (INCLINATION)
Japanese Journal of Aerospace and Environmental Medicine, volume 30, no. 1
[JTN-94-80598] p 3389 N94-28850
Effect of food intake on skin vasomotor responses to head-up tilt in humans p 3390 N94-28854
The influence of appendage vibration on the attitude dynamics of a dual-spin satellite p 3168 N94-29828

ATTITUDE CONTROL
Software engineering methods in the Hermes on-board software p 3414 N94-29326
A gimbaled low noise momentum wheel p 3162 N94-29640
Posture control of goldfishes under microgravity p 3387 N94-29712
Miniature wide field-of-view star trackers for spacecraft attitude sensing and navigation p 3144 N94-29794

ATTITUDE INDICATORS
A comparison of three aircraft attitude display symbology structures
[AD-A275172] p 3150 N94-29048

ATTITUDE STABILITY
The influence of appendage vibration on the attitude dynamics of a dual-spin satellite p 3168 N94-29828

AUDIO EQUIPMENT
Multi-channel spatialization systems for audio signals
[NASA-CASE-ARC-12013-1-CU] p 3245 N94-29364

AUDIO SIGNALS
Data fusion and correlation techniques testbed development audio processing study
[SKD-1600-73-014] p 3241 N94-28532
Multi-channel spatialization systems for audio signals
[NASA-CASE-ARC-12013-1-CU] p 3245 N94-29364

AUDIOMETRY
Evaluation of monitoring audiometry in the United States Air Force Hearing Conservation Program
[AD-A275309] p 3391 N94-29211
Index of NPL acoustics publications 1981-1990
[NPL-RSA(EXT)-0044] p 3480 N94-30786

AUDITORY PERCEPTION
Subjective response to sonic booms having different shapes, rise times, and durations
[NASA-TM-109090] p 3479 N94-29464
AUDITORY SIGNALS
Noise reduction techniques for the restoration of musical recordings
[TELECOM-93-E-019] p 3291 N94-30979
AURORAL ABSORPTION
Initial observation results with imaging riometer at NY-Alesund (L is equal to 16) p 3360 N94-29239
AURORAL ECHOES
Long term variations of radio auroral activity p 3359 N94-29237
New-type echoes observed with the 50 MHz auroral Doppler radar at Showa Station p 3360 N94-29238
AURORAL IRRADIATION
Proceedings of the NIPR Symposium on Upper Atmosphere Physics, no. 6
[JTN-94-80593] p 3359 N94-29233
Aurora stereo observation in Iceland p 3359 N94-29234
Long term variations of radio auroral activity p 3359 N94-29237
New-type echoes observed with the 50 MHz auroral Doppler radar at Showa Station p 3360 N94-29238
AURORAL ZONES
The effects of magnetic storm phases on F-layer irregularities from auroral to equatorial latitudes
[AD-A275203] p 3356 N94-28891
AURORAS
Space-time structure of the morning aurora inferred from coincident DMSP-F6, -F8, and Sondrestrom incoherent scatter radar observations
[AD-A275442] p 3356 N94-28869
Aurora stereo observation in Iceland p 3359 N94-29234
Long term variations of radio auroral activity p 3359 N94-29237
New-type echoes observed with the 50 MHz auroral Doppler radar at Showa Station p 3360 N94-29238
Initial observation results with imaging riometer at NY-Alesund (L is equal to 16) p 3360 N94-29239
A theory of current generator in the magnetosphere-ionosphere coupling p 3360 N94-29240
Scale-length dependence of the ratio between the magnetic and electric field perturbations in the ionospheric field-aligned current region p 3360 N94-29243
Observation of Jovian auroral Ly-alpha line profile and emission variability with a sounding rocket and the IUE archives p 3550 N94-30798
AUSTENITE
Analysis of data by long-time mechanical properties of 08KH18N10T steel irradiated by neutrons
[DE94-605337] p 3202 N94-28551
Toughening mechanisms in ultrahigh-strength steels
[AD-A275439] p 3202 N94-28867
AUSTENITIC STAINLESS STEELS
Joining silicon carbide to austenitic stainless steel through diffusion welding
[PB94-126331] p 3297 N94-28399
Relationship between swelling and irradiation creep in cold-worked PCA stainless steel irradiated to approximately 178 dpa at approximately 400 C
[DE94-004368] p 3201 N94-28456
AUSTIN COMET
Infrared observations of cometary dust by COBE p 3541 N94-29994
AUTOMATA THEORY
Partial support for the Second International Symposium on Artificial Intelligence and Mathematics
[AD-A275199] p 3434 N94-29026
Dynamics of defect ensembles in one-dimensional cellular automata
[PB94-136819] p 3464 N94-29030
On-line search for optimal controller parameters using interconnected learning automata
[MATHS-REPT-A-196] p 3436 N94-29526
Some methodological issues about designing autonomous agents which learn their behaviors: The ELF experience
[REPT-93-068] p 3449 N94-30939
AUTOMATED RADAR TERMINAL SYSTEM
Machine Intelligence in Air Traffic Management
[AGARD-CP-538] p 3136 N94-29558
AUTOMATIC CONTROL
The state transition diagram with path priority and it's applications
[AD-A275524] p 3434 N94-28672
Partial support for the Second International Symposium on Artificial Intelligence and Mathematics
[AD-A275199] p 3434 N94-29026
A concurrent, object-based implementation for the tactical level of the rational behavior model
[AD-A275024] p 3410 N94-29115
Reactive system software concept with automation using the LDS language p 3414 N94-29327
Automation of the NDT diagnostic using neural nets. Application: Inspection of Airbus longitudinal joints during maintenance
[REPT-932-600-104] p 3315 N94-29474
Welding wire pressure sensor assembly
[NASA-CASE-MFS-26216-1-SB] p 3300 N94-29506
Intelligent systems for air space control and management p 3137 N94-29560
Use of GPS in automated air traffic control p 3137 N94-29563
Design of Center-TRACON Automation System p 3138 N94-29568
Simulation of fully automated air traffic control concepts p 3139 N94-29569
ARC2000: Automatic radar control p 3141 N94-29583
Automatic control steps for aircraft taxi guidance p 3141 N94-29584
Control system design for A and R supported microgravity experiments: An experiment payload control development
[AD-B179107] p 3229 N94-30421
The use of interactive computer vision and robot hand controllers for enhancing manufacturing safety p 3314 N94-30442
Programmable Automated Welding System (PAWS): Control of welding through software and hardware p 3314 N94-30443
Task-level control for autonomous robots
[AIAA PAPER 94-1210-CP] p 3444 N94-30561
Using generic tool kits to build intelligent systems
[AIAA PAPER 94-1214-CP] p 3445 N94-30565
A reactive system for open terrain navigation: Performance and limitations
[AIAA PAPER 94-1218-CP] p 3445 N94-30566
The road plan model: Information model for planning road building activities
[AIAA PAPER 94-1219-CP] p 3445 N94-30567
Programmable Automated Welding System (PAWS)
[AIAA PAPER 94-1221-CP] p 3446 N94-30570
AUTOMATION
Reactive system software concept with automation using the LDS language p 3414 N94-29327
Conference on Intelligent Robotics in Field, Factory, Service, and Space (CIRFFSS 1994), volume 1
[NASA-CP-3251] p 3439 N94-30526
Task automation in a successful industrial telerobot
[AIAA PAPER 94-1189-CP] p 3441 N94-30539
The Automated Aircraft Rework System (AARS): A system integration approach
[AIAA PAPER 94-1225-CP] p 3446 N94-30574
Automated inspection of turbine blades: Challenges and opportunities
[AIAA PAPER 94-1226-CP] p 3446 N94-30575
AUTOMOBILE FUELS
Technical analysis of alternative fueled vehicles
[DE94-744238] p 3304 N94-30269
TCM exemptions to promote alternative-fuel vehicles: The good, the bad, and the ugly
[DE94-005924] p 3311 N94-30703
Fuel cycle evaluations of biomass-ethanol and reformulated gasoline
[DE94-000227] p 3226 N94-30818
Investigation of the technology development status of alternate fuel vehicles
[DE94-744237] p 3312 N94-30831
Compressed natural gas fueled vehicles: The Houston experience
[DE94-005804] p 3312 N94-30878
AUTOMOBILES
Technical analysis of alternative fueled vehicles
[DE94-744238] p 3304 N94-30269
Vehicle following controller design for autonomous intelligent vehicles
[AIAA PAPER 94-1203-CP] p 3443 N94-30554
Proceedings of the 1993 Windsor Workshop on Alternative Fuels
[DE94-003908] p 3226 N94-30612
Design of a variable-conductance vacuum insulation
[DE94-000270] p 3268 N94-30819
Investigation of the technology development status of alternate fuel vehicles
[DE94-744237] p 3312 N94-30831
AUTOMORPHISMS
Remarks on Galois symmetry in RCFT
[PB94-138179] p 3467 N94-29147
AUTONOMIC NERVOUS SYSTEM
Analysis of various biological activity parameters during parabolic flight p 3393 N94-29716
AUTONOMOUS NAVIGATION
A concurrent, object-based implementation for the tactical level of the rational behavior model
[AD-A275024] p 3410 N94-29115
Object oriented design of the autonomous fixtaking management system p 3143 N94-29323
Proceedings of the 3rd Conference on Military Robotic Applications
[DRES-SP-149] p 3304 N94-30275
Autonomous intelligent military robots: Army ants, killer bees, and cybernetic soldiers p 3304 N94-30276
The NRC mobile robot project p 3305 N94-30280
Extended occupancy grid method for modelling unknown dynamic environments p 3144 N94-30281
Navigation of military and space unmanned ground vehicles in unstructured terrains p 3144 N94-30282
A generic semi-autonomous ground vehicle control system p 3306 N94-30283
Encoding technique for automated guided vehicle POSE recovery in a structured environment p 3144 N94-30286
Obstacle detection for an autonomous vehicle p 3309 N94-30302
Unmanned vehicle mobility: Limits of autonomous navigation p 3310 N94-30311
Design of an autonomous exterior security robot
[AIAA PAPER 94-1188-CP] p 3441 N94-30538
Controlling multiple security robots in a warehouse environment
[AIAA PAPER 94-1300-CP] p 3441 N94-30540
A Space Station robot walker and its shared control software
[AIAA PAPER 94-1192-CP] p 3442 N94-30543
Vision based object pose estimation for mobile robots
[AIAA PAPER 94-1197-CP] p 3442 N94-30548
Perception system and functions for autonomous navigation in a natural environment
[AIAA PAPER 94-1201-CP] p 3443 N94-30552
The real-world navigator
[AIAA PAPER 94-1204-CP] p 3443 N94-30555
Autonomous mobile robot teams
[AIAA PAPER 94-1207-CP] p 3444 N94-30558
A reactive system for open terrain navigation: Performance and limitations
[AIAA PAPER 94-1218-CP] p 3445 N94-30566
Aspects of vision and planning in a dynamic, uncertain environment p 3448 N94-30803
Iterative removal of boundary minima of harmonic potential function for mobile robot navigation
[REPT-93-059] p 3449 N94-30962
AUTONOMOUS SPACECRAFT CLOCKS
Cesium and rubidium frequency standards status and performance on the GPS program p 3145 N94-30663
Comparison of LASSO and GPS time transfers p 3145 N94-30665
AUTONOMY
Achieving robot autonomy p 3310 N94-30307
Vehicle following controller design for autonomous intelligent vehicles
[AIAA PAPER 94-1203-CP] p 3443 N94-30554
A streamlined software environment for situated skills
[AIAA PAPER 94-1205-CP] p 3444 N94-30556
Situational reaction and planning
[AIAA PAPER 94-1206-CP] p 3444 N94-30557
Autonomous mobile robot teams
[AIAA PAPER 94-1207-CP] p 3444 N94-30558
AUXILIARY POWER SOURCES
Advanced steady-state operating scenarios
[DE94-004810] p 3509 N94-30768
AVALANCHES
Physical processes in snowpacks during rain or melt events
[AD-A275445] p 3325 N94-28881
AVIATION METEOROLOGY
Prototype terminal aerodrome forecasts using a mesoscale model
[AD-A275308] p 3369 N94-29194
AVIATION PSYCHOLOGY
Information presentation for expert systems in future fighter aircraft
[AD-A275126] p 3149 N94-29005
AVIONICS
Aerospace Software Engineering for Advanced Systems Architectures
[AGARD-CP-545] p 3412 N94-29315
Experiences with the HOOD design method on avionics software development p 3414 N94-29325
Potential software failures methodology analysis p 3414 N94-29329
Rome Laboratory software engineering technology program p 3414 N94-29330
A common Ada run-time system for avionics software p 3150 N94-29331
Ada run time system certification for avionics applications p 3150 N94-29332
Design of a thinwire real-time multiprocessor operating system p 3415 N94-29333
On ground system integration and testing: A modern approach p 3150 N94-29334

Software testing practices and their evolution for the 1990's p 3415 N94-29335
Validation and test of complex weapon systems p 3150 N94-29336
Testing Operational Flight Programs (OFPs) p 3415 N94-29337
DSSA-ADAGE: An environment for architecture-based avionics development p 3150 N94-29348
Future manned systems advanced avionics study [NASA-CR-188277] p 3150 N94-29377
KC-135 cockpit modernization study and crew reduction feasibility demonstration [AD-A275230] p 3146 N94-29391
DLR's ATM demonstration programme p 3140 N94-29575
Installation of experimental mode-S data link in commercial aircraft [PB94-138757] p 3254 N94-29998

AXIAL FLOW
Local heat transfer in an enclosed corotating disk with axial throughflow p 3276 N94-29849

AXIAL LOADS
A modeling study of the effect of stress state on void linking during ductile fracture [AD-A275505] p 3317 N94-28811
Cyclic axial-torsional deformation behavior of a cobalt-base superalloy [NASA-TM-106372] p 3203 N94-28921
Granular bases for heavily loaded pavements [AD-A275171] p 3156 N94-29047
Failure strength and mechanism of composite laminates under multiaxial loading conditions p 3182 N94-29875
Experimental and analytical comparison of constraint effects due to biaxial loading and shallow-flaws [DE94-004794] p 3323 N94-30689

AXIAL STRAIN
A modeling study of the effect of stress state on void linking during ductile fracture [AD-A275505] p 3317 N94-28811
Cyclic axial-torsional deformation behavior of a cobalt-base superalloy [NASA-TM-106372] p 3203 N94-28921
Finite element analysis of axisymmetric deformations of thick thermoviscoplastic targets p 3320 N94-29688

AXIAL STRESS
Failure strength and mechanism of composite laminates under multiaxial loading conditions p 3182 N94-29875

AXISYMMETRIC FLOW
Forced generation of solitary waves in a rotating fluid and their stability p 3274 N94-29689

AZOLES
Superior energetic materials that contain carbocations and anions. Energetic materials restricted in composition to C, H, N, and O atoms [AD-A275449] p 3225 N94-29310

B

BACILLUS
Physiology and molecular-genetics of thermus and bacillus [PB94-135571] p 3385 N94-29190

BACKGROUND NOISE
Ion-assisted tropospheric OH measurement technique p 3344 N94-28601
Removal of coherent Extremely Low Frequency (ELF) background noise by adaptive noise cancellation [AD-A275016] p 3243 N94-28898
The Rb 780-nanometer Faraday anomalous dispersion optical filter: Theory and experiment p 3250 N94-29659
The effect of enhanced backscattering on target detection p 3258 N94-30508

BACKGROUND RADIATION
CBSD: The celestial background scene descriptor [AD-A275521] p 3538 N94-28671
Camera artifacts in IUE spectra [NASA-CR-189337] p 3198 N94-29857
High redshift QSOs and the x ray background [NASA-CR-195112] p 3540 N94-29957
Energetic events in the early universe p 3547 N94-30012
An absolute measurement of the cosmic background radiation temperature at 1.4 GHz p 3553 N94-30351

BACKSCATTERING
RL/ERCT automated swept-angle bistatic measurement system [AD-A275763] p 3241 N94-28763
Backscatter haze device for measurement of haze in aircraft transparencies [AD-A275127] p 3146 N94-29042
Considerations in the modelling of seafloor acoustic backscatter [AD-A275404] p 3478 N94-29206
Backscatter Mossbauer Spectrometer (BaMS) for extraterrestrial applications p 3236 N94-29774
The influence of the evaporation duct on the angle of arrival and amplitude of the backscattered signal from targets low above the sea p 3256 N94-30498
The effect of enhanced backscattering on target detection p 3258 N94-30508
Polarimetric backscatter measurements of natural surfaces at millimeter wavelengths p 3259 N94-30509
A hybrid electromagnetic-statistical approach for characterizing MMW scattering by terrain p 3259 N94-30510

BACTERIA
Cellular and molecular approaches to polymer synthesis by bacteria [AD-A275501] p 3212 N94-28661
Studies on bacterial spore ultraviolet light resistance and regulation of the activity of a spore protease [AD-A275448] p 3384 N94-28884
Fundamental studies on the corrosion behavior of weldments in marine microbial environments [AD-A275247] p 3203 N94-28900
Stable RNA sequences as a tool for DNA probes and phylogenetic studies [PB94-135423] p 3385 N94-29156
One carbon metabolism in anaerobic bacteria: Regulation of carbon and electron flow during organic acid production [DE94-004852] p 3386 N94-30180

BALANCE
Disturbance of equilibrium on JAL flight crew p 3390 N94-28856
Space and vertigo: In relation to space motion sickness p 3390 N94-28857
An actively cooled floating element skin friction balance for direct measurement in high enthalpy supersonic flows p 3289 N94-29824

BALL BEARINGS
Parachute Swivel Mechanism for planetary entry p 3162 N94-29643
Rotor instability induced by dead band clearance in bearing supports p 3312 N94-30809

BALLISTICS
Ballistic performance of polycarbonate/polyester and polycarbonate/styrene- acrylonitrile microlayer sheets [AD-A275462] p 3177 N94-28735
Dynamic response of ceramics [AD-A275396] p 3214 N94-29203

BALLOON SOUNDING
Observations of the geomagnetic field by Polar Patrol Balloon (PPB) experiment in Antarctica p 3359 N94-29235
Data transfer system using a multi-ID ARGOS transmitter for the Antarctic polar patrol balloon experiment p 3363 N94-29980

BALLOONING MODES
Higher order collisionless ballooning mode in tokamaks [PPL-143] p 3507 N94-30156
Eigenmode analysis of the destabilized ion acoustic mode in tokamaks [PPL-142] p 3507 N94-30158
Resistive ballooning mode in a gas-dynamic trap [DE94-608328] p 3508 N94-30171
Advanced steady-state operating scenarios [DE94-004810] p 3509 N94-30768

BANACH SPACE
Approximation methods for nonlinear operator equations of the m-accretive type [DE94-608099] p 3467 N94-30065
Comparative semantics for linear arrays of communicating processes [CWI-CS-R9336] p 3426 N94-30491

BAND STRUCTURE OF SOLIDS
Energy gap structure of layered superconductors [DE94-005132] p 3511 N94-28570
Nonadiabatic effects in the quantum Hall regime p 3513 N94-29530
Band structure of superlattice with (delta)-like potential [DE94-608108] p 3516 N94-30072

BANDWIDTH
The Rb 780-nanometer Faraday anomalous dispersion optical filter: Theory and experiment p 3250 N94-29659
Sampling behaviour in a four instrument monitoring task: Effects of signal bandwidth and number of events per signal [AD-B179613] p 3402 N94-30422

BARIUM COMPOUNDS
Normal state resistivity of MBa2Cu3O(7-x) ceramics [DE94-608456] p 3220 N94-30745

BARLEY
Barley cell culture as a producer of heterologous protein [PB94-132339] p 3379 N94-28408

BAROCLINIC INSTABILITY
Physical processes associated with variability in successive operational model forecasts of cyclogenesis [ISBN-0-315-74753-6] p 3371 N94-29751
Multiple weather regimes and baroclinically forced spherical resonance [DM-65] p 3376 N94-30966

BAROCLINIC WAVES
Physical processes associated with variability in successive operational model forecasts of cyclogenesis [ISBN-0-315-74753-6] p 3371 N94-29751
Downstream development of baroclinic waves p 3372 N94-29796

BAROCLINITY
Multiple weather regimes and baroclinically forced spherical resonance [DM-65] p 3376 N94-30966

BAROTROPIC FLOW
Papers in meteorology and geophysics, vol. 44, no.1 [JTN-94-80585] p 3324 N94-28693
On the linear stability of Verkley's modons p 3324 N94-28695

BARRED GALAXIES
Multicolor photometry of barred spiral galaxies p 3541 N94-30270

BARRIER LAYERS
Epitaxial heterojunctions of oxide semiconductors and metals on high temperature superconductors [NASA-CASE-NPO-18483-1-CU] p 3513 N94-29501
Strong overlap and transmission in triple barrier resonant structures [DE94-608103] p 3516 N94-30067

BARYONS
Semileptonic heavy-to-light decays of baryons [DE94-606481] p 3487 N94-29502

BASALT
Motion and development of the Pacific Plate from the Middle Jurassic to the Late Cretaceous p 3362 N94-29939
Geochemical and fluid dynamic investigations into the nature of chemical variability in the Earth's mantle p 3367 N94-30917

BASE FLOW
Development and application of particle image velocimetry in high-speed separated flow: Two-dimensional base cavities p 3282 N94-30791

BATCH PROCESSING
Batch updates and concurrency in B-trees [PB94-136835] p 3530 N94-29167

BATHYMETERS
Considerations in the modelling of seafloor acoustic backscatter [AD-A275404] p 3478 N94-29206

BAYES THEOREM
Bayesian belief networks and conditional independencies [RUU-CS-92-36] p 3465 N94-30376

BEAM CURRENTS
A transmission-loss monitor using current transformers [DE94-003974] p 3267 N94-30716

BEAM INJECTION
Active electron and ion beam experiments in space [AD-A275570] p 3504 N94-28828
A 6MeV heavy ion beam probe for the Large Helical Device [NIFS-272] p 3505 N94-29397
Tuning of AmPS [NIKHEF-K-AMPS-93-01] p 3494 N94-29422
Peculiarities of heat transfer in the experiments of beam injection heating of a plasma at the GOL-3 device [DE94-608357] p 3508 N94-30194
A future, intense source of negative hydrogen ions p 3494 N94-30485

BEAM WAVEGUIDES
Laser beam steering with semiconductor waveguide [AD-A275775] p 3292 N94-28765
X-/Ka-band dichroic plate design and grating lobe study p 3247 N94-29616
A portable X-band front-end test package for beam-waveguide antenna performance evaluation. Part 2: Tests on the antenna p 3247 N94-29620
Gaussian beam and physical optics iteration technique for wideband beam waveguide feed design p 3248 N94-29624
Determining noise temperatures in beam waveguide systems p 3249 N94-29657

BEAMS (RADIATION)
Gaussian beam and physical optics iteration technique for wideband beam waveguide feed design p 3248 N94-29624

BEAMS (SUPPORTS)
Position control of a flexible beam with active damping of vibrations [ISBN-0-315-85841-9] p 3321 N94-30033
Damage identification in composites using built-in piezoelectrics p 3184 N94-30355

Thin-walled orthotropic laminated beam theory
p 3324 N94-30920

BED REST
Leg muscle volume during 30-day 6-degree head-down bed rest with isotonic and isokinetic exercise training
[NASA-TM-4580] p 3385 N94-29401

BEDS (PROCESS ENGINEERING)
Electrochemical incineration of wastes
[NASA-CR-195262] p 3198 N94-29938

BEHAVIOR
Behavior and visual control of cyprinodonts under microgravity p 3387 N94-29713

BELTS
A newly developed snow vehicle (SM100S) for Antarctica. Part 4: Low temperature properties of crawler belt p 3314 N94-29984

BENDING
Numerical and experimental investigation of the bending response of thin-walled composite cylinders
[NASA-CR-195730] p 3317 N94-28801
Interlaminar fracture analysis for laminated composites under combined loading p 3182 N94-29964
Analysis and design of inflatable aerospace structures
p 3403 N94-30799

BENDING MOMENTS
Analysis and design of inflatable aerospace structures
p 3403 N94-30799

BENDING VIBRATION
Position control of a flexible beam with active damping of vibrations
[ISBN-0-315-85841-9] p 3321 N94-30033
Analysis and design of inflatable aerospace structures
p 3403 N94-30799

BENZENE
Polyimides containing the penta fluoro sulfanyl benzene moiety
[NASA-CASE-LAR-15082-1] p 3175 N94-29554

BERYLLIUM
Radiation effects in beryllium used for plasma protection
[DE94-004599] p 3201 N94-28460

BETA FACTOR
Beta enhancement of thermal diffusivity in tokamaks
[PPL-141] p 3508 N94-30159

BEVERAGES
Effects of three hydration beverages on exercise performance during 60 hours of simulated desert exposure p 3383 N94-28448

BIAS
Longitudinal effects and intensity-phase coupling in distributed feedback semiconductor lasers
p 3294 N94-29590

BIBLIOGRAPHIES
Microgravity science and applications. Program tasks and bibliography for FY 1993
[NASA-TM-4569] p 3227 N94-28415
Aeronautical engineering: A cumulative index to a continuing bibliography (supplement 300)
[NASA-SP-7037(300)] p 3121 N94-28537
ARTI Refrigerant Database
[DE94-004906] p 3230 N94-28563
Catalog of Air Force weather technical publications 1992-1993
[AD-A275635] p 3368 N94-28638
TRADOC library and information network (TRALINET). Union list of periodicals (TULIP)
[AD-A275263] p 3529 N94-28903
Defense Technical Information Center cataloging guidelines
[AD-A275100] p 3529 N94-28911
Learning about the Internet bibliography and beginners' guide
[AD-A275205] p 3430 N94-29051
Publications of the NASA Controlled Ecological Life Support System (CELSS) program 1989-1992
[NASA-CR-4603] p 3401 N94-30122
NREL Photovoltaic Program FY 1993 bibliography
[DE94-000272] p 3340 N94-30820

BIG BANG COSMOLOGY
A theory approach for creation of the matter of universe
[DE94-608109] p 3548 N94-30163

BIMETALS
Fundamental studies of hydrogen interaction with supported meta and bimetallic catalysts
[DE94-004887] p 3202 N94-28562

BINARY ALLOYS
Intermetallic growth at the interface between copper and bismuth-tin solder
[AD-A275716] p 3202 N94-28643
Localization in presence of magnetic field in 2-D disordered binary alloys
[DE94-608093] p 3208 N94-30108
Volume averaged model for the mechanics of alloys solidification
[PB94-138617] p 3208 N94-30113
Nature of dissolution of binary tantalum-titanium alloys by molten plutonium
[DE94-005090] p 3210 N94-30776

BINARY CODES
Modifications of the Griesmer bound
p 3247 N94-29618

BINARY DATA
Modifications of the Griesmer bound
p 3247 N94-29618

BINARY MIXTURES
Ionic conduction mechanisms in CaF2 and CaF2-Al2O3 nanocomposite films on Al2O3 substrates
[DE94-004792] p 3520 N94-30773

BINARY PHASE SHIFT KEYING
Communications subsystem for the Petite Amateur Navy Satellite (PANSAT)
[AD-A275532] p 3242 N94-28812

BINARY STARS
Binary-single star scattering: An investigation of a realistic chaotic scattering system p 3543 N94-29719
A study of recycled pulsars in globular clusters
p 3539 N94-29825
Coronal temperatures of unusually active K-dwarf binary systems
[NASA-CR-189335] p 3545 N94-29861

BINARY SYSTEMS (MATERIALS)
Effect of microstructure on the strength and fracture energy of bimaterial interfaces
[AD-A274987] p 3178 N94-29126
Mechanical alloying processing with application to structural materials: ASSERT supplement
[AD-A275400] p 3204 N94-29205

BINOCULAR VISION
Design and control of active vision based mechanisms for intelligent robots
[AIAA PAPER 94-1196-CP] p 3442 N94-30547

BIOASSAY
Microfabricated silicon biosensors for microphysiometry p 3238 N94-29783
Computerized in vitro test for chemical toxicity based on tetrahymena swimming patterns
p 3354 N94-30463

BIOASTRONAUTICS
Hemodynamic measurement during parabolic flight
p 3393 N94-29717
Motion sickness in parabolic flight: Possibility of electrogastrography as an objective index
p 3393 N94-29718

BIOCHEMISTRY
Cellular and molecular approaches to polymer synthesis by bacteria
[AD-A275501] p 3212 N94-28661
Development of novel switchable protein surfaces
[AD-A275510] p 3384 N94-28667
Biodiesel from aquatic species
[DE94-000275] p 3225 N94-30038
One carbon metabolism in anaerobic bacteria: Regulation of carbon and electron flow during organic acid production
[DE94-004852] p 3386 N94-30180
Lattice gas simulations of replicating domains
[DE94-005008] p 3200 N94-30748

BIOCONVERSION
Journal of NIRE, Vol. 2, No. 2
[JTN-94-80552] p 3187 N94-28675
Researches on bioconversion of coal into liquid product p 3187 N94-28677
Fossil energy biotechnology: A research needs assessment
[DE94-004239] p 3338 N94-29953
Fuel cycle evaluations of biomass-ethanol and reformulated gasoline
[DE94-000227] p 3226 N94-30818
Biological conversion of synthesis gas
[DE94-005815] p 3340 N94-30879

BIODEGRADATION
Fossil energy biotechnology: A research needs assessment
[DE94-004239] p 3338 N94-29953

BIOGEOCHEMISTRY
Atmosphere, ocean, and land: Critical gaps in Earth system models p 3350 N94-30617
Towards coupled physical-biogeochemical models of the ocean carbon cycle p 3350 N94-30618
Linkages between terrestrial ecosystems and the atmosphere p 3351 N94-30624
Development of simplified ecosystem models for applications in Earth system studies: The Century experience p 3352 N94-30629
A toy terrestrial carbon flow model
p 3352 N94-30630

BIOINSTRUMENTATION
Microfabricated silicon biosensors for microphysiometry p 3238 N94-29783

BIOLOGICAL EFFECTS
Computerized in vitro test for chemical toxicity based on tetrahymena swimming patterns
p 3354 N94-30463
Electric power lines: Questions and answers on research into health effects
[DE94-005637] p 3353 N94-30757
Role of x ray-induced transcripts in adaptive responses following x rays
[DE94-005412] p 3386 N94-30895

BIOMASS
Impact study on the use of biomass-derived fuels in gas turbines for power generation
[DE94-000261] p 3224 N94-28502
Copepods collected along 33.5 deg E longitude of the Antarctic Ocean in the 1976 summer
p 3358 N94-29082
Caesium-137 in a boreal forest ecosystem: Aspects on the long-term behavior
[PB94-137809] p 3347 N94-29158
Impact of biomass burning on the atmosphere
[DE94-004333] p 3349 N94-29954
The direct observation of alkali vapor species in biomass combustion and gasification
[DE94-000262] p 3339 N94-30606
Annual report and summaries of FY 1993 activities: Division of Energy Biosciences
[DE94-001723] p 3386 N94-30607
Proceedings of the low cost materials of construction for biological processes workshop
[DE94-000218] p 3226 N94-30761

BIOMASS ENERGY PRODUCTION
Annual report and summaries of FY 1993 activities: Division of Energy Biosciences
[DE94-001723] p 3386 N94-30607
Fuel cycle evaluations of biomass-ethanol and reformulated gasoline
[DE94-000227] p 3226 N94-30818

BIOMETRICS
Motion sickness in parabolic flight: Possibility of electrogastrography as an objective index
p 3393 N94-29718
Non-invasive temperature measurements using electron paramagnetic resonance spectroscopy
p 3198 N94-29881

BIOPROCESSING
Researches on bioconversion of coal into liquid product p 3187 N94-28677

BIOREACTORS
Biological conversion of synthesis gas
[DE94-005815] p 3340 N94-30879

BIOSPHERE
Linkages between terrestrial ecosystems and the atmosphere p 3351 N94-30624
Evaluating models of climate and forest vegetation
p 3353 N94-30637
Comprehensive system models: Strategies for evaluation p 3353 N94-30638

BIOSYNTHESIS
Cellular and molecular approaches to polymer synthesis by bacteria
[AD-A275501] p 3212 N94-28661
Biodiesel from aquatic species
[DE94-000275] p 3225 N94-30038
One carbon metabolism in anaerobic bacteria: Regulation of carbon and electron flow during organic acid production
[DE94-004852] p 3386 N94-30180

BIOTECHNOLOGY
Fossil energy biotechnology: A research needs assessment
[DE94-004239] p 3338 N94-29953
Technology 2003: The Fourth National Technology Transfer Conference and Exposition, volume 1
[NASA-CP-3249] p 3555 N94-30440
Composite redesign of obstetrical forceps
p 3397 N94-30457
Dexterity enhancement in microsurgery using telemicro-robotics
[AIAA PAPER 94-1230-CP] p 3447 N94-30579
Annual report and summaries of FY 1993 activities: Division of Energy Biosciences
[DE94-001723] p 3386 N94-30607
Proceedings of the low cost materials of construction for biological processes workshop
[DE94-000218] p 3226 N94-30761

BIOTITE
Studies in Jurassic and Cretaceous North American apparent polar wander p 3362 N94-29940

BIPOLAR TRANSISTORS
Solid-state, active-phased arrays: Some aspects of receiver design
[AD-A275893] p 3527 N94-28779
Effects of oxide charge and surface recombination velocity on the excess base current of BJT's
[DE94-003711] p 3263 N94-29025

A bipolar analog front-end integrated circuit for the SDC silicon tracker
[DE94-005203] p 3267 N94-30711

BIRDS
Development and implementation of a scrub habitat compensation plan for Kennedy Space Center
[NASA-TM-109202] p 3347 N94-29099

BIREFRINGENCE
Experimental and theoretical studies of molecular solids
[AD-A275511] p 3485 N94-28668
Electrooptical and optical evaluation of Pb(Zr,Ti)O3 thin films using waveguide refractometry
[DE94-006374] p 3518 N94-30247

BIRTH
Composite redesign of obstetrical forceps
p 3397 N94-30457

BISMALEIMIDE
Irradiation polymerization of bismaleimide resins
[REPT-932-430-105] p 3215 N94-29441
Correlation between wet ageing, humidity absorption and properties on composite materials based on different resins family
[REPT-932-600-107] p 3179 N94-29462

BISMUTH ALLOYS
Electrodeposition of bismuth alloys by the controlled potential method
[DE94-605318] p 3212 N94-28550
Intermetallic growth at the interface between copper and bismuth-tin solder
[AD-A275716] p 3202 N94-28643
Microstructural development and mechanical behavior of eutectic bismuth-tin and eutectic indium-tin in response to high temperature deformation
[DE94-005202] p 3210 N94-30710

BISMUTH OXIDES
Investigation of the phase equilibria and phase transformations associated with the Bi2Sr2CaCu2O(y) superconductor
[DE94-004889] p 3519 N94-30691

BISPHENOLS
Poly(arylene ether-co-imidazole)s as toughness modifiers for epoxy resins
[NASA-CASE-LAR-15229-1-CU] p 3215 N94-29451

BIT ERROR RATE
Partially coherent detection of PSK signals in Rician channels
[ISBN-0-315-85799-4] p 3254 N94-30031

BIT SYNCHRONIZATION
Decoder synchronization for deep space missions
p 3250 N94-29664

BITS
Influence of clearance and rake angles on the cutting force of rock p 3368 N94-29520

BIVARIATE ANALYSIS
A family of joint probability models for cost and schedule uncertainties
[AD-A275513] p 3463 N94-28670

BLACK BODY RADIATION
Procedures for basic inverse problems: Black body radiation problem and phonon density of states problem
[ISBN-0-315-85757-9] p 3525 N94-30244

BLACK HOLES (ASTRONOMY)
On dyonic black holes and cosmic censorship
p 3546 N94-29912
Physics, astronomy, and astrophysics: A numerical study of the black hole plus Brill wave spacetime
p 3540 N94-29990
A numerical study of gravitational collapse
p 3548 N94-30271

BLACKOUT
Remote control of transcranial Doppler (TCD) probe during centrifuge exposures up to 9 +Gz
[AD-A275253] p 3400 N94-29029

BLANKETS (FUSION REACTORS)
Liquid metal MHD and heat transfer in a tokamak blanket slotted coolant channel
[DE94-004622] p 3506 N94-29510

BLOCH BAND
Nonadiabatic effects in the quantum Hall regime
p 3513 N94-29530

BLOCKS
Information system for flow simulation based on the Navier-Stokes equations vectorization
[AD-B179293] p 3281 N94-30763

BLOOD
Japanese Journal of Aerospace and Environmental Medicine, volume 30, no. 1
[JTN-94-80598] p 3389 N94-28850
Arterial oxygen saturation during +Gz acceleration by short-radius centrifuge p 3389 N94-28852

BLOOD FLOW
A comparison of four methods of rewarming individuals cooled by immersion in cold water p 3382 N94-28442
Effect of food intake on skin vasomotor responses to head-up tilt in humans p 3390 N94-28854
Remote control of transcranial Doppler (TCD) probe during centrifuge exposures up to 9 +Gz
[AD-A275253] p 3400 N94-29029
Effects of make-up on the heat transfer from the head in hyperthermic conditions p 3394 N94-29864

BLOOD PRESSURE
Effect of food intake on skin vasomotor responses to head-up tilt in humans p 3390 N94-28854

BLOOD PUMPS
Rotary blood pump
[NASA-CASE-MSC-22424-1] p 3299 N94-29370
Development of the NASA/Baylor VAD
p 3397 N94-30458

BLOOD VESSELS
Effect of food intake on skin vasomotor responses to head-up tilt in humans p 3390 N94-28854

BLOWING
Numerical study of the trailing vortex of a wing with wing-tip blowing
[NASA-CR-195803] p 3130 N94-29760

BLOWOUTS
Studies of lean blowout in a research combustor
p 3193 N94-29266

BLUE STARS
Globular cluster photometry near the turnoff: Blue stragglers, relative ages, and the horizontal branch
p 3538 N94-29732
Spatially resolved spectroscopy of AG Carinae, and direct evidence for stellar evolution: The central star of NGC 2392
[NASA-CR-189291] p 3545 N94-29871

BODIES OF REVOLUTION
Integral equation analysis of composite bodies of revolution and arbitrary surfaces with application to cavity-backed antennas p 3253 N94-29883

BODY CENTERED CUBIC LATTICES
Failure strength and mechanism of composite laminates under multiaxial loading conditions p 3182 N94-29875
Influence of tungsten alloying additions on the mechanical properties and texture of tantalum
[DE94-004994] p 3210 N94-30774

BODY FLUIDS
Studies on water electrolyte metabolism and endocrine responses at rest and during submaximal exercise at 6,000 m simulated altitude p 3388 N94-28496
Effects of training at simulated altitude of 6,000 m on endocrine responses at rest and during exercise at the same altitude p 3388 N94-28497

BODY KINEMATICS
Determination of acceleration field parameters with linear accelerometers
[PB94-125606] p 3290 N94-30742

BODY TEMPERATURE
Fuelling shivering in humans during cold water immersion p 3379 N94-28426
Biochemical enhancement of cold tolerance
p 3380 N94-28427
Treatment of mild immersion hypothermia by body-to-body and forced-air warming
p 3380 N94-28428
The potential of new textiles in improving survival prospects p 3380 N94-28430
Thermoregulation in the extreme cold environment
p 3381 N94-28438
Physiological investigations of the isolated rat's liver in hypothermia and hypoxia and their relevance in aircraft incidents above the sea p 3382 N94-28439
Rewarming methodologies in the field
p 3382 N94-28441
A comparison of four methods of rewarming individuals cooled by immersion in cold water p 3382 N94-28442
Thermal strain generated by an enhanced anti-G protection system in a hot climate p 3383 N94-28445
Implications of climatic extremes in aircrew NBC operations p 3383 N94-28446
Alleviation of thermal strain in the CF: Keeping our cool during the Gulf conflict p 3383 N94-28449
Test of a new protection suit in a climatic chamber
p 3384 N94-28452
Physiological responses during shipboard firefighting
[AD-A275104] p 3391 N94-28912

BODY WEIGHT
Nutrition and hydration status of aircrew members consuming an improved survival ration during a simulated survival scenario p 3380 N94-28429

BODY-WING CONFIGURATIONS
Numerical analysis of sonic boom in the near field
p 3125 N94-28962
Three-dimensional external flow computations using prismatic grid p 3127 N94-28979
Aircraft aerodynamics with deflected jets in ground effect p 3132 N94-29973

BOEING 737 AIRCRAFT
Dual-Band Infrared (DBIR) imaging inspections of Boeing 737 and KC-135 aircraft panels
[DE94-005700] p 3122 N94-29642

BOLTED JOINTS
Measurement and modelling of bolted joint stress relaxation in plastics
[PB94-124849] p 3318 N94-28841

BOLTS
Test and analysis of a stitched RFI graphite-epoxy panel with a fuel access door
[NASA-TM-108992] p 3178 N94-29100
Bolt and nut evaluator
[NASA-CASE-GSC-13468-1] p 3288 N94-29538

BOMBS (ORDNANCE)
Cockpit video: A low cost BDA source
[AD-A275228] p 3150 N94-29389

BONDED JOINTS
Casting of weldable graphite/magnesium metal matrix composites with built-in metallic inserts
p 3186 N94-30482

BONDING
Crystal structure of La(2-x)Ba(x)CuO4
[DE94-707688] p 3511 N94-28750
Method and apparatus for indicating disbonds in joint regions
[NASA-CASE-LAR-14626-1] p 3315 N94-29548

BORATES
Surface chemistry of boron-doped SiO2 CVD: Enhanced uptake of tetraethyl orthosilicate by hydroxyl groups bonded to boron
[DE94-005428] p 3221 N94-30896

BORIDES
Magnetotransport measurements in magnetic fields up to 50T in SmB6 and FeSi
[DE94-006227] p 3520 N94-30848

BORN-INFELD THEORY
The Klein-Fock equation, minimal surfaces and gravitational fields
[DE94-606340] p 3356 N94-28803

BORN-OPPENHEIMER APPROXIMATION
Low frequency dynamics of CO/Cu-breakdown of Born-Oppenheimer approximation
[DE94-005508] p 3510 N94-28512

BOSONS
Asymptotic coherence of gluons and of q-bosons
[DE94-005417] p 3481 N94-28492
Properties of W + jet events in proton-antiproton collisions at 1.8 TeV
[DE94-004002] p 3482 N94-28524
Path integral for coherent states of the dynamical U(sub 2) group and U(sub 2/1) supergroup
[DE94-606382] p 3466 N94-28785
Twistor-like type 2 superstring and bosonic string
[DE94-606339] p 3523 N94-28802
Measurement of the W mass in the D0 detector
[DE94-006002] p 3490 N94-30103
Space-time symmetries: P and CP violation
[DE94-005012] p 3526 N94-30750

BOUNDARY CONDITIONS
The static and nonstatic electrical solenoids
[DE94-606326] p 3261 N94-28585
Numerical solution of the multichannel scattering problem
[DE94-606297] p 3484 N94-28619
A method for the modelling of porous and solid wind tunnel walls in computational fluid dynamics codes
[NASA-CR-195699] p 3270 N94-28724
Modelling and analysis of creep deformation and fracture in a 1 Cr 1/2 Mo ferritic steel
[PB94-138328] p 3319 N94-29121
A non-local computational boundary condition for duct acoustics
[NASA-TM-109091] p 3478 N94-29382
Stress transfer mechanics for multiple perfectly bonded concentric cylinder models of unidirectional composites
[PB94-138633] p 3181 N94-29524
Boundary-induced phase transitions in equilibrium and non-equilibrium systems
[DE94-608137] p 3199 N94-30111
Three-dimensional free vibration analysis of thick arbitrarily laminated, rectangular, cylindrical and spherical composite panels p 3184 N94-30257

BOUNDARY ELEMENT METHOD
Analysis of 3-D acoustic problems using boundary element method p 3127 N94-28974
Experimental validation of finite element and boundary element methods for predicting structural vibration and radiated noise
[NASA-CR-4561] p 3301 N94-29552
Modal analysis of solar panels using boundary integral equations
[NLT-TP-92218-U] p 3338 N94-30328
Comparison of RCS prediction techniques, computations and measurements
[PB94-125515] p 3256 N94-30392

BOUNDARY INTEGRAL METHOD
A spectral boundary integral equation method for the 2-D Helmholtz equation
[NASA-CR-194890] p 3454 N94-30207

BOUNDARY LAYER CONTROL
Method of reducing hydraulic instability
[NASA-CASE-LEW-15463-1] p 3273 N94-29539
BOUNDARY LAYER FLOW
Boundary layers induced by three-dimensional vortex loops
[AD-A275678] p 3270 N94-28665
Papers in meteorology and geophysics, vol. 44, no.1
[JTN-94-80585] p 3324 N94-28693
Structure of neutrally stratified turbulent Ekman layer as predicted by closure models with prognostic equation for master length scale p 3325 N94-28696
Spin-up in a rectangular cylinder
[AD-A275465] p 3271 N94-28738
A flow visualization study of acoustically enhanced hairpin vortices
[AD-A275467] p 3271 N94-28809
Long-wavelength asymptotics of unstable crossflow modes, including the effect of surface curvature
[NASA-CR-4579] p 3273 N94-29460
The effect of a wavy boundary on turbulent flow p 3280 N94-30272
The effect of pressure gradient on the structure of an equilibrium turbulent boundary layer p 3282 N94-30807
BOUNDARY LAYER SEPARATION
Boundary layers induced by three-dimensional vortex loops
[AD-A275678] p 3270 N94-28665
Fluid dynamic noise in a centrifugal pump
[AD-A275264] p 3477 N94-28904
An experimental study of the flowfield on a semispan rectangular wing with a simulated glaze ice accretion p 3130 N94-29674
The flow field near the body surface with thin filaments p 3234 N94-29706
BOUNDARY LAYER TRANSITION
An experimental study of the flowfield on a semispan rectangular wing with a simulated glaze ice accretion p 3130 N94-29674
Experiments and theoretical considerations regarding the allowable roughness height in laminar flow
[PB94-125556] p 3133 N94-30389
BOUNDARY LAYERS
Boundary layer coherent structures
[AD-A275007] p 3272 N94-29195
The flow field near the body surface with thin filaments p 3234 N94-29706
BOUNDARY VALUE PROBLEMS
A numerical solver for initial and boundary value problems in differential-algebraic systems
[AD-A275447] p 3452 N94-28883
Weighted and unweighted maximum clique algorithms with upper bounds from fractional coloring
[AD-A275328] p 3409 N94-28917
Compound matrix method for multi-point boundary-value problems
[PB94-137791] p 3453 N94-29476
A spectral boundary integral equation method for the 2-D Helmholtz equation
[NASA-CR-194890] p 3454 N94-30207
Accurate finite difference methods for time-harmonic wave propagation
[NASA-CR-194887] p 3454 N94-30209
Process modelling for materials preparation experiments
[NASA-CR-195782] p 3175 N94-30242
A numerical study of gravitational collapse p 3548 N94-30271
Parallel iteration across the steps of high order Runge-Kutta methods for nonstiff initial value problems
[CWI-NM-R9313] p 3433 N94-30730
Generalized Eulerian-Lagrangian formulations in free and moving boundary problems: Processing of viscoelastic polymers and fiber suspensions p 3283 N94-30955
BRAIDED COMPOSITES
Development of braided rope engine seals
[NASA-TM-105902] p 3298 N94-28838
On the dynamic mechanical behavior of 3-D integrated fabric reinforced composites
[AD-A275424] p 3177 N94-28865
3-D braided, continuous fiber ceramic composites produced by chemical vapor infiltration
[AD-A275192] p 3178 N94-29024
BRAIN
Synaptogenesis, selective stabilization, and free association
[AD-A275250] p 3392 N94-29431
Japanese Journal of Aerospace and Environmental Medicine, vol. 30, no. 2
[JTN-94-80599] p 3394 N94-29863
Effects of make-up on the heat transfer from the head in hyperthermic conditions p 3394 N94-29864
BRANCHING (MATHEMATICS)
Parallel quantification
[LP-93-01] p 3422 N94-30318
Three metric domains of processes for bisimulation
[CWI-CS-R9335] p 3459 N94-30427
Hopf bifurcation in viscous, low-speed flows about an airfoil with structural coupling p 3134 N94-30865
BRASSES
Studies of high temperature ternary phases in mixed-metal-rich early transition metal sulfide and phosphide systems
[DE94-006034] p 3209 N94-30336
BREADBOARD MODELS
Design and implementation of a hybrid digital phase-locked loop with a TMS320C25: An application to a transponder receiver breadboard p 3251 N94-29667
Electrochemical incineration of wastes
[NASA-CR-195262] p 3198 N94-29938
Analysis of EDP performance
[NASA-CR-195726] p 3420 N94-29945
BREAKWATERS
Bulletin of National Research Institute of Fisheries Engineering, No. 13
[JTN-94-80596] p 3233 N94-29701
Development of the breakwater with submerged mound for interchanging sea water p 3234 N94-29703
BREATHING APPARATUS
Emergency underwater breathing aids for helicopter passengers and crew p 3381 N94-28437
Decompression sickness risk versus time and altitude
[AD-A275261] p 3391 N94-29071
BREEDING (REPRODUCTION)
Reproduction in the Japanese anchovy (Engraulis japonica) as related to population fluctuation p 3235 N94-29708
BREMSSTRAHLUNG
A measurement of the LMP effect
[DE94-005225] p 3482 N94-28493
Plasma turbulent bremsstrahlung
[PPL-144] p 3507 N94-30157
Quantum-mechanical suppression of bremsstrahlung
[DE94-005223] p 3497 N94-30712
BRIDGES (STRUCTURES)
Study of bridge design and technology
[PB94-137916] p 3121 N94-29160
BRIGHTNESS
Multicolor photometry of barred spiral galaxies p 3541 N94-30270
Optical depth effects in cluster cooling flows p 3541 N94-30800
BRIGHTNESS TEMPERATURE
Inter-comparison of Wildfire and High-resolution Interferometer Sounder (HIS) data from STORM-FEST: An investigation of wildfire spectral channel discrepancies
[NASA-TM-108439] p 3333 N94-29553
Atmospheric moisture fields derived by satellite observations over the tropical Pacific Ocean p 3375 N94-30863
BRINES
Solubility of Nd in brine
[DE94-005099] p 3187 N94-28567
BRITTLE MATERIALS
Estimation of Weibull modulus from dynamic and static fatigue experiments
[PB94-138641] p 3322 N94-30114
BRITTLENESS
Fracture process zone of brittle composites p 3182 N94-29876
Brittle composites modeling: Comparisons with MoSi2/ZrO2
[DE94-004978] p 3182 N94-29933
The role of plastic deformation in brittle and near-brittle cracking behavior p 3322 N94-30226
A class of inclusion problems for the strengthening of brittle and ductile composites p 3186 N94-30959
BROADBAND
Broadband EUV survey spectrometer for short-timescale experiments
[DE94-005459] p 3498 N94-28534
Absolute calibration technique for broadband ultrasonic transducers
[NASA-CASE-LAR-14672-1] p 3287 N94-29199
Gaussian beam and physical optics iteration technique for wideband beam waveguide feed design p 3248 N94-29624
A digital combining-weight estimation algorithm for broadband sources with the array feed compensation system p 3250 N94-29660
Digital combining-weight estimation for broadband sources using maximum-likelihood estimates p 3250 N94-29661
A broad-band microseismometer for planetary operations p 3237 N94-29778
Communications technology for unattended sensors
[DE94-005685] p 3254 N94-30043
II-VI wide band gap semiconductors under hydrostatic pressure
[DE94-608106] p 3516 N94-30070
Microsecond fiber optic delay line
[DE94-607903] p 3500 N94-30075
Performance issues of signalling protocols for broadband ISDN
[MEMO-INF-93-30] p 3255 N94-30374
BROADCASTING
Design and analysis of dynamic leader election protocols in broadcast networks
[MEMO-INF-93-43] p 3260 N94-30520
BROKEN SYMMETRY
Discrete quark-lepton symmetry need not pose a cosmological domain wall problem
[DE94-601606] p 3481 N94-28471
Discrete symmetries, strong CP problem and gravity
[DE94-608091] p 3524 N94-30089
Space-time symmetries: P and CP violation
[DE94-005012] p 3526 N94-30750
BROMINE
Pitting corrosion of titanium
[AD-A274980] p 3203 N94-29089
BROWNIAN MOVEMENTS
Non-Markovian quantum Brownian motion of a harmonic oscillator
[DE94-005922] p 3477 N94-30873
BRYOPHYTES
Estimation of the net production of moss community at Langhovde, East Antarctica p 3358 N94-29081
Japan-China collaboration research program on terrestrial biology at Great Wall Station in King George Island, in the summer of 1990/1991 p 3358 N94-29085
Cellular polarity and interactions in plant graviperception
[NASA-CR-195261] p 3385 N94-29943
BSCCO SUPERCONDUCTORS
Exploratory research for a high temperature superconducting integrated circuit
[AD-A275798] p 3262 N94-28767
BUBBLE CHAMBERS
Weak decays of charged K-mesons and charm particles
[PB94-138062] p 3486 N94-29143
Adaption of the bubble detector for use as a LET spectrometer p 3291 N94-30216
BUBBLES
Analysis of spark-induced bubble experiments using CALE
[DE94-003667] p 3270 N94-28476
Numerical analysis of incompressible viscous flow around a bubble p 3126 N94-28968
BUCKLING
Numerical and experimental investigation of the bending response of thin-walled composite cylinders
[NASA-CR-195730] p 3317 N94-28801
General theory and algorithms for the non-casual inversion, slewing and control of space-based articulated structures
[AD-A275118] p 3167 N94-29002
Computational simulation of composite structures with and without damage
[NASA-CR-194433] p 3183 N94-30190
BUDGETING
Business planning model user's guide
[AD-A274978] p 3409 N94-28895
Financial resource review model user's guide
[AD-A274979] p 3410 N94-29088
BUFFER STORAGE
I/O on the Tera file system
[AD-A275278] p 3530 N94-29182
BUILDINGS
Object-oriented CAD tool implementations for the construction industry
[PB94-132370] p 3407 N94-28411
Exploitation of stereophotogrammetrically derived 3-D wireframe models to produce urban simulations
[AD-A275459] p 3325 N94-28808
Rooftop emergency heliports
[DOT/FAA/RD-93/2] p 3157 N94-29754
Improved ground-penetrating radar, bridge decks
[DE94-004863] p 3254 N94-29929
BULK MODULUS
Measurement of bulk longitudinal modulus and correction for edge effects
[DE94-005581] p 3222 N94-30900
BULKHEADS
Aircraft system aft telescope cavity configuration study for Stratospheric Observatory for Infrared Astronomy (SOFIA), phase 2
[NASA-CR-194266] p 3147 N94-29685
Photovoltaic power without batteries for continuous cathodic protection p 3341 N94-30465
BUOYANCY
Similarity solutions and numerical modeling in buoyancy controlled turbulent diffusion flames
[AD-A275820] p 3188 N94-28777

Development of buoyancy affected laminar flow in a heated pipe p 3128 N94-28988
BUOYS
The velocity field in the Northeast Atlantic from satellite-tracked drifting buoys
[AD-A275704] p 3376 N94-28690
BURNERS
Numerical simulation of radiative heat loss in an experimental burner
[DE94-002016] p 3277 N94-29923
BURNOUT
Experimental and analytical studies of high heat flux components for fusion experimental reactor
[DE94-707671] p 3504 N94-28556
BUTANES
Effects of hydrogen addition on pollutant emissions in a gas turbine combustor p 3195 N94-29275

C

C BAND
Evaluation of dual polarization attenuation of millimeter frequencies through a meteorological radar p 3256 N94-30496
C-135 AIRCRAFT
KC-135 cockpit modernization study and crew reduction feasibility demonstration
[AD-A275230] p 3146 N94-29391
Dual-Band Infrared (DBIR) imaging inspections of Boeing 737 and KC-135 aircraft panels
[DE94-005700] p 3122 N94-29842
CABLES
Unscreened low tension cables scrape abrasion testing. Part 1: An interlaboratory study on scrape abrasion testing according to ISO DP 6722-1
[PB94-135605] p 3264 N94-29191
CADMIUM SELENIDES
Electronic structure of Zn-based quantum wells
[DE94-608104] p 3516 N94-30068
CADMIUM SULFIDES
Optical properties of cadmium sulfide, zinc selenide, and zinc manganese selenide semiconductor films p 3500 N94-29759
CADMIUM TELLURIDES
Modeling the total dose radiation effects of Hg(1-x)Cd(x)Te photodiodes using numerical device simulators
[AD-A275235] p 3263 N94-29028
Vibrational properties of homopolar and heteropolar surfaces and interfaces of the CdTe/HgTe system
[DE94-608105] p 3516 N94-30069
CAFFEINE
Biochemical enhancement of cold tolerance p 3380 N94-28427
CALCIUM FLUORIDES
Ionic conduction mechanisms in CaF2 and CaF2-Al2O3 nanocomposite films on Al2O3 substrates
[DE94-004792] p 3520 N94-30773
CALCIUM OXIDES
Investigation of the phase equilibria and phase transformations associated with the Bi2Sr2CaCu2O(y) superconductor
[DE94-004889] p 3519 N94-30691
CALCULUS
A time reasoning system based on the event calculus for scheduling in aeronautic maintenance
[REPT-932-710-101] p 3122 N94-29463
Completeness of the Lambek calculus with respect to relativized relational semantics
[LP-93-03] p 3455 N94-30326
Models of the untyped lambda-calculus in semi Cartesian closed categories
[ML-93-05] p 3456 N94-30381
The conjoinability relation in Lambek calculus in linear logic
[ML-93-03] p 3457 N94-30397
The secrets of causality
[RUU-CS-93-29] p 3426 N94-30490
More problems on rewriting
[CWI-CS-R9332] p 3428 N94-30734
CALCULUS OF VARIATIONS
Four-dimensional data assimilation using the adjoint method p 3455 N94-30353
CALIBRATING
Testing laboratories as notified bodies
[PB94-132396] p 3160 N94-28413
Absolute calibration technique for broadband ultrasonic transducers
[NASA-CASE-LAR-14672-1] p 3287 N94-29199
Inter-comparison of Wildfire and High-resolution Interferometer Sounder (HIS) data from STORM-FEST: An investigation of wildfire spectral channel discrepancies
[NASA-TM-108439] p 3333 N94-29553
Line-of-sight tropospheric calibration from measurements in arbitrary directions p 3249 N94-29654
Summary report of mission acceleration measurements for Spacehab-01, STS-57 launched 21 June 1993
[NASA-TM-106514] p 3168 N94-29757
Calibration of charge coupled device digital cameras
[ISBN-0-315-85539-8] p 3290 N94-30232
Two-way satellite time transfer: Overview and recent developments p 3469 N94-30646
Remote clocks linked by a fully calibrated two-way timing link p 3471 N94-30659
LASSO experiment: Intercalibrations of the LASSO ranging stations p 3297 N94-30666
Ground control system for the midcourse space experiment UTC clock p 3474 N94-30674
Guidance notes for use with NPL low permeability reference materials
[NPL-DES-121] p 3476 N94-30780
The use of thermistors in the NPL electron-beam calorimeter
[PB94-139334] p 3290 N94-30782
Report on the development of low magnetic permeability reference materials
[NPL-DES-119] p 3476 N94-30783
Determination of photon fluence spectra from the NPL Mobaltron Co-60 unit
[NPL-RSA(EXT)-46] p 3492 N94-30795
Solar measurements from the Airglow-Solar Spectrometer Instrument (ASSI) on the San Marco 5 satellite
[NASA-CR-193815] p 3551 N94-30948
CALIFORNIA
The management issues of implementing telecommuting: A case study
[AD-A275267] p 3527 N94-28905
Site comparison for optical visibility statistics in southern California p 3247 N94-29617
Intermedia transfer factors for fifteen toxic pollutants released to air basins in California
[DE94-005699] p 3349 N94-30044
CALIFORNIUM ISOTOPES
Using Cf-252 for single event upset testing p 3496 N94-30219
CALORIC REQUIREMENTS
Nutrition and hydration status of aircrew members consuming an improved survival ration during a simulated survival scenario p 3380 N94-28429
CALORIMETERS
Elementary particle interactions
[DE94-004238] p 3482 N94-28504
The use of thermistors in the NPL electron-beam calorimeter
[PB94-139334] p 3290 N94-30782
CAMERA SHUTTERS
Three high duty cycle, space-qualified mechanisms p 3162 N94-29642
CAMERAS
Digital camera with apparatus for authentication of images produced from an image file
[NASA-CASE-NPO-19108-1-CU] p 3287 N94-29373
Three high duty cycle, space-qualified mechanisms p 3162 N94-29642
Camera artifacts in IUE spectra
[NASA-CR-189337] p 3198 N94-29857
Calibration of charge coupled device digital cameras
[ISBN-0-315-85539-8] p 3290 N94-30232
Sensing the gas metal arc welding process p 3314 N94-30444
CAMOUFLAGE
Spectral and polarimetric analysis of hyperspectral data collected by an acousto-optic tunable filter system
[AD-A275076] p 3329 N94-29095
Experimental evaluation of camouflage effectiveness in the thermal infrared p 3257 N94-30502
Global approach towards the evaluation of thermal infrared countermeasures p 3258 N94-30504
CANCELLATION
The bootstrapped algorithm: A fast algorithm for blind signal separation
[AD-A275759] p 3408 N94-28760
Method for cancelling expansion waves in a wave rotor
[NASA-CASE-LEW-15218-2] p 3274 N94-29740
CANCER
Conformal external radiotherapy of prostatic carcinoma: Requirements and preliminary results p 3395 N94-30029
CANONICAL FORMS
Canonical-variables multigrid method for steady-state Euler equations
[NASA-CR-194888] p 3454 N94-30208
Two algorithms for finding rectangular duals of planar graphs
[RUU-CS-92-41] p 3423 N94-30345
CANOPIES (VEGETATION)
Fractal approach to computer-analytical modelling of tree crown
[DE94-608089] p 3467 N94-30088
CANTILEVER BEAMS
An actively cooled floating element skin friction balance for direct measurement in high enthalpy supersonic flows p 3289 N94-29824
Fracture process zone of brittle composites p 3182 N94-29876
Delamination growth in composites under cyclic loads p 3183 N94-30256
Delamination of woven E-glass fabric composites
[DE94-003227] p 3185 N94-30827
CAPACITORS
Charge trapping and breakdown in N2O oxides
[DE94-003775] p 3266 N94-30040
Plasma treatment of polymer dielectric films to improve capacitive energy storage p 3223 N94-30479
CAPE KENNEDY LAUNCH COMPLEX
An observational and numerical study of sea/land-breeze circulations in an area of complex coastal heating p 3372 N94-29813
CARBOHYDRATES
Fuelling shivering in humans during cold water immersion p 3379 N94-28426
CARBON
Pull-test adhesion measurements of diamondlike carbon films on silicon carbide, silicon nitride, aluminum oxide, and zirconium oxide
[DE94-005469] p 3211 N94-28536
Silicon germanium carbon heteroepitaxial growth on silicon
[AD-A275197] p 3512 N94-28889
Preparation and structure of amorphous hydrogenated carbon film deposited with RF plasma CVD p 3223 N94-29518
One carbon metabolism in anaerobic bacteria: Regulation of carbon and electron flow during organic acid production
[DE94-004852] p 3386 N94-30180
CARBON CYCLE
Towards coupled physical-biogeochemical models of the ocean carbon cycle p 3350 N94-30618
The carbon cycle revisited p 3350 N94-30622
Ocean-atmospheric linkages p 3350 N94-30623
Linkages between terrestrial ecosystems and the atmosphere p 3351 N94-30624
Four simple ocean carbon models p 3351 N94-30625
A toy terrestrial carbon flow model p 3352 N94-30630
Carbon cycling in high-latitude ecosystems p 3352 N94-30631
Models of atmosphere-ecosystem-hydrology interactions: Approaches and testing p 3353 N94-30636
CARBON DIOXIDE
Peroxy radical measurements with NCAR's chemical amplifier p 3345 N94-28603
Survey on effects of petroleum substitution energy utilization on the global environment
[DE94-732339] p 3346 N94-28630
Computer simulation of molecular interactions in supercritical solvents
[AD-A274977] p 3486 N94-29087
The 1992-1993 advanced design program. Part 1: The Mars methane engine project. Part 2: The Mars oxygen processor new furnace
[NASA-CR-195513] p 3299 N94-29409
Second Japan-U.S. Workshop on Global Change: Environmental Response Technologies for Global Change (Mitigation and Adaptation) p 3354 N94-29522
Large heat pumps using CO2 refrigerant
[PB94-138773] p 3279 N94-29999
Dynamic constraints on CO2 uptake by an iron-fertilized Antarctic p 3350 N94-30619
Four simple ocean carbon models p 3351 N94-30625
CARBON DIOXIDE CONCENTRATION
The carbon cycle revisited p 3350 N94-30622
Ocean-atmospheric linkages p 3350 N94-30623
Linkages between terrestrial ecosystems and the atmosphere p 3351 N94-30624
Four simple ocean carbon models p 3351 N94-30625
The challenge of identifying greenhouse gas-induced climatic change p 3352 N94-30634
CARBON DIOXIDE REMOVAL
Second Japan-U.S. Workshop on Global Change: Environmental Response Technologies for Global Change (Mitigation and Adaptation) p 3354 N94-29522
CARBON FIBER REINFORCED PLASTICS
Assessment of the fibre volume distribution around optical fibres
[FFA-TN-1993-12] p 3179 N94-29425

Intelligent material systems and structures. Part 7: Debonding and pull-out of two optical fibers from two epoxies
[PB94-137767] p 3180 N94-29475

CARBON FIBERS
Formation and chemical reactivity of carbon fibers prepared by defluorination of graphite fluoride
[NASA-TM-106398] p 3174 N94-28747
Polymer infiltration studies
[NASA-CR-195729] p 3213 N94-28748
Graphite intercalation compounds prepared from graphite fluoride
[NASA-TM-106447] p 3174 N94-28924
Preparation of graphite fibers from polyimide
p 3223 N94-29517
Stress transfer mechanics for multiple perfectly bonded concentric cylinder models of unidirectional composites
[PB94-138633] p 3181 N94-29524

CARBON MONOXIDE
Low frequency dynamics of CO/Cu-breakdown of Born-Oppenheimer approximation
[DE94-005508] p 3510 N94-28512
The radiocarbon hydroxyl technique
p 3344 N94-28600
Simulation of pollutant formation in turbulent combustors using an extended coherent flame model
p 3190 N94-29251
Toxicity of carbon monoxide-hydrogen cyanide gas mixtures: Exposure concentration, time-to-incapacitation, carboxyhemoglobin, and blood cyanide parameters
[DOT/FAA/AM-94/7] p 3395 N94-29919

CARBON STEELS
Fatigue of carbon and low-alloy steels in LWR environments
[DE94-005116] p 3207 N94-30021

CARBON 13
Nuclear magnetic relaxation studies of semiconductor nanocrystals and solids
[DE94-006301] p 3520 N94-30842

CARBON 14
Cosmogenic C-14 in Antarctic and non-Antarctic meteorites and lunar samples
[NASA-CR-195795] p 3546 N94-29905
Dynamic constraints on CO2 uptake by an iron-fertilized Antarctic p 3350 N94-30619

CARBON-CARBON COMPOSITES
Damage meso-modeling of 3D evolutive composites
[REPT-932-430-106] p 3179 N94-29442
Performance of CVD and CVR coated carbon-carbon in high temperature hydrogen
[DE94-005451] p 3487 N94-29841
Dynamic fracture mechanics analysis for an edge delamination crack
[NASA-TM-109106] p 3479 N94-29856
Irradiation-induced structure and property changes in tokamak plasma-facing, carbon-carbon composites
[DE94-006046] p 3508 N94-30365
Four advances in carbon-carbon materials technology
p 3186 N94-30481

CARBONATES
Enhanced ion dissociation of LiCF3SO3 by new carbonate plasticizers: Raman and IR studies
[DE94-005448] p 3485 N94-28741
Fundamental stack and system issues in molten carbonate fuel cell development
[DE94-005960] p 3338 N94-30048
Configuration and performance of the indirect-fired fuel cell bottomed turbine cycle
[DE94-005961] p 3338 N94-30313

CARBONIZATION
Structural changes during carbonization and oxidation of coal p 3187 N94-28678

CARBOXYHEMOGLOBIN
Toxicity of carbon monoxide-hydrogen cyanide gas mixtures: Exposure concentration, time-to-incapacitation, carboxyhemoglobin, and blood cyanide parameters
[DOT/FAA/AM-94/7] p 3395 N94-29919

CARBOXYLIC ACIDS
Chemically modified polymeric resins for separation of cations, organic acids, and small polar molecules by high performance liquid chromatography
[DE94-005548] p 3211 N94-28516

CARDIAC OUTPUT
Development of the NASA/Baylor VAD
p 3397 N94-30458

CARDIAC VENTRICLES
Use of snakes to link edge points to create left ventricular boundaries in echocardiographic images
[TELECOM-93-D-016] p 3395 N94-30970

CARDIOVASCULAR SYSTEM
Effects of three hydration beverages on exercise performance during 60 hours of simulated desert exposure p 3383 N94-28448
Japanese Journal of Aerospace and Environmental Medicine, volume 30, no. 1
[JTN-94-80598] p 3389 N94-28850
Effect of food intake on skin vasomotor responses to head-up tilt in humans p 3390 N94-28854
Relaxed tolerance following HSG, high sustained +Gz
[AD-A275204] p 3391 N94-28892
Remote control of transcranial Doppler (TCD) probe during centrifuge exposures up to 9 +Gz
[AD-A275253] p 3400 N94-29029
The MERSS 5th Symposium on Space Medicine: Medical and Physiological Experiment Utilizing Parabolic Flight
[JTN-94-80588] p 3392 N94-29709
Hemodynamic measurement during parabolic flight
p 3393 N94-29717

CARRIER DENSITY (SOLID STATE)
Aggregation equilibria in arsenic doped silicon
[DE94-607269] p 3515 N94-30005

CARRIER MOBILITY
Transport properties of epitaxial lift off films
[NASA-TM-106156] p 3264 N94-29209

CARRIER TRANSPORT (SOLID STATE)
Photoelectronic study of GaAs epilayers and In(x)Ga(1-x)As/GaAs quantum wells
[ISBN-0-315-85756-0] p 3518 N94-30239

CARRIER WAVES
A digital combining-weight estimation algorithm for broadband sources with the array feed compensation system p 3250 N94-29660

CARTESIAN COORDINATES
Large-scale 3-D solutions of the time-dependent Dirac equation
[DE94-005591] p 3454 N94-30317

CARTRIDGES
Ampoule failure sensor time response testing: Experiment 1
[NASA-TM-108449] p 3290 N94-30199

CASCADE FLOW
Application of flow field simulation to turbine vane design p 3127 N94-28978
An elliptic-hyperbolic grid generation method and application to compressor flows p 3128 N94-28981
Mixed Eulerian-Lagrangian finite element solutions of unsteady flow and flutter in transonic cascade
p 3282 N94-30816

CASCADE RANGE (CA-OR-WA)
Analysis of deep seismic reflection and other data from the southern Washington Cascades
[DE94-005915] p 3367 N94-30883

CASE HISTORIES
Advanced development of PV encapsulents
[DE94-000219] p 3336 N94-28500
Development centres: Assessing or developing people
[PB94-138070] p 3536 N94-29144

CASSEGRAIN ANTENNAS
Beam scanning offset Cassegrain reflector antennas by subreflector movement
[NASA-CR-191604] p 3160 N94-28836
A portable X-band front-end test package for beam-waveguide antenna performance evaluation. Part 2: Tests on the antenna p 3247 N94-29620

CASSEGRAIN OPTICS
Determining noise temperatures in beam waveguide systems p 3249 N94-29657

CAST ALLOYS
New inoculants for ductile cast iron
[PB94-138476] p 3206 N94-29947

CASTING
Melt flow during alloy solidification: Dimensional analysis and model problems
[PB94-138625] p 3206 N94-29997
Casting of weldable graphite/magnesium metal matrix composites with built-in metallic inserts
p 3186 N94-30482

CASUALTIES
Aeromedical support for casualties in extremely hot climates p 3382 N94-28443

CATACLYSMIC VARIABLES
The cataclysmic variables from the Palomar-Green survey p 3539 N94-29819

CATALOGS (PUBLICATIONS)
Catalog of Air Force weather technical publications 1992-1993
[AD-A275635] p 3368 N94-28638
TRADOC library and information network (TRALINET). Union list of periodicals (TULIP)
[AD-A275263] p 3529 N94-28903
Defense Technical Information Center cataloging guidelines
[AD-A275100] p 3529 N94-28911

CATALYSIS
Fundamental studies of hydrogen interaction with supported meta and bimetallic catalysts
[DE94-004887] p 3202 N94-28562
Project of the experiment to test the hypothesis on existence of white and black p(mu)-atoms
[DE94-606751] p 3485 N94-28625
Polymer technology publication series no. 16
[PB94-135522] p 3214 N94-29157
Fuel-rich catalytic combustion of a high density fuel
[NASA-TP-3281] p 3197 N94-29356
Theoretical investigation of gas-surface interactions
[NASA-CR-195755] p 3272 N94-29378

CATALYSTS
Catalytic fabric filtration for simultaneous NO(x) and particulate control
[DE94-001660] p 3341 N94-28463
Fundamental studies of hydrogen interaction with supported meta and bimetallic catalysts
[DE94-004887] p 3202 N94-28562
Polymer technology publication series no. 16
[PB94-135522] p 3214 N94-29157
Theoretical investigation of gas-surface interactions
[NASA-CR-195755] p 3272 N94-29378
Catalytic ignitor for regenerative propellant gun
[NASA-CASE-NPO-18987-1-CU] p 3225 N94-29490
The polymerization of epsilon-caprolactone with stannous catalyst and lactide/epsilon-caprolactone (LA/epsilon-CL) and lactide/glycolide (LA/GA) copolymers. Polymer technology publication series no. 15
[PB94-137551] p 3220 N94-30713
Dual cure low-VOC coating process, phase 3
[DE94-003202] p 3221 N94-30826
Studies of supported molybdenum and tungsten
[DE94-006207] p 3210 N94-30839
Transient studies of low temperature catalysts for methane conversion
[DE94-005767] p 3200 N94-30877

CATALYTIC ACTIVITY
Catalytic fabric filtration for simultaneous NO(x) and particulate control
[DE94-001660] p 3341 N94-28463

CATEGORIES
Remarks on the theory of semi-functors
[ML-93-08] p 3457 N94-30384
Commutative Lambek categorial grammars
[ML-93-01] p 3457 N94-30395

CATHODES
Low voltage electron beam lithography
[AD-A275648] p 3262 N94-28650
RF vacuum microelectronics
[AD-A275221] p 3263 N94-28915
Dendrite preventing separator for secondary lithium batteries
[NASA-CASE-NPO-18585-1-CU] p 3265 N94-29411

CATHODIC COATINGS
Photovoltaic power without batteries for continuous cathodic protection p 3341 N94-30465

CATIONS
Chemically modified polymeric resins for separation of cations, organic acids, and small polar molecules by high performance liquid chromatography
[DE94-005548] p 3211 N94-28516

CAUCHY PROBLEM
Approximation of solutions of the cubic NLSE by finite dimensional equations and non-squeezing properties
[PB94-138294] p 3452 N94-29148

CAUCHY-RIEMANN EQUATIONS
Numerical solution of 3-D Navier-Stokes equations in vorticity-velocity form for incompressible flows
p 3276 N94-29843

CAVITIES
Neural network application to Particle Impact Noise Detection p 3437 N94-29840

CAVITY RESONATORS
Hydrogen maser clocks in space for solid-Earth research and time-transfer applications: Experiment overview and evaluation of Russian miniature sapphire loaded cavity
p 3474 N94-30676

CD-ROM
NASA space and Earth science data on CD-ROM
[NASA-TM-109709] p 3528 N94-28414

CELLS (BIOLOGY)
Barley cell culture as a producer of heterologous protein
[PB94-132339] p 3379 N94-28408
Cell culture in space p 3228 N94-28944
Stable RNA sequences as a tool for DNA probes and phylogenetic studies
[PB94-135423] p 3385 N94-29156
Computerized in vitro test for chemical toxicity based on tetrahymena swimming patterns
p 3354 N94-30463

CENTRIFUGAL COMPRESSORS
Numerical study on internal flows of centrifugal compressors p 3127 N94-28977
Method of reducing hydraulic instability
[NASA-CASE-LEW-15463-1] p 3273 N94-29539

CENTRIFUGAL FORCE
Use of magnetic compression to support turbine engine rotors p 3314 N94-30484

CENTRIFUGAL PUMPS
Fluid dynamic noise in a centrifugal pump
[AD-A275264] p 3477 N94-28904
Method of reducing hydraulic instability
[NASA-CASE-LEW-15463-1] p 3273 N94-29539
Experiments on the aerodynamic generation of noise in centrifugal turbomachinery p 3480 N94-30804

CENTRIFUGES
Relaxed tolerance following HSG, high sustained +Gz
[AD-A275204] p 3391 N94-28892
Comparative centrifuge evaluation of the Air Force Advanced Technology Anti-G Suit (ATAGS) and the Navy Enhanced Anti-G Lower Ensemble (EAGLE)
[AD-A275348] p 3400 N94-28996
Remote control of transcranial Doppler (TCD) probe during centrifuge exposures up to 9 +Gz
[AD-A275253] p 3400 N94-29029

CENTRIFUGING
Effect of chronic centrifugation on in vitro fertilization and early development in mice ova
p 3386 N94-28853
Centrifugal atomization of lanthanide materials for cryogenic coolers
[DE94-006035] p 3219 N94-30337

CEPHEID VARIABLES
Pushing the limit: Precision radial velocities, techniques, and applications p 3542 N94-30861

CERAMIC COATINGS
A novel approach to the fabrication of SiC structures of arbitrary shape
[AD-A275475] p 3214 N94-29073
Evaluation of oxide-coated iridium-rhenium chambers
[NASA-TM-106442] p 3172 N94-29097
Plasma sprayed ceramic thermal barrier coating for NiAl-based intermetallic alloys
[NASA-CASE-LEW-15535-1] p 3205 N94-29507
Synthesis and characterization of advanced materials for Navy applications p 3223 N94-30474
Deposition of tantalum carbide coatings on graphite by laser interactions p 3223 N94-30475

CERAMIC FIBERS
3-D braided, continuous fiber ceramic composites produced by chemical vapor infiltration
[AD-A275192] p 3178 N94-29024
Multiple Concentric Cylinder Model (MCCM) user's guide
[NASA-CR-195299] p 3183 N94-30125

CERAMIC MATRIX COMPOSITES
Fatigue behavior of a cross-ply ceramic matrix composite at elevated temperatures under tension-tension loading
[AD-A275466] p 3176 N94-28673
Innovative processing of composites for ultra-high temperature applications, book 1
[AD-A275597] p 3176 N94-28729
Innovative processing of composites for ultra-high temperature applications, book 3
[AD-A275599] p 3177 N94-28731
Superplasticity in fine-grained ceramics
[AD-A275461] p 3212 N94-28733
Static fracture behavior of a ceramic matrix composite at elevated temperatures
[AD-A275363] p 3177 N94-29008
Fatigue behavior of a cross-ply ceramic matrix composite under strain controlled tension-tension and tension-compression loading
[AD-A275374] p 3177 N94-29012
3-D braided, continuous fiber ceramic composites produced by chemical vapor infiltration
[AD-A275192] p 3178 N94-29024
Characterisation and processing of SiC/MAS-L glass ceramic matrix composite
[REPT-932-430-111] p 3179 N94-29412
Glass-ceramic matrix composites
[REPT-932-430-112] p 3179 N94-29413
Microfocus radioscopy, a high resolution means of inspecting composite materials
[REPT-932-430-109] p 3179 N94-29454
Method of producing a ceramic fiber-reinforced glass-ceramic matrix composite
[NASA-CASE-LEW-15264-2] p 3180 N94-29508
Analysis of pressureless densification of ceramic matrix composites p 3216 N94-29766
Interface engineering in alumina fiber/glass composites p 3182 N94-29852
Transient thermal fatigue of ceramic composites
p 3216 N94-29874
Fracture process zone of brittle composites
p 3182 N94-29876
Micromechanics of the dynamic response of ceramics and ceramic composites p 3217 N94-29975
Damage analysis and mechanical response of as-received and heat-treated Nicalon/CAS-2 glass-ceramic matrix composites p 3219 N94-30259
A review of mechanical test methods for ceramic matrix composites
[PB94-147576] p 3184 N94-30524
Effect of fiber coating on mechanical properties of Nicalon fibers and Nicalon-fiber/SiC matrix composites
[DE94-005477] p 3185 N94-30593
Microwave assisted chemical vapor infiltration
[DE94-005005] p 3185 N94-30771
A class of inclusion problems for the strengthening of brittle and ductile composites p 3186 N94-30959

CERAMICS
Adhesion of electrolessly deposited Ni(P) on alumina ceramic
[ETN-94-95358] p 3212 N94-28539
Alumina ceramic: A cost effective replacement for titanium in deep submergence pressure housings
[AD-A275640] p 3212 N94-28641
Superplasticity in fine-grained ceramics
[AD-A275461] p 3212 N94-28733
Nonaqueous slip casting of YBa2Cu3O(7-x) superconductive ceramics
[NASA-CR-4575] p 3512 N94-29101
Effect of surface condition on strength and fatigue behavior of alumina ceramic
[AD-A275053] p 3214 N94-29133
Dynamic response of ceramics
[AD-A275396] p 3214 N94-29203
Advanced microfabrication technologies for microspacecraft p 3171 N94-29782
Inorganic polymer-derived ceramic membranes
[DE94-000082] p 3216 N94-29830
Transient thermal fatigue of ceramic composites
p 3216 N94-29874
Micromechanics of the dynamic response of ceramics and ceramic composites p 3217 N94-29975
The bases for the development of high-temperature integrated SQUID-systems
[DE94-607901] p 3267 N94-30073
Synthesis and characterization of advanced materials for Navy applications p 3223 N94-30474
Normal state resistivity of MBa2Cu3O(7-x) ceramics
[DE94-608456] p 3220 N94-30745
Design of a variable-conductance vacuum insulation
[DE94-000270] p 3268 N94-30819
Material properties and fracture mechanics in relation to ceramic machining
[DE94-006623] p 3221 N94-30829

CEREBRAL CORTEX
Synaptogenesis, selective stabilization, and free association
[AD-A275250] p 3392 N94-29431

CEREBRUM
Remote control of transcranial Doppler (TCD) probe during centrifuge exposures up to 9 +Gz
[AD-A275253] p 3400 N94-29029

CERMETS
Effect of microstructure on the strength and fracture energy of bimaterial interfaces
[AD-A274987] p 3178 N94-29126

CERTIFICATION
Testing laboratories as notified bodies
[PB94-132396] p 3160 N94-28413
Ada run time system certification for avionics applications p 3150 N94-29332

CESIUM
Time and frequency technology at NIST
p 3468 N94-30641
Hydrogen masers and cesium fountains at NRC
p 3297 N94-30664

CESIUM IODIDES
Characteristics of secondary electron emission from CsI induced by x rays with energies up to 100 keV
[DE94-608422] p 3395 N94-30185

CESIUM ISOTOPES
Two-way satellite time transfer: Overview and recent developments p 3469 N94-30646

CESIUM 137
Caesium-137 in a boreal forest ecosystem: Aspects on the long-term behavior
[PB94-137809] p 3347 N94-29158

CF-700 ENGINE
Radar jet engine health monitoring project
[ASSGI-301] p 3153 N94-30130

CHANGE DETECTION
Amazonia: Remote sensing test site and survey
p 3327 N94-28935
Proceedings of the 3rd International Symposium: JERS-1 and Remote Sensing in the Future
[JTN-94-80597] p 3329 N94-29217

CHANNEL FLOW
Wall pressure events from the direct numerical simulation of a turbulent wall-bounded flow
[AD-A275890] p 3271 N94-28778
Glaciohydrologic and glaciohydraulic effects on runoff and sediment yield in glacierized basins
[AD-A275134] p 3361 N94-29286

CHANNELS
Search for the top quark in the electron-electron and electron-muon channels at D0
[DE94-006174] p 3492 N94-30779

CHANNELS (DATA TRANSMISSION)
Preliminary analysis of Asynchronous Transfer Mode (ATM) over microwave channels
[AD-A275214] p 3243 N94-29069
High throughput network for multiprocessor interconnections
[VTT-PUBS-147] p 3245 N94-29468
Extended horizon lifting for periodic gain adjustment in control systems, and for equalization of communication channels
[NASA-CASE-NPO-19166-1-CU] p 3246 N94-29495
Decoder synchronization for deep space missions
p 3250 N94-29664

CHAOS
Research activities of Martin C. Casdagli at SFI September 1989--May 1991
[DE94-005655] p 3463 N94-28548
Controlling chaos in plasma filled diodes
[AD-A275525] p 3504 N94-28686
The lectures in complex systems, volume 5
[AD-A275458] p 3466 N94-28807
Existence of quantum characteristic exponents
[PB94-138161] p 3523 N94-29146
Boundary layer coherent structures
[AD-A275007] p 3272 N94-29195
Effects of diffusion and inertia on chaotic mixing: A computational and experimental study
p 3488 N94-29903
Significant figures and Lyapunov exponents in chaos and constrained divergence of chaotic orbits
p 3467 N94-29910
A semiclassical study of quantum maps
p 3524 N94-29987
On chaos in quantum mechanics: The two meanings of sensitive dependence
[DE94-608069] p 3524 N94-30086
Superdiffusion
[DE94-002333] p 3492 N94-30834

CHAPMAN-ENSKOG THEORY
Large eddy simulations using lattice Boltzmann algorithms
[DE94-005666] p 3270 N94-28549

CHARACTER RECOGNITION
Encoding technique for automated guided vehicle POSE recovery in a structured environment
p 3144 N94-30286

CHARACTERIZATION
Synthesis and characterization of novel ternary and quaternary reduced molybdenum oxides
[DE94-005563] p 3510 N94-28529
A characterization of graphs with interval two-step graphs
[AD-A275652] p 3451 N94-28651
Seafloor characterization using texture
[AD-A275399] p 3377 N94-29204
Glass-ceramic matrix composites
[REPT-932-430-112] p 3179 N94-29413
Radioelectric characterization of materials at 1000 C
[REPT-932-430-104] p 3245 N94-29440

CHARGE CARRIERS
Carrier collection and scattering in quantum well and superlattice devices
[AD-A275443] p 3512 N94-28880
Band structure of superlattice with (delta)-like potential
[DE94-608108] p 3516 N94-30072

CHARGE COUPLED DEVICES
Response of GaAs charge storage devices to transient ionizing radiation
[DE94-005273] p 3510 N94-28484
Monolithic in-based III-V compound semiconductor focal plane array cell with single stage CCD output
[NASA-CASE-NPO-18978-1-CU] p 3265 N94-29488
Lasercom system architecture with reduced complexity
[NASA-CASE-NPO-19069-1-CU] p 3293 N94-29493
Calibration of charge coupled device digital cameras
[ISBN-0-315-85539-8] p 3290 N94-30232
Sensing the gas metal arc welding process
p 3314 N94-30444

CHARGE EXCHANGE
Wave generation by contaminant ions near a large spacecraft
[NASA-CR-195797] p 3169 N94-29917

CHARGE TRANSFER
Crystal structure of La(2-x)Ba(x)CuO4
[DE94-707688] p 3511 N94-28750
Remote pumping of solid state lasers with nuclear driven fluorescers
[DE94-004846] p 3296 N94-30614
Rotator phases in narrow-gap semiconductors
[DE94-005472] p 3521 N94-30897

CHARGED PARTICLES
Energy losses of fast charged particles in thin silicon detectors
[DE94-606065] p 3483 N94-28552
Solution of charged particle transport equation by Monte-Carlo method in the BRANDZ code system
[DE94-606270] p 3484 N94-28614
The proper field of charges and gauge-invariant variables in electrodynamics
[DE94-606405] p 3523 N94-28751
Weak decays of charged K-mesons and charm particles
[PB94-138062] p 3486 N94-29143
Some remarks about pseudo-Hamiltonian
[DE94-003273] p 3487 N94-29700
A Tevatron collider beauty factory
[DE94-004879] p 3488 N94-29930
Fast precise algorithm for simulation of ionization energy losses
[DE94-608010] p 3421 N94-30080
On relativity principle violation in local measurements of spin precession of moving particles
[DE94-608067] p 3489 N94-30085
Superdiffusion
[DE94-002333] p 3492 N94-30834
CHARM (PARTICLE PHYSICS)
Weak decays of charged K-mesons and charm particles
[PB94-138062] p 3486 N94-29143
Charmonium and bottomonium in (-p)p interactions
[DE94-006173] p 3493 N94-30886
CHARON
The Pluto fast flyby mission: Completing the reconnaissance of the solar system
p 3235 N94-29768
CHARPY IMPACT TEST
Single specimen fracture toughness determination procedure using instrumented impact test
[PB94-132040] p 3316 N94-28402
A newly developed snow vehicle (SM100S) for Antarctica. Part 3: Low temperature toughness of the welded joints of the structural steel
p 3364 N94-29983
CHARTS
A model analysis of potential vorticity on isopycnal surfaces for the global ocean
[AD-A275047] p 3377 N94-29164
CHASSIGNITES
Cosmogenic C-14 in Antarctic and non-Antarctic meteorites and lunar samples
[NASA-CR-195795] p 3546 N94-29905
CHASSIS
Acquisition, design modification, assembly, and ground test of NPS Hummingbird remotely piloted helicopter
[AD-A275546] p 3146 N94-28837
A newly developed snow vehicle (SM100S) for Antarctica. Part 3: Low temperature toughness of the welded joints of the structural steel
p 3364 N94-29983
CHEBYSHEV APPROXIMATION
Frequency-domain analysis of nonlinear microwave circuits
[PB94-132024] p 3261 N94-28400
Frequency-domain transfer-function identification using Chebyshev polynomials
[DE94-004777] p 3451 N94-28739
Process modelling for materials preparation experiments
[NASA-CR-195782] p 3175 N94-30242
Sensitivity analysis of the static aeroelastic response of a wing p 3134 N94-30525
CHECKOUT
The MACS-TSA applied in the ISO and SAX spacecraft projects
[PB94-126257] p 3170 N94-30857
CHEMICAL ANALYSIS
Measurement of elemental speciation by liquid chromatography: inductively coupled plasma mass spectrometry (LC-ICP-MS) with the Direct Injection Nebulizer (DIN)
[DE94-005261] p 3187 N94-28483
Harvard ER-2 OH laser-induced fluorescence instrument p 3343 N94-28592
Tropospheric HO2 determination by FAGE
p 3345 N94-28606
Fiscal 1991 geothermal development promotion energy
[DE94-732332] p 3337 N94-28627
Electron microscopy: Metal alloy x ray microanalysis
[REPT-932-600-101] p 3205 N94-29525
Photoelectron diffraction and holography: Some new directions
[DE94-006297] p 3289 N94-30027
Technology 2003: The Fourth National Technology Transfer Conference and Exposition, volume 1
[NASA-CP-3249] p 3555 N94-30440
A modular approach for automated sample preparation and chemical analysis p 3354 N94-30464
Fullerenes as precursors for diamond film growth without hydrogen or oxygen additions
[DE94-004582] p 3519 N94-30718
Method of test for cleanness assessment of metal alloys: The preparation of button specimens by electron beam melting and the characterisation of recovered inclusions
[NPL-DMM(A)-130] p 3210 N94-30796
CHEMICAL BONDS
Development of novel switchable protein surfaces
[AD-A275510] p 3384 N94-28667
Electronic structure and mechanical properties of grain boundaries
[AD-A275198] p 3512 N94-28890
Crosslinking and surface reactions in macromolecules: Spectroscopic FT-IR studies p 3221 N94-30812
CHEMICAL COMPOSITION
Speciation in Water and Soil: A literature review
[PB94-132388] p 3341 N94-28412
ARTI Refrigerant Database
[DE94-004906] p 3230 N94-28563
Effects of pressure on membrane-associated receptors and effector elements
[AD-A275813] p 3384 N94-28829
Method of test for cleanness assessment of metal alloys: The preparation of button specimens by electron beam melting and the characterisation of recovered inclusions
[NPL-DMM(A)-130] p 3210 N94-30796
Chemical composition of insoluble particles in superimposed ice on Storoeya, Svalbard (Sweden)
[CM-82] p 3336 N94-30944
CHEMICAL DEFENSE
Implications of climatic extremes in aircrew NBC operations p 3383 N94-28446
CHEMICAL EFFECTS
Investigations into ultraviolet matrix-assisted laser desorption
[DE94-005265] p 3296 N94-30908
CHEMICAL ENGINEERING
Qualitative vector optimization of a condensate stabilizer process
[PB94-133246] p 3189 N94-28789
CHEMICAL EXPLOSIONS
An emergency response mobile robot for operations in combustible atmospheres
[NASA-CASE-NPO-19020-1-CU] p 3299 N94-29420
XCHEM-1D: A heat transfer/chemical kinetics computer program for multilayered reactive materials
[DE94-005072] p 3226 N94-30615
CHEMICAL PROPERTIES
Gas phase thermochemistry of organogermanium compounds
[DE94-004885] p 3187 N94-28561
High temperature arc-track resistant aerospace insulation p 3167 N94-28716
A 3M high temperature dielectric film
p 3167 N94-28717
CHEMICAL REACTIONS
Low energy ion-molecule reactions and chemiionization kinetics
[DE94-005414] p 3481 N94-28491
The generalized spin-boson model for electron-transfer reactions involving two harmonic potentials with a different force constant
[DE94-005470] p 3482 N94-28509
Ozone production at a rural site in Georgia during the summer 1992 SOS campaign
[DE94-003989] p 3342 N94-28523
Peroxy radical measurements with NCAR's chemical amplifier p 3345 N94-28603
The radical amplifier p 3345 N94-28604
Tropospheric HO2 determination by FAGE
p 3345 N94-28606
Formation and chemical reactivity of carbon fibers prepared by defluorination of graphite fluoride
[NASA-TM-106398] p 3174 N94-28747
Chemical dynamics studies of reactions in energetic materials
[AD-A275607] p 3224 N94-28769
Calculation of propulsive nozzle flowfields in multidiffusing chemically reacting environments
[NASA-TM-106532] p 3271 N94-28835
The effects of molecular orientation geometry and surface anisotropy upon etching
[AD-A275154] p 3486 N94-29032
Tris(trimethylsily)arsine and lithium bis(trimethylsily)arsenide
[AD-A275075] p 3189 N94-29140
Dynamic response of ceramics
[AD-A275396] p 3214 N94-29203
The maximum entropy approach applied to energy exchange, chemical reactions and ionisation in the direct simulation Monte Carlo method for rarefied hypersonic flows
[IC-AERO-93-01] p 3524 N94-29481
Thermodynamic analysis of chemical compatibility of several compounds with Fe-Cr-Al alloys
[NASA-CR-191166] p 3181 N94-29684
Brief summary of accomplishments since our DOE-sponsored radon project commenced
[DE94-004643] p 3348 N94-29926
Reactions of metal ions and their clusters in the gas phase using laser ionization: Fourier transform mass spectrometry
[DE94-006208] p 3207 N94-30024
Application of semiclassical methods to reaction rate theory
[DE94-007041] p 3199 N94-30266
Analysis of infrared radiation heating process considering chemical reaction of material to be heated
[DE94-744116] p 3199 N94-30267
XCHEM-1D: A heat transfer/chemical kinetics computer program for multilayered reactive materials
[DE94-005072] p 3226 N94-30615
Lattice gas simulations of replicating domains
[DE94-005008] p 3200 N94-30748
Theory for electron-transfer reactions involving two Marcus surfaces with a different force constant
[DE94-005925] p 3493 N94-30874
Reinterpretation of rate data for the reaction of ClF and F2
[DE94-005819] p 3200 N94-30880
Theory for electron-transfer reactions in a three-component system: The degenerate regime
[DE94-005919] p 3493 N94-30903
CHEMICAL REACTORS
Plasma enhanced chemical vapor deposition of ZrO2 thin films
[DE94-006031] p 3218 N94-30104
Microwave assisted chemical vapor infiltration
[DE94-005005] p 3185 N94-30771
CHEMICAL VAPOR INFILTRATION
3-D braided, continuous fiber ceramic composites produced by chemical vapor infiltration
[AD-A275192] p 3178 N94-29024
Properties of chemical vapor infiltration diamond deposited in a diamond powder matrix
[DE94-005429] p 3220 N94-30591
Microwave assisted chemical vapor infiltration
[DE94-005005] p 3185 N94-30771
CHEMICAL WARFARE
Development of a new chemical warfare agent protective material p 3381 N94-28432
CHEMILUMINESCENCE
Peroxy radical measurements with NCAR's chemical amplifier p 3345 N94-28603
CHEMISORPTION
The effects of molecular orientation geometry and surface anisotropy upon etching
[AD-A275154] p 3486 N94-29032
Halogen chemisorption on silver(111): Scanning tunneling microscopy of coadsorbed halogen atoms
[AD-A275219] p 3486 N94-29060
Surface chemistry of boron-doped SiO2 CVD: Enhanced uptake of tetraethyl orthosilicate by hydroxyl groups bonded to boron
[DE94-005428] p 3221 N94-30896
CHINA
Study of dynamic characteristics of a monsoon circulation tube
[AD-A275238] p 3370 N94-29394
CHIPS (ELECTRONICS)
Construction of a connectionist network supercomputer
[AD-A275765] p 3405 N94-28764
Design and packaging of fault tolerant optoelectronic multiprocessor computing system
[AD-A275896] p 3405 N94-28798
Digitally programmable composite operational amplifier applications
[AD-A275081] p 3262 N94-28842
NSC 800, 8-bit CMOS microprocessor
[NASA-CR-195736] p 3405 N94-28845
A combined electron beam/optical lithography process step for the fabrication of sub-half-micron-gate-length MMIC chips p 3240 N94-30445
CHIRAL DYNAMICS
One-loop QCD mass effects in the production of polarized bottom and top quarks
[PB94-138104] p 3487 N94-29145
CHLORIDES
Anodization of copper in chloride media
[AD-A275565] p 3202 N94-28793
X ray crystal structures of ((Me3SiCH2)2InCl)2 and ((Me3SiCH2)InCl2)
[AD-A275074] p 3513 N94-29155
CHLORINATION
Non-aqueous cleaning solvent substitution
p 3354 N94-30466

CHLORINE
Convective flow effects on protein crystal growth
[NASA-CR-195785] p 3515 N94-30015
CHLORINE COMPOUNDS
Preparation, characterization, and facile thermolysis of (X2GaP(SiMe3)2) (X = Br, I) and (Cl3Ga2P)n; new precursors to nanocrystalline gallium phosphide
[AD-A275019] p 3513 N94-29130
Non-aqueous cleaning solvent substitution
[DE94-005339] p 3219 N94-30245
CHLORINE FLUORIDES
Reinterpretation of rate data for the reaction of ClF and F2
[DE94-005819] p 3200 N94-30880
CHLOROFLUOROCARBONS
Technology transfer initiatives
[NASA-CR-195151] p 3537 N94-29410
Materials compatibility and lubricants research on CFC-refrigerant substitutes
[DE94-004905] p 3220 N94-30692
CHLOROFLUOROMETHANE
Journal of NIRE, Vol. 2, No. 2
[JTN-94-80552] p 3187 N94-28675
Properties of adsorbents for collection and analysis of trace amount of chlorofluorocarbons in air
p 3188 N94-28680
CHLOROPRENE RESINS
Insulative properties of two thermo-metal neoprenes
[AD-A275209] p 3401 N94-29302
CHORDS (GEOMETRY)
Minimum fill-in for chordal bipartite graphs
[RUU-CS-93-11] p 3458 N94-30404
CHROMATES
Crystallization of silver chromate from ethanol via salt metathesis reactions of solubilized precursors
[AD-A275178] p 3189 N94-29058
CHROMIUM
An improved plating process p 3223 N94-30451
CHROMIUM ALLOYS
Thick thermal barrier coatings for diesel components
[NASA-CR-187111] p 3537 N94-29350
Thermodynamic analysis of chemical compatibility of several compounds with Fe-Cr-Al alloys
[NASA-CR-191166] p 3181 N94-29684
Studies on the optimization of deformation processed metal-metal matrix composites
[DE94-006033] p 3185 N94-30704
CHROMIUM CARBIDES
The organometallic chemical vapor deposition of transition metal carbides: The use of homoleptic alkyls
[DE94-005577] p 3206 N94-30007
CHROMOSPHERE
Surface differential rotation in a sample of cool dwarf stars p 3545 N94-29827
CIRCADIAN RHYTHMS
Strategies to sustain and enhance performance in stressful environments
[AD-A275223] p 3398 N94-29027
Circadian countermeasures for shiftworkers during USMP-2: A report to mission management
[NASA-CR-195260] p 3402 N94-30188
CIRCLES (GEOMETRY)
Treewidth of circle graphs
[RUU-CS-93-12] p 3458 N94-30405
CIRCUIT BOARDS
Screening of flexible cables by nonlinear resistance measurements
[AD-A275193] p 3264 N94-29289
Controlled thermal expansion printed wiring boards based on liquid crystal polymer dielectrics
[NASA-CR-189338] p 3287 N94-29400
Logistics for the implementation of lead-free solders on electronic assemblies
[DE94-004800] p 3206 N94-29936
CIRCUIT RELIABILITY
Self-stressing test structures used for high-frequency electromigration
[DE94-006142] p 3267 N94-30368
CIRCUITS
Cryogenic probe station for use in automated microwave and noise figure measurements
[NASA-TM-106560] p 3286 N94-29000
Guidance on eliminating interference from sensitive electrical circuits
[PB94-139300] p 3268 N94-30784
CIRCULAR CYLINDERS
Numerical and experimental investigation of the bending response of thin-walled composite cylinders
[NASA-CR-195730] p 3317 N94-28801
Flow past a circular cylinder with a permeable wake splitter plate p 3275 N94-29764
CIRCULAR PLATES
Further investigation of curve veering phenomena
p 3460 N94-30515
CIRCULAR TUBES
Mutual similarity of developing laminar flows with secondary streams in ducts: Curved pipe flow and orthogonal rotating pipe flow p 3129 N94-28989
CIRCULATION
Strategies to sustain and enhance performance in stressful environments
[AD-A275223] p 3398 N94-29027
CIRCULATORY SYSTEM
Effects of make-up on the heat transfer from the head in hyperthermic conditions p 3394 N94-29864
CITIES
Exploitation of stereophotogrammetrically derived 3-D wireframe models to produce urban simulations
[AD-A275459] p 3325 N94-28808
Cities for tomorrow: Directions for change
[PB94-136850] p 3537 N94-29168
A laboratory simulation of urban heat-island-induced circulation in a stratified environment
p 3367 N94-30921
CIVIL AVIATION
Effects of repair on structural integrity
[AD-A275756] p 3145 N94-28647
How to control the increase in the complexity of civil aircraft on-board systems p 3150 N94-29316
Ada run time system certification for avionics applications p 3150 N94-29332
CLADDING
A novel approach to the fabrication of SiC structures of arbitrary shape
[AD-A275475] p 3214 N94-29073
CLAMPS
System for the installation and replacement of components in hostile environments
[NASA-CASE-LEW-14906-1-SB] p 3300 N94-29427
CLASSICAL MECHANICS
A semiclassical study of quantum maps
p 3524 N94-29987
CLASSIFICATIONS
A space-based classification system for RF transients
[DE94-003933] p 3240 N94-28522
Defense Technical Information Center cataloging guidelines
[AD-A275100] p 3529 N94-28911
Copepods collected along 33.5 deg E longitude of the Antarctic Ocean in the 1976 summer
p 3358 N94-29082
Seafloor characterization using texture
[AD-A275399] p 3377 N94-29204
CLASSIFIERS
A space-based classification system for RF transients
[DE94-003933] p 3240 N94-28522
CLEAN ROOMS
The 1992 report on the next generation ultra clean technology for advanced microfabrication
[DE94-744171] p 3157 N94-30268
CLEANERS
Regenerating using aqueous cleaners with ozone and electrolysis p 3240 N94-30468
CLEANING
Surface energy changes produced by ultraviolet-ozone irradiation of poly(methylmethacrylate), polycarbone and polytetrafluoroethylene
[NASA-TM-106460] p 3213 N94-28922
Practical applications of plasma surface modification
[DE94-004892] p 3349 N94-29932
Non-aqueous cleaning solvent substitution
[DE94-005339] p 3219 N94-30245
The 1992 report on the next generation ultra clean technology for advanced microfabrication
[DE94-744171] p 3157 N94-30268
Non-aqueous cleaning solvent substitution
p 3354 N94-30466
Supersonic gas-liquid cleaning system
p 3240 N94-30467
Regenerating using aqueous cleaners with ozone and electrolysis p 3240 N94-30468
CLEANLINESS
Supersonic gas-liquid cleaning system
p 3240 N94-30467
CLEARANCES
Influence of clearance and rake angles on the cutting force of rock p 3368 N94-29520
CLIMATE
Prediction of survival times on land in a cold climate
p 3379 N94-28423
Aeromedical support for casualties in extremely hot climates p 3382 N94-28443
Work conditions assessment in pilots and ground personnel under high weather temperatures
p 3382 N94-28444
Thermal strain generated by an enhanced anti-G protection system in a hot climate p 3383 N94-28445
Implications of climatic extremes in aircrew NBC operations p 3383 N94-28446
Global atmospheric and ocean modeling on the connection machine
[DE94-003930] p 3342 N94-28521
Role of satellite observations of sea-surface temperature in the detection of global change
[PB94-138120] p 3329 N94-29107
On the annual cycle of the tropical Pacific atmosphere and ocean p 3371 N94-29763
Interannual-decadal variability in tropical climate systems: Stable isotope records and general circulation model experiments p 3373 N94-29962
Land surface interaction p 3350 N94-30621
Linkages between terrestrial ecosystems and the atmosphere p 3351 N94-30624
A toy model of sea ice growth p 3351 N94-30626
Cryosphere and climate p 3352 N94-30632
Modeling Earth system changes of the past
p 3353 N94-30635
Models of atmosphere-ecosystem-hydrology interactions: Approaches and testing
p 3353 N94-30636
Evaluating models of climate and forest vegetation
p 3353 N94-30637
CLIMATE CHANGE
Global change research: Summaries of research in FY 1993
[DE94-003150] p 3341 N94-28473
Survey on effects of petroleum substitution energy utilization on the global environment
[DE94-732339] p 3346 N94-28630
Role of satellite observations of sea-surface temperature in the detection of global change
[PB94-138120] p 3329 N94-29107
On the effect of emissions from aircraft engines on the state of the atmosphere p 3189 N94-29247
Second Japan-U.S. Workshop on Global Change: Environmental Response Technologies for Global Change (Mitigation and Adaptation) p 3354 N94-29522
GCM studies of the influence of vegetation on the general circulation: The role of albedo in modulating climate change p 3348 N94-29749
Comparison of Savannah River Site's meteorological databases
[DE94-001751] p 3373 N94-29817
Impact of biomass burning on the atmosphere
[DE94-004333] p 3349 N94-29954
Interannual-decadal variability in tropical climate systems: Stable isotope records and general circulation model experiments p 3373 N94-29962
On interannual variability and climate change in the North Pacific p 3374 N94-29963
Global patterns of cloud optical thickness variation with temperature and the implications for climate change
p 3374 N94-29972
PCCM2: A GCM adapted for scalable parallel computers
[DE94-005113] p 3350 N94-30116
Modeling the Earth System, volume 3
[NASA-CR-194256] p 3350 N94-30616
The role of sea ice dynamics in global climate change
p 3350 N94-30620
A toy model of sea ice growth p 3351 N94-30626
Cryosphere and climate p 3352 N94-30632
The challenge of identifying greenhouse gas-induced climatic change p 3352 N94-30634
Modeling Earth system changes of the past
p 3353 N94-30635
CLIMATOLOGY
Global change research: Summaries of research in FY 1993
[DE94-003150] p 3341 N94-28473
Global atmospheric and ocean modeling on the connection machine
[DE94-003930] p 3342 N94-28521
Capabilities, products, and services of USAFETAC (USAF Environmental Technical Applications Center)
[AD-A275654] p 3368 N94-28652
Studies of marine aerosols and their evolution in the eastern North Atlantic
[AD-A275011] p 3377 N94-29128
Sensitivity and feedbacks associated with vegetation-related land surface parameters in a general circulation model p 3348 N94-29800
Interannual temperature variability and cyclone frequency over Eastern Canada and the New England States. A case study: Winter seasons 1931-1932 to 1984-1985
[ISBN-0-315-74841-9] p 3373 N94-29908
On interannual variability and climate change in the North Pacific p 3374 N94-29963
PCCM2: A GCM adapted for scalable parallel computers
[DE94-005113] p 3350 N94-30116
Modeling the Earth System, volume 3
[NASA-CR-194256] p 3350 N94-30616

Towards coupled physical-biogeochemical models of the ocean carbon cycle p 3350 N94-30618
The role of sea ice dynamics in global climate change p 3350 N94-30620
Land surface interaction p 3350 N94-30621
A toy model for estimating N2O emissions from natural soils p 3351 N94-30627
Models of atmosphere-ecosystem-hydrology interactions: Approaches and testing p 3353 N94-30636
Comprehensive system models: Strategies for evaluation p 3353 N94-30638

CLIMBING FLIGHT
The effect of various metallurgical parameters on the flow and fracture behavior of polycrystalline NiAl near the brittle-to-ductile transition
[NASA-TM-106534] p 3205 N94-29758

CLINICAL MEDICINE
Clinical investigation program
[AD-A275025] p 3391 N94-29116
Evaluation of monitoring audiometry in the United States Air Force Hearing Conservation Program
[AD-A275309] p 3391 N94-29211

CLOCKS
Time and frequency technology at NIST p 3468 N94-30641
European PTTI report p 3468 N94-30642
Loran-C time management p 3144 N94-30644
Report on NATO PTTI p 3469 N94-30645
Cascaded clocks measurement and simulation findings p 3469 N94-30649
Time and position accuracy using codeless GPS p 3144 N94-30650
Remote clocks linked by a fully calibrated two-way timing link p 3471 N94-30659
Hydrogen masers and cesium fountains at NRC p 3297 N94-30664
Time maintenance system for the BMDO MSX spacecraft p 3171 N94-30672
Ground control system for the midcourse space experiment UTC clock p 3474 N94-30674
Hydrogen maser clocks in space for solid-Earth research and time-transfer applications: Experiment overview and evaluation of Russian miniature sapphire loaded cavity p 3474 N94-30676
Using GLONASS signal for clock synchronization p 3475 N94-30680
A look into the crystal ball: The next 25 years p 3475 N94-30681
The future of time and frequency dissemination p 3476 N94-30684

CLOSED ECOLOGICAL SYSTEMS
Electrochemical incineration of wastes
[NASA-CR-195262] p 3198 N94-29938
Publications of the NASA Controlled Ecological Life Support System (CELSS) program 1989-1992
[NASA-CR-4603] p 3401 N94-30122

CLOSURE LAW
An alternative assessment of second-order closure models in turbulent shear flows
[NASA-CR-194881] p 3272 N94-29381

CLOTHING
Simulation of the effect of wind on clothing by measurements and calculations
[PB94-132289] p 3399 N94-28406
Deterioration of manual performance in cold and windy climates p 3381 N94-28434

CLOUD COVER
The appearance of the Sun and Moon seen through clouds
[AD-A275338] p 3551 N94-29212
Site comparison for optical visibility statistics in southern California p 3247 N94-29617
Radiation transport in cloudy and aerosol loaded atmospheres p 3366 N94-30805

CLOUD GLACIATION
Remote sensor observations during WISP91: The use of microwave radiometers, RASS, and lidar ceilometers for detection of aircraft icing conditions
[PB94-142106] p 3136 N94-30890

CLOUD HEIGHT INDICATORS
Remote sensor observations during WISP91: The use of microwave radiometers, RASS, and lidar ceilometers for detection of aircraft icing conditions
[PB94-142106] p 3136 N94-30890

CLOUD PHYSICS
Studies of marine aerosols and their evolution in the eastern North Atlantic
[AD-A275011] p 3377 N94-29128
The incorporation and initialization of cloud water/ice in an operational forecast model p 3373 N94-29814
Correlation studies of Pioneer Venus imagery obtained from PV experiments with near IR imagery obtained from ground-based observations during Venus inferior conjunction
[NASA-CR-195772] p 3550 N94-29892
Cloud and aerosol characterization for the ARM central facility: Multiple remote sensor techniques development
[DE94-003523] p 3365 N94-30608

CLOUDS
The effects of man-made smokes and battlefield-induced smokes on the propagation of electromagnetic radiation p 3258 N94-30505

CLOUDS (METEOROLOGY)
Numerical simulations of a mountain thunderstorm. A comparison with Doppler radar observations
[AD-A275296] p 3369 N94-28873
Studies of marine aerosols and their evolution in the eastern North Atlantic
[AD-A275011] p 3377 N94-29128
Global patterns of cloud optical thickness variation with temperature and the implications for climate change p 3374 N94-29972
Cloud and aerosol characterization for the ARM central facility: Multiple remote sensor techniques development
[DE94-003523] p 3365 N94-30608

CLUTTER
Radar returns from a low-flying target over a rough sea surface under multipath and clutter conditions p 3253 N94-29882
Infrared polarization signatures p 3258 N94-30506
A hybrid electromagnetic-statistical approach for characterizing MMW scattering by terrain p 3259 N94-30510
Radar cross sections of ground clutter at 95 GHz for summer and fall conditions p 3259 N94-30512

CMOS
Digitally programmable composite operational amplifier applications
[AD-A275081] p 3262 N94-28842
NSC 800, 8-bit CMOS microprocessor
[NASA-CR-195736] p 3405 N94-28845
Nonvolatile programmable neural network synaptic array
[NASA-CASE-NPO-18578-1-CU] p 3265 N94-29426
Single event upset susceptibilities of latchup immune CMOS process programmable gate arrays p 3495 N94-30214
Multiple single event upsets in CMOS static rams p 3496 N94-30215
Determination of cosmic ray latchup rate in CMOS devices p 3497 N94-30222
Self-stressing test structures used for high-frequency electromigration
[DE94-006142] p 3267 N94-30368
A high rate, low noise, x ray silicon strip detector system
[DE94-004557] p 3268 N94-30717

CNOIDAL WAVES
Dissipation in Hamiltonian systems: Decaying cnoidal waves
[MEMO-1151] p 3460 N94-30738

COAL
Development of the integrated environmental control model: Performance models of selective catalytic reduction NO(x) control systems
[DE94-002151] p 3341 N94-28465
Proceedings of the Joint Contractors Meeting: FE/EE Advanced Turbine Systems Conference FE Fuel Cells and Coal-Fired Heat Engines Conference
[DE93-011308] p 3336 N94-28499
Journal of NIRE, Vol. 2, No. 2
[JTN-94-80552] p 3187 N94-28675
Molecular structure of coal studied by solvent extraction p 3187 N94-28676
Researches on bioconversion of coal into liquid product p 3187 N94-28677
Structural changes during carbonization and oxidation of coal p 3187 N94-28678
Methanol-mediated continuous extraction of phenolic compounds from coal liquid p 3188 N94-28679
Joint research activities with CCMRI (China) p 3240 N94-29521
Corrosion performance of materials for advanced combustion systems
[DE94-006726] p 3207 N94-30057
An electromagnetic noncontacting sensor for thickness measurement in a dispersive medium
[AIAA PAPER 94-1200-CP] p 3443 N94-30551

COAL DERIVED GASES
Biological conversion of synthesis gas
[DE94-005815] p 3340 N94-30879

COAL DERIVED LIQUIDS
Journal of NIRE, Vol. 2, No. 2
[JTN-94-80552] p 3187 N94-28675
Methanol-mediated continuous extraction of phenolic compounds from coal liquid p 3188 N94-28679

COAL LIQUEFACTION
Journal of NIRE, Vol. 2, No. 2
[JTN-94-80552] p 3187 N94-28675
Researches on bioconversion of coal into liquid product p 3187 N94-28677
Methanol-mediated continuous extraction of phenolic compounds from coal liquid p 3188 N94-28679

COASTAL CURRENTS
Objective analysis of a coastal ocean eddy using satellite AVHRR and in situ hydrographic data
[AD-A275715] p 3376 N94-28642
Statistical analysis of a satellite imagery time series: Implications for the study of coastal and estuarine circulation p 3335 N94-30919

COASTAL WATER
Bulletin of National Research Institute of Fisheries Engineering, No. 13
[JTN-94-80596] p 3233 N94-29701
Development of a simple current meter using solution p 3233 N94-29702
Statistical analysis of a satellite imagery time series: Implications for the study of coastal and estuarine circulation p 3335 N94-30919

COASTS
The undrained shear strength characteristics of undisturbed soil from fishing port areas p 3234 N94-29704

COATING
Electrodeposition of bismuth alloys by the controlled potential method
[DE94-605318] p 3212 N94-28550
Dual cure low-VOC coating process, phase 3
[DE94-003202] p 3221 N94-30826

COATINGS
Effect of fiber coating on mechanical properties of Nicalon fibers and Nicalon-fiber/SiC matrix composites
[DE94-005477] p 3185 N94-30593
Nonlinear absorption in high reflector multilayers
[DE94-005818] p 3295 N94-30598
Characterization of defect geometries in multilayer optical coatings
[DE94-005820] p 3501 N94-30599

COBALT
Study on the formation of ultrafine particles of Sm-Co intermetallic compounds using RF thermal plasma p 3211 N94-29516

COBALT ALLOYS
Performance and durability of high emittance heat receiver surfaces for solar dynamic power systems
[NASA-TM-106549] p 3172 N94-28834
Cyclic axial-torsional deformation behavior of a cobalt-base superalloy
[NASA-TM-106372] p 3203 N94-28921
Thick thermal barrier coatings for diesel components
[NASA-CR-187111] p 3537 N94-29350
Giant magnetoresistance and microstructural characteristics of epitaxial Fe-Ag and Co-Ag granular thin films
[DE94-006287] p 3519 N94-30707

COBALT COMPOUNDS
Study on the formation of ultrafine particles of Sm-Co intermetallic compounds using RF thermal plasma p 3211 N94-29516

COBALT OXIDES
Transient studies of low temperature catalysts for methane conversion
[DE94-005767] p 3200 N94-30877

COCKPITS
Thermal strain generated by an enhanced anti-G protection system in a hot climate p 3383 N94-28445
KC-135 cockpit modernization study and crew reduction feasibility demonstration
[AD-A275230] p 3146 N94-29391

CODE DIVISION MULTIPLE ACCESS
The bootstrapped algorithm: A fast algorithm for blind signal separation
[AD-A275759] p 3408 N94-28760

CODERS
Multi-speed multi-phase resolver converter
[NASA-CASE-MFS-28855-1] p 3264 N94-29372
Non-orthogonal subband/transform coder
[NASA-CASE-LEW-15310-1] p 3246 N94-29589

CODING
Video transmission on ATM networks
[NASA-CR-195124] p 3244 N94-29106
Modifications of the Griesmer bound p 3247 N94-29618
Integer cosine transform for image compression p 3247 N94-29619
Convolutional encoding of self-dual codes p 3250 N94-29662
Encoding technique for automated guided vehicle POSE recovery in a structured environment p 3144 N94-30286
Low frame rate video coding for small bandwidth realtime multimedia tele-education systems
[PB94-125531] p 3256 N94-30398
Fast and efficient variable-to-fixed-length coding algorithm
[PB94-125465] p 3424 N94-30400

Two-way satellite time transfer: Overview and recent developments p 3469 N94-30646

COGENERATION

Report of feasibility study on international-cooperation in high efficient energy conversion technology [DE94-732340] p 3337 N94-28631

COGNITION

Toward a model of expert knowledge structure and their role in cognitive task performance [AD-A275641] p 3529 N94-28645

Key cognitive issues in the design of electronic displays of instrument approach procedure charts [AD-A275647] p 3399 N94-28649

Temporal and qualitative decomposition of plausible reasoning [AD-A275073] p 3398 N94-29154

COGNITIVE PSYCHOLOGY

Key cognitive issues in the design of electronic displays of instrument approach procedure charts [AD-A275647] p 3399 N94-28649

Designing for performance: A cognitive systems engineering approach to modifying an AWACS human computer interface [AD-A275187] p 3399 N94-28861

COHERENT LIGHT

Linac Coherent Light Source (LCLS) at 2-4 nm using the SLAC linac [DE94-005235] p 3292 N94-28481

COHERENT RADAR

RL/ERCT automated swept-angle bistatic measurement system [AD-A275763] p 3241 N94-28763

COHERENT RADIATION

Enhanced coherence x ray laser experiments and simulations [DE94-005367] p 3295 N94-30060

COLD FLOW TESTS

An actively cooled floating element skin friction balance for direct measurement in high enthalpy supersonic flows p 3289 N94-29824

COLD PLASMAS

Coulomb field effect on plasma focusing and wake field acceleration [DE94-004937] p 3504 N94-28564

COLD SURFACES

On the temperature distribution near a cold surface [AD-A275162] p 3332 N94-29288

COLD TOLERANCE

Medical support for British operations in the Antarctic p 3379 N94-28421

Prediction of survival times on land in a cold climate p 3379 N94-28423

Fuelling shivering in humans during cold water immersion p 3379 N94-28426

Biochemical enhancement of cold tolerance p 3380 N94-28427

The potential of new textiles in improving survival prospects p 3380 N94-28430

Deterioration of manual performance in cold and windy climates p 3381 N94-28434

COLD WATER

Effect of seasickness on aircrew student survivor ability after ditching in cold water p 3379 N94-28425

Advanced integrated cold protection for aircrew p 3381 N94-28436

Emergency underwater breathing aids for helicopter passengers and crew p 3381 N94-28437

A comparison of four methods of rewarming individuals cooled by immersion in cold water p 3382 N94-28442

COLD WEATHER

Deterioration of manual performance in cold and windy climates p 3381 N94-28434

Effectiveness of protection clothing for cold weather conditions after ejection over sea: A case report p 3381 N94-28435

Thermoregulation in the extreme cold environment p 3381 N94-28438

Physiological investigations of the isolated rat's liver in hypothermia and hypoxia and their relevance in aircraft incidents above the sea p 3382 N94-28439

Rewarming methodologies in the field p 3382 N94-28441

COLD WEATHER TESTS

Simulation of the effect of wind on clothing by measurements and calculations [PB94-132289] p 3399 N94-28406

COLD WORKING

Cold expansion and interference for extending the fatigue life of multi-layer metal joints [AD-A274962] p 3318 N94-29091

A comparison of the evolution of cold and hot deformation microstructures and textures in fcc metals [DE94-005103] p 3210 N94-30777

COLLAGENS

Controlling the material properties of in vitro collagen through directed orientation and cross-linking of fibrils p 3221 N94-30797

COLLISION AVOIDANCE

Collision avoidance and control of multiple revolute manipulators p 3302 N94-29884

An optimal obstacle avoidance path planning algorithm for the Excalibur robot p 3306 N94-30287

COLLISIONAL PLASMAS

Conceptual study of moderately coupled plasmas and experimental comparison of laboratory x ray sources [DE94-005828] p 3506 N94-30045

COLLISIONS

Stellar and gas dynamics of interacting ring galaxies p 3548 N94-30340

COLLOIDS

Inorganic polymer-derived ceramic membranes [DE94-000082] p 3216 N94-29830

Nanosize metal alloy particle formation in Ag and Cu sequentially implanted silica [DE94-005592] p 3207 N94-30042

COLOR

Multicolor photometry of barred spiral galaxies p 3541 N94-30270

Seed viability detection using computerized false-color radiographic image enhancement p 3387 N94-30461

A commercialized, continuous flow fiber optic sensor for trichloroethylene and haloforms p 3502 N94-30462

COLOR-MAGNITUDE DIAGRAM

Globular cluster photometry near the turnoff: Blue stragglers, relative ages, and the horizontal branch p 3538 N94-29732

COMBAT

Thermal strain generated by an enhanced anti-G protection system in a hot climate p 3383 N94-28445

Simulation Networking/Training Requirements Relational Database: User's guide [AD-A275634] p 3528 N94-28637

Effects of endurance training on heat-exercise tolerance in men wearing NBC protective clothing [AD-A275176] p 3391 N94-29049

Autonomous intelligent military robots: Army ants, killer bees, and cybernetic soldiers p 3304 N94-30276

Robotics and the battlefield of the future p 3304 N94-30277

DREV activities related to military vehicles robotization p 3305 N94-30278

Autonomous Robotic Refueling System (ARRS) for rapid aircraft turnaround p 3305 N94-30279

COMBINATIONS (MATHEMATICS)

Higher order recursive program schemes are Turing incomplete [CWI-CS-R9348] p 3425 N94-30414

COMBINATORIAL ANALYSIS

A note on the complexity of local search problems [CT-93-02] p 3456 N94-30370

Perpetual reductions in orthogonal combinatory reduction systems [CWI-CS-R9349] p 3459 N94-30413

Relative length of long paths and cycles in graphs with large degree sums [MEMO-1145] p 3461 N94-30766

COMBUSTIBLE FLOW

Development of a new generation solid rocket motor ignition computer code [NASA-CR-195734] p 3171 N94-28800

Prediction of prompt NO(x) in hydrocarbon air flames p 3190 N94-29250

Flowfield prediction of NO(x) and smoke production in aircraft engines p 3191 N94-29252

Time-resolved measurements in a three dimensional model combustor p 3196 N94-29283

Scramjet CFD methods and analysis. Part 1: Scramjet CFD methods. Numerical simulation of the flow in scramjet duct p 3152 N94-29296

An investigation of the reacting vortex structures associated with pulse combustion p 3200 N94-30911

COMBUSTION

Proceedings of the Joint Contractors Meeting: FE/EE Advanced Turbine Systems Conference FE Fuel Cells and Coal-Fired Heat Engines Conference [DE93-011308] p 3336 N94-28499

Fuels combustion research [AD-A275122] p 3189 N94-29004

Numerical simulation of aerothermal characteristics in gas turbine combustors with complex geometries p 3154 N94-29255

Recent CFD applications in small gas turbine combustion systems development p 3154 N94-29257

Aerothermochemical calculations in afterburners p 3154 N94-29258

Theoretical investigation of gas-surface interactions [NASA-CR-195755] p 3272 N94-29378

An emergency response mobile robot for operations in combustible atmospheres [NASA-CASE-NPO-19020-1-CU] p 3299 N94-29420

Catalytic ignitor for regenerative propellant gun [NASA-CASE-NPO-18987-1-CU] p 3225 N94-29490

Impact of biomass burning on the atmosphere [DE94-004333] p 3349 N94-29954

The direct observation of alkali vapor species in biomass combustion and gasification [DE94-000262] p 3339 N94-30606

An investigation of the reacting vortex structures associated with pulse combustion p 3200 N94-30911

COMBUSTION CHAMBERS

Numerical study on the interaction between scramjet engine modules caused by thermal choke p 3125 N94-28960

Fuels combustion research [AD-A275122] p 3189 N94-29004

Numerical modelling of turbine combustion chambers p 3154 N94-29254

Numerical simulation of aerothermal characteristics in gas turbine combustors with complex geometries p 3154 N94-29255

Application of CFD in combustor design technology p 3154 N94-29256

Recent CFD applications in small gas turbine combustion systems development p 3154 N94-29257

Aerothermochemical calculations in afterburners p 3154 N94-29258

Fuel injector design for high temperature aircraft engine p 3154 N94-29263

The effect of incomplete fuel-air mixing on the lean limit and emissions characteristics of a Lean Prevaporized Premixed (LPP) combustor p 3193 N94-29265

Studies of lean blowout in a research combustor p 3193 N94-29266

Ultra low NO(x) ultra lean gas turbine primary zones with liquid fuels p 3154 N94-29267

Computational and experimental results in high pressure combustions of H2/air and H2/O2/H2O p 3193 N94-29268

Evaluation of the transient operation of advanced gas turbine combustors p 3154 N94-29269

Pollutant emissions from and within a model gas turbine combustor at elevated pressures and temperatures p 3194 N94-29271

Reduction of NO(x) by fuel-staging in gas turbine engines: A commitment to the future p 3194 N94-29272

Chambers of turboreactors with variable geometry: A response to the matrix of pollution in cycles at high temperature, high pressure p 3194 N94-29273

The influence of air distribution on homogeneity and pollutant formation in the primary zone of a tubular combustor p 3194 N94-29274

Effects of hydrogen addition on pollutant emissions in a gas turbine combustor p 3195 N94-29275

Spray combustion experiments and numerical predictions p 3195 N94-29277

Modeling of the phase liquidates in combustion chambers p 3195 N94-29278

Investigation of the two-phase flow in a research combustor under reacting and non-reacting conditions p 3196 N94-29282

Time-resolved measurements in a three dimensional model combustor p 3196 N94-29283

Temperature and combustion analysis of combustor with acoustically controlled primary zone air-jet mixing p 3196 N94-29284

Research and Development of Ram/Scramjets and Turboramjets in Russia [AGARD-LS-194] p 3151 N94-29291

Research and development of ramjets/ramrockets. Part 1: Integral solid propellant ramrockets p 3151 N94-29294

CIAM experimental turboramjets p 3152 N94-29299

Optical flameout detector [NASA-CASE-LAR-14997-1] p 3287 N94-29368

An actively cooled floating element skin friction balance for direct measurement in high enthalpy supersonic flows p 3289 N94-29824

Corrosion performance of materials for advanced combustion systems [DE94-006726] p 3207 N94-30057

Potential capabilities of Reynolds stress turbulence model in the COMMIX-RSM code p 3285 N94-30450

COMBUSTION CHEMISTRY

Fuels combustion research [AD-A275122] p 3189 N94-29004

Fuels and Combustion Technology for Advanced Aircraft Engines [AGARD-CP-536] p 3189 N94-29246

Prediction of prompt NO(x) in hydrocarbon air flames p 3190 N94-29250

Simulation of pollutant formation in turbulent combustors using an extended coherent flame model p 3190 N94-29251
Flowfield prediction of NO(x) and smoke production in aircraft engines p 3191 N94-29252
Numerical prediction of turbulent sooting diffusion flames p 3191 N94-29253
The effect of incomplete fuel-air mixing on the lean limit and emissions characteristics of a Lean Prevaporized Premixed (LPP) combustor p 3193 N94-29265
Computational and experimental results in high pressure combustions of H2/air and H2/O2/H2O p 3193 N94-29268
Computing at the leading edge: Research in the energy sciences
[DE94-006121] p 3563 N94-30844

COMBUSTION CONTROL
Evaluation of the transient operation of advanced gas turbine combustors p 3154 N94-29269
Fuel-rich catalytic combustion of a high density fuel
[NASA-TP-3281] p 3197 N94-29356
Activities of Ishikawajima-Harima Heavy Industries Co. Ltd.
[PB94-137981] p 3555 N94-29798

COMBUSTION PHYSICS
Measurement of volatile metal species at elevated temperatures
[PB94-132321] p 3186 N94-28407
Numerical modelling of turbine combustion chambers p 3154 N94-29254
Numerical simulation of aerothermal characteristics in gas turbine combustors with complex geometries p 3154 N94-29255
Application of CFD in combustor design technology p 3154 N94-29256
Temperature and combustion analysis of combustor with acoustically controlled primary zone air-jet mixing p 3196 N94-29284
Lifted turbulent jet flames p 3198 N94-29676
Computational fluid and combustion dynamics
[DE94-006596] p 3279 N94-30003
XCHEM-1D: A heat transfer/chemical kinetics computer program for multilayered reactive materials
[DE94-005072] p 3226 N94-30615
An investigation of the reacting vortex structures associated with pulse combustion p 3200 N94-30911

COMBUSTION PRODUCTS
Measurement of volatile metal species at elevated temperatures
[PB94-132321] p 3186 N94-28407
Development of the integrated environmental control model: Performance models of selective catalytic reduction NO(x) control systems
[DE94-002151] p 3341 N94-28465
Gas phase thermochemistry of organogermanium compounds
[DE94-004885] p 3187 N94-28561
Advanced diagnostics for reacting flows
[AD-A275057] p 3272 N94-29136
Characterization of air emissions from the simulated open combustion of fiberglass materials
[PB94-136231] p 3347 N94-29192
Fuels and Combustion Technology for Advanced Aircraft Engines
[AGARD-CP-536] p 3189 N94-29246
Simulation of pollutant formation in turbulent combustors using an extended coherent flame model p 3190 N94-29251
Flowfield prediction of NO(x) and smoke production in aircraft engines p 3191 N94-29252
Numerical prediction of turbulent sooting diffusion flames p 3191 N94-29253
The effect of incomplete fuel-air mixing on the lean limit and emissions characteristics of a Lean Prevaporized Premixed (LPP) combustor p 3193 N94-29265
Ultra low NO(x) ultra lean gas turbine primary zones with liquid fuels p 3154 N94-29267
Technology rigs: A tool for afterburner development p 3154 N94-29270
Pollutant emissions from and within a model gas turbine combustor at elevated pressures and temperatures p 3194 N94-29271
Chambers of turboreactors with variable geometry: A response to the matrix of pollution in cycles at high temperature, high pressure p 3194 N94-29273
The influence of air distribution on homogeneity and pollutant formation in the primary zone of a tubular combustor p 3194 N94-29274
Research and development of ramjets/ramrockets. Part 1: Integral solid propellant ramrockets p 3151 N94-29294
Fuel-rich catalytic combustion of a high density fuel
[NASA-TP-3281] p 3197 N94-29356
Fire behavior of aeronautical materials
[REPT-932-600-105] p 3197 N94-29457
A study of low emissions gas turbine combustions
[NASA-CR-195763] p 3152 N94-29660
Toxicity of carbon monoxide-hydrogen cyanide gas mixtures: Exposure concentration, time-to-incapacitation, carboxyhemoglobin, and blood cyanide parameters
[DOT/FAA/AM-94/7] p 3395 N94-29919
Corrosion performance of materials for advanced combustion systems
[DE94-006726] p 3207 N94-30057
The direct observation of alkali vapor species in biomass combustion and gasification
[DE94-000262] p 3339 N94-30606
Application of the extended Kalman filter to the estimation of the char mass in a fluidized bed combustor
[REPT-93-065] p 3200 N94-30938

COMBUSTION STABILITY
Combustion studies under microgravity p 3228 N94-28940
Studies of lean blowout in a research combustor p 3193 N94-29266
Chambers of turboreactors with variable geometry: A response to the matrix of pollution in cycles at high temperature, high pressure p 3194 N94-29273
The influence of air distribution on homogeneity and pollutant formation in the primary zone of a tubular combustor p 3194 N94-29274
Ducted kerosene spray flames p 3195 N94-29276
Liquid-oxygen droplet vaporization and combustion: Analysis of transcritical behavior and application to liquid-rocket combustion instability p 3197 N94-29592

COMBUSTION TEMPERATURE
Combustion for future supersonic transport propulsion p 3190 N94-29249
Temperature and combustion analysis of combustor with acoustically controlled primary zone air-jet mixing p 3196 N94-29284
Numerical simulation of radiative heat loss in an experimental burner
[DE94-002016] p 3277 N94-29923

COMET NUCLEI
Collecting cometary soil samples? Development of the ROSETTA sample acquisition system p 3160 N94-29628

COMET TAILS
Infrared observations of cometary dust by COBE p 3541 N94-29994

COMETS
Collecting cometary soil samples? Development of the ROSETTA sample acquisition system p 3160 N94-29628

COMFORT
The potential of new textiles in improving survival prospects p 3380 N94-28430
Fire-resistant water vapour permeable buoyant insulation p 3380 N94-28431
Human requirements to the indoor air quality and the thermal environment p 3232 N94-29600

COMMAND AND CONTROL
Artificial intelligence technology program at Rome Laboratory p 3414 N94-29328
ACCS Surveillance Exploratory Prototype (ASEP) p 3138 N94-29566
Multi-sensor data fusion and the use of artificial intelligence
[PB94-126216] p 3448 N94-30741

COMMERCE
Spin-off companies as agents of technology transfer: An empirical study of the spin-off companies of the Technical Research Centre of Finland
[PB94-132248] p 3537 N94-28405
Triple Diagonal modeling: A mechanism to focus productivity improvement for business success
[DE94-004309] p 3527 N94-30041

COMMERCIAL AIRCRAFT
Effects of repair on structural integrity
[AD-A275756] p 3145 N94-28647
Ada run time system certification for avionics applications p 3150 N94-29332
Installation of experimental mode-S data link in commercial aircraft
[PB94-138757] p 3254 N94-29998

COMMERCIAL SPACECRAFT
Start of space tourism p 3164 N94-29714

COMMUNICATION
On blocks: Locality and asynchronous communication (extended abstract)
[RUU-CS-92-44] p 3424 N94-30347

COMMUNICATION CABLES
NEMA wire and cable standards development programs p 3166 N94-28706
Standard testing procedures for optical fiber and unshielded twisted pair at Sandia National Laboratories
[DE94-005315] p 3501 N94-30910

COMMUNICATION EQUIPMENT
SPC toolbox: An interactive MATLAB (tm) package for signal modeling, analysis, and communications
[AD-A275617] p 3241 N94-28634
1.8 gigahertz (GHz) digital Low Density Radio Communications Link (LDRCL) Operational Test and Evaluation (OT&E) integration and OT&E operational final test report
[AD-A275800] p 3241 N94-28771
Solid-state, active-phased arrays: Some aspects of receiver design
[AD-A275893] p 3527 N94-28779
The 19th Convention on Radio Science: Abstracts of Papers
[PB94-136868] p 3244 N94-29169
Overview of microoptics: Past, present, and future p 3235 N94-29771
A combined electron beam/optical lithography process step for the fabrication of sub-half-micron-gate-length MMIC chips p 3240 N94-30445
Development status of the Communications and Broadcasting Engineering Test Satellite (COMETS)
[JTN-94-80545] p 3169 N94-30811
Development status of COMETS missions
[JTN-94-80544] p 3170 N94-30932

COMMUNICATION NETWORKS
1.8 gigahertz (GHz) digital Low Density Radio Communications Link (LDRCL) Operational Test and Evaluation (OT&E) integration and OT&E operational final test report
[AD-A275800] p 3241 N94-28771
Evaluation of wireless Local Area Networks
[AD-A275133] p 3243 N94-29064
Video transmission on ATM networks
[NASA-CR-195124] p 3244 N94-29106
High throughput network for multiprocessor interconnections
[VTT-PUBS-147] p 3245 N94-29468
DLR's ATM demonstration programme p 3140 N94-29575
Optimizing the Galileo space communication link p 3250 N94-29663
Decoder synchronization for deep space missions p 3250 N94-29664
Hypra/TR: A tuple oriented recovery method for a continuously available distributed DBMS on a shared nothing multi-computer
[PB94-141264] p 3533 N94-29921
A physical optics model for scattering of HF radiation by irregular terrain
[DE94-006187] p 3255 N94-30106
Performance evaluation of intelligent network services
[MEMO-INF-93-20] p 3438 N94-30373
Performance issues of signalling protocols for broadband ISDN
[MEMO-INF-93-30] p 3255 N94-30374
Customer creation and combination in queueing networks
[MEMO-INF-93-35] p 3438 N94-30375
Design and analysis of dynamic leader election protocols in broadcast networks
[MEMO-INF-93-43] p 3260 N94-30520
Cascaded clocks measurement and simulation findings p 3469 N94-30649
Modeling data throughput on communication networks
[DE94-005077] p 3260 N94-30772

COMMUNICATION SATELLITES
Arcjet system integration development
[NASA-CR-187147] p 3171 N94-28736
TacSats for NATO
[AGARD-AR-322] p 3169 N94-30350
Remote clocks linked by a fully calibrated two-way timing link p 3471 N94-30659

COMMUNICATION THEORY
SPC toolbox: An interactive MATLAB (tm) package for signal modeling, analysis, and communications
[AD-A275617] p 3241 N94-28634

COMMUNICATIONS TECHNOLOGY SATELLITE
Development status of the Communications and Broadcasting Engineering Test Satellite (COMETS)
[JTN-94-80545] p 3169 N94-30811
Development status of COMETS missions
[JTN-94-80544] p 3170 N94-30932

COMMUTER AIRCRAFT
Crashworthiness analysis of commuter aircraft seats
[AD-A275889] p 3135 N94-28799

COMPARISON
Electrical and mechanical testing of wire insulation for space applications p 3166 N94-28710
Evaluation of discretization schemes for advection-diffusion equations
[CWI-NM-R9311] p 3481 N94-30751

COMPARTMENTS
Security aspects of computer supported collaborative work
[AD-A275638] p 3528 N94-28640

COMPATIBILITY
Thermodynamic analysis of chemical compatibility of several compounds with Fe-Cr-Al alloys
[NASA-CR-191166] p 3181 N94-29684
COMPENSATORY TRACKING
Human pilot response during single- and multi-axis tracking tasks
[AD-A275080] p 3398 N94-28887
COMPILERS
Advanced languages for systems software
[AD-A275272] p 3410 N94-29007
Performance of MCNP4A on seven computing platforms
[DE93-040101] p 3419 N94-29816
The MSRC ab initio methods benchmark suite: A measurement of hardware and software performance in the area of electronic structure methods
[DE94-006428] p 3514 N94-30001
Federal grammars and modular compilers
[REPT-93-054] p 3429 N94-30928
COMPLETENESS
Completeness of the Lambek calculus with respect to relativized relational semantics
[LP-93-03] p 3455 N94-30326
A note on the complexity of local search problems
[CT-93-02] p 3456 N94-30370
COMPLEX COMPOUNDS
Journal of NIRE, Vol. 2, No. 2
[JTN-94-80552] p 3187 N94-28675
Ab initio study of vibrational frequency shift upon the 1:1 acetone-iodine complex formation
p 3188 N94-28681
Polymer technology publication series no. 16
[PB94-135522] p 3214 N94-29157
Group transfer and electron transfer reactions of organometallic complexes: Summary of research accomplished in 1993
[DE94-004963] p 3200 N94-30770
COMPLEX SYSTEMS
The lectures in complex systems, volume 5
[AD-A275458] p 3466 N94-28807
Performing specifications for complex systems' software p 3155 N94-29317
Potential software failures methodology analysis
p 3414 N94-29329
Validation and test of complex weapon systems
p 3150 N94-29336
Dependability analysis of parallel systems using a simulation-based approach
[NASA-CR-195762] p 3431 N94-29846
COMPLEXITY
A note on the complexity of local search problems
[CT-93-02] p 3456 N94-30370
Thermodynamics of computation and information distance
[CWI-CS-R9341] p 3526 N94-30433
The Boltzmann entropy and randomness tests
[CWI-CS-R9342] p 3426 N94-30434
Relations between varieties of Kolmogorov complexities
[CWI-CS-R9329] p 3427 N94-30732
COMPONENT RELIABILITY
NAVAIR aircraft wiring standardization and qualification program p 3166 N94-28704
The influence of temperature on microelectronic device failure mechanisms, phase 2
[AD-A275029] p 3265 N94-29511
Neural network application to Particle Impact Noise Detection p 3437 N94-29840
Specialized data analysis of SSME and advanced propulsion system vibration measurements
[NASA-CR-193940] p 3174 N94-29868
COMPOSITE MATERIALS
Safety enhancement of composites via periodic proof testing
[AD-A275662] p 3176 N94-28655
Insulative properties of two thermo-metal neoprenes
[AD-A275209] p 3401 N94-29302
Rules and definition of the range of paints applied on aeronautical structrural composites
[REPT-932-600-106] p 3215 N94-29459
Non-rectangular towpreg architectures
[NASA-CASE-LAR-14863-1-CU] p 3180 N94-29485
Free edge and size effects on failure initiation and ultimate strength of laminates containing a center hole
p 3181 N94-29735
Brittle composites modeling: Comparisons with MoSi2/ZrO2
[DE94-004978] p 3182 N94-29933
Interlaminar fracture analysis for laminated composites under combined loading p 3182 N94-29964
Composite hot drape forming p 3240 N94-30448
Composite redesign of obstetrical forceps
p 3397 N94-30457
Creep behavior of MoSi2-SiC composites
[DE94-004980] p 3185 N94-30693
Ionic conduction mechanisms in CaF2 and CaF2-Al2O3 nanocomposite films on Al2O3 substrates
[DE94-004792] p 3520 N94-30773
COMPOSITE PROPELLANTS
Correlation of cookoff behavior of rocket propellants with thermomechanical and thermochemical properties
[AD-A274983] p 3224 N94-29092
COMPOSITE STRUCTURES
Composite panel failure analysis and improvement plan
[AD-A275655] p 3176 N94-28653
Safety enhancement of composites via periodic proof testing
[AD-A275662] p 3176 N94-28655
Numerical and experimental investigation of the bending response of thin-walled composite cylinders
[NASA-CR-195730] p 3317 N94-28801
A method for the probabilistic design assessment of composite structures
[NASA-TM-106384] p 3319 N94-29384
Review of sonic fatigue technology
[NASA-CR-4587] p 3479 N94-29407
Reliability of composite material structures. Application: High pressure spherical coded tanks
[REPT-932-430-103] p 3180 N94-29478
Composite flexible blanket insulation
[NASA-CASE-ARC-11955-1-CU] p 3180 N94-29509
Active control of delaminations in smart composite structures p 3181 N94-29593
Performance of a higher-order triangular finite element for composite laminated structures
p 3181 N94-29810
Dynamic fracture mechanics analysis for an edge delamination crack
[NASA-TM-109106] p 3479 N94-29856
Integral equation analysis of composite bodies of revolution and arbitrary surfaces with application to cavity-backed antennas p 3253 N94-29883
Physical interpretation and development of ultrasonic nondestructive evaluation techniques applied to the quantitative characterization of textile composite materials
[NASA-CR-195766] p 3183 N94-30016
Computational simulation of composite structures with and without damage
[NASA-CR-194433] p 3183 N94-30190
Three-dimensional free vibration analysis of thick arbitrarily laminated, rectangular, cylindrical and spherical composite panels p 3184 N94-30257
Damage identification in composites using built-in piezoelectrics p 3184 N94-30355
Composite hot drape forming p 3240 N94-30448
Thin-walled orthotropic laminated beam theory
p 3324 N94-30920
COMPRESSIBILITY
On the numerical analysis of shear flows
p 3126 N94-28972
Manufacturing methods for machining spring ends parallel at loaded length
[NASA-CASE-MFS-28767-1] p 3231 N94-29379
COMPRESSIBILITY EFFECTS
An asymptotic analysis for compressible gas lubrication of rough surfaces p 3222 N94-30922
COMPRESSIBLE FLOW
Three dimensional simulation of compressible flow induced by a high-speed train moving into a tunnel
p 3126 N94-28967
An implicit upwind scheme for the three-dimensional Euler equations using a pointwise relaxation method
p 3128 N94-28983
Interaction of multiple spark-generated bubbles in a compressible liquid
[AD-A275037] p 3272 N94-29149
CFD analyses for advanced pump design
[NASA-CR-194866] p 3300 N94-29550
A vorticity transport closure method for turbulent reacting flows p 3274 N94-29761
Numerical solution of the two-dimensional time-dependent incompressible Euler equations
[NASA-CR-195775] p 3277 N94-29859
Numerical comparison of convective heat transfer augmentation devices used in cooling channels of hypersonic vehicles
[NASA-TM-106546] p 3279 N94-30147
Canonical-variables multigrid method for steady-state Euler equations
[NASA-CR-194888] p 3454 N94-30208
Three dimensional compressible turbulent flow computations for a diffusing S-duct with/without vortex generators p 3281 N94-30519
Numerical simulation of leading-edge vortex flow
[AD-B175154] p 3134 N94-30871
Transition to turbulence in confined compressible mixing layers p 3283 N94-30958
COMPRESSIBLE FLUIDS
An interactive educational tool for compressible aerodynamics
[NASA-TM-106568] p 3422 N94-30175
COMPRESSION LOADS
Test and analysis of a stitched RFI graphite-epoxy panel with a fuel access door
[NASA-TM-108992] p 3178 N94-29100
Micromechanics of the dynamic response of ceramics and ceramic composites p 3217 N94-29975
Simulation of composite material response under dynamic compressive loading
[DE94-005272] p 3184 N94-30589
COMPRESSION TESTS
Fabrication and testing of plasma-spray formed MoSi2 and MoSi2 composite tubes
[DE94-004995] p 3175 N94-28581
Fatigue behavior of a cross-ply ceramic matrix composite under strain controlled tension-tension and tension-compression loading
[AD-A275374] p 3177 N94-29012
Numerical analysis of dynamic direct tension and direct compression tests
[AD-A275255] p 3319 N94-29433
Micromechanics of the dynamic response of ceramics and ceramic composites p 3217 N94-29975
COMPRESSIVE STRENGTH
Alumina ceramic: A cost effective replacement for titanium in deep submergence pressure housings
[AD-A275640] p 3212 N94-28641
Manufacturing methods for machining spring ends parallel at loaded length
[NASA-CASE-MFS-28767-1] p 3231 N94-29379
Numerical analysis of dynamic direct tension and direct compression tests
[AD-A275255] p 3319 N94-29433
COMPRESSOR ROTORS
Verification of a three-dimensional viscous flow analysis for a single stage compressor p 3127 N94-28976
An elliptic-hyperbolic grid generation method and application to compressor flows p 3128 N94-28981
COMPRESSORS
Lunar base heat pump, phase 1 draft
[NASA-CR-195211] p 3278 N94-29977
COMPUTATION
Applied analysis/computational mathematics
[DE94-005133] p 3451 N94-28571
Analysis of 3-D acoustic problems using boundary element method p 3127 N94-28974
Digital filter
[DE94-607902] p 3406 N94-30074
Computational balance in real-time cyclic spectral analysis
[DE94-005091] p 3432 N94-30100
Logic of transition systems
[CT-93-03] p 3424 N94-30371
Comparing curried and uncurried rewriting
[CWI-CS-R9350] p 3425 N94-30415
Thermodynamics of computation and information distance
[CWI-CS-R9341] p 3526 N94-30433
Perpetual reductions and strong normalization in orthogonal term rewriting systems
[CWI-CS-R9345] p 3426 N94-30437
Numerical precision and roundoff considerations concerning computer code migration
[DE94-005421] p 3427 N94-30590
Calculation of inelastic mean free path and stopping power for electrons in solids from an optical-data model
[USIP-92-06] p 3494 N94-30980
COMPUTATIONAL CHEMISTRY
Theoretical investigation of gas-surface interactions
[NASA-CR-195755] p 3272 N94-29378
COMPUTATIONAL FLUID DYNAMICS
Large eddy simulations using lattice Boltzmann algorithms
[DE94-005666] p 3270 N94-28549
Aerodynamic design using parallel processors
[AD-A275470] p 3122 N94-28674
A method for the modelling of porous and solid wind tunnel walls in computational fluid dynamics codes
[NASA-CR-195699] p 3270 N94-28724
Development of a new generation solid rocket motor ignition computer code
[NASA-CR-195734] p 3171 N94-28800
Proceedings of the 10th NAL Symposium on Aircraft Computational Aerodynamics
[NAL-SP-19] p 3123 N94-28946
Engineering of systems for application of scientific computing in industry p 3123 N94-28947
Monte Carlo simulation or normal shock wave. Part 2: VHS model and VSS model p 3123 N94-28948
Variable soft sphere molecular model in the Monte Carlo simulation of air species p 3123 N94-28949
Rarefied gas numerical wind tunnel. Part 8: HOPE
p 3123 N94-28950

Numerical simulation of arc heated wind tunnel flow p 3123 N94-28951
Numerical simulation of unsteady aerodynamic heating induced by shock reflections p 3123 N94-28952
Numerical simulation of steady Mach reflection by shock capturing schemes p 3123 N94-28953
Higher-order accurate numerical simulation of 3D supersonic mixing layers p 3124 N94-28954
Numerical simulation of aerothermodynamic heating of hypersonic space transportation vehicles p 3124 N94-28955
ENGRID: A graphical interactive code for the computation of structured grids for blocked flow domains p 3124 N94-28956
Numerical simulation of supersonic flow around space plane with engine installed p 3125 N94-28961
Numerical analysis of sonic boom in the near field p 3125 N94-28962
Role of computational fluid dynamics in aeronautical engineering. Part 10: Numerical analysis of flow around 2-D multi-element HLD p 3125 N94-28964
Numerical solution of inverse problem in aerodynamics p 3125 N94-28965
Code development for hypersonic real-gas flow simulations toward the design of space vehicles, part 2 p 3125 N94-28966
Three dimensional simulation of compressible flow induced by a high-speed train moving into a tunnel p 3126 N94-28967
Numerical analysis of incompressible viscous flow around a bubble p 3126 N94-28968
Unsteady aerodynamic computations around NACA0012 at high angles of attack p 3126 N94-28969
Study of modeling of turbulence of renormalization group analysis p 3126 N94-28970
The upsilon-q method and the psi-q method for incompressible flows p 3126 N94-28971
On the numerical analysis of shear flows p 3126 N94-28972
On approximate Riemann solvers: Improvement of HLLEM scheme and its generalization for chemically reacting flows p 3126 N94-28973
Study on mixing and injection of hydrogen into a supersonic flow p 3127 N94-28975
Verification of a three-dimensional viscous flow analysis for a single stage compressor p 3127 N94-28976
Numerical study on internal flows of centrifugal compressors p 3127 N94-28977
Application of flow field simulation to turbine vane design p 3127 N94-28978
Three-dimensional external flow computations using prismatic grid p 3127 N94-28979
Application of digital control theory to adaptive grid generation p 3127 N94-28980
An elliptic-hyperbolic grid generation method and application to compressor flows p 3128 N94-28981
Upwind method using local interpolation p 3128 N94-28982
An implicit upwind scheme for the three-dimensional Euler equations using a pointwise relaxation method p 3128 N94-28983
Flow and heat transfer in a rotating square sectioned U-bend p 3128 N94-28984
Transonic expanding flow through axially symmetric orifices p 3128 N94-28985
Similarity between turbulent flows through curved pipe and orthogonal rotating pipe p 3128 N94-28986
Numerical analysis of laminar flow in S-curved square duct with inlet and outlet straight region p 3128 N94-28987
Development of buoyancy affected laminar flow in a heated pipe p 3128 N94-28988
Mutual similarity of developing laminar flows with secondary streams in ducts: Curved pipe flow and orthogonal rotating pipe flow p 3129 N94-28989
Parallelization techniques for highly parallel vector computer p 3129 N94-28990
Parallel Fortran programming for NWT p 3129 N94-28991
Performance evaluation of the NWT with parallel Fortran p 3129 N94-28992
A method of user interface for NWT p 3129 N94-28993
A free-wake Euler and Navier-Stokes CFD method and its application to helicopter rotors including dynamic stall [AD-A275416] p 3129 N94-29197
Prediction of prompt NO(x) in hydrocarbon air flames p 3190 N94-29250
Flowfield prediction of NO(x) and smoke production in aircraft engines p 3191 N94-29252
Numerical prediction of turbulent sooting diffusion flames p 3191 N94-29253
Application of CFD in combustor design technology p 3154 N94-29256
Development of global/chemistry model for jet-fuel thermal stability based on observations from static and flowing experiments p 3192 N94-29262
Spray combustion experiments and numerical predictions p 3195 N94-29277
Modeling of the phase liquidates in combustion chambers p 3195 N94-29278
A new Eulerian model for turbulent evaporating sprays in recirculating flows p 3195 N94-29279
Scramjet CFD methods and analysis. Part 1: Scramjet CFD methods. Numerical simulation of the flow in scramjet duct p 3152 N94-29296
Scramjet CFD methods and analysis. Part 2: Scramjet CFD analysis. Numerical simulation of supersonic mixing and combustion applied to scramjet combustor p 3152 N94-29300
A non-local computational boundary condition for duct acoustics [NASA-TM-109091] p 3478 N94-29382
Investigation of advanced counterrotation blade configuration concepts for high speed turboprop systems. Task 2: Unsteady ducted propfan analysis computer program users manual [NASA-CR-187105] p 3152 N94-29438
RNS optimization procedure for three-dimensional composite velocity multi-block applications p 3273 N94-29534
Industrial ventilation p 3232 N94-29604
Computational fluid dynamics in ventilation. 1: Theory and one-dimensional test case p 3232 N94-29606
Computational fluid dynamics in ventilation. 2: Theory and codes p 3233 N94-29607
Computational fluid dynamics in ventilation. 3: The IEA annex 20 work p 3233 N94-29608
Computational fluid dynamics in ventilation. 4: Commercial application of CFD in ventilation p 3233 N94-29609
Computational fluid dynamics in ventilation. 5: New developments in CFD with relevance to ventilation p 3233 N94-29610
Computational fluid dynamics in ventilation: Practical approach p 3233 N94-29611
Finite element method for numerical simulation of turbulent flows. The N3S code p 3233 N94-29612
A vorticity transport closure method for turbulent reacting flows p 3274 N94-29761
Direct and large-eddy simulations of turbulent flow in a square duct p 3275 N94-29809
Numerical solution of 3-D Navier-Stokes equations in vorticity-velocity form for incompressible flows p 3276 N94-29843
Aspects of model-based rocket engine condition monitoring and control [NASA-CR-195116] p 3173 N94-29848
Time-marching aeroelastic and spatial adaptation procedures on triangular and tetrahedral meshes using an unstructured-grid Euler method p 3131 N94-29877
A numerical method for confined unsteady flows related to fluid-structure interactions [ISBN-0-315-74739-0] p 3277 N94-29902
High-resolution algorithms for the Navier-Stokes equations for generalized discretizations p 3278 N94-29965
Aircraft aerodynamics with deflected jets in ground effect p 3132 N94-29973
Computational fluid and combustion dynamics [DE94-006596] p 3279 N94-30003
Aeroacoustic sensitivity analysis and optimal aeroacoustic design of turbomachinery blades [NASA-CR-195786] p 3153 N94-30013
Canonical-variables multigrid method for steady-state Euler equations [NASA-CR-194888] p 3454 N94-30208
Numerical prediction of mixing process in a methane-fueled engine p 3304 N94-30230
The design of a system of codes for industrial calculations of flows around aircraft and other complex aerodynamic configurations [PB94-125598] p 3133 N94-30387
Numerical investigation into high-angle-of-attack leading-edge vortex flow [PB94-125564] p 3133 N94-30388
Aspects of the modeling and numerical simulation of leading-edge vortex flow [AD-B179108] p 3133 N94-30492
A residual correction method applied to 2D multi-point airfoil design and 3D single-point wing design [NLR-TP-92524-U] p 3134 N94-30493
Three dimensional compressible turbulent flow computations for a diffusing S-duct with/without vortex generators p 3281 N94-30519
Prospects of time-linearized unsteady calculation methods for exponentially diverging motions in aeroelasticity [PB94-126224] p 3134 N94-30740
Euler results of the ISNaS compressible multi-block flow solver [AD-B179299] p 3281 N94-30756
Information system for flow simulation based on the Navier-Stokes equations vectorization [AD-B179293] p 3281 N94-30763
Mixed Eulerian-Lagrangian finite element solutions of unsteady flow and flutter in transonic cascade p 3282 N94-30816
Computing at the leading edge: Research in the energy sciences [DE94-006121] p 3563 N94-30844
Grid adaption in computational aerodynamics [PB94-126240] p 3134 N94-30858
Numerical simulation of leading-edge vortex flow [AD-B175154] p 3134 N94-30871
Local two-phase flow simulations including interface tracking with mass transfer p 3283 N94-30954
Generalized Eulerian-Lagrangian formulations in free and moving boundary problems: Processing of viscoelastic polymers and fiber suspensions p 3283 N94-30955
Transition to turbulence in confined compressible mixing layers p 3283 N94-30958
Numerical simulation and prediction of implosion phenomena [GKSS-92/E/99] p 3284 N94-30968

COMPUTATIONAL GEOMETRY

Generation of gear tooth surfaces by application of CNC machines [NASA-CR-195306] p 3303 N94-30205
A deterministic algorithm for the three-dimensional diameter problem [RUU-CS-92-45] p 3424 N94-30348
Generalized hidden surface removal [RUU-CS-93-05] p 3424 N94-30364
Shape from diameter: Negative results [RUU-CS-93-16] p 3458 N94-30407
Shape from diameter: Positive results [RUU-CS-93-17] p 3458 N94-30408
Piecewise linear paths among convex obstacles [RUU-CS-93-20] p 3460 N94-30721
Placing registration marks [RUU-CS-93-21] p 3427 N94-30725
Perfect binary space partitions [RUU-CS-93-23] p 3460 N94-30728
The (n squared)-hard problems in computational geometry [RUU-CS-93-15] p 3461 N94-30747

COMPUTATIONAL GRIDS

Analytic rendering of curvilinear volume data [DE94-004934] p 3407 N94-28506
Numerical simulation of steady Mach reflection by shock capturing schemes p 3123 N94-28953
ENGRID: A graphical interactive code for the computation of structured grids for blocked flow domains p 3124 N94-28956
Numerical analysis of airfoil for helicopter blade at high angle of attack using Navier-Stokes code p 3124 N94-28958
Numerical simulation of supersonic flow around space plane with engine installed p 3125 N94-28961
Numerical analysis of sonic boom in the near field p 3125 N94-28962
Numerical analysis of incompressible viscous flow around a bubble p 3126 N94-28968
Three-dimensional external flow computations using prismatic grid p 3127 N94-28979
Application of digital control theory to adaptive grid generation p 3127 N94-28980
An elliptic-hyperbolic grid generation method and application to compressor flows p 3128 N94-28981
Upwind method using local interpolation p 3128 N94-28982
An implicit upwind scheme for the three-dimensional Euler equations using a pointwise relaxation method p 3128 N94-28983
Time-marching aeroelastic and spatial adaptation procedures on triangular and tetrahedral meshes using an unstructured-grid Euler method p 3131 N94-29877
High-resolution algorithms for the Navier-Stokes equations for generalized discretizations p 3278 N94-29965
PCCM2: A GCM adapted for scalable parallel computers [DE94-005113] p 3350 N94-30116
Accurate finite difference methods for time-harmonic wave propagation [NASA-CR-194887] p 3454 N94-30209
Extended occupancy grid method for modelling unknown dynamic environments p 3144 N94-30281
Grid adaption in computational aerodynamics [PB94-126240] p 3134 N94-30858
Optimal size finite element meshes without obtuse and small angles [RUU-CS-92-39] p 3462 N94-30860

COMPUTER AIDED DESIGN
Object-oriented CAD tool implementations for the construction industry
[PB94-132370] p 3407 N94-28411
Aerodynamic design using parallel processors
[AD-A275470] p 3122 N94-28674
Thermal/structural tailoring of engine blades (T/SEAEBL). Theoretical manual
[NASA-CR-194462] p 3317 N94-28815
Modification of ACSYNT aircraft computer program for preliminary design
[NASA-CR-195737] p 3145 N94-28817
Procedural guide for modelling and analyzing the flight characteristics of a helicopter design using flightlab
[AD-A275077] p 3146 N94-28870
Application of flow field simulation to turbine vane design p 3127 N94-28978
Exploring QDES as a tool for determining limits of achievable performance in aircraft design
[AD-A275359] p 3146 N94-28998
Some efficient procedures for correcting triangulated models
[PB94-136926] p 3452 N94-29171
Engineering document management system
[PB94-136934] p 3530 N94-29172
EXTdesign. Version 1.0: Reference manual
[PB94-136827] p 3411 N94-29193
A case-based approach to creative design
[AD-A275229] p 3417 N94-29390
Animation techniques in BRL-CAD
[AD-A275232] p 3417 N94-29392
Application of FLUIDNET-G software to the preliminary thermal and hydraulic design of Hermes spaceplane
[REPT-932-440-107] p 3168 N94-29543
A variable selection heuristic for solid rocket motor design p 3173 N94-29544
Computational fluid and combustion dynamics
[DE94-006596] p 3279 N94-30003
Calculus of variations applied to 2D multi-point airfoil design
[PB94-125457] p 3133 N94-30401
Hybrid optics for space applications
[ESA-CP-1158] p 3501 N94-30418
A residual correction method applied to 2D multi-point airfoil design and 3D single-point wing design
[NLR-TP-92524-U] p 3134 N94-30493
Realization of function logics by means of transmission gate
[REPT-93-061] p 3429 N94-30936

COMPUTER AIDED MANUFACTURING
Intelligent automated process planning and code generation for computer-controlled inspection
[AD-A275346] p 3409 N94-28920
Numerical simulation of industrial workpiece superplastic forming
[REPT-932-600-102] p 3418 N94-29479
Integration of a path generation algorithm into off-line programming of airbus panels
[REPT-932-600-103] p 3435 N94-29480
Generation of gear tooth surfaces by application of CNC machines
[NASA-CR-195306] p 3303 N94-30205
Programmable Automated Welding System (PAWS)
[AIAA PAPER 94-1221-CP] p 3446 N94-30570
Graphical simulation for aerospace manufacturing
[AIAA PAPER 94-1224-CP] p 3446 N94-30573

COMPUTER AIDED MAPPING
Feature mapping in a photogrammetric GIS
[AD-A275418] p 3325 N94-28863
Application of remote sensing techniques for the seismo-tectonic study of Nahanni earthquake area
[ISBN-0-315-85942-3] p 3334 N94-30037

COMPUTER AIDED TOMOGRAPHY
Computer Assisted Medical Interventions: Application to Conformal Radiotherapy
[RR-912-I] p 3395 N94-30028

COMPUTER ANIMATION
Animation techniques in BRL-CAD
[AD-A275232] p 3417 N94-29392

COMPUTER ASSISTED INSTRUCTION
SPC toolbox: An interactive MATLAB (tm) package for signal modeling, analysis, and communications
[AD-A275617] p 3241 N94-28634
Application of digital video to hypermedia training systems
[AD-A274989] p 3409 N94-28910
Empirical studies of the value of algorithm animation in algorithm understanding
[AD-A275135] p 3412 N94-29287

COMPUTER DESIGN
How to control the increase in the complexity of civil aircraft on-board systems p 3150 N94-29316
Neural network with dynamically adaptable neurons
[NASA-CASE-NPO-17803-1-CU] p 3436 N94-29756

COMPUTER GRAPHICS
Exploitation of stereophotogrammetrically derived 3-D wireframe models to produce urban simulations
[AD-A275459] p 3325 N94-28808
Optimizing ray tracing with visual coherence
[AD-A275218] p 3499 N94-29059
Financial resource review model user's guide
[AD-A274979] p 3410 N94-29088
Empirical studies of the value of algorithm animation in algorithm understanding
[AD-A275135] p 3412 N94-29287
Graphics for ABC
[CWI-CS-R9255] p 3418 N94-29449
PAW using under MS DOS
[DE94-608012] p 3406 N94-30081
Graphics in the Views system
[CWI-CS-R9260] p 3422 N94-30322
Modelling interaction tools in the Views architecture
[CWI-CS-R9261] p 3423 N94-30323
The beauty and the beast
[TR-93-03] p 3423 N94-30331
Generalized hidden surface removal
[RUU-CS-93-05] p 3424 N94-30364

COMPUTER INFORMATION SECURITY
Security aspects of computer supported collaborative work
[AD-A275638] p 3528 N94-28640
Aid to Ada component reuse at Aerospatiale Cannes (France)
[REPT-932-440-102] p 3418 N94-29418
RIPE integrity primitives, part 1 (RACE Integrity Primitives Evaluation)
[CWI-CS-R9324-PT-1] p 3252 N94-29692
RIPE integrity primitives, part 2 (RACE Integrity Primitives Evaluation)
[CWI-CS-R9325-PT-2] p 3252 N94-29693
Secure network databases: Survey and analysis
[PB94-138492] p 3533 N94-29948
Management of PEM public key certificates using X.500 directory service: Some problems and solutions
[DE94-004200] p 3431 N94-29952

COMPUTER NETWORKS
Construction of a connectionist network supercomputer
[AD-A275765] p 3405 N94-28764
TRADOC library and information network (TRALINET). Union list of periodicals (TULIP)
[AD-A275263] p 3529 N94-28903
A porting methodology for parallel database systems
[AD-A275256] p 3529 N94-29053
NPSNET: Integration of Distributed Interactive Simulation (DIS) protocol for communication architecture and information interchange
[AD-A275061] p 3530 N94-29139
A neural network with modular hierarchical learning
[NASA-CASE-NPO-19077-1-CU] p 3435 N94-29492
The Common Modular Simulator (CMS): An architecture test bed for future advanced ATM systems p 3141 N94-29582
Extending the X Window System
[DE94-006496] p 3420 N94-29844
Secure network databases: Survey and analysis
[PB94-138492] p 3533 N94-29948
Management of PEM public key certificates using X.500 directory service: Some problems and solutions
[DE94-004200] p 3431 N94-29952
Customer creation and combination in queueing networks
[MEMO-INF-93-35] p 3438 N94-30375
Self-stabilizing l-exclusion algorithms
[RUU-CS-93-01] p 3424 N94-30379
An all pairs shortest paths distributed algorithm using 2n(exp 2) messages
[RUU-CS-93-19] p 3432 N94-30411
Service independent building blocks-1: Concepts, examples and formal specifications
[CWI-CS-R9326] p 3448 N94-30731
Modeling data throughput on communication networks
[DE94-005077] p 3260 N94-30772
Supercomputing has to be part of an organization-wide automation concept
[AD-B174654] p 3433 N94-30913

COMPUTER PROGRAMMING
A conceptual framework for software technology transition
[AD-A275637] p 3407 N94-28639
Cleanroom engineering handbook. Volume 3: Project execution in the cleanroom environment
[AD-A275860] p 3156 N94-28752
Cleanroom engineering handbook. Volume 4. Specification team practices
[AD-A275861] p 3156 N94-28753
Basic research in computer science
[AD-A275222] p 3405 N94-28916
Advanced languages for systems software
[AD-A275272] p 3410 N94-29007
Reference model for project support environments, version 2.0
[AD-A275191] p 3410 N94-29068
Model-oriented analysis of a communications protocol
[PB94-138146] p 3244 N94-29109
North American jumelage 'type systems'
[AD-A275342] p 3411 N94-29214
Empirical studies of the value of algorithm animation in algorithm understanding
[AD-A275135] p 3412 N94-29287
Program derivation by proof transformation
[AD-A275260] p 3453 N94-29304
Software engineering methods in the Hermes on-board software p 3414 N94-29326
Reactive system software concept with automation using the LDS language p 3414 N94-29327
A common Ada run-time system for avionics software p 3150 N94-29331
Engineering specification editing tools
[AD-A275116] p 3419 N94-29746
Second-order algebraic specification of state semantics
[CWI-CS-R9254] p 3453 N94-29889
The beauty and the beast
[TR-93-03] p 3423 N94-30331
Derivation lengths in term rewriting from interpretations in the naturals
[RUU-CS-92-43] p 3455 N94-30346
On blocks: Locality and asynchronous communication (extended abstract)
[RUU-CS-92-44] p 3424 N94-30347
A deterministic algorithm for the three-dimensional diameter problem
[RUU-CS-92-45] p 3424 N94-30348
Parsing in ISBES
[TR-92-32] p 3432 N94-30363
Models of the untyped lambda-calculus in semi Cartesian closed categories
[ML-93-05] p 3456 N94-30381
Event structures and orthogonal term graph rewriting
[CWI-CS-R9347] p 3459 N94-30412
Higher order recursive program schemes are Turing incomplete
[CWI-CS-R9348] p 3425 N94-30414
The secrets of causality
[RUU-CS-93-29] p 3426 N94-30490
Engineering of systems for application of scientific computing in industry WP project management ISNaS 9209099
[PB94-126232] p 3428 N94-30739
A new programming methodology for lazy functional languages
[MEMO-INF-93-44] p 3429 N94-30765
Federal grammars and modular compilers
[REPT-93-054] p 3429 N94-30928

COMPUTER PROGRAMS
Viscous and elastic-plastic material model in the ABAQUS
[PB94-132347] p 3316 N94-28409
BAG: A code for predicting the performance of a gas bag impact attenuation system for the Pathfinder lander
[DE94-003688] p 3165 N94-28477
SAFSIM theory manual: A computer program for the engineering simulation of flow systems
[DE94-005381] p 3270 N94-28488
Process guide for the Domain-Specific Software Architectures (DSSA) process life cycle
[AD-A275642] p 3407 N94-28648
Software Technology for Adaptable, Reliable Systems (STARS) program
[AD-A275675] p 3407 N94-28664
Cleanroom engineering handbook. Volume 2: Organization and project formation in the cleanroom environment
[AD-A275809] p 3156 N94-28772
Development of a new generation solid rocket motor ignition computer code
[NASA-CR-195734] p 3171 N94-28800
Modification of ACSYNT aircraft computer program for preliminary design
[NASA-CR-195737] p 3145 N94-28817
SOCRATES simulation of the emission at wavelength 6300 A generated by the interaction between the atmosphere and the Space Shuttle exhaust
[AD-A275567] p 3164 N94-28827
Advanced fuel properties: A computer program for estimating property values
[AD-A275248] p 3224 N94-28901
Statistical Modeling and Estimation of Reliability Functions for Software (SMERFS) user's guide, revision 3
[AD-A275390] p 3411 N94-29202
Statistical Modeling and Estimation of Reliability Functions for Software (SMERFS) library access guide, revision 3
[AD-A275405] p 3411 N94-29207

Empirical studies of the value of algorithm animation in algorithm understanding
[AD-A275135] p 3412 N94-29287
Program derivation by proof transformation
[AD-A275260] p 3453 N94-29304
Software engineering methods in the Hermes on-board software p 3414 N94-29326
Artificial intelligence technology program at Rome Laboratory p 3414 N94-29328
Rome Laboratory software engineering technology program p 3414 N94-29330
Investigation of advanced counterrotation blade configuration concepts for high speed turboprop systems. Task 2: Unsteady ducted propfan analysis computer program users manual
[NASA-CR-187105] p 3152 N94-29438
Industrial ventilation p 3232 N94-29604
Computation of vibration mode elastic-rigid and effective weight coefficients from finite-element computer program output p 3247 N94-29615
Software Management Environment (SME) concepts and architecture, revision 1
[NASA-CR-189293] p 3419 N94-29727
AFGWC Dial-In Subsystem (AFDIS) software users manual, version 2.2
[AD-A275844] p 3371 N94-29747
Performance of MCNP4A on seven computing platforms
[DE93-040101] p 3419 N94-29816
Hypra/TR: A tuple oriented recovery method for a continuously available distributed DBMS on a shared nothing multi-computer
[PB94-141264] p 3533 N94-29921
Large-scale computations in analysis of structures
[DE94-004022] p 3321 N94-29951
The MSRC ab initio methods benchmark suite: A measurement of hardware and software performance in the area of electronic structure methods
[DE93-006428] p 3514 N94-30001
Aeroacoustic sensitivity analysis and optimal aeroacoustic design of turbomachinery blades
[NASA-CR-195786] p 3153 N94-30013
GNU debugger internal architecture
[DE94-006665] p 3422 N94-30251
COSMIC monthly progress report
[NASA-CR-195809] p 3422 N94-30273
Activities in machine vision at Imago Manufacturing Ltd. p 3308 N94-30297
The design of a system of codes for industrial calculations of flows around aircraft and other complex aerodynamic configurations
[PB94-125598] p 3133 N94-30387
MANIFOLD version 1.0 programming: Programs and problems
[CWI-CS-R9334] p 3425 N94-30428
A force-controllable macro-micro manipulator and its application to medical robots p 3314 N94-30441
Numerical precision and roundoff considerations concerning computer code migration
[DE94-005421] p 3427 N94-30590
On the unification free PROLOG programs
[CWI-CS-R9331] p 3427 N94-30733

COMPUTER STORAGE DEVICES

Advantages of the LBL 88-inch cyclotron ion beam for SEP studies
[AD-A275142] p 3494 N94-29065
Redundant disk arrays in transaction processing systems
[NASA-CR-195759] p 3418 N94-29404

COMPUTER SYSTEMS DESIGN

Work-oriented development of interactive software tools: Understanding the work of software maintainers and making an interactive software tool for them
[PB94-132032] p 3406 N94-28401
Design and packaging of fault tolerant optoelectronic multiprocessor computing system
[AD-A275896] p 3405 N94-28798
Basic research in computer science
[AD-A275222] p 3405 N94-28916
Algorithms for treating redundancy in repairable and non-repairable systems
[DE94-005289] p 3315 N94-29020
Designing and maintaining decision-making processes p 3412 N94-29318
Embedded expert system: From the mock-up to the real world p 3412 N94-29319
Reactive system software concept with automation using the LDS language p 3414 N94-29327
Validation and test of complex weapon systems p 3150 N94-29336
Information engineering implementation and acceptance p 3530 N94-29533
Design and analysis of concurrency control schemes for heterogeneous database systems p 3531 N94-29591
Using RDD-100 with CoRE. Version 01.00.03
[AD-A275336] p 3419 N94-29797
Design for dependability: A simulation-based approach
[NASA-CR-195757] p 3420 N94-29890
DREV activities related to military vehicles robotization p 3305 N94-30278
Genetic algorithms for optimal database design
[TR-93-01] p 3535 N94-30330
Supercomputing has to be part of an organization-wide automation concept
[AD-B174654] p 3433 N94-30913
View integration: A survey of current developments
[REPT-93-053] p 3536 N94-30927

COMPUTER SYSTEMS PERFORMANCE

Performance analysis of memory hierachies in high performance systems
[DE94-005549] p 3404 N94-28517
Statistical Modeling and Estimation of Reliability Functions for Software (SMERFS) user's guide, revision 3
[AD-A275390] p 3411 N94-29202
Potential software failures methodology analysis p 3414 N94-29329
A common Ada run-time system for avionics software p 3150 N94-29331
A study of the relationship between the performance and dependability of a fault-tolerant computer
[NASA-CR-195758] p 3406 N94-29695
Performance of MCNP4A on seven computing platforms
[DE93-040101] p 3419 N94-29816
Dependability analysis of parallel systems using a simulation-based approach
[NASA-CR-195762] p 3431 N94-29846
Design for dependability: A simulation-based approach
[NASA-CR-195757] p 3420 N94-29890
Modeling systems by probabilistic process algebra: An event structures approach
[MEMO-INF-93-29-REV] p 3425 N94-30416
A user's guide to the Software Testpilot
[CWI-CS-R9343] p 3426 N94-30435
Numerical precision and roundoff considerations concerning computer code migration
[DE94-005421] p 3427 N94-30590
On the unification free PROLOG programs
[CWI-CS-R9331] p 3427 N94-30733
Early experiences with the IBM SP1 and the high-performance switch
[DE94-006261] p 3429 N94-30840

COMPUTER SYSTEMS PROGRAMS

The state transition diagram with path priority and it's applications
[AD-A275524] p 3434 N94-28672
Software systems reengineering process model, version 1.0
[AD-A275711] p 3407 N94-28691
Advanced languages for systems software
[AD-A275272] p 3410 N94-29007
Performing specifications for complex systems' software p 3155 N94-29317
Ada run time system certification for avionics applications p 3150 N94-29332
Integrated formal verification and validation of safety critical software p 3416 N94-29338
Aid to Ada component reuse at Aerospatiale Cannes (France)
[REPT-932-440-102] p 3418 N94-29418
Using RDD-100 with CoRE. Version 01.00.03
[AD-A275336] p 3419 N94-29797
Progress report for the PTUF Project-93 Q1 and Q2
[PB94-138591] p 3431 N94-29995
Relating state transformation semantics and predicate transformer semantics for parallel programs
[CWI-CS-R9339] p 3433 N94-30431

COMPUTER SYSTEMS SIMULATION

Dependability analysis of parallel systems using a simulation-based approach
[NASA-CR-195762] p 3431 N94-29846
Design for dependability: A simulation-based approach
[NASA-CR-195757] p 3420 N94-29890
The MACS-TSA applied in the ISO and SAX spacecraft projects
[PB94-126257] p 3170 N94-30857
Validation experiments with an Ethernet model using the simulation tool 'PROMISE'
[AD-B174795] p 3429 N94-30912

COMPUTER TECHNIQUES

User-centered guidelines for environmental management
[DE94-004313] p 3341 N94-28454
The computer-aided system for the high resolution SQUID-magnetometer
[DE94-606138] p 3286 N94-28553
Capabilities, products, and services of USAFETAC (USAF Environmental Technical Applications Center)
[AD-A275654] p 3368 N94-28652
A reliable and repeatable method for volume calculation of pressurized garments
[AD-A275600] p 3399 N94-28766
DOD Electronic Commerce (EC)/Electronic Data Interchange (EDI) in contracting report
[AD-A275298] p 3242 N94-28874
Automated interface for retrieving reusable software components
[AD-A275004] p 3409 N94-28896
Solution of augmented systems
[PB94-138211] p 3452 N94-29111
Microcomputer-based protective functions in industrial production systems: Assessment method
[PB94-137817] p 3411 N94-29159
The discipline of defining the software product p 3416 N94-29343
A case-based approach to creative design
[AD-A275229] p 3417 N94-29390
Reconfigurable optical interconnections via dynamic computer-generated holograms
[NASA-CASE-NPO-19039-1-CU] p 3499 N94-29491
Stress transfer mechanics for multiple perfectly bonded concentric cylinder models of unidirectional composites
[PB94-138633] p 3181 N94-29524
Information engineering implementation and acceptance p 3530 N94-29533
Automating geographically referenced digital mosaics from aerial videography with area-based feature matching p 3333 N94-29540
Large-scale computations in analysis of structures
[DE94-004022] p 3321 N94-29951
Computer-based linking of thesauri p 3534 N94-29961
Progress report for the PTUF Project-93 Q1 and Q2
[PB94-138591] p 3431 N94-29995
TOTAL user manual
[NASA-TM-109101] p 3432 N94-30160
Total termination of term rewriting
[RUU-CS-92-42] p 3460 N94-30744
A new programming methodology for lazy functional languages
[MEMO-INF-93-44] p 3429 N94-30765
Measuring the impact of investments in information technologies on business performance
[REPT-93-056] p 3536 N94-30929
MPEG-2 video decoding architecture: Analysis and design
[REPT-93-069] p 3260 N94-30940

COMPUTER VISION

A new method for recognizing quadric surfaces from range data and its application to telerobotics and automation, final phase
[NASA-CR-195733] p 3408 N94-28825
Basic research in computer science
[AD-A275184] p 3405 N94-29181
Automating geographically referenced digital mosaics from aerial videography with area-based feature matching p 3333 N94-29540
Airside ground movements surveillance p 3141 N94-29585
Analyses of stationary and growing crack tip deformation by digital image processing p 3320 N94-29690
Stereo imaging based particle velocimeter
[NASA-CR-195800] p 3289 N94-29742
Robotic hand-eye motor learning p 3436 N94-29835
Computer Assisted Medical Interventions: Application to Conformal Radiotherapy
[RR-912-I] p 3395 N94-30028
Pre- and intra-radiotherapy multimodal image registration: Principles and first experiments p 3395 N94-30030
Computational methods for the shape shading problem
[ISBN-0-315-85430-8] p 3421 N94-30136
Encoding technique for automated guided vehicle POSE recovery in a structured environment p 3144 N94-30286
Activities in machine vision at Imago Manufacturing Ltd. p 3308 N94-30297
Thermal imaging for a mobile robot p 3308 N94-30300
Obstacle detection for an autonomous vehicle p 3309 N94-30302
The use of interactive computer vision and robot hand controllers for enhancing manufacturing safety p 3314 N94-30442
Conference on Intelligent Robotics in Field, Factory, Service, and Space (CIRFFSS 1994), volume 1
[NASA-CP-3251] p 3439 N94-30526
VAS: A Vision Advisor System combining agents and object-oriented databases
[AIAA PAPER 94-1181-CP] p 3440 N94-30532

Application of the Modular Automated Reconfigurable Assembly System (MARAS) concept to adaptable vision gauging and parts feading
[AIAA PAPER 94-1182-CP] p 3440 N94-30533
Integration of vision and robotic workcell
[AIAA PAPER 94-1186-CP] p 3440 N94-30536
Design of an autonomous exterior security robot
[AIAA PAPER 94-1188-CP] p 3441 N94-30538
Technology for robotic surface inspection in space
[AIAA PAPER 94-1193-CP] p 3442 N94-30544
Design and control of active vision based mechanisms for intelligent robots
[AIAA PAPER 94-1196-CP] p 3442 N94-30547
Vision based object pose estimation for mobile robots
[AIAA PAPER 94-1197-CP] p 3442 N94-30548
Unsupervised texture image segmentation by improved neural network ART2
[AIAA PAPER 94-1199-CP] p 3442 N94-30549
Microwave vision for robots
[AIAA PAPER 94-0687-CP] p 3443 N94-30550
A reactive system for open terrain navigation: Performance and limitations
[AIAA PAPER 94-1218-CP] p 3445 N94-30566
The Automated Aircraft Rework System (AARS): A system integration approach
[AIAA PAPER 94-1225-CP] p 3446 N94-30574
Placing registration marks
[RUU-CS-93-21] p 3427 N94-30725
Aspects of vision and planning in a dynamic, uncertain environment p 3448 N94-30803

COMPUTERIZED SIMULATION
Speciation in Water and Soil: A literature review
[PB94-132388] p 3341 N94-28412
Analysis of spark-induced bubble experiments using CALE
[DE94-003667] p 3270 N94-28476
BAG: A code for predicting the performance of a gas bag impact attenuation system for the Pathfinder lander
[DE94-003688] p 3165 N94-28477
Computer simulation of martensitic transformations
[DE94-005213] p 3201 N94-28479
SAFSIM theory manual: A computer program for the engineering simulation of flow systems
[DE94-005381] p 3270 N94-28488
Composite load spectra for select space propulsion structural components
[NASA-CR-194476] p 3316 N94-28508
Simulation of experiments on deep inelastic scattering of muons on superconducting magnetic toroidal spectrometer STORS
[DE94-606267] p 3483 N94-28554
Solution of charged particle transport equation by Monte-Carlo method in the BRANDZ code system
[DE94-606270] p 3484 N94-28614
Capabilities, products, and services of USAFETAC (USAF Environmental Technical Applications Center)
[AD-A275654] p 3368 N94-28652
Exploitation of stereophotogrammetrically derived 3-D wireframe models to produce urban simulations
[AD-A275459] p 3325 N94-28808
Modification of ACSYNT aircraft computer program for preliminary design
[NASA-CR-195737] p 3145 N94-28817
SOCRATES simulation of the emission at wavelength 6300 A generated by the interaction between the atmosphere and the Space Shuttle exhaust
[AD-A275567] p 3164 N94-28827
Evaluation of simulated JERS-1 data for geologic mapping at Drum Mountains, Utah, Silver Bell, Arizona, and Wind River, Wyoming under the GEOSAT-ERSDAC/JAPEX/JGI/RESTEC joint studies p 3326 N94-28929
Synthetic image generator model; application of view angle dependent reflectivity components and performance evaluation in the visible region
[AD-A275365] p 3499 N94-29009
A comparison of two computer models of sound propagation for a wedge shaped ocean over a penetrable bottom
[AD-A275031] p 3477 N94-29117
A non-linear simulation for an autonomous unmanned air vehicle
[AD-A275062] p 3146 N94-29200
Computer simulations on development of the fast reconnection mechanism p 3360 N94-29241
Technology rigs: A tool for afterburner development p 3154 N94-29270
Pollutant emissions from and within a model gas turbine combustor at elevated pressures and temperatures p 3194 N94-29271
Scramjet CFD methods and analysis. Part 2: Scramjet CFD analysis. Numerical simulation of supersonic mixing and combustion applied to scramjet combustor p 3152 N94-29300
Testing Operational Flight Programs (OFPs) p 3415 N94-29337
A distributed object-based environment in Ada p 3417 N94-29347
Microvibrations on a GEO telecommunication satellite
[REPT-932-440-101] p 3168 N94-29415
Satellites: Reliability and operation security
[REPT-932-440-108] p 3168 N94-29419
Pyrotechnic shock: Devices in pyrotechnic environment qualification logic
[REPT-932-430-108] p 3225 N94-29429
Numerical simulation of industrial workpiece superplastic forming
[REPT-932-600-102] p 3418 N94-29479
Concurrent simulation and constraint stabilization for flexible multibody systems p 3154 N94-29532
Simulation of fully automated air traffic control concepts p 3139 N94-29569
Radar estimations of atmospheric winds in the troposphere and lower stratosphere p 3370 N94-29697
Microgravity by parabolic flight with MU-300 aircraft p 3392 N94-29710
The role of cloud collisions in N-body simulations of disk galaxies p 3545 N94-29755
Numerical study of the trailing vortex of a wing with wing-tip blowing
[NASA-CR-195803] p 3130 N94-29760
A simulation study of high degree and order geopotential determination using satellite gravity gradiometry p 3333 N94-29762
A pot-pourri of results in QCD from large lattice simulations on the CM5
[DE94-005084] p 3514 N94-29818
Large eddy simulation of subsonic mixing layers p 3276 N94-29851
Radar returns from a low-flying target over a rough sea surface under multipath and clutter conditions p 3253 N94-29882
Numerical simulation of radiative heat loss in an experimental burner
[DE94-002016] p 3277 N94-29923
Large-scale computations in analysis of structures
[DE94-004022] p 3321 N94-29951
Progress report for the PTUF Project-93 Q1 and Q2
[PB94-138591] p 3431 N94-29995
Algorithm and program ORANGE for magnetic field simulation of magnetic system spectrometer STORS
[DE94-608013] p 3421 N94-30083
Fractal approach to computer-analytical modelling of tree crown
[DE94-608089] p 3467 N94-30088
Large eddy simulation of the upper atmospheric surface layer
[ISBN-0-315-85393-X] p 3365 N94-30134
Computer simulation of the interaction of fast hydrogen atoms with a molybdenum containing sorbed hydrogen
[DE94-608419] p 3209 N94-30253
Simulation of lightweight robots and their controllers p 3307 N94-30294
A simulator for multi-radar analysis for realistic traffic
[AD-B179099] p 3142 N94-30439
Biologically-inspired hexapod robot design and simulation
[AIAA PAPER 94-1178-CP] p 3439 N94-30530
Graphical simulation for aerospace manufacturing
[AIAA PAPER 94-1224-CP] p 3446 N94-30573
The second coming of cold dark matter?
[DE94-004992] p 3548 N94-30694
Engineering of systems for application of scientific computing in industry WP project management ISNaS 9209099
[PB94-126232] p 3428 N94-30739
Computing at the leading edge: Research in the energy sciences
[DE94-006121] p 3563 N94-30844
Numerical simulation of a condenser in two-phase heat transport systems: A feasibility study
[AD-B173650] p 3282 N94-30855
Numerical simulation of leading-edge vortex flow
[AD-B175154] p 3134 N94-30871
Application of ALE techniques to metal forming simulations
[DE94-005358] p 3211 N94-30892

COMPUTERS
Basic research in computer science
[AD-A275184] p 3405 N94-29181

CONCATENATED CODES
Convolutional encoding of self-dual codes p 3250 N94-29662

CONCENTRATION (COMPOSITION)
Absolute determination of local tropospheric OH concentrations p 3343 N94-28594
Evaluating models of climate and forest vegetation p 3353 N94-30637
Chemical composition of insoluble particles in superimposed ice on Storoeya, Svalbard (Sweden)
[CM-82] p 3336 N94-30944

CONCENTRATORS
Performance of the Southern California Edison Company Stirling dish
[DE94-004676] p 3337 N94-29018
Methane challenge of high performance molecular sieve oxygen concentrator
[AD-A275155] p 3337 N94-29033

CONCENTRIC CYLINDERS
Stress transfer mechanics for multiple perfectly bonded concentric cylinder models of unidirectional composites
[PB94-138633] p 3181 N94-29524
Multiple Concentric Cylinder Model (MCCM) user's guide
[NASA-CR-195299] p 3183 N94-30125

CONCRETE STRUCTURES
Development of the breakwater with submerged mound for interchanging sea water p 3234 N94-29703

CONCRETES
Asphaltic concrete performance under heavy fighter aircraft loading
[AD-A275046] p 3157 N94-29151
Numerical analysis of dynamic direct tension and direct compression tests
[AD-A275255] p 3319 N94-29433
Contributions of DLR to air traffic capacity enhancement within a terminal area p 3138 N94-29567
Fracture process zone of brittle composites p 3182 N94-29876
Improved ground-penetrating radar, bridge decks
[DE94-004863] p 3254 N94-29929

CONCURRENT PROCESSING
Reasoning about programs by exploiting the environment
[AD-A275852] p 3408 N94-28794
Intelligent automated process planning and code generation for computer-controlled inspection
[AD-A275346] p 3409 N94-28920
Tinkertoy(tm) transactions
[AD-A275271] p 3410 N94-29006
Batch updates and concurrency in B-trees
[PB94-136835] p 3530 N94-29167
Design and analysis of concurrency control schemes for heterogeneous database systems p 3531 N94-29591
Event structures and orthogonal term graph rewriting
[CWI-CS-R9347] p 3459 N94-30412
Three metric domains of processes for bisimulation
[CWI-CS-R9335] p 3459 N94-30427
MANIFOLD version 1.0 programming: Programs and problems
[CWI-CS-R9334] p 3425 N94-30428
Manray: A replicated workers program in MANIFOLD
[CWI-CS-R9337] p 3433 N94-30429
Isomorphisms between predicate and state transformers
[CWI-CS-R9338] p 3459 N94-30430
Topological models for higher order control flow
[CWI-CS-R9340] p 3425 N94-30432
Efficient bounded timestamping using traceable use abstraction: Is writer's guessing better than reader's telling?
[RUU-CS-93-28] p 3426 N94-30489
Validation experiments with an Ethernet model using the simulation tool 'PROMISE'
[AD-B174795] p 3429 N94-30912

CONDENSATES
Qualitative vector optimization of a condensate stabilizer process
[PB94-133246] p 3189 N94-28789

CONDENSERS (LIQUEFIERS)
The influence of wall conductivity of film condensation with integral fin tubes
[AD-A275503] p 3523 N94-28662
Numerical simulation of a condenser in two-phase heat transport systems: A feasibility study
[AD-B173650] p 3282 N94-30855

CONDITIONS
Conditional dependence in probabilistic networks
[RUU-CS-92-34] p 3464 N94-29450

CONDUCTING POLYMERS
Corrosion inhibition by electrodeposited conductive-polymer film
[AD-A275456] p 3213 N94-28806

CONDUCTIVE HEAT TRANSFER
Peculiarities of heat transfer in the experiments of beam injection heating of a plasma at the GOL-3 device
[DE94-608357] p 3508 N94-30194
Unstructured space-time finite element method of heat conduction p 3279 N94-30224

CONDUCTORS
Orbital applications of electrodynamic propulsion
[AD-A275413] p 3173 N94-29216
Screening of flexible cables by nonlinear resistance measurements
[AD-A275193] p 3264 N94-29289

Focused ion beam fabrication of microelectronic structures
[AD-A275384] p 3264 N94-29305
Magnetic field generation by circularly polarized laser light and inertial plasma confinement in a miniature magnetic bottle induced by circularly polarized laser light
[DE94-608353] p 3508 N94-30192

CONES
Filament to mandrel gap analysis: Resulting gap from filament winding over a cone-cylinder transition mandrel (reference NMTP no. 93838)
[DE94-004225] p 3175 N94-28528

CONFERENCES
The Support of Air Operations under Extreme Hot and Cold Weather Conditions
[AGARD-CP-540] p 3379 N94-28420
Proceedings of the Joint Contractors Meeting: FE/EE Advanced Turbine Systems Conference FE Fuel Cells and Coal-Fired Heat Engines Conference
[DE93-011308] p 3336 N94-28499
Proceedings of Japan-US Workshop P-196 on High Heat Flux Components and Plasma Surface Interactions for Next Devices
[DE94-701164] p 3503 N94-28513
Research on elementary particle physics. Task P: Studies in theory and phenomenology of elementary physics
[DE94-004955] p 3483 N94-28566
Local Measurement of Tropospheric HO(x)
[NASA-CP-3245] p 3342 N94-28587
Proceedings of the workshop on quark and lepton mass matrices
[DE94-707692] p 3485 N94-28624
Minutes. Accredited Standards Committee on Acoustics, S1. US tag for ISO/TC 43 acoustics and IEC/TC 29 electroacoustics
[AD-A275702] p 3477 N94-28689
Second NASA Workshop on Wiring for Space Applications
[NASA-CP-3244] p 3165 N94-28697
Minutes: Accredited Standards Committee on Mechanical Vibration and Shock, S2. US TAG for ISO/TC 108 Mechanical Vibration and Shock
[AD-A275591] p 3316 N94-28726
The Seventh Annual National Conference of Black Physics Students
[NASA-CR-195735] p 3526 N94-28746
Computational methods in continuum mechanics
[AD-A275560] p 3451 N94-28792
Proceedings of the International Symposium on Remote Sensing
[JTN-94-80578] p 3325 N94-28925
Partial support for the Second International Symposium on Artificial Intelligence and Mathematics
[AD-A275199] p 3434 N94-29026
Proceedings of the 15th Earth Observation Symposium
[JTN-94-80607] p 3328 N94-29036
The 19th Convention on Radio Science: Abstracts of Papers
[PB94-136868] p 3244 N94-29169
Finnish astronomy days, 1992-1993. Proceedings of the Finnish Astronomical Society
[PB94-136892] p 3538 N94-29170
Proceedings of the 3rd International Symposium: JERS-1 and Remote Sensing in the Future
[JTN-94-80597] p 3329 N94-29217
Proceedings of the NIPR Symposium on Upper Atmosphere Physics, no. 6
[JTN-94-80593] p 3359 N94-29233
Fuels and Combustion Technology for Advanced Aircraft Engines
[AGARD-CP-536] p 3189 N94-29246
Aerospace Software Engineering for Advanced Systems Architectures
[AGARD-CP-545] p 3412 N94-29315
Electrical engineering and industrial electronics education days: Control of asynchronous generators
[PB94-135514] p 3266 N94-29523
Machine Intelligence in Air Traffic Management
[AGARD-CP-538] p 3136 N94-29558
The 27th Aerospace Mechanisms Symposium
[NASA-CP-3205] p 3160 N94-29627
The MERSS 5th Symposium on Space Medicine: Medical and Physiological Experiment Utilizing Parabolic Flight
[JTN-94-80588] p 3392 N94-29709
Proceedings of the Workshop on Microtechnologies and Applications to Space Systems
[NASA-CR-195688] p 3235 N94-29767
The Seventh International Beer Sheva Seminar on MHD Flows and Turbulence
[DE94-607211] p 3506 N94-29831
Proceedings: SISAL 1993
[DE94-006641] p 3420 N94-30056
Proceedings of the 1991 Single Event Upset Symposium
[DSIS-92-00652] p 3495 N94-30211
Proceedings of the 3rd Conference on Military Robotic Applications
[DRES-SP-149] p 3304 N94-30275
Technology 2003: The Fourth National Technology Transfer Conference and Exposition, volume 1
[NASA-CP-3249] p 3555 N94-30440
Conference on Intelligent Robotics in Field, Factory, Service, and Space (CIRFFSS 1994), volume 1
[NASA-CP-3251] p 3439 N94-30526
Proceedings of the 1993 Windsor Workshop on Alternative Fuels
[DE94-003908] p 3226 N94-30612
International Energy and Environmental Congress: Proceedings
[DE93-040609] p 3353 N94-30715
Proceedings of the low cost materials of construction for biological processes workshop
[DE94-000218] p 3226 N94-30761
Index of NPL acoustics publications 1981-1990
[NPL-RSA(EXT)-0044] p 3480 N94-30786
NREL Photovoltaic Program FY 1993 bibliography
[DE94-000272] p 3340 N94-30820
Interagency advanced power group: Solar working group
[DE94-004953] p 3340 N94-30833

CONFIDENCE LIMITS
Ten new checks to assess the statistical quality of Monte Carlo solutions in MCNP
[DE94-006137] p 3465 N94-30366

CONFIGURATION INTERACTION
Numerical study on the interaction between scramjet engine modules caused by thermal choke
p 3125 N94-28960

CONFIGURATION MANAGEMENT
Guide to the Environmental-Language
[AD-A275849] p 3408 N94-28784
Kinematic functions for redundancy resolution using configuration control
[NASA-CASE-NPO-18608-1-CU] p 3436 N94-29504
Software engineering and software management in a distributed UNIX environment
[NLR-TP-92233-U] p 3422 N94-30314

CONFINEMENT
The impact of improved physics on commercial tokamak reactors
[DE94-006103] p 3509 N94-30760

CONFORMAL MAPPING
Reidemeister numbers of equivariant maps
[PB94-138286] p 3452 N94-29118
Remarks on Galois symmetry in RCFT
[PB94-138179] p 3467 N94-29147

CONGRUENCES
Reidemeister numbers of equivariant maps
[PB94-138286] p 3452 N94-29118

CONIFERS
Plant-microbe interactions: Plant hormone production by phylloplane fungi
[PB94-135563] p 3385 N94-29189

CONJUGATE GRADIENT METHOD
Concurrent simulation and constraint stabilization for flexible multibody systems p 3154 N94-29532

CONJUGATE POINTS
Estimation of geomagnetic conjugate points by using Pc5 pulsations p 3357 N94-29079

CONJUGATION
Polymer technology publication series no. 16
[PB94-135522] p 3214 N94-29157

CONNECTION MACHINE
Global atmospheric and ocean modeling on the connection machine
[DE94-003930] p 3342 N94-28521

CONNECTORS
Quick connect fastener
[NASA-CASE-MFS-28829-1] p 3300 N94-29486
Development and testing of the Automated Fluid Interface System p 3161 N94-29636

CONSERVATION
Evaluation of monitoring audiometry in the United States Air Force Hearing Conservation Program
[AD-A275309] p 3391 N94-29211

CONSERVATION EQUATIONS
A new flux-conserving numerical scheme for the steady, incompressible Navier-Stokes equations
[NASA-TM-106520] p 3273 N94-29471
On some general properties of parabolic conservation equations
[DE94-006101] p 3461 N94-30758

CONSERVATION LAWS
A new flux-conserving numerical scheme for the steady, incompressible Navier-Stokes equations
[NASA-TM-106520] p 3273 N94-29471
An investigation into certain geometrical and variational properties of the P(4) theory of gravitation and electromagnetism p 3526 N94-30950

CONSOLIDATION
Mechanical alloying processing with application to structural materials: ASSERT supplement
[AD-A275400] p 3204 N94-29205

CONSTRAINTS
Significant figures and Lyapunov exponents in chaos and constrained divergence of chaotic orbits
p 3467 N94-29910

CONSTRUCTION
Object-oriented CAD tool implementations for the construction industry
[PB94-132370] p 3407 N94-28411
Study of bridge design and technology
[PB94-137916] p 3121 N94-29160
Rooftop emergency heliports
[DOT/FAA/RD-93/2] p 3157 N94-29754
The road plan model: Information model for planning road building activities
[AIAA PAPER 94-1219-CP] p 3445 N94-30567
Local interaction control for space construction
p 3170 N94-30960

CONSTRUCTION INDUSTRY
Object-oriented CAD tool implementations for the construction industry
[PB94-132370] p 3407 N94-28411

CONSTRUCTION MATERIALS
Improved construction materials for polar regions using microcellular thermoplastic foams p 3223 N94-30483

CONTACT LOADS
Force control techniques for robot manipulators and their military applications p 3307 N94-30291

CONTAINERLESS MELTS
Plasma heating for containerless and microgravity materials processing
[NASA-CASE-NPO-18819-1-CU] p 3229 N94-29371

CONTAMINANTS
Speciation in Water and Soil: A literature review
[PB94-132388] p 3341 N94-28412
Methane challenge of high performance molecular sieve oxygen concentrator
[AD-A275155] p 3337 N94-29033
Characterization of air emissions from the simulated open combustion of fiberglass materials
[PB94-136231] p 3347 N94-29192
Simulation of pollutant formation in turbulent combustors using an extended coherent flame model
p 3190 N94-29251
Brief summary of accomplishments since our DOE-sponsored radon project commenced
[DE94-004643] p 3348 N94-29926
Intermedia transfer factors for fifteen toxic pollutants released to air basins in California
[DE94-005699] p 3349 N94-30044
Novel mass spectrometric instrument for gaseous and particulate characterization and monitoring
[DE94-005896] p 3349 N94-30047
Regenerating using aqueous cleaners with ozone and electrolysis p 3240 N94-30468
Dewatering of contaminated river sediments
p 3354 N94-30472

CONTAMINATION
SOCRATES simulation of the emission at wavelength 6300 A generated by the interaction between the atmosphere and the Space Shuttle exhaust
[AD-A275567] p 3164 N94-28827
A modular approach for automated sample preparation and chemical analysis p 3354 N94-30464

CONTEXT FREE LANGUAGES
Increasing the applicability of LR parsing
[TR-93-06] p 3423 N94-30332
Generalized left-corner parsing
[TR-92-21] p 3432 N94-30356

CONTINUITY (MATHEMATICS)
Splines and ocean wave modelling
[PB94-139409] p 3378 N94-30002

CONTINUOUS RADIATION
A space-based classification system for RF transients
[DE94-003933] p 3240 N94-28522
RL/ERCT automated swept-angle bistatic measurement system
[AD-A275763] p 3241 N94-28763
Induced crystallization in CW laser-irradiated sol-gel deposited titania films
[DE94-006527] p 3207 N94-30062

CONTINUOUS SPECTRA
Miln equation for the calculation of the phases and amplitudes of wave functions for continuum spectrum of Coulomb two-center problem
[DE94-606292] p 3522 N94-28616

CONTINUOUS WAVE LASERS
High-power CW diode-laser-array-pumped solid-state lasers and efficient nonlinear optical frequency
[AD-A275394] p 3293 N94-29309

Fission-activated laser as primary power for CW laser propulsion
[DE94-006138] p 3295 N94-30367

CONTINUOUS WAVE RADAR
RL/ERCT automated swept-angle bistatic measurement system
[AD-A275763] p 3241 N94-28763
Radar jet engine health monitoring project
[ASSGI-3U1] p 3153 N94-30130

CONTINUUM MECHANICS
Computational methods in continuum mechanics
[AD-A275560] p 3451 N94-28792
The motion of deforming bodies
[AD-A275224] p 3271 N94-29061
Brittle composites modeling: Comparisons with MoSi2/ZrO2
[DE94-004978] p 3182 N94-29933

CONTOURS
The performance of gloss meters on curving surfaces
[NPL-DMM(A)-111] p 3501 N94-30522
Use of snakes to link edge points to create left ventricular boundaries in echocardiographic images
[TELECOM-93-D-016] p 3395 N94-30970

CONTRACT MANAGEMENT
DOD Electronic Commerce (EC)/Electronic Data Interchange (EDI) in contracting report
[AD-A275298] p 3242 N94-28874

CONTRACTION
Bounded contraction and many-valued semantics
[ML-93-04] p 3456 N94-30380

CONTRACTORS
Proceedings of the Joint Contractors Meeting: FE/EE Advanced Turbine Systems Conference FE Fuel Cells and Coal-Fired Heat Engines Conference
[DE93-011308] p 3336 N94-28499

CONTRAROTATING PROPELLERS
Investigation of advanced counterrotation blade configuration concepts for high speed turboprop systems. Task 2: Unsteady ducted propfan analysis computer program users manual
[NASA-CR-187105] p 3152 N94-29438

CONTROL BOARDS
Micro guidance and control technology overview
p 3144 N94-29772

CONTROL EQUIPMENT
Effects of pressure on membrane-associated receptors and effector elements
[AD-A275813] p 3384 N94-28829
Extended horizon lifting for periodic gain adjustment in control systems, and for equalization of communication channels
[NASA-CASE-NPO-19166-1-CU] p 3246 N94-29495
Micro guidance and control technology overview
p 3144 N94-29772
Control of heating, ventilation and air conditioning (HVAC) systems
[PB94-138807] p 3401 N94-30000
Nearly time-optimal feedback control of a magnetically levitated photolithography positioning system
[DE94-005288] p 3266 N94-30055

CONTROL MOMENT GYROSCOPES
Suspension system for gimbal supported scanning payloads
[NASA-CASE-MFS-28817-1] p 3287 N94-29358

CONTROL SIMULATION
Procedural guide for modelling and analyzing the flight characteristics of a helicopter design using flightlab
[AD-A275077] p 3146 N94-28870
Simulation of fully automated air traffic control concepts p 3139 N94-29569
Elevation control system model for the DSS 13 antenna p 3248 N94-29622
Generation mechanisms of quasi-stationary waves in the Southern Hemisphere p 3365 N94-30789
The MACS-TSA applied in the ISO and SAX spacecraft projects
[PB94-126257] p 3170 N94-30857

CONTROL STABILITY
Experimental evaluation of fuzzy logic control of a flexible arm manipulator
[AD-A275375] p 3434 N94-29013
The development procedures and tools applied for the attitude control software of the Italian satellite SAX
p 3170 N94-29324
Kinematic representations, workspace analysis, and grasp stability in robot arms and multi-fingered hands
p 3301 N94-29847
A design methodology for synthesizing low-order robust controllers for flexible structures p 3302 N94-29870
Robust adaptive control and filtering
p 3437 N94-29895
Vehicle following controller design for autonomous intelligent vehicles
[AIAA PAPER 94-1203-CP] p 3443 N94-30554
Robust adaptive control of a mechanical manipulator
p 3449 N94-30806
A control method for bilateral teleoperating systems
[ISBN-0-315-78705-8] p 3313 N94-30952

CONTROL SURFACES
Experimental investigation of three-dimensional vortex-airfoil interaction in a supersonic stream
[AD-A275107] p 3122 N94-28899
Numerical study of the trailing vortex of a wing with wing-tip blowing
[NASA-CR-195803] p 3130 N94-29760

CONTROL SYSTEMS DESIGN
The development procedures and tools applied for the attitude control software of the Italian satellite SAX
p 3170 N94-29324
Software engineering methods in the Hermes on-board software p 3414 N94-29326
High level language-based robotic control system
[NASA-CASE-NPO-17918-2-CU] p 3435 N94-29465
Extended horizon lifting for periodic gain adjustment in control systems, and for equalization of communication channels
[NASA-CASE-NPO-19166-1-CU] p 3246 N94-29495
Intelligent systems for air space control and management p 3137 N94-29560
Elevation control system model for the DSS 13 antenna p 3248 N94-29622
Formal specification and verification of real-time sequential control systems
[AD-A275776] p 3419 N94-29678
Pulse response based minimum time control of flexible structures p 3436 N94-29720
Control of micromachined deformable mirrors
p 3239 N94-29787
Activities of Ishikawajima-Harima Heavy Industries Co. Ltd.
[PB94-137981] p 3555 N94-29798
Decoupled flight control system design using the singular perturbation method p 3155 N94-29850
A design methodology for synthesizing low-order robust controllers for flexible structures p 3302 N94-29870
Maestro: An open system architecture for multi-robot control p 3306 N94-30288
Elements of supervisory control for military robotic applications p 3309 N94-30303
Aspects of the operator interface for military robotic applications in unstructured environments
p 3309 N94-30304
Supervised autonomous control for Space Station Special Purpose Dextrous Manipulator (SPDM) robot
p 3309 N94-30305
Motion control of mobile robots p 3310 N94-30309
Control system design for A and R supported microgravity experiments: An experiment payload control development
[AD-B179107] p 3229 N94-30421
A direct digital control-law synthesis in the w-domain: W-synthesis methodology p 3438 N94-30517
Design and control of active vision based mechanisms for intelligent robots
[AIAA PAPER 94-1196-CP] p 3442 N94-30547
Predictive sufficiency and the use of stored internal state
[AIAA PAPER 94-1213-CP] p 3445 N94-30564
Using generic tool kits to build intelligent systems
[AIAA PAPER 94-1214-CP] p 3445 N94-30565
A reactive system for open terrain navigation: Performance and limitations
[AIAA PAPER 94-1218-CP] p 3445 N94-30566
The road plan model: Information model for planning road building activities
[AIAA PAPER 94-1219-CP] p 3445 N94-30567
Programmable Automated Welding System (PAWS)
[AIAA PAPER 94-1221-CP] p 3446 N94-30570
Robust adaptive control of a mechanical manipulator
p 3449 N94-30806
A stochastic control approach to flight path monitoring
[AD-B174630] p 3143 N94-30853
Integrated structure/control design of nonrigid robot arms for high-speed manipulation p 3312 N94-30866
Wind tunnel tests of a 5.3 m diameter yaw controlled turbine
[FFA-TN-1993-20] p 3340 N94-30946
A control method for bilateral teleoperating systems
[ISBN-0-315-78705-8] p 3313 N94-30952

CONTROL THEORY
Application of digital control theory to adaptive grid generation p 3127 N94-28980
Air traffic management as principled negotiation between intelligent agents p 3137 N94-29562
A guidance and navigation system for two spacecraft rendezvous in translunar halo orbit
p 3142 N94-29837
Kinematic representations, workspace analysis, and grasp stability in robot arms and multi-fingered hands
p 3301 N94-29847
Decoupled flight control system design using the singular perturbation method p 3155 N94-29850
Robust adaptive control and filtering
p 3437 N94-29895
Stochastic stability and nonlinear control in mechanical systems p 3303 N94-29966
Second order necessary conditions in optimal control
[ISBN-0-315-85443-X] p 3437 N94-30255
A force-controllable macro-micro manipulator and its application to medical robots p 3314 N94-30441
A direct digital control-law synthesis in the w-domain: W-synthesis methodology p 3438 N94-30517
Fuzzy logic based robotic controller
[AIAA PAPER 94-1202-CP] p 3443 N94-30553
Dynamics and control of tethered satellite systems
p 3170 N94-30864
A control method for bilateral teleoperating systems
[ISBN-0-315-78705-8] p 3313 N94-30952
Robust control of robots via linear estimated state-feedback
[MEMO-1153] p 3449 N94-30963

CONTROLLABILITY
Exploring QDES as a tool for determining limits of achievable performance in aircraft design
[AD-A275359] p 3146 N94-28998

CONTROLLERS
Exploring QDES as a tool for determining limits of achievable performance in aircraft design
[AD-A275359] p 3146 N94-28998
Experimental evaluation of fuzzy logic control of a flexible arm manipulator
[AD-A275375] p 3434 N94-29013
Fault tolerant testbed evaluation, phase 1
[NASA-CR-188275] p 3171 N94-29035
An alternate method for achieving temperature control in the -160 to +90 C range
[NASA-CASE-NPO-18995-1-CU] p 3288 N94-29497
Design and test of electromechanical actuators for thrust vector control p 3163 N94-29650
Micro guidance and control synthesis: New components, architectures, and capabilities p 3144 N94-29792
Robotic hand-eye motor learning
p 3436 N94-29835
Integrated propulsion-airframe dynamics and control
p 3147 N94-29854
A design methodology for synthesizing low-order robust controllers for flexible structures p 3302 N94-29870
Application of fuzzy logic to the control of wind tunnel settling chamber temperature
[NASA-TM-109105] p 3157 N94-30200
Experimental sliding mode control of a flexible single link manipulator
[ISBN-0-315-85466-9] p 3304 N94-30238
A fuzzy logic controller for hormone administration using an implantable pump p 3397 N94-30459
A direct digital control-law synthesis in the w-domain: W-synthesis methodology p 3438 N94-30517
Confessions of a robot lobotomist
[AIAA PAPER 94-1185-CP] p 3440 N94-30535
Fuzzy logic based robotic controller
[AIAA PAPER 94-1202-CP] p 3443 N94-30553
Vehicle following controller design for autonomous intelligent vehicles
[AIAA PAPER 94-1203-CP] p 3443 N94-30554
Situational reaction and planning
[AIAA PAPER 94-1206-CP] p 3444 N94-30557
Programmable Automated Welding System (PAWS)
[AIAA PAPER 94-1221-CP] p 3446 N94-30570
Robotic NDE inspection of advanced solid rocket motor casings
[AIAA PAPER 94-1222-CP] p 3446 N94-30571
Local interaction control for space construction
p 3170 N94-30960

CONVECTION
A model analysis of potential vorticity on isopycnal surfaces for the global ocean
[AD-A275047] p 3377 N94-29164
Convective turbulence and transport in stars
p 3546 N94-29913
A laboratory simulation of urban heat-island-induced circulation in a stratified environment
p 3367 N94-30921

CONVECTION CURRENTS
On the origins of low-level tornadic circulations within the remnants of hurricane Andrews
[AD-A275373] p 3369 N94-29011
Hydrodynamics of convection under winter polar leads
[AD-A275182] p 3369 N94-29067
Prototype terminal aerodrome forecasts using a mesoscale model
[AD-A275308] p 3369 N94-29194
Evaluation of the National Meteorological Center mesoscale model for prediction of severe convection over Central Arizona p 3371 N94-29744

CONVECTIVE FLOW
Convective flow effects on protein crystal growth
[NASA-CR-195785] p 3515 N94-30015

CONVECTIVE HEAT TRANSFER
Numerical comparison of convective heat transfer augmentation devices used in cooling channels of hypersonic vehicles
[NASA-TM-106546] p 3279 N94-30147
CONVERGENCE
The bootstrapped algorithm: A fast algorithm for blind signal separation
[AD-A275759] p 3408 N94-28760
A study of the convergence of spherical harmonic expansions of gravity using distributed point-mass Earth models p 3362 N94-29909
Perpetual reductions in orthogonal combinatory reduction systems
[CWI-CS-R9349] p 3459 N94-30413
Eigenvalue analysis of the convergence behaviour of an Euler method
[PB94-1255722-U] p 3281 N94-30743
CONVERGENT-DIVERGENT NOZZLES
Supersonic gas-liquid cleaning system
p 3240 N94-30467
CONVEXITY
Representations of dynamical systems described by behavioral inequalities
[AD-B173649] p 3458 N94-30402
CONVOLUTION INTEGRALS
Convolutional encoding of self-dual codes
p 3250 N94-29662
Decoder synchronization for deep space missions
p 3250 N94-29664
CONVULSIONS
Monitor for status epilepticus seizures
p 3397 N94-30460
COOL STARS
Surface differential rotation in a sample of cool dwarf stars p 3545 N94-29827
COOLANTS
Research and development of high thermal stability fuels p 3192 N94-29261
COOLING
Alleviation of thermal strain in the CF: Keeping our cool during the Gulf conflict p 3383 N94-28449
Electron beam irradiation experiments of monoblock divertor mock-up
[DE94-707497] p 3503 N94-28555
Numerical comparison of convective heat transfer augmentation devices used in cooling channels of hypersonic vehicles
[NASA-TM-106546] p 3279 N94-30147
COOLING FINS
The influence of wall conductivity of film condensation with integral fin tubes
[AD-A275503] p 3523 N94-28662
Numerical comparison of convective heat transfer augmentation devices used in cooling channels of hypersonic vehicles
[NASA-TM-106546] p 3279 N94-30147
COOLING FLOWS (ASTROPHYSICS)
Numerical simulations of cluster cooling flows
p 3544 N94-29725
Optical depth effects in cluster cooling flows
p 3541 N94-30800
COOLING SYSTEMS
Recent Canadian advances in active thermal protection p 3384 N94-28451
Endothermic fuels for hypersonic aviation
p 3197 N94-29285
Liquid metal MHD and heat transfer in a tokamak blanket slotted coolant channel
[DE94-004622] p 3506 N94-29510
An actively cooled floating element skin friction balance for direct measurement in high enthalpy supersonic flows p 3289 N94-29824
TOPAZ 2 system description
[DE94-006230] p 3498 N94-30846
COORDINATES
Variational calculation of the eigenpotential for H(sup -)-system
[DE94-606269] p 3407 N94-28622
Least-squares determination of burst-point coordinates
[AD-A275423] p 3452 N94-28864
Quasi-adiabatic motion of energetic particles in a dipole magnetic field
[DE94-607322] p 3362 N94-29935
COORDINATION
Coordinated control of multiple robot manipulators
p 3306 N94-30289
COPOLYMERIZATION
The polymerization of epsilon-caprolactone with stannous catalyst and lactide/epsilon-caprolactone (LA/epsilon-CL) and lactide/glycolide (LA/GA) copolymers. Polymer technology publication series no. 15
[PB94-137551] p 3220 N94-30713
COPOLYMERS
Polymer technology publication series no. 16
[PB94-135522] p 3214 N94-29157
A new material for removing heavy metals from water
p 3354 N94-30471
The polymerization of epsilon-caprolactone with stannous catalyst and lactide/epsilon-caprolactone (LA/epsilon-CL) and lactide/glycolide (LA/GA) copolymers. Polymer technology publication series no. 15
[PB94-137551] p 3220 N94-30713
COPPER
Low frequency dynamics of CO/Cu-breakdown of Born-Oppenheimer approximation
[DE94-005508] p 3510 N94-28512
Intermetallic growth at the interface between copper and bismuth-tin solder
[AD-A275716] p 3202 N94-28643
Anodization of copper in chloride media
[AD-A275565] p 3202 N94-28793
Properties of graphite fiber reinforced copper matrix composites for space power applications
[NASA-CR-191026] p 3178 N94-29208
Nanosize metal alloy particle formation in Ag and Cu sequentially implanted silica
[DE94-005592] p 3207 N94-30042
Effects of hydrogen on the resistivity of thin Au and Cu films p 3218 N94-30225
Metafusion: A breakthrough in metallurgy
p 3211 N94-30446
COPPER ALLOYS
Directional solidification characteristics of hyper-eutectic Al-Cu alloys under varying gravity conditions
[ISBN-0-315-86108-8] p 3209 N94-30146
Studies on the optimization of deformation processed metal-metal matrix composites
[DE94-006033] p 3185 N94-30704
COPPER CHLORIDES
Anodization of copper in chloride media
[AD-A275565] p 3202 N94-28793
COPPER OXIDES
Influence of doping on the electronic structure of (La, Sr)2CuO4
[DE94-006383] p 3516 N94-30054
Investigation of the phase equilibria and phase transformations associated with the Bi2Sr2CaCu2O(y) superconductor
[DE94-004889] p 3519 N94-30691
Normal state resistivity of MBa2Cu3O(7-x) ceramics
[DE94-608456] p 3220 N94-30745
Intra- versus interlayer pairing in the copper oxide superconductors: Response to a magnetic field
[DE94-005475] p 3521 N94-30898
CORE SAMPLING
Collecting cometary soil samples? Development of the ROSETTA sample acquisition system
p 3160 N94-29628
CORIOLIS EFFECT
Similarity between turbulent flows through curved pipe and orthogonal rotating pipe p 3128 N94-28986
A model analysis of potential vorticity on isopycnal surfaces for the global ocean
[AD-A275047] p 3377 N94-29164
CORN
Frequency dependence of polarization phase difference
[NASA-TM-109737] p 3254 N94-30094
CORNERS
Three-dimensional flow characteristics downstream of a blade endwall corner p 3280 N94-30229
COROTATION
Local heat transfer in an enclosed corotating disk with axial throughflow p 3276 N94-29849
CORRELATION
Exclusive many-particle diffusion in disordered media and correlation functions for random vertex models
[DE94-608134] p 3525 N94-30121
CORRELATORS
A digital combining-weight estimation algorithm for broadband sources with the array feed compensation system p 3250 N94-29660
CORROSION
Fundamental studies on the corrosion behavior of weldments in marine microbial environments
[AD-A275247] p 3203 N94-28900
Portable electronically based method for the nondestructive remote sensing of crevice corrosion
[AD-A275403] p 3318 N94-29057
Dual-Band Infrared (DBIR) imaging inspections of Boeing 737 and KC-135 aircraft panels
[DE94-005700] p 3122 N94-29842
Corrosion performance of materials for advanced combustion systems
[DE94-006726] p 3207 N94-30057
An investigation of the corrosion properties of aluminum-tantalum alloys using electrochemical impedance spectroscopy and local electrochemical impedance spectroscopy p 3209 N94-30521
Dual-band infrared imaging for quantitative corrosion detection in aging aircraft
[DE94-004187] p 3149 N94-30687
CORROSION PREVENTION
Corrosion inhibition by electrodeposited conductive-polymer film
[AD-A275456] p 3213 N94-28806
Electrochemical behavior and surface chemistry of nonequilibrium aluminum alloys: Passivity mechanism and fabrication methods
[AD-A275401] p 3204 N94-29196
Non-chromate talc conversion coatings for aluminum
[DE94-005281] p 3207 N94-30053
Evaluation of corrosion protecting properties of modern aircraft paint systems
[AD-B179388] p 3220 N94-30420
Photovoltaic power without batteries for continuous cathodic protection p 3341 N94-30465
Development of a unique polyurethane primer/topcoat
p 3223 N94-30476
CORROSION RESISTANCE
Corrosion inhibition by electrodeposited conductive-polymer film
[AD-A275456] p 3213 N94-28806
Electrochemical behavior and surface chemistry of nonequilibrium aluminum alloys: Passivity mechanism and fabrication methods
[AD-A275401] p 3204 N94-29196
Performance of CVD and CVR coated carbon-carbon in high temperature hydrogen
[DE94-005451] p 3487 N94-29841
Non-chromate talc conversion coatings for aluminum
[DE94-005281] p 3207 N94-30053
Corrosion performance of materials for advanced combustion systems
[DE94-006726] p 3207 N94-30057
COSINE SERIES
Some remarkable sine and cosine functions
[PB94-137759] p 3453 N94-29439
COSMIC DUST
Dust in the Small Magellanic Cloud
[NASA-CR-195764] p 3543 N94-29696
Infrared properties of obscuring dust tori in active galactic nuclei p 3545 N94-29832
COSMIC GASES
Energetic events in the early universe
p 3547 N94-30012
A single-fluid, self-consistent formulation of particle transport and fluid dynamics p 3280 N94-30352
COSMIC NOISE
Initial observation results with imaging riometer at NY-Alesund (L is equal to 16) p 3360 N94-29239
COSMIC RAY SHOWERS
A study of the ultrahigh-energy cosmic ray mass composition with the MACRO and EAS-TOP experiments p 3552 N94-29687
A study of ultra high-energy radiation associated with Hercules X-1 p 3552 N94-29823
COSMIC RAYS
Production rates of terrestrial in-situ-produced cosmogenic nuclides
[DE94-005156] p 3543 N94-28545
Acceleration in astrophysics
[DE94-004986] p 3552 N94-28580
A study of ultra high-energy radiation associated with Hercules X-1 p 3552 N94-29823
Camera artifacts in IUE spectra
[NASA-CR-189337] p 3198 N94-29857
Determination of cosmic ray latchup rate in CMOS devices p 3497 N94-30222
A single-fluid, self-consistent formulation of particle transport and fluid dynamics p 3280 N94-30352
COSMOCHEMISTRY
Production rates of terrestrial in-situ-produced cosmogenic nuclides
[DE94-005156] p 3543 N94-28545
COSMOLOGY
Cosmogenic C-14 in Antarctic and non-Antarctic meteorites and lunar samples
[NASA-CR-195795] p 3546 N94-29905
On dyonic black holes and cosmic censorship
p 3546 N94-29912
The angular two-point correlation function of galaxies down to 25th mag p 3547 N94-30010
Energetic events in the early universe
p 3547 N94-30012
COST ANALYSIS
A family of joint probability models for cost and schedule uncertainties
[AD-A275513] p 3463 N94-28670

Analysis of cost: CVD diamond deposition and finishing --- Quarterly report
[AD-A275586] p 3212 N94-28725
Aircraft age impact on individual operating and support cost elements
[AD-A275739] p 3121 N94-28732
Business planning model user's guide
[AD-A274978] p 3409 N94-28895
PV Cz silicon manufacturing technology improvements
[DE94-000248] p 3339 N94-30603
Assessment of costs and benefits of flexible and alternative fuel use in the US transportation sector
[DE94-006100] p 3226 N94-30885

COST EFFECTIVENESS
Risk-based prioritization: A comparison of approaches
[DE94-003368] p 3526 N94-28474
Alumina ceramic: A cost effective replacement for titanium in deep submergence pressure housings
[AD-A275640] p 3212 N94-28641
Development of large area RF induction plasma for cost effective diamond
[AD-A275888] p 3504 N94-28776
Application of digital video to hypermedia training systems
[AD-A274989] p 3409 N94-28910
Ventilation cost and air cleaning p 3232 N94-29605
PV Cz silicon manufacturing technology improvements
[DE94-000248] p 3339 N94-30603
Solar photovoltaics for development applications
[DE94-006116] p 3340 N94-30843

COST ESTIMATES
Demonstration of improved software support labor estimation for Air Force operational flight programs through functional orientation
[AD-A275789] p 3121 N94-28743
Business planning model user's guide
[AD-A274978] p 3409 N94-28895
Ventilation cost and air cleaning p 3232 N94-29605
Estimating the cost of large superconducting thin solenoid magnets
[DE94-006289] p 3468 N94-30026
Overview of the US stellarator reactor study
[DE94-006042] p 3508 N94-30339

COST REDUCTION
Photovoltaic power without batteries for continuous cathodic protection p 3341 N94-30465
PV Cz silicon manufacturing technology improvements
[DE94-000248] p 3339 N94-30603

COSTS
Ventilation cost and air cleaning p 3232 N94-29605
Fuel cycle evaluations of biomass-ethanol and reformulated gasoline
[DE94-000227] p 3226 N94-30818
Benchmarking for cost improvement
[DE94-002276] p 3528 N94-30824

COULOMB COLLISIONS
Simulation of experiments on deep inelastic scattering of muons on superconducting magnetic toroidal spectrometer STORS
[DE94-606267] p 3483 N94-28554
Conceptual study of moderately coupled plasmas and experimental comparison of laboratory x ray sources
[DE94-005828] p 3506 N94-30045

COULOMB POTENTIAL
Quasipotential in the fourth order of perturbation theory
[DE94-606299] p 3484 N94-28584

COUNTER ROTATION
Design and fabrication of forward-swept counterrotation blade configuration for wind tunnel testing
[NASA-CR-194868] p 3155 N94-28510

COUNTERMEASURES
NATO SOCMET trials p 3258 N94-30503

COUNTERS
A measurement of the LMP effect
[DE94-005225] p 3482 N94-28493

COUNTING
Photon counting spectroscopy as done with a Thomson scattering diagnostic
[DE94-005543] p 3503 N94-28515

COUPLERS
An investigation of distributed coupling in a nonlinear semiconductor waveguide p 3246 N94-29529

COUPLING
TFTR Ion Cyclotron Range of Frequencies (ICRF) experimental data analysis collaboration
[DE94-004699] p 3504 N94-28575

COUPLING COEFFICIENTS
Dynamics of a coupled solid state laser array p 3294 N94-29551

COUPLINGS
Quick connect fastener
[NASA-CASE-MFS-28829-1] p 3300 N94-29486
Development and testing of the Automated Fluid Interface System p 3161 N94-29636

CRACK CLOSURE
On fatigue crack closure: Analysis and measurement
[ISBN-0-315-74873-7] p 3321 N94-29812

CRACK INITIATION
Single specimen fracture toughness determination procedure using instrumented impact test
[PB94-132040] p 3316 N94-28402
Development of Alternating Current Potential Drop (ACPD) procedures for crack detection in aluminum aircraft panels
[AD-A275755] p 3315 N94-28646
Static fracture behavior of a ceramic matrix composite at elevated temperatures
[AD-A275363] p 3177 N94-29008
Analyses of stationary and growing crack tip deformation by digital image processing p 3320 N94-29690
The role of plastic deformation in brittle and near-brittle cracking behavior p 3322 N94-30226

CRACK OPENING DISPLACEMENT
Single specimen fracture toughness determination procedure using instrumented impact test
[PB94-132040] p 3316 N94-28402
Analyses of stationary and growing crack tip deformation by digital image processing p 3320 N94-29690
On fatigue crack closure: Analysis and measurement
[ISBN-0-315-74873-7] p 3321 N94-29812
Fracture process zone of brittle composites p 3182 N94-29876

CRACK PROPAGATION
Single specimen fracture toughness determination procedure using instrumented impact test
[PB94-132040] p 3316 N94-28402
Development of Alternating Current Potential Drop (ACPD) procedures for crack detection in aluminum aircraft panels
[AD-A275755] p 3315 N94-28646
Full-scale testing and analysis of curved aircraft fuselage panels
[AD-A275666] p 3145 N94-28657
Plane stress stable crack growth and J-integral/HRR field
[AD-A275761] p 3317 N94-28761
Analyses of stationary and growing crack tip deformation by digital image processing p 3320 N94-29690
Mechanisms and effects of heat generation at the tips of dynamic cracks and notches in metals p 3321 N94-29808
Dynamic fracture mechanics analysis for an edge delamination crack
[NASA-TM-109106] p 3479 N94-29856
Fracture process zone of brittle composites p 3182 N94-29876
Acoustic emission monitoring of aging aircraft structures
[DREP-93-17] p 3148 N94-30129
Enhanced fatigue crack detection in aging aircraft using continuous acoustic emission monitoring
[DREP-93-16] p 3148 N94-30131
Time-resolved holography for the microscopic study of crack-tip motion in dynamic fracture p 3290 N94-30254
An investigation of fatigue crack propagation under mode 1 and mixed mode 1/2 loadings p 3323 N94-30814
Fractographic and microstructural analysis of fatigue crack growth in Ti-6Al-4V fan disc forgings
[AD-B174765] p 3153 N94-30914

CRACK TIPS
Plane stress stable crack growth and J-integral/HRR field
[AD-A275761] p 3317 N94-28761
Flux-focusing eddy current probe and method for flaw detection
[NASA-CASE-LAR-15046-1] p 3315 N94-29366
Analyses of stationary and growing crack tip deformation by digital image processing p 3320 N94-29690
Mechanisms and effects of heat generation at the tips of dynamic cracks and notches in metals p 3321 N94-29808
Higher order asymptotic crack tip fields in a power-law hardening material p 3321 N94-29829
Fracture process zone of brittle composites p 3182 N94-29876
Time-resolved holography for the microscopic study of crack-tip motion in dynamic fracture p 3290 N94-30254
Experimental and analytical comparison of constraint effects due to biaxial loading and shallow-flaws
[DE94-004794] p 3323 N94-30689

CRACKING (FRACTURING)
Single specimen fracture toughness determination procedure using instrumented impact test
[PB94-132040] p 3316 N94-28402
Full-scale testing and analysis of curved aircraft fuselage panels
[AD-A275666] p 3145 N94-28657
Fatigue behavior of a cross-ply ceramic matrix composite under strain controlled tension-tension and tension-compression loading
[AD-A275374] p 3177 N94-29012
Effect of microstructure on the strength and fracture energy of bimaterial interfaces
[AD-A274987] p 3178 N94-29126
Analyses of stationary and growing crack tip deformation by digital image processing p 3320 N94-29690

CRACKS
Electron beam irradiation experiments of monoblock divertor mock-up
[DE94-707497] p 3503 N94-28555
Development of Alternating Current Potential Drop (ACPD) procedures for crack detection in aluminum aircraft panels
[AD-A275755] p 3315 N94-28646
Plane stress stable crack growth and J-integral/HRR field
[AD-A275761] p 3317 N94-28761
Fundamental studies on the corrosion behavior of weldments in marine microbial environments
[AD-A275247] p 3203 N94-28900
Effect of surface condition on strength and fatigue behavior of alumina ceramic
[AD-A275053] p 3214 N94-29133
Flux-focusing eddy current probe and method for flaw detection
[NASA-CASE-LAR-15046-1] p 3315 N94-29366
Mechanisms and effects of heat generation at the tips of dynamic cracks and notches in metals p 3321 N94-29808
Dynamic fracture mechanics analysis for an edge delamination crack
[NASA-TM-109106] p 3479 N94-29856
Fracture process zone of brittle composites p 3182 N94-29876
Delamination growth in composites under cyclic loads p 3183 N94-30256

CRASHWORTHINESS
Crashworthiness analysis of commuter aircraft seats
[AD-A275889] p 3135 N94-28799

CRAWLER TRACTORS
Antarctic Record, vol. 36, no. 3
[REPT-108] p 3363 N94-29978
A newly developed snow vehicle (SM100S) for Antarctica. Part 1: Necessity and process of the development p 3314 N94-29981
A newly developed snow vehicle (SM100S) for Antarctica. Part 2: Design of the system p 3314 N94-29982
A newly developed snow vehicle (SM100S) for Antarctica. Part 3: Low temperature toughness of the welded joints of the structural steel p 3364 N94-29983
A newly developed snow vehicle (SM100S) for Antarctica. Part 4: Low temperature properties of crawler belt p 3314 N94-29984
A newly developed snow vehicle (SM100S) for Antarctica. Part 5: Result of general performance tests p 3314 N94-29985

CRAY COMPUTERS
Computational methods in continuum mechanics
[AD-A275560] p 3451 N94-28792

CREATIVITY
A case-based approach to creative design
[AD-A275229] p 3417 N94-29390

CREEP ANALYSIS
The effect of temperature on creep and physical ageing of PVC
[NPL-DMM(A)-93] p 3217 N94-29885
Creep and physical aging of PVC: Dependence on stress and temperature
[NPL-DMM(A)-115] p 3217 N94-29886

CREEP PROPERTIES
Relationship between swelling and irradiation creep in cold-worked PCA stainless steel irradiated to approximately 178 dpa at approximately 400 C
[DE94-004368] p 3201 N94-28456
Effects of thermomechanical processing on tensile and long-time creep behavior of Nb-1 percent Zr-0.1 percent C sheet
[NASA-TM-106319] p 3202 N94-28822
Probabilistic material strength degradation model for Inconel 718 components subjected to high temperature, mechanical fatigue, creep and thermal fatigue effects
[NASA-CR-195284] p 3318 N94-28840
Modelling and analysis of creep deformation and fracture in a 1 Cr 1/2 Mo ferritic steel
[PB94-138328] p 3319 N94-29121
Effects of physical aging on long-term creep of polymers and polymer matrix composites
[NASA-TM-109081] p 3181 N94-29541
Creep and physical aging of PVC: Dependence on stress and temperature
[NPL-DMM(A)-115] p 3217 N94-29886

Creep behavior of MoSi2-SiC composites
[DE94-004980] p 3185 N94-30693
Microstructural development and mechanical behavior of eutectic bismuth-tin and eutectic indium-tin in response to high temperature deformation
[DE94-005202] p 3210 N94-30710

CREEP TESTS
The effect of temperature on creep and physical ageing of PVC
[NPL-DMM(A)-93] p 3217 N94-29885

CRETACEOUS PERIOD
Motion and development of the Pacific Plate from the Middle Jurassic to the Late Cretaceous
p 3362 N94-29939
Studies in Jurassic and Cretaceous North American apparent polar wander p 3362 N94-29940

CRETACEOUS-TERTIARY BOUNDARY
Field guide to Cretaceous-tertiary boundary sections in northeastern Mexico
[NASA-CR-195719] p 3354 N94-28416

CRITERIA
The development and demonstration of the metric assessment tool
[AD-A275788] p 3230 N94-28742

CRITICAL EXPERIMENTS
Experimental and analytical studies of high heat flux components for fusion experimental reactor
[DE94-707671] p 3504 N94-28556

CRITICAL LOADING
Delamination of woven E-glass fabric composites
[DE94-003227] p 3185 N94-30827

CROSS CORRELATION
Reconstruction of stellar images from correlations
[ISBN-0-315-85382-4] p 3541 N94-30133
Providing hydrogen maser timing stability to orbiting VLBI radio telescope observations by post-measurement compensation of linked frequency standard imperfections p 3297 N94-30670

CROSS FLOW
The mixing process in the quenching zone of the rich-lean-combustion concept p 3196 N94-29281
Long-wavelength asymptotics of unstable crossflow modes, including the effect of surface curvature
[NASA-CR-4579] p 3273 N94-29460

CROSS SECTIONS
Calculation of inelastic mean free path and stopping power for electrons in solids from an optical-data model
[USIP-92-06] p 3494 N94-30980

CROSSED FIELDS
The investigation of electron-ion radiative and dielectronic recombination in high-temperature plasmas
[DE94-005150] p 3509 N94-30755

CROSSLINKING
Organic materials that respond to molecules
[AD-A275392] p 3174 N94-29307
Controlling the material properties of in vitro collagen through directed orientation and cross-linking of fibrils
p 3221 N94-30797
Crosslinking and surface reactions in macromolecules: Spectroscopic FT-IR studies p 3221 N94-30812

CRRES (SATELLITE)
Proton switches
[AD-A275150] p 3167 N94-29022
Identification of an unexpected space radiation hazard
[AD-A275170] p 3552 N94-29046

CRUCIBLES
A novel approach to the fabrication of SiC structures of arbitrary shape
[AD-A275475] p 3214 N94-29073

CRUDE OIL
Survey on effects of petroleum substitution energy utilization on the global environment
[DE94-732339] p 3346 N94-28630

CRYOGENIC COOLING
Centrifugal atomization of lanthanide materials for cryogenic coolers
[DE94-006035] p 3219 N94-30337

CRYOGENIC EQUIPMENT
An absolute measurement of the cosmic background radiation temperature at 1.4 GHz p 3553 N94-30351

CRYOGENIC FLUID STORAGE
Cryogenic on-orbit liquid depot storage acquisition and transfer (COLD-SAT) experiment subsystem instrumentation and wire harness design report
[NASA-CR-189172] p 3168 N94-29405
Large scale cryogenic fluid systems testing
[NASA-TM-109735] p 3157 N94-29904

CRYOGENIC FLUIDS
Development and testing of the Automated Fluid Interface System p 3161 N94-29636

CRYOGENIC TEMPERATURE
Cryogenic probe station for use in automated microwave and noise figure measurements
[NASA-TM-106560] p 3286 N94-29000
Collecting cometary soil samples? Development of the ROSETTA sample acquisition system
p 3160 N94-29628
The far-infrared absorption spectrum of low temperature hydrogen gas
[ISBN-0-315-85432-4] p 3199 N94-30137

CRYOGENIC WIND TUNNELS
Analysis of fluctuating static pressure measurements in a large high Reynolds number transonic cryogenic wind tunnel p 3158 N94-30788

CRYOGENICS
ISO overview: General presentation of the satellite, cryogenic aspects
[REPT-932-440-102] p 3231 N94-29416

CRYOPUMPING
Argon frost continuous cryopump for fusion applications
[DE94-004478] p 3230 N94-29017
Application of divertor cryopumping to H-mode density control in DIII-D
[DE94-004859] p 3510 N94-30832

CRYOSTATS
Estimating the cost of large superconducting thin solenoid magnets
[DE94-006289] p 3468 N94-30026

CRYPTOGRAPHY
Digital camera with apparatus for authentication of images produced from an image file
[NASA-CASE-NPO-19108-1-CU] p 3287 N94-29373
RIPE integrity primitives, part 1 (RACE Integrity Primitives Evaluation)
[CWI-CS-R9324-PT-1] p 3252 N94-29692
RIPE integrity primitives, part 2 (RACE Integrity Primitives Evaluation)
[CWI-CS-R9325-PT-2] p 3252 N94-29693

CRYSTAL DEFECTS
Dislocation loops in spinel crystals irradiated successively with deep and shallow ion implants
[DE94-005083] p 3517 N94-30201
The influence of an in-situ electric field on H(+) and He(+) implantation induced defects insil icon
[DE94-006553] p 3518 N94-30249
Fullerenes as precursors for diamond film growth without hydrogen or oxygen additions
[DE94-004582] p 3519 N94-30718

CRYSTAL DISLOCATIONS
Nanodislocation structures generated in shocked crystals p 3514 N94-29915

CRYSTAL FIELD THEORY
Magnetic properties of a transverse spin-1 Ising model with longitudinal crystal field interactions
[DE94-608118] p 3517 N94-30165
Magnetic properties of a transverse spin-1 Ising model with random crystal field interactions
[DE94-608117] p 3517 N94-30181

CRYSTAL GROWTH
Intermetallic growth at the interface between copper and bismuth-tin solder
[AD-A275716] p 3202 N94-28643
Growth condition of an ice layer in freezing soils under applied loads. Part 1: Experiment
[AD-A275215] p 3357 N94-29070
X ray standing wave studies of underpotentially deposited metal monolayers
[AD-A275409] p 3513 N94-29215
Synthesis of diamond in a hydrogen plasma jet: Simulations of XRD patterns of diamond polytypes and boundary layer on a substrate p 3522 N94-29515
A photoemission electron microscope investigation of chemical vapor deposition diamond films and diamond nucleation p 3215 N94-29745
Process modelling for materials preparation experiments
[NASA-CR-195782] p 3175 N94-30242
Strain relaxation and surface roughness as a function of growth temperature in linearly graded In(x)Al(1-x)As (x = 0.05 to 0.25) buffers
[DE94-005430] p 3519 N94-30592
Thin EFG octagons
[DE94-000257] p 3339 N94-30605
Research on the atomic layer-by-layer growth of high-temperature superconductor thin films at the Institute of Scientific and Industrial Research, Japan
[DE94-003739] p 3519 N94-30611
Survey report of JSUP Space Environment Utilization Research Committee in fiscal year 1992: Metallic Materials Session
[JTN-94-80583] p 3159 N94-30794
Study of nucleation and growth in Al-Zn alloys using TEM
[DE94-006312] p 3211 N94-30852
A solid-on-solid invasion percolation model for self-affine interfaces
[DE94-608102] p 3521 N94-30888

CRYSTAL LATTICES
Interstitially stabilized phases in the zirconium-nickel system
[DE94-005561] p 3201 N94-28525
Atomic and magnetic structure of YBa2(Cu(1-x)Fe(x))3O(6+y) at 0.05 less than or equal to x less than or equal to 0.30, y is approximately equal to 1 and y is approximately equal to 0.5
[DE94-606852] p 3513 N94-29210
A pot-pourri of results in QCD from large lattice simulations on the CM5
[DE94-005084] p 3514 N94-29818
The bases for the development of high-temperature integrated SQUID-systems
[DE94-608462] p 3517 N94-30082
Some results on the phase diagram of the antiferromagnetic Potts model in an external magnetic field
[DE94-608115] p 3468 N94-30110
Exclusive many-particle diffusion in disordered media and correlation functions for random vertex models
[DE94-608134] p 3525 N94-30121
Lattice gas simulations of replicating domains
[DE94-005008] p 3200 N94-30748

CRYSTAL OSCILLATORS
Ground control system for the midcourse space experiment UTC clock p 3474 N94-30674

CRYSTAL STRUCTURE
Synthesis and characterization of novel ternary and quaternary reduced molybdenum oxides
[DE94-005563] p 3510 N94-28529
Crystal structure of La(2-x)Ba(x)CuO4
[DE94-707688] p 3511 N94-28750
Preparation, characterization, and facile thermolysis of (X2GaP(SiMe3)2) (X = Br, I) and (Cl3Ga2P)n; new precursors to nanocrystalline gallium phosphide
[AD-A275019] p 3513 N94-29130
Synthesis and molecular structures of R(Me3CCH2)2In-E(SiMe3) (R = Me3CCH2, E = P or As; R = Me, E = P)
[AD-A275020] p 3486 N94-29131
X ray crystal structures of ((Me3SiCH2)2InCl)2 and ((Me3SiCH2)InCl2)
[AD-A275074] p 3513 N94-29155
Nanodislocation structures generated in shocked crystals p 3514 N94-29915
Pit initiation on passivated metal surfaces: Crystallographic orientation and environmental effects
[ISBN-0-315-85433-2] p 3208 N94-30138
Studies of high temperature ternary phases in mixed-metal-rich early transition metal sulfide and phosphide systems
[DE94-006034] p 3209 N94-30336
Fullerenes as precursors for diamond film growth without hydrogen or oxygen additions
[DE94-004582] p 3519 N94-30718

CRYSTAL SURFACES
Strain relaxation and surface roughness as a function of growth temperature in linearly graded In(x)Al(1-x)As (x = 0.05 to 0.25) buffers
[DE94-005430] p 3519 N94-30592

CRYSTALLITES
Crystallization of silver chromate from ethanol via salt metathesis reactions of solubilized precursors
[AD-A275178] p 3189 N94-29058
Bench-scale synthesis of nanoscale materials
p 3240 N94-30473

CRYSTALLIZATION
Crystallization of silver chromate from ethanol via salt metathesis reactions of solubilized precursors
[AD-A275178] p 3189 N94-29058
The thermal consequences of giant impacts in the early solar system p 3543 N94-29698
Convective flow effects on protein crystal growth
[NASA-CR-195785] p 3515 N94-30015
Induced crystallization in CW laser-irradiated sol-gel deposited titania films
[DE94-006527] p 3207 N94-30062
Densification and crystallization of zirconia thin films prepared by sol-gel processing
[DE94-005573] p 3518 N94-30315
Investigation of the phase equilibria and phase transformations associated with the Bi2Sr2CaCu2O(y) superconductor
[DE94-004889] p 3519 N94-30691

CRYSTALLOGRAPHY
Directional solidification studies in Ni-Al alloys
[DE94-005562] p 3201 N94-28527
Pit initiation on passivated metal surfaces: Crystallographic orientation and environmental effects
[ISBN-0-315-85433-2] p 3208 N94-30138
Influence of tungsten alloying additions on the mechanical properties and texture of tantalum
[DE94-004994] p 3210 N94-30774

CRYSTALS
Effect of phonon dispersion on properties of exciton in magnetic field
[DE93-634756] p 3481 N94-28469
Innovative optoelectronic materials and structures using OMVPE
[AD-A275811] p 3511 N94-28773
Protein crystal growth in microgravity p 3228 N94-28943
The appearance of the Sun and Moon seen through clouds
[AD-A275338] p 3551 N94-29212
Magnetic properties of a quantum transverse spin-1 Blume-Emery-Griffiths model
[DE94-608114] p 3517 N94-30109
Overlap of metal clusters and nuclear structure physics
[DE94-608367] p 3517 N94-30183
CUBANE
Cubanes: Super explosives and potential pharmaceutical intermediates p 3227 N94-30454
CUBIC EQUATIONS
Approximation of solutions of the cubic NLSE by finite dimensional equations and non-squeezing properties
[PB94-138294] p 3452 N94-29148
CUBIC LATTICES
Synthesis of diamond in a hydrogen plasma jet: Simulations of XRD patterns of diamond polytypes and boundary layer on a substrate p 3522 N94-29515
CULTIVATION
Overview of space environment utilization science
[JTN-94-80581] p 3227 N94-28938
Cell culture in space p 3228 N94-28944
CULTURE TECHNIQUES
Barley cell culture as a producer of heterologous protein
[PB94-132339] p 3379 N94-28408
Cell culture in space p 3228 N94-28944
Stable RNA sequences as a tool for DNA probes and phylogenetic studies
[PB94-135423] p 3385 N94-29156
CURING
Dual cure low-VOC coating process, phase 3
[DE94-003202] p 3221 N94-30826
CURRENT ALGEBRA
Extended nonabelian symmetries for free fermionic model
[DE94-601554] p 3481 N94-28470
Anomalous algebraic structures in quantum field theories p 3524 N94-29911
CURRENT DENSITY
Fluctuation and transport reduction in a reversed field pinch by inductive poloidal current drive
[DE94-005542] p 3503 N94-28514
Stripline monitor electronics for the bundle position determination in AmPS
[DIGEL-1993-8] p 3495 N94-29888
Application of divertor cryopumping to H-mode density control in DIII-D
[DE94-004859] p 3510 N94-30832
Magnetic flux reconstruction methods for shaped tokamaks
[DE94-005827] p 3510 N94-30882
CURRENT DISTRIBUTION
A physical optics model for scattering of HF radiation by irregular terrain
[DE94-006187] p 3255 N94-30106
CURRENT SHEETS
Tail lobe ion composition at energies of 0.1 to 16 keV/e: Evidence for mass-dependent density gradients
[PAPER-93JA03201] p 3507 N94-30127
Experimental investigation of possible geomagnetic feedback from energetic (0.1 to 16 keV) terrestrial O(+) ions in the magnetotail current sheet
[PAPER-93JA01991] p 3507 N94-30128
CURVATURE
Analytic rendering of curvilinear volume data
[DE94-004934] p 3407 N94-28506
The performance of gloss meters on curving surfaces
[NPL-DMM(A)-111] p 3501 N94-30522
CURVE FITTING
An efficient algorithm for 3D connect-the-dots
[AD-A275431] p 3409 N94-28866
The exact fitting problem in higher dimensions
[RUU-CS-92-37] p 3456 N94-30377
CURVED PANELS
Full-scale testing and analysis of curved aircraft fuselage panels
[AD-A275666] p 3145 N94-28657
CURVES (GEOMETRY)
Trace formulas and dynamical zeta functions in the Nielsen theory
[PB94-138195] p 3467 N94-29163
CUSHIONS
BAG: A code for predicting the performance of a gas bag impact attenuation system for the Pathfinder lander
[DE94-003688] p 3165 N94-28477
CUTTERS
Effect of non-metallic inclusions on the machinability of steel
[PB93-230233] p 3204 N94-29387
Influence of clearance and rake angles on the cutting force of rock p 3368 N94-29520
Metafusion: A breakthrough in metallurgy p 3211 N94-30446
CUTTING
Influence of clearance and rake angles on the cutting force of rock p 3368 N94-29520
CYANATES
Correlation between wet ageing, humidity absorption and properties on composite materials based on different resins family
[REPT-932-600-107] p 3179 N94-29462
CYANIDES
Toxicity of carbon monoxide-hydrogen cyanide gas mixtures: Exposure concentration, time-to-incapacitation, carboxyhemoglobin, and blood cyanide parameters
[DOT/FAA/AM-94/7] p 3395 N94-29919
CYBERNETICS
A lateral inhibition neural network that emulates a winner-takes-all algorithm
[RUU-CS-92-46] p 3438 N94-30334
CYCLES
Effect of surface condition on strength and fatigue behavior of alumina ceramic
[AD-A275053] p 3214 N94-29133
The transient period of a cyclic process: An horizon theorem
[MEMO-1149] p 3427 N94-30585
Modeling Earth system changes of the past p 3353 N94-30635
CYCLIC ACCELERATORS
Some remarks about pseudo-Hamiltonian
[DE94-003273] p 3487 N94-29700
CYCLIC HYDROCARBONS
The active titration method for measuring local hydroxyl radical concentration p 3345 N94-28602
CYCLIC LOADS
Experimental and analytical studies of high heat flux components for fusion experimental reactor
[DE94-707671] p 3504 N94-28556
An analysis of isothermal, bithermal, and thermomechanical fatigue data of Haynes 188 and B1900+Hf by energy considerations
[NASA-TM-106359] p 3317 N94-28819
Granular bases for heavily loaded pavements
[AD-A275171] p 3156 N94-29047
Transient thermal fatigue of ceramic composites p 3216 N94-29874
Delamination growth in composites under cyclic loads p 3183 N94-30256
Damage analysis and mechanical response of as-received and heat-treated Nicalon/CAS-2 glass-ceramic matrix composites p 3219 N94-30259
WISPER and WISPERX: Final definition of two standardised fatigue loading sequences for wind turbine blades
[AD-B175835] p 3324 N94-30872
CYCLOGENESIS
Physical processes associated with variability in successive operational model forecasts of cyclogenesis
[ISBN-0-315-74753-6] p 3371 N94-29751
CYCLONES
Hydrodynamics of convection under winter polar leads
[AD-A275182] p 3369 N94-29067
Interannual temperature variability and cyclone frequency over Eastern Canada and the New England States. A case study: Winter seasons 1931-1932 to 1984-1985
[ISBN-0-315-74841-9] p 3373 N94-29908
CYCLOTRON FREQUENCY
TFTR Ion Cyclotron Range of Frequencies (ICRF) experimental data analysis collaboration
[DE94-004699] p 3504 N94-28575
Wave generation by contaminant ions near a large spacecraft
[NASA-CR-195797] p 3169 N94-29917
CYCLOTRON RADIATION
A study of white dwarf radiative accretion shocks p 3544 N94-29731
ECR plasma synthesis of silicon nitride films on GaAs and InSb
[DE94-005575] p 3515 N94-30006
CYCLOTRON RESONANCE
ECR plasma synthesis of silicon nitride films on GaAs and InSb
[DE94-005575] p 3515 N94-30006
Three-dimensional effects for radio frequency antenna modeling
[DE94-006102] p 3255 N94-30105
CYCLOTRONS
Advantages of the LBL 88-inch cyclotron ion beam for SEP studies
[AD-A275142] p 3494 N94-29065
CYLINDRICAL ANTENNAS
Theoretical and experimental study of a cylindrical microstrip antenna
[REPT-932-440-109] p 3245 N94-29456
CYLINDRICAL BODIES
Filament to mandrel gap analysis: Resulting gap from filament winding over a cone-cylinder transition mandrel (reference NMTP no. 93838)
[DE94-004225] p 3175 N94-28528
Effect of surface condition on strength and fatigue behavior of alumina ceramic
[AD-A275053] p 3214 N94-29133
The flow field near the body surface with thin filaments p 3234 N94-29706
Three-dimensional free vibration analysis of thick arbitrarily laminated, rectangular, cylindrical and spherical composite panels p 3184 N94-30257
CYLINDRICAL SHELLS
Numerical and experimental investigation of the bending response of thin-walled composite cylinders
[NASA-CR-195730] p 3317 N94-28801
CYLINDRICAL TANKS
Reliability of composite material structures. Application: High pressure spherical coded tanks
[REPT-932-430-103] p 3180 N94-29478

D

D LINES
Two-way satellite time transfer: Overview and recent developments p 3469 N94-30646
DAMAGE
Full-scale testing and analysis of curved aircraft fuselage panels
[AD-A275666] p 3145 N94-28657
Asphaltic concrete performance under heavy fighter aircraft loading
[AD-A275046] p 3157 N94-29151
Damage meso-modeling of 3D evolutive composites
[REPT-932-430-106] p 3179 N94-29442
Micromechanics of the dynamic response of ceramics and ceramic composites p 3217 N94-29975
DAMAGE ASSESSMENT
Cockpit video: A low cost BDA source
[AD-A275228] p 3150 N94-29389
Damage analysis and mechanical response of as-received and heat-treated Nicalon/CAS-2 glass-ceramic matrix composites p 3219 N94-30259
Damage identification in composites using built-in piezoelectrics p 3184 N94-30355
Analysis concerning the inspection threshold for multi-site damage
[PB94-142429] p 3149 N94-30905
DAMPING
Identification of the damping ratio relationship of an autovehicle suspension
[REPT-93-063] p 3313 N94-30937
DARK MATTER
The second coming of cold dark matter?
[DE94-004992] p 3548 N94-30694
DATA ACQUISITION
Laser velocimeter data acquisition system for the Langley 14- by 22-foot subsonic tunnel. Software reference guide version 3.3
[NASA-CR-191606] p 3293 N94-28839
The Norwegian seismic array (NORSAR), phase 3
[AD-A275440] p 3356 N94-28868
Performance evaluation of a 22.5/30 kW 270 volts direct current generator system
[AD-A275106] p 3263 N94-28913
Los Angeles international airport instrument landing system approach data collection and reduction, phase 1
[AD-A275115] p 3136 N94-28914
Evaluation of simulated JERS-1 data for geologic mapping at Drum Mountains, Utah, Silver Bell, Arizona, and Wind River, Wyoming under the GEOSAT-ERSDAC/JAPEX/JGI/RESTEC joint studies p 3326 N94-28929
JERS-1 data acquisition and distribution p 3326 N94-28931
Parallelization techniques for highly parallel vector computer p 3129 N94-28990
Principles and application tendency of remote sensing: Its principle, function and utilization p 3328 N94-29037
Status and tendency of earth observation system p 3328 N94-29038

Model-oriented data analysis with applications to lake and soil water simulation
[PB94-136942] p 3329 N94-29173
Application of JERS-1 data to geologic analyses
p 3330 N94-29222
Application of optical sensor data to resource survey
p 3330 N94-29223
Cryogenic on-orbit liquid depot storage acquisition and transfer (COLD-SAT) experiment subsystem instrumentation and wire harness design report
[NASA-CR-189172] p 3168 N94-29405
The Telecommunications and Data Acquisition Report
[NASA-CR-195694] p 3246 N94-29613
Radio science ground data system for the Voyager-Neptune encounter, part 1
p 3248 N94-29623
The Telecommunications and Data Acquisition Report
[NASA-CR-195689] p 3249 N94-29652
Recent results from testing fast ADCs
[DE94-005565] p 3406 N94-30004
Digital filter
[DE94-607902] p 3406 N94-30074
Program SCREEN for acquisition, visualization, processing and output of experimental data
[DE94-608009] p 3534 N94-30079
User's manual for the model interface and plugboard cabinets in the 14- by 22-foot subsonic tunnel
[NASA-TM-109062] p 3133 N94-30176
Air-deployable geophysics package
[DE94-005651] p 3335 N94-30594

DATA BASE MANAGEMENT SYSTEMS
The program for catalogization of magnetic tapes in EXCHARM experiment
[DE94-606271] p 3528 N94-28615
Specialized data base management system for data processing in the experiments at low energies
[DE94-606268] p 3485 N94-28621
A porting methodology for parallel database systems
[AD-A275256] p 3529 N94-29053
Batch updates and concurrency in B-trees
[PB94-136835] p 3530 N94-29167
On conceptual design of active databases
p 3531 N94-29535
Object-oriented database support for scientific data management: A system for experimentation
p 3531 N94-29677
A unified framework for retrieval in image databases
p 3533 N94-29811
Comparison of Savannah River Site's meteorological databases
[DE94-001751] p 3373 N94-29817
Hypra/TR: A tuple oriented recovery method for a continuously available distributed DBMS on a shared nothing multi-computer
[PB94-141264] p 3533 N94-29921
Secure network databases: Survey and analysis
[PB94-138492] p 3533 N94-29948
The evolution of information management
[DE94-004173] p 3535 N94-30179
Taxonomy of gamma ray burster data using a self-organizing neural network
[DE94-006480] p 3553 N94-30248
A user's guide to the Software Testpilot
[CWI-CS-R9343] p 3426 N94-30435

DATA BASES
NASA space and Earth science data on CD-ROM
[NASA-TM-109709] p 3528 N94-28414
ARTI Refrigerant Database
[DE94-004906] p 3230 N94-28563
Specialized data base management system for data processing in the experiments at low energies
[DE94-606268] p 3485 N94-28621
Simulation Networking/Training Requirements Relational Database: User's guide
[AD-A275634] p 3528 N94-28637
Updated deep-tow acoustics/geophysics system compressional velocity database
[AD-A275477] p 3355 N94-28685
Aviation epidemiology data register: Age distribution of U.S. Army aviators stratified by gender and component of service
[AD-A275901] p 3388 N94-28757
Los Angeles international airport instrument landing system approach data collection and reduction, phase 1
[AD-A275115] p 3136 N94-28914
Tinkertoy(tm) transactions
[AD-A275271] p 3410 N94-29006
A porting methodology for parallel database systems
[AD-A275256] p 3529 N94-29053
Reference model for project support environments, version 2.0
[AD-A275191] p 3410 N94-29068
Decompression sickness risk versus time and altitude
[AD-A275261] p 3391 N94-29071
The covering property of the object-oriented data model: Design and implementation issues
[AD-A275048] p 3530 N94-29165
Engineering document management system
[PB94-136934] p 3530 N94-29172
The UNICON approach to through-life support and evolution of software-intensive systems
p 3416 N94-29340
Redundant disk arrays in transaction processing systems
[NASA-CR-195759] p 3418 N94-29404
Tidal atlas software development
[AD-A275251] p 3377 N94-29432
On conceptual design of active databases
p 3531 N94-29535
The effects of inheritance on the properties of physical storage models in object-oriented databases
p 3531 N94-29537
Design and analysis of concurrency control schemes for heterogeneous database systems
p 3531 N94-29591
A unified framework for retrieval in image databases
p 3533 N94-29811
Performance of MCNP4A on seven computing platforms
[DE93-040101] p 3419 N94-29816
Comparison of Savannah River Site's meteorological databases
[DE94-001751] p 3373 N94-29817
Secure network databases: Survey and analysis
[PB94-138492] p 3533 N94-29948
Extrapolation of point data for resource mapping
p 3334 N94-29959
Pausing behavior of end-users in online searching
p 3533 N94-29960
Computer-based linking of thesauri
p 3534 N94-29961
Development of evaluated data bank of physical properties of perspective nuclear engineering steels and alloys
[DE94-607999] p 3207 N94-30076
Genetic algorithms for optimal database design
[TR-93-01] p 3535 N94-30330
DTL: A deductive and typed object-oriented language
[MEMO-INF-93-41] p 3425 N94-30417
VAS: A Vision Advisor System combining agents and object-oriented databases
[AIAA PAPER 94-1181-CP] p 3440 N94-30532
Information-seeking in hypertext: Multiple access methods in a full-text hypertext database
p 3536 N94-30918
View integration: A survey of current developments
[REPT-93-053] p 3536 N94-30927

DATA COMPRESSION
Image-adapted visually weighted quantization matrices for digital image compression
[NASA-CASE-ARC-12015-1] p 3406 N94-29375
Integer cosine transform for image compression
p 3247 N94-29619
Optimizing the Galileo space communication link
p 3250 N94-29663
Extending the X Window System
[DE94-006496] p 3420 N94-29844
Low frame rate video coding for small bandwidth realtime multimedia tele-education systems
[PB94-125531] p 3256 N94-30398
Fast and efficient variable-to-fixed-length coding algorithm
[PB94-125465] p 3424 N94-30400

DATA CORRELATION
Correlation analysis on optical and radio light curves for a large sample of active galactic nuclei
p 3546 N94-29992

DATA FLOW ANALYSIS
Common spaceborne multicomputer operating system and development environment
[NASA-TM-109092] p 3422 N94-30197
Customer creation and combination in queueing networks
[MEMO-INF-93-35] p 3438 N94-30375
Topological models for higher order control flow
[CWI-CS-R9340] p 3425 N94-30432

DATA INTEGRATION
ACCS Surveillance Exploratory Prototype (ASEP)
p 3138 N94-29566
Knowledge combination and data fusion with application to recognition systems p 3259 N94-30513
Multi-sensor data fusion and the use of artificial intelligence
[PB94-126216] p 3448 N94-30741

DATA LINKS
1.8 gigahertz (GHz) digital Low Density Radio Communications Link (LDRCL) Operational Test and Evaluation (OT&E) integration and OT&E operational final test report
[AD-A275800] p 3241 N94-28771
A new information system: Satellite observation
p 3330 N94-29219
Simulation of fully automated air traffic control concepts p 3139 N94-29569
Adaptive power control as a fade countermeasure on satellite links p 3253 N94-29697
Installation of experimental mode-S data link in commercial aircraft
[PB94-138757] p 3254 N94-29998
A physical optics model for scattering of HF radiation by irregular terrain
[DE94-006187] p 3255 N94-30106
Achieving robot autonomy p 3310 N94-30307
A multiplexed two-way solid communications link for teleoperated robots p 3310 N94-30310

DATA MANAGEMENT
NASA space and Earth science data on CD-ROM
[NASA-TM-109709] p 3528 N94-28414
The High Performance Storage System
[DE94-004350] p 3404 N94-28505
Transferable Output ASCII Data (TOAD) editor version 1.0 user's guide
[NASA-CR-187507] p 3408 N94-28818
A survey of geographical information systems applications for the Earth Science and Applications Division, Space Sciences Laboratory, Marshall Space Flight Center
[NASA-TM-108438] p 3529 N94-28820
JERS-1 data acquisition and distribution
p 3326 N94-28931
JERS-1 data and information system for resources exploration p 3327 N94-28932
Principles and application tendency of remote sensing: Its principle, function and utilization
p 3328 N94-29037
A porting methodology for parallel database systems
[AD-A275256] p 3529 N94-29053
Engineering document management system
[PB94-136934] p 3530 N94-29172
MODIS technical report series. Volume 3: MODIS airborne simulator level 1B data user's guide
[NASA-TM-104594] p 3231 N94-29385
Object-oriented database support for scientific data management: A system for experimentation
p 3531 N94-29677
Analysis of EDP performance
[NASA-CR-195726] p 3420 N94-29945
Mapping objects to files: A UNIX file system interface to an object management system
[RUU-CS-93-08] p 3428 N94-30746

DATA PROCESSING
A space-based classification system for RF transients
[DE94-003933] p 3240 N94-28522
Specialized data base management system for data processing in the experiments at low energies
[DE94-606268] p 3485 N94-28621
Defense Technical Information Center cataloging guidelines
[AD-A275100] p 3529 N94-28911
Basic research in computer science
[AD-A275222] p 3405 N94-28916
Operation semantics with read and write frames
[PB94-138138] p 3529 N94-29108
Invariants, frames and postconditions: A comparison of two formal specification notations
[PB94-138153] p 3405 N94-29110
A new information system: Satellite observation
p 3330 N94-29219
Designing and maintaining decision-making processes
p 3412 N94-29318
MODIS technical report series. Volume 3: MODIS airborne simulator level 1B data user's guide
[NASA-TM-104594] p 3231 N94-29385
Installation of experimental mode-S data link in commercial aircraft
[PB94-138757] p 3254 N94-29998
PAW using under MS DOS
[DE94-608012] p 3406 N94-30081

DATA PROCESSING EQUIPMENT
'Real time' and the NLR aerodynamic facilities
[AD-B173626] p 3158 N94-30856

DATA RECORDING
Cockpit video: A low cost BDA source
[AD-A275228] p 3150 N94-29389

DATA REDUCTION
Performance analysis of memory hierachies in high performance systems
[DE94-005549] p 3404 N94-28517
Los Angeles international airport instrument landing system approach data collection and reduction, phase 1
[AD-A275115] p 3136 N94-28914
Image processing for hyperspectral data
p 3326 N94-28930
JERS-1 data acquisition and distribution
p 3326 N94-28931

JERS-1 data and information system for resources exploration p 3327 N94-28932
Application of optical sensor data to resource survey p 3330 N94-29223
NASA Marshall Space Flight Center Solar Observatory report, July - October 1993
[NASA-TM-108448] p 3160 N94-29470
Optimizing the Galileo space communication link p 3250 N94-29663
A study of cloud-to-ground lightning processes with emphasis on data analysis and modeling of the return stroke p 3372 N94-29802
Correction of X hot-wire measurements for gradients normal to the plane of the wires
[PB94-125473] p 3157 N94-30399
The use of the AOA TTR-4P GPS receiver in operation at the BIPM for real-time restitution of GPS time p 3144 N94-30651
A comparison of several GPS data reduction methods p 3145 N94-30662
Altimeter data processing from sea surface topography to horizontal eddy momentum fluxes
[PB94-147550] p 3378 N94-30714
Spatial interpolation, network bias, and terrestrial air temperature variability p 3374 N94-30810

DATA RETRIEVAL
The effects of inheritance on the properties of physical storage models in object-oriented databases p 3531 N94-29537
A unified framework for retrieval in image databases p 3533 N94-29811
Hypra/TR: A tuple oriented recovery method for a continuously available distributed DBMS on a shared nothing multi-computer
[PB94-141264] p 3533 N94-29921
Computer-based linking of thesauri p 3534 N94-29961

DATA SAMPLING
Effects of low sampling rate in the digital data-transition tracking loop p 3251 N94-29669
L(sub)p optimal d dimensional triangulations for piecewise linear interpolation: A new result on data dependent triangulations
[RUU-CS-93-13] p 3458 N94-30406

DATA SIMULATION
Simulation Networking/Training Requirements Relational Database: User's guide
[AD-A275634] p 3528 N94-28637

DATA SMOOTHING
Strategy for the approximation of large scattered data sets
[PB94-138518] p 3420 N94-29949

DATA STORAGE
The High Performance Storage System
[DE94-004350] p 3404 N94-28505
Performance analysis of memory hierachies in high performance systems
[DE94-005549] p 3404 N94-28517
Redundant disk arrays in transaction processing systems
[NASA-CR-195759] p 3418 N94-29404
Nonvolatile programmable neural network synaptic array
[NASA-CASE-NPO-18578-1-CU] p 3265 N94-29426
The effects of inheritance on the properties of physical storage models in object-oriented databases p 3531 N94-29537
Efficient bounded timestamping using traceable use abstraction: Is writer's guessing better than reader's telling?
[RUU-CS-93-28] p 3426 N94-30489

DATA STRUCTURES
Ada, object-oriented techniques, and concurrency in teaching data structures and file management
[AD-A275385] p 3411 N94-29201
On conceptual design of active databases p 3531 N94-29535
Object-oriented database support for scientific data management: A system for experimentation p 3531 N94-29677
A conceptual language for the description and manipulation of complex information models
[TR-92-34] p 3423 N94-30344
Towards a general theory for the evolution of application domains
[TR-92-22] p 3535 N94-30357
A general theory for the evolution of application domains
[TR-92-26] p 3535 N94-30360
Event structures and orthogonal term graph rewriting
[CWI-CS-R9347] p 3459 N94-30412
Modeling systems by probabilistic process algebra: An event structures approach
[MEMO-INF-93-29-REV] p 3425 N94-30416
Homomorphism preserving algebraic specifications require hidden sorts
[CWI-CS-R9344] p 3459 N94-30436
Efficient bounded timestamping using traceable use abstraction: Is writer's guessing better than reader's telling?
[RUU-CS-93-28] p 3426 N94-30489
Dynamic microsets for RAMs
[RUU-CS-93-22] p 3406 N94-30727
A neural network-based technique for structural identification of SISO systems
[REPT-93-076] p 3449 N94-30941

DATA SYSTEMS
Program SCREEN for acquisition, visualization, processing and output of experimental data
[DE94-608009] p 3534 N94-30079
User's manual for the model interface and plugboard cabinets in the 14- by 22-foot subsonic tunnel
[NASA-TM-109062] p 3133 N94-30176
Predictive sufficiency and the use of stored internal state
[AIAA PAPER 94-1213-CP] p 3445 N94-30564

DATA TRANSFER (COMPUTERS)
I/O on the Tera file system
[AD-A275278] p 3530 N94-29182
Redundant disk arrays in transaction processing systems
[NASA-CR-195759] p 3418 N94-29404

DATA TRANSMISSION
The High Performance Storage System
[DE94-004350] p 3404 N94-28505
DOD Electronic Commerce (EC)/Electronic Data Interchange (EDI) in contracting report
[AD-A275298] p 3242 N94-28874
A new information system: Satellite observation p 3330 N94-29219
Observations of the geomagnetic field by Polar Patrol Balloon (PPB) experiment in Antarctica p 3359 N94-29235
RIPE integrity primitives, part 1 (RACE Integrity Primitives Evaluation)
[CWI-CS-R9324-PT-1] p 3252 N94-29692
RIPE integrity primitives, part 2 (RACE Integrity Primitives Evaluation)
[CWI-CS-R9325-PT-2] p 3252 N94-29693
Antarctic Record, vol. 36, no. 3
[REPT-108] p 3363 N94-29978
Data transfer system using a multi-ID ARGOS transmitter for the Antarctic polar patrol balloon experiment p 3363 N94-29980
Installation of experimental mode-S data link in commercial aircraft
[PB94-138757] p 3254 N94-29998
Communications technology for unattended sensors
[DE94-005685] p 3254 N94-30043
Microsecond fiber optic delay line
[DE94-607903] p 3500 N94-30075
Program SCREEN for acquisition, visualization, processing and output of experimental data
[DE94-608009] p 3534 N94-30079
Fast and efficient variable-to-fixed-length coding algorithm
[PB94-125465] p 3424 N94-30400
End-to-end delay reduction in narrow bandwidth real-time multimedia tele-education applications
[AD-B179614] p 3260 N94-30518
Modeling data throughput on communication networks
[DE94-005077] p 3260 N94-30772

DAWN CHORUS
Study of generation mechanisms of magnetospheric VLF/ELF emissions based on the direction findings p 3361 N94-29245

DC GENERATORS
Performance evaluation of a 22.5/30 kW 270 volts direct current generator system
[AD-A275106] p 3263 N94-28913

DEATH
Aeropathological diagnosis of lethal hypothermia p 3382 N94-28440

DEBONDING (MATERIALS)
Intelligent material systems and structures. Part 7: Debonding and pull-out of two optical fibers from two epoxies
[PB94-137767] p 3180 N94-29475
Transient thermal fatigue of ceramic composites p 3216 N94-29874
Damage analysis and mechanical response of as-received and heat-treated Nicalon/CAS-2 glass-ceramic matrix composites p 3219 N94-30259

DEBYE LENGTH
Coulomb field effect on plasma focusing and wake field acceleration
[DE94-004937] p 3504 N94-28564

DECAY RATES
Application of semiclassical methods to reaction rate theory
[DE94-007041] p 3199 N94-30266

DECELERATION
BAG: A code for predicting the performance of a gas bag impact attenuation system for the Pathfinder lander
[DE94-003688] p 3165 N94-28477

DECISION MAKING
Effects of workload on communication processes in decision making teams
[AD-A275894] p 3527 N94-28796
A cognitive model of decision making: Chunking and the radar detection device
[AD-A275185] p 3242 N94-28859
Information presentation for expert systems in future fighter aircraft
[AD-A275126] p 3149 N94-29005
Evaluating the analytic hierarchy process and recommended modifications for its use in multi-attribute decision making
[AD-A275065] p 3527 N94-29153
Temporal and qualitative decomposition of plausible reasoning
[AD-A275073] p 3398 N94-29154
Designing and maintaining decision-making processes p 3412 N94-29318
Advances in development capabilities for intelligent air traffic management systems p 3137 N94-29559
Air traffic management as principled negotiation between intelligent agents p 3137 N94-29562
Decision Making Aids (DMA) in on-line ATC systems p 3139 N94-29570
Cognitive approach to specifications on air traffic controllers' decision assistance systems p 3139 N94-29571
DAISY: A decision aid for an air situation interpretation system p 3139 N94-29574

DECISION THEORY
Subphonetic acoustic modeling for speaker-independent continuous speech recognition
[AD-A275217] p 3244 N94-29303

DECISIONS
Undecidability in diagonalizable algebras
[ML-93-13] p 3463 N94-30976

DECODERS
Non-orthogonal subband/transform coder
[NASA-CASE-LEW-15310-1] p 3246 N94-29589

DECODING
Digital camera with apparatus for authentication of images produced from an image file
[NASA-CASE-NPO-19108-1-CU] p 3287 N94-29373
Optimizing the Galileo space communication link p 3250 N94-29663
MPEG-2 video decoding architecture: Analysis and design
[REPT-93-069] p 3260 N94-30940

DECOMPOSITION
Chemical dynamics studies of reactions in energetic materials
[AD-A275607] p 3224 N94-28769
A new orthogonal decomposition method for turbulent flows p 3281 N94-30494
Influence of surface defects and local structure on oxygenate reaction pathways over metal oxide surfaces
[DE94-005680] p 3522 N94-30901

DECOMPRESSION SICKNESS
Decompression sickness risk versus time and altitude
[AD-A275261] p 3391 N94-29071

DECONGESTANTS
Biochemical enhancement of cold tolerance p 3380 N94-28427

DECONTAMINATION
The 1992 report on the next generation ultra clean technology for advanced microfabrication
[DE94-744171] p 3157 N94-30268

DEDUCTION
Natural deduction for intuitionistic linear logic
[ML-93-09] p 3457 N94-30385
DTL: A deductive and typed object-oriented language
[MEMO-INF-93-41] p 3425 N94-30417

DEEP SPACE
Design and analysis of a low-loss linear analog phase modulator for deep space spacecraft X-band transponder applications p 3248 N94-29625
Decoder synchronization for deep space missions p 3250 N94-29664

DEEP SPACE NETWORK
Combining GPS and VLBI earth-rotation data for improved universal time p 3144 N94-29614
Phasing the Very Large Array on Galileo in the presence of Jupiter's strong radio emission p 3164 N94-29621
Elevation control system model for the DSS 13 antenna p 3248 N94-29622

Radio science ground data system for the Voyager-Neptune encounter, part 1
p 3248 N94-29623
The Telecommunications and Data Acquisition Report
[NASA-CR-195689] p 3249 N94-29652
Toward astrometric tracking with the infrared spatial interferometer p 3249 N94-29653
Determining noise temperatures in beam waveguide systems p 3249 N94-29657
A dual-cavity ruby maser for the Ka-band link experiment p 3250 N94-29658
A digital combining-weight estimation algorithm for broadband sources with the array feed compensation system p 3250 N94-29660
An improved conscan algorithm based on a Kalman filter p 3251 N94-29670

DEEP WATER
Effect of surface condition on strength and fatigue behavior of alumina ceramic
[AD-A275053] p 3214 N94-29133

DEFECTS
Dynamics of defect ensembles in one-dimensional cellular automata
[PB94-136819] p 3464 N94-29030
Flux-focusing eddy current probe and method for flaw detection
[NASA-CASE-LAR-15046-1] p 3315 N94-29366
Improved ground-penetrating radar, bridge decks
[DE94-004863] p 3254 N94-29929
Standardisation requirements for ultrasonic C-scanning of polymer matrix composites: An initial assessment
[PB94-139318] p 3184 N94-30438
Sensing the gas metal arc welding process
p 3314 N94-30444
Characterization of defect geometries in multilayer optical coatings
[DE94-005820] p 3501 N94-30599

DEFENSE INDUSTRY
Technology base enhancement program. Metal matrix composites
[AD-A275531] p 3176 N94-28688

DEFENSE PROGRAM
Security aspects of computer supported collaborative work
[AD-A275638] p 3528 N94-28640
Technology base enhancement program. Metal matrix composites
[AD-A275531] p 3176 N94-28688
Defense Technical Information Center cataloging guidelines
[AD-A275100] p 3529 N94-28911
Towards an information model and mechanisms for design rationale capture and use
[AD-A275060] p 3530 N94-29138
Artificial intelligence technology program at Rome Laboratory p 3414 N94-29328
Triple Diagonal modeling: A mechanism to focus productivity improvement for business success
[DE94-004309] p 3527 N94-30041
A survey of NASA and military standards on fault tolerance and reliability applied to robotics
[AIAA PAPER 94-1211-CP] p 3445 N94-30562
Loran-C time management p 3144 N94-30644

DEFLAGRATION
A study of solid propellants using a microprobe mass spectrometer system
[AD-A275325] p 3224 N94-28879

DEFLECTION
Structural/aerodynamic blade analyzer (SAB) user's guide, version 1.0
[NASA-CR-194460] p 3151 N94-29103

DEFLUORINATION
Formation and chemical reactivity of carbon fibers prepared by defluorination of graphite fluoride
[NASA-TM-106398] p 3174 N94-28747

DEFOCUSING
Defocussing characteristics of the ACTS, T1-VSAT Earth terminal antennas
[NASA-TM-106420] p 3242 N94-28826

DEFORESTATION
Amazonia: Remote sensing test site and survey
p 3327 N94-28935
Utilization of remote sensing data in Southeast Asia
p 3327 N94-28936
GCM studies of the influence of vegetation on the general circulation: The role of albedo in modulating climate change p 3348 N94-29749

DEFORMATION
Failures to model the development of a cube texture during the high temperature compression of Al-Mg alloys
[DE94-005013] p 3201 N94-28544
Cyclic axial-torsional deformation behavior of a cobalt-base superalloy
[NASA-TM-106372] p 3203 N94-28921
Granular bases for heavily loaded pavements
[AD-A275171] p 3156 N94-29047
Modelling and analysis of creep deformation and fracture in a 1 Cr 1/2 Mo ferritic steel
[PB94-138328] p 3319 N94-29121
II-VI wide band gap semiconductors under hydrostatic pressure
[DE94-608106] p 3516 N94-30070
Thin-walled orthotropic laminated beam theory
p 3324 N94-30920
Elements for the recognition of three dimensional deformable shapes: Application to biomedical imagery
[TELECOM-93-E-006] p 3396 N94-30978

DEGENERATE MATTER
Theoretical asteroseismology of white dwarf stars: The encyclopedia Seismologica p 3547 N94-30011

DEGENERATION
Theory for electron-transfer reactions in a three-component system: The degenerate regime
[DE94-005919] p 3493 N94-30903

DEGRADATION
The viability of photovoltaics on the Martian surface
[NASA-TM-106478] p 3338 N94-30196

DEGREES OF FREEDOM
Mechanical flexible joint design document
[NASA-CR-193941] p 3297 N94-28419
Feedback control of a three-link planar under-actuated manipulator using a surge velocity
[AD-A275159] p 3435 N94-29044
A non-linear simulation for an autonomous unmanned air vehicle
[AD-A275062] p 3146 N94-29200
Six-degree-of-freedom parallel minimanipulator with three inextensible limbs
[NASA-CASE-GSC-13485-1] p 3288 N94-29726
A highly redundant robot system for inspection
[AIAA PAPER 94-1194-CP] p 3442 N94-30545

DEHYDRATION
Aeromedical support for casualties in extremely hot climates p 3382 N94-28443
Work conditions assessment in pilots and ground personnel under high weather temperatures
p 3382 N94-28444

DEHYDROGENATION
Endothermic fuels for hypersonic aviation
p 3197 N94-29285

DELAMINATING
Active control of delaminations in smart composite structures p 3181 N94-29593
Dynamic fracture mechanics analysis for an edge delamination crack
[NASA-TM-109106] p 3479 N94-29856
Interlaminar fracture analysis for laminated composites under combined loading p 3182 N94-29964
Computational simulation of composite structures with and without damage
[NASA-CR-194433] p 3183 N94-30190
Delamination growth in composites under cyclic loads
p 3183 N94-30256
Damage analysis and mechanical response of as-received and heat-treated Nicalon/CAS-2 glass-ceramic matrix composites p 3219 N94-30259
Damage identification in composites using built-in piezoelectrics p 3184 N94-30355
Evaluation of corrosion protecting properties of modern aircraft paint systems
[AD-B179388] p 3220 N94-30420
Delamination of woven E-glass fabric composites
[DE94-003227] p 3185 N94-30827

DELAWARE BAY (US)
Statistical analysis of a satellite imagery time series: Implications for the study of coastal and estuarine circulation p 3335 N94-30919

DELAY CIRCUITS
Microsecond fiber optic delay line
[DE94-607903] p 3500 N94-30075

DELAY LINES
Photorefractive adaptive antenna array processor
[AD-A275762] p 3241 N94-28762
Microsecond fiber optic delay line
[DE94-607903] p 3500 N94-30075

DELTA WINGS
Numerical investigation into high-angle-of-attack leading-edge vortex flow
[PB94-125564] p 3133 N94-30388
Numerical simulation of leading-edge vortex flow
[AD-B175154] p 3134 N94-30871

DEMODULATION
Two-way satellite time transfer: Overview and recent developments p 3469 N94-30646

DENSE PLASMAS
Experiments on the two-stage dense plasma heating on the GOL-3 device
[DE94-608356] p 3508 N94-30193
Molecular dynamics simulations of dense plasmas
[DE94-005082] p 3509 N94-30752

DENSIFICATION
Innovative processing of composites for ultra-high temperature applications, book 3
[AD-A275599] p 3177 N94-28731
Analysis of pressureless densification of ceramic matrix composites p 3216 N94-29766
Densification and crystallization of zirconia thin films prepared by sol-gel processing
[DE94-005573] p 3518 N94-30315
Properties of chemical vapor infiltration diamond deposited in a diamond powder matrix
[DE94-005429] p 3220 N94-30591

DENSITY MEASUREMENT
Characterization of structural vibration: Field descriptors based on energy density and intensity
[PB94-132230] p 3316 N94-28404

DEOXIDIZING
Pitting corrosion of titanium
[AD-A274980] p 3203 N94-29089

DEOXYRIBONUCLEIC ACID
Stable RNA sequences as a tool for DNA probes and phylogenetic studies
[PB94-135423] p 3385 N94-29156

DEPENDENCE
Conditional dependence in probabilistic networks
[RUU-CS-92-34] p 3464 N94-29450

DEPENDENT VARIABLES
Conditional dependence in probabilistic networks
[RUU-CS-92-34] p 3464 N94-29450

DEPLOYMENT
Deployable reflector structure
[NASA-CASE-LAR-14513-1-SB] p 3245 N94-29360

DEPOSITION
Silicon-Film (tm) photovoltaic manufacturing technology
[DE94-000258] p 3336 N94-28501
Surface structure and stereochemical properties of self-assembled monolayer materials
[DE94-004960] p 3484 N94-28578
Sweep rate and concentration effects on metastable structures formed in the underpotential deposition of silver on Pt(111)
[AD-A275369] p 3189 N94-29010
Development of global/chemistry model for jet-fuel thermal stability based on observations from static and flowing experiments p 3192 N94-29262
Focused ion beam fabrication of microelectronic structures
[AD-A275384] p 3264 N94-29305
ECR plasma synthesis of silicon nitride films on GaAs and InSb
[DE94-005575] p 3515 N94-30006
The organometallic chemical vapor deposition of transition metal carbides: The use of homoleptic alkyls
[DE94-005577] p 3206 N94-30007
Use of satellite data to improve parameterization of spatial and temporal variations of gaseous dry deposition in regional-scale models
[DE94-005110] p 3334 N94-30022
Properties of chemical vapor infiltration diamond deposited in a diamond powder matrix
[DE94-005429] p 3220 N94-30591

DEPOSITS
Plasma enhanced chemical vapor deposition of ZrO2 thin films
[DE94-006031] p 3218 N94-30104

DERIVATION
Derivation lengths in term rewriting from interpretations in the naturals
[RUU-CS-92-43] p 3455 N94-30346

DESCENT TRAJECTORIES
Advanced air traffic control and flight management system concepts p 3140 N94-29576

DESERTS
Effects of three hydration beverages on exercise performance during 60 hours of simulated desert exposure p 3383 N94-28448

DESIGN ANALYSIS
Systematic safety consideration in product design
[PB94-132354] p 3229 N94-28410
A design of third-generation airfoils for helicopter rotor blades using Navier-Stokes p 3124 N94-28957
Recent CFD applications in small gas turbine combustion systems development p 3154 N94-29257
On conceptual design of active databases
p 3531 N94-29535
A module concept for a cable-mesh deployable antenna p 3161 N94-29631
Advanced vehicle concepts systems and design analysis studies
[NASA-CR-195115] p 3147 N94-29721
EVA glove evaluation methodology and test protocol
p 3401 N94-29729
Using RDD-100 with CoRE. Version 01.00.03
[AD-A275336] p 3419 N94-29797

A newly developed snow vehicle (SM100S) for Antarctica. Part 2: Design of the system p 3314 N94-29982
Composite redesign of obstetrical forceps p 3397 N94-30457
Expanding the waverider design space using arbitrary generating flowfields p 3148 N94-30516
Design and analysis of dynamic leader election protocols in broadcast networks [MEMO-INF-93-43] p 3260 N94-30520
Nonlinear multibody formulation for rotorcraft analysis p 3149 N94-30787

DESORPTION
Influence of surface defects and local structure on oxygenate reaction pathways over metal oxide surfaces [DE94-005680] p 3522 N94-30901
Investigations into ultraviolet matrix-assisted laser desorption [DE94-005265] p 3296 N94-30908

DETECTION
Development of Alternating Current Potential Drop (ACPD) procedures for crack detection in aluminum aircraft panels [AD-A275755] p 3315 N94-28646
Using multiple searchers to locate a randomly moving target [AD-A275602] p 3463 N94-28768
Markov chains for random urinalysis 3: Daily model and drug kinetics [AD-A275540] p 3389 N94-28797
Optical flameout detector [NASA-CASE-LAR-14997-1] p 3287 N94-29368
Computerized in vitro test for chemical toxicity based on tetrahymena swimming patterns p 3354 N94-30463
Granulometry in environments with very small particle concentrations p 3259 N94-30511

DETERGENTS
Regenerating using aqueous cleaners with ozone and electrolysis p 3240 N94-30468

DETERIORATION
Design aspects in small aircraft gas turbine fuel injectors p 3154 N94-29264

DETONATION
Blast overpressure studies with animals and man [AD-A275038] p 3391 N94-29150

DEUTERIUM
Deep inelastic lepton scattering on nuclei: operator product expansion and meson-nucleon theory [DE94-606442] p 3484 N94-28610

DEUTERONS
Deep inelastic lepton scattering on nuclei: operator product expansion and meson-nucleon theory [DE94-606442] p 3484 N94-28610

DEVELOPING NATIONS
Report of feasibility study on international-cooperation in high efficient energy conversion technology [DE94-732340] p 3337 N94-28631
Solar photovoltaics for development applications [DE94-006116] p 3340 N94-30843

DEWATERING
Dewatering of contaminated river sediments p 3354 N94-30472

DIAGNOSIS
Aeropathological diagnosis of lethal hypothermia p 3382 N94-28440
Equilibrium dysfunction in the clinical field p 3390 N94-28858
Advanced diagnostics for reacting flows [AD-A275057] p 3272 N94-29136

DIAMETERS
A deterministic algorithm for the three-dimensional diameter problem [RUU-CS-92-45] p 3424 N94-30348

DIAMOND FILMS
Analysis of cost: CVD diamond deposition and finishing --- Quarterly report [AD-A275586] p 3212 N94-28725
Electron beam analysis for cyclotron harmonic and free-electron laser devices [AD-A275070] p 3293 N94-29179
Synthesis of diamond in a hydrogen plasma jet: Simulations of XRD patterns of diamond polytypes and boundary layer on a substrate p 3522 N94-29515
A photoemission electron microscope investigation of chemical vapor deposition diamond films and diamond nucleation p 3215 N94-29745
Fullerenes as precursors for diamond film growth without hydrogen or oxygen additions [DE94-004582] p 3519 N94-30718

DIAMONDS
Development of large area RF induction plasma for cost effective diamond [AD-A275888] p 3504 N94-28776
A photoemission electron microscope investigation of chemical vapor deposition diamond films and diamond nucleation p 3215 N94-29745
Precision and manufacturing at the Lawrence Livermore National Laboratory p 3240 N94-30449
Properties of chemical vapor infiltration diamond deposited in a diamond powder matrix [DE94-005429] p 3220 N94-30591

DIATOMIC MOLECULES
Theoretical studies of solid-fluid phase equilibria [DE94-006406] p 3226 N94-30708

DICHROISM
X-/Ka-band dichroic plate design and grating lobe study p 3247 N94-29616

DICKE RADIOMETERS
Conceptual radiometer design studies for Earth observations from low Earth orbit [NASA-CR-4588] p 3329 N94-29098

DIELECTRIC PROPERTIES
Experimental and theoretical studies of molecular solids [AD-A275511] p 3485 N94-28668
Breakdown testing of wiring insulation p 3166 N94-28713
Acoustic or electromagnetic scattering from the penetrable wedge [AD-A275259] p 3243 N94-29054
Controlled thermal expansion printed wiring boards based on liquid crystal polymer dielectrics [NASA-CR-189338] p 3287 N94-29400
RF and microwave dielectric measurements upon layered materials using reflectometric coaxial sensor [NPL-DES-125] p 3476 N94-30781

DIELECTRICS
High temperature polymer dielectric film insulation p 3167 N94-28715
A 3M high temperature dielectric film p 3167 N94-28717
Spatial light modulators with arbitrary quantum wells profiles [AD-A275023] p 3499 N94-29114
Low dielectric polyimide fibers [NASA-CASE-LAR-14526-1] p 3214 N94-29359
Controlled thermal expansion printed wiring boards based on liquid crystal polymer dielectrics [NASA-CR-189338] p 3287 N94-29400
Radioelectric characterization of materials at 1000 C [REPT-932-430-104] p 3245 N94-29440
ECR plasma synthesis of silicon nitride films on GaAs and InSb [DE94-005575] p 3515 N94-30006
Conceptual study of moderately coupled plasmas and experimental comparison of laboratory x ray sources [DE94-005828] p 3506 N94-30045
Plasma treatment of polymer dielectric films to improve capacitive energy storage p 3223 N94-30479

DIESEL ENGINES
Feasibility study on introduction of a large methanol engine power generation plant [DE94-732338] p 3224 N94-28629
Thick thermal barrier coatings for diesel components [NASA-CR-187111] p 3537 N94-29350

DIESEL FUELS
Combustion and heat transfer in a high speed diesel engine operating with rape seed oil methyl ester fuel [PB94-137536] p 3301 N94-29679
Biodiesel from aquatic species [DE94-000275] p 3225 N94-30038

DIETS
Work conditions assessment in pilots and ground personnel under high weather temperatures p 3382 N94-28444

DIFFERENCE EQUATIONS
Computational fluid dynamics in ventilation. 1: Theory and one-dimensional test case p 3232 N94-29606
Representations of dynamical systems described by behavioral inequalities [AD-B173649] p 3458 N94-30402

DIFFERENTIAL CALCULUS
GL(sub q)(N)-covariant quantum algebras and covariant differential calculus [DE94-608072] p 3460 N94-30726
Non-commutative geometry [PB94-139342] p 3462 N94-30889

DIFFERENTIAL EQUATIONS
Some constraints and solutions of the Kadomtsev-Petviashvili equation [DE93-634355] p 3466 N94-28467
A numerical solver for initial and boundary value problems in differential-algebraic systems [AD-A275447] p 3452 N94-28883
Approximation of solutions of the cubic NLSE by finite dimensional equations and non-squeezing properties [PB94-138294] p 3452 N94-29148
A free-wake Euler and Navier-Stokes CFD method and its application to helicopter rotors including dynamic stall [AD-A275416] p 3129 N94-29197
Compound matrix method for multi-point boundary-value problems [PB94-137791] p 3453 N94-29476
Computational fluid dynamics in ventilation. 1: Theory and one-dimensional test case p 3232 N94-29606
Splines and ocean wave modelling [PB94-139409] p 3378 N94-30002
Formulas of the Runge-Kutta-Nystroem type [ISBN-0-315-85774-9] p 3454 N94-30241
An evaluation of explicit pseudo-steady-state approximation schemes for stiff ODE systems from chemical kinetics [CWI-NM-R9312] p 3353 N94-30729
Graded Froelicher-Nijenhuis brackets and the theory of recursion operators for super differential equations [MEMO-1147] p 3460 N94-30736
Numerical simulations of piano strings. Part 1: A physical model for a struck string using finite difference methods [TELECOM-93-C-003] p 3481 N94-30972

DIFFERENTIAL GEOMETRY
Non-commutative geometry [PB94-139342] p 3462 N94-30889

DIFFRACTION
Surface structure and stereochemical properties of self-assembled monolayer materials [DE94-004960] p 3484 N94-28578
Backscatter haze device for measurement of haze in aircraft transparencies [AD-A275127] p 3146 N94-29042
Hybrid optics for space applications [ESA-CP-1158] p 3501 N94-30418

DIFFUSION
Remote control of transcranial Doppler (TCD) probe during centrifuge exposures up to 9 +Gz [AD-A275253] p 3400 N94-29029
XCHEM-1D: A heat transfer/chemical kinetics computer program for multilayered reactive materials [DE94-005072] p 3226 N94-30615
Evaluation of discretization schemes for advection-diffusion equations [CWI-NM-R9311] p 3461 N94-30751
On some general properties of parabolic conservation equations [DE94-006101] p 3461 N94-30758
Superdiffusion [DE94-002333] p 3492 N94-30834

DIFFUSION FLAMES
Similarity solutions and numerical modeling in buoyancy controlled turbulent diffusion flames [AD-A275820] p 3188 N94-28777
Numerical prediction of turbulent sooting diffusion flames p 3191 N94-29253
Lifted turbulent jet flames p 3198 N94-29676

DIFFUSION LENGTH
RHEED studies of the nucleation, growth, and mobility of Ag atoms on the Si(111)7 x 7 surface [DE94-005551] p 3521 N94-30899

DIFFUSION WELDING
Joining silicon carbide to austenitic stainless steel through diffusion welding [PB94-126331] p 3297 N94-28399

DIFFUSIVITY
Process modelling for materials preparation experiments [NASA-CR-195782] p 3175 N94-30242

DIFLUORIDES
Plasma treatment of polymer dielectric films to improve capacitive energy storage p 3223 N94-30479

DIGITAL DATA
The Image Digitizing System (IDS) [AD-A275341] p 3329 N94-29213
Digital camera with apparatus for authentication of images produced from an image file [NASA-CASE-NPO-19108-1-CU] p 3287 N94-29373
The uses and limitations of fractal geometry in digital terrain modelling p 3333 N94-29958

DIGITAL ELECTRONICS
Yield and variability optimization of integrated circuits: Principles and practical solutions p 3266 N94-29805

DIGITAL FILTERS
Design and implementation of a hybrid digital phase-locked loop with a TMS320C25: An application to a transponder receiver breadboard p 3251 N94-29667
Digital filter [DE94-607902] p 3406 N94-30074

DIGITAL NAVIGATION
Automatic control steps for aircraft taxi guidance p 3141 N94-29584

DIGITAL RADAR SYSTEMS
Spurs in digital radio frequency memory and applications of DRFM [AD-A275013] p 3243 N94-28897

Digital pulse compression and its application in reducing radar interference
[ISBN-0-315-85767-6] p 3255 N94-30240

DIGITAL SIMULATION
Proceedings of the 10th NAL Symposium on Aircraft Computational Aerodynamics
[NAL-SP-19] p 3123 N94-28946
Engineering of systems for application of scientific computing in industry p 3123 N94-28947
Monte Carlo simulation or normal shock wave. Part 2: VHS model and VSS model p 3123 N94-28948
Variable soft sphere molecular model in the Monte Carlo simulation of air species p 3123 N94-28949
Rarefied gas numerical wind tunnel. Part 8: HOPE p 3123 N94-28950
Numerical simulation of arc heated wind tunnel flow p 3123 N94-28951
Numerical simulation of unsteady aerodynamic heating induced by shock reflections p 3123 N94-28952
Numerical simulation of steady Mach reflection by shock capturing schemes p 3123 N94-28953
Higher-order accurate numerical simulation of 3D supersonic mixing layers p 3124 N94-28954
Numerical simulation of aerothermodynamic heating of hypersonic space transportation vehicles p 3124 N94-28955
Transonic expanding flow through axially symmetric orifices p 3128 N94-28985
Similarity between turbulent flows through curved pipe and orthogonal rotating pipe p 3128 N94-28986
Mutual similarity of developing laminar flows with secondary streams in ducts: Curved pipe flow and orthogonal rotating pipe flow p 3129 N94-28989
Parallelization techniques for highly parallel vector computer p 3129 N94-28990
Parallel Fortran programming for NWT p 3129 N94-28991
Performance evaluation of the NWT with parallel Fortran p 3129 N94-28992
A method of user interface for NWT p 3129 N94-28993
Simulation of lightweight robots and their controllers p 3307 N94-30294
Symbolic generation of dynamics equations for manipulators mounted on moving bases p 3308 N94-30296
Supercomputing has to be part of an organization-wide automation concept
[AD-B174654] p 3433 N94-30913

DIGITAL SYSTEMS
Video transmission on ATM networks
[NASA-CR-195124] p 3244 N94-29106
How to control the increase in the complexity of civil aircraft on-board systems p 3150 N94-29316
On ground system integration and testing: A modern approach p 3150 N94-29334
Digital camera with apparatus for authentication of images produced from an image file
[NASA-CASE-NPO-19108-1-CU] p 3287 N94-29373
Method of implementing digital phase-locked loops
[NASA-CASE-NPO-18757-1-CU] p 3265 N94-29374
Design and implementation of a hybrid digital phase-locked loop with a TMS320C25: An application to a transponder receiver breadboard p 3251 N94-29667
Effects of low sampling rate in the digital data-transition tracking loop p 3251 N94-29669
Performance issues of signalling protocols for broadband ISDN
[MEMO-INF-93-30] p 3255 N94-30374
A direct digital control-law synthesis in the w-domain: W-synthesis methodology p 3438 N94-30517

DIGITAL TECHNIQUES
The Image Digitizing System (IDS)
[AD-A275341] p 3329 N94-29213
Digital camera with apparatus for authentication of images produced from an image file
[NASA-CASE-NPO-19108-1-CU] p 3287 N94-29373
Method of implementing digital phase-locked loops
[NASA-CASE-NPO-18757-1-CU] p 3265 N94-29374
Image-adapted visually weighted quantization matrices for digital image compression
[NASA-CASE-ARC-12015-1] p 3406 N94-29375
A normative frame of reference for the metrology function
[REPT-932-430-102] p 3231 N94-29477
Automating geographically referenced digital mosaics from aerial videography with area-based feature matching p 3333 N94-29540
High-resolution robot tracking and direction finding for space station environment p 3168 N94-29896
A direct digital control-law synthesis in the w-domain: W-synthesis methodology p 3438 N94-30517
Applicability of digital terrain analyses to wind energy prospecting and siting
[DE94-004363] p 3374 N94-30587
The experimental flight management system: An air traffic management research tool
[NLR-TP-92253-U] p 3143 N94-30943

DIGITAL TELEVISION
Application of digital video to hypermedia training systems
[AD-A274989] p 3409 N94-28910

DIGITAL TO ANALOG CONVERTERS
Multi-speed multi-phase resolver converter
[NASA-CASE-MFS-28855-1] p 3264 N94-29372
Program SCREEN for acquisition, visualization, processing and output of experimental data
[DE94-608009] p 3534 N94-30079

DIMENSIONAL ANALYSIS
Melt flow during alloy solidification: Dimensional analysis and model problems
[PB94-138625] p 3206 N94-29997

DIMENSIONAL STABILITY
Irradiation-induced structure and property changes in tokamak plasma-facing, carbon-carbon composites
[DE94-006046] p 3508 N94-30365

DIODES
Near-IR diode laser absorption for measurement of tropospheric HO2 p 3345 N94-28607
Developing a diode array spectrometer for tropospheric chemistry studies p 3362 N94-29752
A commercialized, continuous flow fiber optic sensor for trichloroethylene and haloforms p 3502 N94-30462

DIPOLE ANTENNAS
Waves in space plasma dipole antenna subsystem p 3161 N94-29632

DIRAC EQUATION
Research on elementary particle physics. Task P: Studies in theory and phenomenology of elementary physics
[DE94-004955] p 3483 N94-28566
The (j,0) + (0,j) representation space: Dirac-like construct
[DE94-005011] p 3522 N94-28572
Theoretical investigation of gas-surface interactions
[NASA-CR-195755] p 3272 N94-29378
Theory of fundamental interactions
[DE94-608126] p 3525 N94-30169
Large-scale 3-D solutions of the time-dependent Dirac equation
[DE94-005591] p 3454 N94-30317

DIRECT CURRENT
Performance evaluation of a 22.5/30 kW 270 volts direct current generator system
[AD-A275106] p 3263 N94-28913

DIRECTION FINDING
Study of generation mechanisms of magnetospheric VLF/ELF emissions based on the direction findings p 3361 N94-29245
High-resolution robot tracking and direction finding for space station environment p 3168 N94-29896

DIRECTIONAL CONTROL
Electrical engineering and industrial electronics education days: Control of asynchronous generators
[PB94-135514] p 3266 N94-29523

DIRECTIONAL SOLIDIFICATION (CRYSTALS)
Directional solidification studies in Ni-Al alloys
[DE94-005562] p 3201 N94-28527
Directional solidification characteristics of hyper-eutectic Al-Cu alloys under varying gravity conditions
[ISBN-0-315-86108-8] p 3209 N94-30146
Process modelling for materials preparation experiments
[NASA-CR-195782] p 3175 N94-30242

DIRECTIONAL STABILITY
An experimental investigation of the effect of leading edge extensions on directional stability and the effectiveness of forebody nose strakes p 3155 N94-29728

DIRICHLET PROBLEM
Stability of dynamical systems in the presence of noise
[AD-A275383] p 3243 N94-29072

DISABILITIES
Monitor for status epilepticus seizures p 3397 N94-30460

DISASTERS
Application of remote sensing in prevention of disasters p 3332 N94-29230

DISCOLORATION
Advanced development of PV encapsulents
[DE94-000219] p 3336 N94-28500

DISCONTINUITY
Nonlinear wave packet evolution in a dispersive plasma: Application to rotational discontinuities p 3506 N94-29822

DISCRETE COSINE TRANSFORM
Image-adapted visually weighted quantization matrices for digital image compression
[NASA-CASE-ARC-12015-1] p 3406 N94-29375

DISILICIDES
Characterization of structure and mechanical properties of MoSi2-SiC nanolayer composites
[DE94-004982] p 3175 N94-28579
Innovative processing of composites for ultra-high temperature applications, book 2
[AD-A275598] p 3177 N94-28730

DISK GALAXIES
The role of cloud collisions in N-body simulations of disk galaxies p 3545 N94-29755
Stellar and gas dynamics of interacting ring galaxies p 3548 N94-30340

DISK OPERATING SYSTEM (DOS)
PAW using under MS DOS
[DE94-608012] p 3406 N94-30081

DISLOCATIONS (MATERIALS)
Low temperature behavior of virgin martensite
[PB94-132925] p 3204 N94-29142

DISPERSING
Nonlinear wave packet evolution in a dispersive plasma: Application to rotational discontinuities p 3506 N94-29822

DISPLACEMENT
Toward a molecular scale understanding of frost heaving, phase 1
[AD-A275446] p 3356 N94-28882
Field methods to measure surface displacement and strain with the Video Image Correlation method
[NASA-CR-195796] p 3316 N94-29724

DISPLAY DEVICES
Key cognitive issues in the design of electronic displays of instrument approach procedure charts
[AD-A275647] p 3399 N94-28649
Information presentation for expert systems in future fighter aircraft
[AD-A275126] p 3149 N94-29005
A comparison of three aircraft attitude display symbology structures
[AD-A275172] p 3150 N94-29048
Program SCREEN for acquisition, visualization, processing and output of experimental data
[DE94-608009] p 3534 N94-30079
The use of interactive computer vision and robot hand controllers for enhancing manufacturing safety p 3314 N94-30442
A multi-mode manipulator display system for controlling remote robotic systems
[AIAA PAPER 94-0888-CP] p 3446 N94-30569

DISSOCIATION
Enhanced ion dissociation of LiCF3SO3 by new carbonate plasticizers: Raman and IR studies
[DE94-005448] p 3485 N94-28741
Application of semiclassical methods to reaction rate theory
[DE94-007041] p 3199 N94-30266
Dissociative recombination of H3(+)
[DE94-005356] p 3493 N94-30891

DISSOLVED GASES
Fatigue of carbon and low-alloy steels in LWR environments
[DE94-005116] p 3207 N94-30021

DISSOLVING
Nature of dissolution of binary tantalum-titanium alloys by molten plutonium
[DE94-005090] p 3210 N94-30776

DISTANCE
Three forms of relativity
[DE94-606338] p 3523 N94-28782

DISTRIBUTED FEEDBACK LASERS
Longitudinal effects and intensity-phase coupling in distributed feedback semiconductor lasers p 3294 N94-29590

DISTRIBUTED PROCESSING
A distributed object-based environment in Ada p 3417 N94-29347
Extending the X Window System
[DE94-006496] p 3420 N94-29844
Checkpoint-based forward recovery using lookahead execution and rollback validation in parallel and distributed systems
[NASA-CR-195760] p 3431 N94-29869
Space reclamation for uncoordinated checkpointing in message-passing systems
[NASA-CR-195761] p 3420 N94-29906
Hypra/TR: A tuple oriented recovery method for a continuously available distributed DBMS on a shared nothing multi-computer
[PB94-141264] p 3533 N94-29921
Software engineering and software management in a distributed UNIX environment
[NLR-TP-92233-U] p 3422 N94-30314
Self-stabilizing l-exclusion algorithms
[RUU-CS-93-01] p 3424 N94-30379
An all pairs shortest paths distributed algorithm using 2n(exp 2) messages
[RUU-CS-93-19] p 3432 N94-30411

Modeling systems by probabilistic process algebra: An event structures approach
[MEMO-INF-93-29-REV] p 3425 N94-30416
The secrets of causality
[RUU-CS-93-29] p 3426 N94-30490
On the relation between Unity properties and sequences of states
[RUU-CS-93-07] p 3433 N94-30720

DISTRIBUTION FUNCTIONS
Photon counting spectroscopy as done with a Thomson scattering diagnostic
[DE94-005543] p 3503 N94-28515
Equation of state of stellar plasmas
[DE94-004186] p 3542 N94-28526
Derivation of a Fokker-Planck equation for bunched beams
[DE94-004950] p 3483 N94-28565
The small-x behaviour of parton distribution functions
[DE94-606414] p 3485 N94-28758
Probabilistic material strength degradation model for Inconel 718 components subjected to high temperature, mechanical fatigue, creep and thermal fatigue effects
[NASA-CR-195264] p 3318 N94-28840
The modified Cramer-von mises goodness-of-fit criterion for time series
[AD-A275377] p 3464 N94-29014
A single-fluid, self-consistent formulation of particle transport and fluid dynamics p 3280 N94-30352

DIURNAL VARIATIONS
Ozone production at a rural site in Georgia during the summer 1992 SOS campaign
[DE94-003989] p 3342 N94-28523
Thermal variation in vegetated or snow-covered background scenes and its effect on passive infrared systems
[AD-A275174] p 3325 N94-28849
An observational and numerical study of sea/land-breeze circulations in an area of complex coastal heating p 3372 N94-29813

DIVERTERS
Proceedings of Japan-US Workshop P-196 on High Heat Flux Components and Plasma Surface Interactions for Next Devices
[DE94-701164] p 3503 N94-28513
Electron beam irradiation experiments of monoblock divertor mock-up
[DE94-707497] p 3503 N94-28555
Experimental and analytical studies of high heat flux components for fusion experimental reactor
[DE94-707671] p 3504 N94-28556
Application of divertor cryopumping to H-mode density control in DIII-D
[DE94-004859] p 3510 N94-30832

DIVING (UNDERWATER)
Advanced seal delivery system life support parameters
[AD-A275304] p 3401 N94-29184
Insulative properties of two thermo-metal neoprenes
[AD-A275209] p 3401 N94-29302

DOCUMENTATION
The discipline of defining the software product p 3416 N94-29343
A normative frame of reference for the metrology function
[REPT-932-430-102] p 3231 N94-29477

DOCUMENTS
Engineering document management system
[PB94-136934] p 3530 N94-29172
Modelling interaction tools in the Views architecture
[CWI-CS-R9261] p 3423 N94-30323

DOLPHINS
Design of the biosonar simulator for dolphin's clicks waveform reproduction p 3234 N94-29707

DOMAIN WALL
Discrete quark-lepton symmetry need not pose a cosmological domain wall problem
[DE94-601606] p 3481 N94-28471
Discrete symmetries, strong CP problem and gravity
[DE94-608091] p 3524 N94-30089

DOMAINS
Frequency-domain analysis of nonlinear microwave circuits
[PB94-132024] p 3261 N94-28400
Investigation into formalization of domain-oriented parallel software development
[AD-A275177] p 3430 N94-29050

DOPED CRYSTALS
Electronic structure and mechanical properties of grain boundaries
[AD-A275198] p 3512 N94-28890
Effects of oxide charge and surface recombination velocity on the excess base current of BJT's
[DE94-003711] p 3263 N94-29025
Aggregation equilibria in arsenic doped silicon
[DE94-607269] p 3515 N94-30005

DOPPLER EFFECT
Apparent unambiguousness of relativistic time dilation
[DE94-606328] p 3522 N94-28586
Retarded distances and the Doppler effect
[DE94-606296] p 3523 N94-28618
Annual summary of basic research thermoacoustic heat transport, 1993
[AD-A275751] p 3230 N94-28644
On a direct experimental verification of the elongation formula
[DE94-606329] p 3523 N94-28721
Remote control of transcranial Doppler (TCD) probe during centrifuge exposures up to 9 +Gz
[AD-A275253] p 3400 N94-29029
Theory and observations of horizontal and vertical structure of gravity wave perturbations in the middle atmosphere p 3366 N94-30802

DOPPLER RADAR
Innovative direct detection range-Doppler laser radar
[AD-A275619] p 3292 N94-28635
Numerical simulations of a mountain thunderstorm. A comparison with Doppler radar observations
[AD-A275296] p 3369 N94-28873
New-type echoes observed with the 50 MHz auroral Doppler radar at Showa Station p 3360 N94-29238
Method for ambiguity resolution in range-Doppler measurements
[NASA-CASE-GSC-13542-1] p 3252 N94-29739

DOUBLE BASE ROCKET PROPELLANTS
Correlation of cookoff behavior of rocket propellants with thermomechanical and thermochemical properties
[AD-A274983] p 3224 N94-29092

DOWNLINKING
Design and analysis of a low-loss linear analog phase modulator for deep space spacecraft X-band transponder applications p 3248 N94-29625
A dual-cavity ruby maser for the Ka-band link experiment p 3250 N94-29658
Optimizing the Galileo space communication link p 3250 N94-29663

DRAFT (GAS FLOW)
Human requirements to the indoor air quality and the thermal environment p 3232 N94-29600

DRAG
Three-dimensional finite element modeling of a magnet array spinning above a conductor
[DE94-004573] p 3468 N94-28459

DRAG REDUCTION
Numerical analysis of supersonic transport wings p 3124 N94-28959

DRAINAGE
Glaciohydrologic and glaciohydraulic effects on runoff and sediment yield in glacierized basins
[AD-A275134] p 3361 N94-29286
A coupled approach to spatially derived parameters necessary for ecosystem modeling on the North Slope of Alaska: Appendix A
[DE94-005853] p 3349 N94-30046

DREDGED MATERIALS
Dewatering of contaminated river sediments p 3354 N94-30472

DREDGING
Dewatering of contaminated river sediments p 3354 N94-30472

DRIFT RATE
A comparative study of clock rate and drift estimation p 3473 N94-30669
Ground control system for the midcourse space experiment UTC clock p 3474 N94-30674

DRONE AIRCRAFT
HATT-X: A high performance flying laboratory for autonomous unmanned aircraft research and development p 3149 N94-30293

DROPS (LIQUIDS)
Numerical simulation of aerothermal characteristics in gas turbine combustors with complex geometries p 3154 N94-29255
An experimental investigation of flow patterns and liquid entrainment in a horizontal-tube evaporator p 3277 N94-29899
Near-net-shape manufacturing: Spray-formed metal matrix composites and tooling p 3186 N94-30447

DRUGS
Markov chains for random urinalysis 3: Daily model and drug kinetics
[AD-A275540] p 3389 N94-28797
Microencapsulation of anti-tumor, antibiotic and thrombolytic drugs in microgravity p 3397 N94-30453

DRYING
Use of satellite data to improve parameterization of spatial and temporal variations of gaseous dry deposition in regional-scale models
[DE94-005110] p 3334 N94-30022

DUAL SPIN SPACECRAFT
The influence of appendage vibration on the attitude dynamics of a dual-spin satellite p 3168 N94-29828

DUCTED FANS
Investigation of advanced counterrotation blade configuration concepts for high speed turboprop systems. Task 2: Unsteady ducted propfan analysis computer program users manual
[NASA-CR-187105] p 3152 N94-29438

DUCTED FLOW
Flow and heat transfer in a rotating square sectioned U-bend p 3128 N94-28984
Numerical analysis of laminar flow in S-curved square duct with inlet and outlet straight region p 3128 N94-28987
Ducted kerosene spray flames p 3195 N94-29276
Scramjet CFD methods and analysis. Part 1: Scramjet CFD methods. Numerical simulation of the flow in scramjet duct p 3152 N94-29296
Direct and large-eddy simulations of turbulent flow in a square duct p 3275 N94-29809
Three dimensional compressible turbulent flow computations for a diffusing S-duct with/without vortex generators p 3281 N94-30519

DUCTILE-BRITTLE TRANSITION
The effect of various metallurgical parameters on the flow and fracture behavior of polycrystalline NiAl near the brittle-to-ductile transition
[NASA-TM-106534] p 3205 N94-29758
The role of plastic deformation in brittle and near-brittle cracking behavior p 3322 N94-30226

DUCTILITY
A modeling study of the effect of stress state on void linking during ductile fracture
[AD-A275505] p 3317 N94-28811
An analysis of the microstructure and reinforcement distribution of an extruded particle-reinforced Al 6061-10 volume percent Al2O3 metal matrix composite
[AD-A275050] p 3178 N94-29166
A class of inclusion problems for the strengthening of brittle and ductile composites p 3186 N94-30959

DUCTS
Mutual similarity of developing laminar flows with secondary streams in ducts: Curved pipe flow and orthogonal rotating pipe flow p 3129 N94-28989
Introduction and overview of research and development of solid propellant ramrockets, liquid fuel ramjets and experimental hydrogen ram combustors p 3151 N94-29292

DUMP COMBUSTORS
An investigation of the reacting vortex structures associated with pulse combustion p 3200 N94-30911

DURABILITY
Analysis of data by long-time mechanical properties of 08KH18N10T steel irradiated by neutrons
[DE94-605337] p 3202 N94-28551
Role of microstructure on the fatigue durability of aluminum aircraft alloys
[AD-A275814] p 3202 N94-28830
Performance and durability of high emittance heat receiver surfaces for solar dynamic power systems
[NASA-TM-106549] p 3172 N94-28834
Low Earth orbit durability evaluation of protected silicone for advanced refractive photovoltaic concentrator arrays
[NASA-TM-106543] p 3172 N94-28999
Photovoltaic performance and reliability workshop
[DE94-000236] p 3339 N94-30601

DUST
Joint research activities with CCMRI (China) p 3240 N94-29521

DUST STORMS
The viability of photovoltaics on the Martian surface
[NASA-TM-106478] p 3338 N94-30196

DWARF GALAXIES
Study of the stellar populations of the Fornax dwarf spheroidal galaxy
[ISBN-0-315-85526-6] p 3541 N94-30231

DWARF STARS
Surface differential rotation in a sample of cool dwarf stars p 3545 N94-29827

DYE LASERS
Absolute determination of local tropospheric OH concentrations p 3343 N94-28594
On the possibility of measuring atmospheric OH using intracavity laser spectroscopy p 3344 N94-28597
Advances in tunable powerful lasers: The advanced free-electron laser
[DE94-004997] p 3294 N94-29934

DYES
Measurement of atmospheric OH by titration of near-IR fluorescent dyes p 3344 N94-28599

DYNAMIC CHARACTERISTICS
Dynamics of a coupled solid state laser array p 3294 N94-29551
Elevation control system model for the DSS 13 antenna p 3248 N94-29622
Activities of Ishikawajima-Harima Heavy Industries Co. Ltd.
[PB94-137981] p 3555 N94-29798

Specialized data analysis of SSME and advanced propulsion system vibration measurements
[NASA-CR-193940] p 3174 N94-29868
Analysis and design of inflatable aerospace structures p 3403 N94-30799

DYNAMIC CONTROL
Fluid dynamic noise in a centrifugal pump
[AD-A275264] p 3477 N94-28904
Pulse response based minimum time control of flexible structures p 3436 N94-29720
Integrated propulsion-airframe dynamics and control p 3147 N94-29854
Stochastic stability and nonlinear control in mechanical systems p 3303 N94-29966
Motion control of mobile robots p 3310 N94-30309
Robotic NDE inspection of advanced solid rocket motor casings
[AIAA PAPER 94-1222-CP] p 3446 N94-30571
Kinematic analysis of platform-type robotic manipulators
[ISBN-0-315-78703-1] p 3311 N94-30793

DYNAMIC LOADS
Composite load spectra for select space propulsion structural components
[NASA-CR-194476] p 3316 N94-28508
Granular bases for heavily loaded pavements
[AD-A275171] p 3156 N94-29047
Asphaltic concrete performance under heavy fighter aircraft loading
[AD-A275046] p 3157 N94-29151
Fuzzy logic based robotic controller
[AIAA PAPER 94-1202-CP] p 3443 N94-30553
Simulation of composite material response under dynamic compressive loading
[DE94-005272] p 3184 N94-30589

DYNAMIC MODELS
Miniature linear-to-rotary motion actuator p 3163 N94-29647
Theoretical prediction of the influence coefficients on damped simple flexible rotors using the transfer matrix method
[IMR-TM-TR-002] p 3321 N94-30018
Symbolic generation of dynamics equations for manipulators mounted on moving bases p 3308 N94-30296
Development and validation of a linear recursive order-N algorithm for the simulation of flexible space manipulators dynamics
[AD-B173557] p 3311 N94-30391
Dynamic modeling of multibody flexible structures p 3323 N94-30813
Second-order structural identification via state space-based system realizations p 3323 N94-30815

DYNAMIC PRESSURE
Low-speed longitudinal aerodynamic characteristics of a flat-plate planform model of an advanced fighter configuration
[NASA-TM-109045] p 3130 N94-29443
Method for making a dynamic pressure sensor and a pressure sensor made according to the method
[NASA-CASE-LAR-14029-1] p 3288 N94-29484

DYNAMIC PROGRAMMING
The transient period of a cyclic process: An horizon theorem
[MEMO-1149] p 3427 N94-30585
Use of snakes to link edge points to create left ventricular boundaries in echocardiographic images
[TELECOM-93-D-016] p 3395 N94-30970

DYNAMIC RESPONSE
On the dynamic mechanical behavior of 3-D integrated fabric reinforced composites
[AD-A275424] p 3177 N94-28865
Turbomachinery forced response prediction system (FREPS): User's manual
[NASA-CR-194465] p 3319 N94-29104
Dynamic response of ceramics
[AD-A275396] p 3214 N94-29203
Active control of delaminations in smart composite structures p 3181 N94-29593
Modelling soft impacts for vibrational excitation of civil engineering structures
[PB94-137619] p 3320 N94-29681
Micromechanics of the dynamic response of ceramics and ceramic composites p 3217 N94-29975
Modal analysis of solar panels using boundary integral equations
[NLT-TP-92218-U] p 3338 N94-30328
Damage identification in composites using built-in piezoelectrics p 3184 N94-30355
Sensitivity analysis of the static aeroelastic response of a wing p 3134 N94-30525

DYNAMIC STABILITY
Stability of dynamical systems in the presence of noise
[AD-A275383] p 3243 N94-29072
Dissipation in Hamiltonian systems: Decaying cnoidal waves
[MEMO-1151] p 3460 N94-30738

DYNAMIC STRUCTURAL ANALYSIS
General theory and algorithms for the non-casual inversion, slewing and control of space-based articulated structures
[AD-A275118] p 3167 N94-29002
Turbomachinery forced response prediction system (FREPS): User's manual
[NASA-CR-194465] p 3319 N94-29104
Stiffness-generated rigid-body mode shapes for Lanczos eigensolution with SUPORT DOF by way of a MSC/NASTRAN DMAP alter
[NASA-TM-106537] p 3319 N94-29406
Transient analysis mode participation for modal survey target mode selection using MSC/NASTRAN DMAP
[NASA-TM-106536] p 3319 N94-29469
Concurrent simulation and constraint stabilization for flexible multibody systems p 3154 N94-29532
Experimental validation of finite element and boundary element methods for predicting structural vibration and radiated noise
[NASA-CR-4561] p 3301 N94-29552
Modelling soft impacts for vibrational excitation of civil engineering structures
[PB94-137619] p 3320 N94-29681
Advanced microfabrication technologies for microspacecraft p 3171 N94-29782
Dynamic fracture mechanics analysis for an edge delamination crack
[NASA-TM-109106] p 3479 N94-29856
Specialized data analysis of SSME and advanced propulsion system vibration measurements
[NASA-CR-193940] p 3174 N94-29868
A numerical method for confined unsteady flows related to fluid-structure interactions
[ISBN-0-315-74739-0] p 3277 N94-29902
Position control of a flexible beam with active damping of vibrations
[ISBN-0-315-85841-9] p 3321 N94-30033
A study of the flexible space platform based deployable manipulator
[ISBN-0-315-85410-3] p 3303 N94-30135
Three-dimensional free vibration analysis of thick arbitrarily laminated, rectangular, cylindrical and spherical composite panels p 3184 N94-30257
Sensitivity analysis of the static aeroelastic response of a wing p 3134 N94-30525
Analysis and design of inflatable aerospace structures p 3403 N94-30799
Dynamic modeling of multibody flexible structures p 3323 N94-30813
Second-order structural identification via state space-based system realizations p 3323 N94-30815
Hopf bifurcation in viscous, low-speed flows about an airfoil with structural coupling p 3134 N94-30865

DYNAMIC TESTS
Crashworthiness analysis of commuter aircraft seats
[AD-A275889] p 3135 N94-28799
Analysis and design of inflatable aerospace structures p 3403 N94-30799

DYNAMICAL SYSTEMS
Research activities of Martin C. Casdagli at SFI September 1989--May 1991
[DE94-005655] p 3463 N94-28548
On invariant measures for some infinite-dimensional dynamical systems
[DE94-606342] p 3522 N94-28609
Stability of dynamical systems in the presence of noise
[AD-A275383] p 3243 N94-29072
Boundary layer coherent structures
[AD-A275007] p 3272 N94-29195
On-line search for optimal controller parameters using interconnected learning automata
[MATHS-REPT-A-196] p 3436 N94-29526
Stochastic stability and nonlinear control in mechanical systems p 3303 N94-29966
Representations of dynamical systems described by behavioral inequalities
[AD-B173649] p 3458 N94-30402
Superdiffusion
[DE94-002333] p 3492 N94-30834
Dynamics and control of tethered satellite systems p 3170 N94-30864

DYNAMOMETERS
Deterioration of manual performance in cold and windy climates p 3381 N94-28434

DYSPROSIUM COMPOUNDS
Terfenol: A study of the phase equilibrium diagram and the solidification process
[DE94-004883] p 3209 N94-30690

E

E GLASS
Delamination of woven E-glass fabric composites
[DE94-003227] p 3185 N94-30827

E REGION
Space-time structure of the morning aurora inferred from coincident DMSP-F6, -F8, and Sondrestrom incoherent scatter radar observations
[AD-A275442] p 3356 N94-28869
A study of the thermospheric dynamics of the high-latitude E region using a spectral thermospheric general circulation model p 3362 N94-29743

EARLY WARNING SYSTEMS
Dual-use applications of infrared sensitive materials
[AD-A275140] p 3499 N94-29694

EARTH ATMOSPHERE
On the linear stability of Verkley's modons p 3324 N94-28695
Structure of neutrally stratified turbulent Ekman layer as predicted by closure models with prognostic equation for master length scale p 3325 N94-28696
Activities of the wintering party at Showa Station by the 31st Japanese Antarctic Research Expedition in 1990 p 3358 N94-29083
Activities of the fourth wintering party at Asuka Station by the 31st Japanese Antarctic Research Expedition in 1990 p 3358 N94-29084
Proceedings of the NIPR Symposium on Upper Atmosphere Physics, no. 6
[JTN-94-80593] p 3359 N94-29233
Second Japan-U.S. Workshop on Global Change: Environmental Response Technologies for Global Change (Mitigation and Adaptation) p 3354 N94-29522
Use of satellite data to improve parameterization of spatial and temporal variations of gaseous dry deposition in regional-scale models
[DE94-005110] p 3334 N94-30022
Linkages between terrestrial ecosystems and the atmosphere p 3351 N94-30624
Modeling Earth system changes of the past p 3353 N94-30635
Generation mechanisms of quasi-stationary waves in the Southern Hemisphere p 3365 N94-30789

EARTH CORE
Dislocation theory of melting for iron, revisited
[DE94-002715] p 3355 N94-28538
Electromagnetic core-mantle coupling p 3366 N94-30808

EARTH CRUST
Effects and implications of fault zone heterogeneity and anisotropy on earthquake strong ground motion p 3363 N94-29941

EARTH ENVIRONMENT
Proceedings of the 15th Earth Observation Symposium
[JTN-94-80607] p 3328 N94-29036
Antarctic Record, volume 36, no. 1
[REPT-106-VOL-36-NO-1] p 3357 N94-29078
Activities of the wintering party at Showa Station by the 31st Japanese Antarctic Research Expedition in 1990 p 3358 N94-29083
Activities of the fourth wintering party at Asuka Station by the 31st Japanese Antarctic Research Expedition in 1990 p 3358 N94-29084
Second Japan-U.S. Workshop on Global Change: Environmental Response Technologies for Global Change (Mitigation and Adaptation) p 3354 N94-29522
Modeling the Earth System, volume 3
[NASA-CR-194256] p 3350 N94-30616

EARTH GRAVITATION
A simulation study of high degree and order geopotential determination using satellite gravity gradiometry p 3333 N94-29762

EARTH IONOSPHERE
Antarctic Record, volume 36, no. 1
[REPT-106-VOL-36-NO-1] p 3357 N94-29078
Activities of the wintering party at Showa Station by the 31st Japanese Antarctic Research Expedition in 1990 p 3358 N94-29083
Signatures of dayside solar wind/magnetosphere/ionosphere coupling as revealed by the pace HF radars and associated experiments p 3359 N94-29236
A theory of current generator in the magnetosphere-ionosphere coupling p 3360 N94-29240
Coupled magnetohydrodynamic oscillations in the magnetosphere-ionosphere system: Hall current effect p 3360 N94-29242
Scale-length dependence of the ratio between the magnetic and electric field perturbations in the ionospheric field-aligned current region p 3360 N94-29243
ULF waves and magnetic field characteristics in the polar cusp observed at Godhavn p 3361 N94-29244

Study of generation mechanisms of magnetospheric VLF/ELF emissions based on the direction findings p 3361 N94-29245

EARTH MAGNETOSPHERE

Electron beams at geosynchronous orbit [AD-A275471] p 3355 N94-28684

Identification of an unexpected space radiation hazard [AD-A275170] p 3552 N94-29046

Antarctic Record, volume 36, no. 1 [REPT-106-VOL-36-NO-1] p 3357 N94-29078

Estimation of geomagnetic conjugate points by using Pc5 pulsations p 3357 N94-29079

Activities of the wintering party at Showa Station by the 31st Japanese Antarctic Research Expedition in 1990 p 3358 N94-29083

Observations of the geomagnetic field by Polar Patrol Balloon (PPB) experiment in Antarctica p 3359 N94-29235

Signatures of dayside solar wind/magnetosphere/ionosphere coupling as revealed by the pace HF radars and associated experiments p 3359 N94-29236

A theory of current generator in the magnetosphere-ionosphere coupling p 3360 N94-29240

Coupled magnetohydrodynamic oscillations in the magnetosphere-ionosphere system: Hall current effect p 3360 N94-29242

ULF waves and magnetic field characteristics in the polar cusp observed at Godhavn p 3361 N94-29244

Study of generation mechanisms of magnetospheric VLF/ELF emissions based on the direction findings p 3361 N94-29245

Variations of electron fluxes, low-frequency radiations and plasma density during the geomagnetic storm on 9-12 March, 1979 according to data of the Interkosmos-19 satellites [DE94-607323] p 3365 N94-30223

EARTH MANTLE

Electromagnetic core-mantle coupling p 3366 N94-30808

Geochemical and fluid dynamic investigations into the nature of chemical variability in the Earth's mantle p 3367 N94-30917

EARTH MOVEMENTS

Effects and implications of fault zone heterogeneity and anisotropy on earthquake strong ground motion p 3363 N94-29941

EARTH OBSERVATIONS (FROM SPACE)

Application of remote sensing in prevention of disasters p 3332 N94-29230

Japan's Earth observation satellite programs p 3332 N94-29232

Application of remote sensing techniques for the seismo-tectonic study of Nahanni earthquake area [ISBN-0-315-85942-3] p 3334 N94-30037

EARTH OBSERVING SYSTEM (EOS)

EOS project and ASTER (ITIR) p 3331 N94-29226

EARTH ORBITAL ENVIRONMENTS

Electron beams at geosynchronous orbit [AD-A275471] p 3355 N94-28684

Robust 300 C wire insulation system p 3165 N94-28699

Low Earth orbit durability evaluation of protected silicone for advanced refractive photovoltaic concentrator arrays [NASA-TM-106543] p 3172 N94-28999

Orbital debris radar instrumentation p 3248 N94-29626

Study of activation data of metal samples from LDEF-1 and Spacelab-2 [NASA-CR-195802] p 3205 N94-29736

Wave generation by contaminant ions near a large spacecraft [NASA-CR-195797] p 3169 N94-29917

Simulation of space-energy distributions of hot plasma on a geostationary orbit [DE94-607324] p 3365 N94-30107

EARTH ORIENTATION

Combining GPS and VLBI earth-rotation data for improved universal time p 3144 N94-29614

EARTH RESOURCES

Evaluation of simulated JERS-1 data for geologic mapping at Drum Mountains, Utah, Silver Bell, Arizona, and Wind River, Wyoming under the GEOSAT-ERSDAC/JAPEX/JGI/RESTEC joint studies p 3326 N94-28929

Image processing for hyperspectral data p 3326 N94-28930

JERS-1 data and information system for resources exploration p 3327 N94-28932

Observations by ERS-1 start p 3327 N94-28933

Principles and application tendency of remote sensing: Its principle, function and utilization p 3328 N94-29037

Proceedings of the 3rd International Symposium: JERS-1 and Remote Sensing in the Future [JTN-94-80597] p 3329 N94-29217

Remote sensing and the Earth p 3329 N94-29218

Application of optical sensor data to resource survey p 3330 N94-29223

Radar applications at the Canada Centre for Remote Sensing p 3331 N94-29224

JERS-1 and future remote sensing: Application of remote sensing data to agroecological problems p 3331 N94-29229

Future expectation of remote sensing technology p 3332 N94-29231

Journal of NIRE, vol. 2, no. 3 [JTN-94-80553] p 3553 N94-29512

Extrapolation of point data for resource mapping p 3334 N94-29959

EARTH ROTATION

Hydrodynamics of convection under winter polar leads [AD-A275182] p 3369 N94-29067

Combining GPS and VLBI earth-rotation data for improved universal time p 3144 N94-29614

Towards 10(exp 9) GPS geodesy: Vector baselines, Earth rotation and reference frames [NASA-CR-195768] p 3142 N94-30243

Electromagnetic core-mantle coupling p 3366 N94-30808

EARTH SCIENCES

A survey of geographical information systems applications for the Earth Science and Applications Division, Space Sciences Laboratory, Marshall Space Flight Center [NASA-TM-108438] p 3529 N94-28820

Imaging spectrometry of the Earth and other solar system bodies p 3237 N94-29779

Research and technology, 1992 [NASA-TM-103996] p 3555 N94-29891

EARTH SURFACE

Atmosphere, ocean, and land: Critical gaps in Earth system models p 3350 N94-30617

Models of atmosphere-ecosystem-hydrology interactions: Approaches and testing p 3353 N94-30636

EARTH TERMINALS

Defocussing characteristics of the ACTS, T1-VSAT Earth terminal antennas [NASA-TM-106420] p 3242 N94-28826

The two-way time synchronization system via a satellite voice channel p 3471 N94-30658

EARTH-MOON TRAJECTORIES

Optimal low-thrust, Earth-Moon trajectories p 3159 N94-30961

EARTHQUAKES

Effects and implications of fault zone heterogeneity and anisotropy on earthquake strong ground motion p 3363 N94-29941

The rupture process of large earthquakes along convergent margins: Cast studies from Alaska and Armenia p 3363 N94-29969

Application of remote sensing techniques for the seismo-tectonic study of Nahanni earthquake area [ISBN-0-315-85942-3] p 3334 N94-30037

EATING

Nutrition and hydration status of aircrew members consuming an improved survival ration during a simulated survival scenario p 3380 N94-28429

Some issues on Japan's space food developrnent and relating preliminary experimental study p 3388 N94-28498

Effect of food intake on skin vasomotor responses to head-up tilt in humans p 3390 N94-28854

ECCENTRICS

Metal band drives in spacecraft mechanisms p 3162 N94-29637

ECHOCARDIOGRAPHY

Use of snakes to link edge points to create left ventricular boundaries in echocardiographic images [TELECOM-93-D-016] p 3395 N94-30970

ECHOES

Seafloor characterization using texture [AD-A275399] p 3377 N94-29204

ECOLOGY

JERS-1 and future remote sensing: Application of remote sensing data to agroecological problems p 3331 N94-29229

A coupled approach to spatially derived parameters necessary for ecosystem modeling on the North Slope of Alaska: Appendix A [DE94-005853] p 3349 N94-30046

A bottom-up evolution of terrestrial ecosystem modeling theory, and ideas toward global vegetation modeling p 3351 N94-30628

Development of simplified ecosystem models for applications in Earth system studies: The Century experience p 3352 N94-30629

A toy terrestrial carbon flow model p 3352 N94-30630

ECONOMIC ANALYSIS

Diode-pumped solid-state-laser drivers and the competitiveness of inertial fusion energy [DE94-006654] p 3296 N94-30830

Assessment of costs and benefits of flexible and alternative fuel use in the US transportation sector [DE94-006100] p 3226 N94-30885

ECONOMIC DEVELOPMENT

Spin-off companies as agents of technology transfer: An empirical study of the spin-off companies of the Technical Research Centre of Finland [PB94-132248] p 3537 N94-28405

ECONOMIC IMPACT

Analysis and modeling of environmental and economic impacts of the solar hydrogen energy system p 3348 N94-29901

Solar photovoltaics for development applications [DE94-006116] p 3340 N94-30843

Measuring the impact of investments in information technologies on business performance [REPT-93-056] p 3536 N94-30929

ECONOMICS

Proceedings of the low cost materials of construction for biological processes workshop [DE94-000218] p 3226 N94-30761

ECOSYSTEMS

Development and implementation of a scrub habitat compensation plan for Kennedy Space Center [NASA-TM-109202] p 3347 N94-29099

Caesium-137 in a boreal forest ecosystem: Aspects on the long-term behavior [PB94-137809] p 3347 N94-29158

A coupled approach to spatially derived parameters necessary for ecosystem modeling on the North Slope of Alaska: Appendix A [DE94-005853] p 3349 N94-30046

Linkages between terrestrial ecosystems and the atmosphere p 3351 N94-30624

A bottom-up evolution of terrestrial ecosystem modeling theory, and ideas toward global vegetation modeling p 3351 N94-30628

Development of simplified ecosystem models for applications in Earth system studies: The Century experience p 3352 N94-30629

A toy terrestrial carbon flow model p 3352 N94-30630

Carbon cycling in high-latitude ecosystems p 3352 N94-30631

Models of atmosphere-ecosystem-hydrology interactions: Approaches and testing p 3353 N94-30636

The development and evaluation of a tunable diode laser trace gas sensor for the measurement of N2O and CH4 fluxes using micrometeorological techniques [ISBN-0-315-78975-1] p 3296 N94-30801

EDDY CURRENTS

Three-dimensional finite element modeling of a magnet array spinning above a conductor [DE94-004573] p 3468 N94-28459

Electrical conductivity measurements on a SiCp/Al alloy metal matrix composite [PB94-138310] p 3263 N94-29120

Flux-focusing eddy current probe and method for flaw detection [NASA-CASE-LAR-15046-1] p 3315 N94-29366

Mathematical models of hysteresis [DE94-005681] p 3260 N94-30902

EDDY VISCOSITY

Large eddy simulations using lattice Boltzmann algorithms [DE94-005666] p 3270 N94-28549

EDGE DETECTION

Use of snakes to link edge points to create left ventricular boundaries in echocardiographic images [TELECOM-93-D-016] p 3395 N94-30970

EDGES

Stability properties of inclusive connectivity for graphs [AD-A275360] p 3452 N94-29016

EDITING

Engineering specification editing tools [AD-A275116] p 3419 N94-29746

EDITING ROUTINES (COMPUTERS)

Transferable Output ASCII Data (TOAD) editor version 1.0 user's guide [NASA-CR-187507] p 3408 N94-28818

The ABC structure editor: Structure-based editing for the ABC programming environment [CWI-CS-R9256] p 3418 N94-29487

EDUCATION

Simulation Networking/Training Requirements Relational Database: User's guide [AD-A275634] p 3528 N94-28637

The Seventh Annual National Conference of Black Physics Students
[NASA-CR-195735] p 3526 N94-28746
Summer intern program
[AD-A275194] p 3466 N94-28888
Application of digital video to hypermedia training systems
[AD-A274989] p 3409 N94-28910
An evaluation of techniques for ranking academic information systems journals
[AD-A275179] p 3529 N94-29066
Fundamentals of printing technology
[PB94-132602] p 3530 N94-29141
Ada, object-oriented techniques, and concurrency in teaching data structures and file management
[AD-A275385] p 3411 N94-29201
Empirical studies of the value of algorithm animation in algorithm understanding
[AD-A275135] p 3412 N94-29287
ECSU home-institution support program (1993)
[AD-A275244] p 3431 N94-29396
Electrical engineering and industrial electronics education days: Control of asynchronous generators
[PB94-135514] p 3266 N94-29523
Progress report for the PTUF Project-93 Q1 and Q2
[PB94-138591] p 3431 N94-29995
An interactive, design and educational tool for supersonic external-compression inlets
[NASA-TM-106581] p 3421 N94-30174
An interactive educational tool for compressible aerodynamics
[NASA-TM-106568] p 3422 N94-30175

EGGS
Japanese Journal of Aerospace and Environmental Medicine, volume 30, no. 1
[JTN-94-80598] p 3389 N94-28850
Effect of chronic centrifugation on in vitro fertilization and early development in mice ova
p 3386 N94-28853

EIGENVALUES
Calculation of eigenvalues of Schroedinger operators for arbitrary coupling
[DE94-606302] p 3522 N94-28582
Variational calculation of the eigenpotential for H(sup -)-system
[DE94-606269] p 3407 N94-28622
The bootstrapped algorithm: A fast algorithm for blind signal separation
[AD-A275759] p 3408 N94-28760
Computation of vibration mode elastic-rigid and effective weight coefficients from finite-element computer program output p 3247 N94-29615
Eigenmode analysis of the destabilized ion acoustic mode in tokamaks
[PPL-142] p 3507 N94-30158
Further investigation of curve veering phenomena
p 3460 N94-30515
Eigenvalue analysis of the convergence behaviour of an Euler method
[PB94-1255722-U] p 3281 N94-30743

EIGENVECTORS
Variational calculation of the eigenpotential for H(sup -)-system
[DE94-606269] p 3407 N94-28622
A semiclassical study of quantum maps
p 3524 N94-29987
Further investigation of curve veering phenomena
p 3460 N94-30515

EINSTEIN EQUATIONS
Physics, astronomy, and astrophysics: A numerical study of the black hole plus Brill wave spacetime
p 3540 N94-29990
A numerical study of gravitational collapse
p 3548 N94-30271

EJECTION
Effectiveness of protection clothing for cold weather conditions after ejection over sea: A case report
p 3381 N94-28435
Sputtering of single crystals: Experimental evidence of the ejection process
[AD-A275819] p 3512 N94-28775

EKMAN LAYER
Papers in meteorology and geophysics, vol. 44, no.1
[JTN-94-80585] p 3324 N94-28693
Structure of neutrally stratified turbulent Ekman layer as predicted by closure models with prognostic equation for master length scale p 3325 N94-28696

ELASTIC ANISOTROPY
Thermal expansion and elastic anisotropy in single crystal Al2O3 and SiC reinforcements
[NASA-TM-106516] p 3214 N94-29105

ELASTIC DAMPING
Theoretical prediction of the influence coefficients on damped simple flexible rotors using the transfer matrix method
[IMR-TM-TR-002] p 3321 N94-30018

ELASTIC DEFORMATION
Viscous and elastic-plastic material model in the ABAQUS
[PB94-132347] p 3316 N94-28409
Dynamic modeling of multibody flexible structures
p 3323 N94-30813

ELASTIC MEDIA
A program for rapid computation of multioffset vertical seismic profile synthetic seismograms for layered media
[AD-A275464] p 3355 N94-28737
Numerical modeling and prediction of the thermomechanical behavior of fiber-reinforced composites p 3186 N94-30956

ELASTIC PROPERTIES
Computer simulation of martensitic transformations
[DE94-005213] p 3201 N94-28479
Free vibration of thermally loaded panels including initial imperfections and post-buckling effects
[NASA-TM-109097] p 3479 N94-29461
Preliminary evaluation of hybrid titanium composite laminates
[NASA-TM-109095] p 3180 N94-29472
Thermomechanical properties of 3-D transition metals
[DE94-604015] p 3487 N94-29500
Computation of vibration mode elastic-rigid and effective weight coefficients from finite-element computer program output p 3247 N94-29615
A non-contacting vertical alignment system for mass properties measuring instruments
[DE94-004680] p 3289 N94-29927
High elongation elastomers p 3223 N94-30477
Measurement of bulk longitudinal modulus and correction for edge effects
[DE94-005581] p 3222 N94-30900

ELASTIC SCATTERING
Numerical solution of the multichannel scattering problem
[DE94-606297] p 3484 N94-28619
Incommensurate magnetic order in UNi2Al3
[DE94-005449] p 3209 N94-30246

ELASTIC WAVES
Method for cancelling expansion waves in a wave rotor
[NASA-CASE-LEW-15218-2] p 3274 N94-29740

ELASTOMERS
Polymer technology publication series no. 16
[PB94-135522] p 3214 N94-29157
Novel techniques applied to polymer lifetime predictions
[DE94-005095] p 3218 N94-30102
High elongation elastomers p 3223 N94-30477

ELASTOPLASTICITY
Viscous and elastic-plastic material model in the ABAQUS
[PB94-132347] p 3316 N94-28409
Higher order asymptotic crack tip fields in a power-law hardening material p 3321 N94-29829
Micromechanical analysis of thermo-inelastic multiphase short-fiber composites
[NASA-CR-195290] p 3183 N94-30178
Closed form expressions for a consistent stress material nonlinear finite element p 3322 N94-30258

ELECTRIC ARCS
Second NASA Workshop on Wiring for Space Applications
[NASA-CP-3244] p 3165 N94-28697
Evaluation of pyrolysis and arc tracking on candidate wire insulation designs for space applications
p 3166 N94-28711
A new test method for the assessment of the arc tracking properties of wire insulation in air, oxygen enriched atmospheres and vacuum p 3167 N94-28714
High temperature arc-track resistant aerospace insulation p 3167 N94-28716
Hypervelocity impact induced arcing and Kapton pyrolization in a plasma environment
[NASA-TM-106528] p 3167 N94-28814
Plasma arc welding torch having means for vortexing plasma for exiting the welding torch
[NASA-CASE-MFS-28828-1] p 3298 N94-29351

ELECTRIC AUTOMOBILES
DOE/KEURP site operator program
[DE94-005832] p 3267 N94-30701

ELECTRIC BATTERIES
Battery energy and superconducting magnetic energy storage for utility applications: A qualitative analysis
[DE94-005382] p 3336 N94-28489
Anode for rechargeable ambient temperature lithium cells
[NASA-CASE-NPO-18580-1-CU] p 3265 N94-29505
Electrochemical Power Source (EPS) selection for Energetically Independent Robots (EIR): A systematic approach p 3269 N94-30312
Preliminary detector design ST862-prototype neutron detector
[DE94-004714] p 3491 N94-30695
Design of a variable-conductance vacuum insulation
[DE94-000270] p 3268 N94-30819

ELECTRIC BRIDGES
VHF impedance measurement: A review
[PB94-138682] p 3267 N94-30115

ELECTRIC CHARGE
Charge trapping and breakdown in N2O oxides
[DE94-003775] p 3266 N94-30040

ELECTRIC CONDUCTORS
Three-dimensional finite element modeling of a magnet array spinning above a conductor
[DE94-004573] p 3468 N94-28459
NEMA wire and cable standards development programs p 3166 N94-28706

ELECTRIC CONNECTORS
Intermetallic growth at the interface between copper and bismuth-tin solder
[AD-A275716] p 3202 N94-28543
Three dimensional transient analysis of microstrip circuits in multilayered anisotropic media
[AD-A274995] p 3263 N94-28995
System for the installation and replacement of components in hostile environments
[NASA-CASE-LEW-14906-1-SB] p 3300 N94-29427

ELECTRIC CONTACTS
Current leads and magnetic bearings
[DE94-004607] p 3297 N94-28461

ELECTRIC CURRENT
Correlative analysis of hard and soft x ray observations of solar flares
[NASA-CR-189329] p 3551 N94-29453
The structure of solar magnetic fields and their associated electric currents p 3544 N94-29723

ELECTRIC DISCHARGES
Interaction of multiple spark-generated bubbles in a compressible liquid
[AD-A275037] p 3272 N94-29149

ELECTRIC ENERGY STORAGE
Plasma treatment of polymer dielectric films to improve capacitive energy storage p 3223 N94-30479

ELECTRIC EQUIPMENT
NASA Parts Program Office responsibilities
p 3165 N94-28702

ELECTRIC EQUIPMENT TESTS
A new test method for the assessment of the arc tracking properties of wire insulation in air, oxygen enriched atmospheres and vacuum p 3167 N94-28714

ELECTRIC FIELDS
Fluctuation and transport reduction in a reversed field pinch by inductive poloidal current drive
[DE94-005542] p 3503 N94-28514
On the EKL-effect
[DE94-606325] p 3468 N94-28720
Correlative analysis of hard and soft x ray observations of solar flares
[NASA-CR-189329] p 3551 N94-29453
Nonadiabatic effects in the quantum Hall regime
p 3513 N94-29530
A study of cloud-to-ground lightning processes with emphasis on data analysis and modeling of the return stroke p 3372 N94-29802
Periodic electromagnetic vacuum in the two-dimensional Yang-Mills theory with the Chern-Simons mass
[DE94-608128] p 3525 N94-30170
Langmuir waves in the electron-positron plasma
[DE94-608330] p 3508 N94-30191
The influence of an in-situ electric field on H(+) and He(+) implantation induced defects insil icon
[DE94-006553] p 3518 N94-30249
Missile launch detection electric field perturbation experiment
[DE94-004224] p 3466 N94-30586
Electric power lines: Questions and answers on research into health effects
[DE94-005637] p 3353 N94-30757

ELECTRIC GENERATORS
Overview of space environment utilization science
[JTN-94-80581] p 3227 N94-28938
Electrical engineering and industrial electronics education days: Control of asynchronous generators
[PB94-135514] p 3266 N94-29523
Survey report of JSUP Space Environment Utilization Research Committee in fiscal year 1992: Functional New Materials Session
[JTN-94-80582] p 3159 N94-30162

ELECTRIC HYBRID VEHICLES
Analysis of data from electric and hybrid electric vehicle student competitions
[DE94-000269] p 3302 N94-29922
DOE/KEURP site operator program
[DE94-005832] p 3267 N94-30701

ELECTRIC MOTOR VEHICLES
Fuel Cell Seminar, 1992: Program and abstracts
[DE94-003882] p 3336 N94-28472

Analysis of data from electric and hybrid electric vehicle student competitions
[DE94-000269] p 3302 N94-29922
Technical analysis of alternative fueled vehicles
[DE94-744238] p 3304 N94-30269
DOE/KEURP site operator program
[DE94-005832] p 3267 N94-30701
Investigation of the technology development status of alternate fuel vehicles
[DE94-744237] p 3312 N94-30831

ELECTRIC MOTORS
Three high duty cycle, space-qualified mechanisms p 3162 N94-29642
Design of an electromagnetic accelerator for turbulent hydrodynamic mix studies
[DE94-005821] p 3281 N94-30600

ELECTRIC POTENTIAL
Breakdown testing of wiring insulation p 3166 N94-28713
Performance evaluation of a 22.5/30 kW 270 volts direct current generator system
[AD-A275106] p 3263 N94-28913
Effects of oxide charge and surface recombination velocity on the excess base current of BJT's
[DE94-003711] p 3263 N94-29025
Deexcitation processes in nuclear reactions: The study of hot hadronic matter
[DE94-003396] p 3492 N94-30836
A magnetically coupled quench detector for superconducting magnets
[DE94-006040] p 3268 N94-30904

ELECTRIC POWER PLANTS
Impact study on the use of biomass-derived fuels in gas turbines for power generation
[DE94-000261] p 3224 N94-28502
Performance of the Southern California Edison Company Stirling dish
[DE94-004676] p 3337 N94-29018

ELECTRIC POWER SUPPLIES
Cosmic energy equipment p 3229 N94-28945
Electrochemical Power Source (EPS) selection for Energetically Independent Robots (EIR): A systematic approach p 3269 N94-30312

ELECTRIC POWER TRANSMISSION
Development of an accurate transmission line fault locator using the global positioning system satellites p 3144 N94-30652

ELECTRIC PROPULSION
Arcjet system integration development
[NASA-CR-187147] p 3171 N94-28736
Orbital applications of electrodynamic propulsion
[AD-A275413] p 3173 N94-29216
Non-isolated 30 kW class arcjet PCU
[NASA-CR-189148] p 3173 N94-29444

ELECTRIC SWITCHES
Measurand transient signal suppressor
[NASA-CASE-MSC-22027-1] p 3435 N94-29466

ELECTRIC WIRE
Second NASA Workshop on Wiring for Space Applications
[NASA-CP-3244] p 3165 N94-28697
ESTEC wiring test programme materials related properties p 3165 N94-28698
Robust 300 C wire insulation system p 3165 N94-28699
NASA wiring program: Survey of NASA experiences in wiring system safety p 3165 N94-28700
NASA Parts Project Office: Basic goals p 3166 N94-28703
NAVAIR aircraft wiring standardization and qualification program p 3166 N94-28704
Organized wiring systems p 3166 N94-28705
NEMA wire and cable standards development programs p 3166 N94-28706
MSFC inspections of installed polyimide wire p 3166 N94-28707
Flammability, odor, offgassing, thermal vacuum stability, and compatibility with aerospace fluids of wire insulations p 3166 N94-28709
The effects of propagational factors on quantum wires in close parallel proximity
[ISBN-0-315-86157-6] p 3254 N94-30035

ELECTRICAL ENGINEERING
SPC toolbox: An interactive MATLAB (tm) package for signal modeling, analysis, and communications
[AD-A275617] p 3241 N94-28634
Electrical engineering and industrial electronics education days: Control of asynchronous generators
[PB94-135514] p 3266 N94-29523

ELECTRICAL FAULTS
Investigation of advanced fault insertion and simulator methods
[NASA-CR-195241] p 3261 N94-28511
Non-isolated 30 kW class arcjet PCU
[NASA-CR-189148] p 3173 N94-29444
Development of an accurate transmission line fault locator using the global positioning system satellites p 3144 N94-30652

ELECTRICAL IMPEDANCE
VHF impedance measurement: A review
[PB94-138682] p 3267 N94-30115

ELECTRICAL INSULATION
Second NASA Workshop on Wiring for Space Applications
[NASA-CP-3244] p 3165 N94-28697
Robust 300 C wire insulation system p 3165 N94-28699
Selection of the Space Station Freedom (SSF) Flat Collector Circuit (FCC) insulation material p 3165 N94-28701
NEMA wire and cable standards development programs p 3166 N94-28706
Wiring for space applications program p 3166 N94-28708
Flammability, odor, offgassing, thermal vacuum stability, and compatibility with aerospace fluids of wire insulations p 3166 N94-28709
Electrical and mechanical testing of wire insulation for space applications p 3166 N94-28710
Evaluation of pyrolysis and arc tracking on candidate wire insulation designs for space applications p 3166 N94-28711
Wire insulation degradation and flammability in low gravity p 3166 N94-28712
Breakdown testing of wiring insulation p 3166 N94-28713
A new test method for the assessment of the arc tracking properties of wire insulation in air, oxygen enriched atmospheres and vacuum p 3167 N94-28714
High temperature polymer dielectric film insulation p 3167 N94-28715
High temperature arc-track resistant aerospace insulation p 3167 N94-28716
Screening of flexible cables by nonlinear resistance measurements
[AD-A275193] p 3264 N94-29289
Picosecond response of the quasiparticle current in superconducting tunnel junctions
[DE94-006300] p 3515 N94-30009
Development of radiation resistant electrical cable insulations p 3223 N94-30480
Development of radiation resistant electrical cable insulations
[DE94-005189] p 3222 N94-30906

ELECTRICAL MEASUREMENT
Portable electronically based method for the nondestructive remote sensing of crevice corrosion
[AD-A275403] p 3318 N94-29057
System for improving measurement accuracy of transducer by measuring transducer temperature and resistance change using thermoelectric voltages
[NASA-CASE-ARC-12014-1] p 3287 N94-29361
BPM901N monitor electronics for the determination of the bundle profile in the extraction line of AmPS
[DIGEL-1993-9] p 3495 N94-29467

ELECTRICAL PROPERTIES
ESTEC wiring test programme materials related properties p 3165 N94-28698
Performance evaluation of a 22.5/30 kW 270 volts direct current generator system
[AD-A275106] p 3263 N94-28913
Electroset Technology: On the forefront of manufacturing
[AD-A275166] p 3263 N94-29045
Studies on the optimization of deformation processed metal-metal matrix composites
[DE94-006033] p 3185 N94-30704
Rotator phases in narrow-gap semiconductors
[DE94-005472] p 3521 N94-30897

ELECTRICAL RESISTANCE
Screening of flexible cables by nonlinear resistance measurements
[AD-A275193] p 3264 N94-29289
System for improving measurement accuracy of transducer by measuring transducer temperature and resistance change using thermoelectric voltages
[NASA-CASE-ARC-12014-1] p 3287 N94-29361

ELECTRICAL RESISTIVITY
Electrical conductivity measurements on a SiCp/Al alloy metal matrix composite
[PB94-138310] p 3263 N94-29120
High resistivity buffer layers by oxygen doping
[AD-A274986] p 3513 N94-29125
Focused ion beam fabrication of microelectronic structures
[AD-A275384] p 3264 N94-29305
Aggregation equilibria in arsenic doped silicon
[DE94-607269] p 3515 N94-30005
Non-chromate talc conversion coatings for aluminum
[DE94-005281] p 3207 N94-30053
Localization in presence of magnetic field in 2-D disordered binary alloys
[DE94-608093] p 3208 N94-30108
Resistive ballooning mode in a gas-dynamic trap
[DE94-608328] p 3508 N94-30171
Effects of hydrogen on the resistivity of thin Au and Cu films p 3218 N94-30225
Thermal conductivities, electrical resistivities, and Seebeck coefficients of YBa2Cu3O(7-x) superconductors from 80 to 300 K
[DE94-004796] p 3520 N94-30724
Ionic conduction mechanisms in CaF2 and CaF2-Al2O3 nanocomposite films on Al2O3 substrates
[DE94-004792] p 3520 N94-30773

ELECTRICITY
NEMA wire and cable standards development programs p 3166 N94-28706

ELECTRO-OPTICAL EFFECT
Electrooptical and optical evaluation of Pb(Zr,Ti)O3 thin films using waveguide refractometry
[DE94-006374] p 3518 N94-30247

ELECTRO-OPTICS
Advanced optical A/D converter
[AD-A275663] p 3498 N94-28656
Gordon research conference on optical signal processing and holography
[AD-A275092] p 3499 N94-28848
Reconfigurable optical interconnections via dynamic computer-generated holograms
[NASA-CASE-NPO-19039-1-CU] p 3499 N94-29491
An investigation of distributed coupling in a nonlinear semiconductor waveguide p 3246 N94-29529
Proceedings of the Workshop on Microtechnologies and Applications to Space Systems
[NASA-CR-195688] p 3235 N94-29767
Study of nonlinear optical polymers and their applications in optical waveguides p 3216 N94-29807
Electrooptical and optical evaluation of Pb(Zr,Ti)O3 thin films using waveguide refractometry
[DE94-006374] p 3518 N94-30247
Optoelectronic packaging activities at Sandia National Laboratories
[DE94-005287] p 3501 N94-30261
Photonics at Sandia National Laboratories: From research to applications
[DE94-006463] p 3501 N94-30828

ELECTROACOUSTIC TRANSDUCERS
Absolute calibration technique for broadband ultrasonic transducers
[NASA-CASE-LAR-14672-1] p 3287 N94-29199
Sensing the gas metal arc welding process p 3314 N94-30444

ELECTROACOUSTICS
Minutes. Accredited Standards Committee on Acoustics, S1. US tag for ISO/TC 43 acoustics and IEC/TC 29 electroacoustics
[AD-A275702] p 3477 N94-28689

ELECTROCARDIOGRAPHY
Relaxed tolerance following HSG, high sustained +Gz
[AD-A275204] p 3391 N94-28892

ELECTROCHEMICAL CELLS
Anode for rechargeable ambient temperature lithium cells
[NASA-CASE-NPO-18580-1-CU] p 3265 N94-29505

ELECTROCHEMICAL CORROSION
Pitting corrosion of titanium
[AD-A274980] p 3203 N94-29089
Pit initiation on passivated metal surfaces: Crystallographic orientation and environmental effects
[ISBN-0-315-85433-2] p 3208 N94-30138

ELECTROCHEMICAL OXIDATION
Electrochemical incineration of wastes
[NASA-CR-195262] p 3198 N94-29938

ELECTROCHEMISTRY
Pitting corrosion of titanium
[AD-A274980] p 3203 N94-29089
X ray standing wave studies of underpotentially deposited metal monolayers
[AD-A275409] p 3513 N94-29215
Realtime structural electrochemistry of platinum clusters using dispersive XAFS
[DE94-005093] p 3208 N94-30101
An investigation of the corrosion properties of aluminum-tantalum alloys using electrochemical impedance spectroscopy and local electrochemical impedance spectroscopy p 3209 N94-30521

ELECTRODEPOSITION
Electrodeposition of bismuth alloys by the controlled potential method
[DE94-605318] p 3212 N94-28550
Corrosion inhibition by electrodeposited conductive-polymer film
[AD-A275456] p 3213 N94-28806
X ray standing wave studies of underpotentially deposited metal monolayers
[AD-A275409] p 3513 N94-29215

Template synthesized nanoscopic gold particles: Optical spectra and the effects of particle size and shape
[AD-A275378] p 3197 N94-29312
An improved plating process p 3223 N94-30451

ELECTRODES
Pitting corrosion of titanium
[AD-A274980] p 3203 N94-29089
X ray standing wave studies of underpotentially deposited metal monolayers
[AD-A275409] p 3513 N94-29215
Electrochemical incineration of wastes
[NASA-CR-195262] p 3198 N94-29938
Ionic conduction mechanisms in CaF2 and CaF2-Al2O3 nanocomposite films on Al2O3 substrates
[DE94-004792] p 3520 N94-30773

ELECTRODYNAMICS
The Klein-Fock equation, minimal surfaces and gravitational fields
[DE94-606340] p 3356 N94-28803
Orbital applications of electrodynamic propulsion
[AD-A275413] p 3173 N94-29216
On determination of a momentum of Alfven wave packet
[DE94-608329] p 3255 N94-30172

ELECTROLESS DEPOSITION
Adhesion of electrolessly deposited Ni(P) on alumina ceramic
[ETN-94-95358] p 3212 N94-28539

ELECTROLYSIS
Regenerating using aqueous cleaners with ozone and electrolysis p 3240 N94-30468

ELECTROLYTE METABOLISM
Japanese Journal of Aerospace and Environmental Medicine, vol. 30, no. 3
[JTN-94-80606] p 3387 N94-28495
Studies on water electrolyte metabolism and endocrine responses at rest and during submaximal exercise at 6,000 m simulated altitude p 3388 N94-28496
Effects of training at simulated altitude of 6,000 m on endocrine responses at rest and during exercise at the same altitude p 3388 N94-28497

ELECTROLYTES
Electromagnetic effect on turbulent transport in liquid metals and electrolytes (bath)
[PB94-138450] p 3206 N94-29946

ELECTROLYTIC CELLS
Fuel Cell Seminar, 1992: Program and abstracts
[DE94-003882] p 3336 N94-28472

ELECTROMAGNETIC ABSORPTION
UV laser long-path absorption spectroscopy p 3343 N94-28595
Developing a diode array spectrometer for tropospheric chemistry studies p 3362 N94-29752
Characterization of thermally annealed Sb implanted fused silica
[DE94-005464] p 3219 N94-30335
Nonlinear absorption in high reflector multilayers
[DE94-005818] p 3295 N94-30598
Pushing the limit: Precision radial velocities, techniques, and applications p 3542 N94-30861

ELECTROMAGNETIC COMPATIBILITY
Arcjet system integration development
[NASA-CR-187147] p 3171 N94-28736
Development of electromagnetic compatibility tests
[REPT-932-430-110] p 3245 N94-29421

ELECTROMAGNETIC COUPLING
Printed circuit elements with applications to antennas, scattering, and circuits
[AD-A275512] p 3262 N94-28669
Electromagnetic core-mantle coupling p 3366 N94-30808

ELECTROMAGNETIC FIELDS
The static and nonstatic electrical solenoids
[DE94-606326] p 3261 N94-28585
Potential hazards of magnetic resonance imagers to emergency medical service helicopter operations
[DOT/FAA/RD-92/15] p 3135 N94-29862
Three-dimensional effects for radio frequency antenna modeling
[DE94-006102] p 3255 N94-30105
Theory of fundamental interactions
[DE94-608126] p 3525 N94-30169
Periodic electromagnetic vacuum in the two-dimensional Yang-Mills theory with the Chern-Simons mass
[DE94-608128] p 3525 N94-30170
Mathematical models of hysteresis
[DE94-005681] p 3260 N94-30902

ELECTROMAGNETIC INTERACTIONS
A measurement of the tau polarization at the resonance with the DELPHI detector at LEP
[DE94-005557] p 3482 N94-28520
Masses and mixing of leptons and quarks (Dirac particles)
[DE94-606446] p 3484 N94-28611
High sensitivity tests of the standard model for electroweak interactions
[DE94-005415] p 3490 N94-30262
Theoretical studies in hadronic and nuclear physics
[DE94-003524] p 3492 N94-30838

ELECTROMAGNETIC INTERFERENCE
Analysis of microwave induced interference in pn-diodes
[PB94-136983] p 3243 N94-28906
Digital pulse compression and its application in reducing radar interference
[ISBN-0-315-85767-6] p 3255 N94-30240
Guidance on eliminating interference from sensitive electrical circuits
[PB94-139300] p 3268 N94-30784

ELECTROMAGNETIC NOISE
High Tc superconducting bolometric and nonbolometric infrared (IR) detectors
[NASA-CR-195728] p 3262 N94-28846
Removal of coherent Extremely Low Frequency (ELF) background noise by adaptive noise cancellation
[AD-A275016] p 3243 N94-28898
The effect of enhanced backscattering on target detection p 3258 N94-30508

ELECTROMAGNETIC NOISE MEASUREMENT
Long term variations of radio auroral activity p 3359 N94-29237
New-type echoes observed with the 50 MHz auroral Doppler radar at Showa Station p 3360 N94-29238
Initial observation results with imaging riometer at NY-Alesund (L is equal to 16) p 3360 N94-29239

ELECTROMAGNETIC PROPERTIES
Radioelectric characterization of materials at 1000 C
[REPT-932-430-104] p 3245 N94-29440

ELECTROMAGNETIC PULSES
A space-based classification system for RF transients
[DE94-003933] p 3240 N94-28522
A relativistic solitary wave in electron positron plasma
[DE94-608107] p 3507 N94-30071

ELECTROMAGNETIC RADIATION
Exact spherical wave solutions to Maxwell's equations with applications p 3252 N94-29733
The effects of man-made smokes and battlefield-induced smokes on the propagation of electromagnetic radiation p 3258 N94-30505
Relativistic theory for picosecond time transfer in the vicinity of Earth p 3470 N94-30653

ELECTROMAGNETIC SCATTERING
Acoustic or electromagnetic scattering from the penetrable wedge
[AD-A275259] p 3243 N94-29054

ELECTROMAGNETIC SHIELDING
Flux-focusing eddy current probe and method for flaw detection
[NASA-CASE-LAR-15046-1] p 3315 N94-29366

ELECTROMAGNETIC SPECTRA
VHF impedance measurement: A review
[PB94-138682] p 3267 N94-30115

ELECTROMAGNETIC WAVE TRANSMISSION
Atmospheric Propagation Effects Through Natural and Man-Made Obscurants for Visible to MM-Wave Radiation
[AGARD-CP-542] p 3256 N94-30495
The effects of man-made smokes and battlefield-induced smokes on the propagation of electromagnetic radiation p 3258 N94-30505

ELECTROMAGNETISM
Integral equation analysis of composite bodies of revolution and arbitrary surfaces with application to cavity-backed antennas p 3253 N94-29883
An investigation into certain geometrical and variational properties of the P(4) theory of gravitation and electromagnetism p 3526 N94-30950

ELECTROMECHANICAL DEVICES
NASA Parts Program Office responsibilities p 3165 N94-28702
An emergency response mobile robot for operations in combustible atmospheres
[NASA-CASE-NPO-19020-1-CU] p 3299 N94-29420
Design and test of electromechanical actuators for thrust vector control p 3163 N94-29650
SP-100 control drive assembly development p 3163 N94-29651
Micromanufacturing: Recent developments in this country and abroad p 3235 N94-29769

ELECTROMECHANICS
Three-dimensional finite element modeling of a magnet array spinning above a conductor
[DE94-004573] p 3468 N94-28459

ELECTROMIGRATION
Self-stressing test structures used for high-frequency electromigration
[DE94-006142] p 3267 N94-30368

ELECTRON ACCELERATION
Acceleration in astrophysics
[DE94-004986] p 3552 N94-28580

ELECTRON BEAMS
Electron beam irradiation experiments of monoblock divertor mock-up
[DE94-707497] p 3503 N94-28555
Coulomb field effect on plasma focusing and wake field acceleration
[DE94-004937] p 3504 N94-28564
Low voltage electron beam lithography
[AD-A275648] p 3262 N94-28650
Electron beams at geosynchronous orbit
[AD-A275471] p 3355 N94-28684
Active electron and ion beam experiments in space
[AD-A275570] p 3504 N94-28828
Electron beam analysis for cyclotron harmonic and free-electron laser devices
[AD-A275070] p 3293 N94-29179
BPM901N monitor electronics for the determination of the bundle profile in the extraction line of AmPS
[DIGEL-1993-9] p 3495 N94-29467
Stripline monitor electronics for the bundle position determination in AmPS
[DIGEL-1993-8] p 3495 N94-29888
Experiments on the two-stage dense plasma heating on the GOL-3 device
[DE94-608356] p 3508 N94-30193
Investigations of large area electron beam diodes for excimer lasers
[DE94-005670] p 3295 N94-30595
The use of thermistors in the NPL electron-beam calorimeter
[PB94-139334] p 3290 N94-30782
Atomic physics with highly charged ions
[DE94-003397] p 3492 N94-30837

ELECTRON BUNCHING
Coulomb field effect on plasma focusing and wake field acceleration
[DE94-004937] p 3504 N94-28564

ELECTRON CAPTURE
Analytic cross sections for collisions of H, H2, He and Li atoms and ions with atoms and molecules
[DE94-707686] p 3485 N94-28788
Atomic physics with highly charged ions
[DE94-003397] p 3492 N94-30837

ELECTRON CLOUDS
Controlling chaos in plasma filled diodes
[AD-A275525] p 3504 N94-28686

ELECTRON DENSITY (CONCENTRATION)
A novel spectroscopic measurement method of RF plasma for temperature and electron density diagnoses p 3188 N94-28682
Controlling chaos in plasma filled diodes
[AD-A275525] p 3504 N94-28686
Transport properties of epitaxial lift off films
[NASA-TM-106156] p 3264 N94-29209
Physical conditions in classical H2 regions in the Magellanic Clouds p 3543 N94-29722
Effects of hydrogen on the resistivity of thin Au and Cu films p 3218 N94-30225
Remote pumping of solid state lasers with nuclear driven fluorescers
[DE94-004846] p 3296 N94-30614
Inertial confinement fusion
[DE94-005957] p 3510 N94-30875

ELECTRON DIFFRACTION
Photoelectron diffraction and holography: Some new directions
[DE94-006297] p 3289 N94-30027
RHEED studies of the nucleation, growth, and mobility of Ag atoms on the Si(111)7 x 7 surface
[DE94-005551] p 3521 N94-30899

ELECTRON EMISSION
Electron beam analysis for cyclotron harmonic and free-electron laser devices
[AD-A275070] p 3293 N94-29179
Characteristics of secondary electron emission from CsI induced by x rays with energies up to 100 keV
[DE94-608422] p 3395 N94-30185

ELECTRON ENERGY
Physical conditions in classical H2 regions in the Magellanic Clouds p 3543 N94-29722
Atomic-scale structure and chemistry of interfaces by Z-contrast imaging and electron energy loss spectroscopy in the STEM
[DE94-006563] p 3516 N94-30064
Resistive ballooning mode in a gas-dynamic trap
[DE94-608328] p 3508 N94-30171
Distribution functions of electrons within aluminium oxide thin films
[DE94-608418] p 3490 N94-30184
Peculiarities of heat transfer in the experiments of beam injection heating of a plasma at the GOL-3 device
[DE94-608357] p 3508 N94-30194
Atomic physics with highly charged ions
[DE94-003397] p 3492 N94-30837

ELECTRON FLUX DENSITY
Variations of electron fluxes, low-frequency radiations and plasma density during the geomagnetic storm on 9-12 March, 1979 according to data of the Interkosmos-19 satellites
[DE94-607323] p 3365 N94-30223
ELECTRON GAS
Transport properties of epitaxial lift off films
[NASA-TM-106156] p 3264 N94-29209
ELECTRON IRRADIATION
Irradiation polymerization of bismaleimide resins
[REPT-932-430-105] p 3215 N94-29441
ELECTRON MICROSCOPES
A sub-cm micromachined electron microscope
p 3236 N94-29775
ELECTRON MOBILITY
Effects of hydrogen on the resistivity of thin Au and Cu films p 3218 N94-30225
ELECTRON OSCILLATIONS
The effects of propagational factors on quantum wires in close parallel proximity
[ISBN-0-315-86157-6] p 3254 N94-30035
ELECTRON PARAMAGNETIC RESONANCE
An improved method of measuring tropospheric NO2, NO3, HO2, and RO2 by Matrix Isolation and Electronic Spin Resonance (MIESR) p 3345 N94-28605
Study of iron exchanged zeolites by Moessbauer effect and electron spin resonance spectroscopy
[DE94-605138] p 3514 N94-29691
Non-invasive temperature measurements using electron paramagnetic resonance spectroscopy
p 3198 N94-29881
ELECTRON PHONON INTERACTIONS
Thermal conductivities, electrical resistivities, and Seebeck coefficients of YBa2Cu3O(7-x) superconductors from 80 to 300 K
[DE94-004796] p 3520 N94-30724
ELECTRON PLASMA
Experiments on the two-stage dense plasma heating on the GOL-3 device
[DE94-608356] p 3508 N94-30193
ELECTRON PRECIPITATION
Space-time structure of the morning aurora inferred from coincident DMSP-F6, -F8, and Sondrestrom incoherent scatter radar observations
[AD-A275442] p 3356 N94-28869
ELECTRON RADIATION
Optical depth effects in cluster cooling flows
p 3541 N94-30800
ELECTRON SCATTERING
A measurement of the LMP effect
[DE94-005225] p 3482 N94-28493
Quantum-mechanical suppression of bremsstrahlung
[DE94-005223] p 3497 N94-30712
Dissociative recombination of H3(+)
[DE94-005356] p 3493 N94-30891
ELECTRON SPECTROSCOPY
Study of iron exchanged zeolites by Moessbauer effect and electron spin resonance spectroscopy
[DE94-605138] p 3514 N94-29691
ELECTRON STATES
Electronic structure and mechanical properties of grain boundaries
[AD-A275198] p 3512 N94-28890
ELECTRON TRANSFER
The generalized spin-boson model for electron-transfer reactions involving two harmonic potentials with a different force constant
[DE94-005470] p 3482 N94-28509
Quenching of the excited state of hydrated Europium(3) ions by electron transfer
[DE94-005553] p 3482 N94-28518
Tunnelling hot electron transfer amplifiers
[AD-A275529] p 3262 N94-28687
Conceptual study of moderately coupled plasmas and experimental comparison of laboratory x ray sources
[DE94-005828] p 3506 N94-30045
Photochemistry in constrained spaces: Zeolites and layered double metal hydroxides
[DE94-004958] p 3200 N94-30769
Group transfer and electron transfer reactions of organometallic complexes: Summary of research accomplished in 1993
[DE94-004963] p 3200 N94-30770
Theory for electron-transfer reactions involving two Marcus surfaces with a different force constant
[DE94-005925] p 3493 N94-30874
Theory for electron-transfer reactions in a three-component system: The degenerate regime
[DE94-005919] p 3493 N94-30903
ELECTRON TUNNELING
Tunnelling hot electron transfer amplifiers
[AD-A275529] p 3262 N94-28687
Micromachined electron tunneling infrared sensors
p 3238 N94-29785
The effects of propagational factors on quantum wires in close parallel proximity
[ISBN-0-315-86157-6] p 3254 N94-30035
Strong overlap and transmission in triple barrier resonant structures
[DE94-608103] p 3516 N94-30067
ELECTRON-POSITRON PAIRS
Experiment studies of electron-positron interactions at the Stanford Linear Accelerator Center
[DE94-005877] p 3491 N94-30702
ELECTRON-POSITRON PLASMAS
A relativistic solitary wave in electron positron plasma
[DE94-608107] p 3507 N94-30071
Langmuir waves in the electron-positron plasma
[DE94-608330] p 3508 N94-30191
ELECTRONIC CONTROL
BPM901N monitor electronics for the determination of the bundle profile in the extraction line of AmPS
[DIGEL-1993-9] p 3495 N94-29467
ELECTRONIC COUNTERMEASURES
Spurs in digital radio frequency memory and applications of DRFM
[AD-A275013] p 3243 N94-28897
Analysis of microwave induced interference in pn-diodes
[PB94-136983] p 3243 N94-28906
Detection methods for stealth radio signals: A literature survey
[PB94-137452] p 3244 N94-29176
ELECTRONIC EQUIPMENT
NASA Parts Program Office responsibilities
p 3165 N94-28702
Analysis of microwave induced interference in pn-diodes
[PB94-136983] p 3243 N94-28906
Neural network application to Particle Impact Noise Detection p 3437 N94-29840
Practical applications of plasma surface modification
[DE94-004892] p 3349 N94-29932
Non-aqueous cleaning solvent substitution
[DE94-005339] p 3219 N94-30245
Non-aqueous cleaning solvent substitution
p 3354 N94-30466
ELECTRONIC EQUIPMENT TESTS
The 100 kA, 5000 V solid-state opening switch for inductive energy storage
[AD-A274993] p 3263 N94-28994
Neural network application to Particle Impact Noise Detection p 3437 N94-29840
Self-stressing test structures used for high-frequency electromigration
[DE94-006142] p 3267 N94-30368
Fiber optical solar simulator p 3341 N94-30486
ELECTRONIC MAIL
DOD Electronic Commerce (EC)/Electronic Data Interchange (EDI) in contracting report
[AD-A275298] p 3242 N94-28874
Management of PEM public key certificates using X.500 directory service: Some problems and solutions
[DE94-004200] p 3431 N94-29952
ELECTRONIC MODULES
Design and packaging of fault tolerant optoelectronic multiprocessor computing system
[AD-A275896] p 3405 N94-28798
BPM901N monitor electronics for the determination of the bundle profile in the extraction line of AmPS
[DIGEL-1993-9] p 3495 N94-29467
ELECTRONIC PACKAGING
Design and packaging of fault tolerant optoelectronic multiprocessor computing system
[AD-A275896] p 3405 N94-28798
Optoelectronic packaging activities at Sandia National Laboratories
[DE94-005287] p 3501 N94-30261
ELECTRONIC TRANSDUCERS
Micromachined electron tunneling infrared sensors
p 3238 N94-29785
ELECTRONS
Interband optical absorption in the Wannier-Stark ladder under the electron-LO-phonon resonance condition
[DE94-608097] p 3267 N94-30092
Langmuir waves in the electron-positron plasma
[DE94-608330] p 3508 N94-30191
Search for the top quark in the electron-electron and electron-muon channels at D0
[DE94-006174] p 3492 N94-30779
Self-similar variables and the problem of nonlocal electron heat conductivity
[DE94-005826] p 3493 N94-30881
ELECTRONYSTAGMOGRAPHY
Disturbance of equilibrium on JAL flight crew
p 3390 N94-28856
ELECTROPHORESIS
Instrumental development of novel detection and separation methods for capillary electrophoresis
[DE94-005554] p 3187 N94-28519
Properties of chemical vapor infiltration diamond deposited in a diamond powder matrix
[DE94-005429] p 3220 N94-30591
ELECTROPLATING
Microactuator production via high aspect ratio, high edge acuity metal fabrication technology
p 3235 N94-29770
ELECTROSTATIC CHARGE
The impact of electrically charged microspheres with planar surfaces under vacuum conditions
p 3320 N94-29765
ELECTROSTATIC ENGINES
Development and verification of a model to predict impingement currents for ion thrusters
[NASA-CR-195322] p 3173 N94-29546
ELECTROSTATIC GYROSCOPES
Integrated microgyroscope p 3239 N94-29789
ELECTROSTATICS
Active electron and ion beam experiments in space
[AD-A275570] p 3504 N94-28828
Toward milli-Newton electro- and magneto-static microactuators p 3238 N94-29784
ELECTROWEAK MODEL
High sensitivity tests of the standard model for electroweak interactions
[DE94-005415] p 3490 N94-30262
ELEMENTARY PARTICLE INTERACTIONS
Properties of W + jet events in proton-antiproton collisions at 1.8 TeV
[DE94-004002] p 3482 N94-28524
ELEVATION
Elevation control system model for the DSS 13 antenna p 3248 N94-29622
ELLIPSOIDS
The stability of perfect elliptic disks
p 3545 N94-29834
ELLIPTICAL GALAXIES
The stability of perfect elliptic disks
p 3545 N94-29834
ELLIPTICAL POLARIZATION
Infrared polarization signatures p 3258 N94-30506
EMBEDDED COMPUTER SYSTEMS
Object-based design of embedded software
[PB94-132073] p 3407 N94-28403
Technology transition push. Part 1: A case study of rate monotonic analysis
[AD-A275616] p 3407 N94-28633
Embedded expert system: From the mock-up to the real world p 3412 N94-29319
Experiences with the HOOD design method on avionics software development p 3414 N94-29325
Rome Laboratory software engineering technology program p 3414 N94-29330
Design of a thinwire real-time multiprocessor operating system p 3415 N94-29333
Software testing practices and their evolution for the 1990's p 3415 N94-29335
Integrated formal verification and validation of safety critical software p 3416 N94-29338
A common approach for an aerospace software environment p 3417 N94-29346
Analysis of EDP performance
[NASA-CR-195726] p 3420 N94-29945
Predictive sufficiency and the use of stored internal state
[AIAA PAPER 94-1213-CP] p 3445 N94-30564
EMBEDDING
HYPER-NPSNET: Embedded multimedia in a 3D virtual world
[AD-A275063] p 3410 N94-29152
Embeddings of Heyting algebras
[ML-93-14] p 3463 N94-30977
EMBRITTLEMENT
Radiation effects in beryllium used for plasma protection
[DE94-004599] p 3201 N94-28460
EMBRYOS
Japanese Journal of Aerospace and Environmental Medicine, volume 30, no. 1
[JTN-94-80598] p 3389 N94-28850
Effect of chronic centrifugation on in vitro fertilization and early development in mice ova
p 3386 N94-28853
EMERGENCIES
Rooftop emergency heliports
[DOT/FAA/RD-93/2] p 3157 N94-29754
Potential hazards of magnetic resonance imagers to emergency medical service helicopter operations
[DOT/FAA/RD-92/15] p 3135 N94-29862
EMERGENCY LIFE SUSTAINING SYSTEMS
Emergency underwater breathing aids for helicopter passengers and crew p 3381 N94-28437
Portable ventilatory resuscitation systems
[AD-A274984] p 3401 N94-29093

Lunar surface operations. Volume 1: Lunar surface emergency shelter
[NASA-CR-195551] p 3299 N94-29354

EMISSION
The effects of relativistic neutrons on nonthermal models of active galactic nuclei p 3547 N94-29993

EMISSION SPECTRA
Photon counting spectroscopy as done with a Thomson scattering diagnostic
[DE94-005543] p 3503 N94-28515
Progress in Z-Pinch Research
[IPPCZ-321] p 3505 N94-29074
Investigation of intense XUV emission of nitrogen-puff Z-pinch with small energy input
[PH-23] p 3505 N94-29075
Multichannel x ray spectral measurement of hot plasma evolution in nitrogen-puff Z-pinch
[PH-24] p 3505 N94-29076
X ray emission scaling and energy balance of small gas-puff Z-pinch p 3505 N94-29077
A multi wavelength observational study of the Cartwheel ring galaxy p 3539 N94-29821
Camera artifacts in IUE spectra
[NASA-CR-189337] p 3198 N94-29857
Spatially resolved spectroscopy of AG Carinae, and direct evidence for stellar evolution: The central star of NGC 2392
[NASA-CR-189291] p 3545 N94-29871
Spectral and temporal behavior of low mass x ray binaries observed with the Einstein SSS and MPC, and the Broad Band X Ray Telescope p 3542 N94-30862

EMITTANCE
Minutes. Accredited Standards Committee on Noise, S12. US tag for ISO/TC 43/SC1 noise and ISO/TC 94/SC12 hearing protection
[AD-A275622] p 3477 N94-28636
An experimental and comprehensive method to measure emission characteristics p 3257 N94-30501

EMITTERS
Active electron and ion beam experiments in space
[AD-A275570] p 3504 N94-28828

ENCAPSULATING
Microencapsulation of anti-tumor, antibiotic and thrombolytic drugs in microgravity p 3397 N94-30453

END EFFECTORS
Kinematic functions for redundancy resolution using configuration control
[NASA-CASE-NPO-18608-1-CU] p 3436 N94-29504
Kinematic representations, workspace analysis, and grasp stability in robot arms and multi-fingered hands p 3301 N94-29847
The use of interactive computer vision and robot hand controllers for enhancing manufacturing safety p 3314 N94-30442
A highly redundant robot system for inspection
[AIAA PAPER 94-1194-CP] p 3442 N94-30545
Dexterity enhancement in microsurgery using telemicro-robotics
[AIAA PAPER 94-1230-CP] p 3447 N94-30579
Kinematics and force analysis of a robot hand based on an artificial biological control scheme p 3313 N94-30957

ENDANGERED SPECIES
Development and implementation of a scrub habitat compensation plan for Kennedy Space Center
[NASA-TM-109202] p 3347 N94-29099

ENDOCRINE SYSTEMS
Studies on water electrolyte metabolism and endocrine responses at rest and during submaximal exercise at 6,000 m simulated altitude p 3388 N94-28496
Effects of training at simulated altitude of 6,000 m on endocrine responses at rest and during exercise at the same altitude p 3388 N94-28497

ENDOTHERMIC FUELS
Fuels combustion research
[AD-A275122] p 3189 N94-29004
Endothermic fuels for hypersonic aviation p 3197 N94-29285

ENDOTHERMIC REACTIONS
Dynamic response of ceramics
[AD-A275396] p 3214 N94-29203

ENERGETIC PARTICLES
A study of the ultrahigh-energy cosmic ray mass composition with the MACRO and EAS-TOP experiments p 3552 N94-29687
Quasi-adiabatic motion of energetic particles in a dipole magnetic field
[DE94-607322] p 3362 N94-29935
Energetic heavy-ion tracks in micron sites p 3495 N94-30213
Variations of electron fluxes, low-frequency radiations and plasma density during the geomagnetic storm on 9-12 March, 1979 according to data of the Interkosmos-19 satellites
[DE94-607323] p 3365 N94-30223

ENERGY ABSORPTION
Landing gear energy absorption system
[NASA-CASE-MSC-22277-1] p 3300 N94-29448

ENERGY CONSERVATION
Alternative fuel vehicles for the state fleets: Results of the 5-year planning process
[DE94-004709] p 3224 N94-28577
Survey on effects of petroleum substitution energy utilization on the global environment
[DE94-732339] p 3346 N94-28630
Computational fluid dynamics in ventilation. 3: The IEA annex 20 work p 3233 N94-29608
Analysis of data from electric and hybrid electric vehicle student competitions
[DE94-000269] p 3302 N94-29922
International Energy and Environmental Congress: Proceedings
[DE93-040609] p 3353 N94-30715

ENERGY CONSUMPTION
Survey on effects of petroleum substitution energy utilization on the global environment
[DE94-732339] p 3346 N94-28630
Analysis of data from electric and hybrid electric vehicle student competitions
[DE94-000269] p 3302 N94-29922
Investigation of the technology development status of alternate fuel vehicles
[DE94-744237] p 3312 N94-30831

ENERGY CONVERSION
Report of feasibility study on international-cooperation in high efficient energy conversion technology
[DE94-732340] p 3337 N94-28631
Technology 2003: The Fourth National Technology Transfer Conference and Exposition, volume 1
[NASA-CP-3249] p 3555 N94-30440

ENERGY CONVERSION EFFICIENCY
Performance of the Southern California Edison Company Stirling dish
[DE94-004676] p 3337 N94-29018
Efficiencies of the ICRF minority heating in the CHS and LHD plasmas
[NIFS-270] p 3506 N94-29499
Configuration and performance of the indirect-fired fuel cell bottomed turbine cycle
[DE94-005961] p 3338 N94-30313
Photovoltaic performance and reliabiiity workshop
[DE94-000236] p 3339 N94-30601

ENERGY DISSIPATION
Energy losses of fast charged particles in thin silicon detectors
[DE94-606065] p 3483 N94-28552
Study on mixing and injection of hydrogen into a supersonic flow p 3127 N94-28975
Atomic-scale structure and chemistry of interfaces by Z-contrast imaging and electron energy loss spectroscopy in the STEM
[DE94-006563] p 3516 N94-30064
AC losses for the self field of an AC transport current with a DC transport current offset in high T(c) superconducting magnet coils for MagLev application
[DE94-005187] p 3268 N94-30907
Calculation of inelastic mean free path and stopping power for electrons in solids from an optical-data model
[USIP-92-06] p 3494 N94-30980

ENERGY GAPS (SOLID STATE)
Energy gap structure of layered superconductors
[DE94-005132] p 3511 N94-28570
Silicon germanium carbon heteroepitaxial growth on silicon
[AD-A275197] p 3512 N94-28889
II-VI wide band gap semiconductors under hydrostatic pressure
[DE94-608106] p 3516 N94-30070
Rotator phases in narrow-gap semiconductors
[DE94-005472] p 3521 N94-30897

ENERGY LEVELS
The solving of the relativistic two-body problem with a nonlinear dependence upon a spectrum parameter
[DE94-606343] p 3451 N94-28783
Electronic structure of Zn-based quantum wells
[DE94-608104] p 3516 N94-30068
Reconstruction of spectra in the discrete quantum mechanics (new elements of the lattice quantum engineering)
[DE94-608075] p 3524 N94-30087
Theory for electron-transfer reactions in a three-component system: The degenerate regime
[DE94-005919] p 3493 N94-30903

ENERGY POLICY
Alternative fuel vehicles for the state fleets: Results of the 5-year planning process
[DE94-004709] p 3224 N94-28577
Proceedings of the 1993 Windsor Workshop on Alternative Fuels
[DE94-003908] p 3226 N94-30612
International Energy and Environmental Congress: Proceedings
[DE93-040609] p 3353 N94-30715

ENERGY SOURCES
Report of feasibility study on international-cooperation in high efficient energy conversion technology
[DE94-732340] p 3337 N94-28631

ENERGY SPECTRA
Energy distribution of the leptons in top decay to charged Higgs
[DE94-005231] p 3482 N94-28494
Fast precise algorithm for simulation of ionization energy losses
[DE94-608010] p 3421 N94-30080
Distribution functions of electrons within aluminium oxide thin films
[DE94-608418] p 3490 N94-30184

ENERGY STORAGE
The 100 kA, 5000 V solid-state opening switch for inductive energy storage
[AD-A274993] p 3263 N94-28994
Electrochemical Power Source (EPS) selection for Energetically Independent Robots (EIR): A systematic approach p 3269 N94-30312

ENERGY TECHNOLOGY
Catalytic fabric filtration for simultaneous NO(x) and particulate control
[DE94-001660] p 3341 N94-28463
Development of the integrated environmental control model: Performance models of selective catalytic reduction NO(x) control systems
[DE94-002151] p 3341 N94-28465
Proceedings of the Joint Contractors Meeting: FE/EE Advanced Turbine Systems Conference FE Fuel Cells and Coal-Fired Heat Engines Conference
[DE93-011308] p 3336 N94-28499
Summaries of FY 1993 geosciences research
[DE94-004710] p 3355 N94-28558
Alternative fuel vehicles for the state fleets: Results of the 5-year planning process
[DE94-004709] p 3224 N94-28577
Survey on effects of petroleum substitution energy utilization on the global environment
[DE94-732339] p 3346 N94-28630
Report of feasibility study on international-cooperation in high efficient energy conversion technology
[DE94-732340] p 3337 N94-28631
Energy and Technology Review
[DE94-004472] p 3338 N94-29955
Proceedings: SISAL 1993
[DE94-006641] p 3420 N94-30056
Technical analysis of alternative fueled vehicles
[DE94-744238] p 3304 N94-30269
Technology 2003: The Fourth National Technology Transfer Conference and Exposition, volume 1
[NASA-CP-3249] p 3555 N94-30440
Proceedings of the 1993 Windsor Workshop on Alternative Fuels
[DE94-003908] p 3226 N94-30612
International Energy and Environmental Congress: Proceedings
[DE93-040609] p 3353 N94-30715
Fuel cycle evaluations of biomass-ethanol and reformulated gasoline
[DE94-000227] p 3226 N94-30818
Interagency advanced power group: Solar working group
[DE94-004953] p 3340 N94-30833
Computing at the leading edge: Research in the energy sciences
[DE94-006121] p 3563 N94-30844

ENERGY TRANSFER
Density reduction: A mechanism for amorphization at high ion doses
[DE94-004793] p 3483 N94-28559
SHARC, a model for calculating atmospheric and infrared radiation under non-equilibrium conditions
[AD-A275207] p 3357 N94-28893
Turboramjet engines: Types and performances p 3151 N94-29293
The maximum entropy approach applied to energy exchange, chemical reactions and ionisation in the direct simulation Monte Carlo method for rarefied hypersonic flows
[IC-AERO-93-01] p 3524 N94-29481
Melt flow during alloy solidification: Dimensional analysis and model problems
[PB94-138625] p 3206 N94-29997
Volume averaged model for the mechanics of alloys solidification
[PB94-138617] p 3208 N94-30113
Overview of the US stellarator reactor study
[DE94-006042] p 3508 N94-30339
On the nonlinear dynamics of ocean wave systems p 3378 N94-30790

Atomic physics with highly charged ions
[DE94-003397] p 3492 N94-30837

ENGINE AIRFRAME INTEGRATION
Numerical study on the interaction between scramjet engine modules caused by thermal choke
p 3125 N94-28960
Numerical simulation of supersonic flow around space plane with engine installed p 3125 N94-28961

ENGINE CONTROL
Research and development of ramjets/ramrockets. Part 2: Integral liquid fuel ramjets p 3152 N94-29297
Aspects of model-based rocket engine condition monitoring and control
[NASA-CR-195116] p 3173 N94-29848

ENGINE COOLANTS
Endothermic fuels for hypersonic aviation
p 3197 N94-29285

ENGINE DESIGN
Feasibility study on introduction of a large methanol engine power generation plant
[DE94-732338] p 3224 N94-28629
Fuels and Combustion Technology for Advanced Aircraft Engines
[AGARD-CP-536] p 3189 N94-29246
Combustion technology needs for advanced high pressure cycle engines p 3190 N94-29248
High temperature fuel requirements and payoffs
p 3192 N94-29259
Design aspects in small aircraft gas turbine fuel injectors p 3154 N94-29264
Technology rigs: A tool for afterburner development
p 3154 N94-29270
Pollutant emissions from and within a model gas turbine combustor at elevated pressures and temperatures
p 3194 N94-29271
Reduction of NO(x) by fuel-staging in gas turbine engines: A commitment to the future
p 3194 N94-29272
Spray combustion experiments and numerical predictions p 3195 N94-29277
The mixing process in the quenching zone of the rich-lean-combustion concept p 3196 N94-29281
CIAM experimental turboramjets p 3152 N94-29299
Scramjet CFD methods and analysis. Part 2: Scramjet CFD analysis. Numerical simulation of supersonic mixing and combustion applied to scramjet combustor
p 3152 N94-29300
A variable selection heuristic for solid rocket motor design p 3173 N94-29544
Use of magnetic compression to support turbine engine rotors p 3314 N94-30484

ENGINE FAILURE
Rocket engine system reliability analyses using probabilistic and fuzzy logic techniques
[NASA-TM-106519] p 3173 N94-29403

ENGINE INLETS
Introduction and overview of research and development of solid propellant ramrockets, liquid fuel ramjets and experimental hydrogen ram combustors
p 3151 N94-29292
Turboramjet engines: Types and performances
p 3151 N94-29293

ENGINE TESTING LABORATORIES
The nozzle acoustic test rig: An acoustic and aerodynamic free-jet facility
[NASA-TM-106495] p 3156 N94-28749

ENGINE TESTS
Research and development of high thermal stability fuels p 3192 N94-29261
Technology rigs: A tool for afterburner development
p 3154 N94-29270
CIAM experimental turboramjets p 3152 N94-29299
Some problems of scramjet propulsion for aerospace planes. Part 2: Scramjet: Development and test problems p 3152 N94-29301
Thick thermal barrier coatings for diesel components
[NASA-CR-187111] p 3537 N94-29350
Specialized data analysis of SSME and advanced propulsion system vibration measurements
[NASA-CR-193940] p 3174 N94-29868

ENGINEERING MANAGEMENT
Cleanroom engineering handbook. Volume 2: Organization and project formation in the cleanroom environment
[AD-A275809] p 3156 N94-28772
A generalization of the software engineering maturity model p 3416 N94-29341

ENTHALPY
Differential Scanning Calorimetry (DSC) for planetary surface exploration p 3236 N94-29776
An actively cooled floating element skin friction balance for direct measurement in high enthalpy supersonic flows p 3289 N94-29824

ENTRAINMENT
An experimental investigation of flow patterns and liquid entrainment in a horizontal-tube evaporator
p 3277 N94-29899

ENTRANCES
Three dimensional simulation of compressible flow induced by a high-speed train moving into a tunnel
p 3126 N94-28967

ENTROPY
Nucleon and nuclei at finite temperature, as a phenomenological test of the entropy bound
[DE94-608094] p 3489 N94-30097
Centrifugal atomization of lanthanide materials for cryogenic coolers
[DE94-006035] p 3219 N94-30337
Thermodynamics of computation and information distance
[CWI-CS-R9341] p 3526 N94-30433
The Boltzmann entropy and randomness tests
[CWI-CS-R9342] p 3426 N94-30434
Relations between varieties of Kolmogorov complexities
[CWI-CS-R9329] p 3427 N94-30732

ENTROPY (STATISTICS)
Relations between varieties of Kolmogorov complexities
[CWI-CS-R9329] p 3427 N94-30732

ENVIRONMENT EFFECTS
Fuel Cell Seminar, 1992: Program and abstracts
[DE94-003882] p 3336 N94-28472
Global change research: Summaries of research in FY 1993
[DE94-003150] p 3341 N94-28473
Survey on effects of petroleum substitution energy utilization on the global environment
[DE94-732339] p 3346 N94-28630
Development and implementation of a scrub habitat compensation plan for Kennedy Space Center
[NASA-TM-109202] p 3347 N94-29099
On the effect of emissions from aircraft engines on the state of the atmosphere p 3189 N94-29247
Analysis and modeling of environmental and economic impacts of the solar hydrogen energy system
p 3348 N94-29901
Impact of biomass burning on the atmosphere
[DE94-004333] p 3349 N94-29954
Fatigue of carbon and low-alloy steels in LWR environments
[DE94-005116] p 3207 N94-30021

ENVIRONMENT MANAGEMENT
User-centered guidelines for environmental management
[DE94-004313] p 3341 N94-28454
Environmental Compliance Assessment System (ECAS) --- Japan supplement
[AD-A275549] p 3346 N94-28722
Environmental Compliance Assessment And Management System Program (ECAMP). US Air Force European Economic Community (EEC)
[AD-A275593] p 3346 N94-28727
Environmental Review Guide for Operations (ERGO)
[AD-A275611] p 3346 N94-28774
The European community directive: An alternative environmental impact assessment procedure after Massey?
[AD-A275550] p 3347 N94-28844
Remote sensing and the Earth p 3329 N94-29218
Research report on the potential of ocean development suitable for area characteristics
[JTN-94-80587] p 3377 N94-29595
Benchmarking for cost improvement
[DE94-002276] p 3528 N94-30824

ENVIRONMENT MODELS
Analysis and modeling of environmental and economic impacts of the solar hydrogen energy system
p 3348 N94-29901
A coupled approach to spatially derived parameters necessary for ecosystem modeling on the North Slope of Alaska: Appendix A
[DE94-005853] p 3349 N94-30046
Modeling the Earth System, volume 3
[NASA-CR-194256] p 3350 N94-30616
Atmosphere, ocean, and land: Critical gaps in Earth system models p 3350 N94-30617
Towards coupled physical-biogeochemical models of the ocean carbon cycle p 3350 N94-30618
Dynamic constraints on CO2 uptake by an iron-fertilized Antarctic p 3350 N94-30619
The role of sea ice dynamics in global climate change
p 3350 N94-30620
Land surface interaction p 3350 N94-30621
A toy model for estimating N2O emissions from natural soils p 3351 N94-30627
A bottom-up evolution of terrestrial ecosystem modeling theory, and ideas toward global vegetation modeling
p 3351 N94-30628
Development of simplified ecosystem models for applications in Earth system studies: The Century experience p 3352 N94-30629
A toy terrestrial carbon flow model
p 3352 N94-30630

ENVIRONMENT POLLUTION
Speciation in Water and Soil: A literature review
[PB94-132388] p 3341 N94-28412
Caesium-137 in a boreal forest ecosystem: Aspects on the long-term behavior
[PB94-137809] p 3347 N94-29158

ENVIRONMENT PROTECTION
Environmental Compliance Assessment System (ECAS) --- Japan supplement
[AD-A275549] p 3346 N94-28722
Environmental Compliance Assessment And Management System Program (ECAMP). US Air Force European Economic Community (EEC)
[AD-A275593] p 3346 N94-28727
Environmental Review Guide for Operations (ERGO)
[AD-A275611] p 3346 N94-28774
The European community directive: An alternative environmental impact assessment procedure after Massey?
[AD-A275550] p 3347 N94-28844
Protocol on environmental protection to the Antarctic Treaty and its annexes: International agreement on the comprehensive measures for the protection of Antarctic environment and ecosystems p 3354 N94-29086
Remote sensing and the Earth p 3329 N94-29218

ENVIRONMENT SIMULATION
Simulation of the effect of wind on clothing by measurements and calculations
[PB94-132289] p 3399 N94-28406

ENVIRONMENTAL CHEMISTRY
A modular approach for automated sample preparation and chemical analysis p 3354 N94-30464

ENVIRONMENTAL CONTROL
Development of the integrated environmental control model: Performance models of selective catalytic reduction NO(x) control systems
[DE94-002151] p 3341 N94-28485
Advanced seal delivery system life support parameters
[AD-A275304] p 3401 N94-29184

ENVIRONMENTAL ENGINEERING
Journal of NIRE, vol. 2, no. 3
[JTN-94-80553] p 3553 N94-29512

ENVIRONMENTAL LABORATORIES
A modular approach for automated sample preparation and chemical analysis p 3354 N94-30464

ENVIRONMENTAL MONITORING
Speciation in Water and Soil: A literature review
[PB94-132388] p 3341 N94-28412
Environmental Compliance Assessment System (ECAS) --- Japan supplement
[AD-A275549] p 3346 N94-28722
Proceedings of the International Symposium on Remote Sensing
[JTN-94-80578] p 3325 N94-28925
Research trends on remote sensing at research facilities in Japan: The priority area programme on better understanding of earth environment via satellite
p 3326 N94-28928
Observations by ERS-1 start p 3327 N94-28933
Amazonia: Remote sensing test site and survey
p 3327 N94-28935
Utilization of remote sensing data in Southeast Asia
p 3327 N94-28936
Proceedings of the 15th Earth Observation Symposium
[JTN-94-80607] p 3328 N94-29036
Principles and application tendency of remote sensing: Its principle, function and utilization
p 3328 N94-29037
Tohoku district observed by artificial satellites
p 3328 N94-29041
Activities of the wintering party at Showa Station by the 31st Japanese Antarctic Research Expedition in 1990
p 3358 N94-29083
Activities of the fourth wintering party at Asuka Station by the 31st Japanese Antarctic Research Expedition in 1990 p 3358 N94-29084
Proceedings of the 3rd International Symposium: JERS-1 and Remote Sensing in the Future
[JTN-94-80597] p 3329 N94-29217
Remote sensing and the Earth p 3329 N94-29218
A new information system: Satellite observation
p 3330 N94-29219
Radar applications at the Canada Centre for Remote Sensing p 3331 N94-29224
Earth-observation plan in Europe
p 3331 N94-29227
JERS-1 and future remote sensing: Application of remote sensing data to agroecological problems
p 3331 N94-29229

Application of remote sensing in prevention of disasters p 3332 N94-29230
Future expectation of remote sensing technology p 3332 N94-29231
GOME: Global Ozone Monitoring Experiment [ESA-SP-1151] p 3347 N94-29452
Research report on the potential of ocean development suitable for area characteristics [JTN-94-80587] p 3377 N94-29595
Activities of the wintering party at Syowa Station by the 32nd Japanese Antarctic Research Expedition in 1991 p 3364 N94-29986
FAME: A Forest Assessment and Monitoring Environment scenario [AD-B179106] p 3335 N94-30759
Multitemporal analysis of a braiding river: The advanced study of 1992 [NLR-TP-93100-U] p 3335 N94-30942

ENVIRONMENTAL SURVEYS
The European community directive: An alternative environmental impact assessment procedure after Massey? [AD-A275550] p 3347 N94-28844
A broad-band microseismometer for planetary operations p 3237 N94-29778
Modeling Earth system changes of the past p 3353 N94-30635

ENVIRONMENTAL TESTS
Low Earth orbit durability evaluation of protected silicone for advanced refractive photovoltaic concentrator arrays [NASA-TM-106543] p 3172 N94-28999
Study of activation data of metal samples from LDEF-1 and Spacelab-2 [NASA-CR-195802] p 3205 N94-29736

ENZYMES
Barley cell culture as a producer of heterologous protein [PB94-132339] p 3379 N94-28408
Survey report of JSUP Space Environment Utilization Research Committee in fiscal year 1992: Protein Crystal Growth Session [JTN-94-80584] p 3158 N94-28583
Development of novel switchable protein surfaces [AD-A275510] p 3384 N94-28667
Researches on bioconversion of coal into liquid product p 3187 N94-28677

EPHEMERIDES
GPS common-view time transfer p 3144 N94-30648
A comparison of GPS broadcast and DMA precise ephemerides p 3145 N94-30660

EPIDEMIOLOGY
Aviation epidemiology data register: Age distribution of U.S. Army aviators stratified by gender and component of service [AD-A275901] p 3388 N94-28757

EPILEPSY
Monitor for status epilepticus seizures p 3397 N94-30460

EPITAXY
Optoelectronic integrated circuits fabricated using atomic layer epitaxy [AD-A275454] p 3262 N94-28805
Silicon germanium carbon heteroepitaxial growth on silicon [AD-A275197] p 3512 N94-28889
Transport properties of epitaxial lift off films [NASA-TM-106156] p 3264 N94-29209
Epitaxial heterojunctions of oxide semiconductors and metals on high temperature superconductors [NASA-CASE-NPO-18483-1-CU] p 3513 N94-29501
Retention latch mechanism for the Wake Shield Facility p 3161 N94-29635
Micro-opto-mechanical devices and systems using epitaxial lift off p 3239 N94-29793

EPOXY MATRIX COMPOSITES
Intelligent material systems and structures. Part 7: Debonding and pull-out of two optical fibers from two epoxies [PB94-137767] p 3180 N94-29475
Stress transfer mechanics for multiple perfectly bonded concentric cylinder models of unidirectional composites [PB94-138633] p 3181 N94-29524
Simulation of composite material response under dynamic compressive loading [DE94-005272] p 3184 N94-30589

EPOXY RESINS
Poly(arylene ether-co-imidazole)s as toughness modifiers for epoxy resins [NASA-CASE-LAR-15229-1-CU] p 3215 N94-29451
Correlation between wet ageing, humidity absorption and properties on composite materials based on different resins family [REPT-932-600-107] p 3179 N94-29462

EQUALIZERS (CIRCUITS)
Extended horizon lifting for periodic gain adjustment in control systems, and for equalization of communication channels [NASA-CASE-NPO-19166-1-CU] p 3246 N94-29495

EQUATIONS OF MOTION
A non-linear simulation for an autonomous unmanned air vehicle [AD-A275062] p 3146 N94-29200
Iterative procedure as equation of motion [DE94-608008] p 3453 N94-30078
Theory of fundamental interactions [DE94-608126] p 3525 N94-30169
A new orthogonal decomposition method for turbulent flows p 3281 N94-30494
Evaluation of discretization schemes for advection-diffusion equations [CWI-NM-R9311] p 3461 N94-30751

EQUATIONS OF STATE
Equation of state of neutron star matter, limiting rotational periods of fast pulsars, and the properties of strange stars [DE94-005214] p 3542 N94-28480
Equation of state of stellar plasmas [DE94-004186] p 3542 N94-28526
Dynamic response of ceramics [AD-A275396] p 3214 N94-29203

EQUATORIAL REGIONS
The effects of magnetic storm phases on F-layer irregularities from auroral to equatorial latitudes [AD-A275203] p 3356 N94-28891
Modeling deep equatorial circulation p 3378 N94-29815

EQUILIBRIUM FLOW
The effect of pressure gradient on the structure of an equilibrium turbulent boundary layer p 3282 N94-30807

EQUIPMENT SPECIFICATIONS
Composite redesign of obstetrical forceps p 3397 N94-30457
Development of the NASA/Baylor VAD p 3397 N94-30458
Status of frequency and time support for NASA systems p 3468 N94-30640
Development status of the Communications and Broadcasting Engineering Test Satellite (COMETS) [JTN-94-80545] p 3169 N94-30811
Development status of COMETS missions [JTN-94-80544] p 3170 N94-30932

EQUIVALENCE
The conjoinability relation in Lambek calculus in linear logic [ML-93-03] p 3457 N94-30397
Remarks on uniformly finitely precomplete positive equivalences [ML-93-12] p 3463 N94-30975

EROSION
Modelling erosion damage from low-energy plasma gun simulations of disruptions [DE94-005196] p 3509 N94-30697

ERROR ANALYSIS
Los Angeles international airport instrument landing system approach data collection and reduction, phase 1 [AD-A275115] p 3136 N94-28914
Solution of augmented systems [PB94-138211] p 3452 N94-29111
Error growth in poor ECMWF forecasts over the contiguous United States [AD-A275297] p 3369 N94-29183
Line-of-sight tropospheric calibration from measurements in arbitrary directions p 3249 N94-29654
Enhanced orbit determination filter sensitivity analysis: Error budget development p 3159 N94-29655
Enhanced orbit determination filter: Inclusion of ground system errors as filter parameters p 3159 N94-29656
Engineering specification editing tools [AD-A275116] p 3419 N94-29746
A simulation study of high degree and order geopotential determination using satellite gravity gradiometry p 3333 N94-29762
An analysis of carrier phase jitter in an MPSK receiver utilizing map estimation [NASA-CR-195806] p 3164 N94-29880
The effect of enhanced backscattering on target detection p 3258 N94-30508
Prediction and standard error estimation for a finite universe total when a stratum is not sampled [DE94-004929] p 3465 N94-30696
Systematic error estimation in multisensor fusion systems [AD-B179298] p 3428 N94-30764
Spatial interpolation, network bias, and terrestrial air temperature variability p 3374 N94-30810

ERROR CORRECTING CODES
Convolutional encoding of self-dual codes p 3250 N94-29662

ERROR DETECTION CODES
Animators and error reporters for generated programming environments [CWI-CS-R9253] p 3418 N94-29503
Decoder synchronization for deep space missions p 3250 N94-29664
Checkpoint-based forward recovery using lookahead execution and rollback validation in parallel and distributed systems [NASA-CR-195760] p 3431 N94-29869
Space reclamation for uncoordinated checkpointing in message-passing systems [NASA-CR-195761] p 3420 N94-29906

ERRORS
Los Angeles international airport instrument landing system approach data collection and reduction, phase 1 [AD-A275115] p 3136 N94-28914
Animators and error reporters for generated programming environments [CWI-CS-R9253] p 3418 N94-29503
Significant figures and Lyapunov exponents in chaos and constrained divergence of chaotic orbits p 3467 N94-29910
Numerical precision and roundoff considerations concerning computer code migration [DE94-005421] p 3427 N94-30590

ERS-1 (ESA SATELLITE)
Observations by ERS-1 start p 3327 N94-28933
Sea ice and oceans applications of SAR p 3327 N94-28934
GOME: Global Ozone Monitoring Experiment [ESA-SP-1151] p 3347 N94-29452

ESTERS
Combustion and heat transfer in a high speed diesel engine operating with rape seed oil methyl ester fuel [PB94-137536] p 3301 N94-29679

ESTIMATES
Improved QCD sum rule estimates of the higher twist contributions to polarised and unpolarised nucleon structure functions [PB94-138112] p 3487 N94-29161
Triple Diagonal modeling: A mechanism to focus productivity improvement for business success [DE94-004309] p 3527 N94-30041

ESTIMATING
Advanced fuel properties: A computer program for estimating property values [AD-A275248] p 3224 N94-28901
A complex symbol signal-to-noise ratio estimator and its performance p 3251 N94-29671
Prediction and standard error estimation for a finite universe total when a stratum is not sampled [DE94-004929] p 3465 N94-30696

ESTUARIES
Statistical analysis of a satellite imagery time series: Implications for the study of coastal and estuarine circulation p 3335 N94-30919

ETCHING
Directional solidification studies in Ni-Al alloys [DE94-005562] p 3201 N94-28527
The effects of molecular orientation geometry and surface anisotropy upon etching [AD-A275154] p 3486 N94-29032

ETHERS
Matrix isolation studies of the interactions of BF3 with water and substituted diethyl ethers. Chemical ionization mass spectrometric determination of the proton affinity of (CF3CH2)2O [NASA-TM-106422] p 3189 N94-28832
XPS analysis of 440C steel surfaces lubricated with perfluoropolyethers under sliding conditions in high vacuum [NASA-TM-106548] p 3218 N94-30177

ETHYL ALCOHOL
Crystallization of silver chromate from ethanol via salt metathesis reactions of solubilized precursors [AD-A275178] p 3189 N94-29058
Proceedings of the low cost materials of construction for biological processes workshop [DE94-000218] p 3226 N94-30761

ETHYL COMPOUNDS
Matrix isolation studies of the interactions of BF3 with water and substituted diethyl ethers. Chemical ionization mass spectrometric determination of the proton affinity of (CF3CH2)2O [NASA-TM-106422] p 3189 N94-28832

ETHYLENE COMPOUNDS
Anodization of copper in chloride media [AD-A275565] p 3202 N94-28793

EUCLIDEAN GEOMETRY
A deterministic algorithm for the three-dimensional diameter problem [RUU-CS-92-45] p 3424 N94-30348

Theoretical and experimental analysis of a new algorithm for the Euclidean 1-center problem
[REPT-93-045] p 3429 N94-30924

EULER EQUATIONS OF MOTION
ENGRID: A graphical interactive code for the computation of structured grids for blocked flow domains p 3124 N94-28956
Numerical analysis of supersonic transport wings p 3124 N94-28959
Numerical analysis of sonic boom in the near field p 3125 N94-28962
An implicit upwind scheme for the three-dimensional Euler equations using a pointwise relaxation method p 3128 N94-28983
A new Eulerian model for turbulent evaporating sprays in recirculating flows p 3195 N94-29279
Investigation of advanced counterrotation blade configuration concepts for high speed turboprop systems. Task 2: Unsteady ducted propfan analysis computer program users manual
[NASA-CR-187105] p 3152 N94-29438
Numerical solution of the two-dimensional time-dependent incompressible Euler equations
[NASA-CR-195775] p 3277 N94-29859
Time-marching aeroelastic and spatial adaptation procedures on triangular and tetrahedral meshes using an unstructured-grid Euler method p 3131 N94-29877
High-resolution algorithms for the Navier-Stokes equations for generalized discretizations p 3278 N94-29965
Canonical-variables multigrid method for steady-state Euler equations
[NASA-CR-194888] p 3454 N94-30208
Numerical investigation into high-angle-of-attack leading-edge vortex flow
[PB94-125564] p 3133 N94-30388
Aspects of the modeling and numerical simulation of leading-edge vortex flow
[AD-B179108] p 3133 N94-30492
Eigenvalue analysis of the convergence behaviour of an Euler method
[PB94-1255722-U] p 3281 N94-30743
Euler results of the ISNaS compressible multi-block flow solver
[AD-B179299] p 3281 N94-30756
Mixed Eulerian-Lagrangian finite element solutions of unsteady flow and flutter in transonic cascade p 3282 N94-30816

EUROPE
The European community directive: An alternative environmental impact assessment procedure after Massey?
[AD-A275550] p 3347 N94-28844
European PTTI report p 3468 N94-30642

EUROPEAN AIRBUS
Integration of a path generation algorithm into off-line programming of airbus panels
[REPT-932-600-103] p 3435 N94-29480

EUROPEAN SPACE AGENCY
ESTEC wiring test programme materials related properties p 3165 N94-28698
Earth-observation plan in Europe p 3331 N94-29227

EUROPIUM
Quenching of the excited state of hydrated Europium(3) ions by electron transfer
[DE94-005553] p 3482 N94-28518

EUTECTIC ALLOYS
Directional solidification characteristics of hyper-eutectic Al-Cu alloys under varying gravity conditions
[ISBN-0-315-86108-8] p 3209 N94-30146
Microstructural development and mechanical behavior of eutectic bismuth-tin and eutectic indium-tin in response to high temperature deformation
[DE94-005202] p 3210 N94-30710

EUTECTICS
Directional solidification studies in Ni-Al alloys
[DE94-005562] p 3201 N94-28527

EVACUATING (TRANSPORTATION)
Aircraft evacuations: The effect of a cabin water spray system upon evacuation rates and behaviour
[CAA-PAPER-93008] p 3148 N94-29887

EVALUATION
NAVAIR aircraft wiring standardization and qualification program p 3166 N94-28704
Performance evaluation of a 22.5/30 kW 270 volts direct current generator system
[AD-A275106] p 3263 N94-28913

EVAPORATION
A new Eulerian model for turbulent evaporating sprays in recirculating flows p 3195 N94-29279
The influence of the evaporation duct on the angle of arrival and amplitude of the backscattered signal from targets low above the sea p 3256 N94-30498

EVAPORATORS
An experimental investigation of flow patterns and liquid entrainment in a horizontal-tube evaporator p 3277 N94-29899

EVENT HORIZON
A numerical study of gravitational collapse p 3548 N94-30271

EVOLUTION (DEVELOPMENT)
Modelling the evolution of information systems
[TR-92-36] p 3535 N94-30329

EXCIMER LASERS
Investigations of large area electron beam diodes for excimer lasers
[DE94-005670] p 3295 N94-30595
Remote pumping of solid state lasers with nuclear driven fluorescers
[DE94-004846] p 3296 N94-30614

EXCIMERS
Remote pumping of solid state lasers with nuclear driven fluorescers
[DE94-004846] p 3296 N94-30614

EXCITATION
Quenching of the excited state of hydrated Europium(3) ions by electron transfer
[DE94-005553] p 3482 N94-28518
Search for excited quarks in p(bar p) collisions at the square root of s = 1.8 TeV
[DE94-004658] p 3484 N94-28573
Two-Photon/Laser-Induced Fluorescence (TP/LIF) sensor p 3342 N94-28588
Detection of tropospheric OH and HO2 by laser-induced fluorescence at low pressure using the 308nm excitation of OH p 3343 N94-28591

EXCITONS
Effect of phonon dispersion on properties of exciton in magnetic field
[DE93-634756] p 3481 N94-28469
Comparison of 14 MeV isomer production of Hf-178m1 and Hf-179m2 using Feshbach-Kerman-Koonin and exciton preequilibrium models
[DE94-002640] p 3488 N94-30039
Nonlinear optics response of semiconductor quantum wells under high magnetic fields
[DE94-003244] p 3520 N94-30835

EXERCISE PHYSIOLOGY
Effects of endurance training on heat-exercise tolerance in men wearing NBC protective clothing
[AD-A275176] p 3391 N94-29049

EXHAUST EMISSION
Development of the integrated environmental control model: Performance models of selective catalytic reduction NO(x) control systems
[DE94-002151] p 3341 N94-28465
On the effect of emissions from aircraft engines on the state of the atmosphere p 3189 N94-29247
Ultra low NO(x) ultra lean gas turbine primary zones with liquid fuels p 3154 N94-29267
Pollutant emissions from and within a model gas turbine combustor at elevated pressures and temperatures p 3194 N94-29271
Reduction of NO(x) by fuel-staging in gas turbine engines: A commitment to the future p 3194 N94-29272
Chambers of turboreactors with variable geometry: A response to the matrix of pollution in cycles at high temperature, high pressure p 3194 N94-29273
The influence of air distribution on homogeneity and pollutant formation in the primary zone of a tubular combustor p 3194 N94-29274
Effects of hydrogen addition on pollutant emissions in a gas turbine combustor p 3195 N94-29275
Spray combustion experiments and numerical predictions p 3195 N94-29277
Combustion and heat transfer in a high speed diesel engine operating with rape seed oil methyl ester fuel
[PB94-137536] p 3301 N94-29679
Investigation of the technology development status of alternate fuel vehicles
[DE94-744237] p 3312 N94-30831

EXHAUST GASES
SOCRATES simulation of the emission at wavelength 6300 A generated by the interaction between the atmosphere and the Space Shuttle exhaust
[AD-A275567] p 3164 N94-28827
Methane challenge of high performance molecular sieve oxygen concentrator
[AD-A275155] p 3337 N94-29033
Ultra low NO(x) ultra lean gas turbine primary zones with liquid fuels p 3154 N94-29267
Reduction of NO(x) by fuel-staging in gas turbine engines: A commitment to the future p 3194 N94-29272
Effects of hydrogen addition on pollutant emissions in a gas turbine combustor p 3195 N94-29275
Spray combustion experiments and numerical predictions p 3195 N94-29277
Combustion and heat transfer in a high speed diesel engine operating with rape seed oil methyl ester fuel
[PB94-137536] p 3301 N94-29679
A study of low emissions gas turbine combustions
[NASA-CR-195763] p 3152 N94-29860

EXHAUST NOZZLES
The nozzle acoustic test rig: An acoustic and aerodynamic free-jet facility
[NASA-TM-106495] p 3156 N94-28749

EXISTENCE THEOREMS
Existence of quantum characteristic exponents
[PB94-138161] p 3523 N94-29146

EXOBIOLOGY
A discussion of eye-head coordinative movement under microgravity during parabolic flight p 3393 N94-29715

EXOTHERMIC REACTIONS
Dendrite preventing separator for secondary lithium batteries
[NASA-CASE-NPO-18585-1-CU] p 3265 N94-29411

EXPANDABLE STRUCTURES
Collapsible mechanical joint
[NASA-CASE-MFS-28765-1] p 3299 N94-29367

EXPEDITIONS
Evaluation of life support equipment during an unsupported North Pole expedition p 3379 N94-28422
Activities of the fourth wintering party at Asuka Station by the 31st Japanese Antarctic Research Expedition in 1990 p 3358 N94-29084

EXPERIMENT DESIGN
Model-oriented data analysis with applications to lake and soil water simulation
[PB94-136942] p 3329 N94-29173
Empirical studies of the value of algorithm animation in algorithm understanding
[AD-A275135] p 3412 N94-29287
Cryogenic on-orbit liquid depot storage acquisition and transfer (COLD-SAT) experiment subsystem instrumentation and wire harness design report
[NASA-CR-189172] p 3168 N94-29405
Physiological Anatomical Rodent Experiment (PARE) .04 feasibility test 2
[NASA-CR-195210] p 3385 N94-29968

EXPERT SYSTEMS
Toward a model of expert knowledge structure and their role in cognitive task performance
[AD-A275641] p 3529 N94-28645
Information presentation for expert systems in future fighter aircraft
[AD-A275126] p 3149 N94-29005
Incorporating geometric constraints into rule-based systems using nonlinear optimization
[AD-A275093] p 3452 N94-29063
Propagation of evidence through fuzzy rules
[AD-A275071] p 3411 N94-29180
Embedded expert system: From the mock-up to the real world p 3412 N94-29319
GPS/GNSS for ATM p 3138 N94-29565
DAISY: A decision aid for an air situation interpretation system p 3139 N94-29574
Knowledge based system for identification of gamma sources
[PB94-137742] p 3487 N94-29683
Knowledge combination and data fusion with application to recognition systems p 3259 N94-30513
A Modular Artificial Intelligence Inference Engine System (MAIS) for support of on orbit experiments
[AIAA PAPER 94-1237-CP] p 3448 N94-30584

EXPLOITATION
Fiscal 1991 geothermal development promotion energy
[DE94-732332] p 3337 N94-28627
Fiscal 1990 geothermal development promotion survey
[DE94-732333] p 3337 N94-28628

EXPLORATION
Activities of the wintering party at Syowa Station by the 32nd Japanese Antarctic Research Expedition in 1991 p 3364 N94-29986

EXPLOSIONS
Minutes: Accredited Standards Committee on Mechanical Vibration and Shock, S2. US TAG for ISO/TC 108 Mechanical Vibration and Shock
[AD-A275591] p 3316 N94-28726
Blast overpressure studies with animals and man
[AD-A275038] p 3391 N94-29150
Joint research activities with CCMRI (China) p 3240 N94-29521

EXPLOSIVE DEVICES
Integration of pyrotechnics into aerospace systems p 3161 N94-29634

EXPLOSIVES
Insensitive energetic materials: The importance of physical properties and molecular structure
[AD-A275393] p 3225 N94-29308

Superior energetic materials that contain carbocations and anions. Energetic materials restricted in composition to C, H, N, and O atoms
[AD-A275449] p 3225 N94-29310
The laser approach for sequential pyrotechnic initiation systems: Envisageable chain architecture and concepts
[REPT-932-430-113] p 3225 N94-29414
Cubanes: Super explosives and potential pharmaceutical intermediates p 3227 N94-30454

EXPONENTS
Existence of quantum characteristic exponents
[PB94-138161] p 3523 N94-29146
Significant figures and Lyapunov exponents in chaos and constrained divergence of chaotic orbits
p 3467 N94-29910
The structure of exponentials: Uncovering the dynamics of linear logic proofs
[ML-93-10] p 3430 N94-30973

EXPOSURE
The Support of Air Operations under Extreme Hot and Cold Weather Conditions
[AGARD-CP-540] p 3379 N94-28420
The concept of Royal Navy air operations under extreme environmental conditions p 3379 N94-28424
Deterioration of manual performance in cold and windy climates p 3381 N94-28434
Aeropathological diagnosis of lethal hypothermia
p 3382 N94-28440
Rewarming methodologies in the field
p 3382 N94-28441
Aeromedical support for casualties in extremely hot climates p 3382 N94-28443
The Environmental Symptoms Questionnaire: Assessing reactions to environmental extremes in military operations p 3383 N94-28447
Analysis of selected materials flown on interior locations of the Long Duration Exposure Facility
[NASA-CR-4586] p 3175 N94-29458
An outdoor exposure testing program for optical materials used in solar thermal electric technologies
[DE94-000265] p 3500 N94-29799

EXTENSOMETERS
Experimental determination of orthotropic elastic constants
[FFA-TN-1991-35] p 3215 N94-29424

EXTRAPOLATION
Extrapolation of point data for resource mapping
p 3334 N94-29959

EXTRATERRESTRIAL RADIATION
CBSD: The celestial background scene descriptor
[AD-A275521] p 3538 N94-28671
Proton switches
[AD-A275150] p 3167 N94-29022
Identification of an unexpected space radiation hazard
[AD-A275170] p 3552 N94-29046

EXTRAVEHICULAR ACTIVITY
Extra-vehicular activity translation tool
[NASA-CASE-MSC-21955-1] p 3300 N94-29428
EVA glove evaluation methodology and test protocol
p 3401 N94-29729
Tactility as a function of grasp force: Effects of glove, orientation, pressure, load, and handle
[NASA-TP-3474] p 3402 N94-30210

EXTREME ULTRAVIOLET RADIATION
Broadband EUV survey spectrometer for short-timescale experiments
[DE94-005459] p 3498 N94-28534
Progress in Z-Pinch Research
[IPPCZ-321] p 3505 N94-29074
Investigation of intense XUV emission of nitrogen-puff Z-pinch with small energy input
[PH-23] p 3505 N94-29075
A sounding rocket program in extreme and far ultraviolet interferometry
[NASA-CR-195114] p 3289 N94-29907
Accurate modeling of F-region electron densities
[NASA-CR-195781] p 3364 N94-30014

EXTREMELY HIGH FREQUENCIES
X-/Ka-band dichroic plate design and grating lobe study p 3247 N94-29616
Digital combining-weight estimation for broadband sources using maximum-likelihood estimates
p 3250 N94-29661
A 32 GHz microstrip array antenna for microspacecraft application p 3251 N94-29668
Radar cross sections of ground clutter at 95 GHz for summer and fall conditions p 3259 N94-30512

EXTREMELY LOW FREQUENCIES
Study of generation mechanisms of magnetospheric VLF/ELF emissions based on the direction findings
p 3361 N94-29245

EXTREMELY LOW RADIO FREQUENCIES
Removal of coherent Extremely Low Frequency (ELF) background noise by adaptive noise cancellation
[AD-A275016] p 3243 N94-28898

EXTRUDING
An analysis of the microstructure and reinforcement distribution of an extruded particle-reinforced Al 6061-10 volume percent Al2O3 metal matrix composite
[AD-A275050] p 3178 N94-29166
Controlling the material properties of in vitro collagen through directed orientation and cross-linking of fibrils
p 3221 N94-30797

EYE (ANATOMY)
Dual use of image based tracking techniques: Laser eye surgery and low vision prosthesis p 3397 N94-30455

EYE MOVEMENTS
Digital tracking and control of retinal images
[AD-A275469] p 3389 N94-28810
Non-intrusive gaze tracking using artificial neural networks
[AD-A275186] p 3397 N94-28860
A discussion of eye-head coordinative movement under microgravity during parabolic flight p 3393 N94-29715

F

F REGION
The effects of magnetic storm phases on F-layer irregularities from auroral to equatorial latitudes
[AD-A275203] p 3356 N94-28891
Accurate modeling of F-region electron densities
[NASA-CR-195781] p 3364 N94-30014

F-22 AIRCRAFT
A disciplined approach to software test and evaluation
p 3416 N94-29339

FABRICATION
Practical superconductor development for electrical power applications
[DE94-005378] p 3261 N94-28487
Design and fabrication of forward-swept counterrotation blade configuration for wind tunnel testing
[NASA-CR-194868] p 3155 N94-28510
Filament to mandrel gap analysis: Resulting gap from filament winding over a cone-cylinder transition mandrel (reference NMTP no. 93838)
[DE94-004225] p 3175 N94-28528
Fabrication issues in optimizing YBa(2)Cu(3)O(7-x) flux transformers for low I/f noise
[DE94-005209] p 3261 N94-28546
Fabrication and testing of plasma-spray formed MoSi2 and MoSi2 composite tubes
[DE94-004995] p 3175 N94-28581
Polymer infiltration studies
[NASA-CR-195729] p 3213 N94-28748
A/GATECH DOSP fabrication --- optical programmable logic array
[AD-A275848] p 3430 N94-28781
Optoelectronic integrated circuits fabricated using atomic layer epitaxy
[AD-A275454] p 3262 N94-28805
Development of braided rope engine seals
[NASA-TM-105902] p 3298 N94-28838
3-D braided, continuous fiber ceramic composites produced by chemical vapor infiltration
[AD-A275192] p 3178 N94-29024
Modeling the total dose radiation effects of Hg(1-x)Cd(x)Te photodiodes using numerical device simulators
[AD-A275235] p 3263 N94-29028
A novel approach to the fabrication of SiC structures of arbitrary shape
[AD-A275475] p 3214 N94-29073
Method for forming thin composite solid electrolyte film for lithium batteries
[NASA-CASE-NPO-18877-1-CU] p 3264 N94-29357
Non-rectangular towpreg architectures
[NASA-CASE-LAR-14863-1-CU] p 3180 N94-29485
A module concept for a cable-mesh deployable antenna p 3161 N94-29631
Microactuator production via high aspect ratio, high edge acuity metal fabrication technology
p 3235 N94-29770
Micro-opto-mechanical devices and systems using epitaxial lift off p 3239 N94-29793
Nearly time-optimal feedback control of a magnetically levitated photolithography positioning system
[DE94-005288] p 3266 N94-30055
The machining of fiber metal laminates. Part 1: An inventory of forming processes
[LR-710-PT-1] p 3184 N94-30343
A combined electron beam/optical lithography process step for the fabrication of sub-half-micron-gate-length MMIC chips p 3240 N94-30445
PV Cz silicon manufacturing technology improvements
[DE94-000248] p 3339 N94-30603
Large-area triple-junction a-Si alloy production scale up
[DE94-000249] p 3339 N94-30604
Microwave assisted chemical vapor infiltration
[DE94-005005] p 3185 N94-30771
Controlling the material properties of in vitro collagen through directed orientation and cross-linking of fibrils
p 3221 N94-30797

FABRICS
The potential of new textiles in improving survival prospects p 3380 N94-28430
Development of a new chemical warfare agent protective material p 3381 N94-28432
Catalytic fabric filtration for simultaneous NO(x) and particulate control
[DE94-001660] p 3341 N94-28463
Analysis and design of inflatable aerospace structures
p 3403 N94-30799
Delamination of woven E-glass fabric composites
[DE94-003227] p 3185 N94-30827

FACE (ANATOMY)
Effects of make-up on the heat transfer from the head in hyperthermic conditions p 3394 N94-29864

FACE CENTERED CUBIC LATTICES
A comparison of the evolution of cold and hot deformation microstructures and textures in fcc metals
[DE94-005103] p 3210 N94-30777

FACTOR ANALYSIS
The Environmental Symptoms Questionnaire: Assessing reactions to environmental extremes in military operations p 3383 N94-28447

FAILURE
Identification of components to optimize improvement in system reliability
[DE94-001601] p 3315 N94-28503
Composite panel failure analysis and improvement plan
[AD-A275655] p 3176 N94-28653
Neural network application to Particle Impact Noise Detection p 3437 N94-29840
Failure strength and mechanism of composite laminates under multiaxial loading conditions p 3182 N94-29875
Ampoule failure sensor time response testing: Experiment 1
[NASA-TM-108449] p 3290 N94-30199

FAILURE ANALYSIS
Investigation of advanced fault insertion and simulator methods
[NASA-CR-195241] p 3261 N94-28511
Composite panel failure analysis and improvement plan
[AD-A275655] p 3176 N94-28653
Test and analysis of a stitched RFI graphite-epoxy panel with a fuel access door
[NASA-TM-108992] p 3178 N94-29100
Potential software failures methodology analysis
p 3414 N94-29329
Reliability of composite material structures. Application: High pressure spherical coded tanks
[REPT-932-430-103] p 3180 N94-29478
Lock-up failure of a four-bar linkage deployment mechanism p 3163 N94-29646
Free edge and size effects on failure initiation and ultimate strength of laminates containing a center hole
p 3181 N94-29735
Estimation of Weibull modulus from dynamic and static fatigue experiments
[PB94-138641] p 3322 N94-30114

FAILURE MODES
Investigation of advanced fault insertion and simulator methods
[NASA-CR-195241] p 3261 N94-28511
Static fracture behavior of a ceramic matrix composite at elevated temperatures
[AD-A275363] p 3177 N94-29008
Fatigue behavior of a cross-ply ceramic matrix composite under strain controlled tension-tension and tension-compression loading
[AD-A275374] p 3177 N94-29012
The influence of temperature on microelectronic device failure mechanisms, phase 2
[AD-A275029] p 3265 N94-29511
Interface engineering in alumina fiber/glass composites p 3182 N94-29852
Design for dependability: A simulation-based approach
[NASA-CR-195757] p 3420 N94-29890
Issues arising with the application of optical fiber transmission in class 1E systems in nuclear power plants
[DE94-004743] p 3500 N94-29928

FALKNER-SKAN EQUATION
Experiments and theoretical considerations regarding the allowable roughness height in laminar flow
[PB94-125556] p 3133 N94-30389

FALLOUT
Caesium-137 in a boreal forest ecosystem: Aspects on the long-term behavior
[PB94-137809] p 3347 N94-29158

FAR INFRARED RADIATION
Temperature depencence of the far infrared optical constants of polyethylene
[PB94-124336] p 3213 N94-28795
The far-infrared absorption spectrum of low temperature hydrogen gas
[ISBN-0-315-85432-4] p 3199 N94-30137
FAR ULTRAVIOLET RADIATION
Far ultraviolet images of the nighttime ionosphere
[AD-A275083] p 3356 N94-28843
A sounding rocket program in extreme and far ultraviolet interferometry
[NASA-CR-195114] p 3289 N94-29907
Ablation of polymers by ultraviolet pulsed laser
[DE94-608100] p 3218 N94-30066
FARM CROPS
Frequency dependence of polarization phase difference
[NASA-TM-109737] p 3254 N94-30094
FAST FOURIER TRANSFORMATIONS
Spectral analysis of wave propagation in connected waveguides p 3277 N94-29944
FAST NEUTRONS
Preliminary detector design ST862-prototype neutron detector
[DE94-004714] p 3491 N94-30695
FASTENERS
Development of Alternating Current Potential Drop (ACPD) procedures for crack detection in aluminum aircraft panels
[AD-A275755] p 3315 N94-28646
Cold expansion and interference for extending the fatigue life of multi-layer metal joints
[AD-A274982] p 3318 N94-29091
Quick connect fastener
[NASA-CASE-MFS-28829-1] p 3300 N94-29486
FATIGUE (MATERIALS)
Effects of repair on structural integrity
[AD-A275756] p 3145 N94-28647
A moment plotting method for characterizing aircraft fatigue data population distributions
[AD-A275500] p 3145 N94-28660
Fatigue behavior of a cross-ply ceramic matrix composite at elevated temperatures under tension-tension loading
[AD-A275466] p 3176 N94-28673
On fatigue crack closure: Analysis and measurement
[ISBN-0-315-74873-7] p 3321 N94-29812
Analysis concerning the inspection threshold for multi-site damage
[PB94-142429] p 3149 N94-30905
Fatigue management and verification of airframes
[FFA-TN-1993-55] p 3149 N94-30947
FATIGUE LIFE
A moment plotting method for characterizing aircraft fatigue data population distributions
[AD-A275500] p 3145 N94-28660
An analysis of isothermal, bithermal, and thermomechanical fatigue data of Haynes 188 and B1900+Hf by energy considerations
[NASA-TM-106359] p 3317 N94-28819
Fatigue behavior of a cross-ply ceramic matrix composite under strain controlled tension-tension and tension-compression loading
[AD-A275374] p 3177 N94-29012
Cold expansion and interference for extending the fatigue life of multi-layer metal joints
[AD-A274982] p 3318 N94-29091
Preliminary evaluation of hybrid titanium composite laminates
[NASA-TM-109095] p 3180 N94-29472
The effect of mechanical paint stripping on the fatigue and fracture of thin aluminum airplane skin
p 3205 N94-29900
Surface fatigue life of high temperature gear materials
[NASA-TM-106562] p 3303 N94-30227
Damage analysis and mechanical response of as-received and heat-treated Nicalon/CAS-2 glass-ceramic matrix composites p 3219 N94-30259
FATIGUE TESTS
Fatigue behavior of a cross-ply ceramic matrix composite at elevated temperatures under tension-tension loading
[AD-A275466] p 3176 N94-28673
Fatigue behavior of a cross-ply ceramic matrix composite under strain controlled tension-tension and tension-compression loading
[AD-A275374] p 3177 N94-29012
Cold expansion and interference for extending the fatigue life of multi-layer metal joints
[AD-A274982] p 3318 N94-29091
On fatigue crack closure: Analysis and measurement
[ISBN-0-315-74873-7] p 3321 N94-29812
Fatigue of carbon and low-alloy steels in LWR environments
[DE94-005116] p 3207 N94-30021
Estimation of Weibull modulus from dynamic and static fatigue experiments
[PB94-138641] p 3322 N94-30114
Surface fatigue life of high temperature gear materials
[NASA-TM-106562] p 3303 N94-30227
WISPER and WISPERX: Final definition of two standardised fatigue loading sequences for wind turbine blades
[AD-B175835] p 3324 N94-30872
Fractographic and microstructural analysis of fatigue crack growth in Ti-6Al-4V fan disc forgings
[AD-B174765] p 3153 N94-30914
Fatigue management and verification of airframes
[FFA-TN-1993-55] p 3149 N94-30947
FAULT TOLERANCE
Design and packaging of fault tolerant optoelectronic multiprocessor computing system
[AD-A275896] p 3405 N94-28798
Algorithms for treating redundancy in repairable and non-repairable systems
[DE94-005289] p 3315 N94-29020
Fault tolerant testbed evaluation, phase 1
[NASA-CR-188275] p 3171 N94-29035
Potential software failures methodology analysis
p 3414 N94-29329
Rome Laboratory software engineering technology program p 3414 N94-29330
Distributed applications and failure tolerance programs using a reconfigurable parallel architecture
p 3417 N94-29345
ASSIST internals reference manual
[NASA-TM-109102] p 3431 N94-29494
A study of the relationship between the performance and dependability of a fault-tolerant computer
[NASA-CR-195758] p 3406 N94-29695
Checkpoint-based forward recovery using lookahead execution and rollback validation in parallel and distributed systems
[NASA-CR-195760] p 3431 N94-29869
Design for dependability: A simulation-based approach
[NASA-CR-195757] p 3420 N94-29890
Space reclamation for uncoordinated checkpointing in message-passing systems
[NASA-CR-195761] p 3420 N94-29906
TOTAL user manual
[NASA-TM-109101] p 3432 N94-30160
Self-stabilizing l-exclusion algorithms
[RUU-CS-93-01] p 3424 N94-30379
Design and analysis of dynamic leader election protocols in broadcast networks
[MEMO-INF-93-43] p 3260 N94-30520
A survey of NASA and military standards on fault tolerance and reliability applied to robotics
[AIAA PAPER 94-1211-CP] p 3445 N94-30562
FAULT TREES
Rocket engine system reliability analyses using probabilistic and fuzzy logic techniques
[NASA-TM-106519] p 3173 N94-29403
FEASIBILITY
Feasibility study on introduction of a large methanol engine power generation plant
[DE94-732338] p 3224 N94-28629
FEASIBILITY ANALYSIS
KC-135 cockpit modernization study and crew reduction feasibility demonstration
[AD-A275230] p 3146 N94-29391
Electron microscopy: Metal alloy x ray microanalysis
[REPT-932-600-101] p 3205 N94-29525
Compressed natural gas fueled vehicles: The Houston experience
[DE94-005804] p 3312 N94-30878
FEDERAL BUDGETS
Omnibus Budget Reconciliation Act of 1990
[PUB-LAW-101-508] p 3537 N94-28540
Technology base enhancement program. Metal matrix composites
[AD-A275531] p 3176 N94-28688
FEED SYSTEMS
Gaussian beam and physical optics iteration technique for wideband beam waveguide feed design
p 3248 N94-29624
A digital combining-weight estimation algorithm for broadband sources with the array feed compensation system p 3250 N94-29660
Application of the Modular Automated Reconfigurable Assembly System (MARAS) concept to adaptable vision gauging and parts feeding
[AIAA PAPER 94-1182-CP] p 3440 N94-30533
FEEDBACK
Enhancing performance of full-text retrieval systems using relevance feedback p 3532 N94-29806
Reinforcement learning for robots using neural networks p 3437 N94-29853
Integrated propulsion-airframe dynamics and control
p 3147 N94-29854
Experimental investigation of possible geomagnetic feedback from energetic (0.1 to 16 keV) terrestrial O(+) ions in the magnetotail current sheet
[PAPER-93JA01991] p 3507 N94-30128
FEEDBACK CONTROL
Integrated active and passive control design methodology for the LaRC CSI evolutionary model
[NASA-CR-4580] p 3164 N94-28417
Closed loop vibrational control: Theory and applications
[AD-A275451] p 3154 N94-28632
Feedback control of a three-link planar under-actuated manipulator using a surge velocity
[AD-A275159] p 3435 N94-29044
Extended horizon lifting for periodic gain adjustment in control systems, and for equalization of communication channels
[NASA-CASE-NPO-19166-1-CU] p 3246 N94-29495
Control of micromachined deformable mirrors
p 3239 N94-29787
Decoupled flight control system design using the singular perturbation method p 3155 N94-29850
Integrated propulsion-airframe dynamics and control
p 3147 N94-29854
A design methodology for synthesizing low-order robust controllers for flexible structures p 3302 N94-29870
Robust adaptive control and filtering
p 3437 N94-29895
Nearly time-optimal feedback control of a magnetically levitated photolithography positioning system
[DE94-005288] p 3266 N94-30055
A study of the flexible space platform based deployable manipulator
[ISBN-0-315-85410-3] p 3303 N94-30135
Force control techniques for robot manipulators and their military applications p 3307 N94-30291
The response of flexible manipulators to a new computed torque control strategy: Simulation results
p 3308 N94-30295
Dynamics and control of tethered satellite systems
p 3170 N94-30864
Local interaction control for space construction
p 3170 N94-30960
Robust control of robots via linear estimated state-feedback
[MEMO-1153] p 3449 N94-30963
FEEDFORWARD CONTROL
Non-intrusive gaze tracking using artificial neural networks
[AD-A275186] p 3397 N94-28860
Robotic hand-eye motor learning
p 3436 N94-29835
Vehicle following controller design for autonomous intelligent vehicles
[AIAA PAPER 94-1203-CP] p 3443 N94-30554
FEEDING (SUPPLYING)
Application of the Modular Automated Reconfigurable Assembly System (MARAS) concept to adaptable vision gauging and parts feeding
[AIAA PAPER 94-1182-CP] p 3440 N94-30533
FERMAT PRINCIPLE
Method of Chabauty-Coleman and the second case of Fermat's last theorem for regular primes
[PB94-138187] p 3467 N94-29162
FERMENTATION
One carbon metabolism in anaerobic bacteria: Regulation of carbon and electron flow during organic acid production
[DE94-004852] p 3386 N94-30180
Proceedings of the low cost materials of construction for biological processes workshop
[DE94-000218] p 3226 N94-30761
FERMIONS
Extended nonabelian symmetries for free fermionic model
[DE94-601554] p 3481 N94-28470
Gluon and fermion damping in hot QCD
[ISBN-0-315-85982-2] p 3490 N94-30141
Incommensurate magnetic order in UNi2Al3
[DE94-005449] p 3209 N94-30246
Scaling in heavy-fermion systems
[DE94-005002] p 3492 N94-30775
FERRITIC STAINLESS STEELS
Modelling and analysis of creep deformation and fracture in a 1 Cr 1/2 Mo ferritic steel
[PB94-138328] p 3319 N94-29121
FERROELECTRICITY
Experimental and theoretical studies of molecular solids
[AD-A275511] p 3485 N94-28668
FERROMAGNETIC MATERIALS
Flux-focusing eddy current probe and method for flaw detection
[NASA-CASE-LAR-15046-1] p 3315 N94-29366

Magnetic properties of the three dimensional Ising model with interface single-ion anisotropy
[DE94-608116] p 3525 N94-30164

FERTILIZATION

Japanese Journal of Aerospace and Environmental Medicine, volume 30, no. 1
[JTN-94-80598] p 3389 N94-28850
Effect of chronic centrifugation on in vitro fertilization and early development in mice ova
p 3386 N94-28853
Dynamic constraints on CO2 uptake by an iron-fertilized Antarctic p 3350 N94-30619

FIBER COMPOSITES

Service life prediction of composite structures through fiber testing
[AD-A275661] p 3176 N94-28654
Innovative processing of composites for ultra-high temperature applications, book 1
[AD-A275597] p 3176 N94-28729
Polymer infiltration studies
[NASA-CR-195729] p 3213 N94-28748
Prediction of stress-strain response of SCS-6/Timetal-21S subjected to a hypersonic flight profile
[NASA-TM-109026] p 3177 N94-28823
Static fracture behavior of a ceramic matrix composite at elevated temperatures
[AD-A275363] p 3177 N94-29008
Fatigue behavior of a cross-ply ceramic matrix composite under strain controlled tension-tension and tension-compression loading
[AD-A275374] p 3177 N94-29012
3-D braided, continuous fiber ceramic composites produced by chemical vapor infiltration
[AD-A275192] p 3178 N94-29024
Properties of graphite fiber reinforced copper matrix composites for space power applications
[NASA-CR-191026] p 3178 N94-29208
Intelligent material systems and structures. Part 7: Debonding and pull-out of two optical fibers from two epoxies
[PB94-137767] p 3180 N94-29475
Apparatus for providing a uniform, consolidated, unidirectional, continuous, fiber-reinforced polymeric material and method relating thereto
[NASA-CASE-LAR-15173-1-CU] p 3180 N94-29496
Method of producing a ceramic fiber-reinforced glass-ceramic matrix composite
[NASA-CASE-LEW-15264-2] p 3180 N94-29508
Stress transfer mechanics for multiple perfectly bonded concentric cylinder models of unidirectional composites
[PB94-138633] p 3181 N94-29524
Interface engineering in alumina fiber/glass composites p 3182 N94-29852
Transient thermal fatigue of ceramic composites
p 3216 N94-29874
Failure strength and mechanism of composite laminates under multiaxial loading conditions p 3182 N94-29875
Micromechanical analysis of thermo-inelastic multiphase short-fiber composites
[NASA-CR-195290] p 3183 N94-30178
Delamination growth in composites under cyclic loads
p 3183 N94-30256
The machining of fiber metal laminates. Part 1: An inventory of forming processes
[LR-710-PT-1] p 3184 N94-30343
Effect of fiber coating on mechanical properties of Nicalon fibers and Nicalon-fiber/SiC matrix composites
[DE94-005477] p 3185 N94-30593
Generalized Eulerian-Lagrangian formulations in free and moving boundary problems: Processing of viscoelastic polymers and fiber suspensions p 3283 N94-30955
Numerical modeling and prediction of the thermomechanical behavior of fiber-reinforced composites p 3186 N94-30956

FIBER OPTICS

Broadband EUV survey spectrometer for short-timescale experiments
[DE94-005459] p 3498 N94-28534
Preliminary analysis of Asynchronous Transfer Mode (ATM) over microwave channels
[AD-A275214] p 3243 N94-29069
Three-axis fiber optic vector magnetometer
[AD-D016016] p 3288 N94-29699
Issues arising with the application of optical fiber transmission in class 1E systems in nuclear power plants
[DE94-004743] p 3500 N94-29928
Microsecond fiber optic delay line
[DE94-607903] p 3500 N94-30075
Optoelectronic packaging activities at Sandia National Laboratories
[DE94-005287] p 3501 N94-30261
A commercialized, continuous flow fiber optic sensor for trichloroethylene and haloforms
p 3502 N94-30462
Fiber optical solar simulator p 3341 N94-30486
Optical techniques for time and frequency transfer
p 3469 N94-30647

FIBER ORIENTATION

Generalized Eulerian-Lagrangian formulations in free and moving boundary problems: Processing of viscoelastic polymers and fiber suspensions p 3283 N94-30955

FIBER STRENGTH

Safety enhancement of composites via periodic proof testing
[AD-A275662] p 3176 N94-28655
Effect of fiber coating on mechanical properties of Nicalon fibers and Nicalon-fiber/SiC matrix composites
[DE94-005477] p 3185 N94-30593

FIBER VOLUME FRACTION

Properties of graphite fiber reinforced copper matrix composites for space power applications
[NASA-CR-191026] p 3178 N94-29208
Assessment of the fibre volume distribution around optical fibres
[FFA-TN-1993-12] p 3179 N94-29425

FIBERS

Shortening velocity and calcium sensitivity of single fibers from hindlimb suspended muscle in rats
p 3387 N94-29866

FIELD EFFECT TRANSISTORS

Frequency-domain analysis of nonlinear microwave circuits
[PB94-132024] p 3261 N94-28400
Solid-state, active-phased arrays: Some aspects of receiver design
[AD-A275893] p 3527 N94-28779
A combined electron beam/optical lithography process step for the fabrication of sub-half-micron-gate-length MMIC chips p 3240 N94-30445

FIELD EMISSION

A sub-cm micromachined electron microscope
p 3236 N94-29775

FIELD STRENGTH

Formulae for the calculation of the magnetic field strength in a Helmholtz system with circular coils
[NPL-DES-130] p 3260 N94-30785
An investigation into certain geometrical and variational properties of the P(4) theory of gravitation and electromagnetism p 3526 N94-30950

FIELD THEORY (ALGEBRA)

Is it possible to extend the deformed Weyl algebra W(sub q)(n) to a Hopf algebra?
[DE94-608092] p 3467 N94-30202

FIELD THEORY (PHYSICS)

Extended nonabelian symmetries for free fermionic model
[DE94-601554] p 3481 N94-28470
The (j,0) + (0,j) representation space: Majorna-like construct
[DE94-005010] p 3522 N94-28543
On the EKL-effect
[DE94-606325] p 3468 N94-28720
The Klein-Fock equation, minimal surfaces and gravitational fields
[DE94-606340] p 3356 N94-28803
Remarks on Galois symmetry in RCFT
[PB94-138179] p 3467 N94-29147
Trace formulas and dynamical zeta functions in the Nielsen theory
[PB94-138195] p 3467 N94-29163
Exact spherical wave solutions to Maxwell's equations with applications p 3252 N94-29733
A pot-pourri of results in QCD from large lattice simulations on the CM5
[DE94-005084] p 3514 N94-29818
Anomalous algebraic structures in quantum field theories p 3524 N94-29911
Periodic electromagnetic vacuum in the two-dimensional Yang-Mills theory with the Chern-Simons mass
[DE94-608128] p 3525 N94-30170
Space-time symmetries: P and CP violation
[DE94-005012] p 3526 N94-30750

FIGHTER AIRCRAFT

Information presentation for expert systems in future fighter aircraft
[AD-A275126] p 3149 N94-29005
Asphaltic concrete performance under heavy fighter aircraft loading
[AD-A275046] p 3157 N94-29151
Low-speed longitudinal aerodynamic characteristics of a flat-plate planform model of an advanced fighter configuration
[NASA-TM-109045] p 3130 N94-29443
Autonomous Robotic Refueling System (ARRS) for rapid aircraft turnaround p 3305 N94-30279
Development of a method to predict transonic limit cycle oscillation characteristics of fighter aircraft (continued)
[NLR-TP-92156-U] p 3148 N94-30342
Fatigue management and verification of airframes
[FFA-TN-1993-55] p 3149 N94-30947

FILAMENT WINDING

Filament to mandrel gap analysis: Resulting gap from filament winding over a cone-cylinder transition mandrel (reference NMTP no. 93838)
[DE94-004225] p 3175 N94-28528

FILE MAINTENANCE (COMPUTERS)

Work-oriented development of interactive software tools: Understanding the work of software maintainers and making an interactive software tool for them
[PB94-132032] p 3406 N94-28401
I/O on the Tera file system
[AD-A275278] p 3530 N94-29182
Redundant disk arrays in transaction processing systems
[NASA-CR-195759] p 3418 N94-29404

FILLERS

Fundamental studies on the corrosion behavior of weldments in marine microbial environments
[AD-A275247] p 3203 N94-28900
Welding wire pressure sensor assembly
[NASA-CASE-MFS-26216-1-SB] p 3300 N94-29506
Fusion welding with self-generated filler metal
[NASA-CASE-LEW-15671-1] p 3301 N94-29557

FILM CONDENSATION

The influence of wall conductivity of film condensation with integral fin tubes
[AD-A275503] p 3523 N94-28662

FILM THICKNESS

A novel approach to the fabrication of SiC structures of arbitrary shape
[AD-A275475] p 3214 N94-29073
Effect of fiber coating on mechanical properties of Nicalon fibers and Nicalon-fiber/SiC matrix composites
[DE94-005477] p 3185 N94-30593

FILTRATION

Catalytic fabric filtration for simultaneous NO(x) and particulate control
[DE94-001660] p 3341 N94-28463
Gas stream purifier p 3354 N94-30469

FINANCIAL MANAGEMENT

Business planning model user's guide
[AD-A274978] p 3409 N94-28895
Financial resource review model user's guide
[AD-A274979] p 3410 N94-29088

FINES

Preparation of monodispersed fine particles containing rare metals and rare earths p 3201 N94-29514
Bench-scale synthesis of nanoscale materials
p 3240 N94-30473

FINGERS

Deterioration of manual performance in cold and windy climates p 3381 N94-28434
Effect of food intake on skin vasomotor responses to head-up tilt in humans p 3390 N94-28854

FINISHES

The performance of gloss meters on curving surfaces
[NPL-DMM(A)-111] p 3501 N94-30522

FINITE DIFFERENCE THEORY

Numerical solution of the multichannel scattering problem
[DE94-606297] p 3484 N94-28619
Computational methods in continuum mechanics
[AD-A275560] p 3451 N94-28792
Numerical study of the trailing vortex of a wing with wing-tip blowing
[NASA-CR-195803] p 3130 N94-29760
Large eddy simulation of subsonic mixing layers
p 3276 N94-29851
Unsteady transonic aerodynamics in frequency domain for flutter analysis p 3131 N94-29879
Aeroacoustic sensitivity analysis and optimal aeroacoustic design of turbomachinery blades
[NASA-CR-195786] p 3153 N94-30013
Accurate finite difference methods for time-harmonic wave propagation
[NASA-CR-194887] p 3454 N94-30209
Comparison of RCS prediction techniques, computations and measurements
[PB94-125515] p 3256 N94-30392
Numerical simulations of piano strings. Part 1: A physical model for a struck string using finite difference methods
[TELECOM-93-C-003] p 3481 N94-30972

FINITE ELEMENT METHOD

Viscous and elastic-plastic material model in the ABAQUS
[PB94-132347] p 3316 N94-28409
Three-dimensional finite element modeling of a magnet array spinning above a conductor
[DE94-004573] p 3468 N94-28459
Numerical analysis and computation of nonlinear partial differential equations from applied mathematics
[AD-A275582] p 3451 N94-28723
Numerical simulation of industrial workpiece superplastic forming
[REPT-932-600-102] p 3418 N94-29479

Stress transfer mechanics for multiple perfectly bonded concentric cylinder models of unidirectional composites
[PB94-138633] p 3181 N94-29524
Experimental validation of finite element and boundary element methods for predicting structural vibration and radiated noise
[NASA-CR-4561] p 3301 N94-29552
Finite element method for numerical simulation of turbulent flows. The N3S code p 3233 N94-29612
Computation of vibration mode elastic-rigid and effective weight coefficients from finite-element computer program output p 3247 N94-29615
Elevation control system model for the DSS 13 antenna p 3248 N94-29622
Aircraft system aft telescope cavity configuration study for Stratospheric Observatory for Infrared Astronomy (SOFIA), phase 2
[NASA-CR-194266] p 3147 N94-29685
Finite element analysis of axisymmetric deformations of thick thermoviscoplastic targets p 3320 N94-29688
Analysis of pressureless densification of ceramic matrix composites p 3216 N94-29766
Performance of a higher-order triangular finite element for composite laminated structures p 3181 N94-29810
The h-p adaptive methods for incompressible viscous flow problems p 3275 N94-29836
Dynamic fracture mechanics analysis for an edge delamination crack
[NASA-TM-109106] p 3479 N94-29856
Radiation and scattering from cylindrically conformal printed antennas
[NASA-CR-195546] p 3253 N94-29873
Rotorcraft airframe structural optimization for vibration and dynamic stress reduction including damping treatment p 3147 N94-29878
Computational simulation of composite structures with and without damage
[NASA-CR-194433] p 3183 N94-30190
Unstructured space-time finite element method of heat conduction p 3279 N94-30224
Closed form expressions for a consistent stress material nonlinear finite element p 3322 N94-30258
Plane strain finite element analysis of sheet forming operations including bending effects p 3322 N94-30354
Nonlinear multibody formulation for rotorcraft analysis p 3149 N94-30787
Mixed Eulerian-Lagrangian finite element solutions of unsteady flow and flutter in transonic cascade p 3282 N94-30816
Optimal size finite element meshes without obtuse and small angles
[RUU-CS-92-39] p 3462 N94-30860
Numerical modeling and prediction of the thermomechanical behavior of fiber-reinforced composites p 3186 N94-30956

FINITE VOLUME METHOD
On the numerical analysis of shear flows p 3126 N94-28972
Numerical analysis of laminar flow in S-curved square duct with inlet and outlet straight region p 3128 N94-28987
Numerical solution of the two-dimensional time-dependent incompressible Euler equations
[NASA-CR-195775] p 3277 N94-29859
High-resolution algorithms for the Navier-Stokes equations for generalized discretizations p 3278 N94-29965
Aspects of the modeling and numerical simulation of leading-edge vortex flow
[AD-B179108] p 3133 N94-30492
Local two-phase flow simulations including interface tracking with mass transfer p 3283 N94-30954

FINLAND
Application of high-speed milling to the Finnish manufacturing industry
[PB94-135548] p 3230 N94-29187

FINNED BODIES
The influence of wall conductivity of film condensation with integral fin tubes
[AD-A275503] p 3523 N94-28662
Prediction of fluid flow and heat transfer in internally finned tubes p 3280 N94-30228

FINS
Prediction of fluid flow and heat transfer in internally finned tubes p 3280 N94-30228

FIRE EXTINGUISHERS
Aircraft evacuations: The effect of a cabin water spray system upon evacuation rates and behaviour
[CAA-PAPER-93008] p 3148 N94-29887

FIRE FIGHTING
Comparison of two cool vests on heat-strain reduction while wearing a firefighting ensemble in a hot/humid environment
[AD-A275103] p 3400 N94-28902
Physiological responses during shipboard firefighting
[AD-A275104] p 3391 N94-28912

FIRE PREVENTION
Wire insulation degradation and flammability in low gravity p 3166 N94-28712

FIRES
Similarity solutions and numerical modeling in buoyancy controlled turbulent diffusion flames
[AD-A275820] p 3188 N94-28777
Physiological responses during shipboard firefighting
[AD-A275104] p 3391 N94-28912
Characterization of air emissions from the simulated open combustion of fiberglass materials
[PB94-136231] p 3347 N94-29192
Rooftop emergency heliports
[DOT/FAA/RD-93/2] p 3157 N94-29754
Impact of biomass burning on the atmosphere
[DE94-004333] p 3349 N94-29954

FISHES
Bulletin of National Research Institute of Fisheries Engineering, No. 13
[JTN-94-80596] p 3233 N94-29701
Reproduction in the Japanese anchovy (Engraulis japonica) as related to population fluctuation p 3235 N94-29708
Posture control of goldfishes under microgravity p 3387 N94-29712
Behavior and visual control of cyprinodonts under microgravity p 3387 N94-29713

FISHING
Bulletin of National Research Institute of Fisheries Engineering, No. 13
[JTN-94-80596] p 3233 N94-29701

FISSION
Overlap of metal clusters and nuclear structure physics
[DE94-608387] p 3517 N94-30183

FITTINGS
Root-sum-square structural strength verification approach
[NASA-TM-108453] p 3322 N94-30206

FIXED POINTS (MATHEMATICS)
Reidemeister numbers of equivariant maps
[PB94-138286] p 3452 N94-29118

FIXTURES
A non-contacting vertical alignment system for mass properties measuring instruments
[DE94-004680] p 3289 N94-29927
Root-sum-square structural strength verification approach
[NASA-TM-108453] p 3322 N94-30206

FLAME RETARDANTS
Fire-resistant water vapour permeable buoyant insulation p 3380 N94-28431
Thermal protective performance and instrumented mannequin evaluation of multi-layer garment systems p 3381 N94-28433

FLAME STABILITY
Ultra low NO(x) ultra lean gas turbine primary zones with liquid fuels p 3154 N94-29267
Lifted turbulent jet flames p 3198 N94-29676

FLAMEOUT
Optical flameout detector
[NASA-CASE-LAR-14997-1] p 3287 N94-29368

FLAMMABILITY
Thermal protective performance and instrumented mannequin evaluation of multi-layer garment systems p 3381 N94-28433
Flammability, odor, offgassing, thermal vacuum stability, and compatibility with aerospace fluids of wire insulations p 3166 N94-28709
Wire insulation degradation and flammability in low gravity p 3166 N94-28712

FLAMMABLE GASES
An emergency response mobile robot for operations in combustible atmospheres
[NASA-CASE-NPO-19020-1-CU] p 3299 N94-29420
Joint research activities with CCMRI (China) p 3240 N94-29521

FLANGES
Portable electronically based method for the nondestructive remote sensing of crevice corrosion
[AD-A275403] p 3318 N94-29057

FLARED BODIES
An experimental and theoretical study of the aerodynamic characteristics of some generic missile concepts at Mach numbers from 2 to 6.8
[NASA-TM-109110] p 3130 N94-29473

FLAT CONDUCTORS
Hypervelocity impact induced arcing and Kapton pyrolization in a plasma environment
[NASA-TM-106528] p 3167 N94-28814

FLAT PLATES
Low-speed longitudinal aerodynamic characteristics of a flat-plate planform model of an advanced fighter configuration
[NASA-TM-109045] p 3130 N94-29443
Nominally two-dimensional flow about a normal flat plate p 3275 N94-29838
Rotordynamic analysis of annular honeycomb-stator turbulent gas seals using a new friction-factor model based on flat plate tests p 3302 N94-29916

FLAVOR (PARTICLE PHYSICS)
Operator analysis for quark and lepton masses in SO(10)
[DE94-005201] p 3491 N94-30709
Heavy flavor production at fixed target photo- and hadroproduction
[DE94-004651] p 3491 N94-30719

FLEXIBILITY
Evaluation of corrosion protecting properties of modern aircraft paint systems
[AD-B179388] p 3220 N94-30420
High elongation elastomers p 3223 N94-30477

FLEXIBLE BODIES
Mechanical flexible joint design document
[NASA-CR-193941] p 3297 N94-28419
Collapsible mechanical joint
[NASA-CASE-MFS-28765-1] p 3299 N94-29367
Concurrent simulation and constraint stabilization for flexible multibody systems p 3154 N94-29532
Pulse response based minimum time control of flexible structures p 3436 N94-29720
A design methodology for synthesizing low-order robust controllers for flexible structures p 3302 N94-29870
Theoretical prediction of the influence coefficients on damped simple flexible rotors using the transfer matrix method
[IMR-TM-TR-002] p 3321 N94-30018
Position control of a flexible beam with active damping of vibrations
[ISBN-0-315-85841-9] p 3321 N94-30033
A study of the flexible space platform based deployable manipulator
[ISBN-0-315-85410-3] p 3303 N94-30135
Experimental sliding mode control of a flexible single link manipulator
[ISBN-0-315-85466-9] p 3304 N94-30238
The response of flexible manipulators to a new computed torque control strategy: Simulation results p 3308 N94-30295
Dynamic modeling of multibody flexible structures p 3323 N94-30813
Integrated structure/control design of nonrigid robot arms for high-speed manipulation p 3312 N94-30866

FLEXIBLE SPACECRAFT
Integrated active and passive control design methodology for the LaRC CSI evolutionary model
[NASA-CR-4580] p 3164 N94-28417
Development and validation of a linear recursive order-N algorithm for the simulation of flexible space manipulators dynamics
[AD-B173557] p 3311 N94-30391
Local interaction control for space construction p 3170 N94-30960

FLEXIBLE WINGS
Steady pressure measurements on an Aeroelastic Research Wing (ARW-2)
[NASA-TM-109046] p 3122 N94-28658

FLEXING
Delamination of woven E-glass fabric composites
[DE94-003227] p 3185 N94-30827

FLICKER
Accuracy metrics for judging time scale algorithms p 3471 N94-30656

FLIGHT CLOTHING
Advanced integrated cold protection for aircrew p 3381 N94-28436
Emergency underwater breathing aids for helicopter passengers and crew p 3381 N94-28437
Implications of climatic extremes in aircrew NBC operations p 3383 N94-28446
A reliable and repeatable method for volume calculation of pressurized garments
[AD-A275600] p 3399 N94-28766

FLIGHT CONDITIONS
A non-linear simulation for an autonomous unmanned air vehicle
[AD-A275062] p 3146 N94-29200
Extremely Low Visibility IFR Rotorcraft Approach (ELVIRA) operational concept development. Volume 1: Executive Summary
[DOT/FAA/RD-94/1,I] p 3142 N94-30189
Remote sensor observations during WISP91: The use of microwave radiometers, RASS, and lidar ceilometers for detection of aircraft icing conditions
[PB94-142106] p 3136 N94-30890

FLIGHT CONTROL
Human pilot response during single- and multi-axis tracking tasks
[AD-A275080] p 3398 N94-28887
Exploring QDES as a tool for determining limits of achievable performance in aircraft design
[AD-A275359] p 3146 N94-28998
Flight command software development: RAFALE studies p 3413 N94-29320
On ground system integration and testing: A modern approach p 3150 N94-29334
Decoupled flight control system design using the singular perturbation method p 3155 N94-29850
A novel approach to noise-filtering based on a gain-scheduling neural network architecture
[NASA-TM-106563] p 3155 N94-30204

FLIGHT CREWS
Effect of seasickness on aircrew student survivor ability after ditching in cold water p 3379 N94-28425
Effectiveness of protection clothing for cold weather conditions after ejection over sea: A case report
p 3381 N94-28435
Implications of climatic extremes in aircrew NBC operations p 3383 N94-28446
Alleviation of thermal strain in the CF: Keeping our cool during the Gulf conflict p 3383 N94-28449
Experimental evaluation of two systems of individual air-conditioning p 3384 N94-28450
An evaluation of personality testing and the five-factor model in the selection of landing craft air cushion vehicle crew members
[AD-A275869] p 3397 N94-28754
Aviation epidemiology data register: Age distribution of U.S. Army aviators stratified by gender and component of service
[AD-A275901] p 3388 N94-28757
Disturbance of equilibrium on JAL flight crew
p 3390 N94-28856
Relaxed tolerance following HSG, high sustained +Gz
[AD-A275204] p 3391 N94-28892
Comparative centrifuge evaluation of the Air Force Advanced Technology Anti-G Suit (ATAGS) and the Navy Enhanced Anti-G Lower Ensemble (EAGLE)
[AD-A275348] p 3400 N94-28996

FLIGHT ENVELOPES
Integrated propulsion-airframe dynamics and control
p 3147 N94-29854

FLIGHT HAZARDS
Potential hazards of magnetic resonance imagers to emergency medical service helicopter operations
[DOT/FAA/RD-92/15] p 3135 N94-29862
Vulnerability of manned spacecraft to crew loss from orbital debris penetration
[NASA-TM-108452] p 3169 N94-30161

FLIGHT MANAGEMENT SYSTEMS
Machine Intelligence in Air Traffic Management
[AGARD-CP-538] p 3136 N94-29558
Advances in development capabilities for intelligent air traffic management systems p 3137 N94-29559
Intelligent systems for air space control and management p 3137 N94-29560
Use of advanced technologies in ATM (air traffic management) domain p 3137 N94-29561
Air traffic management as principled negotiation between intelligent agents p 3137 N94-29562
GPS/GNSS for ATM p 3138 N94-29565
Contributions of DLR to air traffic capacity enhancement within a terminal area p 3138 N94-29567
Design of Center-TRACON Automation System
p 3138 N94-29568
Advanced air traffic control and flight management system concepts p 3140 N94-29576
Opportunities for integrating the aircraft FMS, aeronautical operational control centers, and future air traffic management systems in oceanic airspace
p 3140 N94-29577
Profile negotiation: An air/ground automation integration concept for managing arrival traffic
p 3140 N94-29578
Air-ground integration of the ATM system in PHARE
p 3141 N94-29579
Experimental flight management system
p 3141 N94-29580
The PHARE advanced tools p 3141 N94-29581
The experimental flight management system: An air traffic management research tool
[NLR-TP-92253-U] p 3143 N94-30943

FLIGHT PATHS
An efficient algorithm for 3D connect-the-dots
[AD-A275431] p 3409 N94-28866
Decision Making Aids (DMA) in on-line ATC systems
p 3139 N94-29570
Advanced air traffic control and flight management system concepts p 3140 N94-29576
Profile negotiation: An air/ground automation integration concept for managing arrival traffic
p 3140 N94-29578
Air-ground integration of the ATM system in PHARE
p 3141 N94-29579
The PHARE advanced tools p 3141 N94-29581
A simulator for multi-radar analysis for realistic traffic
[AD-B179099] p 3142 N94-30439
A stochastic control approach to flight path monitoring
[AD-B174630] p 3143 N94-30853

FLIGHT PLANS
ACCS Surveillance Exploratory Prototype (ASEP)
p 3138 N94-29566
Opportunities for integrating the aircraft FMS, aeronautical operational control centers, and future air traffic management systems in oceanic airspace
p 3140 N94-29577
A simulator for multi-radar analysis for realistic traffic
[AD-B179099] p 3142 N94-30439

FLIGHT SAFETY
Crashworthiness analysis of commuter aircraft seats
[AD-A275889] p 3135 N94-28799
Integrated formal verification and validation of safety critical software p 3416 N94-29338
Aircraft accident/incident summary report: In-flight loss of control, leading to forced landing and runway overrun, Continental Express, Inc., N24706 Embraer EMB-120 RT, Pine Bluff, Arkansas, 29 April 1993
[PB94-910404] p 3135 N94-29402
The 1993 Federal Aviation Administration Aviation System Capital Investment Plan p 3136 N94-29445
Interactive analysis and planning tools for air traffic and airspace management p 3139 N94-29573
DAISY: A decision aid for an air situation interpretation system p 3139 N94-29574
Development of precision runway monitor system for increasing capacity of parallel runway operations
p 3142 N94-29587
Extremely Low Visibility IFR Rotorcraft Approach (ELVIRA) operational concept development. Volume 1: Executive Summary
[DOT/FAA/RD-94/1,I] p 3142 N94-30189
The TOPAZ 2 space reactor response under accident conditions
[DE94-004998] p 3498 N94-30847

FLIGHT SIMULATION
Modification of ACSYNT aircraft computer program for preliminary design
[NASA-CR-195737] p 3145 N94-28817
Procedural guide for modelling and analyzing the flight characteristics of a helicopter design using flightlab
[AD-A275077] p 3146 N94-28870
A non-linear simulation for an autonomous unmanned air vehicle
[AD-A275062] p 3146 N94-29200
Particle kinetic simulation of high altitude hypervelocity flight
[NASA-CR-194535] p 3131 N94-29893
Physiological Anatomical Rodent Experiment (PARE) .04 feasibility test 2
[NASA-CR-195210] p 3385 N94-29968
Flight simulator evaluation of advanced MLS procedures
[AD-B174270] p 3143 N94-30915

FLIGHT SIMULATORS
Six-degree-of-freedom parallel minimanipulator with three inextensible limbs
[NASA-CASE-GSC-13485-1] p 3288 N94-29726

FLIGHT TESTS
Acquisition, design modification, assembly, and ground test of NPS Hummingbird remotely piloted helicopter
[AD-A275546] p 3146 N94-28837
Some problems of scramjet propulsion for aerospace planes. Part 2: Scramjet: Development and test problems p 3152 N94-29301
Testing Operational Flight Programs (OFPs)
p 3415 N94-29337
Microgravity by parabolic flight with MU-300 aircraft
p 3392 N94-29710

FLOATING
An actively cooled floating element skin friction balance for direct measurement in high enthalpy supersonic flows p 3289 N94-29824

FLOATING POINT ARITHMETIC
Numerical precision and roundoff considerations concerning computer code migration
[DE94-005421] p 3427 N94-30590

FLOCCULATING
Dewatering of contaminated river sediments
p 3354 N94-30472

FLOW CHARACTERISTICS
Study of bridge design and technology
[PB94-137916] p 3121 N94-29160
Recent CFD applications in small gas turbine combustion systems development p 3154 N94-29257
An experimental study of wing tip vortex in the near wake of a rectangular wing
[AD-A275389] p 3129 N94-29306
Prediction of fluid flow and heat transfer in internally finned tubes p 3280 N94-30228

FLOW DISTRIBUTION
Calculation of propulsive nozzle flowfields in multidiffusing chemically reacting environments
[NASA-TM-106532] p 3271 N94-28835
Code development for hypersonic real-gas flow simulations toward the design of space vehicles, part 2
p 3125 N94-28966
Three dimensional simulation of compressible flow induced by a high-speed train moving into a tunnel
p 3126 N94-28967
Numerical analysis of incompressible viscous flow around a bubble p 3126 N94-28968
Transonic expanding flow through axially symmetric orifices p 3128 N94-28985
Numerical analysis of laminar flow in S-curved square duct with inlet and outlet straight region
p 3128 N94-28987
A free-wake Euler and Navier-Stokes CFD method and its application to helicopter rotors including dynamic stall
[AD-A275416] p 3129 N94-29197
Flowfield prediction of NO(x) and smoke production in aircraft engines p 3191 N94-29252
Numerical modelling of turbine combustion chambers
p 3154 N94-29254
Pollutant emissions from and within a model gas turbine combustor at elevated pressures and temperatures
p 3194 N94-29271
The influence of air distribution on homogeneity and pollutant formation in the primary zone of a tubular combustor p 3194 N94-29274
Time-resolved measurements in a three dimensional model combustor p 3196 N94-29283
Fronts at the confluences of spring-fed streams with Joekulsa a Fjoellum: Possibly thermal bars?
[MATHS-REPT-A-198] p 3333 N94-29528
An experimental study of the flowfield on a semispan rectangular wing with a simulated glaze ice accretion
p 3130 N94-29674
An analytical study of unsteady rotor/fuselage interaction in hover and forward flight
p 3131 N94-29826
An experimental investigation of flow patterns and liquid entrainment in a horizontal-tube evaporator
p 3277 N94-29899
Aircraft aerodynamics with deflected jets in ground effect p 3132 N94-29973
The 3-D LDV measurements on a 30-degree swept wing with a simulated ice accretion
[NASA-CR-195327] p 3132 N94-30124
Three-dimensional flow characteristics downstream of a blade endwall corner p 3280 N94-30229
The design of a system of codes for industrial calculations of flows around aircraft and other complex aerodynamic configurations
[PB94-125598] p 3133 N94-30387
The enhancement of compressible turbulent mixing via streamwise vorticity p 3280 N94-30487
Expanding the waverider design space using arbitrary generating flowfields p 3148 N94-30516
In-cylinder gas velocity measurements comparing crankcase and blower scavenging in a fired two-stroke cycle engine
[DE94-005752] p 3311 N94-30596
Experiments on the aerodynamic generation of noise in centrifugal turbomachinery p 3480 N94-30804
Evaluation of flip-flop jet nozzles for use as practical excitation devices
[NASA-TM-106377] p 3135 N94-30949
Generalized Eulerian-Lagrangian formulations in free and moving boundary problems: Processing of viscoelastic polymers and fiber suspensions p 3283 N94-30955

FLOW EQUATIONS
On the linear stability of Verkley's modons
p 3324 N94-28695
Advanced Design of Ventilation Systems
[VKI-LS-1993-07] p 3231 N94-29598
Numerical solution of the two-dimensional time-dependent incompressible Euler equations
[NASA-CR-195775] p 3277 N94-29859
The design of a system of codes for industrial calculations of flows around aircraft and other complex aerodynamic configurations
[PB94-125598] p 3133 N94-30387
Euler results of the ISNaS compressible multi-block flow solver
[AD-B179299] p 3281 N94-30756

FLOW MEASUREMENT
Characterization of structural vibration: Field descriptors based on energy density and intensity
[PB94-132230] p 3316 N94-28404

Development and application of a thermistor current meter
[AD-A275816] p 3286 N94-28831
Improved in-flow acoustic sensor
[NASA-CASE-ARC-12001-1] p 3478 N94-29363
Method for making a dynamic pressure sensor and a pressure sensor made according to the method
[NASA-CASE-LAR-14029-1] p 3288 N94-29484
Development of a simple current meter using solution p 3233 N94-29702
Correction of X hot-wire measurements for gradients normal to the plane of the wires
[PB94-125473] p 3157 N94-30399
Thermal conductivities, electrical resistivities, and Seebeck coefficients of YBa2Cu3O(7-x) superconductors from 80 to 300 K
[DE94-004796] p 3520 N94-30724
Analysis of fluctuating static pressure measurements in a large high Reynolds number transonic cryogenic wind tunnel p 3158 N94-30788

FLOW STABILITY
On the linear stability of Verkley's modons p 3324 N94-28695
Structure of neutrally stratified turbulent Ekman layer as predicted by closure models with prognostic equation for master length scale p 3325 N94-28696
Long-wavelength asymptotics of unstable crossflow modes, including the effect of surface curvature
[NASA-CR-4579] p 3273 N94-29460
Forced generation of solitary waves in a rotating fluid and their stability p 3274 N94-29689
An improvement of the slender body theory for oscillating ships with finite forward speed p 3234 N94-29705
The dynamics of tropical intraseasonal variability p 3371 N94-29741
The h-p adaptive methods for incompressible viscous flow problems p 3275 N94-29836
Hydrodynamic stability analysis of swirling jets p 3278 N94-29974
The instantaneous concentration field in the self-similar region of a high Schmidt number round jet p 3278 N94-29976
Near-critical spherically symmetric accretion by neutron stars p 3546 N94-29991
Potential capabilities of Reynolds stress turbulence model in the COMMIX-RSM code p 3285 N94-30450
An experimental study of nonlinear wave coupling and energy transfer characterizing the transition of a planar jet shear layer p 3282 N94-30953
Transition to turbulence in confined compressible mixing layers p 3283 N94-30958

FLOW VELOCITY
Development of laser velocimetry for the measurements of turbulence intensity and flow velocity ahead of a NGV row in a full-stage rotating turbine
[AD-A275712] p 3270 N94-28692
Qualitative vector optimization of a condensate stabilizer process
[PB94-133246] p 3189 N94-28789
Development and application of a thermistor current meter
[AD-A275816] p 3286 N94-28831
Fluid dynamic noise in a centrifugal pump
[AD-A275264] p 3477 N94-28904
Remote control of transcranial Doppler (TCD) probe during centrifuge exposures up to 9 +Gz
[AD-A275253] p 3400 N94-29029
Methane challenge of high performance molecular sieve oxygen concentrator
[AD-A275155] p 3337 N94-29033
Development of a simple current meter using solution p 3233 N94-29702
Two-phase power-law modeling of pipe flows displaying shear-thinning phenomena
[DE94-005115] p 3279 N94-30020
The effect of a wavy boundary on turbulent flow p 3280 N94-30272
Correction of X hot-wire measurements for gradients normal to the plane of the wires
[PB94-125473] p 3157 N94-30399
In-cylinder gas velocity measurements comparing crankcase and blower scavenging in a fired two-stroke cycle engine
[DE94-005752] p 3311 N94-30596
Development and application of particle image velocimetry in high-speed separated flow: Two-dimensional base cavities p 3282 N94-30791

FLOW VISUALIZATION
Holographic interferometry: A user's guide
[DE94-003136] p 3286 N94-28466
A flow visualization study of acoustically enhanced hairpin vortices
[AD-A275467] p 3271 N94-28809
Evolution of the large-scale vortices in turbulent mixing-layers p 3273 N94-29686
The flow field near the body surface with thin filaments p 3234 N94-29706
An experimental investigation of the effect of leading edge extensions on directional stability and the effectiveness of forebody nose strakes p 3155 N94-29728
Flow past a circular cylinder with a permeable wake splitter plate p 3275 N94-29764
Wall pressure fluctuations in the reattachment region of a supersonic free shear layer
[NASA-CR-195790] p 3132 N94-29920
Development and application of particle image velocimetry in high-speed separated flow: Two-dimensional base cavities p 3282 N94-30791
The execution of wind energy projects 1986 - 1992 between China Aerodynamics Research and Development Centre (CARDC) and The Aeronautical Research Institute of Sweden (FFA)
[FFA-TN-1993-19] p 3340 N94-30945

FLOWMETERS
Development of a simple current meter using solution p 3233 N94-29702

FLUE GASES
Measurement of volatile metal species at elevated temperatures
[PB94-132321] p 3186 N94-28407

FLUENCE
Determination of photon fluence spectra from the NPL Mobaltron Co-60 unit
[NPL-RSA(EXT)-46] p 3492 N94-30795

FLUID DYNAMICS
Fluid and transportation phenomena under microgravity p 3227 N94-28939
The motion of deforming bodies
[AD-A275224] p 3271 N94-29061
Numerical solution of the two-dimensional time-dependent incompressible Euler equations
[NASA-CR-195775] p 3277 N94-29859
A single-fluid, self-consistent formulation of particle transport and fluid dynamics p 3280 N94-30352
A new orthogonal decomposition method for turbulent flows p 3281 N94-30494

FLUID FILTERS
Gas stream purifier p 3354 N94-30469

FLUID FLOW
Holographic interferometry: A user's guide
[DE94-003136] p 3286 N94-28466
Computational methods in continuum mechanics
[AD-A275560] p 3451 N94-28792
Fluid and transportation phenomena under microgravity p 3227 N94-28939
Electromagnetic effect on turbulent transport in liquid metals and electrolytes (bath)
[PB94-138450] p 3206 N94-29946
Computational fluid and combustion dynamics
[DE94-006596] p 3279 N94-30003
A new orthogonal decomposition method for turbulent flows p 3281 N94-30494
Information system for flow simulation based on the Navier-Stokes equations vectorization
[AD-B179293] p 3281 N94-30763

FLUID JETS
Liquid atomization in supersonic flows p 3276 N94-29839

FLUID MANAGEMENT
Cryogenic on-orbit liquid depot storage acquisition and transfer (COLD-SAT) experiment subsystem instrumentation and wire harness design report
[NASA-CR-189172] p 3168 N94-29405
Large scale cryogenic fluid systems testing
[NASA-TM-109735] p 3157 N94-29904
Microgravity fluid science research in Europe
[AD-B179178] p 3229 N94-30409

FLUID MECHANICS
SAFSIM theory manual: A computer program for the engineering simulation of flow systems
[DE94-005381] p 3270 N94-28488
Microgravity fluid science research in Europe
[AD-B179178] p 3229 N94-30409

FLUID PRESSURE
Apparatus for testing high pressure injector elements
[NASA-CASE-MFS-28773-1] p 3299 N94-29365

FLUID-SOLID INTERACTIONS
Flammability, odor, offgassing, thermal vacuum stability, and compatibility with aerospace fluids of wire insulations p 3166 N94-28709
A numerical method for confined unsteady flows related to fluid-structure interactions
[ISBN-0-315-74739-0] p 3277 N94-29902
Theoretical studies of solid-fluid phase equilibria
[DE94-006406] p 3226 N94-30708

FLUIDIZED BED PROCESSORS
Application of the extended Kalman filter to the estimation of the char mass in a fluidized bed combustor
[REPT-93-065] p 3200 N94-30938

FLUORESCENCE
Measurement of atmospheric OH by titration of near-IR fluorescent dyes p 3344 N94-28599

FLUORIDES
Formation and chemical reactivity of carbon fibers prepared by defluorination of graphite fluoride
[NASA-TM-106398] p 3174 N94-28747
Graphite intercalation compounds prepared from graphite fluoride
[NASA-TM-106447] p 3174 N94-28924

FLUORINE
Reinterpretation of rate data for the reaction of ClF and F2
[DE94-005819] p 3200 N94-30880

FLUORINE COMPOUNDS
Non-aqueous cleaning solvent substitution
[DE94-005339] p 3219 N94-30245

FLUORINE ORGANIC COMPOUNDS
XPS analysis of 440C steel surfaces lubricated with perfluoropolyethers under sliding conditions in high vacuum
[NASA-TM-106548] p 3218 N94-30177

FLUORO COMPOUNDS
Polyimides containing the penta fluoro sulfanyl benzene moiety
[NASA-CASE-LAR-15082-1] p 3175 N94-29554

FLUTTER ANALYSIS
Unsteady transonic aerodynamics in frequency domain for flutter analysis p 3131 N94-29879
Development of a method to predict transonic limit cycle oscillation characteristics of fighter aircraft (continued)
[NLR-TP-92156-U] p 3148 N94-30342
Prospects of time-linearized unsteady calculation methods for exponentially diverging motions in aeroelasticity
[PB94-126224] p 3134 N94-30740

FLUX DENSITY
Characterization of structural vibration: Field descriptors based on energy density and intensity
[PB94-132230] p 3316 N94-28404

FLUX PINNING
New evidence for flux cutting in type II superconductors
[ISBN-0-315-85830-3] p 3515 N94-30032

FLYBY MISSIONS
Radio science ground data system for the Voyager-Neptune encounter, part 1 p 3248 N94-29623
The Pluto fast flyby mission: Completing the reconnaissance of the solar system p 3235 N94-29768

FOAMS
Improved construction materials for polar regions using microcellular thermoplastic foams p 3223 N94-30483

FOCAL PLANE DEVICES
Development of ultra-low noise, high performance 3 -5 quantum well infrared photodetectors (QWIPs) for focal plane array staring image sensor systems
[AD-A275745] p 3511 N94-28734
Monolithic in-based III-V compound semiconductor focal plane array cell with single stage CCD output
[NASA-CASE-NPO-18978-1-CU] p 3265 N94-29488
Dual-use applications of infrared sensitive materials
[AD-A275140] p 3499 N94-29694
Smart focal-plane technology for micro-instruments and micro-rovers p 3237 N94-29780
Evolution of miniature detectors and focal plane arrays for infrared sensors p 3237 N94-29781

FOCUSING
Radiation transport and focusing systems for power industrial lasers
[DE94-606817] p 3293 N94-28786
An Earth observation telescope refocusing mechanism
[REPT-932-440-103] p 3332 N94-29417
Smart focal-plane technology for micro-instruments and micro-rovers p 3237 N94-29780

FOG
Multispectral transmittance measurements through man-made water fogs p 3257 N94-30499

FOKKER-PLANCK EQUATION
Derivation of a Fokker-Planck equation for bunched beams
[DE94-004950] p 3483 N94-28565
Conceptual study of moderately coupled plasmas and experimental comparison of laboratory x ray sources
[DE94-005828] p 3506 N94-30045

FOLDING STRUCTURES
Low melting temperature alloy deployment mechanism and recent experiments p 3163 N94-29644

FOOD
Evaluation of life support equipment during an unsupported North Pole expedition p 3379 N94-28422

FOOD PROCESSING
Evaluation of life support equipment during an unsupported North Pole expedition
p 3379 N94-28422
FOOD PRODUCTION (IN SPACE)
Publications of the NASA Controlled Ecological Life Support System (CELSS) program 1989-1992
[NASA-CR-4603] p 3401 N94-30122
FORCE-FREE MAGNETIC FIELDS
The structure of solar magnetic fields and their associated electric currents p 3544 N94-29723
FORCED VIBRATION
Turbomachinery forced response prediction system (FREPS): User's manual
[NASA-CR-194465] p 3319 N94-29104
FORECASTING
Research activities of Martin C. Casdagli at SFI September 1989--May 1991
[DE94-005655] p 3463 N94-28548
FOREST MANAGEMENT
Utilization of remote sensing data in Southeast Asia
p 3327 N94-28936
Tohoku district observed by artificial satellites
p 3328 N94-29041
FAME: A Forest Assessment and Monitoring Environment scenario
[AD-B179106] p 3335 N94-30759
FORESTS
Caesium-137 in a boreal forest ecosystem: Aspects on the long-term behavior
[PB94-137809] p 3347 N94-29158
Frequency dependence of polarization phase difference
[NASA-TM-109737] p 3254 N94-30094
The extraction and representation of forest inventory information using continuous density surfaces
[ISBN-0-315-85658-0] p 3334 N94-30236
A bottom-up evolution of terrestrial ecosystem modeling theory, and ideas toward global vegetation modeling
p 3351 N94-30628
Evaluating models of climate and forest vegetation
p 3353 N94-30637
Atmospheric turbulence within and above a coniferous forest
[ISBN-0-315-75468-0] p 3375 N94-30870
FORMALISM
Operation semantics with read and write frames
[PB94-138138] p 3529 N94-29108
Invariants, frames and postconditions: A comparison of two formal specification notations
[PB94-138153] p 3405 N94-29110
Flight command software development: RAFALE studies p 3413 N94-29320
Formal specification and verification of real-time sequential control systems
[AD-A275776] p 3419 N94-29678
A single-fluid, self-consistent formulation of particle transport and fluid dynamics p 3280 N94-30352
Unravelling nondeterminism: On having the ability to choose
[RUU-CS-93-30] p 3428 N94-30749
Theoretical studies in hadronic and nuclear physics
[DE94-003524] p 3492 N94-30838
FORMAT
Object-oriented CAD tool implementations for the construction industry
[PB94-132370] p 3407 N94-28411
FORMING TECHNIQUES
Apparatus for providing a uniform, consolidated, unidirectional, continuous, fiber-reinforced polymeric material and method relating thereto
[NASA-CASE-LAR-15173-1-CU] p 3180 N94-29496
Plane strain finite element analysis of sheet forming operations including bending effects
p 3322 N94-30354
FORTRAN
Comparing Ada and FORTRAN lines of code: Some experimental results
[AD-A275322] p 3409 N94-28878
Parallel Fortran programming for NWT
p 3129 N94-28991
Performance evaluation of the NWT with parallel Fortran p 3129 N94-28992
FOSSIL FUELS
Development of the integrated environmental control model: Performance models of selective catalytic reduction NO(x) control systems
[DE94-002151] p 3341 N94-28465
Proceedings of the Joint Contractors Meeting: FE/EE Advanced Turbine Systems Conference FE Fuel Cells and Coal-Fired Heat Engines Conference
[DE93-011308] p 3336 N94-28499
Fossil energy biotechnology: A research needs assessment
[DE94-004239] p 3338 N94-29953
FOUR-WAVE MIXING
Interaction of sound with sound by novel mechanisms: Ultrasonic four-wave mixing mediated by a suspension and ultrasonic three-wave mixing at a free surface
p 3479 N94-29988
FOURIER TRANSFORMATION
JPL Fourier transform ultraviolet spectrometer
p 3343 N94-28593
Temperature depencence of the far infrared optical constants of polyethylene
[PB94-124336] p 3213 N94-28795
A new guided wave lens structure and its application
[AD-A275541] p 3499 N94-28813
Reactions of metal ions and their clusters in the gas phase using laser ionization: Fourier transform mass spectrometry
[DE94-006208] p 3207 N94-30024
Meso-optical Fourier transform microscope with double focusing
[DE94-607851] p 3290 N94-30148
Dual use of image based tracking techniques: Laser eye surgery and low vision prosthesis p 3397 N94-30455
FRACTALS
A fractal analysis of near-field atmospheric concentration data
[AD-A275460] p 3355 N94-28728
The uses and limitations of fractal geometry in digital terrain modelling p 3333 N94-29958
Fractal approach to computer-analytical modelling of tree crown
[DE94-608089] p 3467 N94-30088
FRACTOGRAPHY
Fractographic and microstructural analysis of fatigue crack growth in Ti-6Al-4V fan disc forgings
[AD-B174765] p 3153 N94-30914
FRACTURE MECHANICS
Fatigue behavior of a cross-ply ceramic matrix composite at elevated temperatures under tension-tension loading
[AD-A275466] p 3176 N94-28673
Plane stress stable crack growth and J-integral/HRR field
[AD-A275761] p 3317 N94-28761
A modeling study of the effect of stress state on void linking during ductile fracture
[AD-A275505] p 3317 N94-28811
Role of microstructure on the fatigue durability of aluminum aircraft alloys
[AD-A275814] p 3202 N94-28830
Modelling and analysis of creep deformation and fracture in a 1 Cr 1/2 Mo ferritic steel
[PB94-138328] p 3319 N94-29121
Effect of microstructure on the strength and fracture energy of bimaterial interfaces
[AD-A274987] p 3178 N94-29126
Microstructure/property relationships for SCS6/Timetal 21-S composite
[AD-A275056] p 3178 N94-29135
Stress transfer mechanics for multiple perfectly bonded concentric cylinder models of unidirectional composites
[PB94-138633] p 3181 N94-29524
Analyses of stationary and growing crack tip deformation by digital image processing p 3320 N94-29690
The effect of various metallurgical parameters on the flow and fracture behavior of polycrystalline NiAl near the brittle-to-ductile transition
[NASA-TM-106534] p 3205 N94-29758
Dynamic fracture mechanics analysis for an edge delamination crack
[NASA-TM-109106] p 3479 N94-29856
Interlaminar fracture analysis for laminated composites under combined loading p 3182 N94-29964
Microgravity compatible drive system-rider. New technologies
[PB94-138583] p 3229 N94-29996
Estimation of Weibull modulus from dynamic and static fatigue experiments
[PB94-138641] p 3322 N94-30114
Experimental and analytical comparison of constraint effects due to biaxial loading and shallow-flaws
[DE94-004794] p 3323 N94-30689
An investigation of fatigue crack propagation under mode 1 and mixed mode 1/2 loadings p 3323 N94-30814
Material properties and fracture mechanics in relation to ceramic machining
[DE94-006623] p 3221 N94-30829
Fatigue management and verification of airframes
[FFA-TN-1993-55] p 3149 N94-30947
FRACTURE STRENGTH
Single specimen fracture toughness determination procedure using instrumented impact test
[PB94-132040] p 3316 N94-28402
Effects of repair on structural integrity
[AD-A275756] p 3145 N94-28647
Toughening mechanisms in ultrahigh-strength steels
[AD-A275439] p 3202 N94-28867
Effect of microstructure on the strength and fracture energy of bimaterial interfaces
[AD-A274987] p 3178 N94-29126
The effect of mechanical paint stripping on the fatigue and fracture of thin aluminum airplane skin
p 3205 N94-29900
A newly developed snow vehicle (SM100S) for Antarctica. Part 3: Low temperature toughness of the welded joints of the structural steel
p 3364 N94-29983
Surface fatigue life of high temperature gear materials
[NASA-TM-106562] p 3303 N94-30227
A review of mechanical test methods for ceramic matrix composites
[PB94-147576] p 3184 N94-30524
FRACTURES (MATERIALS)
Stress transfer mechanics for multiple perfectly bonded concentric cylinder models of unidirectional composites
[PB94-138633] p 3181 N94-29524
FRACTURING
Static fracture behavior of a ceramic matrix composite at elevated temperatures
[AD-A275363] p 3177 N94-29008
Microstructure/property relationships for SCS6/Timetal 21-S composite
[AD-A275056] p 3178 N94-29135
An analysis of the microstructure and reinforcement distribution of an extruded particle-reinforced Al 6061-10 volume percent Al2O3 metal matrix composite
[AD-A275050] p 3178 N94-29166
Stress transfer mechanics for multiple perfectly bonded concentric cylinder models of unidirectional composites
[PB94-138633] p 3181 N94-29524
The effect of various metallurgical parameters on the flow and fracture behavior of polycrystalline NiAl near the brittle-to-ductile transition
[NASA-TM-106534] p 3205 N94-29758
Fracture process zone of brittle composites
p 3182 N94-29876
Interlaminar fracture analysis for laminated composites under combined loading p 3182 N94-29964
Time-resolved holography for the microscopic study of crack-tip motion in dynamic fracture
p 3290 N94-30254
Experimental and analytical comparison of constraint effects due to biaxial loading and shallow-flaws
[DE94-004794] p 3323 N94-30689
FREDHOLM EQUATIONS
Procedures for basic inverse problems: Black body radiation problem and phonon density of states problem
[ISBN-0-315-85757-9] p 3525 N94-30244
FREE CONVECTION
Finite element method for numerical simulation of turbulent flows. The N3S code p 3233 N94-29612
FREE ELECTRON LASERS
Linac Coherent Light Source (LCLS) at 2-4 nm using the SLAC linac
[DE94-005235] p 3292 N94-28481
Advances in tunable powerful lasers: The advanced free-electron laser
[DE94-004997] p 3294 N94-29934
Towards short wavelengths FELs workshop
[DE94-004346] p 3296 N94-30688
FREE ELECTRONS
Nonadiabatic effects in the quantum Hall regime
p 3513 N94-29530
Calculation of inelastic mean free path and stopping power for electrons in solids from an optical-data model
[USIP-92-06] p 3494 N94-30980
FREE ENERGY
Surface energy changes produced by ultraviolet-ozone irradiation of poly(methylmethacrylate), polycarbone and polytetrafluoroethylene
[NASA-TM-106460] p 3213 N94-28922
Theory for electron-transfer reactions in a three-component system: The degenerate regime
[DE94-005919] p 3493 N94-30903
FREE FLOW
Low-speed longitudinal aerodynamic characteristics of a flat-plate planform model of an advanced fighter configuration
[NASA-TM-109045] p 3130 N94-29443
An interactive, design and educational tool for supersonic external-compression inlets
[NASA-TM-106581] p 3421 N94-30174
FREE JETS
The nozzle acoustic test rig: An acoustic and aerodynamic free-jet facility
[NASA-TM-106495] p 3156 N94-28749
FREE VIBRATION
Free vibration of thermally loaded panels including initial imperfections and post-buckling effects
[NASA-TM-109097] p 3479 N94-29461
Three-dimensional free vibration analysis of thick arbitrarily laminated, rectangular, cylindrical and spherical composite panels p 3184 N94-30257

FREEZE DRYING
Evaluation of life support equipment during an unsupported North Pole expedition p 3379 N94-28422

FREQUENCIES
An absolute measurement of the cosmic background radiation temperature at 1.4 GHz p 3553 N94-30351
Status of frequency and time support for NASA systems p 3468 N94-30640

FREQUENCY ANALYZERS
Frequency-domain analysis of nonlinear microwave circuits
[PB94-132024] p 3261 N94-28400

FREQUENCY MODULATION
Longitudinal effects and intensity-phase coupling in distributed feedback semiconductor lasers p 3294 N94-29590

FREQUENCY RANGES
VHF impedance measurement: A review
[PB94-138682] p 3267 N94-30115
Measurement of bulk longitudinal modulus and correction for edge effects
[DE94-005581] p 3222 N94-30900

FREQUENCY RESPONSE
Identification of the damping ratio relationship of an autovehicle suspension
[REPT-93-063] p 3313 N94-30937

FREQUENCY SHIFT
Journal of NIRE, Vol. 2, No. 2
[JTN-94-80552] p 3187 N94-28675
Ab initio study of vibrational frequency shift upon the 1:1 acetone-iodine complex formation p 3188 N94-28681
Inter-comparison of Wildfire and High-resolution Interferometer Sounder (HIS) data from STORM-FEST: An investigation of wildfire spectral channel discrepancies
[NASA-TM-108439] p 3333 N94-29553

FREQUENCY STABILITY
Accuracy metrics for judging time scale algorithms p 3471 N94-30656
Precision frequency synthesizing sources with excellent time/frequency performances p 3473 N94-30671
Measurement of the frequency stability of responders in aircraft p 3261 N94-30673
Ground control system for the midcourse space experiment UTC clock p 3474 N94-30674

FREQUENCY STANDARDS
The 25th Annual Precise Time and Time Interval (PTTI) Applications and Planning Meeting
[NASA-CP-3267] p 3468 N94-30639
Time and frequency technology at NIST p 3468 N94-30641
European PTTI report p 3468 N94-30642
Report on NATO PTTI p 3469 N94-30645
Optical techniques for time and frequency transfer p 3469 N94-30647
Cesium and rubidium frequency standards status and performance on the GPS program p 3145 N94-30663
Hydrogen masers and cesium fountains at NRC p 3297 N94-30664
Providing hydrogen maser timing stability to orbiting VLBI radio telescope observations by post-measurement compensation of linked frequency standard imperfections p 3297 N94-30670
Measurement of the frequency stability of responders in aircraft p 3261 N94-30673
Russian national time scale long-term stability p 3475 N94-30679
A look into the crystal ball: The next 25 years p 3475 N94-30681
Frequency standards from government laboratories over the next 25 years p 3475 N94-30682
Frequency standards from industry over the next 25 years p 3475 N94-30683
The future of time and frequency dissemination p 3476 N94-30684

FREQUENCY SYNTHESIZERS
Communications technology for unattended sensors
[DE94-005685] p 3254 N94-30043
Precision frequency synthesizing sources with excellent time/frequency performances p 3473 N94-30671

FRESH WATER
Growth condition of an ice layer in freezing soils under applied loads. Part 1: Experiment
[AD-A275215] p 3357 N94-29070

FRESNEL LENSES
Low Earth orbit durability evaluation of protected silicone for advanced refractive photovoltaic concentrator arrays
[NASA-TM-106543] p 3172 N94-28999

FRICTION
A compact roller-gear pitch-yaw joint module: Design and control issues p 3161 N94-29629
Lock-up failure of a four-bar linkage deployment mechanism p 3163 N94-29646
Microgravity compatible drive system-rider. New technologies
[PB94-138583] p 3229 N94-29996

FRICTION FACTOR
Finite element analysis of axisymmetric deformations of thick thermoviscoplastic targets p 3320 N94-29688
Rotordynamic analysis of annular honeycomb-stator turbulent gas seals using a new friction-factor model based on flat plate tests p 3302 N94-29916
Damage analysis and mechanical response of as-received and heat-treated Nicalon/CAS-2 glass-ceramic matrix composites p 3219 N94-30259
Plane strain finite element analysis of sheet forming operations including bending effects p 3322 N94-30354

FRICTION MEASUREMENT
Atomic-scale friction measurements using friction force microscopy. Part 2: Application to magnetic media
[AD-A275202] p 3298 N94-29290
Bolt and nut evaluator
[NASA-CASE-GSC-13468-1] p 3288 N94-29538

FRONTS (METEOROLOGY)
US National Weather experiment STORM-FEST: Waves and turbulence in frontal zones
[AD-A275084] p 3369 N94-28847
Modeling studies of frontogenesis in the upper and middle troposphere p 3375 N94-30868

FROST
Toward a molecular scale understanding of frost heaving, phase 1
[AD-A275446] p 3356 N94-28882
Argon frost continuous cryopump for fusion applications
[DE94-004478] p 3230 N94-29017

FUEL CELL POWER PLANTS
Activities of Ishikawajima-Harima Heavy Industries Co. Ltd.
[PB94-137981] p 3555 N94-29798
Fundamental stack and system issues in molten carbonate fuel cell development
[DE94-005960] p 3338 N94-30048
Configuration and performance of the indirect-fired fuel cell bottomed turbine cycle
[DE94-005961] p 3338 N94-30313

FUEL CELLS
Fuel Cell Seminar, 1992: Program and abstracts
[DE94-003882] p 3336 N94-28472
Proceedings of the Joint Contractors Meeting: FE/EE Advanced Turbine Systems Conference FE Fuel Cells and Coal-Fired Heat Engines Conference
[DE93-011308] p 3336 N94-28499
Fundamental stack and system issues in molten carbonate fuel cell development
[DE94-005960] p 3338 N94-30048
Electrochemical Power Source (EPS) selection for Energetically Independent Robots (EIR): A systematic approach p 3269 N94-30312
Configuration and performance of the indirect-fired fuel cell bottomed turbine cycle
[DE94-005961] p 3338 N94-30313

FUEL COMBUSTION
Overview of space environment utilization science
[JTN-94-80581] p 3227 N94-28938
Combustion studies under microgravity p 3228 N94-28940
Fuels combustion research
[AD-A275122] p 3189 N94-29004
Fuels and Combustion Technology for Advanced Aircraft Engines
[AGARD-CP-536] p 3189 N94-29246
Combustion technology needs for advanced high pressure cycle engines p 3190 N94-29248
Studies of lean blowout in a research combustor p 3193 N94-29266
Computational and experimental results in high pressure combustions of H2/air and H2/O2/H2O p 3193 N94-29268
Ducted kerosene spray flames p 3195 N94-29276
Spray combustion experiments and numerical predictions p 3195 N94-29277
Time-resolved measurements in a three dimensional model combustor p 3196 N94-29283
Temperature and combustion analysis of combustor with acoustically controlled primary zone air-jet mixing p 3196 N94-29284
Endothermic fuels for hypersonic aviation p 3197 N94-29285
Research and development of ramjets/ramrockets. Part 1: Integral solid propellant ramrockets p 3151 N94-29294
Fuel-rich catalytic combustion of a high density fuel
[NASA-TP-3281] p 3197 N94-29356
The 1992-1993 advanced design program. Part 1: The Mars methane engine project. Part 2: The Mars oxygen processor new furnace
[NASA-CR-195513] p 3299 N94-29409
Lifted turbulent jet flames p 3198 N94-29676
Combustion and heat transfer in a high speed diesel engine operating with rape seed oil methyl ester fuel
[PB94-137536] p 3301 N94-29679
A study of low emissions gas turbine combustions
[NASA-CR-195763] p 3152 N94-29860
Corrosion performance of materials for advanced combustion systems
[DE94-006726] p 3207 N94-30057

FUEL CONSUMPTION
Alternative fuel vehicles for the state fleets: Results of the 5-year planning process
[DE94-004709] p 3224 N94-28577
Combustion and heat transfer in a high speed diesel engine operating with rape seed oil methyl ester fuel
[PB94-137536] p 3301 N94-29679
Optimal low-thrust, Earth-Moon trajectories p 3159 N94-30961

FUEL CONTROL
Chambers of turboreactors with variable geometry: A response to the matrix of pollution in cycles at high temperature, high pressure p 3194 N94-29273

FUEL FLOW
Fuel injector design for high temperature aircraft engine p 3154 N94-29263
The effect of incomplete fuel-air mixing on the lean limit and emissions characteristics of a Lean Prevaporized Premixed (LPP) combustor p 3193 N94-29265
Evaluation of the transient operation of advanced gas turbine combustors p 3154 N94-29269

FUEL INJECTION
Fuel injector design for high temperature aircraft engine p 3154 N94-29263
Design aspects in small aircraft gas turbine fuel injectors p 3154 N94-29264
Chambers of turboreactors with variable geometry: A response to the matrix of pollution in cycles at high temperature, high pressure p 3194 N94-29273
Effects of hydrogen addition on pollutant emissions in a gas turbine combustor p 3195 N94-29275
Ducted kerosene spray flames p 3195 N94-29276
A new Eulerian model for turbulent evaporating sprays in recirculating flows p 3195 N94-29279
Experimental studies on effervescent atomizers with wide spray angles p 3196 N94-29280
Investigation of the two-phase flow in a research combustor under reacting and non-reacting conditions p 3196 N94-29282
Apparatus for testing high pressure injector elements
[NASA-CASE-MFS-28773-1] p 3299 N94-29365
Numerical prediction of mixing process in a methane-fueled engine p 3304 N94-30230

FUEL PRODUCTION
Biodiesel from aquatic species
[DE94-000275] p 3225 N94-30038

FUEL PUMPS
Method of reducing hydraulic instability
[NASA-CASE-LEW-15463-1] p 3273 N94-29539

FUEL SPRAYS
Ducted kerosene spray flames p 3195 N94-29276
Spray combustion experiments and numerical predictions p 3195 N94-29277
Modeling of the phase liquidates in combustion chambers p 3195 N94-29278
A new Eulerian model for turbulent evaporating sprays in recirculating flows p 3195 N94-29279
Experimental studies on effervescent atomizers with wide spray angles p 3196 N94-29280

FUEL SYSTEMS
High temperature fuel requirements and payoffs p 3192 N94-29259
Research and development of high thermal stability fuels p 3192 N94-29261
Reduction of NO(x) by fuel-staging in gas turbine engines: A commitment to the future p 3194 N94-29272

FULLERENES
Production of fullerenes with concentrated solar flux
[DE94-000266] p 3514 N94-29801
Fullerenes as precursors for diamond film growth without hydrogen or oxygen additions
[DE94-004582] p 3519 N94-30718

FUNCTION SPACE
Isomorphisms between predicate and state transformers
[CWI-CS-R9338] p 3459 N94-30430

FUNCTIONAL ANALYSIS
Engineering of systems for application of scientific computing in industry p 3123 N94-28947

FUNCTIONAL DESIGN SPECIFICATIONS
Engineering of systems for application of scientific computing in industry p 3123 N94-28947
How to control the increase in the complexity of civil aircraft on-board systems p 3150 N94-29316

Formal specification and verification of real-time sequential control systems
[AD-A275776] p 3419 N94-29678
Development status of the Communications and Broadcasting Engineering Test Satellite (COMETS)
[JTN-94-80545] p 3169 N94-30811
Development status of COMETS missions
[JTN-94-80544] p 3170 N94-30932

FUNCTIONS (MATHEMATICS)
Remarks on the theory of semi-functors
[ML-93-08] p 3457 N94-30384
L(sub)p optimal d dimensional triangulations for piecewise linear interpolation: A new result on data dependent triangulations
[RUU-CS-93-13] p 3458 N94-30406
Comparing curried and uncurried rewriting
[CWI-CS-R9350] p 3425 N94-30415

FUNGI
Barley cell culture as a producer of heterologous protein
[PB94-132339] p 3379 N94-28408
Plant-microbe interactions: Plant hormone production by phylloplane fungi
[PB94-135563] p 3385 N94-29189

FUSELAGES
Closed loop vibrational control: Theory and applications
[AD-A275451] p 3154 N94-28632
An analytical study of unsteady rotor/fuselage interaction in hover and forward flight
p 3131 N94-29826

FUSION REACTORS
Experimental and analytical studies of high heat flux components for fusion experimental reactor
[DE94-707671] p 3504 N94-28556
Argon frost continuous cryopump for fusion applications
[DE94-004478] p 3230 N94-29017
Comparison of 14 MeV isomer production of Hf-178m1 and Hf-179m2 using Feshbach-Kerman-Koonin and exciton preequilibrium models
[DE94-002640] p 3488 N94-30039
The impact of improved physics on commercial tokamak reactors
[DE94-006103] p 3509 N94-30760
Advanced steady-state operating scenarios
[DE94-004810] p 3509 N94-30768
Intercomparison of theoretical calculations of important activation cross sections for fusion reactor technology
[DE94-002642] p 3497 N94-30825
Diode-pumped solid-state-laser drivers and the competitiveness of inertial fusion energy
[DE94-006654] p 3296 N94-30830

FUSION WELDING
Fusion welding with self-generated filler metal
[NASA-CASE-LEW-15671-1] p 3301 N94-29557

FUZZY SETS
Propagation of evidence through fuzzy rules
[AD-A275071] p 3411 N94-29180
Situational reaction and planning
[AIAA PAPER 94-1206-CP] p 3444 N94-30557
Fuzzy-algebra uncertainty analysis for abnormal-environment safety assessment
[DE94-006257] p 3462 N94-30849
ELF: Learning incomplete fuzzy rule sets for an autonomous robot
[REPT-93-043] p 3449 N94-30923

FUZZY SYSTEMS
Experimental evaluation of fuzzy logic control of a flexible arm manipulator
[AD-A275375] p 3434 N94-29013
Propagation of evidence through fuzzy rules
[AD-A275071] p 3411 N94-29180
Rocket engine system reliability analyses using probabilistic and fuzzy logic techniques
[NASA-TM-106519] p 3173 N94-29403
Application of fuzzy logic to the control of wind tunnel settling chamber temperature
[NASA-TM-109105] p 3157 N94-30200
A fuzzy logic controller for hormone administration using an implantable pump p 3397 N94-30459
Knowledge combination and data fusion with application to recognition systems p 3259 N94-30513
Fuzzy logic based robotic controller
[AIAA PAPER 94-1202-CP] p 3443 N94-30553
Situational reaction and planning
[AIAA PAPER 94-1206-CP] p 3444 N94-30557
Some methodological issues about designing autonomous agents which learn their behaviors: The ELF experience
[REPT-93-068] p 3449 N94-30939

G

GALACTIC CLUSTERS
Numerical simulations of cluster cooling flows
p 3544 N94-29725
The angular two-point correlation function of galaxies down to 25th mag p 3547 N94-30010
Optical depth effects in cluster cooling flows
p 3541 N94-30800
Substructure, dynamics and evolution in clusters of galaxies p 3548 N94-30951

GALACTIC EVOLUTION
The angular two-point correlation function of galaxies down to 25th mag p 3547 N94-30010
Energetic events in the early universe
p 3547 N94-30012
Multicolor photometry of barred spiral galaxies
p 3541 N94-30270
Substructure, dynamics and evolution in clusters of galaxies p 3548 N94-30951

GALACTIC RADIATION
Correlation analysis on optical and radio light curves for a large sample of active galactic nuclei
p 3546 N94-29992
The effects of relativistic neutrons on nonthermal models of active galactic nuclei p 3547 N94-29993
Energetic events in the early universe
p 3547 N94-30012

GALACTIC STRUCTURE
Substructure, dynamics and evolution in clusters of galaxies p 3548 N94-30951

GALAXIES
Numerical simulations of cluster cooling flows
p 3544 N94-29725

GALERKIN METHOD
Theoretical study of the incompressible Navier-Stokes equations by the least-squares method
[NASA-TM-106535] p 3272 N94-29096
Unstructured space-time finite element method of heat conduction p 3279 N94-30224
Dynamics and control of tethered satellite systems
p 3170 N94-30864

GALILEO PROJECT
Optimizing the Galileo space communication link
p 3250 N94-29663
Decoder synchronization for deep space missions
p 3250 N94-29664

GALILEO SPACECRAFT
Phasing the Very Large Array on Galileo in the presence of Jupiter's strong radio emission p 3164 N94-29621
A comparison of full-spectrum and complex-symbol combining techniques for the Galileo S-band mission
p 3250 N94-29665

GALLIUM ARSENIDES
Frequency-domain analysis of nonlinear microwave circuits
[PB94-132024] p 3261 N94-28400
Response of GaAs charge storage devices to transient ionizing radiation
[DE94-005273] p 3510 N94-28484
Tunnelling hot electron transfer amplifiers
[AD-A275529] p 3262 N94-28687
Development of ultra-low noise, high performance 3 -5 quantum well infrared photodetectors (QWIPs) for focal plane array staring image sensor systems
[AD-A275745] p 3511 N94-28734
Optoelectronic integrated circuits fabricated using atomic layer epitaxy
[AD-A275454] p 3262 N94-28805
High resistivity buffer layers by oxygen doping
[AD-A274986] p 3513 N94-29125
Quantum interference phenomena and novel switching in split gate high electron mobility transistors
p 3266 N94-29734
Micro-opto-mechanical devices and systems using epitaxial lift off p 3239 N94-29793
ECR plasma synthesis of silicon nitride films on GaAs and InSb
[DE94-005575] p 3515 N94-30006
Structural characterization of semiconductor heterostructures by atomic resolution Z-contrast imaging at 300 kV
[DE94-006561] p 3516 N94-30063
Band structure of superlattice with (delta)-like potential
[DE94-608108] p 3516 N94-30072
Ampoule failure sensor time response testing: Experiment 1
[NASA-TM-108449] p 3290 N94-30199
Photoelectronic study of GaAs epilayers and In(x)Ga(1-x)As/GaAs quantum wells
[ISBN-0-315-85756-0] p 3518 N94-30239
A combined electron beam/optical lithography process step for the fabrication of sub-half-micron-gate-length MMIC chips p 3240 N94-30445
Survey report of JSUP Space Environment Utilization Research Committee in fiscal year 1992: Metallic Materials Session
[JTN-94-80583] p 3159 N94-30794
Ion damage studies in GaAs/Al(0.6)Ga(0.4)As/GaAs heterostructures
[DE94-005384] p 3521 N94-30894

GALLIUM ISOTOPES
Recent results from SAGE
[DE94-006229] p 3551 N94-30845

GALLIUM NITRIDES
MOCVD growth of GaN, AlN and AlGaN for UV photodetector applications
[AD-A275078] p 3512 N94-28871

GALLIUM PHOSPHIDES
Preparation, characterization, and facile thermolysis of (X2GaP(SiMe3)2) (X = Br, I) and (Cl3Ga2P)n; new precursors to nanocrystalline gallium phosphide
[AD-A275019] p 3513 N94-29130

GAME THEORY
Markov chains for random urinalysis 3: Daily model and drug kinetics
[AD-A275540] p 3389 N94-28797
Set games
[MEMO-1148] p 3466 N94-30737

GAMMA RAY ASTRONOMY
A study of ultra high-energy radiation associated with Hercules X-1 p 3552 N94-29823

GAMMA RAY BURSTS
Taxonomy of gamma ray burster data using a self-organizing neural network
[DE94-006480] p 3553 N94-30248

GAMMA RAY SPECTRA
Knowledge based system for identification of gamma sources
[PB94-137742] p 3487 N94-29683
Study of activation data of metal samples from LDEF-1 and Spacelab-2
[NASA-CR-195802] p 3205 N94-29736
Taxonomy of gamma ray burster data using a self-organizing neural network
[DE94-006480] p 3553 N94-30248

GAMMA RAY SPECTROMETERS
Knowledge based system for identification of gamma sources
[PB94-137742] p 3487 N94-29683
Miniaturization in x ray and gamma ray spectroscopy
p 3236 N94-29773

GAMMA RAYS
Preliminary detector design ST862-prototype neutron detector
[DE94-004714] p 3491 N94-30695
Determination of photon fluence spectra from the NPL Mobaltron Co-60 unit
[NPL-RSA(EXT)-46] p 3492 N94-30795

GAPS
Filament to mandrel gap analysis: Resulting gap from filament winding over a cone-cylinder transition mandrel (reference NMTP no. 93838)
[DE94-004225] p 3175 N94-28528

GARMENTS
Thermal protective performance and instrumented mannequin evaluation of multi-layer garment systems
p 3381 N94-28433
A reliable and repeatable method for volume calculation of pressurized garments
[AD-A275600] p 3399 N94-28766

GAS ANALYSIS
New high temperature plasmas and sample introduction systems for analytical atomic emission and mass spectrometry
[DE94-004564] p 3503 N94-28458
Measurement of atmospheric OH by titration of near-IR fluorescent dyes p 3344 N94-28599
Properties of adsorbents for collection and analysis of trace amount of chlorofluorocarbons in air
p 3188 N94-28680
Novel mass spectrometric instrument for gaseous and particulate characterization and monitoring
[DE94-005896] p 3349 N94-30047

GAS BAGS
BAG: A code for predicting the performance of a gas bag impact attenuation system for the Pathfinder lander
[DE94-003688] p 3165 N94-28477

GAS CHROMATOGRAPHY
Properties of adsorbents for collection and analysis of trace amount of chlorofluorocarbons in air
p 3188 N94-28680

GAS COMPOSITION
Evaluating models of climate and forest vegetation
p 3353 N94-30837

GAS DENSITY
Transport properties of epitaxial lift off films
[NASA-TM-106156] p 3264 N94-29209

Experiments on the two-stage dense plasma heating on the GOL-3 device
[DE94-608356] p 3508 N94-30193
Stellar and gas dynamics of interacting ring galaxies p 3548 N94-30340

GAS DETECTORS
The development and evaluation of a tunable diode laser trace gas sensor for the measurement of N2O and CH4 fluxes using micrometeorological techniques
[ISBN-0-315-78975-1] p 3296 N94-30801

GAS DISSOCIATION
Predissociation in N2(C'4, 1 Sigma u +) and other N2 states and its importance in the atmospheres of Titan and Triton
[NASA-CR-195727] p 3549 N94-28816
Models for vibration-dissociation coupling in high-temperature gases p 3273 N94-29675

GAS DYNAMICS
Low energy ion-molecule reactions and chemiionization kinetics
[DE94-005414] p 3481 N94-28491
Dynamic response of ceramics
[AD-A275396] p 3214 N94-29203
Stellar and gas dynamics of interacting ring galaxies p 3548 N94-30340

GAS EXCHANGE
Ocean-atmospheric linkages p 3350 N94-30623

GAS EXPANSION
Tropospheric HO determination by FAGE p 3342 N94-28590

GAS FLOW
Synthesis of diamond in a hydrogen plasma jet: Simulations of XRD patterns of diamond polytypes and boundary layer on a substrate p 3522 N94-29515
A commercialized, continuous flow fiber optic sensor for trichloroethylene and haloforms p 3502 N94-30462

GAS GENERATORS
Research and development of ramjets/ramrockets. Part 1: Integral solid propellant ramrockets p 3151 N94-29294

GAS INJECTION
Study on mixing and injection of hydrogen into a supersonic flow p 3127 N94-28975
Effects of hydrogen addition on pollutant emissions in a gas turbine combustor p 3195 N94-29275
The mixing process in the quenching zone of the rich-lean-combustion concept p 3196 N94-29281

GAS IONIZATION
Reactions of metal ions and their clusters in the gas phase using laser ionization: Fourier transform mass spectrometry
[DE94-006208] p 3207 N94-30024

GAS LASERS
Reactor-pumped laser experimental results
[DE94-005247] p 3292 N94-28482

GAS LUBRICANTS
An asymptotic analysis for compressible gas lubrication of rough surfaces p 3222 N94-30922

GAS MIXTURES
Numerical prediction of mixing process in a methane-fueled engine p 3304 N94-30230
Remote pumping of solid state lasers with nuclear driven fluorescers
[DE94-004846] p 3296 N94-30614

GAS PRESSURE
Design of a variable-conductance vacuum insulation
[DE94-000270] p 3268 N94-30819

GAS STREAMS
Methane challenge of high performance molecular sieve oxygen concentrator
[AD-A275155] p 3337 N94-29033
A commercialized, continuous flow fiber optic sensor for trichloroethylene and haloforms p 3502 N94-30462
Gas stream purifier p 3354 N94-30469
The enhancement of compressible turbulent mixing via streamwise vorticity p 3280 N94-30487

GAS TRANSPORT
XCHEM-1D: A heat transfer/chemical kinetics computer program for multilayered reactive materials
[DE94-005072] p 3226 N94-30615

GAS TURBINE ENGINES
Combustion technology needs for advanced high pressure cycle engines p 3190 N94-29248
High temperature fuel requirements and payoffs p 3192 N94-29259
Design aspects in small aircraft gas turbine fuel injectors p 3154 N94-29264
Pollutant emissions from and within a model gas turbine combustor at elevated pressures and temperatures p 3194 N94-29271
Reduction of NO(x) by fuel-staging in gas turbine engines: A commitment to the future p 3194 N94-29272
The influence of air distribution on homogeneity and pollutant formation in the primary zone of a tubular combustor p 3194 N94-29274
Effects of hydrogen addition on pollutant emissions in a gas turbine combustor p 3195 N94-29275
A study of low emissions gas turbine combustions
[NASA-CR-195763] p 3152 N94-29860
Use of magnetic compression to support turbine engine rotors p 3314 N94-30484

GAS TURBINES
Advanced gas turbine systems research
[DE94-005303] p 3297 N94-28485
Proceedings of the Joint Contractors Meeting: FE/EE Advanced Turbine Systems Conference FE Fuel Cells and Coal-Fired Heat Engines Conference
[DE93-011308] p 3336 N94-28499
Impact study on the use of biomass-derived fuels in gas turbines for power generation
[DE94-000261] p 3224 N94-28502
Numerical modelling of turbine combustion chambers p 3154 N94-29254
Numerical simulation of aerothermal characteristics in gas turbine combustors with complex geometries p 3154 N94-29255
Application of CFD in combustor design technology p 3154 N94-29256
Recent CFD applications in small gas turbine combustion systems development p 3154 N94-29257
Studies of lean blowout in a research combustor p 3193 N94-29266
Ultra low NO(x) ultra lean gas turbine primary zones with liquid fuels p 3154 N94-29267
Computational and experimental results in high pressure combustions of H2/air and H2/O2/H2O p 3193 N94-29268
Evaluation of the transient operation of advanced gas turbine combustors p 3154 N94-29269
Pollutant emissions from and within a model gas turbine combustor at elevated pressures and temperatures p 3194 N94-29271
A study of low emissions gas turbine combustions
[NASA-CR-195763] p 3152 N94-29860
Configuration and performance of the indirect-fired fuel cell bottomed turbine cycle
[DE94-005961] p 3338 N94-30313

GAS-LIQUID INTERACTIONS
Liquid atomization in supersonic flows p 3276 N94-29839
Numerical simulation and prediction of implosion phenomena
[GKSS-92/E/99] p 3284 N94-30968

GAS-SOLID INTERACTIONS
The effects of molecular orientation geometry and surface anisotropy upon etching
[AD-A275154] p 3486 N94-29032
Theoretical investigation of gas-surface interactions
[NASA-CR-195755] p 3272 N94-29378

GASEOUS DIFFUSION
Ocean-atmospheric linkages p 3350 N94-30623

GASEOUS ROCKET PROPELLANTS
Aspects of model-based rocket engine condition monitoring and control
[NASA-CR-195116] p 3173 N94-29848

GASIFICATION
Measurement of volatile metal species at elevated temperatures
[PB94-132321] p 3186 N94-28407
The direct observation of alkali vapor species in biomass combustion and gasification
[DE94-000262] p 3339 N94-30606

GASOHOL (FUEL)
Fuel cycle evaluations of biomass-ethanol and reformulated gasoline
[DE94-000227] p 3226 N94-30818

GASOLINE
Fuel cycle evaluations of biomass-ethanol and reformulated gasoline
[DE94-000227] p 3226 N94-30818

GATES (CIRCUITS)
Realization of function logics by means of transmission gate
[REPT-93-061] p 3429 N94-30936

GAUGE INVARIANCE
The proper field of charges and gauge-invariant variables in electrodynamics
[DE94-606405] p 3523 N94-28751
Twistor-like type 2 superstring and bosonic string
[DE94-606339] p 3523 N94-28802
Anomalous algebraic structures in quantum field theories p 3524 N94-29911
Theory of fundamental interactions
[DE94-608126] p 3525 N94-30169
Space-time symmetries: P and CP violation
[DE94-005012] p 3526 N94-30750

GAUGE THEORY
Extended nonabelian symmetries for free fermionic model
[DE94-601554] p 3481 N94-28470
Gluon and fermion damping in hot QCD
[ISBN-0-315-85982-2] p 3490 N94-30141
Curved-space quantization, and Dirac versus reduced quantization of Poincare gauge theories
[ISBN-0-315-85990-3] p 3525 N94-30142
Glueball and meson dispersion and diffusion relations in compact U(1)(2+1) gauge theory
[ISBN-0-315-85577-0] p 3490 N94-30234
Problems in particle theory
[DE94-003665] p 3491 N94-30685
Research in elementary particle physics
[DE94-001657] p 3491 N94-30762

GEAR TEETH
Microgravity compatible drive system-rider. New technologies
[PB94-138583] p 3229 N94-29996
Generation of gear tooth surfaces by application of CNC machines
[NASA-CR-195306] p 3303 N94-30205

GEARS
Microgravity compatible drive system-rider. New technologies
[PB94-138583] p 3229 N94-29996
Generation of gear tooth surfaces by application of CNC machines
[NASA-CR-195306] p 3303 N94-30205
Surface fatigue life of high temperature gear materials
[NASA-TM-106562] p 3303 N94-30227

GELS
Low dielectric polyimide fibers
[NASA-CASE-LAR-14526-1] p 3214 N94-29359

GENERAL AVIATION AIRCRAFT
National Transportation Safety Board annual review of aircraft accident data. US general aviation, 1990
[PB94-126869] p 3135 N94-29185

GENERAL OVERVIEWS
Keynote address --- Japanese Earth Resources Satellite 1 (JERS-1) and future remote sensing projects p 3326 N94-28926
Review of sonic fatigue technology
[NASA-CR-4587] p 3479 N94-29407
The evolution of information management
[DE94-004173] p 3535 N94-30179
A bottom-up evolution of terrestrial ecosystem modeling theory, and ideas toward global vegetation modeling p 3351 N94-30628

GENES
Role of x ray-induced transcripts in adaptive responses following x rays
[DE94-005412] p 3386 N94-30895

GENETIC ALGORITHMS
Using multiple searchers to locate a randomly moving target
[AD-A275602] p 3463 N94-28768
Partial support for the Second International Symposium on Artificial Intelligence and Mathematics
[AD-A275199] p 3434 N94-29026
Investigation on application of genetic algorithms to optimal reactive power dispatch of power systems
[MATHS-REPT-A-197] p 3266 N94-29527
Genetic algorithms at UC Davis/LLNL
[DE94-006625] p 3421 N94-30117
Genetic algorithms for optimal database design
[TR-93-01] p 3535 N94-30330

GENETIC CODE
Stable RNA sequences as a tool for DNA probes and phylogenetic studies
[PB94-135423] p 3385 N94-29156

GENETIC ENGINEERING
Barley cell culture as a producer of heterologous protein
[PB94-132339] p 3379 N94-28408
Stable RNA sequences as a tool for DNA probes and phylogenetic studies
[PB94-135423] p 3385 N94-29156

GENETICS
Effects of pressure on membrane-associated receptors and effector elements
[AD-A275813] p 3384 N94-28829
Physiology and molecular-genetics of thermus and bacillus
[PB94-135571] p 3385 N94-29190

GEOCHEMISTRY
Speciation in Water and Soil: A literature review
[PB94-132388] p 3341 N94-28412
Summaries of FY 1993 geosciences research
[DE94-004710] p 3355 N94-28558
Motion and development of the Pacific Plate from the Middle Jurassic to the Late Cretaceous p 3362 N94-29939

Geochemical and fluid dynamic investigations into the nature of chemical variability in the Earth's mantle p 3367 N94-30917

GEODESY
A study of the convergence of spherical harmonic expansions of gravity using distributed point-mass Earth models p 3362 N94-29909
Towards 10(exp 9) GPS geodesy: Vector baselines, Earth rotation and reference frames [NASA-CR-195768] p 3142 N94-30243
Time and position accuracy using codeless GPS p 3144 N94-30650

GEODETIC SATELLITES
The effects of altimeter sampling characteristics: Some Geosat examples [AD-A275225] p 3357 N94-29062
New perspectives for high accuracy SLR with second generation geodesic satellites [REPT-932-440-105] p 3336 N94-30965

GEODETIC SURVEYS
Time and position accuracy using codeless GPS p 3144 N94-30650

GEOGRAPHIC INFORMATION SYSTEMS
A survey of geographical information systems applications for the Earth Science and Applications Division, Space Sciences Laboratory, Marshall Space Flight Center [NASA-TM-108438] p 3529 N94-28820
Feature mapping in a photogrammetric GIS [AD-A275418] p 3325 N94-28863
Human and institutional factors in GIS implementation by local governments p 3532 N94-29804

GEOLOGICAL SURVEYS
Evaluation of simulated JERS-1 data for geologic mapping at Drum Mountains, Utah, Silver Bell, Arizona, and Wind River, Wyoming under the GEOSAT-ERSDAC/JAPEX/JGI/RESTEC joint studies p 3326 N94-28929
Activities of the fourth wintering party at Asuka Station by the 31st Japanese Antarctic Research Expedition in 1990 p 3358 N94-29084
Proceedings of the 3rd International Symposium: JERS-1 and Remote Sensing in the Future [JTN-94-80597] p 3329 N94-29217
Application of JERS-1 data to geologic analyses p 3330 N94-29222
Application of optical sensor data to resource survey p 3330 N94-29223
Radar applications at the Canada Centre for Remote Sensing p 3331 N94-29224
Application of remote sensing techniques in petroleum exploration: The Indonesian experience p 3331 N94-29225
Rock identification using thermal infrared data p 3331 N94-29228

GEOLOGY
Updated deep-tow acoustics/geophysics system compressional velocity database [AD-A275477] p 3355 N94-28685
Glaciohydrologic and glaciohydraulic effects on runoff and sediment yield in glacierized basins [AD-A275134] p 3361 N94-29286

GEOMAGNETIC LATITUDE
The effects of magnetic storm phases on F-layer irregularities from auroral to equatorial latitudes [AD-A275203] p 3356 N94-28891

GEOMAGNETISM
Antarctic Record, volume 36, no. 1 [REPT-106-VOL-36-NO-1] p 3357 N94-29078
Estimation of geomagnetic conjugate points by using Pc5 pulsations p 3357 N94-29079
Solar-geophysical data number 592, December 1993. Part 1: Prompt reports. Data for October, November 1993 and late data [PB94-142130] p 3550 N94-29123
Observations of the geomagnetic field by Polar Patrol Balloon (PPB) experiment in Antarctica p 3359 N94-29235
ULF waves and magnetic field characteristics in the polar cusp observed at Godhavn p 3361 N94-29244
Study of generation mechanisms of magnetospheric VLF/ELF emissions based on the direction findings p 3361 N94-29245
Fast gravity, gravity partials, normalized gravity, gravity gradient torque and magnetic field: Derivation, code and data [NASA-CR-188243] p 3361 N94-29588
Quasi-adiabatic motion of energetic particles in a dipole magnetic field [DE94-607322] p 3362 N94-29935
Motion and development of the Pacific Plate from the Middle Jurassic to the Late Cretaceous p 3362 N94-29939
Experimental investigation of possible geomagnetic feedback from energetic (0.1 to 16 keV) terrestrial O(+) ions in the magnetotail current sheet [PAPER-93JA01991] p 3507 N94-30128
Electromagnetic core-mantle coupling p 3366 N94-30808

GEOMETRICAL OPTICS
Gaussian beam and physical optics iteration technique for wideband beam waveguide feed design p 3248 N94-29624

GEOMETRY
Symplectic topology of integrable Hamiltonian systems [DE94-608120] p 3467 N94-30166
The exact fitting problem in higher dimensions [RUU-CS-92-37] p 3458 N94-30377

GEOMORPHOLOGY
The Pluto fast flyby mission: Completing the reconnaissance of the solar system p 3235 N94-29768

GEOPHYSICAL SATELLITES
Outline of JERS-1 system p 3330 N94-29220
Application of remote sensing techniques in petroleum exploration: The Indonesian experience p 3331 N94-29225

GEOPHYSICS
Global atmospheric and ocean modeling on the connection machine [DE94-003930] p 3342 N94-28521
Summaries of FY 1993 geosciences research [DE94-004710] p 3355 N94-28558
Papers in meteorology and geophysics, vol. 44, no.1 [JTN-94-80585] p 3324 N94-28693
Solar-geophysical data number 591, November 1993. Part 1: Prompt reports. Data for September, October 1993 and late data [PB94-140548] p 3550 N94-29122
Solar-geophysical data number 592, December 1993. Part 1: Prompt reports. Data for October, November 1993 and late data [PB94-142130] p 3550 N94-29123
Solar-geophysical data number 592, December 1993. Part 2: Comprehensive reports. Data for June 1993 and miscellaneous [PB94-142148] p 3550 N94-29124
A study of the formation and dynamics of the Earth's plasma sheet using ion composition data [NASA-CR-195119] p 3507 N94-30126
Missile launch detection electric field perturbation experiment [DE94-004224] p 3466 N94-30586
Air-deployable geophysics package [DE94-005651] p 3335 N94-30594
Analysis of deep seismic reflection and other data from the southern Washington Cascades [DE94-005915] p 3367 N94-30883

GEOPOTENTIAL
A simulation study of high degree and order geopotential determination using satellite gravity gradiometry p 3333 N94-29762

GEOSAT SATELLITES
The effects of altimeter sampling characteristics: Some Geosat examples [AD-A275225] p 3357 N94-29062

GEOSTROPHIC WIND
Multiple weather regimes and baroclinically forced spherical resonance [DM-65] p 3376 N94-30966

GEOSYNCHRONOUS ORBITS
Electron beams at geosynchronous orbit [AD-A275471] p 3355 N94-28684
Beam scanning offset Cassegrain reflector antennas by subreflector movement [NASA-CR-191604] p 3160 N94-28836
Simulation of space-energy distributions of hot plasma on a geostationary orbit [DE94-607324] p 3365 N94-30107
Relativistic theory for picosecond time transfer in the vicinity of Earth p 3470 N94-30653
Time transfer using geostationary satellites: Implementation of a Kalman filter p 3471 N94-30657

GEOTHERMAL ENERGY UTILIZATION
Fiscal 1990 geothermal development promotion survey [DE94-732333] p 3337 N94-28628
Geothermal direct-heat utilization assistance [DE94-005831] p 3340 N94-30700

GEOTHERMAL RESOURCES
Fiscal 1991 geothermal development promotion energy [DE94-732332] p 3337 N94-28627
Fiscal 1990 geothermal development promotion survey [DE94-732333] p 3337 N94-28628

GEOTHERMAL TECHNOLOGY
Geothermal direct-heat utilization assistance [DE94-005831] p 3340 N94-30700

GERMANIUM
Silicon germanium carbon heteroepitaxial growth on silicon [AD-A275197] p 3512 N94-28889

GERMANIUM ISOTOPES
Recent results from SAGE [DE94-006229] p 3551 N94-30845

GERMINATION
Seed viability detection using computerized false-color radiographic image enhancement p 3387 N94-30461

GET AWAY SPECIALS (STS)
Retention latch mechanism for the Wake Shield Facility p 3161 N94-29635

GIMBALS
Suspension system for gimbal supported scanning payloads [NASA-CASE-MFS-28817-1] p 3287 N94-29358

GIRDERS
Study of bridge design and technology [PB94-137916] p 3121 N94-29160

GLACIAL DRIFT
Glacial landforms and late Cenozoic history of the western Soer-Rondane mountains p 3357 N94-29080
Fronts at the confluences of spring-fed streams with Joekulsa a Fjoellum: Possibly thermal bars? [MATHS-REPT-A-198] p 3333 N94-29528

GLACIERS
Glacial landforms and late Cenozoic history of the western Soer-Rondane mountains p 3357 N94-29080
Glaciohydrologic and glaciohydraulic effects on runoff and sediment yield in glacierized basins [AD-A275134] p 3361 N94-29286

GLACIOLOGY
Glacial landforms and late Cenozoic history of the western Soer-Rondane mountains p 3357 N94-29080
Glaciohydrologic and glaciohydraulic effects on runoff and sediment yield in glacierized basins [AD-A275134] p 3361 N94-29286

GLASS
Glass studies under microgravity p 3228 N94-28941
Glass-ceramic matrix composites [REPT-932-430-112] p 3179 N94-29413
Method of producing a ceramic fiber-reinforced glass-ceramic matrix composite [NASA-CASE-LEW-15264-2] p 3180 N94-29508
Interface engineering in alumina fiber/glass composites p 3182 N94-29852
Estimation of Weibull modulus from dynamic and static fatigue experiments [PB94-138641] p 3322 N94-30114
Optical studies of dynamical processes in disordered systems [DE94-006751] p 3501 N94-30252
Damage analysis and mechanical response of as-received and heat-treated Nicalon/CAS-2 glass-ceramic matrix composites p 3219 N94-30259

GLASS FIBER REINFORCED PLASTICS
Characterization of air emissions from the simulated open combustion of fiberglass materials [PB94-136231] p 3347 N94-29192
Simulation of composite material response under dynamic compressive loading [DE94-005272] p 3184 N94-30589

GLASS FIBERS
Catalytic fabric filtration for simultaneous NO(x) and particulate control [DE94-001660] p 3341 N94-28463
Development of braided rope engine seals [NASA-TM-105902] p 3298 N94-28838
Characterization of air emissions from the simulated open combustion of fiberglass materials [PB94-136231] p 3347 N94-29192
Analysis of selected materials flown on interior locations of the Long Duration Exposure Facility [NASA-CR-4586] p 3175 N94-29458
Failure strength and mechanism of composite laminates under multiaxial loading conditions p 3182 N94-29875

GLASS TRANSITION TEMPERATURE
Correlation between wet ageing, humidity absorption and properties on composite materials based on different resins family [REPT-932-600-107] p 3179 N94-29462

GLOBAL AIR POLLUTION
Survey on effects of petroleum substitution energy utilization on the global environment [DE94-732339] p 3346 N94-28630

GLOBAL POSITIONING SYSTEM
Theoretical and experimental study of a cylindrical microstrip antenna [REPT-932-440-109] p 3245 N94-29456
Use of GPS in automated air traffic control p 3137 N94-29563
GPS/GNSS for ATM p 3138 N94-29565
Combining GPS and VLBI earth-rotation data for improved universal time p 3144 N94-29614

TOPEX/POSEIDON operational orbit determination results using global positioning satellites p 3160 N94-29666
Application of extended Lagrange series to the precise determination of Global Positioning Satellite orbits [ISBN-0-315-85724-2] p 3159 N94-30237
Towards 10(exp 9) GPS geodesy: Vector baselines, Earth rotation and reference frames [NASA-CR-195768] p 3142 N94-30243
The use of low cost differential mode GPS receivers in unmanned vehicles p 3144 N94-30285
The 25th Annual Precise Time and Time Interval (PTTI) Applications and Planning Meeting [NASA-CP-3267] p 3468 N94-30639
An Operational Control Segment (OCS) update on GPS constellation status and future program directions p 3144 N94-30643
Loran-C time management p 3144 N94-30644
GPS common-view time transfer p 3144 N94-30648
Time and position accuracy using codeless GPS p 3144 N94-30650
The use of the AOA TTR-4P GPS receiver in operation at the BIPM for real-time restitution of GPS time p 3144 N94-30651
Development of an accurate transmission line fault locator using the global positioning system satellites p 3144 N94-30652
A real-time prediction of UTC p 3470 N94-30654
Tropospheric corrections to GPS measurements using locally measured meteorological parameters compared with general tropospheric corrections p 3144 N94-30655
A comparison of GPS broadcast and DMA precise ephemerides p 3145 N94-30660
Some applications of GPS timing information p 3145 N94-30661
A comparison of several GPS data reduction methods p 3145 N94-30662
Comparison of LASSO and GPS time transfers p 3145 N94-30665
Ionospheric corrections to precise time transfer using GPS p 3145 N94-30677
A review of the status and capabilities of Navstar GPS [AD-B174629] p 3143 N94-30854

GLOBAL WARMING
Spatial interpolation, network bias, and terrestrial air temperature variability p 3374 N94-30810

GLOBULAR CLUSTERS
Binary-single star scattering: An investigation of a realistic chaotic scattering system p 3543 N94-29719
Globular cluster photometry near the turnoff: Blue stragglers, relative ages, and the horizontal branch p 3538 N94-29732
Abundance patterns in red-giant CH stars p 3539 N94-29820
A study of recycled pulsars in globular clusters p 3539 N94-29825
Study of the stellar populations of the Fornax dwarf spheroidal galaxy [ISBN-0-315-85526-6] p 3541 N94-30231

GLOVES
EVA glove evaluation methodology and test protocol p 3401 N94-29729
Tactility as a function of grasp force: Effects of glove, orientation, pressure, load, and handle [NASA-TP-3474] p 3402 N94-30210

GLUONS
Asymptotic coherence of gluons and of q-bosons [DE94-005417] p 3481 N94-28492
Research on elementary particle physics. Task P: Studies in theory and phenomenology of elementary physics [DE94-004955] p 3483 N94-28566
The small-x behaviour of parton distribution functions [DE94-606414] p 3485 N94-28758
Statistical description of hot and dense clustering matter [DE94-608155] p 3490 N94-30112
Gluon and fermion damping in hot QCD [ISBN-0-315-85982-2] p 3490 N94-30141
Glueball and meson dispersion and diffusion relations in compact U(1)(2+1) gauge theory [ISBN-0-315-85577-0] p 3490 N94-30234

GLYCOLS
Analysis of infrared radiation heating process considering chemical reaction of material to be heated [DE94-744116] p 3199 N94-30267

GOGGLES
An investigation of stereopsis with AN/AVS-6 night vision goggles at varying levels of illuminance and contrast [AD-A275332] p 3400 N94-28918

GOLAY DETECTOR CELLS
Micromachined electron tunneling infrared sensors p 3238 N94-29785

GOLD
Template synthesized nanoscopic gold particles: Optical spectra and the effects of particle size and shape [AD-A275378] p 3197 N94-29312
Effects of hydrogen on the resistivity of thin Au and Cu films p 3218 N94-30225

GOLD ISOTOPES
Theory of ultra dense matter and the dynamics of high energy interactions involving nuclei [DE94-004178] p 3491 N94-30686

GOODNESS OF FIT
A moment plotting method for characterizing aircraft fatigue data population distributions [AD-A275500] p 3145 N94-28660
The modified Cramer-von mises goodness-of-fit criterion for time series [AD-A275377] p 3464 N94-29014

GOVERNMENT PROCUREMENT
DOD Electronic Commerce (EC)/Electronic Data Interchange (EDI) in contracting report [AD-A275298] p 3242 N94-28874

GOVERNMENT/INDUSTRY RELATIONS
Intelligent robotics can boost America's economic growth [AIAA PAPER 94-1301-CP] p 3439 N94-30527

GOVERNMENTS
Omnibus Budget Reconciliation Act of 1990 [PUB-LAW-101-508] p 3537 N94-28540
Human and institutional factors in GIS implementation by local governments p 3532 N94-29804

GRADIENTS
Tail lobe ion composition at energies of 0.1 to 16 keV/e: Evidence for mass-dependent density gradients [PAPER-93JA03201] p 3507 N94-30127

GRAIN BOUNDARIES
Practical superconductor development for electrical power applications [DE94-005378] p 3261 N94-28487
Electronic structure and mechanical properties of grain boundaries [AD-A275198] p 3512 N94-28890
Mechanical alloying processing with application to structural materials: ASSERT supplement [AD-A275400] p 3204 N94-29205
The effect of various metallurgical parameters on the flow and fracture behavior of polycrystalline NiAl near the brittle-to-ductile transition [NASA-TM-106534] p 3205 N94-29758
First principles pseudopotential calculations on aluminum and aluminum alloys [DE94-004890] p 3206 N94-29931
Atomic-scale structure and chemistry of interfaces by Z-contrast imaging and electron energy loss spectroscopy in the STEM [DE94-006563] p 3516 N94-30064

GRAIN SIZE
On the prediction of HAZ grain size using Monte Carlo simulation [DE94-005465] p 3511 N94-28535
Superplasticity in fine-grained ceramics [AD-A275461] p 3212 N94-28733
An analysis of the microstructure and reinforcement distribution of an extruded particle-reinforced Al 6061-10 volume percent Al2O3 metal matrix composite [AD-A275050] p 3178 N94-29166

GRAMMARS
Commutative Lambek categorial grammars [ML-93-01] p 3457 N94-30395
Federal grammars and modular compilers [REPT-93-054] p 3429 N94-30928

GRAND UNIFIED THEORY
Operator analysis for quark and lepton masses in SO(10) [DE94-005201] p 3491 N94-30709

GRANULAR MATERIALS
Granular bases for heavily loaded pavements [AD-A275171] p 3156 N94-29047

GRAPH THEORY
A characterization of graphs with interval two-step graphs [AD-A275652] p 3451 N94-28651
Stability properties of inclusive connectivity for graphs [AD-A275360] p 3452 N94-29016
Conditional dependence in probabilistic networks [RUU-CS-92-34] p 3464 N94-29450
Only few graphs have bounded treewidth [RUU-CS-92-35] p 3455 N94-30333
Two algorithms for finding rectangular duals of planar graphs [RUU-CS-92-41] p 3423 N94-30345
Bayesian belief networks and conditional independencies [RUU-CS-92-36] p 3465 N94-30376
Minimum fill-in for chordal bipartite graphs [RUU-CS-93-11] p 3458 N94-30404
Treewidth of circle graphs [RUU-CS-93-12] p 3458 N94-30405
Event structures and orthogonal term graph rewriting [CWI-CS-R9347] p 3459 N94-30412
Rectilinear decompositions with low stabbing number [RUU-CS-93-25] p 3459 N94-30425
A more compact visibility representation [RUU-CS-93-26] p 3425 N94-30426
Efficient and constructive algorithms for the pathwidth and treewidth of graphs [RUU-CS-93-27] p 3426 N94-30488
Relative length of long paths and cycles in graphs with large degree sums [MEMO-1145] p 3461 N94-30766
Pancyclicity of Hamiltonian line graphs [MEMO-1146] p 3461 N94-30767
Heuristic algorithms for static and dynamic problems of locating the center and the barycenter of a graph [REPT-93-050] p 3429 N94-30925
The structure of exponentials: Uncovering the dynamics of linear logic proofs [ML-93-10] p 3430 N94-30973

GRAPHIC ARTS
Fundamentals of printing technology [PB94-132602] p 3530 N94-29141

GRAPHICAL USER INTERFACE
Evaluation of access/navigational features of a graphical-user interface installed on a portable maintenance aid [AD-A275791] p 3136 N94-28744
HYPER-NPSNET: Embedded multimedia in a 3D virtual world [AD-A275063] p 3410 N94-29152
Basic research in computer science [AD-A275184] p 3405 N94-29181
Graphics for ABC [CWI-CS-R9255] p 3418 N94-29449
Considerations on graphical user interfaces for intelligent ATM support systems p 3139 N94-29572
The ergonomics of computer interfaces: Designing a system for human use [CWI-CS-R9258] p 3402 N94-30320
Programming aspects of Views: An open-architecture application environment [CWI-CS-R9259] p 3422 N94-30321
Graphics in the Views system [CWI-CS-R9260] p 3422 N94-30322
Maintaining presentation invariants in the Views system [CWI-CS-R9262] p 3423 N94-30324
The beauty and the beast [TR-93-03] p 3423 N94-30331
Object-based task-level control: A hierarchical control architecture for remote operation of space robots [AIAA PAPER 94-1209-CP] p 3444 N94-30560

GRAPHITE
Formation and chemical reactivity of carbon fibers prepared by defluorination of graphite fluoride [NASA-TM-106398] p 3174 N94-28747
Graphite intercalation compounds prepared from graphite fluoride [NASA-TM-106447] p 3174 N94-28924
Properties of graphite fiber reinforced copper matrix composites for space power applications [NASA-CR-191026] p 3178 N94-29208
Preparation of graphite fibers from polyimide p 3223 N94-29517
Deposition of tantalum carbide coatings on graphite by laser interactions p 3223 N94-30475

GRAPHITE-EPOXY COMPOSITES
Numerical and experimental investigation of the bending response of thin-walled composite cylinders [NASA-CR-195730] p 3317 N94-28801
Test and analysis of a stitched RFI graphite-epoxy panel with a fuel access door [NASA-TM-108992] p 3178 N94-29100
Delamination growth in composites under cyclic loads p 3183 N94-30256

GRAPHS (CHARTS)
A characterization of graphs with interval two-step graphs [AD-A275652] p 3451 N94-28651
Only few graphs have bounded treewidth [RUU-CS-92-35] p 3455 N94-30333
Minimum fill-in for chordal bipartite graphs [RUU-CS-93-11] p 3458 N94-30404
Treewidth of circle graphs [RUU-CS-93-12] p 3458 N94-30405
A more compact visibility representation [RUU-CS-93-26] p 3425 N94-30426
Efficient and constructive algorithms for the pathwidth and treewidth of graphs [RUU-CS-93-27] p 3426 N94-30488

GRASHOF NUMBER
Local heat transfer in an enclosed corotating disk with axial throughflow p 3276 N94-29849

GRATINGS (SPECTRA)
Characterization of a diffraction grating as a simulant of a selective frequency antenna for radiometric applications
[AD-A275793] p 3241 N94-28745
Deformed ellipsoidal diffraction grating blank
[NASA-CR-189334] p 3289 N94-29872
Interaction of sound with sound by novel mechanisms: Ultrasonic four-wave mixing mediated by a suspension and ultrasonic three-wave mixing at a free surface
p 3479 N94-29988

GRAVIMETRY
Analysis of crustal structure of Venus utilizing residual Line-of-Sight (LOS) gravity acceleration and surface topography data. A trial of global modeling of Venus gravity field using harmonic spline method
[NASA-CR-195799] p 3549 N94-29737

GRAVITATION
A study of the convergence of spherical harmonic expansions of gravity using distributed point-mass Earth models p 3362 N94-29909
Discrete symmetries, strong CP problem and gravity
[DE94-608091] p 3524 N94-30089
An investigation into certain geometrical and variational properties of the P(4) theory of gravitation and electromagnetism p 3526 N94-30950

GRAVITATIONAL COLLAPSE
A numerical study of gravitational collapse
p 3548 N94-30271

GRAVITATIONAL EFFECTS
Japanese Journal of Aerospace and Environmental Medicine, vol. 30, no. 3
[JTN-94-80606] p 3387 N94-28495
Some issues on Japan's space food development and relating preliminary experimental study
p 3388 N94-28498
Fluid and transportation phenomena under microgravity p 3227 N94-28939
Combustion studies under microgravity
p 3228 N94-28940
Glass studies under microgravity
p 3228 N94-28941
Fabrication of electronic materials in space
p 3228 N94-28942
The thermal consequences of giant impacts in the early solar system p 3543 N94-29698
The MERSS 5th Symposium on Space Medicine: Medical and Physiological Experiment Utilizing Parabolic Flight
[JTN-94-80588] p 3392 N94-29709
Microgravity by parabolic flight with MU-300 aircraft
p 3392 N94-29710
Space movement of Trichinella spiralis under microgravity p 3387 N94-29711
Posture control of goldfishes under microgravity
p 3387 N94-29712
Hemodynamic measurement during parabolic flight
p 3393 N94-29717
Motion sickness in parabolic flight: Possibility of electrogastrography as an objective index
p 3393 N94-29718
Japanese Journal of Aerospace and Environmental Medicine, vol. 30, no. 2
[JTN-94-80599] p 3394 N94-29863
Effect of water immersion on muscle sympathetic nerve response during static muscle contraction
p 3394 N94-29865
Physiological Anatomical Rodent Experiment (PARE) .04 feasibility test 2
[NASA-CR-195210] p 3385 N94-29968
Laser beam welding of AISI 316 stainless steel in microgravity environment: Experiments aboard a KC-135 flight
[ISBN-0-315-86095-2] p 3229 N94-30145
Directional solidification characteristics of hyper-eutectic Al-Cu alloys under varying gravity conditions
[ISBN-0-315-86108-8] p 3209 N94-30146
Theory of fundamental interactions
[DE94-608126] p 3525 N94-30169
Microencapsulation of anti-tumor, antibiotic and thrombolytic drugs in microgravity p 3397 N94-30453
Numerical simulation of a condenser in two-phase heat transport systems: A feasibility study
[AD-B173650] p 3282 N94-30855

GRAVITATIONAL FIELDS
The Klein-Fock equation, minimal surfaces and gravitational fields
[DE94-606340] p 3356 N94-28803
Fast gravity, gravity partials, normalized gravity, gravity gradient torque and magnetic field: Derivation, code and data
[NASA-CR-188243] p 3361 N94-29588
Numerical simulations of cluster cooling flows
p 3544 N94-29725
Analysis of crustal structure of Venus utilizing residual Line-of-Sight (LOS) gravity acceleration and surface topography data. A trial of global modeling of Venus gravity field using harmonic spline method
[NASA-CR-195799] p 3549 N94-29737

GRAVITATIONAL PHYSIOLOGY
Japanese Journal of Aerospace and Environmental Medicine, volume 30, no. 1
[JTN-94-80598] p 3389 N94-28850
Image technology and information analysis of bone change with gravitational exposure
p 3389 N94-28851
Arterial oxygen saturation during +Gz acceleration by short-radius centrifuge p 3389 N94-28852
Effect of chronic centrifugation on in vitro fertilization and early development in mice ova
p 3386 N94-28853
Basic understanding of vertigo p 3390 N94-28855
Relaxed tolerance following HSG, high sustained +Gz
[AD-A275204] p 3391 N94-28892
Portable Linear Sled (PLS) for biomedical research
p 3163 N94-29648
Behavior and visual control of cyprinodonts under microgravity p 3387 N94-29713
A discussion of eye-head coordinative movement under microgravity during parabolic flight p 3393 N94-29715
Analysis of various biological activity parameters during parabolic flight p 3393 N94-29716
Shortening velocity and calcium sensitivity of single fibers from hindlimb suspended muscle in rats
p 3387 N94-29866

GRAVITATIONAL WAVES
Physics, astronomy, and astrophysics: A numerical study of the black hole plus Brill wave spacetime
p 3540 N94-29990

GRAVITROPISM
Cellular polarity and interactions in plant graviperception
[NASA-CR-195261] p 3385 N94-29943

GRAVITY ANOMALIES
Analysis of crustal structure of Venus utilizing residual Line-of-Sight (LOS) gravity acceleration and surface topography data. A trial of global modeling of Venus gravity field using harmonic spline method
[NASA-CR-195799] p 3549 N94-29737

GRAVITY GRADIOMETERS
A simulation study of high degree and order geopotential determination using satellite gravity gradiometry
p 3333 N94-29762

GRAVITY WAVES
US National Weather experiment STORM-FEST: Waves and turbulence in frontal zones
[AD-A275084] p 3369 N94-28847
Theory and observations of horizontal and vertical structure of gravity wave perturbations in the middle atmosphere p 3366 N94-30802

GREASES
Regenerating using aqueous cleaners with ozone and electrolysis p 3240 N94-30468

GREEN'S FUNCTIONS
The solving of the relativistic two-body problem with a nonlinear dependence upon a spectrum parameter
[DE94-606343] p 3451 N94-28783

GREENHOUSE EFFECT
Global change research: Summaries of research in FY 1993
[DE94-003150] p 3341 N94-28473
Role of satellite observations of sea-surface temperature in the detection of global change
[PB94-138120] p 3329 N94-29107
Second Japan-U.S. Workshop on Global Change: Environmental Response Technologies for Global Change (Mitigation and Adaptation) p 3354 N94-29522
Impact of biomass burning on the atmosphere
[DE94-004333] p 3349 N94-29954
Radiative flux calculations at UV and visible wavelengths
[DE94-004278] p 3350 N94-30613
Atmosphere, ocean, and land: Critical gaps in Earth system models p 3350 N94-30617
The challenge of identifying greenhouse gas-induced climatic change p 3352 N94-30634

GRID GENERATION (MATHEMATICS)
Analytic rendering of curvilinear volume data
[DE94-004934] p 3407 N94-28506
ENGRID: A graphical interactive code for the computation of structured grids for blocked flow domains
p 3124 N94-28956
Numerical analysis of airfoil for helicopter blade at high angle of attack using Navier-Stokes code
p 3124 N94-28958
Three-dimensional external flow computations using prismatic grid p 3127 N94-28979
Application of digital control theory to adaptive grid generation p 3127 N94-28980
An elliptic-hyperbolic grid generation method and application to compressor flows p 3128 N94-28981
CFD analyses for advanced pump design
[NASA-CR-194866] p 3300 N94-29550
Time-marching aeroelastic and spatial adaptation procedures on triangular and tetrahedral meshes using an unstructured-grid Euler method p 3131 N94-29877
Computational fluid and combustion dynamics
[DE94-006596] p 3279 N94-30003
The design of a system of codes for industrial calculations of flows around aircraft and other complex aerodynamic configurations
[PB94-125598] p 3133 N94-30387
Grid adaption in computational aerodynamics
[PB94-126240] p 3134 N94-30858
Optimal size finite element meshes without obtuse and small angles
[RUU-CS-92-39] p 3462 N94-30860
Local two-phase flow simulations including interface tracking with mass transfer p 3283 N94-30954

GRINDING (MATERIAL REMOVAL)
Float polishing studies of fused silica
[AD-A275001] p 3213 N94-28886
Material properties and fracture mechanics in relation to ceramic machining
[DE94-006623] p 3221 N94-30829

GROUND BASED CONTROL
Design of Center-TRACON Automation System
p 3138 N94-29568
ARC2000: Automatic radar control
p 3141 N94-29583
A testbed for the development of ground-based control of space-based manipulators p 3309 N94-30306
Ground control system for the midcourse space experiment UTC clock p 3474 N94-30674

GROUND EFFECT (AERODYNAMICS)
Aircraft aerodynamics with deflected jets in ground effect p 3132 N94-29973

GROUND STATIONS
Status and tendency of earth observation system
p 3328 N94-29038
An Operational Control Segment (OCS) update on GPS constellation status and future program directions
p 3144 N94-30643
Two-way satellite time transfer: Overview and recent developments p 3469 N94-30646
Remote clocks linked by a fully calibrated two-way timing link p 3471 N94-30659
LASSO experiment: Intercalibrations of the LASSO ranging stations p 3297 N94-30666

GROUND SUPPORT EQUIPMENT
Autonomous Robotic Refueling System (ARRS) for rapid aircraft turnaround p 3305 N94-30279
The experimental flight management system: An air traffic management research tool
[NLR-TP-92253-U] p 3143 N94-30943

GROUND SUPPORT SYSTEMS
Status and tendency of earth observation system
p 3328 N94-29038
Design and testing of the LITE Variable Field Stop mechanism p 3161 N94-29633

GROUND TESTS
Acquisition, design modification, assembly, and ground test of NPS Hummingbird remotely piloted helicopter
[AD-A275546] p 3146 N94-28837
On ground system integration and testing: A modern approach p 3150 N94-29334
A transmission-loss monitor using current transformers
[DE94-003974] p 3267 N94-30716
TOPAZ 2 system description
[DE94-006230] p 3498 N94-30846

GROUND TRUTH
Environmental characterization for target acquisition. Analysis of thermal and visible imagery
[AD-A275414] p 3242 N94-28862

GROUND WATER
Fiscal 1991 geothermal development promotion energy
[DE94-732332] p 3337 N94-28627
Model-oriented data analysis with applications to lake and soil water simulation
[PB94-136942] p 3329 N94-29173

GROUND WIND
On the annual cycle of the tropical Pacific atmosphere and ocean p 3371 N94-29763
The viability of photovoltaics on the Martian surface
[NASA-TM-106478] p 3338 N94-30196

GROUND-AIR-GROUND COMMUNICATION
Simulation of interference between Earth stations and Earth-orbiting satellites p 3252 N94-29673

GROUP DYNAMICS
Security aspects of computer supported collaborative work
[AD-A275638] p 3528 N94-28640

GROUP THEORY
Remarks on Galois symmetry in RCFT
[PB94-138179] p 3467 N94-29147
Coherent states of SU(l,1) groups
[DE94-603654] p 3524 N94-29498
Non-commutative geometry
[PB94-139342] p 3462 N94-30889
GROWTH
Japanese Journal of Aerospace and Environmental Medicine, volume 30, no. 1
[JTN-94-80598] p 3389 N94-28850
Effect of chronic centrifugation on in vitro fertilization and early development in mice ova
p 3386 N94-28853
GUIDANCE SENSORS
Micro guidance and control technology overview
p 3144 N94-29772
Micro guidance and control synthesis: New components, architectures, and capabilities p 3144 N94-29792
An electromagnetic noncontacting sensor for thickness measurement in a dispersive medium
[AIAA PAPER 94-1200-CP] p 3443 N94-30551
GUN LAUNCHERS
The 100 kA, 5000 V solid-state opening switch for inductive energy storage
[AD-A274993] p 3263 N94-28994
GUN PROPELLANTS
Catalytic ignitor for regenerative propellant gun
[NASA-CASE-NPO-18987-1-CU] p 3225 N94-29490
GUST LOADS
WISPER and WISPERX: Final definition of two standardised fatigue loading sequences for wind turbine blades
[AD-B175835] p 3324 N94-30872
GYROSCOPES
GEC Ferranti piezo vibratory gyroscope
p 3239 N94-29790

H

H ALPHA LINE
Broad H alpha profiles of radio-loud active galactic nuclei and rapid profile variability in Seyfert and radio galaxies
p 3552 N94-29989
H II REGIONS
Physical conditions in classical H2 regions in the Magellanic Clouds p 3543 N94-29722
A multi wavelength observational study of the Cartwheel ring galaxy p 3539 N94-29821
HABITATS
Development and implementation of a scrub habitat compensation plan for Kennedy Space Center
[NASA-TM-109202] p 3347 N94-29099
HADRONS
Issues in light hadron spectroscopy
[PB94-138229] p 3486 N94-29112
A Tevatron collider beauty factory
[DE94-004879] p 3488 N94-29930
Experimental setup for study of hadron and hard photon production in nucleus-nucleus collisions
[DE94-607849] p 3489 N94-30051
Experimental setups and methods to obtain new nuclear data at intermediate and high energies
[DE94-607850] p 3489 N94-30052
Statistical description of hot and dense clustering matter
[DE94-608155] p 3490 N94-30112
Modelling of multiparticle production by dynamical semigroup method
[DE94-608132] p 3490 N94-30120
Heavy flavor production at fixed target photo- and hadroproduction
[DE94-004651] p 3491 N94-30719
Research in elementary particle physics
[DE94-001657] p 3491 N94-30762
Deexcitation processes in nuclear reactions: The study of hot hadronic matter
[DE94-003396] p 3492 N94-30836
Theoretical studies in hadronic and nuclear physics
[DE94-003524] p 3492 N94-30838
HAFNIUM CARBIDES
The organometallic chemical vapor deposition of transition metal carbides: The use of homoleptic alkyls
[DE94-005577] p 3206 N94-30007
HAFNIUM ISOTOPES
Comparison of 14 MeV isomer production of Hf-178m1 and Hf-179m2 using Feshbach-Kerman-Koonin and exciton preequilibrium models
[DE94-002640] p 3488 N94-30039
HALF LIFE
Comparison of 14 MeV isomer production of Hf-178m1 and Hf-179m2 using Feshbach-Kerman-Koonin and exciton preequilibrium models
[DE94-002640] p 3488 N94-30039
HALIDES
Halogen chemisorption on silver(111): Scanning tunneling microscopy of coadsorbed halogen atoms
[AD-A275219] p 3486 N94-29060
Preparation, characterization, and facile thermolysis of (X2GaP(SiMe3)2) (X = Br, I) and (Cl3Ga2P)n; new precursors to nanocrystalline gallium phosphide
[AD-A275019] p 3513 N94-29130
HALL EFFECT
Nonadiabatic effects in the quantum Hall regime
p 3513 N94-29530
Aggregation equilibria in arsenic doped silicon
[DE94-607269] p 3515 N94-30005
Periodic electromagnetic vacuum in the two-dimensional Yang-Mills theory with the Chern-Simons mass
[DE94-608128] p 3525 N94-30170
Effects of hydrogen on the resistivity of thin Au and Cu films p 3218 N94-30225
Problems in particle theory
[DE94-003665] p 3491 N94-30685
HALOGENATION
Group transfer and electron transfer reactions of organometallic complexes: Summary of research accomplished in 1993
[DE94-004963] p 3200 N94-30770
HALOGENS
Halogen chemisorption on silver(111): Scanning tunneling microscopy of coadsorbed halogen atoms
[AD-A275219] p 3486 N94-29060
HAMILTONIAN FUNCTIONS
On invariant measures for some infinite-dimensional dynamical systems
[DE94-606342] p 3522 N94-28609
Path integral for coherent states of the dynamical U(sub 2) group and U(sub 2/1) supergroup
[DE94-606382] p 3466 N94-28785
Some remarks about pseudo-Hamiltonian
[DE94-003273] p 3487 N94-29700
Periodic orbits of n-body type problems: The fixed period case
[DE94-608096] p 3453 N94-30091
Symplectic topology of integrable Hamiltonian systems
[DE94-608120] p 3467 N94-30166
Dissipation in Hamiltonian systems: Decaying cnoidal waves
[MEMO-1151] p 3460 N94-30738
Pancyclicity of Hamiltonian line graphs
[MEMO-1146] p 3461 N94-30767
An intrinsic Hamiltonian formulation of the dynamics of LC-circuits
[MEMO-1154] p 3462 N94-30964
HANDBOOKS
Cleanroom engineering handbook. Volume 3: Project execution in the cleanroom environment
[AD-A275860] p 3156 N94-28752
Cleanroom engineering handbook. Volume 4. Specification team practices
[AD-A275861] p 3156 N94-28753
Cleanroom engineering handbook. Volume 2: Organization and project formation in the cleanroom environment
[AD-A275809] p 3156 N94-28772
SI (Metric) handbook
[NASA-TM-109197] p 3231 N94-29376
HANDLES
Extra-vehicular activity translation tool
[NASA-CASE-MSC-21955-1] p 3300 N94-29428
HARD LANDING
Aircraft accident/incident summary report: In-flight loss of control, leading to forced landing and runway overrun, Continental Express, Inc., N24706 Embraer EMB-120 RT, Pine Bluff, Arkansas, 29 April 1993
[PB94-910404] p 3135 N94-29402
HARDENING (MATERIALS)
Higher order asymptotic crack tip fields in a power-law hardening material p 3321 N94-29829
HARDNESS
The role of plastic deformation in brittle and near-brittle cracking behavior p 3322 N94-30226
HARMONIC ANALYSIS
Frequency-domain analysis of nonlinear microwave circuits
[PB94-132024] p 3261 N94-28400
HARMONIC EXCITATION
Stochastic stability and nonlinear control in mechanical systems p 3303 N94-29966
HARMONIC FUNCTIONS
Analysis of crustal structure of Venus utilizing residual Line-of-Sight (LOS) gravity acceleration and surface topography data. A trial of global modeling of Venus gravity field using harmonic spline method
[NASA-CR-195799] p 3549 N94-29737
Iterative removal of boundary minima of harmonic potential function for mobile robot navigation
[REPT-93-059] p 3449 N94-30962
HARMONIC GENERATIONS
Study of nonlinear optical polymers and their applications in optical waveguides p 3216 N94-29807
Polynomial modeling of analog-to-digital converters
[DE94-005579] p 3406 N94-30008
Studies of interfaces and vapors with Optical Second Harmonic Generation
[DE94-006295] p 3476 N94-30841
HARMONIC OSCILLATION
Development of a method to predict transonic limit cycle oscillation characteristics of fighter aircraft (continued)
[NLR-TP-92156-U] p 3148 N94-30342
HARMONIC OSCILLATORS
Model of polylinear Bose- and Fermi-like oscillator
[DE94-606303] p 3485 N94-28718
Stability of dynamical systems in the presence of noise
[AD-A275383] p 3243 N94-29072
Non-Markovian quantum Brownian motion of a harmonic oscillator
[DE94-005922] p 3477 N94-30873
HARMONICS
Spurs in digital radio frequency memory and applications of DRFM
[AD-A275013] p 3243 N94-28897
Polynomial modeling of analog-to-digital converters
[DE94-005579] p 3406 N94-30008
Accurate finite difference methods for time-harmonic wave propagation
[NASA-CR-194887] p 3454 N94-30209
HARNESSES
MSFC inspections of installed polyimide wire
p 3166 N94-28707
HARTREE APPROXIMATION
Theoretical investigation of gas-surface interactions
[NASA-CR-195755] p 3272 N94-29378
HAZARDOUS MATERIAL DISPOSAL (IN SPACE)
Design reuse experience of space and hazardous operations robots
[AIAA PAPER 94-1220-CP] p 3445 N94-30568
HAZARDS
Systematic safety consideration in product design
[PB94-132354] p 3229 N94-28410
Medical support for British operations in the Antarctic
p 3379 N94-28421
An emergency response mobile robot for operations in combustible atmospheres
[NASA-CASE-NPO-19020-1-CU] p 3299 N94-29420
HAZE
Backscatter haze device for measurement of haze in aircraft transparencies
[AD-A275127] p 3146 N94-29042
HEAD (ANATOMY)
Japanese Journal of Aerospace and Environmental Medicine, volume 30, no. 1
[JTN-94-80598] p 3389 N94-28850
Effect of food intake on skin vasomotor responses to head-up tilt in humans p 3390 N94-28854
Basic understanding of vertigo p 3390 N94-28855
Equilibrium dysfunction in the clinical field
p 3390 N94-28858
HEAD DOWN TILT
Leg muscle volume during 30-day 6-degree head-down bed rest with isotonic and isokinetic exercise training
[NASA-TM-4580] p 3385 N94-29401
HEAD MOVEMENT
A discussion of eye-head coordinative movement under microgravity during parabolic flight p 3393 N94-29715
HEALTH
Non-aqueous cleaning solvent substitution
[DE94-005339] p 3219 N94-30245
Non-aqueous cleaning solvent substitution
p 3354 N94-30466
Electric power lines: Questions and answers on research into health effects
[DE94-005637] p 3353 N94-30757
HEARING
Minutes. Accredited Standards Committee on Noise, S12. US tag for ISO/TC 43/SC1 noise and ISO/TC 94/SC12 hearing protection
[AD-A275622] p 3477 N94-28636
Evaluation of monitoring audiometry in the United States Air Force Hearing Conservation Program
[AD-A275309] p 3391 N94-29211
HEART
Development of the NASA/Baylor VAD
p 3397 N94-30458
HEART FUNCTION
Effects of three hydration beverages on exercise performance during 60 hours of simulated desert exposure p 3383 N94-28448
Relaxed tolerance following HSG, high sustained +Gz
[AD-A275204] p 3391 N94-28892
Development of the NASA/Baylor VAD
p 3397 N94-30458

HEART RATE
Relaxed tolerance following HSG, high sustained +Gz
[AD-A275204] p 3391 N94-28892
Physiological responses during shipboard firefighting
[AD-A275104] p 3391 N94-28912
Spectral analysis of heart rate and psychological state: A review of its validity as a workload index
[AD-B179387] p 3399 N94-30969

HEAT AFFECTED ZONE
On the prediction of HAZ grain size using Monte Carlo simulation
[DE94-005465] p 3511 N94-28535

HEAT ENGINES
Proceedings of the Joint Contractors Meeting: FE/EE Advanced Turbine Systems Conference FE Fuel Cells and Coal-Fired Heat Engines Conference
[DE93-011308] p 3336 N94-28499
Annual summary of basic research thermoacoustic heat transport, 1993
[AD-A275751] p 3230 N94-28644

HEAT EXCHANGERS
Annual summary of basic research thermoacoustic heat transport, 1993
[AD-A275751] p 3230 N94-28644
Qualitative vector optimization of a condensate stabilizer process
[PB94-133246] p 3189 N94-28789
Lunar base heat pump, phase 1 draft
[NASA-CR-195211] p 3278 N94-29977
Configuration and performance of the indirect-fired fuel cell bottomed turbine cycle
[DE94-005961] p 3338 N94-30313
Centrifugal atomization of lanthanide materials for cryogenic coolers
[DE94-006035] p 3219 N94-30337

HEAT FLUX
Prediction of survival times on land in a cold climate
p 3379 N94-28423
Proceedings of Japan-US Workshop P-196 on High Heat Flux Components and Plasma Surface Interactions for Next Devices
[DE94-701164] p 3503 N94-28513
Electron beam irradiation experiments of monoblock divertor mock-up
[DE94-707497] p 3503 N94-28555
Experimental and analytical studies of high heat flux components for fusion experimental reactor
[DE94-707671] p 3504 N94-28556
Heat flux instrumentation for Hyflite thermal protection system
[NASA-CR-195731] p 3286 N94-28824
Development of buoyancy affected laminar flow in a heated pipe p 3128 N94-28988
On some general properties of parabolic conservation equations
[DE94-006101] p 3461 N94-30758
The validation of ocean surface heat fluxes in AMIP
[DE94-001539] p 3378 N94-30823

HEAT GENERATION
Mechanisms and effects of heat generation at the tips of dynamic cracks and notches in metals
p 3321 N94-29808

HEAT ISLANDS
A laboratory simulation of urban heat-island-induced circulation in a stratified environment
p 3367 N94-30921

HEAT MEASUREMENT
Differential Scanning Calorimetry (DSC) for planetary surface exploration p 3236 N94-29776

HEAT OF FORMATION
First principles pseudopotential calculations on aluminum and aluminum alloys
[DE94-004890] p 3206 N94-29931
Thermochemical data for CVD modeling from ab initio calculations
[DE94-005269] p 3222 N94-30909

HEAT PUMPS
Lunar base heat pump, phase 1 draft
[NASA-CR-195211] p 3278 N94-29977
Large heat pumps using CO2 refrigerant
[PB94-138773] p 3279 N94-29999

HEAT RESISTANT ALLOYS
Performance and durability of high emittance heat receiver surfaces for solar dynamic power systems
[NASA-TM-106549] p 3172 N94-28834
Cyclic axial-torsional deformation behavior of a cobalt-base superalloy
[NASA-TM-106372] p 3203 N94-28921
Thermodynamic analysis of chemical compatibility of several compounds with Fe-Cr-Al alloys
[NASA-CR-191166] p 3181 N94-29684
Corrosion performance of materials for advanced combustion systems
[DE94-006726] p 3207 N94-30057

HEAT SINKS
Experimental and analytical studies of high heat flux components for fusion experimental reactor
[DE94-707671] p 3504 N94-28556

HEAT STROKE
Aeromedical support for casualties in extremely hot climates p 3382 N94-28443

HEAT TOLERANCE
The potential of new textiles in improving survival prospects p 3380 N94-28430
Aeromedical support for casualties in extremely hot climates p 3382 N94-28443
Implications of climatic extremes in aircrew NBC operations p 3383 N94-28446
Effects of three hydration beverages on exercise performance during 60 hours of simulated desert exposure p 3383 N94-28448
The use of liquid and air microclimate conditioning systems to alleviate heat stress in helicopter NBC operations p 3384 N94-28453
Comparison of two cool vests on heat-strain reduction while wearing a firefighting ensemble in a hot/humid environment
[AD-A275103] p 3400 N94-28902
Effects of endurance training on heat-exercise tolerance in men wearing NBC protective clothing
[AD-A275176] p 3391 N94-29049

HEAT TRANSFER
Treatment of mild immersion hypothermia by body-to-body and forced-air warming
p 3380 N94-28428
SAFSIM theory manual: A computer program for the engineering simulation of flow systems
[DE94-005381] p 3270 N94-28488
Experimental and analytical studies of high heat flux components for fusion experimental reactor
[DE94-707671] p 3504 N94-28556
Annual summary of basic research thermoacoustic heat transport, 1993
[AD-A275751] p 3230 N94-28644
The influence of wall conductivity of film condensation with integral fin tubes
[AD-A275503] p 3523 N94-28662
Code development for hypersonic real-gas flow simulations toward the design of space vehicles, part 2
p 3125 N94-28966
Development of buoyancy affected laminar flow in a heated pipe p 3128 N94-28988
WINDOW 4.0: Documentation of calculation procedures
[DE94-004935] p 3410 N94-29019
Liquid metal MHD and heat transfer in a tokamak blanket slotted coolant channel
[DE94-004622] p 3506 N94-29510
Combustion and heat transfer in a high speed diesel engine operating with rape seed oil methyl ester fuel
[PB94-137536] p 3301 N94-29679
Local heat transfer in an enclosed corotating disk with axial throughflow p 3276 N94-29849
Particle kinetic simulation of high altitude hypervelocity flight
[NASA-CR-194535] p 3131 N94-29893
Electromagnetic effect on turbulent transport in liquid metals and electrolytes (bath)
[PB94-138450] p 3206 N94-29946
Peculiarities of heat transfer in the experiments of beam injection heating of a plasma at the GOL-3 device
[DE94-608357] p 3508 N94-30194
Prediction of fluid flow and heat transfer in internally finned tubes p 3280 N94-30228
Numerical simulation of a condenser in two-phase heat transport systems: A feasibility study
[AD-B173650] p 3282 N94-30855
Self-similar variables and the problem of nonlocal electron heat conductivity
[DE94-005826] p 3493 N94-30881

HEAT TRANSFER COEFFICIENTS
The influence of wall conductivity of film condensation with integral fin tubes
[AD-A275503] p 3523 N94-28662
Local heat transfer in an enclosed corotating disk with axial throughflow p 3276 N94-29849

HEAT TRANSMISSION
Properties of graphite fiber reinforced copper matrix composites for space power applications
[NASA-CR-191026] p 3178 N94-29208
Differential Scanning Calorimetry (DSC) for planetary surface exploration p 3236 N94-29776
Thermal conductivities, electrical resistivities, and Seebeck coefficients of YBa2Cu3O(7-x) superconductors from 80 to 300 K
[DE94-004796] p 3520 N94-30724

HEAT TREATMENT
Practical superconductor development for electrical power applications
[DE94-005378] p 3261 N94-28487
Low temperature behavior of virgin martensite
[PB94-132925] p 3204 N94-29142
An analysis of the microstructure and reinforcement distribution of an extruded particle-reinforced Al 6061-10 volume percent Al2O3 metal matrix composite
[AD-A275050] p 3178 N94-29166
Mechanical alloying processing with application to structural materials: ASSERT supplement
[AD-A275400] p 3204 N94-29205
Damage analysis and mechanical response of as-received and heat-treated Nicalon/CAS-2 glass-ceramic matrix composites p 3219 N94-30259

HEATING
Rewarming methodologies in the field
p 3382 N94-28441
Free vibration of thermally loaded panels including initial imperfections and post-buckling effects
[NASA-TM-109097] p 3479 N94-29461
Large heat pumps using CO2 refrigerant
[PB94-138773] p 3279 N94-29999
Composite hot drape forming p 3240 N94-30448

HEATING EQUIPMENT
Proceedings of the Joint Contractors Meeting: FE/EE Advanced Turbine Systems Conference FE Fuel Cells and Coal-Fired Heat Engines Conference
[DE93-011308] p 3336 N94-28499

HEAVING
Toward a molecular scale understanding of frost heaving, phase 1
[AD-A275446] p 3356 N94-28882

HEAVY IONS
The induction approach to heavy ion inertial fusion: Accelerator and target considerations
[DE94-005216] p 3494 N94-28507
Derivation of a Fokker-Planck equation for bunched beams
[DE94-004950] p 3483 N94-28565
Relativistic heavy ion research
[DE94-004701] p 3484 N94-28576
A 6MeV heavy ion beam probe for the Large Helical Device
[NIFS-272] p 3505 N94-29397
Energetic heavy-ion tracks in micron sites
p 3495 N94-30213
Kinetics of surface roughening and smoothing during ion sputtering
[DE94-006358] p 3219 N94-30263
Theory of ultra dense matter and the dynamics of high energy interactions involving nuclei
[DE94-004178] p 3491 N94-30686
Deexcitation processes in nuclear reactions: The study of hot hadronic matter
[DE94-003396] p 3492 N94-30836
Inertial confinement fusion
[DE94-005957] p 3510 N94-30875

HEAVY LIFT LAUNCH VEHICLES
Heavy-lift vehicle-launched Space Station method and apparatus
[NASA-CASE-MSC-21760-1] p 3160 N94-29369

HELICOPTER DESIGN
Procedural guide for modelling and analyzing the flight characteristics of a helicopter design using flightlab
[AD-A275077] p 3146 N94-28870
Helicopter mission and rotor performance optimization with quasi-linear inflow theory p 3147 N94-29594
Rotorcraft airframe structural optimization for vibration and dynamic stress reduction including damping treatment p 3147 N94-29878
Nonlinear multibody formulation for rotorcraft analysis
p 3149 N94-30787

HELICOPTER PERFORMANCE
Closed loop vibrational control: Theory and applications
[AD-A275451] p 3154 N94-28632
Boundary layers induced by three-dimensional vortex loops
[AD-A275678] p 3270 N94-28665
Procedural guide for modelling and analyzing the flight characteristics of a helicopter design using flightlab
[AD-A275077] p 3146 N94-28870
Helicopter mission and rotor performance optimization with quasi-linear inflow theory p 3147 N94-29594

HELICOPTER PROPELLER DRIVE
Experimental validation of finite element and boundary element methods for predicting structural vibration and radiated noise
[NASA-CR-4561] p 3301 N94-29552

HELICOPTERS
Closed loop vibrational control: Theory and applications
[AD-A275451] p 3154 N94-28632
Acquisition, design modification, assembly, and ground test of NPS Hummingbird remotely piloted helicopter
[AD-A275546] p 3146 N94-28837

Procedural guide for modelling and analyzing the flight characteristics of a helicopter design using flightlab
[AD-A275077] p 3146 N94-28870
An investigation of stereopsis with AN/AVS-6 night vision goggles at varying levels of illuminance and contrast
[AD-A275332] p 3400 N94-28918
Rooftop emergency heliports
[DOT/FAA/RD-93/2] p 3157 N94-29754
An analytical study of unsteady rotor/fuselage interaction in hover and forward flight
p 3131 N94-29826
Potential hazards of magnetic resonance imagers to emergency medical service helicopter operations
[DOT/FAA/RD-92/15] p 3135 N94-29862
Extremely Low Visibility IFR Rotorcraft Approach (ELVIRA) operational concept development. Volume 1: Executive Summary
[DOT/FAA/RD-94/1,I] p 3142 N94-30189
Computational analysis of high resolution unsteady airloads for rotor aeroacoustics
[NASA-CR-194894] p 3480 N94-30274

HELIOSPHERE
Remote sensing of inner heliospheric plasmas
[AD-A275021] p 3550 N94-29132

HELIOTRONS
A 6MeV heavy ion beam probe for the Large Helical Device
[NIFS-272] p 3505 N94-29397
The effect of magnetic field configuration on particle pinch velocity in Compact Helical System (CHS)
[NIFS-267] p 3505 N94-29398
Efficiencies of the ICRF minority heating in the CHS and LHD plasmas
[NIFS-270] p 3506 N94-29499

HELIPORTS
Rooftop emergency heliports
[DOT/FAA/RD-93/2] p 3157 N94-29754

HELIUM ATOMS
Analytic cross sections for collisions of H, H2, He and Li atoms and ions with atoms and molecules
[DE94-707686] p 3485 N94-28788

HELIUM IONS
Analytic cross sections for collisions of H, H2, He and Li atoms and ions with atoms and molecules
[DE94-707686] p 3485 N94-28788
Optical field ionization of atoms and ions using ultrashort laser pulses
[DE94-006643] p 3488 N94-29845

HELIUM ISOTOPES
Acoustic and optical investigations of superfluid (3)He
[PB94-135415] p 3477 N94-29186

HELIUM PLASMA
New high temperature plasmas and sample introduction systems for analytical atomic emission and mass spectrometry
[DE94-004564] p 3503 N94-28458

HELMHOLTZ EQUATIONS
Analysis of 3-D acoustic problems using boundary element method p 3127 N94-28974

HELMHOLTZ VORTICITY EQUATION
A spectral boundary integral equation method for the 2-D Helmholtz equation
[NASA-CR-194890] p 3454 N94-30207
Accurate finite difference methods for time-harmonic wave propagation
[NASA-CR-194887] p 3454 N94-30209

HEMODYNAMICS
Hemodynamic measurement during parabolic flight
p 3393 N94-29717

HEMOLYSIS
Rotary blood pump
[NASA-CASE-MSC-22424-1] p 3299 N94-29370

HERMES MANNED SPACEPLANE
Software engineering methods in the Hermes on-board software p 3414 N94-29326
Application of FLUIDNET-G software to the preliminary thermal and hydraulic design of Hermes spaceplane
[REPT-932-440-107] p 3168 N94-29543

HETEROGENEITY
Fundamental studies of hydrogen interaction with supported meta and bimetallic catalysts
[DE94-004887] p 3202 N94-28562
Effects and implications of fault zone heterogeneity and anisotropy on earthquake strong ground motion
p 3363 N94-29941

HETEROJUNCTIONS
Epitaxial heterojunctions of oxide semiconductors and metals on high temperature superconductors
[NASA-CASE-NPO-18483-1-CU] p 3513 N94-29501
Quantum interference phenomena and novel switching in split gate high electron mobility transistors
p 3266 N94-29734
Structural characterization of semiconductor heterostructures by atomic resolution Z-contrast imaging at 300 kV
[DE94-006561] p 3516 N94-30063
Electronic structure of Zn-based quantum wells
[DE94-608104] p 3516 N94-30068
Ion damage studies in GaAs/Al(0.6)Ga(0.4)As/GaAs heterostructures
[DE94-005384] p 3521 N94-30894

HEURISTIC METHODS
Using multiple searchers to locate a randomly moving target
[AD-A275602] p 3463 N94-28768
Weighted and unweighted maximum clique algorithms with upper bounds from fractional coloring
[AD-A275328] p 3409 N94-28917
A variable selection heuristic for solid rocket motor design p 3173 N94-29544
Knowledge combination and data fusion with application to recognition systems p 3259 N94-30513
Heuristic algorithms for static and dynamic problems of locating the center and the barycenter of a graph
[REPT-93-050] p 3429 N94-30925

HEWLETT-PACKARD COMPUTERS
'Real time' and the NLR aerodynamic facilities
[AD-B173626] p 3158 N94-30856

HEXAGONAL CELLS
Synthesis of diamond in a hydrogen plasma jet: Simulations of XRD patterns of diamond polytypes and boundary layer on a substrate p 3522 N94-29515

HIERARCHIES
Evaluating the analytic hierarchy process and recommended modifications for its use in multi-attribute decision making
[AD-A275065] p 3527 N94-29153
The covering property of the object-oriented data model: Design and implementation issues
[AD-A275048] p 3530 N94-29165
Hierarchical structures and asymmetric stochastic processes on p-adics and adeles
[PB94-138203] p 3464 N94-29178
Hierarchical Object Oriented Design (HOOD): Possibilities, limitations, and challenges
p 3413 N94-29322
A neural network with modular hierarchical learning
[NASA-CASE-NPO-19077-1-CU] p 3435 N94-29492

HIGH ALTITUDE
SHARC, a model for calculating atmospheric and infrared radiation under non-equilibrium conditions
[AD-A275207] p 3357 N94-28893
Particle kinetic simulation of high altitude hypervelocity flight
[NASA-CR-194535] p 3131 N94-29893

HIGH ALTITUDE ENVIRONMENTS
Japanese Journal of Aerospace and Environmental Medicine, vol. 30, no. 3
[JTN-94-80606] p 3387 N94-28495
Studies on water electrolyte metabolism and endocrine responses at rest and during submaximal exercise at 6,000 m simulated altitude p 3388 N94-28496
Effects of training at simulated altitude of 6,000 m on endocrine responses at rest and during exercise at the same altitude p 3388 N94-28497

HIGH ASPECT RATIO
Microactuator production via high aspect ratio, high edge acuity metal fabrication technology
p 3235 N94-29770

HIGH DISPERSION SPECTROGRAPHS
Camera artifacts in IUE spectra
[NASA-CR-189337] p 3198 N94-29857

HIGH ELECTRON MOBILITY TRANSISTORS
Quantum interference phenomena and novel switching in split gate high electron mobility transistors
p 3266 N94-29734

HIGH ENERGY ELECTRONS
Quantum-mechanical suppression of bremsstrahlung
[DE94-005223] p 3497 N94-30712

HIGH ENERGY INTERACTIONS
US/Japan cooperation in high energy physics
[DE94-005376] p 3494 N94-28486
Elementary particle interactions
[DE94-004238] p 3482 N94-28504
Research on elementary particle physics. Task P: Studies in theory and phenomenology of elementary physics
[DE94-004955] p 3483 N94-28566
Theory of ultra dense matter and the dynamics of high energy interactions involving nuclei
[DE94-004178] p 3491 N94-30686
Experiment studies of electron-positron interactions at the Stanford Linear Accelerator Center
[DE94-005877] p 3491 N94-30702
A search for rapidity gap events in p(bar p) collisions at D(0)
[DE94-004654] p 3491 N94-30722
Research in elementary particle physics
[DE94-001657] p 3491 N94-30762

HIGH LEVEL LANGUAGES
Advanced languages for systems software
[AD-A275272] p 3410 N94-29007
The covering property of the object-oriented data model: Design and implementation issues
[AD-A275048] p 3530 N94-29165
High level language-based robotic control system
[NASA-CASE-NPO-17918-2-CU] p 3435 N94-29465

HIGH POLYMERS
Molecular structure of coal studied by solvent extraction p 3187 N94-28676

HIGH POWER LASERS
Radiation transport and focusing systems for power industrial lasers
[DE94-606817] p 3293 N94-28786
High-power CW diode-laser-array-pumped solid-state lasers and efficient nonlinear optical frequency
[AD-A275394] p 3293 N94-29309
Space debris removal using a high-power ground-based laser
[DE94-006363] p 3169 N94-30264
Reactor-pumped laser facility at DOE's Nevada Test Site
[DE94-006371] p 3295 N94-30265

HIGH PRESSURE
Synthesis and neutron diffraction study of Na3WN3 and Na3MoN3
[AD-A275158] p 3203 N94-29043
Combustion technology needs for advanced high pressure cycle engines p 3190 N94-29248
Computational and experimental results in high pressure combustions of H2/air and H2/O2/H2O
p 3193 N94-29268
Pollutant emissions from and within a model gas turbine combustor at elevated pressures and temperatures
p 3194 N94-29271
Chambers of turboreactors with variable geometry: A response to the matrix of pollution in cycles at high temperature, high pressure p 3194 N94-29273
Apparatus for testing high pressure injector elements
[NASA-CASE-MFS-28773-1] p 3299 N94-29365

HIGH RESOLUTION
System requirements review for the High-Resolution Ozone Imager (HIROIG)
[AD-A275151] p 3347 N94-29023
Microfocus radioscopy, a high resolution means of inspecting composite materials
[REPT-932-430-109] p 3179 N94-29454
A simulation study of high degree and order geopotential determination using satellite gravity gradiometry
p 3333 N94-29762
Evolution of miniature detectors and focal plane arrays for infrared sensors p 3237 N94-29781
Computational analysis of high resolution unsteady airloads for rotor aeroacoustics
[NASA-CR-194894] p 3480 N94-30274

HIGH REYNOLDS NUMBER
Analysis of fluctuating static pressure measurements in a large high Reynolds number transonic cryogenic wind tunnel p 3158 N94-30788

HIGH STRENGTH
Alumina ceramic: A cost effective replacement for titanium in deep submergence pressure housings
[AD-A275640] p 3212 N94-28641
Innovative processing of composites for ultra-high temperature applications, book 2
[AD-A275598] p 3177 N94-28730
Collapsible mechanical joint
[NASA-CASE-MFS-28765-1] p 3299 N94-29367

HIGH STRENGTH STEELS
Toughening mechanisms in ultrahigh-strength steels
[AD-A275439] p 3202 N94-28867
Fatigue of carbon and low-alloy steels in LWR environments
[DE94-005116] p 3207 N94-30021

HIGH TEMPERATURE
Measurement of volatile metal species at elevated temperatures
[PB94-132321] p 3186 N94-28407
Breakdown testing of wiring insulation
p 3166 N94-28713
High temperature arc-track resistant aerospace insulation p 3167 N94-28716
A 3M high temperature dielectric film
p 3167 N94-28717
Innovative processing of composites for ultra-high temperature applications, book 2
[AD-A275598] p 3177 N94-28730
Innovative processing of composites for ultra-high temperature applications, book 3
[AD-A275599] p 3177 N94-28731

Comparison of two cool vests on heat-strain reduction while wearing a firefighting ensemble in a hot/humid environment
[AD-A275103] p 3400 N94-28902
Static fracture behavior of a ceramic matrix composite at elevated temperatures
[AD-A275363] p 3177 N94-29008
High temperature fuel requirements and payoffs p 3192 N94-29259
Fuel injector design for high temperature aircraft engine p 3154 N94-29263
Pollutant emissions from and within a model gas turbine combustor at elevated pressures and temperatures p 3194 N94-29271
Chambers of turboreactors with variable geometry: A response to the matrix of pollution in cycles at high temperature, high pressure p 3194 N94-29273
Low dielectric polyimide fibers
[NASA-CASE-LAR-14526-1] p 3214 N94-29359
Radioelectric characterization of materials at 1000 C
[REPT-932-430-104] p 3245 N94-29440
The influence of temperature on microelectronic device failure mechanisms, phase 2
[AD-A275029] p 3265 N94-29511
Particle kinetic simulation of high altitude hypervelocity flight
[NASA-CR-194535] p 3131 N94-29893
Lunar base heat pump, phase 1 draft
[NASA-CR-195211] p 3278 N94-29977
Surface fatigue life of high temperature gear materials
[NASA-TM-106562] p 3303 N94-30227
Studies of high temperature ternary phases in mixed-metal-rich early transition metal sulfide and phosphide systems
[DE94-006034] p 3209 N94-30336

HIGH TEMPERATURE ENVIRONMENTS
The Support of Air Operations under Extreme Hot and Cold Weather Conditions
[AGARD-CP-540] p 3379 N94-28420
The concept of Royal Navy air operations under extreme environmental conditions p 3379 N94-28424
Experimental evaluation of two systems of individual air-conditioning p 3384 N94-28450
Recent Canadian advances in active thermal protection p 3384 N94-28451
Innovative processing of composites for ultra-high temperature applications, book 1
[AD-A275597] p 3176 N94-28729
Innovative processing of composites for ultra-high temperature applications, book 2
[AD-A275598] p 3177 N94-28730
Innovative processing of composites for ultra-high temperature applications, book 3
[AD-A275599] p 3177 N94-28731
Measurement and modelling of bolted joint stress relaxation in plastics
[PB94-124849] p 3318 N94-28841

HIGH TEMPERATURE GAS COOLED REACTORS
Overview of shielding analyses for the MHTGR from 1986 to 1991
[DE94-002448] p 3495 N94-29924

HIGH TEMPERATURE GASES
Models for vibration-dissociation coupling in high-temperature gases p 3273 N94-29675
Performance of CVD and CVR coated carbon-carbon in high temperature hydrogen
[DE94-005451] p 3487 N94-29841

HIGH TEMPERATURE LUBRICANTS
Matrix isolation studies of the interactions of BF3 with water and substituted diethyl ethers. Chemical ionization mass spectrometric determination of the proton affinity of (CF3CH2)2O
[NASA-TM-106422] p 3189 N94-28832

HIGH TEMPERATURE PLASMAS
New high temperature plasmas and sample introduction systems for analytical atomic emission and mass spectrometry
[DE94-004564] p 3503 N94-28458
Multichannel x ray spectral measurement of hot plasma evolution in nitrogen-puff Z-pinch
[PH-24] p 3505 N94-29076
X ray emission scaling and energy balance of small gas-puff Z-pinch p 3505 N94-29077
Transient internal probe
[AD-A275054] p 3505 N94-29134
Coronal temperatures of unusually active K-dwarf binary systems
[NASA-CR-189335] p 3545 N94-29861
Simulation of space-energy distributions of hot plasma on a geostationary orbit
[DE94-607324] p 3365 N94-30107
Magnetic field generation by circularly polarized laser light and inertial plasma confinement in a miniature magnetic bottle induced by circularly polarized laser light
[DE94-608353] p 3508 N94-30192
Experiments on the two-stage dense plasma heating on the GOL-3 device
[DE94-608356] p 3508 N94-30193
Molecular dynamics simulations of dense plasmas
[DE94-005082] p 3509 N94-30752
The investigation of electron-ion radiative and dielectronic recombination in high-temperature plasmas
[DE94-005150] p 3509 N94-30755

HIGH TEMPERATURE SUPERCONDUCTORS
Current leads and magnetic bearings
[DE94-004607] p 3297 N94-28461
Practical superconductor development for electrical power applications
[DE94-005378] p 3261 N94-28487
Energy gap structure of layered superconductors
[DE94-005132] p 3511 N94-28570
Crystal structure of La(2-x)Ba(x)CuO4
[DE94-707688] p 3511 N94-28750
High Tc superconducting bolometric and nonbolometric infrared (IR) detectors
[NASA-CR-195728] p 3262 N94-28846
Nonaqueous slip casting of YBa2Cu3O(7-x) superconductive ceramics
[NASA-CR-4575] p 3512 N94-29101
Epitaxial heterojunctions of oxide semiconductors and metals on high temperature superconductors
[NASA-CASE-NPO-18483-1-CU] p 3513 N94-29501
New evidence for flux cutting in type II superconductors
[ISBN-0-315-85830-3] p 3515 N94-30032
The bases for the development of high-temperature integrated SQUID-systems
[DE94-607901] p 3267 N94-30073
The bases for the development of high-temperature integrated SQUID-systems
[DE94-608462] p 3517 N94-30082
Butterfly and scaling law in YBa2Cu4O8
[DE94-006037] p 3519 N94-30338
Research on the atomic layer-by-layer growth of high-temperature superconductor thin films at the Institute of Scientific and Industrial Research, Japan
[DE94-003739] p 3519 N94-30611
Investigation of the phase equilibria and phase transformations associated with the Bi2Sr2CaCu2O(y) superconductor
[DE94-004889] p 3519 N94-30691
Normal state resistivity of MBa2Cu3O(7-x) ceramics
[DE94-608456] p 3220 N94-30745
Scaling in heavy-fermion systems
[DE94-005002] p 3492 N94-30775
Intra- versus interlayer pairing in the copper oxide superconductors: Response to a magnetic field
[DE94-005475] p 3521 N94-30898
AC losses for the self field of an AC transport current with a DC transport current offset in high T(c) superconducting magnet coils for MagLev application
[DE94-005187] p 3268 N94-30907

HIGH TEMPERATURE TESTS
Measurement of volatile metal species at elevated temperatures
[PB94-132321] p 3186 N94-28407
Fatigue behavior of a cross-ply ceramic matrix composite at elevated temperatures under tension-tension loading
[AD-A275466] p 3176 N94-28673
Static fracture behavior of a ceramic matrix composite at elevated temperatures
[AD-A275363] p 3177 N94-29008
A review of mechanical test methods for ceramic matrix composites
[PB94-147576] p 3184 N94-30524

HIGH VOLTAGES
Non-isolated 30 kW class arcjet PCU
[NASA-CR-189148] p 3173 N94-29444

HILSCH TUBES
Large eddy simulation of subsonic mixing layers p 3276 N94-29851

HISS
Study of generation mechanisms of magnetospheric VLF/ELF emissions based on the direction findings p 3361 N94-29245

HISTORIES
Perspectives of earth observing techniques: Expectation of earth observation in space development history p 3328 N94-29039
Fishermans Bend: A centre of Australian aviation
[AD-A274981] p 3121 N94-29090
Energy and Technology Review
[DE94-004472] p 3338 N94-29955
The evolution of information management
[DE94-004173] p 3535 N94-30179

HMX
Insensitive energetic materials: The importance of physical properties and molecular structure
[AD-A275393] p 3225 N94-29308

HODOGRAPHS
Transonic expanding flow through axially symmetric orifices p 3128 N94-28985

HOLES (ELECTRON DEFICIENCIES)
Nonlinear optics response of semiconductor quantum wells under high magnetic fields
[DE94-003244] p 3520 N94-30835

HOLES (MECHANICS)
Test and analysis of a stitched RFI graphite-epoxy panel with a fuel access door
[NASA-TM-108992] p 3178 N94-29100

HOLLOW CATHODES
Vacuum vapor deposition
[NASA-CASE-MFS-28652-1] p 3215 N94-29446

HOLOGRAMMETRY
Reconfigurable optical interconnections via dynamic computer-generated holograms
[NASA-CASE-NPO-19039-1-CU] p 3499 N94-29491

HOLOGRAPHIC INTERFEROMETRY
Holographic interferometry: A user's guide
[DE94-003136] p 3286 N94-28466

HOLOGRAPHY
Holographic interferometry: A user's guide
[DE94-003136] p 3286 N94-28466
Innovative optoelectronic materials and structures using OMVPE
[AD-A275811] p 3511 N94-28773
Gordon research conference on optical signal processing and holography
[AD-A275092] p 3499 N94-28848
Reconfigurable optical interconnections via dynamic computer-generated holograms
[NASA-CASE-NPO-19039-1-CU] p 3499 N94-29491
Vacuum chamber and adaptors for shearography and holography
[NASA-CR-192467] p 3157 N94-29956
Photoelectron diffraction and holography: Some new directions
[DE94-006297] p 3289 N94-30027
Enhanced coherence x ray laser experiments and simulations
[DE94-005367] p 3295 N94-30060
Time-resolved holography for the microscopic study of crack-tip motion in dynamic fracture p 3290 N94-30254

HOMING DEVICES
Dual-use applications of infrared sensitive materials
[AD-A275140] p 3499 N94-29694

HOMOGENEITY
Microfocus radioscopy, a high resolution means of inspecting composite materials
[REPT-932-430-109] p 3179 N94-29454

HOMOGENEOUS TURBULENCE
Spherical model for turbulence p 3274 N94-29730

HOMOMORPHISMS
Homomorphism preserving algebraic specifications require hidden sorts
[CWI-CS-R9344] p 3459 N94-30436

HONEYCOMB STRUCTURES
Composite flexible blanket insulation
[NASA-CASE-ARC-11955-1-CU] p 3180 N94-29509
Rotordynamic analysis of annular honeycomb-stator turbulent gas seals using a new friction-factor model based on flat plate tests p 3302 N94-29916

HORIZON
The transient period of a cyclic process: An horizon theorem
[MEMO-1149] p 3427 N94-30585

HORIZONTAL FLIGHT
An analytical study of unsteady rotor/fuselage interaction in hover and forward flight p 3131 N94-29826

HORMONES
Plant-microbe interactions: Plant hormone production by phylloplane fungi
[PB94-135563] p 3385 N94-29189
A fuzzy logic controller for hormone administration using an implantable pump p 3397 N94-30459

HORN ANTENNAS
An absolute measurement of the cosmic background radiation temperature at 1.4 GHz p 3553 N94-30351

HORSESHOE VORTICES
A flow visualization study of acoustically enhanced hairpin vortices
[AD-A275467] p 3271 N94-28809

HOSPITALS
Clinical investigation program
[AD-A275025] p 3391 N94-29116
An update on Lab Rover: A hospital material transporter
[AIAA PAPER 94-1228-CP] p 3447 N94-30577

HOT ELECTRONS
Tunnelling hot electron transfer amplifiers
[AD-A275529] p 3262 N94-28687

Conceptual study of moderately coupled plasmas and experimental comparison of laboratory x ray sources
[DE94-005828] p 3506 N94-30045
Experiments on the two-stage dense plasma heating on the GOL-3 device
[DE94-608356] p 3508 N94-30193
Optical depth effects in cluster cooling flows p 3541 N94-30800

HOT ISOSTATIC PRESSING
Effect of non-metallic inclusions on the machinability of steel
[PB93-230233] p 3204 N94-29387

HOT WORKING
Numerical simulation of industrial workpiece superplastic forming
[REPT-932-600-102] p 3418 N94-29479
Composite hot drape forming p 3240 N94-30448
A comparison of the evolution of cold and hot deformation microstructures and textures in fcc metals
[DE94-005103] p 3210 N94-30777

HOT-WIRE FLOWMETERS
Correction of X hot-wire measurements for gradients normal to the plane of the wires
[PB94-125473] p 3157 N94-30399

HOUSINGS
Alumina ceramic: A cost effective replacement for titanium in deep submergence pressure housings
[AD-A275640] p 3212 N94-28641
Rotary blood pump
[NASA-CASE-MSC-22424-1] p 3299 N94-29370

HOVERING
An analytical study of unsteady rotor/fuselage interaction in hover and forward flight p 3131 N94-29826

HTPB PROPELLANTS
Correlation of cookoff behavior of rocket propellants with thermomechanical and thermochemical properties
[AD-A274983] p 3224 N94-29092

HUMAN BEINGS
A discussion of eye-head coordinative movement under microgravity during parabolic flight p 3393 N94-29715

HUMAN BODY
Effects of endurance training on heat-exercise tolerance in men wearing NBC protective clothing
[AD-A275176] p 3391 N94-29049

HUMAN FACTORS ENGINEERING
Test of a new protection suit in a climatic chamber p 3384 N94-28452
Key cognitive issues in the design of electronic displays of instrument approach procedure charts
[AD-A275647] p 3399 N94-28649
Designing for performance: A cognitive systems engineering approach to modifying an AWACS human computer interface
[AD-A275187] p 3399 N94-28861
Relaxed tolerance following HSG, high sustained +Gz
[AD-A275204] p 3391 N94-28892
The management issues of implementing telecommuting: A case study
[AD-A275267] p 3527 N94-28905
Procedures and metrics for anti-G suit evaluations
[AD-A275349] p 3400 N94-28997
Information presentation for expert systems in future fighter aircraft
[AD-A275126] p 3149 N94-29005
Stress and ergonomic design and evaluation of person-machine systems
[AD-A275156] p 3400 N94-29034
A comparison of three aircraft attitude display symbology structures
[AD-A275172] p 3150 N94-29048
The 1993 Federal Aviation Administration Aviation System Capital Investment Plan p 3136 N94-29445
Aircraft evacuations: The effect of a cabin water spray system upon evacuation rates and behaviour
[CAA-PAPER-93008] p 3148 N94-29887
The use of task network simulation in workload prediction
[DCIEM-92-32] p 3402 N94-30132
Tactility as a function of grasp force: Effects of glove, orientation, pressure, load, and handle
[NASA-TP-3474] p 3402 N94-30210
The ergonomics of computer interfaces: Designing a system for human use
[CWI-CS-R9258] p 3402 N94-30320
Graphics in the Views system
[CWI-CS-R9260] p 3422 N94-30322
Maintaining presentation invariants in the Views system
[CWI-CS-R9262] p 3423 N94-30324
The Views application environment
[CWI-CS-R9257] p 3423 N94-30341

HUMAN PATHOLOGY
Aeropathological diagnosis of lethal hypothermia p 3382 N94-28440

HUMAN PERFORMANCE
Deterioration of manual performance in cold and windy climates p 3381 N94-28434
Toward a model of expert knowledge structure and their role in cognitive task performance
[AD-A275641] p 3529 N94-28645
Effects of workload on communication processes in decision making teams
[AD-A275894] p 3527 N94-28796
Disturbance of equilibrium on JAL flight crew p 3390 N94-28856
Equilibrium dysfunction in the clinical field p 3390 N94-28858
Cognitive approach to specifications on air traffic controllers' decision assistance systems p 3139 N94-29571
Scanning and monitoring performance: Effects of the reinforcement values of the events being monitored
[DOT/FAA/AM-94/8] p 3398 N94-29918
Dexterity enhancement in microsurgery using telemicro-robotics
[AIAA PAPER 94-1230-CP] p 3447 N94-30579
Maintaining vigilance on a simulated ATC monitoring task across repeated sessions
[DOT/FAA/AM-94/6] p 3143 N94-30933

HUMAN REACTIONS
Human pilot response during single- and multi-axis tracking tasks
[AD-A275080] p 3398 N94-28887
The MSRC ab initio methods benchmark suite: A measurement of hardware and software performance in the area of electronic structure methods
[DE94-006428] p 3514 N94-30001

HUMAN RESOURCES
Development centres: Assessing or developing people
[PB94-138070] p 3536 N94-29144

HUMAN TOLERANCES
Medical support for British operations in the Antarctic p 3379 N94-28421
Biochemical enhancement of cold tolerance p 3380 N94-28427
Crashworthiness analysis of commuter aircraft seats
[AD-A275889] p 3135 N94-28799

HUMAN WASTES
Electrochemical incineration of wastes
[NASA-CR-195262] p 3198 N94-29938

HUMAN-COMPUTER INTERFACE
Work-oriented development of interactive software tools: Understanding the work of software maintainers and making an interactive software tool for them
[PB94-132032] p 3406 N94-28401
Evaluation of access/navigational features of a graphical-user interface installed on a portable maintenance aid
[AD-A275791] p 3136 N94-28744
Designing for performance: A cognitive systems engineering approach to modifying an AWACS human computer interface
[AD-A275187] p 3399 N94-28861
A method of user interface for NWT p 3129 N94-28993
Information presentation for expert systems in future fighter aircraft
[AD-A275126] p 3149 N94-29005
Reference model for project support environments, version 2.0
[AD-A275191] p 3410 N94-29068
Advances in development capabilities for intelligent air traffic management systems p 3137 N94-29559
Intelligent systems for air space control and management p 3137 N94-29560
Use of advanced technologies in ATM (air traffic management) domain p 3137 N94-29561
ACCS Surveillance Exploratory Prototype (ASEP) p 3138 N94-29566
Decision Making Aids (DMA) in on-line ATC systems p 3139 N94-29570
Considerations on graphical user interfaces for intelligent ATM support systems p 3139 N94-29572
Aspects of the operator interface for military robotic applications in unstructured environments p 3309 N94-30304
The ergonomics of computer interfaces: Designing a system for human use
[CWI-CS-R9258] p 3402 N94-30320
Programming aspects of Views: An open-architecture application environment
[CWI-CS-R9259] p 3422 N94-30321
Graphics in the Views system
[CWI-CS-R9260] p 3422 N94-30322

HUMIDITY
Correlation between wet ageing, humidity absorption and properties on composite materials based on different resins family
[REPT-932-600-107] p 3179 N94-29462
Atmospheric turbulence within and above a coniferous forest
[ISBN-0-315-75468-0] p 3375 N94-30870

HUMIDITY MEASUREMENT
Micro-sensors for in-situ meteorological measurements p 3236 N94-29777

HURRICANES
On the origins of low-level tornadic circulations within the remnants of hurricane Andrews
[AD-A275373] p 3369 N94-29011

HYBRID COMPOSITES
Preliminary evaluation of hybrid titanium composite laminates
[NASA-TM-109095] p 3180 N94-29472

HYDRATION
Nutrition and hydration status of aircrew members consuming an improved survival ration during a simulated survival scenario p 3380 N94-28429
Effects of three hydration beverages on exercise performance during 60 hours of simulated desert exposure p 3383 N94-28448

HYDRAULIC ANALOGIES
Glaciohydrologic and glaciohydraulic effects on runoff and sediment yield in glacierized basins
[AD-A275134] p 3361 N94-29286

HYDRAULIC EQUIPMENT
Application of FLUIDNET-G software to the preliminary thermal and hydraulic design of Hermes spaceplane
[REPT-932-440-107] p 3168 N94-29543
Miniature linear-to-rotary motion actuator p 3163 N94-29647

HYDRAULIC FLUIDS
Finite element method for numerical simulation of turbulent flows. The N3S code p 3233 N94-29612

HYDRAULIC JETS
The instantaneous concentration field in the self-similar region of a high Schmidt number round jet p 3278 N94-29976

HYDROCARBON COMBUSTION
Prediction of prompt NO(x) in hydrocarbon air flames p 3190 N94-29250
Simulation of pollutant formation in turbulent combustors using an extended coherent flame model p 3190 N94-29251
Numerical prediction of turbulent sooting diffusion flames p 3191 N94-29253
Time-resolved measurements in a three dimensional model combustor p 3196 N94-29283
Fuel-rich catalytic combustion of a high density fuel
[NASA-TP-3281] p 3197 N94-29356
Measurements and predictions of the combustion characteristics of enclosed swirl-stabilized propane flames
[IECE-CFE-TR-001] p 3198 N94-30017

HYDROCARBON FUEL PRODUCTION
Researches on bioconversion of coal into liquid product p 3187 N94-28677
Structural changes during carbonization and oxidation of coal p 3187 N94-28678

HYDROCARBON FUELS
Fuel-rich catalytic combustion of a high density fuel
[NASA-TP-3281] p 3197 N94-29356
Combustion and heat transfer in a high speed diesel engine operating with rape seed oil methyl ester fuel
[PB94-137536] p 3301 N94-29679

HYDROCARBONS
X ray crystal structures of ((Me3SiCH2)2InCl)2 and ((Me3SiCH2)InCl2)
[AD-A275074] p 3513 N94-29155
Fullerenes as precursors for diamond film growth without hydrogen or oxygen additions
[DE94-004582] p 3519 N94-30718

HYDROCYANIC ACID
Toxicity of carbon monoxide-hydrogen cyanide gas mixtures: Exposure concentration, time-to-incapacitation, carboxyhemoglobin, and blood cyanide parameters
[DOT/FAA/AM-94/7] p 3395 N94-29919

HYDRODYNAMICS
Analysis of spark-induced bubble experiments using CALE
[DE94-003667] p 3270 N94-28476
Hydrodynamics of convection under winter polar leads
[AD-A275182] p 3369 N94-29067
Interaction of multiple spark-generated bubbles in a compressible liquid
[AD-A275037] p 3272 N94-29149
Bulletin of National Research Institute of Fisheries Engineering, No. 13
[JTN-94-80596] p 3233 N94-29701
Numerical simulations of cluster cooling flows p 3544 N94-29725
Hydrodynamic stability analysis of swirling jets p 3278 N94-29974
Two-phase power-law modeling of pipe flows displaying shear-thinning phenomena
[DE94-005115] p 3279 N94-30020

Enhanced coherence x ray laser experiments and simulations
[DE94-005367] p 3295 N94-30060

HYDROGEN
Equation of state of stellar plasmas
[DE94-004186] p 3542 N94-28526
Fundamental studies of hydrogen interaction with supported meta and bimetallic catalysts
[DE94-004887] p 3202 N94-28562
Analytic cross sections for collisions of H, H2, He and Li atoms and ions with atoms and molecules
[DE94-707686] p 3485 N94-28788
Study on mixing and injection of hydrogen into a supersonic flow p 3127 N94-28975
Fuels combustion research
[AD-A275122] p 3189 N94-29004
Effects of hydrogen addition on pollutant emissions in a gas turbine combustor p 3195 N94-29275
The far-infrared absorption spectrum of low temperature hydrogen gas
[ISBN-0-315-85432-4] p 3199 N94-30137
Effects of hydrogen on the resistivity of thin Au and Cu films p 3218 N94-30225
Fullerenes as precursors for diamond film growth without hydrogen or oxygen additions
[DE94-004582] p 3519 N94-30718

HYDROGEN ATOMS
Analytic cross sections for collisions of H, H2, He and Li atoms and ions with atoms and molecules
[DE94-707686] p 3485 N94-28788
Computer simulation of the interaction of fast hydrogen atoms with a molybdenum containing sorbed hydrogen
[DE94-608419] p 3209 N94-30253

HYDROGEN BONDS
Structure of ordinary ice I(sub h). Part 1: Ideal structure of ice
[AD-A275149] p 3486 N94-29021

HYDROGEN COMPOUNDS
Local Measurement of Tropospheric HO(x)
[NASA-CP-3245] p 3342 N94-28587
The radical amplifier p 3345 N94-28604

HYDROGEN EMBRITTLEMENT
Performance of CVD and CVR coated carbon-carbon in high temperature hydrogen
[DE94-005451] p 3487 N94-29841

HYDROGEN FUELS
Computational and experimental results in high pressure combustions of H2/air and H2/O2/H2O p 3193 N94-29268
Research and development of ramjets/ramrockets. Part 3: The study of gaseous hydrogen ram combustors p 3152 N94-29298

HYDROGEN IONS
Variational calculation of the eigenpotential for H(sup -)-system
[DE94-606269] p 3407 N94-28622
Analytic cross sections for collisions of H, H2, He and Li atoms and ions with atoms and molecules
[DE94-707686] p 3485 N94-28788
A future, intense source of negative hydrogen ions p 3494 N94-30485
Dissociative recombination of H3(+)
[DE94-005356] p 3493 N94-30891

HYDROGEN MASERS
Accuracy metrics for judging time scale algorithms p 3471 N94-30656
Hydrogen masers and cesium fountains at NRC p 3297 N94-30664
A comparative study of clock rate and drift estimation p 3473 N94-30669
Hydrogen maser clocks in space for solid-Earth research and time-transfer applications: Experiment overview and evaluation of Russian miniature sapphire loaded cavity p 3474 N94-30676

HYDROGEN OXYGEN ENGINES
Calculation of propulsive nozzle flowfields in multidiffusing chemically reacting environments
[NASA-TM-106532] p 3271 N94-28835

HYDROGEN PLASMA
Molecular dynamics simulations of dense plasmas
[DE94-005082] p 3509 N94-30752

HYDROGEN PRODUCTION
Analysis and modeling of environmental and economic impacts of the solar hydrogen energy system p 3348 N94-29901
Biological conversion of synthesis gas
[DE94-005815] p 3340 N94-30879

HYDROGEN SULFIDE
Biological conversion of synthesis gas
[DE94-005815] p 3340 N94-30879

HYDROGEN-BASED ENERGY
Analysis and modeling of environmental and economic impacts of the solar hydrogen energy system p 3348 N94-29901

HYDROGENATION
Pull-test adhesion measurements of diamondlike carbon films on silicon carbide, silicon nitride, aluminum oxide, and zirconium oxide
[DE94-005469] p 3211 N94-28536
Preparation and structure of amorphous hydrogenated carbon film deposited with RF plasma CVD p 3223 N94-29518
Group transfer and electron transfer reactions of organometallic complexes: Summary of research accomplished in 1993
[DE94-004963] p 3200 N94-30770

HYDROGRAPHY
Objective analysis of a coastal ocean eddy using satellite AVHRR and in situ hydrographic data
[AD-A275715] p 3376 N94-28642
Considerations in the modelling of seafloor acoustic backscatter
[AD-A275404] p 3478 N94-29206
Tidal atlas software development
[AD-A275251] p 3377 N94-29432

HYDROLOGICAL CYCLE
Land surface interaction p 3350 N94-30621
Models of atmosphere-ecosystem-hydrology interactions: Approaches and testing p 3353 N94-30636

HYDROLOGY
Glaciohydrologic and glaciohydraulic effects on runoff and sediment yield in glacierized basins
[AD-A275134] p 3361 N94-29286
Atmosphere, ocean, and land: Critical gaps in Earth system models p 3350 N94-30617
Models of atmosphere-ecosystem-hydrology interactions: Approaches and testing p 3353 N94-30636

HYDROLOGY MODELS
Comprehensive system models: Strategies for evaluation p 3353 N94-30638

HYDROSTATIC PRESSURE
Effects of pressure on membrane-associated receptors and effector elements
[AD-A275813] p 3384 N94-28829
II-VI wide band gap semiconductors under hydrostatic pressure
[DE94-608106] p 3516 N94-30070

HYDROSTATICS
Four-dimensional data assimilation using the adjoint method p 3455 N94-30353
Parameter identification of the rotordynamic coefficients of high-Reynolds-number hydrostatic bearings p 3311 N94-30792

HYDROTHERMAL SYSTEMS
Fiscal 1991 geothermal development promotion energy
[DE94-732332] p 3337 N94-28627

HYDROXIDES
Photochemistry in constrained spaces: Zeolites and layered double metal hydroxides
[DE94-004958] p 3200 N94-30769

HYDROXYL COMPOUNDS
The radiocarbon hydroxyl technique p 3344 N94-28600

HYDROXYL EMISSION
Mesopause winds and OH intensities at Mid-Latitudes-Fabry-Perot interferometer observations of the OH emission at 8430 A from bear lake observatory
[AD-A275246] p 3361 N94-29430

HYDROXYL RADICALS
Local Measurement of Tropospheric HO(x)
[NASA-CP-3245] p 3342 N94-28587
Two-Photon/Laser-Induced Fluorescence (TP/LIF) sensor p 3342 N94-28588
In situ detection of tropospheric OH and HO2 by laser-induced fluorescence in a detection chamber at low pressure p 3342 N94-28589
Tropospheric HO determination by FAGE p 3342 N94-28590
Detection of tropospheric OH and HO2 by laser-induced fluorescence at low pressure using the 308nm excitation of OH p 3343 N94-28591
Harvard ER-2 OH laser-induced fluorescence instrument p 3343 N94-28592
JPL Fourier transform ultraviolet spectrometer p 3343 N94-28593
Absolute determination of local tropospheric OH concentrations p 3343 N94-28594
UV laser long-path absorption spectroscopy p 3343 N94-28595
Measurement of tropospheric OH by laser long-path absorption spectroscopy p 3343 N94-28596
On the possibility of measuring atmospheric OH using intracavity laser spectroscopy p 3344 N94-28597
NOAA Aeronomy Laboratory long-path OH experiment, Fritz Peak Observatory, Colorado p 3344 N94-28598
Measurement of atmospheric OH by titration of near-IR fluorescent dyes p 3344 N94-28599
The active titration method for measuring local hydroxyl radical concentration p 3345 N94-28602
Tropospheric HO2 determination by FAGE p 3345 N94-28606
Direct measurement of the reactivity of NH and OH on a silicon nitride surface
[DE94-005286] p 3199 N94-30260

HYPERBARIC CHAMBERS
Advanced seal delivery system life support parameters
[AD-A275304] p 3401 N94-29184

HYPERPLANES
The exact fitting problem in higher dimensions
[RUU-CS-92-37] p 3456 N94-30377
Perfect binary space partitions
[RUU-CS-93-23] p 3460 N94-30728

HYPERSONIC FLIGHT
Introduction and overview of research and development of solid propellant ramrockets, liquid fuel ramjets and experimental hydrogen ram combustors p 3151 N94-29292
Turboramjet engines: Types and performances p 3151 N94-29293
Particle kinetic simulation of high altitude hypervelocity flight
[NASA-CR-194535] p 3131 N94-29893
Potential of the ramjet engine for hypersonic flight speeds p 3153 N94-30935

HYPERSONIC FLOW
Numerical analysis of two dimensional/axisymmetric non-equilibrium hypersonic flow p 3125 N94-28963
Code development for hypersonic real-gas flow simulations toward the design of space vehicles, part 2 p 3125 N94-28966
The maximum entropy approach applied to energy exchange, chemical reactions and ionisation in the direct simulation Monte Carlo method for rarefied hypersonic flows
[IC-AERO-93-01] p 3524 N94-29481
Particle kinetic simulation of high altitude hypervelocity flight
[NASA-CR-194535] p 3131 N94-29893

HYPERSONIC SPEED
An actively cooled floating element skin friction balance for direct measurement in high enthalpy supersonic flows p 3289 N94-29824
Potential of the ramjet engine for hypersonic flight speeds p 3153 N94-30935

HYPERSONIC VEHICLES
Development of braided rope engine seals
[NASA-TM-105902] p 3298 N94-28838
Advanced vehicle concepts systems and design analysis studies
[NASA-CR-195115] p 3147 N94-29721
Numerical comparison of convective heat transfer augmentation devices used in cooling channels of hypersonic vehicles
[NASA-TM-106546] p 3279 N94-30147
Expanding the waverider design space using arbitrary generating flowfields p 3148 N94-30516

HYPERSONIC WIND TUNNELS
Holographic interferometry: A user's guide
[DE94-003136] p 3286 N94-28466

HYPERSONICS
Some problems of scramjet propulsion for aerospace planes. Part 2: Scramjet: Development and test problems p 3152 N94-29301
Models for vibration-dissociation coupling in high-temperature gases p 3273 N94-29675

HYPERSPACES
Perfect binary space partitions
[RUU-CS-93-23] p 3460 N94-30728

HYPERSPHERES
The exact fitting problem in higher dimensions
[RUU-CS-92-37] p 3456 N94-30377

HYPERTHERMIA
The Support of Air Operations under Extreme Hot and Cold Weather Conditions
[AGARD-CP-540] p 3379 N94-28420
Thermoregulation in the extreme cold environment p 3381 N94-28438

HYPERVELOCITY IMPACT
Hypervelocity impact induced arcing and Kapton pyrolization in a plasma environment
[NASA-TM-106528] p 3167 N94-28814
Hypervelocity impact testing of Space Station Freedom solar cells
[NASA-TM-106509] p 3167 N94-29383

HYPERVELOCITY PROJECTILES
Microwave Michelson interferometer system report of first use on a railgun, Green Farm, San Diego, CA
[DE94-005294] p 3289 N94-30059

HYPERVENTILATION
Emergency underwater breathing aids for helicopter passengers and crew p 3381 N94-28437

HYPOBARIC ATMOSPHERES
Studies on water electrolyte metabolism and endocrine responses at rest and during submaximal exercise at 6,000 m simulated altitude p 3388 N94-28496
Effects of training at simulated altitude of 6,000 m on endocrine responses at rest and during exercise at the same altitude p 3388 N94-28497
Decompression sickness risk versus time and altitude [AD-A275261] p 3391 N94-29071
HYPOKINESIA
Shortening velocity and calcium sensitivity of single fibers from hindlimb suspended muscle in rats p 3387 N94-29866
HYPOTHERMIA
The Support of Air Operations under Extreme Hot and Cold Weather Conditions [AGARD-CP-540] p 3379 N94-28420
Fuelling shivering in humans during cold water immersion p 3379 N94-28426
Biochemical enhancement of cold tolerance p 3380 N94-28427
Treatment of mild immersion hypothermia by body-to-body and forced-air warming p 3380 N94-28428
Advanced integrated cold protection for aircrew p 3381 N94-28436
Emergency underwater breathing aids for helicopter passengers and crew p 3381 N94-28437
Thermoregulation in the extreme cold environment p 3381 N94-28438
Physiological investigations of the isolated rat's liver in hypothermia and hypoxia and their relevance in aircraft incidents above the sea p 3382 N94-28439
Aeropathological diagnosis of lethal hypothermia p 3382 N94-28440
Rewarming methodologies in the field p 3382 N94-28441
A comparison of four methods of rewarming individuals cooled by immersion in cold water p 3382 N94-28442
HYPOTHESES
Selecting model complexity in learning problems [DE94-000764] p 3461 N94-30821
HYPOXIA
Physiological investigations of the isolated rat's liver in hypothermia and hypoxia and their relevance in aircraft incidents above the sea p 3382 N94-28439
HYSTERESIS
Hysteresis phenomena at spin-flop transition induced by the pulsed magnetic field [DE94-606851] p 3511 N94-28626
Butterfly and scaling law in YBa2Cu4O8 [DE94-006037] p 3519 N94-30338
Mathematical models of hysteresis [DE94-005681] p 3260 N94-30902

I

I BEAMS
Composite hot drape forming p 3240 N94-30448
IBM COMPUTERS
Early experiences with the IBM SP1 and the high-performance switch [DE94-006261] p 3429 N94-30840
IBM PERSONAL COMPUTERS
PAW using under MS DOS [DE94-608012] p 3406 N94-30081
ICE
Structure of ordinary ice I(sub h). Part 1: Ideal structure of ice [AD-A275149] p 3486 N94-29021
Growth condition of an ice layer in freezing soils under applied loads. Part 1: Experiment [AD-A275215] p 3357 N94-29070
On the temperature distribution near a cold surface [AD-A275162] p 3332 N94-29288
The thermal consequences of giant impacts in the early solar system p 3543 N94-29698
Propagation modeling of moist air and suspended water/ice particles at frequencies below 1000 GHz p 3256 N94-30497
ICE CLOUDS
Laboratory studies of chemical and photochemical processes relevant to stratospheric ozone [NASA-CR-195779] p 3347 N94-29549
ICE ENVIRONMENTS
Simulation of the effect of wind on clothing by measurements and calculations [PB94-132289] p 3399 N94-28406
Evaluation of life support equipment during an unsupported North Pole expedition p 3379 N94-28422
Thermoregulation in the extreme cold environment p 3381 N94-28438
A newly developed snow vehicle (SM100S) for Antarctica. Part 1: Necessity and process of the development p 3314 N94-29981
A newly developed snow vehicle (SM100S) for Antarctica. Part 2: Design of the system p 3314 N94-29982
ICE FLOES
The role of sea ice dynamics in global climate change p 3350 N94-30620
ICE FORMATION
Growth condition of an ice layer in freezing soils under applied loads. Part 1: Experiment [AD-A275215] p 3357 N94-29070
A toy model of sea ice growth p 3351 N94-30626
Remote sensor observations during WISP91: The use of microwave radiometers, RASS, and lidar ceilometers for detection of aircraft icing conditions [PB94-142106] p 3136 N94-30890
ICE MAPPING
Sea ice and oceans applications of SAR p 3327 N94-28934
IDENTITIES
Identity: Quarrelling with an unproblematic notion [LP-93-04] p 3455 N94-30327
IFF SYSTEMS (IDENTIFICATION)
A cognitive model of decision making: Chunking and the radar detection device [AD-A275185] p 3242 N94-28859
Incorporating geometric constraints into rule-based systems using nonlinear optimization [AD-A275093] p 3452 N94-29063
IGNITERS
Catalytic ignitor for regenerative propellant gun [NASA-CASE-NPO-18987-1-CU] p 3225 N94-29490
IGNITION
Combustion studies under microgravity p 3228 N94-28940
XCHEM-1D: A heat transfer/chemical kinetics computer program for multilayered reactive materials [DE94-005072] p 3226 N94-30615
IGNITION SYSTEMS
The laser approach for sequential pyrotechnic initiation systems: Envisageable chain architecture and concepts [REPT-932-430-113] p 3225 N94-29414
ILL-POSED PROBLEMS (MATHEMATICS)
Numerical solution of inverse problem in aerodynamics p 3125 N94-28965
Computational methods for the shape shading problem [ISBN-0-315-85430-8] p 3421 N94-30136
ILLUMINANCE
An investigation of stereopsis with AN/AVS-6 night vision goggles at varying levels of illuminance and contrast [AD-A275332] p 3400 N94-28918
IMAGE ANALYSIS
A new method for recognizing quadric surfaces from range data and its application to telerobotics and automation, final phase [NASA-CR-195733] p 3408 N94-28825
Far ultraviolet images of the nighttime ionosphere [AD-A275083] p 3356 N94-28843
Image technology and information analysis of bone change with gravitational exposure p 3389 N94-28851
Environmental characterization for target acquisition. Analysis of thermal and visible imagery [AD-A275414] p 3242 N94-28862
Proceedings of the International Symposium on Remote Sensing [JTN-94-80578] p 3325 N94-28925
Image processing for hyperspectral data p 3326 N94-28930
JERS-1 data acquisition and distribution p 3326 N94-28931
JERS-1 data and information system for resources exploration p 3327 N94-28932
Application of optical sensor data to resource survey p 3330 N94-29223
Initial observation results with imaging riometer at NY-Alesund (L is equal to 16) p 3360 N94-29239
The extraction and representation of forest inventory information using continuous density surfaces [ISBN-0-315-85658-0] p 3334 N94-30236
Activities in machine vision at Imago Manufacturing Ltd. p 3308 N94-30297
VAS: A Vision Advisor System combining agents and object-oriented databases [AIAA PAPER 94-1181-CP] p 3440 N94-30532
Application of the Modular Automated Reconfigurable Assembly System (MARAS) concept to adaptable vision gauging and parts feeding [AIAA PAPER 94-1182-CP] p 3440 N94-30533
Vision based object pose estimation for mobile robots [AIAA PAPER 94-1197-CP] p 3442 N94-30548
Statistical analysis of a satellite imagery time series: Implications for the study of coastal and estuarine circulation p 3335 N94-30919
Multitemporal analysis of a braiding river: The advanced study of 1992 [NLR-TP-93100-U] p 3335 N94-30942
Elements for the recognition of three dimensional deformable shapes: Application to biomedical imagery [TELECOM-93-E-006] p 3396 N94-30978
IMAGE CLASSIFICATION
Extrapolation of point data for resource mapping p 3334 N94-29959
A multiscale approach to image segmentation using Kohonen networks [RUU-CS-93-06] p 3438 N94-30349
Unsupervised texture image segmentation by improved neural network ART2 [AIAA PAPER 94-1199-CP] p 3442 N94-30549
Use of bad training data for better predictions [DE94-006233] p 3427 N94-30705
IMAGE CORRELATORS
Field methods to measure surface displacement and strain with the Video Image Correlation method [NASA-CR-195796] p 3316 N94-29724
IMAGE ENHANCEMENT
Automatic focus and registration of synthetic aperture radar images p 3246 N94-29536
Motion and structure from planar motion in noisy monocular image sequences p 3308 N94-30299
Seed viability detection using computerized false-color radiographic image enhancement p 3387 N94-30461
IMAGE PROCESSING
Fusion of range and luminance data from laser radar systems [AD-A275608] p 3292 N94-28770
Image technology and information analysis of bone change with gravitational exposure p 3389 N94-28851
Aberrated point-spread functions and beam quality for optical systems with annular pupils [AD-A275311] p 3499 N94-28875
Lead detection and mapping with reference to relationships between scale, sensor characteristics, surface conditions and atmospheric properties [AD-A275321] p 3377 N94-28877
Image processing for hyperspectral data p 3326 N94-28930
JERS-1 data acquisition and distribution p 3326 N94-28931
JERS-1 data and information system for resources exploration p 3327 N94-28932
Quadruplet expansion of the acoustic pressure field in a wedge shaped ocean [AD-A275121] p 3477 N94-29003
Synthetic image generator model; application of view angle dependent reflectivity components and performance evaluation in the visible region [AD-A275365] p 3499 N94-29009
Optimizing ray tracing with visual coherence [AD-A275218] p 3499 N94-29059
Spectral and polarimetric analysis of hyperspectral data collected by an acousto-optic tunable filter system [AD-A275076] p 3329 N94-29095
The appearance of the Sun and Moon seen through clouds [AD-A275338] p 3551 N94-29212
The Image Digitizing System (IDS) [AD-A275341] p 3329 N94-29213
A new information system: Satellite observation p 3330 N94-29219
Application of optical sensor data to resource survey p 3330 N94-29223
Initial observation results with imaging riometer at NY-Alesund (L is equal to 16) p 3360 N94-29239
Digital camera with apparatus for authentication of images produced from an image file [NASA-CASE-NPO-19108-1-CU] p 3287 N94-29373
Image-adapted visually weighted quantization matrices for digital image compression [NASA-CASE-ARC-12015-1] p 3406 N94-29375
Automating geographically referenced digital mosaics from aerial videography with area-based feature matching p 3333 N94-29540
Airside ground movements surveillance p 3141 N94-29585
Integer cosine transform for image compression p 3247 N94-29619
Analyses of stationary and growing crack tip deformation by digital image processing p 3320 N94-29690
Field methods to measure surface displacement and strain with the Video Image Correlation method [NASA-CR-195796] p 3316 N94-29724
Stereo imaging based particle velocimeter [NASA-CR-195800] p 3289 N94-29742
Camera artifacts in IUE spectra [NASA-CR-189337] p 3198 N94-29857

Computer Assisted Medical Interventions: Application to Conformal Radiotherapy
[RR-912-I] p 3395 N94-30028
Conformal external radiotherapy of prostatic carcinoma: Requirements and preliminary results
p 3395 N94-30029
Application of remote sensing techniques for the seismo-tectonic study of Nahanni earthquake area
[ISBN-0-315-85942-3] p 3334 N94-30037
Structural characterization of semiconductor heterostructures by atomic resolution Z-contrast imaging at 300 kV
[DE94-006561] p 3516 N94-30063
Computational methods for the shape shading problem
[ISBN-0-315-85430-8] p 3421 N94-30136
Meso-optical Fourier transform microscope with double focusing
[DE94-607851] p 3290 N94-30148
Activities in machine vision at Imago Manufacturing Ltd. p 3308 N94-30297
Variable-resolution stereo matching
p 3308 N94-30298
Unmanned vehicle mobility: Limits of autonomous navigation p 3310 N94-30311
A multiscale approach to image segmentation using Kohonen networks
[RUU-CS-93-06] p 3438 N94-30349
The use of interactive computer vision and robot hand controllers for enhancing manufacturing safety
p 3314 N94-30442
Dual use of image based tracking techniques: Laser eye surgery and low vision prosthesis p 3397 N94-30455
Analysis and an image recovery algorithm for ultrasonic tomography system p 3397 N94-30456
Design and control of active vision based mechanisms for intelligent robots
[AIAA PAPER 94-1196-CP] p 3442 N94-30547
Using stereoscopic imaging for visualization applications
[DE94-006247] p 3536 N94-30706
Use of snakes to link edge points to create left ventricular boundaries in echocardiographic images
[TELECOM-93-D-016] p 3395 N94-30970
Elements for the recognition of three dimensional deformable shapes: Application to biomedical imagery
[TELECOM-93-E-006] p 3396 N94-30978

IMAGE RECONSTRUCTION

Fusion of range and luminance data from laser radar systems
[AD-A275608] p 3292 N94-28770
Reconstruction of stellar images from correlations
[ISBN-0-315-85382-4] p 3541 N94-30133
Computational methods for the shape shading problem
[ISBN-0-315-85430-8] p 3421 N94-30136
A locally synchronous globally asynchronous Vertex-8 processing element for image reconstruction on a mesh
[ISBN-0-315-86005-7] p 3432 N94-30143

IMAGE RESOLUTION

Optimizing ray tracing with visual coherence
[AD-A275218] p 3499 N94-29059
Image-adapted visually weighted quantization matrices for digital image compression
[NASA-CASE-ARC-12015-1] p 3406 N94-29375
Variable-resolution stereo matching
p 3308 N94-30298
Motion and structure from planar motion in noisy monocular image sequences p 3308 N94-30299
Thermal imaging for a mobile robot
p 3308 N94-30300
Development and application of particle image velocimetry in high-speed separated flow: Two-dimensional base cavities p 3282 N94-30791

IMAGES

The appearance of the Sun and Moon seen through clouds
[AD-A275338] p 3551 N94-29212
A unified framework for retrieval in image databases
p 3533 N94-29811
Camera artifacts in IUE spectra
[NASA-CR-189337] p 3198 N94-29857

IMAGING RADAR

Synthetic aperture radar applications: Now and in the future p 3260 N94-28927
Improved ground-penetrating radar, bridge decks
[DE94-004863] p 3254 N94-29929

IMAGING SPECTROMETERS

Imaging spectrometry of the Earth and other solar system bodies p 3237 N94-29779

IMAGING TECHNIQUES

Exploitation of stereophotogrammetrically derived 3-D wireframe models to produce urban simulations
[AD-A275459] p 3325 N94-28808
Image technology and information analysis of bone change with gravitational exposure
p 3389 N94-28851
System requirements review for the High-Resolution Ozone Imager (HIROIG)
[AD-A275151] p 3347 N94-29023
Spectral and polarimetric analysis of hyperspectral data collected by an acousto-optic tunable filter system
[AD-A275076] p 3329 N94-29095
Fundamentals of printing technology
[PB94-132602] p 3530 N94-29141
Seafloor characterization using texture
[AD-A275399] p 3377 N94-29204
Digital camera with apparatus for authentication of images produced from an image file
[NASA-CASE-NPO-19108-1-CU] p 3287 N94-29373
Near-ultraviolet laser photoemission: Scanning microscopy, buried interfaces and image-potential states
p 3294 N94-29531
Field methods to measure surface displacement and strain with the Video Image Correlation method
[NASA-CR-195796] p 3316 N94-29724
Stereo imaging based particle velocimeter
[NASA-CR-195800] p 3289 N94-29742
Imaging spectrometry of the Earth and other solar system bodies p 3237 N94-29779
Smart focal-plane technology for micro-instruments and micro-rovers p 3237 N94-29780
Potential hazards of magnetic resonance imagers to emergency medical service helicopter operations
[DOT/FAA/RD-92/15] p 3135 N94-29862
Accurate modeling of F-region electron densities
[NASA-CR-195781] p 3364 N94-30014
Physical interpretation and development of ultrasonic nondestructive evaluation techniques applied to the quantitative characterization of textile composite materials
[NASA-CR-195766] p 3183 N94-30016
Computer Assisted Medical Interventions: Application to Conformal Radiotherapy
[RR-912-I] p 3395 N94-30028
Conformal external radiotherapy of prostatic carcinoma: Requirements and preliminary results
p 3395 N94-30029
Pre- and intra-radiotherapy multimodal image registration: Principles and first experiments
p 3395 N94-30030
Structural characterization of semiconductor heterostructures by atomic resolution Z-contrast imaging at 300 kV
[DE94-006561] p 3516 N94-30063
Atomic-scale structure and chemistry of interfaces by Z-contrast imaging and electron energy loss spectroscopy in the STEM
[DE94-006563] p 3516 N94-30064
Study of the problems of nonuniformity of heating in infrared vision applied to the inspection of materials having non-planar relief
[ISBN-0-315-85637-8] p 3316 N94-30235
Direct measurement of the reactivity of NH and OH on a silicon nitride surface
[DE94-005286] p 3199 N94-30260
Thermal imaging for a mobile robot
p 3308 N94-30300
Analysis and an image recovery algorithm for ultrasonic tomography system p 3397 N94-30456
Calculation of turbulence degraded point spread function of an imaging system p 3260 N94-30514
An electromagnetic noncontacting sensor for thickness measurement in a dispersive medium
[AIAA PAPER 94-1200-CP] p 3443 N94-30551
Using stereoscopic imaging for visualization applications
[DE94-006247] p 3536 N94-30706

IMPACT

The thermal consequences of giant impacts in the early solar system p 3543 N94-29698
The impact of electrically charged microspheres with planar surfaces under vacuum conditions
p 3320 N94-29765

IMPACT DAMAGE

Test and analysis of a stitched RFI graphite-epoxy panel with a fuel access door
[NASA-TM-108992] p 3178 N94-29100
Hypervelocity impact testing of Space Station Freedom solar cells
[NASA-TM-106509] p 3167 N94-29383
Cockpit video: A low cost BDA source
[AD-A275228] p 3150 N94-29389

IMPACT MELTS

The thermal consequences of giant impacts in the early solar system p 3543 N94-29698

IMPACT RESISTANCE

Ballistic performance of polycarbonate/polyester and polycarbonate/styrene- acrylonitrile microlayer sheets
[AD-A275462] p 3177 N94-28735
Air-deployable geophysics package
[DE94-005651] p 3335 N94-30594

IMPACT STRENGTH

On the dynamic mechanical behavior of 3-D integrated fabric reinforced composites
[AD-A275424] p 3177 N94-28865

IMPACT TESTS

Single specimen fracture toughness determination procedure using instrumented impact test
[PB94-132040] p 3316 N94-28402
Hypervelocity impact induced arcing and Kapton pyrolization in a plasma environment
[NASA-TM-106528] p 3167 N94-28814
Hypervelocity impact testing of Space Station Freedom solar cells
[NASA-TM-106509] p 3167 N94-29383
Modelling soft impacts for vibrational excitation of civil engineering structures
[PB94-137619] p 3320 N94-29681
The impact of electrically charged microspheres with planar surfaces under vacuum conditions
p 3320 N94-29765
Micromechanics of the dynamic response of ceramics and ceramic composites p 3217 N94-29975

IMPEDANCE MEASUREMENT

VHF impedance measurement: A review
[PB94-138682] p 3267 N94-30115

IMPELLERS

Fluid dynamic noise in a centrifugal pump
[AD-A275264] p 3477 N94-28904
Numerical study on internal flows of centrifugal compressors p 3127 N94-28977
Rotary blood pump
[NASA-CASE-MSC-22424-1] p 3299 N94-29370
CFD analyses for advanced pump design
[NASA-CR-194866] p 3300 N94-29550

IMPINGEMENT

Development and verification of a model to predict impingement currents for ion thrusters
[NASA-CR-195322] p 3173 N94-29546

IMPLOSIONS

Turbulence models and their application in implosion analyses with two-phase flow
[GKSS-92/E/98] p 3284 N94-30967
Numerical simulation and prediction of implosion phenomena
[GKSS-92/E/99] p 3284 N94-30968

IMPURITIES

Silicon-Film (tm) photovoltaic manufacturing technology
[DE94-000258] p 3336 N94-28501
Directional solidification studies in Ni-Al alloys
[DE94-005562] p 3201 N94-28527
First principles pseudopotential calculations on aluminum and aluminum alloys
[DE94-004890] p 3206 N94-29931
Chemical composition of insoluble particles in superimposed ice on Storoeya, Svalbard (Sweden)
[CM-82] p 3336 N94-30944

IN SITU MEASUREMENT

X ray standing wave studies of underpotentially deposited metal monolayers
[AD-A275409] p 3513 N94-29215
Micro-sensors for in-situ meteorological measurements p 3236 N94-29777

INCENTIVES

TCM exemptions to promote alternative-fuel vehicles: The good, the bad, and the ugly
[DE94-005924] p 3311 N94-30703

INCINERATORS

Measurement of volatile metal species at elevated temperatures
[PB94-132321] p 3186 N94-28407
Electrochemical incineration of wastes
[NASA-CR-195262] p 3198 N94-29938

INCLUSIONS

Effect of non-metallic inclusions on the machinability of steel
[PB93-230233] p 3204 N94-29387
Analysis of pressureless densification of ceramic matrix composites p 3216 N94-29766
Method of test for cleanness assessment of metal alloys: The preparation of button specimens by electron beam melting and the characterisation of recovered inclusions
[NPL-DMM(A)-130] p 3210 N94-30796
A class of inclusion problems for the strengthening of brittle and ductile composites p 3186 N94-30959

INCOHERENT SCATTER RADAR

Space-time structure of the morning aurora inferred from coincident DMSP-F6, -F8, and Sondrestrom incoherent scatter radar observations
[AD-A275442] p 3356 N94-28869

INCOMPRESSIBLE FLOW

Modeling turbulence in flows with a strong rotational component
[DE94-003577] p 3270 N94-28475

Large eddy simulations using lattice Boltzmann algorithms
[DE94-005666] p 3270 N94-28549
Numerical analysis of incompressible viscous flow around a bubble p 3126 N94-28968
The upsilon-q method and the psi-q method for incompressible flows p 3126 N94-28971
Theoretical study of the incompressible Navier-Stokes equations by the least-squares method
[NASA-TM-106535] p 3272 N94-29096
A new flux-conserving numerical scheme for the steady, incompressible Navier-Stokes equations
[NASA-TM-106520] p 3273 N94-29471
CFD analyses for advanced pump design
[NASA-CR-194866] p 3300 N94-29550
The h-p adaptive methods for incompressible viscous flow problems p 3275 N94-29836
Numerical solution of 3-D Navier-Stokes equations in vorticity-velocity form for incompressible flows p 3276 N94-29843
Hopf bifurcation in viscous, low-speed flows about an airfoil with structural coupling p 3134 N94-30865

INCOMPRESSIBLE FLUIDS
Forced generation of solitary waves in a rotating fluid and their stability p 3274 N94-29689

INCONEL (TRADEMARK)
Probabilistic material strength degradation model for Inconel 718 components subjected to high temperature, mechanical fatigue, creep and thermal fatigue effects
[NASA-CR-195284] p 3318 N94-28840

INDENTATION
The role of plastic deformation in brittle and near-brittle cracking behavior p 3322 N94-30226
Creep behavior of MoSi2-SiC composites
[DE94-004980] p 3185 N94-30693

INDEPENDENT VARIABLES
A variable selection heuristic for solid rocket motor design p 3173 N94-29544

INDEXES (DOCUMENTATION)
Aeronautical engineering: A cumulative index to a continuing bibliography (supplement 300)
[NASA-SP-7037(300)] p 3121 N94-28537
Catalog of Air Force weather technical publications 1992-1993
[AD-A275635] p 3368 N94-28638
TRADOC library and information network (TRALINET). Union list of periodicals (TULIP)
[AD-A275263] p 3529 N94-28903
Index of NPL acoustics publications 1981-1990
[NPL-RSA(EXT)-0044] p 3480 N94-30786

INDIUM ALLOYS
Microstructural development and mechanical behavior of eutectic bismuth-tin and eutectic indium-tin in response to high temperature deformation
[DE94-005202] p 3210 N94-30710

INDIUM ANTIMONIDES
InTlSb for long-wavelength infrared photodetectors and arrays
[AD-A275079] p 3512 N94-28872
The growth of InAsSb/InGaAs strained-layer superlattices by metal-organic chemical vapor deposition
[DE94-005576] p 3518 N94-30316

INDIUM ARSENIDES
Tunnelling hot electron transfer amplifiers
[AD-A275529] p 3282 N94-28687
Development of ultra-low noise, high performance 3 -5 quantum well infrared photodetectors (QWIPs) for focal plane array staring image sensor systems
[AD-A275745] p 3511 N94-28734
Photoelectronic study of GaAs epilayers and In(x)Ga(1-x)As/GaAs quantum wells
[ISBN-0-315-85756-0] p 3518 N94-30239
The growth of InAsSb/InGaAs strained-layer superlattices by metal-organic chemical vapor deposition
[DE94-005576] p 3518 N94-30316
Strain relaxation and surface roughness as a function of growth temperature in linearly graded In(x)Al(1-x)As (x = 0.05 to 0.25) buffers
[DE94-005430] p 3519 N94-30592

INDIUM COMPOUNDS
Synthesis and molecular structures of R(Me3CCH2)2In-E(SiMe3) (R = Me3CCH2, E = P or As; R = Me, E = P)
[AD-A275020] p 3486 N94-29131
X ray crystal structures of ((Me3SiCH2)2InCl)2 and ((Me3SiCH2)InCl2)
[AD-A275074] p 3513 N94-29155
Monolithic in-based III-V compound semiconductor focal plane array cell with single stage CCD output
[NASA-CASE-NPO-18978-1-CU] p 3265 N94-29488

INDIUM PHOSPHIDES
Micro-opto-mechanical devices and systems using epitaxial lift off p 3239 N94-29793

INDOOR AIR POLLUTION
Human requirements to the indoor air quality and the thermal environment p 3232 N94-29600
Theory of age distribution p 3232 N94-29602
Computational fluid dynamics in ventilation: Practical approach p 3233 N94-29611
Brief summary of accomplishments since our DOE-sponsored radon project commenced
[DE94-004643] p 3348 N94-29926
Using spacecraft trace contaminant control systems to cure sick building syndrome p 3354 N94-30470

INDUCTION (MATHEMATICS)
Bisimulations and predicate logic
[CWI-CS-R9333] p 3460 N94-30735
A structural co-induction theorem
[CWI-CS-R9346] p 3461 N94-30753

INDUCTORS
Non-isolated 30 kW class arcjet PCU
[NASA-CR-189148] p 3173 N94-29444

INDUSTRIAL MANAGEMENT
Realizing the productivity potential of expeditious operations
[PB94-135555] p 3230 N94-29188
Agile manufacturing: The factory of the future
[AIAA PAPER 94-1184-CP] p 3440 N94-30534

INDUSTRIAL PLANTS
Agile manufacturing: The factory of the future
[AIAA PAPER 94-1184-CP] p 3440 N94-30534

INDUSTRIAL SAFETY
Systematic safety consideration in product design
[PB94-132354] p 3229 N94-28410
Microcomputer-based protective functions in industrial production systems: Assessment method
[PB94-137817] p 3411 N94-29159
Computational fluid dynamics in ventilation: Practical approach p 3233 N94-29611

INDUSTRIES
Spin-off companies as agents of technology transfer: An empirical study of the spin-off companies of the Technical Research Centre of Finland
[PB94-132248] p 3537 N94-28405
Nuclear energy related research
[DE94-606286] p 3494 N94-28623
Application of high-speed milling to the Finnish manufacturing industry
[PB94-135548] p 3230 N94-29187
Industrial ventilation p 3232 N94-29604
Scientific and technical information transfer: Promoting information acquisition in the Saudi Arabian industrial sector p 3532 N94-29803

INELASTIC COLLISIONS
Analytic cross sections for collisions of H, H2, He and Li atoms and ions with atoms and molecules
[DE94-707686] p 3485 N94-28788
Calculation of inelastic mean free path and stopping power for electrons in solids from an optical-data model
[USIP-92-06] p 3494 N94-30980

INELASTIC SCATTERING
Results on structure functions from fixed-target experiments
[DE94-005233] p 3482 N94-28541
Determination of the neutron spin-structure function
[DE94-005234] p 3483 N94-28542
Simulation of experiments on deep inelastic scattering of muons on superconducting magnetic toroidal spectrometer STORS
[DE94-606267] p 3483 N94-28554
Physics at HERA
[DE94-005117] p 3483 N94-28569
Deep inelastic lepton scattering on nuclei: operator product expansion and meson-nucleon theory
[DE94-606442] p 3484 N94-28610
Numerical solution of the multichannel scattering problem
[DE94-606297] p 3484 N94-28619
Optical field ionization of atoms and ions using ultrashort laser pulses
[DE94-006643] p 3488 N94-29845

INEQUALITIES
Representations of dynamical systems described by behavioral inequalities
[AD-B173649] p 3458 N94-30402

INERTIAL CONFINEMENT FUSION
Conceptual study of moderately coupled plasmas and experimental comparison of laboratory x ray sources
[DE94-005828] p 3506 N94-30045
Inertial confinement fusion
[DE94-005957] p 3510 N94-30875

INERTIAL FUSION (REACTOR)
The induction approach to heavy ion inertial fusion: Accelerator and target considerations
[DE94-005216] p 3494 N94-28507
A review of the ablative stabilization of the Rayleigh-Taylor instability in regimes relevant to ICF
[DE94-005809] p 3509 N94-30597
Diode-pumped solid-state-laser drivers and the competitiveness of inertial fusion energy
[DE94-006654] p 3296 N94-30830

INFERENCE
Index expression belief networks for information disclosure
[TR-92-23] p 3465 N94-30358

INFLATABLE STRUCTURES
Analysis and design of inflatable aerospace structures p 3403 N94-30799

INFLUENCE COEFFICIENT
Theoretical prediction of the influence coefficients on damped simple flexible rotors using the transfer matrix method
[IMR-TM-TR-002] p 3321 N94-30018

INFORMATION
Temporal and qualitative decomposition of plausible reasoning
[AD-A275073] p 3398 N94-29154
A conceptual language for the description and manipulation of complex information models
[TR-92-34] p 3423 N94-30344

INFORMATION DISSEMINATION
NASA space and Earth science data on CD-ROM
[NASA-TM-109709] p 3528 N94-28414
Defense Technical Information Center cataloging guidelines
[AD-A275100] p 3529 N94-28911
Information center assessment p 3533 N94-29855
NASA/DOD Aerospace Knowledge Diffusion Research Project. Report 23: The communications practices of US aerospace engineering faculty and students: Results of the phase 3 survey
[NASA-TM-109085] p 3534 N94-30149
NASA/DOD Aerospace Knowledge Diffusion Research Project. Report 22: US academic librarians and technical information specialists as information intermediaries: Results of the phase 3 survey
[NASA-TM-109067] p 3534 N94-30150
DOE New Technology: Sharing New Frontiers, April 1, 1993 - September 30, 1993
[DE93-041289] p 3535 N94-30699
Marketing tools for increasing proactivity in technical information centers
[AGARD-AR-326] p 3528 N94-30934

INFORMATION FLOW
A streamlined software environment for situated skills
[AIAA PAPER 94-1205-CP] p 3444 N94-30556

INFORMATION MANAGEMENT
The program for catalogization of magnetic tapes in EXCHARM experiment
[DE94-606271] p 3528 N94-28615
Software systems reengineering process model, version 1.0
[AD-A275711] p 3407 N94-28691
NASA Parts Program Office responsibilities p 3165 N94-28702
A survey of geographical information systems applications for the Earth Science and Applications Division, Space Sciences Laboratory, Marshall Space Flight Center
[NASA-TM-108438] p 3529 N94-28820
Engineering document management system
[PB94-136934] p 3530 N94-29172
Application of information management methodologies for project quality improvement in a changing environment p 3416 N94-29342
Information center assessment p 3533 N94-29855
Smart Document System (SDS) used in managing DOE order's with electronic Engineering Procedures
[DE94-005076] p 3534 N94-30099
The evolution of information management
[DE94-004173] p 3535 N94-30179
COSMIC monthly progress report
[NASA-CR-195809] p 3422 N94-30273

INFORMATION PROCESSING (BIOLOGY)
Temporal and qualitative decomposition of plausible reasoning
[AD-A275073] p 3398 N94-29154
The MERSS 5th Symposium on Space Medicine: Medical and Physiological Experiment Utilizing Parabolic Flight
[JTN-94-80588] p 3392 N94-29709
Analysis of various biological activity parameters during parabolic flight p 3393 N94-29716

INFORMATION RETRIEVAL
Automated interface for retrieving reusable software components
[AD-A275004] p 3409 N94-28896
Enhancing performance of full-text retrieval systems using relevance feedback p 3532 N94-29806
Pausing behavior of end-users in online searching p 3533 N94-29960
Computer-based linking of thesauri p 3534 N94-29961
Index expression belief networks for information disclosure
[TR-92-23] p 3465 N94-30358

Information-seeking in hypertext: Multiple access methods in a full-text hypertext database p 3536 N94-30918

INFORMATION SYSTEMS
User-centered guidelines for environmental management
[DE94-004313] p 3341 N94-28454
TRADOC library and information network (TRALINET). Union list of periodicals (TULIP)
[AD-A275263] p 3529 N94-28903
Defense Technical Information Center cataloging guidelines
[AD-A275100] p 3529 N94-28911
A comparison of three aircraft attitude display symbology structures
[AD-A275172] p 3150 N94-29048
Evaluation of wireless Local Area Networks
[AD-A275133] p 3243 N94-29064
Designing and maintaining decision-making processes p 3412 N94-29318
Information engineering implementation and acceptance p 3530 N94-29533
The Telecommunications and Data Acquisition Report
[NASA-CR-195694] p 3246 N94-29613
Evaluation of the Resource Library System in Finland
[PB94-137734] p 3532 N94-29682
RIPE integrity primitives, part 1 (RACE Integrity Primitives Evaluation)
[CWI-CS-R9324-PT-1] p 3252 N94-29692
RIPE integrity primitives, part 2 (RACE Integrity Primitives Evaluation)
[CWI-CS-R9325-PT-2] p 3252 N94-29693
Information center assessment p 3533 N94-29855
COSMIC monthly progress report
[NASA-CR-195809] p 3422 N94-30273
Modelling the evolution of information systems
[TR-92-36] p 3535 N94-30329
Towards a general theory for the evolution of application domains
[TR-92-22] p 3535 N94-30357
Evolving information systems: Meeting the ever-changing environment
[TR-92-24] p 3535 N94-30359
A general theory for the evolution of application domains
[TR-92-26] p 3535 N94-30360
A framework for comparing conceptual modelling languages
[TR-92-29] p 3535 N94-30361
A note on schema equivalence
[TR-92-30] p 3535 N94-30362
Information-seeking in hypertext: Multiple access methods in a full-text hypertext database p 3536 N94-30918
Measuring the impact of investments in information technologies on business performance
[REPT-93-056] p 3536 N94-30929
Marketing tools for increasing proactivity in technical information centers
[AGARD-AR-326] p 3528 N94-30934

INFORMATION THEORY
SPC toolbox: An interactive MATLAB (tm) package for signal modeling, analysis, and communications
[AD-A275617] p 3241 N94-28634
Fast and efficient variable-to-fixed-length coding algorithm
[PB94-125465] p 3424 N94-30400
Thermodynamics of computation and information distance
[CWI-CS-R9341] p 3526 N94-30433
Relations between varieties of Kolmogorov complexities
[CWI-CS-R9329] p 3427 N94-30732

INFORMATION TRANSFER
NASA Parts Project Office: Basic goals p 3166 N94-28703
Technology transfer initiatives
[NASA-CR-195151] p 3537 N94-29410
Scientific and technical information transfer: Promoting information acquisition in the Saudi Arabian industrial sector p 3532 N94-29803
NASA/DOD Aerospace Knowledge Diffusion Research Project. Report 23: The communications practices of US aerospace engineering faculty and students: Results of the phase 3 survey
[NASA-TM-109085] p 3534 N94-30149
NASA/DOD Aerospace Knowledge Diffusion Research Project. Report 22: US academic librarians and technical information specialists as information intermediaries: Results of the phase 3 survey
[NASA-TM-109067] p 3534 N94-30150

INFRARED ABSORPTION
HO2 detection by near infrared absorption using tunable diode lasers p 3346 N94-28608
Analysis of infrared radiation heating process considering chemical reaction of material to be heated
[DE94-744116] p 3199 N94-30267

INFRARED ASTRONOMY
Infrared observations of cometary dust by COBE p 3541 N94-29994

INFRARED DETECTORS
Development of ultra-low noise, high performance 3 -5 quantum well infrared photodetectors (QWIPs) for focal plane array staring image sensor systems
[AD-A275745] p 3511 N94-28734
High Tc superconducting bolometric and nonbolometric infrared (IR) detectors
[NASA-CR-195728] p 3262 N94-28846
Thermal variation in vegetated or snow-covered background scenes and its effect on passive infrared systems
[AD-A275174] p 3325 N94-28849
InTlSb for long-wavelength infrared photodetectors and arrays
[AD-A275079] p 3512 N94-28872
Keynote address --- Japanese Earth Resources Satellite 1 (JERS-1) and future remote sensing projects p 3326 N94-28926
Modeling the total dose radiation effects of Hg(1-x)Cd(x)Te photodiodes using numerical device simulators
[AD-A275235] p 3263 N94-29028
Dual-use applications of infrared sensitive materials
[AD-A275140] p 3499 N94-29694
Evolution of miniature detectors and focal plane arrays for infrared sensors p 3237 N94-29781
Micromachined electron tunneling infrared sensors p 3238 N94-29785
Mechanisms and effects of heat generation at the tips of dynamic cracks and notches in metals p 3321 N94-29808

INFRARED IMAGERY
Environmental characterization for target acquisition. Analysis of thermal and visible imagery
[AD-A275414] p 3242 N94-28862
Dual-use applications of infrared sensitive materials
[AD-A275140] p 3499 N94-29694
Dual-Band Infrared (DBIR) imaging inspections of Boeing 737 and KC-135 aircraft panels
[DE94-005700] p 3122 N94-29842
Correlation studies of Pioneer Venus imagery obtained from PV experiments with near IR imagery obtained from ground-based observations during Venus inferior conjunction
[NASA-CR-195772] p 3550 N94-29892
Study of the problems of nonuniformity of heating in infrared vision applied to the inspection of materials having non-planar relief
[ISBN-0-315-85637-8] p 3316 N94-30235
Dual-band infrared imaging for quantitative corrosion detection in aging aircraft
[DE94-004187] p 3149 N94-30687

INFRARED INSPECTION
Study of the problems of nonuniformity of heating in infrared vision applied to the inspection of materials having non-planar relief
[ISBN-0-315-85637-8] p 3316 N94-30235

INFRARED INSTRUMENTS
Near-IR diode laser absorption for measurement of tropospheric HO2 p 3345 N94-28607

INFRARED INTERFEROMETERS
Toward astrometric tracking with the infrared spatial interferometer p 3249 N94-29653

INFRARED LASERS
Reactor-pumped laser experimental results
[DE94-005247] p 3292 N94-28482

INFRARED RADIATION
SHARC, a model for calculating atmospheric and infrared radiation under non-equilibrium conditions
[AD-A275207] p 3357 N94-28893
Evaluation of wireless Local Area Networks
[AD-A275133] p 3243 N94-29064
Infrared observations of cometary dust by COBE p 3541 N94-29994
Analysis of infrared radiation heating process considering chemical reaction of material to be heated
[DE94-744116] p 3199 N94-30267
The influence of the evaporation duct on the angle of arrival and amplitude of the backscattered signal from targets low above the sea p 3256 N94-30498
Multispectral transmittance measurements through man-made water fogs p 3257 N94-30499
Global approach towards the evaluation of thermal infrared countermeasures p 3258 N94-30504

INFRARED RADIOMETERS
Rock identification using thermal infrared data p 3331 N94-29228
Optical Chopper Assembly for the Mars Observer p 3162 N94-29639

INFRARED SIGNATURES
An experimental and comprehensive method to measure emission characteristics p 3257 N94-30501
Experimental evaluation of camouflage effectiveness in the thermal infrared p 3257 N94-30502
Infrared polarization signatures p 3258 N94-30506

INFRARED SPACE OBSERVATORY (ISO)
ISO overview: General presentation of the satellite, cryogenic aspects
[REPT-932-440-102] p 3231 N94-29416

INFRARED SPECTRA
SHARC, a model for calculating atmospheric and infrared radiation under non-equilibrium conditions
[AD-A275207] p 3357 N94-28893
Inter-comparison of Wildfire and High-resolution Interferometer Sounder (HIS) data from STORM-FEST: An investigation of wildfire spectral channel discrepancies
[NASA-TM-108439] p 3333 N94-29553
The far-infrared absorption spectrum of low temperature hydrogen gas
[ISBN-0-315-85432-4] p 3199 N94-30137

INFRARED SPECTROMETERS
MODIS technical report series. Volume 3: MODIS airborne simulator level 1B data user's guide
[NASA-TM-104594] p 3231 N94-29385
Imaging spectrometry of the Earth and other solar system bodies p 3237 N94-29779

INFRARED SPECTROSCOPY
Temperature depencence of the far infrared optical constants of polyethylene
[PB94-124336] p 3213 N94-28795

INFRARED STARS
A near-infrared survey of the star forming region NGC 2264 p 3540 N94-29971

INHIBITORS
Plant-microbe interactions: Plant hormone production by phylloplane fungi
[PB94-135563] p 3385 N94-29189
Four advances in carbon-carbon materials technology p 3186 N94-30481

INITIATORS (EXPLOSIVES)
Pyrotechnic shock: Devices in pyrotechnic environment qualification logic
[REPT-932-430-108] p 3225 N94-29429

INJECTION MOLDING
Generalized Eulerian-Lagrangian formulations in free and moving boundary problems: Processing of viscoelastic polymers and fiber suspensions p 3283 N94-30955

INJECTORS
Ducted kerosene spray flames p 3195 N94-29276
Apparatus for testing high pressure injector elements
[NASA-CASE-MFS-28773-1] p 3299 N94-29385
Laminar Flow Supersonic Wind Tunnel primary air injector p 3158 N94-29649

INJURIES
Blast overpressure studies with animals and man
[AD-A275038] p 3391 N94-29150

INLET AIRFRAME CONFIGURATIONS
Numerical study on the interaction between scramjet engine modules caused by thermal choke p 3125 N94-28960

INLET FLOW
Fluid dynamic noise in a centrifugal pump
[AD-A275264] p 3477 N94-28904
Scramjet CFD methods and analysis. Part 1: Scramjet CFD methods. Numerical simulation of the flow in scramjet duct p 3152 N94-29296

INLET TEMPERATURE
Surface fatigue life of high temperature gear materials
[NASA-TM-106562] p 3303 N94-30227

INOCULATION
New inoculants for ductile cast iron
[PB94-138476] p 3206 N94-29947

INORGANIC COATINGS
Non-chromate talc conversion coatings for aluminum
[DE94-005281] p 3207 N94-30053

INPUT/OUTPUT ROUTINES
Operation semantics with read and write frames
[PB94-138138] p 3529 N94-29108
I/O on the Tera file system
[AD-A275278] p 3530 N94-29182
Redundant disk arrays in transaction processing systems
[NASA-CR-195759] p 3418 N94-29404
The beauty and the beast
[TR-93-03] p 3423 N94-30331
Efficient bounded timestamping using traceable use abstraction: Is writer's guessing better than reader's telling?
[RUU-CS-93-28] p 3426 N94-30489

INSERTS
Casting of weldable graphite/magnesium metal matrix composites with built-in metallic inserts p 3186 N94-30482

INSOLATION
Advanced development of PV encapsulents
[DE94-000219] p 3336 N94-28500
INSPECTION
MSFC inspections of installed polyimide wire
p 3166 N94-28707
Intelligent automated process planning and code generation for computer-controlled inspection
[AD-A275346] p 3409 N94-28920
Improved ground-penetrating radar, bridge decks
[DE94-004863] p 3254 N94-29929
Radar jet engine health monitoring project
[ASSGI-301] p 3153 N94-30130
Teleoperated systems for nuclear reactors: Inspection and maintenance
[AIAA PAPER 94-1176-CP] p 3439 N94-30528
Technology for robotic surface inspection in space
[AIAA PAPER 94-1193-CP] p 3442 N94-30544
Robotic NDE inspection of advanced solid rocket motor casings
[AIAA PAPER 94-1222-CP] p 3446 N94-30571
Automation for nondestructive inspection of aircraft
[AIAA PAPER 94-1223-CP] p 3446 N94-30572
Automated inspection of turbine blades: Challenges and opportunities
[AIAA PAPER 94-1226-CP] p 3446 N94-30575
INSTALLING
System for the installation and replacement of components in hostile environments
[NASA-CASE-LEW-14906-1-SB] p 3300 N94-29427
Installation of experimental mode-S data link in commercial aircraft
[PB94-138757] p 3254 N94-29998
INSTRUMENT APPROACH
Key cognitive issues in the design of electronic displays of instrument approach procedure charts
[AD-A275647] p 3399 N94-28649
INSTRUMENT ERRORS
Inter-comparison of Wildfire and High-resolution Interferometer Sounder (HIS) data from STORM-FEST: An investigation of wildfire spectral channel discrepancies
[NASA-TM-108439] p 3333 N94-29553
Correction of X hot-wire measurements for gradients normal to the plane of the wires
[PB94-125473] p 3157 N94-30399
A comparative study of clock rate and drift estimation
p 3473 N94-30669
Systematic error estimation in multisensor fusion systems
[AD-B179298] p 3428 N94-30764
INSTRUMENT FLIGHT RULES
Extremely Low Visibility IFR Rotorcraft Approach (ELVIRA) operational concept development. Volume 1: Executive Summary
[DOT/FAA/RD-94/1,I] p 3142 N94-30189
INSTRUMENT LANDING SYSTEMS
Los Angeles international airport instrument landing system approach data collection and reduction, phase 1
[AD-A275115] p 3136 N94-28914
Ground independent landing system
p 3137 N94-29564
INSTRUMENT PACKAGES
The Pluto fast flyby mission: Completing the reconnaissance of the solar system
p 3235 N94-29768
Air-deployable geophysics package
[DE94-005651] p 3335 N94-30594
INTEGRAL EQUATIONS
Applied analysis/computational mathematics
[DE94-005133] p 3451 N94-28571
The solving of the relativistic two-body problem with a nonlinear dependence upon a spectrum parameter
[DE94-606343] p 3451 N94-28783
Numerical solution of inverse problem in aerodynamics p 3125 N94-28965
A note on the Poisson brackets associated with Lax operators
[MATHS-REPT-A-195] p 3464 N94-29482
Integral equation analysis of composite bodies of revolution and arbitrary surfaces with application to cavity-backed antennas p 3253 N94-29883
A spectral boundary integral equation method for the 2-D Helmholtz equation
[NASA-CR-194890] p 3454 N94-30207
Modal analysis of solar panels using boundary integral equations
[NLT-TP-92218-U] p 3338 N94-30328
INTEGRAL ROCKET RAMJETS
Research and development of ramjets/ramrockets. Part 2: Integral liquid fuel ramjets p 3152 N94-29297
Research and development of ramjets/ramrockets. Part 3: The study of gaseous hydrogen ram combustors
p 3152 N94-29298
INTEGRALS
Path integral for coherent states of the dynamical U(sub 2) group and U(sub 2/1) supergroup
[DE94-606382] p 3466 N94-28785
INTEGRATED CIRCUITS
Frequency-domain analysis of nonlinear microwave circuits
[PB94-132024] p 3261 N94-28400
Exploratory research for a high temperature superconducting integrated circuit
[AD-A275798] p 3262 N94-28767
Innovative optoelectronic materials and structures using OMVPE
[AD-A275811] p 3511 N94-28773
Optoelectronic integrated circuits fabricated using atomic layer epitaxy
[AD-A275454] p 3262 N94-28805
Focused ion beam fabrication of microelectronic structures
[AD-A275384] p 3264 N94-29305
Multi-speed multi-phase resolver converter
[NASA-CASE-MFS-28855-1] p 3264 N94-29372
Yield and variability optimization of integrated circuits: Principles and practical solutions p 3266 N94-29805
Nearly time-optimal feedback control of a magnetically levitated photolithography positioning system
[DE94-005288] p 3266 N94-30055
A locally synchronous globally asynchronous Vertex-8 processing element for image reconstruction on a mesh
[ISBN-0-315-86005-7] p 3432 N94-30143
Optoelectronic packaging activities at Sandia National Laboratories
[DE94-005287] p 3501 N94-30261
A combined electron beam/optical lithography process step for the fabrication of sub-half-micron-gate-length MMIC chips p 3240 N94-30445
A bipolar analog front-end integrated circuit for the SDC silicon tracker
[DE94-005203] p 3267 N94-30711
A high rate, low noise, x ray silicon strip detector system
[DE94-004557] p 3268 N94-30717
INTEGRATED OPTICS
A new guided wave lens structure and its application
[AD-A275541] p 3499 N94-28813
Reconfigurable optical interconnections via dynamic computer-generated holograms
[NASA-CASE-NPO-19039-1-CU] p 3499 N94-29491
INTEGRATORS
BPM901N monitor electronics for the determination of the bundle profile in the extraction line of AmPS
[DIGEL-1993-9] p 3495 N94-29467
INTELSAT SATELLITES
Two-way satellite time transfer: Overview and recent developments p 3469 N94-30646
INTERACTING GALAXIES
Stellar and gas dynamics of interacting ring galaxies
p 3548 N94-30340
INTERACTIONAL AERODYNAMICS
Experimental investigation of three-dimensional vortex-airfoil interaction in a supersonic stream
[AD-A275107] p 3122 N94-28899
RNS optimization procedure for three-dimensional composite velocity multi-block applications
p 3273 N94-29534
An analytical study of unsteady rotor/fuselage interaction in hover and forward flight
p 3131 N94-29826
Aerodynamic analysis of slipstream/wing/nacelle interference for preliminary design of aircraft configurations
[AD-B173651] p 3135 N94-30916
INTERACTIVE CONTROL
Work-oriented development of interactive software tools: Understanding the work of software maintainers and making an interactive software tool for them
[PB94-132032] p 3406 N94-28401
The use of interactive computer vision and robot hand controllers for enhancing manufacturing safety
p 3314 N94-30442
INTERCALATION
Graphite intercalation compounds prepared from graphite fluoride
[NASA-TM-106447] p 3174 N94-28924
INTERFACIAL TENSION
Surface tension of tin and its alloys with particular reference to solders
[PB94-138302] p 3204 N94-29119
INTERFERENCE FIT
Cold expansion and interference for extending the fatigue life of multi-layer metal joints
[AD-A274982] p 3318 N94-29091
INTERFEROMETERS
Innovative direct detection range-Doppler laser radar
[AD-A275619] p 3292 N94-28635
Radar estimations of atmospheric winds in the troposphere and lower stratosphere
p 3370 N94-29697
Three-axis fiber optic vector magnetometer
[AD-D016016] p 3288 N94-29699
A sounding rocket program in extreme and far ultraviolet interferometry
[NASA-CR-195114] p 3289 N94-29907
INTERFEROMETRY
Longitudinal effects and intensity-phase coupling in distributed feedback semiconductor lasers
p 3294 N94-29590
Enhanced coherence x ray laser experiments and simulations
[DE94-005367] p 3295 N94-30060
INTERLAMINAR STRESS
Correlation between wet ageing, humidity absorption and properties on composite materials based on different resins family
[REPT-932-600-107] p 3179 N94-29462
Interlaminar fracture analysis for laminated composites under combined loading p 3182 N94-29964
INTERLAYERS
Development of a new chemical warfare agent protective material p 3381 N94-28432
Pull-test adhesion measurements of diamondlike carbon films on silicon carbide, silicon nitride, aluminum oxide, and zirconium oxide
[DE94-005469] p 3211 N94-28536
Effect of microstructure on the strength and fracture energy of bimaterial interfaces
[AD-A274987] p 3178 N94-29126
Intra- versus interlayer pairing in the copper oxide superconductors: Response to a magnetic field
[DE94-005475] p 3521 N94-30898
INTERMETALLICS
Directional solidification studies in Ni-Al alloys
[DE94-005562] p 3201 N94-28527
Intermetallic growth at the interface between copper and bismuth-tin solder
[AD-A275716] p 3202 N94-28643
Innovative processing of composites for ultra-high temperature applications, book 2
[AD-A275598] p 3177 N94-28730
Study on the formation of ultrafine particles of Sm-Co intermetallic compounds using RF thermal plasma
p 3211 N94-29516
Fusion welding with self-generated filler metal
[NASA-CASE-LEW-15671-1] p 3301 N94-29557
The effect of various metallurgical parameters on the flow and fracture behavior of polycrystalline NiAl near the brittle-to-ductile transition
[NASA-TM-106534] p 3205 N94-29758
INTERNAL COMBUSTION ENGINES
The 1992-1993 advanced design program. Part 1: The Mars methane engine project. Part 2: The Mars oxygen processor new furnace
[NASA-CR-195513] p 3299 N94-29409
Numerical prediction of mixing process in a methane-fueled engine p 3304 N94-30230
In-cylinder gas velocity measurements comparing crankcase and blower scavenging in a fired two-stroke cycle engine
[DE94-005752] p 3311 N94-30596
INTERNAL FRICTION
Low temperature behavior of virgin martensite
[PB94-132925] p 3204 N94-29142
INTERNATIONAL COOPERATION
US/Japan cooperation in high energy physics
[DE94-005376] p 3494 N94-28486
Report of feasibility study on international-cooperation in high efficient energy conversion technology
[DE94-732340] p 3337 N94-28631
Journal of NIRE, Vol. 2, No. 2
[JTN-94-80552] p 3187 N94-28675
On United States-Japan Conference on Development and Utilization of Natural Resources: Report of the 14th Joint Meeting of U. S. and Japan Marine Mining Panel
p 3188 N94-28683
Protocol on environmental protection to the Antarctic Treaty and its annexes: International agreement on the comprehensive measures for the protection of Antarctic environment and ecosystems p 3354 N94-29086
Second Japan-U.S. Workshop on Global Change: Environmental Response Technologies for Global Change (Mitigation and Adaptation) p 3354 N94-29522
European PTTI report p 3468 N94-30642
INTERNATIONAL LAW
Protocol on environmental protection to the Antarctic Treaty and its annexes: International agreement on the comprehensive measures for the protection of Antarctic environment and ecosystems p 3354 N94-29086
INTERNATIONAL SUN EARTH EXPLORER 1
A study of the formation and dynamics of the Earth's plasma sheet using ion composition data
[NASA-CR-195119] p 3507 N94-30126

Tail lobe ion composition at energies of 0.1 to 16 keV/e: Evidence for mass-dependent density gradients
[PAPER-93JA03201] p 3507 N94-30127
Experimental investigation of possible geomagnetic feedback from energetic (0.1 to 16 keV) terrestrial O(+) ions in the magnetotail current sheet
[PAPER-93JA01991] p 3507 N94-30128

INTERNATIONAL SYSTEM OF UNITS
SI (Metric) handbook
[NASA-TM-109197] p 3231 N94-29376

INTERNETS
Learning about the Internet bibliography and beginners' guide
[AD-A275205] p 3430 N94-29051
The NIST Internet time service p 3475 N94-30678

INTERPLANETARY NAVIGATION
Enhanced orbit determination filter: Inclusion of ground system errors as filter parameters p 3159 N94-29656

INTERPOLATION
Upwind method using local interpolation p 3128 N94-28982
Closed form expressions for a consistent stress material nonlinear finite element p 3322 N94-30258
L(sub)p optimal d dimensional triangulations for piecewise linear interpolation: A new result on data dependent triangulations
[RUU-CS-93-13] p 3458 N94-30406
Noise and drift analysis of non-equally spaced timing data p 3472 N94-30667
Spatial interpolation, network bias, and terrestrial air temperature variability p 3374 N94-30810

INTERPROCESSOR COMMUNICATION
The management issues of implementing telecommuting: A case study
[AD-A275267] p 3527 N94-28905
Model-oriented analysis of a communications protocol
[PB94-138146] p 3244 N94-29109
Invariants, frames and postconditions: A comparison of two formal specification notations
[PB94-138153] p 3405 N94-29110
NPSNET: Integration of Distributed Interactive Simulation (DIS) protocol for communication architecture and information interchange
[AD-A275061] p 3530 N94-29139
High throughput network for multiprocessor interconnections
[VTT-PUBS-147] p 3245 N94-29468
Space reclamation for uncoordinated checkpointing in message-passing systems
[NASA-CR-195761] p 3420 N94-29906
An all pairs shortest paths distributed algorithm using 2n(exp 2) messages
[RUU-CS-93-19] p 3432 N94-30411
MANIFOLD version 1.0 programming: Programs and problems
[CWI-CS-R9334] p 3425 N94-30428
Manray: A replicated workers program in MANIFOLD
[CWI-CS-R9337] p 3433 N94-30429
Comparative semantics for linear arrays of communicating processes
[CWI-CS-R9336] p 3426 N94-30491
Parallel iteration across the steps of high order Runge-Kutta methods for nonstiff initial value problems
[CWI-NM-R9313] p 3433 N94-30730

INTERSTELLAR EXTINCTION
Dust in the Small Magellanic Cloud
[NASA-CR-195764] p 3543 N94-29696
Physical conditions in classical H2 regions in the Magellanic Clouds p 3543 N94-29722
Multicolor photometry of barred spiral galaxies p 3541 N94-30270

INTERSTELLAR GAS
The kinematics of molecular gas and dust in the nearby galaxies Centaurus A and M82 p 3544 N94-29738
A multi wavelength observational study of the Cartwheel ring galaxy p 3539 N94-29821

INTERSTELLAR MATTER
Dust in the Small Magellanic Cloud
[NASA-CR-195764] p 3543 N94-29696
The kinematics of molecular gas and dust in the nearby galaxies Centaurus A and M82 p 3544 N94-29738

INTERSTITIALS
Interstitially stabilized phases in the zirconium-nickel system
[DE94-005561] p 3201 N94-28525

INTERVALS
A characterization of graphs with interval two-step graphs
[AD-A275652] p 3451 N94-28651

INVARIANCE
On determination of a momentum of Alfven wave packet
[DE94-608329] p 3255 N94-30172
On some general properties of parabolic conservation equations
[DE94-006101] p 3461 N94-30758

INVENTIONS
DOE New Technology: Sharing New Frontiers, April 1, 1993 - September 30, 1993
[DE93-041289] p 3535 N94-30699

INVERSE KINEMATICS
Design and construction of the Aerobot Robotic Manipulator (ARM)
[AD-A275362] p 3298 N94-28894
Kinematics and force analysis of a robot hand based on an artificial biological control scheme p 3313 N94-30957

INVERSIONS
General theory and algorithms for the non-casual inversion, slewing and control of space-based articulated structures
[AD-A275118] p 3167 N94-29002

INVISCID FLOW
Numerical simulation of supersonic flow around space plane with engine installed p 3125 N94-28961
An implicit upwind scheme for the three-dimensional Euler equations using a pointwise relaxation method p 3128 N94-28983
Forced generation of solitary waves in a rotating fluid and their stability p 3274 N94-29689
Hydrodynamic stability analysis of swirling jets p 3278 N94-29974
An interactive, design and educational tool for supersonic external-compression inlets
[NASA-TM-106581] p 3421 N94-30174
Canonical-variables multigrid method for steady-state Euler equations
[NASA-CR-194888] p 3454 N94-30208

IO
Phasing the Very Large Array on Galileo in the presence of Jupiter's strong radio emission p 3164 N94-29621

IODINE
Ab initio study of vibrational frequency shift upon the 1:1 acetone-iodine complex formation p 3188 N94-28681

ION ACCELERATORS
The induction approach to heavy ion inertial fusion: Accelerator and target considerations
[DE94-005216] p 3494 N94-28507
Advantages of the LBL 88-inch cyclotron ion beam for SEP studies
[AD-A275142] p 3494 N94-29065
McMaster accelerator facility p 3496 N94-30217
Inertial confinement fusion
[DE94-005957] p 3510 N94-30875

ION ACOUSTIC WAVES
Large amplitude Langmuir and ion-acoustic waves in a relativistic two-fluid plasma
[NIFS-271] p 3506 N94-29547
Eigenmode analysis of the destabilized ion acoustic mode in tokamaks
[PPL-142] p 3507 N94-30158

ION ATOM INTERACTIONS
Energetic heavy-ion tracks in micron sites p 3495 N94-30213

ION BEAMS
The induction approach to heavy ion inertial fusion: Accelerator and target considerations
[DE94-005216] p 3494 N94-28507
Active electron and ion beam experiments in space
[AD-A275570] p 3504 N94-28828
Advantages of the LBL 88-inch cyclotron ion beam for SEP studies
[AD-A275142] p 3494 N94-29065
Focused ion beam fabrication of microelectronic structures
[AD-A275384] p 3264 N94-29305
A 6MeV heavy ion beam probe for the Large Helical Device
[NIFS-272] p 3505 N94-29397
Development and verification of a model to predict impingement currents for ion thrusters
[NASA-CR-195322] p 3173 N94-29546
Wave generation by contaminant ions near a large spacecraft
[NASA-CR-195797] p 3169 N94-29917
ECR plasma synthesis of silicon nitride films on GaAs and InSb
[DE94-005575] p 3515 N94-30006
A transmission-loss monitor using current transformers
[DE94-003974] p 3267 N94-30716
Atomic physics with highly charged ions
[DE94-003397] p 3492 N94-30837
Inertial confinement fusion
[DE94-005957] p 3510 N94-30875

ION CURRENTS
A future, intense source of negative hydrogen ions p 3494 N94-30485
Ionic conduction mechanisms in CaF2 and CaF2-Al2O3 nanocomposite films on Al2O3 substrates
[DE94-004792] p 3520 N94-30773

ION CYCLOTRON RADIATION
TFTR Ion Cyclotron Range of Frequencies (ICRF) experimental data analysis collaboration
[DE94-004699] p 3504 N94-28575
Efficiencies of the ICRF minority heating in the CHS and LHD plasmas
[NIFS-270] p 3506 N94-29499
Wave generation by contaminant ions near a large spacecraft
[NASA-CR-195797] p 3169 N94-29917

ION DISTRIBUTION
Tail lobe ion composition at energies of 0.1 to 16 keV/e: Evidence for mass-dependent density gradients
[PAPER-93JA03201] p 3507 N94-30127

ION EMISSION
Progress in Z-Pinch Research
[IPPCZ-321] p 3505 N94-29074
Investigation of intense XUV emission of nitrogen-puff Z-pinch with small energy input
[PH-23] p 3505 N94-29075
Multichannel x ray spectral measurement of hot plasma evolution in nitrogen-puff Z-pinch
[PH-24] p 3505 N94-29076
X ray emission scaling and energy balance of small gas-puff Z-pinch p 3505 N94-29077

ION ENGINES
Development and verification of a model to predict impingement currents for ion thrusters
[NASA-CR-195322] p 3173 N94-29546

ION EXCHANGING
Study of iron exchanged zeolites by Moessbauer effect and electron spin resonance spectroscopy
[DE94-605138] p 3514 N94-29691
A new material for removing heavy metals from water p 3354 N94-30471

ION IMPACT
Development and verification of a model to predict impingement currents for ion thrusters
[NASA-CR-195322] p 3173 N94-29546

ION IMPLANTATION
Silicon-Film (tm) photovoltaic manufacturing technology
[DE94-000258] p 3336 N94-28501
Density reduction: A mechanism for amorphization at high ion doses
[DE94-004793] p 3483 N94-28559
Silicon germanium carbon heteroepitaxial growth on silicon
[AD-A275197] p 3512 N94-28889
Nanosize metal alloy particle formation in Ag and Cu sequentially implanted silica
[DE94-005592] p 3207 N94-30042
Dislocation loops in spinel crystals irradiated successively with deep and shallow ion implants
[DE94-005083] p 3517 N94-30201
The influence of an in-situ electric field on H(+) and He(+) implantation induced defects insil icon
[DE94-006553] p 3518 N94-30249
Synthesis of (SiC)3N4 thin films by ion implantation
[DE94-006311] p 3521 N94-30851

ION IRRADIATION
Ion damage studies in GaAs/Al(0.6)Ga(0.4)As/GaAs heterostructures
[DE94-005384] p 3521 N94-30894

ION PROPULSION
A transportronic solution to the problem of interorbital transportation
[NASA-CR-191152] p 3164 N94-29355

ION RECOMBINATION
Dissociative recombination of H3(+)
[DE94-005356] p 3493 N94-30891

ION SCATTERING
Pulse height response of Si surface barrier detectors p 3497 N94-30221

ION SOURCES
A future, intense source of negative hydrogen ions p 3494 N94-30485
Inertial confinement fusion
[DE94-005957] p 3510 N94-30875

ION TEMPERATURE
Resistive ballooning mode in a gas-dynamic trap
[DE94-608328] p 3508 N94-30171

IONIC COLLISIONS
Reactions of metal ions and their clusters in the gas phase using laser ionization: Fourier transform mass spectrometry
[DE94-006208] p 3207 N94-30024

IONIC DIFFUSION
Ion channeling peculiarities in YBa2Cu3 O7 monocrystal
[DE94-606885] p 3512 N94-28787

IONIC REACTIONS
Low energy ion-molecule reactions and chemiionization kinetics
[DE94-005414] p 3481 N94-28491

Relativistic heavy ion research
[DE94-004701] p 3484 N94-28576

IONIZATION
Energy losses of fast charged particles in thin silicon detectors
[DE94-606065] p 3483 N94-28552
Enhanced ion dissociation of LiCF3SO3 by new carbonate plasticizers: Raman and IR studies
[DE94-005448] p 3485 N94-28741
Investigation of intense XUV emission of nitrogen-puff Z-pinch with small energy input
[PH-23] p 3505 N94-29075
The maximum entropy approach applied to energy exchange, chemical reactions and ionisation in the direct simulation Monte Carlo method for rarefied hypersonic flows
[IC-AERO-93-01] p 3524 N94-29481
Fast precise algorithm for simulation of ionization energy losses
[DE94-608010] p 3421 N94-30080

IONIZATION CROSS SECTIONS
Analytic cross sections for collisions of H, H2, He and Li atoms and ions with atoms and molecules
[DE94-707686] p 3485 N94-28788

IONIZING RADIATION
Response of GaAs charge storage devices to transient ionizing radiation
[DE94-005273] p 3510 N94-28484
Recent results from testing fast ADCs
[DE94-005565] p 3406 N94-30004
Role of x ray-induced transcripts in adaptive responses following x rays
[DE94-005412] p 3386 N94-30895

IONOSPHERIC DISTURBANCES
The effects of magnetic storm phases on F-layer irregularities from auroral to equatorial latitudes
[AD-A275203] p 3356 N94-28891

IONOSPHERIC ELECTRON DENSITY
Space-time structure of the morning aurora inferred from coincident DMSP-F6, -F8, and Sondrestrom incoherent scatter radar observations
[AD-A275442] p 3356 N94-28869
Accurate modeling of F-region electron densities
[NASA-CR-195781] p 3364 N94-30014

IONOSPHERIC ION DENSITY
Space-time structure of the morning aurora inferred from coincident DMSP-F6, -F8, and Sondrestrom incoherent scatter radar observations
[AD-A275442] p 3356 N94-28869

IONOSPHERIC PROPAGATION
Ionospheric corrections to precise time transfer using GPS p 3145 N94-30677

IONOSPHERIC SOUNDING
Proceedings of the NIPR Symposium on Upper Atmosphere Physics, no. 6
[JTN-94-80593] p 3359 N94-29233
Aurora stereo observation in Iceland
p 3359 N94-29234

IONS
Ion-assisted tropospheric OH measurement technique
p 3344 N94-28601
Enhanced ion dissociation of LiCF3SO3 by new carbonate plasticizers: Raman and IR studies
[DE94-005448] p 3485 N94-28741
Wave generation by contaminant ions near a large spacecraft
[NASA-CR-195797] p 3169 N94-29917
Brief summary of accomplishments since our DOE-sponsored radon project commenced
[DE94-004643] p 3348 N94-29926
Tail lobe ion composition at energies of 0.1 to 16 keV/e: Evidence for mass-dependent density gradients
[PAPER-93JA03201] p 3507 N94-30127
Experimental investigation of possible geomagnetic feedback from energetic (0.1 to 16 keV) terrestrial O(+) ions in the magnetotail current sheet
[PAPER-93JA01991] p 3507 N94-30128
Atomic physics with highly charged ions
[DE94-003397] p 3492 N94-30837

IRIDIUM
Evaluation of oxide-coated iridium-rhenium chambers
[NASA-TM-106442] p 3172 N94-29097

IRON
Dislocation theory of melting for iron, revisited
[DE94-002715] p 3355 N94-28538
Study of iron exchanged zeolites by Moessbauer effect and electron spin resonance spectroscopy
[DE94-605138] p 3514 N94-29691
Photovoltaic power without batteries for continuous cathodic protection p 3341 N94-30465
Dynamic constraints on CO2 uptake by an iron-fertilized Antarctic p 3350 N94-30619

IRON ALLOYS
Thermodynamic analysis of chemical compatibility of several compounds with Fe-Cr-Al alloys
[NASA-CR-191166] p 3181 N94-29684
New inoculants for ductile cast iron
[PB94-138476] p 3206 N94-29947
Terfenol: A study of the phase equilibrium diagram and the solidification process
[DE94-004883] p 3209 N94-30690
Giant magnetoresistance and microstructural characteristics of epitaxial Fe-Ag and Co-Ag granular thin films
[DE94-006287] p 3519 N94-30707

IRON CHLORIDES
Graphite intercalation compounds prepared from graphite fluoride
[NASA-TM-106447] p 3174 N94-28924

IRON COMPOUNDS
Study of iron exchanged zeolites by Moessbauer effect and electron spin resonance spectroscopy
[DE94-605138] p 3514 N94-29691
Magnetotransport measurements in magnetic fields up to 50T in SmB6 and FeSi
[DE94-006227] p 3520 N94-30848

IRON ISOTOPES
A high rate, low noise, x ray silicon strip detector system
[DE94-004557] p 3268 N94-30717

IRON 57
Backscatter Mossbauer Spectrometer (BaMS) for extraterrestrial applications p 3236 N94-29774

IRRADIANCE
The automated rotating shadowband spectroradiometer
[DE94-001878] p 3269 N94-28464

IRRADIATION
Electron beam irradiation experiments of monoblock divertor mock-up
[DE94-707497] p 3503 N94-28555
Surface energy changes produced by ultraviolet-ozone irradiation of poly(methylmethacrylate), polycarbone and polytetrafluoroethylene
[NASA-TM-106460] p 3213 N94-28922
Modeling the total dose radiation effects of Hg(1-x)Cd(x)Te photodiodes using numerical device simulators
[AD-A275235] p 3263 N94-29028
Induced crystallization in CW laser-irradiated sol-gel deposited titania films
[DE94-006527] p 3207 N94-30062
Dislocation loops in spinel crystals irradiated successively with deep and shallow ion implants
[DE94-005083] p 3517 N94-30201

ISING MODEL
Magnetic properties of a quantum transverse spin-1 Blume-Emery-Griffiths model
[DE94-608114] p 3517 N94-30109
Some results on the phase diagram of the antiferromagnetic Potts model in an external magnetic field
[DE94-608115] p 3468 N94-30110
Magnetic properties of the three dimensional Ising model with interface single-ion anisotropy
[DE94-608116] p 3525 N94-30164
Magnetic properties of a transverse spin-1 Ising model with longitudinal crystal field interactions
[DE94-608118] p 3517 N94-30165
The bond diluted spin-1 Blume-Emery-Griffiths model in a transverse field
[DE94-608121] p 3525 N94-30167
Magnetic properties of a transverse spin-1 Ising model with random crystal field interactions
[DE94-608117] p 3517 N94-30181

ISOMERS
Comparison of 14 MeV isomer production of Hf-178m1 and Hf-179m2 using Feshbach-Kerman-Koonin and exciton preequilibrium models
[DE94-002640] p 3488 N94-30039

ISOMORPHISM
Isomorphisms between predicate and state transformers
[RUU-CS-93-09] p 3458 N94-30403
Isomorphisms between predicate and state transformers
[CWI-CS-R9338] p 3459 N94-30430
Relating state transformation semantics and predicate transformer semantics for parallel programs
[CWI-CS-R9339] p 3433 N94-30431
Remarks on uniformly finitely precomplete positive equivalences
[ML-93-12] p 3463 N94-30975

ISOTHERMAL LAYERS
On the temperature distribution near a cold surface
[AD-A275162] p 3332 N94-29288

ISOTOPES
Interannual-decadal variability in tropical climate systems: Stable isotope records and general circulation model experiments p 3373 N94-29962

ISOTOPIC LABELING
Geochemical and fluid dynamic investigations into the nature of chemical variability in the Earth's mantle
p 3367 N94-30917

ISOTROPIC TURBULENCE
Spherical model for turbulence p 3274 N94-29730

ISRAEL
Research laboratories annual report 1992
[DE94-608124] p 3555 N94-30168

ITERATION
Gaussian beam and physical optics iteration technique for wideband beam waveguide feed design
p 3248 N94-29624
Iterative procedure as equation of motion
[DE94-608008] p 3453 N94-30078
Categorial generalization of algebraic recursion theory
[ML-93-06] p 3456 N94-30382
Parallel iteration across the steps of high order Runge-Kutta methods for nonstiff initial value problems
[CWI-NM-R9313] p 3433 N94-30730
On the unification free PROLOG programs
[CWI-CS-R9331] p 3427 N94-30733

ITERATIVE SOLUTION
Applied analysis/computational mathematics
[DE94-005133] p 3451 N94-28571
Computational fluid dynamics in ventilation. 1: Theory and one-dimensional test case p 3232 N94-29606
Approximation methods for nonlinear operator equations of the m-accretive type
[DE94-608099] p 3467 N94-30065
Iterative procedure as equation of motion
[DE94-608008] p 3453 N94-30078
Calculus of variations applied to 2D multi-point airfoil design
[PB94-125457] p 3133 N94-30401
A residual correction method applied to 2D multi-point airfoil design and 3D single-point wing design
[NLR-TP-92524-U] p 3134 N94-30493

IUE
Camera artifacts in IUE spectra
[NASA-CR-189337] p 3198 N94-29857

J

J INTEGRAL
Plane stress stable crack growth and J-integral/HRR field
[AD-A275761] p 3317 N94-28761
Dynamic fracture mechanics analysis for an edge delamination crack
[NASA-TM-109106] p 3479 N94-29856

J-85 ENGINE
Radar jet engine health monitoring project
[ASSGI-301] p 3153 N94-30130

JACOBI INTEGRAL
Method of Chabauty-Coleman and the second case of Fermat's last theorem for regular primes
[PB94-138187] p 3467 N94-29162

JACOBI MATRIX METHOD
Eigenvalue analysis of the convergence behaviour of an Euler method
[PB94-1255722-U] p 3281 N94-30743

JAMMING
Spurs in digital radio frequency memory and applications of DRFM
[AD-A275013] p 3243 N94-28897

JAPAN
On United States-Japan Conference on Development and Utilization of Natural Resources: Report of the 14th Joint Meeting of U. S. and Japan Marine Mining Panel
p 3188 N94-28683

JAPANESE SPACECRAFT
Keynote address --- Japanese Earth Resources Satellite 1 (JERS-1) and future remote sensing projects
p 3326 N94-28926
JERS-1 data acquisition and distribution
p 3326 N94-28931
Outline of JERS-1 system p 3330 N94-29220
Observatory system of Earth Resources Satellite-1
p 3330 N94-29221
Application of remote sensing techniques in petroleum exploration: The Indonesian experience
p 3331 N94-29225
Japan's Earth observation satellite programs
p 3332 N94-29232

JET AIRCRAFT
Information presentation for expert systems in future fighter aircraft
[AD-A275126] p 3149 N94-29005

JET ENGINE FUELS
High temperature fuel requirements and payoffs
p 3192 N94-29259
High temperature resistant jet fuels
p 3192 N94-29260

Research and development of high thermal stability fuels p 3192 N94-29261
Development of global/chemistry model for jet-fuel thermal stability based on observations from static and flowing experiments p 3192 N94-29262
The effect of incomplete fuel-air mixing on the lean limit and emissions characteristics of a Lean Prevaporized Premixed (LPP) combustor p 3193 N94-29265
Endothermic fuels for hypersonic aviation p 3197 N94-29285
Liquid atomization in supersonic flows p 3276 N94-29839

JET ENGINES
Combustion for future supersonic transport propulsion p 3190 N94-29249
Automated inspection of turbine blades: Challenges and opportunities
[AIAA PAPER 94-1226-CP] p 3446 N94-30575

JET FLOW
Transonic expanding flow through axially symmetric orifices p 3128 N94-28985
Lifted turbulent jet flames p 3198 N94-29676
Hydrodynamic stability analysis of swirling jets p 3278 N94-29974
The instantaneous concentration field in the self-similar region of a high Schmidt number round jet p 3278 N94-29976
An experimental study of nonlinear wave coupling and energy transfer characterizing the transition of a planar jet shear layer p 3282 N94-30953

JET IMPINGEMENT
Aircraft aerodynamics with deflected jets in ground effect p 3132 N94-29973

JET MIXING FLOW
Study on mixing and injection of hydrogen into a supersonic flow p 3127 N94-28975
The mixing process in the quenching zone of the rich-lean-combustion concept p 3196 N94-29281
Temperature and combustion analysis of combustor with acoustically controlled primary zone air-jet mixing p 3196 N94-29284
Scramjet CFD methods and analysis. Part 2: Scramjet CFD analysis. Numerical simulation of supersonic mixing and combustion applied to scramjet combustor p 3152 N94-29300

JET PROPULSION
Combustion for future supersonic transport propulsion p 3190 N94-29249

JETS
Properties of events containing a photon and several jets seen in p(bar p) collisions at (radical)s = 1.8 TeV
[DE94-005596] p 3482 N94-28531

JOINTS (JUNCTIONS)
Mechanical flexible joint design document
[NASA-CR-193941] p 3297 N94-28419
Collapsible mechanical joint
[NASA-CASE-MFS-28765-1] p 3299 N94-29367
Method and apparatus for indicating disbonds in joint regions
[NASA-CASE-LAR-14626-1] p 3315 N94-29548

JOSEPHSON JUNCTIONS
Exploratory research for a high temperature superconducting integrated circuit
[AD-A275798] p 3262 N94-28767
Epitaxial heterojunctions of oxide semiconductors and metals on high temperature superconductors
[NASA-CASE-NPO-18483-1-CU] p 3513 N94-29501
The bases for the development of high-temperature integrated SQUID-systems
[DE94-607901] p 3267 N94-30073
The bases for the development of high-temperature integrated SQUID-systems
[DE94-608462] p 3517 N94-30082

JOURNAL BEARINGS
Effects of diffusion and inertia on chaotic mixing: A computational and experimental study p 3488 N94-29903

JP-8 JET FUEL
Research and development of high thermal stability fuels p 3192 N94-29261

JUDGMENTS
Subjective response to sonic booms having different shapes, rise times, and durations
[NASA-TM-109090] p 3479 N94-29464

JUNCTION DIODES
Analysis of microwave induced interference in pn-diodes
[PB94-136983] p 3243 N94-28906

JUNCTION TRANSISTORS
Effects of oxide charge and surface recombination velocity on the excess base current of BJT's
[DE94-003711] p 3263 N94-29025

JUPITER (PLANET)
Phasing the Very Large Array on Galileo in the presence of Jupiter's strong radio emission p 3164 N94-29621

JUPITER ATMOSPHERE
Observation of Jovian auroral Ly-alpha line profile and emission variability with a sounding rocket and the IUE archives p 3550 N94-30798

K

K LINES
Surface differential rotation in a sample of cool dwarf stars p 3545 N94-29827

K-EPSILON TURBULENCE MODEL
Modeling turbulence in flows with a strong rotational component
[DE94-003577] p 3270 N94-28475
Numerical simulation of aerothermal characteristics in gas turbine combustors with complex geometries p 3154 N94-29255

KALMAN FILTERS
An improved conscan algorithm based on a Kalman filter p 3251 N94-29670
The use of the AOA TTR-4P GPS receiver in operation at the BIPM for real-time restitution of GPS time p 3144 N94-30651
Time transfer using geostationary satellites: Implementation of a Kalman filter p 3471 N94-30657
A comparison of GPS broadcast and DMA precise ephemerides p 3145 N94-30660
Application of the extended Kalman filter to the estimation of the char mass in a fluidized bed combustor
[REPT-93-065] p 3200 N94-30938

KAONS
Weak decays of charged K-mesons and charm particles
[PB94-138062] p 3486 N94-29143

KAPTON (TRADEMARK)
Selection of the Space Station Freedom (SSF) Flat Collector Circuit (FCC) insulation material p 3165 N94-28701
Ablation of polymers by ultraviolet pulsed laser
[DE94-608100] p 3218 N94-30066

KELVIN-HELMHOLTZ INSTABILITY
Transition to turbulence in confined compressible mixing layers p 3283 N94-30958

KERNEL FUNCTIONS
Method of Chabauty-Coleman and the second case of Fermat's last theorem for regular primes
[PB94-138187] p 3467 N94-29162
The MSRC ab initio methods benchmark suite: A measurement of hardware and software performance in the area of electronic structure methods
[DE94-006428] p 3514 N94-30001
Euler results of the ISNaS compressible multi-block flow solver
[AD-B179299] p 3281 N94-30756

KEROSENE
High temperature resistant jet fuels p 3192 N94-29260
Ducted kerosene spray flames p 3195 N94-29276

KINEMATICS
Kinematic functions for redundancy resolution using configuration control
[NASA-CASE-NPO-18608-1-CU] p 3436 N94-29504
Kinematic representations, workspace analysis, and grasp stability in robot arms and multi-fingered hands p 3301 N94-29847
Fuzzy logic based robotic controller
[AIAA PAPER 94-1202-CP] p 3443 N94-30553
Kinematic analysis of platform-type robotic manipulators
[ISBN-0-315-78703-1] p 3311 N94-30793

KINESTHESIA
Basic understanding of vertigo p 3390 N94-28855

KINETIC ENERGY
Volume averaged model for the mechanics of alloys solidification
[PB94-138617] p 3208 N94-30113

KINETIC EQUATIONS
Self-similar variables and the problem of nonlocal electron heat conductivity
[DE94-005826] p 3493 N94-30881

KIRCHHOFF LAW OF NETWORKS
An intrinsic Hamiltonian formulation of the dynamics of LC-circuits
[MEMO-1154] p 3462 N94-30964

KITS
Using generic tool kits to build intelligent systems
[AIAA PAPER 94-1214-CP] p 3445 N94-30565

KLEIN-GORDON EQUATION
On dyonic black holes and cosmic censorship p 3546 N94-29912

KNOWLEDGE BASED SYSTEMS
Toward a model of expert knowledge structure and their role in cognitive task performance
[AD-A275641] p 3529 N94-28645
A cognitive model of decision making: Chunking and the radar detection device
[AD-A275185] p 3242 N94-28859
Investigation into formalization of domain-oriented parallel software development
[AD-A275177] p 3430 N94-29050
Neural network solutions to logic programs with geometric constraints
[AD-A275419] p 3435 N94-29198
Designing and maintaining decision-making processes p 3412 N94-29318
Embedded expert system: From the mock-up to the real world p 3412 N94-29319
Object oriented design of the autonomous fixtaking management system p 3143 N94-29323
Artificial intelligence technology program at Rome Laboratory p 3414 N94-29328
Advances in development capabilities for intelligent air traffic management systems p 3137 N94-29559
Airside ground movements surveillance p 3141 N94-29585
Pearl's belief propagation: The proofs
[RUU-CS-92-47] p 3456 N94-30378
Multi-sensor data fusion and the use of artificial intelligence
[PB94-126216] p 3448 N94-30741

KNOWLEDGE BASES (ARTIFICIAL INTELLIGENCE)
Incorporating geometric constraints into rule-based systems using nonlinear optimization
[AD-A275093] p 3452 N94-29063

KNOWLEDGE REPRESENTATION
Pearl's belief propagation: The proofs
[RUU-CS-92-47] p 3456 N94-30378

KOLMOGOROV THEORY
Hierarchical structures and asymmetric stochastic processes on p-adics and adeles
[PB94-138203] p 3464 N94-29178
Spherical model for turbulence p 3274 N94-29730
Thermodynamics of computation and information distance
[CWI-CS-R9341] p 3526 N94-30433
The Boltzmann entropy and randomness tests
[CWI-CS-R9342] p 3426 N94-30434

KOLMOGOROV-SMIRNOV TEST
Relations between varieties of Kolmogorov complexities
[CWI-CS-R9329] p 3427 N94-30732

KONDO EFFECT
Scaling in heavy-fermion systems
[DE94-005002] p 3492 N94-30775

KORTEWEG-DEVRIES EQUATION
Forced generation of solitary waves in a rotating fluid and their stability p 3274 N94-29689
Graded Froelicher-Nijenhuis brackets and the theory of recursion operators for super differential equations
[MEMO-1147] p 3460 N94-30736
Dissipation in Hamiltonian systems: Decaying cnoidal waves
[MEMO-1151] p 3460 N94-30738

L

LABORATORIES
Testing laboratories as notified bodies
[PB94-132396] p 3160 N94-28413
High Tc superconducting bolometric and nonbolometric infrared (IR) detectors
[NASA-CR-195728] p 3262 N94-28846
Artificial intelligence technology program at Rome Laboratory p 3414 N94-29328

LAGRANGE MULTIPLIERS
An investigation into certain geometrical and variational properties of the P(4) theory of gravitation and electromagnetism p 3526 N94-30950

LAGRANGIAN FUNCTION
The Klein-Fock equation, minimal surfaces and gravitational fields
[DE94-606340] p 3356 N94-28803
On determination of a momentum of Alfven wave packet
[DE94-608329] p 3255 N94-30172
Plane strain finite element analysis of sheet forming operations including bending effects p 3322 N94-30354
Nonlinear multibody formulation for rotorcraft analysis p 3149 N94-30787
Application of ALE techniques to metal forming simulations
[DE94-005358] p 3211 N94-30892
An investigation into certain geometrical and variational properties of the P(4) theory of gravitation and electromagnetism p 3526 N94-30950

LAKE MICHIGAN
The suitability of low-cost urban airshed modeling in the Chicago area
[DE94-005114] p 3349 N94-30023
LAKES
Model-oriented data analysis with applications to lake and soil water simulation
[PB94-136942] p 3329 N94-29173
LAMINAR BOUNDARY LAYER
Experiments and theoretical considerations regarding the allowable roughness height in laminar flow
[PB94-125556] p 3133 N94-30389
LAMINAR FLOW
Flow and heat transfer in a rotating square sectioned U-bend p 3128 N94-28984
Numerical analysis of laminar flow in S-curved square duct with inlet and outlet straight region p 3128 N94-28987
Development of buoyancy affected laminar flow in a heated pipe p 3128 N94-28988
Mutual similarity of developing laminar flows with secondary streams in ducts: Curved pipe flow and orthogonal rotating pipe flow p 3129 N94-28989
Laminar Flow Supersonic Wind Tunnel primary air injector p 3158 N94-29649
Prediction of fluid flow and heat transfer in internally finned tubes p 3280 N94-30226
LAMINAR HEAT TRANSFER
Flow and heat transfer in a rotating square sectioned U-bend p 3128 N94-28984
LAMINATES
Development of a new chemical warfare agent protective material p 3381 N94-28432
Characterization of structure and mechanical properties of MoSi2-SiC nanolayer composites
[DE94-004962] p 3175 N94-28579
Fabrication and testing of plasma-spray formed MoSi2 and MoSi2 composite tubes
[DE94-004995] p 3175 N94-28581
Numerical and experimental investigation of the bending response of thin-walled composite cylinders
[NASA-CR-195730] p 3317 N94-28801
Prediction of stress-strain response of SCS-6/Timetal-21S subjected to a hypersonic flight profile
[NASA-TM-109026] p 3177 N94-28823
Fatigue behavior of a cross-ply ceramic matrix composite under strain controlled tension-tension and tension-compression loading
[AD-A275374] p 3177 N94-29012
Assessment of the fibre volume distribution around optical fibres
[FFA-TN-1993-12] p 3179 N94-29425
Preliminary evaluation of hybrid titanium composite laminates
[NASA-TM-109095] p 3180 N94-29472
Effects of physical aging on long-term creep of polymers and polymer matrix composites
[NASA-TM-109081] p 3181 N94-29541
Active control of delaminations in smart composite structures p 3181 N94-29593
Free edge and size effects on failure initiation and ultimate strength of laminates containing a center hole p 3181 N94-29735
Performance of a higher-order triangular finite element for composite laminated structures p 3181 N94-29810
Failure strength and mechanism of composite laminates under multiaxial loading conditions p 3182 N94-29875
Interlaminar fracture analysis for laminated composites under combined loading p 3182 N94-29964
Computational simulation of composite structures with and without damage
[NASA-CR-194433] p 3183 N94-30190
Three-dimensional free vibration analysis of thick arbitrarily laminated, rectangular, cylindrical and spherical composite panels p 3184 N94-30257
Damage analysis and mechanical response of as-received and heat-treated Nicalon/CAS-2 glass-ceramic matrix composites p 3219 N94-30259
The machining of fiber metal laminates. Part 1: An inventory of forming processes
[LR-710-PT-1] p 3184 N94-30343
Damage identification in composites using built-in piezoelectrics p 3184 N94-30355
Four advances in carbon-carbon materials technology p 3186 N94-30481
RF and microwave dielectric measurements upon layered materials using reflectometric coaxial sensor
[NPL-DES-125] p 3476 N94-30781
Thin-walled orthotropic laminated beam theory p 3324 N94-30920
LAND ICE
Glacial landforms and late Cenozoic history of the western Soer-Rondane mountains p 3357 N94-29080
Chemical composition of insoluble particles in superimposed ice on Storoeya, Svalbard (Sweden)
[CM-82] p 3336 N94-30944
LAND MANAGEMENT
Utilization of remote sensing data in Southeast Asia p 3327 N94-28936
Remote sensing and global management p 3328 N94-28937
Tohoku district observed by artificial satellites p 3328 N94-29041
Radar applications at the Canada Centre for Remote Sensing p 3331 N94-29224
JERS-1 and future remote sensing: Application of remote sensing data to agroecological problems p 3331 N94-29229
Application of remote sensing in prevention of disasters p 3332 N94-29230
Future expectation of remote sensing technology p 3332 N94-29231
LAND USE
Development and implementation of a scrub habitat compensation plan for Kennedy Space Center
[NASA-TM-109202] p 3347 N94-29099
Extrapolation of point data for resource mapping p 3334 N94-29959
LANDFORMS
The uses and limitations of fractal geometry in digital terrain modelling p 3333 N94-29958
A coupled approach to spatially derived parameters necessary for ecosystem modeling on the North Slope of Alaska: Appendix A
[DE94-005853] p 3349 N94-30046
LANDING GEAR
BAG: A code for predicting the performance of a gas bag impact attenuation system for the Pathfinder lander
[DE94-003688] p 3165 N94-28477
Landing gear energy absorption system
[NASA-CASE-MSC-22277-1] p 3300 N94-29448
LANDING LOADS
Landing gear energy absorption system
[NASA-CASE-MSC-22277-1] p 3300 N94-29448
LANDING MATS
Composite panel failure analysis and improvement plan
[AD-A275655] p 3176 N94-28653
LANDING SIMULATION
Flight simulator evaluation of advanced MLS procedures
[AD-B174270] p 3143 N94-30915
LANGEVIN FORMULA
Derivation of a Fokker-Planck equation for bunched beams
[DE94-004950] p 3483 N94-28565
Non-Markovian quantum Brownian motion of a harmonic oscillator
[DE94-005922] p 3477 N94-30873
LANGUAGE PROGRAMMING
Comparative semantics for linear arrays of communicating processes
[CWI-CS-R9336] p 3426 N94-30491
LANGUAGES
A framework for comparing conceptual modelling languages
[TR-92-29] p 3535 N94-30361
LANTHANUM COMPOUNDS
Centrifugal atomization of lanthanide materials for cryogenic coolers
[DE94-006035] p 3219 N94-30337
LANTHANUM OXIDES
influence of doping on the electronic structure of (La, Sr)2CuO4
[DE94-006383] p 3516 N94-30054
Transient studies of low temperature catalysts for methane conversion
[DE94-005767] p 3200 N94-30877
LAP JOINTS
Full-scale testing and analysis of curved aircraft fuselage panels
[AD-A275666] p 3145 N94-28657
Analysis concerning the inspection threshold for multi-site damage
[PB94-142429] p 3149 N94-30905
LARGE SCALE INTEGRATION
Investigation of advanced fault insertion and simulator methods
[NASA-CR-195241] p 3261 N94-28511
The 1992 report on the next generation ultra clean technology for advanced microfabrication
[DE94-744171] p 3157 N94-30268
LARGE SPACE STRUCTURES
General theory and algorithms for the non-casual inversion, slewing and control of space-based articulated structures
[AD-A275118] p 3167 N94-29002
Concurrent simulation and constraint stabilization for flexible multibody systems p 3154 N94-29532
The 27th Aerospace Mechanisms Symposium
[NASA-CP-3205] p 3160 N94-29627
LASER ABLATION
Laser-material interactions: A study of laser energy coupling with solids
[DE94-005212] p 3292 N94-28478
Ablation of polymers by ultraviolet pulsed laser
[DE94-608100] p 3218 N94-30066
LASER APPLICATIONS
Annual summary of basic research thermoacoustic heat transport, 1993
[AD-A275751] p 3230 N94-28644
Digital tracking and control of retinal images
[AD-A275469] p 3389 N94-28810
The laser approach for sequential pyrotechnic initiation systems: Envisageable chain architecture and concepts
[REPT-932-430-113] p 3225 N94-29414
Lasercom system architecture with reduced complexity
[NASA-CASE-NPO-19069-1-CU] p 3293 N94-29493
Solid state laser systems for space application
[NASA-CR-195777] p 3294 N94-29914
Research laboratories annual report 1992
[DE94-608124] p 3555 N94-30168
Development of high time-resolution laser flash equipment for thermal diffusivity measurements using miniature-size specimens
[NIFS-268] p 3295 N94-30186
Space debris removal using a high-power ground-based laser
[DE94-006363] p 3169 N94-30264
Sensing the gas metal arc welding process p 3314 N94-30444
Dual use of image based tracking techniques: Laser eye surgery and low vision prosthesis p 3397 N94-30455
Optical techniques for time and frequency transfer p 3469 N94-30647
Relativistic theory for picosecond time transfer in the vicinity of Earth p 3470 N94-30653
LASER ARRAYS
Dynamics of a coupled solid state laser array p 3294 N94-29551
LASER BEAMS
Laser-material interactions: A study of laser energy coupling with solids
[DE94-005212] p 3292 N94-28478
Laser beam steering with semiconductor waveguide
[AD-A275775] p 3292 N94-28765
Radiation transport and focusing systems for power industrial lasers
[DE94-606817] p 3293 N94-28786
Aberrated point-spread functions and beam quality for optical systems with annular pupils
[AD-A275311] p 3499 N94-28875
Lasercom system architecture with reduced complexity
[NASA-CASE-NPO-19069-1-CU] p 3293 N94-29493
Advances in tunable powerful lasers: The advanced free-electron laser
[DE94-004997] p 3294 N94-29934
Research on the atomic layer-by-layer growth of high-temperature superconductor thin films at the Institute of Scientific and Industrial Research, Japan
[DE94-003739] p 3519 N94-30611
LASER CAVITIES
Visible vertical cavity surface emitting lasers
[AD-A275334] p 3293 N94-28919
LASER CUTTING
Thin EFG octagons
[DE94-000257] p 3339 N94-30605
LASER DAMAGE
Characterization of defect geometries in multilayer optical coatings
[DE94-005820] p 3501 N94-30599
LASER DEPOSITION
Optoelectronic integrated circuits fabricated using atomic layer epitaxy
[AD-A275454] p 3262 N94-28805
Deposition of tantalum carbide coatings on graphite by laser interactions p 3223 N94-30475
LASER DOPPLER VELOCIMETERS
Development of laser velocimetry for the measurements of turbulence intensity and flow velocity ahead of a NGV row in a full-stage rotating turbine
[AD-A275712] p 3270 N94-28692
Laser velocimeter data acquisition system for the Langley 14- by 22-foot subsonic tunnel. Software reference guide version 3.3
[NASA-CR-191606] p 3293 N94-28839
The enhancement of compressible turbulent mixing via streamwise vorticity p 3280 N94-30487
LASER FUSION
Diode-pumped solid-state-laser drivers and the competitiveness of inertial fusion energy
[DE94-006654] p 3296 N94-30830

LASER HEATING
Laser-material interactions: A study of laser energy coupling with solids
[DE94-005212] p 3292 N94-28478
Deposition of tantalum carbide coatings on graphite by laser interactions p 3223 N94-30475
LASER INDUCED FLUORESCENCE
Instrumental development of novel detection and separation methods for capillary electrophoresis
[DE94-005554] p 3187 N94-28519
Two-Photon/Laser-Induced Fluorescence (TP/LIF) sensor p 3342 N94-28588
In situ detection of tropospheric OH and HO2 by laser-induced fluorescence in a detection chamber at low pressure p 3342 N94-28589
Tropospheric HO determination by FAGE p 3342 N94-28590
Detection of tropospheric OH and HO2 by laser-induced fluorescence at low pressure using the 308nm excitation of OH p 3343 N94-28591
Harvard ER-2 OH laser-induced fluorescence instrument p 3343 N94-28592
JPL Fourier transform ultraviolet spectrometer p 3343 N94-28593
Tropospheric HO2 determination by FAGE p 3345 N94-28606
Advanced diagnostics for reacting flows
[AD-A275057] p 3272 N94-29136
LASER INTERFEROMETRY
Toward astrometric tracking with the infrared spatial interferometer p 3249 N94-29653
LASER MATERIALS
Optical studies of dynamical processes in disordered systems
[DE94-006751] p 3501 N94-30252
LASER MICROSCOPY
Near-ultraviolet laser photoemission: Scanning microscopy, buried interfaces and image-potential states p 3294 N94-29531
LASER OUTPUTS
Advances in tunable powerful lasers: The advanced free-electron laser
[DE94-004997] p 3294 N94-29934
LASER PLASMAS
Enhanced coherence x ray laser experiments and simulations
[DE94-005367] p 3295 N94-30060
Magnetic field generation by circularly polarized laser light and inertial plasma confinement in a miniature magnetic bottle induced by circularly polarized laser light
[DE94-608353] p 3508 N94-30192
LASER POWER BEAMING
Space debris removal using a high-power ground-based laser
[DE94-006363] p 3169 N94-30264
Reactor-pumped laser facility at DOE's Nevada Test Site
[DE94-006371] p 3295 N94-30265
Fission-activated laser as primary power for CW laser propulsion
[DE94-006138] p 3295 N94-30367
LASER PROPULSION
Fission-activated laser as primary power for CW laser propulsion
[DE94-006138] p 3295 N94-30367
LASER PUMPING
Reactor-pumped laser experimental results
[DE94-005247] p 3292 N94-28482
High-power CW diode-laser-array-pumped solid-state lasers and efficient nonlinear optical frequency
[AD-A275394] p 3293 N94-29309
Time and frequency technology at NIST p 3468 N94-30641
LASER RANGE FINDERS
Fusion of range and luminance data from laser radar systems
[AD-A275608] p 3292 N94-28770
GLRS-R 2-colour retroreflector target design and predicted performance
[REPT-932-440-106] p 3246 N94-29542
LASSO experiment: Intercalibrations of the LASSO ranging stations p 3297 N94-30666
New perspectives for high accuracy SLR with second generation geodesic satellites
[REPT-932-440-105] p 3336 N94-30965
LASER SPECTROMETERS
Measurement of tropospheric OH by laser long-path absorption spectroscopy p 3343 N94-28596
NOAA Aeronomy Laboratory long-path OH experiment, Fritz Peak Observatory, Colorado p 3344 N94-28598
LASER SPECTROSCOPY
UV laser long-path absorption speciroscopy p 3343 N94-28595
Measurement of tropospheric OH by laser long-path absorption spectroscopy p 3343 N94-28596
On the possibility of measuring atmospheric OH using intracavity laser spectroscopy p 3344 N94-28597
NOAA Aeronomy Laboratory long-path OH experiment, Fritz Peak Observatory, Colorado p 3344 N94-28598
Near-IR diode laser absorption for measurement of tropospheric HO2 p 3345 N94-28607
HO2 detection by near infrared absorption using tunable diode lasers p 3346 N94-28608
Advanced diagnostics for reacting flows
[AD-A275057] p 3272 N94-29136
Magnetic field generation by circularly polarized laser light and inertial plasma confinement in a miniature magnetic bottle induced by circularly polarized laser light
[DE94-608353] p 3508 N94-30192
LASER TARGETS
GLRS-R 2-colour retroreflector target design and predicted performance
[REPT-932-440-106] p 3246 N94-29542
Enhanced coherence x ray laser experiments and simulations
[DE94-005367] p 3295 N94-30060
LASER WELDING
Laser beam welding of AISI 316 stainless steel in microgravity environment: Experiments aboard a KC-135 flight
[ISBN-0-315-86095-2] p 3229 N94-30145
LASERS
Photonic devices and systems for optical signal processing
[AD-A275818] p 3498 N94-28804
Spatial light modulators with arbitrary quantum wells profiles
[AD-A275023] p 3499 N94-29114
LASING
Linac Coherent Light Source (LCLS) at 2-4 nm using the SLAC linac
[DE94-005235] p 3292 N94-28481
Visible vertical cavity surface emitting lasers
[AD-A275334] p 3293 N94-28919
Dynamics of a coupled solid state laser array p 3294 N94-29551
LATCH-UP
Advantages of the LBL 88-inch cyclotron ion beam for SEP studies
[AD-A275142] p 3494 N94-29065
Single event upset and latchup measurements at Brookhaven National Laboratory p 3495 N94-30212
Single event upset susceptibilities of latchup immune CMOS process programmable gate arrays p 3495 N94-30214
Determination of cosmic ray latchup rate in CMOS devices p 3497 N94-30222
LATTICE PARAMETERS
Crystal structure of La(2-x)Ba(x)CuO4
[DE94-707688] p 3511 N94-28750
Research on the improvement of shape-memory and magnetostrictive materials
[AD-A275397] p 3203 N94-29056
LATTICE VIBRATIONS
Vibrational properties of homopolar and heteropolar surfaces and interfaces of the CdTe/HgTe system
[DE94-608105] p 3516 N94-30069
LATTICES (MATHEMATICS)
Codes on the unit sphere
[PB94-136991] p 3453 N94-29174
Reconstruction of spectra in the discrete quantum mechanics (new elements of the lattice quantum engineering)
[DE94-608075] p 3524 N94-30087
LAUNCH VEHICLES
Advanced vehicle concepts systems and design analysis studies
[NASA-CR-195115] p 3147 N94-29721
Fission-activated laser as primary power for CW laser propulsion
[DE94-006138] p 3295 N94-30367
LAUNCHING
The laser approach for sequential pyrotechnic initiation systems: Envisageable chain architecture and concepts
[REPT-932-430-113] p 3225 N94-29414
Missile launch detection electric field perturbation experiment
[DE94-004224] p 3466 N94-30586
LAW (JURISPRUDENCE)
The European community directive: An alternative environmental impact assessment procedure after Massey?
[AD-A275550] p 3347 N94-28844
LAWS
Omnibus Budget Reconciliation Act of 1990
[PUB-LAW-101-508] p 3537 N94-28540
LAY-UP
Composite hot drape forming p 3240 N94-30448
LC CIRCUITS
An intrinsic Hamiltonian formulation of the dynamics of LC-circuits
[MEMO-1154] p 3462 N94-30964
LEAD ALLOYS
Logistics for the implementation of lead-free solders on electronic assemblies
[DE94-004800] p 3206 N94-29936
LEAD COMPOUNDS
Measurement of elemental speciation by liquid chromatography: Inductively coupled plasma mass spectrometry (LC-ICP-MS) with the Direct Injection Nebulizer (DIN)
[DE94-005261] p 3187 N94-28483
LEADING EDGES
Experimental investigation of three-dimensional vortex-airfoil interaction in a supersonic stream
[AD-A275107] p 3122 N94-28899
An experimental investigation of the effect of leading edge extensions on directional stability and the effectiveness of forebody nose strakes p 3155 N94-29728
An experimental study of the aerodynamics of a swept and unswept semispan wing with a simulated glaze ice accretion
[NASA-CR-195330] p 3133 N94-30152
LEAST SQUARES METHOD
Least-squares determination of burst-point coordinates
[AD-A275423] p 3452 N94-28864
Theoretical study of the incompressible Navier-Stokes equations by the least-squares method
[NASA-TM-106535] p 3272 N94-29096
Prediction and standard error estimation for a finite universe total when a stratum is not sampled
[DE94-004929] p 3465 N94-30696
LECTURES
The (j,0) + (0,j) representation space: Dirac-like construct
[DE94-005011] p 3522 N94-28572
Research and Development of Ram/Scramjets and Turboramjets in Russia
[AGARD-LS-194] p 3151 N94-29291
Introduction and overview of research and development of solid propellant ramrockets, liquid fuel ramjets and experimental hydrogen ram combustors p 3151 N94-29292
LEG (ANATOMY)
Leg muscle volume during 30-day 6-degree head-down bed rest with isotonic and isokinetic exercise training
[NASA-TM-4580] p 3385 N94-29401
LEGENDRE FUNCTIONS
Fast gravity, gravity partials, normalized gravity, gravity gradient torque and magnetic field: Derivation, code and data
[NASA-CR-188243] p 3361 N94-29588
LENS DESIGN
Hybrid optics for space applications
[ESA-CP-1158] p 3501 N94-30418
LENSES
A new guided wave lens structure and its application
[AD-A275541] p 3499 N94-28813
LENTICULAR BODIES
Low temperature behavior of virgin martensite
[PB94-132925] p 3204 N94-29142
LEPTONS
Discrete quark-lepton symmetry need not pose a cosmological domain wall problem
[DE94-601606] p 3481 N94-28471
Energy distribution of the leptons in top decay to charged Higgs
[DE94-005231] p 3482 N94-28494
A measurement of the tau polarization at the resonance with the DELPHI detector at LEP
[DE94-005557] p 3482 N94-28520
Deep inelastic lepton scattering on nuclei: operator product expansion and meson-nucleon theory
[DE94-606442] p 3484 N94-28610
Masses and mixing of leptons and quarks (Dirac particles)
[DE94-606446] p 3484 N94-28611
Proceedings of the workshop on quark and lepton mass matrices
[DE94-707692] p 3485 N94-28624
Measurement of the W mass in the D0 detector
[DE94-006002] p 3490 N94-30103
High sensitivity tests of the standard model for electroweak interactions
[DE94-005415] p 3490 N94-30262
Operator analysis for quark and lepton masses in SO(10)
[DE94-005201] p 3491 N94-30709
LESIONS
Digital tracking and control of retinal images
[AD-A275469] p 3389 N94-28810

LEVITATION
Nearly time-optimal feedback control of a magnetically levitated photolithography positioning system
[DE94-005288] p 3266 N94-30055
Neural network based time-optimal control of a magnetically levitated precision positioning system
[DE94-006573] p 3437 N94-30250

LEVITATION MELTING
Plasma heating for containerless and microgravity materials processing
[NASA-CASE-NPO-18819-1-CU] p 3229 N94-29371

LIAPUNOV FUNCTIONS
On the linear stability of Verkley's modons
p 3324 N94-28695
Stability of dynamical systems in the presence of noise
[AD-A275383] p 3243 N94-29072
Existence of quantum characteristic exponents
[PB94-138161] p 3523 N94-29146
Significant figures and Lyapunov exponents in chaos and constrained divergence of chaotic orbits
p 3467 N94-29910
Dynamics and control of tethered satellite systems
p 3170 N94-30864

LIBRARIES
TRADOC library and information network (TRALINET). Union list of periodicals (TULIP)
[AD-A275263] p 3529 N94-28903
Evaluation of the Resource Library System in Finland
[PB94-137734] p 3532 N94-29682
Information center assessment p 3533 N94-29855
NASA/DOD Aerospace Knowledge Diffusion Research Project. Report 22: US academic librarians and technical information specialists as information intermediaries: Results of the phase 3 survey
[NASA-TM-109067] p 3534 N94-30150
Marketing tools for increasing proactivity in technical information centers
[AGARD-AR-326] p 3528 N94-30934

LIE GROUPS
Extended nonabelian symmetries for free fermionic model
[DE94-601554] p 3481 N94-28470
Path integral for coherent states of the dynamical U(sub 2) group and U(sub 2/1) supergroup
[DE94-606382] p 3466 N94-28785

LIFE (DURABILITY)
Process guide for the Domain-Specific Software Architectures (DSSA) process life cycle
[AD-A275642] p 3407 N94-28648
Service life prediction of composite structures through fiber testing
[AD-A275661] p 3176 N94-28654
Novel techniques applied to polymer lifetime predictions
[DE94-005095] p 3218 N94-30102

LIFE CYCLE COSTS
Aircraft age impact on individual operating and support cost elements
[AD-A275739] p 3121 N94-28732
Demonstration of improved software support labor estimation for Air Force operational flight programs through functional orientation
[AD-A275789] p 3121 N94-28743
Towards an information model and mechanisms for design rationale capture and use
[AD-A275060] p 3530 N94-29138

LIFE SCIENCES
Research and technology, 1992
[NASA-TM-103996] p 3555 N94-29891

LIFE SUPPORT SYSTEMS
Evaluation of life support equipment during an unsupported North Pole expedition
p 3379 N94-28422
Advanced seal delivery system life support parameters
[AD-A275304] p 3401 N94-29184

LIFT
Unsteady aerodynamic computations around NACA0012 at high angles of attack
p 3126 N94-28969
Aerodynamic characteristics of a propeller-powered high-lift semispan wing
[NASA-TM-4541] p 3132 N94-29937
Computation of wind tunnel wall effects for complex models using a low-order panel method
[NASA-TM-104019] p 3132 N94-30151
Aerodynamic analysis of slipstream/wing/nacelle interference for preliminary design of aircraft configurations
[AD-B173651] p 3135 N94-30916

LIFT AUGMENTATION
Numerical study of the trailing vortex of a wing with wing-tip blowing
[NASA-CR-195803] p 3130 N94-29760
Aerodynamic characteristics of a propeller-powered high-lift semispan wing
[NASA-TM-4541] p 3132 N94-29937

LIFT DEVICES
Role of computational fluid dynamics in aeronautical engineering. Part 10: Numerical analysis of flow around 2-D multi-element HLD p 3125 N94-28964

LIFT DRAG RATIO
Numerical analysis of supersonic transport wings
p 3124 N94-28959

LIFTING ROTORS
A design of third-generation airfoils for helicopter rotor blades using Navier-Stokes p 3124 N94-28957

LIGANDS
Development of novel switchable protein surfaces
[AD-A275510] p 3384 N94-28667
Anodization of copper in chloride media
[AD-A275565] p 3202 N94-28793

LIGHT (VISIBLE RADIATION)
Estimation of the net production of moss community at Langhovde, East Antarctica p 3358 N94-29081
Deployable reflector structure
[NASA-CASE-LAR-14513-1-SB] p 3245 N94-29360
Optical field ionization of atoms and ions using ultrashort laser pulses
[DE94-006643] p 3488 N94-29845
Correlation analysis on optical and radio light curves for a large sample of active galactic nuclei
p 3546 N94-29992
Circadian countermeasures for shiftworkers during USMP-2: A report to mission management
[NASA-CR-195260] p 3402 N94-30188

LIGHT AMPLIFIERS
Photonic devices and systems for optical signal processing
[AD-A275818] p 3498 N94-28804

LIGHT BEAMS
Advances in tunable powerful lasers: The advanced free-electron laser
[DE94-004997] p 3294 N94-29934

LIGHT CURVE
On observing neutron star oscillations
p 3538 N94-29795
Correlation analysis on optical and radio light curves for a large sample of active galactic nuclei
p 3546 N94-29992

LIGHT EMISSION
A study of white dwarf radiative accretion shocks
p 3544 N94-29731
A multiwavelength study of two prototypical supernova remnants p 3540 N94-29833

LIGHT GAS GUNS
Transient internal probe
[AD-A275054] p 3505 N94-29134

LIGHT IONS
Ion channeling peculiarities in YBa2Cu3 O7 monocrystal
[DE94-606885] p 3512 N94-28787
Kinetics of surface roughening and smoothing during ion sputtering
[DE94-006358] p 3219 N94-30263

LIGHT MODULATION
Spatial light modulators with arbitrary quantum wells profiles
[AD-A275023] p 3499 N94-29114
Reconfigurable optical interconnections via dynamic computer-generated holograms
[NASA-CASE-NPO-19039-1-CU] p 3499 N94-29491
Optical Chopper Assembly for the Mars Observer
p 3162 N94-29639
Optical techniques for time and frequency transfer
p 3469 N94-30647

LIGHT SCATTERING
Experimental and theoretical studies of molecular solids
[AD-A275511] p 3485 N94-28668
CBSD: The celestial background scene descriptor
[AD-A275521] p 3538 N94-28671
Backscatter haze device for measurement of haze in aircraft transparencies
[AD-A275127] p 3146 N94-29042
Deformed ellipsoidal diffraction grating blank
[NASA-CR-189334] p 3289 N94-29872
The enhancement of compressible turbulent mixing via streamwise vorticity p 3280 N94-30487

LIGHT SCATTERING METERS
Granulometry in environments with very small particle concentrations p 3259 N94-30511

LIGHT SOURCES
Linac Coherent Light Source (LCLS) at 2-4 nm using the SLAC linac
[DE94-005235] p 3292 N94-28481
Backscatter haze device for measurement of haze in aircraft transparencies
[AD-A275127] p 3146 N94-29042

LIGHT SPEED
On the importance of the Michelson-Morley experiment
[DE94-606298] p 3523 N94-28620

LIGHT TRANSMISSION
UV laser long-path absorption spectroscopy
p 3343 N94-28595
Optical modeling of visibility and visibility instrumentation using stratified Mie theory p 3348 N94-29750
Developing a diode array spectrometer for tropospheric chemistry studies p 3362 N94-29752
Characterization of thermally annealed Sb implanted fused silica
[DE94-005464] p 3219 N94-30335
Estimation of transmittance from satellite imagery
p 3257 N94-30500
Calculation of turbulence degraded point spread function of an imaging system p 3260 N94-30514

LIGHTNING
A space-based classification system for RF transients
[DE94-003933] p 3240 N94-28522
A study of cloud-to-ground lightning processes with emphasis on data analysis and modeling of the return stroke p 3372 N94-29802

LIMESTONE
Influence of clearance and rake angles on the cutting force of rock p 3368 N94-29520

LINE SPECTRA
UV laser long-path absorption spectroscopy
p 3343 N94-28595
Camera artifacts in IUE spectra
[NASA-CR-189337] p 3198 N94-29857
Spectral and temporal behavior of low mass x ray binaries observed with the Einstein SSS and MPC, and the Broad Band X Ray Telescope p 3542 N94-30862

LINEAR ACCELERATORS
Linac Coherent Light Source (LCLS) at 2-4 nm using the SLAC linac
[DE94-005235] p 3292 N94-28481
Towards short wavelengths FELs workshop
[DE94-004346] p 3296 N94-30688
Experiment studies of electron-positron interactions at the Stanford Linear Accelerator Center
[DE94-005877] p 3491 N94-30702
A transmission-loss monitor using current transformers
[DE94-003974] p 3267 N94-30716
Atomic physics with highly charged ions
[DE94-003397] p 3492 N94-30837

LINEAR ARRAYS
Analysis of spark-induced bubble experiments using CALE
[DE94-003667] p 3270 N94-28476
Broadband EUV survey spectrometer for short-timescale experiments
[DE94-005459] p 3498 N94-28534
Physical interpretation and development of ultrasonic nondestructive evaluation techniques applied to the quantitative characterization of textile composite materials
[NASA-CR-195766] p 3183 N94-30016
Comparative semantics for linear arrays of communicating processes
[CWI-CS-R9336] p 3426 N94-30491

LINEAR CIRCUITS
Digitally programmable composite operational amplifier applications
[AD-A275081] p 3262 N94-28842

LINEAR ENERGY TRANSFER (LET)
Adaption of the bubble detector for use as a LET spectrometer p 3291 N94-30216
Using Cf-252 for single event upset testing
p 3496 N94-30219

LINEAR EQUATIONS
Frequency-domain transfer-function identification using Chebyshev polynomials
[DE94-004777] p 3451 N94-28739
Solution of augmented systems
[PB94-138211] p 3452 N94-29111

LINEAR FILTERS
A novel approach to noise-filtering based on a gain-scheduling neural network architecture
[NASA-TM-106563] p 3155 N94-30204

LINEAR POLARIZATION
Infrared polarization signatures p 3258 N94-30506

LINEAR PROGRAMMING
Weighted and unweighted maximum clique algorithms with upper bounds from fractional coloring
[AD-A275328] p 3409 N94-28917
Solution of augmented systems
[PB94-138211] p 3452 N94-29111
Center for Parallel Optimization
[AD-A274988] p 3431 N94-29127
Natural deduction for intuitionistic linear logic
[ML-93-09] p 3457 N94-30385

LINEAR QUADRATIC GAUSSIAN CONTROL
A stochastic control approach to flight path monitoring
[AD-B174630] p 3143 N94-30853
LINEAR SYSTEMS
Design and analysis of a low-loss linear analog phase modulator for deep space spacecraft X-band transponder applications p 3248 N94-29625
Microgravity compatible drive system-rider. New technologies
[PB94-138583] p 3229 N94-29996
Robust control of robots via linear estimated state-feedback
[MEMO-1153] p 3449 N94-30963
LINEAR TRANSFORMATIONS
Path integral for coherent states of the dynamical U(sub 2) group and U(sub 2/1) supergroup
[DE94-606382] p 3466 N94-28785
LINEARIZATION
The structure of exponentials: Uncovering the dynamics of linear logic proofs
[ML-93-10] p 3430 N94-30973
LINES OF FORCE
New evidence for flux cutting in type II superconductors
[ISBN-0-315-85830-3] p 3515 N94-30032
LINGUISTICS
An architecturally-based theory of human sentence comprehension
[AD-A275380] p 3398 N94-29313
Interrogatives and adverbs of quantification
[LP-92-14] p 3456 N94-30372
Commutative Lambek categorial grammars
[ML-93-01] p 3457 N94-30395
LININGS
Evaluation of life support equipment during an unsupported North Pole expedition
p 3379 N94-28422
LINKAGES
Simplified and symmetrical five-bar linkage driver for manipulating a six-degree-of-freedom parallel minimanipulator with three inextensible limbs
[NASA-CASE-GSC-13485-2] p 3301 N94-29556
Lock-up failure of a four-bar linkage deployment mechanism p 3163 N94-29646
LINKS
A design methodology for synthesizing low-order robust controllers for flexible structures p 3302 N94-29870
LIOUVILLE THEOREM
The generalized spin-boson model for electron-transfer reactions involving two harmonic potentials with a different force constant
[DE94-005470] p 3482 N94-28509
Theory for electron-transfer reactions involving two Marcus surfaces with a different force constant
[DE94-005925] p 3493 N94-30874
LIPIDS
Biodiesel from aquatic species
[DE94-000275] p 3225 N94-30038
LIPSCHITZ CONDITION
Complicated problem solution techniques in optimal parameter searching
[DE94-608007] p 3421 N94-30077
LIQUEFIED GASES
On possibility to create the scintillation trigger for liquid-argon neutrino detector
[DE94-607844] p 3489 N94-30050
LIQUEFIED NATURAL GAS
Assessment of costs and benefits of flexible and alternative fuel use in the US transportation sector
[DE94-006100] p 3226 N94-30885
LIQUID ATOMIZATION
Modeling of the phase liquidates in combustion chambers p 3195 N94-29278
Investigation of the two-phase flow in a research combustor under reacting and non-reacting conditions
p 3196 N94-29282
Liquid atomization in supersonic flows
p 3276 N94-29839
LIQUID CHROMATOGRAPHY
Measurement of elemental speciation by liquid chromatography: Inductively coupled plasma mass spectrometry (LC-ICP-MS) with the Direct Injection Nebulizer (DIN)
[DE94-005261] p 3187 N94-28483
Chemically modified polymeric resins for separation of cations, organic acids, and small polar molecules by high performance liquid chromatography
[DE94-005548] p 3211 N94-28516
Structural analysis of amorphous phosphates using high performance liquid chromatography
[DE94-004791] p 3199 N94-30723
LIQUID COOLING
The use of liquid and air microclimate conditioning systems to alleviate heat stress in helicopter NBC operations p 3384 N94-28453
LIQUID CRYSTALS
Controlled thermal expansion printed wiring boards based on liquid crystal polymer dielectrics
[NASA-CR-189338] p 3287 N94-29400
LIQUID FILLED SHELLS
Spin-up in a rectangular cylinder
[AD-A275465] p 3271 N94-28738
LIQUID FLOW
Spin-up in a rectangular cylinder
[AD-A275465] p 3271 N94-28738
LIQUID FUELS
Impact study on the use of biomass-derived fuels in gas turbines for power generation
[DE94-000261] p 3224 N94-28502
Ultra low NO(x) ultra lean gas turbine primary zones with liquid fuels p 3154 N94-29267
Research and development of ramjets/ramrockets. Part 1: Integral solid propellant ramrockets
p 3151 N94-29294
Biodiesel from aquatic species
[DE94-000275] p 3225 N94-30038
LIQUID HELIUM
Argon frost continuous cryopump for fusion applications
[DE94-004478] p 3230 N94-29017
Acoustic and optical investigations of superfluid (3)He
[PB94-135415] p 3477 N94-29186
LIQUID INJECTION
Investigation of the two-phase flow in a research combustor under reacting and non-reacting conditions
p 3196 N94-29282
Liquid atomization in supersonic flows
p 3276 N94-29839
LIQUID METALS
Liquid metal MHD and heat transfer in a tokamak blanket slotted coolant channel
[DE94-004622] p 3506 N94-29510
Electromagnetic effect on turbulent transport in liquid metals and electrolytes (bath)
[PB94-138450] p 3206 N94-29946
On the structure and atomic motions in liquid sodium
[DE94-608386] p 3490 N94-30182
Near-net-shape manufacturing: Spray-formed metal matrix composites and tooling p 3186 N94-30447
Nature of dissolution of binary tantalum-titanium alloys by molten plutonium
[DE94-005090] p 3210 N94-30776
LIQUID NITROGEN
An alternate method for achieving temperature control in the -160 to +90 C range
[NASA-CASE-NPO-18995-1-CU] p 3288 N94-29497
LIQUID OXYGEN
Liquid-oxygen droplet vaporization and combustion: Analysis of transcritical behavior and application to liquid-rocket combustion instability p 3197 N94-29592
LIQUID PHASE SINTERING
Innovative processing of composites for ultra-high temperature applications, book 3
[AD-A275599] p 3177 N94-28731
LIQUID PHASES
Modeling of the phase liquidates in combustion chambers p 3195 N94-29278
LIQUID ROCKET PROPELLANTS
Introduction and overview of research and development of solid propellant ramrockets, liquid fuel ramjets and experimental hydrogen ram combustors
p 3151 N94-29292
Research and development of ramjets/ramrockets. Part 2: Integral liquid fuel ramjets p 3152 N94-29297
Catalytic ignitor for regenerative propellant gun
[NASA-CASE-NPO-18987-1-CU] p 3225 N94-29490
Aspects of model-based rocket engine condition monitoring and control
[NASA-CR-195116] p 3173 N94-29848
LIQUID SLOSHING
Determination of acceleration field parameters with linear accelerometers
[PB94-125606] p 3290 N94-30742
LIQUID SODIUM
On the structure and atomic motions in liquid sodium
[DE94-608386] p 3490 N94-30182
LIQUID SURFACES
Liquid atomization in supersonic flows
p 3276 N94-29839
LIQUID-SOLID INTERFACES
A solid-on-solid invasion percolation model for self-affine interfaces
[DE94-608102] p 3521 N94-30888
LIQUID-VAPOR INTERFACES
Liquid atomization in supersonic flows
p 3276 N94-29839
Local two-phase flow simulations including interface tracking with mass transfer p 3283 N94-30954
LIQUIDS
Interaction of multiple spark-generated bubbles in a compressible liquid
[AD-A275037] p 3272 N94-29149
LITHIUM
Analytic cross sections for collisions of H, H2, He and Li atoms and ions with atoms and molecules
[DE94-707686] p 3485 N94-28788
Tris(trimethylsily)arsine and lithium bis(trimethylsily)arsenide
[AD-A275075] p 3189 N94-29140
Dendrite preventing separator for secondary lithium batteries
[NASA-CASE-NPO-18585-1-CU] p 3265 N94-29411
Anode for rechargeable ambient temperature lithium cells
[NASA-CASE-NPO-18580-1-CU] p 3265 N94-29505
LITHIUM HYDRIDES
A future, intense source of negative hydrogen ions
p 3494 N94-30485
LITHIUM ISOTOPES
Neutronics of a D-Li neutron source: An overview
[DE94-005372] p 3493 N94-30893
LITHOGRAPHY
Low voltage electron beam lithography
[AD-A275648] p 3262 N94-28650
Focused ion beam fabrication of microelectronic structures
[AD-A275384] p 3264 N94-29305
Microactuator production via high aspect ratio, high edge acuity metal fabrication technology
p 3235 N94-29770
A combined electron beam/optical lithography process step for the fabrication of sub-half-micron-gate-length MMIC chips p 3240 N94-30445
LIVER
Physiological investigations of the isolated rat's liver in hypothermia and hypoxia and their relevance in aircraft incidents above the sea p 3382 N94-28439
LOAD DISTRIBUTION (FORCES)
Coordinated control of multiple robot manipulators
p 3306 N94-30289
LOAD TESTS
Static fracture behavior of a ceramic matrix composite at elevated temperatures
[AD-A275363] p 3177 N94-29008
Root-sum-square structural strength verification approach
[NASA-TM-108453] p 3322 N94-30206
WISPER and WISPERX: Final definition of two standardised fatigue loading sequences for wind turbine blades
[AD-B175835] p 3324 N94-30872
LOADS (FORCES)
Performance evaluation of a 22.5/30 kW 270 volts direct current generator system
[AD-A275106] p 3263 N94-28913
Growth condition of an ice layer in freezing soils under applied loads. Part 1: Experiment
[AD-A275215] p 3357 N94-29070
Rotary blood pump
[NASA-CASE-MSC-22424-1] p 3299 N94-29370
A compact roller-gear pitch-yaw joint module: Design and control issues p 3161 N94-29629
Closed form expressions for a consistent stress material nonlinear finite element p 3322 N94-30258
LOCAL AREA NETWORKS
Evaluation of wireless Local Area Networks
[AD-A275133] p 3243 N94-29064
Remote observatory access via the advanced communications technology satellite
p 3253 N94-29894
Validation experiments with an Ethernet model using the simulation tool 'PROMISE'
[AD-B174795] p 3429 N94-30912
LOCAL THERMODYNAMIC EQUILIBRIUM
SHARC, a model for calculating atmospheric and infrared radiation under non-equilibrium conditions
[AD-A275207] p 3357 N94-28893
Abundance patterns in red-giant CH stars
p 3539 N94-29820
LOCI
Further investigation of curve veering phenomena
p 3460 N94-30515
LOCOMOTION
Computerized in vitro test for chemical toxicity based on tetrahymena swimming patterns
p 3354 N94-30463
Biologically-inspired hexapod robot design and simulation
[AIAA PAPER 94-1178-CP] p 3439 N94-30530
ODYSSEUS autonomous walking robot: The leg/arm design
[AIAA PAPER 94-1180-CP] p 3439 N94-30531

LOGIC CIRCUITS
Three dimensional transient analysis of microstrip circuits in multilayered anisotropic media
[AD-A274995] p 3263 N94-28995
LOGIC DESIGN
Program derivation by proof transformation
[AD-A275260] p 3453 N94-29304
Yield and variability optimization of integrated circuits: Principles and practical solutions p 3266 N94-29805
LOGIC PROGRAMMING
Partial support for the Second International Symposium on Artificial Intelligence and Mathematics
[AD-A275199] p 3434 N94-29026
Incorporating geometric constraints into rule-based systems using nonlinear optimization
[AD-A275093] p 3452 N94-29063
Neural network solutions to logic programs with geometric constraints
[AD-A275419] p 3435 N94-29198
Logic of transition systems
[CT-93-03] p 3424 N94-30371
Algorithmic problems concerning first-order definability of modal formulas on the class of all finite frames
[ML-93-07] p 3456 N94-30383
Remarks on the theory of semi-functors
[ML-93-08] p 3457 N94-30384
The Vanilla meta-interpreter for definite logic programs and ambivalent syntax
[CT-93-01] p 3424 N94-30386
Isomorphisms between predicate and state transformers
[CWI-CS-R9338] p 3459 N94-30430
Comparative semantics for linear arrays of communicating processes
[CWI-CS-R9336] p 3426 N94-30491
Unravelling nondeterminism: On having the ability to choose
[RUU-CS-93-30] p 3428 N94-30749
LOGISTICS
The 1993 Federal Aviation Administration Aviation System Capital Investment Plan p 3136 N94-29445
LOGISTICS MANAGEMENT
DOD Electronic Commerce (EC)/Electronic Data Interchange (EDI) in contracting report
[AD-A275298] p 3242 N94-28874
LONG DURATION EXPOSURE FACILITY
Analysis of selected materials flown on interior locations of the Long Duration Exposure Facility
[NASA-CR-4586] p 3175 N94-29458
Study of activation data of metal samples from LDEF-1 and Spacelab-2
[NASA-CR-195802] p 3205 N94-29736
LONGITUDINAL STABILITY
An experimental and theoretical study of the aerodynamic characteristics of some generic missile concepts at Mach numbers from 2 to 6.8
[NASA-TM-109110] p 3130 N94-29473
LOOP ANTENNAS
Three-dimensional effects for radio frequency antenna modeling
[DE94-006102] p 3255 N94-30105
LOOPS
Method of implementing digital phase-locked loops
[NASA-CASE-NPO-18757-1-CU] p 3265 N94-29374
Butterfly and scaling law in YBa2Cu4O8
[DE94-006037] p 3519 N94-30338
LORAN C
Loran-C time management p 3144 N94-30644
LORENTZ TRANSFORMATIONS
Possible explanation of the interaction cross-section growth at high energies
[DE94-606457] p 3494 N94-28612
LOSSES
Broad geoacoustic assessment of some regional areas
[AD-A275504] p 3356 N94-28791
AC losses for the self field of an AC transport current with a DC transport current offset in high T(c) superconducting magnet coils for MagLev application
[DE94-005187] p 3268 N94-30907
LOUDNESS
Subjective response to sonic booms having different shapes, rise times, and durations
[NASA-TM-109090] p 3479 N94-29464
LOVE WAVES
Extension of love wave transformation theory to laterally heterogeneous structures
[DE94-608098] p 3365 N94-30093
LOW CONCENTRATIONS
Granulometry in environments with very small particle concentrations p 3259 N94-30511
LOW CONDUCTIVITY
Properties of graphite fiber reinforced copper matrix composites for space power applications
[NASA-CR-191026] p 3178 N94-29208
LOW COST
NPSNET: Integration of Distributed Interactive Simulation (DIS) protocol for communication architecture and information interchange
[AD-A275061] p 3530 N94-29139
The suitability of low-cost urban airshed modeling in the Chicago area
[DE94-005114] p 3349 N94-30023
Proceedings of the low cost materials of construction for biological processes workshop
[DE94-000218] p 3226 N94-30761
LOW GRAVITY MANUFACTURING
Survey report of JSUP Space Environment Utilization Research Committee in fiscal year 1992: Protein Crystal Growth Session
[JTN-94-80584] p 3158 N94-28583
Fluid and transportation phenomena under microgravity p 3227 N94-28939
Combustion studies under microgravity p 3228 N94-28940
Glass studies under microgravity p 3228 N94-28941
Fabrication of electronic materials in space p 3228 N94-28942
Protein crystal growth in microgravity p 3228 N94-28943
Cell culture in space p 3228 N94-28944
Cosmic energy equipment p 3229 N94-28945
Survey report of JSUP Space Environment Utilization Research Committee in fiscal year 1992: Functional New Materials Session
[JTN-94-80582] p 3159 N94-30162
Survey report of JSUP Space Environment Utilization Research Committee in fiscal year 1992: Metallic Materials Session
[JTN-94-80583] p 3159 N94-30794
LOW MOLECULAR WEIGHTS
Solventless, curable fluid oligomeric systems for high performance microwave, acoustical and mechanical applications p 3223 N94-30478
LOW NOISE
A gimbaled low noise momentum wheel p 3162 N94-29640
A high rate, low noise, x ray silicon strip detector system
[DE94-004557] p 3268 N94-30717
LOW PRESSURE
Studies on water electrolyte metabolism and endocrine responses at rest and during submaximal exercise at 6,000 m simulated altitude p 3388 N94-28496
Effects of training at simulated altitude of 6,000 m on endocrine responses at rest and during exercise at the same altitude p 3388 N94-28497
Metal inert gas welding system for use in vacuum
[NASA-CASE-MFS-28808-1] p 3298 N94-29352
Large eddy simulation of subsonic mixing layers p 3276 N94-29851
LOW SPEED
Hopf bifurcation in viscous, low-speed flows about an airfoil with structural coupling p 3134 N94-30865
LOW TEMPERATURE
Low temperature behavior of virgin martensite
[PB94-132925] p 3204 N94-29142
A newly developed snow vehicle (SM100S) for Antarctica. Part 3: Low temperature toughness of the welded joints of the structural steel p 3364 N94-29983
Centrifugal atomization of lanthanide materials for cryogenic coolers
[DE94-006035] p 3219 N94-30337
LOW TEMPERATURE ENVIRONMENTS
The Support of Air Operations under Extreme Hot and Cold Weather Conditions
[AGARD-CP-540] p 3379 N94-28420
Medical support for British operations in the Antarctic p 3379 N94-28421
The concept of Royal Navy air operations under extreme environmental conditions p 3379 N94-28424
Toward a molecular scale understanding of frost heaving, phase 1
[AD-A275446] p 3356 N94-28882
Antarctic Record, vol. 36, no. 3
[REPT-108] p 3363 N94-29978
A newly developed snow vehicle (SM100S) for Antarctica. Part 1: Necessity and process of the development p 3314 N94-29981
A newly developed snow vehicle (SM100S) for Antarctica. Part 2: Design of the system p 3314 N94-29982
A newly developed snow vehicle (SM100S) for Antarctica. Part 4: Low temperature properties of crawler belt p 3314 N94-29984
A newly developed snow vehicle (SM100S) for Antarctica. Part 5: Result of general performance tests p 3314 N94-29985
Activities of the wintering party at Syowa Station by the 32nd Japanese Antarctic Research Expedition in 1991 p 3364 N94-29986
LOW TEMPERATURE TESTS
Cryogenic probe station for use in automated microwave and noise figure measurements
[NASA-TM-106560] p 3286 N94-29000
Low temperature behavior of virgin martensite
[PB94-132925] p 3204 N94-29142
Evaluation of corrosion protecting properties of modern aircraft paint systems
[AD-B179388] p 3220 N94-30420
Improved construction materials for polar regions using microcellular thermoplastic foams p 3223 N94-30483
LOW THRUST PROPULSION
Determination of pressure response times for gaseous flow in a tube
[AD-A275274] p 3272 N94-29435
LOW VISIBILITY
Extremely Low Visibility IFR Rotorcraft Approach (ELVIRA) operational concept development. Volume 1: Executive Summary
[DOT/FAA/RD-94/1,I] p 3142 N94-30189
LOW VOLTAGE
Low voltage electron beam lithography
[AD-A275648] p 3262 N94-28650
LUBRICANT TESTS
The use of screening tests in spacecraft lubricant evaluation p 3162 N94-29641
LUBRICANTS
The use of screening tests in spacecraft lubricant evaluation p 3162 N94-29641
Lubricant rheology at high shear rates p 3217 N94-29967
Materials compatibility and lubricants research on CFC-refrigerant substitutes
[DE94-004905] p 3220 N94-30692
LUBRICATION
Lubrication of space systems
[NASA-TM-106392] p 3214 N94-29399
An asymptotic analysis for compressible gas lubrication of rough surfaces p 3222 N94-30922
LUBRICATION SYSTEMS
Lubrication of space systems
[NASA-TM-106392] p 3214 N94-29399
LUMINANCE
Fusion of range and luminance data from laser radar systems
[AD-A275608] p 3292 N94-28770
LUMINOSITY
Physical conditions in classical H2 regions in the Magellanic Clouds p 3543 N94-29722
A multiwavelength study of two prototypical supernova remnants p 3540 N94-29833
High redshift QSOs and the x ray background
[NASA-CR-195112] p 3540 N94-29957
LUMINOUS INTENSITY
Absolute determination of local tropospheric OH concentrations p 3343 N94-28594
Strategies to sustain and enhance performance in stressful environments
[AD-A275223] p 3398 N94-29027
Optical flameout detector
[NASA-CASE-LAR-14997-1] p 3287 N94-29368
LUNAR MINING
Lunar surface operations. Volume 4: Lunar rover trailer
[NASA-CR-195554] p 3299 N94-29386
LUNAR ROVING VEHICLES
Lunar surface operations. Volume 4: Lunar rover trailer
[NASA-CR-195554] p 3299 N94-29386
LUNAR SHELTERS
Lunar surface operations. Volume 1: Lunar surface emergency shelter
[NASA-CR-195551] p 3299 N94-29354
LUNAR SURFACE
Lunar surface operations. Volume 4: Lunar rover trailer
[NASA-CR-195554] p 3299 N94-29386
Backscatter Mossbauer Spectrometer (BaMS) for extraterrestrial applications p 3236 N94-29774
LYMAN ALPHA RADIATION
Physical conditions in classical H2 regions in the Magellanic Clouds p 3543 N94-29722
Observation of Jovian auroral Ly-alpha line profile and emission variability with a sounding rocket and the IUE archives p 3550 N94-30798
LYSOZYME
Convective flow effects on protein crystal growth
[NASA-CR-195785] p 3515 N94-30015

M

MACH NUMBER
Large amplitude Langmuir and ion-acoustic waves in a relativistic two-fluid plasma
[NIFS-271] p 3506 N94-29547
Analysis of fluctuating static pressure measurements in a large high Reynolds number transonic cryogenic wind tunnel p 3158 N94-30788

MACHINE LEARNING
A neural network with modular hierarchical learning
[NASA-CASE-NPO-19077-1-CU] p 3435 N94-29492
On-line search for optimal controller parameters using interconnected learning automata
[MATHS-REPT-A-196] p 3436 N94-29526
Nonlinear PCA: Algorithms and applications
[PB94-137544] p 3419 N94-29680
Robotic hand-eye motor learning p 3436 N94-29835
Reinforcement learning for robots using neural networks p 3437 N94-29853
Unsupervised learning in analog networks
[ISBN-0-315-85959-8] p 3432 N94-30140
A lateral inhibition neural network that emulates a winner-takes-all algorithm
[RUU-CS-92-46] p 3438 N94-30334
An intelligent robotic aid system for human services
[AIAA PAPER 94-1232-CP] p 3447 N94-30580
Use of bad training data for better predictions
[DE94-006233] p 3427 N94-30705
ELF: Learning incomplete fuzzy rule sets for an autonomous robot
[REPT-93-043] p 3449 N94-30923
Some methodological issues about designing autonomous agents which learn their behaviors: The ELF experience
[REPT-93-068] p 3449 N94-30939

MACHINE TOOLS
Application of high-speed milling to the Finnish manufacturing industry
[PB94-135548] p 3230 N94-29187
Effect of non-metallic inclusions on the machinability of steel
[PB93-230233] p 3204 N94-29387
Generation of gear tooth surfaces by application of CNC machines
[NASA-CR-195306] p 3303 N94-30205
Precision and manufacturing at the Lawrence Livermore National Laboratory p 3240 N94-30449

MACHINING
Effect of non-metallic inclusions on the machinability of steel
[PB93-230233] p 3204 N94-29387
The machining of fiber metal laminates. Part 1: An inventory of forming processes
[LR-710-PT-1] p 3184 N94-30343
Confessions of a robot lobotomist
[AIAA PAPER 94-1185-CP] p 3440 N94-30535
Material properties and fracture mechanics in relation to ceramic machining
[DE94-006623] p 3221 N94-30829

MACROMOLECULES
Molecular structure of coal studied by solvent extraction p 3187 N94-28676
Crosslinking and surface reactions in macromolecules: Spectroscopic FT-IR studies p 3221 N94-30812

MACROSCOPIC EQUATIONS
Volume averaged model for the mechanics of alloys solidification
[PB94-138617] p 3208 N94-30113

MAGELLANIC CLOUDS
Dust in the Small Magellanic Cloud
[NASA-CR-195764] p 3543 N94-29696
Physical conditions in classical H2 regions in the Magellanic Clouds p 3543 N94-29722

MAGMA
The thermal consequences of giant impacts in the early solar system p 3543 N94-29698
Studies in Jurassic and Cretaceous North American apparent polar wander p 3362 N94-29940

MAGNESIUM ALLOYS
Failures to model the development of a cube texture during the high temperature compression of Al-Mg alloys
[DE94-005013] p 3201 N94-28544
Casting of weldable graphite/magnesium metal matrix composites with built-in metallic inserts p 3186 N94-30482

MAGNET COILS
AC losses for the self field of an AC transport current with a DC transport current offset in high T(c) superconducting magnet coils for MagLev application
[DE94-005187] p 3268 N94-30907

MAGNETIC ANOMALIES
Observations of the geomagnetic field by Polar Patrol Balloon (PPB) experiment in Antarctica p 3359 N94-29235

MAGNETIC BEARINGS
Current leads and magnetic bearings
[DE94-004607] p 3297 N94-28461
A gimbaled low noise momentum wheel p 3162 N94-29640

MAGNETIC COILS
Formulae for the calculation of the magnetic field strength in a Helmholtz system with circular coils
[NPL-DES-130] p 3260 N94-30785

MAGNETIC COMPRESSION
Use of magnetic compression to support turbine engine rotors p 3314 N94-30484

MAGNETIC CONTROL
The effect of magnetic field configuration on particle pinch velocity in Compact Helical System (CHS)
[NIFS-267] p 3505 N94-29398

MAGNETIC DISKS
Atomic-scale friction measurements using friction force microscopy. Part 2: Application to magnetic media
[AD-A275202] p 3298 N94-29290

MAGNETIC EFFECTS
Potential hazards of magnetic resonance imagers to emergency medical service helicopter operations
[DOT/FAA/RD-92/15] p 3135 N94-29862
Electromagnetic effect on turbulent transport in liquid metals and electrolytes (bath)
[PB94-138450] p 3206 N94-29946
Localization in presence of magnetic field in 2-D disordered binary alloys
[DE94-608093] p 3208 N94-30108
Magnetic properties of a transverse spin-1 Ising model with longitudinal crystal field interactions
[DE94-608118] p 3517 N94-30165

MAGNETIC ENERGY STORAGE
Battery energy and superconducting magnetic energy storage for utility applications: A qualitative analysis
[DE94-005382] p 3336 N94-28489

MAGNETIC EQUATOR
The effects of magnetic storm phases on F-layer irregularities from auroral to equatorial latitudes
[AD-A275203] p 3356 N94-28891

MAGNETIC FIELD CONFIGURATIONS
Atomic and magnetic structure of YBa2(Cu(1-x)Fe(x))3O(6+y) at 0.05 less than or equal to x less than or equal to 0.30, y is approximately equal to 1 and y is approximately equal to 0.5
[DE94-606852] p 3513 N94-29210
A 6MeV heavy ion beam probe for the Large Helical Device
[NIFS-272] p 3505 N94-29397
The effect of magnetic field configuration on particle pinch velocity in Compact Helical System (CHS)
[NIFS-267] p 3505 N94-29398
Magnetic field generation by circularly polarized laser light and inertial plasma confinement in a miniature magnetic bottle induced by circularly polarized laser light
[DE94-608353] p 3508 N94-30192

MAGNETIC FIELD RECONNECTION
Computer simulations on development of the fast reconnection mechanism p 3360 N94-29241

MAGNETIC FIELDS
Three-dimensional finite element modeling of a magnet array spinning above a conductor
[DE94-004573] p 3468 N94-28459
Effect of phonon dispersion on properties of exciton in magnetic field
[DE93-634756] p 3481 N94-28469
Estimation of geomagnetic conjugate points by using Pc5 pulsations p 3357 N94-29079
Transient internal probe
[AD-A275054] p 3505 N94-29134
Orbital applications of electrodynamic propulsion
[AD-A275413] p 3173 N94-29216
Observations of the geomagnetic field by Polar Patrol Balloon (PPB) experiment in Antarctica p 3359 N94-29235
Formation and self-healing of magnetic islands in finite-beta helias equilibria
[NIFS-269] p 3505 N94-29483
Nonadiabatic effects in the quantum Hall regime p 3513 N94-29530
Fast gravity, gravity partials, normalized gravity, gravity gradient torque and magnetic field: Derivation, code and data
[NASA-CR-188243] p 3361 N94-29588
Three-axis fiber optic vector magnetometer
[AD-D016016] p 3288 N94-29699
Potential hazards of magnetic resonance imagers to emergency medical service helicopter operations
[DOT/FAA/RD-92/15] p 3135 N94-29962
Quasi-adiabatic motion of energetic particles in a dipole magnetic field
[DE94-607322] p 3362 N94-29935
Electromagnetic effect on turbulent transport in liquid metals and electrolytes (bath)
[PB94-138450] p 3206 N94-29946
Estimating the cost of large superconducting thin solenoid magnets
[DE94-006289] p 3468 N94-30026
Algorithm and program ORANGE for magnetic field simulation of magnetic system spectrometer STORS
[DE94-608013] p 3421 N94-30083
Localization in presence of magnetic field in 2-D disordered binary alloys
[DE94-608093] p 3208 N94-30108
Some results on the phase diagram of the antiferromagnetic Potts model in an external magnetic field
[DE94-608115] p 3468 N94-30110
Periodic electromagnetic vacuum in the two-dimensional Yang-Mills theory with the Chern-Simons mass
[DE94-608128] p 3525 N94-30170
Resistive ballooning mode in a gas-dynamic trap
[DE94-608328] p 3508 N94-30171
Magnetic field generation by circularly polarized laser light and inertial plasma confinement in a miniature magnetic bottle induced by circularly polarized laser light
[DE94-608353] p 3508 N94-30192
Electric power lines: Questions and answers on research into health effects
[DE94-005637] p 3353 N94-30757
Formulae for the calculation of the magnetic field strength in a Helmholtz system with circular coils
[NPL-DES-130] p 3260 N94-30785
Nonlinear optics response of semiconductor quantum wells under high magnetic fields
[DE94-003244] p 3520 N94-30835
Magnetotransport measurements in magnetic fields up to 50T in SmB6 and FeSi
[DE94-006227] p 3520 N94-30848
Calculating the J(c), B, T surface for commercial niobium tin conductors using a reduced state model
[DE94-006296] p 3520 N94-30850
Intra- versus interlayer pairing in the copper oxide superconductors: Response to a magnetic field
[DE94-005475] p 3521 N94-30898

MAGNETIC FILMS
Giant magnetoresistance and microstructural characteristics of epitaxial Fe-Ag and Co-Ag granular thin films
[DE94-006287] p 3519 N94-30707

MAGNETIC FLUX
The structure of solar magnetic fields and their associated electric currents p 3544 N94-29723
New evidence for flux cutting in type II superconductors
[ISBN-0-315-85830-3] p 3515 N94-30032
Periodic electromagnetic vacuum in the two-dimensional Yang-Mills theory with the Chern-Simons mass
[DE94-608128] p 3525 N94-30170
Magnetic flux reconstruction methods for shaped tokamaks
[DE94-005827] p 3510 N94-30882
Solar measurements from the Airglow-Solar Spectrometer Instrument (ASSI) on the San Marco 5 satellite
[NASA-CR-193815] p 3551 N94-30948

MAGNETIC LENSES
Third-order beam optics of real solenoid magnetic lens
[DE94-608014] p 3500 N94-30084

MAGNETIC MATERIALS
Report on the development of low magnetic permeability reference materials
[NPL-DES-119] p 3476 N94-30783

MAGNETIC MEASUREMENT
Observations of the geomagnetic field by Polar Patrol Balloon (PPB) experiment in Antarctica p 3359 N94-29235
Three-axis fiber optic vector magnetometer
[AD-D016016] p 3288 N94-29699
The structure of solar magnetic fields and their associated electric currents p 3544 N94-29723
Guidance notes for use with NPL low permeability reference materials
[NPL-DES-121] p 3476 N94-30780
Magnetic flux reconstruction methods for shaped tokamaks
[DE94-005827] p 3510 N94-30882

MAGNETIC MIRRORS
Experiments on the two-stage dense plasma heating on the GOL-3 device
[DE94-608356] p 3508 N94-30193

MAGNETIC MOMENTS
Quasi-adiabatic motion of energetic particles in a dipole magnetic field
[DE94-607322] p 3362 N94-29935

MAGNETIC PERMEABILITY
Scaling in heavy-fermion systems
[DE94-005002] p 3492 N94-30775
Guidance notes for use with NPL low permeability reference materials
[NPL-DES-121] p 3476 N94-30780
Report on the development of low magnetic permeability reference materials
[NPL-DES-119] p 3476 N94-30783

MAGNETIC PROPERTIES
Magnetic properties of a quantum transverse spin-1 Blume-Emery-Griffiths model
[DE94-608114] p 3517 N94-30109
Magnetic properties of the three dimensional Ising model with interface single-ion anisotropy
[DE94-608116] p 3525 N94-30164
Magnetic properties of a transverse spin-1 Ising model with longitudinal crystal field interactions
[DE94-608118] p 3517 N94-30165
The bond diluted spin-1 Blume-Emery-Griffiths model in a transverse field
[DE94-608121] p 3525 N94-30167
Magnetic properties of a transverse spin-1 Ising model with random crystal field interactions
[DE94-608117] p 3517 N94-30181
MuSR measurement of the magnetic penetration depth and coherence length in the high-Tc superconductor YBa2Cu3O(6.95)
[ISBN-0-315-85385-9] p 3517 N94-30203

MAGNETIC RELAXATION
On the (mu)SR activity at LNP JINR phasotron
[DE94-608385] p 3517 N94-30195
Nuclear magnetic relaxation studies of semiconductor nanocrystals and solids
[DE94-006301] p 3520 N94-30842

MAGNETIC RESONANCE
Potential hazards of magnetic resonance imagers to emergency medical service helicopter operations
[DOT/FAA/RD-92/15] p 3135 N94-29862

MAGNETIC SPECTROSCOPY
Simulation of experiments on deep inelastic scattering of muons on superconducting magnetic toroidal spectrometer STORS
[DE94-606267] p 3483 N94-28554
Experimental setups and methods to obtain new nuclear data at intermediate and high energies
[DE94-607850] p 3489 N94-30052
Spectroscopic and dynamical studies of highly energized small polyatomic molecules
[DE94-006509] p 3489 N94-30061
Algorithm and program ORANGE for magnetic field simulation of magnetic system spectrometer STORS
[DE94-608013] p 3421 N94-30083

MAGNETIC STARS
Convective turbulence and transport in stars
p 3546 N94-29913

MAGNETIC STORMS
The effects of magnetic storm phases on F-layer irregularities from auroral to equatorial latitudes
[AD-A275203] p 3356 N94-28891
Accurate modeling of F-region electron densities
[NASA-CR-195781] p 3364 N94-30014
Variations of electron fluxes, low-frequency radiations and plasma density during the geomagnetic storm on 9-12 March, 1979 according to data of the Interkosmos-19 satellites
[DE94-607323] p 3365 N94-30223

MAGNETIC SUSPENSION
Neural network based time-optimal control of a magnetically levitated precision positioning system
[DE94-006573] p 3437 N94-30250

MAGNETIC TAPES
The program for catalogization of magnetic tapes in EXCHARM experiment
[DE94-606271] p 3528 N94-28615
Atomic-scale friction measurements using friction force microscopy. Part 2: Application to magnetic media
[AD-A275202] p 3298 N94-29290

MAGNETIC VARIATIONS
Mesopause winds and OH intensities at Mid-Latitudes-Fabry-Perot interferometer observations of the OH emission at 8430 A from bear lake observatory
[AD-A275246] p 3361 N94-29430

MAGNETIZATION
Observation of the phase shift of the wave function of the neutron under total reflection
[DE94-608244] p 3489 N94-30096
Magnetic properties of a quantum transverse spin-1 Blume-Emery-Griffiths model
[DE94-608114] p 3517 N94-30109
Magnetic properties of the three dimensional Ising model with interface single-ion anisotropy
[DE94-608116] p 3525 N94-30164
Magnetic properties of a transverse spin-1 Ising model with longitudinal crystal field interactions
[DE94-608118] p 3517 N94-30165
The bond diluted spin-1 Blume-Emery-Griffiths model in a transverse field
[DE94-608121] p 3525 N94-30167
Magnetic properties of a transverse spin-1 Ising model with random crystal field interactions
[DE94-608117] p 3517 N94-30181
Butterfly and scaling law in YBa2Cu4O8
[DE94-006037] p 3519 N94-30338

MAGNETO-OPTICS
Transient internal probe
[AD-A275054] p 3505 N94-29134

MAGNETOHYDRODYNAMIC FLOW
Proceedings of the NIPR Symposium on Upper Atmosphere Physics, no. 6
[JTN-94-80593] p 3359 N94-29233
Computer simulations on development of the fast reconnection mechanism p 3360 N94-29241
The Seventh International Beer Sheva Seminar on MHD Flows and Turbulence
[DE94-607211] p 3506 N94-29831

MAGNETOHYDRODYNAMIC STABILITY
Nonlinear magnetohydrodynamics
[DE94-005654] p 3503 N94-28547
Active electron and ion beam experiments in space
[AD-A275570] p 3504 N94-28828
Towards experimental verification and device applications of current driven plasma instabilities in solid state systems
[AD-A275395] p 3504 N94-29055
Proceedings of the NIPR Symposium on Upper Atmosphere Physics, no. 6
[JTN-94-80593] p 3359 N94-29233
Computer simulations on development of the fast reconnection mechanism p 3360 N94-29241
Coupled magnetohydrodynamic oscillations in the magnetosphere-ionosphere system: Hall current effect
p 3360 N94-29242
Scale-length dependence of the ratio between the magnetic and electric field perturbations in the ionospheric field-aligned current region p 3360 N94-29243
Formation and self-healing of magnetic islands in finite-beta helias equilibria
[NIFS-269] p 3505 N94-29483
The structure of solar magnetic fields and their associated electric currents p 3544 N94-29723
Higher order collisionless ballooning mode in tokamaks
[PPL-143] p 3507 N94-30156
Eigenmode analysis of the destabilized ion acoustic mode in tokamaks
[PPL-142] p 3507 N94-30158
Resistive ballooning mode in a gas-dynamic trap
[DE94-608328] p 3508 N94-30171
Langmuir waves in the electron-positron plasma
[DE94-608330] p 3508 N94-30191
A review of the ablative stabilization of the Rayleigh-Taylor instability in regimes relevant to ICF
[DE94-005809] p 3509 N94-30597
Advanced steady-state operating scenarios
[DE94-004810] p 3509 N94-30768
On the nonlinear dynamics of ocean wave systems
p 3378 N94-30790
Inertial confinement fusion
[DE94-005957] p 3510 N94-30875

MAGNETOHYDRODYNAMIC TURBULENCE
Acceleration in astrophysics
[DE94-004986] p 3552 N94-28580
The Seventh International Beer Sheva Seminar on MHD Flows and Turbulence
[DE94-607211] p 3506 N94-29831

MAGNETOHYDRODYNAMIC WAVES
Proceedings of the NIPR Symposium on Upper Atmosphere Physics, no. 6
[JTN-94-80593] p 3359 N94-29233
Coupled magnetohydrodynamic oscillations in the magnetosphere-ionosphere system: Hall current effect
p 3360 N94-29242
Scale-length dependence of the ratio between the magnetic and electric field perturbations in the ionospheric field-aligned current region p 3360 N94-29243
ULF waves and magnetic field characteristics in the polar cusp observed at Godhavn p 3361 N94-29244
Study of generation mechanisms of magnetospheric VLF/ELF emissions based on the direction findings
p 3361 N94-29245
Nonlinear wave packet evolution in a dispersive plasma: Application to rotational discontinuities
p 3506 N94-29822
On determination of a momentum of Alfven wave packet
[DE94-608329] p 3255 N94-30172

MAGNETOHYDRODYNAMICS
Nonlinear magnetohydrodynamics
[DE94-005654] p 3503 N94-28547
Acceleration in astrophysics
[DE94-004986] p 3552 N94-28580
Formation and self-healing of magnetic islands in finite-beta helias equilibria
[NIFS-269] p 3505 N94-29483
Liquid metal MHD and heat transfer in a tokamak blanket slotted coolant channel
[DE94-004622] p 3506 N94-29510
A relativistic solitary wave in electron positron plasma
[DE94-608107] p 3507 N94-30071
Advanced steady-state operating scenarios
[DE94-004810] p 3509 N94-30768

MAGNETOMETERS
Fabrication issues in optimizing YBa(2)Cu(3)O(7-x) flux transformers for low I/f noise
[DE94-005209] p 3261 N94-28546
The computer-aided system for the high resolution SQUID-magnetometer
[DE94-606138] p 3286 N94-28553
NASA Marshall Space Flight Center Solar Observatory report, July - October 1993
[NASA-TM-108448] p 3160 N94-29470
Three-axis fiber optic vector magnetometer
[AD-D016016] p 3288 N94-29699

MAGNETORESISTIVITY
Giant magnetoresistance and microstructural characteristics of epitaxial Fe-Ag and Co-Ag granular thin films
[DE94-006287] p 3519 N94-30707
Magnetotransport measurements in magnetic fields up to 50T in SmB6 and FeSi
[DE94-006227] p 3520 N94-30848

MAGNETOSPHERE-IONOSPHERE COUPLING
Proceedings of the NIPR Symposium on Upper Atmosphere Physics, no. 6
[JTN-94-80593] p 3359 N94-29233
Signatures of dayside solar wind/magnetosphere/ionosphere coupling as revealed by the pace HF radars and associated experiments
p 3359 N94-29236
A theory of current generator in the magnetosphere-ionosphere coupling
p 3360 N94-29240
Coupled magnetohydrodynamic oscillations in the magnetosphere-ionosphere system: Hall current effect
p 3360 N94-29242

MAGNETOSTATICS
Toward milli-Newton electro- and magneto-static microactuators p 3238 N94-29784

MAGNETOSTRICTION
Research on the improvement of shape-memory and magnetostrictive materials
[AD-A275397] p 3203 N94-29056

MAIN SEQUENCE STARS
Globular cluster photometry near the turnoff: Blue stragglers, relative ages, and the horizontal branch
p 3538 N94-29732
Surface differential rotation in a sample of cool dwarf stars p 3545 N94-29827

MAINTENANCE
Towards an information model and mechanisms for design rationale capture and use
[AD-A275060] p 3530 N94-29138
A compact roller-gear pitch-yaw joint module: Design and control issues p 3161 N94-29629
Teleoperated systems for nuclear reactors: Inspection and maintenance
[AIAA PAPER 94-1176-CP] p 3439 N94-30528

MALFUNCTIONS
Lock-up failure of a four-bar linkage deployment mechanism p 3163 N94-29646

MAN MACHINE SYSTEMS
Systematic safety consideration in product design
[PB94-132354] p 3229 N94-28410
Engineering of systems for application of scientific computing in industry p 3123 N94-28947
Stress and ergonomic design and evaluation of person-machine systems
[AD-A275156] p 3400 N94-29034
Future manned systems advanced avionics study
[NASA-CR-188277] p 3150 N94-29377
Cognitive approach to specifications on air traffic controllers' decision assistance systems
p 3139 N94-29571
Elements of supervisory control for military robotic applications p 3309 N94-30303
Supervised autonomous control for Space Station Special Purpose Dextrous Manipulator (SPDM) robot
p 3309 N94-30305
Aiding the operator in the manual control of a space manipulator
[PB94-125549] p 3402 N94-30390
A force-controllable macro-micro manipulator and its application to medical robots p 3314 N94-30441
Task automation in a successful industrial telerobot
[AIAA PAPER 94-1189-CP] p 3441 N94-30539

MANAGEMENT INFORMATION SYSTEMS
Software systems reengineering process model, version 1.0
[AD-A275711] p 3407 N94-28691
Environmental Compliance Assessment And Management System Program (ECAMP). US Air Force European Economic Community (EEC)
[AD-A275593] p 3346 N94-28727
An evaluation of techniques for ranking academic information systems journals
[AD-A275179] p 3529 N94-29066
Software engineering and software management in a distributed UNIX environment
[NLR-TP-92233-U] p 3422 N94-30314
MANAGEMENT METHODS
Risk-based prioritization: A comparison of approaches
[DE94-003368] p 3526 N94-28474
The development and demonstration of the metric assessment tool
[AD-A275788] p 3230 N94-28742
A generalization of the software engineering maturity model p 3416 N94-29341
Application of information management methodologies for project quality improvement in a changing environment p 3416 N94-29342
Information engineering implementation and acceptance p 3530 N94-29533
Report on NATO PTTI p 3469 N94-30645
Why TQM fails (and what you can do about it)
[DE93-018945] p 3527 N94-30698
MANAGEMENT PLANNING
Financial resource review model user's guide
[AD-A274979] p 3410 N94-29088
Software Management Environment (SME) concepts and architecture, revision 1
[NASA-CR-189293] p 3419 N94-29727
Triple Diagonal modeling: A mechanism to focus productivity improvement for business success
[DE94-004309] p 3527 N94-30041
Graphical simulation for aerospace manufacturing
[AIAA PAPER 94-1224-CP] p 3446 N94-30573
MANAGEMENT SYSTEMS
Environmental Compliance Assessment And Management System Program (ECAMP). US Air Force European Economic Community (EEC)
[AD-A275593] p 3346 N94-28727
Object oriented design of the autonomous fixtaking management system p 3143 N94-29323
A common Ada run-time system for avionics software p 3150 N94-29331
DLR's ATM demonstration programme p 3140 N94-29575
ARC2000: Automatic radar control p 3141 N94-29583
Software Management Environment (SME) concepts and architecture, revision 1
[NASA-CR-189293] p 3419 N94-29727
Analysis of EDP performance
[NASA-CR-195726] p 3420 N94-29945
MANDRELS
Filament to mandrel gap analysis: Resulting gap from filament winding over a cone-cylinder transition mandrel (reference NMTP no. 93838)
[DE94-004225] p 3175 N94-28528
Composite hot drape forming p 3240 N94-30448
MANEUVERABILITY
Exploring QDES as a tool for determining limits of achievable performance in aircraft design
[AD-A275359] p 3146 N94-28998
MANGANESE COMPOUNDS
Optical properties of cadmium sulfide, zinc selenide, and zinc manganese selenide semiconductor films p 3500 N94-29759
MANIFOLDS (MATHEMATICS)
Symplectic topology of integrable Hamiltonian systems
[DE94-608120] p 3467 N94-30166
Elements for the recognition of three dimensional deformable shapes: Application to biomedical imagery
[TELECOM-93-E-006] p 3396 N94-30978
MANIPULATORS
Design and construction of the Aerobot Robotic Manipulator (ARM)
[AD-A275362] p 3298 N94-28894
Experimental evaluation of fuzzy logic control of a flexible arm manipulator
[AD-A275375] p 3434 N94-29013
Feedback control of a three-link planar under-actuated manipulator using a surge velocity
[AD-A275159] p 3435 N94-29044
Kinematic functions for redundancy resolution using configuration control
[NASA-CASE-NPO-18608-1-CU] p 3436 N94-29504
Simplified and symmetrical five-bar linkage driver for manipulating a six-degree-of-freedom parallel minimanipulator with three inextensible limbs
[NASA-CASE-GSC-13485-2] p 3301 N94-29556
A compact roller-gear pitch-yaw joint module: Design and control issues p 3161 N94-29629
Six-degree-of-freedom parallel minimanipulator with three inextensible limbs
[NASA-CASE-GSC-13485-1] p 3288 N94-29726
Collision avoidance and control of multiple revolute manipulators p 3302 N94-29884
A study of the flexible space platform based deployable manipulator
[ISBN-0-315-85410-3] p 3303 N94-30135
Experimental sliding mode control of a flexible single link manipulator
[ISBN-0-315-85466-9] p 3304 N94-30238
Coordinated control of multiple robot manipulators p 3306 N94-30289
Force control techniques for robot manipulators and their military applications p 3307 N94-30291
An inverse kinematics algorithm for the DREP/Philips real-time radiographic manipulator system p 3307 N94-30292
Simulation of lightweight robots and their controllers p 3307 N94-30294
The response of flexible manipulators to a new computed torque control strategy: Simulation results p 3308 N94-30295
Symbolic generation of dynamics equations for manipulators mounted on moving bases p 3308 N94-30296
Supervised autonomous control for Space Station Special Purpose Dextrous Manipulator (SPDM) robot p 3309 N94-30305
A testbed for the development of ground-based control of space-based manipulators p 3309 N94-30306
Aiding the operator in the manual control of a space manipulator
[PB94-125549] p 3402 N94-30390
Development and validation of a linear recursive order-N algorithm for the simulation of flexible space manipulators dynamics
[AD-B173557] p 3311 N94-30391
A force-controllable macro-micro manipulator and its application to medical robots p 3314 N94-30441
Programmable Automated Welding System (PAWS): Control of welding through software and hardware p 3314 N94-30443
Space flight manipulator technologies and requirements for the NASA Flight Telerobotic Servicer (FTS)
[AIAA PAPER 94-1191-CP] p 3441 N94-30542
A highly redundant robot system for inspection
[AIAA PAPER 94-1194-CP] p 3442 N94-30545
Fuzzy logic based robotic controller
[AIAA PAPER 94-1202-CP] p 3443 N94-30553
Robotic NDE inspection of advanced solid rocket motor casings
[AIAA PAPER 94-1222-CP] p 3446 N94-30571
An intelligent robotic aid system for human services
[AIAA PAPER 94-1232-CP] p 3447 N94-30580
Kinematic analysis of platform-type robotic manipulators
[ISBN-0-315-78703-1] p 3311 N94-30793
Robust adaptive control of a mechanical manipulator p 3449 N94-30806
Kinematics and force analysis of a robot hand based on an artificial biological control scheme p 3313 N94-30957
MANNED LUNAR SURFACE VEHICLES
Lunar surface operations. Volume 1: Lunar surface emergency shelter
[NASA-CR-195551] p 3299 N94-29354
MANNED MARS MISSIONS
Nuclear electric propulsion: A better, safer, cheaper transportation system for human exploration of Mars
[NASA-TM-106406] p 3171 N94-28833
MANNED SPACE FLIGHT
Start of space tourism p 3164 N94-29714
MANNED SPACECRAFT
ESTEC wiring test programme materials related properties p 3165 N94-28698
Vulnerability of manned spacecraft to crew loss from orbital debris penetration
[NASA-TM-108452] p 3169 N94-30161
MANUAL CONTROL
Tactility as a function of grasp force: Effects of glove, orientation, pressure, load, and handle
[NASA-TP-3474] p 3402 N94-30210
Aiding the operator in the manual control of a space manipulator
[PB94-125549] p 3402 N94-30390
MANUALS
Defense Technical Information Center cataloging guidelines
[AD-A275100] p 3529 N94-28911
Fundamentals of printing technology
[PB94-132602] p 3530 N94-29141
User's manual for the model interface and plugboard cabinets in the 14- by 22-foot subsonic tunnel
[NASA-TM-109062] p 3133 N94-30176
MANUFACTURING
Silicon-Film (tm) photovoltaic manufacturing technology
[DE94-000258] p 3336 N94-28501
NEMA wire and cable standards development programs p 3166 N94-28706
Electroset Technology: On the forefront of manufacturing
[AD-A275166] p 3263 N94-29045
Application of high-speed milling to the Finnish manufacturing industry
[PB94-135548] p 3230 N94-29187
Realizing the productivity potential of expeditious operations
[PB94-135555] p 3230 N94-29188
Technology transfer initiatives
[NASA-CR-195151] p 3537 N94-29410
Micromanufacturing: Recent developments in this country and abroad p 3235 N94-29769
Practical applications of plasma surface modification
[DE94-004892] p 3349 N94-29932
Logistics for the implementation of lead-free solders on electronic assemblies
[DE94-004800] p 3206 N94-29936
Non-aqueous cleaning solvent substitution
[DE94-005339] p 3219 N94-30245
The 1992 report on the next generation ultra clean technology for advanced microfabrication
[DE94-744171] p 3157 N94-30268
Technology 2003: The Fourth National Technology Transfer Conference and Exposition, volume 1
[NASA-CP-3249] p 3555 N94-30440
The use of interactive computer vision and robot hand controllers for enhancing manufacturing safety p 3314 N94-30442
Near-net-shape manufacturing: Spray-formed metal matrix composites and tooling p 3186 N94-30447
Precision and manufacturing at the Lawrence Livermore National Laboratory p 3240 N94-30449
Conference on Intelligent Robotics in Field, Factory, Service, and Space (CIRFFSS 1994), volume 1
[NASA-CP-3251] p 3439 N94-30526
Agile manufacturing: The factory of the future
[AIAA PAPER 94-1184-CP] p 3440 N94-30534
Confessions of a robot lobotomist
[AIAA PAPER 94-1185-CP] p 3440 N94-30535
PV Cz silicon manufacturing technology improvements
[DE94-000248] p 3339 N94-30603
Large-area triple-junction a-Si alloy production scale up
[DE94-000249] p 3339 N94-30604
Thin EFG octagons
[DE94-000257] p 3339 N94-30605
MANY BODY PROBLEM
Equation of state of stellar plasmas
[DE94-004186] p 3542 N94-28526
The role of cloud collisions in N-body simulations of disk galaxies p 3545 N94-29755
The stability of perfect elliptic disks p 3545 N94-29834
Periodic orbits of n-body type problems: The fixed period case
[DE94-608096] p 3453 N94-30091
Exclusive many-particle diffusion in disordered media and correlation functions for random vertex models
[DE94-608134] p 3525 N94-30121
MAPPING
The uses and limitations of fractal geometry in digital terrain modelling p 3333 N94-29958
A monotonicity conjecture for real cubic maps
[DE94-003969] p 3335 N94-30610
MARANGONI CONVECTION
Survey report of JSUP Space Environment Utilization Research Committee in fiscal year 1992: Metallic Materials Session
[JTN-94-80583] p 3159 N94-30794
MARINE CHEMISTRY
The carbon cycle revisited p 3350 N94-30622
MARINE ENVIRONMENTS
Fundamental studies on the corrosion behavior of weldments in marine microbial environments
[AD-A275247] p 3203 N94-28900
Oceanic survey utilizing satellites p 3328 N94-29040
Tohoku district observed by artificial satellites p 3328 N94-29041
The effects of altimeter sampling characteristics: Some Geosat examples
[AD-A275225] p 3357 N94-29062
Research report on the potential of ocean development suitable for area characteristics
[JTN-94-80587] p 3377 N94-29595

MARINE METEOROLOGY
Studies of marine aerosols and their evolution in the eastern North Atlantic
[AD-A275011] p 3377 N94-29128
MARINE RESOURCES
On United States-Japan Conference on Development and Utilization of Natural Resources: Report of the 14th Joint Meeting of U. S. and Japan Marine Mining Panel
p 3188 N94-28683
Research report on the potential of ocean development suitable for area characteristics
[JTN-94-80587] p 3377 N94-29595
Reproduction in the Japanese anchovy (Engraulis japonica) as related to population fluctuation
p 3235 N94-29708
MARINE TECHNOLOGY
Fundamental studies on the corrosion behavior of weldments in marine microbial environments
[AD-A275247] p 3203 N94-28900
Research report on the potential of ocean development suitable for area characteristics
[JTN-94-80587] p 3377 N94-29595
Development of the breakwater with submerged mound for interchanging sea water p 3234 N94-29703
Photovoltaic power without batteries for continuous cathodic protection p 3341 N94-30465
MARKARIAN GALAXIES
Finnish astronomy days, 1992-1993. Proceedings of the Finnish Astronomical Society
[PB94-136892] p 3538 N94-29170
MARKET RESEARCH
Marketing tools for increasing proactivity in technical information centers
[AGARD-AR-326] p 3528 N94-30934
MARKETING
Marketing tools for increasing proactivity in technical information centers
[AGARD-AR-326] p 3528 N94-30934
MARKOV CHAINS
Markov chains for random urinalysis 3: Daily model and drug kinetics
[AD-A275540] p 3389 N94-28797
MARKOV PROCESSES
Stability of dynamical systems in the presence of noise
[AD-A275383] p 3243 N94-29072
U-statistics of random-size samples and limit theorems for systems of Markovian particles with non-Poisson initial distributions
[AD-A275018] p 3464 N94-29129
Hierarchical structures and asymmetric stochastic processes on p-adics and adeles
[PB94-138203] p 3464 N94-29178
Subphonetic acoustic modeling for speaker-independent continuous speech recognition
[AD-A275217] p 3244 N94-29303
ASSIST internals reference manual
[NASA-TM-109102] p 3431 N94-29494
MARS (PLANET)
MUADEE: Mars Upper Atmosphere Dynamics, Energetics, and Evolution discovery mission. Executive summary volume
[NASA-CR-195732] p 3549 N94-28418
BAG: A code for predicting the performance of a gas bag impact attenuation system for the Pathfinder lander
[DE94-003688] p 3165 N94-28477
MARS ATMOSPHERE
MUADEE: Mars Upper Atmosphere Dynamics, Energetics, and Evolution discovery mission. Executive summary volume
[NASA-CR-195732] p 3549 N94-28418
The 1992-1993 advanced design program. Part 1: The Mars methane engine project. Part 2: The Mars oxygen processor new furnace
[NASA-CR-195513] p 3299 N94-29409
The viability of photovoltaics on the Martian surface
[NASA-TM-106478] p 3338 N94-30196
MARS ENVIRONMENT
The viability of photovoltaics on the Martian surface
[NASA-TM-106478] p 3338 N94-30196
MARS LANDING
BAG: A code for predicting the performance of a gas bag impact attenuation system for the Pathfinder lander
[DE94-003688] p 3165 N94-28477
MARS OBSERVER
Optical Chopper Assembly for the Mars Observer
p 3162 N94-29639
MARS PROBES
Parachute Swivel Mechanism for planetary entry
p 3162 N94-29643
MARS SURFACE
Mars rover mechanisms designed for Rocky 4
p 3161 N94-29630
Backscatter Mossbauer Spectrometer (BaMS) for extraterrestrial applications p 3236 N94-29774
A broad-band microseismometer for planetary operations p 3237 N94-29778
The viability of photovoltaics on the Martian surface
[NASA-TM-106478] p 3338 N94-30196
MARS SURFACE SAMPLES
Thermal imaging for a mobile robot
p 3308 N94-30300
MARTENSITE
Computer simulation of martensitic transformations
[DE94-005213] p 3201 N94-28479
Research on the improvement of shape-memory and magnetostrictive materials
[AD-A275397] p 3203 N94-29056
Low temperature behavior of virgin martensite
[PB94-132925] p 3204 N94-29142
MARTENSITIC STAINLESS STEELS
Toughening mechanisms in ultrahigh-strength steels
[AD-A275439] p 3202 N94-28867
MARTENSITIC TRANSFORMATION
Computer simulation of martensitic transformations
[DE94-005213] p 3201 N94-28479
MASERS
A dual-cavity ruby maser for the Ka-band link experiment p 3250 N94-29658
X-band ultralow-noise maser amplifier performance
p 3251 N94-29672
MASKS
RF vacuum microelectronics
[AD-A275221] p 3263 N94-28915
MASS
A compact roller-gear pitch-yaw joint module: Design and control issues p 3161 N94-29629
A non-contacting vertical alignment system for mass properties measuring instruments
[DE94-004680] p 3289 N94-29927
MASS FLOW RATE
Advanced diagnostics for reacting flows
[AD-A275057] p 3272 N94-29136
MASS RATIOS
Large amplitude Langmuir and ion-acoustic waves in a relativistic two-fluid plasma
[NIFS-271] p 3506 N94-29547
MASS SPECTRA
Measurement of the W mass in the D0 detector
[DE94-006002] p 3490 N94-30103
Overlap of metal clusters and nuclear structure physics
[DE94-608387] p 3517 N94-30183
MASS SPECTROMETERS
New high temperature plasmas and sample introduction systems for analytical atomic emission and mass spectrometry
[DE94-004564] p 3503 N94-28458
A study of solid propellants using a microprobe mass spectrometer system
[AD-A275325] p 3224 N94-28879
Adaption of the bubble detector for use as a LET spectrometer p 3291 N94-30216
MASS SPECTROSCOPY
New high temperature plasmas and sample introduction systems for analytical atomic emission and mass spectrometry
[DE94-004564] p 3503 N94-28458
Measurement of elemental speciation by liquid chromatography: Inductively coupled plasma mass spectrometry (LC-ICP-MS) with the Direct Injection Nebulizer (DIN)
[DE94-005261] p 3187 N94-28483
Matrix isolation studies of the interactions of BF3 with water and substituted diethyl ethers. Chemical ionization mass spectrometric determination of the proton affinity of (CF3CH2)2O
[NASA-TM-106422] p 3189 N94-28832
Reactions of metal ions and their clusters in the gas phase using laser ionization: Fourier transform mass spectrometry
[DE94-006208] p 3207 N94-30024
Novel mass spectrometric instrument for gaseous and particulate characterization and monitoring
[DE94-005896] p 3349 N94-30047
MASS TRANSFER
Volume averaged model for the mechanics of alloys solidification
[PB94-138617] p 3208 N94-30113
On the structure and atomic motions in liquid sodium
[DE94-608386] p 3490 N94-30182
Local two-phase flow simulations including interface tracking with mass transfer p 3283 N94-30954
MASSIVE STARS
Physical conditions in classical H2 regions in the Magellanic Clouds p 3543 N94-29722
A multi wavelength observational study of the Cartwheel ring galaxy p 3539 N94-29821
MASSIVELY PARALLEL PROCESSORS
Rome Laboratory software engineering technology program p 3414 N94-29330
Progress report for the PTUF Project-93 Q1 and Q2
[PB94-138591] p 3431 N94-29995
MATCHED FILTERS
Output statistics of the SALFAS FM normalizer Smoothing/Prediction function
[AD-A275758] p 3463 N94-28759
MATCHING
Variable-resolution stereo matching
p 3308 N94-30298
On the unification free PROLOG programs
[CWI-CS-R9331] p 3427 N94-30733
MATERIALS SCIENCE
Report on smart materials
[PB94-137528] p 3203 N94-29015
Journal of NIRE, vol. 2, no. 3
[JTN-94-80553] p 3553 N94-29512
Research laboratories annual report 1992
[DE94-608124] p 3555 N94-30168
Technology 2003: The Fourth National Technology Transfer Conference and Exposition, volume 1
[NASA-CP-3249] p 3555 N94-30440
MATHEMATICAL LOGIC
Parallel quantification
[LP-93-01] p 3422 N94-30318
Dynamic generalized quantifiers and monotonicity
[LP-93-02] p 3454 N94-30319
A smart child of Peano's
[ML-92-10] p 3455 N94-30325
Completeness of the Lambek calculus with respect to relativized relational semantics
[LP-93-03] p 3455 N94-30326
Identity: Quarrelling with an unproblematic notion
[LP-93-04] p 3455 N94-30327
A note on schema equivalence
[TR-92-30] p 3535 N94-30362
Logic of transition systems
[CT-93-03] p 3424 N94-30371
Bounded contraction and many-valued semantics
[ML-93-04] p 3456 N94-30380
Models of the untyped lambda-calculus in semi Cartesian closed categories
[ML-93-05] p 3456 N94-30381
Categorial generalization of algebraic recursion theory
[ML-93-06] p 3456 N94-30382
Algorithmic problems concerning first-order definability of modal formulas on the class of all finite frames
[ML-93-07] p 3456 N94-30383
Remarks on the theory of semi-functors
[ML-93-08] p 3457 N94-30384
Natural deduction for intuitionistic linear logic
[ML-93-09] p 3457 N94-30385
The conjoinability relation in Lambek calculus in linear logic
[ML-93-03] p 3457 N94-30397
Termination of term rewriting by semantic labelling
[RUU-CS-93-24] p 3459 N94-30424
Three metric domains of processes for bisimulation
[CWI-CS-R9335] p 3459 N94-30427
Perpetual reductions and strong normalization in orthogonal term rewriting systems
[CWI-CS-R9345] p 3426 N94-30437
Comparative semantics for linear arrays of communicating processes
[CWI-CS-R9336] p 3426 N94-30491
Design and analysis of dynamic leader election protocols in broadcast networks
[MEMO-INF-93-43] p 3260 N94-30520
A monotonicity conjecture for real cubic maps
[DE94-003969] p 3335 N94-30610
Unravelling nondeterminism: On having the ability to choose
[RUU-CS-93-30] p 3428 N94-30749
Termination of term rewriting by semantic labelling
[RUU-CS-92-38] p 3462 N94-30859
The structure of exponentials: Uncovering the dynamics of linear logic proofs
[ML-93-10] p 3430 N94-30973
Inventory of fragments and exact models in intuitionistic proportional logic
[ML-93-11] p 3463 N94-30974
Remarks on uniformly finitely precomplete positive equivalences
[ML-93-12] p 3463 N94-30975
MATHEMATICAL MODELS
Filament to mandrel gap analysis: Resulting gap from filament winding over a cone-cylinder transition mandrel (reference NMTP no. 93838)
[DE94-004225] p 3175 N94-28528
Applied analysis/computational mathematics
[DE94-005133] p 3451 N94-28571
Dissipative quantum dynamics and nonlinear sigma-model
[DE94-606295] p 3523 N94-28617
A family of joint probability models for cost and schedule uncertainties
[AD-A275513] p 3463 N94-28670

Controlling chaos in plasma filled diodes
[AD-A275525] p 3504 N94-28686
On the linear stability of Verkley's modons
p 3324 N94-28695
Similarity solutions and numerical modeling in buoyancy controlled turbulent diffusion flames
[AD-A275820] p 3188 N94-28777
Modeling, analysis, and simulation of an optical time-division multiple-access network architecture
[AD-A275847] p 3498 N94-28780
The lectures in complex systems, volume 5
[AD-A275458] p 3466 N94-28807
Approximation of solutions of the cubic NLSE by finite dimensional equations and non-squeezing properties
[PB94-138294] p 3452 N94-29148
Model-oriented data analysis with applications to lake and soil water simulation
[PB94-136942] p 3329 N94-29173
Computer simulations on development of the fast reconnection mechanism p 3360 N94-29241
Flowfield prediction of NO(x) and smoke production in aircraft engines p 3191 N94-29252
Numerical prediction of turbulent sooting diffusion flames p 3191 N94-29253
Numerical modelling of turbine combustion chambers
p 3154 N94-29254
Modeling of the phase liquidates in combustion chambers p 3195 N94-29278
Scramjet CFD methods and analysis. Part 2: Scramjet CFD analysis. Numerical simulation of supersonic mixing and combustion applied to scramjet combustor
p 3152 N94-29300
Attenuation of outdoor sound propagation levels by a snow cover
[AD-A275387] p 3478 N94-29314
Damage meso-modeling of 3D evolutive composites
[REPT-932-430-106] p 3179 N94-29442
On-line search for optimal controller parameters using interconnected learning automata
[MATHS-REPT-A-196] p 3436 N94-29526
Development and verification of a model to predict impingement currents for ion thrusters
[NASA-CR-195322] p 3173 N94-29546
Introduction to the design of ventilation systems
p 3231 N94-29599
Ventilation models p 3232 N94-29603
Models for vibration-dissociation coupling in high-temperature gases p 3273 N94-29675
Spherical model for turbulence p 3274 N94-29730
Control of micromachined deformable mirrors
p 3239 N94-29787
On fatigue crack closure: Analysis and measurement
[ISBN-0-315-74873-7] p 3321 N94-29812
An analytical study of unsteady rotor/fuselage interaction in hover and forward flight
p 3131 N94-29826
Radiation and scattering from cylindrically conformal printed antennas
[NASA-CR-195546] p 3253 N94-29873
Acceptance sampling methods for sample results verification
[DE94-002882] p 3465 N94-29925
Microgravity compatible drive system-rider. New technologies
[PB94-138583] p 3229 N94-29996
Melt flow during alloy solidification: Dimensional analysis and model problems
[PB94-138625] p 3206 N94-29997
Polynomial modeling of analog-to-digital converters
[DE94-005579] p 3406 N94-30008
Triple Diagonal modeling: A mechanism to focus productivity improvement for business success
[DE94-004309] p 3527 N94-30041
Boundary-induced phase transitions in equilibrium and non-equilibrium systems
[DE94-608137] p 3199 N94-30111
Statistical description of hot and dense clustering matter
[DE94-608155] p 3490 N94-30112
Volume averaged model for the mechanics of alloys solidification
[PB94-138617] p 3208 N94-30113
Generalized augmented space theorem for correlated disorder and cluster coherent potential approximation
[DE94-608110] p 3208 N94-30118
Modelling of multiparticle production by dynamical semigroup method
[DE94-608132] p 3490 N94-30120
A framework for comparing conceptual modelling languages
[TR-92-29] p 3535 N94-30361
Logic of transition systems
[CT-93-03] p 3424 N94-30371
Bounded contraction and many-valued semantics
[ML-93-04] p 3456 N94-30380
Models of the untyped lambda-calculus in semi Cartesian closed categories
[ML-93-05] p 3456 N94-30381
The secrets of causality
[RUU-CS-93-29] p 3426 N94-30490
Free-floating dual-arm robots for space assembly
[AIAA PAPER 94-1195-CP] p 3442 N94-30546
The road plan model: Information model for planning road building activities
[AIAA PAPER 94-1219-CP] p 3445 N94-30567
Simulation of composite material response under dynamic compressive loading
[DE94-005272] p 3184 N94-30589
An evaluation of explicit pseudo-steady-state approximation schemes for stiff ODE systems from chemical kinetics
[CWI-NM-R9312] p 3353 N94-30729
Engineering of systems for application of scientific computing in industry WP project management ISNaS 9209099
[PB94-126232] p 3428 N94-30739
Modeling data throughput on communication networks
[DE94-005077] p 3260 N94-30772
Formulae for the calculation of the magnetic field strength in a Helmholtz system with circular coils
[NPL-DES-130] p 3260 N94-30785
Using the log-normal distribution in analyzing aerosols: The mathematical reasoning underlying the various diameters used and the plotting procedure
[DE94-006459] p 3461 N94-30817
Selecting model complexity in learning problems
[DE94-000764] p 3461 N94-30821
Numerical simulation of a condenser in two-phase heat transport systems: A feasibility study
[AD-B173650] p 3282 N94-30855
A solid-on-solid invasion percolation model for self-affine interfaces
[DE94-608102] p 3521 N94-30888
Mathematical models of hysteresis
[DE94-005681] p 3260 N94-30902
An investigation of the reacting vortex structures associated with pulse combustion p 3200 N94-30911
An asymptotic analysis for compressible gas lubrication of rough surfaces p 3222 N94-30922
Optimization techniques for a dial-a-ride transportation system in urban environment
[REPT-93-051] p 3537 N94-30926
Identification of the damping ratio relationship of an autovehicle suspension
[REPT-93-063] p 3313 N94-30937
Application of the extended Kalman filter to the estimation of the char mass in a fluidized bed combustor
[REPT-93-065] p 3200 N94-30938
Numerical modeling and prediction of the thermomechanical behavior of fiber-reinforced composites p 3186 N94-30956
Numerical simulations of piano strings. Part 1: A physical model for a struck string using finite difference methods
[TELECOM-93-C-003] p 3481 N94-30972
Elements for the recognition of three dimensional deformable shapes: Application to biomedical imagery
[TELECOM-93-E-006] p 3396 N94-30978

MATHEMATICAL PROGRAMMING
North American jumelage 'type systems'
[AD-A275342] p 3411 N94-29214
Program derivation by proof transformation
[AD-A275260] p 3453 N94-29304
A structural co-induction theorem
[CWI-CS-R9346] p 3461 N94-30753

MATRICES (MATHEMATICS)
Improved QCD sum rule estimates of the higher twist contributions to polarised and unpolarised nucleon structure functions
[PB94-138112] p 3487 N94-29161
Integer cosine transform for image compression
p 3247 N94-29619
The Stroemberg wavelet on the interval and the Franklin system
[TELECOM-93-C-002] p 3462 N94-30971

MATRIX MATERIALS
Innovative processing of composites for ultra-high temperature applications, book 2
[AD-A275598] p 3177 N94-28730
3-D braided, continuous fiber ceramic composites produced by chemical vapor infiltration
[AD-A275192] p 3178 N94-29024
Microwave assisted chemical vapor infiltration
[DE94-005005] p 3185 N94-30771

MATRIX METHODS
Compound matrix method for multi-point boundary-value problems
[PB94-137791] p 3453 N94-29476

MATTER (PHYSICS)
Equation of state of neutron star matter, limiting rotational periods of fast pulsars, and the properties of strange stars
[DE94-005214] p 3542 N94-28480
Theoretical studies in hadronic and nuclear physics
[DE94-003524] p 3492 N94-30838

MAXIMUM ENTROPY METHOD
The maximum entropy approach applied to energy exchange, chemical reactions and ionisation in the direct simulation Monte Carlo method for rarefied hypersonic flows
[IC-AERO-93-01] p 3524 N94-29481
Procedures for basic inverse problems: Black body radiation problem and phonon density of states problem
[ISBN-0-315-85757-9] p 3525 N94-30244

MAXIMUM LIKELIHOOD ESTIMATES
Digital combining-weight estimation for broadband sources using maximum-likelihood estimates
p 3250 N94-29661

MAXIMUM PRINCIPLE
On some general properties of parabolic conservation equations
[DE94-006101] p 3461 N94-30758

MAXWELL EQUATION
Exact spherical wave solutions to Maxwell's equations with applications p 3252 N94-29733
Theory of fundamental interactions
[DE94-608126] p 3525 N94-30169

MEASURE AND INTEGRATION
On invariant measures for some infinite-dimensional dynamical systems
[DE94-606342] p 3522 N94-28609

MEASUREMENT
The development and demonstration of the metric assessment tool
[AD-A275788] p 3230 N94-28742

MEASURING INSTRUMENTS
Single specimen fracture toughness determination procedure using instrumented impact test
[PB94-132040] p 3316 N94-28402
Development and application of a thermistor current meter
[AD-A275816] p 3286 N94-28831
Improved in-flow acoustic sensor
[NASA-CASE-ARC-12001-1] p 3478 N94-29363
Stereo imaging based particle velocimeter
[NASA-CR-195800] p 3289 N94-29742
A non-contacting vertical alignment system for mass properties measuring instruments
[DE94-004680] p 3289 N94-29927
VHF impedance measurement: A review
[PB94-138682] p 3267 N94-30115
Theory of fundamental interactions
[DE94-608126] p 3525 N94-30169
User's manual for the model interface and plugboard cabinets in the 14- by 22-foot subsonic tunnel
[NASA-TM-109062] p 3133 N94-30176
Monitor for status epilepticus seizures
p 3397 N94-30460
The performance of gloss meters on curving surfaces
[NPL-DMM(A)-111] p 3501 N94-30522
Guidance notes for use with NPL low permeability reference materials
[NPL-DES-121] p 3476 N94-30780
Report on the development of low magnetic permeability reference materials
[NPL-DES-119] p 3476 N94-30783
Guidance on eliminating interference from sensitive electrical circuits
[PB94-139300] p 3268 N94-30784

MECHANICAL DEVICES
An Earth observation telescope refocusing mechanism
[REPT-932-440-103] p 3332 N94-29417
Rotary actuator
[NASA-CASE-MFS-28581-1] p 3205 N94-29447
Metal band drives in spacecraft mechanisms
p 3162 N94-29637
Proceedings of the Workshop on Microtechnologies and Applications to Space Systems
[NASA-CR-195688] p 3235 N94-29767

MECHANICAL DRIVES
Electrical engineering and industrial electronics education days: Control of asynchronous generators
[PB94-135514] p 3266 N94-29523
Mars rover mechanisms designed for Rocky 4
p 3161 N94-29630
SP-100 control drive assembly development
p 3163 N94-29651
Microgravity compatible drive system-rider. New technologies
[PB94-138583] p 3229 N94-29996

MECHANICAL ENGINEERING
Filament to mandrel gap analysis: Resulting gap from filament winding over a cone-cylinder transition mandrel (reference NMTP no. 93838)
[DE94-004225] p 3175 N94-28526
MECHANICAL MEASUREMENT
Shape from diameter: Negative results
[RUU-CS-93-16] p 3458 N94-30407
Shape from diameter: Positive results
[RUU-CS-93-17] p 3458 N94-30408
MECHANICAL PROPERTIES
Joining silicon carbide to austenitic stainless steel through diffusion welding
[PB94-126331] p 3297 N94-28399
Viscous and elastic-plastic material model in the ABAQUS
[PB94-132347] p 3316 N94-28409
Analysis of data by long-time mechanical properties of 08KH18N10T steel irradiated by neutrons
[DE94-605337] p 3202 N94-28551
Robust 300 C wire insulation system
p 3165 N94-28699
Electrical and mechanical testing of wire insulation for space applications p 3166 N94-28710
Innovative processing of composites for ultra-high temperature applications, book 1
[AD-A275597] p 3176 N94-28729
Probabilistic material strength degradation model for Inconel 718 components subjected to high temperature, mechanical fatigue, creep and thermal fatigue effects
[NASA-CR-195284] p 3318 N94-28840
On the dynamic mechanical behavior of 3-D integrated fabric reinforced composites
[AD-A275424] p 3177 N94-28865
Electronic structure and mechanical properties of grain boundaries
[AD-A275198] p 3512 N94-28890
Microstructure/property relationships for SCS6/Timetal 21-S composite
[AD-A275056] p 3178 N94-29135
Characterisation and processing of SiC/MAS-L glass ceramic matrix composite
[REPT-932-430-111] p 3179 N94-29412
Glass-ceramic matrix composites
[REPT-932-430-112] p 3179 N94-29413
The effect of various metallurgical parameters on the flow and fracture behavior of polycrystalline NiAl near the brittle-to-ductile transition
[NASA-TM-106534] p 3205 N94-29758
Estimation of Weibull modulus from dynamic and static fatigue experiments
[PB94-138641] p 3322 N94-30114
High elongation elastomers p 3223 N94-30477
Simulation of composite material response under dynamic compressive loading
[DE94-005272] p 3184 N94-30589
Effect of fiber coating on mechanical properties of Nicalon fibers and Nicalon-fiber/SiC matrix composites
[DE94-005477] p 3185 N94-30593
Studies on the optimization of deformation processed metal-metal matrix composites
[DE94-006033] p 3185 N94-30704
Influence of tungsten alloying additions on the mechanical properties and texture of tantalum
[DE94-004994] p 3210 N94-30774
Numerical modeling and prediction of the thermomechanical behavior of fiber-reinforced composites p 3186 N94-30956
MECHANICAL SHOCK
Minutes: Accredited Standards Committee on Mechanical Vibration and Shock, S2. US TAG for ISO/TC 108 Mechanical Vibration and Shock
[AD-A275591] p 3316 N94-28726
MEDIA
Development of novel switchable protein surfaces
[AD-A275510] p 3384 N94-28667
MEDICAL EQUIPMENT
Technology 2003: The Fourth National Technology Transfer Conference and Exposition, volume 1
[NASA-CP-3249] p 3555 N94-30440
A force-controllable macro-micro manipulator and its application to medical robots p 3314 N94-30441
Composite redesign of obstetrical forceps
p 3397 N94-30457
A fuzzy logic controller for hormone administration using an implantable pump p 3397 N94-30459
MEDICAL PERSONNEL
Aeromedical support for casualties in extremely hot climates p 3382 N94-28443
MEDICAL SCIENCE
Clinical investigation program
[AD-A275025] p 3391 N94-29116
MEDICAL SERVICES
Clinical investigation program
[AD-A275025] p 3391 N94-29116
Potential hazards of magnetic resonance imagers to emergency medical service helicopter operations
[DOT/FAA/RD-92/15] p 3135 N94-29862
MEDIUM SCALE INTEGRATION
Investigation of advanced fault insertion and simulator methods
[NASA-CR-195241] p 3261 N94-28511
MELTING
Laser-material interactions: A study of laser energy coupling with solids
[DE94-005212] p 3292 N94-28478
Dislocation theory of melting for iron, revisited
[DE94-002715] p 3355 N94-28538
Melt flow during alloy solidification: Dimensional analysis and model problems
[PB94-138625] p 3206 N94-29997
A toy model of sea ice growth p 3351 N94-30626
MELTING POINTS
Directional solidification studies in Ni-Al alloys
[DE94-005562] p 3201 N94-28527
Dislocation theory of melting for iron, revisited
[DE94-002715] p 3355 N94-28538
On the temperature distribution near a cold surface
[AD-A275162] p 3332 N94-29288
MELTS (CRYSTAL GROWTH)
A novel approach to the fabrication of SiC structures of arbitrary shape
[AD-A275475] p 3214 N94-29073
Process modelling for materials preparation experiments
[NASA-CR-195782] p 3175 N94-30242
Investigation of the phase equilibria and phase transformations associated with the Bi2Sr2CaCu2O(y) superconductor
[DE94-004889] p 3519 N94-30691
MEMBRANES
Polyaniline membranes for gas and liquid separation
[AD-A275851] p 3408 N94-28790
Effects of pressure on membrane-associated receptors and effector elements
[AD-A275813] p 3384 N94-28829
Inorganic polymer-derived ceramic membranes
[DE94-000082] p 3216 N94-29830
MEMORY (COMPUTERS)
Performance analysis of memory hierachies in high performance systems
[DE94-005549] p 3404 N94-28517
A common Ada run-time system for avionics software
p 3150 N94-29331
Multi-speed multi-phase resolver converter
[NASA-CASE-MFS-28855-1] p 3264 N94-29372
MENTAL PERFORMANCE
Toward a model of expert knowledge structure and their role in cognitive task performance
[AD-A275641] p 3529 N94-28645
Designing for performance: A cognitive systems engineering approach to modifying an AWACS human computer interface
[AD-A275187] p 3399 N94-28861
Temporal and qualitative decomposition of plausible reasoning
[AD-A275073] p 3398 N94-29154
Spectral analysis of heart rate and psychological state: A review of its validity as a workload index
[AD-B179387] p 3399 N94-30969
MERCURY (METAL)
Measurement of volatile metal species at elevated temperatures
[PB94-132321] p 3186 N94-28407
MERCURY CADMIUM TELLURIDES
Modeling the total dose radiation effects of Hg(1-x)Cd(x)Te photodiodes using numerical device simulators
[AD-A275235] p 3263 N94-29028
Dual-use applications of infrared sensitive materials
[AD-A275140] p 3499 N94-29694
MERCURY COMPOUNDS
Measurement of volatile metal species at elevated temperatures
[PB94-132321] p 3186 N94-28407
Measurement of elemental speciation by liquid chromatography: Inductively coupled plasma mass spectrometry (LC-ICP-MS) with the Direct Injection Nebulizer (DIN)
[DE94-005261] p 3187 N94-28483
MERCURY TELLURIDES
Vibrational properties of homopolar and heteropolar surfaces and interfaces of the CdTe/HgTe system
[DE94-608105] p 3516 N94-30069
MERRITT ISLAND (FL)
Development and implementation of a scrub habitat compensation plan for Kennedy Space Center
[NASA-TM-109202] p 3347 N94-29099
MESOMETEOROLOGY
Evaluation of the National Meteorological Center mesoscale model for prediction of severe convection over Central Arizona p 3371 N94-29744
An observational and numerical study of sea/land-breeze circulations in an area of complex coastal heating p 3372 N94-29813
MESON RESONANCE
Issues in light hadron spectroscopy
[PB94-138229] p 3486 N94-29112
MESON-NUCLEON INTERACTIONS
Deep inelastic lepton scattering on nuclei: operator product expansion and meson-nucleon theory
[DE94-606442] p 3484 N94-28610
Possible explanation of the interaction cross-section growth at high energies
[DE94-606457] p 3494 N94-28612
MESONS
B production and B(0)(bar B)(0) mixing at DO
[DE94-004664] p 3484 N94-28574
Glueball and meson dispersion and diffusion relations in compact U(1)(2+1) gauge theory
[ISBN-0-315-85577-0] p 3490 N94-30234
Heavy flavor production at fixed target photo- and hadroproduction
[DE94-004651] p 3491 N94-30719
Theoretical studies in hadronic and nuclear physics
[DE94-003524] p 3492 N94-30838
MESOPAUSE
Mesopause winds and OH intensities at Mid-Latitudes-Fabry-Perot interferometer observations of the OH emission at 8430 A from bear lake observatory
[AD-A275246] p 3361 N94-29430
MESOSCALE PHENOMENA
Objective analysis of a coastal ocean eddy using satellite AVHRR and in situ hydrographic data
[AD-A275715] p 3376 N94-28642
Prototype terminal aerodrome forecasts using a mesoscale model
[AD-A275308] p 3369 N94-29194
Evaluation of the National Meteorological Center mesoscale model for prediction of severe convection over Central Arizona p 3371 N94-29744
Four-dimensional data assimilation using the adjoint method p 3455 N94-30353
MESSAGE PROCESSING
An all pairs shortest paths distributed algorithm using 2n(exp 2) messages
[RUU-CS-93-19] p 3432 N94-30411
MESSAGES
Security aspects of computer supported collaborative work
[AD-A275638] p 3528 N94-28640
METABOLISM
Prediction of survival times on land in a cold climate
p 3379 N94-28423
Physiological investigations of the isolated rat's liver in hypothermia and hypoxia and their relevance in aircraft incidents above the sea p 3382 N94-28439
METAL BONDING
Joining silicon carbide to austenitic stainless steel through diffusion welding
[PB94-126331] p 3297 N94-28399
METAL CLUSTERS
Realtime structural electrochemistry of platinum clusters using dispersive XAFS
[DE94-005093] p 3208 N94-30101
Generalized augmented space theorem for correlated disorder and cluster coherent potential approximation
[DE94-608110] p 3208 N94-30118
Overlap of metal clusters and nuclear structure physics
[DE94-608387] p 3517 N94-30183
METAL COATINGS
Electrodeposition of bismuth alloys by the controlled potential method
[DE94-605318] p 3212 N94-28550
Anodization of copper in chloride media
[AD-A275565] p 3202 N94-28793
Thick thermal barrier coatings for diesel components
[NASA-CR-187111] p 3537 N94-29350
Metafusion: A breakthrough in metallurgy
p 3211 N94-30446
METAL CRYSTALS
Pit initiation on passivated metal surfaces: Crystallographic orientation and environmental effects
[ISBN-0-315-85433-2] p 3208 N94-30138
METAL CUTTING
Effect of non-metallic inclusions on the machinability of steel
[PB93-230233] p 3204 N94-29387
METAL DRAWING
Plane strain finite element analysis of sheet forming operations including bending effects
p 3322 N94-30354

METAL FATIGUE
An analysis of isothermal, bithermal, and thermomechanical fatigue data of Haynes 188 and B1900+Hf by energy considerations
[NASA-TM-106359] p 3317 N94-28819
Role of microstructure on the fatigue durability of aluminum aircraft alloys
[AD-A275814] p 3202 N94-28830
Cyclic axial-torsional deformation behavior of a cobalt-base superalloy
[NASA-TM-106372] p 3203 N94-28921
Cold expansion and interference for extending the fatigue life of multi-layer metal joints
[AD-A274982] p 3318 N94-29091
The effect of mechanical paint stripping on the fatigue and fracture of thin aluminum airplane skin
p 3205 N94-29900
Fatigue of carbon and low-alloy steels in LWR environments
[DE94-005116] p 3207 N94-30021
An investigation of fatigue crack propagation under mode 1 and mixed mode 1/2 loadings p 3323 N94-30814
Fractographic and microstructural analysis of fatigue crack growth in Ti-6Al-4V fan disc forgings
[AD-B174765] p 3153 N94-30914

METAL FILMS
Geometric structures of thin film: Pt on Pd(110) and NiO on Ni(100)
[DE94-005564] p 3211 N94-28530
Sweep rate and concentration effects on metastable structures formed in the underpotential deposition of silver on Pt(111)
[AD-A275369] p 3189 N94-29010
Vacuum vapor deposition
[NASA-CASE-MFS-28652-1] p 3215 N94-29446
Microstructure and mechanical properties of nitrided molybdenum silicide coatings
[DE94-006249] p 3217 N94-30025
Effects of hydrogen on the resistivity of thin Au and Cu films p 3218 N94-30225
Giant magnetoresistance and microstructural characteristics of epitaxial Fe-Ag and Co-Ag granular thin films
[DE94-006287] p 3519 N94-30707

METAL IONS
Study of iron exchanged zeolites by Moessbauer effect and electron spin resonance spectroscopy
[DE94-605138] p 3514 N94-29691
Reactions of metal ions and their clusters in the gas phase using laser ionization: Fourier transform mass spectrometry
[DE94-006208] p 3207 N94-30024
Nanosize metal alloy particle formation in Ag and Cu sequentially implanted silica
[DE94-005592] p 3207 N94-30042
Rotator phases in narrow-gap semiconductors
[DE94-005472] p 3521 N94-30897

METAL JOINTS
Cold expansion and interference for extending the fatigue life of multi-layer metal joints
[AD-A274982] p 3318 N94-29091
Automation of the NDT diagnostic using neural nets. Application: Inspection of Airbus longitudinal joints during maintenance
[REPT-932-600-104] p 3315 N94-29474

METAL MATRIX COMPOSITES
Technology base enhancement program. Metal matrix composites
[AD-A275531] p 3176 N94-28688
Innovative processing of composites for ultra-high temperature applications, book 1
[AD-A275597] p 3176 N94-28729
Innovative processing of composites for ultra-high temperature applications, book 2
[AD-A275598] p 3177 N94-28730
An anisotropic extension of Bodner's model of viscoplasticity: Model development
[NASA-CR-195289] p 3318 N94-28821
Prediction of stress-strain response of SCS-6/Timetal-21S subjected to a hypersonic flight profile
[NASA-TM-109026] p 3177 N94-28823
Electrical conductivity measurements on a SiCp/Al alloy metal matrix composite
[PB94-138310] p 3263 N94-29120
Microstructure/property relationships for SCS6/Timetal 21-S composite
[AD-A275056] p 3178 N94-29135
An analysis of the microstructure and reinforcement distribution of an extruded particle-reinforced Al 6061-10 volume percent Al2O3 metal matrix composite
[AD-A275050] p 3178 N94-29166
Properties of graphite fiber reinforced copper matrix composites for space power applications
[NASA-CR-191026] p 3178 N94-29208
Thermodynamic analysis of chemical compatibility of several compounds with Fe-Cr-Al alloys
[NASA-CR-191166] p 3181 N94-29684
Multiple Concentric Cylinder Model (MCCM) user's guide
[NASA-CR-195299] p 3183 N94-30125
The machining of fiber metal laminates. Part 1: An inventory of forming processes
[LR-710-PT-1] p 3184 N94-30343
Particulate metal matrix composites: Draft procedure for tensile tests at ambient temperature
[NPL-DMM(A)-100] p 3184 N94-30419
Near-net-shape manufacturing: Spray-formed metal matrix composites and tooling p 3186 N94-30447
Casting of weldable graphite/magnesium metal matrix composites with built-in metallic inserts
p 3186 N94-30482
Studies on the optimization of deformation processed metal-metal matrix composites
[DE94-006033] p 3185 N94-30704
A class of inclusion problems for the strengthening of brittle and ductile composites p 3186 N94-30959

METAL NITRIDES
Synthesis and neutron diffraction study of Na3WN3 and Na3MoN3
[AD-A275158] p 3203 N94-29043

METAL OXIDE SEMICONDUCTORS
Nonvolatile programmable neural network synaptic array
[NASA-CASE-NPO-18578-1-CU] p 3265 N94-29426
Charge collection spectroscopy applied to MOS RAM's p 3201 N94-30220

METAL OXIDES
Epitaxial heterojunctions of oxide semiconductors and metals on high temperature superconductors
[NASA-CASE-NPO-18483-1-CU] p 3513 N94-29501
Bench-scale synthesis of nanoscale materials
p 3240 N94-30473
Influence of surface defects and local structure on oxygenate reaction pathways over metal oxide surfaces
[DE94-005680] p 3522 N94-30901

METAL PARTICLES
Template synthesized nanoscopic gold particles: Optical spectra and the effects of particle size and shape
[AD-A275378] p 3197 N94-29312
Study on the formation of ultrafine particles of Sm-Co intermetallic compounds using RF thermal plasma
p 3211 N94-29516
Nanosize metal alloy particle formation in Ag and Cu sequentially implanted silica
[DE94-005592] p 3207 N94-30042

METAL PLATES
Electrical conductivity measurements on a SiCp/Al alloy metal matrix composite
[PB94-138310] p 3263 N94-29120

METAL POWDER
Mechanical alloying processing with application to structural materials: ASSERT supplement
[AD-A275400] p 3204 N94-29205
Studies of high temperature ternary phases in mixed-metal-rich early transition metal sulfide and phosphide systems
[DE94-006034] p 3209 N94-30336
Centrifugal atomization of lanthanide materials for cryogenic coolers
[DE94-006035] p 3219 N94-30337

METAL SHEETS
Electrical conductivity measurements on a SiCp/Al alloy metal matrix composite
[PB94-138310] p 3263 N94-29120
Delamination growth in composites under cyclic loads
p 3183 N94-30256
Plane strain finite element analysis of sheet forming operations including bending effects
p 3322 N94-30354
Photovoltaic power without batteries for continuous cathodic protection p 3341 N94-30465
Design of a variable-conductance vacuum insulation
[DE94-000270] p 3268 N94-30819

METAL SURFACES
Sweep rate and concentration effects on metastable structures formed in the underpotential deposition of silver on Pt(111)
[AD-A275369] p 3189 N94-29010
X ray standing wave studies of underpotentially deposited metal monolayers
[AD-A275409] p 3513 N94-29215
Pit initiation on passivated metal surfaces: Crystallographic orientation and environmental effects
[ISBN-0-315-85433-2] p 3208 N94-30138
XPS analysis of 440C steel surfaces lubricated with perfluoropolyethers under sliding conditions in high vacuum
[NASA-TM-106548] p 3218 N94-30177
Effects of hydrogen on the resistivity of thin Au and Cu films p 3218 N94-30225
Computer simulation of the interaction of fast hydrogen atoms with a molybdenum containing sorbed hydrogen
[DE94-608419] p 3209 N94-30253
An investigation of the corrosion properties of aluminum-tantalum alloys using electrochemical impedance spectroscopy and local electrochemical impedance spectroscopy p 3209 N94-30521

METAL VAPORS
Studies of interfaces and vapors with Optical Second Harmonic Generation
[DE94-006295] p 3476 N94-30841

METAL WORKING
Plane strain finite element analysis of sheet forming operations including bending effects
p 3322 N94-30354
Application of ALE techniques to metal forming simulations
[DE94-005358] p 3211 N94-30892

METALLICITY
Globular cluster photometry near the turnoff: Blue stragglers, relative ages, and the horizontal branch
p 3538 N94-29732
Study of the stellar populations of the Fornax dwarf spheroidal galaxy
[ISBN-0-315-85526-6] p 3541 N94-30231

METALLIZING
X ray standing wave studies of underpotentially deposited metal monolayers
[AD-A275409] p 3513 N94-29215
Vacuum vapor deposition
[NASA-CASE-MFS-28652-1] p 3215 N94-29446
The organometallic chemical vapor deposition of transition metal carbides: The use of homoleptic alkyls
[DE94-005577] p 3206 N94-30007

METALLOGRAPHY
Development of evaluated data bank of physical properties of perspective nuclear engineering steels and alloys
[DE94-607999] p 3207 N94-30076
Nature of dissolution of binary tantalum-titanium alloys by molten plutonium
[DE94-005090] p 3210 N94-30776
Method of test for cleanness assessment of metal alloys: The preparation of button specimens by electron beam melting and the characterisation of recovered inclusions
[NPL-DMM(A)-130] p 3210 N94-30796

METALLURGY
Metafusion: A breakthrough in metallurgy
p 3211 N94-30446

METALORGANIC CHEMICAL VAPOR DEPOSITION
MOCVD growth of GaN, AlN and AlGaN for UV photodetector applications
[AD-A275078] p 3512 N94-28871
InTlSb for long-wavelength infrared photodetectors and arrays
[AD-A275079] p 3512 N94-28872

METALS
Speciation in Water and Soil: A literature review
[PB94-132388] p 3341 N94-28412
Dislocation theory of melting for iron, revisited
[DE94-002715] p 3355 N94-28538
Study of activation data of metal samples from LDEF-1 and Spacelab-2
[NASA-CR-195802] p 3205 N94-29736
Microactuator production via high aspect ratio, high edge acuity metal fabrication technology
p 3235 N94-29770
Mechanisms and effects of heat generation at the tips of dynamic cracks and notches in metals
p 3321 N94-29808
Novel mass spectrometric instrument for gaseous and particulate characterization and monitoring
[DE94-005896] p 3349 N94-30047
A new material for removing heavy metals from water
p 3354 N94-30471
A comparison of the evolution of cold and hot deformation microstructures and textures in fcc metals
[DE94-005103] p 3210 N94-30777

METAMORPHISM (GEOLOGY)
Geochemical and fluid dynamic investigations into the nature of chemical variability in the Earth's mantle
p 3367 N94-30917

METASTABLE STATE
Directional solidification studies in Ni-Al alloys
[DE94-005562] p 3201 N94-28527
Laboratory studies of chemical and photochemical processes relevant to stratospheric ozone
[NASA-CR-195779] p 3347 N94-29549

METEOROLOGICAL INSTRUMENTS
Micro-sensors for in-situ meteorological measurements p 3236 N94-29777
Comparison of Savannah River Site's meteorological databases
[DE94-001751] p 3373 N94-29817

METEOROLOGICAL PARAMETERS
A global forecast model comparison study - year 1
[AD-A275674] p 3369 N94-28663
Lead detection and mapping with reference to relationships between scale, sensor characteristics, surface conditions and atmospheric properties
[AD-A275321] p 3377 N94-28877
Oceanic survey utilizing satellites
p 3328 N94-29040
Antarctic Record, volume 36, no. 1
[REPT-106-VOL-36-NO-1] p 3357 N94-29078
Micro-sensors for in-situ meteorological measurements p 3236 N94-29777
The incorporation and initialization of cloud water/ice in an operational forecast model p 3373 N94-29814
Atmospheric Propagation Effects Through Natural and Man-Made Obscurants for Visible to MM-Wave Radiation
[AGARD-CP-542] p 3256 N94-30495
Propagation modeling of moist air and suspended water/ice particles at frequencies below 1000 GHz
p 3256 N94-30497
Tropospheric corrections to GPS measurements using locally measured meteorological parameters compared with general tropospheric corrections
p 3144 N94-30655

METEOROLOGICAL RADAR
Numerical simulations of a mountain thunderstorm. A comparison with Doppler radar observations
[AD-A275296] p 3369 N94-28873
A study of precipitation in the coastal area of Antarctica as observed at Syowa Station using a vertical pointing radar p 3363 N94-29979
Evaluation of dual polarization attenuation of millimeter frequencies through a meteorological radar
p 3256 N94-30496

METEOROLOGICAL SATELLITES
TacSats for NATO
[AGARD-AR-322] p 3169 N94-30350

METEOROLOGICAL SERVICES
AFGWC Dial-In Subsystem (AFDIS) software users manual, version 2.2
[AD-A275844] p 3371 N94-29747

METEOROLOGY
The active titration method for measuring local hydroxyl radical concentration p 3345 N94-28602
Catalog of Air Force weather technical publications 1992-1993
[AD-A275635] p 3368 N94-28638
Papers in meteorology and geophysics, vol. 44, no.1
[JTN-94-80585] p 3324 N94-28693
Activities report of the International Meteorological Institute
[ETN-94-95524] p 3370 N94-29423
Comparison of Savannah River Site's meteorological databases
[DE94-001751] p 3373 N94-29817
The suitability of low-cost urban airshed modeling in the Chicago area
[DE94-005114] p 3349 N94-30023
Multiple weather regimes and baroclinically forced spherical resonance
[DM-65] p 3376 N94-30966

METHANE
Methane challenge of high performance molecular sieve oxygen concentrator
[AD-A275155] p 3337 N94-29033
Prediction of prompt NO(x) in hydrocarbon air flames
p 3190 N94-29250
The 1992-1993 advanced design program. Part 1: The Mars methane engine project. Part 2: The Mars oxygen processor new furnace
[NASA-CR-195513] p 3299 N94-29409
Preparation and structure of amorphous hydrogenated carbon film deposited with RF plasma CVD
p 3223 N94-29518
Numerical prediction of mixing process in a methane-fueled engine p 3304 N94-30230
The development and evaluation of a tunable diode laser trace gas sensor for the measurement of N2O and CH4 fluxes using micrometeorological techniques
[ISBN-0-315-78975-1] p 3296 N94-30801
Transient studies of low temperature catalysts for methane conversion
[DE94-005767] p 3200 N94-30877
An investigation of the reacting vortex structures associated with pulse combustion p 3200 N94-30911

METHOD OF CHARACTERISTICS
Transonic expanding flow through axially symmetric orifices p 3128 N94-28985

METHOD OF MOMENTS
Integral equation analysis of composite bodies of revolution and arbitrary surfaces with application to cavity-backed antennas p 3253 N94-29883

METHYL ALCOHOL
Feasibility study on introduction of a large methanol engine power generation plant
[DE94-732338] p 3224 N94-28629
Methanol-mediated continuous extraction of phenolic compounds from coal liquid p 3188 N94-28679
Technical analysis of alternative fueled vehicles
[DE94-744238] p 3304 N94-30269
Fuel cycle evaluations of biomass-ethanol and reformulated gasoline
[DE94-000227] p 3226 N94-30818
Investigation of the technology development status of alternate fuel vehicles
[DE94-744237] p 3312 N94-30831
Assessment of costs and benefits of flexible and alternative fuel use in the US transportation sector
[DE94-006100] p 3226 N94-30885

METHYL COMPOUNDS
Tris(trimethylsily)arsine and lithium bis(trimethylsily)arsenide
[AD-A275075] p 3189 N94-29140
X ray crystal structures of ((Me3SiCH2)2InCl)2 and ((Me3SiCH2)InCl2)
[AD-A275074] p 3513 N94-29155
Combustion and heat transfer in a high speed diesel engine operating with rape seed oil methyl ester fuel
[PB94-137536] p 3301 N94-29679
Group transfer and electron transfer reactions of organometallic complexes: Summary of research accomplished in 1993
[DE94-004963] p 3200 N94-30770

METHYL POLYSILOXANES
Crosslinking and surface reactions in macromolecules: Spectroscopic FT-IR studies p 3221 N94-30812

METHYLATION
Group transfer and electron transfer reactions of organometallic complexes: Summary of research accomplished in 1993
[DE94-004963] p 3200 N94-30770

METRIC SPACE
Three metric domains of processes for bisimulation
[CWI-CS-R9335] p 3459 N94-30427
Topological models for higher order control flow
[CWI-CS-R9340] p 3425 N94-30432
Comparative semantics for linear arrays of communicating processes
[CWI-CS-R9336] p 3426 N94-30491
A structural co-induction theorem
[CWI-CS-R9346] p 3461 N94-30753

METRICATION
SI (Metric) handbook
[NASA-TM-109197] p 3231 N94-29376

METROLOGY
SI (Metric) handbook
[NASA-TM-109197] p 3231 N94-29376
A normative frame of reference for the metrology function
[REPT-932-430-102] p 3231 N94-29477
Solid state laser systems for space application
[NASA-CR-195777] p 3294 N94-29914
European PTTI report p 3468 N94-30642
Russian national time scale long-term stability
p 3475 N94-30679

MEXICO
Field guide to Cretaceous-tertiary boundary sections in northeastern Mexico
[NASA-CR-195719] p 3354 N94-28416

MICHELSON INTERFEROMETERS
On the importance of the Michelson-Morley experiment
[DE94-606298] p 3523 N94-28620
Three high duty cycle, space-qualified mechanisms
p 3162 N94-29642
Solid state laser systems for space application
[NASA-CR-195777] p 3294 N94-29914
Microwave Michelson interferometer system report of first use on a railgun, Green Farm, San Diego, CA
[DE94-005294] p 3289 N94-30059

MICROANALYSIS
A study of solid propellants using a microprobe mass spectrometer system
[AD-A275325] p 3224 N94-28879
Electron microscopy: Metal alloy x ray microanalysis
[REPT-932-600-101] p 3205 N94-29525
Atomic-scale structure and chemistry of interfaces by Z-contrast imaging and electron energy loss spectroscopy in the STEM
[DE94-006563] p 3516 N94-30064

MICROBIOLOGY
Physiology and molecular-genetics of thermus and bacillus
[PB94-135571] p 3385 N94-29190

MICROCLIMATOLOGY
The use of liquid and air microclimate conditioning systems to alleviate heat stress in helicopter NBC operations p 3384 N94-28453

MICROCOMPUTERS
Microcomputer-based protective functions in industrial production systems: Assessment method
[PB94-137817] p 3411 N94-29159

MICROCRACKS
Brittle composites modeling: Comparisons with MoSi2/ZrO2
[DE94-004978] p 3182 N94-29933
Micromechanics of the dynamic response of ceramics and ceramic composites p 3217 N94-29975

MICROELECTRONICS
RF vacuum microelectronics
[AD-A275221] p 3263 N94-28915
Focused ion beam fabrication of microelectronic structures
[AD-A275384] p 3264 N94-29305
The influence of temperature on microelectronic device failure mechanisms, phase 2
[AD-A275029] p 3265 N94-29511
Proceedings of the Workshop on Microtechnologies and Applications to Space Systems
[NASA-CR-195688] p 3235 N94-29767
Micromanufacturing: Recent developments in this country and abroad p 3235 N94-29769
Overview of microoptics: Past, present, and future
p 3235 N94-29771
Micro guidance and control technology overview
p 3144 N94-29772
Micro guidance and control synthesis: New components, architectures, and capabilities p 3144 N94-29792
The bases for the development of high-temperature integrated SQUID-systems
[DE94-607901] p 3267 N94-30073
The bases for the development of high-temperature integrated SQUID-systems
[DE94-608462] p 3517 N94-30082
Proceedings of the 1991 Single Event Upset Symposium
[DSIS-92-00652] p 3495 N94-30211
Advanced development of the Spectrum Sciences Model 5005-TF, single event test fixture
p 3291 N94-30218
Direct measurement of the reactivity of NH and OH on a silicon nitride surface
[DE94-005286] p 3199 N94-30260
Optoelectronic packaging activities at Sandia National Laboratories
[DE94-005287] p 3501 N94-30261
A combined electron beam/optical lithography process step for the fabrication of sub-half-micron-gate-length MMIC chips p 3240 N94-30445

MICROGRAVITY
Microgravity science and applications. Program tasks and bibliography for FY 1993
[NASA-TM-4569] p 3227 N94-28415
Japanese Journal of Aerospace and Environmental Medicine, vol. 30, no. 3
[JTN-94-80606] p 3387 N94-28495
Some issues on Japan's space food development and relating preliminary experimental study
p 3388 N94-28498
Japanese Journal of Aerospace and Environmental Medicine, volume 30, no. 1
[JTN-94-80598] p 3389 N94-28850
Image technology and information analysis of bone change with gravitational exposure
p 3389 N94-28851
Overview of space environment utilization science
[JTN-94-80581] p 3227 N94-28938
Fluid and transportation phenomena under microgravity p 3227 N94-28939
Combustion studies under microgravity
p 3228 N94-28940
Glass studies under microgravity
p 3228 N94-28941
Fabrication of electronic materials in space
p 3228 N94-28942
Protein crystal growth in microgravity
p 3228 N94-28943
Cell culture in space p 3228 N94-28944
Cosmic energy equipment p 3229 N94-28945
The MERSS 5th Symposium on Space Medicine: Medical and Physiological Experiment Utilizing Parabolic Flight
[JTN-94-80588] p 3392 N94-29709
Microgravity by parabolic flight with MU-300 aircraft
p 3392 N94-29710
Space movement of Trichinella spiralis under microgravity p 3387 N94-29711
Posture control of goldfishes under microgravity
p 3387 N94-29712
Behavior and visual control of cyprinodonts under microgravity p 3387 N94-29713
A discussion of eye-head coordinative movement under microgravity during parabolic flight p 3393 N94-29715

Analysis of various biological activity parameters during parabolic flight p 3393 N94-29716
Hemodynamic measurement during parabolic flight p 3393 N94-29717
Motion sickness in parabolic flight: Possibility of electrogastrography as an objective index p 3393 N94-29718
Summary report of mission acceleration measurements for Spacehab-01, STS-57 launched 21 June 1993 [NASA-TM-106514] p 3168 N94-29757
Japanese Journal of Aerospace and Environmental Medicine, vol. 30, no. 2 [JTN-94-80599] p 3394 N94-29863
Effect of water immersion on muscle sympathetic nerve response during static muscle contraction p 3394 N94-29865
Shortening velocity and calcium sensitivity of single fibers from hindlimb suspended muscle in rats p 3387 N94-29866
Microgravity compatible drive system-rider. New technologies [PB94-138583] p 3229 N94-29996
Laser beam welding of AISI 316 stainless steel in microgravity environment: Experiments aboard a KC-135 flight [ISBN-0-315-86095-2] p 3229 N94-30145
Directional solidification characteristics of hyper-eutectic Al-Cu alloys under varying gravity conditions [ISBN-0-315-86108-8] p 3209 N94-30146
Survey report of JSUP Space Environment Utilization Research Committee in fiscal year 1992: Functional New Materials Session [JTN-94-80582] p 3159 N94-30162
Microgravity fluid science research in Europe [AD-B179178] p 3229 N94-30409
Control system design for A and R supported microgravity experiments: An experiment payload control development [AD-B179107] p 3229 N94-30421
Microencapsulation of anti-tumor, antibiotic and thrombolytic drugs in microgravity p 3397 N94-30453
Survey report of JSUP Space Environment Utilization Research Committee in fiscal year 1992: Metallic Materials Session [JTN-94-80583] p 3159 N94-30794

MICROGRAVITY APPLICATIONS
Microgravity science and applications. Program tasks and bibliography for FY 1993 [NASA-TM-4569] p 3227 N94-28415
Plasma heating for containerless and microgravity materials processing [NASA-CASE-NPO-18819-1-CU] p 3229 N94-29371
Summary report of mission acceleration measurements for Spacehab-01, STS-57 launched 21 June 1993 [NASA-TM-106514] p 3168 N94-29757
Survey report of JSUP Space Environment Utilization Research Committee in fiscal year 1992: Functional New Materials Session [JTN-94-80582] p 3159 N94-30162

MICROHARDNESS
Characterization of structure and mechanical properties of MoSi2-SiC nanolayer composites [DE94-004982] p 3175 N94-28579

MICROINSTRUMENTATION
Micro-sensors for in-situ meteorological measurements p 3236 N94-29777
Smart focal-plane technology for micro-instruments and micro-rovers p 3237 N94-29780
Microfabricated silicon biosensors for microphysiometry p 3238 N94-29783

MICROMACHINING
Proceedings of the Workshop on Microtechnologies and Applications to Space Systems [NASA-CR-195688] p 3235 N94-29767
Micromanufacturing: Recent developments in this country and abroad p 3235 N94-29769
Microactuator production via high aspect ratio, high edge acuity metal fabrication technology p 3235 N94-29770
Micro guidance and control technology overview p 3144 N94-29772
A broad-band microseismometer for planetary operations p 3237 N94-29778
Macro, mini, micro and nano (M(sup 3)N) technologies for the future p 3238 N94-29786
Emerging technologies in microguidance and control p 3144 N94-29788
The application of micromachined sensors to manned space systems p 3171 N94-29791

MICROMECHANICS
Prediction of stress-strain response of SCS-6/Timetal-21S subjected to a hypersonic flight profile [NASA-TM-109026] p 3177 N94-28823
Proceedings of the Workshop on Microtechnologies and Applications to Space Systems [NASA-CR-195688] p 3235 N94-29767
Microactuator production via high aspect ratio, high edge acuity metal fabrication technology p 3235 N94-29770
Toward milli-Newton electro- and magneto-static microactuators p 3238 N94-29784
Macro, mini, micro and nano (M(sup 3)N) technologies for the future p 3238 N94-29786
Integrated microgyroscope p 3239 N94-29789
Micro-opto-mechanical devices and systems using epitaxial lift off p 3239 N94-29793
Micromechanics of the dynamic response of ceramics and ceramic composites p 3217 N94-29975
Multiple Concentric Cylinder Model (MCCM) user's guide [NASA-CR-195299] p 3183 N94-30125
Micromechanical analysis of thermo-inelastic multiphase short-fiber composites [NASA-CR-195290] p 3183 N94-30178
Simulation of composite material response under dynamic compressive loading [DE94-005272] p 3184 N94-30589
Numerical modeling and prediction of the thermomechanical behavior of fiber-reinforced composites p 3186 N94-30956
A class of inclusion problems for the strengthening of brittle and ductile composites p 3186 N94-30959

MICROMETEOROIDS
Hypervelocity impact induced arcing and Kapton pyrolization in a plasma environment [NASA-TM-106528] p 3167 N94-28814

MICROMETEOROLOGY
On the temperature distribution near a cold surface [AD-A275162] p 3332 N94-29288

MICROMINIATURIZATION
Toward milli-Newton electro- and magneto-static microactuators p 3238 N94-29784
Macro, mini, micro and nano (M(sup 3)N) technologies for the future p 3238 N94-29786
Emerging technologies in microguidance and control p 3144 N94-29788
Micro guidance and control synthesis: New components, architectures, and capabilities p 3144 N94-29792
The universal applications of microtubes and microtube composites p 3186 N94-30452

MICROMINIATURIZED ELECTRONIC DEVICES
Microfabricated silicon biosensors for microphysiometry p 3238 N94-29783
Macro, mini, micro and nano (M(sup 3)N) technologies for the future p 3238 N94-29786
Control of micromachined deformable mirrors p 3239 N94-29787
Emerging technologies in microguidance and control p 3144 N94-29788
The application of micromachined sensors to manned space systems p 3171 N94-29791
Micro guidance and control synthesis: New components, architectures, and capabilities p 3144 N94-29792
Single event upset and latchup measurements at Brookhaven National Laboratory p 3495 N94-30212

MICROMOTORS
Microactuator production via high aspect ratio, high edge acuity metal fabrication technology p 3235 N94-29770

MICROORGANISMS
Researches on bioconversion of coal into liquid product p 3187 N94-28677
Fundamental studies on the corrosion behavior of weldments in marine microbial environments [AD-A275247] p 3203 N94-28900
Stable RNA sequences as a tool for DNA probes and phylogenetic studies [PB94-135423] p 3385 N94-29156
Growth of hydrocarbon-rich microalga Botryococcus braunii in secondarily treated sewage and its consumption of nitrate ion and phosphate ion p 3387 N94-29519
Microfabricated silicon biosensors for microphysiometry p 3238 N94-29783
Biodiesel from aquatic species [DE94-000275] p 3225 N94-30038

MICROPARTICLES
The impact of electrically charged microspheres with planar surfaces under vacuum conditions p 3320 N94-29765
Microencapsulation of anti-tumor, antibiotic and thrombolytic drugs in microgravity p 3397 N94-30453

MICROPHONES
Improved in-flow acoustic sensor [NASA-CASE-ARC-12001-1] p 3478 N94-29363

MICROPROCESSORS
Data fusion and correlation techniques testbed development audio processing study [SKD-1600-73-014] p 3241 N94-28532
NSC 800, 8-bit CMOS microprocessor [NASA-CR-195736] p 3405 N94-28845
Microcomputer-based protective functions in industrial production systems: Assessment method [PB94-137817] p 3411 N94-29159
On ground system integration and testing: A modern approach p 3150 N94-29334
Communications technology for unattended sensors [DE94-005685] p 3254 N94-30043
Maestro: An open system architecture for multi-robot control p 3306 N94-30288

MICROSTRIP ANTENNAS
Printed circuit elements with applications to antennas, scattering, and circuits [AD-A275512] p 3262 N94-28669
Three dimensional transient analysis of microstrip circuits in multilayered anisotropic media [AD-A274995] p 3263 N94-28995
Theoretical and experimental study of a cylindrical microstrip antenna [REPT-932-440-109] p 3245 N94-29456
A 32 GHz microstrip array antenna for microspacecraft application p 3251 N94-29668
Radiation and scattering from cylindrically conformal printed antennas [NASA-CR-195546] p 3253 N94-29873
Radial microstrip slotline feed network for circular mobile communications array [NASA-TM-106540] p 3267 N94-30198

MICROSTRIP TRANSMISSION LINES
Three dimensional transient analysis of microstrip circuits in multilayered anisotropic media [AD-A274995] p 3263 N94-28995

MICROSTRUCTURE
Computer simulation of martensitic transformations [DE94-005213] p 3201 N94-28479
Directional solidification studies in Ni-Al alloys [DE94-005562] p 3201 N94-28527
On the prediction of HAZ grain size using Monte Carlo simulation [DE94-005465] p 3511 N94-28535
Failures to model the development of a cube texture during the high temperature compression of Al-Mg alloys [DE94-005013] p 3201 N94-28544
Characterization of structure and mechanical properties of MoSi2-SiC nanolayer composites [DE94-004982] p 3175 N94-28579
Role of microstructure on the fatigue durability of aluminum aircraft alloys [AD-A275814] p 3202 N94-28830
Toughening mechanisms in ultrahigh-strength steels [AD-A275439] p 3202 N94-28867
Research on the improvement of shape-memory and magnetostrictive materials [AD-A275397] p 3203 N94-29056
Effect of microstructure on the strength and fracture energy of bimaterial interfaces [AD-A274987] p 3178 N94-29126
Microstructure/property relationships for SCS6/Timetal 21-S composite [AD-A275056] p 3178 N94-29135
Low temperature behavior of virgin martensite [PB94-132925] p 3204 N94-29142
An analysis of the microstructure and reinforcement distribution of an extruded particle-reinforced Al 6061-10 volume percent Al2O3 metal matrix composite [AD-A275050] p 3178 N94-29166
Mechanical alloying processing with application to structural materials: ASSERT supplement [AD-A275400] p 3204 N94-29205
Characterisation and processing of SiC/MAS-L glass ceramic matrix composite [REPT-932-430-111] p 3179 N94-29412
Assessment of the fibre volume distribution around optical fibres [FFA-TN-1993-12] p 3179 N94-29425
Microstructure and mechanical properties of nitrided molybdenum silicide coatings [DE94-006249] p 3217 N94-30025
Development of evaluated data bank of physical properties of perspective nuclear engineering steels and alloys [DE94-607999] p 3207 N94-30076
Plasma enhanced chemical vapor deposition of ZrO2 thin films [DE94-006031] p 3218 N94-30104
On the structure and atomic motions in liquid sodium [DE94-608386] p 3490 N94-30182
Dislocation loops in spinel crystals irradiated successively with deep and shallow ion implants [DE94-005083] p 3517 N94-30201
Studies on the optimization of deformation processed metal-metal matrix composites [DE94-006033] p 3185 N94-30704

Giant magnetoresistance and microstructural characteristics of epitaxial Fe-Ag and Co-Ag granular thin films
[DE94-006287] p 3519 N94-30707
Microstructural development and mechanical behavior of eutectic bismuth-tin and eutectic indium-tin in response to high temperature deformation
[DE94-005202] p 3210 N94-30710
A comparison of the evolution of cold and hot deformation microstructures and textures in fcc metals
[DE94-005103] p 3210 N94-30777
Fractographic and microstructural analysis of fatigue crack growth in Ti-6Al-4V fan disc forgings
[AD-B174765] p 3153 N94-30914

MICROWAVE AMPLIFIERS
Towards experimental verification and device applications of current driven plasma instabilities in solid state systems
[AD-A275395] p 3504 N94-29055
X-band ultralow-noise maser amplifier performance p 3251 N94-29672

MICROWAVE ANTENNAS
A digital combining-weight estimation algorithm for broadband sources with the array feed compensation system p 3250 N94-29660
Digital combining-weight estimation for broadband sources using maximum-likelihood estimates p 3250 N94-29661
A 32 GHz microstrip array antenna for microspacecraft application p 3251 N94-29668

MICROWAVE ATTENUATION
Evaluation of dual polarization attenuation of millimeter frequencies through a meteorological radar p 3256 N94-30496

MICROWAVE CIRCUITS
Frequency-domain analysis of nonlinear microwave circuits
[PB94-132024] p 3261 N94-28400
Three dimensional transient analysis of microstrip circuits in multilayered anisotropic media
[AD-A274995] p 3263 N94-28995
Towards experimental verification and device applications of current driven plasma instabilities in solid state systems
[AD-A275395] p 3504 N94-29055
A combined electron beam/optical lithography process step for the fabrication of sub-half-micron-gate-length MMIC chips p 3240 N94-30445
Precision frequency synthesizing sources with excellent time/frequency performances p 3473 N94-30671

MICROWAVE EQUIPMENT
Photoconductive switching for high power microwave generation
[PB94-137460] p 3244 N94-29177
Hydrogen maser clocks in space for solid-Earth research and time-transfer applications: Experiment overview and evaluation of Russian miniature sapphire loaded cavity p 3474 N94-30676

MICROWAVE FILTERS
X-/Ka-band dichroic plate design and grating lobe study p 3247 N94-29616

MICROWAVE FREQUENCIES
Cryogenic probe station for use in automated microwave and noise figure measurements
[NASA-TM-106560] p 3286 N94-29000
RF and microwave dielectric measurements upon layered materials using reflectometric coaxial sensor
[NPL-DES-125] p 3476 N94-30781

MICROWAVE HOLOGRAPHY
Automated inspection of turbine blades: Challenges and opportunities
[AIAA PAPER 94-1226-CP] p 3446 N94-30575

MICROWAVE IMAGERY
Model for the simulation of atmospheric effects on targets to background passive signatures p 3258 N94-30507
Polarimetric backscatter measurements of natural surfaces at millimeter wavelengths p 3259 N94-30509

MICROWAVE INTERFEROMETERS
Microwave Michelson interferometer system report of first use on a railgun, Green Farm, San Diego, CA
[DE94-005294] p 3289 N94-30059

MICROWAVE LANDING SYSTEMS
Ground independent landing system p 3137 N94-29564
Flight simulator evaluation of advanced MLS procedures
[AD-B174270] p 3143 N94-30915

MICROWAVE OSCILLATORS
Synchronization of microwave oscillators by direct optical injection
[ISBN-0-315-85546-0] p 3500 N94-30233

MICROWAVE POWER BEAMING
A transportronic solution to the problem of interorbital transportation
[NASA-CR-191152] p 3164 N94-29355

MICROWAVE RADIOMETERS
Conceptual radiometer design studies for Earth observations from low Earth orbit
[NASA-CR-4588] p 3329 N94-29098
On the relation between SMMR 37-GHz polarization difference and the rainfall over Africa and Australia
[NASA-TM-104598] p 3370 N94-29408
Model for the simulation of atmospheric effects on targets to background passive signatures p 3258 N94-30507
Remote sensor observations during WISP91: The use of microwave radiometers, RASS, and lidar ceilometers for detection of aircraft icing conditions
[PB94-142106] p 3136 N94-30890

MICROWAVE SCATTERING
A hybrid electromagnetic-statistical approach for characterizing MMW scattering by terrain p 3259 N94-30510

MICROWAVE SENSORS
Conceptual radiometer design studies for Earth observations from low Earth orbit
[NASA-CR-4588] p 3329 N94-29098

MICROWAVE SIGNATURES
Model for the simulation of atmospheric effects on targets to background passive signatures p 3258 N94-30507

MICROWAVE SPECTRA
Evaluation of wireless Local Area Networks
[AD-A275133] p 3243 N94-29064

MICROWAVE SWITCHING
Photoconductive switching for high power microwave generation
[PB94-137460] p 3244 N94-29177

MICROWAVE TRANSMISSION
Preliminary analysis of Asynchronous Transfer Mode (ATM) over microwave channels
[AD-A275214] p 3243 N94-29069
Propagation modeling of moist air and suspended water/ice particles at frequencies below 1000 GHz p 3256 N94-30497
The influence of the evaporation duct on the angle of arrival and amplitude of the backscattered signal from targets low above the sea p 3256 N94-30498

MICROWAVES
Analysis of microwave induced interference in pn-diodes
[PB94-136983] p 3243 N94-28906
Deployable reflector structure
[NASA-CASE-LAR-14513-1-SB] p 3245 N94-29360
Energetic events in the early universe p 3547 N94-30012
Microwave vision for robots
[AIAA PAPER 94-0687-CP] p 3443 N94-30550
Remote pumping of solid state lasers with nuclear driven fluorescers
[DE94-004846] p 3296 N94-30614

MIDAIR COLLISIONS
Effectiveness of protection clothing for cold weather conditions after ejection over sea: A case report p 3381 N94-28435

MIDDLE ATMOSPHERE
Theory and observations of horizontal and vertical structure of gravity wave perturbations in the middle atmosphere p 3366 N94-30802

MIE SCATTERING
Template synthesized nanoscopic gold particles: Optical spectra and the effects of particle size and shape
[AD-A275378] p 3197 N94-29312
Optical modeling of visibility and visibility instrumentation using stratified Mie theory p 3348 N94-29750

MILITARY OPERATIONS
The Support of Air Operations under Extreme Hot and Cold Weather Conditions
[AGARD-CP-540] p 3379 N94-28420
The concept of Royal Navy air operations under extreme environmental conditions p 3379 N94-28424
The Environmental Symptoms Questionnaire: Assessing reactions to environmental extremes in military operations p 3383 N94-28447
The management issues of implementing telecommuting: A case study
[AD-A275267] p 3527 N94-28905
Clinical investigation program
[AD-A275025] p 3391 N94-29116
TacSats for NATO
[AGARD-AR-322] p 3169 N94-30350
Report on NATO PTTI p 3469 N94-30645

MILITARY SPACECRAFT
TacSats for NATO
[AGARD-AR-322] p 3169 N94-30350

MILITARY TECHNOLOGY
The management issues of implementing telecommuting: A case study
[AD-A275267] p 3527 N94-28905
Spectral and polarimetric analysis of hyperspectral data collected by an acousto-optic tunable filter system
[AD-A275076] p 3329 N94-29095
NPSNET: Integration of Distributed Interactive Simulation (DIS) protocol for communication architecture and information interchange
[AD-A275061] p 3530 N94-29139
Software testing practices and their evolution for the 1990's p 3415 N94-29335
A disciplined approach to software test and evaluation p 3416 N94-29339
Proceedings of the 3rd Conference on Military Robotic Applications
[DRES-SP-149] p 3304 N94-30275
Autonomous intelligent military robots: Army ants, killer bees, and cybernetic soldiers p 3304 N94-30276
Robotics and the battlefield of the future p 3304 N94-30277
DREV activities related to military vehicles robotization p 3305 N94-30278
Autonomous Robotic Refueling System (ARRS) for rapid aircraft turnaround p 3305 N94-30279
Force control techniques for robot manipulators and their military applications p 3307 N94-30291
Elements of supervisory control for military robotic applications p 3309 N94-30303
Aspects of the operator interface for military robotic applications in unstructured environments p 3309 N94-30304
Cubanes: Super explosives and potential pharmaceutical intermediates p 3227 N94-30454

MILLIMETER WAVES
Characterization of a diffraction grating as a simulant of a selective frequency antenna for radiometric applications
[AD-A275793] p 3241 N94-28745
A combined electron beam/optical lithography process step for the fabrication of sub-half-micron-gate-length MMIC chips p 3240 N94-30445
Evaluation of dual polarization attenuation of millimeter frequencies through a meteorological radar p 3256 N94-30496
Propagation modeling of moist air and suspended water/ice particles at frequencies below 1000 GHz p 3256 N94-30497
Model for the simulation of atmospheric effects on targets to background passive signatures p 3258 N94-30507
Polarimetric backscatter measurements of natural surfaces at millimeter wavelengths p 3259 N94-30509
A hybrid electromagnetic-statistical approach for characterizing MMW scattering by terrain p 3259 N94-30510

MILLING (MACHINING)
Application of high-speed milling to the Finnish manufacturing industry
[PB94-135548] p 3230 N94-29187

MILNE METHOD
Miln equation for the calculation of the phases and amplitudes of wave functions for continuum spectrum of Coulomb two-center problem
[DE94-606292] p 3522 N94-28616

MIMD (COMPUTERS)
Building brains for bodies
[AIAA PAPER 94-1208-CP] p 3444 N94-30559

MIMO (CONTROL SYSTEMS)
Integrated active and passive control design methodology for the LaRC CSI evolutionary model
[NASA-CR-4580] p 3164 N94-28417

MINERAL DEPOSITS
On United States-Japan Conference on Development and Utilization of Natural Resources: Report of the 14th Joint Meeting of U. S. and Japan Marine Mining Panel p 3188 N94-28683

MINERALS
Image processing for hyperspectral data p 3326 N94-28930
JERS-1 data and information system for resources exploration p 3327 N94-28932

MINES (EXCAVATIONS)
Joint research activities with CCMRI (China) p 3240 N94-29521

MINIATURE ELECTRONIC EQUIPMENT
Micromachined electron tunneling infrared sensors p 3238 N94-29785
Integrated microgyroscope p 3239 N94-29789

MINIATURIZATION
Miniaturization in x ray and gamma ray spectroscopy p 3236 N94-29773
A sub-cm micromachined electron microscope p 3236 N94-29775
Micromachined electron tunneling infrared sensors p 3238 N94-29785
Miniature wide field-of-view star trackers for spacecraft attitude sensing and navigation p 3144 N94-29794

MINIMA
Modifications of the Griesmer bound
p 3247 N94-29618
MINIMAL SURFACES
The Klein-Fock equation, minimal surfaces and gravitational fields
[DE94-606340] p 3356 N94-28803
MINIMAX TECHNIQUE
The transient period of a cyclic process: An horizon theorem
[MEMO-1149] p 3427 N94-30585
MINING
On United States-Japan Conference on Development and Utilization of Natural Resources: Report of the 14th Joint Meeting of U. S. and Japan Marine Mining Panel
p 3188 N94-28683
An electromagnetic noncontacting sensor for thickness measurement in a dispersive medium
[AIAA PAPER 94-1200-CP] p 3443 N94-30551
MINORITIES
The Seventh Annual National Conference of Black Physics Students
[NASA-CR-195735] p 3526 N94-28746
MIRRORS
Design and testing of the LITE Variable Field Stop mechanism p 3161 N94-29633
Determining noise temperatures in beam waveguide systems p 3249 N94-29657
Control of micromachined deformable mirrors
p 3239 N94-29787
Nonlinear absorption in high reflector multilayers
[DE94-005818] p 3295 N94-30598
Characterization of defect geometries in multilayer optical coatings
[DE94-005820] p 3501 N94-30599
MISSILE DEFENSE
Laser beam steering with semiconductor waveguide
[AD-A275775] p 3292 N94-28765
MISSILE DESIGN
An experimental and theoretical study of the aerodynamic characteristics of some generic missile concepts at Mach numbers from 2 to 6.8
[NASA-TM-109110] p 3130 N94-29473
MISSILE DETECTION
Missile launch detection electric field perturbation experiment
[DE94-004224] p 3466 N94-30586
MISSILES
Experimental investigation of three-dimensional vortex-airfoil interaction in a supersonic stream
[AD-A275107] p 3122 N94-28899
MISSION PLANNING
MUADEE: Mars Upper Atmosphere Dynamics, Energetics, and Evolution discovery mission. Executive summary volume
[NASA-CR-195732] p 3549 N94-28418
Proceedings of the 3rd International Symposium: JERS-1 and Remote Sensing in the Future
[JTN-94-80597] p 3329 N94-29217
A capacity planning model for Canadian military airlift requests
[ISBN-0-315-86079-0] p 3136 N94-30144
Development status of the Communications and Broadcasting Engineering Test Satellite (COMETS)
[JTN-94-80545] p 3169 N94-30811
MIXED OXIDES
Synthesis and characterization of novel ternary and quaternary reduced molybdenum oxides
[DE94-005563] p 3510 N94-28529
Nonaqueous slip casting of YBa2Cu3O(7-x) superconductive ceramics
[NASA-CR-4575] p 3512 N94-29101
MIXERS
Frequency-domain analysis of nonlinear microwave circuits
[PB94-132024] p 3261 N94-28400
MIXING
Methods of testing parameterizations: Vertical ocean mixing p 3352 N94-30633
MIXING LAYERS (FLUIDS)
A random distribution reacting mixing layer model
[NASA-TM-106517] p 3150 N94-28923
Evolution of the large-scale vortices in turbulent mixing-layers p 3273 N94-29686
Large eddy simulation of subsonic mixing layers
p 3276 N94-29851
The enhancement of compressible turbulent mixing via streamwise vorticity p 3280 N94-30487
Transition to turbulence in confined compressible mixing layers p 3283 N94-30958
MOBILE COMMUNICATION SYSTEMS
Evaluation of wireless Local Area Networks
[AD-A275133] p 3243 N94-29064
Radial microstrip slotline feed network for circular mobile communications array
[NASA-TM-106540] p 3267 N94-30198
MOBILITY
RHEED studies of the nucleation, growth, and mobility of Ag atoms on the Si(111)7 x 7 surface
[DE94-005551] p 3521 N94-30899
MODAL RESPONSE
Stiffness-generated rigid-body mode shapes for Lanczos eigensolution with SUPORT DOF by way of a MSC/NASTRAN DMAP alter
[NASA-TM-106537] p 3319 N94-29406
Transient analysis mode participation for modal survey target mode selection using MSC/NASTRAN DMAP
[NASA-TM-106536] p 3319 N94-29469
Modelling soft impacts for vibrational excitation of civil engineering structures
[PB94-137619] p 3320 N94-29681
Pulse response based minimum time control of flexible structures p 3436 N94-29720
Modal analysis of solar panels using boundary integral equations
[NLT-TP-92218-U] p 3338 N94-30328
Second-order structural identification via state space-based system realizations p 3323 N94-30815
MODEL REFERENCE ADAPTIVE CONTROL
Using generic tool kits to build intelligent systems
[AIAA PAPER 94-1214-CP] p 3445 N94-30565
MODELS
Molecular structure of coal studied by solvent extraction p 3187 N94-28676
Reference model for project support environments, version 2.0
[AD-A275191] p 3410 N94-29068
MODEMS
Two-way satellite time transfer: Overview and recent developments p 3469 N94-30646
MODES (STANDING WAVES)
Experiments on the aerodynamic generation of noise in centrifugal turbomachinery p 3480 N94-30804
MODULATION
Tropospheric HO2 determination by FAGE
p 3345 N94-28606
MODULATORS
Spatial light modulators with arbitrary quantum wells profiles
[AD-A275023] p 3499 N94-29114
Design and analysis of a low-loss linear analog phase modulator for deep space spacecraft X-band transponder applications p 3248 N94-29625
Optical Chopper Assembly for the Mars Observer
p 3162 N94-29639
MODULES
A modular approach for automated sample preparation and chemical analysis p 3354 N94-30464
MODULUS OF ELASTICITY
Alumina ceramic: A cost effective replacement for titanium in deep submergence pressure housings
[AD-A275640] p 3212 N94-28641
Thermal expansion and elastic anisotropy in single crystal Al2O3 and SiC reinforcements
[NASA-TM-106516] p 3214 N94-29105
Experimental determination of orthotropic elastic constants
[FFA-TN-1991-35] p 3215 N94-29424
Creep and physical aging of PVC: Dependence on stress and temperature
[NPL-DMM(A)-115] p 3217 N94-29886
Resonant ultrasound spectroscopy for elastic constant measurements
[DE94-005016] p 3480 N94-30098
A class of inclusion problems for the strengthening of brittle and ductile composites p 3186 N94-30959
MOIRE EFFECTS
Plane stress stable crack growth and J-integral/HRR field
[AD-A275761] p 3317 N94-28761
MOIRE INTERFEROMETRY
Plane stress stable crack growth and J-integral/HRR field
[AD-A275761] p 3317 N94-28761
Fracture process zone of brittle composites
p 3182 N94-29876
MOISTURE CONTENT
Global patterns of cloud optical thickness variation with temperature and the implications for climate change
p 3374 N94-29972
MOISTURE RESISTANCE
Polyimides containing pendent siloxane groups
[NASA-CASE-LAR-14638-1] p 3215 N94-29555
MOLECULAR BEAM EPITAXY
Exploratory research for a high temperature superconducting integrated circuit
[AD-A275798] p 3262 N94-28767
Spatial light modulators with arbitrary quantum wells profiles
[AD-A275023] p 3499 N94-29114
Research on the atomic layer-by-layer growth of high-temperature superconductor thin films at the Institute of Scientific and Industrial Research, Japan
[DE94-003739] p 3519 N94-30611
MOLECULAR BEAMS
Surface structure and stereochemical properties of self-assembled monolayer materials
[DE94-004960] p 3484 N94-28578
RHEED studies of the nucleation, growth, and mobility of Ag atoms on the Si(111)7 x 7 surface
[DE94-005551] p 3521 N94-30899
MOLECULAR BIOLOGY
Biodiesel from aquatic species
[DE94-000275] p 3225 N94-30038
Lattice gas simulations of replicating domains
[DE94-005008] p 3200 N94-30748
MOLECULAR CLOUDS
The role of cloud collisions in N-body simulations of disk galaxies p 3545 N94-29755
MOLECULAR DIFFUSION
Molecular aspects of transport in thin films of controlled architecture
[DE94-004552] p 3211 N94-28457
Effects of diffusion and inertia on chaotic mixing: A computational and experimental study
p 3488 N94-29903
Lattice gas simulations of replicating domains
[DE94-005008] p 3200 N94-30748
MOLECULAR DYNAMICS
Experimental and theoretical studies of molecular solids
[AD-A275511] p 3485 N94-28668
Computer simulation of molecular interactions in supercritical solvents
[AD-A274977] p 3486 N94-29087
Nanodislocation structures generated in shocked crystals p 3514 N94-29915
Exclusive many-particle diffusion in disordered media and correlation functions for random vertex models
[DE94-608134] p 3525 N94-30121
Theoretical studies of solid-fluid phase equilibria
[DE94-006406] p 3226 N94-30708
Molecular dynamics simulations of dense plasmas
[DE94-005082] p 3509 N94-30752
MOLECULAR ENERGY LEVELS
Predissociation in N2(C'4, 1 Sigma u +) and other N2 states and its importance in the atmospheres of Titan and Triton
[NASA-CR-195727] p 3549 N94-28816
MOLECULAR EXCITATION
Spectroscopic and dynamical studies of highly energized small polyatomic molecules
[DE94-006509] p 3489 N94-30061
MOLECULAR GASES
The kinematics of molecular gas and dust in the nearby galaxies Centaurus A and M82 p 3544 N94-29738
MOLECULAR INTERACTIONS
Low energy ion-molecule reactions and chemiionization kinetics
[DE94-005414] p 3481 N94-28491
Monte Carlo simulation or normal shock wave. Part 2: VHS model and VSS model p 3123 N94-28948
Computer simulation of molecular interactions in supercritical solvents
[AD-A274977] p 3486 N94-29087
Theoretical studies of solid-fluid phase equilibria
[DE94-006406] p 3226 N94-30708
MOLECULAR IONS
Experimental and theoretical studies of molecular solids
[AD-A275511] p 3485 N94-28668
MOLECULAR ORBITALS
Ab initio study of vibrational frequency shift upon the 1:1 acetone-iodine complex formation
p 3188 N94-28681
MOLECULAR SPECTRA
Ab initio study of vibrational frequency shift upon the 1:1 acetone-iodine complex formation
p 3188 N94-28681
MOLECULAR STRUCTURE
Journal of NIRE, Vol. 2, No. 2
[JTN-94-80552] p 3187 N94-28675
Molecular structure of coal studied by solvent extraction p 3187 N94-28676
Structural changes during carbonization and oxidation of coal p 3187 N94-28678
Ab initio study of vibrational frequency shift upon the 1:1 acetone-iodine complex formation
p 3188 N94-28681
Structure of ordinary ice I(sub h). Part 1: Ideal structure of ice
[AD-A275149] p 3486 N94-29021
Synthesis and molecular structures of R(Me3CCH2)2In-E(SiMe3) (R = Me3CCH2, E = P or As; R = Me, E = P)
[AD-A275020] p 3486 N94-29131

Polymer technology publication series no. 16
[PB94-135522] p 3214 N94-29157
Organic materials that respond to molecules
[AD-A275392] p 3174 N94-29307
Insensitive energetic materials: The importance of physical properties and molecular structure
[AD-A275393] p 3225 N94-29308
Theoretical investigation of gas-surface interactions
[NASA-CR-195755] p 3272 N94-29378

MOLECULES
Influence of surface defects and local structure on oxygenate reaction pathways over metal oxide surfaces
[DE94-005680] p 3522 N94-30901

MOLNIYA SATELLITES
Orbital applications of electrodynamic propulsion
[AD-A275413] p 3173 N94-29216

MOLTEN SALT ELECTROLYTES
Fundamental stack and system issues in molten carbonate fuel cell development
[DE94-005960] p 3338 N94-30048

MOLYBDENUM
A photoemission electron microscope investigation of chemical vapor deposition diamond films and diamond nucleation p 3215 N94-29745
Brittle composites modeling: Comparisons with MoSi2/ZrO2
[DE94-004978] p 3182 N94-29933
Microstructure and mechanical properties of nitrided molybdenum silicide coatings
[DE94-006249] p 3217 N94-30025
Computer simulation of the interaction of fast hydrogen atoms with a molybdenum containing sorbed hydrogen
[DE94-608419] p 3209 N94-30253
Creep behavior of MoSi2-SiC composites
[DE94-004980] p 3185 N94-30693
Studies of supported molybdenum and tungsten
[DE94-006207] p 3210 N94-30839

MOLYBDENUM ALLOYS
Innovative processing of composites for ultra-high temperature applications, book 2
[AD-A275598] p 3177 N94-28730

MOLYBDENUM COMPOUNDS
Characterization of structure and mechanical properties of MoSi2-SiC nanolayer composites
[DE94-004982] p 3175 N94-28579
Fabrication and testing of plasma-spray formed MoSi2 and MoSi2 composite tubes
[DE94-004995] p 3175 N94-28581

MOLYBDENUM OXIDES
Synthesis and characterization of novel ternary and quaternary reduced molybdenum oxides
[DE94-005563] p 3510 N94-28529

MOMENTS OF INERTIA
Theory of fundamental interactions
[DE94-608126] p 3525 N94-30169

MOMENTUM
Melt flow during alloy solidification: Dimensional analysis and model problems
[PB94-138625] p 3206 N94-29997
On determination of a momentum of Alfven wave packet
[DE94-608329] p 3255 N94-30172
Deexcitation processes in nuclear reactions: The study of hot hadronic matter
[DE94-003396] p 3492 N94-30836

MOMENTUM TRANSFER
Volume averaged model for the mechanics of alloys solidification
[PB94-138617] p 3208 N94-30113
On determination of a momentum of Alfven wave packet
[DE94-608329] p 3255 N94-30172
On the structure and atomic motions in liquid sodium
[DE94-608386] p 3490 N94-30182

MONITORS
Monitor for status epilepticus seizures
p 3397 N94-30460
A transmission-loss monitor using current transformers
[DE94-003974] p 3267 N94-30716

MONOCULAR VISION
Motion and structure from planar motion in noisy monocular image sequences p 3308 N94-30299

MONOMOLECULAR FILMS
Surface structure and stereochemical properties of self-assembled monolayer materials
[DE94-004960] p 3484 N94-28578

MONOPULSE RADAR
Radar cross sections of ground clutter at 95 GHz for summer and fall conditions p 3259 N94-30512

MONSOONS
Study of dynamic characteristics of a monsoon circulation tube
[AD-A275238] p 3370 N94-29394

MONTE CARLO METHOD
A measurement of the LMP effect
[DE94-005225] p 3482 N94-28493
On the prediction of HAZ grain size using Monte Carlo simulation
[DE94-005465] p 3511 N94-28535
Energy losses of fast charged particles in thin silicon detectors
[DE94-606065] p 3483 N94-28552
Solution of charged particle transport equation by Monte-Carlo method in the BRANDZ code system
[DE94-606270] p 3484 N94-28614
A family of joint probability models for cost and schedule uncertainties
[AD-A275513] p 3463 N94-28670
SOCRATES simulation of the emission at wavelength 6300 A generated by the interaction between the atmosphere and the Space Shuttle exhaust
[AD-A275567] p 3164 N94-28827
Proceedings of the 10th NAL Symposium on Aircraft Computational Aerodynamics
[NAL-SP-19] p 3123 N94-28946
Monte Carlo simulation or normal shock wave. Part 2: VHS model and VSS model p 3123 N94-28948
Variable soft sphere molecular model in the Monte Carlo simulation of air species p 3123 N94-28949
The appearance of the Sun and Moon seen through clouds
[AD-A275338] p 3551 N94-29212
Focused ion beam fabrication of microelectronic structures
[AD-A275384] p 3264 N94-29305
The maximum entropy approach applied to energy exchange, chemical reactions and ionisation in the direct simulation Monte Carlo method for rarefied hypersonic flows
[IC-AERO-93-01] p 3524 N94-29481
Efficiencies of the ICRF minority heating in the CHS and LHD plasmas
[NIFS-270] p 3506 N94-29499
Performance of MCNP4A on seven computing platforms
[DE93-040101] p 3419 N94-29816
Particle kinetic simulation of high altitude hypervelocity flight
[NASA-CR-194535] p 3131 N94-29893
Measurement of the W mass in the D0 detector
[DE94-006002] p 3490 N94-30103
Estimation of Weibull modulus from dynamic and static fatigue experiments
[PB94-138641] p 3322 N94-30114
Ten new checks to assess the statistical quality of Monte Carlo solutions in MCNP
[DE94-006137] p 3465 N94-30366
Systematic error estimation in multisensor fusion systems
[AD-B179298] p 3428 N94-30764

MOON
The appearance of the Sun and Moon seen through clouds
[AD-A275338] p 3551 N94-29212

MORALE
Stress and ergonomic design and evaluation of person-machine systems
[AD-A275156] p 3400 N94-29034

MORNING
Space-time structure of the morning aurora inferred from coincident DMSP-F6, -F8, and Sondrestrom incoherent scatter radar observations
[AD-A275442] p 3356 N94-28869

MORPHOLOGY
Elements for the recognition of three dimensional deformable shapes: Application to biomedical imagery
[TELECOM-93-E-006] p 3396 N94-30978

MOSAICS
Automating geographically referenced digital mosaics from aerial videography with area-based feature matching p 3333 N94-29540

MOSSBAUER EFFECT
Atomic and magnetic structure of YBa2(Cu(1-x)Fe(x))3O(6+y) at 0.05 less than or equal to x less than or equal to 0.30, y is approximately equal to 1 and y is approximately equal to 0.5
[DE94-606852] p 3513 N94-29210
Study of iron exchanged zeolites by Moessbauer effect and electron spin resonance spectroscopy
[DE94-605138] p 3514 N94-29691
Backscatter Mossbauer Spectrometer (BaMS) for extraterrestrial applications p 3236 N94-29774

MOTION PERCEPTION
Motion and structure from planar motion in noisy monocular image sequences p 3308 N94-30299
Obstacle detection for an autonomous vehicle
p 3309 N94-30302
Aspects of vision and planning in a dynamic, uncertain environment p 3448 N94-30803

MOTION PICTURES
Animation techniques in BRL-CAD
[AD-A275232] p 3417 N94-29392

MOTION SICKNESS
Effect of seasickness on aircrew student survivor ability after ditching in cold water p 3379 N94-28425
Japanese Journal of Aerospace and Environmental Medicine, volume 30, no. 1
[JTN-94-80598] p 3389 N94-28850
Disturbance of equilibrium on JAL flight crew
p 3390 N94-28856
Space and vertigo: In relation to space motion sickness p 3390 N94-28857
The MERSS 5th Symposium on Space Medicine: Medical and Physiological Experiment Utilizing Parabolic Flight
[JTN-94-80588] p 3392 N94-29709
Motion sickness in parabolic flight: Possibility of electrogastrography as an objective index
p 3393 N94-29718

MOTION STABILITY
Some remarks about pseudo-Hamiltonian
[DE94-003273] p 3487 N94-29700

MOTOR VEHICLES
TCM exemptions to promote alternative-fuel vehicles: The good, the bad, and the ugly
[DE94-005924] p 3311 N94-30703

MOUNTAINS
Glacial landforms and late Cenozoic history of the western Soer-Rondane mountains p 3357 N94-29080

MOUNTING
RF vacuum microelectronics
[AD-A275221] p 3263 N94-28915

MTBF
Algorithms for treating redundancy in repairable and non-repairable systems
[DE94-005289] p 3315 N94-29020

MULTIGRID METHODS
ENGRID: A graphical interactive code for the computation of structured grids for blocked flow domains
p 3124 N94-28956
An elliptic-hyperbolic grid generation method and application to compressor flows p 3128 N94-28981
RNS optimization procedure for three-dimensional composite velocity multi-block applications
p 3273 N94-29534
Computational methods for the shape shading problem
[ISBN-0-315-85430-8] p 3421 N94-30136
Canonical-variables multigrid method for steady-state Euler equations
[NASA-CR-194888] p 3454 N94-30208

MULTIMEDIA
Application of digital video to hypermedia training systems
[AD-A274989] p 3409 N94-28910
HYPER-NPSNET: Embedded multimedia in a 3D virtual world
[AD-A275063] p 3410 N94-29152
End-to-end delay reduction in narrow bandwidth real-time multimedia tele-education applications
[AD-B179614] p 3260 N94-30518

MULTIPATH TRANSMISSION
Radar returns from a low-flying target over a rough sea surface under multipath and clutter conditions
p 3253 N94-29882

MULTIPLE ACCESS
Validation experiments with an Ethernet model using the simulation tool 'PROMISE'
[AD-B174795] p 3429 N94-30912
Information-seeking in hypertext: Multiple access methods in a full-text hypertext database
p 3536 N94-30918

MULTIPLEXING
A multiplexed two-way solid communications link for teleoperated robots p 3310 N94-30310

MULTIPROCESSING (COMPUTERS)
Design and packaging of fault tolerant optoelectronic multiprocessor computing system
[AD-A275896] p 3405 N94-28798
Model-oriented analysis of a communications protocol
[PB94-138146] p 3244 N94-29109
NPSNET: Integration of Distributed Interactive Simulation (DIS) protocol for communication architecture and information interchange
[AD-A275061] p 3530 N94-29139
Design of a thinwire real-time multiprocessor operating system p 3415 N94-29333
High throughput network for multiprocessor interconnections
[VTT-PUBS-147] p 3245 N94-29468
Hypra/TR: A tuple oriented recovery method for a continuously available distributed DBMS on a shared nothing multi-computer
[PB94-141264] p 3533 N94-29921
Computational balance in real-time cyclic spectral analysis
[DE94-005091] p 3432 N94-30100

A locally synchronous globally asynchronous Vertex-8 processing element for image reconstruction on a mesh
[ISBN-0-315-86005-7] p 3432 N94-30143
Common spaceborne multicomputer operating system and development environment
[NASA-TM-109092] p 3422 N94-30197
Maestro: An open system architecture for multi-robot control p 3306 N94-30288
Improving the execution speed of robot control computations: An allocation scheme for heterogeneous multiprocessors p 3310 N94-30308

MULTISENSOR APPLICATIONS
ACCS Surveillance Exploratory Prototype (ASEP) p 3138 N94-29566
Multi-sensor data fusion and the use of artificial intelligence
[PB94-126216] p 3448 N94-30741
Systematic error estimation in multisensor fusion systems
[AD-B179298] p 3428 N94-30764

MULTISTATIC RADAR
RL/ERCT automated swept-angle bistatic measurement system
[AD-A275763] p 3241 N94-28763
Synchronization in multistatic radar
[PB94-136975] p 3242 N94-28885
Synchronization, positioning, and communication in multistatic radar systems for air defence
[PB94-137478] p 3243 N94-28908
Simulator for multistatic radar
[PB94-135506] p 3245 N94-29311

MULTIVARIATE STATISTICAL ANALYSIS
Noise and drift analysis of non-equally spaced timing data p 3472 N94-30667

MUON SPIN ROTATION
On the (mu)SR activity at LNP JINR phasotron
[DE94-608385] p 3517 N94-30195
MuSR measurement of the magnetic penetration depth and coherence length in the high-Tc superconductor YBa2Cu3O(6.95)
[ISBN-0-315-85385-9] p 3517 N94-30203

MUONS
Simulation of experiments on deep inelastic scattering of muons on superconducting magnetic toroidal spectrometer STORS
[DE94-606267] p 3483 N94-28554
B production and B(0)(bar B)(0) mixing at DO
[DE94-004664] p 3484 N94-28574
Project of the experiment to test the hypothesis on existence of white and black p(mu)-atoms
[DE94-606751] p 3485 N94-28625
A study of the ultrahigh-energy cosmic ray mass composition with the MACRO and EAS-TOP experiments p 3552 N94-29687
On the (mu)SR activity at LNP JINR phasotron
[DE94-608385] p 3517 N94-30195
Search for the top quark in the electron-electron and electron-muon channels at D0
[DE94-006174] p 3492 N94-30779
Inclusive single muon production in D0
[DE94-006175] p 3493 N94-30887

MUSCLES
Leg muscle volume during 30-day 6-degree head-down bed rest with isotonic and isokinetic exercise training
[NASA-TM-4580] p 3385 N94-29401
Japanese Journal of Aerospace and Environmental Medicine, vol. 30, no. 2
[JTN-94-80599] p 3394 N94-29863
Effect of water immersion on muscle sympathetic nerve response during static muscle contraction p 3394 N94-29865
Shortening velocity and calcium sensitivity of single fibers from hindlimb suspended muscle in rats p 3387 N94-29866

MUSCULAR FUNCTION
Japanese Journal of Aerospace and Environmental Medicine, vol. 30, no. 2
[JTN-94-80599] p 3394 N94-29863
Shortening velocity and calcium sensitivity of single fibers from hindlimb suspended muscle in rats p 3387 N94-29866

MUSCULOSKELETAL SYSTEM
Shortening velocity and calcium sensitivity of single fibers from hindlimb suspended muscle in rats p 3387 N94-29866

MUSIC
Numerical simulations of piano strings. Part 1: A physical model for a struck string using finite difference methods
[TELECOM-93-C-003] p 3481 N94-30972
Noise reduction techniques for the restoration of musical recordings
[TELECOM-93-E-019] p 3291 N94-30979

N

NAKHLITES
Cosmogenic C-14 in Antarctic and non-Antarctic meteorites and lunar samples
[NASA-CR-195795] p 3546 N94-29905

NAPHTHALENE
Computer simulation of molecular interactions in supercritical solvents
[AD-A274977] p 3486 N94-29087

NASA PROGRAMS
NASA space and Earth science data on CD-ROM
[NASA-TM-109709] p 3528 N94-28414
BAG: A code for predicting the performance of a gas bag impact attenuation system for the Pathfinder lander
[DE94-003688] p 3165 N94-28477
NASA Parts Program Office responsibilities p 3165 N94-28702
NASA Parts Project Office: Basic goals p 3166 N94-28703
Research and technology, 1992
[NASA-TM-103996] p 3555 N94-29891
A survey of NASA and military standards on fault tolerance and reliability applied to robotics
[AIAA PAPER 94-1211-CP] p 3445 N94-30562
Terrestrial applications of NASA space telerobotics technologies
[AIAA PAPER 94-1235-CP] p 3448 N94-30582

NASA SPACE PROGRAMS
Status of frequency and time support for NASA systems p 3468 N94-30640

NASTRAN
Stiffness-generated rigid-body mode shapes for Lanczos eigensolution with SUPORT DOF by way of a MSC/NASTRAN DMAP alter
[NASA-TM-106537] p 3319 N94-29406
Transient analysis mode participation for modal survey target mode selection using MSC/NASTRAN DMAP
[NASA-TM-106536] p 3319 N94-29469

NATIONAL AIRSPACE SYSTEM
1.8 gigahertz (GHz) digital Low Density Radio Communications Link (LDRCL) Operational Test and Evaluation (OT&E) integration and OT&E operational final test report
[AD-A275800] p 3241 N94-28771
The 1993 Federal Aviation Administration Aviation System Capital Investment Plan p 3136 N94-29445
Loran-C time management p 3144 N94-30644

NATURAL GAS
Numerical prediction of mixing process in a methane-fueled engine p 3304 N94-30230
Technical analysis of alternative fueled vehicles
[DE94-744238] p 3304 N94-30269
Configuration and performance of the indirect-fired fuel cell bottomed turbine cycle
[DE94-005961] p 3338 N94-30313
Investigation of the technology development status of alternate fuel vehicles
[DE94-744237] p 3312 N94-30831
Compressed natural gas fueled vehicles: The Houston experience
[DE94-005804] p 3312 N94-30878
Assessment of costs and benefits of flexible and alternative fuel use in the US transportation sector
[DE94-006100] p 3226 N94-30885

NATURAL LANGUAGE (COMPUTERS)
Engineering specification editing tools
[AD-A275116] p 3419 N94-29746

NATURAL LANGUAGE PROCESSING
An architecturally-based theory of human sentence comprehension
[AD-A275380] p 3398 N94-29313
Generalized left-corner parsing
[TR-92-21] p 3432 N94-30356
Interrogatives and adverbs of quantification
[LP-92-14] p 3456 N94-30372

NAVIER-STOKES EQUATION
Large eddy simulations using lattice Boltzmann algorithms
[DE94-005666] p 3270 N94-28549
Numerical simulation of unsteady aerodynamic heating induced by shock reflections p 3123 N94-28952
ENGRID: A graphical interactive code for the computation of structured grids for blocked flow domains p 3124 N94-28956
A design of third-generation airfoils for helicopter rotor blades using Navier-Stokes p 3124 N94-28957
Unsteady aerodynamic computations around NACA0012 at high angles of attack p 3126 N94-28969
Study of modeling of turbulence of renormalization group analysis p 3126 N94-28970
The upsilon-q method and the psi-q method for incompressible flows p 3126 N94-28971
Theoretical study of the incompressible Navier-Stokes equations by the least-squares method
[NASA-TM-106535] p 3272 N94-29096
A free-wake Euler and Navier-Stokes CFD method and its application to helicopter rotors including dynamic stall
[AD-A275416] p 3129 N94-29197
Investigation of advanced counterrotation blade configuration concepts for high speed turboprop systems. Task 2: Unsteady ducted propfan analysis computer program users manual
[NASA-CR-187105] p 3152 N94-29438
A new flux-conserving numerical scheme for the steady, incompressible Navier-Stokes equations
[NASA-TM-106520] p 3273 N94-29471
RNS optimization procedure for three-dimensional composite velocity multi-block applications p 3273 N94-29534
Finite element method for numerical simulation of turbulent flows. The N3S code p 3233 N94-29612
Spherical model for turbulence p 3274 N94-29730
Numerical study of the trailing vortex of a wing with wing-tip blowing
[NASA-CR-195803] p 3130 N94-29760
Direct and large-eddy simulations of turbulent flow in a square duct p 3275 N94-29809
The h-p adaptive methods for incompressible viscous flow problems p 3275 N94-29836
Numerical solution of 3-D Navier-Stokes equations in vorticity-velocity form for incompressible flows p 3276 N94-29843
Algorithm and code development for unsteady three-dimensional Navier-Stokes equations
[NASA-CR-195774] p 3277 N94-29942
High-resolution algorithms for the Navier-Stokes equations for generalized discretizations p 3278 N94-29965
Aircraft aerodynamics with deflected jets in ground effect p 3132 N94-29973
Three dimensional compressible turbulent flow computations for a diffusing S-duct with/without vortex generators p 3281 N94-30519
Euler results of the ISNaS compressible multi-block flow solver
[AD-B179299] p 3281 N94-30756
Information system for flow simulation based on the Navier-Stokes equations vectorization
[AD-B179293] p 3281 N94-30763

NAVIGATION
Micro guidance and control synthesis: New components, architectures, and capabilities p 3144 N94-29792
ARK: Autonomous mobile robot in an industrial environment
[AIAA PAPER 94-1177-CP] p 3439 N94-30529
Meeting the challenges of installing a mobile robotic system
[AIAA PAPER 94-1187-CP] p 3440 N94-30537

NAVIGATION AIDS
Software engineering methods in the Hermes on-board software p 3414 N94-29326
Ground independent landing system p 3137 N94-29564
GPS/GNSS for ATM p 3138 N94-29565

NAVIGATION INSTRUMENTS
An electromagnetic noncontacting sensor for thickness measurement in a dispersive medium
[AIAA PAPER 94-1200-CP] p 3443 N94-30551

NAVIGATION SATELLITES
GPS/GNSS for ATM p 3138 N94-29565
TacSats for NATO
[AGARD-AR-322] p 3169 N94-30350
The 25th Annual Precise Time and Time Interval (PTTI) Applications and Planning Meeting
[NASA-CP-3267] p 3468 N94-30639

NAVSTAR SATELLITES
Cesium and rubidium frequency standards status and performance on the GPS program p 3145 N94-30663
A review of the status and capabilities of Navstar GPS
[AD-B174629] p 3143 N94-30854

NAVY
Communications subsystem for the Petite Amateur Navy Satellite (PANSAT)
[AD-A275532] p 3242 N94-28812

NEAR FIELDS
Measurement basis of near fields in spherical coordinates in the 100 MHz to 6 GHz band
[REPT-932-430-107] p 3255 N94-30153

NEAR INFRARED RADIATION
Measurement of atmospheric OH by titration of near-IR fluorescent dyes p 3344 N94-28599
Near-IR diode laser absorption for measurement of tropospheric HO2 p 3345 N94-28607
HO2 detection by near infrared absorption using tunable diode lasers p 3346 N94-28608
Imaging spectrometry of the Earth and other solar system bodies p 3237 N94-29779

Evolution of miniature detectors and focal plane arrays for infrared sensors p 3237 N94-29781
Infrared properties of obscuring dust tori in active galactic nuclei p 3545 N94-29832
Correlation studies of Pioneer Venus imagery obtained from PV experiments with near IR imagery obtained from ground-based observations during Venus inferior conjunction
[NASA-CR-195772] p 3550 N94-29892
A near-infrared survey of the star forming region NGC 2264 p 3540 N94-29971

NEAR ULTRAVIOLET RADIATION
Near-ultraviolet laser photoemission: Scanning microscopy, buried interfaces and image-potential states p 3294 N94-29531

NEAR WAKES
An experimental study of wing tip vortex in the near wake of a rectangular wing
[AD-A275389] p 3129 N94-29306
Flow past a circular cylinder with a permeable wake splitter plate p 3275 N94-29764

NEGATIVE ELECTRON AFFINITY
Electron beam analysis for cyclotron harmonic and free-electron laser devices
[AD-A275070] p 3293 N94-29179

NEGATIVE IONS
A future, intense source of negative hydrogen ions p 3494 N94-30485

NEODYMIUM
Solubility of Nd in brine
[DE94-005099] p 3187 N94-28567

NEON
Computer simulation of molecular interactions in supercritical solvents
[AD-A274977] p 3466 N94-29087
Optical field ionization of atoms and ions using ultrashort laser pulses
[DE94-006643] p 3488 N94-29845

NEPTUNE (PLANET)
Radio science ground data system for the Voyager-Neptune encounter, part 1 p 3248 N94-29623

NERVOUS SYSTEM
Effect of food intake on skin vasomotor responses to head-up tilt in humans p 3390 N94-28854

NETS
Conditional dependence in probabilistic networks
[RUU-CS-92-34] p 3464 N94-29450
Pearl's belief propagation: The proofs
[RUU-CS-92-47] p 3456 N94-30378

NETWORK ANALYSIS
Modeling, analysis, and simulation of an optical time-division multiple-access network architecture
[AD-A275847] p 3498 N94-28780
Digitally programmable composite operational amplifier applications
[AD-A275081] p 3262 N94-28842
High throughput network for multiprocessor interconnections
[VTT-PUBS-147] p 3245 N94-29468
Customer creation and combination in queueing networks
[MEMO-INF-93-35] p 3438 N94-30375
An intrinsic Hamiltonian formulation of the dynamics of LC-circuits
[MEMO-1154] p 3462 N94-30964

NETWORK CONTROL
Video transmission on ATM networks
[NASA-CR-195124] p 3244 N94-29106
High throughput network for multiprocessor interconnections
[VTT-PUBS-147] p 3245 N94-29468
Remote observatory access via the advanced communications technology satellite p 3253 N94-29894
Performance evaluation of intelligent network services
[MEMO-INF-93-20] p 3438 N94-30373
Self-stabilizing l-exclusion algorithms
[RUU-CS-93-01] p 3424 N94-30379
An all pairs shortest paths distributed algorithm using 2n(exp 2) messages
[RUU-CS-93-19] p 3432 N94-30411

NETWORKS
Bayesian belief networks and conditional independencies
[RUU-CS-92-36] p 3465 N94-30376

NEURAL NETS
A space-based classification system for RF transients
[DE94-003933] p 3240 N94-28522
Track filtering by robust neural network
[DE94-606067] p 3434 N94-28613
Modeling, analysis, and simulation of an optical time-division multiple-access network architecture
[AD-A275847] p 3498 N94-28780
Non-intrusive gaze tracking using artificial neural networks
[AD-A275186] p 3397 N94-28860
Intelligent automated process planning and code generation for computer-controlled inspection
[AD-A275346] p 3409 N94-28920
Initial wave-type identification with neural networks and its contribution to automated processing in IMS version 3.0
[AD-A275058] p 3359 N94-29137
Neural network solutions to logic programs with geometric constraints
[AD-A275419] p 3435 N94-29198
Nonvolatile programmable neural network synaptic array
[NASA-CASE-NPO-18578-1-CU] p 3265 N94-29426
Automation of the NDT diagnostic using neural nets. Application: Inspection of Airbus longitudinal joints during maintenance
[REPT-932-600-104] p 3315 N94-29474
A neural network with modular hierarchical learning
[NASA-CASE-NPO-19077-1-CU] p 3435 N94-29492
Nonlinear PCA: Algorithms and applications
[PB94-137544] p 3419 N94-29680
Stereo imaging based particle velocimeter
[NASA-CR-195800] p 3289 N94-29742
Neural network with dynamically adaptable neurons
[NASA-CASE-NPO-17803-1-CU] p 3436 N94-29756
Activities of Ishikawajima-Harima Heavy Industries Co. Ltd.
[PB94-137981] p 3555 N94-29798
Robotic hand-eye motor learning p 3436 N94-29835
Neural network application to Particle Impact Noise Detection p 3437 N94-29840
Reinforcement learning for robots using neural networks p 3437 N94-29853
Genetic algorithms at UC Davis/LLNL
[DE94-006625] p 3421 N94-30117
Unsupervised learning in analog networks
[ISBN-0-315-85959-8] p 3432 N94-30140
A novel approach to noise-filtering based on a gain-scheduling neural network architecture
[NASA-TM-106563] p 3155 N94-30204
Taxonomy of gamma ray burster data using a self-organizing neural network
[DE94-006480] p 3553 N94-30248
Neural network based time-optimal control of a magnetically levitated precision positioning system
[DE94-006573] p 3437 N94-30250
A lateral inhibition neural network that emulates a winner-takes-all algorithm
[RUU-CS-92-46] p 3438 N94-30334
A multiscale approach to image segmentation using Kohonen networks
[RUU-CS-93-06] p 3438 N94-30349
Microwave vision for robots
[AIAA PAPER 94-0887-CP] p 3443 N94-30550
A neural network-based technique for structural identification of SISO systems
[REPT-93-076] p 3449 N94-30941

NEUROLOGY
Monitor for status epilepticus seizures p 3397 N94-30460

NEURONS
Synaptogenesis, selective stabilization, and free association
[AD-A275250] p 3392 N94-29431
A lateral inhibition neural network that emulates a winner-takes-all algorithm
[RUU-CS-92-46] p 3438 N94-30334

NEUTRAL ATMOSPHERES
The Pluto fast flyby mission: Completing the reconnaissance of the solar system p 3235 N94-29768

NEUTRINOS
Emission of supersymmetric neutron pair by charged lepton in magnetic field
[DE93-634365] p 3481 N94-28468
Properties of W + jet events in proton-antiproton collisions at 1.8 TeV
[DE94-004002] p 3482 N94-28524
Proceedings of the workshop on quark and lepton mass matrices
[DE94-707692] p 3485 N94-28624
A Tevatron collider beauty factory
[DE94-004879] p 3488 N94-29930
On possibility to create the scintillation trigger for liquid-argon neutrino detector
[DE94-607844] p 3489 N94-30050
Search for heavy neutrinos at the IHEP-JINR neutrino detector
[DE94-608175] p 3489 N94-30095
Research in elementary particle physics
[DE94-001657] p 3491 N94-30762

NEUTRON COUNTERS
Preliminary detector design ST862-prototype neutron detector
[DE94-004714] p 3491 N94-30695

NEUTRON DIFFRACTION
Hysteresis phenomena at spin-flop transition induced by the pulsed magnetic field
[DE94-606851] p 3511 N94-28626
Synthesis and neutron diffraction study of Na3WN3 and Na3MoN3
[AD-A275158] p 3203 N94-29043

NEUTRON IRRADIATION
Relationship between swelling and irradiation creep in cold-worked PCA stainless steel irradiated to approximately 178 dpa at approximately 400 C
[DE94-004368] p 3201 N94-28456
Radiation effects in beryllium used for plasma protection
[DE94-004599] p 3201 N94-28460
Irradiation-induced structure and property changes in tokamak plasma-facing, carbon-carbon composites
[DE94-006046] p 3508 N94-30365

NEUTRON SCATTERING
Hysteresis phenomena at spin-flop transition induced by the pulsed magnetic field
[DE94-606851] p 3511 N94-28626
Double-crystal analyser system for the PRISMA spectrometer: Test of a prototype
[PB94-138245] p 3286 N94-29113
Incommensurate magnetic order in UNi2Al3
[DE94-005449] p 3209 N94-30246

NEUTRON SOURCES
Double-crystal analyser system for the PRISMA spectrometer: Test of a prototype
[PB94-138245] p 3286 N94-29113
Neutronics of a D-Li neutron source: An overview
[DE94-005372] p 3493 N94-30893

NEUTRON SPECTROMETERS
Double-crystal analyser system for the PRISMA spectrometer: Test of a prototype
[PB94-138245] p 3286 N94-29113
Experimental setups and methods to obtain new nuclear data at intermediate and high energies
[DE94-607850] p 3489 N94-30052

NEUTRON STARS
Equation of state of neutron star matter, limiting rotational periods of fast pulsars, and the properties of strange stars
[DE94-005214] p 3542 N94-28480
On observing neutron star oscillations p 3538 N94-29795
Near-critical spherically symmetric accretion by neutron stars p 3546 N94-29991

NEUTRONS
Results on structure functions from fixed-target experiments
[DE94-005233] p 3482 N94-28541
Determination of the neutron spin-structure function
[DE94-005234] p 3483 N94-28542
The effects of relativistic neutrons on nonthermal models of active galactic nuclei p 3547 N94-29993
Experimental setups and methods to obtain new nuclear data at intermediate and high energies
[DE94-607850] p 3489 N94-30052
Observation of the phase shift of the wave function of the neutron under total reflection
[DE94-608244] p 3489 N94-30096
Intercomparison of theoretical calculations of important activation cross sections for fusion reactor technology
[DE94-002642] p 3497 N94-30825

NEWTON METHODS
Numerical solution of the two-dimensional time-dependent incompressible Euler equations
[NASA-CR-195775] p 3277 N94-29859

NICKEL
Geometric structures of thin film: Pt on Pd(110) and NiO on Ni(100)
[DE94-005564] p 3211 N94-28530
Pit initiation on passivated metal surfaces: Crystallographic orientation and environmental effects
[ISBN-0-315-85433-2] p 3208 N94-30138

NICKEL ALLOYS
Directional solidification studies in Ni-Al alloys
[DE94-005562] p 3201 N94-28527
Fusion welding with self-generated filler metal
[NASA-CASE-LEW-15671-1] p 3301 N94-29557
The effect of various metallurgical parameters on the flow and fracture behavior of polycrystalline NiAl near the brittle-to-ductile transition
[NASA-TM-106534] p 3205 N94-29758
Incommensurate magnetic order in UNi2Al3
[DE94-005449] p 3209 N94-30246

NICKEL COATINGS
Adhesion of electrolessly deposited Ni(P) on alumina ceramic
[ETN-94-95358] p 3212 N94-28539

NICKEL COMPOUNDS
Interstitially stabilized phases in the zirconium-nickel system
[DE94-005561] p 3201 N94-28525
NICKEL OXIDES
Interstitially stabilized phases in the zirconium-nickel system
[DE94-005561] p 3201 N94-28525
Geometric structures of thin film: Pt on Pd(110) and NiO on Ni(100)
[DE94-005564] p 3211 N94-28530
Transient studies of low temperature catalysts for methane conversion
[DE94-005767] p 3200 N94-30877
NIGHT VISION
An investigation of stereopsis with AN/AVS-6 night vision goggles at varying levels of illuminance and contrast
[AD-A275332] p 3400 N94-28918
NIOBIUM ALLOYS
Effects of thermomechanical processing on tensile and long-time creep behavior of Nb-1 percent Zr-0.1 percent C sheet
[NASA-TM-106319] p 3202 N94-28822
Calculating the J(c), B, T surface for commercial niobium tin conductors using a reduced state model
[DE94-006296] p 3520 N94-30850
NITRAMINE PROPELLANTS
Insensitive energetic materials: The importance of physical properties and molecular structure
[AD-A275393] p 3225 N94-29308
NITRATES
Growth of hydrocarbon-rich microalga Botryococcus braunii in secondarily treated sewage and its consumption of nitrate ion and phosphate ion p 3387 N94-29519
NITRIC OXIDE
Ozone production at a rural site in Georgia during the summer 1992 SOS campaign
[DE94-003989] p 3342 N94-28523
Simulation of pollutant formation in turbulent combustors using an extended coherent flame model
p 3190 N94-29251
Flowfield prediction of NO(x) and smoke production in aircraft engines p 3191 N94-29252
NITRIDING
Microstructure and mechanical properties of nitrided molybdenum silicide coatings
[DE94-006249] p 3217 N94-30025
Charge trapping and breakdown in N2O oxides
[DE94-003775] p 3266 N94-30040
NITRO COMPOUNDS
Superior energetic materials that contain carbocations and anions. Energetic materials restricted in composition to C, H, N, and O atoms
[AD-A275449] p 3225 N94-29310
NITROGEN
Peroxy radical measurements with NCAR's chemical amplifier p 3345 N94-28603
Predissociation in N2(C'4, 1 Sigma u +) and other N2 states and its importance in the atmospheres of Titan and Triton
[NASA-CR-195727] p 3549 N94-28816
Microstructure and mechanical properties of nitrided molybdenum silicide coatings
[DE94-006249] p 3217 N94-30025
NITROGEN DIOXIDE
The radical amplifier p 3345 N94-28604
NITROGEN OXIDES
Catalytic fabric filtration for simultaneous NO(x) and particulate control
[DE94-001660] p 3341 N94-28463
The radical amplifier p 3345 N94-28604
Fuels and Combustion Technology for Advanced Aircraft Engines
[AGARD-CP-536] p 3189 N94-29246
On the effect of emissions from aircraft engines on the state of the atmosphere p 3189 N94-29247
Prediction of prompt NO(x) in hydrocarbon air flames
p 3190 N94-29250
Ultra low NO(x) ultra lean gas turbine primary zones with liquid fuels p 3154 N94-29267
Reduction of NO(x) by fuel-staging in gas turbine engines: A commitment to the future
p 3194 N94-29272
Chambers of turboreactors with variable geometry: A response to the matrix of pollution in cycles at high temperature, high pressure p 3194 N94-29273
The influence of air distribution on homogeneity and pollutant formation in the primary zone of a tubular combustor p 3194 N94-29274
Effects of hydrogen addition on pollutant emissions in a gas turbine combustor p 3195 N94-29275
Charge trapping and breakdown in N2O oxides
[DE94-003775] p 3266 N94-30040
NITROGEN PLASMA
Investigation of intense XUV emission of nitrogen-puff Z-pinch with small energy input
[PH-23] p 3505 N94-29075
Multichannel x ray spectral measurement of hot plasma evolution in nitrogen-puff Z-pinch
[PH-24] p 3505 N94-29076
NITROGEN POLYMERS
Ballistic performance of polycarbonate/polyester and polycarbonate/styrene- acrylonitrile microlayer sheets
[AD-A275462] p 3177 N94-28735
NITROUS OXIDES
Ozone production at a rural site in Georgia during the summer 1992 SOS campaign
[DE94-003989] p 3342 N94-28523
An improved method of measuring tropospheric NO2, NO3, HO2, and RO2 by Matrix Isolation and Electronic Spin Resonance (MIESR) p 3345 N94-28605
Charge trapping and breakdown in N2O oxides
[DE94-003775] p 3266 N94-30040
A toy model for estimating N2O emissions from natural soils p 3351 N94-30627
The development and evaluation of a tunable diode laser trace gas sensor for the measurement of N2O and CH4 fluxes using micrometeorological techniques
[ISBN-0-315-78975-1] p 3296 N94-30801
NOISE (SOUND)
Minutes. Accredited Standards Committee on Noise, S12. US tag for ISO/TC 43/SC1 noise and ISO/TC 94/SC12 hearing protection
[AD-A275622] p 3477 N94-28636
Evaluation of monitoring audiometry in the United States Air Force Hearing Conservation Program
[AD-A275309] p 3391 N94-29211
Neural network application to Particle Impact Noise Detection p 3437 N94-29840
Parameter identification of the rotordynamic coefficients of high-Reynolds-number hydrostatic bearings
p 3311 N94-30792
NOISE GENERATORS
Fluid dynamic noise in a centrifugal pump
[AD-A275264] p 3477 N94-28904
Experiments on the aerodynamic generation of noise in centrifugal turbomachinery p 3480 N94-30804
NOISE INTENSITY
Subjective response to sonic booms having different shapes, rise times, and durations
[NASA-TM-109090] p 3479 N94-29464
NOISE MEASUREMENT
Report of National Institute for Resources and Environment. No. 8: Research on blasting sound related to it's measurement, propagation prediction, control and evaluation
[JTN-94-80605] p 3479 N94-29597
A high rate, low noise, x ray silicon strip detector system
[DE94-004557] p 3268 N94-30717
NOISE PREDICTION
Report of National Institute for Resources and Environment. No. 8: Research on blasting sound related to it's measurement, propagation prediction, control and evaluation
[JTN-94-80605] p 3479 N94-29597
NOISE PREDICTION (AIRCRAFT)
Experimental validation of finite element and boundary element methods for predicting structural vibration and radiated noise
[NASA-CR-4561] p 3301 N94-29552
NOISE PROPAGATION
Attenuation of outdoor sound propagation levels by a snow cover
[AD-A275387] p 3478 N94-29314
Report of National Institute for Resources and Environment. No. 8: Research on blasting sound related to it's measurement, propagation prediction, control and evaluation
[JTN-94-80605] p 3479 N94-29597
NOISE REDUCTION
Removal of coherent Extremely Low Frequency (ELF) background noise by adaptive noise cancellation
[AD-A275016] p 3243 N94-28898
Fluid dynamic noise in a centrifugal pump
[AD-A275264] p 3477 N94-28904
Boundary layer control device for duct silencers
[NASA-CASE-ARC-12030-1] p 3478 N94-29362
A novel approach to noise-filtering based on a gain-scheduling neural network architecture
[NASA-TM-106563] p 3155 N94-30204
Noise reduction techniques for the restoration of musical recordings
[TELECOM-93-E-019] p 3291 N94-30979
NOISE SPECTRA
Parameter identification of the rotordynamic coefficients of high-Reynolds-number hydrostatic bearings
p 3311 N94-30792
NOISE TEMPERATURE
Determining noise temperatures in beam waveguide systems p 3249 N94-29657
A dual-cavity ruby maser for the Ka-band link experiment p 3250 N94-29658
X-band ultralow-noise maser amplifier performance
p 3251 N94-29672
NONADIABATIC CONDITIONS
Nonadiabatic effects in the quantum Hall regime
p 3513 N94-29530
Theory for electron-transfer reactions in a three-component system: The degenerate regime
[DE94-005919] p 3493 N94-30903
NONDESTRUCTIVE TESTS
Portable electronically based method for the nondestructive remote sensing of crevice corrosion
[AD-A275403] p 3318 N94-29057
Automation of the NDT diagnostic using neural nets. Application: Inspection of Airbus longitudinal joints during maintenance
[REPT-932-600-104] p 3315 N94-29474
Bolt and nut evaluator
[NASA-CASE-GSC-13468-1] p 3288 N94-29538
Method and apparatus for indicating disbonds in joint regions
[NASA-CASE-LAR-14626-1] p 3315 N94-29548
Improved ground-penetrating radar, bridge decks
[DE94-004863] p 3254 N94-29929
Vacuum chamber and adaptors for shearography and holography
[NASA-CR-192467] p 3157 N94-29956
Physical interpretation and development of ultrasonic nondestructive evaluation techniques applied to the quantitative characterization of textile composite materials
[NASA-CR-195766] p 3183 N94-30016
Development of evaluated data bank of physical properties of perspective nuclear engineering steels and alloys
[DE94-607999] p 3207 N94-30076
Resonant ultrasound spectroscopy for elastic constant measurements
[DE94-005016] p 3480 N94-30098
Radar jet engine health monitoring project
[ASSGI-301] p 3153 N94-30130
Robotic NDE inspection of advanced solid rocket motor casings
[AIAA PAPER 94-1222-CP] p 3446 N94-30571
Automation for nondestructive inspection of aircraft
[AIAA PAPER 94-1223-CP] p 3446 N94-30572
NONEQUILIBRIUM CONDITIONS
Models for vibration-dissociation coupling in high-temperature gases p 3273 N94-29675
NONEQUILIBRIUM FLOW
Numerical analysis of two dimensional/axisymmetric non-equilibrium hypersonic flow p 3125 N94-28963
On approximate Riemann solvers: Improvement of HLLEM scheme and its generalization for chemically reacting flows p 3126 N94-28973
Models for vibration-dissociation coupling in high-temperature gases p 3273 N94-29675
NONINTRUSIVE MEASUREMENT
Non-intrusive gaze tracking using artificial neural networks
[AD-A275186] p 3397 N94-28860
An actively cooled floating element skin friction balance for direct measurement in high enthalpy supersonic flows p 3289 N94-29824
Non-invasive temperature measurements using electron paramagnetic resonance spectroscopy
p 3198 N94-29881
NONLINEAR EQUATIONS
Numerical analysis and computation of nonlinear partial differential equations from applied mathematics
[AD-A275582] p 3451 N94-28723
Approximation of solutions of the cubic NLSE by finite dimensional equations and non-squeezing properties
[PB94-138294] p 3452 N94-29148
A non-linear simulation for an autonomous unmanned air vehicle
[AD-A275062] p 3146 N94-29200
Nonlinear wave packet evolution in a dispersive plasma: Application to rotational discontinuities
p 3506 N94-29822
Approximation methods for nonlinear operator equations of the m-accretive type
[DE94-608099] p 3467 N94-30065
Fuzzy logic based robotic controller
[AIAA PAPER 94-1202-CP] p 3443 N94-30553
NONLINEAR FILTERS
A novel approach to noise-filtering based on a gain-scheduling neural network architecture
[NASA-TM-106563] p 3155 N94-30204

NONLINEAR OPTICS
High-power CW diode-laser-array-pumped solid-state lasers and efficient nonlinear optical frequency
[AD-A275394] p 3293 N94-29309
Study of nonlinear optical polymers and their applications in optical waveguides p 3216 N94-29807
Nonlinear absorption in high reflector multilayers
[DE94-005818] p 3295 N94-30598
Nonlinear optics response of semiconductor quantum wells under high magnetic fields
[DE94-003244] p 3520 N94-30835

NONLINEAR PROGRAMMING
Center for Parallel Optimization
[AD-A274988] p 3431 N94-29127
Investigation on application of genetic algorithms to optimal reactive power dispatch of power systems
[MATHS-REPT-A-197] p 3266 N94-29527

NONLINEAR SYSTEMS
Frequency-domain analysis of nonlinear microwave circuits
[PB94-132024] p 3261 N94-28400
Nonlinear magnetohydrodynamics
[DE94-005654] p 3503 N94-28547
Annual summary of basic research thermoacoustic heat transport, 1993
[AD-A275751] p 3230 N94-28644
The solving of the relativistic two-body problem with a nonlinear dependence upon a spectrum parameter
[DE94-606343] p 3451 N94-28783
General theory and algorithms for the non-casual inversion, slewing and control of space-based articulated structures
[AD-A275118] p 3167 N94-29002
Incorporating geometric constraints into rule-based systems using nonlinear optimization
[AD-A275093] p 3452 N94-29063
Evolution of the large-scale vortices in turbulent mixing-layers p 3273 N94-29686
Large-scale computations in analysis of structures
[DE94-004022] p 3321 N94-29951
Stochastic stability and nonlinear control in mechanical systems p 3303 N94-29966
On the nonlinear dynamics of ocean wave systems p 3378 N94-30790
An experimental study of nonlinear wave coupling and energy transfer characterizing the transition of a planar jet shear layer p 3282 N94-30953

NONLINEARITY
Dissipative quantum dynamics and nonlinear sigma-model
[DE94-606295] p 3523 N94-28617
Computational methods in continuum mechanics
[AD-A275560] p 3451 N94-28792
A non-linear simulation for an autonomous unmanned air vehicle
[AD-A275062] p 3146 N94-29200
Screening of flexible cables by nonlinear resistance measurements
[AD-A275193] p 3264 N94-29289
An investigation of distributed coupling in a nonlinear semiconductor waveguide p 3246 N94-29529
Large amplitude Langmuir and ion-acoustic waves in a relativistic two-fluid plasma
[NIFS-271] p 3506 N94-29547
Nonlinear wave packet evolution in a dispersive plasma: Application to rotational discontinuities p 3506 N94-29822
Robotic hand-eye motor learning p 3436 N94-29835
A guidance and navigation system for two spacecraft rendezvous in translunar halo orbit p 3142 N94-29837
Large-scale computations in analysis of structures
[DE94-004022] p 3321 N94-29951
Closed form expressions for a consistent stress material nonlinear finite element p 3322 N94-30258
Nonlinear multibody formulation for rotorcraft analysis p 3149 N94-30787

NORMALIZING
Comparing curried and uncurried rewriting
[CWI-CS-R9350] p 3425 N94-30415
Perpetual reductions and strong normalization in orthogonal term rewriting systems
[CWI-CS-R9345] p 3426 N94-30437

NORMALIZING (STATISTICS)
Output statistics of the SALFAS FM normalizer Smoothing/Prediction function
[AD-A275758] p 3463 N94-28759
Perpetual reductions in orthogonal combinatory reduction systems
[CWI-CS-R9349] p 3459 N94-30413
Higher order recursive program schemes are Turing incomplete
[CWI-CS-R9348] p 3425 N94-30414
Comparing curried and uncurried rewriting
[CWI-CS-R9350] p 3425 N94-30415

NORTH ATLANTIC TREATY ORGANIZATION (NATO)
Report on NATO PTTI p 3469 N94-30645

NORWAY
The Norwegian seismic array (NORSAR), phase 3
[AD-A275440] p 3356 N94-28868

NOSES (FOREBODIES)
An experimental investigation of the effect of leading edge extensions on directional stability and the effectiveness of forebody nose strakes p 3155 N94-29728

NOTCHES
Mechanisms and effects of heat generation at the tips of dynamic cracks and notches in metals p 3321 N94-29808

NOZZLE DESIGN
Fuel injector design for high temperature aircraft engine p 3154 N94-29263

NOZZLE FLOW
Calculation of propulsive nozzle flowfields in multidiffusing chemically reacting environments
[NASA-TM-106532] p 3271 N94-28835
Fuel injector design for high temperature aircraft engine p 3154 N94-29263
Scramjet CFD methods and analysis. Part 1: Scramjet CFD methods. Numerical simulation of the flow in scramjet duct p 3152 N94-29296
Particle kinetic simulation of high altitude hypervelocity flight
[NASA-CR-194535] p 3131 N94-29893
Eigenvalue analysis of the convergence behaviour of an Euler method
[PB94-125722-U] p 3281 N94-30743
Evaluation of flip-flop jet nozzles for use as practical excitation devices
[NASA-TM-106377] p 3135 N94-30949

NUCLEAR BINDING ENERGY
The bond diluted spin-1 Blume-Emery-Griffiths model in a transverse field
[DE94-608121] p 3525 N94-30167

NUCLEAR DEFORMATION
Overlap of metal clusters and nuclear structure physics
[DE94-608387] p 3517 N94-30183

NUCLEAR ELECTRIC POWER GENERATION
Research laboratories annual report 1992
[DE94-608124] p 3555 N94-30168

NUCLEAR ELECTRIC PROPULSION
Nuclear electric propulsion: A better, safer, cheaper transportation system for human exploration of Mars
[NASA-TM-106406] p 3171 N94-28833

NUCLEAR EMULSIONS
Meso-optical Fourier transform microscope with double focusing
[DE94-607851] p 3290 N94-30148

NUCLEAR ENERGY
Cosmic energy equipment p 3229 N94-28945

NUCLEAR FUSION
Broadband EUV survey spectrometer for short-timescale experiments
[DE94-005459] p 3498 N94-28534
Project of the experiment to test the hypothesis on existence of white and black p(mu)-atoms
[DE94-606751] p 3485 N94-28625
Transient internal probe
[AD-A275054] p 3505 N94-29134
Comparison of 14 MeV isomer production of Hf-178m1 and Hf-179m2 using Feshbach-Kerman-Koonin and exciton preequilibrium models
[DE94-002640] p 3488 N94-30039
Overview of the US stellarator reactor study
[DE94-006042] p 3508 N94-30339

NUCLEAR INTERACTIONS
Experimental setup for study of hadron and hard photon production in nucleus-nucleus collisions
[DE94-607849] p 3489 N94-30051
Experimental setups and methods to obtain new nuclear data at intermediate and high energies
[DE94-607850] p 3489 N94-30052
Theory of ultra dense matter and the dynamics of high energy interactions involving nuclei
[DE94-004178] p 3491 N94-30686

NUCLEAR MAGNETIC RESONANCE
Fundamental studies of hydrogen interaction with supported meta and bimetallic catalysts
[DE94-004887] p 3202 N94-28562
Structural changes during carbonization and oxidation of coal p 3187 N94-28678
Nuclear magnetic relaxation studies of semiconductor nanocrystals and solids
[DE94-006301] p 3520 N94-30842

NUCLEAR MODELS
Nucleon and nuclei at finite temperature, as a phenomenological test of the entropy bound
[DE94-608094] p 3489 N94-30097

NUCLEAR PHYSICS
Research laboratories annual report 1992
[DE94-608124] p 3555 N94-30168
Overlap of metal clusters and nuclear structure physics
[DE94-608387] p 3517 N94-30183
Theoretical studies in hadronic and nuclear physics
[DE94-003524] p 3492 N94-30838

NUCLEAR POWER PLANTS
Issues arising with the application of optical fiber transmission in class 1E systems in nuclear power plants
[DE94-004743] p 3500 N94-29928
Risk measures in living probabilistic safety assessment
[VTT-PUBS-146] p 3465 N94-30154
Diode-pumped solid-state-laser drivers and the competitiveness of inertial fusion energy
[DE94-006654] p 3296 N94-30830

NUCLEAR PROPULSION
Small low mass advanced PBR's for propulsion
[DE94-005142] p 3497 N94-30588

NUCLEAR PUMPING
Reactor-pumped laser experimental results
[DE94-005247] p 3292 N94-28482
Reactor-pumped laser facility at DOE's Nevada Test Site
[DE94-006371] p 3295 N94-30265
Remote pumping of solid state lasers with nuclear driven fluorescers
[DE94-004846] p 3296 N94-30614

NUCLEAR RADIATION
Infrared properties of obscuring dust tori in active galactic nuclei p 3545 N94-29832

NUCLEAR REACTIONS
Comparison of 14 MeV isomer production of Hf-178m1 and Hf-179m2 using Feshbach-Kerman-Koonin and exciton preequilibrium models
[DE94-002640] p 3488 N94-30039
Intercomparison of theoretical calculations of important activation cross sections for fusion reactor technology
[DE94-002642] p 3497 N94-30825
Deexcitation processes in nuclear reactions: The study of hot hadronic matter
[DE94-003396] p 3492 N94-30836
Neutronics of a D-Li neutron source: An overview
[DE94-005372] p 3493 N94-30893

NUCLEAR REACTOR CONTROL
SP-100 control drive assembly development p 3163 N94-29651

NUCLEAR REACTORS
Single specimen fracture toughness determination procedure using instrumented impact test
[PB94-132040] p 3316 N94-28402
Teleoperated systems for nuclear reactors: Inspection and maintenance
[AIAA PAPER 94-1176-CP] p 3439 N94-30528
Small low mass advanced PBR's for propulsion
[DE94-005142] p 3497 N94-30588

NUCLEAR STRUCTURE
Overlap of metal clusters and nuclear structure physics
[DE94-608387] p 3517 N94-30183

NUCLEATION
A photoemission electron microscope investigation of chemical vapor deposition diamond films and diamond nucleation p 3215 N94-29745
Study of nucleation and growth in Al-Zn alloys using TEM
[DE94-006312] p 3211 N94-30852
RHEED studies of the nucleation, growth, and mobility of Ag atoms on the Si(111)7 x 7 surface
[DE94-005551] p 3521 N94-30899

NUCLEI (NUCLEAR PHYSICS)
Nucleon and nuclei at finite temperature, as a phenomenological test of the entropy bound
[DE94-608094] p 3489 N94-30097

NUCLEONS
Improved QCD sum rule estimates of the higher twist contributions to polarised and unpolarised nucleon structure functions
[PB94-138112] p 3487 N94-29161
Nucleon and nuclei at finite temperature, as a phenomenological test of the entropy bound
[DE94-608094] p 3489 N94-30097
Theoretical studies in hadronic and nuclear physics
[DE94-003524] p 3492 N94-30838

NUCLIDES
Production rates of terrestrial in-situ-produced cosmogenic nuclides
[DE94-005156] p 3543 N94-28545

NUMERICAL ANALYSIS
Frequency-domain analysis of nonlinear microwave circuits
[PB94-132024] p 3261 N94-28400

Applied analysis/computational mathematics
[DE94-005133] p 3451 N94-28571
On the linear stability of Verkley's modons
p 3324 N94-28695
Numerical analysis and computation of nonlinear partial differential equations from applied mathematics
[AD-A275582] p 3451 N94-28723
Computational methods in continuum mechanics
[AD-A275560] p 3451 N94-28792
A numerical solver for initial and boundary value problems in differential-algebraic systems
[AD-A275447] p 3452 N94-28883
Numerical analysis of airfoil for helicopter blade at high angle of attack using Navier-Stokes code
p 3124 N94-28958
Modeling the total dose radiation effects of Hg(1-x)Cd(x)Te photodiodes using numerical device simulators
[AD-A275235] p 3263 N94-29028
Scale-length dependence of the ratio between the magnetic and electric field perturbations in the ionospheric field-aligned current region p 3360 N94-29243
An improvement of the slender body theory for oscillating ships with finite forward speed p 3234 N94-29705
Investigations of dispersion characteristics of microwave/optical guided wave structures by using transmission line matrix method
[ISBN-0-315-85856-7] p 3254 N94-30034

NUMERICAL CONTROL
Digital tracking and control of retinal images
[AD-A275469] p 3389 N94-28810
Intelligent automated process planning and code generation for computer-controlled inspection
[AD-A275346] p 3409 N94-28920
Reactive system software concept with automation using the LDS language p 3414 N94-29327
Communications technology for unattended sensors
[DE94-005685] p 3254 N94-30043
Application of fuzzy logic to the control of wind tunnel settling chamber temperature
[NASA-TM-109105] p 3157 N94-30200
Generation of gear tooth surfaces by application of CNC machines
[NASA-CR-195306] p 3303 N94-30205
Maestro: An open system architecture for multi-robot control p 3306 N94-30288
An inverse kinematics algorithm for the DREP/Philips real-time radiographic manipulator system
p 3307 N94-30292
Simulation of lightweight robots and their controllers
p 3307 N94-30294
Elements of supervisory control for military robotic applications p 3309 N94-30303
Supervised autonomous control for Space Station Special Purpose Dextrous Manipulator (SPDM) robot
p 3309 N94-30305
A testbed for the development of ground-based control of space-based manipulators p 3309 N94-30306
Achieving robot autonomy p 3310 N94-30307
Improving the execution speed of robot control computations: An allocation scheme for heterogeneous multiprocessors p 3310 N94-30308
Programmable Automated Welding System (PAWS): Control of welding through software and hardware
p 3314 N94-30443
Confessions of a robot lobotomist
[AIAA PAPER 94-1185-CP] p 3440 N94-30535
Controlling multiple security robots in a warehouse environment
[AIAA PAPER 94-1300-CP] p 3441 N94-30540
Object-based task-level control: A hierarchical control architecture for remote operation of space robots
[AIAA PAPER 94-1209-CP] p 3444 N94-30560

NUMERICAL FLOW VISUALIZATION
Analytic rendering of curvilinear volume data
[DE94-004934] p 3407 N94-28506

NUMERICAL STABILITY
Concurrent simulation and constraint stabilization for flexible multibody systems p 3154 N94-29532
Aspects of the modeling and numerical simulation of leading-edge vortex flow
[AD-B179108] p 3133 N94-30492
Numerical precision and roundoff considerations concerning computer code migration
[DE94-005421] p 3427 N94-30590

NUMERICAL WEATHER FORECASTING
A global forecast model comparison study - year 1
[AD-A275674] p 3369 N94-28663
Error growth in poor ECMWF forecasts over the contiguous United States
[AD-A275297] p 3369 N94-29183
Prototype terminal aerodrome forecasts using a mesoscale model
[AD-A275308] p 3369 N94-29194
Evaluation of the National Meteorological Center mesoscale model for prediction of severe convection over Central Arizona p 3371 N94-29744
Physical processes associated with variability in successive operational model forecasts of cyclogenesis
[ISBN-0-315-74753-6] p 3371 N94-29751
An observational and numerical study of sea/land-breeze circulations in an area of complex coastal heating p 3372 N94-29813
The incorporation and initialization of cloud water/ice in an operational forecast model p 3373 N94-29814

NUSSELT NUMBER
Local heat transfer in an enclosed corotating disk with axial throughflow p 3276 N94-29849

NUTRITION
Nutrition and hydration status of aircrew members consuming an improved survival ration during a simulated survival scenario p 3380 N94-28429

NUTRITIONAL REQUIREMENTS
Nutrition and hydration status of aircrew members consuming an improved survival ration during a simulated survival scenario p 3380 N94-28429

NUTS (FASTENERS)
Bolt and nut evaluator
[NASA-CASE-GSC-13468-1] p 3288 N94-29538

NYLON (TRADEMARK)
Analysis of selected materials flown on interior locations of the Long Duration Exposure Facility
[NASA-CR-4586] p 3175 N94-29458

NYSTAGMUS
Disturbance of equilibrium on JAL flight crew
p 3390 N94-28856

O

OBJECT PROGRAMS
Maestro: An open system architecture for multi-robot control p 3306 N94-30288
The Vanilla meta-interpreter for definite logic programs and ambivalent syntax
[CT-93-01] p 3424 N94-30386

OBJECT-ORIENTED PROGRAMMING
Object-based design of embedded software
[PB94-132073] p 3407 N94-28403
Object-oriented CAD tool implementations for the construction industry
[PB94-132370] p 3407 N94-28411
A concurrent, object-based implementation for the tactical level of the rational behavior model
[AD-A275024] p 3410 N94-29115
The covering property of the object-oriented data model: Design and implementation issues
[AD-A275048] p 3530 N94-29165
Basic research in computer science
[AD-A275184] p 3405 N94-29181
Aerospace Software Engineering for Advanced Systems Architectures
[AGARD-CP-545] p 3412 N94-29315
Object versus functional oriented design
p 3413 N94-29321
Hierarchical Object Oriented Design (HOOD): Possibilities, limitations, and challenges
p 3413 N94-29322
Object oriented design of the autonomous fixtaking management system p 3143 N94-29323
A distributed object-based environment in Ada
p 3417 N94-29347
Constrained objects
[AD-A275273] p 3418 N94-29434
The effects of inheritance on the properties of physical storage models in object-oriented databases
p 3531 N94-29537
Object-oriented database support for scientific data management: A system for experimentation
p 3531 N94-29677
Maestro: An open system architecture for multi-robot control p 3306 N94-30288
DTL: A deductive and typed object-oriented language
[MEMO-INF-93-41] p 3425 N94-30417
Mapping objects to files: A UNIX file system interface to an object management system
[RUU-CS-93-08] p 3428 N94-30746

OBLATE SPHEROIDS
Orbital applications of electrodynamic propulsion
[AD-A275413] p 3173 N94-29216

OBLIQUE SHOCK WAVES
Experimental investigation of three-dimensional vortex-airfoil interaction in a supersonic stream
[AD-A275107] p 3122 N94-28899

OBSERVATORIES
Site comparison for optical visibility statistics in southern California p 3247 N94-29617

OBSTACLE AVOIDANCE
Collision avoidance and control of multiple revolute manipulators p 3302 N94-29884
Extended occupancy grid method for modelling unknown dynamic environments p 3144 N94-30281
Navigation of military and space unmanned ground vehicles in unstructured terrains p 3144 N94-30282
An optimal obstacle avoidance path planning algorithm for the Excalibur robot p 3306 N94-30287
Sonar sensing and obstable detection
p 3309 N94-30301
Obstacle detection for an autonomous vehicle
p 3309 N94-30302
Motion control of mobile robots p 3310 N94-30309
A probabilistic approach to motion planning for car-like robots
[RUU-CS-93-18] p 3438 N94-30410
A robotic wheelchair
[AIAA PAPER 94-1229-CP] p 3447 N94-30578
Piecewise linear paths among convex obstacles
[RUU-CS-93-20] p 3460 N94-30721
Iterative removal of boundary minima of harmonic potential function for mobile robot navigation
[REPT-93-059] p 3449 N94-30962

OCEAN BOTTOM
Updated deep-tow acoustics/geophysics system compressional velocity database
[AD-A275477] p 3355 N94-28685
Seafloor characterization using texture
[AD-A275399] p 3377 N94-29204
Considerations in the modelling of seafloor acoustic backscatter
[AD-A275404] p 3478 N94-29206

OCEAN CURRENTS
Global atmospheric and ocean modeling on the connection machine
[DE94-003930] p 3342 N94-28521
The velocity field in the Northeast Atlantic from satellite-tracked drifting buoys
[AD-A275704] p 3376 N94-28690
Papers in meteorology and geophysics, vol. 44, no.1
[JTN-94-80585] p 3324 N94-28693
The Japan Sea proper water and water circulation in the Japan Sea p 3324 N94-28694
Development and application of a thermistor current meter
[AD-A275816] p 3286 N94-28831
A model analysis of potential vorticity on isopycnal surfaces for the global ocean
[AD-A275047] p 3377 N94-29164
SAR-related stress variability in the Marine Atmospheric Boundary Layer (MABL)
[AD-A275275] p 3377 N94-29436
Modeling deep equatorial circulation
p 3378 N94-29815
Atmosphere, ocean, and land: Critical gaps in Earth system models p 3350 N94-30617
Cryosphere and climate p 3352 N94-30632
Methods of testing parameterizations: Vertical ocean mixing p 3352 N94-30633
Altimeter data processing from sea surface topography to horizontal eddy momentum fluxes
[PB94-147550] p 3378 N94-30714

OCEAN DATA ACQUISITIONS SYSTEMS
Global Acoustic Mapping of Ocean Temperatures (GAMOT)
[AD-A275777] p 3376 N94-28740

OCEAN DYNAMICS
A model analysis of potential vorticity on isopycnal surfaces for the global ocean
[AD-A275047] p 3377 N94-29164
The dynamics of tropical intraseasonal variability
p 3371 N94-29741
Modeling deep equatorial circulation
p 3378 N94-29815
Modeling the Earth System, volume 3
[NASA-CR-194256] p 3350 N94-30616
Towards coupled physical-biogeochemical models of the ocean carbon cycle p 3350 N94-30618
Dynamic constraints on CO2 uptake by an iron-fertilized Antarctic p 3350 N94-30619
The role of sea ice dynamics in global climate change
p 3350 N94-30620
On the nonlinear dynamics of ocean wave systems
p 3378 N94-30790

OCEAN MODELS
Global atmospheric and ocean modeling on the connection machine
[DE94-003930] p 3342 N94-28521
Global Acoustic Mapping of Ocean Temperatures (GAMOT)
[AD-A275777] p 3376 N94-28740
A model analysis of potential vorticity on isopycnal surfaces for the global ocean
[AD-A275047] p 3377 N94-29164
The dynamics of tropical intraseasonal variability
p 3371 N94-29741
On the annual cycle of the tropical Pacific atmosphere and ocean p 3371 N94-29763

Modeling deep equatorial circulation p 3378 N94-29815
Splines and ocean wave modelling [PB94-139409] p 3378 N94-30002
Modeling the Earth System, volume 3 [NASA-CR-194256] p 3350 N94-30616
Atmosphere, ocean, and land: Critical gaps in Earth system models p 3350 N94-30617
Towards coupled physical-biogeochemical models of the ocean carbon cycle p 3350 N94-30618
Dynamic constraints on CO2 uptake by an iron-fertilized Antarctic p 3350 N94-30619
The role of sea ice dynamics in global climate change p 3350 N94-30620
Four simple ocean carbon models p 3351 N94-30625
Methods of testing parameterizations: Vertical ocean mixing p 3352 N94-30633
Comprehensive system models: Strategies for evaluation p 3353 N94-30638

OCEAN SURFACE
Sea ice and oceans applications of SAR p 3327 N94-28934
Tohoku district observed by artificial satellites p 3328 N94-29041
A model analysis of potential vorticity on isopycnal surfaces for the global ocean [AD-A275047] p 3377 N94-29164
SAR-related stress variability in the Marine Atmospheric Boundary Layer (MABL) [AD-A275275] p 3377 N94-29436
Radar returns from a low-flying target over a rough sea surface under multipath and clutter conditions p 3253 N94-29882
Splines and ocean wave modelling [PB94-139409] p 3378 N94-30002
The influence of the evaporation duct on the angle of arrival and amplitude of the backscattered signal from targets low above the sea p 3256 N94-30498
Altimeter data processing from sea surface topography to horizontal eddy momentum fluxes [PB94-147550] p 3378 N94-30714
The validation of ocean surface heat fluxes in AMIP [DE94-001539] p 3378 N94-30823

OCEAN TEMPERATURE
Global Acoustic Mapping of Ocean Temperatures (GAMOT) [AD-A275777] p 3376 N94-28740

OCEANOGRAPHIC PARAMETERS
Proceedings of the 15th Earth Observation Symposium [JTN-94-80607] p 3328 N94-29036
Oceanic survey utilizing satellites p 3328 N94-29040
The effects of altimeter sampling characteristics: Some Geosat examples [AD-A275225] p 3357 N94-29062
Tidal atlas software development [AD-A275251] p 3377 N94-29432

OCEANOGRAPHY
Global change research: Summaries of research in FY 1993 [DE94-003150] p 3341 N94-28473
Papers in meteorology and geophysics, vol. 44, no.1 [JTN-94-80585] p 3324 N94-28693
A model analysis of potential vorticity on isopycnal surfaces for the global ocean [AD-A275047] p 3377 N94-29164
Modeling the Earth System, volume 3 [NASA-CR-194256] p 3350 N94-30616
Towards coupled physical-biogeochemical models of the ocean carbon cycle p 3350 N94-30618

OCEANS
Quadruplet expansion of the acoustic pressure field in a wedge shaped ocean [AD-A275121] p 3477 N94-29003
Atmosphere, ocean, and land: Critical gaps in Earth system models p 3350 N94-30617
The carbon cycle revisited p 3350 N94-30622
Ocean-atmospheric linkages p 3350 N94-30623
Four simple ocean carbon models p 3351 N94-30625

OCULOMOTOR NERVES
Japanese Journal of Aerospace and Environmental Medicine, volume 30, no. 1 [JTN-94-80598] p 3389 N94-28850
Basic understanding of vertigo p 3390 N94-28855
Equilibrium dysfunction in the clinical field p 3390 N94-28858

ODORS
Flammability, odor, offgassing, thermal vacuum stability, and compatibility with aerospace fluids of wire insulations p 3166 N94-28709

OFFGASSING
Flammability, odor, offgassing, thermal vacuum stability, and compatibility with aerospace fluids of wire insulations p 3166 N94-28709

OIL EXPLORATION
Application of remote sensing techniques in petroleum exploration: The Indonesian experience p 3331 N94-29225

OILS
Biodiesel from aquatic species [DE94-000275] p 3225 N94-30038

OKAZAKI-LEVY-RUDENKO COMET
Infrared observations of cometary dust by COBE p 3541 N94-29994

OLIGOMERS
Synthesis and characterization of novel ternary and quaternary reduced molybdenum oxides [DE94-005563] p 3510 N94-28529
Solventless, curable fluid oligomeric systems for high performance microwave, acoustical and mechanical applications p 3223 N94-30478

ON-LINE SYSTEMS
Defense Technical Information Center cataloging guidelines [AD-A275100] p 3529 N94-28911
Decision Making Aids (DMA) in on-line ATC systems p 3139 N94-29570
AFGWC Dial-In Subsystem (AFDIS) software users manual, version 2.2 [AD-A275844] p 3371 N94-29747
Pausing behavior of end-users in online searching p 3533 N94-29960

ONBOARD DATA PROCESSING
Software engineering methods in the Hermes on-board software p 3414 N94-29326
GPS/GNSS for ATM p 3138 N94-29565
Unmanned vehicle mobility: Limits of autonomous navigation p 3310 N94-30311

ONE DIMENSIONAL FLOW
Eigenvalue analysis of the convergence behaviour of an Euler method [PB94-1255722-U] p 3281 N94-30743

OPEN CLUSTERS
A near-infrared survey of the star forming region NGC 2264 p 3540 N94-29971

OPERATING COSTS
Aircraft age impacts on maintenance requirements [AD-A275701] p 3121 N94-28666
Aircraft age impact on individual operating and support cost elements [AD-A275739] p 3121 N94-28732
The 1993 Federal Aviation Administration Aviation System Capital Investment Plan p 3136 N94-29445
Ventilation cost and air cleaning p 3232 N94-29605

OPERATING SYSTEMS (COMPUTERS)
Object-based design of embedded software [PB94-132073] p 3407 N94-28403
Reference model for project support environments, version 2.0 [AD-A275191] p 3410 N94-29068
Design of a thinwire real-time multiprocessor operating system p 3415 N94-29333

OPERATING TEMPERATURE
The influence of temperature on microelectronic device failure mechanisms, phase 2 [AD-A275029] p 3265 N94-29511

OPERATIONAL AMPLIFIERS
Digitally programmable composite operational amplifier applications [AD-A275081] p 3262 N94-28842
A magnetically coupled quench detector for superconducting magnets [DE94-006040] p 3268 N94-30904

OPERATIONS RESEARCH
Realizing the productivity potential of expeditious operations [PB94-135555] p 3230 N94-29188
A capacity planning model for Canadian military airlift requests [ISBN-0-315-86079-0] p 3136 N94-30144

OPERATOR PERFORMANCE
Designing for performance: A cognitive systems engineering approach to modifying an AWACS human computer interface [AD-A275187] p 3399 N94-28861
Aiding the operator in the manual control of a space manipulator [PB94-125549] p 3402 N94-30390
Sampling behaviour in a four instrument monitoring task: Effects of signal bandwidth and number of events per signal [AD-B179613] p 3402 N94-30422

OPERATORS (MATHEMATICS)
Calculation of eigenvalues of Schroedinger operators for arbitrary coupling [DE94-606302] p 3522 N94-28582
A note on the Poisson brackets associated with Lax operators [MATHS-REPT-A-195] p 3464 N94-29482
Approximation methods for nonlinear operator equations of the m-accretive type [DE94-608099] p 3467 N94-30065
Graded Froelicher-Nijenhuis brackets and the theory of recursion operators for super differential equations [MEMO-1147] p 3460 N94-30736

OPHTHALMOLOGY
Digital tracking and control of retinal images [AD-A275469] p 3389 N94-28810

OPTICAL COMMUNICATION
Lasercom system architecture with reduced complexity [NASA-CASE-NPO-19069-1-CU] p 3293 N94-29493
Site comparison for optical visibility statistics in southern California p 3247 N94-29617
The Rb 780-nanometer Faraday anomalous dispersion optical filter: Theory and experiment p 3250 N94-29659
Overview of microoptics: Past, present, and future p 3235 N94-29771
Photonics at Sandia National Laboratories: From research to applications [DE94-006463] p 3501 N94-30828
Standard testing procedures for optical fiber and unshielded twisted pair at Sandia National Laboratories [DE94-005315] p 3501 N94-30910

OPTICAL COMPUTERS
Photorefractive adaptive antenna array processor [AD-A275762] p 3241 N94-28762
A/GATECH DOSP fabrication --- optical programmable logic array [AD-A275848] p 3430 N94-28781
Overview of microoptics: Past, present, and future p 3235 N94-29771

OPTICAL COUNTERMEASURES
Atmospheric Propagation Effects Through Natural and Man-Made Obscurants for Visible to MM-Wave Radiation [AGARD-CP-542] p 3256 N94-30495
Experimental evaluation of camouflage effectiveness in the thermal infrared p 3257 N94-30502
NATO SOCMET trials p 3258 N94-30503
Global approach towards the evaluation of thermal infrared countermeasures p 3258 N94-30504
The effects of man-made smokes and battlefield-induced smokes on the propagation of electromagnetic radiation p 3258 N94-30505

OPTICAL COUPLING
An investigation of distributed coupling in a nonlinear semiconductor waveguide p 3246 N94-29529

OPTICAL DATA PROCESSING
Modeling, analysis, and simulation of an optical time-division multiple-access network architecture [AD-A275847] p 3498 N94-28780
Photonic devices and systems for optical signal processing [AD-A275818] p 3498 N94-28804
Gordon research conference on optical signal processing and holography [AD-A275092] p 3499 N94-28848
Overview of microoptics: Past, present, and future p 3235 N94-29771

OPTICAL DENSITY
Temperature depencence of the far infrared optical constants of polyethylene [PB94-124336] p 3213 N94-28795

OPTICAL EQUIPMENT
Aberrated point-spread functions and beam quality for optical systems with annular pupils [AD-A275311] p 3499 N94-28875
Lasercom system architecture with reduced complexity [NASA-CASE-NPO-19069-1-CU] p 3293 N94-29493
Design and testing of the LITE Variable Field Stop mechanism p 3161 N94-29633
Optical Chopper Assembly for the Mars Observer p 3162 N94-29639
Overview of microoptics: Past, present, and future p 3235 N94-29771
Hybrid optics for space applications [ESA-CP-1158] p 3501 N94-30418
Precision and manufacturing at the Lawrence Livermore National Laboratory p 3240 N94-30449

OPTICAL FIBERS
Optical flameout detector [NASA-CASE-LAR-14997-1] p 3287 N94-29368
Assessment of the fibre volume distribution around optical fibres [FFA-TN-1993-12] p 3179 N94-29425
Intelligent material systems and structures. Part 7: Debonding and pull-out of two optical fibers from two epoxies [PB94-137767] p 3180 N94-29475

A sub-cm micromachined electron microscope
p 3236 N94-29775
Issues arising with the application of optical fiber transmission in class 1E systems in nuclear power plants
[DE94-004743] p 3500 N94-29928
Optical studies of dynamical processes in disordered systems
[DE94-006751] p 3501 N94-30252
Standard testing procedures for optical fiber and unshielded twisted pair at Sandia National Laboratories
[DE94-005315] p 3501 N94-30910

OPTICAL FILTERS
The Rb 780-nanometer Faraday anomalous dispersion optical filter: Theory and experiment
p 3250 N94-29659

OPTICAL MATERIALS
Dual-use applications of infrared sensitive materials
[AD-A275140] p 3499 N94-29694
An outdoor exposure testing program for optical materials used in solar thermal electric technologies
[DE94-000265] p 3500 N94-29799
Study of nonlinear optical polymers and their applications in optical waveguides p 3216 N94-29807
Nonlinear absorption in high reflector multilayers
[DE94-005818] p 3295 N94-30598
Characterization of defect geometries in multilayer optical coatings
[DE94-005820] p 3501 N94-30599
Remote pumping of solid state lasers with nuclear driven fluorescers
[DE94-004846] p 3296 N94-30614

OPTICAL MEASUREMENT
Optical flameout detector
[NASA-CASE-LAR-14997-1] p 3287 N94-29368
An experimental and comprehensive method to measure emission characteristics p 3257 N94-30501

OPTICAL MEASURING INSTRUMENTS
A novel spectroscopic measurement method of RF plasma for temperature and electron density diagnoses
p 3188 N94-28682
Three-axis fiber optic vector magnetometer
[AD-D016016] p 3288 N94-29699
Overview of microoptics: Past, present, and future
p 3235 N94-29771
A commercialized, continuous flow fiber optic sensor for trichloroethylene and haloforms
p 3502 N94-30462

OPTICAL MEMORY (DATA STORAGE)
Photonic devices and systems for optical signal processing
[AD-A275818] p 3498 N94-28804
Gordon research conference on optical signal processing and holography
[AD-A275092] p 3499 N94-28848

OPTICAL MICROSCOPES
Meso-optical Fourier transform microscope with double focusing
[DE94-607851] p 3290 N94-30148

OPTICAL POLARIZATION
Dust in the Small Magellanic Cloud
[NASA-CR-195764] p 3543 N94-29696

OPTICAL PROPERTIES
High damage threshold anti-reflectors by physical vapor deposited amorphous fluoropolymer
[DE94-004865] p 3212 N94-28560
Experimental and theoretical studies of molecular solids
[AD-A275511] p 3485 N94-28668
WINDOW 4.0: Documentation of calculation procedures
[DE94-004935] p 3410 N94-29019
Template synthesized nanoscopic gold particles: Optical spectra and the effects of particle size and shape
[AD-A275378] p 3197 N94-29312
Optical properties of cadmium sulfide, zinc selenide, and zinc manganese selenide semiconductor films
p 3500 N94-29759
Nanosize metal alloy particle formation in Ag and Cu sequentially implanted silica
[DE94-005592] p 3207 N94-30042
Optical studies of dynamical processes in disordered systems
[DE94-006751] p 3501 N94-30252
Hybrid optics for space applications
[ESA-CP-1158] p 3501 N94-30418
Nonlinear optics response of semiconductor quantum wells under high magnetic fields
[DE94-003244] p 3520 N94-30835

OPTICAL PUMPING
Visible vertical cavity surface emitting lasers
[AD-A275334] p 3293 N94-28919

OPTICAL RADAR
Innovative direct detection range-Doppler laser radar
[AD-A275619] p 3292 N94-28635
Laser beam steering with semiconductor waveguide
[AD-A275775] p 3292 N94-28765
Fusion of range and luminance data from laser radar systems
[AD-A275608] p 3292 N94-28770
Design and testing of the LITE Variable Field Stop mechanism p 3161 N94-29633
Automated inspection of turbine blades: Challenges and opportunities
[AIAA PAPER 94-1226-CP] p 3446 N94-30575
Cloud and aerosol characterization for the ARM central facility: Multiple remote sensor techniques development
[DE94-003523] p 3365 N94-30608
Remote sensor observations during WISP91: The use of microwave radiometers, RASS, and lidar ceilometers for detection of aircraft icing conditions
[PB94-142106] p 3136 N94-30890

OPTICAL REFLECTION
The performance of gloss meters on curving surfaces
[NPL-DMM(A)-111] p 3501 N94-30522

OPTICAL SWITCHING
Advanced optical A/D converter
[AD-A275663] p 3498 N94-28656
Photonic devices and systems for optical signal processing
[AD-A275818] p 3498 N94-28804
Photoconductive switching for high power microwave generation
[PB94-137460] p 3244 N94-29177

OPTICAL THICKNESS
The appearance of the Sun and Moon seen through clouds
[AD-A275338] p 3551 N94-29212
Global patterns of cloud optical thickness variation with temperature and the implications for climate change
p 3374 N94-29972
Optical depth effects in cluster cooling flows
p 3541 N94-30800

OPTICAL TRACKING
The 25th Annual Precise Time and Time Interval (PTTI) Applications and Planning Meeting
[NASA-CP-3267] p 3468 N94-30639

OPTICAL TRANSFER FUNCTION
Calculation of turbulence degraded point spread function of an imaging system p 3260 N94-30514

OPTICAL WAVEGUIDES
Laser beam steering with semiconductor waveguide
[AD-A275775] p 3292 N94-28765
A new guided wave lens structure and its application
[AD-A275541] p 3499 N94-28813
An investigation of distributed coupling in a nonlinear semiconductor waveguide p 3246 N94-29529
Study of nonlinear optical polymers and their applications in optical waveguides p 3216 N94-29807

OPTIMAL CONTROL
Application of digital control theory to adaptive grid generation p 3127 N94-28980
On-line search for optimal controller parameters using interconnected learning automata
[MATHS-REPT-A-196] p 3436 N94-29526
Reinforcement learning for robots using neural networks p 3437 N94-29853
Second order necessary conditions in optimal control
[ISBN-0-315-85443-X] p 3437 N94-30255
An optimal obstacle avoidance path planning algorithm for the Excalibur robot p 3306 N94-30287
Coordinated control of multiple robot manipulators
p 3306 N94-30289
Calculus of variations applied to 2D multi-point airfoil design
[PB94-125457] p 3133 N94-30401
A stochastic control approach to flight path monitoring
[AD-B174630] p 3143 N94-30853
Integrated structure/control design of nonrigid robot arms for high-speed manipulation p 3312 N94-30866
Optimal low-thrust, Earth-Moon trajectories
p 3159 N94-30961

OPTIMIZATION
Aerodynamic design using parallel processors
[AD-A275470] p 3122 N94-28674
Thermal/structural tailoring of engine blades (T/SEAEBL). Theoretical manual
[NASA-CR-194462] p 3317 N94-28815
Incorporating geometric constraints into rule-based systems using nonlinear optimization
[AD-A275093] p 3452 N94-29063
Investigation on application of genetic algorithms to optimal reactive power dispatch of power systems
[MATHS-REPT-A-197] p 3266 N94-29527
Yield and variability optimization of integrated circuits: Principles and practical solutions p 3266 N94-29805
Complicated problem solution techniques in optimal parameter searching
[DE94-608007] p 3421 N94-30077
A note on the complexity of local search problems
[CT-93-02] p 3456 N94-30370
Hybrid optics for space applications
[ESA-CP-1158] p 3501 N94-30418
Optimization techniques for a dial-a-ride transportation system in urban environment
[REPT-93-051] p 3537 N94-30926

OPTOELECTRONIC DEVICES
Innovative optoelectronic materials and structures using OMVPE
[AD-A275811] p 3511 N94-28773
Optoelectronic integrated circuits fabricated using atomic layer epitaxy
[AD-A275454] p 3262 N94-28805
Gordon research conference on optical signal processing and holography
[AD-A275092] p 3499 N94-28848
Carrier collection and scattering in quantum well and superlattice devices
[AD-A275443] p 3512 N94-28880
An investigation of distributed coupling in a nonlinear semiconductor waveguide p 3246 N94-29529
Overview of microoptics: Past, present, and future
p 3235 N94-29771
Micro guidance and control technology overview
p 3144 N94-29772
Micro-opto-mechanical devices and systems using epitaxial lift off p 3239 N94-29793
Synchronization of microwave oscillators by direct optical injection
[ISBN-0-315-85546-0] p 3500 N94-30233
Optoelectronic packaging activities at Sandia National Laboratories
[DE94-005287] p 3501 N94-30261

ORBIT CALCULATION
Enhanced orbit determination filter sensitivity analysis: Error budget development p 3159 N94-29655
Enhanced orbit determination filter: Inclusion of ground system errors as filter parameters p 3159 N94-29656
TOPEX/POSEIDON operational orbit determination results using global positioning satellites
p 3160 N94-29666
Application of extended Lagrange series to the precise determination of Global Positioning Satellite orbits
[ISBN-0-315-85724-2] p 3159 N94-30237
Time transfer using geostationary satellites: Implementation of a Kalman filter p 3471 N94-30657

ORBIT TRANSFER VEHICLES
A transportronic solution to the problem of interorbital transportation
[NASA-CR-191152] p 3164 N94-29355

ORBITAL ASSEMBLY
Free-floating dual-arm robots for space assembly
[AIAA PAPER 94-1195-CP] p 3442 N94-30546

ORBITAL ELEMENTS
Time transfer using geostationary satellites: Implementation of a Kalman filter p 3471 N94-30657

ORBITAL MANEUVERS
Orbital applications of electrodynamic propulsion
[AD-A275413] p 3173 N94-29216

ORBITAL MECHANICS
Symplectic topology of integrable Hamiltonian systems
[DE94-608120] p 3467 N94-30166

ORBITAL POSITION ESTIMATION
TOPEX/POSEIDON operational orbit determination results using global positioning satellites
p 3160 N94-29666
Time transfer using geostationary satellites: Implementation of a Kalman filter p 3471 N94-30657

ORBITAL RENDEZVOUS
Orbital applications of electrodynamic propulsion
[AD-A275413] p 3173 N94-29216

ORBITAL RESONANCES (CELESTIAL MECHANICS)
Binary-single star scattering: An investigation of a realistic chaotic scattering system p 3543 N94-29719

ORBITAL SERVICING
System for the installation and replacement of components in hostile environments
[NASA-CASE-LEW-14906-1-SB] p 3300 N94-29427
Development and testing of the Automated Fluid Interface System p 3161 N94-29636
Technology transfer and evaluation for Space Station telerobotics
[AIAA PAPER 94-1190-CP] p 3441 N94-30541
Space flight manipulator technologies and requirements for the NASA Flight Telerobotic Servicer (FTS)
[AIAA PAPER 94-1191-CP] p 3441 N94-30542
A Space Station robot walker and its shared control software
[AIAA PAPER 94-1192-CP] p 3442 N94-30543
Technology for robotic surface inspection in space
[AIAA PAPER 94-1193-CP] p 3442 N94-30544
On-orbit spacecraft servicing: An element in the evolution of space robotics applications
[AIAA PAPER 94-1236-CP] p 3448 N94-30583

ORBITS
A semiclassical study of quantum maps
p 3524 N94-29987

Periodic orbits of n-body type problems: The fixed period case
[DE94-608096] p 3453 N94-30091

ORDER-DISORDER TRANSFORMATIONS
First principles pseudopotential calculations on aluminum and aluminum alloys
[DE94-004890] p 3206 N94-29931
Structural analysis of amorphous phosphates using high performance liquid chromatography
[DE94-004791] p 3199 N94-30723

ORGANIC COMPOUNDS
Surface structure and stereochemical properties of self-assembled monolayer materials
[DE94-004960] p 3484 N94-28578
Advanced fuel properties: A computer program for estimating property values
[AD-A275248] p 3224 N94-28901
Novel mass spectrometric instrument for gaseous and particulate characterization and monitoring
[DE94-005896] p 3349 N94-30047

ORGANIC MATERIALS
Organic materials that respond to molecules
[AD-A275392] p 3174 N94-29307

ORGANIC SULFUR COMPOUNDS
Nuclear magnetic relaxation studies of semiconductor nanocrystals and solids
[DE94-006301] p 3520 N94-30842

ORGANIZATIONS
Measuring the impact of investments in information technologies on business performance
[REPT-93-056] p 3536 N94-30929

ORGANOMETALLIC COMPOUNDS
Alkylene-bridged polygerm- and polygermsilsesqui-oxanes: New hybrid organic-inorganic materials
[DE94-005096] p 3174 N94-28557
Gas phase thermochemistry of organogermanium compounds
[DE94-004885] p 3187 N94-28561
Innovative optoelectronic materials and structures using OMVPE
[AD-A275811] p 3511 N94-28773
Polymer technology publication series no. 16
[PB94-135522] p 3214 N94-29157
The organometallic chemical vapor deposition of transition metal carbides: The use of homoleptic alkyls
[DE94-005577] p 3206 N94-30007
Plasma enhanced chemical vapor deposition of ZrO2 thin films
[DE94-006031] p 3218 N94-30104
Group transfer and electron transfer reactions of organometallic complexes: Summary of research accomplished in 1993
[DE94-004963] p 3200 N94-30770

ORIFICE FLOW
Transonic expanding flow through axially symmetric orifices p 3128 N94-28985

ORTHOGONAL FUNCTIONS
Statistical analysis of a satellite imagery time series: Implications for the study of coastal and estuarine circulation p 3335 N94-30919
The Stroemberg wavelet on the interval and the Franklin system
[TELECOM-93-C-002] p 3462 N94-30971

ORTHOGONALITY
Event structures and orthogonal term graph rewriting
[CWI-CS-R9347] p 3459 N94-30412
Perpetual reductions in orthogonal combinatory reduction systems
[CWI-CS-R9349] p 3459 N94-30413
Perpetual reductions and strong normalization in orthogonal term rewriting systems
[CWI-CS-R9345] p 3426 N94-30437
A new orthogonal decomposition method for turbulent flows p 3281 N94-30494

ORTHONORMAL FUNCTIONS
The Stroemberg wavelet on the interval and the Franklin system
[TELECOM-93-C-002] p 3462 N94-30971

ORTHOTROPISM
Experimental determination of orthotropic elastic constants
[FFA-TN-1991-35] p 3215 N94-29424
Approximate estimation of the effects of asymmetry on the testing of tensile specimens
[NPL-DMM(A)-117] p 3322 N94-30523

OSCILLATION DAMPERS
Tuned mass damper for integrally bladed turbine rotor
[NASA-CASE-MFS-28697-1] p 3298 N94-29353

OSCILLATIONS
An improvement of the slender body theory for oscillating ships with finite forward speed p 3234 N94-29705

OSCILLATORS
Research on elementary particle physics. Task P: Studies in theory and phenomenology of elementary physics
[DE94-004955] p 3483 N94-28566
Time and frequency technology at NIST p 3468 N94-30641
Accuracy metrics for judging time scale algorithms p 3471 N94-30656
Noise and drift analysis of non-equally spaced timing data p 3472 N94-30667
Frequency standards from industry over the next 25 years p 3475 N94-30683

OUTCROPS
Field guide to Cretaceous-tertiary boundary sections in northeastern Mexico
[NASA-CR-195719] p 3354 N94-28416

OUTGASSING
ESTEC wiring test programme materials related properties p 3165 N94-28698

OVERPRESSURE
Blast overpressure studies with animals and man
[AD-A275038] p 3391 N94-29150

OXIDATION
Structural changes during carbonization and oxidation of coal p 3187 N94-28678
Polymer technology publication series no. 16
[PB94-135522] p 3214 N94-29157
Simulation of pollutant formation in turbulent combustors using an extended coherent flame model p 3190 N94-29251
Charge trapping and breakdown in N2O oxides
[DE94-003775] p 3266 N94-30040
Studies of supported molybdenum and tungsten
[DE94-006207] p 3210 N94-30839
Transient studies of low temperature catalysts for methane conversion
[DE94-005767] p 3200 N94-30877

OXIDATION RESISTANCE
Selection of the Space Station Freedom (SSF) Flat Collector Circuit (FCC) insulation material p 3165 N94-28701
Evaluation of oxide-coated iridium-rhenium chambers
[NASA-TM-106442] p 3172 N94-29097
Polyimides containing pendent siloxane groups
[NASA-CASE-LAR-14638-1] p 3215 N94-29555
Development of radiation resistant electrical cable insulations p 3223 N94-30480
Four advances in carbon-carbon materials technology p 3186 N94-30481

OXIDATION-REDUCTION REACTIONS
Quenching of the excited state of hydrated Europium(3) ions by electron transfer
[DE94-005553] p 3482 N94-28518
Realtime structural electrochemistry of platinum clusters using dispersive XAFS
[DE94-005093] p 3208 N94-30101

OXIDE FILMS
Pull-test adhesion measurements of diamondlike carbon films on silicon carbide, silicon nitride, aluminum oxide, and zirconium oxide
[DE94-005469] p 3211 N94-28536
Low Earth orbit durability evaluation of protected silicone for advanced refractive photovoltaic concentrator arrays
[NASA-TM-106543] p 3172 N94-28999
Pitting corrosion of titanium
[AD-A274980] p 3203 N94-29089
Distribution functions of electrons within aluminium oxide thin films
[DE94-608418] p 3490 N94-30184
Ionic conduction mechanisms in CaF2 and CaF2-Al2O3 nanocomposite films on Al2O3 substrates
[DE94-004792] p 3520 N94-30773

OXIDES
The radical amplifier p 3345 N94-28604
Effects of oxide charge and surface recombination velocity on the excess base current of BJT's
[DE94-003711] p 3263 N94-29025
Dislocation loops in spinel crystals irradiated successively with deep and shallow ion implants
[DE94-005083] p 3517 N94-30201
Remote pumping of solid state lasers with nuclear driven fluorescers
[DE94-004846] p 3296 N94-30614

OXYGEN
Peroxy radical measurements with NCAR's chemical amplifier p 3345 N94-28603
Japanese Journal of Aerospace and Environmental Medicine, volume 30, no. 1
[JTN-94-80598] p 3389 N94-28850
Arterial oxygen saturation during +Gz acceleration by short-radius centrifuge p 3389 N94-28852
Methane challenge of high performance molecular sieve oxygen concentrator
[AD-A275155] p 3337 N94-29033
High resistivity buffer layers by oxygen doping
[AD-A274986] p 3513 N94-29125
Fullerenes as precursors for diamond film growth without hydrogen or oxygen additions
[DE94-004582] p 3519 N94-30718

OXYGEN ATOMS
Low Earth orbit durability evaluation of protected silicone for advanced refractive photovoltaic concentrator arrays
[NASA-TM-106543] p 3172 N94-28999

OXYGEN BREATHING
Decompression sickness risk versus time and altitude
[AD-A275261] p 3391 N94-29071

OXYGEN IONS
Low energy ion-molecule reactions and chemiionization kinetics
[DE94-005414] p 3481 N94-28491

OXYGEN MASKS
Portable ventilatory resuscitation systems
[AD-A274984] p 3401 N94-29093

OXYGEN PRODUCTION
The 1992-1993 advanced design program. Part 1: The Mars methane engine project. Part 2: The Mars oxygen processor new furnace
[NASA-CR-195513] p 3299 N94-29409

OXYGENATION
Fatigue of carbon and low-alloy steels in LWR environments
[DE94-005116] p 3207 N94-30021

OXYNITRIDES
The synthesis and structural characterization of Na3WO3N
[AD-A275243] p 3204 N94-29395

OZONE
Ozone production at a rural site in Georgia during the summer 1992 SOS campaign
[DE94-003989] p 3342 N94-28523
Harvard ER-2 OH laser-induced fluorescence instrument p 3343 N94-28592
Peroxy radical measurements with NCAR's chemical amplifier p 3345 N94-28603
Surface energy changes produced by ultraviolet-ozone irradiation of poly(methylmethacrylate), polycarbone and polytetrafluoroethylene
[NASA-TM-106460] p 3213 N94-28922
System requirements review for the High-Resolution Ozone Imager (HIROIG)
[AD-A275151] p 3347 N94-29023
Activities of the wintering party at Showa Station by the 31st Japanese Antarctic Research Expedition in 1990 p 3358 N94-29083
GOME: Global Ozone Monitoring Experiment
[ESA-SP-1151] p 3347 N94-29452
Laboratory studies of chemical and photochemical processes relevant to stratospheric ozone
[NASA-CR-195779] p 3347 N94-29549
The suitability of low-cost urban airshed modeling in the Chicago area
[DE94-005114] p 3349 N94-30023
Regenerating using aqueous cleaners with ozone and electrolysis p 3240 N94-30468
Radiative flux calculations at UV and visible wavelengths
[DE94-004278] p 3350 N94-30613
Tropospheric radiative forcing of O3 for the 1994 IPCC report
[DE94-005698] p 3367 N94-30876

OZONE DEPLETION
System requirements review for the High-Resolution Ozone Imager (HIROIG)
[AD-A275151] p 3347 N94-29023

OZONOMETRY
Activities of the wintering party at Showa Station by the 31st Japanese Antarctic Research Expedition in 1990 p 3358 N94-29083

OZONOSPHERE
System requirements review for the High-Resolution Ozone Imager (HIROIG)
[AD-A275151] p 3347 N94-29023
Radiative flux calculations at UV and visible wavelengths
[DE94-004278] p 3350 N94-30613

P

P WAVES
Initial wave-type identification with neural networks and its contribution to automated processing in IMS version 3.0
[AD-A275058] p 3359 N94-29137

P-N JUNCTIONS
Analysis of microwave induced interference in pn-diodes
[PB94-136983] p 3243 N94-28906

The influence of an in-situ electric field on H(+) and He(+) implantation induced defects insil icon
[DE94-006553] p 3518 N94-30249

PACIFIC OCEAN
Global Acoustic Mapping of Ocean Temperatures (GAMOT)
[AD-A275777] p 3376 N94-28740
On the annual cycle of the tropical Pacific atmosphere and ocean p 3371 N94-29763
On interannual variability and climate change in the North Pacific p 3374 N94-29963
Satellite estimation of the global distribution and interannual variability of photosynthetically active radiation p 3334 N94-29970

PACKAGING
Codes on the unit sphere
[PB94-136991] p 3453 N94-29174

PACKET TRANSMISSION
Video transmission on ATM networks
[NASA-CR-195124] p 3244 N94-29106

PAINTS
Rules and definition of the range of paints applied on aeronautical structrural composites
[REPT-932-600-106] p 3215 N94-29459
Effects of make-up on the heat transfer from the head in hyperthermic conditions p 3394 N94-29864
The effect of mechanical paint stripping on the fatigue and fracture of thin aluminum airplane skin p 3205 N94-29900
Evaluation of corrosion protecting properties of modern aircraft paint systems
[AD-B179388] p 3220 N94-30420
Development of a unique polyurethane primer/topcoat p 3223 N94-30476

PAIR PRODUCTION
Emission of supersymmetric neutron pair by charged lepton in magnetic field
[DE93-634365] p 3481 N94-28468

PALEOCLIMATOLOGY
Impact of biomass burning on the atmosphere
[DE94-004333] p 3349 N94-29954
Modeling Earth system changes of the past p 3353 N94-30635

PALEOMAGNETISM
Motion and development of the Pacific Plate from the Middle Jurassic to the Late Cretaceous p 3362 N94-29939

PALLADIUM
Geometric structures of thin film: Pt on Pd(110) and NiO on Ni(100)
[DE94-005564] p 3211 N94-28530

PANEL METHOD (FLUID DYNAMICS)
Aircraft aerodynamics with deflected jets in ground effect p 3132 N94-29973
Computation of wind tunnel wall effects for complex models using a low-order panel method
[NASA-TM-104019] p 3132 N94-30151
Aerodynamic analysis of slipstream/wing/nacelle interference for preliminary design of aircraft configurations
[AD-B173651] p 3135 N94-30916

PANELS
Development of Alternating Current Potential Drop (ACPD) procedures for crack detection in aluminum aircraft panels
[AD-A275755] p 3315 N94-28646
Composite panel failure analysis and improvement plan
[AD-A275655] p 3176 N94-28653
Test and analysis of a stitched RFI graphite-epoxy panel with a fuel access door
[NASA-TM-108992] p 3178 N94-29100
Deployable reflector structure
[NASA-CASE-LAR-14513-1-SB] p 3245 N94-29360
Free vibration of thermally loaded panels including initial imperfections and post-buckling effects
[NASA-TM-109097] p 3479 N94-29461
Preliminary evaluation of hybrid titanium composite laminates
[NASA-TM-109095] p 3180 N94-29472
Dual-Band Infrared (DBIR) imaging inspections of Boeing 737 and KC-135 aircraft panels
[DE94-005700] p 3122 N94-29842
Three-dimensional free vibration analysis of thick arbitrarily laminated, rectangular, cylindrical and spherical composite panels p 3184 N94-30257

PAPERS
Index of NPL acoustics publications 1981-1990
[NPL-RSA(EXT)-0044] p 3480 N94-30786

PARABOLIC DIFFERENTIAL EQUATIONS
Unstructured space-time finite element method of heat conduction p 3279 N94-30224
On some general properties of parabolic conservation equations
[DE94-006101] p 3461 N94-30758

PARABOLIC FLIGHT
The MERSS 5th Symposium on Space Medicine: Medical and Physiological Experiment Utilizing Parabolic Flight
[JTN-94-80588] p 3392 N94-29709
Microgravity by parabolic flight with MU-300 aircraft p 3392 N94-29710
A discussion of eye-head coordinative movement under microgravity during parabolic flight p 3393 N94-29715
Determination of acceleration field parameters with linear accelerometers
[PB94-125606] p 3290 N94-30742

PARABOLIC REFLECTORS
Performance of the Southern California Edison Company Stirling dish
[DE94-004676] p 3337 N94-29018

PARACHUTE DESCENT
Parachute Swivel Mechanism for planetary entry p 3162 N94-29643

PARACHUTES
Parachute Swivel Mechanism for planetary entry p 3162 N94-29643

PARALLEL COMPUTERS
The High Performance Storage System
[DE94-004350] p 3404 N94-28505
Rome Laboratory software engineering technology program p 3414 N94-29330
Dependability analysis of parallel systems using a simulation-based approach
[NASA-CR-195762] p 3431 N94-29846
PCCM2: A GCM adapted for scalable parallel computers
[DE94-005113] p 3350 N94-30116
Early experiences with the IBM SP1 and the high-performance switch
[DE94-006261] p 3429 N94-30840

PARALLEL PROCESSING (COMPUTERS)
The High Performance Storage System
[DE94-004350] p 3404 N94-28505
Performance analysis of memory hierachies in high performance systems
[DE94-005549] p 3404 N94-28517
Design of parallel systems for signal processing
[AD-A275490] p 3430 N94-28659
Aerodynamic design using parallel processors
[AD-A275470] p 3122 N94-28674
Parallelization techniques for highly parallel vector computer p 3129 N94-28990
Parallel Fortran programming for NWT p 3129 N94-28991
Performance evaluation of the NWT with parallel Fortran p 3129 N94-28992
A method of user interface for NWT p 3129 N94-28993
A porting methodology for parallel database systems
[AD-A275256] p 3529 N94-29053
Center for Parallel Optimization
[AD-A274988] p 3431 N94-29127
Rome Laboratory software engineering technology program p 3414 N94-29330
Distributed applications and failure tolerance programs using a reconfigurable parallel architecture p 3417 N94-29345
ECSU home-institution support program (1993)
[AD-A275244] p 3431 N94-29396
Stereo imaging based particle velocimeter
[NASA-CR-195800] p 3289 N94-29742
Checkpoint-based forward recovery using lookahead execution and rollback validation in parallel and distributed systems
[NASA-CR-195760] p 3431 N94-29869
First principles pseudopotential calculations on aluminum and aluminum alloys
[DE94-004890] p 3206 N94-29931
Progress report for the PTUF Project-93 Q1 and Q2
[PB94-138591] p 3431 N94-29995
Computational fluid and combustion dynamics
[DE94-006596] p 3279 N94-30003
Computational balance in real-time cyclic spectral analysis
[DE94-005091] p 3432 N94-30100
PCCM2: A GCM adapted for scalable parallel computers
[DE94-005113] p 3350 N94-30116
A locally synchronous globally asynchronous Vertex-8 processing element for image reconstruction on a mesh
[ISBN-0-315-86005-7] p 3432 N94-30143
Common spaceborne multicomputer operating system and development environment
[NASA-TM-109092] p 3422 N94-30197
Large-scale 3-D solutions of the time-dependent Dirac equation
[DE94-005591] p 3454 N94-30317
Manray: A replicated workers program in MANIFOLD
[CWI-CS-R9337] p 3433 N94-30429
Parallel iteration across the steps of high order Runge-Kutta methods for nonstiff initial value problems
[CWI-NM-R9313] p 3433 N94-30730
Parallel language constructs for paradigm integration and deterministic computations
[DE94-005119] p 3428 N94-30754
Early experiences with the IBM SP1 and the high-performance switch
[DE94-006261] p 3429 N94-30840
Computing at the leading edge: Research in the energy sciences
[DE94-006121] p 3563 N94-30844

PARALLEL PROGRAMMING
Global atmospheric and ocean modeling on the connection machine
[DE94-003930] p 3342 N94-28521
Reasoning about programs by exploiting the environment
[AD-A275852] p 3408 N94-28794
Investigation into formalization of domain-oriented parallel software development
[AD-A275177] p 3430 N94-29050
Progress report for the PTUF Project-93 Q1 and Q2
[PB94-138591] p 3431 N94-29995
Three metric domains of processes for bisimulation
[CWI-CS-R9335] p 3459 N94-30427
MANIFOLD version 1.0 programming: Programs and problems
[CWI-CS-R9334] p 3425 N94-30428
Manray: A replicated workers program in MANIFOLD
[CWI-CS-R9337] p 3433 N94-30429
Isomorphisms between predicate and state transformers
[CWI-CS-R9338] p 3459 N94-30430
Relating state transformation semantics and predicate transformer semantics for parallel programs
[CWI-CS-R9339] p 3433 N94-30431
Topological models for higher order control flow
[CWI-CS-R9340] p 3425 N94-30432
Comparative semantics for linear arrays of communicating processes
[CWI-CS-R9336] p 3426 N94-30491
On the relation between Unity properties and sequences of states
[RUU-CS-93-07] p 3433 N94-30720
Parallel iteration across the steps of high order Runge-Kutta methods for nonstiff initial value problems
[CWI-NM-R9313] p 3433 N94-30730
Parallel language constructs for paradigm integration and deterministic computations
[DE94-005119] p 3428 N94-30754

PARAMECIA
Space movement of Trichinella spiralis under microgravity p 3387 N94-29711

PARAMETER IDENTIFICATION
A variable selection heuristic for solid rocket motor design p 3173 N94-29544
Parameter identification of the rotordynamic coefficients of high-Reynolds-number hydrostatic bearings p 3311 N94-30792

PARAMETERIZATION
An observational and numerical study of sea/land-breeze circulations in an area of complex coastal heating p 3372 N94-29813
The incorporation and initialization of cloud water/ice in an operational forecast model p 3373 N94-29814
Use of satellite data to improve parameterization of spatial and temporal variations of gaseous dry deposition in regional-scale models
[DE94-005110] p 3334 N94-30022
Methods of testing parameterizations: Vertical ocean mixing p 3352 N94-30633

PARITY
Space-time symmetries: P and CP violation
[DE94-005012] p 3526 N94-30750

PARKING ORBITS
Optimal low-thrust, Earth-Moon trajectories p 3159 N94-30961

PARSING ALGORITHMS
Engineering specification editing tools
[AD-A275116] p 3419 N94-29746
Maintaining presentation invariants in the Views system
[CWI-CS-R9262] p 3423 N94-30324
Increasing the applicability of LR parsing
[TR-93-06] p 3423 N94-30332
Generalized left-corner parsing
[TR-92-21] p 3432 N94-30356
Parsing in ISBES
[TR-92-32] p 3432 N94-30363

PARTIAL DIFFERENTIAL EQUATIONS
Applied analysis/computational mathematics
[DE94-005133] p 3451 N94-28571
Numerical analysis and computation of nonlinear partial differential equations from applied mathematics
[AD-A275582] p 3451 N94-28723

On approximate Riemann solvers: Improvement of HLLEM scheme and its generalization for chemically reacting flows p 3126 N94-28973
A design methodology for synthesizing low-order robust controllers for flexible structures p 3302 N94-29870

PARTICLE ACCELERATION
Acceleration in astrophysics
[DE94-004986] p 3552 N94-28580
A single-fluid, self-consistent formulation of particle transport and fluid dynamics p 3280 N94-30352

PARTICLE ACCELERATOR TARGETS
Heavy flavor production at fixed target photo- and hadroproduction
[DE94-004651] p 3491 N94-30719

PARTICLE ACCELERATORS
A Tevatron collider beauty factory
[DE94-004879] p 3488 N94-29930

PARTICLE BEAMS
Third-order beam optics of real solenoid magnetic lens
[DE94-608014] p 3500 N94-30084

PARTICLE COLLISIONS
Properties of W + jet events in proton-antiproton collisions at 1.8 TeV
[DE94-004002] p 3482 N94-28524
Properties of events containing a photon and several jets seen in p(bar p) collisions at (radical)s = 1.8 TeV
[DE94-005596] p 3482 N94-28531
Search for excited quarks in p(bar p) collisions at the square root of s = 1.8 TeV
[DE94-004658] p 3484 N94-28573
B production and B(0)(bar B)(0) mixing at DO
[DE94-004664] p 3484 N94-28574
A Tevatron collider beauty factory
[DE94-004879] p 3488 N94-29930
Inclusive jet and direct photon production at the D0 experiment
[DE94-006001] p 3488 N94-30049
Direct anti-b b production in anti-pp collisions at the square root of s = 1.8 TeV
[DE94-006167] p 3491 N94-30369
A search for rapidity gap events in p(bar p) collisions at D(0)
[DE94-004654] p 3491 N94-30722
Deexcitation processes in nuclear reactions: The study of hot hadronic matter
[DE94-003396] p 3492 N94-30836
Atomic physics with highly charged ions
[DE94-003397] p 3492 N94-30837

PARTICLE DENSITY (CONCENTRATION)
A study of the ultrahigh-energy cosmic ray mass composition with the MACRO and EAS-TOP experiments p 3552 N94-29687

PARTICLE DIFFUSION
Boundary-induced phase transitions in equilibrium and non-equilibrium systems
[DE94-608137] p 3199 N94-30111
Exclusive many-particle diffusion in disordered media and correlation functions for random vertex models
[DE94-608134] p 3525 N94-30121
Glueball and meson dispersion and diffusion relations in compact U(1)(2+1) gauge theory
[ISBN-0-315-85577-0] p 3490 N94-30234

PARTICLE IMAGE VELOCIMETRY
Evolution of the large-scale vortices in turbulent mixing-layers p 3273 N94-29686
Development and application of particle image velocimetry in high-speed separated flow: Two-dimensional base cavities p 3282 N94-30791

PARTICLE INTERACTIONS
Energy distribution of the leptons in top decay to charged Higgs
[DE94-005231] p 3482 N94-28494
Theory of fundamental interactions
[DE94-608126] p 3525 N94-30169
Atomic physics with highly charged ions
[DE94-003397] p 3492 N94-30837

PARTICLE MASS
Operator analysis for quark and lepton masses in SO(10)
[DE94-005201] p 3491 N94-30709

PARTICLE MOTION
The effect of magnetic field configuration on particle pinch velocity in Compact Helical System (CHS)
[NIFS-267] p 3505 N94-29398

PARTICLE PRODUCTION
Report of the subgroup on the top quark
[DE94-004624] p 3481 N94-28462
Properties of W + jet events in proton-antiproton collisions at 1.8 TeV
[DE94-004002] p 3482 N94-28524
Properties of events containing a photon and several jets seen in p(bar p) collisions at (radical)s = 1.8 TeV
[DE94-005596] p 3482 N94-28531
B production and B(0)(bar B)(0) mixing at DO
[DE94-004664] p 3484 N94-28574
Experimental setup for study of hadron and hard photon production in nucleus-nucleus collisions
[DE94-607849] p 3489 N94-30051
Experimental setups and methods to obtain new nuclear data at intermediate and high energies
[DE94-607850] p 3489 N94-30052
Search for heavy neutrinos at the IHEP-JINR neutrino detector
[DE94-608175] p 3489 N94-30095
Modelling of multiparticle production by dynamical semigroup method
[DE94-608132] p 3490 N94-30120
Direct anti-b b production in anti-pp collisions at the square root of s = 1.8 TeV
[DE94-006167] p 3491 N94-30369
Heavy flavor production at fixed target photo- and hadroproduction
[DE94-004651] p 3491 N94-30719
Search for the top quark in the electron-electron and electron-muon channels at D0
[DE94-006174] p 3492 N94-30779
Charmonium and bottomonium in (-p)p interactions
[DE94-006173] p 3493 N94-30886
Inclusive single muon production in D0
[DE94-006175] p 3493 N94-30887

PARTICLE SIZE DISTRIBUTION
Using the log-normal distribution in analyzing aerosols: The mathematical reasoning underlying the various diameters used and the plotting procedure
[DE94-006459] p 3461 N94-30817

PARTICLE SPIN
Determination of the neutron spin-structure function
[DE94-005234] p 3483 N94-28542
On relativity principle violation in local measurements of spin precession of moving particles
[DE94-608067] p 3489 N94-30085
Magnetic properties of a quantum transverse spin-1 Blume-Emery-Griffiths model
[DE94-608114] p 3517 N94-30109

PARTICLE THEORY
Twistor-like type 2 superstring and bosonic string
[DE94-606339] p 3523 N94-28802
Statistical description of hot and dense clustering matter
[DE94-608155] p 3490 N94-30112
Modelling of multiparticle production by dynamical semigroup method
[DE94-608132] p 3490 N94-30120
Problems in particle theory
[DE94-003665] p 3491 N94-30685

PARTICLE TRACKS
Track filtering by robust neural network
[DE94-606067] p 3434 N94-28613
Meso-optical Fourier transform microscope with double focusing
[DE94-607851] p 3290 N94-30148

PARTICLE TRAJECTORIES
A 6MeV heavy ion beam probe for the Large Helical Device
[NIFS-272] p 3505 N94-29397
Some remarks about pseudo-Hamiltonian
[DE94-003273] p 3487 N94-29700
The impact of electrically charged microspheres with planar surfaces under vacuum conditions p 3320 N94-29765

PARTICULATES
Catalytic fabric filtration for simultaneous NO(x) and particulate control
[DE94-001660] p 3341 N94-28463
Novel mass spectrometric instrument for gaseous and particulate characterization and monitoring
[DE94-005896] p 3349 N94-30047
Centrifugal atomization of lanthanide materials for cryogenic coolers
[DE94-006035] p 3219 N94-30337
Particulate metal matrix composites: Draft procedure for tensile tests at ambient temperature
[NPL-DMM(A)-100] p 3184 N94-30419

PARTITIONS (MATHEMATICS)
Codes on the unit sphere
[PB94-136991] p 3453 N94-29174
Rectilinear decompositions with low stabbing number
[RUU-CS-93-25] p 3459 N94-30425
Dynamic microsets for RAMs
[RUU-CS-93-22] p 3406 N94-30727
Perfect binary space partitions
[RUU-CS-93-23] p 3460 N94-30728

PARTONS
The small-x behaviour of parton distribution functions
[DE94-606414] p 3485 N94-28758
Inclusive jet and direct photon production at the D0 experiment
[DE94-006001] p 3488 N94-30049

PASSIVITY
Pit initiation on passivated metal surfaces: Crystallographic orientation and environmental effects
[ISBN-0-315-85433-2] p 3208 N94-30138
An investigation of the corrosion properties of aluminum-tantalum alloys using electrochemical impedance spectroscopy and local electrochemical impedance spectroscopy p 3209 N94-30521

PATIENTS
Aeromedical support for casualties in extremely hot climates p 3382 N94-28443

PATTERN RECOGNITION
A new method for recognizing quadric surfaces from range data and its application to telerobotics and automation, final phase
[NASA-CR-195733] p 3408 N94-28825
Animators and error reporters for generated programming environments
[CWI-CS-R9253] p 3418 N94-29503
A locally synchronous globally asynchronous Vertex-8 processing element for image reconstruction on a mesh
[ISBN-0-315-86005-7] p 3432 N94-30143
Shape from diameter: Negative results
[RUU-CS-93-16] p 3458 N94-30407
Shape from diameter: Positive results
[RUU-CS-93-17] p 3458 N94-30408
The use of interactive computer vision and robot hand controllers for enhancing manufacturing safety p 3314 N94-30442
Unsupervised texture image segmentation by improved neural network ART2
[AIAA PAPER 94-1199-CP] p 3442 N94-30549
Use of bad training data for better predictions
[DE94-006233] p 3427 N94-30705
Placing registration marks
[RUU-CS-93-21] p 3427 N94-30725
Elements for the recognition of three dimensional deformable shapes: Application to biomedical imagery
[TELECOM-93-E-008] p 3396 N94-30978

PATTERN REGISTRATION
Automatic focus and registration of synthetic aperture radar images p 3246 N94-29536
Pre- and intra-radiotherapy multimodal image registration: Principles and first experiments p 3395 N94-30030

PAVEMENTS
Granular bases for heavily loaded pavements
[AD-A275171] p 3156 N94-29047
Asphaltic concrete performance under heavy fighter aircraft loading
[AD-A275046] p 3157 N94-29151

PAYLOAD CONTROL
Control system design for A and R supported microgravity experiments: An experiment payload control development
[AD-B179107] p 3229 N94-30421

PAYLOAD TRANSFER
A transportronic solution to the problem of interorbital transportation
[NASA-CR-191152] p 3164 N94-29355

PAYLOADS
BAG: A code for predicting the performance of a gas bag impact attenuation system for the Pathfinder lander
[DE94-003688] p 3165 N94-28477
Suspension system for gimbal supported scanning payloads
[NASA-CASE-MFS-28817-1] p 3287 N94-29358
GOME: Global Ozone Monitoring Experiment
[ESA-SP-1151] p 3347 N94-29452
Imaging spectrometry of the Earth and other solar system bodies p 3237 N94-29779
Root-sum-square structural strength verification approach
[NASA-TM-108453] p 3322 N94-30206

PENETRATION
Finite element analysis of axisymmetric deformations of thick thermoviscoplastic targets p 3320 N94-29688

PERFORATED PLATES
X-/Ka-band dichroic plate design and grating lobe study p 3247 N94-29616

PERFORMANCE PREDICTION
Development of the integrated environmental control model: Performance models of selective catalytic reduction NO(x) control systems
[DE94-002151] p 3341 N94-28465
BAG: A code for predicting the performance of a gas bag impact attenuation system for the Pathfinder lander
[DE94-003688] p 3165 N94-28477
Simulation Networking/Training Requirements Relational Database: User's guide
[AD-A275634] p 3528 N94-28637
Effects of workload on communication processes in decision making teams
[AD-A275894] p 3527 N94-28796

Role of microstructure on the fatigue durability of aluminum aircraft alloys
[AD-A275814] p 3202 N94-28830
GLRS-R 2-colour retroreflector target design and predicted performance
[REPT-932-440-106] p 3246 N94-29542
Performance evaluation of intelligent network services
[MEMO-INF-93-20] p 3438 N94-30373

PERFORMANCE TESTS
Thermal protective performance and instrumented mannequin evaluation of multi-layer garment systems
p 3381 N94-28433
Rewarming methodologies in the field
p 3382 N94-28441
Environmental characterization for target acquisition. Analysis of thermal and visible imagery
[AD-A275414] p 3242 N94-28862
Performance evaluation of a 22.5/30 kW 270 volts direct current generator system
[AD-A275106] p 3263 N94-28913
Stress and ergonomic design and evaluation of person-machine systems
[AD-A275156] p 3400 N94-29034
Some problems of scramjet propulsion for aerospace planes. Part 2: Scramjet: Development and test problems p 3152 N94-29301
Software testing practices and their evolution for the 1990's p 3415 N94-29335
A disciplined approach to software test and evaluation
p 3416 N94-29339
Development of electromagnetic compatibility tests
[REPT-932-430-110] p 3245 N94-29421
A portable X-band front-end test package for beam-waveguide antenna performance evaluation. Part 2: Tests on the antenna p 3247 N94-29620
The use of screening tests in spacecraft lubricant evaluation p 3162 N94-29641
A study of the relationship between the performance and dependability of a fault-tolerant computer
[NASA-CR-195758] p 3406 N94-29695
Remote observatory access via the advanced communications technology satellite
p 3253 N94-29894
Scanning and monitoring performance: Effects of the reinforcement values of the events being monitored
[DOT/FAA/AM-94/8] p 3398 N94-29918
A newly developed snow vehicle (SM100S) for Antarctica. Part 5: Result of general performance tests
p 3314 N94-29985
A user's guide to the Software Testpilot
[CWI-CS-R9343] p 3426 N94-30435
NATO SOCMET trials p 3258 N94-30503
A performance analysis method for distributed real-time robotic systems: A case study of remote teleoperation
[AIAA PAPER 94-1212-CP] p 3445 N94-30563
Status of frequency and time support for NASA systems p 3468 N94-30640

PERIDOTITE
Studies in Jurassic and Cretaceous North American apparent polar wander p 3362 N94-29940
Geochemical and fluid dynamic investigations into the nature of chemical variability in the Earth's mantle
p 3367 N94-30917

PERIODIC VARIATIONS
Long term variations of radio auroral activity
p 3359 N94-29237
Extended horizon lifting for periodic gain adjustment in control systems, and for equalization of communication channels
[NASA-CASE-NPO-19166-1-CU] p 3246 N94-29495
On observing neutron star oscillations
p 3538 N94-29795
Interannual-decadal variability in tropical climate systems: Stable isotope records and general circulation model experiments p 3373 N94-29962
Satellite estimation of the global distribution and interannual variability of photosynthetically active radiation p 3334 N94-29970

PERIODICALS
TRADOC library and information network (TRALINET). Union list of periodicals (TULIP)
[AD-A275263] p 3529 N94-28903

PERMAFROST
Growth condition of an ice layer in freezing soils under applied loads. Part 1: Experiment
[AD-A275215] p 3357 N94-29070
On the temperature distribution near a cold surface
[AD-A275162] p 3332 N94-29288

PERMEABILITY
Fire-resistant water vapour permeable buoyant insulation p 3380 N94-28431
Flow past a circular cylinder with a permeable wake splitter plate p 3275 N94-29764
Melt flow during alloy solidification: Dimensional analysis and model problems
[PB94-138625] p 3206 N94-29997

PEROXIDES
In situ detection of tropospheric OH and HO2 by laser-induced fluorescence in a detection chamber at low pressure p 3342 N94-28589
Detection of tropospheric OH and HO2 by laser-induced fluorescence at low pressure using the 308nm excitation of OH p 3343 N94-28591
Harvard ER-2 OH laser-induced fluorescence instrument p 3343 N94-28592
Peroxy radical measurements with NCAR's chemical amplifier p 3345 N94-28603
An improved method of measuring tropospheric NO2, NO3, HO2, and RO2 by Matrix Isolation and Electronic Spin Resonance (MIESR) p 3345 N94-28605
Tropospheric HO2 determination by FAGE
p 3345 N94-28606
Near-IR diode laser absorption for measurement of tropospheric HO2 p 3345 N94-28607
HO2 detection by near infrared absorption using tunable diode lasers p 3346 N94-28608

PERSONAL COMPUTERS
Evaluation of access/navigational features of a graphical-user interface installed on a portable maintenance aid
[AD-A275791] p 3136 N94-28744

PERSONALITY
An evaluation of personality testing and the five-factor model in the selection of landing craft air cushion vehicle crew members
[AD-A275869] p 3397 N94-28754

PERSONALITY TESTS
An evaluation of personality testing and the five-factor model in the selection of landing craft air cushion vehicle crew members
[AD-A275869] p 3397 N94-28754

PERSONNEL
Recent Canadian advances in active thermal protection p 3384 N94-28451
Effects of workload on communication processes in decision making teams
[AD-A275894] p 3527 N94-28796

PERSONNEL DEVELOPMENT
Development centres: Assessing or developing people
[PB94-138070] p 3536 N94-29144

PERSONNEL MANAGEMENT
The management issues of implementing telecommuting: A case study
[AD-A275267] p 3527 N94-28905

PERSONNEL SELECTION
An evaluation of personality testing and the five-factor model in the selection of landing craft air cushion vehicle crew members
[AD-A275869] p 3397 N94-28754
Naval aviation vision standards research at the naval aerospace medical research laboratory: The long view
[AD-A275885] p 3388 N94-28756
Scanning and monitoring performance: Effects of the reinforcement values of the events being monitored
[DOT/FAA/AM-94/8] p 3398 N94-29918

PERSPIRATION
Simulation of the effect of wind on clothing by measurements and calculations
[PB94-132289] p 3399 N94-28406

PERTURBATION
Missile launch detection electric field perturbation experiment
[DE94-004224] p 3466 N94-30586

PERTURBATION THEORY
Quasipotential in the fourth order of perturbation theory
[DE94-606299] p 3484 N94-28584
Decoupled flight control system design using the singular perturbation method p 3155 N94-29850
Physics, astronomy, and astrophysics: A numerical study of the black hole plus Brill wave spacetime
p 3540 N94-29990
Reconstruction of spectra in the discrete quantum mechanics (new elements of the lattice quantum engineering)
[DE94-608075] p 3524 N94-30087
Dissipation in Hamiltonian systems: Decaying cnoidal waves
[MEMO-1151] p 3460 N94-30738

PETRI NETS
On conceptual design of active databases
p 3531 N94-29535

PHARMACOLOGY
Cubanes: Super explosives and potential pharmaceutical intermediates p 3227 N94-30454

PHASE COHERENCE
Dynamics of a coupled solid state laser array
p 3294 N94-29551

PHASE CONJUGATION
Estimation of geomagnetic conjugate points by using Pc5 pulsations p 3357 N94-29079

PHASE DETECTORS
An analysis of carrier phase jitter in an MPSK receiver utilizing map estimation
[NASA-CR-195806] p 3164 N94-29880

PHASE DEVIATION
Design and analysis of a low-loss linear analog phase modulator for deep space spacecraft X-band transponder applications p 3248 N94-29625

PHASE DIAGRAMS
Crystal structure of La(2-x)Ba(x)CuO4
[DE94-707688] p 3511 N94-28750
Structure of ordinary ice I(sub h). Part 1: Ideal structure of ice
[AD-A275149] p 3486 N94-29021
Some results on the phase diagram of the antiferromagnetic Potts model in an external magnetic field
[DE94-608115] p 3468 N94-30110
Boundary-induced phase transitions in equilibrium and non-equilibrium systems
[DE94-608137] p 3199 N94-30111
Terfenol: A study of the phase equilibrium diagram and the solidification process
[DE94-004883] p 3209 N94-30690
Theoretical studies of solid-fluid phase equilibria
[DE94-006406] p 3226 N94-30708

PHASE ERROR
Automatic focus and registration of synthetic aperture radar images p 3246 N94-29536
Effects of low sampling rate in the digital data-transition tracking loop p 3251 N94-29669
An analysis of carrier phase jitter in an MPSK receiver utilizing map estimation
[NASA-CR-195806] p 3164 N94-29880

PHASE LOCKED SYSTEMS
Method of implementing digital phase-locked loops
[NASA-CASE-NPO-18757-1-CU] p 3265 N94-29374
Dynamics of a coupled solid state laser array
p 3294 N94-29551
Design and implementation of a hybrid digital phase-locked loop with a TMS320C25: An application to a transponder receiver breadboard
p 3251 N94-29667
Precision frequency synthesizing sources with excellent time/frequency performances p 3473 N94-30671

PHASE MODULATION
Longitudinal effects and intensity-phase coupling in distributed feedback semiconductor lasers
p 3294 N94-29590
Design and analysis of a low-loss linear analog phase modulator for deep space spacecraft X-band transponder applications p 3248 N94-29625
Two-way satellite time transfer: Overview and recent developments p 3469 N94-30646

PHASE SHIFT
Derivation of a Fokker-Planck equation for bunched beams
[DE94-004950] p 3483 N94-28565
Observation of the phase shift of the wave function of the neutron under total reflection
[DE94-608244] p 3489 N94-30096

PHASE SHIFT KEYING
An analysis of carrier phase jitter in an MPSK receiver utilizing map estimation
[NASA-CR-195806] p 3164 N94-29880
Partially coherent detection of PSK signals in Rician channels
[ISBN-0-315-85799-4] p 3254 N94-30031

PHASE STABILITY (MATERIALS)
Interstitially stabilized phases in the zirconium-nickel system
[DE94-005561] p 3201 N94-28525

PHASE TRANSFORMATIONS
Directional solidification studies in Ni-Al alloys
[DE94-005562] p 3201 N94-28527
Experimental and theoretical studies of molecular solids
[AD-A275511] p 3485 N94-28668
Crystal structure of La(2-x)Ba(x)CuO4
[DE94-707688] p 3511 N94-28750
Structure of ordinary ice I(sub h). Part 1: Ideal structure of ice
[AD-A275149] p 3486 N94-29021
Differential Scanning Calorimetry (DSC) for planetary surface exploration p 3236 N94-29776
Boundary-induced phase transitions in equilibrium and non-equilibrium systems
[DE94-608137] p 3199 N94-30111
Investigation of the phase equilibria and phase transformations associated with the Bi2Sr2CaCu2O(y) superconductor
[DE94-004889] p 3519 N94-30691

PHASED ARRAYS
Solid-state, active-phased arrays: Some aspects of receiver design
[AD-A275893] p 3527 N94-28779

Pointing mechanisms for the Shuttle Radar Laboratory p 3162 N94-29638
A combined electron beam/optical lithography process step for the fabrication of sub-half-micron-gate-length MMIC chips p 3240 N94-30445

PHENOLIC RESINS
Measurement and modelling of bolted joint stress relaxation in plastics [PB94-124849] p 3318 N94-28841

PHENOLS
Journal of NIRE, Vol. 2, No. 2 [JTN-94-80552] p 3187 N94-28675
Methanol-mediated continuous extraction of phenolic compounds from coal liquid p 3188 N94-28679

PHENOMENOLOGY
Research on elementary particle physics. Task P: Studies in theory and phenomenology of elementary physics [DE94-004955] p 3483 N94-28566

PHILOSOPHY
Identity: Quarrelling with an unproblematic notion [LP-93-04] p 3455 N94-30327

PHONETICS
Subphonetic acoustic modeling for speaker-independent continuous speech recognition [AD-A275217] p 3244 N94-29303

PHONONS
Effect of phonon dispersion on properties of exciton in magnetic field [DE93-634756] p 3481 N94-28469
Vibrational properties of homopolar and heteropolar surfaces and interfaces of the CdTe/HgTe system [DE94-608105] p 3516 N94-30069
Interband optical absorption in the Wannier-Stark ladder under the electron-LO-phonon resonance condition [DE94-608097] p 3267 N94-30092
Procedures for basic inverse problems: Black body radiation problem and phonon density of states problem [ISBN-0-315-85757-9] p 3525 N94-30244

PHOSPHATES
Growth of hydrocarbon-rich microalga Botryococcus braunii in secondarily treated sewage and its consumption of nitrate ion and phosphate ion p 3387 N94-29519
Structural analysis of amorphous phosphates using high performance liquid chromatography [DE94-004791] p 3199 N94-30723

PHOSPHIDES
Studies of high temperature ternary phases in mixed-metal-rich early transition metal sulfide and phosphide systems [DE94-006034] p 3209 N94-30336

PHOSPHORUS COMPOUNDS
Synthesis and molecular structures of R(Me3CCH2)2In-E(SiMe3) (R = Me3CCH2, E = P or As; R = Me, E = P) [AD-A275020] p 3486 N94-29131

PHOTOCHEMICAL REACTIONS
Ozone production at a rural site in Georgia during the summer 1992 SOS campaign [DE94-003989] p 3342 N94-28523
Laboratory studies of chemical and photochemical processes relevant to stratospheric ozone [NASA-CR-195779] p 3347 N94-29549
Developing a diode array spectrometer for tropospheric chemistry studies p 3362 N94-29752
Photochemistry in constrained spaces: Zeolites and layered double metal hydroxides [DE94-004958] p 3200 N94-30769

PHOTOCONDUCTIVITY
Transport properties of epitaxial lift off films [NASA-TM-106156] p 3264 N94-29209
Study of the ultraviolet absorption and photoconduction spectra of polyimide films fabricated at various curing temperatures [ISBN-0-315-85923-7] p 3218 N94-30036

PHOTOCONDUCTORS
InTlSb for long-wavelength infrared photodetectors and arrays [AD-A275079] p 3512 N94-28872
Photoconductive switching for high power microwave generation [PB94-137460] p 3244 N94-29177

PHOTODIODES
The automated rotating shadowband spectroradiometer [DE94-001878] p 3269 N94-28464
Broadband EUV survey spectrometer for short-timescale experiments [DE94-005459] p 3498 N94-28534
UV laser long-path absorption spectroscopy p 3343 N94-28595
Modeling the total dose radiation effects of Hg(1-x)Cd(x)Te photodiodes using numerical device simulators [AD-A275235] p 3263 N94-29028
Miniaturization in x ray and gamma ray spectroscopy p 3236 N94-29773

PHOTODISSOCIATION
Radiation transport in cloudy and aerosol loaded atmospheres p 3365 N94-30805

PHOTOELECTRIC EFFECT
Photoelectron diffraction and holography: Some new directions [DE94-006297] p 3289 N94-30027

PHOTOELECTRIC EMISSION
Near-ultraviolet laser photoemission: Scanning microscopy, buried interfaces and image-potential states p 3294 N94-29531
A photoemission electron microscope investigation of chemical vapor deposition diamond films and diamond nucleation p 3215 N94-29745
Characteristics of secondary electron emission from CsI induced by x rays with energies up to 100 keV [DE94-608422] p 3395 N94-30185
Influence of surface defects and local structure on oxygenate reaction pathways over metal oxide surfaces [DE94-005680] p 3522 N94-30901

PHOTOELECTROMAGNETIC EFFECTS
Photoelectronic study of GaAs epilayers and In(x)Ga(1-x)As/GaAs quantum wells [ISBN-0-315-85756-0] p 3518 N94-30239

PHOTOELECTRON SPECTROSCOPY
Structure of ordinary ice I(sub h). Part 1: Ideal structure of ice [AD-A275149] p 3486 N94-29021
XPS analysis of 440C steel surfaces lubricated with perfluoropolyethers under sliding conditions in high vacuum [NASA-TM-106548] p 3218 N94-30177

PHOTOELECTRONS
Photoelectron diffraction and holography: Some new directions [DE94-006297] p 3289 N94-30027
Photochemistry in constrained spaces: Zeolites and layered double metal hydroxides [DE94-004958] p 3200 N94-30769

PHOTOEXCITATION
Predissociation in N2(C'4, 1 Sigma u +) and other N2 states and its importance in the atmospheres of Titan and Triton [NASA-CR-195727] p 3549 N94-28816

PHOTOGRAMMETRY
Exploitation of stereophotogrammetrically derived 3-D wireframe models to produce urban simulations [AD-A275459] p 3325 N94-28808
Feature mapping in a photogrammetric GIS [AD-A275418] p 3325 N94-28863
The use of digital stereo photogrammetric methods in historical photo analysis [AD-A275287] p 3288 N94-29437
Calibration of charge coupled device digital cameras [ISBN-0-315-85539-8] p 3290 N94-30232

PHOTOINTERPRETATION
The use of digital stereo photogrammetric methods in historical photo analysis [AD-A275287] p 3288 N94-29437

PHOTOIONIZATION
Optical field ionization of atoms and ions using ultrashort laser pulses [DE94-006643] p 3488 N94-29845
Optical depth effects in cluster cooling flows p 3541 N94-30800

PHOTOLITHOGRAPHY
Nearly time-optimal feedback control of a magnetically levitated photolithography positioning system [DE94-005288] p 3266 N94-30055
Neural network based time-optimal control of a magnetically levitated precision positioning system [DE94-006573] p 3437 N94-30250

PHOTOLUMINESCENCE
ECR plasma synthesis of silicon nitride films on GaAs and InSb [DE94-005575] p 3515 N94-30006

PHOTOMETERS
Development of ultra-low noise, high performance 3 -5 quantum well infrared photodetectors (QWIPs) for focal plane array staring image sensor systems [AD-A275745] p 3511 N94-28734
MOCVD growth of GaN, AlN and AlGaN for UV photodetector applications [AD-A275078] p 3512 N94-28871
InTlSb for long-wavelength infrared photodetectors and arrays [AD-A275079] p 3512 N94-28872
Remote sensing of inner heliospheric plasmas [AD-A275021] p 3550 N94-29132
Issues arising with the application of optical fiber transmission in class 1E systems in nuclear power plants [DE94-004743] p 3500 N94-29928

PHOTOMETRY
Multicolor photometry of barred spiral galaxies p 3541 N94-30270

PHOTOMULTIPLIER TUBES
Photon counting spectroscopy as done with a Thomson scattering diagnostic [DE94-005543] p 3503 N94-28515
On possibility to create the scintillation trigger for liquid-argon neutrino detector [DE94-607844] p 3489 N94-30050

PHOTON BEAMS
Activity report of Synchrotron Radiation Laboratory 1992 [JTN-94-80600] p 3495 N94-29596

PHOTON-ELECTRON INTERACTION
Quantum-mechanical suppression of bremsstrahlung [DE94-005223] p 3497 N94-30712

PHOTONICS
Photonic devices and systems for optical signal processing [AD-A275818] p 3498 N94-28804
Optoelectronic packaging activities at Sandia National Laboratories [DE94-005287] p 3501 N94-30261
Photonics at Sandia National Laboratories: From research to applications [DE94-006463] p 3501 N94-30828

PHOTONS
Photon counting spectroscopy as done with a Thomson scattering diagnostic [DE94-005543] p 3503 N94-28515
Properties of events containing a photon and several jets seen in p(bar p) collisions at (radical)s = 1.8 TeV [DE94-005596] p 3482 N94-28531
Advanced diagnostics for reacting flows [AD-A275057] p 3272 N94-29136
Physical conditions in classical H2 regions in the Magellanic Clouds p 3543 N94-29722
Inclusive jet and direct photon production at the D0 experiment [DE94-006001] p 3488 N94-30049
Experimental setup for study of hadron and hard photon production in nucleus-nucleus collisions [DE94-607849] p 3489 N94-30051
Experimental setups and methods to obtain new nuclear data at intermediate and high energies [DE94-607850] p 3489 N94-30052
Quantum-mechanical suppression of bremsstrahlung [DE94-005223] p 3497 N94-30712

PHOTONUCLEAR REACTIONS
Heavy flavor production at fixed target photo- and hadroproduction [DE94-004651] p 3491 N94-30719

PHOTOPRODUCTION
A measurement of the LMP effect [DE94-005225] p 3482 N94-28493
Elementary particle interactions [DE94-004238] p 3482 N94-28504
Properties of events containing a photon and several jets seen in p(bar p) collisions at (radical)s = 1.8 TeV [DE94-005596] p 3482 N94-28531
Inclusive jet and direct photon production at the D0 experiment [DE94-006001] p 3488 N94-30049
Heavy flavor production at fixed target photo- and hadroproduction [DE94-004651] p 3491 N94-30719

PHOTOSPHERE
The structure of solar magnetic fields and their associated electric currents p 3544 N94-29723

PHOTOSYNTHESIS
Estimation of the net production of moss community at Langhovde, East Antarctica p 3358 N94-29081
Satellite estimation of the global distribution and interannual variability of photosynthetically active radiation p 3334 N94-29970

PHOTOTHERMAL CONVERSION
Quality and efficiency of solar collectors in Sweden [PB94-137486] p 3337 N94-28909

PHOTOVOLTAIC CELLS
The viability of photovoltaics on the Martian surface [NASA-TM-106478] p 3338 N94-30196
Large-area triple-junction a-Si alloy production scale up [DE94-000249] p 3339 N94-30604
Solar photovoltaics for development applications [DE94-006116] p 3340 N94-30843

PHOTOVOLTAIC CONVERSION
Advanced development of PV encapsulents [DE94-000219] p 3336 N94-28500
Photovoltaic power without batteries for continuous cathodic protection p 3341 N94-30465
Photovoltaic performance and reliability workshop [DE94-000236] p 3339 N94-30601

Large-area triple-junction a-Si alloy production scale up
[DE94-000249] p 3339 N94-30604
NREL Photovoltaic Program FY 1993 bibliography
[DE94-000272] p 3340 N94-30820
Solar photovoltaics for development applications
[DE94-006116] p 3340 N94-30843

PHYSICAL EXERCISE
Effects of three hydration beverages on exercise performance during 60 hours of simulated desert exposure p 3383 N94-28448
Studies on water electrolyte metabolism and endocrine responses at rest and during submaximal exercise at 6,000 m simulated altitude p 3388 N94-28496
Effects of training at simulated altitude of 6,000 m on endocrine responses at rest and during exercise at the same altitude p 3388 N94-28497
Effects of endurance training on heat-exercise tolerance in men wearing NBC protective clothing
[AD-A275176] p 3391 N94-29049
Leg muscle volume during 30-day 6-degree head-down bed rest with isotonic and isokinetic exercise training
[NASA-TM-4580] p 3385 N94-29401

PHYSICAL FACTORS
Modeling data throughput on communication networks
[DE94-005077] p 3260 N94-30772

PHYSICAL OPTICS
Gaussian beam and physical optics iteration technique for wideband beam waveguide feed design p 3248 N94-29624
A physical optics model for scattering of HF radiation by irregular terrain
[DE94-006187] p 3255 N94-30106

PHYSICAL SCIENCES
The Seventh Annual National Conference of Black Physics Students
[NASA-CR-195735] p 3526 N94-28746

PHYSIOLOGICAL ACCELERATION
Portable Linear Sled (PLS) for biomedical research p 3163 N94-29648

PHYSIOLOGICAL EFFECTS
Physiological investigations of the isolated rat's liver in hypothermia and hypoxia and their relevance in aircraft incidents above the sea p 3382 N94-28439
Japanese Journal of Aerospace and Environmental Medicine, vol. 30, no. 3
[JTN-94-80606] p 3387 N94-28495
Studies on water electrolyte metabolism and endocrine responses at rest and during submaximal exercise at 6,000 m simulated altitude p 3388 N94-28496
Effects of training at simulated altitude of 6,000 m on endocrine responses at rest and during exercise at the same altitude p 3388 N94-28497
Some issues on Japan's space food development and relating preliminary experimental study p 3388 N94-28498
Effects of pressure on membrane-associated receptors and effector elements
[AD-A275813] p 3384 N94-28829
Japanese Journal of Aerospace and Environmental Medicine, volume 30, no. 1
[JTN-94-80598] p 3389 N94-28850
Image technology and information analysis of bone change with gravitational exposure p 3389 N94-28851
Arterial oxygen saturation during +Gz acceleration by short-radius centrifuge p 3389 N94-28852
Effect of chronic centrifugation on in vitro fertilization and early development in mice ova p 3386 N94-28853
Disturbance of equilibrium on JAL flight crew p 3390 N94-28856
Equilibrium dysfunction in the clinical field p 3390 N94-28858
The MERSS 5th Symposium on Space Medicine: Medical and Physiological Experiment Utilizing Parabolic Flight
[JTN-94-80588] p 3392 N94-29709
Space movement of Trichinella spiralis under microgravity p 3387 N94-29711
Posture control of goldfishes under microgravity p 3387 N94-29712
Behavior and visual control of cyprinodonts under microgravity p 3387 N94-29713
A discussion of eye-head coordinative movement under microgravity during parabolic flight p 3393 N94-29715
Analysis of various biological activity parameters during parabolic flight p 3393 N94-29716
Hemodynamic measurement during parabolic flight p 3393 N94-29717
Motion sickness in parabolic flight: Possibility of electrogastrography as an objective index p 3393 N94-29718
Japanese Journal of Aerospace and Environmental Medicine, vol. 30, no. 2
[JTN-94-80599] p 3394 N94-29863
Effect of water immersion on muscle sympathetic nerve response during static muscle contraction p 3394 N94-29865
Shortening velocity and calcium sensitivity of single fibers from hindlimb suspended muscle in rats p 3387 N94-29866
Toxicity of carbon monoxide-hydrogen cyanide gas mixtures: Exposure concentration, time-to-incapacitation, carboxyhemoglobin, and blood cyanide parameters
[DOT/FAA/AM-94/7] p 3395 N94-29919
Physiological Anatomical Rodent Experiment (PARE).04 feasibility test 2
[NASA-CR-195210] p 3385 N94-29968

PHYSIOLOGICAL FACTORS
Psychophysiological study on the effects of co-existence of lines for detecting dot target p 3394 N94-29867

PHYSIOLOGICAL RESPONSES
Prediction of survival times on land in a cold climate p 3379 N94-28423
Treatment of mild immersion hypothermia by body-to-body and forced-air warming p 3380 N94-28428
Thermoregulation in the extreme cold environment p 3381 N94-28438
Rewarming methodologies in the field p 3382 N94-28441
A comparison of four methods of rewarming individuals cooled by immersion in cold water p 3382 N94-28442
Work conditions assessment in pilots and ground personnel under high weather temperatures p 3382 N94-28444
Effects of three hydration beverages on exercise performance during 60 hours of simulated desert exposure p 3383 N94-28448
Alleviation of thermal strain in the CF: Keeping our cool during the Gulf conflict p 3383 N94-28449
Relaxed tolerance following HSG, high sustained +Gz
[AD-A275204] p 3391 N94-28892
Physiological responses during shipboard firefighting
[AD-A275104] p 3391 N94-28912
Effect of water immersion on muscle sympathetic nerve response during static muscle contraction p 3394 N94-29865

PHYSIOLOGY
Thermoregulation in the extreme cold environment p 3381 N94-28438
Physiological investigations of the isolated rat's liver in hypothermia and hypoxia and their relevance in aircraft incidents above the sea p 3382 N94-28439
Physiological Anatomical Rodent Experiment (PARE).04 feasibility test 2
[NASA-CR-195210] p 3385 N94-29968
A fuzzy logic controller for hormone administration using an implantable pump p 3397 N94-30459

PHYTOTRONS
Seed viability detection using computerized false-color radiographic image enhancement p 3387 N94-30461

PIEZOELECTRIC CERAMICS
GEC Ferranti piezo vibratory gyroscope p 3239 N94-29790
Damage identification in composites using built-in piezoelectrics p 3184 N94-30355

PIEZOELECTRIC GAGES
Damage identification in composites using built-in piezoelectrics p 3184 N94-30355

PILOT PERFORMANCE
Disturbance of equilibrium on JAL flight crew p 3390 N94-28856
Human pilot response during single- and multi-axis tracking tasks
[AD-A275080] p 3398 N94-28887
Information presentation for expert systems in future fighter aircraft
[AD-A275126] p 3149 N94-29005
Aircraft accident/incident summary report: In-flight loss of control, leading to forced landing and runway overrun, Continental Express, Inc., N24706 Embraer EMB-120 RT, Pine Bluff, Arkansas, 29 April 1993
[PB94-910404] p 3135 N94-29402
Japanese Journal of Aerospace and Environmental Medicine, vol. 30, no. 2
[JTN-94-80599] p 3394 N94-29863
Psychophysiological study on the effects of co-existence of lines for detecting dot target p 3394 N94-29867
Flight simulator evaluation of advanced MLS procedures
[AD-B174270] p 3143 N94-30915

PILOTLESS AIRCRAFT
Payload central control for unmanned aircraft p 3155 N94-30284

PILOTS (PERSONNEL)
Work conditions assessment in pilots and ground personnel under high weather temperatures p 3382 N94-28444
Human pilot response during single- and multi-axis tracking tasks
[AD-A275080] p 3398 N94-28887

PIONEER VENUS SPACECRAFT
Correlation studies of Pioneer Venus imagery obtained from PV experiments with near IR imagery obtained from ground-based observations during Venus inferior conjunction
[NASA-CR-195772] p 3550 N94-29892
Taxonomy of gamma ray burster data using a self-organizing neural network
[DE94-006480] p 3553 N94-30248

PIPE FLOW
Development of buoyancy affected laminar flow in a heated pipe p 3128 N94-28988
Mutual similarity of developing laminar flows with secondary streams in ducts: Curved pipe flow and orthogonal rotating pipe flow p 3129 N94-28989
Two-phase power-law modeling of pipe flows displaying shear-thinning phenomena
[DE94-005115] p 3279 N94-30020
Controlling the material properties of in vitro collagen through directed orientation and cross-linking of fibrils p 3221 N94-30797

PIPES (TUBES)
Fabrication and testing of plasma-spray formed MoSi2 and MoSi2 composite tubes
[DE94-004995] p 3175 N94-28581
The influence of wall conductivity of film condensation with integral fin tubes
[AD-A275503] p 3523 N94-28662
Similarity between turbulent flows through curved pipe and orthogonal rotating pipe p 3128 N94-28986
Two-phase power-law modeling of pipe flows displaying shear-thinning phenomena
[DE94-005115] p 3279 N94-30020
The universal applications of microtubes and microtube composites p 3186 N94-30452

PITCHING MOMENTS
An experimental and theoretical study of the aerodynamic characteristics of some generic missile concepts at Mach numbers from 2 to 6.8
[NASA-TM-109110] p 3130 N94-29473

PITTING
Pitting corrosion of titanium
[AD-A274980] p 3203 N94-29089
Pit initiation on passivated metal surfaces: Crystallographic orientation and environmental effects
[ISBN-0-315-85433-2] p 3208 N94-30138

PIVOTS
Mars rover mechanisms designed for Rocky 4 p 3161 N94-29630

PIXELS
A multiscale approach to image segmentation using Kohonen networks
[RUU-CS-93-06] p 3438 N94-30349

PLANAR STRUCTURES
Printed circuit elements with applications to antennas, scattering, and circuits
[AD-A275512] p 3262 N94-28669

PLANE STRAIN
Plane strain finite element analysis of sheet forming operations including bending effects p 3322 N94-30354
An investigation of fatigue crack propagation under mode 1 and mixed mode 1/2 loadings p 3323 N94-30814

PLANE STRESS
Plane stress stable crack growth and J-integral/HRR field
[AD-A275761] p 3317 N94-28761
A modeling study of the effect of stress state on void linking during ductile fracture
[AD-A275505] p 3317 N94-28811
Approximate estimation of the effects of asymmetry on the testing of tensile specimens
[NPL-DMM(A)-117] p 3322 N94-30523
An investigation of fatigue crack propagation under mode 1 and mixed mode 1/2 loadings p 3323 N94-30814

PLANETARY ATMOSPHERES
The Pluto fast flyby mission: Completing the reconnaissance of the solar system p 3235 N94-29768
The far-infrared absorption spectrum of low temperature hydrogen gas
[ISBN-0-315-85432-4] p 3199 N94-30137

PLANETARY EVOLUTION
The thermal consequences of giant impacts in the early solar system p 3543 N94-29698

PLANETARY GEOLOGY
Venus Data Analysis Program: Directory of Research Projects (1993-1994)
[NASA-CR-195742] p 3549 N94-29102
The Pluto fast flyby mission: Completing the reconnaissance of the solar system p 3235 N94-29768

PLANETARY GRAVITATION
Analysis of crustal structure of Venus utilizing residual Line-of-Sight (LOS) gravity acceleration and surface topography data. A trial of global modeling of Venus gravity field using harmonic spline method
[NASA-CR-195799] p 3549 N94-29737
PLANETARY IONOSPHERES
Venus Data Analysis Program: Directory of Research Projects (1993-1994)
[NASA-CR-195742] p 3549 N94-29102
PLANETARY MAGNETOSPHERES
Observation of Jovian auroral Ly-alpha line profile and emission variability with a sounding rocket and the IUE archives p 3550 N94-30798
PLANETARY MAGNETOTAILS
Experimental investigation of possible geomagnetic feedback from energetic (0.1 to 16 keV) terrestrial O(+) ions in the magnetotail current sheet
[PAPER-93JA01991] p 3507 N94-30128
PLANETARY MAPPING
The Pluto fast flyby mission: Completing the reconnaissance of the solar system
p 3235 N94-29768
PLANETARY NEBULAE
Spatially resolved spectroscopy of AG Carinae, and direct evidence for stellar evolution: The central star of NGC 2392
[NASA-CR-189291] p 3545 N94-29871
PLANETARY SURFACES
The thermal consequences of giant impacts in the early solar system p 3543 N94-29698
Differential Scanning Calorimetry (DSC) for planetary surface exploration p 3236 N94-29776
PLANETARY WAVES
Papers in meteorology and geophysics, vol. 44, no.1
[JTN-94-80585] p 3324 N94-28693
On the linear stability of Verkley's modons
p 3324 N94-28695
Generation mechanisms of quasi-stationary waves in the Southern Hemisphere p 3365 N94-30789
PLANFORMS
Numerical solution of inverse problem in aerodynamics p 3125 N94-28965
Low-speed longitudinal aerodynamic characteristics of a flat-plate planform model of an advanced fighter configuration
[NASA-TM-109045] p 3130 N94-29443
PLANNING
A time reasoning system based on the event calculus for scheduling in aeronautic maintenance
[REPT-932-710-101] p 3122 N94-29463
Interactive analysis and planning tools for air traffic and airspace management p 3139 N94-29573
PLASMA ANTENNAS
Waves in space plasma dipole antenna subsystem
p 3161 N94-29632
PLASMA ARC WELDING
Plasma arc welding torch having means for vortexing plasma for exiting the welding torch
[NASA-CASE-MFS-28828-1] p 3298 N94-29351
Metal inert gas welding system for use in vacuum
[NASA-CASE-MFS-28808-1] p 3298 N94-29352
Chamber free fusion welding root side purging method and apparatus
[NASA-CASE-MFS-28832-1] p 3204 N94-29380
Ternary arc gas plasma welding torch
[NASA-CASE-MFS-28857-1] p 3303 N94-30173
PLASMA BUBBLES
Interaction of multiple spark-generated bubbles in a compressible liquid
[AD-A275037] p 3272 N94-29149
PLASMA CHEMISTRY
Direct measurement of the reactivity of NH and OH on a silicon nitride surface
[DE94-005286] p 3199 N94-30260
PLASMA CLOUDS
Experiments on the two-stage dense plasma heating on the GOL-3 device
[DE94-608356] p 3508 N94-30193
PLASMA COMPOSITION
A study of the formation and dynamics of the Earth's plasma sheet using ion composition data
[NASA-CR-195119] p 3507 N94-30126
PLASMA CONDUCTIVITY
Resistive ballooning mode in a gas-dynamic trap
[DE94-608328] p 3508 N94-30171
PLASMA CONTROL
Progress in Z-Pinch Research
[IPPCZ-321] p 3505 N94-29074
A 6MeV heavy ion beam probe for the Large Helical Device
[NIFS-272] p 3505 N94-29397
The effect of magnetic field configuration on particle pinch velocity in Compact Helical System (CHS)
[NIFS-267] p 3505 N94-29398
Formation and self-healing of magnetic islands in finite-beta helias equilibria
[NIFS-269] p 3505 N94-29483
Magnetic field generation by circularly polarized laser light and inertial plasma confinement in a miniature magnetic bottle induced by circularly polarized laser light
[DE94-608353] p 3508 N94-30192
The impact of improved physics on commercial tokamak reactors
[DE94-006103] p 3509 N94-30760
Application of divertor cryopumping to H-mode density control in DIII-D
[DE94-004859] p 3510 N94-30832
PLASMA COOLING
Peculiarities of heat transfer in the experiments of beam injection heating of a plasma at the GOL-3 device
[DE94-608357] p 3508 N94-30194
PLASMA CURRENTS
Theoretical reversed field pinch and tokamak studies
[DE94-005409] p 3503 N94-28490
Fluctuation and transport reduction in a reversed field pinch by inductive poloidal current drive
[DE94-005542] p 3503 N94-28514
Three-dimensional effects for radio frequency antenna modeling
[DE94-006102] p 3255 N94-30105
Advanced steady-state operating scenarios
[DE94-004810] p 3509 N94-30768
Application of divertor cryopumping to H-mode density control in DIII-D
[DE94-004859] p 3510 N94-30832
PLASMA DENSITY
Wave generation by contaminant ions near a large spacecraft
[NASA-CR-195797] p 3169 N94-29917
Magnetic field generation by circularly polarized laser light and inertial plasma confinement in a miniature magnetic bottle induced by circularly polarized laser light
[DE94-608353] p 3508 N94-30192
Experiments on the two-stage dense plasma heating on the GOL-3 device
[DE94-608356] p 3508 N94-30193
Peculiarities of heat transfer in the experiments of beam injection heating of a plasma at the GOL-3 device
[DE94-608357] p 3508 N94-30194
Variations of electron fluxes, low-frequency radiations and plasma density during the geomagnetic storm on 9-12 March, 1979 according to data of the Interkosmos-19 satellites
[DE94-607323] p 3365 N94-30223
Application of divertor cryopumping to H-mode density control in DIII-D
[DE94-004859] p 3510 N94-30832
PLASMA DIAGNOSTICS
New high temperature plasmas and sample introduction systems for analytical atomic emission and mass spectrometry
[DE94-004564] p 3503 N94-28458
Photon counting spectroscopy as done with a Thomson scattering diagnostic
[DE94-005543] p 3503 N94-28515
Broadband EUV survey spectrometer for short-timescale experiments
[DE94-005459] p 3498 N94-28534
Journal of NIRE, Vol. 2, No. 2
[JTN-94-80552] p 3187 N94-28675
A novel spectroscopic measurement method of RF plasma for temperature and electron density diagnoses
p 3188 N94-28682
Transient internal probe
[AD-A275054] p 3505 N94-29134
Experiments on the two-stage dense plasma heating on the GOL-3 device
[DE94-608356] p 3508 N94-30193
Inertial confinement fusion
[DE94-005957] p 3510 N94-30875
Magnetic flux reconstruction methods for shaped tokamaks
[DE94-005827] p 3510 N94-30882
PLASMA DIODES
Controlling chaos in plasma filled diodes
[AD-A275525] p 3504 N94-28686
PLASMA DRIFT
Space-time structure of the morning aurora inferred from coincident DMSP-F6, -F8, and Sondrestrom incoherent scatter radar observations
[AD-A275442] p 3356 N94-28869
PLASMA DYNAMICS
Molecular dynamics simulations of dense plasmas
[DE94-005082] p 3509 N94-30752
PLASMA FREQUENCIES
Practical applications of plasma surface modification
[DE94-004892] p 3349 N94-29932
PLASMA GUNS
Modelling erosion damage from low-energy plasma gun simulations of disruptions
[DE94-005196] p 3509 N94-30697
PLASMA HEATING
Electron beam irradiation experiments of monoblock divertor mock-up
[DE94-707497] p 3503 N94-28555
Experimental and analytical studies of high heat flux components for fusion experimental reactor
[DE94-707671] p 3504 N94-28556
TFTR Ion Cyclotron Range of Frequencies (ICRF) experimental data analysis collaboration
[DE94-004699] p 3504 N94-28575
Plasma heating for containerless and microgravity materials processing
[NASA-CASE-NPO-18819-1-CU] p 3229 N94-29371
Efficiencies of the ICRF minority heating in the CHS and LHD plasmas
[NIFS-270] p 3506 N94-29499
Three-dimensional effects for radio frequency antenna modeling
[DE94-006102] p 3255 N94-30105
Experiments on the two-stage dense plasma heating on the GOL-3 device
[DE94-608356] p 3508 N94-30193
Peculiarities of heat transfer in the experiments of beam injection heating of a plasma at the GOL-3 device
[DE94-608357] p 3508 N94-30194
PLASMA INTERACTIONS
Proceedings of Japan-US Workshop P-196 on High Heat Flux Components and Plasma Surface Interactions for Next Devices
[DE94-701164] p 3503 N94-28513
Active electron and ion beam experiments in space
[AD-A275570] p 3504 N94-28828
PLASMA JETS
Synthesis of diamond in a hydrogen plasma jet: Simulations of XRD patterns of diamond polytypes and boundary layer on a substrate p 3522 N94-29515
PLASMA LAYERS
Plasma sprayed ceramic thermal barrier coating for NiAl-based intermetallic alloys
[NASA-CASE-LEW-15535-1] p 3205 N94-29507
A study of the formation and dynamics of the Earth's plasma sheet using ion composition data
[NASA-CR-195119] p 3507 N94-30126
Tail lobe ion composition at energies of 0.1 to 16 keV/e: Evidence for mass-dependent density gradients
[PAPER-93JA03201] p 3507 N94-30127
PLASMA OSCILLATIONS
Resistive ballooning mode in a gas-dynamic trap
[DE94-608328] p 3508 N94-30171
PLASMA PHYSICS
Controlling chaos in plasma filled diodes
[AD-A275525] p 3504 N94-28686
A 6MeV heavy ion beam probe for the Large Helical Device
[NIFS-272] p 3505 N94-29397
The effect of magnetic field configuration on particle pinch velocity in Compact Helical System (CHS)
[NIFS-267] p 3505 N94-29398
Nonlinear wave packet evolution in a dispersive plasma: Application to rotational discontinuities
p 3506 N94-29822
ECR plasma synthesis of silicon nitride films on GaAs and InSb
[DE94-005575] p 3515 N94-30006
The investigation of electron-ion radiative and dielectronic recombination in high-temperature plasmas
[DE94-005150] p 3509 N94-30755
The impact of improved physics on commercial tokamak reactors
[DE94-006103] p 3509 N94-30760
Self-similar variables and the problem of nonlocal electron heat conductivity
[DE94-005826] p 3493 N94-30881
PLASMA PRESSURE
Formation and self-healing of magnetic islands in finite-beta helias equilibria
[NIFS-269] p 3505 N94-29483
Experiments on the two-stage dense plasma heating on the GOL-3 device
[DE94-608356] p 3508 N94-30193
PLASMA SPECTRA
Coronal temperatures of unusually active K-dwarf binary systems
[NASA-CR-189335] p 3545 N94-29881
PLASMA SPRAYING
Fabrication and testing of plasma-spray formed MoSi2 and MoSi2 composite tubes
[DE94-004995] p 3175 N94-28581
Plasma sprayed ceramic thermal barrier coating for NiAl-based intermetallic alloys
[NASA-CASE-LEW-15535-1] p 3205 N94-29507

PLASMA TEMPERATURE
Resistive ballooning mode in a gas-dynamic trap
[DE94-608328] p 3508 N94-30171
Peculiarities of heat transfer in the experiments of beam injection heating of a plasma at the GOL-3 device
[DE94-608357] p 3508 N94-30194
PLASMA TORCHES
Plasma arc welding torch having means for vortexing plasma for exiting the welding torch
[NASA-CASE-MFS-28828-1] p 3298 N94-29351
Metal inert gas welding system for use in vacuum
[NASA-CASE-MFS-28808-1] p 3298 N94-29352
Plasma heating for containerless and microgravity materials processing
[NASA-CASE-NPO-18819-1-CU] p 3229 N94-29371
Ternary arc gas plasma welding torch
[NASA-CASE-MFS-28857-1] p 3303 N94-30173
PLASMA TURBULENCE
Plasma turbulent bremsstrahlung
[PPL-144] p 3507 N94-30157
PLASMA WAVES
Coulomb field effect on plasma focusing and wake field acceleration
[DE94-004937] p 3504 N94-28564
Towards experimental verification and device applications of current driven plasma instabilities in solid state systems
[AD-A275395] p 3504 N94-29055
Wave generation by contaminant ions near a large spacecraft
[NASA-CR-195797] p 3169 N94-29917
A relativistic solitary wave in electron positron plasma
[DE94-608107] p 3507 N94-30071
Plasma turbulent bremsstrahlung
[PPL-144] p 3507 N94-30157
Langmuir waves in the electron-positron plasma
[DE94-608330] p 3508 N94-30191
PLASMA-PARTICLE INTERACTIONS
A 6MeV heavy ion beam probe for the Large Helical Device
[NIFS-272] p 3505 N94-29397
PLASMAS (PHYSICS)
Nonlinear magnetohydrodynamics
[DE94-005654] p 3503 N94-28547
Experimental and analytical studies of high heat flux components for fusion experimental reactor
[DE94-707671] p 3504 N94-28556
A novel spectroscopic measurement method of RF plasma for temperature and electron density diagnoses
p 3188 N94-28682
Development of large area RF induction plasma for cost effective diamond
[AD-A275886] p 3504 N94-28776
Advanced diagnostics for reacting flows
[AD-A275057] p 3272 N94-29136
Plasma arc welding torch having means for vortexing plasma for exiting the welding torch
[NASA-CASE-MFS-28828-1] p 3298 N94-29351
Chamber free fusion welding root side purging method and apparatus
[NASA-CASE-MFS-28832-1] p 3204 N94-29380
Preparation and structure of amorphous hydrogenated carbon film deposited with RF plasma CVD
p 3223 N94-29518
Nonlinear wave packet evolution in a dispersive plasma: Application to rotational discontinuities
p 3506 N94-29822
Practical applications of plasma surface modification
[DE94-004892] p 3349 N94-29932
Magnetic field generation by circularly polarized laser light and inertial plasma confinement in a miniature magnetic bottle induced by circularly polarized laser light
[DE94-608353] p 3508 N94-30192
Direct measurement of the reactivity of NH and OH on a silicon nitride surface
[DE94-005286] p 3199 N94-30260
Plasma treatment of polymer dielectric films to improve capacitive energy storage p 3223 N94-30479
Advanced steady-state operating scenarios
[DE94-004810] p 3509 N94-30768
Deexcitation processes in nuclear reactions: The study of hot hadronic matter
[DE94-003396] p 3492 N94-30836
Self-similar variables and the problem of nonlocal electron heat conductivity
[DE94-005826] p 3493 N94-30881
PLASMASPHERE
Electron beams at geosynchronous orbit
[AD-A275471] p 3355 N94-28684
PLASTIC DEFORMATION
Superplasticity in fine-grained ceramics
[AD-A275461] p 3212 N94-28733
Finite element analysis of axisymmetric deformations of thick thermoviscoplastic targets p 3320 N94-29688
The effect of various metallurgical parameters on the flow and fracture behavior of polycrystalline NiAl near the brittle-to-ductile transition
[NASA-TM-106534] p 3205 N94-29758
Higher order asymptotic crack tip fields in a power-law hardening material p 3321 N94-29829
Nanodislocation structures generated in shocked crystals p 3514 N94-29915
The role of plastic deformation in brittle and near-brittle cracking behavior p 3322 N94-30226
PLASTIC PROPERTIES
Toughening mechanisms in ultrahigh-strength steels
[AD-A275439] p 3202 N94-28867
Preliminary evaluation of hybrid titanium composite laminates
[NASA-TM-109095] p 3180 N94-29472
PLASTICIZERS
Development of novel switchable protein surfaces
[AD-A275510] p 3384 N94-28667
Enhanced ion dissociation of LiCF3SO3 by new carbonate plasticizers: Raman and IR studies
[DE94-005448] p 3485 N94-28741
High elongation elastomers p 3223 N94-30477
PLASTICS
Ballistic performance of polycarbonate/polyester and polycarbonate/styrene- acrylonitrile microlayer sheets
[AD-A275462] p 3177 N94-28735
PLATENS
Neural network based time-optimal control of a magnetically levitated precision positioning system
[DE94-006573] p 3437 N94-30250
PLATING
An improved plating process p 3223 N94-30451
PLATINUM
Geometric structures of thin film: Pt on Pd(110) and NiO on Ni(100)
[DE94-005564] p 3211 N94-28530
Realtime structural electrochemistry of platinum clusters using dispersive XAFS
[DE94-005093] p 3208 N94-30101
PLAYBACKS
Noise reduction techniques for the restoration of musical recordings
[TELECOM-93-E-019] p 3291 N94-30979
PLUMES
SOCRATES simulation of the emission at wavelength 6300 A generated by the interaction between the atmosphere and the Space Shuttle exhaust
[AD-A275567] p 3164 N94-28827
A laboratory simulation of urban heat-island-induced circulation in a stratified environment
p 3367 N94-30921
PLUTO (PLANET)
The Pluto fast flyby mission: Completing the reconnaissance of the solar system
p 3235 N94-29768
PLUTONIUM
Nature of dissolution of binary tantalum-titanium alloys by molten plutonium
[DE94-005090] p 3210 N94-30776
PLY ORIENTATION
Microstructure/property relationships for SCS6/Timetal 21-S composite
[AD-A275056] p 3178 N94-29135
Free edge and size effects on failure initiation and ultimate strength of laminates containing a center hole
p 3181 N94-29735
POINT SOURCES
A study of the convergence of spherical harmonic expansions of gravity using distributed point-mass Earth models p 3362 N94-29909
POINT SPREAD FUNCTIONS
Aberrated point-spread functions and beam quality for optical systems with annular pupils
[AD-A275311] p 3499 N94-28875
Calculation of turbulence degraded point spread function of an imaging system p 3260 N94-30514
POINTING CONTROL SYSTEMS
Lasercom system architecture with reduced complexity
[NASA-CASE-NPO-19069-1-CU] p 3293 N94-29493
The 27th Aerospace Mechanisms Symposium
[NASA-CP-3205] p 3160 N94-29627
Design and control of active vision based mechanisms for intelligent robots
[AIAA PAPER 94-1196-CP] p 3442 N94-30547
POISSON DENSITY FUNCTIONS
Photon counting spectroscopy as done with a Thomson scattering diagnostic
[DE94-005543] p 3503 N94-28515
Modelling of multiparticle production by dynamical semigroup method
[DE94-608132] p 3490 N94-30120
An intrinsic Hamiltonian formulation of the dynamics of LC-circuits
[MEMO-1154] p 3462 N94-30964
POISSON EQUATION
The upsilon-q method and the psi-q method for incompressible flows p 3126 N94-28971
A note on the Poisson brackets associated with Lax operators
[MATHS-REPT-A-195] p 3464 N94-29482
POISSON RATIO
Experimental determination of orthotropic elastic constants
[FFA-TN-1991-35] p 3215 N94-29424
POLAR CAPS
On observing neutron star oscillations
p 3538 N94-29795
POLAR CUSPS
ULF waves and magnetic field characteristics in the polar cusp observed at Godhavn p 3361 N94-29244
POLAR METEOROLOGY
Laboratory studies of chemical and photochemical processes relevant to stratospheric ozone
[NASA-CR-195779] p 3347 N94-29549
POLAR REGIONS
The effects of magnetic storm phases on F-layer irregularities from auroral to equatorial latitudes
[AD-A275203] p 3356 N94-28891
Hydrodynamics of convection under winter polar leads
[AD-A275182] p 3369 N94-29067
Signatures of dayside solar wind/magnetosphere/ionosphere coupling as revealed by the pace HF radars and associated experiments
p 3359 N94-29236
ULF waves and magnetic field characteristics in the polar cusp observed at Godhavn p 3361 N94-29244
Laboratory studies of chemical and photochemical processes relevant to stratospheric ozone
[NASA-CR-195779] p 3347 N94-29549
A study of the thermospheric dynamics of the high-latitude E region using a spectral thermospheric general circulation model p 3362 N94-29743
Cryosphere and climate p 3352 N94-30632
POLARIMETRY
Spectral and polarimetric analysis of hyperspectral data collected by an acousto-optic tunable filter system
[AD-A275076] p 3329 N94-29095
Transient internal probe
[AD-A275054] p 3505 N94-29134
Frequency dependence of polarization phase difference
[NASA-TM-109737] p 3254 N94-30094
Polarimetric backscatter measurements of natural surfaces at millimeter wavelengths p 3259 N94-30509
POLARIZATION (SPIN ALIGNMENT)
One-loop QCD mass effects in the production of polarized bottom and top quarks
[PB94-138104] p 3487 N94-29145
Improved QCD sum rule estimates of the higher twist contributions to polarised and unpolarised nucleon structure functions
[PB94-138112] p 3487 N94-29161
POLARIZATION (WAVES)
Evaluation of dual polarization attenuation of millimeter frequencies through a meteorological radar
p 3256 N94-30496
POLARIZATION CHARACTERISTICS
On the relation between SMMR 37-GHz polarization difference and the rainfall over Africa and Australia
[NASA-TM-104598] p 3370 N94-29408
POLARIZED ELECTROMAGNETIC RADIATION
On the relation between SMMR 37-GHz polarization difference and the rainfall over Africa and Australia
[NASA-TM-104598] p 3370 N94-29408
Radar cross sections of ground clutter at 95 GHz for summer and fall conditions p 3259 N94-30512
POLARIZED LIGHT
One-loop QCD mass effects in the production of polarized bottom and top quarks
[PB94-138104] p 3487 N94-29145
POLARONS
Interband optical absorption in the Wannier-Stark ladder under the electron-LO-phonon resonance condition
[DE94-608097] p 3267 N94-30092
POLICIES
Fuel cycle evaluations of biomass-ethanol and reformulated gasoline
[DE94-000227] p 3226 N94-30818
POLISHING
Analysis of cost: CVD diamond deposition and finishing --- Quarterly report
[AD-A275586] p 3212 N94-28725
Float polishing studies of fused silica
[AD-A275001] p 3213 N94-28886
POLLUTION CONTROL
Speciation in Water and Soil: A literature review
[PB94-132388] p 3341 N94-28412
Reduction of NO(x) by fuel-staging in gas turbine engines: A commitment to the future
p 3194 N94-29272

Chambers of turboreactors with variable geometry: A response to the matrix of pollution in cycles at high temperature, high pressure p 3194 N94-29273
Ventilation cost and air cleaning p 3232 N94-29605
A study of low emissions gas turbine combustions [NASA-CR-195763] p 3152 N94-29860
Technology 2003: The Fourth National Technology Transfer Conference and Exposition, volume 1 [NASA-CP-3249] p 3555 N94-30440
International Energy and Environmental Congress: Proceedings [DE93-040609] p 3353 N94-30715
Biological conversion of synthesis gas [DE94-005815] p 3340 N94-30879

POLLUTION MONITORING
Intermedia transfer factors for fifteen toxic pollutants released to air basins in California [DE94-005699] p 3349 N94-30044
Novel mass spectrometric instrument for gaseous and particulate characterization and monitoring [DE94-005896] p 3349 N94-30047
Computerized in vitro test for chemical toxicity based on tetrahymena swimming patterns p 3354 N94-30463
Granulometry in environments with very small particle concentrations p 3259 N94-30511

POLLUTION TRANSPORT
Intermedia transfer factors for fifteen toxic pollutants released to air basins in California [DE94-005699] p 3349 N94-30044
Evaluation of discretization schemes for advection-diffusion equations [CWI-NM-R9311] p 3461 N94-30751

POLYACRYLONITRILE
Preparation of graphite fibers from polyimide p 3223 N94-29517

POLYATOMIC MOLECULES
Chemical dynamics studies of reactions in energetic materials [AD-A275607] p 3224 N94-28769
Theoretical investigation of gas-surface interactions [NASA-CR-195755] p 3272 N94-29378
Spectroscopic and dynamical studies of highly energized small polyatomic molecules [DE94-006509] p 3489 N94-30061

POLYBUTADIENE
Correlation of cookoff behavior of rocket propellants with thermomechanical and thermochemical properties [AD-A274983] p 3224 N94-29092
A newly developed snow vehicle (SM100S) for Antarctica. Part 4: Low temperature properties of crawler belt p 3314 N94-29984
Solventless, curable fluid oligomeric systems for high performance microwave, acoustical and mechanical applications p 3223 N94-30478

POLYCARBONATES
Ballistic performance of polycarbonate/polyester and polycarbonate/styrene- acrylonitrile microlayer sheets [AD-A275462] p 3177 N94-28735
Surface energy changes produced by ultraviolet-ozone irradiation of poly(methylmethacrylate), polycarbone and polytetrafluoroethylene [NASA-TM-106460] p 3213 N94-28922
Ablation of polymers by ultraviolet pulsed laser [DE94-608100] p 3218 N94-30066
Improved construction materials for polar regions using microcellular thermoplastic foams p 3223 N94-30483

POLYCRYSTALS
An improved method of measuring tropospheric NO2, NO3, HO2, and RO2 by Matrix Isolation and Electronic Spin Resonance (MIESR) p 3345 N94-28605
The effect of various metallurgical parameters on the flow and fracture behavior of polycrystalline NiAl near the brittle-to-ductile transition [NASA-TM-106534] p 3205 N94-29758
The bases for the development of high-temperature integrated SQUID-systems [DE94-607901] p 3267 N94-30073
Plasma enhanced chemical vapor deposition of ZrO2 thin films [DE94-006031] p 3218 N94-30104
Electrooptical and optical evaluation of Pb(Zr,Ti)O3 thin films using waveguide refractometry [DE94-006374] p 3518 N94-30247

POLYESTERS
The polymerization of epsilon-caprolactone with stannous catalyst and lactide/epsilon-caprolactone (LA/epsilon-CL) and lactide/glycolide (LA/GA) copolymers. Polymer technology publication series no. 15 [PB94-137551] p 3220 N94-30713

POLYETHYLENE TEREPHTHALATE
Ablation of polymers by ultraviolet pulsed laser [DE94-608100] p 3218 N94-30066

POLYETHYLENES
Temperature depencence of the far infrared optical constants of polyethylene [PB94-124336] p 3213 N94-28795
Analysis of infrared radiation heating process considering chemical reaction of material to be heated [DE94-744116] p 3199 N94-30267
Development of radiation resistant electrical cable insulations p 3223 N94-30480
Development of radiation resistant electrical cable insulations [DE94-005189] p 3222 N94-30906

POLYGONS
Shape from diameter: Negative results [RUU-CS-93-16] p 3458 N94-30407
Shape from diameter: Positive results [RUU-CS-93-17] p 3458 N94-30408
Rectilinear decompositions with low stabbing number [RUU-CS-93-25] p 3459 N94-30425

POLYHEDRONS
Representations of dynamical systems described by behavioral inequalities [AD-B173649] p 3458 N94-30402

POLYIMIDE RESINS
Low dielectric polyimide fibers [NASA-CASE-LAR-14526-1] p 3214 N94-29359
Irradiation polymerization of bismaleimide resins [REPT-932-430-105] p 3215 N94-29441

POLYIMIDES
Breakdown testing of wiring insulation p 3166 N94-28713
High temperature polymer dielectric film insulation p 3167 N94-28715
Low dielectric polyimide fibers [NASA-CASE-LAR-14526-1] p 3214 N94-29359
Composite flexible blanket insulation [NASA-CASE-ARC-11955-1-CU] p 3180 N94-29509
Preparation of graphite fibers from polyimide p 3223 N94-29517
Polyimides containing the penta fluoro sulfanyl benzene moiety [NASA-CASE-LAR-15082-1] p 3175 N94-29554
Polyimides containing pendent siloxane groups [NASA-CASE-LAR-14638-1] p 3215 N94-29555
Study of the ultraviolet absorption and photoconduction spectra of polyimide films fabricated at various curing temperatures [ISBN-0-315-85923-7] p 3218 N94-30036

POLYISOPRENES
A newly developed snow vehicle (SM100S) for Antarctica. Part 4: Low temperature properties of crawler belt p 3314 N94-29984

POLYMER BLENDS
Ballistic performance of polycarbonate/polyester and polycarbonate/styrene- acrylonitrile microlayer sheets [AD-A275462] p 3177 N94-28735

POLYMER CHEMISTRY
Cellular and molecular approaches to polymer synthesis by bacteria [AD-A275501] p 3212 N94-28661
High temperature arc-track resistant aerospace insulation p 3167 N94-28716
Polymer Technology Seminar, 1993. Kem-100.600 [PB94-137593] p 3213 N94-29031
Polymer technology publication series no. 16 [PB94-135522] p 3214 N94-29157
Polyimides containing the penta fluoro sulfanyl benzene moiety [NASA-CASE-LAR-15082-1] p 3175 N94-29554
Polyimides containing pendent siloxane groups [NASA-CASE-LAR-14638-1] p 3215 N94-29555
Solventless, curable fluid oligomeric systems for high performance microwave, acoustical and mechanical applications p 3223 N94-30478
The polymerization of epsilon-caprolactone with stannous catalyst and lactide/epsilon-caprolactone (LA/epsilon-CL) and lactide/glycolide (LA/GA) copolymers. Polymer technology publication series no. 15 [PB94-137551] p 3220 N94-30713
Crosslinking and surface reactions in macromolecules: Spectroscopic FT-IR studies p 3221 N94-30812

POLYMER MATRIX COMPOSITES
Apparatus for providing a uniform, consolidated, unidirectional, continuous, fiber-reinforced polymeric material and method relating thereto [NASA-CASE-LAR-15173-1-CU] p 3180 N94-29496
Effects of physical aging on long-term creep of polymers and polymer matrix composites [NASA-TM-109081] p 3181 N94-29541
Standardisation requirements for ultrasonic C-scanning of polymer matrix composites: An initial assessment [PB94-139318] p 3184 N94-30438
High elongation elastomers p 3223 N94-30477
Generalized Eulerian-Lagrangian formulations in free and moving boundary problems: Processing of viscoelastic polymers and fiber suspensions p 3283 N94-30955

POLYMER PHYSICS
Organic materials that respond to molecules [AD-A275392] p 3174 N94-29307

POLYMERIC FILMS
Molecular aspects of transport in thin films of controlled architecture [DE94-004552] p 3211 N94-28457
High temperature polymer dielectric film insulation p 3167 N94-28715
A 3M high temperature dielectric film p 3167 N94-28717
Polyaniline membranes for gas and liquid separation [AD-A275851] p 3408 N94-28790
Corrosion inhibition by electrodeposited conductive-polymer film [AD-A275456] p 3213 N94-28806
Composite flexible blanket insulation [NASA-CASE-ARC-11955-1-CU] p 3180 N94-29509
Study of nonlinear optical polymers and their applications in optical waveguides p 3216 N94-29807
Ablation of polymers by ultraviolet pulsed laser [DE94-608100] p 3218 N94-30066
Plasma treatment of polymer dielectric films to improve capacitive energy storage p 3223 N94-30479

POLYMERIZATION
Alkylene-bridged polygerm- and polygermsilsesqui-oxanes: New hybrid organic-inorganic materials [DE94-005096] p 3174 N94-28557
Cellular and molecular approaches to polymer synthesis by bacteria [AD-A275501] p 3212 N94-28661
Polymer Technology Seminar, 1993. Kem-100.600 [PB94-137593] p 3213 N94-29031
Polymer technology publication series no. 16 [PB94-135522] p 3214 N94-29157
Irradiation polymerization of bismaleimide resins [REPT-932-430-105] p 3215 N94-29441
Polyimides containing the penta fluoro sulfanyl benzene moiety [NASA-CASE-LAR-15082-1] p 3175 N94-29554
Polyimides containing pendent siloxane groups [NASA-CASE-LAR-14638-1] p 3215 N94-29555

POLYMERS
Alkylene-bridged polygerm- and polygermsilsesqui-oxanes: New hybrid organic-inorganic materials [DE94-005096] p 3174 N94-28557
High temperature arc-track resistant aerospace insulation p 3167 N94-28716
Polymer Technology Seminar, 1993. Kem-100.600 [PB94-137593] p 3213 N94-29031
Measurement of bulk longitudinal modulus and correction for edge effects [DE94-005581] p 3222 N94-30900

POLYMETHYL METHACRYLATE
Surface energy changes produced by ultraviolet-ozone irradiation of poly(methylmethacrylate), polycarbone and polytetrafluoroethylene [NASA-TM-106460] p 3213 N94-28922
Ablation of polymers by ultraviolet pulsed laser [DE94-608100] p 3218 N94-30066

POLYNOMIALS
Upwind method using local interpolation p 3128 N94-28982
Splines and ocean wave modelling [PB94-139409] p 3378 N94-30002
Polynomial modeling of analog-to-digital converters [DE94-005579] p 3406 N94-30008
Homogeneous Poisson structures [DE94-608112] p 3453 N94-30119
Derivation lengths in term rewriting from interpretations in the naturals [RUU-CS-92-43] p 3455 N94-30346
A note on the complexity of local search problems [CT-93-02] p 3456 N94-30370

POLYPROPYLENE
Dendrite preventing separator for secondary lithium batteries [NASA-CASE-NPO-18585-1-CU] p 3265 N94-29411

POLYSTYRENE
Ablation of polymers by ultraviolet pulsed laser [DE94-608100] p 3218 N94-30066
Improved construction materials for polar regions using microcellular thermoplastic foams p 3223 N94-30483

POLYTETRAFLUOROETHYLENE
Surface energy changes produced by ultraviolet-ozone irradiation of poly(methylmethacrylate), polycarbone and polytetrafluoroethylene [NASA-TM-106460] p 3213 N94-28922

POLYURETHANE RESINS
Development of a unique polyurethane primer/topcoat p 3223 N94-30476

POLYVINYL ALCOHOL
A new material for removing heavy metals from water p 3354 N94-30471
POLYVINYL CHLORIDE
The effect of temperature on creep and physical ageing of PVC
[NPL-DMM(A)-93] p 3217 N94-29885
Creep and physical aging of PVC: Dependence on stress and temperature
[NPL-DMM(A)-115] p 3217 N94-29886
Improved construction materials for polar regions using microcellular thermoplastic foams p 3223 N94-30483
POPULATIONS
Reproduction in the Japanese anchovy (Engraulis japonica) as related to population fluctuation p 3235 N94-29708
POROSITY
Computational methods in continuum mechanics
[AD-A275560] p 3451 N94-28792
Microfocus radioscopy, a high resolution means of inspecting composite materials
[REPT-932-430-109] p 3179 N94-29454
Non-chromate talc conversion coatings for aluminum
[DE94-005281] p 3207 N94-30053
POROUS BOUNDARY LAYER CONTROL
Boundary layer control device for duct silencers
[NASA-CASE-ARC-12030-1] p 3478 N94-29362
POROUS PLATES
Boundary layer control device for duct silencers
[NASA-CASE-ARC-12030-1] p 3478 N94-29362
POROUS WALLS
A method for the modelling of porous and solid wind tunnel walls in computational fluid dynamics codes
[NASA-CR-195699] p 3270 N94-28724
PORPHYRINS
Photochemistry in constrained spaces: Zeolites and layered double metal hydroxides
[DE94-004958] p 3200 N94-30769
PORTABLE EQUIPMENT
Evaluation of access/navigational features of a graphical-user interface installed on a portable maintenance aid
[AD-A275791] p 3136 N94-28744
Radiation transport and focusing systems for power industrial lasers
[DE94-606817] p 3293 N94-28786
Portable electronically based method for the nondestructive remote sensing of crevice corrosion
[AD-A275403] p 3318 N94-29057
Portable Linear Sled (PLS) for biomedical research p 3163 N94-29648
PORTABLE LIFE SUPPORT SYSTEMS
Portable ventilatory resuscitation systems
[AD-A274984] p 3401 N94-29093
Lunar surface operations. Volume 1: Lunar surface emergency shelter
[NASA-CR-195551] p 3299 N94-29354
POSEIDON SATELLITE
TOPEX/POSEIDON operational orbit determination results using global positioning satellites p 3160 N94-29666
POSITION (LOCATION)
Testing for a signal with unknown location and scale in a stationary Gaussian random field
[AD-A275320] p 3464 N94-28876
Stability properties of inclusive connectivity for graphs
[AD-A275360] p 3452 N94-29016
Development of an accurate transmission line fault locator using the global positioning system satellites p 3144 N94-30652
Placing registration marks
[RUU-CS-93-21] p 3427 N94-30725
POSITION ERRORS
Time and position accuracy using codeless GPS p 3144 N94-30650
POSITION SENSING
Stripline monitor electronics for the bundle position determination in AmPS
[DIGEL-1993-8] p 3495 N94-29888
Computer Assisted Medical Interventions: Application to Conformal Radiotherapy
[RR-912-I] p 3395 N94-30028
Conformal external radiotherapy of prostatic carcinoma: Requirements and preliminary results p 3395 N94-30029
Pre- and intra-radiotherapy multimodal image registration: Principles and first experiments p 3395 N94-30030
Encoding technique for automated guided vehicle POSE recovery in a structured environment p 3144 N94-30286
POSITIONING
Synchronization, positioning, and communication in multistatic radar systems for air defence
[PB94-137478] p 3243 N94-28908
Position control of a flexible beam with active damping of vibrations
[ISBN-0-315-85841-9] p 3321 N94-30033
Nearly time-optimal feedback control of a magnetically levitated photolithography positioning system
[DE94-005288] p 3266 N94-30055
Neural network based time-optimal control of a magnetically levitated precision positioning system
[DE94-006573] p 3437 N94-30250
POSITIONING DEVICES (MACHINERY)
Three methods to improve the accuracy of a PUMA 560 robot p 3307 N94-30290
POSITIVE FEEDBACK
Sensitivity and feedbacks associated with vegetation-related land surface parameters in a general circulation model p 3348 N94-29800
Modeling studies of frontogenesis in the upper and middle troposphere p 3375 N94-30868
POSITRON ANNIHILATION
Influence of doping on the electronic structure of (La, Sr)2CuO4
[DE94-006383] p 3516 N94-30054
Experiment studies of electron-positron interactions at the Stanford Linear Accelerator Center
[DE94-005877] p 3491 N94-30702
POSITRONS
Langmuir waves in the electron-positron plasma
[DE94-608330] p 3508 N94-30191
POTASSIUM ALLOYS
Thermodynamics of molten K-TE alloys
[DE94-608095] p 3208 N94-30090
POTASSIUM COMPOUNDS
Experimental and theoretical studies of molecular solids
[AD-A275511] p 3485 N94-28668
POTENTIAL FLOW
A residual correction method applied to 2D multi-point airfoil design and 3D single-point wing design
[NLR-TP-92524-U] p 3134 N94-30493
POTENTIAL THEORY
Quasipotential in the fourth order of perturbation theory
[DE94-606299] p 3484 N94-28584
POWDER (PARTICLES)
Synthesis and neutron diffraction study of Na3WN3 and Na3MoN3
[AD-A275158] p 3203 N94-29043
Bench-scale synthesis of nanoscale materials p 3240 N94-30473
Properties of chemical vapor infiltration diamond deposited in a diamond powder matrix
[DE94-005429] p 3220 N94-30591
POWER AMPLIFIERS
Miniaturization in x ray and gamma ray spectroscopy p 3236 N94-29773
Communications technology for unattended sensors
[DE94-005685] p 3254 N94-30043
POWER CONDITIONING
Non-isolated 30 kW class arcjet PCU
[NASA-CR-189148] p 3173 N94-29444
POWER EFFICIENCY
Investigation on application of genetic algorithms to optimal reactive power dispatch of power systems
[MATHS-REPT-A-197] p 3266 N94-29527
POWER LINES
Electric power lines: Questions and answers on research into health effects
[DE94-005637] p 3353 N94-30757
POWER REACTORS
Advanced steady-state operating scenarios
[DE94-004810] p 3509 N94-30768
POWER SERIES
Method of Chabauty-Coleman and the second case of Fermat's last theorem for regular primes
[PB94-138187] p 3467 N94-29162
POWER SPECTRA
Parameter identification of the rotordynamic coefficients of high-Reynolds-number hydrostatic bearings p 3311 N94-30792
Theory and observations of horizontal and vertical structure of gravity wave perturbations in the middle atmosphere p 3366 N94-30802
POWER SUPPLIES
Investigation on application of genetic algorithms to optimal reactive power dispatch of power systems
[MATHS-REPT-A-197] p 3266 N94-29527
POWER SUPPLY CIRCUITS
Selection of the Space Station Freedom (SSF) Flat Collector Circuit (FCC) insulation material p 3165 N94-28701
Electric power system test and verification program
[NASA-TM-106405] p 3169 N94-30123
PREAMPLIFIERS
A high rate, low noise, x ray silicon strip detector system
[DE94-004557] p 3268 N94-30717
A low noise silicon detector preamplifier system for room temperature x ray spectroscopy
[REPT-93-058] p 3291 N94-30930
PRECESSION
On relativity principle violation in local measurements of spin precession of moving particles
[DE94-608067] p 3489 N94-30085
PRECIPITATION (METEOROLOGY)
Sensitivity and feedbacks associated with vegetation-related land surface parameters in a general circulation model p 3348 N94-29800
The incorporation and initialization of cloud water/ice in an operational forecast model p 3373 N94-29814
A study of precipitation in the coastal area of Antarctica as observed at Syowa Station using a vertical pointing radar p 3363 N94-29979
PRECIPITATION HARDENING
Toughening mechanisms in ultrahigh-strength steels
[AD-A275439] p 3202 N94-28867
PRECISION
An Earth observation telescope refocusing mechanism
[REPT-932-440-103] p 3332 N94-29417
Precision and manufacturing at the Lawrence Livermore National Laboratory p 3240 N94-30449
Time and position accuracy using codeless GPS p 3144 N94-30650
PREDICATE CALCULUS
Commutative Lambek categorial grammars
[ML-93-01] p 3457 N94-30395
Modal quantification over structured domains
[ML-93-02] p 3457 N94-30396
Isomorphisms between predicate and state transformers
[CWI-CS-R9338] p 3459 N94-30430
Relating state transformation semantics and predicate transformer semantics for parallel programs
[CWI-CS-R9339] p 3433 N94-30431
PREDICATE LOGIC
Interrogatives and adverbs of quantification
[LP-92-14] p 3456 N94-30372
The Vanilla meta-interpreter for definite logic programs and ambivalent syntax
[CT-93-01] p 3424 N94-30386
Commutative Lambek categorial grammars
[ML-93-01] p 3457 N94-30395
Modal quantification over structured domains
[ML-93-02] p 3457 N94-30396
Isomorphisms between predicate and state transformers
[RUU-CS-93-09] p 3458 N94-30403
Isomorphisms between predicate and state transformers
[CWI-CS-R9338] p 3459 N94-30430
Relating state transformation semantics and predicate transformer semantics for parallel programs
[CWI-CS-R9339] p 3433 N94-30431
Bisimulations and predicate logic
[CWI-CS-R9333] p 3460 N94-30735
PREDICTION ANALYSIS TECHNIQUES
Modeling turbulence in flows with a strong rotational component
[DE94-003577] p 3270 N94-28475
BAG: A code for predicting the performance of a gas bag impact attenuation system for the Pathfinder lander
[DE94-003688] p 3165 N94-28477
Role of microstructure on the fatigue durability of aluminum aircraft alloys
[AD-A275814] p 3202 N94-28830
Decompression sickness risk versus time and altitude
[AD-A275261] p 3391 N94-29071
Spray combustion experiments and numerical predictions p 3195 N94-29277
Free edge and size effects on failure initiation and ultimate strength of laminates containing a center hole p 3181 N94-29735
Theoretical prediction of the influence coefficients on damped simple flexible rotors using the transfer matrix method
[IMR-TM-TR-002] p 3321 N94-30018
Development of a method to predict transonic limit cycle oscillation characteristics of fighter aircraft (continued)
[NLR-TP-92156-U] p 3148 N94-30342
Comparison of RCS prediction techniques, computations and measurements
[PB94-125515] p 3256 N94-30392
Predictive sufficiency and the use of stored internal state
[AIAA PAPER 94-1213-CP] p 3445 N94-30564
A real-time prediction of UTC p 3470 N94-30654
Numerical simulation and prediction of implosion phenomena
[GKSS-92/E/99] p 3284 N94-30968
PREDICTIONS
Significant figures and Lyapunov exponents in chaos and constrained divergence of chaotic orbits p 3467 N94-29910

A real-time prediction of UTC p 3470 N94-30654
PREFORMS
3-D braided, continuous fiber ceramic composites produced by chemical vapor infiltration
[AD-A275192] p 3178 N94-29024
Microwave assisted chemical vapor infiltration
[DE94-005005] p 3185 N94-30771
PREGNANCY
Physiological Anatomical Rodent Experiment (PARE) .04 feasibility test 2
[NASA-CR-195210] p 3385 N94-29968
PRELAUNCH TESTS
Electric power system test and verification program
[NASA-TM-106405] p 3169 N94-30123
PREMIXED FLAMES
Prediction of prompt NO(x) in hydrocarbon air flames p 3190 N94-29250
Simulation of pollutant formation in turbulent combustors using an extended coherent flame model p 3190 N94-29251
Ducted kerosene spray flames p 3195 N94-29276
PREMIXING
The effect of incomplete fuel-air mixing on the lean limit and emissions characteristics of a Lean Prevaporized Premixed (LPP) combustor p 3193 N94-29265
Effects of hydrogen addition on pollutant emissions in a gas turbine combustor p 3195 N94-29275
Numerical prediction of mixing process in a methane-fueled engine p 3304 N94-30230
PREPREGS
Polymer infiltration studies
[NASA-CR-195729] p 3213 N94-28748
Non-rectangular towpreg architectures
[NASA-CASE-LAR-14863-1-CU] p 3180 N94-29485
Apparatus for providing a uniform, consolidated, unidirectional, continuous, fiber-reinforced polymeric material and method relating thereto
[NASA-CASE-LAR-15173-1-CU] p 3180 N94-29496
PRESSING (FORMING)
Generalized Eulerian-Lagrangian formulations in free and moving boundary problems: Processing of viscoelastic polymers and fiber suspensions p 3283 N94-30955
PRESSURE
Scaling in heavy-fermion systems
[DE94-005002] p 3492 N94-30775
PRESSURE BREATHING
Comparative centrifuge evaluation of the Air Force Advanced Technology Anti-G Suit (ATAGS) and the Navy Enhanced Anti-G Lower Ensemble (EAGLE)
[AD-A275348] p 3400 N94-28996
PRESSURE CHAMBERS
Numerical simulation and prediction of implosion phenomena
[GKSS-92/E/99] p 3284 N94-30968
PRESSURE DEPENDENCE
Dislocation theory of melting for iron, revisited
[DE94-002715] p 3355 N94-28538
Crystal structure of La(2-x)Ba(x)CuO4
[DE94-707688] p 3511 N94-28750
Synthesis and neutron diffraction study of Na3WN3 and Na3MoN3
[AD-A275158] p 3203 N94-29043
Scaling in heavy-fermion systems
[DE94-005002] p 3492 N94-30775
Studies of interfaces and vapors with Optical Second Harmonic Generation
[DE94-006295] p 3476 N94-30841
PRESSURE DISTRIBUTION
Fluid dynamic noise in a centrifugal pump
[AD-A275264] p 3477 N94-28904
Quadruplet expansion of the acoustic pressure field in a wedge shaped ocean
[AD-A275121] p 3477 N94-29003
Wall pressure fluctuations in the reattachment region of a supersonic free shear layer
[NASA-CR-195790] p 3132 N94-29920
Computation of wind tunnel wall effects for complex models using a low-order panel method
[NASA-TM-104019] p 3132 N94-30151
An interactive, design and educational tool for supersonic external-compression inlets
[NASA-TM-106581] p 3421 N94-30174
Three-dimensional flow characteristics downstream of a blade endwall corner p 3280 N94-30229
Calculus of variations applied to 2D multi-point airfoil design
[PB94-125457] p 3133 N94-30401
Sensitivity analysis of the static aeroelastic response of a wing p 3134 N94-30525
Design of a variable-conductance vacuum insulation
[DE94-000270] p 3268 N94-30819
PRESSURE EFFECTS
Dislocation theory of melting for iron, revisited
[DE94-002715] p 3355 N94-28538
Effects of pressure on membrane-associated receptors and effector elements
[AD-A275813] p 3384 N94-28829
Pollutant emissions from and within a model gas turbine combustor at elevated pressures and temperatures p 3194 N94-29271
Formation and self-healing of magnetic islands in finite-beta helias equilibria
[NIFS-269] p 3505 N94-29483
The effect of pressure gradient on the structure of an equilibrium turbulent boundary layer p 3282 N94-30807
PRESSURE GRADIENTS
The effect of pressure gradient on the structure of an equilibrium turbulent boundary layer p 3282 N94-30807
Atmospheric turbulence within and above a coniferous forest
[ISBN-0-315-75468-0] p 3375 N94-30870
PRESSURE MEASUREMENT
Steady pressure measurements on an Aeroelastic Research Wing (ARW-2)
[NASA-TM-109046] p 3122 N94-28658
Method for making a dynamic pressure sensor and a pressure sensor made according to the method
[NASA-CASE-LAR-14029-1] p 3288 N94-29484
Micro-sensors for in-situ meteorological measurements p 3236 N94-29777
Analysis of fluctuating static pressure measurements in a large high Reynolds number transonic cryogenic wind tunnel p 3158 N94-30788
The execution of wind energy projects 1986 - 1992 between China Aerodynamics Research and Development Centre (CARDC) and The Aeronautical Research Institute of Sweden (FFA)
[FFA-TN-1993-19] p 3340 N94-30945
PRESSURE MODULATOR RADIOMETERS
Optical Chopper Assembly for the Mars Observer p 3162 N94-29639
PRESSURE OSCILLATIONS
Wall pressure fluctuations in the reattachment region of a supersonic free shear layer
[NASA-CR-195790] p 3132 N94-29920
PRESSURE RATIO
Evaluation of flip-flop jet nozzles for use as practical excitation devices
[NASA-TM-106377] p 3135 N94-30949
PRESSURE REGULATORS
Determination of pressure response times for gaseous flow in a tube
[AD-A275274] p 3272 N94-29435
Measurand transient signal suppressor
[NASA-CASE-MSC-22027-1] p 3435 N94-29466
PRESSURE SENSORS
Method for making a dynamic pressure sensor and a pressure sensor made according to the method
[NASA-CASE-LAR-14029-1] p 3288 N94-29484
PRESSURE SUITS
A reliable and repeatable method for volume calculation of pressurized garments
[AD-A275600] p 3399 N94-28766
Comparative centrifuge evaluation of the Air Force Advanced Technology Anti-G Suit (ATAGS) and the Navy Enhanced Anti-G Lower Ensemble (EAGLE)
[AD-A275348] p 3400 N94-28996
Procedures and metrics for anti-G suit evaluations
[AD-A275349] p 3400 N94-28997
Decompression sickness risk versus time and altitude
[AD-A275261] p 3391 N94-29071
EVA glove evaluation methodology and test protocol p 3401 N94-29729
PRESSURE VESSELS
Single specimen fracture toughness determination procedure using instrumented impact test
[PB94-132040] p 3316 N94-28402
Experimental and analytical comparison of constraint effects due to biaxial loading and shallow-flaws
[DE94-004794] p 3323 N94-30689
PREVENTION
Application of remote sensing in prevention of disasters p 3332 N94-29230
PRIMERS (COATINGS)
Development of a unique polyurethane primer/topcoat p 3223 N94-30476
PRIMITIVE EQUATIONS
Modeling studies of frontogenesis in the upper and middle troposphere p 3375 N94-30868
PRINCIPAL COMPONENTS ANALYSIS
Nonlinear PCA: Algorithms and applications
[PB94-137544] p 3419 N94-29680
PRINTED CIRCUITS
Printed circuit elements with applications to antennas, scattering, and circuits
[AD-A275512] p 3262 N94-28669
Screening of flexible cables by nonlinear resistance measurements
[AD-A275193] p 3264 N94-29289
Controlled thermal expansion printed wiring boards based on liquid crystal polymer dielectrics
[NASA-CR-189338] p 3287 N94-29400
PRINTING
Fundamentals of printing technology
[PB94-132602] p 3530 N94-29141
PRIORITIES
Risk-based prioritization: A comparison of approaches
[DE94-003368] p 3526 N94-28474
PRIVACY
Management of PEM public key certificates using X.500 directory service: Some problems and solutions
[DE94-004200] p 3431 N94-29952
PROBABILITY DENSITY FUNCTIONS
Ten new checks to assess the statistical quality of Monte Carlo solutions in MCNP
[DE94-006137] p 3465 N94-30366
PROBABILITY DISTRIBUTION FUNCTIONS
A moment plotting method for characterizing aircraft fatigue data population distributions
[AD-A275500] p 3145 N94-28660
A family of joint probability models for cost and schedule uncertainties
[AD-A275513] p 3463 N94-28670
A method for the probabilistic design assessment of composite structures
[NASA-TM-106384] p 3319 N94-29384
Rocket engine system reliability analyses using probabilistic and fuzzy logic techniques
[NASA-TM-106519] p 3173 N94-29403
Pearl's belief propagation: The proofs
[RUU-CS-92-47] p 3456 N94-30378
PROBABILITY THEORY
Risk-based prioritization: A comparison of approaches
[DE94-003368] p 3526 N94-28474
Identification of components to optimize improvement in system reliability
[DE94-001601] p 3315 N94-28503
A family of joint probability models for cost and schedule uncertainties
[AD-A275513] p 3463 N94-28670
Markov chains for random urinalysis 3: Daily model and drug kinetics
[AD-A275540] p 3389 N94-28797
The effects of molecular orientation geometry and surface anisotropy upon etching
[AD-A275154] p 3486 N94-29032
Stability of dynamical systems in the presence of noise
[AD-A275383] p 3243 N94-29072
Boundary layer coherent structures
[AD-A275007] p 3272 N94-29195
A method for the probabilistic design assessment of composite structures
[NASA-TM-106384] p 3319 N94-29384
Conditional dependence in probabilistic networks
[RUU-CS-92-34] p 3464 N94-29450
Reliability of composite material structures. Application: High pressure spherical coded tanks
[REPT-932-430-103] p 3180 N94-29478
Comparison of Savannah River Site's meteorological databases
[DE94-001751] p 3373 N94-29817
Risk measures in living probabilistic safety assessment
[VTT-PUBS-146] p 3465 N94-30154
Vulnerability of manned spacecraft to crew loss from orbital debris penetration
[NASA-TM-108452] p 3169 N94-30161
Bayesian belief networks and conditional independencies
[RUU-CS-92-36] p 3465 N94-30376
A probabilistic approach to motion planning for car-like robots
[RUU-CS-93-18] p 3438 N94-30410
Modeling systems by probabilistic process algebra: An event structures approach
[MEMO-INF-93-29-REV] p 3425 N94-30416
Thermodynamics of computation and information distance
[CWI-CS-R9341] p 3526 N94-30433
PROBLEM SOLVING
A cognitive model of decision making: Chunking and the radar detection device
[AD-A275185] p 3242 N94-28859
Incorporating geometric constraints into rule-based systems using nonlinear optimization
[AD-A275093] p 3452 N94-29063
Propagation of evidence through fuzzy rules
[AD-A275071] p 3411 N94-29180
Neural network solutions to logic programs with geometric constraints
[AD-A275419] p 3435 N94-29198

More problems on rewriting
[CWI-CS-R9332] p 3428 N94-30734
The (n squared)-hard problems in computational geometry
[RUU-CS-93-15] p 3461 N94-30747

PROCEDURES
Environmental Compliance Assessment System (ECAS) --- Japan supplement
[AD-A275549] p 3346 N94-28722
Cleanroom engineering handbook. Volume 4. Specification team practices
[AD-A275861] p 3156 N94-28753
Tuning of AmPS
[NIKHEF-K-AMPS-93-01] p 3494 N94-29422

PROCESS CONTROL (INDUSTRY)
The development and demonstration of the metric assessment tool
[AD-A275788] p 3230 N94-28742
Effect of non-metallic inclusions on the machinability of steel
[PB93-230233] p 3204 N94-29387
Formal specification and verification of real-time sequential control systems
[AD-A275776] p 3419 N94-29678
Yield and variability optimization of integrated circuits: Principles and practical solutions p 3266 N94-29805

PROCUREMENT
Reference model for project support environments, version 2.0
[AD-A275191] p 3410 N94-29068

PRODUCT DEVELOPMENT
Systematic safety consideration in product design
[PB94-132354] p 3229 N94-28410
A conceptual framework for software technology transition
[AD-A275637] p 3407 N94-28639
Cleanroom engineering handbook. Volume 2: Organization and project formation in the cleanroom environment
[AD-A275809] p 3156 N94-28772
Comparative centrifuge evaluation of the Air Force Advanced Technology Anti-G Suit (ATAGS) and the Navy Enhanced Anti-G Lower Ensemble (EAGLE)
[AD-A275348] p 3400 N94-28996
The UNICON approach to through-life support and evolution of software-intensive systems
p 3416 N94-29340
The discipline of defining the software product
p 3416 N94-29343
A common approach for an aerospace software environment p 3417 N94-29346

PRODUCTION COSTS
Large-area triple-junction a-Si alloy production scale up
[DE94-000249] p 3339 N94-30604

PRODUCTION ENGINEERING
Microcomputer-based protective functions in industrial production systems: Assessment method
[PB94-137817] p 3411 N94-29159

PRODUCTION MANAGEMENT
Technology transfer initiatives
[NASA-CR-195151] p 3537 N94-29410

PRODUCTIVITY
Realizing the productivity potential of expeditious operations
[PB94-135555] p 3230 N94-29188
Triple Diagonal modeling: A mechanism to focus productivity improvement for business success
[DE94-004309] p 3527 N94-30041

PROGRAM VERIFICATION (COMPUTERS)
Software Technology for Adaptable, Reliable Systems (STARS) program
[AD-A275675] p 3407 N94-28664
Reasoning about programs by exploiting the environment
[AD-A275852] p 3408 N94-28794
Microcomputer-based protective functions in industrial production systems: Assessment method
[PB94-137817] p 3411 N94-29159
Program derivation by proof transformation
[AD-A275260] p 3453 N94-29304
Object versus functional oriented design
p 3413 N94-29321
Software testing practices and their evolution for the 1990's p 3415 N94-29335
Validation and test of complex weapon systems
p 3150 N94-29336
Integrated formal verification and validation of safety critical software p 3416 N94-29338
Animators and error reporters for generated programming environments
[CWI-CS-R9253] p 3418 N94-29503
Formal specification and verification of real-time sequential control systems
[AD-A275776] p 3419 N94-29678
Electric power system test and verification program
[NASA-TM-106405] p 3169 N94-30123
GNU debugger internal architecture
[DE94-006665] p 3422 N94-30251
Isomorphisms between predicate and state transformers
[CWI-CS-R9338] p 3459 N94-30430
A user's guide to the Software Testpilot
[CWI-CS-R9343] p 3426 N94-30435
The MACS-TSA applied in the ISO and SAX spacecraft projects
[PB94-126257] p 3170 N94-30857

PROGRAMMABLE LOGIC DEVICES
A/GATECH DOSP fabrication --- optical programmable logic array
[AD-A275848] p 3430 N94-28781

PROGRAMMING ENVIRONMENTS
Guide to the Environmental-Language
[AD-A275849] p 3408 N94-28784
SDE's for the year 2000 and beyond: An EF perspective p 3417 N94-29344
A common approach for an aerospace software environment p 3417 N94-29346
A distributed object-based environment in Ada
p 3417 N94-29347
DSSA-ADAGE: An environment for architecture-based avionics development p 3150 N94-29348
Entreprise 2: A PCTE integrated project support environment p 3417 N94-29349
The ABC structure editor: Structure-based editing for the ABC programming environment
[CWI-CS-R9256] p 3418 N94-29487
Animators and error reporters for generated programming environments
[CWI-CS-R9253] p 3418 N94-29503
Considerations on graphical user interfaces for intelligent ATM support systems p 3139 N94-29572
Programming aspects of Views: An open-architecture application environment
[CWI-CS-R9259] p 3422 N94-30321
Modelling interaction tools in the Views architecture
[CWI-CS-R9261] p 3423 N94-30323
Maintaining presentation invariants in the Views system
[CWI-CS-R9262] p 3423 N94-30324

PROGRAMMING LANGUAGES
Guide to the Environmental-Language
[AD-A275849] p 3408 N94-28784
Summer intern program
[AD-A275194] p 3466 N94-28888
Tinkertoy(tm) transactions
[AD-A275271] p 3410 N94-29006
Advanced languages for systems software
[AD-A275272] p 3410 N94-29007
North American jumelage 'type systems'
[AD-A275342] p 3411 N94-29214
Constrained objects
[AD-A275273] p 3418 N94-29434
Graphics for ABC
[CWI-CS-R9255] p 3418 N94-29449
The ABC structure editor: Structure-based editing for the ABC programming environment
[CWI-CS-R9256] p 3418 N94-29487
Proceedings: SISAL 1993
[DE94-006641] p 3420 N94-30056
Programming aspects of Views: An open-architecture application environment
[CWI-CS-R9259] p 3422 N94-30321
A conceptual language for the description and manipulation of complex information models
[TR-92-34] p 3423 N94-30344
On blocks: Locality and asynchronous communication (extended abstract)
[RUU-CS-92-44] p 3424 N94-30347
A note on the Smyth powerdomain construction
[RUU-CS-93-02] p 3457 N94-30393
Algebraic domains, chain completion, and the Plotkin powerdomain construction
[RUU-CS-93-03] p 3457 N94-30394
Modeling systems by probabilistic process algebra: An event structures approach
[MEMO-INF-93-29-REV] p 3425 N94-30416
Three metric domains of processes for bisimulation
[CWI-CS-R9335] p 3459 N94-30427
MANIFOLD version 1.0 programming: Programs and problems
[CWI-CS-R9334] p 3425 N94-30428
Manray: A replicated workers program in MANIFOLD
[CWI-CS-R9337] p 3433 N94-30429
Topological models for higher order control flow
[CWI-CS-R9340] p 3425 N94-30432
Comparative semantics for linear arrays of communicating processes
[CWI-CS-R9336] p 3426 N94-30491
A streamlined software environment for situated skills
[AIAA PAPER 94-1205-CP] p 3444 N94-30556
On the relation between Unity properties and sequences of states
[RUU-CS-93-07] p 3433 N94-30720
Parallel language constructs for paradigm integration and deterministic computations
[DE94-005119] p 3428 N94-30754
A new programming methodology for lazy functional languages
[MEMO-INF-93-44] p 3429 N94-30765
Federal grammars and modular compilers
[REPT-93-054] p 3429 N94-30928

PROJECT MANAGEMENT
NASA Parts Program Office responsibilities
p 3165 N94-28702
NAVAIR aircraft wiring standardization and qualification program p 3166 N94-28704
Cleanroom engineering handbook. Volume 2: Organization and project formation in the cleanroom environment
[AD-A275809] p 3156 N94-28772
Application of information management methodologies for project quality improvement in a changing environment p 3416 N94-29342
SDE's for the year 2000 and beyond: An EF perspective p 3417 N94-29344
The 1993 Federal Aviation Administration Aviation System Capital Investment Plan p 3136 N94-29445
Crystalline-silicon solar cell development sponsored by the US Department of Energy
[DE94-003783] p 3340 N94-30609
Benchmarking for cost improvement
[DE94-002276] p 3528 N94-30824

PROJECT PLANNING
Intelligent automated process planning and code generation for computer-controlled inspection
[AD-A275346] p 3409 N94-28920
EOS project and ASTER (ITIR) p 3331 N94-29226
Earth-observation plan in Europe
p 3331 N94-29227
Japan's Earth observation satellite programs
p 3332 N94-29232
Artificial intelligence technology program at Rome Laboratory p 3414 N94-29328
An Operational Control Segment (OCS) update on GPS constellation status and future program directions
p 3144 N94-30643
Development status of the Communications and Broadcasting Engineering Test Satellite (COMETS)
[JTN-94-80545] p 3169 N94-30811

PROJECT SETI
The Telecommunications and Data Acquisition Report
[NASA-CR-195694] p 3246 N94-29613

PROLOG (PROGRAMMING LANGUAGE)
On the unification free PROLOG programs
[CWI-CS-R9331] p 3427 N94-30733

PROP-FAN TECHNOLOGY
Investigation of advanced counterrotation blade configuration concepts for high speed turboprop systems. Task 2: Unsteady ducted propfan analysis computer program users manual
[NASA-CR-187105] p 3152 N94-29438

PROPANE
Measurements and predictions of the combustion characteristics of enclosed swirl-stabilized propane flames
[IECE-CFE-TR-001] p 3198 N94-30017

PROPELLANT ADDITIVES
A study of low emissions gas turbine combustions
[NASA-CR-195763] p 3152 N94-29860

PROPELLANT CHEMISTRY
Fuels combustion research
[AD-A275122] p 3189 N94-29004
Superior energetic materials that contain carbocations and anions. Energetic materials restricted in composition to C, H, N, and O atoms
[AD-A275449] p 3225 N94-29310

PROPELLANT COMBUSTION
Fuel-rich catalytic combustion of a high density fuel
[NASA-TP-3281] p 3197 N94-29356
Liquid-oxygen droplet vaporization and combustion: Analysis of transcritical behavior and application to liquid-rocket combustion instability p 3197 N94-29592

PROPELLANT PROPERTIES
Advanced fuel properties: A computer program for estimating property values
[AD-A275248] p 3224 N94-28901
Correlation of cookoff behavior of rocket propellants with thermomechanical and thermochemical properties
[AD-A274983] p 3224 N94-29092

PROPELLANT SENSITIVITY
Insensitive energetic materials: The importance of physical properties and molecular structure
[AD-A275393] p 3225 N94-29308

PROPELLANT STORAGE
Large scale cryogenic fluid systems testing
[NASA-TM-109735] p 3157 N94-29904

PROPELLANT TANKS
Large scale cryogenic fluid systems testing
[NASA-TM-109735] p 3157 N94-29904
PROPELLANT TESTS
Correlation of cookoff behavior of rocket propellants with thermomechanical and thermochemical properties
[AD-A274983] p 3224 N94-29092
PROPELLANT TRANSFER
Development and testing of the Automated Fluid Interface System p 3161 N94-29636
PROPELLANTS
Superior energetic materials that contain carbocations and anions. Energetic materials restricted in composition to C, H, N, and O atoms
[AD-A275449] p 3225 N94-29310
PROPELLER SLIPSTREAMS
Aerodynamic characteristics of a propeller-powered high-lift semispan wing
[NASA-TM-4541] p 3132 N94-29937
Aerodynamic analysis of slipstream/wing/nacelle interference for preliminary design of aircraft configurations
[AD-B173651] p 3135 N94-30916
PROPELLERS
Aerodynamic characteristics of a propeller-powered high-lift semispan wing
[NASA-TM-4541] p 3132 N94-29937
PROPOSALS
Advanced gas turbine systems research
[DE94-005303] p 3297 N94-28485
PROPULSION SYSTEM CONFIGURATIONS
Nuclear electric propulsion: A better, safer, cheaper transportation system for human exploration of Mars
[NASA-TM-106406] p 3171 N94-28833
Research and Development of Ram/Scramjets and Turboramjets in Russia
[AGARD-LS-194] p 3151 N94-29291
Turboramjet engines: Types and performances p 3151 N94-29293
Fission-activated laser as primary power for CW laser propulsion
[DE94-006138] p 3295 N94-30367
PROPULSION SYSTEM PERFORMANCE
Nuclear electric propulsion: A better, safer, cheaper transportation system for human exploration of Mars
[NASA-TM-106406] p 3171 N94-28833
Fuels combustion research
[AD-A275122] p 3189 N94-29004
Orbital applications of electrodynamic propulsion
[AD-A275413] p 3173 N94-29216
Combustion for future supersonic transport propulsion p 3190 N94-29249
Research and Development of Ram/Scramjets and Turboramjets in Russia
[AGARD-LS-194] p 3151 N94-29291
Turboramjet engines: Types and performances p 3151 N94-29293
Some problems of scramjet propulsion for aerospace planes. Part 1: Scramjet: Aims and features p 3151 N94-29295
CIAM experimental turboramjets p 3152 N94-29299
Some problems of scramjet propulsion for aerospace planes. Part 2: Scramjet: Development and test problems p 3152 N94-29301
Aspects of model-based rocket engine condition monitoring and control
[NASA-CR-195116] p 3173 N94-29848
PROPYLENE
Enhanced ion dissociation of LiCF3SO3 by new carbonate plasticizers: Raman and IR studies
[DE94-005448] p 3485 N94-28741
PROSTATE GLAND
Conformal external radiotherapy of prostatic carcinoma: Requirements and preliminary results p 3395 N94-30029
PROTEASE
Studies on bacterial spore ultraviolet light resistance and regulation of the activity of a spore protease
[AD-A275448] p 3384 N94-28884
PROTECTION
Development of a new chemical warfare agent protective material p 3381 N94-28432
PROTECTIVE CLOTHING
The Support of Air Operations under Extreme Hot and Cold Weather Conditions
[AGARD-CP-540] p 3379 N94-28420
Evaluation of life support equipment during an unsupported North Pole expedition p 3379 N94-28422
The potential of new textiles in improving survival prospects p 3380 N94-28430
Fire-resistant water vapour permeable buoyant insulation p 3380 N94-28431
Thermal protective performance and instrumented mannequin evaluation of multi-layer garment systems p 3381 N94-28433
Effectiveness of protection clothing for cold weather conditions after ejection over sea: A case report p 3381 N94-28435
Advanced integrated cold protection for aircrew p 3381 N94-28436
Thermal strain generated by an enhanced anti-G protection system in a hot climate p 3383 N94-28445
Implications of climatic extremes in aircrew NBC operations p 3383 N94-28446
Test of a new protection suit in a climatic chamber p 3384 N94-28452
A reliable and repeatable method for volume calculation of pressurized garments
[AD-A275600] p 3399 N94-28766
Comparison of two cool vests on heat-strain reduction while wearing a firefighting ensemble in a hot/humid environment
[AD-A275103] p 3400 N94-28902
Physiological responses during shipboard firefighting
[AD-A275104] p 3391 N94-28912
Comparative centrifuge evaluation of the Air Force Advanced Technology Anti-G Suit (ATAGS) and the Navy Enhanced Anti-G Lower Ensemble (EAGLE)
[AD-A275348] p 3400 N94-28996
Procedures and metrics for anti-G suit evaluations
[AD-A275349] p 3400 N94-28997
Effects of endurance training on heat-exercise tolerance in men wearing NBC protective clothing
[AD-A275176] p 3391 N94-29049
Insulative properties of two thermo-metal neoprenes
[AD-A275209] p 3401 N94-29302
PROTECTIVE COATINGS
Selection of the Space Station Freedom (SSF) Flat Collector Circuit (FCC) insulation material p 3165 N94-28701
Corrosion inhibition by electrodeposited conductive-polymer film
[AD-A275456] p 3213 N94-28806
Heat flux instrumentation for Hyflite thermal protection system
[NASA-CR-195731] p 3286 N94-28824
Low Earth orbit durability evaluation of protected silicone for advanced refractive photovoltaic concentrator arrays
[NASA-TM-106543] p 3172 N94-28999
Evaluation of oxide-coated iridium-rhenium chambers
[NASA-TM-106442] p 3172 N94-29097
Electrochemical behavior and surface chemistry of nonequilibrium aluminum alloys: Passivity mechanism and fabrication methods
[AD-A275401] p 3204 N94-29196
Insulative properties of two thermo-metal neoprenes
[AD-A275209] p 3401 N94-29302
Thick thermal barrier coatings for diesel components
[NASA-CR-187111] p 3537 N94-29350
Rules and definition of the range of paints applied on aeronautical structrural composites
[REPT-932-600-106] p 3215 N94-29459
Plasma sprayed ceramic thermal barrier coating for NiAl-based intermetallic alloys
[NASA-CASE-LEW-15535-1] p 3205 N94-29507
Polyimides containing pendent siloxane groups
[NASA-CASE-LAR-14638-1] p 3215 N94-29555
Performance of CVD and CVR coated carbon-carbon in high temperature hydrogen
[DE94-005451] p 3487 N94-29841
Non-chromate talc conversion coatings for aluminum
[DE94-005281] p 3207 N94-30053
Evaluation of corrosion protecting properties of modern aircraft paint systems
[AD-B179388] p 3220 N94-30420
Deposition of tantalum carbide coatings on graphite by laser interactions p 3223 N94-30475
Development of a unique polyurethane primer/topcoat p 3223 N94-30476
Four advances in carbon-carbon materials technology p 3186 N94-30481
The performance of gloss meters on curving surfaces
[NPL-DMM(A)-111] p 3501 N94-30522
PROTEIN CRYSTAL GROWTH
Survey report of JSUP Space Environment Utilization Research Committee in fiscal year 1992: Protein Crystal Growth Session
[JTN-94-80584] p 3158 N94-28583
Overview of space environment utilization science
[JTN-94-80581] p 3227 N94-28938
Protein crystal growth in microgravity p 3228 N94-28943
Thermal enclosure system functional simulation user's manual
[NASA-TM-109094] p 3466 N94-29489
Convective flow effects on protein crystal growth
[NASA-CR-195785] p 3515 N94-30015
PROTEINS
Barley cell culture as a producer of heterologous protein
[PB94-132339] p 3379 N94-28408
Survey report of JSUP Space Environment Utilization Research Committee in fiscal year 1992: Protein Crystal Growth Session
[JTN-94-80584] p 3158 N94-28583
Development of novel switchable protein surfaces
[AD-A275510] p 3384 N94-28667
Protein crystal growth in microgravity p 3228 N94-28943
PROTOCOL (COMPUTERS)
Design of parallel systems for signal processing
[AD-A275490] p 3430 N94-28659
Preliminary analysis of Asynchronous Transfer Mode (ATM) over microwave channels
[AD-A275214] p 3243 N94-29069
Model-oriented analysis of a communications protocol
[PB94-138146] p 3244 N94-29109
Invariants, frames and postconditions: A comparison of two formal specification notations
[PB94-138153] p 3405 N94-29110
NPSNET: Integration of Distributed Interactive Simulation (DIS) protocol for communication architecture and information interchange
[AD-A275061] p 3530 N94-29139
Space reclamation for uncoordinated checkpointing in message-passing systems
[NASA-CR-195761] p 3420 N94-29906
Performance issues of signalling protocols for broadband ISDN
[MEMO-INF-93-30] p 3255 N94-30374
End-to-end delay reduction in narrow bandwidth real-time multimedia tele-education applications
[AD-B179614] p 3260 N94-30518
Design and analysis of dynamic leader election protocols in broadcast networks
[MEMO-INF-93-43] p 3260 N94-30520
The NIST Internet time service p 3475 N94-30678
Validation experiments with an Ethernet model using the simulation tool 'PROMISE'
[AD-B174795] p 3429 N94-30912
An UIO-based method for protocol conformance testing
[REPT-93-060] p 3429 N94-30931
PROTON BEAMS
Physics at HERA
[DE94-005117] p 3483 N94-28569
Search for heavy neutrinos at the IHEP-JINR neutrino detector
[DE94-608175] p 3489 N94-30095
PROTON DENSITY (CONCENTRATION)
Variations of electron fluxes, low-frequency radiations and plasma density during the geomagnetic storm on 9-12 March, 1979 according to data of the Interkosmos-19 satellites
[DE94-607323] p 3365 N94-30223
PROTON ENERGY
Proton switches
[AD-A275150] p 3167 N94-29022
PROTONS
Properties of W + jet events in proton-antiproton collisions at 1.8 TeV
[DE94-004002] p 3482 N94-28524
Results on structure functions from fixed-target experiments
[DE94-005233] p 3482 N94-28541
Proton switches
[AD-A275150] p 3167 N94-29022
Inclusive jet and direct photon production at the D0 experiment
[DE94-006001] p 3488 N94-30049
A search for rapidity gap events in p(bar p) collisions at D(0)
[DE94-004654] p 3491 N94-30722
PROTOTYPES
Automated interface for retrieving reusable software components
[AD-A275004] p 3409 N94-28896
Fundamental studies on the corrosion behavior of weldments in marine microbial environments
[AD-A275247] p 3203 N94-28900
Mars rover mechanisms designed for Rocky 4 p 3161 N94-29630
Test of prototype liquid-water-content meter for aircraft use
[NASA-CR-189304] p 3374 N94-30187
PSEUDONOISE
Acquisition time analysis of noncoherent PN sequence acquisition schemes
[AD-A275017] p 3244 N94-29094
PSEUDOPOTENTIALS
First principles pseudopotential calculations on aluminum and aluminum alloys
[DE94-004890] p 3206 N94-29931
PSYCHOACOUSTICS
Subjective response to sonic booms having different shapes, rise times, and durations
[NASA-TM-109090] p 3479 N94-29464

PSYCHOLOGICAL EFFECTS
Some issues on Japan's space food development and relating preliminary experimental study
p 3388 N94-28498
PSYCHOLOGICAL FACTORS
The management issues of implementing telecommuting: A case study
[AD-A275267] p 3527 N94-28905
PSYCHOMOTOR PERFORMANCE
Experimental evaluation of two systems of individual air-conditioning p 3384 N94-28450
An evaluation of personality testing and the five-factor model in the selection of landing craft air cushion vehicle crew members
[AD-A275869] p 3397 N94-28754
PSYCHOPHYSIOLOGY
Psychophysiological study on the effects of co-existence of lines for detecting dot target p 3394 N94-29867
PUBLIC LAW
Loran-C time management p 3144 N94-30644
PULSARS
Equation of state of neutron star matter, limiting rotational periods of fast pulsars, and the properties of strange stars
[DE94-005214] p 3542 N94-28480
A study of recycled pulsars in globular clusters
p 3539 N94-29825
PULSE AMPLITUDE
Coronal temperatures of unusually active K-dwarf binary systems
[NASA-CR-189335] p 3545 N94-29861
Pulse height response of Si surface barrier detectors
p 3497 N94-30221
PULSE COMMUNICATION
1.8 gigahertz (GHz) digital Low Density Radio Communications Link (LDRCL) Operational Test and Evaluation (OT&E) integration and OT&E operational final test report
[AD-A275800] p 3241 N94-28771
PULSE COMPRESSION
Digital pulse compression and its application in reducing radar interference
[ISBN-0-315-85767-6] p 3255 N94-30240
PULSE DOPPLER RADAR
Theory and application of a Radio-Acoustic Sounding System (RASS) p 3367 N94-30869
PULSE MODULATION
Measurement of the frequency stability of responders in aircraft p 3261 N94-30673
PULSE RADAR
Digital pulse compression and its application in reducing radar interference
[ISBN-0-315-85767-6] p 3255 N94-30240
PULSED LASERS
Design and testing of the LITE Variable Field Stop mechanism p 3161 N94-29633
Optical field ionization of atoms and ions using ultrashort laser pulses
[DE94-006643] p 3488 N94-29845
Optical techniques for time and frequency transfer
p 3469 N94-30647
PULSED RADIATION
Tuning of AmPS
[NIKHEF-K-AMPS-93-01] p 3494 N94-29422
PUMP IMPELLERS
Experiments on the aerodynamic generation of noise in centrifugal turbomachinery p 3480 N94-30804
PUMPS
Argon frost continuous cryopump for fusion applications
[DE94-004478] p 3230 N94-29017
PUPILS
Analysis of various biological activity parameters during parabolic flight p 3393 N94-29716
PURGING
Chamber free fusion welding root side purging method and apparatus
[NASA-CASE-MFS-28832-1] p 3204 N94-29380
PURIFICATION
Development of novel switchable protein surfaces
[AD-A275510] p 3384 N94-28667
Fossil energy biotechnology: A research needs assessment
[DE94-004239] p 3338 N94-29953
Gas stream purifier p 3354 N94-30469
A new material for removing heavy metals from water
p 3354 N94-30471
PURITY
Method of test for cleanness assessment of metal alloys: The preparation of button specimens by electron beam melting and the characterisation of recovered inclusions
[NPL-DMM(A)-130] p 3210 N94-30796
PYRENES
Computer simulation of molecular interactions in supercritical solvents
[AD-A274977] p 3486 N94-29087
Photochemistry in constrained spaces: Zeolites and layered double metal hydroxides
[DE94-004958] p 3200 N94-30769
PYROLYSIS
Gas phase thermochemistry of organogermanium compounds
[DE94-004885] p 3187 N94-28561
Evaluation of pyrolysis and arc tracking on candidate wire insulation designs for space applications
p 3166 N94-28711
Hypervelocity impact induced arcing and Kapton pyrolization in a plasma environment
[NASA-TM-106528] p 3167 N94-28814
A study of solid propellants using a microprobe mass spectrometer system
[AD-A275325] p 3224 N94-28879
Endothermic fuels for hypersonic aviation
p 3197 N94-29285
PYROTECHNICS
Pyrotechnic shock: Devices in pyrotechnic environment qualification logic
[REPT-932-430-108] p 3225 N94-29429
The 27th Aerospace Mechanisms Symposium
[NASA-CP-3205] p 3160 N94-29627
Integration of pyrotechnics into aerospace systems
p 3161 N94-29634

Q

Q SWITCHED LASERS
Development of high time-resolution laser flash equipment for thermal diffusivity measurements using miniature-size specimens
[NIFS-268] p 3295 N94-30186
QUADRATIC EQUATIONS
Convolutional encoding of self-dual codes
p 3250 N94-29662
L(sub)p optimal d dimensional triangulations for piecewise linear interpolation: A new result on data dependent triangulations
[RUU-CS-93-13] p 3458 N94-30406
QUADRUPOLES
Magnetic properties of a quantum transverse spin-1 Blume-Emery-Griffiths model
[DE94-608114] p 3517 N94-30109
QUALIFICATIONS
NAVAIR aircraft wiring standardization and qualification program p 3166 N94-28704
Organized wiring systems p 3166 N94-28705
Pyrotechnic shock: Devices in pyrotechnic environment qualification logic
[REPT-932-430-108] p 3225 N94-29429
Fire behavior of aeronautical materials
[REPT-932-600-105] p 3197 N94-29457
Logistics for the implementation of lead-free solders on electronic assemblies
[DE94-004800] p 3206 N94-29936
QUALITATIVE ANALYSIS
Knowledge based system for identification of gamma sources
[PB94-137742] p 3487 N94-29683
QUALITY CONTROL
Testing laboratories as notified bodies
[PB94-132396] p 3160 N94-28413
NAVAIR aircraft wiring standardization and qualification program p 3166 N94-28704
Organized wiring systems p 3166 N94-28705
Cleanroom engineering handbook. Volume 3: Project execution in the cleanroom environment
[AD-A275860] p 3156 N94-28752
A reliable and repeatable method for volume calculation of pressurized garments
[AD-A275600] p 3399 N94-28766
Screening of flexible cables by nonlinear resistance measurements
[AD-A275193] p 3264 N94-29289
Application of information management methodologies for project quality improvement in a changing environment p 3416 N94-29342
The discipline of defining the software product
p 3416 N94-29343
A normative frame of reference for the metrology function
[REPT-932-430-102] p 3231 N94-29477
The 1992 report on the next generation ultra clean technology for advanced microfabrication
[DE94-744171] p 3157 N94-30268
A user's guide to the Software Testpilot
[CWI-CS-R9343] p 3426 N94-30435
QUANTUM CHROMODYNAMICS
Report of the subgroup on the top quark
[DE94-004624] p 3481 N94-28462
Properties of W + jet events in proton-antiproton collisions at 1.8 TeV
[DE94-004002] p 3482 N94-28524
Properties of events containing a photon and several jets seen in p(bar p) collisions at (radical)s = 1.8 TeV
[DE94-005596] p 3482 N94-28531
Proceedings of the workshop on quark and lepton mass matrices
[DE94-707692] p 3485 N94-28624
One-loop QCD mass effects in the production of polarized bottom and top quarks
[PB94-138104] p 3487 N94-29145
Improved QCD sum rule estimates of the higher twist contributions to polarised and unpolarised nucleon structure functions
[PB94-138112] p 3487 N94-29161
A pot-pourri of results in QCD from large lattice simulations on the CM5
[DE94-005084] p 3514 N94-29818
Inclusive jet and direct photon production at the D0 experiment
[DE94-006001] p 3488 N94-30049
Gluon and fermion damping in hot QCD
[ISBN-0-315-85982-2] p 3490 N94-30141
Direct anti-b b production in anti-pp collisions at the square root of s = 1.8 TeV
[DE94-006167] p 3491 N94-30369
Problems in particle theory
[DE94-003665] p 3491 N94-30685
Theory of ultra dense matter and the dynamics of high energy interactions involving nuclei
[DE94-004178] p 3491 N94-30686
Heavy flavor production at fixed target photo- and hadroproduction
[DE94-004651] p 3491 N94-30719
Research in elementary particle physics
[DE94-001657] p 3491 N94-30762
Theoretical studies in hadronic and nuclear physics
[DE94-003524] p 3492 N94-30838
Computing at the leading edge: Research in the energy sciences
[DE94-006121] p 3563 N94-30844
QUANTUM ELECTRODYNAMICS
The proper field of charges and gauge-invariant variables in electrodynamics
[DE94-606405] p 3523 N94-28751
Curved-space quantization, and Dirac versus reduced quantization of Poincare gauge theories
[ISBN-0-315-85990-3] p 3525 N94-30142
QUANTUM ELECTRONICS
The effects of propagational factors on quantum wires in close parallel proximity
[ISBN-0-315-86157-6] p 3254 N94-30035
Electronic structure of Zn-based quantum wells
[DE94-608104] p 3516 N94-30068
QUANTUM MECHANICS
Miln equation for the calculation of the phases and amplitudes of wave functions for continuum spectrum of Coulomb two-center problem
[DE94-606292] p 3522 N94-28616
Dissipative quantum dynamics and nonlinear sigma-model
[DE94-606295] p 3523 N94-28617
Classical interpretation of quantum mechanics
[DE94-606304] p 3523 N94-28719
Electronic structure and mechanical properties of grain boundaries
[AD-A275198] p 3512 N94-28890
Existence of quantum characteristic exponents
[PB94-138161] p 3523 N94-29146
Coherent states of SU(l,1) groups
[DE94-603654] p 3524 N94-29498
Nonadiabatic effects in the quantum Hall regime
p 3513 N94-29530
Quantum interference phenomena and novel switching in split gate high electron mobility transistors
p 3266 N94-29734
A semiclassical study of quantum maps
p 3524 N94-29987
The MSRC ab initio methods benchmark suite: A measurement of hardware and software performance in the area of electronic structure methods
[DE94-006428] p 3514 N94-30001
On chaos in quantum mechanics: The two meanings of sensitive dependence
[DE94-608069] p 3524 N94-30086
Reconstruction of spectra in the discrete quantum mechanics (new elements of the lattice quantum engineering)
[DE94-608075] p 3524 N94-30087
Quantum-mechanical suppression of bremsstrahlung
[DE94-005223] p 3497 N94-30712
Molecular dynamics simulations of dense plasmas
[DE94-005082] p 3509 N94-30752
Non-Markovian quantum Brownian motion of a harmonic oscillator
[DE94-005922] p 3477 N94-30873
Non-commutative geometry
[PB94-139342] p 3462 N94-30889

QUANTUM STATISTICS
Equation of state of stellar plasmas
[DE94-004186] p 3542 N94-28526
QUANTUM THEORY
The (j,0) + (0,j) representation space: Dirac-like construct
[DE94-005011] p 3522 N94-28572
On invariant measures for some infinite-dimensional dynamical systems
[DE94-606342] p 3522 N94-28609
Anomalous algebraic structures in quantum field theories p 3524 N94-29911
A Tevatron collider beauty factory
[DE94-004879] p 3488 N94-29930
Discrete symmetries, strong CP problem and gravity
[DE94-608091] p 3524 N94-30089
Modelling of multiparticle production by dynamical semigroup method
[DE94-608132] p 3490 N94-30120
A theory approach for creation of the matter of universe
[DE94-608109] p 3548 N94-30163
GL(sub q)(N)-covariant quantum algebras and covariant differential calculus
[DE94-608072] p 3460 N94-30726
Space-time symmetries: P and CP violation
[DE94-005012] p 3526 N94-30750
Non-commutative geometry
[PB94-139342] p 3462 N94-30889
QUANTUM WELLS
Development of ultra-low noise, high performance 3 -5 quantum well infrared photodetectors (QWIPs) for focal plane array staring image sensor systems
[AD-A275745] p 3511 N94-28734
Photonic devices and systems for optical signal processing
[AD-A275818] p 3498 N94-28804
Carrier collection and scattering in quantum well and superlattice devices
[AD-A275443] p 3512 N94-28880
Visible vertical cavity surface emitting lasers
[AD-A275334] p 3293 N94-28919
Spatial light modulators with arbitrary quantum wells profiles
[AD-A275023] p 3499 N94-29114
The effects of propagational factors on quantum wires in close parallel proximity
[ISBN-0-315-86157-6] p 3254 N94-30035
Electronic structure of Zn-based quantum wells
[DE94-608104] p 3516 N94-30068
Photoelectronic study of GaAs epilayers and In(x)Ga(1-x)As/GaAs quantum wells
[ISBN-0-315-85756-0] p 3518 N94-30239
Nonlinear optics response of semiconductor quantum wells under high magnetic fields
[DE94-003244] p 3520 N94-30835
QUARK MODELS
Search for excited quarks in p(bar p) collisions at the square root of s = 1.8 TeV
[DE94-004658] p 3484 N94-28573
Semileptonic heavy-to-light decays of baryons
[DE94-606481] p 3487 N94-29502
QUARK PARTON MODEL
Determination of the neutron spin-structure function
[DE94-005234] p 3483 N94-28542
QUARKS
Report of the subgroup on the top quark
[DE94-004624] p 3481 N94-28462
Discrete quark-lepton symmetry need not pose a cosmological domain wall problem
[DE94-601606] p 3481 N94-28471
Properties of W + jet events in proton-antiproton collisions at 1.8 TeV
[DE94-004002] p 3482 N94-28524
Research on elementary particle physics. Task P: Studies in theory and phenomenology of elementary physics
[DE94-004955] p 3483 N94-28566
Search for excited quarks in p(bar p) collisions at the square root of s = 1.8 TeV
[DE94-004658] p 3484 N94-28573
Masses and mixing of leptons and quarks (Dirac particles)
[DE94-606446] p 3484 N94-28611
Proceedings of the workshop on quark and lepton mass matrices
[DE94-707692] p 3485 N94-28624
The small-x behaviour of parton distribution functions
[DE94-606414] p 3485 N94-28758
One-loop QCD mass effects in the production of polarized bottom and top quarks
[PB94-136104] p 3487 N94-29145
Semileptonic heavy-to-light decays of baryons
[DE94-606481] p 3487 N94-29502
Statistical description of hot and dense clustering matter
[DE94-608155] p 3490 N94-30112
Direct anti-b b production in anti-pp collisions at the square root of s = 1.8 TeV
[DE94-006167] p 3491 N94-30369
Operator analysis for quark and lepton masses in SO(10)
[DE94-005201] p 3491 N94-30709
Search for the top quark in the electron-electron and electron-muon channels at D0
[DE94-006174] p 3492 N94-30779
Theoretical studies in hadronic and nuclear physics
[DE94-003524] p 3492 N94-30838
Charmonium and bottomonium in (-p)p interactions
[DE94-006173] p 3493 N94-30886
QUASARS
Infrared properties of obscuring dust tori in active galactic nuclei p 3545 N94-29832
High redshift QSOs and the x ray background
[NASA-CR-195112] p 3540 N94-29957
Broad H alpha profiles of radio-loud active galactic nuclei and rapid profile variability in Seyfert and radio galaxies p 3552 N94-29989
QUENCHING (ATOMIC PHYSICS)
Quenching of the excited state of hydrated Europium(3) ions by electron transfer
[DE94-005553] p 3482 N94-28518
QUERY LANGUAGES
Automated interface for retrieving reusable software components
[AD-A275004] p 3409 N94-28696
DTL: A deductive and typed object-oriented language
[MEMO-INF-93-41] p 3425 N94-30417
QUEUEING THEORY
M-interference queue analysis by decomposition method
[ISBN-0-315-85795-1] p 3453 N94-30139
Performance evaluation of intelligent network services
[MEMO-INF-93-20] p 3438 N94-30373
Customer creation and combination in queueing networks
[MEMO-INF-93-35] p 3438 N94-30375

R

RACKS (GEARS)
Metal band drives in spacecraft mechanisms p 3162 N94-29637
RADAR ANTENNAS
Printed circuit elements with applications to antennas, scattering, and circuits
[AD-A275512] p 3262 N94-28669
Orbital debris radar instrumentation p 3248 N94-29626
Radar estimations of atmospheric winds in the troposphere and lower stratosphere p 3370 N94-29697
RADAR APPROACH CONTROL
Design of Center-TRACON Automation System p 3138 N94-29568
Development of precision runway monitor system for increasing capacity of parallel runway operations p 3142 N94-29587
RADAR ASTRONOMY
The Telecommunications and Data Acquisition Report
[NASA-CR-195694] p 3246 N94-29613
RADAR CROSS SECTIONS
Printed circuit elements with applications to antennas, scattering, and circuits
[AD-A275512] p 3262 N94-28669
RL/ERCT automated swept-angle bistatic measurement system
[AD-A275763] p 3241 N94-28763
Comparison of RCS prediction techniques, computations and measurements
[PB94-125515] p 3256 N94-30392
The influence of the evaporation duct on the angle of arrival and amplitude of the backscattered signal from targets low above the sea p 3256 N94-30498
Polarimetric backscatter measurements of natural surfaces at millimeter wavelengths p 3259 N94-30509
Radar cross sections of ground clutter at 95 GHz for summer and fall conditions p 3259 N94-30512
RADAR DETECTION
Radar returns from a low-flying target over a rough sea surface under multipath and clutter conditions p 3253 N94-29882
An electromagnetic noncontacting sensor for thickness measurement in a dispersive medium
[AIAA PAPER 94-1200-CP] p 3443 N94-30551
RADAR ECHOES
Long term variations of radio auroral activity p 3359 N94-29237
New-type echoes observed with the 50 MHz auroral Doppler radar at Showa Station p 3360 N94-29238
RADAR EQUIPMENT
Orbital debris radar instrumentation p 3248 N94-29626
RADAR IMAGERY
Fusion of range and luminance data from laser radar systems
[AD-A275608] p 3292 N94-28770
SAR-related stress variability in the Marine Atmospheric Boundary Layer (MABL)
[AD-A275275] p 3377 N94-29436
Automatic focus and registration of synthetic aperture radar images p 3246 N94-29536
Pointing mechanisms for the Shuttle Radar Laboratory p 3162 N94-29638
Application of remote sensing techniques for the seismo-tectonic study of Nahanni earthquake area
[ISBN-0-315-85942-3] p 3334 N94-30037
Frequency dependence of polarization phase difference
[NASA-TM-109737] p 3254 N94-30094
RADAR MEASUREMENT
RL/ERCT automated swept-angle bistatic measurement system
[AD-A275763] p 3241 N94-28763
New-type echoes observed with the 50 MHz auroral Doppler radar at Showa Station p 3360 N94-29238
Radar estimations of atmospheric winds in the troposphere and lower stratosphere p 3370 N94-29697
Antarctic Record, vol. 36, no. 3
[REPT-108] p 3363 N94-29978
RADAR NAVIGATION
Ground independent landing system p 3137 N94-29564
ARC2000: Automatic radar control p 3141 N94-29583
RADAR NETWORKS
A novel near-range radar network for airport surface control p 3142 N94-29586
A simulator for multi-radar analysis for realistic traffic
[AD-B179099] p 3142 N94-30439
RADAR RANGE
Retarded distances and the Doppler effect
[DE94-606296] p 3523 N94-28618
Orbital debris radar instrumentation p 3248 N94-29626
Method for ambiguity resolution in range-Doppler measurements
[NASA-CASE-GSC-13542-1] p 3252 N94-29739
RADAR RECEIVERS
Synchronization in multistatic radar
[PB94-136975] p 3242 N94-28885
Ground independent landing system p 3137 N94-29564
RADAR SCATTERING
Printed circuit elements with applications to antennas, scattering, and circuits
[AD-A275512] p 3262 N94-28669
Radar returns from a low-flying target over a rough sea surface under multipath and clutter conditions p 3253 N94-29882
RADAR SIGNATURES
Radar jet engine health monitoring project
[ASSGI-301] p 3153 N94-30130
RADAR TARGETS
RL/ERCT automated swept-angle bistatic measurement system
[AD-A275763] p 3241 N94-28763
Method for ambiguity resolution in range-Doppler measurements
[NASA-CASE-GSC-13542-1] p 3252 N94-29739
RADAR TRACKING
Laser beam steering with semiconductor waveguide
[AD-A275775] p 3292 N94-28765
Numerical simulations of a mountain thunderstorm. A comparison with Doppler radar observations
[AD-A275296] p 3369 N94-28873
Synchronization, positioning, and communication in multistatic radar systems for air defence
[PB94-137478] p 3243 N94-28908
Simulation of fully automated air traffic control concepts p 3139 N94-29569
Orbital debris radar instrumentation p 3248 N94-29626
A simulator for multi-radar analysis for realistic traffic
[AD-B179099] p 3142 N94-30439
Systematic error estimation in multisensor fusion systems
[AD-B179298] p 3428 N94-30764
RADAR TRANSMISSION
Atmospheric Propagation Effects Through Natural and Man-Made Obscurants for Visible to MM-Wave Radiation
[AGARD-CP-542] p 3256 N94-30495

The influence of the evaporation duct on the angle of arrival and amplitude of the backscattered signal from targets low above the sea p 3256 N94-30498

RADAR TRANSMITTERS

Ground independent landing system p 3137 N94-29564

RADARSCOPES

Designing for performance: A cognitive systems engineering approach to modifying an AWACS human computer interface [AD-A275187] p 3399 N94-28861

RADIAL FLOW

Fluid dynamic noise in a centrifugal pump [AD-A275264] p 3477 N94-28904

Near-critical spherically symmetric accretion by neutron stars p 3546 N94-29991

RADIAL VELOCITY

Convective turbulence and transport in stars p 3546 N94-29913

Pushing the limit: Precision radial velocities, techniques, and applications p 3542 N94-30861

RADIANCE

CBSD: The celestial background scene descriptor [AD-A275521] p 3538 N94-28671

SHARC, a model for calculating atmospheric and infrared radiation under non-equilibrium conditions [AD-A275207] p 3357 N94-28893

RADIANT COOLING

Numerical simulation of radiative heat loss in an experimental burner [DE94-002016] p 3277 N94-29923

Thermal conductivities, electrical resistivities, and Seebeck coefficients of YBa2Cu3O(7-x) superconductors from 80 to 300 K [DE94-004796] p 3520 N94-30724

RADIANT HEATING

Analysis of infrared radiation heating process considering chemical reaction of material to be heated [DE94-744116] p 3199 N94-30267

RADIATION ABSORPTION

TFTR Ion Cyclotron Range of Frequencies (ICRF) experimental data analysis collaboration [DE94-004699] p 3504 N94-28575

RADIATION BELTS

Identification of an unexpected space radiation hazard [AD-A275170] p 3552 N94-29046

RADIATION COUNTERS

Elementary particle interactions [DE94-004238] p 3482 N94-28504

Adaption of the bubble detector for use as a LET spectrometer p 3291 N94-30216

A bipolar analog front-end integrated circuit for the SDC silicon tracker [DE94-005203] p 3267 N94-30711

Research in elementary particle physics [DE94-001657] p 3491 N94-30762

RADIATION DAMAGE

Proceedings of Japan-US Workshop P-196 on High Heat Flux Components and Plasma Surface Interactions for Next Devices [DE94-701164] p 3503 N94-28513

Analysis of data by long-time mechanical properties of 08KH18N10T steel irradiated by neutrons [DE94-605337] p 3202 N94-28551

Electron beam irradiation experiments of monoblock divertor mock-up [DE94-707497] p 3503 N94-28555

Dislocation loops in spinel crystals irradiated successively with deep and shallow ion implants [DE94-005083] p 3517 N94-30201

Irradiation-induced structure and property changes in tokamak plasma-facing, carbon-carbon composites [DE94-006046] p 3508 N94-30365

Ion damage studies in GaAs/Al(0.6)Ga(0.4)As/GaAs heterostructures [DE94-005384] p 3521 N94-30894

RADIATION DETECTORS

Proton switches [AD-A275150] p 3167 N94-29022

Backscatter haze device for measurement of haze in aircraft transparencies [AD-A275127] p 3146 N94-29042

A Tevatron collider beauty factory [DE94-004879] p 3488 N94-29930

Deexcitation processes in nuclear reactions: The study of hot hadronic matter [DE94-003396] p 3492 N94-30836

RADIATION DISTRIBUTION

Caesium-137 in a boreal forest ecosystem: Aspects on the long-term behavior [PB94-137809] p 3347 N94-29158

RADIATION DOSAGE

Modeling the total dose radiation effects of Hg(1-x)Cd(x)Te photodiodes using numerical device simulators [AD-A275235] p 3263 N94-29028

Recent results from testing fast ADCs [DE94-005565] p 3406 N94-30004

RADIATION EFFECTS

Relationship between swelling and irradiation creep in cold-worked PCA stainless steel irradiated to approximately 178 dpa at approximately 400 C [DE94-004368] p 3201 N94-28456

Radiation effects in beryllium used for plasma protection [DE94-004599] p 3201 N94-28460

Response of GaAs charge storage devices to transient ionizing radiation [DE94-005273] p 3510 N94-28484

Proceedings of Japan-US Workshop P-196 on High Heat Flux Components and Plasma Surface Interactions for Next Devices [DE94-701164] p 3503 N94-28513

Analysis of data by long-time mechanical properties of 08KH18N10T steel irradiated by neutrons [DE94-605337] p 3202 N94-28551

Modeling the total dose radiation effects of Hg(1-x)Cd(x)Te photodiodes using numerical device simulators [AD-A275235] p 3263 N94-29028

Identification of an unexpected space radiation hazard [AD-A275170] p 3552 N94-29046

Charge trapping and breakdown in N2O oxides [DE94-003775] p 3266 N94-30040

Research laboratories annual report 1992 [DE94-608124] p 3555 N94-30168

Dislocation loops in spinel crystals irradiated successively with deep and shallow ion implants [DE94-005083] p 3517 N94-30201

Computer simulation of the interaction of fast hydrogen atoms with a molybdenum containing sorbed hydrogen [DE94-608419] p 3209 N94-30253

Role of x ray-induced transcripts in adaptive responses following x rays [DE94-005412] p 3386 N94-30895

Development of radiation resistant electrical cable insulations [DE94-005189] p 3222 N94-30906

Investigations into ultraviolet matrix-assisted laser desorption [DE94-005265] p 3296 N94-30908

RADIATION HARDENING

Elementary particle interactions [DE94-004238] p 3482 N94-28504

Recent results from testing fast ADCs [DE94-005565] p 3406 N94-30004

Development of radiation resistant electrical cable insulations p 3223 N94-30480

Silica scintillating materials prepared by sol-gel methods [DE94-005123] p 3220 N94-30778

Development of radiation resistant electrical cable insulations [DE94-005189] p 3222 N94-30906

RADIATION HAZARDS

Identification of an unexpected space radiation hazard [AD-A275170] p 3552 N94-29046

Caesium-137 in a boreal forest ecosystem: Aspects on the long-term behavior [PB94-137809] p 3347 N94-29158

RADIATION MEASUREMENT

The automated rotating shadowband spectroradiometer [DE94-001878] p 3269 N94-28464

Measurement basis of near fields in spherical coordinates in the 100 MHz to 6 GHz band [REPT-932-430-107] p 3255 N94-30153

Determination of photon fluence spectra from the NPL Mobaltron Co-60 unit [NPL-RSA(EXT)-46] p 3492 N94-30795

Solar neutrino experiments: An update [DE94-006061] p 3551 N94-30884

RADIATION MEASURING INSTRUMENTS

Solar neutrino experiments: An update [DE94-006061] p 3551 N94-30884

RADIATION PRESSURE

Infrared properties of obscuring dust tori in active galactic nuclei p 3545 N94-29832

RADIATION PROTECTION

Nuclear energy related research [DE94-606286] p 3494 N94-28623

Selection of the Space Station Freedom (SSF) Flat Collector Circuit (FCC) insulation material p 3165 N94-28701

RADIATION SOURCES

Determination of photon fluence spectra from the NPL Mobaltron Co-60 unit [NPL-RSA(EXT)-46] p 3492 N94-30795

RADIATION SPECTRA

Remote pumping of solid state lasers with nuclear driven fluorescers [DE94-004846] p 3296 N94-30614

Determination of photon fluence spectra from the NPL Mobaltron Co-60 unit [NPL-RSA(EXT)-46] p 3492 N94-30795

RADIATION THERAPY

Computer Assisted Medical Interventions: Application to Conformal Radiotherapy. [RR-912-I] p 3395 N94-30028

Conformal external radiotherapy of prostatic carcinoma: Requirements and preliminary results p 3395 N94-30029

Pre- and intra-radiotherapy multimodal image registration: Principles and first experiments p 3395 N94-30030

RADIATION TOLERANCE

Studies on bacterial spore ultraviolet light resistance and regulation of the activity of a spore protease [AD-A275448] p 3384 N94-28884

Development of radiation resistant electrical cable insulations [DE94-005189] p 3222 N94-30906

RADIATION TRANSPORT

Performance of MCNP4A on seven computing platforms [DE93-040101] p 3419 N94-29816

Radiative flux calculations at UV and visible wavelengths [DE94-004278] p 3350 N94-30613

Modelling erosion damage from low-energy plasma gun simulations of disruptions [DE94-005196] p 3509 N94-30697

Radiation transport in cloudy and aerosol loaded atmospheres p 3366 N94-30805

RADIATIVE HEAT TRANSFER

Numerical simulation of radiative heat loss in an experimental burner [DE94-002016] p 3277 N94-29923

Measurements and predictions of the combustion characteristics of enclosed swirl-stabilized propane flames [IECE-CFE-TR-001] p 3198 N94-30017

Thermal conductivities, electrical resistivities, and Seebeck coefficients of YBa2Cu3O(7-x) superconductors from 80 to 300 K [DE94-004796] p 3520 N94-30724

RADIATIVE RECOMBINATION

The investigation of electron-ion radiative and dielectronic recombination in high-temperature plasmas [DE94-005150] p 3509 N94-30755

RADIATIVE TRANSFER

Lead detection and mapping with reference to relationships between scale, sensor characteristics, surface conditions and atmospheric properties [AD-A275321] p 3377 N94-28877

Infrared properties of obscuring dust tori in active galactic nuclei p 3545 N94-29832

Radiative flux calculations at UV and visible wavelengths [DE94-004278] p 3350 N94-30613

Optical depth effects in cluster cooling flows p 3541 N94-30800

Tropospheric radiative forcing of O3 for the 1994 IPCC report [DE94-005698] p 3367 N94-30876

RADICALS

Peroxy radical measurements with NCAR's chemical amplifier p 3345 N94-28603

The radical amplifier p 3345 N94-28604

An improved method of measuring tropospheric NO2, NO3, HO2, and RO2 by Matrix Isolation and Electronic Spin Resonance (MIESR) p 3345 N94-28605

HO2 detection by near infrared absorption using tunable diode lasers p 3346 N94-28608

Direct measurement of the reactivity of NH and OH on a silicon nitride surface [DE94-005286] p 3199 N94-30260

RADIO ALTIMETERS

Altimeter data processing from sea surface topography to horizontal eddy momentum fluxes [PB94-147550] p 3378 N94-30714

RADIO ANTENNAS

Active antennas, a review [PB94-137445] p 3243 N94-28907

Three-dimensional effects for radio frequency antenna modeling [DE94-006102] p 3255 N94-30105

RADIO ASTRONOMY

The Telecommunications and Data Acquisition Report [NASA-CR-195694] p 3246 N94-29613

Radio science ground data system for the Voyager-Neptune encounter, part 1 p 3248 N94-29623

A multi wavelength observational study of the Cartwheel ring galaxy p 3539 N94-29821

A study of recycled pulsars in globular clusters p 3539 N94-29825

RADIO ATTENUATION
Adaptive power control as a fade countermeasure on satellite links p 3253 N94-29897
RADIO COMMUNICATION
1.8 gigahertz (GHz) digital Low Density Radio Communications Link (LDRCL) Operational Test and Evaluation (OT&E) integration and OT&E operational final test report
[AD-A275800] p 3241 N94-28771
Acquisition time analysis of noncoherent PN sequence acquisition schemes
[AD-A275017] p 3244 N94-29094
Optimizing the Galileo space communication link p 3250 N94-29663
Simulation of interference between Earth stations and Earth-orbiting satellites p 3252 N94-29673
RADIO EMISSION
Phasing the Very Large Array on Galileo in the presence of Jupiter's strong radio emission p 3164 N94-29621
On observing neutron star oscillations p 3538 N94-29795
RADIO EQUIPMENT
1.8 gigahertz (GHz) digital Low Density Radio Communications Link (LDRCL) Operational Test and Evaluation (OT&E) integration and OT&E operational final test report
[AD-A275800] p 3241 N94-28771
Communications technology for unattended sensors
[DE94-005685] p 3254 N94-30043
RADIO FREQUENCIES
A space-based classification system for RF transients
[DE94-003933] p 3240 N94-28522
Derivation of a Fokker-Planck equation for bunched beams
[DE94-004950] p 3483 N94-28565
A novel spectroscopic measurement method of RF plasma for temperature and electron density diagnoses p 3188 N94-28682
Development of large area RF induction plasma for cost effective diamond
[AD-A275888] p 3504 N94-28776
RF vacuum microelectronics
[AD-A275221] p 3263 N94-28915
Preliminary analysis of Asynchronous Transfer Mode (ATM) over microwave channels
[AD-A275214] p 3243 N94-29069
Waves in space plasma dipole antenna subsystem p 3161 N94-29632
Communications technology for unattended sensors
[DE94-005685] p 3254 N94-30043
Three-dimensional effects for radio frequency antenna modeling
[DE94-006102] p 3255 N94-30105
RF and microwave dielectric measurements upon layered materials using reflectometric coaxial sensor
[NPL-DES-125] p 3476 N94-30781
RADIO FREQUENCY HEATING
TFTR Ion Cyclotron Range of Frequencies (ICRF) experimental data analysis collaboration
[DE94-004699] p 3504 N94-28575
Efficiencies of the ICRF minority heating in the CHS and LHD plasmas
[NIFS-270] p 3506 N94-29499
RADIO FREQUENCY INTERFERENCE
Simulation of interference between Earth stations and Earth-orbiting satellites p 3252 N94-29673
RADIO GALAXIES
The kinematics of molecular gas and dust in the nearby galaxies Centaurus A and M82 p 3544 N94-29738
Broad H alpha profiles of radio-loud active galactic nuclei and rapid profile variability in Seyfert and radio galaxies p 3552 N94-29989
RADIO NAVIGATION
The Telecommunications and Data Acquisition Report
[NASA-CR-195694] p 3246 N94-29613
The Telecommunications and Data Acquisition Report
[NASA-CR-195689] p 3249 N94-29652
The use of low cost differential mode GPS receivers in unmanned vehicles p 3144 N94-30285
An Operational Control Segment (OCS) update on GPS constellation status and future program directions p 3144 N94-30643
RADIO PROBING
Theory and application of a Radio-Acoustic Sounding System (RASS) p 3367 N94-30869
RADIO RECEIVERS
Acquisition time analysis of noncoherent PN sequence acquisition schemes
[AD-A275017] p 3244 N94-29094
Design and implementation of a hybrid digital phase-locked loop with a TMS320C25: An application to a transponder receiver breadboard p 3251 N94-29667
Effects of low sampling rate in the digital data-transition tracking loop p 3251 N94-29669
Communications technology for unattended sensors
[DE94-005685] p 3254 N94-30043
Towards 10(exp 9) GPS geodesy: Vector baselines, Earth rotation and reference frames
[NASA-CR-195768] p 3142 N94-30243
The use of low cost differential mode GPS receivers in unmanned vehicles p 3144 N94-30285
RADIO SIGNALS
Spurs in digital radio frequency memory and applications of DRFM
[AD-A275013] p 3243 N94-28897
Detection methods for stealth radio signals: A literature survey
[PB94-137452] p 3244 N94-29176
RADIO TELESCOPES
Phasing the Very Large Array on Galileo in the presence of Jupiter's strong radio emission p 3164 N94-29621
Providing hydrogen maser timing stability to orbiting VLBI radio telescope observations by post-measurement compensation of linked frequency standard imperfections p 3297 N94-30670
RADIO TRACKING
High-resolution robot tracking and direction finding for space station environment p 3168 N94-29896
RADIO TRANSMISSION
Data transfer system using a multi-ID ARGOS transmitter for the Antarctic polar patrol balloon experiment p 3363 N94-29980
RADIO WAVES
Correlation analysis on optical and radio light curves for a large sample of active galactic nuclei p 3546 N94-29992
RADIOACTIVE DECAY
Report of the subgroup on the top quark
[DE94-004624] p 3481 N94-28462
Weak decays of charged K-mesons and charm particles
[PB94-138062] p 3486 N94-29143
Search for heavy neutrinos at the IHEP-JINR neutrino detector
[DE94-608175] p 3489 N94-30095
Measurement of the W mass in the D0 detector
[DE94-006002] p 3490 N94-30103
RADIOACTIVE ISOTOPES
Production rates of terrestrial in-situ-produced cosmogenic nuclides
[DE94-005156] p 3543 N94-28545
Caesium-137 in a boreal forest ecosystem: Aspects on the long-term behavior
[PB94-137809] p 3347 N94-29158
Knowledge based system for identification of gamma sources
[PB94-137742] p 3487 N94-29683
Intercomparison of theoretical calculations of important activation cross sections for fusion reactor technology
[DE94-002642] p 3497 N94-30825
The long-range transport of aerosol particles over the North Atlantic Ocean p 3366 N94-30867
RADIOACTIVE WASTES
Nuclear energy related research
[DE94-606286] p 3494 N94-28623
Novel mass spectrometric instrument for gaseous and particulate characterization and monitoring
[DE94-005896] p 3349 N94-30047
A modular approach for automated sample preparation and chemical analysis p 3354 N94-30464
Design reuse experience of space and hazardous operations robots
[AIAA PAPER 94-1220-CP] p 3445 N94-30568
RADIOACTIVITY
Comparison of 14 MeV isomer production of Hf-178m1 and Hf-179m2 using Feshbach-Kerman-Koonin and exciton preequilibrium models
[DE94-002640] p 3488 N94-30039
Conceptual study of moderately coupled plasmas and experimental comparison of laboratory x ray sources
[DE94-005828] p 3506 N94-30045
Complex source rate estimation for atmospheric transport and dispersion models
[DE94-000958] p 3354 N94-30822
RADIOCHEMISTRY
Research laboratories annual report 1992
[DE94-608124] p 3555 N94-30168
Recent results from SAGE
[DE94-006229] p 3551 N94-30845
RADIOGRAPHY
Microfocus radioscopy, a high resolution means of inspecting composite materials
[REPT-932-430-109] p 3179 N94-29454
Characteristics of secondary electron emission from CsI induced by x rays with energies up to 100 keV
[DE94-608422] p 3395 N94-30185
An inverse kinematics algorithm for the DREP/Philips real-time radiographic manipulator system p 3307 N94-30292
Seed viability detection using computerized false-color radiographic image enhancement p 3387 N94-30461
RADIOMETERS
Observations by ERS-1 start p 3327 N94-28933
Principles and application tendency of remote sensing: Its principle, function and utilization p 3328 N94-29037
Observatory system of Earth Resources Satellite-1 p 3330 N94-29221
Application of JERS-1 data to geologic analyses p 3330 N94-29222
EOS project and ASTER (ITIR) p 3331 N94-29226
An absolute measurement of the cosmic background radiation temperature at 1.4 GHz p 3553 N94-30351
RADON
Brief summary of accomplishments since our DOE-sponsored radon project commenced
[DE94-004643] p 3348 N94-29926
The long-range transport of aerosol particles over the North Atlantic Ocean p 3366 N94-30867
RAIL TRANSPORTATION
Electrical engineering and industrial electronics education days: Control of asynchronous generators
[PB94-135514] p 3266 N94-29523
RAILGUN ACCELERATORS
The 100 kA, 5000 V solid-state opening switch for inductive energy storage
[AD-A274993] p 3263 N94-28994
Microwave Michelson interferometer system report of first use on a railgun, Green Farm, San Diego, CA
[DE94-005294] p 3289 N94-30059
Design of an electromagnetic accelerator for turbulent hydrodynamic mix studies
[DE94-005821] p 3281 N94-30600
RAIN
Physical processes in snowpacks during rain or melt events
[AD-A275445] p 3325 N94-28881
On the relation between SMMR 37-GHz polarization difference and the rainfall over Africa and Australia
[NASA-TM-104598] p 3370 N94-29408
GCM studies of the influence of vegetation on the general circulation: The role of albedo in modulating climate change p 3348 N94-29749
Evaluation of dual polarization attenuation of millimeter frequencies through a meteorological radar p 3256 N94-30496
RAINDROPS
The appearance of the Sun and Moon seen through clouds
[AD-A275338] p 3551 N94-29212
RAMAN SPECTROSCOPY
Enhanced ion dissociation of LiCF3SO3 by new carbonate plasticizers: Raman and IR studies
[DE94-005448] p 3485 N94-28741
RAMJET ENGINES
Research and development of ramjets/ramrockets. Part 1: Integral solid propellant ramrockets p 3151 N94-29294
Research and development of ramjets/ramrockets. Part 2: Integral liquid fuel ramjets p 3152 N94-29297
Research and development of ramjets/ramrockets. Part 3: The study of gaseous hydrogen ram combustors p 3152 N94-29298
CIAM experimental turboramjets p 3152 N94-29299
Potential of the ramjet engine for hypersonic flight speeds p 3153 N94-30935
RAMPS (STRUCTURES)
Numerical simulation of unsteady aerodynamic heating induced by shock reflections p 3123 N94-28952
RANDOM ACCESS
Dynamic microsets for RAMs
[RUU-CS-93-22] p 3406 N94-30727
RANDOM ACCESS MEMORY
Advantages of the LBL 88-inch cyclotron ion beam for SEP studies
[AD-A275142] p 3494 N94-29065
Multiple single event upsets in CMOS static rams p 3496 N94-30215
Using Cf-252 for single event upset testing p 3496 N94-30219
Charge collection spectroscopy applied to MOS RAM's p 3201 N94-30220
RANDOM ERRORS
A comparative study of clock rate and drift estimation p 3473 N94-30669
RANDOM NOISE
Testing for a signal with unknown location and scale in a stationary Gaussian random field
[AD-A275320] p 3464 N94-28876
RANDOM PROCESSES
Polynomial modeling of analog-to-digital converters
[DE94-005579] p 3406 N94-30008
Thermodynamics of computation and information distance
[CWI-CS-R9341] p 3526 N94-30433

The Boltzmann entropy and randomness tests
[CWI-CS-R9342] p 3426 N94-30434

RANDOM SAMPLING
U-statistics of random-size samples and limit theorems for systems of Markovian particles with non-Poisson initial distributions
[AD-A275018] p 3464 N94-29129

RANDOM VARIABLES
U-statistics of random-size samples and limit theorems for systems of Markovian particles with non-Poisson initial distributions
[AD-A275018] p 3464 N94-29129

RANDOM VIBRATION
Root-sum-square structural strength verification approach
[NASA-TM-108453] p 3322 N94-30206

RANDOM WALK
Accuracy metrics for judging time scale algorithms
p 3471 N94-30656

RANGEFINDING
Simulation of fully automated air traffic control concepts p 3139 N94-29569
Orbital debris radar instrumentation
p 3248 N94-29626
Method for ambiguity resolution in range-Doppler measurements
[NASA-CASE-GSC-13542-1] p 3252 N94-29739

RANKING
Evaluating the analytic hierarchy process and recommended modifications for its use in multi-attribute decision making
[AD-A275065] p 3527 N94-29153

RAPID QUENCHING (METALLURGY)
Near-net-shape manufacturing: Spray-formed metal matrix composites and tooling p 3186 N94-30447

RAPID TRANSIT SYSTEMS
Electrical engineering and industrial electronics education days: Control of asynchronous generators
[PB94-135514] p 3266 N94-29523

RARE EARTH COMPOUNDS
Normal state resistivity of MBa2Cu3O(7-x) ceramics
[DE94-608456] p 3220 N94-30745

RARE EARTH ELEMENTS
Preparation of monodispersed fine particles containing rare metals and rare earths p 3201 N94-29514

RARE GASES
Metal inert gas welding system for use in vacuum
[NASA-CASE-MFS-28808-1] p 3298 N94-29352
Chamber free fusion welding root side purging method and apparatus
[NASA-CASE-MFS-28832-1] p 3204 N94-29380

RAREFIED GASES
Monte Carlo simulation or normal shock wave. Part 2: VHS model and VSS model p 3123 N94-28948
The maximum entropy approach applied to energy exchange, chemical reactions and ionisation in the direct simulation Monte Carlo method for rarefied hypersonic flows
[IC-AERO-93-01] p 3524 N94-29481

RATES (PER TIME)
Complex source rate estimation for atmospheric transport and dispersion models
[DE94-000958] p 3354 N94-30822

RATIONAL FUNCTIONS
Frequency-domain analysis of nonlinear microwave circuits
[PB94-132024] p 3261 N94-28400
Trace formulas and dynamical zeta functions in the Nielsen theory
[PB94-138195] p 3467 N94-29163

RATIONS
Nutrition and hydration status of aircrew members consuming an improved survival ration during a simulated survival scenario p 3380 N94-28429

RATS
Physiological investigations of the isolated rat's liver in hypothermia and hypoxia and their relevance in aircraft incidents above the sea p 3382 N94-28439
Shortening velocity and calcium sensitivity of single fibers from hindlimb suspended muscle in rats
p 3387 N94-29866

RAY TRACING
Synthetic image generator model; application of view angle dependent reflectivity components and performance evaluation in the visible region
[AD-A275365] p 3499 N94-29009
Optimizing ray tracing with visual coherence
[AD-A275218] p 3499 N94-29059

RAYLEIGH SCATTERING
Considerations in the modelling of seafloor acoustic backscatter
[AD-A275404] p 3478 N94-29206

RDX
Chemical dynamics studies of reactions in energetic materials
[AD-A275607] p 3224 N94-28769
Correlation of cookoff behavior of rocket propellants with thermomechanical and thermochemical properties
[AD-A274983] p 3224 N94-29092
Insensitive energetic materials: The importance of physical properties and molecular structure
[AD-A275393] p 3225 N94-29308

REACTING FLOW
A random distribution reacting mixing layer model
[NASA-TM-106517] p 3150 N94-28923
On approximate Riemann solvers: Improvement of HLLEM scheme and its generalization for chemically reacting flows p 3126 N94-28973
Advanced diagnostics for reacting flows
[AD-A275057] p 3272 N94-29136
A vorticity transport closure method for turbulent reacting flows p 3274 N94-29761
An evaluation of explicit pseudo-steady-state approximation schemes for stiff ODE systems from chemical kinetics
[CWI-NM-R9312] p 3353 N94-30729

REACTION KINETICS
SAFSIM theory manual: A computer program for the engineering simulation of flow systems
[DE94-005381] p 3270 N94-28488
Ozone production at a rural site in Georgia during the summer 1992 SOS campaign
[DE94-003989] p 3342 N94-28523
Ion-assisted tropospheric OH measurement technique
p 3344 N94-28601
Chemical dynamics studies of reactions in energetic materials
[AD-A275607] p 3224 N94-28769
High temperature resistant jet fuels
p 3192 N94-29260
Development of global/chemistry model for jet-fuel thermal stability based on observations from static and flowing experiments p 3192 N94-29262
Application of semiclassical methods to reaction rate theory
[DE94-007041] p 3199 N94-30266
XCHEM-1D: A heat transfer/chemical kinetics computer program for multilayered reactive materials
[DE94-005072] p 3226 N94-30615
An evaluation of explicit pseudo-steady-state approximation schemes for stiff ODE systems from chemical kinetics
[CWI-NM-R9312] p 3353 N94-30729
Lattice gas simulations of replicating domains
[DE94-005008] p 3200 N94-30748
Theory for electron-transfer reactions involving two Marcus surfaces with a different force constant
[DE94-005925] p 3493 N94-30874
Reinterpretation of rate data for the reaction of ClF and F2
[DE94-005819] p 3200 N94-30880
Role of x ray-induced transcripts in adaptive responses following x rays
[DE94-005412] p 3386 N94-30895
Surface chemistry of boron-doped SiO2 CVD: Enhanced uptake of tetraethyl orthosilicate by hydroxyl groups bonded to boron
[DE94-005428] p 3221 N94-30896
Influence of surface defects and local structure on oxygenate reaction pathways over metal oxide surfaces
[DE94-005680] p 3522 N94-30901

REACTION PRODUCTS
Dynamic response of ceramics
[AD-A275396] p 3214 N94-29203

REACTION TIME
Strategies to sustain and enhance performance in stressful environments
[AD-A275223] p 3398 N94-29027

REACTION WHEELS
Suspension system for gimbal supported scanning payloads
[NASA-CASE-MFS-28817-1] p 3287 N94-29358
A gimbaled low noise momentum wheel
p 3162 N94-29640

REACTIVITY
SAFSIM theory manual: A computer program for the engineering simulation of flow systems
[DE94-005381] p 3270 N94-28488
Dendrite preventing separator for secondary lithium batteries
[NASA-CASE-NPO-18585-1-CU] p 3265 N94-29411
Direct measurement of the reactivity of NH and OH on a silicon nitride surface
[DE94-005286] p 3199 N94-30260
XCHEM-1D: A heat transfer/chemical kinetics computer program for multilayered reactive materials
[DE94-005072] p 3226 N94-30615

REACTOR DESIGN
The organometallic chemical vapor deposition of transition metal carbides: The use of homoleptic alkyls
[DE94-005577] p 3206 N94-30007
Small low mass advanced PBR's for propulsion
[DE94-005142] p 3497 N94-30588

REACTOR MATERIALS
Relationship between swelling and irradiation creep in cold-worked PCA stainless steel irradiated to approximately 178 dpa at approximately 400 C
[DE94-004368] p 3201 N94-28456
Radiation effects in beryllium used for plasma protection
[DE94-004599] p 3201 N94-28460
Proceedings of Japan-US Workshop P-196 on High Heat Flux Components and Plasma Surface Interactions for Next Devices
[DE94-701164] p 3503 N94-28513
Analysis of data by long-time mechanical properties of 08KH18N10T steel irradiated by neutrons
[DE94-605337] p 3202 N94-28551
Fatigue of carbon and low-alloy steels in LWR environments
[DE94-005116] p 3207 N94-30021
Development of evaluated data bank of physical properties of perspective nuclear engineering steels and alloys
[DE94-607999] p 3207 N94-30076
Irradiation-induced structure and property changes in tokamak plasma-facing, carbon-carbon composites
[DE94-006046] p 3508 N94-30365
Development of radiation resistant electrical cable insulations p 3223 N94-30480
Modelling erosion damage from low-energy plasma gun simulations of disruptions
[DE94-005196] p 3509 N94-30697
Neutronics of a D-Li neutron source: An overview
[DE94-005372] p 3493 N94-30893

REACTOR SAFETY
Single specimen fracture toughness determination procedure using instrumented impact test
[PB94-132040] p 3316 N94-28402
Nuclear energy related research
[DE94-606286] p 3494 N94-28623
Risk measures in living probabilistic safety assessment
[VTT-PUBS-146] p 3465 N94-30154
The TOPAZ 2 space reactor response under accident conditions
[DE94-004998] p 3498 N94-30847

REACTOR TECHNOLOGY
Nuclear energy related research
[DE94-606286] p 3494 N94-28623
Development of evaluated data bank of physical properties of perspective nuclear engineering steels and alloys
[DE94-607999] p 3207 N94-30076
Intercomparison of theoretical calculations of important activation cross sections for fusion reactor technology
[DE94-002642] p 3497 N94-30825

REAGENTS
A commercialized, continuous flow fiber optic sensor for trichloroethylene and haloforms
p 3502 N94-30462

REAL TIME OPERATION
Technology transition push. Part 1: A case study of rate monotonic analysis
[AD-A275616] p 3407 N94-28633
The bootstrapped algorithm: A fast algorithm for blind signal separation
[AD-A275759] p 3408 N94-28760
Information presentation for expert systems in future fighter aircraft
[AD-A275126] p 3149 N94-29005
NPSNET: Integration of Distributed Interactive Simulation (DIS) protocol for communication architecture and information interchange
[AD-A275061] p 3530 N94-29139
A common Ada run-time system for avionics software
p 3150 N94-29331
Design of a thinwire real-time multiprocessor operating system p 3415 N94-29333
Validation and test of complex weapon systems
p 3150 N94-29336
GPS/GNSS for ATM p 3138 N94-29565
ACCS Surveillance Exploratory Prototype (ASEP)
p 3138 N94-29566
Formal specification and verification of real-time sequential control systems
[AD-A275776] p 3419 N94-29678
Hypra/TR: A tuple oriented recovery method for a continuously available distributed DBMS on a shared nothing multi-computer
[PB94-141264] p 3533 N94-29921
Novel mass spectrometric instrument for gaseous and particulate characterization and monitoring
[DE94-005896] p 3349 N94-30047
Computational balance in real-time cyclic spectral analysis
[DE94-005091] p 3432 N94-30100

Common spaceborne multicomputer operating system and development environment
[NASA-TM-109092] p 3422 N94-30197
Sensing the gas metal arc welding process
p 3314 N94-30444
ARK: Autonomous mobile robot in an industrial environment
[AIAA PAPER 94-1177-CP] p 3439 N94-30529
A performance analysis method for distributed real-time robotic systems: A case study of remote teleoperation
[AIAA PAPER 94-1212-CP] p 3445 N94-30563
Predictive sufficiency and the use of stored internal state
[AIAA PAPER 94-1213-CP] p 3445 N94-30564
The use of the AOA TTR-4P GPS receiver in operation at the BIPM for real-time restitution of GPS time
p 3144 N94-30651
A real-time prediction of UTC p 3470 N94-30654
'Real time' and the NLR aerodynamic facilities
[AD-B173626] p 3158 N94-30856

REATTACHED FLOW
An experimental study of the flowfield on a semispan rectangular wing with a simulated glaze ice accretion
p 3130 N94-29674

RECEIVERS
Output statistics of the SALFAS FM normalizer Smoothing/Prediction function
[AD-A275758] p 3463 N94-28759
Performance and durability of high emittance heat receiver surfaces for solar dynamic power systems
[NASA-TM-106549] p 3172 N94-28834
An analysis of carrier phase jitter in an MPSK receiver utilizing map estimation
[NASA-CR-195806] p 3164 N94-29880
An absolute measurement of the cosmic background radiation temperature at 1.4 GHz p 3553 N94-30351
Time and position accuracy using codeless GPS
p 3144 N94-30650
The use of the AOA TTR-4P GPS receiver in operation at the BIPM for real-time restitution of GPS time
p 3144 N94-30651

RECEPTORS (PHYSIOLOGY)
Effects of pressure on membrane-associated receptors and effector elements
[AD-A275813] p 3384 N94-28829

RECESSES
Portable electronically based method for the nondestructive remote sensing of crevice corrosion
[AD-A275403] p 3318 N94-29057

RECHARGING
Anode for rechargeable ambient temperature lithium cells
[NASA-CASE-NPO-18580-1-CU] p 3265 N94-29505

RECIRCULATIVE FLUID FLOW
A new Eulerian model for turbulent evaporating sprays in recirculating flows p 3195 N94-29279
An experimental study of the flowfield on a semispan rectangular wing with a simulated glaze ice accretion
p 3130 N94-29674

RECOMBINATION REACTIONS
Reinterpretation of rate data for the reaction of ClF and F2
[DE94-005819] p 3200 N94-30880

RECONNAISSANCE
The Pluto fast flyby mission: Completing the reconnaissance of the solar system
p 3235 N94-29768

RECORDING
Noise reduction techniques for the restoration of musical recordings
[TELECOM-93-E-019] p 3291 N94-30979

RECORDS MANAGEMENT
The evolution of information management
[DE94-004173] p 3535 N94-30179

RECRYSTALLIZATION
On the prediction of HAZ grain size using Monte Carlo simulation
[DE94-005465] p 3511 N94-28535
Failures to model the development of a cube texture during the high temperature compression of Al-Mg alloys
[DE94-005013] p 3201 N94-28544

RECTANGLES
Rectilinear decompositions with low stabbing number
[RUU-CS-93-25] p 3459 N94-30425

RECTANGULAR PLATES
Further investigation of curve veering phenomena
p 3460 N94-30515

RECTANGULAR WINGS
An experimental study of wing tip vortex in the near wake of a rectangular wing
[AD-A275389] p 3129 N94-29306
An experimental study of the flowfield on a semispan rectangular wing with a simulated glaze ice accretion
p 3130 N94-29674

RECURSIVE FUNCTIONS
Categorial generalization of algebraic recursion theory
[ML-93-06] p 3456 N94-30382
Development and validation of a linear recursive order-N algorithm for the simulation of flexible space manipulators dynamics
[AD-B173557] p 3311 N94-30391
Higher order recursive program schemes are Turing incomplete
[CWI-CS-R9348] p 3425 N94-30414

RED GIANT STARS
Abundance patterns in red-giant CH stars
p 3539 N94-29820

RED SHIFT
High redshift QSOs and the x ray background
[NASA-CR-195112] p 3540 N94-29957
Broad H alpha profiles of radio-loud active galactic nuclei and rapid profile variability in Seyfert and radio galaxies
p 3552 N94-29989

REDUCED ORDER FILTERS
Enhanced orbit determination filter sensitivity analysis: Error budget development p 3159 N94-29655
Enhanced orbit determination filter: Inclusion of ground system errors as filter parameters p 3159 N94-29656

REDUCTION
Perpetual reductions and strong normalization in orthogonal term rewriting systems
[CWI-CS-R9345] p 3426 N94-30437

REDUNDANCY
Algorithms for treating redundancy in repairable and non-repairable systems
[DE94-005289] p 3315 N94-29020
Kinematic functions for redundancy resolution using configuration control
[NASA-CASE-NPO-18608-1-CU] p 3436 N94-29504

REDUNDANCY ENCODING
Software engineering methods in the Hermes on-board software p 3414 N94-29326
Checkpoint-based forward recovery using lookahead execution and rollback validation in parallel and distributed systems
[NASA-CR-195760] p 3431 N94-29869

REDUNDANT COMPONENTS
Redundant disk arrays in transaction processing systems
[NASA-CR-195759] p 3418 N94-29404
An algorithm for the Italian atomic time scale
p 3473 N94-30668

REED-SOLOMON CODES
Optimizing the Galileo space communication link
p 3250 N94-29663
Decoder synchronization for deep space missions
p 3250 N94-29664

REFINING
Near-net-shape manufacturing: Spray-formed metal matrix composites and tooling p 3186 N94-30447

REFLECTANCE
Synthetic image generator model; application of view angle dependent reflectivity components and performance evaluation in the visible region
[AD-A275365] p 3499 N94-29009
Satellite estimation of the global distribution and interannual variability of photosynthetically active radiation p 3334 N94-29970
Electrooptical and optical evaluation of Pb(Zr,Ti)O3 thin films using waveguide refractometry
[DE94-006374] p 3518 N94-30247
Characterization of thermally annealed Sb implanted fused silica
[DE94-005464] p 3219 N94-30335
The performance of gloss meters on curving surfaces
[NPL-DMM(A)-111] p 3501 N94-30522

REFLECTED WAVES
Method for cancelling expansion waves in a wave rotor
[NASA-CASE-LEW-15218-2] p 3274 N94-29740

REFLECTION
Observation of the phase shift of the wave function of the neutron under total reflection
[DE94-608244] p 3489 N94-30096
Hybrid optics for space applications
[ESA-CP-1158] p 3501 N94-30418

REFLECTOMETERS
VHF impedance measurement: A review
[PB94-138682] p 3267 N94-30115
RF and microwave dielectric measurements upon layered materials using reflectometric coaxial sensor
[NPL-DES-125] p 3476 N94-30781

REFLECTOR ANTENNAS
Defocussing characteristics of the ACTS, T1-VSAT Earth terminal antennas
[NASA-TM-106420] p 3242 N94-28826
Beam scanning offset Cassegrain reflector antennas by subreflector movement
[NASA-CR-191604] p 3160 N94-28836
GLRS-R 2-colour retroreflector target design and predicted performance
[REPT-932-440-106] p 3246 N94-29542

REFLECTORS
Deployable reflector structure
[NASA-CASE-LAR-14513-1-SB] p 3245 N94-29360
Optical Chopper Assembly for the Mars Observer
p 3162 N94-29639
Overview of shielding analyses for the MHTGR from 1986 to 1991
[DE94-002448] p 3495 N94-29924
Nonlinear absorption in high reflector multilayers
[DE94-005818] p 3295 N94-30598

REFRACTION
Hybrid optics for space applications
[ESA-CP-1158] p 3501 N94-30418

REFRACTIVITY
High damage threshold anti-reflectors by physical vapor deposited amorphous fluoropolymer
[DE94-004865] p 3212 N94-28560
Electrooptical and optical evaluation of Pb(Zr,Ti)O3 thin films using waveguide refractometry
[DE94-006374] p 3518 N94-30247
Characterization of thermally annealed Sb implanted fused silica
[DE94-005464] p 3219 N94-30335

REFRACTORY COATINGS
A novel approach to the fabrication of SiC structures of arbitrary shape
[AD-A275475] p 3214 N94-29073

REFRACTORY MATERIALS
Thermal expansion and elastic anisotropy in single crystal Al2O3 and SiC reinforcements
[NASA-TM-106516] p 3214 N94-29105
Method of producing a ceramic fiber-reinforced glass-ceramic matrix composite
[NASA-CASE-LEW-15264-2] p 3180 N94-29508
Surface fatigue life of high temperature gear materials
[NASA-TM-106562] p 3303 N94-30227

REFRIGERANTS
ARTI Refrigerant Database
[DE94-004906] p 3230 N94-28563
An experimental investigation of flow patterns and liquid entrainment in a horizontal-tube evaporator
p 3277 N94-29899
Lunar base heat pump, phase 1 draft
[NASA-CR-195211] p 3278 N94-29977
Large heat pumps using CO2 refrigerant
[PB94-138773] p 3279 N94-29999
Materials compatibility and lubricants research on CFC-refrigerant substitutes
[DE94-004905] p 3220 N94-30692

REFRIGERATING
ARTI Refrigerant Database
[DE94-004906] p 3230 N94-28563

REFRIGERATORS
Annual summary of basic research thermoacoustic heat transport, 1993
[AD-A275751] p 3230 N94-28644

REFUELING
Development and testing of the Automated Fluid Interface System p 3161 N94-29636
Autonomous Robotic Refueling System (ARRS) for rapid aircraft turnaround p 3305 N94-30279

REGRESSION ANALYSIS
Least-squares determination of burst-point coordinates
[AD-A275423] p 3452 N94-28864
Atmospheric moisture fields derived by satellite observations over the tropical Pacific Ocean
p 3375 N94-30863

REGRESSION COEFFICIENTS
Estimation of the net production of moss community at Langhovde, East Antarctica p 3358 N94-29081

REGULATIONS
Effects of repair on structural integrity
[AD-A275756] p 3145 N94-28647
Environmental Compliance Assessment System (ECAS) --- Japan supplement
[AD-A275549] p 3346 N94-28722
Environmental Compliance Assessment And Management System Program (ECAMP). US Air Force European Economic Community (EEC)
[AD-A275593] p 3346 N94-28727
Environmental Review Guide for Operations (ERGO)
[AD-A275611] p 3346 N94-28774
Crashworthiness analysis of commuter aircraft seats
[AD-A275889] p 3135 N94-28799
Evaluation of monitoring audiometry in the United States Air Force Hearing Conservation Program
[AD-A275309] p 3391 N94-29211
Non-aqueous cleaning solvent substitution
[DE94-005339] p 3219 N94-30245
Non-aqueous cleaning solvent substitution
p 3354 N94-30466

TCM exemptions to promote alternative-fuel vehicles: The good, the bad, and the ugly
[DE94-005924] p 3311 N94-30703
REGULATORS
Non-isolated 30 kW class arcjet PCU
[NASA-CR-189148] p 3173 N94-29444
REGULATORY MECHANISMS (BIOLOGY)
Japanese Journal of Aerospace and Environmental Medicine, vol. 30, no. 2
[JTN-94-80599] p 3394 N94-29863
Effects of make-up on the heat transfer from the head in hyperthermic conditions p 3394 N94-29864
REINFORCING FIBERS
Innovative processing of composites for ultra-high temperature applications, book 1
[AD-A275597] p 3176 N94-28729
Thermal expansion and elastic anisotropy in single crystal Al2O3 and SiC reinforcements
[NASA-TM-106516] p 3214 N94-29105
Damage meso-modeling of 3D evolutive composites
[REPT-932-430-106] p 3179 N94-29442
Method of producing a ceramic fiber-reinforced glass-ceramic matrix composite
[NASA-CASE-LEW-15264-2] p 3180 N94-29508
REINFORCING MATERIALS
Technology base enhancement program. Metal matrix composites
[AD-A275531] p 3176 N94-28688
Controlled thermal expansion printed wiring boards based on liquid crystal polymer dielectrics
[NASA-CR-189338] p 3287 N94-29400
Thermodynamic analysis of chemical compatibility of several compounds with Fe-Cr-Al alloys
[NASA-CR-191166] p 3181 N94-29684
A review of mechanical test methods for ceramic matrix composites
[PB94-147576] p 3184 N94-30524
RELATIVISTIC EFFECTS
Apparent unambiguousness of relativistic time dilation
[DE94-606328] p 3522 N94-28586
On a direct experimental verification of the elongation formula
[DE94-606329] p 3523 N94-28721
Theoretical investigation of gas-surface interactions
[NASA-CR-195755] p 3272 N94-29378
Large amplitude Langmuir and ion-acoustic waves in a relativistic two-fluid plasma
[NIFS-271] p 3506 N94-29547
RELATIVISTIC ELECTRON BEAMS
Experiments on the two-stage dense plasma heating on the GOL-3 device
[DE94-608356] p 3508 N94-30193
Peculiarities of heat transfer in the experiments of beam injection heating of a plasma at the GOL-3 device
[DE94-608357] p 3508 N94-30194
RELATIVISTIC PARTICLES
The effects of relativistic neutrons on nonthermal models of active galactic nuclei p 3547 N94-29993
On relativity principle violation in local measurements of spin precession of moving particles
[DE94-608067] p 3489 N94-30085
RELATIVISTIC PLASMAS
Large amplitude Langmuir and ion-acoustic waves in a relativistic two-fluid plasma
[NIFS-271] p 3506 N94-29547
A relativistic solitary wave in electron positron plasma
[DE94-608107] p 3507 N94-30071
RELATIVISTIC THEORY
The solving of the relativistic two-body problem with a nonlinear dependence upon a spectrum parameter
[DE94-606343] p 3451 N94-28783
Relativistic theory for picosecond time transfer in the vicinity of Earth p 3470 N94-30653
RELATIVITY
Apparent unambiguousness of relativistic time dilation
[DE94-606328] p 3522 N94-28586
Retarded distances and the Doppler effect
[DE94-606296] p 3523 N94-28618
On the importance of the Michelson-Morley experiment
[DE94-606298] p 3523 N94-28620
Three forms of relativity
[DE94-606338] p 3523 N94-28782
On dyonic black holes and cosmic censorship p 3546 N94-29912
On relativity principle violation in local measurements of spin precession of moving particles
[DE94-608067] p 3489 N94-30085
RELAXATION (MECHANICS)
Strain relaxation and surface roughness as a function of growth temperature in linearly graded In(x)Al(1-x)As (x = 0.05 to 0.25) buffers
[DE94-005430] p 3519 N94-30592
RELAXATION METHOD (MATHEMATICS)
Numerical analysis of two dimensional/axisymmetric non-equilibrium hypersonic flow p 3125 N94-28963
An implicit upwind scheme for the three-dimensional Euler equations using a pointwise relaxation method p 3128 N94-28983
Numerical solution of the two-dimensional time-dependent incompressible Euler equations
[NASA-CR-195775] p 3277 N94-29859
RELIABILITY
Identification of components to optimize improvement in system reliability
[DE94-001601] p 3315 N94-28503
Rocket engine system reliability analyses using probabilistic and fuzzy logic techniques
[NASA-TM-106519] p 3173 N94-29403
ASSIST internals reference manual
[NASA-TM-109102] p 3431 N94-29494
Issues arising with the application of optical fiber transmission in class 1E systems in nuclear power plants
[DE94-004743] p 3500 N94-29928
RELIABILITY ANALYSIS
Identification of components to optimize improvement in system reliability
[DE94-001601] p 3315 N94-28503
Statistical Modeling and Estimation of Reliability Functions for Software (SMERFS) user's guide, revision 3
[AD-A275390] p 3411 N94-29202
Statistical Modeling and Estimation of Reliability Functions for Software (SMERFS) library access guide, revision 3
[AD-A275405] p 3411 N94-29207
Rocket engine system reliability analyses using probabilistic and fuzzy logic techniques
[NASA-TM-106519] p 3173 N94-29403
Reliability of composite material structures. Application: High pressure spherical coded tanks
[REPT-932-430-103] p 3180 N94-29478
ASSIST internals reference manual
[NASA-TM-109102] p 3431 N94-29494
Dependability analysis of parallel systems using a simulation-based approach
[NASA-CR-195762] p 3431 N94-29846
Estimation of Weibull modulus from dynamic and static fatigue experiments
[PB94-138641] p 3322 N94-30114
TOTAL user manual
[NASA-TM-109101] p 3432 N94-30160
Modeling systems by probabilistic process algebra: An event structures approach
[MEMO-INF-93-29-REV] p 3425 N94-30416
A survey of NASA and military standards on fault tolerance and reliability applied to robotics
[AIAA PAPER 94-1211-CP] p 3445 N94-30562
Photovoltaic performance and reliability workshop
[DE94-000236] p 3339 N94-30601
RELIABILITY ENGINEERING
Advanced languages for systems software
[AD-A275272] p 3410 N94-29007
Satellites: Reliability and operation security
[REPT-932-440-108] p 3168 N94-29419
A survey of NASA and military standards on fault tolerance and reliability applied to robotics
[AIAA PAPER 94-1211-CP] p 3445 N94-30562
RELIEF MAPS
The Image Digitizing System (IDS)
[AD-A275341] p 3329 N94-29213
REMOTE CONTROL
Remote control of transcranial Doppler (TCD) probe during centrifuge exposures up to 9 +Gz
[AD-A275253] p 3400 N94-29029
An emergency response mobile robot for operations in combustible atmospheres
[NASA-CASE-NPO-19020-1-CU] p 3299 N94-29420
Simplified and symmetrical five-bar linkage driver for manipulating a six-degree-of-freedom parallel minimanipulator with three inextensible limbs
[NASA-CASE-GSC-13485-2] p 3301 N94-29556
Remote observatory access via the advanced communications technology satellite p 3253 N94-29894
Aspects of the operator interface for military robotic applications in unstructured environments p 3309 N94-30304
A multiplexed two-way solid communications link for teleoperated robots p 3310 N94-30310
Task automation in a successful industrial telerobot
[AIAA PAPER 94-1189-CP] p 3441 N94-30539
Object-based task-level control: A hierarchical control architecture for remote operation of space robots
[AIAA PAPER 94-1209-CP] p 3444 N94-30560
A performance analysis method for distributed real-time robotic systems: A case study of remote teleoperation
[AIAA PAPER 94-1212-CP] p 3445 N94-30563
A multi-mode manipulator display system for controlling remote robotic systems
[AIAA PAPER 94-0888-CP] p 3446 N94-30569
REMOTE HANDLING
A multiplexed two-way solid communications link for teleoperated robots p 3310 N94-30310
Aiding the operator in the manual control of a space manipulator
[PB94-125549] p 3402 N94-30390
REMOTE MANIPULATOR SYSTEM
A multi-mode manipulator display system for controlling remote robotic systems
[AIAA PAPER 94-0888-CP] p 3446 N94-30569
REMOTE SENSING
Objective analysis of a coastal ocean eddy using satellite AVHRR and in situ hydrographic data
[AD-A275715] p 3376 N94-28642
Proceedings of the International Symposium on Remote Sensing
[JTN-94-80578] p 3325 N94-28925
Keynote address --- Japanese Earth Resources Satellite 1 (JERS-1) and future remote sensing projects p 3326 N94-28926
Synthetic aperture radar applications: Now and in the future p 3260 N94-28927
Research trends on remote sensing at research facilities in Japan: The priority area programme on better understanding of earth environment via satellite p 3326 N94-28928
Evaluation of simulated JERS-1 data for geologic mapping at Drum Mountains, Utah, Silver Bell, Arizona, and Wind River, Wyoming under the GEOSAT-ERSDAC/JAPEX/JGI/RESTEC joint studies p 3326 N94-28929
Image processing for hyperspectral data p 3326 N94-28930
JERS-1 data and information system for resources exploration p 3327 N94-28932
Observations by ERS-1 start p 3327 N94-28933
Sea ice and oceans applications of SAR p 3327 N94-28934
Amazonia: Remote sensing test site and survey p 3327 N94-28935
Utilization of remote sensing data in Southeast Asia p 3327 N94-28936
Remote sensing and global management p 3328 N94-28937
Synthetic image generator model; application of view angle dependent reflectivity components and performance evaluation in the visible region
[AD-A275365] p 3499 N94-29009
Proceedings of the 15th Earth Observation Symposium
[JTN-94-80607] p 3328 N94-29036
Principles and application tendency of remote sensing: Its principle, function and utilization p 3328 N94-29037
Status and tendency of earth observation system p 3328 N94-29038
Perspectives of earth observing techniques: Expectation of earth observation in space development history p 3328 N94-29039
Oceanic survey utilizing satellites p 3328 N94-29040
Tohoku district observed by artificial satellites p 3328 N94-29041
Portable electronically based method for the nondestructive remote sensing of crevice corrosion
[AD-A275403] p 3318 N94-29057
Activities of the wintering party at Showa Station by the 31st Japanese Antarctic Research Expedition in 1990 p 3358 N94-29083
Role of satellite observations of sea-surface temperature in the detection of global change
[PB94-138120] p 3329 N94-29107
Remote sensing of inner heliospheric plasmas
[AD-A275021] p 3550 N94-29132
Proceedings of the 3rd International Symposium: JERS-1 and Remote Sensing in the Future
[JTN-94-80597] p 3329 N94-29217
Remote sensing and the Earth p 3329 N94-29218
A new information system: Satellite observation p 3330 N94-29219
Application of optical sensor data to resource survey p 3330 N94-29223
Radar applications at the Canada Centre for Remote Sensing p 3331 N94-29224
Earth-observation plan in Europe p 3331 N94-29227
Rock identification using thermal infrared data p 3331 N94-29228
JERS-1 and future remote sensing: Application of remote sensing data to agroecological problems p 3331 N94-29229
Application of remote sensing in prevention of disasters p 3332 N94-29230
Future expectation of remote sensing technology p 3332 N94-29231

Japan's Earth observation satellite programs
p 3332 N94-29232
Imaging spectrometry of the Earth and other solar system bodies p 3237 N94-29779
Evolution of miniature detectors and focal plane arrays for infrared sensors p 3237 N94-29781
Frequency dependence of polarization phase difference
[NASA-TM-109737] p 3254 N94-30094
The extraction and representation of forest inventory information using continuous density surfaces
[ISBN-0-315-85658-0] p 3334 N94-30236
Cloud and aerosol characterization for the ARM central facility: Multiple remote sensor techniques development
[DE94-003523] p 3365 N94-30608
FAME: A Forest Assessment and Monitoring Environment scenario
[AD-B179106] p 3335 N94-30759
Multitemporal analysis of a braiding river: The advanced study of 1992
[NLR-TP-93100-U] p 3335 N94-30942

REMOTE SENSORS
Beam scanning offset Cassegrain reflector antennas by subreflector movement
[NASA-CR-191604] p 3160 N94-28836
Proceedings of the International Symposium on Remote Sensing
[JTN-94-80578] p 3325 N94-28925
Conceptual radiometer design studies for Earth observations from low Earth orbit
[NASA-CR-4588] p 3329 N94-29098
Proceedings of the 3rd International Symposium: JERS-1 and Remote Sensing in the Future
[JTN-94-80597] p 3329 N94-29217
Outline of JERS-1 system p 3330 N94-29220
Observatory system of Earth Resources Satellite-1
p 3330 N94-29221
Application of JERS-1 data to geologic analyses
p 3330 N94-29222
Rock identification using thermal infrared data
p 3331 N94-29228
Remote sensor observations during WISP91: The use of microwave radiometers, RASS, and lidar ceilometers for detection of aircraft icing conditions
[PB94-142106] p 3136 N94-30890

REMOTELY PILOTED VEHICLES
Acquisition, design modification, assembly, and ground test of NPS Hummingbird remotely piloted helicopter
[AD-A275546] p 3146 N94-28837
A non-linear simulation for an autonomous unmanned air vehicle
[AD-A275062] p 3146 N94-29200
Navigation of military and space unmanned ground vehicles in unstructured terrains p 3144 N94-30282
A generic semi-autonomous ground vehicle control system p 3306 N94-30283
The use of low cost differential mode GPS receivers in unmanned vehicles p 3144 N94-30285
HATT-X: A high performance flying laboratory for autonomous unmanned aircraft research and development p 3149 N94-30293

RENDEZVOUS SPACECRAFT
A guidance and navigation system for two spacecraft rendezvous in translunar halo orbit
p 3142 N94-29837

RENORMALIZATION GROUP METHODS
Study of modeling of turbulence of renormalization group analysis p 3126 N94-28970

REPLACING
Alumina ceramic: A cost effective replacement for titanium in deep submergence pressure housings
[AD-A275640] p 3212 N94-28641
Technology transfer initiatives
[NASA-CR-195151] p 3537 N94-29410

REPRODUCTION (BIOLOGY)
Reproduction in the Japanese anchovy (Engraulis japonica) as related to population fluctuation
p 3235 N94-29708

REPRODUCTION (COPYING)
Fundamentals of printing technology
[PB94-132602] p 3530 N94-29141

REQUIREMENTS
Development of electromagnetic compatibility tests
[REPT-932-430-110] p 3245 N94-29421

RESCUE OPERATIONS
Effectiveness of protection clothing for cold weather conditions after ejection over sea: A case report
p 3381 N94-28435

RESEARCH
Venus Data Analysis Program: Directory of Research Projects (1993-1994)
[NASA-CR-195742] p 3549 N94-29102
Basic research in computer science
[AD-A275184] p 3405 N94-29181
Activities report of the International Meteorological Institute
[ETN-94-95524] p 3370 N94-29423
Antarctic Record, vol. 36, no. 3
[REPT-108] p 3363 N94-29978
Activities of the wintering party at Syowa Station by the 32nd Japanese Antarctic Research Expedition in 1991
p 3364 N94-29986

RESEARCH AIRCRAFT
The radiocarbon hydroxyl technique
p 3344 N94-28600
Design and construction of the Aerobot Robotic Manipulator (ARM)
[AD-A275362] p 3298 N94-28894
HATT-X: A high performance flying laboratory for autonomous unmanned aircraft research and development p 3149 N94-30293

RESEARCH AND DEVELOPMENT
Glass-ceramic matrix composites
[REPT-932-430-112] p 3179 N94-29413
Journal of NIRE, vol. 2, no. 3
[JTN-94-80553] p 3553 N94-29512
Activity report of Synchrotron Radiation Laboratory 1992
[JTN-94-80600] p 3495 N94-29596
Proceedings: SISAL 1993
[DE94-006641] p 3420 N94-30056
NASA/DOD Aerospace Knowledge Diffusion Research Project. Report 23: The communications practices of US aerospace engineering faculty and students: Results of the phase 3 survey
[NASA-TM-109085] p 3534 N94-30149
NASA/DOD Aerospace Knowledge Diffusion Research Project. Report 22: US academic librarians and technical information specialists as information intermediaries: Results of the phase 3 survey
[NASA-TM-109067] p 3534 N94-30150
Proceedings of the 3rd Conference on Military Robotic Applications
[DRES-SP-149] p 3304 N94-30275
Intelligent robotics can boost America's economic growth
[AIAA PAPER 94-1301-CP] p 3439 N94-30527
Geothermal direct-heat utilization assistance
[DE94-005831] p 3340 N94-30700
Photonics at Sandia National Laboratories: From research to applications
[DE94-006463] p 3501 N94-30828

RESEARCH FACILITIES
Physics at HERA
[DE94-005117] p 3483 N94-28569
Antarctic Record, volume 36, no. 1
[REPT-106-VOL-36-NO-1] p 3357 N94-29078
Fishermans Bend: A centre of Australian aviation
[AD-A274981] p 3121 N94-29090
Joint research activities with CCMRI (China)
p 3240 N94-29521
Portable Linear Sled (PLS) for biomedical research
p 3163 N94-29648
Research and technology, 1992
[NASA-TM-103996] p 3555 N94-29891
Energy and Technology Review
[DE94-004472] p 3338 N94-29955
On the (mu)SR activity at LNP JINR phasotron
[DE94-608385] p 3517 N94-30195
Microgravity fluid science research in Europe
[AD-B179178] p 3229 N94-30409

RESEARCH MANAGEMENT
Spin-off companies as agents of technology transfer: An empirical study of the spin-off companies of the Technical Research Centre of Finland
[PB94-132248] p 3537 N94-28405
Fundamental studies on the corrosion behavior of weldments in marine microbial environments
[AD-A275247] p 3203 N94-28900
Basic research in computer science
[AD-A275222] p 3405 N94-28916

RESEARCH PROJECTS
Advanced gas turbine systems research
[DE94-005303] p 3297 N94-28485
US/Japan cooperation in high energy physics
[DE94-005376] p 3494 N94-28486
Summaries of FY 1993 geosciences research
[DE94-004710] p 3355 N94-28558
Relativistic heavy ion research
[DE94-004701] p 3484 N94-28576
Annual summary of basic research thermoacoustic heat transport, 1993
[AD-A275751] p 3230 N94-28644
The Norwegian seismic array (NORSAR), phase 3
[AD-A275440] p 3356 N94-28868
Annual report and summaries of FY 1993 activities: Division of Energy Biosciences
[DE94-001723] p 3386 N94-30607
Crystalline-silicon solar cell development sponsored by the US Department of Energy
[DE94-003783] p 3340 N94-30609

RESERVOIRS
Fiscal 1990 geothermal development promotion survey
[DE94-732333] p 3337 N94-28628

RESIDUAL STRENGTH
Full-scale testing and analysis of curved aircraft fuselage panels
[AD-A275666] p 3145 N94-28657

RESIDUAL STRESS
Prediction of stress-strain response of SCS-6/Timetal-21S subjected to a hypersonic flight profile
[NASA-TM-109026] p 3177 N94-28823
Multiple Concentric Cylinder Model (MCCM) user's guide
[NASA-CR-195299] p 3183 N94-30125

RESIN MATRIX COMPOSITES
Polymer infiltration studies
[NASA-CR-195729] p 3213 N94-28748
On the dynamic mechanical behavior of 3-D integrated fabric reinforced composites
[AD-A275424] p 3177 N94-28865

RESINS
Chemically modified polymeric resins for separation of cations, organic acids, and small polar molecules by high performance liquid chromatography
[DE94-005548] p 3211 N94-28516
Electroset Technology: On the forefront of manufacturing
[AD-A275166] p 3263 N94-29045

RESOLUTION
Kinematic functions for redundancy resolution using configuration control
[NASA-CASE-NPO-18608-1-CU] p 3436 N94-29504
Method for ambiguity resolution in range-Doppler measurements
[NASA-CASE-GSC-13542-1] p 3252 N94-29739

RESOLVERS
Multi-speed multi-phase resolver converter
[NASA-CASE-MFS-28855-1] p 3264 N94-29372

RESONANCE
A measurement of the tau polarization at the resonance with the DELPHI detector at LEP
[DE94-005557] p 3482 N94-28520
Overlap of metal clusters and nuclear structure physics
[DE94-608387] p 3517 N94-30183
Multiple weather regimes and baroclinically forced spherical resonance
[DM-65] p 3376 N94-30966

RESONANCE FLUORESCENCE
Activity report of Synchrotron Radiation Laboratory 1992
[JTN-94-80600] p 3495 N94-29596

RESONANCE LINES
The investigation of electron-ion radiative and dielectronic recombination in high-temperature plasmas
[DE94-005150] p 3509 N94-30755

RESONANT FREQUENCIES
Rotor instability induced by dead band clearance in bearing supports p 3312 N94-30809

RESONANT TUNNELING
Strong overlap and transmission in triple barrier resonant structures
[DE94-608103] p 3516 N94-30067

RESOURCES MANAGEMENT
On United States-Japan Conference on Development and Utilization of Natural Resources: Report of the 14th Joint Meeting of U. S. and Japan Marine Mining Panel
p 3188 N94-28683
Remote sensing and global management
p 3328 N94-28937
Remote sensing and the Earth p 3329 N94-29218
Future expectation of remote sensing technology
p 3332 N94-29231
Research report on the potential of ocean development suitable for area characteristics
[JTN-94-80587] p 3377 N94-29595

RESPIRATORS
Portable ventilatory resuscitation systems
[AD-A274984] p 3401 N94-29093

RESPIRATORY RATE
Estimation of the net production of moss community at Langhovde, East Antarctica p 3358 N94-29081

RESPIRATORY SYSTEM
Blast overpressure studies with animals and man
[AD-A275038] p 3391 N94-29150

RESTORATION
Development and implementation of a scrub habitat compensation plan for Kennedy Space Center
[NASA-TM-109202] p 3347 N94-29099
Benchmarking for cost improvement
[DE94-002276] p 3528 N94-30824

RESUSCITATION
Portable ventilatory resuscitation systems
[AD-A274984] p 3401 N94-29093
RETENTION (PSYCHOLOGY)
Key cognitive issues in the design of electronic displays of instrument approach procedure charts
[AD-A275647] p 3399 N94-28649
RETINA
Digital tracking and control of retinal images
[AD-A275469] p 3389 N94-28810
RETINAL IMAGES
Digital tracking and control of retinal images
[AD-A275469] p 3389 N94-28810
RETROREFLECTION
Transient internal probe
[AD-A275054] p 3505 N94-29134
New perspectives for high accuracy SLR with second generation geodesic satellites
[REPT-932-440-105] p 3336 N94-30965
REVERSE ENGINEERING
The UNICON approach to through-life support and evolution of software-intensive systems
p 3416 N94-29340
REVERSE FIELD PINCH
Theoretical reversed field pinch and tokamak studies
[DE94-005409] p 3503 N94-28490
Fluctuation and transport reduction in a reversed field pinch by inductive poloidal current drive
[DE94-005542] p 3503 N94-28514
The effect of magnetic field configuration on particle pinch velocity in Compact Helical System (CHS)
[NIFS-267] p 3505 N94-29398
REVERSING
Granular bases for heavily loaded pavements
[AD-A275171] p 3156 N94-29047
REYNOLDS NUMBER
Direct and large-eddy simulations of turbulent flow in a square duct p 3275 N94-29809
The h-p adaptive methods for incompressible viscous flow problems p 3275 N94-29836
Local heat transfer in an enclosed corotating disk with axial throughflow p 3276 N94-29849
A modernised HST of NLR
[AD-B179220] p 3158 N94-30423
REYNOLDS STRESS
Modeling turbulence in flows with a strong rotational component
[DE94-003577] p 3270 N94-28475
Potential capabilities of Reynolds stress turbulence model in the COMMIX-RSM code p 3285 N94-30450
RHENIUM
Evaluation of oxide-coated iridium-rhenium chambers
[NASA-TM-106442] p 3172 N94-29097
RHEOLOGY
Lubricant rheology at high shear rates
p 3217 N94-29967
The role of sea ice dynamics in global climate change
p 3350 N94-30620
RHEOMETERS
Lubricant rheology at high shear rates
p 3217 N94-29967
RIBBONS
Non-rectangular towpreg architectures
[NASA-CASE-LAR-14863-1-CU] p 3180 N94-29485
RIBONUCLEIC ACIDS
Stable RNA sequences as a tool for DNA probes and phylogenetic studies
[PB94-135423] p 3385 N94-29156
RIGID ROTOR HELICOPTERS
Numerical analysis of airfoil for helicopter blade at high angle of attack using Navier-Stokes code
p 3124 N94-28958
RIGID STRUCTURES
Collapsible mechanical joint
[NASA-CASE-MFS-28765-1] p 3299 N94-29367
Stiffness-generated rigid-body mode shapes for Lanczos eigensolution with SUPORT DOF by way of a MSC/NASTRAN DMAP alter
[NASA-TM-106537] p 3319 N94-29406
Computation of vibration mode elastic-rigid and effective weight coefficients from finite-element computer program output p 3247 N94-29615
Theory of fundamental interactions
[DE94-608126] p 3525 N94-30169
Determination of acceleration field parameters with linear accelerometers
[PB94-125606] p 3290 N94-30742
RING GALAXIES
A multi wavelength observational study of the Cartwheel ring galaxy p 3539 N94-29821
Stellar and gas dynamics of interacting ring galaxies
p 3548 N94-30340
RINGS (MATHEMATICS)
Remarks on Galois symmetry in RCFT
[PB94-138179] p 3467 N94-29147
Hierarchical structures and asymmetric stochastic processes on p-adics and adeles
[PB94-138203] p 3464 N94-29178
RIOMETERS
Initial observation results with imaging riometer at NY-Alesund (L is equal to 16) p 3360 N94-29239
RISK
Risk-based prioritization: A comparison of approaches
[DE94-003368] p 3526 N94-28474
Identification of components to optimize improvement in system reliability
[DE94-001601] p 3315 N94-28503
Risk measures in living probabilistic safety assessment
[VTT-PUBS-146] p 3465 N94-30154
Fuzzy-algebra uncertainty analysis for abnormal-environment safety assessment
[DE94-006257] p 3462 N94-30849
RIVERS
Glaciohydrologic and glaciohydraulic effects on runoff and sediment yield in glacierized basins
[AD-A275134] p 3361 N94-29286
Dewatering of contaminated river sediments
p 3354 N94-30472
Multitemporal analysis of a braiding river: The advanced study of 1992
[NLR-TP-93100-U] p 3335 N94-30942
RIVETS
Full-scale testing and analysis of curved aircraft fuselage panels
[AD-A275666] p 3145 N94-28657
ROADS
The road plan model: Information model for planning road building activities
[AIAA PAPER 94-1219-CP] p 3445 N94-30567
ROBOT ARMS
Design and construction of the Aerobot Robotic Manipulator (ARM)
[AD-A275362] p 3298 N94-28894
Experimental evaluation of fuzzy logic control of a flexible arm manipulator
[AD-A275375] p 3434 N94-29013
Feedback control of a three-link planar under-actuated manipulator using a surge velocity
[AD-A275159] p 3435 N94-29044
High level language-based robotic control system
[NASA-CASE-NPO-17918-2-CU] p 3435 N94-29465
Simplified and symmetrical five-bar linkage driver for manipulating a six-degree-of-freedom parallel minimanipulator with three inextensible limbs
[NASA-CASE-GSC-13485-2] p 3301 N94-29556
Kinematic representations, workspace analysis, and grasp stability in robot arms and multi-fingered hands
p 3301 N94-29847
Three methods to improve the accuracy of a PUMA 560 robot p 3307 N94-30290
Aiding the operator in the manual control of a space manipulator
[PB94-125549] p 3402 N94-30390
The use of interactive computer vision and robot hand controllers for enhancing manufacturing safety
p 3314 N94-30442
ODYSSEUS autonomous walking robot: The leg/arm design
[AIAA PAPER 94-1180-CP] p 3439 N94-30531
A highly redundant robot system for inspection
[AIAA PAPER 94-1194-CP] p 3442 N94-30545
An intelligent robotic aid system for human services
[AIAA PAPER 94-1232-CP] p 3447 N94-30580
Kinematic analysis of platform-type robotic manipulators
[ISBN-0-315-78703-1] p 3311 N94-30793
Robust adaptive control of a mechanical manipulator
p 3449 N94-30806
Integrated structure/control design of nonrigid robot arms for high-speed manipulation p 3312 N94-30866
Kinematics and force analysis of a robot hand based on an artificial biological control scheme
p 3313 N94-30957
ROBOT CONTROL
The state transition diagram with path priority and it's applications
[AD-A275524] p 3434 N94-28672
Experimental evaluation of fuzzy logic control of a flexible arm manipulator
[AD-A275375] p 3434 N94-29013
High level language-based robotic control system
[NASA-CASE-NPO-17918-2-CU] p 3435 N94-29465
Integration of a path generation algorithm into off-line programming of airbus panels
[REPT-932-600-103] p 3435 N94-29480
Robotic hand-eye motor learning
p 3436 N94-29835
Collision avoidance and control of multiple revolute manipulators p 3302 N94-29884
A study of the flexible space platform based deployable manipulator
[ISBN-0-315-85410-3] p 3303 N94-30135
DREV activities related to military vehicles robotization
p 3305 N94-30278
The NRC mobile robot project p 3305 N94-30280
A generic semi-autonomous ground vehicle control system p 3306 N94-30283
An optimal obstacle avoidance path planning algorithm for the Excalibur robot p 3306 N94-30287
Maestro: An open system architecture for multi-robot control p 3306 N94-30288
Coordinated control of multiple robot manipulators
p 3306 N94-30289
An inverse kinematics algorithm for the DREP/Philips real-time radiographic manipulator system
p 3307 N94-30292
Simulation of lightweight robots and their controllers
p 3307 N94-30294
Elements of supervisory control for military robotic applications p 3309 N94-30303
Supervised autonomous control for Space Station Special Purpose Dextrous Manipulator (SPDM) robot
p 3309 N94-30305
A testbed for the development of ground-based control of space-based manipulators p 3309 N94-30306
Achieving robot autonomy p 3310 N94-30307
Improving the execution speed of robot control computations: An allocation scheme for heterogeneous multiprocessors p 3310 N94-30308
Motion control of mobile robots p 3310 N94-30309
Control system design for A and R supported microgravity experiments: An experiment payload control development
[AD-B179107] p 3229 N94-30421
A force-controllable macro-micro manipulator and its application to medical robots p 3314 N94-30441
The use of interactive computer vision and robot hand controllers for enhancing manufacturing safety
p 3314 N94-30442
Programmable Automated Welding System (PAWS): Control of welding through software and hardware
p 3314 N94-30443
Conference on Intelligent Robotics in Field, Factory, Service, and Space (CIRFFSS 1994), volume 1
[NASA-CP-3251] p 3439 N94-30526
ARK: Autonomous mobile robot in an industrial environment
[AIAA PAPER 94-1177-CP] p 3439 N94-30529
Integration of vision and robotic workcell
[AIAA PAPER 94-1186-CP] p 3440 N94-30536
Meeting the challenges of installing a mobile robotic system
[AIAA PAPER 94-1187-CP] p 3440 N94-30537
Controlling multiple security robots in a warehouse environment
[AIAA PAPER 94-1300-CP] p 3441 N94-30540
A Space Station robot walker and its shared control software
[AIAA PAPER 94-1192-CP] p 3442 N94-30543
Perception system and functions for autonomous navigation in a natural environment
[AIAA PAPER 94-1201-CP] p 3443 N94-30552
A streamlined software environment for situated skills
[AIAA PAPER 94-1205-CP] p 3444 N94-30556
Object-based task-level control: A hierarchical control architecture for remote operation of space robots
[AIAA PAPER 94-1209-CP] p 3444 N94-30560
Task-level control for autonomous robots
[AIAA PAPER 94-1210-CP] p 3444 N94-30561
A performance analysis method for distributed real-time robotic systems: A case study of remote teleoperation
[AIAA PAPER 94-1212-CP] p 3445 N94-30563
Using generic tool kits to build intelligent systems
[AIAA PAPER 94-1214-CP] p 3445 N94-30565
A reactive system for open terrain navigation: Performance and limitations
[AIAA PAPER 94-1218-CP] p 3445 N94-30566
The road plan model: Information model for planning road building activities
[AIAA PAPER 94-1219-CP] p 3445 N94-30567
Programmable Automated Welding System (PAWS)
[AIAA PAPER 94-1221-CP] p 3446 N94-30570
Robotic NDE inspection of advanced solid rocket motor casings
[AIAA PAPER 94-1222-CP] p 3446 N94-30571
Piecewise linear paths among convex obstacles
[RUU-CS-93-20] p 3460 N94-30721
Robust adaptive control of a mechanical manipulator
p 3449 N94-30806
ELF: Learning incomplete fuzzy rule sets for an autonomous robot
[REPT-93-043] p 3449 N94-30923
Kinematics and force analysis of a robot hand based on an artificial biological control scheme
p 3313 N94-30957

Iterative removal of boundary minima of harmonic potential function for mobile robot navigation
[REPT-93-059] p 3449 N94-30962
Robust control of robots via linear estimated state-feedback
[MEMO-1153] p 3449 N94-30963

ROBOT DYNAMICS
Integration of a path generation algorithm into off-line programming of airbus panels
[REPT-932-600-103] p 3435 N94-29480
Kinematic representations, workspace analysis, and grasp stability in robot arms and multi-fingered hands
p 3301 N94-29847
Motion control of mobile robots p 3310 N94-30309
Development and validation of a linear recursive order-N algorithm for the simulation of flexible space manipulators dynamics
[AD-B173557] p 3311 N94-30391
A probabilistic approach to motion planning for car-like robots
[RUU-CS-93-18] p 3438 N94-30410
Biologically-inspired hexapod robot design and simulation
[AIAA PAPER 94-1178-CP] p 3439 N94-30530
ODYSSEUS autonomous walking robot: The leg/arm design
[AIAA PAPER 94-1180-CP] p 3439 N94-30531
Free-floating dual-arm robots for space assembly
[AIAA PAPER 94-1195-CP] p 3442 N94-30546
Aspects of vision and planning in a dynamic, uncertain environment p 3448 N94-30803
Integrated structure/control design of nonrigid robot arms for high-speed manipulation p 3312 N94-30866
Kinematics and force analysis of a robot hand based on an artificial biological control scheme
p 3313 N94-30957

ROBOT SENSORS
DREV activities related to military vehicles robotization
p 3305 N94-30278
The NRC mobile robot project p 3305 N94-30280
Thermal imaging for a mobile robot
p 3308 N94-30300
Sonar sensing and obstable detection
p 3309 N94-30301
Conference on Intelligent Robotics in Field, Factory, Service, and Space (CIRFFSS 1994), volume 1
[NASA-CP-3251] p 3439 N94-30526
TRC research products: Components for service robots
[AIAA PAPER 94-1227-CP] p 3447 N94-30576

ROBOTICS
Design and construction of the Aerobot Robotic Manipulator (ARM)
[AD-A275362] p 3298 N94-28894
High level language-based robotic control system
[NASA-CASE-NPO-17918-2-CU] p 3435 N94-29465
The 27th Aerospace Mechanisms Symposium
[NASA-CP-3205] p 3160 N94-29627
A compact roller-gear pitch-yaw joint module: Design and control issues p 3161 N94-29629
Kinematic representations, workspace analysis, and grasp stability in robot arms and multi-fingered hands
p 3301 N94-29847
Collision avoidance and control of multiple revolute manipulators p 3302 N94-29884
Robotics and the battlefield of the future
p 3304 N94-30277
DREV activities related to military vehicles robotization
p 3305 N94-30278
A generic semi-autonomous ground vehicle control system p 3306 N94-30283
An inverse kinematics algorithm for the DREP/Philips real-time radiographic manipulator system
p 3307 N94-30292
Sonar sensing and obstable detection
p 3309 N94-30301
Shape from diameter: Negative results
[RUU-CS-93-16] p 3458 N94-30407
Shape from diameter: Positive results
[RUU-CS-93-17] p 3458 N94-30408
Control system design for A and R supported microgravity experiments: An experiment payload control development
[AD-B179107] p 3229 N94-30421
A force-controllable macro-micro manipulator and its application to medical robots p 3314 N94-30441
The use of interactive computer vision and robot hand controllers for enhancing manufacturing safety
p 3314 N94-30442
Programmable Automated Welding System (PAWS): Control of welding through software and hardware
p 3314 N94-30443
Conference on Intelligent Robotics in Field, Factory, Service, and Space (CIRFFSS 1994), volume 1
[NASA-CP-3251] p 3439 N94-30526
Intelligent robotics can boost America's economic growth
[AIAA PAPER 94-1301-CP] p 3439 N94-30527
Teleoperated systems for nuclear reactors: Inspection and maintenance
[AIAA PAPER 94-1176-CP] p 3439 N94-30528
A highly redundant robot system for inspection
[AIAA PAPER 94-1194-CP] p 3442 N94-30545
Microwave vision for robots
[AIAA PAPER 94-0887-CP] p 3443 N94-30550
Fuzzy logic based robotic controller
[AIAA PAPER 94-1202-CP] p 3443 N94-30553
The real-world navigator
[AIAA PAPER 94-1204-CP] p 3443 N94-30555
Autonomous mobile robot teams
[AIAA PAPER 94-1207-CP] p 3444 N94-30558
A survey of NASA and military standards on fault tolerance and reliability applied to robotics
[AIAA PAPER 94-1211-CP] p 3445 N94-30562
Design reuse experience of space and hazardous operations robots
[AIAA PAPER 94-1220-CP] p 3445 N94-30568
A multi-mode manipulator display system for controlling remote robotic systems
[AIAA PAPER 94-0888-CP] p 3446 N94-30569
Robotic NDE inspection of advanced solid rocket motor casings
[AIAA PAPER 94-1222-CP] p 3446 N94-30571
Automation for nondestructive inspection of aircraft
[AIAA PAPER 94-1223-CP] p 3446 N94-30572
The Automated Aircraft Rework System (AARS): A system integration approach
[AIAA PAPER 94-1225-CP] p 3446 N94-30574
A robotic wheelchair
[AIAA PAPER 94-1229-CP] p 3447 N94-30578
An intelligent robotic aid system for human services
[AIAA PAPER 94-1232-CP] p 3447 N94-30580
On-orbit spacecraft servicing: An element in the evolution of space robotics applications
[AIAA PAPER 94-1236-CP] p 3448 N94-30583
Kinematic analysis of platform-type robotic manipulators
[ISBN-0-315-78703-1] p 3311 N94-30793
Integrated structure/control design of nonrigid robot arms for high-speed manipulation p 3312 N94-30866
Kinematics and force analysis of a robot hand based on an artificial biological control scheme
p 3313 N94-30957

ROBOTS
Feedback control of a three-link planar under-actuated manipulator using a surge velocity
[AD-A275159] p 3435 N94-29044
An emergency response mobile robot for operations in combustible atmospheres
[NASA-CASE-NPO-19020-1-CU] p 3299 N94-29420
Robotic hand-eye motor learning
p 3436 N94-29835
High-resolution robot tracking and direction finding for space station environment p 3168 N94-29896
Proceedings of the 3rd Conference on Military Robotic Applications
[DRES-SP-149] p 3304 N94-30275
Autonomous intelligent military robots: Army ants, killer bees, and cybernetic soldiers p 3304 N94-30276
Autonomous Robotic Refueling System (ARRS) for rapid aircraft turnaround p 3305 N94-30279
The NRC mobile robot project p 3305 N94-30280
An optimal obstacle avoidance path planning algorithm for the Excalibur robot p 3306 N94-30287
Maestro: An open system architecture for multi-robot control p 3306 N94-30288
Coordinated control of multiple robot manipulators
p 3306 N94-30289
Three methods to improve the accuracy of a PUMA 560 robot p 3307 N94-30290
Force control techniques for robot manipulators and their military applications p 3307 N94-30291
Simulation of lightweight robots and their controllers
p 3307 N94-30294
Thermal imaging for a mobile robot
p 3308 N94-30300
Aspects of the operator interface for military robotic applications in unstructured environments
p 3309 N94-30304
Achieving robot autonomy p 3310 N94-30307
Improving the execution speed of robot control computations: An allocation scheme for heterogeneous multiprocessors p 3310 N94-30308
Motion control of mobile robots p 3310 N94-30309
Electrochemical Power Source (EPS) selection for Energetically Independent Robots (EIR): A systematic approach p 3269 N94-30312
Conference on Intelligent Robotics in Field, Factory, Service, and Space (CIRFFSS 1994), volume 1
[NASA-CP-3251] p 3439 N94-30526
ARK: Autonomous mobile robot in an industrial environment
[AIAA PAPER 94-1177-CP] p 3439 N94-30529
Biologically-inspired hexapod robot design and simulation
[AIAA PAPER 94-1178-CP] p 3439 N94-30530
ODYSSEUS autonomous walking robot: The leg/arm design
[AIAA PAPER 94-1180-CP] p 3439 N94-30531
VAS: A Vision Advisor System combining agents and object-oriented databases
[AIAA PAPER 94-1181-CP] p 3440 N94-30532
Application of the Modular Automated Reconfigurable Assembly System (MARAS) concept to adaptable vision gauging and parts feeding
[AIAA PAPER 94-1182-CP] p 3440 N94-30533
Confessions of a robot lobotomist
[AIAA PAPER 94-1185-CP] p 3440 N94-30535
Integration of vision and robotic workcell
[AIAA PAPER 94-1186-CP] p 3440 N94-30536
Meeting the challenges of installing a mobile robotic system
[AIAA PAPER 94-1187-CP] p 3440 N94-30537
Design of an autonomous exterior security robot
[AIAA PAPER 94-1188-CP] p 3441 N94-30538
Task automation in a successful industrial telerobot
[AIAA PAPER 94-1189-CP] p 3441 N94-30539
Free-floating dual-arm robots for space assembly
[AIAA PAPER 94-1195-CP] p 3442 N94-30546
Vision based object pose estimation for mobile robots
[AIAA PAPER 94-1197-CP] p 3442 N94-30548
Microwave vision for robots
[AIAA PAPER 94-0887-CP] p 3443 N94-30550
Perception system and functions for autonomous navigation in a natural environment
[AIAA PAPER 94-1201-CP] p 3443 N94-30552
Fuzzy logic based robotic controller
[AIAA PAPER 94-1202-CP] p 3443 N94-30553
The real-world navigator
[AIAA PAPER 94-1204-CP] p 3443 N94-30555
A streamlined software environment for situated skills
[AIAA PAPER 94-1205-CP] p 3444 N94-30556
Situational reaction and planning
[AIAA PAPER 94-1206-CP] p 3444 N94-30557
Autonomous mobile robot teams
[AIAA PAPER 94-1207-CP] p 3444 N94-30558
Building brains for bodies
[AIAA PAPER 94-1208-CP] p 3444 N94-30559
Object-based task-level control: A hierarchical control architecture for remote operation of space robots
[AIAA PAPER 94-1209-CP] p 3444 N94-30560
Task-level control for autonomous robots
[AIAA PAPER 94-1210-CP] p 3444 N94-30561
A survey of NASA and military standards on fault tolerance and reliability applied to robotics
[AIAA PAPER 94-1211-CP] p 3445 N94-30562
Using generic tool kits to build intelligent systems
[AIAA PAPER 94-1214-CP] p 3445 N94-30565
The road plan model: Information model for planning road building activities
[AIAA PAPER 94-1219-CP] p 3445 N94-30567
Design reuse experience of space and hazardous operations robots
[AIAA PAPER 94-1220-CP] p 3445 N94-30568
Automation for nondestructive inspection of aircraft
[AIAA PAPER 94-1223-CP] p 3446 N94-30572
Graphical simulation for aerospace manufacturing
[AIAA PAPER 94-1224-CP] p 3446 N94-30573
TRC research products: Components for service robots
[AIAA PAPER 94-1227-CP] p 3447 N94-30576
An update on Lab Rover: A hospital material transporter
[AIAA PAPER 94-1228-CP] p 3447 N94-30577
An intelligent robot for helping astronauts
[AIAA PAPER 94-1233-CP] p 3447 N94-30581
On-orbit spacecraft servicing: An element in the evolution of space robotics applications
[AIAA PAPER 94-1236-CP] p 3448 N94-30583
Aspects of vision and planning in a dynamic, uncertain environment p 3448 N94-30803
ELF: Learning incomplete fuzzy rule sets for an autonomous robot
[REPT-93-043] p 3449 N94-30923
Iterative removal of boundary minima of harmonic potential function for mobile robot navigation
[REPT-93-059] p 3449 N94-30962

ROBUSTNESS (MATHEMATICS)
Track filtering by robust neural network
[DE94-606067] p 3434 N94-28613
A design methodology for synthesizing low-order robust controllers for flexible structures p 3302 N94-29870
Robust adaptive control and filtering
p 3437 N94-29895
Robust adaptive control of a mechanical manipulator
p 3449 N94-30806

ROCK INTRUSIONS
Studies in Jurassic and Cretaceous North American apparent polar wander p 3362 N94-29940
ROCKET ENGINES
Rocket engine system reliability analyses using probabilistic and fuzzy logic techniques
[NASA-TM-106519] p 3173 N94-29403
Method of reducing hydraulic instability
[NASA-CASE-LEW-15463-1] p 3273 N94-29539
CFD analyses for advanced pump design
[NASA-CR-194866] p 3300 N94-29550
Aspects of model-based rocket engine condition monitoring and control
[NASA-CR-195116] p 3173 N94-29848
ROCKET EXHAUST
SOCRATES simulation of the emission at wavelength 6300 A generated by the interaction between the atmosphere and the Space Shuttle exhaust
[AD-A275567] p 3164 N94-28827
ROCKET SOUNDING
Time series comparisons of satellite and rocketsonde temperatures in 1978-1979
[NASA-TP-3409] p 3370 N94-29455
A sounding rocket program in extreme and far ultraviolet interferometry
[NASA-CR-195114] p 3289 N94-29907
ROCKS
Speciation in Water and Soil: A literature review
[PB94-132388] p 3341 N94-28412
ROOFS
Rooftop emergency heliports
[DOT/FAA/RD-93/2] p 3157 N94-29754
ROOM TEMPERATURE
Anode for rechargeable ambient temperature lithium cells
[NASA-CASE-NPO-18580-1-CU] p 3265 N94-29505
ROOT-MEAN-SQUARE ERRORS
Error growth in poor ECMWF forecasts over the contiguous United States
[AD-A275297] p 3369 N94-29183
ROSAT MISSION
Coronal temperatures of unusually active K-dwarf binary systems
[NASA-CR-189335] p 3545 N94-29861
ROTARY GYROSCOPES
Emerging technologies in microguidance and control p 3144 N94-29788
ROTARY STABILITY
Rotor instability induced by dead band clearance in bearing supports p 3312 N94-30809
ROTARY WING AIRCRAFT
Nonlinear multibody formulation for rotorcraft analysis p 3149 N94-30787
ROTARY WINGS
Boundary layers induced by three-dimensional vortex loops
[AD-A275678] p 3270 N94-28665
A free-wake Euler and Navier-Stokes CFD method and its application to helicopter rotors including dynamic stall
[AD-A275416] p 3129 N94-29197
Helicopter mission and rotor performance optimization with quasi-linear inflow theory p 3147 N94-29594
Numerical study of the trailing vortex of a wing with wing-tip blowing
[NASA-CR-195803] p 3130 N94-29760
Computational analysis of high resolution unsteady airloads for rotor aeroacoustics
[NASA-CR-194894] p 3480 N94-30274
Nonlinear multibody formulation for rotorcraft analysis p 3149 N94-30787
ROTATING BODIES
Flow and heat transfer in a rotating square sectioned U-bend p 3128 N94-28984
ROTATING DISKS
Local heat transfer in an enclosed corotating disk with axial throughflow p 3276 N94-29849
ROTATING FLUIDS
Modeling turbulence in flows with a strong rotational component
[DE94-003577] p 3270 N94-28475
Acoustic and optical investigations of superfluid (3)He
[PB94-135415] p 3477 N94-29186
Forced generation of solitary waves in a rotating fluid and their stability p 3274 N94-29689
ROTATING SHAFTS
Rotary actuator
[NASA-CASE-MFS-28581-1] p 3205 N94-29447
ROTATION
Spin-up in a rectangular cylinder
[AD-A275465] p 3271 N94-28738
Similarity between turbulent flows through curved pipe and orthogonal rotating pipe p 3128 N94-28986
Mutual similarity of developing laminar flows with secondary streams in ducts: Curved pipe flow and orthogonal rotating pipe flow p 3129 N94-28989
Suspension system for gimbal supported scanning payloads
[NASA-CASE-MFS-28817-1] p 3287 N94-29358
Dynamic modeling of multibody flexible structures p 3323 N94-30813
ROTOR AERODYNAMICS
A design of third-generation airfoils for helicopter rotor blades using Navier-Stokes p 3124 N94-28957
Numerical analysis of airfoil for helicopter blade at high angle of attack using Navier-Stokes code p 3124 N94-28958
Verification of a three-dimensional viscous flow analysis for a single stage compressor p 3127 N94-28976
International collaborative research in wind turbine rotor aerodynamics
[DE94-000244] p 3339 N94-30602
ROTOR BLADES
Numerical study of the trailing vortex of a wing with wing-tip blowing
[NASA-CR-195803] p 3130 N94-29760
ROTOR BLADES (TURBOMACHINERY)
Fluid dynamic noise in a centrifugal pump
[AD-A275264] p 3477 N94-28904
Verification of a three-dimensional viscous flow analysis for a single stage compressor p 3127 N94-28976
Tuned mass damper for integrally bladed turbine rotor
[NASA-CASE-MFS-28697-1] p 3298 N94-29353
ROTOR BODY INTERACTIONS
An analytical study of unsteady rotor/fuselage interaction in hover and forward flight p 3131 N94-29826
ROTOR DYNAMICS
Rotordynamic analysis of annular honeycomb-stator turbulent gas seals using a new friction-factor model based on flat plate tests p 3302 N94-29916
Theoretical prediction of the influence coefficients on damped simple flexible rotors using the transfer matrix method
[IMR-TM-TR-002] p 3321 N94-30018
Parameter identification of the rotordynamic coefficients of high-Reynolds-number hydrostatic bearings p 3311 N94-30792
Rotor instability induced by dead band clearance in bearing supports p 3312 N94-30809
ROTOR LIFT
A design of third-generation airfoils for helicopter rotor blades using Navier-Stokes p 3124 N94-28957
ROTORS
Acquisition, design modification, assembly, and ground test of NPS Hummingbird remotely piloted helicopter
[AD-A275546] p 3146 N94-28837
Rotary blood pump
[NASA-CASE-MSC-22424-1] p 3299 N94-29370
Method for cancelling expansion waves in a wave rotor
[NASA-CASE-LEW-15218-2] p 3274 N94-29740
Theoretical prediction of the influence coefficients on damped simple flexible rotors using the transfer matrix method
[IMR-TM-TR-002] p 3321 N94-30018
Use of magnetic compression to support turbine engine rotors p 3314 N94-30484
Rotor instability induced by dead band clearance in bearing supports p 3312 N94-30809
ROVING VEHICLES
Mars rover mechanisms designed for Rocky 4 p 3161 N94-29630
Smart focal-plane technology for micro-instruments and micro-rovers p 3237 N94-29780
Navigation of military and space unmanned ground vehicles in unstructured terrains p 3144 N94-30282
RUBBER
A newly developed snow vehicle (SM100S) for Antarctica. Part 4: Low temperature properties of crawler belt p 3314 N94-29984
Novel techniques applied to polymer lifetime predictions
[DE94-005095] p 3218 N94-30102
RUBIDIUM
Time and frequency technology at NIST p 3468 N94-30641
RUBY
A dual-cavity ruby maser for the Ka-band link experiment p 3250 N94-29658
RULES
ELF: Learning incomplete fuzzy rule sets for an autonomous robot
[REPT-93-043] p 3449 N94-30923
RUNGE-KUTTA METHOD
Formulas of the Runge-Kutta-Nystroem type
[ISBN-0-315-85774-9] p 3454 N94-30241
Parallel iteration across the steps of high order Runge-Kutta methods for nonstiff initial value problems
[CWI-NM-R9313] p 3433 N94-30730
Eigenvalue analysis of the convergence behaviour of an Euler method
[PB94-1255722-U] p 3281 N94-30743
RUNWAYS
Contributions of DLR to air traffic capacity enhancement within a terminal area p 3138 N94-29567
RURAL AREAS
Report of feasibility study on international-cooperation in high efficient energy conversion technology
[DE94-732340] p 3337 N94-28631
RUSSIAN FEDERATION
Research and Development of Ram/Scramjets and Turboramjets in Russia
[AGARD-LS-194] p 3151 N94-29291
Russian national time scale long-term stability p 3475 N94-30679

S

S WAVES
Initial wave-type identification with neural networks and its contribution to automated processing in IMS version 3.0
[AD-A275058] p 3359 N94-29137
SABOT PROJECTILES
Transient internal probe
[AD-A275054] p 3505 N94-29134
SAFETY
Safety enhancement of composites via periodic proof testing
[AD-A275662] p 3176 N94-28655
Non-aqueous cleaning solvent substitution
[DE94-005339] p 3219 N94-30245
Non-aqueous cleaning solvent substitution p 3354 N94-30466
Fuzzy-algebra uncertainty analysis for abnormal-environment safety assessment
[DE94-006257] p 3462 N94-30849
SAFETY DEVICES
Comparison of two cool vests on heat-strain reduction while wearing a firefighting ensemble in a hot/humid environment
[AD-A275103] p 3400 N94-28902
Microcomputer-based protective functions in industrial production systems: Assessment method
[PB94-137817] p 3411 N94-29159
The use of interactive computer vision and robot hand controllers for enhancing manufacturing safety p 3314 N94-30442
SAFETY FACTORS
Systematic safety consideration in product design
[PB94-132354] p 3229 N94-28410
NASA wiring program: Survey of NASA experiences in wiring system safety p 3165 N94-28700
Advanced steady-state operating scenarios
[DE94-004810] p 3509 N94-30768
SAFETY MANAGEMENT
Evaluation of monitoring audiometry in the United States Air Force Hearing Conservation Program
[AD-A275309] p 3391 N94-29211
Joint research activities with CCMRI (China) p 3240 N94-29521
Risk measures in living probabilistic safety assessment
[VTT-PUBS-146] p 3465 N94-30154
SALINITY
Cryosphere and climate p 3352 N94-30632
SAMARIUM
Study on the formation of ultrafine particles of Sm-Co intermetallic compounds using RF thermal plasma p 3211 N94-29516
SAMARIUM COMPOUNDS
Study on the formation of ultrafine particles of Sm-Co intermetallic compounds using RF thermal plasma p 3211 N94-29516
Magnetotransport measurements in magnetic fields up to 50T in SmB6 and FeSi
[DE94-006227] p 3520 N94-30848
SAMPLING
Fiscal 1991 geothermal development promotion energy
[DE94-732332] p 3337 N94-28627
Acceptance sampling methods for sample results verification
[DE94-002882] p 3465 N94-29925
Sampling behaviour in a four instrument monitoring task: Effects of signal bandwidth and number of events per signal
[AD-B179613] p 3402 N94-30422
Prediction and standard error estimation for a finite universe total when a stratum is not sampled
[DE94-004929] p 3465 N94-30696

SAPPHIRE
MOCVD growth of GaN, AlN and AlGaN for UV photodetector applications
[AD-A275078] p 3512 N94-28871
Thermal expansion and elastic anisotropy in single crystal Al2O3 and SiC reinforcements
[NASA-TM-106516] p 3214 N94-29105
SATELLITE ALTIMETRY
The effects of altimeter sampling characteristics: Some Geosat examples
[AD-A275225] p 3357 N94-29062
SATELLITE ANTENNAS
Screening of flexible cables by nonlinear resistance measurements
[AD-A275193] p 3264 N94-29289
SATELLITE ATMOSPHERES
Predissociation in N2(C'4, 1 Sigma u +) and other N2 states and its importance in the atmospheres of Titan and Triton
[NASA-CR-195727] p 3549 N94-28816
SATELLITE ATTITUDE CONTROL
The development procedures and tools applied for the attitude control software of the Italian satellite SAX
p 3170 N94-29324
The influence of appendage vibration on the attitude dynamics of a dual-spin satellite p 3168 N94-29828
The MACS-TSA applied in the ISO and SAX spacecraft projects
[PB94-126257] p 3170 N94-30857
SATELLITE COMMUNICATION
Communications subsystem for the Petite Amateur Navy Satellite (PANSAT)
[AD-A275532] p 3242 N94-28812
Microvibrations on a GEO telecommunication satellite
[REPT-932-440-101] p 3168 N94-29415
Simulation of interference between Earth stations and Earth-orbiting satellites p 3252 N94-29673
Remote observatory access via the advanced communications technology satellite
p 3253 N94-29894
Adaptive power control as a fade countermeasure on satellite links p 3253 N94-29897
Communications technology for unattended sensors
[DE94-005685] p 3254 N94-30043
Radial microstrip slotline feed network for circular mobile communications array
[NASA-TM-106540] p 3267 N94-30198
The two-way time synchronization system via a satellite voice channel p 3471 N94-30658
Providing hydrogen maser timing stability to orbiting VLBI radio telescope observations by post-measurement compensation of linked frequency standard imperfections p 3297 N94-30670
SATELLITE CONSTELLATIONS
An Operational Control Segment (OCS) update on GPS constellation status and future program directions
p 3144 N94-30643
SATELLITE CONTROL
Dynamics and control of tethered satellite systems
p 3170 N94-30864
SATELLITE DESIGN
Outline of JERS-1 system p 3330 N94-29220
Development status of the Communications and Broadcasting Engineering Test Satellite (COMETS)
[JTN-94-80545] p 3169 N94-30811
Development status of COMETS missions
[JTN-94-80544] p 3170 N94-30932
New perspectives for high accuracy SLR with second generation geodesic satellites
[REPT-932-440-105] p 3336 N94-30965
SATELLITE GROUND SUPPORT
Site comparison for optical visibility statistics in southern California p 3247 N94-29617
SATELLITE IMAGERY
Far ultraviolet images of the nighttime ionosphere
[AD-A275083] p 3356 N94-28843
Lead detection and mapping with reference to relationships between scale, sensor characteristics, surface conditions and atmospheric properties
[AD-A275321] p 3377 N94-28877
Proceedings of the International Symposium on Remote Sensing
[JTN-94-80578] p 3325 N94-28925
Synthetic aperture radar applications: Now and in the future p 3260 N94-28927
Evaluation of simulated JERS-1 data for geologic mapping at Drum Mountains, Utah, Silver Bell, Arizona, and Wind River, Wyoming under the GEOSAT-ERSDAC/JAPEX/JGI/RESTEC joint studies
p 3326 N94-28929
Image processing for hyperspectral data
p 3326 N94-28930
JERS-1 data acquisition and distribution
p 3326 N94-28931
JERS-1 data and information system for resources exploration p 3327 N94-28932
Observations by ERS-1 start p 3327 N94-28933
Sea ice and oceans applications of SAR
p 3327 N94-28934
Amazonia: Remote sensing test site and survey
p 3327 N94-28935
Utilization of remote sensing data in Southeast Asia
p 3327 N94-28936
Remote sensing and global management
p 3328 N94-28937
Proceedings of the 15th Earth Observation Symposium
[JTN-94-80607] p 3328 N94-29036
Principles and application tendency of remote sensing: Its principle, function and utilization
p 3328 N94-29037
Oceanic survey utilizing satellites
p 3328 N94-29040
Proceedings of the 3rd International Symposium: JERS-1 and Remote Sensing in the Future
[JTN-94-80597] p 3329 N94-29217
A new information system: Satellite observation
p 3330 N94-29219
Observatory system of Earth Resources Satellite-1
p 3330 N94-29221
Application of JERS-1 data to geologic analyses
p 3330 N94-29222
Application of optical sensor data to resource survey
p 3330 N94-29223
Radar applications at the Canada Centre for Remote Sensing p 3331 N94-29224
Application of remote sensing techniques in petroleum exploration: The Indonesian experience
p 3331 N94-29225
JERS-1 and future remote sensing: Application of remote sensing data to agroecological problems
p 3331 N94-29229
Application of remote sensing in prevention of disasters p 3332 N94-29230
Future expectation of remote sensing technology
p 3332 N94-29231
Japan's Earth observation satellite programs
p 3332 N94-29232
Extrapolation of point data for resource mapping
p 3334 N94-29959
Application of remote sensing techniques for the seismo-tectonic study of Nahanni earthquake area
[ISBN-0-315-85942-3] p 3334 N94-30037
Estimation of transmittance from satellite imagery
p 3257 N94-30500
Statistical analysis of a satellite imagery time series: Implications for the study of coastal and estuarine circulation p 3335 N94-30919
Multitemporal analysis of a braiding river: The advanced study of 1992
[NLR-TP-93100-U] p 3335 N94-30942
SATELLITE INSTRUMENTS
EOS project and ASTER (ITIR) p 3331 N94-29226
The 25th Annual Precise Time and Time Interval (PTTI) Applications and Planning Meeting
[NASA-CP-3267] p 3468 N94-30639
Development status of the Communications and Broadcasting Engineering Test Satellite (COMETS)
[JTN-94-80545] p 3169 N94-30811
SATELLITE NAVIGATION SYSTEMS
Use of GPS in automated air traffic control
p 3137 N94-29563
An Operational Control Segment (OCS) update on GPS constellation status and future program directions
p 3144 N94-30643
A review of the status and capabilities of Navstar GPS
[AD-B174629] p 3143 N94-30854
SATELLITE OBSERVATION
Lead detection and mapping with reference to relationships between scale, sensor characteristics, surface conditions and atmospheric properties
[AD-A275321] p 3377 N94-28877
Proceedings of the International Symposium on Remote Sensing
[JTN-94-80578] p 3325 N94-28925
Keynote address --- Japanese Earth Resources Satellite 1 (JERS-1) and future remote sensing projects
p 3326 N94-28926
Synthetic aperture radar applications: Now and in the future p 3260 N94-28927
Research trends on remote sensing at research facilities in Japan: The priority area programme on better understanding of earth environment via satellite
p 3326 N94-28928
Evaluation of simulated JERS-1 data for geologic mapping at Drum Mountains, Utah, Silver Bell, Arizona, and Wind River, Wyoming under the GEOSAT-ERSDAC/JAPEX/JGI/RESTEC joint studies
p 3326 N94-28929
JERS-1 data acquisition and distribution
p 3326 N94-28931
Observations by ERS-1 start p 3327 N94-28933
Sea ice and oceans applications of SAR
p 3327 N94-28934
Amazonia: Remote sensing test site and survey
p 3327 N94-28935
Utilization of remote sensing data in Southeast Asia
p 3327 N94-28936
Remote sensing and global management
p 3328 N94-28937
Proceedings of the 15th Earth Observation Symposium
[JTN-94-80607] p 3328 N94-29036
Principles and application tendency of remote sensing: Its principle, function and utilization
p 3328 N94-29037
Status and tendency of earth observation system
p 3328 N94-29038
Perspectives of earth observing techniques: Expectation of earth observation in space development history
p 3328 N94-29039
Oceanic survey utilizing satellites
p 3328 N94-29040
Tohoku district observed by artificial satellites
p 3328 N94-29041
Antarctic Record, volume 36, no. 1
[REPT-106-VOL-36-NO-1] p 3357 N94-29078
Activities of the wintering party at Showa Station by the 31st Japanese Antarctic Research Expedition in 1990
p 3358 N94-29083
Conceptual radiometer design studies for Earth observations from low Earth orbit
[NASA-CR-4588] p 3329 N94-29098
Role of satellite observations of sea-surface temperature in the detection of global change
[PB94-138120] p 3329 N94-29107
Proceedings of the 3rd International Symposium: JERS-1 and Remote Sensing in the Future
[JTN-94-80597] p 3329 N94-29217
Remote sensing and the Earth p 3329 N94-29218
A new information system: Satellite observation
p 3330 N94-29219
Outline of JERS-1 system p 3330 N94-29220
Application of JERS-1 data to geologic analyses
p 3330 N94-29222
Application of optical sensor data to resource survey
p 3330 N94-29223
Radar applications at the Canada Centre for Remote Sensing p 3331 N94-29224
Application of remote sensing techniques in petroleum exploration: The Indonesian experience
p 3331 N94-29225
EOS project and ASTER (ITIR) p 3331 N94-29226
Earth-observation plan in Europe
p 3331 N94-29227
Rock identification using thermal infrared data
p 3331 N94-29228
JERS-1 and future remote sensing: Application of remote sensing data to agroecological problems
p 3331 N94-29229
Application of remote sensing in prevention of disasters p 3332 N94-29230
Future expectation of remote sensing technology
p 3332 N94-29231
Japan's Earth observation satellite programs
p 3332 N94-29232
On the relation between SMMR 37-GHz polarization difference and the rainfall over Africa and Australia
[NASA-TM-104598] p 3370 N94-29408
A simulation study of high degree and order geopotential determination using satellite gravity gradiometry
p 3333 N94-29762
Satellite estimation of the global distribution and interannual variability of photosynthetically active radiation p 3334 N94-29970
Estimation of transmittance from satellite imagery
p 3257 N94-30500
Altimeter data processing from sea surface topography to horizontal eddy momentum fluxes
[PB94-147550] p 3378 N94-30714
FAME: A Forest Assessment and Monitoring Environment scenario
[AD-B179106] p 3335 N94-30759
Atmospheric moisture fields derived by satellite observations over the tropical Pacific Ocean
p 3375 N94-30863
Multitemporal analysis of a braiding river: The advanced study of 1992
[NLR-TP-93100-U] p 3335 N94-30942
SATELLITE ORBITS
TOPEX/POSEIDON operational orbit determination results using global positioning satellites
p 3160 N94-29666
Application of extended Lagrange series to the precise determination of Global Positioning Satellite orbits
[ISBN-0-315-85724-2] p 3159 N94-30237

Towards 10(exp 9) GPS geodesy: Vector baselines, Earth rotation and reference frames
[NASA-CR-195768] p 3142 N94-30243

SATELLITE ORIENTATION
Towards 10(exp 9) GPS geodesy: Vector baselines, Earth rotation and reference frames
[NASA-CR-195768] p 3142 N94-30243
Time transfer using geostationary satellites: Implementation of a Kalman filter p 3471 N94-30657

SATELLITE PERTURBATION
The influence of appendage vibration on the attitude dynamics of a dual-spin satellite p 3168 N94-29828
Application of extended Lagrange series to the precise determination of Global Positioning Satellite orbits
[ISBN-0-315-85724-2] p 3159 N94-30237

SATELLITE POWER TRANSMISSION
Reactor-pumped laser facility at DOE's Nevada Test Site
[DE94-006371] p 3295 N94-30265

SATELLITE ROTATION
The Solar Anomalous and Magnetospheric Particle Explorer (SAMPEX) yo-yo despin and solar array deployment mechanism p 3163 N94-29645

SATELLITE SOUNDING
Objective analysis of a coastal ocean eddy using satellite AVHRR and in situ hydrographic data
[AD-A275715] p 3376 N94-28642
Far ultraviolet images of the nighttime ionosphere
[AD-A275083] p 3356 N94-28843
Proceedings of the 15th Earth Observation Symposium
[JTN-94-80607] p 3328 N94-29036
Principles and application tendency of remote sensing: Its principle, function and utilization p 3328 N94-29037
Status and tendency of earth observation system p 3328 N94-29038

SATELLITE TRACKING
The velocity field in the Northeast Atlantic from satellite-tracked drifting buoys
[AD-A275704] p 3376 N94-28690
Towards 10(exp 9) GPS geodesy: Vector baselines, Earth rotation and reference frames
[NASA-CR-195768] p 3142 N94-30243
A comparison of GPS broadcast and DMA precise ephemerides p 3145 N94-30660

SATELLITE TRANSMISSION
A new information system: Satellite observation p 3330 N94-29219
Data transfer system using a multi-ID ARGOS transmitter for the Antarctic polar patrol balloon experiment p 3363 N94-29980

SATELLITE-BORNE PHOTOGRAPHY
Far ultraviolet images of the nighttime ionosphere
[AD-A275083] p 3356 N94-28843

SATURATION (CHEMISTRY)
Arterial oxygen saturation during +Gz acceleration by short-radius centrifuge p 3389 N94-28852

SAUDI ARABIA
Scientific and technical information transfer: Promoting information acquisition in the Saudi Arabian industrial sector p 3532 N94-29803

SCALARS
Numerical modelling of turbine combustion chambers p 3154 N94-29254

SCALE MODELS
Catalytic fabric filtration for simultaneous NO(x) and particulate control
[DE94-001660] p 3341 N94-28463

SCALING LAWS
Butterfly and scaling law in YBa2Cu4O8
[DE94-006037] p 3519 N94-30338
Experiments and theoretical considerations regarding the allowable roughness height in laminar flow
[PB94-125556] p 3133 N94-30389
Scaling in heavy-fermion systems
[DE94-005002] p 3492 N94-30775

SCANNERS
Beam scanning offset Cassegrain reflector antennas by subreflector movement
[NASA-CR-191604] p 3160 N94-28836
Suspension system for gimbal supported scanning payloads
[NASA-CASE-MFS-28817-1] p 3287 N94-29358
MODIS technical report series. Volume 3: MODIS airborne simulator level 1B data user's guide
[NASA-TM-104594] p 3231 N94-29385

SCANNING
Three methods to improve the accuracy of a PUMA 560 robot p 3307 N94-30290
Standardisation requirements for ultrasonic C-scanning of polymer matrix composites: An initial assessment
[PB94-139318] p 3184 N94-30438

SCANNING ELECTRON MICROSCOPY
Electron microscopy: Metal alloy x ray microanalysis
[REPT-932-600-101] p 3205 N94-29525
A sub-cm micromachined electron microscope p 3236 N94-29775
Atomic-scale structure and chemistry of interfaces by Z-contrast imaging and electron energy loss spectroscopy in the STEM
[DE94-006563] p 3516 N94-30064

SCANNING TUNNELING MICROSCOPY
Halogen chemisorption on silver(111): Scanning tunneling microscopy of coadsorbed halogen atoms
[AD-A275219] p 3486 N94-29060

SCATTERING
Printed circuit elements with applications to antennas, scattering, and circuits
[AD-A275512] p 3262 N94-28669
Carrier collection and scattering in quantum well and superlattice devices
[AD-A275443] p 3512 N94-28880
A physical optics model for scattering of HF radiation by irregular terrain
[DE94-006187] p 3255 N94-30106

SCATTERING CROSS SECTIONS
Radiation transport in cloudy and aerosol loaded atmospheres p 3366 N94-30805

SCATTEROMETERS
Observations by ERS-1 start p 3327 N94-28933

SCAVENGING
In-cylinder gas velocity measurements comparing crankcase and blower scavenging in a fired two-stroke cycle engine
[DE94-005752] p 3311 N94-30596

SCENE ANALYSIS
Synthetic image generator model; application of view angle dependent reflectivity components and performance evaluation in the visible region
[AD-A275365] p 3499 N94-29009
Unmanned vehicle mobility: Limits of autonomous navigation p 3310 N94-30311
Vision based object pose estimation for mobile robots
[AIAA PAPER 94-1197-CP] p 3442 N94-30548
Multi-sensor data fusion and the use of artificial intelligence
[PB94-126216] p 3448 N94-30741

SCHEDULES
A family of joint probability models for cost and schedule uncertainties
[AD-A275513] p 3463 N94-28670
Circadian countermeasures for shiftworkers during USMP-2: A report to mission management
[NASA-CR-195260] p 3402 N94-30188

SCHEDULING
Technology transition push. Part 1: A case study of rate monotonic analysis
[AD-A275616] p 3407 N94-28633
Artificial intelligence technology program at Rome Laboratory p 3414 N94-29328
A time reasoning system based on the event calculus for scheduling in aeronautic maintenance
[REPT-932-710-101] p 3122 N94-29463

SCHMIDT NUMBER
The instantaneous concentration field in the self-similar region of a high Schmidt number round jet p 3278 N94-29976

SCHOOLS
An evaluation of techniques for ranking academic information systems journals
[AD-A275179] p 3529 N94-29066

SCHROEDINGER EQUATION
Calculation of eigenvalues of Schroedinger operators for arbitrary coupling
[DE94-606302] p 3522 N94-28582
Miln equation for the calculation of the phases and amplitudes of wave functions for continuum spectrum of Coulomb two-center problem
[DE94-606292] p 3522 N94-28616
Dissipative quantum dynamics and nonlinear sigma-model
[DE94-606295] p 3523 N94-28617
Numerical solution of the multichannel scattering problem
[DE94-606297] p 3484 N94-28619
Variational calculation of the eigenpotential for H(sup -)-system
[DE94-606269] p 3407 N94-28622
The solving of the relativistic two-body problem with a nonlinear dependence upon a spectrum parameter
[DE94-606343] p 3451 N94-28783
Reconstruction of spectra in the discrete quantum mechanics (new elements of the lattice quantum engineering)
[DE94-608075] p 3524 N94-30087
Graded Froelicher-Nijenhuis brackets and the theory of recursion operators for super differential equations
[MEMO-1147] p 3460 N94-30736

SCHWARZSCHILD METRIC
Physics, astronomy, and astrophysics: A numerical study of the black hole plus Brill wave spacetime p 3540 N94-29990

SCHWASSMANN-WACHMANN COMET
Infrared observations of cometary dust by COBE p 3541 N94-29994

SCIENTIFIC SATELLITES
The development procedures and tools applied for the attitude control software of the Italian satellite SAX p 3170 N94-29324

SCIENTIFIC VISUALIZATION
Analytic rendering of curvilinear volume data
[DE94-004934] p 3407 N94-28506
Using stereoscopic imaging for visualization applications
[DE94-006247] p 3536 N94-30706

SCINTILLATION
On possibility to create the scintillation trigger for liquid-argon neutrino detector
[DE94-607844] p 3489 N94-30050
Preliminary detector design ST862-prototype neutron detector
[DE94-004714] p 3491 N94-30695
Silica scintillating materials prepared by sol-gel methods
[DE94-005123] p 3220 N94-30778

SCINTILLATION COUNTERS
On possibility to create the scintillation trigger for liquid-argon neutrino detector
[DE94-607844] p 3489 N94-30050
Preliminary detector design ST862-prototype neutron detector
[DE94-004714] p 3491 N94-30695
Silica scintillating materials prepared by sol-gel methods
[DE94-005123] p 3220 N94-30778

SCREWS
Kinematic analysis of platform-type robotic manipulators
[ISBN-0-315-78703-1] p 3311 N94-30793

SCRUBBERS
Gas stream purifier p 3354 N94-30469

SEA BREEZE
An observational and numerical study of sea/land-breeze circulations in an area of complex coastal heating p 3372 N94-29813

SEA ICE
Lead detection and mapping with reference to relationships between scale, sensor characteristics, surface conditions and atmospheric properties
[AD-A275321] p 3377 N94-28877
Sea ice and oceans applications of SAR p 3327 N94-28934
Dynamic constraints on CO2 uptake by an iron-fertilized Antarctic p 3350 N94-30619
The role of sea ice dynamics in global climate change p 3350 N94-30620
A toy model of sea ice growth p 3351 N94-30626
Cryosphere and climate p 3352 N94-30632

SEA LEVEL
Altimeter data processing from sea surface topography to horizontal eddy momentum fluxes
[PB94-147550] p 3378 N94-30714

SEA OF JAPAN
Papers in meteorology and geophysics, vol. 44, no.1
[JTN-94-80585] p 3324 N94-28693
The Japan Sea proper water and water circulation in the Japan Sea p 3324 N94-28694

SEA SURFACE TEMPERATURE
Role of satellite observations of sea-surface temperature in the detection of global change
[PB94-138120] p 3329 N94-29107
On the annual cycle of the tropical Pacific atmosphere and ocean p 3371 N94-29763
On interannual variability and climate change in the North Pacific p 3374 N94-29963
The validation of ocean surface heat fluxes in AMIP
[DE94-001539] p 3378 N94-30823

SEALERS
Mechanical flexible joint design document
[NASA-CR-193941] p 3297 N94-28419

SEALS (STOPPERS)
Development of braided rope engine seals
[NASA-TM-105902] p 3298 N94-28838
Rotordynamic analysis of annular honeycomb-stator turbulent gas seals using a new friction-factor model based on flat plate tests p 3302 N94-29916

SEAMS (JOINTS)
Chamber free fusion welding root side purging method and apparatus
[NASA-CASE-MFS-28832-1] p 3204 N94-29380

SEARCH PROFILES
A unified framework for retrieval in image databases p 3533 N94-29811

Knowledge combination and data fusion with application to recognition systems p 3259 N94-30513

SEARCHING

Using multiple searchers to locate a randomly moving target
[AD-A275602] p 3463 N94-28768

Enhancing performance of full-text retrieval systems using relevance feedback p 3532 N94-29806

A note on the complexity of local search problems
[CT-93-02] p 3456 N94-30370

SEAS

The validation of ocean surface heat fluxes in AMIP
[DE94-001539] p 3378 N94-30823

SEAT BELTS

Crashworthiness analysis of commuter aircraft seats
[AD-A275889] p 3135 N94-28799

SEATS

Crashworthiness analysis of commuter aircraft seats
[AD-A275889] p 3135 N94-28799

SECONDARY EMISSION

Characteristics of secondary electron emission from CsI induced by x rays with energies up to 100 keV
[DE94-608422] p 3395 N94-30185

SECONDARY FLOW

Flow and heat transfer in a rotating square sectioned U-bend p 3128 N94-28984

SECULAR VARIATIONS

Electromagnetic core-mantle coupling
p 3366 N94-30808

SECURITY

Security aspects of computer supported collaborative work
[AD-A275638] p 3528 N94-28640

Design of an autonomous exterior security robot
[AIAA PAPER 94-1188-CP] p 3441 N94-30538

Controlling multiple security robots in a warehouse environment
[AIAA PAPER 94-1300-CP] p 3441 N94-30540

SEDIMENT TRANSPORT

Glaciohydrologic and glaciohydraulic effects on runoff and sediment yield in glacierized basins
[AD-A275134] p 3361 N94-29286

SEDIMENTARY ROCKS

Field guide to Cretaceous-tertiary boundary sections in northeastern Mexico
[NASA-CR-195719] p 3354 N94-28416

SEDIMENTS

Glaciohydrologic and glaciohydraulic effects on runoff and sediment yield in glacierized basins
[AD-A275134] p 3361 N94-29286

The undrained shear strength characteristics of undisturbed soil from fishing port areas
p 3234 N94-29704

Dewatering of contaminated river sediments
p 3354 N94-30472

SEEBECK EFFECT

Thermal conductivities, electrical resistivities, and Seebeck coefficients of YBa2Cu3O(7-x) superconductors from 80 to 300 K
[DE94-004796] p 3520 N94-30724

SEEDS

Seed viability detection using computerized false-color radiographic image enhancement p 3387 N94-30461

SEISMIC WAVES

Initial wave-type identification with neural networks and its contribution to automated processing in IMS version 3.0
[AD-A275058] p 3359 N94-29137

Statistical characterization of rugged propagation paths with application to Rg scattering study
[AD-A275237] p 3361 N94-29393

Effects and implications of fault zone heterogeneity and anisotropy on earthquake strong ground motion
p 3363 N94-29941

The rupture process of large earthquakes along convergent margins: Cast studies from Alaska and Armenia p 3363 N94-29969

Extension of love wave transformation theory to laterally heterogeneous structures
[DE94-608098] p 3365 N94-30093

SEISMOGRAMS

A program for rapid computation of multioffset vertical seismic profile synthetic seismograms for layered media
[AD-A275464] p 3355 N94-28737

Effects and implications of fault zone heterogeneity and anisotropy on earthquake strong ground motion
p 3363 N94-29941

SEISMOGRAPHS

A broad-band microseismometer for planetary operations p 3237 N94-29778

Air-deployable geophysics package
[DE94-005651] p 3335 N94-30594

SEISMOLOGY

A program for rapid computation of multioffset vertical seismic profile synthetic seismograms for layered media
[AD-A275464] p 3355 N94-28737

The Norwegian seismic array (NORSAR), phase 3
[AD-A275440] p 3356 N94-28868

Initial wave-type identification with neural networks and its contribution to automated processing in IMS version 3.0
[AD-A275058] p 3359 N94-29137

Statistical characterization of rugged propagation paths with application to Rg scattering study
[AD-A275237] p 3361 N94-29393

A broad-band microseismometer for planetary operations p 3237 N94-29778

The rupture process of large earthquakes along convergent margins: Cast studies from Alaska and Armenia p 3363 N94-29969

Theoretical asteroseismology of white dwarf stars: The encyclopedia Seismologica p 3547 N94-30011

Application of remote sensing techniques for the seismo-tectonic study of Nahanni earthquake area
[ISBN-0-315-85942-3] p 3334 N94-30037

SEIZURES

Monitor for status epilepticus seizures
p 3397 N94-30460

SELECTION

Unravelling nondeterminism: On having the ability to choose
[RUU-CS-93-30] p 3428 N94-30749

SELENIDES

Studies of high temperature ternary phases in mixed-metal-rich early transition metal sulfide and phosphide systems
[DE94-006034] p 3209 N94-30336

SELENIUM

The long-range transport of aerosol particles over the North Atlantic Ocean p 3366 N94-30867

SELENIUM OXIDES

Experimental and theoretical studies of molecular solids
[AD-A275511] p 3485 N94-28668

SELF FOCUSING

Automatic focus and registration of synthetic aperture radar images p 3246 N94-29536

SELF ORGANIZING SYSTEMS

Taxonomy of gamma ray burster data using a self-organizing neural network
[DE94-006480] p 3553 N94-30248

A lateral inhibition neural network that emulates a winner-takes-all algorithm
[RUU-CS-92-46] p 3438 N94-30334

SEMANTICS

Operation semantics with read and write frames
[PB94-138138] p 3529 N94-29108

North American jumelage 'type systems'
[AD-A275342] p 3411 N94-29214

Second-order algebraic specification of state semantics
[CWI-CS-R9254] p 3453 N94-29889

A^c smart child of Peano's
[ML-92-10] p 3455 N94-30325

Completeness of the Lambek calculus with respect to relativized relational semantics
[LP-93-03] p 3455 N94-30326

Identity: Quarrelling with an unproblematic notion
[LP-93-04] p 3455 N94-30327

On blocks: Locality and asynchronous communication (extended abstract)
[RUU-CS-92-44] p 3424 N94-30347

Index expression belief networks for information disclosure
[TR-92-23] p 3465 N94-30358

Parsing in ISBES
[TR-92-32] p 3432 N94-30363

Interrogatives and adverbs of quantification
[LP-92-14] p 3456 N94-30372

Bounded contraction and many-valued semantics
[ML-93-04] p 3456 N94-30380

Models of the untyped lambda-calculus in semi Cartesian closed categories
[ML-93-05] p 3456 N94-30381

Algorithmic problems concerning first-order definability of modal formulas on the class of all finite frames
[ML-93-07] p 3456 N94-30383

The Vanilla meta-interpreter for definite logic programs and ambivalent syntax
[CT-93-01] p 3424 N94-30386

A note on the Smyth powerdomain construction
[RUU-CS-93-02] p 3457 N94-30393

Algebraic domains, chain completion, and the Plotkin powerdomain construction
[RUU-CS-93-03] p 3457 N94-30394

Modal quantification over structured domains
[ML-93-02] p 3457 N94-30396

Isomorphisms between predicate and state transformers
[RUU-CS-93-09] p 3458 N94-30403

Modeling systems by probabilistic process algebra: An event structures approach
[MEMO-INF-93-29-REV] p 3425 N94-30416

Termination of term rewriting by semantic labelling
[RUU-CS-93-24] p 3459 N94-30424

Three metric domains of processes for bisimulation
[CWI-CS-R9335] p 3459 N94-30427

Isomorphisms between predicate and state transformers
[CWI-CS-R9338] p 3459 N94-30430

Relating state transformation semantics and predicate transformer semantics for parallel programs
[CWI-CS-R9339] p 3433 N94-30431

Topological models for higher order control flow
[CWI-CS-R9340] p 3425 N94-30432

Comparative semantics for linear arrays of communicating processes
[CWI-CS-R9336] p 3426 N94-30491

On the relation between Unity properties and sequences of states
[RUU-CS-93-07] p 3433 N94-30720

Bisimulations and predicate logic
[CWI-CS-R9333] p 3460 N94-30735

Unravelling nondeterminism: On having the ability to choose
[RUU-CS-93-30] p 3428 N94-30749

A structural co-induction theorem
[CWI-CS-R9346] p 3461 N94-30753

Termination of term rewriting by semantic labelling
[RUU-CS-92-38] p 3462 N94-30859

Inventory of fragments and exact models in intuitionistic proportional logic
[ML-93-11] p 3463 N94-30974

SEMICIRCULAR CANALS

Basic understanding of vertigo p 3390 N94-28855

SEMICONDUCTING FILMS

Optical properties of cadmium sulfide, zinc selenide, and zinc manganese selenide semiconductor films
p 3500 N94-29759

SEMICONDUCTOR DEVICES

Investigation of advanced fault insertion and simulator methods
[NASA-CR-195241] p 3261 N94-28511

Innovative optoelectronic materials and structures using OMVPE
[AD-A275811] p 3511 N94-28773

Optoelectronic integrated circuits fabricated using atomic layer epitaxy
[AD-A275454] p 3262 N94-28805

Cryogenic probe station for use in automated microwave and noise figure measurements
[NASA-TM-106560] p 3286 N94-29000

Effects of oxide charge and surface recombination velocity on the excess base current of BJT's
[DE94-003711] p 3263 N94-29025

Towards experimental verification and device applications of current driven plasma instabilities in solid state systems
[AD-A275395] p 3504 N94-29055

Proceedings of the Workshop on Microtechnologies and Applications to Space Systems
[NASA-CR-195688] p 3235 N94-29767

Micro-opto-mechanical devices and systems using epitaxial lift off p 3239 N94-29793

Photonics at Sandia National Laboratories: From research to applications
[DE94-006463] p 3501 N94-30828

SEMICONDUCTOR JUNCTIONS

Strong overlap and transmission in triple barrier resonant structures
[DE94-608103] p 3516 N94-30067

SEMICONDUCTOR LASERS

Near-IR diode laser absorption for measurement of tropospheric HO2 p 3345 N94-28607

HO2 detection by near infrared absorption using tunable diode lasers p 3346 N94-28608

Visible vertical cavity surface emitting lasers
[AD-A275334] p 3293 N94-28919

High-power CW diode-laser-array-pumped solid-state lasers and efficient nonlinear optical frequency
[AD-A275394] p 3293 N94-29309

Dynamics of a coupled solid state laser array
p 3294 N94-29551

Longitudinal effects and intensity-phase coupling in distributed feedback semiconductor lasers
p 3294 N94-29590

Time and frequency technology at NIST
p 3468 N94-30641

Diode-pumped solid-state-laser drivers and the competitiveness of inertial fusion energy
[DE94-006654] p 3296 N94-30830

SEMICONDUCTORS (MATERIALS)

Laser beam steering with semiconductor waveguide
[AD-A275775] p 3292 N94-28765

Innovative optoelectronic materials and structures using OMVPE
[AD-A275811] p 3511 N94-28773
Electroset Technology: On the forefront of manufacturing
[AD-A275166] p 3263 N94-29045
High resistivity buffer layers by oxygen doping
[AD-A274986] p 3513 N94-29125
Preparation, characterization, and facile thermolysis of (X2GaP(SiMe3)2) (X = Br, I) and (Cl3Ga2P)n; new precursors to nanocrystalline gallium phosphide
[AD-A275019] p 3513 N94-29130
Monolithic in-based III-V compound semiconductor focal plane array cell with single stage CCD output
[NASA-CASE-NPO-18978-1-CU] p 3265 N94-29488
Epitaxial heterojunctions of oxide semiconductors and metals on high temperature superconductors
[NASA-CASE-NPO-18483-1-CU] p 3513 N94-29501
Near-ultraviolet laser photoemission: Scanning microscopy, buried interfaces and image-potential states p 3294 N94-29531
Optical properties of cadmium sulfide, zinc selenide, and zinc manganese selenide semiconductor films p 3500 N94-29759
Overview of microoptics: Past, present, and future p 3235 N94-29771
ECR plasma synthesis of silicon nitride films on GaAs and InSb
[DE94-005575] p 3515 N94-30006
Structural characterization of semiconductor heterostructures by atomic resolution Z-contrast imaging at 300 kV
[DE94-006561] p 3516 N94-30063
Vibrational properties of homopolar and heteropolar surfaces and interfaces of the CdTe/HgTe system
[DE94-608105] p 3516 N94-30069
II-VI wide band gap semiconductors under hydrostatic pressure
[DE94-608106] p 3516 N94-30070
Band structure of superlattice with (delta)-like potential
[DE94-608108] p 3516 N94-30072
Survey report of JSUP Space Environment Utilization Research Committee in fiscal year 1992: Functional New Materials Session
[JTN-94-80582] p 3159 N94-30162
The 1992 report on the next generation ultra clean technology for advanced microfabrication
[DE94-744171] p 3157 N94-30268
Nonlinear optics response of semiconductor quantum wells under high magnetic fields
[DE94-003244] p 3520 N94-30835
Nuclear magnetic relaxation studies of semiconductor nanocrystals and solids
[DE94-006301] p 3520 N94-30842
Rotator phases in narrow-gap semiconductors
[DE94-005472] p 3521 N94-30897

SENSITIVITY
Insensitive energetic materials: The importance of physical properties and molecular structure
[AD-A275393] p 3225 N94-29308
Sensitivity analysis of the static aeroelastic response of a wing p 3134 N94-30525

SENSORIMOTOR PERFORMANCE
Deterioration of manual performance in cold and windy climates p 3381 N94-28434
Human pilot response during single- and multi-axis tracking tasks
[AD-A275080] p 3398 N94-28887

SENSORS
The application of micromachined sensors to manned space systems p 3171 N94-29791
Micro guidance and control synthesis: New components, architectures, and capabilities p 3144 N94-29792
Air-deployable geophysics package
[DE94-005651] p 3335 N94-30594

SENSORY PERCEPTION
Basic understanding of vertigo p 3390 N94-28855
Disturbance of equilibrium on JAL flight crew p 3390 N94-28856
Space and vertigo: In relation to space motion sickness p 3390 N94-28857

SENTENCES
An architecturally-based theory of human sentence comprehension
[AD-A275380] p 3398 N94-29313

SEPARATED FLOW
Role of computational fluid dynamics in aeronautical engineering. Part 10: Numerical analysis of flow around 2-D multi-element HLD p 3125 N94-28964
Aspects of the modeling and numerical simulation of leading-edge vortex flow
[AD-B179108] p 3133 N94-30492
Development and application of particle image velocimetry in high-speed separated flow: Two-dimensional base cavities p 3282 N94-30791
Numerical simulation of leading-edge vortex flow
[AD-B175154] p 3134 N94-30871

SEPARATORS
Specialized data base management system for data processing in the experiments at low energies
[DE94-606268] p 3485 N94-28621
Polyaniline membranes for gas and liquid separation
[AD-A275851] p 3408 N94-28790
Dendrite preventing separator for secondary lithium batteries
[NASA-CASE-NPO-18585-1-CU] p 3265 N94-29411

SEQUENCING
Stable RNA sequences as a tool for DNA probes and phylogenetic studies
[PB94-135423] p 3385 N94-29156
A time reasoning system based on the event calculus for scheduling in aeronautic maintenance
[REPT-932-710-101] p 3122 N94-29463

SEQUENTIAL ANALYSIS
North American jumelage 'type systems'
[AD-A275342] p 3411 N94-29214

SEQUENTIAL CONTROL
High level language-based robotic control system
[NASA-CASE-NPO-17918-2-CU] p 3435 N94-29465
Formal specification and verification of real-time sequential control systems
[AD-A275776] p 3419 N94-29678
Topological models for higher order control flow
[CWI-CS-R9340] p 3425 N94-30432

SERIES EXPANSION
Higher order asymptotic crack tip fields in a power-law hardening material p 3321 N94-29829

SERUMS
Strategies to sustain and enhance performance in stressful environments
[AD-A275223] p 3398 N94-29027

SERVICE LIFE
Advanced development of PV encapsulents
[DE94-000219] p 3336 N94-28500
Service life prediction of composite structures through fiber testing
[AD-A275661] p 3176 N94-28654
Aircraft age impacts on maintenance requirements
[AD-A275701] p 3121 N94-28666
Aircraft age impact on individual operating and support cost elements
[AD-A275739] p 3121 N94-28732
Performance and durability of high emittance heat receiver surfaces for solar dynamic power systems
[NASA-TM-106549] p 3172 N94-28834
Measurement and modelling of bolted joint stress relaxation in plastics
[PB94-124849] p 3318 N94-28841
An outdoor exposure testing program for optical materials used in solar thermal electric technologies
[DE94-000265] p 3500 N94-29799
Space flight manipulator technologies and requirements for the NASA Flight Telerobotic Servicer (FTS)
[AIAA PAPER 94-1191-CP] p 3441 N94-30542

SET THEORY
On blocks: Locality and asynchronous communication (extended abstract)
[RUU-CS-92-44] p 3424 N94-30347
A note on the Smyth powerdomain construction
[RUU-CS-93-02] p 3457 N94-30393
Algebraic domains, chain completion, and the Plotkin powerdomain construction
[RUU-CS-93-03] p 3457 N94-30394
Commutative Lambek categorial grammars
[ML-93-01] p 3457 N94-30395
Representations of dynamical systems described by behavioral inequalities
[AD-B173649] p 3458 N94-30402
Isomorphisms between predicate and state transformers
[RUU-CS-93-09] p 3458 N94-30403
Isomorphisms between predicate and state transformers
[CWI-CS-R9338] p 3459 N94-30430
Dynamic microsets for RAMs
[RUU-CS-93-22] p 3406 N94-30727
Set games
[MEMO-1148] p 3466 N94-30737
Total termination of term rewriting
[RUU-CS-92-42] p 3460 N94-30744
A structural co-induction theorem
[CWI-CS-R9346] p 3461 N94-30753
Non-commutative geometry
[PB94-139342] p 3462 N94-30889
Remarks on uniformly finitely precomplete positive equivalences
[ML-93-12] p 3463 N94-30975

SEWAGE TREATMENT
Growth of hydrocarbon-rich microalga Botryococcus braunii in secondarily treated sewage and its consumption of nitrate ion and phosphate ion p 3387 N94-29519

SEYFERT GALAXIES
Infrared properties of obscuring dust tori in active galactic nuclei p 3545 N94-29832
Broad H alpha profiles of radio-loud active galactic nuclei and rapid profile variability in Seyfert and radio galaxies p 3552 N94-29989

SHAFTS (MACHINE ELEMENTS)
Multi-speed multi-phase resolver converter
[NASA-CASE-MFS-28855-1] p 3264 N94-29372

SHAKERS
Root-sum-square structural strength verification approach
[NASA-TM-108453] p 3322 N94-30206

SHAKING
Monitor for status epilepticus seizures p 3397 N94-30460

SHALLOW WATER
Broad geoacoustic assessment of some regional areas
[AD-A275504] p 3356 N94-28791

SHAPE CONTROL
Control of micromachined deformable mirrors p 3239 N94-29787

SHAPE MEMORY ALLOYS
Report on smart materials
[PB94-137528] p 3203 N94-29015
Research on the improvement of shape-memory and magnetostrictive materials
[AD-A275397] p 3203 N94-29056
Rotary actuator
[NASA-CASE-MFS-28581-1] p 3205 N94-29447

SHARP LEADING EDGES
Numerical investigation into high-angle-of-attack leading-edge vortex flow
[PB94-125564] p 3133 N94-30388
Aspects of the modeling and numerical simulation of leading-edge vortex flow
[AD-B179108] p 3133 N94-30492
Numerical simulation of leading-edge vortex flow
[AD-B175154] p 3134 N94-30871

SHEAR FLOW
On the numerical analysis of shear flows p 3126 N94-28972
An alternative assessment of second-order closure models in turbulent shear flows
[NASA-CR-194881] p 3272 N94-29381
Lubricant rheology at high shear rates p 3217 N94-29967
Potential capabilities of Reynolds stress turbulence model in the COMMIX-RSM code p 3285 N94-30450
Evaluation of flip-flop jet nozzles for use as practical excitation devices
[NASA-TM-106377] p 3135 N94-30949

SHEAR LAYERS
A random distribution reacting mixing layer model
[NASA-TM-106517] p 3150 N94-28923
Wall pressure fluctuations in the reattachment region of a supersonic free shear layer
[NASA-CR-195790] p 3132 N94-29920
The effect of a wavy boundary on turbulent flow p 3280 N94-30272
Numerical simulation of leading-edge vortex flow
[AD-B175154] p 3134 N94-30871
An experimental study of nonlinear wave coupling and energy transfer characterizing the transition of a planar jet shear layer p 3282 N94-30953

SHEAR PROPERTIES
Experimental determination of orthotropic elastic constants
[FFA-TN-1991-35] p 3215 N94-29424
Performance of a higher-order triangular finite element for composite laminated structures p 3181 N94-29810
Lubricant rheology at high shear rates p 3217 N94-29967

SHEAR STRAIN
Cyclic axial-torsional deformation behavior of a cobalt-base superalloy
[NASA-TM-106372] p 3203 N94-28921
Interlaminar fracture analysis for laminated composites under combined loading p 3182 N94-29964
Thin-walled orthotropic laminated beam theory p 3324 N94-30920

SHEAR STRENGTH
The undrained shear strength characteristics of undisturbed soil from fishing port areas p 3234 N94-29704
Delamination growth in composites under cyclic loads p 3183 N94-30256
Four advances in carbon-carbon materials technology p 3186 N94-30481

SHEAR STRESS
Cyclic axial-torsional deformation behavior of a cobalt-base superalloy
[NASA-TM-106372] p 3203 N94-28921

Granular bases for heavily loaded pavements
[AD-A275171] p 3156 N94-29047
Performance of a higher-order triangular finite element for composite laminated structures
p 3181 N94-29810
Nanodislocation structures generated in shocked crystals p 3514 N94-29915
Vacuum chamber and adaptors for shearography and holography
[NASA-CR-192467] p 3157 N94-29956
On interannual variability and climate change in the North Pacific p 3374 N94-29963

SHEEP
Blast overpressure studies with animals and man
[AD-A275038] p 3391 N94-29150

SHELL THEORY
Plane strain finite element analysis of sheet forming operations including bending effects
p 3322 N94-30354

SHERGOTTITES
Cosmogenic C-14 in Antarctic and non-Antarctic meteorites and lunar samples
[NASA-CR-195795] p 3546 N94-29905

SHIELDING
Overview of shielding analyses for the MHTGR from 1986 to 1991
[DE94-002448] p 3495 N94-29924

SHIP HULLS
An improvement of the slender body theory for oscillating ships with finite forward speed p 3234 N94-29705

SHIP TERMINALS
Orbital applications of electrodynamic propulsion
[AD-A275413] p 3173 N94-29216

SHIPS
Physiological responses during shipboard firefighting
[AD-A275104] p 3391 N94-28912
An improvement of the slender body theory for oscillating ships with finite forward speed p 3234 N94-29705

SHIVERING
Fuelling shivering in humans during cold water immersion p 3379 N94-28426

SHOCK ABSORBERS
Landing gear energy absorption system
[NASA-CASE-MSC-22277-1] p 3300 N94-29448
Identification of the damping ratio relationship of an autovehicle suspension
[REPT-93-063] p 3313 N94-30937

SHOCK FRONTS
Experimental investigation of three-dimensional vortex-airfoil interaction in a supersonic stream
[AD-A275107] p 3122 N94-28899
Nanodislocation structures generated in shocked crystals p 3514 N94-29915

SHOCK HEATING
Numerical simulation of unsteady aerodynamic heating induced by shock reflections p 3123 N94-28952
A study of low emissions gas turbine combustions
[NASA-CR-195763] p 3152 N94-29860

SHOCK LOADS
Pyrotechnic shock: Devices in pyrotechnic environment qualification logic
[REPT-932-430-108] p 3225 N94-29429

SHOCK WAVE INTERACTION
Wall pressure fluctuations in the reattachment region of a supersonic free shear layer
[NASA-CR-195790] p 3132 N94-29920

SHOCK WAVE PROFILES
Numerical simulation of unsteady aerodynamic heating induced by shock reflections p 3123 N94-28952
Numerical simulation of steady Mach reflection by shock capturing schemes p 3123 N94-28953

SHOCK WAVE PROPAGATION
Numerical simulation of steady Mach reflection by shock capturing schemes p 3123 N94-28953

SHOCK WAVES
Dislocation theory of melting for iron, revisited
[DE94-002715] p 3355 N94-28538
Acceleration in astrophysics
[DE94-004986] p 3552 N94-28580
Report of National Institute for Resources and Environment. No. 8: Research on blasting sound related to it's measurement, propagation prediction, control and evaluation
[JTN-94-80605] p 3479 N94-29597
A multiwavelength study of two prototypical supernova remnants p 3540 N94-29833
Wall pressure fluctuations in the reattachment region of a supersonic free shear layer
[NASA-CR-195790] p 3132 N94-29920
An interactive, design and educational tool for supersonic external-compression inlets
[NASA-TM-106581] p 3421 N94-30174

SHORT CIRCUITS
A new test method for the assessment of the arc tracking properties of wire insulation in air, oxygen enriched atmospheres and vacuum p 3167 N94-28714

SHORT WAVE RADIATION
A physical optics model for scattering of HF radiation by irregular terrain
[DE94-006187] p 3255 N94-30106

SHRINKAGE
Innovative processing of composites for ultra-high temperature applications, book 3
[AD-A275599] p 3177 N94-28731
Measurement and modelling of bolted joint stress relaxation in plastics
[PB94-124849] p 3318 N94-28841

SHUTTLE IMAGING RADAR
Pointing mechanisms for the Shuttle Radar Laboratory
p 3162 N94-29638

SIDELOBES
A new guided wave lens structure and its application
[AD-A275541] p 3499 N94-28813

SIEVES
Methane challenge of high performance molecular sieve oxygen concentrator
[AD-A275155] p 3337 N94-29033

SIGNAL ANALYSIS
SPC toolbox: An interactive MATLAB (tm) package for signal modeling, analysis, and communications
[AD-A275617] p 3241 N94-28634
The Stroemberg wavelet on the interval and the Franklin system
[TELECOM-93-C-002] p 3462 N94-30971

SIGNAL DETECTION
Acquisition time analysis of noncoherent PN sequence acquisition schemes
[AD-A275017] p 3244 N94-29094
Detection methods for stealth radio signals: A literature survey
[PB94-137452] p 3244 N94-29176
A review of signal detection using the bispectrum with applications in underwater acoustics
[AD-A275227] p 3478 N94-29388
Partially coherent detection of PSK signals in Rician channels
[ISBN-0-315-85799-4] p 3254 N94-30031
Sampling behaviour in a four instrument monitoring task: Effects of signal bandwidth and number of events per signal
[AD-B179613] p 3402 N94-30422
Some applications of GPS timing information
p 3145 N94-30661

SIGNAL DETECTORS
A magnetically coupled quench detector for superconducting magnets
[DE94-006040] p 3268 N94-30904

SIGNAL DISTORTION
Three dimensional transient analysis of microstrip circuits in multilayered anisotropic media
[AD-A274995] p 3263 N94-28995

SIGNAL ENCODING
Non-orthogonal subband/transform coder
[NASA-CASE-LEW-15310-1] p 3246 N94-29589

SIGNAL FADING
Adaptive power control as a fade countermeasure on satellite links p 3253 N94-29897

SIGNAL MIXING
Multi-channel spatialization systems for audio signals
[NASA-CASE-ARC-12013-1-CU] p 3245 N94-29364

SIGNAL PROCESSING
A space-based classification system for RF transients
[DE94-003933] p 3240 N94-28522
Data fusion and correlation techniques testbed development audio processing study
[SKD-1600-73-014] p 3241 N94-28532
Data fusion and correlation techniques testbed development. Phase 1: Interim report
[SKD-1600-73-015] p 3405 N94-28533
SPC toolbox: An interactive MATLAB (tm) package for signal modeling, analysis, and communications
[AD-A275617] p 3241 N94-28634
Advanced optical A/D converter
[AD-A275663] p 3498 N94-28656
Design of parallel systems for signal processing
[AD-A275490] p 3430 N94-28659
The bootstrapped algorithm: A fast algorithm for blind signal separation
[AD-A275759] p 3408 N94-28760
Modeling, analysis, and simulation of an optical time-division multiple-access network architecture
[AD-A275847] p 3498 N94-28780
Testing for a signal with unknown location and scale in a stationary Gaussian random field
[AD-A275320] p 3464 N94-28876
Spurs in digital radio frequency memory and applications of DRFM
[AD-A275013] p 3243 N94-28897
Removal of coherent Extremely Low Frequency (ELF) background noise by adaptive noise cancellation
[AD-A275016] p 3243 N94-28898
Backscatter haze device for measurement of haze in aircraft transparencies
[AD-A275127] p 3146 N94-29042
Multi-channel spatialization systems for audio signals
[NASA-CASE-ARC-12013-1-CU] p 3245 N94-29364
Measurand transient signal suppressor
[NASA-CASE-MSC-22027-1] p 3435 N94-29466
Orbital debris radar instrumentation
p 3248 N94-29626
A comparison of full-spectrum and complex-symbol combining techniques for the Galileo S-band mission
p 3250 N94-29665
A complex symbol signal-to-noise ratio estimator and its performance p 3251 N94-29671
Method for ambiguity resolution in range-Doppler measurements
[NASA-CASE-GSC-13542-1] p 3252 N94-29739
High-resolution robot tracking and direction finding for space station environment p 3168 N94-29896
A novel approach to noise-filtering based on a gain-scheduling neural network architecture
[NASA-TM-106563] p 3155 N94-30204
An electromagnetic noncontacting sensor for thickness measurement in a dispersive medium
[AIAA PAPER 94-1200-CP] p 3443 N94-30551
Noise and drift analysis of non-equally spaced timing data p 3472 N94-30667
A bipolar analog front-end integrated circuit for the SDC silicon tracker
[DE94-005203] p 3267 N94-30711
The Stroemberg wavelet on the interval and the Franklin system
[TELECOM-93-C-002] p 3462 N94-30971
Noise reduction techniques for the restoration of musical recordings
[TELECOM-93-E-019] p 3291 N94-30979

SIGNAL RECEPTION
Solid-state, active-phased arrays: Some aspects of receiver design
[AD-A275893] p 3527 N94-28779
A comparison of full-spectrum and complex-symbol combining techniques for the Galileo S-band mission
p 3250 N94-29665
A combined electron beam/optical lithography process step for the fabrication of sub-half-micron-gate-length MMIC chips p 3240 N94-30445
Remote clocks linked by a fully calibrated two-way timing link p 3471 N94-30659
Some applications of GPS timing information
p 3145 N94-30661

SIGNAL REFLECTION
Three dimensional transient analysis of microstrip circuits in multilayered anisotropic media
[AD-A274995] p 3263 N94-28995

SIGNAL TO NOISE RATIOS
Decoder synchronization for deep space missions
p 3250 N94-29664
A comparison of full-spectrum and complex-symbol combining techniques for the Galileo S-band mission
p 3250 N94-29665
A complex symbol signal-to-noise ratio estimator and its performance p 3251 N94-29671
An analysis of carrier phase jitter in an MPSK receiver utilizing map estimation
[NASA-CR-195806] p 3164 N94-29880
The bases for the development of high-temperature integrated SQUID-systems
[DE94-607901] p 3267 N94-30073

SIGNAL TRANSMISSION
Considerations in the modelling of seafloor acoustic backscatter
[AD-A275404] p 3478 N94-29206
The Rb 780-nanometer Faraday anomalous dispersion optical filter: Theory and experiment
p 3250 N94-29659
Performance issues of signalling protocols for broadband ISDN
[MEMO-INF-93-30] p 3255 N94-30374
The 25th Annual Precise Time and Time Interval (PTTI) Applications and Planning Meeting
[NASA-CP-3267] p 3468 N94-30639
Optical techniques for time and frequency transfer
p 3469 N94-30647
Some applications of GPS timing information
p 3145 N94-30661

SIGNATURES
Energy distribution of the leptons in top decay to charged Higgs
[DE94-005231] p 3482 N94-28494
Digital camera with apparatus for authentication of images produced from an image file
[NASA-CASE-NPO-19108-1-CU] p 3287 N94-29373

SIGNS AND SYMPTOMS
The Environmental Symptoms Questionnaire: Assessing reactions to environmental extremes in military operations p 3383 N94-28447

SILANES
Silica scintillating materials prepared by sol-gel methods
[DE94-005123] p 3220 N94-30778
SILENCERS
Boundary layer control device for duct silencers
[NASA-CASE-ARC-12030-1] p 3478 N94-29362
SILICA GLASS
Float polishing studies of fused silica
[AD-A275001] p 3213 N94-28886
Characterisation and processing of SiC/MAS-L glass ceramic matrix composite
[REPT-932-430-111] p 3179 N94-29412
Characterization of thermally annealed Sb implanted fused silica
[DE94-005464] p 3219 N94-30335
SILICATES
Layered polysilicate: Properties and perspectives in applications p 3223 N94-29513
SILICIDES
Fabrication and testing of plasma-spray formed MoSi2 and MoSi2 composite tubes
[DE94-004995] p 3175 N94-28581
Brittle composites modeling: Comparisons with MoSi2/ZrO2
[DE94-004978] p 3182 N94-29933
Microstructure and mechanical properties of nitrided molybdenum silicide coatings
[DE94-006249] p 3217 N94-30025
Creep behavior of MoSi2-SiC composites
[DE94-004980] p 3185 N94-30693
Magnetotransport measurements in magnetic fields up to 50T in SmB6 and FeSi
[DE94-006227] p 3520 N94-30848
SILICON
NSC 800, 8-bit CMOS microprocessor
[NASA-CR-195736] p 3405 N94-28845
Silicon germanium carbon heteroepitaxial growth on silicon
[AD-A275197] p 3512 N94-28889
Preparation and structure of amorphous hydrogenated carbon film deposited with RF plasma CVD p 3223 N94-29518
A sub-cm micromachined electron microscope p 3236 N94-29775
A broad-band microseismometer for planetary operations p 3237 N94-29778
Aggregation equilibria in arsenic doped silicon
[DE94-607269] p 3515 N94-30005
The role of plastic deformation in brittle and near-brittle cracking behavior p 3322 N94-30226
The influence of an in-situ electric field on H(+) and He(+) implantation induced defects insil icon
[DE94-006553] p 3518 N94-30249
Thin EFG octagons
[DE94-000257] p 3339 N94-30605
A high rate, low noise, x ray silicon strip detector system
[DE94-004557] p 3268 N94-30717
SILICON ALLOYS
Large-area triple-junction a-Si alloy production scale up
[DE94-000249] p 3339 N94-30604
SILICON CARBIDES
Joining silicon carbide to austenitic stainless steel through diffusion welding
[PB94-126331] p 3297 N94-28399
Pull-test adhesion measurements of diamondlike carbon films on silicon carbide, silicon nitride, aluminum oxide, and zirconium oxide
[DE94-005469] p 3211 N94-28536
Characterization of structure and mechanical properties of MoSi2-SiC nanolayer composites
[DE94-004982] p 3175 N94-28579
MOCVD growth of GaN, AlN and AlGaN for UV photodetector applications
[AD-A275078] p 3512 N94-28871
A novel approach to the fabrication of SiC structures of arbitrary shape
[AD-A275475] p 3214 N94-29073
Thermal expansion and elastic anisotropy in single crystal Al2O3 and SiC reinforcements
[NASA-TM-106516] p 3214 N94-29105
Electrical conductivity measurements on a SiCp/Al alloy metal matrix composite
[PB94-138310] p 3263 N94-29120
Method of producing a ceramic fiber-reinforced glass-ceramic matrix composite
[NASA-CASE-LEW-15264-2] p 3180 N94-29508
Composite flexible blanket insulation
[NASA-CASE-ARC-11955-1-CU] p 3180 N94-29509
Effect of fiber coating on mechanical properties of Nicalon fibers and Nicalon-fiber/SiC matrix composites
[DE94-005477] p 3185 N94-30593
Creep behavior of MoSi2-SiC composites
[DE94-004980] p 3185 N94-30693
Synthesis of (SiC)3N4 thin films by ion implantation
[DE94-006311] p 3521 N94-30851
SILICON COMPOUNDS
Alkylene-bridged polygerm- and polygermsilsesqui-oxanes: New hybrid organic-inorganic materials
[DE94-005096] p 3174 N94-28557
X ray crystal structures of ((Me3SiCH2)2InCl)2 and ((Me3SiCH2)InCl2)
[AD-A275074] p 3513 N94-29155
Thermochemical data for CVD modeling from ab initio calculations
[DE94-005269] p 3222 N94-30909
SILICON DIOXIDE
Development of novel switchable protein surfaces
[AD-A275510] p 3384 N94-28667
Float polishing studies of fused silica
[AD-A275001] p 3213 N94-28886
Inorganic polymer-derived ceramic membranes
[DE94-000082] p 3216 N94-29830
Nanosize metal alloy particle formation in Ag and Cu sequentially implanted silica
[DE94-005592] p 3207 N94-30042
Kinetics of surface roughening and smoothing during ion sputtering
[DE94-006358] p 3219 N94-30263
Silica scintillating materials prepared by sol-gel methods
[DE94-005123] p 3220 N94-30778
Surface chemistry of boron-doped SiO2 CVD: Enhanced uptake of tetraethyl orthosilicate by hydroxyl groups bonded to boron
[DE94-005428] p 3221 N94-30896
SILICON FILMS
Silicon-Film (tm) photovoltaic manufacturing technology
[DE94-000258] p 3336 N94-28501
Energy losses of fast charged particles in thin silicon detectors
[DE94-606065] p 3483 N94-28552
SILICON JUNCTIONS
The influence of an in-situ electric field on H(+) and He(+) implantation induced defects insil icon
[DE94-006553] p 3518 N94-30249
SILICON NITRIDES
Pull-test adhesion measurements of diamondlike carbon films on silicon carbide, silicon nitride, aluminum oxide, and zirconium oxide
[DE94-005469] p 3211 N94-28536
ECR plasma synthesis of silicon nitride films on GaAs and InSb
[DE94-005575] p 3515 N94-30006
Sliding friction and wear between titanium nitride, M50 steel and silicon nitride (round 3 of VAMAS wear test program)
[IMR-TM-TR-003] p 3303 N94-30019
Direct measurement of the reactivity of NH and OH on a silicon nitride surface
[DE94-005286] p 3199 N94-30260
Synthesis of (SiC)3N4 thin films by ion implantation
[DE94-006311] p 3521 N94-30851
SILICON OXIDES
Selection of the Space Station Freedom (SSF) Flat Collector Circuit (FCC) insulation material p 3165 N94-28701
Charge trapping and breakdown in N2O oxides
[DE94-003775] p 3266 N94-30040
SILICON POLYMERS
Layered polysilicate: Properties and perspectives in applications p 3223 N94-29513
Inorganic polymer-derived ceramic membranes
[DE94-000082] p 3216 N94-29830
SILICON RADIATION DETECTORS
Energy losses of fast charged particles in thin silicon detectors
[DE94-606065] p 3483 N94-28552
Pulse height response of Si surface barrier detectors p 3497 N94-30221
A low noise silicon detector preamplifier system for room temperature x ray spectroscopy
[REPT-93-058] p 3291 N94-30930
SILICONES
Low Earth orbit durability evaluation of protected silicone for advanced refractive photovoltaic concentrator arrays
[NASA-TM-106543] p 3172 N94-28999
SILOXANES
Polyimides containing pendent siloxane groups
[NASA-CASE-LAR-14638-1] p 3215 N94-29555
SILVER
Sweep rate and concentration effects on metastable structures formed in the underpotential deposition of silver on Pt(111)
[AD-A275369] p 3189 N94-29010
Crystallization of silver chromate from ethanol via salt metathesis reactions of solubilized precursors
[AD-A275178] p 3189 N94-29058
Haiogen chemisorption on silver(111): Scanning tunneling microscopy of coadsorbed halogen atoms
[AD-A275219] p 3486 N94-29060
Nanosize metal alloy particle formation in Ag and Cu sequentially implanted silica
[DE94-005592] p 3207 N94-30042
SILVER ALLOYS
Giant magnetoresistance and microstructural characteristics of epitaxial Fe-Ag and Co-Ag granular thin films
[DE94-006287] p 3519 N94-30707
SIMULATED ANNEALING
Use of snakes to link edge points to create left ventricular boundaries in echocardiographic images
[TELECOM-93-D-016] p 3395 N94-30970
SIMULATION
CBSD: The celestial background scene descriptor
[AD-A275521] p 3538 N94-28671
Simulator for multistatic radar
[PB94-135506] p 3245 N94-29311
A coupled approach to spatially derived parameters necessary for ecosystem modeling on the North Slope of Alaska: Appendix A
[DE94-005853] p 3349 N94-30046
Logic of transition systems
[CT-93-03] p 3424 N94-30371
Three metric domains of processes for bisimulation
[CWI-CS-R9335] p 3459 N94-30427
A structural co-induction theorem
[CWI-CS-R9346] p 3461 N94-30753
A laboratory simulation of urban heat-island-induced circulation in a stratified environment p 3367 N94-30921
SIMULATORS
Fiscal 1990 geothermal development promotion survey
[DE94-732333] p 3337 N94-28628
Simulator for multistatic radar
[PB94-135506] p 3245 N94-29311
Simulation of fully automated air traffic control concepts p 3139 N94-29569
The Common Modular Simulator (CMS): An architecture test bed for future advanced ATM systems p 3141 N94-29582
A simulator for multi-radar analysis for realistic traffic
[AD-B179099] p 3142 N94-30439
SINE SERIES
Some remarkable sine and cosine functions
[PB94-137759] p 3453 N94-29439
SINE WAVES
Multi-speed multi-phase resolver converter
[NASA-CASE-MFS-28855-1] p 3264 N94-29372
Polynomial modeling of analog-to-digital converters
[DE94-005579] p 3406 N94-30008
SINGLE CHANNEL PER CARRIER TRANSMISSION
The two-way time synchronization system via a satellite voice channel p 3471 N94-30658
SINGLE CRYSTALS
Interstitially stabilized phases in the zirconium-nickel system
[DE94-005561] p 3201 N94-28525
Hysteresis phenomena at spin-flop transition induced by the pulsed magnetic field
[DE94-606851] p 3511 N94-28626
Sputtering of single crystals: Experimental evidence of the ejection process
[AD-A275819] p 3512 N94-28775
Ion channeling peculiarities in YBa2Cu3 O7 monocrystal
[DE94-606885] p 3512 N94-28787
Synthesis and neutron diffraction study of Na3WN3 and Na3MoN3
[AD-A275158] p 3203 N94-29043
Thermal expansion and elastic anisotropy in single crystal Al2O3 and SiC reinforcements
[NASA-TM-106516] p 3214 N94-29105
X ray standing wave studies of underpotentially deposited metal monolayers
[AD-A275409] p 3513 N94-29215
Anode for rechargeable ambient temperature lithium cells
[NASA-CASE-NPO-18580-1-CU] p 3265 N94-29505
Dislocation loops in spinel crystals irradiated successively with deep and shallow ion implants
[DE94-005083] p 3517 N94-30201
Incommensurate magnetic order in UNi2Al3
[DE94-005449] p 3209 N94-30246
Studies of high temperature ternary phases in mixed-metal-rich early transition metal sulfide and phosphide systems
[DE94-006034] p 3209 N94-30336
Butterfly and scaling law in YBa2Cu4O8
[DE94-006037] p 3519 N94-30338
Magnetotransport measurements in magnetic fields up to 50T in SmB6 and FeSi
[DE94-006227] p 3520 N94-30848

SINGLE EVENT UPSETS
Advantages of the LBL 88-inch cyclotron ion beam for SEP studies
[AD-A275142] p 3494 N94-29065
Proceedings of the 1991 Single Event Upset Symposium
[DSIS-92-00652] p 3495 N94-30211
Single event upset and latchup measurements at Brookhaven National Laboratory p 3495 N94-30212
Single event upset susceptibilities of latchup immune CMOS process programmable gate arrays p 3495 N94-30214
Multiple single event upsets in CMOS static rams p 3496 N94-30215
McMaster accelerator facility p 3496 N94-30217
Advanced development of the Spectrum Sciences Model 5005-TF, single event test fixture p 3291 N94-30218
Using Cf-252 for single event upset testing p 3496 N94-30219
Charge collection spectroscopy applied to MOS RAM's p 3201 N94-30220

SINTERING
Analysis of pressureless densification of ceramic matrix composites p 3216 N94-29766

SIS (SUPERCONDUCTORS)
Picosecond response of the quasiparticle current in superconducting tunnel junctions
[DE94-006300] p 3515 N94-30009

SISO (CONTROL SYSTEMS)
A neural network-based technique for structural identification of SISO systems
[REPT-93-076] p 3449 N94-30941

SITE SELECTION
Site comparison for optical visibility statistics in southern California p 3247 N94-29617

SKID LANDINGS
Aircraft accident/incident summary report: In-flight loss of control, leading to forced landing and runway overrun, Continental Express, Inc., N24706 Embraer EMB-120 RT, Pine Bluff, Arkansas, 29 April 1993
[PB94-910404] p 3135 N94-29402

SKIN (ANATOMY)
Effects of make-up on the heat transfer from the head in hyperthermic conditions p 3394 N94-29864

SKIN FRICTION
An actively cooled floating element skin friction balance for direct measurement in high enthalpy supersonic flows p 3289 N94-29824

SKIN TEMPERATURE (BIOLOGY)
Simulation of the effect of wind on clothing by measurements and calculations
[PB94-132289] p 3399 N94-28406
A comparison of four methods of rewarming individuals cooled by immersion in cold water p 3382 N94-28442
Thermal strain generated by an enhanced anti-G protection system in a hot climate p 3383 N94-28445
Physiological responses during shipboard firefighting
[AD-A275104] p 3391 N94-28912
Effects of make-up on the heat transfer from the head in hyperthermic conditions p 3394 N94-29864

SKY SURVEYS (ASTRONOMY)
X ray studies of the Hyades cluster
[NASA-CR-189325] p 3538 N94-29001
A study of recycled pulsars in globular clusters p 3539 N94-29825
A near-infrared survey of the star forming region NGC 2264 p 3540 N94-29971

SKY WAVES
A physical optics model for scattering of HF radiation by irregular terrain
[DE94-006187] p 3255 N94-30106

SLEDS
Portable Linear Sled (PLS) for biomedical research p 3163 N94-29648

SLENDER BODIES
An improvement of the slender body theory for oscillating ships with finite forward speed p 3234 N94-29705

SLEWING
General theory and algorithms for the non-casual inversion, slewing and control of space-based articulated structures
[AD-A275118] p 3167 N94-29002

SLIDING FRICTION
Atomic-scale friction measurements using friction force microscopy. Part 2: Application to magnetic media
[AD-A275202] p 3298 N94-29290
Sliding friction and wear between titanium nitride, M50 steel and silicon nitride (round 3 of VAMAS wear test program)
[IMR-TM-TR-003] p 3303 N94-30019
XPS analysis of 440C steel surfaces lubricated with perfluoropolyethers under sliding conditions in high vacuum
[NASA-TM-106548] p 3218 N94-30177

SLIP CASTING
Nonaqueous slip casting of YBa2Cu3O(7-x) superconductive ceramics
[NASA-CR-4575] p 3512 N94-29101

SLOPES
Influence of clearance and rake angles on the cutting force of rock p 3368 N94-29520
A coupled approach to spatially derived parameters necessary for ecosystem modeling on the North Slope of Alaska: Appendix A
[DE94-005853] p 3349 N94-30046

SLOT ANTENNAS
Printed circuit elements with applications to antennas, scattering, and circuits
[AD-A275512] p 3262 N94-28669
Radial microstrip slotline feed network for circular mobile communications array
[NASA-TM-106540] p 3267 N94-30198

SLOTTED WIND TUNNELS
Experimental studies of transonic flow field near a longitudinally slotted wind tunnel wall
[NASA-TP-3392] p 3130 N94-29545

SLURRIES
Dewatering of contaminated river sediments p 3354 N94-30472

SMART STRUCTURES
Collocated tunable wavenumber sensor/actuators for smart structures
[AD-A275872] p 3241 N94-28755
Report on smart materials
[PB94-137528] p 3203 N94-29015
Assessment of the fibre volume distribution around optical fibres
[FFA-TN-1993-12] p 3179 N94-29425
Intelligent material systems and structures. Part 7: Debonding and pull-out of two optical fibers from two epoxies
[PB94-137767] p 3180 N94-29475
Active control of delaminations in smart composite structures p 3181 N94-29593

SMOKE
Flowfield prediction of NO(x) and smoke production in aircraft engines p 3191 N94-29252
The influence of air distribution on homogeneity and pollutant formation in the primary zone of a tubular combustor p 3194 N94-29274
NATO SOCMET trials p 3258 N94-30503
The effects of man-made smokes and battlefield-induced smokes on the propagation of electromagnetic radiation p 3258 N94-30505

SMOOTHING
Output statistics of the SALFAS FM normalizer Smoothing/Prediction function
[AD-A275758] p 3463 N94-28759
The use of the AOA TTR-4P GPS receiver in operation at the BIPM for real-time restitution of GPS time p 3144 N94-30651

SNOW
On the temperature distribution near a cold surface
[AD-A275162] p 3332 N94-29288

SNOW COVER
Physical processes in snowpacks during rain or melt events
[AD-A275445] p 3325 N94-28881
On the temperature distribution near a cold surface
[AD-A275162] p 3332 N94-29288
Attenuation of outdoor sound propagation levels by a snow cover
[AD-A275387] p 3478 N94-29314
A newly developed snow vehicle (SM100S) for Antarctica. Part 5: Result of general performance tests p 3314 N94-29985
The role of sea ice dynamics in global climate change p 3350 N94-30620

SODIUM
Convective flow effects on protein crystal growth
[NASA-CR-195785] p 3515 N94-30015

SOFIA (AIRBORNE OBSERVATORY)
Aircraft system aft telescope cavity configuration study for Stratospheric Observatory for Infrared Astronomy (SOFIA), phase 2
[NASA-CR-194266] p 3147 N94-29685

SOFTWARE ENGINEERING
Technology transition push. Part 1: A case study of rate monotonic analysis
[AD-A275616] p 3407 N94-28633
A conceptual framework for software technology transition
[AD-A275637] p 3407 N94-28639
Software Technology for Adaptable, Reliable Systems (STARS) program
[AD-A275675] p 3407 N94-28664
Software systems reengineering process model, version 1.0
[AD-A275711] p 3407 N94-28691
Demonstration of improved software support labor estimation for Air Force operational flight programs through functional orientation
[AD-A275789] p 3121 N94-28743
Cleanroom engineering handbook. Volume 3: Project execution in the cleanroom environment
[AD-A275860] p 3156 N94-28752
Cleanroom engineering handbook. Volume 4. Specification team practices
[AD-A275861] p 3156 N94-28753
Construction of a connectionist network supercomputer
[AD-A275765] p 3405 N94-28764
Cleanroom engineering handbook. Volume 2: Organization and project formation in the cleanroom environment
[AD-A275809] p 3156 N94-28772
Guide to the Environmental-Language
[AD-A275849] p 3408 N94-28784
Automated interface for retrieving reusable software components
[AD-A275004] p 3409 N94-28896
Advanced languages for systems software
[AD-A275272] p 3410 N94-29007
Investigation into formalization of domain-oriented parallel software development
[AD-A275177] p 3430 N94-29050
Reference model for project support environments, version 2.0
[AD-A275191] p 3410 N94-29068
A concurrent, object-based implementation for the tactical level of the rational behavior model
[AD-A275024] p 3410 N94-29115
Towards an information model and mechanisms for design rationale capture and use
[AD-A275060] p 3530 N94-29138
Ada, object-oriented techniques, and concurrency in teaching data structures and file management
[AD-A275385] p 3411 N94-29201
Aerospace Software Engineering for Advanced Systems Architectures
[AGARD-CP-545] p 3412 N94-29315
Object versus functional oriented design p 3413 N94-29321
Experiences with the HOOD design method on avionics software development p 3414 N94-29325
Software engineering methods in the Hermes on-board software p 3414 N94-29326
Rome Laboratory software engineering technology program p 3414 N94-29330
A common Ada run-time system for avionics software p 3150 N94-29331
Software testing practices and their evolution for the 1990's p 3415 N94-29335
Validation and test of complex weapon systems p 3150 N94-29336
Testing Operational Flight Programs (OFPs) p 3415 N94-29337
Integrated formal verification and validation of safety critical software p 3416 N94-29338
A disciplined approach to software test and evaluation p 3416 N94-29339
The UNICON approach to through-life support and evolution of software-intensive systems p 3416 N94-29340
Application of information management methodologies for project quality improvement in a changing environment p 3416 N94-29342
The discipline of defining the software product p 3416 N94-29343
SDE's for the year 2000 and beyond: An EF perspective p 3417 N94-29344
A common approach for an aerospace software environment p 3417 N94-29346
DSSA-ADAGE: An environment for architecture-based avionics development p 3150 N94-29348
Entreprise 2: A PCTE integrated project support environment p 3417 N94-29349
Information engineering implementation and acceptance p 3530 N94-29533
Software Management Environment (SME) concepts and architecture, revision 1
[NASA-CR-189293] p 3419 N94-29727
Engineering specification editing tools
[AD-A275116] p 3419 N94-29746
Using RDD-100 with CoRE. Version 01.00.03
[AD-A275336] p 3419 N94-29797
Research and technology, 1992
[NASA-TM-103996] p 3555 N94-29891
Progress report for the PTUF Project-93 Q1 and Q2
[PB94-138591] p 3431 N94-29995
Software engineering and software management in a distributed UNIX environment
[NLR-TP-92233-U] p 3422 N94-30314

The ergonomics of computer interfaces: Designing a system for human use
[CWI-CS-R9258] p 3402 N94-30320
Graphics in the Views system
[CWI-CS-R9260] p 3422 N94-30322
The Views application environment
[CWI-CS-R9257] p 3423 N94-30341
The real-world navigator
[AIAA PAPER 94-1204-CP] p 3443 N94-30555

SOFTWARE RELIABILITY
Demonstration of improved software support labor estimation for Air Force operational flight programs through functional orientation
[AD-A275789] p 3121 N94-28743
Advanced languages for systems software
[AD-A275272] p 3410 N94-29007
Fault tolerant testbed evaluation, phase 1
[NASA-CR-188275] p 3171 N94-29035
Microcomputer-based protective functions in industrial production systems: Assessment method
[PB94-137817] p 3411 N94-29159
Statistical Modeling and Estimation of Reliability Functions for Software (SMERFS) user's guide, revision 3
[AD-A275390] p 3411 N94-29202
Statistical Modeling and Estimation of Reliability Functions for Software (SMERFS) library access guide, revision 3
[AD-A275405] p 3411 N94-29207
Object versus functional oriented design
p 3413 N94-29321
The development procedures and tools applied for the attitude control software of the Italian satellite SAX
p 3170 N94-29324
Potential software failures methodology analysis
p 3414 N94-29329
A user's guide to the Software Testpilot
[CWI-CS-R9343] p 3426 N94-30435

SOFTWARE REUSE
Automated interface for retrieving reusable software components
[AD-A275004] p 3409 N94-28896
Advanced languages for systems software
[AD-A275272] p 3410 N94-29007
Program derivation by proof transformation
[AD-A275260] p 3453 N94-29304
A common Ada run-time system for avionics software
p 3150 N94-29331
DSSA-ADAGE: An environment for architecture-based avionics development p 3150 N94-29348
Aid to Ada component reuse at Aerospatiale Cannes (France)
[REPT-932-440-102] p 3418 N94-29418
Design reuse experience of space and hazardous operations robots
[AIAA PAPER 94-1220-CP] p 3445 N94-30568

SOFTWARE TOOLS
Work-oriented development of interactive software tools: Understanding the work of software maintainers and making an interactive software tool for them
[PB94-132032] p 3406 N94-28401
Transferable Output ASCII Data (TOAD) editor version 1.0 user's guide
[NASA-CR-187507] p 3408 N94-28818
Business planning model user's guide
[AD-A274978] p 3409 N94-28895
Fault tolerant testbed evaluation, phase 1
[NASA-CR-188275] p 3171 N94-29035
HYPER-NPSNET: Embedded multimedia in a 3D virtual world
[AD-A275063] p 3410 N94-29152
The development procedures and tools applied for the attitude control software of the Italian satellite SAX
p 3170 N94-29324
Rome Laboratory software engineering technology program p 3414 N94-29330
Design of a thinwire real-time multiprocessor operating system p 3415 N94-29333
The UNICON approach to through-life support and evolution of software-intensive systems
p 3416 N94-29340
SDE's for the year 2000 and beyond: An EF perspective p 3417 N94-29344
DSSA-ADAGE: An environment for architecture-based avionics development p 3150 N94-29348
Entreprise 2: A PCTE integrated project support environment p 3417 N94-29349
Microvibrations on a GEO telecommunication satellite
[REPT-932-440-101] p 3168 N94-29415
Aid to Ada component reuse at Aerospatiale Cannes (France)
[REPT-932-440-102] p 3418 N94-29418
ASSIST internals reference manual
[NASA-TM-109102] p 3431 N94-29494
Application of FLUIDNET-G software to the preliminary thermal and hydraulic design of Hermes spaceplane
[REPT-932-440-107] p 3168 N94-29543
A study of the relationship between the performance and dependability of a fault-tolerant computer
[NASA-CR-195758] p 3406 N94-29695
Extending the X Window System
[DE94-006496] p 3420 N94-29844
Addendum to the final report for the investigation of proof techniques within the EVES verification technology
[TR-93-5451-03] p 3421 N94-30155
GNU debugger internal architecture
[DE94-006665] p 3422 N94-30251
Software engineering and software management in a distributed UNIX environment
[NLR-TP-92233-U] p 3422 N94-30314
Modelling interaction tools in the Views architecture
[CWI-CS-R9261] p 3423 N94-30323
A user's guide to the Software Testpilot
[CWI-CS-R9343] p 3426 N94-30435
A simulator for multi-radar analysis for realistic traffic
[AD-B179099] p 3142 N94-30439
A streamlined software environment for situated skills
[AIAA PAPER 94-1205-CP] p 3444 N94-30556
Engineering of systems for application of scientific computing in industry WP project management ISNaS 9209099
[PB94-126232] p 3428 N94-30739

SOHO MISSION
Three high duty cycle, space-qualified mechanisms
p 3162 N94-29642

SOI (SEMICONDUCTORS)
An investigation of distributed coupling in a nonlinear semiconductor waveguide p 3246 N94-29529

SOIL MECHANICS
Toward a molecular scale understanding of frost heaving, phase 1
[AD-A275446] p 3356 N94-28882
The undrained shear strength characteristics of undisturbed soil from fishing port areas
p 3234 N94-29704

SOIL MOISTURE
Sensitivity and feedbacks associated with vegetation-related land surface parameters in a general circulation model p 3348 N94-29800

SOIL SCIENCE
Speciation in Water and Soil: A literature review
[PB94-132388] p 3341 N94-28412
A toy model for estimating N2O emissions from natural soils p 3351 N94-30627
Development of simplified ecosystem models for applications in Earth system studies: The Century experience p 3352 N94-30629
A toy terrestrial carbon flow model
p 3352 N94-30630

SOILS
Speciation in Water and Soil: A literature review
[PB94-132388] p 3341 N94-28412
Growth condition of an ice layer in freezing soils under applied loads. Part 1: Experiment
[AD-A275215] p 3357 N94-29070
Collecting cometary soil samples? Development of the ROSETTA sample acquisition system
p 3160 N94-29628
The undrained shear strength characteristics of undisturbed soil from fishing port areas
p 3234 N94-29704
A toy model for estimating N2O emissions from natural soils p 3351 N94-30627
Development of simplified ecosystem models for applications in Earth system studies: The Century experience p 3352 N94-30629

SOL-GEL PROCESSES
Densification and crystallization of zirconia thin films prepared by sol-gel processing
[DE94-005573] p 3518 N94-30315
Synthesis and characterization of advanced materials for Navy applications p 3223 N94-30474
Silica scintillating materials prepared by sol-gel methods
[DE94-005123] p 3220 N94-30778

SOLAR ACTIVITY
The effects of magnetic storm phases on F-layer irregularities from auroral to equatorial latitudes
[AD-A275203] p 3356 N94-28891
Solar-geophysical data number 591, November 1993. Part 1: Prompt reports. Data for September, October 1993 and late data
[PB94-140548] p 3550 N94-29122
Solar-geophysical data number 592, December 1993. Part 1: Prompt reports. Data for October, November 1993 and late data
[PB94-142130] p 3550 N94-29123
Solar-geophysical data number 592, December 1993. Part 2: Comprehensive reports. Data for June 1993 and miscellaneous
[PB94-142148] p 3550 N94-29124
Solar measurements from the Airglow-Solar Spectrometer Instrument (ASSI) on the San Marco 5 satellite
[NASA-CR-193815] p 3551 N94-30948

SOLAR ACTIVITY EFFECTS
Solar-geophysical data number 591, November 1993. Part 1: Prompt reports. Data for September, October 1993 and late data
[PB94-140548] p 3550 N94-29122
ULF waves and magnetic field characteristics in the polar cusp observed at Godhavn p 3361 N94-29244

SOLAR ARRAYS
Selection of the Space Station Freedom (SSF) Flat Collector Circuit (FCC) insulation material
p 3165 N94-28701
Hypervelocity impact induced arcing and Kapton pyrolization in a plasma environment
[NASA-TM-106528] p 3167 N94-28814
Low Earth orbit durability evaluation of protected silicone for advanced refractive photovoltaic concentrator arrays
[NASA-TM-106543] p 3172 N94-28999
Hypervelocity impact testing of Space Station Freedom solar cells
[NASA-TM-106509] p 3167 N94-29383
The Solar Anomalous and Magnetospheric Particle Explorer (SAMPEX) yo-yo despin and solar array deployment mechanism p 3163 N94-29645
Modal analysis of solar panels using boundary integral equations
[NLT-TP-92218-U] p 3338 N94-30328

SOLAR ATMOSPHERE
The structure of solar magnetic fields and their associated electric currents p 3544 N94-29723

SOLAR CELLS
Advanced development of PV encapsulents
[DE94-000219] p 3336 N94-28500
Silicon-Film (tm) photovoltaic manufacturing technology
[DE94-000258] p 3336 N94-28501
Hypervelocity impact testing of Space Station Freedom solar cells
[NASA-TM-106509] p 3167 N94-29383
Fiber optical solar simulator p 3341 N94-30486
Photovoltaic performance and reliability workshop
[DE94-000236] p 3339 N94-30601
PV Cz silicon manufacturing technology improvements
[DE94-000248] p 3339 N94-30603
Thin EFG octagons
[DE94-000257] p 3339 N94-30605
Crystalline-silicon solar cell development sponsored by the US Department of Energy
[DE94-003783] p 3340 N94-30609
NREL Photovoltaic Program FY 1993 bibliography
[DE94-000272] p 3340 N94-30820

SOLAR COLLECTORS
Quality and efficiency of solar collectors in Sweden
[PB94-137486] p 3337 N94-28909
Low Earth orbit durability evaluation of protected silicone for advanced refractive photovoltaic concentrator arrays
[NASA-TM-106543] p 3172 N94-28999
Performance of the Southern California Edison Company Stirling dish
[DE94-004676] p 3337 N94-29018
Crystalline-silicon solar cell development sponsored by the US Department of Energy
[DE94-003783] p 3340 N94-30609

SOLAR CORONA
Remote sensing of inner heliospheric plasmas
[AD-A275021] p 3550 N94-29132
Correlative analysis of hard and soft x ray observations of solar flares
[NASA-CR-189329] p 3551 N94-29453
Coronal abundances and their variation
[NASA-CR-195767] p 3551 N94-29858

SOLAR CYCLES
Experimental investigation of possible geomagnetic feedback from energetic (0.1 to 16 keV) terrestrial O(+) ions in the magnetotail current sheet
[PAPER-93JA01991] p 3507 N94-30128

SOLAR DYNAMIC POWER SYSTEMS
Performance and durability of high emittance heat receiver surfaces for solar dynamic power systems
[NASA-TM-106549] p 3172 N94-28834

SOLAR ELECTRONS
Correlative analysis of hard and soft x ray observations of solar flares
[NASA-CR-189329] p 3551 N94-29453

SOLAR ENERGY
Cosmic energy equipment p 3229 N94-28945
Analysis and modeling of environmental and economic impacts of the solar hydrogen energy system
p 3348 N94-29901

Interagency advanced power group: Solar working group
[DE94-004953] p 3340 N94-30833
SOLAR ENERGY CONVERSION
Performance of the Southern California Edison Company Stirling dish
[DE94-004676] p 3337 N94-29018
SOLAR FLARES
Identification of an unexpected space radiation hazard
[AD-A275170] p 3552 N94-29046
Remote sensing of inner heliospheric plasmas
[AD-A275021] p 3550 N94-29132
Correlative analysis of hard and soft x ray observations of solar flares
[NASA-CR-189329] p 3551 N94-29453
SOLAR FLUX
The effects of magnetic storm phases on F-layer irregularities from auroral to equatorial latitudes
[AD-A275203] p 3356 N94-28891
Production of fullerenes with concentrated solar flux
[DE94-000266] p 3514 N94-29801
Radiative flux calculations at UV and visible wavelengths
[DE94-004278] p 3350 N94-30613
Recent results from SAGE
[DE94-006229] p 3551 N94-30845
SOLAR FLUX DENSITY
Accurate modeling of F-region electron densities
[NASA-CR-195781] p 3364 N94-30014
SOLAR FURNACES
Production of fullerenes with concentrated solar flux
[DE94-000266] p 3514 N94-29801
SOLAR INSTRUMENTS
NASA Marshall Space Flight Center Solar Observatory report, July - October 1993
[NASA-TM-108448] p 3160 N94-29470
Solar neutrino experiments: An update
[DE94-006061] p 3551 N94-30884
SOLAR MAGNETIC FIELD
Solar-geophysical data number 591, November 1993. Part 1: Prompt reports. Data for September, October 1993 and late data
[PB94-140548] p 3550 N94-29122
The structure of solar magnetic fields and their associated electric currents p 3544 N94-29723
Solar measurements from the Airglow-Solar Spectrometer Instrument (ASSI) on the San Marco 5 satellite
[NASA-CR-193815] p 3551 N94-30948
SOLAR NEUTRINOS
Recent results from SAGE
[DE94-006229] p 3551 N94-30845
Solar neutrino experiments: An update
[DE94-006061] p 3551 N94-30884
SOLAR OBSERVATORIES
NASA Marshall Space Flight Center Solar Observatory report, July - October 1993
[NASA-TM-108448] p 3160 N94-29470
SOLAR PHYSICS
Solar-geophysical data number 591, November 1993. Part 1: Prompt reports. Data for September, October 1993 and late data
[PB94-140548] p 3550 N94-29122
Solar-geophysical data number 592, December 1993. Part 1: Prompt reports. Data for October, November 1993 and late data
[PB94-142130] p 3550 N94-29123
Solar-geophysical data number 592, December 1993. Part 2: Comprehensive reports. Data for June 1993 and miscellaneous
[PB94-142148] p 3550 N94-29124
SOLAR PLANETARY INTERACTIONS
ULF waves and magnetic field characteristics in the polar cusp observed at Godhavn p 3361 N94-29244
SOLAR RADIATION
The automated rotating shadowband spectroradiometer
[DE94-001878] p 3269 N94-28464
Solar measurements from the Airglow-Solar Spectrometer Instrument (ASSI) on the San Marco 5 satellite
[NASA-CR-193815] p 3551 N94-30948
SOLAR RADIATION SHIELDING
Lunar surface operations. Volume 1: Lunar surface emergency shelter
[NASA-CR-195551] p 3299 N94-29354
SOLAR RADIO EMISSION
The Rb 780-nanometer Faraday anomalous dispersion optical filter: Theory and experiment p 3250 N94-29659
SOLAR REFLECTORS
An outdoor exposure testing program for optical materials used in solar thermal electric technologies
[DE94-000265] p 3500 N94-29799
SOLAR SIMULATORS
Fiber optical solar simulator p 3341 N94-30486
SOLAR SPECTRA
Fiber optical solar simulator p 3341 N94-30486
Solar measurements from the Airglow-Solar Spectrometer Instrument (ASSI) on the San Marco 5 satellite
[NASA-CR-193815] p 3551 N94-30948
SOLAR SPECTROMETERS
Solar measurements from the Airglow-Solar Spectrometer Instrument (ASSI) on the San Marco 5 satellite
[NASA-CR-193815] p 3551 N94-30948
SOLAR SYSTEM
Imaging spectrometry of the Earth and other solar system bodies p 3237 N94-29779
SOLAR TERRESTRIAL INTERACTIONS
Solar-geophysical data number 591, November 1993. Part 1: Prompt reports. Data for September, October 1993 and late data
[PB94-140548] p 3550 N94-29122
A study of the formation and dynamics of the Earth's plasma sheet using ion composition data
[NASA-CR-195119] p 3507 N94-30126
Experimental investigation of possible geomagnetic feedback from energetic (0.1 to 16 keV) terrestrial O(+) ions in the magnetotail current sheet
[PAPER-93JA01991] p 3507 N94-30128
SOLAR THERMAL ELECTRIC POWER PLANTS
An outdoor exposure testing program for optical materials used in solar thermal electric technologies
[DE94-000265] p 3500 N94-29799
SOLAR WIND
Identification of an unexpected space radiation hazard
[AD-A275170] p 3552 N94-29046
Remote sensing of inner heliospheric plasmas
[AD-A275021] p 3550 N94-29132
Proceedings of the NIPR Symposium on Upper Atmosphere Physics, no. 6
[JTN-94-80593] p 3359 N94-29233
Signatures of dayside solar wind/magnetosphere/ionosphere coupling as revealed by the pace HF radars and associated experiments p 3359 N94-29236
A theory of current generator in the magnetosphere-ionosphere coupling p 3360 N94-29240
A study of the formation and dynamics of the Earth's plasma sheet using ion composition data
[NASA-CR-195119] p 3507 N94-30126
SOLAR X-RAYS
Solar-geophysical data number 592, December 1993. Part 2: Comprehensive reports. Data for June 1993 and miscellaneous
[PB94-142148] p 3550 N94-29124
Coronal abundances and their variation
[NASA-CR-195767] p 3551 N94-29858
SOLDERED JOINTS
Surface tension of tin and its alloys with particular reference to solders
[PB94-138302] p 3204 N94-29119
Microstructural development and mechanical behavior of eutectic bismuth-tin and eutectic indium-tin in response to high temperature deformation
[DE94-005202] p 3210 N94-30710
SOLDERING
Intermetallic growth at the interface between copper and bismuth-tin solder
[AD-A275716] p 3202 N94-28643
Logistics for the implementation of lead-free solders on electronic assemblies
[DE94-004800] p 3206 N94-29936
SOLDERS
Intermetallic growth at the interface between copper and bismuth-tin solder
[AD-A275716] p 3202 N94-28643
Surface tension of tin and its alloys with particular reference to solders
[PB94-138302] p 3204 N94-29119
Logistics for the implementation of lead-free solders on electronic assemblies
[DE94-004800] p 3206 N94-29936
Microstructural development and mechanical behavior of eutectic bismuth-tin and eutectic indium-tin in response to high temperature deformation
[DE94-005202] p 3210 N94-30710
SOLENOIDS
The static and nonstatic electrical solenoids
[DE94-606326] p 3261 N94-28585
Estimating the cost of large superconducting thin solenoid magnets
[DE94-006289] p 3468 N94-30026
Third-order beam optics of real solenoid magnetic lens
[DE94-608014] p 3500 N94-30084
SOLID ELECTROLYTES
Fuel Cell Seminar, 1992: Program and abstracts
[DE94-003882] p 3336 N94-28472
Enhanced ion dissociation of LiCF3SO3 by new carbonate plasticizers: Raman and IR studies
[DE94-005448] p 3485 N94-28741
Method for forming thin composite solid electrolyte film for lithium batteries
[NASA-CASE-NPO-18877-1-CU] p 3264 N94-29357
SOLID LUBRICANTS
XPS analysis of 440C steel surfaces lubricated with perfluoropolyethers under sliding conditions in high vacuum
[NASA-TM-106548] p 3218 N94-30177
SOLID PHASES
Interstitially stabilized phases in the zirconium-nickel system
[DE94-005561] p 3201 N94-28525
Directional solidification studies in Ni-Al alloys
[DE94-005562] p 3201 N94-28527
Experimental and theoretical studies of molecular solids
[AD-A275511] p 3485 N94-28668
SOLID PROPELLANT IGNITION
Development of a new generation solid rocket motor ignition computer code
[NASA-CR-195734] p 3171 N94-28800
A study of solid propellants using a microprobe mass spectrometer system
[AD-A275325] p 3224 N94-28879
Correlation of cookoff behavior of rocket propellants with thermomechanical and thermochemical properties
[AD-A274983] p 3224 N94-29092
SOLID PROPELLANT ROCKET ENGINES
Research and development of ramjets/ramrockets. Part 1: Integral solid propellant ramrockets p 3151 N94-29294
A variable selection heuristic for solid rocket motor design p 3173 N94-29544
SOLID PROPELLANTS
A study of solid propellants using a microprobe mass spectrometer system
[AD-A275325] p 3224 N94-28879
SOLID ROCKET PROPELLANTS
Introduction and overview of research and development of solid propellant ramrockets, liquid fuel ramjets and experimental hydrogen ram combustors p 3151 N94-29292
Research and development of ramjets/ramrockets. Part 1: Integral solid propellant ramrockets p 3151 N94-29294
SOLID STATE DEVICES
Solid-state, active-phased arrays: Some aspects of receiver design
[AD-A275893] p 3527 N94-28779
Fabrication of electronic materials in space p 3228 N94-28942
The 100 kA, 5000 V solid-state opening switch for inductive energy storage
[AD-A274993] p 3263 N94-28994
Miniaturization in x ray and gamma ray spectroscopy p 3236 N94-29773
SOLID STATE LASERS
Dynamics of a coupled solid state laser array p 3294 N94-29551
Solid state laser systems for space application
[NASA-CR-195777] p 3294 N94-29914
Remote pumping of solid state lasers with nuclear driven fluorescers
[DE94-004846] p 3296 N94-30614
Diode-pumped solid-state-laser drivers and the competitiveness of inertial fusion energy
[DE94-006654] p 3296 N94-30830
SOLID-SOLID INTERFACES
Effect of microstructure on the strength and fracture energy of bimaterial interfaces
[AD-A274987] p 3178 N94-29126
Interface engineering in alumina fiber/glass composites p 3182 N94-29852
A solid-on-solid invasion percolation model for self-affine interfaces
[DE94-608102] p 3521 N94-30888
SOLIDIFICATION
Melt flow during alloy solidification: Dimensional analysis and model problems
[PB94-138625] p 3206 N94-29997
Volume averaged model for the mechanics of alloys solidification
[PB94-138617] p 3208 N94-30113
Near-net-shape manufacturing: Spray-formed metal matrix composites and tooling p 3186 N94-30447
Terfenol: A study of the phase equilibrium diagram and the solidification process
[DE94-004883] p 3209 N94-30690
Survey report of JSUP Space Environment Utilization Research Committee in fiscal year 1992: Metallic Materials Session
[JTN-94-80583] p 3159 N94-30794

SOLIDS
Laser-material interactions: A study of laser energy coupling with solids
[DE94-005212] p 3292 N94-28478
Two-phase power-law modeling of pipe flows displaying shear-thinning phenomena
[DE94-005115] p 3279 N94-30020
Calculation of inelastic mean free path and stopping power for electrons in solids from an optical-data model
[USIP-92-06] p 3494 N94-30980
SOLITARY WAVES
Papers in meteorology and geophysics, vol. 44, no.1
[JTN-94-80585] p 3324 N94-28693
On the linear stability of Verkley's modons
p 3324 N94-28695
A note on the Poisson brackets associated with Lax operators
[MATHS-REPT-A-195] p 3464 N94-29482
Forced generation of solitary waves in a rotating fluid and their stability p 3274 N94-29689
A relativistic solitary wave in electron positron plasma
[DE94-608107] p 3507 N94-30071
Langmuir waves in the electron-positron plasma
[DE94-608330] p 3508 N94-30191
SOLUBILITY
Solubility of Nd in brine
[DE94-005099] p 3187 N94-28567
Crystallization of silver chromate from ethanol via salt metathesis reactions of solubilized precursors
[AD-A275178] p 3189 N94-29058
SOLUTIONS
Computer simulation of molecular interactions in supercritical solvents
[AD-A274977] p 3486 N94-29087
SOLVENT EXTRACTION
Molecular structure of coal studied by solvent extraction p 3187 N94-28676
Methanol-mediated continuous extraction of phenolic compounds from coal liquid p 3188 N94-28679
SOLVENTS
Solubility of Nd in brine
[DE94-005099] p 3187 N94-28567
Computer simulation of molecular interactions in supercritical solvents
[AD-A274977] p 3486 N94-29087
Poly(arylene ether-co-imidazole)s as toughness modifiers for epoxy resins
[NASA-CASE-LAR-15229-1-CU] p 3215 N94-29451
Non-aqueous cleaning solvent substitution
[DE94-005339] p 3219 N94-30245
Non-aqueous cleaning solvent substitution
p 3354 N94-30466
Supersonic gas-liquid cleaning system
p 3240 N94-30467
Regenerating using aqueous cleaners with ozone and electrolysis p 3240 N94-30468
Theory for electron-transfer reactions involving two Marcus surfaces with a different force constant
[DE94-005925] p 3493 N94-30874
SONAR
Seafloor characterization using texture
[AD-A275399] p 3377 N94-29204
Design of the biosonar simulator for dolphin's clicks waveform reproduction p 3234 N94-29707
Sonar sensing and obstable detection
p 3309 N94-30301
Iterative removal of boundary minima of harmonic potential function for mobile robot navigation
[REPT-93-059] p 3449 N94-30962
SONIC BOOMS
Numerical analysis of sonic boom in the near field
p 3125 N94-28962
Subjective response to sonic booms having different shapes, rise times, and durations
[NASA-TM-109090] p 3479 N94-29464
SOOT
Numerical prediction of turbulent sooting diffusion flames p 3191 N94-29253
Measurements and predictions of the combustion characteristics of enclosed swirl-stabilized propane flames
[IECE-CFE-TR-001] p 3198 N94-30017
SOUND DETECTING AND RANGING
A review of signal detection using the bispectrum with applications in underwater acoustics
[AD-A275227] p 3478 N94-29388
SOUND FIELDS
Characterization of structural vibration: Field descriptors based on energy density and intensity
[PB94-132230] p 3316 N94-28404
SOUND GENERATORS
Analysis of spark-induced bubble experiments using CALE
[DE94-003667] p 3270 N94-28476
Design of the biosonar simulator for dolphin's clicks waveform reproduction p 3234 N94-29707
Experiments on the aerodynamic generation of noise in centrifugal turbomachinery p 3480 N94-30804
SOUND INTENSITY
Minutes. Accredited Standards Committee on Noise, S12. US tag for ISO/TC 43/SC1 noise and ISO/TC 94/SC12 hearing protection
[AD-A275622] p 3477 N94-28636
Subjective response to sonic booms having different shapes, rise times, and durations
[NASA-TM-109090] p 3479 N94-29464
SOUND PRESSURE
Quadruplet expansion of the acoustic pressure field in a wedge shaped ocean
[AD-A275121] p 3477 N94-29003
A comparison of two computer models of sound propagation for a wedge shaped ocean over a penetrable bottom
[AD-A275031] p 3477 N94-29117
Determination of sound power levels of air terminal units according to ISO 5135-Nordic inter-laboratory tests, Nordtest project no. 968-91
[PB94-137411] p 3477 N94-29175
Report of National Institute for Resources and Environment. No. 8: Research on blasting sound related to it's measurement, propagation prediction, control and evaluation
[JTN-94-80605] p 3479 N94-29597
Modal analysis of solar panels using boundary integral equations
[NLT-TP-92218-U] p 3338 N94-30328
SOUND PROPAGATION
A comparison of two computer models of sound propagation for a wedge shaped ocean over a penetrable bottom
[AD-A275031] p 3477 N94-29117
Attenuation of outdoor sound propagation levels by a snow cover
[AD-A275387] p 3478 N94-29314
A non-local computational boundary condition for duct acoustics
[NASA-TM-109091] p 3478 N94-29382
Report of National Institute for Resources and Environment. No. 8: Research on blasting sound related to it's measurement, propagation prediction, control and evaluation
[JTN-94-80605] p 3479 N94-29597
SOUND RANGING
Sonar sensing and obstable detection
p 3309 N94-30301
SOUND TRANSDUCERS
Design of the biosonar simulator for dolphin's clicks waveform reproduction p 3234 N94-29707
Sensing the gas metal arc welding process
p 3314 N94-30444
SOUND TRANSMISSION
A comparison of two computer models of sound propagation for a wedge shaped ocean over a penetrable bottom
[AD-A275031] p 3477 N94-29117
SOUND WAVES
Broad geoacoustic assessment of some regional areas
[AD-A275504] p 3356 N94-28791
Analysis of 3-D acoustic problems using boundary element method p 3127 N94-28974
Quadruplet expansion of the acoustic pressure field in a wedge shaped ocean
[AD-A275121] p 3477 N94-29003
Considerations in the modelling of seafloor acoustic backscatter
[AD-A275404] p 3478 N94-29206
Improved in-flow acoustic sensor
[NASA-CASE-ARC-12001-1] p 3478 N94-29363
A non-local computational boundary condition for duct acoustics
[NASA-TM-109091] p 3478 N94-29382
Report of National Institute for Resources and Environment. No. 8: Research on blasting sound related to it's measurement, propagation prediction, control and evaluation
[JTN-94-80605] p 3479 N94-29597
Design of the biosonar simulator for dolphin's clicks waveform reproduction p 3234 N94-29707
Convective turbulence and transport in stars
p 3546 N94-29913
SOUNDING ROCKETS
Time series comparisons of satellite and rocketsonde temperatures in 1978-1979
[NASA-TP-3409] p 3370 N94-29455
SOUTHERN HEMISPHERE
Generation mechanisms of quasi-stationary waves in the Southern Hemisphere p 3365 N94-30789
SOUTHERN OSCILLATION
Interannual-decadal variability in tropical climate systems: Stable isotope records and general circulation model experiments p 3373 N94-29962
On interannual variability and climate change in the North Pacific p 3374 N94-29963
Satellite estimation of the global distribution and interannual variability of photosynthetically active radiation p 3334 N94-29970
SPACE ADAPTATION SYNDROME
Japanese Journal of Aerospace and Environmental Medicine, volume 30, no. 1
[JTN-94-80598] p 3389 N94-28850
Space and vertigo: In relation to space motion sickness p 3390 N94-28857
The MERSS 5th Symposium on Space Medicine: Medical and Physiological Experiment Utilizing Parabolic Flight
[JTN-94-80588] p 3392 N94-29709
SPACE BASED RADAR
Ground independent landing system
p 3137 N94-29564
Pointing mechanisms for the Shuttle Radar Laboratory
p 3162 N94-29638
SPACE COMMERCIALIZATION
The MERSS 5th Symposium on Space Medicine: Medical and Physiological Experiment Utilizing Parabolic Flight
[JTN-94-80588] p 3392 N94-29709
Start of space tourism p 3164 N94-29714
SPACE COMMUNICATION
Lasercom system architecture with reduced complexity
[NASA-CASE-NPO-19069-1-CU] p 3293 N94-29493
The Telecommunications and Data Acquisition Report
[NASA-CR-195694] p 3246 N94-29613
Design and analysis of a low-loss linear analog phase modulator for deep space spacecraft X-band transponder applications p 3248 N94-29625
The Rb 780-nanometer Faraday anomalous dispersion optical filter: Theory and experiment
p 3250 N94-29659
Optimizing the Galileo space communication link
p 3250 N94-29663
Decoder synchronization for deep space missions
p 3250 N94-29664
SPACE DEBRIS
Orbital debris radar instrumentation
p 3248 N94-29626
Vulnerability of manned spacecraft to crew loss from orbital debris penetration
[NASA-TM-108452] p 3169 N94-30161
Space debris removal using a high-power ground-based laser
[DE94-006363] p 3169 N94-30264
SPACE ENVIRONMENT SIMULATION
Technology for robotic surface inspection in space
[AIAA PAPER 94-1193-CP] p 3442 N94-30544
SPACE ERECTABLE STRUCTURES
Deployable reflector structure
[NASA-CASE-LAR-14513-1-SB] p 3245 N94-29360
A module concept for a cable-mesh deployable antenna p 3161 N94-29631
Low melting temperature alloy deployment mechanism and recent experiments p 3163 N94-29644
SPACE EXPLORATION
MUADEE: Mars Upper Atmosphere Dynamics, Energetics, and Evolution discovery mission. Executive summary volume
[NASA-CR-195732] p 3549 N94-28418
The Pluto fast flyby mission: Completing the reconnaissance of the solar system
p 3235 N94-29768
Smart focal-plane technology for micro-instruments and micro-rovers p 3237 N94-29780
SPACE FLIGHT
NASA space and Earth science data on CD-ROM
[NASA-TM-109709] p 3528 N94-28414
SPACE FLIGHT FEEDING
Japanese Journal of Aerospace and Environmental Medicine, vol. 30, no. 3
[JTN-94-80606] p 3387 N94-28495
Some issues on Japan's space food development and relating preliminary experimental study
p 3388 N94-28498
SPACE HABITATS
Summary report of mission acceleration measurements for Spacehab-01, STS-57 launched 21 June 1993
[NASA-TM-106514] p 3168 N94-29757
SPACE HEATING (BUILDINGS)
Maintaining acceptable thermal comfort with a low air temperature by means of local heating
[PB94-138526] p 3401 N94-29950
Control of heating, ventilation and air conditioning (HVAC) systems
[PB94-138807] p 3401 N94-30000
SPACE MAINTENANCE
System for the installation and replacement of components in hostile environments
[NASA-CASE-LEW-14906-1-SB] p 3300 N94-29427

Extra-vehicular activity translation tool
[NASA-CASE-MSC-21955-1] p 3300 N94-29428
SPACE MANUFACTURING
Overview of space environment utilization science
[JTN-94-80581] p 3227 N94-28938
Fluid and transportation phenomena under microgravity p 3227 N94-28939
Combustion studies under microgravity p 3228 N94-28940
Glass studies under microgravity p 3228 N94-28941
Fabrication of electronic materials in space p 3228 N94-28942
Protein crystal growth in microgravity p 3228 N94-28943
Cell culture in space p 3228 N94-28944
Cosmic energy equipment p 3229 N94-28945
Laser beam welding of AISI 316 stainless steel in microgravity environment: Experiments aboard a KC-135 flight
[ISBN-0-315-86095-2] p 3229 N94-30145
Survey report of JSUP Space Environment Utilization Research Committee in fiscal year 1992: Functional New Materials Session
[JTN-94-80582] p 3159 N94-30162
Survey report of JSUP Space Environment Utilization Research Committee in fiscal year 1992: Metallic Materials Session
[JTN-94-80583] p 3159 N94-30794
SPACE MISSIONS
MUADEE: Mars Upper Atmosphere Dynamics, Energetics, and Evolution discovery mission. Executive summary volume
[NASA-CR-195732] p 3549 N94-28418
Decoder synchronization for deep space missions p 3250 N94-29664
SPACE NAVIGATION
Fault tolerant testbed evaluation, phase 1
[NASA-CR-188275] p 3171 N94-29035
Enhanced orbit determination filter sensitivity analysis: Error budget development p 3159 N94-29655
Miniature wide field-of-view star trackers for spacecraft attitude sensing and navigation p 3144 N94-29794
A guidance and navigation system for two spacecraft rendezvous in translunar halo orbit p 3142 N94-29837
SPACE OBSERVATIONS (FROM EARTH)
Correlation studies of Pioneer Venus imagery obtained from PV experiments with near IR imagery obtained from ground-based observations during Venus inferior conjunction
[NASA-CR-195772] p 3550 N94-29892
SPACE PERCEPTION
Disturbance of equilibrium on JAL flight crew p 3390 N94-28856
An investigation of stereopsis with AN/AVS-6 night vision goggles at varying levels of illuminance and contrast
[AD-A275332] p 3400 N94-28918
Extended occupancy grid method for modelling unknown dynamic environments p 3144 N94-30281
Using stereoscopic imaging for visualization applications
[DE94-006247] p 3536 N94-30706
SPACE PLASMAS
Equation of state of stellar plasmas
[DE94-004186] p 3542 N94-28526
Electron beams at geosynchronous orbit
[AD-A275471] p 3355 N94-28684
Active electron and ion beam experiments in space
[AD-A275570] p 3504 N94-28828
Computer simulations on development of the fast reconnection mechanism p 3360 N94-29241
Waves in space plasma dipole antenna subsystem p 3161 N94-29632
Coronal temperatures of unusually active K-dwarf binary systems
[NASA-CR-189335] p 3545 N94-29861
Simulation of space-energy distributions of hot plasma on a geostationary orbit
[DE94-607324] p 3365 N94-30107
A single-fluid, self-consistent formulation of particle transport and fluid dynamics p 3260 N94-30352
SPACE POWER REACTORS
SP-100 control drive assembly development p 3163 N94-29651
Performance of CVD and CVR coated carbon-carbon in high temperature hydrogen
[DE94-005451] p 3487 N94-29841
Small low mass advanced PBR's for propulsion
[DE94-005142] p 3497 N94-30588
TOPAZ 2 system description
[DE94-006230] p 3498 N94-30846
The TOPAZ 2 space reactor response under accident conditions
[DE94-004998] p 3498 N94-30847
SPACE PROCESSING
Survey report of JSUP Space Environment Utilization Research Committee in fiscal year 1992: Protein Crystal Growth Session
[JTN-94-80584] p 3158 N94-28583
Overview of space environment utilization science
[JTN-94-80581] p 3227 N94-28938
Fluid and transportation phenomena under microgravity p 3227 N94-28939
Combustion studies under microgravity p 3228 N94-28940
Glass studies under microgravity p 3228 N94-28941
Fabrication of electronic materials in space p 3228 N94-28942
Protein crystal growth in microgravity p 3228 N94-28943
Cell culture in space p 3228 N94-28944
Cosmic energy equipment p 3229 N94-28945
Plasma heating for containerless and microgravity materials processing
[NASA-CASE-NPO-18819-1-CU] p 3229 N94-29371
The 1992-1993 advanced design program. Part 1: The Mars methane engine project. Part 2: The Mars oxygen processor new furnace
[NASA-CR-195513] p 3299 N94-29409
Thermal enclosure system functional simulation user's manual
[NASA-TM-109094] p 3466 N94-29489
Directional solidification characteristics of hyper-eutectic Al-Cu alloys under varying gravity conditions
[ISBN-0-315-86108-8] p 3209 N94-30146
Survey report of JSUP Space Environment Utilization Research Committee in fiscal year 1992: Functional New Materials Session
[JTN-94-80582] p 3159 N94-30162
Survey report of JSUP Space Environment Utilization Research Committee in fiscal year 1992: Metallic Materials Session
[JTN-94-80583] p 3159 N94-30794
SPACE RENDEZVOUS
A guidance and navigation system for two spacecraft rendezvous in translunar halo orbit p 3142 N94-29837
SPACE SHUTTLE BOOSTERS
Development of a new generation solid rocket motor ignition computer code
[NASA-CR-195734] p 3171 N94-28800
Development of a unique polyurethane primer/topcoat p 3223 N94-30476
SPACE SHUTTLE MAIN ENGINE
Mechanical flexible joint design document
[NASA-CR-193941] p 3297 N94-28419
Composite load spectra for select space propulsion structural components
[NASA-CR-194476] p 3316 N94-28508
Specialized data analysis of SSME and advanced propulsion system vibration measurements
[NASA-CR-193940] p 3174 N94-29868
SPACE SHUTTLE MISSIONS
Summary report of mission acceleration measurements for Spacehab-01, STS-57 launched 21 June 1993
[NASA-TM-106514] p 3168 N94-29757
SPACE SHUTTLE ORBITERS
Extra-vehicular activity translation tool
[NASA-CASE-MSC-21955-1] p 3300 N94-29428
Waves in space plasma dipole antenna subsystem p 3161 N94-29632
SPACE SHUTTLE PAYLOADS
Retention latch mechanism for the Wake Shield Facility p 3161 N94-29635
Pointing mechanisms for the Shuttle Radar Laboratory p 3162 N94-29638
Summary report of mission acceleration measurements for Spacehab-01, STS-57 launched 21 June 1993
[NASA-TM-106514] p 3168 N94-29757
SPACE SHUTTLES
SOCRATES simulation of the emission at wavelength 6300 A generated by the interaction between the atmosphere and the Space Shuttle exhaust
[AD-A275567] p 3164 N94-28827
Wind tunnel testing and research
[NASA-CR-188273] p 3156 N94-29052
Wave generation by contaminant ions near a large spacecraft
[NASA-CR-195797] p 3169 N94-29917
Local interaction control for space construction p 3170 N94-30960
SPACE STATION FREEDOM
Selection of the Space Station Freedom (SSF) Flat Collector Circuit (FCC) insulation material p 3165 N94-28701
Hypervelocity impact testing of Space Station Freedom solar cells
[NASA-TM-106509] p 3167 N94-29383
Electric power system test and verification program
[NASA-TM-106405] p 3169 N94-30123
A Space Station robot walker and its shared control software
[AIAA PAPER 94-1192-CP] p 3442 N94-30543
SPACE STATION POWER SUPPLIES
Hypervelocity impact induced arcing and Kapton pyrolization in a plasma environment
[NASA-TM-106528] p 3167 N94-28814
Electric power system test and verification program
[NASA-TM-106405] p 3169 N94-30123
SPACE STATIONS
Heavy-lift vehicle-launched Space Station method and apparatus
[NASA-CASE-MSC-21760-1] p 3160 N94-29369
Technology transfer and evaluation for Space Station telerobotics
[AIAA PAPER 94-1190-CP] p 3441 N94-30541
Local interaction control for space construction p 3170 N94-30960
SPACE STORAGE
Large scale cryogenic fluid systems testing
[NASA-TM-109735] p 3157 N94-29904
SPACE TEMPERATURE
Determining noise temperatures in beam waveguide systems p 3249 N94-29657
SPACE TOOLS
Extra-vehicular activity translation tool
[NASA-CASE-MSC-21955-1] p 3300 N94-29428
SPACE TRANSPORTATION
A transportronic solution to the problem of interorbital transportation
[NASA-CR-191152] p 3164 N94-29355
SPACE TRANSPORTATION SYSTEM FLIGHTS
Physiological Anatomical Rodent Experiment (PARE) .04 feasibility test 2
[NASA-CR-195210] p 3385 N94-29968
SPACE VEHICLE CHECKOUT PROGRAM
The MACS-TSA applied in the ISO and SAX spacecraft projects
[PB94-126257] p 3170 N94-30857
SPACE-TIME FUNCTIONS
Numerical analysis and computation of nonlinear partial differential equations from applied mathematics
[AD-A275582] p 3451 N94-28723
Three forms of relativity
[DE94-606338] p 3523 N94-28782
Anomalous algebraic structures in quantum field theories p 3524 N94-29911
On dyonic black holes and cosmic censorship p 3546 N94-29912
Physics, astronomy, and astrophysics: A numerical study of the black hole plus Brill wave spacetime p 3540 N94-29990
Theory of fundamental interactions
[DE94-608126] p 3525 N94-30169
SPACEBORNE EXPERIMENTS
Overview of space environment utilization science
[JTN-94-80581] p 3227 N94-28938
Cryogenic on-orbit liquid depot storage acquisition and transfer (COLD-SAT) experiment subsystem instrumentation and wire harness design report
[NASA-CR-189172] p 3168 N94-29405
GOME: Global Ozone Monitoring Experiment
[ESA-SP-1151] p 3347 N94-29452
Analysis of selected materials flown on interior locations of the Long Duration Exposure Facility
[NASA-CR-4586] p 3175 N94-29458
Thermal enclosure system functional simulation user's manual
[NASA-TM-109094] p 3466 N94-29489
Retention latch mechanism for the Wake Shield Facility p 3161 N94-29635
Study of activation data of metal samples from LDEF-1 and Spacelab-2
[NASA-CR-195802] p 3205 N94-29736
Summary report of mission acceleration measurements for Spacehab-01, STS-57 launched 21 June 1993
[NASA-TM-106514] p 3168 N94-29757
Microgravity fluid science research in Europe
[AD-B179178] p 3229 N94-30409
Microencapsulation of anti-tumor, antibiotic and thrombolytic drugs in microgravity p 3397 N94-30453
A Modular Artificial Intelligence Inference Engine System (MAIS) for support of on orbit experiments
[AIAA PAPER 94-1237-CP] p 3448 N94-30584
SPACEBORNE LASERS
Lasercom system architecture with reduced complexity
[NASA-CASE-NPO-19069-1-CU] p 3293 N94-29493
GLRS-R 2-colour retroreflector target design and predicted performance
[REPT-932-440-106] p 3246 N94-29542
The Rb 780-nanometer Faraday anomalous dispersion optical filter: Theory and experiment p 3250 N94-29659

Solid state laser systems for space application
[NASA-CR-195777] p 3294 N94-29914

SPACEBORNE TELESCOPES
An Earth observation telescope refocusing mechanism
[REPT-932-440-103] p 3332 N94-29417
Providing hydrogen maser timing stability to orbiting VLBI radio telescope observations by post-measurement compensation of linked frequency standard imperfections p 3297 N94-30670

SPACECRAFT ANTENNAS
A comparison of full-spectrum and complex-symbol combining techniques for the Galileo S-band mission p 3250 N94-29665

SPACECRAFT CHARGING
Active electron and ion beam experiments in space
[AD-A275570] p 3504 N94-28828

SPACECRAFT COMMUNICATION
The Telecommunications and Data Acquisition Report
[NASA-CR-195689] p 3249 N94-29652
High-resolution robot tracking and direction finding for space station environment p 3168 N94-29896

SPACECRAFT COMPONENTS
Second NASA Workshop on Wiring for Space Applications
[NASA-CP-3244] p 3165 N94-28697
ESTEC wiring test programme materials related properties p 3165 N94-28698
Robust 300 C wire insulation system p 3165 N94-28699
NASA wiring program: Survey of NASA experiences in wiring system safety p 3165 N94-28700
Metal band drives in spacecraft mechanisms p 3162 N94-29637
The use of screening tests in spacecraft lubricant evaluation p 3162 N94-29641
Advanced microfabrication technologies for microspacecraft p 3171 N94-29782

SPACECRAFT CONSTRUCTION MATERIALS
NASA Parts Project Office: Basic goals p 3166 N94-28703
Electrical and mechanical testing of wire insulation for space applications p 3166 N94-28710
Evaluation of pyrolysis and arc tracking on candidate wire insulation designs for space applications p 3166 N94-28711
Wire insulation degradation and flammability in low gravity p 3166 N94-28712
Advanced microfabrication technologies for microspacecraft p 3171 N94-29782
Survey report of JSUP Space Environment Utilization Research Committee in fiscal year 1992: Functional New Materials Session
[JTN-94-80582] p 3159 N94-30162
Composite hot drape forming p 3240 N94-30448
Casting of weldable graphite/magnesium metal matrix composites with built-in metallic inserts p 3186 N94-30482

SPACECRAFT CONTROL
General theory and algorithms for the non-casual inversion, slewing and control of space-based articulated structures
[AD-A275118] p 3167 N94-29002
Software engineering methods in the Hermes on-board software p 3414 N94-29326
Micro guidance and control technology overview p 3144 N94-29772
Miniature wide field-of-view star trackers for spacecraft attitude sensing and navigation p 3144 N94-29794
Activities of Ishikawajima-Harima Heavy Industries Co. Ltd.
[PB94-137981] p 3555 N94-29798
Local interaction control for space construction p 3170 N94-30960

SPACECRAFT DESIGN
ESTEC wiring test programme materials related properties p 3165 N94-28698
Code development for hypersonic real-gas flow simulations toward the design of space vehicles, part 2 p 3125 N94-28966
The Solar Anomalous and Magnetospheric Particle Explorer (SAMPEX) yo-yo despin and solar array deployment mechanism p 3163 N94-29645
Analysis of EDP performance
[NASA-CR-195726] p 3420 N94-29945
The MACS-TSA applied in the ISO and SAX spacecraft projects
[PB94-126257] p 3170 N94-30857

SPACECRAFT DOCKING
Development and testing of the Automated Fluid Interface System p 3161 N94-29636
Local interaction control for space construction p 3170 N94-30960

SPACECRAFT ELECTRONIC EQUIPMENT
Time maintenance system for the BMDO MSX spacecraft p 3171 N94-30672

SPACECRAFT ENVIRONMENTS
Analysis of selected materials flown on interior locations of the Long Duration Exposure Facility
[NASA-CR-4586] p 3175 N94-29458

SPACECRAFT EQUIPMENT
Observations by ERS-1 start p 3327 N94-28933
Outline of JERS-1 system p 3330 N94-29220
Observatory system of Earth Resources Satellite-1 p 3330 N94-29221
Pyrotechnic shock: Devices in pyrotechnic environment qualification logic
[REPT-932-430-108] p 3225 N94-29429
Development status of the Communications and Broadcasting Engineering Test Satellite (COMETS)
[JTN-94-80545] p 3169 N94-30811
Development status of COMETS missions
[JTN-94-80544] p 3170 N94-30932

SPACECRAFT GUIDANCE
Fault tolerant testbed evaluation, phase 1
[NASA-CR-188275] p 3171 N94-29035
Micro guidance and control technology overview p 3144 N94-29772
Miniature wide field-of-view star trackers for spacecraft attitude sensing and navigation p 3144 N94-29794
A guidance and navigation system for two spacecraft rendezvous in translunar halo orbit p 3142 N94-29837

SPACECRAFT INSTRUMENTS
Outline of JERS-1 system p 3330 N94-29220
Future manned systems advanced avionics study
[NASA-CR-188277] p 3150 N94-29377
Three high duty cycle, space-qualified mechanisms p 3162 N94-29642
Miniature wide field-of-view star trackers for spacecraft attitude sensing and navigation p 3144 N94-29794
Ground control system for the midcourse space experiment UTC clock p 3474 N94-30674

SPACECRAFT LANDING
BAG: A code for predicting the performance of a gas bag impact attenuation system for the Pathfinder lander
[DE94-003688] p 3165 N94-28477
Landing gear energy absorption system
[NASA-CASE-MSC-22277-1] p 3300 N94-29448

SPACECRAFT LAUNCHING
Heavy-lift vehicle-launched Space Station method and apparatus
[NASA-CASE-MSC-21760-1] p 3160 N94-29369
Advanced microfabrication technologies for microspacecraft p 3171 N94-29782
Neural network application to Particle Impact Noise Detection p 3437 N94-29840
Fission-activated laser as primary power for CW laser propulsion
[DE94-006138] p 3295 N94-30367
Measurement of the frequency stability of responders in aircraft p 3261 N94-30673
The TOPAZ 2 space reactor response under accident conditions
[DE94-004998] p 3498 N94-30847

SPACECRAFT MAINTENANCE
On-orbit spacecraft servicing: An element in the evolution of space robotics applications
[AIAA PAPER 94-1236-CP] p 3448 N94-30583

SPACECRAFT MODELS
Wind tunnel testing and research
[NASA-CR-188273] p 3156 N94-29052

SPACECRAFT POWER SUPPLIES
Selection of the Space Station Freedom (SSF) Flat Collector Circuit (FCC) insulation material p 3165 N94-28701
TOPAZ 2 system description
[DE94-006230] p 3498 N94-30846
The TOPAZ 2 space reactor response under accident conditions
[DE94-004998] p 3498 N94-30847

SPACECRAFT PROPULSION
Nuclear electric propulsion: A better, safer, cheaper transportation system for human exploration of Mars
[NASA-TM-106406] p 3171 N94-28833
Some problems of scramjet propulsion for aerospace planes. Part 1: Scramjet: Aims and features p 3151 N94-29295
Research and development of ramjets/ramrockets. Part 2: Integral liquid fuel ramjets p 3152 N94-29297
Research and development of ramjets/ramrockets. Part 3: The study of gaseous hydrogen ram combustors p 3152 N94-29298
Some problems of scramjet propulsion for aerospace planes. Part 2: Scramjet: Development and test problems p 3152 N94-29301
A transportronic solution to the problem of interorbital transportation
[NASA-CR-191152] p 3164 N94-29355
Determination of pressure response times for gaseous flow in a tube
[AD-A275274] p 3272 N94-29435
Specialized data analysis of SSME and advanced propulsion system vibration measurements
[NASA-CR-193940] p 3174 N94-29868
Small low mass advanced PBR's for propulsion
[DE94-005142] p 3497 N94-30588

SPACECRAFT RADIATORS
Numerical simulation of a condenser in two-phase heat transport systems: A feasibility study
[AD-B173650] p 3282 N94-30855

SPACECRAFT REENTRY
Numerical simulation of aerothermodynamic heating of hypersonic space transportation vehicles p 3124 N94-28955

SPACECRAFT STABILITY
A gimbaled low noise momentum wheel p 3162 N94-29640

SPACECRAFT STRUCTURES
Reliability of composite material structures. Application: High pressure spherical coded tanks
[REPT-932-430-103] p 3180 N94-29478
Composite hot drape forming p 3240 N94-30448

SPACECRAFT SURVIVABILITY
Vulnerability of manned spacecraft to crew loss from orbital debris penetration
[NASA-TM-108452] p 3169 N94-30161

SPACECRAFT TRACKING
Radio science ground data system for the Voyager-Neptune encounter, part 1 p 3248 N94-29623
The Telecommunications and Data Acquisition Report
[NASA-CR-195689] p 3249 N94-29652
Toward astrometric tracking with the infrared spatial interferometer p 3249 N94-29653
Line-of-sight tropospheric calibration from measurements in arbitrary directions p 3249 N94-29654
Enhanced orbit determination filter sensitivity analysis: Error budget development p 3159 N94-29655
Enhanced orbit determination filter: Inclusion of ground system errors as filter parameters p 3159 N94-29656
A dual-cavity ruby maser for the Ka-band link experiment p 3250 N94-29658
Status of frequency and time support for NASA systems p 3468 N94-30640

SPACECRAFT TRAJECTORIES
Software engineering methods in the Hermes on-board software p 3414 N94-29326

SPACELAB
Study of activation data of metal samples from LDEF-1 and Spacelab-2
[NASA-CR-195802] p 3205 N94-29736

SPANWISE BLOWING
Numerical study of the trailing vortex of a wing with wing-tip blowing
[NASA-CR-195803] p 3130 N94-29760

SPARKS
Analysis of spark-induced bubble experiments using CALE
[DE94-003667] p 3270 N94-28476

SPATIAL DISTRIBUTION
U-statistics of random-size samples and limit theorems for systems of Markovian particles with non-Poisson initial distributions
[AD-A275018] p 3464 N94-29129
Multi-channel spatialization systems for audio signals
[NASA-CASE-ARC-12013-1-CU] p 3245 N94-29364
Use of satellite data to improve parameterization of spatial and temporal variations of gaseous dry deposition in regional-scale models
[DE94-005110] p 3334 N94-30022

SPATIAL FILTERING
Enhanced coherence x ray laser experiments and simulations
[DE94-005367] p 3295 N94-30060

SPATIAL RESOLUTION
Satellite estimation of the global distribution and interannual variability of photosynthetically active radiation p 3334 N94-29970

SPECIFIC HEAT
Endothermic fuels for hypersonic aviation p 3197 N94-29285
Centrifugal atomization of lanthanide materials for cryogenic coolers
[DE94-006035] p 3219 N94-30337
Scaling in heavy-fermion systems
[DE94-005002] p 3492 N94-30775

SPECIFICATIONS
Impact study on the use of biomass-derived fuels in gas turbines for power generation
[DE94-000261] p 3224 N94-28502
Cleanroom engineering handbook. Volume 4. Specification team practices
[AD-A275861] p 3156 N94-28753
Invariants, frames and postconditions: A comparison of two formal specification notations
[PB94-138153] p 3405 N94-29110

Engineering specification editing tools
[AD-A275116] p 3419 N94-29746
Using RDD-100 with CoRE. Version 01.00.03
[AD-A275336] p 3419 N94-29797
Second-order algebraic specification of state semantics
[CWI-CS-R9254] p 3453 N94-29889
Homomorphism preserving algebraic specifications require hidden sorts
[CWI-CS-R9344] p 3459 N94-30436
Service independent building blocks-1: Concepts, examples and formal specifications
[CWI-CS-R9326] p 3448 N94-30731

SPECTRAL BANDS
Temperature depencence of the far infrared optical constants of polyethylene
[PB94-124336] p 3213 N94-28795
Imaging spectrometry of the Earth and other solar system bodies p 3237 N94-29779
Evolution of miniature detectors and focal plane arrays for infrared sensors p 3237 N94-29781

SPECTRAL ENERGY DISTRIBUTION
Parameter identification of the rotordynamic coefficients of high-Reynolds-number hydrostatic bearings p 3311 N94-30792

SPECTRAL METHODS
A global forecast model comparison study - year 1
[AD-A275674] p 3369 N94-28663
Spectral analysis of wave propagation in connected waveguides p 3277 N94-29944
A spectral boundary integral equation method for the 2-D Helmholtz equation
[NASA-CR-194890] p 3454 N94-30207
Process modelling for materials preparation experiments
[NASA-CR-195782] p 3175 N94-30242
An experimental study of nonlinear wave coupling and energy transfer characterizing the transition of a planar jet shear layer p 3282 N94-30953
Transition to turbulence in confined compressible mixing layers p 3283 N94-30958

SPECTRAL RESOLUTION
Evolution of miniature detectors and focal plane arrays for infrared sensors p 3237 N94-29781

SPECTROMETERS
Inter-comparison of Wildfire and High-resolution Interferometer Sounder (HIS) data from STORM-FEST: An investigation of wildfire spectral channel discrepancies
[NASA-TM-108439] p 3333 N94-29553
Developing a diode array spectrometer for tropospheric chemistry studies p 3362 N94-29752
Backscatter Mossbauer Spectrometer (BaMS) for extraterrestrial applications p 3236 N94-29774
A Tevatron collider beauty factory
[DE94-004879] p 3488 N94-29930
Algorithm and program ORANGE for magnetic field simulation of magnetic system spectrometer STORS
[DE94-608013] p 3421 N94-30083

SPECTRORADIOMETERS
The automated rotating shadowband spectroradiometer
[DE94-001878] p 3269 N94-28464

SPECTROSCOPIC ANALYSIS
Measurement of tropospheric OH by laser long-path absorption spectroscopy p 3343 N94-28596
On the possibility of measuring atmospheric OH using intracavity laser spectroscopy p 3344 N94-28597
An improved method of measuring tropospheric NO2, NO3, HO2, and RO2 by Matrix Isolation and Electronic Spin Resonance (MIESR) p 3345 N94-28605
A novel spectroscopic measurement method of RF plasma for temperature and electron density diagnoses p 3188 N94-28682
Issues in light hadron spectroscopy
[PB94-138229] p 3486 N94-29112
Knowledge based system for identification of gamma sources
[PB94-137742] p 3487 N94-29683
Nanosize metal alloy particle formation in Ag and Cu sequentially implanted silica
[DE94-005592] p 3207 N94-30042
Crosslinking and surface reactions in macromolecules: Spectroscopic FT-IR studies p 3221 N94-30812

SPECTROSCOPY
Issues in light hadron spectroscopy
[PB94-138229] p 3486 N94-29112
Knowledge based system for identification of gamma sources
[PB94-137742] p 3487 N94-29683
Backscatter Mossbauer Spectrometer (BaMS) for extraterrestrial applications p 3236 N94-29774
Non-invasive temperature measurements using electron paramagnetic resonance spectroscopy p 3198 N94-29881
Charge collection spectroscopy applied to MOS RAM's p 3201 N94-30220

SPECTRUM ANALYSIS
Journal of NIRE, Vol. 2, No. 2
[JTN-94-80552] p 3187 N94-28675
A novel spectroscopic measurement method of RF plasma for temperature and electron density diagnoses p 3188 N94-28682
Principles and application tendency of remote sensing: Its principle, function and utilization p 3328 N94-29037
Investigation of intense XUV emission of nitrogen-puff Z-pinch with small energy input
[PH-23] p 3505 N94-29075
Multichannel x ray spectral measurement of hot plasma evolution in nitrogen-puff Z-pinch
[PH-24] p 3505 N94-29076
Spectral and polarimetric analysis of hyperspectral data collected by an acousto-optic tunable filter system
[AD-A275076] p 3329 N94-29095
Double-crystal analyser system for the PRISMA spectrometer: Test of a prototype
[PB94-138245] p 3286 N94-29113
A review of signal detection using the bispectrum with applications in underwater acoustics
[AD-A275227] p 3478 N94-29388
High redshift QSOs and the x ray background
[NASA-CR-195112] p 3540 N94-29957
Computational balance in real-time cyclic spectral analysis
[DE94-005091] p 3432 N94-30100
Theory and observations of horizontal and vertical structure of gravity wave perturbations in the middle atmosphere p 3366 N94-30802
Spectral analysis of heart rate and psychological state: A review of its validity as a workload index
[AD-B179387] p 3399 N94-30969
Noise reduction techniques for the restoration of musical recordings
[TELECOM-93-E-019] p 3291 N94-30979

SPEECH RECOGNITION
Subphonetic acoustic modeling for speaker-independent continuous speech recognition
[AD-A275217] p 3244 N94-29303

SPHERES
A study of the convergence of spherical harmonic expansions of gravity using distributed point-mass Earth models p 3362 N94-29909

SPHERICAL COORDINATES
Analytic rendering of curvilinear volume data
[DE94-004934] p 3407 N94-28506
Exact spherical wave solutions to Maxwell's equations with applications p 3252 N94-29733

SPHERICAL WAVES
Exact spherical wave solutions to Maxwell's equations with applications p 3252 N94-29733

SPIN
Hysteresis phenomena at spin-flop transition induced by the pulsed magnetic field
[DE94-606851] p 3511 N94-28626

SPIN DYNAMICS
Extended nonabelian symmetries for free fermionic model
[DE94-601554] p 3481 N94-28470

SPIN REDUCTION
One-loop QCD mass effects in the production of polarized bottom and top quarks
[PB94-138104] p 3487 N94-29145
The Solar Anomalous and Magnetospheric Particle Explorer (SAMPEX) yo-yo despin and solar array deployment mechanism p 3163 N94-29645

SPINE
Image technology and information analysis of bone change with gravitational exposure p 3389 N94-28851

SPINEL
Dislocation loops in spinel crystals irradiated successively with deep and shallow ion implants
[DE94-005083] p 3517 N94-30201

SPIRAL GALAXIES
Multicolor photometry of barred spiral galaxies p 3541 N94-30270

SPLINE FUNCTIONS
Analysis of crustal structure of Venus utilizing residual Line-of-Sight (LOS) gravity acceleration and surface topography data. A trial of global modeling of Venus gravity field using harmonic spline method
[NASA-CR-195799] p 3549 N94-29737
Splines and ocean wave modelling
[PB94-139409] p 3378 N94-30002

SPORES
Studies on bacterial spore ultraviolet light resistance and regulation of the activity of a spore protease
[AD-A275448] p 3384 N94-28884

SPRAY CHARACTERISTICS
Experimental studies on effervescent atomizers with wide spray angles p 3196 N94-29280
Apparatus for testing high pressure injector elements
[NASA-CASE-MFS-28773-1] p 3299 N94-29365

SPRAYED COATINGS
Plasma sprayed ceramic thermal barrier coating for NiAl-based intermetallic alloys
[NASA-CASE-LEW-15535-1] p 3205 N94-29507
Dual cure low-VOC coating process, phase 3
[DE94-003202] p 3221 N94-30826

SPRAYERS
Ducted kerosene spray flames p 3195 N94-29276
Spray combustion experiments and numerical predictions p 3195 N94-29277
Experimental studies on effervescent atomizers with wide spray angles p 3196 N94-29280
Aircraft evacuations: The effect of a cabin water spray system upon evacuation rates and behaviour
[CAA-PAPER-93008] p 3148 N94-29887
Near-net-shape manufacturing: Spray-formed metal matrix composites and tooling p 3186 N94-30447

SPRAYING
Modeling of the phase liquidates in combustion chambers p 3195 N94-29278
Experimental studies on effervescent atomizers with wide spray angles p 3196 N94-29280
Investigation of the two-phase flow in a research combustor under reacting and non-reacting conditions p 3196 N94-29282

SPREAD SPECTRUM TRANSMISSION
Communications subsystem for the Petite Amateur Navy Satellite (PANSAT)
[AD-A275532] p 3242 N94-28812
Evaluation of wireless Local Area Networks
[AD-A275133] p 3243 N94-29064
Acquisition time analysis of noncoherent PN sequence acquisition schemes
[AD-A275017] p 3244 N94-29094
High-resolution robot tracking and direction finding for space station environment p 3168 N94-29896

SPRINGS (ELASTIC)
Manufacturing methods for machining spring ends parallel at loaded length
[NASA-CASE-MFS-28767-1] p 3231 N94-29379

SPRINGS (WATER)
Fronts at the confluences of spring-fed streams with Joekulsa a Fjoellum: Possibly thermal bars?
[MATHS-REPT-A-198] p 3333 N94-29528

SPUTTERING
Sputtering of single crystals: Experimental evidence of the ejection process
[AD-A275819] p 3512 N94-28775
Kinetics of surface roughening and smoothing during ion sputtering
[DE94-006358] p 3219 N94-30263

SQUID (DETECTORS)
Fabrication issues in optimizing YBa(2)Cu(3)O(7-x) flux transformers for low I/f noise
[DE94-005209] p 3261 N94-28546
The computer-aided system for the high resolution SQUID-magnetometer
[DE94-606138] p 3286 N94-28553
The bases for the development of high-temperature integrated SQUID-systems
[DE94-607901] p 3267 N94-30073
The bases for the development of high-temperature integrated SQUID-systems
[DE94-608462] p 3517 N94-30082

STABILITY
Stability properties of inclusive connectivity for graphs
[AD-A275360] p 3452 N94-29016
Improved QCD sum rule estimates of the higher twist contributions to polarised and unpolarised nucleon structure functions
[PB94-138112] p 3487 N94-29161
The stability of perfect elliptic disks p 3545 N94-29834
Russian national time scale long-term stability p 3475 N94-30679

STAINLESS STEELS
Fundamental studies on the corrosion behavior of weldments in marine microbial environments
[AD-A275247] p 3203 N94-28900
Insulative properties of two thermo-metal neoprenes
[AD-A275209] p 3401 N94-29302
The organometallic chemical vapor deposition of transition metal carbides: The use of homoleptic alkyls
[DE94-005577] p 3206 N94-30007
Laser beam welding of AISI 316 stainless steel in microgravity environment: Experiments aboard a KC-135 flight
[ISBN-0-315-86095-2] p 3229 N94-30145

STANDARD DEVIATION
Probabilistic material strength degradation model for Inconel 718 components subjected to high temperature, mechanical fatigue, creep and thermal fatigue effects
[NASA-CR-195284] p 3318 N94-28840

STANDARD MODEL (PARTICLE PHYSICS)
Report of the subgroup on the top quark
[DE94-004624] p 3481 N94-28462
Search for the top quark in the electron-electron and electron-muon channels at D0
[DE94-006174] p 3492 N94-30779
STANDARDIZATION
NASA Parts Program Office responsibilities
p 3165 N94-28702
NASA Parts Project Office: Basic goals
p 3166 N94-28703
NAVAIR aircraft wiring standardization and qualification program p 3166 N94-28704
Organized wiring systems p 3166 N94-28705
SI (Metric) handbook
[NASA-TM-109197] p 3231 N94-29376
A normative frame of reference for the metrology function
[REPT-932-430-102] p 3231 N94-29477
Neural network application to Particle Impact Noise Detection p 3437 N94-29840
Standardisation requirements for ultrasonic C-scanning of polymer matrix composites: An initial assessment
[PB94-139318] p 3184 N94-30438
Cascaded clocks measurement and simulation findings p 3469 N94-30649
STANDARDS
NAVAIR aircraft wiring standardization and qualification program p 3166 N94-28704
Unscreened low tension cables scrape abrasion testing. Part 1: An interlaboratory study on scrape abrasion testing according to ISO DP 6722-1
[PB94-135605] p 3264 N94-29191
A normative frame of reference for the metrology function
[REPT-932-430-102] p 3231 N94-29477
A survey of NASA and military standards on fault tolerance and reliability applied to robotics
[AIAA PAPER 94-1211-CP] p 3445 N94-30562
The 25th Annual Precise Time and Time Interval (PTTI) Applications and Planning Meeting
[NASA-CP-3267] p 3468 N94-30639
Time and frequency technology at NIST
p 3468 N94-30641
European PTTI report p 3468 N94-30642
Report on NATO PTTI p 3469 N94-30645
Guidance notes for use with NPL low permeability reference materials
[NPL-DES-121] p 3476 N94-30780
STANDING WAVES
X ray standing wave studies of underpotentially deposited metal monolayers
[AD-A275409] p 3513 N94-29215
STAR CLUSTERS
X ray studies of the Hyades cluster
[NASA-CR-189325] p 3538 N94-29001
STAR FORMATION
The role of cloud collisions in N-body simulations of disk galaxies p 3545 N94-29755
A multi wavelength observational study of the Cartwheel ring galaxy p 3539 N94-29821
Multicolor photometry of barred spiral galaxies
p 3541 N94-30270
Stellar and gas dynamics of interacting ring galaxies
p 3548 N94-30340
STAR TRACKERS
Miniature wide field-of-view star trackers for spacecraft attitude sensing and navigation p 3144 N94-29794
STARBURST GALAXIES
The kinematics of molecular gas and dust in the nearby galaxies Centaurus A and M82 p 3544 N94-29738
A multi wavelength observational study of the Cartwheel ring galaxy p 3539 N94-29821
STATE ESTIMATION
Systematic error estimation in multisensor fusion systems
[AD-B179298] p 3428 N94-30764
Robust control of robots via linear estimated state-feedback
[MEMO-1153] p 3449 N94-30963
STATIC LOADS
Root-sum-square structural strength verification approach
[NASA-TM-108453] p 3322 N94-30206
STATIC PRESSURE
Blast overpressure studies with animals and man
[AD-A275038] p 3391 N94-29150
Analysis of fluctuating static pressure measurements in a large high Reynolds number transonic cryogenic wind tunnel p 3158 N94-30788
STATIC STABILITY
An experimental and theoretical study of the aerodynamic characteristics of some generic missile concepts at Mach numbers from 2 to 6.8
[NASA-TM-109110] p 3130 N94-29473
STATIC TESTS
Estimation of Weibull modulus from dynamic and static fatigue experiments
[PB94-138641] p 3322 N94-30114
Analysis and design of inflatable aerospace structures
p 3403 N94-30799
STATISTICAL ANALYSIS
Equation of state of stellar plasmas
[DE94-004186] p 3542 N94-28526
Probabilistic material strength degradation model for Inconel 718 components subjected to high temperature, mechanical fatigue, creep and thermal fatigue effects
[NASA-CR-195284] p 3318 N94-28840
U-statistics of random-size samples and limit theorems for systems of Markovian particles with non-Poisson initial distributions
[AD-A275018] p 3464 N94-29129
Statistical Modeling and Estimation of Reliability Functions for Software (SMERFS) user's guide, revision 3
[AD-A275390] p 3411 N94-29202
Statistical Modeling and Estimation of Reliability Functions for Software (SMERFS) library access guide, revision 3
[AD-A275405] p 3411 N94-29207
Statistical characterization of rugged propagation paths with application to Rg scattering study
[AD-A275237] p 3361 N94-29393
Simulation of interference between Earth stations and Earth-orbiting satellites p 3252 N94-29673
Evolution of the large-scale vortices in turbulent mixing-layers p 3273 N94-29686
Yield and variability optimization of integrated circuits: Principles and practical solutions p 3266 N94-29805
Comparison of Savannah River Site's meteorological databases
[DE94-001751] p 3373 N94-29817
Acceptance sampling methods for sample results verification
[DE94-002882] p 3465 N94-29925
Comparison of 14 MeV isomer production of Hf-178m1 and Hf-179m2 using Feshbach-Kerman-Koonin and exciton preequilibrium models
[DE94-002640] p 3488 N94-30039
Statistical description of hot and dense clustering matter
[DE94-608155] p 3490 N94-30112
Prediction and standard error estimation for a finite universe total when a stratum is not sampled
[DE94-004929] p 3465 N94-30696
Statistical analysis of a satellite imagery time series: Implications for the study of coastal and estuarine circulation p 3335 N94-30919
Substructure, dynamics and evolution in clusters of galaxies p 3548 N94-30951
STATISTICAL DISTRIBUTIONS
A random distribution reacting mixing layer model
[NASA-TM-106517] p 3150 N94-28923
Conditional dependence in probabilistic networks
[RUU-CS-92-34] p 3464 N94-29450
STATISTICAL MECHANICS
Thermodynamics of computation and information distance
[CWI-CS-R9341] p 3526 N94-30433
The Boltzmann entropy and randomness tests
[CWI-CS-R9342] p 3426 N94-30434
STATISTICAL TESTS
A moment plotting method for characterizing aircraft fatigue data population distributions
[AD-A275500] p 3145 N94-28660
Comparison of Savannah River Site's meteorological databases
[DE94-001751] p 3373 N94-29817
The Boltzmann entropy and randomness tests
[CWI-CS-R9342] p 3426 N94-30434
STATORS
Numerical study on internal flows of centrifugal compressors p 3127 N94-28977
Rotary blood pump
[NASA-CASE-MSC-22424-1] p 3299 N94-29370
Rotordynamic analysis of annular honeycomb-stator turbulent gas seals using a new friction-factor model based on flat plate tests p 3302 N94-29916
STEADY FLOW
Steady pressure measurements on an Aeroelastic Research Wing (ARW-2)
[NASA-TM-109046] p 3122 N94-28658
Nominally two-dimensional flow about a normal flat plate p 3275 N94-29838
Numerical solution of the two-dimensional time-dependent incompressible Euler equations
[NASA-CR-195775] p 3277 N94-29859
Aeroacoustic sensitivity analysis and optimal aeroacoustic design of turbomachinery blades
[NASA-CR-195786] p 3153 N94-30013
Numerical comparison of convective heat transfer augmentation devices used in cooling channels of hypersonic vehicles
[NASA-TM-106546] p 3279 N94-30147
Canonical-variables multigrid method for steady-state Euler equations
[NASA-CR-194888] p 3454 N94-30208
A new orthogonal decomposition method for turbulent flows p 3281 N94-30494
Numerical simulation of leading-edge vortex flow
[AD-B175154] p 3134 N94-30871
STEADY STATE
Frequency-domain analysis of nonlinear microwave circuits
[PB94-132024] p 3261 N94-28400
Non-isolated 30 kW class arcjet PCU
[NASA-CR-189148] p 3173 N94-29444
Numerical simulations of cluster cooling flows
p 3544 N94-29725
Two-phase power-law modeling of pipe flows displaying shear-thinning phenomena
[DE94-005115] p 3279 N94-30020
Advanced steady-state operating scenarios
[DE94-004810] p 3509 N94-30768
STEAM
Configuration and performance of the indirect-fired fuel cell bottomed turbine cycle
[DE94-005961] p 3338 N94-30313
STEEL STRUCTURES
Photovoltaic power without batteries for continuous cathodic protection p 3341 N94-30465
STEELS
Analysis of data by long-time mechanical properties of 08KH18N10T steel irradiated by neutrons
[DE94-605337] p 3202 N94-28551
Corrosion inhibition by electrodeposited conductive-polymer film
[AD-A275456] p 3213 N94-28806
Low temperature behavior of virgin martensite
[PB94-132925] p 3204 N94-29142
Effect of non-metallic inclusions on the machinability of steel
[PB93-230233] p 3204 N94-29387
Sliding friction and wear between titanium nitride, M50 steel and silicon nitride (round 3 of VAMAS wear test program)
[IMR-TM-TR-003] p 3303 N94-30019
Development of evaluated data bank of physical properties of perspective nuclear engineering steels and alloys
[DE94-607999] p 3207 N94-30076
XPS analysis of 440C steel surfaces lubricated with perfluoropolyethers under sliding conditions in high vacuum
[NASA-TM-106548] p 3218 N94-30177
Metafusion: A breakthrough in metallurgy
p 3211 N94-30446
Photovoltaic power without batteries for continuous cathodic protection p 3341 N94-30465
Experimental and analytical comparison of constraint effects due to biaxial loading and shallow-flaws
[DE94-004794] p 3323 N94-30689
Design of a variable-conductance vacuum insulation
[DE94-000270] p 3268 N94-30819
STEERING
Characterization of a diffraction grating as a simulant of a selective frequency antenna for radiometric applications
[AD-A275793] p 3241 N94-28745
STELLAR ACTIVITY
Surface differential rotation in a sample of cool dwarf stars p 3545 N94-29827
STELLAR ATMOSPHERES
Abundance patterns in red-giant CH stars
p 3539 N94-29820
STELLAR COMPOSITION
Abundance patterns in red-giant CH stars
p 3539 N94-29820
Coronal abundances and their variation
[NASA-CR-195767] p 3551 N94-29858
Study of the stellar populations of the Fornax dwarf spheroidal galaxy
[ISBN-0-315-85526-6] p 3541 N94-30231
STELLAR CORONAS
Coronal temperatures of unusually active K-dwarf binary systems
[NASA-CR-189335] p 3545 N94-29861
STELLAR EVOLUTION
Binary-single star scattering: An investigation of a realistic chaotic scattering system p 3543 N94-29719
Convective turbulence and transport in stars
p 3546 N94-29913
Theoretical asteroseismology of white dwarf stars: The encyclopedia Seismologica p 3547 N94-30011

STELLAR LUMINOSITY
Globular cluster photometry near the turnoff: Blue stragglers, relative ages, and the horizontal branch p 3538 N94-29732
Spatially resolved spectroscopy of AG Carinae, and direct evidence for stellar evolution: The central star of NGC 2392
[NASA-CR-189291] p 3545 N94-29871
A near-infrared survey of the star forming region NGC 2264 p 3540 N94-29971
Near-critical spherically symmetric accretion by neutron stars p 3546 N94-29991
Spectral and temporal behavior of low mass x ray binaries observed with the Einstein SSS and MPC, and the Broad Band X Ray Telescope p 3542 N94-30862
STELLAR MAGNITUDE
Globular cluster photometry near the turnoff: Blue stragglers, relative ages, and the horizontal branch p 3538 N94-29732
STELLAR MASS
A study of recycled pulsars in globular clusters p 3539 N94-29825
Theoretical asteroseismology of white dwarf stars: The encyclopedia Seismologica p 3547 N94-30011
STELLAR MASS ACCRETION
A study of white dwarf radiative accretion shocks p 3544 N94-29731
Near-critical spherically symmetric accretion by neutron stars p 3546 N94-29991
STELLAR MASS EJECTION
Remote sensing of inner heliospheric plasmas
[AD-A275021] p 3550 N94-29132
STELLAR MODELS
Equation of state of neutron star matter, limiting rotational periods of fast pulsars, and the properties of strange stars
[DE94-005214] p 3542 N94-28480
Equation of state of stellar plasmas
[DE94-004186] p 3542 N94-28526
CBSD: The celestial background scene descriptor
[AD-A275521] p 3538 N94-28671
Abundance patterns in red-giant CH stars p 3539 N94-29820
Near-critical spherically symmetric accretion by neutron stars p 3546 N94-29991
Theoretical asteroseismology of white dwarf stars: The encyclopedia Seismologica p 3547 N94-30011
STELLAR ORBITS
A study of recycled pulsars in globular clusters p 3539 N94-29825
STELLAR OSCILLATIONS
On observing neutron star oscillations p 3538 N94-29795
Near-critical spherically symmetric accretion by neutron stars p 3546 N94-29991
Theoretical asteroseismology of white dwarf stars: The encyclopedia Seismologica p 3547 N94-30011
STELLAR RADIATION
A study of white dwarf radiative accretion shocks p 3544 N94-29731
On observing neutron star oscillations p 3538 N94-29795
A study of ultra high-energy radiation associated with Hercules X-1 p 3552 N94-29823
Coronal temperatures of unusually active K-dwarf binary systems
[NASA-CR-189335] p 3545 N94-29861
Spatially resolved spectroscopy of AG Carinae, and direct evidence for stellar evolution: The central star of NGC 2392
[NASA-CR-189291] p 3545 N94-29871
STELLAR ROTATION
Equation of state of neutron star matter, limiting rotational periods of fast pulsars, and the properties of strange stars
[DE94-005214] p 3542 N94-28480
Surface differential rotation in a sample of cool dwarf stars p 3545 N94-29827
Convective turbulence and transport in stars p 3546 N94-29913
STELLAR SPECTRA
The role of cloud collisions in N-body simulations of disk galaxies p 3545 N94-29755
Surface differential rotation in a sample of cool dwarf stars p 3545 N94-29827
Coronal temperatures of unusually active K-dwarf binary systems
[NASA-CR-189335] p 3545 N94-29861
Inhomogeneities in the wind from Wolf-Rayet stars
[ISBN-0-315-85893-1] p 3548 N94-30058
Reconstruction of stellar images from correlations
[ISBN-0-315-85382-4] p 3541 N94-30133
Spectral and temporal behavior of low mass x ray binaries observed with the Einstein SSS and MPC, and the Broad Band X Ray Telescope p 3542 N94-30862
STELLAR SYSTEMS
Study of the stellar populations of the Fornax dwarf spheroidal galaxy
[ISBN-0-315-85526-6] p 3541 N94-30231
STELLAR TEMPERATURE
Coronal temperatures of unusually active K-dwarf binary systems
[NASA-CR-189335] p 3545 N94-29861
STELLAR WINDS
Inhomogeneities in the wind from Wolf-Rayet stars
[ISBN-0-315-85893-1] p 3548 N94-30058
STELLARATORS
A 6MeV heavy ion beam probe for the Large Helical Device
[NIFS-272] p 3505 N94-29397
The effect of magnetic field configuration on particle pinch velocity in Compact Helical System (CHS)
[NIFS-267] p 3505 N94-29398
Efficiencies of the ICRF minority heating in the CHS and LHD plasmas
[NIFS-270] p 3506 N94-29499
Overview of the US stellarator reactor study
[DE94-006042] p 3508 N94-30339
STEREOPHOTOGRAPHY
The use of digital stereo photogrammetric methods in historical photo analysis
[AD-A275267] p 3288 N94-29437
STEREOSCOPIC VISION
An investigation of stereopsis with AN/AVS-6 night vision goggles at varying levels of illuminance and contrast
[AD-A275332] p 3400 N94-28918
Automating geographically referenced digital mosaics from aerial videography with area-based feature matching p 3333 N94-29540
Stereo imaging based particle velocimeter
[NASA-CR-195800] p 3289 N94-29742
Navigation of military and space unmanned ground vehicles in unstructured terrains p 3144 N94-30282
Variable-resolution stereo matching p 3308 N94-30298
Obstacle detection for an autonomous vehicle p 3309 N94-30302
STEREOSCOPY
Aurora stereo observation in Iceland p 3359 N94-29234
Using stereoscopic imaging for visualization applications
[DE94-006247] p 3536 N94-30706
STIFFNESS
Performance of a higher-order triangular finite element for composite laminated structures p 3181 N94-29810
Transient thermal fatigue of ceramic composites p 3216 N94-29874
STIFFNESS MATRIX
Stiffness-generated rigid-body mode shapes for Lanczos eigensolution with SUPORT DOF by way of a MSC/NASTRAN DMAP alter
[NASA-TM-106537] p 3319 N94-29406
Experimental determination of orthotropic elastic constants
[FFA-TN-1991-35] p 3215 N94-29424
Closed form expressions for a consistent stress material nonlinear finite element p 3322 N94-30258
STIMULATED EMISSION
Spectroscopic and dynamical studies of highly energized small polyatomic molecules
[DE94-006509] p 3489 N94-30061
STIRLING CYCLE
Performance of the Southern California Edison Company Stirling dish
[DE94-004676] p 3337 N94-29018
STIRLING ENGINES
Performance of the Southern California Edison Company Stirling dish
[DE94-004676] p 3337 N94-29018
STOCHASTIC PROCESSES
Research activities of Martin C. Casdagli at SFI September 1989--May 1991
[DE94-005655] p 3463 N94-28548
Derivation of a Fokker-Planck equation for bunched beams
[DE94-004950] p 3483 N94-28565
The lectures in complex systems, volume 5
[AD-A275458] p 3466 N94-28807
The modified Cramer-von mises goodness-of-fit criterion for time series
[AD-A275377] p 3464 N94-29014
Stability of dynamical systems in the presence of noise
[AD-A275383] p 3243 N94-29072
Hierarchical structures and asymmetric stochastic processes on p-adics and adeles
[PB94-138203] p 3464 N94-29178
On-line search for optimal controller parameters using interconnected learning automata
[MATHS-REPT-A-196] p 3436 N94-29526
Effects of diffusion and inertia on chaotic mixing: A computational and experimental study p 3488 N94-29903
Stochastic stability and nonlinear control in mechanical systems p 3303 N94-29966
Exclusive many-particle diffusion in disordered media and correlation functions for random vertex models
[DE94-608134] p 3525 N94-30121
Langmuir waves in the electron-positron plasma
[DE94-608330] p 3508 N94-30191
A stochastic control approach to flight path monitoring
[AD-B174630] p 3143 N94-30853
Theory for electron-transfer reactions involving two Marcus surfaces with a different force constant
[DE94-005925] p 3493 N94-30874
Theory for electron-transfer reactions in a three-component system: The degenerate regime
[DE94-005919] p 3493 N94-30903
STOICHIOMETRY
Terfenol: A study of the phase equilibrium diagram and the solidification process
[DE94-004883] p 3209 N94-30690
Influence of surface defects and local structure on oxygenate reaction pathways over metal oxide surfaces
[DE94-005680] p 3522 N94-30901
STOPPING POWER
Calculation of inelastic mean free path and stopping power for electrons in solids from an optical-data model
[USIP-92-06] p 3494 N94-30980
STORAGE BATTERIES
Method for forming thin composite solid electrolyte film for lithium batteries
[NASA-CASE-NPO-18877-1-CU] p 3264 N94-29357
Dendrite preventing separator for secondary lithium batteries
[NASA-CASE-NPO-18585-1-CU] p 3265 N94-29411
STORAGE RINGS (PARTICLE ACCELERATORS)
Physics at HERA
[DE94-005117] p 3483 N94-28569
Tuning of AmPS
[NIKHEF-K-AMPS-93-01] p 3494 N94-29422
BPM901N monitor electronics for the determination of the bundle profile in the extraction line of AmPS
[DIGEL-1993-9] p 3495 N94-29467
Activity report of Synchrotron Radiation Laboratory 1992
[JTN-94-80600] p 3495 N94-29596
Stripline monitor electronics for the bundle position determination in AmPS
[DIGEL-1993-8] p 3495 N94-29888
STORAGE TANKS
Large scale cryogenic fluid systems testing
[NASA-TM-109735] p 3157 N94-29904
STORMS
Remote sensor observations during WISP91: The use of microwave radiometers, RASS, and lidar ceilometers for detection of aircraft icing conditions
[PB94-142106] p 3136 N94-30890
STRAIN DISTRIBUTION
Plane stress stable crack growth and J-integral/HRR field
[AD-A275761] p 3317 N94-28761
Analyses of stationary and growing crack tip deformation by digital image processing p 3320 N94-29690
Field methods to measure surface displacement and strain with the Video Image Correlation method
[NASA-CR-195796] p 3316 N94-29724
STRAIN ENERGY METHODS
Integrated active and passive control design methodology for the LaRC CSI evolutionary model
[NASA-CR-4580] p 3164 N94-28417
An analysis of isothermal, bithermal, and thermomechanical fatigue data of Haynes 188 and B1900+Hf by energy considerations
[NASA-TM-106359] p 3317 N94-28819
STRAIN ENERGY RELEASE RATE
Plane stress stable crack growth and J-integral/HRR field
[AD-A275761] p 3317 N94-28761
Transient thermal fatigue of ceramic composites p 3216 N94-29874
Computational simulation of composite structures with and without damage
[NASA-CR-194433] p 3183 N94-30190
STRAIN GAGES
Damage identification in composites using built-in piezoelectrics p 3184 N94-30355
STRAIN HARDENING
A modeling study of the effect of stress state on void linking during ductile fracture
[AD-A275505] p 3317 N94-28811

STRAIN MEASUREMENT
Experimental determination of orthotropic elastic constants
[FFA-TN-1991-35] p 3215 N94-29424
STRAIN RATE
Failures to model the development of a cube texture during the high temperature compression of Al-Mg alloys
[DE94-005013] p 3201 N94-28544
Numerical analysis of dynamic direct tension and direct compression tests
[AD-A275255] p 3319 N94-29433
The effect of various metallurgical parameters on the flow and fracture behavior of polycrystalline NiAl near the brittle-to-ductile transition
[NASA-TM-106534] p 3205 N94-29758
Mechanisms and effects of heat generation at the tips of dynamic cracks and notches in metals
p 3321 N94-29808
Nanodislocation structures generated in shocked crystals p 3514 N94-29915
Fatigue of carbon and low-alloy steels in LWR environments
[DE94-005116] p 3207 N94-30021
Influence of tungsten alloying additions on the mechanical properties and texture of tantalum
[DE94-004994] p 3210 N94-30774
STRAKES
An experimental investigation of the effect of leading edge extensions on directional stability and the effectiveness of forebody nose strakes
p 3155 N94-29728
STRANGE ATTRACTORS
Controlling chaos in plasma filled diodes
[AD-A275525] p 3504 N94-28686
Boundary layer coherent structures
[AD-A275007] p 3272 N94-29195
STRANGENESS
Equation of state of neutron star matter, limiting rotational periods of fast pulsars, and the properties of strange stars
[DE94-005214] p 3542 N94-28480
Weak decays of charged K-mesons and charm particles
[PB94-138062] p 3486 N94-29143
STRATIFICATION
Modeling deep equatorial circulation
p 3378 N94-29815
STRATIGRAPHY
Field guide to Cretaceous-tertiary boundary sections in northeastern Mexico
[NASA-CR-195719] p 3354 N94-28416
STRATOSPHERE
Harvard ER-2 OH laser-induced fluorescence instrument p 3343 N94-28592
Time series comparisons of satellite and rocketsonde temperatures in 1978-1979
[NASA-TP-3409] p 3370 N94-29455
Laboratory studies of chemical and photochemical processes relevant to stratospheric ozone
[NASA-CR-195779] p 3347 N94-29549
Radar estimations of atmospheric winds in the troposphere and lower stratosphere
p 3370 N94-29697
STRATUS CLOUDS
The appearance of the Sun and Moon seen through clouds
[AD-A275338] p 3551 N94-29212
STREAMS
Development and application of a thermistor current meter
[AD-A275816] p 3286 N94-28831
Fronts at the confluences of spring-fed streams with Joekulsa a Fjoellum: Possibly thermal bars?
[MATHS-REPT-A-198] p 3333 N94-29528
STRESS (PHYSIOLOGY)
Implications of climatic extremes in aircrew NBC operations p 3383 N94-28446
Physiological responses during shipboard firefighting
[AD-A275104] p 3391 N94-28912
Stress and ergonomic design and evaluation of person-machine systems
[AD-A275156] p 3400 N94-29034
Effects of endurance training on heat-exercise tolerance in men wearing NBC protective clothing
[AD-A275176] p 3391 N94-29049
STRESS (PSYCHOLOGY)
Strategies to sustain and enhance performance in stressful environments
[AD-A275223] p 3398 N94-29027
Stress and ergonomic design and evaluation of person-machine systems
[AD-A275156] p 3400 N94-29034
Spectral analysis of heart rate and psychological state: A review of its validity as a workload index
[AD-B179387] p 3399 N94-30969
STRESS ANALYSIS
Viscous and elastic-plastic material model in the ABAQUS
[PB94-132347] p 3316 N94-28409
A modeling study of the effect of stress state on void linking during ductile fracture
[AD-A275505] p 3317 N94-28811
An anisotropic extension of Bodner's model of viscoplasticity: Model development
[NASA-CR-195289] p 3318 N94-28821
Modelling and analysis of creep deformation and fracture in a 1 Cr 1/2 Mo ferritic steel
[PB94-138328] p 3319 N94-29121
Low temperature behavior of virgin martensite
[PB94-132925] p 3204 N94-29142
Numerical analysis of dynamic direct tension and direct compression tests
[AD-A275255] p 3319 N94-29433
Stress transfer mechanics for multiple perfectly bonded concentric cylinder models of unidirectional composites
[PB94-138633] p 3181 N94-29524
Free edge and size effects on failure initiation and ultimate strength of laminates containing a center hole
p 3181 N94-29735
Performance of a higher-order triangular finite element for composite laminated structures
p 3181 N94-29810
Higher order asymptotic crack tip fields in a power-law hardening material p 3321 N94-29829
Estimation of Weibull modulus from dynamic and static fatigue experiments
[PB94-138641] p 3322 N94-30114
Multiple Concentric Cylinder Model (MCCM) user's guide
[NASA-CR-195299] p 3183 N94-30125
Micromechanical analysis of thermo-inelastic multiphase short-fiber composites
[NASA-CR-195290] p 3183 N94-30178
Potential capabilities of Reynolds stress turbulence model in the COMMIX-RSM code p 3285 N94-30450
Approximate estimation of the effects of asymmetry on the testing of tensile specimens
[NPL-DMM(A)-117] p 3322 N94-30523
An investigation of fatigue crack propagation under mode 1 and mixed mode 1/2 loadings p 3323 N94-30814
Fatigue management and verification of airframes
[FFA-TN-1993-55] p 3149 N94-30947
Numerical modeling and prediction of the thermomechanical behavior of fiber-reinforced composites p 3186 N94-30956
STRESS DISTRIBUTION
Damage meso-modeling of 3D evolutive composites
[REPT-932-430-106] p 3179 N94-29442
Stress transfer mechanics for multiple perfectly bonded concentric cylinder models of unidirectional composites
[PB94-138633] p 3181 N94-29524
Higher order asymptotic crack tip fields in a power-law hardening material p 3321 N94-29829
Delamination of woven E-glass fabric composites
[DE94-003227] p 3185 N94-30827
STRESS INTENSITY FACTORS
Estimation of Weibull modulus from dynamic and static fatigue experiments
[PB94-138641] p 3322 N94-30114
STRESS MEASUREMENT
Vacuum chamber and adaptors for shearography and holography
[NASA-CR-192467] p 3157 N94-29956
STRESS RELAXATION
Measurement and modelling of bolted joint stress relaxation in plastics
[PB94-124849] p 3318 N94-28841
STRESS WAVES
Dynamic response of ceramics
[AD-A275396] p 3214 N94-29203
STRESS-STRAIN RELATIONSHIPS
Viscous and elastic-plastic material model in the ABAQUS
[PB94-132347] p 3316 N94-28409
Prediction of stress-strain response of SCS-6/Timetal-21S subjected to a hypersonic flight profile
[NASA-TM-109026] p 3177 N94-28823
Granular bases for heavily loaded pavements
[AD-A275171] p 3156 N94-29047
Fatigue of carbon and low-alloy steels in LWR environments
[DE94-005116] p 3207 N94-30021
STRETCHING
On some general properties of parabolic conservation equations
[DE94-006101] p 3461 N94-30758
STRING THEORY
Twistor-like type 2 superstring and bosonic string
[DE94-606339] p 3523 N94-28802
Problems in particle theory
[DE94-003665] p 3491 N94-30685
STRINGS
Controlling the material properties of in vitro collagen through directed orientation and cross-linking of fibrils
p 3221 N94-30797
STRONGLY COUPLED PLASMAS
Conceptual study of moderately coupled plasmas and experimental comparison of laboratory x ray sources
[DE94-005828] p 3506 N94-30045
STRONTIUM OXIDES
Influence of doping on the electronic structure of (La, Sr)2CuO4
[DE94-006383] p 3516 N94-30054
Investigation of the phase equilibria and phase transformations associated with the Bi2Sr2CaCu2O(y) superconductor
[DE94-004889] p 3519 N94-30691
STRUCTURAL ANALYSIS
Viscous and elastic-plastic material model in the ABAQUS
[PB94-132347] p 3316 N94-28409
Composite load spectra for select space propulsion structural components
[NASA-CR-194476] p 3316 N94-28508
Effects of repair on structural integrity
[AD-A275756] p 3145 N94-28647
Service life prediction of composite structures through fiber testing
[AD-A275661] p 3176 N94-28654
Thermal/structural tailoring of engine blades (T/SEAEBL). Theoretical manual
[NASA-CR-194462] p 3317 N94-28815
Structural/aerodynamic blade analyzer (SAB) user's guide, version 1.0
[NASA-CR-194460] p 3151 N94-29103
Study of bridge design and technology
[PB94-137916] p 3121 N94-29160
Performing specifications for complex systems' software p 3155 N94-29317
A method for the probabilistic design assessment of composite structures
[NASA-TM-106384] p 3319 N94-29384
Large-scale computations in analysis of structures
[DE94-004022] p 3321 N94-29951
Root-sum-square structural strength verification approach
[NASA-TM-108453] p 3322 N94-30206
Sensitivity analysis of the static aeroelastic response of a wing p 3134 N94-30525
Fullerenes as precursors for diamond film growth without hydrogen or oxygen additions
[DE94-004582] p 3519 N94-30718
Structural analysis of amorphous phosphates using high performance liquid chromatography
[DE94-004791] p 3199 N94-30723
Thin-walled orthotropic laminated beam theory
p 3324 N94-30920
STRUCTURAL DESIGN
Study of bridge design and technology
[PB94-137916] p 3121 N94-29160
Review of sonic fatigue technology
[NASA-CR-4587] p 3479 N94-29407
Field methods to measure surface displacement and strain with the Video Image Correlation method
[NASA-CR-195796] p 3316 N94-29724
Dynamic fracture mechanics analysis for an edge delamination crack
[NASA-TM-109106] p 3479 N94-29856
Rotorcraft airframe structural optimization for vibration and dynamic stress reduction including damping treatment p 3147 N94-29878
Improved ground-penetrating radar, bridge decks
[DE94-004863] p 3254 N94-29929
Hopf bifurcation in viscous, low-speed flows about an airfoil with structural coupling p 3134 N94-30865
Integrated structure/control design of nonrigid robot arms for high-speed manipulation p 3312 N94-30866
STRUCTURAL DESIGN CRITERIA
A method for the probabilistic design assessment of composite structures
[NASA-TM-106384] p 3319 N94-29384
STRUCTURAL FAILURE
Effects of repair on structural integrity
[AD-A275756] p 3145 N94-28647
Numerical and experimental investigation of the bending response of thin-walled composite cylinders
[NASA-CR-195730] p 3317 N94-28801
Test and analysis of a stitched RFI graphite-epoxy panel with a fuel access door
[NASA-TM-108992] p 3178 N94-29100
STRUCTURAL MEMBERS
Advanced microfabrication technologies for microspacecraft p 3171 N94-29782

STRUCTURAL PROPERTIES (GEOLOGY)
Application of remote sensing techniques for the seismo-tectonic study of Nahanni earthquake area
[ISBN-0-315-85942-3] p 3334 N94-30037
Analysis of deep seismic reflection and other data from the southern Washington Cascades
[DE94-005915] p 3367 N94-30883
STRUCTURAL RELIABILITY
A method for the probabilistic design assessment of composite structures
[NASA-TM-106384] p 3319 N94-29384
STRUCTURAL STABILITY
Study of bridge design and technology
[PB94-137916] p 3121 N94-29160
Modelling soft impacts for vibrational excitation of civil engineering structures
[PB94-137619] p 3320 N94-29681
STRUCTURAL VIBRATION
Characterization of structural vibration: Field descriptors based on energy density and intensity
[PB94-132230] p 3316 N94-28404
Study of bridge design and technology
[PB94-137916] p 3121 N94-29160
Experimental validation of finite element and boundary element methods for predicting structural vibration and radiated noise
[NASA-CR-4561] p 3301 N94-29552
Modelling soft impacts for vibrational excitation of civil engineering structures
[PB94-137619] p 3320 N94-29681
Rotorcraft airframe structural optimization for vibration and dynamic stress reduction including damping treatment p 3147 N94-29878
Spectral analysis of wave propagation in connected waveguides p 3277 N94-29944
Analysis and design of inflatable aerospace structures p 3403 N94-30799
STRUCTURED PROGRAMMING
Object-based design of embedded software
[PB94-132073] p 3407 N94-28403
The ABC structure editor: Structure-based editing for the ABC programming environment
[CWI-CS-R9256] p 3418 N94-29487
STRUTS
Mars rover mechanisms designed for Rocky 4 p 3161 N94-29630
STUDENTS
Summer intern program
[AD-A275194] p 3466 N94-28888
Application of digital video to hypermedia training systems
[AD-A274989] p 3409 N94-28910
An interactive, design and educational tool for supersonic external-compression inlets
[NASA-TM-106581] p 3421 N94-30174
An interactive educational tool for compressible aerodynamics
[NASA-TM-106568] p 3422 N94-30175
STYRENES
Ballistic performance of polycarbonate/polyester and polycarbonate/styrene- acrylonitrile microlayer sheets
[AD-A275462] p 3177 N94-28735
SUBDUCTION (GEOLOGY)
The rupture process of large earthquakes along convergent margins: Cast studies from Alaska and Armenia p 3363 N94-29969
SUBJECTS
Catalog of Air Force weather technical publications 1992-1993
[AD-A275635] p 3368 N94-28638
SUBREFLECTORS
Beam scanning offset Cassegrain reflector antennas by subreflector movement
[NASA-CR-191604] p 3160 N94-28836
SUBROUTINE LIBRARIES (COMPUTERS)
Program derivation by proof transformation
[AD-A275260] p 3453 N94-29304
SUBSONIC FLOW
The 3-D LDV measurements on a 30-degree swept wing with a simulated ice accretion
[NASA-CR-195327] p 3132 N94-30124
Canonical-variables multigrid method for steady-state Euler equations
[NASA-CR-194888] p 3454 N94-30208
Numerical investigation into high-angle-of-attack leading-edge vortex flow
[PB94-125564] p 3133 N94-30388
Aspects of the modeling and numerical simulation of leading-edge vortex flow
[AD-B179108] p 3133 N94-30492
A residual correction method applied to 2D multi-point airfoil design and 3D single-point wing design
[NLR-TP-92524-U] p 3134 N94-30493
SUBSONIC WIND TUNNELS
The nozzle acoustic test rig: An acoustic and aerodynamic free-jet facility
[NASA-TM-106495] p 3156 N94-28749
User's manual for the model interface and plugboard cabinets in the 14- by 22-foot subsonic tunnel
[NASA-TM-109062] p 3133 N94-30176
SUBSTITUTES
Alternative fuel vehicles for the state fleets: Results of the 5-year planning process
[DE94-004709] p 3224 N94-28577
Practical applications of plasma surface modification
[DE94-004892] p 3349 N94-29932
Logistics for the implementation of lead-free solders on electronic assemblies
[DE94-004800] p 3206 N94-29936
Non-aqueous cleaning solvent substitution
[DE94-005339] p 3219 N94-30245
Non-aqueous cleaning solvent substitution p 3354 N94-30466
Proceedings of the 1993 Windsor Workshop on Alternative Fuels
[DE94-003908] p 3226 N94-30612
SUBSTRATES
Pull-test adhesion measurements of diamondlike carbon films on silicon carbide, silicon nitride, aluminum oxide, and zirconium oxide
[DE94-005469] p 3211 N94-28536
Development of large area RF induction plasma for cost effective diamond
[AD-A275888] p 3504 N94-28776
MOCVD growth of GaN, AlN and AlGaN for UV photodetector applications
[AD-A275078] p 3512 N94-28871
Silicon germanium carbon heteroepitaxial growth on silicon
[AD-A275197] p 3512 N94-28889
Dual-use applications of infrared sensitive materials
[AD-A275140] p 3499 N94-29694
Ionic conduction mechanisms in CaF2 and CaF2-Al2O3 nanocomposite films on Al2O3 substrates
[DE94-004792] p 3520 N94-30773
Surface chemistry of boron-doped SiO2 CVD: Enhanced uptake of tetraethyl orthosilicate by hydroxyl groups bonded to boron
[DE94-005428] p 3221 N94-30896
SUDDEN IONOSPHERIC DISTURBANCES
Solar-geophysical data number 591, November 1993. Part 1: Prompt reports. Data for September, October 1993 and late data
[PB94-140548] p 3550 N94-29122
SUGARS
Instrumental development of novel detection and separation methods for capillary electrophoresis
[DE94-005554] p 3187 N94-28519
SUITS
Insulative properties of two thermo-metal neoprenes
[AD-A275209] p 3401 N94-29302
SULFIDES
Interstitially stabilized phases in the zirconium-nickel system
[DE94-005561] p 3201 N94-28525
Studies of high temperature ternary phases in mixed-metal-rich early transition metal sulfide and phosphide systems
[DE94-006034] p 3209 N94-30336
SULFONES
Poly(arylene ether-co-imidazole)s as toughness modifiers for epoxy resins
[NASA-CASE-LAR-15229-1-CU] p 3215 N94-29451
SULFUR COMPOUNDS
Polyimides containing the penta fluoro sulfanyl benzene moiety
[NASA-CASE-LAR-15082-1] p 3175 N94-29554
SULFURIC ACID
Ion-assisted tropospheric OH measurement technique p 3344 N94-28601
SUM RULES
Improved QCD sum rule estimates of the higher twist contributions to polarised and unpolarised nucleon structure functions
[PB94-138112] p 3487 N94-29161
Theoretical studies in hadronic and nuclear physics
[DE94-003524] p 3492 N94-30838
SUMMER
Summer intern program
[AD-A275194] p 3466 N94-28888
SUN
The appearance of the Sun and Moon seen through clouds
[AD-A275338] p 3551 N94-29212
SUNSPOT CYCLE
Surface differential rotation in a sample of cool dwarf stars p 3545 N94-29827
SUPERCOMPUTERS
The High Performance Storage System
[DE94-004350] p 3404 N94-28505
Construction of a connectionist network supercomputer
[AD-A275765] p 3405 N94-28764
Parallel Fortran programming for NWT p 3129 N94-28991
A method of user interface for NWT p 3129 N94-28993
A porting methodology for parallel database systems
[AD-A275256] p 3529 N94-29053
Progress report for the PTUF Project-93 Q1 and Q2
[PB94-138591] p 3431 N94-29995
Engineering of systems for application of scientific computing in industry WP project management ISNaS 9209099
[PB94-126232] p 3428 N94-30739
Information system for flow simulation based on the Navier-Stokes equations vectorization
[AD-B179293] p 3281 N94-30763
Modeling data throughput on communication networks
[DE94-005077] p 3260 N94-30772
Computing at the leading edge: Research in the energy sciences
[DE94-006121] p 3563 N94-30844
Supercomputing has to be part of an organization-wide automation concept
[AD-B174654] p 3433 N94-30913
SUPERCONDUCTING DEVICES
Epitaxial heterojunctions of oxide semiconductors and metals on high temperature superconductors
[NASA-CASE-NPO-18483-1-CU] p 3513 N94-29501
SUPERCONDUCTING FILMS
Fabrication issues in optimizing YBa(2)Cu(3)O(7-x) flux transformers for low I/f noise
[DE94-005209] p 3261 N94-28546
Exploratory research for a high temperature superconducting integrated circuit
[AD-A275798] p 3262 N94-28767
Ion channeling peculiarities in YBa2Cu3 O7 monocrystal
[DE94-606885] p 3512 N94-28787
High Tc superconducting bolometric and nonbolometric infrared (IR) detectors
[NASA-CR-195728] p 3262 N94-28846
The bases for the development of high-temperature integrated SQUID-systems
[DE94-607901] p 3267 N94-30073
The bases for the development of high-temperature integrated SQUID-systems
[DE94-608462] p 3517 N94-30082
Research on the atomic layer-by-layer growth of high-temperature superconductor thin films at the Institute of Scientific and Industrial Research, Japan
[DE94-003739] p 3519 N94-30611
SUPERCONDUCTING MAGNETS
Battery energy and superconducting magnetic energy storage for utility applications: A qualitative analysis
[DE94-005382] p 3336 N94-28489
Estimating the cost of large superconducting thin solenoid magnets
[DE94-006289] p 3468 N94-30026
Algorithm and program ORANGE for magnetic field simulation of magnetic system spectrometer STORS
[DE94-608013] p 3421 N94-30083
A magnetically coupled quench detector for superconducting magnets
[DE94-006040] p 3268 N94-30904
AC losses for the self field of an AC transport current with a DC transport current offset in high T(c) superconducting magnet coils for MagLev application
[DE94-005187] p 3268 N94-30907
SUPERCONDUCTIVITY
Normal state resistivity of MBa2Cu3O(7-x) ceramics
[DE94-608456] p 3220 N94-30745
On some general properties of parabolic conservation equations
[DE94-006101] p 3461 N94-30758
SUPERCONDUCTORS
Computing at the leading edge: Research in the energy sciences
[DE94-006121] p 3563 N94-30844
Calculating the J(c), B, T surface for commercial niobium tin conductors using a reduced state model
[DE94-006296] p 3520 N94-30850
Mathematical models of hysteresis
[DE94-005681] p 3260 N94-30902
SUPERCRITICAL AIRFOILS
Steady pressure measurements on an Aeroelastic Research Wing (ARW-2)
[NASA-TM-109046] p 3122 N94-28658
SUPERCRITICAL FLUIDS
Computer simulation of molecular interactions in supercritical solvents
[AD-A274977] p 3486 N94-29087

SUPERFLUIDITY
Acoustic and optical investigations of superfluid (3)He
[PB94-135415] p 3477 N94-29186
SUPERHEATING
An experimental investigation of flow patterns and liquid entrainment in a horizontal-tube evaporator
p 3277 N94-29899
SUPERHIGH FREQUENCIES
X-/Ka-band dichroic plate design and grating lobe study p 3247 N94-29616
A portable X-band front-end test package for beam-waveguide antenna performance evaluation. Part 2: Tests on the antenna p 3247 N94-29620
Design and analysis of a low-loss linear analog phase modulator for deep space spacecraft X-band transponder applications p 3248 N94-29625
Optimizing the Galileo space communication link
p 3250 N94-29663
X-band ultralow-noise maser amplifier performance
p 3251 N94-29672
Adaptive power control as a fade countermeasure on satellite links p 3253 N94-29897
Measurement basis of near fields in spherical coordinates in the 100 MHz to 6 GHz band
[REPT-932-430-107] p 3255 N94-30153
SUPERLATTICES
Carrier collection and scattering in quantum well and superlattice devices
[AD-A275443] p 3512 N94-28880
Band structure of superlattice with (delta)-like potential
[DE94-608108] p 3516 N94-30072
Interband optical absorption in the Wannier-Stark ladder under the electron-LO-phonon resonance condition
[DE94-608097] p 3267 N94-30092
The growth of InAsSb/InGaAs strained-layer superlattices by metal-organic chemical vapor deposition
[DE94-005576] p 3518 N94-30316
SUPERNOVA REMNANTS
A multiwavelength study of two prototypical supernova remnants p 3540 N94-29833
SUPERPLASTICITY
Superplasticity in fine-grained ceramics
[AD-A275461] p 3212 N94-28733
Numerical simulation of industrial workpiece superplastic forming
[REPT-932-600-102] p 3418 N94-29479
SUPERSONIC AIRCRAFT
Advanced fuel properties: A computer program for estimating property values
[AD-A275248] p 3224 N94-28901
Numerical analysis of supersonic transport wings
p 3124 N94-28959
SUPERSONIC COMBUSTION
Scramjet CFD methods and analysis. Part 2: Scramjet CFD analysis. Numerical simulation of supersonic mixing and combustion applied to scramjet combustor
p 3152 N94-29300
Fuel-rich catalytic combustion of a high density fuel
[NASA-TP-3281] p 3197 N94-29356
SUPERSONIC COMBUSTION RAMJET ENGINES
Numerical study on the interaction between scramjet engine modules caused by thermal choke
p 3125 N94-28960
Research and Development of Ram/Scramjets and Turboramjets in Russia
[AGARD-LS-194] p 3151 N94-29291
Introduction and overview of research and development of solid propellant ramrockets, liquid fuel ramjets and experimental hydrogen ram combustors
p 3151 N94-29292
Some problems of scramjet propulsion for aerospace planes. Part 1: Scramjet: Aims and features
p 3151 N94-29295
Scramjet CFD methods and analysis. Part 1: Scramjet CFD methods. Numerical simulation of the flow in scramjet duct p 3152 N94-29296
Scramjet CFD methods and analysis. Part 2: Scramjet CFD analysis. Numerical simulation of supersonic mixing and combustion applied to scramjet combustor
p 3152 N94-29300
Some problems of scramjet propulsion for aerospace planes. Part 2: Scramjet: Development and test problems p 3152 N94-29301
Liquid atomization in supersonic flows
p 3276 N94-29839
SUPERSONIC FLIGHT
Experimental investigation of three-dimensional vortex-airfoil interaction in a supersonic stream
[AD-A275107] p 3122 N94-28899
SUPERSONIC FLOW
Experimental investigation of three-dimensional vortex-airfoil interaction in a supersonic stream
[AD-A275107] p 3122 N94-28899
Higher-order accurate numerical simulation of 3D supersonic mixing layers p 3124 N94-28954
Numerical simulation of supersonic flow around space plane with engine installed p 3125 N94-28961
Study on mixing and injection of hydrogen into a supersonic flow p 3127 N94-28975
Scramjet CFD methods and analysis. Part 2: Scramjet CFD analysis. Numerical simulation of supersonic mixing and combustion applied to scramjet combustor
p 3152 N94-29300
An actively cooled floating element skin friction balance for direct measurement in high enthalpy supersonic flows p 3289 N94-29824
Liquid atomization in supersonic flows
p 3276 N94-29839
An interactive educational tool for compressible aerodynamics
[NASA-TM-106568] p 3422 N94-30175
The enhancement of compressible turbulent mixing via streamwise vorticity p 3280 N94-30487
SUPERSONIC HEAT TRANSFER
Numerical simulation of aerothermodynamic heating of hypersonic space transportation vehicles
p 3124 N94-28955
SUPERSONIC INLETS
An interactive, design and educational tool for supersonic external-compression inlets
[NASA-TM-106581] p 3421 N94-30174
SUPERSONIC JET FLOW
Liquid atomization in supersonic flows
p 3276 N94-29839
SUPERSONIC NOZZLES
Supersonic gas-liquid cleaning system
p 3240 N94-30467
SUPERSONIC TRANSPORTS
Combustion for future supersonic transport propulsion
p 3190 N94-29249
A study of low emissions gas turbine combustions
[NASA-CR-195763] p 3152 N94-29860
SUPERSONIC WAKES
Numerical study on internal flows of centrifugal compressors p 3127 N94-28977
SUPERSONIC WIND TUNNELS
Laminar Flow Supersonic Wind Tunnel primary air injector p 3158 N94-29649
SUPERSYMMETRY
Emission of supersymmetric neutron pair by charged lepton in magnetic field
[DE93-634365] p 3481 N94-28468
Model of polylinear Bose- and Fermi-like oscillator
[DE94-606303] p 3485 N94-28718
Twistor-like type 2 superstring and bosonic string
[DE94-606339] p 3523 N94-28802
Operator analysis for quark and lepton masses in SO(10)
[DE94-005201] p 3491 N94-30709
Graded Froelicher-Nijenhuis brackets and the theory of recursion operators for super differential equations
[MEMO-1147] p 3460 N94-30736
SUPPORT SYSTEMS
Flight command software development: RAFALE studies p 3413 N94-29320
A Modular Artificial Intelligence Inference Engine System (MAIS) for support of on orbit experiments
[AIAA PAPER 94-1237-CP] p 3448 N94-30584
SUPPORTS
Rotor instability induced by dead band clearance in bearing supports p 3312 N94-30809
SUPPRESSORS
Measurand transient signal suppressor
[NASA-CASE-MSC-22027-1] p 3435 N94-29466
SURFACE COOLING
The thermal consequences of giant impacts in the early solar system p 3543 N94-29698
SURFACE DEFECTS
Influence of surface defects and local structure on oxygenate reaction pathways over metal oxide surfaces
[DE94-005680] p 3522 N94-30901
SURFACE EMITTING LASERS
Visible vertical cavity surface emitting lasers
[AD-A275334] p 3293 N94-28919
SURFACE ENERGY
Surface energy changes produced by ultraviolet-ozone irradiation of poly(methylmethacrylate), polycarbone and polytetrafluoroethylene
[NASA-TM-106460] p 3213 N94-28922
SURFACE FINISHING
Analysis of cost: CVD diamond deposition and finishing --- Quarterly report
[AD-A275586] p 3212 N94-28725
Float polishing studies of fused silica
[AD-A275001] p 3213 N94-28886
Practical applications of plasma surface modification
[DE94-004892] p 3349 N94-29932
Logistics for the implementation of lead-free solders on electronic assemblies
[DE94-004800] p 3206 N94-29936
Evaluation of corrosion protecting properties of modern aircraft paint systems
[AD-B179388] p 3220 N94-30420
SURFACE LAYERS
Large eddy simulation of the upper atmospheric surface layer
[ISBN-0-315-85393-X] p 3365 N94-30134
SURFACE NAVIGATION
Automatic control steps for aircraft taxi guidance
p 3141 N94-29584
Navigation of military and space unmanned ground vehicles in unstructured terrains p 3144 N94-30282
A probabilistic approach to motion planning for car-like robots
[RUU-CS-93-18] p 3438 N94-30410
SURFACE PROPERTIES
Geometric structures of thin film: Pt on Pd(110) and NiO on Ni(100)
[DE94-005564] p 3211 N94-28530
Density reduction: A mechanism for amorphization at high ion doses
[DE94-004793] p 3483 N94-28559
Surface structure and stereochemical properties of self-assembled monolayer materials
[DE94-004960] p 3484 N94-28578
Lead detection and mapping with reference to relationships between scale, sensor characteristics, surface conditions and atmospheric properties
[AD-A275321] p 3377 N94-28877
Near-ultraviolet laser photoemission: Scanning microscopy, buried interfaces and image-potential states
p 3294 N94-29531
The performance of gloss meters on curving surfaces
[NPL-DMM(A)-111] p 3501 N94-30522
Nuclear magnetic relaxation studies of semiconductor nanocrystals and solids
[DE94-006301] p 3520 N94-30842
Influence of surface defects and local structure on oxygenate reaction pathways over metal oxide surfaces
[DE94-005680] p 3522 N94-30901
SURFACE REACTIONS
Development of novel switchable protein surfaces
[AD-A275510] p 3384 N94-28667
The effects of molecular orientation geometry and surface anisotropy upon etching
[AD-A275154] p 3486 N94-29032
Electrochemical behavior and surface chemistry of nonequilibrium aluminum alloys: Passivity mechanism and fabrication methods
[AD-A275401] p 3204 N94-29196
Theoretical investigation of gas-surface interactions
[NASA-CR-195755] p 3272 N94-29378
Effect of non-metallic inclusions on the machinability of steel
[PB93-230233] p 3204 N94-29387
Computer simulation of the interaction of fast hydrogen atoms with a molybdenum containing sorbed hydrogen
[DE94-608419] p 3209 N94-30253
Direct measurement of the reactivity of NH and OH on a silicon nitride surface
[DE94-005286] p 3199 N94-30260
An investigation of the corrosion properties of aluminum-tantalum alloys using electrochemical impedance spectroscopy and local electrochemical impedance spectroscopy p 3209 N94-30521
Modelling erosion damage from low-energy plasma gun simulations of disruptions
[DE94-005196] p 3509 N94-30697
Crosslinking and surface reactions in macromolecules: Spectroscopic FT-IR studies p 3221 N94-30812
Surface chemistry of boron-doped SiO2 CVD: Enhanced uptake of tetraethyl orthosilicate by hydroxyl groups bonded to boron
[DE94-005428] p 3221 N94-30896
SURFACE ROUGHNESS
Considerations in the modelling of seafloor acoustic backscatter
[AD-A275404] p 3478 N94-29206
Sensitivity and feedbacks associated with vegetation-related land surface parameters in a general circulation model p 3348 N94-29800
Radar returns from a low-flying target over a rough sea surface under multipath and clutter conditions
p 3253 N94-29882
Observation of the phase shift of the wave function of the neutron under total reflection
[DE94-608244] p 3489 N94-30096
An experimental study of the aerodynamics of a swept and unswept semispan wing with a simulated glaze ice accretion
[NASA-CR-195330] p 3133 N94-30152
Kinetics of surface roughening and smoothing during ion sputtering
[DE94-006358] p 3219 N94-30263

Experiments and theoretical considerations regarding the allowable roughness height in laminar flow
[PB94-125556] p 3133 N94-30389
Strain relaxation and surface roughness as a function of growth temperature in linearly graded In(x)Al(1-x)As (x = 0.05 to 0.25) buffers
[DE94-005430] p 3519 N94-30592
An asymptotic analysis for compressible gas lubrication of rough surfaces p 3222 N94-30922

SURFACE TEMPERATURE
Prediction of survival times on land in a cold climate p 3379 N94-28423
Objective analysis of a coastal ocean eddy using satellite AVHRR and in situ hydrographic data
[AD-A275715] p 3376 N94-28642
Thermal variation in vegetated or snow-covered background scenes and its effect on passive infrared systems
[AD-A275174] p 3325 N94-28849
The effects of molecular orientation geometry and surface anisotropy upon etching
[AD-A275154] p 3486 N94-29032
On the temperature distribution near a cold surface
[AD-A275162] p 3332 N94-29288
Dual-Band Infrared (DBIR) imaging inspections of Boeing 737 and KC-135 aircraft panels
[DE94-005700] p 3122 N94-29842
Nonlinear absorption in high reflector multilayers
[DE94-005818] p 3295 N94-30598
Dual-band infrared imaging for quantitative corrosion detection in aging aircraft
[DE94-004187] p 3149 N94-30687
RHEED studies of the nucleation, growth, and mobility of Ag atoms on the Si(111)7 x 7 surface
[DE94-005551] p 3521 N94-30899

SURFACE TREATMENT
Fuel injector design for high temperature aircraft engine p 3154 N94-29263
The effect of mechanical paint stripping on the fatigue and fracture of thin aluminum airplane skin p 3205 N94-29900
Practical applications of plasma surface modification
[DE94-004892] p 3349 N94-29932
Ablation of polymers by ultraviolet pulsed laser
[DE94-608100] p 3218 N94-30066
Plasma treatment of polymer dielectric films to improve capacitive energy storage p 3223 N94-30479

SURFACE VEHICLES
Three dimensional simulation of compressible flow induced by a high-speed train moving into a tunnel p 3126 N94-28967
A generic semi-autonomous ground vehicle control system p 3306 N94-30283
Encoding technique for automated guided vehicle POSE recovery in a structured environment p 3144 N94-30286

SURFACE WAVES
The rupture process of large earthquakes along convergent margins: Cast studies from Alaska and Armenia p 3363 N94-29969
On the nonlinear dynamics of ocean wave systems p 3378 N94-30790

SURFACTANTS
Regenerating using aqueous cleaners with ozone and electrolysis p 3240 N94-30468

SURGERY
Digital tracking and control of retinal images
[AD-A275469] p 3389 N94-28810
A force-controllable macro-micro manipulator and its application to medical robots p 3314 N94-30441
Dual use of image based tracking techniques: Laser eye surgery and low vision prosthesis p 3397 N94-30455
Dexterity enhancement in microsurgery using telemicro-robotics
[AIAA PAPER 94-1230-CP] p 3447 N94-30579

SURVEILLANCE
Cockpit video: A low cost BDA source
[AD-A275228] p 3150 N94-29389
ACCS Surveillance Exploratory Prototype (ASEP) p 3138 N94-29566
Airside ground movements surveillance p 3141 N94-29585
TacSats for NATO
[AGARD-AR-322] p 3169 N94-30350

SURVEILLANCE RADAR
GPS/GNSS for ATM p 3138 N94-29565
Development of precision runway monitor system for increasing capacity of parallel runway operations p 3142 N94-29587

SURVEYS
Advanced development of PV encapsulents
[DE94-000219] p 3336 N94-28500
NASA wiring program: Survey of NASA experiences in wiring system safety p 3165 N94-28700
An evaluation of techniques for ranking academic information systems journals
[AD-A275179] p 3529 N94-29066
Statistical Modeling and Estimation of Reliability Functions for Software (SMERFS) library access guide, revision 3
[AD-A275405] p 3411 N94-29207
A survey of NASA and military standards on fault tolerance and reliability applied to robotics
[AIAA PAPER 94-1211-CP] p 3445 N94-30562

SURVIVAL
Prediction of survival times on land in a cold climate p 3379 N94-28423
Effectiveness of protection clothing for cold weather conditions after ejection over sea: A case report p 3381 N94-28435
Advanced integrated cold protection for aircrew p 3381 N94-28436
Thermoregulation in the extreme cold environment p 3381 N94-28438

SUSPENSION SYSTEMS (VEHICLES)
Identification of the damping ratio relationship of an autovehicle suspension
[REPT-93-063] p 3313 N94-30937

SWELLING
Relationship between swelling and irradiation creep in cold-worked PCA stainless steel irradiated to approximately 178 dpa at approximately 400 C
[DE94-004368] p 3201 N94-28456
Molecular aspects of transport in thin films of controlled architecture
[DE94-004552] p 3211 N94-28457
Radiation effects in beryllium used for plasma protection
[DE94-004599] p 3201 N94-28460

SWEPT WINGS
Steady pressure measurements on an Aeroelastic Research Wing (ARW-2)
[NASA-TM-109046] p 3122 N94-28658
The 3-D LDV measurements on a 30-degree swept wing with a simulated ice accretion
[NASA-CR-195327] p 3132 N94-30124
An experimental study of the aerodynamics of a swept and unswept semispan wing with a simulated glaze ice accretion
[NASA-CR-195330] p 3133 N94-30152

SWEPTBACK WINGS
Design and fabrication of forward-swept counterrotation blade configuration for wind tunnel testing
[NASA-CR-194868] p 3155 N94-28510

SWIRLING
Modeling turbulence in flows with a strong rotational component
[DE94-003577] p 3270 N94-28475
Hydrodynamic stability analysis of swirling jets p 3278 N94-29974

SWITCHES
The 100 kA, 5000 V solid-state opening switch for inductive energy storage
[AD-A274993] p 3263 N94-28994
Proton switches
[AD-A275150] p 3167 N94-29022

SWITCHING
Quantum interference phenomena and novel switching in split gate high electron mobility transistors p 3266 N94-29734

SWITCHING CIRCUITS
Photoconductive switching for high power microwave generation
[PB94-137460] p 3244 N94-29177

SWIVELS
Parachute Swivel Mechanism for planetary entry p 3162 N94-29643

SYMBOLS
A comparison of three aircraft attitude display symbology structures
[AD-A275172] p 3150 N94-29048

SYMMETRY
Some constraints and solutions of the Kadomtsev-Petviashvili equation
[DE93-634355] p 3466 N94-28467
Extended nonabelian symmetries for free fermionic model
[DE94-601554] p 3481 N94-28470
Remarks on Galois symmetry in RCFT
[PB94-138179] p 3467 N94-29147
A numerical study of gravitational collapse p 3548 N94-30271

SYMPATHETIC NERVOUS SYSTEM
Japanese Journal of Aerospace and Environmental Medicine, vol. 30, no. 2
[JTN-94-80599] p 3394 N94-29863
Effect of water immersion on muscle sympathetic nerve response during static muscle contraction p 3394 N94-29865

SYMPTOMOLOGY
The Environmental Symptoms Questionnaire: Assessing reactions to environmental extremes in military operations p 3383 N94-28447

SYNAPSES
Synaptogenesis, selective stabilization, and free association
[AD-A275250] p 3392 N94-29431

SYNCHROCYCLOTRONS
On the (mu)SR activity at LNP JINR phasotron
[DE94-608385] p 3517 N94-30195

SYNCHRONISM
Synchronization in multistatic radar
[PB94-136975] p 3242 N94-28885
Acquisition time analysis of noncoherent PN sequence acquisition schemes
[AD-A275017] p 3244 N94-29094
Synchronization of microwave oscillators by direct optical injection
[ISBN-0-315-85546-0] p 3500 N94-30233
On blocks: Locality and asynchronous communication (extended abstract)
[RUU-CS-92-44] p 3424 N94-30347
The 25th Annual Precise Time and Time Interval (PTTI) Applications and Planning Meeting
[NASA-CP-3267] p 3468 N94-30639
Loran-C time management p 3144 N94-30644
Optical techniques for time and frequency transfer p 3469 N94-30647
Relativistic theory for picosecond time transfer in the vicinity of Earth p 3470 N94-30653
The two-way time synchronization system via a satellite voice channel p 3471 N94-30658
LASSO experiment: Intercalibrations of the LASSO ranging stations p 3297 N94-30666
Time synchronized video systems p 3261 N94-30675
Using GLONASS signal for clock synchronization p 3475 N94-30680

SYNCHRONOUS PLATFORMS
Time transfer using geostationary satellites: Implementation of a Kalman filter p 3471 N94-30657

SYNCHRONOUS SATELLITES
Microvibrations on a GEO telecommunication satellite
[REPT-932-440-101] p 3168 N94-29415

SYNCHROPHASOTRONS
Experimental setups and methods to obtain new nuclear data at intermediate and high energies
[DE94-607850] p 3489 N94-30052

SYNCHROTRON RADIATION
Activity report of Synchrotron Radiation Laboratory 1992
[JTN-94-80600] p 3495 N94-29596
Photoelectron diffraction and holography: Some new directions
[DE94-006297] p 3289 N94-30027
A high rate, low noise, x ray silicon strip detector system
[DE94-004557] p 3268 N94-30717

SYNCHROTRONS
Measurement of the W mass in the D0 detector
[DE94-006002] p 3490 N94-30103
Search for the top quark in the electron-electron and electron-muon channels at D0
[DE94-006174] p 3492 N94-30779

SYNTAX
Models of the untyped lambda-calculus in semi Cartesian closed categories
[ML-93-05] p 3456 N94-30381
The Vanilla meta-interpreter for definite logic programs and ambivalent syntax
[CT-93-01] p 3424 N94-30386
The conjoinability relation in Lambek calculus in linear logic
[ML-93-03] p 3457 N94-30397
Comparative semantics for linear arrays of communicating processes
[CWI-CS-R9336] p 3426 N94-30491
Federal grammars and modular compilers
[REPT-93-054] p 3429 N94-30928

SYNTHESIS (CHEMISTRY)
Synthesis and characterization of novel ternary and quaternary reduced molybdenum oxides
[DE94-005563] p 3510 N94-28529
Preparation, characterization, and facile thermolysis of (X2GaP(SiMe3)2) (X = Br, I) and (Cl3Ga2P)n; new precursors to nanocrystalline gallium phosphide
[AD-A275019] p 3513 N94-29130
Synthesis and molecular structures of R(Me3CCH2)2In-E(SiMe3) (R = Me3CCH2, E = P or As; R = Me, E = P)
[AD-A275020] p 3486 N94-29131
Tris(trimethylsily)arsine and lithium bis(trimethylsily)arsenide
[AD-A275075] p 3189 N94-29140

The synthesis and structural characterization of Na3WO3N
[AD-A275243] p 3204 N94-29395
Preparation of monodispersed fine particles containing rare metals and rare earths p 3201 N94-29514
Study on the formation of ultrafine particles of Sm-Co intermetallic compounds using RF thermal plasma p 3211 N94-29516
Preparation of graphite fibers from polyimide p 3223 N94-29517
Production of fullerenes with concentrated solar flux
[DE94-000266] p 3514 N94-29801
Bench-scale synthesis of nanoscale materials p 3240 N94-30473
Synthesis and characterization of advanced materials for Navy applications p 3223 N94-30474

SYNTHETIC APERTURE RADAR
Proceedings of the International Symposium on Remote Sensing
[JTN-94-80578] p 3325 N94-28925
Keynote address --- Japanese Earth Resources Satellite 1 (JERS-1) and future remote sensing projects p 3326 N94-28926
Synthetic aperture radar applications: Now and in the future p 3260 N94-28927
Observations by ERS-1 start p 3327 N94-28933
Sea ice and oceans applications of SAR p 3327 N94-28934
Observatory system of Earth Resources Satellite-1 p 3330 N94-29221
Application of JERS-1 data to geologic analyses p 3330 N94-29222
SAR-related stress variability in the Marine Atmospheric Boundary Layer (MABL)
[AD-A275275] p 3377 N94-29436
Automatic focus and registration of synthetic aperture radar images p 3246 N94-29536
Pointing mechanisms for the Shuttle Radar Laboratory p 3162 N94-29638
Analysis and an image recovery algorithm for ultrasonic tomography system p 3397 N94-30456

SYNTHETIC FIBERS
Preparation of graphite fibers from polyimide p 3223 N94-29517
The flow field near the body surface with thin filaments p 3234 N94-29706

SYNTHETIC FUELS
Proceedings of the 1993 Windsor Workshop on Alternative Fuels
[DE94-003908] p 3226 N94-30612
Proceedings of the low cost materials of construction for biological processes workshop
[DE94-000218] p 3226 N94-30761

SYSTEM FAILURES
Algorithms for treating redundancy in repairable and non-repairable systems
[DE94-005289] p 3315 N94-29020
Potential software failures methodology analysis p 3414 N94-29329
Distributed applications and failure tolerance programs using a reconfigurable parallel architecture p 3417 N94-29345
TOTAL user manual
[NASA-TM-109101] p 3432 N94-30160
Flight simulator evaluation of advanced MLS procedures
[AD-B174270] p 3143 N94-30915

SYSTEM IDENTIFICATION
A neural network-based technique for structural identification of SISO systems
[REPT-93-076] p 3449 N94-30941

SYSTEMS ANALYSIS
SAFSIM theory manual: A computer program for the engineering simulation of flow systems
[DE94-005381] p 3270 N94-28488
Identification of components to optimize improvement in system reliability
[DE94-001601] p 3315 N94-28503
Rome Laboratory software engineering technology program p 3414 N94-29330
Dependability analysis of parallel systems using a simulation-based approach
[NASA-CR-195762] p 3431 N94-29846
Modelling the evolution of information systems
[TR-92-36] p 3535 N94-30329
Evolving information systems: Meeting the ever-changing environment
[TR-92-24] p 3535 N94-30359

SYSTEMS ENGINEERING
Design of parallel systems for signal processing
[AD-A275490] p 3430 N94-28659
NASA wiring program: Survey of NASA experiences in wiring system safety p 3165 N94-28700
Cleanroom engineering handbook. Volume 3: Project execution in the cleanroom environment
[AD-A275860] p 3156 N94-28752
Designing for performance: A cognitive systems engineering approach to modifying an AWACS human computer interface
[AD-A275187] p 3399 N94-28861
Towards an information model and mechanisms for design rationale capture and use
[AD-A275060] p 3530 N94-29138
Artificial intelligence technology program at Rome Laboratory p 3414 N94-29328
Rome Laboratory software engineering technology program p 3414 N94-29330
On ground system integration and testing: A modern approach p 3150 N94-29334
A disciplined approach to software test and evaluation p 3416 N94-29339
A generalization of the software engineering maturity model p 3416 N94-29341
A common approach for an aerospace software environment p 3417 N94-29346
ISO overview: General presentation of the satellite, cryogenic aspects
[REPT-932-440-102] p 3231 N94-29416
The Common Modular Simulator (CMS): An architecture test bed for future advanced ATM systems p 3141 N94-29582
Advanced Design of Ventilation Systems
[VKI-LS-1993-07] p 3231 N94-29598
Introduction to the design of ventilation systems p 3231 N94-29599
Industrial ventilation p 3232 N94-29604
Advanced vehicle concepts systems and design analysis studies
[NASA-CR-195115] p 3147 N94-29721
A performance analysis method for distributed real-time robotic systems: A case study of remote teleoperation
[AIAA PAPER 94-1212-CP] p 3445 N94-30563
Engineering of systems for application of scientific computing in industry WP project management ISNaS 9209099
[PB94-126232] p 3428 N94-30739
Solar photovoltaics for development applications
[DE94-006116] p 3340 N94-30843
A review of the status and capabilities of Navstar GPS
[AD-B174629] p 3143 N94-30854
Validation experiments with an Ethernet model using the simulation tool 'PROMISE'
[AD-B174795] p 3429 N94-30912

SYSTEMS INTEGRATION
Arcjet system integration development
[NASA-CR-187147] p 3171 N94-28736
On ground system integration and testing: A modern approach p 3150 N94-29334
Future manned systems advanced avionics study
[NASA-CR-188277] p 3150 N94-29377
Automation of the NDT diagnostic using neural nets. Application: Inspection of Airbus longitudinal joints during maintenance
[REPT-932-600-104] p 3315 N94-29474
Air-ground integration of the ATM system in PHARE p 3141 N94-29579
Integration of pyrotechnics into aerospace systems p 3161 N94-29634
Programmable Automated Welding System (PAWS)
[AIAA PAPER 94-1221-CP] p 3446 N94-30570
Robotic NDE inspection of advanced solid rocket motor casings
[AIAA PAPER 94-1222-CP] p 3446 N94-30571
The Automated Aircraft Rework System (AARS): A system integration approach
[AIAA PAPER 94-1225-CP] p 3446 N94-30574
View integration: A survey of current developments
[REPT-93-053] p 3536 N94-30927

SYSTEMS MANAGEMENT
Publications of the NASA Controlled Ecological Life Support System (CELSS) program 1989-1992
[NASA-CR-4603] p 3401 N94-30122

SYSTEMS SIMULATION
Thermal enclosure system functional simulation user's manual
[NASA-TM-109094] p 3466 N94-29489
The Common Modular Simulator (CMS): An architecture test bed for future advanced ATM systems p 3141 N94-29582
The use of task network simulation in workload prediction
[DCIEM-92-32] p 3402 N94-30132

SYSTEMS STABILITY
Stability of dynamical systems in the presence of noise
[AD-A275383] p 3243 N94-29072
Self-stabilizing l-exclusion algorithms
[RUU-CS-93-01] p 3424 N94-30379
Dynamics and control of tethered satellite systems p 3170 N94-30864
Local interaction control for space construction p 3170 N94-30960

T

TABLES (DATA)
Transferable Output ASCII Data (TOAD) editor version 1.0 user's guide
[NASA-CR-187507] p 3408 N94-28818

TACTILE DISCRIMINATION
Tactility as a function of grasp force: Effects of glove, orientation, pressure, load, and handle
[NASA-TP-3474] p 3402 N94-30210

TAIL ROTORS
Acquisition, design modification, assembly, and ground test of NPS Hummingbird remotely piloted helicopter
[AD-A275546] p 3146 N94-28837

TALC
Non-chromate talc conversion coatings for aluminum
[DE94-005281] p 3207 N94-30053

TANKER AIRCRAFT
Effectiveness of protection clothing for cold weather conditions after ejection over sea: A case report p 3381 N94-28435

TANTALUM
Influence of tungsten alloying additions on the mechanical properties and texture of tantalum
[DE94-004994] p 3210 N94-30774

TANTALUM ALLOYS
An investigation of the corrosion properties of aluminum-tantalum alloys using electrochemical impedance spectroscopy and local electrochemical impedance spectroscopy p 3209 N94-30521
Influence of tungsten alloying additions on the mechanical properties and texture of tantalum
[DE94-004994] p 3210 N94-30774
Nature of dissolution of binary tantalum-titanium alloys by molten plutonium
[DE94-005090] p 3210 N94-30776

TANTALUM CARBIDES
Deposition of tantalum carbide coatings on graphite by laser interactions p 3223 N94-30475

TARGET ACQUISITION
Using multiple searchers to locate a randomly moving target
[AD-A275602] p 3463 N94-28768
Environmental characterization for target acquisition. Analysis of thermal and visible imagery
[AD-A275414] p 3242 N94-28862
GLRS-R 2-colour retroreflector target design and predicted performance
[REPT-932-440-106] p 3246 N94-29542
ACCS Surveillance Exploratory Prototype (ASEP) p 3138 N94-29566
Radar returns from a low-flying target over a rough sea surface under multipath and clutter conditions p 3253 N94-29882
Infrared polarization signatures p 3258 N94-30506
Model for the simulation of atmospheric effects on targets to background passive signatures p 3258 N94-30507
The effect of enhanced backscattering on target detection p 3258 N94-30508
A hybrid electromagnetic-statistical approach for characterizing MMW scattering by terrain p 3259 N94-30510
Radar cross sections of ground clutter at 95 GHz for summer and fall conditions p 3259 N94-30512

TARGET RECOGNITION
Environmental characterization for target acquisition. Analysis of thermal and visible imagery
[AD-A275414] p 3242 N94-28862
Spectral and polarimetric analysis of hyperspectral data collected by an acousto-optic tunable filter system
[AD-A275076] p 3329 N94-29095
ACCS Surveillance Exploratory Prototype (ASEP) p 3138 N94-29566
Psychophysiological study on the effects of co-existence of lines for detecting dot target p 3394 N94-29867
Knowledge combination and data fusion with application to recognition systems p 3259 N94-30513

TARGET THICKNESS
An electromagnetic noncontacting sensor for thickness measurement in a dispersive medium
[AIAA PAPER 94-1200-CP] p 3443 N94-30551

TARGETS
Psychophysiological study on the effects of co-existence of lines for detecting dot target p 3394 N94-29867
Experimental evaluation of camouflage effectiveness in the thermal infrared p 3257 N94-30502

TASK PLANNING (ROBOTICS)
A Space Station robot walker and its shared control software
[AIAA PAPER 94-1192-CP] p 3442 N94-30543
Task-level control for autonomous robots
[AIAA PAPER 94-1210-CP] p 3444 N94-30561
Using generic tool kits to build intelligent systems
[AIAA PAPER 94-1214-CP] p 3445 N94-30565

A reactive system for open terrain navigation: Performance and limitations
| AIAA PAPER 94-1218-CP | p 3445 N94-30566
The road plan model: Information model for planning road building activities
| AIAA PAPER 94-1219-CP | p 3445 N94-30567

TASKS
Simulation Networking/Training Requirements Relational Database: User's guide
| AD-A275634 | p 3528 N94-28637
Toward a model of expert knowledge structure and their role in cognitive task performance
| AD-A275641 | p 3529 N94-28645
Cognitive approach to specifications on air traffic controllers' decision assistance systems p 3139 N94-29571
Considerations on graphical user interfaces for intelligent ATM support systems p 3139 N94-29572
The use of task network simulation in workload prediction
| DCIEM-92-32 | p 3402 N94-30132

TASTE
Some issues on Japan's space food development and relating preliminary experimental study p 3388 N94-28498

TAXIING
Automatic control steps for aircraft taxi guidance p 3141 N94-29584
Airside ground movements surveillance p 3141 N94-29585
A novel near-range radar network for airport surface control p 3142 N94-29586

TAYLOR INSTABILITY
Dynamic response of ceramics
| AD-A275396 | p 3214 N94-29203
A review of the ablative stabilization of the Rayleigh-Taylor instability in regimes relevant to ICF
| DE94-005809 | p 3509 N94-30597
Design of an electromagnetic accelerator for turbulent hydrodynamic mix studies
| DE94-005821 | p 3281 N94-30600

TEACHING MACHINES
Reinforcement learning for robots using neural networks p 3437 N94-29853
Use of bad training data for better predictions
| DE94-006233 | p 3427 N94-30705

TECHNOLOGIES
Proceedings: SISAL 1993
| DE94-006641 | p 3420 N94-30056

TECHNOLOGY ASSESSMENT
A conceptual framework for software technology transition
| AD-A275637 | p 3407 N94-28639
Technology base enhancement program. Metal matrix composites
| AD-A275531 | p 3176 N94-28688
Report on smart materials
| PB94-137528 | p 3203 N94-29015
Combustion technology needs for advanced high pressure cycle engines p 3190 N94-29248
Proceedings of the Workshop on Microtechnologies and Applications to Space Systems
| NASA-CR-195688 | p 3235 N94-29767
Micro guidance and control technology overview p 3144 N94-29772
Technical analysis of alternative fueled vehicles
| DE94-744238 | p 3304 N94-30269
A look into the crystal ball: The next 25 years p 3475 N94-30681
Frequency standards from government laboratories over the next 25 years p 3475 N94-30682
Frequency standards from industry over the next 25 years p 3475 N94-30683
The future of time and frequency dissemination p 3476 N94-30684
DOE New Technology: Sharing New Frontiers, April 1, 1993 - September 30, 1993
| DE93-041289 | p 3535 N94-30699
DOE/KEURP site operator program
| DE94-005832 | p 3267 N94-30701
Investigation of the technology development status of alternate fuel vehicles
| DE94-744237 | p 3312 N94-30831
A review of the status and capabilities of Navstar GPS
| AD-B174629 | p 3143 N94-30854
Compressed natural gas fueled vehicles: The Houston experience
| DE94-005804 | p 3312 N94-30878

TECHNOLOGY TRANSFER
Spin-off companies as agents of technology transfer: An empirical study of the spin-off companies of the Technical Research Centre of Finland
| PB94-132248 | p 3537 N94-28405
Cleanroom engineering handbook. Volume 3: Project execution in the cleanroom environment
| AD-A275860 | p 3156 N94-28752
Cleanroom engineering handbook. Volume 4: Specification team practices
| AD-A275861 | p 3156 N94-28753
Technology transfer initiatives
| NASA-CR-195151 | p 3537 N94-29410
Overview of microoptics: Past, present, and future p 3235 N94-29771
Technology 2003: The Fourth National Technology Transfer Conference and Exposition, volume 1
| NASA-CP-3249 | p 3555 N94-30440
Precision and manufacturing at the Lawrence Livermore National Laboratory p 3240 N94-30449
Technology transfer and evaluation for Space Station telerobotics
| AIAA PAPER 94-1190-CP | p 3441 N94-30541
DOE New Technology: Sharing New Frontiers, April 1, 1993 - September 30, 1993
| DE93-041289 | p 3535 N94-30699
Geothermal direct-heat utilization assistance
| DE94-005831 | p 3340 N94-30700

TECHNOLOGY UTILIZATION
Spin-off companies as agents of technology transfer: An empirical study of the spin-off companies of the Technical Research Centre of Finland
| PB94-132248 | p 3537 N94-28405
Current leads and magnetic bearings
| DE94-004607 | p 3297 N94-28461
Survey report of JSUP Space Environment Utilization Research Committee in fiscal year 1992: Protein Crystal Growth Session
| JTN-94-80584 | p 3158 N94-28583
Remote sensing and global management p 3328 N94-28937
Computational fluid dynamics in ventilation. 4: Commercial application of CFD in ventilation p 3233 N94-29609
A 32 GHz microstrip array antenna for microspacecraft application p 3251 N94-29668
Human and institutional factors in GIS implementation by local governments p 3532 N94-29804
Robotics and the battlefield of the future p 3304 N94-30277
Hybrid optics for space applications
| ESA-CP-1158 | p 3501 N94-30418
Cubanes: Super explosives and potential pharmaceutical intermediates p 3227 N94-30454
Dual use of image based tracking techniques: Laser eye surgery and low vision prosthesis p 3397 N94-30455
Composite redesign of obstetrical forceps p 3397 N94-30457
Intelligent robotics can boost America's economic growth
| AIAA PAPER 94-1301-CP | p 3439 N94-30527
On-orbit spacecraft servicing: An element in the evolution of space robotics applications
| AIAA PAPER 94-1236-CP | p 3448 N94-30583
DOE New Technology: Sharing New Frontiers, April 1, 1993 - September 30, 1993
| DE93-041289 | p 3535 N94-30699

TECTONICS
Studies in Jurassic and Cretaceous North American apparent polar wander p 3362 N94-29940
The rupture process of large earthquakes along convergent margins: Cast studies from Alaska and Armenia p 3363 N94-29969

TEFLON (TRADEMARK)
High damage threshold anti-reflectors by physical vapor deposited amorphous fluoropolymer
| DE94-004865 | p 3212 N94-28560

TELECOMMUNICATION
The Telecommunications and Data Acquisition Report
| NASA-CR-195694 | p 3246 N94-29613
Hypra/TR: A tuple oriented recovery method for a continuously available distributed DBMS on a shared nothing multi-computer
| PB94-141264 | p 3533 N94-29921

TELECONFERENCING
Security aspects of computer supported collaborative work
| AD-A275638 | p 3528 N94-28640

TELEMETRY
A space-based classification system for RF transients
| DE94-003933 | p 3240 N94-28522
Phasing the Very Large Array on Galileo in the presence of Jupiter's strong radio emission p 3164 N94-29621
Design and analysis of a low-loss linear analog phase modulator for deep space spacecraft X-band transponder applications p 3248 N94-29625
A dual-cavity ruby maser for the Ka-band link experiment p 3250 N94-29658
A digital combining-weight estimation algorithm for broadband sources with the array feed compensation system p 3250 N94-29660

TELEOPERATORS
Teleoperated systems for nuclear reactors: Inspection and maintenance
| AIAA PAPER 94-1176-CP | p 3439 N94-30528
Object-based task-level control: A hierarchical control architecture for remote operation of space robots
| AIAA PAPER 94-1209-CP | p 3444 N94-30560
A performance analysis method for distributed real-time robotic systems: A case study of remote teleoperation
| AIAA PAPER 94-1212-CP | p 3445 N94-30563
A control method for bilateral teleoperating systems
| ISBN-0-315-78705-8 | p 3313 N94-30952

TELEROBOTICS
A new method for recognizing quadric surfaces from range data and its application to telerobotics and automation, final phase
| NASA-CR-195733 | p 3408 N94-28825
Thermal enclosure system functional simulation user's manual
| NASA-TM-109094 | p 3466 N94-29489
Aspects of the operator interface for military robotic applications in unstructured environments p 3309 N94-30304
A multiplexed two-way solid communications link for teleoperated robots p 3310 N94-30310
Task automation in a successful industrial telerobot
| AIAA PAPER 94-1189-CP | p 3441 N94-30539
Technology transfer and evaluation for Space Station telerobotics
| AIAA PAPER 94-1190-CP | p 3441 N94-30541
Space flight manipulator technologies and requirements for the NASA Flight Telerobotic Servicer (FTS)
| AIAA PAPER 94-1191-CP | p 3441 N94-30542
A Space Station robot walker and its shared control software
| AIAA PAPER 94-1192-CP | p 3442 N94-30543
Technology for robotic surface inspection in space
| AIAA PAPER 94-1193-CP | p 3442 N94-30544
Object-based task-level control: A hierarchical control architecture for remote operation of space robots
| AIAA PAPER 94-1209-CP | p 3444 N94-30560
A performance analysis method for distributed real-time robotic systems: A case study of remote teleoperation
| AIAA PAPER 94-1212-CP | p 3445 N94-30563
Dexterity enhancement in microsurgery using telemicro-robotics
| AIAA PAPER 94-1230-CP | p 3447 N94-30579
Terrestrial applications of NASA space telerobotics technologies
| AIAA PAPER 94-1235-CP | p 3448 N94-30582
A control method for bilateral teleoperating systems
| ISBN-0-315-78705-8 | p 3313 N94-30952

TELESCOPES
NASA Marshall Space Flight Center Solar Observatory report, July - October 1993
| NASA-TM-108448 | p 3160 N94-29470
Aircraft system aft telescope cavity configuration study for Stratospheric Observatory for Infrared Astronomy (SOFIA), phase 2
| NASA-CR-194266 | p 3147 N94-29685

TELEVISION SYSTEMS
A space-based classification system for RF transients
| DE94-003933 | p 3240 N94-28522

TELLURIUM ALLOYS
Thermodynamics of molten K-TE alloys
| DE94-608095 | p 3208 N94-30090

TEMPERATURE
Estimation of the net production of moss community at Langhovde, East Antarctica p 3358 N94-29081

TEMPERATURE CONTROL
Fuels combustion research
| AD-A275122 | p 3189 N94-29004
An alternate method for achieving temperature control in the -160 to +90 C range
| NASA-CASE-NPO-18995-1-CU | p 3288 N94-29497
Maintaining acceptable thermal comfort with a low air temperature by means of local heating
| PB94-138526 | p 3401 N94-29950
Numerical comparison of convective heat transfer augmentation devices used in cooling channels of hypersonic vehicles
| NASA-TM-106546 | p 3279 N94-30147
Application of fuzzy logic to the control of wind tunnel settling chamber temperature
| NASA-TM-109105 | p 3157 N94-30200
Process modelling for materials preparation experiments
| NASA-CR-195782 | p 3175 N94-30242

TEMPERATURE DEPENDENCE
Experimental and analytical studies of high heat flux components for fusion experimental reactor
| DE94-707671 | p 3504 N94-28556

Atomic and magnetic structure of YBa2(Cu(1-x)Fe(x))3O(6+y) at 0.05 less than or equal to x less than or equal to 0.30, y is approximately equal to 1 and y is approximately equal to 0.5
[DE94-606852] p 3513 N94-29210
Creep and physical aging of PVC: Dependence on stress and temperature
[NPL-DMM(A)-115] p 3217 N94-29886
Particle kinetic simulation of high altitude hypervelocity flight
[NASA-CR-194535] p 3131 N94-29893
Global patterns of cloud optical thickness variation with temperature and the implications for climate change
p 3374 N94-29972
Study of the ultraviolet absorption and photoconduction spectra of polyimide films fabricated at various curing temperatures
[ISBN-0-315-85923-7] p 3218 N94-30036
The bases for the development of high-temperature integrated SQUID-systems
[DE94-607901] p 3267 N94-30073
On the structure and atomic motions in liquid sodium
[DE94-608386] p 3490 N94-30182
Peculiarities of heat transfer in the experiments of beam injection heating of a plasma at the GOL-3 device
[DE94-608357] p 3508 N94-30194
Strain relaxation and surface roughness as a function of growth temperature in linearly graded In(x)Al(1-x)As (x = 0.05 to 0.25) buffers
[DE94-005430] p 3519 N94-30592
Terfenol: A study of the phase equilibrium diagram and the solidification process
[DE94-004883] p 3209 N94-30690
Scaling in heavy-fermion systems
[DE94-005002] p 3492 N94-30775

TEMPERATURE DISTRIBUTION
Objective analysis of a coastal ocean eddy using satellite AVHRR and in situ hydrographic data
[AD-A275715] p 3376 N94-28642
A novel spectroscopic measurement method of RF plasma for temperature and electron density diagnoses
p 3188 N94-28682
A random distribution reacting mixing layer model
[NASA-TM-106517] p 3150 N94-28923
The mixing process in the quenching zone of the rich-lean-combustion concept p 3196 N94-29281
On the temperature distribution near a cold surface
[AD-A275162] p 3332 N94-29288
Four-dimensional data assimilation using the adjoint method p 3455 N94-30353
Intra- versus interlayer pairing in the copper oxide superconductors: Response to a magnetic field
[DE94-005475] p 3521 N94-30898

TEMPERATURE EFFECTS
Measurement of volatile metal species at elevated temperatures
[PB94-132321] p 3186 N94-28407
Physiological investigations of the isolated rat's liver in hypothermia and hypoxia and their relevance in aircraft incidents above the sea p 3382 N94-28439
High temperature polymer dielectric film insulation
p 3167 N94-28715
Probabilistic material strength degradation model for Inconel 718 components subjected to high temperature, mechanical fatigue, creep and thermal fatigue effects
[NASA-CR-195284] p 3318 N94-28840
Low temperature behavior of virgin martensite
[PB94-132925] p 3204 N94-29142
Pollutant emissions from and within a model gas turbine combustor at elevated pressures and temperatures
p 3194 N94-29271
The influence of temperature on microelectronic device failure mechanisms, phase 2
[AD-A275029] p 3265 N94-29511
Finite element analysis of axisymmetric deformations of thick thermoviscoplastic targets p 3320 N94-29688
Mechanisms and effects of heat generation at the tips of dynamic cracks and notches in metals
p 3321 N94-29808
An actively cooled floating element skin friction balance for direct measurement in high enthalpy supersonic flows p 3289 N94-29824
The effect of temperature on creep and physical ageing of PVC
[NPL-DMM(A)-93] p 3217 N94-29885
Antarctic Record, vol. 36, no. 3
[REPT-108] p 3363 N94-29978
Theory and application of a Radio-Acoustic Sounding System (RASS) p 3367 N94-30869

TEMPERATURE GRADIENTS
Lock-up failure of a four-bar linkage deployment mechanism p 3163 N94-29646
Theory and application of a Radio-Acoustic Sounding System (RASS) p 3367 N94-30869

TEMPERATURE MEASUREMENT
Objective analysis of a coastal ocean eddy using satellite AVHRR and in situ hydrographic data
[AD-A275715] p 3376 N94-28642
Global Acoustic Mapping of Ocean Temperatures (GAMOT)
[AD-A275777] p 3376 N94-28740
Heat flux instrumentation for Hyflite thermal protection system
[NASA-CR-195731] p 3286 N94-28824
System for improving measurement accuracy of transducer by measuring transducer temperature and resistance change using thermoelectric voltages
[NASA-CASE-ARC-12014-1] p 3287 N94-29361
Determining noise temperatures in beam waveguide systems p 3249 N94-29657
Non-invasive temperature measurements using electron paramagnetic resonance spectroscopy
p 3198 N94-29881
A low noise silicon detector preamplifier system for room temperature x ray spectroscopy
[REPT-93-058] p 3291 N94-30930

TEMPERATURE PROFILES
On the temperature distribution near a cold surface
[AD-A275162] p 3332 N94-29288
Fronts at the confluences of spring-fed streams with Joekulsa a Fjoellum: Possibly thermal bars?
[MATHS-REPT-A-198] p 3333 N94-29528
Atmospheric moisture fields derived by satellite observations over the tropical Pacific Ocean
p 3375 N94-30863

TEMPERATURE SENSORS
Heat flux instrumentation for Hyflite thermal protection system
[NASA-CR-195731] p 3286 N94-28824

TEMPLATES
Template synthesized nanoscopic gold particles: Optical spectra and the effects of particle size and shape
[AD-A275378] p 3197 N94-29312

TEMPORAL DISTRIBUTION
Use of satellite data to improve parameterization of spatial and temporal variations of gaseous dry deposition in regional-scale models
[DE94-005110] p 3334 N94-30022
Time and frequency technology at NIST
p 3468 N94-30641

TEMPORAL RESOLUTION
Evolution of miniature detectors and focal plane arrays for infrared sensors p 3237 N94-29781
Development of high time-resolution laser flash equipment for thermal diffusivity measurements using miniature-size specimens
[NIFS-268] p 3295 N94-30186
Multitemporal analysis of a braiding river: The advanced study of 1992
[NLR-TP-93100-U] p 3335 N94-30942

TENSILE CREEP
The effect of temperature on creep and physical ageing of PVC
[NPL-DMM(A)-93] p 3217 N94-29885

TENSILE PROPERTIES
Effects of thermomechanical processing on tensile and long-time creep behavior of Nb-1 percent Zr-0.1 percent C sheet
[NASA-TM-106319] p 3202 N94-28822
An analysis of the microstructure and reinforcement distribution of an extruded particle-reinforced Al 6061-10 volume percent Al2O3 metal matrix composite
[AD-A275050] p 3178 N94-29166
Low dielectric polyimide fibers
[NASA-CASE-LAR-14526-1] p 3214 N94-29359

TENSILE STRENGTH
Microstructure/property relationships for SCS6/Timetal 21-S composite
[AD-A275056] p 3178 N94-29135
Numerical analysis of dynamic direct tension and direct compression tests
[AD-A275255] p 3319 N94-29433
Preliminary evaluation of hybrid titanium composite laminates
[NASA-TM-109095] p 3180 N94-29472
Delamination growth in composites under cyclic loads
p 3183 N94-30256
Controlling the material properties of in vitro collagen through directed orientation and cross-linking of fibrils
p 3221 N94-30797

TENSILE STRESS
Micromechanics of the dynamic response of ceramics and ceramic composites p 3217 N94-29975

TENSILE TESTS
Fatigue behavior of a cross-ply ceramic matrix composite at elevated temperatures under tension-tension loading
[AD-A275466] p 3176 N94-28673
Fatigue behavior of a cross-ply ceramic matrix composite under strain controlled tension-tension and tension-compression loading
[AD-A275374] p 3177 N94-29012
Microstructure/property relationships for SCS6/Timetal 21-S composite
[AD-A275056] p 3178 N94-29135
The effect of temperature on creep and physical ageing of PVC
[NPL-DMM(A)-93] p 3217 N94-29885
Particulate metal matrix composites: Draft procedure for tensile tests at ambient temperature
[NPL-DMM(A)-100] p 3184 N94-30419
Approximate estimation of the effects of asymmetry on the testing of tensile specimens
[NPL-DMM(A)-117] p 3322 N94-30523

TENSORS
Modeling turbulence in flows with a strong rotational component
[DE94-003577] p 3270 N94-28475
A note on the Poisson brackets associated with Lax operators
[MATHS-REPT-A-195] p 3464 N94-29482
Anomalous algebraic structures in quantum field theories p 3524 N94-29911
Homogeneous Poisson structures
[DE94-608112] p 3453 N94-30119

TERBIUM COMPOUNDS
Terfenol: A study of the phase equilibrium diagram and the solidification process
[DE94-004883] p 3209 N94-30690

TERMINAL BALLISTICS
Least-squares determination of burst-point coordinates
[AD-A275423] p 3452 N94-28864

TERMS
Index expression belief networks for information disclosure
[TR-92-23] p 3465 N94-30358
Total termination of term rewriting
[RUU-CS-92-42] p 3460 N94-30744

TERNARY ALLOYS
Terfenol: A study of the phase equilibrium diagram and the solidification process
[DE94-004883] p 3209 N94-30690

TERNARY SYSTEMS
The synthesis and structural characterization of Na3WO3N
[AD-A275243] p 3204 N94-29395
Studies of high temperature ternary phases in mixed-metal-rich early transition metal sulfide and phosphide systems
[DE94-006034] p 3209 N94-30336

TERRAIN
Environmental characterization for target acquisition. Analysis of thermal and visible imagery
[AD-A275414] p 3242 N94-28862
Feature mapping in a photogrammetric GIS
[AD-A275418] p 3325 N94-28863
The uses and limitations of fractal geometry in digital terrain modelling p 3333 N94-29958
A physical optics model for scattering of HF radiation by irregular terrain
[DE94-006187] p 3255 N94-30106
A hybrid electromagnetic-statistical approach for characterizing MMW scattering by terrain
p 3259 N94-30510

TERRAIN ANALYSIS
The uses and limitations of fractal geometry in digital terrain modelling p 3333 N94-29958
Applicability of digital terrain analyses to wind energy prospecting and siting
[DE94-004363] p 3374 N94-30587

TEST CHAMBERS
Vacuum chamber and adaptors for shearography and holography
[NASA-CR-192467] p 3157 N94-29956
A modernised HST of NLR
[AD-B179220] p 3158 N94-30423

TEST EQUIPMENT
Modelling soft impacts for vibrational excitation of civil engineering structures
[PB94-137619] p 3320 N94-29681

TEST FACILITIES
Testing laboratories as notified bodies
[PB94-132396] p 3160 N94-28413
Data fusion and correlation techniques testbed development. Phase 1: Interim report
[SKD-1600-73-015] p 3405 N94-28533
Cryogenic probe station for use in automated microwave and noise figure measurements
[NASA-TM-106560] p 3286 N94-29000
CIAM experimental turboramjets p 3152 N94-29299
Development of electromagnetic compatibility tests
[REPT-932-430-110] p 3245 N94-29421
McMaster accelerator facility p 3496 N94-30217

Advanced development of the Spectrum Sciences Model 5005-TF, single event test fixture p 3291 N94-30218
Using Cf-252 for single event upset testing p 3496 N94-30219
A testbed for the development of ground-based control of space-based manipulators p 3309 N94-30306
Technology transfer and evaluation for Space Station telerobotics [AIAA PAPER 94-1190-CP] p 3441 N94-30541
Free-floating dual-arm robots for space assembly [AIAA PAPER 94-1195-CP] p 3442 N94-30546
The MACS-TSA applied in the ISO and SAX spacecraft projects [PB94-126257] p 3170 N94-30857

TEST PATTERN GENERATORS
An UIO-based method for protocol conformance testing [REPT-93-060] p 3429 N94-30931

TEST STANDS
Technology rigs: A tool for afterburner development p 3154 N94-29270

TEST VEHICLES
Mars rover mechanisms designed for Rocky 4 p 3161 N94-29630
DOE/KEURP site operator program [DE94-005832] p 3267 N94-30701

TESTING TIME
Validation and test of complex weapon systems p 3150 N94-29336

TETHERED SATELLITES
Dynamics and control of tethered satellite systems p 3170 N94-30864

TETRAETHYL ORTHOSILICATE
Surface chemistry of boron-doped SiO2 CVD: Enhanced uptake of tetraethyl orthosilicate by hydroxyl groups bonded to boron [DE94-005428] p 3221 N94-30896

TETRAHEDRONS
Rotator phases in narrow-gap semiconductors [DE94-005472] p 3521 N94-30897

TEXTILES
The potential of new textiles in improving survival prospects p 3380 N94-28430
Fire-resistant water vapour permeable buoyant insulation p 3380 N94-28431
Development of braided rope engine seals [NASA-TM-105902] p 3298 N94-28838
Low dielectric polyimide fibers [NASA-CASE-LAR-14526-1] p 3214 N94-29359
Physical interpretation and development of ultrasonic nondestructive evaluation techniques applied to the quantitative characterization of textile composite materials [NASA-CR-195766] p 3183 N94-30016

TEXTURES
Failures to model the development of a cube texture during the high temperature compression of Al-Mg alloys [DE94-005013] p 3201 N94-28544
Seafloor characterization using texture [AD-A275399] p 3377 N94-29204
Unsupervised texture image segmentation by improved neural network ART2 [AIAA PAPER 94-1199-CP] p 3442 N94-30549
Influence of tungsten alloying additions on the mechanical properties and texture of tantalum [DE94-004994] p 3210 N94-30774
A comparison of the evolution of cold and hot deformation microstructures and textures in fcc metals [DE94-005103] p 3210 N94-30777

THAILAND
Utilization of remote sensing data in Southeast Asia p 3327 N94-28936

THALLIUM COMPOUNDS
InTlSb for long-wavelength infrared photodetectors and arrays [AD-A275079] p 3512 N94-28872

THEMATIC MAPPING
Evaluation of simulated JERS-1 data for geologic mapping at Drum Mountains, Utah, Silver Bell, Arizona, and Wind River, Wyoming under the GEOSAT-ERSDAC/JAPEX/JGI/RESTEC joint studies p 3326 N94-28929
Extrapolation of point data for resource mapping p 3334 N94-29959

THEOREM PROVING
Partial support for the Second International Symposium on Artificial Intelligence and Mathematics [AD-A275199] p 3434 N94-29026
Program derivation by proof transformation [AD-A275260] p 3453 N94-29304
Addendum to the final report for the investigation of proof techniques within the EVES verification technology [TR-93-5451-03] p 3421 N94-30155
A smart child of Peano's [ML-92-10] p 3455 N94-30325
Only few graphs have bounded treewidth [RUU-CS-92-35] p 3455 N94-30333
Two algorithms for finding rectangular duals of planar graphs [RUU-CS-92-41] p 3423 N94-30345
Derivation lengths in term rewriting from interpretations in the naturals [RUU-CS-92-43] p 3455 N94-30346
The transient period of a cyclic process: An horizon theorem [MEMO-1149] p 3427 N94-30585
Bisimulations and predicate logic [CWI-CS-R9333] p 3460 N94-30735

THEOREMS
Dynamic generalized quantifiers and monotonicity [LP-93-02] p 3454 N94-30319
Modal quantification over structured domains [ML-93-02] p 3457 N94-30396
The transient period of a cyclic process: An horizon theorem [MEMO-1149] p 3427 N94-30585
Perfect binary space partitions [RUU-CS-93-23] p 3460 N94-30728
The structure of exponentials: Uncovering the dynamics of linear logic proofs [ML-93-10] p 3430 N94-30973
Inventory of fragments and exact models in intuitionistic proportional logic [ML-93-11] p 3463 N94-30974
Undecidability in diagonalizable algebras [ML-93-13] p 3463 N94-30976

THEORETICAL PHYSICS
Specialized data base management system for data processing in the experiments at low energies [DE94-606268] p 3485 N94-28621
Weak decays of charged K-mesons and charm particles [PB94-138062] p 3486 N94-29143
Magnetic properties of a quantum transverse spin-1 Blume-Emery-Griffiths model [DE94-608114] p 3517 N94-30109
Research laboratories annual report 1992 [DE94-608124] p 3555 N94-30168

THERMAL ANALYSIS
Thermal/structural tailoring of engine blades (T/SEAEBL). Theoretical manual [NASA-CR-194462] p 3317 N94-28815
Modelling and analysis of creep deformation and fracture in a 1 Cr 1/2 Mo ferritic steel [PB94-138328] p 3319 N94-29121
Application of FLUIDNET-G software to the preliminary thermal and hydraulic design of Hermes spaceplane [REPT-932-440-107] p 3168 N94-29543
Study of iron exchanged zeolites by Moessbauer effect and electron spin resonance spectroscopy [DE94-605138] p 3514 N94-29691
Analysis of infrared radiation heating process considering chemical reaction of material to be heated [DE94-744116] p 3199 N94-30267
Terfenol: A study of the phase equilibrium diagram and the solidification process [DE94-004883] p 3209 N94-30690

THERMAL BOUNDARY LAYER
Hydrodynamics of convection under winter polar leads [AD-A275182] p 3369 N94-29067

THERMAL BUCKLING
Free vibration of thermally loaded panels including initial imperfections and post-buckling effects [NASA-TM-109097] p 3479 N94-29461

THERMAL COMFORT
Thermal strain generated by an enhanced anti-G protection system in a hot climate p 3383 N94-28445
Recent Canadian advances in active thermal protection p 3384 N94-28451
Maintaining acceptable thermal comfort with a low air temperature by means of local heating [PB94-138526] p 3401 N94-29950

THERMAL CONDUCTIVITY
Properties of graphite fiber reinforced copper matrix composites for space power applications [NASA-CR-191026] p 3178 N94-29208
Insulative properties of two thermo-metal neoprenes [AD-A275209] p 3401 N94-29302
Prediction of fluid flow and heat transfer in internally finned tubes p 3280 N94-30228
Irradiation-induced structure and property changes in tokamak plasma-facing, carbon-carbon composites [DE94-006046] p 3508 N94-30365
Thermal conductivities, electrical resistivities, and Seebeck coefficients of YBa2Cu3O(7-x) superconductors from 80 to 300 K [DE94-004796] p 3520 N94-30724
Design of a variable-conductance vacuum insulation [DE94-000270] p 3268 N94-30819
Self-similar variables and the problem of nonlocal electron heat conductivity [DE94-005826] p 3493 N94-30881

THERMAL CONTROL COATINGS
Thick thermal barrier coatings for diesel components [NASA-CR-187111] p 3537 N94-29350
Plasma sprayed ceramic thermal barrier coating for NiAl-based intermetallic alloys [NASA-CASE-LEW-15535-1] p 3205 N94-29507

THERMAL CYCLING TESTS
Electron beam irradiation experiments of monoblock divertor mock-up [DE94-707497] p 3503 N94-28555
Performance and durability of high emittance heat receiver surfaces for solar dynamic power systems [NASA-TM-106549] p 3172 N94-28834
Static fracture behavior of a ceramic matrix composite at elevated temperatures [AD-A275363] p 3177 N94-29008
Evaluation of oxide-coated iridium-rhenium chambers [NASA-TM-106442] p 3172 N94-29097
Performance of CVD and CVR coated carbon-carbon in high temperature hydrogen [DE94-005451] p 3487 N94-29841

THERMAL DECOMPOSITION
Peroxy radical measurements with NCAR's chemical amplifier p 3345 N94-28603
Insensitive energetic materials: The importance of physical properties and molecular structure [AD-A275393] p 3225 N94-29308
Bench-scale synthesis of nanoscale materials p 3240 N94-30473

THERMAL DEGRADATION
Advanced development of PV encapsulents [DE94-000219] p 3336 N94-28500

THERMAL DIFFUSION
Calculation of propulsive nozzle flowfields in multidiffusing chemically reacting environments [NASA-TM-106532] p 3271 N94-28835
RHEED studies of the nucleation, growth, and mobility of Ag atoms on the Si(111)7 x 7 surface [DE94-005551] p 3521 N94-30899

THERMAL DIFFUSIVITY
Beta enhancement of thermal diffusivity in tokamaks [PPL-141] p 3508 N94-30159
Development of high time-resolution laser flash equipment for thermal diffusivity measurements using miniature-size specimens [NIFS-268] p 3295 N94-30186

THERMAL DISSOCIATION
Preparation, characterization, and facile thermolysis of (X2GaP(SiMe3)2) (X = Br, I) and (Cl3Ga2P)n; new precursors to nanocrystalline gallium phosphide [AD-A275019] p 3513 N94-29130

THERMAL EMISSION
Global approach towards the evaluation of thermal infrared countermeasures p 3258 N94-30504

THERMAL ENERGY
Development of global/chemistry model for jet-fuel thermal stability based on observations from static and flowing experiments p 3192 N94-29262

THERMAL EXPANSION
Thermal expansion and elastic anisotropy in single crystal Al2O3 and SiC reinforcements [NASA-TM-106516] p 3214 N94-29105
Properties of graphite fiber reinforced copper matrix composites for space power applications [NASA-CR-191026] p 3178 N94-29208
Controlled thermal expansion printed wiring boards based on liquid crystal polymer dielectrics [NASA-CR-189338] p 3287 N94-29400
Scaling in heavy-fermion systems [DE94-005002] p 3492 N94-30775

THERMAL FATIGUE
An analysis of isothermal, bithermal, and thermomechanical fatigue data of Haynes 188 and B1900+Hf by energy considerations [NASA-TM-106359] p 3317 N94-28819
Probabilistic material strength degradation model for Inconel 718 components subjected to high temperature, mechanical fatigue, creep and thermal fatigue effects [NASA-CR-195284] p 3318 N94-28840
Transient thermal fatigue of ceramic composites p 3216 N94-29874

THERMAL INSULATION
Fire-resistant water vapour permeable buoyant insulation p 3380 N94-28431
Selection of the Space Station Freedom (SSF) Flat Collector Circuit (FCC) insulation material p 3165 N94-28701
High temperature arc-track resistant aerospace insulation p 3167 N94-28716
Quality and efficiency of solar collectors in Sweden [PB94-137486] p 3337 N94-28909
Insulative properties of two thermo-metal neoprenes [AD-A275209] p 3401 N94-29302

Composite flexible blanket insulation
[NASA-CASE-ARC-11955-1-CU] p 3180 N94-29509
Design of a variable-conductance vacuum insulation
[DE94-000270] p 3268 N94-30819

THERMAL MAPPING
Evolution of miniature detectors and focal plane arrays for infrared sensors p 3237 N94-29781
Thermal imaging for a mobile robot
p 3308 N94-30300

THERMAL PLASMAS
Coulomb field effect on plasma focusing and wake field acceleration
[DE94-004937] p 3504 N94-28564
Study on the formation of ultrafine particles of Sm-Co intermetallic compounds using RF thermal plasma
p 3211 N94-29516

THERMAL PROTECTION
Alleviation of thermal strain in the CF: Keeping our cool during the Gulf conflict p 3383 N94-28449
Recent Canadian advances in active thermal protection p 3384 N94-28451
Test of a new protection suit in a climatic chamber
p 3384 N94-28452
Heat flux instrumentation for Hyflite thermal protection system
[NASA-CR-195731] p 3286 N94-28824
Fuel injector design for high temperature aircraft engine p 3154 N94-29263
Numerical comparison of convective heat transfer augmentation devices used in cooling channels of hypersonic vehicles
[NASA-TM-106546] p 3279 N94-30147

THERMAL RADIATION
Thermal variation in vegetated or snow-covered background scenes and its effect on passive infrared systems
[AD-A275174] p 3325 N94-28849

THERMAL RESISTANCE
Simulation of the effect of wind on clothing by measurements and calculations
[PB94-132289] p 3399 N94-28406
Evaluation of oxide-coated iridium-rhenium chambers
[NASA-TM-106442] p 3172 N94-29097
Insulative properties of two thermo-metal neoprenes
[AD-A275209] p 3401 N94-29302

THERMAL SHOCK
Evaluation of oxide-coated iridium-rhenium chambers
[NASA-TM-106442] p 3172 N94-29097

THERMAL STABILITY
Barley cell culture as a producer of heterologous protein
[PB94-132339] p 3379 N94-28408
Flammability, odor, offgassing, thermal vacuum stability, and compatibility with aerospace fluids of wire insulations p 3166 N94-28709
High temperature resistant jet fuels
p 3192 N94-29260
Research and development of high thermal stability fuels p 3192 N94-29261
Development of global/chemistry model for jet-fuel thermal stability based on observations from static and flowing experiments p 3192 N94-29262
Insensitive energetic materials: The importance of physical properties and molecular structure
[AD-A275393] p 3225 N94-29308

THERMAL STRESSES
Thermal strain generated by an enhanced anti-G protection system in a hot climate p 3383 N94-28445
Composite load spectra for select space propulsion structural components
[NASA-CR-194476] p 3316 N94-28508
An analysis of isothermal, bithermal, and thermomechanical fatigue data of Haynes 188 and B1900+Hf by energy considerations
[NASA-TM-106359] p 3317 N94-28819
Prediction of stress-strain response of SCS-6/Timetal-21S subjected to a hypersonic flight profile
[NASA-TM-109026] p 3177 N94-28823
Research and development of high thermal stability fuels p 3192 N94-29261
The influence of temperature on microelectronic device failure mechanisms, phase 2
[AD-A275029] p 3265 N94-29511
Transient thermal fatigue of ceramic composites
p 3216 N94-29874
Multiple Concentric Cylinder Model (MCCM) user's guide
[NASA-CR-195299] p 3183 N94-30125

THERMAL VACUUM TESTS
Arcjet system integration development
[NASA-CR-187147] p 3171 N94-28736
An alternate method for achieving temperature control in the -160 to +90 C range
[NASA-CASE-NPO-18995-1-CU] p 3288 N94-29497

THERMIONIC CONVERTERS
TOPAZ 2 system description
[DE94-006230] p 3498 N94-30846

THERMIONIC DIODES
Investigations of large area electron beam diodes for excimer lasers
[DE94-005670] p 3295 N94-30595

THERMIONIC POWER GENERATION
TOPAZ 2 system description
[DE94-006230] p 3498 N94-30846
The TOPAZ 2 space reactor response under accident conditions
[DE94-004998] p 3498 N94-30847

THERMISTORS
Development and application of a thermistor current meter
[AD-A275816] p 3286 N94-28831
The use of thermistors in the NPL electron-beam calorimeter
[PB94-139334] p 3290 N94-30782

THERMOCHEMICAL PROPERTIES
Advanced fuel properties: A computer program for estimating property values
[AD-A275248] p 3224 N94-28901

THERMOCHEMISTRY
Gas phase thermochemistry of organogermanium compounds
[DE94-004885] p 3187 N94-28561
Brief summary of accomplishments since our DOE-sponsored radon project commenced
[DE94-004643] p 3348 N94-29926

THERMOCOUPLES
System for improving measurement accuracy of transducer by measuring transducer temperature and resistance change using thermoelectric voltages
[NASA-CASE-ARC-12014-1] p 3287 N94-29361

THERMODYNAMIC CYCLES
Chambers of turboreactors with variable geometry: A response to the matrix of pollution in cycles at high temperature, high pressure p 3194 N94-29273
Lunar base heat pump, phase 1 draft
[NASA-CR-195211] p 3278 N94-29977

THERMODYNAMIC EFFICIENCY
Feasibility study on introduction of a large methanol engine power generation plant
[DE94-732338] p 3224 N94-28629
Quality and efficiency of solar collectors in Sweden
[PB94-137486] p 3337 N94-28909

THERMODYNAMIC EQUILIBRIUM
Theoretical studies of solid-fluid phase equilibria
[DE94-006406] p 3226 N94-30708

THERMODYNAMIC PROPERTIES
Innovative processing of composites for ultra-high temperature applications, book 3
[AD-A275599] p 3177 N94-28731
WINDOW 4.0: Documentation of calculation procedures
[DE94-004935] p 3410 N94-29019
Surface tension of tin and its alloys with particular reference to solders
[PB94-138302] p 3204 N94-29119
Mechanical alloying processing with application to structural materials: ASSERT supplement
[AD-A275400] p 3204 N94-29205
Thermomechanical properties of 3-D transition metals
[DE94-604015] p 3487 N94-29500
The influence of temperature on microelectronic device failure mechanisms, phase 2
[AD-A275029] p 3265 N94-29511
Aspects of model-based rocket engine condition monitoring and control
[NASA-CR-195116] p 3173 N94-29848
Transient thermal fatigue of ceramic composites
p 3216 N94-29874
Particle kinetic simulation of high altitude hypervelocity flight
[NASA-CR-194535] p 3131 N94-29893
Thermodynamics of molten K-TE alloys
[DE94-608095] p 3208 N94-30090
Volume averaged model for the mechanics of alloys solidification
[PB94-138617] p 3208 N94-30113
The role of sea ice dynamics in global climate change
p 3350 N94-30620

THERMODYNAMICS
Dynamic response of ceramics
[AD-A275396] p 3214 N94-29203
Thermodynamic analysis of chemical compatibility of several compounds with Fe-Cr-Al alloys
[NASA-CR-191166] p 3181 N94-29684
Statistical description of hot and dense clustering matter
[DE94-608155] p 3490 N94-30112
Thermodynamics of computation and information distance
[CWI-CS-R9341] p 3526 N94-30433
The Boltzmann entropy and randomness tests
[CWI-CS-R9342] p 3426 N94-30434
The role of sea ice dynamics in global climate change
p 3350 N94-30620

THERMOGRAPHY
Dual-Band Infrared (DBIR) imaging inspections of Boeing 737 and KC-135 aircraft panels
[DE94-005700] p 3122 N94-29842
Study of the problems of nonuniformity of heating in infrared vision applied to the inspection of materials having non-planar relief
[ISBN-0-315-85637-8] p 3316 N94-30235
Dual-band infrared imaging for quantitative corrosion detection in aging aircraft
[DE94-004187] p 3149 N94-30687

THERMOGRAVIMETRY
Study of iron exchanged zeolites by Moessbauer effect and electron spin resonance spectroscopy
[DE94-605138] p 3514 N94-29691

THERMOMECHANICAL TREATMENT
Effects of thermomechanical processing on tensile and long-time creep behavior of Nb-1 percent Zr-0.1 percent C sheet
[NASA-TM-106319] p 3202 N94-28822

THERMONUCLEAR POWER GENERATION
Overview of the US stellarator reactor study
[DE94-006042] p 3508 N94-30339

THERMOPHYSICAL PROPERTIES
Characterisation and processing of SiC/MAS-L glass ceramic matrix composite
[REPT-932-430-111] p 3179 N94-29412
Glass-ceramic matrix composites
[REPT-932-430-112] p 3179 N94-29413

THERMOPLASTIC RESINS
Polymer infiltration studies
[NASA-CR-195729] p 3213 N94-28748
Composite redesign of obstetrical forceps
p 3397 N94-30457
Improved construction materials for polar regions using microcellular thermoplastic foams p 3223 N94-30483

THERMOPLASTICITY
Finite element analysis of axisymmetric deformations of thick thermoviscoplastic targets p 3320 N94-29688

THERMOREGULATION
Prediction of survival times on land in a cold climate
p 3379 N94-28423
Fuelling shivering in humans during cold water immersion p 3379 N94-28426
Biochemical enhancement of cold tolerance
p 3380 N94-28427
Treatment of mild immersion hypothermia by body-to-body and forced-air warming
p 3380 N94-28428
The potential of new textiles in improving survival prospects p 3380 N94-28430
Thermoregulation in the extreme cold environment
p 3381 N94-28438
Thermal strain generated by an enhanced anti-G protection system in a hot climate p 3383 N94-28445
Alleviation of thermal strain in the CF: Keeping our cool during the Gulf conflict p 3383 N94-28449
Japanese Journal of Aerospace and Environmental Medicine, vol. 30, no. 2
[JTN-94-80599] p 3394 N94-29863
Effects of make-up on the heat transfer from the head in hyperthermic conditions p 3394 N94-29864

THERMOSPHERE
A study of the thermospheric dynamics of the high-latitude E region using a spectral thermospheric general circulation model p 3362 N94-29743

THESAURI
Computer-based linking of thesauri
p 3534 N94-29961

THICK PLATES
Further investigation of curve veering phenomena
p 3460 N94-30515

THICKNESS
Dual-Band Infrared (DBIR) imaging inspections of Boeing 737 and KC-135 aircraft panels
[DE94-005700] p 3122 N94-29842
Three-dimensional free vibration analysis of thick arbitrarily laminated, rectangular, cylindrical and spherical composite panels p 3184 N94-30257
An electromagnetic noncontacting sensor for thickness measurement in a dispersive medium
[AIAA PAPER 94-1200-CP] p 3443 N94-30551

THIN AIRFOILS
A new flux-conserving numerical scheme for the steady, incompressible Navier-Stokes equations
[NASA-TM-106520] p 3273 N94-29471

THIN FILMS
Molecular aspects of transport in thin films of controlled architecture
[DE94-004552] p 3211 N94-28457

Silicon-Film (tm) photovoltaic manufacturing technology
[DE94-000258] p 3336 N94-28501
Geometric structures of thin film: Pt on Pd(110) and NiO on Ni(100)
[DE94-005564] p 3211 N94-28530
A 3M high temperature dielectric film
p 3167 N94-28717
Ion channeling peculiarities in YBa2Cu3 O7 monocrystal
[DE94-606885] p 3512 N94-28787
MOCVD growth of GaN, AlN and AlGaN for UV photodetector applications
[AD-A275078] p 3512 N94-28871
Method for forming thin composite solid electrolyte film for lithium batteries
[NASA-CASE-NPO-18877-1-CU] p 3264 N94-29357
Vacuum vapor deposition
[NASA-CASE-MFS-28652-1] p 3215 N94-29446
Preparation and structure of amorphous hydrogenated carbon film deposited with RF plasma CVD
p 3223 N94-29518
Retention latch mechanism for the Wake Shield Facility p 3161 N94-29635
Optical properties of cadmium sulfide, zinc selenide, and zinc manganese selenide semiconductor films
p 3500 N94-29759
Micro-opto-mechanical devices and systems using epitaxial lift off p 3239 N94-29793
Lubricant rheology at high shear rates
p 3217 N94-29967
ECR plasma synthesis of silicon nitride films on GaAs and InSb
[DE94-005575] p 3515 N94-30006
The organometallic chemical vapor deposition of transition metal carbides: The use of homoleptic alkyls
[DE94-005577] p 3206 N94-30007
Study of the ultraviolet absorption and photoconduction spectra of polyimide films fabricated at various curing temperatures
[ISBN-0-315-85923-7] p 3218 N94-30036
The bases for the development of high-temperature integrated SQUID-systems
[DE94-608462] p 3517 N94-30082
Plasma enhanced chemical vapor deposition of ZrO2 thin films
[DE94-006031] p 3218 N94-30104
Distribution functions of electrons within aluminium oxide thin films
[DE94-608418] p 3490 N94-30184
Effects of hydrogen on the resistivity of thin Au and Cu films p 3218 N94-30225
Electrooptical and optical evaluation of Pb(Zr,Ti)O3 thin films using waveguide refractometry
[DE94-006374] p 3518 N94-30247
Densification and crystallization of zirconia thin films prepared by sol-gel processing
[DE94-005573] p 3518 N94-30315
Metafusion: A breakthrough in metallurgy
p 3211 N94-30446
Research on the atomic layer-by-layer growth of high-temperature superconductor thin films at the Institute of Scientific and Industrial Research, Japan
[DE94-003739] p 3519 N94-30611
Ionic conduction mechanisms in CaF2 and CaF2-Al2O3 nanocomposite films on Al2O3 substrates
[DE94-004792] p 3520 N94-30773
Synthesis of (SiC)3N4 thin films by ion implantation
[DE94-006311] p 3521 N94-30851
RHEED studies of the nucleation, growth, and mobility of Ag atoms on the Si(111)7 x 7 surface
[DE94-005551] p 3521 N94-30899

THIN PLATES
Performance of a higher-order triangular finite element for composite laminated structures
p 3181 N94-29810

THIN WALLS
Numerical and experimental investigation of the bending response of thin-walled composite cylinders
[NASA-CR-195730] p 3317 N94-28801
Thin-walled orthotropic laminated beam theory
p 3324 N94-30920

THOMSON SCATTERING
Photon counting spectroscopy as done with a Thomson scattering diagnostic
[DE94-005543] p 3503 N94-28515

THREE BODY PROBLEM
A guidance and navigation system for two spacecraft rendezvous in translunar halo orbit
p 3142 N94-29837
Optimal low-thrust, Earth-Moon trajectories
p 3159 N94-30961

THREE DIMENSIONAL BODIES
Comparison of RCS prediction techniques, computations and measurements
[PB94-125515] p 3256 N94-30392

THREE DIMENSIONAL BOUNDARY LAYER
Long-wavelength asymptotics of unstable crossflow modes, including the effect of surface curvature
[NASA-CR-4579] p 3273 N94-29460

THREE DIMENSIONAL COMPOSITES
On the dynamic mechanical behavior of 3-D integrated fabric reinforced composites
[AD-A275424] p 3177 N94-28865

THREE DIMENSIONAL FLOW
Boundary layers induced by three-dimensional vortex loops
[AD-A275678] p 3270 N94-28665
Proceedings of the 10th NAL Symposium on Aircraft Computational Aerodynamics
[NAL-SP-19] p 3123 N94-28946
On the numerical analysis of shear flows
p 3126 N94-28972
Verification of a three-dimensional viscous flow analysis for a single stage compressor p 3127 N94-28976
Application of flow field simulation to turbine vane design p 3127 N94-28978
Three-dimensional external flow computations using prismatic grid p 3127 N94-28979
An elliptic-hyperbolic grid generation method and application to compressor flows p 3128 N94-28981
An implicit upwind scheme for the three-dimensional Euler equations using a pointwise relaxation method
p 3128 N94-28983
A free-wake Euler and Navier-Stokes CFD method and its application to helicopter rotors including dynamic stall
[AD-A275416] p 3129 N94-29197
Numerical simulation of aerothermal characteristics in gas turbine combustors with complex geometries
p 3154 N94-29255
Time-resolved measurements in a three dimensional model combustor p 3196 N94-29283
RNS optimization procedure for three-dimensional composite velocity multi-block applications
p 3273 N94-29534
An improvement of the slender body theory for oscillating ships with finite forward speed p 3234 N94-29705
Direct and large-eddy simulations of turbulent flow in a square duct p 3275 N94-29809
Numerical solution of 3-D Navier-Stokes equations in vorticity-velocity form for incompressible flows
p 3276 N94-29843
Unsteady transonic aerodynamics in frequency domain for flutter analysis p 3131 N94-29879
The 3-D LDV measurements on a 30-degree swept wing with a simulated ice accretion
[NASA-CR-195327] p 3132 N94-30124
Three-dimensional flow characteristics downstream of a blade endwall corner p 3280 N94-30229
The design of a system of codes for industrial calculations of flows around aircraft and other complex aerodynamic configurations
[PB94-125598] p 3133 N94-30387
Three dimensional compressible turbulent flow computations for a diffusing S-duct with/without vortex generators p 3281 N94-30519

THREE DIMENSIONAL MODELS
Three-dimensional finite element modeling of a magnet array spinning above a conductor
[DE94-004573] p 3468 N94-28459
Exploitation of stereophotogrammetrically derived 3-D wireframe models to produce urban simulations
[AD-A275459] p 3325 N94-28808
Active electron and ion beam experiments in space
[AD-A275570] p 3504 N94-28828
Higher-order accurate numerical simulation of 3D supersonic mixing layers p 3124 N94-28954
Three dimensional simulation of compressible flow induced by a high-speed train moving into a tunnel
p 3126 N94-28967
Some efficient procedures for correcting triangulated models
[PB94-136926] p 3452 N94-29171
Damage meso-modeling of 3D evolutive composites
[REPT-932-430-106] p 3179 N94-29442
Computational fluid dynamics in ventilation. 3: The IEA annex 20 work p 3233 N94-29608
Effects and implications of fault zone heterogeneity and anisotropy on earthquake strong ground motion
p 3363 N94-29941
Three-dimensional effects for radio frequency antenna modeling
[DE94-006102] p 3255 N94-30105
Magnetic properties of the three dimensional Ising model with interface single-ion anisotropy
[DE94-608116] p 3525 N94-30164
Magnetic properties of a transverse spin-1 Ising model with longitudinal crystal field interactions
[DE94-608118] p 3517 N94-30165
A deterministic algorithm for the three-dimensional diameter problem
[RUU-CS-92-45] p 3424 N94-30348
Three dimensional compressible turbulent flow computations for a diffusing S-duct with/without vortex generators p 3281 N94-30519
Sensitivity analysis of the static aeroelastic response of a wing p 3134 N94-30525
A laboratory simulation of urban heat-island-induced circulation in a stratified environment
p 3367 N94-30921

THREE DIMENSIONAL MOTION
Nominally two-dimensional flow about a normal flat plate p 3275 N94-29838
Dynamic modeling of multibody flexible structures
p 3323 N94-30813

THROTTLING
Method of reducing hydraulic instability
[NASA-CASE-LEW-15463-1] p 3273 N94-29539

THRUST BEARINGS
Parachute Swivel Mechanism for planetary entry
p 3162 N94-29643

THRUST CHAMBERS
Evaluation of oxide-coated iridium-rhenium chambers
[NASA-TM-106442] p 3172 N94-29097

THRUST VECTOR CONTROL
Design and test of electromechanical actuators for thrust vector control p 3163 N94-29650

THRUST-WEIGHT RATIO
Small low mass advanced PBR's for propulsion
[DE94-005142] p 3497 N94-30588

THUNDERSTORMS
Numerical simulations of a mountain thunderstorm. A comparison with Doppler radar observations
[AD-A275296] p 3369 N94-28873

TIDES
Tidal atlas software development
[AD-A275251] p 3377 N94-29432

TIMBER IDENTIFICATION
The extraction and representation of forest inventory information using continuous density surfaces
[ISBN-0-315-85658-0] p 3334 N94-30236

TIMBER INVENTORY
The extraction and representation of forest inventory information using continuous density surfaces
[ISBN-0-315-85658-0] p 3334 N94-30236

TIME
A time reasoning system based on the event calculus for scheduling in aeronautic maintenance
[REPT-932-710-101] p 3122 N94-29463

TIME CONSTANT
Electron beam irradiation experiments of monoblock divertor mock-up
[DE94-707497] p 3503 N94-28555

TIME DEPENDENCE
Feasibility study on introduction of a large methanol engine power generation plant
[DE94-732338] p 3224 N94-28629
The h-p adaptive methods for incompressible viscous flow problems p 3275 N94-29836
Numerical solution of the two-dimensional time-dependent incompressible Euler equations
[NASA-CR-195775] p 3277 N94-29859
Large-scale 3-D solutions of the time-dependent Dirac equation
[DE94-005591] p 3454 N94-30317

TIME DIVISION MULTIPLE ACCESS
Modeling, analysis, and simulation of an optical time-division multiple-access network architecture
[AD-A275847] p 3498 N94-28780
M-interference queue analysis by decomposition method
[ISBN-0-315-85795-1] p 3453 N94-30139

TIME FUNCTIONS
The Stroemberg wavelet on the interval and the Franklin system
[TELECOM-93-C-002] p 3462 N94-30971

TIME LAG
Development of a method to predict transonic limit cycle oscillation characteristics of fighter aircraft (continued)
[NLR-TP-92156-U] p 3148 N94-30342
End-to-end delay reduction in narrow bandwidth real-time multimedia tele-education applications
[AD-B179614] p 3260 N94-30518
Tropospheric corrections to GPS measurements using locally measured meteorological parameters compared with general tropospheric corrections
p 3144 N94-30655
A comparison of several GPS data reduction methods
p 3145 N94-30662
Ionospheric corrections to precise time transfer using GPS p 3145 N94-30677

TIME MARCHING
Time-marching aeroelastic and spatial adaptation procedures on triangular and tetrahedral meshes using an unstructured-grid Euler method p 3131 N94-29877
Three dimensional compressible turbulent flow computations for a diffusing S-duct with/without vortex generators p 3281 N94-30519

TIME MEASUREMENT
Cosmogenic C-14 in Antarctic and non-Antarctic meteorites and lunar samples
[NASA-CR-195795] p 3546 N94-29905
The MSRC ab initio methods benchmark suite: A measurement of hardware and software performance in the area of electronic structure methods
[DE94-006428] p 3514 N94-30001
The 25th Annual Precise Time and Time Interval (PTTI) Applications and Planning Meeting
[NASA-CP-3267] p 3468 N94-30639
Status of frequency and time support for NASA systems p 3468 N94-30640
Time and frequency technology at NIST p 3468 N94-30641
European PTTI report p 3468 N94-30642
Loran-C time management p 3144 N94-30644
Report on NATO PTTI p 3469 N94-30645
GPS common-view time transfer p 3144 N94-30648
Cascaded clocks measurement and simulation findings p 3469 N94-30649
Time and position accuracy using codeless GPS p 3144 N94-30650
Relativistic theory for picosecond time transfer in the vicinity of Earth p 3470 N94-30653
Tropospheric corrections to GPS measurements using locally measured meteorological parameters compared with general tropospheric corrections p 3144 N94-30655
The two-way time synchronization system via a satellite voice channel p 3471 N94-30658
Remote clocks linked by a fully calibrated two-way timing link p 3471 N94-30659
Some applications of GPS timing information p 3145 N94-30661
A comparison of several GPS data reduction methods p 3145 N94-30662
Cesium and rubidium frequency standards status and performance on the GPS program p 3145 N94-30663
Comparison of LASSO and GPS time transfers p 3145 N94-30665
Noise and drift analysis of non-equally spaced timing data p 3472 N94-30667
An algorithm for the Italian atomic time scale p 3473 N94-30668
A comparative study of clock rate and drift estimation p 3473 N94-30669
Time maintenance system for the BMDO MSX spacecraft p 3171 N94-30672
Hydrogen maser clocks in space for solid-Earth research and time-transfer applications: Experiment overview and evaluation of Russian miniature sapphire loaded cavity p 3474 N94-30676
Russian national time scale long-term stability p 3475 N94-30679
Using GLONASS signal for clock synchronization p 3475 N94-30680
A look into the crystal ball: The next 25 years p 3475 N94-30681
The future of time and frequency dissemination p 3476 N94-30684

TIME OF FLIGHT SPECTROMETERS
Experimental setup for study of hadron and hard photon production in nucleus-nucleus collisions
[DE94-607849] p 3489 N94-30051

TIME OPTIMAL CONTROL
Pulse response based minimum time control of flexible structures p 3436 N94-29720
Nearly time-optimal feedback control of a magnetically levitated photolithography positioning system
[DE94-005288] p 3266 N94-30055
Neural network based time-optimal control of a magnetically levitated precision positioning system
[DE94-006573] p 3437 N94-30250

TIME RESPONSE
The two-way time synchronization system via a satellite voice channel p 3471 N94-30658

TIME SERIES ANALYSIS
Research activities of Martin C. Casdagli at SFI September 1989--May 1991
[DE94-005655] p 3463 N94-28548
A fractal analysis of near-field atmospheric concentration data
[AD-A275460] p 3355 N94-28728
The modified Cramer-von mises goodness-of-fit criterion for time series
[AD-A275377] p 3464 N94-29014
Time series comparisons of satellite and rocketsonde temperatures in 1978-1979
[NASA-TP-3409] p 3370 N94-29455
Surface differential rotation in a sample of cool dwarf stars p 3545 N94-29827
Statistical analysis of a satellite imagery time series: Implications for the study of coastal and estuarine circulation p 3335 N94-30919

TIME SIGNALS
The 25th Annual Precise Time and Time Interval (PTTI) Applications and Planning Meeting
[NASA-CP-3267] p 3468 N94-30639
Two-way satellite time transfer: Overview and recent developments p 3469 N94-30646
Optical techniques for time and frequency transfer p 3469 N94-30647
Time transfer using geostationary satellites: Implementation of a Kalman filter p 3471 N94-30657
Comparison of LASSO and GPS time transfers p 3145 N94-30665
Time maintenance system for the BMDO MSX spacecraft p 3171 N94-30672
Time synchronized video systems p 3261 N94-30675
Ionospheric corrections to precise time transfer using GPS p 3145 N94-30677
The NIST Internet time service p 3475 N94-30678
Using GLONASS signal for clock synchronization p 3475 N94-30680

TIME TEMPERATURE PARAMETER
Performance of CVD and CVR coated carbon-carbon in high temperature hydrogen
[DE94-005451] p 3487 N94-29841
XCHEM-1D: A heat transfer/chemical kinetics computer program for multilayered reactive materials
[DE94-005072] p 3226 N94-30615

TIMING DEVICES
Status of frequency and time support for NASA systems p 3468 N94-30640
Time and frequency technology at NIST p 3468 N94-30641
European PTTI report p 3468 N94-30642
Report on NATO PTTI p 3469 N94-30645
LASSO experiment: Intercalibrations of the LASSO ranging stations p 3297 N94-30666

TIN
Intermetallic growth at the interface between copper and bismuth-tin solder
[AD-A275716] p 3202 N94-28643
Pit initiation on passivated metal surfaces: Crystallographic orientation and environmental effects
[ISBN-0-315-85433-2] p 3208 N94-30138
Calculating the J(c), B, T surface for commercial niobium tin conductors using a reduced state model
[DE94-006296] p 3520 N94-30850

TIN ALLOYS
Surface tension of tin and its alloys with particular reference to solders
[PB94-138302] p 3204 N94-29119
Logistics for the implementation of lead-free solders on electronic assemblies
[DE94-004800] p 3206 N94-29936
Microstructural development and mechanical behavior of eutectic bismuth-tin and eutectic indium-tin in response to high temperature deformation
[DE94-005202] p 3210 N94-30710
Calculating the J(c), B, T surface for commercial niobium tin conductors using a reduced state model
[DE94-006296] p 3520 N94-30850

TIN COMPOUNDS
The polymerization of epsilon-caprolactone with stannous catalyst and lactide/epsilon-caprolactone (LA/epsilon-CL) and lactide/glycolide (LA/GA) copolymers. Polymer technology publication series no. 15
[PB94-137551] p 3220 N94-30713

TIN OXIDES
Interface engineering in alumina fiber/glass composites p 3182 N94-29852

TIRES
Asphaltic concrete performance under heavy fighter aircraft loading
[AD-A275046] p 3157 N94-29151

TITANIUM
Corrosion inhibition by electrodeposited conductive-polymer film
[AD-A275456] p 3213 N94-28806
Insulative properties of two thermo-metal neoprenes
[AD-A275209] p 3401 N94-29302
Preliminary evaluation of hybrid titanium composite laminates
[NASA-TM-109095] p 3180 N94-29472

TITANIUM ALLOYS
Effect of surface condition on strength and fatigue behavior of alumina ceramic
[AD-A275053] p 3214 N94-29133
Nature of dissolution of binary tantalum-titanium alloys by molten plutonium
[DE94-005090] p 3210 N94-30776
Fractographic and microstructural analysis of fatigue crack growth in Ti-6Al-4V fan disc forgings
[AD-B174765] p 3153 N94-30914

TITANIUM CARBIDES
The organometallic chemical vapor deposition of transition metal carbides: The use of homoleptic alkyls
[DE94-005577] p 3206 N94-30007
Metafusion: A breakthrough in metallurgy p 3211 N94-30446

TITANIUM NITRIDES
Sliding friction and wear between titanium nitride, M50 steel and silicon nitride (round 3 of VAMAS wear test program)
[IMR-TM-TR-003] p 3303 N94-30019

TITANIUM OXIDES
Pitting corrosion of titanium
[AD-A274980] p 3203 N94-29089
Induced crystallization in CW laser-irradiated sol-gel deposited titania films
[DE94-006527] p 3207 N94-30062

TITRATION
Measurement of atmospheric OH by titration of near-IR fluorescent dyes p 3344 N94-28599
The active titration method for measuring local hydroxyl radical concentration p 3345 N94-28602

TOKAMAK DEVICES
Theoretical reversed field pinch and tokamak studies
[DE94-005409] p 3503 N94-28490
Proceedings of Japan-US Workshop P-196 on High Heat Flux Components and Plasma Surface Interactions for Next Devices
[DE94-701164] p 3503 N94-28513
Electron beam irradiation experiments of monoblock divertor mock-up
[DE94-707497] p 3503 N94-28555
TFTR Ion Cyclotron Range of Frequencies (ICRF) experimental data analysis collaboration
[DE94-004699] p 3504 N94-28575
Argon frost continuous cryopump for fusion applications
[DE94-004478] p 3230 N94-29017
Liquid metal MHD and heat transfer in a tokamak blanket slotted coolant channel
[DE94-004622] p 3506 N94-29510
Higher order collisionless ballooning mode in tokamaks
[PPL-143] p 3507 N94-30156
Eigenmode analysis of the destabilized ion acoustic mode in tokamaks
[PPL-142] p 3507 N94-30158
Beta enhancement of thermal diffusivity in tokamaks
[PPL-141] p 3508 N94-30159
The impact of improved physics on commercial tokamak reactors
[DE94-006103] p 3509 N94-30760
Advanced steady-state operating scenarios
[DE94-004810] p 3509 N94-30768
Application of divertor cryopumping to H-mode density control in DIII-D
[DE94-004859] p 3510 N94-30832
Superdiffusion
[DE94-002333] p 3492 N94-30834
Magnetic flux reconstruction methods for shaped tokamaks
[DE94-005827] p 3510 N94-30882

TOLUENE
Fuels combustion research
[AD-A275122] p 3189 N94-29004

TOMOGRAPHY
Dual-Band Infrared (DBIR) imaging inspections of Boeing 737 and KC-135 aircraft panels
[DE94-005700] p 3122 N94-29842
Analysis and an image recovery algorithm for ultrasonic tomography system p 3397 N94-30456

TOOLING
Near-net-shape manufacturing: Spray-formed metal matrix composites and tooling p 3186 N94-30447

TOPEX
TOPEX/POSEIDON operational orbit determination results using global positioning satellites p 3160 N94-29666

TOPOGRAPHY
Objective analysis of a coastal ocean eddy using satellite AVHRR and in situ hydrographic data
[AD-A275715] p 3376 N94-28642
Exploitation of stereophotogrammetrically derived 3-D wireframe models to produce urban simulations
[AD-A275459] p 3325 N94-28808
Feature mapping in a photogrammetric GIS
[AD-A275418] p 3325 N94-28863
Statistical characterization of rugged propagation paths with application to Rg scattering study
[AD-A275237] p 3361 N94-29393
Applicability of digital terrain analyses to wind energy prospecting and siting
[DE94-004363] p 3374 N94-30587

TOPOLOGY
Reidemeister numbers of equivariant maps
[PB94-138286] p 3452 N94-29118

High throughput network for multiprocessor interconnections
[VTT-PUBS-147] p 3245 N94-29468
Symplectic topology of integrable Hamiltonian systems
[DE94-608120] p 3467 N94-30166
Topological models for higher order control flow
[CWI-CS-R9340] p 3425 N94-30432
A monotonicity conjecture for real cubic maps
[DE94-003969] p 3335 N94-30610
Non-commutative geometry
[PB94-139342] p 3462 N94-30889

TORCHES
Vacuum vapor deposition
[NASA-CASE-MFS-28652-1] p 3215 N94-29446

TORNADOES
Effectiveness of protection clothing for cold weather conditions after ejection over sea: A case report
p 3481 N94-28435
On the origins of low-level tornadic circulations within the remnants of hurricane Andrews
[AD-A275373] p 3369 N94-29011
Dynamics of tornado-like vortices
p 3371 N94-29753

TOROIDAL PLASMAS
A 6MeV heavy ion beam probe for the Large Helical Device
[NIFS-272] p 3505 N94-29397
Formation and self-healing of magnetic islands in finite-beta helias equilibria
[NIFS-269] p 3505 N94-29483

TORQUE
Bolt and nut evaluator
[NASA-CASE-GSC-13468-1] p 3288 N94-29538
The response of flexible manipulators to a new computed torque control strategy: Simulation results
p 3308 N94-30295

TORQUE MOTORS
Suspension system for gimbal supported scanning payloads
[NASA-CASE-MFS-28817-1] p 3287 N94-29358

TORQUEMETERS
Bolt and nut evaluator
[NASA-CASE-GSC-13468-1] p 3288 N94-29538

TORSION
Cyclic axial-torsional deformation behavior of a cobalt-base superalloy
[NASA-TM-106372] p 3203 N94-28921
Interlaminar fracture analysis for laminated composites under combined loading p 3182 N94-29964

TORUSES
Infrared properties of obscuring dust tori in active galactic nuclei p 3545 N94-29832

TOTAL QUALITY MANAGEMENT
The development and demonstration of the metric assessment tool
[AD-A275788] p 3230 N94-28742
An evaluation of techniques for ranking academic information systems journals
[AD-A275179] p 3529 N94-29066
Why TQM fails (and what you can do about it)
[DE93-018945] p 3527 N94-30698

TOUGHNESS
Toughening mechanisms in ultrahigh-strength steels
[AD-A275439] p 3202 N94-28867
Poly(arylene ether-co-imidazole)s as toughness modifiers for epoxy resins
[NASA-CASE-LAR-15229-1-CU] p 3215 N94-29451

TOWED BODIES
Nominally two-dimensional flow about a normal flat plate p 3275 N94-29838

TOWERS
Study of bridge design and technology
[PB94-137916] p 3121 N94-29160

TOXIC HAZARDS
Characterization of air emissions from the simulated open combustion of fiberglass materials
[PB94-136231] p 3347 N94-29192
Toxicity of carbon monoxide-hydrogen cyanide gas mixtures: Exposure concentration, time-to-incapacitation, carboxyhemoglobin, and blood cyanide parameters
[DOT/FAA/AM-94/7] p 3395 N94-29919

TOXICITY
Toxicity of carbon monoxide-hydrogen cyanide gas mixtures: Exposure concentration, time-to-incapacitation, carboxyhemoglobin, and blood cyanide parameters
[DOT/FAA/AM-94/7] p 3395 N94-29919
Intermedia transfer factors for fifteen toxic pollutants released to air basins in California
[DE94-005699] p 3349 N94-30044
Computerized in vitro test for chemical toxicity based on tetrahymena swimming patterns
p 3354 N94-30463

TOXICITY AND SAFETY HAZARD
Fire behavior of aeronautical materials
[REPT-932-600-105] p 3197 N94-29457

TOXINS AND ANTITOXINS
Effects of pressure on membrane-associated receptors and effector elements
[AD-A275813] p 3384 N94-28829

TRACE CONTAMINANTS
Developing a diode array spectrometer for tropospheric chemistry studies p 3362 N94-29752
Using spacecraft trace contaminant control systems to cure sick building syndrome p 3354 N94-30470
A new material for removing heavy metals from water
p 3354 N94-30471

TRACE ELEMENTS
JPL Fourier transform ultraviolet spectrometer
p 3343 N94-28593
Absolute determination of local tropospheric OH concentrations p 3343 N94-28594
Developing a diode array spectrometer for tropospheric chemistry studies p 3362 N94-29752
Use of satellite data to improve parameterization of spatial and temporal variations of gaseous dry deposition in regional-scale models
[DE94-005110] p 3334 N94-30022
Evaluating models of climate and forest vegetation
p 3353 N94-30637
The development and evaluation of a tunable diode laser trace gas sensor for the measurement of N2O and CH4 fluxes using micrometeorological techniques
[ISBN-0-315-78975-1] p 3296 N94-30801
Geochemical and fluid dynamic investigations into the nature of chemical variability in the Earth's mantle
p 3367 N94-30917

TRACKED VEHICLES
A newly developed snow vehicle (SM100S) for Antarctica. Part 1: Necessity and process of the development p 3314 N94-29981
A newly developed snow vehicle (SM100S) for Antarctica. Part 2: Design of the system
p 3314 N94-29982
A newly developed snow vehicle (SM100S) for Antarctica. Part 3: Low temperature toughness of the welded joints of the structural steel
p 3364 N94-29983
A newly developed snow vehicle (SM100S) for Antarctica. Part 4: Low temperature properties of crawler belt p 3314 N94-29984
A newly developed snow vehicle (SM100S) for Antarctica. Part 5: Result of general performance tests
p 3314 N94-29985

TRACKING (POSITION)
Digital tracking and control of retinal images
[AD-A275469] p 3389 N94-28810
Non-intrusive gaze tracking using artificial neural networks
[AD-A275186] p 3397 N94-28860
General theory and algorithms for the non-casual inversion, slewing and control of space-based articulated structures
[AD-A275118] p 3167 N94-29002
ACCS Surveillance Exploratory Prototype (ASEP)
p 3138 N94-29566
An improved conscan algorithm based on a Kalman filter p 3251 N94-29670

TRACKING NETWORKS
The 25th Annual Precise Time and Time Interval (PTTI) Applications and Planning Meeting
[NASA-CP-3267] p 3468 N94-30639

TRACKING STATIONS
Radio science ground data system for the Voyager-Neptune encounter, part 1
p 3248 N94-29623

TRAILERS
Lunar surface operations. Volume 4: Lunar rover trailer
[NASA-CR-195554] p 3299 N94-29386

TRAILING EDGES
Numerical analysis of airfoil for helicopter blade at high angle of attack using Navier-Stokes code
p 3124 N94-28958

TRAINING DEVICES
A cognitive model of decision making: Chunking and the radar detection device
[AD-A275185] p 3242 N94-28859

TRAINING SIMULATORS
Data fusion and correlation techniques testbed development. Phase 1: Interim report
[SKD-1600-73-015] p 3405 N94-28533
Simulation Networking/Training Requirements Relational Database: User's guide
[AD-A275634] p 3528 N94-28637

TRAJECTORIES
Iterative procedure as equation of motion
[DE94-608008] p 3453 N94-30078
Fast precise algorithm for simulation of ionization energy losses
[DE94-608010] p 3421 N94-30080

TRAJECTORY ANALYSIS
General theory and algorithms for the non-casual inversion, slewing and control of space-based articulated structures
[AD-A275118] p 3167 N94-29002
Advanced air traffic control and flight management system concepts p 3140 N94-29576
Experimental flight management system
p 3141 N94-29580
Optimal low-thrust, Earth-Moon trajectories
p 3159 N94-30961

TRAJECTORY CONTROL
A 6MeV heavy ion beam probe for the Large Helical Device
[NIFS-272] p 3505 N94-29397
Profile negotiation: An air/ground automation integration concept for managing arrival traffic
p 3140 N94-29578
Optimal low-thrust, Earth-Moon trajectories
p 3159 N94-30961

TRAJECTORY MEASUREMENT
A simulator for multi-radar analysis for realistic traffic
[AD-B179099] p 3142 N94-30439

TRAJECTORY OPTIMIZATION
Profile negotiation: An air/ground automation integration concept for managing arrival traffic
p 3140 N94-29578
Optimal low-thrust, Earth-Moon trajectories
p 3159 N94-30961

TRAJECTORY PLANNING
Integration of a path generation algorithm into off-line programming of airbus panels
[REPT-932-600-103] p 3435 N94-29480
Air-ground integration of the ATM system in PHARE
p 3141 N94-29579
Experimental flight management system
p 3141 N94-29580
The PHARE advanced tools p 3141 N94-29581
Collision avoidance and control of multiple revolute manipulators p 3302 N94-29884
The NRC mobile robot project p 3305 N94-30280
An optimal obstacle avoidance path planning algorithm for the Excalibur robot p 3306 N94-30287
Motion control of mobile robots p 3310 N94-30309
Unmanned vehicle mobility: Limits of autonomous navigation p 3310 N94-30311
A probabilistic approach to motion planning for car-like robots
[RUU-CS-93-18] p 3438 N94-30410
Fuzzy logic based robotic controller
[AIAA PAPER 94-1202-CP] p 3443 N94-30553
Aspects of vision and planning in a dynamic, uncertain environment p 3448 N94-30803
The experimental flight management system: An air traffic management research tool
[NLR-TP-92253-U] p 3143 N94-30943

TRANSATMOSPHERIC VEHICLES
Numerical study on the interaction between scramjet engine modules caused by thermal choke
p 3125 N94-28960

TRANSDUCERS
Characterization of structural vibration: Field descriptors based on energy density and intensity
[PB94-132230] p 3316 N94-28404
System for improving measurement accuracy of transducer by measuring transducer temperature and resistance change using thermoelectric voltages
[NASA-CASE-ARC-12014-1] p 3287 N94-29361
Method and apparatus for indicating disbonds in joint regions
[NASA-CASE-LAR-14626-1] p 3315 N94-29548

TRANSFER FUNCTIONS
Frequency-domain transfer-function identification using Chebyshev polynomials
[DE94-004777] p 3451 N94-28739
Polynomial modeling of analog-to-digital converters
[DE94-005579] p 3406 N94-30008

TRANSFORMATIONS (MATHEMATICS)
Reidemeister numbers of equivariant maps
[PB94-138286] p 3452 N94-29118
Trace formulas and dynamical zeta functions in the Nielsen theory
[PB94-138195] p 3467 N94-29163
Integer cosine transform for image compression
p 3247 N94-29619
Parsing in ISBES
[TR-92-32] p 3432 N94-30363
Isomorphisms between predicate and state transformers
[RUU-CS-93-09] p 3458 N94-30403
Termination of term rewriting by semantic labelling
[RUU-CS-93-24] p 3459 N94-30424
Isomorphisms between predicate and state transformers
[CWI-CS-R9338] p 3459 N94-30430

Relating state transformation semantics and predicate transformer semantics for parallel programs
[CWI-CS-R9339] p 3433 N94-30431

TRANSFORMERS
Fabrication issues in optimizing YBa(2)Cu(3)O(7-x) flux transformers for low l/f noise
[DE94-005209] p 3261 N94-28546

TRANSIENT LOADS
Stiffness-generated rigid-body mode shapes for Lanczos eigensolution with SUPORT DOF by way of a MSC/NASTRAN DMAP alter
[NASA-TM-106537] p 3319 N94-29406
Transient analysis mode participation for modal survey target mode selection using MSC/NASTRAN DMAP
[NASA-TM-106536] p 3319 N94-29469
Transient thermal fatigue of ceramic composites
p 3216 N94-29874

TRANSIENT RESPONSE
A space-based classification system for RF transients
[DE94-003933] p 3240 N94-28522
Performance evaluation of a 22.5/30 kW 270 volts direct current generator system
[AD-A275106] p 3263 N94-28913
Evaluation of the transient operation of advanced gas turbine combustors p 3154 N94-29269
Transient analysis mode participation for modal survey target mode selection using MSC/NASTRAN DMAP
[NASA-TM-106536] p 3319 N94-29469
Concurrent simulation and constraint stabilization for flexible multibody systems p 3154 N94-29532

TRANSISTORS
Tunnelling hot electron transfer amplifiers
[AD-A275529] p 3262 N94-28687
Nonvolatile programmable neural network synaptic array
[NASA-CASE-NPO-18578-1-CU] p 3265 N94-29426
Charge trapping and breakdown in N2O oxides
[DE94-003775] p 3266 N94-30040

TRANSITION FLOW
Long-wavelength asymptotics of unstable crossflow modes, including the effect of surface curvature
[NASA-CR-4579] p 3273 N94-29460
An experimental study of nonlinear wave coupling and energy transfer characterizing the transition of a planar jet shear layer p 3282 N94-30953
Transition to turbulence in confined compressible mixing layers p 3283 N94-30958

TRANSITION METALS
Polymer technology publication series no. 16
[PB94-135522] p 3214 N94-29157
Thermomechanical properties of 3-D transition metals
[DE94-604015] p 3487 N94-29500
The organometallic chemical vapor deposition of transition metal carbides: The use of homoleptic alkyls
[DE94-005577] p 3206 N94-30007
Studies of high temperature ternary phases in mixed-metal-rich early transition metal sulfide and phosphide systems
[DE94-006034] p 3209 N94-30336

TRANSITION TEMPERATURE
Atomic and magnetic structure of YBa2(Cu(1-x)Fe(x))3O(6+y) at 0.05 less than or equal to x less than or equal to 0.30, y is approximately equal to 1 and y is approximately equal to 0.5
[DE94-606852] p 3513 N94-29210
The effect of various metallurgical parameters on the flow and fracture behavior of polycrystalline NiAl near the brittle-to-ductile transition
[NASA-TM-106534] p 3205 N94-29758
Calculating the J(c), B, T surface for commercial niobium tin conductors using a reduced state model
[DE94-006296] p 3520 N94-30850

TRANSLATING
More problems on rewriting
[CWI-CS-R9332] p 3428 N94-30734

TRANSMISSION
A combined electron beam/optical lithography process step for the fabrication of sub-half-micron-gate-length MMIC chips p 3240 N94-30445

TRANSMISSION EFFICIENCY
End-to-end delay reduction in narrow bandwidth real-time multimedia tele-education applications
[AD-B179614] p 3260 N94-30518

TRANSMISSION LINES
Preliminary analysis of Asynchronous Transfer Mode (ATM) over microwave channels
[AD-A275214] p 3243 N94-29069
Development of an accurate transmission line fault locator using the global positioning system satellites
p 3144 N94-30652
Electric power lines: Questions and answers on research into health effects
[DE94-005637] p 3353 N94-30757

TRANSMISSION LOSS
Investigation on application of genetic algorithms to optimal reactive power dispatch of power systems
[MATHS-REPT-A-197] p 3266 N94-29527
A transmission-loss monitor using current transformers
[DE94-003974] p 3267 N94-30716

TRANSMISSIONS (MACHINE ELEMENTS)
Experimental validation of finite element and boundary element methods for predicting structural vibration and radiated noise
[NASA-CR-4561] p 3301 N94-29552
Metal band drives in spacecraft mechanisms
p 3162 N94-29637

TRANSMITTANCE
SHARC, a model for calculating atmospheric and infrared radiation under non-equilibrium conditions
[AD-A275207] p 3357 N94-28893
Multispectral transmittance measurements through man-made water fogs p 3257 N94-30499
Estimation of transmittance from satellite imagery
p 3257 N94-30500

TRANSMITTER RECEIVERS
Solid-state, active-phased arrays: Some aspects of receiver design
[AD-A275893] p 3527 N94-28779
Ground independent landing system
p 3137 N94-29564
A commercialized, continuous flow fiber optic sensor for trichloroethylene and haloforms
p 3502 N94-30462

TRANSMITTERS
A space-based classification system for RF transients
[DE94-003933] p 3240 N94-28522

TRANSOCEANIC FLIGHT
Opportunities for integrating the aircraft FMS, aeronautical operational control centers, and future air traffic management systems in oceanic airspace
p 3140 N94-29577

TRANSONIC FLOW
Steady pressure measurements on an Aeroelastic Research Wing (ARW-2)
[NASA-TM-109046] p 3122 N94-28658
Numerical solution of inverse problem in aerodynamics p 3125 N94-28965
Verification of a three-dimensional viscous flow analysis for a single stage compressor p 3127 N94-28976
Investigation of advanced counterrotation blade configuration concepts for high speed turboprop systems. Task 2: Unsteady ducted propfan analysis computer program users manual
[NASA-CR-187105] p 3152 N94-29438
Experimental studies of transonic flow field near a longitudinally slotted wind tunnel wall
[NASA-TP-3392] p 3130 N94-29545
Unsteady transonic aerodynamics in frequency domain for flutter analysis p 3131 N94-29879
Development of a method to predict transonic limit cycle oscillation characteristics of fighter aircraft (continued)
[NLR-TP-92156-U] p 3148 N94-30342
A residual correction method applied to 2D multi-point airfoil design and 3D single-point wing design
[NLR-TP-92524-U] p 3134 N94-30493
Mixed Eulerian-Lagrangian finite element solutions of unsteady flow and flutter in transonic cascade
p 3282 N94-30816

TRANSONIC FLUTTER
Prospects of time-linearized unsteady calculation methods for exponentially diverging motions in aeroelasticity
[PB94-126224] p 3134 N94-30740
Mixed Eulerian-Lagrangian finite element solutions of unsteady flow and flutter in transonic cascade
p 3282 N94-30816

TRANSONIC WIND TUNNELS
Experimental studies of transonic flow field near a longitudinally slotted wind tunnel wall
[NASA-TP-3392] p 3130 N94-29545
A modernised HST of NLR
[AD-B179220] p 3158 N94-30423
Analysis of fluctuating static pressure measurements in a large high Reynolds number transonic cryogenic wind tunnel p 3158 N94-30788

TRANSPARENCE
Backscatter haze device for measurement of haze in aircraft transparencies
[AD-A275127] p 3146 N94-29042

TRANSPIRATION
Calculation of propulsive nozzle flowfields in multidiffusing chemically reacting environments
[NASA-TM-106532] p 3271 N94-28835

TRANSPONDERS
Design and analysis of a low-loss linear analog phase modulator for deep space spacecraft X-band transponder applications p 3248 N94-29625
Design and implementation of a hybrid digital phase-locked loop with a TMS320C25: An application to a transponder receiver breadboard
p 3251 N94-29667
Measurement of the frequency stability of responders in aircraft p 3261 N94-30673

TRANSPORT AIRCRAFT
Numerical analysis of supersonic transport wings
p 3124 N94-28959
Advanced vehicle concepts systems and design analysis studies
[NASA-CR-195115] p 3147 N94-29721

TRANSPORT PROPERTIES
Molecular aspects of transport in thin films of controlled architecture
[DE94-004552] p 3211 N94-28457
Transport properties of epitaxial lift off films
[NASA-TM-106156] p 3264 N94-29209
The effect of magnetic field configuration on particle pinch velocity in Compact Helical System (CHS)
[NIFS-267] p 3505 N94-29398
Nonadiabatic effects in the quantum Hall regime
p 3513 N94-29530
Conceptual study of moderately coupled plasmas and experimental comparison of laboratory x ray sources
[DE94-005828] p 3506 N94-30045
Volume averaged model for the mechanics of alloys solidification
[PB94-138617] p 3208 N94-30113
Process modelling for materials preparation experiments
[NASA-CR-195782] p 3175 N94-30242
The long-range transport of aerosol particles over the North Atlantic Ocean p 3386 N94-30867

TRANSPORT THEORY
Solution of charged particle transport equation by Monte-Carlo method in the BRANDZ code system
[DE94-606270] p 3484 N94-28614
A vorticity transport closure method for turbulent reacting flows p 3274 N94-29761
Overview of the US stellarator reactor study
[DE94-006042] p 3508 N94-30339
Ten new checks to assess the statistical quality of Monte Carlo solutions in MCNP
[DE94-006137] p 3465 N94-30366
Theory of ultra dense matter and the dynamics of high energy interactions involving nuclei
[DE94-004178] p 3491 N94-30686
Superdiffusion
[DE94-002333] p 3492 N94-30834

TRANSPORTATION
Electrical engineering and industrial electronics education days: Control of asynchronous generators
[PB94-135514] p 3266 N94-29523
TCM exemptions to promote alternative-fuel vehicles: The good, the bad, and the ugly
[DE94-005924] p 3311 N94-30703
Fuel cycle evaluations of biomass-ethanol and reformulated gasoline
[DE94-000227] p 3226 N94-30818

TRANSPORTER
An update on Lab Rover: A hospital material transporter
[AIAA PAPER 94-1228-CP] p 3447 N94-30577

TRAPPED PARTICLES
Charge trapping and breakdown in N2O oxides
[DE94-003775] p 3266 N94-30040
Langmuir waves in the electron-positron plasma
[DE94-608330] p 3508 N94-30191

TRAPPING
Charge trapping and breakdown in N2O oxides
[DE94-003775] p 3266 N94-30040
Langmuir waves in the electron-positron plasma
[DE94-608330] p 3508 N94-30191

TRAVELING WAVES
Annual summary of basic research thermoacoustic heat transport, 1993
[AD-A275751] p 3230 N94-28644
Langmuir waves in the electron-positron plasma
[DE94-608330] p 3508 N94-30191
Development of an accurate transmission line fault locator using the global positioning system satellites
p 3144 N94-30652
On some general properties of parabolic conservation equations
[DE94-006101] p 3461 N94-30758

TREES
Seed viability detection using computerized false-color radiographic image enhancement p 3387 N94-30461

TREES (MATHEMATICS)
Only few graphs have bounded treewidth
[RUU-CS-92-35] p 3455 N94-30333
Pearl's belief propagation: The proofs
[RUU-CS-92-47] p 3456 N94-30378
Treewidth of circle graphs
[RUU-CS-93-12] p 3458 N94-30405

A more compact visibility representation
[RUU-CS-93-26] p 3425 N94-30426
Efficient and constructive algorithms for the pathwidth and treewidth of graphs
[RUU-CS-93-27] p 3426 N94-30488
TREES (PLANTS)
Caesium-137 in a boreal forest ecosystem: Aspects on the long-term behavior
[PB94-137809] p 3347 N94-29158
Fractal approach to computer-analytical modelling of tree crown
[DE94-608089] p 3467 N94-30088
TRENDS
Interannual temperature variability and cyclone frequency over Eastern Canada and the New England States. A case study: Winter seasons 1931-1932 to 1984-1985
[ISBN-0-315-74841-9] p 3373 N94-29908
TRIANGULATION
Some efficient procedures for correcting triangulated models
[PB94-136926] p 3452 N94-29171
L(sub)p optimal d dimensional triangulations for piecewise linear interpolation: A new result on data dependent triangulations
[RUU-CS-93-13] p 3458 N94-30406
Optimal size finite element meshes without obtuse and small angles
[RUU-CS-92-39] p 3462 N94-30860
TRIAXIAL STRESSES
A modeling study of the effect of stress state on void linking during ductile fracture
[AD-A275505] p 3317 N94-28811
Granular bases for heavily loaded pavements
[AD-A275171] p 3156 N94-29047
TRIBOLOGY
Atomic-scale friction measurements using friction force microscopy. Part 2: Application to magnetic media
[AD-A275202] p 3298 N94-29290
Lubrication of space systems
[NASA-TM-106392] p 3214 N94-29399
The 27th Aerospace Mechanisms Symposium
[NASA-CP-3205] p 3160 N94-29627
Metal band drives in spacecraft mechanisms p 3162 N94-29637
The use of screening tests in spacecraft lubricant evaluation p 3162 N94-29641
An asymptotic analysis for compressible gas lubrication of rough surfaces p 3222 N94-30922
TRIGGER CIRCUITS
Recent results from testing fast ADCs
[DE94-005565] p 3406 N94-30004
TRIGONOMETRIC FUNCTIONS
Some remarkable sine and cosine functions
[PB94-137759] p 3453 N94-29439
TRIMETHYL COMPOUNDS
Tris(trimethylsily)arsine and lithium bis(trimethylsily)arsenide
[AD-A275075] p 3189 N94-29140
Surface chemistry of boron-doped SiO2 CVD: Enhanced uptake of tetraethyl orthosilicate by hydroxyl groups bonded to boron
[DE94-005428] p 3221 N94-30896
TRITIUM
Argon frost continuous cryopump for fusion applications
[DE94-004478] p 3230 N94-29017
TROPICAL METEOROLOGY
Satellite estimation of the global distribution and interannual variability of photosynthetically active radiation p 3334 N94-29970
TROPICAL REGIONS
The dynamics of tropical intraseasonal variability p 3371 N94-29741
On the annual cycle of the tropical Pacific atmosphere and ocean p 3371 N94-29763
Interannual-decadal variability in tropical climate systems: Stable isotope records and general circulation model experiments p 3373 N94-29962
FAME: A Forest Assessment and Monitoring Environment scenario
[AD-B179106] p 3335 N94-30759
TROPOSPHERE
Local Measurement of Tropospheric HO(x)
[NASA-CP-3245] p 3342 N94-28587
In situ detection of tropospheric OH and HO2 by laser-induced fluorescence in a detection chamber at low pressure p 3342 N94-28589
Tropospheric HO determination by FAGE p 3342 N94-28590
Detection of tropospheric OH and HO2 by laser-induced fluorescence at low pressure using the 308nm excitation of OH p 3343 N94-28591
Absolute determination of local tropospheric OH concentrations p 3343 N94-28594
UV laser long-path abscrption spectroscopy p 3343 N94-28595
Measurement of tropospheric OH by laser long-path absorption spectroscopy p 3343 N94-28596
Ion-assisted tropospheric OH measurement technique p 3344 N94-28601
An improved method of measuring tropospheric NO2, NO3, HO2, and RO2 by Matrix Isolation and Electronic Spin Resonance (MIESR) p 3345 N94-28605
Tropospheric HO2 determination by FAGE p 3345 N94-28606
Near-IR diode laser absorption for measurement of tropospheric HO2 p 3345 N94-28607
Line-of-sight tropospheric calibration from measurements in arbitrary directions p 3249 N94-29654
Radar estimations of atmospheric winds in the troposphere and lower stratosphere p 3370 N94-29697
Developing a diode array spectrometer for tropospheric chemistry studies p 3362 N94-29752
Radiative flux calculations at UV and visible wavelengths
[DE94-004278] p 3350 N94-30613
Tropospheric corrections to GPS measurements using locally measured meteorological parameters compared with general tropospheric corrections p 3144 N94-30655
Modeling studies of frontogenesis in the upper and middle troposphere p 3375 N94-30868
Tropospheric radiative forcing of O3 for the 1994 IPCC report
[DE94-005698] p 3367 N94-30876
TRUCKS
Prediction and standard error estimation for a finite universe total when a stratum is not sampled
[DE94-004929] p 3465 N94-30696
Compressed natural gas fueled vehicles: The Houston experience
[DE94-005804] p 3312 N94-30878
TUNABLE LASERS
Near-IR diode laser absorption for measurement of tropospheric HO2 p 3345 N94-28607
HO2 detection by near infrared absorption using tunable diode lasers p 3346 N94-28608
Advances in tunable powerful lasers: The advanced free-electron laser
[DE94-004997] p 3294 N94-29934
TUNGSTEN
Influence of tungsten alloying additions on the mechanical properties and texture of tantalum
[DE94-004994] p 3210 N94-30774
Studies of supported molybdenum and tungsten
[DE94-006207] p 3210 N94-30839
TUNGSTEN ALLOYS
Electrochemical behavior and surface chemistry of nonequilibrium aluminum alloys: Passivity mechanism and fabrication methods
[AD-A275401] p 3204 N94-29196
Influence of tungsten alloying additions on the mechanical properties and texture of tantalum
[DE94-004994] p 3210 N94-30774
TUNGSTEN CARBIDES
Metafusion: A breakthrough in metallurgy p 3211 N94-30446
TUNGSTEN COMPOUNDS
Interstitially stabilized phases in the zirconium-nickel system
[DE94-005561] p 3201 N94-28525
TUNING
Tuning of AmPS
[NIKHEF-K-AMPS-93-01] p 3494 N94-29422
TUNING FORK GYROSCOPES
Emerging technologies in microguidance and control p 3144 N94-29788
TUNNEL JUNCTIONS
Picosecond response of the quasiparticle current in superconducting tunnel junctions
[DE94-006300] p 3515 N94-30009
Strong overlap and transmission in triple barrier resonant structures
[DE94-608103] p 3516 N94-30067
TUNNELS
Three dimensional simulation of compressible flow induced by a high-speed train moving into a tunnel p 3126 N94-28967
TURBIDITY
Statistical analysis of a satellite imagery time series: Implications for the study of coastal and estuarine circulation p 3335 N94-30919
TURBINE BLADES
Design and fabrication of forward-swept counterrotation blade configuration for wind tunnel testing
[NASA-CR-194868] p 3155 N94-28510
Thermal/structural tailoring of engine blades (T/SEAEBL). Theoretical manual
[NASA-CR-194462] p 3317 N94-28815
Application of flow field simulation to turbine vane design p 3127 N94-28978
Automated inspection of turbine blades: Challenges and opportunities
[AIAA PAPER 94-1226-CP] p 3446 N94-30575
WISPER and WISPERX: Final definition of two standardised fatigue loading sequences for wind turbine blades
[AD-B175835] p 3324 N94-30872
TURBINE PUMPS
CFD analyses for advanced pump design
[NASA-CR-194866] p 3300 N94-29550
TURBINES
Development of laser velocimetry for the measurements of turbulence intensity and flow velocity ahead of a NGV row in a full-stage rotating turbine
[AD-A275712] p 3270 N94-28692
TURBOFAN ENGINES
Spray combustion experiments and numerical predictions p 3195 N94-29277
Integrated propulsion-airframe dynamics and control p 3147 N94-29854
TURBOJET ENGINES
Aerothermochemical calculations in afterburners p 3154 N94-29258
CIAM experimental turboramjets p 3152 N94-29299
TURBOMACHINE BLADES
Structural/aerodynamic blade analyzer (SAB) user's guide, version 1.0
[NASA-CR-194460] p 3151 N94-29103
Turbomachinery forced response prediction system (FREPS): User's manual
[NASA-CR-194465] p 3319 N94-29104
Aeroacoustic sensitivity analysis and optimal aeroacoustic design of turbomachinery blades
[NASA-CR-195786] p 3153 N94-30013
Mixed Eulerian-Lagrangian finite element solutions of unsteady flow and flutter in transonic cascade p 3282 N94-30816
TURBOMACHINERY
A numerical method for confined unsteady flows related to fluid-structure interactions
[ISBN-0-315-74739-0] p 3277 N94-29902
TURBOPROP ENGINES
Aerodynamic characteristics of a propeller-powered high-lift semispan wing
[NASA-TM-4541] p 3132 N94-29937
TURBORAMJET ENGINES
Research and Development of Ram/Scramjets and Turboramjets in Russia
[AGARD-LS-194] p 3151 N94-29291
Introduction and overview of research and development of solid propellant ramrockets, liquid fuel ramjets and experimental hydrogen ram combustors p 3151 N94-29292
Turboramjet engines: Types and performances p 3151 N94-29293
Research and development of ramjets/ramrockets. Part 3: The study of gaseous hydrogen ram combustors p 3152 N94-29298
TURBULENCE
Evolution of the large-scale vortices in turbulent mixing-layers p 3273 N94-29686
Dynamics of tornado-like vortices p 3371 N94-29753
Convective turbulence and transport in stars p 3546 N94-29913
Correction of X hot-wire measurements for gradients normal to the plane of the wires
[PB94-125473] p 3157 N94-30399
A laboratory simulation of urban heat-island-induced circulation in a stratified environment p 3367 N94-30921
Transition to turbulence in confined compressible mixing layers p 3283 N94-30958
TURBULENCE EFFECTS
Study of bridge design and technology
[PB94-137916] p 3121 N94-29160
Theory and application of a Radio-Acoustic Sounding System (RASS) p 3367 N94-30869
TURBULENCE MODELS
Study of modeling of turbulence of renormalization group analysis p 3126 N94-28970
An alternative assessment of second-order closure models in turbulent shear flows
[NASA-CR-194881] p 3272 N94-29381
A vorticity transport closure method for turbulent reacting flows p 3274 N94-29761
Direct and large-eddy simulations of turbulent flow in a square duct p 3275 N94-29809
Potential capabilities of Reynolds stress turbulence model in the COMMIX-RSM code p 3285 N94-30450

Three dimensional compressible turbulent flow computations for a diffusing S-duct with/without vortex generators p 3281 N94-30519
Turbulence models and their application in implosion analyses with two-phase flow
[GKSS-92/E/98] p 3284 N94-30967

TURBULENT BOUNDARY LAYER
Wall pressure events from the direct numerical simulation of a turbulent wall-bounded flow
[AD-A275890] p 3271 N94-28778
A flow visualization study of acoustically enhanced hairpin vortices
[AD-A275467] p 3271 N94-28809
An alternative assessment of second-order closure models in turbulent shear flows
[NASA-CR-194881] p 3272 N94-29381
The effect of pressure gradient on the structure of an equilibrium turbulent boundary layer
p 3282 N94-30807

TURBULENT COMBUSTION
A random distribution reacting mixing layer model
[NASA-TM-106517] p 3150 N94-28923
Simulation of pollutant formation in turbulent combustors using an extended coherent flame model
p 3190 N94-29251
Numerical prediction of turbulent sooting diffusion flames p 3191 N94-29253
Lifted turbulent jet flames p 3198 N94-29676
A vorticity transport closure method for turbulent reacting flows p 3274 N94-29761
An investigation of the reacting vortex structures associated with pulse combustion p 3200 N94-30911

TURBULENT DIFFUSION
Similarity solutions and numerical modeling in buoyancy controlled turbulent diffusion flames
[AD-A275820] p 3188 N94-28777

TURBULENT FLOW
New parameters for characterizing turbulence at a potential wind site
[DE94-004355] p 3368 N94-28455
Modeling turbulence in flows with a strong rotational component
[DE94-003577] p 3270 N94-28475
Development of laser velocimetry for the measurements of turbulence intensity and flow velocity ahead of a NGV row in a full-stage rotating turbine
[AD-A275712] p 3270 N94-28692
Papers in meteorology and geophysics, vol. 44, no.1
[JTN-94-80585] p 3324 N94-28693
Structure of neutrally stratified turbulent Ekman layer as predicted by closure models with prognostic equation for master length scale p 3325 N94-28696
Wall pressure events from the direct numerical simulation of a turbulent wall-bounded flow
[AD-A275890] p 3271 N94-28778
Study of modeling of turbulence of renormalization group analysis p 3126 N94-28970
Similarity between turbulent flows through curved pipe and orthogonal rotating pipe p 3128 N94-28986
Hydrodynamics of convection under winter polar leads
[AD-A275182] p 3369 N94-29067
Numerical modelling of turbine combustion chambers
p 3154 N94-29254
Numerical simulation of aerothermal characteristics in gas turbine combustors with complex geometries
p 3154 N94-29255
A new Eulerian model for turbulent evaporating sprays in recirculating flows p 3195 N94-29279
Time-resolved measurements in a three dimensional model combustor p 3196 N94-29283
An alternative assessment of second-order closure models in turbulent shear flows
[NASA-CR-194881] p 3272 N94-29381
Finite element method for numerical simulation of turbulent flows. The N3S code p 3233 N94-29612
Spherical model for turbulence p 3274 N94-29730
A vorticity transport closure method for turbulent reacting flows p 3274 N94-29761
Direct and large-eddy simulations of turbulent flow in a square duct p 3275 N94-29809
A numerical method for confined unsteady flows related to fluid-structure interactions
[ISBN-0-315-74739-0] p 3277 N94-29902
Wall pressure fluctuations in the reattachment region of a supersonic free shear layer
[NASA-CR-195790] p 3132 N94-29920
Electromagnetic effect on turbulent transport in liquid metals and electrolytes (bath)
[PB94-138450] p 3206 N94-29946
Prediction of fluid flow and heat transfer in internally finned tubes p 3280 N94-30228
The effect of a wavy boundary on turbulent flow
p 3280 N94-30272
Potential capabilities of Reynolds stress turbulence model in the COMMIX-RSM code p 3285 N94-30450
The enhancement of compressible turbulent mixing via streamwise vorticity p 3280 N94-30487
A new orthogonal decomposition method for turbulent flows p 3281 N94-30494
Three dimensional compressible turbulent flow computations for a diffusing S-duct with/without vortex generators p 3281 N94-30519
Development and application of particle image velocimetry in high-speed separated flow: Two-dimensional base cavities p 3282 N94-30791
The effect of pressure gradient on the structure of an equilibrium turbulent boundary layer
p 3282 N94-30807
Hopf bifurcation in viscous, low-speed flows about an airfoil with structural coupling p 3134 N94-30865
Turbulence models and their application in implosion analyses with two-phase flow
[GKSS-92/E/98] p 3284 N94-30967

TURBULENT HEAT TRANSFER
A flow visualization study of acoustically enhanced hairpin vortices
[AD-A275467] p 3271 N94-28809
Potential capabilities of Reynolds stress turbulence model in the COMMIX-RSM code p 3285 N94-30450

TURBULENT JETS
Lifted turbulent jet flames p 3198 N94-29676
The instantaneous concentration field in the self-similar region of a high Schmidt number round jet
p 3278 N94-29976

TURBULENT MIXING
Higher-order accurate numerical simulation of 3D supersonic mixing layers p 3124 N94-28954
Study on mixing and injection of hydrogen into a supersonic flow p 3127 N94-28975
Modeling of the phase liquidates in combustion chambers p 3195 N94-29278
A new Eulerian model for turbulent evaporating sprays in recirculating flows p 3195 N94-29279
Computational fluid dynamics in ventilation. 5: New developments in CFD with relevance to ventilation
p 3233 N94-29610
Evolution of the large-scale vortices in turbulent mixing-layers p 3273 N94-29686
Effects of diffusion and inertia on chaotic mixing: A computational and experimental study
p 3488 N94-29903
The enhancement of compressible turbulent mixing via streamwise vorticity p 3280 N94-30487
Design of an electromagnetic accelerator for turbulent hydrodynamic mix studies
[DE94-005821] p 3281 N94-30600

TURING MACHINES
A note on the complexity of local search problems
[CT-93-02] p 3456 N94-30370

TVD SCHEMES
A design of third-generation airfoils for helicopter rotor blades using Navier-Stokes p 3124 N94-28957
Numerical analysis of sonic boom in the near field
p 3125 N94-28962
Numerical analysis of two dimensional/axisymmetric non-equilibrium hypersonic flow p 3125 N94-28963
Role of computational fluid dynamics in aeronautical engineering. Part 10: Numerical analysis of flow around 2-D multi-element HLD p 3125 N94-28964

TWO BODY PROBLEM
Quasipotential in the fourth order of perturbation theory
[DE94-606299] p 3484 N94-28584
The solving of the relativistic two-body problem with a nonlinear dependence upon a spectrum parameter
[DE94-606343] p 3451 N94-28783

TWO DIMENSIONAL FLOW
Nominally two-dimensional flow about a normal flat plate p 3275 N94-29838
Calculus of variations applied to 2D multi-point airfoil design
[PB94-125457] p 3133 N94-30401

TWO DIMENSIONAL MODELS
Active electron and ion beam experiments in space
[AD-A275570] p 3504 N94-28828
Role of computational fluid dynamics in aeronautical engineering. Part 10: Numerical analysis of flow around 2-D multi-element HLD p 3125 N94-28964
Computational fluid dynamics in ventilation. 2: Theory and codes p 3233 N94-29607
Computational fluid dynamics in ventilation. 3: The IEA annex 20 work p 3233 N94-29608

TWO FLUID MODELS
A single-fluid, self-consistent formulation of particle transport and fluid dynamics p 3280 N94-30352

TWO PHASE FLOW
Numerical simulation of aerothermal characteristics in gas turbine combustors with complex geometries
p 3154 N94-29255
Modeling of the phase liquidates in combustion chambers p 3195 N94-29278
A new Eulerian model for turbulent evaporating sprays in recirculating flows p 3195 N94-29279
Experimental studies on effervescent atomizers with wide spray angles p 3196 N94-29280
Investigation of the two-phase flow in a research combustor under reacting and non-reacting conditions
p 3196 N94-29282
An experimental investigation of flow patterns and liquid entrainment in a horizontal-tube evaporator
p 3277 N94-29899
Two-phase power-law modeling of pipe flows displaying shear-thinning phenomena
[DE94-005115] p 3279 N94-30020
Numerical simulation of a condenser in two-phase heat transport systems: A feasibility study
[AD-B173650] p 3282 N94-30855
Local two-phase flow simulations including interface tracking with mass transfer p 3283 N94-30954
Turbulence models and their application in implosion analyses with two-phase flow
[GKSS-92/E/98] p 3284 N94-30967
Numerical simulation and prediction of implosion phenomena
[GKSS-92/E/99] p 3284 N94-30968

TWO-WAVELENGTH LASERS
Investigations of large area electron beam diodes for excimer lasers
[DE94-005670] p 3295 N94-30595

U

U BENDS
Flow and heat transfer in a rotating square sectioned U-bend p 3128 N94-28984

ULTRAHIGH FREQUENCIES
ULF waves and magnetic field characteristics in the polar cusp observed at Godhavn p 3361 N94-29244
Precision frequency synthesizing sources with excellent time/frequency performances p 3473 N94-30671

ULTRAHIGH VACUUM
Retention latch mechanism for the Wake Shield Facility p 3161 N94-29635

ULTRASONIC FLAW DETECTION
Physical interpretation and development of ultrasonic nondestructive evaluation techniques applied to the quantitative characterization of textile composite materials
[NASA-CR-195766] p 3183 N94-30016
Standardisation requirements for ultrasonic C-scanning of polymer matrix composites: An initial assessment
[PB94-139318] p 3184 N94-30438
Sensing the gas metal arc welding process
p 3314 N94-30444

ULTRASONIC RADIATION
Absolute calibration technique for broadband ultrasonic transducers
[NASA-CASE-LAR-14672-1] p 3287 N94-29199
Interaction of sound with sound by novel mechanisms: Ultrasonic four-wave mixing mediated by a suspension and ultrasonic three-wave mixing at a free surface
p 3479 N94-29988
Analysis and an image recovery algorithm for ultrasonic tomography system p 3397 N94-30456

ULTRASONIC SCANNERS
Conformal external radiotherapy of prostatic carcinoma: Requirements and preliminary results
p 3395 N94-30029
Three methods to improve the accuracy of a PUMA 560 robot p 3307 N94-30290
Standardisation requirements for ultrasonic C-scanning of polymer matrix composites: An initial assessment
[PB94-139318] p 3184 N94-30438

ULTRASONIC SPECTROSCOPY
Resonant ultrasound spectroscopy for elastic constant measurements
[DE94-005016] p 3480 N94-30098

ULTRASONIC TESTS
Physical interpretation and development of ultrasonic nondestructive evaluation techniques applied to the quantitative characterization of textile composite materials
[NASA-CR-195766] p 3183 N94-30016
Resonant ultrasound spectroscopy for elastic constant measurements
[DE94-005016] p 3480 N94-30098

ULTRASONIC WAVE TRANSDUCERS
Absolute calibration technique for broadband ultrasonic transducers
[NASA-CASE-LAR-14672-1] p 3287 N94-29199

ULTRASONICS
Acoustic and optical investigations of superfluid (3)He
[PB94-135415] p 3477 N94-29186

Interaction of sound with sound by novel mechanisms: Ultrasonic four-wave mixing mediated by a suspension and ultrasonic three-wave mixing at a free surface p 3479 N94-29988

ULTRAVIOLET ABSORPTION

Optical modeling of visibility and visibility instrumentation using stratified Mie theory p 3348 N94-29750

Study of the ultraviolet absorption and photoconduction spectra of polyimide films fabricated at various curing temperatures

[ISBN-0-315-85923-7] p 3218 N94-30036

ULTRAVIOLET ASTRONOMY

Observation of Jovian auroral Ly-alpha line profile and emission variability with a sounding rocket and the IUE archives p 3550 N94-30798

ULTRAVIOLET DETECTORS

MOCVD growth of GaN, AlN and AlGaN for UV photodetector applications

[AD-A275078] p 3512 N94-28871

ULTRAVIOLET EMISSION

A multiwavelength study of two prototypical supernova remnants p 3540 N94-29833

Observation of Jovian auroral Ly-alpha line profile and emission variability with a sounding rocket and the IUE archives p 3550 N94-30798

ULTRAVIOLET LASERS

UV laser long-path absorption spectroscopy p 3343 N94-28595

On the possibility of measuring atmospheric OH using intracavity laser spectroscopy p 3344 N94-28597

Ablation of polymers by ultraviolet pulsed laser

[DE94-608100] p 3218 N94-30066

Investigations into ultraviolet matrix-assisted laser desorption

[DE94-005265] p 3296 N94-30908

ULTRAVIOLET MICROSCOPY

Near-ultraviolet laser photoemission: Scanning microscopy, buried interfaces and image-potential states p 3294 N94-29531

ULTRAVIOLET PHOTOGRAPHY

Far ultraviolet images of the nighttime ionosphere

[AD-A275083] p 3356 N94-28843

ULTRAVIOLET RADIATION

Studies on bacterial spore ultraviolet light resistance and regulation of the activity of a spore protease

[AD-A275448] p 3384 N94-28884

Radiative flux calculations at UV and visible wavelengths

[DE94-004278] p 3350 N94-30613

Radiation transport in cloudy and aerosol loaded atmospheres p 3366 N94-30805

ULTRAVIOLET REFLECTION

Deformed ellipsoidal diffraction grating blank

[NASA-CR-189334] p 3289 N94-29872

ULTRAVIOLET SPECTRA

Spatially resolved spectroscopy of AG Carinae, and direct evidence for stellar evolution: The central star of NGC 2392

[NASA-CR-189291] p 3545 N94-29871

Study of the ultraviolet absorption and photoconduction spectra of polyimide films fabricated at various curing temperatures

[ISBN-0-315-85923-7] p 3218 N94-30036

ULTRAVIOLET SPECTROMETERS

Broadband EUV survey spectrometer for short-timescale experiments

[DE94-005459] p 3498 N94-28534

JPL Fourier transform ultraviolet spectrometer p 3343 N94-28593

A multiwavelength study of two prototypical supernova remnants p 3540 N94-29833

Deformed ellipsoidal diffraction grating blank

[NASA-CR-189334] p 3289 N94-29872

A sounding rocket program in extreme and far ultraviolet interferometry

[NASA-CR-195114] p 3289 N94-29907

ULTRAVIOLET SPECTROSCOPY

Structure of ordinary ice I(sub h). Part 1: Ideal structure of ice

[AD-A275149] p 3486 N94-29021

UNDERWATER ACOUSTICS

Analysis of spark-induced bubble experiments using CALE

[DE94-003667] p 3270 N94-28476

Global Acoustic Mapping of Ocean Temperatures (GAMOT)

[AD-A275777] p 3376 N94-28740

Broad geoacoustic assessment of some regional areas

[AD-A275504] p 3356 N94-28791

Quadruplet expansion of the acoustic pressure field in a wedge shaped ocean

[AD-A275121] p 3477 N94-29003

A review of signal detection using the bispectrum with applications in underwater acoustics

[AD-A275227] p 3478 N94-29388

Bulletin of National Research Institute of Fisheries Engineering, No. 13

[JTN-94-80596] p 3233 N94-29701

Design of the biosonar simulator for dolphin's clicks waveform reproduction p 3234 N94-29707

Interaction of sound with sound by novel mechanisms: Ultrasonic four-wave mixing mediated by a suspension and ultrasonic three-wave mixing at a free surface p 3479 N94-29988

UNDERWATER BREATHING APPARATUS

Advanced seal delivery system life support parameters

[AD-A275304] p 3401 N94-29184

UNDERWATER EXPLOSIONS

Analysis of spark-induced bubble experiments using CALE

[DE94-003667] p 3270 N94-28476

UNDERWATER RESOURCES

Journal of NIRE, Vol. 2, No. 2

[JTN-94-80552] p 3187 N94-28675

On United States-Japan Conference on Development and Utilization of Natural Resources: Report of the 14th Joint Meeting of U. S. and Japan Marine Mining Panel p 3188 N94-28683

UNDERWATER STRUCTURES

Development of the breakwater with submerged mound for interchanging sea water p 3234 N94-29703

UNDERWATER VEHICLES

Alumina ceramic: A cost effective replacement for titanium in deep submergence pressure housings

[AD-A275640] p 3212 N94-28641

The state transition diagram with path priority and it's applications

[AD-A275524] p 3434 N94-28672

A concurrent, object-based implementation for the tactical level of the rational behavior model

[AD-A275024] p 3410 N94-29115

Effect of surface condition on strength and fatigue behavior of alumina ceramic

[AD-A275053] p 3214 N94-29133

Advanced seal delivery system life support parameters

[AD-A275304] p 3401 N94-29184

UNIFIED FIELD THEORY

Experimental and theoretical studies of molecular solids

[AD-A275511] p 3485 N94-28668

UNIFORM FLOW

Flow past a circular cylinder with a permeable wake splitter plate p 3275 N94-29764

UNIQUENESS

Some results on the phase diagram of the antiferromagnetic Potts model in an external magnetic field

[DE94-608115] p 3468 N94-30110

UNITED STATES

On United States-Japan Conference on Development and Utilization of Natural Resources: Report of the 14th Joint Meeting of U. S. and Japan Marine Mining Panel p 3188 N94-28683

The European community directive: An alternative environmental impact assessment procedure after Massey?

[AD-A275550] p 3347 N94-28844

National Transportation Safety Board annual review of aircraft accident data. US general aviation, 1990

[PB94-126869] p 3135 N94-29185

Prediction and standard error estimation for a finite universe total when a stratum is not sampled

[DE94-004929] p 3465 N94-30696

UNITS OF MEASUREMENT

SI (Metric) handbook

[NASA-TM-109197] p 3231 N94-29376

UNIVERSAL TIME

Combining GPS and VLBI earth-rotation data for improved universal time p 3144 N94-29614

Loran-C time management p 3144 N94-30644

Report on NATO PTTI p 3469 N94-30645

A real-time prediction of UTC p 3470 N94-30654

UNIVERSE

Energetic events in the early universe p 3547 N94-30012

A theory approach for creation of the matter of universe

[DE94-608109] p 3548 N94-30163

UNIX (OPERATING SYSTEM)

Summer intern program

[AD-A275194] p 3466 N94-28888

The MSRC ab initio methods benchmark suite: A measurement of hardware and software performance in the area of electronic structure methods

[DE94-006428] p 3514 N94-30001

Comparative semantics for linear arrays of communicating processes

[CWI-CS-R9336] p 3426 N94-30491

Mapping objects to files: A UNIX file system interface to an object management system

[RUU-CS-93-08] p 3428 N94-30746

UNSTEADY AERODYNAMICS

Numerical study on the interaction between scramjet engine modules caused by thermal choke p 3125 N94-28960

Unsteady aerodynamic computations around NACA0012 at high angles of attack p 3126 N94-28969

Unsteady transonic aerodynamics in frequency domain for flutter analysis p 3131 N94-29879

Algorithm and code development for unsteady three-dimensional Navier-Stokes equations

[NASA-CR-195774] p 3277 N94-29942

Aeroacoustic sensitivity analysis and optimal aeroacoustic design of turbomachinery blades

[NASA-CR-195786] p 3153 N94-30013

Computational analysis of high resolution unsteady airloads for rotor aeroacoustics

[NASA-CR-194894] p 3480 N94-30274

Development of a method to predict transonic limit cycle oscillation characteristics of fighter aircraft (continued)

[NLR-TP-92156-U] p 3148 N94-30342

UNSTEADY FLOW

Boundary layers induced by three-dimensional vortex loops

[AD-A275678] p 3270 N94-28665

An experimental study of wing tip vortex in the near wake of a rectangular wing

[AD-A275389] p 3129 N94-29306

Investigation of advanced counterrotation blade configuration concepts for high speed turboprop systems. Task 2: Unsteady ducted propfan analysis computer program users manual

[NASA-CR-187105] p 3152 N94-29438

Numerical solution of the two-dimensional time-dependent incompressible Euler equations

[NASA-CR-195775] p 3277 N94-29859

A numerical method for confined unsteady flows related to fluid-structure interactions

[ISBN-0-315-74739-0] p 3277 N94-29902

Effects of diffusion and inertia on chaotic mixing: A computational and experimental study p 3488 N94-29903

Aeroacoustic sensitivity analysis and optimal aeroacoustic design of turbomachinery blades

[NASA-CR-195786] p 3153 N94-30013

A new orthogonal decomposition method for turbulent flows p 3281 N94-30494

Prospects of time-linearized unsteady calculation methods for exponentially diverging motions in aeroelasticity

[PB94-126224] p 3134 N94-30740

Development and application of particle image velocimetry in high-speed separated flow: Two-dimensional base cavities p 3282 N94-30791

Experiments on the aerodynamic generation of noise in centrifugal turbomachinery p 3480 N94-30804

Mixed Eulerian-Lagrangian finite element solutions of unsteady flow and flutter in transonic cascade p 3282 N94-30816

UNSWEPT WINGS

An experimental study of the aerodynamics of a swept and unswept semispan wing with a simulated glaze ice accretion

[NASA-CR-195330] p 3133 N94-30152

UPLINKING

Adaptive power control as a fade countermeasure on satellite links p 3253 N94-29897

Providing hydrogen maser timing stability to orbiting VLBI radio telescope observations by post-measurement compensation of linked frequency standard imperfections p 3297 N94-30670

Time maintenance system for the BMDO MSX spacecraft p 3171 N94-30672

UPPER ATMOSPHERE

Predissociation in N2(C'4, 1 Sigma u +) and other N2 states and its importance in the atmospheres of Titan and Triton

[NASA-CR-195727] p 3549 N94-28816

Far ultraviolet images of the nighttime ionosphere

[AD-A275083] p 3356 N94-28843

US National Weather experiment STORM-FEST: Waves and turbulence in frontal zones

[AD-A275084] p 3369 N94-28847

Large eddy simulation of the upper atmospheric surface layer

[ISBN-0-315-85393-X] p 3365 N94-30134

Atmosphere, ocean, and land: Critical gaps in Earth system models p 3350 N94-30617

UPSTREAM

Wall pressure events from the direct numerical simulation of a turbulent wall-bounded flow

[AD-A275890] p 3271 N94-28778

Experimental investigation of three-dimensional vortex-airfoil interaction in a supersonic stream

[AD-A275107] p 3122 N94-28899

UPWIND SCHEMES (MATHEMATICS)
Code development for hypersonic real-gas flow simulations toward the design of space vehicles, part 2 p 3125 N94-28966
On the numerical analysis of shear flows p 3126 N94-28972
Upwind method using local interpolation p 3128 N94-28982
An implicit upwind scheme for the three-dimensional Euler equations using a pointwise relaxation method p 3128 N94-28983
Time-marching aeroelastic and spatial adaptation procedures on triangular and tetrahedral meshes using an unstructured-grid Euler method p 3131 N94-29877
URANIUM ALLOYS
Incommensurate magnetic order in UNi2Al3 [DE94-005449] p 3209 N94-30246
URANUS (PLANET)
Radio science ground data system for the Voyager-Neptune encounter, part 1 p 3248 N94-29623
URBAN DEVELOPMENT
Cities for tomorrow: Directions for change [PB94-136850] p 3537 N94-29168
URBAN PLANNING
Cities for tomorrow: Directions for change [PB94-136850] p 3537 N94-29168
URBAN RESEARCH
The suitability of low-cost urban airshed modeling in the Chicago area [DE94-005114] p 3349 N94-30023
URBAN TRANSPORTATION
Optimization techniques for a dial-a-ride transportation system in urban environment [REPT-93-051] p 3537 N94-30926
URINALYSIS
Markov chains for random urinalysis 3: Daily model and drug kinetics [AD-A275540] p 3389 N94-28797
USER MANUALS (COMPUTER PROGRAMS)
A program for rapid computation of multioffset vertical seismic profile synthetic seismograms for layered media [AD-A275464] p 3355 N94-28737
Thermal/structural tailoring of engine blades (T/SEAEBL). Theoretical manual [NASA-CR-194462] p 3317 N94-28815
Transferable Output ASCII Data (TOAD) editor version 1.0 user's guide [NASA-CR-187507] p 3408 N94-28818
Laser velocimeter data acquisition system for the Langley 14- by 22-foot subsonic tunnel. Software reference guide version 3.3 [NASA-CR-191606] p 3293 N94-28839
Procedural guide for modelling and analyzing the flight characteristics of a helicopter design using flightlab [AD-A275077] p 3146 N94-28870
Business planning model user's guide [AD-A274978] p 3409 N94-28895
Learning about the Internet bibliography and beginners' guide [AD-A275205] p 3430 N94-29051
Financial resource review model user's guide [AD-A274979] p 3410 N94-29088
Structural/aerodynamic blade analyzer (SAB) user's guide, version 1.0 [NASA-CR-194460] p 3151 N94-29103
Turbomachinery forced response prediction system (FREPS): User's manual [NASA-CR-194465] p 3319 N94-29104
EXTdesign. Version 1.0: Reference manual [PB94-136827] p 3411 N94-29193
Statistical Modeling and Estimation of Reliability Functions for Software (SMERFS) user's guide, revision 3 [AD-A275390] p 3411 N94-29202
Animation techniques in BRL-CAD [AD-A275232] p 3417 N94-29392
Thermal enclosure system functional simulation user's manual [NASA-TM-109094] p 3466 N94-29489
ASSIST internals reference manual [NASA-TM-109102] p 3431 N94-29494
RIPE integrity primitives, part 1 (RACE Integrity Primitives Evaluation) [CWI-CS-R9324-PT-1] p 3252 N94-29692
RIPE integrity primitives, part 2 (RACE Integrity Primitives Evaluation) [CWI-CS-R9325-PT-2] p 3252 N94-29693
AFGWC Dial-In Subsystem (AFDIS) software users manual, version 2.2 [AD-A275844] p 3371 N94-29747
Multiple Concentric Cylinder Model (MCCM) user's guide [NASA-CR-195299] p 3183 N94-30125
TOTAL user manual [NASA-TM-109101] p 3432 N94-30160
A user's guide to the Software Testpilot [CWI-CS-R9343] p 3426 N94-30435
USER REQUIREMENTS
User-centered guidelines for environmental management [DE94-004313] p 3341 N94-28454
A survey of geographical information systems applications for the Earth Science and Applications Division, Space Sciences Laboratory, Marshall Space Flight Center [NASA-TM-108438] p 3529 N94-28820
Aid to Ada component reuse at Aerospatiale Cannes (France) [REPT-932-440-102] p 3418 N94-29418
Information engineering implementation and acceptance p 3530 N94-29533
Use of advanced technologies in ATM (air traffic management) domain p 3137 N94-29561
Information center assessment p 3533 N94-29855
Pausing behavior of end-users in online searching p 3533 N94-29960
UTILITIES
Nuclear energy related research [DE94-606286] p 3494 N94-28623
UTILIZATION
The universal applications of microtubes and microtube composites p 3186 N94-30452

V

V-22 AIRCRAFT
Organized wiring systems p 3166 N94-28705
V/STOL AIRCRAFT
Computation of wind tunnel wall effects for complex models using a low-order panel method [NASA-TM-104019] p 3132 N94-30151
VACUUM
RF vacuum microelectronics [AD-A275221] p 3263 N94-28915
Fabrication of electronic materials in space p 3228 N94-28942
Metal inert gas welding system for use in vacuum [NASA-CASE-MFS-28808-1] p 3298 N94-29352
Collecting cometary soil samples? Development of the ROSETTA sample acquisition system p 3160 N94-29628
Periodic electromagnetic vacuum in the two-dimensional Yang-Mills theory with the Chern-Simons mass [DE94-608128] p 3525 N94-30170
Survey report of JSUP Space Environment Utilization Research Committee in fiscal year 1992: Metallic Materials Session [JTN-94-80583] p 3159 N94-30794
Design of a variable-conductance vacuum insulation [DE94-000270] p 3268 N94-30819
VACUUM APPARATUS
Composite hot drape forming p 3240 N94-30448
VACUUM CHAMBERS
Vacuum chamber and adaptors for shearography and holography [NASA-CR-192467] p 3157 N94-29956
VACUUM DEPOSITION
Vacuum vapor deposition [NASA-CASE-MFS-28652-1] p 3215 N94-29446
Research on the atomic layer-by-layer growth of high-temperature superconductor thin films at the Institute of Scientific and Industrial Research, Japan [DE94-003739] p 3519 N94-30611
VACUUM EFFECTS
Fabrication of electronic materials in space p 3228 N94-28942
The impact of electrically charged microspheres with planar surfaces under vacuum conditions p 3320 N94-29765
VACUUM SYSTEMS
Argon frost continuous cryopump for fusion applications [DE94-004478] p 3230 N94-29017
VACUUM TESTS
Flammability, odor, offgassing, thermal vacuum stability, and compatibility with aerospace fluids of wire insulations p 3166 N94-28709
VALENCE
Band structure of superlattice with (delta)-like potential [DE94-608108] p 3516 N94-30072
VALLEYS
Glacial landforms and late Cenozoic history of the western Soer-Rondane mountains p 3357 N94-29080
VANELESS DIFFUSERS
Fluid dynamic noise in a centrifugal pump [AD-A275264] p 3477 N94-28904
VANES
Thermal/structural tailoring of engine blades (T/SEAEBL). Theoretical manual [NASA-CR-194462] p 3317 N94-28815
VAPOR BARRIER CLOTHING
Development of a new chemical warfare agent protective material p 3381 N94-28432
VAPOR DEPOSITION
High damage threshold anti-reflectors by physical vapor deposited amorphous fluoropolymer [DE94-004865] p 3212 N94-28560
Analysis of cost: CVD diamond deposition and finishing --- Quarterly report [AD-A275586] p 3212 N94-28725
Development of large area RF induction plasma for cost effective diamond [AD-A275888] p 3504 N94-28776
Method of producing a ceramic fiber-reinforced glass-ceramic matrix composite [NASA-CASE-LEW-15264-2] p 3180 N94-29508
Synthesis of diamond in a hydrogen plasma jet: Simulations of XRD patterns of diamond polytypes and boundary layer on a substrate p 3522 N94-29515
Preparation and structure of amorphous hydrogenated carbon film deposited with RF plasma CVD p 3223 N94-29518
A photoemission electron microscope investigation of chemical vapor deposition diamond films and diamond nucleation p 3215 N94-29745
Performance of CVD and CVR coated carbon-carbon in high temperature hydrogen [DE94-005451] p 3487 N94-29841
The organometallic chemical vapor deposition of transition metal carbides: The use of homoleptic alkyls [DE94-005577] p 3206 N94-30007
Plasma enhanced chemical vapor deposition of ZrO2 thin films [DE94-006031] p 3218 N94-30104
The growth of InAsSb/InGaAs strained-layer superlattices by metal-organic chemical vapor deposition [DE94-005576] p 3518 N94-30316
Large-area triple-junction a-Si alloy production scale up [DE94-000249] p 3339 N94-30604
Fullerenes as precursors for diamond film growth without hydrogen or oxygen additions [DE94-004582] p 3519 N94-30718
Surface chemistry of boron-doped SiO2 CVD: Enhanced uptake of tetraethyl orthosilicate by hydroxyl groups bonded to boron [DE94-005428] p 3221 N94-30896
Thermochemical data for CVD modeling from ab initio calculations [DE94-005269] p 3222 N94-30909
VAPOR PHASE EPITAXY
Innovative optoelectronic materials and structures using OMVPE [AD-A275811] p 3511 N94-28773
High resistivity buffer layers by oxygen doping [AD-A274986] p 3513 N94-29125
VAPOR PHASES
Gas phase thermochemistry of organogermanium compounds [DE94-004885] p 3187 N94-28561
Ion-assisted tropospheric OH measurement technique p 3344 N94-28601
Numerical simulation of aerothermal characteristics in gas turbine combustors with complex geometries p 3154 N94-29255
Laboratory studies of chemical and photochemical processes relevant to stratospheric ozone [NASA-CR-195779] p 3347 N94-29549
Reactions of metal ions and their clusters in the gas phase using laser ionization: Fourier transform mass spectrometry [DE94-006208] p 3207 N94-30024
Investigations into ultraviolet matrix-assisted laser desorption [DE94-005265] p 3296 N94-30908
VAPOR PRESSURE
Laboratory studies of chemical and photochemical processes relevant to stratospheric ozone [NASA-CR-195779] p 3347 N94-29549
Studies of interfaces and vapors with Optical Second Harmonic Generation [DE94-006295] p 3476 N94-30841
VAPORIZING
Liquid-oxygen droplet vaporization and combustion: Analysis of transcritical behavior and application to liquid-rocket combustion instability p 3197 N94-29592
VAPORS
Interaction of multiple spark-generated bubbles in a compressible liquid [AD-A275037] p 3272 N94-29149
VARIABILITY
The dynamics of tropical intraseasonal variability p 3371 N94-29741
Yield and variability optimization of integrated circuits: Principles and practical solutions p 3266 N94-29805

Interannual temperature variability and cyclone frequency over Eastern Canada and the New England States. A case study: Winter seasons 1931-1932 to 1984-1985
[ISBN-0-315-74841-9] p 3373 N94-29908
Interannual-decadal variability in tropical climate systems: Stable isotope records and general circulation model experiments p 3373 N94-29962
On interannual variability and climate change in the North Pacific p 3374 N94-29963
Satellite estimation of the global distribution and interannual variability of photosynthetically active radiation p 3334 N94-29970
Seed viability detection using computerized false-color radiographic image enhancement p 3387 N94-30461

VARIANCE (STATISTICS)
Ten new checks to assess the statistical quality of Monte Carlo solutions in MCNP
[DE94-006137] p 3465 N94-30366

VARIATIONAL PRINCIPLES
Dissipative quantum dynamics and nonlinear sigma-model
[DE94-606295] p 3523 N94-28617

VECTOR PROCESSING (COMPUTERS)
Parallelization techniques for highly parallel vector computer p 3129 N94-28990
Performance evaluation of the NWT with parallel Fortran p 3129 N94-28992
A method of user interface for NWT p 3129 N94-28993
Information system for flow simulation based on the Navier-Stokes equations vectorization
[AD-B179293] p 3281 N94-30763

VECTOR QUANTIZATION
Low frame rate video coding for small bandwidth realtime multimedia tele-education systems
[PB94-125531] p 3256 N94-30398

VECTOR SPACES
Homogeneous Poisson structures
[DE94-608112] p 3453 N94-30119

VEGETATION
GCM studies of the influence of vegetation on the general circulation: The role of albedo in modulating climate change p 3348 N94-29749
Sensitivity and feedbacks associated with vegetation-related land surface parameters in a general circulation model p 3348 N94-29800
Use of satellite data to improve parameterization of spatial and temporal variations of gaseous dry deposition in regional-scale models
[DE94-005110] p 3334 N94-30022
A coupled approach to spatially derived parameters necessary for ecosystem modeling on the North Slope of Alaska: Appendix A
[DE94-005853] p 3349 N94-30046
Frequency dependence of polarization phase difference
[NASA-TM-109737] p 3254 N94-30094
A bottom-up evolution of terrestrial ecosystem modeling theory, and ideas toward global vegetation modeling p 3351 N94-30628
Development of simplified ecosystem models for applications in Earth system studies: The Century experience p 3352 N94-30629
Evaluating models of climate and forest vegetation p 3353 N94-30637

VEGETATION GROWTH
Plant-microbe interactions: Plant hormone production by phylloplane fungi
[PB94-135563] p 3385 N94-29189
Cellular polarity and interactions in plant graviperception
[NASA-CR-195261] p 3385 N94-29943

VELOCITY DISTRIBUTION
Characterization of structural vibration: Field descriptors based on energy density and intensity
[PB94-132230] p 3316 N94-28404
Annual summary of basic research thermoacoustic heat transport, 1993
[AD-A275751] p 3230 N94-28644
The velocity field in the Northeast Atlantic from satellite-tracked drifting buoys
[AD-A275704] p 3376 N94-28690
Development and application of a thermistor current meter
[AD-A275816] p 3286 N94-28831
A random distribution reacting mixing layer model
[NASA-TM-106517] p 3150 N94-28923
Electron beam analysis for cyclotron harmonic and free-electron laser devices
[AD-A275070] p 3293 N94-29179
Spherical model for turbulence p 3274 N94-29730
Tail lobe ion composition at energies of 0.1 to 16 keV/e: Evidence for mass-dependent density gradients
[PAPER-93JA03201] p 3507 N94-30127
Computational analysis of high resolution unsteady airloads for rotor aeroacoustics
[NASA-CR-194894] p 3480 N94-30274
A single-fluid, self-consistent formulation of particle transport and fluid dynamics p 3280 N94-30352

VELOCITY ERRORS
Pushing the limit: Precision radial velocities, techniques, and applications p 3542 N94-30861

VELOCITY MEASUREMENT
Annual summary of basic research thermoacoustic heat transport, 1993
[AD-A275751] p 3230 N94-28644
Development and application of a thermistor current meter
[AD-A275816] p 3286 N94-28831
Stereo imaging based particle velocimeter
[NASA-CR-195800] p 3289 N94-29742
Flow past a circular cylinder with a permeable wake splitter plate p 3275 N94-29764
The impact of electrically charged microspheres with planar surfaces under vacuum conditions p 3320 N94-29765
The effect of a wavy boundary on turbulent flow p 3280 N94-30272
Pushing the limit: Precision radial velocities, techniques, and applications p 3542 N94-30861

VENTILATION
Advanced Design of Ventilation Systems
[VKI-LS-1993-07] p 3231 N94-29598
Introduction to the design of ventilation systems p 3231 N94-29599
Human requirements to the indoor air quality and the thermal environment p 3232 N94-29600
Ventilation systems p 3232 N94-29601
Theory of age distribution p 3232 N94-29602
Ventilation models p 3232 N94-29603
Industrial ventilation p 3232 N94-29604
Ventilation cost and air cleaning p 3232 N94-29605
Computational fluid dynamics in ventilation. 1: Theory and one-dimensional test case p 3232 N94-29606
Computational fluid dynamics in ventilation. 2: Theory and codes p 3233 N94-29607
Computational fluid dynamics in ventilation. 3: The IEA annex 20 work p 3233 N94-29608
Computational fluid dynamics in ventilation. 4: Commercial application of CFD in ventilation p 3233 N94-29609
Computational fluid dynamics in ventilation. 5: New developments in CFD with relevance to ventilation p 3233 N94-29610
Computational fluid dynamics in ventilation: Practical approach p 3233 N94-29611
Control of heating, ventilation and air conditioning (HVAC) systems
[PB94-138807] p 3401 N94-30000
Using spacecraft trace contaminant control systems to cure sick building syndrome p 3354 N94-30470

VENTILATION FANS
Comparison of two cool vests on heat-strain reduction while wearing a firefighting ensemble in a hot/humid environment
[AD-A275103] p 3400 N94-28902

VENTILATORS
Determination of sound power levels of air terminal units according to ISO 5135-Nordic inter-laboratory tests, Nordtest project no. 968-91
[PB94-137411] p 3477 N94-29175
Advanced Design of Ventilation Systems
[VKI-LS-1993-07] p 3231 N94-29598
Introduction to the design of ventilation systems p 3231 N94-29599
Ventilation models p 3232 N94-29603
Ventilation cost and air cleaning p 3232 N94-29605

VENUS (PLANET)
Venus Data Analysis Program: Directory of Research Projects (1993-1994)
[NASA-CR-195742] p 3549 N94-29102
Analysis of crustal structure of Venus utilizing residual Line-of-Sight (LOS) gravity acceleration and surface topography data. A trial of global modeling of Venus gravity field using harmonic spline method
[NASA-CR-195799] p 3549 N94-29737
Correlation studies of Pioneer Venus imagery obtained from PV experiments with near IR imagery obtained from ground-based observations during Venus inferior conjunction
[NASA-CR-195772] p 3550 N94-29892

VENUS ATMOSPHERE
Venus Data Analysis Program: Directory of Research Projects (1993-1994)
[NASA-CR-195742] p 3549 N94-29102

VENUS CLOUDS
Correlation studies of Pioneer Venus imagery obtained from PV experiments with near IR imagery obtained from ground-based observations during Venus inferior conjunction
[NASA-CR-195772] p 3550 N94-29892

VENUS SURFACE
Venus Data Analysis Program: Directory of Research Projects (1993-1994)
[NASA-CR-195742] p 3549 N94-29102

VERTICAL AIR CURRENTS
On eddy accumulation with limited conditional sampling to measure air-surface exchange
[DE94-005112] p 3368 N94-28568
On the origins of low-level tornadic circulations within the remnants of hurricane Andrews
[AD-A275373] p 3369 N94-29011
A study of the thermospheric dynamics of the high-latitude E region using a spectral thermospheric general circulation model p 3362 N94-29743
Evaluation of the National Meteorological Center mesoscale model for prediction of severe convection over Central Arizona p 3371 N94-29744

VERTICAL DISTRIBUTION
Theory and observations of horizontal and vertical structure of gravity wave perturbations in the middle atmosphere p 3366 N94-30802
Atmospheric turbulence within and above a coniferous forest
[ISBN-0-315-75468-0] p 3375 N94-30870

VERTIGO
Basic understanding of vertigo p 3390 N94-28855
Space and vertigo: In relation to space motion sickness p 3390 N94-28857
Equilibrium dysfunction in the clinical field p 3390 N94-28858

VERY HIGH FREQUENCIES
A space-based classification system for RF transients
[DE94-003933] p 3240 N94-28522
VHF impedance measurement: A review
[PB94-138682] p 3267 N94-30115
Measurement basis of near fields in spherical coordinates in the 100 MHz to 6 GHz band
[REPT-932-430-107] p 3255 N94-30153

VERY LARGE ARRAY (VLA)
Phasing the Very Large Array on Galileo in the presence of Jupiter's strong radio emission p 3164 N94-29621

VERY LARGE SCALE INTEGRATION
Construction of a connectionist network supercomputer
[AD-A275765] p 3405 N94-28764
Nonvolatile programmable neural network synaptic array
[NASA-CASE-NPO-18578-1-CU] p 3265 N94-29426
Micromanufacturing: Recent developments in this country and abroad p 3235 N94-29769
Self-stressing test structures used for high-frequency electromigration
[DE94-006142] p 3267 N94-30368

VERY LONG BASE INTERFEROMETRY
Combining GPS and VLBI earth-rotation data for improved universal time p 3144 N94-29614
Line-of-sight tropospheric calibration from measurements in arbitrary directions p 3249 N94-29654
Providing hydrogen maser timing stability to orbiting VLBI radio telescope observations by post-measurement compensation of linked frequency standard imperfections p 3297 N94-30670

VERY LOW FREQUENCIES
Study of generation mechanisms of magnetospheric VLF/ELF emissions based on the direction findings p 3361 N94-29245

VESTIBULAR NYSTAGMUS
Equilibrium dysfunction in the clinical field p 3390 N94-28858

VESTIBULAR TESTS
Equilibrium dysfunction in the clinical field p 3390 N94-28858
Portable Linear Sled (PLS) for biomedical research p 3163 N94-29648

VESTIBULES
Basic understanding of vertigo p 3390 N94-28855
Posture control of goldfishes under microgravity p 3387 N94-29712

VESTS
Comparison of two cool vests on heat-strain reduction while wearing a firefighting ensemble in a hot/humid environment
[AD-A275103] p 3400 N94-28902

VIBRATION
Characterization of structural vibration: Field descriptors based on energy density and intensity
[PB94-132230] p 3316 N94-28404

Closed loop vibrational control: Theory and applications
[AD-A275451] p 3154 N94-28632
Minutes: Accredited Standards Committee on Mechanical Vibration and Shock, S2. US TAG for ISO/TC 108 Mechanical Vibration and Shock
[AD-A275591] p 3316 N94-28726
Index of NPL acoustics publications 1981-1990
[NPL-RSA(EXT)-0044] p 3480 N94-30786
Rotor instability induced by dead band clearance in bearing supports p 3312 N94-30809
Numerical simulations of piano strings. Part 1: A physical model for a struck string using finite difference methods
[TELECOM-93-C-003] p 3481 N94-30972

VIBRATION DAMPING
Integrated active and passive control design methodology for the LaRC CSI evolutionary model
[NASA-CR-4580] p 3164 N94-28417
Closed loop vibrational control: Theory and applications
[AD-A275451] p 3154 N94-28632
General theory and algorithms for the non-casual inversion, slewing and control of space-based articulated structures
[AD-A275118] p 3167 N94-29002
Study of bridge design and technology
[PB94-137916] p 3121 N94-29160
Tuned mass damper for integrally bladed turbine rotor
[NASA-CASE-MFS-28697-1] p 3298 N94-29353
Position control of a flexible beam with active damping of vibrations
[ISBN-0-315-85841-9] p 3321 N94-30033
Analysis and design of inflatable aerospace structures p 3403 N94-30799
Second-order structural identification via state space-based system realizations p 3323 N94-30815

VIBRATION EFFECTS
The influence of appendage vibration on the attitude dynamics of a dual-spin satellite p 3168 N94-29828

VIBRATION ISOLATORS
Tuned mass damper for integrally bladed turbine rotor
[NASA-CASE-MFS-28697-1] p 3298 N94-29353
Activities of Ishikawajima-Harima Heavy Industries Co. Ltd.
[PB94-137981] p 3555 N94-29798

VIBRATION MEASUREMENT
Specialized data analysis of SSME and advanced propulsion system vibration measurements
[NASA-CR-193940] p 3174 N94-29868

VIBRATION MODE
Stiffness-generated rigid-body mode shapes for Lanczos eigensolution with SUPORT DOF by way of a MSC/NASTRAN DMAP alter
[NASA-TM-106537] p 3319 N94-29406
Computation of vibration mode elastic-rigid and effective weight coefficients from finite-element computer program output p 3247 N94-29615
Vibrational properties of homopolar and heteropolar surfaces and interfaces of the CdTe/HgTe system
[DE94-608105] p 3516 N94-30069
Three-dimensional free vibration analysis of thick arbitrarily laminated, rectangular, cylindrical and spherical composite panels p 3184 N94-30257
Second-order structural identification via state space-based system realizations p 3323 N94-30815

VIBRATION TESTS
Microvibrations on a GEO telecommunication satellite
[REPT-932-440-101] p 3168 N94-29415

VIBRATIONAL SPECTRA
Journal of NIRE, Vol. 2, No. 2
[JTN-94-80552] p 3187 N94-28675
Ab initio study of vibrational frequency shift upon the 1:1 acetone-iodine complex formation p 3188 N94-28681

VIBRATIONAL STATES
Low frequency dynamics of CO/Cu-breakdown of Born-Oppenheimer approximation
[DE94-005508] p 3510 N94-28512
SHARC, a model for calculating atmospheric and infrared radiation under non-equilibrium conditions
[AD-A275207] p 3357 N94-28893
Models for vibration-dissociation coupling in high-temperature gases p 3273 N94-29675
Spectroscopic and dynamical studies of highly energized small polyatomic molecules
[DE94-006509] p 3489 N94-30061
Application of semiclassical methods to reaction rate theory
[DE94-007041] p 3199 N94-30266

VIDEO COMMUNICATION
Video transmission on ATM networks
[NASA-CR-195124] p 3244 N94-29106
Low frame rate video coding for small bandwidth realtime multimedia tele-education systems
[PB94-125531] p 3256 N94-30398

VIDEO COMPRESSION
MPEG-2 video decoding architecture: Analysis and design
[REPT-93-069] p 3260 N94-30940

VIDEO DATA
Video transmission on ATM networks
[NASA-CR-195124] p 3244 N94-29106
Automating geographically referenced digital mosaics from aerial videography with area-based feature matching p 3333 N94-29540
Low frame rate video coding for small bandwidth realtime multimedia tele-education systems
[PB94-125531] p 3256 N94-30398
Time synchronized video systems p 3261 N94-30675
MPEG-2 video decoding architecture: Analysis and design
[REPT-93-069] p 3260 N94-30940

VIDEO TAPE RECORDERS
Cockpit video: A low cost BDA source
[AD-A275228] p 3150 N94-29389

VIEW EFFECTS
Synthetic image generator model; application of view angle dependent reflectivity components and performance evaluation in the visible region
[AD-A275365] p 3499 N94-29009

VIKING LANDER SPACECRAFT
BAG: A code for predicting the performance of a gas bag impact attenuation system for the Pathfinder lander
[DE94-003688] p 3165 N94-28477

VINYL POLYMERS
Plasma treatment of polymer dielectric films to improve capacitive energy storage p 3223 N94-30479

VINYLIDENE
Plasma treatment of polymer dielectric films to improve capacitive energy storage p 3223 N94-30479

VIRTUAL REALITY
HYPER-NPSNET: Embedded multimedia in a 3D virtual world
[AD-A275063] p 3410 N94-29152

VISCOELASTIC DAMPING
Advanced microfabrication technologies for microspacecraft p 3171 N94-29782

VISCOELASTICITY
Viscous and elastic-plastic material model in the ABAQUS
[PB94-132347] p 3316 N94-28409
Measurement and modelling of bolted joint stress relaxation in plastics
[PB94-124849] p 3318 N94-28841
Effects of physical aging on long-term creep of polymers and polymer matrix composites
[NASA-TM-109081] p 3181 N94-29541
Analysis of pressureless densification of ceramic matrix composites p 3216 N94-29766
On the structure and atomic motions in liquid sodium
[DE94-608386] p 3490 N94-30182
Generalized Eulerian-Lagrangian formulations in free and moving boundary problems: Processing of viscoelastic polymers and fiber suspensions p 3283 N94-30955

VISCOPLASTICITY
An anisotropic extension of Bodner's model of viscoplasticity: Model development
[NASA-CR-195289] p 3318 N94-28821
Prediction of stress-strain response of SCS-6/Timetal-21S subjected to a hypersonic flight profile
[NASA-TM-109026] p 3177 N94-28823
Finite element analysis of axisymmetric deformations of thick thermoviscoplastic targets p 3320 N94-29688
Micromechanical analysis of thermo-inelastic multiphase short-fiber composites
[NASA-CR-195290] p 3183 N94-30178

VISCOSITY
The motion of deforming bodies
[AD-A275224] p 3271 N94-29061
Numerical modelling of turbine combustion chambers p 3154 N94-29254
Electromagnetic effect on turbulent transport in liquid metals and electrolytes (bath)
[PB94-138450] p 3206 N94-29946
Two-phase power-law modeling of pipe flows displaying shear-thinning phenomena
[DE94-005115] p 3279 N94-30020

VISCOUS DAMPING
Low melting temperature alloy deployment mechanism and recent experiments p 3163 N94-29644

VISCOUS FLOW
Innovative processing of composites for ultra-high temperature applications, book 3
[AD-A275599] p 3177 N94-28731
Numerical analysis of incompressible viscous flow around a bubble p 3126 N94-28968
Verification of a three-dimensional viscous flow analysis for a single stage compressor p 3127 N94-28976
Three-dimensional external flow computations using prismatic grid p 3127 N94-28979
The motion of deforming bodies
[AD-A275224] p 3271 N94-29061
CFD analyses for advanced pump design
[NASA-CR-194866] p 3300 N94-29550
The h-p adaptive methods for incompressible viscous flow problems p 3275 N94-29836
Hopf bifurcation in viscous, low-speed flows about an airfoil with structural coupling p 3134 N94-30865

VISCOUS FLUIDS
Low melting temperature alloy deployment mechanism and recent experiments p 3163 N94-29644

VISIBILITY
The appearance of the Sun and Moon seen through clouds
[AD-A275338] p 3551 N94-29212
Optical modeling of visibility and visibility instrumentation using stratified Mie theory p 3348 N94-29750

VISION
Naval aviation vision standards research at the naval aerospace medical research laboratory: The long view
[AD-A275885] p 3388 N94-28756
Dual use of image based tracking techniques: Laser eye surgery and low vision prosthesis p 3397 N94-30455

VISUAL ACUITY
An investigation of stereopsis with AN/AVS-6 night vision goggles at varying levels of illuminance and contrast
[AD-A275332] p 3400 N94-28918
Backscatter haze device for measurement of haze in aircraft transparencies
[AD-A275127] p 3146 N94-29042

VISUAL DISCRIMINATION
Japanese Journal of Aerospace and Environmental Medicine, vol. 30, no. 2
[JTN-94-80599] p 3394 N94-29883
Psychophysiological study on the effects of co-existence of lines for detecting dot target p 3394 N94-29867

VISUAL PERCEPTION
Naval aviation vision standards research at the naval aerospace medical research laboratory: The long view
[AD-A275885] p 3388 N94-28756
An investigation of stereopsis with AN/AVS-6 night vision goggles at varying levels of illuminance and contrast
[AD-A275332] p 3400 N94-28918
The appearance of the Sun and Moon seen through clouds
[AD-A275338] p 3551 N94-29212
Empirical studies of the value of algorithm animation in algorithm understanding
[AD-A275135] p 3412 N94-29287
Behavior and visual control of cyprinodonts under microgravity p 3367 N94-29713
Psychophysiological study on the effects of co-existence of lines for detecting dot target p 3394 N94-29867

VISUAL TASKS
Scanning and monitoring performance: Effects of the reinforcement values of the events being monitored
[DOT/FAA/AM-94/8] p 3398 N94-29918
Sampling behaviour in a four instrument monitoring task: Effects of signal bandwidth and number of events per signal
[AD-B179613] p 3402 N94-30422
Maintaining vigilance on a simulated ATC monitoring task across repeated sessions
[DOT/FAA/AM-94/6] p 3143 N94-30933

VITERBI DECODERS
Convolutional encoding of self-dual codes p 3250 N94-29662
Decoder synchronization for deep space missions p 3250 N94-29664

VOIDS
A modeling study of the effect of stress state on void linking during ductile fracture
[AD-A275505] p 3317 N94-28811

VOLATILITY
Measurement of volatile metal species at elevated temperatures
[PB94-132321] p 3186 N94-28407

VOLCANOLOGY
Studies in Jurassic and Cretaceous North American apparent polar wander p 3362 N94-29940

VORTEX BREAKDOWN
Dynamics of tornado-like vortices p 3371 N94-29753
Numerical investigation into high-angle-of-attack leading-edge vortex flow
[PB94-125564] p 3133 N94-30388
Aspects of the modeling and numerical simulation of leading-edge vortex flow
[AD-B179108] p 3133 N94-30492

VORTEX FILAMENTS
The instantaneous concentration field in the self-similar region of a high Schmidt number round jet p 3278 N94-29976
VORTEX GENERATORS
Evolution of the large-scale vortices in turbulent mixing-layers p 3273 N94-29686
Three dimensional compressible turbulent flow computations for a diffusing S-duct with/without vortex generators p 3281 N94-30519
VORTEX INJECTORS
The enhancement of compressible turbulent mixing via streamwise vorticity p 3280 N94-30487
VORTEX SHEDDING
An investigation of the reacting vortex structures associated with pulse combustion p 3200 N94-30911
VORTICES
Modeling turbulence in flows with a strong rotational component
[DE94-003577] p 3270 N94-28475
Large eddy simulations using lattice Boltzmann algorithms
[DE94-005686] p 3270 N94-28549
Objective analysis of a coastal ocean eddy using satellite AVHRR and in situ hydrographic data
[AD-A275715] p 3376 N94-28642
Boundary layers induced by three-dimensional vortex loops
[AD-A275678] p 3270 N94-28665
Spin-up in a rectangular cylinder
[AD-A275465] p 3271 N94-28738
Experimental investigation of three-dimensional vortex-airfoil interaction in a supersonic stream
[AD-A275107] p 3122 N94-28899
A model analysis of potential vorticity on isopycnal surfaces for the global ocean
[AD-A275047] p 3377 N94-29164
Long-wavelength asymptotics of unstable crossflow modes, including the effect of surface curvature
[NASA-CR-4579] p 3273 N94-29460
Evolution of the large-scale vortices in turbulent mixing-layers p 3273 N94-29686
Forced generation of solitary waves in a rotating fluid and their stability p 3274 N94-29689
An experimental investigation of the effect of leading edge extensions on directional stability and the effectiveness of forebody nose strakes p 3155 N94-29728
Dynamics of tornado-like vortices p 3371 N94-29753
Numerical study of the trailing vortex of a wing with wing-tip blowing
[NASA-CR-195803] p 3130 N94-29760
Flow past a circular cylinder with a permeable wake splitter plate p 3275 N94-29764
Direct and large-eddy simulations of turbulent flow in a square duct p 3275 N94-29809
Nominally two-dimensional flow about a normal flat plate p 3275 N94-29838
Large eddy simulation of subsonic mixing layers p 3276 N94-29851
Hydrodynamic stability analysis of swirling jets p 3278 N94-29974
Large eddy simulation of the upper atmospheric surface layer
[ISBN-0-315-85393-X] p 3365 N94-30134
Computational analysis of high resolution unsteady airloads for rotor aeroacoustics
[NASA-CR-194894] p 3480 N94-30274
Numerical investigation into high-angle-of-attack leading-edge vortex flow
[PB94-125564] p 3133 N94-30388
The enhancement of compressible turbulent mixing via streamwise vorticity p 3280 N94-30487
Aspects of the modeling and numerical simulation of leading-edge vortex flow
[AD-B179108] p 3133 N94-30492
Three dimensional compressible turbulent flow computations for a diffusing S-duct with/without vortex generators p 3281 N94-30519
Experiments on the aerodynamic generation of noise in centrifugal turbomachinery p 3480 N94-30804
Numerical simulation of leading-edge vortex flow
[AD-B175154] p 3134 N94-30871
An investigation of the reacting vortex structures associated with pulse combustion p 3200 N94-30911
VORTICITY
On the origins of low-level tornadic circulations within the remnants of hurricane Andrews
[AD-A275373] p 3369 N94-29011
A model analysis of potential vorticity on isopycnal surfaces for the global ocean
[AD-A275047] p 3377 N94-29164
Evolution of the large-scale vortices in turbulent mixing-layers p 3273 N94-29686
Physical processes associated with variability in successive operational model forecasts of cyclogenesis
[ISBN-0-315-74753-6] p 3371 N94-29751
A vorticity transport closure method for turbulent reacting flows p 3274 N94-29761
Numerical solution of 3-D Navier-Stokes equations in vorticity-velocity form for incompressible flows p 3276 N94-29843
Large eddy simulation of subsonic mixing layers p 3276 N94-29851
The enhancement of compressible turbulent mixing via streamwise vorticity p 3280 N94-30487
VOYAGER PROJECT
Radio science ground data system for the Voyager-Neptune encounter, part 1 p 3248 N94-29623
VULNERABILITY
Vulnerability of manned spacecraft to crew loss from orbital debris penetration
[NASA-TM-108452] p 3169 N94-30161

W

WAFERS
Silicon-Film (tm) photovoltaic manufacturing technology
[DE94-000258] p 3336 N94-28501
A sub-cm micromachined electron microscope p 3236 N94-29775
WAKES
Coulomb field effect on plasma focusing and wake field acceleration
[DE94-004937] p 3504 N94-28564
Boundary layers induced by three-dimensional vortex loops
[AD-A275678] p 3270 N94-28665
A new flux-conserving numerical scheme for the steady, incompressible Navier-Stokes equations
[NASA-TM-106520] p 3273 N94-29471
Nominally two-dimensional flow about a normal flat plate p 3275 N94-29838
Three-dimensional flow characteristics downstream of a blade endwall corner p 3280 N94-30229
Computational analysis of high resolution unsteady airloads for rotor aeroacoustics
[NASA-CR-194894] p 3480 N94-30274
WALKING MACHINES
Biologically-inspired hexapod robot design and simulation
[AIAA PAPER 94-1178-CP] p 3439 N94-30530
ODYSSEUS autonomous walking robot: The leg/arm design
[AIAA PAPER 94-1180-CP] p 3439 N94-30531
WALL FLOW
A method for the modelling of porous and solid wind tunnel walls in computational fluid dynamics codes
[NASA-CR-195699] p 3270 N94-28724
Experimental studies of transonic flow field near a longitudinally slotted wind tunnel wall
[NASA-TP-3392] p 3130 N94-29545
WALL PRESSURE
Wall pressure events from the direct numerical simulation of a turbulent wall-bounded flow
[AD-A275890] p 3271 N94-28778
Method for making a dynamic pressure sensor and a pressure sensor made according to the method
[NASA-CASE-LAR-14029-1] p 3268 N94-29484
Wall pressure fluctuations in the reattachment region of a supersonic free shear layer
[NASA-CR-195790] p 3132 N94-29920
WALL TEMPERATURE
Development of buoyancy affected laminar flow in a heated pipe p 3128 N94-28988
WALLS
Proceedings of Japan-US Workshop P-196 on High Heat Flux Components and Plasma Surface Interactions for Next Devices
[DE94-701164] p 3503 N94-28513
Wall pressure events from the direct numerical simulation of a turbulent wall-bounded flow
[AD-A275890] p 3271 N94-28778
The effect of a wavy boundary on turbulent flow p 3280 N94-30272
WARFARE
Autonomous intelligent military robots: Army ants, killer bees, and cybernetic soldiers p 3304 N94-30276
Robotics and the battlefield of the future p 3304 N94-30277
DREV activities related to military vehicles robotization p 3305 N94-30278
Autonomous Robotic Refueling System (ARRS) for rapid aircraft turnaround p 3305 N94-30279
WARNING SYSTEMS
Minutes. Accredited Standards Committee on Noise, S12. US tag for ISO/TC 43/SC1 noise and ISO/TC 94/SC12 hearing protection
[AD-A275622] p 3477 N94-28636
Initial wave-type identification with neural networks and its contribution to automated processing in IMS version 3.0
[AD-A275058] p 3359 N94-29137
TacSats for NATO
[AGARD-AR-322] p 3169 N94-30350
WASHERS (SPACERS)
Bolt and nut evaluator
[NASA-CASE-GSC-13468-1] p 3288 N94-29538
WASHINGTON
Analysis of deep seismic reflection and other data from the southern Washington Cascades
[DE94-005915] p 3367 N94-30883
WASTE DISPOSAL
Novel mass spectrometric instrument for gaseous and particulate characterization and monitoring
[DE94-005896] p 3349 N94-30047
A modular approach for automated sample preparation and chemical analysis p 3354 N94-30464
Benchmarking for cost improvement
[DE94-002276] p 3528 N94-30824
WASTE ENERGY UTILIZATION
Feasibility study on introduction of a large methanol engine power generation plant
[DE94-732338] p 3224 N94-28629
WASTE TREATMENT
Electrochemical incineration of wastes
[NASA-CR-195262] p 3198 N94-29938
Novel mass spectrometric instrument for gaseous and particulate characterization and monitoring
[DE94-005896] p 3349 N94-30047
Benchmarking for cost improvement
[DE94-002276] p 3528 N94-30824
WASTE UTILIZATION
Electrochemical incineration of wastes
[NASA-CR-195262] p 3198 N94-29938
Publications of the NASA Controlled Ecological Life Support System (CELSS) program 1989-1992
[NASA-CR-4603] p 3401 N94-30122
WASTE WATER
Growth of hydrocarbon-rich microalga Botryococcus braunii in secondarily treated sewage and its consumption of nitrate ion and phosphate ion p 3387 N94-29519
WATER
Speciation in Water and Soil: A literature review
[PB94-132388] p 3341 N94-28412
Aeromedical support for casualties in extremely hot climates p 3382 N94-28443
Development of novel switchable protein surfaces
[AD-A275510] p 3384 N94-28667
Nominally two-dimensional flow about a normal flat plate p 3275 N94-29838
Wave generation by contaminant ions near a large spacecraft
[NASA-CR-195797] p 3169 N94-29917
Fatigue of carbon and low-alloy steels in LWR environments
[DE94-005116] p 3207 N94-30021
Regenerating using aqueous cleaners with ozone and electrolysis p 3240 N94-30468
WATER CONSUMPTION
Nutrition and hydration status of aircrew members consuming an improved survival ration during a simulated survival scenario p 3380 N94-28429
WATER CURRENTS
Development and application of a thermistor current meter
[AD-A275816] p 3286 N94-28831
Development of a simple current meter using solution p 3233 N94-29702
WATER DEPTH
Tidal atlas software development
[AD-A275251] p 3377 N94-29432
WATER FLOW
Papers in meteorology and geophysics, vol. 44, no.1
[JTN-94-80585] p 3324 N94-28693
The Japan Sea proper water and water circulation in the Japan Sea p 3324 N94-28694
Development and application of a thermistor current meter
[AD-A275816] p 3286 N94-28831
Fronts at the confluences of spring-fed streams with Joekulsa a Fjoellum: Possibly thermal bars?
[MATHS-REPT-A-198] p 3333 N94-29528
Development of a simple current meter using solution p 3233 N94-29702
The flow field near the body surface with thin filaments p 3234 N94-29706
WATER IMMERSION
Fuelling shivering in humans during cold water immersion p 3379 N94-28426

Advanced integrated cold protection for aircrew p 3381 N94-28436
Emergency underwater breathing aids for helicopter passengers and crew p 3381 N94-28437
A comparison of four methods of rewarming individuals cooled by immersion in cold water p 3382 N94-28442

WATER MANAGEMENT
Bulletin of National Research Institute of Fisheries Engineering, No. 13
[JTN-94-80596] p 3233 N94-29701
Development of the breakwater with submerged mound for interchanging sea water p 3234 N94-29703

WATER MASERS
Finnish astronomy days, 1992-1993. Proceedings of the Finnish Astronomical Society
[PB94-136892] p 3538 N94-29170

WATER RECLAMATION
An improved plating process p 3223 N94-30451

WATER RESOURCES
Fiscal 1991 geothermal development promotion energy
[DE94-732332] p 3337 N94-28627
Fiscal 1990 geothermal development promotion survey
[DE94-732333] p 3337 N94-28628
Model-oriented data analysis with applications to lake and soil water simulation
[PB94-136942] p 3329 N94-29173
Glaciohydrologic and glaciohydraulic effects on runoff and sediment yield in glacierized basins
[AD-A275134] p 3361 N94-29286

WATER RUNOFF
Glaciohydrologic and glaciohydraulic effects on runoff and sediment yield in glacierized basins
[AD-A275134] p 3361 N94-29286

WATER TEMPERATURE
Effectiveness of protection clothing for cold weather conditions after ejection over sea: A case report p 3381 N94-28435

WATER TREATMENT
A new material for removing heavy metals from water p 3354 N94-30471

WATER TUNNEL TESTS
Low-speed longitudinal aerodynamic characteristics of a flat-plate planform model of an advanced fighter configuration
[NASA-TM-109045] p 3130 N94-29443

WATER VAPOR
Fire-resistant water vapour permeable buoyant insulation p 3380 N94-28431
Low energy ion-molecule reactions and chemiionization kinetics
[DE94-005414] p 3481 N94-28491
On the effect of emissions from aircraft engines on the state of the atmosphere p 3189 N94-29247
Propagation modeling of moist air and suspended water/ice particles at frequencies below 1000 GHz p 3256 N94-30497
Estimation of transmittance from satellite imagery p 3257 N94-30500
Atmospheric moisture fields derived by satellite observations over the tropical Pacific Ocean p 3375 N94-30863

WATER WAVES
An improvement of the slender body theory for oscillating ships with finite forward speed p 3234 N94-29705
The dynamics of tropical intraseasonal variability p 3371 N94-29741
Splines and ocean wave modelling
[PB94-139409] p 3378 N94-30002
On the nonlinear dynamics of ocean wave systems p 3378 N94-30790

WATERPROOFING
Simulation of the effect of wind on clothing by measurements and calculations
[PB94-132289] p 3399 N94-28406

WATERSHEDS
Glaciohydrologic and glaciohydraulic effects on runoff and sediment yield in glacierized basins
[AD-A275134] p 3361 N94-29286

WATERWAYS
Glaciohydrologic and glaciohydraulic effects on runoff and sediment yield in glacierized basins
[AD-A275134] p 3361 N94-29286

WAVE ATTENUATION
Method for cancelling expansion waves in a wave rotor
[NASA-CASE-LEW-15218-2] p 3274 N94-29740

WAVE DIFFRACTION
Characterization of a diffraction grating as a simulant of a selective frequency antenna for radiometric applications
[AD-A275793] p 3241 N94-28745

WAVE DISPERSION
Investigations of dispersion characteristics of microwave/optical guided wave structures by using transmission line matrix method
[ISBN-0-315-85856-7] p 3254 N94-30034
Resistive ballooning mode in a gas-dynamic trap
[DE94-608328] p 3508 N94-30171
Theory and observations of horizontal and vertical structure of gravity wave perturbations in the middle atmosphere p 3366 N94-30802

WAVE EQUATIONS
The (j,0) + (0,j) representation space: Majorna-like construct
[DE94-005010] p 3522 N94-28543
Exact spherical wave solutions to Maxwell's equations with applications p 3252 N94-29733
A numerical study of gravitational collapse p 3548 N94-30271
Numerical simulations of piano strings. Part 1: A physical model for a struck string using finite difference methods
[TELECOM-93-C-003] p 3481 N94-30972

WAVE FUNCTIONS
The (j,0) + (0,j) representation space: Dirac-like construct
[DE94-005011] p 3522 N94-28572
Miln equation for the calculation of the phases and amplitudes of wave functions for continuum spectrum of Coulomb two-center problem
[DE94-606292] p 3522 N94-28616
Classical interpretation of quantum mechanics
[DE94-606304] p 3523 N94-28719
The solving of the relativistic two-body problem with a nonlinear dependence upon a spectrum parameter
[DE94-606343] p 3451 N94-28783
Observation of the phase shift of the wave function of the neutron under total reflection
[DE94-608244] p 3489 N94-30096

WAVE GENERATION
Forced generation of solitary waves in a rotating fluid and their stability p 3274 N94-29689
Wave generation by contaminant ions near a large spacecraft
[NASA-CR-195797] p 3169 N94-29917

WAVE INTERACTION
Interaction of sound with sound by novel mechanisms: Ultrasonic four-wave mixing mediated by a suspension and ultrasonic three-wave mixing at a free surface p 3479 N94-29988
On the nonlinear dynamics of ocean wave systems p 3378 N94-30790
An experimental study of nonlinear wave coupling and energy transfer characterizing the transition of a planar jet shear layer p 3282 N94-30953

WAVE PACKETS
Nonlinear wave packet evolution in a dispersive plasma: Application to rotational discontinuities p 3506 N94-29822
On determination of a momentum of Alfven wave packet
[DE94-608329] p 3255 N94-30172

WAVE PROPAGATION
Characterization of structural vibration: Field descriptors based on energy density and intensity
[PB94-132230] p 3316 N94-28404
Broad geoacoustic assessment of some regional areas
[AD-A275504] p 3356 N94-28791
Quadruplet expansion of the acoustic pressure field in a wedge shaped ocean
[AD-A275121] p 3477 N94-29003
Dynamic response of ceramics
[AD-A275396] p 3214 N94-29203
Statistical characterization of rugged propagation paths with application to Rg scattering study
[AD-A275237] p 3361 N94-29393
The dynamics of tropical intraseasonal variability p 3371 N94-29741
Nonlinear wave packet evolution in a dispersive plasma: Application to rotational discontinuities p 3506 N94-29822
Spectral analysis of wave propagation in connected waveguides p 3277 N94-29944
The effects of propagational factors on quantum wires in close parallel proximity
[ISBN-0-315-86157-6] p 3254 N94-30035
A relativistic solitary wave in electron positron plasma
[DE94-608107] p 3507 N94-30071
Extension of love wave transformation theory to laterally heterogeneous structures
[DE94-608098] p 3365 N94-30093
On determination of a momentum of Alfven wave packet
[DE94-608329] p 3255 N94-30172
Accurate finite difference methods for time-harmonic wave propagation
[NASA-CR-194887] p 3454 N94-30209

WAVE REFLECTION
Quadruplet expansion of the acoustic pressure field in a wedge shaped ocean
[AD-A275121] p 3477 N94-29003

WAVE SCATTERING
Statistical characterization of rugged propagation paths with application to Rg scattering study
[AD-A275237] p 3361 N94-29393
A spectral boundary integral equation method for the 2-D Helmholtz equation
[NASA-CR-194890] p 3454 N94-30207

WAVEFORMS
Laser beam steering with semiconductor waveguide
[AD-A275775] p 3292 N94-28765
Design of the biosonar simulator for dolphin's clicks waveform reproduction p 3234 N94-29707
Numerical simulations of piano strings. Part 1: A physical model for a struck string using finite difference methods
[TELECOM-93-C-003] p 3481 N94-30972

WAVEGUIDE ANTENNAS
Printed circuit elements with applications to antennas, scattering, and circuits
[AD-A275512] p 3262 N94-28669
X-/Ka-band dichroic plate design and grating lobe study p 3247 N94-29616
A portable X-band front-end test package for beam-waveguide antenna performance evaluation. Part 2: Tests on the antenna p 3247 N94-29620
Determining noise temperatures in beam waveguide systems p 3249 N94-29657

WAVEGUIDES
Three dimensional transient analysis of microstrip circuits in multilayered anisotropic media
[AD-A274995] p 3263 N94-28995
A comparison of two computer models of sound propagation for a wedge shaped ocean over a penetrable bottom
[AD-A275031] p 3477 N94-29117
Spectral analysis of wave propagation in connected waveguides p 3277 N94-29944
Investigations of dispersion characteristics of microwave/optical guided wave structures by using transmission line matrix method
[ISBN-0-315-85856-7] p 3254 N94-30034
Electrooptical and optical evaluation of Pb(Zr,Ti)O3 thin films using waveguide refractometry
[DE94-006374] p 3518 N94-30247

WAVELET ANALYSIS
Taxonomy of gamma ray burster data using a self-organizing neural network
[DE94-006480] p 3553 N94-30248
The Stroemberg wavelet on the interval and the Franklin system
[TELECOM-93-C-002] p 3482 N94-30971
Noise reduction techniques for the restoration of musical recordings
[TELECOM-93-E-019] p 3291 N94-30979

WAVERIDERS
Advanced vehicle concepts systems and design analysis studies
[NASA-CR-195115] p 3147 N94-29721
Expanding the waverider design space using arbitrary generating flowfields p 3148 N94-30516

WEAK INTERACTIONS (FIELD THEORY)
A measurement of the tau polarization at the resonance with the DELPHI detector at LEP
[DE94-005557] p 3482 N94-28520
Weak decays of charged K-mesons and charm particles
[PB94-138062] p 3486 N94-29143
A Tevatron collider beauty factory
[DE94-004879] p 3488 N94-29930
High sensitivity tests of the standard model for electroweak interactions
[DE94-005415] p 3490 N94-30262

WEAPON SYSTEMS
A common Ada run-time system for avionics software p 3150 N94-29331
Validation and test of complex weapon systems p 3150 N94-29336
Testing Operational Flight Programs (OFPs) p 3415 N94-29337
A disciplined approach to software test and evaluation p 3416 N94-29339

WEAPONS DELIVERY
Characterization of a diffraction grating as a simulant of a selective frequency antenna for radiometric applications
[AD-A275793] p 3241 N94-28745

WEAR
Lubrication of space systems
[NASA-TM-106392] p 3214 N94-29399

WEAR RESISTANCE
Development of braided rope engine seals
[NASA-TM-105902] p 3298 N94-28838

Unscreened low tension cables scrape abrasion testing. Part 1: An interlaboratory study on scrape abrasion testing according to ISO DP 6722-1
[PB94-135605] p 3264 N94-29191

WEAR TESTS
Unscreened low tension cables scrape abrasion testing. Part 1: An interlaboratory study on scrape abrasion testing according to ISO DP 6722-1
[PB94-135605] p 3264 N94-29191
Sliding friction and wear between titanium nitride, M50 steel and silicon nitride (round 3 of VAMAS wear test program)
[IMR-TM-TR-003] p 3303 N94-30019

WEATHER
Catalog of Air Force weather technical publications 1992-1993
[AD-A275635] p 3368 N94-28638
Capabilities, products, and services of USAFETAC (USAF Environmental Technical Applications Center)
[AD-A275654] p 3368 N94-28652
AFGWC Dial-In Subsystem (AFDIS) software users manual, version 2.2
[AD-A275844] p 3371 N94-29747
Micro-sensors for in-situ meteorological measurements p 3236 N94-29777

WEATHER STATIONS
Spatial interpolation, network bias, and terrestrial air temperature variability p 3374 N94-30810

WEATHERING
An outdoor exposure testing program for optical materials used in solar thermal electric technologies
[DE94-000265] p 3500 N94-29799

WEDGES
Quadruplet expansion of the acoustic pressure field in a wedge shaped ocean
[AD-A275121] p 3477 N94-29003
A comparison of two computer models of sound propagation for a wedge shaped ocean over a penetrable bottom
[AD-A275031] p 3477 N94-29117

WEIBULL DENSITY FUNCTIONS
Estimation of Weibull modulus from dynamic and static fatigue experiments
[PB94-138641] p 3322 N94-30114

WEIGHT INDICATORS
A non-contacting vertical alignment system for mass properties measuring instruments
[DE94-004680] p 3289 N94-29927

WEIGHT REDUCTION
Advanced microfabrication technologies for microspacecraft p 3171 N94-29782
Use of magnetic compression to support turbine engine rotors p 3314 N94-30484

WEIGHTING FUNCTIONS
Track filtering by robust neural network
[DE94-606067] p 3434 N94-28613
Weighted and unweighted maximum clique algorithms with upper bounds from fractional coloring
[AD-A275328] p 3409 N94-28917

WEIGHTLESSNESS SIMULATION
Free-floating dual-arm robots for space assembly
[AIAA PAPER 94-1195-CP] p 3442 N94-30546

WELD STRENGTH
A newly developed snow vehicle (SM100S) for Antarctica. Part 3: Low temperature toughness of the welded joints of the structural steel
p 3364 N94-29983

WELDABILITY
Casting of weldable graphite/magnesium metal matrix composites with built-in metallic inserts
p 3186 N94-30482

WELDED JOINTS
Fundamental studies on the corrosion behavior of weldments in marine microbial environments
[AD-A275247] p 3203 N94-28900
Chamber free fusion welding root side purging method and apparatus
[NASA-CASE-MFS-28832-1] p 3204 N94-29380
Fusion welding with self-generated filler metal
[NASA-CASE-LEW-15671-1] p 3301 N94-29557
A newly developed snow vehicle (SM100S) for Antarctica. Part 3: Low temperature toughness of the welded joints of the structural steel
p 3364 N94-29983

WELDING
On the prediction of HAZ grain size using Monte Carlo simulation
[DE94-005465] p 3511 N94-28535
Programmable Automated Welding System (PAWS): Control of welding through software and hardware
p 3314 N94-30443
Metafusion: A breakthrough in metallurgy
p 3211 N94-30446
Programmable Automated Welding System (PAWS)
[AIAA PAPER 94-1221-CP] p 3446 N94-30570

WELLS
Fiscal 1991 geothermal development promotion energy
[DE94-732332] p 3337 N94-28627

WENTZEL-KRAMER-BRILLOUIN METHOD
Application of semiclassical methods to reaction rate theory
[DE94-007041] p 3199 N94-30266

WETTABILITY
Logistics for the implementation of lead-free solders on electronic assemblies
[DE94-004800] p 3206 N94-29936

WHARVES
The undrained shear strength characteristics of undisturbed soil from fishing port areas
p 3234 N94-29704

WHEELCHAIRS
A robotic wheelchair
[AIAA PAPER 94-1229-CP] p 3447 N94-30578

WHISKER COMPOSITES
Technology base enhancement program. Metal matrix composites
[AD-A275531] p 3176 N94-28688
Superplasticity in fine-grained ceramics
[AD-A275461] p 3212 N94-28733

WHISTLERS
Active electron and ion beam experiments in space
[AD-A275570] p 3504 N94-28828

WHITE DWARF STARS
A study of white dwarf radiative accretion shocks
p 3544 N94-29731
Theoretical asteroseismology of white dwarf stars: The encyclopedia Seismologica p 3547 N94-30011

WHITE NOISE
Stability of dynamical systems in the presence of noise
[AD-A275383] p 3243 N94-29072
Partially coherent detection of PSK signals in Rician channels
[ISBN-0-315-85799-4] p 3254 N94-30031

WILDLIFE
Development and implementation of a scrub habitat compensation plan for Kennedy Space Center
[NASA-TM-109202] p 3347 N94-29099

WIND (METEOROLOGY)
On the linear stability of Verkley's modons
p 3324 N94-28695
Radar estimations of atmospheric winds in the troposphere and lower stratosphere
p 3370 N94-29697
On interannual variability and climate change in the North Pacific p 3374 N94-29963
Test of prototype liquid-water-content meter for aircraft use
[NASA-CR-189304] p 3374 N94-30187

WIND DIRECTION
The active titration method for measuring local hydroxyl radical concentration p 3345 N94-28602

WIND EFFECTS
Simulation of the effect of wind on clothing by measurements and calculations
[PB94-132289] p 3399 N94-28406
Deterioration of manual performance in cold and windy climates p 3381 N94-28434

WIND MEASUREMENT
Simulation of the effect of wind on clothing by measurements and calculations
[PB94-132289] p 3399 N94-28406
New parameters for characterizing turbulence at a potential wind site
[DE94-004355] p 3368 N94-28455
Radar estimations of atmospheric winds in the troposphere and lower stratosphere
p 3370 N94-29697
Four-dimensional data assimilation using the adjoint method p 3455 N94-30353

WIND TUNNEL APPARATUS
Laminar Flow Supersonic Wind Tunnel primary air injector p 3158 N94-29649
'Real time' and the NLR aerodynamic facilities
[AD-B173626] p 3158 N94-30856

WIND TUNNEL CALIBRATION
Experimental studies of transonic flow field near a longitudinally slotted wind tunnel wall
[NASA-TP-3392] p 3130 N94-29545

WIND TUNNEL MODELS
Variable soft sphere molecular model in the Monte Carlo simulation of air species p 3123 N94-28949
Rarefied gas numerical wind tunnel. Part 8: HOPE
p 3123 N94-28950
Numerical simulation of arc heated wind tunnel flow
p 3123 N94-28951
Numerical simulation of aerothermodynamic heating of hypersonic space transportation vehicles
p 3124 N94-28955
Wind tunnel testing and research
[NASA-CR-188273] p 3156 N94-29052
Low-speed longitudinal aerodynamic characteristics of a flat-plate planform model of an advanced fighter configuration
[NASA-TM-109045] p 3130 N94-29443
Miniature linear-to-rotary motion actuator
p 3163 N94-29647

WIND TUNNEL TESTS
Simulation of the effect of wind on clothing by measurements and calculations
[PB94-132289] p 3399 N94-28406
Design and fabrication of forward-swept counterrotation blade configuration for wind tunnel testing
[NASA-CR-194868] p 3155 N94-28510
Steady pressure measurements on an Aeroelastic Research Wing (ARW-2)
[NASA-TM-109046] p 3122 N94-28658
A method for the modelling of porous and solid wind tunnel walls in computational fluid dynamics codes
[NASA-CR-195699] p 3270 N94-28724
A flow visualization study of acoustically enhanced hairpin vortices
[AD-A275467] p 3271 N94-28809
Laser velocimeter data acquisition system for the Langley 14- by 22-foot subsonic tunnel. Software reference guide version 3.3
[NASA-CR-191606] p 3293 N94-28839
Wind tunnel testing and research
[NASA-CR-188273] p 3156 N94-29052
An experimental study of wing tip vortex in the near wake of a rectangular wing
[AD-A275389] p 3129 N94-29306
Experimental studies of transonic flow field near a longitudinally slotted wind tunnel wall
[NASA-TP-3392] p 3130 N94-29545
An experimental study of the flowfield on a semispan rectangular wing with a simulated glaze ice accretion
p 3130 N94-29674
An experimental investigation of the effect of leading edge extensions on directional stability and the effectiveness of forebody nose strakes
p 3155 N94-29728
Algorithm and code development for unsteady three-dimensional Navier-Stokes equations
[NASA-CR-195774] p 3277 N94-29942
The 3-D LDV measurements on a 30-degree swept wing with a simulated ice accretion
[NASA-CR-195327] p 3132 N94-30124
Computation of wind tunnel wall effects for complex models using a low-order panel method
[NASA-TM-104019] p 3132 N94-30151
Three-dimensional flow characteristics downstream of a blade endwall corner p 3280 N94-30229
The enhancement of compressible turbulent mixing via streamwise vorticity p 3280 N94-30487
The effect of pressure gradient on the structure of an equilibrium turbulent boundary layer
p 3282 N94-30807
The execution of wind energy projects 1986 - 1992 between China Aerodynamics Research and Development Centre (CARDC) and The Aeronautical Research Institute of Sweden (FFA)
[FFA-TN-1993-19] p 3340 N94-30945
Wind tunnel tests of a 5.3 m diameter yaw controlled turbine
[FFA-TN-1993-20] p 3340 N94-30946

WIND TUNNEL WALLS
A method for the modelling of porous and solid wind tunnel walls in computational fluid dynamics codes
[NASA-CR-195699] p 3270 N94-28724
Computation of wind tunnel wall effects for complex models using a low-order panel method
[NASA-TM-104019] p 3132 N94-30151

WIND TUNNELS
Holographic interferometry: A user's guide
[DE94-003136] p 3286 N94-28466
Performance evaluation of the NWT with parallel Fortran p 3129 N94-28992
Application of fuzzy logic to the control of wind tunnel settling chamber temperature
[NASA-TM-109105] p 3157 N94-30200
The effect of pressure gradient on the structure of an equilibrium turbulent boundary layer
p 3282 N94-30807

WIND TURBINES
New parameters for characterizing turbulence at a potential wind site
[DE94-004355] p 3368 N94-28455
International collaborative research in wind turbine rotor aerodynamics
[DE94-000244] p 3339 N94-30602
WISPER and WISPERX: Final definition of two standardised fatigue loading sequences for wind turbine blades
[AD-B175835] p 3324 N94-30872

The execution of wind energy projects 1986 - 1992 between China Aerodynamics Research and Development Centre (CARDC) and The Aeronautical Research Institute of Sweden (FFA)
[FFA-TN-1993-19] p 3340 N94-30945
Wind tunnel tests of a 5.3 m diameter yaw controlled turbine
[FFA-TN-1993-20] p 3340 N94-30946

WIND VELOCITY
Simulation of the effect of wind on clothing by measurements and calculations
[PB94-132289] p 3399 N94-28406
Prediction of survival times on land in a cold climate p 3379 N94-28423
The viability of photovoltaics on the Martian surface
[NASA-TM-106478] p 3338 N94-30196
Atmospheric turbulence within and above a coniferous forest
[ISBN-0-315-75468-0] p 3375 N94-30870

WIND VELOCITY MEASUREMENT
Micro-sensors for in-situ meteorological measurements p 3236 N94-29777

WINDOWS (APERTURES)
WINDOW 4.0: Documentation of calculation procedures
[DE94-004935] p 3410 N94-29019

WINDOWS (COMPUTER PROGRAMS)
Extending the X Window System
[DE94-006496] p 3420 N94-29844
The Views application environment
[CWI-CS-R9257] p 3423 N94-30341

WINDPOWER UTILIZATION
Applicability of digital terrain analyses to wind energy prospecting and siting
[DE94-004363] p 3374 N94-30587
The execution of wind energy projects 1986 - 1992 between China Aerodynamics Research and Development Centre (CARDC) and The Aeronautical Research Institute of Sweden (FFA)
[FFA-TN-1993-19] p 3340 N94-30945
Wind tunnel tests of a 5.3 m diameter yaw controlled turbine
[FFA-TN-1993-20] p 3340 N94-30946

WINDS ALOFT
Mesopause winds and OH intensities at Mid-Latitudes-Fabry-Perot interferometer observations of the OH emission at 8430 A from bear lake observatory
[AD-A275246] p 3361 N94-29430

WINDSHIELDS
Backscatter haze device for measurement of haze in aircraft transparencies
[AD-A275127] p 3146 N94-29042

WING NACELLE CONFIGURATIONS
Aerodynamic analysis of slipstream/wing/nacelle interference for preliminary design of aircraft configurations
[AD-B173651] p 3135 N94-30916

WING OSCILLATIONS
Development of a method to predict transonic limit cycle oscillation characteristics of fighter aircraft (continued)
[NLR-TP-92156-U] p 3148 N94-30342
Prospects of time-linearized unsteady calculation methods for exponentially diverging motions in aeroelasticity
[PB94-126224] p 3134 N94-30740

WING PROFILES
Numerical analysis of supersonic transport wings p 3124 N94-28959
Numerical solution of inverse problem in aerodynamics p 3125 N94-28965

WING TIP VORTICES
Experimental investigation of three-dimensional vortex-airfoil interaction in a supersonic stream
[AD-A275107] p 3122 N94-28899
An experimental study of wing tip vortex in the near wake of a rectangular wing
[AD-A275389] p 3129 N94-29306

WING TIPS
Experimental investigation of three-dimensional vortex-airfoil interaction in a supersonic stream
[AD-A275107] p 3122 N94-28899

WINGS
Experimental investigation of three-dimensional vortex-airfoil interaction in a supersonic stream
[AD-A275107] p 3122 N94-28899
Numerical study of the trailing vortex of a wing with wing-tip blowing
[NASA-CR-195803] p 3130 N94-29760
Aerodynamic characteristics of a propeller-powered high-lift semispan wing
[NASA-TM-4541] p 3132 N94-29937
Sensitivity analysis of the static aeroelastic response of a wing p 3134 N94-30525

WINTER
Hydrodynamics of convection under winter polar leads
[AD-A275182] p 3369 N94-29067
Interannual temperature variability and cyclone frequency over Eastern Canada and the New England States. A case study: Winter seasons 1931-1932 to 1984-1985
[ISBN-0-315-74841-9] p 3373 N94-29908

WIRE
Welding wire pressure sensor assembly
[NASA-CASE-MFS-26216-1-SB] p 3300 N94-29506

WIRE CLOTH
Flow past a circular cylinder with a permeable wake splitter plate p 3275 N94-29764

WIRE WINDING
Rotary actuator
[NASA-CASE-MFS-28581-1] p 3205 N94-29447

WIRELESS COMMUNICATION
Evaluation of wireless Local Area Networks
[AD-A275133] p 3243 N94-29064
The 19th Convention on Radio Science: Abstracts of Papers
[PB94-136868] p 3244 N94-29169

WIRING
Second NASA Workshop on Wiring for Space Applications
[NASA-CP-3244] p 3165 N94-28697
ESTEC wiring test programme materials related properties p 3165 N94-28698
NASA wiring program: Survey of NASA experiences in wiring system safety p 3165 N94-28700
NAVAIR aircraft wiring standardization and qualification program p 3166 N94-28704
Organized wiring systems p 3166 N94-28705
MSFC inspections of installed polyimide wire p 3166 N94-28707
Wiring for space applications program p 3166 N94-28708
Cryogenic on-orbit liquid depot storage acquisition and transfer (COLD-SAT) experiment subsystem instrumentation and wire harness design report
[NASA-CR-189172] p 3168 N94-29405

WOLF-RAYET STARS
Inhomogeneities in the wind from Wolf-Rayet stars
[ISBN-0-315-85893-1] p 3548 N94-30058

WORD PROCESSING
Smart Document System (SDS) used in managing DOE order's with electronic Engineering Procedures
[DE94-005076] p 3534 N94-30099

WORK CAPACITY
Circadian countermeasures for shiftworkers during USMP-2: A report to mission management
[NASA-CR-195260] p 3402 N94-30188

WORK FUNCTIONS
Engineering of systems for application of scientific computing in industry p 3123 N94-28947

WORKING FLUIDS
ARTI Refrigerant Database
[DE94-004906] p 3230 N94-28563
Method for cancelling expansion waves in a wave rotor
[NASA-CASE-LEW-15218-2] p 3274 N94-29740

WORKLOADS (PSYCHOPHYSIOLOGY)
Effects of workload on communication processes in decision making teams
[AD-A275894] p 3527 N94-28796
Information presentation for expert systems in future fighter aircraft
[AD-A275126] p 3149 N94-29005
Stress and ergonomic design and evaluation of person-machine systems
[AD-A275156] p 3400 N94-29034
The use of task network simulation in workload prediction
[DCIEM-92-32] p 3402 N94-30132
Spectral analysis of heart rate and psychological state: A review of its validity as a workload index
[AD-B179387] p 3399 N94-30969

WORKSTATIONS
The High Performance Storage System
[DE94-004350] p 3404 N94-28505
Data fusion and correlation techniques testbed development. Phase 1: Interim report
[SKD-1600-73-015] p 3405 N94-28533
ACCS Surveillance Exploratory Prototype (ASEP) p 3138 N94-29566
Performance of MCNP4A on seven computing platforms
[DE93-040101] p 3419 N94-29816
PAW using under MS DOS
[DE94-608012] p 3406 N94-30081
An interactive educational tool for compressible aerodynamics
[NASA-TM-106568] p 3422 N94-30175

WOVEN COMPOSITES
Delamination of woven E-glass fabric composites
[DE94-003227] p 3185 N94-30827

WROUGHT ALLOYS
Cyclic axial-torsional deformation behavior of a cobalt-base superalloy
[NASA-TM-106372] p 3203 N94-28921

WURTZITE
The synthesis and structural characterization of Na3WO3N
[AD-A275243] p 3204 N94-29395

X

X RAY ABSORPTION
A novel approach to the fabrication of SiC structures of arbitrary shape
[AD-A275475] p 3214 N94-29073

X RAY ANALYSIS
Interstitially stabilized phases in the zirconium-nickel system
[DE94-005561] p 3201 N94-28525
A novel approach to the fabrication of SiC structures of arbitrary shape
[AD-A275475] p 3214 N94-29073
Electron microscopy: Metal alloy x ray microanalysis
[REPT-932-600-101] p 3205 N94-29525

X RAY ASTRONOMY
X ray studies of the Hyades cluster
[NASA-CR-189325] p 3538 N94-29001
Coronal temperatures of unusually active K-dwarf binary systems
[NASA-CR-189335] p 3545 N94-29861
Spectral and temporal behavior of low mass x ray binaries observed with the Einstein SSS and MPC, and the Broad Band X Ray Telescope p 3542 N94-30862

X RAY BINARIES
A study of ultra high-energy radiation associated with Hercules X-1 p 3552 N94-29823
Spectral and temporal behavior of low mass x ray binaries observed with the Einstein SSS and MPC, and the Broad Band X Ray Telescope p 3542 N94-30862

X RAY DETECTORS
A high rate, low noise, x ray silicon strip detector system
[DE94-004557] p 3268 N94-30717

X RAY DIFFRACTION
Structure of ordinary ice I(sub h). Part 1: Ideal structure of ice
[AD-A275149] p 3486 N94-29021

X RAY INSPECTION
Microfocus radioscopy, a high resolution means of inspecting composite materials
[REPT-932-430-109] p 3179 N94-29454

X RAY IRRADIATION
Irradiation polymerization of bismaleimide resins
[REPT-932-430-105] p 3215 N94-29441

X RAY LASERS
Linac Coherent Light Source (LCLS) at 2-4 nm using the SLAC linac
[DE94-005235] p 3292 N94-28481
Enhanced coherence x ray laser experiments and simulations
[DE94-005367] p 3295 N94-30060

X RAY SOURCES
Correlative analysis of hard and soft x ray observations of solar flares
[NASA-CR-189329] p 3551 N94-29453
On observing neutron star oscillations p 3538 N94-29795
High redshift QSOs and the x ray background
[NASA-CR-195112] p 3540 N94-29957
Conceptual study of moderately coupled plasmas and experimental comparison of laboratory x ray sources
[DE94-005828] p 3506 N94-30045

X RAY SPECTRA
Coronal abundances and their variation
[NASA-CR-195767] p 3551 N94-29858
A high rate, low noise, x ray silicon strip detector system
[DE94-004557] p 3268 N94-30717

X RAY SPECTROSCOPY
Structure of ordinary ice I(sub h). Part 1: Ideal structure of ice
[AD-A275149] p 3486 N94-29021
Miniaturization in x ray and gamma ray spectroscopy p 3236 N94-29773
Aggregation equilibria in arsenic doped silicon
[DE94-607269] p 3515 N94-30005
XPS analysis of 440C steel surfaces lubricated with perfluoropolyethers under sliding conditions in high vacuum
[NASA-TM-106548] p 3218 N94-30177
A low noise silicon detector preamplifier system for room temperature x ray spectroscopy
[REPT-93-058] p 3291 N94-30930

X RAYS
Progress in Z-Pinch Research
[IPPCZ-321] p 3505 N94-29074
Multichannel x ray spectral measurement of hot plasma evolution in nitrogen-puff Z-pinch
[PH-24] p 3505 N94-29076
X ray emission scaling and energy balance of small gas-puff Z-pinch p 3505 N94-29077
X ray crystal structures of ((Me3SiCH2)2InCl)2 and ((Me3SiCH2)InCl2)
[AD-A275074] p 3513 N94-29155
X ray standing wave studies of underpotentially deposited metal monolayers
[AD-A275409] p 3513 N94-29215
Correlative analysis of hard and soft x ray observations of solar flares
[NASA-CR-189329] p 3551 N94-29453
Microactuator production via high aspect ratio, high edge acuity metal fabrication technology
p 3235 N94-29770
Characteristics of secondary electron emission from CsI induced by x rays with energies up to 100 keV
[DE94-608422] p 3395 N94-30185
Determination of photon fluence spectra from the NPL Mobaltron Co-60 unit
[NPL-RSA(EXT)-46] p 3492 N94-30795
Role of x ray-induced transcripts in adaptive responses following x rays
[DE94-005412] p 3386 N94-30895
XANTHINES
Biochemical enhancement of cold tolerance
p 3380 N94-28427
XENON
Computer simulation of molecular interactions in supercritical solvents
[AD-A274977] p 3486 N94-29087
Remote pumping of solid state lasers with nuclear driven fluorescers
[DE94-004846] p 3296 N94-30614

Y

YAG LASERS
Laser beam steering with semiconductor waveguide
[AD-A275775] p 3292 N94-28765
High-power CW diode-laser-array-pumped solid-state lasers and efficient nonlinear optical frequency
[AD-A275394] p 3293 N94-29309
The laser approach for sequential pyrotechnic initiation systems: Envisageable chain architecture and concepts
[REPT-932-430-113] p 3225 N94-29414
YANG-MILLS THEORY
Theory of fundamental interactions
[DE94-608126] p 3525 N94-30169
Periodic electromagnetic vacuum in the two-dimensional Yang-Mills theory with the Chern-Simons mass
[DE94-608128] p 3525 N94-30170
YARNS
Development of braided rope engine seals
[NASA-TM-105902] p 3298 N94-28838
YAW
The execution of wind energy projects 1986 - 1992 between China Aerodynamics Research and Development Centre (CARDC) and The Aeronautical Research Institute of Sweden (FFA)
[FFA-TN-1993-19] p 3340 N94-30945
Wind tunnel tests of a 5.3 m diameter yaw controlled turbine
[FFA-TN-1993-20] p 3340 N94-30946
YBCO SUPERCONDUCTORS
Fabrication issues in optimizing YBa(2)Cu(3)O(7-x) flux transformers for low I/f noise
[DE94-005209] p 3261 N94-28546
Ion channeling peculiarities in YBa2Cu3 O7 monocrystal
[DE94-606885] p 3512 N94-28787
Atomic and magnetic structure of YBa2(Cu(1-x)Fe(x))3O(6+y) at 0.05 less than or equal to x less than or equal to 0.30, y is approximately equal to 1 and y is approximately equal to 0.5
[DE94-606852] p 3513 N94-29210
MuSR measurement of the magnetic penetration depth and coherence length in the high-Tc superconductor YBa2Cu3O(6.95)
[ISBN-0-315-85385-9] p 3517 N94-30203
Thermal conductivities, electrical resistivities, and Seebeck coefficients of YBa2Cu3O(7-x) superconductors from 80 to 300 K
[DE94-004796] p 3520 N94-30724
YEAST
Plant-microbe interactions: Plant hormone production by phylloplane fungi
[PB94-135563] p 3385 N94-29189
YIELD POINT
High damage threshold anti-reflectors by physical vapor deposited amorphous fluoropolymer
[DE94-004865] p 3212 N94-28560
YIELD STRENGTH
Bolt and nut evaluator
[NASA-CASE-GSC-13468-1] p 3288 N94-29538
YO-YO DEVICES
The Solar Anomalous and Magnetospheric Particle Explorer (SAMPEX) yo-yo despin and solar array deployment mechanism p 3163 N94-29645
YTTRIA-STABILIZED ZIRCONIA
Superplasticity in fine-grained ceramics
[AD-A275461] p 3212 N94-28733
YTTRIUM ALLOYS
Studies on the optimization of deformation processed metal-metal matrix composites
[DE94-006033] p 3185 N94-30704
YUKAWA POTENTIAL
Possible explanation of the interaction cross-section growth at high energies
[DE94-606457] p 3494 N94-28612

Z

ZEOLITES
Study of iron exchanged zeolites by Moessbauer effect and electron spin resonance spectroscopy
[DE94-605138] p 3514 N94-29691
Photochemistry in constrained spaces: Zeolites and layered double metal hydroxides
[DE94-004958] p 3200 N94-30769
ZETA PINCH
Progress in Z-Pinch Research
[IPPCZ-321] p 3505 N94-29074
Investigation of intense XUV emission of nitrogen-puff Z-pinch with small energy input
[PH-23] p 3505 N94-29075
Multichannel x ray spectral measurement of hot plasma evolution in nitrogen-puff Z-pinch
[PH-24] p 3505 N94-29076
X ray emission scaling and energy balance of small gas-puff Z-pinch p 3505 N94-29077
ZINC
Pit initiation on passivated metal surfaces: Crystallographic orientation and environmental effects
[ISBN-0-315-85433-2] p 3208 N94-30138
ZINC ALLOYS
Study of nucleation and growth in Al-Zn alloys using TEM
[DE94-006312] p 3211 N94-30852
ZINC SELENIDES
Optical properties of cadmium sulfide, zinc selenide, and zinc manganese selenide semiconductor films
p 3500 N94-29759
Electronic structure of Zn-based quantum wells
[DE94-608104] p 3516 N94-30068
ZINC TELLURIDES
Dual-use applications of infrared sensitive materials
[AD-A275140] p 3499 N94-29694
ZINCBLENDE
II-VI wide band gap semiconductors under hydrostatic pressure
[DE94-608106] p 3516 N94-30070
ZIRCONIUM ALLOYS
Effects of thermomechanical processing on tensile and long-time creep behavior of Nb-1 percent Zr-0.1 percent C sheet
[NASA-TM-106319] p 3202 N94-28822
ZIRCONIUM CARBIDES
The organometallic chemical vapor deposition of transition metal carbides: The use of homoleptic alkyls
[DE94-005577] p 3206 N94-30007
ZIRCONIUM COMPOUNDS
Interstitially stabilized phases in the zirconium-nickel system
[DE94-005561] p 3201 N94-28525
ZIRCONIUM OXIDES
Interstitially stabilized phases in the zirconium-nickel system
[DE94-005561] p 3201 N94-28525
Pull-test adhesion measurements of diamondlike carbon films on silicon carbide, silicon nitride, aluminum oxide, and zirconium oxide
[DE94-005469] p 3211 N94-28536
Thick thermal barrier coatings for diesel components
[NASA-CR-187111] p 3537 N94-29350
Brittle composites modeling: Comparisons with MoSi2/ZrO2
[DE94-004978] p 3182 N94-29933
Plasma enhanced chemical vapor deposition of ZrO2 thin films
[DE94-006031] p 3218 N94-30104
Densification and crystallization of zirconia thin films prepared by sol-gel processing
[DE94-005573] p 3518 N94-30315
ZODIACAL DUST
Infrared observations of cometary dust by COBE
p 3541 N94-29994
ZODIACAL LIGHT
CBSD: The celestial background scene descriptor
[AD-A275521] p 3538 N94-28671
ZOOPLANKTON
Copepods collected along 33.5 deg E longitude of the Antarctic Ocean in the 1976 summer
p 3358 N94-29082

Typical Personal Author Index Listing

ALEXOPOULOS, JIM S. ..... p 436 N94-12023

PERSONAL AUTHOR | PAGE NUMBER | ACCESSION NUMBER

Listings in this index are arranged alphabetically by personal author. The page number helps you locate the citation in the abstract section. The accession number denotes the number by which the citation is identified.

A

AARONS, JULES ..... p 3356 N94-28891
AARTS, H. F. M. ..... p 3466 N94-30737
ABBASCHIAN, REZA ..... p 3176 N94-28729
p 3177 N94-28730
p 3177 N94-28731
ABDALLAH, AYMAN A. ..... p 3319 N94-29406
ABDEL-KADER, W. G. ..... p 3201 N94-30220
ABDULAZIZ, M. ..... p 3154 N94-29267
ABDULHUSSAIN, U. S. ..... p 3154 N94-29267
ABE, MINORU ..... p 3359 N94-29234
ABER, G. S. ..... p 3397 N94-30458
ABER, GREG S. ..... p 3299 N94-29370
ABJEAN, P. ..... p 3179 N94-29462
ABOUDI, JACOB ..... p 3183 N94-30178
ABRUNA, H. D. ..... p 3189 N94-29010
p 3513 N94-29215
ACEVEDO, D. ..... p 3513 N94-29215
ACHEROY, MARC ..... p 3259 N94-30513
ACHTEN, PETER ..... p 3423 N94-30331
ACKERMAN, M. Y. ..... p 3381 N94-28433
ACKERMANN, M. R. ..... p 3291 N94-30218
ADACHI, KUMIKO ..... p 3234 N94-29706
ADACHI, NAOHITO ..... p 3124 N94-28958
ADAM, STEVEN J. ..... p 3354 N94-30469
ADAM, V. ..... p 3140 N94-29575
p 3141 N94-29580
ADAMS, CATHERINE A. ..... p 3142 N94-30189
ADAMS, J. W. ..... p 3487 N94-29841
ADAMS, R. L. ..... p 3501 N94-30910
ADAMS, RICHARD J. ..... p 3142 N94-30189
ADATTE, THIERRY ..... p 3354 N94-28416
ADELMAN, HENRY G. ..... p 3152 N94-29860
ADELMAN, LEONARD ..... p 3399 N94-28861
ADELSON, S. J. ..... p 3536 N94-30706
ADJARDOUZOV, P. A. K. ..... p 3152 N94-29299
ADLER, S. L. ..... p 3491 N94-30685
ADRIAN, FREDERIC W. ..... p 3347 N94-29099
AFANASEV, G. N. ..... p 3261 N94-28585
AFFES, H. ..... p 3270 N94-28665
AFFINITO, J. D. ..... p 3491 N94-30695
AGAH, ARVIN ..... p 3444 N94-30558
AGARDH, L. ..... p 3320 N94-29681
AGER, C. I. ..... p 3476 N94-30780
p 3476 N94-30783
AGINS, DAVID M. ..... p 3177 N94-29008
AGRAWAL, SUNIL KUMAR ..... p 3442 N94-30546
AGRESTI, D. G. ..... p 3236 N94-29774
AGRONIN, M. L. ..... p 3239 N94-29787
AGUIRRECAMPUZANO, C. E. ..... p 3514 N94-29691
AHLUWALIA, D. V. ..... p 3522 N94-28543
p 3522 N94-28572
p 3526 N94-30750
AHMED, ALAUDDIN ..... p 3283 N94-30955
AHRENS, THOMAS J. ..... p 3214 N94-29203
AI, REBECCA X. ..... p 3517 N94-30201
AISSI, SLIM ..... p 3273 N94-29686
AITKEN, V. C. ..... p 3308 N94-30299
AKAMATSU, TOMONARI ..... p 3233 N94-29701
p 3234 N94-29707
AKHIL, A. A. ..... p 3336 N94-28489
AKIBA, MASATO ..... p 3503 N94-28555
AKIMOV, K. YU. ..... p 3483 N94-28552
AKIN, DAVID ..... p 3162 N94-29642
AKINLADE, O. ..... p 3208 N94-30090
AKIYAMA, TSUYOSHI ..... p 3331 N94-29229
AKKERMAN, A. ..... p 3395 N94-30185
AKKERMAN, J. W. ..... p 3397 N94-30458
AKKERMAN, JAMES W. ..... p 3299 N94-29370
AL-HASHEM, MOHAMMED YOUSSEF ..... p 3280 N94-30228
ALBERT, DONALD G. ..... p 3478 N94-29314
ALDERFER, DAVID W. ..... p 3287 N94-29368
ALECHINA, NATASHA ..... p 3457 N94-30396
ALEKSEEV, I. A. ..... p 3293 N94-28786
ALEXANDER, J. IWAN D. ..... p 3175 N94-30242
ALEXANDER, NORMAN ..... p 3171 N94-29782
ALEXOPOULOS, N. G. ..... p 3262 N94-28669
ALGRA, T. ..... p 3256 N94-30398
p 3424 N94-30400
ALGRA, THEO ..... p 3260 N94-30518
ALHO, K. ..... p 3530 N94-29172
ALHORN, DEAN ..... p 3264 N94-29372
ALINIKULA, P. ..... p 3244 N94-29169
ALIPPI, CESARE ..... p 3313 N94-30937
ALIZADEH, S. ..... p 3191 N94-29252
ALKABIE, H. S. ..... p 3154 N94-29267
ALLAN, DAVID W. ..... p 3470 N94-30654
ALLEN, CHRISTOPHER S. ..... p 3478 N94-29363
ALLEN, M. ..... p 3239 N94-29793
ALLEN, M. R. ..... p 3329 N94-29107
ALLEN, P. G. ..... p 3208 N94-30101
ALLEN, S. NICHOLAS ..... p 3381 N94-28432
ALLEN, TERRY ..... p 3162 N94-29639
ALLIX, O. ..... p 3179 N94-29442
ALLOUCHE, R. ..... p 3139 N94-29574
ALM, A. ..... p 3243 N94-28908
p 3245 N94-29311
ALMAHROOS, HUSSAIN MOHAMED HASAN ..... p 3273 N94-29534
ALOGLA, SULAIMAN IBN SALEH ..... p 3532 N94-29803
ALSHINA, A. P. ..... p 3475 N94-30679
ALTAII, ABDULKARIM A. J. ABDULLA ..... p 3280 N94-30229
ALTEROVITZ, S. A. ..... p 3264 N94-29209
ALTEROVITZ, SAMUEL A. ..... p 3286 N94-29000
ALTINTAS, A. ..... p 3260 N94-30514
ALTNER, BRUCE ..... p 3545 N94-29871
ALVAREZ, L. S. ..... p 3250 N94-29659
ALVAREZ, LOPEZ F. J. ..... p 3212 N94-28550
ALVERTOS, NICOLAS ..... p 3408 N94-28825
ALVIN, KENNETH F. ..... p 3323 N94-30815
AMANO, KANICHI ..... p 3125 N94-28964
AMATUNI, A. TS. ..... p 3504 N94-28564
AMRO, JOE P. ..... p 3205 N94-29900
ANDERS, CARL J. ..... p 3448 N94-30583
ANDERSON, JAMES G. ..... p 3343 N94-28592
ANDERSON, KARL F. ..... p 3287 N94-29361
ANDERSON, M. ..... p 3209 N94-30690
ANDERSON, PENNY ..... p 3453 N94-29304
ANDERSON, S. D. ..... p 3192 N94-29261
ANDERSON, STUART BRUCE ..... p 3539 N94-29825
ANDERSON, T. A. ..... p 3207 N94-30042
ANDERSON, T. W. ..... p 3464 N94-29014
ANDERSON, WILLIAM J. ..... p 3161 N94-29629
ANDERSSON, G. ..... p 3244 N94-29176
ANDO, NORIYUKI ..... p 3129 N94-28990
ANDRE, S. ..... p 3168 N94-29543
ANDREEV, A. N. ..... p 3485 N94-28621
ANDREEV, V. V. ..... p 3500 N94-30084
ANDRESEN, G. ..... p 3477 N94-29175
ANDREWS, C. C. ..... p 3318 N94-29057
ANDREWS, G. E. ..... p 3154 N94-29267
ANDRIOLE, STEPHEN J. ..... p 3399 N94-28861
ANDRIOLO, MIGUEL ..... p 3452 N94-28864
ANDROSENKO, A. A. ..... p 3484 N94-28614
ANDROSENKO, P. A. ..... p 3484 N94-28614
ANDRUKITIS, RONALD J. ..... p 3471 N94-30659
ANGELL, P. ..... p 3203 N94-28900
ANSARI, HOMAYOON ..... p 3293 N94-29493
ANSART, D. ..... p 3194 N94-29273
ANSELL, H. ..... p 3149 N94-30947
ANTHONY, P. ..... p 3482 N94-28493
p 3497 N94-30712
ANTONESCU, C. ..... p 3500 N94-29928
ANTOUN, SAMI JAMIL ..... p 3153 N94-30935
ANTTONEN, HANNU ..... p 3399 N94-28406
AOKI, SHIGERU ..... p 3442 N94-30543
AOYAGI, YUKITOSHI ..... p 3391 N94-29049
AOYAMA, JUNICHI ..... p 3169 N94-30811
APBLETT, CHRISTOPHER ALAN ..... p 3218 N94-30225
APPELBE, WILLIAM ..... p 3466 N94-28888
APPLIN, ZACHARY T. ..... p 3132 N94-29937
APT, KRYSZTOF R. ..... p 3427 N94-30733
ARAKI, MASANORI ..... p 3503 N94-28555
p 3504 N94-28556
ARASTEH, D. K. ..... p 3410 N94-29019
ARBAB, F. ..... p 3433 N94-30429
ARBUCKLE, P. DOUGLAS ..... p 3140 N94-29578
ARBUZOVA, ELENA V. ..... p 3481 N94-28468
ARCHULETA, J. I. ..... p 3210 N94-30776
ARGE, E. ..... p 3420 N94-29949
ARICI, MEHMET EMIN ..... p 3304 N94-30230
ARIZMENDI, C. M. ..... p 3521 N94-30888
ARMENDARIZ, M. G. ..... p 3501 N94-30261
ARMENTROUT, JEFFREY J. ..... p 3400 N94-28918
ARMERDING, WOLFGANG ..... p 3343 N94-28594
ARMITAGE, JAMES W. ..... p 3407 N94-28648
ARTAKI, I. ..... p 3206 N94-29936
ARTAMONOV, S. N. ..... p 3484 N94-28614
ARTUSA, ELISA A. ..... p 3231 N94-29376
ASANO, KATSUMI ..... p 3388 N94-28496
p 3388 N94-28497
ASENSIO, SANTIAGO ..... p 3192 N94-29260
ASHBY, C. I. H. ..... p 3515 N94-30006
ASHBY, DALE L. ..... p 3132 N94-30151
ASHIDA, TAMAICHI ..... p 3158 N94-28583
ASHOUR-ABDALLA, M. ..... p 3504 N94-28828
ASKENFELT, ANDERS ..... p 3481 N94-30972
ASKEW, ELDON W. ..... p 3380 N94-28429
ASKEW, JOHN C. ..... p 3223 N94-30451
ASKEW, ROBERT B. ..... p 3133 N94-30176
ASKEW, T. R. ..... p 3261 N94-28487
ASMAR, S. W. ..... p 3248 N94-29623
ASO, SHIGERU ..... p 3123 N94-28952
ASO, TAKEHIKO ..... p 3359 N94-29234
ASUKATA, ICHIRO ..... p 3387 N94-28495
p 3389 N94-28850
p 3394 N94-29863
ATAKA, MITSUO ..... p 3158 N94-28583
p 3228 N94-28943
ATCHLEY, ANTHONY A. ..... p 3230 N94-28644
ATKINS, DONALD J. ..... p 3231 N94-29379
ATKINS, JOEL ..... p 3315 N94-29020
ATLAS, S. R. ..... p 3342 N94-28521
ATTIA, ALAN I. ..... p 3264 N94-29357
p 3265 N94-29505
ATTIA, F. ..... p 3443 N94-30553
AUBERTIN, G. ..... p 3231 N94-29599
AUBUCHON, STEVEN R. ..... p 3513 N94-29130
p 3189 N94-29140
AUKIN, M. ..... p 3152 N94-29296
AUTIO, ERKKO ..... p 3537 N94-28405
AXLER, K. M. ..... p 3210 N94-30776
AYLWARD, JUDY M. ..... p 3380 N94-28429
AZINHAL, RAFAELA K. ..... p 3445 N94-30567

B

BAALBERGEN, E. H. ..... p 3422 N94-30314
BABAI, MAJID ..... p 3446 N94-30573
BACAK, J. W. ..... p 3397 N94-30458
BACAK, JAMES W. ..... p 3299 N94-29370
BAER, H. ..... p 3481 N94-28462
BAER, M. R. ..... p 3226 N94-30615
BAGCHI, S. ..... p 3447 N94-30580
BAGEPALLI, B. ..... p 3171 N94-29782
BAGINYAN, S. A. ..... p 3434 N94-28613
BAILEY, JOHN W. ..... p 3409 N94-28878
BAIRD, ROBERT W. ..... p 3166 N94-28706
BAJAJ, KRISHAN K. ..... p 3499 N94-29114
BAKER, J. ..... p 3254 N94-30043

BAKSHI, P. p 3504 N94-29055
BAKUNIN, O. G. p 3493 N94-30881
BAL, C. M. RENE p 3425 N94-30417
BALABANOVIC, MARKO p 3443 N94-30555
BALACHANDRAN, U. p 3261 N94-28487
BALAGUROV, A. M. p 3513 N94-29210
BALARAM, J. p 3442 N94-30544
BALAS, EGON p 3409 N94-28917
BALDI, PIERRE F. p 3435 N94-29492
BALDINI, L. p 3256 N94-30496
BALDO, P. p 3521 N94-30894
BALDWIN, ULF I. p 3400 N94-29029
BALL, DAVID W. p 3189 N94-28832
BALL, ROY p 3308 N94-30297
BALLAL, D. R. p 3193 N94-29266
BALLANTYNE, M. J. p 3383 N94-28449
BALMER, G. J. p 3258 N94-30508
BALMI, P. J. p 3382 N94-28442
BALOMEY, J. C. p 3255 N94-30153
BALSTERS, HERMAN p 3425 N94-30417
BALUJA, SHUMEET p 3397 N94-28860
BANDAK, FARIS AFIF p 3514 N94-29915
BANE, CHUCK H., JR. p 3527 N94-28905
BANE, K. p 3292 N94-28481
BANERDT, W. B. p 3237 N94-29778
BANERJEE, V. p 3306 N94-30287
BANGERTER, R. O. p 3494 N94-28507
BANSAL, NAROTTAM P. p 3180 N94-29508
BANTA, G. p 3391 N94-28912
BANTLE, GERHARD p 3138 N94-29565
BAO, JIAN-WEN p 3455 N94-30353
BAQUERO, R. p 3516 N94-30070
BAR-NESS, YEHESKEL p 3408 N94-28760
BARAD, HERB p 3377 N94-29204
BARAER, P. p 3225 N94-29414
BARANOV, G. A. p 3293 N94-28786
BARANOV, S. A. p 3489 N94-30095
BARBIER, PIERRE p 3231 N94-29477
BARBIR, FRANO p 3348 N94-29901
BARBOUR, J. C. p 3515 N94-30006
BARCLAY, REBECCA O. p 3534 N94-30149
p 3534 N94-30150
BARFIELD, LON G. p 3422 N94-30322
BARIETTA, R. E. p 3223 N94-30475
BARKEY, DALE P. p 3213 N94-28806
BARLETTA, R. E. p 3487 N94-29841
BARNARD, J. C. p 3368 N94-28455
BARNETT, ALAN R. p 3319 N94-29406
p 3319 N94-29469
BARNHART, JOHN STEVEN p 3277 N94-29899
BARRETT, STEVEN F. p 3389 N94-28810
BARTELL, RICHARD J. p 3146 N94-29042
BARTKNECHT, A. T. p 3515 N94-30009
BARTMAN, R. p 3239 N94-29787
BARTRAM, M. E. p 3221 N94-30896
BARWICK, MICHAEL p 3268 N94-29437
BASHIR-HASHEMI, A. p 3227 N94-30454
BASORE, P. A. p 3340 N94-30509
BASS, B. R. p 3323 N94-30689
BAST, CALLIE CORINNE SCHEIDT p 3318 N94-28840
BASU, ANUP p 3308 N94-30298
BASU, R. p 3340 N94-30879
BATCHELOR, D. B. p 3255 N94-30105
BATES, J. B. p 3520 N94-30773
BATHKER, D. A. p 3248 N94-29624
BATUR, CELAL p 3289 N94-29742
BATUSOV, YU. A. p 3489 N94-30095
p 3290 N94-30148
BAUCOM, K. C. p 3518 N94-30316
BAUCOM, ROBERT M. p 3180 N94-29485
BAUDRILLARD, GILLES p 3315 N94-29474
BAUER, DANIEL H. p 3400 N94-28997
BAUM, AARON p 3262 N94-28650
BAUMGART, C. p 3240 N94-28522
BAUMGART, C. W. p 3553 N94-30248
BAUMONT, F. p 3145 N94-30665
BAUMONT, FRANCOISE p 3469 N94-30647
BAUNE, SCOTT A. p 3272 N94-29435
BAYARD, DAVID S. p 3246 N94-29495
BAYO, E. p 3167 N94-29002
BAYOUMI, M. M. p 3308 N94-30295
BEARD, P. p 3195 N94-29278
BEAUCHAMP, DOMINIQUE p 3541 N94-30231
BEAUDET, WILLIAM p 3241 N94-28762
BEAULIEU, CHRISTIAN p 3500 N94-30233
BEAUMONT, M. p 3384 N94-28450
BEAUVAIS, W. J. p 3201 N94-30220
BECKER-SZENDY, R. p 3482 N94-28493
p 3497 N94-30712
BECKER, C. p 3205 N94-29525
BECKER, CRAIG p 3443 N94-30555
BECKER, M. p 3496 N94-30219
BECKLER, TINA M. p 3346 N94-28727
p 3346 N94-28774
BEDARD, ROGER p 3144 N94-30282
BEDDOES, M. P. p 3309 N94-30302
BEELER, R. H. p 3136 N94-30890
BEGAULT, DURAND R. p 3245 N94-29364
BEHRENS, RICHARD, JR. p 3225 N94-29308
BEIK, M. A. p 3269 N94-28464
BEKEY, GEORGE A. p 3444 N94-30558
BELANGER, FRANCOIS p 3277 N94-29902
BELIKOV, S. V. p 3489 N94-30050
BELL, J. A. p 3498 N94-28656
BELONGIE, M. L. p 3250 N94-29664
BELYAEV, V. B. p 3407 N94-28622
BELYAKOV, V. A. p 3494 N94-28612
BEMENT, LAURENCE J. p 3161 N94-29634
BEN-ZVI, I. p 3296 N94-30688
BENDER, ROBERT J. p 3381 N94-28432
BENHARRATS, N. p 3218 N94-30066
BENJAMIN, CLIVE L. p 3150 N94-29331
BENKOWSKI, ROBERT J. p 3299 N94-29370
BENNETT, BRAD L. p 3400 N94-28902
p 3391 N94-28912
BENNETT, CHARLES H. p 3526 N94-30433
BENOIT, ANDRE p 3136 N94-29558
p 3139 N94-29570
BENOIT, MICHAEL J. p 3446 N94-30574
BENSON, D. K. p 3268 N94-30819
BENSON, DWAYNE M. p 3231 N94-29379
BENSON, THOMAS J. p 3421 N94-30174
p 3422 N94-30175
BENT, PAUL HENRY p 3480 N94-30804
BENYOUSSEF, A. p 3468 N94-30110
p 3525 N94-30164
p 3517 N94-30165
p 3517 N94-30181
BENZEL, D. M. p 3254 N94-30043
BEREZHIANI, V. I. p 3507 N94-30071
BEREZOVSKAYA, F. S. p 3467 N94-30088
BERGER, M. p 3451 N94-28571
BERGER, M. J. p 3279 N94-30003
BERGEY, JOHN K. p 3416 N94-29343
BERGHUIS, HARRY p 3449 N94-30963
BERGMAN, R. p 3347 N94-29158
BERGREN, TODD EDWARD p 3221 N94-30797
BERGSTRA, J. A. p 3459 N94-30436
BERGSTRA, JAN p 3424 N94-30371
BERKA, REGINALD B. p 3160 N94-29369
BERMAN, M. p 3326 N94-28930
BERNARD, DENYS p 3122 N94-29463
BERNIER, L. G. p 3474 N94-30676
BERNSTEIN, DAVID HAROLD p 3540 N94-29990
BERNSTEIN, H. p 3224 N94-28502
BERNSTEIN, L. S. p 3357 N94-28893
BERTA, Y. p 3521 N94-30851
BERTHAUD, P. p 3255 N94-30153
BESHTOEV, KH. M. p 3484 N94-28611
BEST, SARA p 3529 N94-28911
BEST, STEVE R. p 3167 N94-28814
p 3167 N94-29383
BESTER, M. p 3249 N94-29653
BETERMIER, J. M. p 3168 N94-29415
BETHEL, WES p 3407 N94-28506
BETHKE, K.-H. p 3142 N94-29586
BETTADPUR, SRINIVAS VISWANATH p 3333 N94-29762
BETTERTON, ERIC A. p 3344 N94-28599
BETTNER, JAMES L. p 3152 N94-29438
BEURRIER, D. p 3413 N94-29320
BEUTNER, THOMAS JOHN p 3270 N94-28724
BEYER, R. p 3139 N94-29572
BEZIERS, DANIEL p 3215 N94-29441
BHARDWAJ, R. C. p 3198 N94-29938
BHAT, ISWARA p 3263 N94-29028
BHATIA, S. p 3202 N94-28562
BHATT, PRAFUL P. p 3370 N94-29455
BHATTACHARYA, T. p 3514 N94-29818
BHUSHAN, BHARAT p 3298 N94-29290
BICARREGUI, J. p 3405 N94-29110
BICARREGUI, J. C. p 3529 N94-29108
p 3244 N94-29109
BICHAT, N. p 3139 N94-29574
BICHLER, U. p 3162 N94-29640
BICKEL, T. C. p 3336 N94-28489
BIDDLE, TEDD B. p 3192 N94-29259
BIDLACK, CLINT p 3442 N94-30548
BIDOT, T. p 3233 N94-29612
BIEFELD, R. M. p 3518 N94-30316
BIEN, CHRISTOPHER p 3446 N94-30573
BIERS, DAVID W. p 3150 N94-29048
BIESEMAN, T. p 3144 N94-30286
BIEZAD, DANIEL J. p 3145 N94-28817
BILBRO, GRIFF L. p 3292 N94-28770
BILLER, STEVEN DOUGLAS p 3552 N94-29823
BINDER, M. p 3223 N94-30479
BINGEL, BRADFORD D. p 3408 N94-28818
BINGERT, S. R. p 3210 N94-30774
BINGHAM, C. p 3514 N94-29801
BIRCH, J. R. p 3213 N94-28795
BIRD, CHRISTINA MARIE p 3548 N94-30951
BIRKETT, P. R. p 3417 N94-29347
BIRN, M. B. p 3374 N94-30587
BIRNER, R. p 3162 N94-29643
BISHOP, D. F. p 3252 N94-29673
BISHOP, J. p 3469 N94-30645
BISHU, RAM R. p 3402 N94-30210
BISSON, R. U. p 3382 N94-28443
BLACK, D. B. p 3506 N94-29510
BLAKE, BILL p 3140 N94-29577
BLAKE, J. B. p 3167 N94-29022
p 3552 N94-29046
BLANAS, PANAGIOTIS p 3186 N94-30956
BLANCHETTE, MARTIN p 3255 N94-30240
BLECHMAN, BARRY M. p 3499 N94-29694
BLISS, DONALD B. p 3480 N94-30274
BLIZARD, KENT p 3287 N94-29400
BLOCK, R. C. p 3496 N94-30219
BLOCK, ROBERT C. p 3263 N94-29028
BLOM, A. F. p 3149 N94-30947
BLOM, H. A. P. p 3428 N94-30764
p 3143 N94-30853
BLOM, HENK A. P. p 3141 N94-29581
BLOM, KEES L. p 3425 N94-30428
BLUMEN, WILLIAM p 3369 N94-28847
BOATNER, L. A. p 3199 N94-30723
BOBBITT, PERCY J. p 3130 N94-29545
BOCKRIS, J. O. M. p 3198 N94-29938
BODLAENDER, HANS L. p 3426 N94-30488
BOERSCHLEIN, DAVID P. p 3431 N94-29494
p 3432 N94-30160
BOERSTOEL, J. W. p 3133 N94-30387
BOEVE, EDDY D. G. p 3423 N94-30323
BOGDANOV, PYOTR P. p 3475 N94-30680
BOHEMIER, ALBERT p 3379 N94-28425
BOHNEN, H. G. M. p 3402 N94-30422
BOISSET, J. P. p 3245 N94-29456
BOITEN, EERKE A. p 3432 N94-30363
BOJKOVA, N. A. p 3484 N94-28584
BOLAENDER, H. p 3455 N94-30333
BOLIN, BERT p 3350 N94-30622
BOLLA, M. p 3395 N94-30028
p 3395 N94-30029
BOLLA, MICHEL p 3395 N94-30030
BOLLWEG, A. p 3378 N94-30714
BOLY, J. P. p 3252 N94-29692
p 3252 N94-29693
BOMMARITO, G. M. p 3513 N94-29215
BONACUSE, PETER J. p 3203 N94-28921
BONARINI, ANDREA p 3449 N94-30923
p 3449 N94-30939
BONNARD, M. p 3137 N94-29561
BONSANGUE, MARCELLO p 3458 N94-30403
p 3459 N94-30430
BONYUSHKINA, A. YU. p 3483 N94-28554
BOOGERS, J. A. M. p 3220 N94-30420
BOOTH, T. E. p 3465 N94-30366
BOOTHMAN, D. A. p 3386 N94-30895
BORAH, BOLINDRA N. p 3451 N94-28792
BORDANO, ALDO p 3171 N94-29791
BORDEN, ANDREW p 3412 N94-29318
BORDES, NICOLE p 3517 N94-30201
BORG, STEPHEN E. p 3287 N94-29368
BORGHI, GIUSEPPE p 3449 N94-30962
BORIES, A. p 3139 N94-29574
BORISOV, A. A. p 3489 N94-30095
BORISOV, I. p 3152 N94-29300
BORN, GEORGE p 3357 N94-29062
BOROVIK, A. S. p 3512 N94-28787
BOS, J. F. T. p 3402 N94-30390
BOSC, J. J. p 3414 N94-29327
BOSSELAERS, A. p 3252 N94-29692
p 3252 N94-29693
BOSSI, L. L. p 3383 N94-28449
BOSSIEUX, T. A. p 3440 N94-30536
BOSSIEUX, TERRY A. p 3440 N94-30534
BOSTED, P. p 3497 N94-30712
BOSTED, P. E. p 3482 N94-28493
BOTTENBERG, W. R. p 3336 N94-28501
BOTTOMLEY, D. M. p 3148 N94-29887
BOTTONI, M. p 3285 N94-30450
BOUCKAERT, REMCO R. p 3464 N94-29450
p 3465 N94-30376
BOULANGER, J.-S. p 3471 N94-30656
p 3297 N94-30664
BOURBAKIS, N. G. p 3439 N94-30531
BOURDAIS, PH. p 3413 N94-29320
BOURGAIN, J. p 3452 N94-29148
BOURGEOIS, BRIAN S. p 3377 N94-29204
p 3478 N94-29206
BOURIANOFF, G. p 3487 N94-29700
BOUSSE, L. J. p 3238 N94-29783
BOWEN, DAVID p 3137 N94-29560
BOWERS, CLINT A. p 3527 N94-28796
BOWIN, CARL p 3549 N94-29737
BOWLES, ED E. p 3263 N94-28994

BOWSER, JAMES R. p 3513 N94-29130
BOYCE, R. p 3292 N94-28481
BOYD, IAIN p 3131 N94-29893
BOYD, PATRICIA THERESE p 3543 N94-29719
BOYER, JOSEPH H. p 3225 N94-29310
BOYLE, JAMES P. p 3389 N94-28797
BOYLE, T. J. p 3518 N94-30315
BOZADA, CHRISTOPHER A. p 3240 N94-30445
BOZEMAN, R. J., JR. p 3397 N94-30458
BOZEMAN, RICHARD J. p 3299 N94-29370
BOZEMAN, RICHARD J., JR. p 3435 N94-29466
BOZOVIC, I. p 3262 N94-28767
BRABBS, THEODORE A. p 3197 N94-29356
BRABY, RICHARD p 3409 N94-28910
BRADLEY, JAMES G. p 3236 N94-29773
BRADLEY, PAUL ANDREW p 3547 N94-30011
BRADSHAW, JOHN D. p 3342 N94-28588
BRADT, RICHARD C. p 3214 N94-29105
BRADY, V. L. p 3223 N94-30477
BRAGG, MICHAEL B. p 3132 N94-30124
p 3133 N94-30152
BRAITHWAITE, R. NEIL p 3309 N94-30302
BRAMHAM, E. p 3381 N94-28436
p 3381 N94-28437
BRAMMER, KARL G. p 3416 N94-29341
BRANCH, D. p 3223 N94-30475
BRAND, M. G. E. p 3256 N94-30392
BRANDT, J. p 3252 N94-29692
p 3252 N94-29693
BRASWELL, DOROTHY O. p 3130 N94-29473
BRASWELL, WILLIAM DANNY p 3362 N94-29909
BRAUERS, THEO p 3343 N94-28595
BRAUN, HANS MARTIN p 3137 N94-29564
BRAUN, RON p 3440 N94-30532
BRAWLEY, STEPHEN C. p 3122 N94-28674
BREAKIRON, LEE A. p 3473 N94-30669
BREEDVELD, P. C. p 3462 N94-30964
BREILAND, W. G. p 3199 N94-30260
BREININGER, DAVID R. p 3347 N94-29099
BREMER, P. p 3411 N94-29159
BRENKOSH, J. P. p 3420 N94-29844
BRESE, N. E. p 3203 N94-29043
BRESKIN, A. p 3395 N94-30185
BRETHERTON, FRANCIS p 3351 N94-30624
BREZINI, A. p 3218 N94-30066
p 3208 N94-30108
BREZINSKY, KENNETH p 3189 N94-29004
BRILL, JAMES H. p 3416 N94-29341
BRINDAMOUR, MARTIN p 3290 N94-30232
BRINKER, C. J. p 3216 N94-29830
BRINSON, L. CATHERINE p 3181 N94-29541
BRISTOW, GERALD K. p 3380 N94-28428
BRITT, EDWARD J. p 3173 N94-29444
BROCKENBROUGH, J. R. p 3202 N94-28830
BROCKHOFF, R. C. p 3419 N94-29816
BROECKER, WALLACE S. p 3350 N94-30619
BROEK, D. p 3145 N94-28647
p 3149 N94-30905
BROKOF, U. p 3138 N94-29567
BRONKEMA, LISA A. p 3402 N94-30210
BROOKS, RODNEY ALLEN p 3444 N94-30559
BROOKSHAW, L. p 3277 N94-29923
BROUSSET, CHRISTINE p 3315 N94-29474
BROWALL, K. p 3171 N94-29782
BROWN, ALAN p 3410 N94-29068
BROWN, ARNOLD O., III p 3242 N94-28812
BROWN, BEN p 3442 N94-30543
BROWN, DENNIS W. p 3241 N94-28634
BROWN, K. W. p 3317 N94-28815
BROWN, L. M. p 3225 N94-30038
BROWN, LORETTA p 3529 N94-28911
BROWN, ROGER O. p 3325 N94-28863
BROWN, S. F. p 3156 N94-29047
BROWN, WILLIAM C. p 3164 N94-29355
BROWNE, P. A. p 3384 N94-28451
BROWNING, J. S. p 3291 N94-30218
BROWNING, N. D. p 3516 N94-30064
BRUCKER, G. J. p 3496 N94-30215
BRUDANIN, V. B. p 3485 N94-28625
BRUDNICKI, MYRON p 3205 N94-29447
BRUEGGEN, JOB p 3143 N94-30943
BRUEGMAN, O. W. p 3198 N94-29857
BRUNE, WILLIAM H. p 3342 N94-28589
BRUNEKREEF, JACOB p 3260 N94-30520
BRUNIE, L. p 3395 N94-30028
BRUNIE, LIONEL p 3395 N94-30030
BRUZA, P. D. p 3465 N94-30358
BRYANT, R. p 3405 N94-28916
BRYGIER, JACQUES p 3150 N94-29332
BRYSON, J. W. p 3323 N94-30689
BUCCI, R. J. p 3202 N94-28830
BUCHAN, K. p 3309 N94-30306
BUCHAN, KEIR p 3310 N94-30307
BUCHANAN, R. A. p 3203 N94-28900
BUCHELNIKOVA, N. S. p 3508 N94-30191
BUCHHEIT, C. D. p 3518 N94-30315
BUCHHEIT, R. G. p 3207 N94-30053
BUCHOLTZ, FRANK p 3288 N94-29699
BUCHOLZ, J. A. p 3495 N94-29924
BUDIC, ZORICA D. p 3532 N94-29804
BUEHLER, M. F. p 3240 N94-30473
BUESCHER, K. L. p 3461 N94-30821
BUGG, W. M. p 3482 N94-28504
BULMER, R. H. p 3509 N94-30768
BULZAN, DANIEL L. p 3195 N94-29277
BURALLI, B. p 3245 N94-29456
BURCHELL, T. D. p 3508 N94-30365
BURDAKOV, A. V. p 3508 N94-30193
p 3508 N94-30194
BURDEN, HUBERT W. p 3385 N94-29968
BURGESS, D. E. p 3270 N94-28475
BURGESS, EDWIN B. p 3529 N94-28903
BURGESS, LYLE p 3326 N94-28929
BURGGRAF, O. R. p 3270 N94-28665
BURKE, CHRISTOPHER A. p 3172 N94-28834
BURKE, G. J. p 3255 N94-30106
BURKHARDT, LINDA A. p 3166 N94-28710
BURKHARDT, RAYMOND p 3288 N94-29538
BURKHART, P. D. p 3159 N94-29655
BURKY, ALBERT J. p 3286 N94-28831
BURNETT, RON p 3261 N94-30675
BURNS, D. T. p 3290 N94-30782
BURNS, JOHN W. p 3400 N94-28996
BURR, G. S. p 3546 N94-29905
BUSCA, G. p 3474 N94-30676
BUSS, R. J. p 3199 N94-30260
BUTLER, G. F. p 3417 N94-29347
BUTLER, K. A. p 3529 N94-28820
BUTLER, LEE A. p 3417 N94-29392
BUTLER, P. p 3336 N94-28489
BUTLER, ROBERT PAUL p 3542 N94-30861
BUTT, D. P. p 3185 N94-30693
BUTTERFIELD, C. P. p 3339 N94-30602
BUYERS, W. J. L. p 3209 N94-30246
BY, ANDRE BERNARD p 3440 N94-30533
BYER, ROBERT L. p 3293 N94-29309
BYSTRITSKIJ, V. M. p 3485 N94-28625

C

CAGEAO, R. P. p 3343 N94-28593
CAGNACHE, FREDERIC p 3412 N94-29319
CAHILL, C. J. p 3382 N94-28442
CAI, XIAOMING p 3365 N94-30134
CAI, ZHONG p 3298 N94-28838
CAILLAS, CLAUDE p 3308 N94-30300
CAIMI, RAOUL E. B. p 3240 N94-30467
CAIN, D. p 3400 N94-28902
CALDWELL, J. LYNN p 3384 N94-28453
CALL, D. p 3240 N94-28522
CALLOWAY, TERRY MARSHALL p 3246 N94-29536
CALM, J. M. p 3230 N94-28563
CALUORI, V., JR. p 3171 N94-29035
CALVERT, JACK G. p 3345 N94-28603
CAMACHO, B. A. p 3516 N94-30068
p 3516 N94-30069
CAMBIAGGIO, E. p 3245 N94-29456
CAMPBELL, CYNTHIA A. p 3230 N94-28742
CAMPBELL, D. V. p 3267 N94-30368
CAMPBELL, I. G. p 3198 N94-30017
CAMPBELL, J. p 3315 N94-28503
CAMPBELL, JAMES E. p 3315 N94-29020
CAMPBELL, MALCOLM J. p 3344 N94-28600
CAMPBELL, ROBERT J. p 3157 N94-29956
CAMPBELL, STEPHEN L. p 3452 N94-28883
CAMPERI-GINESTET, C. p 3239 N94-29793
CANDEL, S. p 3190 N94-29251
CANNON, R. H. p 3444 N94-30560
CANTRELL, CHRISTOPHER p 3345 N94-28603
CANTRELL, JOHN H. p 3287 N94-29199
CAPPE, OLIVIER p 3291 N94-30979
CARDELL, GREGORY SCOTT p 3275 N94-29764
CARDELLA, A. p 3503 N94-28555
CARLEY, KATHLEEN p 3242 N94-28859
CARLSON, G. S. p 3333 N94-29553
CARLSON, N. M. p 3314 N94-30444
CARLSSON, TORBOJOERN p 3341 N94-28412
CARMAN, E. J. p 3263 N94-29120
CARNEY, DAVID p 3410 N94-29068
CARNEY, LISA A. p 3136 N94-28744
CARON p 3266 N94-29523
CARON, KEN p 3440 N94-30533
CARR, L. PHILIP p 3153 N94-30130
CARRE, DAVID p 3162 N94-29641
CARRIERE, B. p 3197 N94-29457
CARSON, R. F. p 3501 N94-30261
CARTER, M. D. p 3255 N94-30105
CARTER, PAUL M. p 3421 N94-30136
CARUFEL, JEAN DE p 3321 N94-30033
CARVALHO, M. G. p 3191 N94-29253
CASILLAS, NORBERTO p 3203 N94-29089
CASSANTO, JOHN p 3397 N94-30453
CASSIGNEUL, V. p 3150 N94-29316
CASTELLANO, C. C. p 3374 N94-30587
CASTNER, RAYMOND S. p 3156 N94-28749
CASTONGUAY, ARTHUR p 3306 N94-30288
CASTRO, EDGAR O. p 3160 N94-29369
CASTRO, R. G. p 3175 N94-28581
CATO, GAVIN R. p 3498 N94-28780
CAULFIELD, H. J. p 3430 N94-28781
CAVALLARO, JOSEPH R. p 3445 N94-30562
CAVALLI-SFORZA, M. p 3482 N94-28493
p 3497 N94-30712
CAYLOR, MICHAEL JOSEPH p 3320 N94-29765
CAZEMIER, W. p 3281 N94-30743
CELMINS, AIVARS p 3452 N94-28864
CHA, Y. S. p 3261 N94-28487
CHAARA, EL MOUEZ AHMED p 3490 N94-30234
CHABAL, Y. J. p 3510 N94-28512
CHADSEY, H. p 3145 N94-30662
CHADWICK, KENNETH MICHAEL p 3289 N94-29824
CHADWICK, M. B. p 3488 N94-30039
p 3497 N94-30825
CHAGROV, A. V. p 3456 N94-30383
CHAGROVA, L. A. p 3456 N94-30383
CHAIGNE, ANTOINE p 3481 N94-30972
CHAKOUMAKOS, B. C. p 3199 N94-30723
CHAKRABARTI, S. p 3289 N94-29907
CHAKRABARTY, S. p 3489 N94-30097
CHAMIS, CHRISTOS C. p 3319 N94-29384
CHAN, ANTONIO WONG p 3482 N94-28520
CHAN, LAI-HIM p 3491 N94-30762
CHAN, W. K. p 3156 N94-29047
CHANDY, K. M. p 3428 N94-30754
CHANET, P. p 3150 N94-29316
CHANG, EDMUMD KAR-MAN p 3372 N94-29796
CHANG, F. C. p 3285 N94-30450
CHANG, PAUL p 3259 N94-30509
CHANG, SHIH-HSIAO MARK p 3436 N94-29720
CHAPMAN, B. E. p 3498 N94-28534
CHARLEBOIS, STEVEN J. p 3203 N94-29089
CHARLES, STEVE p 3447 N94-30579
CHARMEAU, M. C. p 3168 N94-29415
CHASON, E. p 3219 N94-30263
CHATILA, RAJA p 3443 N94-30552
CHATURVEDI, ARVIND K. p 3395 N94-29919
CHAUM, D. p 3252 N94-29692
p 3252 N94-29693
CHAUVIN, T. H. p 3250 N94-29664
CHECHIK, R. p 3395 N94-30185
CHELOTTI, J. N. p 3168 N94-29543
CHEMLA, D. S. p 3520 N94-30835
CHEN, CHIEN-CHUNG p 3293 N94-29493
CHEN, GUANGGING p 3214 N94-29203
CHEN, J. p 3284 N94-30968
CHEN, J. C. p 3247 N94-29616
p 3248 N94-29624
CHEN, J. F. p 3187 N94-28567
CHEN, J. G. p 3284 N94-30967
CHEN, KUO-HUEY p 3195 N94-29277
CHEN, M. Y. p 3442 N94-30546
CHEN, N. X. p 3303 N94-30205
CHEN, R. p 3496 N94-30219
CHEN, S. P. p 3182 N94-29933
CHEN, S. R. p 3210 N94-30774
CHEN, SHUH RONG p 3201 N94-28544
CHEN, X. p 3504 N94-28686
CHEN, XINGJU p 3320 N94-29688
CHEN, YONG MING p 3216 N94-29807
CHEN, YUN-CHUNG p 3244 N94-29106
CHERATZU, F. D. p 3417 N94-29346
CHESNEY, R. H. p 3155 N94-30284
CHETTY, N. p 3206 N94-29931
CHEUNG, K.-M. p 3247 N94-29619
p 3250 N94-29664
CHEUNG, TERRY C. p 3431 N94-29952
CHIAO, F. F. p 3349 N94-30044
CHIDUME, C. E. p 3467 N94-30065
CHIEN, C. C. p 3443 N94-30554
CHIKALOV, V. V. p 3523 N94-28802
CHILTON, JIMMIE HERBERT p 3526 N94-30950
CHISHOLM, M. F. p 3516 N94-30064
CHISLOW, DON p 3469 N94-30649
CHLADEK, JOHN T. p 3441 N94-30542
CHO, SOO YONG p 3281 N94-30519
CHO, UK YOUN p 3322 N94-30354
CHOI, S.-K. p 3300 N94-29550
CHOI, WOOYOUNG p 3274 N94-29689
CHOPPIN, G. R. p 3187 N94-28567
CHOPRA, O. K. p 3207 N94-30021
CHOU, TIAN p 3466 N94-28467
CHOUDHARI, MEELAN p 3273 N94-29460
CHOUDHURY, BHASKAR J. p 3370 N94-29408
CHOW, R. p 3212 N94-28560
p 3501 N94-30599
CHRISTENSEN, K. p 3482 N94-28518
CHRISTENSON, T. R. p 3235 N94-29770

CHRISTIAN, DAMIAN JOSEPH ... p 3542 N94-30862
CHRISTIE, ROBERT J. ... p 3167 N94-28814
p 3167 N94-29383
CHRISTOPHE, F. ... p 3258 N94-30507
CHRYSTALL, K. ... p 3307 N94-30291
p 3309 N94-30303
p 3309 N94-30304
p 3309 N94-30308
CHU, GOU-DON ... p 3181 N94-29735
CHU, HUAN CHANG ... p 3282 N94-30953
CHUFO, ROBERT L. ... p 3443 N94-30551
CHUMBINHO, ROGERIO P. ... p 3376 N94-28642
CHUNG, HYOSANG ... p 3375 N94-30863
CHURCH, RONALD H. ... p 3354 N94-30472
CICCIA, P. ... p 3194 N94-29273
CINQIN, J. ... p 3179 N94-29462
CINQUE, G. ... p 3154 N94-29255
CINQUIN, P. ... p 3395 N94-30028
p 3395 N94-30029
CINQUIN, PHILIPPE ... p 3395 N94-30030
CITENO, J. V. ... p 3193 N94-29265
CIUCCI, ALESSANDRO ... p 3171 N94-28800
CLARK, A. N. ... p 3141 N94-29585
CLARK, JAMES R. ... p 3157 N94-29956
CLARK, JAMES S. ... p 3353 N94-30637
CLARK, JOHN S. ... p 3171 N94-28833
CLARK, KENNETH D. ... p 3452 N94-28883
CLARK, MICHAEL L. ... p 3354 N94-30464
CLARKE, J. ... p 3261 N94-28546
CLARKE, R. N. ... p 3476 N94-30781
CLARKSON, B. L. ... p 3479 N94-29407
CLAUSEN, E. C. ... p 3340 N94-30879
CLAY, MELANIE C. ... p 3399 N94-28649
CLEMENTS, SANDRA DENISE ... p 3546 N94-29992
CLENDENIN, C. GERALD ... p 3315 N94-29366
CLERE, J. M. ... p 3384 N94-28450
CLEVENGER, W. B. ... p 3317 N94-28815
CLOUGH, R. L. ... p 3218 N94-30102
CLOUSER, S. ... p 3154 N94-29263
CLOUSER, STEPHEN D. ... p 3190 N94-29248
CLOUTMAN, L. D. ... p 3277 N94-29923
CLUZEL, C. ... p 3179 N94-29442
COBB, RICHARD H. ... p 3407 N94-28664
p 3156 N94-28752
p 3156 N94-28753
COBB, ROBERT L. ... p 3523 N94-28662
COCHRAN, WILLIAM L. ... p 3298 N94-28894
COELHO, P. J. ... p 3191 N94-29253
COFFEY, BENJAMIN J. ... p 3398 N94-28887
COFFEY, H. E. ... p 3550 N94-29122
p 3550 N94-29123
p 3550 N94-29124
COFFIN, THOMAS ... p 3174 N94-29868
COGAN, JAMES ... p 3257 N94-30500
COGAN, JAMES L. ... p 3257 N94-30499
COGGIOLA, M. J. ... p 3349 N94-30047
COGLIANESE, LOUIS H. ... p 3150 N94-29348
COHEN, J. M. ... p 3154 N94-29269
COHEN, T. D. ... p 3492 N94-30838
COLANGELI, PAOLO ... p 3414 N94-29326
COLE, DAVID A. ... p 3326 N94-28929
COLE, J. K. ... p 3165 N94-28477
COLE, JULIA ELLEN ... p 3373 N94-29962
COLEMAN, J. J. ... p 3521 N94-30894
COLES, L. STEPHEN ... p 3397 N94-30459
COLESHAW, S. R. K. ... p 3379 N94-28421
COLGATE, STIRLING A. ... p 3552 N94-28580
COLLAUDIN, BERNARD ... p 3231 N94-29416
COLLINS, AMY ... p 3326 N94-28929
COLLINS, L. A. ... p 3509 N94-30752
COLLINS, T. ... p 3267 N94-30711
COLORNI, A. ... p 3537 N94-30926
COMBES, P. F. ... p 3258 N94-30507
COMBS, W. E. ... p 3263 N94-29025
COMEDI, D. ... p 3497 N94-30221
COMES, FRANZ-JOSEF ... p 3343 N94-28594
CONDO, G. T. ... p 3482 N94-28504
CONKLIN, JEANINE A. ... p 3408 N94-28790
CONLIN, DAVID B. ... p 3529 N94-28903
CONLISK, A. T. ... p 3270 N94-28665
CONNELL, JOHN W. ... p 3215 N94-29451
p 3215 N94-29555
CONNES, A. ... p 3462 N94-30889
CONRADSON, S. D. ... p 3208 N94-30101
CONTRASTANO, L. ... p 3414 N94-29329
CONWAY, H. ... p 3325 N94-28881
COOK, A. ... p 3318 N94-28841
p 3501 N94-30522
COOK, JEFFREY A. ... p 3272 N94-29149
COOPER, ELIZABETH A. ... p 3517 N94-30201
COOPER, J. A. ... p 3462 N94-30849
COPELAND, RICHARD A. ... p 3549 N94-28816
COPPOLA, D. ... p 3414 N94-29329
CORBIN, M. J. ... p 3417 N94-29347
CORDARA, F. ... p 3473 N94-30668
CORDARA, FRANCO ... p 3468 N94-30642
CORNELIUS, DAVID M. ... p 3135 N94-30949
CORRALL, D. R. ... p 3141 N94-29585
COSKUN, FEZA ... p 3253 N94-29882
COSTANTINE, A. G. ... p 3496 N94-30219
COSTE, A. ... p 3467 N94-29147
COSTE, P. A. ... p 3160 N94-29628
COSTES, B. ... p 3197 N94-29457
COTE, MARC G. ... p 3241 N94-28763
COTTARD, G. ... p 3255 N94-30153
COTTON, J. D. ... p 3210 N94-30776
COTTON, M. G. ... p 3256 N94-30497
COTTRELL, D. ... p 3261 N94-28511
COUCH, R. ... p 3211 N94-30892
COURNUT, F. ... p 3205 N94-29525
COURTNEY, T. H. ... p 3204 N94-29205
COUSINS, T. ... p 3291 N94-30216
p 3496 N94-30217
COUTU, STEPHANE ... p 3552 N94-29687
COVINO, J. ... p 3223 N94-30474
COWAN, J. R. ... p 3163 N94-29650
COWLES, K. ... p 3247 N94-29617
COX, D. F. ... p 3522 N94-30901
COX, J. M. ... p 3322 N94-30114
COYNE, R. A. ... p 3404 N94-28505
CRABTREE, G. W. ... p 3519 N94-30338
CRAIG, M. ... p 3326 N94-28930
CRAIN, W. R. ... p 3495 N94-30214
CRAVER, WILLIAM M. ... p 3441 N94-30542
CRAWFORD, K. B. ... p 3495 N94-30214
CRAWLEY, GERARD M. ... p 3526 N94-28746
CRAWLEY, H. B. ... p 3406 N94-30004
CRAYMER, L. G. ... p 3422 N94-30197
CRENSHAW, D. M. ... p 3198 N94-29857
CRESPI-REGHIZZI, STEFANO ... p 3429 N94-30928
CREWE, A. V. ... p 3236 N94-29775
CREWE, D. A. ... p 3236 N94-29775
CRIBB, DAVID W. ... p 3452 N94-29016
CRIMINSKI, DAVID A. ... p 3263 N94-28913
CRISP, DAVID ... p 3236 N94-29777
CROMACK, K. R. ... p 3220 N94-30778
CRONISE, RAYMOND J. ... p 3354 N94-30463
CROSLEY, DAVID R. ... p 3342 N94-28587
CROSWELL, BENNETT M. ... p 3192 N94-29259
CROUSE, GILBERT LEWIS, JR. ... p 3131 N94-29826
CROWELL, RONALD A. ... p 3262 N94-28842
CROWN, E. M. ... p 3381 N94-28433
CRUICKSHANK, ALEXANDER ... p 3499 N94-28848
CRUSH, D. F. ... p 3417 N94-29347
CUNNINGHAM, ATLEE M., JR. ... p 3148 N94-30342
CUNNINGHAM, DANIEL J. ... p 3223 N94-30483
CUNNINGHAM, THOMAS J. ... p 3265 N94-29488
CURTIS, ERIC ... p 3144 N94-29794
CUSHMAN, JOHN H. ... p 3356 N94-28882
CUSTER, J. S. ... p 3515 N94-30006
CUTLER, LEONARD S. ... p 3475 N94-30683
CUTRI, R. M. ... p 3538 N94-28671
CZICHY, REINHARD H. ... p 3501 N94-30418

D

DAANEN, H. A. M. ... p 3381 N94-28434
DABROWSKI, B. ... p 3519 N94-30338
DAEHLEN, M. ... p 3420 N94-29949
DAGNINO, A. ... p 3309 N94-30303
p 3309 N94-30306
DAHLEN, CHRISTIAN ULF ... p 3183 N94-30256
DAHLSTROM, R. K. ... p 3259 N94-30512
DAHMANI, RACHID ... p 3500 N94-29759
DAIGUJI, HISAAKI ... p 3124 N94-28954
DAILEY, R. ... p 3341 N94-28454
DAILY, VIC ... p 3297 N94-28419
DALE, J. D. ... p 3381 N94-28433
DALLEDONNE, M. ... p 3201 N94-28460
DALLING, ROBERT HAL ... p 3467 N94-29910
DALSOGLIO, S. ... p 3395 N94-30029
DAMGAARD, I. ... p 3252 N94-29692
p 3252 N94-29693
DAMM, G. A. ... p 3397 N94-30458
DAMM, Z. ... p 3220 N94-30745
DANCHI, W. C. ... p 3249 N94-29653
DANIEHL, A. V. ... p 3489 N94-30051
DANIELS, J. I. ... p 3349 N94-30044
DANOS, VINCENT ... p 3430 N94-30973
DANTSKER, E. ... p 3261 N94-28546
DAOUST, MARIO ... p 3373 N94-29908
DAPKUS, P. D. ... p 3262 N94-28805
DARAB, J. G. ... p 3240 N94-30473
DASS, S. M. ... p 3157 N94-29151
DASS, W. C. ... p 3157 N94-29151
DATTA, AJOY KUMAR ... p 3424 N94-30379
DAVENPORT, J. W. ... p 3206 N94-29931
DAVIES, J. ... p 3497 N94-30221
DAVIES, J. A. ... p 3496 N94-30217
DAVIS, G. D. ... p 3204 N94-29196
DAVIS, STAN ... p 3121 N94-28732
DAVIS, THOMAS J. ... p 3138 N94-29568
DAWSON, A. J. ... p 3263 N94-29120
DAWSON, D. ... p 3318 N94-28841
DAWSON, P. R. ... p 3201 N94-28544
DAWSON, S. P. ... p 3335 N94-30610
p 3200 N94-30748
DAY, R. L. ... p 3349 N94-30046
DAYTON, D. C. ... p 3339 N94-30606
DCUNHA, IVAN ... p 3408 N94-28825
DEAN, G. D. ... p 3217 N94-29885
p 3217 N94-29886
DEAN, GARFIELD ... p 3141 N94-29581
DEBAKKER, J. W. ... p 3425 N94-30432
p 3426 N94-30491
DEBENEDETTI, P. G. ... p 3486 N94-29087
DEBERG, MARK ... p 3424 N94-30364
p 3459 N94-30425
p 3460 N94-30721
p 3460 N94-30728
DEBOER, A. ... p 3311 N94-30391
DEBOER, F. S. ... p 3424 N94-30347
DEBRUIN, A. ... p 3426 N94-30491
DEBRUIN, A. C. ... p 3133 N94-30389
DECEW, ALAN E., JR. ... p 3289 N94-29872
DECOCK, K. M. J. ... p 3134 N94-30858
DECORTE, CELESTE ... p 3440 N94-30537
DECOSS, R. ... p 3516 N94-30070
DEGABAI, D. ... p 3418 N94-29418
DEGROH, KIM K. ... p 3172 N94-28834
p 3172 N94-28999
DEGROOT, MARKO ... p 3460 N94-30728
DEICK, A. ... p 3196 N94-29282
DEJEU, C. ... p 3154 N94-29258
DEJONG, F. J. ... p 3300 N94-29550
DEJONG, GERRIT ... p 3469 N94-30646
DEJONG, S. ... p 3422 N94-30314
DEJONGH, DICK ... p 3463 N94-30977
DEKKER, G. J. ... p 3170 N94-29324
DELABEAUJARDIERE, O. ... p 3356 N94-28869
DELAFUENTE, HORATIO ... p 3160 N94-29369
DELANEY, ROBERT A. ... p 3152 N94-29438
DELAUS, M. ... p 3263 N94-29025
DELFOUR, A. ... p 3259 N94-30511
DELGRANDE, N. K. ... p 3122 N94-29842
p 3149 N94-30687
DELHAYE, F. ... p 3155 N94-29317
DELOMBARD, RICHARD ... p 3168 N94-29757
DELPLANQUE, JEAN-PIERRE ... p 3197 N94-29592
DELUCA, J. A. ... p 3261 N94-28487
DEMARQUILLY, DOMINIQUE ... p 3168 N94-29419
DEMATHELIN, MICHEL ... p 3259 N94-30513
DENBOER, B. ... p 3252 N94-29692
p 3252 N94-29693
DENBRAVEN, WIM ... p 3139 N94-29569
p 3140 N94-29578
DENG, LITAO ... p 3371 N94-29753
DENHARTOG, D. J. ... p 3503 N94-28515
DENISOV, D. ... p 3484 N94-28574
DENIZOT, VINCENT ... p 3215 N94-29441
DEPOOTER, K. ... p 3198 N94-30017
DERDOUR, M. ... p 3515 N94-30005
DERKS, G. L. A. ... p 3460 N94-30738
DERKSEN, J. J. ... p 3338 N94-30328
DERMOTT, S. F. ... p 3538 N94-28671
DERRICK, M. ... p 3483 N94-28569
DERSHOWITZ, NACHUM ... p 3428 N94-30734
DESARIO, MARCO ... p 3442 N94-30549
DESBAT, L. ... p 3395 N94-30028
p 3395 N94-30029
DEVETSIKIOTIS, MICHAEL ... p 3498 N94-28780
DEVLIN, D. J. ... p 3185 N94-30771
DEVRIES, F. J. ... p 3459 N94-30412
DEVRIES, FER-JAN ... p 3425 N94-30415
DEVY, MICHEL ... p 3443 N94-30552
DEXIN, HE ... p 3340 N94-30945
DEY, J. ... p 3489 N94-30097
DEY, M. ... p 3489 N94-30097
DEYOUNG, JAMES A. ... p 3471 N94-30659
DICARLO, PATRIZIA ... p 3415 N94-29335
DICELLO, J. F. ... p 3495 N94-30213
DICHTL, M. ... p 3252 N94-29692
p 3252 N94-29693
DICKINSON, ROBERT E. ... p 3350 N94-30621
p 3351 N94-30624
DIDZIULIS, STEPHEN ... p 3162 N94-29641
DIELEMAN, P. ... p 3229 N94-30421
DIEMUNSCH, JOSEPH ... p 3143 N94-29323
DIERKS, J. F. ... p 3211 N94-28536
DIETRICH, R. A. ... p 3284 N94-30967
p 3284 N94-30968
DIFTLER, MYRON A. ... p 3441 N94-30541
DIGIANDOMENICO, B. ... p 3150 N94-29334
DIGIROLAMO, NICOLO E. ... p 3370 N94-29408
DIGNON, J. ... p 3349 N94-29954
DIJKSTRA, ATZE ... p 3428 N94-30746
DILLER, T. E. ... p 3286 N94-28824

DILLMAN, ROBERT A. p 3161 N94-29633
DIMARTINO, P. p 3154 N94-29255
DIMONTE, G. p 3281 N94-30600
DIMOS, D. p 3518 N94-30247
DINC, ABDULKADIR p 3408 N94-28760
DINESH, T. B. p 3418 N94-29503
DING, JIANMIN p 3279 N94-30020
DINI, DINO p 3193 N94-29268
DIPIETRO, E. p 3503 N94-28555
DIPPE, D. p 3138 N94-29567
DIRMEYER, PAUL ALAN p 3348 N94-29749
DISALVO, F. J. p 3203 N94-29043
p 3204 N94-29395
DIXON, R. D. p 3480 N94-30098
DJAVDAN, E. p 3190 N94-29251
DO, KIM HYONG p 3406 N94-30074
DOBRANICH, DEAN p 3270 N94-28488
DODDS, W. J. p 3154 N94-29263
DOERR, TH. p 3196 N94-29281
DOHERTY, MICHAEL P. p 3171 N94-28833
DOHERTY, PATRICIA H. p 3145 N94-30677
DOHNAL, M. p 3189 N94-28789
DOHNALOVA, J. p 3189 N94-28789
DOHRING, MARK E. p 3161 N94-29629
DOI, MAKOTO p 3388 N94-28498
DOLAN, K. W. p 3122 N94-29842
DOLCE, JAMES L. p 3300 N94-29427
DOLENC, A. p 3452 N94-29171
DOLGOFF, SCOTT J. p 3409 N94-28896
DOLLINS, ANDREW B. p 3398 N94-29027
DOMENGE, J. J. p 3225 N94-29429
DONAHUE, D. J. p 3546 N94-29905
DONAHUE, ROBERT ANDREW p 3545 N94-29827
DONAL, VALERIE p 3418 N94-29479
DONALDSON, ROBERT R. p 3240 N94-30449
DONNADILLE, P. p 3195 N94-29278
DONNER, J. T. p 3224 N94-28901
DONZAC, J. M. p 3179 N94-29412
DORN, HANS-PETER p 3343 N94-28595
DOROGY, WILLIAM p 3167 N94-28716
DOROGY, WILLIAM E., JR. p 3214 N94-29359
DOROKHOV, D. V. p 3439 N94-30528
DOROKHOV, V. P. p 3439 N94-30528
DORRIS, S. E. p 3261 N94-28487
DOTE, YUTAKA p 3387 N94-29519
DOU, LIXIN p 3525 N94-30244
DOUGLAS, R. J. p 3471 N94-30656
p 3297 N94-30664
DOWLING, MARGARET p 3401 N94-29093
DOWN, B. p 3439 N94-30529
DOXSEE, KENNETH M. p 3189 N94-29058
DOYAL, ROY p 3391 N94-29150
DOYCHAK, JOSEPH p 3205 N94-29507
DOYLE, JAMES F. p 3479 N94-29856
DOYLE, THOMAS E. p 3314 N94-30443
DRAGONETTE, RICHARD p 3474 N94-30674
DRAIN, T. p 3160 N94-29666
DRAKE, A. E. p 3476 N94-30780
p 3476 N94-30783
DRAKE, J. p 3350 N94-30116
DRAVID, V. P. p 3516 N94-30064
DRENNAN, S. A. p 3194 N94-29271
DRESNER, L. p 3461 N94-30758
DREWIEN, C. A. p 3207 N94-30053
DROBIN, V. M. p 3220 N94-30745
DROPKIN, H. p 3259 N94-30512
DROUICHE, K. p 3462 N94-30971
DRUCKER, R. B. p 3482 N94-28524
DSOUZA, M. V. p 3198 N94-30017
DUANE, S. p 3492 N94-30795
DUBLINEAU, P. p 3215 N94-29459
DUC, DUONG ANH p 3548 N94-30163
DUCHARME, MICHAEL B. p 3401 N94-29302
DUCLOS, J. M. p 3190 N94-29251
DUDEK, GREGORY p 3309 N94-30301
DUDENEY, J. R. p 3359 N94-29236
DUFF, I. S. p 3452 N94-29111
DUFF, J. W. p 3357 N94-28893
DUGINOV, V. N. p 3517 N94-30195
DUMSER, T. p 3382 N94-28439
DUNAHAY, T. G. p 3225 N94-30038
DUNCAN, B. C. p 3318 N94-28841
p 3501 N94-30522
DUNCAN, BREAN W. p 3347 N94-29099
DUNHAM, G. E. p 3341 N94-28463
DUNN, C. E. p 3144 N94-30650
DUNN, LAWRENCE BENNET p 3371 N94-29744
DUNN, M. L. p 3185 N94-30827
DUNN, W. R. p 3261 N94-28511
DUPONT, VALERIE p 3190 N94-29250
DURBIN, P. F. p 3122 N94-29842
DURFEE, EDMUND H. p 3445 N94-30564
DURHAM, TIMOTHY E. p 3253 N94-29883
DUSEK, J. T. p 3261 N94-28487
DUSSERRE, A. p 3395 N94-30028
p 3395 N94-30029
DUTTA, P. K. p 3200 N94-30769
DUTTA, PRADIP p 3488 N94-29903
DUWE, R. p 3503 N94-28555
DVOEGLAZOV, V. V. p 3484 N94-28584
DYACHENKO, P. P. p 3490 N94-30184
DYALL, KENNETH G. p 3272 N94-29378
DYE, DENNIS GENE p 3334 N94-29970
DYSON, B. F. p 3319 N94-29121

E

EARL, C. p 3306 N94-30287
EASH, D. p 3175 N94-29458
EBIHARA, BEN T. p 3286 N94-29000
ECHER, C. p 3519 N94-30707
ECKARDT, T. p 3162 N94-29640
ECKBURG, JOSEPH JOHN p 3198 N94-29881
ECKSTEIN, J. N. p 3262 N94-28767
ECKSTROM, CLINTON V. p 3122 N94-28658
EDDY, D. p 3309 N94-30306
EDDY, TRAVIS p 3400 N94-29029
EDKINS, CRAIG R. p 3398 N94-28887
EDWARDS, BENJAMIN I., II p 3369 N94-29194
EDWARDS, DANIEL p 3288 N94-29437
EDWARDS, GRANT CARLETON p 3296 N94-30801
EDWARDS, L. L. p 3354 N94-30822
EDWARDS, LAWRENCE G. p 3168 N94-29405
EDWARDS, T. p 3192 N94-29261
EFIMOV, G. V. p 3487 N94-29502
EGAMI, KOICHI p 3125 N94-28964
EGIKYAN, R. S. p 3421 N94-30083
EGUCHI, HOSHIO p 3387 N94-29713
EHMAN, D. p 3155 N94-30284
EHRHART, JOHN E., JR. p 3146 N94-29391
EHST, D. A. p 3509 N94-30697
EICKHOFF, H. p 3196 N94-29282
EIDEN, MICHAEL p 3160 N94-29628
EIKE, D. R. p 3341 N94-28454
EILBERT, JAMES L. p 3440 N94-30532
EIRICH, RON p 3306 N94-30283
EISELE, FRED L. p 3344 N94-28601
EJIRI, MASAKI p 3357 N94-29078
p 3359 N94-29233
p 3359 N94-29234
p 3359 N94-29235
p 3361 N94-29244
p 3363 N94-29978
EL-GUEBALY, L. p 3508 N94-30339
EL-RAYYES, L. p 3308 N94-30296
ELACHI, CHARLES p 3260 N94-28927
ELBAKIAN, S. S. p 3504 N94-28564
ELDER, S. H. p 3204 N94-29395
ELDRED, D. B. p 3251 N94-29670
ELDRED, LLOYD BYRON p 3134 N94-30525
ELDRIDGE, J. M. p 3260 N94-30772
ELDRIDGE, NORMAN R. p 3334 N94-30236
ELGAZZAR, SHADIA p 3306 N94-30288
ELKENZ, A. p 3525 N94-30164
ELLINGSON, W. A. p 3261 N94-28487
ELLIOTT, D. H. p 3381 N94-28437
ELLIS, DAVID L. p 3178 N94-29208
ELLIS, S. p 3385 N94-29401
ELLIS, T. W. p 3185 N94-30704
ELLIS, WILLIAM GRENVILLE, JR. p 3366 N94-30867
ELORANTA, K. p 3464 N94-29030
ELZARKI, MAGDA p 3438 N94-30375
EMERSON, DAWN p 3165 N94-28701
EMERSON, J. E. p 3261 N94-28487
EMERSON, JANET M. p 3146 N94-29391
ENAMI, KAZUYUKI p 3229 N94-28945
ENDECOTT, BOYD R. p 3395 N94-29919
ENDSLEY, MICA R. p 3149 N94-29005
ENGEL, J. P. p 3187 N94-28561
ENGLMEIER, H. P. p 3254 N94-29998
ENOMOTO, HIKOE p 3461 N94-30766
EPERIN, A. P. p 3439 N94-30528
EPIFANOV, A. A. p 3512 N94-28787
EPP, RICHARD J. p 3525 N94-30142
ERACLEOUS, MICHAEL p 3552 N94-29989
ERCK, R. A. p 3211 N94-28536
ERDEN, F. p 3260 N94-30514
ERFAN, ZOHREH p 3302 N94-29884
ERICKSON, J. D. p 3447 N94-30581
ERICKSON, JON D. p 3439 N94-30526
p 3439 N94-30527
ERKELENS, L. J. J. p 3143 N94-30915
ERMAKOV, V. A. p 3406 N94-30074
EROKHIN, Y. N. p 3518 N94-30249
ERZBERGER, HEINZ p 3138 N94-29568
ESPENSCHIED, KENNETH S. p 3439 N94-30530
ESPINOSA, HORACIO DANTE p 3217 N94-29975
ESTABROOK, CHARLES HERSHEY p 3363 N94-29969
ESTEFAN, J. A. p 3159 N94-29655
ESTES, TODD G. p 3530 N94-29165
ETALLE, SANDRO p 3427 N94-30733
EUSSEN, B. J. G. p 3134 N94-30740
EVANS, ANTHONY G. p 3178 N94-29126
EVERETT, H. R. p 3441 N94-30540
EVERHART, JOEL L. p 3130 N94-29545
EVTUSHENKO, I. A. p 3506 N94-29510
EWING, R. C. p 3517 N94-30201
EXARHOS, G. J. p 3207 N94-30062
EZ-ZAHRAOUY, H. p 3517 N94-30109
p 3468 N94-30110
p 3525 N94-30164
p 3517 N94-30165
p 3525 N94-30167
p 3517 N94-30181

F

FABINY, LARRY p 3294 N94-29551
FACHERIS, L. p 3256 N94-30496
FADLEY, C. S. p 3406 N94-30027
FAIZOV, E. L. p 3551 N94-30845
FAJN, V. EH. p 3406 N94-30081
FALKENBERG, E. D. p 3535 N94-30329
p 3535 N94-30359
FAN, LONG-SHENG p 3238 N94-29784
FANG, MING p 3549 N94-29737
FANGER, P. OLE p 3232 N94-29600
FARGUES, MONIQUE P. p 3241 N94-28634
FARIAS, T. L. p 3191 N94-29253
FARNWORTH, BRIAN p 3380 N94-28431
FAROOQ, M. p 3306 N94-30287
p 3308 N94-30295
p 3310 N94-30308
FARR, WILLIAM H. p 3411 N94-29202
p 3411 N94-29207
FARRAR, JAMES M. p 3481 N94-28491
FARROW, R. F. C. p 3519 N94-30707
FATYGA, M. p 3492 N94-30779
FAUCHER p 3266 N94-29523
FAUSTOV, R. N. p 3484 N94-28584
FEAGUE, ROY p 3442 N94-30548
FEARNSIDES, JOHN J. p 3137 N94-29559
FEDOR, L. S. p 3136 N94-30890
FEDOROV, F. I. p 3356 N94-28803
FEENSTRA, R. p 3519 N94-30611
FEIGHAN, P. p 3309 N94-30303
p 3309 N94-30304
p 3309 N94-30306
FEINERMAN, A. D. p 3236 N94-29775
FEITH, S. p 3382 N94-28441
FELDMAN, RAISA E. p 3464 N94-29129
FELLER, D. F. p 3514 N94-30001
FELSHTYN, A. p 3452 N94-29118
p 3467 N94-29163
FELTHAM, S. p 3474 N94-30676
FENG, RUQIANG p 3217 N94-29967
FENZI, M. p 3160 N94-29628
FEO, J. T. p 3420 N94-30056
FERGUSON, FREDERICK p 3148 N94-30516
FERGUSON, R. J. p 3307 N94-30294
FERIA, Y. p 3251 N94-29671
FERNANDEZ-BACA, J. A. p 3511 N94-28750
FERNANDEZ-VAREA, J. M. p 3494 N94-30980
FERNANDO, H. J. p 3369 N94-29067
FERNANDO, R. TIM P. p 3460 N94-30735
FERNAU, M. E. p 3349 N94-30023
FERRARO, NED W. p 3225 N94-29490
FERREIRA, M. C. F. p 3460 N94-30744
FERRISS, D. H. p 3322 N94-30523
FERRO, A. p 3168 N94-29543
FERRON, J. R. p 3510 N94-30832
FERSCHL, TONY p 3224 N94-29092
FETEIH, SALAH p 3299 N94-29354
p 3299 N94-29386
FICK, GREGORY J. p 3146 N94-28837
FIELD, CHRISTOPHER p 3353 N94-30638
FIELD, R. W. p 3489 N94-30061
FIELDS, C. p 3514 N94-29801
FILLIUS, R. W. p 3552 N94-29046
FINCH, J. L. p 3207 N94-30053
FINK, D. p 3543 N94-28545
FINKELSTEIN, ROBERT p 3304 N94-30276
FINLAYSON, E. U. p 3410 N94-29019
FINLEY, BRIAN p 3168 N94-29757
FINNEMORE, D. K. p 3519 N94-30338
FINNEY, J. M. p 3318 N94-29091
FIORINO, STEVEN T. p 3369 N94-29011
FIRSOV, V. G. p 3517 N94-30195
FISCHER, SOPHIE p 3456 N94-30370
FISHER, E. R. p 3199 N94-30260
FISK, Z. p 3492 N94-30775
p 3520 N94-30848
FITCHETT, JEFFREY W. p 3432 N94-30143
FITTINGHOFF, D. N. p 3488 N94-29845

FIX, LIMOR ..... p 3408 N94-23794
FIXLER, RICHARD S. ..... p 3157 N94-29754
FLATEBO, MITCHELL ..... p 3424 N94-30379
FLEETWOOD, D. M. ..... p 3263 N94-29025
p 3266 N94-30040
FLEISCHAUER, PAUL ..... p 3162 N94-29641
FLORENTINE, ROBERT A. ..... p 3178 N94-29024
FLORIJN, GERT ..... p 3428 N94-30746
FLUSS, M. J. ..... p 3516 N94-30054
FOLINSBEE, TERRY ..... p 3308 N94-30297
FOLLSTAEDT, D. M. ..... p 3518 N94-30316
FONCK, R. J. ..... p 3498 N94-28534
FONTAINE, J. R. ..... p 3233 N94-29611
FONTAINE, SCOTT A. ..... p 3142 N94-30189
FOOTE, MARC C. ..... p 3513 N94-29501
FORBES, D. V. ..... p 3521 N94-30894
FORBES, JOHN C. ..... p 3299 N94-29365
FORD, W. ..... p 3240 N94-28522
FOREMAN, JIM ..... p 3223 N94-30478
FORNASIERI, C. ..... p 3207 N94-30057
FORSTEN, JARL ..... p 3160 N94-28413
FORSTER, R. A. ..... p 3465 N94-30366
FORTIN, LOUIS ..... p 3316 N94-30235
FORTNER, BRAND IRVING ..... p 3546 N94-29991
FORTNER, J. ..... p 3521 N94-30897
FOSS, COLBY A., JR. ..... p 3197 N94-29312
FOSSUM, ERIC R. ..... p 3265 N94-29488
p 3237 N94-29780
FOSTER, C. A. ..... p 3230 N94-29017
FOSTER, I. ..... p 3350 N94-30116
FOSTER, I. T. ..... p 3428 N94-30754
FOSTER, WINFRED A., JR. ..... p 3171 N94-28800
FOUREU, JOHN ..... p 3224 N94-29092
FOWLER, PRISCILLA ..... p 3407 N94-28633
p 3407 N94-28639
FOX, J. A. ..... p 3341 N94-28454
FRABOUL, CH. ..... p 3417 N94-29345
FRAGONAS, E. ..... p 3255 N94-30153
FRANCALANCI, C. ..... p 3536 N94-30927
p 3536 N94-30929
FRANCINI, R. ..... p 3145 N94-28647
FRANCO, M. ..... p 3249 N94-29657
FRANCO, M. M. ..... p 3247 N94-29620
FRANK, J. P. ..... p 3258 N94-30508
FRANKEN, L. J. N. ..... p 3438 N94-30373
FRANO, GLENN ..... p 3288 N94-29437
FRAZIER, THOMAS P. ..... p 3409 N94-28878
FREEDMAN, A. P. ..... p 3144 N94-29614
FREER, HARRISON C. ..... p 3144 N94-30643
FREISER, B. S. ..... p 3207 N94-30024
FRENCH, DONALD A. ..... p 3451 N94-28723
FRENCH, R. J. ..... p 3339 N94-30606
FREY, H. C. ..... p 3341 N94-28465
FRIDELANCE, P. ..... p 3145 N94-30665
FRIEDL, R. R. ..... p 3343 N94-28593
FRIEDMAN, GARY L. ..... p 3287 N94-29373
FRIEDMAN, ROBERT ..... p 3166 N94-28712
FRIEDRICH, CRAIG R. ..... p 3235 N94-29769
p 3238 N94-29786
FRIM, J. ..... p 3383 N94-28449
FRIM, JOHN ..... p 3401 N94-29302
FRITZ, I. J. ..... p 3519 N94-30592
FROLKING, STEPHEN ..... p 3352 N94-30631
FRON, XAVIER ..... p 3141 N94-29583
FU, AN-KUO ..... p 3155 N94-29728
FUCHS, J. P. ..... p 3317 N94-28801
FUESS, D. A. ..... p 3254 N94-30043
FUJII, KOZO ..... p 3125 N94-28961
p 3125 N94-28966
FUJII, RYOICHI ..... p 3126 N94-28967
p 3359 N94-29235
FUJII, SHOICHI ..... p 3363 N94-29980
FUJII, YOSHIYUKI ..... p 3125 N94-28962
FUJIMORI, HIROYASU ..... p 3364 N94-29986
FUJISAWA, A. ..... p 3495 N94-29596
FUJISAWA, MASAMI ..... p 3505 N94-29397
FUJITA, SHIGERU ..... p 3495 N94-29596
FUKUDA, MASAHIRO ..... p 3360 N94-29242
p 3127 N94-28976
p 3129 N94-28991
FULFORD, JAMES K. ..... p 3129 N94-28992
FULLER, R. C. ..... p 3356 N94-28791
FUMMI, FRANCO ..... p 3212 N94-28661
FUMY, W. ..... p 3429 N94-30931
p 3252 N94-29692
FUNAHASHI, SATORU ..... p 3252 N94-29693
FUNAKI, Y. ..... p 3511 N94-28750
FUNG, INEZ ..... p 3466 N94-30737
p 3350 N94-30622
p 3351 N94-30624
FURLAN, G. ..... p 3351 N94-30627
FURUKAWA, MASATO ..... p 3515 N94-30005
FUSARO, ROBERT L. ..... p 3128 N94-28983
p 3214 N94-29399

G

GABOURY, SCOTT RICHARD ..... p 3221 N94-30812
GABRIELIAN, ARMEN ..... p 3419 N94-29678
GACS, PETER ..... p 3526 N94-30433
p 3426 N94-30434
GADDY, J. L. ..... p 3340 N94-30879
GAEBLER, K. ..... p 3138 N94-29566
GAGNE, M.-C. ..... p 3297 N94-30664
GAIER, JAMES R. ..... p 3338 N94-30196
GAIGEROV, B. A. ..... p 3475 N94-30679
GAIGNEBET, J. ..... p 3145 N94-30665
p 3297 N94-30666
GAIGNEBET, JEAN ..... p 3469 N94-30647
GAJENTAAN, ANKA ..... p 3461 N94-30747
GALAMBOS, J. D. ..... p 3509 N94-30760
GALEEVA, R. ..... p 3335 N94-30610
GALLIS, MICHAEL A. ..... p 3524 N94-29481
GANNON, T. ..... p 3467 N94-29147
GANZEVOORT, JOB ..... p 3423 N94-30324
GAO, ROBERT X. ..... p 3235 N94-29769
p 3238 N94-29786
GAO, WEI-GANG ..... p 3334 N94-30022
GARCIA-CALDERON, G. ..... p 3516 N94-30067
GARCIA, DISHAYNE ..... p 3402 N94-30210
GARCIAALCON, J. L. ..... p 3382 N94-28444
GARDNER, D. ..... p 3497 N94-30825
GARDNER, M. ..... p 3497 N94-30825
GARNER, F. A. ..... p 3201 N94-28456
GARNER, T. ..... p 3187 N94-28519
GARNIER, C. ..... p 3168 N94-29415
GARNIER, F. ..... p 3203 N94-29015
GARRETT, J. D. ..... p 3209 N94-30246
GARVEY, PAUL R. ..... p 3463 N94-28670
GASHIMZADE, F. M. ..... p 3516 N94-30072
GASHIMZADE, N. F. ..... p 3516 N94-30072
GAST, KARL ..... p 3344 N94-28599
GATES, THOMAS S. ..... p 3181 N94-29541
GATLIN, GREGORY M. ..... p 3130 N94-29443
GATSKI, THOMAS B. ..... p 3272 N94-29381
GAULIN, B. D. ..... p 3209 N94-30246
GAUTHIER, CHARLES ..... p 3415 N94-29333
GAUTVIK, W. ..... p 3379 N94-28422
GAVRIN, V. N. ..... p 3551 N94-30845
GAW, RAYMOND C. ..... p 3355 N94-28684
GAWRONSKI, W. ..... p 3248 N94-29622
GAYGEROV, B. A. ..... p 3474 N94-30676
GEFERT, LEON P. ..... p 3171 N94-28833
GEHLING, RUSSEL N. ..... p 3164 N94-28417
GEILING, D. W. ..... p 3336 N94-28499
GEISELMAN, ERIC E. ..... p 3150 N94-29048
GELLES, D. S. ..... p 3201 N94-28460
GELTMACHER, A. B. ..... p 3317 N94-28811
GENCHEV, V. I. ..... p 3483 N94-28554
GENTRY, GARL L., JR. ..... p 3132 N94-29937
GEORGE, JEFFREY A. ..... p 3171 N94-28833
GEORGE, L. A. ..... p 3342 N94-28590
p 3345 N94-28606
GEORGHIOU, GEORGHIOS ANDREOU
p 3253 N94-29894
GEORGIEV, D. ..... p 3511 N94-28626
GERAGHTY, P. ..... p 3175 N94-28528
GERBER, HERMANN E. ..... p 3374 N94-30187
GERBER, RICHARD ALAN ..... p 3548 N94-30340
GERGEL, V. P. ..... p 3421 N94-30077
GETTRUST, JOSEPH F. ..... p 3355 N94-28685
GETTY, WARD D. ..... p 3293 N94-29179
GEVORKYAN, ARVID G. ..... p 3475 N94-30680
GHEZZO, M. ..... p 3171 N94-29782
GHIO, G. ..... p 3245 N94-29456
GIAMBRA, JULIA A. ..... p 3513 N94-29130
GIANNETTI, PAOLO ..... p 3376 N94-28690
GIBBONS, K. A. ..... p 3193 N94-29265
GIBREKHTERMAN, A. ..... p 3395 N94-30185
GIESBRECHT, GORDON G. ..... p 3380 N94-28428
GIFFORD, FRANKLIN A. ..... p 3355 N94-28728
GILBREATH, G. A. ..... p 3441 N94-30540
GILCHRIST, A. RICHARD ..... p 3163 N94-29651
GILLEN, K. T. ..... p 3218 N94-30102
GILPATRICK, J. D. ..... p 3267 N94-30716
GILPIN, ROGER K. ..... p 3384 N94-28667
GINSBERG, I. W. BILL ..... p 3326 N94-28929
GIOVANONI, PETER MICHAEL ..... p 3547 N94-29993
GITMAN, D. M. ..... p 3524 N94-29498
GIUDICELLI, PHILIPPE ..... p 3168 N94-29419
GIULI, D. ..... p 3256 N94-30496
GLASS, G. W. ..... p 3251 N94-29672
GLASS, K. C. ..... p 3383 N94-28449
GLASS, KEVIN ..... p 3409 N94-28910
GLASSMAN, IRVIN ..... p 3189 N94-29004
GLEASON, THOMAS ..... p 3163 N94-29651
GLECKLER, P. J. ..... p 3378 N94-30823
GLENDENNING, N. K. ..... p 3542 N94-28480
GLENDINNING, S. G. ..... p 3509 N94-30597
GLOVER, DANIEL R. ..... p 3246 N94-29589
GODWIN, D. S. ..... p 3220 N94-30692
GOEL, ASHOK ..... p 3417 N94-29390
GOG, T. ..... p 3513 N94-29215
GOLDBERG, KENNETH Y. ..... p 3458 N94-30407
p 3458 N94-30408
p 3427 N94-30725
GOLDMAN, G. ..... p 3259 N94-30512
GOLDMAN, JEFFREY H. ..... p 3278 N94-29977
GOLDMAN, T. ..... p 3522 N94-28543
p 3522 N94-28572
p 3526 N94-30750
GOLDSTEIN, J. L. F. ..... p 3210 N94-30710
GOLDSTEIN, RICHARD M. ..... p 3248 N94-29626
GOLUBEV, A. V. ..... p 3505 N94-29076
GOMES, I. C. ..... p 3493 N94-30893
GONZALES, DAVID ALBERT ..... p 3273 N94-29675
GOOD, PHILIP GRAHAM ..... p 3170 N94-30960
GOODEN, J. H. M. ..... p 3157 N94-30399
GOODFELLOW, H. D. ..... p 3232 N94-29604
p 3232 N94-29605
GOODING, JAMES L. ..... p 3236 N94-29776
GOODNIGHT, THOMAS W. ..... p 3319 N94-29469
GOODWIN, D. J. ..... p 3417 N94-29344
GORDAN, ANDREW L. ..... p 3300 N94-29427
GORDON, HENRY G. ..... p 3411 N94-29201
GORDON, J. LEA ..... p 3416 N94-29339
GORETTA, KENNETH C. ..... p 3261 N94-28487
GORVAD, M. R. ..... p 3122 N94-29842
GOSWAMI, KUMAR K. ..... p 3406 N94-29695
p 3420 N94-29890
GOTT, REBECCA M. ..... p 3478 N94-29206
GOTTESFELD, S. ..... p 3208 N94-30101
GOTTLIEB, ROBERT G. ..... p 3361 N94-29588
GOTTSHALL, R. MARC ..... p 3440 N94-30535
GOUDREAU, G. L. ..... p 3321 N94-29951
GOUZHVA, YURI G. ..... p 3475 N94-30680
GOVINDAN, T. R. ..... p 3300 N94-29550
GOVOROV, A. O. ..... p 3267 N94-30092
GOWER, G. L. ..... p 3374 N94-30587
GRAF, JOHN C. ..... p 3354 N94-30470
GRAF, T. ..... p 3520 N94-30848
GRAHAM, R. ..... p 3534 N94-30099
GRAHN, P. ..... p 3245 N94-29311
GRANDI, E. ..... p 3414 N94-29325
GRANLEY, DARCY ..... p 3398 N94-28887
GRANT, EDWARD ..... p 3447 N94-30578
GRANT, K. E. ..... p 3350 N94-30613
p 3367 N94-30876
GRAUX, L. ..... p 3435 N94-29480
GRAVES, DAVID ..... p 3241 N94-28762
GRAVESTEIJN, H. ..... p 3256 N94-30498
GRAY, G. T., III ..... p 3210 N94-30774
GREBINNIK, V. G. ..... p 3517 N94-30195
GREEN, ANDREW A. ..... p 3326 N94-28930
GREEN, DAVID ..... p 3305 N94-30280
GREEN, M. A. ..... p 3468 N94-30026
p 3520 N94-30850
GREEN, R. M. ..... p 3311 N94-30596
GREEN, STEVEN ..... p 3138 N94-29568
GREEN, STEVEN M. ..... p 3140 N94-29578
GREENLEAF, J. E. ..... p 3385 N94-29401
GREENWOOD, D. ..... p 3289 N94-30059
GREGORY, A. P. ..... p 3476 N94-30781
GREGUS, M. M. ..... p 3451 N94-28783
GRENIER-LOUSTALOT, MARIE-FLORENCE
p 3215 N94-29441
GRIFFIN, J. J. ..... p 3492 N94-30838
GRIFFITH, L. V. ..... p 3221 N94-30829
GRIGGS, D. ..... p 3286 N94-28466
GRIGOREV, A. N. ..... p 3500 N94-30075
GRIMALDI, SABRINA ..... p 3468 N94-30642
GRIMM, K. A. ..... p 3447 N94-30581
GRISHAGIN, V. A. ..... p 3421 N94-30077
GRODSINSKY, CARLOS ..... p 3168 N94-29757
GRODSKI, J. J. ..... p 3310 N94-30310
GROENENDIJK, JEROEN ..... p 3456 N94-30372
GRONG, O. ..... p 3206 N94-29947
GROPP, W. ..... p 3429 N94-30840
GROSS, R. J. ..... p 3226 N94-30615
GROSSMAN, A. S. ..... p 3350 N94-30613
p 3367 N94-30876
GROSSMAN, T. ..... p 3427 N94-30705
GRUDLER, P. ..... p 3145 N94-30665
GRUDZEVICH, O. T. ..... p 3497 N94-30825
GRUEN, D. M. ..... p 3519 N94-30718
GRUNINGER, J. H. ..... p 3357 N94-28893
GU, L. ..... p 3206 N94-29946
GUARDIANI, FRANK ..... p 3384 N94-28453
GUBER, A. F. ..... p 3508 N94-30193
GUCKEL, H. ..... p 3235 N94-29770
GUDAITIS, JAMES J. ..... p 3177 N94-29012
GUDIVADA, VENKAT NAIDU ..... p 3533 N94-29811
GUESS, T. R. ..... p 3185 N94-30827
GUIBAS, LEONIDAS J. ..... p 3456 N94-30377
GUILLAME, B. ..... p 3259 N94-30511
GUINN, J. ..... p 3160 N94-29666

GULEC, K. p 3508 N94-30339
GUMLEY, LIAM E. p 3231 N94-29385
GUMMADI, LAKSHMANA NAGESH BABU p 3181 N94-29593
GUNDLACH, JAMES PHILLIP p 3362 N94-29743
GUO, RUIJIN p 3208 N94-30138
GUO, YIN p 3524 N94-29987
GUPTA, R. p 3514 N94-29818
GUREVICH, I. I. p 3517 N94-30195
GURZHIEV, S. N. p 3489 N94-30050
GUSEV, A. A. p 3365 N94-30223
GUSSENHOVEN, M. S. p 3552 N94-29046
GUTIERREZ, D. J. p 3347 N94-29023
GUTTERMAN, GREGORY M. p 3230 N94-28742
GUYENNE, T. D. p 3347 N94-29452
GWALTNEY, DAVID A. p 3157 N94-30200
GYULASSY, M. p 3491 N94-30686

H

HA, CHEOLKEUN p 3438 N94-30517
HA, TAE WOONG p 3302 N94-29916
HAAN, S. W. p 3509 N94-30597
HAAS, BRIAN L. p 3131 N94-29893
HACK, J. J. p 3350 N94-30116
HACKETT, MICHAEL p 3555 N94-30440
HADAEGH, F. Y. p 3239 N94-29787
HADAEGH, FRED Y. p 3144 N94-29772
p 3144 N94-29792
HAGAN, R. D. p 3400 N94-28902
p 3391 N94-28912
HAGEN, M. p 3286 N94-29113
HAGMEIJER, R. p 3134 N94-30858
HAHN, R. L. p 3551 N94-30884
HAILA, A. p 3537 N94-29168
HAINES, NICHOLAS p 3410 N94-29006
HAJIEV, A. T. p 3516 N94-30072
HAKULINEN, T. T. p 3487 N94-29683
HALDAR, S. p 3432 N94-30411
p 3426 N94-30489
HALE, M. J. p 3514 N94-29801
HALFORD, GARY R. p 3317 N94-28819
HALL, EDWARD J. p 3152 N94-29438
HALL, KENNETH C. p 3153 N94-30013
HALL, L. J. p 3491 N94-30709
HALLDEN, A. p 3411 N94-29159
HALLMANN, M. p 3195 N94-29279
HALPERT, GERALD p 3265 N94-29411
p 3265 N94-29505
HALPIN, T. A. p 3535 N94-30361
HAMADA, Y. p 3505 N94-29397
HAMAKAWA, YOSHIHIRO p 3228 N94-28942
p 3159 N94-30162
HAMAZAKI, HIROSHI p 3127 N94-28978
HAMDACHE, F. p 3218 N94-30066
HAMEETMAN, G. J. p 3170 N94-29324
HAMILTON, A. D. p 3174 N94-29307
HAMILTON, M. C. p 3498 N94-28656
HAMMEL, B. A. p 3509 N94-30597
HAMMER, JAY ALAN p 3198 N94-29676
HAMMONS, B. E. p 3519 N94-30592
HAMMOUD, AHMAD p 3166 N94-28708
HAMPL, EDWARD, JR. p 3167 N94-28717
HAMSHAR, JASON p 3408 N94-28784
HAN, GANG p 3320 N94-29690
HANCOCK, JOHN p 3143 N94-29323
HANCOCK, THOMAS M., III p 3448 N94-30584
HANDLER, T. p 3482 N94-28504
HANEY, S. p 3509 N94-30760
HANEY, S. W. p 3509 N94-30768
HANNA, D. M. p 3310 N94-30311
HANNUS, MATTI p 3407 N94-28411
HANSEL, S. J. p 3495 N94-30214
HANSEN, CHRISTOPHER P. p 3300 N94-29448
HANSEN, N. p 3210 N94-30777
HANSEN, T. H. p 3431 N94-29995
HANSON, L. K. p 3485 N94-28741
HANSON, R. K. p 3272 N94-29136
HANSSON, HANS-CHRISTEN p 3336 N94-30944
HANSSON, MARGARETA E. p 3336 N94-30944
HARA, MASAHIRO p 3324 N94-28693
HARARI, ISAAC p 3454 N94-30209
HARBEN, P. E. p 3335 N94-30594
HARD, THOMAS M. p 3342 N94-28590
p 3345 N94-28606
HARDY, G. R. p 3307 N94-30290
HARDY, JOHN R. p 3485 N94-28668
HARDY, M. B. p 3157 N94-29151
HARDY, TERRY L. p 3173 N94-29403
HARING, S. p 3438 N94-30349
HAROUTUNIAN, GEORGE V., JR. p 3528 N94-28640
HARPER, ROBERT p 3410 N94-29007
HARPER, SAMUEL E., JR. p 3287 N94-29368
HARRE, M. p 3384 N94-28452
HARRINGTON, RICHARD F. p 3329 N94-29098
HARRIS, SCOTT H. p 3132 N94-30151
HARRIS, WALTER MICHAEL p 3550 N94-30798
HARRISON, CATHERINE p 3153 N94-30130
HARRISON, L. p 3269 N94-28464
HARRISON, W. E. p 3192 N94-29261
HARROP, JOSEPH D. p 3527 N94-28779
HART, E. L. p 3482 N94-28504
HART, R. L. p 3368 N94-28568
HARTL, PHILIPP p 3137 N94-29564
HARTLEY, DANA p 3350 N94-30617
HARTOG, D. J. DEN p 3498 N94-28534
HARTZ, LESLIE S. p 3300 N94-29428
HARUYAMA, YUKIO p 3332 N94-29232
HARVEY, A. p 3278 N94-29977
HARVEY, JOHN K. p 3524 N94-29481
HASEGAWA, KATSUO p 3233 N94-29701
HASHIBA, MOTOYUKI p 3390 N94-28855
HASHIMOTO, KEISUKE p 3127 N94-28976
HASHIMOTO, TAKESHI p 3359 N94-29234
HASSA, C. p 3196 N94-29282
HASSANEIN, A. p 3509 N94-30697
HASSLACHER, B. p 3200 N94-30748
HASTIE, D. R. p 3345 N94-28604
HATAKEYAMA, YOSHIMI p 3234 N94-29707
HATAMA, HARUO p 3129 N94-28993
HATAT, J.-L. p 3297 N94-30666
HATORI, HIROAKI p 3223 N94-29517
HAUG, E. p 3206 N94-29997
HAUG, S. p 3533 N94-29948
HAUGLAND, E. J. p 3264 N94-29209
HAURI, ERIK HAROLD p 3367 N94-30917
HAUTIER p 3266 N94-29523
HAVERKORT, B. R. p 3438 N94-30373
HAVEY, GARY p 3171 N94-29791
HAWKE, R. S. p 3289 N94-30059
p 3281 N94-30600
HAWKEY, TIMOTHY J. p 3239 N94-29789
HAWTHORNE, H. M. p 3303 N94-30019
HAYAKAWA, MASASHI p 3361 N94-29245
HAYASHI, MASANORI p 3123 N94-28952
HAYASHI, T. p 3505 N94-29483
HAYATI, SAMAD p 3442 N94-30545
HAYDEN, LINDA p 3431 N94-29396
HAYES, D. M. p 3210 N94-30796
HAYES, JULIE p 3402 N94-30188
HAYES, P. J. p 3422 N94-30197
HAYES, TEDDIANN S. p 3529 N94-29066
HAYMAKER, R. p 3491 N94-30762
HAYS, G. N. p 3292 N94-28482
HE, XIN p 3423 N94-30345
HEADLEY, T. J. p 3216 N94-29830
HEALY, M. D. p 3206 N94-30007
HEATH-PASTORE, T. A. p 3441 N94-30540
HEBERT, M. p 3445 N94-30566
HEBNER, G. A. p 3292 N94-28482
HEBRARD, P. p 3195 N94-29278
HECHT, J. H. p 3347 N94-29023
HEDBY, G. p 3453 N94-29174
HEEMSKERK, H. J. M. p 3256 N94-30498
HEEREMA, F. p 3142 N94-30439
HEERING, J. p 3459 N94-30436
HEERING, JAN p 3453 N94-29889
HEGELS, HERMANN F. p 3137 N94-29563
HEIJENK, GEERT p 3438 N94-30375
HEIJSTEK, J. J. p 3338 N94-30328
HEINTZENBERG, JOST p 3336 N94-30944
HEISE, T. W. p 3296 N94-30908
HEKMAN, THOMAS P. p 3356 N94-28843
HELLE, AINO p 3204 N94-29387
HELLMAN, J. R. p 3175 N94-28581
HELLWIG, HELMUT p 3475 N94-30681
HELMICKI, ARTHUR J. p 3173 N94-29848
HELTON, K. T. p 3397 N94-28754
HENDERS, M. G. p 3155 N94-30284
HENDERSON, D. O. p 3219 N94-30335
HENDERSON, F. B., III p 3328 N94-28937
HENDERSON, FREDERIC B., III p 3326 N94-28929
HENDRICK, ROBERT p 3419 N94-29727
HENDRICKS, J. S. p 3419 N94-29816
HENDRIKS, LEX p 3463 N94-30974
HENDRY, R. C. p 3504 N94-28776
HENDY, KEITH C. p 3402 N94-30132
HENEGHAN, S. P. p 3193 N94-29266
HENG-QIU, ZHENG p 3471 N94-30658
HENKEL, M. p 3199 N94-30111
HENLINE, D. M. p 3535 N94-30699
HENNECKE, D. K. p 3196 N94-29281
HENN!NGER, SANDRA p 3157 N94-29754
HENRIKSSON, ANDERS p 3215 N94-29424
HENRY, PAUL K. p 3235 N94-29768
HERGENROTHER, PAUL M. p 3215 N94-29555
HERMES, MARTIN J. p 3171 N94-30672
HERNANDEZ, R. p 3199 N94-30266
HERRB, MATTHIEU p 3443 N94-30552
HERRERA-FIERRO, PILAR p 3218 N94-30177
HERRING, ROBERT W. p 3149 N94-30293
HERTZBACH, S. S. p 3491 N94-30702
HESS, N. J. p 3207 N94-30062
HESSLINK, R. L. p 3382 N94-28441
HETHERINGTON, D. L. p 3510 N94-28484
HEVNER, ALAN R. p 3156 N94-28752
p 3156 N94-28753
HEYMSFIELD, GERALD M. p 3252 N94-29739
HEYSE, MARK W. p 3263 N94-28994
HIBLER, WILLIAM D., III p 3350 N94-30620
p 3352 N94-30632
HICKS, WILLIAM p 3391 N94-29150
HIGDON, JAMES LLOYD p 3539 N94-29821
HILDRE, H. P. p 3229 N94-29996
HILJANEN, M. p 3220 N94-30713
HILL, A. G. p 3141 N94-29585
HILL, N. p 3302 N94-29922
HILL, R. p 3452 N94-29118
p 3467 N94-29163
HILL, RONALD C. p 3400 N94-28996
HILLS, C. R. p 3220 N94-30591
HILTON, MIKE p 3162 N94-29641
HILTUNEN, ESA p 3399 N94-28406
HINEDI, S. p 3250 N94-29665
p 3251 N94-29669
HINKE, PATRICK THOMAS p 3231 N94-29379
HINKLE, A. J. p 3202 N94-28830
HINKS, D. G. p 3519 N94-30338
HINMAN-SWEENEY, ELAINE MARIE p 3401 N94-29729
HIRAI, ATSUO p 3390 N94-28854
p 3394 N94-29864
HIRAKAWA, KAZUOMI p 3357 N94-29080
HIRASAWA, TAKEO p 3357 N94-29078
p 3359 N94-29233
p 3363 N94-29978
HIRASHITA, MASAMI p 3394 N94-29864
HIRATA, KOZO p 3394 N94-29864
HIRATA, YUTAKA p 3393 N94-29716
HIROI, YOSHIKUNI p 3357 N94-29078
p 3363 N94-29978
HIROSE, A. p 3507 N94-30156
p 3507 N94-30158
p 3508 N94-30159
HIROSE, AKIRA p 3507 N94-30157
HIROSE, NAOKI p 3124 N94-28958
HIRSCH, DAVID p 3166 N94-28709
HIRSCHMUGL, C. p 3510 N94-28512
HIRVONEN, J. P. p 3175 N94-28579
p 3217 N94-30025
HITCHENS, G. D. p 3318 N94-29057
HLIBOWICKI, ANDRZEJ p 3137 N94-29560
HO, HING W. p 3316 N94-28508
HO, P. p 3199 N94-30260
p 3222 N94-30909
HO, SOOK Y. p 3224 N94-29092
HOADLEY, D. p 3145 N94-28657
HOANG, P. p 3136 N94-28914
HOBBS, M. L. p 3226 N94-30615
HOBBS, PETER V. p 3377 N94-29128
HOBERMAN, CHARLES p 3245 N94-29360
HODGE, STEVE L. p 3478 N94-29382
HODGETTS, T. E. p 3476 N94-30781
HODKO, D. p 3318 N94-29057
HOEBEL, LOUIS J. p 3414 N94-29328
HOEDE, C. p 3466 N94-30737
HOEIJMAKERS, H. W. M. p 3133 N94-30388
p 3133 N94-30492
p 3134 N94-30871
HOEKMAN, DIRK H. p 3335 N94-30759
HOEKSTRA, WILLEM E. p 3137 N94-29563
HOEPER, J. p 3382 N94-28439
HOFFMAN, FREDERICK p 3434 N94-29026
HOFFMAN, WESLEY P. p 3186 N94-30452
HOFLER, ALICIA S. p 3408 N94-28818
HOFZUMAHAUS, ANDREAS p 3343 N94-28591
HOGENDOORN, R. A. p 3142 N94-30439
HOKIN, S. A. p 3503 N94-28514
HOLESINGER, T. p 3519 N94-30691
HOLLAND, ELIZABETH p 3352 N94-30631
HOLLAND, FRANK p 3343 N94-28591
HOLLEY, W. H. p 3336 N94-28500
HOLLIS, PATRICK p 3299 N94-29354
p 3299 N94-29386
HOLLOWAY, L. E. p 3483 N94-28566
HOLMBERG, JAN p 3465 N94-30154
HOLMSTROEM, J. p 3230 N94-29188
HOLTET, JAN A. p 3360 N94-29239
HONG, WEI p 3216 N94-29766
HONG, YANHUA p 3148 N94-30131
HOOFMAN, RAYMOND p 3456 N94-30381
p 3457 N94-30384
HOOKER, MATTHEW W. p 3512 N94-29101
HOOPES, JOAN E. p 3533 N94-29855
HOOVER, SCOTT p 3299 N94-29409
HORBER. RALPH p 3162 N94-29642
HORI, TAKANOBU p 3159 N94-30162
p 3159 N94-30794

HORIGOME, SHINICHI p 3386 N94-28853
HORIKOSHI, NOBUYUKI p 3234 N94-29704
HORN, BRUCE p 3418 N94-29434
HORNYAK, GABOR L. p 3197 N94-29312
HORRIGAN, D. J., JR. p 3383 N94-28448
HORST, WILLIAM DOUGLAS p 3541 N94-30270
HORTON, CHARLES M. p 3316 N94-29724
p 3157 N94-29956
HOSHIAI, TAKAO p 3357 N94-29078
p 3363 N94-29978
HOSOYA, MASAYUKI p 3314 N94-29981
p 3314 N94-29982
p 3314 N94-29985
HOSTETLER, CHRIS ALAN p 3366 N94-30802
HOU, XINLI p 3255 N94-30374
HOUNJET, M. H. J. p 3134 N94-30740
HOURAHAN, G. C. p 3220 N94-30692
HOWARD, A. J. p 3515 N94-30006
p 3219 N94-30263
p 3519 N94-30592
HOWARD, DAVID p 3264 N94-29372
HOWARD, J. W. p 3496 N94-30219
HOWARD, JAMES W. p 3263 N94-29028
HOWELL, R. H. p 3516 N94-30054
HOWELLS, W. S. p 3521 N94-30897
HOYT, J. J. p 3211 N94-30852
HRILJAC, J. A. p 3204 N94-29395
HROVAT, KENNETH p 3166 N94-28711
HSIAO, CHINGTENG p 3282 N94-30816
HSIEH, D. P. H. p 3349 N94-30044
HSU, ELTON P. p 3243 N94-29072
HSU, Y. L. p 3377 N94-29432
HU, E. L. p 3519 N94-30592
HU, FANG Q. p 3454 N94-30207
HU, T. C. J. p 3154 N94-29257
HUA, T. Q. p 3506 N94-29510
HUANG, CHEN-KUO p 3265 N94-29411
p 3265 N94-29505
HUANG, HO-SHUENN p 3283 N94-30958
HUANG, J. p 3251 N94-29668
HUANG, KUAN HONG p 3184 N94-30257
HUANG, L.-M. p 3194 N94-29272
HUANG, MU-HSUAN p 3533 N94-29960
HUANG, SHU-CHUAN p 3408 N94-28790
HUANG, YONG p 3276 N94-29843
HUBANKS, PAUL A. p 3231 N94-29385
HUDSON, JOHN DALE p 3280 N94-30272
HUEY, K. A. p 3400 N94-28902
HUFFORD, G. A. p 3256 N94-30497
HUGHES, D. A. p 3210 N94-30777
HUGHES, E. p 3482 N94-28541
HUGHES, MARY L. p 3319 N94-29433
HUGHES, R. C. p 3510 N94-28484
HUGHES, THOMAS C. p 3146 N94-29391
HUGHLOCK, B. W. p 3291 N94-30218
HUIZENGA, C. p 3410 N94-29019
HULEN, H. p 3404 N94-28505
HULL, ANTHONY p 3144 N94-29794
HULL, J. R. p 3468 N94-28459
p 3297 N94-28461
HUMPHREYS, GREGORY L. p 3157 N94-30200
HUNDLEY, M. F. p 3520 N94-30848
HUNG, CHING-CHEH p 3174 N94-28747
p 3174 N94-28924
HUNT, BRIAN D. p 3513 N94-29501
HUNTER, IAIN p 3395 N94-30970
HUNTER, R. D. p 3141 N94-29579
HUNTER, S. L. p 3335 N94-30594
HUOT, CAROLINE p 3159 N94-30237
HURME, M. p 3189 N94-28789
HURT, TINA M. p 3346 N94-28722
HUSKEY, WINNIE L. p 3529 N94-29066
HUTCHINS, D. R. p 3259 N94-30512
HUYNH, LOC C. p 3147 N94-29721
HVASSHOVD, S. p 3533 N94-29921
HVASSHOVD, S. O. p 3533 N94-29948
HWANG, MEI-YUH p 3244 N94-29303
HYATT, A. W. p 3510 N94-30832
HYER, M. W. p 3317 N94-28801

I

IANOVSKI, LEONID S. p 3197 N94-29285
IBARAKI, SEIICHI p 3128 N94-28983
IBRAHIM, OMAR M. p 3319 N94-29469
IDA, K. p 3505 N94-29398
IEMORI, TOSHIHIKO p 3360 N94-29243
IGARASHI, KIYOSHI p 3360 N94-29238
IGARASHI, YUMINOBU p 3128 N94-28985
IGNATOVICH, V. K. p 3523 N94-28719
IGNATYUK, A. V. p 3497 N94-30825
IGOE, WILLIAM B. p 3158 N94-30788
IGUCHI, H. p 3505 N94-29397
p 3505 N94-29398
IIDA, TAKEHIRO p 3328 N94-29038
IIJIMA, HIGASHI p 3332 N94-29231
IJIRI, KENICHI p 3387 N94-29713
IKAWA, SACHIO p 3387 N94-28495
p 3389 N94-28850
p 3394 N94-29863
IKEDA, MIZUHO p 3169 N94-30811
ILIN, V. D. p 3362 N94-29935
ILVESOKSA, J. p 3385 N94-29189
IMAIZUMI, HIROYUKI p 3479 N94-29597
IMAMOTO, S. S. p 3167 N94-29022
IMBRIALE, W. p 3249 N94-29657
IMLAY, R. p 3491 N94-30762
IMMEGA, GUY p 3309 N94-30305
IMPEY, CHRIS p 3540 N94-29957
INAGAWA, MASARU p 3324 N94-28694
INAMURA, KINSAKU p 3394 N94-29865
INATANI, TOSHIHIRO p 3159 N94-30794
ING, H. p 3291 N94-30216
INGLE, G. p 3141 N94-29580
INGRAHAM, R. L. p 3524 N94-30086
INO, YOSHIO p 3358 N94-29081
INOUE, MASAHIRO p 3128 N94-28983
INOUE, SEIICHI p 3387 N94-29519
IRWIN, TROY p 3173 N94-29216
ISA, HIIZU p 3377 N94-29595
ISAEV, A. P. p 3460 N94-30726
ISEI, TAKEHIRO p 3479 N94-29597
ISHIGAKI, HIROSHI p 3128 N94-28984
p 3128 N94-28986
p 3128 N94-28987
p 3128 N94-28988
p 3129 N94-28989
ISHIGAMI, HIROSHI p 3326 N94-28931
ISHIGURO, MITSUO p 3124 N94-28958
ISHIHARA, OSAMU p 3507 N94-30157
ISHII, KEN p 3234 N94-29707
ISHII, KIMIHIRO p 3495 N94-29596
ISHII, MAMORU p 3360 N94-29243
ISHII, MASANORI p 3390 N94-28857
ISHII, RYUJI p 3126 N94-28968
ISHII, YOSHINORI p 3328 N94-28937
p 3329 N94-29218
p 3332 N94-29231
ISHIJIMA, YOSHIRO p 3386 N94-28853
ISHIKAWA, YOJI p 3159 N94-30162
ISHIKURA, SEIZO p 3393 N94-29717
ISHIWADA, YASUAKI p 3332 N94-29231
ISHIZAKA, KOICHI p 3124 N94-28954
ISHIZAWA, KENJI p 3314 N94-29981
ISKAROUS, M. p 3447 N94-30580
ITO, KATSUHIRO p 3123 N94-28953
ITO, MASAO p 3388 N94-28498
p 3389 N94-28852
p 3386 N94-28853
ITO, RINSUKE p 3485 N94-28788
ITOH, K. p 3505 N94-29398
ITOH, S.-I. p 3505 N94-29398
IVANCHENKO, I. M. p 3483 N94-28554
IVANOV, M. A. p 3487 N94-29502
IVANOV, V. V. p 3483 N94-28552
IVANSSON, S. p 3453 N94-29476
IWANCZYK, JAN S. p 3236 N94-29773
IWASAKI, KENICHI p 3389 N94-28852
p 3386 N94-28853
IWASE, SATOSHI p 3394 N94-29865
IWATA, YOSHIHIRO p 3159 N94-30794

J

JAARSMA, F. p 3158 N94-30423
JABLONSKI, D. A. p 3315 N94-28646
JACKSON, BERNARD V. p 3550 N94-29132
JACKSON, C. p 3536 N94-29144
JACKSON, E. p 3305 N94-30279
p 3309 N94-30306
JACKSON, ERIC p 3310 N94-30307
JACKSON, JOEL p 3434 N94-29013
JACOB, THOMAS p 3138 N94-29565
JACOBS, I. p 3379 N94-28426
JACOBS, PIETER A. M. p 3257 N94-30502
JACOBS, V. L. p 3509 N94-30755
JACOBSON, J. p 3411 N94-29159
JACOBUS, CHARLES J. p 3314 N94-30442
JACQUES, C. p 3471 N94-30656
JAIN, ABHINANDAN p 3435 N94-29465
JAIN, M. p 3386 N94-30180
JAKEMAN, E. p 3258 N94-30508
JAKLEVIC, J. p 3268 N94-30717
JAMES, DALE A. p 3405 N94-29181
JAMES, G. H., III p 3289 N94-29927
JAMES, RICHARD D. p 3203 N94-29056
JAMET, JEAN F. p 3179 N94-29413
JAMISON, G. M. p 3174 N94-28557
JANICKA, J. p 3154 N94-29254
JANSEN, C. J. A. p 3252 N94-29692
p 3252 N94-29693
JANSEN, R. H. p 3213 N94-28922
JARBOE, THOMAS R. p 3505 N94-29134
JARVIS, E. E. p 3225 N94-30038
JASIOBEDZKI, P. p 3439 N94-30529
JASKIERNY, W. p 3268 N94-30904
JASON, A. J. p 3267 N94-30716
JAYARAJ, K. p 3287 N94-29400
JECKEL, R. p 3196 N94-29283
JEDLOVEC, G. J. p 3333 N94-29553
JEE, J. p 3160 N94-29666
JEFFERSON, D. C. p 3144 N94-30650
JEGLEY, DAWN C. p 3178 N94-29100
JEN, FU-HUA p 3301 N94-29847
JENDEN, C. M. p 3258 N94-30503
JENKIN, M. p 3439 N94-30529
JENKIN, MICHAEL p 3309 N94-30301
JENKINS, RHONALD M. p 3171 N94-28800
JEPSON, A. p 3439 N94-30529
JERVIS, T. R. p 3175 N94-28579
p 3217 N94-30025
JESSE, C. A. p 3465 N94-29925
JESTER, T. p 3339 N94-30603
JI, H. p 3503 N94-28514
JI, Y. p 3451 N94-28792
JIA, WEI p 3126 N94-28971
JIANG, BO-NAN p 3272 N94-29096
JIANG, WEN-XIN p 3524 N94-29911
JIH, RONG-SONG p 3361 N94-29393
JIN, MICHAEL Y. p 3397 N94-30456
JOANNOPOULOS, JOHN D. p 3512 N94-28890
JOHANSEN, JAMES D. p 3189 N94-29140
JOHANSEN, S. T. p 3206 N94-29946
JOHANSON, GUNNAR p 3465 N94-30154
JOHANSSON, E. M. p 3254 N94-29929
JOHNSON, D. L. p 3251 N94-29672
JOHNSON, DANIEL L. p 3391 N94-29150
JOHNSON, HARRY p 3166 N94-28709
JOHNSON, J. A. p 3314 N94-30444
JOHNSON, J. M. p 3451 N94-28739
JOHNSON, JACQUELINE U. p 3354 N94-30463
JOHNSON, JOHN p 3121 N94-28666
JOHNSON, KENNETH R. p 3288 N94-29497
JOHNSON, M. B. p 3522 N94-28543
p 3522 N94-28572
p 3526 N94-30750
JOHNSON, M. L. p 3290 N94-30199
JOHNSON, MARK p 3397 N94-30460
JOHNSON, MARK A. p 3392 N94-29431
JOHNSON, MARK D. p 3502 N94-30462
JOHNSON, RICHARD F. p 3383 N94-28447
JOHNSON, S. p 3240 N94-28522
JOHNSON, SALLY C. p 3431 N94-29494
p 3432 N94-30160
JOHNSON, SHELBY D. p 3171 N94-28800
JOHNSON, W. S. p 3180 N94-29472
JOHNSON, W. STEVEN p 3177 N94-28823
JOINET, JEAN-BAPTISTE p 3430 N94-30973
JOKERST, N. M. p 3239 N94-29793
JONASSON, H. G. p 3477 N94-29175
JONES, BRIAN LEIGH p 3142 N94-29837
JONES, E. G. p 3192 N94-29262
JONES, LEONIDAS J., III p 3486 N94-29131
p 3513 N94-29155
JONES, LORI p 3241 N94-28755
JONES, R. L. p 3422 N94-30197
JONES, RICHARD A. p 3150 N94-28923
JONES, ROBERT J. p 3167 N94-28715
JONES, SAMMY L. p 3441 N94-30539
JONES, TANYA E. p 3380 N94-28429
JONES, W. R., JR. p 3213 N94-28922
JONES, WILLIAM R., JR. p 3218 N94-30177
JONG, YEN-YI p 3174 N94-29868
JONSSON, STIG p 3336 N94-30944
JORDAN, D. L. p 3258 N94-30506
JORDAN, PERNELL A. p 3435 N94-29044
JORGENSEN, G. p 3500 N94-29799
JORNA, P. G. A. M. p 3399 N94-30969
JOSEPH, ADRIAN A. p 3211 N94-30446
JOUANNAUD, JEAN-PIERRE p 3428 N94-30734
JOYCE, MICHAEL D. p 3477 N94-29003
JUBRINK, H. G. p 3242 N94-28885
JUDAY, RICHARD D. p 3397 N94-30455
JUDD, M. D. p 3165 N94-28698
JULL, A. J. TIMOTHY p 3546 N94-29905
JUMPER, JUDITH K. p 3293 N94-28839
JUN, OH-SUNG p 3321 N94-30018
JUNCHAT, ALAIN P. p 3259 N94-30511
JUNGLING, K. C. p 3213 N94-28886
JUSTICE, CHARLES p 3144 N94-30644

K

KABAMBA, PIERRE T. p 3154 N94-28632
KACYNSKI, KENNETH JOHN p 3271 N94-28835
KAESE, J. p 3162 N94-29643

KAHLE, ANNE B. p 3331 N94-29228
KAISER, J. H. p 3516 N94-30054
KAISER, W. p 3239 N94-29787
KAISER, W. J. p 3237 N94-29778
p 3238 N94-29785
KAISER, WILLIAM J. p 3236 N94-29777
KAJI, SHOJIRO p 3125 N94-28960
p 3127 N94-28975
KAKIMOTO, YUKIKO p 3387 N94-28495
p 3389 N94-28850
p 3394 N94-29863
KALAYCIOGLU, S. p 3306 N94-30289
KALAYCLOGLU, S. p 3310 N94-30309
KALEJS, J. P. p 3339 N94-30605
KALIKHOV, A. V. p 3551 N94-30845
KALINOWSKI, JOSEPH M. p 3301 N94-29557
KALKHORAN, IRAJ M. p 3122 N94-28899
KALLURI, SREERAMESH p 3317 N94-28819
p 3203 N94-28921
KALMUS, G. E. p 3486 N94-29143
KALOGERAS, CHRIS p 3162 N94-29641
KALSBEEK, MARIANNE p 3424 N94-30386
KAMAI, TAKESHI p 3240 N94-29521
KAMBURYAN, A. F. p 3528 N94-28615
KAMEL, RAAFAT p 3408 N94-28760
KAMEYAMA, YUICHI p 3386 N94-28853
KAMIN, RICHARD A. p 3190 N94-29248
KAMINUMA, KATSUTADA p 3357 N94-29078
p 3363 N94-29978
KAMIO, AKIHIKO p 3159 N94-30794
KAN, LIN p 3218 N94-30036
KANAI, TOSHINOBU p 3495 N94-29596
KANAZAWA, CHRISTINE H. p 3178 N94-29135
KANAZAWA, MAKOTO p 3454 N94-30319
KANDA, SHUJI p 3388 N94-28498
KANDA, TAKESHI p 3123 N94-28953
KANDULSKI, MACIEJ p 3457 N94-30395
KANE, J. p 3480 N94-30786
KANE, R. J. p 3466 N94-30586
KANEHISA, HIROTADA p 3324 N94-28695
KANEKO, ATSUSHI p 3461 N94-30766
KANEKO, NORIHIKO p 3377 N94-29595
KANER, RICHARD B. p 3408 N94-28790
KANEYOSHI, T. p 3525 N94-30164
KANG, NAM KOOK p 3149 N94-30787
KANSAKU, HIROSHI p 3387 N94-28495
p 3389 N94-28850
p 3394 N94-29863
KANT, GOOS p 3423 N94-30345
p 3425 N94-30426
KAPTARI, L. P. p 3484 N94-28610
KARADI, C. p 3515 N94-30009
KARAOGLU, B. p 3487 N94-29500
KARASAWA, HIROKAZU p 3368 N94-29520
KAREV, G. P. p 3467 N94-30088
KARHUMEN, J. p 3419 N94-29680
KARLSSON, T. p 3180 N94-29475
KARMANN, B. p 3384 N94-28452
KARR, GERALD R. p 3173 N94-29848
KARSTILA, KARI p 3407 N94-28411
KARTAVTSEV, O. I. p 3407 N94-28622
KARUBE, YUKIHIRO p 3129 N94-28993
KASHALIKAR, UDAY p 3186 N94-30482
KATAHIRA, TADAMI p 3328 N94-28937
KATANO, SUSUMU p 3511 N94-28750
KATEB, D. p 3462 N94-30971
KATKERE, ARUN p 3442 N94-30548
KATO, KENICHI p 3361 N94-29244
KATO, HIROYASU p 3234 N94-29706
KATO, KEN-ICHI p 3357 N94-29079
KATO, TAKAKUNI p 3390 N94-28856
KATOEN, JOOST-PIETER p 3425 N94-30416
p 3260 N94-30520
KATTA, V. R. p 3192 N94-29262
KATTELUS, H. p 3217 N94-30025
KAUPPINEN, V. p 3230 N94-29187
KAWAGUCHI, MASAYOSHI p 3169 N94-30811
KAWAGUCHI, SADAO p 3357 N94-29078
p 3363 N94-29978
KAWAMATA, SHIGERU p 3233 N94-29702
KAWAMURA, H. p 3201 N94-28460
KAWAMURA, K. p 3447 N94-30580
KAWASHIMA, HIROYUKI p 3187 N94-28678
KAWASHIMA, TOSHIHIKO p 3233 N94-29701
p 3234 N94-29706
KAY, ANTHONY p 3333 N94-29528
KAY, RICHARD B. p 3294 N94-29914
KEAN, ELIZABETH S. p 3414 N94-29330
KEENE, B. J. p 3204 N94-29119
KEILERS, CHARLES HENRY, JR. p 3184 N94-30355
KEITH, JOYCE p 3529 N94-28911
KELLER, GERTA p 3354 N94-28416
KELLER, L. p 3497 N94-30712
KELLER, L. P. p 3482 N94-28493
KELLEY, L. p 3497 N94-30712
KELLEY, L. A. p 3482 N94-28493
KELLOGG, JAMES W. p 3163 N94-29645
p 3267 N94-30198
KELLY, ERON S. p 3381 N94-28432
KELLY, TERRI L. p 3504 N94-29055
KEMPA, K. p 3253 N94-29873
KEMPEL, LEO C. p 3211 N94-30852
KENIK, E. A. p 3459 N94-30412
KENNAWAY, J. R. p 3425 N94-30415
KENNAWAY, J. RICHARD p 3538 N94-28671
KENNEALY, J. P. p 3534 N94-30149
KENNEDY, JOHN M. p 3534 N94-30150
p 3237 N94-29778
KENNY, T. W. p 3238 N94-29785
p 3121 N94-29090
KEPERT, J. L. p 3484 N94-28573
KEPHART, R. D. p 3170 N94-30857
KEPPEL, HENK p 3132 N94-30124
KERHO, MICHAEL K. p 3288 N94-29538
KERLEY, JAMES J. p 3426 N94-30435
KERSTEN, M. L. p 3460 N94-30736
KERSTEN, P. H. M. p 3411 N94-29180
KERSTEN, P. R. p 3329 N94-29173
KETTUNEN, J. p 3377 N94-28877
KEY, J. p 3187 N94-28567
KHALILI, F. p 3147 N94-29594
KHAN, AZHAR MANSUR p 3463 N94-28759
KHAN, FYZODEEN p 3203 N94-28900
KHAN, K. K. p 3459 N94-30413
KHASIDASHVILI, ZURAB p 3425 N94-30414
p 3426 N94-30437
p 3194 N94-29271
KHATIB, F. M. p 3467 N94-30088
KHLEBOPROS, R. G. p 3130 N94-29674
KHODADOUST, ABDOLLAH p 3451 N94-28783
KHOROMSKIJ, B. N. p 3255 N94-30172
KHUDIK, V. N. p 3268 N94-30784
KIBBLE, B. P. p 3187 N94-28675
KIDO, NOBUO p 3553 N94-29512
p 3407 N94-28411
KIHLMAN, MARKKU p 3357 N94-29078
KIKUCHI, KATSUHIRO p 3127 N94-28976
KIKUCHI, KAZUO p 3127 N94-28978
p 3188 N94-28682
KIKUKAWA, NOBUYUKI p 3522 N94-29515
p 3211 N94-29516
KILKENNY, J. D. p 3509 N94-30597
KILLEEN, TIMOTHY L. p 3549 N94-28418
KILROY, PATRICK L. p 3165 N94-28702
KIM, CHI-KYUNG p 3279 N94-30224
KIM, EUISOK p 3170 N94-30864
KIM, JOHN p 3409 N94-28866
KIM, MAN GUEN p 3313 N94-30957
KIM, PAUL Y. p 3321 N94-30018
KIM, SOO YONG p 3276 N94-29849
KIM, YOUNG W. p 3239 N94-29793
KINBARA, AKIRA p 3159 N94-30162
KINCAID, P. p 3382 N94-28441
KINDRED, DARRELL p 3410 N94-29006
KING, DANIEL P. p 3430 N94-29050
KINO, ATSUSHI p 3314 N94-29981
KINOSHITA, MICHIAKI p 3479 N94-29597
KINOSHITA, NOBUYUKI p 3325 N94-28696
KINZER, K. E. p 3221 N94-30826
KIPNIS, I. p 3267 N94-30711
p 3268 N94-30717
KIRCHER, C. J. p 3262 N94-28687
KIRCHNER, D. p 3144 N94-30655
KIRILLOV, I. R. p 3506 N94-29510
KIRIS, ESIN O. p 3149 N94-29005
KIRK, M. A. p 3521 N94-30894
KIRK, RICHARD A. p 3419 N94-29797
KIRSTETTER, B. p 3141 N94-29579
KIRTMAN, BENJAMIN PAUL p 3371 N94-29741
KISEL, I. V. p 3434 N94-28613
KISLIUK, O. F. p 3467 N94-30088
KISSEL, GLEN J. p 3144 N94-29772
KISTLER, DAVID p 3419 N94-29727
KISUGI, SHIN p 3377 N94-29595
KITTEL, TIMOTHY G. F. p 3352 N94-30629
KLARIC, MARIO p 3545 N94-29755
KLASSON, K. T. p 3340 N94-30879
KLEIN, GARY p 3399 N94-28861
KLEIN, S. p 3497 N94-30712
KLEIN, S. R. p 3482 N94-28493
KLEINMAN, L. I. p 3342 N94-28523
KLEM, J. F. p 3510 N94-28484
KLEMM, R. A. p 3511 N94-28570
p 3521 N94-30898
KLENKE, S. E. p 3222 N94-30900
KLEPCZYNSKI, W. J. p 3145 N94-30665
KLEPCZYNSKI, WILLIAM J. p 3297 N94-30666
KLINE, MARTIN D. p 3314 N94-30443
p 3446 N94-30570
KLINGER, DAVID W. p 3399 N94-28861
KLINGLER, KERRY M. p 3354 N94-30464
KLINKER, F. p 3256 N94-30392
KLOBUCHAR, JOHN A. p 3145 N94-30677
KLOKS, T. p 3455 N94-30333
p 3458 N94-30404
p 3458 N94-30405
KLOKS, TON p 3426 N94-30488
KLOP, J. W. p 3459 N94-30412
KLOP, JAN WILLEM p 3425 N94-30415
p 3428 N94-30734
KLOSTERMANN, E. p 3140 N94-29575
KLOTZ, JAMES M. p 3223 N94-30476
KLUEVER, CRAIG ALLEN p 3159 N94-30961
KLUKEN, A. O. p 3206 N94-29947
KLUMPAR, D. M. p 3507 N94-30128
KLUSENER, A. STEVEN p 3448 N94-30731
KLUTE, GLENN p 3402 N94-30210
KNAFELC, M. E. p 3401 N94-29184
KNAPPE, S. p 3261 N94-28546
KNAUER, J. P. p 3509 N94-30597
KNIJNENBURG, PETER p 3457 N94-30393
p 3457 N94-30394
KNIPE, RICHARD LEE p 3322 N94-30258
KNOLL, THOMAS E. p 3287 N94-29400
KNOWLTON, LAWRENCE W. p 3369 N94-28663
KO, FRANK K. p 3298 N94-28838
p 3177 N94-28865
KOBAYAKAWA, MAKOTO p 3127 N94-28980
KOBAYASHI, A. S. p 3317 N94-28761
KOBAYASHI, MIKIO p 3187 N94-28675
p 3553 N94-29512
p 3201 N94-29514
p 3211 N94-29516
KOBAYASHI, SHUNICHI p 3363 N94-29978
KOBAYASHI, TAKAHISA p 3324 N94-28693
KOBAYASHI, TAKAO p 3178 N94-29135
KOBLISH, T. R. p 3154 N94-29263
KOBRICK, JOHN L. p 3383 N94-28447
KOCH, H. p 3261 N94-28546
KOCHETKOV, V. I. p 3489 N94-30050
KOCHETOV, E. A. p 3466 N94-28785
KOCHKIN, V. I. p 3407 N94-28622
KOCIEMBA, P. L. p 3435 N94-29480
KOCKS, U. F. p 3201 N94-28544
KODAIRA, NOBUHIKO p 3332 N94-29231
KODAL, ALI p 3281 N94-30494
KODERA, YOICHI p 3188 N94-28679
KODIYALAM, S. p 3171 N94-29782
KOELINK, H. T. p 3338 N94-30328
KOELLE, D. p 3261 N94-28546
KOENIG, DIETER p 3167 N94-28714
KOERNER, J. G. p 3487 N94-29145
KOFLER, R. R. p 3491 N94-30702
KOGA, KAZUO p 3393 N94-29715
p 3394 N94-29865
KOGA, KEI-ICHI p 3511 N94-28750
KOGA, R. p 3495 N94-30214
KOGA, ROCKY p 3494 N94-29065
KOHLMAN, WILLIAM G. p 3177 N94-28735
KOIDE, YOSHIO p 3485 N94-28624
KOK, J. N. p 3438 N94-30334
p 3424 N94-30347
p 3438 N94-30349
p 3433 N94-30720
KOK, JOOST N. p 3458 N94-30403
p 3459 N94-30430
KOKUBUN, SUSUMU p 3357 N94-29078
p 3359 N94-29233
p 3363 N94-29978
KOLAWOLE, JOSHUA p 3263 N94-28994
KOLB, C. E. p 3344 N94-28597
KOLB, CHARLES E. p 3347 N94-29549
KOLBAS, ROBERT M. p 3498 N94-28780
p 3512 N94-28880
KOLKA, E. p 3508 N94-30192
KOLLER, F. p 3162 N94-29643
KOLODNER, JANET L. p 3417 N94-29390
KON, YOSHIHARU p 3377 N94-29595
KONDO, HIROAKI p 3187 N94-28675
p 3553 N94-29512
KONG, J. A. p 3263 N94-28995
KONISHI, HIROYUKI p 3363 N94-29979
KONO, MICHIKATA p 3228 N94-28940
KONOR, CELAL SUKRU p 3375 N94-30868
KONOTOPSKAYA, E. V. p 3434 N94-28613
KOO, KEE P. p 3288 N94-29699
KOOSH, V. F. p 3268 N94-30907
KOPCHENOV, V. p 3152 N94-29296
p 3152 N94-29300
KORBA, LARRY p 3305 N94-30280
KOREN, B. p 3461 N94-30751
KORHAM, C. p 3171 N94-29782
KORNEEV, D. A. p 3512 N94-28787
KOROBOV, V. I. p 3484 N94-28619
KORSAH, K. p 3500 N94-29928
KORZEKWA, D. A. p 3185 N94-30693
KOSHELYAEVSKY, N. B. p 3475 N94-30679
KOSIER, S. L. p 3263 N94-29025

KOSS, D. A. p 3317 N94-28811
KOSTENKO, B. F. p 3490 N94-30120
KOSUDA, MICHINORI p 3295 N94-30186
KOSUGE, KATSUNORI p 3223 N94-29513
KOTCHER, J. p 3488 N94-30049
KOTIKOV, A. V. p 3485 N94-28758
KOUBEK, RICHARD p 3529 N94-28645
KOUCHAKDJIAN, ARA p 3407 N94-28664
p 3156 N94-28752
p 3156 N94-28753
KOURA, KATSUHISA p 3123 N94-28948
p 3123 N94-28949
p 3123 N94-28950
KOURTIDES, DEMETRIUS A. p 3180 N94-29509
KOVACS, A. p 3203 N94-28900
KOVALENKO, A. D. p 3489 N94-30052
KOVESHNIKOV, S. p 3518 N94-30249
KOVTYUKH, A. S. p 3365 N94-30107
KOWBEL, WITOLD p 3186 N94-30481
KOYMANS, RON p 3260 N94-30520
KOZLOWSKI, M. R. p 3212 N94-28560
p 3501 N94-30599
KRABACH, TIMOTHY N. p 3265 N94-29488
KRAEMER, M. p 3381 N94-28435
p 3382 N94-28439
p 3382 N94-28440
KRAFT, MICHAEL p 3343 N94-28596
KRAMER, ALAN p 3306 N94-30283
KRANENBERG, C. F. p 3213 N94-28886
KRASHENINNIKOV, S. I. p 3493 N94-30881
KRASILSHCHIK, I. S. p 3460 N94-30736
KRASNOPEROV, E. P. p 3517 N94-30195
KRAUSS, A. R. p 3519 N94-30718
KREJCI, ALES p 3505 N94-29075
p 3505 N94-29076
p 3505 N94-29077
KREKELBERG, B. p 3438 N94-30334
KRESS, J. D. p 3509 N94-30752
KRIHA, K. R. p 3224 N94-28901
KRISHNAN, K. M. p 3519 N94-30707
KRISS, JORDAN R. p 3146 N94-29391
KRISTALINSKI, A. p 3268 N94-30904
KRJUKOV, V. p 3152 N94-29296
KROMODIMOELJO, SENTOT p 3421 N94-30155
KROOKS, DAVID A. p 3346 N94-28722
KROUSKY, E. p 3505 N94-29076
KRUETZ, KENNETH K. p 3435 N94-29465
KRUGERS, J. P. H. M. p 3297 N94-28399
KRUZINAUSKAS, JOHN, JR. p 3398 N94-28887
KUDRYASHOV, O. E. p 3490 N94-30182
KUECHENMEISTER, DAVID R. p 3146 N94-29200
KUHNLE, PAUL F. p 3468 N94-30640
KUKHTIN, V. V. p 3421 N94-30077
KULANDER, K. C. p 3493 N94-30891
KULIMANOVA, N. B. p 3487 N94-29502
KUMAR, P. R. p 3461 N94-30821
KUMAZAKI, YASUHITO p 3388 N94-28496
p 3388 N94-28497
KUMMEL, ANDREW C. p 3486 N94-29032
KUNG, H. p 3175 N94-28579
p 3217 N94-30025
p 3185 N94-30693
KUNIMATSU, SUNAO p 3479 N94-29597
KUNITAKE, MANABU p 3360 N94-29238
KUPIEC, STEVEN p 3430 N94-28781
KUPRIYANOV, A. S. p 3209 N94-30253
KURAS, C. p 3197 N94-29457
KURIBAYASHI, KAZUHIKO p 3159 N94-30794
KURODA, SHINICHI p 3125 N94-28961
KUROTAKI, TAKUJI p 3125 N94-28963
KUROTANI, AKEMI p 3387 N94-29713
KURSINSKI, E. R. p 3248 N94-29623
KURTZ, S. R. p 3518 N94-30316
KUSAKAWA, TSUNE p 3377 N94-29595
KUSHMEIDER, PAUL J. p 3468 N94-30640
KUTZBACH, JOHN E. p 3353 N94-30635
p 3353 N94-30638
KUZNETSOV, S. N. p 3362 N94-29935
KWAKKEL, F. p 3426 N94-30435
KWAN, S. p 3491 N94-30719
KWON, I. p 3509 N94-30752
KWON, OHBIN p 3274 N94-29761
KYLLING, ARVE p 3366 N94-30805
KYRILLIDIS, A. p 3451 N94-28792

L

LAAKKO, T. p 3411 N94-29193
LAANANEN, DAVID H. p 3135 N94-28799
LABINI, G. SYLOS p 3442 N94-30549
LABRUJERE, T. E. p 3133 N94-30401
p 3134 N94-30493
LACAN, PHILIPPE p 3414 N94-29326
LACERDA, A. p 3520 N94-30848
LACROIX, SIMON p 3443 N94-30552
LACY, LEE p 3409 N94-28910
LADEVEZE, P. p 3179 N94-29442
LAGATTUTA, F. p 3160 N94-29666
LAGHARI, JAVAID R. p 3166 N94-28713
LAHAYE, R. J. p 3510 N94-30832
LAHITTE, P. p 3255 N94-30153
LAI, M. C. p 3443 N94-30554
LAIEB, N. p 3395 N94-30028
p 3395 N94-30029
LAIRD, C. E. p 3205 N94-29736
LAIRD, R. T. p 3441 N94-30540
LAKEOU, SAMUEL p 3262 N94-28846
LAM, C.-M. GORDON p 3480 N94-30274
LAMBERT, KEVIN M. p 3242 N94-28826
LAMOUREUX, J. p 3491 N94-30369
LANDERS, JOE C. p 3166 N94-28707
LANG, SHERMAN p 3305 N94-30280
LANGE, MICHAEL p 3241 N94-28762
LANGER, D. p 3445 N94-30566
LANGERAK, ROM p 3425 N94-30416
LANGLOIS, B. p 3435 N94-29480
LANNI, THOMAS ROBERT p 3362 N94-29752
LANSING, MATTHEW D. p 3316 N94-29724
LANTZ, E. p 3472 N94-30667
LAPEAN, JAMES W., JR. p 3160 N94-28836
LAPEDES, A. p 3427 N94-30705
LAPOUTRE, J. A. p 3406 N94-30727
LAPPALAINEN, R. p 3217 N94-30025
LARJAVA, KARI p 3186 N94-28407
LARKINA, V. I. p 3365 N94-30223
LARNAC, G. p 3179 N94-29412
LARSEN, E. D. p 3314 N94-30444
LARSEN, R. P. p 3302 N94-29922
LASKE, JANEEN A. p 3189 N94-29140
LATAITIS, RICHARD JOSEPH p 3367 N94-30869
LATALLA, DIEGO p 3425 N94-30416
LAU, D. D. p 3495 N94-30214
LAU, J. H. p 3198 N94-30017
LAU, WAI-MAN p 3401 N94-29093
LAUDAL, D. L. p 3341 N94-28463
LAUER, STEPHEN p 3299 N94-29409
LAUGHON, G. L. p 3510 N94-30832
LAVADOUX, M. p 3332 N94-29417
LAVALLEE, S. p 3395 N94-30028
LAVALLEE, STEPHANE p 3395 N94-30030
LAVERGNE, G. p 3195 N94-29278
LAVERY, DAVE p 3448 N94-30582
LAVERY, DAVID p 3144 N94-30282
LAWRENCE, ANDREA W. p 3412 N94-29287
LAWRENCE, J. M. p 3492 N94-30775
LAWRENCE, LORI p 3299 N94-29409
LAWRENCE, ROBERT M. p 3287 N94-29368
LAWSON, DANIEL E. p 3361 N94-29286
LAWSON, SETH W. p 3397 N94-30457
LAX, P. p 3451 N94-28571
LAYMON, C. A. p 3529 N94-28820
LEBLANC, DAVID p 3515 N94-30032
LEE, B. S. p 3223 N94-30480
p 3222 N94-30906
LEE, CHIN C. p 3499 N94-28813
LEE, D. H. p 3521 N94-30851
LEE, EDWARD A. p 3430 N94-28659
LEE, H. S. p 3485 N94-28741
LEE, HARRY p 3144 N94-30652
LEE, HENRY M. p 3322 N94-30206
LEE, I. p 3223 N94-30474
LEE, JE-HYUN p 3201 N94-28527
LEE, JONATHAN A. p 3186 N94-30482
LEE, P. L. p 3385 N94-29401
LEE, PETER p 3410 N94-29007
LEE, RICHARD Q. p 3267 N94-30198
LEE, S. R. p 3519 N94-30592
LEE, SHIN STEVEN p 3219 N94-30259
LEE, SING H. p 3405 N94-28798
LEE, THOMAS S. p 3442 N94-30545
LEE, XUHUI p 3375 N94-30870
LEE, YIN-NAN p 3342 N94-28523
LEEP, D. A. p 3498 N94-28656
LEERMAKERS, M. A. M. p 3402 N94-30422
LEEVER, P. J. E. p 3438 N94-30373
LEFAVE, G. M. p 3223 N94-30478
LEFEBVRE, A. H. p 3196 N94-29280
LEFEBVRE, D. R. p 3445 N94-30563
LEGUILLOU, MARC p 3141 N94-29581
LEH, M. p 3510 N94-30832
LEHTINEN, K. p 3538 N94-29170
LEI, TING-KWO p 3282 N94-30807
LEJEUNE, D. p 3384 N94-28450
LEMORTON, J. p 3258 N94-30507
LENGSFIELD, B. H., III p 3493 N94-30891
LENNARTSSON, O. W. p 3507 N94-30126
p 3507 N94-30127
p 3507 N94-30128
LENTZ, C. p 3144 N94-30655
LENZ, ROBERT W. p 3212 N94-28661
LEROUX, MARCEL p 3139 N94-29571
LESCHIUTTA, SIGFRIDO p 3468 N94-30642
LESCOE, PAUL p 3144 N94-30282
LESH, JAMES R. p 3293 N94-29493
LESNIAREK-HAMID, J. L. p 3184 N94-30438
LEUNG, EMILY W. p 3229 N94-29371
LEVA, ALBERTO p 3449 N94-30941
LEVIN, KERRY M. p 3137 N94-29559
LEVIN, KLAS p 3179 N94-29425
LEVINE, JUDAH p 3475 N94-30678
p 3476 N94-30684
LEVINE, L. O. p 3527 N94-30041
LEVINE, LINDA p 3407 N94-28633
p 3407 N94-28639
LEVINE, STEPHEN E. p 3545 N94-29834
LEVY, R. p 3247 N94-29615
LEW, H. p 3481 N94-28471
LEWANDOWSKI, A. p 3514 N94-29801
LEWANDOWSKI, LEON p 3443 N94-30550
LEWANDOWSKI, W. p 3144 N94-30648
p 3145 N94-30665
LEWIS, B. F. p 3422 N94-30197
LEWIS, G. p 3258 N94-30506
LEWIS, RICHARD L. p 3398 N94-29313
LI, BO p 3334 N94-30037
LI, C. p 3506 N94-30045
LI, JIAN p 3182 N94-29964
LI, JIYUE J. p 3378 N94-30790
LI, MING p 3526 N94-30433
LI, SHENG S. p 3511 N94-28734
LI, TIANMING p 3371 N94-29763
LI, ZHUANG p 3214 N94-29105
LIAW, CHYUAN-HSYAN PAUL p 3132 N94-29973
LIBBY, J. M. p 3238 N94-29783
LIBBY, S. B. p 3295 N94-30060
LIBBY, STUART I. p 3498 N94-28804
LICHTEN, S. M. p 3144 N94-30650
LIEBE, H. J. p 3256 N94-30497
LIEBERMAN, HARRIS B. p 3398 N94-29027
LIEBSCHER, PETER p 3536 N94-30918
LIEN, T. K. p 3229 N94-29996
LIEU, D. K. p 3468 N94-28459
LIGHSTONE, LEONARD p 3153 N94-30130
LILIENTHAL, GERALD W. p 3162 N94-29638
LILJEQUIST, D. p 3494 N94-30980
LILLARD, ROBERT SCOTT p 3209 N94-30521
LIM, HOCK-BIN p 3130 N94-29760
LIM, WILLIAM p 3440 N94-30532
LIN, GANG p 3235 N94-29769
p 3238 N94-29786
LIN, HAI p 3473 N94-30671
LIN, J. P. p 3498 N94-28656
LIN, LONG-JI p 3437 N94-29853
LIN, Y. p 3220 N94-30778
LIN, YAO-QUN p 3312 N94-30809
LINDL, J. D. p 3509 N94-30597
LINDQVIST, P. p 3453 N94-29439
LINDSAY, P. A. p 3504 N94-28686
LINDWALL, DENNIS p 3355 N94-28737
LINEHAN, J. C. p 3240 N94-30473
LINJAMA, JUKKA p 3316 N94-28404
LINSKENS, JEFFREY R. p 3551 N94-29212
LIPINSKI, R. J. p 3295 N94-30265
LISCANO, RAMIRO p 3305 N94-30280
LISOSKI, DEREK LEE ASHTON p 3275 N94-29838
LISSE, CAREY MICHAEL p 3541 N94-29994
LITVIN, F. L. p 3303 N94-30205
LITVINENKO, E. I. p 3286 N94-28553
LITZINGER, THOMAS A. p 3224 N94-28879
LIU, HUA-KUANG p 3499 N94-29491
LIU, S. p 3519 N94-30718
LIU, S. H. p 3511 N94-28570
LIU, SAMUEL H. p 3521 N94-30898
LIU, XIAOFAN p 3261 N94-30673
LOB, W. STUART p 3447 N94-30576
LOEVE, W. p 3123 N94-28947
p 3428 N94-30739
p 3433 N94-30913
LOEW, G. p 3292 N94-28481
LOFGREN, BRENT MELVIN p 3348 N94-29800
LOH, CHING Y. p 3272 N94-29096
LOIBL, JOSEPH M. p 3440 N94-30534
LOKENSGARD, ROLF M. p 3145 N94-28660
LOMBARDO, CHARLES P. p 3410 N94-29152
LOMKOV, K. p 3152 N94-29296
p 3152 N94-29300
LONCLE, M. p 3384 N94-28450
LONG, CLAUDINE p 3529 N94-28911
LONG, DAVID WILLIAM p 3334 N94-29959
LONG, JUNSHENG p 3431 N94-29869
LONGENECKER, FREDRIC W. p 3178 N94-29166
LONGSINE, DENNIS E. p 3315 N94-29020
LOOFBOURROW, NATHAN p 3499 N94-29059
LOOGER, LOREN L. p 3354 N94-30463
LOOIJE, C. E. W. p 3153 N94-30914
LOOKE, T. D. p 3306 N94-30287
p 3308 N94-30295

LOOMIS, G. E. ..... p 3212 N94-28560
LOOMIS, H. H., JR. ..... p 3432 N94-30100
LOOYEN, WIM J. ..... p 3335 N94-30759
LOPEZ, C. W. ..... p 3337 N94-29018
LOPEZ, G. ..... p 3195 N94-29275
LOPEZ, P. C. ..... p 3210 N94-30776
LORD, J. D. ..... p 3184 N94-30419
LORENTZEN, G. ..... p 3279 N94-29999
LORIMER, W. L. ..... p 3468 N94-28459
LOTT, JAMES A. ..... p 3293 N94-28919
LOTZ, W. G. ..... p 3383 N94-28448
LOUBET, DANIEL ..... p 3179 N94-29454
LOVE, JEFFREY JAMES ..... p 3366 N94-30808
LOVEJOY, M. L. ..... p 3515 N94-30006
LOVELL, T. ..... p 3278 N94-29977
LOWDEN, R. A. ..... p 3185 N94-30593
LOWE, DAVID M. ..... p 3180 N94-29509
LOWE, DONALD R. ..... p 3354 N94-28416
LOWER, M. C. ..... p 3148 N94-29887
LOWRIE, B. W. ..... p 3190 N94-29249
LOY, D. A. ..... p 3174 N94-28557
LU, JIE ..... p 3367 N94-30921
LUBBEN, D. ..... p 3520 N94-30773
LUCASIUS, C. B. ..... p 3535 N94-30330
LUDEWIG, H. ..... p 3497 N94-30588
LUDEWIGT, B. ..... p 3268 N94-30717
LUDWIG, F. ..... p 3261 N94-28546
LUEPTOW, RICHARD M. ..... p 3271 N94-28778
LUFKIN, ERIC ANDREW ..... p 3544 N94-29725
LUHMANN, H.-J. ..... p 3162 N94-29643
LUM, G. K. ..... p 3291 N94-30218
LUNA-ACOSTA, G. A. ..... p 3524 N94-30086
LUND, GLENN ..... p 3246 N94-29542
p 3336 N94-30965
LUNDGREN, J. R. ..... p 3451 N94-28651
LUNDGREN, L. ..... p 3244 N94-29177
LUNDIN, C. D. ..... p 3203 N94-28900
LUNTZ, MICHAEL ..... p 3241 N94-28762
LUO, J. ..... p 3519 N94-30718
LUSH, SCOTT C. ..... p 3499 N94-29694
LUSSIER, J. G. ..... p 3209 N94-30246
LUTES, C. C. ..... p 3347 N94-29192
LUTTON, MARK JOHN ..... p 3134 N94-30865
LYAPIN, V. G. ..... p 3489 N94-30051
LYCZKOWSKI, R. W. ..... p 3279 N94-30020
LYENGAR, A. ..... p 3204 N94-29196
LYNCH, D. L. ..... p 3509 N94-30752
LYNCH, HARRY J. ..... p 3398 N94-29027
LYON, J. F. ..... p 3508 N94-30339
LYUBOVITSKIJ, V. E. ..... p 3487 N94-29502
LYUBUTIN, I. S. ..... p 3513 N94-29210

M

MA, D. I. ..... p 3266 N94-30040
MA, J. T. ..... p 3266 N94-29527
MAAHS, HOWARD G. ..... p 3186 N94-30481
MAAS, M. ..... p 3439 N94-30531
MAAS, P. A. ..... p 3482 N94-28531
MAAS, R. ..... p 3494 N94-29422
MABRY, D. J. ..... p 3347 N94-29023
MACCRACKEN, MICHAEL C. ..... p 3352 N94-30634
p 3353 N94-30638
MACIASZEK, T. ..... p 3168 N94-29543
MACIEL, A. K. A. ..... p 3493 N94-30887
MACKAY, D. J. ..... p 3308 N94-30296
MACKAY, DAVID J. ..... p 3304 N94-30275
MACKAY, R. A. ..... p 3201 N94-28525
MACKENZIE, D. R. ..... p 3223 N94-30480
p 3222 N94-30906
MACLEOD, NORMAN ..... p 3354 N94-28416
MACMILLAN, A. J. F. ..... p 3383 N94-28446
MACPHEE, JOHN ANTHONY ..... p 3187 N94-28678
MADABHUSHI, RAVI KUMAR ..... p 3275 N94-29809
MADARAS, ERIC I. ..... p 3315 N94-29548
MADDEN, M. J. ..... p 3163 N94-29644
MADDUX, GARY A. ..... p 3316 N94-29724
MAEDA, TAKASHI ..... p 3386 N94-28853
MAEDA, YUKIO ..... p 3295 N94-30186
MAEKAWA, ETSUJI ..... p 3314 N94-29984
MAEKELAE, I. ..... p 3452 N94-29171
MAENNISTOE, T. ..... p 3530 N94-29172
MAENO, HIDEO ..... p 3360 N94-29238
MAENTYLAE, M. ..... p 3411 N94-29193
MAES, CARL F. ..... p 3499 N94-28875
MAGALHAES, ANTONIO MARIO ..... p 3543 N94-29696
MAGGIOLINI, P. ..... p 3536 N94-30929
MAGNUSEN, P. E. ..... p 3202 N94-28830
MAGRUDER, R. H., III ..... p 3207 N94-30042
p 3219 N94-30335
MAHAJAN, S. ..... p 3507 N94-30071
MAHDAVI, M. A. ..... p 3510 N94-30832
MAHLICH, S. E. ..... p 3139 N94-29573
MAIDHOF, S. ..... p 3154 N94-29254
MAIDMENT, G. ..... p 3379 N94-28423
MAIN, JOHN ALAN ..... p 3403 N94-30799
MAINETTI, LUCA ..... p 3260 N94-30940
MAINGI, R. ..... p 3510 N94-30832
MAITRE, HENRI ..... p 3395 N94-30970
MAJKOWSKI, PATRICIA ..... p 3186 N94-30482
MAK, KIN WAH ..... p 3490 N94-30141
MAKARENKO, T. M. ..... p 3451 N94-28783
MAKIHARA, MASAKI ..... p 3228 N94-28941
MAKINO, MITSUO ..... p 3522 N94-29515
MAKITA, KAZUO ..... p 3361 N94-29244
MAKOFSKE, W. J. ..... p 3349 N94-30023
MALA, W. ..... p 3414 N94-29325
MALDONADO, JAIME J. ..... p 3279 N94-30147
MALEK, F. ..... p 3453 N94-30119
MALEK, FADI ..... p 3454 N94-30241
MALEKI, L. ..... p 3475 N94-30682
MALILA, WILLIAM ..... p 3326 N94-28929
MALITSKY, N. ..... p 3487 N94-29700
MALLICK, SUBHASHIS ..... p 3355 N94-28737
MALOY, S. A. ..... p 3185 N94-30693
MALTSEVA, S. M. ..... p 3485 N94-28621
MALYSHEVSKIJ, V. S. ..... p 3512 N94-28787
MAMEDOV, T. N. ..... p 3517 N94-30195
MAMMONE, R. J. ..... p 3223 N94-30479
MAN, KIN F. ..... p 3229 N94-29371
MANABE, MOTOHUMI ..... p 3234 N94-29703
MANCINI, RON ..... p 3160 N94-29627
MANDREKAS, J. ..... p 3509 N94-30760
MANDRUS, D. ..... p 3520 N94-30848
MANELLA, RICHARD T. ..... p 3319 N94-29406
MANGASARIAN, OLVI L. ..... p 3431 N94-29127
MANGIN, J. F. ..... p 3297 N94-30666
MANICKAM, J. ..... p 3509 N94-30768
MANNINEN, A. ..... p 3477 N94-29186
MANNONEN, L. ..... p 3379 N94-28408
MANO, TADAAKI ..... p 3387 N94-28495
p 3389 N94-28850
p 3394 N94-29863
MANO, TAKAICHI ..... p 3394 N94-29865
p 3389 N94-28852
p 3386 N94-28853
MANORE, MICHAEL J. ..... p 3327 N94-28934
MANZ, ALLAN ..... p 3305 N94-30280
MARACAS, GEORGE N. ..... p 3499 N94-29114
MARBLE, DOUGLAS C. ..... p 3377 N94-29164
MARCHAL, R. ..... p 3257 N94-30501
MARCHELLO, JOSEPH M. ..... p 3213 N94-28748
p 3180 N94-29485
MARCHMENT, A. D. ..... p 3194 N94-29274
MAREFAT, MICHAEL M. ..... p 3442 N94-30547
MAREK, C. JOHN ..... p 3150 N94-28923
MARKING, G. A. ..... p 3209 N94-30336
MARKO, MICHAEL ..... p 3387 N94-30461
MARKOV, ALEX B. ..... p 3149 N94-30293
MARKS, R. F. ..... p 3519 N94-30707
MAROM, ITSHAK ..... p 3303 N94-30135
MARR, R. B. ..... p 3206 N94-29931
MARRA, JOHN J. ..... p 3298 N94-29353
MARRON, JOSEPH C. ..... p 3446 N94-30575
MARSHALL, CRAIG ..... p 3341 N94-30486
MARTIN, CHARLES R. ..... p 3197 N94-29312
MARTIN, H. O. ..... p 3521 N94-30888
MARTINEZ, ANDREW B. ..... p 3377 N94-29204
p 3478 N94-29206
MARU, RURIKO ..... p 3386 N94-28853
MARUYAMA, KATSUHISA ..... p 3522 N94-29515
MARZWELL, NEVILLE I. ..... p 3314 N94-30441
p 3314 N94-30442
MASCHKE, B. M. ..... p 3462 N94-30964
MASLANIK, J. A. ..... p 3377 N94-28877
MASON, JAMES JOSEPH ..... p 3321 N94-29808
MASON, KEVIN T. ..... p 3388 N94-28757
MASON, NORM ..... p 3144 N94-30644
MASSIMINO, MICHAEL J. ..... p 3446 N94-30569
MASSON, J. ..... p 3225 N94-29414
MAST, J. E. ..... p 3254 N94-29929
MASTERS, W. C. ..... p 3159 N94-29656
MASUDA, HIROSHI ..... p 3233 N94-29701
MASUDA, MAKOTO ..... p 3387 N94-28495
p 3389 N94-28850
p 3394 N94-29863
MASUKO, MASABUMI ..... p 3218 N94-30177
MASUOKA, EDWARD J. ..... p 3231 N94-29385
MASUYA, TOSHIKAZU ..... p 3234 N94-29705
MATHER, JAMES ..... p 3342 N94-28589
MATIC, P. ..... p 3317 N94-28811
MATOCHKIN, E. P. ..... p 3508 N94-30191
MATOUSEK, JIRI ..... p 3424 N94-30348
p 3460 N94-30721
MATSON, D. W. ..... p 3240 N94-30473
MATSOS, HELEN C. ..... p 3354 N94-30463
MATSUHIRO, DENNIS ..... p 3163 N94-29648
MATSUMOTO, HIROAKI ..... p 3123 N94-28948
p 3123 N94-28949
p 3123 N94-28950
MATSUMURA, AKIMITSU ..... p 3188 N94-28679
MATSUNAGA, KOJI ..... p 3127 N94-28978
MATSUO, EITO ..... p 3128 N94-28983
MATSUOKA, AKINORI ..... p 3127 N94-28976
MATSUOKA, K. ..... p 3505 N94-29398
MATSUZAKI, TATSUYA ..... p 3129 N94-28992
MATTABONI, PAUL ..... p 3447 N94-30577
MATTEODA, ANNA MARIA ..... p 3335 N94-30919
MATTICK, ARTHUR T. ..... p 3505 N94-29134
MATTSSON, J. ..... p 3385 N94-29156
MAUDRY, BERNARD ..... p 3141 N94-29583
MAUS, DARYL ..... p 3162 N94-29637
MAUW, SJOUKE ..... p 3260 N94-30520
MAY, G. B. ..... p 3317 N94-28761
MAYBEE, JOHN S. ..... p 3451 N94-28651
MAYER, JAMES W. ..... p 3512 N94-28889
MAYER, T. M. ..... p 3219 N94-30263
MAYERGOYZ, I. D. ..... p 3260 N94-30902
MAYFIELD, M. J. ..... p 3338 N94-30048
MAYOL, R. ..... p 3494 N94-30980
MAYR, B. ..... p 3381 N94-28435
MAYR, R. ..... p 3443 N94-30554
MAZUR, V. S. ..... p 3500 N94-30075
MAZZETTI, P. ..... p 3256 N94-30496
MCALLISTER, S. W. ..... p 3270 N94-28476
MCBEE, CHARLES L. ..... p 3243 N94-29064
MCBREEN, J. ..... p 3485 N94-28741
MCBRIDE, S. L. ..... p 3148 N94-30129
MCBRIDE, STUART L. ..... p 3148 N94-30131
MCCAIN, J. WAYNE ..... p 3173 N94-29544
MCCAIN, WAYNE ..... p 3537 N94-29410
MCCALDON, K. ..... p 3154 N94-29264
MCCALLEN, D. B. ..... p 3321 N94-29951
MCCALLEN, R. ..... p 3211 N94-30892
MCCALLUM, J. C. ..... p 3199 N94-30723
MCCALLUM, W. G. ..... p 3467 N94-29162
MCCARTNEY, L. N. ..... p 3181 N94-29524
MCCARTY, WILLIAM ..... p 3144 N94-29794
MCCOLLUM, TIMOTHY A. ..... p 3172 N94-28999
MCCORMAC, A. W. ..... p 3310 N94-30311
MCCUBIN, L. ..... p 3297 N94-30666
MCCURDY, DAVID A. ..... p 3479 N94-29464
MCCURDY, H. C. ..... p 3230 N94-29017
MCDANIEL, PATRICIA D. ..... p 3215 N94-29451
MCELIECE, R. J. ..... p 3247 N94-29618
MCEWEN, M. R. ..... p 3290 N94-30782
MCFEE, J. ..... p 3310 N94-30311
MCGEE, WILLIAM F. ..... p 3298 N94-29351
p 3204 N94-29380
p 3303 N94-30173
MCGIBBON, A. J. ..... p 3516 N94-30063
MCGIBBON, M. M. ..... p 3516 N94-30064
MCGINNESS, MICHAEL P. ..... p 3240 N94-30468
MCGRATH, BRIAN E. ..... p 3130 N94-29443
MCHUGH, KEVIN M. ..... p 3186 N94-30447
MCHUGH, PAUL D. ..... p 3347 N94-28844
MCINTOSH, ROBERT ..... p 3259 N94-30509
MCKAY, M. ..... p 3310 N94-30308
MCKAY, R. L. ..... p 3406 N94-30004
MCKENZIE, D. L. ..... p 3347 N94-29023
MCKINNEY, R. G. ..... p 3194 N94-29272
MCKONE, T. E. ..... p 3349 N94-30044
MCLELLAN, TOM M. ..... p 3391 N94-29049
MCMANUS, J. BARRY ..... p 3344 N94-28597
MCMATH, W. S. ..... p 3144 N94-30286
MCNAMARA, DAVID K. ..... p 3176 N94-28653
MCNEELEGE, GLENN E. ..... p 3446 N94-30571
MCNEELY, MARY ..... p 3398 N94-28887
MCNEIL, R. ..... p 3491 N94-30762
MCNEILL, DEAN KEVIN ..... p 3432 N94-30140
MCNEILL, STEPHEN R. ..... p 3316 N94-29724
MCNULTY, P. J. ..... p 3201 N94-30220
MCPHAIL, ANDREW T. ..... p 3513 N94-29130
p 3486 N94-29131
p 3513 N94-29155
MCQUAIL, WILLIAM H. ..... p 3527 N94-29153
MCVANEY, GARY P. ..... p 3146 N94-28870
MEAD, JAMES ..... p 3259 N94-30509
MEADOWS, J. W. ..... p 3497 N94-30825
MEARST, J. O. ..... p 3515 N94-30009
MEDVED, S. V. ..... p 3500 N94-30075
MEERKOV, SEMYON M. ..... p 3154 N94-28632
MEERTENS, LAMBERT G. L. T. ..... p 3418 N94-29487
p 3402 N94-30320
MEEUSSEN, V. C. S. ..... p 3455 N94-30346
MEGURO, AKIRA ..... p 3161 N94-29631
MEHLUM, E. ..... p 3378 N94-30002
MEHTA, MANISH ..... p 3446 N94-30575
MEIER, G. J. ..... p 3219 N94-30245
MEIER, GERALD J. ..... p 3354 N94-30466
MEIJER, JOS J. ..... p 3148 N94-30342
MEINER, THOMAS ..... p 3166 N94-28704
p 3166 N94-28705
MEISENHEIMER, CHARLES C. ..... p 3477 N94-29117
MEKJAVIC, IGOR B. ..... p 3380 N94-28428
MELILLO, MICHAEL R. ..... p 3241 N94-28771

MELISSARATOS, ELEFTERIOS A. p 3458 N94-30406
p 3462 N94-30860
MELIUS, C. F. p 3222 N94-30909
MELIZA, LARRY L. p 3528 N94-28637
MELLO, MARK D. p 3178 N94-29024
MELLSTROM, J. A. p 3248 N94-29622
MELNGAILIS, JOHN p 3264 N94-29305
MENA, R. A. p 3264 N94-29209
MENDELSOHN, JAY p 3440 N94-30532
MENDES, R. V. p 3523 N94-29146
p 3464 N94-29178
MENDEZ, J. p 3180 N94-29478
MENDILLO, MICHAEL p 3356 N94-28891
MENGUY, Y. p 3395 N94-30028
p 3395 N94-30029
MENON, M. M. p 3510 N94-30832
MENON, RAMESH GOPAL p 3154 N94-29532
MERKEL, P. p 3505 N94-29483
MERKULOV, L. A. p 3421 N94-30083
MERRILL, W. p 3155 N94-30204
MERRITT, SYLVIA A. p 3197 N94-29356
MERWIN, L. p 3223 N94-30477
MERZ, SARAH K. p 3451 N94-28651
MESCHLER, MICHAEL F. p 3446 N94-30569
MESSER-YARON, HAGIT p 3408 N94-28760
METCALF, W. p 3491 N94-30762
METTLER, EDWARD p 3144 N94-29792
MEUNIER, S. p 3154 N94-29258
p 3194 N94-29273
MEYER-HILBERG, JOCHEN p 3138 N94-29565
MEYER, F. p 3471 N94-30657
MEYER, J. p 3501 N94-30828
MEYER, J. J. C. p 3428 N94-30749
MEYER, L. G. p 3383 N94-28448
MEYER, W. T. p 3406 N94-30004
MICHALAKES, J. p 3350 N94-30116
MICHALSKY, J. J. p 3269 N94-28464
MICHAUD, W. F. p 3207 N94-30021
MICHELI, P. L. p 3338 N94-30313
MICHELIN, P. p 3215 N94-29459
MICKELSON, MARK p 3369 N94-28663
MICOUIN, PATRICE M. p 3413 N94-29322
MIELKE, ROLAND p 3408 N94-28825
MIGLIORI, A. p 3480 N94-30098
MIKAMI, HISASHI p 3128 N94-28985
MIKI, KEIJI p 3187 N94-28677
MIKLICH, A. H. p 3261 N94-28546
MIKULAS, MARTIN, JR. p 3245 N94-29360
MILEANT, A. p 3251 N94-29669
MILES, E. S. p 3444 N94-30560
MILES, P. C. p 3311 N94-30596
MILIOS, E. p 3439 N94-30529
MILIOS, EVANGELOS p 3309 N94-30301
MILITELLO, LAURA G. p 3399 N94-28861
MILLER-WAY, CHRISTINE A. p 3286 N94-28831
MILLER, CLYDE p 3140 N94-29577
MILLER, DAVID J. p 3445 N94-30565
MILLER, DAVID P. p 3444 N94-30556
p 3447 N94-30578
MILLER, G. F. p 3322 N94-30523
MILLER, GEORGE W. p 3337 N94-29033
MILLER, J. L. p 3180 N94-29472
MILLER, JAMES G. p 3183 N94-30016
MILLER, JOSEPH p 3140 N94-29577
MILLER, L. p 3152 N94-29296
MILLER, LEE S. p 3252 N94-29739
MILLER, P. p 3422 N94-30251
MILLER, R. L. p 3508 N94-30339
MILLER, ROBERT A. p 3205 N94-29507
MILLER, ROBERT P. p 3319 N94-29406
MILLER, S. D. p 3491 N94-30695
MILLIES, P. p 3435 N94-29480
MILLION, S. p 3250 N94-29665
p 3251 N94-29669
MILLS, S. p 3193 N94-29265
MILLY, PETER F., SR. p 3300 N94-29506
MILNE, T. A. p 3339 N94-30606
MILNOR, J. p 3335 N94-30610
MILTON, MARTHA E. p 3161 N94-29636
MINEEV, YU. V. p 3365 N94-30223
MING, DOUGLAS W. p 3236 N94-29776
MINODA, TAKASHI p 3358 N94-29082
MINOWA, TOMOAKI p 3387 N94-29519
MINSON, C. p 3400 N94-28902
MINTZ, M. p 3311 N94-30703
MIODUSZEWSKI, P. K. p 3510 N94-30832
MIRDAMADI, MASSOUD p 3177 N94-28823
MIRIN, A. A. p 3563 N94-30844
MIRZAEI, MAJID p 3321 N94-29812
MISAWA, SHIGEO p 3368 N94-29520
MISIRLIOGLU, LEVENT p 3244 N94-29094
MISRA, AJAY K. p 3181 N94-29684
MISSOUM, AZZEDINE p 3276 N94-29839
MITCHELL, BRIAN T. p 3314 N94-30442
MITCHELL, CURTIS RANDALL p 3278 N94-29965
MITCHELL, T. E. p 3175 N94-28579
MITSUI, YUKIO p 3158 N94-28583
MIWA, CHIHIRO p 3394 N94-29865
MIYAJIMA, DAISUKE p 3170 N94-30932
MIYAMOTO, AKIRA p 3388 N94-28498
p 3393 N94-29717
MIYANAGA, T. p 3199 N94-30267
MIYAOKA, HIROSHI p 3359 N94-29234
MIYASATO, S. M. p 3202 N94-28830
MIYATA, KAZUHITO p 3126 N94-28969
MIYATA, YASUNORI p 3227 N94-28939
MIYAUCHI, MASAMI p 3159 N94-30794
MIYAZAKI, AKIRA p 3187 N94-28675
p 3553 N94-29512
MIZUGUCHI, K. p 3397 N94-30458
MIZUMOTO, KIYOSHI p 3394 N94-29867
MIZUNO, KOH p 3388 N94-28496
p 3388 N94-28497
MIZUNO, KOICHI p 3187 N94-28675
p 3553 N94-29512
MIZUNO, TAKANORI p 3324 N94-28694
MIZUNO, TATEKI p 3354 N94-29522
MOAK, E. p 3535 N94-30179
MOCHIZUKI, MUNEKAZU p 3128 N94-28987
p 3128 N94-28988
MODINE, F. A. p 3520 N94-30773
MODLIN, NORMAN R. p 3369 N94-29183
MOEHLENKAMP, KLAUS p 3141 N94-29584
MOERDIJK, IEKE p 3457 N94-30384
MOFFAT, H. K. p 3221 N94-30896
MOLEZZI, MICHAEL JOSEPH p 3282 N94-30791
MONACO, LISA A. p 3515 N94-30015
MONACO, M. p 3245 N94-29456
MONDAY, SUSAN D. p 3527 N94-28796
MONGIA, HUKAM C. p 3154 N94-29256
MONHEISER, JEFFERY p 3173 N94-29546
MONROE, D. K. p 3169 N94-30264
p 3295 N94-30367
MONSON, P. A. p 3226 N94-30708
MONTASER, A. p 3503 N94-28458
MONTGOMERY, ROBERT p 3241 N94-28762
MONTMINY, B. p 3305 N94-30278
MOOKERJEE, A. p 3208 N94-30118
MOON, SUNG BEEN p 3532 N94-29806
MOORE, BERRIEN, III p 3351 N94-30624
p 3351 N94-30625
MOORE, K. R. p 3240 N94-28522
MOORE, THOMAS J. p 3301 N94-29557
MOREL, M. R. p 3151 N94-29103
p 3319 N94-29104
MORELLA, G. L. p 3478 N94-29388
MORENO, J. C. p 3295 N94-30060
MORENOVAZQUEZ, J. M. p 3382 N94-28444
MORGAN, BEN B., JR. p 3527 N94-28796
MORGAN, D. p 3486 N94-29112
MORGAN, S. H. p 3219 N94-30335
MORGAN, WILLIAM p 3144 N94-29794
MORGENTHALER, DANIEL R. p 3164 N94-28417
MORI, NOBUO p 3511 N94-28750
MORIGUCHI, AKIHIKO p 3234 N94-29703
MORIN, GREGORY S. p 3176 N94-28654
MORIOKA, SHIGEKI p 3126 N94-28968
MORISHIGE, HIROSHI p 3129 N94-28993
MORITA, YASUO p 3233 N94-29701
MORITA, YUHEI p 3158 N94-28583
MORIWAKI, KIICHI p 3357 N94-29080
MORRELL, R. p 3322 N94-30114
p 3184 N94-30524
MORRIS, A. TERRY p 3466 N94-29489
MORRIS, D. p 3297 N94-30664
MORRIS, DEBRA A. p 3530 N94-29138
MORRIS, J. B. p 3211 N94-28516
MORRIS, R. V. p 3236 N94-29774
MORRIS, TIMOTHY B. p 3300 N94-29506
MORRIS, V. R. p 3368 N94-28455
MORRISETT, J. G. p 3410 N94-29006
MORRISON, DENNIS R. p 3397 N94-30453
MORRISON, J. p 3289 N94-30059
MORRISON, J. J. p 3281 N94-30600
MORSE, SARAH K. p 3443 N94-30555
MORTON, P. p 3292 N94-28481
MOSES, C. A. p 3224 N94-28502
MOSES, CLIFFORD p 3197 N94-29285
MOSIER, BENJAMIN p 3397 N94-30453
MOSS, J. B. p 3191 N94-29252
MOTEGI, TETSUICHI p 3159 N94-30794
MOU, CHUNG-YU p 3274 N94-29730
MOUCHOT, MARIE-CATHERINE p 3327 N94-28934
MOUNT, GEORGE H. p 3344 N94-28598
MOURA-PIRES, FERNANDO p 3445 N94-30567
MOURAD, ANTOINE NAGIB p 3418 N94-29404
MRIG, L. p 3339 N94-30601
MUEHL, W. W., SR. p 3341 N94-30465
MUEHLNER, E. p 3162 N94-29643
MUELLER, ERIC M. p 3530 N94-29165
MUELLER, R. O. p 3248 N94-29625
MUGNUOLO, R. p 3442 N94-30549
MUIR, H. C. p 3148 N94-29887
MUJIBURRAHMAN, S. M. p 3487 N94-29500
MUKHANOV, O. p 3262 N94-28767
MULARZ, EDWARD J. p 3195 N94-29277
MULCAHY, T. M. p 3468 N94-28459
MULLEN, E. G. p 3552 N94-29046
MULLIN, C. S. p 3476 N94-30841
MUNRO, D. p 3509 N94-30597
MURA, T. p 3202 N94-28867
MURAKAMI, AKIRA p 3387 N94-29711
MURAKAMI, S. p 3506 N94-29499
MURAKOSHI, HEITA p 3188 N94-28680
MURAO, RINICHI p 3126 N94-28969
MURASE, TAKEO p 3129 N94-28992
MURDZA, CHRISTINE p 3417 N94-29392
MURPHY, K. D. p 3479 N94-29461
MURPHY, O. J. p 3318 N94-29057
MURPHY, P. W. p 3510 N94-30875
MURTHY, D. V. p 3319 N94-29104
MUSLINER, DAVID J. p 3445 N94-30564
MUTHARASAN, RAJAKKANNU p 3298 N94-28838
MUTOH, T. p 3506 N94-29499
MUTTER, SUSAN H. p 3380 N94-28429
MYERS, B. p 3405 N94-28916
MYERS, D. R. p 3501 N94-30828
MYERS, D. W. p 3254 N94-30043
MYERS, SCOTT D. p 3441 N94-30538
MYERS, WILLIAM NEILL p 3299 N94-29365
MYHRE, CRAIG A. p 3167 N94-28814
p 3167 N94-29383
MYRABO, LEIK N. p 3150 N94-28923
MYSOOR, N. R. p 3248 N94-29625

N

NADEL, LYNN p 3466 N94-28807
NAERHI, T. p 3261 N94-28400
NAGAMATSU, HENRY T. p 3150 N94-28923
NAGAMIYA, S. p 3484 N94-28576
NAGAOKA, SHUNJI p 3387 N94-29713
p 3393 N94-29717
NAGASAKA, TETSUO p 3394 N94-29864
NAGASHIMA, NOBUYA p 3158 N94-28583
NAGASHIMA, TOSHIO p 3127 N94-28977
NAGASUBRAMANIAN, GANESAN p 3264 N94-29357
NAGATOMO, MAKOTO p 3164 N94-29714
NAGY, KORNEL p 3160 N94-29369
NAIK, SANJEEV MANUBHAI p 3437 N94-29895
NAIRN, DONALD p 3416 N94-29340
NAIRUS, JOHN G. p 3165 N94-28699
p 3263 N94-28913
NAITO, YASUHIKO p 3357 N94-29078
p 3358 N94-29083
p 3363 N94-29978
NAKADA, HIDEAKI p 3377 N94-29595
NAKADATE, MASAAKI p 3124 N94-28957
NAKAGAWA, SHINJI p 3324 N94-28693
NAKAHASHI, KAZUHIRO p 3125 N94-28962
p 3127 N94-28979
NAKAIZUMI, MASAMITSU p 3234 N94-29703
NAKAJIMA, MASASHI p 3314 N94-29982
p 3364 N94-29983
NAKAJIMA, N. p 3506 N94-29499
NAKAMICHI, JIRO p 3126 N94-28969
NAKAMURA, KINUYO p 3129 N94-28990
NAKAMURA, MASAKAZU p 3188 N94-28682
p 3211 N94-29516
NAKAMURA, SHINGO p 3125 N94-28964
NAKAMURA, SHUICHI p 3129 N94-28991
p 3129 N94-28992
NAKAMURA, TAKASHI p 3129 N94-28991
p 3129 N94-28992
NAKAMURA, YOSHIAKI p 3126 N94-28971
NAKANO, Y. p 3199 N94-30267
NAKANO, YOSHISUKE p 3357 N94-29070
NAKAO, MASAHIRO p 3124 N94-28958
p 3125 N94-28966
NAKATSUBO, TAKAYUKI p 3358 N94-29085
NAKAYAMA, KATSUYA p 3328 N94-28937
p 3332 N94-29231
NAKAYAMA, YOSHIO p 3479 N94-29597
NAKAZATO, SHOZO p 3170 N94-30932
NAMBA, CHUSEI p 3295 N94-30186
NARASIMHAN, S. p 3206 N94-29931
NASR, HATEM p 3171 N94-29791
NASTASI, M. p 3175 N94-28579
p 3217 N94-30025
NASTASI, MICHAEL p 3517 N94-30201
NATESAN, K. p 3207 N94-30057
NATH, BIMAN BIHARI p 3547 N94-30012
NAUGHTON, JONATHAN WAYNE p 3280 N94-30487
NAWIJN, W. M. p 3427 N94-30585

NECSULESCU, D. S. ..... p 3306 N94-30289
p 3310 N94-30309
NEDERHOF, MARK-JAN ..... p 3423 N94-30332
p 3432 N94-30356
NEGANOV, B. S. ..... p 3489 N94-30085
NEHRKORN, THOMAS ..... p 3369 N94-28663
NEISLER, H. M. ..... p 3383 N94-28448
NEJOH, Y. ..... p 3506 N94-29547
NELIN, P. ..... p 3347 N94-29158
NELSON, C. A. ..... p 3481 N94-28492
NELSON, DAVID ..... p 3346 N94-28608
NELSON, DAVID D. ..... p 3347 N94-29549
NELSON, K. M. ..... p 3175 N94-29458
NELSON, S. D. ..... p 3254 N94-29929
NEMARICH, J. ..... p 3259 N94-30512
NEMETH, D. T. ..... p 3261 N94-28546
NESS, S. R. ..... p 3341 N94-28463
NESSETT, D. ..... p 3422 N94-30251
NESTERENKO, V. O. ..... p 3517 N94-30183
NETTLES, SCOTT M. ..... p 3410 N94-29006
NEUHART, DAN H. ..... p 3130 N94-29443
NEUROTH, RUDOLF ..... p 3343 N94-28595
NEUSCHAEFER, LYMAN WADE . p 3547 N94-30010
NEVINS, W. M. ..... p 3509 N94-30768
NEWBERRY, T. ..... p 3171 N94-29035
NEWELL, JAMES F. ..... p 3316 N94-28508
NEWMAN, ROBERT B. ..... p 3135 N94-29862
NEWMAN, WYATT S. ..... p 3161 N94-29629
NGUYEN, T. M. ..... p 3251 N94-29667
NICHOLS, F. A. ..... p 3211 N94-28536
NICHOLS, G. H. ..... p 3155 N94-28510
NICKERSON, S. B. ..... p 3439 N94-30529
NICKS, ORAN W. ..... p 3156 N94-29052
NICOLAON, JEAN-PIERRE ..... p 3141 N94-29583
NIEH, T. G. ..... p 3212 N94-28733
NIELSEN, PETER V. ..... p 3232 N94-29606
p 3233 N94-29607
p 3233 N94-29608
p 3233 N94-29609
p 3233 N94-29610
NIEMEGEERS, IGNAS ..... p 3438 N94-30375
NIEMEGEERS, IGNAS G. ..... p 3255 N94-30374
NIEMELAE, ILKKA ..... p 3465 N94-30154
NIEMI, G. ..... p 3482 N94-28493
p 3497 N94-30712
NIEMINEN, I. ..... p 3230 N94-29187
NIJMEIJER, HENK ..... p 3449 N94-30963
NIKIFOROVA, M. G. ..... p 3365 N94-30223
NIKITIN, V. F. ..... p 3485 N94-28621
NIKITINA, V. I. ..... p 3485 N94-28621
NIKOLSKY, B. A. ..... p 3517 N94-30195
NIKONOV, EH. G. ..... p 3421 N94-30083
NIRASAWA, HIROSHI ..... p 3324 N94-28693
NISHI, NAOKI ..... p 3129 N94-28990
NISHIMURA, HITOSHI ..... p 3377 N94-29595
NISHIMURA, KOSUKE ..... p 3389 N94-28851
NISHINO, MASANORI ..... p 3360 N94-29239
NISHISU, YOSHIHIRO ..... p 3201 N94-29514
NISHIYAMA, KATSUNOBU ..... p 3324 N94-28693
p 3324 N94-28694
NISSAN, R. ..... p 3223 N94-30477
NITTS, V. V. ..... p 3511 N94-28626
NITYANANDA, B. V. ..... p 3243 N94-28897
NOAH, P. V. ..... p 3538 N94-28671
NOBILI, D. ..... p 3515 N94-30005
NODULMAN, L. ..... p 3481 N94-28462
NOEBE, RONALD D. ..... p 3205 N94-29758
NOEVER, DAVID A. ..... p 3354 N94-30463
NOGARINO, M. ..... p 3414 N94-29329
NOMA, TOSHIBUMI ..... p 3233 N94-29701
NONTASAK, T. ..... p 3397 N94-28754
NOON, G. P. ..... p 3397 N94-30458
NOORBERGEN, H. H. S. ..... p 3335 N94-30942
NORDSTROEM, K. M. ..... p 3385 N94-29190
NORMAN, J. N. ..... p 3379 N94-28421
NOSE, Y. ..... p 3397 N94-30458
NOULTY, R. ..... p 3291 N94-30216
NOURBAKHSH, ILLAH R. ..... p 3443 N94-30555
NOVAK, HOWARD L. ..... p 3223 N94-30476
NOVAK, M. ..... p 3318 N94-29057
NOZAKI, OSAMU ..... p 3127 N94-28976
p 3127 N94-28978
NUEHRENBERG, J. ..... p 3505 N94-29483
NUHN, H. D. ..... p 3292 N94-28481
NUNNELEY, S. A. ..... p 3382 N94-28443
NUTTALL, J. D. ..... p 3239 N94-29790
NYLEN, T. ..... p 3347 N94-29158

O

OBARA, HIROYUKI ..... p 3479 N94-29597
OBAYASHI, SHIGERU ..... p 3277 N94-29942
OBERACKER, V. E. ..... p 3454 N94-30317
OBERNDORF, PATRICIA ..... p 3410 N94-29068
OBRIEN, ROBERT J. ..... p 3342 N94-28590
p 3345 N94-28606
OBUKATA, MASAHIRO ..... p 3124 N94-28957
OBUKHOV, YU. V. ..... p 3286 N94-28553
OCCELLI, P. ..... p 3413 N94-29321
OCONNOR, E. M. ..... p 3383 N94-28445
ODAKA, TOSHIKAZU ..... p 3324 N94-28693
ODGERS, J. ..... p 3196 N94-29284
ODOWD, J. ..... p 3339 N94-30604
OEI, J. L. H. ..... p 3535 N94-30329
p 3535 N94-30359
p 3535 N94-30361
OESTERLUND, RALF ..... p 3399 N94-28406
OESTLUND, H. G. ..... p 3350 N94-30619
OEVEL, W. ..... p 3464 N94-29482
OFTEDAL, T. A. ..... p 3379 N94-28422
OGATA, YUJI ..... p 3479 N94-29597
OGAWA, SATORU ..... p 3126 N94-28972
OGAWA, TADAHIKO ..... p 3360 N94-29238
OGAWA, TAKANOBU ..... p 3126 N94-28967
OGAWA, TOMOYA ..... p 3158 N94-28583
OGISU, YOSHIHIRO ..... p 3187 N94-28675
p 3553 N94-29512
OGUTI, TAKASI ..... p 3360 N94-29239
OHALLORAN, T. A. ..... p 3483 N94-28566
OHKAWA, HITOMI ..... p 3531 N94-29677
OHLHAUSEN, JOHN H. ..... p 3399 N94-28766
OHM, TIMOTHY R. ..... p 3299 N94-29420
OHMAKI, SEIKI ..... p 3234 N94-29704
OHMS, TIM ..... p 3442 N94-30545
OHYAMA, KENICHI ..... p 3123 N94-28952
OISHI, KATSUMI ..... p 3169 N94-30811
OITTINEN, P. T. ..... p 3530 N94-29141
OJA, E. ..... p 3419 N94-29680
OJIMA, DENNIS ..... p 3350 N94-30616
OJIMA, DENNIS S. ..... p 3352 N94-30629
OKADA, SHIGENOBU ..... p 3159 N94-30162
OKADA, SHIN ..... p 3129 N94-28991
OKAMOTO, M. ..... p 3506 N94-29499
OKAMURA, S. ..... p 3505 N94-29398
OKEEFFE, M. ..... p 3203 N94-29043
OKUBO, JIN ..... p 3390 N94-28858
OLANDER, L. ..... p 3232 N94-29601
OLGUIN, D. ..... p 3516 N94-30070
OLIVERA, ARGELIO M. ..... p 3162 N94-29636
OLIVIER, GERARD ..... p 3417 N94-29349
OLLEVIER, THOMAS E. ..... p 3144 N94-30285
OLOFSSON, LARS MAGNUS ..... p 3294 N94-29590
OLSEN, J. A. ..... p 3519 N94-30592
OLSHEVSKY, V. G. ..... p 3517 N94-30195
OLSON, CHRISTINE A. ..... p 3528 N94-30934
OLSON, G. B. ..... p 3202 N94-28867
ONEIL, BRIAN P. ..... p 3319 N94-29433
ONEIL, P. GRAHAM ..... p 3445 N94-30568
ONEIL, PAT ..... p 3130 N94-29443
ONO, KAZUHIKO ..... p 3363 N94-29980
ONO, NOBUO ..... p 3357 N94-29078
ONO, TAKAYUKI ..... p 3359 N94-29234
ONO, TETSUJI ..... p 3368 N94-29520
ONODERA, TAKUO ..... p 3125 N94-28960
ONUMA, T. ..... p 3199 N94-30267
OREL, A. E. ..... p 3493 N94-30891
ORENSTEIN, J. O. ..... p 3515 N94-30009
ORIEL, JOHN T. ..... p 3419 N94-29746
OROURKE, P. J. ..... p 3270 N94-28475
ORTENDAHL, D. A. ..... p 3385 N94-29401
ORTH, C. D. ..... p 3296 N94-30830
ORTIZ, G. G. ..... p 3251 N94-29672
OSAKA, TOSHIAKI ..... p 3495 N94-29596
OSBORNE, ALLEN W., III ..... p 3145 N94-30677
OSBORNE, HAYWOOD S. ..... p 3419 N94-29797
OSBORNE, M. G. ..... p 3219 N94-30337
OSBORNE, WILLIAM P. ..... p 3164 N94-29880
OSGERBY, D. ..... p 3319 N94-29121
OSGOOD, ROBERT K. ..... p 3150 N94-29048
OSHIDA, KAZUHIKO ..... p 3169 N94-30811
p 3170 N94-30932
OSHIMA, MASAMITSU ..... p 3387 N94-28495
p 3389 N94-28850
p 3394 N94-29863
OSILIKE, M. O. ..... p 3467 N94-30065
OSKAM, B. ..... p 3135 N94-30916
OSOSKOV, G. A. ..... p 3434 N94-28613
OSTERYOUNG, JANET G. ..... p 3202 N94-28793
OSWALD, R. ..... p 3339 N94-30604
OTA, SHIGEO ..... p 3363 N94-29980
OTAKA, KAZUHIRO ..... p 3359 N94-29237
OTAKE, KAZUHIKO ..... p 3328 N94-28937
OTANI, SHUJI ..... p 3358 N94-29085
OTERO, I. ..... p 3211 N94-30892
OTOSHI, T. ..... p 3249 N94-29657
OTOSHI, T. Y. ..... p 3247 N94-29620
OTT, THOMAS ..... p 3240 N94-30448
OUCHI, CHIHARU ..... p 3170 N94-30932
OVCHINNIKOV, I. E. ..... p 3490 N94-30182
OVCHINNIKOV, VITALY V. ..... p 3475 N94-30680
OVERMARS, MARK H. ..... p 3456 N94-30377
p 3460 N94-30728
p 3461 N94-30747
OVSIEW, PHYLLIS L. ..... p 3430 N94-29051
OWE, J. O. ..... p 3379 N94-28422
OWYOUNG, A. ..... p 3501 N94-30828
OYAMA, SHIGERU ..... p 3159 N94-30744
OZAKI, MASAO ..... p 3360 N94-29240
OZAWA, KEISUKE ..... p 3169 N94-30811

P

PACETTI, RANDOLPH ..... p 3354 N94-30464
PACK, R. T. ..... p 3447 N94-30580
PACO, TINA M. ..... p 3530 N94-29138
PADEN, B. ..... p 3167 N94-29002
PADUANO, C. ..... p 3154 N94-29255
PADUREANU, I. ..... p 3490 N94-30182
PAGE, DOUGLAS ARTHUR ..... p 3513 N94-29530
PAINTON, L. ..... p 3315 N94-28503
PALAMIDESSI, C. ..... p 3424 N94-30347
PALEV, T. D. ..... p 3467 N94-30202
PALO, T. ..... p 3347 N94-29158
PAN, HUANG-HSING ..... p 3186 N94-30959
PAN, X. ..... p 3519 N94-30718
PAN, Z. ..... p 3219 N94-30335
PANASYUK, M. I. ..... p 3365 N94-30107
PANEBRATSEV, YU. A. ..... p 3489 N94-30052
PANITZ, J. K. G. ..... p 3220 N94-30591
PANKRATEV, NIKOLAI ..... p 3455 N94-30326
PANZA, G. F. ..... p 3365 N94-30093
PAPAGEORGIOU, CONSTANTINE P. p 3242 N94-28859
PAPARISTODEMOU, CHRISTOS ..... p 3299 N94-29409
PAQUOT, D. ..... p 3155 N94-29317
PARCE, J. W. ..... p 3238 N94-29783
PARIKH, JO A. ..... p 3435 N94-29198
PARIKH, JO ANN ..... p 3452 N94-29063
PARISE, J. B. ..... p 3204 N94-29395
PARK, B. ..... p 3521 N94-30851
PARK, JAHNG-HYON ..... p 3312 N94-30866
PARK, KI OOK ..... p 3222 N94-30922
PARK, S. Y. ..... p 3219 N94-30335
PARK, SUKJUNE ..... p 3155 N94-29850
PARKE, MICHAEL E. ..... p 3357 N94-29062
PARKER, ALLEN R., JR. ..... p 3287 N94-29361
PARKER, C. A. ..... p 3224 N94-28901
PARKER, MICHAEL A. ..... p 3498 N94-28804
PARKIN, S. S. P. ..... p 3519 N94-30707
PARMETER, J. E. ..... p 3206 N94-30007
PARO, J. ..... p 3230 N94-29187
PARSONS, E. L., JR. ..... p 3338 N94-30048
p 3338 N94-30313
PARTIN, D. ..... p 3203 N94-29043
PARTON, WILLIAM J. ..... p 3352 N94-30629
p 3352 N94-30630
PASCIAK, J. E. ..... p 3206 N94-29931
PASE, BILL ..... p 3421 N94-30155
PASHNEV, A. I. ..... p 3523 N94-28802
PATERSON, J. ..... p 3292 N94-28481
PATIN, J. F. ..... p 3332 N94-29417
PATNAIK, GAGAN B. ..... p 3359 N94-29137
PATOZ, C. ..... p 3205 N94-29525
PAUL, TAPAN KUMAR ..... p 3323 N94-30814
PAXSON, DANIEL E. ..... p 3274 N94-29740
PAYNE, T. ..... p 3240 N94-28522
PEACE, GEORGE M. ..... p 3446 N94-30575
PEARLSTEIN, L. D. ..... p 3509 N94-30768
PEARSON, J. E. ..... p 3200 N94-30748
PEASE, R. F. ..... p 3262 N94-28650
PECHT, MICHAEL ..... p 3265 N94-29511
PECK, LINDAMAE ..... p 3325 N94-28849
PEDERSON, S. P. ..... p 3465 N94-30366
PEIERLS, R. F. ..... p 3206 N94-29931
PELISCHEK, TIMOTHY E. ..... p 3160 N94-29369
PELKOWITZ, LIONEL ..... p 3308 N94-30297
PELLOSNIEMI, JUKKA ..... p 3407 N94-28411
PELOCHE, LUIS M. ..... p 3192 N94-29260
PELTONEN, H. ..... p 3530 N94-29172
PEMBERTON, STEVEN ..... p 3418 N94-29487
p 3402 N94-30320
p 3422 N94-30321
p 3423 N94-30341
PENDLETON, T. W. ..... p 3447 N94-30581
PENG, TSUNG-HUNG ..... p 3350 N94-30619
PENNYCOOK, S. J. ..... p 3516 N94-30063
p 3516 N94-30064
PENTUS, MATI ..... p 3457 N94-30397
PEPPER, STEPHEN V. ..... p 3218 N94-30177
PEREIRA, J. C. F. ..... p 3191 N94-29253
PEREIRADACUNHA, ROBERTO . p 3327 N94-28935
PERES, P. ..... p 3179 N94-29412
p 3179 N94-29442
PEREZ-DAVIS, MARLA E. ..... p 3338 N94-30196
PEREZ-ORTIZ, R. M. ..... p 3195 N94-29276
PEREZ-SABORID, MIGUEL ..... p 3546 N94-29913
PEREZ, RICARDO, III ..... p 3399 N94-28766
PEREZ, RICHARDO, III ..... p 3400 N94-28997

PEREZ, RONALD A. p 3147 N94-29854
PERKINS, L. J. p 3509 N94-30760
PERL, M. p 3497 N94-30712
PERL, M. L. p 3482 N94-28493
PERNEEL, CHRISTIAAN p 3259 N94-30513
PERNER, D. p 3343 N94-28596
PERNG, D. C. p 3236 N94-29775
PERNICI, B. p 3536 N94-30927
PERRY, MICHAEL A. p 3501 N94-30418
PESONEN, PEKKA p 3407 N94-28403
PESTOV, A. B. p 3525 N94-30169
PETERSEN, G. W. p 3349 N94-30046
PETERSON, C. O. p 3194 N94-29271
PETIT, G. p 3470 N94-30653
p 3145 N94-30665
PETIT, GERARD p 3145 N94-30660
PETRATOS, G. G. p 3483 N94-28542
PETRE, ERIC p 3141 N94-29581
PETRENKO, VICTOR F. p 3486 N94-29021
PETRILLO, C. p 3286 N94-29113
PETRIU, E. p 3144 N94-30286
PETROSKY, JAMES C. p 3263 N94-29028
PETROVIC, J. J. p 3185 N94-30693
PETTITI, V. p 3473 N94-30668
PEURACH, THOMAS M. p 3314 N94-30442
PFLUGER, NATHAN p 3444 N94-30557
PHANEUF, R. A. p 3485 N94-28788
PHI, DUONG VAN p 3548 N94-30163
PHILIPP, WARREN H., JR. p 3354 N94-30471
PHILLIPS, M. R. p 3322 N94-30114
PIANETTA, P. p 3292 N94-28481
PICARD, D. p 3255 N94-30153
PICHE, FRANCOIS p 3540 N94-29971
PIEDBOEUF, J.-C. p 3307 N94-30294
PIER, EDWARD A. p 3545 N94-29832
PIERCE, D. G. p 3267 N94-30368
PIERS, W. J. p 3135 N94-30916
PIERSON, MITCHELL p 3288 N94-29437
PIETIKAEINEN, JUHA p 3204 N94-29387
PIETIKAEINEN, P. p 3214 N94-29157
PIFFL, V. p 3505 N94-29075
p 3505 N94-29076
PILAFTSIS, A. p 3487 N94-29145
PILMANIS, ANDREW A. p 3391 N94-29071
PIMPERL, M. M. p 3236 N94-29774
PINDERA, MAREK-JERZY p 3183 N94-30125
PINELLI, THOMAS E. p 3534 N94-30149
p 3534 N94-30150
PING, K. F. p 3213 N94-28795
PINKERTON, STEVEN D. p 3494 N94-29065
PINNA, G. M. p 3328 N94-28937
PINNA, GIANMARIA M. p 3327 N94-28933
PINSKY, MARK A. p 3243 N94-29072
PIPPIN, H. G. p 3175 N94-29458
PIRODDI, LUIGI p 3200 N94-30938
p 3449 N94-30941
PITARYS, MARC J. p 3150 N94-29331
PITTS, R. p 3514 N94-29801
PIZZILLO, THOMAS J. p 3241 N94-28745
PLANCHON, P. p 3137 N94-29561
PLANTE, JEANNETTE p 3166 N94-28703
PLASMEIJER, RINUS p 3423 N94-30331
PLATONOV, YU. YA. p 3505 N94-29076
PLESHANOV, N. K. p 3489 N94-30096
PODOSEK, J. A. p 3238 N94-29785
POEPPEL, ROGER B. p 3261 N94-28487
POH, ENG-KEE p 3154 N94-28632
POHJOLAINEN, S. p 3538 N94-29170
POHLE, L. p 3340 N94-30820
POIRIER, J. P. p 3355 N94-28538
POKER, D. B. p 3521 N94-30851
POLITES, MICHAEL E. p 3287 N94-29358
POLITZER, PETER p 3225 N94-29310
POLLACK, J. p 3349 N94-30046
POLLARA, F. p 3247 N94-29619
POLLARD, M. D. p 3148 N94-30129
POLLARD, MICHAEL p 3148 N94-30131
POLLARI-MALMI, K. p 3530 N94-29167
POLLOCK, GERRY DARREN p 3324 N94-30920
POLUSHKIN, V. N. p 3267 N94-30073
p 3517 N94-30082
POMAROL, A. p 3482 N94-28494
POMERET, JEAN-MARC p 3139 N94-29570
POMERLEAU, DEAN p 3397 N94-28860
POMFRET, CHRIS J. p 3314 N94-30484
POMJAKUSHIN, V. YU. p 3517 N94-30195
PONGRATZ, H. p 3384 N94-28452
PONOMAREV, A. N. p 3517 N94-30195
PONTER, A. B. p 3213 N94-28922
POORMAN, RICHARD M. p 3215 N94-29446
POPESCU, I. p 3490 N94-30182
PORDES, S. p 3493 N94-30886
PORILE, N. T. p 3492 N94-30836
PORRA, V. p 3244 N94-29169
POSNER, EDWARD C. p 3246 N94-29613
POSTUPAEV, V. V. p 3508 N94-30194
POTREBENIKOV, YU. K. p 3528 N94-28615
POTTER, B. G., JR. p 3518 N94-30247
POTTER, T. F. p 3268 N94-30819
POURKASHANIAN, M. p 3190 N94-29250
POVINELLI, LOUIS A. p 3272 N94-29096
POWELL, J. R. p 3497 N94-30588
POWELL, K. p 3305 N94-30279
POWER, J. F. p 3267 N94-30716
POWERS, JANET V. p 3401 N94-30122
POZOS, R. S. p 3382 N94-28441
PRACHE, BRIGITTE p 3245 N94-29440
PRAGER, S. C. p 3503 N94-28514
PRASAD, R. p 3208 N94-30118
PRATHER, MICHAEL p 3351 N94-30624
PREEN, PHILIP J. p 3399 N94-28766
PRELAS, M. A. p 3296 N94-30614
PRELEWITZ, DAVID FLOYD p 3246 N94-29529
PRICE, CHARLES R. p 3441 N94-30541
PRICE, D. L. p 3521 N94-30897
PRIJATELJ, ANDREJA p 3456 N94-30380
PRINCIPE, E. L. p 3204 N94-29196
PRINN, RONALD G. p 3345 N94-28602
p 3350 N94-30617
PRITCHETT, P. L. p 3504 N94-28828
PROCIW, L. A. p 3154 N94-29257
p 3154 N94-29264
PROGAR, D. J. p 3180 N94-29472
PROPER, H. A. p 3535 N94-30329
p 3423 N94-30344
p 3535 N94-30357
p 3535 N94-30359
p 3535 N94-30360
p 3535 N94-30362
PROVOST p 3266 N94-29523
PSAILA, GIUSEPPE p 3429 N94-30928
PUGACHEVA, G. I. p 3365 N94-30223
PULLIA, A. p 3291 N94-30930
PUSHKIN, S. B. p 3475 N94-30679
PUZYNIN, V. I. p 3522 N94-28616
PYATOV, P. N. p 3460 N94-30726

Q

QIAN, TIMOTHY WEI TIE p 3304 N94-30238
QIU, BING p 3254 N94-30034
QUACKENBUSH, TODD R. p 3480 N94-30274
QUESTED, P. N. p 3210 N94-30796
QUILLEN, ALICE C. p 3544 N94-29738
QUINIOU, BERTRAND OLIVIER MARIE p 3294 N94-29531
QUINN, J. M. p 3507 N94-30128
QUINN, P. J. p 3548 N94-30694
QUINN, R. B. p 3250 N94-29658
QUINN, ROGER D. p 3439 N94-30530
QUINTANAR, IGNACIO-ARTURO p 3365 N94-30789
QUINTO, P. FRANK p 3133 N94-30176
QUINTO, ROGER A. p 3136 N94-28744
QUIRK, W. J. p 3338 N94-29955
QUIROGA, L. p 3516 N94-30069

R

RAATIKAINEN, PERTTI p 3245 N94-29468
RABKIN, J. p 3250 N94-29664
RACHEV, SVETLOZAR p 3464 N94-29129
RADHAKRISHNAN, B. p 3511 N94-28535
RADHAKRISHNAN, V. M. p 3317 N94-28819
RADKE, KATHIE p 3150 N94-29377
RAFFENSBERGER, MARK E. p 3369 N94-28873
RAFFERTY, RUSSELL P. p 3529 N94-28903
RAGENT, BORIS p 3550 N94-29892
RAHMAN, S. p 3145 N94-28647
RAINER, F. p 3212 N94-28560
RAISTRICK, I. D. p 3208 N94-30101
RAJULU, SUDHAKAR p 3402 N94-30210
RAMAKER, DAVID E. p 3188 N94-28777
RAMAN, GANESH p 3135 N94-30949
RAMAN, N. p 3216 N94-29830
RAMANATHAN, V. p 3353 N94-30638
RAMAPRIAN, B. R. p 3129 N94-29306
RAMESH, V. p 3196 N94-29284
RAMEY, J. O. p 3199 N94-30723
RANDALL, D. A. p 3378 N94-30823
RANDOLPH, L. W. p 3248 N94-29626
RAO, ANIL S. p 3458 N94-30407
p 3458 N94-30408
p 3427 N94-30725
RAO, K. S. p 3254 N94-30094
RAO, Y. S. p 3254 N94-30094
RAPP, DOUGLAS C. p 3173 N94-29403
RASHED, HUSSAIN YOUSEF p 3544 N94-29731
RASHEVSKIJ, A. V. p 3534 N94-30079
RASMUSSEN, CRAIG W. p 3451 N94-28651
RASMUSSEN, P. G. p 3398 N94-29918
RAUBENHEIMER, T. p 3292 N94-28481
RAUCH, P. E. p 3203 N94-29043
RAUS, J. p 3505 N94-29075
p 3505 N94-29076
RAUSCH, RUSS DAVID p 3131 N94-29877
RAVEU, B. p 3245 N94-29421
RAVI, J. p 3518 N94-30249
RAVIKUMAR, V. p 3516 N94-30064
RAWLINGS, R. p 3141 N94-29580
RAYMOND, M. p 3255 N94-30153
RAZEGHI, MANIJEH p 3512 N94-28871
p 3512 N94-28872
READ, B. E. p 3217 N94-29885
p 3217 N94-29886
READ, K. p 3482 N94-28504
READING, J. p 3382 N94-28441
READINGS, C. p 3347 N94-29452
REBELSKY, L. p 3209 N94-30246
REDING, T. p 3535 N94-30179
REDMOND, J. p 3266 N94-30055
p 3437 N94-30250
REECE, M. J. p 3322 N94-30114
REED, BRIAN D. p 3172 N94-29097
REED, C. B. p 3506 N94-29510
REED, CHARLES p 3529 N94-28911
REED, R. p 3223 N94-30477
REEDY, E. D., JR. p 3185 N94-30827
REEDY, R. C. p 3543 N94-28545
REES, B. J. p 3204 N94-29196
REHN, L. E. p 3521 N94-30894
REICHERT, PAUL G. p 3335 N94-30759
REIDINGER, MARK F. p 3146 N94-28998
REIJMERINK, R. A. J. p 3438 N94-30373
REILLY, M. S. p 3410 N94-29019
REITZ, RONALD P. p 3263 N94-29045
RELWANI, RACHNA A. p 3354 N94-30463
REMINGTON, B. A. p 3509 N94-30597
p 3281 N94-30600
REMSBERG, ELLIS E. p 3370 N94-29455
REN-HUAN, ZHANG p 3471 N94-30658
RENNER, O. p 3505 N94-29076
RESSLER, H. p 3144 N94-30655
REUNANEN, MARKKU p 3229 N94-28410
REVZIN, A. M. p 3398 N94-29918
REY-GONZALES, R. p 3516 N94-30069
REYNAUD, JUAN F. p 3377 N94-29432
REYNOLDS, J. p 3405 N94-28916
REYNOLDS, J. K. p 3238 N94-29785
RIAHI, H. p 3453 N94-30091
RICCARDI, G. p 3154 N94-29270
RICE, EDWARD J. p 3135 N94-30949
RICE, R. p 3145 N94-28647
RICHARD-FOY, MARC p 3150 N94-29332
RICHARD, P. p 3492 N94-30837
RICHARDS, E. H. p 3340 N94-30843
RICHARDS, KENNETH E., JR. p 3164 N94-28417
RICHARDS, P. L. p 3515 N94-30009
RICHARDSON, J. W. p 3521 N94-30897
RICHARDSON, J. W., JR. p 3204 N94-29395
RICKARDS, RONALD ROBERT p 3348 N94-29750
RICKEFS, R. p 3297 N94-30666
RICKMAN, D. p 3529 N94-28820
RICKMAN, STEVEN L. p 3160 N94-29369
RIDEAU, P. p 3168 N94-29415
RIDLER, N. M. p 3267 N94-30115
RIECK, A. p 3384 N94-28452
RIETMAN, F. p 3426 N94-30490
RIGAKIS, K. B. p 3381 N94-28433
RIGHINI, G. p 3537 N94-30926
RIGHINI, GIOVANNI p 3429 N94-30924
p 3429 N94-30925
RINGWALD, F. A. p 3539 N94-29819
RINTAMAA, R. p 3494 N94-28623
RINTAMAA, RAUNO p 3316 N94-28402
RINTOUL, STEPHEN R. p 3350 N94-30618
p 3350 N94-30623
RIPLEY, GRADY L. p 3400 N94-28997
RISEMAN, TANYA MARIA p 3517 N94-30203
RITCHIE, B. p 3405 N94-29110
RITTER, ROXANE M. p 3395 N94-29919
RIVELLINI, TOMMASO P. p 3161 N94-29630
RIVERA, SALVADOR, JR. p 3242 N94-28862
RIZZI, S. A. p 3479 N94-29461
RIZZI, STEPHEN A. p 3479 N94-29856
ROBBINS, D. p 3534 N94-30099
ROBBINS, WILLIAM E. p 3288 N94-29484
ROBERGE, P. R. p 3269 N94-30312
ROBERT, CARMELLE p 3548 N94-30058
ROBERT, JEAN-MARC p 3456 N94-30377
ROBERTS, R. G. p 3487 N94-29161
ROBERTS, R. S. p 3432 N94-30100
ROBERTSON, GLEN A. p 3299 N94-29367
ROBERTSON, I. M. p 3521 N94-30894
ROBESON, SCOTT MICHAEL p 3374 N94-30810
ROBINS, GLENN M. p 3288 N94-29484
ROBINSON, DAVID N. p 3318 N94-28821

ROBINSON, FRANK, JR. p 3169 N94-30123
ROBINSON, I. A. p 3268 N94-30784
ROCHESTER, L. p 3497 N94-30712
ROCHESTER, L. S. p 3482 N94-28493
ROCK, S. J. p 3444 N94-30560
ROCKSTAD, H. K. p 3238 N94-29785
RODEMICH, E. R. p 3250 N94-29660
p 3250 N94-29661
RODRIGUEZ, ALBERTO A. p 3446 N94-30569
RODRIGUEZ, GUILLERMO p 3435 N94-29465
RODRIGUEZ, J. F. p 3513 N94-29215
ROE, L. H. p 3480 N94-30098
ROEBBER, PAUL J. p 3371 N94-29751
ROEBUCK, B. p 3263 N94-29120
p 3184 N94-30419
ROEDE, B. p 3142 N94-29586
ROESCH, WINIFRED p 3138 N94-29565
ROESSLER, P. G. p 3225 N94-30038
ROGACKI, K. p 3220 N94-30745
ROGATNEVA, E. A. p 3421 N94-30077
ROGERS, F. J. p 3542 N94-28526
ROGERS, HARRY C. p 3177 N94-28865
ROHN, DOUGLAS A. p 3161 N94-29629
ROIG, DAVID M. p 3172 N94-28834
ROJOS-OVIEDO, RUBEN p 3145 N94-28817
ROLLBUHLER, R. J. p 3196 N94-29280
ROMANELLI, F. p 3365 N94-30093
ROMANOFSKY, ROBERT R. p 3286 N94-29000
ROMO, R. p 3516 N94-30067
ROOS, K. R. p 3521 N94-30899
ROOS, MAURITS p 3329 N94-29213
p 3288 N94-29437
ROQUEMORE, W. M. p 3192 N94-29261
p 3192 N94-29262
ROSENBERG, E. I. p 3406 N94-30004
ROSENBERGER, FRANZ p 3515 N94-30015
p 3175 N94-30242
ROSENBLATT, J. p 3445 N94-30566
ROSENFELD, M. p 3145 N94-28647
ROSENQVIST, H. p 3385 N94-29189
ROSFJORD, T. J. p 3154 N94-29269
ROSS, G. G. p 3487 N94-29161
ROSS, M. N. p 3347 N94-29023
ROSSING, T. D. p 3468 N94-28459
ROSSINGTON, C. p 3268 N94-30717
ROTARESCU, GH. p 3490 N94-30182
ROTH, D. R. p 3201 N94-30220
ROTHENBERG, MICHAEL p 3440 N94-30533
ROUDAKOV, A. p 3151 N94-29295
p 3152 N94-29301
ROUGON, NICOLAS p 3396 N94-30978
ROUVAS, CONSTANTINOS p 3311 N94-30792
ROWE, MARY M. p 3355 N94-28685
ROY, CLAUDE H. p 3448 N94-30583
ROZGONYI, G. A. p 3518 N94-30249
RUAN, JU-AI p 3298 N94-29290
RUBERTI, ROBERT N. p 3414 N94-29328
RUBIANO, R. R. p 3206 N94-30007
RUBIN, LESLIE S. p 3287 N94-29400
RUBIN, M. D. p 3410 N94-29019
RUDDER, R. A. p 3504 N94-28776
RUDENKO, A. I. p 3500 N94-30075
RUEB, K. p 3305 N94-30279
RUEGSEGGER, STEVEN M. p 3409 N94-28920
RUGGIERO, ALESSANDRO G. p 3483 N94-28565
RULEV, I. p 3152 N94-29296
RUNNING, STEVEN W. p 3351 N94-30624
p 3351 N94-30628
p 3352 N94-30630
RUOFF, CARL FREDERICK p 3436 N94-29835
RUPPERT, D. E. p 3503 N94-28515
RUST, S. p 3145 N94-28647
RUTTEN, J. J. M. M. p 3424 N94-30347
p 3461 N94-30753
RYAN, J. V. p 3347 N94-29192
RYBICKI, DANIEL J. p 3298 N94-29351
p 3204 N94-29380
p 3303 N94-30173
RYKOV, V. A. p 3490 N94-30184
RYLICKI, DANIEL S. p 3169 N94-30123
RYNNE, T. M. p 3466 N94-30586

S

SAAD, A. p 3447 N94-30580
SAALTINK, MARK p 3421 N94-30155
SAARELMA, H. J. p 3530 N94-29141
SABA, JULIA L. R. p 3551 N94-29858
SABOL, BRUCE M. p 3242 N94-28862
SABOUNGI, M. L. p 3521 N94-30897
SACCHETTI, F. p 3286 N94-29113
SACHLEBEN, J. R. p 3520 N94-30842
SACK, FRED D. p 3385 N94-29943
SACKS, R. A. p 3510 N94-30875
SAEKI, CHIKAKO p 3389 N94-28852
SAGER, J. p 3154 N94-29263
SAITO, AKIRA p 3461 N94-30786
SAITO, IKUO p 3187 N94-28678
SAITO, MASAHIRO p 3553 N94-29512
SAITO, MASAYOSHI p 3187 N94-28675
SAITO, MITSURU p 3394 N94-29865
p 3314 N94-29985
SAITO, SHIGEBUMI p 3326 N94-28926
SAITO, THEODORE T. p 3240 N94-30449
SAKAMOTO, HIROSHI p 3211 N94-29516
SAKATA, TOSHIBUMI p 3328 N94-28937
p 3328 N94-29039
p 3330 N94-29219
p 3332 N94-29231
SAKO, TOSHITSUGU p 3377 N94-29595
SAKS, N. S. p 3266 N94-30040
SAKUI, SHIN p 3364 N94-29983
SAKURADA, SOTARO p 3390 N94-28854
SAKURAI, TORU p 3361 N94-29244
SALEM, JONATHAN A. p 3214 N94-29105
SALES, B. C. p 3199 N94-30723
SALES, VIC p 3440 N94-30533
SALICE, FABIO p 3429 N94-30936
SALMON, DAVID KURT p 3374 N94-29963
SALMON, J. K. p 3548 N94-30694
SALVA, J. p 3195 N94-29275
SALVAT, F. p 3494 N94-30980
SAMAVEDAM, G. p 3145 N94-28657
SAMPATH, P. p 3154 N94-29264
SAMPSON, JAMES B. p 3383 N94-28447
SAMPSON, ROBERT E. p 3446 N94-30575
SAMPSON, WILLIAM T., III p 3157 N94-29754
SAMUELSEN, G. S. p 3194 N94-29271
SANADA, ESTER p 3386 N94-28853
SANCHEZ, J. R. p 3521 N94-30888
SANDER, STANLEY P. p 3343 N94-28593
SANDERS, B. p 3196 N94-29284
SANDERS, DONALD C. p 3395 N94-29919
SANDERSON, A. C. p 3445 N94-30563
SANDFORD, MAYNARD C. p 3122 N94-28658
SANDOW, S. p 3525 N94-30121
SANDRELLI, FABRIZIO p 3416 N94-29342
SANDUSKY, DONALD A. p 3180 N94-29485
p 3180 N94-29496
SANHET p 3266 N94-29523
SANJEEVI, AMBA p 3534 N94-29961
SANO, KENICHI p 3159 N94-30162
SANTAOJA, KARI p 3316 N94-28409
SANTAVICCA, D. A. p 3193 N94-29265
SANTOS, ALMIR G. p 3463 N94-28768
SANUKI, H. p 3505 N94-29398
p 3506 N94-29547
SAPLAKOGLU, G. p 3260 N94-30514
SARABANDI, KAMAL p 3259 N94-30510
SARAJEDINI, ATA p 3538 N94-29732
SARANTOS, CHRIS p 3446 N94-30571
SARAVANAN, K. p 3218 N94-30104
SARBO, JANOS J. p 3423 N94-30332
SAREEN, ASHISH KUMAR p 3147 N94-29878
SARFF, J. S. p 3503 N94-28514
SARGINSON, T. G. p 3295 N94-30598
SARRAO, J. L. p 3520 N94-30848
SASAKI, MITSUO p 3387 N94-28495
p 3389 N94-28850
p 3394 N94-29863
SASAKI, TORU p 3324 N94-28693
SASAO, M. p 3505 N94-29397
SASSEN, K. p 3365 N94-30608
SATO, ATSUSHIGE p 3228 N94-28944
SATO, KATSUAKI p 3495 N94-29596
SATO, MASARU p 3188 N94-28681
SATO, MITSUO p 3392 N94-29710
SATO, NAOKI p 3169 N94-30811
SATO, NATSUO p 3357 N94-29079
p 3359 N94-29233
SATO, T. p 3361 N94-29244
SATOH, KAZUYOSHI p 3505 N94-29483
SATOU, MAMORU p 3503 N94-28555
SATTERTHWAITE, CHARLES P. p 3124 N94-28958
SAUCLER, D. R. p 3415 N94-29337
SAUER, M. C., JR. p 3397 N94-30458
SAUER, P. p 3220 N94-30778
SAUVAN, M. p 3142 N94-30439
SAWAMURA, BOB p 3245 N94-29456
SAWAYAMA, SHIGEKI p 3150 N94-29377
SAWYER, DARREN CHARLES p 3387 N94-29519
SCAGLIONE, LOIS JEAN p 3431 N94-29846
SCANLON, RAYMOND D. p 3437 N94-29840
SCARSTEIN, ROBERT W. p 3392 N94-29431
SCEDROV, ANDRE p 3243 N94-29054
SCHACHAM, S. E. p 3411 N94-29214
SCHAENZER, GUNTHER p 3264 N94-29209
SCHARER, J. E. p 3141 N94-29584
SCHAUB, RON p 3504 N94-28575
SCHEERES, D. J. p 3147 N94-29099
SCHEINER, BERNARD J. p 3159 N94-29656
SCHELL, DONNA J. p 3354 N94-30472
p 3346 N94-28727
p 3346 N94-28774
SCHELLINX, HAROLD p 3456 N94-30381
p 3430 N94-30973
SCHEURLEN, M. p 3195 N94-29279
SCHILDMEYER, F. p 3289 N94-30059
SCHIMEK, G. L. p 3510 N94-28529
SCHIMEL, DAVID S. p 3352 N94-30629
p 3353 N94-30636
SCHIMMEL, MORRY L. p 3161 N94-29634
SCHIPPERS, H. p 3338 N94-30328
p 3256 N94-30392
SCHLEICH, D. P. p 3510 N94-30875
SCHLEISLING, JOHN A. p 3160 N94-29369
SCHMALZER, PAUL A. p 3347 N94-29099
SCHMEHL, R. p 3195 N94-29279
SCHMIDLIN, FRANCIS J. p 3370 N94-29455
SCHMIDT, C. R. p 3482 N94-28494
SCHMIDT, CHARLES G. p 3178 N94-29135
SCHMIDT, HORST p 3138 N94-29565
SCHMITZ, ERIC p 3164 N94-28417
SCHMITZ, FREDRIC H. p 3478 N94-29362
SCHNEIDER, FRED B. p 3408 N94-28794
SCHNEIDER, M. p 3142 N94-29586
SCHOFIELD, R. J. p 3224 N94-28901
SCHOLZ, THOMAS p 3434 N94-28672
SCHOONE, ANNEKE A. p 3424 N94-30379
SCHOTT, JOACHIM H. p 3486 N94-29060
SCHRIMPF, R. D. p 3263 N94-29025
SCHRIVER, D. p 3504 N94-28828
SCHROEDER, A. p 3209 N94-30246
SCHROEDER, D. J. p 3143 N94-30933
SCHROEDER, MARC p 3380 N94-28428
SCHROER, BERNARD J. p 3537 N94-29410
SCHROTH, A. p 3142 N94-29586
SCHUABEL, K. M. p 3510 N94-30832
SCHUBERT, M. p 3138 N94-29567
p 3140 N94-29575
SCHUCK, MARY MARGARET p 3402 N94-30132
SCHUETZ, G. p 3199 N94-30111
p 3525 N94-30121
SCHULTZ, J. L. p 3154 N94-29258
SCHULTZ, ROBERT L. p 3140 N94-29576
SCHULZ, THERESA Y. p 3391 N94-29211
SCHUMANN, U. p 3189 N94-29247
SCHUNK, P. R. p 3216 N94-29830
SCHUSTER, GARY p 3163 N94-29651
SCHUTZ, BOB E. p 3142 N94-30243
SCHWARTZ, H. M. p 3308 N94-30299
SCHWARTZ, R. W. p 3518 N94-30247
p 3518 N94-30315
SCHWARZKOPF, OTFRIED p 3424 N94-30348
p 3460 N94-30721
SCHWENN, U. p 3505 N94-29483
SCHWIDERSKI, ERNST W. p 3377 N94-29432
SCHWINKENDORF, K. N. p 3427 N94-30590
SCOTT, EWELL M. p 3299 N94-29365
SCOTT, JAMES R. p 3273 N94-29471
SEDREL, STEVE p 3150 N94-29331
SEEMAN, J. T. p 3292 N94-28481
SEFCIK, ROBERT J. p 3171 N94-28833
SEGALL, A. E. p 3175 N94-28581
SEGALMAN, D. J. p 3222 N94-30900
SEGALMAN, I. p 3194 N94-29272
SEHGAL, R. p 3216 N94-29830
SEIDEL, DAVID A. p 3122 N94-28658
SEIGAL, P. K. p 3501 N94-30261
SEKHPOSSIAN, E. V. p 3504 N94-28564
SEKI, TSUYOSHI p 3314 N94-29985
SEKIGUCHI, CHIHARU p 3388 N94-28498
SELF, HERSCHEL C. p 3400 N94-29034
SELF, MARK F. p 3486 N94-29131
p 3189 N94-29140
p 3513 N94-29155
SELZER, R. H. p 3385 N94-29401
SEMENOV, B. YU. p 3534 N94-30079
SEMERARO, B. D. p 3350 N94-30116
SEMIZ, IBRAHIM p 3546 N94-29912
SENJANOVIC, G. p 3524 N94-30089
SEPPAELAE, J. V. p 3214 N94-29157
SERAJI, HOMAYOUN p 3436 N94-29504
SERDYUKOVA, S. I. p 3524 N94-30087
SEREN, KARL-JOHAN p 3407 N94-28411
SERENO, THOMAS J., JR. p 3359 N94-29137
SERLING, J. D. p 3270 N94-28549
SERNYAEV, G. A. p 3201 N94-28460
SERVICE, J. R. R. p 3439 N94-30529
SESSLER, DANIEL I. p 3380 N94-28428
SETAYESH, A. p 3164 N94-28627
SETLOW, PETER p 3384 N94-28884
SETOKUCHI, OSAMU p 3188 N94-28681
SEVERGIN, YU. p 3487 N94-29700
SEVERIN, JAN WILLEM p 3212 N94-28539
SEWELL, JAMES S. p 3240 N94-30445
SEYBERT, A. F. p 3301 N94-29552

SHA, W. T. p 3279 N94-30020
SHABANOV, S. V. p 3523 N94-28751
SHACK, W. J. p 3207 N94-30021
SHADOAN, MICHAEL D. p 3299 N94-29365
SHAFEIDEHABAD, A. p 3453 N94-30119
SHAFER, S. p 3405 N94-28916
SHAFER, STEVEN A. p 3499 N94-29059
SHAFFSTAFF, ROBERT M. p 3391 N94-28892
SHAH, B. p 3250 N94-29665
SHAH, DILIPKUMAR R. p 3172 N94-28834
SHAHRABI, KAMAL p 3168 N94-29896
SHAHSHAHANI, M. p 3247 N94-29619
SHAKOCIUS, AARON M. p 3337 N94-29033
SHANENKO, A. A. p 3490 N94-30112
SHANKARLINGHAM, S. p 3451 N94-28792
SHANKLAND, T. J. p 3355 N94-28538
SHANNON, MARK ALAN p 3292 N94-28478
SHANNON, S. G. p 3388 N94-28757
SHAPIRO, A. B. p 3122 N94-29842
SHAPIRO, A. M. p 3506 N94-29510
SHAPIRO, S. M. p 3209 N94-30246
SHARMA, R. D. p 3357 N94-28893
SHARMA, RAJEEV p 3448 N94-30803
SHARP, R. p 3211 N94-30892
SHATOKHIN, V. N. p 3286 N94-28553
SHATTIL, STEVE p 3145 N94-30660
SHAVOKHINA, N. S. p 3356 N94-28803
SHAVRUKOV, V. Y. p 3455 N94-30325
p 3463 N94-30975
p 3463 N94-30976
SHAW, B. A. p 3204 N94-29196
SHAY, T. M. p 3250 N94-29659
SHEA, ANNE L. p 3408 N94-28818
SHEA, K. J. p 3174 N94-28557
SHEALY, JAMES R. p 3511 N94-28773
SHEEN, SHAW-CHING p 3276 N94-29851
SHEFFIELD, R. p 3294 N94-29934
SHELEPIN, A. L. p 3524 N94-29498
SHELFER, T. D. p 3236 N94-29774
SHELL, J. p 3250 N94-29658
SHELLEMAN, D. L. p 3175 N94-28581
SHELLEY, E. G. p 3507 N94-30128
SHEN, ALEXANDER p 3427 N94-30732
SHEN, DAVID H. p 3265 N94-29411
SHEN, M. H. p 3236 N94-29774
SHEPHARD, ROY J. p 3391 N94-29049
SHEPPARD, EMORY LAMAR p 3370 N94-29697
SHEPPARD, JOHN C. p 3344 N94-28600
SHEPPERD, L. W. p 3340 N94-30843
SHERMAN, KENNETH E. p 3391 N94-29116
SHETTER, RICHARD p 3345 N94-28603
SHI, XIAOLUN p 3311 N94-30793
SHI, XIAOTIAN p 3541 N94-30133
SHIAO, MICHAEL C. p 3319 N94-29384
SHIELDS, JOHN W. p 3529 N94-28903
SHIELDS, WILLIAM p 3299 N94-29354
p 3299 N94-29386
SHIGEHARA, KOJI p 3324 N94-28693
SHIGETA, JUNICHI p 3158 N94-28583
SHIKAMA, TATSUO p 3295 N94-30186
SHIMA, EIJI p 3125 N94-28964
SHIMANSKIIJ, S. S. p 3489 N94-30052
SHIN, HYUNGJAE p 3322 N94-30226
SHIN, KANG G. p 3445 N94-30564
SHINE, ROBERT J. p 3293 N94-29309
SHINOHARA, JOJI p 3159 N94-30162
SHIOTA, MASAZUMI p 3479 N94-29597
SHIPLEY, D. R. p 3492 N94-30795
SHIPTON, M. S. p 3480 N94-30786
SHIRAI, TOSHIZO p 3485 N94-28788
SHIRAISHI, KAZUYUKI p 3358 N94-29084
SHIRAISHI, LORI R. p 3162 N94-29638
SHIRAISHI, MINORU p 3522 N94-29515
p 3223 N94-29517
p 3223 N94-29518
SHIRAYAMA, SUSUMU p 3128 N94-28982
SHIRER, HAMPTON N. p 3272 N94-29195
p 3377 N94-29436
SHOAF, S. E. p 3236 N94-29775
SHOCKEY, DONALD A. p 3178 N94-29135
SHOCKLEY, D. R. p 3520 N94-30724
SHOGA, M. A. p 3497 N94-30222
SHORE, STEVEN N. p 3545 N94-29871
SHUL, R. J. p 3515 N94-30006
SHUM, S. p 3187 N94-28483
SHUXIN, YIN p 3370 N94-29394
SICKAFUS, KURT E. p 3517 N94-30201
SIDORENKOV, S. I. p 3506 N94-29510
SIEBENALLER, JOSEPH F. p 3384 N94-28829
SIEFKEN, HUGH p 3494 N94-30485
SIEGEL, M. W. p 3446 N94-30572
SIEGMUND, DAVID O. p 3464 N94-28876
SIERRA, V. p 3160 N94-29666
SIGEL, GEORGE H., JR. p 3288 N94-29699
SILBEY, R. J. p 3489 N94-30061
SILLING, S. A. p 3184 N94-30589
SILVESTRI, GUY G. p 3252 N94-29733
SILVESTRIN, P. p 3474 N94-30676
SILVIOUS, J. L. p 3259 N94-30512
SIMKINS, THOMAS p 3397 N94-30460
SIMMONS, REID p 3444 N94-30561
SIMMS, D. A. p 3339 N94-30602
SIMONS, RAINEE N. p 3267 N94-30198
SIMONSON, S. C., III p 3270 N94-28476
SIMPSON, HARRY JAY p 3479 N94-29988
SIMPSON, JOHN W. p 3315 N94-29366
SIMS, G. D. p 3184 N94-30438
SINCLAIR, M. B. p 3518 N94-30247
SINDELAR, PAVEL p 3179 N94-29425
SINGER, S. p 3294 N94-29934
SINGH, D. p 3185 N94-30593
SINGH, J. P. p 3185 N94-30593
SINGH, N. p 3169 N94-29917
SINGHAL, SURENDRA N. p 3319 N94-29384
SINHA, ARVIND K. p 3216 N94-29874
SIQUEIRA, PAUL p 3259 N94-30510
SIRON, P. p 3417 N94-29345
SIROTIN, A. P. p 3511 N94-28626
SISK, D. R. p 3491 N94-30695
SITTROP, H. p 3256 N94-30498
SITUMORANG, B. p 3331 N94-29225
SIVASEGARAM, S. p 3195 N94-29276
SIVESKI, ZORAN p 3408 N94-28760
SKAARET, EIMUND p 3232 N94-29602
p 3232 N94-29603
SKACHKOV, N. B. p 3451 N94-28783
SKALOZUB, V. V. p 3525 N94-30170
SKARKA, V. p 3507 N94-30071
SKOWRONSKI, MAREK p 3513 N94-29125
SLACK, MARC G. p 3444 N94-30556
SLANEY, V. R. p 3331 N94-29224
SLANGER, TOM G. p 3549 N94-28816
SLATER, K. p 3380 N94-28430
SLAVEN, MIKE p 3409 N94-28910
SLAVIN, JAMES A. p 3360 N94-29243
SLEEP, M. R. p 3459 N94-30412
SLEEP, M. RONAN p 3425 N94-30415
SMARTT, H. B. p 3314 N94-30444
SMELTZER, STAN S. p 3397 N94-30457
SMID, I. p 3503 N94-28555
SMIRNOVA, O. G. p 3406 N94-30081
SMITH, BROOKE EDWARD p 3158 N94-29649
SMITH, CARL W. p 3354 N94-30472
SMITH, D. C. p 3206 N94-30007
SMITH, D. L. p 3493 N94-30893
SMITH, DE PASS p 3409 N94-28910
SMITH, E. C. p 3497 N94-30222
SMITH, EDWARD E. p 3398 N94-29154
SMITH, H. A. p 3175 N94-29458
SMITH, J. p 3158 N94-30423
SMITH, J. E. p 3160 N94-29470
SMITH, KEVIN W. p 3150 N94-29389
SMITH, L. S. p 3496 N94-30219
SMITH, M. D. p 3349 N94-29932
SMITH, OLIVER D. p 3411 N94-29202
p 3411 N94-29207
SMITH, R. K. p 3527 N94-30698
SMITH, S. p 3145 N94-28647
SMITS, ALEXANDER J. p 3132 N94-29920
SMOLYAKOV, A. I. p 3508 N94-30159
SMYRL, WILLIAM H. p 3203 N94-29089
SNIDER, J. B. p 3136 N94-30890
SNOW, ROBERT W. p 3145 N94-30677
SNYDER, E. S. p 3267 N94-30368
SOBREMONTE, MICHAEL ABELLERA p 3530 N94-29533
SODERMAN, PAUL T. p 3478 N94-29362
SOEPENBERG, LEO p 3428 N94-30746
SOERLIE, R. p 3401 N94-29950
SOISALON-SOININEN, E. p 3530 N94-29167
SOLEM, ERIK p 3304 N94-30277
SOLI, G. A. p 3496 N94-30219
SOLOMON, ELIEZER N. p 3150 N94-29331
SOLOMON, G. p 3247 N94-29618
p 3250 N94-29662
SOLOMON, O. M., JR. p 3406 N94-30008
SOLONIN, V. I. p 3152 N94-29299
SOLOVEV, A. D. p 3421 N94-30083
SOLOVEV, V. A. p 3202 N94-28551
p 3207 N94-30076
SOMA, HISASHI p 3377 N94-29595
SOMMEIJER, B. P. p 3433 N94-30730
SONG, BYUNG-KEUN p 3302 N94-29870
SONNENSCHEIN, FRANS J. p 3170 N94-30857
SOO, P. p 3223 N94-30480
p 3222 N94-30906
SOPORI, BHUSHAN L. p 3341 N94-30486
SOPOV, O. V. p 3202 N94-28551
p 3207 N94-30076
SORENSEN, JOHN p 3140 N94-29577
SOROKACH, MICHAEL R., JR. p 3163 N94-29647
SOROKO, L. M. p 3290 N94-30148
SOSIN, K. A. p 3269 N94-30312
SOSOUNOV, V. p 3151 N94-29292
p 3151 N94-29294
p 3152 N94-29297
SOSOUNOV, V. A. p 3152 N94-29298
SOUTH, D. W. p 3349 N94-30023
SOVINEC, C. R. p 3503 N94-28514
SOWA, W. A. p 3194 N94-29271
SOWOOD, P. J. p 3383 N94-28445
SPAAN, MARTIJN p 3422 N94-30318
SPEARMAN, M. LEROY p 3130 N94-29473
SPECHT, E. D. p 3483 N94-28559
SPEKREIJSE, S. P. p 3124 N94-28956
p 3133 N94-30387
SPELT, PHILIP F. p 3441 N94-30539
SPENCE, H. E. p 3356 N94-28869
SPENCER, K. p 3240 N94-28522
SPEZIALE, CHARLES G. p 3272 N94-29381
SPIELER, H. p 3267 N94-30711
p 3268 N94-30717
SPILG, L. p 3264 N94-29191
SPILLING, P. p 3433 N94-30429
SPOONER, S. p 3211 N94-30852
SPRAGGE, M. K. p 3212 N94-28560
SPRAGUE, S. p 3225 N94-30038
SPRENGNETHER, MICHELE p 3345 N94-28602
SPRINGER, R. W. p 3206 N94-30007
SPRINGETT, JAMES C. p 3297 N94-30670
SPRINGLE, G. p 3309 N94-30306
SPRINGSTON, S. R. p 3342 N94-28523
SQUIRE, K. R. p 3224 N94-28901
SRINIVASAN, GANAPATHI R. p 3129 N94-29197
SRINIVASAN, GOPALAKRISHNAN p 3277 N94-29944
ST.CLAIR, ANNA K. p 3175 N94-29554
ST.CLAIR, ANNE K. p 3214 N94-29359
ST.CLAIR, T. L. p 3180 N94-29472
ST.CLAIR, TERRY L. p 3175 N94-29554
p 3215 N94-29555
ST.LORANT, S. J. p 3468 N94-30026
STABB, MARK CHANNING p 3168 N94-29828
STACHIW, JERRY D. p 3212 N94-28641
STAGGS, SUZANNE THERESE p 3553 N94-30351
STALEY, D. J. p 3220 N94-30591
STALLER, CRAIG O. p 3265 N94-29488
STALLINGS, D. C. p 3255 N94-30105
STAMPE, D. p 3310 N94-30310
STANKOV, B. B. p 3136 N94-30890
STANLEY, W. D. p 3367 N94-30883
STANNARD, BARRY ANTHONY p 3136 N94-30144
STANTON, ALAN C. p 3345 N94-28607
STANTON, LEO p 3223 N94-30478
STARK, J. W. p 3496 N94-30217
STARK, RICHARD B. p 3499 N94-29009
STARNES, J. H., JR. p 3317 N94-28801
STARTSEV, V. S. p 3489 N94-30050
STASSEN, H. G. p 3402 N94-30390
STASSINOPOULOS, E. G. p 3496 N94-30215
STATMAN, J. I. p 3250 N94-29663
p 3250 N94-29664
STAUBER, M. C. p 3496 N94-30219
STAVNES, MARK W. p 3165 N94-28700
STECKENRIDER, JOHN SCOTT p 3290 N94-30254
STEELE-PERKINS, A. P. p 3379 N94-28424
STEELE, J. H. p 3210 N94-30776
STEIGENBERGER, U. p 3286 N94-29113
STEIN, CHARLES p 3494 N94-30485
STEIN, DANIEL L. p 3466 N94-28807
STEIN, LYNN ANDREA p 3444 N94-30559
STEINBERGER, R. L. p 3193 N94-29265
STEINETZ, BRUCE M. p 3298 N94-28838
STENGEL, ROBERT p 3137 N94-29562
STEPANOV, V. p 3152 N94-29296
STEPHENS, M. A. p 3464 N94-29014
STEPHENS, SCOTT A. p 3265 N94-29374
STEPHENSON, MARK M. p 3150 N94-29336
STERN, J. A. p 3143 N94-30933
STERN, ROBERT A. p 3538 N94-29001
p 3545 N94-29861
STERNE, P. A. p 3516 N94-30054
STERRINO, V. J. p 3495 N94-30212
STEVENS, H. D. p 3444 N94-30560
STEVENS, PHILIP S. p 3342 N94-28589
STEWART, DAWN L. p 3271 N94-28738
STEWART, KAREN T. p 3402 N94-30188
STEWART, S. R. p 3247 N94-29620
STICKLES, R. W. p 3154 N94-29263
STINNESBECK, WOLFGANG p 3354 N94-28416
STOCKERT, JON A. p 3197 N94-29312
STOCKS, CHARLES D. p 3298 N94-29352
STOKES, LEBARIAN p 3441 N94-30541
STOKHOF, MARTIN p 3456 N94-30372
STOLIAROV, N. p 3143 N94-30933
STOLL, LAURENCE p 3121 N94-28732
STOLZ, C. J. p 3295 N94-30598
STONE, HENRY W. p 3299 N94-29420

STONE, K. W. p 3337 N94-29018
STONE, R. S. p 3377 N94-28877
STONER, G. E. p 3207 N94-30053
STOUT, M. G. p 3317 N94-28811
STOWERS, IRVING F. p 3240 N94-30449
STRAIT, R. S. p 3526 N94-28474
STRANGE, SAMUEL J. p 3243 N94-28898
STRASSBERG, YESAYAHU p 3313 N94-30952
STRAYER, M. R. p 3454 N94-30317
STREET, D. R., JR. p 3397 N94-28754
STREET, KENNETH W., JR. p 3354 N94-30471
STREETS, K. T. p 3491 N94-30722
STRELTSOV, V. N. p 3522 N94-28586
p 3494 N94-28612
p 3523 N94-28618
p 3523 N94-28620
p 3468 N94-28720
p 3523 N94-28721
p 3523 N94-28782
STRICKLER, WALTER M. p 3242 N94-28826
STRIGANOV, S. I. p 3421 N94-30080
STRIZH, T. A. p 3406 N94-30081
STROHMAYER, TOD E. p 3538 N94-29795
STRONGIN, R. G. p 3421 N94-30077
STRUCKMAN, KEITH p 3443 N94-30550
STUDENIKIN, A. I. p 3481 N94-28468
STUEBER, THOMAS J. p 3166 N94-28711
STUPIAN, G. W. p 3264 N94-29289
STURGEON, MELISSA A. p 3329 N94-29095
STURGESS, G. J. p 3193 N94-29266
p 3194 N94-29272
STUTZMAN, WARREN L. p 3160 N94-28836
SU, WEI-JOU p 3363 N94-29941
SUAZO, J. E. p 3289 N94-29927
SUBRAHAMANIAN, V. S. p 3435 N94-29198
SUBRAMANIAM, SURESH p 3377 N94-29204
SUEMATSU, KAZUYO p 3129 N94-28993
SUEMATSU, SHUNJI p 3129 N94-28993
SUES, R. H. p 3157 N94-29151
SUGANO, MINORU p 3126 N94-28968
SUGANUMA, ISAO p 3388 N94-28496
p 3388 N94-28497
SUGASAWA, MASAMI p 3188 N94-28682
p 3211 N94-29516
SUGIURA, MASAHISA p 3360 N94-29243
SUITIALA, RISTO p 3406 N94-28401
SULKOWSKI, C. p 3220 N94-30745
SULLIVAN, D. B. p 3468 N94-30641
SULLIVAN, TIMOTHY L. p 3319 N94-29469
SULONEN, R. p 3530 N94-29172
SUN, SHANG-WEN p 3548 N94-30271
SUN, TAI-HSING TOM p 3131 N94-29879
SUNDAR, G. p 3211 N94-30852
SUNDBERG, R. L. p 3357 N94-28893
SUNI, I. p 3217 N94-30025
SURAMPUDI, SUBBARAO p 3265 N94-29411
p 3265 N94-29505
SUSOEFF, A. R. p 3281 N94-30600
SUSZKO, S. F. p 3405 N94-28845
SUTHERLAND, ROBERT A. p 3257 N94-30499
SUZUKI, HAJIME p 3389 N94-28852
SUZUKI, HIROYUKI p 3393 N94-29718
SUZUKI, SATOSHI p 3503 N94-28555
SUZUKI, SINJI p 3170 N94-30932
SUZUKI, TAKASHI p 3330 N94-29220
SUZUKI, YOSHIMI p 3324 N94-28693
SVANDRLIK, J. p 3487 N94-29841
SVEDIN, J. p 3243 N94-28906
SVEJKOVSKY, P. A. p 3397 N94-30458
SVEJKOVSKY, PAUL A. p 3299 N94-29370
SVENSSON, M. C. p 3401 N94-30000
SVESTKA, PETR p 3438 N94-30410
SVOBODA, R. p 3491 N94-30762
SWANSON, PAUL D. p 3498 N94-28804
SWANSON, S. E. p 3267 N94-30368
SWANSON, WAYNE L. p 3174 N94-29868
SWEENEY, DENNIS GIVENS p 3253 N94-29897
SWIERSTRA, SIP p 3139 N94-29570
SWINNEY, DAVID A. p 3398 N94-29154
SYDNOR, RICHARD L. p 3468 N94-30639
SYMEOPOULOS, V. p 3187 N94-28567
SYMM, G. T. p 3476 N94-30781
SYTSMA, H. A. p 3133 N94-30388
SZYMANSKI, RAYMOND p 3150 N94-29348
SZYMURSKI, S. R. p 3220 N94-30692

T

TAASAN, SHLOMO p 3454 N94-30208
TABATA, TATSUO p 3485 N94-28788
TACONI, NOLAN E., JR. p 3263 N94-28994
TAGGART, DOUG p 3144 N94-30644
TAGUCHI, YASUKO p 3387 N94-29713
TAGUIROV, R. p 3152 N94-29296
TAHMASEBI, FARHAD p 3301 N94-29556
p 3288 N94-29726
TAKABAYASHI, AKIRA p 3387 N94-29712
TAKAGI, KANICHI p 3389 N94-28850
p 3394 N94-29863
TAKAGI, KENICHI p 3387 N94-28495
TAKAGI, MIKIO p 3326 N94-28928
TAKAHASHI, KEIICHI p 3387 N94-29711
TAKAHASHI, MASAHIRO p 3123 N94-28953
TAKAHASHI, YOSHIKAZU p 3223 N94-29517
TAKAHASI, MINORU p 3170 N94-30932
TAKAHIRA, MIKINARI p 3123 N94-28949
p 3123 N94-28950
TAKAKI, RYOJI p 3123 N94-28951
TAKAKURA, HIDEYUKI p 3159 N94-30162
TAKAKURA, YOKO p 3126 N94-28972
TAKALLU, M. A. p 3132 N94-29937
TAKANASHI, KOKI p 3495 N94-29596
TAKANASHI, SUSUMU p 3125 N94-28965
TAKANASHI, WAKO p 3126 N94-28970
TAKANO, ISAO p 3324 N94-28693
TAKEDA, KANAME p 3328 N94-29037
TAKEDA, KAZUO p 3357 N94-29070
TAKEI, MITSURU p 3330 N94-29221
TAKENAGA, H. p 3505 N94-29398
TAKEUCHI, HISAO p 3127 N94-28978
TAKEUCHI, SADAO p 3314 N94-29981
TAKIMOTO, HIROSHI p 3159 N94-30162
TAKRIFF, M. p 3340 N94-30879
TALLANT, D. R. p 3220 N94-30591
TALWAR, SANJIV p 3303 N94-29966
TAMURA, A. T. p 3535 N94-30699
TAMURA, ATSUHIRO p 3127 N94-28976
TAMURA, HIROSHI p 3128 N94-28984
TAMURA, YOSHIAKI p 3126 N94-28967
TANABE, MINORU p 3390 N94-28854
TANAKA, ASTERIO KIYOSHI p 3531 N94-29535
TANAKA, ATSUSHIGE p 3127 N94-28978
TANAKA, MAKOTO p 3240 N94-29521
p 3479 N94-29597
TANAKA, NOBUO p 3158 N94-28583
TANAKA, TAKASHI p 3359 N94-29237
p 3360 N94-29238
TANAKA, TOSHIYUKI p 3188 N94-28680
TANAKA, YOSHIHITO p 3360 N94-29239
TANG, J. p 3482 N94-28509
p 3477 N94-30873
p 3493 N94-30903
TANG, JAU p 3493 N94-30874
TANI, KOUICHIRO p 3123 N94-28953
TANIIKE, A. p 3505 N94-29397
TANIMURA, ATSUSHI p 3358 N94-29082
TANJI, AKIRA p 3159 N94-30794
TARASOV, V. E. p 3523 N94-28617
TARTAKOVSKY, E. A. p 3220 N94-30778
TASCILLO, A. p 3439 N94-30531
TASK, H. L. p 3146 N94-29042
TASSELLI, A. p 3154 N94-29270
TATARENKOV, V. M. p 3474 N94-30676
TATCHYN, R. p 3292 N94-28481
TAUB, SUSAN R. p 3286 N94-29000
p 3267 N94-30198
TAUTZ, M. F. p 3164 N94-28827
TAVELLA, P. p 3473 N94-30668
TAWEL, RAOUL p 3265 N94-29426
p 3436 N94-29756
TAYLOR, C. R. p 3405 N94-29181
TAYLOR, D. L. p 3189 N94-29010
TAYLOR, DOUG p 3299 N94-29409
TAYLOR, J. R. p 3295 N94-30598
TAYLOR, LAFAYETTE K. p 3277 N94-29859
TAYLOR, P. A. p 3184 N94-30589
TAYLOR, P. L. p 3314 N94-30444
TAYLOR, THEODORE D. p 3512 N94-29101
TCELNIKER, YU. L. p 3467 N94-30088
TEDESCO, E. F. p 3538 N94-28671
TEDESCO, JOSEPH W. p 3319 N94-29433
TEMME, LEONARD A. p 3388 N94-28756
TEMPLE, JOHN p 3163 N94-29648
TENCH, R. J. p 3501 N94-30599
TENDAM, A. A. p 3458 N94-30402
p 3282 N94-30855
TENHAVE, A. A. p 3324 N94-30872
TENNAKOON, C. L. K. p 3198 N94-29938
TERAYAMA, YOSHIHIDE p 3314 N94-29984
TERESHCHENKO, V. V. p 3290 N94-30148
TERHOFSTEDE, A. H. M. p 3423 N94-30344
p 3535 N94-30362
TERZOPOULOS, D. p 3439 N94-30529
THACKRAY, R. p 3143 N94-30933
THADHANI, N. N. p 3521 N94-30851
THANGARAJ, N. p 3519 N94-30707
THART, W. G. J. p 3220 N94-30420
THAXTON, ERIC A. p 3240 N94-30467
THEISS, T. J. p 3323 N94-30689
THEVIK, H. J. p 3206 N94-29997
p 3208 N94-30113
THOMAS, CLAUDINE p 3144 N94-30651
p 3470 N94-30654
THOMAS, I. M. p 3212 N94-28560
THOMAS, J. p 3136 N94-28914
THOMAS, J. B. p 3144 N94-30650
THOMAS, JESS BROOKS, JR. p 3265 N94-29374
THOMAS, W. D. p 3406 N94-30004
THOMPSON, B. p 3305 N94-30279
THOMPSON, DANIEL C. p 3240 N94-30449
THOMPSON, DONALD L. p 3224 N94-28769
THOMPSON, J. D. p 3492 N94-30775
p 3520 N94-30848
THOMPSON, THEODORE J. p 3389 N94-28797
THOMSON, D. p 3145 N94-28657
THOMSON, MARK p 3161 N94-29632
THOMSON, R. E. p 3261 N94-28546
THOR, SVEN-ERIK p 3340 N94-30945
THORNDIKE, ALAN S. p 3351 N94-30626
p 3352 N94-30632
THORNTON, FREDERICK P., JR. p 3410 N94-29115
THORNTON, ROBERT p 3384 N94-28453
THOTTAPPILLIL, RAJEEV p 3372 N94-29802
THUAIRE, A. p 3168 N94-29543
THURMAN, S. W. p 3159 N94-29656
TIESSEN, HOLM p 3351 N94-30624
TILLMAN, JAMES E. p 3236 N94-29777
TILSTON, J. R. p 3194 N94-29274
TIMIAN, D. A. p 3157 N94-29151
TIMOTEO, D. p 3136 N94-28914
TIP, F. p 3418 N94-29503
TIPTON, M. J. p 3381 N94-28436
p 3381 N94-28437
p 3382 N94-28442
TIPTON, R. p 3211 N94-30892
TITRAN, ROBERT H. p 3202 N94-28822
TOBA, YOSHIAKI p 3328 N94-29040
TOBIAS, M. L. p 3461 N94-30817
TOCHILOV, V. N. p 3500 N94-30075
TODOSOW, M. p 3497 N94-30588
TOERNUDD, E. p 3532 N94-29682
TOGAMI, YUJI p 3495 N94-29596
TOLOCZKO, M. B. p 3201 N94-28456
TOLSTAYA, E. D. p 3365 N94-30223
TOMLINS, P. E. p 3217 N94-29885
p 3217 N94-29886
TONEGAWA, YUTAKA p 3357 N94-29079
p 3361 N94-29244
TONKS, WILLIAM BRIAN p 3543 N94-29698
TOOGOOD, R. W. p 3308 N94-30296
TOOMARIAN, NIKZAD p 3435 N94-29492
TOONEN, B. p 3350 N94-30116
TORRE, J. M. p 3297 N94-30686
TORRI, P. p 3217 N94-30025
TORTI, RICHARD P. p 3239 N94-29789
TOUCHSTONE, R. M. p 3143 N94-30933
TOWHEED, SYED S. p 3528 N94-28414
TOWNES, C. H. p 3249 N94-29653
TOWNSEND, ALAN p 3352 N94-30631
TOWNSEND, DENNIS P. p 3303 N94-30227
TOWNSEND, J. K. p 3498 N94-28780
TOYAMA, FUMIO p 3359 N94-29235
TRACK, E. K. p 3262 N94-28767
TRACY, C. E. p 3268 N94-30819
TRESSER, C. p 3335 N94-30610
TREUHAFT, R. N. p 3249 N94-29653
TRICHET, P. p 3195 N94-29278
TRIEBNIG, G. p 3331 N94-29227
TRIF, N. p 3144 N94-30286
TRIFUNAC, A. D. p 3220 N94-30778
TROCCAZ, J. p 3395 N94-30028
p 3395 N94-30029
TROCCAZ, JOCELYNE p 3395 N94-30030
TROELSTRA, A. S. p 3457 N94-30385
TROUDET, T. p 3155 N94-30204
TROULLIER, N. p 3509 N94-30752
TROVATI, A. p 3154 N94-29270
TROWBRIDGE, L. D. p 3200 N94-30880
TRUDNOWSKI, D. J. p 3451 N94-28739
TSACOYEANES, W. C. p 3291 N94-30218
TSAI, JEENHUEI p 3460 N94-30515
TSAI, LUNG-WEN p 3301 N94-29556
p 3288 N94-29726
TSAO, J. Y. p 3519 N94-30592
p 3501 N94-30828
TSE, D. G. p 3477 N94-28904
TSELIOUDIS, GEORGE p 3374 N94-29972
TSIDULKO, YU. A. p 3508 N94-30171
TSKHOVREBOV, M. M. p 3151 N94-29293
p 3152 N94-29299
TSOTSOS, J. p 3439 N94-30529
TSU, HIROJI p 3331 N94-29226
TSUBOTA, T. K. p 3495 N94-30214
TSUBOTA, YUKIO p 3234 N94-29704
TSUCHIYA, MASAKO p 3129 N94-28993
TSUI, CHI-WA p 3510 N94-30882
TSUNASHIMA, ATSUMU p 3223 N94-29513
TSURUSAKI, KATSUYA p 3187 N94-28675
p 3553 N94-29512

TSURUTA, YOSHINARI p 3233 N94-29701
p 3235 N94-29708
TSUTAYA, TSUTOMU p 3495 N94-29596
TSUZUKIYAMA, KOJI p 3495 N94-29596
TSVETKOV, I. O. p 3489 N94-30051
TSYBIN, I. YA. p 3500 N94-30075
TU, HU QI p 3481 N94-28469
TUCKER, S. p 3437 N94-30250
TUMELIN, JEAN-CLAUDE p 3141 N94-29583
TUNCA, YASAR p 3254 N94-30031
TUNG, M. M. p 3487 N94-29145
TUNIZ, C. p 3543 N94-28545
TUOMI, T. p 3385 N94-29189
TURKEL, ELI p 3454 N94-30209
TURKOT, B. A. p 3521 N94-30894
TURNER, TERRY D. p 3354 N94-30464
TURUNEN, R. p 3301 N94-29679
TUTTLE, B. A. p 3518 N94-30247
TUZNIK, RICHARD J. p 3176 N94-28673
TVEITO, A. p 3420 N94-29949
TYBURCZY, JAMES A. p 3214 N94-29203
TYLER, TONY R. p 3161 N94-29636
TYSON, K. S. p 3226 N94-30818
TYUKHTYAEV, YU. N. p 3484 N94-28584
TZAVARAS, ATHANASIOS E. p 3271 N94-29061
TZIPERMAN, ELI p 3352 N94-30633

U

UBEAUD, DANIEL J. p 3413 N94-29322
UCHIDA, HIDENOBU p 3479 N94-29597
UCHIDA, TAKASHI p 3124 N94-28959
UDINK, R. T. p 3433 N94-30720
UECKER, DARRIN R. p 3314 N94-30441
UEDA, YUTAKA p 3511 N94-28750
UEHARA, SHIGETSUGU p 3332 N94-29230
UGAI, MASAYUKI p 3360 N94-29241
UGLENE, WENDELL p 3380 N94-28431
UKEGAWA, KOJI p 3188 N94-28679
UKETA, YOSHIE p 3390 N94-28854
ULABY, FAWWAZ T. p 3259 N94-30510
ULEN, ESKIL p 3340 N94-30946
ULLMAN, FRANK G. p 3485 N94-28668
ULVESTAD, J. S. p 3164 N94-29621
UMAR, A. S. p 3454 N94-30317
UMNIKOV, A. YU. p 3484 N94-28610
UNGER, SHELDON E. p 3146 N94-29042
UPADHYA, KAMLESHWAR p 3186 N94-30452
UPADHYAYA, M. p 3443 N94-30553
URBAN, JULIE M. p 3527 N94-28796
USAMI, TAKESHI p 3187 N94-28675
p 3188 N94-28683
p 3553 N94-29512
USLU, C. p 3521 N94-30851
USPENSKY, VLADIMIR A. p 3427 N94-30732
USUI, SHIRO p 3393 N94-29716
UZ, MEHMET p 3202 N94-28822

V

VACHON, PARIS W. p 3327 N94-28934
VADNAIS, CAROLYN M. p 3361 N94-29430
VAEINOELAE, REIMA p 3204 N94-29387
VAIC, H. p 3384 N94-28452
VAKATOV, D. V. p 3485 N94-28621
VALETT, JON p 3419 N94-29727
VALLERAND, A. L. p 3380 N94-28427
VALLOTTON, WILL p 3163 N94-29648
VANBEEK, C. M. p 3135 N94-30916
VANBENTHEM, JOHAN p 3424 N94-30371
p 3457 N94-30396
VANBLANKEN, E. p 3461 N94-30767
VANBOCKSTAL, L. p 3520 N94-30848
VANBOMMEL, P. p 3535 N94-30330
VANBREUGEL, F. p 3425 N94-30432
p 3426 N94-30491
VANBREUGEL, FRANCK p 3459 N94-30427
VANBRUEGEL, FRANCK p 3433 N94-30431
VANCURA, OLAF p 3540 N94-29833
VANDAMM, GEORGE A. p 3299 N94-29370
VANDEBERG, J. I. p 3282 N94-30855
VANDENBERG, J. I. p 3133 N94-30388
p 3281 N94-30743
VANDENBOS, HANS p 3139 N94-29569
VANDENBROEK, P. M. p 3429 N94-30765
VANDENBURG, GERT p 3335 N94-30759
VANDENHEUVEL, J. P. M. p 3461 N94-30767
VANDENHEUVEL, JAN P. M. p 3461 N94-30766
VANDERDRAAI, R. K. p 3158 N94-30423
p 3158 N94-30856
VANDERGAAG, L. C. p 3465 N94-30358
VANDERGAAG, LINDA p 3456 N94-30378
VANDERHAM, M. p 3252 N94-29692
p 3252 N94-29693
VANDERHOEK, W. p 3428 N94-30749
VANDERHOUWEN, P. J. p 3433 N94-30730
VANDERSANDEN, JOOST J. p 3335 N94-30759
VANDERSCHAFT, A. J. p 3462 N94-30964
VANDERVEEN, W. A. p 3433 N94-30730
VANDERVOOREN, J. p 3133 N94-30401
p 3134 N94-30493
VANDERWEIDE, T. P. p 3535 N94-30330
p 3423 N94-30344
p 3535 N94-30357
p 3535 N94-30360
p 3535 N94-30362
VANDEWAL, ANTHONY p 3258 N94-30505
VANDEWINCKEL, C. p 3439 N94-30531
VANDOORN, B. A. p 3428 N94-30764
p 3143 N94-30853
VANDRIEL, N. p 3143 N94-30854
VANDRONKELAAR, J. H. p 3143 N94-30915
VANDYKE, P. T. p 3563 N94-30844
VANE, GREGG p 3237 N94-29779
VANEWIJK, L. J. p 3256 N94-30392
VANFOSSEN, MICKEY CHARLES p 3362 N94-29940
VANGGAARD, LEIF p 3381 N94-28438
VANGILST, F. A. p 3429 N94-30765
VANGROESEN, E. W. C. p 3460 N94-30738
VANGSNESS, M. D. p 3193 N94-29266
VANIER, P. E. p 3487 N94-29841
p 3223 N94-30475
VANKREVELD, MARC p 3459 N94-30425
VANLEEUWEN, JACQUES p 3455 N94-30327
VANLINDER, B. p 3428 N94-30749
VANLOON, M. p 3353 N94-30729
VANLUNTEREN, A. p 3402 N94-30390
VANMELLE, M. J. p 3145 N94-30663
VANMOURIK, P. A. p 3281 N94-30763
VANPRAAG, R. p 3184 N94-30343
VANROSSUM, GUIDO p 3418 N94-29487
VANTURE, ANDREW DOUGLAS p 3539 N94-29820
VANVLIJMEN, BAS p 3448 N94-30731
VANWAVEREN, ARJAN p 3448 N94-30731
VANWOERKOM, P. T. L. M. p 3311 N94-30391
VANZANDT, T. p 3237 N94-29778
VANZANDT, THOMAS R. p 3236 N94-29777
VARGA, R. C. p 3289 N94-29927
VASQUEZ, BERNARD JOHN p 3506 N94-29822
VASQUEZ, RICHARD P. p 3513 N94-29501
VASSAL, P. p 3395 N94-30028
p 3395 N94-30029
VAUGHN, WALLACE L. p 3186 N94-30481
VEILLET, C. p 3145 N94-30665
VELDKAMP, WILFRID B. p 3235 N94-29771
VELDMAN, A. E. P. p 3281 N94-30743
VELDMAN, H. J. p 3461 N94-30767
VELIGDAN, JAMES p 3223 N94-30475
VELTEN, J. R. p 3141 N94-29582
VEMURI, V. R. p 3421 N94-30117
VENDRELY, TIMOTHY G. p 3161 N94-29635
VENEMA, JAN CEES p 3335 N94-30759
VENEMANS, P. J. p 3402 N94-30422
VENKATESH, RAMANAN p 3182 N94-29852
VERDON, C. P. p 3509 N94-30597
VERES, JOSEPH P. p 3273 N94-29539
VERGHESE, S. p 3515 N94-30009
VERGNOL, F. p 3413 N94-29320
VERKOOIJEN, H. p 3495 N94-29467
p 3495 N94-29888
VERLINDE, PATRICK p 3258 N94-30504
VERMEER, G. S. p 3438 N94-30373
VERMEULEN, P. J. p 3196 N94-29284
VERNOTTE, F. p 3472 N94-30667
VERUTTIPONG, W. p 3248 N94-29624
p 3249 N94-29657
VERWER, J. G. p 3353 N94-30729
VESELSKY, M. p 3485 N94-28621
VEYNANTE, D. p 3190 N94-29251
VIANCO, P. T. p 3206 N94-29936
VIBULSRESTH, SUVIT p 3327 N94-28936
p 3328 N94-28937
VIERGEVER, M. A. p 3438 N94-30349
VIGOUREUX, P. p 3260 N94-30785
VIGUE, Y. p 3144 N94-30650
VILENSKY, S. A. p 3525 N94-30170
VILLAREAL, L. D. p 3527 N94-30041
VILNROTTER, V. A. p 3250 N94-29660
p 3250 N94-29661
VINER, M. R. p 3148 N94-30129
VINOGRADOV, V. p 3152 N94-29296
VIRGIN, L. N. p 3479 N94-29461
VIRSHUP, G. F. p 3262 N94-28767
VISSER, A. T. p 3268 N94-30904
VISSER, ALBERT p 3463 N94-30977
VITAGLIANO, P. L. p 3133 N94-30387
VITANYI, PAUL M. R. B. p 3526 N94-30433
VIZIO, G. p 3473 N94-30668
VLADIMIROVA, N. M. p 3220 N94-30745
VOECKS, GERALD E. p 3225 N94-29490
VOELCKERS, U. p 3138 N94-29567
VOELCKERS, UWE p 3141 N94-29581
VOGELS, M. E. S. p 3281 N94-30756
VOIGT, J. A. p 3518 N94-30315
VOLAKIS, JOHN L. p 3253 N94-29873
VOLKAS, R. R. p 3481 N94-28471
VOLLWEILER, FRED O. p 3202 N94-28643
VOLPE, RICHARD p 3442 N94-30544
VOROPAEV, S. G. p 3508 N94-30193
VOSS, S. S. p 3498 N94-30846
p 3498 N94-30847
VOTH, CHRISTOPHER T. p 3164 N94-28417
VOZZO, J. A. p 3387 N94-30461
VREEBURG, J. P. B. p 3229 N94-30409
p 3290 N94-30742
VREUGDENHIL, C. B. p 3461 N94-30751
VU, NGOCOANH p 3395 N94-29919
VYSOTSKAYA, I. N. p 3421 N94-30077

W

WACHSPRESS, DANIEL A. p 3480 N94-30274
WADA, MAKOTO p 3363 N94-29979
WADA, YASUHIRO p 3123 N94-28951
p 3126 N94-28973
WADA, YOSHIRO p 3393 N94-29718
WADDOUPS, M. A. p 3314 N94-30444
WADE, DONALD C. p 3160 N94-29369
WAGENAAR, W. p 3281 N94-30756
WALD, JERRY p 3171 N94-29791
WALDRON, DOUGLAS J. p 3303 N94-30173
WALKER, BRIAN p 3352 N94-30630
WALKER, DAVID H. p 3278 N94-29977
WALKER, IAN D. p 3445 N94-30562
WALKO, D. A. p 3483 N94-28559
WALLEZ, C. p 3258 N94-30507
WALLICK, BRIAN PAUL p 3362 N94-29939
WAN, A. S. p 3295 N94-30060
WANG, CONGJUN p 3215 N94-29745
WANG, DAILIN p 3378 N94-29815
WANG, GUOQING p 3229 N94-30145
WANG, J. R. p 3254 N94-30094
WANG, JERRY ZHIQI p 3182 N94-29875
WANG, P. K. C. p 3239 N94-29787
WANG, YE p 3518 N94-30239
WANG, YI-MIN p 3420 N94-29906
WANG, YULUN p 3314 N94-30441
WANG, YUZHONG J. p 3236 N94-29773
WANG, ZHILING p 3442 N94-30549
WANGERMANN, JOHN p 3137 N94-29562
WANHILL, R. J. H. p 3153 N94-30914
WARD, B. F. L. p 3482 N94-28504
WARD, N. J. p 3416 N94-29338
WARD, R. L. p 3212 N94-28560
WARDRIP, S. CLARK p 3468 N94-30640
WARHUS, J. P. p 3254 N94-29929
WARNER, RONALD R., JR. p 3121 N94-28743
WARREN, M. S. p 3548 N94-30694
WARREN, O. L. p 3211 N94-28530
WARRINGTON, ROBERT O. p 3235 N94-29769
p 3238 N94-29786
WARWOWSKI, W. p 3464 N94-29178
WASILEWSKI, Z. p 3516 N94-30063
WASLEY, RICHARD J. p 3240 N94-30449
WATANABE, HIROSHI p 3330 N94-29223
WATANABE, KOJI p 3158 N94-28583
WATANABE, SATORU p 3393 N94-29718
WATANABE, YASUO p 3123 N94-28951
WATERMANN, J. p 3356 N94-28869
WATERS, MARK H. p 3147 N94-29721
WATERS, W. ALLEN, JR. p 3178 N94-29100
WATKINS, A. D. p 3314 N94-30444
WATKINS, J. p 3504 N94-28686
WATKINS, STANLEY H. p 3529 N94-29053
WATRING, D. A. p 3290 N94-30199
WATSON, ANDREW B. p 3406 N94-29375
WATSON, R. p 3404 N94-28505
WATSON, WILLIE R. p 3478 N94-29382
WATTS, LOUIS A. p 3237 N94-29781
WAWRYSCUK, J. p 3485 N94-28625
WAY, CARL M. p 3286 N94-28831
WAYE, D. E. p 3165 N94-28477
WEAVER, H. T. p 3510 N94-28484
WEBB, JAMES T. p 3391 N94-29071
WEBBER, ROBERT E. p 3144 N94-30281
WEBER, A. H. p 3373 N94-29817
WEBER, F. p 3542 N94-28480
WEBER, G. F. p 3341 N94-28463
WEBER, S. G. p 3174 N94-29307
WEBER, S. V. p 3509 N94-30597
WEDDENDORF, BRUCE p 3300 N94-29486
WEDLOCK, M. I. p 3194 N94-29274
WEDZINGA, G. p 3429 N94-30912
WEEKS, JACK L. p 3215 N94-29446
WEEKS, M. D. p 3291 N94-30218

WEEKS, R. A. p 3219 N94-30335
WEI, A. p 3263 N94-29025
WEI, GU SHI p 3481 N94-28469
WEILER, D. R. p 3155 N94-30284
WEINBERG, MARC S. p 3144 N94-29788
WEINERT, M. p 3206 N94-29931
WEIR, RAE ANN p 3163 N94-29650
WEISS, MARC A. p 3145 N94-30660
WELCH, SAMUEL WILLIAMSON JOHN
p 3283 N94-30954
WELLMAN, R. J. p 3259 N94-30512
WELLS, GEORGE H., JR. p 3397 N94-30459
WELLS, J. C. p 3454 N94-30317
WELLS, JAMES C. p 3502 N94-30462
WELLS, RICHARD D. p 3486 N94-29131
WELLS, RICHARD L. p 3513 N94-29130
p 3189 N94-29140
p 3513 N94-29155
WENDELIN, T. p 3500 N94-29799
WENDELL, L. L. p 3368 N94-28455
p 3374 N94-30587
WENK, CARL J. p 3463 N94-28759
WENNBERG, PAUL O. p 3343 N94-28592
WENNERHOLM, H. p 3337 N94-28909
WERCHAN, PAUL p 3400 N94-29029
WERKHEISER, ANNE p 3452 N94-29063
p 3435 N94-29198
WERST, D. W. p 3220 N94-30778
WESELY, M. L. p 3368 N94-28568
p 3334 N94-30022
WESSELSKI, CLARENCE J. p 3160 N94-29369
WEST, JAMES W. p 3287 N94-29368
WESTERLING, J. p 3243 N94-28907
WESTINGA, EDUARD p 3335 N94-30759
WESTWATER, E. R. p 3136 N94-30890
WEYMOUTH, TERRY p 3442 N94-30548
WHEELER, HOWARD A. p 3142 N94-30189
WHITE, C. W. p 3518 N94-30249
WHITE, HENRY S. p 3486 N94-29060
p 3203 N94-29089
WHITE, J. KEVIN p 3300 N94-29506
WHITE, ROBERT E. p 3451 N94-28792
WHITE, STEVEN p 3288 N94-29538
WHITELAW, J. H. p 3477 N94-28904
p 3195 N94-29276
WHITFIELD, DAVID L. p 3277 N94-29859
WHITLOW, J. D. p 3196 N94-29280
WHITTAKER, JAMES A. p 3407 N94-28664
p 3156 N94-28752
p 3156 N94-28753
WHYTE, STEPHEN A. p 3271 N94-28809
WIANT, J. p 3145 N94-30665
p 3297 N94-30666
WIDRICK, TIMOTHY W. p 3319 N94-29406
WIKNER, D. A. p 3259 N94-30512
WILCOTS, ERIC MATTHEW p 3543 N94-29722
WILCOX, J. Z. p 3249 N94-29654
WILCZEK, F. p 3491 N94-30685
WILKERSON, J. F. p 3240 N94-28522
WILKES, D. p 3439 N94-30529
WILKES, DAVID p 3309 N94-30301
WILKINSON, LADYE KATHRYN p 3544 N94-29723
WILKINSON, S. p 3239 N94-29793
WILLIAMS, A. p 3190 N94-29250
WILLIAMS, A. J. p 3290 N94-30782
WILLIAMS, DAVID p 3257 N94-30500
WILLIAMS, DAVID H. p 3140 N94-29578
WILLIAMS, F. p 3391 N94-28912
WILLIAMS, G. P. p 3510 N94-28512
WILLIAMS, LANCE LEE p 3280 N94-30352
WILLIAMS, M. C. p 3338 N94-30048
p 3338 N94-30313
WILLIAMS, O. R. p 3305 N94-30279
WILLIAMS, OWEN p 3310 N94-30307
WILLIAMS, R. K. p 3520 N94-30724
WILLIAMS, TODD O. p 3183 N94-30125
WILLIAMSEN, J. E. p 3169 N94-30161
WILLIAMSON, D. L. p 3350 N94-30116
WILLS, E. L. p 3236 N94-29774
WILLSHIRE, MARY JANE p 3531 N94-29537
WILMS, PHILIPPE p 3258 N94-30504
WILSON, B. A. p 3235 N94-29767
WILSON, DAVID A. p 3254 N94-30035
WILSON, K. N. p 3503 N94-28513
WILSON, M. S. p 3208 N94-30101
WILT, THOMAS F. p 3183 N94-30190
WING, J. p 3405 N94-28916
WING, JEANNETTE M. p 3410 N94-29006
WINICK, H. p 3296 N94-30688
WINOGRAD, N. p 3512 N94-28775
WIPKE, K. B. p 3302 N94-29922
WIPPICH, HEINZ-GEORG p 3138 N94-29565
WISE, J. p 3218 N94-30102
WISE, MICHAEL WAYNE p 3541 N94-30800
WISE, NICHOLAS p 3153 N94-30130
WISHNOW, EDWARD HYMAN p 3199 N94-30137
WITTE, TOM p 3325 N94-28808
WITTIG, J. E. p 3207 N94-30042
WITTIG, S. p 3195 N94-29279
p 3196 N94-29283
WITZE, P. O. p 3311 N94-30596
WOJCIK, P. p 3307 N94-30291
p 3309 N94-30304
WOLF, E. E. p 3200 N94-30877
WOLF, MARTIN F. p 3214 N94-29073
WOLF, P. p 3470 N94-30653
WOLFF, P. p 3160 N94-29666
WOLFSON, JAKE p 3162 N94-29642
WONG, GENE A. p 3142 N94-29587
WONG, P. p 3452 N94-29118
WONG, SEE-POK p 3173 N94-29444
WOODS, THOMAS N. p 3551 N94-30948
WOODWARD, JOSEPH H. p 3176 N94-28655
WORLEY, P. p 3350 N94-30116
WORSLEY, KEITH J. p 3464 N94-28876
WORSNOP, DOUGLAS R. p 3347 N94-29549
WORTLEY, C. p 3310 N94-30308
WRIGHT, DARREL L. p 3121 N94-28743
WRIGHT, S. I. p 3210 N94-30774
WRIGHT, T. p 3465 N94-30696
WU, ANNIE p 3442 N94-30548
WU, CHARLES CHENGZHI p 3278 N94-29974
WU, JONG-CHING p 3266 N94-29734
WU, LIWEI p 3442 N94-30547
WU, Q. H. p 3436 N94-29526
p 3266 N94-29527
WU, T. W. p 3301 N94-29552
WU, WEIHAN ROBERT p 3275 N94-29836
WU, X. F. p 3301 N94-29552
WU, Y. p 3494 N94-29422
WUEBBLES, D. J. p 3350 N94-30613
p 3367 N94-30876
WUNNEBURGER, DOUGLAS FRANK
p 3333 N94-29540
WURTMAN, RICHARD J. p 3398 N94-29027
WYNN, TOM p 3163 N94-29648

X

XIA, ZONG-GUO p 3333 N94-29958
XIANGDE, XU p 3370 N94-29394
XIAO, H. p 3521 N94-30894
XIAO, ZHENHUA p 3270 N94-28665
XU, JIECHI p 3323 N94-30813
XU, MING p 3519 N94-30338
XU, PING p 3201 N94-28479
XU, YANGSHENG p 3442 N94-30543
XUE, JUE p 3409 N94-28917

Y

YABU, TETSURO p 3359 N94-29234
YAJIMA, KAZUYOSHI p 3388 N94-28498
p 3389 N94-28852
p 3386 N94-28853
YAJIMA, NOBUYUKI p 3359 N94-29235
YAKOVENKO, N. A. p 3286 N94-28553
YAKOVLEV, R. M. p 3489 N94-30051
p 3489 N94-30052
YAMADA, EITARO p 3127 N94-28980
YAMADA, H. p 3505 N94-29398
YAMADA, HITOSHI p 3128 N94-28987
YAMADA, I. p 3505 N94-29398
YAMADA, OSAMU p 3187 N94-28676
YAMADA, SATOSHI p 3358 N94-29082
YAMADA, YOSHIO p 3187 N94-28675
p 3187 N94-28678
p 3553 N94-29512
p 3223 N94-29517
p 3223 N94-29518
YAMAGISHI, HISAO p 3359 N94-29233
p 3360 N94-29239
p 3361 N94-29244
YAMAGUCHI, SHIZUKO p 3388 N94-28498
YAMAGUCHI, YASUSHI p 3129 N94-28993
p 3330 N94-29222
YAMALEEV, R. M. p 3485 N94-28718
YAMAMOTO, KAZUOMI p 3128 N94-28981
YAMAMOTO, MASAAKI p 3233 N94-29701
p 3234 N94-29703
YAMAMOTO, RYUTARO p 3233 N94-29701
p 3234 N94-29704
YAMAMOTO, SATORU p 3124 N94-28954
YAMAMOTO, SHINICHI p 3360 N94-29238
YAMAMOTO, TAKASHI p 3360 N94-29240
YAMAMOTO, YOSHINOBU p 3159 N94-30162
YAMAMOTO, YUKIMITU p 3124 N94-28955
YAMANE, TAKASHI p 3127 N94-28977
YAMASHINA, T. p 3503 N94-28513
YAMASHITA, KATSUMASA p 3387 N94-29866
YAMASHITA, MASAMICHI p 3387 N94-29713
YAMASHITA, YASUMASA p 3187 N94-28678
YAMAWAKI, RURIKO p 3127 N94-28978
YAMAZAKI, MICHIO p 3159 N94-30794
YAMAZAKI, TETSUO p 3124 N94-28959
YAN, ZANYU p 3449 N94-30806
YANAGIZAWA, MITSUNORI p 3127 N94-28974
YANEZ-HERRERO, M. p 3207 N94-30057
YANG, SHAORUI p 3321 N94-29829
YANG, SHUTING p 3376 N94-30966
YANG, X. Q. p 3485 N94-28741
YAO, XIAO-XIONG p 3453 N94-30139
YARBROUGH, D. W. p 3520 N94-30724
YEARWOOD, MICHAEL p 3440 N94-30532
YEATES, J. p 3536 N94-29144
YEE, YOUNG P. p 3257 N94-30499
YEH, H.-G. p 3251 N94-29667
YELVERTON, JOHN T. p 3391 N94-29150
YEN, JOHN p 3444 N94-30557
YEN, W. M. p 3501 N94-30252
YEN, YIN-CHAO p 3332 N94-29288
YEOM, HEON YOUNG p 3531 N94-29591
YEUNG, K. K. p 3307 N94-30292
YEUNG, S. K. p 3144 N94-30286
YIALIZIS, A. p 3223 N94-30479
YICK, S. K. p 3303 N94-30019
YIN, B. p 3250 N94-29659
YLIKANGAS, I. p 3220 N94-30713
YLOENEN, T. p 3530 N94-29167
YODA, MINAMI p 3278 N94-29976
YOGESH, A. p 3404 N94-28517
YOKOBORI, SAKAE p 3387 N94-28495
p 3389 N94-28850
p 3394 N94-29863
YOKOTA, KAZUHIKO p 3127 N94-28975
YOKOTA, TOYOHACHI p 3170 N94-30932
YOKOUCHI, NORIHISA p 3377 N94-29595
YOKOYAMA, KENJI p 3503 N94-28555
YOKOYAMA, RYUZO p 3328 N94-29041
YONG-HUI, HU p 3471 N94-30658
YONG, FU XIN p 3481 N94-28469
YONG, L. p 3204 N94-29142
YONUSHONIS, T. M. p 3537 N94-29350
YOSHIDA, AKIHIKO p 3125 N94-28962
YOSHIDA, JIRO p 3314 N94-29981
YOSHIDA, MASAHIRO p 3129 N94-28991
p 3129 N94-28992
YOSHIDA, TETSUJI p 3442 N94-30543
YOSHIDA, YOSHIO p 3354 N94-29086
YOSHIKAWA, SHINYA p 3158 N94-28583
YOSHIMURA, KENJIRO p 3387 N94-29711
YOSHIOKA, TOSHITADA p 3387 N94-29866
YOSHIZAWA, NORIKO p 3223 N94-29518
YOST, WILLIAM T. p 3287 N94-29199
YOUNG, GEORGE S. p 3272 N94-29195
p 3377 N94-29436
YOUNG, L. E. p 3144 N94-30650
YOUNG, MELISSA L. p 3409 N94-28878
YOUNG, P. G. p 3264 N94-29209
p 3488 N94-30039
YOUNG, PAUL G. p 3286 N94-29000
YU, CHANG-TE p 3182 N94-29876
YU, CHRISTOPHER C. p 3243 N94-29069
YU, HAO p 3181 N94-29810
YU, HONG p 3209 N94-30146
YU, SOPHIA T. p 3444 N94-30556
YUAN, C. P. p 3481 N94-28462
YUDIN, I. P. p 3421 N94-30083
p 3500 N94-30084
YUEN, JOSEPH H. p 3249 N94-29652
YUKALOV, V. I. p 3522 N94-28582
p 3453 N94-30078
p 3490 N94-30112
YUKALOVA, E. P. p 3522 N94-28582
p 3453 N94-30078
p 3490 N94-30112
YUMIKURA, SEI p 3388 N94-28498
YUNG, Y. L. p 3343 N94-28593
YUREVICH, V. I. p 3489 N94-30051
p 3489 N94-30052
YUSHKOV, B. YU. p 3362 N94-29935

Z

ZACHARIA, T. p 3511 N94-28535
ZACHAROV, N. p 3152 N94-29296
ZAFRAN, SIDNEY p 3171 N94-28736
ZAHNISER, MARK S. p 3346 N94-28608
p 3347 N94-29549
ZAIDER, M. p 3495 N94-30213
ZAIKOV, R. P. p 3481 N94-28470
ZAITSEV, S. p 3152 N94-29300
ZAKHAREV, B. N. p 3524 N94-30087
ZALAMANSKY, G. p 3472 N94-30667
ZAMPETTI, GEORGE p 3469 N94-30649

ZANTEMA, H. ..... p 3455 N94-30346
p 3459 N94-30424
p 3460 N94-30744
p 3462 N94-30859
ZARRO, DOMINIC M. ..... p 3551 N94-29453
ZASHEV, J. ..... p 3456 N94-30382
ZASLAVSKY, A. YU. ..... p 3525 N94-30170
ZASLAVSKY, G. M. ..... p 3492 N94-30834
ZEHE, MICHAEL J. ..... p 3189 N94-28832
ZEIKUS, J. G. ..... p 3386 N94-30180
ZEILER, K. G. ..... p 3225 N94-30038
ZEKRI, N. ..... p 3208 N94-30108
ZELKOWITZ, MARVIN ..... p 3410 N94-29068
ZENDER, G. ..... p 3174 N94-28557
ZEPPENFELDT, FRANK O. ..... p 3335 N94-30759
ZESWITZ, STEVEN R. ..... p 3530 N94-29139
ZHANG, JIAN CHENG ..... p 3266 N94-29805
ZHANG, K. ..... p 3519 N94-30338
ZHANG, L. ..... p 3507 N94-30156
p 3507 N94-30158
ZHANG, YINBAI ..... p 3145 N94-30661
ZHANG, YUE-FENG ..... p 3144 N94-30281
ZHAO, QINGYUN ..... p 3373 N94-29814
ZHENG, HARRY HUIHENG ..... p 3437 N94-30255
ZHENG, YOUXIN ..... p 3129 N94-29306
ZHIDKOV, E. P. ..... p 3451 N94-28783
p 3421 N94-30083
ZHIDKOV, P. E. ..... p 3522 N94-28609
ZHONG, SHIYUAN ..... p 3372 N94-29813
ZHOU, LIREN ..... p 3473 N94-30671
ZHOU, QUING G. ..... p 3498 N94-28780
ZHOU, SHAOMIN ..... p 3499 N94-29491
ZHU, QIANG ..... p 3490 N94-30103
ZIDBECK, JUHA ..... p 3245 N94-29468
ZIEMKE, M. CARL ..... p 3537 N94-29410
ZINCHENKO, A. K. ..... p 3293 N94-28786
ZINKLE, S. J. ..... p 3483 N94-28559
ZINN, MICHAEL ..... p 3163 N94-29646
ZINOV, V. G. ..... p 3500 N94-30075
ZIPPERIAN, T. E. ..... p 3501 N94-30828
ZIVKOVIC, MARINA ..... p 3369 N94-28663
ZORUMSKI, WILLIAM E. ..... p 3478 N94-29382
ZSAK, THOMAS WILLIAM ..... p 3200 N94-30911
ZUCKERWAR, ALLAN J. ..... p 3288 N94-29484
ZUHR, R. A. ..... p 3207 N94-30042
p 3219 N94-30335
p 3199 N94-30723
ZUIDGEEST, RENE G. ..... p 3448 N94-30741
ZUNG, NGUYEN TIEN ..... p 3467 N94-30166
ZUREK, W. H. ..... p 3548 N94-30694
ZUREK, WOJCIECH H. ..... p 3526 N94-30433
ZWAAN, JAAP ..... p 3418 N94-29449
ZWART, ROLF ..... p 3418 N94-29449

Typical Corporate Source Index Listing

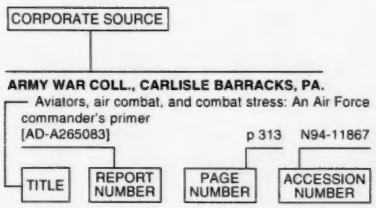

Listings in this index are arranged alphabetically by corporate source. The title of the document provides the user with a brief description of the subject matter. The report number helps to indicate the type of document cited (e.g., NASA report, translation, NASA contractor report). The accession number denotes the number by which the citation is identified. The page number helps you locate the citation in the abstract section. The titles are arranged under each corporate source in ascending accession number order.

A

AALBORG UNIV. (DENMARK).
Computational fluid dynamics in ventilation. 1: Theory and one-dimensional test case p 3232 N94-29606
Computational fluid dynamics in ventilation. 2: Theory and codes p 3233 N94-29607
Computational fluid dynamics in ventilation. 3: The IEA annex 20 work p 3233 N94-29608
Computational fluid dynamics in ventilation. 4: Commercial application of CFD in ventilation p 3233 N94-29609
Computational fluid dynamics in ventilation. 5: New developments in CFD with relevance to ventilation p 3233 N94-29610

ABACUS TECHNOLOGY CORP., CHEVY CHASE, MD.
Alternative fuel vehicles for the state fleets: Results of the 5-year planning process
[DE94-004709] p 3224 N94-28577

ACADEMY OF SCIENCES OF THE ARMENIAN SSR, ERIVAN.
Coulomb field effect on plasma focusing and wake field acceleration
[DE94-004937] p 3504 N94-28564

ACADEMY OF SCIENCES (USSR), LENINGRAD.
Observation of the phase shift of the wave function of the neutron under total reflection
[DE94-608244] p 3489 N94-30096

ACADEMY OF SCIENCES (USSR), NOVOSIBIRSK.
Resistive ballooning mode in a gas-dynamic trap
[DE94-608328] p 3508 N94-30171
On determination of a momentum of Alfven wave packet
[DE94-608329] p 3255 N94-30172
Langmuir waves in the electron-positron plasma
[DE94-608330] p 3508 N94-30191
Experiments on the two-stage dense plasma heating on the GOL-3 device
[DE94-608356] p 3508 N94-30193
Peculiarities of heat transfer in the experiments of beam injection heating of a plasma at the GOL-3 device
[DE94-608357] p 3508 N94-30194
Computer simulation of the interaction of fast hydrogen atoms with a molybdenum containing sorbed hydrogen
[DE94-608419] p 3209 N94-30253

ACOUSTICAL SOCIETY OF AMERICA, NEW YORK, NY.
Minutes. Accredited Standards Committee on Noise, S12. US tag for ISO/TC 43/SC1 noise and ISO/TC 94/SC12 hearing protection
[AD-A275622] p 3477 N94-28636
Minutes. Accredited Standards Committee on Acoustics, S1. US tag for ISO/TC 43 acoustics and IEC/TC 29 electroacoustics
[AD-A275702] p 3477 N94-28689
Minutes: Accredited Standards Committee on Mechanical Vibration and Shock, S2. US TAG for ISO/TC 108 Mechanical Vibration and Shock
[AD-A275591] p 3316 N94-28726

ACUREX CORP., RESEARCH TRIANGLE PARK, NC.
Characterization of air emissions from the simulated open combustion of fiberglass materials
[PB94-136231] p 3347 N94-29192

ADVANCED AVIATION CONCEPTS, JUPITER, FL.
Extremely Low Visibility IFR Rotorcraft Approach (ELVIRA) operational concept development. Volume 1: Executive Summary
[DOT/FAA/RD-94/1,I] p 3142 N94-30189

ADVISORY GROUP FOR AEROSPACE RESEARCH AND DEVELOPMENT, NEUILLY-SUR-SEINE (FRANCE).
The Support of Air Operations under Extreme Hot and Cold Weather Conditions
[AGARD-CP-540] p 3379 N94-28420
Fuels and Combustion Technology for Advanced Aircraft Engines
[AGARD-CP-536] p 3189 N94-29246
Research and Development of Ram/Scramjets and Turboramjets in Russia
[AGARD-LS-194] p 3151 N94-29291
Aerospace Software Engineering for Advanced Systems Architectures
[AGARD-CP-545] p 3412 N94-29315
Machine Intelligence in Air Traffic Management
[AGARD-CP-538] p 3136 N94-29558
TacSats for NATO
[AGARD-AR-322] p 3169 N94-30350
Atmospheric Propagation Effects Through Natural and Man-Made Obscurants for Visible to MM-Wave Radiation
[AGARD-CP-542] p 3256 N94-30495
Marketing tools for increasing proactivity in technical information centers
[AGARD-AR-326] p 3528 N94-30934

AERODYNE RESEARCH, INC., BILLERICA, MA.
On the possibility of measuring atmospheric OH using intracavity laser spectroscopy p 3344 N94-28597
HO2 detection by near infrared absorption using tunable diode lasers p 3346 N94-28608
Laboratory studies of chemical and photochemical processes relevant to stratospheric ozone
[NASA-CR-195779] p 3347 N94-29549

AERONAUTICAL RESEARCH INST. OF SWEDEN, STOCKHOLM.
Experimental determination of orthotropic elastic constants
[FFA-TN-1991-35] p 3215 N94-29424
Assessment of the fibre volume distribution around optical fibres
[FFA-TN-1993-12] p 3179 N94-29425
The execution of wind energy projects 1986 - 1992 between China Aerodynamics Research and Development Centre (CARDC) and The Aeronautical Research Institute of Sweden (FFA)
[FFA-TN-1993-19] p 3340 N94-30945
Wind tunnel tests of a 5.3 m diameter yaw controlled turbine
[FFA-TN-1993-20] p 3340 N94-30946
Fatigue management and verification of airframes
[FFA-TN-1993-55] p 3149 N94-30947

AERONAUTICAL RESEARCH LABS., MELBOURNE (AUSTRALIA).
Fishermans Bend: A centre of Australian aviation
[AD-A274981] p 3121 N94-29090
Cold expansion and interference for extending the fatigue life of multi-layer metal joints
[AD-A274982] p 3318 N94-29091

AERONAUTICAL SYSTEMS DIV., WRIGHT-PATTERSON AFB, OH.
KC-135 cockpit modernization study and crew reduction feasibility demonstration
[AD-A275230] p 3146 N94-29391

AEROSPACE CORP., EL SEGUNDO, CA.
Space-time structure of the morning aurora inferred from coincident DMSP-F6, -F8, and Sondrestrom incoherent scatter radar observations
[AD-A275442] p 3356 N94-28869
Proton switches
[AD-A275150] p 3167 N94-29022
System requirements review for the High-Resolution Ozone Imager (HIROIG)
[AD-A275151] p 3347 N94-29023
Identification of an unexpected space radiation hazard
[AD-A275170] p 3552 N94-29046
Advantages of the LBL 88-inch cyclotron ion beam for SEP studies
[AD-A275142] p 3494 N94-29065
Screening of flexible cables by nonlinear resistance measurements
[AD-A275193] p 3264 N94-29289
The use of screening tests in spacecraft lubricant evaluation p 3162 N94-29641
Single event upset susceptibilities of latchup immune CMOS process programmable gate arrays p 3495 N94-30214

AEROSPACE MEDICAL RESEARCH LABS., BROOKS AFB, TX.
Aeromedical support for casualties in extremely hot climates p 3382 N94-28443
Comparative centrifuge evaluation of the Air Force Advanced Technology Anti-G Suit (ATAGS) and the Navy Enhanced Anti-G Lower Ensemble (EAGLE)
[AD-A275348] p 3400 N94-28996

AEROSPATIALE, BORDEAUX (FRANCE).
Irradiation polymerization of bismaleimide resins
[REPT-932-430-105] p 3215 N94-29441

AEROSPATIALE, CANNES (FRANCE).
Microvibrations on a GEO telecommunication satellite
[REPT-932-440-101] p 3168 N94-29415
ISO overview: General presentation of the satellite, cryogenic aspects
[REPT-932-440-102] p 3231 N94-29416
An Earth observation telescope refocusing mechanism
[REPT-932-440-103] p 3332 N94-29417
Aid to Ada component reuse at Aerospatiale Cannes (France)
[REPT-932-440-102] p 3418 N94-29418
Satellites: Reliability and operation security
[REPT-932-440-108] p 3168 N94-29419
Theoretical and experimental study of a cylindrical microstrip antenna
[REPT-932-440-109] p 3245 N94-29456
GLRS-R 2-colour retroreflector target design and predicted performance
[REPT-932-440-106] p 3246 N94-29542
Application of FLUIDNET-G software to the preliminary thermal and hydraulic design of Hermes spaceplane
[REPT-932-440-107] p 3168 N94-29543
New perspectives for high accuracy SLR with second generation geodesic satellites
[REPT-932-440-105] p 3336 N94-30965

AEROSPATIALE, CHATILLON (FRANCE).
Electron microscopy: Metal alloy x ray microanalysis
[REPT-932-600-101] p 3205 N94-29525

AEROSPATIALE, LES MUREAUX (FRANCE).
The laser approach for sequential pyrotechnic initiation systems: Envisageable chain architecture and concepts
[REPT-932-430-113] p 3225 N94-29414

AEROSPATIALE, PARIS (FRANCE).
A time reasoning system based on the event calculus for scheduling in aeronautic maintenance
[REPT-932-710-101] p 3122 N94-29463

AEROSPATIALE, SURESNES (FRANCE).
Fire behavior of aeronautical materials
[REPT-932-600-105] p 3197 N94-29457
Rules and definition of the range of paints applied on aeronautical structrural composites
[REPT-932-600-106] p 3215 N94-29459
Correlation between wet ageing, humidity absorption and properties on composite materials based on different resins family
[REPT-932-600-107] p 3179 N94-29462
Automation of the NDT diagnostic using neural nets. Application: Inspection of Airbus longitudinal joints during maintenance
[REPT-932-600-104] p 3315 N94-29474
Numerical simulation of industrial workpiece superplastic forming
[REPT-932-600-102] p 3418 N94-29479
Integration of a path generation algorithm into off-line programming of airbus panels
[REPT-932-600-103] p 3435 N94-29480
AEROSPATIALE, TOULOUSE (FRANCE).
How to control the increase in the complexity of civil aircraft on-board systems p 3150 N94-29316
AEROSPATIALE AQUITAINE, SAINT-MEDARD EN JALLES (FRANCE).
Characterisation and processing of SiC/MAS-L glass ceramic matrix composite
[REPT-932-430-111] p 3179 N94-29412
Glass-ceramic matrix composites
[REPT-932-430-112] p 3179 N94-29413
Development of electromagnetic compatibility tests
[REPT-932-430-110] p 3245 N94-29421
Pyrotechnic shock: Devices in pyrotechnic environment qualification logic
[REPT-932-430-108] p 3225 N94-29429
Radioelectric characterization of materials at 1000 C
[REPT-932-430-104] p 3245 N94-29440
Damage meso-modeling of 3D evolutive composites
[REPT-932-430-106] p 3179 N94-29442
Microfocus radioscopy, a high resolution means of inspecting composite materials
[REPT-932-430-109] p 3179 N94-29454
A normative frame of reference for the metrology function
[REPT-932-430-102] p 3231 N94-29477
Reliability of composite material structures. Application: High pressure spherical coded tanks
[REPT-932-430-103] p 3180 N94-29478
Measurement basis of near fields in spherical coordinates in the 100 MHz to 6 GHz band
[REPT-932-430-107] p 3255 N94-30153
AEROSPATIALE ETABLISSEMENT DES MUREAUX (FRANCE).
Software engineering methods in the Hermes on-board software p 3414 N94-29326
AICHI FISHERIES RESEARCH INST., MINATO (JAPAN).
Copepods collected along 33.5 deg E longitude of the Antarctic Ocean in the 1976 summer p 3358 N94-29082
AIR-CONDITIONING AND REFRIGERATION TECHNOLOGY INST., INC., ARLINGTON, VA.
Materials compatibility and lubricants research on CFC-refrigerant substitutes
[DE94-004905] p 3220 N94-30692
AIR FORCE CIVIL ENGINEERING CENTER, TYNDALL AFB, FL.
Asphaltic concrete performance under heavy fighter aircraft loading
[AD-A275046] p 3157 N94-29151
AIR FORCE ENVIRONMENTAL TECHNICAL APPLICATIONS CENTER, SCOTT AFB, IL.
Catalog of Air Force weather technical publications 1992-1993
[AD-A275635] p 3368 N94-28638
Capabilities, products, and services of USAFETAC (USAF Environmental Technical Applications Center)
[AD-A275654] p 3368 N94-28652
AIR FORCE INST. OF TECH., WRIGHT-PATTERSON AFB, OH.
Fatigue behavior of a cross-ply ceramic matrix composite at elevated temperatures under tension-tension loading
[AD-A275466] p 3176 N94-28673
Spin-up in a rectangular cylinder
[AD-A275465] p 3271 N94-28738
The development and demonstration of the metric assessment tool
[AD-A275788] p 3230 N94-28742
Demonstration of improved software support labor estimation for Air Force operational flight programs through functional orientation
[AD-A275789] p 3121 N94-28743
Evaluation of access/navigational features of a graphical-user interface installed on a portable maintenance aid
[AD-A275791] p 3136 N94-28744
A flow visualization study of acoustically enhanced hairpin vortices
[AD-A275467] p 3271 N94-28809
Digital tracking and control of retinal images
[AD-A275469] p 3389 N94-28810
The European community directive: An alternative environmental impact assessment procedure after Massey?
[AD-A275550] p 3347 N94-28844
Numerical simulations of a mountain thunderstorm. A comparison with Doppler radar observations
[AD-A275296] p 3369 N94-28873
Aberrated point-spread functions and beam quality for optical systems with annular pupils
[AD-A275311] p 3499 N94-28875
Design and construction of the Aerobot Robotic Manipulator (ARM)
[AD-A275362] p 3298 N94-28894
An investigation of stereopsis with AN/AVS-6 night vision goggles at varying levels of illuminance and contrast
[AD-A275332] p 3400 N94-28918
Visible vertical cavity surface emitting lasers
[AD-A275334] p 3293 N94-28919
Exploring QDES as a tool for determining limits of achievable performance in aircraft design
[AD-A275359] p 3146 N94-28998
Static fracture behavior of a ceramic matrix composite at elevated temperatures
[AD-A275363] p 3177 N94-29008
Synthetic image generator model; application of view angle dependent reflectivity components and performance evaluation in the visible region
[AD-A275365] p 3499 N94-29009
On the origins of low-level tornadic circulations within the remnants of hurricane Andrews
[AD-A275373] p 3369 N94-29011
Fatigue behavior of a cross-ply ceramic matrix composite under strain controlled tension-tension and tension-compression loading
[AD-A275374] p 3177 N94-29012
Experimental evaluation of fuzzy logic control of a flexible arm manipulator
[AD-A275375] p 3434 N94-29013
Stability properties of inclusive connectivity for graphs
[AD-A275360] p 3452 N94-29016
Investigation into formalization of domain-oriented parallel software development
[AD-A275177] p 3430 N94-29050
Error growth in poor ECMWF forecasts over the contiguous United States
[AD-A275297] p 3369 N94-29183
Prototype terminal aerodrome forecasts using a mesoscale model
[AD-A275308] p 3369 N94-29194
Evaluation of monitoring audiometry in the United States Air Force Hearing Conservation Program
[AD-A275309] p 3391 N94-29211
The appearance of the Sun and Moon seen through clouds
[AD-A275338] p 3551 N94-29212
Orbital applications of electrodynamic propulsion
[AD-A275413] p 3173 N94-29216
Mesopause winds and OH intensities at Mid-Latitudes-Fabry-Perot interferometer observations of the OH emission at 8430 A from bear lake observatory
[AD-A275246] p 3361 N94-29430
Determination of pressure response times for gaseous flow in a tube
[AD-A275274] p 3272 N94-29435
Hopf bifurcation in viscous, low-speed flows about an airfoil with structural coupling p 3134 N94-30865
AIR FORCE OFFICE OF SCIENTIFIC RESEARCH, BOLLING AFB, WASHINGTON, DC.
A look into the crystal ball: The next 25 years p 3475 N94-30681
AIR FORCE SYSTEMS COMMAND, FALCON AFB, CO.
An Operational Control Segment (OCS) update on GPS constellation status and future program directions p 3144 N94-30643
AIR FORCE SYSTEMS COMMAND, WRIGHT-PATTERSON AFB, OH.
Stress and ergonomic design and evaluation of person-machine systems
[AD-A275156] p 3400 N94-29034
A disciplined approach to software test and evaluation p 3416 N94-29339
Study of dynamic characteristics of a monsoon circulation tube
[AD-A275238] p 3370 N94-29394
A combined electron beam/optical lithography process step for the fabrication of sub-half-micron-gate-length MMIC chips p 3240 N94-30445
AIR FORCE TEST PILOT SCHOOL, EDWARDS AFB, CA.
Human pilot response during single- and multi-axis tracking tasks
[AD-A275080] p 3398 N94-28887
AIR UNIV., MAXWELL AFB, AL.
Cockpit video: A low cost BDA source
[AD-A275228] p 3150 N94-29389
AKRON UNIV., OH.
An anisotropic extension of Bodner's model of viscoplasticity: Model development
[NASA-CR-195289] p 3318 N94-28821
Stereo imaging based particle velocimeter
[NASA-CR-195800] p 3289 N94-29742
Computational simulation of composite structures with and without damage
[NASA-CR-194433] p 3183 N94-30190
ALABAMA UNIV., HUNTSVILLE.
A/GATECH DOSP fabrication
[AD-A275848] p 3430 N94-28781
Technology transfer initiatives
[NASA-CR-195151] p 3537 N94-29410
A variable selection heuristic for solid rocket motor design p 3173 N94-29544
The structure of solar magnetic fields and their associated electric currents p 3544 N94-29723
Field methods to measure surface displacement and strain with the Video Image Correlation method
[NASA-CR-195796] p 3316 N94-29724
The role of cloud collisions in N-body simulations of disk galaxies p 3545 N94-29755
Aspects of model-based rocket engine condition monitoring and control
[NASA-CR-195116] p 3173 N94-29848
Wave generation by contaminant ions near a large spacecraft
[NASA-CR-195797] p 3169 N94-29917
Vacuum chamber and adaptors for shearography and holography
[NASA-CR-192467] p 3157 N94-29956
Computer-based linking of thesauri p 3534 N94-29961
Accurate modeling of F-region electron densities
[NASA-CR-195781] p 3364 N94-30014
Convective flow effects on protein crystal growth
[NASA-CR-195785] p 3515 N94-30015
Process modelling for materials preparation experiments
[NASA-CR-195782] p 3175 N94-30242
ALABAMA UNIV., TUSCALOOSA.
Unstructured space-time finite element method of heat conduction p 3279 N94-30224
ALABAMA UNIV., UNIVERSITY.
Acoustic or electromagnetic scattering from the penetrable wedge
[AD-A275259] p 3243 N94-29054
ALASKA UNIV., FAIRBANKS.
On interannual variability and climate change in the North Pacific p 3374 N94-29963
Radiation transport in cloudy and aerosol loaded atmospheres p 3366 N94-30805
ALBERTA RESEARCH COUNCIL, EDMONTON.
Proceedings of the 3rd Conference on Military Robotic Applications
[DRES-SP-149] p 3304 N94-30275
Force control techniques for robot manipulators and their military applications p 3307 N94-30291
Elements of supervisory control for military robotic applications p 3309 N94-30303
Aspects of the operator interface for military robotic applications in unstructured environments p 3309 N94-30304
ALBERTA UNIV., CALGARY.
Symbolic generation of dynamics equations for manipulators mounted on moving bases p 3308 N94-30296
ALBERTA UNIV., EDMONTON.
Thermal protective performance and instrumented mannequin evaluation of multi-layer garment systems p 3381 N94-28433
Variable-resolution stereo matching p 3308 N94-30298
ALCATEL ISR, EVRY (FRANCE).
DAISY: A decision aid for an air situation interpretation system p 3139 N94-29574
ALENIA, NERVIANO (ITALY).
Potential software failures methodology analysis p 3414 N94-29329
ALENIA, TORINO (ITALY).
On ground system integration and testing: A modern approach p 3150 N94-29334
Software testing practices and their evolution for the 1990's p 3415 N94-29335
A common approach for an aerospace software environment p 3417 N94-29346

ALENIA SPAZIO S.P.A., ROME (ITALY).
ENGRID: A graphical interactive code for the computation of structured grids for blocked flow domains p 3124 N94-28956
Application of information management methodologies for project quality improvement in a changing environment p 3416 N94-29342
ALENIA SPAZIO S.P.A., TURIN (ITALY).
Object versus functional oriented design p 3413 N94-29321
ALFA ROMEO S.P.A., NAPLES (ITALY).
Numerical simulation of aerothermal characteristics in gas turbine combustors with complex geometries p 3154 N94-29255
ALL-UNION RESEARCH INST. FOR PHYSICAL AND RADIOTECHNICAL MEASUREMENTS, MENDELEEVO (USSR).
Russian national time scale long-term stability p 3475 N94-30679
ALLIED-SIGNAL AEROSPACE CO., DES PLAINES, IL.
Advanced fuel properties: A computer program for estimating property values
[AD-A275248] p 3224 N94-28901
ALLIED-SIGNAL AEROSPACE CO., KANSAS CITY, MO.
Practical applications of plasma surface modification
[DE94-004892] p 3349 N94-29932
Non-aqueous cleaning solvent substitution
[DE94-005339] p 3219 N94-30245
ALLIED-SIGNAL CORP., KANSAS CITY, MO.
Non-aqueous cleaning solvent substitution p 3354 N94-30466
ALSYS, INC., SAINT CLOUD (FRANCE).
Ada run time system certification for avionics applications p 3150 N94-29332
ALUMINUM CO. OF AMERICA, ALCOA CENTER, PA.
Role of microstructure on the fatigue durability of aluminum aircraft alloys
[AD-A275814] p 3202 N94-28830
AMERICAN UNIV., WASHINGTON, DC.
Solid state laser systems for space application
[NASA-CR-195777] p 3294 N94-29914
AMES LAB., IA.
Measurement of elemental speciation by liquid chromatography: Inductively coupled plasma mass spectrometry (LC-ICP-MS) with the Direct Injection Nebulizer (DIN)
[DE94-005261] p 3187 N94-28483
Chemically modified polymeric resins for separation of cations, organic acids, and small polar molecules by high performance liquid chromatography
[DE94-005548] p 3211 N94-28516
Performance analysis of memory hierachies in high performance systems
[DE94-005549] p 3404 N94-28517
Quenching of the excited state of hydrated Europium(3) ions by electron transfer
[DE94-005553] p 3482 N94-28518
Instrumental development of novel detection and separation methods for capillary electrophoresis
[DE94-005554] p 3187 N94-28519
A measurement of the tau polarization at the resonance with the DELPHI detector at LEP
[DE94-005557] p 3482 N94-28520
Interstitially stabilized phases in the zirconium-nickel system
[DE94-005561] p 3201 N94-28525
Directional solidification studies in Ni-Al alloys
[DE94-005562] p 3201 N94-28527
Synthesis and characterization of novel ternary and quaternary reduced molybdenum oxides
[DE94-005563] p 3510 N94-28529
Geometric structures of thin film: Pt on Pd(110) and NiO on Ni(100)
[DE94-005564] p 3211 N94-28530
Gas phase thermochemistry of organogermanium compounds
[DE94-004885] p 3187 N94-28561
Fundamental studies of hydrogen interaction with supported meta and bimetallic catalysts
[DE94-004887] p 3202 N94-28562
Recent results from testing fast ADCs
[DE94-005565] p 3406 N94-30004
Plasma enhanced chemical vapor deposition of ZrO2 thin films
[DE94-006031] p 3218 N94-30104
Studies of high temperature ternary phases in mixed-metal-rich early transition metal sulfide and phosphide systems
[DE94-006034] p 3209 N94-30336
Centrifugal atomization of lanthanide materials for cryogenic coolers
[DE94-006035] p 3219 N94-30337
Butterfly and scaling law in YBa2Cu4O8
[DE94-006037] p 3519 N94-30338
Studies on the optimization of deformation processed metal-metal matrix composites
[DE94-006033] p 3185 N94-30704
RHEED studies of the nucleation, growth, and mobility of Ag atoms on the Si(111)7 x 7 surface
[DE94-005551] p 3521 N94-30899
Investigations into ultraviolet matrix-assisted laser desorption
[DE94-005265] p 3296 N94-30908
AMSTERDAM UNIV. (NETHERLANDS).
Parallel quantification
[LP-93-01] p 3422 N94-30318
Dynamic generalized quantifiers and monotonicity
[LP-93-02] p 3454 N94-30319
A smart child of Peano's
[ML-92-10] p 3455 N94-30325
Completeness of the Lambek calculus with respect to relativized relational semantics
[LP-93-03] p 3455 N94-30326
Identity: Quarrelling with an unproblematic notion
[LP-93-04] p 3455 N94-30327
A note on the complexity of local search problems
[CT-93-02] p 3456 N94-30370
Logic of transition systems
[CT-93-03] p 3424 N94-30371
Interrogatives and adverbs of quantification
[LP-92-14] p 3456 N94-30372
Bounded contraction and many-valued semantics
[ML-93-04] p 3456 N94-30380
Models of the untyped lambda-calculus in semi Cartesian closed categories
[ML-93-05] p 3456 N94-30381
Categorial generalization of algebraic recursion theory
[ML-93-06] p 3456 N94-30382
Algorithmic problems concerning first-order definability of modal formulas on the class of all finite frames
[ML-93-07] p 3456 N94-30383
Remarks on the theory of semi-functors
[ML-93-08] p 3457 N94-30384
Natural deduction for intuitionistic linear logic
[ML-93-09] p 3457 N94-30385
The Vanilla meta-interpreter for definite logic programs and ambivalent syntax
[CT-93-01] p 3424 N94-30386
Commutative Lambek categorial grammars
[ML-93-01] p 3457 N94-30395
Modal quantification over structured domains
[ML-93-02] p 3457 N94-30396
The conjoinability relation in Lambek calculus in linear logic
[ML-93-03] p 3457 N94-30397
The structure of exponentials: Uncovering the dynamics of linear logic proofs
[ML-93-10] p 3430 N94-30973
Inventory of fragments and exact models in intuitionistic proportional logic
[ML-93-11] p 3463 N94-30974
Remarks on uniformly finitely precomplete positive equivalences
[ML-93-12] p 3463 N94-30975
Undecidability in diagonalizable algebras
[ML-93-13] p 3463 N94-30976
Embeddings of Heyting algebras
[ML-93-14] p 3463 N94-30977
ANALEX CORP., BROOK PARK, OH.
Cryogenic on-orbit liquid depot storage acquisition and transfer (COLD-SAT) experiment subsystem instrumentation and wire harness design report
[NASA-CR-189172] p 3168 N94-29405
APPLIED RESEARCH CORP., LANDOVER, MD.
Correlative analysis of hard and soft x ray observations of solar flares
[NASA-CR-189329] p 3551 N94-29453
Spatially resolved spectroscopy of AG Carinae, and direct evidence for stellar evolution: The central star of NGC 2392
[NASA-CR-189291] p 3545 N94-29871
ARGONNE NATIONAL LAB., IDAHO FALLS, ID.
Potential capabilities of Reynolds stress turbulence model in the COMMIX-RSM code p 3285 N94-30450
ARGONNE NATIONAL LAB., IL.
Three-dimensional finite element modeling of a magnet array spinning above a conductor
[DE94-004573] p 3468 N94-28459
Current leads and magnetic bearings
[DE94-004607] p 3297 N94-28461
Report of the subgroup on the top quark
[DE94-004624] p 3481 N94-28462
Practical superconductor development for electrical power applications
[DE94-005378] p 3261 N94-28487
The generalized spin-boson model for electron-transfer reactions involving two harmonic potentials with a different force constant
[DE94-005470] p 3482 N94-28509
Pull-test adhesion measurements of diamondlike carbon films on silicon carbide, silicon nitride, aluminum oxide, and zirconium oxide
[DE94-005469] p 3211 N94-28536
On eddy accumulation with limited conditional sampling to measure air-surface exchange
[DE94-005112] p 3368 N94-28565
Physics at HERA
[DE94-005117] p 3483 N94-28569
Energy gap structure of layered superconductors
[DE94-005132] p 3511 N94-28570
Liquid metal MHD and heat transfer in a tokamak blanket slotted coolant channel
[DE94-004622] p 3506 N94-29510
Two-phase power-law modeling of pipe flows displaying shear-thinning phenomena
[DE94-005115] p 3279 N94-30020
Fatigue of carbon and low-alloy steels in LWR environments
[DE94-005116] p 3207 N94-30021
Use of satellite data to improve parameterization of spatial and temporal variations of gaseous dry deposition in regional-scale models
[DE94-005110] p 3334 N94-30022
The suitability of low-cost urban airshed modeling in the Chicago area
[DE94-005114] p 3349 N94-30023
Corrosion performance of materials for advanced combustion systems
[DE94-006726] p 3207 N94-30057
PCCM2: A GCM adapted for scalable parallel computers
[DE94-005113] p 3350 N94-30116
Effect of fiber coating on mechanical properties of Nicalon fibers and Nicalon-fiber/SiC matrix composites
[DE94-005477] p 3185 N94-30593
Modelling erosion damage from low-energy plasma gun simulations of disruptions
[DE94-005196] p 3509 N94-30697
TCM exemptions to promote alternative-fuel vehicles: The good, the bad, and the ugly
[DE94-005924] p 3311 N94-30703
Fullerenes as precursors for diamond film growth without hydrogen or oxygen additions
[DE94-004582] p 3519 N94-30718
Parallel language constructs for paradigm integration and deterministic computations
[DE94-005119] p 3428 N94-30754
Silica scintillating materials prepared by sol-gel methods
[DE94-005123] p 3220 N94-30778
Early experiences with the IBM SP1 and the high-performance switch
[DE94-006261] p 3429 N94-30840
Non-Markovian quantum Brownian motion of a harmonic oscillator
[DE94-005922] p 3477 N94-30873
Theory for electron-transfer reactions involving two Marcus surfaces with a different force constant
[DE94-005925] p 3493 N94-30874
Neutronics of a D-Li neutron source: An overview
[DE94-005372] p 3493 N94-30893
Ion damage studies in GaAs/Al(0.6)Ga(0.4)As/GaAs heterostructures
[DE94-005384] p 3521 N94-30894
Rotator phases in narrow-gap semiconductors
[DE94-005472] p 3521 N94-30897
Intra- versus interlayer pairing in the copper oxide superconductors: Response to a magnetic field
[DE94-005475] p 3521 N94-30898
Theory for electron-transfer reactions in a three-component system: The degenerate regime
[DE94-005919] p 3493 N94-30903
ARIZONA STATE UNIV., TEMPE.
Crashworthiness analysis of commuter aircraft seats
[AD-A275889] p 3135 N94-28799
Silicon germanium carbon heteroepitaxial growth on silicon
[AD-A275197] p 3512 N94-28889
Hydrodynamics of convection under winter polar leads
[AD-A275182] p 3369 N94-29067
Spatial light modulators with arbitrary quantum wells profiles
[AD-A275023] p 3499 N94-29114
The angular two-point correlation function of galaxies down to 25th mag p 3547 N94-30010
ARIZONA UNIV., TUCSON.
Measurement of atmospheric OH by titration of near-IR fluorescent dyes p 3344 N94-28599
The thermal consequences of giant impacts in the early solar system p 3543 N94-29698
Cosmogenic C-14 in Antarctic and non-Antarctic meteorites and lunar samples
[NASA-CR-195795] p 3546 N94-29905
High redshift QSOs and the x ray background
[NASA-CR-195112] p 3540 N94-29957

A single-fluid, self-consistent formulation of particle transport and fluid dynamics p 3280 N94-30352
Design and control of active vision based mechanisms for intelligent robots
[AIAA PAPER 94-1196-CP] p 3442 N94-30547
Land surface interaction p 3350 N94-30621

ARKANSAS UNIV., FAYETTEVILLE.
Biological conversion of synthesis gas
[DE94-005815] p 3340 N94-30879

ARMY AEROMEDICAL RESEARCH LAB., FORT RUCKER, AL.
The use of liquid and air microclimate conditioning systems to alleviate heat stress in helicopter NBC operations p 3384 N94-28453
Aviation epidemiology data register: Age distribution of U.S. Army aviators stratified by gender and component of service
[AD-A275901] p 3388 N94-28757

ARMY ARMAMENT MUNITIONS AND CHEMICAL COMMAND, WATERVLIET, NY.
An improved plating process p 3223 N94-30451

ARMY ARMAMENT RESEARCH, DEVELOPMENT AND ENGINEERING CENTER, WATERVLIET, NY.
Synaptogenesis, selective stabilization, and free association
[AD-A275250] p 3392 N94-29431
Monitor for status epilepticus seizures p 3397 N94-30460

ARMY COLD REGIONS RESEARCH AND ENGINEERING LAB., HANOVER, NH.
Thermal variation in vegetated or snow-covered background scenes and its effect on passive infrared systems
[AD-A275174] p 3325 N94-28849
Growth condition of an ice layer in freezing soils under applied loads. Part 1: Experiment
[AD-A275215] p 3357 N94-29070
Glaciohydrologic and glaciohydraulic effects on runoff and sediment yield in glacierized basins
[AD-A275134] p 3361 N94-29286
On the temperature distribution near a cold surface
[AD-A275162] p 3332 N94-29288
Attenuation of outdoor sound propagation levels by a snow cover
[AD-A275387] p 3478 N94-29314

ARMY CONSTRUCTION ENGINEERING RESEARCH LAB., CHAMPAIGN, IL.
Environmental Compliance Assessment System (ECAS)
[AD-A275549] p 3346 N94-28722
Environmental Compliance Assessment And Management System Program (ECAMP). US Air Force European Economic Community (EEC)
[AD-A275593] p 3346 N94-28727
Environmental Review Guide for Operations (ERGO)
[AD-A275611] p 3346 N94-28774

ARMY ENGINEER WATERWAYS EXPERIMENT STATION, VICKSBURG, MS.
Development and application of a thermistor current meter
[AD-A275816] p 3286 N94-28831
Environmental characterization for target acquisition. Analysis of thermal and visible imagery
[AD-A275414] p 3242 N94-28862

ARMY MEDICAL CENTER, AURORA, CO.
Clinical investigation program
[AD-A275025] p 3391 N94-29116

ARMY NATICK LABS., MA.
Ballistic performance of polycarbonate/polyester and polycarbonate/styrene- acrylonitrile microlayer sheets
[AD-A275462] p 3177 N94-28735

ARMY NATICK RESEARCH AND DEVELOPMENT COMMAND, MA.
Nutrition and hydration status of aircrew members consuming an improved survival ration during a simulated survival scenario p 3380 N94-28429

ARMY RESEARCH INST. FOR THE BEHAVIORAL AND SOCIAL SCIENCES, ALEXANDRIA, VA.
Simulation Networking/Training Requirements Relational Database: User's guide
[AD-A275634] p 3528 N94-28637

ARMY RESEARCH INST. OF ENVIRONMENTAL MEDICINE, NATICK, MA.
Nutrition and hydration status of aircrew members consuming an improved survival ration during a simulated survival scenario p 3380 N94-28429
The Environmental Symptoms Questionnaire: Assessing reactions to environmental extremes in military operations p 3383 N94-28447

ARMY RESEARCH LAB., ABERDEEN PROVING GROUND, MD.
Least-squares determination of burst-point coordinates
[AD-A275423] p 3452 N94-28864
Animation techniques in BRL-CAD
[AD-A275232] p 3417 N94-29392
The effects of man-made smokes and battlefield-induced smokes on the propagation of electromagnetic radiation p 3258 N94-30505

ARMY RESEARCH LAB., ADELPHI, MD.
Characterization of a diffraction grating as a simulant of a selective frequency antenna for radiometric applications
[AD-A275793] p 3241 N94-28745
Radar cross sections of ground clutter at 95 GHz for summer and fall conditions p 3259 N94-30512

ARMY RESEARCH LAB., WHITE SANDS MISSLE RANGE, NM.
Multispectral transmittance measurements through man-made water fogs p 3257 N94-30499
Estimation of transmittance from satellite imagery p 3257 N94-30500

ARMY TOPOGRAPHIC ENGINEERING CENTER, FORT BELVOIR, VA.
Exploitation of stereophotogrammetrically derived 3-D wireframe models to produce urban simulations
[AD-A275459] p 3325 N94-28808
Feature mapping in a photogrammetric GIS
[AD-A275418] p 3325 N94-28863
An efficient algorithm for 3D connect-the-dots
[AD-A275431] p 3409 N94-28866
Incorporating geometric constraints into rule-based systems using nonlinear optimization
[AD-A275093] p 3452 N94-29063
Neural network solutions to logic programs with geometric constraints
[AD-A275419] p 3435 N94-29198
The Image Digitizing System (IDS)
[AD-A275341] p 3329 N94-29213
The use of digital stereo photogrammetric methods in historical photo analysis
[AD-A275287] p 3288 N94-29437

ARMY TRAINING AND DOCTRINE COMMAND, FORT MONROE, VA.
TRADOC library and information network (TRALINET). Union list of periodicals (TULIP)
[AD-A275263] p 3529 N94-28903

ARSENAL DU MATERIEL MECHANIQUE ET DE L'ARMEMENT, ROCOURT (BELGIUM).
An experimental and comprehensive method to measure emission characteristics p 3257 N94-30501

ASSOCIATION OF ENERGY ENGINEERS, ATLANTA, GA.
International Energy and Environmental Congress: Proceedings
[DE93-040609] p 3353 N94-30715

ASTRO AEROSPACE CORP., CARPINTERIA, CA.
Waves in space plasma dipole antenna subsystem p 3161 N94-29632

ASTROPOWER, INC., NEWARK, DE.
Silicon-Film (tm) photovoltaic manufacturing technology
[DE94-000258] p 3336 N94-28501

ATLANTIS SCIENTIFIC SYSTEMS GROUP, INC., OTTAWA (ONTARIO).
Radar jet engine health monitoring project
[ASSGI-301] p 3153 N94-30130

ATMOSPHERIC AND ENVIRONMENTAL RESEARCH, INC., CAMBRIDGE, MA.
A global forecast model comparison study - year 1
[AD-A275674] p 3369 N94-28663

AUBURN UNIV., AL.
Development of a new generation solid rocket motor ignition computer code
[NASA-CR-195734] p 3171 N94-28800
Numerical analysis of dynamic direct tension and direct compression tests
[AD-A275255] p 3319 N94-29433

AXIOMATICS CORP., WOBURN, MA.
Improved construction materials for polar regions using microcellular thermoplastic foams p 3223 N94-30483

B

BABCOCK AND WILCOX CO., LYNCHBURG, VA.
Programmable Automated Welding System (PAWS): Control of welding through software and hardware p 3314 N94-30443
Programmable Automated Welding System (PAWS)
[AIAA PAPER 94-1221-CP] p 3446 N94-30570
Robotic NDE inspection of advanced solid rocket motor casings
[AIAA PAPER 94-1222-CP] p 3446 N94-30571

BANDO CHEMICAL INDUSTRIES LTD., KOBE (JAPAN).
A newly developed snow vehicle (SM100S) for Antarctica. Part 4: Low temperature properties of crawler belt p 3314 N94-29984

BATTELLE COLUMBUS LABS., OH.
Effects of repair on structural integrity
[AD-A275756] p 3145 N94-28647

BDM CORP., MCLEAN, VA.
Technology base enhancement program. Metal matrix composites
[AD-A275531] p 3176 N94-28688

BEIJING INST. OF RADIO METROLOGY AND MEASUREMENTS (CHINA).
Some applications of GPS timing information p 3145 N94-30661
Precision frequency synthesizing sources with excellent time/frequency performances p 3473 N94-30671
Measurement of the frequency stability of responders in aircraft p 3261 N94-30673

BELGIAN ARMY, PEUTIE.
Global approach towards the evaluation of thermal infrared countermeasures p 3258 N94-30504

BILKENT UNIV., ANKARA (TURKEY).
Calculation of turbulence degraded point spread function of an imaging system p 3260 N94-30514

BINGHAMTON UNIV., NY.
ODYSSEUS autonomous walking robot: The leg/arm design
[AIAA PAPER 94-1180-CP] p 3439 N94-30531

BIONETICS CORP., COCOA BEACH, FL.
Development and implementation of a scrub habitat compensation plan for Kennedy Space Center
[NASA-TM-109202] p 3347 N94-29099

BOEING CO., SEATTLE, WA.
Confessions of a robot lobotomist
[AIAA PAPER 94-1185-CP] p 3440 N94-30535

BOEING DEFENSE AND SPACE GROUP, PHILADELPHIA, PA.
Composite hot drape forming p 3240 N94-30448

BOEING DEFENSE AND SPACE GROUP, SEATTLE, WA.
Advanced optical A/D converter
[AD-A275663] p 3498 N94-28656
Fault tolerant testbed evaluation, phase 1
[NASA-CR-188275] p 3171 N94-29035
Analysis of selected materials flown on interior locations of the Long Duration Exposure Facility
[NASA-CR-4586] p 3175 N94-29458

BOSTON COLL., CHESTNUT HILL, MA.
Towards experimental verification and device applications of current driven plasma instabilities in solid state systems
[AD-A275395] p 3504 N94-29055

BOSTON UNIV., MA.
The effects of magnetic storm phases on F-layer irregularities from auroral to equatorial latitudes
[AD-A275203] p 3356 N94-28891

BRITISH AEROSPACE DEFENCE LTD., PRESTON (ENGLAND).
SDE's for the year 2000 and beyond: An EF perspective p 3417 N94-29344

BRITISH ANTARCTIC SURVEY, CAMBRIDGE (ENGLAND).
Signatures of dayside solar wind/magnetosphere/ionosphere coupling as revealed by the pace HF radars and associated experiments p 3359 N94-29236

BRITISH COLUMBIA UNIV., VANCOUVER.
Reconstruction of stellar images from correlations
[ISBN-0-315-85382-4] p 3541 N94-30133
Large eddy simulation of the upper atmospheric surface layer
[ISBN-0-315-85393-X] p 3365 N94-30134
A study of the flexible space platform based deployable manipulator
[ISBN-0-315-85410-3] p 3303 N94-30135
Computational methods for the shape shading problem
[ISBN-0-315-85430-8] p 3421 N94-30136
The far-infrared absorption spectrum of low temperature hydrogen gas
[ISBN-0-315-85432-4] p 3199 N94-30137
Pit initiation on passivated metal surfaces: Crystallographic orientation and environmental effects
[ISBN-0-315-85433-2] p 3208 N94-30138
MuSR measurement of the magnetic penetration depth and coherence length in the high-Tc superconductor YBa2Cu3O(6.95)
[ISBN-0-315-85385-9] p 3517 N94-30203
Experimental sliding mode control of a flexible single link manipulator
[ISBN-0-315-85466-9] p 3304 N94-30238
Second order necessary conditions in optimal control
[ISBN-0-315-85443-X] p 3437 N94-30255
Obstacle detection for an autonomous vehicle p 3309 N94-30302
Atmospheric turbulence within and above a coniferous forest
[ISBN-0-315-75468-0] p 3375 N94-30870

BROOKHAVEN NATIONAL LAB., UPTON, NY.
Computer simulation of martensitic transformations
[DE94-005213] p 3201 N94-28479

Low frequency dynamics of CO/Cu-breakdown of Born-Oppenheimer approximation
[DE94-005508] p 3510 N94-28512
Ozone production at a rural site in Georgia during the summer 1992 SOS campaign
[DE94-003989] p 3342 N94-28523
Derivation of a Fokker-Planck equation for bunched beams
[DE94-004950] p 3483 N94-28565
Enhanced ion dissociation of LiCF3SO3 by new carbonate plasticizers: Raman and IR studies
[DE94-005448] p 3485 N94-28741
Performance of CVD and CVR coated carbon-carbon in high temperature hydrogen
[DE94-005451] p 3487 N94-29841
First principles pseudopotential calculations on aluminum and aluminum alloys
[DE94-004890] p 3206 N94-29931
Incommensurate magnetic order in UNi2Al3
[DE94-005449] p 3209 N94-30246
Deposition of tantalum carbide coatings on graphite by laser interactions p 3223 N94-30475
Development of radiation resistant electrical cable insulations p 3223 N94-30480
Small low mass advanced PBR's for propulsion
[DE94-005142] p 3497 N94-30588
Towards short wavelengths FELs workshop
[DE94-004346] p 3296 N94-30688
Solar neutrino experiments: An update
[DE94-006061] p 3551 N94-30884
Development of radiation resistant electrical cable insulations
[DE94-005189] p 3222 N94-30906
AC losses for the self field of an AC transport current with a DC transport current offset in high T(c) superconducting magnet coils for MagLev application
[DE94-005187] p 3268 N94-30907

BROWN UNIV., PROVIDENCE, RI.
Micromechanics of the dynamic response of ceramics and ceramic composites p 3217 N94-29975

BRTRC, INC., VIENNA, VA.
Business planning model user's guide
[AD-A274978] p 3409 N94-28895
Financial resource review model user's guide
[AD-A274979] p 3410 N94-29088

BUBBLE TECHNOLOGY INDUSTRIES, INC., CHALK RIVER (ONTARIO).
Adaption of the bubble detector for use as a LET spectrometer p 3291 N94-30216

BUREAU INTERNATIONAL DES POIDS ET MESURES, SEVRES (FRANCE).
GPS common-view time transfer p 3144 N94-30648
The use of the AOA TTR-4P GPS receiver in operation at the BIPM for real-time restitution of GPS time p 3144 N94-30651
Relativistic theory for picosecond time transfer in the vicinity of Earth p 3470 N94-30653
A real-time prediction of UTC p 3470 N94-30654
Comparison of LASSO and GPS time transfers p 3145 N94-30665

BUREAU OF MINES, PITTSBURGH, PA.
An electromagnetic noncontacting sensor for thickness measurement in a dispersive medium
[AIAA PAPER 94-1200-CP] p 3443 N94-30551

BUREAU OF MINES, TUSCALOOSA, AL.
Dewatering of contaminated river sediments p 3354 N94-30472

C

CALGARY UNIV. (ALBERTA).
Temperature and combustion analysis of combustor with acoustically controlled primary zone air-jet mixing p 3196 N94-29284

CALIFORNIA INST. OF TECH., PASADENA.
Dynamic response of ceramics
[AD-A275396] p 3214 N94-29203
Lifted turbulent jet flames p 3198 N94-29676
A study of the ultrahigh-energy cosmic ray mass composition with the MACRO and EAS-TOP experiments p 3552 N94-29687
Forced generation of solitary waves in a rotating fluid and their stability p 3274 N94-29689
Spherical model for turbulence p 3274 N94-29730
The kinematics of molecular gas and dust in the nearby galaxies Centaurus A and M82 p 3544 N94-29738
Flow past a circular cylinder with a permeable wake splitter plate p 3275 N94-29764
Mechanisms and effects of heat generation at the tips of dynamic cracks and notches in metals p 3321 N94-29808
A study of recycled pulsars in globular clusters p 3539 N94-29825
Robotic hand-eye motor learning p 3436 N94-29835
Nominally two-dimensional flow about a normal flat plate p 3275 N94-29838
An investigation of the reacting vortex structures associated with pulse combustion p 3200 N94-30911

CALIFORNIA POLYTECHNIC STATE UNIV., SAN LUIS OBISPO.
Modification of ACSYNT aircraft computer program for preliminary design
[NASA-CR-195737] p 3145 N94-28817

CALIFORNIA UNIV., BERKELEY.
Design of parallel systems for signal processing
[AD-A275490] p 3430 N94-28659
Construction of a connectionist network supercomputer
[AD-A275765] p 3405 N94-28764
A sounding rocket program in extreme and far ultraviolet interferometry
[NASA-CR-195114] p 3289 N94-29907

CALIFORNIA UNIV., BERKELEY. LAWRENCE BERKELEY LAB.
Laser-material interactions: A study of laser energy coupling with solids
[DE94-005212] p 3292 N94-28478
Equation of state of neutron star matter, limiting rotational periods of fast pulsars, and the properties of strange stars
[DE94-005214] p 3542 N94-28480
Analytic rendering of curvilinear volume data
[DE94-004934] p 3407 N94-28506
The induction approach to heavy ion inertial fusion: Accelerator and target considerations
[DE94-005216] p 3494 N94-28507
Properties of W + jet events in proton-antiproton collisions at 1.8 TeV
[DE94-004002] p 3482 N94-28524
Fabrication issues in optimizing YBa(2)Cu(3)O(7-x) flux transformers for low I/f noise
[DE94-005209] p 3261 N94-28546
Coulomb field effect on plasma focusing and wake field acceleration
[DE94-004937] p 3504 N94-28564
WINDOW 4.0: Documentation of calculation procedures
[DE94-004935] p 3410 N94-29019
Picosecond response of the quasiparticle current in superconducting tunnel junctions
[DE94-006300] p 3515 N94-30009
Estimating the cost of large superconducting thin solenoid magnets
[DE94-006289] p 3468 N94-30026
Photoelectron diffraction and holography: Some new directions
[DE94-006297] p 3289 N94-30027
Application of semiclassical methods to reaction rate theory
[DE94-007041] p 3199 N94-30266
Giant magnetoresistance and microstructural characteristics of epitaxial Fe-Ag and Co-Ag granular thin films
[DE94-006287] p 3519 N94-30707
Operator analysis for quark and lepton masses in SO(10)
[DE94-005201] p 3491 N94-30709
Microstructural development and mechanical behavior of eutectic bismuth-tin and eutectic indium-tin in response to high temperature deformation
[DE94-005202] p 3210 N94-30710
A bipolar analog front-end integrated circuit for the SDC silicon tracker
[DE94-005203] p 3267 N94-30711
A high rate, low noise, x ray silicon strip detector system
[DE94-004557] p 3268 N94-30717
Nonlinear optics response of semiconductor quantum wells under high magnetic fields
[DE94-003244] p 3520 N94-30835
Studies of interfaces and vapors with Optical Second Harmonic Generation
[DE94-006295] p 3476 N94-30841
Nuclear magnetic relaxation studies of semiconductor nanocrystals and solids
[DE94-006301] p 3520 N94-30842
Calculating the J(c), B, T surface for commercial niobium tin conductors using a reduced state model
[DE94-006296] p 3520 N94-30850

CALIFORNIA UNIV., DAVIS.
Optical modeling of visibility and visibility instrumentation using stratified Mie theory p 3348 N94-29750
The effect of pressure gradient on the structure of an equilibrium turbulent boundary layer p 3282 N94-30807

CALIFORNIA UNIV., IRVINE.
A new guided wave lens structure and its application
[AD-A275541] p 3499 N94-28813

Pollutant emissions from and within a model gas turbine combustor at elevated pressures and temperatures p 3194 N94-29271
Liquid-oxygen droplet vaporization and combustion: Analysis of transcritical behavior and application to liquid-rocket combustion instability p 3197 N94-29592
A study of ultra high-energy radiation associated with Hercules X-1 p 3552 N94-29823

CALIFORNIA UNIV., LOS ANGELES.
Printed circuit elements with applications to antennas, scattering, and circuits
[AD-A275512] p 3262 N94-28669
Polyaniline membranes for gas and liquid separation
[AD-A275851] p 3408 N94-28790
Active electron and ion beam experiments in space
[AD-A275570] p 3504 N94-28828
Generation mechanisms of quasi-stationary waves in the Southern Hemisphere p 3365 N94-30789
Mixed Eulerian-Lagrangian finite element solutions of unsteady flow and flutter in transonic cascade p 3282 N94-30816
Modeling studies of frontogenesis in the upper and middle troposphere p 3375 N94-30868

CALIFORNIA UNIV., SAN DIEGO, LA JOLLA.
Design and packaging of fault tolerant optoelectronic multiprocessor computing system
[AD-A275896] p 3405 N94-28798
Remote sensing of inner heliospheric plasmas
[AD-A275021] p 3550 N94-29132

CALIFORNIA UNIV., SANTA BARBARA.
General theory and algorithms for the non-casual inversion, slewing and control of space-based articulated structures
[AD-A275118] p 3167 N94-29002
The effects of molecular orientation geometry and surface anisotropy upon etching
[AD-A275154] p 3486 N94-29032
Effect of microstructure on the strength and fracture energy of bimaterial interfaces
[AD-A274987] p 3178 N94-29126
U-statistics of random-size samples and limit theorems for systems of Markovian particles with non-Poisson initial distributions
[AD-A275018] p 3464 N94-29129
On the nonlinear dynamics of ocean wave systems p 3378 N94-30790

CALM (JAMES M.), GREAT FALLS, VA.
ARTI Refrigerant Database
[DE94-004906] p 3230 N94-28563

CALSPAN-BUFFALO UNIV. RESEARCH CENTER, NY.
Development of laser velocimetry for the measurements of turbulence intensity and flow velocity ahead of a NGV row in a full-stage rotating turbine
[AD-A275712] p 3270 N94-28692

CANADA CENTRE FOR REMOTE SENSING, OTTAWA (ONTARIO).
Sea ice and oceans applications of SAR p 3327 N94-28934
Radar applications at the Canada Centre for Remote Sensing p 3331 N94-29224

CANTONAL OBSERVATORY, NEUCHATEL (SWITZERLAND).
Hydrogen maser clocks in space for solid-Earth research and time-transfer applications: Experiment overview and evaluation of Russian miniature sapphire loaded cavity p 3474 N94-30676

CARNEGIE INSTITUTION OF WASHINGTON, STANFORD, CA.
Comprehensive system models: Strategies for evaluation p 3353 N94-30638

CARNEGIE-MELLON UNIV., PITTSBURGH, PA.
Development of the integrated environmental control model: Performance models of selective catalytic reduction NO(x) control systems
[DE94-002151] p 3341 N94-28465
Technology transition push. Part 1: A case study of rate monotonic analysis
[AD-A275616] p 3407 N94-28633
A conceptual framework for software technology transition
[AD-A275637] p 3407 N94-28639
Process guide for the Domain-Specific Software Architectures (DSSA) process life cycle
[AD-A275642] p 3407 N94-28648
A cognitive model of decision making: Chunking and the radar detection device
[AD-A275185] p 3242 N94-28859
Non-intrusive gaze tracking using artificial neural networks
[AD-A275186] p 3397 N94-28860
Basic research in computer science
[AD-A275222] p 3405 N94-28916
Weighted and unweighted maximum clique algorithms with upper bounds from fractional coloring
[AD-A275328] p 3409 N94-28917

Tinkertoy(tm) transactions
[AD-A275271] p 3410 N94-29006
Advanced languages for systems software
[AD-A275272] p 3410 N94-29007
Optimizing ray tracing with visual coherence
[AD-A275218] p 3499 N94-29059
Reference model for project support environments, version 2.0
[AD-A275191] p 3410 N94-29068
High resistivity buffer layers by oxygen doping
[AD-A274986] p 3513 N94-29125
Basic research in computer science
[AD-A275184] p 3405 N94-29181
Subphonetic acoustic modeling for speaker-independent continuous speech recognition
[AD-A275217] p 3244 N94-29303
Program derivation by proof transformation
[AD-A275260] p 3453 N94-29304
An architecturally-based theory of human sentence comprehension
[AD-A275380] p 3398 N94-29313
Constrained objects
[AD-A275273] p 3418 N94-29434
Reinforcement learning for robots using neural networks p 3437 N94-29853
A Space Station robot walker and its shared control software
[AIAA PAPER 94-1192-CP] p 3442 N94-30543
Task-level control for autonomous robots
[AIAA PAPER 94-1210-CP] p 3444 N94-30561
A reactive system for open terrain navigation: Performance and limitations
[AIAA PAPER 94-1218-CP] p 3445 N94-30566
Automation for nondestructive inspection of aircraft
[AIAA PAPER 94-1223-CP] p 3446 N94-30572

CASE WESTERN RESERVE UNIV., CLEVELAND, OH.
Intelligent automated process planning and code generation for computer-controlled inspection
[AD-A275346] p 3409 N94-28920
Properties of graphite fiber reinforced copper matrix composites for space power applications
[NASA-CR-191026] p 3178 N94-29208
Three dimensional compressible turbulent flow computations for a diffusing S-duct with/without vortex generators p 3281 N94-30519
Biologically-inspired hexapod robot design and simulation
[AIAA PAPER 94-1178-CP] p 3439 N94-30530

CATHOLIC UNIV. OF AMERICA, WASHINGTON, DC.
Kinematics and force analysis of a robot hand based on an artificial biological control scheme p 3313 N94-30957

CENTER FOR MATHEMATICS AND COMPUTER SCIENCE, AMSTERDAM (NETHERLANDS).
Graphics for ABC
[CWI-CS-R9255] p 3418 N94-29449
The ABC structure editor: Structure-based editing for the ABC programming environment
[CWI-CS-R9256] p 3418 N94-29487
Animators and error reporters for generated programming environments
[CWI-CS-R9253] p 3418 N94-29503
RIPE integrity primitives, part 1 (RACE Integrity Primitives Evaluation)
[CWI-CS-R9324-PT-1] p 3252 N94-29692
RIPE integrity primitives, part 2 (RACE Integrity Primitives Evaluation)
[CWI-CS-R9325-PT-2] p 3252 N94-29693
Second-order algebraic specification of state semantics
[CWI-CS-R9254] p 3453 N94-29889
The ergonomics of computer interfaces: Designing a system for human use
[CWI-CS-R9258] p 3402 N94-30320
Programming aspects of Views: An open-architecture application environment
[CWI-CS-R9259] p 3422 N94-30321
Graphics in the Views system
[CWI-CS-R9260] p 3422 N94-30322
Modelling interaction tools in the Views architecture
[CWI-CS-R9261] p 3423 N94-30323
Maintaining presentation invariants in the Views system
[CWI-CS-R9262] p 3423 N94-30324
The Views application environment
[CWI-CS-R9257] p 3423 N94-30341
Event structures and orthogonal term graph rewriting
[CWI-CS-R9347] p 3459 N94-30412
Perpetual reductions in orthogonal combinatory reduction systems
[CWI-CS-R9349] p 3459 N94-30413
Higher order recursive program schemes are Turing incomplete
[CWI-CS-R9348] p 3425 N94-30414
Comparing curried and uncurried rewriting
[CWI-CS-R9350] p 3425 N94-30415
Three metric domains of processes for bisimulation
[CWI-CS-R9335] p 3459 N94-30427
MANIFOLD version 1.0 programming: Programs and problems
[CWI-CS-R9334] p 3425 N94-30428
Manray: A replicated workers program in MANIFOLD
[CWI-CS-R9337] p 3433 N94-30429
Isomorphisms between predicate and state transformers
[CWI-CS-R9338] p 3459 N94-30430
Relating state transformation semantics and predicate transformer semantics for parallel programs
[CWI-CS-R9339] p 3433 N94-30431
Topological models for higher order control flow
[CWI-CS-R9340] p 3425 N94-30432
Thermodynamics of computation and information distance
[CWI-CS-R9341] p 3526 N94-30433
The Boltzmann entropy and randomness tests
[CWI-CS-R9342] p 3426 N94-30434
A user's guide to the Software Testpilot
[CWI-CS-R9343] p 3426 N94-30435
Homomorphism preserving algebraic specifications require hidden sorts
[CWI-CS-R9344] p 3459 N94-30436
Perpetual reductions and strong normalization in orthogonal term rewriting systems
[CWI-CS-R9345] p 3426 N94-30437
Comparative semantics for linear arrays of communicating processes
[CWI-CS-R9336] p 3426 N94-30491
An evaluation of explicit pseudo-steady-state approximation schemes for stiff ODE systems from chemical kinetics
[CWI-NM-R9312] p 3353 N94-30729
Parallel iteration across the steps of high order Runge-Kutta methods for nonstiff initial value problems
[CWI-NM-R9313] p 3433 N94-30730
Service independent building blocks-1: Concepts, examples and formal specifications
[CWI-CS-R9326] p 3448 N94-30731
Relations between varieties of Kolmogorov complexities
[CWI-CS-R9329] p 3427 N94-30732
On the unification free PROLOG programs
[CWI-CS-R9331] p 3427 N94-30733
More problems on rewriting
[CWI-CS-R9332] p 3428 N94-30734
Bisimulations and predicate logic
[CWI-CS-R9333] p 3460 N94-30735
Evaluation of discretization schemes for advection-diffusion equations
[CWI-NM-R9311] p 3461 N94-30751
A structural co-induction theorem
[CWI-CS-R9346] p 3461 N94-30753

CENTRAL AND TECHNICAL ESTABLISHMENT FOR ARMAMENT, ARCUEIL (FRANCE).
Thermal imaging for a mobile robot p 3308 N94-30300

CENTRAL INST. OF AVIATION MOTORS, MOSCOW (RUSSIA).
Endothermic fuels for hypersonic aviation p 3197 N94-29285
Introduction and overview of research and development of solid propellant ramrockets, liquid fuel ramjets and experimental hydrogen ram combustors p 3151 N94-29292
Turboramjet engines: Types and performances p 3151 N94-29293
Research and development of ramjets/ramrockets. Part 1: Integral solid propellant ramrockets p 3151 N94-29294
Some problems of scramjet propulsion for aerospace planes. Part 1: Scramjet: Aims and features p 3151 N94-29295
Scramjet CFD methods and analysis. Part 1: Scramjet CFD methods. Numerical simulation of the flow in scramjet duct p 3152 N94-29296
Research and development of ramjets/ramrockets. Part 2: Integral liquid fuel ramjets p 3152 N94-29297
Research and development of ramjets/ramrockets. Part 3: The study of gaseous hydrogen ram combustors p 3152 N94-29298
CIAM experimental turboramjets p 3152 N94-29299
Scramjet CFD methods and analysis. Part 2: Scramjet CFD analysis. Numerical simulation of supersonic mixing and combustion applied to scramjet combustor p 3152 N94-29300
Some problems of scramjet propulsion for aerospace planes. Part 2: Scramjet: Development and test problems p 3152 N94-29301

CENTRAL RESEARCH INST. OF ELECTRIC POWER INDUSTRY, TOKYO (JAPAN).
Analysis of infrared radiation heating process considering chemical reaction of material to be heated
[DE94-744116] p 3199 N94-30267

CENTRE D'ETUDES DE LA NAVIGATION AERIENNE, TOULOUSE (FRANCE).
Use of advanced technologies in ATM (air traffic management) domain p 3137 N94-29561
Cognitive approach to specifications on air traffic controllers' decision assistance systems p 3139 N94-29571
The Common Modular Simulator (CMS): An architecture test bed for future advanced ATM systems p 3141 N94-29582

CENTRE D'ETUDES ET DE RECHERCHES, TOULOUSE (FRANCE).
Modeling of the phase liquidates in combustion chambers p 3195 N94-29278
Distributed applications and failure tolerance programs using a reconfigurable parallel architecture p 3417 N94-29345
Model for the simulation of atmospheric effects on targets to background passive signatures p 3258 N94-30507
Granulometry in environments with very small particle concentrations p 3259 N94-30511

CENTRE NATIONAL DE LA RECHERCHE SCIENTIFIQUE, PARIS (FRANCE).
Simulation of pollutant formation in turbulent combustors using an extended coherent flame model p 3190 N94-29251

CENTRE NATIONAL DE LA RECHERCHE SCIENTIFIQUE, THIAIS (FRANCE).
Report on smart materials
[PB94-137528] p 3203 N94-29015

CENTRE NATIONAL DE LA RECHERCHE SCIENTIFIQUE, TOULOUSE (FRANCE).
Perception system and functions for autonomous navigation in a natural environment
[AIAA PAPER 94-1201-CP] p 3443 N94-30552

CENTRO APPLICAZIONI MILITARI DELL'ENERGIA NUCLEARE, PISA (ITALY).
Computational and experimental results in high pressure combustions of H2/air and H2/O2/H2O p 3193 N94-29268

CHINESE AERODYNAMIC RESEARCH AND DEVELOPMENT CENTER, MIANYANG.
Wind tunnel tests of a 5.3 m diameter yaw controlled turbine
[FFA-TN-1993-20] p 3340 N94-30946

CINCINNATI UNIV., OH.
Numerical analysis and computation of nonlinear partial differential equations from applied mathematics
[AD-A275582] p 3451 N94-28723
RNS optimization procedure for three-dimensional composite velocity multi-block applications p 3273 N94-29534
Numerical solution of 3-D Navier-Stokes equations in vorticity-velocity form for incompressible flows p 3276 N94-29843

CITY UNIV. OF NEW YORK, NY.
Temporal and qualitative decomposition of plausible reasoning
[AD-A275073] p 3398 N94-29154
High-resolution robot tracking and direction finding for space station environment p 3168 N94-29896
The uses and limitations of fractal geometry in digital terrain modelling p 3333 N94-29958
Three-dimensional flow characteristics downstream of a blade endwall corner p 3280 N94-30229

CIVIL AEROMEDICAL INST., OKLAHOMA CITY, OK.
Maintaining vigilance on a simulated ATC monitoring task across repeated sessions
[DOT/FAA/AM-94/6] p 3143 N94-30933

CIVIL AVIATION AUTHORITY, LONDON (ENGLAND).
Aircraft evacuations: The effect of a cabin water spray system upon evacuation rates and behaviour
[CAA-PAPER-93008] p 3148 N94-29887

CLARKSON UNIV., POTSDAM, NY.
Energetic heavy-ion tracks in micron sites p 3495 N94-30213

CLEMSON UNIV., SC.
Advanced gas turbine systems research
[DE94-005303] p 3297 N94-28485
Nonaqueous slip casting of YBa2Cu3O(7-x) superconductive ceramics
[NASA-CR-4575] p 3512 N94-29101
Radar estimations of atmospheric winds in the troposphere and lower stratosphere p 3370 N94-29697
A study of the thermospheric dynamics of the high-latitude E region using a spectral thermospheric general circulation model p 3362 N94-29743
Charge collection spectroscopy applied to MOS RAM's p 3201 N94-30220

CLEVELAND STATE UNIV., OH.
Neural network application to Particle Impact Noise Detection p 3437 N94-29840

COAST GUARD, WASHINGTON, DC.
Loran-C time management p 3144 N94-30644

COGENERATION AND COMPETITIVE POWER INST.
International Energy and Environmental Congress: Proceedings
[DE93-040609] p 3353 N94-30715
COLORADO STATE UNIV., FORT COLLINS.
Template synthesized nanoscopic gold particles: Optical spectra and the effects of particle size and shape
[AD-A275378] p 3197 N94-29312
Development and verification of a model to predict impingement currents for ion thrusters
[NASA-CR-195322] p 3173 N94-29546
Development of simplified ecosystem models for applications in Earth system studies: The Century experience p 3352 N94-30629
A toy terrestrial carbon flow model p 3352 N94-30630
COLORADO UNIV., BOULDER.
US National Weather experiment STORM-FEST: Waves and turbulence in frontal zones
[AD-A275084] p 3369 N94-28847
Lead detection and mapping with reference to relationships between scale, sensor characteristics, surface conditions and atmospheric properties
[AD-A275321] p 3377 N94-28877
The NIST Internet time service p 3475 N94-30678
Controlling the material properties of in vitro collagen through directed orientation and cross-linking of fibrils p 3221 N94-30797
Second-order structural identification via state space-based system realizations p 3323 N94-30815
Theory and application of a Radio-Acoustic Sounding System (RASS) p 3367 N94-30869
Local two-phase flow simulations including interface tracking with mass transfer p 3283 N94-30954
Local interaction control for space construction p 3170 N94-30960
COLORADO UNIV., DENVER.
A characterization of graphs with interval two-step graphs
[AD-A275652] p 3451 N94-28651
COLUMBIA UNIV., NEW YORK, NY.
Relativistic heavy ion research
[DE94-004701] p 3484 N94-28576
Near-ultraviolet laser photoemission: Scanning microscopy, buried interfaces and image-potential states p 3294 N94-29531
Kinematic representations, workspace analysis, and grasp stability in robot arms and multi-fingered hands p 3301 N94-29847
Effects of diffusion and inertia on chaotic mixing: A computational and experimental study p 3488 N94-29903
Studies in Jurassic and Cretaceous North American apparent polar wander p 3362 N94-29940
Interannual-decadal variability in tropical climate systems: Stable isotope records and general circulation model experiments p 3373 N94-29962
The rupture process of large earthquakes along convergent margins: Cast studies from Alaska and Armenia p 3363 N94-29969
Global patterns of cloud optical thickness variation with temperature and the implications for climate change p 3374 N94-29972
Broad H alpha profiles of radio-loud active galactic nuclei and rapid profile variability in Seyfert and radio galaxies p 3552 N94-29989
Theory of ultra dense matter and the dynamics of high energy interactions involving nuclei
[DE94-004178] p 3491 N94-30686
COM:ONE DEVICES, INC., SAN JOSE, CA.
A novel approach to the fabrication of SiC structures of arbitrary shape
[AD-A275475] p 3214 N94-29073
COMBUSTION DYNAMICS LTD., MEDICINE HAT (ALBERTA).
Payload central control for unmanned aircraft p 3155 N94-30284
COMMONWEALTH SCIENTIFIC AND INDUSTRIAL RESEARCH ORGANIZATION, HOBART (AUSTRALIA).
Towards coupled physical-biogeochemical models of the ocean carbon cycle p 3350 N94-30618
Ocean-atmospheric linkages p 3350 N94-30623
COMMONWEALTH SCIENTIFIC AND INDUSTRIAL RESEARCH ORGANIZATION, PARKSIDE (AUSTRALIA).
Image processing for hyperspectral data p 3326 N94-28930
COMPENGSERV LTD., OTTAWA (ONTARIO).
Intelligent systems for air space control and management p 3137 N94-29560
COMPUTER SCIENCES CORP., HAMPTON, VA.
Transferable Output ASCII Data (TOAD) editor version 1.0 user's guide
[NASA-CR-187507] p 3408 N94-28818
Laser velocimeter data acquisition system for the Langley 14- by 22-foot subsonic tunnel. Software reference guide version 3.3
[NASA-CR-191606] p 3293 N94-28839
COMPUTER SOFTWARE MANAGEMENT AND INFORMATION CENTER, ATHENS, GA.
COSMIC monthly progress report
[NASA-CR-195809] p 3422 N94-30273
CONGRESS OF THE UNITED STATES, WASHINGTON, DC.
Omnibus Budget Reconciliation Act of 1990
[PUB-LAW-101-508] p 3537 N94-28540
CONNECTICUT UNIV., FARMINGTON.
Studies on bacterial spore ultraviolet light resistance and regulation of the activity of a spore protease
[AD-A275448] p 3384 N94-28884
CONNECTICUT UNIV., STORRS.
Effects and implications of fault zone heterogeneity and anisotropy on earthquake strong ground motion p 3363 N94-29941
CONTINUUM DYNAMICS, INC., PRINCETON, NJ.
Computational analysis of high resolution unsteady airloads for rotor aeroacoustics
[NASA-CR-194894] p 3480 N94-30274
CORNELL UNIV., ITHACA, NY.
Innovative optoelectronic materials and structures using OMVPE
[AD-A275811] p 3511 N94-28773
Reasoning about programs by exploiting the environment
[AD-A275852] p 3408 N94-28794
Sweep rate and concentration effects on metastable structures formed in the underpotential deposition of silver on Pt(111)
[AD-A275369] p 3189 N94-29010
Synthesis and neutron diffraction study of Na3WN3 and Na3MoN3
[AD-A275158] p 3203 N94-29043
X ray standing wave studies of underpotentially deposited metal monolayers
[AD-A275409] p 3513 N94-29215
The synthesis and structural characterization of Na3WO3N
[AD-A275243] p 3204 N94-29395
COURTESY ASSOCIATES, INC., WASHINGTON, DC.
Fuel Cell Seminar, 1992: Program and abstracts
[DE94-003882] p 3336 N94-28472
CRANFIELD INST. OF TECH., BEDFORD (ENGLAND).
Flowfield prediction of NO(x) and smoke production in aircraft engines p 3191 N94-29252
CRYOGENIC APPLICATIONS F, INC., CLINTON, TN.
Argon frost continuous cryopump for fusion applications
[DE94-004478] p 3230 N94-29017
CUMMINS ENGINE CO., INC., COLUMBUS, IN.
Thick thermal barrier coatings for diesel components
[NASA-CR-187111] p 3537 N94-29350
CUSTOM PROCESS SYSTEMS AND SERVICE CO., PASADENA, TX.
Regenerating using aqueous cleaners with ozone and electrolysis p 3240 N94-30468
CYBEROMOTION, INC., SALEM, VA.
Meeting the challenges of installing a mobile robotic system
[AIAA PAPER 94-1187-CP] p 3440 N94-30537
CYBEROTICS, INC., WALTHAM, MA
An update on Lab Rover: A hospital material transporter
[AIAA PAPER 94-1228-CP] p 3447 N94-30577

D

DARTMOUTH COLL., HANOVER, NH.
Nonlinear magnetohydrodynamics
[DE94-005654] p 3503 N94-28547
Structure of ordinary ice I(sub h). Part 1: Ideal structure of ice
[AD-A275149] p 3486 N94-29021
The cataclysmic variables from the Palomar-Green survey p 3539 N94-29819
The role of sea ice dynamics in global climate change p 3350 N94-30620
Cryosphere and climate p 3352 N94-30632
DASSAULT-BREGUET AVIATION, SAINT CLOUD (FRANCE).
Flight command software development: RAFALE studies p 3413 N94-29320
DAYTON UNIV., OH.
Studies of lean blowout in a research combustor p 3193 N94-29266
DEFENCE AND CIVIL INST. OF ENVIRONMENTAL MEDICINE, DOWNSVIEW (ONTARIO).
Effects of endurance training on heat-exercise tolerance in men wearing NBC protective clothing
[AD-A275176] p 3391 N94-29049
Insulative properties of two thermo-metal neoprenes
[AD-A275209] p 3401 N94-29302
The use of task network simulation in workload prediction
[DCIEM-92-32] p 3402 N94-30132
DEFENCE AND CIVIL INST. OF ENVIRONMENTAL MEDICINE, NORTH YORK (ONTARIO).
Fuelling shivering in humans during cold water immersion p 3379 N94-28426
Biochemical enhancement of cold tolerance p 3380 N94-28427
Alleviation of thermal strain in the CF: Keeping our cool during the Gulf conflict p 3383 N94-28449
DEFENCE AND CIVIL INST. OF ENVIRONMENTAL MEDICINE, TORONTO (ONTARIO).
A multiplexed two-way solid communications link for teleoperated robots p 3310 N94-30310
DEFENCE RESEARCH AGENCY, FARNBOROUGH (ENGLAND).
The influence of air distribution on homogeneity and pollutant formation in the primary zone of a tubular combustor p 3194 N94-29274
A distributed object-based environment in Ada p 3417 N94-29347
DEFENCE RESEARCH AGENCY, MALVERN (ENGLAND).
Infrared polarization signatures p 3258 N94-30506
The effect of enhanced backscattering on target detection p 3258 N94-30508
DEFENCE RESEARCH AGENCY, PORTLAND (ENGLAND).
The UNICON approach to through-life support and evolution of software-intensive systems p 3416 N94-29340
DEFENCE RESEARCH ESTABLISHMENT, OTTAWA (ONTARIO).
Proceedings of the 1991 Single Event Upset Symposium
[DSIS-92-00652] p 3495 N94-30211
McMaster accelerator facility p 3496 N94-30217
Advanced development of the Spectrum Sciences Model 5005-TF, single event test fixture p 3291 N94-30218
DEFENCE RESEARCH ESTABLISHMENT PACIFIC, VICTORIA (BRITISH COLUMBIA).
Three methods to improve the accuracy of a PUMA 560 robot p 3307 N94-30290
An inverse kinematics algorithm for the DREP/Philips real-time radiographic manipulator system p 3307 N94-30292
DEFENCE RESEARCH ESTABLISHMENT SUFFIELD, MEDICINE HAT (ALBERTA).
Proceedings of the 3rd Conference on Military Robotic Applications
[DRES-SP-149] p 3304 N94-30275
A generic semi-autonomous ground vehicle control system p 3308 N94-30283
The use of low cost differential mode GPS receivers in unmanned vehicles p 3144 N94-302R5
Motion and structure from planar motion in noisy monocular image sequences p 3308 N94-30299
Unmanned vehicle mobility: Limits of autonomous navigation p 3310 N94-30311
DEFENCE RESEARCH ESTABLISHMENT SUFFIELD, RALSTON (ALBERTA).
HATT-X: A high performance flying laboratory for autonomous unmanned aircraft research and development p 3149 N94-30293
DEFENCE RESEARCH ESTABLISHMENT VALCARTIER (QUEBEC).
DREV activities related to military vehicles robotization p 3305 N94-30278
DEFENSE FORECASTS, INC., WASHINGTON, DC.
Dual-use applications of infrared sensitive materials
[AD-A275140] p 3499 N94-29694
DEFENSE INFORMATION SYSTEMS AGENCY, ARLINGTON, VA.
Software systems reengineering process model, version 1.0
[AD-A275711] p 3407 N94-28691
DEFENSE TECHNICAL INFORMATION CENTER, ALEXANDRIA, VA.
Defense Technical Information Center cataloging guidelines
[AD-A275100] p 3529 N94-28911
Learning about the Internet bibliography and beginners' guide
[AD-A275205] p 3430 N94-29051
DELAWARE UNIV., NEWARK.
Robust adaptive control of a mechanical manipulator p 3449 N94-30806
Spatial interpolation, network bias, and terrestrial air temperature variability p 3374 N94-30810
Statistical analysis of a satellite imagery time series: Implications for the study of coastal and estuarine circulation p 3335 N94-30919

DEMAND-SIDE MANAGEMENT SOCIETY.
International Energy and Environmental Congress: Proceedings
[DE93-040609] p 3353 N94-30715
DEPARTMENT OF AGRICULTURE, STARKVILLE, MS.
Seed viability detection using computerized false-color radiographic image enhancement p 3387 N94-30461
DEPARTMENT OF ENERGY, OAK RIDGE, TN.
DOE New Technology: Sharing New Frontiers, April 1, 1993 - September 30, 1993
[DE93-041289] p 3535 N94-30699
DEPARTMENT OF ENERGY, PORTLAND, OR.
Electric power lines: Questions and answers on research into health effects
[DE94-005637] p 3353 N94-30757
DEPARTMENT OF ENERGY, WASHINGTON, DC.
Global change research: Summaries of research in FY 1993
[DE94-003150] p 3341 N94-28473
US/Japan cooperation in high energy physics
[DE94-005376] p 3494 N94-28486
Summaries of FY 1993 geosciences research
[DE94-004710] p 3355 N94-28558
Effects of thermomechanical processing on tensile and long-time creep behavior of Nb-1 percent Zr-0.1 percent C sheet
[NASA-TM-106319] p 3202 N94-28822
Fossil energy biotechnology: A research needs assessment
[DE94-004239] p 3338 N94-29953
Annual report and summaries of FY 1993 activities: Division of Energy Biosciences
[DE94-001723] p 3386 N94-30607
Benchmarking for cost improvement
[DE94-002276] p 3528 N94-30824
Assessment of costs and benefits of flexible and alternative fuel use in the US transportation sector
[DE94-006100] p 3226 N94-30885
DEPARTMENT OF NATIONAL DEFENCE, OTTAWA (ONTARIO).
Robotics and the battlefield of the future
p 3304 N94-30277
DEPARTMENT OF THE NAVY, WASHINGTON, DC.
Three-axis fiber optic vector magnetometer
[AD-D016016] p 3288 N94-29699
DEUTSCHE AEROSPACE A.G., MUNICH (GERMANY).
Parachute Swivel Mechanism for planetary entry
p 3162 N94-29643
DEUTSCHE AEROSPACE A.G., ULM (GERMANY).
GPS/GNSS for ATM p 3138 N94-29565
DEUTSCHE FORSCHUNGS- UND VERSUCHSANSTALT FUER LUFT- UND RAUMFAHRT, COLOGNE (GERMANY).
Investigation of the two-phase flow in a research combustor under reacting and non-reacting conditions
p 3196 N94-29282
DEUTSCHE FORSCHUNGSANSTALT FUER LUFT- UND RAUMFAHRT, BRUNSWICK (GERMANY).
Contributions of DLR to air traffic capacity enhancement within a terminal area p 3138 N94-29567
Considerations on graphical user interfaces for intelligent ATM support systems p 3139 N94-29572
Interactive analysis and planning tools for air traffic and airspace management p 3139 N94-29573
DLR's ATM demonstration programme
p 3140 N94-29575
Experimental flight management system
p 3141 N94-29580
DEUTSCHE FORSCHUNGSANSTALT FUER LUFT- UND RAUMFAHRT, OBERPFAFFENHOFEN (GERMANY).
On the effect of emissions from aircraft engines on the state of the atmosphere p 3189 N94-29247
DEUTSCHE FORSCHUNGSANSTALT FUER LUFT- UND RAUMFAHRT, WESSLING (GERMANY).
A novel near-range radar network for airport surface control p 3142 N94-29586
DIAMOND AIR SERVICE, INC. (JAPAN).
Microgravity by parabolic flight with MU-300 aircraft
p 3392 N94-29710
DISTRICT OF COLUMBIA UNIV., WASHINGTON, DC.
High Tc superconducting bolometric and nonbolometric infrared (IR) detectors
[NASA-CR-195728] p 3262 N94-28846
DRAPER (CHARLES STARK) LAB., INC., CAMBRIDGE, MA.
Emerging technologies in microguidance and control
p 3144 N94-29788
DREXEL UNIV., PHILADELPHIA, PA.
On the dynamic mechanical behavior of 3-D integrated fabric reinforced composites
[AD-A275424] p 3177 N94-28865
Binary-single star scattering: An investigation of a realistic chaotic scattering system p 3543 N94-29719
DUKE UNIV., DURHAM, NC.
Preparation, characterization, and facile thermolysis of (X2GaP(SiMe3)2) (X = Br, I) and (Cl3Ga2P)n; new precursors to nanocrystalline gallium phosphide
[AD-A275019] p 3513 N94-29130
Synthesis and molecular structures of R(Me3CCH2)2In-E(SiMe3) (R = Me3CCH2, E = P or As; R = Me, E = P)
[AD-A275020] p 3486 N94-29131
Tris(trimethylsily)arsine and lithium bis(trimethylsily)arsenide
[AD-A275075] p 3189 N94-29140
X ray crystal structures of ((Me3SiCH2)2InCl)2 and ((Me3SiCH2)InCl2)
[AD-A275074] p 3513 N94-29155
Aeroacoustic sensitivity analysis and optimal aeroacoustic design of turbomachinery blades
[NASA-CR-195786] p 3153 N94-30013

E

EAGLE TECHNOLOGY, INC., WINTER PARK, FL.
Application of digital video to hypermedia training systems
[AD-A274989] p 3409 N94-28910
EARTH RESOURCES SATELLITE DATA ANALYSIS CENTER, TOKYO (JAPAN).
Proceedings of the International Symposium on Remote Sensing
[JTN-94-80578] p 3325 N94-28925
JERS-1 data and information system for resources exploration p 3327 N94-28932
Proceedings of the 3rd International Symposium: JERS-1 and Remote Sensing in the Future
[JTN-94-80597] p 3329 N94-29217
EAST CAROLINA UNIV., GREENVILLE, NC.
Physiological Anatomical Rodent Experiment (PARE) .04 feasibility test 2
[NASA-CR-195210] p 3385 N94-29968
ECOLE NATIONALE SUPERIEURE DES TELECOMMUNICATIONS, PARIS (FRANCE).
Use of snakes to link edge points to create left ventricular boundaries in echocardiographic images
[TELECOM-93-D-016] p 3395 N94-30970
The Stroemberg wavelet on the interval and the Franklin system
[TELECOM-93-C-002] p 3462 N94-30971
Numerical simulations of piano strings. Part 1: A physical model for a struck string using finite difference methods
[TELECOM-93-C-003] p 3481 N94-30972
Elements for the recognition of three dimensional deformable shapes: Application to biomedical imagery
[TELECOM-93-E-006] p 3396 N94-30978
Noise reduction techniques for the restoration of musical recordings
[TELECOM-93-E-019] p 3291 N94-30979
EDGERTON, GERMESHAUSEN AND GRIER, INC., ALBUQUERQUE, NM.
Blast overpressure studies with animals and man
[AD-A275038] p 3391 N94-29150
EDGERTON, GERMESHAUSEN AND GRIER, INC., IDAHO FALLS, ID.
Acceptance sampling methods for sample results verification
[DE94-002882] p 3465 N94-29925
Why TQM fails (and what you can do about it)
[DE93-018945] p 3527 N94-30698
EG AND G ENERGY MEASUREMENTS, INC., LOS ALAMOS, NM.
Taxonomy of gamma ray burster data using a self-organizing neural network
[DE94-006480] p 3553 N94-30248
EHIME UNIV., MATSUYAMA (JAPAN).
Computer simulations on development of the fast reconnection mechanism p 3360 N94-29241
ELECTRO-OPTICAL SCIENCES, INC., IRVINGTON, NY.
Innovative direct detection range-Doppler laser radar
[AD-A275619] p 3292 N94-28635
ELECTRONIC SYSTEM G.M.B.H., MUNICH (GERMANY).
Experiences with the HOOD design method on avionics software development p 3414 N94-29325
A generalization of the software engineering maturity model p 3416 N94-29341
ELIZABETH CITY STATE UNIV., NC.
ECSU home-institution support program (1993)
[AD-A275244] p 3431 N94-29396
ELORET CORP., PALO ALTO, CA.
Theoretical investigation of gas-surface interactions
[NASA-CR-195755] p 3272 N94-29378
Advanced vehicle concepts systems and design analysis studies
[NASA-CR-195115] p 3147 N94-29721
A study of low emissions gas turbine combustions
[NASA-CR-195763] p 3152 N94-29860
Particle kinetic simulation of high altitude hypervelocity flight
[NASA-CR-194535] p 3131 N94-29893
ENTREPRISE 2 SOFTWARE, SAINT-CLOUD (FRANCE).
Entreprise 2: A PCTE integrated project support environment p 3417 N94-29349
ENVIRONMENTAL ENGINEERS AND MANAGERS INST.
International Energy and Environmental Congress: Proceedings
[DE93-040609] p 3353 N94-30715
ENVIRONMENTAL RESEARCH INST. OF MICHIGAN, ANN ARBOR.
Automated inspection of turbine blades: Challenges and opportunities
[AIAA PAPER 94-1226-CP] p 3446 N94-30575
ERLANGEN-NUREMBERG UNIV. CHILDRENS HOSPITAL (GERMANY).
Physiological investigations of the isolated rat's liver in hypothermia and hypoxia and their relevance in aircraft incidents above the sea p 3382 N94-28439
ESE/SEKAI, SANTA FE SPRINGS, CA.
Time synchronized video systems
p 3261 N94-30675
EUROCONTROL EXPERIMENTAL CENTRE, BRETIGNY (FRANCE).
ARC2000: Automatic radar control
p 3141 N94-29583
Installation of experimental mode-S data link in commercial aircraft
[PB94-138757] p 3254 N94-29998
EUROPEAN ORGANIZATION FOR THE SAFETY OF AIR NAVIGATION, BRUSSELS (BELGIUM).
Decision Making Aids (DMA) in on-line ATC systems
p 3139 N94-29570
Air-ground integration of the ATM system in PHARE
p 3141 N94-29579
EUROPEAN SPACE AGENCY, PARIS (FRANCE).
GOME: Global Ozone Monitoring Experiment
[ESA-SP-1151] p 3347 N94-29452
Hybrid optics for space applications
[ESA-CP-1158] p 3501 N94-30418
EUROPEAN SPACE AGENCY. EUROPEAN SPACE RESEARCH AND TECHNOLOGY CENTER, ESTEC, NOORDWIJK (NETHERLANDS).
ESTEC wiring test programme materials related properties p 3165 N94-28698
Collecting cometary soil samples? Development of the ROSETTA sample acquisition system
p 3160 N94-29628
EUROPEAN SPACE RESEARCH INST., FRASCATI (ITALY).
Observations by ERS-1 start p 3327 N94-28933
Earth-observation plan in Europe
p 3331 N94-29227
EXOTEMP SYSTEMS, INC., STITTSVILLE (ONTARIO).
Recent Canadian advances in active thermal protection p 3384 N94-28451

F

FEDERAL AVIATION ADMINISTRATION, ATLANTIC CITY, NJ.
1.8 gigahertz (GHz) digital Low Density Radio Communications Link (LDRCL) Operational Test and Evaluation (OT&E) integration and OT&E operational final test report
[AD-A275800] p 3241 N94-28771
Los Angeles international airport instrument landing system approach data collection and reduction, phase 1
[AD-A275115] p 3136 N94-28914
FEDERAL AVIATION ADMINISTRATION, CAMBRIDGE, MA.
Key cognitive issues in the design of electronic displays of instrument approach procedure charts
[AD-A275647] p 3399 N94-28649
FEDERAL AVIATION ADMINISTRATION, OKLAHOMA CITY, OK.
Scanning and monitoring performance: Effects of the reinforcement values of the events being monitored
[DOT/FAA/AM-94/8] p 3398 N94-29918
Toxicity of carbon monoxide-hydrogen cyanide gas mixtures: Exposure concentration, time-to-incapacitation, carboxyhemoglobin, and blood cyanide parameters
[DOT/FAA/AM-94/7] p 3395 N94-29919
FEDERAL AVIATION ADMINISTRATION, WASHINGTON, DC.
The 1993 Federal Aviation Administration Aviation System Capital Investment Plan p 3136 N94-29445
Opportunities for integrating the aircraft FMS, aeronautical operational control centers, and future air traffic management systems in oceanic airspace
p 3140 N94-29577
Development of precision runway monitor system for increasing capacity of parallel runway operations
p 3142 N94-29587

FERMI NATIONAL ACCELERATOR LAB., BATAVIA, IL.
Search for excited quarks in p(bar p) collisions at the square root of s = 1.8 TeV
[DE94-004658] p 3484 N94-28573
B production and B(0)(bar B)(0) mixing at DO
[DE94-004664] p 3484 N94-28574
Inclusive jet and direct photon production at the D0 experiment
[DE94-006001] p 3488 N94-30049
Measurement of the W mass in the D0 detector
[DE94-006002] p 3490 N94-30103
Heavy flavor production at fixed target photo- and hadroproduction
[DE94-004651] p 3491 N94-30719
A search for rapidity gap events in p(bar p) collisions at D(0)
[DE94-004654] p 3491 N94-30722
Search for the top quark in the electron-electron and electron-muon channels at D0
[DE94-006174] p 3492 N94-30779
Charmonium and bottomonium in (-p)p interactions
[DE94-006173] p 3493 N94-30886
Inclusive single muon production in D0
[DE94-006175] p 3493 N94-30887
A magnetically coupled quench detector for superconducting magnets
[DE94-006040] p 3268 N94-30904

FIAT AVIAZIONE S.P.A., TURIN (ITALY).
Technology rigs: A tool for afterburner development p 3154 N94-29270

FLORENCE UNIV. (ITALY).
Evaluation of dual polarization attenuation of millimeter frequencies through a meteorological radar p 3256 N94-30496

FLORIDA ATLANTIC UNIV., BOCA RATON.
Partial support for the Second International Symposium on Artificial Intelligence and Mathematics
[AD-A275199] p 3434 N94-29026

FLORIDA STATE UNIV., TALLAHASSEE.
Lunar surface operations. Volume 1: Lunar surface emergency shelter
[NASA-CR-195551] p 3299 N94-29354
Lunar surface operations. Volume 4: Lunar rover trailer
[NASA-CR-195554] p 3299 N94-29386

FLORIDA UNIV., GAINESVILLE.
Innovative processing of composites for ultra-high temperature applications, book 1
[AD-A275597] p 3176 N94-28729
Innovative processing of composites for ultra-high temperature applications, book 2
[AD-A275598] p 3177 N94-28730
Innovative processing of composites for ultra-high temperature applications, book 3
[AD-A275599] p 3177 N94-28731
Development of ultra-low noise, high performance 3 -5 quantum well infrared photodetectors (QWIPs) for focal plane array staring image sensor systems
[AD-A275745] p 3511 N94-28734
A study of cloud-to-ground lightning processes with emphasis on data analysis and modeling of the return stroke p 3372 N94-29802
Correlation analysis on optical and radio light curves for a large sample of active galactic nuclei p 3546 N94-29992

FLUID POLYMERS, INC., LAS VEGAS, NV.
Solventless, curable fluid oligomeric systems for high performance microwave, acoustical and mechanical applications p 3223 N94-30478

FOKKER SPACE AND SYSTEMS, AMSTERDAM (NETHERLANDS).
Aiding the operator in the manual control of a space manipulator
[PB94-125549] p 3402 N94-30390

FORD MOTOR CO., DEARBORN, MI.
Agile manufacturing: The factory of the future
[AIAA PAPER 94-1184-CP] p 3440 N94-30534
Integration of vision and robotic workcell
[AIAA PAPER 94-1186-CP] p 3440 N94-30536

FORSCHUNGSZENTRUM JUELICH G.M.B.H. (GERMANY).
Detection of tropospheric OH and HO2 by laser-induced fluorescence at low pressure using the 308nm excitation of OH p 3343 N94-28591
UV laser long-path absorption spectroscopy p 3343 N94-28595

FOSTER-MILLER ASSOCIATES, INC., WALTHAM, MA.
Full-scale testing and analysis of curved aircraft fuselage panels
[AD-A275666] p 3145 N94-28657
High temperature arc-track resistant aerospace insulation p 3167 N94-28716
Controlled thermal expansion printed wiring boards based on liquid crystal polymer dielectrics
[NASA-CR-189338] p 3287 N94-29400
Lunar base heat pump, phase 1 draft
[NASA-CR-195211] p 3278 N94-29977

FRACTURESEARCH, INC., GALENA, OH.
Analysis concerning the inspection threshold for multi-site damage
[PB94-142429] p 3149 N94-30905

FUJI HEAVY INDUSTRIES LTD., TOKYO (JAPAN).
A design of third-generation airfoils for helicopter rotor blades using Navier-Stokes p 3124 N94-28957
Numerical analysis of supersonic transport wings p 3124 N94-28959

FUJITA HEALTH UNIV., TOYOHASHI (JAPAN).
Posture control of goldfishes under microgravity p 3387 N94-29712

FUJITSU LTD., TOKYO (JAPAN).
Parallel Fortran programming for NWT p 3129 N94-28991
Performance evaluation of the NWT with parallel Fortran p 3129 N94-28992

G

GEC FERRANTI, EDINBURGH (SCOTLAND).
GEC Ferranti piezo vibratory gyroscope p 3239 N94-29790

GENERAL ATOMIC CO., SAN DIEGO, CA.
The 100 kA, 5000 V solid-state opening switch for inductive energy storage
[AD-A274993] p 3263 N94-28994

GENERAL ATOMICS TECHNOLOGIES CORP., SAN DIEGO, CA.
Application of divertor cryopumping to H-mode density control in DIII-D
[DE94-004859] p 3510 N94-30832

GENERAL ELECTRIC CO., CINCINNATI, OH.
Design and fabrication of forward-swept counterrotation blade configuration for wind tunnel testing
[NASA-CR-194868] p 3155 N94-28510
Fuel injector design for high temperature aircraft engine p 3154 N94-29263

GENERAL ELECTRIC CO., SAN JOSE, CA.
SP-100 control drive assembly development p 3163 N94-29651

GENERAL ELECTRIC CO., SCHENECTADY, NY.
Advanced microfabrication technologies for microspacecraft p 3171 N94-29782

GENERAL MOTORS CORP., INDIANAPOLIS, IN.
Application of CFD in combustor design technology p 3154 N94-29256
Investigation of advanced counterrotation blade configuration concepts for high speed turboprop systems. Task 2: Unsteady ducted propfan analysis computer program users manual
[NASA-CR-187105] p 3152 N94-29438

GEO-CENTERS, INC., LAKE HOPATCONG, NJ.
Cubanes: Super explosives and potential pharmaceutical intermediates p 3227 N94-30454

GEOLOGICAL SURVEY OF JAPAN, IBARAKI.
Application of JERS-1 data to geologic analyses p 3330 N94-29222
EOS project and ASTER (ITIR) p 3331 N94-29226

GEORGE WASHINGTON UNIV., WASHINGTON, DC.
New high temperature plasmas and sample introduction systems for analytical atomic emission and mass spectrometry
[DE94-004564] p 3503 N94-28458
Similarity solutions and numerical modeling in buoyancy controlled turbulent diffusion flames
[AD-A275820] p 3188 N94-28777
Publications of the NASA Controlled Ecological Life Support System (CELSS) program 1989-1992
[NASA-CR-4603] p 3401 N94-30122
Analysis of fluctuating static pressure measurements in a large high Reynolds number transonic cryogenic wind tunnel p 3158 N94-30788

GEORGIA INST. OF TECH., ATLANTA.
Two-Photon/Laser-Induced Fluorescence (TP/LIF) sensor p 3342 N94-28588
Ion-assisted tropospheric OH measurement technique p 3344 N94-28601
Summer intern program
[AD-A275194] p 3466 N94-28888
Empirical studies of the value of algorithm animation in algorithm understanding
[AD-A275135] p 3412 N94-29287
A case-based approach to creative design
[AD-A275229] p 3417 N94-29390
On conceptual design of active databases p 3531 N94-29535
The effects of inheritance on the properties of physical storage models in object-oriented databases p 3531 N94-29537
Dynamics of a coupled solid state laser array p 3294 N94-29551
Active control of delaminations in smart composite structures p 3181 N94-29593
Helicopter mission and rotor performance optimization with quasi-linear inflow theory p 3147 N94-29594
Micro-opto-mechanical devices and systems using epitaxial lift off p 3239 N94-29793
Rotorcraft airframe structural optimization for vibration and dynamic stress reduction including damping treatment p 3147 N94-29878
Interlaminar fracture analysis for laminated composites under combined loading p 3182 N94-29964

GEORGIA UNIV., ATHENS.
Optical studies of dynamical processes in disordered systems
[DE94-006751] p 3501 N94-30252
Evaluating models of climate and forest vegetation p 3353 N94-30637

GEOSAT COMMITTEE, INC., NORMAN, OK.
Evaluation of simulated JERS-1 data for geologic mapping at Drum Mountains, Utah, Silver Bell, Arizona, and Wind River, Wyoming under the GEOSAT-ERSDAC/JAPEX/JGI/RESTEC joint studies p 3326 N94-28929

GERBER SCIENTIFIC, INC., RESTON, VA.
Test of prototype liquid-water-content meter for aircraft use
[NASA-CR-189304] p 3374 N94-30187

GERMAN AIR FORCE, FUERSTENFELDBRUK (GERMANY).
Effectiveness of protection clothing for cold weather conditions after ejection over sea: A case report p 3381 N94-28435

GIFFORD (F. A.), OAK RIDGE, TN.
A fractal analysis of near-field atmospheric concentration data
[AD-A275460] p 3355 N94-28728

GKSS-FORSCHUNGSZENTRUM GEESTHACHT (GERMANY).
Turbulence models and their application in implosion analyses with two-phase flow
[GKSS-92/E/98] p 3284 N94-30967
Numerical simulation and prediction of implosion phenomena
[GKSS-92/E/99] p 3284 N94-30968

GOODFELLOW CONSULTANTS, INC., MISSISSAUGA (ONTARIO).
Industrial ventilation p 3232 N94-29604
Ventilation cost and air cleaning p 3232 N94-29605

GORE (W. L.) AND ASSOCIATES, INC., ELKTON, MD.
Development of a new chemical warfare agent protective material p 3381 N94-28432

GOSUDARSTVENNYI KOMITET PO ISPOLZOVANIYU ATOMNOI ENERGII, OBNINSK (USSR).
Analysis of data by long-time mechanical properties of 08KH18N10T steel irradiated by neutrons
[DE94-605337] p 3202 N94-28551
Solution of charged particle transport equation by Monte-Carlo method in the BRANDZ code system
[DE94-606270] p 3484 N94-28614
Miln equation for the calculation of the phases and amplitudes of wave functions for continuum spectrum of Coulomb two-center problem
[DE94-606292] p 3522 N94-28616
Development of evaluated data bank of physical properties of perspective nuclear engineering steels and alloys
[DE94-607999] p 3207 N94-30076
Fast precise algorithm for simulation of ionization energy losses
[DE94-608010] p 3421 N94-30080
Distribution functions of electrons within aluminium oxide thin films
[DE94-608418] p 3490 N94-30184

GOSUDARSTVENNYI KOMITET PO ISPOLZOVANIYU ATOMNOI ENERGII, SERPUKHOV (USSR).
On possibility to create the scintillation trigger for liquid-argon neutrino detector
[DE94-607844] p 3489 N94-30050

GOVERNMENT INDUSTRIAL RESEARCH INST., CHUGOKU (JAPAN).
Future expectation of remote sensing technology p 3332 N94-29231

GOVERNMENT INDUSTRIAL RESEARCH INST., OSAKA (JAPAN).
Glass studies under microgravity p 3228 N94-28941

GRAZ UNIV. (AUSTRIA).
Tropospheric corrections to GPS measurements using locally measured meteorological parameters compared with general tropospheric corrections p 3144 N94-30655

GREENVILLE COLL., IL.
A future, intense source of negative hydrogen ions p 3494 N94-30485

GRENOBLE-1 UNIV. (FRANCE).
Computer Assisted Medical Interventions: Application to Conformal Radiotherapy
[RR-912-I] p 3395 N94-30028
Conformal external radiotherapy of prostatic carcinoma: Requirements and preliminary results
p 3395 N94-30029
Pre- and intra-radiotherapy multimodal image registration: Principles and first experiments
p 3395 N94-30030
GRUMMAN AEROSPACE CORP., BETHPAGE, NY.
VAS: A Vision Advisor System combining agents and object-oriented databases
[AIAA PAPER 94-1181-CP] p 3440 N94-30532
GUELPH UNIV. (ONTARIO).
The potential of new textiles in improving survival prospects p 3380 N94-28430
The development and evaluation of a tunable diode laser trace gas sensor for the measurement of N2O and CH4 fluxes using micrometeorological techniques
[ISBN-0-315-78975-1] p 3296 N94-30801

H

HAMAMATSU UNIV., SHIZUOKA (JAPAN).
Space movement of Trichinella spiralis under microgravity p 3387 N94-29711
HARRIS CORP., MELBOURNE, FL.
Photorefractive adaptive antenna array processor
[AD-A275762] p 3241 N94-28762
HARVARD UNIV., CAMBRIDGE, MA.
Harvard ER-2 OH laser-induced fluorescence instrument p 3343 N94-28592
Electromagnetic core-mantle coupling
p 3366 N94-30808
HAWAII UNIV., HONOLULU.
On the annual cycle of the tropical Pacific atmosphere and ocean p 3371 N94-29763
Modeling deep equatorial circulation
p 3378 N94-29815
HELSINKI UNIV. OF TECHNOLOGY, ESPOO (FINLAND).
Qualitative vector optimization of a condensate stabilizer process
[PB94-133246] p 3189 N94-28789
Dynamics of defect ensembles in one-dimensional cellular automata
[PB94-136819] p 3464 N94-29030
Polymer Technology Seminar, 1993. Kem-100.600
[PB94-137593] p 3213 N94-29031
Fundamentals of printing technology
[PB94-132602] p 3530 N94-29141
Low temperature behavior of virgin martensite
[PB94-132925] p 3204 N94-29142
Polymer technology publication series no. 16
[PB94-135522] p 3214 N94-29157
Batch updates and concurrency in B-trees
[PB94-136835] p 3530 N94-29167
Cities for tomorrow: Directions for change
[PB94-136850] p 3537 N94-29168
The 19th Convention on Radio Science: Abstracts of Papers
[PB94-136868] p 3244 N94-29169
Some efficient procedures for correcting triangulated models
[PB94-136926] p 3452 N94-29171
Engineering document management system
[PB94-136934] p 3530 N94-29172
Model-oriented data analysis with applications to lake and soil water simulation
[PB94-136942] p 3329 N94-29173
Acoustic and optical investigations of superfluid (3)He
[PB94-135415] p 3477 N94-29186
Application of high-speed milling to the Finnish manufacturing industry
[PB94-135548] p 3230 N94-29187
Realizing the productivity potential of expeditious operations
[PB94-135555] p 3230 N94-29188
Plant-microbe interactions: Plant hormone production by phylloplane fungi
[PB94-135563] p 3385 N94-29189
Physiology and molecular-genetics of thermus and bacillus
[PB94-135571] p 3385 N94-29190
EXTdesign. Version 1.0: Reference manual
[PB94-136827] p 3411 N94-29193
Effect of non-metallic inclusions on the machinability of steel
[PB93-230233] p 3204 N94-29387
Some remarkable sine and cosine functions
[PB94-137759] p 3453 N94-29439
Combustion and heat transfer in a high speed diesel engine operating with rape seed oil methyl ester fuel
[PB94-137536] p 3301 N94-29679
Nonlinear PCA: Algorithms and applications
[PB94-137544] p 3419 N94-29680
Evaluation of the Resource Library System in Finland
[PB94-137734] p 3532 N94-29682
Knowledge based system for identification of gamma sources
[PB94-137742] p 3487 N94-29683
The polymerization of epsilon-caprolactone with stannous catalyst and lactide/epsilon-caprolactone (LA/epsilon-CL) and lactide/glycolide (LA/GA) copolymers. Polymer technology publication series no. 15
[PB94-137551] p 3220 N94-30713
HELSINKI UNIV. OF TECHNOLOGY, KYLMAELAE (FINLAND).
Finnish astronomy days, 1992-1993. Proceedings of the Finnish Astronomical Society
[PB94-136892] p 3538 N94-29170
HEWLETT-PACKARD LABS., PALO ALTO, CA.
Frequency standards from industry over the next 25 years p 3475 N94-30683
HIGH TECHNOLOGY CORP., HAMPTON, VA.
Long-wavelength asymptotics of unstable crossflow modes, including the effect of surface curvature
[NASA-CR-4579] p 3273 N94-29460
HIROSHIMA INST. OF TECH. (JAPAN).
Remote sensing and global management
p 3328 N94-28937
HONEYWELL, INC., GLENDALE, AZ.
Optical Chopper Assembly for the Mars Observer
p 3162 N94-29639
HONEYWELL, INC., MINNEAPOLIS, MN.
Advanced air traffic control and flight management system concepts p 3140 N94-29576
HONEYWELL INFORMATION SYSTEMS, INC., MINNEAPOLIS, MN.
Future manned systems advanced avionics study
[NASA-CR-188277] p 3150 N94-29377
HORIZON DATA CORP., RESTON, VA.
Interagency advanced power group: Solar working group
[DE94-004953] p 3340 N94-30833
HOUSTON UNIV., CLEAR LAKE, TX.
Field guide to Cretaceous-tertiary boundary sections in northeastern Mexico
[NASA-CR-195719] p 3354 N94-28416
HOUSTON UNIV., TX.
Fuzzy logic based robotic controller
[AIAA PAPER 94-1202-CP] p 3443 N94-30553
HUGHES AIRCRAFT CO., LOS ANGELES, CA.
Determination of cosmic ray latchup rate in CMOS devices p 3497 N94-30222
HUGHES SPACE AND COMMUNICATIONS GROUP, EL SEGUNDO, CA.
Low melting temperature alloy deployment mechanism and recent experiments p 3163 N94-29644
HYDRO-ELECTRIC POWER COMMISSION, BURNABY (BRITISH COLUMBIA).
Development of an accurate transmission line fault locator using the global positioning system satellites
p 3144 N94-30652
HYPRES, INC., ELMSFORD, NY.
Exploratory research for a high temperature superconducting integrated circuit
[AD-A275798] p 3262 N94-28767

I

IBIS ASSOCIATES, INC., WELLESLEY, MA.
Analysis of cost: CVD diamond deposition and finishing
[AD-A275586] p 3212 N94-28725
IBM FEDERAL SYSTEMS DIV., GAITHERSBURG, MD.
Software Technology for Adaptable, Reliable Systems (STARS) program
[AD-A275675] p 3407 N94-28664
Cleanroom engineering handbook. Volume 3: Project execution in the cleanroom environment
[AD-A275860] p 3156 N94-28752
Cleanroom engineering handbook. Volume 4. Specification team practices
[AD-A275861] p 3156 N94-28753
Cleanroom engineering handbook. Volume 2: Organization and project formation in the cleanroom environment
[AD-A275809] p 3156 N94-28772
IDAHO NATIONAL ENGINEERING LAB., IDAHO FALLS.
Sensing the gas metal arc welding process
p 3314 N94-30444
Near-net-shape manufacturing: Spray-formed metal matrix composites and tooling p 3186 N94-30447
A modular approach for automated sample preparation and chemical analysis p 3354 N94-30464
ILLINOIS UNIV., CHICAGO.
A sub-cm micromachined electron microscope
p 3236 N94-29775
Generation of gear tooth surfaces by application of CNC machines
[NASA-CR-195306] p 3303 N94-30205
ILLINOIS UNIV., URBANA.
Molecular aspects of transport in thin films of controlled architecture
[DE94-004552] p 3211 N94-28457
Research on elementary particle physics. Task P: Studies in theory and phenomenology of elementary physics
[DE94-004955] p 3483 N94-28566
ILLINOIS UNIV., URBANA-CHAMPAIGN.
Redundant disk arrays in transaction processing systems
[NASA-CR-195759] p 3418 N94-29404
An experimental study of the flowfield on a semispan rectangular wing with a simulated glaze ice accretion
p 3130 N94-29674
A study of the relationship between the performance and dependability of a fault-tolerant computer
[NASA-CR-195758] p 3406 N94-29695
Direct and large-eddy simulations of turbulent flow in a square duct p 3275 N94-29809
Dependability analysis of parallel systems using a simulation-based approach
[NASA-CR-195762] p 3431 N94-29846
Checkpoint-based forward recovery using lookahead execution and rollback validation in parallel and distributed systems
[NASA-CR-195760] p 3431 N94-29869
Failure strength and mechanism of composite laminates under multiaxial loading conditions p 3182 N94-29875
Non-invasive temperature measurements using electron paramagnetic resonance spectroscopy
p 3198 N94-29881
Design for dependability: A simulation-based approach
[NASA-CR-195757] p 3420 N94-29890
Robust adaptive control and filtering
p 3437 N94-29895
An experimental investigation of flow patterns and liquid entrainment in a horizontal-tube evaporator
p 3277 N94-29899
Space reclamation for uncoordinated checkpointing in message-passing systems
[NASA-CR-195761] p 3420 N94-29906
Stochastic stability and nonlinear control in mechanical systems p 3303 N94-29966
Physics, astronomy, and astrophysics: A numerical study of the black hole plus Brill wave spacetime
p 3540 N94-29990
Near-critical spherically symmetric accretion by neutron stars p 3546 N94-29991
The 3-D LDV measurements on a 30-degree swept wing with a simulated ice accretion
[NASA-CR-195327] p 3132 N94-30124
An experimental study of the aerodynamics of a swept and unswept semispan wing with a simulated glaze ice accretion
[NASA-CR-195330] p 3133 N94-30152
The effect of a wavy boundary on turbulent flow
p 3280 N94-30272
Stellar and gas dynamics of interacting ring galaxies
p 3548 N94-30340
Development and application of particle image velocimetry in high-speed separated flow: Two-dimensional base cavities p 3282 N94-30791
Theory and observations of horizontal and vertical structure of gravity wave perturbations in the middle atmosphere p 3366 N94-30802
Thin-walled orthotropic laminated beam theory
p 3324 N94-30920
IMAGO MFG. LTD., OTTAWA (ONTARIO).
Activities in machine vision at Imago Manufacturing Ltd. p 3308 N94-30297
IMPERIAL COLL. OF SCIENCE AND TECHNOLOGY, LONDON (ENGLAND).
Ducted kerosene spray flames p 3195 N94-29276
The maximum entropy approach applied to energy exchange, chemical reactions and ionisation in the direct simulation Monte Carlo method for rarefied hypersonic flows
[IC-AERO-93-01] p 3524 N94-29481
INDIANA UNIV., BLOOMINGTON.
Scientific and technical information transfer: Promoting information acquisition in the Saudi Arabian industrial sector p 3532 N94-29803
INSTITUT DE RECHERCHE DE L'HYDRO-ONTARIO, TORONTO.
ARK: Autonomous mobile robot in an industrial environment
[AIAA PAPER 94-1177-CP] p 3439 N94-30529

INSTITUT DES HAUTES ETUDES SCIENTIFIQUES, BURES-SUR-YVETTE (FRANCE).
Reidemeister numbers of equivariant maps
[PB94-138286] p 3452 N94-29118
Existence of quantum characteristic exponents
[PB94-138161] p 3523 N94-29146
Remarks on Galois symmetry in RCFT
[PB94-138179] p 3467 N94-29147
Approximation of solutions of the cubic NLSE by finite dimensional equations and non-squeezing properties
[PB94-138294] p 3452 N94-29148
Method of Chabauty-Coleman and the second case of Fermat's last theorem for regular primes
[PB94-138187] p 3467 N94-29162
Trace formulas and dynamical zeta functions in the Nielsen theory
[PB94-138195] p 3467 N94-29163
Hierarchical structures and asymmetric stochastic processes on p-adics and adeles
[PB94-138203] p 3464 N94-29178
Non-commutative geometry
[PB94-139342] p 3462 N94-30889

INSTITUT NATIONAL DE RECHERCHE ET DE SECURITE POUR LA PREVENTION DES ACCIDENTS DU TRAVAIL ET DES MALADIES PROFESSIONNELLES, VANDOEUVRE (FRANCE).
Introduction to the design of ventilation systems p 3231 N94-29599
Computational fluid dynamics in ventilation: Practical approach p 3233 N94-29611

INSTITUTE FOR ADVANCED STUDY, PRINCETON, NJ.
Problems in particle theory
[DE94-003665] p 3491 N94-30685

INSTITUTE FOR COMPUTER APPLICATIONS IN SCIENCE AND ENGINEERING, HAMPTON, VA.
An alternative assessment of second-order closure models in turbulent shear flows
[NASA-CR-194881] p 3272 N94-29381
A spectral boundary integral equation method for the 2-D Helmholtz equation
[NASA-CR-194890] p 3454 N94-30207
Canonical-variables multigrid method for steady-state Euler equations
[NASA-CR-194888] p 3454 N94-30208
Accurate finite difference methods for time-harmonic wave propagation
[NASA-CR-194887] p 3454 N94-30209

INSTITUTE FOR DEFENSE ANALYSES, ALEXANDRIA, VA.
Comparing Ada and FORTRAN lines of code: Some experimental results
[AD-A275322] p 3409 N94-28878

INSTITUTE FOR PERCEPTION RVO-TNO, SOESTERBERG (NETHERLANDS).
Deterioration of manual performance in cold and windy climates p 3381 N94-28434

INSTITUTE OF AVIATION MEDICINE, FUERSTENFELDBRUCK (GERMANY).
Aeropathological diagnosis of lethal hypothermia p 3382 N94-28440

INSTITUTE OF AVIATION MEDICINE, MANCHING (GERMANY).
Test of a new protection suit in a climatic chamber p 3384 N94-28452

INSTITUTE OF PLASMA PHYSICS, PRAGUE (CZECHOSLOVAKIA).
Progress in Z-Pinch Research
[IPPCZ-321] p 3505 N94-29074
Investigation of intense XUV emission of nitrogen-puff Z-pinch with small energy input
[PH-23] p 3505 N94-29075
Multichannel x ray spectral measurement of hot plasma evolution in nitrogen-puff Z-pinch
[PH-24] p 3505 N94-29076
X ray emission scaling and energy balance of small gas-puff Z-pinch p 3505 N94-29077

INSTITUTO DE PESQUISAS ESPACIAIS, SAO JOSE DOS CAMPOS (BRAZIL).
Amazonia: Remote sensing test site and survey p 3327 N94-28935

INSTITUTO NACIONAL DE TECNICA AEROESPACIAL, MADRID (SPAIN).
High temperature resistant jet fuels p 3192 N94-29260

INSTRON CORP., CANTON, MA.
Development of Alternating Current Potential Drop (ACPD) procedures for crack detection in aluminum aircraft panels
[AD-A275755] p 3315 N94-28646

INTERNATIONAL BUSINESS MACHINES CORP., OWEGO, NY.
DSSA-ADAGE: An environment for architecture-based avionics development p 3150 N94-29348

INTERNATIONAL BUSINESS MACHINES CORP., SAN JOSE, CA.
Toward milli-Newton electro- and magneto-static microactuators p 3238 N94-29784

INTERNATIONAL BUSINESS MACHINES CORP., YORKTOWN HEIGHTS, NY.
Tunnelling hot electron transfer amplifiers
[AD-A275529] p 3262 N94-28687

INTERNATIONAL CENTRE FOR THEORETICAL PHYSICS, TRIESTE (ITALY).
Some constraints and solutions of the Kadomtsev-Petviashvili equation
[DE93-634355] p 3466 N94-28467
Emission of supersymmetric neutron pair by charged lepton in magnetic field
[DE93-634365] p 3481 N94-28468
Effect of phonon dispersion on properties of exciton in magnetic field
[DE93-634756] p 3481 N94-28469
Extended nonabelian symmetries for free fermionic model
[DE94-601554] p 3481 N94-28470
Coherent states of SU(l,1) groups
[DE94-603654] p 3524 N94-29498
Thermomechanical properties of 3-D transition metals
[DE94-604015] p 3487 N94-29500
Aggregation equilibria in arsenic doped silicon
[DE94-607269] p 3515 N94-30005
Approximation methods for nonlinear operator equations of the m-accretive type
[DE94-608099] p 3467 N94-30065
Ablation of polymers by ultraviolet pulsed laser
[DE94-608100] p 3218 N94-30066
Strong overlap and transmission in triple barrier resonant structures
[DE94-608103] p 3516 N94-30067
Electronic structure of Zn-based quantum wells
[DE94-608104] p 3516 N94-30068
Vibrational properties of homopolar and heteropolar surfaces and interfaces of the CdTe/HgTe system
[DE94-608105] p 3516 N94-30069
II-VI wide band gap semiconductors under hydrostatic pressure
[DE94-608106] p 3516 N94-30070
A relativistic solitary wave in electron positron plasma
[DE94-608107] p 3507 N94-30071
Band structure of superlattice with (delta)-like potential
[DE94-608108] p 3516 N94-30072
On chaos in quantum mechanics: The two meanings of sensitive dependence
[DE94-608069] p 3524 N94-30086
Fractal approach to computer-analytical modelling of tree crown
[DE94-608089] p 3467 N94-30088
Discrete symmetries, strong CP problem and gravity
[DE94-608091] p 3524 N94-30089
Thermodynamics of molten K-TE alloys
[DE94-608095] p 3208 N94-30090
Periodic orbits of n-body type problems: The fixed period case
[DE94-608096] p 3453 N94-30091
Interband optical absorption in the Wannier-Stark ladder under the electron-LO-phonon resonance condition
[DE94-608097] p 3267 N94-30092
Extension of love wave transformation theory to laterally heterogeneous structures
[DE94-608098] p 3365 N94-30093
Frequency dependence of polarization phase difference
[NASA-TM-109737] p 3254 N94-30094
Nucleon and nuclei at finite temperature, as a phenomenological test of the entropy bound
[DE94-608094] p 3489 N94-30097
Localization in presence of magnetic field in 2-D disordered binary alloys
[DE94-608093] p 3208 N94-30108
Magnetic properties of a quantum transverse spin-1 Blume-Emery-Griffiths model
[DE94-608114] p 3517 N94-30109
Some results on the phase diagram of the antiferromagnetic Potts model in an external magnetic field
[DE94-608115] p 3468 N94-30110
Generalized augmented space theorem for correlated disorder and cluster coherent potential approximation
[DE94-608110] p 3208 N94-30118
Homogeneous Poisson structures
[DE94-608112] p 3453 N94-30119
A theory approach for creation of the matter of universe
[DE94-608109] p 3548 N94-30163
Magnetic properties of the three dimensional Ising model with interface single-ion anisotropy
[DE94-608116] p 3525 N94-30164
Magnetic properties of a transverse spin-1 Ising model with longitudinal crystal field interactions
[DE94-608118] p 3517 N94-30165
Symplectic topology of integrable Hamiltonian systems
[DE94-608120] p 3467 N94-30166
The bond diluted spin-1 Blume-Emery-Griffiths model in a transverse field
[DE94-608121] p 3525 N94-30167
Periodic electromagnetic vacuum in the two-dimensional Yang-Mills theory with the Chern-Simons mass
[DE94-608128] p 3525 N94-30170
Magnetic properties of a transverse spin-1 Ising model with random crystal field interactions
[DE94-608117] p 3517 N94-30181
Is it possible to extend the deformed Weyl algebra W(sub q)(n) to a Hopf algebra?
[DE94-608092] p 3467 N94-30202
A solid-on-solid invasion percolation model for self-affine interfaces
[DE94-608102] p 3521 N94-30888

INTERNATIONAL METEOROLOGICAL INST., STOCKHOLM (SWEDEN).
Activities report of the International Meteorological Institute
[ETN-94-95524] p 3370 N94-29423

INTERNATIONAL SUBMARINE ENGINEERING LTD., PORT COQUITLAM (BRITISH COLUMBIA).
Autonomous Robotic Refueling System (ARRS) for rapid aircraft turnaround p 3305 N94-30279
A testbed for the development of ground-based control of space-based manipulators p 3309 N94-30306
Achieving robot autonomy p 3310 N94-30307

IOWA STATE UNIV. OF SCIENCE AND TECHNOLOGY, AMES.
An observational and numerical study of sea/land-breeze circulations in an area of complex coastal heating p 3372 N94-29813
Terfenol: A study of the phase equilibrium diagram and the solidification process
[DE94-004883] p 3209 N94-30690
Investigation of the phase equilibria and phase transformations associated with the Bi2Sr2CaCu2O(y) superconductor
[DE94-004889] p 3519 N94-30691
Dynamic modeling of multibody flexible structures p 3323 N94-30813
Optimal low-thrust, Earth-Moon trajectories p 3159 N94-30961

ISHIKAWAJIMA-HARIMA HEAVY INDUSTRIES CO. LTD., TOKYO (JAPAN).
Numerical simulation of supersonic flow around space plane with engine installed p 3125 N94-28961
Unsteady aerodynamic computations around NACA0012 at high angles of attack p 3126 N94-28969
Application of flow field simulation to turbine vane design p 3127 N94-28978
Activities of Ishikawajima-Harima Heavy Industries Co. Ltd.
[PB94-137981] p 3555 N94-29798

ISRAEL ACADEMY OF SCIENCES AND HUMANITIES, JERUSALEM.
The Seventh International Beer Sheva Seminar on MHD Flows and Turbulence
[DE94-607211] p 3506 N94-29831

ISRAEL ATOMIC ENERGY COMMISSION, TEL AVIV.
Research laboratories annual report 1992
[DE94-608124] p 3555 N94-30168

ISRAEL ATOMIC ENERGY COMMISSION, YAVNEH.
Magnetic field generation by circularly polarized laser light and inertial plasma confinement in a miniature magnetic bottle induced by circularly polarized laser light
[DE94-608353] p 3508 N94-30192

ISTITUTO ELETTROTECNICO NAZIONALE, TURIN (ITALY).
European PTTI report p 3468 N94-30642

ISTITUTO ELETTROTECNICO NAZIONALE (GALILEO FERRARIS), TURIN (ITLAY).
An algorithm for the Italian atomic time scale p 3473 N94-30668

ISTITUTO NAZIONALE DI FISICA NUCLEARE, FRASCATI (ITALY).
Double-crystal analyser system for the PRISMA spectrometer: Test of a prototype
[PB94-138245] p 3286 N94-29113

ITALIAN SPACE AGENCY, MATERA.
Unsupervised texture image segmentation by improved neural network ART2
[AIAA PAPER 94-1199-CP] p 3442 N94-30549

IWATE UNIV., MORIOKA (JAPAN).
Tohoku district observed by artificial satellites p 3328 N94-29041

J

JAI ASSOCIATES, INC., MOUNTAIN VIEW, CA.
A free-wake Euler and Navier-Stokes CFD method and its application to helicopter rotors including dynamic stall
[AD-A275416] p 3129 N94-29197

JAPAN AIR LINES CO. LTD., TOKYO.
Disturbance of equilibrium on JAL flight crew
p 3390 N94-28856

JAPAN ATOMIC ENERGY RESEARCH INST., TOKYO.
Electron beam irradiation experiments of monoblock divertor mock-up
[DE94-707497] p 3503 N94-28555
Experimental and analytical studies of high heat flux components for fusion experimental reactor
[DE94-707671] p 3504 N94-28556
Crystal structure of La(2-x)Ba(x)CuO4
[DE94-707688] p 3511 N94-28750
Analytic cross sections for collisions of H, H2, He and Li atoms and ions with atoms and molecules
[DE94-707686] p 3485 N94-28788

JAPAN MACHINERY FEDERATION, TOKYO.
The 1992 report on the next generation ultra clean technology for advanced microfabrication
[DE94-744171] p 3157 N94-30268

JAPAN MARINE SCIENCE AND TECHNOLOGY CENTER, TOKYO.
Research report on the potential of ocean development suitable for area characteristics
[JTN-94-80587] p 3377 N94-29595

JAPAN RESOURCES OBSERVATION SYSTEM ORGANIZATION.
Observatory system of Earth Resources Satellite-1
p 3330 N94-29221

JAPAN SOCIETY OF AEROSPACE AND ENVIRONMENTAL MEDICINE, TOKYO.
Japanese Journal of Aerospace and Environmental Medicine, vol. 30, no. 3
[JTN-94-80606] p 3387 N94-28495
Japanese Journal of Aerospace and Environmental Medicine, volume 30, no. 1
[JTN-94-80598] p 3389 N94-28850
Japanese Journal of Aerospace and Environmental Medicine, vol. 30, no. 2
[JTN-94-80599] p 3394 N94-29863

JAPAN SPACE UTILIZATION PROMOTION CENTER, TOKYO.
Survey report of JSUP Space Environment Utilization Research Committee in fiscal year 1992: Protein Crystal Growth Session
[JTN-94-80584] p 3158 N94-28583
Overview of space environment utilization science
[JTN-94-80581] p 3227 N94-28938
Survey report of JSUP Space Environment Utilization Research Committee in fiscal year 1992: Functional New Materials Session
[JTN-94-80582] p 3159 N94-30162
Survey report of JSUP Space Environment Utilization Research Committee in fiscal year 1992: Metallic Materials Session
[JTN-94-80583] p 3159 N94-30794

JAPEX GEOSCIENCE INST., TOKYO (JAPAN).
Application of optical sensor data to resource survey
p 3330 N94-29223

JET PROPULSION LAB., CALIFORNIA INST. OF TECH., PASADENA.
JPL Fourier transform ultraviolet spectrometer
p 3343 N94-28593
NSC 800, 8-bit CMOS microprocessor
[NASA-CR-195736] p 3405 N94-28845
Synthetic aperture radar applications: Now and in the future p 3260 N94-28927
Rock identification using thermal infrared data
p 3331 N94-29228
Method for forming thin composite solid electrolyte film for lithium batteries
[NASA-CASE-NPO-18877-1-CU] p 3264 N94-29357
Plasma heating for containerless and microgravity materials processing
[NASA-CASE-NPO-18819-1-CU] p 3229 N94-29371
Digital camera with apparatus for authentication of images produced from an image file
[NASA-CASE-NPO-19108-1-CU] p 3287 N94-29373
Method of implementing digital phase-locked loops
[NASA-CASE-NPO-18757-1-CU] p 3265 N94-29374
Dendrite preventing separator for secondary lithium batteries
[NASA-CASE-NPO-18585-1-CU] p 3265 N94-29411
An emergency response mobile robot for operations in combustible atmospheres
[NASA-CASE-NPO-19020-1-CU] p 3299 N94-29420
Nonvolatile programmable neural network synaptic array
[NASA-CASE-NPO-18578-1-CU] p 3265 N94-29426
High level language-based robotic control system
[NASA-CASE-NPO-17918-2-CU] p 3435 N94-29465
Monolithic in-based III-V compound semiconductor focal plane array cell with single stage CCD output
[NASA-CASE-NPO-18978-1-CU] p 3265 N94-29488
Catalytic ignitor for regenerative propellant gun
[NASA-CASE-NPO-18987-1-CU] p 3225 N94-29490
Reconfigurable optical interconnections via dynamic computer-generated holograms
[NASA-CASE-NPO-19039-1-CU] p 3499 N94-29491
A neural network with modular hierarchical learning
[NASA-CASE-NPO-19077-1-CU] p 3435 N94-29492
Lasercom system architecture with reduced complexity
[NASA-CASE-NPO-19069-1-CU] p 3293 N94-29493
Extended horizon lifting for periodic gain adjustment in control systems, and for equalization of communication channels
[NASA-CASE-NPO-19166-1-CU] p 3246 N94-29495
An alternate method for achieving temperature control in the -160 to +90 C range
[NASA-CASE-NPO-18995-1-CU] p 3288 N94-29497
Epitaxial heterojunctions of oxide semiconductors and metals on high temperature superconductors
[NASA-CASE-NPO-18483-1-CU] p 3513 N94-29501
Kinematic functions for redundancy resolution using configuration control
[NASA-CASE-NPO-18608-1-CU] p 3436 N94-29504
Anode for rechargeable ambient temperature lithium cells
[NASA-CASE-NPO-18580-1-CU] p 3265 N94-29505
The Telecommunications and Data Acquisition Report
[NASA-CR-195694] p 3246 N94-29613
Combining GPS and VLBI earth-rotation data for improved universal time p 3144 N94-29614
Computation of vibration mode elastic-rigid and effective weight coefficients from finite-element computer program output p 3247 N94-29615
X-/Ka-band dichroic plate design and grating lobe study p 3247 N94-29616
Site comparison for optical visibility statistics in southern California p 3247 N94-29617
Modifications of the Griesmer bound
p 3247 N94-29618
Integer cosine transform for image compression
p 3247 N94-29619
A portable X-band front-end test package for beam-waveguide antenna performance evaluation. Part 2: Tests on the antenna p 3247 N94-29620
Phasing the Very Large Array on Galileo in the presence of Jupiter's strong radio emission p 3164 N94-29621
Elevation control system model for the DSS 13 antenna p 3248 N94-29622
Radio science ground data system for the Voyager-Neptune encounter, part 1
p 3248 N94-29623
Gaussian beam and physical optics iteration technique for wideband beam waveguide feed design
p 3248 N94-29624
Design and analysis of a low-loss linear analog phase modulator for deep space spacecraft X-band transponder applications p 3248 N94-29625
Orbital debris radar instrumentation
p 3248 N94-29626
Mars rover mechanisms designed for Rocky 4
p 3161 N94-29630
Pointing mechanisms for the Shuttle Radar Laboratory
p 3162 N94-29638
The Telecommunications and Data Acquisition Report
[NASA-CR-195689] p 3249 N94-29652
Toward astrometric tracking with the infrared spatial interferometer p 3249 N94-29653
Line-of-sight tropospheric calibration from measurements in arbitrary directions
p 3249 N94-29654
Enhanced orbit determination filter sensitivity analysis: Error budget development p 3159 N94-29655
Enhanced orbit determination filter: Inclusion of ground system errors as filter parameters p 3159 N94-29656
Determining noise temperatures in beam waveguide systems p 3249 N94-29657
A dual-cavity ruby maser for the Ka-band link experiment p 3250 N94-29658
A digital combining-weight estimation algorithm for broadband sources with the array feed compensation system p 3250 N94-29660
Digital combining-weight estimation for broadband sources using maximum-likelihood estimates
p 3250 N94-29661
Optimizing the Galileo space communication link
p 3250 N94-29663
Decoder synchronization for deep space missions
p 3250 N94-29664
A comparison of full-spectrum and complex-symbol combining techniques for the Galileo S-band mission
p 3250 N94-29665
TOPEX/POSEIDON operational orbit determination results using global positioning satellites
p 3160 N94-29666
Design and implementation of a hybrid digital phase-locked loop with a TMS320C25: An application to a transponder receiver breadboard
p 3251 N94-29667
A 32 GHz microstrip array antenna for microspacecraft application p 3251 N94-29668
Effects of low sampling rate in the digital data-transition tracking loop p 3251 N94-29669
An improved conscan algorithm based on a Kalman filter p 3251 N94-29670
A complex symbol signal-to-noise ratio estimator and its performance p 3251 N94-29671
X-band ultralow-noise maser amplifier performance
p 3251 N94-29672
Simulation of interference between Earth stations and Earth-orbiting satellites p 3252 N94-29673
Neural network with dynamically adaptable neurons
[NASA-CASE-NPO-17803-1-CU] p 3436 N94-29756
Proceedings of the Workshop on Microtechnologies and Applications to Space Systems
[NASA-CR-195688] p 3235 N94-29767
The Pluto fast flyby mission: Completing the reconnaissance of the solar system
p 3235 N94-29768
Micro guidance and control technology overview
p 3144 N94-29772
Miniaturization in x ray and gamma ray spectroscopy
p 3236 N94-29773
Micro-sensors for in-situ meteorological measurements p 3236 N94-29777
A broad-band microseismometer for planetary operations p 3237 N94-29778
Imaging spectrometry of the Earth and other solar system bodies p 3237 N94-29779
Smart focal-plane technology for micro-instruments and micro-rovers p 3237 N94-29780
Micromachined electron tunneling infrared sensors
p 3238 N94-29785
Control of micromachined deformable mirrors
p 3239 N94-29787
Micro guidance and control synthesis: New components, architectures, and capabilities p 3144 N94-29792
Common spaceborne multicomputer operating system and development environment
[NASA-TM-109092] p 3422 N94-30197
A force-controllable macro-micro manipulator and its application to medical robots p 3314 N94-30441
The use of interactive computer vision and robot hand controllers for enhancing manufacturing safety
p 3314 N94-30442
Analysis and an image recovery algorithm for ultrasonic tomography system p 3397 N94-30456
A fuzzy logic controller for hormone administration using an implantable pump p 3397 N94-30459
Technology for robotic surface inspection in space
[AIAA PAPER 94-1193-CP] p 3442 N94-30544
A highly redundant robot system for inspection
[AIAA PAPER 94-1194-CP] p 3442 N94-30545
Status of frequency and time support for NASA systems p 3468 N94-30640
Time and position accuracy using codeless GPS
p 3144 N94-30650
Frequency standards from government laboratories over the next 25 years p 3475 N94-30682

JIKEI UNIV., TOKYO (JAPAN).
Space and vertigo: In relation to space motion sickness p 3390 N94-28857

JOHANN-WOLFGANG-GOETHE-UNIV., FRANKFURT AM MAIN (GERMANY).
Absolute determination of local tropospheric OH concentrations p 3343 N94-28594

JOHNS HOPKINS UNIV., BALTIMORE, MD.
Infrared properties of obscuring dust tori in active galactic nuclei p 3545 N94-29832
A multiwavelength study of two prototypical supernova remnants p 3540 N94-29833
Nanodislocation structures generated in shocked crystals p 3514 N94-29915
Lubricant rheology at high shear rates
p 3217 N94-29967
Time-resolved holography for the microscopic study of crack-tip motion in dynamic fracture
p 3290 N94-30254
An investigation of the corrosion properties of aluminum-tantalum alloys using electrochemical impedance spectroscopy and local electrochemical impedance spectroscopy p 3209 N94-30521

JOHNS HOPKINS UNIV., COLUMBIA, MD.
Time maintenance system for the BMDO MSX spacecraft p 3171 N94-30672
Ground control system for the midcourse space experiment UTC clock p 3474 N94-30674

JOINT INST. FOR LAB. ASTROPHYSICS, BOULDER, CO.
The NIST Internet time service p 3475 N94-30678
JOINT INST. FOR NUCLEAR RESEARCH, DUBNA (USSR).
Energy losses of fast charged particles in thin silicon detectors
[DE94-606065] p 3483 N94-28552
The computer-aided system for the high resolution SQUID-magnetometer
[DE94-606138] p 3286 N94-28553
Simulation of experiments on deep inelastic scattering of muons on superconducting magnetic toroidal spectrometer STORS
[DE94-606267] p 3483 N94-28554
Calculation of eigenvalues of Schroedinger operators for arbitrary coupling
[DE94-606302] p 3522 N94-28582
Quasipotential in the fourth order of perturbation theory
[DE94-606299] p 3484 N94-28584
The static and nonstatic electrical solenoids
[DE94-606326] p 3261 N94-28585
Apparent unambiguousness of relativistic time dilation
[DE94-606328] p 3522 N94-28586
On invariant measures for some infinite-dimensional dynamical systems
[DE94-606342] p 3522 N94-28609
Deep inelastic lepton scattering on nuclei: operator product expansion and meson-nucleon theory
[DE94-606442] p 3484 N94-28610
Masses and mixing of leptons and quarks (Dirac particles)
[DE94-606446] p 3484 N94-28611
Possible explanation of the interaction cross-section growth at high energies
[DE94-606457] p 3494 N94-28612
Track filtering by robust neural network
[DE94-606067] p 3434 N94-28613
The program for catalogization of magnetic tapes in EXCHARM experiment
[DE94-606271] p 3528 N94-28615
Retarded distances and the Doppler effect
[DE94-606296] p 3523 N94-28618
Numerical solution of the multichannel scattering problem
[DE94-606297] p 3484 N94-28619
On the importance of the Michelson-Morley experiment
[DE94-606298] p 3523 N94-28620
Specialized data base management system for data processing in the experiments at low energies
[DE94-606268] p 3485 N94-28621
Variational calculation of the eigenpotential for H(sup -)-system
[DE94-606269] p 3407 N94-28622
Project of the experiment to test the hypothesis on existence of white and black p(mu)-atoms
[DE94-606751] p 3485 N94-28625
Hysteresis phenomena at spin-flop transition induced by the pulsed magnetic field
[DE94-606851] p 3511 N94-28626
Model of polylinear Bose- and Fermi-like oscillator
[DE94-606303] p 3485 N94-28718
Classical interpretation of quantum mechanics
[DE94-606304] p 3523 N94-28719
On the EKL-effect
[DE94-606325] p 3468 N94-28720
On a direct experimental verification of the elongation formula
[DE94-606329] p 3523 N94-28721
The proper field of charges and gauge-invariant variables in electrodynamics
[DE94-606405] p 3523 N94-28751
The small-x behaviour of parton distribution functions
[DE94-606414] p 3485 N94-28758
Three forms of relativity
[DE94-606338] p 3523 N94-28782
The solving of the relativistic two-body problem with a nonlinear dependence upon a spectrum parameter
[DE94-606343] p 3451 N94-28783
Path integral for coherent states of the dynamical U(sub 2) group and U(sub 2/1) supergroup
[DE94-606382] p 3466 N94-28785
Ion channeling peculiarities in YBa2Cu3 O7 monocrystal
[DE94-606885] p 3512 N94-28787
Twistor-like type 2 superstring and bosonic string
[DE94-606339] p 3523 N94-28802
The Klein-Fock equation, minimal surfaces and gravitational fields
[DE94-606340] p 3356 N94-28803
Atomic and magnetic structure of YBa2(Cu(1-x)Fe(x))3O(6+y) at 0.05 less than or equal to x less than or equal to 0.30, y is approximately equal to 1 and y is approximately equal to 0.5
[DE94-606852] p 3513 N94-29210
Semileptonic heavy-to-light decays of baryons
[DE94-606481] p 3487 N94-29502
Experimental setup for study of hadron and hard photon production in nucleus-nucleus collisions
[DE94-607849] p 3489 N94-30051
Experimental setups and methods to obtain new nuclear data at intermediate and high energies
[DE94-607850] p 3489 N94-30052
The bases for the development of high-temperature integrated SQUID-systems
[DE94-607901] p 3267 N94-30073
Digital filter
[DE94-607902] p 3406 N94-30074
Microsecond fiber optic delay line
[DE94-607903] p 3500 N94-30075
Complicated problem solution techniques in optimal parameter searching
[DE94-608007] p 3421 N94-30077
Iterative procedure as equation of motion
[DE94-608008] p 3453 N94-30078
Program SCREEN for acquisition, visualization, processing and output of experimental data
[DE94-608009] p 3534 N94-30079
PAW using under MS DOS
[DE94-608012] p 3406 N94-30081
The bases for the development of high-temperature integrated SQUID-systems
[DE94-608462] p 3517 N94-30082
Algorithm and program ORANGE for magnetic field simulation of magnetic system spectrometer STORS
[DE94-608013] p 3421 N94-30083
Third-order beam optics of real solenoid magnetic lens
[DE94-608014] p 3500 N94-30084
On relativity principle violation in local measurements of spin precession of moving particles
[DE94-608067] p 3489 N94-30085
Reconstruction of spectra in the discrete quantum mechanics (new elements of the lattice quantum engineering)
[DE94-608075] p 3524 N94-30087
Search for heavy neutrinos at the IHEP-JINR neutrino detector
[DE94-608175] p 3489 N94-30095
Statistical description of hot and dense clustering matter
[DE94-608155] p 3490 N94-30112
Modelling of multiparticle production by dynamical semigroup method
[DE94-608132] p 3490 N94-30120
Meso-optical Fourier transform microscope with double focusing
[DE94-607851] p 3290 N94-30148
Theory of fundamental interactions
[DE94-608126] p 3525 N94-30169
On the structure and atomic motions in liquid sodium
[DE94-608386] p 3490 N94-30182
Overlap of metal clusters and nuclear structure physics
[DE94-608387] p 3517 N94-30183
On the (mu)SR activity at LNP JINR phasotron
[DE94-608385] p 3517 N94-30195
GL(sub q)(N)-covariant quantum algebras and covariant differential calculus
[DE94-608072] p 3460 N94-30726
Normal state resistivity of MBa2Cu3O(7-x) ceramics
[DE94-608456] p 3220 N94-30745

K

KANAGAWA PREFECTUAL COLL. (JAPAN).
Image technology and information analysis of bone change with gravitational exposure p 3389 N94-28851
KANAZAWA WOMAN'S JUNIOR COLL. (JAPAN).
Effect of food intake on skin vasomotor responses to head-up tilt in humans p 3390 N94-28854
Effects of make-up on the heat transfer from the head in hyperthermic conditions p 3394 N94-29864
KANSAS STATE UNIV., MANHATTAN.
DOE/KEURP site operator program
[DE94-005832] p 3267 N94-30701
Atomic physics with highly charged ions
[DE94-003397] p 3492 N94-30837
KANSAS UNIV., LAWRENCE.
An experimental investigation of the effect of leading edge extensions on directional stability and the effectiveness of forebody nose strakes p 3155 N94-29728
Unsteady transonic aerodynamics in frequency domain for flutter analysis p 3131 N94-29879
Aircraft aerodynamics with deflected jets in ground effect p 3132 N94-29973
Hydrodynamic stability analysis of swirling jets p 3278 N94-29974
KARLSRUHE UNIV. (GERMANY).
A new Eulerian model for turbulent evaporating sprays in recirculating flows p 3195 N94-29279
Time-resolved measurements in a three dimensional model combustor p 3196 N94-29283
KAWASAKI HEAVY INDUSTRIES LTD., GIFU (JAPAN).
Role of computational fluid dynamics in aeronautical engineering. Part 10: Numerical analysis of flow around 2-D multi-element HLD p 3125 N94-28964
KAWASAKI HEAVY INDUSTRIES LTD., TOKYO (JAPAN).
Some issues on Japan's space food development and relating preliminary experimental study p 3388 N94-28498
Verification of a three-dimensional viscous flow analysis for a single stage compressor p 3127 N94-28976
KEELE UNIV. (ENGLAND).
Double-crystal analyser system for the PRISMA spectrometer: Test of a prototype
[PB94-138245] p 3286 N94-29113
KENT STATE UNIV., OH.
Development of novel switchable protein surfaces
[AD-A275510] p 3384 N94-28667
KENTUCKY UNIV., LEXINGTON.
Experimental validation of finite element and boundary element methods for predicting structural vibration and radiated noise
[NASA-CR-4561] p 3301 N94-29552
KINETIC SCIENCES, INC., VANCOUVER (BRITISH COLUMBIA).
Supervised autonomous control for Space Station Special Purpose Dextrous Manipulator (SPDM) robot p 3309 N94-30305
KINGS COLL., LONDON (ENGLAND).
Controlling chaos in plasma filled diodes
[AD-A275525] p 3504 N94-28686
KISS INST. FOR PRACTICAL ROBOTICS, RESTON, VA.
A robotic wheelchair
[AIAA PAPER 94-1229-CP] p 3447 N94-30578
KLEIN ASSOICIATES, INC., FAIRBORN, OH.
Designing for performance: A cognitive systems engineering approach to modifying an AWACS human computer interface
[AD-A275187] p 3399 N94-28861
KRUG LIFE SCIENCES, INC., SAN ANTONIO, TX.
A reliable and repeatable method for volume calculation of pressurized garments
[AD-A275600] p 3399 N94-28766
Relaxed tolerance following HSG, high sustained +Gz
[AD-A275204] p 3391 N94-28892
Procedures and metrics for anti-G suit evaluations
[AD-A275349] p 3400 N94-28997
Methane challenge of high performance molecular sieve oxygen concentrator
[AD-A275155] p 3337 N94-29033
Decompression sickness risk versus time and altitude
[AD-A275261] p 3391 N94-29071
KUTZTOWN STATE COLL., PA.
Ada, object-oriented techniques, and concurrency in teaching data structures and file management
[AD-A275385] p 3411 N94-29201
KYORIN UNIV., TOKYO (JAPAN).
Psychophysiological study on the effects of co-existence of lines for detecting dot target p 3394 N94-29867
KYOTO UNIV., SAKYOKU (JAPAN).
Numerical analysis of incompressible viscous flow around a bubble p 3126 N94-28968
Application of digital control theory to adaptive grid generation p 3127 N94-28980
Aurora stereo observation in Iceland p 3359 N94-29234
KYUSHU UNIV., FUKUOKA (JAPAN).
Numerical simulation of unsteady aerodynamic heating induced by shock reflections p 3123 N94-28952
An implicit upwind scheme for the three-dimensional Euler equations using a pointwise relaxation method p 3128 N94-28983

L

LABORATOIRE DE MEDECINE AEROSPATIALE, BRETIGNY-SUR-ORGE (FRANCE).
Experimental evaluation of two systems of individual air-conditioning p 3384 N94-28450
LAKEHEAD UNIV., PORT ARTHUR (ONTARIO).
The effects of propagational factors on quantum wires in close parallel proximity
[ISBN-0-315-86157-6] p 3254 N94-30035

LAMONT-DOHERTY GEOLOGICAL OBSERVATORY, PALISADES, NY.
Dynamic constraints on CO2 uptake by an iron-fertilized Antarctic p 3350 N94-30619
LAVAL UNIV. (QUEBEC).
Study of the stellar populations of the Fornax dwarf spheroidal galaxy
[ISBN-0-315-85526-6] p 3541 N94-30231
Calibration of charge coupled device digital cameras
[ISBN-0-315-85539-8] p 3290 N94-30232
Synchronization of microwave oscillators by direct optical injection
[ISBN-0-315-85546-0] p 3500 N94-30233
Glueball and meson dispersion and diffusion relations in compact U(1)(2+1) gauge theory
[ISBN-0-315-85577-0] p 3490 N94-30234
Study of the problems of nonuniformity of heating in infrared vision applied to the inspection of materials having non-planar relief
[ISBN-0-315-85637-8] p 3316 N94-30235
The extraction and representation of forest inventory information using continuous density surfaces
[ISBN-0-315-85658-0] p 3334 N94-30236
Application of extended Lagrange series to the precise determination of Global Positioning Satellite orbits
[ISBN-0-315-85724-2] p 3159 N94-30237
LAWRENCE LIVERMORE NATIONAL LAB., CA.
Risk-based prioritization: A comparison of approaches
[DE94-003368] p 3526 N94-28474
Analysis of spark-induced bubble experiments using CALE
[DE94-003667] p 3270 N94-28476
The High Performance Storage System
[DE94-004350] p 3404 N94-28505
Equation of state of stellar plasmas
[DE94-004186] p 3542 N94-28526
Filament to mandrel gap analysis: Resulting gap from filament winding over a cone-cylinder transition mandrel (reference NMTP no. 93838)
[DE94-004225] p 3175 N94-28528
High damage threshold anti-reflectors by physical vapor deposited amorphous fluoropolymer
[DE94-004865] p 3212 N94-28560
Superplasticity in fine-grained ceramics
[AD-A275461] p 3212 N94-28733
Dual-Band Infrared (DBIR) imaging inspections of Boeing 737 and KC-135 aircraft panels
[DE94-005700] p 3122 N94-29842
Optical field ionization of atoms and ions using ultrashort laser pulses
[DE94-006643] p 3488 N94-29845
Numerical simulation of radiative heat loss in an experimental burner
[DE94-002016] p 3277 N94-29923
Improved ground-penetrating radar, bridge decks
[DE94-004863] p 3254 N94-29929
Large-scale computations in analysis of structures
[DE94-004022] p 3321 N94-29951
Management of PEM public key certificates using X.500 directory service: Some problems and solutions
[DE94-004200] p 3431 N94-29952
Impact of biomass burning on the atmosphere
[DE94-004333] p 3349 N94-29954
Energy and Technology Review
[DE94-004472] p 3338 N94-29955
Communications technology for unattended sensors
[DE94-005685] p 3254 N94-30043
Intermedia transfer factors for fifteen toxic pollutants released to air basins in California
[DE94-005699] p 3349 N94-30044
Influence of doping on the electronic structure of (La, Sr)2CuO4
[DE94-006383] p 3516 N94-30054
Proceedings: SISAL 1993
[DE94-006641] p 3420 N94-30056
Microwave Michelson interferometer system report of first use on a railgun, Green Farm, San Diego, CA
[DE94-005294] p 3289 N94-30059
Enhanced coherence x ray laser experiments and simulations
[DE94-005367] p 3295 N94-30060
A physical optics model for scattering of HF radiation by irregular terrain
[DE94-006187] p 3255 N94-30106
Genetic algorithms at UC Davis/LLNL
[DE94-006625] p 3421 N94-30117
GNU debugger internal architecture
[DE94-006665] p 3422 N94-30251
Precision and manufacturing at the Lawrence Livermore National Laboratory p 3240 N94-30449
Missile launch detection electric field perturbation experiment
[DE94-004224] p 3466 N94-30586
Air-deployable geophysics package
[DE94-005651] p 3335 N94-30594
A review of the ablative stabilization of the Rayleigh-Taylor instability in regimes relevant to ICF
[DE94-005809] p 3509 N94-30597
Nonlinear absorption in high reflector multilayers
[DE94-005818] p 3295 N94-30598
Characterization of defect geometries in multilayer optical coatings
[DE94-005820] p 3501 N94-30599
Design of an electromagnetic accelerator for turbulent hydrodynamic mix studies
[DE94-005821] p 3281 N94-30600
Radiative flux calculations at UV and visible wavelengths
[DE94-004278] p 3350 N94-30613
The challenge of identifying greenhouse gas-induced climatic change p 3352 N94-30634
Dual-band infrared imaging for quantitative corrosion detection in aging aircraft
[DE94-004187] p 3149 N94-30687
Advanced steady-state operating scenarios
[DE94-004810] p 3509 N94-30768
Complex source rate estimation for atmospheric transport and dispersion models
[DE94-000958] p 3354 N94-30822
The validation of ocean surface heat fluxes in AMIP
[DE94-001539] p 3378 N94-30823
Material properties and fracture mechanics in relation to ceramic machining
[DE94-006623] p 3221 N94-30829
Diode-pumped solid-state-laser drivers and the competitiveness of inertial fusion energy
[DE94-006654] p 3296 N94-30830
Computing at the leading edge: Research in the energy sciences
[DE94-006121] p 3563 N94-30844
Inertial confinement fusion
[DE94-005957] p 3510 N94-30875
Tropospheric radiative forcing of O3 for the 1994 IPCC report
[DE94-005698] p 3367 N94-30876
Dissociative recombination of H3(+)
[DE94-005356] p 3493 N94-30891
Application of ALE techniques to metal forming simulations
[DE94-005358] p 3211 N94-30892
LEEDS UNIV. (ENGLAND).
Prediction of prompt NO(x) in hydrocarbon air flames p 3190 N94-29250
Ultra low NO(x) ultra lean gas turbine primary zones with liquid fuels p 3154 N94-29267
LEMIGAS RESEARCH AND DEVELOPMENT CENTRE FOR OIL AND GAS TECHNOLOGY, JAKARTA (INDONESIA).
Application of remote sensing techniques in petroleum exploration: The Indonesian experience p 3331 N94-29225
LOCKHEED AIRCRAFT CORP., PALO ALTO, CA.
X ray studies of the Hyades cluster
[NASA-CR-189325] p 3538 N94-29001
LOCKHEED AIRCRAFT SERVICE, INC., ONTARIO, CA.
Aircraft system aft telescope cavity configuration study for Stratospheric Observatory for Infrared Astronomy (SOFIA), phase 2
[NASA-CR-194266] p 3147 N94-29685
LOCKHEED ENGINEERING AND SCIENCES CO., HOUSTON, TX.
Design reuse experience of space and hazardous operations robots
[AIAA PAPER 94-1220-CP] p 3445 N94-30568
LOCKHEED MISSILES AND SPACE CO., PALO ALTO, CA.
Three high duty cycle, space-qualified mechanisms p 3162 N94-29642
Coronal abundances and their variation
[NASA-CR-195767] p 3551 N94-29858
Coronal temperatures of unusually active K-dwarf binary systems
[NASA-CR-189335] p 3545 N94-29861
A study of the formation and dynamics of the Earth's plasma sheet using ion composition data
[NASA-CR-195119] p 3507 N94-30126
Tail lobe ion composition at energies of 0.1 to 16 keV/e: Evidence for mass-dependent density gradients
[PAPER-93JA03201] p 3507 N94-30127
Experimental investigation of possible geomagnetic feedback from energetic (0.1 to 16 keV) terrestrial O(+) ions in the magnetotail current sheet
[PAPER-93JA01991] p 3507 N94-30128
LOCKHEED MISSILES AND SPACE CO., SUNNYVALE, CA.
Lock-up failure of a four-bar linkage deployment mechanism p 3163 N94-29646
LOCKHEED SANDERS, INC., NASHUA, NH.
Microwave vision for robots
[AIAA PAPER 94-0887-CP] p 3443 N94-30550
LOGICON, INC., DAYTON, OH.
Backscatter haze device for measurement of haze in aircraft transparencies
[AD-A275127] p 3146 N94-29042
A comparison of three aircraft attitude display symbology structures
[AD-A275172] p 3150 N94-29048
LORAL SPACE INFORMATION SYSTEMS, HOUSTON, TX.
Analysis of EDP performance
[NASA-CR-195726] p 3420 N94-29945
LOS ALAMOS NATIONAL LAB., NM.
Modeling turbulence in flows with a strong rotational component
[DE94-003577] p 3270 N94-28475
Global atmospheric and ocean modeling on the connection machine
[DE94-003930] p 3342 N94-28521
A space-based classification system for RF transients
[DE94-003933] p 3240 N94-28522
Dislocation theory of melting for iron, revisited
[DE94-002715] p 3355 N94-28538
The (j,0) + (0,j) representation space: Majorna-like construct
[DE94-005010] p 3522 N94-28543
Failures to model the development of a cube texture during the high temperature compression of Al-Mg alloys
[DE94-005013] p 3201 N94-28544
Production rates of terrestrial in-situ-produced cosmogenic nuclides
[DE94-005156] p 3543 N94-28545
Research activities of Martin C. Casdagli at SFI September 1989--May 1991
[DE94-005655] p 3463 N94-28548
Large eddy simulations using lattice Boltzmann algorithms
[DE94-005666] p 3270 N94-28549
The (j,0) + (0,j) representation space: Dirac-like construct
[DE94-005011] p 3522 N94-28572
Characterization of structure and mechanical properties of MoSi2-SiC nanolayer composites
[DE94-004982] p 3175 N94-28579
Acceleration in astrophysics
[DE94-004986] p 3552 N94-28580
Fabrication and testing of plasma-spray formed MoSi2 and MoSi2 composite tubes
[DE94-004995] p 3175 N94-28581
Performance of MCNP4A on seven computing platforms
[DE93-040101] p 3419 N94-29816
A pot-pourri of results in QCD from large lattice simulations on the CM5
[DE94-005084] p 3514 N94-29818
Brittle composites modeling: Comparisons with MoSi2/ZrO2
[DE94-004978] p 3182 N94-29933
Advances in tunable powerful lasers: The advanced free-electron laser
[DE94-004997] p 3294 N94-29934
Microstructure and mechanical properties of nitrided molybdenum silicide coatings
[DE94-006249] p 3217 N94-30025
Comparison of 14 MeV isomer production of Hf-178m1 and Hf-179m2 using Feshbach-Kerman-Koonin and exciton preequilibrium models
[DE94-002640] p 3488 N94-30039
Resonant ultrasound spectroscopy for elastic constant measurements
[DE94-005016] p 3480 N94-30098
Computational balance in real-time cyclic spectral analysis
[DE94-005091] p 3432 N94-30100
Realtime structural electrochemistry of platinum clusters using dispersive XAFS
[DE94-005093] p 3208 N94-30101
Dislocation loops in spinel crystals irradiated successively with deep and shallow ion implants
[DE94-005083] p 3517 N94-30201
Ten new checks to assess the statistical quality of Monte Carlo solutions in MCNP
[DE94-006137] p 3465 N94-30366
Investigations of large area electron beam diodes for excimer lasers
[DE94-005670] p 3295 N94-30595
A monotonicity conjecture for real cubic maps
[DE94-003969] p 3335 N94-30610
Creep behavior of MoSi2-SiC composites
[DE94-004980] p 3185 N94-30693
The second coming of cold dark matter?
[DE94-004992] p 3548 N94-30694
Use of bad training data for better predictions
[DE94-006233] p 3427 N94-30705
Using stereoscopic imaging for visualization applications
[DE94-006247] p 3536 N94-30706

A transmission-loss monitor using current transformers
[DE94-003974] p 3267 N94-30716
Lattice gas simulations of replicating domains
[DE94-005008] p 3200 N94-30748
Space-time symmetries: P and CP violation
[DE94-005012] p 3526 N94-30750
Molecular dynamics simulations of dense plasmas
[DE94-005082] p 3509 N94-30752
Microwave assisted chemical vapor infiltration
[DE94-005005] p 3185 N94-30771
Influence of tungsten alloying additions on the mechanical properties and texture of tantalum
[DE94-004994] p 3210 N94-30774
Scaling in heavy-fermion systems
[DE94-005002] p 3492 N94-30775
Nature of dissolution of binary tantalum-titanium alloys by molten plutonium
[DE94-005090] p 3210 N94-30776
Selecting model complexity in learning problems
[DE94-000764] p 3461 N94-30821
Intercomparison of theoretical calculations of important activation cross sections for fusion reactor technology
[DE94-002642] p 3497 N94-30825
Recent results from SAGE
[DE94-006229] p 3551 N94-30845
TOPAZ 2 system description
[DE94-006230] p 3498 N94-30846
The TOPAZ 2 space reactor response under accident conditions
[DE94-004998] p 3498 N94-30847
Magnetotransport measurements in magnetic fields up to 50T in SmB6 and FeSi
[DE94-006227] p 3520 N94-30848

LOUGHBOROUGH UNIV. OF TECHNOLOGY (ENGLAND).

A note on the Poisson brackets associated with Lax operators
[MATHS-REPT-A-195] p 3464 N94-29482
On-line search for optimal controller parameters using interconnected learning automata
[MATHS-REPT-A-196] p 3436 N94-29526
Investigation on application of genetic algorithms to optimal reactive power dispatch of power systems
[MATHS-REPT-A-197] p 3266 N94-29527
Fronts at the confluences of spring-fed streams with Joekulsa a Fjoellum: Possibly thermal bars?
[MATHS-REPT-A-198] p 3333 N94-29528

LOUISIANA STATE UNIV., BATON ROUGE.

Effects of pressure on membrane-associated receptors and effector elements
[AD-A275813] p 3384 N94-28829
Research in elementary particle physics
[DE94-001657] p 3491 N94-30762

LOUISIANA TECH UNIV., RUSTON.

Micromanufacturing: Recent developments in this country and abroad p 3235 N94-29769
Macro, mini, micro and nano (M(sup 3)N) technologies for the future p 3238 N94-29786

LUNAR AND PLANETARY INST., HOUSTON, TX.

Field guide to Cretaceous-tertiary boundary sections in northeastern Mexico
[NASA-CR-195719] p 3354 N94-28416
Venus Data Analysis Program: Directory of Research Projects (1993-1994)
[NASA-CR-195742] p 3549 N94-29102

LYNNTECH, INC., COLLEGE STATION, TX.

Portable electronically based method for the nondestructive remote sensing of crevice corrosion
[AD-A275403] p 3318 N94-29057

M

MANITOBA UNIV., WINNIPEG.

Treatment of mild immersion hypothermia by body-to-body and forced-air warming p 3380 N94-28428
Study of the ultraviolet absorption and photoconduction spectra of polyimide films fabricated at various curing temperatures
[ISBN-0-315-85923-7] p 3218 N94-30036
Application of remote sensing techniques for the seismo-tectonic study of Nahanni earthquake area
[ISBN-0-315-85942-3] p 3334 N94-30037
Unsupervised learning in analog networks
[ISBN-0-315-85959-8] p 3432 N94-30140
Gluon and fermion damping in hot QCD
[ISBN-0-315-85982-2] p 3490 N94-30141
Curved-space quantization, and Dirac versus reduced quantization of Poincare gauge theories
[ISBN-0-315-85990-3] p 3525 N94-30142
A locally synchronous globally asynchronous Vertex-8 processing element for image reconstruction on a mesh
[ISBN-0-315-86005-7] p 3432 N94-30143
A capacity planning model for Canadian military airlift requests
[ISBN-0-315-86079-0] p 3136 N94-30144
Laser beam welding of AISI 316 stainless steel in microgravity environment: Experiments aboard a KC-135 flight
[ISBN-0-315-86095-2] p 3229 N94-30145
Directional solidification characteristics of hyper-eutectic Al-Cu alloys under varying gravity conditions
[ISBN-0-315-86108-8] p 3209 N94-30146

MARCONI RADAR SYSTEMS LTD., CHELMSFORD (ENGLAND).

Airside ground movements surveillance p 3141 N94-29585

MARTIN MARIETTA CORP., DENVER, CO.

Integrated active and passive control design methodology for the LaRC CSI evolutionary model
[NASA-CR-4580] p 3164 N94-28417

MARTIN MARIETTA LABS., BALTIMORE, MD.

Composite panel failure analysis and improvement plan
[AD-A275655] p 3176 N94-28853
Collocated tunable wavenumber sensor/actuators for smart structures
[AD-A275872] p 3241 N94-28755
Electrochemical behavior and surface chemistry of nonequilibrium aluminum alloys: Passivity mechanism and fabrication methods
[AD-A275401] p 3204 N94-29196

MARYLAND UNIV., COLLEGE PARK.

The dynamics of tropical intraseasonal variability p 3371 N94-29741
GCM studies of the influence of vegetation on the general circulation: The role of albedo in modulating climate change p 3348 N94-29749
Optical properties of cadmium sulfide, zinc selenide, and zinc manganese selenide semiconductor films p 3500 N94-29759
A vorticity transport closure method for turbulent reacting flows p 3274 N94-29761
Nonlinear wave packet evolution in a dispersive plasma: Application to rotational discontinuities p 3506 N94-29822
An analytical study of unsteady rotor/fuselage interaction in hover and forward flight p 3131 N94-29826
Pausing behavior of end-users in online searching p 3533 N94-29960
Satellite estimation of the global distribution and interannual variability of photosynthetically active radiation p 3334 N94-29970
A semiclassical study of quantum maps p 3524 N94-29987
The effects of relativistic neutrons on nonthermal models of active galactic nuclei p 3547 N94-29993
Infrared observations of cometary dust by COBE p 3541 N94-29994
Energetic events in the early universe p 3547 N94-30012
The role of plastic deformation in brittle and near-brittle cracking behavior p 3322 N94-30226
Three-dimensional free vibration analysis of thick arbitrarily laminated, rectangular, cylindrical and spherical composite panels p 3184 N94-30257
Expanding the waverider design space using arbitrary generating flowfields p 3148 N94-30516
Predictive sufficiency and the use of stored internal state
[AIAA PAPER 94-1213-CP] p 3445 N94-30564
Aspects of vision and planning in a dynamic, uncertain environment p 3448 N94-30803
Theoretical studies in hadronic and nuclear physics
[DE94-003524] p 3492 N94-30838
Pushing the limit: Precision radial velocities, techniques, and applications p 3542 N94-30861
Spectral and temporal behavior of low mass x ray binaries observed with the Einstein SSS and MPC, and the Broad Band X Ray Telescope p 3542 N94-30862
Mathematical models of hysteresis
[DE94-005681] p 3260 N94-30902
Information-seeking in hypertext: Multiple access methods in a full-text hypertext database p 3536 N94-30918

MASSACHUSETTS INST. OF TECH., CAMBRIDGE.

The active titration method for measuring local hydroxyl radical concentration p 3345 N94-28602
Electronic structure and mechanical properties of grain boundaries
[AD-A275198] p 3512 N94-28890
Three dimensional transient analysis of microstrip circuits in multilayered anisotropic media
[AD-A274995] p 3263 N94-28995
Strategies to sustain and enhance performance in stressful environments
[AD-A275223] p 3398 N94-29027
Focused ion beam fabrication of microelectronic structures
[AD-A275384] p 3264 N94-29305
Conceptual study of moderately coupled plasmas and experimental comparison of laboratory x ray sources
[DE94-005828] p 3506 N94-30045
Spectroscopic and dynamical studies of highly energized small polyatomic molecules
[DE94-006509] p 3489 N94-30061
Building brains for bodies
[AIAA PAPER 94-1208-CP] p 3444 N94-30559
Atmosphere, ocean, and land: Critical gaps in Earth system models p 3350 N94-30617
Integrated structure/control design of nonrigid robot arms for high-speed manipulation p 3312 N94-30866
Self-similar variables and the problem of nonlocal electron heat conductivity
[DE94-005826] p 3493 N94-30881
Magnetic flux reconstruction methods for shaped tokamaks
[DE94-005827] p 3510 N94-30882
Geochemical and fluid dynamic investigations into the nature of chemical variability in the Earth's mantle p 3367 N94-30917

MASSACHUSETTS INST. OF TECH., LEXINGTON.

Overview of microoptics: Past, present, and future p 3235 N94-29771
Single event upset and latchup measurements at Brookhaven National Laboratory p 3495 N94-30212

MASSACHUSETTS UNIV., AMHERST.

Cellular and molecular approaches to polymer synthesis by bacteria
[AD-A275501] p 3212 N94-28661
Polarimetric backscatter measurements of natural surfaces at millimeter wavelengths p 3259 N94-30509
Experiment studies of electron-positron interactions at the Stanford Linear Accelerator Center
[DE94-005877] p 3491 N94-30702
Theoretical studies of solid-fluid phase equilibria
[DE94-006406] p 3226 N94-30708

MASSACHUSETTS UNIV., LOWELL.

Study of nonlinear optical polymers and their applications in optical waveguides p 3216 N94-29807
Numerical modeling and prediction of the thermomechanical behavior of fiber-reinforced composites p 3186 N94-30956

MATERIALS RESEARCH LABS., ASCOT VALE (AUSTRALIA).

Correlation of cookoff behavior of rocket propellants with thermomechanical and thermochemical properties
[AD-A274983] p 3224 N94-29092
Portable ventilatory resuscitation systems
[AD-A274984] p 3401 N94-29093

MAX-PLANCK-INST. FUER CHEMIE, MAINZ (GERMANY).

Measurement of tropospheric OH by laser long-path absorption spectroscopy p 3343 N94-28596

MCAT INST., SAN JOSE, CA.

Algorithm and code development for unsteady three-dimensional Navier-Stokes equations
[NASA-CR-195774] p 3277 N94-29942

MCDONNELL-DOUGLAS AEROSPACE, SAINT LOUIS, MO.

Electrical and mechanical testing of wire insulation for space applications p 3166 N94-28710

MCDONNELL-DOUGLAS CORP., HOUSTON, TX.

A multi-mode manipulator display system for controlling remote robotic systems
[AIAA PAPER 94-0888-CP] p 3446 N94-30569

MCDONNELL-DOUGLAS CORP., HUNTINGTON BEACH, CA.

Gas stream purifier p 3354 N94-30469

MCDONNELL-DOUGLAS SPACE SYSTEMS CO., HOUSTON, TX.

Fast gravity, gravity partials, normalized gravity, gravity gradient torque and magnetic field: Derivation, code and data
[NASA-CR-188243] p 3361 N94-29588

MCGILL UNIV., MONTREAL (QUEBEC).

Physical processes associated with variability in successive operational model forecasts of cyclogenesis
[ISBN-0-315-74753-6] p 3371 N94-29751
On fatigue crack closure: Analysis and measurement
[ISBN-0-315-74873-7] p 3321 N94-29812
A numerical method for confined unsteady flows related to fluid-structure interactions
[ISBN-0-315-74739-0] p 3277 N94-29902
Interannual temperature variability and cyclone frequency over Eastern Canada and the New England States. A case study: Winter seasons 1931-1932 to 1984-1985
[ISBN-0-315-74841-9] p 3373 N94-29908
Sonar sensing and obstable detection p 3309 N94-30301

MCMASTER UNIV., HAMILTON (ONTARIO).
Pulse height response of Si surface barrier detectors p 3497 N94-30221
MELBOURNE UNIV., PARKVILLE (AUSTRALIA).
Discrete quark-lepton symmetry need not pose a cosmological domain wall problem
[DE94-601606] p 3481 N94-28471
MERCER UNIV., MACON, GA.
The Automated Aircraft Rework System (AARS): A system integration approach
[AIAA PAPER 94-1225-CP] p 3446 N94-30574
META RESEARCH, INC., RICHMOND (BRITISH COLUMBIA).
Fire-resistant water vapour permeable buoyant insulation p 3380 N94-28431
METAFUSE CORP., LOS ANGELES, CA.
Metafusion: A breakthrough in metallurgy p 3211 N94-30446
METEOROLOGICAL RESEARCH INST., TSUKUBA (JAPAN).
Papers in meteorology and geophysics, vol. 44, no.1
[JTN-94-80585] p 3324 N94-28693
The Japan Sea proper water and water circulation in the Japan Sea p 3324 N94-28694
On the linear stability of Verkley's modons p 3324 N94-28695
Structure of neutrally stratified turbulent Ekman layer as predicted by closure models with prognostic equation for master length scale p 3325 N94-28696
MIAMI UNIV., CORAL GABLES, FL.
Analysis and modeling of environmental and economic impacts of the solar hydrogen energy system p 3348 N94-29901
MICHIGAN BIOTECHNOLOGY INST., LANSING.
One carbon metabolism in anaerobic bacteria: Regulation of carbon and electron flow during organic acid production
[DE94-004852] p 3386 N94-30180
MICHIGAN STATE UNIV., EAST LANSING.
The Seventh Annual National Conference of Black Physics Students
[NASA-CR-195735] p 3526 N94-28746
MICHIGAN UNIV., ANN ARBOR.
MUADEE: Mars Upper Atmosphere Dynamics, Energetics, and Evolution discovery mission. Executive summary volume
[NASA-CR-195732] p 3549 N94-28418
Closed loop vibrational control: Theory and applications
[AD-A275451] p 3154 N94-28632
Electron beam analysis for cyclotron harmonic and free-electron laser devices
[AD-A275070] p 3293 N94-29179
Evolution of the large-scale vortices in turbulent mixing-layers p 3273 N94-29686
Radiation and scattering from cylindrically conformal printed antennas
[NASA-CR-195546] p 3253 N94-29873
A new orthogonal decomposition method for turbulent flows p 3281 N94-30494
A hybrid electromagnetic-statistical approach for characterizing MMW scattering by terrain p 3259 N94-30510
Vision based object pose estimation for mobile robots
[AIAA PAPER 94-1197-CP] p 3442 N94-30548
Investigations of large area electron beam diodes for excimer lasers
[DE94-005670] p 3295 N94-30595
Observation of Jovian auroral Ly-alpha line profile and emission variability with a sounding rocket and the IUE archives p 3550 N94-30798
Role of x ray-induced transcripts in adaptive responses following x rays
[DE94-005412] p 3386 N94-30895
An asymptotic analysis for compressible gas lubrication of rough surfaces p 3222 N94-30922
MICRO-DEXTERITY SYSTEMS, INC., MEMPHIS, TN.
Dexterity enhancement in microsurgery using telemicro-robotics
[AIAA PAPER 94-1230-CP] p 3447 N94-30579
MIDWEST RESEARCH INST., GOLDEN, CO.
Advanced development of PV encapsulents
[DE94-000219] p 3336 N94-28500
Silicon-Film (tm) photovoltaic manufacturing technology
[DE94-000258] p 3336 N94-28501
Impact study on the use of biomass-derived fuels in gas turbines for power generation
[DE94-000261] p 3224 N94-28502
An outdoor exposure testing program for optical materials used in solar thermal electric technologies
[DE94-000265] p 3500 N94-29799
Production of fullerenes with concentrated solar flux
[DE94-000266] p 3514 N94-29801
Analysis of data from electric and hybrid electric vehicle student competitions
[DE94-000269] p 3302 N94-29922
Biodiesel from aquatic species
[DE94-000275] p 3225 N94-30038
Fiber optical solar simulator p 3341 N94-30486
Photovoltaic performance and reliability workshop
[DE94-000236] p 3339 N94-30601
International collaborative research in wind turbine rotor aerodynamics
[DE94-000244] p 3339 N94-30602
PV Cz silicon manufacturing technology improvements
[DE94-000248] p 3339 N94-30603
Large-area triple-junction a-Si alloy production scale up
[DE94-000249] p 3339 N94-30604
Thin EFG octagons
[DE94-000257] p 3339 N94-30605
The direct observation of alkali vapor species in biomass combustion and gasification
[DE94-000262] p 3339 N94-30606
Proceedings of the low cost materials of construction for biological processes workshop
[DE94-000218] p 3226 N94-30761
Fuel cycle evaluations of biomass-ethanol and reformulated gasoline
[DE94-000227] p 3226 N94-30818
Design of a variable-conductance vacuum insulation
[DE94-000270] p 3268 N94-30819
NREL Photovoltaic Program FY 1993 bibliography
[DE94-000272] p 3340 N94-30820
MINISTRY OF AGRICULTURE, FORESTRY, AND FISHERIES, IBARAKI (JAPAN).
Bulletin of National Research Institute of Fisheries Engineering, No. 13
[JTN-94-80596] p 3233 N94-29701
Development of a simple current meter using solution p 3233 N94-29702
Development of the breakwater with submerged mound for interchanging sea water p 3234 N94-29703
The undrained shear strength characteristics of undisturbed soil from fishing port areas p 3234 N94-29704
An improvement of the slender body theory for oscillating ships with finite forward speed p 3234 N94-29705
The flow field near the body surface with thin filaments p 3234 N94-29706
Reproduction in the Japanese anchovy (Engraulis japonica) as related to population fluctuation p 3235 N94-29708
MINISTRY OF DEFENCE, LONDON (ENGLAND).
NATO SOCMET trials p 3258 N94-30503
Report on NATO PTTI p 3469 N94-30645
MINISTRY OF EDUCATION, SCIENCE AND CULTURE, SAGAMIHARA (JAPAN).
Start of space tourism p 3164 N94-29714
MINISTRY OF INTERNATIONAL TRADE AND INDUSTRY, TSUKUBA (JAPAN).
Protein crystal growth in microgravity p 3228 N94-28943
MINISTRY OF POSTS AND TELECOMMUNICATIONS, TOKYO (JAPAN).
Long term variations of radio auroral activity p 3359 N94-29237
New-type echoes observed with the 50 MHz auroral Doppler radar at Showa Station p 3360 N94-29238
MINISTRY OF TRANSPORTATION, CHIBA (JAPAN).
Coupled magnetohydrodynamic oscillations in the magnetosphere-ionosphere system: Hall current effect p 3360 N94-29242
MINNESOTA MINING AND MFG. CO., SAINT PAUL.
A 3M high temperature dielectric film p 3167 N94-28717
Dual cure low-VOC coating process, phase 3
[DE94-003202] p 3221 N94-30826
MINNESOTA UNIV., MINNEAPOLIS.
Research on the improvement of shape-memory and magnetostrictive materials
[AD-A275397] p 3203 N94-29056
Substructure, dynamics and evolution in clusters of galaxies p 3548 N94-30951
MISSION RESEARCH CORP., NASHUA, NH.
CBSD: The celestial background scene descriptor
[AD-A275521] p 3538 N94-28671
MISSISSIPPI STATE UNIV., MISSISSIPPI STATE.
Numerical solution of the two-dimensional time-dependent incompressible Euler equations
[NASA-CR-195775] p 3277 N94-29859
MISSOURI UNIV., COLUMBIA.
Multicolor photometry of barred spiral galaxies p 3541 N94-30270
Remote pumping of solid state lasers with nuclear driven fluorescers
[DE94-004846] p 3296 N94-30614
MISSOURI UNIV., ROLLA.
Finite element analysis of axisymmetric deformations of thick thermoviscoplastic targets p 3320 N94-29688
Analysis of pressureless densification of ceramic matrix composites p 3216 N94-29766
Liquid atomization in supersonic flows p 3276 N94-29839
MITRE CORP., BEDFORD, MA.
A family of joint probability models for cost and schedule uncertainties
[AD-A275513] p 3463 N94-28670
MITRE CORP., MCLEAN, VA.
Advances in development capabilities for intelligent air traffic management systems p 3137 N94-29559
A streamlined software environment for situated skills
[AIAA PAPER 94-1205-CP] p 3444 N94-30556
MITSUBISHI ELECTRIC CORP., KAMAKURA (JAPAN).
Numerical analysis of two dimensional/axisymmetric non-equilibrium hypersonic flow p 3125 N94-28963
MITSUBISHI HEAVY INDUSTRIES LTD., TOKYO (JAPAN).
Numerical analysis of airfoil for helicopter blade at high angle of attack using Navier-Stokes code p 3124 N94-28958
Code development for hypersonic real-gas flow simulations toward the design of space vehicles, part 2 p 3125 N94-28966
MOLECULAR DEVICES CORP., MENLO PARK, CA.
Microfabricated silicon biosensors for microphysiometry p 3238 N94-29783
MONTANA UNIV., MISSOULA.
A bottom-up evolution of terrestrial ecosystem modeling theory, and ideas toward global vegetation modeling p 3351 N94-30628
MONTREAL UNIV. (QUEBEC).
Inhomogeneities in the wind from Wolf-Rayet stars
[ISBN-0-315-85893-1] p 3548 N94-30058
MORGANTOWN TECHNOLOGY CENTER, WV.
Proceedings of the Joint Contractors Meeting: FE/EE Advanced Turbine Systems Conference FE Fuel Cells and Coal-Fired Heat Engines Conference
[DE93-011308] p 3336 N94-28499
Fundamental stack and system issues in molten carbonate fuel cell development
[DE94-005960] p 3338 N94-30048
Configuration and performance of the indirect-fired fuel cell bottomed turbine cycle
[DE94-005961] p 3338 N94-30313
Analysis of deep seismic reflection and other data from the southern Washington Cascades
[DE94-005915] p 3367 N94-30883
MOSCOW STATE UNIV. (RUSSIA).
Dissipative quantum dynamics and nonlinear sigma-model
[DE94-606295] p 3523 N94-28617
Quasi-adiabatic motion of energetic particles in a dipole magnetic field
[DE94-607322] p 3362 N94-29935
Simulation of space-energy distributions of hot plasma on a geostationary orbit
[DE94-607324] p 3365 N94-30107
Variations of electron fluxes, low-frequency radiations and plasma density during the geomagnetic storm on 9-12 March, 1979 according to data of the Interkosmos-19 satellites
[DE94-607323] p 3365 N94-30223

N

NAGAOKA TECHNOLOGICAL UNIV., NIIGATA (JAPAN).
Fluid and transportation phenomena under microgravity p 3227 N94-28939
NAGOYA CITY UNIV. (JAPAN).
Basic understanding of vertigo p 3390 N94-28855
NAGOYA UNIV. (JAPAN).
The upsilon-q method and the psi-q method for incompressible flows p 3126 N94-28971
A discussion of eye-head coordinative movement under microgravity during parabolic flight p 3393 N94-29715
Motion sickness in parabolic flight: Possibility of electrogastrography as an objective index p 3393 N94-29718
NAGOYA UNIV., TOYOKAWA (JAPAN).
Initial observation results with imaging riometer at NY-Alesund (L is equal to 16) p 3360 N94-29239
NATIONAAL INST. VOOR KERNFYSICA EN HOGE ENERGIEFYSICA, AMSTERDAM (NETHERLANDS).
Tuning of AmPS
[NIKHEF-K-AMPS-93-01] p 3494 N94-29422
BPM901N monitor electronics for the determination of the bundle profile in the extraction line of AmPS
[DIGEL-1993-9] p 3495 N94-29467
Stripline monitor electronics for the bundle position determination in AmPS
[DIGEL-1993-8] p 3495 N94-29888

NATIONAL AERONAUTICS AND SPACE ADMINISTRATION, WASHINGTON, DC.
Microgravity science and applications. Program tasks and bibliography for FY 1993
[NASA-TM-4569] p 3227 N94-28415
Aeronautical engineering: A cumulative index to a continuing bibliography (supplement 300)
[NASA-SP-7037(300)] p 3121 N94-28537
Navigation of military and space unmanned ground vehicles in unstructured terrains p 3144 N94-30282
Technology 2003: The Fourth National Technology Transfer Conference and Exposition, volume 1
[NASA-CP-3249] p 3555 N94-30440
Terrestrial applications of NASA space telerobotics technologies
[AIAA PAPER 94-1235-CP] p 3448 N94-30582

NATIONAL AERONAUTICS AND SPACE ADMINISTRATION. AMES RESEARCH CENTER, MOFFETT FIELD, CA.
System for improving measurement accuracy of transducer by measuring transducer temperature and resistance change using thermoelectric voltages
[NASA-CASE-ARC-12014-1] p 3287 N94-29361
Boundary layer control device for duct silencers
[NASA-CASE-ARC-12030-1] p 3478 N94-29362
Improved in-flow acoustic sensor
[NASA-CASE-ARC-12001-1] p 3478 N94-29363
Multi-channel spatialization systems for audio signals
[NASA-CASE-ARC-12013-1-CU] p 3245 N94-29364
Image-adapted visually weighted quantization matrices for digital image compression
[NASA-CASE-ARC-12015-1] p 3406 N94-29375
Leg muscle volume during 30-day 6-degree head-down bed rest with isotonic and isokinetic exercise training
[NASA-TM-4580] p 3385 N94-29401
Composite flexible blanket insulation
[NASA-CASE-ARC-11955-1-CU] p 3180 N94-29509
Design of Center-TRACON Automation System p 3138 N94-29568
The 27th Aerospace Mechanisms Symposium
[NASA-CP-3205] p 3160 N94-29627
Portable Linear Sled (PLS) for biomedical research p 3163 N94-29648
Laminar Flow Supersonic Wind Tunnel primary air injector p 3158 N94-29649
Research and technology, 1992
[NASA-TM-103996] p 3555 N94-29891
Computation of wind tunnel wall effects for complex models using a low-order panel method
[NASA-TM-104019] p 3132 N94-30151

NATIONAL AERONAUTICS AND SPACE ADMINISTRATION. GODDARD INST. FOR SPACE STUDIES, NEW YORK, NY.
The carbon cycle revisited p 3350 N94-30622
Linkages between terrestrial ecosystems and the atmosphere p 3351 N94-30624
A toy model for estimating N2O emissions from natural soils p 3351 N94-30627

NATIONAL AERONAUTICS AND SPACE ADMINISTRATION. GODDARD SPACE FLIGHT CENTER, GREENBELT, MD.
NASA space and Earth science data on CD-ROM
[NASA-TM-109709] p 3528 N94-28414
NASA Parts Program Office responsibilities p 3165 N94-28702
Scale-length dependence of the ratio between the magnetic and electric field perturbations in the ionospheric field-aligned current region p 3360 N94-29243
MODIS technical report series. Volume 3: MODIS airborne simulator level 1B data user's guide
[NASA-TM-104594] p 3231 N94-29385
On the relation between SMMR 37-GHz polarization difference and the rainfall over Africa and Australia
[NASA-TM-104598] p 3370 N94-29408
Bolt and nut evaluator
[NASA-CASE-GSC-13468-1] p 3288 N94-29538
Simplified and symmetrical five-bar linkage driver for manipulating a six-degree-of-freedom parallel minimanipulator with three inextensible limbs
[NASA-CASE-GSC-13485-2] p 3301 N94-29556
The Solar Anomalous and Magnetospheric Particle Explorer (SAMPEX) yo-yo despin and solar array deployment mechanism p 3163 N94-29645
Six-degree-of-freedom parallel minimanipulator with three inextensible limbs
[NASA-CASE-GSC-13485-1] p 3288 N94-29726
Software Management Environment (SME) concepts and architecture, revision 1
[NASA-CR-189293] p 3419 N94-29727
Method for ambiguity resolution in range-Doppler measurements
[NASA-CASE-GSC-13542-1] p 3252 N94-29739
Multiple single event upsets in CMOS static rams p 3496 N94-30215
The 25th Annual Precise Time and Time Interval (PTTI) Applications and Planning Meeting
[NASA-CP-3267] p 3468 N94-30639

NATIONAL AERONAUTICS AND SPACE ADMINISTRATION. JOHN F. KENNEDY SPACE CENTER, COCOA BEACH, FL.
SI (Metric) handbook
[NASA-TM-109197] p 3231 N94-29376
Supersonic gas-liquid cleaning system p 3240 N94-30467

NATIONAL AERONAUTICS AND SPACE ADMINISTRATION. LYNDON B. JOHNSON SPACE CENTER, HOUSTON, TX.
Heavy-lift vehicle-launched Space Station method and apparatus
[NASA-CASE-MSC-21760-1] p 3160 N94-29369
Rotary blood pump
[NASA-CASE-MSC-22424-1] p 3299 N94-29370
Extra-vehicular activity translation tool
[NASA-CASE-MSC-21955-1] p 3300 N94-29428
Landing gear energy absorption system
[NASA-CASE-MSC-22277-1] p 3300 N94-29448
Measurand transient signal suppressor
[NASA-CASE-MSC-22027-1] p 3435 N94-29466
Backscatter Mossbauer Spectrometer (BaMS) for extraterrestrial applications p 3236 N94-29774
Differential Scanning Calorimetry (DSC) for planetary surface exploration p 3236 N94-29776
The application of micromachined sensors to manned space systems p 3171 N94-29791
Tactility as a function of grasp force: Effects of glove, orientation, pressure, load, and handle
[NASA-TP-3474] p 3402 N94-30210
Microencapsulation of anti-tumor, antibiotic and thrombolytic drugs in microgravity p 3397 N94-30453
Dual use of image based tracking techniques: Laser eye surgery and low vision prosthesis p 3397 N94-30455
Development of the NASA/Baylor VAD p 3397 N94-30458
Using spacecraft trace contaminant control systems to cure sick building syndrome p 3354 N94-30470
Conference on Intelligent Robotics in Field, Factory, Service, and Space (CIRFFSS 1994), volume 1
[NASA-CP-3251] p 3439 N94-30526
Intelligent robotics can boost America's economic growth
[AIAA PAPER 94-1301-CP] p 3439 N94-30527
Technology transfer and evaluation for Space Station telerobotics
[AIAA PAPER 94-1190-CP] p 3441 N94-30541
Space flight manipulator technologies and requirements for the NASA Flight Telerobotic Servicer (FTS)
[AIAA PAPER 94-1191-CP] p 3441 N94-30542
An intelligent robot for helping astronauts
[AIAA PAPER 94-1233-CP] p 3447 N94-30581

NATIONAL AERONAUTICS AND SPACE ADMINISTRATION. LANGLEY RESEARCH CENTER, HAMPTON, VA.
Steady pressure measurements on an Aeroelastic Research Wing (ARW-2)
[NASA-TM-109046] p 3122 N94-28658
Prediction of stress-strain response of SCS-6/Timetal-21S subjected to a hypersonic flight profile
[NASA-TM-109026] p 3177 N94-28823
Test and analysis of a stitched RFI graphite-epoxy panel with a fuel access door
[NASA-TM-108992] p 3178 N94-29100
Absolute calibration technique for broadband ultrasonic transducers
[NASA-CASE-LAR-14672-1] p 3287 N94-29199
Low dielectric polyimide fibers
[NASA-CASE-LAR-14526-1] p 3214 N94-29359
Deployable reflector structure
[NASA-CASE-LAR-14513-1-SB] p 3245 N94-29360
Flux-focusing eddy current probe and method for flaw detection
[NASA-CASE-LAR-15046-1] p 3315 N94-29366
Optical flameout detector
[NASA-CASE-LAR-14997-1] p 3287 N94-29368
A non-local computational boundary condition for duct acoustics
[NASA-TM-109091] p 3478 N94-29382
Low-speed longitudinal aerodynamic characteristics of a flat-plate planform model of an advanced fighter configuration
[NASA-TM-109045] p 3130 N94-29443
Poly(arylene ether-co-imidazole)s as toughness modifiers for epoxy resins
[NASA-CASE-LAR-15229-1-CU] p 3215 N94-29451
Time series comparisons of satellite and rocketsonde temperatures in 1978-1979
[NASA-TP-3409] p 3370 N94-29455
Free vibration of thermally loaded panels including initial imperfections and post-buckling effects
[NASA-TM-109097] p 3479 N94-29461
Subjective response to sonic booms having different shapes, rise times, and durations
[NASA-TM-109090] p 3479 N94-29464
Preliminary evaluation of hybrid titanium composite laminates
[NASA-TM-109095] p 3180 N94-29472
An experimental and theoretical study of the aerodynamic characteristics of some generic missile concepts at Mach numbers from 2 to 6.8
[NASA-TM-109110] p 3130 N94-29473
Method for making a dynamic pressure sensor and a pressure sensor made according to the method
[NASA-CASE-LAR-14029-1] p 3288 N94-29484
Non-rectangular towpreg architectures
[NASA-CASE-LAR-14863-1-CU] p 3180 N94-29485
Thermal enclosure system functional simulation user's manual
[NASA-TM-109094] p 3466 N94-29489
ASSIST internals reference manual
[NASA-TM-109102] p 3431 N94-29494
Apparatus for providing a uniform, consolidated, unidirectional, continuous, fiber-reinforced polymeric material and method relating thereto
[NASA-CASE-LAR-15173-1-CU] p 3180 N94-29496
Effects of physical aging on long-term creep of polymers and polymer matrix composites
[NASA-TM-109081] p 3181 N94-29541
Experimental studies of transonic flow field near a longitudinally slotted wind tunnel wall
[NASA-TP-3392] p 3130 N94-29545
Method and apparatus for indicating disbonds in joint regions
[NASA-CASE-LAR-14626-1] p 3315 N94-29548
Polyimides containing the penta fluoro sulfanyl benzene moiety
[NASA-CASE-LAR-15082-1] p 3175 N94-29554
Polyimides containing pendent siloxane groups
[NASA-CASE-LAR-14638-1] p 3215 N94-29555
Profile negotiation: An air/ground automation integration concept for managing arrival traffic p 3140 N94-29578
Design and testing of the LITE Variable Field Stop mechanism p 3161 N94-29633
Integration of pyrotechnics into aerospace systems p 3161 N94-29634
Miniature linear-to-rotary motion actuator p 3163 N94-29647
Dynamic fracture mechanics analysis for an edge delamination crack
[NASA-TM-109106] p 3479 N94-29856
Aerodynamic characteristics of a propeller-powered high-lift semispan wing
[NASA-TM-4541] p 3132 N94-29937
NASA/DOD Aerospace Knowledge Diffusion Research Project. Report 23: The communications practices of US aerospace engineering faculty and students: Results of the phase 3 survey
[NASA-TM-109085] p 3534 N94-30149
NASA/DOD Aerospace Knowledge Diffusion Research Project. Report 22: US academic librarians and technical information specialists as information intermediaries: Results of the phase 3 survey
[NASA-TM-109067] p 3534 N94-30150
TOTAL user manual
[NASA-TM-109101] p 3432 N94-30160
User's manual for the model interface and plugboard cabinets in the 14- by 22-foot subsonic tunnel
[NASA-TM-109062] p 3133 N94-30176
Application of fuzzy logic to the control of wind tunnel settling chamber temperature
[NASA-TM-109105] p 3157 N94-30200
Four advances in carbon-carbon materials technology p 3186 N94-30481

NATIONAL AERONAUTICS AND SPACE ADMINISTRATION. LEWIS RESEARCH CENTER, CLEVELAND, OH.
Second NASA Workshop on Wiring for Space Applications
[NASA-CP-3244] p 3165 N94-28697
Selection of the Space Station Freedom (SSF) Flat Collector Circuit (FCC) insulation material p 3165 N94-28701
Wire insulation degradation and flammability in low gravity p 3166 N94-28712
Formation and chemical reactivity of carbon fibers prepared by defluorination of graphite fluoride
[NASA-TM-106398] p 3174 N94-28747
The nozzle acoustic test rig: An acoustic and aerodynamic free-jet facility
[NASA-TM-106495] p 3156 N94-28749
Hypervelocity impact induced arcing and Kapton pyrolization in a plasma environment
[NASA-TM-106528] p 3167 N94-28814

An analysis of isothermal, bithermal, and thermomechanical fatigue data of Haynes 188 and B1900+Hf by energy considerations
[NASA-TM-106359] p 3317 N94-28819
Effects of thermomechanical processing on tensile and long-time creep behavior of Nb-1 percent Zr-0.1 percent C sheet
[NASA-TM-106319] p 3202 N94-28822
Defocussing characteristics of the ACTS, T1-VSAT Earth terminal antennas
[NASA-TM-106420] p 3242 N94-28826
Matrix isolation studies of the interactions of BF3 with water and substituted diethyl ethers. Chemical ionization mass spectrometric determination of the proton affinity of (CF3CH2)2O
[NASA-TM-106422] p 3189 N94-28832
Nuclear electric propulsion: A better, safer, cheaper transportation system for human exploration of Mars
[NASA-TM-106406] p 3171 N94-28833
Performance and durability of high emittance heat receiver surfaces for solar dynamic power systems
[NASA-TM-106549] p 3172 N94-28834
Calculation of propulsive nozzle flowfields in multidiffusing chemically reacting environments
[NASA-TM-106532] p 3271 N94-28835
Development of braided rope engine seals
[NASA-TM-105902] p 3298 N94-28838
Cyclic axial-torsional deformation behavior of a cobalt-base superalloy
[NASA-TM-106372] p 3203 N94-28921
Surface energy changes produced by ultraviolet-ozone irradiation of poly(methylmethacrylate), polycarbone and polytetrafluoroethylene
[NASA-TM-106460] p 3213 N94-28922
A random distribution reacting mixing layer model
[NASA-TM-106517] p 3150 N94-28923
Graphite intercalation compounds prepared from graphite fluoride
[NASA-TM-106447] p 3174 N94-28924
Low Earth orbit durability evaluation of protected silicone for advanced refractive photovoltaic concentrator arrays
[NASA-TM-106543] p 3172 N94-28999
Cryogenic probe station for use in automated microwave and noise figure measurements
[NASA-TM-106560] p 3286 N94-29000
Theoretical study of the incompressible Navier-Stokes equations by the least-squares method
[NASA-TM-106535] p 3272 N94-29096
Evaluation of oxide-coated iridium-rhenium chambers
[NASA-TM-106442] p 3172 N94-29097
Thermal expansion and elastic anisotropy in single crystal Al2O3 and SiC reinforcements
[NASA-TM-106516] p 3214 N94-29105
Transport properties of epitaxial lift off films
[NASA-TM-106156] p 3264 N94-29209
Spray combustion experiments and numerical predictions p 3195 N94-29277
Experimental studies on effervescent atomizers with wide spray angles p 3196 N94-29280
Thick thermal barrier coatings for diesel components
[NASA-CR-187111] p 3537 N94-29350
Fuel-rich catalytic combustion of a high density fuel
[NASA-TP-3281] p 3197 N94-29356
Hypervelocity impact testing of Space Station Freedom solar cells
[NASA-TM-106509] p 3167 N94-29383
A method for the probabilistic design assessment of composite structures
[NASA-TM-106384] p 3319 N94-29384
Lubrication of space systems
[NASA-TM-106392] p 3214 N94-29399
Rocket engine system reliability analyses using probabilistic and fuzzy logic techniques
[NASA-TM-106519] p 3173 N94-29403
Stiffness-generated rigid-body mode shapes for Lanczos eigensolution with SUPORT DOF by way of a MSC/NASTRAN DMAP alter
[NASA-TM-106537] p 3319 N94-29406
System for the installation and replacement of components in hostile environments
[NASA-CASE-LEW-14906-1-SB] p 3300 N94-29427
Transient analysis mode participation for modal survey target mode selection using MSC/NASTRAN DMAP
[NASA-TM-106536] p 3319 N94-29469
A new flux-conserving numerical scheme for the steady, incompressible Navier-Stokes equations
[NASA-TM-106520] p 3273 N94-29471
Plasma sprayed ceramic thermal barrier coating for NiAl-based intermetallic alloys
[NASA-CASE-LEW-15535-1] p 3205 N94-29507
Method of producing a ceramic fiber-reinforced glass-ceramic matrix composite
[NASA-CASE-LEW-15264-2] p 3180 N94-29508
Method of reducing hydraulic instability
[NASA-CASE-LEW-15463-1] p 3273 N94-29539
Fusion welding with self-generated filler metal
[NASA-CASE-LEW-15671-1] p 3301 N94-29557
Non-orthogonal subband/transform coder
[NASA-CASE-LEW-15310-1] p 3246 N94-29589
A compact roller-gear pitch-yaw joint module: Design and control issues p 3161 N94-29629
Method for cancelling expansion waves in a wave rotor
[NASA-CASE-LEW-15218-2] p 3274 N94-29740
Summary report of mission acceleration measurements for Spacehab-01, STS-57 launched 21 June 1993
[NASA-TM-106514] p 3168 N94-29757
The effect of various metallurgical parameters on the flow and fracture behavior of polycrystalline NiAl near the brittle-to-ductile transition
[NASA-TM-106534] p 3205 N94-29758
Large scale cryogenic fluid systems testing
[NASA-TM-109735] p 3157 N94-29904
Electric power system test and verification program
[NASA-TM-106405] p 3169 N94-30123
Numerical comparison of convective heat transfer augmentation devices used in cooling channels of hypersonic vehicles
[NASA-TM-106546] p 3279 N94-30147
An interactive, design and educational tool for supersonic external-compression inlets
[NASA-TM-106581] p 3421 N94-30174
An interactive educational tool for compressible aerodynamics
[NASA-TM-106568] p 3422 N94-30175
XPS analysis of 440C steel surfaces lubricated with perfluoropolyethers under sliding conditions in high vacuum
[NASA-TM-106548] p 3218 N94-30177
The viability of photovoltaics on the Martian surface
[NASA-TM-106478] p 3338 N94-30196
Radial microstrip slotline feed network for circular mobile communications array
[NASA-TM-106540] p 3267 N94-30198
A novel approach to noise-filtering based on a gain-scheduling neural network architecture
[NASA-TM-106563] p 3155 N94-30204
Surface fatigue life of high temperature gear materials
[NASA-TM-106562] p 3303 N94-30227
A new material for removing heavy metals from water p 3354 N94-30471
Evaluation of flip-flop jet nozzles for use as practical excitation devices
[NASA-TM-106377] p 3135 N94-30949

NATIONAL AERONAUTICS AND SPACE ADMINISTRATION. MARSHALL SPACE FLIGHT CENTER, HUNTSVILLE, AL.

MSFC inspections of installed polyimide wire p 3166 N94-28707
A survey of geographical information systems applications for the Earth Science and Applications Division, Space Sciences Laboratory, Marshall Space Flight Center
[NASA-TM-108438] p 3529 N94-28820
Plasma arc welding torch having means for vortexing plasma for exiting the welding torch
[NASA-CASE-MFS-28828-1] p 3298 N94-29351
Metal inert gas welding system for use in vacuum
[NASA-CASE-MFS-28808-1] p 3298 N94-29352
Tuned mass damper for integrally bladed turbine rotor
[NASA-CASE-MFS-28697-1] p 3298 N94-29353
Suspension system for gimbal supported scanning payloads
[NASA-CASE-MFS-28817-1] p 3287 N94-29358
Apparatus for testing high pressure injector elements
[NASA-CASE-MFS-28773-1] p 3299 N94-29365
Collapsible mechanical joint
[NASA-CASE-MFS-28765-1] p 3299 N94-29367
Multi-speed multi-phase resolver converter
[NASA-CASE-MFS-28855-1] p 3264 N94-29372
Manufacturing methods for machining spring ends parallel at loaded length
[NASA-CASE-MFS-28767-1] p 3231 N94-29379
Chamber free fusion welding root side purging method and apparatus
[NASA-CASE-MFS-28832-1] p 3204 N94-29380
Vacuum vapor deposition
[NASA-CASE-MFS-28652-1] p 3215 N94-29446
Rotary actuator
[NASA-CASE-MFS-28581-1] p 3205 N94-29447
NASA Marshall Space Flight Center Solar Observatory report, July - October 1993
[NASA-TM-108448] p 3160 N94-29470
Quick connect fastener
[NASA-CASE-MFS-28829-1] p 3300 N94-29486
Welding wire pressure sensor assembly
[NASA-CASE-MFS-26216-1-SB] p 3300 N94-29506
Inter-comparison of Wildfire and High-resolution Interferometer Sounder (HIS) data from STORM-FEST: An investigation of wildfire spectral channel discrepancies
[NASA-TM-108429] p 3333 N94-29553
Development and testing of the Automated Fluid Interface System p 3161 N94-29636
Design and test of electromechanical actuators for thrust vector control p 3163 N94-29650
Vulnerability of manned spacecraft to crew loss from orbital debris penetration
[NASA-TM-108452] p 3169 N94-30161
Ternary arc gas plasma welding torch
[NASA-CASE-MFS-28857-1] p 3303 N94-30173
Ampoule failure sensor time response testing: Experiment 1
[NASA-TM-108449] p 3290 N94-30199
Root-sum-square structural strength verification approach
[NASA-TM-108453] p 3322 N94-30206
Composite redesign of obstetrical forceps p 3397 N94-30457
Computerized in vitro test for chemical toxicity based on tetrahymena swimming patterns p 3354 N94-30463
Casting of weldable graphite/magnesium metal matrix composites with built-in metallic inserts p 3186 N94-30482
Graphical simulation for aerospace manufacturing
[AIAA PAPER 94-1224-CP] p 3446 N94-30573

NATIONAL AERONAUTICS AND SPACE ADMINISTRATION. PASADENA OFFICE, CA.

Method for forming thin composite solid electrolyte film for lithium batteries
[NASA-CASE-NPO-18877-1-CU] p 3264 N94-29357
Plasma heating for containerless and microgravity materials processing
[NASA-CASE-NPO-18819-1-CU] p 3229 N94-29371
Digital camera with apparatus for authentication of images produced from an image file
[NASA-CASE-NPO-19108-1-CU] p 3287 N94-29373
Method of implementing digital phase-locked loops
[NASA-CASE-NPO-18757-1-CU] p 3265 N94-29374
Dendrite preventing separator for secondary lithium batteries
[NASA-CASE-NPO-18585-1-CU] p 3265 N94-29411
An emergency response mobile robot for operations in combustible atmospheres
[NASA-CASE-NPO-19020-1-CU] p 3299 N94-29420
Nonvolatile programmable neural network synaptic array
[NASA-CASE-NPO-18578-1-CU] p 3265 N94-29426
High level language-based robotic control system
[NASA-CASE-NPO-17918-2-CU] p 3435 N94-29465
Monolithic in-based III-V compound semiconductor focal plane array cell with single stage CCD output
[NASA-CASE-NPO-18978-1-CU] p 3265 N94-29488
Catalytic ignitor for regenerative propellant gun
[NASA-CASE-NPO-18987-1-CU] p 3225 N94-29490
Reconfigurable optical interconnections via dynamic computer-generated holograms
[NASA-CASE-NPO-19039-1-CU] p 3499 N94-29491
A neural network with modular hierarchical learning
[NASA-CASE-NPO-19077-1-CU] p 3435 N94-29492
Lasercom system architecture with reduced complexity
[NASA-CASE-NPO-19069-1-CU] p 3293 N94-29493
Extended horizon lifting for periodic gain adjustment in control systems, and for equalization of communication channels
[NASA-CASE-NPO-19166-1-CU] p 3246 N94-29495
An alternate method for achieving temperature control in the -160 to +90 C range
[NASA-CASE-NPO-18995-1-CU] p 3288 N94-29497
Epitaxial heterojunctions of oxide semiconductors and metals on high temperature superconductors
[NASA-CASE-NPO-18483-1-CU] p 3513 N94-29501
Kinematic functions for redundancy resolution using configuration control
[NASA-CASE-NPO-18608-1-CU] p 3436 N94-29504
Anode for rechargeable ambient temperature lithium cells
[NASA-CASE-NPO-18580-1-CU] p 3265 N94-29505
Neural network with dynamically adaptable neurons
[NASA-CASE-NPO-17803-1-CU] p 3436 N94-29756

NATIONAL AERONAUTICS AND SPACE ADMINISTRATION. WHITE SANDS TEST FACILITY, NM.

Flammability, odor, offgassing, thermal vacuum stability, and compatibility with aerospace fluids of wire insulations p 3166 N94-28709

NATIONAL AEROSPACE LAB., AMSTERDAM (NETHERLANDS).

Engineering of systems for application of scientific computing in industry p 3123 N94-28947
ENGRID: A graphical interactive code for the computation of structured grids for blocked flow domains p 3124 N94-28956
The development procedures and tools applied for the attitude control software of the Italian satellite SAX p 3170 N94-29324

Simulation of fully automated air traffic control concepts p 3139 N94-29569
The PHARE advanced tools p 3141 N94-29581
Software engineering and software management in a distributed UNIX environment
[NLR-TP-92233-U] p 3422 N94-30314
Modal analysis of solar panels using boundary integral equations
[NLT-TP-92218-U] p 3338 N94-30328
Development of a method to predict transonic limit cycle oscillation characteristics of fighter aircraft (continued)
[NLR-TP-92156-U] p 3148 N94-30342
The design of a system of codes for industrial calculations of flows around aircraft and other complex aerodynamic configurations
[PB94-125598] p 3133 N94-30387
Numerical investigation into high-angle-of-attack leading-edge vortex flow
[PB94-125564] p 3133 N94-30388
Aiding the operator in the manual control of a space manipulator
[PB94-125549] p 3402 N94-30390
Development and validation of a linear recursive order-N algorithm for the simulation of flexible space manipulators dynamics
[AD-B173557] p 3311 N94-30391
Comparison of RCS prediction techniques, computations and measurements
[PB94-125515] p 3256 N94-30392
Low frame rate video coding for small bandwidth realtime multimedia tele-education systems
[PB94-125531] p 3256 N94-30398
Correction of X hot-wire measurements for gradients normal to the plane of the wires
[PB94-125473] p 3157 N94-30399
Fast and efficient variable-to-fixed-length coding algorithm
[PB94-125465] p 3424 N94-30400
Calculus of variations applied to 2D multi-point airfoil design
[PB94-125457] p 3133 N94-30401
Representations of dynamical systems described by behavioral inequalities
[AD-B173649] p 3458 N94-30402
Microgravity fluid science research in Europe
[AD-B179178] p 3229 N94-30409
Evaluation of corrosion protecting properties of modern aircraft paint systems
[AD-B179388] p 3220 N94-30420
Control system design for A and R supported microgravity experiments: An experiment payload control development
[AD-B179107] p 3229 N94-30421
Sampling behaviour in a four instrument monitoring task: Effects of signal bandwidth and number of events per signal
[AD-B179613] p 3402 N94-30422
A modernised HST of NLR
[AD-B179220] p 3158 N94-30423
A simulator for multi-radar analysis for realistic traffic
[AD-B179099] p 3142 N94-30439
Aspects of the modeling and numerical simulation of leading-edge vortex flow
[AD-B179108] p 3133 N94-30492
A residual correction method applied to 2D multi-point airfoil design and 3D single-point wing design
[NLR-TP-92524-U] p 3134 N94-30493
End-to-end delay reduction in narrow bandwidth real-time multimedia tele-education applications
[AD-B179614] p 3260 N94-30518
Engineering of systems for application of scientific computing in industry WP project management ISNaS 9209099
[PB94-126232] p 3428 N94-30739
Prospects of time-linearized unsteady calculation methods for exponentially diverging motions in aeroelasticity
[PB94-126224] p 3134 N94-30740
Multi-sensor data fusion and the use of artificial intelligence
[PB94-126216] p 3448 N94-30741
Determination of acceleration field parameters with linear accelerometers
[PB94-125606] p 3290 N94-30742
Eigenvalue analysis of the convergence behaviour of an Euler method
[PB94-1255722-U] p 3281 N94-30743
Euler results of the ISNaS compressible multi-block flow solver
[AD-B179299] p 3281 N94-30756
FAME: A Forest Assessment and Monitoring Environment scenario
[AD-B179106] p 3335 N94-30759
Information system for flow simulation based on the Navier-Stokes equations vectorization
[AD-B179293] p 3281 N94-30763
Systematic error estimation in multisensor fusion systems
[AD-B179298] p 3428 N94-30764
A stochastic control approach to flight path monitoring
[AD-B174630] p 3143 N94-30853
A review of the status and capabilities of Navstar GPS
[AD-B174629] p 3143 N94-30854
Numerical simulation of a condenser in two-phase heat transport systems: A feasibility study
[AD-B173650] p 3282 N94-30855
'Real time' and the NLR aerodynamic facilities
[AD-B173626] p 3158 N94-30856
Grid adaption in computational aerodynamics
[PB94-126240] p 3134 N94-30858
Numerical simulation of leading-edge vortex flow
[AD-B175154] p 3134 N94-30871
WISPER and WISPERX: Final definition of two standardised fatigue loading sequences for wind turbine blades
[AD-B175835] p 3324 N94-30872
Validation experiments with an Ethernet model using the simulation tool 'PROMISE'
[AD-B174795] p 3429 N94-30912
Supercomputing has to be part of an organization-wide automation concept
[AD-B174654] p 3433 N94-30913
Fractographic and microstructural analysis of fatigue crack growth in Ti-6Al-4V fan disc forgings
[AD-B174765] p 3153 N94-30914
Flight simulator evaluation of advanced MLS procedures
[AD-B174270] p 3143 N94-30915
Aerodynamic analysis of slipstream/wing/nacelle interference for preliminary design of aircraft configurations
[AD-B173651] p 3135 N94-30916
Multitemporal analysis of a braiding river: The advanced study of 1992
[NLR-TP-93100-U] p 3335 N94-30942
The experimental flight management system: An air traffic management research tool
[NLR-TP-92253-U] p 3143 N94-30943
Spectral analysis of heart rate and psychological state: A review of its validity as a workload index
[AD-B179387] p 3399 N94-30969

NATIONAL AEROSPACE LAB., EMMELOORD (NETHERLANDS).

Experiments and theoretical considerations regarding the allowable roughness height in laminar flow
[PB94-125556] p 3133 N94-30389
The MACS-TSA applied in the ISO and SAX spacecraft projects
[PB94-126257] p 3170 N94-30857

NATIONAL AEROSPACE LAB., KAKUDA (JAPAN).

Numerical simulation of steady Mach reflection by shock capturing schemes p 3123 N94-28953
Flow and heat transfer in a rotating square sectioned U-bend p 3128 N94-28984
Similarity between turbulent flows through curved pipe and orthogonal rotating pipe p 3128 N94-28986
Numerical analysis of laminar flow in S-curved square duct with inlet and outlet straight region p 3128 N94-28987
Development of buoyancy affected laminar flow in a heated pipe p 3128 N94-28988
Mutual similarity of developing laminar flows with secondary streams in ducts: Curved pipe flow and orthogonal rotating pipe flow p 3129 N94-28989

NATIONAL AEROSPACE LAB., TOKYO (JAPAN).

Proceedings of the 10th NAL Symposium on Aircraft Computational Aerodynamics
[NAL-SP-19] p 3123 N94-28946
Monte Carlo simulation or normal shock wave. Part 2: VHS model and VSS model p 3123 N94-28948
Variable soft sphere molecular model in the Monte Carlo simulation of air species p 3123 N94-28949
Rarefied gas numerical wind tunnel. Part 8: HOPE p 3123 N94-28950
Numerical simulation of arc heated wind tunnel flow p 3123 N94-28951
Numerical simulation of aerothermodynamic heating of hypersonic space transportation vehicles p 3124 N94-28955
Numerical solution of inverse problem in aerodynamics p 3125 N94-28965
On the numerical analysis of shear flows p 3126 N94-28972
On approximate Riemann solvers: Improvement of HLLEM scheme and its generalization for chemically reacting flows p 3126 N94-28973
Numerical study on internal flows of centrifugal compressors p 3127 N94-28977
An elliptic-hyperbolic grid generation method and application to compressor flows p 3128 N94-28981
Parallelization techniques for highly parallel vector computer p 3129 N94-28990

Parallel Fortran programming for NWT p 3129 N94-28991
Performance evaluation of the NWT with parallel Fortran p 3129 N94-28992
A method of user interface for NWT p 3129 N94-28993

NATIONAL BOARD OF OCCUPATIONAL SAFETY AND HEALTH, STOCKHOLM (SWEDEN).

Ventilation systems p 3232 N94-29601

NATIONAL CENTER FOR ATMOSPHERIC RESEARCH, BOULDER, CO.

Peroxy radical measurements with NCAR's chemical amplifier p 3345 N94-28603
Models of atmosphere-ecosystem-hydrology interactions: Approaches and testing p 3353 N94-30636
Solar measurements from the Airglow-Solar Spectrometer Instrument (ASSI) on the San Marco 5 satellite
[NASA-CR-193815] p 3551 N94-30948

NATIONAL DEFENCE RESEARCH ESTABLISHMENT, LINKOEPING (SWEDEN).

Synchronization in multistatic radar
[PB94-136975] p 3242 N94-28885
Analysis of microwave induced interference in pn-diodes
[PB94-136983] p 3243 N94-28906
Active antennas, a review
[PB94-137445] p 3243 N94-28907
Synchronization, positioning, and communication in multistatic radar systems for air defence
[PB94-137478] p 3243 N94-28908
Quality and efficiency of solar collectors in Sweden
[PB94-137486] p 3337 N94-28909
Codes on the unit sphere
[PB94-136991] p 3453 N94-29174
Detection methods for stealth radio signals: A literature survey
[PB94-137452] p 3244 N94-29176
Simulator for multistatic radar
[PB94-135506] p 3245 N94-29311

NATIONAL DEFENCE RESEARCH ESTABLISHMENT, STOCKHOLM (SWEDEN).

Photoconductive switching for high power microwave generation
[PB94-137460] p 3244 N94-29177
Intelligent material systems and structures. Part 7: Debonding and pull-out of two optical fibers from two epoxies
[PB94-137767] p 3180 N94-29475
Compound matrix method for multi-point boundary-value problems
[PB94-137791] p 3453 N94-29476

NATIONAL DEFENCE RESEARCH ESTABLISHMENT, UMEA (SWEDEN).

Caesium-137 in a boreal forest ecosystem: Aspects on the long-term behavior
[PB94-137809] p 3347 N94-29158

NATIONAL ELECTRICAL MFRS. ASSOCIATION, WASHINGTON, DC.

NEMA wire and cable standards development programs p 3166 N94-28706

NATIONAL GEOPHYSICAL DATA CENTER, BOULDER, CO.

Solar-geophysical data number 591, November 1993. Part 1: Prompt reports. Data for September, October 1993 and late data
[PB94-140548] p 3550 N94-29122
Solar-geophysical data number 592, December 1993. Part 1: Prompt reports. Data for October, November 1993 and late data
[PB94-142130] p 3550 N94-29123
Solar-geophysical data number 592, December 1993. Part 2: Comprehensive reports. Data for June 1993 and miscellaneous
[PB94-142148] p 3550 N94-29124

NATIONAL INST. FOR FUSION SCIENCE, NAGOYA (JAPAN).

Proceedings of Japan-US Workshop P-196 on High Heat Flux Components and Plasma Surface Interactions for Next Devices
[DE94-701164] p 3503 N94-28513
A 6MeV heavy ion beam probe for the Large Helical Device
[NIFS-272] p 3505 N94-29397
The effect of magnetic field configuration on particle pinch velocity in Compact Helical System (CHS)
[NIFS-267] p 3505 N94-29398
Formation and self-healing of magnetic islands in finite-beta helias equilibria
[NIFS-269] p 3505 N94-29483
Efficiencies of the ICRF minority heating in the CHS and LHD plasmas
[NIFS-270] p 3506 N94-29499

Large amplitude Langmuir and ion-acoustic waves in a relativistic two-fluid plasma
[NIFS-271] p 3506 N94-29547
Development of high time-resolution laser flash equipment for thermal diffusivity measurements using miniature-size specimens
[NIFS-268] p 3295 N94-30186

NATIONAL INST. FOR RESOURCES AND ENVIRONMENT, IBARAKI (JAPAN).
Journal of NIRE, Vol. 2, No. 2
[JTN-94-80552] p 3187 N94-28675
Molecular structure of coal studied by solvent extraction p 3187 N94-28676
Researches on bioconversion of coal into liquid product p 3187 N94-28677
Structural changes during carbonization and oxidation of coal p 3187 N94-28678
Methanol-mediated continuous extraction of phenolic compounds from coal liquid p 3188 N94-28679
Properties of adsorbents for collection and analysis of trace amount of chlorofluorocarbons in air p 3188 N94-28680
Ab initio study of vibrational frequency shift upon the 1:1 acetone-iodine complex formation p 3188 N94-28681
A novel spectroscopic measurement method of RF plasma for temperature and electron density diagnoses p 3188 N94-28682
On United States-Japan Conference on Development and Utilization of Natural Resources: Report of the 14th Joint Meeting of U. S. and Japan Marine Mining Panel p 3188 N94-28683
Journal of NIRE, vol. 2, no. 3
[JTN-94-80553] p 3553 N94-29512
Layered polysilicate: Properties and perspectives in applications p 3223 N94-29513
Preparation of monodispersed fine particles containing rare metals and rare earths p 3201 N94-29514
Synthesis of diamond in a hydrogen plasma jet: Simulations of XRD patterns of diamond polytypes and boundary layer on a substrate p 3522 N94-29515
Study on the formation of ultrafine particles of Sm-Co intermetallic compounds using RF thermal plasma p 3211 N94-29516
Preparation of graphite fibers from polyimide p 3223 N94-29517
Preparation and structure of amorphous hydrogenated carbon film deposited with RF plasma CVD p 3223 N94-29518
Growth of hydrocarbon-rich microalga Botryococcus braunii in secondarily treated sewage and its consumption of nitrate ion and phosphate ion p 3387 N94-29519
Influence of clearance and rake angles on the cutting force of rock p 3368 N94-29520
Joint research activities with CCMRI (China) p 3240 N94-29521
Second Japan-U.S. Workshop on Global Change: Environmental Response Technologies for Global Change (Mitigation and Adaptation) p 3354 N94-29522
Report of National Institute for Resources and Environment. No. 8: Research on blasting sound related to it's measurement, propagation prediction, control and evaluation
[JTN-94-80605] p 3479 N94-29597

NATIONAL INST. OF AGRO-ENVIRONMENTAL SCIENCE, IBARAKI (JAPAN).
JERS-1 and future remote sensing: Application of remote sensing data to agroecological problems p 3331 N94-29229

NATIONAL INST. OF POLAR RESEARCH, TOKYO (JAPAN).
Antarctic Record, volume 36, no. 1
[REPT-106-VOL-36-NO-1] p 3357 N94-29078
Glacial landforms and late Cenozoic history of the western Soer-Rondane mountains p 3357 N94-29080
Activities of the wintering party at Showa Station by the 31st Japanese Antarctic Research Expedition in 1990 p 3358 N94-29083
Activities of the fourth wintering party at Asuka Station by the 31st Japanese Antarctic Research Expedition in 1990 p 3358 N94-29084
Japan-China collaboration research program on terrestrial biology at Great Wall Station in King George Island, in the summer of 1990/1991 p 3358 N94-29085
Protocol on environmental protection to the Antarctic Treaty and its annexes: International agreement on the comprehensive measures for the protection of Antarctic environment and ecosystems p 3354 N94-29086
Proceedings of the NIPR Symposium on Upper Atmosphere Physics, no. 6
[JTN-94-80593] p 3359 N94-29233
Antarctic Record, vol. 36, no. 3
[REPT-106] p 3363 N94-29978
A study of precipitation in the coastal area of Antarctica as observed at Syowa Station using a vertical pointing radar p 3363 N94-29979
Data transfer system using a multi-ID ARGOS transmitter for the Antarctic polar patrol balloon experiment p 3363 N94-29980
A newly developed snow vehicle (SM100S) for Antarctica. Part 1: Necessity and process of the development p 3314 N94-29981
Activities of the wintering party at Syowa Station by the 32nd Japanese Antarctic Research Expedition in 1991 p 3364 N94-29986

NATIONAL INST. OF STANDARDS AND TECHNOLOGY, BOULDER, CO.
Time and frequency technology at NIST p 3468 N94-30641
A comparison of GPS broadcast and DMA precise ephemerides p 3145 N94-30660
The NIST Internet time service p 3475 N94-30678
The future of time and frequency dissemination p 3476 N94-30684

NATIONAL OCEANIC AND ATMOSPHERIC ADMINISTRATION, BOULDER, CO.
NOAA Aeronomy Laboratory long-path OH experiment, Fritz Peak Observatory, Colorado p 3344 N94-28598
Remote sensor observations during WISP91: The use of microwave radiometers, RASS, and lidar ceilometers for detection of aircraft icing conditions
[PB94-142106] p 3136 N94-30890

NATIONAL PHYSICAL LAB., TEDDINGTON (ENGLAND).
Temperature depencence of the far infrared optical constants of polyethylene
[PB94-124336] p 3213 N94-28795
Measurement and modelling of bolted joint stress relaxation in plastics
[PB94-124849] p 3318 N94-28841
Surface tension of tin and its alloys with particular reference to solders
[PB94-138302] p 3204 N94-29119
Electrical conductivity measurements on a SiCp/Al alloy metal matrix composite
[PB94-138310] p 3263 N94-29120
Modelling and analysis of creep deformation and fracture in a 1 Cr 1/2 Mo ferritic steel
[PB94-138328] p 3319 N94-29121
Stress transfer mechanics for multiple perfectly bonded concentric cylinder models of unidirectional composites
[PB94-138633] p 3181 N94-29524
The effect of temperature on creep and physical ageing of PVC
[NPL-DMM(A)-93] p 3217 N94-29885
Creep and physical aging of PVC: Dependence on stress and temperature
[NPL-DMM(A)-115] p 3217 N94-29886
Estimation of Weibull modulus from dynamic and static fatigue experiments
[PB94-138641] p 3322 N94-30114
VHF impedance measurement: A review
[PB94-138682] p 3267 N94-30115
Particulate metal matrix composites: Draft procedure for tensile tests at ambient temperature
[NPL-DMM(A)-100] p 3184 N94-30419
Standardisation requirements for ultrasonic C-scanning of polymer matrix composites: An initial assessment
[PB94-139318] p 3184 N94-30438
The performance of gloss meters on curving surfaces
[NPL-DMM(A)-111] p 3501 N94-30522
Approximate estimation of the effects of asymmetry on the testing of tensile specimens
[NPL-DMM(A)-117] p 3322 N94-30523
A review of mechanical test methods for ceramic matrix composites
[PB94-147576] p 3184 N94-30524
Guidance notes for use with NPL low permeability reference materials
[NPL-DES-121] p 3476 N94-30780
RF and microwave dielectric measurements upon layered materials using reflectometric coaxial sensor
[NPL-DES-125] p 3476 N94-30781
The use of thermistors in the NPL electron-beam calorimeter
[PB94-139334] p 3290 N94-30782
Report on the development of low magnetic permeability reference materials
[NPL-DES-119] p 3476 N94-30783
Guidance on eliminating interference from sensitive electrical circuits
[PB94-139300] p 3268 N94-30784
Formulae for the calculation of the magnetic field strength in a Helmholtz system with circular coils
[NPL-DES-130] p 3260 N94-30785
Index of NPL acoustics publications 1981-1990
[NPL-RSA(EXT)-0044] p 3480 N94-30786
Determination of photon fluence spectra from the NPL Mobaltron Co-60 unit
[NPL-RSA(EXT)-46] p 3492 N94-30795
Method of test for cleanness assessment of metal alloys: The preparation of button specimens by electron beam melting and the characterisation of recovered inclusions
[NPL-DMM(A)-130] p 3210 N94-30796

NATIONAL RESEARCH COUNCIL, BANGKOK (THAILAND).
Utilization of remote sensing data in Southeast Asia p 3327 N94-28936

NATIONAL RESEARCH COUNCIL OF CANADA, OTTAWA (ONTARIO).
Design of a thinwire real-time multiprocessor operating system p 3415 N94-29333
Measurements and predictions of the combustion characteristics of enclosed swirl-stabilized propane flames
[IECE-CFE-TR-001] p 3198 N94-30017
Theoretical prediction of the influence coefficients on damped simple flexible rotors using the transfer matrix method
[IMR-TM-TR-002] p 3321 N94-30018
Sliding friction and wear between titanium nitride, M50 steel and silicon nitride (round 3 of VAMAS wear test program)
[IMR-TM-TR-003] p 3303 N94-30019
The NRC mobile robot project p 3305 N94-30280
Maestro: An open system architecture for multi-robot control p 3306 N94-30288
Accuracy metrics for judging time scale algorithms p 3471 N94-30656
Hydrogen masers and cesium fountains at NRC p 3297 N94-30664

NATIONAL RESEARCH INST. FOR EARTH SCIENCE AND DISASTER PREVENTION, TSUKUBA (JAPAN).
Application of remote sensing in prevention of disasters p 3332 N94-29230

NATIONAL RESEARCH INST. OF FISHERIES ENGINEERING, TOKYO (JAPAN).
Design of the biosonar simulator for dolphin's clicks waveform reproduction p 3234 N94-29707

NATIONAL SCIENCE FOUNDATION, WASHINGTON, DC.
Method of Chabauty-Coleman and the second case of Fermat's last theorem for regular primes
[PB94-138187] p 3467 N94-29162

NATIONAL SERVICE OF METROLOGY, DELFT (NETHERLANDS).
Two-way satellite time transfer: Overview and recent developments p 3469 N94-30646

NATIONAL SPACE DEVELOPMENT AGENCY, OHASHI (JAPAN).
Status and tendency of earth observation system p 3328 N94-29038

NATIONAL SPACE DEVELOPMENT AGENCY, TOKYO (JAPAN).
Proceedings of the 15th Earth Observation Symposium
[JTN-94-80607] p 3328 N94-29036
Outline of JERS-1 system p 3330 N94-29220
Japan's Earth observation satellite programs p 3332 N94-29232
Hemodynamic measurement during parabolic flight p 3393 N94-29717
Development status of the Communications and Broadcasting Engineering Test Satellite (COMETS)
[JTN-94-80545] p 3169 N94-30811
Development status of COMETS missions
[JTN-94-80544] p 3170 N94-30932

NATIONAL TELECOMMUNICATIONS AND INFORMATION ADMINISTRATION, BOULDER, CO.
Propagation modeling of moist air and suspended water/ice particles at frequencies below 1000 GHz p 3256 N94-30497

NATIONAL TRANSPORTATION SAFETY BOARD, WASHINGTON, DC.
National Transportation Safety Board annual review of aircraft accident data. US general aviation, 1990
[PB94-126869] p 3135 N94-29185
Aircraft accident/incident summary report: In-flight loss of control, leading to forced landing and runway overrun, Continental Express, Inc., N24706 Embraer EMB-120 RT, Pine Bluff, Arkansas, 29 April 1993
[PB94-910404] p 3135 N94-29402

NAUCHNO-ISSLEDOVATELSKII INST. EHLEKTROFIZICHESKOJ APPARATURY, LENINGRAD (USSR).
Radiation transport and focusing systems for power industrial lasers
[DE94-606817] p 3293 N94-28786

NAVAL AEROSPACE MEDICAL RESEARCH LAB., PENSACOLA, FL.
Effects of three hydration beverages on exercise performance during 60 hours of simulated desert exposure p 3383 N94-28448

An evaluation of personality testing and the five-factor model in the selection of landing craft air cushion vehicle crew members
[AD-A275869] p 3397 N94-28754
Naval aviation vision standards research at the naval aerospace medical research laboratory: The long view
[AD-A275885] p 3388 N94-28756

NAVAL AIR WARFARE CENTER, CHINA LAKE, CA.
Synthesis and characterization of advanced materials for Navy applications p 3223 N94-30474
High elongation elastomers p 3223 N94-30477

NAVAL AIR WARFARE CENTER, INDIANAPOLIS, IN.
NAVAIR aircraft wiring standardization and qualification program p 3166 N94-28704
Organized wiring systems p 3166 N94-28705

NAVAL AIR WARFARE CENTER, ORLANDO, FL.
Engineering specification editing tools
[AD-A275116] p 3419 N94-29746

NAVAL AIR WARFARE CENTER, TRENTON, NJ.
Combustion technology needs for advanced high pressure cycle engines p 3190 N94-29248

NAVAL AIR WARFARE CENTER, WARMINSTER, PA.
The discipline of defining the software product p 3416 N94-29343

NAVAL AVIATION HQ, YEOVIL (ENGLAND).
The concept of Royal Navy air operations under extreme environmental conditions p 3379 N94-28424

NAVAL AVIATION LOGISTICS CENTER, PATUXENT RIVER, MD.
Aircraft age impacts on maintenance requirements
[AD-A275701] p 3121 N94-28666
Aircraft age impact on individual operating and support cost elements
[AD-A275739] p 3121 N94-28732

NAVAL COMMAND, CONTROL AND OCEAN SURVEILLANCE CENTER, SAN DIEGO, CA.
Alumina ceramic: A cost effective replacement for titanium in deep submergence pressure housings
[AD-A275640] p 3212 N94-28641
Effect of surface condition on strength and fatigue behavior of alumina ceramic
[AD-A275053] p 3214 N94-29133
Controlling multiple security robots in a warehouse environment
[AIAA PAPER 94-1300-CP] p 3441 N94-30540

NAVAL HEALTH RESEARCH CENTER, SAN DIEGO, CA.
Rewarming methodologies in the field p 3382 N94-28441
Comparison of two cool vests on heat-strain reduction while wearing a firefighting ensemble in a hot/humid environment
[AD-A275103] p 3400 N94-28902
Physiological responses during shipboard firefighting
[AD-A275104] p 3391 N94-28912

NAVAL OBSERVATORY, WASHINGTON, DC.
Remote clocks linked by a fully calibrated two-way timing link p 3471 N94-30659
A comparison of several GPS data reduction methods p 3145 N94-30662
A comparative study of clock rate and drift estimation p 3473 N94-30669

NAVAL POSTGRADUATE SCHOOL, MONTEREY, CA.
SPC toolbox: An interactive MATLAB (tm) package for signal modeling, analysis, and communications
[AD-A275617] p 3241 N94-28634
Security aspects of computer supported collaborative work
[AD-A275638] p 3528 N94-28640
Objective analysis of a coastal ocean eddy using satellite AVHRR and in situ hydrographic data
[AD-A275715] p 3376 N94-28642
Intermetallic growth at the interface between copper and bismuth-tin solder
[AD-A275716] p 3202 N94-28643
Annual summary of basic research thermoacoustic heat transport, 1993
[AD-A275751] p 3230 N94-28644
Service life prediction of composite structures through fiber testing
[AD-A275661] p 3176 N94-28654
Safety enhancement of composites via periodic proof testing
[AD-A275662] p 3176 N94-28655
A moment plotting method for characterizing aircraft fatigue data population distributions
[AD-A275500] p 3145 N94-28660
The influence of wall conductivity of film condensation with integral fin tubes
[AD-A275503] p 3523 N94-28662
The state transition diagram with path priority and it's applications
[AD-A275524] p 3434 N94-28672
Aerodynamic design using parallel processors
[AD-A275470] p 3122 N94-28674
Electron beams at geosynchronous orbit
[AD-A275471] p 3355 N94-28684
The velocity field in the Northeast Atlantic from satellite-tracked drifting buoys
[AD-A275704] p 3376 N94-28690
Using multiple searchers to locate a randomly moving target
[AD-A275602] p 3463 N94-28768
Communications subsystem for the Petite Amateur Navy Satellite (PANSAT)
[AD-A275532] p 3242 N94-28812
Acquisition, design modification, assembly, and ground test of NPS Hummingbird remotely piloted helicopter
[AD-A275546] p 3146 N94-28837
Digitally programmable composite operational amplifier applications
[AD-A275081] p 3262 N94-28842
Far ultraviolet images of the nighttime ionosphere
[AD-A275083] p 3356 N94-28843
Procedural guide for modelling and analyzing the flight characteristics of a helicopter design using flightlab
[AD-A275077] p 3146 N94-28870
Automated interface for retrieving reusable software components
[AD-A275004] p 3409 N94-28896
Spurs in digital radio frequency memory and applications of DRFM
[AD-A275013] p 3243 N94-28897
Removal of coherent Extremely Low Frequency (ELF) background noise by adaptive noise cancellation
[AD-A275016] p 3243 N94-28898
The management issues of implementing telecommuting: A case study
[AD-A275267] p 3527 N94-28905
Quadruplet expansion of the acoustic pressure field in a wedge shaped ocean
[AD-A275121] p 3477 N94-29003
Feedback control of a three-link planar under-actuated manipulator using a surge velocity
[AD-A275159] p 3435 N94-29044
A porting methodology for parallel database systems
[AD-A275256] p 3529 N94-29053
Evaluation of wireless Local Area Networks
[AD-A275133] p 3243 N94-29064
An evaluation of techniques for ranking academic information systems journals
[AD-A275179] p 3529 N94-29066
Acquisition time analysis of noncoherent PN sequence acquisition schemes
[AD-A275017] p 3244 N94-29094
Spectral and polarimetric analysis of hyperspectral data collected by an acousto-optic tunable filter system
[AD-A275076] p 3329 N94-29095
A concurrent, object-based implementation for the tactical level of the rational behavior model
[AD-A275024] p 3410 N94-29115
A comparison of two computer models of sound propagation for a wedge shaped ocean over a penetrable bottom
[AD-A275031] p 3477 N94-29117
Towards an information model and mechanisms for design rationale capture and use
[AD-A275060] p 3530 N94-29138
NPSNET: Integration of Distributed Interactive Simulation (DIS) protocol for communication architecture and information interchange
[AD-A275061] p 3530 N94-29139
HYPER-NPSNET: Embedded multimedia in a 3D virtual world
[AD-A275063] p 3410 N94-29152
Evaluating the analytic hierarchy process and recommended modifications for its use in multi-attribute decision making
[AD-A275065] p 3527 N94-29153
A model analysis of potential vorticity on isopycnal surfaces for the global ocean
[AD-A275047] p 3377 N94-29164
The covering property of the object-oriented data model: Design and implementation issues
[AD-A275048] p 3530 N94-29165
An analysis of the microstructure and reinforcement distribution of an extruded particle-reinforced Al 6061-10 volume percent Al2O3 metal matrix composite
[AD-A275050] p 3178 N94-29166
A non-linear simulation for an autonomous unmanned air vehicle
[AD-A275062] p 3146 N94-29200

NAVAL RESEARCH LAB., BAY SAINT LOUIS, MS.
Updated deep-tow acoustics/geophysics system compressional velocity database
[AD-A275477] p 3355 N94-28685
A program for rapid computation of multioffset vertical seismic profile synthetic seismograms for layered media
[AD-A275464] p 3355 N94-28737
Broad geoacoustic assessment of some regional areas
[AD-A275504] p 3356 N94-28791
The effects of altimeter sampling characteristics: Some Geosat examples
[AD-A275225] p 3357 N94-29062
Seafloor characterization using texture
[AD-A275399] p 3377 N94-29204
Considerations in the modelling of seafloor acoustic backscatter
[AD-A275404] p 3478 N94-29206
Tidal atlas software development
[AD-A275251] p 3377 N94-29432

NAVAL RESEARCH LAB., WASHINGTON, DC.
Preliminary analysis of Asynchronous Transfer Mode (ATM) over microwave channels
[AD-A275214] p 3243 N94-29069
The investigation of electron-ion radiative and dielectronic recombination in high-temperature plasmas
[DE94-005150] p 3509 N94-30755

NAVAL SURFACE WARFARE CENTER, DAHLGREN, VA.
Solid-state, active-phased arrays: Some aspects of receiver design
[AD-A275893] p 3527 N94-28779
Statistical Modeling and Estimation of Reliability Functions for Software (SMERFS) user's guide, revision 3
[AD-A275390] p 3411 N94-29202
Statistical Modeling and Estimation of Reliability Functions for Software (SMERFS) library access guide, revision 3
[AD-A275405] p 3411 N94-29207

NAVAL SURFACE WARFARE CENTER, PANAMA CITY, FL.
Photovoltaic power without batteries for continuous cathodic protection p 3341 N94-30465

NAVAL SURFACE WARFARE CENTER, SILVER SPRING, MD.
Electroset Technology: On the forefront of manufacturing
[AD-A275166] p 3263 N94-29045

NAVAL UNDERSEA WARFARE CENTER, NEW LONDON, CT.
Output statistics of the SALFAS FM normalizer Smoothing/Prediction function
[AD-A275758] p 3463 N94-28759

NAVAL UNDERSEA WARFARE CENTER, NEWPORT, RI.
Wall pressure events from the direct numerical simulation of a turbulent wall-bounded flow
[AD-A275890] p 3271 N94-28778
Propagation of evidence through fuzzy rules
[AD-A275071] p 3411 N94-29180

NAVY EXPERIMENTAL DIVING UNIT, PANAMA CITY, FL.
Advanced seal delivery system life support parameters
[AD-A275304] p 3401 N94-29184

NAVY PERSONNEL RESEARCH AND DEVELOPMENT CENTER, SAN DIEGO, CA.
Markov chains for random urinalysis 3: Daily model and drug kinetics
[AD-A275540] p 3389 N94-28797

NEBRASKA UNIV., LINCOLN.
Experimental and theoretical studies of molecular solids
[AD-A275511] p 3485 N94-28668
Video transmission on ATM networks
[NASA-CR-195124] p 3244 N94-29106
Performance of a higher-order triangular finite element for composite laminated structures p 3181 N94-29810

NEOCOMM SYSTEMS, INC., LA CANADA-FLINTRIDGE, CA.
Providing hydrogen maser timing stability to orbiting VLBI radio telescope observations by post-measurement compensation of linked frequency standard imperfections p 3297 N94-30670

NETHERLANDS AGENCY FOR AEROSPACE PROGRAMS, DELFT.
ENGRID: A graphical interactive code for the computation of structured grids for blocked flow domains p 3124 N94-28956

NEW ENERGY AND INDUSTRIAL TECHNOLOGY DEVELOPMENT ORGANIZATION, TOKYO (JAPAN).
Fiscal 1991 geothermal development promotion energy
[DE94-732332] p 3337 N94-28627
Fiscal 1990 geothermal development promotion survey
[DE94-732333] p 3337 N94-28628
Feasibility study on introduction of a large methanol engine power generation plant
[DE94-732338] p 3224 N94-28629
Survey on effects of petroleum substitution energy utilization on the global environment
[DE94-732339] p 3346 N94-28630

Report of feasibility study on international-cooperation in high efficient energy conversion technology
[DE94-732340] p 3337 N94-28631
Technical analysis of alternative fueled vehicles
[DE94-744238] p 3304 N94-30269
Investigation of the technology development status of alternate fuel vehicles
[DE94-744237] p 3312 N94-30831

NEW HAMPSHIRE UNIV., DURHAM.
Corrosion inhibition by electrodeposited conductive-polymer film
[AD-A275456] p 3213 N94-28806
Four simple ocean carbon models
p 3351 N94-30625

NEW JERSEY INST. OF TECH., NEWARK.
The bootstrapped algorithm: A fast algorithm for blind signal separation
[AD-A275759] p 3408 N94-28760

NEW MEXICO INST. OF MINING AND TECHNOLOGY, SOCORRO.
Interface engineering in alumina fiber/glass composites p 3182 N94-29852

NEW MEXICO STATE UNIV., LAS CRUCES.
The Rb 780-nanometer Faraday anomalous dispersion optical filter: Theory and experiment
p 3250 N94-29659
An analysis of carrier phase jitter in an MPSK receiver utilizing map estimation
[NASA-CR-195806] p 3164 N94-29880
Remote observatory access via the advanced communications technology satellite
p 3253 N94-29894
Significant figures and Lyapunov exponents in chaos and constrained divergence of chaotic orbits
p 3467 N94-29910

NEW MEXICO STATE UNIV., UNIVERSITY PARK.
Surface differential rotation in a sample of cool dwarf stars p 3545 N94-29827

NEW MEXICO UNIV., ALBUQUERQUE.
Float polishing studies of fused silica
[AD-A275001] p 3213 N94-28886
Automatic focus and registration of synthetic aperture radar images p 3246 N94-29536

NEW ORLEANS UNIV., LA.
Superior energetic materials that contain carbocations and anions. Energetic materials restricted in composition to C, H, N, and O atoms
[AD-A275449] p 3225 N94-29310

NEW TECHNOLOGY, INC., HUNTSVILLE, AL.
A Modular Artificial Intelligence Inference Engine System (MAIS) for support of on orbit experiments
[AIAA PAPER 94-1237-CP] p 3448 N94-30584

NEW YORK UNIV., NEW YORK.
Applied analysis/computational mathematics
[DE94-005133] p 3451 N94-28571
Computational fluid and combustion dynamics
[DE94-006596] p 3279 N94-30003
Superdiffusion
[DE94-002333] p 3492 N94-30834

NIHON UNIV., TOKYO (JAPAN).
Arterial oxygen saturation during +Gz acceleration by short-radius centrifuge p 3389 N94-28852
Effect of chronic centrifugation on in vitro fertilization and early development in mice ova
p 3386 N94-28853

NIJMEGEN UNIV. (NETHERLANDS).
Modelling the evolution of information systems
[TR-92-36] p 3535 N94-30329
Genetic algorithms for optimal database design
[TR-93-01] p 3535 N94-30330
The beauty and the beast
[TR-93-03] p 3423 N94-30331
Increasing the applicability of LR parsing
[TR-93-06] p 3423 N94-30332
A conceptual language for the description and manipulation of complex information models
[TR-92-34] p 3423 N94-30344
Generalized left-corner parsing
[TR-92-21] p 3432 N94-30356
Towards a general theory for the evolution of application domains
[TR-92-22] p 3535 N94-30357
Index expression belief networks for information disclosure
[TR-92-23] p 3465 N94-30358
Evolving information systems: Meeting the ever-changing environment
[TR-92-24] p 3535 N94-30359
A general theory for the evolution of application domains
[TR-92-26] p 3535 N94-30360
A framework for comparing conceptual modelling languages
[TR-92-29] p 3535 N94-30361
A note on schema equivalence
[TR-92-30] p 3535 N94-30362
Parsing in ISBES
[TR-92-32] p 3432 N94-30363

NIPPON KOKAN K. K., KAWASAKI (JAPAN).
A newly developed snow vehicle (SM100S) for Antarctica. Part 3: Low temperature toughness of the welded joints of the structural steel
p 3364 N94-29983

NIPPON TELEGRAPH AND TELEPHONE PUBLIC CORP., YOKOSUKA (JAPAN).
A module concept for a cable-mesh deployable antenna p 3161 N94-29631

NORGES TEKNISKE HOEGSKOLE, TRONDHEIM.
Progress report for the PTUF Project-93 Q1 and Q2
[PB94-138591] p 3431 N94-29995

NORSK DATA A.S., OSLO.
Progress report for the PTUF Project-93 Q1 and Q2
[PB94-138591] p 3431 N94-29995

NORTH CAROLINA AGRICULTURAL AND TECHNICAL STATE UNIV., GREENSBORO.
Computational methods in continuum mechanics
[AD-A275560] p 3451 N94-28792

NORTH CAROLINA STATE UNIV., RALEIGH.
Fusion of range and luminance data from laser radar systems
[AD-A275608] p 3292 N94-28770
Modeling, analysis, and simulation of an optical time-division multiple-access network architecture
[AD-A275847] p 3498 N94-28780
Anodization of copper in chloride media
[AD-A275565] p 3202 N94-28793
Carrier collection and scattering in quantum well and superlattice devices
[AD-A275443] p 3512 N94-28880
A numerical solver for initial and boundary value problems in differential-algebraic systems
[AD-A275447] p 3452 N94-28883
A laboratory simulation of urban heat-island-induced circulation in a stratified environment
p 3367 N94-30921
An investigation into certain geometrical and variational properties of the P(4) theory of gravitation and electromagnetism p 3526 N94-30950

NORTH CAROLINA UNIV., CHAPEL HILL.
Human and institutional factors in GIS implementation by local governments p 3532 N94-29804
Enhancing performance of full-text retrieval systems using relevance feedback p 3532 N94-29806

NORTH DAKOTA STATE UNIV., FARGO.
Crosslinking and surface reactions in macromolecules: Spectroscopic FT-IR studies p 3221 N94-30812

NORTH DAKOTA UNIV., GRAND FORKS.
Catalytic fabric filtration for simultaneous NO(x) and particulate control
[DE94-001660] p 3341 N94-28463

NORTHEASTERN UNIV., BOSTON, MA.
Radar returns from a low-flying target over a rough sea surface under multipath and clutter conditions
p 3253 N94-29882

NORTHWESTERN UNIV., EVANSTON, IL.
Toughening mechanisms in ultrahigh-strength steels
[AD-A275439] p 3202 N94-28867
MOCVD growth of GaN, AlN and AlGaN for UV photodetector applications
[AD-A275078] p 3512 N94-28871
InTlSb for long-wavelength infrared photodetectors and arrays
[AD-A275079] p 3512 N94-28872
Stability of dynamical systems in the presence of noise
[AD-A275383] p 3243 N94-29072

NORWEGIAN BUILDING RESEARCH INST., OSLO.
Theory of age distribution p 3232 N94-29602
Ventilation models p 3232 N94-29603

NORWEGIAN TRANSARCTIC EXPEDITION, HIS.
Evaluation of life support equipment during an unsupported North Pole expedition
p 3379 N94-28422

NOTRE DAME UNIV., IN.
The impact of electrically charged microspheres with planar surfaces under vacuum conditions
p 3320 N94-29765
Transient studies of low temperature catalysts for methane conversion
[DE94-005767] p 3200 N94-30877
An experimental study of nonlinear wave coupling and energy transfer characterizing the transition of a planar jet shear layer p 3282 N94-30953

NOTTINGHAM UNIV. (ENGLAND).
Granular bases for heavily loaded pavements
[AD-A275171] p 3156 N94-29047

O

OAK RIDGE K-25 SITE, TN.
Reinterpretation of rate data for the reaction of ClF and F2
[DE94-005819] p 3200 N94-30880

OAK RIDGE NATIONAL LAB., TN.
On the prediction of HAZ grain size using Monte Carlo simulation
[DE94-005465] p 3511 N94-28535
Density reduction: A mechanism for amorphization at high ion doses
[DE94-004793] p 3483 N94-28559
Overview of shielding analyses for the MHTGR from 1986 to 1991
[DE94-002448] p 3495 N94-29924
Issues arising with the application of optical fiber transmission in class 1E systems in nuclear power plants
[DE94-004743] p 3500 N94-29928
Nanosize metal alloy particle formation in Ag and Cu sequentially implanted silica
[DE94-005592] p 3207 N94-30042
Structural characterization of semiconductor heterostructures by atomic resolution Z-contrast imaging at 300 kV
[DE94-006561] p 3516 N94-30063
Atomic-scale structure and chemistry of interfaces by Z-contrast imaging and electron energy loss spectroscopy in the STEM
[DE94-006563] p 3516 N94-30064
Three-dimensional effects for radio frequency antenna modeling
[DE94-006102] p 3255 N94-30105
The influence of an in-situ electric field on H(+) and He(+) implantation induced defects insil icon
[DE94-006553] p 3518 N94-30249
Large-scale 3-D solutions of the time-dependent Dirac equation
[DE94-005591] p 3454 N94-30317
Characterization of thermally annealed Sb implanted fused silica
[DE94-005464] p 3219 N94-30335
Overview of the US stellarator reactor study
[DE94-006042] p 3508 N94-30339
Irradiation-induced structure and property changes in tokamak plasma-facing, carbon-carbon composites
[DE94-006046] p 3508 N94-30365
Task automation in a successful industrial telerobot
[AIAA PAPER 94-1189-CP] p 3441 N94-30539
Research on the atomic layer-by-layer growth of high-temperature superconductor thin films at the Institute of Scientific and Industrial Research, Japan
[DE94-003739] p 3519 N94-30611
Experimental and analytical comparison of constraint effects due to biaxial loading and shallow-flaws
[DE94-004794] p 3323 N94-30689
Prediction and standard error estimation for a finite universe total when a stratum is not sampled
[DE94-004929] p 3465 N94-30696
Structural analysis of amorphous phosphates using high performance liquid chromatography
[DE94-004791] p 3199 N94-30723
Thermal conductivities, electrical resistivities, and Seebeck coefficients of YBa2Cu3O(7-x) superconductors from 80 to 300 K
[DE94-004796] p 3520 N94-30724
On some general properties of parabolic conservation equations
[DE94-006101] p 3461 N94-30758
The impact of improved physics on commercial tokamak reactors
[DE94-006103] p 3509 N94-30760
Ionic conduction mechanisms in CaF2 and CaF2-Al2O3 nanocomposite films on Al2O3 substrates
[DE94-004792] p 3520 N94-30773
Using the log-normal distribution in analyzing aerosols: The mathematical reasoning underlying the various diameters used and the plotting procedure
[DE94-006459] p 3461 N94-30817
Fuel cycle evaluations of biomass-ethanol and reformulated gasoline
[DE94-000227] p 3226 N94-30818
Synthesis of (SiC)3N4 thin films by ion implantation
[DE94-006311] p 3521 N94-30851
Study of nucleation and growth in Ai-Zn alloys using TEM
[DE94-006312] p 3211 N94-30852

OBSERVATOIRE DE BESANCON (FRANCE).
Time transfer using geostationary satellites: Implementation of a Kalman filter p 3471 N94-30657
Noise and drift analysis of non-equally spaced timing data p 3472 N94-30667

OBSERVATOIRE DE LA COTE D'AZUR, GRASSE (FRANCE).
Optical techniques for time and frequency transfer p 3469 N94-30647
LASSO experiment: Intercalibrations of the LASSO ranging stations p 3297 N94-30666
OCA APPLIED OPTICS, INC., GARDEN GROVE, CA.
Miniature wide field-of-view star trackers for spacecraft attitude sensing and navigation p 3144 N94-29794
OFFICE OF RESEARCH ANALYSES, OTTAWA (ONTARIO).
Addendum to the final report for the investigation of proof techniques within the EVES verification technology [TR-93-5451-03] p 3421 N94-30155
OFFICE OF THE UNDER SECRETARY OF DEFENSE (ACQUISITIONS), WASHINGTON, DC.
DOD Electronic Commerce (EC)/Electronic Data Interchange (EDI) in contracting report [AD-A275298] p 3242 N94-28874
OHARA CORP., NAGAOKA (JAPAN).
A newly developed snow vehicle (SM100S) for Antarctica. Part 2: Design of the system p 3314 N94-29982
A newly developed snow vehicle (SM100S) for Antarctica. Part 5: Result of general performance tests p 3314 N94-29985
OHIO STATE UNIV., COLUMBUS.
Boundary layers induced by three-dimensional vortex loops [AD-A275678] p 3270 N94-28665
Atomic-scale friction measurements using friction force microscopy. Part 2: Application to magnetic media [AD-A275202] p 3298 N94-29290
Cellular polarity and interactions in plant graviperception [NASA-CR-195261] p 3385 N94-29943
Plane strain finite element analysis of sheet forming operations including bending effects p 3322 N94-30354
Further investigation of curve veering phenomena p 3460 N94-30515
Photochemistry in constrained spaces: Zeolites and layered double metal hydroxides [DE94-004958] p 3200 N94-30769
Potential of the ramjet engine for hypersonic flight speeds p 3153 N94-30935
OHIO UNIV., ATHENS.
A photoemission electron microscope investigation of chemical vapor deposition diamond films and diamond nucleation p 3215 N94-29745
Free-floating dual-arm robots for space assembly [AIAA PAPER 94-1195-CP] p 3442 N94-30546
OKLAHOMA STATE UNIV., STILLWATER.
Chemical dynamics studies of reactions in energetic materials [AD-A275607] p 3224 N94-28769
OKLAHOMA UNIV., NORMAN.
Dynamics of tornado-like vortices p 3371 N94-29753
The incorporation and initialization of cloud water/ice in an operational forecast model p 3373 N94-29814
A Tevatron collider beauty factory [DE94-004879] p 3488 N94-29930
An investigation of fatigue crack propagation under mode 1 and mixed mode 1/2 loadings p 3323 N94-30814
OLD DOMINION UNIV., NORFOLK, VA.
Polymer infiltration studies [NASA-CR-195729] p 3213 N94-28748
A new method for recognizing quadric surfaces from range data and its application to telerobotics and automation, final phase [NASA-CR-195733] p 3408 N94-28825
Conceptual radiometer design studies for Earth observations from low Earth orbit [NASA-CR-4588] p 3329 N94-29098
Review of sonic fatigue technology [NASA-CR-4587] p 3479 N94-29407
The 1992-1993 advanced design program. Part 1: The Mars methane engine project. Part 2: The Mars oxygen processor new furnace [NASA-CR-195513] p 3299 N94-29409
OMITRON, INC., GREENBELT, MD.
Camera artifacts in IUE spectra [NASA-CR-189337] p 3198 N94-29857
OREGON GRADUATE INST. OF SCIENCE AND TECHNOLOGY, BEAVERTON.
Object-oriented database support for scientific data management: A system for experimentation p 3531 N94-29677
Exact spherical wave solutions to Maxwell's equations with applications p 3252 N94-29733
OREGON INST. OF TECH., KLAMATH FALLS.
Geothermal direct-heat utilization assistance [DE94-005831] p 3340 N94-30700
OREGON UNIV., EUGENE.
Crystallization of silver chromate from ethanol via salt metathesis reactions of solubilized precursors [AD-A275178] p 3189 N94-29058
A study of white dwarf radiative accretion shocks p 3544 N94-29731
Quantum interference phenomena and novel switching in split gate high electron mobility transistors p 3266 N94-29734
ORTECH INTERNATIONAL, MISSISSAUGA (ONTARIO).
Proceedings of the 1993 Windsor Workshop on Alternative Fuels [DE94-003908] p 3226 N94-30612
OSAKA PREFECTURE UNIV., SAKAI (JAPAN).
Numerical analysis of sonic boom in the near field p 3125 N94-28962
Three-dimensional external flow computations using prismatic grid p 3127 N94-28979
OSAKA UNIV., TOYONAKA (JAPAN).
Fabrication of electronic materials in space p 3228 N94-28942
OSBORNE (ALLEN) ASSOCIATES, WESTLAKE VILLAGE, CA.
Ionospheric corrections to precise time transfer using GPS p 3145 N94-30677
OTTAWA UNIV. (ONTARIO).
Partially coherent detection of PSK signals in Rician channels [ISBN-0-315-85799-4] p 3254 N94-30031
New evidence for flux cutting in type II superconductors [ISBN-0-315-85830-3] p 3515 N94-30032
Position control of a flexible beam with active damping of vibrations [ISBN-0-315-85841-9] p 3321 N94-30033
Investigations of dispersion characteristics of microwave/optical guided wave structures by using transmission line matrix method [ISBN-0-315-85856-7] p 3254 N94-30034
M-interference queue analysis by decomposition method [ISBN-0-315-85795-1] p 3453 N94-30139
Photoelectronic study of GaAs epilayers and In(x)Ga(1-x)As/GaAs quantum wells [ISBN-0-315-85756-0] p 3518 N94-30239
Digital pulse compression and its application in reducing radar interference [ISBN-0-315-85767-6] p 3255 N94-30240
Formulas of the Runge-Kutta-Nystroem type [ISBN-0-315-85774-9] p 3454 N94-30241
Procedures for basic inverse problems: Black body radiation problem and phonon density of states problem [ISBN-0-315-85757-9] p 3525 N94-30244
Encoding technique for automated guided vehicle POSE recovery in a structured environment p 3144 N94-30286
Motion control of mobile robots p 3310 N94-30309
OXFORD UNIV. (ENGLAND).
Improved QCD sum rule estimates of the higher twist contributions to polarised and unpolarised nucleon structure functions [PB94-138112] p 3487 N94-29161

P

PACIFIC NORTHWEST LAB., RICHLAND, WA.
User-centered guidelines for environmental management [DE94-004313] p 3341 N94-28454
New parameters for characterizing turbulence at a potential wind site [DE94-004355] p 3368 N94-28455
Relationship between swelling and irradiation creep in cold-worked PCA stainless steel irradiated to approximately 178 dpa at approximately 400 C [DE94-004368] p 3201 N94-28456
Radiation effects in beryllium used for plasma protection [DE94-004599] p 3201 N94-28460
Frequency-domain transfer-function identification using Chebyshev polynomials [DE94-004777] p 3451 N94-28739
The MSRC ab initio methods benchmark suite: A measurement of hardware and software performance in the area of electronic structure methods [DE94-006428] p 3514 N94-30001
Triple Diagonal modeling: A mechanism to focus productivity improvement for business success [DE94-004309] p 3527 N94-30041
Induced crystallization in CW laser-irradiated sol-gel deposited titania films [DE94-006527] p 3207 N94-30062
Bench-scale synthesis of nanoscale materials p 3240 N94-30473
Applicability of digital terrain analyses to wind energy prospecting and siting [DE94-004363] p 3374 N94-30587
Preliminary detector design ST862-prototype neutron detector [DE94-004714] p 3491 N94-30695
PARAMAX SYSTEMS CORP., LANHAM, MD.
NASA Parts Project Office: Basic goals p 3166 N94-28703
PENNSYLVANIA STATE UNIV., UNIVERSITY PARK.
In situ detection of tropospheric OH and HO2 by laser-induced fluorescence in a detection chamber at low pressure p 3342 N94-28589
Sputtering of single crystals: Experimental evidence of the ejection process [AD-A275819] p 3512 N94-28775
A modeling study of the effect of stress state on void linking during ductile fracture [AD-A275505] p 3317 N94-28811
A study of solid propellants using a microprobe mass spectrometer system [AD-A275325] p 3224 N94-28879
Boundary layer coherent structures [AD-A275007] p 3272 N94-29195
The effect of incomplete fuel-air mixing on the lean limit and emissions characteristics of a Lean Prevaporized Premixed (LPP) combustor p 3193 N94-29265
A review of signal detection using the bispectrum with applications in underwater acoustics [AD-A275227] p 3478 N94-29388
SAR-related stress variability in the Marine Atmospheric Boundary Layer (MABL) [AD-A275275] p 3377 N94-29436
Brief summary of accomplishments since our DOE-sponsored radon project commenced [DE94-004643] p 3348 N94-29926
A coupled approach to spatially derived parameters necessary for ecosystem modeling on the North Slope of Alaska: Appendix A [DE94-005853] p 3349 N94-30046
Four-dimensional data assimilation using the adjoint method p 3455 N94-30353
The enhancement of compressible turbulent mixing via streamwise vorticity p 3280 N94-30487
Experiments on the aerodynamic generation of noise in centrifugal turbomachinery p 3480 N94-30804
PENNSYLVANIA UNIV., PHILADELPHIA.
North American jumelage 'type systems' [AD-A275342] p 3411 N94-29214
PHILIPS GLOEILAMPENFABRIEKEN N.V., EINDHOVEN (NETHERLANDS).
Adhesion of electrolessly deposited Ni(P) on alumina ceramic [ETN-94-95358] p 3212 N94-28539
PHILLIPS LAB., EDWARDS AFB, CA.
The universal applications of microtubes and microtube composites p 3186 N94-30452
PHILLIPS LAB., HANSCOM AFB, MA.
SHARC, a model for calculating atmospheric and infrared radiation under non-equilibrium conditions [AD-A275207] p 3357 N94-28893
PHYSICS AND ELECTRONICS LAB. TNO, THE HAGUE (NETHERLANDS).
The influence of the evaporation duct on the angle of arrival and amplitude of the backscattered signal from targets low above the sea p 3256 N94-30498
Experimental evaluation of camouflage effectiveness in the thermal infrared p 3257 N94-30502
PITTSBURGH UNIV., PA.
Organic materials that respond to molecules [AD-A275392] p 3174 N94-29307
Studies of supported molybdenum and tungsten [DE94-006207] p 3210 N94-30839
POLITECNICO DI MILANO (ITALY).
ELF: Learning incomplete fuzzy rule sets for an autonomous robot [REPT-93-043] p 3449 N94-30923
Theoretical and experimental analysis of a new algorithm for the Euclidean 1-center problem [REPT-93-045] p 3429 N94-30924
Heuristic algorithms for static and dynamic problems of locating the center and the barycenter of a graph [REPT-93-050] p 3429 N94-30925
Optimization techniques for a dial-a-ride transportation system in urban environment [REPT-93-051] p 3537 N94-30926
View integration: A survey of current developments [REPT-93-053] p 3536 N94-30927
Federal grammars and modular compilers [REPT-93-054] p 3429 N94-30928
Measuring the impact of investments in information technologies on business performance [REPT-93-056] p 3536 N94-30929
A low noise silicon detector preamplifier system for room temperature x ray spectroscopy [REPT-93-058] p 3291 N94-30930

An UIO-based method for protocol conformance testing
[REPT-93-060] p 3429 N94-30931
Realization of function logics by means of transmission gate
[REPT-93-061] p 3429 N94-30936
Identification of the damping ratio relationship of an autovehicle suspension
[REPT-93-063] p 3313 N94-30937
Application of the extended Kalman filter to the estimation of the char mass in a fluidized bed combustor
[REPT-93-065] p 3200 N94-30938
Some methodological issues about designing autonomous agents which learn their behaviors: The ELF experience
[REPT-93-068] p 3449 N94-30939
MPEG-2 video decoding architecture: Analysis and design
[REPT-93-069] p 3260 N94-30940
A neural network-based technique for structural identification of SISO systems
[REPT-93-076] p 3449 N94-30941
Iterative removal of boundary minima of harmonic potential function for mobile robot navigation
[REPT-93-059] p 3449 N94-30962

POLYTECHNIC UNIV., BROOKLYN, NY.
Experimental investigation of three-dimensional vortex-airfoil interaction in a supersonic stream
[AD-A275107] p 3122 N94-28899

PORTLAND STATE UNIV., OR.
Tropospheric HO determination by FAGE
p 3342 N94-28590
Tropospheric HO2 determination by FAGE
p 3345 N94-28606

PRATT AND WHITNEY AIRCRAFT, EAST HARTFORD, CT.
Thermal/structural tailoring of engine blades (T/SEAEBL). Theoretical manual
[NASA-CR-194462] p 3317 N94-28815
Reduction of NO(x) by fuel-staging in gas turbine engines: A commitment to the future
p 3194 N94-29272

PRATT AND WHITNEY AIRCRAFT, WEST PALM BEACH, FL.
High temperature fuel requirements and payoffs
p 3192 N94-29259

PRATT AND WHITNEY AIRCRAFT OF CANADA LTD., MISSISSAUGA (ONTARIO).
Recent CFD applications in small gas turbine combustion systems development p 3154 N94-29257
Design aspects in small aircraft gas turbine fuel injectors p 3154 N94-29264

PRINCETON UNIV., NJ.
Surface structure and stereochemical properties of self-assembled monolayer materials
[DE94-004960] p 3484 N94-28578
Fuels combustion research
[AD-A275122] p 3189 N94-29004
Computer simulation of molecular interactions in supercritical solvents
[AD-A274977] p 3486 N94-29087
Air traffic management as principled negotiation between intelligent agents p 3137 N94-29562
Downstream development of baroclinic waves
p 3372 N94-29796
Sensitivity and feedbacks associated with vegetation-related land surface parameters in a general circulation model p 3348 N94-29800
Wall pressure fluctuations in the reattachment region of a supersonic free shear layer
[NASA-CR-195790] p 3132 N94-29920
An absolute measurement of the cosmic background radiation temperature at 1.4 GHz p 3553 N94-30351
Towards coupled physical-biogeochemical models of the ocean carbon cycle p 3350 N94-30618

PUGET SOUND UNIV., TACOMA, WA.
A toy model of sea ice growth p 3351 N94-30626

PURDUE UNIV., WEST LAFAYETTE, IN.
Toward a model of expert knowledge structure and their role in cognitive task performance
[AD-A275641] p 3529 N94-28645
Toward a molecular scale understanding of frost heaving, phase 1
[AD-A275446] p 3356 N94-28882
Free edge and size effects on failure initiation and ultimate strength of laminates containing a center hole
p 3181 N94-29735
Integrated propulsion-airframe dynamics and control
p 3147 N94-29854
Transient thermal fatigue of ceramic composites
p 3216 N94-29874
Time-marching aeroelastic and spatial adaptation procedures on triangular and tetrahedral meshes using an unstructured-grid Euler method p 3131 N94-29877
Collision avoidance and control of multiple revolute manipulators p 3302 N94-29884
A study of the convergence of spherical harmonic expansions of gravity using distributed point-mass Earth models p 3362 N94-29909
Motion and development of the Pacific Plate from the Middle Jurassic to the Late Cretaceous
p 3362 N94-29939
Spectral analysis of wave propagation in connected waveguides p 3277 N94-29944
Reactions of metal ions and their clusters in the gas phase using laser ionization: Fourier transform mass spectrometry
[DE94-006208] p 3207 N94-30024
Deexcitation processes in nuclear reactions: The study of hot hadronic matter
[DE94-003396] p 3492 N94-30836

PURUS, INC., SAN JOSE, CA.
A commercialized, continuous flow fiber optic sensor for trichloroethylene and haloforms
p 3502 N94-30462

Q

QUADRAX ADVANCED MATERIALS SYSTEMS, INC., PORTSMOUTH, RI.
3-D braided, continuous fiber ceramic composites produced by chemical vapor infiltration
[AD-A275192] p 3178 N94-29024

R

RADEX, INC., BEDFORD, MA.
SOCRATES simulation of the emission at wavelength 6300 A generated by the interaction between the atmosphere and the Space Shuttle exhaust
[AD-A275567] p 3164 N94-28827

RAMSEARCH CO., CROFTON, MD.
The influence of temperature on microelectronic device failure mechanisms, phase 2
[AD-A275029] p 3265 N94-29511

RAUMFAHRT SYSTEMTECHNIK G.M.B.H., SALEM (GERMANY).
Ground independent landing system
p 3137 N94-29564

RAYTHEON CO., LEXINGTON, MA.
RF vacuum microelectronics
[AD-A275221] p 3263 N94-28915

RAYTHEON CO., WALTHAM, MA.
A transportronic solution to the problem of interorbital transportation
[NASA-CR-191152] p 3164 N94-29355

REMOTE SENSING TECHNOLOGY CENTER, TOKYO (JAPAN).
Proceedings of the International Symposium on Remote Sensing
[JTN-94-80578] p 3325 N94-28925
JERS-1 data acquisition and distribution
p 3326 N94-28931
Proceedings of the 15th Earth Observation Symposium
[JTN-94-80607] p 3328 N94-29036
Principles and application tendency of remote sensing: Its principle, function and utilization
p 3328 N94-29037

RENSSELAER POLYTECHNIC INST., TROY, NY.
Modeling the total dose radiation effects of Hg(1-x)Cd(x)Te photodiodes using numerical device simulators
[AD-A275235] p 3263 N94-29028
Nonadiabatic effects in the quantum Hall regime
p 3513 N94-29530
Using Cf-252 for single event upset testing
p 3496 N94-30219
Effects of hydrogen on the resistivity of thin Au and Cu films p 3218 N94-30225
A performance analysis method for distributed real-time robotic systems: A case study of remote teleoperation
[AIAA PAPER 94-1212-CP] p 3445 N94-30563
Nonlinear multibody formulation for rotorcraft analysis
p 3149 N94-30787

RESEARCH TRIANGLE INST., RESEARCH TRIANGLE PARK, NC.
Development of large area RF induction plasma for cost effective diamond
[AD-A275888] p 3504 N94-28776

RHODE ISLAND UNIV., KINGSTON.
Gordon research conference on optical signal processing and holography
[AD-A275092] p 3499 N94-28848
The long-range transport of aerosol particles over the North Atlantic Ocean p 3366 N94-30867

RICE UNIV., HOUSTON, TX.
A survey of NASA and military standards on fault tolerance and reliability applied to robotics
[AIAA PAPER 94-1211-CP] p 3445 N94-30562

ROBERT GORDON'S INST. OF TECH., ABERDEEN (SCOTLAND).
Medical support for British operations in the Antarctic
p 3379 N94-28421

ROBOTIC SYSTEMS TECHNOLOGY, WESTMINSTER, MD.
Design of an autonomous exterior security robot
[AIAA PAPER 94-1188-CP] p 3441 N94-30538

ROBOTIC TECHNOLOGY, INC., POTOMAC, MD.
Autonomous intelligent military robots: Army ants, killer bees, and cybernetic soldiers p 3304 N94-30276

ROCHESTER UNIV., NY.
Low energy ion-molecule reactions and chemiionization kinetics
[DE94-005414] p 3481 N94-28491
An investigation of distributed coupling in a nonlinear semiconductor waveguide p 3246 N94-29529
Longitudinal effects and intensity-phase coupling in distributed feedback semiconductor lasers
p 3294 N94-29590
On observing neutron star oscillations
p 3538 N94-29795

ROCKWELL INTERNATIONAL CORP., CANOGA PARK, CA.
Composite load spectra for select space propulsion structural components
[NASA-CR-194476] p 3316 N94-28508

ROCKWELL INTERNATIONAL CORP., COLORADO SPRINGS, CO.
Cesium and rubidium frequency standards status and performance on the GPS program p 3145 N94-30663

ROLLS-ROYCE LTD., BRISTOL (ENGLAND).
Combustion for future supersonic transport propulsion
p 3190 N94-29249

ROME LAB., GRIFFISS AFB, NY.
Guide to the Environmental-Language
[AD-A275849] p 3408 N94-28784
Photonic devices and systems for optical signal processing
[AD-A275818] p 3498 N94-28804
Artificial intelligence technology program at Rome Laboratory p 3414 N94-29328
Rome Laboratory software engineering technology program p 3414 N94-29330

ROME LAB., HANSCOM AFB, MA.
RL/ERCT automated swept-angle bistatic measurement system
[AD-A275763] p 3241 N94-28763

ROYAL AIR FORCE, FARNBOROUGH (ENGLAND).
Prediction of survival times on land in a cold climate
p 3379 N94-28423
Thermal strain generated by an enhanced anti-G protection system in a hot climate p 3383 N94-28445
Implications of climatic extremes in aircrew NBC operations p 3383 N94-28446

ROYAL DANISH NAVY, GENTOFTE.
Thermoregulation in the extreme cold environment
p 3381 N94-28438

ROYAL MILITARY ACADEMY, BRUSSELS (BELGIUM).
Knowledge combination and data fusion with application to recognition systems p 3259 N94-30513

ROYAL MILITARY COLL. OF CANADA, KINGSTON (ONTARIO).
Acoustic emission monitoring of aging aircraft structures
[DREP-93-17] p 3148 N94-30129
Enhanced fatigue crack detection in aging aircraft using continuous acoustic emission monitoring
[DREP-93-16] p 3148 N94-30131
An optimal obstacle avoidance path planning algorithm for the Excalibur robot p 3306 N94-30287
Simulation of lightweight robots and their controllers
p 3307 N94-30294
The response of flexible manipulators to a new computed torque control strategy: Simulation results
p 3308 N94-30295
Improving the execution speed of robot control computations: An allocation scheme for heterogeneous multiprocessors p 3310 N94-30308
Electrochemical Power Source (EPS) selection for Energetically Independent Robots (EIR): A systematic approach p 3269 N94-30312

ROYAL NAVAL HOSPITAL, HASLAR (ENGLAND).
A comparison of four methods of rewarming individuals cooled by immersion in cold water p 3382 N94-28442

ROYAL NORWEGIAN COUNCIL FOR SCIENTIFIC AND INDUSTRIAL RESEARCH, KJELLER.
The Norwegian seismic array (NORSAR), phase 3
[AD-A275440] p 3356 N94-28868

RUSH-PRESBYTERIAN-SAINT LUKE'S MEDICAL CENTER, CHICAGO, IL.
Circadian countermeasures for shiftworkers during USMP-2: A report to mission management
[NASA-CR-195260] p 3402 N94-30188

RUSSIAN INST. OF RADIONAVIGATION AND TIME, SAINT PETERSBURG.
Using GLONASS signal for clock synchronization
p 3475 N94-30680
RUTGERS - THE STATE UNIV., NEW BRUNSWICK, NJ.
A class of inclusion problems for the strengthening of brittle and ductile composites p 3186 N94-30959
RUTHERFORD APPLETON LAB., CHILTON (ENGLAND).
Role of satellite observations of sea-surface temperature in the detection of global change
[PB94-138120] p 3329 N94-29107
Operation semantics with read and write frames
[PB94-138138] p 3529 N94-29108
Model-oriented analysis of a communications protocol
[PB94-138146] p 3244 N94-29109
Invariants, frames and postconditions: A comparison of two formal specification notations
[PB94-138153] p 3405 N94-29110
Solution of augmented systems
[PB94-138211] p 3452 N94-29111
Issues in light hadron spectroscopy
[PB94-138229] p 3486 N94-29112
Double-crystal analyser system for the PRISMA spectrometer: Test of a prototype
[PB94-138245] p 3286 N94-29113
Weak decays of charged K-mesons and charm particles
[PB94-138062] p 3486 N94-29143
One-loop QCD mass effects in the production of polarized bottom and top quarks
[PB94-138104] p 3487 N94-29145
Improved QCD sum rule estimates of the higher twist contributions to polarised and unpolarised nucleon structure functions
[PB94-138112] p 3487 N94-29161
RYUKOKU UNIV., KYOTO (JAPAN).
Cosmic energy equipment p 3229 N94-28945

S

SAINT MARIANNA UNIV., KAWASAKI (JAPAN).
Shortening velocity and calcium sensitivity of single fibers from hindlimb suspended muscle in rats
p 3387 N94-29866
SAN JOSE STATE UNIV., CA.
Correlation studies of Pioneer Venus imagery obtained from PV experiments with near IR imagery obtained from ground-based observations during Venus inferior conjunction
[NASA-CR-195772] p 3550 N94-29892
SANDIA NATIONAL LABS., ALBUQUERQUE, NM.
Holographic interferometry: A user's guide
[DE94-003136] p 3286 N94-28466
BAG: A code for predicting the performance of a gas bag impact attenuation system for the Pathfinder lander
[DE94-003688] p 3165 N94-28477
Reactor-pumped laser experimental results
[DE94-005247] p 3292 N94-28482
Response of GaAs charge storage devices to transient ionizing radiation
[DE94-005273] p 3510 N94-28484
SAFSIM theory manual: A computer program for the engineering simulation of flow systems
[DE94-005381] p 3270 N94-28488
Battery energy and superconducting magnetic energy storage for utility applications: A qualitative analysis
[DE94-005382] p 3336 N94-28489
Identification of components to optimize improvement in system reliability
[DE94-001601] p 3315 N94-28503
Alkylene-bridged polygerm- and polygermsilsesqui-oxanes: New hybrid organic-inorganic materials
[DE94-005096] p 3174 N94-28557
Solubility of Nd in brine
[DE94-005099] p 3187 N94-28567
Performance of the Southern California Edison Company Stirling dish
[DE94-004676] p 3337 N94-29018
Algorithms for treating redundancy in repairable and non-repairable systems
[DE94-005289] p 3315 N94-29020
Effects of oxide charge and surface recombination velocity on the excess base current of BJT's
[DE94-003711] p 3263 N94-29025
Inorganic polymer-derived ceramic membranes
[DE94-000082] p 3216 N94-29830
Extending the X Window System
[DE94-006496] p 3420 N94-29844
A non-contacting vertical alignment system for mass properties measuring instruments
[DE94-004680] p 3289 N94-29927
Logistics for the implementation of lead-free solders on electronic assemblies
[DE94-004800] p 3206 N94-29936
ECR plasma synthesis of silicon nitride films on GaAs and InSb
[DE94-005575] p 3515 N94-30006
The organometallic chemical vapor deposition of transition metal carbides: The use of homoleptic alkyls
[DE94-005577] p 3206 N94-30007
Polynomial modeling of analog-to-digital converters
[DE94-005579] p 3406 N94-30008
Charge trapping and breakdown in N2O oxides
[DE94-003775] p 3266 N94-30040
Non-chromate talc conversion coatings for aluminum
[DE94-005281] p 3207 N94-30053
Nearly time-optimal feedback control of a magnetically levitated photolithography positioning system
[DE94-005288] p 3266 N94-30055
Smart Document System (SDS) used in managing DOE order's with electronic Engineering Procedures
[DE94-005076] p 3534 N94-30099
Novel techniques applied to polymer lifetime predictions
[DE94-005095] p 3218 N94-30102
Electrooptical and optical evaluation of Pb(Zr,Ti)O3 thin films using waveguide refractometry
[DE94-006374] p 3518 N94-30247
Neural network based time-optimal control of a magnetically levitated precision positioning system
[DE94-006573] p 3437 N94-30250
Direct measurement of the reactivity of NH and OH on a silicon nitride surface
[DE94-005286] p 3199 N94-30260
Optoelectronic packaging activities at Sandia National Laboratories
[DE94-005287] p 3501 N94-30261
Kinetics of surface roughening and smoothing during ion sputtering
[DE94-006358] p 3219 N94-30263
Space debris removal using a high-power ground-based laser
[DE94-006363] p 3169 N94-30264
Reactor-pumped laser facility at DOE's Nevada Test Site
[DE94-006371] p 3295 N94-30265
Densification and crystallization of zirconia thin films prepared by sol-gel processing
[DE94-005573] p 3518 N94-30315
The growth of InAsSb/InGaAs strained-layer superlattices by metal-organic chemical vapor deposition
[DE94-005576] p 3518 N94-30316
Fission-activated laser as primary power for CW laser propulsion
[DE94-006138] p 3295 N94-30367
Self-stressing test structures used for high-frequency electromigration
[DE94-006142] p 3267 N94-30368
Using generic tool kits to build intelligent systems
[AIAA PAPER 94-1214-CP] p 3445 N94-30565
Simulation of composite material response under dynamic compressive loading
[DE94-005272] p 3184 N94-30589
Properties of chemical vapor infiltration diamond deposited in a diamond powder matrix
[DE94-005429] p 3220 N94-30591
Strain relaxation and surface roughness as a function of growth temperature in linearly graded In(x)Al(1-x)As (x = 0.05 to 0.25) buffers
[DE94-005430] p 3519 N94-30592
Crystalline-silicon solar cell development sponsored by the US Department of Energy
[DE94-003783] p 3340 N94-30609
XCHEM-1D: A heat transfer/chemical kinetics computer program for multilayered reactive materials
[DE94-005072] p 3226 N94-30615
Modeling data throughput on communication networks
[DE94-005077] p 3260 N94-30772
A comparison of the evolution of cold and hot deformation microstructures and textures in fcc metals
[DE94-005103] p 3210 N94-30777
Delamination of woven E-glass fabric composites
[DE94-003227] p 3185 N94-30827
Photonics at Sandia National Laboratories: From research to applications
[DE94-006463] p 3501 N94-30828
Solar photovoltaics for development applications
[DE94-006116] p 3340 N94-30843
Fuzzy-algebra uncertainty analysis for abnormal-environment safety assessment
[DE94-006257] p 3462 N94-30849
Surface chemistry of boron-doped SiO2 CVD: Enhanced uptake of tetraethyl orthosilicate by hydroxyl groups bonded to boron
[DE94-005428] p 3221 N94-30896
Measurement of bulk longitudinal modulus and correction for edge effects
[DE94-005581] p 3222 N94-30900
Thermochemical data for CVD modeling from ab initio calculations
[DE94-005269] p 3222 N94-30909
Standard testing procedures for optical fiber and unshielded twisted pair at Sandia National Laboratories
[DE94-005315] p 3501 N94-30910
SANDIA NATIONAL LABS., LIVERMORE, CA.
Insensitive energetic materials: The importance of physical properties and molecular structure
[AD-A275393] p 3225 N94-29308
In-cylinder gas velocity measurements comparing crankcase and blower scavenging in a fired two-stroke cycle engine
[DE94-005752] p 3311 N94-30596
SANTA FE INST., NM.
Research activities of Martin C. Casdagli at SFI September 1989--May 1991
[DE94-005655] p 3463 N94-28548
The lectures in complex systems, volume 5
[AD-A275458] p 3466 N94-28807
SAO PAULO UNIV. (BRAZIL).
Dust in the Small Magellanic Cloud
[NASA-CR-195764] p 3543 N94-29696
SASKATCHEWAN UNIV., SASKATOON.
Higher order collisionless ballooning mode in tokamaks
[PPL-143] p 3507 N94-30156
Eigenmode analysis of the destabilized ion acoustic mode in tokamaks
[PPL-142] p 3507 N94-30158
Beta enhancement of thermal diffusivity in tokamaks
[PPL-141] p 3508 N94-30159
SATCON TECHNOLOGY CORP., CAMBRIDGE, MA.
Integrated microgyroscope p 3239 N94-29789
SCIENCE APPLICATIONS INTERNATIONAL CORP., SAN DIEGO, CA.
Initial wave-type identification with neural networks and its contribution to automated processing in IMS version 3.0
[AD-A275058] p 3359 N94-29137
SCIENCE APPLICATIONS INTERNATIONAL CORP., SANTA BARBARA, CA.
Evolution of miniature detectors and focal plane arrays for infrared sensors p 3237 N94-29781
SCIENCE UNIV. OF TOKYO (JAPAN).
Analysis of 3-D acoustic problems using boundary element method p 3127 N94-28974
SCIENTIFIC RESEARCH ASSOCIATES, INC., GLASTONBURY, CT.
Fluid dynamic noise in a centrifugal pump
[AD-A275264] p 3477 N94-28904
CFD analyses for advanced pump design
[NASA-CR-194866] p 3300 N94-29550
SELSKAPET FOR INDUSTRIELL OG TEKNISK FORSKNING, TRONDHEIM (NORWAY).
Hypra/TR: A tuple oriented recovery method for a continuously available distributed DBMS on a shared nothing multi-computer
[PB94-141264] p 3533 N94-29921
Electromagnetic effect on turbulent transport in liquid metals and electrolytes (bath)
[PB94-138450] p 3206 N94-29946
New inoculants for ductile cast iron
[PB94-138476] p 3206 N94-29947
Secure network databases: Survey and analysis
[PB94-138492] p 3533 N94-29948
Strategy for the approximation of large scattered data sets
[PB94-138518] p 3420 N94-29949
Maintaining acceptable thermal comfort with a low air temperature by means of local heating
[PB94-138526] p 3401 N94-29950
Progress report for the PTUF Project-93 Q1 and Q2
[PB94-138591] p 3431 N94-29995
Microgravity compatible drive system-rider. New technologies
[PB94-138583] p 3229 N94-29996
Melt flow during alloy solidification: Dimensional analysis and model problems
[PB94-138625] p 3206 N94-29997
Large heat pumps using CO2 refrigerant
[PB94-138773] p 3279 N94-29999
Control of heating, ventilation and air conditioning (HVAC) systems
[PB94-138807] p 3401 N94-30000
Splines and ocean wave modelling
[PB94-139409] p 3378 N94-30002
Volume averaged model for the mechanics of alloys solidification
[PB94-138617] p 3208 N94-30113
SHAANXI ASTRONOMICAL OBSERVATORY, LINTONG (CHINA).
The two-way time synchronization system via a satellite voice channel p 3471 N94-30658

SHAPE TECHNICAL CENTER, THE HAGUE (NETHERLANDS).
Designing and maintaining decision-making processes p 3412 N94-29318
Use of GPS in automated air traffic control p 3137 N94-29563
ACCS Surveillance Exploratory Prototype (ASEP) p 3138 N94-29566
SHARK GROUP OF COMPANIES, MORPETH (ENGLAND).
Advanced integrated cold protection for aircrew p 3381 N94-28436
SHIMIZU CORP. (JAPAN).
Three dimensional simulation of compressible flow induced by a high-speed train moving into a tunnel p 3126 N94-28967
Study of modeling of turbulence of renormalization group analysis p 3126 N94-28970
SIGMA LABS., INC., TUCSON, AZ.
Plasma treatment of polymer dielectric films to improve capacitive energy storage p 3223 N94-30479
SIMULOG, VALBONNE (FRANCE).
Finite element method for numerical simulation of turbulent flows. The N3S code p 3233 N94-29612
SOCIETE DE FABRICATION D'INSTRUMENTS DE MESURE, MASSY (FRANCE).
Performing specifications for complex systems' software p 3155 N94-29317
SOCIETE DES ELECTRICIENS ET ELECTRONICIENS, PARIS (FRANCE).
Electrical engineering and industrial electronics education days: Control of asynchronous generators [PB94-135514] p 3266 N94-29523
SOCIETE NATIONALE D'ETUDE ET DE CONSTRUCTION DE MOTEURS D'AVIATION, MOISSY-CRAMAYEL (FRANCE).
Aerothermochemical calculations in afterburners p 3154 N94-29258
Chambers of turboreactors with variable geometry: A response to the matrix of pollution in cycles at high temperature, high pressure p 3194 N94-29273
SOCIETY OF MEDICAL RESEACRH FOR SPACE STATION, NAGOYA (JAPAN).
The MERSS 5th Symposium on Space Medicine: Medical and Physiological Experiment Utilizing Parabolic Flight [JTN-94-80588] p 3392 N94-29709
SOFTEK SYSTEMS, INC., TOKYO (JAPAN).
Upwind method using local interpolation p 3128 N94-28982
SOFTWARE KINETICS LTD., STITTSVILLE (ONTARIO).
Data fusion and correlation techniques testbed development audio processing study [SKD-1600-73-014] p 3241 N94-28532
Data fusion and correlation techniques testbed development. Phase 1: Interim report [SKD-1600-73-015] p 3405 N94-28533
SOFTWARE PRODUCTIVITY CONSORTIUM, HERNDON, VA.
Using RDD-100 with CoRE. Version 01.00.03 [AD-A275336] p 3419 N94-29797
SOLOMON (G.), PASADENA, CA.
Convolutional encoding of self-dual codes p 3250 N94-29662
SOUTH CAROLINA UNIV., COLUMBIA.
Analyses of stationary and growing crack tip deformation by digital image processing p 3320 N94-29690
Higher order asymptotic crack tip fields in a power-law hardening material p 3321 N94-29829
SOUTHEASTERN CENTER FOR ELECTRICAL ENGINEERING EDUCATION, INC., SAINT CLOUD, FL.
Remote control of transcranial Doppler (TCD) probe during centrifuge exposures up to 9 +Gz [AD-A275253] p 3400 N94-29029
SOUTHERN COLORADO STATE COLL., PUEBLO.
Investigation of advanced fault insertion and simulator methods [NASA-CR-195241] p 3261 N94-28511
SOUTHWEST RESEARCH INST., SAN ANTONIO, TX.
Impact study on the use of biomass-derived fuels in gas turbines for power generation [DE94-000261] p 3224 N94-28502
SOUTHWEST SCIENCES, INC., SANTA FE, NM.
Near-IR diode laser absorption for measurement of tropospheric HO2 p 3345 N94-28607
SPACE INDUSTRIES, INC., LEAGUE CITY, TX.
Retention latch mechanism for the Wake Shield Facility p 3161 N94-29635
SPACE OPTICS RESEARCH LABS., INC., CHELMSFORD, MA.
Deformed ellipsoidal diffraction grating blank [NASA-CR-189334] p 3289 N94-29872
SPACE POWER, INC., SAN JOSE, CA.
Non-isolated 30 kW class arcjet PCU [NASA-CR-189148] p 3173 N94-29444
SPANISH AIR FORCE, TALAVERA AFB.
Work conditions assessment in pilots and ground personnel under high weather temperatures p 3382 N94-28444
SPAR AEROSPACE LTD., BRAMPTON (ONTARIO).
On-orbit spacecraft servicing: An element in the evolution of space robotics applications [AIAA PAPER 94-1236-CP] p 3448 N94-30583
SPIRE CORP., BEDFORD, MA.
Laser beam steering with semiconductor waveguide [AD-A275775] p 3292 N94-28765
SPRINGBORN LABS., INC., ENFIELD, CT.
Advanced development of PV encapsulents [DE94-000219] p 3336 N94-28500
SRI INTERNATIONAL CORP., MENLO PARK, CA.
Local Measurement of Tropospheric HO(x) [NASA-CP-3245] p 3342 N94-28587
An improved method of measuring tropospheric NO2, NO3, HO2, and RO2 by Matrix Isolation and Electronic Spin Resonance (MIESR) p 3345 N94-28605
Predissociation in N2(C'4, 1 Sigma u +) and other N2 states and its importance in the atmospheres of Titan and Triton [NASA-CR-195727] p 3549 N94-28816
Microstructure/property relationships for SCS6/Timetal 21-S composite [AD-A275056] p 3178 N94-29135
Novel mass spectrometric instrument for gaseous and particulate characterization and monitoring [DE94-005896] p 3349 N94-30047
STANFORD LINEAR ACCELERATOR CENTER, CA.
Linac Coherent Light Source (LCLS) at 2-4 nm using the SLAC linac [DE94-005235] p 3292 N94-28481
A measurement of the LMP effect [DE94-005225] p 3482 N94-28493
Energy distribution of the leptons in top decay to charged Higgs [DE94-005231] p 3482 N94-28494
Results on structure functions from fixed-target experiments [DE94-005233] p 3482 N94-28541
Determination of the neutron spin-structure function [DE94-005234] p 3483 N94-28542
Quantum-mechanical suppression of bremsstrahlung [DE94-005223] p 3497 N94-30712
STANFORD UNIV., CA.
Low voltage electron beam lithography [AD-A275648] p 3262 N94-28650
A method for the modelling of porous and solid wind tunnel walls in computational fluid dynamics codes [NASA-CR-195699] p 3270 N94-28724
Testing for a signal with unknown location and scale in a stationary Gaussian random field [AD-A275320] p 3464 N94-28876
The modified Cramer-von mises goodness-of-fit criterion for time series [AD-A275377] p 3464 N94-29014
Advanced diagnostics for reacting flows [AD-A275057] p 3272 N94-29136
High-power CW diode-laser-array-pumped solid-state lasers and efficient nonlinear optical frequency [AD-A275394] p 3293 N94-29309
Numerical study of the trailing vortex of a wing with wing-tip blowing [NASA-CR-195803] p 3130 N94-29760
The instantaneous concentration field in the self-similar region of a high Schmidt number round jet p 3278 N94-29976
Delamination growth in composites under cyclic loads p 3183 N94-30256
Damage identification in composites using built-in piezoelectrics p 3184 N94-30355
The real-world navigator [AIAA PAPER 94-1204-CP] p 3443 N94-30555
Object-based task-level control: A hierarchical control architecture for remote operation of space robots [AIAA PAPER 94-1209-CP] p 3444 N94-30560
Carbon cycling in high-latitude ecosystems p 3352 N94-30631
STARSYS RESEARCH CORP., BOULDER, CO.
Metal band drives in spacecraft mechanisms p 3162 N94-29637
STATE UNIV. OF NEW YORK, ALBANY.
The automated rotating shadowband spectroradiometer [DE94-001878] p 3269 N94-28464
Developing a diode array spectrometer for tropospheric chemistry studies p 3362 N94-29752
STATE UNIV. OF NEW YORK, BINGHAMTON.
Asymptotic coherence of gluons and of q-bosons [DE94-005417] p 3481 N94-28492
Information center assessment p 3533 N94-29855
STATE UNIV. OF NEW YORK, BUFFALO.
Breakdown testing of wiring insulation p 3166 N94-28713
Group transfer and electron transfer reactions of organometallic complexes: Summary of research accomplished in 1993 [DE94-004963] p 3200 N94-30770
STERIA MEDITERRANEE, VITROLLES (FRANCE).
Hierarchical Object Oriented Design (HOOD): Possibilities, limitations, and challenges p 3413 N94-29322
STERLING SOFTWARE, INC., BELLEVUE, NE.
AFGWC Dial-In Subsystem (AFDIS) software users manual, version 2.2 [AD-A275844] p 3371 N94-29747
STEVENS INST. OF TECH., HOBOKEN, NJ.
A numerical study of gravitational collapse p 3548 N94-30271
STOCKHOLM UNIV. (SWEDEN).
Chemical composition of insoluble particles in superimposed ice on Storoeya, Svalbard (Sweden) [CM-82] p 3336 N94-30944
Multiple weather regimes and baroclinically forced spherical resonance [DM-65] p 3376 N94-30966
Calculation of inelastic mean free path and stopping power for electrons in solids from an optical-data model [USIP-92-06] p 3494 N94-30980
SUMITOMO HEAVY INDUSTRIES LTD., TOKYO (JAPAN).
Study of bridge design and technology [PB94-137916] p 3121 N94-29160
SUOMEN AKATEMIA, HELSINKI (FINLAND).
Batch updates and concurrency in B-trees [PB94-136835] p 3530 N94-29167
SUPERCONDUCTING SUPER COLLIDER LAB., DALLAS, TX.
Some remarks about pseudo-Hamiltonian [DE94-003273] p 3487 N94-29700
SURREY UNIV., GUILDFORD (ENGLAND).
Emergency underwater breathing aids for helicopter passengers and crew p 3381 N94-28437
SURVIVAL SYSTEMS LTD., DARTMOUTH (NOVA SCOTIA).
Effect of seasickness on aircrew student survivor ability after ditching in cold water p 3379 N94-28425
SUSSEX UNIV., BRIGHTON (ENGLAND).
Development centres: Assessing or developing people [PB94-138070] p 3536 N94-29144
SVERDRUP TECHNOLOGY, INC., BROOK PARK, OH.
NASA wiring program: Survey of NASA experiences in wiring system safety p 3165 N94-28700
Evaluation of pyrolysis and arc tracking on candidate wire insulation designs for space applications p 3166 N94-28711
Structural/aerodynamic blade analyzer (SAB) user's guide, version 1.0 [NASA-CR-194460] p 3151 N94-29103
Turbomachinery forced response prediction system (FREPS): User's manual [NASA-CR-194465] p 3319 N94-29104
Thermodynamic analysis of chemical compatibility of several compounds with Fe-Cr-Al alloys [NASA-CR-191166] p 3181 N94-29684
SVERDRUP TECHNOLOGY, INC., CLEVELAND, OH.
Wiring for space applications program p 3166 N94-28708
SVERDRUP TECHNOLOGY, INC., HUNTSVILLE, AL.
Mechanical flexible joint design document [NASA-CR-193941] p 3297 N94-28419
SVERIGES LANTBRUKSUNIV., UPPSALA.
Stable RNA sequences as a tool for DNA probes and phylogenetic studies [PB94-135423] p 3385 N94-29156
SWEDISH INST. FOR MATERIALS TESTING, BORAS.
Microcomputer-based protective functions in industrial production systems: Assessment method [PB94-137817] p 3411 N94-29159
Determination of sound power levels of air terminal units according to ISO 5135-Nordic inter-laboratory tests, Nordtest project no. 968-91 [PB94-137411] p 3477 N94-29175
Unscreened low tension cables scrape abrasion testing. Part 1: An interlaboratory study on scrape abrasion testing according to ISO DP 6722-1 [PB94-135605] p 3264 N94-29191
Modelling soft impacts for vibrational excitation of civil engineering structures [PB94-137619] p 3320 N94-29681
SYSTEMS CONTROL TECHNOLOGY, INC., ARLINGTON, VA.
Rooftop emergency heliports [DOT/FAA/RD-93/2] p 3157 N94-29754
Potential hazards of magnetic resonance imagers to emergency medical service helicopter operations [DOT/FAA/RD-92/15] p 3135 N94-29862

SYSTEMS RESEARCH LABS., INC., DAYTON, OH.
Development of global/chemistry model for jet-fuel thermal stability based on observations from static and flowing experiments p 3192 N94-29262

T

TA CONSULTANCY SERVICES LTD., FARNHAM (ENGLAND).
Integrated formal verification and validation of safety critical software p 3416 N94-29338
TECHNICAL RESEARCH CENTRE OF FINLAND, ESPOO.
Frequency-domain analysis of nonlinear microwave circuits
[PB94-132024] p 3261 N94-28400
Work-oriented development of interactive software tools: Understanding the work of software maintainers and making an interactive software tool for them
[PB94-132032] p 3406 N94-28401
Single specimen fracture toughness determination procedure using instrumented impact test
[PB94-132040] p 3316 N94-28402
Characterization of structural vibration: Field descriptors based on energy density and intensity
[PB94-132230] p 3316 N94-28404
Spin-off companies as agents of technology transfer: An empirical study of the spin-off companies of the Technical Research Centre of Finland
[PB94-132248] p 3537 N94-28405
Measurement of volatile metal species at elevated temperatures
[PB94-132321] p 3186 N94-28407
Barley cell culture as a producer of heterologous protein
[PB94-132339] p 3379 N94-28408
Viscous and elastic-plastic material model in the ABAQUS
[PB94-132347] p 3316 N94-28409
Object-oriented CAD tool implementations for the construction industry
[PB94-132370] p 3407 N94-28411
Speciation in Water and Soil: A literature review
[PB94-132388] p 3341 N94-28412
Testing laboratories as notified bodies
[PB94-132396] p 3160 N94-28413
Nuclear energy related research
[DE94-606286] p 3494 N94-28623
Application of high-speed milling to the Finnish manufacturing industry
[PB94-135548] p 3230 N94-29187
High throughput network for multiprocessor interconnections
[VTT-PUBS-147] p 3245 N94-29468
Risk measures in living probabilistic safety assessment
[VTT-PUBS-146] p 3465 N94-30154
TECHNICAL RESEARCH CENTRE OF FINLAND, OULU.
Object-based design of embedded software
[PB94-132073] p 3407 N94-28403
TECHNICAL RESEARCH CENTRE OF FINLAND, TAMPERE.
Simulation of the effect of wind on clothing by measurements and calculations
[PB94-132289] p 3399 N94-28406
Systematic safety consideration in product design
[PB94-132354] p 3229 N94-28410
TECHNICAL UNIV. OF DENMARK, LYNGBY.
Human requirements to the indoor air quality and the thermal environment p 3232 N94-29600
TECHNICAL UNIV. OF LISBON (PORTUGAL).
Numerical prediction of turbulent sooting diffusion flames p 3191 N94-29253
TECHNIKA, SAINT PETERSBURG (RUSSIA).
Teleoperated systems for nuclear reactors: Inspection and maintenance
[AIAA PAPER 94-1176-CP] p 3439 N94-30528
TECHNISCHE HOCHSCHULE, DARMSTADT (GERMANY).
Numerical modelling of turbine combustion chambers p 3154 N94-29254
The mixing process in the quenching zone of the rich-lean-combustion concept p 3196 N94-29281
TECHNISCHE UNIV., BRUNSWICK (GERMANY).
Automatic control steps for aircraft taxi guidance p 3141 N94-29584
TECHNISCHE UNIV., DARMSTADT (GERMANY).
A new test method for the assessment of the arc tracking properties of wire insulation in air, oxygen enriched atmospheres and vacuum p 3167 N94-28714
TECHNISCHE UNIV., DELFT (NETHERLANDS).
Joining silicon carbide to austenitic stainless steel through diffusion welding
[PB94-126331] p 3297 N94-28399
The machining of fiber metal laminates. Part 1: An inventory of forming processes
[LR-710-PT-1] p 3184 N94-30343
Altimeter data processing from sea surface topography to horizontal eddy momentum fluxes
[PB94-147550] p 3378 N94-30714
TECHNISCHE UNIV., EINDHOVEN (NETHERLANDS).
Adhesion of electrolessly deposited Ni(P) on alumina ceramic
[ETN-94-95358] p 3212 N94-28539
TELDIX LUFTFAHRT-AUSRUESTUNGS G.M.B.H., HEIDELBERG (GERMANY).
A gimbaled low noise momentum wheel p 3162 N94-29640
TELECOM SOLUTIONS LTD., SAN JOSE, CA.
Cascaded clocks measurement and simulation findings p 3469 N94-30649
TELEDYNE GEOTECHNICAL, ALEXANDRIA, VA.
Statistical characterization of rugged propagation paths with application to Rg scattering study
[AD-A275237] p 3361 N94-29393
TENNESSEE UNIV., KNOXVILLE.
Elementary particle interactions
[DE94-004238] p 3482 N94-28504
Fundamental studies on the corrosion behavior of weldments in marine microbial environments
[AD-A275247] p 3203 N94-28900
TERA COMPUTER CO., SEATTLE, WA.
I/O on the Tera file system
[AD-A275278] p 3530 N94-29182
TEXAS A&M UNIV., COLLEGE STATION.
Wind tunnel testing and research
[NASA-CR-188273] p 3156 N94-29052
Concurrent simulation and constraint stabilization for flexible multibody systems p 3154 N94-29532
Automating geographically referenced digital mosaics from aerial videography with area-based feature matching p 3333 N94-29540
Design and analysis of concurrency control schemes for heterogeneous database systems p 3531 N94-29591
Yield and variability optimization of integrated circuits: Principles and practical solutions p 3266 N94-29805
Local heat transfer in an enclosed corotating disk with axial throughflow p 3276 N94-29849
A design methodology for synthesizing low-order robust controllers for flexible structures p 3302 N94-29870
Rotordynamic analysis of annular honeycomb-stator turbulent gas seals using a new friction-factor model based on flat plate tests p 3302 N94-29916
Electrochemical incineration of wastes
[NASA-CR-195262] p 3198 N94-29938
Extrapolation of point data for resource mapping p 3334 N94-29959
Situational reaction and planning
[AIAA PAPER 94-1206-CP] p 3444 N94-30557
Parameter identification of the rotordynamic coefficients of high-Reynolds-number hydrostatic bearings p 3311 N94-30792
Rotor instability induced by dead band clearance in bearing supports p 3312 N94-30809
Atmospheric moisture fields derived by satellite observations over the tropical Pacific Ocean p 3375 N94-30863
Dynamics and control of tethered satellite systems p 3170 N94-30864
TEXAS TECHNOLOGICAL UNIV., LUBBOCK.
Plasma turbulent bremsstrahlung
[PPL-144] p 3507 N94-30157
Numerical prediction of mixing process in a methane-fueled engine p 3304 N94-30230
TEXAS UNIV., ARLINGTON.
Information presentation for expert systems in future fighter aircraft
[AD-A275126] p 3149 N94-29005
Closed form expressions for a consistent stress material nonlinear finite element p 3322 N94-30258
TEXAS UNIV., AUSTIN.
Interaction of multiple spark-generated bubbles in a compressible liquid
[AD-A275037] p 3272 N94-29149
Models for vibration-dissociation coupling in high-temperature gases p 3273 N94-29675
Pulse response based minimum time control of flexible structures p 3436 N94-29720
A simulation study of high degree and order geopotential determination using satellite gravity gradiometry p 3333 N94-29762
A multi wavelength observational study of the Cartwheel ring galaxy p 3539 N94-29821
The h-p adaptive methods for incompressible viscous flow problems p 3275 N94-29836
A guidance and navigation system for two spacecraft rendezvous in translunar halo orbit p 3142 N94-29837
Theoretical asteroseismology of white dwarf stars: The encyclopedia Seismologica p 3547 N94-30011
Towards 10(exp 9) GPS geodesy: Vector baselines, Earth rotation and reference frames
[NASA-CR-195768] p 3142 N94-30243
TEXAS UNIV., SAN ANTONIO.
Probabilistic material strength degradation model for Inconel 718 components subjected to high temperature, mechanical fatigue, creep and thermal fatigue effects
[NASA-CR-195284] p 3318 N94-28840
THOMSON-CSF, BOULOGNE-BILLANCOURT (FRANCE).
Reactive system software concept with automation using the LDS language p 3414 N94-29327
THOMSON-CSF, MALAKOFF (FRANCE).
Embedded expert system: From the mock-up to the real world p 3412 N94-29319
THOMSON-CSF SYSTEMS CANADA, INC., OTTAWA (ONTARIO).
Coordinated control of multiple robot manipulators p 3308 N94-30289
TOBISHIMA CORP., TOKYO (JAPAN).
Report of National Institute for Resources and Environment. No. 8: Research on blasting sound related to it's measurement, propagation prediction, control and evaluation
[JTN-94-80605] p 3479 N94-29597
TOHOKU AEROSPACE DEVELOPMENT PROMOTION ASSOCIATION, MIYAGI (JAPAN).
Proceedings of the 15th Earth Observation Symposium
[JTN-94-80607] p 3328 N94-29036
TOHOKU UNIV., SENDAI (JAPAN).
Higher-order accurate numerical simulation of 3D supersonic mixing layers p 3124 N94-28954
Oceanic survey utilizing satellites p 3328 N94-29040
TOKAI UNIV., HIRATSUKA (JAPAN).
Estimation of geomagnetic conjugate points by using Pc5 pulsations p 3357 N94-29079
Observations of the geomagnetic field by Polar Patrol Balloon (PPB) experiment in Antarctica p 3359 N94-29235
ULF waves and magnetic field characteristics in the polar cusp observed at Godhavn p 3361 N94-29244
TOKAI UNIV., TOKYO (JAPAN).
Perspectives of earth observing techniques: Expectation of earth observation in space development history p 3328 N94-29039
A new information system: Satellite observation p 3330 N94-29219
TOKYO INST. OF TECH. (JAPAN).
Transonic expanding flow through axially symmetric orifices p 3128 N94-28985
TOKYO MEDICAL AND DENTAL UNIV. (JAPAN).
Equilibrium dysfunction in the clinical field p 3390 N94-28858
Cell culture in space p 3228 N94-28944
TOKYO UNIV. (JAPAN).
Proceedings of the workshop on quark and lepton mass matrices
[DE94-707692] p 3485 N94-28624
Keynote address p 3326 N94-28926
Research trends on remote sensing at research facilities in Japan: The priority area programme on better understanding of earth environment via satellite p 3326 N94-28928
Combustion studies under microgravity p 3228 N94-28940
Numerical study on the interaction between scramjet engine modules caused by thermal choke p 3125 N94-28960
Study on mixing and injection of hydrogen into a supersonic flow p 3127 N94-28975
Remote sensing and the Earth p 3329 N94-29218
A theory of current generator in the magnetosphere-ionosphere coupling p 3360 N94-29240
Behavior and visual control of cyprinodonts under microgravity p 3387 N94-29713
TOKYO UNIV., TANASHI (JAPAN).
Activity report of Synchrotron Radiation Laboratory 1992
[JTN-94-80600] p 3495 N94-29596
TORAY INDUSTRIES, INC., OTSU (JAPAN).
The flow field near the body surface with thin filaments p 3234 N94-29706
The flow field near the body surface with thin filaments p 3234 N94-29706
TORONTO UNIV. (ONTARIO).
Kinematic analysis of platform-type robotic manipulators
[ISBN-0-315-78703-1] p 3311 N94-30793
A control method for bilateral teleoperating systems
[ISBN-0-315-78705-8] p 3313 N94-30952

TOYOHASHI UNIV. OF TECHNOLOGY, AICHI (JAPAN).
Analysis of various biological activity parameters during parabolic flight p 3393 N94-29716
TOYOTA COLL. OF TECHNOLOGY (JAPAN).
Effect of water immersion on muscle sympathetic nerve response during static muscle contraction p 3394 N94-29865
TOYOTA MOTOR CO., AICHI (JAPAN).
Numerical analysis of incompressible viscous flow around a bubble p 3125 N94-28968
TRANSITION RESEARCH, INC., DANBURY, CT.
TRC research products: Components for service robots
[AIAA PAPER 94-1227-CP] p 3447 N94-30576
TRW, INC., REDONDO BEACH, CA.
High temperature polymer dielectric film insulation p 3167 N94-28715
Arcjet system integration development
[NASA-CR-187147] p 3171 N94-28736
TRW ENVIRONMENTAL SERVICES, LAS VEGAS, NV.
The evolution of information management
[DE94-004173] p 3535 N94-30179
TSUKUBA UNIV., IBARAKI (JAPAN).
Studies on water electrolyte metabolism and endocrine responses at rest and during submaximal exercise at 6,000 m simulated altitude p 3388 N94-28496
Effects of training at simulated altitude of 6,000 m on endocrine responses at rest and during exercise at the same altitude p 3388 N94-28497
TUFTS UNIV., MEDFORD, MA.
Application of the Modular Automated Reconfigurable Assembly System (MARAS) concept to adaptable vision gauging and parts feeding
[AIAA PAPER 94-1182-CP] p 3440 N94-30533

U

UNION COLL., SCHENECTADY, NY.
Information engineering implementation and acceptance p 3530 N94-29533
UNITED TECHNOLOGIES RESEARCH CENTER, EAST HARTFORD, CT.
Evaluation of the transient operation of advanced gas turbine combustors p 3154 N94-29269
UNIVERSIDAD AUTONOMA DEL ESTADO DE MEXICO, TOLUCA.
Study of iron exchanged zeolites by Moessbauer effect and electron spin resonance spectroscopy
[DE94-605138] p 3514 N94-29691
UNIVERSIDAD NACIONAL AUTONOMA DE MEXICO, MEXICO CITY.
Electrodeposition of bismuth alloys by the controlled potential method
[DE94-605316] p 3212 N94-28550
UNIVERSIDAD POLITECNICA DE MADRID (SPAIN).
Effects of hydrogen addition on pollutant emissions in a gas turbine combustor p 3195 N94-29275
UNIVERSIDADE NOVA DE LISBOA (PORTUGAL).
The road plan model: Information model for planning road building activities
[AIAA PAPER 94-1219-CP] p 3445 N94-30567
UNIVERSITEIT TWENTE, ENSCHEDE (NETHERLANDS).
Performance evaluation of intelligent network services
[MEMO-INF-93-20] p 3438 N94-30373
Performance issues of signalling protocols for broadband ISDN
[MEMO-INF-93-30] p 3255 N94-30374
Customer creation and combination in queueing networks
[MEMO-INF-93-35] p 3438 N94-30375
Modeling systems by probabilistic process algebra: An event structures approach
[MEMO-INF-93-29-REV] p 3425 N94-30416
DTL: A deductive and typed object-oriented language
[MEMO-INF-93-41] p 3425 N94-30417
Design and analysis of dynamic leader election protocols in broadcast networks
[MEMO-INF-93-43] p 3260 N94-30520
The transient period of a cyclic process: An horizon theorem
[MEMO-1149] p 3427 N94-30585
Graded Froelicher-Nijenhuis brackets and the theory of recursion operators for super differential equations
[MEMO-1147] p 3460 N94-30736
Set games
[MEMO-1148] p 3466 N94-30737
Dissipation in Hamiltonian systems: Decaying cnoidal waves
[MEMO-1151] p 3460 N94-30738
A new programming methodology for lazy functional languages
[MEMO-INF-93-44] p 3429 N94-30765
Relative length of long paths and cycles in graphs with large degree sums
[MEMO-1145] p 3461 N94-30766
Pancyclicity of Hamiltonian line graphs
[MEMO-1146] p 3451 N94-30767
Robust control of robots via linear estimated state-feedback
[MEMO-1153] p 3449 N94-30963
An intrinsic Hamiltonian formulation of the dynamics of LC-circuits
[MEMO-1154] p 3462 N94-30964
UNIVERSITY CORP. FOR ATMOSPHERIC RESEARCH, BOULDER, CO.
Modeling the Earth System, volume 3
[NASA-CR-194256] p 3350 N94-30616
UNIVERSITY OF CENTRAL FLORIDA, ORLANDO.
Effects of workload on communication processes in decision making teams
[AD-A275894] p 3527 N94-28796
Integral equation analysis of composite bodies of revolution and arbitrary surfaces with application to cavity-backed antennas p 3253 N94-29883
UNIVERSITY OF EASTERN KENTUCKY, RICHMOND.
Study of activation data of metal samples from LDEF-1 and Spacelab-2
[NASA-CR-195802] p 3205 N94-29736
UNIVERSITY OF ELECTRO-COMMUNICATIONS, CHOFU (JAPAN).
Study of generation mechanisms of magnetospheric VLF/ELF emissions based on the direction findings p 3361 N94-29245
UNIVERSITY OF SOUTHERN CALIFORNIA, LOS ANGELES.
Optoelectronic integrated circuits fabricated using atomic layer epitaxy
[AD-A275454] p 3262 N94-28805
Vehicle following controller design for autonomous intelligent vehicles
[AIAA PAPER 94-1203-CP] p 3443 N94-30554
Autonomous mobile robot teams
[AIAA PAPER 94-1207-CP] p 3444 N94-30558
UNIVERSITY OF SOUTHWESTERN LOUISIANA, LAFAYETTE.
A unified framework for retrieval in image databases p 3533 N94-29811
UNIVERSITY OF WESTERN ONTARIO, LONDON.
Extended occupancy grid method for modelling unknown dynamic environments p 3144 N94-30281
UNIVIEW SYSTEMS, MOUNTAIN VIEW, CA.
Formal specification and verification of real-time sequential control systems
[AD-A275776] p 3419 N94-29678
URBAN CONSORTIUM FOR TECHNOLOGY INITIATIVES.
Compressed natural gas fueled vehicles: The Houston experience
[DE94-005804] p 3312 N94-30878
USBI BOOSTER PRODUCTION CO., TITUSVILLE, FL.
Development of a unique polyurethane primer/topcoat p 3223 N94-30476
UTAH UNIV., SALT LAKE CITY.
Halogen chemisorption on silver(111): Scanning tunneling microscopy of coadsorbed halogen atoms
[AD-A275219] p 3486 N94-29060
Pitting corrosion of titanium
[AD-A274980] p 3203 N94-29089
Evaluation of the National Meteorological Center mesoscale model for prediction of severe convection over Central Arizona p 3371 N94-29744
Cloud and aerosol characterization for the ARM central facility: Multiple remote sensor techniques development
[DE94-003523] p 3365 N94-30608
UTRECHT STATE UNIV. (NETHERLANDS).
Conditional dependence in probabilistic networks
[RUU-CS-92-34] p 3464 N94-29450
Only few graphs have bounded treewidth
[RUU-CS-92-35] p 3455 N94-30333
A lateral inhibition neural network that emulates a winner-takes-all algorithm
[RUU-CS-92-46] p 3438 N94-30334
Two algorithms for finding rectangular duals of planar graphs
[RUU-CS-92-41] p 3423 N94-30345
Derivation lengths in term rewriting from interpretations in the naturals
[RUU-CS-92-43] p 3455 N94-30346
On blocks: Locality and asynchronous communication (extended abstract)
[RUU-CS-92-44] p 3424 N94-30347
A deterministic algorithm for the three-dimensional diameter problem
[RUU-CS-92-45] p 3424 N94-30348
A multiscale approach to image segmentation using Kohonen networks
[RUU-CS-93-06] p 3438 N94-30349
Generalized hidden surface removal
[RUU-CS-93-05] p 3424 N94-30364
Bayesian belief networks and conditional independencies
[RUU-CS-92-36] p 3465 N94-30376
The exact fitting problem in higher dimensions
[RUU-CS-92-37] p 3456 N94-30377
Pearl's belief propagation: The proofs
[RUU-CS-92-47] p 3456 N94-30378
Self-stabilizing l-exclusion algorithms
[RUU-CS-93-01] p 3424 N94-30379
A note on the Smyth powerdomain construction
[RUU-CS-93-02] p 3457 N94-30393
Algebraic domains, chain completion, and the Plotkin powerdomain construction
[RUU-CS-93-03] p 3457 N94-30394
Isomorphisms between predicate and state transformers
[RUU-CS-93-09] p 3458 N94-30403
Minimum fill-in for chordal bipartite graphs
[RUU-CS-93-11] p 3458 N94-30404
Treewidth of circle graphs
[RUU-CS-93-12] p 3458 N94-30405
L(sub)p optimal d dimensional triangulations for piecewise linear interpolation: A new result on data dependent triangulations
[RUU-CS-93-13] p 3458 N94-30406
Shape from diameter: Negative results
[RUU-CS-93-16] p 3458 N94-30407
Shape from diameter: Positive results
[RUU-CS-93-17] p 3458 N94-30408
A probabilistic approach to motion planning for car-like robots
[RUU-CS-93-18] p 3438 N94-30410
An all pairs shortest paths distributed algorithm using 2n(exp 2) messages
[RUU-CS-93-19] p 3432 N94-30411
Termination of term rewriting by semantic labelling
[RUU-CS-93-24] p 3459 N94-30424
Rectilinear decompositions with low stabbing number
[RUU-CS-93-25] p 3459 N94-30425
A more compact visibility representation
[RUU-CS-93-26] p 3425 N94-30426
Efficient and constructive algorithms for the pathwidth and treewidth of graphs
[RUU-CS-93-27] p 3426 N94-30488
Efficient bounded timestamping using traceable use abstraction: Is writer's guessing better than reader's telling?
[RUU-CS-93-28] p 3426 N94-30489
The secrets of causality
[RUU-CS-93-29] p 3426 N94-30490
On the relation between Unity properties and sequences of states
[RUU-CS-93-07] p 3433 N94-30720
Piecewise linear paths among convex obstacles
[RUU-CS-93-20] p 3460 N94-30721
Placing registration marks
[RUU-CS-93-21] p 3427 N94-30725
Dynamic microsets for RAMs
[RUU-CS-93-22] p 3406 N94-30727
Perfect binary space partitions
[RUU-CS-93-23] p 3460 N94-30728
Total termination of term rewriting
[RUU-CS-92-42] p 3460 N94-30744
Mapping objects to files: A UNIX file system interface to an object management system
[RUU-CS-93-08] p 3428 N94-30746
The (n squared)-hard problems in computational geometry
[RUU-CS-93-15] p 3461 N94-30747
Unravelling nondeterminism: On having the ability to choose
[RUU-CS-93-30] p 3428 N94-30749
Termination of term rewriting by semantic labelling
[RUU-CS-92-38] p 3462 N94-30859
Optimal size finite element meshes without obtuse and small angles
[RUU-CS-92-39] p 3462 N94-30860

V

VALPARAISO UNIV., IN.
High sensitivity tests of the standard model for electroweak interactions
[DE94-005415] p 3490 N94-30262
VANDERBILT UNIV., NASHVILLE, TN.
EVA glove evaluation methodology and test protocol p 3401 N94-29729
Prediction of fluid flow and heat transfer in internally finned tubes p 3280 N94-30228
An intelligent robotic aid system for human services
[AIAA PAPER 94-1232-CP] p 3447 N94-30580
Analysis and design of inflatable aerospace structures p 3403 N94-30799

VIRGINIA CENTER OF EXCELLANCE FOR SOFTWARE REUSE AND TECHNOLOGY TRANSFER, HERNDON.
Using RDD-100 with CoRE. Version 01.00.03
[AD-A275336] p 3419 N94-29737
VIRGINIA POLYTECHNIC INST. AND STATE UNIV., BLACKSBURG.
Numerical and experimental investigation of the bending response of thin-walled composite cylinders
[NASA-CR-195730] p 3317 N94-28801
Heat flux instrumentation for Hyflite thermal protection system
[NASA-CR-195731] p 3286 N94-28824
Beam scanning offset Cassegrain reflector antennas by subreflector movement
[NASA-CR-191604] p 3160 N94-28836
An actively cooled floating element skin friction balance for direct measurement in high enthalpy supersonic flows p 3289 N94-29824
Large eddy simulation of subsonic mixing layers p 3276 N94-29851
Adaptive power control as a fade countermeasure on satellite links p 3253 N94-29897
High-resolution algorithms for the Navier-Stokes equations for generalized discretizations p 3278 N94-29965
Damage analysis and mechanical response of as-received and heat-treated Nicalon/CAS-2 glass-ceramic matrix composites p 3219 N94-30259
Sensitivity analysis of the static aeroelastic response of a wing p 3134 N94-30525
Influence of surface defects and local structure on oxygenate reaction pathways over metal oxide surfaces
[DE94-005680] p 3522 N94-30901
VIRGINIA UNIV., CHARLOTTESVILLE.
Mechanical alloying processing with application to structural materials: ASSERT supplement
[AD-A275400] p 3204 N94-29205
Numerical simulations of cluster cooling flows p 3544 N94-29725
Multiple Concentric Cylinder Model (MCCM) user's guide
[NASA-CR-195299] p 3183 N94-30125
Micromechanical analysis of thermo-inelastic multiphase short-fiber composites
[NASA-CR-195290] p 3183 N94-30178
Optical depth effects in cluster cooling flows p 3541 N94-30800
VON KARMAN INST. FOR FLUID DYNAMICS, RHODE-SAINT-GENESE (BELGIUM).
Advanced Design of Ventilation Systems
[VKI-LS-1993-07] p 3231 N94-29598

W

WASEDA UNIV., TOKYO (JAPAN).
Estimation of the net production of moss community at Langhovde, East Antarctica p 3358 N94-29081
WASHINGTON STATE UNIV., PULLMAN.
The radiocarbon hydroxyl technique p 3344 N94-28600
An experimental study of wing tip vortex in the near wake of a rectangular wing
[AD-A275389] p 3129 N94-29306
Interaction of sound with sound by novel mechanisms: Ultrasonic four-wave mixing mediated by a suspension and ultrasonic three-wave mixing at a free surface p 3479 N94-29988
WASHINGTON UNIV., SAINT LOUIS, MO.
Physical interpretation and development of ultrasonic nondestructive evaluation techniques applied to the quantitative characterization of textile composite materials
[NASA-CR-195766] p 3183 N94-30016
WASHINGTON UNIV., SEATTLE.
Plane stress stable crack growth and J-integral/HRR field
[AD-A275761] p 3317 N94-28761
Physical processes in snowpacks during rain or melt events
[AD-A275445] p 3325 N94-28881
Studies of marine aerosols and their evolution in the eastern North Atlantic
[AD-A275011] p 3377 N94-29128
Transient internal probe
[AD-A275054] p 3505 N94-29134
Physical conditions in classical H2 regions in the Magellanic Clouds p 3543 N94-29722
Abundance patterns in red-giant CH stars p 3539 N94-29820
Fracture process zone of brittle composites p 3182 N94-29876
A near-infrared survey of the star forming region NGC 2264 p 3540 N94-29971
A direct digital control-law synthesis in the w-domain: W-synthesis methodology p 3438 N94-30517
Transition to turbulence in confined compressible mixing layers p 3283 N94-30958
WEIZMANN INST. OF SCIENCE, REHOVOTH (ISRAEL).
Boundary-induced phase transitions in equilibrium and non-equilibrium systems
[DE94-608137] p 3199 N94-30111
Exclusive many-particle diffusion in disordered media and correlation functions for random vertex models
[DE94-608134] p 3525 N94-30121
Characteristics of secondary electron emission from CsI induced by x rays with energies up to 100 keV
[DE94-608422] p 3395 N94-30185
Methods of testing parameterizations: Vertical ocean mixing p 3352 N94-30633
WESTINGHOUSE HANFORD CO., RICHLAND, WA.
Numerical precision and roundoff considerations concerning computer code migration
[DE94-005421] p 3427 N94-30590
WESTINGHOUSE SAVANNAH RIVER CO., AIKEN, SC.
Comparison of Savannah River Site's meteorological databases
[DE94-001751] p 3373 N94-29817
WICHITA STATE UNIV., KS.
Decoupled flight control system design using the singular perturbation method p 3155 N94-29850
The effect of mechanical paint stripping on the fatigue and fracture of thin aluminum airplane skin p 3205 N94-29900
WISCONSIN UNIV., MADISON.
Theoretical reversed field pinch and tokamak studies
[DE94-005409] p 3503 N94-28490
Fluctuation and transport reduction in a reversed field pinch by inductive poloidal current drive
[DE94-005542] p 3503 N94-28514
Photon counting spectroscopy as done with a Thomson scattering diagnostic
[DE94-005543] p 3503 N94-28515
Properties of events containing a photon and several jets seen in p(bar p) collisions at (radical)s = 1.8 TeV
[DE94-005596] p 3482 N94-28531
Broadband EUV survey spectrometer for short-timescale experiments
[DE94-005459] p 3498 N94-28534
TFTR Ion Cyclotron Range of Frequencies (ICRF) experimental data analysis collaboration
[DE94-004699] p 3504 N94-28575
The motion of deforming bodies
[AD-A275224] p 3271 N94-29061
Center for Parallel Optimization
[AD-A274988] p 3431 N94-29127
Microactuator production via high aspect ratio, high edge acuity metal fabrication technology p 3235 N94-29770
The influence of appendage vibration on the attitude dynamics of a dual-spin satellite p 3168 N94-29828
The stability of perfect elliptic disks p 3545 N94-29834
Direct anti-b b production in anti-pp collisions at the square root of s = 1.8 TeV
[DE94-006167] p 3491 N94-30369
Modeling Earth system changes of the past p 3353 N94-30635
WOODS HOLE OCEANOGRAPHIC INST., MA.
Global Acoustic Mapping of Ocean Temperatures (GAMOT)
[AD-A275777] p 3376 N94-28740
Analysis of crustal structure of Venus utilizing residual Line-of-Sight (LOS) gravity acceleration and surface topography data. A trial of global modeling of Venus gravity field using harmonic spline method
[NASA-CR-195799] p 3549 N94-29737
WORCESTER POLYTECHNIC INST., MA.
Generalized Eulerian-Lagrangian formulations in free and moving boundary problems: Processing of viscoelastic polymers and fiber suspensions p 3283 N94-30955
WRIGHT LAB., WRIGHT-PATTERSON AFB, OH.
Robust 300 C wire insulation system p 3165 N94-28699
Performance evaluation of a 22.5/30 kW 270 volts direct current generator system
[AD-A275106] p 3263 N94-28913
Research and development of high thermal stability fuels p 3192 N94-29261
Object oriented design of the autonomous fixtaking management system p 3143 N94-29323
A common Ada run-time system for avionics software p 3150 N94-29331
Validation and test of complex weapon systems p 3150 N94-29336
Testing Operational Flight Programs (OFPs) p 3415 N94-29337
Use of magnetic compression to support turbine engine rotors p 3314 N94-30484
WYLE LABS., INC., HUNTSVILLE, AL.
Specialized data analysis of SSME and advanced propulsion system vibration measurements
[NASA-CR-193940] p 3174 N94-29868

Y

YALE UNIV., NEW HAVEN, CT.
Globular cluster photometry near the turnoff: Blue stragglers, relative ages, and the horizontal branch p 3538 N94-29732
Anomalous algebraic structures in quantum field theories p 3524 N94-29911
On dyonic black holes and cosmic censorship p 3546 N94-29912
Convective turbulence and transport in stars p 3546 N94-29913
YORK UNIV. (ONTARIO).
The radical amplifier p 3345 N94-28604

Typical Contract Number Index Listing

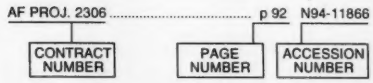

Listings in this index are arranged alphanumerically by contract number. Under each contract number the accession numbers denoting documents that have been produced as a result of research done under that contract are arranged in ascending order. The page number helps to locate the citation in the abstract section. The accession number denotes the number by which the citation is identified.

AERO-0018-C(H) ..... p 3134 N94-30858
AERO-1082 ..... p 3134 N94-30493
AF PROJ. 4600 ..... p 3241 N94-28763
AF PROJ. 5581 ..... p 3408 N94-28784
AF PROJ. 7184 ..... p 3400 N94-29034
p 3146 N94-29042
AF PROJ. 9201 ..... p 3346 N94-28727
AF-AFOSR-0067-89 ..... p 3272 N94-29136
AF-AFOSR-0091-91 ..... p 3550 N94-29132
AF-AFOSR-0118-90 ..... p 3499 N94-29114
AF-AFOSR-0125-90 ..... p 3398 N94-29027
AF-AFOSR-0145-90 ..... p 3213 N94-28886
AF-AFOSR-0225-91 ..... p 3398 N94-29154
AF-AFOSR-0276-90 ..... p 3512 N94-28890
AF-AFOSR-0345-90 ..... p 3505 N94-29134
AF-AFOSR-0373-91 ..... p 3513 N94-29125
AF-AFOSR-0390-89 ..... p 3486 N94-29032
AF-AFOSR-0410-89 ..... p 3431 N94-29127
AF-AFOSR-0431-91 ..... p 3189 N94-29004
ARO-MIPR-130-93 ..... p 3225 N94-29308
ARPA ORDER 6266 ..... p 3359 N94-29137
ARPA ORDER 7597 ..... p 3499 N94-29059
p 3405 N94-29181
p 3453 N94-29304
p 3418 N94-29434
ARPA ORDER 8313 ..... p 3410 N94-29007
ARPA ORDER 9537 ..... p 3498 N94-28656
BD/860/90-IB ..... p 3191 N94-29253
BRITE/EURAM-1019 ..... p 3194 N94-29274
CNR-203.15.3 ..... p 3458 N94-30403
p 3459 N94-30430
CSC-468969 ..... p 3406 N94-29695
DA PROJ. 1L1-62211-A-47-A ..... p 3303 N94-30205
p 3303 N94-30227
DA PROJ. 1L1-62211-A-47A ..... p 3301 N94-29552
DA PROJ. 1L1-62618-AH-80 ..... p 3452 N94-28864
p 3417 N94-29392
DA PROJ. 1L1-62786-AH-98 ..... p 3177 N94-28735
DA PROJ. 3M1-62787-A-879 ..... p 3388 N94-28757
DA PROJ. 4A1-61102-AT-24 ..... p 3357 N94-29070
DA PROJ. 4A7-62730-AT-24 ..... p 3478 N94-29314
DA PROJ. 4A7-62730-AT-42 ..... p 3478 N94-29314
DA PROJ. 4A7-62784-AT-42 ..... p 3325 N94-28849
DAAA08-91-D-0008 ..... p 3176 N94-28688
DAAE07-90-C-R059 ..... p 3445 N94-30566
DAAH04-93-C-0002 ..... p 3355 N94-28728
DAAH04-93-C-0023 ..... p 3214 N94-29073
DAAK70-90-C-0019 ..... p 3176 N94-28653
DAAK70-92-D-0003 ..... p 3409 N94-28895
p 3410 N94-29088
DAAL01-91-C-0142 ..... p 3265 N94-29511
DAAL03-86-G-0069 ..... p 3177 N94-28865
DAAL03-89-D-0003 ..... p 3292 N94-28770
p 3452 N94-28883
DAAL03-89-G-0081 ..... p 3203 N94-29056
DAAL03-89-K-0052 ..... p 3224 N94-28769
DAAL03-89-K-0072 ..... p 3262 N94-28805
DAAL03-89-K-0095 ..... p 3270 N94-28665
DAAL03-89-K-0138 ..... p 3213 N94-28806
DAAL03-89-K-0152 ..... p 3202 N94-28867
DAAL03-90-C-0013 ..... p 3129 N94-29197
DAAL03-90-G-0004 ..... p 3154 N94-28632
DAAL03-90-G-0051 ..... p 3174 N94-29307
DAAL03-90-G-0061 ..... p 3384 N94-28667
DAAL03-90-G-0074 ..... p 3356 N94-28882
DAAL03-90-G-0110 ..... p 3384 N94-28884
DAAL03-90-G-0112 ..... p 3485 N94-28668
DAAL03-90-G-0118 ..... p 3512 N94-28880
DAAL03-90-G-0182 ..... p 3262 N94-28669
DAAL03-90-G-0205 ..... p 3225 N94-29310
DAAL03-90-G-0216 ..... p 3451 N94-28792
DAAL03-90-G-0223 ..... p 3264 N94-29305
DAAL03-91-G-0010 ..... p 3451 N94-28723
DAAL03-91-G-0026 ..... p 3129 N94-29306
DAAL03-91-G-0121 ..... p 3504 N94-29055
DAAL03-91-G-0143 ..... p 3325 N94-28881
DAAL03-91-G-0164 ..... p 3486 N94-29021
DAAL03-91-G-0311 ..... p 3243 N94-29072
DAAL03-92-G-0096 ..... p 3204 N94-29205
DAAL03-92-G-0218 ..... p 3214 N94-29203
DAAL03-92-G-0413 ..... p 3411 N94-29201
DAAL03-93-G-0415 ..... p 3293 N94-29309
DAAL04-91-C-0004 ..... p 3178 N94-29024
DACA76-89-C-0014 ..... p 3445 N94-30566
DAMD17-88-C-8141 ..... p 3391 N94-29150
DE-AC01-90CE-90053 ..... p 3340 N94-30833
DE-AC01-91ER-30156 ..... p 3338 N94-29953
DE-AC01-91RW-00134 ..... p 3535 N94-30179
DE-AC02-76CH-00016 ..... p 3510 N94-28512
p 3342 N94-28523
p 3483 N94-28565
p 3485 N94-28741
p 3487 N94-29841
p 3206 N94-29931
p 3209 N94-30246
p 3223 N94-30475
p 3497 N94-30588
p 3296 N94-30688
p 3551 N94-30884
p 3222 N94-30906
p 3268 N94-30907
DE-AC02-76CH-03000 ..... p 3484 N94-28573
p 3484 N94-28574
p 3488 N94-30049
p 3490 N94-30103
p 3491 N94-30719
p 3491 N94-30722
p 3492 N94-30779
p 3493 N94-30886
p 3493 N94-30887
p 3268 N94-30904
DE-AC02-76ER-00881 ..... p 3482 N94-28531
p 3491 N94-30369
DE-AC02-78ET-51013 ..... p 3510 N94-30882
DE-AC02-83CH-10093 ..... p 3336 N94-28500
p 3336 N94-28501
p 3224 N94-28502
p 3500 N94-29799
p 3514 N94-29801
p 3302 N94-29922
p 3225 N94-30038
p 3341 N94-30486
p 3339 N94-30601
p 3339 N94-30602
p 3339 N94-30603
p 3339 N94-30604
p 3339 N94-30605
p 3339 N94-30606
p 3226 N94-30761
p 3226 N94-30818
p 3268 N94-30819
p 3340 N94-30820
DE-AC03-76SF-00098 ..... p 3292 N94-28478
p 3201 N94-28479
p 3542 N94-28480
p 3407 N94-28506
p 3494 N94-28507
p 3482 N94-28524
p 3261 N94-28546
p 3504 N94-28564
p 3410 N94-29019
p 3515 N94-30009
p 3468 N94-30026
p 3289 N94-30027
p 3199 N94-30266
p 3519 N94-30707
p 3491 N94-30709
p 3210 N94-30710
p 3267 N94-30711
p 3268 N94-30717
p 3520 N94-30835
p 3476 N94-30841
p 3520 N94-30842
p 3520 N94-30850
DE-AC03-76SF-00515 ..... p 3292 N94-28481
p 3482 N94-28493
p 3482 N94-28494
p 3482 N94-28541
p 3483 N94-28542
p 3497 N94-30712
DE-AC03-89ER-51114 ..... p 3510 N94-30832
DE-AC04-76DP-00613 ..... p 3349 N94-29932
p 3219 N94-30245
p 3354 N94-30466
DE-AC04-76DP-00789 ..... p 3216 N94-29830
p 3406 N94-30008
p 3219 N94-30263
p 3184 N94-30589
p 3311 N94-30596
DE-AC04-76DR-00789 ..... p 3210 N94-30777
DE-AC04-88ID-12692 ..... p 3221 N94-30826
DE-AC04-94AL-85000 ..... p 3286 N94-28466
p 3165 N94-28477
p 3292 N94-28482
p 3510 N94-28484
p 3270 N94-28488
p 3336 N94-28489
p 3315 N94-28503
p 3174 N94-28557
p 3187 N94-28567
p 3337 N94-29018
p 3315 N94-29020
p 3263 N94-29025
p 3420 N94-29844
p 3289 N94-29927
p 3206 N94-29936
p 3515 N94-30006
p 3206 N94-30007
p 3266 N94-30040
p 3207 N94-30053
p 3266 N94-30055
p 3534 N94-30099
p 3218 N94-30102
p 3518 N94-30247
p 3437 N94-30250
p 3199 N94-30260
p 3501 N94-30261
p 3169 N94-30264
p 3295 N94-30265
p 3518 N94-30315
p 3518 N94-30316
p 3295 N94-30367
p 3267 N94-30368
p 3445 N94-30565
p 3184 N94-30589
p 3220 N94-30591
p 3519 N94-30592
p 3340 N94-30609
p 3226 N94-30615
p 3260 N94-30772
p 3185 N94-30827
p 3501 N94-30828
p 3340 N94-30843
p 3462 N94-30849
p 3221 N94-30896
p 3222 N94-30900
p 3222 N94-30909
p 3501 N94-30910
DE-AC05-76OR-00033 ..... p 3211 N94-30852
DE-AC05-84OR-21400 ..... p 3511 N94-28535
p 3483 N94-28559
p 3511 N94-28570
p 3495 N94-29924
p 3500 N94-29928
p 3207 N94-30042
p 3516 N94-30063
p 3516 N94-30064

DE-AC06-76RL-01830 ..... p 3255 N94-30105
p 3518 N94-30249
p 3454 N94-30317
p 3219 N94-30335
p 3508 N94-30339
p 3508 N94-30365
p 3441 N94-30539
p 3519 N94-30611
p 3350 N94-30619
p 3323 N94-30689
p 3465 N94-30696
p 3199 N94-30723
p 3520 N94-30724
p 3461 N94-30758
p 3509 N94-30760
p 3520 N94-30773
p 3461 N94-30817
p 3510 N94-30832
p 3521 N94-30851
p 3211 N94-30852
p 3200 N94-30880
p 3521 N94-30898
p 3341 N94-28454
p 3368 N94-28455
p 3201 N94-28456
p 3201 N94-28460
p 3269 N94-28464
p 3451 N94-28739
p 3514 N94-30001
p 3527 N94-30041
p 3207 N94-30062
p 3240 N94-30473
p 3374 N94-30587
p 3491 N94-30695
DE-AC06-87RL-10930 ..... p 3427 N94-30590
DE-AC07-76ID-01570 ..... p 3465 N94-29925
p 3314 N94-30444
p 3186 N94-30447
p 3527 N94-30698
DE-AC08-93NV-11265 ..... p 3553 N94-30248
DE-AC09-89SR-18035 ..... p 3373 N94-29817
DE-AC21-92MC-29116 ..... p 3349 N94-30047
DE-AC22-90PC-90361 ..... p 3341 N94-28463
DE-AC22-92PC-91346 ..... p 3341 N94-28465
DE-AC35-89ER-40486 ..... p 3487 N94-29700
DE-AI01-86CE-50162 ..... p 3537 N94-29350
DE-AI05-89ER-53281 ..... p 3509 N94-30755
DE-AS05-80ER-10629 ..... p 3488 N94-29930
DE-AT21-92MC-29267 ..... p 3367 N94-30883
DE-FC07-91ID-13074 ..... p 3267 N94-30701
DE-FC21-92MC-29061 ..... p 3297 N94-28485
DE-FG02-85ER-53194 ..... p 3503 N94-28547
DE-FG02-85ER-53198 ..... p 3503 N94-28514
p 3503 N94-28515
p 3498 N94-28534
DE-FG02-85ER-53212 ..... p 3503 N94-28490
DE-FG02-86ER-13491 ..... p 3492 N94-30837
DE-FG02-86ER-40281 ..... p 3484 N94-28576
DE-FG02-86ER-40291 ..... p 3481 N94-28492
DE-FG02-87ER-13671 ..... p 3489 N94-30061
DE-FG02-87ER-13719 ..... p 3386 N94-30180
DE-FG02-87ER-13766 ..... p 3207 N94-30024
DE-FG02-87ER-13775 ..... p 3200 N94-30770
DE-FG02-87ER-13781 ..... p 3210 N94-30839
DE-FG02-88ER-13849 ..... p 3481 N94-28491
DE-FG02-88ER-13949 ..... p 3211 N94-28457
DE-FG02-88ER-25053 ..... p 3451 N94-28571
DE-FG02-88ER-40408 ..... p 3492 N94-30836
DE-FG02-88ER-40416 ..... p 3490 N94-30262
DE-FG02-88ER-60668 ..... p 3348 N94-29926
DE-FG02-89ER-60760 ..... p 3349 N94-30046
DE-FG02-90CE-27504 ..... p 3312 N94-30878
DE-FG02-90ER-13029 ..... p 3296 N94-30614
DE-FG02-90ER-14105 ..... p 3200 N94-30769
DE-FG02-90ER-14150 ..... p 3226 N94-30708
DE-FG02-90ER-40542 ..... p 3491 N94-30685
DE-FG02-90ER-61059 ..... p 3365 N94-30608
DE-FG02-90ER-61072 ..... p 3269 N94-28464
DE-FG02-91CE-23810 ..... p 3230 N94-28563
p 3220 N94-30692
DE-FG02-91ER-40677 ..... p 3483 N94-28566
DE-FG02-91ER-45439 ..... p 3521 N94-30894
DE-FG02-91ER-54109 ..... p 3506 N94-30045
p 3493 N94-30881
DE-FG02-91ER-61256 ..... p 3386 N94-30895
DE-FG02-92ER-25139 ..... p 3279 N94-30003
DE-FG02-92ER-40715 ..... p 3491 N94-30702
DE-FG02-92ER-54184 ..... p 3492 N94-30834
DE-FG02-93ER-14320 ..... p 3503 N94-28458
DE-FG02-93ER-40762 ..... p 3492 N94-30838
DE-FG02-93ER-40764 ..... p 3491 N94-30686
DE-FG02-93ER-45503 ..... p 3484 N94-28578
DE-FG02-93ER-54196 ..... p 3504 N94-28575
DE-FG05-88ER-13846 ..... p 3260 N94-30902
DE-FG05-90ER-14129 ..... p 3522 N94-30901
DE-FG05-91ER-40617 ..... p 3491 N94-30762
DE-FG05-91ER-40627 ..... p 3482 N94-28504
DE-FG05-91ER-81236 ..... p 3230 N94-29017
DE-FG06-89ER-75522 ..... p 3201 N94-28456
p 3451 N94-28739
DE-FG07-90ID-13040 ..... p 3340 N94-30700
DE-FG09-87ER-45291 ..... p 3501 N94-30252
DE-FG21-90MC-27225 ..... p 3340 N94-30879
DE-FG22-92PC-92529 ..... p 3200 N94-30877
DEN3-331 ..... p 3537 N94-29350
DT-FA01-92-G-0011 ..... p 3137 N94-29562
DTFA01-87-C-00014 ..... p 3157 N94-29754
p 3135 N94-29862
DTFA01-89-C-00016 ..... p 3142 N94-30189
DTFA02-90-R-00149 ..... p 3143 N94-30933
DTFA03-90-P-00447 ..... p 3135 N94-28799
DTRS57-89-C-00006 ..... p 3145 N94-28647
DTRS57-89-D-00007 ..... p 3315 N94-28646
DTRS57-89-D-00009 ..... p 3145 N94-28657
DTRS57-91-P-80859 ..... p 3149 N94-30905
EC-3075 ..... p 3426 N94-30488
EC-7141 ..... p 3423 N94-30345
p 3406 N94-30727
p 3460 N94-30728
EPA-68-DO-0141 ..... p 3347 N94-29192
EPRI PROJ. 8004-11 ..... p 3344 N94-28599
FMI PROJ. NAS-9614 ..... p 3278 N94-29977
FMV52700-90-066-16-001 ..... p 3179 N94-29425
F04701-88-C-0089 ..... p 3356 N94-28869
p 3167 N94-29022
p 3347 N94-29023
p 3552 N94-29046
p 3494 N94-29065
p 3264 N94-29289
p 3162 N94-29641
F08635-90-C-0100 ..... p 3194 N94-29271
F08635-90-C-0241 ..... p 3263 N94-28994
F08635-92-C-0019 ..... p 3444 N94-30561
F11623-92-D-0003 ..... p 3371 N94-29747
F19628-88-C-0014 ..... p 3538 N94-28671
F19628-88-C-0032 ..... p 3156 N94-28752
F19628-88-D-0032 ..... p 3407 N94-28664
p 3156 N94-28753
p 3156 N94-28772
F19628-88-K-0011 ..... p 3504 N94-28828
F19628-90-C-0003 ..... p 3407 N94-28633
p 3407 N94-28639
p 3407 N94-28648
p 3410 N94-29068
F19628-91-C-0168 ..... p 3410 N94-29007
F19628-92-C-0092 ..... p 3369 N94-28663
F19628-93-C-0023 ..... p 3164 N94-28827
F29601-91-C-DB23 ..... p 3361 N94-29393
F30602-88-D-0025 ..... p 3408 N94-28760
p 3430 N94-28781
p 3241 N94-28762
F30602-91-C-0005 ..... p 3498 N94-28780
F30602-92-C-0016 ..... p 3270 N94-28692
F33615-85-C-2566 ..... p 3224 N94-28901
F33615-87-C-2709 ..... p 3409 N94-28920
F33615-87-C-5250 ..... p 3400 N94-29029
F33615-87-D-0609 ..... p 3150 N94-29048
F33615-89-C-0532 ..... p 3399 N94-28861
F33615-90-C-0533 ..... p 3262 N94-28767
F33615-90-C-1456 ..... p 3405 N94-28916
F33615-90-C-1465 ..... p 3499 N94-29059
p 3405 N94-29181
p 3453 N94-29304
p 3418 N94-29434
F33615-90-C-2033 ..... p 3192 N94-29262
F33615-91-C-0003 ..... p 3409 N94-28910
F33615-92-C-0018 ..... p 3399 N94-28766
p 3391 N94-28892
p 3400 N94-28997
p 3337 N94-29033
F33615-92-C-2207 ..... p 3391 N94-29071
F33615-93-1-1330 ..... p 3193 N94-29266
p 3410 N94-29006
p 3398 N94-29313
F33616-89-C-0532 ..... p 3149 N94-29005
F49620-91-C-0095 ..... p 3167 N94-29002
F49620-92-C-0063 ..... p 3178 N94-29135
F49620-92-J-0120 ..... p 3434 N94-29026
F49620-92-J-0137 ..... p 3369 N94-28847
F49620-92-J-0219 ..... p 3504 N94-28686
F49620-92-J-0420 ..... p 3512 N94-28889
F49620-93-I-0040 ..... p 3486 N94-29087
F49620-93-I-0348 ..... p 3499 N94-28848
F49620-93-1-0009 ..... p 3122 N94-28899
GSFC PROJ. 913-44468 ..... p 3374 N94-30187
I-32-91 ..... p 3456 N94-30382
MDA972-91-C-0032 ..... p 3263 N94-28915
MDA972-91-C-0046 ..... p 3499 N94-29694
MDA972-92-C-0005 ..... p 3238 N94-29783
MDA972-92-C-0026 ..... p 3359 N94-29137
MDA972-92-J-1010 ..... p 3446 N94-30572
MDA972-92-J-1018 ..... p 3419 N94-29797
MDA972-93-1-0004 ..... p 3376 N94-28740
MIPR-ARO-131-93 ..... p 3212 N94-28733
MIPR-ARO-132-91 ..... p 3499 N94-28813
MIPR-92-501 ..... p 3263 N94-29028
MOD-01689029811 ..... p 3448 N94-30741
NAGW-1175 ..... p 3444 N94-30561
NAGW-1333 ..... p 3445 N94-30563
NAGW-1779 ..... p 3198 N94-29938
NAGW-252 ..... p 3351 N94-30628
NAGW-3214 ..... p 3526 N94-28746
NAGW-3581 ..... p 3549 N94-28816
NAGW-996 ..... p 3364 N94-30014
NAG1-1067 ..... p 3213 N94-28748
NAG1-1072 ..... p 3132 N94-29920
NAG1-1223 ..... p 3408 N94-28825
NAG1-1538 ..... p 3286 N94-28824
NAG1-343 ..... p 3317 N94-28801
NAG1-363 ..... p 3479 N94-29407
NAG1-613 ..... p 3418 N94-29404
p 3406 N94-29695
p 3431 N94-29846
p 3431 N94-29869
p 3420 N94-29890
p 3420 N94-29906
NAG1-859 ..... p 3160 N94-28836
NAG10-0085 ..... p 3385 N94-29943
NAG2-581 ..... p 3443 N94-30555
NAG2-681 ..... p 3550 N94-29892
NAG2-768 ..... p 3549 N94-29737
NAG3-1124 ..... p 3194 N94-29271
NAG3-1134 ..... p 3132 N94-30124
p 3133 N94-30152
NAG3-1157 ..... p 3277 N94-29859
NAG3-1206 ..... p 3173 N94-29546
NAG3-1263 ..... p 3303 N94-30205
NAG3-1373 ..... p 3169 N94-29917
NAG3-1377 ..... p 3183 N94-30178
NAG3-1433 ..... p 3153 N94-30013
NAG3-1669 ..... p 3319 N94-29104
NAG3-28 ..... p 3133 N94-30152
NAG3-379 ..... p 3318 N94-28821
NAG3-50 ..... p 3183 N94-30190
NAG3-867 ..... p 3318 N94-28840
NAG3-912 ..... p 3301 N94-29552
NAG5-1319 ..... p 3294 N94-29914
NAG5-1463 ..... p 3543 N94-29696
NAG5-1491 ..... p 3164 N94-29880
NAG5-1612 ..... p 3244 N94-29106
NAG5-1867 ..... p 3540 N94-29957
NAG5-1936 ..... p 3142 N94-30243
NAG5-2250 ..... p 3549 N94-28418
NAG5-2348 ..... p 3262 N94-28846
NAG5-675 ..... p 3289 N94-29907
NAG8-212 ..... p 3173 N94-29848
NAG8-683 ..... p 3171 N94-28800
NAG8-790 ..... p 3175 N94-30242
NAG8-950 ..... p 3515 N94-30015
NAG9-233 ..... p 3546 N94-29905
NASA ORDER H-13012-D ..... p 3402 N94-30188
NASA ORDER H-13029-D ..... p 3205 N94-29736
NASA ORDER S-97242-E ..... p 3551 N94-30948
NASW-4324 ..... p 3401 N94-30122
NASW-4435 ..... p 3299 N94-29354
p 3299 N94-29386
p 3299 N94-29409
NASW-4492 ..... p 3236 N94-29773
NASW-4574 ..... p 3354 N94-28416
p 3549 N94-29102
NASW-4670 ..... p 3422 N94-30273
NASW-4814 ..... p 3551 N94-29858
NAS1-18224 ..... p 3175 N94-29458
NAS1-18584 ..... p 3329 N94-29098
NAS1-19038 ..... p 3408 N94-28818
NAS1-19247 ..... p 3175 N94-29458
NAS1-19299 ..... p 3273 N94-29460
NAS1-19303 ..... p 3480 N94-30274
NAS1-19371 ..... p 3164 N94-28417
NAS1-19480 ..... p 3272 N94-29381
p 3454 N94-30207
p 3454 N94-30208
p 3454 N94-30209
NAS1-20048 ..... p 3293 N94-28839
NAS10-11624 ..... p 3347 N94-29099
NAS2-13210 ..... p 3478 N94-29363
NAS2-13758 ..... p 3420 N94-29945
NAS2-13872 ..... p 3147 N94-29685
NAS3-22525 ..... p 3317 N94-28815
NAS3-25066 ..... p 3164 N94-29355
NAS3-25266 ..... p 3317 N94-28819
p 3203 N94-28921
p 3151 N94-29103
p 3319 N94-29104
p 3181 N94-29684
p 3168 N94-29757
p 3267 N94-30198
p 3155 N94-30204

NAS3-25269 p 3155 N94-28510
NAS3-25270 p 3152 N94-29438
NAS3-25603 p 3171 N94-28736
NAS3-25609 p 3173 N94-29444
NAS3-25776 p 3242 N94-28826
p 3168 N94-29405
p 3319 N94-29406
p 3319 N94-29469
NAS3-26371 p 3316 N94-28508
NAS3-26571 p 3183 N94-30125
NAS3-27186 p 3135 N94-30949
NAS5-26813 p 3162 N94-29642
NAS5-30386 p 3162 N94-29642
NAS5-30565 p 3507 N94-30128
NAS5-30920 p 3351 N94-30628
NAS5-31000 p 3468 N94-30639
NAS5-31209 p 3507 N94-30126
NAS5-31234 p 3198 N94-29857
NAS5-31790 p 3289 N94-29872
NAS5-31838 p 3545 N94-29871
NAS5-31847 p 3347 N94-29549
NAS5-31996 p 3287 N94-29400
NAS5-32064 p 3551 N94-29453
NAS5-32070 p 3538 N94-29001
NAS5-32079 p 3545 N94-29861
NAS5-33045 p 3236 N94-29773
NAS5-33047 p 3507 N94-30127
p 3507 N94-30128
NAS7-1149 p 3314 N94-30441
NAS7-1189 p 3314 N94-30442
NAS7-1260 p 3264 N94-29357
p 3265 N94-29488
p 3225 N94-29490
p 3499 N94-29491
p 3435 N94-29492
p 3293 N94-29493
p 3246 N94-29495
NAS7-918 p 3229 N94-29371
p 3287 N94-29373
p 3265 N94-29374
p 3265 N94-29411
p 3299 N94-29420
p 3288 N94-29497
p 3246 N94-29613
p 3249 N94-29652
p 3235 N94-29767
NAS8-37334 p 3162 N94-29642
NAS8-37814 p 3297 N94-28419
NAS8-38156 p 3174 N94-29868
NAS8-38609 p 3316 N94-29724
p 3157 N94-29956
NAS8-38866 p 3300 N94-29550
NAS9-17885 p 3361 N94-29588
NAS9-18261 p 3156 N94-29052
NAS9-18819 p 3278 N94-29977
NAS9-18878 p 3171 N94-29035
NCA2-839 p 3253 N94-29873
NCC2-303 p 3261 N94-28511
NCC2-552 p 3272 N94-29378
NCC2-55 p 3270 N94-28724
NCC2-582 p 3131 N94-29693
NCC2-605 p 3277 N94-29942
NCC2-699 p 3152 N94-29860
NCC2-746 p 3147 N94-29721
NCC2-810 p 3385 N94-29968
NCC2-834 p 3145 N94-28817
NCC3-231 p 3289 N94-29742
NCC3-233 p 3272 N94-29096
NCC3-94 p 3178 N94-29208
NCC8-18 p 3537 N94-29410
NF-102/62-356 p 3454 N94-30319
p 3457 N94-30397
p 3460 N94-30735
NF-62-376 p 3424 N94-30379
p 3432 N94-30411
p 3526 N94-30433
p 3426 N94-30434
p 3426 N94-30489
NF-62-518 p 3426 N94-30490
NF-63/62-518 p 3432 N94-30363
NGT-10000 p 3445 N94-30563
NGT-50548 p 3512 N94-29101
NIH-5R01-GM37161 p 3236 N94-29773
NIVR-01506N p 3133 N94-30389
NIVR-01604N p 3133 N94-30387
NIVR-02003N p 3338 N94-30328
NIVR-02506N p 3311 N94-30391
NIVR-07801N p 3148 N94-30342
NR PROJ. H12-92 p 3356 N94-28791
NR PROJ. 032-02 p 3355 N94-28737
NSERC-A-7801 p 3196 N94-29284
NSERC-ISE-0046203 p 3526 N94-30433
NSERC-OGP-046506 p 3526 N94-30433
NSF ATM-92-07345 p 3374 N94-30187
NSF BCS-91-20655 p 3445 N94-30566
NSF BSR-88-17965 p 3351 N94-30628
NSF CCR-88-03549 p 3462 N94-30860
NSF CCR-90-02614 p 3526 N94-30433
p 3426 N94-30434
NSF CCR-90-07195 p 3428 N94-30734
NSF CCR-90-11214 p 3423 N94-30345
NSF CCR-90-24271 p 3428 N94-30734
NSF CCR-91-0473 p 3462 N94-30860
NSF DDM-92-01340 p 3409 N94-28917
NSF DDM-92-10018 p 3442 N94-30547
NSF DDM-93-19208 p 3442 N94-30547
NSF DMR-88-21625 p 3235 N94-29770
NSF DMS-90-02095 p 3467 N94-29162
NSF DMS-91-03452 p 3464 N94-29129
NSF DMS-91-04432 p 3464 N94-28876
p 3464 N94-29014
NSF EET-88-15285 p 3235 N94-29770
NSF IRI-91-08638 p 3452 N94-29063
NSF IRI-91-23747 p 3458 N94-30407
p 3458 N94-30408
p 3427 N94-30725
NSF IRI-91-58473 p 3445 N94-30564
NSF IRI-92-09031 p 3445 N94-30564
NSF NCR-91-15055 p 3475 N94-30678
NSF RIA-90-09842 p 3236 N94-29775
NSF STC-88-09648 p 3462 N94-30860
NSG-1601 p 3183 N94-30016
NWO-00-62-518 p 3423 N94-30332
p 3432 N94-30356
N00014-C-93-0007 p 3204 N94-29196
N00014-82-K-0612 p 3197 N94-29312
N00014-85-K-0198 p 3409 N94-28917
N00014-87-C-0709 p 3262 N94-28687
N00014-88-C-0285 p 3498 N94-28656
N00014-89-J-1276 p 3317 N94-28761
N00014-89-J-1311 p 3511 N94-28773
N00014-89-J-1545 p 3513 N94-29130
p 3486 N94-29131
p 3189 N94-29140
p 3513 N94-29155
N00014-89-J-1721 p 3195 N94-29276
N00014-89-J-1754 p 3356 N94-28891
N00014-89-J-1865 p 3384 N94-28829
N00014-89-J-1870 p 3464 N94-29129
N00014-90-J-1002 p 3263 N94-28995
N00014-90-J-1045 p 3369 N94-29067
N00014-90-J-1065 p 3293 N94-29179
N00014-90-J-1300 p 3178 N94-29126
N00014-90-J-1531 p 3212 N94-28661
N00014-90-J-1533 p 3443 N94-30555
N00014-90-J-1840 p 3377 N94-28877
N00014-90-J-4012 p 3377 N94-29436
N00014-91-C-0128 p 3202 N94-28830
N00014-91-C-0172 p 3477 N94-28904
N00014-91-J-1116 p 3406 N94-29695
p 3431 N94-29846
p 3420 N94-29890
N00014-91-J-1145 p 3451 N94-28651
N00014-91-J-1219 p 3408 N94-28794
N00014-91-J-1269 p 3203 N94-29043
p 3204 N94-29395
N00014-91-J-1283 p 3418 N94-29404
p 3431 N94-29869
p 3431 N94-29396
N00014-91-J-1308 p 3272 N94-29149
N00014-91-J-1366 p 3512 N94-28775
N00014-91-J-1410 p 3317 N94-28811
N00014-91-J-1414 p 3235 N94-29770
N00014-91-J-1876 p 3486 N94-29060
N00014-91-J-1927 p 3203 N94-29089
p 3405 N94-28798
N00014-91-J-1988 p 3176 N94-28729
N00014-91-J-4075 p 3177 N94-28730
p 3177 N94-28731
N00014-92-C-0214 p 3241 N94-28755
N00014-92-C-6004 p 3243 N94-29054
N00014-92-J-1153 p 3529 N94-28645
N00014-92-J-1234 p 3417 N94-29390
N00014-92-J-1264 p 3464 N94-28876
p 3464 N94-29014
N00014-92-J-1455 p 3466 N94-28807
N00014-92-J-1587 p 3377 N94-29128
N00014-92-J-1617 p 3405 N94-28764
N00014-92-J-1809 p 3443 N94-30555
N00014-92-J-1828 p 3466 N94-28888
N00014-92-J-1951 p 3512 N94-28872
N00014-92-J-1996 p 3262 N94-28650
N00014-92-J-4116 p 3203 N94-28900
N00014-92-J-6004 p 3357 N94-29062
N00014-93-C-0067 p 3318 N94-29057
N00014-93-C-0100 p 3419 N94-29678
N00014-93-C-0147 p 3292 N94-28635
N00014-93-C-2044 p 3212 N94-28725
N00014-93-I-G019 p 3477 N94-28689
N00014-93-J-0018 p 3272 N94-29149
N00014-93-1-G014 p 3188 N94-28777
N00014-93-1-0015 p 3271 N94-29061
N00014-93-1-0080 p 3224 N94-28879
N00014-93-1-0102 p 3411 N94-29214
N00014-93-1-0235 p 3512 N94-28871
N00014-93-1-0375 p 3202 N94-28793
N00014-93-1-0409 p 3512 N94-28872
N00014-93-1-0806 p 3397 N94-28860
N00014-93-1-1307 p 3408 N94-28790
N00014-93-1-2005 p 3244 N94-29303
N00014-94-C-0030 p 3504 N94-28776
N00039-92-C-0100 p 3478 N94-29388
N00140-87-C-6321 p 3154 N94-29263
N00140-87-C-9902 p 3154 N94-29269
RTOP 142-20-14-02 p 3512 N94-29101
RTOP 199-16-12-17 p 3163 N94-29648
RTOP 199-16-12-19 p 3163 N94-29648
RTOP 199-18-12-07 p 3385 N94-29401
RTOP 199-90-63-20 p 3163 N94-29648
RTOP 232-01-0B p 3319 N94-29104
RTOP 233-01-03-22 p 3160 N94-28836
p 3329 N94-29098
RTOP 233-01-03 p 3422 N94-30197
RTOP 233-03-02-04 p 3175 N94-29458
RTOP 233-03-03-03 p 3466 N94-29489
RTOP 235-01-0B p 3286 N94-29000
RTOP 310-10-60-90-03 p 3249 N94-29653
RTOP 310-10-60-93-01 p 3249 N94-29654
RTOP 310-10-61-87-02 p 3144 N94-29614
RTOP 310-10-63-50-00 p 3159 N94-29655
p 3159 N94-29656
RTOP 310-20-64-89-01 p 3247 N94-29616
RTOP 310-20-65-86-04 p 3247 N94-29615
RTOP 310-20-65-86-08 p 3249 N94-29657
RTOP 310-20-66-53-00 p 3251 N94-29672
RTOP 310-20-66-87-02 p 3250 N94-29658
RTOP 310-20-67-88-03 p 3247 N94-29617
RTOP 310-20-67-92-02 p 3250 N94-29659
RTOP 310-30-69-88-04 p 3247 N94-29620
RTOP 310-30-70-89-01 p 3250 N94-29660
p 3250 N94-29661
RTOP 310-30-71-83-02 p 3247 N94-29618
p 3247 N94-29619
p 3250 N94-29662
RTOP 314-30-43-10-18 p 3251 N94-29670
RTOP 314-30-50-12-78 p 3248 N94-29624
RTOP 314-30-55-30-01 p 3248 N94-29625
RTOP 314-30-61-02-01 p 3250 N94-29663
p 3250 N94-29664
RTOP 314-30-61-02-10 p 3251 N94-29671
RTOP 314-30-63-03-19 p 3250 N94-29665
RTOP 314-40-22-42-05 p 3160 N94-29666
RTOP 314-40-31-30-03 p 3164 N94-29621
RTOP 314-40-41-10-13 p 3248 N94-29623
RTOP 314-40-41-11-06 p 3251 N94-29669
RTOP 314-40-42-10-40 p 3248 N94-29622
RTOP 315-90-31-00-02 p 3252 N94-29673
RTOP 315-91-10-13-08 p 3251 N94-29667
RTOP 315-91-50-20-04 p 3251 N94-29668
RTOP 323-57-4A p 3165 N94-28697
RTOP 324-02-03 p 3480 N94-30274
RTOP 464-54-03-70 p 3342 N94-28587
RTOP 474-12-10 p 3169 N94-30123
RTOP 474-46-10 p 3167 N94-28814
p 3167 N94-29383
RTOP 505-59-10-03 p 3408 N94-28818
RTOP 505-59-10-13 p 3133 N94-30176
RTOP 505-59-36-01 p 3293 N94-28839
RTOP 505-59-52 p 3478 N94-29382
RTOP 505-59-53 p 3132 N94-30151
RTOP 505-62-10 p 3151 N94-29103
p 3301 N94-29552
RTOP 505-62-36 p 3303 N94-30205
p 3303 N94-30227
RTOP 505-62-52 p 3150 N94-28923
p 3197 N94-29356
p 3273 N94-29471
p 3421 N94-30174
p 3422 N94-30175
p 3135 N94-30949
RTOP 505-62-84 p 3156 N94-28749
RTOP 505-63-12 p 3318 N94-28821
p 3183 N94-30125
p 3183 N94-30178
RTOP 505-63-5A p 3189 N94-28832
p 3213 N94-28922
p 3218 N94-30177
RTOP 505-63-5B p 3317 N94-28815
p 3317 N94-28819
p 3151 N94-29103
p 3183 N94-30190
RTOP 505-63-50-04 p 3177 N94-28823
p 3180 N94-29472
p 3181 N94-29541
RTOP 505-63-50-10 p 3479 N94-29461
p 3479 N94-29856
RTOP 505-63-50-15 p 3122 N94-28658
RTOP 505-63-52 p 3205 N94-29758

RTOP 505-63-58 ..... p 3319 N94-29104
RTOP 505-64-10-07 ..... p 3431 N94-29494
p 3432 N94-30160
RTOP 505-68-10 ..... p 3132 N94-30124
p 3133 N94-30152
RTOP 505-68-70-05 ..... p 3130 N94-29443
RTOP 505-69-20-01 ..... p 3130 N94-29473
RTOP 505-70-59-03 ..... p 3157 N94-30200
RTOP 505-70-69 ..... p 3279 N94-30147
RTOP 505-90-00 ..... p 3534 N94-30149
p 3534 N94-30150
RTOP 505-90-5K ..... p 3272 N94-29096
RTOP 505-90-52-01 ..... p 3272 N94-29381
p 3454 N94-30207
p 3454 N94-30208
p 3454 N94-30209
RTOP 506-40-41-01 ..... p 3130 N94-29545
RTOP 506-41-11 ..... p 3172 N94-28999
RTOP 506-41-41 ..... p 3174 N94-28747
p 3174 N94-28924
RTOP 506-42-31 ..... p 3171 N94-28736
p 3172 N94-29097
p 3173 N94-29444
RTOP 506-42-72 ..... p 3271 N94-28835
p 3173 N94-29403
RTOP 506-43-41 ..... p 3214 N94-29399
RTOP 506-43-61-02 ..... p 3175 N94-29458
RTOP 506-44-2C ..... p 3267 N94-30198
RTOP 506-48-00 ..... p 3168 N94-29405
RTOP 506-49-21 ..... p 3235 N94-29767
RTOP 506-72-1B ..... p 3264 N94-29209
RTOP 506-72-1C ..... p 3242 N94-28826
RTOP 510-01-50 ..... p 3181 N94-29684
RTOP 510-02-12-01 ..... p 3178 N94-29100
RTOP 510-02-12 ..... p 3319 N94-29384
RTOP 535-03-10-02 ..... p 3132 N94-29937
RTOP 535-03-10 ..... p 3151 N94-29103
p 3152 N94-29438
RTOP 537-03-21-03 ..... p 3479 N94-29464
RTOP 538-05-15-03 ..... p 3273 N94-29460
RTOP 579-21-44-70 ..... p 3370 N94-29455
RTOP 583-02-21 ..... p 3202 N94-28822
p 3338 N94-30196
RTOP 584-03-11 ..... p 3316 N94-28508
p 3318 N94-28840
p 3203 N94-28921
p 3155 N94-30204
RTOP 585-03-21 ..... p 3172 N94-28834
RTOP 590-13-11 ..... p 3178 N94-29208
RTOP 590-14-91-52 ..... p 3164 N94-28417
RTOP 593-71-00 ..... p 3171 N94-28833
RTOP 694-03-011 ..... p 3168 N94-29757
RTOP 763-22-2J ..... p 3298 N94-28838
RTOP 763-23-45-70 ..... p 3479 N94-29407
RTOP 906-76-40-43-01 ..... p 3248 N94-29626
SBIR-02.09-9282 ..... p 3480 N94-30274
SERC-GR/F-91582 ..... p 3459 N94-30412
p 3425 N94-30415
SERC-92314900 ..... p 3395 N94-30970
SION-612-317-107 ..... p 3433 N94-30720
SRC-88-MC-507 ..... p 3235 N94-29770
SRI PROJ. 4725 ..... p 3549 N94-28816
W-31-109-ENG-38 ..... p 3468 N94-28459
p 3297 N94-28461
p 3481 N94-28462
p 3261 N94-28487
p 3482 N94-28509
p 3211 N94-28536
p 3368 N94-28568
p 3483 N94-28569
p 3511 N94-28570
p 3506 N94-29510
p 3279 N94-30020
p 3207 N94-30021
p 3334 N94-30022
p 3349 N94-30023
p 3207 N94-30057
p 3350 N94-30116
p 3519 N94-30338
p 3185 N94-30593
p 3509 N94-30697
p 3311 N94-30703
p 3519 N94-30718
p 3428 N94-30754
p 3220 N94-30778
p 3429 N94-30840
p 3477 N94-30873
p 3493 N94-30874
p 3493 N94-30893
p 3521 N94-30894
p 3521 N94-30897
p 3521 N94-30898
p 3493 N94-30903
W-7405-ENG-36 ..... p 3270 N94-28475
p 3342 N94-28521
p 3240 N94-28522
p 3355 N94-28538
p 3522 N94-28543
p 3201 N94-28544
p 3543 N94-28545
p 3463 N94-28548
p 3270 N94-28549
p 3522 N94-28572
p 3175 N94-28579
p 3552 N94-28580
p 3175 N94-28581
p 3419 N94-29816
p 3514 N94-29818
p 3182 N94-29933
p 3294 N94-29934
p 3217 N94-30025
p 3488 N94-30039
p 3480 N94-30098
p 3432 N94-30100
p 3208 N94-30101
p 3517 N94-30201
p 3465 N94-30366
p 3295 N94-30595
p 3335 N94-30610
p 3185 N94-30693
p 3548 N94-30694
p 3427 N94-30705
p 3536 N94-30706
p 3267 N94-30716
p 3200 N94-30748
p 3526 N94-30750
p 3509 N94-30752
p 3185 N94-30771
p 3210 N94-30774
p 3492 N94-30775
p 3210 N94-30776
p 3461 N94-30821
p 3497 N94-30825
p 3551 N94-30845
p 3498 N94-30846
p 3498 N94-30847
p 3520 N94-30848
W-7405-ENG-48 ..... p 3526 N94-28474
p 3270 N94-28476
p 3482 N94-28493
p 3404 N94-28505
p 3542 N94-28526
p 3175 N94-28528
p 3212 N94-28560
p 3122 N94-29842
p 3488 N94-29845
p 3277 N94-29923
p 3254 N94-29929
p 3321 N94-29951
p 3431 N94-29952
p 3349 N94-29954
p 3338 N94-29955
p 3254 N94-30043
p 3349 N94-30044
p 3506 N94-30045
p 3516 N94-30054
p 3420 N94-30056
p 3289 N94-30059
p 3295 N94-30060
p 3255 N94-30106
p 3421 N94-30117
p 3422 N94-30251
p 3240 N94-30449
p 3466 N94-30586
p 3335 N94-30594
p 3509 N94-30597
p 3295 N94-30598
p 3501 N94-30599
p 3281 N94-30600
p 3350 N94-30613
p 3352 N94-30634
p 3149 N94-30687
p 3497 N94-30712
p 3509 N94-30768
p 3354 N94-30822
p 3378 N94-30823
p 3497 N94-30825
p 3221 N94-30829
p 3296 N94-30830
p 3563 N94-30844
p 3510 N94-30875
p 3367 N94-30876
p 3493 N94-30891
p 3211 N94-30892
W-7405-ENG-82 ..... p 3187 N94-28483
p 3211 N94-28516
p 3404 N94-28517
p 3482 N94-28518
p 3187 N94-28519
p 3482 N94-28520
p 3201 N94-28525
p 3201 N94-28527
p 3510 N94-28529
p 3211 N94-28530
p 3187 N94-28561
p 3202 N94-28562
p 3406 N94-30004
p 3218 N94-30104
p 3209 N94-30336
p 3219 N94-30337
p 3519 N94-30338
p 3209 N94-30690
p 3519 N94-30691
p 3185 N94-30704
p 3521 N94-30899
p 3296 N94-30908

Typical Report Number Index Listing

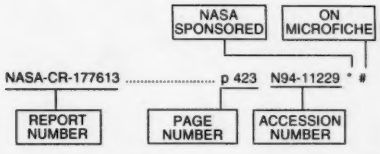

Listings in this index are arranged alphanumerically by report number. The accession number denotes the number by which the citation is identified. The page number helps to locate the citation in the abstract section. An asterisk (*) indicates that the item is a NASA report. A pound sign (#) indicates that the item is available on microfiche.

A-93030 ..... p 3555 N94-29891 * #
A-93053 ..... p 3160 N94-29627 * #
A-93077 ..... p 3132 N94-30151 * #
A-94054 ..... p 3385 N94-29401 * #

AD-A274977 ..... p 3486 N94-29087 #
AD-A274978 ..... p 3409 N94-28895 #
AD-A274979 ..... p 3410 N94-29088 #
AD-A274980 ..... p 3203 N94-29089 #
AD-A274981 ..... p 3121 N94-29090
AD-A274982 ..... p 3318 N94-29091
AD-A274983 ..... p 3224 N94-29092
AD-A274984 ..... p 3401 N94-29093
AD-A274986 ..... p 3513 N94-29125 #
AD-A274987 ..... p 3178 N94-29126 #
AD-A274988 ..... p 3431 N94-29127 #
AD-A274989 ..... p 3409 N94-28910 #
AD-A274993 ..... p 3263 N94-28994 #
AD-A274995 ..... p 3263 N94-28995 #
AD-A275001 ..... p 3213 N94-28886 #
AD-A275004 ..... p 3409 N94-28896
AD-A275007 ..... p 3272 N94-29195 #
AD-A275011 ..... p 3377 N94-29128 #
AD-A275013 ..... p 3243 N94-28897 #
AD-A275016 ..... p 3243 N94-28898 #
AD-A275017 ..... p 3244 N94-29094 #
AD-A275018 ..... p 3464 N94-29129 #
AD-A275019 ..... p 3513 N94-29130 #
AD-A275020 ..... p 3486 N94-29131 #
AD-A275021 ..... p 3550 N94-29132 #
AD-A275023 ..... p 3499 N94-29114 #
AD-A275024 ..... p 3410 N94-29115 #
AD-A275025 ..... p 3391 N94-29116 #
AD-A275029 ..... p 3265 N94-29511 #
AD-A275031 ..... p 3477 N94-29117 #
AD-A275037 ..... p 3272 N94-29149 #
AD-A275038 ..... p 3391 N94-29150 #
AD-A275046 ..... p 3157 N94-29151 #
AD-A275047 ..... p 3377 N94-29164 #
AD-A275048 ..... p 3530 N94-29165 #
AD-A275050 ..... p 3178 N94-29166 #
AD-A275053 ..... p 3214 N94-29133 #
AD-A275054 ..... p 3505 N94-29134 #
AD-A275056 ..... p 3178 N94-29135 #
AD-A275057 ..... p 3272 N94-29136 #
AD-A275058 ..... p 3359 N94-29137 #
AD-A275060 ..... p 3530 N94-29138 #
AD-A275061 ..... p 3530 N94-29139 #
AD-A275062 ..... p 3146 N94-29200 #
AD-A275063 ..... p 3410 N94-29152 #
AD-A275065 ..... p 3527 N94-29153 #
AD-A275070 ..... p 3293 N94-29179
AD-A275071 ..... p 3411 N94-29180
AD-A275073 ..... p 3398 N94-29154 #
AD-A275074 ..... p 3513 N94-29155 #
AD-A275075 ..... p 3189 N94-29140 #
AD-A275076 ..... p 3329 N94-29095 #
AD-A275077 ..... p 3146 N94-28870 #
AD-A275078 ..... p 3512 N94-28871 #
AD-A275079 ..... p 3512 N94-28872 #
AD-A275080 ..... p 3398 N94-28887 #
AD-A275081 ..... p 3262 N94-28842
AD-A275083 ..... p 3356 N94-28843 #
AD-A275084 ..... p 3369 N94-28847
AD-A275092 ..... p 3499 N94-28848 #
AD-A275093 ..... p 3452 N94-29063 #
AD-A275100 ..... p 3529 N94-28911
AD-A275103 ..... p 3400 N94-28902 #
AD-A275104 ..... p 3391 N94-28912 #
AD-A275106 ..... p 3263 N94-28913 #
AD-A275107 ..... p 3122 N94-28899 #
AD-A275115 ..... p 3136 N94-28914 #
AD-A275116 ..... p 3419 N94-29746 #
AD-A275118 ..... p 3167 N94-29002 #
AD-A275121 ..... p 3477 N94-29003 #
AD-A275122 ..... p 3189 N94-29004 #
AD-A275126 ..... p 3149 N94-29005 #
AD-A275127 ..... p 3146 N94-29042 #
AD-A275133 ..... p 3243 N94-29064 #
AD-A275134 ..... p 3361 N94-29286 #
AD-A275135 ..... p 3412 N94-29287 #
AD-A275140 ..... p 3499 N94-29694 #
AD-A275142 ..... p 3494 N94-29065
AD-A275149 ..... p 3486 N94-29021 #
AD-A275150 ..... p 3167 N94-29022 #
AD-A275151 ..... p 3347 N94-29023 #
AD-A275154 ..... p 3486 N94-29032 #
AD-A275155 ..... p 3337 N94-29033 #
AD-A275156 ..... p 3400 N94-29034 #
AD-A275158 ..... p 3203 N94-29043 #
AD-A275159 ..... p 3435 N94-29044 #
AD-A275162 ..... p 3332 N94-29288
AD-A275166 ..... p 3263 N94-29045 #
AD-A275170 ..... p 3552 N94-29046 #
AD-A275171 ..... p 3156 N94-29047 #
AD-A275172 ..... p 3150 N94-29048 #
AD-A275174 ..... p 3325 N94-28849
AD-A275176 ..... p 3391 N94-29049 #
AD-A275177 ..... p 3430 N94-29050 #
AD-A275178 ..... p 3189 N94-29058 #
AD-A275179 ..... p 3529 N94-29066 #
AD-A275182 ..... p 3369 N94-29067 #
AD-A275184 ..... p 3405 N94-29181 #
AD-A275185 ..... p 3242 N94-28859 #
AD-A275186 ..... p 3397 N94-28860 #
AD-A275187 ..... p 3399 N94-28861 #
AD-A275191 ..... p 3410 N94-29068 #
AD-A275192 ..... p 3178 N94-29024 #
AD-A275193 ..... p 3264 N94-29289 #
AD-A275194 ..... p 3466 N94-28888
AD-A275197 ..... p 3512 N94-28889
AD-A275198 ..... p 3512 N94-28890
AD-A275199 ..... p 3434 N94-29026
AD-A275202 ..... p 3298 N94-29290 #
AD-A275203 ..... p 3356 N94-28891
AD-A275204 ..... p 3391 N94-28892
AD-A275205 ..... p 3430 N94-29051
AD-A275207 ..... p 3357 N94-28893
AD-A275209 ..... p 3401 N94-29302 #
AD-A275214 ..... p 3243 N94-29069 #
AD-A275215 ..... p 3357 N94-29070 #
AD-A275217 ..... p 3244 N94-29303 #
AD-A275218 ..... p 3499 N94-29059 #
AD-A275219 ..... p 3486 N94-29060 #
AD-A275221 ..... p 3263 N94-28915
AD-A275222 ..... p 3405 N94-28916
AD-A275223 ..... p 3398 N94-29027
AD-A275224 ..... p 3271 N94-29061 #
AD-A275225 ..... p 3357 N94-29062 #
AD-A275227 ..... p 3478 N94-29388 #
AD-A275228 ..... p 3150 N94-29389 #
AD-A275229 ..... p 3417 N94-29390 #
AD-A275230 ..... p 3146 N94-29391 #
AD-A275232 ..... p 3417 N94-29392 #
AD-A275235 ..... p 3263 N94-29028
AD-A275237 ..... p 3361 N94-29393 #
AD-A275238 ..... p 3370 N94-29394 #
AD-A275243 ..... p 3204 N94-29395 #
AD-A275244 ..... p 3431 N94-29396 #
AD-A275246 ..... p 3361 N94-29430 #
AD-A275247 ..... p 3203 N94-28900
AD-A275248 ..... p 3224 N94-28901
AD-A275250 ..... p 3392 N94-29431 #
AD-A275251 ..... p 3377 N94-29432 #
AD-A275253 ..... p 3400 N94-29029
AD-A275255 ..... p 3319 N94-29433 #
AD-A275256 ..... p 3529 N94-29053 #
AD-A275259 ..... p 3243 N94-29054 #
AD-A275260 ..... p 3453 N94-29304 #
AD-A275261 ..... p 3391 N94-29071
AD-A275263 ..... p 3529 N94-28903 #
AD-A275264 ..... p 3477 N94-28904 #
AD-A275267 ..... p 3527 N94-28905 #
AD-A275271 ..... p 3410 N94-29006 #
AD-A275272 ..... p 3410 N94-29007 #
AD-A275273 ..... p 3418 N94-29434 #
AD-A275274 ..... p 3272 N94-29435 #
AD-A275275 ..... p 3377 N94-29436 #
AD-A275278 ..... p 3530 N94-29182
AD-A275287 ..... p 3288 N94-29437 #
AD-A275296 ..... p 3369 N94-28873 #
AD-A275297 ..... p 3369 N94-29183
AD-A275298 ..... p 3242 N94-28874 #
AD-A275304 ..... p 3401 N94-29184
AD-A275308 ..... p 3369 N94-29194
AD-A275309 ..... p 3391 N94-29211
AD-A275311 ..... p 3499 N94-28875 #
AD-A275320 ..... p 3464 N94-28876 #
AD-A275321 ..... p 3377 N94-28877 #
AD-A275322 ..... p 3409 N94-28878 #
AD-A275325 ..... p 3224 N94-28879 #
AD-A275328 ..... p 3409 N94-28917 #
AD-A275332 ..... p 3400 N94-28918 #
AD-A275334 ..... p 3293 N94-28919 #
AD-A275336 ..... p 3419 N94-29797 #
AD-A275338 ..... p 3551 N94-29212
AD-A275341 ..... p 3329 N94-29213
AD-A275342 ..... p 3411 N94-29214
AD-A275346 ..... p 3409 N94-28920 #
AD-A275348 ..... p 3400 N94-28996 #
AD-A275349 ..... p 3400 N94-28997 #
AD-A275359 ..... p 3146 N94-28998 #
AD-A275360 ..... p 3452 N94-29016 #
AD-A275362 ..... p 3298 N94-28894 #
AD-A275363 ..... p 3177 N94-29008 #
AD-A275365 ..... p 3499 N94-29009 #
AD-A275369 ..... p 3189 N94-29010 #
AD-A275373 ..... p 3369 N94-29011 #
AD-A275374 ..... p 3177 N94-29012 #
AD-A275375 ..... p 3434 N94-29013 #
AD-A275377 ..... p 3464 N94-29014 #
AD-A275378 ..... p 3197 N94-29312 #
AD-A275380 ..... p 3398 N94-29313 #
AD-A275383 ..... p 3243 N94-29072 #
AD-A275384 ..... p 3264 N94-29305 #
AD-A275385 ..... p 3411 N94-29201
AD-A275387 ..... p 3478 N94-29314 #
AD-A275389 ..... p 3129 N94-29306 #
AD-A275390 ..... p 3411 N94-29202
AD-A275392 ..... p 3174 N94-29307 #
AD-A275393 ..... p 3225 N94-29308 #
AD-A275394 ..... p 3293 N94-29309 #
AD-A275395 ..... p 3504 N94-29055 #
AD-A275396 ..... p 3214 N94-29203
AD-A275397 ..... p 3203 N94-29056 #
AD-A275399 ..... p 3377 N94-29204
AD-A275400 ..... p 3204 N94-29205
AD-A275401 ..... p 3204 N94-29196
AD-A275403 ..... p 3318 N94-29057 #
AD-A275404 ..... p 3478 N94-29206
AD-A275405 ..... p 3411 N94-29207
AD-A275409 ..... p 3513 N94-29215
AD-A275413 ..... p 3173 N94-29216
AD-A275414 ..... p 3242 N94-28862 #
AD-A275416 ..... p 3129 N94-29197
AD-A275418 ..... p 3325 N94-28863 #
AD-A275419 ..... p 3435 N94-29198
AD-A275423 ..... p 3452 N94-28864 #
AD-A275424 ..... p 3177 N94-28865 #
AD-A275431 ..... p 3409 N94-28866 #
AD-A275439 ..... p 3202 N94-28867 #

AD-A275440 ..... p 3356 N94-28868 #
AD-A275442 ..... p 3356 N94-28869 #
AD-A275443 ..... p 3512 N94-28880 #
AD-A275445 ..... p 3325 N94-28881 #
AD-A275446 ..... p 3356 N94-28882 #
AD-A275447 ..... p 3452 N94-28883 #
AD-A275448 ..... p 3384 N94-28884 #
AD-A275449 ..... p 3225 N94-29310 #
AD-A275451 ..... p 3154 N94-28632 #
AD-A275454 ..... p 3262 N94-28805 #
AD-A275456 ..... p 3213 N94-28806 #
AD-A275458 ..... p 3466 N94-28807
AD-A275459 ..... p 3325 N94-28808 #
AD-A275460 ..... p 3355 N94-28728 #
AD-A275461 ..... p 3212 N94-28733 #
AD-A275462 ..... p 3177 N94-28735
AD-A275464 ..... p 3355 N94-28737 #
AD-A275465 ..... p 3271 N94-28738 #
AD-A275466 ..... p 3176 N94-28673
AD-A275467 ..... p 3271 N94-28809
AD-A275469 ..... p 3389 N94-28810 #
AD-A275470 ..... p 3122 N94-28674 #
AD-A275471 ..... p 3355 N94-28684 #
AD-A275475 ..... p 3214 N94-29073 #
AD-A275477 ..... p 3355 N94-28685 #
AD-A275490 ..... p 3430 N94-28659 #
AD-A275500 ..... p 3145 N94-28660 #
AD-A275501 ..... p 3212 N94-28661 #
AD-A275503 ..... p 3523 N94-28662 #
AD-A275504 ..... p 3356 N94-28791 #
AD-A275505 ..... p 3317 N94-28811
AD-A275510 ..... p 3384 N94-28667
AD-A275511 ..... p 3485 N94-28668
AD-A275512 ..... p 3262 N94-28669
AD-A275513 ..... p 3463 N94-28670
AD-A275521 ..... p 3538 N94-28671 #
AD-A275524 ..... p 3434 N94-28672
AD-A275525 ..... p 3504 N94-28686
AD-A275529 ..... p 3262 N94-28687
AD-A275531 ..... p 3176 N94-28688
AD-A275532 ..... p 3242 N94-28812
AD-A275540 ..... p 3389 N94-28797 #
AD-A275541 ..... p 3499 N94-28813 #
AD-A275546 ..... p 3146 N94-28837 #
AD-A275549 ..... p 3346 N94-28722
AD-A275550 ..... p 3347 N94-28684 #
AD-A275560 ..... p 3451 N94-28792 #
AD-A275565 ..... p 3202 N94-28793 #
AD-A275567 ..... p 3164 N94-28827 #
AD-A275570 ..... p 3504 N94-28828 #
AD-A275582 ..... p 3451 N94-28723 #
AD-A275586 ..... p 3212 N94-28725
AD-A275591 ..... p 3316 N94-28726
AD-A275593 ..... p 3346 N94-28727
AD-A275597 ..... p 3176 N94-28729
AD-A275598 ..... p 3177 N94-28730
AD-A275599 ..... p 3177 N94-28731
AD-A275600 ..... p 3399 N94-28766 #
AD-A275602 ..... p 3463 N94-28768
AD-A275607 ..... p 3224 N94-28769
AD-A275608 ..... p 3292 N94-28770
AD-A275611 ..... p 3346 N94-28774 #
AD-A275616 ..... p 3407 N94-28633
AD-A275617 ..... p 3241 N94-28634 #
AD-A275619 ..... p 3292 N94-28635
AD-A275622 ..... p 3477 N94-28636 #
AD-A275634 ..... p 3528 N94-28637 #
AD-A275635 ..... p 3368 N94-28638 #
AD-A275637 ..... p 3407 N94-28639 #
AD-A275638 ..... p 3528 N94-28640
AD-A275640 ..... p 3212 N94-28641 #
AD-A275641 ..... p 3529 N94-28645
AD-A275642 ..... p 3407 N94-28648 #
AD-A275647 ..... p 3399 N94-28649 #
AD-A275648 ..... p 3262 N94-28650
AD-A275652 ..... p 3451 N94-28651 #
AD-A275654 ..... p 3368 N94-28652 #
AD-A275655 ..... p 3176 N94-28653 #
AD-A275661 ..... p 3176 N94-28654 #
AD-A275662 ..... p 3176 N94-28655 #
AD-A275663 ..... p 3498 N94-28656 #
AD-A275666 ..... p 3145 N94-28657 #
AD-A275674 ..... p 3369 N94-28663
AD-A275675 ..... p 3407 N94-28664 #
AD-A275678 ..... p 3270 N94-28665 #
AD-A275701 ..... p 3121 N94-28666 #
AD-A275702 ..... p 3477 N94-28689 #
AD-A275704 ..... p 3376 N94-28690 #
AD-A275711 ..... p 3407 N94-28691 #
AD-A275712 ..... p 3270 N94-28692 #
AD-A275715 ..... p 3376 N94-28642 #
AD-A275716 ..... p 3202 N94-28643 #
AD-A275739 ..... p 3121 N94-28732 #
AD-A275745 ..... p 3511 N94-28734 #
AD-A275751 ..... p 3230 N94-28644
AD-A275755 ..... p 3315 N94-28646 #
AD-A275756 ..... p 3145 N94-28647 #
AD-A275758 ..... p 3463 N94-28759 #
AD-A275759 ..... p 3408 N94-28760 #
AD-A275761 ..... p 3317 N94-28761 #
AD-A275762 ..... p 3241 N94-28762 #
AD-A275763 ..... p 3241 N94-28763 #
AD-A275765 ..... p 3405 N94-28764 #
AD-A275775 ..... p 3292 N94-28765 #
AD-A275776 ..... p 3419 N94-29678 #
AD-A275777 ..... p 3376 N94-28740 #
AD-A275788 ..... p 3230 N94-28742 #
AD-A275789 ..... p 3121 N94-28743 #
AD-A275791 ..... p 3136 N94-28744 #
AD-A275793 ..... p 3241 N94-28745
AD-A275798 ..... p 3262 N94-28767 #
AD-A275800 ..... p 3241 N94-28771 #
AD-A275809 ..... p 3156 N94-28772
AD-A275811 ..... p 3511 N94-28773
AD-A275813 ..... p 3384 N94-28829
AD-A275814 ..... p 3202 N94-28830
AD-A275816 ..... p 3286 N94-28831
AD-A275818 ..... p 3498 N94-28804
AD-A275819 ..... p 3512 N94-28775
AD-A275820 ..... p 3188 N94-28777
AD-A275844 ..... p 3371 N94-29747 #
AD-A275847 ..... p 3498 N94-28780
AD-A275848 ..... p 3430 N94-28781 #
AD-A275849 ..... p 3408 N94-28784
AD-A275851 ..... p 3408 N94-28790 #
AD-A275852 ..... p 3408 N94-28794 #
AD-A275860 ..... p 3156 N94-28752 #
AD-A275861 ..... p 3156 N94-28753 #
AD-A275869 ..... p 3397 N94-28754 #
AD-A275872 ..... p 3241 N94-28755 #
AD-A275885 ..... p 3388 N94-28756 #
AD-A275888 ..... p 3504 N94-28776 #
AD-A275889 ..... p 3135 N94-28799 #
AD-A275890 ..... p 3271 N94-28778 #
AD-A275893 ..... p 3527 N94-28779 #
AD-A275894 ..... p 3527 N94-28796 #
AD-A275896 ..... p 3405 N94-28798
AD-A275901 ..... p 3388 N94-28757 #
AD-A276593 ..... p 3149 N94-30905

AD-B173557 ..... p 3311 N94-30391
AD-B173626 ..... p 3158 N94-30856
AD-B173649 ..... p 3458 N94-30402
AD-B173650 ..... p 3282 N94-30855
AD-B173651 ..... p 3135 N94-30916 #
AD-B173696L ..... p 3503 N94-28513 #
AD-B174270 ..... p 3143 N94-30915
AD-B174629 ..... p 3143 N94-30854
AD-B174630 ..... p 3143 N94-30853
AD-B174654 ..... p 3433 N94-30913
AD-B174765 ..... p 3153 N94-30914
AD-B174795 ..... p 3429 N94-30912
AD-B175154 ..... p 3134 N94-30871
AD-B175835 ..... p 3324 N94-30872
AD-B179099 ..... p 3142 N94-30439
AD-B179106 ..... p 3335 N94-30759
AD-B179107 ..... p 3229 N94-30421
AD-B179108 ..... p 3133 N94-30492
AD-B179178 ..... p 3229 N94-30409
AD-B179220 ..... p 3158 N94-30423
AD-B179293 ..... p 3281 N94-30763
AD-B179298 ..... p 3428 N94-30764
AD-B179299 ..... p 3281 N94-30756
AD-B179387 ..... p 3399 N94-30969
AD-B179388 ..... p 3220 N94-30420
AD-B179613 ..... p 3402 N94-30422
AD-B179614 ..... p 3260 N94-30518

AD-D016016 ..... p 3288 N94-29699

AD-E201743 ..... p 3504 N94-28828 #
AD-E201744 ..... p 3164 N94-28827 #
AD-E501740 ..... p 3409 N94-28878 #

AFCESA/CEL-TR-91-06 ..... p 3156 N94-29047 #

AFCESA/ESL-TR-91-26 ..... p 3157 N94-29151 #
AFCESA/ESL-TR-91-41 ..... p 3319 N94-29433 #

AFFTC-TLR-93-41 ..... p 3398 N94-28887 #

AFGWC-TN-93/001 ..... p 3371 N94-29747 #

AFIT/CI/CIA-93-1170 ..... p 3272 N94-29435 #
AFIT/CI/CIA-93-147 ..... p 3551 N94-29212
AFIT/CI/CIA-93-148 ..... p 3369 N94-29011 #
AFIT/CI/CIA-93-150 ..... p 3499 N94-28875 #
AFIT/CI/CIA-93-154 ..... p 3369 N94-29183
AFIT/CI/CIA-93-155 ..... p 3369 N94-28873 #
AFIT/CI/CIA-93-156 ..... p 3369 N94-29194
AFIT/CI/CIA-93-157 ..... p 3361 N94-29430 #
AFIT/CI/CIA-93-158 ..... p 3499 N94-29009 #
AFIT/CI/CIA-93-160 ..... p 3400 N94-28918 #
AFIT/CI/CIA-93-163 ..... p 3271 N94-28738 #
AFIT/CI/CIA-93-164 ..... p 3271 N94-28809
AFIT/CI/CIA-93-23D ..... p 3293 N94-28919 #
AFIT/CI/CIA-93-24D ..... p 3391 N94-29211
AFIT/CI/CIA-93-28D ..... p 3389 N94-28810 #
AFIT/CI/CIA-93-29D ..... p 3452 N94-29016 #

AFIT/CI/CIA/93-167 ..... p 3434 N94-29013 #

AFIT/GA/ENY-93D-2 ..... p 3298 N94-28894 #

AFIT/GA/ENY/93D-4 ..... p 3173 N94-29216

AFIT/GAE/ENY/93D-17 ..... p 3177 N94-29012 #
AFIT/GAE/ENY/93D-1 ..... p 3177 N94-29008 #
AFIT/GAE/ENY/93D-23 ..... p 3146 N94-28998 #
AFIT/GAE/ENY/93D-28 ..... p 3176 N94-28673

AFIT/GCE/ENG/93D-08 ..... p 3430 N94-29050 #

AFIT/GCM/LAS/93S-3 ..... p 3230 N94-28742 #

AFIT/GLM/LAL/93S-9 ..... p 3136 N94-28744 #

AFIT/GSS/LAS/93D-7 ..... p 3121 N94-28743 #

AFOSR-94-0002TR ..... p 3398 N94-29154 #
AFOSR-94-0004TR ..... p 3369 N94-28847
AFOSR-94-0004TR ..... p 3550 N94-29132 #
AFOSR-94-0015TR ..... p 3167 N94-29002 #
AFOSR-94-0017TR ..... p 3431 N94-29127 #
AFOSR-94-0019TR ..... p 3499 N94-29114 #
AFOSR-94-0020TR ..... p 3213 N94-28886 #
AFOSR-94-0021-TR ..... p 3512 N94-28890
AFOSR-94-0022TR ..... p 3505 N94-29134 #
AFOSR-94-0023TR ..... p 3513 N94-29125 #
AFOSR-94-0026TR ..... p 3499 N94-28848 #
AFOSR-94-0027TR ..... p 3122 N94-28899 #
AFOSR-94-0028TR ..... p 3512 N94-28889
AFOSR-94-0029-TR ..... p 3434 N94-29026
AFOSR-94-0030TR ..... p 3272 N94-29136 #
AFOSR-94-0032TR ..... p 3189 N94-29004 #
AFOSR-94-0034TR ..... p 3178 N94-29135 #
AFOSR-94-0036TR ..... p 3486 N94-29087 #
AFOSR-94-0038-TR ..... p 3398 N94-29027
AFOSR-94-0039TR ..... p 3486 N94-29032 #

AGARD-AR-322 ..... p 3169 N94-30350 #
AGARD-AR-326 ..... p 3528 N94-30934 #

AGARD-CP-536 ..... p 3189 N94-29246 #
AGARD-CP-538 ..... p 3136 N94-29558 #
AGARD-CP-540 ..... p 3379 N94-28420 #
AGARD-CP-542 ..... p 3256 N94-30495 #
AGARD-CP-545 ..... p 3412 N94-29315 #

AGARD-LS-194 ..... p 3151 N94-29291 #

AIAA PAPER 92-2600-CP ..... p 3133 N94-30388
AIAA PAPER 92-2619-CP ..... p 3133 N94-30387
AIAA PAPER 94-0374 ..... p 3172 N94-28999 * #
AIAA PAPER 94-0887-CP ..... p 3443 N94-30550 * #
AIAA PAPER 94-0888-CP ..... p 3446 N94-30569 * #
AIAA PAPER 94-1176-CP ..... p 3439 N94-30528 * #
AIAA PAPER 94-1177-CP ..... p 3439 N94-30529 * #
AIAA PAPER 94-1178-CP ..... p 3439 N94-30530 * #
AIAA PAPER 94-1180-CP ..... p 3439 N94-30531 * #
AIAA PAPER 94-1181-CP ..... p 3440 N94-30532 * #
AIAA PAPER 94-1182-CP ..... p 3440 N94-30533 * #
AIAA PAPER 94-1184-CP ..... p 3440 N94-30534 * #
AIAA PAPER 94-1185-CP ..... p 3440 N94-30535 * #
AIAA PAPER 94-1186-CP ..... p 3440 N94-30536 * #
AIAA PAPER 94-1187-CP ..... p 3440 N94-30537 * #
AIAA PAPER 94-1188-CP ..... p 3441 N94-30538 * #
AIAA PAPER 94-1189-CP ..... p 3441 N94-30539 * #
AIAA PAPER 94-1190-CP ..... p 3441 N94-30541 * #
AIAA PAPER 94-1191-CP ..... p 3441 N94-30542 * #
AIAA PAPER 94-1192-CP ..... p 3442 N94-30543 * #
AIAA PAPER 94-1193-CP ..... p 3442 N94-30544 * #
AIAA PAPER 94-1194-CP ..... p 3442 N94-30545 * #
AIAA PAPER 94-1195-CP ..... p 3442 N94-30546 * #
AIAA PAPER 94-1196-CP ..... p 3442 N94-30547 * #
AIAA PAPER 94-1197-CP ..... p 3442 N94-30548 * #
AIAA PAPER 94-1199-CP ..... p 3442 N94-30549 * #
AIAA PAPER 94-1200-CP ..... p 3443 N94-30551 * #
AIAA PAPER 94-1201-CP ..... p 3443 N94-30552 * #
AIAA PAPER 94-1202-CP ..... p 3443 N94-30553 * #
AIAA PAPER 94-1203-CP ..... p 3443 N94-30554 * #
AIAA PAPER 94-1204-CP ..... p 3443 N94-30555 * #
AIAA PAPER 94-1205-CP ..... p 3444 N94-30556 * #
AIAA PAPER 94-1206-CP ..... p 3444 N94-30557 * #
AIAA PAPER 94-1207-CP ..... p 3444 N94-30558 * #
AIAA PAPER 94-1208-CP ..... p 3444 N94-30559 * #
AIAA PAPER 94-1209-CP ..... p 3444 N94-30560 * #
AIAA PAPER 94-1210-CP ..... p 3444 N94-30561 * #

AIAA PAPER 94-1211-CP ..... p 3445 N94-30562 * #
AIAA PAPER 94-1212-CP ..... p 3445 N94-30563 * #
AIAA PAPER 94-1213-CP ..... p 3445 N94-30564 * #
AIAA PAPER 94-1214-CP ..... p 3445 N94-30565 * #
AIAA PAPER 94-1218-CP ..... p 3445 N94-30566 * #
AIAA PAPER 94-1219-CP ..... p 3445 N94-30567 * #
AIAA PAPER 94-1220-CP ..... p 3445 N94-30568 * #
AIAA PAPER 94-1221-CP ..... p 3446 N94-30570 * #
AIAA PAPER 94-1222-CP ..... p 3446 N94-30571 * #
AIAA PAPER 94-1223-CP ..... p 3446 N94-30572 * #
AIAA PAPER 94-1224-CP ..... p 3446 N94-30573 * #
AIAA PAPER 94-1225-CP ..... p 3446 N94-30574 * #
AIAA PAPER 94-1226-CP ..... p 3446 N94-30575 * #
AIAA PAPER 94-1227-CP ..... p 3447 N94-30576 * #
AIAA PAPER 94-1228-CP ..... p 3447 N94-30577 * #
AIAA PAPER 94-1229-CP ..... p 3447 N94-30578 * #
AIAA PAPER 94-1230-CP ..... p 3447 N94-30579 * #
AIAA PAPER 94-1232-CP ..... p 3447 N94-30580 * #
AIAA PAPER 94-1233-CP ..... p 3447 N94-30581 * #
AIAA PAPER 94-1235-CP ..... p 3448 N94-30582 * #
AIAA PAPER 94-1236-CP ..... p 3448 N94-30583 * #
AIAA PAPER 94-1237-CP ..... p 3448 N94-30584 * #
AIAA PAPER 94-1300-CP ..... p 3441 N94-30540 * #
AIAA PAPER 94-1301-CP ..... p 3439 N94-30527 * #
AIAA PAPER 94-2565 ..... p 3156 N94-28749 * #
AIAA PAPER 94-2750 ..... p 3173 N94-29403 * #
AIAA PAPER 94-3050 ..... p 3150 N94-28923 * #
AIAA PAPER 94-3078 ..... p 3303 N94-30227 * #

AL/CF-PC-1993-0039 ..... p 3391 N94-29071
AL/CF-PC-1993-0042 ..... p 3391 N94-28892
AL/CF-PC-1993-0043 ..... p 3400 N94-28997 #
AL/CF-PC-1993-0045 ..... p 3337 N94-29033 #
AL/CF-PC-1993-0046 ..... p 3400 N94-29029
AL/CF-PC-1993-0051 ..... p 3399 N94-28766 #
AL/CF-PC-1993-0052 ..... p 3400 N94-28996 #

AL/CF-SR-1993-0008 ..... p 3400 N94-29034 #

AL/CF-TR-1993-0093 ..... p 3399 N94-28861 #
AL/CF-TR-1993-0102 ..... p 3146 N94-29042 #
AL/CF-TR-1993-0134 ..... p 3150 N94-29048 #
AL/CF-TR-1993-0164 ..... p 3149 N94-29005 #

AL/HR-TR-1993-0132 ..... p 3409 N94-28910 #

ALENIA-TR-57X92054 ..... p 3133 N94-30387

ANL-HEP-CP-93-105 ..... p 3483 N94-28569 #
ANL-HEP-CP-93-94 ..... p 3481 N94-28462 #

ANL-93/33 ..... p 3261 N94-28487 #
ANL-93/41 ..... p 3429 N94-30840

ANL/CHM/CP-81640 ..... p 3220 N94-30778 #

ANL/CHM/PP-79434 ..... p 3477 N94-30873 #
ANL/CHM/PP-79990 ..... p 3493 N94-30903 #
ANL/CHM/PP-80227 ..... p 3493 N94-30874 #
ANL/CHM/PP-80389 ..... p 3482 N94-28509 #
ANL/CHM/PP-81072 ..... p 3519 N94-30718 #

ANL/DIS/CP-81382 ..... p 3349 N94-30023

ANL/EP/CP-79739-REV ..... p 3493 N94-30893 #
ANL/EP/CP-79904 ..... p 3506 N94-29510 #

ANL/ER/CP-80341 ..... p 3368 N94-28568 #
ANL/ER/CP-80787 ..... p 3334 N94-30022 #

ANL/ES/VU-81732 ..... p 3311 N94-30703

ANL/ET/CP-80135 ..... p 3207 N94-30021 #
ANL/ET/CP-80555 ..... p 3185 N94-30593
ANL/ET/CP-80624 ..... p 3279 N94-30020
ANL/ET/CP-81277 ..... p 3468 N94-28459 #
ANL/ET/CP-81504 ..... p 3297 N94-28461 #
ANL/ET/CP-81579 ..... p 3211 N94-28536 #

ANL/FE-93/1 ..... p 3207 N94-30057 #

ANL/FPP/TM-268 ..... p 3509 N94-30697

ANL/MCS/CP-81098 ..... p 3350 N94-30116
ANL/MCS/CP-81591 ..... p 3428 N94-30754 #

ANL/MSD/CP-78012 ..... p 3521 N94-30898 #
ANL/MSD/CP-79750 ..... p 3521 N94-30897 #
ANL/MSD/CP-80230 ..... p 3511 N94-28570 #
ANL/MSD/CP-80260 ..... p 3521 N94-30894

ARC-R93-207 ..... p 3545 N94-29871 * #

ARCCB-TR-93039 ..... p 3392 N94-29431 #

ARI-RP-94-01 ..... p 3528 N94-28637 #

ARI-RR-1072 ..... p 3347 N94-29549 * #

ARL-CR-109 ..... p 3301 N94-29552 * #
ARL-CR-111 ..... p 3178 N94-29024 #
ARL-CR-145 ..... p 3303 N94-30205 * #

ARL-GD-39 ..... p 3121 N94-29090

ARL-MR-113 ..... p 3203 N94-28921 * #

ARL-RR-17 ..... p 3318 N94-29091

ARL-TR-303 ..... p 3241 N94-28745
ARL-TR-313 ..... p 3417 N94-29392 #
ARL-TR-321 ..... p 3452 N94-28864 #
ARL-TR-401 ..... p 3303 N94-30227 * #
ARL-TR-93-10 ..... p 3272 N94-29149 #

ARO-23798.2-MS-F ..... p 3177 N94-28865 #
ARO-26106.23-CH ..... p 3224 N94-28769
ARO-26449.4-MS ..... p 3213 N94-28806 #
ARO-26595.7-EG ..... p 3270 N94-28665 #
ARO-26898.1-EL-SDI ..... p 3262 N94-28805 #
ARO-27063.12-MA-SM ..... p 3203 N94-29056 #
ARO-27163.5-MS ..... p 3202 N94-28867 #
ARO-27316.7-GS ..... p 3356 N94-28882 #
ARO-27510.3-EG ..... p 3154 N94-28632 #
ARO-27695.21-CH-SM ..... p 3384 N94-28667
ARO-27724-6-MS-SM ..... p 3174 N94-29307 #
ARO-27752.8-EG-S ..... p 3129 N94-29197
ARO-27780.18-PH ..... p 3485 N94-28668
ARO-27786.20-MA ..... p 3452 N94-28883 #
ARO-27887.6-CH ..... p 3225 N94-29306 #
ARO-27904.16-EL ..... p 3262 N94-28669
ARO-27956.17-LS ..... p 3384 N94-28884 #
ARO-28070.1-EL-SDI ..... p 3512 N94-28880 #
ARO-28096.7-CH-SAH ..... p 3225 N94-29310 #
ARO-28099.2-EL ..... p 3292 N94-28770
ARO-28159.6-EG ..... p 3129 N94-29306 #
ARO-28186.9-MA ..... p 3451 N94-28792 #
ARO-28344.1-GS ..... p 3325 N94-28881 #
ARO-28345.5-EL ..... p 3264 N94-29305 #
ARO-28535.7-MA ..... p 3451 N94-28723 #
ARO-28587.1-PH ..... p 3499 N94-28813 #
ARO-28652.4-PH ..... p 3504 N94-29055 #
ARO-28884.5-MS ..... p 3214 N94-29203
ARO-28905.6-MA ..... p 3243 N94-29072 #
ARO-29192.1-GS-S ..... p 3355 N94-28728 #
ARO-29728.1-MS-AAS ..... p 3204 N94-29205
ARO-30995.1-MA ..... p 3411 N94-29201
ARO-31207.1-MS ..... p 3212 N94-28733 #
ARO-32129.1-MS-SBI ..... p 3214 N94-29073 #
ARO-32311.1-PH ..... p 3293 N94-29309 #

ASC-TR-93-5023 ..... p 3146 N94-29391 #

ASSGI-301 ..... p 3153 N94-30130 #

AU-ARI-93-1 ..... p 3150 N94-29389 #

B-0426 ..... p 3157 N94-29904 * #

BER-583-162 ..... p 3243 N94-29054 #

BNL-48999 ..... p 3485 N94-28741 #
BNL-49231 ..... p 3342 N94-28523 #
BNL-49299 ..... p 3487 N94-29841 #
BNL-49554-REV ..... p 3483 N94-28565 #
BNL-49651 ..... p 3296 N94-30688 #
BNL-49696 ..... p 3497 N94-30588 #
BNL-49706 ..... p 3268 N94-30907 #
BNL-49718 ..... p 3206 N94-29931 #
BNL-49720 ..... p 3209 N94-30246 #
BNL-49748 ..... p 3222 N94-30906 #
BNL-49777 ..... p 3510 N94-28512 #
BNL-49971 ..... p 3551 N94-30884 #

CAA-PAPER-93008 ..... p 3148 N94-29887

CAR-94-02 ..... p 3537 N94-29410 * #

CCMS-93-19 ..... p 3317 N94-28801 * #

CDI-93-12 ..... p 3480 N94-30274 * #

CERL-SR-EC-93/10 ..... p 3346 N94-28774 #
CERL-SR-EC-93/12 ..... p 3346 N94-28727
CERL-SR-EC-94/04 ..... p 3346 N94-28722

CIRA-DLC-EST-271 ..... p 3133 N94-30387

CM-82 ..... p 3336 N94-30944 #

CMU-CS-93-154 ..... p 3418 N94-29434 #
CMU-CS-93-202 ..... p 3410 N94-29006 #
CMU-CS-93-206 ..... p 3453 N94-29304 #
CMU-CS-93-209 ..... p 3499 N94-29059 #
CMU-CS-93-226 ..... p 3398 N94-29313 #
CMU-CS-93-228 ..... p 3242 N94-28859 #
CMU-CS-93-229 ..... p 3405 N94-29181 #
CMU-CS-93-230 ..... p 3244 N94-29303 #
CMU-CS-94-102 ..... p 3397 N94-28860 #
CMU-CS-94-104 ..... p 3410 N94-29007 #

CMU/SEI-93-SR-21 ..... p 3407 N94-28648 #
CMU/SEI-93-TR-23 ..... p 3410 N94-29068 #
CMU/SEI-93-TR-29 ..... p 3407 N94-28633
CMU/SEI-93-TR-31 ..... p 3407 N94-28639 #

CONF-921114 ..... p 3336 N94-28472
CONF-9211262 ..... p 3503 N94-28513 #
CONF-921296 ..... p 3485 N94-28624 #
CONF-930216 ..... p 3506 N94-29831 #
CONF-9303250-1 ..... p 3349 N94-29954 #
CONF-930346-5 ..... p 3269 N94-28464 #
CONF-9304117-6 ..... p 3206 N94-29936 #
CONF-9304181-4 ..... p 3497 N94-30825 #
CONF-9305136-16 ..... p 3494 N94-28507 #
CONF-9305276-2 ..... p 3406 N94-30004 #
CONF-9305307 ..... p 3296 N94-30688 #
CONF-9305309-2 ..... p 3491 N94-30709 #
CONF-9305310 ..... p 3226 N94-30761
CONF-9306140-2 ..... p 3481 N94-28492 #
CONF-9306176-20 ..... p 3481 N94-28462 #
CONF-9306176-22 ..... p 3482 N94-28494 #
CONF-9306251-2 ..... p 3482 N94-28541 #
CONF-9306285-1 ..... p 3342 N94-28521 #
CONF-9306286-1 ..... p 3335 N94-30610 #
CONF-9306287-1 ..... p 3542 N94-28526 #
CONF-9306291-1 ..... p 3184 N94-30589 #
CONF-9306294-1 ..... p 3200 N94-30748 #
CONF-930637-13 ..... p 3483 N94-28542 #
CONF-930676-63 ..... p 3355 N94-28538 #
CONF-930696 ..... p 3226 N94-30612 #
CONF-930703-42 ..... p 3468 N94-30026 #
CONF-930703-44 ..... p 3520 N94-30850 #
CONF-930710-5 ..... p 3516 N94-30054 #
CONF-9307114-2 ..... p 3551 N94-30884 #
CONF-9307156-1 ..... p 3520 N94-30835 #
CONF-930722-56 ..... p 3292 N94-28481 #
CONF-930726-6 ..... p 3374 N94-30587 #
CONF-930726-7 ..... p 3368 N94-28455 #
CONF-930761-6 ..... p 3491 N94-30722 #
CONF-930767-1 ..... p 3497 N94-30712 #
CONF-930801-13 ..... p 3515 N94-30009
CONF-9308124-2 ..... p 3341 N94-28454 #
CONF-9308154-3 ..... p 3289 N94-30027 #
CONF-9308206-1 ..... p 3552 N94-28580 #
CONF-930823-18 ..... p 3482 N94-28493 #
CONF-930863-3 ..... p 3261 N94-28546 #
CONF-930865-12 ..... p 3209 N94-30246 #
CONF-930893 ..... p 3336 N94-28499 #
CONF-930895 ..... p 3353 N94-30715 #
CONF-9309168-2 ..... p 3527 N94-30041
CONF-9309176-4 ..... p 3454 N94-30317 #
CONF-9309188 ..... p 3339 N94-30601 #
CONF-9309231-6 ..... p 3201 N94-28544 #
CONF-930928-18 ..... p 3201 N94-28460 #
CONF-930928-19 ..... p 3201 N94-28456 #
CONF-930928-6-REV ..... p 3493 N94-30893 #
CONF-9309289-1 ..... p 3240 N94-28522 #
CONF-9309292-2 ..... p 3484 N94-28574 #
CONF-9309292-3 ..... p 3491 N94-30719 #
CONF-9309292-4 ..... p 3493 N94-30886 #
CONF-9309293-1 ..... p 3535 N94-30179 #
CONF-9309296-2 ..... p 3551 N94-30845
CONF-9309297-2 ..... p 3483 N94-28569 #
CONF-9309297-3 ..... p 3497 N94-30712 #
CONF-9309304-1 ..... p 3522 N94-28543 #
CONF-9309304-2 ..... p 3522 N94-28572 #
CONF-9309310-1 ..... p 3279 N94-30020
CONF-9309317-1 ..... p 3493 N94-30891 #
CONF-9309318-1 ..... p 3521 N94-30897 #
CONF-9309319-1 ..... p 3428 N94-30754 #
CONF-9309320-1 ..... p 3509 N94-30752 #
CONF-9309321-1 ..... p 3492 N94-30775 #
CONF-9309322-1 ..... p 3526 N94-30750 #
CONF-930960-7 ..... p 3543 N94-28545 #
CONF-930999-4 ..... p 3542 N94-28480 #
CONF-931009-16 ..... p 3206 N94-29931 #
CONF-931013-3 ..... p 3468 N94-28459 #
CONF-931018-73 ..... p 3506 N94-29510 #
CONF-931018-74 ..... p 3230 N94-29017 #
CONF-931018-75 ..... p 3510 N94-30832 #
CONF-931018-78 ..... p 3508 N94-30339 #
CONF-9310193-10-REV ..... p 3483 N94-28565 #
CONF-9310204-13 ..... p 3267 N94-30716 #
CONF-9310206 ..... p 3420 N94-30056 #
CONF-9310238-1 ..... p 3263 N94-29025 #
CONF-931024-7 ..... p 3485 N94-28741 #
CONF-9310247-1 ..... p 3484 N94-28573 #
CONF-9310247-5 ..... p 3492 N94-30779 #

CONF-9310247-6 ..... p 3493 N94-30887 #
CONF-9310247-8 ..... p 3490 N94-30103 #
CONF-9310247-9 ..... p 3488 N94-30049 #
CONF-9310250-5 ..... p 3514 N94-29818 #
CONF-9310251-SUMM ..... p 3340 N94-30833 #
CONF-9310260-1 ..... p 3210 N94-30777 #
CONF-9310261-2 ..... p 3220 N94-30778 #
CONF-931048-2 ..... p 3294 N94-29934 #
CONF-931048-4 ..... p 3295 N94-30060 #
CONF-931048-5 ..... p 3296 N94-30830 #
CONF-931054-2 ..... p 3212 N94-28560 #
CONF-931054-4 ..... p 3501 N94-30599
CONF-931054-6 ..... p 3295 N94-30598
CONF-931076-1 ..... p 3277 N94-29923 #
CONF-931079-15 ..... p 3500 N94-29928
CONF-931079-16 ..... p 3207 N94-30021 #
CONF-931107-23 ..... p 3268 N94-30717 #
CONF-931107-32 ..... p 3267 N94-30711 #
CONF-931108-29 ..... p 3199 N94-30723 #
CONF-931108-30 ..... p 3185 N94-30693 #
CONF-931108-32 ..... p 3210 N94-30774 #
CONF-931108-33 ..... p 3175 N94-28579 #
CONF-931108-34 ..... p 3517 N94-30201 #
CONF-931108-35 ..... p 3175 N94-28581 #
CONF-931108-39 ..... p 3222 N94-30909 #
CONF-931108-40 ..... p 3520 N94-30773 #
CONF-931108-41 ..... p 3221 N94-30896 #
CONF-931108-42 ..... p 3521 N94-30894
CONF-931108-43 ..... p 3182 N94-29933 #
CONF-931108-43 ..... p 3199 N94-30260 #
CONF-931108-44 ..... p 3487 N94-29841 #
CONF-931108-44 ..... p 3219 N94-30335 #
CONF-931108-46 ..... p 3208 N94-30101 #
CONF-931108-47 ..... p 3515 N94-30006 #
CONF-931108-48 ..... p 3518 N94-30316 #
CONF-931108-49 ..... p 3206 N94-30007 #
CONF-931108-50 ..... p 3207 N94-30042 #
CONF-931108-57 ..... p 3519 N94-30592
CONF-931108-64 ..... p 3219 N94-30263 #
CONF-931108-66 ..... p 3217 N94-30025 #
CONF-931108-68 ..... p 3516 N94-30063 #
CONF-931108-69 ..... p 3516 N94-30064 #
CONF-931108-71 ..... p 3518 N94-30249 #
CONF-931108-72 ..... p 3207 N94-30062 #
CONF-931108-74 ..... p 3521 N94-30851 #
CONF-931108-75 ..... p 3211 N94-30852 #
CONF-9311104-16 ..... p 3510 N94-28512 #
CONF-9311104-17 ..... p 3211 N94-28536 #
CONF-9311104-19 ..... p 3220 N94-30591
CONF-9311114-6 ..... p 3268 N94-30717 #
CONF-9311131-2 ..... p 3520 N94-30724 #
CONF-9311134-1 ..... p 3340 N94-30609 #
CONF-931115-13-REV-1 ..... p 3404 N94-28505 #
CONF-9311153-1 ..... p 3483 N94-28559 #
CONF-9311156-1 ..... p 3548 N94-30694 #
CONF-9311164-1 ..... p 3349 N94-29932 #
CONF-9311171-1 ..... p 3427 N94-30705
CONF-931118-1 ..... p 3323 N94-30689
CONF-931121-36 ..... p 3211 N94-30892 #
CONF-931132-1 ..... p 3509 N94-30597
CONF-931133-7 ..... p 3519 N94-30707
CONF-931142-5 ..... p 3518 N94-30315 #
CONF-931142-7 ..... p 3518 N94-30247 #
CONF-931156-25 ..... p 3216 N94-29830 #
CONF-931164-6 ..... p 3338 N94-30313 #
CONF-931164-7 ..... p 3338 N94-30048 #
CONF-931193-1 ..... p 3149 N94-30687
CONF-931201-10 ..... p 3187 N94-28567 #
CONF-931230-1 ..... p 3510 N94-28484 #
CONF-931233-1 ..... p 3461 N94-30821 #
CONF-931233-3 ..... p 3451 N94-28739
CONF-931234-4 ..... p 3511 N94-28535 #
CONF-931234-5 ..... p 3480 N94-30098 #
CONF-931238-2 ..... p 3297 N94-28461 #
CONF-931244-1 ..... p 3219 N94-30245 #
CONF-931244-2 ..... p 3222 N94-30906 #
CONF-931247-6 ..... p 3520 N94-30848 #
CONF-940101-30 ..... p 3497 N94-30588 #
CONF-940113-6 ..... p 3339 N94-30602 #
CONF-940114-1 ..... p 3292 N94-28482 #
CONF-940115-13 ..... p 3342 N94-28523 #
CONF-940115-19 ..... p 3368 N94-28568 #
CONF-940115-20 ..... p 3334 N94-30022 #
CONF-940115-21 ..... p 3349 N94-30023
CONF-940115-5 ..... p 3378 N94-30823 #
CONF-940121-1 ..... p 3511 N94-28570 #
CONF-940121-2 ..... p 3521 N94-30898 #
CONF-940122-1 ..... p 3519 N94-30338 #
CONF-940127-1 ..... p 3527 N94-30698 #
CONF-940128-5-VUGRAPHS ..... p 3311 N94-30703
CONF-940131-3 ..... p 3350 N94-30116
CONF-940135-2 ..... p 3185 N94-30593
CONF-940142-12 ..... p 3295 N94-30265 #
CONF-940142-5 ..... p 3295 N94-30367 #
CONF-940142-6 ..... p 3169 N94-30264 #
CONF-940151-1 ..... p 3406 N94-30008 #
CONF-940206-1 ..... p 3266 N94-30055 #
CONF-940206-2 ..... p 3222 N94-30900 #
CONF-940214-7 ..... p 3498 N94-30846
CONF-940215-3 ..... p 3210 N94-30776
CONF-940222-10 ..... p 3207 N94-30053 #
CONF-940240-1 ..... p 3431 N94-29952 #
CONF-940241-1 ..... p 3254 N94-29929
CONF-940242-1 ..... p 3302 N94-29922 #
CONF-940242-2 ..... p 3311 N94-30596
CONF-940242-3 ..... p 3268 N94-30819
CONF-940247-1 ..... p 3536 N94-30706
CONF-940301-5 ..... p 3174 N94-28557 #
CONF-940312-22 ..... p 3315 N94-28503 #
CONF-940312-47 ..... p 3526 N94-28474 #
CONF-940326-7 ..... p 3514 N94-29801 #
CONF-940326-8 ..... p 3500 N94-29799 #
CONF-940363-1 ..... p 3501 N94-30261 #
CONF-940363-2 ..... p 3501 N94-30828
CONF-940366-1 ..... p 3255 N94-30106 #
CONF-940369-1 ..... p 3267 N94-30368 #
CONF-940402-2 ..... p 3498 N94-30847 #
CONF-940412-1 ..... p 3185 N94-30827 #
CONF-940412-2 ..... p 3218 N94-30102
CONF-940412-3 ..... p 3508 N94-30365 #
CONF-940424-1 ..... p 3419 N94-29816 #
CONF-940424-5 ..... p 3495 N94-29924 #
CONF-940424-8 ..... p 3465 N94-30366 #
CONF-940432-1 ..... p 3437 N94-30250 #
CONF-940453-1 ..... p 3266 N94-30040
CONF-940456-6 ..... p 3427 N94-30590
CONF-940459-1 ..... p 3497 N94-30825 #
CONF-940459-2 ..... p 3488 N94-30039
CONF-940466-2 ..... p 3321 N94-29951 #
CONF-940476-1 ..... p 3432 N94-30100
CONF-940481-2 ..... p 3281 N94-30600
CONF-940483-3 ..... p 3553 N94-30248 #

CR-R-91012 ..... p 3135 N94-28799 #

CRHC-93-24 ..... p 3420 N94-29906 * #
CRHC-94-01 ..... p 3431 N94-29869 * #
CRHC-94-02 ..... p 3431 N94-29846 * #
CRHC-94-03 ..... p 3420 N94-29890 * #
CRHC-94-04 ..... p 3406 N94-29695 * #
CRHC-94-07 ..... p 3418 N94-29404 * #

CRIE-T-92039 ..... p 3199 N94-30267 #

CRREL-MONO93-2 ..... p 3361 N94-29286 #

CRREL-SR-93-25 ..... p 3486 N94-29021 #

CRREL-93-19 ..... p 3332 N94-29288
CRREL-93-20 ..... p 3478 N94-29314 #
CRREL-93-21 ..... p 3357 N94-29070 #
CRREL-93-22 ..... p 3325 N94-28849

CT-93-01 ..... p 3424 N94-30386 #
CT-93-02 ..... p 3456 N94-30370 #
CT-93-03 ..... p 3424 N94-30371 #

CTN-94-61126 ..... p 3241 N94-28532
CTN-94-61128 ..... p 3405 N94-28533
CTN-94-61129 ..... p 3495 N94-30211
CTN-94-61130 ..... p 3304 N94-30275
CTN-94-61131 ..... p 3198 N94-30017 #
CTN-94-61132 ..... p 3548 N94-30058
CTN-94-61133 ..... p 3321 N94-30018 #
CTN-94-61134 ..... p 3303 N94-30019 #
CTN-94-61135 ..... p 3148 N94-30129 #
CTN-94-61136 ..... p 3153 N94-30130 #
CTN-94-61137 ..... p 3148 N94-30131 #
CTN-94-61138 ..... p 3402 N94-30132 #
CTN-94-61139 ..... p 3421 N94-30155 #
CTN-94-61140 ..... p 3507 N94-30156 #
CTN-94-61141 ..... p 3507 N94-30157 #
CTN-94-61142 ..... p 3507 N94-30158 #
CTN-94-61143 ..... p 3508 N94-30159 #
CTN-94-61146 ..... p 3541 N94-30231
CTN-94-61147 ..... p 3290 N94-30232
CTN-94-61148 ..... p 3500 N94-30233
CTN-94-61149 ..... p 3490 N94-30234
CTN-94-61150 ..... p 3316 N94-30235
CTN-94-61151 ..... p 3334 N94-30236
CTN-94-61152 ..... p 3159 N94-30237
CTN-94-61153 ..... p 3541 N94-30133
CTN-94-61154 ..... p 3517 N94-30203
CTN-94-61155 ..... p 3365 N94-30134
CTN-94-61156 ..... p 3303 N94-30135
CTN-94-61157 ..... p 3421 N94-30136
CTN-94-61158 ..... p 3199 N94-30137
CTN-94-61159 ..... p 3208 N94-30138
CTN-94-61160 ..... p 3437 N94-30255
CTN-94-61161 ..... p 3304 N94-30238
CTN-94-61162 ..... p 3518 N94-30239
CTN-94-61163 ..... p 3525 N94-30244
CTN-94-61164 ..... p 3255 N94-30240
CTN-94-61165 ..... p 3454 N94-30241
CTN-94-61166 ..... p 3453 N94-30139
CTN-94-61167 ..... p 3254 N94-30031
CTN-94-61168 ..... p 3515 N94-30032
CTN-94-61169 ..... p 3321 N94-30033
CTN-94-61170 ..... p 3254 N94-30034
CTN-94-61171 ..... p 3254 N94-30035
CTN-94-61172 ..... p 3218 N94-30036
CTN-94-61173 ..... p 3334 N94-30037
CTN-94-61174 ..... p 3432 N94-30140
CTN-94-61175 ..... p 3490 N94-30141
CTN-94-61176 ..... p 3525 N94-30142
CTN-94-61177 ..... p 3432 N94-30143
CTN-94-61178 ..... p 3136 N94-30144
CTN-94-61179 ..... p 3229 N94-30145
CTN-94-61180 ..... p 3209 N94-30146

CWI-CS-R9253 ..... p 3418 N94-29503
CWI-CS-R9254 ..... p 3453 N94-29889
CWI-CS-R9255 ..... p 3418 N94-29449
CWI-CS-R9256 ..... p 3418 N94-29487
CWI-CS-R9257 ..... p 3423 N94-30341
CWI-CS-R9258 ..... p 3402 N94-30320
CWI-CS-R9259 ..... p 3422 N94-30321
CWI-CS-R9260 ..... p 3422 N94-30322
CWI-CS-R9261 ..... p 3423 N94-30323
CWI-CS-R9262 ..... p 3423 N94-30324
CWI-CS-R9324-PT-1 ..... p 3252 N94-29692 #
CWI-CS-R9325-PT-2 ..... p 3252 N94-29693
CWI-CS-R9326 ..... p 3448 N94-30731
CWI-CS-R9329 ..... p 3427 N94-30732
CWI-CS-R9331 ..... p 3427 N94-30733
CWI-CS-R9332 ..... p 3428 N94-30734
CWI-CS-R9333 ..... p 3460 N94-30735
CWI-CS-R9334 ..... p 3425 N94-30428
CWI-CS-R9335 ..... p 3459 N94-30427
CWI-CS-R9336 ..... p 3426 N94-30491
CWI-CS-R9337 ..... p 3433 N94-30429
CWI-CS-R9338 ..... p 3459 N94-30430
CWI-CS-R9339 ..... p 3433 N94-30431
CWI-CS-R9340 ..... p 3425 N94-30432 #
CWI-CS-R9341 ..... p 3526 N94-30433
CWI-CS-R9342 ..... p 3426 N94-30434
CWI-CS-R9343 ..... p 3426 N94-30435
CWI-CS-R9344 ..... p 3459 N94-30436
CWI-CS-R9345 ..... p 3426 N94-30437
CWI-CS-R9346 ..... p 3461 N94-30753
CWI-CS-R9347 ..... p 3459 N94-30412
CWI-CS-R9348 ..... p 3425 N94-30414
CWI-CS-R9349 ..... p 3459 N94-30413
CWI-CS-R9350 ..... p 3425 N94-30415

CWI-NM-R9311 ..... p 3461 N94-30751
CWI-NM-R9312 ..... p 3353 N94-30729 #
CWI-NM-R9313 ..... p 3433 N94-30730

DCIEM-92-32 ..... p 3402 N94-30132 #
DCIEM-93-46 ..... p 3391 N94-29049 #
DCIEM-93-53 ..... p 3401 N94-29302 #

DCR/M-61546/C-92 ..... p 3197 N94-29457 #

DE93-011308 ..... p 3336 N94-28499 #
DE93-018945 ..... p 3527 N94-30698 #
DE93-040101 ..... p 3419 N94-29816 #
DE93-040609 ..... p 3353 N94-30715 #
DE93-041289 ..... p 3535 N94-30699 #
DE93-634355 ..... p 3466 N94-28467
DE93-634365 ..... p 3481 N94-28468
DE93-634756 ..... p 3481 N94-28469
DE94-000082 ..... p 3216 N94-29830 #
DE94-000218 ..... p 3226 N94-30761
DE94-000219 ..... p 3336 N94-28500 #
DE94-000227 ..... p 3226 N94-30818
DE94-000236 ..... p 3339 N94-30601 #
DE94-000244 ..... p 3339 N94-30602 #
DE94-000248 ..... p 3339 N94-30603 #
DE94-000249 ..... p 3339 N94-30604 #
DE94-000257 ..... p 3339 N94-30605
DE94-000258 ..... p 3336 N94-28501 #
DE94-000261 ..... p 3224 N94-28502 #
DE94-000262 ..... p 3339 N94-30606 #
DE94-000265 ..... p 3500 N94-29799 #
DE94-000266 ..... p 3514 N94-29801 #
DE94-000269 ..... p 3302 N94-29922 #
DE94-000270 ..... p 3268 N94-30819
DE94-000272 ..... p 3340 N94-30820 #
DE94-000275 ..... p 3225 N94-30038
DE94-000764 ..... p 3461 N94-30821 #
DE94-000958 ..... p 3354 N94-30822 #
DE94-001539 ..... p 3378 N94-30823 #
DE94-001601 ..... p 3315 N94-28503 #
DE94-001657 ..... p 3491 N94-30762 #
DE94-001660 ..... p 3341 N94-28463 #
DE94-001723 ..... p 3386 N94-30607 #

DE94-001751 ..... p 3373 N94-29817 #
DE94-001878 ..... p 3269 N94-28464 #
DE94-002016 ..... p 3277 N94-29923 #
DE94-002151 ..... p 3341 N94-28465 #
DE94-002276 ..... p 3528 N94-30824
DE94-002333 ..... p 3492 N94-30834
DE94-002448 ..... p 3495 N94-29924 #
DE94-002640 ..... p 3488 N94-30039
DE94-002642 ..... p 3497 N94-30825 #
DE94-002715 ..... p 3355 N94-28538 #
DE94-002882 ..... p 3465 N94-29925 #
DE94-003136 ..... p 3286 N94-28466 #
DE94-003150 ..... p 3341 N94-28473 #
DE94-003202 ..... p 3221 N94-30826 #
DE94-003227 ..... p 3185 N94-30827 #
DE94-003244 ..... p 3520 N94-30835 #
DE94-003273 ..... p 3487 N94-29700 #
DE94-003368 ..... p 3526 N94-28474 #
DE94-003396 ..... p 3492 N94-30836
DE94-003397 ..... p 3492 N94-30837 #
DE94-003523 ..... p 3365 N94-30608 #
DE94-003524 ..... p 3492 N94-30838 #
DE94-003577 ..... p 3270 N94-28475 #
DE94-003665 ..... p 3491 N94-30685 #
DE94-003667 ..... p 3270 N94-28476 #
DE94-003688 ..... p 3165 N94-28477 #
DE94-003711 ..... p 3263 N94-29025 #
DE94-003739 ..... p 3519 N94-30611 #
DE94-003775 ..... p 3266 N94-30040
DE94-003783 ..... p 3340 N94-30609 #
DE94-003882 ..... p 3336 N94-28472
DE94-003908 ..... p 3226 N94-30612 #
DE94-003930 ..... p 3342 N94-28521 #
DE94-003933 ..... p 3240 N94-28522 #
DE94-003969 ..... p 3335 N94-30610 #
DE94-003974 ..... p 3267 N94-30716 #
DE94-003989 ..... p 3342 N94-28523 #
DE94-004002 ..... p 3482 N94-28524 #
DE94-004022 ..... p 3321 N94-29951 #
DE94-004173 ..... p 3535 N94-30179 #
DE94-004178 ..... p 3491 N94-30686 #
DE94-004186 ..... p 3542 N94-28526 #
DE94-004187 ..... p 3149 N94-30687
DE94-004200 ..... p 3431 N94-29952 #
DE94-004224 ..... p 3466 N94-30586 #
DE94-004225 ..... p 3175 N94-28528 #
DE94-004238 ..... p 3482 N94-28504 #
DE94-004239 ..... p 3338 N94-29953 #
DE94-004278 ..... p 3350 N94-30613 #
DE94-004309 ..... p 3527 N94-30041
DE94-004313 ..... p 3341 N94-28454 #
DE94-004333 ..... p 3349 N94-29954 #
DE94-004346 ..... p 3296 N94-30688 #
DE94-004350 ..... p 3404 N94-28505 #
DE94-004355 ..... p 3368 N94-28455 #
DE94-004363 ..... p 3374 N94-30587 #
DE94-004368 ..... p 3201 N94-28456 #
DE94-004472 ..... p 3338 N94-29955 #
DE94-004478 ..... p 3230 N94-29017 #
DE94-004552 ..... p 3211 N94-28457 #
DE94-004557 ..... p 3268 N94-30717 #
DE94-004564 ..... p 3503 N94-28458 #
DE94-004573 ..... p 3468 N94-28459 #
DE94-004582 ..... p 3519 N94-30718 #
DE94-004599 ..... p 3201 N94-28460 #
DE94-004607 ..... p 3297 N94-28461 #
DE94-004622 ..... p 3506 N94-29510 #
DE94-004624 ..... p 3481 N94-28462 #
DE94-004643 ..... p 3348 N94-29926 #
DE94-004651 ..... p 3491 N94-30719 #
DE94-004654 ..... p 3491 N94-30722 #
DE94-004658 ..... p 3484 N94-28573 #
DE94-004664 ..... p 3484 N94-28574 #
DE94-004676 ..... p 3337 N94-29018 #
DE94-004680 ..... p 3289 N94-29927 #
DE94-004699 ..... p 3504 N94-28575 #
DE94-004701 ..... p 3484 N94-28576 #
DE94-004709 ..... p 3224 N94-28577 #
DE94-004710 ..... p 3355 N94-28558
DE94-004714 ..... p 3491 N94-30695
DE94-004743 ..... p 3500 N94-29928
DE94-004777 ..... p 3451 N94-28739
DE94-004791 ..... p 3199 N94-30723 #
DE94-004792 ..... p 3520 N94-30773 #
DE94-004793 ..... p 3483 N94-28559 #
DE94-004794 ..... p 3323 N94-30689
DE94-004796 ..... p 3520 N94-30724 #
DE94-004800 ..... p 3206 N94-29936 #
DE94-004810 ..... p 3509 N94-30768 #
DE94-004846 ..... p 3296 N94-30614
DE94-004852 ..... p 3386 N94-30180
DE94-004859 ..... p 3510 N94-30832 #
DE94-004863 ..... p 3254 N94-29929
DE94-004865 ..... p 3212 N94-28560 #
DE94-004879 ..... p 3488 N94-29930
DE94-004883 ..... p 3209 N94-30690 #
DE94-004885 ..... p 3187 N94-28561 #
DE94-004887 ..... p 3202 N94-28562 #
DE94-004889 ..... p 3519 N94-30691
DE94-004890 ..... p 3206 N94-29931 #
DE94-004892 ..... p 3349 N94-29932 #
DE94-004905 ..... p 3220 N94-30692 #
DE94-004906 ..... p 3230 N94-28563 #
DE94-004929 ..... p 3465 N94-30696
DE94-004934 ..... p 3407 N94-28506 #
DE94-004935 ..... p 3410 N94-29019 #
DE94-004937 ..... p 3504 N94-28564 #
DE94-004950 ..... p 3483 N94-28565 #
DE94-004953 ..... p 3340 N94-30833 #
DE94-004955 ..... p 3483 N94-28566 #
DE94-004958 ..... p 3200 N94-30769 #
DE94-004960 ..... p 3484 N94-28578 #
DE94-004963 ..... p 3200 N94-30770 #
DE94-004978 ..... p 3182 N94-29933 #
DE94-004980 ..... p 3185 N94-30693 #
DE94-004982 ..... p 3175 N94-28579 #
DE94-004986 ..... p 3552 N94-28580 #
DE94-004992 ..... p 3548 N94-30694 #
DE94-004994 ..... p 3210 N94-30774 #
DE94-004995 ..... p 3175 N94-28581 #
DE94-004997 ..... p 3294 N94-29934 #
DE94-004998 ..... p 3498 N94-30847 #
DE94-005002 ..... p 3492 N94-30775 #
DE94-005005 ..... p 3185 N94-30771 #
DE94-005008 ..... p 3200 N94-30748 #
DE94-005010 ..... p 3522 N94-28543 #
DE94-005011 ..... p 3522 N94-28572 #
DE94-005012 ..... p 3526 N94-30750 #
DE94-005013 ..... p 3201 N94-28544 #
DE94-005016 ..... p 3480 N94-30098 #
DE94-005072 ..... p 3226 N94-30615 #
DE94-005076 ..... p 3534 N94-30099 #
DE94-005077 ..... p 3260 N94-30772
DE94-005082 ..... p 3509 N94-30752 #
DE94-005083 ..... p 3517 N94-30201 #
DE94-005084 ..... p 3514 N94-29818 #
DE94-005090 ..... p 3210 N94-30776
DE94-005091 ..... p 3432 N94-30100
DE94-005093 ..... p 3208 N94-30101 #
DE94-005095 ..... p 3218 N94-30102
DE94-005096 ..... p 3174 N94-28557 #
DE94-005099 ..... p 3187 N94-28567 #
DE94-005103 ..... p 3210 N94-30777 #
DE94-005110 ..... p 3334 N94-30022 #
DE94-005112 ..... p 3368 N94-28568 #
DE94-005113 ..... p 3350 N94-30116
DE94-005114 ..... p 3349 N94-30023
DE94-005115 ..... p 3279 N94-30020
DE94-005116 ..... p 3207 N94-30021 #
DE94-005117 ..... p 3483 N94-28569 #
DE94-005119 ..... p 3428 N94-30754 #
DE94-005123 ..... p 3220 N94-30778 #
DE94-005132 ..... p 3511 N94-28570 #
DE94-005133 ..... p 3451 N94-28571 #
DE94-005142 ..... p 3497 N94-30588 #
DE94-005150 ..... p 3509 N94-30755 #
DE94-005156 ..... p 3543 N94-28545 #
DE94-005187 ..... p 3268 N94-30907 #
DE94-005189 ..... p 3222 N94-30906 #
DE94-005196 ..... p 3509 N94-30697
DE94-005201 ..... p 3491 N94-30709 #
DE94-005202 ..... p 3210 N94-30710 #
DE94-005203 ..... p 3267 N94-30711 #
DE94-005209 ..... p 3261 N94-28546 #
DE94-005212 ..... p 3292 N94-28478 #
DE94-005213 ..... p 3201 N94-28479 #
DE94-005214 ..... p 3542 N94-28480 #
DE94-005216 ..... p 3494 N94-28507 #
DE94-005223 ..... p 3497 N94-30712 #
DE94-005225 ..... p 3482 N94-28493 #
DE94-005231 ..... p 3482 N94-28494 #
DE94-005233 ..... p 3482 N94-28541 #
DE94-005234 ..... p 3483 N94-28542 #
DE94-005235 ..... p 3292 N94-28481 #
DE94-005247 ..... p 3292 N94-28482 #
DE94-005261 ..... p 3187 N94-28483 #
DE94-005265 ..... p 3296 N94-30908 #
DE94-005269 ..... p 3222 N94-30909 #
DE94-005272 ..... p 3184 N94-30589 #
DE94-005273 ..... p 3510 N94-28484 #
DE94-005281 ..... p 3207 N94-30053 #
DE94-005286 ..... p 3199 N94-30260 #
DE94-005287 ..... p 3501 N94-30261 #
DE94-005288 ..... p 3266 N94-30055 #
DE94-005289 ..... p 3315 N94-29020 #
DE94-005294 ..... p 3289 N94-30059
DE94-005303 ..... p 3297 N94-28485 #
DE94-005315 ..... p 3501 N94-30910
DE94-005339 ..... p 3219 N94-30245 #
DE94-005356 ..... p 3493 N94-30891 #
DE94-005358 ..... p 3211 N94-30892 #
DE94-005367 ..... p 3295 N94-30060 #
DE94-005372 ..... p 3493 N94-30893 #
DE94-005376 ..... p 3494 N94-28486 #
DE94-005378 ..... p 3261 N94-28487 #
DE94-005381 ..... p 3270 N94-28488 #
DE94-005382 ..... p 3336 N94-28489 #
DE94-005384 ..... p 3521 N94-30894
DE94-005409 ..... p 3503 N94-28490 #
DE94-005412 ..... p 3386 N94-30895
DE94-005414 ..... p 3481 N94-28491 #
DE94-005415 ..... p 3490 N94-30262 #
DE94-005417 ..... p 3481 N94-28492 #
DE94-005421 ..... p 3427 N94-30590
DE94-005428 ..... p 3221 N94-30896 #
DE94-005429 ..... p 3220 N94-30591
DE94-005430 ..... p 3519 N94-30592
DE94-005448 ..... p 3485 N94-28741 #
DE94-005449 ..... p 3209 N94-30246 #
DE94-005451 ..... p 3487 N94-29841 #
DE94-005459 ..... p 3498 N94-28534 #
DE94-005464 ..... p 3219 N94-30335 #
DE94-005465 ..... p 3511 N94-28535 #
DE94-005469 ..... p 3211 N94-28536 #
DE94-005470 ..... p 3482 N94-28509 #
DE94-005472 ..... p 3521 N94-30897 #
DE94-005475 ..... p 3521 N94-30898 #
DE94-005477 ..... p 3185 N94-30593
DE94-005508 ..... p 3510 N94-28512 #
DE94-005542 ..... p 3503 N94-28514 #
DE94-005543 ..... p 3503 N94-28515 #
DE94-005548 ..... p 3211 N94-28516 #
DE94-005549 ..... p 3404 N94-28517 #
DE94-005551 ..... p 3521 N94-30899 #
DE94-005553 ..... p 3482 N94-28518 #
DE94-005554 ..... p 3187 N94-28519 #
DE94-005557 ..... p 3482 N94-28520 #
DE94-005561 ..... p 3201 N94-28525 #
DE94-005562 ..... p 3201 N94-28527 #
DE94-005563 ..... p 3510 N94-28529 #
DE94-005564 ..... p 3211 N94-28530 #
DE94-005565 ..... p 3406 N94-30004 #
DE94-005573 ..... p 3518 N94-30315 #
DE94-005575 ..... p 3515 N94-30006 #
DE94-005576 ..... p 3518 N94-30316 #
DE94-005577 ..... p 3206 N94-30007 #
DE94-005579 ..... p 3406 N94-30008 #
DE94-005581 ..... p 3222 N94-30900 #
DE94-005591 ..... p 3454 N94-30317 #
DE94-005592 ..... p 3207 N94-30042 #
DE94-005596 ..... p 3482 N94-28531 #
DE94-005637 ..... p 3353 N94-30757 #
DE94-005651 ..... p 3335 N94-30594
DE94-005654 ..... p 3503 N94-28547 #
DE94-005655 ..... p 3463 N94-28548 #
DE94-005666 ..... p 3270 N94-28549 #
DE94-005670 ..... p 3295 N94-30595
DE94-005680 ..... p 3522 N94-30901 #
DE94-005681 ..... p 3260 N94-30902 #
DE94-005685 ..... p 3254 N94-30043 #
DE94-005698 ..... p 3367 N94-30876 #
DE94-005699 ..... p 3349 N94-30044 #
DE94-005700 ..... p 3122 N94-29842 #
DE94-005752 ..... p 3311 N94-30596
DE94-005767 ..... p 3200 N94-30877 #
DE94-005804 ..... p 3312 N94-30878
DE94-005809 ..... p 3509 N94-30597
DE94-005815 ..... p 3340 N94-30879 #
DE94-005818 ..... p 3295 N94-30598
DE94-005819 ..... p 3200 N94-30880 #
DE94-005820 ..... p 3501 N94-30599
DE94-005821 ..... p 3281 N94-30600
DE94-005826 ..... p 3493 N94-30881 #
DE94-005827 ..... p 3510 N94-30882 #
DE94-005828 ..... p 3506 N94-30045 #
DE94-005831 ..... p 3340 N94-30700
DE94-005832 ..... p 3267 N94-30701
DE94-005853 ..... p 3349 N94-30046 #
DE94-005877 ..... p 3491 N94-30702 #
DE94-005896 ..... p 3349 N94-30047 #
DE94-005915 ..... p 3367 N94-30883
DE94-005919 ..... p 3493 N94-30903 #
DE94-005922 ..... p 3477 N94-30873 #
DE94-005924 ..... p 3311 N94-30703
DE94-005925 ..... p 3493 N94-30874 #
DE94-005957 ..... p 3510 N94-30875 #
DE94-005960 ..... p 3338 N94-30048 #
DE94-005961 ..... p 3338 N94-30313 #
DE94-006001 ..... p 3488 N94-30049 #
DE94-006002 ..... p 3490 N94-30103 #
DE94-006031 ..... p 3218 N94-30104 #
DE94-006033 ..... p 3185 N94-30704
DE94-006034 ..... p 3209 N94-30336 #
DE94-006035 ..... p 3219 N94-30337 #
DE94-006037 ..... p 3519 N94-30338 #
DE94-006040 ..... p 3268 N94-30904
DE94-006042 ..... p 3508 N94-30339 #
DE94-006046 ..... p 3508 N94-30365 #

DE94-006061 ..... p 3551 N94-30884 #
DE94-006100 ..... p 3226 N94-30885 #
DE94-006101 ..... p 3461 N94-30758 #
DE94-006102 ..... p 3255 N94-30105 #
DE94-006103 ..... p 3509 N94-30760 #
DE94-006116 ..... p 3340 N94-30843
DE94-006121 ..... p 3563 N94-30844
DE94-006137 ..... p 3465 N94-30366 #
DE94-006138 ..... p 3295 N94-30367 #
DE94-006142 ..... p 3267 N94-30368 #
DE94-006167 ..... p 3491 N94-30369 #
DE94-006173 ..... p 3493 N94-30886 #
DE94-006174 ..... p 3492 N94-30779 #
DE94-006175 ..... p 3493 N94-30887 #
DE94-006187 ..... p 3255 N94-30106 #
DE94-006207 ..... p 3210 N94-30839 #
DE94-006208 ..... p 3207 N94-30024 #
DE94-006227 ..... p 3520 N94-30848 #
DE94-006229 ..... p 3551 N94-30845
DE94-006230 ..... p 3498 N94-30846
DE94-006233 ..... p 3427 N94-30705
DE94-006247 ..... p 3536 N94-30706
DE94-006249 ..... p 3217 N94-30025 #
DE94-006257 ..... p 3462 N94-30849 #
DE94-006261 ..... p 3429 N94-30840
DE94-006287 ..... p 3519 N94-30707
DE94-006289 ..... p 3468 N94-30026 #
DE94-006295 ..... p 3476 N94-30841 #
DE94-006296 ..... p 3520 N94-30850 #
DE94-006297 ..... p 3289 N94-30027 #
DE94-006300 ..... p 3515 N94-30009
DE94-006301 ..... p 3520 N94-30842 #
DE94-006311 ..... p 3521 N94-30851 #
DE94-006312 ..... p 3211 N94-30852 #
DE94-006358 ..... p 3219 N94-30263 #
DE94-006363 ..... p 3169 N94-30264 #
DE94-006371 ..... p 3295 N94-30265 #
DE94-006374 ..... p 3518 N94-30247 #
DE94-006383 ..... p 3516 N94-30054 #
DE94-006406 ..... p 3226 N94-30708
DE94-006428 ..... p 3514 N94-30001
DE94-006459 ..... p 3461 N94-30817 #
DE94-006463 ..... p 3501 N94-30828
DE94-006480 ..... p 3553 N94-30248 #
DE94-006496 ..... p 3420 N94-29844 #
DE94-006509 ..... p 3489 N94-30061 #
DE94-006527 ..... p 3207 N94-30062 #
DE94-006553 ..... p 3518 N94-30249 #
DE94-006561 ..... p 3516 N94-30063 #
DE94-006583 ..... p 3516 N94-30064 #
DE94-006573 ..... p 3437 N94-30250 #
DE94-006596 ..... p 3279 N94-30003
DE94-006623 ..... p 3221 N94-30829
DE94-006625 ..... p 3421 N94-30117
DE94-006641 ..... p 3420 N94-30056 #
DE94-006643 ..... p 3488 N94-29845 #
DE94-006654 ..... p 3296 N94-30830 #
DE94-006665 ..... p 3422 N94-30251 #
DE94-006726 ..... p 3207 N94-30057 #
DE94-006751 ..... p 3501 N94-30252 #
DE94-007041 ..... p 3199 N94-30266 #
DE94-601554 ..... p 3481 N94-28470
DE94-601606 ..... p 3481 N94-28471
DE94-603654 ..... p 3524 N94-29498
DE94-604015 ..... p 3487 N94-29500
DE94-605138 ..... p 3514 N94-29691
DE94-605318 ..... p 3212 N94-28550 #
DE94-605337 ..... p 3202 N94-28551
DE94-606065 ..... p 3483 N94-28552 #
DE94-606067 ..... p 3434 N94-28613
DE94-606138 ..... p 3286 N94-28553 #
DE94-606267 ..... p 3483 N94-28554 #
DE94-606268 ..... p 3485 N94-28621
DE94-606269 ..... p 3407 N94-28622
DE94-606270 ..... p 3484 N94-28614
DE94-606271 ..... p 3528 N94-28615
DE94-606286 ..... p 3494 N94-28623
DE94-606292 ..... p 3522 N94-28616
DE94-606295 ..... p 3523 N94-28617
DE94-606296 ..... p 3523 N94-28618
DE94-606297 ..... p 3484 N94-28619
DE94-606298 ..... p 3523 N94-28620
DE94-606299 ..... p 3484 N94-28584
DE94-606302 ..... p 3522 N94-28582 #
DE94-606303 ..... p 3485 N94-28718 #
DE94-606304 ..... p 3523 N94-28719 #
DE94-606325 ..... p 3468 N94-28720 #
DE94-606326 ..... p 3261 N94-28585
DE94-606328 ..... p 3522 N94-28586
DE94-606329 ..... p 3523 N94-28721 #
DE94-606338 ..... p 3523 N94-28782 #
DE94-606339 ..... p 3523 N94-28802 #
DE94-606340 ..... p 3356 N94-28803 #
DE94-606342 ..... p 3522 N94-28609
DE94-606343 ..... p 3451 N94-28783 #
DE94-606382 ..... p 3466 N94-28785 #
DE94-606405 ..... p 3523 N94-28751 #
DE94-606414 ..... p 3485 N94-28758 #
DE94-606442 ..... p 3484 N94-28610
DE94-606446 ..... p 3484 N94-28611
DE94-606457 ..... p 3494 N94-28612
DE94-606481 ..... p 3487 N94-29502 #
DE94-606751 ..... p 3485 N94-28625
DE94-606817 ..... p 3293 N94-28786 #
DE94-606851 ..... p 3511 N94-28626
DE94-606852 ..... p 3513 N94-29210 #
DE94-606885 ..... p 3512 N94-28787 #
DE94-607211 ..... p 3506 N94-29831 #
DE94-607269 ..... p 3515 N94-30005
DE94-607322 ..... p 3362 N94-29935
DE94-607323 ..... p 3365 N94-30223
DE94-607324 ..... p 3365 N94-30107
DE94-607844 ..... p 3489 N94-30050
DE94-607849 ..... p 3489 N94-30051
DE94-607850 ..... p 3489 N94-30052
DE94-607851 ..... p 3290 N94-30148
DE94-607901 ..... p 3267 N94-30073
DE94-607902 ..... p 3406 N94-30074
DE94-607903 ..... p 3500 N94-30075
DE94-607999 ..... p 3207 N94-30076
DE94-608007 ..... p 3421 N94-30077
DE94-608008 ..... p 3453 N94-30078
DE94-608009 ..... p 3534 N94-30079
DE94-608010 ..... p 3421 N94-30090
DE94-608012 ..... p 3406 N94-30081
DE94-608013 ..... p 3421 N94-30083
DE94-608014 ..... p 3500 N94-30084
DE94-608067 ..... p 3489 N94-30085
DE94-608069 ..... p 3524 N94-30086
DE94-608072 ..... p 3460 N94-30726
DE94-608075 ..... p 3524 N94-30087
DE94-608089 ..... p 3467 N94-30088
DE94-608091 ..... p 3524 N94-30089
DE94-608092 ..... p 3467 N94-30202
DE94-608093 ..... p 3208 N94-30108
DE94-608094 ..... p 3489 N94-30097
DE94-608095 ..... p 3208 N94-30090
DE94-608096 ..... p 3453 N94-30091
DE94-608097 ..... p 3267 N94-30092
DE94-608098 ..... p 3365 N94-30093
DE94-608099 ..... p 3467 N94-30065
DE94-608100 ..... p 3218 N94-30066
DE94-608102 ..... p 3521 N94-30888
DE94-608103 ..... p 3516 N94-30067
DE94-608104 ..... p 3516 N94-30068
DE94-608105 ..... p 3516 N94-30069
DE94-608106 ..... p 3516 N94-30070
DE94-608107 ..... p 3507 N94-30071
DE94-608108 ..... p 3516 N94-30072
DE94-608109 ..... p 3548 N94-30163
DE94-608110 ..... p 3208 N94-30118
DE94-608112 ..... p 3453 N94-30119
DE94-608113 ..... p 3254 N94-30094 *
DE94-608114 ..... p 3517 N94-30109
DE94-608115 ..... p 3468 N94-30110
DE94-608116 ..... p 3525 N94-30164
DE94-608117 ..... p 3517 N94-30181
DE94-608118 ..... p 3517 N94-30165
DE94-608120 ..... p 3467 N94-30166
DE94-608121 ..... p 3525 N94-30167
DE94-608124 ..... p 3555 N94-30168
DE94-608126 ..... p 3525 N94-30169
DE94-608128 ..... p 3525 N94-30170
DE94-608132 ..... p 3490 N94-30120
DE94-608134 ..... p 3525 N94-30121
DE94-608137 ..... p 3199 N94-30111 #
DE94-608155 ..... p 3490 N94-30112
DE94-608175 ..... p 3489 N94-30095
DE94-608244 ..... p 3489 N94-30096
DE94-608328 ..... p 3508 N94-30171
DE94-608329 ..... p 3255 N94-30172
DE94-608330 ..... p 3508 N94-30191
DE94-608353 ..... p 3508 N94-30192
DE94-608356 ..... p 3508 N94-30193
DE94-608357 ..... p 3508 N94-30194
DE94-608385 ..... p 3517 N94-30195
DE94-608386 ..... p 3490 N94-30182
DE94-608387 ..... p 3517 N94-30183
DE94-608418 ..... p 3490 N94-30184
DE94-608419 ..... p 3209 N94-30253
DE94-608422 ..... p 3395 N94-30185 #
DE94-608456 ..... p 3220 N94-30745
DE94-608462 ..... p 3517 N94-30082
DE94-701164 ..... p 3503 N94-28513 #
DE94-707497 ..... p 3503 N94-28555
DE94-707671 ..... p 3504 N94-28556
DE94-707686 ..... p 3485 N94-28788 #
DE94-707688 ..... p 3511 N94-28750 #
DE94-707692 ..... p 3485 N94-28624 #
DE94-732332 ..... p 3337 N94-28627
DE94-732333 ..... p 3337 N94-28628 #
DE94-732338 ..... p 3224 N94-28629
DE94-732339 ..... p 3346 N94-28630 #
DE94-732340 ..... p 3337 N94-28631 #
DE94-744116 ..... p 3199 N94-30267 #
DE94-744171 ..... p 3157 N94-30268 #
DE94-744237 ..... p 3312 N94-30831
DE94-744238 ..... p 3304 N94-30269 #
DIGEL-1993-8 ..... p 3495 N94-29888 #
DIGEL-1993-9 ..... p 3495 N94-29467 #
DM-65 ..... p 3376 N94-30966
DMM(A)-109 ..... p 3318 N94-28841
DNA-TR-93-50 ..... p 3263 N94-29028
DODA-AR-008-278 ..... p 3224 N94-29092
DODA-AR-008-369 ..... p 3318 N94-29091
DODA-AR-008-377 ..... p 3121 N94-29090
DODA-AR-008-575 ..... p 3401 N94-29093
DOE/BP-2081 ..... p 3353 N94-30757 #
DOE/CE-23810/22E ..... p 3230 N94-28563 #
DOE/CE-23810/22 ..... p 3220 N94-30692 #
DOE/CE-27504/T11 ..... p 3312 N94-30878
DOE/EE-0007 ..... p 3224 N94-28577 #
DOE/EM-0106P ..... p 3528 N94-30824
DOE/ER-00881/T5 ..... p 3482 N94-28531 #
DOE/ER-00881/T6 ..... p 3491 N94-30369 #
DOE/ER-0535P-3 ..... p 3535 N94-30699 #
DOE/ER-0597P ..... p 3355 N94-28558
DOE/ER-0597T ..... p 3341 N94-28473 #
DOE/ER-0602P ..... p 3386 N94-30607 #
DOE/ER-0607T ..... p 3494 N94-28486 #
DOE/ER-10629/T9 ..... p 3488 N94-29930
DOE/ER-13029/T3 ..... p 3296 N94-30614
DOE/ER-13491/641 ..... p 3492 N94-30837 #
DOE/ER-13671/7 ..... p 3489 N94-30061 #
DOE/ER-13719/5 ..... p 3386 N94-30180
DOE/ER-13766/11 ..... p 3207 N94-30024 #
DOE/ER-13775/5 ..... p 3200 N94-30770 #
DOE/ER-13781/7 ..... p 3210 N94-30839 #
DOE/ER-13846/6 ..... p 3260 N94-30902 #
DOE/ER-13849/6 ..... p 3481 N94-28491 #
DOE/ER-13949/5 ..... p 3211 N94-28457 #
DOE/ER-14105/4 ..... p 3200 N94-30769 #
DOE/ER-14129/3 ..... p 3522 N94-30901 #
DOE/ER-14150/3 ..... p 3226 N94-30708
DOE/ER-14320/1 ..... p 3503 N94-28458 #
DOE/ER-25053/T2 ..... p 3451 N94-28571 #
DOE/ER-25139/1 ..... p 3279 N94-30003
DOE/ER-30156/H1 ..... p 3338 N94-29953 #
DOE/ER-40281/8 ..... p 3484 N94-28576 #
DOE/ER-40291/20 ..... p 3481 N94-28492 #
DOE/ER-40408/8 ..... p 3492 N94-30836
DOE/ER-40416/6 ..... p 3490 N94-30262 #
DOE/ER-40542/88 ..... p 3491 N94-30685 #
DOE/ER-40617/158 ..... p 3491 N94-30762 #
DOE/ER-40627/3 ..... p 3482 N94-28504 #
DOE/ER-40677/2-PT-1 ..... p 3483 N94-28566 #
DOE/ER-40715/2 ..... p 3491 N94-30702 #
DOE/ER-40762/010 ..... p 3492 N94-30838 #
DOE/ER-40764/1 ..... p 3491 N94-30686 #
DOE/ER-45291/6 ..... p 3501 N94-30252 #
DOE/ER-45503/1 ..... p 3484 N94-28578 #
DOE/ER-53194/6 ..... p 3503 N94-28547 #
DOE/ER-53198/229 ..... p 3498 N94-28534 #
DOE/ER-53198/230 ..... p 3503 N94-28515 #
DOE/ER-53198/231 ..... p 3503 N94-28514 #
DOE/ER-53212/T2 ..... p 3503 N94-28490 #
DOE/ER-53281/T3 ..... p 3509 N94-30755 #
DOE/ER-54184/1 ..... p 3492 N94-30834
DOE/ER-54196/1 ..... p 3504 N94-28575 #
DOE/ER-60668/7 ..... p 3348 N94-29926 #
DOE/ER-60760/5-APP-A ..... p 3349 N94-30046 #
DOE/ER-61059/2 ..... p 3365 N94-30608 #
DOE/ER-61072/7 ..... p 3269 N94-28464 #
DOE/ER-61256/T2 ..... p 3386 N94-30895
DOE/ET-51013/304 ..... p 3510 N94-30882 #
DOE/ID-12692/5-PHASE-3 ..... p 3221 N94-30826 #
DOE/ID-13040/T21 ..... p 3340 N94-30700
DOE/ID-13074/T10 ..... p 3267 N94-30701
DOE/MC-27225/3602 ..... p 3340 N94-30879 #
DOE/MC-29061/3566 ..... p 3297 N94-28485 #
DOE/MC-29116/3575 ..... p 3349 N94-30047 #
DOE/MC-29267/3523 ..... p 3367 N94-30883
DOE/METC-C/94/7117 ..... p 3338 N94-30313 #
DOE/METC-C/94/7118 ..... p 3338 N94-30048 #

DOE/METC-93-6132 ..... p 3336 N94-28499 #

DOE/NASA/0331-1 ..... p 3537 N94-29350 * #
DOE/NASA/26310-19 ..... p 3202 N94-28822 * #

DOE/PC-90361/T11 ..... p 3341 N94-28463 #
DOE/PC-91346/3 ..... p 3341 N94-28465 #
DOE/PC-92529/T4 ..... p 3200 N94-30877 #

DOE/PO-0009 ..... p 3226 N94-30885 #

DOT-VNTSC-FAA-93-10 ..... p 3145 N94-28657 #
DOT-VNTSC-FAA-93-11 ..... p 3145 N94-28647 #
DOT-VNTSC-FAA-93-18 ..... p 3399 N94-28649 #
DOT-VNTSC-FAA-93-7 ..... p 3149 N94-30905
DOT-VNTSC-FAA-93-9 ..... p 3315 N94-28646 #

DOT/FAA/AM-94/6 ..... p 3143 N94-30933 #
DOT/FAA/AM-94/7 ..... p 3395 N94-29919 #
DOT/FAA/AM-94/8 ..... p 3398 N94-29918 #

DOT/FAA/CT-TN-91/28 ..... p 3135 N94-28799 #

DOT/FAA/CT-TN93/12 ..... p 3136 N94-28914 #
DOT/FAA/CT-TN93/41 ..... p 3241 N94-28771 #

DOT/FAA/CT-93/76 ..... p 3315 N94-28646 #
DOT/FAA/CT-93/77 ..... p 3149 N94-30905
DOT/FAA/CT-93/78 ..... p 3145 N94-28657 #
DOT/FAA/CT-93/79 ..... p 3145 N94-28647 #

DOT/FAA/RD-92/15 ..... p 3135 N94-29862 #
DOT/FAA/RD-93/2 ..... p 3157 N94-29754 #
DOT/FAA/RD-93/39 ..... p 3399 N94-28649 #
DOT/FAA/RD-94/1,I ..... p 3142 N94-30189 #

DREP-93-16 ..... p 3148 N94-30131 #
DREP-93-17 ..... p 3148 N94-30129 #

DRES-SP-149 ..... p 3304 N94-30275

DSIS-92-00652 ..... p 3495 N94-30211
DSIS-94-00150 ..... p 3241 N94-28532
DSIS-94-00233 ..... p 3405 N94-28533

DTIC/TR-91/5 ..... p 3529 N94-28911
DTIC/TR-94-4 ..... p 3430 N94-29051
DTIC/TR-94/3 ..... p 3529 N94-28911

DU/DC/TR-36 ..... p 3513 N94-29155 #
DU/DC/TR-37 ..... p 3486 N94-29131 #
DU/DC/TR-38 ..... p 3513 N94-29130 #
DU/DC/TR-39 ..... p 3189 N94-29140 #

DWA-1764 ..... p 3499 N94-29114 #

E-7298 ..... p 3197 N94-29356 * #
E-7426 ..... p 3173 N94-29444 * #
E-7491 ..... p 3178 N94-29208 * #
E-7806-1 ..... p 3213 N94-28922 * #
E-7842 ..... p 3264 N94-29209 * #
E-8009 ..... p 3181 N94-29684 * #
E-8065 ..... p 3202 N94-28822 * #
E-8098 ..... p 3168 N94-29405 * #
E-8153 ..... p 3317 N94-28819 * #
E-8182 ..... p 3203 N94-28921 * #
E-8190 ..... p 3135 N94-30949 * #
E-8204 ..... p 3319 N94-29384 * #
E-8217 ..... p 3214 N94-29399 * #
E-8228 ..... p 3174 N94-28747 * #
E-8240 ..... p 3183 N94-30190 * #
E-8241 ..... p 3169 N94-30123 * #
E-8242 ..... p 3171 N94-28833 * #
E-8257 ..... p 3242 N94-28826 * #
E-8259 ..... p 3189 N94-28832 * #
E-8264 ..... p 3301 N94-29552 * #
E-8286 ..... p 3172 N94-29097 * #
E-8294 ..... p 3165 N94-28697 * #
E-8299 ..... p 3174 N94-28924 * #
E-8407 ..... p 3338 N94-30196 * #
E-8485 ..... p 3156 N94-28749 * #
E-8490 ..... p 3151 N94-29103 * #
E-8495 ..... p 3317 N94-28815 * #
E-8518 ..... p 3319 N94-29104 * #
E-8618 ..... p 3167 N94-29383 * #
E-8621 ..... p 3316 N94-28508 * #
E-8629 ..... p 3318 N94-28840 * #
E-8631 ..... p 3168 N94-29757 * #
E-8635 ..... p 3214 N94-29105 * #
E-8636 ..... p 3150 N94-28923 * #
E-8639 ..... p 3298 N94-28838 * #
E-8640 ..... p 3173 N94-29403 * #
E-8642 ..... p 3273 N94-29471 * #
E-8649 ..... p 3318 N94-28821 * #
E-8650 ..... p 3183 N94-30178 * #
E-8655 ..... p 3171 N94-28736 * #
E-8656 ..... p 3167 N94-28814 * #
E-8665 ..... p 3271 N94-28835 * #
E-8669 ..... p 3205 N94-29758 * #
E-8670 ..... p 3272 N94-29096 * #
E-8674 ..... p 3319 N94-29469 * #
E-8676 ..... p 3319 N94-29406 * #
E-8683 ..... p 3267 N94-30198 * #
E-8687 ..... p 3172 N94-28999 * #
E-8689 ..... p 3183 N94-30125 * #
E-8695 ..... p 3279 N94-30147 * #
E-8699 ..... p 3218 N94-30177 * #
E-8700 ..... p 3172 N94-28834 * #
E-8712 ..... p 3303 N94-30205 * #
E-8726 ..... p 3286 N94-29000 * #
E-8738 ..... p 3303 N94-30227 * #
E-8739 ..... p 3155 N94-30204 * #
E-8756 ..... p 3173 N94-29546 * #
E-8768 ..... p 3422 N94-30175 * #
E-8778 ..... p 3132 N94-30124 * #
E-8813 ..... p 3133 N94-30152 * #
E-8841 ..... p 3421 N94-30174 * #

EEC/NOTE-18/93 ..... p 3254 N94-29998

EGG-ER-10792 ..... p 3465 N94-29925 #

EGG-M-93253 ..... p 3527 N94-30698 #

EGG-11265-5012 ..... p 3553 N94-30248 #

EOARD-TR-94-02 ..... p 3504 N94-28686

EPA/600/R-93/239 ..... p 3347 N94-29192 #

ER-60900-93-F ..... p 3174 N94-29868 * #

ESA-CP-1158 ..... p 3501 N94-30418 #

ESA-SP-1151 ..... p 3347 N94-29452 #

ESC-TR-93-199 ..... p 3410 N94-29068 #
ESC-TR-93-203 ..... p 3407 N94-28633
ESC-TR-93-317 ..... p 3407 N94-28639 #

ETDE/JP-MF-94732332 ..... p 3337 N94-28627
ETDE/JP-MF-94732333 ..... p 3337 N94-28628 #
ETDE/JP-MF-94744171 ..... p 3157 N94-30268 #
ETDE/JP-MF-94744237 ..... p 3312 N94-30831
ETDE/JP-MF-94744238 ..... p 3304 N94-30269 #

ETN-94-95000 ..... p 3395 N94-30028 #
ETN-94-95358 ..... p 3212 N94-28539 #
ETN-94-95437 ..... p 3252 N94-29692 #
ETN-94-95438 ..... p 3252 N94-29693
ETN-94-95458 ..... p 3347 N94-29452 #
ETN-94-95460 ..... p 3231 N94-29477 #
ETN-94-95461 ..... p 3180 N94-29478 #
ETN-94-95462 ..... p 3245 N94-29440 #
ETN-94-95463 ..... p 3215 N94-29441 #
ETN-94-95464 ..... p 3179 N94-29442 #
ETN-94-95465 ..... p 3255 N94-30153 #
ETN-94-95466 ..... p 3225 N94-29429 #
ETN-94-95467 ..... p 3179 N94-29454 #
ETN-94-95468 ..... p 3245 N94-29421 #
ETN-94-95469 ..... p 3179 N94-29412 #
ETN-94-95470 ..... p 3179 N94-29413 #
ETN-94-95471 ..... p 3225 N94-29414 #
ETN-94-95472 ..... p 3168 N94-29415 #
ETN-94-95473 ..... p 3231 N94-29416 #
ETN-94-95474 ..... p 3332 N94-29417 #
ETN-94-95475 ..... p 3418 N94-29418 #
ETN-94-95476 ..... p 3246 N94-29542 #
ETN-94-95477 ..... p 3168 N94-29543 #
ETN-94-95478 ..... p 3168 N94-29419 #
ETN-94-95479 ..... p 3245 N94-29456 #
ETN-94-95480 ..... p 3205 N94-29525 #
ETN-94-95481 ..... p 3418 N94-29479 #
ETN-94-95482 ..... p 3435 N94-29480 #
ETN-94-95483 ..... p 3315 N94-29474 #
ETN-94-95484 ..... p 3197 N94-29457 #
ETN-94-95485 ..... p 3215 N94-29459 #
ETN-94-95486 ..... p 3179 N94-29462 #
ETN-94-95487 ..... p 3122 N94-29463 #
ETN-94-95488 ..... p 3231 N94-29598 #
ETN-94-95504 ..... p 3217 N94-29885
ETN-94-95507 ..... p 3217 N94-29886
ETN-94-95508 ..... p 3524 N94-29481 #
ETN-94-95510 ..... p 3464 N94-29482 #
ETN-94-95511 ..... p 3436 N94-29526 #
ETN-94-95512 ..... p 3266 N94-29527 #
ETN-94-95513 ..... p 3333 N94-29528 #
ETN-94-95514 ..... p 3148 N94-29887
ETN-94-95515 ..... p 3495 N94-29888 #
ETN-94-95516 ..... p 3495 N94-29467 #
ETN-94-95517 ..... p 3494 N94-29422 #
ETN-94-95521 ..... p 3465 N94-30154 #
ETN-94-95522 ..... p 3245 N94-29468 #
ETN-94-95524 ..... p 3370 N94-29423 #
ETN-94-95525 ..... p 3215 N94-29424 #
ETN-94-95526 ..... p 3179 N94-29425 #
ETN-94-95527 ..... p 3184 N94-30343
ETN-94-95535 ..... p 3418 N94-29503
ETN-94-95536 ..... p 3453 N94-29889
ETN-94-95537 ..... p 3418 N94-29449
ETN-94-95538 ..... p 3418 N94-29487
ETN-94-95539 ..... p 3423 N94-30341
ETN-94-95540 ..... p 3402 N94-30320
ETN-94-95541 ..... p 3422 N94-30321
ETN-94-95542 ..... p 3422 N94-30322
ETN-94-95543 ..... p 3423 N94-30323
ETN-94-95544 ..... p 3423 N94-30324
ETN-94-95545 ..... p 3455 N94-30325
ETN-94-95546 ..... p 3457 N94-30395
ETN-94-95547 ..... p 3457 N94-30396
ETN-94-95548 ..... p 3457 N94-30397
ETN-94-95549 ..... p 3456 N94-30380
ETN-94-95550 ..... p 3456 N94-30381
ETN-94-95551 ..... p 3456 N94-30382
ETN-94-95552 ..... p 3456 N94-30383
ETN-94-95553 ..... p 3457 N94-30384
ETN-94-95554 ..... p 3457 N94-30385
ETN-94-95555 ..... p 3424 N94-30386 #
ETN-94-95556 ..... p 3456 N94-30370 #
ETN-94-95557 ..... p 3424 N94-30371 #
ETN-94-95557 ..... p 3428 N94-30739
ETN-94-95558 ..... p 3456 N94-30372 #
ETN-94-95559 ..... p 3422 N94-30318
ETN-94-95560 ..... p 3454 N94-30319 #
ETN-94-95561 ..... p 3455 N94-30326
ETN-94-95562 ..... p 3455 N94-30327
ETN-94-95563 ..... p 3429 N94-30912
ETN-94-95564 ..... p 3433 N94-30913
ETN-94-95565 ..... p 3153 N94-30914
ETN-94-95566 ..... p 3143 N94-30915
ETN-94-95567 ..... p 3135 N94-30916 #
ETN-94-95568 ..... p 3134 N94-30871
ETN-94-95569 ..... p 3324 N94-30872
ETN-94-95570 ..... p 3143 N94-30853
ETN-94-95571 ..... p 3143 N94-30854
ETN-94-95572 ..... p 3282 N94-30855
ETN-94-95573 ..... p 3158 N94-30856
ETN-94-95574 ..... p 3170 N94-30857
ETN-94-95575 ..... p 3134 N94-30858
ETN-94-95576 ..... p 3148 N94-30342
ETN-94-95578 ..... p 3134 N94-30740
ETN-94-95579 ..... p 3448 N94-30741
ETN-94-95580 ..... p 3290 N94-30742
ETN-94-95581 ..... p 3133 N94-30387
ETN-94-95582 ..... p 3338 N94-30328
ETN-94-95583 ..... p 3281 N94-30743
ETN-94-95584 ..... p 3133 N94-30388
ETN-94-95585 ..... p 3133 N94-30389
ETN-94-95586 ..... p 3402 N94-30390
ETN-94-95587 ..... p 3256 N94-30398
ETN-94-95589 ..... p 3311 N94-30391
ETN-94-95590 ..... p 3256 N94-30392
ETN-94-95591 ..... p 3422 N94-30314
ETN-94-95592 ..... p 3157 N94-30399
ETN-94-95593 ..... p 3424 N94-30400
ETN-94-95594 ..... p 3133 N94-30401
ETN-94-95595 ..... p 3458 N94-30402
ETN-94-95596 ..... p 3438 N94-30373
ETN-94-95602 ..... p 3255 N94-30374
ETN-94-95604 ..... p 3438 N94-30375
ETN-94-95610 ..... p 3432 N94-30356
ETN-94-95611 ..... p 3535 N94-30357
ETN-94-95612 ..... p 3465 N94-30358
ETN-94-95613 ..... p 3535 N94-30359
ETN-94-95614 ..... p 3535 N94-30360
ETN-94-95616 ..... p 3535 N94-30361
ETN-94-95617 ..... p 3535 N94-30362
ETN-94-95618 ..... p 3432 N94-30363
ETN-94-95619 ..... p 3423 N94-30344 #
ETN-94-95620 ..... p 3535 N94-30329
ETN-94-95621 ..... p 3535 N94-30330
ETN-94-95622 ..... p 3423 N94-30331
ETN-94-95623 ..... p 3423 N94-30332
ETN-94-95624 ..... p 3464 N94-29450
ETN-94-95625 ..... p 3455 N94-30333
ETN-94-95626 ..... p 3465 N94-30376
ETN-94-95627 ..... p 3456 N94-30377 #
ETN-94-95628 ..... p 3462 N94-30859
ETN-94-95629 ..... p 3462 N94-30860 #
ETN-94-95631 ..... p 3423 N94-30345
ETN-94-95632 ..... p 3460 N94-30744
ETN-94-95633 ..... p 3455 N94-30346
ETN-94-95634 ..... p 3424 N94-30347
ETN-94-95635 ..... p 3424 N94-30348
ETN-94-95636 ..... p 3438 N94-30334
ETN-94-95637 ..... p 3456 N94-30378
ETN-94-95638 ..... p 3424 N94-30379
ETN-94-95639 ..... p 3457 N94-30393

ETN-94-95640 ..... p 3457 N94-30394
ETN-94-95642 ..... p 3424 N94-30364
ETN-94-95643 ..... p 3438 N94-30349
ETN-94-95644 ..... p 3433 N94-30720
ETN-94-95645 ..... p 3428 N94-30746
ETN-94-95646 ..... p 3458 N94-30403
ETN-94-95648 ..... p 3458 N94-30404 #
ETN-94-95649 ..... p 3458 N94-30405 #
ETN-94-95650 ..... p 3458 N94-30406
ETN-94-95652 ..... p 3461 N94-30747
ETN-94-95653 ..... p 3458 N94-30407
ETN-94-95654 ..... p 3458 N94-30408
ETN-94-95655 ..... p 3438 N94-30410
ETN-94-95656 ..... p 3432 N94-30411
ETN-94-95657 ..... p 3460 N94-30721
ETN-94-95658 ..... p 3427 N94-30725
ETN-94-95659 ..... p 3406 N94-30727
ETN-94-95660 ..... p 3460 N94-30728
ETN-94-95661 ..... p 3459 N94-30424
ETN-94-95662 ..... p 3459 N94-30425
ETN-94-95663 ..... p 3425 N94-30426
ETN-94-95664 ..... p 3426 N94-30488
ETN-94-95665 ..... p 3426 N94-30489
ETN-94-95666 ..... p 3426 N94-30490
ETN-94-95667 ..... p 3428 N94-30749
ETN-94-95668 ..... p 3461 N94-30751
ETN-94-95669 ..... p 3353 N94-30729 #
ETN-94-95670 ..... p 3433 N94-30730
ETN-94-95671 ..... p 3448 N94-30731
ETN-94-95672 ..... p 3427 N94-30732
ETN-94-95673 ..... p 3427 N94-30733
ETN-94-95674 ..... p 3428 N94-30734
ETN-94-95675 ..... p 3460 N94-30735
ETN-94-95676 ..... p 3425 N94-30428
ETN-94-95677 ..... p 3459 N94-30427
ETN-94-95678 ..... p 3426 N94-30491
ETN-94-95679 ..... p 3433 N94-30429
ETN-94-95680 ..... p 3459 N94-30430
ETN-94-95681 ..... p 3433 N94-30431
ETN-94-95682 ..... p 3425 N94-30432 #
ETN-94-95683 ..... p 3526 N94-30433
ETN-94-95684 ..... p 3426 N94-30434
ETN-94-95685 ..... p 3426 N94-30435
ETN-94-95686 ..... p 3459 N94-30436
ETN-94-95687 ..... p 3426 N94-30437
ETN-94-95688 ..... p 3461 N94-30753
ETN-94-95689 ..... p 3459 N94-30412
ETN-94-95690 ..... p 3459 N94-30413
ETN-94-95691 ..... p 3425 N94-30414
ETN-94-95692 ..... p 3425 N94-30415
ETN-94-95714 ..... p 3425 N94-30416
ETN-94-95715 ..... p 3425 N94-30417
ETN-94-95717 ..... p 3260 N94-30520
ETN-94-95718 ..... p 3429 N94-30765 #
ETN-94-95719 ..... p 3461 N94-30766
ETN-94-95720 ..... p 3461 N94-30767
ETN-94-95721 ..... p 3460 N94-30736
ETN-94-95722 ..... p 3466 N94-30737
ETN-94-95723 ..... p 3427 N94-30585 #
ETN-94-95725 ..... p 3460 N94-30738
ETN-94-95727 ..... p 3449 N94-30963
ETN-94-95728 ..... p 3462 N94-30964
ETN-94-95798 ..... p 3501 N94-30418 #
ETN-94-95812 ..... p 3449 N94-30923
ETN-94-95813 ..... p 3429 N94-30924
ETN-94-95815 ..... p 3429 N94-30925
ETN-94-95816 ..... p 3537 N94-30926
ETN-94-95817 ..... p 3536 N94-30927
ETN-94-95818 ..... p 3429 N94-30928
ETN-94-95819 ..... p 3536 N94-30929
ETN-94-95820 ..... p 3291 N94-30930
ETN-94-95821 ..... p 3449 N94-30962
ETN-94-95822 ..... p 3429 N94-30931
ETN-94-95823 ..... p 3429 N94-30936
ETN-94-95824 ..... p 3313 N94-30937
ETN-94-95825 ..... p 3200 N94-30938
ETN-94-95826 ..... p 3449 N94-30939
ETN-94-95827 ..... p 3260 N94-30940
ETN-94-95828 ..... p 3449 N94-30941
ETN-94-95829 ..... p 3184 N94-30419
ETN-94-95830 ..... p 3184 N94-30438
ETN-94-95835 ..... p 3501 N94-30522
ETN-94-95839 ..... p 3322 N94-30523
ETN-94-95841 ..... p 3184 N94-30524
ETN-94-95843 ..... p 3476 N94-30783
ETN-94-95844 ..... p 3476 N94-30780
ETN-94-95845 ..... p 3476 N94-30781
ETN-94-95847 ..... p 3268 N94-30784
ETN-94-95848 ..... p 3260 N94-30785
ETN-94-95849 ..... p 3290 N94-30782
ETN-94-95851 ..... p 3336 N94-30944 #
ETN-94-95853 ..... p 3480 N94-30786
ETN-94-95854 ..... p 3492 N94-30795
ETN-94-95855 ..... p 3210 N94-30796
ETN-94-95856 ..... p 3340 N94-30945 #
ETN-94-95857 ..... p 3340 N94-30946 #
ETN-94-95858 ..... p 3149 N94-30947 #
ETN-94-95953 ..... p 3336 N94-30965
ETN-94-95954 ..... p 3376 N94-30966
ETN-94-95956 ..... p 3284 N94-30967
ETN-94-95957 ..... p 3284 N94-30968
ETN-94-95958 ..... p 3220 N94-30420
ETN-94-95959 ..... p 3229 N94-30421
ETN-94-95960 ..... p 3402 N94-30422
ETN-94-95961 ..... p 3158 N94-30423
ETN-94-95962 ..... p 3229 N94-30409
ETN-94-95963 ..... p 3281 N94-30756
ETN-94-95964 ..... p 3142 N94-30439
ETN-94-95965 ..... p 3133 N94-30492
ETN-94-95966 ..... p 3134 N94-30493
ETN-94-95967 ..... p 3335 N94-30759
ETN-94-95968 ..... p 3260 N94-30518
ETN-94-95969 ..... p 3281 N94-30763
ETN-94-95970 ..... p 3428 N94-30764
ETN-94-95971 ..... p 3335 N94-30942 #
ETN-94-95972 ..... p 3143 N94-30943
ETN-94-95975 ..... p 3399 N94-30969
ETN-94-95976 ..... p 3395 N94-30970 #
ETN-94-95977 ..... p 3462 N94-30971
ETN-94-95978 ..... p 3481 N94-30972 #
ETN-94-95981 ..... p 3396 N94-30978
ETN-94-95983 ..... p 3291 N94-30979
ETN-94-95984 ..... p 3494 N94-30980
ETN-94-95986 ..... p 3430 N94-30973
ETN-94-95987 ..... p 3463 N94-30974
ETN-94-95988 ..... p 3463 N94-30975
ETN-94-95989 ..... p 3463 N94-30976
ETN-94-95990 ..... p 3463 N94-30977

FASTC-ID(RS)T-0332-93 ..... p 3370 N94-29394 #

FEI-2244 ..... p 3484 N94-28614
FEI-2246 ..... p 3207 N94-30076
FEI-2247 ..... p 3202 N94-28551
FEI-2255 ..... p 3490 N94-30184

FFA-TN-1991-35 ..... p 3215 N94-29424 #
FFA-TN-1993-12 ..... p 3179 N94-29425 #
FFA-TN-1993-19 ..... p 3340 N94-30945 #
FFA-TN-1993-20 ..... p 3340 N94-30946 #
FFA-TN-1993-55 ..... p 3149 N94-30947 #

FNAL-TM-1870 ..... p 3268 N94-30904

FNAL/C-93/333 ..... p 3491 N94-30719 #
FNAL/C-93/347-E ..... p 3484 N94-28573 #
FNAL/C-93/349-E ..... p 3491 N94-30722 #
FNAL/C-93/352-E ..... p 3484 N94-28574 #
FNAL/C-93/383 ..... p 3493 N94-30886 #
FNAL/C-93/385-E ..... p 3492 N94-30779 #
FNAL/C-93/387-E ..... p 3488 N94-30049 #
FNAL/C-93/395-E ..... p 3493 N94-30887 #
FNAL/C-93/396-E ..... p 3490 N94-30103 #

FOA-A-30082-3.3 ..... p 3243 N94-28908
FOA-A-30082-8.4 ..... p 3243 N94-28908

FOA-C-20945-8.4-PT-7 ..... p 3180 N94-29475
FOA-C-20948-2.2 ..... p 3453 N94-29476
FOA-C-30718-3.3 ..... p 3245 N94-29311
FOA-C-30718-8.4 ..... p 3245 N94-29311
FOA-C-30719-8.3,3.2,3.3 ..... p 3244 N94-29177
FOA-C-30720-3.2 ..... p 3243 N94-28906
FOA-C-30720-8.3 ..... p 3243 N94-28906
FOA-C-30722-3.2 ..... p 3243 N94-28907
FOA-C-30724-8.3 ..... p 3244 N94-29176
FOA-C-30727-8.4 ..... p 3242 N94-28885
FOA-C-30728-3.5 ..... p 3453 N94-29174
FOA-C-40284-4.3 ..... p 3347 N94-29158

F254278 ..... p 3507 N94-30126 * #

GA-A-21501 ..... p 3510 N94-30832 #

GKSS-92/E/98 ..... p 3284 N94-30967
GKSS-92/E/99 ..... p 3284 N94-30968

GL-5130 ..... p 3293 N94-29309 #

HIFAN-577 ..... p 3494 N94-28507 #

IA-1480 ..... p 3508 N94-30192
IA-1481 ..... p 3555 N94-30168

IAF-PAPER-92-0030 ..... p 3311 N94-30391

IAF-92-0966 ..... p 3229 N94-30421

IC-AERO-93-01 ..... p 3524 N94-29481 #

IC-92/267 ..... p 3467 N94-30088
IC-93/113 ..... p 3524 N94-30089
IC-93/163 ..... p 3467 N94-30202
IC-93/169 ..... p 3481 N94-28468
IC-93/171 ..... p 3525 N94-30170
IC-93/172 ..... p 3466 N94-28467
IC-93/212 ..... p 3524 N94-29498
IC-93/229 ..... p 3487 N94-29500
IC-93/237 ..... p 3481 N94-28470
IC-93/253 ..... p 3208 N94-30108
IC-93/254 ..... p 3489 N94-30097
IC-93/255 ..... p 3208 N94-30090
IC-93/256 ..... p 3453 N94-30091
IC-93/258 ..... p 3267 N94-30092
IC-93/259 ..... p 3365 N94-30093
IC-93/260 ..... p 3467 N94-30065
IC-93/264 ..... p 3218 N94-30066
IC-93/265 ..... p 3515 N94-30005
IC-93/270 ..... p 3524 N94-30086
IC-93/273 ..... p 3521 N94-30888
IC-93/274 ..... p 3516 N94-30067
IC-93/279 ..... p 3516 N94-30068
IC-93/280 ..... p 3516 N94-30069
IC-93/281 ..... p 3516 N94-30070
IC-93/282 ..... p 3507 N94-30071
IC-93/283 ..... p 3516 N94-30072
IC-93/284 ..... p 3548 N94-30163
IC-93/286 ..... p 3208 N94-30118
IC-93/291 ..... p 3453 N94-30119
IC-93/292 ..... p 3254 N94-30094 *
IC-93/298 ..... p 3517 N94-30109
IC-93/299 ..... p 3468 N94-30110
IC-93/300 ..... p 3525 N94-30164
IC-93/301 ..... p 3517 N94-30181
IC-93/302 ..... p 3517 N94-30165
IC-93/305 ..... p 3467 N94-30166
IC-93/306 ..... p 3525 N94-30167
IC-93/44 ..... p 3481 N94-28469

ICASE-94-10 ..... p 3272 N94-29381 * #
ICASE-94-13 ..... p 3454 N94-30209 * #
ICASE-94-14 ..... p 3454 N94-30208 * #
ICASE-94-15 ..... p 3454 N94-30207 * #

ICOMP-94-04 ..... p 3272 N94-29096 * #

IDA-P-2899 ..... p 3409 N94-28878 #

IDA/HQ-93-044552 ..... p 3409 N94-28878 #

IECE-CFE-TR-001 ..... p 3198 N94-30017 #

IFVE-OMVT-92-119 ..... p 3522 N94-28616

IFVE-ONF-92-24 ..... p 3489 N94-30050

IHEP-OEIUNK-92-80 ..... p 3421 N94-30080

IHES/M-93/54 ..... p 3462 N94-30889

IHES/M/93/57 ..... p 3467 N94-29147
IHES/M/93/58 ..... p 3523 N94-29146
IHES/M/93/61 ..... p 3452 N94-29148
IHES/M/93/62 ..... p 3467 N94-29162
IHES/M/93/64 ..... p 3452 N94-29118 #
IHES/M/93/65 ..... p 3464 N94-29178
IHES/M/93/67 ..... p 3467 N94-29163

IMR-TM-TR-002 ..... p 3321 N94-30018 #
IMR-TM-TR-003 ..... p 3303 N94-30019 #

IMS-261 ..... p 3536 N94-29144

INIS-MF-13718 ..... p 3514 N94-29691
INIS-MF-13725 ..... p 3212 N94-28550 #
INIS-MF-13737 ..... p 3506 N94-29831 #

INP-MSU-92-33-282 ..... p 3523 N94-28617

INS-J-176 ..... p 3485 N94-28624 #

INT-PATENT-CLASS-B22F-7/00 . p 3205 N94-29507 *
INT-PATENT-CLASS-B23K-31/02 p 3301 N94-29557 *
INT-PATENT-CLASS-B23K-9/12 . p 3300 N94-29506 *
INT-PATENT-CLASS-B25J-11/00 p 3288 N94-29726 *

INT-PATENT-CLASS-C03C-10/06 p 3180 N94-29508 *
INT-PATENT-CLASS-C03C-14/00 p 3180 N94-29508 *

INT-PATENT-CLASS-E05B-1/00 . p 3300 N94-29428 *

INT-PATENT-CLASS-F02C-3/02 . p 3274 N94-29740 *
INT-PATENT-CLASS-F04D-29/68 p 3273 N94-29539 *

INT-PATENT-CLASS-G01D-7/02 . p 3288 N94-29538 *
INT-PATENT-CLASS-G01N-29/10 p 3315 N94-29548 *
INT-PATENT-CLASS-G01N-29/28 p 3315 N94-29548 *
INT-PATENT-CLASS-G01S-13/58 p 3252 N94-29739 *

INT-PATENT-CLASS-G05B-19/00 p 3435 N94-29465 *
INT-PATENT-CLASS-G05B-19/42 p 3436 N94-29504 *
INT-PATENT-CLASS-G05G-11/00 p 3301 N94-29556 *
INT-PATENT-CLASS-G05G-11/00 p 3288 N94-29726 *
INT-PATENT-CLASS-G06F-15/18 p 3436 N94-29756 *
INT-PATENT-CLASS-G06G-7/19 p 3436 N94-29756 *

INT-PATENT-CLASS-H01L-39/22 p 3513 N94-29501 *
INT-PATENT-CLASS-H01M-4/58 p 3265 N94-29505 *
INT-PATENT-CLASS-H03K-19/08 p 3265 N94-29426 *

IPPCZ-321 ..... p 3505 N94-29074 #

IS-M-752 ..... p 3406 N94-30004 #
IS-M-779 ..... p 3519 N94-30338 #

IS-T-1424 ..... p 3218 N94-30104 #
IS-T-1614 ..... p 3187 N94-28519 #
IS-T-1631 ..... p 3519 N94-30691
IS-T-1644 ..... p 3187 N94-28483 #
IS-T-1646 ..... p 3209 N94-30336 #
IS-T-1647 ..... p 3201 N94-28525 #
IS-T-1651 ..... p 3510 N94-28529 #
IS-T-1653 ..... p 3201 N94-28527 #
IS-T-1654 ..... p 3482 N94-28520 #
IS-T-1657 ..... p 3296 N94-30908 #
IS-T-1660 ..... p 3211 N94-28530 #
IS-T-1664 ..... p 3521 N94-30899 #
IS-T-1667 ..... p 3211 N94-28516 #
IS-T-1673 ..... p 3404 N94-28517 #
IS-T-1674 ..... p 3482 N94-28518 #
IS-T-1676 ..... p 3185 N94-30704
IS-T-1679 ..... p 3219 N94-30337 #
IS-T-1682 ..... p 3202 N94-28562 #
IS-T-1687 ..... p 3187 N94-28561 #
IS-T-1688 ..... p 3209 N94-30690 #

ISBN-0-315-74739-0 ..... p 3277 N94-29902
ISBN-0-315-74753-6 ..... p 3371 N94-29751
ISBN-0-315-74841-9 ..... p 3373 N94-29908
ISBN-0-315-74873-7 ..... p 3321 N94-29812
ISBN-0-315-75468-0 ..... p 3375 N94-30870
ISBN-0-315-78703-1 ..... p 3311 N94-30793
ISBN-0-315-78705-8 ..... p 3313 N94-30952
ISBN-0-315-78975-1 ..... p 3296 N94-30801
ISBN-0-315-85382-4 ..... p 3541 N94-30133
ISBN-0-315-85385-9 ..... p 3517 N94-30203
ISBN-0-315-85393-X ..... p 3365 N94-30134
ISBN-0-315-85410-3 ..... p 3303 N94-30135
ISBN-0-315-85430-8 ..... p 3421 N94-30136
ISBN-0-315-85432-4 ..... p 3199 N94-30137
ISBN-0-315-85433-2 ..... p 3208 N94-30138
ISBN-0-315-85443-X ..... p 3437 N94-30255
ISBN-0-315-85466-9 ..... p 3304 N94-30238
ISBN-0-315-85526-6 ..... p 3541 N94-30231
ISBN-0-315-85539-8 ..... p 3290 N94-30232
ISBN-0-315-85546-0 ..... p 3500 N94-30233
ISBN-0-315-85577-0 ..... p 3490 N94-30234
ISBN-0-315-85637-8 ..... p 3316 N94-30235
ISBN-0-315-85658-0 ..... p 3334 N94-30236
ISBN-0-315-85724-2 ..... p 3159 N94-30237
ISBN-0-315-85756-0 ..... p 3518 N94-30239
ISBN-0-315-85757-9 ..... p 3525 N94-30244
ISBN-0-315-85767-6 ..... p 3255 N94-30240
ISBN-0-315-85774-9 ..... p 3454 N94-30241
ISBN-0-315-85795-1 ..... p 3453 N94-30139
ISBN-0-315-85799-4 ..... p 3254 N94-30031
ISBN-0-315-85830-3 ..... p 3515 N94-30032
ISBN-0-315-85841-9 ..... p 3321 N94-30033
ISBN-0-315-85856-7 ..... p 3254 N94-30034
ISBN-0-315-85893-1 ..... p 3548 N94-30058
ISBN-0-315-85923-7 ..... p 3218 N94-30036
ISBN-0-315-85942-3 ..... p 3334 N94-30037
ISBN-0-315-85959-8 ..... p 3432 N94-30140
ISBN-0-315-85982-2 ..... p 3490 N94-30141
ISBN-0-315-85990-3 ..... p 3525 N94-30142
ISBN-0-315-86005-7 ..... p 3432 N94-30143
ISBN-0-315-86079-0 ..... p 3136 N94-30144
ISBN-0-315-86095-2 ..... p 3229 N94-30145
ISBN-0-315-86108-8 ..... p 3209 N94-30146
ISBN-0-315-86157-6 ..... p 3254 N94-30035
ISBN-0-86039-547-2 ..... p 3148 N94-29887
ISBN-9-29-092069-6 ..... p 3501 N94-30418 #
ISBN-91-7848-335-2 ..... p 3264 N94-29191 #
ISBN-91-7848-437-5 ..... p 3411 N94-29159
ISBN-92-835-0719-3 ..... p 3189 N94-29246 #
ISBN-92-835-0721-5 ..... p 3379 N94-28420 #
ISBN-92-835-0724-X ..... p 3136 N94-29558 #
ISBN-92-835-0725-8 ..... p 3412 N94-29315 #
ISBN-92-835-0727-4 ..... p 3256 N94-30495 #
ISBN-92-835-0732-0 ..... p 3151 N94-29291 #
ISBN-92-835-0733-9 ..... p 3169 N94-30350 #
ISBN-92-835-0737-1 ..... p 3528 N94-30934 #
ISBN-92-9092-041-6 ..... p 3347 N94-29452 #
ISBN-95-576-4755-0 ..... p 3385 N94-29156 #
ISBN-951-22-1536-5 ..... p 3204 N94-29387

ISBN-951-22-1594-2 ..... p 3453 N94-29439 #
ISBN-951-22-1629-9 ..... p 3204 N94-29142 #
ISBN-951-22-1633-7 ..... p 3385 N94-29190
ISBN-951-22-1636-1 ..... p 3464 N94-29030
ISBN-951-22-1671-X ..... p 3385 N94-29189
ISBN-951-22-1692-2 ..... p 3530 N94-29141 #
ISBN-951-22-1698-1 ..... p 3537 N94-29168
ISBN-951-22-1699-X ..... p 3220 N94-30713 #
ISBN-951-22-1707-4 ..... p 3213 N94-29031
ISBN-951-22-1710-4 ..... p 3301 N94-29679
ISBN-951-22-1712-0 ..... p 3214 N94-29157 #
ISBN-951-22-1716-3 ..... p 3419 N94-29680
ISBN-951-22-1725-2 ..... p 3538 N94-29170
ISBN-951-22-1773-2 ..... p 3230 N94-29188
ISBN-951-22-1786-4 ..... p 3244 N94-29169
ISBN-951-221762-7 ..... p 3329 N94-29173 #
ISBN-951-38-4251-7 ..... p 3399 N94-28406 #
ISBN-951-38-4255-X ..... p 3186 N94-28407 #
ISBN-951-38-4257-6 ..... p 3406 N94-28401 #
ISBN-951-38-4258-4 ..... p 3316 N94-28402 #
ISBN-951-38-4285-8 ..... p 3245 N94-29468 #
ISBN-951-38-4348-3 ..... p 3341 N94-28412 #
ISBN-951-38-4352-1 ..... p 3160 N94-28413 #
ISBN-951-38-4354-8 ..... p 3407 N94-28411 #
ISBN-951-38-4382-3 ..... p 3316 N94-28409 #
ISBN-951-38-4383-1 ..... p 3229 N94-28410 #
ISBN-951-38-4384-X ..... p 3465 N94-30154 #
ISBN-951-38-4386-6 ..... p 3261 N94-28400 #
ISBN-951-38-4389-0 ..... p 3537 N94-28405 #
ISBN-951-38-4390-4 ..... p 3316 N94-28404 #

IYAF-92-10 ..... p 3508 N94-30171
IYAF-92-12 ..... p 3508 N94-30193
IYAF-92-15 ..... p 3255 N94-30172
IYAF-92-23 ..... p 3209 N94-30253
IYAF-92-27 ..... p 3508 N94-30191
IYAF-92-9 ..... p 3508 N94-30194

JAERI-M-93-058 ..... p 3503 N94-28555
JAERI-M-93-073 ..... p 3504 N94-28556
JAERI-M-93-117 ..... p 3485 N94-28788 #
JAERI-M-93-131 ..... p 3511 N94-28750 #

JIAA-TR-111 ..... p 3270 N94-28724 * #
JIAA-TR-112 ..... p 3130 N94-29760 * #

JINR-D-13-92-339 ..... p 3517 N94-30082
JINR-D-13-92-340 ..... p 3267 N94-30073
JINR-D-15-92-327 ..... p 3485 N94-28625
JINR-D-2-92-114 ..... p 3522 N94-28586
JINR-D-2-92-147 ..... p 3523 N94-28618
JINR-D-2-92-196 ..... p 3468 N94-28720 #
JINR-D-2-92-446 ..... p 3489 N94-30085
JINR-D-2-92-63 ..... p 3523 N94-28782 #
JINR-D-2-92-70 ..... p 3523 N94-28721 #

JINR-E-1-92-249 ..... p 3489 N94-30051
JINR-E-1-92-250 ..... p 3489 N94-30052
JINR-E-1-93-115 ..... p 3483 N94-28552 #
JINR-E-10-93-86 ..... p 3434 N94-28613
JINR-E-11-92-218 ..... p 3421 N94-30077
JINR-E-11-92-357 ..... p 3484 N94-28619
JINR-E-13-92-179 ..... p 3290 N94-30148
JINR-E-14-92-574 ..... p 3517 N94-30195
JINR-E-14-92-79 ..... p 3490 N94-30182
JINR-E-17-92-412 ..... p 3466 N94-28785 #
JINR-E-2-92-106 ..... p 3487 N94-29502 #
JINR-E-2-92-132 ..... p 3261 N94-28585
JINR-E-2-92-136 ..... p 3523 N94-28751 #
JINR-E-2-92-160 ..... p 3523 N94-28620
JINR-E-2-92-337 ..... p 3523 N94-28802 #
JINR-E-2-92-361 ..... p 3485 N94-28758 #
JINR-E-2-92-368 ..... p 3494 N94-28612
JINR-E-2-92-377 ..... p 3356 N94-28803 #
JINR-E-2-92-378 ..... p 3490 N94-30112
JINR-E-2-92-388 ..... p 3484 N94-28610
JINR-E-2-92-440 ..... p 3484 N94-28584
JINR-E-2-92-477 ..... p 3460 N94-30726
JINR-E-2-92-537 ..... p 3525 N94-30169
JINR-E-4-92-529 ..... p 3517 N94-30183
JINR-E-5-92-202 ..... p 3522 N94-28582 #
JINR-E-5-92-395 ..... p 3522 N94-28609
JINR-E-5-92-428 ..... p 3453 N94-30078

JINR-R-1-92-494 ..... p 3489 N94-30095
JINR-R-10-92-188 ..... p 3286 N94-28553 #
JINR-R-10-92-220 ..... p 3534 N94-30079
JINR-R-10-92-370 ..... p 3483 N94-28554 #
JINR-R-10-93-15 ..... p 3485 N94-28621
JINR-R-10-93-40 ..... p 3528 N94-28615
JINR-R-11-92-142 ..... p 3451 N94-28783 #
JINR-R-11-92-416 ..... p 3406 N94-30081
JINR-R-11-92-488 ..... p 3421 N94-30083
JINR-R-13-92-112 ..... p 3406 N94-30074
JINR-R-13-92-489 ..... p 3500 N94-30075
JINR-R-14-92-396 ..... p 3512 N94-28787 #

JINR-R-14-92-401 ..... p 3511 N94-28626
JINR-R-14-92-579 ..... p 3513 N94-29210 #
JINR-R-14-92-65 ..... p 3220 N94-30745
JINR-R-2-92-580 ..... p 3490 N94-30120
JINR-R-2-92-66 ..... p 3485 N94-28718 #
JINR-R-2-93-44 ..... p 3484 N94-28611
JINR-R-4-92-10 ..... p 3524 N94-30087
JINR-R-4-92-297 ..... p 3407 N94-28622
JINR-R-4-92-389 ..... p 3523 N94-28719 #
JINR-R-9-92-53 ..... p 3500 N94-30084

JPL-D-11525 ..... p 3422 N94-30197 * #
JPL-D-1272 ..... p 3405 N94-28845 * #

JPL-PUBL-93-8 ..... p 3235 N94-29767 * #

JPL-TDA-PR-42-105 ..... p 3246 N94-29613 * #

JTN-94-80544 ..... p 3170 N94-30932 #
JTN-94-80545 ..... p 3169 N94-30811 #
JTN-94-80552 ..... p 3187 N94-28675 #
JTN-94-80553 ..... p 3553 N94-29512 #
JTN-94-80578 ..... p 3325 N94-28925 #
JTN-94-80581 ..... p 3227 N94-28938 #
JTN-94-80582 ..... p 3159 N94-30162 #
JTN-94-80583 ..... p 3159 N94-30794 #
JTN-94-80584 ..... p 3158 N94-28583 #
JTN-94-80585 ..... p 3324 N94-28693 #
JTN-94-80587 ..... p 3377 N94-29595 #
JTN-94-80588 ..... p 3392 N94-29709 #
JTN-94-80589 ..... p 3357 N94-29078 #
JTN-94-80591 ..... p 3363 N94-29978 #
JTN-94-80593 ..... p 3359 N94-29233 #
JTN-94-80596 ..... p 3233 N94-29701 #
JTN-94-80597 ..... p 3329 N94-29217 #
JTN-94-80598 ..... p 3389 N94-28850 #
JTN-94-80599 ..... p 3394 N94-29863 #
JTN-94-80600 ..... p 3495 N94-29596 #
JTN-94-80605 ..... p 3479 N94-29597 #
JTN-94-80606 ..... p 3387 N94-28495 #
JTN-94-80607 ..... p 3328 N94-29036 #
JTN-94-80612 ..... p 3123 N94-28946 #

K/TCD-1091 ..... p 3200 N94-30880 #

KCP-613-5331 ..... p 3349 N94-29932 #
KCP-613-5345 ..... p 3219 N94-30245 #

KSC-DM-3673 ..... p 3231 N94-29376 * #

L-16423 ..... p 3130 N94-29545 * #
L-17250 ..... p 3370 N94-29455 * #
L-17259 ..... p 3132 N94-29937 * #
L-17370 ..... p 3342 N94-28587 * #

LA-SUB-93-207 ..... p 3295 N94-30595
LA-SUB-93-223 ..... p 3463 N94-28548 #
LA-SUB-94-1 ..... p 3270 N94-28549 #

LA-UR-93-2968 ..... p 3419 N94-29816 #
LA-UR-93-3381 ..... p 3461 N94-30821 #
LA-UR-93-3632 ..... p 3488 N94-30039
LA-UR-93-3633 ..... p 3497 N94-30825 #
LA-UR-93-3658 ..... p 3355 N94-28538 #
LA-UR-93-3704 ..... p 3267 N94-30716 #
LA-UR-93-3844 ..... p 3335 N94-30610 #
LA-UR-93-4185 ..... p 3240 N94-28522 #
LA-UR-93-4224 ..... p 3342 N94-28521 #
LA-UR-93-4230 ..... p 3175 N94-28581 #
LA-UR-93-4231 ..... p 3210 N94-30774 #
LA-UR-93-4240 ..... p 3548 N94-30694 #
LA-UR-93-4262 ..... p 3552 N94-28580 #
LA-UR-93-4274 ..... p 3175 N94-28579 #
LA-UR-93-4288 ..... p 3185 N94-30693 #
LA-UR-93-4307 ..... p 3182 N94-29933 #
LA-UR-93-4314 ..... p 3526 N94-30750 #
LA-UR-93-4315 ..... p 3522 N94-28572 #
LA-UR-93-4316 ..... p 3522 N94-28543 #
LA-UR-93-4331 ..... p 3200 N94-30748 #
LA-UR-93-4343 ..... p 3185 N94-30771 #
LA-UR-93-4344 ..... p 3492 N94-30775 #
LA-UR-93-4397 ..... p 3543 N94-28545 #
LA-UR-93-4409 ..... p 3498 N94-30847 #
LA-UR-93-4410 ..... p 3294 N94-29934 #
LA-UR-93-4428 ..... p 3208 N94-30101 #
LA-UR-93-4435 ..... p 3432 N94-30100
LA-UR-93-4436 ..... p 3210 N94-30776
LA-UR-93-4459 ..... p 3514 N94-29818 #
LA-UR-93-4464 ..... p 3517 N94-30201 #
LA-UR-93-4474 ..... p 3509 N94-30752 #
LA-UR-93-4477 ..... p 3480 N94-30098 #
LA-UR-93-4521 ..... p 3201 N94-28544 #
LA-UR-94-0116 ..... p 3536 N94-30706
LA-UR-94-111 ..... p 3427 N94-30705
LA-UR-94-227 ..... p 3465 N94-30366 #
LA-UR-94-25 ..... p 3551 N94-30845

LA-UR-94-308 ..... p 3217 N94-30025 #
LA-UR-94-40 ..... p 3520 N94-30848 #
LA-UR-94-4 ..... p 3498 N94-30846

LA-12552-MS ..... p 3270 N94-28475 #

LBL-33456 ..... p 3292 N94-28481 #
LBL-33798 ..... p 3494 N94-28507 #
LBL-33808 ..... p 3407 N94-28506 #
LBL-33943 ..... p 3410 N94-29019 #
LBL-34060 ..... p 3268 N94-30717 #
LBL-34434 ..... p 3520 N94-30835 #
LBL-34587 ..... p 3519 N94-30707
LBL-34738 ..... p 3482 N94-28524 #
LBL-34783 ..... p 3542 N94-28480 #
LBL-34797 ..... p 3491 N94-30709 #
LBL-34836 ..... p 3504 N94-28564 #
LBL-34864 ..... p 3267 N94-30711 #
LBL-34878 ..... p 3261 N94-28546 #
LBL-34884 ..... p 3520 N94-30842 #
LBL-34889 ..... p 3292 N94-28478 #
LBL-34908 ..... p 3201 N94-28479 #
LBL-34909 ..... p 3210 N94-30710 #
LBL-34925 ..... p 3199 N94-30266 #
LBL-35001 ..... p 3520 N94-30850 #
LBL-35002 ..... p 3468 N94-30026 #
LBL-35028 ..... p 3476 N94-30841 #
LBL-35035 ..... p 3515 N94-30009
LBL-35051 ..... p 3289 N94-30027 #

LIYAF-1691 ..... p 3489 N94-30096

LP-92-14 ..... p 3456 N94-30372 #
LP-93-01 ..... p 3422 N94-30318
LP-93-02 ..... p 3454 N94-30319 #
LP-93-03 ..... p 3455 N94-30326
LP-93-04 ..... p 3455 N94-30327

LPI-CONTRIB-827 ..... p 3354 N94-28416 * #

LPI-TR-94-01 ..... p 3549 N94-29102 * #

LR-710-PT-1 ..... p 3184 N94-30343

MATHS-REPT-A-195 ..... p 3464 N94-29482 #
MATHS-REPT-A-196 ..... p 3436 N94-29526 #
MATHS-REPT-A-197 ..... p 3266 N94-29527 #
MATHS-REPT-A-198 ..... p 3333 N94-29528 #

MCAT-94-002 ..... p 3277 N94-29942 * #

MEMO-INF-93-20 ..... p 3438 N94-30373
MEMO-INF-93-29-REV ..... p 3425 N94-30416
MEMO-INF-93-30 ..... p 3255 N94-30374
MEMO-INF-93-35 ..... p 3438 N94-30375
MEMO-INF-93-41 ..... p 3425 N94-30417
MEMO-INF-93-43 ..... p 3260 N94-30520
MEMO-INF-93-44 ..... p 3429 N94-30765 #

MEMO-1145 ..... p 3461 N94-30766
MEMO-1146 ..... p 3461 N94-30767
MEMO-1147 ..... p 3460 N94-30736
MEMO-1148 ..... p 3466 N94-30737
MEMO-1149 ..... p 3427 N94-30585 #
MEMO-1151 ..... p 3460 N94-30738
MEMO-1153 ..... p 3449 N94-30963
MEMO-1154 ..... p 3462 N94-30964

ML-92-10 ..... p 3455 N94-30325
ML-93-01 ..... p 3457 N94-30395
ML-93-02 ..... p 3457 N94-30396
ML-93-03 ..... p 3457 N94-30397
ML-93-04 ..... p 3456 N94-30380
ML-93-05 ..... p 3456 N94-30381
ML-93-06 ..... p 3456 N94-30382
ML-93-07 ..... p 3456 N94-30383
ML-93-08 ..... p 3457 N94-30384
ML-93-09 ..... p 3457 N94-30385
ML-93-10 ..... p 3430 N94-30973
ML-93-11 ..... p 3463 N94-30974
ML-93-12 ..... p 3463 N94-30975
ML-93-13 ..... p 3463 N94-30976
ML-93-14 ..... p 3463 N94-30977

MMAP-STS-57 ..... p 3168 N94-29757 * #

MME-TF-93-1 ..... p 3129 N94-29306 #

MML-TM-94-02 ..... p 3241 N94-28755 #

MML-TR-93-17 ..... p 3176 N94-28653 #
MML-TR-94-02 ..... p 3204 N94-29196

MRL-TN-649 ..... p 3401 N94-29093

MRL-TR-93-15 ..... p 3224 N94-29092

MSRR-590 ..... p 3409 N94-28917 #

NAL-SP-19 ..... p 3123 N94-28946 #

NAMRL-SR-93-2 ..... p 3388 N94-28756 #

NAMRL-1385 ..... p 3397 N94-28754 #

NAS 1.15:103996 ..... p 3555 N94-29891 * #
NAS 1.15:104019 ..... p 3132 N94-30151 * #
NAS 1.15:104594 ..... p 3231 N94-29385 * #
NAS 1.15:104598 ..... p 3370 N94-29408 * #
NAS 1.15:105902 ..... p 3298 N94-28838 * #
NAS 1.15:106156 ..... p 3264 N94-29209 * #
NAS 1.15:106319 ..... p 3202 N94-28822 * #
NAS 1.15:106359 ..... p 3317 N94-28819 * #
NAS 1.15:106372 ..... p 3203 N94-28921 * #
NAS 1.15:106377 ..... p 3135 N94-30949 * #
NAS 1.15:106384 ..... p 3319 N94-29384 * #
NAS 1.15:106392 ..... p 3214 N94-29399 * #
NAS 1.15:106398 ..... p 3174 N94-28747 * #
NAS 1.15:106405 ..... p 3169 N94-30123 * #
NAS 1.15:106406 ..... p 3171 N94-28833 * #
NAS 1.15:106420 ..... p 3242 N94-28826 * #
NAS 1.15:106422 ..... p 3189 N94-28832 * #
NAS 1.15:106442 ..... p 3172 N94-29097 * #
NAS 1.15:106447 ..... p 3174 N94-28924 * #
NAS 1.15:106460 ..... p 3213 N94-28922 * #
NAS 1.15:106478 ..... p 3338 N94-30196 * #
NAS 1.15:106495 ..... p 3156 N94-28749 * #
NAS 1.15:106509 ..... p 3167 N94-29383 * #
NAS 1.15:106514 ..... p 3168 N94-29757 * #
NAS 1.15:106516 ..... p 3214 N94-29105 * #
NAS 1.15:106517 ..... p 3150 N94-28923 * #
NAS 1.15:106519 ..... p 3173 N94-29403 * #
NAS 1.15:106520 ..... p 3273 N94-29471 * #
NAS 1.15:106528 ..... p 3167 N94-28814 * #
NAS 1.15:106532 ..... p 3271 N94-28835 * #
NAS 1.15:106534 ..... p 3205 N94-29758 * #
NAS 1.15:106535 ..... p 3272 N94-29096 * #
NAS 1.15:106536 ..... p 3319 N94-29469 * #
NAS 1.15:106537 ..... p 3319 N94-29406 * #
NAS 1.15:106540 ..... p 3267 N94-30198 * #
NAS 1.15:106543 ..... p 3172 N94-28999 * #
NAS 1.15:106546 ..... p 3279 N94-30147 * #
NAS 1.15:106548 ..... p 3218 N94-30177 * #
NAS 1.15:106549 ..... p 3172 N94-28834 * #
NAS 1.15:106560 ..... p 3286 N94-29000 * #
NAS 1.15:106562 ..... p 3303 N94-30227 * #
NAS 1.15:106563 ..... p 3155 N94-30204 * #
NAS 1.15:106568 ..... p 3422 N94-30175 * #
NAS 1.15:106581 ..... p 3421 N94-30174 * #
NAS 1.15:108438 ..... p 3529 N94-28820 * #
NAS 1.15:108439 ..... p 3333 N94-29553 * #
NAS 1.15:108448 ..... p 3160 N94-29470 * #
NAS 1.15:108449 ..... p 3290 N94-30199 * #
NAS 1.15:108452 ..... p 3169 N94-30161 * #
NAS 1.15:108453 ..... p 3322 N94-30206 * #
NAS 1.15:108992 ..... p 3178 N94-29100 * #
NAS 1.15:109026 ..... p 3177 N94-28823 * #
NAS 1.15:109045 ..... p 3130 N94-29443 * #
NAS 1.15:109046 ..... p 3122 N94-28658 * #
NAS 1.15:109062 ..... p 3133 N94-30176 * #
NAS 1.15:109067 ..... p 3534 N94-30150 * #
NAS 1.15:109081 ..... p 3181 N94-29541 * #
NAS 1.15:109085 ..... p 3534 N94-30149 * #
NAS 1.15:109090 ..... p 3479 N94-29464 * #
NAS 1.15:109091 ..... p 3478 N94-29382 * #
NAS 1.15:109092 ..... p 3422 N94-30197 * #
NAS 1.15:109094 ..... p 3466 N94-29489 * #
NAS 1.15:109095 ..... p 3180 N94-29472 * #
NAS 1.15:109097 ..... p 3479 N94-29461 * #
NAS 1.15:109101 ..... p 3432 N94-30160 * #
NAS 1.15:109102 ..... p 3431 N94-29494 * #
NAS 1.15:109105 ..... p 3157 N94-30200 * #
NAS 1.15:109106 ..... p 3479 N94-29856 * #
NAS 1.15:109110 ..... p 3130 N94-29473 * #
NAS 1.15:109197 ..... p 3231 N94-29376 * #
NAS 1.15:109202 ..... p 3347 N94-29099 * #
NAS 1.15:109735 ..... p 3157 N94-29904 * #
NAS 1.15:109737 ..... p 3254 N94-30094 *
NAS 1.15:109790 ..... p 3528 N94-28414 * #
NAS 1.15:4541 ..... p 3132 N94-29937 * #
NAS 1.15:4569 ..... p 3227 N94-28415 * #
NAS 1.15:4580 ..... p 3385 N94-29401 * #
NAS 1.21:7037(300) ..... p 3121 N94-28537 *
NAS 1.26:187105 ..... p 3152 N94-29438 * #
NAS 1.26:187111 ..... p 3537 N94-29350 * #
NAS 1.26:187147 ..... p 3171 N94-28736 * #
NAS 1.26:187507 ..... p 3408 N94-28818 * #
NAS 1.26:188243 ..... p 3361 N94-29588 * #
NAS 1.26:188273 ..... p 3156 N94-29052 * #
NAS 1.26:188275 ..... p 3171 N94-29035 * #
NAS 1.26:188277 ..... p 3150 N94-29377 * #
NAS 1.26:189148 ..... p 3173 N94-29444 * #
NAS 1.26:189172 ..... p 3168 N94-29405 * #

NAS 1.26:189291 ..... p 3545 N94-29871 * #
NAS 1.26:189293 ..... p 3419 N94-29727 * #
NAS 1.26:189304 ..... p 3374 N94-30187 * #
NAS 1.26:189325 ..... p 3538 N94-29001 * #
NAS 1.26:189329 ..... p 3551 N94-29453 * #
NAS 1.26:189334 ..... p 3289 N94-29872 * #
NAS 1.26:189335 ..... p 3545 N94-29861 * #
NAS 1.26:189337 ..... p 3198 N94-29857 * #
NAS 1.26:189338 ..... p 3287 N94-29400 * #
NAS 1.26:191026 ..... p 3178 N94-29208 * #
NAS 1.26:191152 ..... p 3164 N94-29355 * #
NAS 1.26:191166 ..... p 3181 N94-29684 * #
NAS 1.26:191604 ..... p 3160 N94-28836 * #
NAS 1.26:191606 ..... p 3293 N94-28839 * #
NAS 1.26:192467 ..... p 3157 N94-29956 * #
NAS 1.26:193815 ..... p 3551 N94-30948 * #
NAS 1.26:193940 ..... p 3174 N94-29868 * #
NAS 1.26:193941 ..... p 3297 N94-28419 * #
NAS 1.26:194256 ..... p 3350 N94-30616 * #
NAS 1.26:194266 ..... p 3147 N94-29685 * #
NAS 1.26:194433 ..... p 3183 N94-30190 * #
NAS 1.26:194460 ..... p 3151 N94-29103 * #
NAS 1.26:194462 ..... p 3317 N94-28815 * #
NAS 1.26:194465 ..... p 3319 N94-29104 * #
NAS 1.26:194476 ..... p 3316 N94-28508 * #
NAS 1.26:194535 ..... p 3131 N94-29893 * #
NAS 1.26:194866 ..... p 3300 N94-29550 * #
NAS 1.26:194868 ..... p 3155 N94-28510 * #
NAS 1.26:194881 ..... p 3272 N94-29381 * #
NAS 1.26:194887 ..... p 3454 N94-30209 * #
NAS 1.26:194888 ..... p 3454 N94-30208 * #
NAS 1.26:194890 ..... p 3454 N94-30207 * #
NAS 1.26:194894 ..... p 3480 N94-30274 * #
NAS 1.26:195112 ..... p 3540 N94-29957 * #
NAS 1.26:195114 ..... p 3289 N94-29907 * #
NAS 1.26:195115 ..... p 3147 N94-29721 * #
NAS 1.26:195116 ..... p 3173 N94-29848 * #
NAS 1.26:195119 ..... p 3507 N94-30126 * #
NAS 1.26:195124 ..... p 3244 N94-29106 * #
NAS 1.26:195151 ..... p 3537 N94-29410 * #
NAS 1.26:195210 ..... p 3385 N94-29968 * #
NAS 1.26:195211 ..... p 3278 N94-29977 * #
NAS 1.26:195241 ..... p 3261 N94-28511 * #
NAS 1.26:195260 ..... p 3402 N94-30188 * #
NAS 1.26:195261 ..... p 3385 N94-29943 * #
NAS 1.26:195262 ..... p 3198 N94-29938 * #
NAS 1.26:195284 ..... p 3318 N94-28840 * #
NAS 1.26:195289 ..... p 3318 N94-28821 * #
NAS 1.26:195290 ..... p 3183 N94-30178 * #
NAS 1.26:195299 ..... p 3183 N94-30125 * #
NAS 1.26:195306 ..... p 3303 N94-30205 * #
NAS 1.26:195322 ..... p 3173 N94-29546 * #
NAS 1.26:195327 ..... p 3132 N94-30124 * #
NAS 1.26:195330 ..... p 3133 N94-30152 * #
NAS 1.26:195513 ..... p 3299 N94-29409 * #
NAS 1.26:195546 ..... p 3253 N94-29873 * #
NAS 1.26:195551 ..... p 3299 N94-29354 * #
NAS 1.26:195554 ..... p 3299 N94-29386 * #
NAS 1.26:195688 ..... p 3235 N94-29767 * #
NAS 1.26:195689 ..... p 3249 N94-29652 * #
NAS 1.26:195694 ..... p 3246 N94-29613 * #
NAS 1.26:195699 ..... p 3270 N94-28724 * #
NAS 1.26:195719 ..... p 3354 N94-28416 * #
NAS 1.26:195726 ..... p 3420 N94-29945 * #
NAS 1.26:195727 ..... p 3549 N94-28816 * #
NAS 1.26:195728 ..... p 3262 N94-28846 * #
NAS 1.26:195729 ..... p 3213 N94-28748 * #
NAS 1.26:195730 ..... p 3317 N94-28801 * #
NAS 1.26:195731 ..... p 3286 N94-28824 * #
NAS 1.26:195732 ..... p 3549 N94-28418 * #
NAS 1.26:195733 ..... p 3408 N94-28825 * #
NAS 1.26:195734 ..... p 3171 N94-28800 * #
NAS 1.26:195735 ..... p 3526 N94-28746 * #
NAS 1.26:195736 ..... p 3405 N94-28845 * #
NAS 1.26:195737 ..... p 3145 N94-28817 * #
NAS 1.26:195742 ..... p 3549 N94-29102 * #
NAS 1.26:195755 ..... p 3272 N94-29378 * #
NAS 1.26:195757 ..... p 3420 N94-29890 * #
NAS 1.26:195758 ..... p 3406 N94-29695 * #
NAS 1.26:195759 ..... p 3418 N94-29404 * #
NAS 1.26:195760 ..... p 3431 N94-29869 * #
NAS 1.26:195761 ..... p 3420 N94-29906 * #
NAS 1.26:195762 ..... p 3431 N94-29846 * #
NAS 1.26:195763 ..... p 3152 N94-29860 * #
NAS 1.26:195764 ..... p 3543 N94-29696 * #
NAS 1.26:195766 ..... p 3183 N94-30016 * #
NAS 1.26:195767 ..... p 3551 N94-29858 * #
NAS 1.26:195768 ..... p 3142 N94-30243 * #
NAS 1.26:195772 ..... p 3550 N94-29892 * #
NAS 1.26:195774 ..... p 3277 N94-29942 * #
NAS 1.26:195775 ..... p 3277 N94-29859 * #
NAS 1.26:195777 ..... p 3294 N94-29914 * #
NAS 1.26:195779 ..... p 3347 N94-29549 * #
NAS 1.26:195781 ..... p 3364 N94-30014 * #
NAS 1.26:195782 ..... p 3175 N94-30242 * #
NAS 1.26:195785 ..... p 3515 N94-30015 * #

NAS 1.26:195786 ..... p 3153 N94-30013 * #
NAS 1.26:195790 ..... p 3132 N94-29920 * #
NAS 1.26:195795 ..... p 3546 N94-29905 * #
NAS 1.26:195796 ..... p 3316 N94-29724 * #
NAS 1.26:195797 ..... p 3169 N94-29917 * #
NAS 1.26:195799 ..... p 3549 N94-29737 * #
NAS 1.26:195800 ..... p 3289 N94-29742 * #
NAS 1.26:195802 ..... p 3205 N94-29736 * #
NAS 1.26:195803 ..... p 3130 N94-29760 * #
NAS 1.26:195806 ..... p 3164 N94-29880 * #
NAS 1.26:195809 ..... p 3422 N94-30273 * #
NAS 1.26:4561 ..... p 3301 N94-29552 * #
NAS 1.26:4575 ..... p 3512 N94-29101 * #
NAS 1.26:4579 ..... p 3273 N94-29460 * #
NAS 1.26:4580 ..... p 3164 N94-28417 * #
NAS 1.26:4586 ..... p 3175 N94-29458 * #
NAS 1.26:4587 ..... p 3479 N94-29407 * #
NAS 1.26:4588 ..... p 3329 N94-29098 * #
NAS 1.26:4603 ..... p 3401 N94-30122 * #
NAS 1.55:3205 ..... p 3160 N94-29627 * #
NAS 1.55:3244 ..... p 3165 N94-28697 * #
NAS 1.55:3245 ..... p 3342 N94-28587 * #
NAS 1.55:3249 ..... p 3555 N94-30440 * #
NAS 1.55:3251 ..... p 3439 N94-30526 * #
NAS 1.55:3267 ..... p 3468 N94-30639 * #
NAS 1.60:3281 ..... p 3197 N94-29356 * #
NAS 1.60:3392 ..... p 3130 N94-29545 * #
NAS 1.60:3409 ..... p 3370 N94-29455 * #
NAS 1.60:3474 ..... p 3402 N94-30210 * #
NAS 1.71:ARC-12001-1 ..... p 3478 N94-29363 * #
NAS 1.71:ARC-12013-1-CU ..... p 3245 N94-29364 * #
NAS 1.71:ARC-12014-1 ..... p 3287 N94-29361 * #
NAS 1.71:ARC-12015-1 ..... p 3406 N94-29375 * #
NAS 1.71:ARC-12030-1 ..... p 3478 N94-29362 * #
NAS 1.71:LAR-14029-1 ..... p 3288 N94-29484 * #
NAS 1.71:LAR-14513-1-SB ..... p 3245 N94-29360 * #
NAS 1.71:LAR-14526-1 ..... p 3214 N94-29359 * #
NAS 1.71:LAR-14672-1 ..... p 3287 N94-29199 * #
NAS 1.71:LAR-14863-1-CU ..... p 3180 N94-29485 * #
NAS 1.71:LAR-14997-1 ..... p 3287 N94-29368 * #
NAS 1.71:LAR-15046-1 ..... p 3315 N94-29366 * #
NAS 1.71:LAR-15173-1-CU ..... p 3180 N94-29496 * #
NAS 1.71:LAR-15229-1-CU ..... p 3215 N94-29451 * #
NAS 1.71:LEW-15310-1 ..... p 3246 N94-29589 * #
NAS 1.71:MFS-28581-1 ..... p 3205 N94-29447 * #
NAS 1.71:MFS-28652-1 ..... p 3215 N94-29446 * #
NAS 1.71:MFS-28697-1 ..... p 3298 N94-29353 * #
NAS 1.71:MFS-28765-1 ..... p 3299 N94-29367 * #
NAS 1.71:MFS-28767-1 ..... p 3231 N94-29379 * #
NAS 1.71:MFS-28773-1 ..... p 3299 N94-29365 * #
NAS 1.71:MFS-28808-1 ..... p 3298 N94-29352 * #
NAS 1.71:MFS-28817-1 ..... p 3287 N94-29358 * #
NAS 1.71:MFS-28828-1 ..... p 3298 N94-29351 * #
NAS 1.71:MFS-28829-1 ..... p 3300 N94-29486 * #
NAS 1.71:MFS-28832-1 ..... p 3204 N94-29380 * #
NAS 1.71:MFS-28855-1 ..... p 3264 N94-29372 * #
NAS 1.71:MFS-28857-1 ..... p 3303 N94-30173 * #
NAS 1.71:MSC-21760-1 ..... p 3160 N94-29369 * #
NAS 1.71:MSC-22277-1 ..... p 3300 N94-29448 * #
NAS 1.71:MSC-22424-1 ..... p 3299 N94-29370 * #
NAS 1.71:NPO-18585-1-CU ..... p 3265 N94-29411 * #
NAS 1.71:NPO-18757-1-CU ..... p 3265 N94-29374 * #
NAS 1.71:NPO-18819-1-CU ..... p 3229 N94-29371 * #
NAS 1.71:NPO-18877-1-CU ..... p 3264 N94-29357 * #
NAS 1.71:NPO-18978-1-CU ..... p 3265 N94-29488 * #
NAS 1.71:NPO-18987-1-CU ..... p 3225 N94-29490 * #
NAS 1.71:NPO-18995-1-CU ..... p 3288 N94-29497 * #
NAS 1.71:NPO-19020-1-CU ..... p 3299 N94-29420 * #
NAS 1.71:NPO-19039-1-CU ..... p 3499 N94-29491 * #
NAS 1.71:NPO-19069-1-CU ..... p 3293 N94-29493 * #
NAS 1.71:NPO-19077-1-CU ..... p 3435 N94-29492 * #
NAS 1.71:NPO-19108-1-CU ..... p 3287 N94-29373 * #
NAS 1.71:NPO-19166-1-CU ..... p 3246 N94-29495 * #

NAS-8819-FM-9614-820 ..... p 3278 N94-29977 * #

NASA-CASE-ARC-11955-1-CU ..... p 3180 N94-29509 *
NASA-CASE-ARC-12001-1 ..... p 3478 N94-29363 * #
NASA-CASE-ARC-12013-1-CU ..... p 3245 N94-29364 * #
NASA-CASE-ARC-12014-1 ..... p 3287 N94-29361 * #
NASA-CASE-ARC-12015-1 ..... p 3406 N94-29375 * #
NASA-CASE-ARC-12030-1 ..... p 3478 N94-29362 * #

NASA-CASE-GSC-13468-1 ..... p 3288 N94-29538 *
NASA-CASE-GSC-13485-1 ..... p 3288 N94-29726 *
NASA-CASE-GSC-13485-2 ..... p 3301 N94-29556 *
NASA-CASE-GSC-13542-1 ..... p 3252 N94-29739 *

NASA-CASE-LAR-14029-1 ..... p 3288 N94-29484 * #
NASA-CASE-LAR-14513-1-SB ..... p 3245 N94-29360 * #
NASA-CASE-LAR-14526-1 ..... p 3214 N94-29359 * #
NASA-CASE-LAR-14626-1 ..... p 3315 N94-29548 *
NASA-CASE-LAR-14638-1 ..... p 3215 N94-29555 *
NASA-CASE-LAR-14672-1 ..... p 3287 N94-29199 * #
NASA-CASE-LAR-14863-1-CU ..... p 3180 N94-29485 * #
NASA-CASE-LAR-14997-1 ..... p 3287 N94-29368 * #
NASA-CASE-LAR-15046-1 ..... p 3315 N94-29366 * #
NASA-CASE-LAR-15082-1 ..... p 3175 N94-29554 *
NASA-CASE-LAR-15173-1-CU ..... p 3180 N94-29496 * #
NASA-CASE-LAR-15229-1-CU ..... p 3215 N94-29451 * #

NASA-CASE-LEW-14906-1-SB ..... p 3300 N94-29427 *
NASA-CASE-LEW-15218-2 ..... p 3274 N94-29740 *
NASA-CASE-LEW-15264-2 ..... p 3180 N94-29508 *
NASA-CASE-LEW-15310-1 ..... p 3246 N94-29589 * #
NASA-CASE-LEW-15463-1 ..... p 3273 N94-29539 *
NASA-CASE-LEW-15535-1 ..... p 3205 N94-29507 *
NASA-CASE-LEW-15671-1 ..... p 3301 N94-29557 *

NASA-CASE-MFS-26216-1-SB ..... p 3300 N94-29506 *
NASA-CASE-MFS-28581-1 ..... p 3205 N94-29447 * #
NASA-CASE-MFS-28652-1 ..... p 3215 N94-29446 * #
NASA-CASE-MFS-28697-1 ..... p 3298 N94-29353 * #
NASA-CASE-MFS-28765-1 ..... p 3299 N94-29367 * #
NASA-CASE-MFS-28767-1 ..... p 3231 N94-29379 * #
NASA-CASE-MFS-28773-1 ..... p 3299 N94-29365 * #
NASA-CASE-MFS-28808-1 ..... p 3298 N94-29352 * #
NASA-CASE-MFS-28817-1 ..... p 3287 N94-29358 * #
NASA-CASE-MFS-28828-1 ..... p 3298 N94-29351 * #
NASA-CASE-MFS-28829-1 ..... p 3300 N94-29486 * #
NASA-CASE-MFS-28832-1 ..... p 3204 N94-29380 * #
NASA-CASE-MFS-28855-1 ..... p 3264 N94-29372 * #
NASA-CASE-MFS-28857-1 ..... p 3303 N94-30173 * #

NASA-CASE-MSC-21760-1 ..... p 3160 N94-29369 * #
NASA-CASE-MSC-21955-1 ..... p 3300 N94-29428 *
NASA-CASE-MSC-22027-1 ..... p 3435 N94-29466 *
NASA-CASE-MSC-22277-1 ..... p 3300 N94-29448 * #
NASA-CASE-MSC-22424-1 ..... p 3299 N94-29370 * #

NASA-CASE-NPO-17803-1-CU ..... p 3436 N94-29756 *
NASA-CASE-NPO-17918-2-CU ..... p 3435 N94-29465 *
NASA-CASE-NPO-18483-1-CU ..... p 3513 N94-29501 *
NASA-CASE-NPO-18578-1-CU ..... p 3265 N94-29426 *
NASA-CASE-NPO-18580-1-CU ..... p 3265 N94-29505 *
NASA-CASE-NPO-18585-1-CU ..... p 3265 N94-29411 * #
NASA-CASE-NPO-18608-1-CU ..... p 3436 N94-29504 *
NASA-CASE-NPO-18757-1-CU ..... p 3265 N94-29374 * #
NASA-CASE-NPO-18819-1-CU ..... p 3229 N94-29371 * #
NASA-CASE-NPO-18877-1-CU ..... p 3264 N94-29357 * #
NASA-CASE-NPO-18978-1-CU ..... p 3265 N94-29488 * #
NASA-CASE-NPO-18987-1-CU ..... p 3225 N94-29490 * #
NASA-CASE-NPO-18995-1-CU ..... p 3288 N94-29497 * #
NASA-CASE-NPO-19020-1-CU ..... p 3299 N94-29420 * #
NASA-CASE-NPO-19039-1-CU ..... p 3499 N94-29491 * #
NASA-CASE-NPO-19069-1-CU ..... p 3293 N94-29493 * #
NASA-CASE-NPO-19077-1-CU ..... p 3435 N94-29492 * #
NASA-CASE-NPO-19108-1-CU ..... p 3287 N94-29373 * #
NASA-CASE-NPO-19166-1-CU ..... p 3246 N94-29495 * #

NASA-CP-3205 ..... p 3160 N94-29627 * #
NASA-CP-3244 ..... p 3165 N94-28697 * #
NASA-CP-3245 ..... p 3342 N94-28587 * #
NASA-CP-3249 ..... p 3555 N94-30440 * #
NASA-CP-3251 ..... p 3439 N94-30526 * #
NASA-CP-3267 ..... p 3468 N94-30639 * #

NASA-CR-187105 ..... p 3152 N94-29438 * #
NASA-CR-187111 ..... p 3537 N94-29350 * #
NASA-CR-187147 ..... p 3171 N94-28736 * #
NASA-CR-187507 ..... p 3408 N94-28818 * #
NASA-CR-188243 ..... p 3361 N94-29588 * #
NASA-CR-188273 ..... p 3156 N94-29052 * #
NASA-CR-188275 ..... p 3171 N94-29035 * #
NASA-CR-188277 ..... p 3150 N94-29377 * #
NASA-CR-189148 ..... p 3173 N94-29444 * #
NASA-CR-189172 ..... p 3168 N94-29405 * #
NASA-CR-189291 ..... p 3545 N94-29871 * #
NASA-CR-189293 ..... p 3419 N94-29727 * #
NASA-CR-189304 ..... p 3374 N94-30187 * #
NASA-CR-189325 ..... p 3538 N94-29001 * #
NASA-CR-189329 ..... p 3551 N94-29453 * #
NASA-CR-189334 ..... p 3289 N94-29872 * #
NASA-CR-189335 ..... p 3545 N94-29861 * #
NASA-CR-189337 ..... p 3198 N94-29857 * #
NASA-CR-189338 ..... p 3287 N94-29400 * #
NASA-CR-191026 ..... p 3178 N94-29208 * #
NASA-CR-191152 ..... p 3164 N94-29355 * #
NASA-CR-191166 ..... p 3181 N94-29684 * #
NASA-CR-191604 ..... p 3160 N94-28836 * #
NASA-CR-191606 ..... p 3293 N94-28839 * #
NASA-CR-192467 ..... p 3157 N94-29956 * #
NASA-CR-193815 ..... p 3551 N94-30948 * #
NASA-CR-193940 ..... p 3174 N94-29868 * #
NASA-CR-193941 ..... p 3297 N94-28419 * #
NASA-CR-194256 ..... p 3350 N94-30616 * #
NASA-CR-194266 ..... p 3147 N94-29685 * #
NASA-CR-194433 ..... p 3183 N94-30190 * #
NASA-CR-194460 ..... p 3151 N94-29103 * #
NASA-CR-194462 ..... p 3317 N94-28815 * #
NASA-CR-194465 ..... p 3319 N94-29104 * #
NASA-CR-194476 ..... p 3316 N94-28508 * #
NASA-CR-194535 ..... p 3131 N94-29893 * #
NASA-CR-194866 ..... p 3300 N94-29550 * #
NASA-CR-194868 ..... p 3155 N94-28510 * #
NASA-CR-194881 ..... p 3272 N94-29381 * #
NASA-CR-194887 ..... p 3454 N94-30209 * #
NASA-CR-194888 ..... p 3454 N94-30208 * #
NASA-CR-194890 ..... p 3454 N94-30207 * #
NASA-CR-194894 ..... p 3480 N94-30274 * #
NASA-CR-195112 ..... p 3540 N94-29957 * #
NASA-CR-195114 ..... p 3289 N94-29907 * #
NASA-CR-195115 ..... p 3147 N94-29721 * #
NASA-CR-195116 ..... p 3173 N94-29848 * #
NASA-CR-195119 ..... p 3507 N94-30126 * #
NASA-CR-195124 ..... p 3244 N94-29106 * #
NASA-CR-195151 ..... p 3537 N94-29410 * #
NASA-CR-195210 ..... p 3385 N94-29968 * #
NASA-CR-195211 ..... p 3278 N94-29977 * #
NASA-CR-195241 ..... p 3261 N94-28511 * #
NASA-CR-195260 ..... p 3402 N94-30188 * #
NASA-CR-195261 ..... p 3385 N94-29943 * #
NASA-CR-195262 ..... p 3198 N94-29938 * #
NASA-CR-195284 ..... p 3318 N94-28840 * #
NASA-CR-195289 ..... p 3318 N94-28821 * #
NASA-CR-195290 ..... p 3183 N94-30178 * #
NASA-CR-195299 ..... p 3183 N94-30125 * #
NASA-CR-195306 ..... p 3303 N94-30205 * #
NASA-CR-195322 ..... p 3173 N94-29546 * #
NASA-CR-195327 ..... p 3132 N94-30124 * #
NASA-CR-195330 ..... p 3133 N94-30152 * #
NASA-CR-195513 ..... p 3299 N94-29409 * #
NASA-CR-195546 ..... p 3253 N94-29873 * #
NASA-CR-195551 ..... p 3299 N94-29354 * #
NASA-CR-195554 ..... p 3299 N94-29386 * #
NASA-CR-195688 ..... p 3235 N94-29767 * #
NASA-CR-195689 ..... p 3249 N94-29652 * #
NASA-CR-195694 ..... p 3246 N94-29613 * #
NASA-CR-195699 ..... p 3270 N94-28724 * #
NASA-CR-195719 ..... p 3354 N94-28416 * #
NASA-CR-195726 ..... p 3420 N94-29945 * #
NASA-CR-195727 ..... p 3549 N94-28816 * #
NASA-CR-195728 ..... p 3262 N94-28846 * #
NASA-CR-195729 ..... p 3213 N94-28748 * #
NASA-CR-195730 ..... p 3317 N94-28801 * #
NASA-CR-195731 ..... p 3286 N94-28824 * #
NASA-CR-195732 ..... p 3549 N94-28418 * #
NASA-CR-195733 ..... p 3408 N94-28825 * #
NASA-CR-195734 ..... p 3171 N94-28800 * #
NASA-CR-195735 ..... p 3526 N94-28746 * #
NASA-CR-195736 ..... p 3405 N94-28845 * #
NASA-CR-195737 ..... p 3145 N94-28817 * #
NASA-CR-195742 ..... p 3549 N94-29102 * #
NASA-CR-195755 ..... p 3272 N94-29378 * #
NASA-CR-195757 ..... p 3420 N94-29890 * #
NASA-CR-195758 ..... p 3406 N94-29695 * #
NASA-CR-195759 ..... p 3418 N94-29404 * #
NASA-CR-195760 ..... p 3431 N94-29869 * #
NASA-CR-195761 ..... p 3420 N94-29906 * #
NASA-CR-195762 ..... p 3431 N94-29846 * #
NASA-CR-195763 ..... p 3152 N94-29860 * #
NASA-CR-195764 ..... p 3543 N94-29696 * #
NASA-CR-195766 ..... p 3183 N94-30016 * #
NASA-CR-195767 ..... p 3551 N94-29858 * #
NASA-CR-195768 ..... p 3142 N94-30243 * #
NASA-CR-195772 ..... p 3550 N94-29892 * #
NASA-CR-195774 ..... p 3277 N94-29942 * #
NASA-CR-195775 ..... p 3277 N94-29859 * #
NASA-CR-195777 ..... p 3294 N94-29914 * #
NASA-CR-195779 ..... p 3347 N94-29549 * #
NASA-CR-195781 ..... p 3364 N94-30014 * #
NASA-CR-195782 ..... p 3175 N94-30242 * #
NASA-CR-195785 ..... p 3515 N94-30015 * #
NASA-CR-195786 ..... p 3153 N94-30013 * #
NASA-CR-195790 ..... p 3132 N94-29920 * #
NASA-CR-195795 ..... p 3546 N94-29905 * #
NASA-CR-195796 ..... p 3316 N94-29724 * #
NASA-CR-195797 ..... p 3169 N94-29917 * #
NASA-CR-195799 ..... p 3549 N94-29737 * #
NASA-CR-195800 ..... p 3289 N94-29742 * #
NASA-CR-195802 ..... p 3205 N94-29736 * #
NASA-CR-195803 ..... p 3130 N94-29760 * #
NASA-CR-195806 ..... p 3164 N94-29880 * #
NASA-CR-195809 ..... p 3422 N94-30273 * #
NASA-CR-4561 ..... p 3301 N94-29552 * #
NASA-CR-4575 ..... p 3512 N94-29101 * #
NASA-CR-4579 ..... p 3273 N94-29460 * #
NASA-CR-4580 ..... p 3164 N94-28417 * #
NASA-CR-4586 ..... p 3175 N94-29458 * #
NASA-CR-4587 ..... p 3479 N94-29407 * #
NASA-CR-4588 ..... p 3329 N94-29096 * #
NASA-CR-4603 ..... p 3401 N94-30122 * #

NASA-SP-7037(300) ..... p 3121 N94-28537 *

NASA-TM-103996 ..... p 3555 N94-29891 * #
NASA-TM-104019 ..... p 3132 N94-30151 * #
NASA-TM-104594 ..... p 3231 N94-29385 * #

NASA-TM-104598 ..... p 3370 N94-29408 * #
NASA-TM-105902 ..... p 3298 N94-28838 * #
NASA-TM-106156 ..... p 3264 N94-29209 * #
NASA-TM-106319 ..... p 3202 N94-28822 * #
NASA-TM-106359 ..... p 3317 N94-28819 * #
NASA-TM-106372 ..... p 3203 N94-28921 * #
NASA-TM-106377 ..... p 3135 N94-30949 * #
NASA-TM-106384 ..... p 3319 N94-29384 * #
NASA-TM-106392 ..... p 3214 N94-29399 * #
NASA-TM-106398 ..... p 3174 N94-28747 * #
NASA-TM-106405 ..... p 3169 N94-30123 * #
NASA-TM-106406 ..... p 3171 N94-28833 * #
NASA-TM-106420 ..... p 3242 N94-28826 * #
NASA-TM-106422 ..... p 3189 N94-28832 * #
NASA-TM-106442 ..... p 3172 N94-29097 * #
NASA-TM-106447 ..... p 3174 N94-28924 * #
NASA-TM-106460 ..... p 3213 N94-28922 * #
NASA-TM-106478 ..... p 3338 N94-30196 * #
NASA-TM-106495 ..... p 3156 N94-28749 * #
NASA-TM-106509 ..... p 3167 N94-29383 * #
NASA-TM-106514 ..... p 3168 N94-29757 * #
NASA-TM-106516 ..... p 3214 N94-29105 * #
NASA-TM-106517 ..... p 3150 N94-28923 * #
NASA-TM-106519 ..... p 3173 N94-29403 * #
NASA-TM-106520 ..... p 3273 N94-29471 * #
NASA-TM-106528 ..... p 3167 N94-28814 * #
NASA-TM-106532 ..... p 3271 N94-28835 * #
NASA-TM-106534 ..... p 3205 N94-29758 * #
NASA-TM-106535 ..... p 3272 N94-29096 * #
NASA-TM-106536 ..... p 3319 N94-29469 * #
NASA-TM-106537 ..... p 3319 N94-29406 * #
NASA-TM-106540 ..... p 3267 N94-30198 * #
NASA-TM-106543 ..... p 3172 N94-28999 * #
NASA-TM-106546 ..... p 3279 N94-30147 * #
NASA-TM-106548 ..... p 3218 N94-30177 * #
NASA-TM-106549 ..... p 3172 N94-28834 * #
NASA-TM-106560 ..... p 3286 N94-29000 * #
NASA-TM-106562 ..... p 3303 N94-30227 * #
NASA-TM-106563 ..... p 3155 N94-30204 * #
NASA-TM-106568 ..... p 3422 N94-30175 * #
NASA-TM-106581 ..... p 3421 N94-30174 * #
NASA-TM-108438 ..... p 3529 N94-28820 * #
NASA-TM-108439 ..... p 3333 N94-29553 * #
NASA-TM-108448 ..... p 3160 N94-29470 * #
NASA-TM-108449 ..... p 3290 N94-30199 * #
NASA-TM-108452 ..... p 3169 N94-30161 * #
NASA-TM-108453 ..... p 3322 N94-30206 * #
NASA-TM-108992 ..... p 3178 N94-29100 * #
NASA-TM-109026 ..... p 3177 N94-28823 * #
NASA-TM-109045 ..... p 3130 N94-29443 * #
NASA-TM-109046 ..... p 3122 N94-28658 * #
NASA-TM-109062 ..... p 3133 N94-30176 * #
NASA-TM-109067 ..... p 3534 N94-30150 * #
NASA-TM-109081 ..... p 3181 N94-29541 * #
NASA-TM-109085 ..... p 3534 N94-30149 * #
NASA-TM-109090 ..... p 3479 N94-29464 * #
NASA-TM-109091 ..... p 3478 N94-29382 * #
NASA-TM-109092 ..... p 3422 N94-30197 * #
NASA-TM-109094 ..... p 3466 N94-29489 * #
NASA-TM-109095 ..... p 3180 N94-29472 * #
NASA-TM-109097 ..... p 3479 N94-29461 * #
NASA-TM-109101 ..... p 3432 N94-30160 * #
NASA-TM-109102 ..... p 3431 N94-29494 * #
NASA-TM-109105 ..... p 3157 N94-30200 * #
NASA-TM-109106 ..... p 3479 N94-29856 * #
NASA-TM-109110 ..... p 3130 N94-29473 * #
NASA-TM-109197 ..... p 3231 N94-29376 * #
NASA-TM-109202 ..... p 3347 N94-29099 * #
NASA-TM-109709 ..... p 3528 N94-28414 * #
NASA-TM-109735 ..... p 3157 N94-29904 * #
NASA-TM-109737 ..... p 3254 N94-30094 *
NASA-TM-4541 ..... p 3132 N94-29937 * #
NASA-TM-4569 ..... p 3227 N94-28415 * #
NASA-TM-4580 ..... p 3385 N94-29401 * #

NASA-TP-3281 ..... p 3197 N94-29356 * #
NASA-TP-3392 ..... p 3130 N94-29545 * #
NASA-TP-3409 ..... p 3370 N94-29455 * #
NASA-TP-3474 ..... p 3402 N94-30210 * #

NATICK/TR-94/005 ..... p 3177 N94-28735

NAVSWC-TR-84-373 ..... p 3411 N94-29202

NAVSWC/TR-84-371-REV-2 ..... p 3411 N94-29207

NAWCTSD-TR-93-022 ..... p 3419 N94-29746 #

NCCOSC/RDT/E-TD-2582 ..... p 3212 N94-28641 #
NCCOSC/RDT/E-TD-2584 ..... p 3214 N94-29133 #

NEDO-P-9224 ..... p 3224 N94-28629
NEDO-P-9228 ..... p 3346 N94-28630 #
NEDO-P-9255 ..... p 3337 N94-28631 #

NEDU-2-94 ..... p 3401 N94-29184

NHRC-93-10 ..... p 3400 N94-28902 #
NHRC-93-9 ..... p 3391 N94-28912 #

NIFS-PROC-12 ..... p 3503 N94-28513 #

NIFS-267 ..... p 3505 N94-29398 #
NIFS-268 ..... p 3295 N94-30186 #
NIFS-269 ..... p 3505 N94-29483 #
NIFS-270 ..... p 3506 N94-29499 #
NIFS-271 ..... p 3506 N94-29547 #
NIFS-272 ..... p 3505 N94-29397 #

NIIEFA-P-0908 ..... p 3293 N94-28786 #

NIIYAF-MGU-92-23-272 ..... p 3362 N94-29935
NIIYAF-MGU-92-24-273 ..... p 3365 N94-30223
NIIYAF-**GU-92-28-277 ..... p 3365 N94-30107
NIIYAF-MGU-92-33-282 ..... p 3523 N94-28617

NIKHEF-K-AMPS-93-01 ..... p 3494 N94-29422 #

NLPN-93-428 ..... p 3286 N94-28824 * #

NLR-TP-126232 ..... p 3428 N94-30739
NLR-TP-89191-U ..... p 3429 N94-30912
NLR-TP-90376-U ..... p 3433 N94-30913
NLR-TP-91142-U ..... p 3153 N94-30914
NLR-TP-91446-U ..... p 3143 N94-30915
NLR-TP-91453 ..... p 3135 N94-30916 #
NLR-TP-91460-U ..... p 3220 N94-30420
NLR-TP-91471-U ..... p 3134 N94-30871
NLR-TP-91476-U ..... p 3324 N94-30872
NLR-TP-92020-U ..... p 3143 N94-30853
NLR-TP-92042-U ..... p 3143 N94-30854
NLR-TP-92081-U ..... p 3282 N94-30855
NLR-TP-92134-U ..... p 3170 N94-30857
NLR-TP-92139-U ..... p 3134 N94-30858
NLR-TP-92156-U ..... p 3148 N94-30342
NLR-TP-92163 ..... p 3134 N94-30740
NLR-TP-92174-U ..... p 3448 N94-30741
NLR-TP-92184-U ..... p 3290 N94-30742
NLR-TP-92190-UP ..... p 3133 N94-30387
NLR-TP-92222-U ..... p 3281 N94-30743
NLR-TP-92233-U ..... p 3422 N94-30314
NLR-TP-92248-U ..... p 3133 N94-30388
NLR-TP-92252-U ..... p 3133 N94-30389
NLR-TP-92253-U ..... p 3143 N94-30943
NLR-TP-92261-U ..... p 3402 N94-30390
NLR-TP-92270-U ..... p 3256 N94-30398
NLR-TP-92284-U ..... p 3311 N94-30391
NLR-TP-92288-U ..... p 3256 N94-30392
NLR-TP-92327-U ..... p 3229 N94-30421
NLR-TP-92353-U ..... p 3424 N94-30400
NLR-TP-92361-U ..... p 3133 N94-30401
NLR-TP-92386-U ..... p 3402 N94-30422
NLR-TP-92408-U ..... p 3458 N94-30402
NLR-TP-92420-U ..... p 3158 N94-30423
NLR-TP-92443-U ..... p 3281 N94-30756
NLR-TP-92481-U ..... p 3142 N94-30439
NLR-TP-92521-U ..... p 3133 N94-30492
NLR-TP-92524-U ..... p 3134 N94-30493
NLR-TP-93034-U ..... p 3399 N94-30969
NLR-TP-93047-U ..... p 3335 N94-30759
NLR-TP-93069-U ..... p 3260 N94-30518
NLR-TP-93082-U ..... p 3281 N94-30763
NLR-TP-93094-U ..... p 3428 N94-30764
NLR-TP-93100-U ..... p 3335 N94-30942 #
NLR-TP-93426-U ..... p 3229 N94-30409
NLR-TP-95592 ..... p 3157 N94-30399

NLR-94-92113-U ..... p 3158 N94-30856

NLT-TP-92218-U ..... p 3338 N94-30328

NOAA-TM-ERL-ETL-236 ..... p 3136 N94-30890

NPL-DES-119 ..... p 3476 N94-30783
NPL-DES-121 ..... p 3476 N94-30780
NPL-DES-125 ..... p 3476 N94-30781
NPL-DES-127 ..... p 3267 N94-30115
NPL-DES-128 ..... p 3213 N94-28795
NPL-DES-129 ..... p 3268 N94-30784
NPL-DES-130 ..... p 3260 N94-30785

NPL-DMM(A)-100 ..... p 3184 N94-30419
NPL-DMM(A)-105 ..... p 3184 N94-30438
NPL-DMM(A)-108 ..... p 3322 N94-30114
NPL-DMM(A)-111 ..... p 3501 N94-30522
NPL-DMM(A)-113 ..... p 3204 N94-29119
NPL-DMM(A)-115 ..... p 3217 N94-29886
NPL-DMM(A)-116 ..... p 3319 N94-29121
NPL-DMM(A)-117 ..... p 3322 N94-30523
NPL-DMM(A)-122 ..... p 3184 N94-30524
NPL-DMM(A)-129 ..... p 3181 N94-29524
NPL-DMM(A)-130 ..... p 3210 N94-30796
NPL-DMM(A)-93 ..... p 3217 N94-29885

NPL-DMM(A)85 ..... p 3263 N94-29120

NPL-RSA(EXT)-0044 ..... p 3480 N94-30786
NPL-RSA(EXT)-41 ..... p 3290 N94-30782
NPL-RSA(EXT)-46 ..... p 3492 N94-30795

NPRDC-TN-94-12 ..... p 3389 N94-28797 #

NPS-EC-93-017 ..... p 3241 N94-28634 #

NPS-MA-93-021 ..... p 3451 N94-28651 #

NPS-PH-94-003 ..... p 3230 N94-28644

NRC-36246 ..... p 3198 N94-30017 #

NREL/CP-410-6033 ..... p 3339 N94-30601 #
NREL/CP-420-6032 ..... p 3226 N94-30761

NREL/TP-411-5800 ..... p 3336 N94-28500 #
NREL/TP-411-6010 ..... p 3339 N94-30603 #
NREL/TP-411-6046 ..... p 3339 N94-30605
NREL/TP-411-6047 ..... p 3339 N94-30604 #
NREL/TP-411-6110 ..... p 3336 N94-28501 #
NREL/TP-411-6270 ..... p 3340 N94-30820 #
NREL/TP-422-5726 ..... p 3225 N94-30038
NREL/TP-430-5597 ..... p 3339 N94-30606 #
NREL/TP-430-6085 ..... p 3224 N94-28502 #
NREL/TP-441-5810 ..... p 3339 N94-30602 #
NREL/TP-452-5814 ..... p 3268 N94-30819
NREL/TP-463-4950 ..... p 3226 N94-30818
NREL/TP-471-5864 ..... p 3514 N94-29801 #
NREL/TP-471-5865 ..... p 3500 N94-29799 #
NREL/TP-473-6227 ..... p 3302 N94-29922 #

NRL-CR/7181-93-0002 ..... p 3243 N94-29054 #
NRL-CR/7320-93-0002 ..... p 3357 N94-29062 #

NRL/MR/7175-93-7055 ..... p 3356 N94-28791 #
NRL/MR/7432-93-7022 ..... p 3355 N94-28737 #
NRL/MR/7432-93-7081 ..... p 3355 N94-28685 #
NRL/MR/7442-93-7060 ..... p 3377 N94-29432 #
NRL/MR/8121-93-7417 ..... p 3243 N94-29069 #

NRL/PP/7441-92-0002 ..... p 3478 N94-29206
NRL/PP/7441-93-0013 ..... p 3377 N94-29204

NSSDC-WDC-A-R/S-93-27 ..... p 3528 N94-28414 * #

NSWCDD-TR-84-373-REV-3 ..... p 3411 N94-29202

NSWCDD/TR-84-371-REV-3 ..... p 3411 N94-29207
NSWCDD/TR-93249 ..... p 3527 N94-28779 #

NTSB/AAR-94/02/SUM ..... p 3135 N94-29402 #

NTSB/ARG-93/02 ..... p 3135 N94-29185

NUWC-NL-TM-931139 ..... p 3463 N94-28759 #

NUWC-NPT-TR-10222 ..... p 3411 N94-29180
NUWC-NPT-TR-10481 ..... p 3271 N94-28778 #

ORNL/FTR-4840 ..... p 3519 N94-30611 #

ORNL/TM-12379 ..... p 3465 N94-30696
ORNL/TM-12464 ..... p 3255 N94-30105 #
ORNL/TM-12483 ..... p 3509 N94-30760 #
ORNL/TM-12509 ..... p 3461 N94-30758 #
ORNL/TM-12669 ..... p 3461 N94-30817 #

OSURF-724742 ..... p 3385 N94-29943 * #

OTA-KIRJASTO-A17 ..... p 3532 N94-29682 #

OZ-92/22 ..... p 3481 N94-28471

PAPER-93JA01991 ..... p 3507 N94-30128 * #
PAPER-93JA03201 ..... p 3507 N94-30127 * #

PB93-230233 ..... p 3204 N94-29387
PB94-124336 ..... p 3213 N94-28795
PB94-124849 ..... p 3318 N94-28841
PB94-125457 ..... p 3133 N94-30401
PB94-125465 ..... p 3424 N94-30400
PB94-125473 ..... p 3157 N94-30399
PB94-125481 ..... p 3134 N94-30871
PB94-125515 ..... p 3256 N94-30392
PB94-125531 ..... p 3256 N94-30398
PB94-125549 ..... p 3402 N94-30390
PB94-125556 ..... p 3133 N94-30389
PB94-125564 ..... p 3133 N94-30388
PB94-1255722-U ..... p 3281 N94-30743
PB94-125598 ..... p 3133 N94-30387
PB94-125606 ..... p 3290 N94-30742
PB94-126216 ..... p 3448 N94-30741

PB94-126224 ..... p 3134 N94-30740
PB94-126232 ..... p 3428 N94-30739
PB94-126240 ..... p 3134 N94-30858
PB94-126257 ..... p 3170 N94-30857
PB94-126281 ..... p 3143 N94-30854
PB94-126331 ..... p 3297 N94-28399
PB94-126869 ..... p 3135 N94-29185
PB94-132024 ..... p 3261 N94-28400 #
PB94-132032 ..... p 3406 N94-28401 #
PB94-132040 ..... p 3316 N94-28402 #
PB94-132073 ..... p 3407 N94-28403 #
PB94-132230 ..... p 3316 N94-28404 #
PB94-132248 ..... p 3537 N94-28405 #
PB94-132289 ..... p 3399 N94-28406 #
PB94-132321 ..... p 3186 N94-28407 #
PB94-132339 ..... p 3379 N94-28408
PB94-132347 ..... p 3316 N94-28409 #
PB94-132354 ..... p 3229 N94-28410 #
PB94-132370 ..... p 3407 N94-28411 #
PB94-132388 ..... p 3341 N94-28412 #
PB94-132396 ..... p 3160 N94-28413 #
PB94-132602 ..... p 3530 N94-29141 #
PB94-132925 ..... p 3204 N94-29142 #
PB94-133246 ..... p 3189 N94-28789 #
PB94-135415 ..... p 3477 N94-29186
PB94-135423 ..... p 3385 N94-29156 #
PB94-135506 ..... p 3245 N94-29311
PB94-135514 ..... p 3266 N94-29523
PB94-135522 ..... p 3214 N94-29157 #
PB94-135548 ..... p 3230 N94-29187 #
PB94-135555 ..... p 3230 N94-29188
PB94-135563 ..... p 3385 N94-29189
PB94-135571 ..... p 3385 N94-29190
PB94-135605 ..... p 3264 N94-29191 #
PB94-136231 ..... p 3347 N94-29192 #
PB94-136819 ..... p 3464 N94-29030
PB94-136827 ..... p 3411 N94-29193
PB94-136835 ..... p 3530 N94-29167 #
PB94-136850 ..... p 3537 N94-29168
PB94-136868 ..... p 3244 N94-29169
PB94-136892 ..... p 3538 N94-29170
PB94-136926 ..... p 3452 N94-29171 #
PB94-136934 ..... p 3530 N94-29172
PB94-136942 ..... p 3329 N94-29173 #
PB94-136975 ..... p 3242 N94-28885
PB94-136983 ..... p 3243 N94-28906
PB94-136991 ..... p 3453 N94-29174
PB94-137411 ..... p 3477 N94-29175 #
PB94-137445 ..... p 3243 N94-28907
PB94-137452 ..... p 3244 N94-29176
PB94-137460 ..... p 3244 N94-29177
PB94-137478 ..... p 3243 N94-28908
PB94-137486 ..... p 3337 N94-28909
PB94-137528 ..... p 3203 N94-29015
PB94-137536 ..... p 3301 N94-29679
PB94-137544 ..... p 3419 N94-29680
PB94-137551 ..... p 3220 N94-30713 #
PB94-137593 ..... p 3213 N94-29031
PB94-137619 ..... p 3320 N94-29681 #
PB94-137734 ..... p 3532 N94-29682 #
PB94-137742 ..... p 3487 N94-29683
PB94-137759 ..... p 3453 N94-29439 #
PB94-137767 ..... p 3180 N94-29475
PB94-137791 ..... p 3453 N94-29476
PB94-137809 ..... p 3347 N94-29158
PB94-137817 ..... p 3411 N94-29159
PB94-137916 ..... p 3121 N94-29160
PB94-137981 ..... p 3555 N94-29798
PB94-138062 ..... p 3486 N94-29143
PB94-138070 ..... p 3536 N94-29144
PB94-138104 ..... p 3487 N94-29145
PB94-138112 ..... p 3487 N94-29161
PB94-138120 ..... p 3329 N94-29107
PB94-138138 ..... p 3529 N94-29108
PB94-138146 ..... p 3244 N94-29109
PB94-138153 ..... p 3405 N94-29110
PB94-138161 ..... p 3523 N94-29146
PB94-138179 ..... p 3467 N94-29147
PB94-138187 ..... p 3467 N94-29162
PB94-138195 ..... p 3467 N94-29163
PB94-138203 ..... p 3464 N94-29178
PB94-138211 ..... p 3452 N94-29111
PB94-138229 ..... p 3486 N94-29112
PB94-138245 ..... p 3286 N94-29113
PB94-138286 ..... p 3452 N94-29118 #
PB94-138294 ..... p 3452 N94-29148
PB94-138302 ..... p 3204 N94-29119
PB94-138310 ..... p 3263 N94-29120
PB94-138328 ..... p 3319 N94-29121
PB94-138450 ..... p 3206 N94-29946
PB94-138476 ..... p 3206 N94-29947
PB94-138492 ..... p 3533 N94-29948
PB94-138518 ..... p 3420 N94-29949
PB94-138526 ..... p 3401 N94-29950
PB94-138583 ..... p 3229 N94-29996
PB94-138591 ..... p 3431 N94-29995
PB94-138617 ..... p 3208 N94-30113
PB94-138625 ..... p 3206 N94-29997
PB94-138633 ..... p 3181 N94-29524
PB94-138641 ..... p 3322 N94-30114
PB94-138682 ..... p 3267 N94-30115
PB94-138757 ..... p 3254 N94-29998
PB94-138773 ..... p 3279 N94-29999
PB94-138807 ..... p 3401 N94-30000
PB94-139300 ..... p 3268 N94-30784
PB94-139318 ..... p 3184 N94-30438
PB94-139334 ..... p 3290 N94-30782
PB94-139342 ..... p 3462 N94-30889
PB94-139409 ..... p 3378 N94-30002
PB94-140548 ..... p 3550 N94-29122 #
PB94-141264 ..... p 3533 N94-29921
PB94-142106 ..... p 3136 N94-30890
PB94-142130 ..... p 3550 N94-29123
PB94-142148 ..... p 3550 N94-29124
PB94-142429 ..... p 3149 N94-30905
PB94-142551 ..... p 3145 N94-28657 #
PB94-143336 ..... p 3145 N94-28647 #
PB94-147550 ..... p 3378 N94-30714 #
PB94-147576 ..... p 3184 N94-30524
PB94-910404 ..... p 3135 N94-29402 #

PFC/RR-93-05 ..... p 3510 N94-30882 #
PFC/RR-93-4 ..... p 3493 N94-30881 #
PFC/RR-93-6 ..... p 3506 N94-30045 #

PH-23 ..... p 3505 N94-29075 #
PH-24 ..... p 3505 N94-29076 #

PL-TR-93-2112 ..... p 3504 N94-28828 #
PL-TR-93-2186 ..... p 3164 N94-28827 #
PL-TR-93-2203 ..... p 3369 N94-28663
PL-TR-93-2215 ..... p 3538 N94-28671 #
PL-TR-94-2010 ..... p 3357 N94-28893

PNL-SA-21413 ..... p 3527 N94-30041
PNL-SA-22117 ..... p 3374 N94-30587 #
PNL-SA-22124 ..... p 3368 N94-28455 #
PNL-SA-22420 ..... p 3341 N94-28454 #
PNL-SA-22456 ..... p 3201 N94-28456 #
PNL-SA-22668 ..... p 3201 N94-28460 #
PNL-SA-22790 ..... p 3207 N94-30062 #
PNL-SA-22915 ..... p 3451 N94-28739

PNL-8670 ..... p 3514 N94-30001
PNL-8957 ..... p 3491 N94-30695

POLY-AE-93-8 ..... p 3122 N94-28899 #

PPL-141 ..... p 3508 N94-30159 #
PPL-142 ..... p 3507 N94-30158 #
PPL-143 ..... p 3507 N94-30156 #
PPL-144 ..... p 3507 N94-30157 #

PSU/ARL-TR-94-03 ..... p 3478 N94-29388 #

PT-7452 ..... p 3164 N94-29355 * #

PUB-LAW-101-508 ..... p 3537 N94-28540 #

PURD-TH-92/10 ..... p 3481 N94-28471

RACE-1040-PT-1 ..... p 3252 N94-29692 #
RACE-1040-PT-2 ..... p 3252 N94-29693

RAL-93-078 ..... p 3486 N94-29112
RAL-93-084 ..... p 3452 N94-29111
RAL-93-087 ..... p 3486 N94-29143
RAL-93-091 ..... p 3286 N94-29113
RAL-93-092 ..... p 3487 N94-29161
RAL-93-095 ..... p 3329 N94-29107
RAL-93-098 ..... p 3529 N94-29108
RAL-93-099 ..... p 3244 N94-29109
RAL-93-100 ..... p 3405 N94-29110

RAL/93-81 ..... p 3487 N94-29145

RAY/RD/S-4955 ..... p 3263 N94-28915

REPT-05503-004 ..... p 3407 N94-28664 #
REPT-0650-300-L407 ..... p 3243 N94-29072 #
REPT-106-VOL-36-NO-1 ..... p 3357 N94-29078 #
REPT-108 ..... p 3363 N94-29978 #
REPT-11 ..... p 3189 N94-28789 #
REPT-2-92/93 ..... p 3356 N94-28868 #
REPT-31522-LS ..... p 3384 N94-28884 #
REPT-324-005-93-041 ..... p 3297 N94-28419 * #
REPT-5/1993/MTR ..... p 3204 N94-29142 #
REPT-879.01.4 ..... p 3409 N94-28910 #
REPT-93-043 ..... p 3449 N94-30923
REPT-93-045 ..... p 3429 N94-30924
REPT-93-050 ..... p 3429 N94-30925
REPT-93-051 ..... p 3537 N94-30926
REPT-93-053 ..... p 3536 N94-30927
REPT-93-054 ..... p 3429 N94-30928
REPT-93-056 ..... p 3536 N94-30929
REPT-93-058 ..... p 3291 N94-30930
REPT-93-059 ..... p 3449 N94-30962
REPT-93-060 ..... p 3429 N94-30931
REPT-93-061 ..... p 3429 N94-30936
REPT-93-063 ..... p 3313 N94-30937
REPT-93-065 ..... p 3200 N94-30938
REPT-93-068 ..... p 3449 N94-30939
REPT-93-069 ..... p 3260 N94-30940
REPT-93-076 ..... p 3449 N94-30941
REPT-932-430-102 ..... p 3231 N94-29477 #
REPT-932-430-103 ..... p 3180 N94-29478 #
REPT-932-430-104 ..... p 3245 N94-29440 #
REPT-932-430-105 ..... p 3215 N94-29441 #
REPT-932-430-106 ..... p 3179 N94-29442 #
REPT-932-430-107 ..... p 3255 N94-30153 #
REPT-932-430-108 ..... p 3225 N94-29429 #
REPT-932-430-109 ..... p 3179 N94-29454 #
REPT-932-430-110 ..... p 3245 N94-29421 #
REPT-932-430-111 ..... p 3179 N94-29412 #
REPT-932-430-112 ..... p 3179 N94-29413 #
REPT-932-430-113 ..... p 3225 N94-29414 #
REPT-932-440-101 ..... p 3168 N94-29415 #
REPT-932-440-102 ..... p 3231 N94-29416 #
REPT-932-440-102 ..... p 3418 N94-29418 #
REPT-932-440-103 ..... p 3332 N94-29417 #
REPT-932-440-105 ..... p 3336 N94-30965
REPT-932-440-106 ..... p 3246 N94-29542 #
REPT-932-440-107 ..... p 3168 N94-29543 #
REPT-932-440-108 ..... p 3168 N94-29419 #
REPT-932-440-109 ..... p 3245 N94-29456 #
REPT-932-600-101 ..... p 3205 N94-29525 #
REPT-932-600-102 ..... p 3418 N94-29479 #
REPT-932-600-103 ..... p 3435 N94-29480 #
REPT-932-600-104 ..... p 3315 N94-29474 #
REPT-932-600-105 ..... p 3197 N94-29457 #
REPT-932-600-106 ..... p 3215 N94-29459 #
REPT-932-600-107 ..... p 3179 N94-29462 #
REPT-932-710-101 ..... p 3122 N94-29463 #
REPT-94B00049 ..... p 3370 N94-29408 * #
REPT-94B00063 ..... p 3468 N94-30639 * #
REPT-94B00065 ..... p 3231 N94-29385 * #

RF-767440/722045 ..... p 3270 N94-28665 #

RL-TR-93-157 ..... p 3498 N94-28804
RL-TR-93-203 ..... p 3408 N94-28784
RL-TR-93-224 ..... p 3430 N94-28781 #
RL-TR-93-225 ..... p 3498 N94-28780
RL-TR-93-236 ..... p 3408 N94-28760 #
RL-TR-93-245 ..... p 3241 N94-28762 #
RL-TR-93-52 ..... p 3241 N94-28763 #

RR-912-I ..... p 3395 N94-30028 #

RTI-83U-5676 ..... p 3504 N94-28776 #

RUU-CS-92-34 ..... p 3464 N94-29450
RUU-CS-92-35 ..... p 3455 N94-30333
RUU-CS-92-36 ..... p 3465 N94-30376
RUU-CS-92-37 ..... p 3456 N94-30377 #
RUU-CS-92-38 ..... p 3459 N94-30424
RUU-CS-92-38 ..... p 3462 N94-30859
RUU-CS-92-39 ..... p 3462 N94-30860 #
RUU-CS-92-41 ..... p 3423 N94-30345
RUU-CS-92-42 ..... p 3460 N94-30744
RUU-CS-92-43 ..... p 3455 N94-30346
RUU-CS-92-44 ..... p 3424 N94-30347
RUU-CS-92-45 ..... p 3424 N94-30348
RUU-CS-92-46 ..... p 3438 N94-30334
RUU-CS-92-47 ..... p 3456 N94-30378
RUU-CS-93-01 ..... p 3424 N94-30379
RUU-CS-93-02 ..... p 3457 N94-30393
RUU-CS-93-03 ..... p 3457 N94-30394
RUU-CS-93-05 ..... p 3424 N94-30364
RUU-CS-93-06 ..... p 3438 N94-30349
RUU-CS-93-07 ..... p 3433 N94-30720
RUU-CS-93-08 ..... p 3428 N94-30746
RUU-CS-93-09 ..... p 3458 N94-30403
RUU-CS-93-11 ..... p 3458 N94-30404 #
RUU-CS-93-12 ..... p 3458 N94-30405 #
RUU-CS-93-13 ..... p 3458 N94-30406
RUU-CS-93-15 ..... p 3461 N94-30747
RUU-CS-93-16 ..... p 3458 N94-30407
RUU-CS-93-17 ..... p 3458 N94-30408
RUU-CS-93-18 ..... p 3438 N94-30410
RUU-CS-93-19 ..... p 3432 N94-30411
RUU-CS-93-20 ..... p 3460 N94-30721
RUU-CS-93-21 ..... p 3427 N94-30725
RUU-CS-93-22 ..... p 3406 N94-30727
RUU-CS-93-23 ..... p 3460 N94-30728
RUU-CS-93-24 ..... p 3459 N94-30424
RUU-CS-93-25 ..... p 3459 N94-30425
RUU-CS-93-26 ..... p 3425 N94-30426

RUU-CS-93-27 ..... p 3426 N94-30488
RUU-CS-93-28 ..... p 3426 N94-30489
RUU-CS-93-29 ..... p 3426 N94-30490
RUU-CS-93-30 ..... p 3428 N94-30749

RXR-93082 ..... p 3164 N94-28827 #

R54045007 ..... p 3147 N94-29685 * #
R93-9245-F ..... p 3477 N94-28904 #
R94-9081-F ..... p 3300 N94-29550 * #

S-754-VOL-1 ..... p 3439 N94-30526 * #
S-761 ..... p 3402 N94-30210 * #

SAIC-93/1219 ..... p 3359 N94-29137 #

SAND-92-0693 ..... p 3270 N94-28488 #
SAND-92-2909 ..... p 3286 N94-28466 #
SAND-92-2926 ..... p 3534 N94-30099 #
SAND-93-0226C ..... p 3206 N94-29936 #
SAND-93-0871 ..... p 3260 N94-30772
SAND-93-0974C ..... p 3518 N94-30247 #
SAND-93-0975C ..... p 3518 N94-30315 #
SAND-93-1076 ..... p 3501 N94-30910
SAND-93-1425 ..... p 3289 N94-29927 #
SAND-93-1442C ..... p 3185 N94-30827 #
SAND-93-1447C ..... p 3219 N94-30263 #
SAND-93-1456C ..... p 3199 N94-30260 #
SAND-93-1457C ..... p 3218 N94-30102
SAND-93-1462C ..... p 3519 N94-30592
SAND-93-1483C ..... p 3518 N94-30316 #
SAND-93-1490C ..... p 3184 N94-30589 #
SAND-93-1497C ..... p 3221 N94-30896 #
SAND-93-1523C ..... p 3169 N94-30264 #
SAND-93-1524C ..... p 3295 N94-30367 #
SAND-93-1603 ..... p 3226 N94-30615 #
SAND-93-1642 ..... p 3340 N94-30843
SAND-93-1662C ..... p 3515 N94-30006 #
SAND-93-1822 ..... p 3315 N94-29020 #
SAND-93-1870C ..... p 3263 N94-29025 #
SAND-93-2058C ..... p 3222 N94-30900 #
SAND-93-2133 ..... p 3165 N94-28477 #
SAND-93-2311C ..... p 3510 N94-28484 #
SAND-93-2420C ..... p 3315 N94-28503 #
SAND-93-2449C ..... p 3266 N94-30040
SAND-93-2477 ..... p 3336 N94-28489 #
SAND-93-2514C ..... p 3174 N94-28557 #
SAND-93-2533C ..... p 3207 N94-30053 #
SAND-93-2594C ..... p 3220 N94-30591
SAND-93-2665 ..... p 3462 N94-30849 #
SAND-93-2744C ..... p 3340 N94-30609 #
SAND-93-3842C ..... p 3222 N94-30909 #
SAND-93-3984C ..... p 3266 N94-30055 #
SAND-93-3993C ..... p 3292 N94-28482 #
SAND-93-4029C ..... p 3501 N94-30261 #
SAND-93-4079C ..... p 3206 N94-30007 #
SAND-93-4100 ..... p 3420 N94-29844 #
SAND-93-7098 ..... p 3337 N94-29018 #
SAND-93-7113C ..... p 3187 N94-28567 #
SAND-94-0011C ..... p 3406 N94-30008 #
SAND-94-0074C ..... p 3295 N94-30265 #
SAND-94-0132C ..... p 3501 N94-30828
SAND-94-0248C ..... p 3267 N94-30368 #
SAND-94-0417C ..... p 3437 N94-30250 #
SAND-94-8487C ..... p 3210 N94-30777 #
SAND-94-8521C ..... p 3311 N94-30596

SATCOM-93-19 ..... p 3160 N94-28836 * #

SCT-92RR-14 ..... p 3135 N94-29862 #

SEL-89-103-REV-1 ..... p 3419 N94-29727 * #

SGD-591-PT-1 ..... p 3550 N94-29122 #
SGD-592-PT-1 ..... p 3550 N94-29123
SGD-592-PT-2 ..... p 3550 N94-29124

SKD-1600-73-014 ..... p 3241 N94-28532
SKD-1600-73-015 ..... p 3405 N94-28533

SLAC-PUB-6400 ..... p 3497 N94-30712 #

SLU-MIKRO-R-57-SE ..... p 3385 N94-29156 #

SMC-TR-93-56 ..... p 3264 N94-29289 #
SMC-TR-93-59 ..... p 3494 N94-29065
SMC-TR-93-60 ..... p 3552 N94-29046 #
SMC-TR-93-61 ..... p 3167 N94-29022 #
SMC-TR-93-62 ..... p 3347 N94-29023 #
SMC-TR-93-63 ..... p 3356 N94-28869 #

SP-RAPP-1993-43 ..... p 3477 N94-29175 #
SP-RAPP-1993:17 ..... p 3337 N94-28909
SP-RAPP-1993:50 ..... p 3320 N94-29681 #
SP-RAPP-1993:51 ..... p 3411 N94-29159

SPC-93099-CMC ..... p 3419 N94-29797 #

SPI-39-10 ..... p 3173 N94-29444 * #

SSCL-648 ..... p 3487 N94-29700 #

STF10-A93015 ..... p 3431 N94-29995
STF11-A93017 ..... p 3279 N94-29999
STF11-A93056 ..... p 3401 N94-30000
STF15-A93053 ..... p 3401 N94-29950
STF20-A93105 ..... p 3229 N94-29996
STF28-A93053 ..... p 3208 N94-30113
STF33-A93015 ..... p 3420 N94-29949
STF33-A93019 ..... p 3206 N94-29997
STF34-A93136 ..... p 3206 N94-29947
STF34-A93169 ..... p 3206 N94-29946
STF40-A93074 ..... p 3533 N94-29948
STF40-A93085 ..... p 3533 N94-29921
STF82-595-7759-3 ..... p 3378 N94-30002

SU-SLAC-PUB-6312 ..... p 3292 N94-28481 #
SU-SLAC-PUB-6329 ..... p 3483 N94-28542 #
SU-SLAC-PUB-6347 ..... p 3482 N94-28541 #
SU-SLAC-PUB-6354 ..... p 3482 N94-28494 #
SU-SLAC-PUB-6378 ..... p 3482 N94-28493 #

TA-309 ..... p 3410 N94-29019 #

TDA-PR-42-116 ..... p 3249 N94-29652 * #

TEC-R-204 ..... p 3452 N94-29063 #
TEC-R-206 ..... p 3435 N94-29198
TEC-R-209 ..... p 3329 N94-29213
TEC-R-210 ..... p 3409 N94-28866 #
TEC-R-211 ..... p 3325 N94-28863 #
TEC-R-214 ..... p 3325 N94-28808 #

TELECOM-93-C-002 ..... p 3462 N94-30971
TELECOM-93-C-003 ..... p 3481 N94-30972 #
TELECOM-93-D-016 ..... p 3395 N94-30970 #
TELECOM-93-E-006 ..... p 3396 N94-30978
TELECOM-93-E-019 ..... p 3291 N94-30979

TGAL-93-07 ..... p 3361 N94-29393 #

TIOS-93-11 ..... p 3438 N94-30373
TIOS-93-17 ..... p 3425 N94-30416
TIOS-93-18 ..... p 3255 N94-30374
TIOS-93-25 ..... p 3438 N94-30375
TIOS-93-26 ..... p 3260 N94-30520

TKK-F-B147 ..... p 3487 N94-29683

TKK-V-B85 ..... p 3204 N94-29387

TKO-B106 ..... p 3530 N94-29167 #
TKO-B108 ..... p 3452 N94-29171 #
TKO-B109 ..... p 3530 N94-29172

TKO-C63 ..... p 3411 N94-29193

TR-0091(6940-05)-4 ..... p 3494 N94-29065
TR-0091(6940-05)-7 ..... p 3167 N94-29022 #
TR-18 ..... p 3204 N94-29395 #
TR-1 ..... p 3202 N94-28793 #
TR-28 ..... p 3203 N94-29089 #
TR-477 ..... p 3464 N94-28876 #
TR-478 ..... p 3464 N94-29014 #
TR-70 ..... p 3512 N94-28775
TR-8 ..... p 3317 N94-28811
TR-91 ..... p 3197 N94-29312 #
TR-92(2940)-12 ..... p 3552 N94-29046 #
TR-92(2940)-4 ..... p 3356 N94-28869 #
TR-92-21 ..... p 3432 N94-30356
TR-92-22 ..... p 3535 N94-30357
TR-92-23 ..... p 3465 N94-30358
TR-92-24 ..... p 3535 N94-30359
TR-92-26 ..... p 3535 N94-30360
TR-92-29 ..... p 3535 N94-30361
TR-92-30 ..... p 3535 N94-30362
TR-92-32 ..... p 3432 N94-30363
TR-92-34 ..... p 3423 N94-30344 #
TR-92-36 ..... p 3535 N94-30329
TR-93(3231)-2 ..... p 3347 N94-29023 #
TR-93(3404)-1 ..... p 3264 N94-29289 #
TR-93-01 ..... p 3527 N94-28796 #
TR-93-01 ..... p 3129 N94-29197
TR-93-01 ..... p 3535 N94-30330
TR-93-03 ..... p 3423 N94-30331
TR-93-06 ..... p 3423 N94-30332
TR-93-5451-03 ..... p 3421 N94-30155 #

UAH-5-30175 ..... p 3173 N94-29848 * #
UAH-5-32902 ..... p 3157 N94-29956 * #
UAH-5-33282 ..... p 3316 N94-29724 * #

UCRL-CR-115237 ..... p 3122 N94-29842 #
UCRL-CR-115620 ..... p 3349 N94-30044 #
UCRL-CR-116116 ..... p 3212 N94-28733 #

UCRL-ID-114079 ..... p 3254 N94-30043 #
UCRL-ID-114322 ..... p 3466 N94-30586 #
UCRL-ID-115264 ..... p 3354 N94-30822 #
UCRL-ID-115283 ..... p 3270 N94-28476 #
UCRL-ID-115336 ..... p 3350 N94-30613 #
UCRL-ID-115370 ..... p 3335 N94-30594
UCRL-ID-115689 ..... p 3221 N94-30829
UCRL-ID-115694 ..... p 3289 N94-30059
UCRL-ID-115701 ..... p 3175 N94-28528 #
UCRL-ID-115827 ..... p 3367 N94-30876 #
UCRL-ID-115904 ..... p 3509 N94-30768 #
UCRL-ID-115982 ..... p 3421 N94-30117

UCRL-JC-114022 ..... p 3493 N94-30891 #
UCRL-JC-114155 ..... p 3516 N94-30054 #
UCRL-JC-114374 ..... p 3431 N94-29952 #
UCRL-JC-114684 ..... p 3378 N94-30823 #
UCRL-JC-114805 ..... p 3281 N94-30600
UCRL-JC-114832 ..... p 3295 N94-30060 #
UCRL-JC-114841 ..... p 3212 N94-28560 #
UCRL-JC-114851 ..... p 3211 N94-30892 #
UCRL-JC-114902 ..... p 3296 N94-30830 #
UCRL-JC-114983 ..... p 3295 N94-30598
UCRL-JC-114999 ..... p 3501 N94-30599
UCRL-JC-115048 ..... p 3277 N94-29923 #
UCRL-JC-115082 ..... p 3349 N94-29954 #
UCRL-JC-115167 ..... p 3149 N94-30687
UCRL-JC-115223 ..... p 3321 N94-29951 #
UCRL-JC-115239 ..... p 3497 N94-30825 #
UCRL-JC-115241 ..... p 3255 N94-30106 #
UCRL-JC-115244 ..... p 3526 N94-28474 #
UCRL-JC-115318-REV-1 ..... p 3404 N94-28505 #
UCRL-JC-115463 ..... p 3254 N94-29929
UCRL-JC-115537 ..... p 3509 N94-30597
UCRL-JC-115702 ..... p 3542 N94-28526 #

UCRL-LR-105821-93-4 ..... p 3510 N94-30875 #
UCRL-LR-115496 ..... p 3488 N94-29845 #

UCRL-MA-115656 ..... p 3422 N94-30251 #

UCRL-TB-111084 ..... p 3563 N94-30844

UCRL-52000-93-8 ..... p 3338 N94-29955 #

UILU-ENG-93-2251 ..... p 3420 N94-29906 * #
UILU-ENG-94-2201 ..... p 3431 N94-29869 * #
UILU-ENG-94-2203 ..... p 3431 N94-29846 * #
UILU-ENG-94-2204 ..... p 3420 N94-29890 * #
UILU-ENG-94-2205 ..... p 3406 N94-29695 * #
UILU-ENG-94-2208 ..... p 3418 N94-29404 * #

UM-P-92/70 ..... p 3481 N94-28471

UMICH-031173-2T ..... p 3253 N94-29873 * #

US-PATENT-APPL-SN-000163 ..... p 3273 N94-29539 *
US-PATENT-APPL-SN-028091 ..... p 3252 N94-29739 *
US-PATENT-APPL-SN-063222 ..... p 3301 N94-29557 *
US-PATENT-APPL-SN-070132 ..... p 3300 N94-29506 *
US-PATENT-APPL-SN-071206 ..... p 3436 N94-29756 *
US-PATENT-APPL-SN-077132 ..... p 3175 N94-29554 *
US-PATENT-APPL-SN-084058 ..... p 3180 N94-29508 *
US-PATENT-APPL-SN-086581 ..... p 3274 N94-29740 *
US-PATENT-APPL-SN-110181 ..... p 3301 N94-29556 *
US-PATENT-APPL-SN-117511 ..... p 3287 N94-29199 * #
US-PATENT-APPL-SN-117587 ..... p 3299 N94-29365 * #
US-PATENT-APPL-SN-123629 ..... p 3287 N94-29358 * #
US-PATENT-APPL-SN-123945 ..... p 3298 N94-29352 * #
US-PATENT-APPL-SN-125888 ..... p 3287 N94-29361 * #
US-PATENT-APPL-SN-126286 ..... p 3245 N94-29360 * #
US-PATENT-APPL-SN-130948 ..... p 3245 N94-29364 * #
US-PATENT-APPL-SN-134441 ..... p 3205 N94-29447 * #
US-PATENT-APPL-SN-134443 ..... p 3298 N94-29353 * #
US-PATENT-APPL-SN-134444 ..... p 3315 N94-29366 * #
US-PATENT-APPL-SN-138046 ..... p 3288 N94-29484 * #
US-PATENT-APPL-SN-141292 ..... p 3180 N94-29496 * #
US-PATENT-APPL-SN-141293 ..... p 3180 N94-29485 * #
US-PATENT-APPL-SN-141294 ..... p 3287 N94-29368 * #
US-PATENT-APPL-SN-141797 ..... p 3265 N94-29374 * #
US-PATENT-APPL-SN-143601 ..... p 3299 N94-29367 * #
US-PATENT-APPL-SN-149889 ..... p 3231 N94-29379 * #
US-PATENT-APPL-SN-149896 ..... p 3478 N94-29363 * #
US-PATENT-APPL-SN-151690 ..... p 3478 N94-29362 * #
US-PATENT-APPL-SN-152631 ..... p 3288 N94-29497 * #
US-PATENT-APPL-SN-153595 ..... p 3299 N94-29370 * #
US-PATENT-APPL-SN-153933 ..... p 3229 N94-29371 * #
US-PATENT-APPL-SN-153934 ..... p 3299 N94-29420 * #
US-PATENT-APPL-SN-154322 ..... p 3265 N94-29411 * #
US-PATENT-APPL-SN-158327 ..... p 3298 N94-29351 * #
US-PATENT-APPL-SN-158331 ..... p 3204 N94-29380 * #
US-PATENT-APPL-SN-159606 ..... p 3300 N94-29448 * #

US-PATENT-APPL-SN-159980 ..... p 3287 N94-29373 * #
US-PATENT-APPL-SN-161038 ..... p 3160 N94-29369 * #
US-PATENT-APPL-SN-167107 ..... p 3246 N94-29589 * #
US-PATENT-APPL-SN-172961 ..... p 3303 N94-30173 * #
US-PATENT-APPL-SN-186054 ..... p 3215 N94-29451 * #
US-PATENT-APPL-SN-186183 ..... p 3264 N94-29357 * #
US-PATENT-APPL-SN-186185 ..... p 3265 N94-29488 * #
US-PATENT-APPL-SN-186366 ..... p 3406 N94-29375 * #
US-PATENT-APPL-SN-187032 ..... p 3300 N94-29486 * #
US-PATENT-APPL-SN-191309 ..... p 3215 N94-29446 * #
US-PATENT-APPL-SN-192476 ..... p 3499 N94-29491 * #
US-PATENT-APPL-SN-199924 ..... p 3264 N94-29372 * #
US-PATENT-APPL-SN-200785 ..... p 3225 N94-29490 * #
US-PATENT-APPL-SN-222762 ..... p 3246 N94-29495 * #
US-PATENT-APPL-SN-223938 ..... p 3293 N94-29493 * #
US-PATENT-APPL-SN-223953 ..... p 3435 N94-29492 * #
US-PATENT-APPL-SN-410576 ..... p 3180 N94-29509 *
US-PATENT-APPL-SN-459438 ..... p 3435 N94-29465 *
US-PATENT-APPL-SN-473024 ..... p 3436 N94-29756 *
US-PATENT-APPL-SN-700368 ..... p 3180 N94-29509 *
US-PATENT-APPL-SN-739026 ..... p 3180 N94-29509 *
US-PATENT-APPL-SN-751489 ..... p 3315 N94-29548 *
US-PATENT-APPL-SN-755207 ..... p 3175 N94-29554 *
US-PATENT-APPL-SN-767955 ..... p 3288 N94-29699
US-PATENT-APPL-SN-786499 ..... p 3435 N9x-29465 *
US-PATENT-APPL-SN-852620 ..... p 3513 N94-29501 *
US-PATENT-APPL-SN-870003 ..... p 3214 N94-29359 * #
US-PATENT-APPL-SN-872262 ..... p 3180 N94-29508 *
US-PATENT-APPL-SN-885697 ..... p 3288 N94-29538 *
US-PATENT-APPL-SN-889003 ..... p 3274 N94-29740 *
US-PATENT-APPL-SN-889572 ..... p 3300 N94-29427 *
US-PATENT-APPL-SN-905061 ..... p 3436 N94-29756 *
US-PATENT-APPL-SN-912956 ..... p 3265 N94-29426 *
US-PATENT-APPL-SN-915567 ..... p 3301 N94-29556 *
US-PATENT-APPL-SN-915567 ..... p 3288 N94-29726 *
US-PATENT-APPL-SN-931468 ..... p 3300 N94-29428 *
US-PATENT-APPL-SN-955801 ..... p 3435 N94-29466 *
US-PATENT-APPL-SN-959858 ..... p 3265 N94-29505 *
US-PATENT-APPL-SN-967083 ..... p 3436 N94-29504 *
US-PATENT-APPL-SN-970669 ..... p 3205 N94-29507 *
US-PATENT-APPL-SN-970755 ..... p 3215 N94-29555 *

US-PATENT-CLASS-112-415 ..... p 3180 N94-29509 *
US-PATENT-CLASS-112-420 ..... p 3180 N94-29509 *
US-PATENT-CLASS-112-440 ..... p 3180 N94-29509 *
US-PATENT-CLASS-139-420A .... p 3180 N94-29509 *
US-PATENT-CLASS-148-512 ..... p 3301 N94-29557 *
US-PATENT-CLASS-16-114R ..... p 3300 N94-29428 *
US-PATENT-CLASS-16-125 ..... p 3300 N94-29428 *
US-PATENT-CLASS-219-137.71 .. p 3300 N94-29506 *
US-PATENT-CLASS-228-203 ..... p 3301 N94-29557 *
US-PATENT-CLASS-228-211 ..... p 3301 N94-29557 *
US-PATENT-CLASS-228-232 ..... p 3301 N94-29557 *
US-PATENT-CLASS-24-513 ..... p 3300 N94-29427 *
US-PATENT-CLASS-248-205.3 .... p 3300 N94-29428 *
US-PATENT-CLASS-252-182.1 .... p 3265 N94-29505 *
US-PATENT-CLASS-257-323 ..... p 3265 N94-29426 *
US-PATENT-CLASS-257-33 ..... p 3513 N94-29501 *
US-PATENT-CLASS-257-35 ..... p 3513 N94-29501 *
US-PATENT-CLASS-264-58 ..... p 3180 N94-29508 *
US-PATENT-CLASS-269-238 ..... p 3300 N94-29427 *
US-PATENT-CLASS-269-242 ..... p 3300 N94-29427 *
US-PATENT-CLASS-269-94 ..... p 3300 N94-29427 *
US-PATENT-CLASS-294-1.1 ..... p 3300 N94-29428 *
US-PATENT-CLASS-307-118 ..... p 3435 N94-29466 *
US-PATENT-CLASS-307-201 ..... p 3265 N94-29426 *
US-PATENT-CLASS-307-234 ..... p 3435 N94-29466 *
US-PATENT-CLASS-307-308 ..... p 3435 N94-29466 *
US-PATENT-CLASS-307-542.1 .... p 3435 N94-29466 *
US-PATENT-CLASS-318-561 ..... p 3436 N94-29504 *
US-PATENT-CLASS-318-568.1 .... p 3436 N94-29504 *
US-PATENT-CLASS-318-628 ..... p 3436 N94-29504 *
US-PATENT-CLASS-318-646 ..... p 3436 N94-29504 *
US-PATENT-CLASS-328-1 ..... p 3435 N94-29466 *
US-PATENT-CLASS-340-309.15 .. p 3435 N94-29466 *
US-PATENT-CLASS-340-507 ..... p 3435 N94-29466 *
US-PATENT-CLASS-342-112 ..... p 3252 N94-29739 *
US-PATENT-CLASS-342-116 ..... p 3252 N94-29739 *
US-PATENT-CLASS-395-23 ..... p 3436 N94-29756 *
US-PATENT-CLASS-395-24 ..... p 3265 N94-29426 *
US-PATENT-CLASS-395-24 ..... p 3436 N94-29756 *
US-PATENT-CLASS-395-25 ..... p 3265 N94-29426 *
US-PATENT-CLASS-395-80 ..... p 3435 N94-29465 *
US-PATENT-CLASS-395-89 ..... p 3435 N94-29465 *
US-PATENT-CLASS-395-95 ..... p 3436 N94-29504 *
US-PATENT-CLASS-395-99 ..... p 3435 N94-29465 *
US-PATENT-CLASS-403-322 ..... p 3300 N94-29427 *
US-PATENT-CLASS-415-115 ..... p 3273 N94-29539 *
US-PATENT-CLASS-415-206 ..... p 3273 N94-29539 *
US-PATENT-CLASS-415-914 ..... p 3273 N94-29539 *
US-PATENT-CLASS-423-324 ..... p 3265 N94-29505 *
US-PATENT-CLASS-424-218 ..... p 3265 N94-29505 *
US-PATENT-CLASS-427-62 ..... p 3513 N94-29501 *
US-PATENT-CLASS-428-116 ..... p 3180 N94-29509 *
US-PATENT-CLASS-428-552 ..... p 3205 N94-29507 *
US-PATENT-CLASS-428-553 ..... p 3205 N94-29507 *
US-PATENT-CLASS-428-565 ..... p 3205 N94-29507 *
US-PATENT-CLASS-428-610 ..... p 3301 N94-29557 *
US-PATENT-CLASS-429-194 ..... p 3265 N94-29505 *
US-PATENT-CLASS-501-32 ..... p 3180 N94-29508 *
US-PATENT-CLASS-501-8 ..... p 3180 N94-29508 *
US-PATENT-CLASS-501-95 ..... p 3180 N94-29508 *
US-PATENT-CLASS-505-190 ..... p 3513 N94-29501 *
US-PATENT-CLASS-505-702 ..... p 3513 N94-29501 *
US-PATENT-CLASS-505-785 ..... p 3513 N94-29501 *
US-PATENT-CLASS-528-125 ..... p 3175 N94-29554 *
US-PATENT-CLASS-528-128 ..... p 3175 N94-29554 *
US-PATENT-CLASS-528-170 ..... p 3175 N94-29554 *
US-PATENT-CLASS-528-172 ..... p 3175 N94-29554 *
US-PATENT-CLASS-528-173 ..... p 3175 N94-29554 *
US-PATENT-CLASS-528-22 ..... p 3215 N94-29555 *
US-PATENT-CLASS-528-26 ..... p 3215 N94-29555 *
US-PATENT-CLASS-528-28 ..... p 3215 N94-29555 *
US-PATENT-CLASS-528-32 ..... p 3215 N94-29555 *
US-PATENT-CLASS-528-33 ..... p 3215 N94-29555 *
US-PATENT-CLASS-528-34 ..... p 3215 N94-29555 *
US-PATENT-CLASS-528-353 ..... p 3175 N94-29554 *
US-PATENT-CLASS-528-353 ..... p 3215 N94-29555 *
US-PATENT-CLASS-60-39.02 ..... p 3274 N94-29740 *
US-PATENT-CLASS-73-588 ..... p 3315 N94-29548 *
US-PATENT-CLASS-73-644 ..... p 3315 N94-29548 *
US-PATENT-CLASS-73-761 ..... p 3288 N94-29538 *
US-PATENT-CLASS-73-789 ..... p 3288 N94-29538 *
US-PATENT-CLASS-74-436 ..... p 3300 N94-29427 *
US-PATENT-CLASS-74-469 ..... p 3301 N94-29556 *
US-PATENT-CLASS-74-479B ..... p 3301 N94-29556 *
US-PATENT-CLASS-74-479B ..... p 3288 N94-29726 *
US-PATENT-CLASS-74-479PF .... p 3288 N94-29726 *
US-PATENT-CLASS-74-479PP .... p 3301 N94-29556 *
US-PATENT-CLASS-74-89.15 ..... p 3300 N94-29427 *
US-PATENT-CLASS-901-14 ..... p 3301 N94-29556 *
US-PATENT-CLASS-901-14 ..... p 3288 N94-29726 *
US-PATENT-CLASS-901-19 ..... p 3301 N94-29556 *
US-PATENT-CLASS-901-19 ..... p 3288 N94-29726 *
US-PATENT-CLASS-901-9 ..... p 3436 N94-29504 *

US-PATENT-5,243,403 ..... p 3288 N94-29699
US-PATENT-5,276,453 ..... p 3252 N94-29739 *
US-PATENT-5,277,959 ..... p 3180 N94-29509 *
US-PATENT-5,279,176 ..... p 3288 N94-29726 *
US-PATENT-5,280,722 ..... p 3315 N94-29548 *
US-PATENT-5,281,559 ..... p 3180 N94-29508 *
US-PATENT-5,284,290 ..... p 3301 N94-29557 *
US-PATENT-5,286,162 ..... p 3273 N94-29539 *
US-PATENT-5,287,747 ..... p 3288 N94-29538 *
US-PATENT-5,289,614 ..... p 3300 N94-29428 *
US-PATENT-5,290,121 ..... p 3300 N94-29427 *
US-PATENT-5,294,503 ..... p 3265 N94-29505 *
US-PATENT-5,294,873 ..... p 3436 N94-29504 *
US-PATENT-5,296,750 ..... p 3435 N94-29466 *
US-PATENT-5,297,384 ..... p 3274 N94-29740 *
US-PATENT-5,298,796 ..... p 3265 N94-29426 *
US-PATENT-5,299,285 ..... p 3436 N94-29756 *
US-PATENT-5,301,566 ..... p 3301 N94-29556 *
US-PATENT-5,302,465 ..... p 3205 N94-29507 *
US-PATENT-5,302,692 ..... p 3175 N94-29554 *
US-PATENT-5,302,805 ..... p 3300 N94-29506 *
US-PATENT-5,303,384 ..... p 3435 N94-29465 *
US-PATENT-5,304,538 ..... p 3513 N94-29501 *
US-PATENT-5,304,627 ..... p 3215 N94-29555 *

USAARL-94-4 ..... p 3388 N94-28757 #

USAFETAC/TC-94/001 ..... p 3368 N94-28638 #

USAFETAC/TN-94/0001 ..... p 3368 N94-28652 #

USIP-92-06 ..... p 3494 N94-30980

UWA/DME/TR-93-74 ..... p 3317 N94-28761 #

VKI-LS-1993-07 ..... p 3231 N94-29598 #

VPI-E-93-11 ..... p 3317 N94-28801 * #

VTT-EKA-B-9 ..... p 3494 N94-28623

VTT-PUBS-146 ..... p 3465 N94-30154 #
VTT-PUBS-147 ..... p 3245 N94-29468 #

VTT/PUB-133 ..... p 3399 N94-28406 #
VTT/PUB-137 ..... p 3186 N94-28407 #
VTT/PUB-138 ..... p 3379 N94-28408
VTT/PUB-139 ..... p 3406 N94-28401 #
VTT/PUB-140 ..... p 3316 N94-28402 #
VTT/PUB-143 ..... p 3407 N94-28403 #
VTT/PUB-144 ..... p 3316 N94-28409 #
VTT/PUB-145 ..... p 3229 N94-28410 #
VTT/PUB-148 ..... p 3261 N94-28400 #
VTT/PUB-151 ..... p 3537 N94-28405 #
VTT/PUB-152 ..... p 3316 N94-28404 #

VTT/RN-1455 ..... p 3341 N94-28412 #
VTT/RN-1458 ..... p 3160 N94-28413 #

VTT/TIED-1460 ..... p 3407 N94-28411 #

WES/TR-EL-94-1 ..... p 3286 N94-28831

WES/TR/EL-93-9-2 ..... p 3242 N94-28862 #

WHC-SA-2178 ..... p 3427 N94-30590

WIS-PH-93-46 ..... p 3525 N94-30121
WIS-PH-93-60 ..... p 3395 N94-30185 #
WIS-PH-93-73 ..... p 3199 N94-30111 #

WL-TP-93-005 ..... p 3263 N94-28994 #

WL-TR-93-1142 ..... p 3405 N94-28916
WL-TR-93-2025 ..... p 3263 N94-28913 #
WL-TR-93-2086 ..... p 3224 N94-28901
WL-TR-93-5031 ..... p 3262 N94-28767 #
WL-TR-94-2008 ..... p 3270 N94-28692 #
WL-TR-94-4002 ..... p 3409 N94-28920 #

WSRC-RP-93-269 ..... p 3373 N94-29817 #

XC-AFCESA/ESL ..... p 3157 N94-29151 #

APPENDIX

NASA SCIENTIFIC AND TECHNICAL INFORMATION PROGRAM PRODUCTS AND SERVICES

The NASA Scientific and Technical Information (STI) Program provides for the collection and announcement of aerospace-related reports and literature obtained worldwide through agreements and exchanges. The result of the collection is the comprehensive NASA STI Database that covers aeronautics, space, and supporting disciplines.

The STI Database, documents generated or obtained by NASA, and products and services derived from or supporting the database are made available to the NASA research community and to the public. Descriptions and sources of these items are presented in the following pages.

Scientific and Technical Aerospace Reports (STAR) is an abstract journal, listing citations with abstracts for aerospace-related reports obtained from worldwide sources. *STAR* is issued on the first of each month, and announces current documents that have been entered into the NASA STI Database during the previous month. The reports are of the following types:

- NASA, NASA contractor, and NASA grantee reports;
- Reports issued by other U.S. Government agencies, domestic and foreign institutions, universities, and private firms;
- Translations in report form;
- NASA-owned patents and patent applications
- Other U.S. Government agency and foreign patents and patent applications
- Domestic and foreign dissertations and theses.

Journal, book, and conference literature, journal translations, and certain foreign dissertations having the same subject scope as *STAR* are announced in a companion journal, *NASA Open Volumes on Aerospace (NOVA). NOVA* is issued on the 15th of each month and is available from the NASA Center for AeroSpace Information, at the address below.

ELIGIBILITY AND REGISTRATION FOR NASA STI PRODUCTS AND SERVICES

Organizations of the type listed below that have registered with NASA can receive products and services.

- NASA offices and installations, contractors, subcontractors, grantees, and consultants;
- Other U.S. Government agencies and their contractors;
- Libraries in the United States that have arrangements with NASA to maintain collections of NASA documents for public reference;
- Other organizations in the United States having a need for NASA documents in work related to aeronautics and space research;
- Organizations abroad that have established reciprocal documents exchange arrangements with NASA.

The central service points—central points of document acquisition and control within qualified organizations—or individuals are eligible to register for NASA STI products and services. Domestic organizations or individuals may be eligible to receive various classes of NASA publications and services and should address their requests for registration or further information to:

ATTN: Registration Services
NASA Center for AeroSpace Information
800 Elkridge Landing Road
Linthicum Heights, MD 21090-2934
301-621-0390

Organizations abroad should direct requests to:

National Aeronautics and Space Administration
Scientific and Technical Information Program (JTT)
International STI Program
Washington, DC 20546-0001
USA
703-271-5640

SUBJECT SCOPE

The subject scope of *STAR* and *NOVA* includes all aspects of aeronautics and space research and development, supporting basic and applied research, and applications. Aerospace aspects of Earth resources, energy development, conservation, oceanography, environmental protection, urban transportation, and other topics of high national priority are also covered.

HOW TO USE *STAR* SUBJECT CATEGORIES

Abstracts in *STAR* are categorized by 10 major subject divisions that are divided further into 76 specific subject categories. The subject divisions and categories are listed in the Table of Contents together with a note for each that defines its scope and provides any cross-references. For example:

16 SPACE TRANSPORTATION

Includes passenger and cargo space transportation, e.g., shuttle operations; and space rescue techniques. For related information see also *03 Air Transportation and Safety* and *18 Spacecraft Design, Testing and Performance.* For space suits see *54 Man/System Technology and Life Support.*

CROSS-REFERENCES

Individual *STAR* abstracts are not ordinarily cross-referenced, except for certain conference reports or book translations that have had separate abstracts written for their component papers or chapters. Citations and abstracts of the components follow immediately after those of the parent document. When the subject content of a component differs sufficiently from the general content of the parent, a cross-reference citation also is printed at the end of the category to which it normally would have been assigned if it were independent.

DOCUMENTS ON MICROFICHE

Documents available on microfiche are designated by a pound sign (#) following the accession number.

LIMITED REPRODUCIBILITY

A note of limited reproducibility appears in the citation, if there are factors affecting the reproducibility of more than 20% of the document. These factors include faint or broken type, color photographs, black and white photographs, foldouts, dot matrix print, or some other factor that limits the reproducibility of the document. This notation also appears on the microfiche header.

COLOR COPIES

An increasing number of NASA scientific and technical reports are being produced with color graphs, charts, illustrations, and photographs. An indication that a document has color pages follows the source and pricing (SAP) information in the *STAR* citation.

Registered users of the NASA Scientific and Technical Information Program will receive ordered documents with color at no additional cost, as long as stock copies of the document are available. Otherwise, an additional fee of $2.00 per color page will be charged. The NASA Center for AeroSpace Information staff will contact registered users to determine individual user's needs.

NASA PATENTS AND PATENT APPLICATIONS

Patents and patent applications owned by NASA are announced in *STAR* under appropriate subject categories and are referenced in the *STAR* indexes. In the Report Number Index, patents are indexed by the NASA Case Number, and the U.S. Patent Class. Patent applications are indexed by the NASA Case Number and the U.S. Patent Application Serial Number.

Printed copies of patents (which are not microfiched) are available for purchase from the U.S. Patent and Trademark Office.

When ordering patents, the U.S. Patent Number should be used, and payment must be remitted in advance, by money order or check payable to the Commissioner of Patents and Trademarks. Prepaid purchase coupons for ordering are also available from the U.S. Patent and Trademark Office.

NASA patent application specifications are sold in both paper copy and microfiche by the NASA Center for AeroSpace Information (CASI). The N accession number should be used in ordering either paper copy or microfiche from CASI.

The patents and patent applications announced in *STAR* are owned by NASA and are available for royalty-free licensing. Requests for licensing terms and further information should be addressed to:

National Aeronautics and Space Administration
Associate General Counsel for Intellectual Property
Code GP
Washington, DC 20546-0001

SOURCES FOR DOCUMENTS

One or more sources from which a document announced in *STAR* is available to the public is ordinarily given on the last line of the citation. The most commonly indicated sources and their acronyms or abbreviations are listed below, and their addresses are listed on page A-6. If the publication is available from a source other than those listed, the publisher and his address will be displayed on the availability line or in combination with the corporate source line.

Avail: CASI. Sold by the NASA Center for AeroSpace Information. Prices for hard copy (HC) and microfiche (MF) are indicated by a price code following the letters HC or MF in the *STAR* citation. Current values for the price codes are given in the tables on page A-7.

NOTE ON ORDERING DOCUMENTS: When ordering publications from CASI, use the N accession number or other report number. It is also advisable to cite the title and other bibliographic identification.

Avail: SOD (or GPO). Sold by the Superintendent of Documents, U.S. Government Printing Office, in hard copy.

Avail: BLL (formerly NLL): British Library Lending Division, Boston Spa, Wetherby, Yorkshire, England. Photocopies available from this organization at the price shown. (If none is given, inquiry should be addressed to the BLL.)

Avail: DOE Depository Libraries. Organizations in U.S. cities and abroad that maintain collections of Department of Energy reports, usually in microfiche form, are listed in *Energy Research Abstracts*. Services available from the DOE and its depositories are described in a booklet, *DOE Technical Information Center - Its Functions and Services* (TID-4660), which may be obtained without charge from the DOE Technical Information Center.

Avail: ESDU. Pricing information on specific data, computer programs, and details on Engineering Sciences Data Unit (ESDU) topic categories can be obtained from ESDU International Ltd. Requesters in North America should use the Virginia address while all other requesters should use the London address, both of which are on page A-6.

Avail: Fachinformationszentrum Karlsruhe. Gesellschaft für wissenschaftlich-technische Information mbH 76344 Eggenstein-Leopoldshafen, Germany.

Avail: HMSO. Publications of Her Majesty's Stationery Office are sold in the U.S. by Pendragon House, Inc. (PHI), Redwood City, CA. The U.S. price (including a service and mailing charge) is given, or a conversion table may be obtained from PHI.

Avail: Issuing Activity, or Corporate Author, or no indication of availability. Inquiries as to the availability of these documents should be addressed to the organization shown in the citation as the corporate author of the document.

Avail: NASA Public Document Rooms. Documents so indicated may be examined at or purchased from the National Aeronautics and Space Administration (JBD-4), Public Documents Room (Room 1H23), Washington, DC 20546-0001, or public document rooms located at NASA installations, and the NASA Pasadena Office at the Jet Propulsion Laboratory.

Avail: NTIS. Sold by the National Technical Information Service. Initially distributed microfiche under the NTIS SRIM (Selected Research in Microfiche) are available. For information concerning this service, consult the NTIS Subscription Section, Springfield, VA 22161.

Avail: Univ. Microfilms. Documents so indicated are dissertations selected from *Dissertation Abstracts* and are sold by University Microfilms as xerographic copy (HC) and microfilm. All requests should cite the author and the Order Number as they appear in the citation.

Avail: US Patent and Trademark Office. Sold by Commissioner of Patents and Trademarks, U.S. Patent and Trademark Office, at the standard price of $1.50 each, postage free. (See discussion of NASA patents and patent applications on page A-3.)

Avail: (US Sales Only). These foreign documents are available to users within the United States from the National Technical Information Service (NTIS). They are available to users outside the United States through the International Nuclear Information Service (INIS) representative in their country, or by applying directly to the issuing organization.

Avail: USGS. Originals of many reports from the U.S. Geological Survey, which may contain color illustrations, or otherwise may not have the quality of illustrations preserved in the microfiche or facsimile reproduction, may be examined by the public at the libraries of the USGS field offices whose addresses are listed on page A-6. The libraries may be queried concerning the availability of specific documents and the possible utilization of local copying services, such as color reproduction.

FEDERAL DEPOSITORY LIBRARY PROGRAM

In order to provide the general public with greater access to U.S. Government publications, Congress established the Federal Depository Library Program under the Government Printing Office (GPO), with 53 regional depositories responsible for permanent retention of material, inter-library loan, and reference services. At least one copy of nearly every NASA and NASA-sponsored publication, either in printed or microfiche format, is received and retained by the 53 regional depositories. A list of the regional GPO libraries, arranged alphabetically by state, appears on page A-8. These libraries are *not* sales outlets. A local library can contact a regional depository to help locate specific reports, or direct contact may be made by an individual.

PUBLIC COLLECTION OF NASA DOCUMENTS

An extensive collection of NASA and NASA-sponsored publications is maintained by the British Library Lending Division, Boston Spa, Wetherby, Yorkshire, England for public access. The British Library Lending Division also has available many of the non-NASA publications cited in *STAR*. European requesters may purchase facsimile copy or microfiche of NASA and NASA-sponsored documents, those identified by both the symbols # and * from ESA — Information Retrieval Service European Space Agency, 8-10 rue Mario-Nikis, 75738 CEDEX 15, France.

SUBMITTING DOCUMENTS

All users of this abstract service are urged to forward reports to be considered for announcement in *STAR*. This will aid NASA in its efforts to provide the fullest possible coverage of all scientific and technical publications that might support aeronautics and space research and development. If you have prepared relevant reports (other than those you will transmit to NASA, DOD, or DOE through the usual contract- or grant-reporting channels), please send them for consideration to the NASA Center for AeroSpace Information, 800 Elkridge Landing Road, Linthicum Heights, MD 21090-2934.

Reprints of journal articles, book chapters, and conference papers are also welcome. These will be considered for announcement in *STAR's* companion journal, *NOVA*.

You may specify a particular source to be included in a report announcement if you wish; otherwise the report will be placed on a public sale at the NASA Center for AeroSpace Information. Copyrighted publications will be announced but not distributed or sold.

PURCHASE OF *STAR*

STAR is publicly available on annual subscription from the NASA Center for AeroSpace Information (CASI) at $94.00/domestic, $117.00/foreign. Single copy prices: $33.00/domestic, $41.00/foreign.

An annual, cumulative *STAR Index* is also available at $54.00/domestic, $65.00/foreign.

STAR is available to registered users on annual subscription from the NASA Center for AeroSpace Information, ATTN: Registration Services, 800 Elkridge Landing Road, Linthicum Heights, MD 21090-2934.

ADDRESSES OF ORGANIZATIONS

British Library Lending Division
Boston Spa, Wetherby, Yorkshire
England

Commissioner of Patents and Trademarks
U.S. Patent and Trademark Office
Washington, DC 20231

Department of Energy
Technical Information Center
P.O. Box 62
Oak Ridge, TN 37830

European Space Agency-
Information Retrieval Service ESRIN
Via Galileo Galilei
00044 Frascati (Rome) Italy

Engineering Sciences Data Unit International
P.O. Box 1633
Manassas, VA 22110

Engineering Sciences Data Unit
International, Ltd.
251-259 Regent Street
London, W1R 7AD, England

Fachinformationszentrum Karlsruhe
Gesellschaft für wissenschaftlich-technische
Information mbH
76344 Eggenstein-Leopoldshafen, Germany

Her Majesty's Stationery Office
P.O. Box 569, S.E. 1
London, England

NASA Center for AeroSpace Information
800 Elkridge Landing Road
Linthicum Heights, MD 21090-2934

National Aeronautics and Space Administration
Scientific and Technical Information Program
(JTT)
Washington, DC 20546-0001

National Technical Information Service
5285 Port Royal Road
Springfield, VA 22161

Pendragon House, Inc.
899 Broadway Avenue
Redwood City, CA 94063

Superintendent of Documents
U.S. Government Printing Office
Washington, DC 20402

University Microfilms
A Xerox Company
300 North Zeeb Road
Ann Arbor, MI 48106

University Microfilms, Ltd.
Tylers Green
London, England

U.S. Geological Survey Library National Center
MS 950
12201 Sunrise Valley Drive
Reston, VA 22092

U.S. Geological Survey Library
2255 North Gemini Drive
Flagstaff, AZ 86001

U.S. Geological Survey
345 Middlefield Road
Menlo Park, CA 94025

U.S. Geological Survey Library
Box 25046
Denver Federal Center, MS914
Denver, CO 80225

CASI PRICE TABLES

(Effective August 1, 1993)

STANDARD PRICE DOCUMENTS

PRICE CODE	NORTH AMERICAN PRICE	FOREIGN PRICE
A01	$ 9.00	$ 18.00
A02	12.50	25.00
A03	17.50	35.00
A04-A05	19.50	39.00
A06-A09	27.00	54.00
A10-A13	36.50	73.00
A14-A17	44.50	89.00
A18-A21	52.00	104.00
A22-A25	61.00	122.00
A99	Call For Price	Call For Price

MICROFICHE

PRICE CODE	NORTH AMERICAN PRICE	FOREIGN PRICE
A01	$ 9.00	$ 18.00
A02	12.50	25.00
A03	17.50	35.00
A04	19.50	39.00
A06	27.00	54.00
A10	36.50	73.00

IMPORTANT NOTICE

CASI Shipping and Handling Charges
U.S.—ADD $3.00 per TOTAL ORDER
Canada and Mexico—ADD $3.50 per TOTAL ORDER
All Other Countries—ADD $7.50 per TOTAL ORDER
Does NOT apply to orders
requesting CASI RUSH HANDLING.
CASI accepts most credit/charge cards.

NASA Center for AeroSpace Information
800 Elkridge Landing Road
Linthicum Heights, MD 21090-2934
Telephone: (301) 621-0390
E-mail: help@sti.nasa.gov
Fax: (301) 621-0134

FEDERAL REGIONAL DEPOSITORY LIBRARIES

ALABAMA

AUBURN UNIV. AT MONTGOMERY LIBRARY
Documents Dept.
7300 University Dr.
Montgomery, AL 36117-3596
(205) 244-3650 Fax: (205) 244-0678

UNIV. OF ALABAMA
Amelia Gayle Gorgas Library
Govt. Documents
Box 870266
Tuscaloosa, AL 35487-0266
(205) 348-6046 Fax: (205) 348-8833

ARIZONA

DEPT. OF LIBRARY, ARCHIVES, AND PUBLIC RECORDS
Federal Documents
Third Floor State Capitol
1700 West Washington
Phoenix, AZ 85007
(602) 542-4121 Fax: (602) 542-4400, 542-4500

ARKANSAS

ARKANSAS STATE LIBRARY
State Library Services
One Capitol Mall
Little Rock, AR 72201
(501) 682-2869

CALIFORNIA

CALIFORNIA STATE LIBRARY
Govt. Publications Section
914 Capitol Mall - P.O. Box 942837
Sacramento, CA 94237-0001
(916) 322-4572 Fax: (916) 324-8120

COLORADO

UNIV. OF COLORADO - BOULDER
Norlin Library
Govt. Publications
Campus Box 184
Boulder, CO 83309-0184
(303) 492-8834 Fax: (303) 492-2185

DENVER PUBLIC LIBRARY
Govt. Publications Dept. BS/GPD
1357 Broadway
Denver, CO 80203
(303) 571-2135

CONNECTICUT

CONNECTICUT STATE LIBRARY
231 Capitol Avenue
Hartford, CT 06106
(203) 566-4971 Fax: (203) 566-3322

FLORIDA

UNIV. OF FLORIDA LIBRARIES
Documents Dept.
Library West
Gainesville, FL 32611-2048
(904) 392-0366 Fax: (904) 392-7251

GEORGIA

UNIV. OF GEORGIA LIBRARIES
Govt. Documents Dept.
Jackson Street
Athens, GA 30602
(404) 542-8949 Fax: (404) 542-6522

HAWAII

UNIV. OF HAWAII
Hamilton Library
Govt. Documents Collection
2550 The Mall
Honolulu, HI 96822
(808) 948-8230 Fax: (808) 956-5968

IDAHO

UNIV. OF IDAHO LIBRARY
Documents Section
Moscow, ID 83843
(208) 885-6344 Fax: (208) 885-6817

ILLINOIS

ILLINOIS STATE LIBRARY
Reference Dept.
300 South Second
Springfield, IL 62701-1796
(217) 782-7596 Fax: (217) 524-0041

INDIANA

INDIANA STATE LIBRARY
Serials/Documents Section
140 North Senate Avenue
Indianapolis, IN 46204
(317) 232-3678 Fax: (317) 232-3728

IOWA

UNIV. OF IOWA LIBRARIES
Govt. Publications Dept.
Washington & Madison Streets
Iowa City, IA 52242
(319) 335-5926 Fax: (319) 335-5830

KANSAS

UNIV. OF KANSAS
Govt. Documents & Map Library
6001 Malatt Hall
Lawrence, KS 66045-2800
(913) 864-4660 Fax: (913) 864-5380

KENTUCKY

UNIV. OF KENTUCKY LIBRARIES
Govt. Publications/Maps Dept.
Lexington, KY 40506-0039
(606) 257-3139 Fax: (606) 257-1563, 257-8379

LOUISIANA

LOUISIANA STATE UNIV.
Middleton Library
Govt. Documents Dept.
Baton Rouge, LA 70803
(504) 388-2570 Fax: (504) 388-6992

LOUISIANA TECHNICAL UNIV.
Prescott Memorial Library
Govt. Documents Dept.
305 Wisteria Street
Ruston, LA 71270-9985
(318) 257-4962 Fax: (318) 257-2447

MAINE

TRI-STATE DOCUMENTS DEPOS.
Raymond H. Fogler Library
Govt. Documents & Microforms Dept.
Univ. of Maine
Orono, ME 04469
(207) 581-1680

MARYLAND

UNIV. OF MARYLAND
Hornbake Library
Govt. Documents/Maps Unit
College Park, MD 20742
(301) 454-3034 Fax: (301) 454-4985

MASSACHUSETTS

BOSTON PUBLIC LIBRARY
Govt. Documents Dept.
666 Boylston Street
Boston, MA 02117
(617) 536-5400 ext. 226
Fax: (617) 267-8273, 267-8248

MICHIGAN

DETROIT PUBLIC LIBRARY
5201 Woodward Avenue
Detroit, MI 48202-4093
(313) 833-1440, 833-1409
Fax: (313) 833-5039

LIBRARY OF MICHIGAN
Govt. Documents Unit
P.O. Box 30007
Lansing, MI 48909
(517) 373-0640 Fax: (517) 373-3381

MINNESOTA

UNIV. OF MINNESOTA
Wilson Library
Govt. Publications Library
309 19th Avenue South
Minneapolis, MN 55455
(612) 624-5073 Fax: (612) 626-9353

MISSISSIPPI

UNIV. OF MISSISSIPPI
J.D. Williams Library
Federal Documents Dept.
106 Old Gym Bldg.
University, MS 38677
(601) 232-5857 Fax: (601) 232-5453

MISSOURI

UNIV. OF MISSOURI - COLUMBIA
Ellis Library
Govt. Documents
Columbia, MO 65201
(314) 882-6733 Fax: (314) 882-8044

MONTANA

UNIV. OF MONTANA
Maureen & Mike Mansfield Library
Documents Div.
Missoula, MT 59812-1195
(406)243-6700 Fax: (406) 243-2060

NEBRASKA

UNIV. OF NEBRASKA - LINCOLN
D.L. Love Memorial Library
Documents Dept.
Lincoln, NE 68588
(402) 472-2562

NEVADA

UNIV. OF NEVADA
Reno Library
Govt. Publications Dept.
Reno, NV 89557
(702) 784-6579 Fax: (702) 784-1751

NEW JERSEY

NEWARK PUBLIC LIBRARY
U.S. Documents Div.
5 Washington Street -
P.O. Box 630
Newark, NJ 07101-0630
(201) 733-7812 Fax: (201) 733-5648

NEW MEXICO

UNIV. OF NEW MEXICO
General Library
Govt. Publications Dept.
Albuquerque, NM 87131-1466
(505) 277-5441 Fax: (505) 277-6019

NEW MEXICO STATE LIBRARY
325 Don Gaspar Avenue
Santa Fe, NM 87503
(505) 827-3826 Fax: (505) 827-3820

NEW YORK

NEW YORK STATE LIBRARY
Documents/Gift & Exchange Section
Federal Depository Program
Cultural Education Center
Albany, NY 12230
(518) 474-5563 Fax: (518) 474-5786

NORTH CAROLINA

UNIV. OF NORTH CAROLINA - CHAPEL HILL
CB#3912, Davis Library
BA/SS Dept. - Documents
Chapel Hill, NC 27599
(919) 962-1151 Fax: (919) 962-0484

NORTH DAKOTA

NORTH DAKOTA STATE UNIV. LIB.
Documents Office
Fargo, ND 58105
(701) 237-8886 Fax: (701) 237-7138
In cooperation with Univ. of North Dakota, Chester Fritz Library
Grand Forks

OHIO

STATE LIBRARY OF OHIO
Documents Dept.
65 South Front Street
Columbus, OH 43266
(614) 644-7051 Fax: (614) 752-9178

OKLAHOMA

OKLAHOMA DEPT. OF LIBRARIES
U.S. Govt. Information Div.
200 NE 18th Street
Oklahoma City, OK 73105-3298
(405) 521-2502, ext. 252, 253
Fax: (405) 525-7804

OKLAHOMA STATE UNIV.
Edmon Low Library
Documents Dept.
Stillwater, OK 74078
(405) 744-6546 Fax: (405) 744-5183

OREGON

PORTLAND STATE UNIV.
Millar Library
934 SW Harrison - P.O. Box 1151
Portland, OR 97207
(503) 725-3673 Fax: (503) 725-4527

PENNSYLVANIA

STATE LIBRARY OF PENN.
Govt. Publications Section
Walnut St. & Commonwealth Ave. -
P.O. Box 1601
Harrisburg, PA 17105
(717) 787-3752

SOUTH CAROLINA

CLEMSON UNIV.
Cooper Library
Public Documents Unit
Clemson, SC 29634-3001
(803) 656-5174 Fax: (803) 656-3025
In cooperation with Univ. of South Carolina, Thomas Cooper Library, Columbia

TENNESSEE

MEMPHIS STATE UNIV. LIBRARIES
Govt. Documents
Memphis, TN 38152
(901) 678-2586 Fax: (901) 678-2511

TEXAS

TEXAS STATE LIBRARY
United States Documents
P.O. Box 12927 - 1201 Brazos
Austin, TX 78711
(512) 463-5455 Fax: (512) 463-5436

TEXAS TECH. UNIV. LIBRARY
Documents Dept.
Lubbock, TX 79409
(806) 742-2268 Fax: (806) 742-1920

UTAH

UTAH STATE UNIV.
Merrill Library & Learning Resources Center, UMC-3000
Documents Dept.
Logan, UT 84322-3000
(801) 750-2684 Fax: (801) 750-2677

VIRGINIA

UNIV. OF VIRGINIA
Alderrman Library
Govt. Documents
Charlottesville, VA 22903-2498
(804) 824-3133 Fax: (804) 924-4337

WASHINGTON

WASHINGTON STATE LIBRARY
Document Section
MS AJ-11
Olympia, WA 98504-0111
(206) 753-4027 Fax: (206) 753-3546

WEST VIRGINIA

WEST VIRGINIA UNIV. LIBRARY
Govt. Documents Section
P.O. Box 6069
Morgantown, WV 26506
(304) 293-3640

WISCONSIN

ST. HIST. SOC. OF WISCONSIN LIBRARY
Govt. Publications Section
816 State Street
Madison, WI 53706
(608) 262-2781 Fax: (608) 262-4711
In cooperation with Univ. of Wisconsin - Madison, Memorial Library

MILWAUKEE PUBLIC LIBRARY
Documents Div.
814 West Wisconsin Avenue
Milwaukee, WI 53233
(414) 278-2167 Fax: (414) 278-2137

•U.S. GOVERNMENT PRINTING OFFICE: 1994-301-249/00007

SCAN Goes Electronic!

If you have NASA Mail or if you can access the Internet you can get biweekly issues of *SCAN* delivered to your desktop — absolutely *free*!

Electronic SCAN takes advantage of computer technology to alert you to the latest aerospace-related, worldwide scientific and technical information that has been published.

No more waiting while the paper copy is printed and mailed to you. You can review *Electronic SCAN* the same day it is released! And you get all 191 — or any combination of — subject areas of announcements with abstracts to browse at your leisure. When you locate a publication of interest, you can print the announcement or electronically add it to your publication order list.

Start your free access to *Electronic SCAN* today. Over 1,000 announcements of new reports, books, conference proceedings, journal articles . . . and more — delivered to your computer every two weeks.

Electronic SCAN.
Timely.
Flexible.
Complete.
Free!

For instant access via Internet:
ftp.sti.nasa.gov
gopher.sti.nasa.gov
listserv@sti.nasa.gov

For additional information:
e-mail: help@sti.nasa.gov
scan@sti.nasa.gov
(Enter this address on the "To" line. Leave the subject line blank and send. You will receive an automatic reply with instructions in minutes.)
phone: 301-621-0390
fax: 301-621-0134
write: NASA Access Help Desk
NASA STI Program
NASA Center for AeroSpace Information
800 Elkridge Landing Road
Linthicum Heights, MD 21090-2934

NASA STI PROGRAM
SCIENTIFIC & TECHNICAL INFORMATION

SCAN *and* Electronic SCAN *are products of the NASA Scientific & Technical Information Program.*

9/93

POSTMASTER
Address Correction Requested
(Sections 137 and 159 Post Manual)

National Aeronautics and
Space Administration
Code JTT
Washington, DC 20546-0001

Official Business
Penalty for Private Use, $300

BULK RATE
POSTAGE & FEES PAID
NASA
PERMIT No. G-27

NASA

POSTMASTER: If Undeliverable (Section 158 Postal Manual) Do Not Return

Please circulate this publication to other colleagues within your organization.

NASA STI PROGRAM
SCIENTIFIC &
TECHNICAL
INFORMATION